The Big Book of Abstracts

vASB2020

Virtual 44th Meeting of the
American Society of Biomechanics

We would like to thank our sponsors:

!

TABLE OF CONTENTS

(Click on Session title to jump to that group of abstracts)

AB# 1st Author: Title

Wednesday, August 5, 2020: 11:00am-12:30pm
Podium Session 1 - Balance and Falls 1
Moderator: Dr. Peter Fino
150 Wei Liu: Biomechanical Mechanisms of Tai-Chi Gait for Preventing Falls 19
275 Kurt Beschorner: A hydrodynamics model to predict under-shoe fluid pressures based on the dimensions of a worn region 20
673 Corbin Rasmussen: Slipping Foot and Recovery Step Yaw After a Turning Slip: A Balance Recovery Mechanism? 21
672 Kyra Twohy: Impact of an Ankle-Foot Orthosis on Reactive Stepping in Young Adults 22
187 Chuyi Cui: Sensitivity of Toe Height to Joint Angles of the Bipedal Linked Chain during Obstacle Crossing 23
536 Noah Rosenblatt: The impact of obesity on trunk control following trip-like treadmill perturbations while standing 24
397 Kari Loverro: Females have greater local dynamic stability than males when walking with military-relevant loads. 25
667 Chang Liu: Does the Reference Axis for Computing Angular Momentum Affect Inferences about Dynamic Balance? 26
278 Gabriella Small: The Influence of Cognitive Load on Dynamic Balance During Steady State Walking 27
50 Daniel Liss: Young Adults Can Perceive Very Small Locomotor Disturbances Even When Distracted 28
365 Brian Selgrade: Susceptibility to Optical Flow Balance Perturbations in Older Adults Prevails Despite Cognitive Distraction 29
441 Chase Rock: Neuromuscular Adaptation after Exposure to Simulated Hypogravity 30

Podium Session 2 - Sport/Performance 1
Moderator: Dr. Wouter Hoogkamer
588 Sarah Wilson: Application of Inertial Measurement Units and Statistical Parametric Mapping for Assessing Alpine Skiing 31
192 Meredith Wells: A Biomechanical Analysis of the Triple Step in Recreational Swing Dancers 32
805 Joseph Passafiume: Real-Time Visual Feedback on Breathing during Treadmill Running to Exhaustion 33
847 Justin Angelo Ortega: Metabolic Power During Running In Vaporfly Shoes With Intact vs. Cut Carbon-Fiber Plates 34
169 Eric Honert: Foot and ankle kinetics and their interplay during a long duration run 35
266 Torstein Dahlin: Examining the Role of the Toe Flexors in Opposing Foot Arch Deformation 36
586 Matthew Pain: Energy dissipation due to soft tissue movement of the thigh during forefoot and rearfoot impacts at different running velocities 37
414 Micah Garcia: Running Symmetry is not different in Youth Runners with Low, Moderate and High Muscular Symmetry 38
472 Kara Ashcraft: Characterizing Strut Stiffness in Running-Specific Ankle-Foot Orthoses 39
329 Ryan Alcantara: Curve Sprinting With A Split-Toe Running Specific Prosthesis: A Pilot Study, University of Colorado Boulder 40
276 Hiroto Murata: External mechanical work during running after unilateral transfemoral amputation 41
375 Janet Zhang: Effects of a Paralympian With Transfemoral Amputation Using a Prosthesis With & Without a Knee 42

Podium Session 3 - Locomotion
Moderator: Dr. Jessica Allen
616 Matthew Salzano: Moment Arm Plasticity in Response to Loading History during Growth 43
705 Jeffery Olberding: Reconstructing contractile dynamics from muscle length change 44
859 Emily Abbott: Mechanosensation by muscle spindles during active muscle-tendon work loops 45
627 Samuel Kwak: Muscle Fascicle Dynamics During Collisional Phase of Walking and the Relation to Push-off Phase 46
353 Bryan Schlink: High-Density EMG Reveals Lower Limb Spatial Activity during Walking and Running 47
374 M. Janneke Schwaner: In vivo hind limb muscle function during walking on hard and soft substrates in rats (Rattus norvegicus) 48
95 Daniel Kuhman: The effects of advanced age and walking speed on mechanical functions of the ankle plantarflexors 49
708 Jonaz Moreno Jaramillo: Are Muscles Tuned to the Preferred Stride Frequency of Walking? 50
484 Alex Denton: Effects of Varying Tendon Stiffness on the Metabolic Cost of Walking 51
66 Noah Pieper: The Metabolic and Mechanical Consequences of Altered Propulsive Force Generation During Walking 52
609 Talayah Johnson: Develpmental Plasticity of Locomotor Economy in an Avian Bipedal Model 53
194 Daisey Vega: Reducing the Metabolic Cost of Walking by Using the Arms to Drive the Legs 54

Thursday, August 6, 2020: 11:00am-12:30pm
Podium Session 4 - Balance and Falls 2 Neurologic
Moderator: Manuel Hernandez
71 James Tracy: Stroke Survivors Exhibit Little Total Arm Contribution to Standing, Posterior Balance Reactions 55
126 Daniel Kuhman: The effects of advanced age and walking speed on mechanical functions of the ankle plantarflexors 56
220 Leila Alizadehsaravi: Are Improvements of Balance Performance after Short- and Long-term Balance Training in Older Adults associated with changes in H-Reflex Excitability and Muscle Co-Contraction 57

801 Seung Yun Song: Preliminary Study of Spasticity Using the Portable Position, Velocity, and Resistance Meter 58
613 Yang Hu: The Effect of Pain on the Cognitive Control of Balance During the Motor Control Test in Older Women with Osteoarthritis. 59
190 Aiden Payne: People With Worse Balance Have Larger Perturbation-Evoked Cortical Responses 60
495 Gu Eon Kang: Effects of Fear of Falling on Gait and Balance in Chemotherapy-Induced Peripheral Neuropathy 61
341 Brett Meyer: Deep Learning to Classify Fall Risk from Wearable Accelerometer Data During Standing in Persons with Multiple Sclerosis 62
133 Hannah Frame: The Influence of Mediolateral Stabilization on Balance Control during Walking in Individuals Post-stroke 63
700 Carolin Curtze: Dynamics of Turning in People with Parkinson's Disease 64
644 Luis Nolasco: Dynamic Balance During 90-degree Turns in People with a Unilateral Transtibial Amputation 65
750 Peter Fino: Centripetal Acceleration During Turning and its Relationship with Autonomic Function in Mild Traumatic Brain Injury 66

Podium Session 5 -- Computational Modeling
Moderator: Dr. Brooke Odle
641 Amy Lenz: Talocrural Morphology: A Statistical Shape Modeling Multi-Articulation Joint Approach 67
295 Yu Zhou: Pose-matching MRI-CT co-registration via dynamic X-ray for creating subject-specific neck musculoskeletal models 68
212 Megan Mancuso: Bone Strain Distribution, Not Magnitude, is Affected by Execution of a Forearm Loading Task 69
720 Geng Li: Effect of Pelvis Geometry Personalization on Hip Kinematics and Dynamics 70
42 Reed Gurchiek: Estimating Unmeasured Muscle Excitations: NNMF vs Gaussian Process-Based Synergy Models 71
114 Kiisa Nishikawa: Isometric force-length and isotonic force-velocity properties and Hill-type models contain little information needed to predict in vivo muscle forces. 72
727 Benjamin Binder-Markey: Whole Muscle Passive Mechanics Do Not Simply Scale by Architectural Properties 73
434 William Clark: Imaging and Simulation of Inter-Muscular Triceps Surae Contributions to Forward Propulsion During Walking 74
653 William Ferriell: Parametric Analysis and Validation of 3D American Football Faceguard Structural Stiffness Models 75
638 Thanh Tran: Simulation of Speech Muscle Biomechanics to Explains Differences in Corrective Surgery Outcomes 76
690 Julia K. Butterfield: A Split-Belt Rimless Wheel Can Passively Walk Steadily on a Split-Belt Treadmill 77
782 Mingxiao Liu: An Instrumented Glove to Induce Agency-based Performance of Secure Grasp 78

Podium Session 6 -- Prosthetics/Orthotics/Robotics
Moderator: Dr. Karl Zelik
388 Adam Yoder: Trunk Control during Walking with Below-Knee Amputation: Effects of Prosthetic Ankle-Foot Actuation 79
183 Genki Hisano: Whole-body angular momentum during walking in persons with unilateral transfemoral amputation 80
433 Alexandra Voloshina: Effects of exoskeleton assistance in individuals with unilateral transtibial amputation 81
737 Jay Kim: The Effects of Powered Ankles on Gait Initiation and Termination in Daily Life 82
469 Kara Ashcraft: Characterizing Strut Stiffness in Running-Specific Ankle-Foot Orthoses 83
819 Gwendolyn Bryan: Optimized hip-knee-ankle exoskeleton assistance at different speeds 84
410 Inseung Kang: A biomechanical analysis of adaptive assistance strategy for uphill walking using a powered hip exoskeleton 85
475 Patrick Franks: Hip, Knee, Ankle and Multi-Joint Exoskeleton Assistance Can Reduce Metabolic Cost 86
249 Sarah Bass: Biomechanics of individuals with and without lower limb amputation during dual-task walking 87
287 Katherine Poggensee: How Training, Adaptation, and Customization Contribute to Exoskeleton Assistance 88
772 Dylan Schmitz: Achilles Shear-Wave Tensiometry During Walking With a Passive Exoskeleton: A Proof-of-Concept 89
793 John Chomack: Effects of Prosthetic Socket Design on Residual Limb Motion Using Dynamic Stereo X-Ray 90

Awards Session
Young Scientist Pre-doctoral Award: 11:00am -11:15am
391 Joshua Leonardis: Neuromuscular Compensation Strategies Adopted at the Shoulder Following Bilateral Subpectoral Implant Breast Reconstruction 91
Young Scientist Post-doctoral Award: 11:15am-11:30 am
Eni Halilaj: An open-source dataset for modeling human pose priors 92
CLINICAL BIOMECHANICS AWARD 11:30am-12:00pm
322 Mark Geil: Are Gait Kinematics Different in Young Children Who Receive Working Prosthetic Knees? 93
789 Nicholas Kreter:Preparations for Expected Underfoot Perturbations in Healthy and Concussed Individuals 94
JOURNAL OF BIOMECHANICS AWARD 12:30pm-1:00pm
423 Thomas Sandercock: Stress Provides a Lower-Bound Estimate of Shear Wave Velocity in Skeletal Muscle 95
842 Katherine Knaus: 3D Model of the Soleus Reveals Complex Muscle Fascicle and Aponeuroses Deformations during Passive Stretch 96

Thursday, August 6, 2020: 1:00am-2:30pm
Podium Session 7 - Orthopaedics 1

Moderator: Dr. Jared Kaiser
702 Benjamin Binder-Markey: Whole Muscle Passive Mechanics Do Not Simply Scale by Architectural Properties 97
502 Lomas Persad: In vivo measurement of gracilis muscle-tendon characteristics 98
678 Kristen Jakubowski: Muscle stiffness exceeds tendon stiffness at physiologically relevant levels of muscle activation 99
499 Joshua Pataky: The Effect of Rotator Cuff Tear Severity on Joint Loading During Dynamic Tasks 100
456 Sabreen Megherhi: The Effects of Osteoarthritis and Unicompartmental Knee Arthroplasty on Hip, Knee, and Ankle Joint Kinematics 101
462 Rebekah Koehn: Modular Control and Patient Function in Individuals with Knee Osteoarthritis and Total Knee Arthroplasty 102
470 Ahmad Raeisi Najafi: Effects of age-related changes on fracture resistance of human cortical bone 103
262 Meir M. Barak: Trabecular bone stiffness and yield are not declined after exposure to Staphylococcus aureus 104
487 Sevda Gharehbaghi: Joint Acoustic Emissions as a Biomarker for Knee Health Assessment in Loaded and Unloaded Exercises 105
573 Hope Davis-Wilson: Association Between Daily Steps, Moderate-Vigorous Physical Activity, and Femoral Articular Cartilage Composition in Individuals with Anterior Cruciate Ligament Reconstruction 106
10 Nathan Schilaty: Linear Discriminant Analysis Predicts Knee Injury Outcome from Biomechanical Variables 107
449 Melissa Boswell: Mindsets are related to reductions in pain after a gait modification intervention for people with osteoarthritis, Stanford University 108

Podium Session 8 - Locomotion

Moderator: Dr. James Finley
553 Emily McCain: Isolating the Energetic Consequences of Mechanically Imposed Reductions in Ankle and Knee Flexion during Gait 109
500 Nicole Rendos: Real-Time Gait Biofeedback Enhances Dynamic Ankle Stiffness and Propulsion in Healthy and Post-Stroke Participants 110
106 Natalia Sanchez: Using visual guidance to acquire work from the treadmill during split-belt walking does not accelerate adaptation 111
69 Jan Stenum: Step time asymmetry optimizes energy cost of split-belt treadmill walking 112
551 Rebecca Krupenevich: The Effects of Age and Locomotor Demand on Foot Mechanics During Walking 113
562 Anahid Ebrahimi: On the Use of Shear Wave Speed to Assess Tendon Loading in Children with Cerebral Palsy 114
483 Skyler Levine: Effects of Ankle Weights During Overground Walking Using a Bodyweight Support System 115
601 Christopher Hurt: Split-belt walking against resistance increases walking propulsion asymmetrically 116
149 Scott Uhlrich: Muscle coordination retraining reduces knee contact force during gait 117
131 E. Dan Syrett: Peak Knee Joint Forces During Asymmetric Split-Belt Treadmill Walking: A Preliminary Study 118
833 Paul DeVita: Surface stiffness affects knee joint kinetics during decline but not level running 119
850 Keaton Scherpereel: Estimating Knee Joint Load with Joint Acoustic Emissions During Walking 120

Podium session 9- Injury and Injury Prevention

Moderator: Dr. Zachary Domire
173 Zachary Merrill: Predictive Modeling of Serious Injury Risk in Frontal Crashes 121
747 Mohammad Homayounpour: Force and Linear Acceleration Differences after Head Impacts with Clenched and Relaxed Neck Muscles 122
390 Joshua Leonardis: Choosing Mastectomy and Breast Reconstruction or Breast Conserving Therapy: Implications for Pectoralis Major Function 123
398 Whitney Wolff: Quantifying Sternocleidomastoid Material Properties after Definitive Chemoradiation for Head and Neck Cancer 124
238 Emily Matijevich: Estimating Lumbar Loading with Wearable Sensors over a Broad Range of Manual Lifting Tasks 125
530 Jacob Banks: Lower Back Demands During Induced Lower Limb Gait Asymmetries 126
152 Blake Johnson: Material Properties of Human Testicles under Unconfined Compression and Probing with Varying Strain Rate 127
405 Jonathan (FJ) Goodwin: Vertical Stiffness Asymmetry in NCAA Division I Athletes 128
491 Dhruv Gupta: Optimizing whole-body kinematics using OpenSim Moco to reduce peak non-sagittal plane knee loads and ACL injury risk during single leg jump landing 129
529 Brian Diefenbach: Development of an In-Vivo Ligament Loading Device 130
440 Kavya Katugam: Achilles Tendon Material Properties are Resilient to Variations in Load During Growth 131
540 Matthew Ruder: Running Exposure is Associated with Achilles Tendon Shear Wave Speed 132

Friday, August 7, 2020: 1:00am-2:30pm

Podium Session 10 - Orthopaedics

Moderator: Dr. Jessica Goetz
420 Elizabeth Bjornsen: Increased Cervical Spine Musculotendon Strain with Enlarged External Occipital Protuberances 133
356 Julian Acasio: Trunk-Pelvic Coordination during Unstable Sitting at Varying Task Demand 134
431 Tara Diesbourg: The Impact of Sitting on Active Trunk Stiffness and the Mitigating Effect of Age 135

138 Alexa Johnson: Connecting the Pieces: How Low Back Pain Alters Lower Exremity Mechanics in Active Individuals 136
599 Donald Prible: Thoracolumbar and Pelvis Kinematics are Associated with Paretic Force Production 137
686 Emily Levy: Kinetic and Kinematic Comparison of Multiple Hip Pathologies during Sloped and Level Walking 138
195 Ke Song: Periacetabular Osteotomy for Hip Dysplasia Alters Dynamic Flexor and Abductor Muscle Moment Arms and Lines of Action 139
685 Michael Samaan: Hip Joint Muscle and Contact Forces During Sit-to-Stand and Stand-to-Sit Tasks in Patients with Femoroacetabular Impingement Syndrome 140
493 Cara Lewis: Bone-to-bone Distance Changes Are Larger in Patients with Cam Femoroacetabular Impingement Syndrome 141
656 Amber Vocelle: The effect of osteoarthritis on three-dimensional thumb motions and force production 142
107 Bardiya Akhbari: Contact Pattern of Total Wrist Arthroplasty Changes with the Direction of Motion: In-Vivo Study 143
447 Mark Carl Miller: Crista Volume Shows a Relationship to Sesamoid Station 144
72 Junjun Zhu: Development of Injury Risk Functions for Lisfranc Injury 145

Podium Session 11 -- Prosthetics/Orthotics/Robotics

Moderator: Dr. Elisa Arch

51 Ying Fang: Step Length Biofeedback with Exoskeleton Assistance Can Improve Walking Function and Gait Mechanics in Cerebral Palsy 146
377 Dean Molinaro: Estimating Biological Hip Torque During Overground Ambulation: A Machine Learning Approach 147
577 Dawit Lee: Reducing Human Energetics Using a Bilateral Knee Exoskeleton 148
844 Sabrina Abram: People explore gait dimensions, and reduce this exploration, as they learn to walk with exoskeleton assistance.
795 Yi-Tesn Pan: The Biomechanical Effect of Bilateral Assistance for Hemiparetic Gait Poststroke Using a Powered Hip Exoskeleton 149 150
577 Corey Koller: A Case Series Examining the Effects of Wearing a Quantitatively-Prescribed Passive-Dynamic Ankle-Foot Orthosis Compared to Standard-of-Care Ankle-Foot Orthosis 151
151 Tatiana Djafar: Longitudinal Assessment of Gait Quality for Servicemembers with Transtibial Amputation: A Case Series 152
704 Jay Kim: The Effects of Powered Ankles on Gait Initiation and Termination in Daily Life 153
74 Tom Gale: Motion of the Residual Femur Within the Socket During Gait is Associated with Patient-Reported Problems in Transfemoral Amputees 154
488 Christina Lee: The Performance of Implantable Electrodes on the Control of a Myoelectric Prosthesis Over One Year Post-Implantation 155
526 Alexander Klishko: Stimulation of residual sensory nerve modulates walking mechanics in the cat with bone-anchored transtibial prosthesis 156
596 Sarah Hood: Open Dataset of 18 Above-Knee Amputees Walking at 5 Different Speeds with their Prescribed Prostheses 157

Podium Session 12 - Sport/Performance

Moderator: Dr. Kristin Morgan

19 Glenn Fleisig: Should Baseball Adjust the Mound Height and Pitching Distance? 158
282 Kate Harrison: Influence of Alternative Shoe Fit Configuration on Athlete Biomechanics 159
764 Alex Lurski: Performance Evaluation of Rate Activated Tether (RAT) Football Helmet 160
867 Chenxi Yan: Tibial Bone Strains in Basketball Players during Dynamic Tasks 161
754 Cherice Hughes-Oliver: Racial Differences in Running and Landing Measures Associated with Injury Risk Vary by Gender 162
429 Joshua Weinhandl: Anticipation and an External Target Alter Knee Biomechanics in Volleyball-Specific Task 163
544 Lauren Biscardi: Running to Fractal-Like Stimulus Preserves the Complexity of Stride-To-Stride Fluctuations 164
361 Namwoong Kim: Muscle Contributions to Knee Joint Reaction Forces and Moments during Single-Leg Landing 165
255 Anna Ursiny: Does Sex Influence Interpretations of Control Complexity via Muscle Synergy Analysis? 166
380 Mitchell St. Pierre: Effect of Transcutaneous Vagus Nerve Stimulation on Visuomotor Skill Learning in Humans 167
401 Aakash Bajpai: Human Reaction and Movement Enhancement via Audial, Tactile, and Visual Perceptual Cues 168
432 Anvesh S. Naik: Should I stay or should I go? Stability of digit forces is lowered to enhance maneuverability when expecting to move a pinched object 169

Posters:

Wednesday, August 5

Animal, Comparative, and Evolutionary Biomechanics

333 Patrick Hall: Rabbit Hindlimb Ankle Kinematics During Stance Phase of Hopping Gait 170
345 Robert Catena: Gestational Lumbopelvic Postural Changes and Joint Loads in Standing and Walking 171
395 Siwoo Jeong: The effect of active shortening velocity on the ratio of muscle stiffness to muscle force 172
436 Emma Gilmore: Shape Characterization of Bighorn Sheep Horns for Bending and Impact Implications 173
457 Brian Hamilton: Perturbations to the classic force-length relationship of skeletal muscle 174
463 Brooke Christensen: Impact of Surface Grade on Hindlimb Muscle Function in Desert Kangaroo Rats (Dipodomys deserti) 175
549 Jarrod Petersen: Dynamic changes in force modulate pennate muscle architecture 176
676 Alex Duman: Landing on Compliant Surfaces: Lessons from an animal model of landing control 177

742 Yonghee Lee: EXPLORING HOW FUNCTIONAL IMPROVEMENT IS RELATED TO INTERACTION BETWEEN CHILDREN WITH CEREBRAL PALSY AND HORSES DURING EQUINE-ASSISTED THERAPY: A PILOT STUDY 178
781 Adrien Arias: Limb joint mechanics during quadrupedal walking in alligators 179
808 Nathan Kirkpatrick: DeepLabCut Increases Markerless Tracking Efficiency in Bi-Planar X-Ray Video Analysis of Rat Kinematics 180

Balance and Falls - General

8 MU QIAO: How do Leg Joint Stiffness Affect Dynamics of Backward Falling: A Simulation Work 181
27 Mituniewicz Austin: Evaluation of an app for vestibular rehabilitation of older adults with motion controlled games and remote monitoring 182
34 Gordon Alderink: Analysis of Coherence between Electromyographic (EMG) signals of Tibialis Anterior, Soleus and Gastrocnemius during Standing Balance Tasks: A Pilot Study 183
59 Mengnan Wu: Human-human hand interactions assist beam-walking balance by haptic communication, not mechanical support 184
73 Caroline Simpkins: Dance Interventions Improving Balance in People with Parkinson's Disease: A Meta-Analysis 185
86 Gordon Alderink: Margin of Stability during Tandem Stance with Dominant Limb Placed Back or Forward: A Pilot Study 186
97 Jocelyn F Hafer: Coordination Responses to a Change in Walking Speed Do Not Differ with Age or Knee Osteoarthritis 187
209 Jiyun Ahn: Effects of Sole Thickness on Recovery from an Unexpected Slip during Standing 188
216 Kitaek Lim: Muscle activation pattern during a fall from standing height 189
239 Farahnaz Fallahtafti: Speed of Walking, as well as Walking Mode (Treadmill vs. Overground), can affect Margin of Stability 190
245 Bummo Koo: Ranking Algorithm for ANN-Based Post-Fall Detection 191
256 Lydia Brough: Biomechanical Response to Altered Foot Placement During Walking 192
294 Heather Vanderhoof: Advancing Stages of Pregnancy on Postural Sway Range in Healthy Females 193
348 Tyler Wood: The Potential Implications of Co-Contraction Index of Neck Muscles on Traumatic Brain Injuries 194
378 Michael Christensen: The Effect of a Reduced Marker Set on the Margin of Stability During Gait 195
379 Jiyeon Kim: Association between Activities-specific Balance Confidence, Dynamic Gait Index, and Physical Activity in People with Parkinson's Disease 196
482 Bianca Tovar: The Effect of Advancing Pregnancy on Postural Sway Velocity in Bilateral and Unilateral Standing 197
519 Erika Pliner: Behavioral risk predicts maximum lateral reach during a roof gutter clearing task 198
524 Bailey Petersen: Characterization of Posturography and Sensory Loss in Lower-limb Amputees. 199
563 Dorien Butter: Influence of Object Characteristics on Patient Safety and Stability During Ambulation 200
570 Claire Zai: Evaluation of the Four Square Step Test as an outcome measure in a novel clinical fall prevention program 201
604 Tom Van Wouwe: Causes of increased step incidence in response to perturbations in older adults 202
629 Claire Martin: Locomotor Response of Older Persons with and without Transtibial Amputation to a Trip Disturbance 203
631 Nicole Stoehr: Balance Control and Muscle Asymmetry in Persons with Lower-limb Amputation During Yoga Poses 204
651 Luis Nolasco: Segment Angular Momenta in People with a Unilateral Transtibial Amputation During 90-degree Turns 205
697 Sydni Wilhoite: Relationship between Postural Control and Lower Body Physical Function in Children with Cerebral Palsy 206
724 Michael Jayson: Foot Structure and Postural Stability in Healthy Young Individuals 207
726 Sam Wilson: The Effects of Golf Specific Footwear on Postural Perturbations 208
730 Sara Elnahhas: Preliminary Investigation of Limb Load Symmetry During Quiet Stance & Sit-to-Stand 209
746 Meghan Kazanski: Physical and Perceived Abilities and Motor Planning of Older Adults During A Virtual Beam-Walking Task 210
753 Riley Sheehan: Step Width Variables are not Meaningfully Correlated with Stumble or Fall Incidence in a High Functioning Population with Lower Limb Trauma 211
759 Mitchell Tillman: Early Testing of a Real-Time Balance Sonification System In Single Leg Stance 212
779 Kreg Gruben: A novel measure of standing balance coordination demonstrates greater consistency than traditional measures 213
794 Jennifer Leestma: Spatiotemporal recovery responses used to combat translational platform perturbations during walking 214
814 ABDERRAHMAN OUATTAS: Implimenting A Double-Limb Slip Training Protocol To Reduce Falls And Improve Slip Recovery: A Pilot Study 215
816 Lisa Zukowski: Acute Effects of Virtual Reality Treadmill Training on Gait and Cognition in Older Adults 216
822 Riley Horn: Identification of specific somatosensation and location to predict postural control outcomes 217
851 Meghan Kazanski: Mediolateral Margins of Stability of Older Adults During A Virtual Beam-Walking Task 218
860 Mei Huang: Effect of a multicomponent home-based training on gait performance in older adults with hip fracture: a randomized control trial 219

Ergonomics and Occupational Biomechanics

57 John Wu: Improvement of Shock Absorption Performance of Construction Helmet using Air-bubble Cushioning- A Preliminary Study 220
58 Emily Miller: Assessment of Surgeon Muscle Fatigue during Microsurgery using a Rat Model 221
68 Joseph Langenderfer: Non-linear analysis of effects of inertial properties on hammer movement variability 222
93 Erika Nelson-Wong: Office Workers Maintain Decreased Sitting Time Long Term When Provided Sit-Stand Workstations 223
98 Stacy Loushin: Surgeon Hand Tremor during Microsurgery using a Rat Model 224

193 Jazmin Cruz: Verifying Joint Space-Based Metabolic Energy Expenditure Models 225
251 John Wu: The Effects of Posterior Shank/Thigh Contact on the Knee Joint Loading during Deep Squatting 226
260 Liying Zheng: Evaluation of a Powered Lumbar-Support Exoskeleton during a Pace-Controlled Lifting Task: A Pilot Study 227
394 Archana Lamsal: Comparison of a Mid-Seated Posture with Seated and Standing Postures 228
415 Matthew Hanks: Glenohumeral Joint Motion Variability during Wheelchair Propulsion in Children and Adults with Spinal Cord Injury 229
416 Caleb Burruss: Neck Kinematic Differences Between Six Computer Monitor Configurations 230
427 Tara Diesbourg: If Sitting Does Not Cause Low Back Pain in Healthy Working Adults, What Does? 231
480 Mustafa Yerebakan: EMG Based Biomechanical Analysis of the Effect Different Writing Surfaces and Postures Have on Forearm Muscles 232
481 Jason Gillette: Exoskeleton Usage, Arm Posture, and Tool Weight Changes Shoulder Fatigue Risk 233
503 Onebin Lim: Effects of a Footrest on the Lumbo-Pelvic-Hip Kinematics and Kinetics, and Low Back Pain during Prolonged Standing Work 234
659 Garrett Weidig: An Engineering and Ergonomic Analysis of Shoulder Posture in a Seated Position Through the Use of an Avatar 235

Locomotion - Running

94 Li Jin: Relationship between Joint Stiffness and Limb Stiffness in Running Across Speeds 236
176 Yo Shih: Lower Extremity Support Moment and Distribution of Joint Moments during Sloped Running 237
285 Kathryn Harrison: Training effects on frontal plane kinematics and coordination in novice runners 238
386 Caelyn Hirschman: How Do Net Mechanical Joint Work and Stiffness Change on Slopes During Running 239
448 Mikaela Smith: Beat the Streets: Music-based Stride Length Intervention to Decrease Injury Risk in Runners 240
461 AmirAli Jafarnezhadgero: Long term training on sand changes foot posture and running kinetics in active individuals with over-pronated feet 241
494 Kim Hébert-Losier: Running in the Nike Vaporfly, Saucony Racing Flats, and Own Shoes: Who Wins the Race? 242
511 Heather Hamilton: Coordination Variability in Injured and Uninjured Runners: A Systematic Review 243
513 Victoria Bode: Can Running Shoes be Used for All Activities During Basic Training? 244
518 Jessica Hunter: Novice runners maintain cumulative loads during steady-state running 245
552 Matthew Seeley: EFFECTS OF EXPERIMENTAL ANTERIOR KNEE PAIN ON RUNNING NEUROMECHANICS: A PILOT STUDY 246
592 Allison Hoffee: Relationship Between the Single-Leg Step-Down and Lower Extremity Loading in Adolescent Runners 247
716 Drew Rutherford: Effect of Increasing Running Cadence on Impact Force in an Outdoor Environment 248
717 Laura Healey: Biomechanics during running in Vaporfly shoes with intact vs. cut carbon-fiber plates 249
751 JJ Hannigan: The Effect of Carbon-Fiber Plate Racing Shoes on Running Biomechanics 250
785 Daniel Davis: Application of automatic segment filtering procedure to the kinematics of running 251
826 Bryan Conrad: Visualizing Variation in Vertical Ground Reaction Forces During Running 252
828 Justin Wager: Maximum voluntary ankle plantarflexion moments are unaffected by extension of the metatarsophalangeal joints 253

Neurorehabilitation - Stroke, TBI

142 Lindsey Lewallen: Assessment of Turning Performance and Coordination in Individuals Post-Stroke 254
186 Hogene Kim: 3D Scanned Foot Image: A Potential Biomarker of Spastistic Foot Deformity in Chronic Stroke 255
299 Mara Thompson: Narrow walking alters qualitative measures of COM movement in TBI vs. Control subjects 256
366 Shraddha Srivastava: Relationship Between Walking Coordination and Motor Pathways Recovery Following Stroke 257
409 Nicole Rendos: Verbal Instructions and Feedback Enhance Motor Learning During Post-Stroke Gait Retraining 258
531 Ashley Rice: Combination of Ankle Muscle Functional Electrical Stimulation (FES) & Fast Treadmill Walking Therapy Effect on Post-Stroke Motor Control 259
556 Peter Fino: Turning Speed and Performance During a Simulated Urban Patrol Task in People with Mild Traumatic Brain Injury 260
600 Hannah Christianson: Is Faster Always Better? A Subgroup Analysis of the Effects of Walking Speed on Post-Stroke Gait Biomechanics 261
626 Russell Johnson: Simulation-based Predictions of Gait Patterns with Muscle Strength Asymmetries 262
635 Keng-Hung Shen: Neuromechanical Control of Ankle Joint during Forced Lower Limb Loading in Individuals with Chronic Stroke 263
671 Erica Hedrick: Functional Level Alters the Impact of Assistive Device Use on Propulsive Impulse Post-Stroke 264
709 Zhenxuan Zhang: Arm reaching controlled by a tongue-operated exoskeleton system: Implications for stroke rehabilitation 265
776 Kyung Koh: Abnormal coordinataion of the multiple upper-limb joints during passive movement 266

Sport and Performance - Pitching and Swinging

11 Kyle Wasserberger: Humeral Energy Transfer and Glenohumeral Rotation Strength in Adolescent Baseball Pitchers 267
12 Kristen Nicholson: The Relationship Between Pitch Velocity and Arm Kinetics in Collegiate and High School Pitchers 268
13 Megan Stewart: Does Lead and Rear Foot Placement Affect Pitching Biomechanics? 269

14 Megan Stewart: The Effect of Pronation on Break of The Curveball 270
40 Jonathan Slowik: The Relationship between Fastball Velocity and Elbow Varus Torque in Professional Baseball Pitchers 271
41 Jonathan Slowik: Biomechanical Differences between Overhand, Three-Quarter, and Sidearm Baseball Pitching 272
101 Alek Diffendaffer: The relationship between variability in baseball pitching kinematics and consistency in pitch location 273
122 Jessica Downs: Hip Range of Motion and Isometric Strength Differences Between High and Low Batted Ball Velocity Hitters 274
134 Michael Haischer: Movement Patterns of the Torso Predict Upper Extremity Joint Loading in Little League Pitchers 275
139 Hannah Stokes: Shoulder External Rotation ROM During Physical Exam Is Related to Joint Loading During Baseball Pitching 276
140 Hannah Stokes: External Shoulder Flexibility During Physical Exam Is Related to Shoulder Joint Loading During Baseball Pitching 277
141 Hannah Stokes: Shoulder Rotational Properties During Physical Exam Are Related to Performance and Injury During Baseball Pitching 278
180 Kevin Giordano: Knee Kinetics in Baseball Hitting and Their Implication for Return to Play After Anterior Cruciate Ligament Reconstruction 279
181 Nicole Bordelon: THE RELATIONSHIP BETWEEN HUMERAL SEGMENT ENERGY AND HAND ANGULAR VELOCITY IN SOFTBALL HITTING 280
283 Arnel Aguinaldo: Segmental components of induced velocity and power of a pitched baseball in collegiate baseball players 281
446 Wendi Weimar: Proximal to Distal Sequence is Predicted by the Fibonacci Sequence 282
512 Michael Rose: Using IMUs to Quantify Throw Counts and Intensities in Youth Baseball Players 283
736 Andrew Oliver: Effect of Real-Time Feedback on Baseball Pitching Mechanics Using Inertial Measurement Units 284
769 Andrew Bryan: Utilizing Kinematic Motion Capture Data to Visually Improve Lower Extremity Mechanics of a Pitching Motion 285
786 Quinn Guzman: Biomechanical Effects Of The Draw Shot Golf Swing 286
824 Stephen Cain: A Comparison of Filtering Techniques applied to Baseball Pitching Data 287
868 Christopher Wendt: Comparison of Hip Biomechanics During a Half and Full Golf Swing in Male Amateur Golfers 288

Teaching and Outreach

15 Brian Wallace: Problem-based learning improves student learning in undergraduate biomechanics 289
28 Kayt Frisch: Teaching Undergraduate Biomechanics using Project Based Learning: A Case Study 290
228 Scott Monfort: The Impact of National Biomechanics Day on Student Perceptions toward Biomechanics: A Multisite Pilot Study 291
271 Amelia S. Lanier: Teacher Content Knowledge and Confidence in Youth Biomechanics Education 292
516 Shunafrica White: Teaching Methods to FEA of Human Gastrocnemius for STEM Early College Senior Research Project 293
840 Johanna O'Day: Biomechanics On Our Minds (BOOM): Learnings from a biomechanics podcast 294

Thursday, August 7

Balance and Falls - Neurologic

89 Yunju Lee: Effects of assistive devices on postural sway during a simulated forward fall 295
91 Will Pitt: Gait Event Specific IMU-Based Kinematic Metrics are able to Identify Balance Control Deficits in Acutely Concussed Young Adults 296
109 Eryn Gerber: An Investigation of Rambling-Trembling Trajectories with Somatosensory Deficit 297
125 Seo-hyun Kim: The Effects of Augmented Somatosensory Feedback on Postural Sway and Muscle Co-contraction 298
182 Meng-Wei Lin: Effects of vibration training in reducing falls in people with multiple sclerosis 299
243 Paris Nichols: Quantifying Somatosensory Deficits Using Sample Entropy and Fuzzy Sample Entropy 300
288 Sara Klein: Gait changes in young onset Parkinson's disease before and after medication 301
327 Christian Witkop: Detecting lingering effects on postural control using linear metrics following TBI 302
328 Christian Witkop: Correlating postural control metrics with Neurocom functional scores 303
598 Ashwini Sansare: Walking Balance Control is Delayed in Children with Cerebral Palsy 304
640 Brittany Sommers: Examining Effects of Cognitive Task Difficulty on Postural Stability via Wavelet Transforms 305

Locomotion - General

7 MU QIAO: Leg Joint Mechanics When Hopping at Different Frequencies 306
83 Kundan Joshi: Methods of Estimating Foot Power in Takeoff Phase of Standing Vertical Jump 307
225 Joseph Wasser: Movement Patterns During Single-Leg Hopping in Individuals with Lower Limb Loss 308
261 Owen Beck: Cyclically Producing the Same Average Muscle-Tendon Force with a Smaller Duty Increases Metabolic Rate 309
352 Nicholas Blonski: Kinetic Energy for Chair Mobility in Individuals with Functional Limitations 310
430 Emma Neuendorff: Performing Multi-Terrain Transient Locomotion Influence Changes in Joint Coordination of Individuals with Early-Stage Parkinson's Disease 311
479 Nathan Frakes: Effects of Gravitational and Inertial Forces on Determinants of Gait Transitions 312
505 Christopher Wilburn: The Effect of Arch Types on Propulsive Forces During Jumping and Hopping Tasks 313
534 Jonathan Camargo: Opensource biomechanics for locomotion in stairs, ramps and level-ground 314

582 Camille Johnson: Forced Marching Alters Plantar Force Distribution Compared to Running and Walking 315
583 Hannah Carey: Young Adults Recruit Similar Motor Modules Across Walking, Turning, and Chair Transfers 316
619 Ana Gutierrez: Association between Foot Thermal Responses and Shear Forces during Turning Gait 317
682 Pawel Golyski: Are biceps femoris muscle length changes influenced by in-series compliance across locomotor demand? 318
707 Pooja Moolchandani: Escape Motions for Real-World Scenarios: A Kinematic and Kinetic Investigation of Rapid, Dynamic Movements 319
729 Gaura Saini: Shoulder Kinematics using an Ergonomic Wheelchair 320
770 Jonathan Gosyne: The Effect of Frequency on the Energetics of Hopping in Dissipative Terrain 321
832 Zachary Mercer: Predicting Human Bouncing Behavior from Trajectory Optimization of Minimal Models 322

Locomotion - Walking

22 Claire Rodman: Quantification of Spatiotemporal Parameter Behavior During Walking Speed Transitions 323
25 Kyoung Jae Kim: A Comparison of Gait Characteristics between Extravehicular Activity Training Environments 324
35 Chun-Hao Huang: Step Length Asymmetry is Associated with Gait Efficiency in Older Women with Hip Osteoarthritis 325
84 Seyoung Kim: Zero power but positive acceleration at the end of a single-support phase in human walking 326
102 Szu-Hua (Teresa) Chen: Gait Balance Control After Fatigue: Effects of Age and Cognitive Demand 327
115 Emily Chavez: Treadmill Walking Does Not Elicit Increased Tripping Risks in Children with Autism 328
129 Yujin Kwon: Gait adaptation of individuals with limited dorsiflexion ROM during incline walking 329
130 Rebecca Krupenevich: Older Adults Overcome Reduced Triceps Surae Structural Stiffness to Preserve Ankle Joint Quasi-Stiffness 330
145 Alyssa Olivas: Responses to Incremental Loads in a Weighted Vest in Children with Autism Spectrum Disorder 331
153 Cherice Hughes-Oliver: Spatial Step and Joint Angular Kinematics Differ between Racial Groups 332
168 Tara Cornwell: Using Movement Amplification to Explore the Effect of Walking Speed on Stability in iSCI 333
172 Milad Zarei: Plantar Force During Walking Is Associated with Arch Structure and Walking Surface 334
211 Nicole Zaino: Transient Dynamics of Energy Consumption During Walking in Cerebral Palsy 335
213 Daniel Kuhman: It's time to start talking about timing of locomotor propulsion 336
219 Taylor Trentadue: Interpreting vertical ground reaction force impact spikes using Fourier analysis 337
240 Farahnaz Fallahtafti: Sampling Frequency Influences the Calculation of Temporal, but not Spatial, Regularity of Walking 338
254 Vivian Rose: The Cost and Spring-like Behavior of Walking: Are Children Scaled Down Adults? 339
265 Katie Conway: The Effects of a 6-week Horizontal Impeding Force Training Protocol on Push-off Intensity in Older Adults 340
279 Mark Geil: Effectiveness of a Gamification Intervention to Limit the Hawthorne Effect in Pediatric Gait Analysis 341
289 Ricky Pimentel: Muscle Metabolic Energy Costs While Modifying Propulsive Force Generation During Walking 342
309 Tasos Karakostas: The relationship between pelvic-hip musculature and functional ambulation in patients with Myelomeningocele 343
310 Moira van Leeuwen: Step width and frequency to modulate: Active foot placement control ensures stable gait 344
311 Natalie Egginton: Accuracy of Machine Learning to Determine Gait Events from Electromyography Signals 345
316 Song Li: LSTM Deep Learning and IMU Based Irregular Surface Gait Alteration Recognition 346
323 Taniel Winner: Do Switched Linear Dynamical Systems Provide Robust Kinematic Predictions of Healthy Treadmill Gait at Different Speeds? 347
338 Haneol Kim: Effect of Unilateral Ankle Loading on Spatiotemporal Gait Parameters during Treadmill Walking 348
346 Gena Henderson: Correlation Between Forward and Backward Treadmill Walking in School-aged Children 349
349 Sarah Brinkerhoff: Type of Physical Activity Affects Spatiotemporal Adaptation Strategy 350
362 Janki Patel:
Correlations Between Clinical Pain Measures And Lower Extremity Kinematics Among Individuals With Low Back Pain 351
376 Kevin Dames: Normalizing Kinetic Data Alters Conclusions Based on Obesity 352
392 Hang "Frankie" Qu: Effects of Marker Placement and Body Sizes on Frontal Plane Center of Mass Motion During Walking: A Preliminary Study 353
393 Patrick Monaghan: The Influence of an Expert Audience on Gait Initiation Performance 354
399 Shakiba Rafiee: Dorsiflexion Restriction Highlights the Role of Early-Stance Modulation of Tibialis Anterior in Forward Body Propulsion 355
450 Sidney Baudendistel: Length vs time: Dominant strategies to increase speed in older adults 356
464 Stephanie Molitor: Comparison of Joint Mechanics of the Dominant vs. Non-Dominant Lower Limbs During Locomotion 357
476 JUTALUK KONGSUK: Decreased Balance Confidence Related with Limits Maximum Speed among Older Adults. 358
486 Yue Luo: Effects of Smartphone Operation on Pedastrains' Gait Performance: An Outdoor Study 359
509 Mhairi MacLean: Ankle, knee, and hip dynamics during overground walking with bodyweight support 360
514 Kayla Pariser: Real-time Adaptive Treadmill Controller Optimization: A Parameter Sensitivity Study 361
521 Ashwini Kulkarni: Step length synergy is stabilized during adaptive gait tasks in young adults 362
533 Emily Dooley: The Effect of Cervical Spondylotic Myelopathy on the Dynamic Stability of Gait 363
542 HyeYoung Cho: Task Challenge Affects Both Gait and Reaction Time Performance in Young Adults 364
564 Anna Render: People Can Voluntarily Change Their Lateral Stepping Regulation During Goal-Directed Walking 365
571 Kali Shamaly: Impact of flip-flops on foot and ankle biomechanics 366
578 Cesar Castano: Self-pace treadmill controllers influence gait variability but not average walking speed 367

603 Ganesh Bapat: Roll-over Characteristics Remain Invariant in Patients with Peripheral Artery Disease 368
610 Kate Havens: Infant Transportation: Ground Reaction Forces during Gait 369
621 Rohan Gupta: Stride Time and Variability in Older Adults Walking on an Uneven Terrain Treadmill 370
625 Anahita Qashqai: Ankle Power and Stiffness during Gait in Children with Hypermobile Ehlers-Danlos Syndrome 371
642 Pouria Nozari Porshokouhi: A Data-Driven Low-Dimensional Optimization Framework Using Dynamical Movement Primitives Produces Human-Like Relationships between Walking Speed and Energetic Cost 372
648 Jillian Hawkins: Walking biomechanics before and after 30 minutes of walking in young adult women 373
661 Anne Marie Severyn: Biomechanical Analysis of Hippotherapy Using 3-D Motion Capture and Surface Electromyography 374
679 Safoura Sadegh Pour Aji Bishe: Developing a Synergistic Control Strategy for Knee and Ankle Exoskeleton Assistance 375
680 Sheridan Parker: Kinematic Response to Adaptive Speed Treadmill versus Fixed Speed Treadmill Walking in Older Adults 376
694 Allison Kinney: Influence of Added Mass on Overground Kinematics and Kinetics in Young Adults 377
696 Pawel Golyski: Treadmill Belt Acceleration Timing Affects Stability During Walking 378
711 John Willson: Foot and Ankle Kinetics During Walking in People with Plantar Fasciitis 379
722 Grace Kellaher: Gait variability during treadmill walking in older adults with high and low cognitive status 380
773 Xuan Liu: Adaptation to multi-session real-time visual feedback training of knee joint pattern in pediatric cerebral palsy: a case report 381
812 Wendy Nevarez-Sanchez: Can EMG accurately predict metabolically optimal step frequency? 382
821 Angel Bu: Musculoskeletal Model of Muscle Characteristics with Varied Bodyweight Support 383
830 Andre Alvarez: Propulsion timing affects the relationship between paretic propulsion and long-distance walking function after stroke 384
837 Dustin Bruening: Plantar Shear Stress Increases with Added Body Mass 385
846 Michael Browne: Asymmetric Gait Training with a Tied-Belt Treadmill 386
853 Jinfeng Li: Locomotor adaptation to visual cueing of impending mechanical perturbations during treadmill walking 387

Neurorehabilitation - General

54 Conner, Benjamin 388
165 Paul Kline: Compensations during Step Ascent Contribute to Stair Climbing Ability in Multiple Sclerosis 389
242 Charlotte Caskey: Gait Coordination in Adults with Spinal Cord Injury Receiving Spinal Stimulation 390
305 Diego Ferreira: Acute effects of whole-body vibration on stair ascent in children with Down syndrome 391
342 Margaret Finley: Movement coordination during humeral elevation in individuals with newly acquired spinal cord injury 392
497 Christopher Hurt: Changes to Walk Speed: Programming Deep Brain Stimulators for Parkinson's Patients 393
546 Daniel Richie: Gait and Balance Characteristics for Adults with Degenerative Cervical Myelopathy 394
569 Krista Nunn: Gait Variability in Persons with Parkinson's disease after Individualized Physical Therapy 395
589 Zachary Ripic: Differences in Knee Joint Angle Between Parkinson's Disease "on" and "off" Medication Across Varying Levels of Visual Flow 396
620 Isaiah Lachica: A Novel Augmented Reality Platform Delivers Sensory Cues to Improve Parkinsonian Gait 397
681 Daniel Free: Intermuscular Coherence within the Upper Limb in Persons with Essential Tremor 398
695 Clayton Wauneka: ECG Artifact Subtraction from Instramuscular Diaphragm EMGs in Humans with Acute Spinal Cord Injuries 399
719 Christopher Hurt: Dynamic task performance for Parkinson's patients with a novel deep brain stimulator 400

Orthopaedics - Lower Extremity

9 Nate Bates: Cadaveric ACL Reconstruction Mechanics during Simulated Landings: A Pilot Investigation 401
18 Camila Grant: Patellofemoral Kinematics in Patellofemoral Pain Syndrome: The Influence of Demographic Factors 402
49 Samuel Acuña: Increased Task Demand Differentiates Knee Muscle Forces after ACL-Reconstruction 403
90 Shangcheng Wang: Optimal Placement of Suspension Fixation Tunnel to Restore Proximal Tibiofibular Joint Stability: A Finite Element Study 404
105 Alex Peebles: Risk Factors for Second ACL Injury can be Objectively Measured in a Clinical Setting 405
108 Katie Collins: Drop-Landing Asymmetries in Young Individuals 6-Months Following ACL Reconstruction 406
124 April McPherson: Quadriceps Musculature Motor Unit Characteristics between Injured and Non-Injured Limb after ACL Reconstruction 407
132 Benjamin Wheatley: Modeling the Effect of Femoral Anteversion on Knee Extensor Muscle Force and Anterior Knee Mechanics 408
136 Tanner Thorsen: Lower Extremity Muscle Force Adaptation to Increased Q-Factor in Stationary Cycling 409
171 Alyssa Evans-Pickett: Serum Cartilage Oligomeric Matrix Protein Response to Braced and Non-braced Walking in Individuals with an Anterior Cruciate Ligament Reconstruction 410
196 Nahir Habet: Biomechanical Evaluation of a Novel, All-Inside Posterior Medial Meniscus Root Repair via Fixation to the Posterior Cruciate Ligament 411
221 Michelle Ramsey: Seasonal Variations in Vertical Stiffness and Jump Height in NCAA Division-I Soccer Athletes 412
229 Scott Monfort: Influence of Baseline Cognitive Function on Knee Mechanics during Dual-Task Sidestep Cutting 413
241 STEVEN GARCIA: Gait asymmetries are more apparent at faster walking speeds in individuals with acute anterior cruciate ligament reconstruction 414

252 Shumeng Yang: Asymmetry and Sex Differences in Ankle and Hindfoot Kinematics During Gait 415
300 Lindsey Remski: Use of Nonlinear Dynamics to Characterize Force Control during Leg Press 416
313 Brian Pietrosimone: Linking Greater Type II Collagen Turnover Following Anterior Cruciate Ligament Injury to a Stiffened-Knee Gait Strategy 417
317 Safeer Siddicky: Does the Pavlik harness treatment cause lower extremity biomechanical changes in infants? 418
354 Jeonghoon Oh: Estimated Ground Reaction Forces in Stair Climbing After ACL Reconstruction Using a Single Depth Sensor-Driven Musculoskeletal Model 419
357 Seung-Min Baik: EFFECT OF SIDE PLANK EXERCISE USING A SLING WITH DIFFERENT HIP ROTATIONS 420
373 Jacqueline Foody: Evaluation of Running as a Means to Identify Limb Symmetry After ACL Reconstruction 421
400 Naoaki Ito: LATENCY BETWEEN PEAK VASTUS MEDIALIS ACTIVATION AND PEAK KNEE FLEXION MOMENT DURING GAIT IS LONGER IN KNEES AFTER ANTERIOR CRUCIATE LIGAMENT RECONSTRUCTION WITH A BONE-PATELLAR TENDON-BONE GRAFT 422
467 Jack R. Williams: Asymmetries in Patellofemoral Gait Mechanics Are Detectable 3 Months after ACL Reconstruction 423
501 Bingfei Fan: 3D knee joint angle estimation during drop landing using inertial sensors: Towards ACL injury risk assessment 424
520 Matthew Seeley: PATIENT-REPORTED OUTCOMES FOR ANTERIOR CRUCIATE LIGAMENT RECONSTRUCTION PATIENTS CLUSTERED ON FUNCTIONAL AND DISCRETE WALKING BIOMECHANICS 425
561 John Mead: Effect of Antegrade vs. Retrograde Femoral Nailing After Traumatic Femur Fracture on Lower Body Kinematics and Kinetics 426
574 Kelsey Neal: Knee Biomechanical Asymmetries Improve 3 to 6 months After ACLR, but Continue to Persist at 6 Months 427
575 Nathan Robey: Effects of Stroboscopic Vision on Single-limb Postural Stability Measures in ACLR and Healthy Individuals 428
624 Micah Garcia: The Relationship among Hip Strength and Hip Kinematics during Single-Leg Tasks: A Systematic Review and Meta-Analysis 429
699 Abdulmajeed Alfayyadh: Women Walk With Higher Muscle Co-Contraction Indices 3 Months after Anterior Cruciate Ligament Reconstruction 430
710 Logan Moore: Joint Angular Impulse and Neuromuscular Control during the Y Balance Test™ in ACL Reconstructed Individuals 431
725 Callan Luetkemeyer: Fiber Splay Obscures Macroscopic Mechanical Measurements of Ligament Stiffness: Implications for ACL Graft Selection 432
756 Eric Thorhauer: Kinematics of the foot sesamoids in a cadaver model during simulated activities 433
758 Stephanie Cone: Iliotibial Band Wave Speed Modulates with Hip Abduction Moments 434
767 Luca Rigamonti: Hamstrings Training Program improves Drop Vertical Jump performance and efficacy of movement in female athletes 435
790 Maxine Wold: Ground Reaction Force Distribution Algorithm for a Kinetic Segmental Foot Model 436
797 Donald Anderson: Weight Bearing CT Detects Early Changes in 3D Joint Space Width after Tibial Pilon Fractures 437
862 Bryan Tanner: Custom Orthosis Prescription is Needed to Reliably Reduce Harmful Contact Stress after Intra-Articular Fracture 438
871 Tarang Jain: Medio-Lateral Ankle Fluency In People With Chronic Ankle Instability During Dynamic Movement Trials 439

Orthopaedics - Upper Extremity

99 Bardiya Akhbari: Higher Volar Tilt of a Total Wrist Arthroplasty is Associated with Larger Range-Of-Motion 440
100 Kimberly Kontson: Establishing an Age-Matched, Healthy Control Dataset of Joint Kinematics for Comparison to rTSA Patient Joint Kinematics 441
111 Kate Spitzley: Effects of Sex and Vision on Shoulder Position Sense 442
135 Matt Petersen: Body Position Effect on Scapulohumeral Rhythm 443
257 Clarissa LeVasseur: Glenoid Lateralization Increases Abduction ROM and Strength After Reverse Shoulder Arthroplasty 444
286 Aaron Trunt: Glenohumeral Rotation and Strength Characteristics Related to Shoulder Stress in Collegiate Pitchers 445
387 Omid Jahanian: Rotator Cuff Tears and Humeral Elevation in Manual Wheelchair Users with Spinal Cord Injury and Able-bodied Controls 446
523 R. Tyler Richardson: A Comparison of Methods to Estimate Scapular Kinematics for Brachial Plexus Birth Injuries 447
545 Emily Fawcett: Macrostructural bone deformity following brachial plexus birth injury cannot be explained solely by limb disuse 448
550 Emily Fawcett: Adaptations in trabecular microstructure following brachial plexus birth injury are not due solely to limb disuse 449
738 Alyssa Schnorenberg: Normalization of Thoracohumeral Kinematics Following Rotator Cuff Repair 450
835 Giovanni Oppizzi: CHARACTERIZING STIFFNESS COUPLING IN FINGERS DURING PASSIVE MOVEMENT 451

Prosthetics, Orthotics, & Robotics

39 Kinyata Cooper: Back squat mechanics in persons with a unilateral transtibial amputation: A case study 452
87 Coral Ben David: Evaluation of a Passive Knee Exoskeleton for Vertical Jumping 453
118 Therese Parr: Development and Testing of a Linear Adjustable Lower-Limb Prosthesis 454
119 Shane Murphy: Influence of Asymmetry on the Metabolic Costs of Walking 455

143 Harrison Bartlett: Ankle Exhibits Consistent External Quasi-Stiffness Behavior Across Level, Sloped, and Uneven Terrain: Implications for Prosthesis Design 456
163 Cory Christiansen: Repeated Error-Based Gait Training for Non-Traumatic Amputation: Proof of Concept Study 457
164 Wyatt Ihmels: Effect of Intrepid Dynamic Exoskeletal Orthosis (IDEO) Design on Knee Total Joint Moment and Gait Parameters. 458
203 Jacob Misch: Effects of incremental mass changes on wheelchair motion using robotic tester 459
244 Taehee Kim: Finger gesture recognition of forearm amputee according to the sampling rate 460
250 Adrienne Henderson: Modulating Distal Foot Energetics Using A Customized Deformable Foot Orthosis 461
259 Elizabeth Russell Esposito: Impact Biomechanics in Individuals Using a Custom Carbon Ankle-foot Orthosis during Running 462
269 Arash Mohammadzadeh Gonabadi: Designing and developing a new semi-rigid bilateral exoskeleton to assist hip joint motion 463
270 Arash Mohammadzadeh Gonabadi: Development of a system for assistance at the center of mass 464
272 Morteza Asgari: Biomechanical Evaluation of a Wearable Passive Shoulder Exoskeleton 465
274 David Ziemnicki: Combining an Artificial Gastrocnemius and Powered Ankle Prosthesis: Effects on Transtibial Prosthesis User Gait 466
297 Zane Colvin: Leg Muscle Activity when Using Powered and Passive Prostheses for Sloped Walking 467
303 Jenny Kent: Knee flexion damping affects several key features of the prosthetic limb swing phase 468
315 Anna Pace: A Simple Walking Model to Optimize Prosthetic Knee and Foot Combinations for Prosthetic Limb Stability 469
320 Fatemeh Zahedi: Characterization of human arm stability in relation to unstable viscous environments 470
324 Michael Poppo: Ankle Roll-over Shape Comparisons of Different Prosthetic Foot Types 471
358 Arian Vistamehr: The Influence of Articulated AFOs on Mediolateral Balance Control and Forward Propulsion during Walking Post Stroke 472
372 Rachel Teater: Asymmetry, Instability and Functional Deficits in Transtibial Prosthesis Users During Squatting, Lifting and Sit-to-Stand 473
406 Rachel Hybart: MYOELECTRIC CONTROL OF A COMMERCIALLY AVAILABLE ANKLE EXOSKELETON IN CONTINUOUS AND DISCRETE MOVEMENTS 474
411 Amber Gatto: The Design and Development of a Wrist Hand Orthosis 475
422 Cara Welker: Teleoperation of an Ankle-Foot Prosthesis with a Wrist Exoskeleton 476
428 Maura Eveld: Stumble recovery strategies for healthy individuals and transfemoral prosthesis users 477
437 Bailey McLain: EMG-Informed Neuromusculoskeletal Model for Knee Joint Load Estimation with a Powered Knee Exoskeleton 478
439 Kinsey Herrin: An automatic human-in-the-loop tuning algorithm for a robotic ankle prosthesis depends on an understanding of gait quality 479
444 Leila Rahnama: Use of Nearly-Invisible, Non-restrictive Sensory Insoles as Treatment for Idiopathic Toe Walking: A Case Series 480
460 Matthew Major: Biomechanics of Women with Transtibial Limb Loss Walking with Heel Height Adjustable Feet 481
466 Woolim Hong: Effects of material of the 3D printed foot on ankle kinematics/kinetics and toe joint bending during prosthetic walking 482
473 Joshua Tacca: Adjustable prosthetic socket improves symmetry of transfemoral amputees during walking 483
492 Paige Paulus: A Comparison of Ground Reaction Forces During Treadmill and Overground Walking in Transfemoral Amputees 484
526 Krishan Bhakta: Restoring Functional Gait of Individuals with Transfemoral Amputation using a Powered Prosthesis 485
538 Matthew Mulligan: Leveraging Machine Learning for Real-Time Metabolic Cost Prediction 486
543 Namita Anil Kumar: Impedance Control of the Knee Mechanism of a Transfemoral Prosthetic for Level Walking 487
547 Noah Rosenblatt: THE ASSOCIATION BETWEEN PHYSICAL ACTIVITY PARAMETERS, SELF-EFFICACY, QUALITY OF LIFE AND COMMUNITY PARTICIPATION IN USERS OF UNILATERAL TRANSTIBIAL PROSTHESES 488
567 Nicole Stafford: Proportional Myoelectric Control of a Bionic Lower Limb with a Series Elastic Actuator 489
615 Elizabeth Halsne: Measured Forefoot Stiffness Across Prosthetic Foot Stiffness Categories 490
623 Shane King: Development and evaluation of a powered knee stumble recovery controller for transfemoral prosthesis users 491
634 Leif Hasselquist: Does the use of a Powered Assistive Ankle Exo Device Augment Cost of Transport 492
663 Jared Li: Reduction of Trunk Extensor Muscle Activation using a Cable-Driven Back Exosuit 493
665 Sameer Amarnath Upadhye: Design & Control of a novel modular stiffness spring Ankle prosthesis with embedded ball screw powered prosthesis 494
674 Grace Hunt: Volitional Control of Powered Knee-Ankle Prosthesis During Sit-to-Stand 495
675 Myrriah Laine Dyreson: Immediate Effects of a Hydraulic Slope Adaptive Prosthetic Foot-Ankle System When Standing on Slopes 496
698 Luke Nigro: Providing Rate-Responsive Bending Stiffness to a Passive Ankle-Foot Orthosis with Shear-Thickening Fluid Elements 497
701 Gabriel Rios: Biomimicry of the Gastrocnemius During Gait for Transtibial Amputees 498
721 Aaron Fleming: Regularity of Center of Pressure Excursion with Proportional Myoelectric Control of a Powered Prosthetic Ankle after Training 499

733 Santiago Canete: The Effects of a Powered Pneumatic Ankle Exoskeleton on Balance Control 500
757 Kieran Nichols: Sensitivity of Mechanical Outcomes to Various Stiffnesses of Variable Stiffness Foot (VSF) 501
760 Connor Phillips: Muscle Response During Interaction with a Variable Damping Controlled Robotic Arm 502
761 Yinan Pei: Biomechanical Design and Preliminary Evaluation of an Ankle-Foot Simulator for Ankle Clonus Assessment Training 503
762 Jairo Maldonado-Contreras: User- and Speed-Independent Slope Estimation for Lower-Extremity Wearable Devices 504
777 Seth Higgins: Performance Evaluation of a Robotic Knee Exoskeleton 505
788 Shaniel Bowen: Biomechanical Analysis of Device-Assisted Sit-to-Stand Transfers in Young Adult 506
803 Jinwon Lee: Gait Phase Estimation of Powered Transfemoral Prosthesis using RNN 507
857 Krista Cyr: Lower Limb Response of Transtibial Amputees Stepping on a Coronally Uneven Surface 508

Friday, August 8

Clinical and Real World Applications

30 Chi-Whan Choi: Comparison of Trunk Muscle Activity during Modified Side-Bridge Exercises and Traditional Side Bridge Exercise 509
60 Seth Donahue: Semi-Unsupervised Machine Learning System for Gait Event Detection, Locomotion Mode Classification and Prediction 510
65 Adam Luftglass: The Impact of Standardized Footwear on Load and Load Symmetry 511
77 Jeff Eggleston: Live animation biofeedback responses between children with autism and children with typical development 512
103 Alex Peebles: Automated 2D Video Analysis is Reliable for Assessing Knee Kinematics During Landing 513
155 Cherice Hughes-Oliver: Discrete Projection and Similarity Analysis in Total Ankle Replacement Patients 514
159 Jongseok Hwang: Comparative Effects of Abdominal Breathing and Dynamic Neuromuscular Stabilization Breathing on Diaphragmatic Movement and Pulmonary Function in Chronic Obstructive Pulmonary Disease 515
161 Hunter Bennett: Lower Extremity Biomechanics during Running in Persons Who are Blind: A Preliminary Report 516
208 Ajit Chaudhari: Biomechanics In The Real World: Design and Evaluation of a Clinical Balance Tool 517
236 Malaka (Graci) Finco: Lower Limb Kinematic Asymmetries and Correlation to Clinical Measures in Individuals with Parkinson's Disease 518
301 Ajit Chaudhari: Core Stability in Patients Awaiting Hernia Repair 519
332 Trevor Kingsbury: Evaluation of Running Biomechanics, CHAMP Performance, and Patient Reported Outcomes of Servicemembers with Lower Extremity Fracture Utilizing an IDEO 520
306 Diego Ferreira: Effect of body position and external load on knee joint kinematics and muscle activity in healthy young adults during the pendulum test 521
367 I-Chieh (EJ) Lee: Kinematics features and experience in differentiating above-knee amputee gait 522
419 Inbar Kima: Near Infra-Red Spectroscopy Used for Muscles Hemodynamic of Adults with Cerebral Palsy versus Adults with No Physical Impairment 523
438 Jenny Perry: Dynamic Joint Stiffness During Single Leg Drop in FAIS Participants 524
532 Jacob Banks: Are Lower Back Demands Optimal in People with Unilateral Amputation? 525
580 Alex Dzewaltowski: Faster walking following revascularization not accompanied by an increase in joint work 526
614 Sumire Sato: Spatiotemporal gait characteristics in multiple sclerosis subtypes during timed-25-foot-walk 527
622 Cecile Smeesters: Force Applied to a Grab Bar During Bathtub Transfers 528
645 Ryan Wedge: Speed Effects of Knee Joint Loading in People with Unilateral Transtibial Amputation 529
668 David Bazett-Jones: Depth of Squat Influences the Two-Dimensional Analysis of Knee, Hip, and Pelvis Frontal Plane Motion in Pain-Free Women 530

Computational Modeling

43 Hoon Kim: Muscle Forces of the Lower Extremity During Dynamic Tasks in People With and Without Chronic Ankle Instability 531
88 barak ostraich: Simulation of passive knee exoskeleton for vertical jumping 532
92 Michael McGeehan: A Computational Gait Model With Lower Limb Loss and a Semi-Active Variable-Stiffness Foot Prosthesis 533
144 Timothy Zehnbauer: Comparison of Vertex Influence Weight Algorithms for Repositioning of 3D Medical Models 534
198 Elijah Kuska: Soleus Weakness Necessitates Increased Control Complexity For Unimpaired Gait 535
227 Suzanne Cox: Moment Arms for Velocity Optimization Vary with Muscle OFL and Resistive Forces 536
277 Shihao Li: A Subject-Specific Finite-Element Musculoskeletal Model for Analysis of Lower Limb Biomechanics 537
293 Brecca Gaffney: Effect of Movement Training on the Location of Acetabular Loading in Developmental Dysplasia of the Hip 538
339 Mettler Jeff: A Comparison of Ligament Strain Estimations Using Bone Pins and Skin Markers 539
413 Todd Leutzinger: Walking with a cane alters plantarflexor muscle forces during walking in an individual post-stroke 540
443 Katelyn Burkhart: Between-session Reliability of Subject-Specific Musculoskeletal Models of the Spine Derived from Optoelectronic Motion Capture Data 541
453 Brianna Karpowicz: A self-correcting spiking network model for motor unit coordination during force production 542
471 Ebrahim Maghami: Fracture resistance analysis in human dentin microstructure 543

508 Ajay Goyal: MODELING WOVEN BONE DISTRIBUTION IN RESPONSE TO EXOGENEOUS PURE BENDING OF RAT TIBIA 544
510 Tom Van Wouwe: Contributions of co-contraction and sensory feedback to deal with unstable musculoskeletal dynamics 545
554 Heonsu Kim: 3D-Printable Prosthetic Foot with Human Toe-Joint Property 546
557 Huijin Um: Structural behavior evaluation of prosthetic foot using the auxetic structure via finite element analysis 547
558 Jente Willaert: Simulations of pendulum test kinematics can estimate underlying parameters to joint hyper-resistance 548
585 Giovanni Martino: Differential effect of spindle gamma drive and reflex gain in passive lower limb movements: a simulation study 549
591 Joseph Dranetz: Identifying the Role of Residual Gastrocnemius in Isometric Knee Flexion of Below Knee Amputees 550
605 Jonathon Blank: Effects of End-User and Design Parameters on Shear Wave Propagation: A High-Throughput Parametric Modeling Study 551
628 Muhammad Salman: Harmonic excitation approach to determine system identification of a mannequin 552
639 Di Ao: Effect of Muscle Passive Force Minimization on EMG-driven Model Calibration 553
652 Marleny Arones: Musculoskeletal Model Calibration Affects Metabolic Cost Estimates for Walking 554
657 Owen Pearl: Is My Musculoskeletal Model Complex Enough? The Implications of Six Degree of Freedom Lower Limb Joints for Dynamic Consistency and Biomechanical Relevance 555
666 Christian DeBuys: Minimizing Angular Momentum Yields More Robust Walking Trajectories in Five-Link Biped 556
683 Daniel McFarland: Sensitivity of Simulated Grip Strength to Wrist Posture 557
713 Rodolfo Amezcua: An Approach to Simulate Control and Dynamics of Land and Stop Tasks Performed by Humans 558
718 Veronica Knisley: Optimal Bipedal Walking Gaits Found with Different Direct Collocation Settings 559
723 Adrienne Williams: A 3D Computational Model to Simulate 2D Ultrasound Measurements of Medial Gastrocnemius Architecture 560
731 Stephanie Rossman: The Contribution of Spinal Erector Muscle Strength and Facet Contact in Reducing Disc Herniation Risk During Forward Bending 561
735 Megan Auger: Discrepancy Modeling for Human Locomotion 562
749 Spencer Baker: Which Muscles are Most Responsible for Tremor? Principles from Computer Simulations 563
755 Stephanie Rossman: The Importance of Spinal Erector Muscle Strength and Facet Contact in Establishing Sagittal Balance and Reducing Disc Loads During Standing and Forward Bending 564
774 Sydney Ward: Using System Identification to Determine how Tremor Propagates in the Upper Limb 565
780 Emily Dooley: Comparison of Three Unique Foot Models Over One Step 566
807 Mohammad Shourijeh: Mohammad Shourijeh Static Optimization Personalization for the Muscle Redundancy Problem 567
811 Pilwon Hur: A Framework for Bipedal Walking Research in Biomechanics from Robotics 568
817 Jinhyuk Kim: Analysis the Strain of Plantar Fascia with Different Plantar Fascia Thickness and Tendon Loading in 3D FE Foot Model 569
820 Michael Rosenberg: Investigating Whole-Leg Contributions to Center-of-Mass Acceleration During Gait 570
823 John Rogers: Bungee Method for Augmenting Human Treadmill Running 571
827 Marleny Arones: Predicted Gait Alterations due to Reduced Paretic Leg Muscle Synergy Complexity 572
854 Thendral Govindaraj: The Influence of Inter-joint Force-dependent Feedback on Whole Limb Impedance Over a Range of Frequencies 573
861 Ian Syndergaard: A Novel Closed-Loop MIMO Model for Studying the Effects of Spinal Afferents on Tremor 574
864 Sepehr Ramezani: Validation of Musculoskelatal Models Using Single Degree of Freedom Analysis 575

Injury and Injury Prevention

31 Jaroslav Hruby: Experimental Head Injury Investigation of Head Impact Caused by Unsecured Object in Vehicle during Vehicle Frontal Crash 576
63 Kyle Van Housen: Evaluation and Modeling of Falls onto Poured Rubber Playground Surfaces 577
117 Shelby Walford: The Relationship Between the Hand Pattern Used During Fast Propulsion and Shoulder Pain Development 578
120 Justin Scott: Relationships Between Blood Perfusion and Pressure: A Study with Wheelchair Users and Able-Bodied Individuals 579
123 Phillips David: Females Exhibit Higher Hamstring Activation Prior to Landing and Reduced Activation After Acute Fatigue 580
127 Haneul Jung: A Threshold-based Algorithm for the Detection of Pre-impact Falls-from-Height 581
147 Yannis Halkiadakis: A Predictive Model for Stress Fractures in Runners 582
178 Paige Cordts: Pressure Relief in Wheelchair Users with Static Posture Changes 583
188 Jeff Barfield: Bilateral Differences in Lumbopelvic-Hip Complex Kinematics during the CKCUEST 584
191 Rebecca Ban: ACUTE EFFECT OF AN INTERVENTION TO IMPROVE ANKLE DORSIFLEXION AMONG INDIVIDUALS WHO DISPLAY MEDIAL KNEE DISPLACEMENT 585
199 Lauren Schroeder: Increased Ankle Range of Motion Reduces Knee Loads during Landing in Healthy Adults 586
200 Kristin Morgan: Force and Rate Metrics Provide Return-To-Sport Criterion after ACL Reconstruction 587
253 Jaeho Jang: Dynamic Joint Stiffness of the Ankle in Chronic Ankle Instability Patients 588
268 Kathryn Farina: Kinematic and Kinetic Differences Pre- and Post- Femoral Stress Reaction Injury: A Case Study 589
280 Rachel Tanczos: Modeling of Feet First Falls into Protective Water Pits in the Context of OCRs 590

298 Christian Sanchez: Prophylactic Ankle Braces Did Not Elict Changes Associated with Injury or Compromise Performance in Sports Specific Movements 591
314 Takashi Nagai: Effects of 15-Minute Dynamic Warm-Up Program on Hamstrings Muscle Strength, Flexibility, Stiffness, and Jump Performance in High School Basketball Athletes 592
318 Mark Jesunathadas: Impactor Geometry May Obscure The Blunt Impact Performance of a Commuter Bicycle Helmet 593
319 Mark Jesunathadas: The Influence of Headform Pose on the Blunt Impact Performance of American Football Helmets 594
330 Ryan Alcantara: Loading Asymmetry Before and After Metatarsal Stress Fracture: A Case Study 595
344 Ryan Neice: Analysis of a Combat Helmet in a Head-to-Ground Impact Scenario 596
347 Shayne York: Kinematic Response of Different Head-Helmet Interface Friction Conditions 597
371 Gina Garcia: Dorsiflexion shoes affect landing mechanics related to lower extremity injury risk 598
383 Jacob Larson: Evaluating Limb Stiffness and Local Dynamic Stability in Cutting and Landing Movements of Female Athletes 599
408 Mohsen Safaei: Mechanical Stimulation as a Non-invasive Tool for Monitoring Meniscus Tear 600
418 Kimi Dahl: Kinematic Evaluation of Return-to-Play Hop Tests in a Healthy Population 601
421 Kimi Dahl: Do Power, Strength, and Lower Extremity Kinematics Correlate with Maximum Hop Distance in a Healthy Population? 602
425 Sarah Moudy: The effect of landing coordination and amputation on high limb loading during bilateral landings 603
442 William Taylor: Bilateral Asymmetry in Leg Stiffness During Dynamic Activities 604
452 Lukas Krumpl: Relationship Between Clinical Assessments of Health and Fitness and Field-Based Physical Fitness Tests in Reserve Officer Training Corps (ROTC) Cadets 605
458 Eric Shumski: No Difference in Knee Biomechanics During Landing Between Individuals with and without a History of Concussion 606
459 Hillary Holmes: Lower Extremity Stiffness is Altered During Decision-Making Drop Jumps in Males and Females 607
474 Jason Brunet: The Effects of Foot Position on Gluteus Maximus Activation During Jump Tasks 608
496 Junsig Wang: Do inclined sleeping surfaces impact infants' upper body muscle activity and movement? 609
515 Kyle Murdock: Bone Architecture and Foot Muscle Strength are not Different in Healthy Male Versus Female Runners 610
527 Jake Melaro: Sex and Leg Differences in ACL Stress during Unilateral Drop Landing 611
579 Mostafa Hegazy: The relationship between Hip and Core Muscular Endurance and Lower Extremity Injuries in Division II Women's Soccer 612
595 Joshua Winters: Pre-Deployment Loading Patterns in Military Personnel with a History of Low Back Injuries 613
606 Ashleigh Fults: Peak Elbow Angles in Independent Wheelchair Transfer A Prelim Study 614
646 Christina Rohlf: Influence of Arena Surface Mechanics on Equine Fetlock Joint Motion for a Jump 615
655 Mohammed Alamri: Spatiotemporal Gait Parameters in Middle Age Adults with Persistent Ankle Pain 616
664 Nate Bates: Effect of Targeted Hamstrings Intervention on Vertical Ground Reaction Force Asymmetries during Takeoff and Landing 617
684 Dovin Kiernan: Bad Vibes? Preliminary data on shock attenuation in injured and uninjured runners 618
732 Courtney Butowicz: Comparison of trunk neuromuscular control strategies between athletes with and without a shoulder injury 619
741 Suzanne Konz: An investigation into the head accelerations and forces experienced by clay-target shooters 620
745 Amanda Morris: The Influence of Concussion History on Reactive Balance Performance 621
771 Jereme Outerleys: Change In Running Impacts Following a Fatigue Run in Female Runners with Single and Multiple Stress Fractures 622
783 Adam Yoder: Brace Yourself: Sensitivity of Simulated Ankle Inversion Sprains to Neuromuscular Versus External Factors 623
799 Brody Hicks: Modeling Rodent Gait Compensation Strategies After Lateral Gastrocnemius Volumetric Muscle Loss Injury 624
806 Stephen Cobb: Variability of Spatiotemporal Gait Metrics in Middle-Aged Adults with Persistent Ankle Pain 625
818 Taylor Cycenas: The Effects of Recreational Dance Experience on Landing Mechanics 626

Measurement & Validation, Worn Sensors

24 Kyoung Jae Kim: Characterization of Activities and Postures during Planetary Extravehicular Activities via Inertial Measurement Units 627
36 Katherine Hsieh: Assessing Postural Control with Smartphone Accelerometery in People with Multiple Sclerosis 628
61 Seth Donahue: Estimation of Normal Ground Reaction Forces in a Real-World Environment Using Machine Learning 629
78 Gordon Alderink: Comparison of Hara and Harrington Hip Joint Center Location and Influence on Hip Moments during Gait 630
81 Scot Carpenter: Frequency Characterization of Thigh Soft Tissue Artifact During a Relaxed and Activated State 631
85 Youngmin Chun: Application of Quadratic Regression Model in the Calculation of Lower Extremity Joint Stiffness 632
128 David Chiasson: An Investigation of Human Movement IMU Data Compression Methods 633
157 Tian Tan: Magnetometer-Free, Inertial-Sensor-Based Foot Progression Angle Estimation 634
166 Julie Burland: Reliability of Wearable Sensors to Assess Impact Metrics during Sport Specific Tasks 635
179 Hui-Ting Shih: Description and Validation of a Ground Reaction Force Triggered Treadmill Protocol for Simulation of Tripping Falls 636
184 Soyong Shin: Combined Deep learning and Top-Down Optimization for Estimation of Kinematics from IMUs 637
206 Eric Brannock: Comparing IMU and Motion Capture Kinematics for Jumping Jacks 638

246 Jongman Kim: sEMG-based Finger Posture Recognition Considering the Electrode Shift 639
248 Caleb Johnson: A comparison of attachment methods of skin mounted inertial measurement units on tibial accelerations 640
281 Pratham Singh: Determining Stride Length of Runners using an Ultrawide Bandwidth Local Positioning System equipped with an Inertial Measurement Unit 641
296 Wei Yin: A novel use of flexible sensors for ambulatory measurement of gait kinematics 642
326 Michael Zabala: Knee Flexion Prediction from a Neural Network Algorithm with Various Sources of Training Data 643
351 Sara Harper: Wearable Tendon Kinetics 644
360 Naomi Frankston: How Accurately Can Motion Capture Identify the Hip Joint Center During Deep Hip Flexion? 645
381 Brianna Goodwin: The Accuracy of Machine Learning Models for Detecting Propulsion from an Inertial Measurement Unit Worn on the Arm of Manual Wheelchair Users 646
389 Ruopeng Sun: IMU-Based Sit-To-Stand Performance Measurement among Patients with Musculoskeletal Pain 647
396 Yun-An Lin: Human Motion Monitoring using Smart Nanocomposite Kinesiology Tape 648
407 Michael Potter: IMU-based Kinematic Estimates for a Simplified Model of the Human Lower-limbs: Simulation and Experiment 649
485 Jing-Sheng Li: The effect of footwear on hindfoot tracking: A marker-based biplane fluoroscopy study 650
489 Kathryn Akmal: Machine Learning and Optimization Tool for the Classification of Human Movement 651
490 Josiah Mercer: Pennation Angle Changes During Successive Loading Cycles 652
498 BJ Fregly: Coordinate Projection vs Unscented Filtering for IMU-based Motion Measurement 653
537 Matthew Ruder: Preliminary Assessment of Shoulder Activity After Rotator Cuff Repair 654
560 Otto Buchholz: Comparison of Dynamic Stability Measures Based on Planar Torque Versus Ground Reaction Force 655
565 Omer Inan: Knee Joint Acoustic Signatures in Healthy Collegiate Athletes: Sex Differences 656
568 Dheepak Arumukhom Revi: Beyond walking distance: Evaluating propulsion function during the 6-minute walk test with wearable inertial sensors 657
607 Yu-Pin Liang: Center of Mass Accelerations Estimated by Wearable Sensor Technology and Motion Capture System: Are We Measuring the Same Thing? 658
691 Md Sanzid Bin Hossain: Predicting lower limb 3D kinematics during gait using reduced number of wearable sensors via deep learning 659
706 Zachary Bons: Soft-tissue Artifact Compensation for Electromagnetic Motion Capture 660
715 Adriana Miltko: Validity of Peak Tibial Acceleration Obtained from a Wearable IMU during Running 661
740 Eric Thorhauer: Uncertainty propagation in validating bone kinematics from biplane fluoroscopy 662
754 Eli Dawson: Surface-Excited Wave Dispersion in the Achilles Tendon During Walking 663
784 Peter Barrance: Validation of IMU-derived knee flexion angle measurements for use in visual kinematic feedback 664
787 Seung Yun (Leo) Song: Simple and Low-Cost Methods of Computing Joint Angles Using Inertial Measurement Units 665
796 Zachary Katzman: Acceleration Signals and Peaks During Running Vary with IMU Placement 666
800 Robert Creath: Improving Center of Pressure Estimation Using a Simple Optimization Method 667
810 Loubna Baroudi: Estimating Walking Speed in the Wild 668
813 Kaleb Burch: Reliability of One-Size-Fits-All In-Shoe Force Sensors Across Various Walking Speeds 669
815 Patrick Currin: A Preliminary Study of a Motion Capture System Using Smartphones for the Ankle Joint Analysis 670
843 Scott Boebinger: Diffuse Optical Spectroscopy Assessment of Oxygen Metabolism in Leg Musculature 671
845 Zachary White: Reliability of Maximum Voluntary Isometric Contractions 672

Motor Control and Learning

76 Szu-Hua (Teresa) Chen: Inter-Joint Coordination Variability When Fatiguing With a Repetitive Sit-to-Stand Task 673
170 Charles Sloan: Autocorrelation and Probability Distributions in Gait-Metronome Synchronization 674
210 Courtney Shell: Sensory Neuroprosthesis Feedback Impacts Movement Planning in Obstacle Clearing 675
215 Sumire Sato: Effects of reinforcement feedback on locomotor adaptation with a 'virtual' split-belt paradigm 676
232 Huaqing Liang: Older Adults Retain the Ability to Predict External Perturbations Using Auditory Cues Only 677
233 Huaqing Liang: Young Adults Can Learn to Predict Unexpected Posterior Perturbations Using an Auditory Cue 678
235 Nathan Schilaty: Sex Differences of Motor Units Associated with ACL Injury and Arthrogenic Muscle Inhibition 679
325 Junmo An: Vibrotactile cueing improves kinematic recovery after unexpected slip perturbations induced by a split-belt treadmill 680
336 Haneol Kim: Perceptual Motor Abilities of Professional eSports Gamers 681
337 Matthew Beerse: The patterning of local variability during the acquisition of a whole-body continuous motor skill in young adults 682
370 Brian Selgrade: Adaptation of Leg Forces due to Gradually Introduced Split-Belt Walking in People with Trans-Tibial Amputation 683
412 Paige Thompson: Structure of Variance in Finger Forces Changes with Uncertainty in Force Tracking Tasks 684
465 Sumire Sato: Effects of asymmetrical footwear height on gait kinetics and kinematics 685
528 Xenia Demenchuk: Movement Variability During Single Leg Drop In Individuals After Anterior Cruciate Ligament Reconstruction 686
576 Kellen Krajewski: Load Magnitude and Forced Marching Impairs Locomotor System Function in Recruit Aged Females 687
608 Mia Caminita: Interpersonal and Interlimb Synergies in Handling of a Heavy Object Motor Task 688

611 Christopher Hasson: Robotic Augmentation of Human Trainers to Investigate the Role of Trainer Manipulative Variability on Patient Learning 689
647 Xianlian Zhou: Exoskeleton Hip Assistance during Walking: Assisting Flexion or Extension? 690
660 Kathy Reyes: A comparison of kicking kinematics among college students with and without Autism Spectrum Disorder 691
670 Alyssa Spomer: Motor Complexity is Reduced During Emulation of Cerebral Palsy Gait Patterns 692
692 Ahmed Ramadan: Temporal Hempiparetic Gait Symmetry Altered by a Nonparetic-Leg Weight 693
734 Sean Sanford: Multi-Sensory Feedback for Myoelectric Control 694
739 Wentao Liu: Functional connectivity analysis during direct EMG prosthesis control 695
763 Nathan Schilaty: Psychological Readiness is Evident in Motor Unit Action Potentials with ACL Injury 696
778 Seyed Yahya Shirazi: Use-dependent learning, not error-based learning, occurs during perturbed recumbent stepping 697
791 Ashley Williams: OPTIMAL-Based Virtual Reality Feedback to Reduce Dual-Task Balance Cost 698
836 Ahmed Ramadan: Sensory-Motor Assessment of the Lower Extremity in Tibial Rotation: Towards Knee Osteoarthritis Rehabilitation 699
838 Grace Han: Evaluating Activation Patterns of the Hand and Wrist During Dynamic Tasks Using a Similarity Index 700

Orthopaedics - General

112 Kayla Seymore: Clinical Improvements Relate to Gait Function in Patients with Achilles Tendinopathy 701
137 Scott Crawford: Shear Wave Speed Measurement Reliability in the Hamstring Muscles 702
207 Shadman Tahmid: Development and Validation of a Finite Element Model of the Cervical Spine 703
234 Kazandra Rodriguez: Quadriceps Muscle Morphology Predicts Vertical Ground Reaction Forces Following ACL Injury 704
258 Clarissa LeVasseur: The Effects of Pathology and Surgery on the Instant Center of Rotation in the Cervical Spine 705
304 Curran Reddy: Neck Muscle Size-Strength Relationships and Sex Differences 706
312 Takashi Nagai: Neck Neuromuscular Characteristics in Response to Multidirectional Visual Cues in Healthy Young Adults: Test-Retest Reliability Study 707
331 Tae Soo Bae: Biomechanical Effect of Valgus/Varus Knee Joint Alignment on ACL Reconstruction Surgery 708
350 Andrea Rossman: Evaluation of Texture Features from Micro-Computed Tomography of Osteogenesis Imperfecta Bone Specimens 709
368 Alexander Hooke: Auxetic Behavior of Achilles Tendons while Loading to Failure 710
402 Luca Fuller: Material Properties of Bighorn Sheep Horncore Bone for Energy Absorption 711
417 Edward Owens: Padding on the support table affects spinal posterior-to-anterior stiffness measurements 712
435 Nathan Lehr: The Effects of Triceps Surae Muscle Stimulation on Localized Achilles Subtendon Tissue Displacements 713
504 Grace Rozanski: Regional Differences in Shear Wave Velocity in the Short and Long Head of Biceps Brachii 714
566 Patrick Williamson: Preliminary Evaluation of Articular-Sided Supraspinatus Surface Strain for Varying Infraspinatus Loads 715
597 Craig Kage: Chronic Neck Pain: In Vivo Cervical Spine Kinematics 716
632 Ridhi Sahani: Skeletal muscle fibrosis involves changes in collagen organization in Duchenne muscular dystrophy 717
643 Hunter Wallace: Changes in Active and Passive Mechanics of the Diaphragm During the Progression of Duchenne Muscular Dystrophy 718
654 Tanetta Curenton: Biomechanical Assessment of Bone Staples: Effect of Declining Bone Mechanical Properties 719
662 Laura Hallock: The OpenArm Project: Exploring Deformation as a Measure of Muscle Force 720
669 Moein Nazifi: Can entropy of muscle synergies help track the gait improvements in ADS patients? 721
687 Sujata Khandare: How Do Dry Needling and High-Intensity Focused Ultrasound Affect Tendon Strain Pattern? 722
703 Matthew MacEwen: Dynamic Arthrokinematic Assessment of the Sacroiliac Joint 723
712 Christopher Weathers: Knee Valgus Angle: MRI versus Motion Capture 724
728 Halime Gulle: Graded Loading Challenge test for clinical assessment of foot pain: reliability and validity study. 725
768 Michael Polanco: The Utilization of Porcine Ligament Properties as a Substitute for Human Ligaments in a Spinal Finite Element Model 726
809 Dustin Bruening: Investigating Energy Transfer due to the Windlass Mechanism: A Pilot Study 727
825 Cribb Matthew: Tensile Testing of Spinal Ligaments 728
839 Jordyn Schroeder: Relative Contribution of Material and Morphological Properties to Altered Achilles Tendon Stiffness in Aging 729
841 Caleb Stubbs: Mechanical Testing of System for Anchoring a Synthetic Tendon to Replace the Achilles Tendon in a Rabbit Model 730
865 Yuhui Zhu: Factors Influencing Ambulatory Function Following Internal Hemipelvectomy 731
873 Karen Troy: Exoskeleton-Assisted Walking Therapy Increases Muscle Volume in People with Spinal Cord Injury (SCI) 732

Orthopaedics - Osteoarthritis & Joint Replacement

48 Amanda Munsch: The Association Between Altered Peak Knee Extensor Moments and Articular Contact Forces During Walking 733
75 Burcu Aydemir: Spatial gait characteristics are related to impaired hip abductor strength in women with hip osteoarthritis 734
104 Amy Morton: A Classifier for the Categorization of Thumb Carpometacarpal Osteoarthritis 735

156 Kyung Min Kim: Image-Based Optimization of Articular Cartilage Material Properties for The Isotropic Poroelastic Cartilage Model with Strain-Dependent Permeability 736
189 Trey Crisco: On Computing and Measuring Osteophyte Formation in the Progression of Thumb Osteoarthritis 737
197 Kirsten Seagers: The effect of toe-in and toe-out gait on hip moments in people with medial knee osteoarthritis 738
202 Nathan Webb: Total Ankle Replacement Wear Testing: ISO 22622 vs. Previous Wear Testing 739
217 Francesca Wade: Changes in the Plantarflexion Moment Arm of the Achilles Tendon Following Total Ankle Arthroplasty 740
218 Francesca Wade: Locomotor Function and Pain in Total Ankle Arthroplasty Patients at 6-Months Follow-up 741
230 Nicole Stark: Ankle Osteoarthritis Causes Hip Extension Asymmetry Compared to Healthy Controls 742
247 Skylar Holmes: Influence of Pain on Knee Extensor Function in Individuals With Knee Osteoarthritis 743
290 Songning Zhang: Are Level Walking Knee Biomechanics Different Between Bilateral and Unilateral Total Knee Replacement Patients? 744
291 Derek Yocum: Knee Joint Kinetic Differences in Bilateral and Unilateral TKR Patients During Stair Negotiation 745
340 Daniel Hochman: Exploring the Viability of Collecting Joint Acoustic Emissions Around the Wrist 746
359 Hannah Stokes: Patient Perceived Pain and Function Measures Are Related to Biomechanical Measures in TKA Patients 747
364 Daniel Kasman: Invasive and Non-invasive Methods for Humeral Head and Glenohumeral Joint Center Localization 748
384 Jarred Kaiser: Exercise may Mediate Post-Traumatic Osteoarthritis Through Restoration of Joint Homeostasis 749
424 Rebecca Weiss: A Comparison of Modular Control of the Lower Limbs during Gait Following Total Knee Arthroplasty 750
455 Abigail Schmitt: Does osteoarthritis impact gait and balance abilities in people with Parkinson's Disease? 751
677 Kenechukwu Okoye: AP laxity after TKA does not predict long-term quadriceps strength 752
714 Rachel Hall: Muscle Forces & Contributions to Acceleration During Chair-Rise in Individuals with Total Knee Arthroplasty 753
744 Melvin Mejia: Incremental lateral wedging for medial knee osteoarthritis: effects on frontal moment arm of the ground reaction force 754
855 Laura Linsley: A Biomechanical Processing Comparison between Frontal Plane Kinetics and Kinematics following Total Knee Arthroplasty 755
856 Raziyeh Baghi: Total Knee Moment Tracking During Elliptical Stepping with different foot progression angle 756

Sport and Performance - General

26 John Krzyszkowski: Countermovement Jump Phase-Specific Differences Between Fast and Slow Jumpers in Division 1 Collegiate Male Basketball Players 757
47 Kristof Kipp: Bivariate Functional Principal Component Analysis of Bar Trajectories during the Snatch 758
82 Ben Meyer: The Effects of Isokinetic Testing Speed on Ham:Quad Ratios and Asymmetry Indexes 759
121 Corina Kaufman: Shoulder, hip, and trunk sagittal plane kinematics during stand up paddle boarding 760
162 Grace Crowder: Validation of a Portable Force System for Assessing Jump Performance 761
205 Shelby Peel: The effects of fatigue on knee mechanics during a landing and cutting task in healthy females: a statistical parametric mapping approach 762
231 Paul Slaughter: Cutting Down on Cutting Injuries: Knee Flexion and ACL Injury Risk at Different Levels of Competitive Women's Ultimate Frisbee 763
237 Meghan Haser: Relationships Between Vertical Stiffness and Jump Performance in NCAA Division-I Athletes 764
267 Brittany Warren: Differences in Vertical Stiffness as A Function of Sex and Sport 765
302 Youngmin Chun: Effects of Box Height on Instantaneous Lower Extremity Joint Stiffness during Drop Vertical Jump 766
363 Nicole Arnold: Fabrication of a Hand Brace for a Collegiate Basketball Player Following Surgery: Identification of Hand Forces During Dribbling and Passing 767
426 Brandi Decoux: Inter-segmental coordination variability during hopping and running on natural and synthetic turf surfaces 768
445 Abby Blocker: Simulated Exercise Device Vibration Isolation System for Spaceflight Applications 769
451 Sarah Wilson: Use of Inertial Measurement Units to Quantify Performance in Alpine Skiing 770
572 Patrick Fischer: Assessing the Generalizability of Dual-Task Effects across Different Movements 771
581 Beau Kewley: Dynamic Simulation Analysis and Optimization of a Standing Power Throw 772
584 Patrick Fischer: Elucidating the Spectrum of Cognitive-Motor Relationships during a Sidestep Cut 773
590 Meredith Owen: Golf Swing Consistency and Balance Improvements Following Eight Week Balance Intervention 774
593 Casey Wiens: Coordination of Upper Extremity and Center of Mass Trajectory During Basketball Shots from Varying Distances 775
594 Elizabeth Euiler: Reliability of muscle activity during adaptive rowing: A pilot study 776
618 Matt Wagner: Blood Flow Restriction Exercise Limb Occlusion Pressure in Hypertensive and Normotensive Participants 777
689 John H Challis: Mass Distribution and Jump Performance 778
743 Suzanne Konz: An investigation into the release factors of the hammer throw 779
766 Abigail Swenson: Head Impact Exposure in Youth Hockey 780
792 Mei Zhen Huang: Familiarization time of novel footwear for treadmill running tests 781
834 Caitlin Mazurek: Lower-extremity Inter-segment Coordination during Ice Hockey Skating Starts 782
863 Hamidreza Barnamehei: Motor control evaluation of front kick (Ap Chagi) with kinematics pattern executed by professional kyorugi Taekwondo players 783
869 Maria Rodriguez: 2D kinematics of skating on a slide board versus skating on a treadmill 784

Biomechanical Mechanisms of Tai-Chi Gait for Preventing Falls

Feng Yang.[1] and Wei Liu [2]
[1]Department of Kinesiology and Health, Georgia State University, Atlanta, GA 30303
[2]Division of Osteopathic Rehabilitation, Edward Via College of Osteopathic Medicine, Auburn, AL, 36832
Email: fyang@gsu.edu

Introduction

Falls are a threat to the health of older adults and people with neurological dysfucntions. Tremendous efforts have been devoted in developing fall prevention progams. Tai-Chi (TC) practice, as an approach for preventing falls, is growing in popularity worldwide. TC is an ancient Chinese traditional mind-body exercise of self-cultivation and energy preservation. During TC practice, the players focus on slow, gentle, and fluid body movements and breathing. Despite the potential health benefits from TC practice, the underlying biomechanical mechanisms of TC practice reducing the risk of falls are still uncler. Previous TC-based clinical trials adopted certain selected TC forms. However, the scientific rationals of the forms selection is lacking. Without a thorough understanding of such mechanisms, it is difficult to accurately identify and effectively implement optimal TC forms into interventions for preventing falls.

TC gait is a basic and common lower extremity TC movements. Given that the majority of outdoor falls occur during locomotion, like walking, the purpose of this study was to examine the influence of TC gait on dynamic gait stability compared with regular walking gait in adults. As dynamic gait stabitliy is a key risk factor fo falls (Yang et al., 2009), examining the impact of TC gait on dynamic gait stability may provide valuable insight into the mechanisms of TC reducing the risk of falls.

Methods

Ten healthy adults (five males, 58.4 ± 13.1 years) with at least two-year experience of TC practice were enrolled into this cross-sectional study approved by the Institutional Reviw Board. After three-five trials of regular walking over a linear pathway embedded with two force plates (AMTI, MA) at self-selected speed and manner, all participants performed five trials of Yang-style TC gait. Full-body kinematics and ground reaction force were synchronously collected from reflective markers using a motion capture system (Vicon, UK) and the force plates, respectively (Liu et al., 2016).

The last TC gait trial was chosen as the representative one and analyzed. Two events: touchdown (TD) and liftoff (LO), were identified based on the ground reaction force. The filtered marker paths were used to calculate the body COM kinematics (de Leva, 1996). The two components of the COM motion state (i.e., its position and velocity) were calculated relative to the rear of the BOS and normalized by the foot length (l_{BOS}) and the square root of the product of the body height (bh) and gravitational acceleration (g), respectively. Dynamic gait stability at both events was calculated as the shortest distance from the COM motion state to the limit against backward balance loss (Fig. 1a) (Yang and Pai, 2010). The dependent variable (dynamic stabitliy at TD and LO) was compared between TC and regular gait using paired t-tests with SPSS 24 (IBM) and a significance level of 0.05 was applied.

Results and Discussion

During stance phase, the COM motion trajectory was lower for TC gait than the regular gait (Fig. 1a). Both types of gait covered a similar range of COM position but COM velocity was lower during TC gait than the regular gait. Notably, COM during the regular gait continuously travelled forward relative to the BOS while it reversed the moving direction four times in TC gait. Overall, participants were less stable when practicing TC gait than in normal gait. Specifically, individuals were less stable during TC gait in comparison with regular gait at both events (Fig. 1b): 0.038 ± 0.018 vs. 0.190 ± 0.029, $p < 0.001$ at TD; and -0.201 ± 0.053 vs. -0.041 ± 0.037, $p < 0.001$ at LO.

Our results revealed that individuals are less stable during TC gait than regular gait. A lower stability represents more challenging to the body's postural control system and increase the risk of falling. To respond to the challenge, the body must adaptively develop neuromuscular control strategies to maintain and improve body balance. Improvements in body balance could signify a reduced fall risk. From this perspective, TC practice reflects the overload practice principle (i.e., to increase the difficulty of tasks during practice). This could in part account for the observed TC-induced balance improvements among older adults in previous clinical trials (Lomas-Vega et al., 2017).

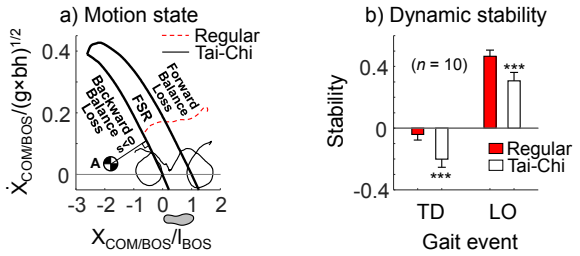

Figure 1: a) Demonstration of dynamic gait stability defined within the conceptual framework of Feasible Stabiity Region (FSR). Also shown are the COM motion state trajectories during the stance phase in TC and regular gaits for a representative participant. b) Comparison beween TC and regular gaits for dynamic gait stabitliy at TD and LO. ***: $p < 0.001$.

Significance

Our study represents the first attempt to inspect the biomechanical impact of TC movements on fall risk. A clear understanding of how each TC form affects body biomechanics will lay a solid scientific foundation for future efforts to optimize the effectiveness of TC practice on preventing falls.

Acknowledgements

This work was in part supported by NIH (K23AT009568 to Liu).

References

de Leva, P. (1996). *Journal of Biomechanics*, 29, 1223-1230.
Liu, W. et al. *Journal of Alternative and Complementary Medicine*, 22, 818-823.
Lomas-Vega, R. et al. (2017). *Journal of American Geriatrics Society*, 65, 2037-2043.
Yang, F., et al. (2009). *Journal of Biomechanics*, 42, 1903-1908.
Yang, F. et al. (2010). *Journal of Biomechanics*, 43, 397-404.

A hydrodynamics model to predict under-shoe fluid pressures based on the dimensions of a worn region

Sarah L. Hemler[1], Vani H. Sundaram[2], and Kurt E. Beschorner[1]
[1] Department of Bioengineering, University of Pittsburgh, [2] Department of Mechanical Engineering, University of Colorado, Boulder,
Email: *slh148@pitt.edu

Introduction

Slips and falls are a major cause of injury in the workplace. As slips occur at the shoe-floor interface in the presence of a lubricant, footwear is an important factor for preventing slips. Previous research has shown that donning completely worn shoes presents a higher slip risk than wearing new shoes [1] and that switching to a new pair of shoes lowers slip risk [2]. While these studies establish wear as a relevant risk factor for slips, the literature fails to present a method of predicting slip risk based on the physical conidition of the shoe. Lubrication theory may provide important information on the impact of the size of the worn region relative to the under-shoe performance in the presence of liquid contaminants. As the size of the worn region grows, the drainage ability decreases leading to increased under-shoe fluid pressures and subsequent increased slip risk [3]. The purpose of this study is to assess the ability to predict under-shoe fluid pressures based on shoe wear geometry applied to a theoretical hydrodynamics solution.

Methods

This study analyzes data from three previous experiments (E1-simulated shoe wear [3], E2-progressive shoe wear [4], and E3-human slipping trials [5]). In each experiment, under-shoe fluid pressures are predicted by a solution of Reynolds equation based on shoe wear geometry measurements.

E1: Four right shoes were systematically abraded to simulate wear during gait. At baseline and after each wear cycle, under-shoe peak fluid pressures were measured as shoes were slid across a contamined surface.

E2: 13 participants wore two pairs of shoes in the workplace for one month at a time (n_{shoes}=22). At baseline and after each month of wear, fluid pressures were measured for both sides (L/R).

E3: 57 participants experienced a slippery condition, while wearing their own worn shoes. The liquid contaminant was spread across an array of pressure sensors. Under-shoe fluid pressures were measured during the unexpected slipping condition.

For all shoes, the size of the worn region (length, *l*, and width *b*) was measured based on the largest region without tread on the heel of the shoe. Measurements were repeated for each wear cycle and month of wear for E1 and E2. The tapered-wedge bearing solution of the Reynold's equation was used to predict the minimum film thickness (PFT) based on the size of the worn region along with the dynamic viscosity of the 90% glycerol used in all experiments ($\mu = 214\ cP$), the sliding speed ($u_{E1,E2} = 0.3\frac{m}{s}, u_{E3} = 0.1\frac{m}{s}$ [6]), normal force ($F_{E1,E2} = 250\ N, F_{E3} = 179\ N$ [6]), a wedge incline factor ($K_p = 0.025$) [7], and a wedge-fluid, side leakage factor (η) which was dependent on the worn region size (Eq. 1).

$$PFT = \sqrt{\frac{6\mu u l^2 b \eta K_p}{F}} \quad (1)$$

Three statistical models were used to test the effect of PFT on the peak fluid pressures. Specifically, two repeated-measures regression models (E1 and E2) and one linear regression model (E3) were used where the independent variables were PFT (E1-3), shoe type (E2), and side (E2), and the dependent variable was the peak fluid pressure (E1-3). Random variables of shoe type (E1) and participant (E2) were included in the models.

Results and Discussion

PFT predicted peak fluid pressure for all three models: E1 - $F_{1,75}$ =95.7, $p<.001$, E2 - $F_{1,180}$=47.9, $p<.001$, and E3 - $F_{1,55}$=16.5, $p<.001$.

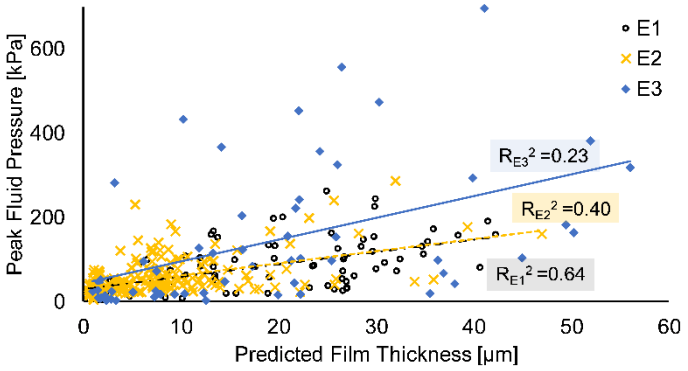

Figure 1: Peak fluid pressure with respect to the PFT across E1, E2, & E3. Trendlines per experiment and respective R^2 values are shown.

This research validates the use of PFT based on the tapered-wedge solution of Reynolds equation to predict under-shoe fluid pressure in multiple experimental contexts. Consequently, the size of the worn region of the shoe outsole wear is a good indicator of under-shoe hydrodynamics.

Significance

Shoe traction performance is dependent on effective drainage that minimizes under-shoe fluid pressures. By applying fluid mechanics to a simple metric of shoe wear, this research supplies a clearer understanding of how shoe outsole wear geometry influences under-shoe fluid pressures. This research provides a foundation for developing a measurement tool to assess the worn region of shoe outsoles and supply replacement recommendations. Such a tool would guide appropriate shoe replacement, enhance the performance of workplace footwear [5], and thus reduce slip and fall accidents [5,6].

Acknowledgments

This study was funded by the following grants: NIOSH R01 OH 010940, NSF GRFP DGE1747452 and DGE1650115, R43AR064111, NCRR S10RR027102.

References

[1] Beschorner, et al. J Biomech, 2014. 47(2).
[2] Verma, et al. Ergo, 2014. 57(12).
[3] Hemler, et al. App Ergo, 2019. 80.
[4] Hemler, et al. *Traction Performance.* J Saf Res, in review.
[5] Sundaram, et al. *Worn Region Size*. J Biomech, in review.
[6] Iraqi, et al. J Biomech, 2018. 74.
[7] Fuller, D. *Theory & Practice*. 1956

Slipping Foot and Recovery Step Yaw After a Turning Slip: A Balance Recovery Mechanism?

Corbin M. Rasmussen[1] and Nathaniel H. Hunt[1]
[1]Department of Biomechanics, University of Nebraska at Omaha, Omaha, NE USA
Email: cmrasmussen@unomaha.edu

Introduction

A wealth of research has focused on factors and behaviors key to slip recovery and fall prevention, such as trunk angle, recovery steps (RS), and arm swing,[1,2] but little attention has been paid to the role of foot yaw. Side-specific adjustments to foot yaw occur during turning[3] and it is considered a balance strategy in response to small deviations during walking.[4] Whether this extends to larger perturbations like slips has not been explored, possibly due to the mechanical constraints of commonly used slipping methods in the lab. We recently developed a wearable device (WASP) that delivers unconstrained slips, allowing the sliding foot to move and rotate freely.[5] Using this device, we aimed to determine how slipping foot (SF) and RS yaw changes during slips of different contexts, and to investigate the influence of slip severity (i.e. slip distance) on the degree of SF and RS yaw.

Methods

18 young adults (22.72±2.89 yrs., 9 females) were outfitted with a safety harness, full-body marker set, athletic shoes, and a pair of WASP devices.[4] Subjects were slipped via WASP during early (0-33%), mid (34-67%), or late (68-100%) stance phase of the inside or outside foot as they followed 180° curvilinear turns of 1.0 or 2.0 meter radius. Twelve trials were performed randomly to observe all possible combinations of phase, foot, and radius, however only early stance slips are reported here. All trials were recorded by a 17-camera motion capture system at 200 Hz.

Gait events[6], slip onset, and slip cessation were determined from kinematics. Foot segments were simplified to a line between the calcaneus and 2nd metatarsal head markers. SF yaw change was calculated as the continuous angle between the SF segment throughout the slip and the foot's position at slip onset. Peak external and internal rotation angles were extracted from the resulting time series, and the one with the largest magnitude was entered into the SF analysis. For RS yaw, the angle between the RS foot segment and the center of mass (CoM) velocity vector at step touchdown was derived. The same method was used to obtain unperturbed step (US) yaw at the left and right heel-strike before slip onset.[3] The average US yaw angle for each set of contexts was then calculated and subtracted from RS values under the same contexts to obtain the RS yaw change. Finally, slip distance was the difference between the SF CoM positions at slip onset and cessation. Positive values correspond to external rotation and negative to internal rotation.[3]

Linear mixed effects models were built to examine the effect of curvature and foot on SF and RS yaw. These contexts were treated as fixed effects, and subject as a random effect. Spearman rank correlation coefficients were derived to quantify the relationship between slip distance and SF and RS yaw.

Results and Discussion

Figure 1 illustrates the following results. Inside SF max yaw was more externally rotated than that of the outside SF ($t(85)=2.07$, $p=0.042$). The effect of turn curvature ($t(85)=2.13$, $p=0.036$) was qualified by foot, with wider turns reducing and increasing external rotation during inside and outside SF respectively ($t(85)=-2.18$, $p=0.032$). In terms of RS yaw change from US, outside foot RS were more internally rotated, while inside foot RS were externally rotated ($t(82)=-4.29$, $p<0.001$). Sharper turn curvature increased the degree of this trend ($t(82)=-2.25$, $p=0.027$). Regardless of foot, SF max yaw tended to be more externally rotated with increasing slip severity (Outside: $\rho=0.4683$, $p<0.001$; Inside: $\rho=0.3823$, $p=0.041$). RS yaw change tended to increase in magnitude with slip severity, as outside and inside foot slips exhibited externally and internally rotated RS respectively, however the latter was not significant (Outside: $\rho=0.5797$, $p<0.001$; Inside: $\rho=-0.3187$, $p=0.092$).

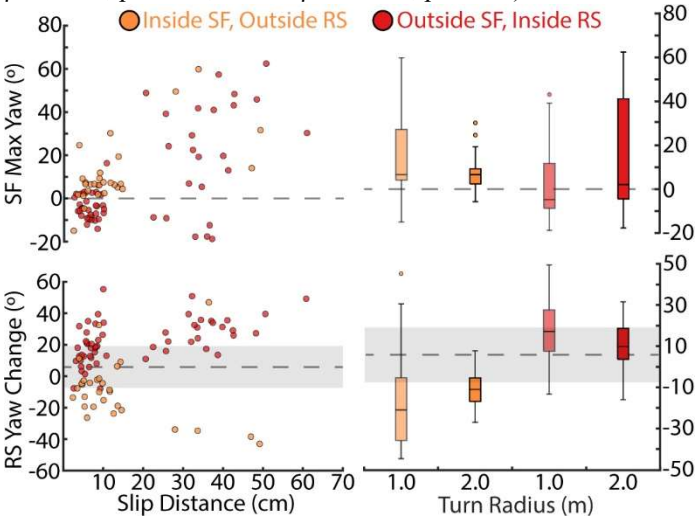

Figure 1: Plots illustrating SF and RS yaws' association with slip severity and context. Shaded areas represent the mean US yaw ± 1 SD.

Significance

To our knowledge, this is the first examination of foot yaw during and after a slip perturbation. Our RS results support the notion of foot yaw as a balance strategy,[4] as the magnitude of RS yaw increased with slip severity. RS yaw, particularly if in the direction of a fall, may act to extend the base of support in that direction with a shorter required RS length. The function of SF yaw, specifically whether it is beneficial or detrimental to recovery, is unclear and should be the topic of future research. Overall, these findings should encourage further study of foot yaw's role in slip recovery in fall-prone populations, and to what degree it can be altered by fall-prevention training.

Acknowledgments

Study funded by NIH grants R15AG063106 and P20GM109090.

References

1. Grabiner MD et al. (2012). *Med Sci Sports Exerc,* **44**: 2410-4.
2. Marigold DS et al. (2003). *J Neurophysiol,* **89**: 1727-37.
3. Courtine G et al. (2003). *Eur J Neurosci,* **18**: 177-90.
4. Rebula JR et al. (2017). *J Biomech,* **53**: 1-8.
5. Rasmussen CM et al. (2019). *J Neuroeng Rehabil,* **16**: 118.
6. Zeni Jr. JA et al. (2008). *Gait Posture,* **27**: 710-4.

Impact of an Ankle-Foot Orthosis on Reactive Stepping in Young Adults

Kyra E. Twohy[1], Kurt Jackson[1], and Kimberly E. Bigelow[1]
[1]University of Dayton, Dayton, OH
Email: twohyk1@udayton.edu

Introduction

Ankle-foot orthoses (AFOs) are commonly prescribed to individuals with conditions such as stroke and multiple sclerosis to assist with foot drop and other gait deficits [1]. While AFOs have obvious benefits, there is believed to be some tradeoffs. In particular, the rigidity and support provided by AFOs may restrict ankle movements, which could be helpful for tasks such as sit-to-stand or recovery upon a slip or trip. While there are numerous studies examining reactive stepping after a perturbation to better understand fall mechanisms and fall recovery strategies [2,3], to date, these studies have not included individuals wearing AFOs.

The goal of this pilot study was to examine, first in healthy young adults, differences in step recovery when an AFO was worn compared to a no-AFO condition, using a lean-and-release paradigm. We hypothesized that individuals would prefer to step with the leg not wearing the AFO, and that the presence of an AFO on either the stepping or stance leg would increase the overall time it took to step.

Methods

Twenty healthy young adults (Age: 23.7 ± 2.3 years, Gender: 14 Male, 6 Female) participated in this study. All individuals gave written informed consent and all study procedures were approved by the University of Dayton Institutional Review Board.

The lean-and-release system followed previous research and set to a 15º forward lean, confirmed with an anglometer [2,3]. To determine release, 2 retro-reflective markers were attached to the harness, which would separate upon release. Each foot was placed on a Bertec in-ground force plate [Models 4060 and 4080].

A total of 30 reactive stepping trials were completed using a lean-and-release set up. No AFO was present for the first 10 trials. Following this, a total of 20 trials with an off-the-shelf traditional plastic AFO were completed (10 per leg, randomized in sets of two). Study participants were instructed to do whatever was necessary to regain their balance. Each participant had retro-reflective markers placed on anatomical locations of the back, hips, thighs, shank, and feet. All trials were recorded with a VICON motion capture system at 150 Hz.

Visual 3D was used to calculate step length, reaction time, step time, and maximum joint angles identified by previous lean-and release-research [2,3]. Other variables studied included step length and stepping foot preference. Differences between reactive stepping with and without an AFO present was determined by running a one-way ANOVA with a Tukey post-hoc in SPSS to compare the no AFO condition to the AFO on the stepping leg and to the AFO on the stance leg.

Results and Discussion

Participants, on average, stepped 1.4 times more frequently with the leg not wearing the AFO. This indicates that an AFO does change stepping foot preference to favor keeping the AFO leg in stance. It may be that individuals find the AFO's weight and movement restrictions are less conducive to the speed and adaptability that a reactive step requires; future work will determine how this changes for those in true need of an AFO.

Results of timing and kinematic variables are displayed in Table 1, below. Reaction time was significantly increased in trials without an AFO present as compared to either the AFO worn on the stance or the stepping leg. Differences in step time were not significant, however.

Step length was significantly shorter in the stance and stepping leg AFO conditions, as compared to the no AFO condition. This could be due to a preference for landing flat footed. As the knee extends to complete the step the toes are brought further up with the ankle constrained by the AFO. A shorter step is then needed to minimize ankle extension to be able to land flat footed.

Both the maximum joint angle of the ankle and the knee were significantly different when the AFO was on the swing leg. This difference was expected because the AFO does limit the range of motion at the ankle and as a result the knee angle would be adjusted to account for the change. However, this did not carry up to the hip joint. Future work may also want to examine muscle activation during a reactive step with and without an AFO to understand the underlying adjustments in muscle activation levels and timing needed to alter a stepping reponse.

Significance

This is the first known study to examine stepping reactions while an AFO is worn. The findings of this study lay the foundation for future studies focused on assessment of stepping reactions on impaired populations wearing AFOs and, if needed, interventions to improve the likelihood of a successful recovery step.

Acknowledgments

The authors acknowledge UD DPT research assistants for their help with data collection.

References

[1] Pohl, M, et al. Clinical rehabilitation. 324-330, 2006.
[2] Do, M, et al. Journal of Biomechanics. 933-939, 1982.
[3] Hsiao-Wecksler, E. Journal of Electromyography and Kinesiology. 179-187, 2008.

Table 1: Summary of Stepping Variables

		Reaction Time (sec)	Step Time (sec)	Step Length (m)	Ankle Angle (°)	Knee Angle (°)	Hip Angle (°)
AFO Condition	No AFO	0.33 ± 0.08	0.19 ± 0.03	0.64 ± 0.1	-20.5 ± 3.6	61.6 ± 9.8	54.3 ± 11.0
	AFO on Stance Leg	0.30 ± 0.06 †	0.19 ± 0.04	0.61 ± 0.13 *	-21.1 ± 3.8	61.6 ± 9.6	56.1 ± 12.7
	AFO on Swing Leg	0.29 ± 0.05 †	0.18 ± 0.03	0.56 ± 0.12 †	-18.2 ± 3.3 †	58.9 ± 9.8 *	53.0 ± 11.1

Significance as compared to No AFO condition: * $p < 0.05$, ‡ $p < 0.01$, † $p < 0.001$

Sensitivity of Toe Height to Joint Angles of the Bipedal Linked Chain during Obstacle Crossing

Chuyi Cui[1], B.C. Muir[2,3], S. Rietdyk[1], J.M. Haddad[1], R.E.A. van Emmerik[4], and S. Ambike[1]
[1]Purdue University, Department of Health and Kinesiology, West Lafayette, IN, USA
Email: cui111@purdue.edu

Introduction

Tripping while walking is a main contributor to falls [1]. Trip frequency is related not only to the elevation of the swing toe above the ground or an obstacle, but also to the variance in the swing toe clearance [2]. To identify the source of this variance, the sensitivity of the swing toe height to changes in the limb joints has been quantified. However, previous sensitivity calculations have been restricted to only sagittal-plane angles [3], swing limb [3], or unobstructed walking [3,4]. Therefore, the aims of the present study are to (1) quantify the sensitivity of swing toe height to sagittal and frontal plane joint angles during overground walking and while crossing obstacles of varying height, and (2) compare the sensitivity of toe height to angles that are grouped as follows: the frontal plane vs. sagittal plane angles, and the swing vs. stance limb angles.

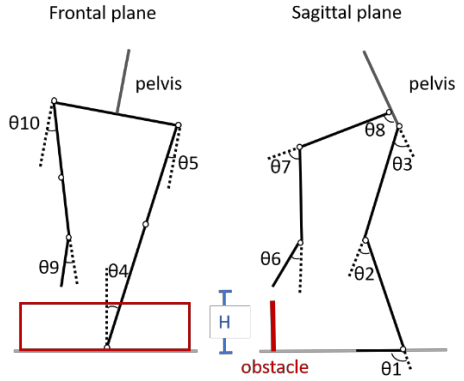

Fig. 1: Lower-limb joint angles that influence toe height.

Methods

Ten subjects (23.8±3.4 years, 3 female) crossed obstacles on a 15 m walkway. Ten trials of each condition were recorded (unobstructed, 3, 10, 26 cm obstacle). Whole-body kinematics were measured using a Qualysis motion capture system. Sensitivity of toe height to the lower-limb joint angles was determined at the instant of minimum toe clearance for unobstructed gait and the instant when the first and second foot crossed the obstacle (lead and trail subtasks).

The function relating toe height (H) to the lower-limb joint angles (θ_i, i=1 to 10; Fig. 1) was written: H=f($\underline{\theta}$). The Jacobian of f was derived: $J=[\partial H/\partial\theta_1 \ \partial H/\partial\theta_2 \ \dots \ \partial H/\partial\theta_{10}]$ and evaluated by substituting the measured values of the joint angles. The values in J are the changes in H due to a unit change in an angle, i.e., the sensitivities of H to individual angles.

Sensitivity of H to groups of angles within the (1) sagittal vs frontal planes and (2) stance vs swing limbs were compared. Senitivity to a group of angles was quantified as the singular value of the Jacobian comprising of the partial derivatives with respect to those angles. For example, the singular value of $J_{frontal}=[\partial H/\partial\theta_4 \ \partial H/\partial\theta_5 \ \partial H/\partial\theta_9 \ \partial H/\partial\theta_{10}]$ yields the maximum possible change in H due to the vector $[\partial\theta_4 \ \partial\theta_5 \ \partial\theta_9 \ \partial\theta_{10}]$ of unit magnitude, and it is defined as the sensitivity of H to the frontal plane angles. ANOVAs were used to determine if sensitivity was affected by individual joint angles (*angle* × *subtask* × *obst_height)*, and by angle groups across planes ($group_{plane}$ × *subtask* × *obst_height*) and across limbs ($group_{limb}$ × *subtask* × *obst_height).*

Results and Discussion

For individual angles, toe height was most sensitive to stance hip ab/adduction, consistent with [4]. Toe height was also sensitive to stance ankle flex/extension and ab/adduction, and least sensitive to swing ankle ab/adduction. Sensitivity to individual angles was not consistent across the lead and trail subtasks during obstacle crossing (3-way interaction: $F_{(27,711)}$=6.65; p<.01; Fig. 2). For example, sensitivity for the trail subtask was higher than the lead subtask for the swing knee flex/extension, but lower for swing hip flex/extension.

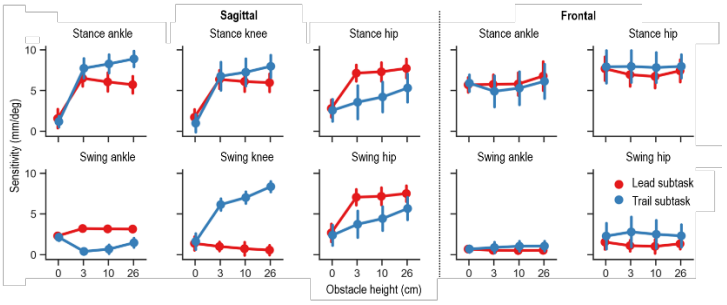

Fig. 2: Mean±SD of toe height sensitivity to individual joint angles.

For groups of angles, toe height was more sensitive to frontal plane angles than sagittal plane angles for unobstructed gait (0 cm obstacle), but this relation is reversed during obstacle crossing ($group_{plane}$×*obst_height*: $F_{(3,135)}$=53.06, p<.01; Fig. 3A). Toe height was more sensitive to the stance limb joint angles than the swing limb joint angles for all obstacle heights ($group_{limb}$: $F_{(1,135)}$=912.9, p<.01; Fig. 3B).

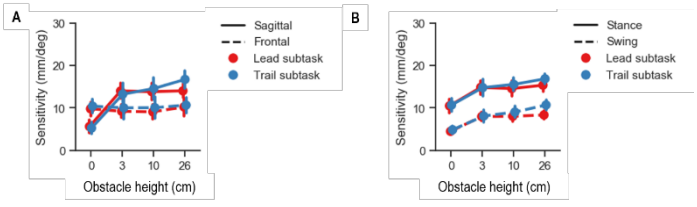

Fig. 3: Mean±SD of toe height sensitivity to groups of joint angles in two planes (A) and in two limbs (B).

Significance

When individuals/patients report increased frequency of tripping, one should consider weakness or impaired coordination in the ab/adductors as potential sources of the issue. Furthermore, interventions should not be limited to the swing limb, as the stance limb angles, as a group, had greater influence than the swing limb angles, as a group, on swing toe height (Fig. 3B).

References

[1] Begg et al., 1997. *Age and Ageing*, *26*(4), 261-268.
[2] Barrett et al., 2010. *Gait & Posture*, *32*(4), 429-435.
[3] Moosabhoy and Gard, 2006. *Gait & Posture*, *24*(4), 493-501.
[4] Winter, 1992. *Physical Therapy*, *72*(1), 45-53.

The impact of obesity on trunk control following trip-like treadmill perturbations while standing

Noah J. Rosenblatt.[1]*, Michael L. Madigan[2]
[1] Rosalind Franklin University of Medicine and Science, North Chicago, IL; [2] Virginia Tech, Blackburg, VA
Email: *noah.rosenblatt@rosalindfranklin.edu

Introduction

The 30% of older Americans (65+ years of age) who are obese (body mass index (BMI) ≥30 kg^2/m) are up to 50% more likely to fall[1] and are at greater odds of sustaining a fall-related injury[2], than normal weight (BMI: 17.5-25 kg2/m) older adults (NW). Obese older adults (OB) may fall at higher rates than NW following a lab-induced trip[3]. A large initial change in angular velocity, such as that imparted by a trip, may present a greater challenge to OB due to a greater increase angular momentum (i.e. more massive trunk)[5]. This may increase the likelihood of a fall, i.e. increase trunk flexion and trunk angular velocity at the instant of recovery step completion[4]. Similarly, increased inertia may be beneficial to balance when there is little initial angular velocity[6]. The purpose of this study was to quantify the effects of obesity on biomechanics of balance recovery in older adults. We hypothesized that following trip-like treadmill perturbations, differences in trunk angle and angular velocity between OB and NW older adults would increase in proportion to the perturbation acceleration. We also explored the extent to which obesity-related impaired trunk control was related to functional mobility.

Methods

We recruited 29 OB and 30 NW with self-reported ability to walk one mile at any pace and normal range of motion in the lower limbs and trunk. Participants were excluded for use of a cane/walker, artificial joint replacement, self-reported history of conditions that interfere with gait or diabetic peripheral neuropathy or osteoporosis. Participants completed the following functional tests: 10m walk at maximum speed (10mW), Timed-up-and-go (TUG), figure of eight walk (F8W), single-limb stance for a maximum of 30 s (SLS), and standing balance using the NIH toolbox. During a separate session they completed 30 perturbation trials, after five practice trials. For each trial, participants stood on a motorized treadmill (C-Mill; Motekforcelink, Netherlands) which suddenly accelerated for 150s in the posterior direction, and then decelerated. There were 10 different accelerations, 1.5-3.75 m/s^2 in increments of 0.25 m/s^2, each of which was provided three times (all practice trials were performed at 1.75 m/s^2). The order of accelerations was randomized. A 6 camera motion capture system (Vicon, UK) tracked body movements. For each trial we calculated the angle of the trunk at the instant that the first and second recovery step contacted the treadmill belt (θ_1 and θ_2, respectively) as well as the associated trunk angular velocities (ω_1 and ω_2, respectively). A mixed model analysis (within subject factor: acceleration; between subject factor: group - OB vs NW, referenced to OB; random factor: subject) was used to determine the relationship between trunk kinematics and treadmill acceleration. In the event of a significant effect of subject, we correlated subject-specific slopes with functional measures.

Results and Discussion

Consistent with our hypothesis, we found significant group x acceleration interactions for all trunk kinematics (Table 1). NW exhibited a smaller θ_1 and θ_2 than OB at low accelerations (negative Beta for group), and the rate of increase in θ_1 with increasing acceleration was nearly 25% greater for OB vs NW (Beta for acceleration for OB is 1.26 vs. 0.96 (1.26-0.30) for NW). With regard to ω_1 at low treadmill accelerations OB had greater extension velocities (more negative values; positive Beta for group), but ω_1 increased more quickly with increasing treadmill acceleration (Figure 1). Despite having different ω_1 at low treadmill accelerations, ω_2 was similar for both groups at low accelerations ($p>0.05$ for group term). Both OB and NW demonstrated increasing trunk extension velocities on the second step with increasing treadmill acceleration, but OB increased extension velocity at a greater rate than NW, perhaps to compensate for differences during the first step. Multiple functional measures were correlated with subject-specific slopes (Table 1). While trunk control strategies for balance recovery. i.e., scaling of kinematics in response to increasing perturbations magnitudes, are thought to be completely distinct from other capabilities, to some extent they may exploit strength and coordination patterns that also facilitate performance of functional tasks. In absence of perturbation paradigms, a battery of such tasks could help predict fall recovery abilities.

Mixed model - p-value; Beta				
	θ_1	θ_2	ω_1	ω_2
Subject	0.08	0.005	0.007	0.012
Group x Acceleration	0.003; -0.30	<0.001; -0.30	<0.001 -3.72	<0.001 2.15
Acceleration	<0.001; 1.26	<0.001; 1.94	<0.001; 4.17	<0.001; -7.07
Group	<0.001; -6.4	<0.001; -4.3	<0.001 22.25	0.56
Correlation coefficients				
10mW	--	-0.56	-0.55	0.32
F8W	--	0.48	0.40	--
Balance	--	-.36	--	--
TUG	--	0.58	0.48	-0.44
4SS	--	0.42	0.39	--
SSL	--	-0.58	-0.31	0.34

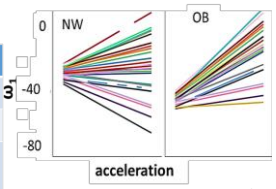

Table 1 (left): Results from mixed model and correlations; Betas and coefficients shown only for $p<0.05$. **Figure 1 (top)**: Example group x acceleration interaction. Each colored line represents the model fit of the ω_1 vs acceleration data for a given subject. OB and NW have similar intercepts ($p>0.05$ for group) but for NW the slope is 7.07 (deg/s)/(m/s^2) less.

Significance

We confirm that obesity provides protection against falls at low velocities (e.g., bumped while standing) but not high velocities (e.g., trips or slips). Perturbation based interventions that have been shown to improve trunk control and reduce trip-related falls in NW may be effective at reducing falls by OB. Such intervention could also improve functional mobility in this population.

Acknowledgements

The work was funded by 1R03AR066326-01A1

References

1. Himes & Reynold. PMID: 22150343; 2. Finkelstein, et al, PMID 17515011; 3. Rosenblatt & Grabiner, PMID 22218136; 4. Matrangola & Madigan, PMID 21470705; 5. Pavol et al. PMID 11445602; 6. Rogers et al, PMID 860

Females have greater local dynamic stability than males when walking with military-relevant loads.

[1] Kari L. Loverro, PhD, [2] Elliot Saltzman, PhD, and [2] Cara L. Lewis, PT, PhD
[1] Combat Capabilities Development Command Soldier Center, Natick, MA, USA [2] Boston University, Boston, MA, USA
email: kari.l.loverro.civ@mail.mil

Introduction

In the military, load carriage is an unavoidable task. Previous research suggests that kinematic adaptations made in response to added load increases stability during gait. Yet, the stability measures typically used do not quantify a gait pattern's dynamic stability, but rather its kinematic variability. [1] The *local divergence exponent* (LDE) provides a nonlinear measure of gait's *local dynamic stability*. [2] We have reported that LDE (and hence local dynamic stability) is affected by military relevant loads and speeds [3] and that females alter average gait mechanics differently than males in response to these loads. [4] No previous research has investigated if standardized military loads affect local dynamic stability of males and females similarly. As females now have access to all US military occupations, often carrying similar loads to males, it is important to assess if these loads affect the stability of females differently than males. The purpose of this analysis was to determine if local dynamic stability is similarly affected in both males and females when carrying standardized military loads. We hypothesized that local dynamic stability would differ between females and males, with females having lower local dynamic stability compared to males as load increased.

Methods

Fifteen females (age: 26.0±5.1 yrs, height: 1.65±0.1 m, mass: 67.6±9.4 kg) and fifteen males (age: 26.0±4.8 yrs, height: 1.78±0.08 m, mass: 79.8±9.1 kg) completed 2-minute walking trials on a treadmill under three load conditions (unloaded: 1.2 kg, light: 15 kg, and heavy: 27 kg) at 1.35 m/s. Loads and walking speed were selected based on Army doctrine recommendations. Two minutes of marker data from the trunk (C7) and pelvis (sacrum) segments were collected and low-pass filtered (10Hz). The first-time derivative (velocity) time series was used for analysis. Rosenstein's algorithm was used to calculate LDE for the trunk and pelvis velocity time series in all directions (mediolateral, anteroposterior, vertical), where a larger LDE indicates decreased local dynamic stability. We used a 3x2 repeated measures ANOVA with sex as a between-subject factor, load as a within subject factor, and included the interaction of sex and load. Post-hoc analyses were run if significant interactions of load and sex were detected.

Results and Discussion

We found no significant interactions of load and sex for LDE of the trunk or pelvis ($p>0.05$), but did detect main effects of load and sex for all directions of the trunk ($p\leq0.03$) and in the vertical direction of the pelvis ($p\leq0.01$). In all directions of the trunk and in the vertical direction of the pelvis, females had significantly lower LDE compared males indicating greater local dynamic stability than males across load. LDE significantly increased with each load in the anteroposterior and vertical directions ($p<0.01$) of the trunk and the vertical direction of the pelvis ($p<0.01$). Mediolateral LDE of the trunk was significantly greater at the heaviest load condition compared to the medium and unloaded conditions ($p\leq0.002$). These results indicate that females have greater local dynamic stability of the trunk than males regardless of load. Local dynamic stability of the trunk is decreased with load in all directions while stability of the pelvis is only affected by load in the vertical direction.

Significance

Female Soldiers are generally shorter and lighter than their male counterparts. We previously reported that females alter their gait mechanics differently than males when wearing standardized loads, likely due to differences in relative mass carried. We have also reported that increasing load decreases local dynamic stability. We hypothesized that local dynamic stability in females would therefore decrease more with load than males given the higher relative mass carried. However, we found that females had greater local dynamic stability than males regardless of load. The excess load decreases this stability in both males and females, but further analysis is needed to determine if the rates of change in stability differs between females and males.

References

[1] Stergiou & Decker,. Hum Mov Sci, 30(5): 869-888. (2011)
[2] Bruijn et al., J. R. Soc. Interface, 10(83): 20120999. (2013)
[3] Loverro et al., MSSE, 50(S5) 816. (2018)
[4] Loverro et al., JoB, 95:109280. (2019)

ACKNOWLEDGEMENTS

This work was supported by the Dudley Allen Sargent Research Fund and the DOE sponsored SMART Scholarship-for-service program. Approved for unlimited distribution: U20-1997

Table 1: Mean±SD of Local Divergence Exponent (LDE) for each load by sex condition in each direction.

		Unloaded		Medium Load		Heavy Load	
	Direction	Female	Male	Female	Male	Female	Male
Trunk	Anteroposterior*†	0.36±0.05	0.45±0.05	0.35±0.04	0.45±0.05	0.37±0.04	0.48±0.06
	Mediolateral*†	0.36±0.04	0.38±0.05	0.41±0.05	0.44±0.03	0.43±0.04	0.46±0.03
	Vertical*†	0.59±0.08	0.68±0.11	0.63±0.10	0.73±0.14	0.71±0.09	0.78±0.14
Pelvis	Anteroposterior	0.33±0.06	0.34±0.04	0.33±0.06	0.34±0.05	0.34±0.07	0.35±0.06
	Mediolateral	0.30±0.05	0.33±0.07	0.29±0.08	0.34±0.09	0.32±0.07	0.35±0.10
	Vertical*†	0.46±0.09	0.57±0.09	0.50±0.13	0.62±0.13	0.56±0.12	0.66±0.13

Note: *Indicates significant ($p < 0.05$) main effect for load, †Indicates significant ($p < 0.05$) main effect of sex

Does the Reference Axis for Computing Angular Momentum Affect Inferences about Dynamic Balance?

Chang Liu[1], Sungwoo Park[2], and James Finley[1,3]
[1]Department of Biomedical Engineering, University of Southern California, Los Angeles, USA
[2]School of Engineering and Applied Sciences, Harvard Univeristy, Boston, USA
[3]Division of Biokinesiology and Physical Therapy, University of Southern California, Los Angeles, USA
Email: jmfinley@usc.edu

Introduction

One common measure of dynamic balance in human walking is whole-body angular momentum (WBAM). To compute angular momentum, one must specify a reference axis about which momentum is calculated. Momentum-based controllers for humanoid robots may use axes that project through either the center of mass (CoM) or the center of pressure [1]. However, biomechanists primarily compute angular momentum about an axis projecting through the CoM to quantify balance during walking [2]–[4]. Here, we asked if the choice of the reference axis influences interpretations of dynamic balance control.

Methods

Four healthy young individuals walked on a dual-belt treadmill at their self-selected speed. Sudden treadmill accelerations of different magnitude and direction were remotely triggered at foot strike, and belt speed returned to the self-selected speed during swing. Full body kinematics were captured using a 10-camera Qualisys Oqus system. From this data, we estimated whole-body angular momentum (WBAM) as the sum of all segmental angular momenta in the sagittal plane (Eqn.1).

$$\overrightarrow{WBAM_{ref}} = \sum_i [\, m_i(\vec{r}^{\,i}_{ref-i} \times \vec{v}^{\,i}_{ref-i}) + I^i\omega^i \,] \quad (1)$$

Here, m_i is segmental mass, $\vec{r}^{\,i}_{ref-i}$ is a vector from the segment's center of mass to the reference axis, I is the segmental moment of inertia about its center of mass, ω is the segmental angular velocity, and the index i corresponds to each limb segment. Two reference axes were used for computing WBAM: a mediolateral axis projecting through 1) the CoM or 2) the leading edge of the base of support (BoS) as estimated by a marker on the first phalanx. Both axes were defined as positive to the person's right.

For both metrics, we used the maximum value of $WBAM_{COM}$ and $WBAM_{BoS}$ during single support of the perturbation step to quantify the effect of perturbations. Negative values represented forward rotation, and positive values represented backward rotation. Each measure was normalized by weight, height, and walking speed [2].

We used a linear mixed effect model to determine if the maximum $WBAM_{COM}$ and $WBAM_{BoS}$ during the perturbation was associated with perturbation magnitude. The significance level was set at $p<0.05$.

Results and Discussion

WBAM during the perturbation step deviated from the trajectory during the pre-perturbation step (Fig 1A & B). During treadmill acceleration, WBAM during the perturbation step became more negative than the pre-perturbation step as the body rotated forward. During treadmill deceleration, WBAM became more positive as the body rotated backward. $WBAM_{BoS}$ magnitude was higher than $WBAM_{COM}$ as a result of the larger distance between most segments and the reference axis. The maximum $WBAM_{COM}$ and $WBAM_{BoS}$ during the perturbation steps were both negatively correlated with perturbation size ($p <0.001$) (Fig 1C & 1D). Thus, peak WBAM is negatively correlated with perturbation size regardless of the reference axis.

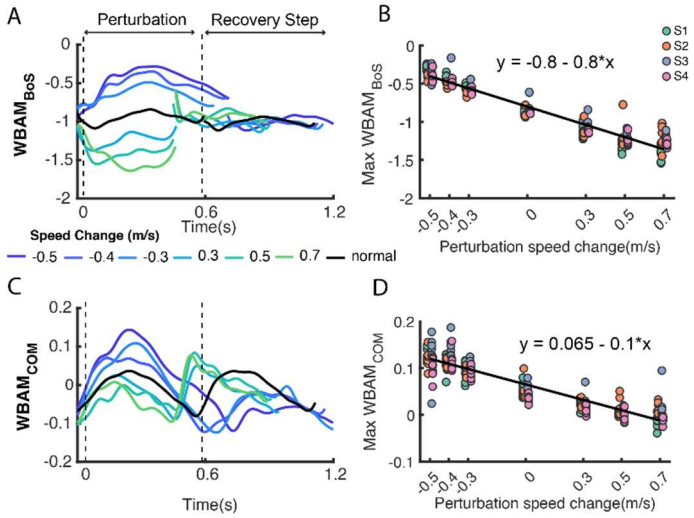

Figure 1: $WBAM_{BoS}$ (A) and $WBAM_{COM}$ (C) over time. Maximum $WBAM_{BoS}$ (B) and $WBAM_{COM}$ (D) were negatively correlated with perturbation size.

One advantage of using a reference axis that projects through the COM is that it is easier to identify the degree of segmental angular momentum cancellation during perturbation responses as perfect limb cancellation will result in zero angular momentum. Whereas, for $WBAM_{BoS}$, one needs to compare the values with the angular momentum generated by the CoM about the contact point with the ground using an inverted pendulum model to quantify the degree of limb cancellation.

Significance

Our future analysis will determine whether errors in approximating CoM dynamics using simplified kinematic model increase when perturbation magnitude increases. During perturbation responses, coordination of the lower extremities and trunk might change relative to unperturbed walking such that estimating the position of the CoM using pelvis motion may be increasingly inaccurate. We will also whether the choice of reference axis influences our interpretations of how intersegmental coordination patterns contribute to regulation of angular momentum during perturbation recovery.

Acknowledgment

This work is supported by NIH NICHD grant R01HD091184.

References

[1] S.-H. Lee et al., *Angular Momentum Based Balance Control*. 2018.
[2] H. M. Herr and M. Popovic, *J. Exp. Biol.211, 467-81 (2008)*
[3] D. Martelli et al. *IEEE Trans. Biomed. Eng. 60(7), 1785-1795 (2013)*
[4] C. Liu et al. *Front. Hum. Neurosci.* 12. *251 (2018)*

The Influence of Cognitive Load on Dynamic Balance During Steady State Walking

Gabriella H. Small, Lydia G. Brough and Richard R. Neptune
Walker Department of Mechanical Engineering, The University of Texas at Austin, Austin, TX
Email: gsmall@utexas.edu

Introduction

Previous research has used a variety of dual-task (DT) paradigms to exacerbate motor impairments and influence gait performance (e.g., walking while performing a mental task) [1], with most research focusing on the influence of DTs on walking speed and stride length [e.g., 2, 3]. However, these studies may not have used sufficiently challenging cognitive tasks [4]. In addition, only limited research has examined the influence of DTs on controlling dynamic balance, which is critical in preventing falls. The purpose of this study was to assess how healthy individuals prioritize their cognitive resources and control dynamic balance during challenging DT conditions. We hypothesize that as the DT load increases, the control of dynamic balance will decrease.

Methods

A 10 camera system (VICON, Los Angeles, USA) recorded full body kinematics during steady state treadmill walking for 15 young healthy subjects (age 25 ± 4 years, 9 females) using four increasing levels of cognitive load: no load, passive listening, spelling short 5 letter words backwards and spelling long 10 letter words backwards [4]. Subjects first performed the spelling trials while standing (single task (ST) condition) to create a cognitive baseline. Then they walked on a treadmill at their self selected speed (SS, speed = 1.35 ± 0.1 m/s) and at a fixed speed (1 m/s) while performing the dual task (DT) conditions in a randomized order. Motion data was then analyzed in Visual3D (C-Motion, Germantown, MD) and MATLAB (Mathworks Inc., Natick, MA, USA) to determine changes in dynamic balance across conditions. Dynamic balance was quantified using whole-body angular momentum (H), where a higher range of H correlates with lower clinical balance scores (poorer balance control) [5]. Audio data was examined to detect percent error and correct response rate for the cognitive responses.

Results and Discussion

As the cognitive load increased in difficulty, peak-to-peak frontal plane H increased (Fig. 1). No differences were observed in sagittal plane H between any of the cognitive conditions or walking speeds. Significant increases in H occurred between the no-load (H = 0.0291 ± 0.009) and long word trials at 1 m/s (H = 0.0332 ± 0.010) ($p < 0.001$) and between the no-load (H = 0.0249 ± 0.008) and long word trials at the SS speed (H = 0.0288 ± 0.010) ($p < 0.001$). Smaller but still significant differences were also found between the no-load and the short word trials for both speeds ($p < 0.001$). These observed increases in H indicate that as the cognitive load increases, balance control decreases at both fixed and self-selected walking speeds.

Regarding the cognitive task performance, spelling performance did not change between the ST and two DT conditions as measured by the number of errors and response rate ($p = 0.3$). While there was variability in spelling ability between subjects, overall the percent error increased from 3% to 11%, and the response rate dropped by almost half between the short and long word tasks (short word response rate = 1.79 ± 0.5 letter/s, long word response rate = 0.98 ± 0.4 letter/s) ($p < 0.001$), confirming that performance was indeed worse in the longer word (higher cognitive load) task.

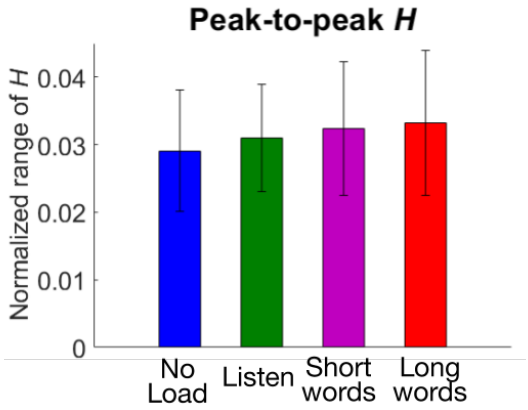

Figure 1: Normalized peak-to-peak difference in whole body angular momentum (H, normalized by height, mass and speed of each individual) in the frontal plane for the 4 cognitive loads at the 1 m/s speed.

Significance

Consistent with previous research, our results suggest that frontal plane balance, as measured by H, requires more active control than sagittal plane balance [6], and subsequently decreases with higher cognitive loads. Thus, in order to see an influence of cognitive load on balance control in healthy individuals, a sufficiently challenging mental task is needed. A decrease in dynamic balance when walking with increased cognitive loads may increase the risk of falling. Furthermore, the cognitive performance did not change between the ST and DT conditions, which suggests that healthy subjects may prioritize a cognitive task over their balance control during steady state walking. These results provide additional insight into the automaticity of walking and task prioritization in healthy individuals [7], which provides the basis for future studies to determine differences in neurologically impaired populations such as individuals post-stroke.

Acknowledgments

This project was supported in part by the Dr. J. Parker Lamb Endowed Presidential Fellowship in Mechanical Engineering.

References

[1] MacAulay, R., et al., *J. Int.Neuropsychol. Soc.,* 23(6), 493-50, 2017.
[2] Kannape, O. A., et al., *PLoS ONE*, 2014.
[3] Al-Yahya, E., et al., *Neurosci. Biobehav. Rev.,* 35(6), 715-728, 2011.
[4] Hollman, J., et al., *Gait & Posture* 32(1), 23-28, 2010.
[5] Nott, C., et al., *Gait & Posture* 39(1), 129-134, 2014.
[6] Bauby, C., et al., *J Biomech* 33(11), 1433-1440, 2000.
[7] Clark, D., *Front. Hum. Neurosci.* 9(1), 246, 2015.

Young Adults Can Perceive Very Small Locomotor Disturbances Even When Distracted

Daniel J. Liss[1], Jessica L. Allen[1]
[1]West Virginia University, Morgantown, WV
Email: jessica.allen@mail.wvu.edu

Introduction

Falls during walking are a leading cause of injuries in both young and older adults (65+ years old).[1,2] Although it is known that concurrent performance of a cognitive task negatively affects both postural control and locomotion,[3,4] the role of cognitive processes in the sensorimotor control of locomotor balance remains unclear. As a first step towards unravelling this role, the purpose of this study was to identify in young adults 1) the threshold of conscious perception of locomotor disturbances (e.g., how small of a locomotor disturbance can be perceived), and 2) the effect of a secondary cognitive distractive task. We hypothesized that performing a cognitive distractive task would impair the ability to perceive small locomotor disturbances.

Methods

11 young adults (3 M, 22.4±3.1 yrs old) walked on a split-belt instrumented treadmill (Bertec, Inc.) at their self-selected walking speed (SSWS) while randomly experiencing balance disturbances every 8-12 strides. Balance disturbances were imposed through a short duration decrease in velocity of the treadmill belt (dV) triggered at heel-strike. The belt was disturbed to speeds of SSWS–dV, where dV was 0, 0.02, 0.05, 0.1, 0.15, 0.2, 0.3, 0.4 m/s, and returned to SSWS during the subsequent swing phase. Disturbances were randomized and repeated 5 times on the dominant leg with disturbances to the nondominant leg interspersed to reduce learning effects. After each disturbance, subjects were asked if they perceived a balance disturbance and responded "yes" or "no". Subjects wore noise cancelling headphones to prevent auditory feedback. The conscious perception threshold was determined by fitting a psychometric curve to the proportion correct responses for each dV (Fig. 1A). A subset of subjects (8 subjects, 3M) repeated the same protocol while performing a secondary cognitive distractive task (i.e., counting backwards by 3), and a second conscious perception threshold was calculated. To test our hypothesis that a cognitive distractive task would impair the ability to perceive small locomotor disturbances, we used a one-sample t-test to identify if the change in the conscious perception threshold with addition of the distractive task was significantly different than zero.

Results and Discussion

Young adults were able to perceive very small locomotor disturbances. Subjects walked at SSWS 1.16 ± 0.08 m/s and perceived disturbances of 0.08 ± 0.04 m/s (7.4 ± 4.0% of the SSWS) during stance. Such low perception thresholds are unsurprising given their intact sensorimotor systems. We expect the ability to perceive locomotor disturbances to get worse with age due to deteriorations in sensory and motor systems.

Young adults maintained the ability to perceive small locomotor disturbances even with the addition of a cognitive distractive task. The average change in conscious perception thresholds between tasks was 0.005 ± 0.027 m/s. In contrast to our hypothesis, the change in perception threshold with the addition of the secondary cognitive distract task was not significantly different than zero (p value = 0.59). This result is consistent with prior studies demonstrating high cognitive reserves in young adults. Due to cognitive declines[5], we expect the cognitive distractive task will have a larger effect on the perception of locomotor disturbances in older adults.

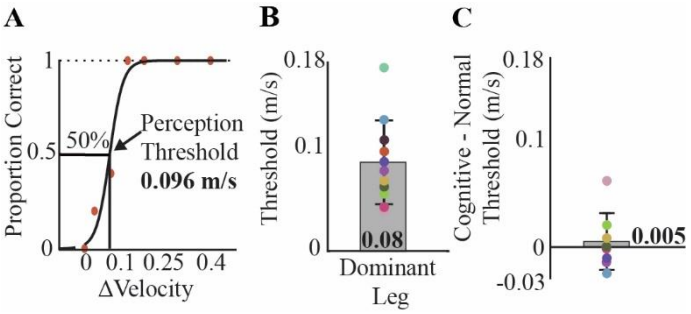

Figure 1: A) Example psychometric curve fitting to identify conscious perception threshold. B) Perception threshold of locomotor disturbances. C) Change in perception threshold with cognitive distractive task. Individual subjects are labeled by a single color.

Open questions remain about what sensory feedback is being utilized by young adults to perceive these small locomotor disturbances. For example, are they estimating changes in task-level variables such as body center of mass and/or sensing joint-level changes (i.e., changes in muscle length). Determining where this localization occurs and changes due to aging may provide targets for rehabilitation aimed at improving the ability to maintain balance during locomotion.

In summary, young adults were able to detect very small locomotor disturbances even when performing a secondary cognitive distractive task. We expect that ability to perceive locomotor disturbances will be reduced in older adults due to declines in their sensory, motor, and cognitive systems.

Significance

Using small level locomotor disturbances, we are investigating the sensorimotor mechanisms responsible for the active control of locomotor balance. Understanding the ability to perceive locomotor disturbances, the sensorimotor contributions to this perception, and changes due to normal aging may provide targets for rehabilitation aimed at improving locomotor balance.

Acknowledgments

Research reported in this publication was supported by NIH NIGMS under Award Number 5U54GM104942-04. The content is solely the responsibility of the authors and does not necessarily represent the official views of the NIH.

References

1. Cigolle et al. *JAMA Intern Med.,* 175:443-445. 2015.
2. Seidler et al. *Neurosci Biobehav R,* 34, 721-733. 2010.
3. Lockhard et al. *Hum Factors* 47, 708-729. 2005.
4. Montero-Odasso et al. *Arch Phys Med Rehabil,* 93, 293-299. 2012.
5. Springer et al. *Mov. Disord.*, 21, 950-957. 2006.

Susceptibility to Optical Flow Balance Perturbations in Older Adults Prevails Despite Cognitive Distraction

Brian P. Selgrade[1,*], Prudence Plummer[2], and Jason R. Franz[3]
[1] Department of Movement Science, Westfield State University [2]MGH Institute of Health Professions
[3]Joint Department of Biomedical Engineering, UNC Chapel Hill and North Carolina State University
Email: *bselgrade@westfield.ma.edu

Introduction

Optical flow perturbations increase gait variability, especially in older adults who rely more on vision to maintain balance [1]. Furthermore, gait variability in older adults is much more susceptible to optical flow perturbations than to a cognitive dual-task [2]. However, cognitive tasks can interfere with motor tasks during walking, reducing gait speed and increasing step width [3]. Those effects are explained by cognitive-motor interference due to the redirection of limited attention to cognitive processing. However, the combined effect of optical flow perturbations and cognitive tasks has yet to be systematically explored; an important gap due to the potential involvement of cognitive resources to either (*i*) reduce attention and attenuate the impact of, or (*ii*) disrupt older adult's ability to appropriately respond to, optical flow perturbations during walking. The purpose of this study was to determine the effect of a cognitive task on gait variability in the presence of optical flow balance perturbations. We anticipated that adding a cognitive task would reduce attention to optical flow perturbations; thus, we hypothesized that gait variability in the presence of optical flow perturbations would decrease when performing a cognitive task.

Methods

Nine older adults (2 male, age: 75.1±3.8 years) gave written informed consent and participated in this study. For each subject, experiments were performed on two different days in randomized order. After participants acclimated to the treadmill over 5 minutes, they completed all walking trials at their preferred speed while viewing optical flow in the form of a virtual hallway projected onto a semi-circular, curved screen in front of the treadmill. Subjects completed four, 2-minute walking conditions: a control trial, a dual-task trial while performing an auditory Stroop task [4], a trial with mediolateral optical flow perturbations, and a trial including both mediolateral optical flow perturbations and the auditory Stroop task. To mitigate any within-subject effect of perturbation training, the perturbation trial performed with the auditory Stroop task was performed in a random order on a different day, separated by one week. Briefly, the auditory Stroop task involved hearing a voice say the words "low" and "high" in a low or high pitch and responding by saying the pitch rather than the word [4] . For all trials, we found step width (SW) by taking the distance between heel markers and calculated step width variability (SWV) and trunk variability quantified as the standard deviation in mediolateral position of the seventh cervical vertebra. A one-way, repeated measures ANOVA with post-hoc t-tests compared condition effects.

Results and Discussion

There were significant main effects of condition on SWV and mediolateral trunk variability ($p=0.003$ and $p=0.002$, respectively) but not SW ($p=0.228$). Specifically, post-hoc tests revealed significant increases due to the presence of optical flow perturbations whether participants were engaged in the Stroop task ($p=0.004$ for SWV, $p=0.006$ for trunk variability) or not ($p=0.008$ for SWV, $p=0.018$ for trunk variability). However, we found no significant effects of the Stroop task on SWV (Fig. 1) or mediolateral trunk variability ($p\geq0.43$).

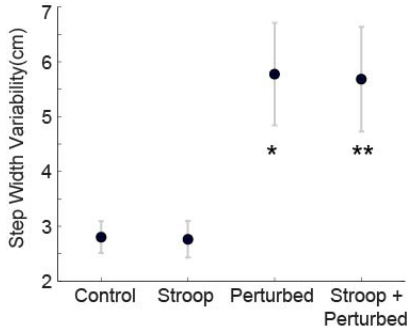

Figure 1. Effects of a Stroop task on step width variability when walking without (control and Stroop trials) and with perturbed optical flow. Significant difference from control (*) and Stroop trial (**).

Our hypothesis that the auditory Stroop task would reduce gait variability in the presence of optical flow perturbations was not supported. Indeed, the Stroop task had no effect on SW, SWV, or trunk variability, niether when performed during normal walking nor in the presence of perturbed optical flow. These findings are consistent with some prior studies [4, 5]. However, we chose the auditory Stroop task to deliberately exclude the visuomotor pathways presumably involved when responding to optical flow preturbations. Together, our results allude to a strategy in which attention to balance is prioritized equal to or above cognitive task performance. Adding a Stroop task can cause older adults to reduce gait speed during obstacle negotiation, but this occurred only when subjects walked at faster than preferred speeds [6]. Accordingly, including a more difficult cognitive task or enforcing a faster walking speed could have increased the prevalence of dual-task interference.

Significance

This study shows that susceptibility to optical flow balance perturbations in older adults prevails even in the presence of distraction from a cognitive dual task. Our findings suggests that walking balance is prioritized over cognitive dual-task performance when walking with balance perturbations.

Acknowledgments

This work was funded by the National Institutes of Health (R56AG054797).

References

1. Franz, JR, et al. 2015. Hum Mov Sci 40:381-392.
2. Francis, CA, et al. 2015. Gait Post 42:380-385.
3. Patel, P, Lamar, M, Bhatt, T. 2014. Neurosci 260:140-148.
4. Siu, K, et al. 2008. Exp Brain Res 184:115-120.
5. Worden, TA, Vallis, LA. 2016. Exp Brain Res 234:387-396.
6. Plummer-D'Amato, P, et al. 2012. J Aging Res. ID 583894.

Neuromuscular Adaptation after Exposure to Simulated Hypogravity

Chase G. Rock[1], Angela Luo[1], Kristy S. Yun[2], and Young-Hui Chang[1,2]
[1]School of Biological Sciences, Georgia Institute of Technology, Atlanta, GA, USA
[2] BioEngineering Program, Georgia Institute of Technology, Atlanta, GA, USA
Email: crock@gatech.edu

Introduction

When falling from a drop or jump, people and other animals preactivate their leg muscles in preparation for landing (*1*, *2*). This preactivation occurs prior to ground contact, indicating it relies on a prediction of the time and force of landing. People are skilled at such predictions, as they readily alter preactivation timing and magnitude to accommodate different jump heights (*3*). The ability to accurately predict the time and force of landing indicates an implicit understanding of the physics affecting the jump, including the acceleration due to gravity.

We aimed to affect these gravity-based predictions by exposing participants to simulated hypogravity in a targeted jumping task. We hypothesized exposure to hypogravity would result in a delayed preactivation time and lower preactivation magnitude, reflecting an expectation of lower gravity.

Methods

Ten participants (6 female; Age: 21.8 ± 4.0 yrs; Height: 1.74 ± 0.11 m; Weight: 615 ± 98 N) gave informed consent prior to participating in this Georgia Tech IRB approved study. They each performed targeted countermovement jumps before (Pre), during, and after (Post) exposure to simulated hypogravity. A 0.5G environment was simulated using constant force springs mounted above the participant and attached at their hips. Muscle activity (Vastus Medialis (VM), Lateral (LG) and Medial (MG) Gastrocnemius, and Soleus (SOL): 960 Hz), kinetics, and kinematics data were collected on both legs for each jump.

Preactivation timing was calculated as the time prior to landing when build-up of muscle activity began (*3*). Preactivation magnitude was calculated as the integrated electromyographic activity between preactivation onset and contact with the ground.

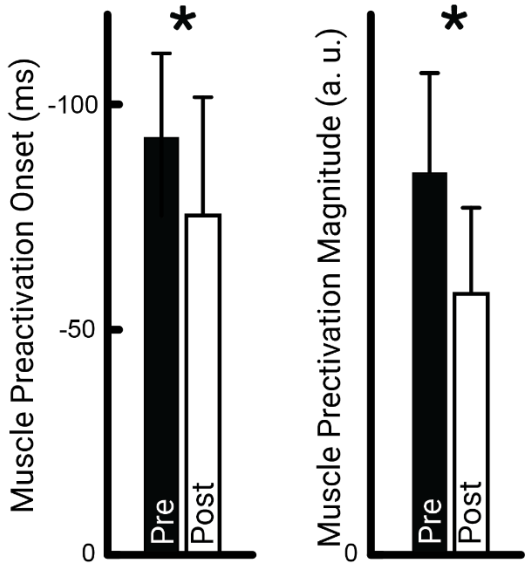

Figure 1: Average preactivation onset timing and magnitude for the LG on the non-dominant leg. Preactivation onset timing (prior to landing) and activation magnitude were larger in jumps before hypogravity exposure (Pre; black bar) compared to after hypogravity exposure (Post; white bar). * denotes $p < 0.05$, paired t-test.

Results and Discussion

Prior to landing from each jump, participants preactivated the knee and ankle extensor muscles to prepare for landing. Following hypogravity exposure, preactivation onset timing was delayed (compared to Pre) in most muscles by about 15-30 ms (Fig. 1; $p < 0.05$ for non-dominant VM, LG, MG and dominant VM & SOL). This delay agrees with our hypothesis and suggests the expectation of a longer airtime due to hypogravity.

Preactivation magnitude was significantly reduced ($p < 0.05$) by about half (32 – 52%) in most muscles, except in the dominant leg SOL & LG. A 50% reduction is reasonable as the hypogravity exposure was targeted at reducing participants' body weight by half. This reduction in preactivation magnitude is also in agreement with our hypothesis and likely represents the expectation of a lower muscle load during landing.

Taken together, our results indicate that people adapt both timing and magnitude of muscle activity in jumping to match the requirements of hypogravity exposure. Such adaptation suggests that people are able to successfully adapt to accelerations that do not match the typical acceleration due to Earth's gravity.

Significance

While previous research has shown humans and other animals can predict the timing of landing from a fall under Earth's gravity (*1*, *2*), very few have investigated altered gravities (*4*). The current study expands on previous hypogravity locomotion paradigms (*5*, *6*) to assess aspects of neural adaptation through the investigation of neuromechanical aftereffects. This new paradigm can be used to explore if this adaptation is isolated to the muscles directly involved in task performance, which may provide important insights on the general nature of how gravity is accounted for during movement control.

Acknowledgments

The authors would like to thank Dhruv Modi for his assistance with data collection and analysis. This material is based upon work supported by the NSF GRFP to CGR under Grant No. DGE-1650044. Any opinions, findings, and conclusions or recommendations expressed in this material are those of the authors and do not necessarily reflect the views of the NSF.

References

1. R. Greenwood, A. Hopkins, *J. Physiol.* **254**, 507–518 (1976).
2. A. M. Laursen, P. Dyhre-Poulsen, A. Djørup, H. Jahnsen, *Acta Physiol. Scand.* **102**, 492–494 (1978).
3. M. Santello, M. J. N. Mcdonagh, *Exp. Physiol.* **83**, 857–874 (1998).
4. J. Avela, P. M. Santos, H. Kyrolainen, P. V. Komi, *Aviat. Sp. Environ. Med.* **65**, 301–308 (1994).
5. Y. H. Chang, H. W. Huang, C. M. Hamerski, R. Kram, *J. Exp. Biol.* **203**, 229–38 (2000).
6. R. Ritzmann, A. Krause, K. Freyler, A. Gollhofer, *Microgravity Sci. Technol.* **29**, 9–18 (2017).

Application of Inertial Measurement Units and Statistical Parametric Mapping for Assessing Alpine Skiing

Sarah A. Wilson[1], Jacqueline N. Foody[1], Amanda L. Vinson[1], Madeleine G. DeClercq[1], and Scott Tashman[1]
[1]Steadman Philippon Research Institute, Vail, CO
Email: swilson@sprivail.org

Introduction

Alpine skiing has high rates of orthopaedic injury, but is impractical to study in a laboratory environment. Skiing biomechanics are best assessed with wearable technologies that can be used in the field, such as Inertial Measurement Units (IMUs). While methods exist to determine ski turn transitions using gyroscope signals [1], there is no consensus in the literature of which other timepoints are most relevant to study. Therefore, it is necessary to evaluate the entire turn cycle. Statistical parametric mapping (SPM) allows evaluation of timeseries data, and avoids some biases found in other statistical methods [2].

This study serves as an early proof-of-concept approach to analyzing IMU data with SPM in alpine skiers, while providing analysis framework for future snowsports biomechanics research.

Methods

Four advanced recreational skiers (aged 27.5 ± 4.6 years, 2 female, no prior lower extremity surgery or injury) consented to participate in this IRB approved protocol. Each skier was instrumented with eight IMUs (APDM, Portland OR, 128hz) secured to the feet, legs, and trunk. Skiers completed four runs through a 10-turn giant slalom style course on moderate terrain.

Gyroscope data was used to determine the start and end times of the middle three turns in each direction from each trial, as previously described [1]. Joint angles were calculated with the IMU manufacturer's software and corrected for offsets in means to account for differences in calibration poses and drift. Kinematics and raw gyroscope data for each turn were filtered at 2hz (per residual analysis [3]) and resampled to 256 points per turn. Foot gyroscope data in the roll (edging) and yaw (turning) axes, and knee flexion, were considered in this analysis example.

SPM analyses were conducted in MATLAB (spm1d.org) to explore three anticipated future use cases: 1) 1-way repeated-measure ANOVAs to determine whether all of a skier's right (or left) turns were performed similarly; 2) 1-way ANOVA to quantify differences between skiers; 3) paired t-test to quantify side-to-side differences within a skier. In all tests, statistically significant results over portions of the turn shorter than 3% were deemed not clinically significant and were disregarded.

Results and Discussion

No within-subject differences were found between turns in a repeated-measures ANOVA for roll (Figure 1a), yaw, or knee flexion. These results are course specific; turn-to-turn similarity must be checked for all future skiing biomechanics research study courses before assuming uniformity.

Between skiers, slight differences were observed in roll and yaw over periods shorter than 6% of the turn cycle. However, a 1-way ANOVA revealed differences in kinematics from 0-55% and 67-100% of the turn cycle. In post-hoc t-tests, there were differences in every pair of skiers' knee flexion angles (Figure 1b), and two pairs were significantly different over more than half of the turn cycle.

Side-to-side asymmetries were observed in kinematics of the inside knee between left and right turns for Skier 1 only (Figure 1c). Asymmetries in gyroscope data were observed in three skiers but for less than 9% of the turn in all cases. Side-to-side asymmetry is widely identified as an injury risk factor in other sports, and may be a valuable comparison in future studies.

The discrepancy between the extent of gyroscope and kinematic differences between skiers and limbs suggests that skiers can employ different body position and movement strategies to achieve similar edging and turning mechanics.

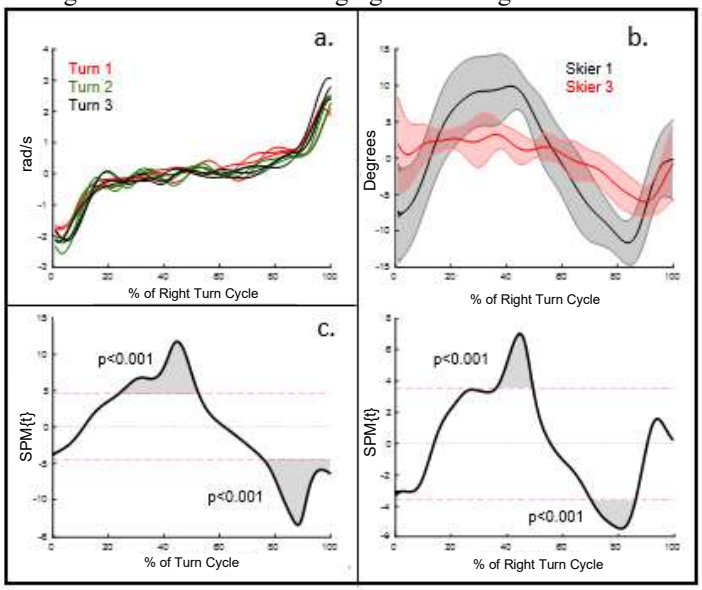

Figure 1: a) Within-subject repeatability of roll signals between turns on multiple runs. **b)** Mean and standard deviation of knee flexion angles of two skiers (top) and associated post-hoc t-test (bottom) highlights significant differences as shaded regions that exceed the F* threshold. **c)** Paired t-test found right/left asymmetry in Skier 1 with increased right knee flexion near the turn apex and decreased flexion at turn finish.

These results are preliminary and limited by a small sample size. Additionally, testing for each participant occurred on a different day; while every effort was made to replicate course gate locations, slight differences between turn position and snow conditions for each skier were inevitable.

Significance

Even with a small sample size in a complex, dynamic sport, significant differences in movement technique can be observed both between and within skiers. This supports the continued use of IMU sensors in the field, and the application of SPM analysis in future skiing biomechanics applications.

Acknowledgments

Funding, in-kind support, and guidance were provided by Lyda Hill Philanthropies, FCFH Lattner Foundation, Double Diamond Ski Shop, Vail Mountain Race Department, and Jeannie Thoren.

References

[1] Martínez et al., fspor, 1:18, 2019
[2] Pataky et al., J.Biomechanics, 46(14):2394-401, 2013
[3] Winter D. "Biomechanics and motor control…" Wiley, 1990a

A Biomechanical Analysis of the Triple Step in Recreational Swing Dancers

Meredith D. Wells[1] and Feng Yang[1]
[1]Department of Kinesiology and Health, Georgia State University, Atlanta, GA, USA
Email: mwells19@student.gsu.edu

Introduction

Traditionally used to refer to the type of jazz music, swing dancing today refers to a cluster of dances developed between the 1920s and 1940s to the swing style of music, including the Lindy hop [1]. Swing dancing is still popular today and continues to draw individuals to it with its lively music and social atmosphere [2]. Yet, dance requires high levels of aerobic power, strength, endurance, and flexibility, making injuries common [3]. There is limited research on the biomechanics of the swing movements which restricts our ability to prevent injuries. Although swing dancing is performed with a partner, it is meaningful to understand whether the biomechanics of swing dancing differ with and without a partner to better develop training protocols.

In swing dancing, the triple step is a common dance element that accounts for the syncopated rhythm of the music and translates it into body movement. This step can be performed by both men and women to the right and left. This step is performed in an upbeat manner with an element of bounce to it. Given the presentative features of the triple step, it is important to analyse the biomechanics underlying this key swing dance element.

The main purpose of this study was to analyse the triple step in recreational swing dancers to determine the biomechanics of the movement and to assess where the greatest risk for injury may lie. It was hypothesized that 1) dancing with and without a partner would not yield biomechanical differences, and 2) that the third step of the triple step would result in the greatest risk for injury.

Methods

Eight recreational swing dancers who completed 50 sessions of swing dancing within the prior year (age: 30.9 ± 4.7 years; height: 1.73 ± 0.07 m; mass: 73.6 ± 13.1 kg; swing dancing experience: 4.1 ± 3.1 years) participated in the study.

Participants completed a 5-minute dance warm-up of their choosing, and then performed a triple step to both the right and the left with and without a partner in a random order. Three trials were collected for each. Participants performed the dance elements on a vinyl floor wearing a standardized pair of socks.

Three-dimensional lower extremity kinematics and ground reaction force (GRF) were collected via 20 reflective markers using an 8-camera motion capture system (Vicon, UK) and two embedded force plates (AMTI, MA), respectively. Joint power at ankle was calculated using inverse dynamcis. The outcome variables (peak vertical GRF and peak ankle power) were identified for all three steps. They were then compared between partnered and non-partnered conditions using paired *t*-tests, and among the three steps using a one-way ANOVA with repeated measures in SPSS v.24 (IBM, NY) with an alpha level of 0.05. Post-hoc tests were run when significant differences were found.

Results and Discussion

There were no significant differences in the peak vertical GRF between partnered vs non-partnered ($p > 0.05$), which supports our first hypothesis (Table 1). The ANOVA indicates an overall significant difference in GRF among groups ($p < 0.05$). Follow-up post-hoc analyses further indicated that the first and second steps had significantly greater peak GRF compared to the third step ($p < 0.05$), but were not significantly different from each other ($p > 0.05$). This contradicts our second hypothesis.

Ankle power showed no difference between partnered and non-partnered ($p > 0.05$ for both), which further supports the first hypothesis. The first and second step showed the greatest amount of propulsion compared to the third step ($p < 0.05$). This is sensible since the dancers paused after the third step and did not move into another step, whereas the first and second step led into consecutive steps making propulsion necessary to keep moving. With ankle power absorption, the second step resulted in the greatest amount of absorption ($p < 0.05$) which contradicts our second hypothesis. However, this is reasonable because when performing a triple step, dancers take a small step to either the right or left, a second step that brings the second foot to meet the first, and then a third step apart again. This element is performed with bounce, so the first and third steps are smoother while the transition from the first to the second step is bouncier as the dancers go up and down when switching from the first to the second foot.

Table 1. Mean ± SD of the peak vertical GRF (/BW) and ankle power (watts/kg) propulsion and absorption for each of the three steps in the triple step element to the left and right individually (TSL & TSR) and with a partner (TSLP &TSRP).

Element	Step	Outcome		
		GRF	Propulsion	Absorption
TSL	1	1.41 ± 0.13	4.38 ± 1.23	-1.61 ± 0.56
	2	1.39 ± 0.12	1.76 ± 1.13	-3.50 ± 0.96
	3	1.11 ± 0.11	0.40 ± 0.22	-1.15 ± 0.64
TSLP	1	1.31 ± 0.12	3.78 ± 1.71	-1.26 ± 0.55
	2	1.37 ± 0.13	1.49 ± 0.48	-3.50 ± 1.34
	3	1.07 ± 0.08	0.42 ± 0.40	-0.70 ± 0.36
TSR	1	1.37 ± 0.14	4.04 ± 1.46	-1.28 ± 0.53
	2	1.38 ± 0.08	1.59 ± 0.82	-3.44 ± 1.03
	3	1.10 ± 0.10	0.52 ± 0.36	-1.15 ± 0.64
TSRP	1	1.30 ± 0.10	3.32 ± 1.08	-1.20 ± 0.60
	2	1.36 ± 0.13	1.67 ± 1.10	-2.98 ± 0.86
	3	1.04 ± 0.06	0.41 ± 0.35	-0.96 ± 0.49

Significance

To the best of our knowledge, this is the first study to analyze the biomechanics of swing dancers. Due to the popularity of swing dancing and the potential resulting injuries it is important to understand the internal and external forces acting on the dancers in order to prevent injury and improve performance. This knowledge will be beneficial for the design of future studies to systematically examine the biomechanical aspect of swing dance.

References

[1] Spring H. (1997). *American Music,* 15(2)*,* 183-207.
[2] Fuller J. (2019). *Swing History.* CentralHome.com.
[3] Kelly A. (2010). *Pediatric Annals*, 39(5), 279-285.

Real-Time Visual Feedback on Breathing during Treadmill Running to Exhaustion

Joseph A. Passfiume.[1],Nelson A. Glover[1], Anne R. Crecelius[2], Ajit M.W. Chaudhari[1]
[1]The Ohio State University, Columbus, OH, USA, [2]University of Dayton, Dayton, OH, USA
Email: glover.262@osu.edu

Introduction

Respiratory inductance plethysmography (RIP) is a method of monitoring breathing through the placement of elastic belts around the chest and abdomen, with the most efficient breathing entailing the chest and abdomen expanding and contracting at the same time (in-phase). It is non-invasive and is shown to be reliable and accurate when compared to other measurements of ventilation [1,2]. Because running is such a popular recreational sport, additional knowledge on how breathing efficiency could help runners become more resistant to fatigue may be able to improve overall performance.

In this study, we tested the effect of visual breathing feedback on breathing patterns and time to exhaustion. We hypothesized that receiving visual feedback would encourage more in-phase breathing and longer times to fatigue.

Methods

13 adult runners (8F,5M; age 25.5±6.5 yrs), who run between 5-20 miles per week, participated in this study. The participants were tested on two days, separated by at least one week, one where they received visual feedback and one without.

On each day, two RIP bands were placed around the chest and abdomen. A neoprene belt holding a BioRadio (Great Lakes NeuroTechnologies, Cleveland OH) was placed around the waist. A chest harness was worn for safety. The participant then ran at a self-selected speed (2.04 ±0.084 m/s) for 5 minutes. After a break, the participants began the fatiguing protocol. The treadmill was inclined to 3°, and speed started at 2.25 m/s. Each minute, the treadmill sped up by 0.083 m/s until the participant signaled they could no longer continue (volitional exhaustion). During this fatiguing protocol, real-time visual feedback was provided on one day (**Fig. 1**) and not on the other. Breathing data (voltage based on the circumference of the RIP bands) were collected during the 5-minute warm up and during the fatiguing protocol at 250 Hz. Phase angle, a quantity between 0 and 180 degrees (representing the synchrony of the chest and abdomen) [3,4], and time to exhaustion were calculated. The effects of visual feedback and phase angle were analyzed with single-variable regressions for their effects on time to exhaustion.

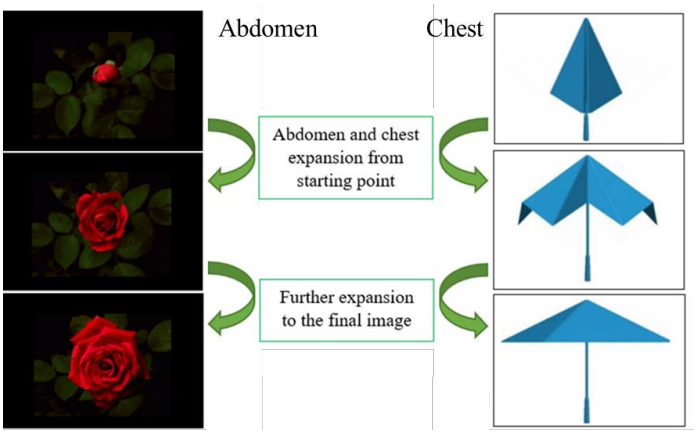

Figure 1: Real-time visualization of the expansion of the chest and abdomen.

Results and Discussion

Time to exhaustion was not significantly predicted by phase angle (p=0.853), nor to having visual feedback (p=1). Pearson pairwise correlation coefficients showed that phase angle and having visual feedback provided did have a negative correlation, although not significant (r=-0.089). This suggests that having visual feedback decreased the phase angle.

These results suggest that providing visual feedback may be able reduce the phase angle to create more synchronous breathing. This however, did not improve the time to exhaustion, which was a hypothesized outcome. **Figure 2** provides a visualization of each participant's change in phase angle and time to exhaustion with the addition of having visual feedback. One major limitation was the methodology for the run to fatigue. Some participants seemed to ask to end the session due to the speed of the treadmill and participant comfort instead of fatigue.

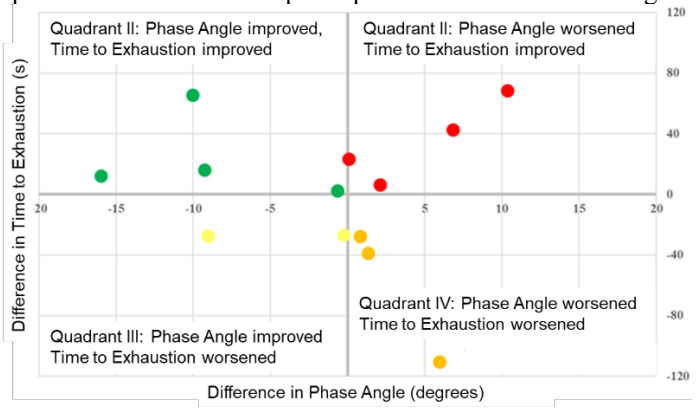

Figure 2: The difference of visual feedback compared to no visual feedback: time to exhaustion versus phase angle for each participant.

Significance

An improvement in phase angle did not ultimately lead to an improvement in time to exhaustion. Looking only at participants that improved phase angle with visual feedback, there is a possibility that time to exhaustion could be improved with further breathing training. However, because not all participants improved phase angle with visual feedback, the largest obstacle that lies ahead is finding a way to more effectively improve the phase angle. Allowing for time to teach the breathing method and a familiarization with visual feedback prior to running should be implemented in the future in an effort to improve phase angle.

Acknowledgments

The authors thank Maggie Abrams, Bernard Tarver, Nihit Tyagi, and Menglin Xu for their help with this work.

References

[1] Carry & Baconnier. Chest, vol. 111, no. 4, 1997
[2] Stick & Ellis. Pediatr. Pulmonol., vol 14, no.3, Nov. 1992
[3] Johnson & Suratt Methods Enzymol., vol. 384, 2004.
[4] Clarenbach et. al. Chest, vol. 128, no. 3, Sep. 2005

Metabolic Power During Running In Vaporfly Shoes With Intact vs. Cut Carbon-Fiber Plates

Justin Angelo O. Ortega[1]*, Laura A.Healey[1], Dale Haavind-Berman[1], and Wouter Hoogkamer[1]
[1]University of Massachusetts Amherst, Department of Kinesiology
Email: * joortega@umass.edu

Introduction

Recently, long distance running has been overwhelmed by athletes zooming past finish lines wearing the Nike Vaporfly 4%, which has been shown to lower metabolic power during running by 4% on average (Hoogkamer et al., 2018). The Nike Vaporfly utilizes a full-length curved carbon fiber plate embedded in a lightweight Pebax foam that is both compliant and resilient. These elements together provide a 4% reduction in energetic cost, but it is unknown how much of the metabolic benefits are specifically related to the increased longitudinal bending stiffness (LBS) provided by the carbon fiber plate. We hypothesized that reducing longitudinal bending stiffness by cutting through the carbon fiber plate of the Nike Vaporfly 4% would increase metabolic power during running by about 2%.

Methods

Ten male participants (23.5±4.5 yrs, 70.0±5.0 kg, 174.0±2.5 cm) ran in two versions of the Nike Vaporfly 4% (size US9.5): 1) a standard, unaltered pair (VF), and 2) a pair where the midsole and carbon fiber plate were cut (CVF) (Figure 1). Participants gave written informed consent that followed the guidelines of the University of Massachusetts Amherst Institutional Review Board. Participants completed a 5-minute warm-up trial at a self-selected pace, while breathing through the expired-gas analysis system to allow familiarization. Participants then completed four 5-minute trials at 14 km/h on a force-measuring treadmill (Treadmetrix) while we measured submaximal rates of oxygen uptake and carbon dioxide production (True One 2400, Parvo Medics). Participants ran twice in each shoe condition in a mirrored order that was counterbalanced and randomly assigned. We used shoe covers to blind participants from the condition and we changed the shoes for the participants during 5-minute breaks between trials. Metabolic power was calculated over the last two minutes of each trial using the Peronnet & Massicotte equation (Peronnet & Massicotte, 1991). The average of the two trials in each shoe was used for all metrics. We used two-tailed paired t-tests to compare shoes with a traditional significance level of $\alpha < 0.05$.

Figure 1: Shoe conditions: VF (baseline), CVF (decreased LBS)

Results and Discussion

Contrary to our hypothesis, metabolic power was statistically similar between the VF and CVF shoes (13.91±0.74 W/kg vs. 13.98±0.76 W/kg; p=0.24; $\Delta = 0.55 \pm 1.38\%$; Figure 2). In the CVF condition, subjects ran with shorter contact times (p=0.001) compared to the VF condition (Table 1). Step frequency, braking impulse, and propulsive impulse were all statistically similar between the VF and CVF shoes (all p>0.17). Our data suggests that the metabolic savings from the LBS function of the carbon-fiber plate are small. A next step is to quantify the LBS of the two shoe conditions with a materials testing machine, to verify that residual LBS in the CVF was indeed minimal. At this point, our data suggests that the midsole foam and geometry are the main contributors to the metabolic savings, in line with our earlier observations that the midsole returns about 50 times more energy in compression than the plate and midsole combined in bending (Hoogkamer et al., 2019). In addition, the individual sections of carbon-fiber plate between the cuts could enhance the function of the foam by increasing the midsole stability and spreading out the vertical ground reaction forces over a larger foam area.

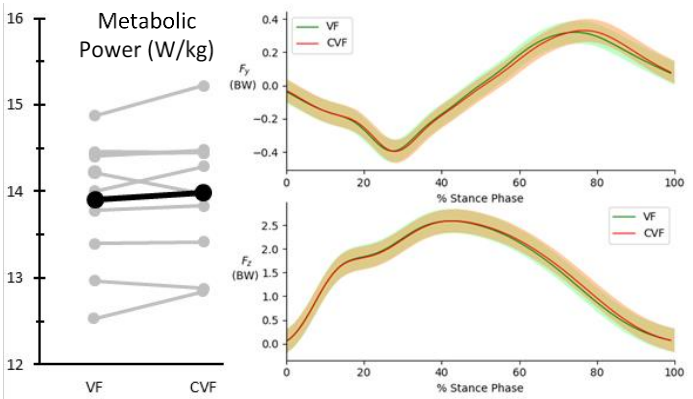

Figure 2: Metabolic power was statistically similar (p = 0.24) between the VF (13.91±0.74 W/kg) and CVF shoes (13.98±0.76 W/kg) with $\Delta = 0.55 \pm 1.38\%$.

	VF	CVF
Contact Time (ms) *	212±2	208±2
Step Frequency (Hz)	3.01±0.12	3.01±0.12
Braking Impulse (N·s)	-0.021±0.002	-0.021±0.002
Propulsive Impulse (N·s)	0.021±0.002	0.021±0.002

Table 1: Contact time was significantly shorter in the CVF shoe compared to VF (p=0.001). Step frequency, braking impulse, and propulsive impulse were all statistically similar (all p>0.17).

Significance

As carbon-fiber plates are introduced into more running footwear, it is important to understand how they affect performance. Although opponents often use words as “spring-plates” and “mechanical doping,” our results indicate that the contributions of the longitudinal bending stiffness of carbon-fiber plates to the overall metabolic savings of Vaporfly shoes are minimal.

References

Hoogkamer et al. (2018). *Sports Med*, **48:** 1009-19.
Hoogkamer et al. (2019). *Sports Med,* **49:** 133-43.
Peronnet & Massicotte (1991). *Can J Sport Sci*, **16**: 23-29

Foot and ankle kinetics and their interplay during a long duration run

Eric C. Honert[1*], Florian Ostermair[1,2], Frieder C. Krafft[1,2], Vinzenz Von Tscharner[1], and Benno M. Nigg[1]
[1]University of Calgary, Calgary, Canada
[2]Karlsruhe Institute of Technology, Karlsruhe, Germany
Email: *eric.honert@ucalgary.ca

Introduction

With the advent of high performance shoes for long distance running, there is a need to understand the kinetic contributions of the lower limbs and how they change throughout longer duration runs. During a long duration run, there may be a re-distribution of ankle-knee-hip joint work from distal joints to proximal joints [1]. However, the power and work contributions from the foot have been neglected when examining such runs even though studies have shown that there are signficiant kinetic contributions from the foot during walking [2,3] and running [4]. Additionally, the interactions between the foot and the ankle have been largely neglected during running. The foot and the ankle are traditionally treated as separate work sources due to inverse dynamics asssumptions. Yet, there are many multiartucular structures that span the foot and the ankle (e.g., flexor hallucis longus) which can cause kinetic interplay [5]. Evaluating how the ankle and foot interact during running can provide insights into the role of multiarticular connections between the ankle and foot and insights for future prosthetic technology. In total, the purpose of this study is to characterize the kinetic interplay between the ankle joint and the foot during a long duration run.

Methods

Fourteen recreationally active, heel-strike running, subjects (7 male, 7 female, 25±3 yrs, 1.72±0.08 m tall, 67.7±6.3 kg) provided informed consent and participanted in this study. Subjects ran continuously for 58 minutes while we collected kinematic marker data, ground reaction forces and electromyography (EMG). The running speed was randomly varied around the subject's self-reported 10k pace to simulate a typical run. Additionally, subjects ran at 2.8 m/s during four time points in the run: 6, 23, 40 and 57 min. Data were collected for one min. at each speed throughought the run. For simplicity, we present the kinetics from the 2.8 m/s running bouts. We computed six degree-of-freedom ankle joint complex (termed here Ankle), distal-to-rearfoot (termed here Foot) and combined Ankle+Foot power [2]. The Foot power is a net estimate from all structures within the foot as well as the shoe. Positive and negative work for each of the power metrics was computed during stance phase. Friedman and Wilcoxon signed-rank tests with a Holm-Sidak correction were used evaluate differences in work metrics throughout the run (α=0.05).

Results and Discussion

We observed during the positive Ankle work decreased by 17% (6.8 J, p<0.001), on average, and positive Foot work increased by 36% (3.4 J, p=0.001), on average (Fig. 1) from min. six to min. 57. There was no difference in the combined Ankle+Foot work, negative Foot and negative Ankle work (Fig. 1, p>0.05).

Runners did not change how work was absorbed, but rather modulated how work was generated throughout a long run at the Ankle and Foot. The consistent negative work by the Foot throughout the run may indicate that runners do not change how they utilize rearfoot midsole cushioning, as this is one of the structures that can absorb work in the Foot [3]. However, runners were ulitizing more positive Foot work sources during the run which can be attributed to mid-tarsal and metatarsalphalangeal joint positive work [4]. When this Foot work was considered with the positive Ankle work, the Ankle+Foot work was consistent during the run which may indicate kinetic interplay due to multiarticular structures between the Ankle and Foot [5]. Additionally, the Ankle+Foot work provides a realistic expectation, rather than only considering Ankle work, for how running prostheses should perform throughout a run.

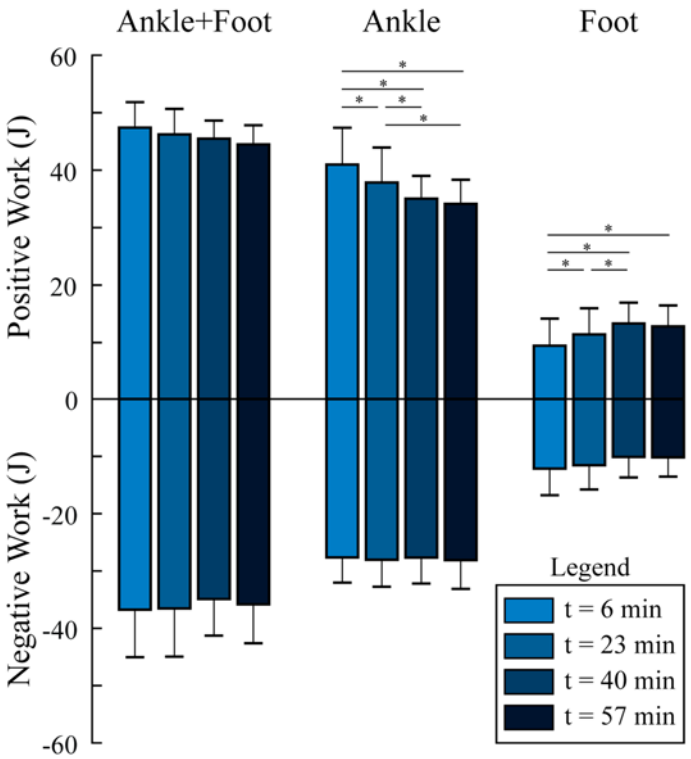

Figure 1: Positive and negative work for the Ankle+Foot, Ankle and Foot throughout the daily-type run. Asterisks indicate significant differenences (p<0.006) between different times in the run.

Significance

This is the first study to characterize the work contributions from the Foot and Ankle+Foot during running over a long period of time. Understanding how work is being performed by the structures of the foot in combination with the shoe can be used to optimize how these structures are interacting to enhance performance. Furthermore, the characterization of the Ankle+Foot can provide design criteria for running prostheses to enhance running performance for persons with amputation.

References

[1] Sanno et al. (2018). *Med Sci Sport Exer*, **50**: 2507-2517.
[2] Zelik and Honert (2018). *J Biomech*, **75**: 1-12.
[3] Honert and Zelik (2019). *Hum Movement Sci*, **64**: 191-202
[4] Bruening et al. (2019). *J Biomech*, **73**: 185-191.
[5] Honert and Zelik (2016). *PLoS One*, **11**: e0163169.

Examining the role of the toe flexors in opposing foot arch deformation

Torstein E. Dæhlin[1], Loren Z.F. Chiu[1]
[1]Faculty of Kinesiology, Sport, and Recreation, University of Alberta, Edmonton, AB, Canada
Email: eriksend@ualberta.ca

Introduction

The foot arch may deform when acted upon by external and calcaneal tendon forces [1, 2]. The amount of desirable arch deformation varies between different tasks. To modulate arch deformation, the toe flexor muscles may exert forces to support the arch. Although previous research has found that these muscles may oppose foot arch deformation from external loads, little is known about their capacity to oppose arch deformation caused by combined external load and internal muscle force [1].

Therefore, the purpose of this study was to investigate the role of the toe flexor muscles, by examining the midfoot joint angle and net joint moment (NJM), in opposing arch deformation due to calcaneal tendon forces that exert ankle plantar flexor NJM.

Methods

A repeated measures design was used to investigate the effect of maximally voluntarily contracting (MVC) the toe flexor muscles on midfoot angle and NJM while the foot was subject to external and calcaneal tendon forces.

Six male and 6 female healthy adults provided informed consent to participate. Eleven retroreflective markers were placed on their right leg and foot, and recorded using stereophotogrammetry (100 Hz). Ground reaction forces were simultaneously recorded using a force platform (1000 Hz). Participants were seated with the hip and knee flexed approximately 90 degrees and the forefoot resting on the force platform, which was elevated 10 cm from the floor. Loads from 0% to 150% of body mass were applied to the participants' distal thigh in 50% increments in two experimental conditions. In the first condition, participants were intructed to relax their toe flexors. In the second condition, participants performed a toe flexor MVC by pressing their toes as hard as possible against the force platform. To create a condition that would activate triceps surae, participants were instructed to maintain their foot parallel to the ground while the loads were applied.

Repeated-measures ANOVAs with Bonferroni corrected post hoc t-tests were used to analyse the effect of external load and toe flexor MVC on midfoot angle and NJM (α-level = 0.05).

Results and Discussion

A condition-by-load interaction and accompanying post hoc tests demonstrated that midfoot angle was lower for each increase in external load ($p = 0.002$; Figure 1). Moreover, midfoot angle was lower in the relaxed compared to MVC condition during the first 50% body mass increment in load.

Further, there was a significant main effect for condition in midfoot NJM, indicating that toe flexor MVC results in larger midfoot elevator NJM than in the relaxed condition ($p < 0.001$; Figure 1). Similarly, there was a significant main effect for load in midfoot NJM ($p < 0.001$; Figure 1). Post hoc comparisons demonstrated that midfoot elevator NJM increased with larger load ($p < 0.001$).

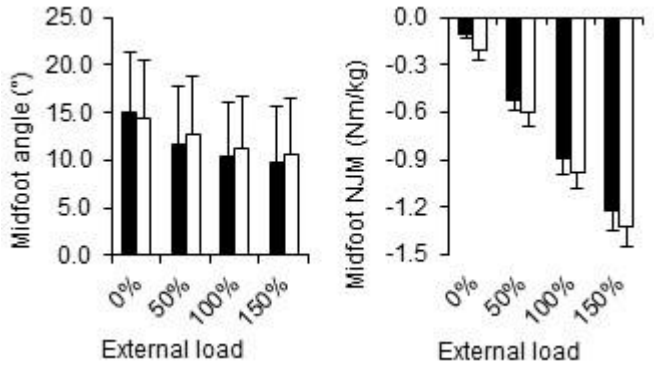

Figure 1: Mean and standard deviation midfoot angle (left panel) and NJM (right panel) across the external loads and conditions (black bars = relaxed, white bars = maximal voluntary). Positive values indicate midfoot elevation angle and NJMs, respectively.

Maximal voluntary activation of the toe flexor muscles resulted in smaller decreases in midfoot angle through greater midfoot elevator NJMs. This suggests that the toe flexor muscles have the capacity to oppose foot arch deformation due to combined external and calcaneal tendon forces. However, the magnitude of the differences in midfoot angle and NJM with toe flexor MVC was small. This may be due to the toe flexor muscles also exerting considerable force during the "relaxed" condition. Indeed, Kelly et al. [1] have demonstrated that the intrinsic toe flexor muscles may activate in response to external loading alone. Future research is therefore necessary to determine the practical importance of the toe flexors for opposing arch deformation.

In summary, it appears that the toe flexor muscles may oppose arch deformation resulting from combined external loads and internal muscle forces.

Significance

The present study provides further insight to the role of the toe flexor muscles in opposing foot arch deformation. Understanding how these muscles operate may help coaches and practitioners develop training protocols for strengthening these muscles in order to maintain normal foot function or enhance performance.

Acknowledgments

The first author is supported with a Vanier Canada Graduate Scholarship.

References

[1] Kelly LA et al. (2014). *J. R. Soc. Interface.* **11:**93 20131188.
[2] Thordarson DB et al. (1995). *Clin. Orthop. Relat. Res.* **316:** 165-172.

Energy dissipation due to soft tissue movement of the thigh during forefoot and rearfoot impacts at different running velocities

Matthew T.G. Pain, Dimitrios Voukelatos, and Laura-Anne M. Furlong
School of Sport, Exercise, and Health Sciences, Loughborough University, UK
Email: m.t.g.pain@lboro.ac.uk

Introduction

Soft tissue deformation has been reported to account for up to 70% of the energy lost in some segments during impacts [1]. Despite the rigid body assumption not holding during dynamic tasks only one single subject study using 2D video analysis has tried to directly calculate energy dissipation in the soft tissues of the thigh during running [2]. The aim of this study was to directly determine energies associated with deforming soft tissue of the thigh during forefoot (FF) and rearfoot (RF) landings whilst running at different velocities using 3D motion analysis.

Methods

Following university ethical approval and written informed consent, seven healthy, university level runners (age: 25 ± 4.5 years, height: 1.80 ± 0.06 m, mass: 70.1 ± 6.6 kg) participated in this study. Seventy-two retro-reflective 6.4 mm diameter markers were attached around the thigh segment of the right limb, in a 9 x 8 array. This covered 85% of the thigh segment length, defined using markers attached to the pelvis and femoral epicondyles. A triangular area about the size of a hand was left unmarked on the inner thigh as markers were occluded and knocked off when placed here. Marker positions in 3D space were determined using an 18 camera high-speed motion analysis system (750 Hz, Vicon Vantage, Oxford Metrics PLC., Oxford, UK) as subjects ran on a motorised treadmill (HP Cosmos Saturn, Traunstein, Germany) in racing flat shoes at four testing velocities (ascending order of 11, 14, 17 and 20 km/hr). Trials at each velocity were performed with a FF (landing on ball of foot) or RF (landing on heel) strike pattern in a counterbalanced order.

One stance with good marker visibility, correct foot strike and a typical stride length was selected for analysis from each person at each speed. Data were reconstructed, labelled and gap filled using Nexus 2.7 (Oxford Metrics PLC, Oxford, UK). Further post-processing was completed using custom-written Matlab code (MathWorks, Natick, MA., USA), including low pass filter at 100 Hz with a 4th order, zero lag Butterworth filter. The change in distance between the fixed segment centre of mass (COM), based on joint markers, and the soft tissue COM, calculated using a Delaunay triangulation representation of the soft tissue [3], was determined. The relative angles between the principle axes of the rigid segment and the soft tissue segment of the thigh were calculate using quaternions for every frame.

Energy loss due to soft tissue motion was calculated for both rotational and angular motions by first fitting a damped simple harmonic curve to the relative linear and angular motion of the soft tissue to the rigid segment thus obtaining the amplitude, frequency and exponential decay of the oscillation. Subsequently the total energy of oscillation was calculated as the sum of the kinetic and potential energies, using those terms.

Results and Discussion

The mass of the soft tissue of the thigh calculated from the marker arrays was on average 6.1 kg. As these subjects would typically have a total thigh mass of just over 7 kg [4] it seems that this is a decent estimate of the soft tissue mass. Overall group mean results showed that energy losses associated with the damped soft tissue motion were greater during RF than FF strike and greater at higher velocities (Table 1). These values reflect the same pattern seen for the shank [5] during these same running trials for the same subjects. However, for these subjects, the energy losses in the thigh are 3-4 times greater than seen in the shank [5] and thus are proportionately greater once segment size is accounted for. Energy losses of up to 17 J per foot strike are not inconsequential in the overall energetics of the system, both from a mechanical perspective of how much work is being done and where, but also from the metabolic perspective.

Assuming typical GRF and kinematics as those previously observed for RF and FF striking, these data support previous suggestions that both magnitude and direction of force applied play an important role in establishing the role of soft tissue motion. This is further highlighted by the fact that the majority of the energy lost was due to rotational oscillations about all three axes not linear oscillations. Standard deviations are high, probably due to a combination of low subject numbers, differences in subject mass and possibly ease or comfort of landing with a RF strike at different velocities for different subjects.

Table 1. Energy in the thigh segment during running with a forefoot-strike and rearfoot-strike at 11, 14, 17 and 20 km/hr.

Running speed (km/hr)	Forefoot (J)	Rearfoot (J)
11	5.7 ± 1.8	7.1 ± 1.9
14	8.9 ± 3.9	8.3 ± 3.7
17	9.1 ± 4.1	13.2 ± 6.7
20	11.2 ± 5.2	17.1 ± 12.2

Significance

Measurement of marker arrays can determine substantial changes in soft tissue motion of the thigh relative to a rigid segment during running. These energy losses are typically unaccounted for in traditional analyses, both with regard to mechanical work and metabolic processes. Given that the energy lost during the damped oscillation of the thigh soft tissue is unlikely to be recoverable to any great extent these losses should be given consideration when dealing with the energetics of running.

References

[1] Pain MTG & Challis JH. 2002. J App Biomech, 18: 231-242.
[2] Schmitt & Gunther. 2011. M. Arch Appl Mech, 81: 887-897.
[3] Furlong et al. 2020. J. Biomech, 99, 109488.
[4] Dempster, 1955. Wright-Patterson Air Force Base, Ohio.
[5] Pain MTG. et al. 2019. Proceed. ISB, Calgary Canada.

Running Symmetry is not different in Youth Runners with Low, Moderate and High Muscular Symmetry

Micah C. Garcia[1], David M. Bazett-Jones[1], Jeffery A. Taylor-Haas[2], Kevin R. Ford[3], and Jason T. Long[2]
[1]University of Toledo, Toledo, OH, USA
[2]Cincinnati Children's Hospital Medical Center, Cincinnati, OH, USA
[3]High Point University, High Point, NC, USA

Email: micah.garcia@rockets.utoledo.edu

Introduction

Unimpaired gait is assumed to be symmetrical [1]. However, some magnitude of asymmetry is normal as side-to-side differences in lower extremity kinematics have been reported in youth runners [2]. Sagittal plane patterns demonstrate very strong side-to-side symmetry in uninjured youth runners, but substantial variability was observed in non-sagittal plane symmetries [2]. A previous study comparing landing mechanics in youth found athletes with a history of ACL reconstruction had greater lower extremity muscular strength asymmetries and greater biomechanical asymmetries during a single-leg landing task than uninjured counterparts [3]. This finding suggests muscular asymmetries may be related to asymmetric movement patterns and injury risk; however, this relationship is unknown in youth runners. The purpose of this study was to investigate if uninjured youth runners with higher muscular symmetry demonstrate higher frontal and transverse plane lower extremity running kinematic symmetry than youth runners with lower muscular symmetries. It was hypothesized runners with high muscular symmetries would have higher running kinematic symmetries than runners with low muscular symmetries.

Methods

Uninjured youth ages 9-19 who participated in long-distance running activities were recruited for the study (m=60, female=75 age=13.5±2.7 years, height=1.58±1.42 m, mass=48.0±13.5 kg). Bilateral muscular testing included side plank, hip abduction (HABDS), and hip extension (HEXTS). Isometric hip abduction strength was measured side-lying using a handheld dynamometer and isokinetic hip extension strength (60 °/s) was measured prone using an isokinetic dynamometer. To assess symmetry, the absolute Normalized Symmetry Index (NSI) [5] was calculated for the duration of side plank holds and peak hip strength. The NSI reports percent asymmetry between sides where NSI=100% indicates perfect asymmetry. To convert NSI to the magnitude of symmetry, the NSI was subtracted from 100%.

Participants underwent 3D motion analysis while running at a self-selected speed on a non-instrumented treadmill. Participants were instrumented with reflective markers and measured using a 12-camera system (Raptor4; Motion Analysis Corp.; Rohnert Park, CA). Lower extremity kinematic symmetries during stance phase were calculated for frontal plane hip and knee motion as well as transverse plane hip and ankle motion using the Linear Fit Model (LFM) [2, 5]. The LFM provides an R^2 symmetry value where R^2=1 is perfect symmetry.

For analysis, participants were stratified into low, moderate, and high muscular symmetry terciles for side plank, HABDS and HEXTS NSIs, respectively. Measures were found to be non-normally distributed and Kruskal-Wallis tests (P<0.05) compared the mean rank of lower extremity R^2 values for each kinematic measure across muscular symmetry groups.

Results and Discussion

No significant differences in running symmetries were found among low, moderate, and high muscular symmetry groups. A previous study reported a relationship between hip extension strength and hip rotation during running [7] but our current study found hip rotation running symmetry was not different across HEXT muscular symmetry groups (low=0.52±0.35, moderate=0.58±0.33, high=0.64±0.33; p=0.269). Running biomechanics do not appear to be influenced by hip abduction strength [8] and our results indicate the same is true for HABDS symmetry (hip adduction symmetry: low=0.55±0.34, moderate=0.63±0.34, high=0.56±0.33; p=0.195).

Our hypothesis that youth runners with high muscular symmetries would have higher running kinematic symmetries than youth runners with low muscular symmetries was not supported. While some level of asymmetry is expected in uninjured populations, previous work demonstrated greater lower extremity strength and single-leg landing asymmetries in youth returning from injury compared to uninjured controls [3]. To our knowledge, the current study is the first to investigate muscular symmetry and waveform symmetry in youth runners. Results from our study indicate running symmetry is not different across varying levels of muscular symmetry in uninjured youth runners. Musculature weakness has been linked to altered running patterns in injured runners [6]. In the current study, muscular symmetry measures did not account for potential musculature weakness as the NSI only quantifies the similarities in strength between sides. When assessing for injury risk, it may be more appropriate to consider the collective influence of muscular strength and side-to-side muscular symmetry on movement symmetry.

Significance

The importance of running symmetry is unknown, especially in a population of uninjured youth runners. As running injuries are multifactorial, isolated muscular symmetries do not appear to influence running symmetry. Further prospective research is warranted to determine the causes of running asymmetries in youth runners and the factors associated with these asymmetries as they relate to running injuries and performance.

Acknowledgments

Thank you to Cincinnati Children's Hospital 2019 Patient Services Grant for supporting this work.

References

[1] Zifchock RA et al. 2008. *J Biomech.*
[2] Garcia MC et al. 2020. *Gait & Posture.*
[3] Ithurburn MP et al. 2015. *Am J Sports Med.*
[4] Queen R et al. 2020. *J Biomech.*
[5] Iosa MA et al. 2014. *Biomed Res Int.*
[6] Fredericson M et al. 2000 *Clin J Sports Med.*
[7] Taylor-Haas JA et al. 2014. *IJSPT.*
[8] Brund RBK et al. 2018. *Scand J Med Sci Sports.*

Effects of Take-off Board Stiffness on Long Jump Performance

Kara Ashcraft[1] & Alena M. Grabowski[1]
[1]University of Colorado, Boulder, CO, USA
Email: Kara.Ashcraft@colorado.edu

Introduction

Long jump has been a standard component of the Olympic games since their birth in Ancient Greece, and by modern competition rules includes a horizontal jump for distance preceded by a run-up of self-selected length. The factors that determine jump distance are a combination of the horizontal velocity developed in the run-up and the horizontal and vertical velocity at take-off, with maximum run-up velocity being the strongest correlate (R^2 = 0.7 – 0.9) with jump distance in non-amputee athletes.[1]

Athletes with leg amputations compete in the long jump using carbon fiber running-specific prostheses (RSPs) that are attached to their residual limb by a rigid socket. Use of RSPs limit force generation during sprinting, which likely limits run-up velocity and may limit the take-off leg's ability to redirect the downward and forward velocity at initial contact into upward and forward velocity at take-off.[2] Willwacher et al. found that use of an RSP by an athlete with a transtibial amputation resulted in a slower run-up velocity but an enhanced take-off technique compared to non-amputees with similar jump distances.[3]

Thus, long jump performance is influenced by maximum horizontal run-up velocity, vertical and horizontal take-off velocity, and likely the in-series RSP stiffness. RSPs are passive-elastic springs that act in-series with the residual limb. To better understand how in-series stiffness affects long jump distance, we measured the effect of take-off platform stiffness (k_{surf}) on long jump distance in non-amputees. We hypothesized that regardless of the run-up velocity, decreasing k_{surf} of the take-off platform would result in longer jump distance by enhancing take-off technique through energy storage and return within the take-off surface.

Methods

Eight competitive collegiate long jump athletes (5 M, 3 F) gave informed written consent and participated in a 3-day protocol that involved maximum effort jumps on 3 take-off platforms with stiffness values of 84 kN/m, 90 kN/m, and 1628 kN/m. These k_{surf} were similar to the stiffness values of two typical RSPs, and a regulation track surface, respectively. Each subject completed 4-6 maximum effort long jumps on each of the 3 take-off platforms. We measured ground reaction forces during the take-off step from force platforms (AMTI; 1000 Hz) installed beneath the track and platform surface. We measured maximum run-up and take-off velocities using a radar gun (Stalker; 47 Hz), two high speed video cameras (Casio; 240 Hz), and the force platforms. Jump distances were measured for all completed jumps with a tape measure. We averaged jump distances from 4 jumps per athlete.

We varied take-off k_{surf} by custom-building a springy platform installed between two force platforms. We used a different number of springs to create two compliant conditions (84 kN/m and 90 kN/m; Fig.1). When a subject landed on the take-off platform, the force applied was distributed between two force plates. We performed a two-way ANOVA to compare jump distance between platforms and used correlations to associate maximum run-up velocity with jump distance.

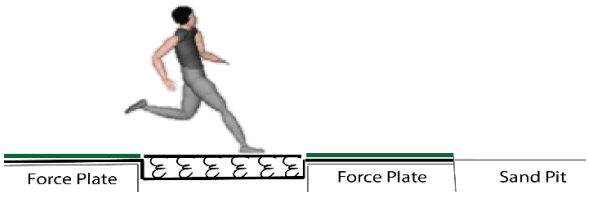

Figure 1. Custom-built take-off platform installed between two force plates. As a subject lands on the platform during the take-off step, the forces produced are recorded by both force plates.

Results and Discussion

There were no differences in the average maximum run-up velocity attained between platform stiffnesses (p = 0.40). There was a moderate correlation between maximum run-up speed and jump distance (R^2 = 0.61; Fig.2B). However, average jump distance was longer for the k_{surf} of 84 kN/m (6.02 ± 0.09 m) compared to the k_{surf} of 1628 kN/m (5.69 ± 0.08 m; Fig 2A), but was not different between these surfaces and a k_{surf} of 90 kN/m. This suggests that jump distance increases with decreased k_{surf} independent of maximum run-up speed.

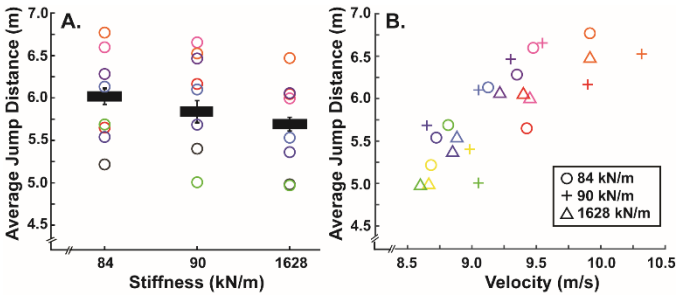

Figure 2. **A.** Average ± SE jump distance (black horizontal bars) and each athlete's jump distance (colored circles) for a given take-off k_{surf}. Jump distance was 5% longer for a k_{surf} of 84 kN/m compared to 1628 kN/m. **B.** Average jump distance versus run-up velocity for a k_{surf} of 84 kN/m, 90 kN/m and 1628 kN/m.

Conclusion

The in-series surface stiffness of the take-off platform affects long jump distance. Though athletes with transtibial amputation using RSPs have a slower maximum run-up velocity compared to non-amputees, the in-series stiffness of an RSP during the take-off step likely affects long jump distance. Future research is planned to better understand the interaction of run-up velocity and the effects of in-series stiffness on take-off technique for the long jump.

References

1. Hay. *Exerc. Sport Sci. Rev.* **14**, 401–446 (1986).
2. Kerdok et al. *J. Appl. Physiol.* **92**, 469–478 (2002).
3. Willwacher et al. *Nature Sic Reports* **7**, (2017).

Curve Sprinting With A Split-Toe Running Specific Prosthesis: A Pilot Study

Ryan S. Alcantara[1]
[1]University of Colorado, Boulder, CO, USA
Email: ryan.alcantara@colorado.edu

Introduction

For athletic track events like the 400 m sprint, over half the race is completed along a curve. Sprinting along a curve imposes different force production requirements [1] and elicits slower maximum sprinting velocity compared to a straightaway [2]. Faster curve sprinting may improve overall performance in these athletic events. Sprinters with transtibial amputations use a passive-elastic running-specific prosthesis (RSP) that is typically made with a solid piece of carbon fiber and torsionally stiff, and thus resists frontal plane rotation during running. Fillauer Composites (Salt Lake City, UT) manufactures an RSP with a "split-toe" design, where a distal portion of the RSP is cut longitudinally, which allows the medial and lateral sides of the RSP to bend independently, reduces torsional stiffness, and potentially increases traction when running on a curve (Fig. 1).

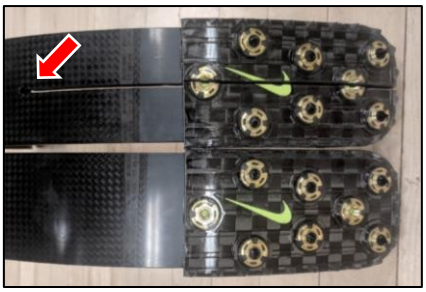

Figure 1. Split-toe (top) and solid (bottom) RSPs. Arrow indicates the proximal end of the split.

We hypothesized that maximum sprinting velocity would be faster using the split-toe compared to solid RSP on curves but would be similar between RSP designs on the straightaway. We also hypothesized that participants would elicit greater affected leg stance-average centripetal ground reaction forces (GRFs) on a curve when using the split-toe compared to solid RSP to achieve faster velocities.

Methods

Three individuals (2 M, 1 F; mean ± SD mass: 72.92 ± 10.72 kg; height: 1.80 ± 0.06 m; age: 25 ± 9 yrs) with a right transtibial amputation participated. Subjects had at least one year of experience competing using an RSP in a sprint event (400 m or shorter) within the past two years. The split-toe and solid RSP had identical shapes, height, and sagittal plane stiffness.

Participants completed a randomized series of 40 m sprints on a flat indoor track. We instructed participants to run as fast as possible for each trial and provided ≥8-min rest between trials. Participants performed clockwise and counterclockwise sprints along curves with radii of 36.5 m and 17.2 m and straightaway sprints over 40 m. Athletes ran across two adjacent force plates (1000 Hz) embedded beneath the track surface. We recorded 3D kinematics using high-speed motion capture cameras (100 Hz). The force plates and capture volume were located halfway along the runway. Trials were repeated until athletes successfully landed on the force plates at least once. Participants were not blinded to the RSP designs.

We measured maximum sprinting velocity using average pelvis marker velocity over the length of the force plates (2.4 m). We calculated stance-average centripetal force for the affected leg. We constructed linear mixed-effects models to determine the effect of RSP design on sprinting velocity and centripetal force production.

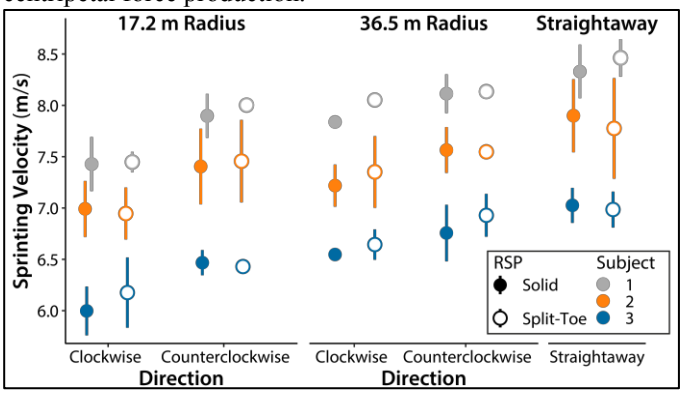

Figure 2. Mean ± SD velocity across conditions. Sprinting velocity using the split-toe running-specific prosthesis (RSP) was 0.13 m/s faster than the solid RSP across curve conditions and directions, but similar during the straightaway. Velocity was 0.34 m/s slower when sprinting in the clockwise compared to counterclockwise direction and 0.33 m/s faster with increased curve radius across directions.

Results and Discussion

Mean (± SE) sprinting velocity with the split-toe RSP was 0.13 ± 0.04 m/s faster compared to the solid RSP for a given curve radii and direction ($p < 0.001$; Fig. 2). Using the split-toe RSP did not affect maximum sprinting velocity on the straightaway compared to the solid RSP ($p = 0.705$).

Stance-average centripetal force was significantly affected by curve condition ($p < 0.001$) and sprinting velocity ($p < 0.001$), but not RSP design ($p = 0.180$) or running direction ($p = 0.746$). Mean stance-average centripetal force for the affected leg on the 17.2 m radius curve was 0.43 ± 0.15 BW and decreased by 0.19 ± 0.02 BW in the 35.2 m radius curve for both directions.

Centripetal (radial) force (Fc) equals mv^2/r, where m is mass, v is tangential velocity, and r is curve radius. Sprinters running on a curve must apply Fc to stay within their lane and achieve a fast velocity. We observed statistically significant increases in sprint velocities with the split-toe RSP, but no change in Fc. Although participants ran along 36.5 m and 17.2 m curve radii, the 1.22 m lane width allows athletes to vary their path traveled for a given curve condition. We suspect that participants decreased the effective radius of the curve they traveled along within the lane when using the split-toe compared to solid RSP, which may potentially explain the faster sprinting velocity without significant increases in Fc.

Significance

Sprinters with a unilateral transtibial amputation may be able to achieve faster curve sprinting velocities using an RSP with a split-toe design compared to a traditional, solid RSP.

References

1. Luo & Stefanyshyn *J Exp Biol* **215**, 4314-21, 2013.
2. Greene *J Biomech Eng* **107**, 96-103, 1985.

External mechanical work during running after unilateral transfemoral amputation

Hiroto Murata[1,3], Genki Hisano[2,3], Ryo Amma[1,3], Brian S Baum[4], Hiroshi Takemura[1] and Hiroaki Hobara[3]
[1]Tokyo University of Science, Chiba, Japan, [2]Tokyo Institute of Technology, Tokyo, Japan
[3]National Institute of Advanced Industrial Science and Technology (AIST), Tokyo, Japan, [4]Regis University, CO, USA
Email: murata-hiroto@aist.go.jp

Introduction

Prevalence of running-specific prostheses (RSPs) have allowed unilateral transfemoral amputees (UTFAs) to run by regaining a spring-like leg function in their affected limbs. When non-amputees run at constant speed on level ground, the mechanical energy of the whole body center of mass (COM) is absorbed during the negative work phase and restored during the subsequent positive work phase [1]. Negative external work is equal to positive external work for each step in order to maintain a symmetrical bouncing gait [1]. However, little is known about mechanical work of the body in UTFAs using RSPs. This study aimed to investigate external mechanical work at different running speeds in UTFAs with RSPs.

Methods

Eight UTFAs wearing RSPs (age: 27 ± 11 years, mass: 64.5 ± 8.1 kg, 100-m personal records: 15.65 ± 1.03 s, mean ± SD) ran on an instrumented-treadmill (FTMH-1244WA, Tec Gihan, Kyoto, Japan) at incremental speeds (30%, 40%, 50%, 60%, 70% and 80% of the average speed of their 100-m personal records). The mechanical energy of the COM (E_{ext}) was calculated from the vertical and horizontal ground reaction forces (GRF, sampled at 1000 Hz) [2]. External mechanical power (P_{ext}) was calculated as the dot product of the GRF and COM velocity, and E_{ext} was the time integral of P_{ext}. The negative (W^-_{ext}) and positive external work (W^+_{ext}) per step were computed as the sum of the negative and positive increments of E_{ext} curves, respectively [3]. Further, net external work (W_{net}) was calculated as the difference between W^-_{ext} and W^+_{ext} [3]. We analysed 10 consecutive steps and averaged five steps of each limb to determine the representative values for each speed. Two-way ANOVA (two limbs × six speeds) was performed to compare variables between the unaffected (UL) and affected (AL) limbs at six speeds. If significant main effects were observed, Bonferroni post-hoc multiple comparisons were performed. Statistical significance was set to $P < 0.05$.

Results and Discussion

As shown in Figure1-A, there was a significant main effect of speed ($P < 0.01$) on W^-_{ext}. However, no significant effect of interaction was observed. Although it did not reach a statistical significance in limb, W^-_{ext} of the AL tended to be smaller than that of the UL across a range of running speeds. E_{ext} is mainly absorbed by knee extensor muscles during the negative work phase [4], but UTFAs have lost the function of these muscles in the AL due to amputation. Therefore, the AL with RSPs may exhibit less capability to absorb the E_{ext} compared to the UL.

W^+_{ext} had significant main effects of speed ($P < 0.01$) and interaction ($P < 0.01$); whereas, no significant main effect of limb was observed (Figure 1-B). W^+_{ext} in the AL was equal to or greater than the UL across a range of running speeds. These results suggest that the AL could perform W^+_{ext} as well as the UL using energy storing and return capabilities of RSPs.

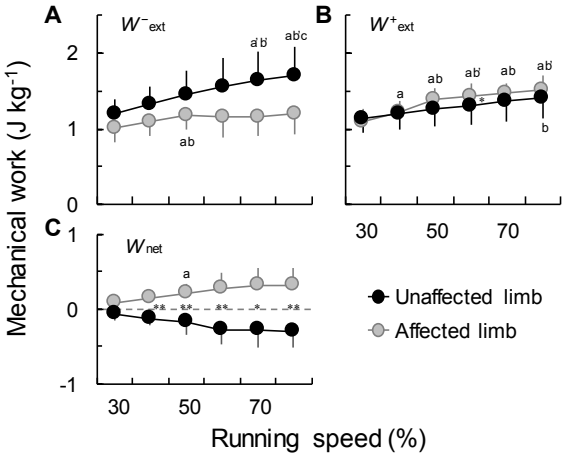

Figure 1: The mass-specific external mechanical work per step. W^-_{ext} (A), W^+_{ext} (B) and W_{net} (C) of unaffected (black) and affected (gray) limbs across six running speeds. Error bars represent 1 SD. The asterisks (*, **) indicate significant differences between the limbs at each speed, at $P < 0.05$ and $P < 0.01$, respectively. Alphabets (a', b', c' and a, b, c) indicate significant differences from 30%, 40% and 50% speed, at $P < 0.05$ and $P < 0.01$, respectively.

Further, statistical analysis revealed significant main effects of limb ($P < 0.01$) and interaction ($P < 0.01$), but no significant main effect of speed on W_{net} (Figure 1-C). While the W_{net} of the UL was negative, the W_{net} of the AL was positive across a range of running speeds. These results indicate that the COM of UTFAs is decelerated in the UL and accelerated in the AL at each step. In this case, the simple spring-mass model (SMM) could not be applied because the W_{net} is not zero for the UL or AL.

We observed that external mechanical work during running in UTFAs is not the same for the both limbs. UTFAs with RSPs maintain their bouncing steps with a limb-specific strategy.

Significance

Generally, the simple SMM has been applied to describe the bouncing mechanism in human running. However, current results suggest that bouncing mechanism in UTFAs should not be described using the simple SMM. Therefore, mechanical energy fluctuations could reveal better biomechanical models to analyse UTFAs with RSPs.

Acknowledgments

This work was partly supported by JSPS KAKENHI [grant Number 19K11338]. The authors thank Mr. Hiroyuki Sakata, Tokyo University of Science, for initial data analyses.

References

[1] Margaria R. (1968). *Z. Angew. Physiol* 25, 339-351
[2] Cavagna GA. (1975). *J Appl Physiol* 39(1), 174-179
[3] Dewolf AH., et al. (2016). *J Exp Biol* 219, 2276-2288
[4] Liew XWB., et al. (2016). *J Biomech* 49, 3275-3280

EFFECTS OF A PARALYMPIAN WITH TRANSFEMORAL AMPUTATION USING A PROSTHESIS WITH & WITHOUT A KNEE

Janet Zhang[1], and Alena Grabowski[1]
[1]University of Colorado, Boulder, CO, USA
Email: Hanwen.Zhang@coloradu.edu

Introduction

Runners with transfemoral amputation using a prosthesis with an articulating knee combined with a running-specific prosthetic foot (blade) have a lower metabolic cost compared to using a prosthesis with a blade only [1]. However, the biomechanical changes induced by using a prosthesis with a knee are unclear. We compared biomechanics from a Paralympic athlete with a transfemoral amputation who ran using two prostheses, one with a knee and one without.

We hypothesized that the 1) prosthesis with a knee would reduce leg stiffness, increase hysteresis, and reduce peak hip abduction during leg swing in the affected leg (AL) compared to the prosthesis without a knee; 2) biomechanics of the unaffected leg (UL) would not differ between the two conditions; 3) peak vertical ground reaction force (vGRF) would be lower in the knee versus no-knee condition.

Methods

A female with a left transfemoral amputation ran on a force-measuring treadmill (Treadmetrix, Park City, UT) at 3.58 m/s, 3.70 m/s, 3.83 m/s, and 3.97 m/s using two running prostheses. The prosthesis with a knee (Ottobock, Berlin, Germany) was 3.0 kg (knee); the prosthesis without knee (Fillauer Composites, Utah, USA) was 1.2 kg (no-knee).

We measured motion at 100 Hz and vGRF at 1000 Hz (Vicon, Oxford, UK) during each trial and normalized vGRFs to body weight in each corresponding prosthesis. Ten steps from each leg were extracted from each trial. We used the spring-mass model to calculate leg stiffness [2] and calculated hysteresis of the leg spring to compare energy loss during the stance phase [3]. To assess the mechanism underlying leg stiffness, we compared the peak vGRF from each leg. We also calculated peak hip abduction angle during the swing phase. We did not perform statistical analyses for this case study.

Results and Discussion

In the knee condition, leg stiffness decreased by 14.6-16.3% in the AL, and 3.9-6.8% in the UL compared to the no-knee condition (Fig. 1). At speeds from 3.58-3.83 m/s, the difference in hysteresis between each condition was within 3.6% in the AL. At 3.9 m/s, the prosthesis with a knee increased energy return (lower hysteresis) of the AL by 16.2% but increased hysteresis of the UL by 32.5% compared to the no-knee condition. In the knee condition, peak vGRF decreased by 3.4-6.3% in the AL and by 3.8-5.3% in the UL compared to the no-knee condition. The AL had lower peak hip abduction angles in the knee condition (7.7-9.8°) versus the no-knee condition (30.0-35.1°) and the UL peak hip abduction angles were similar between conditions (Fig 1).

Lower leg stiffness has been associated with reduced metabolic cost in athletes with transtibial amputation [3]. We found that a triathlete with transfemoral amputation had lower

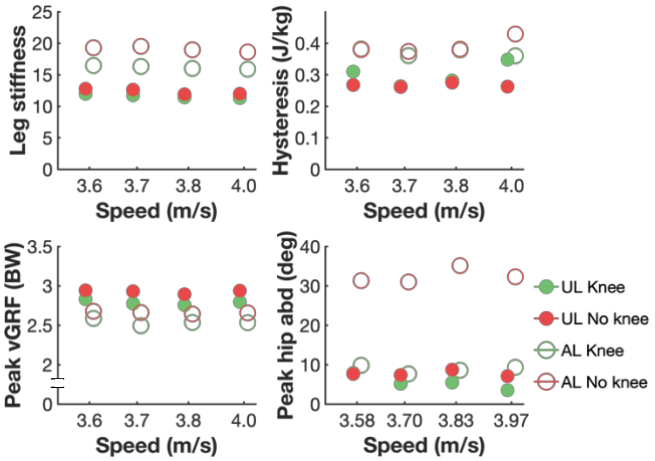

Figure 1. Leg stiffness*, hysteresis, peak vGRF, and peak hip abduction (abd) between prosthetic conditions for the Unaffected Leg (UL) and Affected Leg (AL) during running. (*Leg stiffness was normalized to body weight (N) and leg length (m) in each prosthetic condition.)

leg stiffness when running with the knee versus no-knee condition. The difference between amputation levels limits the application of our findings. However, the results might explain the lower metabolic cost in participants with transfemoral amputation walking or running (1.12 to 2.01 m/s) using a prosthesis with a knee versus without a knee [1].

In the knee versus no-knee condition, the UL had less of a reduction in leg stiffness compared to the AL. However, the UL and AL had similar reductions in peak vGRF in the knee versus no-knee condition. Thus, changes in AL leg stiffness are likely due to changes in leg compression rather than in peak vGRF. Specifically, the AL was more compliant, and UL was stiffer during stance in the knee versus no-knee condition.

The higher peak hip abduction during swing phase in the AL is likely due to the circumduction required to clear the ground in the no-knee condition. A previous study reported similar findings [4]. Moreover, peak hip abduction was more symmetric in the knee compared to no-knee condition.

Significance

We compared the biomechanics of a Paralympian with transfemoral amputation using a prosthesis with and without a knee and found that use of a prosthesis with a knee resulted in biomechanics that would presumably lower metabolic cost and improve running performance.

References

1. Highsmith et al., *Technol Innov*, **18**, 2:3, 2016
2. Farley and Gonzalez, *J Biomechanics*, **29**, 181-186, 1996
3. Beck et al., *J Appl Physiol*, **122**, 976-984, 2017
4. Nelson, Master's thesis, 2018

Moment Arm Plasticity in Response to Loading History during Growth

Matthew Q. Salzano[1,2*], Suzanne M. Cox[1], Stephen J. Piazza[1], and Jonas Rubenson[1,2]
[1]Biomechanics Laboratory, Dept. of Kinesiology, The Pennsylvania State University, University Park, PA 16802
[2]Integrative & Biomedical Physiology, The Pennsylvania State University, University Park, PA 16802
Email: *salzano@psu.edu

Introduction

A muscle's moment arm influences locomotor function since it determines the joint moments produced by a given muscle force and the muscle's shortening velocity for a given rate of joint rotation. While moment arms have been found to vary with locomotor specialization [1], it is not clear how much of this variation is due to nature versus nurture. Here, we investigate whether muscle moment arms are modulated in response to loading history during the growth period in an animal model.

Methods

Guinea fowl (N = 23, *Numida meleagris*) were split evenly into three groups at 4 weeks of age: exercise (EXE), sedentary (SED), and botox (BTX). EXE birds were housed in large pen (3.14 m^2), with ample room for running and perches for jumping. SED and BTX birds were house in small pens (1 m^2) with low ceilings to restrict movement and jumping. BTX birds were also given bilateral injections of botulinum toxin-A (4 units (LD50)/kg) in both gastrocnemius muscles every 5 weeks to promote further disuse, while SED and EXE received sham saline injections. The protocol lasted until birds were 6 months-old, for a total of 4 injections for each group, at which point they were sacrificed.

A tendon travel protocol was used to measure plantarflexion moment arms of the Achilles tendon. Retroreflective markers were placed on dissected limbs to track their movement and calculate joint angles. The Achilles tendon was attached to a linear transducer to measure excursion. Third-order polynomials were fit to the excursion-angle data in order to calculate moment arm as the derivative of excusrsion with respect to angle. Moment arms were found across the range of motion corresponding to that seen during the stance phase of running (30°-90°) [2].

Linear mixed models were run to find the effect of group on moment arm and any interaction between group and angle. The model was run twice: once classifying angle as a continuous variable, to analyze the moment arm curves, and again with angle classified as a categorical variable (at 30°, 60°, and 90°) to permit mean comparisons at each of the three chosen angles.

Results and Discussion

While there were no large, clear differences in moment arm between groups, there were several indications of moment arm plasticity during the growth period. There were significant group ($p = 0.040$) and interaction ($p < 0.001$) effects when the model was run with angle as a continuous variable, in which the EXE group appears to have a slightly larger moment arm than the other two groups. When angle was treated as a categorical variable, however, no significant interaction or group effect was found ($p = 0.104$ and $p = 0.092$, respectively; Fig. 2). This seemed to indicate no difference between groups but might be explained a lack of statistical power due to a small sample size. Our findings are suggestive of moment arm plasticity and adaption in response to loading during growth, but the amibiguous results from statistical tests suggest that caution should be taken when interpreting these results.

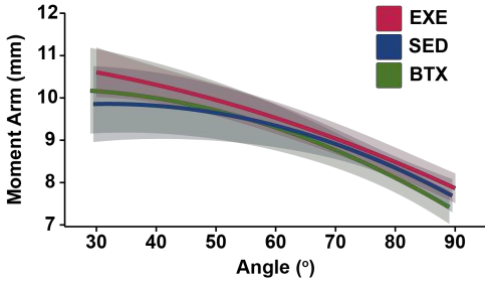

Figure 1: Moment arm plotted versus joint angle. Solid lines represent mean moment arm for each group. Shaded regions: ± 1 SD of the mean.

Significance

These data are among the first to indicate that muscle moment arms may be affected by loading history across growth. The functional consequences of increases in moment arm remain unresolved. On one hand, muscle moment generating capacity increases with increasing moment arm. This could permit high moments with smaller muscle mass, an advantage for reducing the energy required to grow and maintain muscle tissue. But muscle force capacity may also decrease due to a greater influence of force-velocity effects with a larger moment arm. Further work is required to quantify which of these factors dominates.

We encourage future studies exploring developmental plasticity of muscle moment arms. These studies will benefit from addressing deficiencies in statistical power and examining the mechanisms underlying links to locomotor function.

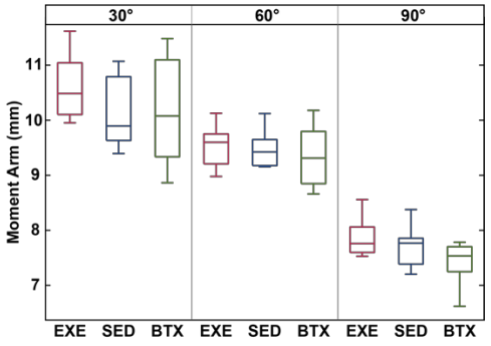

Figure 2: Boxplots of moment arms at 30°, 60°, and 90°. Box represents 25th-75th percentiles. Line within box represents median.

Acknowledgments

This study was supported by NIH (NIAMS) R21AR071588.

References

[1] Lee SS & Piazza SJ. (2009). *J Exp Biol*, 212(22):3700-7.
[2] Ellerby DJ & Marsh RL. (2010). *J Exp Biol*, 213(13):2201-8.

Reconstructing contractile dynamics from muscle length change

Jeffrey P. Olberding, Emanuel Azizi, Monica A. Daley
University of California, Irvine
Email: olberdij@uci.edu

Introduction

Understanding *in vivo* muscle dynamics requires knowledge of both force and length changes, but even indirect measures of muscle force prove difficult or imprecise in many systems. One solution has been to model *in vivo* strain profiles and apply them to isolated muscles, commonly seen in sinusoidal work-loop experiments [1]. While sine waves are reasonable approximations of some movements like insect flight and swimming, they fail to adequately capture the complexity of unsteady movement and particularly terrestrial locomotion. An alternative approach is imposing *in vivo* strain and activation on an isolated muscle and measuring the resulting forces, because strain can be measured in most systems for the whole MTU and sometimes for muscle fascicles. However, it has not been directly demonstrated that forces measured during contractions against reproduced strain profiles are similar to those produced during contractions with dynamic external loads.

Here we measure a strain profile for a muscle stimuatled to contract against a modeled inertia load moving against gravity through a lever system. We then stimulate the same muscle to contract against the strain profile from the first trial and ask whether the force, power, and work generated are similar to the original contraction.

Methods

The plantaris longus and sartorius muscles were isolated from bullfrogs (*Lithobates catesbeianus*) and stimulated them to contract against a dual-mode muscle servomotor. Because the plantaris has significant aponeuroses and tendon, sonomicrometry crystals were implanted to measure muscle fascicle length. All muscles were supramaximally stimulated for 500 ms and rested for 5 min between stimulations. First, muscles contracted against the motor while it was controlled via a feedback controller programed to simulate the motion of a simplified jumper (see [2]). The length changes resulting from that contraction were used for the subsequent trial with identical stimulation and initial length conditions. The force and length of matched pairs of contractions were used to calculate and compare the mechanical output of these two different techniques.

Results and Discussion

There were virtually no differences bewteen the force and length or resulting power and work calculated for muscles contracting against a simulated inertial load compared with muscle contracting against a prescribed length change. This was true for both the parallel-fibered sartorius muscle, which lacks aponeuroses and tendons, and for the pennate plantaris, which has significant elastic connective tissues.

This experiment creates the best possible conditions for applying a strain profile to recreate contractile dynamics: the same muscle, with identical intial conditions and activation pattrens. However, variation introduced to any of those factors could disrupt the tight correlation. Future experiments will explore the sensitivity of the results to variation introduced to initial conditions by varying the starting length of the muscle between a model-driven contraction and the subsequent length-driven contraction.

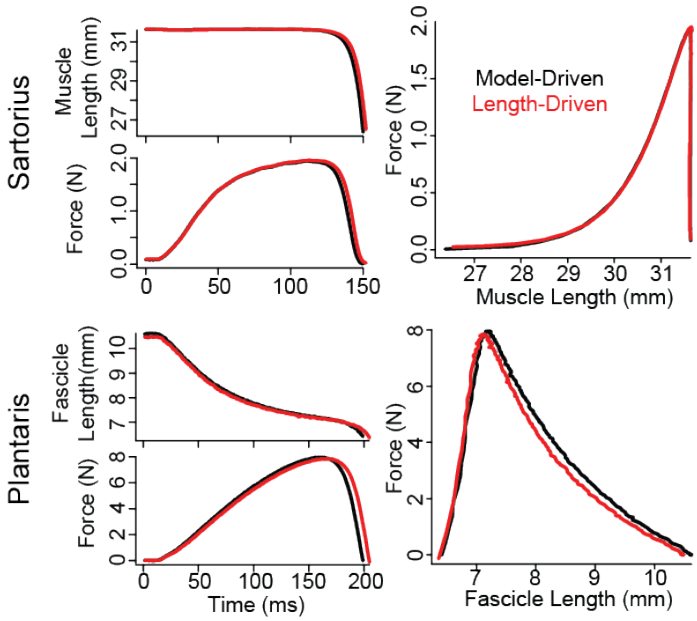

Figure 1: Model-driven and length-driven force and length profiles are identical, even for the plantaris with significant series elastic elements.

Significance

This study confirms that applying *in vivo* strain profiles can recreate the dynamics of a muscle contracting against dynamic load. Muscle contractile dynamics result from external forces acting on a muscle interacting with patterns of stimulation and other conditions. From the perspective of the muscle itself, it does not matter how the patterns of external forces are determined, as long as they are the same.

However, the validity of this approach depends on many other conditions being matched between *in vivo* and *in vitro* measurments, including: level of organization, activation patterns, and initial force/length conditions. The degree to which accurately replicating contractile dynamics depends on these factors will be explored in future experiments.

Additionally, when both *in vivo* strain profiles and a dynamic model are available and other conditions are matched, a comparison between these two types of isolated muscle contractions could be used to validate the dynamic model as an accurate representation of *in vivo* loading conditions.

Acknowledgments

Thanks to T. Whitacre, E. Mendoza, and I. Battoo for help with data collection.

References

1. Josephson, 1985 *J Exp Biol* **114** 493-512
2. Olberding et al., 2019 *Integr Comp Biol* **59:6** 1515–1524

Mechanosensation by muscle spindles during active muscle-tendon work loops

Emily M. Abbott[1,2], Paul Nardelli[1], Timothy Cope[1], Gregory S. Sawicki[1,2]
[1]School of Biological Sciences, Georgia Institute of Technology, Atlanta, GA, USA
[2]The George W. Woodruff School of Mechanical Engineering, Georgia Institute of Technology, Atlanta, GA, USA
Email: emily.abbott@me.gatech.edu

Introduction

While mechanosensation of muscle state is crucial for motor control, our understanding of what mechanosensors encode may be deeply flawed. Classic studies of mechanosenation used passive stretching paradigms and these foundational works concluded that primary muscle spindle receptors (1a afferent nerves) encoded muscle length or velocity while Golgi tendon organs (1b afferent nerves) encoded muscle force[1]. Unfortunately, these results may not accurately represent muscle-tendon functions in a freely moving animal. First, locomotive muscles are not always passive. In a passive stretch a muscle fiber and its associated elastic structure both lengthen, thus force and length are *coupled* in directionality. However, active muscle fibers function with elastic structures such as tendons and aponeuroses. During an active contraction a muscle fiber is activated, it produces force and if the force is great enough, the fiber will shorten and lengthen the elastic structure. Thus, force and length are *decoupled* in directionality[2]. Lastly, during locomotion muscle fiber length change patterns are cyclical and emerge from the interaction of muscle-tendon forces and body dynamics[3]. This perspective motivates us to reavalute the roles of mechanosensors in encoding sensory information.

Methods

We combined in situ muscle-tendon (MT) preparations with simultaneous intra-axonal recordings in female Wistar rats (IACUC #A18042; Fig. 1). We compared two dynamic protocols. 1) A passive condition where the MT interacts with a virtual body mass that is dropped and stretches the MT until the mass position is damped. 2) An active work loop protocol where stimulation is applied at a set frequency and the servomotor applies MT length change according to dynamics of a mass in gravity (Fig. 2).

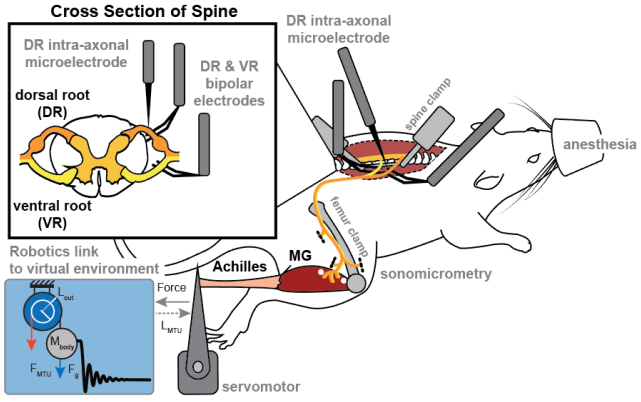

Figure 1: Medial gastrocnemius (MG) activated by stimulation of ventral root and instrumented with sonomicrometry crystals to measure muscle fascicle length. Instantaneous firing rate (IFR) of proprioceptors measured with intra-axonal microelectrode in the dorsal root and physiologically characterized as a muscle spindle[4].

Results and Discussion

Our long-term goal is to establish a bench top framework for re-evaluating the roles of muscle receptors in encoding sensory information during locomotion.

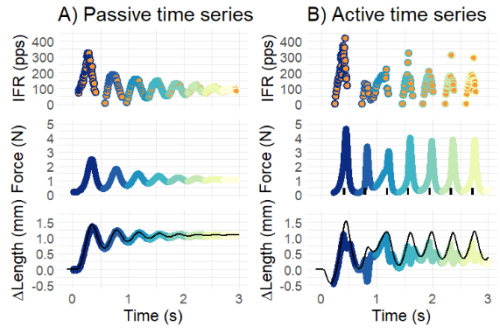

Figure 2: Two real-world conditions with the same muscle spindle recordings. A) passive condition where the MT damps a virtual mass and B) an active condition where MT is stimulated at 2.6Hz. In the bottom panel, muscle fiber lengths are represented with a color line while MT length is represented with a black line.

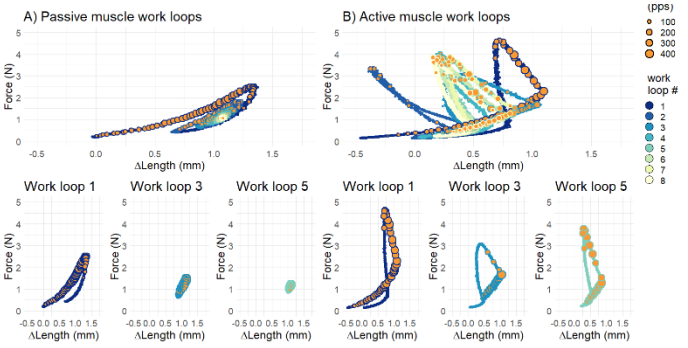

Figure 3: Work loop dynamics observed under the two conditions with the same muscle spindle recordings. Note that for the same forces or muscle fiber lengths, the muscle spindle responds differently (size = IFR in peaks per second)

Under novel real world conditions where the muscle is active, the fiber length is decoupled from force and it interacts with a virtual body mass, we observe that a muscle spindle operates differently than it does in passive conditions. Specifically, muscle spindles respond to increases in force even when the fiber is shortening. Furthermore, these work loops demonstrate that a muscle spindle response is more complex than a simple stretch receptor.

Significance

Here, we demonstrate the feasibility of in situ experiments that employ muscle-tendon work loops[2,3] in combination with direct recordings from muscle spindle receptors[4].

References

1. Gandevia. Kinesthesia: Roles for Afferent Signals and Motor Commands. *Compr. Physiol.* (2011).
2. Sawicki, *et al.* Timing matters: Tuning the mechanics of a muscle-tendon unit by adjusting stimulation phase during cyclic contractions. *J. Exp. Biol.* **218**, 3150–3159 (2015).
3. Robertson & Sawicki. Unconstrained muscle-tendon workloops indicate resonance tuning as a mechanism for elastic limb behavior during terrestrial locomotion. *Proc. Natl. Acad. Sci.* **112**, (2015).
4. Vincent, *et al.* Muscle Proprioceptors in Adult Rat: Mechanosensory Signaling and Synapse Distribution in Spinal Cord. *J. Neurophysiol.* jn.00497.2017 (2017).

Muscle fascicle dynamics during collisional phase of walking and the relation to push-off phase

Samuel T. Kwak[1*], Ashley Tran[2], and Young-Hui Chang[1]
[1]School of Biological Sciences, Georgia Institute of Technology, Atlanta, GA, USA
[2]Agnes Scott College, Decatur, GA, USA
Email: *skwak@gatech.edu

Introduction

People make rapid gait adjustments, minimizing metabolic cost without direct metabolic sensors, yet the mechanism is not known (1). Negative work done during the collisional phase of walking is a major determinant of metabolic cost, with the tibialis anterior (TA) muscle playing an important role in this energy absorption (2,3). Increased push-off work by the trailing leg can reduce the negative work in the collisional phase, heel strike to foot flat (4).

The aim of this study was to understand muscle dynamics during the collisional phase of gait under different gait conditions. We hypothesized that TA muscle fascicles would act isometrically across conditions within a small range of length change (±0.5 mm). We also predicted if significant lengthening occured, it would correlate with the subsequent ipsilateral push-off impulse as would increases in TA muscle force.

Methods

Eleven subjects (6 male, 22.8±3.6 years, 64.4±9.7 kg) gave written, informed consent prior to undergoing five walking conditions: fast (1.5 m/s) and slow (0.5 m/s) speeds at preferred step frequency (PSF), and medium speed (1.0 m/s) at 80%, 100%, and 120% of PSF. Kinematics, kinetics, and TA muscle ultrasound (60 Hz) data were collected. Preliminary data on five subjects are presented here. Fascicle length changes for 69±4 steps per condition were manually digitized in ultrasound images containing the initial contact and foot flat gait events (Echo Wave II, Telemed). Push-off impulses were calculated by integrating the positive portion of the anterior-posterior ground reaction force (GRF) for each step and normalized for each subject's body weight and PSF. Peak muscle forces were estimated using the GRF vector and TA muscle-tendon unit vector acting on the ankle joint and normalized for subject body weight.

Results and Discussion

Rather than being isometric across all steps, TA fascicles lengthened on average during the collisional phase of gait across all conditions. The 80% PSF condition had the most lengthening (0.9±0.9 mm, while also showing isometric and shortening fascicle behavior from step to step (Fig. 1). All conditions with a greater range of fascicle length change than predicted for a subject in each given condition (2.3±0.7 mm).

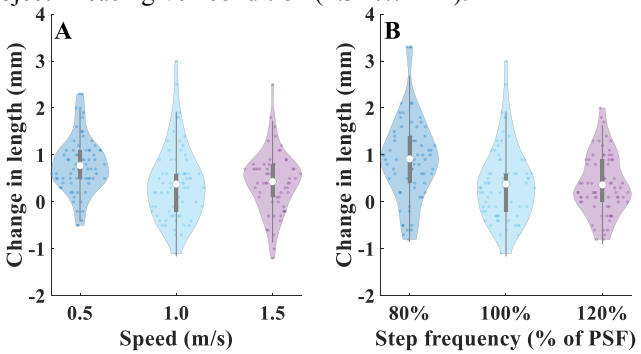

Figure 1. Fascicle length change due to speed (A) and step frequency (B). Violin plots with distrubuted values (colored dots) are shown with the mean (white dot), 25-75% quartiles (box), and ±2SD (whiskers).

For the 80% PSF condition, which can be considered the most novel condition experienced (slow, long steps), change in the dorsiflexor muscle fascicle length did not correlate with the ipsilateral push-off impulse (R^2=0.06, Fig. 2A). However, peak TA muscle force had a strong correlation with the subsequent ipsilateral push-off impulse (R^2=0.82, Fig. 2B). The contralateral leg push-off impulse showed a smaller correlation with TA muscle force (R^2 = 0.64). This correlation was not observed at the less novel 100% or 120% PSF (R^2=0.13 and 0.11, respectively).

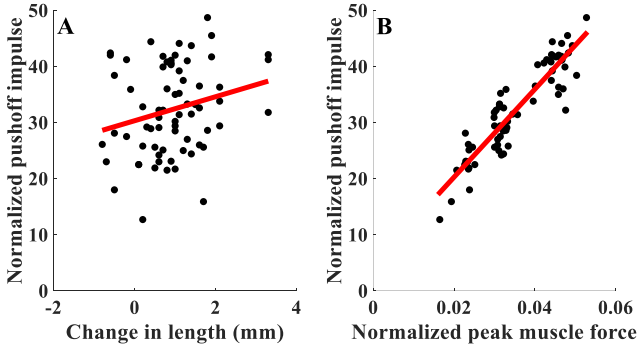

Figure 2. Fascicle length change (A) and peak TA muscle force (B) compared to the subsequent ipsilateral push-off impulse for the 80% PSF condition with a linear regression (red).

Our data show that TA fascicles on average lengthen slightly during early stance, but are variable enough to also regularly exhibit shortening and isometric behaviour on successive steps. Fascicle length feedback appears to be an unreliable parameter for making step-to-step gait adjustments on the subsequent push-off to control speed or minimize energetic cost. Instead, muscle force feedback may be important for these adjustments.

Significance

Although TA muscle spindles are sensitive to small length changes (5), this sensitivity may be task-dependent. During the collisional phase of walking, muscle length feedback may not be used for gait adjustments in the same way they are used in standing balance (6). Muscle force feedback may be a more likely candidate for making propulsive adjustments during gait.

Acknowledgments

The authors would like to thank Erika Sheng for assisting in data collections. This work was funded by the NIH HD055180 T32 Fellowship.

References

1. Selinger, J.C. et al. *Curr. Biol.* **25**, 2452-2456 (2015).
2. Donelan. J.M. et al. *J. Exp. Biol.* **205**, 3717-3727 (2002).
3. Maharaj. J.N. et al. *J. Exp. Biol.* **222**, jeb191247 (2019).
4. Kuo, A.D. et al. *Hum. Mov. Sci.* **26**, 617-656 (2007).
5. Day, J. et al. *J Neurophysiol.* **117**, 1489-1498 (2017).
6. Day, J. et al. *J. App. Physiol.* **115**, 1742-1750 (2013).

High-Density EMG Reveals Lower Limb Spatial Activity during Walking and Running

Bryan R. Schlink[1], Andrew D. Nordin[1], and Daniel P. Ferris[1]
[1]J. Crayton Pruitt Family Department of Biomedical Engineering, University of Florida, Gainesville, FL, USA
Email: *bschlink@ufl.edu

Introduction

High-density electromyography (EMG) is a useful technology that records electrical muscle activity using an array of microelectrodes. Although traditionally used in relatively stationary conditions, recent studies have shown the potential of high-density EMG during locomotion. Two of these studies recorded lateral gastrocnemius and biceps femoris muscles during locomotion and found vast differences in peak activation levels across the muscle bellies [1,2]. This suggests that spatial myoelectric activity widely varies within individual muscles.

The goal of this research was to determine if there are similar spatial EMG activity patterns across multiple lower limb muscles at a range of speeds. We hypothesized that: 1) spatial patterns of EMG activity will vary across different muscles, and 2) spatial EMG activation patterns within each muscle will not change as gait speed increases.

Methods

We recorded high-density surface EMG from five major lower limb muscles from the right leg of 9 healthy subjects (7 M, 2 F) using a 64-channel electrode array. The muscles were the medial and lateral gastrocnemii, vastus medialis, tibialis anterior, and biceps femoris. Subjects walked (1.2 m/s and 1.6 m/s) and ran (2.0, 3.0, 4.0, and 5.0 m/s) on an instrumented treadmill for a duration of twenty strides per leg.

We used canonical correlation analysis to decompose the EMG signals and filter the components from each muscle to remove motion artifacts [3]. We averaged the data from the primary phase of the gait cycle that each muscle is active (stance: medial/lateral gastrocnemii, vastus medialis; swing: tibialis anterior, biceps femoris). We calculated the average root mean square (RMS) value in the target gait phase for each electrode of the array within each speed and normalized the data within each subject to the peak RMS value found across all gait speeds.

Results and Discussion

The spatial EMG activity patterns differed across muscles, but each muscle's individual pattern was relatively consistent across the different speeds (Figure 1). In all muscles, we observed the highest EMG-RMS activity in the fastest trial (5.0 m/s). The highest EMG amplitude in the medial and lateral gastrocnemii during stance phase was at the distal portion of the muscle, consistent with previous research [2]. There was also increased EMG activity in the distal regions of the vastus medialis and biceps femoris, although the overall pattern of EMG activity was less localized than the gastrocnemii. Tibialis anterior EMG activity was more uniform across the entire muscle, and the change in EMG-RMS amplitude across speeds for this muscle was smaller than the other muscles.

The differences in EMG spatial patterns may be explained by multiple factors. The gastrocnemii typically have a higher percentage of fast-twitch fibers [4], and there may be a larger grouping of these fibers in the distal portion of the muscle that act together during locomotion. Conversely, the tibialis anterior muscle has a higher percentage of slow twitch fibers and a circumpennate fiber structure. The relative mechanical capabilities of these muscles may also influence the spatial EMG activity. Muscles with greater relative loading during locomotion may have a more distinct focus of EMG activity compared to those with lower relative loading.

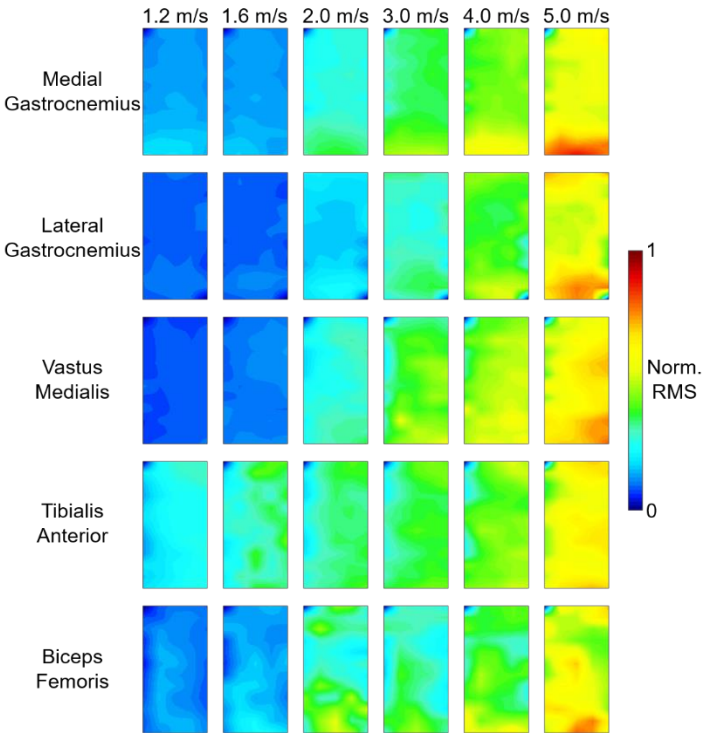

Figure 1: Average EMG-RMS spatial distribution for all muscles (rows) across all walking and running speeds (columns). RMS values for each subject were normalized to the peak RMS value during running at 5.0 m/s. The EMG profiles for the medial and lateral gastrocnemii and vastus medialis were averaged over the stance phase. The tibialis anterior and biceps femoris EMG patterns were averaged over the swing phase.

Significance

Our results indicate heterogenous spatial activation for a range of lower limb muscles across locomotion speeds in healthy individuals. It's not clear if this heterogenous activation pattern equates to a heterogenous force loading pattern across the muscle. Understanding the spatial variety in myoelectric patterns may help researchers, clinicians, and therapists develop intervention and rehabilitation programs that target specific muscle regions.

Acknowledgments

Research supported by CAN-CTA ARL W911NF-10-2-0022.

References

[1] Hegyi et al. (2019). *Med Sci Sports Exerc,* 51(11): 2274-2285.
[2] Cronin et al. (2015). *Neuroscience*, 300: 19-28.
[3] Nordin et al. (2019). *IEEE Tran Biomed Eng,* 67(3): 842-853.
[4] Johnson et al. (1973). *J Neurol Sci*, 18: 111-129.

In vivo hind limb muscle function during walking on hard and soft substrates in rats (*Rattus norvegicus*)

Schwaner, M J [1], Christensen, B A[1], and McGowan, C P [1, 2]
[1]Comparative Neuromuscular Biomechanics Lab, Department of Biological Sciences, University of Idaho, Moscow, ID USA
[2]WWAMI Medical Education Program, Moscow, ID USA
e-mail: janneke.schwaner@gmail.com, web: http://www.webpages.uidaho.edu/McGowanLab/Research.htm

Introduction

Movement is a necessity for animals to find mates, forage, or to prevent becoming food. Most laboratory locomotion studies of animals concern locomotion over solid surfaces [1], which do not reflect complex environments and the variety of unsteady terrains animals experience in the wild.

In this study, we used *in vivo* sonomicrometry (SONO) and electromyography (EMG) techniques to obtain strain and activation patterns of the Vastus Lateralis (VL), a major knee extensor, and the Lateral Gastrocnemius (LG), a major ankle extensor muscle, to elucidate these muscles' role in walking on solid and sandy surfaces in white rats (*Rattus norvegicus*).

Methods

We collected data while rats (N = 4) where walking at 0.7 m/s on a Variable Surface Rotary Treadmill (VSRT) with and without a 2 cm layer of sand. SONO and EMG data were collected at 2000Hz. Walking trials were recorded at 200 frames s^{-1} using a high-speed camera (Xcitex Inc, Woburn, MA, USA), positioned perpendicular to the experimental set up. Video data were digitized using ProAnalyst (Xcitex Inc, Woburn, MA, USA), after which the complete dataset was analyzed using a customized analysis script for Matlab (2015a, MathWorks, Natick, MA, USA).

Results and Discussion

Our data shows that during the stance phase, the VL undergoes more net lengthening, due to a decrease in shortening strain during the stance cycle, when an animal walks on sand versus on a hard surface (Figure 1). Alternatively, the LG shows an increase in net shortening, due to a decrease in lengthening and an increase in shortening, during stance while animals walk on a sandy surface.

These preliminary data suggest that rats accommodate for locomotion on soft sand by increasing muscle shortening by the LG, and therefore increase its mechanical output, and less shortening by the VL. Further investigation of swing phase strain patterns, joint kinematics and gait analysis will provide more detailed insight in how rats accommodate changes in surface compliance and increase of mechanical demand.

Significance

Locomotion is widely studied topic, muscle responses to unsteady, dynamic locomotion tasks less so. Elducidating the role muscles play in adapting to variation in surface substrates provides a frameswork for assessing how animals meet changes in demand and mechanical outputs while moving through their natural environment. It also sets the stage for future bioinspired designs of dynamic robotic devices that are able to navigate through very complex and variable terrain.

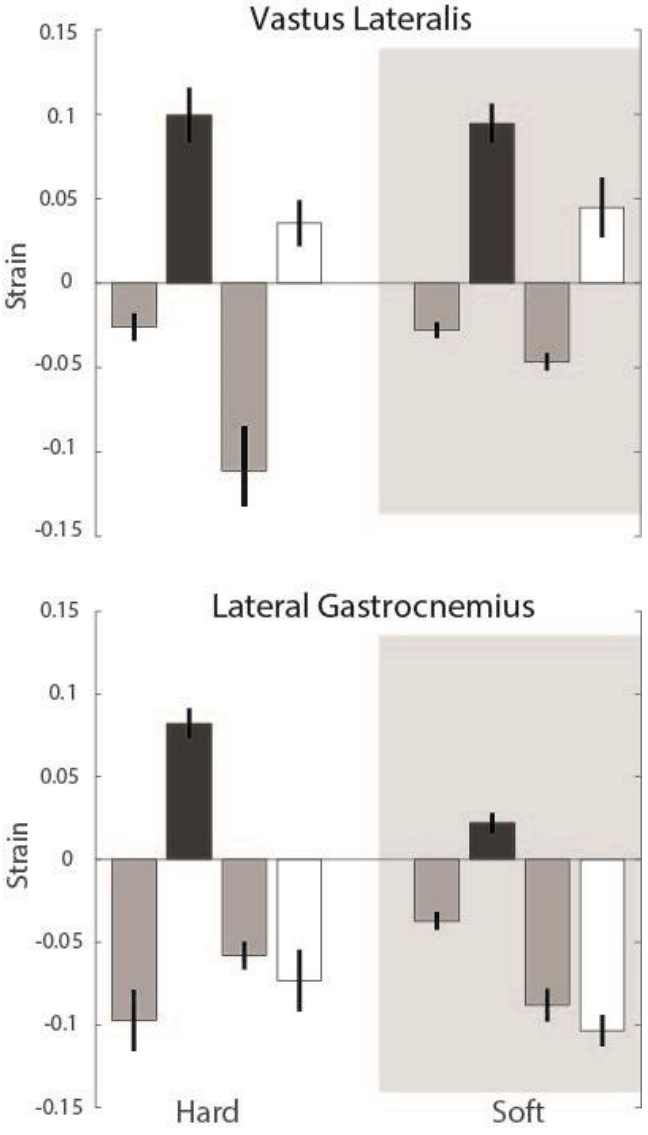

Figure 1. Muscle strain patterns of the Vastus Lateralis (top) and Lateral Gastrocnemius (bottom) during walking on hard (left) and soft (shaded right) substrates during stance phase. During stance phase shortening (light grey), lengthening (dark grey), and net shortening (white) were characterized.

Acknowledgements

This work was supported by NSF grant 1553550 (CPM) and ARO grant 66554-EG (CPM). All procedures were approved by the University of Idaho Institutional Animal Care and Use Committee (IACUC).

Reference

1. Gillis and Biewener, (2001), J Exp Biol 204, 17 -

The effects of advanced age and walking speed on mechanical functions of the ankle plantarflexors

Daniel J. Kuhman[1], Jutaluk Kongsuk[1], and Christopher P. Hurt[1]
[1]University of Alabama at Birmingham, Birmingham, AL, U.S.A.
Email: dkuhman@uab.edu

Introduction

Advanced age is associated with decreased ankle plantarflexor (PF) and increased hip mechanical output during walking [1]. The magnitude of this distal-to-proximal mechanical redistribution increases with task difficulty. For example, old adults disproportionately increase mechanical output at the hip compared to the ankle during maximal versus comfortable speed walking [2] and during uphill versus level-ground walking [1]. In young adults, increasing speed and uphill slope during walking both result in decreased negative and increased positive joint work at the ankle, resulting in more motor-like behavior during these more challenging tasks [3]. Unfortunately, age-related structural (e.g., fiber type) and functional (e.g., decreased strength) changes to muscles and other tissues spanning the ankle may impair their ability to act effectively as mechanical motors [4]. Inability to adapt mechanical behavior of the ankle during more challenging walking tasks may limit the ability of old adults to perform walking tasks which require motor-like behavior (fast, uphill, or accelerated walking). The purpose of this study was to determine the effects of age and walking speed on mechanical behavior of the ankle PFs. We hypothesized that motor-like behavior would increase more in response to increased walking speed in young compared to old adults.

Methods

Healthy young (n = 15, age = 25 ± 2 years) and old (n = 8, age = 69 ± 2 years) adults walked on a dual-belt force-instrumented treadmill at 0.8, 1.2, and 1.6ms^{-1}. For each support phase, we quantified strut-, spring-, motor-, and damper-like behavior of the ankle PFs using the functional indexing approach [3]. Each functional index is calculated as a percentage such that the sum of all indices equals 100. To capture the magnitude of the age-related distal-to-proximal shift with a single variable, we used the following ratio: (ipsilateral hip flexor + contralateral hip extensor positive work) / ankle PF positive work. Higher ratios indicate lager reliance on hip relative to ankle joint mechanical output. We used 2-way repeated measures ANOVAs to determine the effects of age, speed, and their interaction on the magnitude of mechanical redistribution and each functional index. Statistical analyses were conducted in R (lme4 package) and the threshold for statistical significance was $p < 0.05$.

Results and Discussion

We found significant main effects of age ($p < 0.01$) and speed ($p < 0.001$) on the magnitude of mechanical redistribution, confirming that the well-established, age-related redistribution of mechanical output existed in our sample. Significant age-by-speed interactions were observed for spring ($p < 0.05$), motor ($p < 0.01$), and damper ($p < 0.01$) indices, indicating between-group differences in response to changes in walking speeds. Supporting our previous work [3], we observed increased motor-like behavior with increased walking speed in young adults (Fig. 1B). Supporting our hypothesis, old adults displayed the same behavior, but not to the same extent as young adults (age x speed interaction effect). Rather, old adults tended to maintain spring- and strut-like behavior at faster speeds. Age-related structural and functional changes to the ankle PFs may limit their ability to serve as effective motors at faster speeds. Others have reported decreased Achilles tendon stiffness with advanced age, which would theoretically improve its capacity to act as a mechanical spring [5]. This may explain the relative maintenance of spring-like behavior observed here (Fig. 1A). Walking speed and spring index shared an inverted-U shaped relationship in both age groups, which may partially explain lower metabolic costs previously observed at intermediate speeds in both age groups [6].

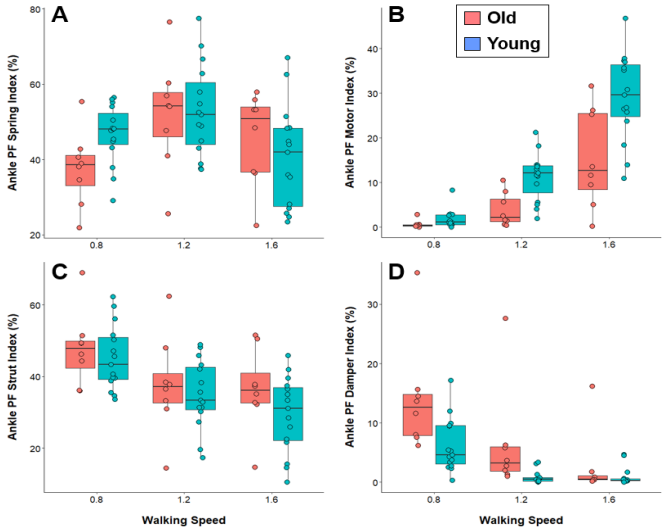

Figure 1: Spring (A), motor (B), strut (C), and damper (D) functional indices across walking speeds in old and young adults.

Significance

Our results suggest that advanced age is associated with a reduced capacity to utilize the ankle PFs as mechanical motors when task difficulty is increased. Inability to utilize the ankle PFs as motors may limit the ability of old adults to walk at faster speeds or perform other walking tasks which require motor-like behavior (e.g., uphill walking, accelerated walking). Enhancing motor-like behavior of the ankle PFs (e.g., via exercise, exoskeletons) may improve mobility in the aging population.

References

1. Kuhman et al., *J Biomech* **69**, 90-96, 2018
2. Kuhman et al., *J Biomech* **79**, 112-118, 2018
3. Kuhman et al., *J Exp Biol* **222(20)**, jeb206383, 2019
4. Porter et al., *Scand J Med & Sci Sport* **5(3)**, 129-142, 1995
5. Stenroth et al., *Appl Phys* **113(10)**, 1537-1544, 2012
6. Peterson & Martin, *Gait Posture* **31(3)**, 355-359, 2010

Are Muscles Tuned to the Preferred Stride Frequency of Walking?

Jonaz Moreno Jaramillo[1], Brian R. Umberger[2]
[1]Department of Kinesiology, University of Massachusetts, Amherst MA.
[2] School of Kinesiology, University of Michigan, Ann Arbor MI.
Email: umberger@umich.edu

Introduction

The energy expended in human locomotion has been an important topic in the field of biomechanics. When humans walk at their preferred walking speed[1] and stride frequency[2], the metabolic cost of transport (mCoT) is minimized relative to other speeds or stride frequencies. However, mCoT provides no muscle-specific information on why cost is minimized for preferred conditions. Previous studies have considered muscle activation as an indirect way to gain insight into the contributions of individual muscles to the total mCoT during walking[1,2].

The purpose of this study was to investigate the impact of stride frequency on activation of the major lower limb muscles during level, fixed-speed walking. Based on previous studies[1,2], we hypothesize that: total muscle activation will demonstrate a U-shaped response to stride frequency with a minimum value at the preferred stride frequency (PSF), while the activation of individual muscles will be minizmied at a range of stride frequencies, reflecting the mechanical demands of walking.

Methods

20 healthy young adults (10 males, 24.5±5.5 yr, 68.6±10.7 kg, 1.71±0.11 m.) walked at a fixed speed (1.3 $m \cdot s^{-1}$) and five different stride frequencies for 2 miutes each with 1 minute rest between conditions. The conditions were PSF, ±12.5% PSF, and ±25% PSF[2,3]. A metronome was used to pace the target stride frequencies. Electromyography (EMG) data were collected during the final 30 s of each condition from eight muscles of the right lower limb: gluteus maximus, gluteus medius, long head of biceps femoris, vastus lateralis, gastrocnemius, soleus, and tibialis anterior. Participants practiced all of the conditions before data collection, and the order of trials was randomized.

Raw EMG signals were DC-bias corrected, full-waved rectified, and low-pass filtered with a Butterworth digital filter at 5 Hz cut-off frequency to create linear envelopes. The linear envelopes were scaled based on the peak EMG amplitudes observed across all conditions and averaged across 10 strides. Scaled EMG signals within a muscle were integrated with respect to time, and then divided by the total time to create the average EMG amplitude for each muscle, for each participant, for each condition. Total average muscle activation was obtained by summing the average EMG amplitude across muscles for each condition, and dividing by the toal number of muscles. We ran orthogonal polynomial contrast on individual muscle activations, and the total activation, to determine the appropriate order polynomial for trend-line fitting. We determined the predicted minimum activation stride frequnencies from the trend-lines for comparison with the preferred stride frequency for individual muscles, and the total actiaviton. Paired t-test were used to determine significant difference between the predicted minimum and preferred stride frequencies ($\alpha = 0.05$).

Results and Discussion

Total muscle actvation was minimized at the PSF (Fig. 1E), in support of our first hypothesis and consistent with results for mCoT[2,3]. Individual muscle activations were not all minimized at PSF. Specifically, activation was minimizied in four out of eight muscles at significantly different ($p<0.05$) frequencies from the PSF, with moderate effect sizes (d=0.62-0.87) (Fig. 1A-D). The muscle-specific responses for rectus femoris and tibialis anterior across stride frequencies (Fig. 1C,D) were similar to a previous study that included only four muscles[2]. Our analysis included a more complete representation of lower limb muscles, and generalizes the finding that total muscle activation is minizmied at the PSF (Fig 1E.), mirroring the result for mCoT.

Although individual muscle activations were not all minimized at the PSF, predicted minima stride frequencies were all within 8% of the PSF, and total muscle activation was only modestly increased at ±12.5% of PSF. Thus there is some flexibility to adjust stride frequency without excessive demands being placed on any specific muscle.

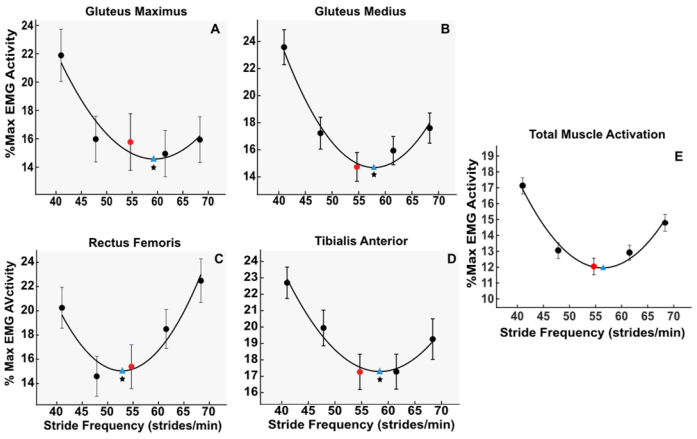

Figure 1: Average muscle activations as a percent of the maximum observed value across stride frequencies. Red dots indicate preferred stride frequency; blue triangles indicate the predicted optimal stride frequency Error bars are are standard errors. The ★ indicates significant differences ($p<0.05$) between predicted and preferred values.

Significance

Minimization of total muscle activation may be a primary reason why mCoT is minimized at the PSF in human walking. Moreover, the relatively shallow slope of the U-shaped mCoT curve around the PSF may be due to individual muscle responses. The individual-muscle activation minima at different stride frequencies provides some flexilibity to adjust walking to the environment without a large increase in mCoT.

Acknowledgments

We would like to thank the UMass Amherst SPHHS Dean's PhD Fellowship and Graduate Diversity Award for funding.

References

1. Carrier et al. (2011) *PNAS,* 108: 18631-36.
2. Russell & Apatoczky (2016) *Gait & Post.* 45: 181-186.
3. Umberger & Martin (2007) *J Exp. Bio.* 210: 3255-65.

Effects of Varying Tendon Stiffness on the Metabolic Cost of Walking

Alex N. Denton and Brian R. Umberger
Locomotion Research Laboratory, School of Kinesiology, University of Michigan, Ann Arbor, MI.
Email: umberger@umich.edu

Introduction

Tendons are compliant structures responsible for transferring muscle force to bone to produce movement. During walking, the triceps surae tendon has been shown to store and return mechanical strain energy as positive work during push-off, reducing the work done by the active muscles.[2] The muscle energetics during walking are sensitive to the stiffness of tendinous tissues.[3] Thus, tendon stiffness should be a factor affecting the metabolic cost of walking.

The triceps surae is often the focus when studying the effects of tendon dynamics on muscle energetics during locomotion due to its superficial and accessible nature. However, the plantar flexors represent only ~25% of the net cost of walking[6], and the effects of tendon stiffness across all major muscles of the lower limb on the energetics and kinematics of walking are unknown. Tendon stiffness should be expected to affect not only energy cost, but also movement patterns. For example, in simulations of vertical jumping, movement amplitude increased as the triceps surae tendon stiffness decreased.[1] In the present study, we use a similar modeling and simulation approach to estimate the effects of tendon stiffness on walking energetics and kinematics, which would be challenging or impossible to do experimentally.

Thus, the purpose of this study was to investigate the effects of tendon stiffness on the COT and kinematics of walking, to enhance the understanding of musculoskeletal function in locomotion. Based on data in the literature[1,4], we hypothesized: (1) tendons with the stiffness reported experimentally (5% tendon strain at peak isometric force) will yield minimum COT and (2) joint range of motion (ROM) will vary inversely with tendon stiffness.

Methods

Predictive simulations of walking (1.3 m/s) were generated using direct collocation with a planar model consisting of 9 segments, 11 degrees of freedom, and 18 musculotendon actuators (nine for each leg).[5] The objective function included terms for stability, smoothness, and muscle activation.[5] Tendon stiffness was characterized as percent strain produced at peak isometric force and was varied between 3 and 20% across all muscles in the model. Metabolic COT was predicted using a model of muscle energy consumption.[6]

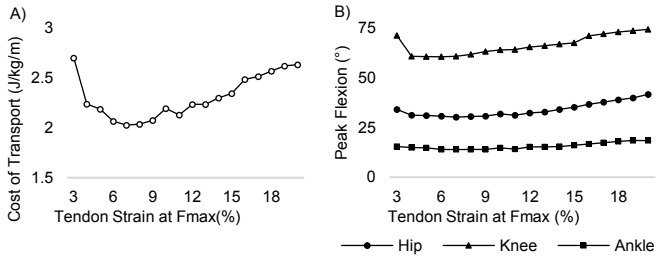

Figure 1: A) Cost of transport and B) peak joint angles of the lower extremities for walking with a wide range of different tendon stiffness.

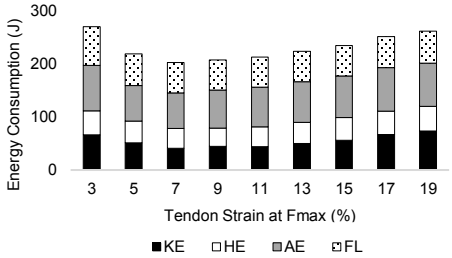

Figure 2: The distribution of energy consumption across muscle groups for walking with different tendon stiffnesses. HE (hip extensors), KE (knee extensors), AE (ankle extensors), and FL (flexors of all joints).

Results and Discussion

Metabolic COT was minimized at the stiffness corresponding to 7% tendon strain at peak isometric force (Fig 1A). COT gradually increased with tendon stiffness above 7%, whereas the COT rapidly increased with tendon stiffness below 7%. The optimal tendon stiffness was close to, though slightly greater than we predicted, yet fit within the range of reported in vivo measurements.[4] The overall trend in COT (Fig 1A) was driven mostly by the knee extensor muscles, which exhibited a minimum at around 7% (Fig 2).

Over most of the tested range, lower limb tendon stiffness resulted in greater joint ROM at the hip, knee, and ankle (Fig 1B). Peak hip flexion had the strongest correlation with decreased tendon stiffness ($R^2 = 0.70$). Consequently, as tendon stiffness decreased, the optimal step length and distance traveled in the direction of motion per step increased. Thus, there is an interaction among tendon stiffness, metabolic cost, and optimal movement patterns.

Significance

While the predicted optimal tendon stiffness value was similar to the biological value from the literature[4], the slight difference between the literature (~5%) and optimal (7%) values may reflect trade-offs associated with task demands beside level walking at preferred speeds. While most attention in the literature has been on the triceps surae[2,3], minimum cost at optimal stiffness was due primarily to the knee extensor muscles. Additionally, the simulations indicate that optimal gait kinematics depend on tendon stiffness.

References

1. Bobbert, M. (2001). *J Exp Biol*, *204*, 533-542.
2. Fukunaga, T., Kubo, K., Kawakami, Y., Fukashiro, S., Kanehisa, H., & Maganaris, C. N. (2001). *Proc. R. Soc. Lond. B.*, *268*, 229-233.
3. Lichtwark, G. & Wilson, A. (2007). *J. Biomech.*, *40*, 1768-1775.
4. Maganaris, C., & Paul, J. (2002). *J. Biomech.*, *35*, 1639-1646.
5. Nguyen, V., Johnson, R., Sup, F., and Umberger, B. (2019). IEEE TNSRE, *27*, 1426-1435.
6. Umberger, B., & Rubenson, J. (2011). *Exerc Sport Sci Rev*, *39*, 59-67.

The Metabolic and Mechanical Consequences of Altered Propulsive Force Generation in Walking

Noah L. Pieper[1], Sidney T. Baudendistel[2], Chris J. Hass[2], Gabriela B. Diaz[1], Rebecca L. Krupenevich[1], and Jason R. Franz[1]
[1]UNC Chapel Hill and NC State University, Chapel Hill, NC
[2]University of Florida, Gainesville, FL
Email: jrfranz@email.unc.edu, web: http://abl.web.unc.edu

Introduction

Compared to young adults walking at the same speed, older adults consume oxygen ~20% faster for reasons that are poorly understood [1]. Simultaneously, older adults exert smaller peak anterior (i.e., propulsive) ground reaction forces (F_p) and, despite no change in total positive work, exhibit a characteristic distal-to-proximal redistribution of leg muscle workload [2]. We suspect that more proximal leg muscles, with their longer fascicles and shorter tendons, are less economical for powering the mechanical demands of walking. We recently used a real-time biofeedback paradigm to reveal that young adults targeting smaller than normal F_p do so by redistributing mechanical workload from the distal to proximal musculature without changing total positive leg joint work [3]. These findings allude to an experimental paradigm that would enable us to study the extent to which a distal-to-proximal contributes to increased metabolic energy cost in the absence of other known age-related changes. Here, we quantified the metabolic and limb- and joint-level mechanical energy costs associated with modulating propulsive forces during the push-off phase of walking. We first hypothesized that when walking with larger than normal F_p, metabolic energy cost would increase in a manner consistent with (*i.e.*, accompanied by) increases in total positive leg joint work. Conversely, second, we hypothesized that total positive leg joint work would not increase when walking with smaller than normal F_p, and that metabolic energy cost would instead increase in a manner consistent with (i.e., accompanied by) a redistribution to muscles spanning the hip for power generation.

Methods

12 young adults (age: 23.3±3.1 years, 8F/4M) completed a series of 5-min walking trials on a dual-belt, instrumented treadmill at their preferred overground walking speed (1.37±0.15 m/s). Immediately following a normal walking trial, a custom Matlab script estimated and stored the stride-averaged F_p for use in subsequent biofeedback trials. Specifically, subjects then walked while receiving visual biofeedback of their step-by-step F_p values with instructions to match those values to, in randomized order, target values corresponding to ±20% and ±40% of values from normal walking (Fig. 1A). We report the following outcomes averaged across the final 2 min of each walking trial: net (*i.e.,* walking-standing) rate of oxygen consumption ($\dot{V}O_2$), net metabolic power [4], and, from the integral of their respective joint power curves divided by stride time, positive stance phase leg joint mechanical work rates.

Results and Discussion

Biofeedback alone (i.e., targeting normal Fp) did not alter metabolic cost (p=0.990). Compared to walking normally, subjects increased net metabolic power by an average of up to 47% when targeting larger than normal F_p (p<0.001; Fig. 1B). As hypothesized, this metabolic response was accompanied by and positively correlated with up to an 13% increase in total positive leg joint work rate (p=0.003, R^2=0.29; Fig. 1C). Conversely, when targeting smaller than normal F_p, subjects increased net metabolic power by up to 58% (p<0.001) but without changing total positive work rate (p=0.693) (Fig. 1B). Rather, as hypothesized, this metabolic response was accompanied by up to an 31% increase in positive hip joint work rate (p=0.002), offset by modest 10% decreases in positive ankle/knee work rates that did not reach significance.

Significance

Our findings suggest that the distal-to-proximal redistribution of leg muscle workload due to aging may contribute to the higher metabolic energy cost of walking in older adults.

References

1. Ortega, JD & Farley, CT. *J Appl Physiol* 102(6), 2007.
2. DeVita, P & Hortobagyi, T. *J Appl Physiol* 88(5), 2000.
3. Browne & Franz. *J Biomech* 55, 2017.
4. Brockway JM. *Hum Nutr: Clin Nutr,* 41C, 1987.

Acknowledgements

This work was supported by grants from the National Institutes of Health (R01AG058615) and the Parkinson's Foundation (PF-VSA-SFW-1908).

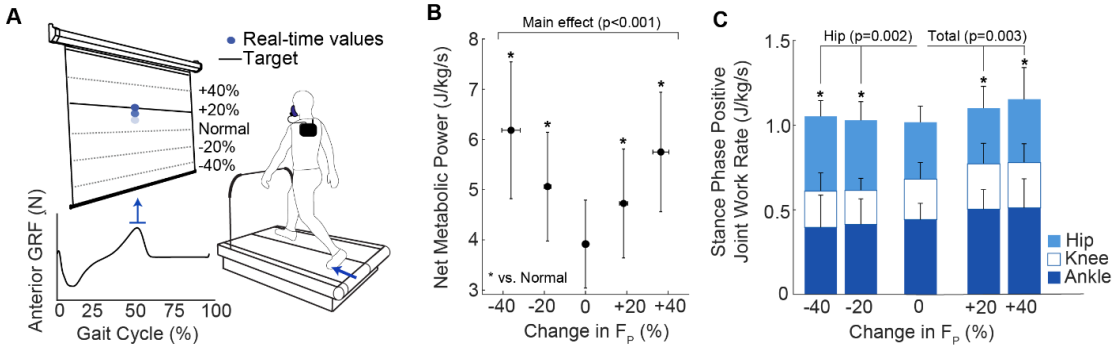

Figure 1. (A) Biofeedback paradigm and experimental conditions. (B) Metabolic and (C) limb and joint level biomechanical responses to altered propulsive force generation in walking. Main effects shown with asterisks (*) indicating significant pairwise difference versus normal walking.

Develpmental Plasticity of Locomotor Economy in an Avian Bipedal Model

Talayah Johnson, Kavya Katugam, Ian Dechene, Suzanne M. Cox, Stephen J. Piazza, Jonas Rubenson
Biomechanics Laboratory, Department of Kinesiology, The Pennsylvania State University, University Park, PA, USA
Email: taj5199@psu.edu

Introduction

Over an evolutionary time scale, natural selection has resulted in specializations for locomotor economy in cursorial species [1]. Whether adaptatations in locomotor economy occur accross an individual's life span, however, remains less clear. For example, it remains debated how and if running economy in humans is altered due to training [2]. A recent study that eliminated high-intensity activity during the growth period in an animal model showed no effect on locomotor economy [3]. The results of this study suggest that locomotor economy might not respond plastically to altered amounts of exercise during growth and may be robust to changes in life history.

To understand better the scope of deveplomental placticity of locomotor economy, we adopted a bipedal model (guinea fowl) that permitted drastic alteration of musculoskeletal loads across the growth span. We achieved this by increasing distal limb mass experimentatly by a factor of ~ 2.5x over the maturation period. We hypothesized that animals subject to habitual increased limb mass would be more economical at carrying extra limb mass compared to a habitually unloaded control group. We also hypothesized that the limb-loaded animals would have worse economy when walking unloaded when compared to controls.

Methods

Twelve 1-day old guinea fowl (*Numida meleagris*) were obtained for this experiment (Privett Hatchery, Portales, NM). All birds were raised in large circular floor pens with constant access to food and water. At one week of age, animals were randomly assigned to a control group (CON, n=6) and a loaded experimental group (EXP, n=6). A lead strip with mass equal to 3.75% of the individual's body mass was chronically added to the right leg of the CON group throughout growth. This leg weight was adjusted weekly to maintain 3.75% of body mass (~ 2.5x biological distal limb mass). Starting at three weeks of age, each group was exercised three times per week by herding animals around a circular course in four 5-minute intervals for a total of 20 minutes.

Metabolic power was measured during standing and during treadmill walking (0.5 m·s^{-1}) using a flow-through metabolic chamber system [2]. Metabolic power was measured in the habitual condition (CON= unloaded , EXP=loaded) as well as in their novel condition where an equivalent leg mass (3.75% body mass) was added to the CON group and the load was removed from the EXP group. Between 3-5 trials were record per condition and the order of conditions was randomized.

Results and Discussion

At the time of this abstract submission, preliminary analysis of data from three EXP and four CON animals have been made. Average net metabolic power in the limb-loaded condition trended lower in these EXP animals (4.1 ± 0.6 W·kg^{-1}) compared to the CON animals (5.3 ± 0.9 W·kg^{-1}) ($p = 0.11$), but appears more similar in the unloaded condition; EXP (4.4 ± 1.3 W·kg^{-1}) vs. CON (4.0 ± 0.9 W·kg^{-1}) ($p = 0.65$). The average delta cost of added limb mass was significantly higher in CON vs EXP ($p = 0.02$; Fig 1a). Data for each animal are depicted in Fig 1b.

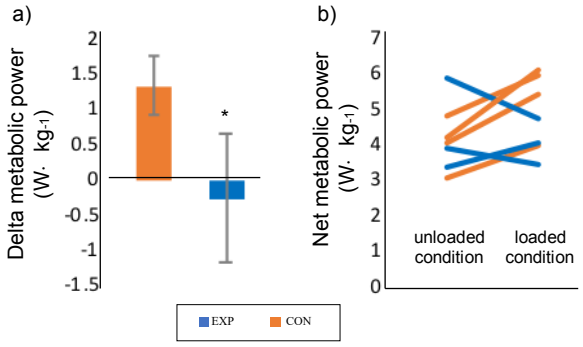

Figure 1: (a) Mean change in net body-mass specific metabolic power between unloaded and limb-loaded (3.75% body mass) walking. Error bars represent standard deviation. (b) Net body-mass specific metabolic power in the unloaded and limb-loaded conditions for each animal. Orange = CON; Blue = EXP.

These preliminary data generally support our first hypothesis; the examined EXP animals exhibit a trend towards lower mean limb-loaded walking economy and exhibit a much lower delta economy of added limb mass. Our preliminary data do not, however, support our second hypothesis that the EXP group would have a higher unloaded walking economy compared to CON. It is interesting to note that for 2/3 EXP animals, walking economy was negatively affected by removing the limb mass. This is surprising given the presumably large reduction in the mechanical work associated with lifting and accelerating the limb. These preliminary data suggest that locomotor economy may be affected by loading history during growth and may be tuned to the habitual loading environment. At present, we have analyzed data from only a small number of animals, so these results must be interpreted with a great deal of caution. Whether sub-optimal locomotor economy in the novel loading environent is the result of musculoskeletal factors or poor motor control and coordination remains to be established.

Significance

Here we provide new evidence that locomotor economy may be altered based on the loading history during growth. These data have important implications for understanding the long-term effects of childhood activity and inactivity. Further analysis may determine the importance of the growth period on permanent adult locomotor energetics and biomechanics.

Acknowledgments

Supported through NIH Grant R21AR071588.

References

[1] Alexander, R.M. (2003). *Principles of Animal Locomotion,* Princeton University Press, Princeton NJ.
[2] Fletcher, J.R. et al. (2017). *Front Physiol,* 8: art 433, p 1-15.
[3] Cox et al (2020). *J. Appl. Physiol.*, 128:1, p 50-8.

Reducing the Metabolic Cost of Walking by Using the Arms to Drive the Legs

Daisey Vega[1], and Christopher J. Arellano[2]
[1, 2]Department of Health and Human Performance, University of Houston
dvega4@uh.edu

Introduction

Experiments on recumbent stepping have provided insight into the neural benefits that may arise from coupling the arms and the legs [1], but how we can achieve this coupling effect during walking has remained elusive. Given the out of phase relation between the limbs, we designed a simple, rope-pulley system that facilitates the active use of the arms to drive the legs during walking.

From a biomechanical perspective, we investigated a metabolic trade-off that may arise from coupling the arms and legs during walking. For instance, the cost of leg swing has been estimated to be between 10% and 33% [2-3], which can be explained by an underlying muscular demand. On the contrary, the cost of arm swing has been considered negligible and explained by its passive dynamics [4]. Given these insights, we explored the use of a direct linkage system where individuals directly use the arms to generate an assistive force to drive the legs, whereby arm swing retraction provides an assistive force via a rope to drive the ipsilateral leg forward. While generating arm forces may incur a metabolic cost, we suspected this would be offset by the reduction in muscular demand needed to swing the leg—yielding a net reduction in cost. Therefore, we hypothesized that using the arms to drive the legs would reduce the demand for net metabolic power during walking.

Methods

Eight subjects participated in this study (3 women and 5 men; mean±s.d.; age: 23.25±3.37 years, mass: 73.86±18.46 kg, height: 173.84±13.95 cm). Subjects performed two randomized trials: (1) Normal Walking and (2) Assistive Walking on a dual belt force measuring treadmill at 1.25 m/s. Each trial was 7 minutes in duration and the following data were collected: rate of metabolic energy consumption, surface electromyography, and ground reaction forces. In addition, arm pulling forces during the assistive walking trial were measured with load cells that attached to the rope-pulley device (Fig. 1A).

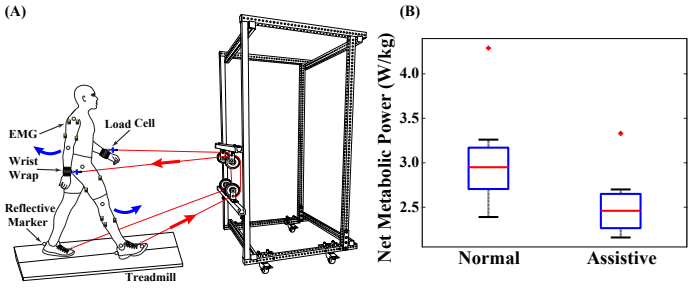

Figure 1. (**A**) Subjects walk with an assistive device that allows them to use the arms to drive the legs via a rope-pulley system. Arrows indicate direction of limb motion (blue) and pulling forces directed along the rope (red). (**B**) Boxplot of net metabolic power for normal and assistive walking trials.

Results and Discussion

When compared to normal walking (median = 2.95 W/kg), we found that using the arms to drive the legs reduced the demand for net metabolic power by ~17% (median = 2.46 W/kg); Wilcoxon Signed Ranks test, $p = 0.006$ (Fig. 1B).

In support of our hypothesis, our results show that using the arms to drive the legs during walking reduces net metabolic power, providing proof-of-concept that our method of coupling the arms and legs reduces the overall effort to walk. Further analyses will focus on the potential changes in neuromuscular demand and ground reaction forces. Such insights will enhance our understanding of the biomechanical trade-off that facilitated the reduction in cost during walking. In addition, it may provide future guidance in optimizing the device for a greater reduction in cost, or modifying the system to lower leg demand at different phases of walking.

Significance

Reducing the effort to walk has implications in a rehabilitation setting for individuals who do not have the endurance and/or neuromuscular strength to do so, and therefore, must rely on manual assistance from physical therapists or more costly robotic devices. In addition, our findings pave the way for future studies to investiage further questions: Can this device be used to promote neural plasticity at crucial stages of locomotor training? Can this device enhance patient autonomy during locomotor training? These questions remain to be answered, but the device shows promise given that an individual can actively use their arms to drive their own legs during walking.

In summary, this device could be used as a simple, but effective means to couple the arms and legs, which may promote neural benefits and help restore an individual's walking ability.

Acknowledgments

We thank the University of Houston's Office of Undergraduate Research for their support.

References

[1] H. J. Huang, and D. P. Ferris,"Neural coupling between upper and lower limbs during recumbent stepping," J. Appl. Physiol., 97: 1299-1308, 2004.
[2] J. S. Gottschall, and R. Kram, "Energy cost and muscular activity required for leg swing during walking," J. Appl. Physiol., 99: 23-30, 2005.
[3] J. Doke, J. M. Donelan, and A. D. Kuo, "Mechanics and energetics of swinging the human leg," J. Exp. Biol., 208: 439, 2005.
[4] S. H. Collins, P. G. Adamczyk, and A. D. Kuo, "Dynamic arm swinging in human walking," Proc. R. Soc., 276: 3679-3688, 2009.

Stroke survivors exhibit little total arm contribution to standing, posterior balance reactions

James B. Tracy[1], Drew A. Petersen[1,2], Elizabeth A. Rapp van Roden[1,3], Jamie Pigman[1,4], Benjamin C. Conner[1,5], R. Tyler Richardson[6], Darcy Reisman[1], Kurt Manal[1], and *Jeremy R. Crenshaw[1]
[1]University of Delaware, Newark, DE; [2]Drexel University, Philadelphia, PA; [3]Exponent, Philadelphia, PA; [4]Monmouth University, West Long Branch, NJ; [5]University of Arizona, Phoenix, AZ; [6]Penn State Harrisburg, Middletown, PA
Email: *crenshaw@udel.edu

Introduction

Stroke survivors often have deficient reactive postural control [1] and impaired upper extremity function [2]. These factors are related, as reduced arm function has been associated with falls in stroke survivors [2]. We previously validated a measure of how the arms contribute to posterior balance reactions [3] through counter-rotation about the whole-body COM [4]. The purpose of this study was to test the hypothesis that, compared to those with no neuromuscular impairment, stroke survivors would have a diminished arm contribution in response to standing posterior perturbations.

Methods

Stroke survivors (n = 10, mean (SD) age = 64.0 (8.8) years, BMI = 30.8 (4.5) $kg \cdot m^{-2}$) and young adults without neuromuscular impairment (n = 11, age = 22.2 (2.3) years, BMI = 22.4 (3.0) $kg \cdot m^{-2}$) participated in this study. All participants completed a single-stepping threshold evaluation on a computer-controlled treadmill to determine the smallest perturbation magnitude that consistently elicited a posterior step [5]. Whole-body, three-dimensional motion was recorded for near-threshold level perturbations to explore the arm contributions and shoulder kinematic responses during recovery.

The rate of change in angular momentum of the body was represented as a compound pendulum (M_{TOTAL}, Equation 1), where r_{COM}, $r_{COM'}$, m, a_{COM}, I_{BODY}, and α_{COM} are the COM position, vertical projection of the COM onto the treadmill surface, body mass, linear acceleration of the COM, whole-body moment of inertia about the COM, and angular acceleration of the vector connecting the whole-body COM to the midpoint of ankle-joint centers.

The rate of change of arm-segment angular momentum with respect to the whole-body COM was calculated (M_{ARMS}, Equation 2), where r_i, m_i, a_i, I_i, and α_i are the position, mass, linear acceleration, moment of inertia, and angular acceleration of the "i^{th}" segment within the arms (i.e. four total segments), R_i is the column vector from the whole body COM to the COM of segment I, and E_3 is the 3 by 3 identity matrix.

The total arm contribution (β_{ARMS}, Equation 3) was quantified from the total-least-squares regression of M_{ARMS} onto M_{TOTAL} and compared using an independent t-test.

[Equation 1] $$M_{TOTAL} = (r_{COM} - r_{COM'}) \times m(a_{COM}) + I_{BODY}\alpha_{COM}$$

[Equation 2] $$M_{ARMS} = \sum\{(r_i - r_{COM}) \times m_i(a_i - a_{COM})\} + \sum I_i(\alpha_i - \alpha_{COM}) - \sum\left\{m_i\left(\left(R_i{}^T R_i\right)E_3 - \left(R_i R_i{}^T\right)\right)\alpha_{COM}\right\}$$

[Equation 3] $$M_{ARMS} = \beta_{ARMS} \cdot M_{TOTAL}$$

Results and Discussion

In support of our hypothesis, those with chronic stroke had substantially less total arm contribution (mean (SD) = -0.1 (0.6) %) than those with no history of stroke (6.3 (6.6) %, $p < 0.01$, Figure 1). In follow-up analyses of shoulder kinematics, we did not detect between-group differences in the peak shoulder flexion velocity of the "faster" ($p = 0.82$, Glass's $\Delta = 0.10$) or "slower" ($p = 0.20$, Glass's $\Delta = 0.48$) arms. Group differences in the arm-contribution measure may be due to the timing of arm motion, the orientation of the arms, and/or the relative contribution of other recovery mechanisms (i.e. altering the COP location or using the force from deceleration of the treadmill belt).

Those with chronic stroke, and older average age, exhibited little total contribution of the arms when reacting to a posterior perturbation. Shoulder kinematics could not explain this deficit.

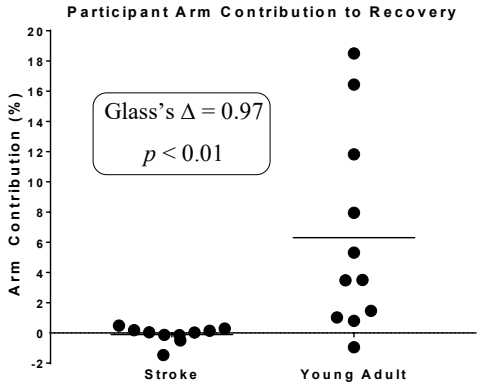

Figure 1: **Arm contribution values for all participants.** Stroke survivors showed little total arm contribution (mean (SD) = -0.1 (0.6) %) during slip perturbation recovery while non-stroke participants measured a significantly greater total arm contribution (6.3 (6.6) %, $p < 0.01$, Glass's Δ effect size = 0.97).

Significance

This study provides evidence that impaired reactive balance in those with chronic stroke may be due to an altered "whole-body" response, not just that of the lower extremities. This study also demonstrates the utility of the arms-contribution measure in detecting impairments when shoulder kinematics failed to do so.

Perturbation-based training has improved reactive balance in those with chronic stroke [6, 7]. We do not know if it specifically benefits the use of the arms in such reactions. Our arm-contribution measure represents a modifiable target for such interventions. It is clear from the shoulder flexion velocities that those with stroke moved their arms; therefore, we are optimistic that such motions can be modified in a manner as to improve their contribution.

Acknowledgments

Funding from the UD Research Foundation, ASB Junior Faculty Research Award, NIGMS (2P20 GM103446), and State of DE.

References

[1] Ikai T., 2003. *Phys Med &* Rehab, 82, 463-469.
[2] Hyndman, D., 2002. *Arch Phys Med & Rehab*, 83, 165-170.
[3] Rapp van Roden, E.A., 2018. *J of Biomech*, 78, 102-108.
[4] Hof, A.L., 2007. *J of Biomech*, 40, 451-457.
[5] Crenshaw, J.R., 2014. *Gait & Posture*, 39, 810-815.
[6] Pigman, J., 2019. *Clinical Biomechanics*, 69, 205-214.
[7] Mansfield, A., 2018. *BMJ Open*, 8, e021510.

Dopamine medication and motor adaptability improve postural control in Parkinson's disease

Daniel J. Kuhman[1], Harrison Walker[1], Carla Lima[1], Christopher Gonzalez[1], Christopher P. Hurt[1]
[1]University of Alabama at Birmingham, Birmingham, AL, U.S.A.
Email: dkuhman@uab.edu

Introduction

Postural instability is a hallmark motor symptom of Parkinson's disease (PD). In PD, progressive loss of dopamine-producing neurons disrupts cortical-basal ganglia-thalamocortical "loops" [1]. These neural circuits play an important role in sensorimotor integration [2], a process of the nervous system that uses multimodal sensory feedback to guide and modify motor outputs. Inability to accurately sense and integrate contexts of postural perturbations and/or generate appropriate motor outputs to control the body's center of mass (CoM) (i.e., impaired sensorimotor integration) may underpin postural instability in the PD population. If true, two hypotheses can be considered. First, medication which regulates basal ganglia function (e.g., carbidopa-levodopa) should improve CoM control during postural perturbations in PD. Second, individuals with well-functioning sensorimotor integration should display better CoM control than individuals with poorer sensorimotor integration. The purpose of this study was to test these hypotheses.

Methods

21 individuals with idiopathic PD performed a step threshold assessment on a dual-belt, force-instrumented treadmill off (≥12 hours; "OFF") and on dopamine medication ("ON"). Posteriorly directed postural perturbations were delivered via progressively larger treadmill belt accelerations [3]. Perturbations consisted of 200ms acceleration and deceleration phases (400ms total), resulting in triangular waveform velocity profiles with larger peak velocities at higher rates of acceleration. Individuals were explicitly instructed to avoid stepping to recover balance. If the participant did not step to recover balance, the perturbation magnitude was increased; if the participant stepped, the same magnitude perturbation was delivered again. Perturbations began at $0.5ms^{-1}$ and increased in steps of $0.5ms^{-1}$ until the participant could not recover balance without stepping on four consecutive trials (i.e., the "step threshold"). The largest perturbation magnitude at which each participant could recover balance using a non-stepping response is referred to here as the maximum sub-threshold. To quantify CoM control, we used minimum margin of stability (MoS) [4] during maximum sub-threshold trials. This measure provides an estimate of the maximum amount of instability each participant could withstand without stepping. To address hypothesis 1, a paired-samples t-test was used to compare minimum MoS between OFF and ON conditions. To address hypothesis 2, we compared minimum MoS between individuals who exhibited adaptive motor behavior ("adapters"; switched from a stepping to a non-stepping response at a sub-threshold perturbation magnitude) and those who did not ("non-adapters") using a Students t-test.

Results and Discussion

In support of our first hypothesis, minimum MoS during maximal sub-thresholds were significantly more negative in the ON compared to OFF medication state ($p = 0.006$, Fig 1A). This finding indicates that individuals were able to withstand larger amounts of instability without stepping (i.e., had greater control over CoM) during the ON state. During ON testing, nearly half (10 of 21) of the participants exhibited adaptive behavior at a sub-threshold perturbation magnitude – that is, they switched from a stepping to a non-stepping response across multiple trials at the same perturbation magnitude. In support of our second hypothesis, minimum MoS were significantly more negative in adapters compared to non-adapters ($p = 0.031$, Fig 1B). This finding indicates that individuals with well-functioning sensorimotor integration (measured behaviorally) had greater control over the CoM during postural perturbations.

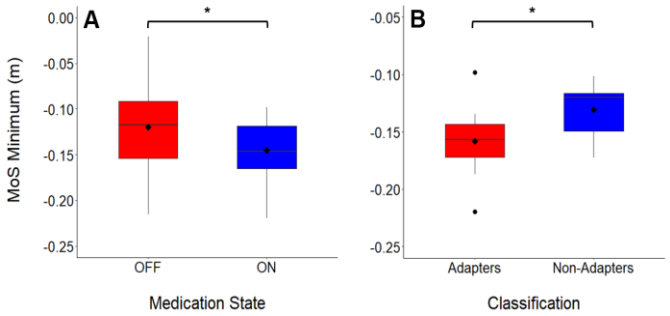

Figure 1: Minimum MoS captured during maximum sub-threshold trials in OFF versus ON medication states (A) and in adapters versus non-adapters (B). More negative minimum MoS values indicate larger "amounts" of instability and greater CoM control.

Significance

Our results suggest that higher-level, transcortical pathways (e.g., cortical-basal ganglia-thalamocortical neural loops) and processes (e.g., sensorimotor integration) play important roles in CoM control during postural perturbations. If true, interventions seeking to improve postural stability – and CoM control more generally – should incorporate tasks that target such central components. For example, the step threshold assessment used here includes an explicit task goal ("avoid stepping to recover balance") which specifies a "successful" response and may challenge higher-level processes of the nervous system. Results from our comparison of adapters and non-adapters also suggest that challenging motor adaptability (and thus, sensorimotor integration) may be a beneficial intervention strategy.

References

1. Berardelli et al., *Brain* **124(11)**, 2131-2146, 2001
2. Abbruzzese & Berardelli, *Mov Disord* **18(3)**, 231-240, 2003
3. Crenshaw & Kaufman, *Gait Posture* **39(2)**, 810-815, 2014
4. Kongsuk et al., *Gait Posture* **73**, 86-92, 2019

Are Improvements of Balance Performance after Short- and Long-term Balance Training in Older Adults associated with changes in H-Reflex Excitability and Muscle Co-Contraction

Leila Alizadehsaravi, Sjoerd M. Bruijn, Jaap H. van Dieën
Department of Human Movement Sciences, Faculty of Behavioural and Movement Sciences, Vrije Universiteit Amsterdam,The Netherlands.
Email: L.alizadehsaravi@vu.nl

Introduction

Balance training leads to improved balance control in both young and older adults (Muehlbauer et al. 2015). However, the mechanisms underlying balance improvements are unclear, especially in older adults. Therefore, we investigated the influence of balance training (BT) on balance performance, spinal excitability, and muscle co-contraction in older adults. It is well accepted that due to ageing, older adults show poorer balance performance, higher co-contraction and lower H-reflex gains. We hypothesized that after the balance training, balance performance improves and that improvements in balance performance in older adults over time are associated with lower co-contraction and higher spinal reflexes gains.

Methods

Twenty-two older adults participated in a 3-weeks balance training program. Balance performance was quantified as the mean absolute mediolateral center of mass velocity in perturbed and unperturbed unipedal stance on a robot-controlled platform, before and after the first session (SBT) and after ten sessions (LBT). In addition, durations of co-contraction in soleus and gastrocnemius lateralis (SOL/GL), as well as gluteus medius and adductor longus (GM/AL) muscles were assessed in perturbed and unperturbed unipedal balancing. H-max was acquired from a recruitment curve during bipedal stance. H-reflex gains (H-reflex/background EMG activity 100 ms prior to the stimulus) were acquired at H-max stimulus intensity during bipedal stance.

Results and Discussion

We found decreased vCOM representing an improved balance performance in perturbed stance after SBT ($t_{19} = 3.015, p = 0.006$) and improvement after LBT in both perturbed and unperturbed conditions ($t_{19} = 3.324, p = 0.003$; $t_{19} = 2.64, p = 0.015$ $respectively$; $Figure. 1$). After SBT, duration of co-contraction of SOL/GL was increased in perturbed balancing ($t_{19} = -2.99, p = 0.007$), but duration of SOL/GL and GM/AL was decreased in unperturbed balancing ($t_{19} = 2.76, p = 0.011$; $t_{19} = 2.57, p = 0.018$ respectively) and, after LBT co-contraction durations had returned to baseline values. H-reflex gains did not change with training.

Correlational analysis indicated that increasing co-contraction coincided with smaller improvements in balance performance ($r = 0.517, p = 0.02, Figure. 2$) and increasing H-reflex gains coincided with bigger improvements in balance performance ($r = -0.518, p = 0.019, Figure. 3$).

Significance

Our result indicate that as a result of balance training older adults rapidly improved balance performance, while LBT only slightly increased the improvement acquired. However the mechanisms underlying the improved performance appear to differ between SBT and LBT. After SBT decreased co-contraction and increased spinal excitability, and after LBT decreased co-contraction coincided with larger improvements in balance performance. This might suggest a higher spinal excitability as a fast solution and, improved skills reflected in lower co-contraction as a long-term solution adopted in balance training by older adults.

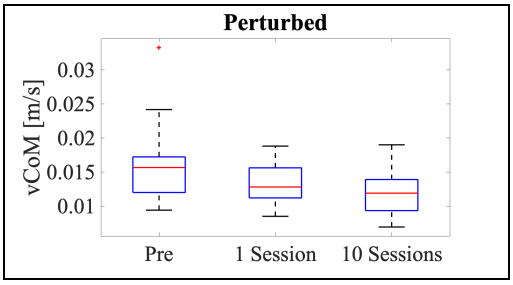

Figure *1*: The vCOM at the three time points; vCOM decreased after Short- and Long-term training.

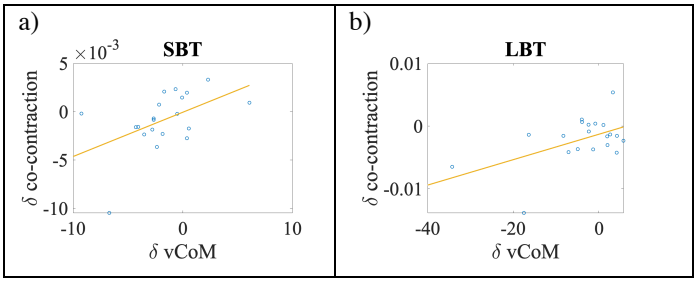

Figure *2*: Decreased vCOM was associated with decreased co-contraction of SOL/GL in unperturbed testing conditions a) after Short-term training and b) after Long-term training.

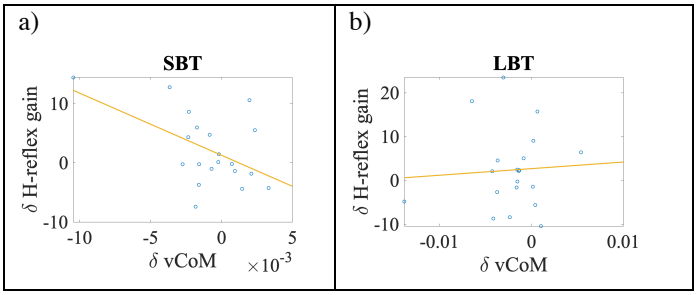

Figure *3*: The decreased vCOM after SBT was associated with increased H-reflex gains in unperturbed testing conditions.

Acknowledgments

This project has received funding from the European Union's Horizon 2020 research and innovation programme under the Marie Skłodowska-Curie grant agreement No 721577.

References

Muehlbauer T, Gollhofer A, Lesinski M, et al (2015) Effects of Balance Training on Balance Performance in Healthy Older Adults : A Systematic Review and Meta-analysis. Sport Med 45:1721–1738.

Preliminary Study of Spasticity Using the Portable Position, Velocity, and Resistance Meter (PVRM)

Seung Yun Song.[1], Yinan Pei[1], Christopher M. Zallek[2], and Elizabeth T. Hsiao-Wecksler[1]
[1]Department of Mechanical Science and Engineering, University of Illinois at Urbana-Champaign, Urbana, IL 61801
[2] Department of Neurology, OSF HealthCare Illinois Neurological Institute, Peoria, IL Email: ethw@illinois.edu

Introduction

Clinical evaluation of spasticity involves direct examiner assessment and grading with qualitative scales, such as the Modified Ashworth Scale (MAS). However, this subjective method heavily relies on the rater's personal experience/ interpretation and usually results in poor consistency and low reliability [1]. Quantitative measurement of muscle tone and joint kinematic behaviors could provide objective data for tracking patient progress.

The Position, Velocity, and Resistance Meter (PVRM) can be used to assess joint kinematics and muscle tone during clinical evaluation of patients with neurological conditions, e.g., spasticity or rigidity, or orthopedic conditions, e.g., joint replacement or recovery from injury (Fig 1**)** [2]–[4]. The PVRM includes a load cell and two inertial measurement unit (IMUs) to measure muscle tone (resistive torque) and joint kinematics (angular position, angular velocity). Two electromyographic (EMG) sensors are monitored to ensure passive movements during joint evaluation.

The goal of this study was to perform a preliminary study using the PVRM to characterize measured muscle tone and joint kinematics for different levels of spasticity, as noted by the MAS.

Methods

Fifteen patients with spasticity (62.19±12.9 yrs, 9f, 6m, MAS 1: n=3, MAS 2: n=4, MAS 3: n=4, MAS 4: n=3) and 12 age and sex matched healthy control subjects (60.4±12.9 yrs, 7f, 5m) were evaluated during passive elbow extension at four different speeds (slow (5˚/s - 20˚/s), medium (20˚/s - 80˚/s), fast (> 80˚/s), and clinician's preferred speed) while wearing the PVRM. Each subject's MAS score for biceps were rated by a certified clinician (CMZ) prior to testing. The PVRM collected kinetic and kinematic movement data (i.e., joint angular position (θ), velocity (ω), and muscle resistance (τ)), as well as monitoring muscle activity during clinical assessments to ensure a passive stretch. The changes of muscle tone and speed across the range of motion were computed to observe any kinetic and kinematic differences between spastic and healthy test groups.

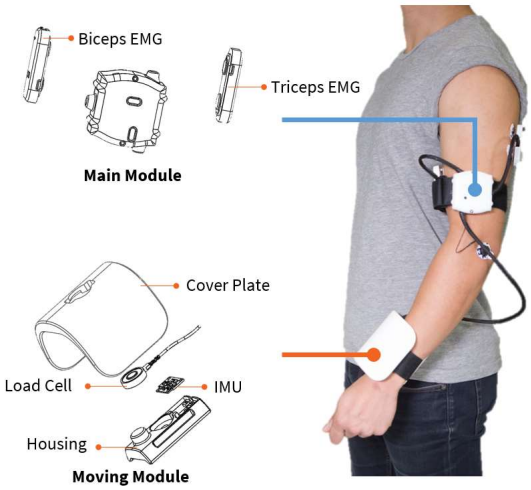

Figure 1: Main and moving modules of the PVRM.

Results and Discussion

Spasticity patients clearly displayed different kinetic and kinematic behaviors compared to healthy subjects (Fig 2, Table 1). First, the spasticity patients exhibited stretch speed dependent muscle behavior, as expected. The muscle tone increased as the stretch speed increased after a certain angular velocity was reached. Second, the spasticity patients, especially the more severely spastic patients, demonstrated less range of motion. Finally, the spaticity patients had a distinct catch-release behavior of muscle tone that were more distinct for patients with severe spasticity.

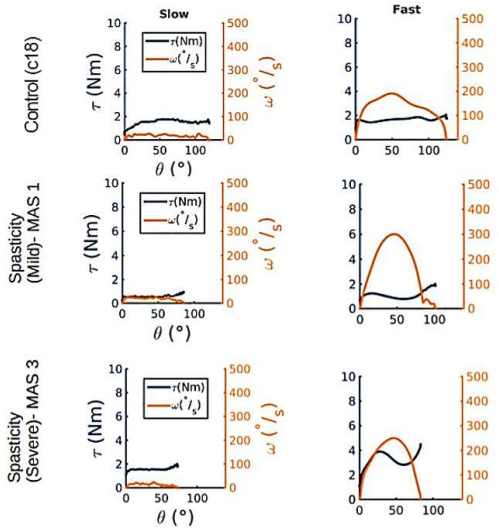

Figure 2: Representative example data of a healthy (top), mildly spastic (middle), and severely spastic (bottom) collected using the PVRM during passive elbow extension at slow and fast speeds.

Table 1: Average τ and ROM for different levels of spasticity patients.

	τ_{avg}(Nm)	ROM (%)
Healthy	2.5	105
MAS 1	4.5	93
MAS 2	5.0	98
MAS 3	6.0	67
MAS 4	7.4	77

Significance

The PVRM and collected data can allow clinicians to make more reliable assessments, and also help researchers gain additional insights into the quantification of spasticity.

Acknowledgments

Funding provided by the Jump ARCHES partnership between OSF HealthCare and the University of Illinois. Special thanks to Shannon Fraikes, Jane Goeken, and Nate Cairns.

References

[1] Blackburn, M., et al.,Phys.Ther.,doi:10.1093/ptj/82.1.25 2002
[2] Song, S.Y., et al., Front Biomed Dev, V001T11A020, 2017
[3] Song, S.Y., et al., Design of Med Dev Conf, 2018
[4] Song, S.Y., Thesis, http://hdl.handle.net/2142/104925. 2019

The Effect of Pain on the Cognitive Control of Balance During the Motor Control Test in Older Women with Osteoarthritis.

Yang Hu[1*], Alka Bishnoi[1], and Manuel Hernandez[1]
[1] University of Illinois at Urbana - Champaign, Department of Kinesiology and Community Health, Urbana, Illinois.
Email: *yangh3@illinois.edu

Introduction

Osteoarthritis (OA) is a musculoskeletal disease that affects balance control in older adults [1]. The ability to restore balance following sudden, unexpected perturbations is critical to avoid falls [1], particularly for persons with OA. However, a significant gap exists in our understanding of reflexive postural control changes due to OA, and the mechanisms underlying these changes. Thus, the objective of this study is to 1) investigate the postural control differences between older women with and without OA in the Motor Control Task (MCT); and 2) explore the relationship between postural control, pain, and attention, as measured by prefrontal cortex (PFC) activation, in older women with OA, given the significant contributions of the PFC in the control of balance [2]. We hypothesize that 1) older women with OA will demonstrate different reflexive postural control responses after anterior and posterior translations perturbations in force and COP pattern compared to age-matched healthy controls (HOA); 2) COP sway will be positively correlated with pain and negatively correlated with PFC activations in OA, while there will be no relationship between PFC activation, pain and COP sway among HOA.

Methods

Ten older women with and without lower extremity OA with a mean age of 66.1 years, Western Ontario and McMaster Universities Arthritis Index (WOMAC) score of 10.5, and BMI of 25kg/m$_2$ participated in this study. Participants went through the MCT task on Neurocom (Natus Medical Inc), which involved small, medium and large perturbations in both forward(FP) and backward directions(BP). Ground reaction force and COP data were collected by the Neurocom force plate. PFC activation was recorded by a Functional Near Infrared Spectroscopy (fNIRS) system (fNIR Devices LLC, Potomac, MD) during the tasks. Pain was assessed by the first five questions of WOMAC(WS). Custom MATLAB scripts were designed to calculate average oxygenated hemoglobin (HbO_2) levels from fNIRS raw data, and extract COP sway features (Strength symmetry (SS), absolute anterior-posterior sway amplitude (ABS), COP root mean square (COPrms) in both resultant sway (Y) and anterior-posterior sway (XY), and Max Amplitude XY (MA)). All statistical analyses were performed using RStudio (Version 1.2.1335, RStudio, Inc). A linear mixed model (lmer) appropriate for repeated measures data was specified for each of the main outcomes was fitted to the data with cohort (OA or HOA), direction (forward or backward), condition (small, medium, and large), and their interactions as fixed effects with the subject as a random effect. For HbO_2 data, the location of the optodes was set as an additional fixed effect, and its interaction with the subject has set as an additional random effect.

Results and Discussion

We found significant cohort effects, cohort x direction(Dir) interactions, or cohort x condition(Cond) interactions in HbO_2, SS, MA, ABS, COPrmsY and COPrmsXY lmers(**Table 1**). In addition to the model results, post-hoc test illustrated the specific differences between groups. Significantly higher HbO_2 levels were observed in BP, relative to FP, in both HOA ($p < 0.001$) and OA ($p < 0.001$) groups. Further, HOA had significantly lower SS scores than OA in overall ($p = 0.0336$), and during BP($p = 0.0109$). These findings indicate that OA adults prefer right foot strategy with an average total deviation of 11 and BP deviation of 13.6. HOA prefers left foot strategy with an average overall deviation of 10 and BP deviation of 13.5.

Outcome	Effects	F-value	P-value
HbO_2	Cohort*Dir	18.3421	<0.001
SS	Cohort	7.1216	0.0235
	Cohort*Dir	4.2876	0.0436
MA	Cohort*Dir	5.9212	0.0160
ABS	Cohort*Dir	6.8625	0.0096
COPrmsY	Cohort*Cond	3.9315	0.0214
COPrmsXY	Cohort*Cond	3.3239	0.0384

Table 1:Significant effects from linear mixed effect models.

Post-hoc tests also indicate that OA group has higher MA ($p = 0.0295$) and ABS ($p = 0.0134$) in FP compared to BP. Significantly higher COPrms were observed as perturbation levels increased in both groups ($p <0.001$). No other significant differences were found.

In the anterior direction, we found that there was a significant negative correlation between SS and WS scores among OA adults ($r = -0.99$, $p < 0.01$), which indicates higher WS is associated with greater asymmetry. At the same time, there are significant positive correlations between MA and WS ($r = 0.96$, $p < 0.05$), and between ABS and WS ($r = 0.96$, $p < 0.05$). In terms of condition, OA adults showed a significant correlation between COP sway in Y ($r = 0.97$, $p < 0.05$) and XY ($r = 0.97$, $p < 0.05$), with WS score in medium perturbation conditions, while similar trends were also observed in large perturbation conditions. No other significant correlations were found.

Consistent with our findings of higher postural sway as pain increased in older women with OA, older adults with "symptomatic" OA, relative to healthy controls, without a history of recent falls demonstrated deficits in postural control [3]. Even though higher PFC activations were observed alone with better postural control in BP compared to FP within OA group, no significant cognitive contribution was found.

Significance

This is the first study investigating reflexive postural control and its mechanisms in lower extremity OA. This work completes the investigation and confirmed OA's impact on both volitional and passive postural control and illustrates the pain mechanism underneath. Due to the small sample size of this study, future verification on the role of cognitive control needs to be done with a bigger sample size.

Acknowledgments

We would like to thank all of the subjects and the MFPRL OA research team for their contributions to the study.

References

[1] Hinman et al. *Rheumatology*. 2002;41:1388–1394.
[2] Mihara et al. *NeuroImage*. 2008; 43:329–336.
[3] Sumaiyah et al. *J Rehabil Med*. 2017; 49: 258–263.

PEOPLE WITH WORSE BALANCE HAVE LARGER PERTURBATION-EVOKED CORTICAL N1 RESPONSES

Aiden M. Payne.[1], Lena H. Ting[1,2]*
[1]Wallace H. Coulter Department of Biomedical Engineering at Georgia Tech and Emory University
[2]Department of Rehabilitation, Division of Physical Therapy, Emory University
Email: *lting@emory.edu

Introduction

A balance disturbance elicits automatic brainstem-mediated corrective motor reactions that can be followed by cortically-mediated control at longer latencies (Jacobs 2007). People with similar biomechanical reactions may differ in the extent to which they rely on automatic vs. cortical control. Dual-task interference studies suggest that older adults with worse balance rely more on cortical control (Shumway-Cook 1997). It is unclear whether cortical involvement differs with balance ability in young adults.

We hypothesized that young adults with worse walking balance ability would have greater cortical activation in response to standing balance perturbations. We measured walking balance ability in a difficult beam-walking task, observing a wide range of performance levels. We measured cortical activation of the N1 response to standing balance perturbations via electroencephalography (EEG). We recently observed greater perturbation-evoked N1 responses in individuals who were unable to recover balance without stepping (Payne 2019). We now test whether the N1 responses are associated with (1) balance ability or (2) stepping behaviors.

Methods

In 20 healthy young adults (11 female, ages 19-38) we measured individual differences in balance ability based on the ability to walk across a narrow (0.5-inch wide) 12-foot beam (Sawers 2015). We measured the cortical N1 response (Cz-EEG, peak amplitude 100-200ms) evoked by 48 backward translational support-surface perturbations of unpredictable timing and amplitude. Perturbations included a small (8 cm) perturbation that was identical across participants, as well as medium (13-15 cm) and large (18-22 cm) perturbations scaled to participant height to control for height-related differences in perturbation difficulty (Payne 2019). On half of trials we asked participants to take steps, and to keep feet in place otherwise.

We assessed correlations between cortical N1 amplitudes and balance ability across subjects. In large perturbations, we compared N1 amplitudes between stepping and non-stepping reactions, and between planned and accidental stepping reactions, to test for effects of step execution and step planning.

Results and Discussion

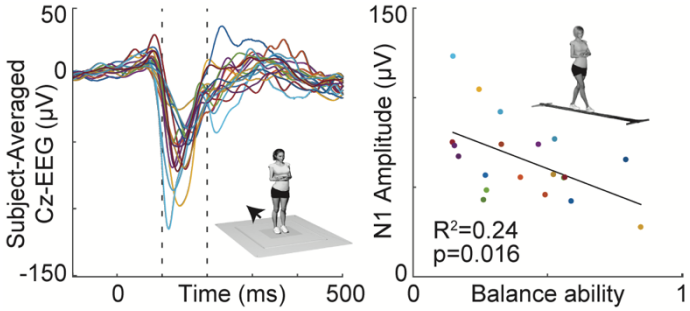

Figure 1. Individuals with worse balance had larger N1 amplitudes.

Cortical N1 peak amplitudes (54 μV, SD 18) in response to standing balance perturbations were inversely correlated to the distance traveled in the difficult beam-walking task (R^2=0.20, p=0.029), suggesting individuals with worse balance have greater cortical activation during reactive balance recovery. The relationship to balance ability was greatest in the difficult large perturbations (Figure 1; R^2=0.24, p=0.016).

Additionally, cortical N1 responses were 11% (SD 25%) larger when executing planned stepping reactions (Figure2; black vs. yellow, p=0.020), suggesting a possible relationship between the cortical N1 response and subsequent compensatory stepping behavior. The increase in N1 amplitude when stepping could not be attributed to an effect of prior planning because cortical N1 amplitudes did not differ between planned and accidental steps (Figure 2; yellow vs. red, p>0.05).

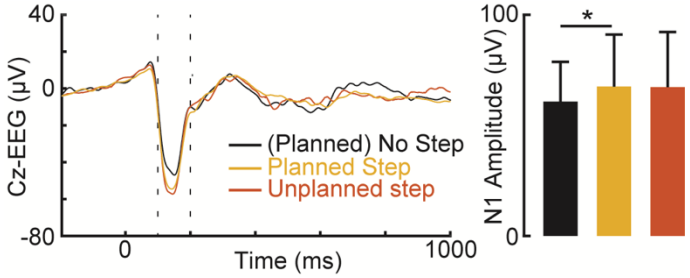

Figure 2. N1 amplitudes were larger when executing stepping responses (black vs. yellow). When stepping, there was no effect of planning on the N1 amplitudes (yellow vs. red).

Significance

Larger cortical N1 amplitudes in individuals with lower balance ability may be related to greater perceived threat (Adkin 2008) or attention to balance (Quant 2004, Little 2015). However, the within-subjects increase in cortical N1 amplitudes when stepping suggests a potential relationship to subsequent balance recovery behavior.

Acknowledgments

This work was supported by the NIH (5T90DA032466, 1P50NS098685, and R01 HD46922-10), the NSF (1137229), and the Andy Zebrowitz Memorial Brain Research Fellowship Award (2017-2018).

References

Jacobs and Horak (2007) J Neural Transm, 114(10): 1339-48. Shumway-Cook et al. (1997) J Gerontol A Biol Sci Med Sci, 54(2): M232-40. Payne et al. (2019) J Neurophysiol, 121(3): 867-80. Sawers and Ting (2015) Gait and Posture, 41(2): 619-23. Adkin et al. (2008) Neurosci Lett, 435(2): 120-5. Quant et al. (2004) BMC Neuroscience, 5(18): 1-12. Little and Woollacott (2015) Exp Brain Res, 233(1): 27-37.

Ab# 495

Effects of Fear of Falling on Gait and Balance in Chemotherapy-Induced Peripheral Neuropathy

Gu Eon Kang[1,*], Tamiko K. Murphy[1], Aanand D. Naik[2,3], Mark E. Kunik[2,3],
Hoda J. Badr[3], Biruh T. Workeneh[4], Savari V. Yellapragada[2,3], Yvonne H. Sada[2,3], and Bijan Najafi[1,**]
[1] Interdisciplinary Consortium on Advanced Motion Performance, Department of Surgery, Baylor College of Medicine, Houston, TX
[2] Michael E. DeBakey VA Medical Center, Houston, TX
[3] Department of Medicine, Baylor College of Medicine, Houston, TX
[4] Department of Emergency Medicine, The University of Texas MD Anderson Cancer Center, Houston, TX
*Email: gueon.kang@bcm.edu, **Email: bijan.najafi@bcm.edu

Introduction

Chemotherapy-induced peripheral neuropathy (CIPN) is a common side effect of neurotoxic chemotherapy that affects up to 70% of people undergoing chemotherapy [1]. People with CIPN often have foot numbness [2] and are at increasesed risk of fall [3], which is likely to develop fear of falling (FoF) [4]. The development of FoF may further increase risk of fall [5], however its underlying mechanism is not well understood. We aimed to investigate the effect of FoF on habitual gait and postural sway in older adults with CIPN using inertial measurement units (IMUs). We hypothesized that FoF would negatively affect habitual gait and postural sway.

Methods

We recruited 35 older adults with CIPN (≥65 years) that had numbness in their foot. The CIPN group did not have a history of a neurological condition such as Parkinson's disease, stroke and dementia. We also recrtuied 16 older adults (≥65 years) with no history of cancer, diabetes, a neurological condition and fall in the past 12 months as the control group (CON).

We assessed FoF using the Falls Efficacy Scale-International (FES-I; on a scale of 16-64 with 16 indicating no FoF), and used a cut-off score of 28 to classify a group with high FoF [6]. We also assessed foot numbness based on vibration perception threshold using a Biothesiometer (Bio-Medical Instrument, Newbury, OH). We evaluated habitual gait and postural sway using previously validated IMUs (100 Hz, BioSensics, Newton, MA) [7,8]. For habitual gait, two IMUs were attached on the shanks, and participants were asked to walk over 40 feet at their normal pace. For postural sway, two IMUs were attached on the lower back and right shank, and participants were asked to stand quietly for 30 seconds with eyes-open and eyes-closed conditions. Data for habitual gait and postural sway were analysed using commercial software (LEGSys and BalanSens, respectively, Biosensic, Newton, MA). Primary outcomes were gait speed, stride length and cadence for habitual gait, and ankle, hip and center-of-mass (COM) sway area for postural sway.

Among the groups of CIPN with high FoF (CIPN FoF+), CIPN without high FoF (CIPN FoF-) and CON, we compared age, FES-I scores and gait parameters using one-way analysis of variance (ANOVA), and body-mass index and postural sway parameters using Kruskal-Wallis tests. Between CIPN FoF+ and CIPN FoF-, we compared vibration perception threshold and time since a cancer diagnosis using Mann Whitney U tests.

Results and Discussion

As expected, the FES-I scores were significantly different among the CIPN FoF+ (40.2±10.7), CIPN FoF- (21.9±3.0) and CON (19.1±2.0) ($p<0.05$). Age and body-mass index did not significantly differ among the CIPN FoF+ (74.1±5.8 years; 27.25±4.67 kg/m^2, respectively), CIPN FoF- (72.1±4.6 years; 24.57±3.46 kg/m^2, respectively) and CON (75.3±6.8 years; 27.25±4.67 kg/m^2, respectively) (all $p>0.05$). The vibration perception threshold and time since a cancer diagnosis were not significantly different between the CIPN FoF+ (41.5±10.7 volts; 5.5±6.1 years, respectively) and CIPN FoF- (36.6±14.1 volts; 4.6±5.1 years, respectively) (all $p>0.05$). Table 1 shows results for habitual gait and postural sway. There were significanty differences among the three groups across the tasks.

Table 1. Characteristics for habitual gait and postural sway.

	CIPN FoF+ (N=16)	CIPN FoF- (N=19)	CON (N=16)	P-value (ANOVA)
Habitual gait				
Gait speed, m/s	0.78±0.21	0.93±0.17	1.17±0.13	<0.001
Stride length, m	0.99±0.22	1.13±0.15	1.26±0.10	<0.001
Cadence, steps/min	47.09±7.06	49.47±4.99	56.00±4.48	<0.001
Postural sway-eyes open condition				
Ankle sway, deg^2	2.60±4.05	1.85±1.22	0.52±0.34	0.001
Hip sway, deg^2	1.84±2.71	1.77±1.79	0.59±0.37	0.036
COM sway, cm^2	0.49±0.87	0.31±0.19	0.10±0.09	0.003
Postural sway-eyes closed condition				
Ankle sway, deg^2	4.79±6.44	2.98±2.02	1.37±1.09	0.039
Hip sway, deg^2	2.45±2.31	3.45±3.34	1.32±0.77	0.076
COM sway, cm^2	3.83±9.50	2.23±2.88	0.25±0.19	0.001

Significance

Slower habitual gait speed and corresponding deterioration in stride length and cadence, and poorer postural sway are indicators of increased fal risk. Thus, our findings may reveal how development of FoF further increases risk of fall in CIPN.

Acknowledgments

This study was funded, in part, by the National Heart, Lung, and Blood Institute (5T32HL139430-02) and by the National Cancer Institute (1R21CA190933-01A1).

References

[1] Ward et al. J Geriatr Oncol. 2014;5:57-64.
[2] Miltenburg and Boogerd. Cancer Treat Rev. 2014;40:872-82.
[3] Winters-Stone et al. J Clin Oncol. 2017;35:2604-12.
[4] Kolb et al. JAMA Neurol. 2016;73:860-66.
[5] Reelick et al. Age Ageing. 2009;38:435-40.
[6] Delbaere et al. Age Ageing. 2010;39:210-16.
[7] Najafi et al. J Diabetes Sci Technol. 2010;4:780-91.
[8] Aminian et al. J Biomech. 2002;53:689-99.

Deep Learning to Classify Fall Risk from Wearable Accelerometer Data During Standing in Persons with Multiple Sclerosis

Brett M. Meyer[1], Lindsey J. Tulipani[1], Reed D. Gurchiek[1], Dakota A. Allen[1], Lukas Adomowicz[1], Dale Larie[1], Andrew J. Solomon[1], Nick Cheney[1], and Ryan S. McGinnis[1]
[1]University of Vermont, Burlington, VT 05405 USA
Email: ryan.mcginnis@uvm.edu

Introduction

Falls are a significant problem for persons with multiple sclerosis (PwMS). Fall risk assessments are reactive, which prevents deployment of preventative interventions and motivates development of new assessments in this population. Previous research has identified measures of postural sway that differ between PwMS who have fallen and those who have not, but many of these biomechanical indices require the use of laboratory-based measurement technologies, preventing deployment outside of research contexts. Wearable sensors may enable characterization of these postural sway metrics outside of the laboratory and subsequently the development of fall risk assessments that can be deployed during daily life. The primary objective of this work was to determine if machine learning methods could be used to develop statistical models for fall risk that are able to differentiate PwMS who have fallen from those who have not.

Methods

Thirty-six PwMS (18 fallers, 18 non-fallers with mean EDSS scores of 3.41±1.39 and 2.48±1.29 respectively; fall history assessed during the 6-mo immediately preceding the study visit) completed a series of daily life activities and functional assessments. Each subject performed several standing tasks including tandem standing, normal standing, and standing with eyes closed (each for at least 2 minutes). Subjects were instrumented with MC10 BioStamp sensors secured to the chest and anterior aspect of the thigh and set to record three components of accelerometer data (31.25 Hz, ± 16G). Following the approach described in [1], a support vector machine activity classifier was used to identify all 4-second windows when the subject was standing within the test session, including but not limited to data recorded during the prescribed standing tasks.

Several statistical models were trained to identify if windows of standing data had been recorded from a faller or non-faller using a supervised machine learning approach. Specifically, we trained a deep learning (DL) model that uses an LSTM layer to extract features followed by a Bi-LSTM layer to peform the faller/non-faller classification. For comparison, we also trained a random forest (RF) model that took as input postural sway features from previous work investigating postural sway and fall risk [2], [3] and provided the same faller/non-faller classification. Performance, as determined via area under the receiver operating characteristic curve (AUC), of both modelling approaches was established using leave one subject out cross validation. We further explored the impact of different lengths of input data by considering 4, 8, 12, and 16 second windows of conseutive standing data.

Results and Discussion

The best fall risk classification performance was observed with the DL model using 4-second windows, which achieved an AUC of 0.89 (Table 1). In contrast, the best performing RF model achieved an AUC of 0.61 with 16-second windows.

Table 1: Performance (AUC) of deep learning and random forest models as a function of the window size (in seconds) of input data.

Window Size (s)	DL	RF	Dataset Size
4	0.89	0.49	7864
8	0.80	0.54	3725
12	0.77	0.58	2378
16	0.76	0.62	1705

The decrease in DL performance with increasing window size is likely due to the model architecture, which requires more observations to effectively learn the relationship between raw input data and the faller/non-faller labels (longer windows reduce the amount of available training data). The increase in RF performance with increasing window size is likely due to the time and frequency domain features used for making the classification, which require longer window sizes. Previous work on characterizing postural sway with wearable accelerometers has considered a minimum of 30 seconds of data [3]. The shorter window size considered here (max of 16 s) could explain the relatively poor performance of the RF classifier.

Significance

The results presented herein suggest that deep learning models are able to effectively classify fall risk based on accelerometer measurements during standing. As seen in the presented results, the deep learning methods were able to far outperform the random forest for all window sizes considered here, which are small compared to existing literature, despite these features showing statistically significant differences between persons with Parkinson's Disease and controls [3]. This suggests that the model may be learning novel postural sway measures within the accelerometer signal that are not captured with established metrics. Comparing to other literature in PwMS, Sun et al. found a random forest using force plate data to be 50% accurate when classifying between PwMS with low and moderate fall risk [2]. We found comparable performance (58% accuracy) using RF classification in this study, despite smaller differences in EDSS between groups (1.07 in this study compared to 4.00 in Sun et al). Even still, our results suggest far superior performance using DL classification (81% accuracy). Additionally, the methods presented in Sun et al. require a force plate to collect data, thus limiting potential for deployment. The results presented in this study are broadly useful outside of the laboratory environtment as they only require two-wearable sensors and a four-second standing period to provide a very accurate classification of fall risk.

Acknowledgments

This work was supported in part by NIH under Grant R21EB027852.

References

[1] R. D. Gurchiek *et al. (2019)*, *Sci. Rep.* **9**(1)
[2] R. Sun *et al.* (2019). *Sci. Rep.* **9**(1)
[3] M. Mancini *et al.* (2012). *J. NeuroEngineering Rehabil.*, **9**(1)

The Influence of Mediolateral Stabilization on Balance Control during Walking in Individuals Post-stroke

Hannah B. Frame[1], Christian Finetto[2], Jesse C. Dean[2], Richard R. Neptune[1]
[1]Department of Mechanical Engineering, The University of Texas at Austin, Austin, TX, USA
[2]Department of Health Professions, Medical University of South Carolina, Charleston, SC, USA
Email: hannahbframe@gmail.com

Introduction

Individuals post-stroke experience higher rates of falls than the healthy elderly [1]. As a result, one goal of post-stroke rehabilitation is to improve functional mobility and reduce fall risk in individuals post-stroke. To reduce fall risk, there is need for evidence-based therapies that target and improve balance control [2]. Mediolateral stabilization (*MLS*) reduces the need to actively control frontal plane balance in healthy adults [3], but it is unknown how individuals post-stroke will respond to *MLS* and whether it will improve walking performance.

The purpose of this study was to quantify the effects of *MLS* on balance control in individuals post-stoke. We hypothesized that *MLS* will improve balance control as evidenced by a reduction in the range of frontal plane whole body angular momentum (*H*), which has been shown to be correlated with clinical balance scores [4].

Methods

Kinematic data were collected from 20 individuals post-stroke (10 right hemiparesis, 9 male, age: 50 ± 16 yrs) during steady state walking on a dual-belt, instrumented treadmill (Bertec Corp.). Subjects walked for three 30-second trials un-aided (normal) and three 30-second trials with *MLS* (stabilized) at their self-selected walking speed. We focused on those subjects who responded to the *MLS*, i.e., those who reduced their step width between the normal and stabilized conditions as determined by a two-tailed t-test ($p < 0.05$).

H was calculated using a 13-segment inverse dynamics model, which summed the angular momentum of each segment about the whole-body center of mass (*CoM*) and was normalized by subject mass, walking speed and height. The range of frontal plane *H* was defined as the peak-to-peak difference in frontal plane *H* and pelvis sway was defined as the peak-to-peak difference in the lateral pelvis *CoM* location, both over the paretic stride. Separate paired t-tests assessed for significant differences in metrics between normal and stabilized conditions with $\alpha = 0.05$.

Results and Discussion

Thirteen of the 20 post-stroke subjects responded to the *MLS* through a significant reduction in step width (Responders). The *MLS* successfully stabilized the pelvis by significantly decreasing pelvis *CoM* sway (Table 1), yet range of frontal plane *H* significantly increased (Table 1). Applying *MLS* decreased dynamic balance control, thus our hypothesis was not supported. To investigate this significant increase, we examined the contributions of each body segment to overall frontal plane *H*.

We found that an increase in the segmental contributions of the trunk and head were the main causes of the increase in peak-to-peak frontal plane *H* while stabilized. These increases were driven by a significantly larger range of relative mediolateral velocity between the head and body *CoM*s (Table 1) and the trunk and body *CoM*s (Table 1) during the stabilized trials.

The reduction in step width and pelvis sway in response to *MLS* is consistent with previous work in neurologically intact [4]–[6] and incomplete spinal cord injury [5] populations. Yet, those reductions did not lead to a corresponding decrease in the range of frontal plane *H*. This study explored *MLS*'s effects on dynamic balance control by examining the intersegmental dynamics that contribute to an increase in the range of frontal plane *H*. While *MLS* may have decreased the absolute motion of the pelvis, it increased the relative motion between the body *CoM* and upper body segments.

Significance

The increased range of frontal plane *H* with *MLS* observed in this study has important clinical implications particularly for gait therapies that constrain the pelvis, such as body weight supported walking. Limiting pelvis sway during gait without also taking care to limit the relative motion between the pelvis and upper body segments may have unintended consequences of destabilizing patients and reducing balance control.

Future work should explore how altered pelvis motion affects segmental contributions to frontal plane *H* and dynamic balance control. Subjects were not instructed how to adapt to *MLS* and future studies should determine if training with the *MLS* over an extended period of time and with feedback would improve balance control.

Acknowledgments

This study was supported by NIH Grant R21 HD083964.

References

[1] L Jorgensen and BK Jacobsen. *Stroke.* 2002.
[2] CM Dean et al. *Neurorehabil. Neural Repair*. 2012.
[3] JC Dean, et al. *IEEE Trans. Biomed. Eng*. 2007.
[4] CR Nott, et al. *Gait Posture*. 2014.
[5] M Wu, et al. *Gait Posture*.2017.
[6] JM Donelan, et al. *J. Biomech*. 2004.

Table 1. Average balance metrics for Responders (n = 13). Values are presented as mean ± standard deviation.

		Normal	Stabilized	p-value
Pelvis sway (m)		0.10 ± 0.02	0.08 ± 0.03	0.03
Range of frontal plane *H* (unitless)		0.11 ± 0.04	0.14 ± 0.06	0.001
Range of relative mediolateral velocity (m/s)	Head	0.21 ± 0.06	0.35 ± 0.10	0.0004
	Trunk	0.13 ± 0.03	0.17 ± 0.05	0.002

Dynamics of Turning in People with Parkinson's Disease

Carolin Curtze[1], Peter C. Fino[2], Patty Carlson-Kuhta[3], Jay Nutt[3], and Fay B. Horak[3]
[1]Department of Biomechanics, University of Nebraska at Omaha
[2]Department of Health, Kinesiology, and Recreation, University of Utah
[3]Department of Neurology, Oregon Health and Science University
Email: ccurtze@unomaha.edu

Introduction

In one of our recent studies, we have shown that when people with Parkinson's disease (PD) take levodopa they walk and turn more quickly, but become unstable during standing and fall more in daily life [1]. Unsafe turning may occur when patients become disinhibited after levodopa intake.

The aim of this study is to determine the effect of antiparkinsonian medication on the dynamics of turning in people with PD.

Methods

We recruited a total of 23 participants with idiopathic Parkinson's disease. Participants were tested in the morning in their practical OFF state, that is, at least 12 hours after their last intake of antiparkinsonian medications. Subsequently, they were retested in the ON state, that is, 1 hour after a L-dopa challenge dose that was approximately 1.25-fold of their regular L-dopa dose.

Participants performed a series of turns (45°, 90°, 135°, and 180°) to the left and right at normal and fast speed (Figure 1). Synchronized inertial sensors (Opal v1, APDM Inc., Portland, OR) attached to the lumbar and feet were used to calculate the centripetal acceleration and yaw angular velocity on a step to step basis [2].

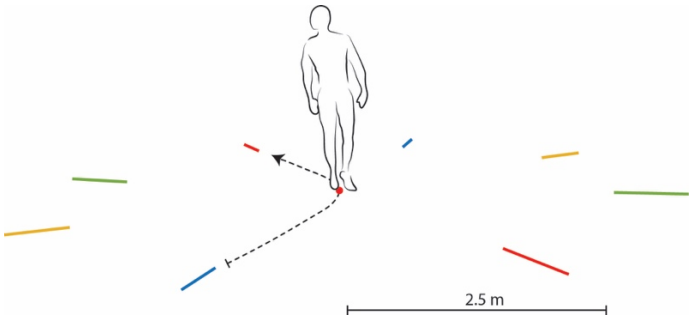

Figure 1: Schematic of the experimental protocol.

To determine the effect of antiparkinsonian medication on turning dynamics, linear mixed-effects models were fit for centripetal acceleration for the left, right, inside, outside limb, separately. Each linear mixed-effects model contained fixed effects of angular velocity, the angular velocity x medication interaction and random intercepts for medication state and subject.

Results and Discussion

In the ON state people with PD exhibited a greater increase in centripetal acceleration as angular rate increased on the inside limb (Figure 2). On the outside limb this interaction effect was absent. Instead, the centripetal acceleration shifted closer to zero for outside limb in the ON medication state. This increase in centripetal acceleration on the inside limb can be interpreted as a greater translation of the center-of-mass lateral to the stance limb and therefore outside of the base of support.

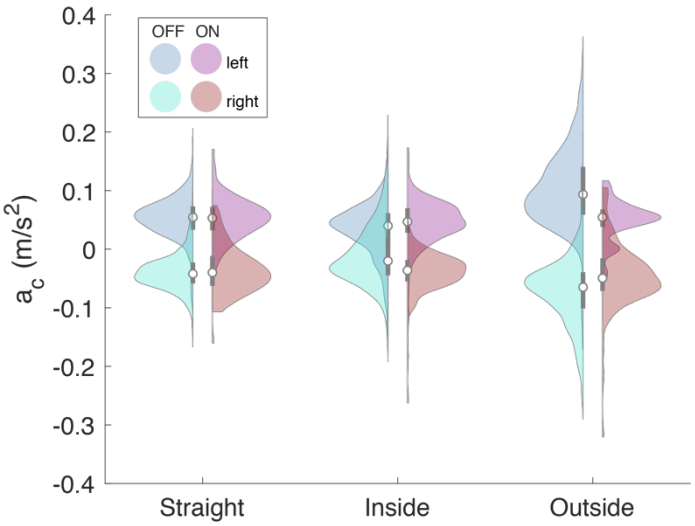

Figure 2: Violin plot depicting the distribution of centripetal acceleration during straight walking and turning stratified by limb for the OFF and ON medication state.

Significance

Our results suggest that inhibitory control is compromised in the ON medication state, leading to an increase in centripetal accelerations generated on the inside stance limb during turning. This increase in centripetal accelerations generated by the inside limb may put people with PD at a higher risk of falls in the ON medication state.

Acknowledgments

This study was supported by the Medical Research Foundation of Oregon (PI: Curtze).

Conflict of Interest

F. B. Horak has a significant financial interest in APDM, a company that may have a commercial interest in the results of this research and technology. This potential conflict has been reviewed and managed by OHSU. All other authors declare that the research was conducted in the absence of any commercial or financial relationships that could be construed as a potential conflict of interest.

References

[1] Curtze C, et al. *Movement Disorders* **30,** 1361-1370, 2015.
[2] Fino PC, Horak FB, Curtze C. *IEEE TNRSE,* **28:3,** 629 – 636, 2020.

Dynamic Balance During 90-degree Turns in People with a Unilateral Transtibial Amputation

Luis A. Nolasco[1], Jenna Livingston[2], Anne K. Silverman[3], and Deanna H. Gates[1]
[1]School of Kinesiology, [2]Department of Mechanical Engineering, University of Michigan, Ann Arbor, MI
[3]Department of Mechanical Engineering, Colorado School of Mines, Golden, CO
Email: lnolasco@umich.edu

Introduction

Ankle muscles play an important role in regulating dynamic balance during walking. The force modulation of ankle muscles also faciliate changing direction while walking. Specifically during circular turns, plantarflexors contribute to accelerating the center of mass laterally toward the center of curvature [1]. This force modulation likely contributes to the greater whole-body angular momentum during 90° turns compared to straight-line walking [2]. However, inner leg ankle muscles have greater contribution than the outer leg ankle muscles [1]. Thus, for people with a transtibial amputation (TTA), the lack of active ankle control, particularly for the inner leg, may affect their ability to regulate whole-body angular momentum during turning. People with TTA also have reduced prosthetic side ground reaction impulses compared to people without an amputation, regardless of whether the prosthesis is on the inside or outside of the turn [3], indicating that turns are challenging for this population. Thus, the purpose of this study was to determine the influence on turn direction on whole-body angular momentum in 90° turns in people with and without TTA.

Methods

Eight individuals with TTA (1F/7M; 52 ± 15 years; 99.5 ± 17.9 kg; 1.77 ± 0.08 m) and eight controls (2F/6M; 39±15 years; 80.7±19.5 kg; 1.77±0.09 m) performed straight-line walking and 90° step turns on level ground. Participants made turns with their prosthetic side on the outside and inside of the turn.

Full body kinematics were tracked with 79 reflective markers at 120 Hz using a 20-camera motion capture system. Kinematics were low-pass filtered using a 4th-order Butterworth filter (f_C = 6 Hz). A 13-segment model was created in Visual3D. To account for the inertial properties of the prosthesis differing from that of a biological limb, the inertial properties of the prosthesis were adjusted according to [4].

We summed all segment angular momenta about the center of mass to calculate whole-body angular momentum (**H_{WB}**). We then normalized by height, mass, and speed across each stride to obtain a unitless measure. For turning, the angular momentum vector was rotated from the lab reference frame to the center of mass reference frame. Turns were divided into initiation, continuation, and termination strides. We compared the average **H_{WB}** between groups (TTA, Controls) and turn type (prosthetic inside/right, prosthetic outside/left) using a series of 2x2 repeated-measures ANOVAs for each plane and stride. A Bonferroni correction was applied to post-hoc tests following significant main effects and interactions.

Results and Discussion

There were no differences between left and right turns for controls ($p > 0.41$). In the sagittal plane, people with TTA generated greater **H_{WB}** during initiation and continuation compared to controls ($p = 0.02$) while controls generated greater **H_{WB}** during termination ($p = 0.02$) regardless of turn direction. In the transverse plane, people with TTA generated greater **H_{WB}** toward the inside of the turn with the prosthesis on the inside compared to controls ($p = 0.005$) and turning with the prosthesis on the outside ($p < 0.001$) for all turning strides.

People with TTA generated greater **H_{WB}** when turning with the prosthesis on the inside compared to when the prosthesis was on the outside of the turn and to controls. As greater force modulation is used with the inside leg during circular turning [1], the inability to modulate forces with the prosthesis likely requires greater generation of **H_{WB}** to succesfully change direction when the prosthesis is on the inside.

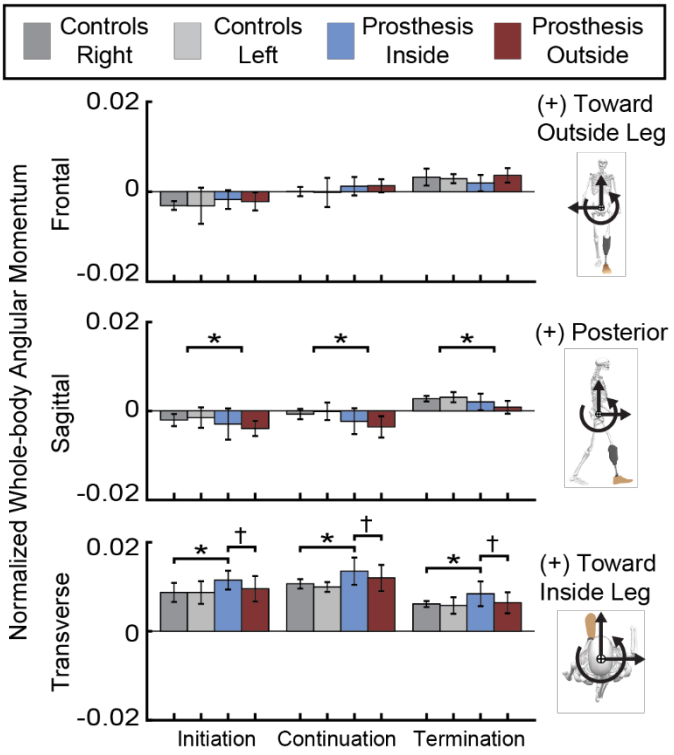

Figure 1: Average **H_{WB}** over a turning strides across individuals. Significant differences between groups ('*') and turns ('†').

Significance

Reduced ability to modulate ground reaction forces with a prosthesis suggests the need for rehabilitation to focus on turning toward the prosthetic side. In addition, this information may be useful for powered prosthetic device development as 3D ground reaction force modulation is important for controlling whole-body angular momentum [5]. Future work should investigate muscle activity and compensatory movements people with TTA use to perform 90° turns.

References

[1] Ventura J, et al. J Biomech, 48, 1067-1074, 2015
[2] Nolasco LA, et al. Gait Posture, 70, 12-19, 2019
[3] Ventura J, et al. Gait Posture, 34, 307-312, 2011
[4] Ferris A, et al. J Biomech, 54, 44-48, 2017
[5] D'Andrea S, et al. Clin Orth Rel Res, 472, 3044-3054

Centripetal Acceleration During Turning and its Relationship with Autonomic Function in Mild Traumatic Brain Injury

Peter C. Fino[1], Leah Millsap[2], Ryan Pelo[3], Benjamin Cassidy[1], Lee E. Dibble[3], Melissa M. Cortez[2]
[1]Department of Health, Kinesiology, and Recreation, University of Utah
[2]Department of Neurology, University of Utah
[3]Department of Physical Therapy & Athletic Training, University of Utah
Email: peter.fino@utah.edu

Introduction

Over 40% of daily steps are turns that require sophisticated integration of time-varying gravitoinertial forces with dynamic changes in heading angle to propel the center-of-mass (CoM) in a new direction of travel.[1] Because turns are ubiquitous in daily life and complex, they can be a useful indicator of mobility.

In people with mild traumatic brain injury (mTBI), abnormal turning is often attributed to sensory integration or vestibular dysfunction.[2] Specifically, we have previously speculated that slower axial rotation during turning may be a strategy to limit symptoms from visual motion and vestibular afferents from the semi-circular canals.[3] However, previous interpretations only considered rates of axial rotation given the reliance on inertial sensors. Rather than turning strictly through upright axial rotation, ambulatory turns are often accomplished through asymmetrical loading and lateral ground reaction forces to generate centripetal force, with corresponding lateral lean to counteract the moment caused by the centripetal force.[4]

Centripetal acceleration, a_c, during turning also suggests that the integrity of the autonomic nervous system (ANS) may influence turning behaviour. Nausea and headache are elicited when the ANS cannot maintain constant cerebral blood flow in the presence of hydrostatic changes caused by centrifugal acceleration of blood within the circulatory system.[5]

Therefore, the purpose of this study was to examine potential differences in a_c during turning between individuals with mTBI and healthy control subjects. Additionally, we sought to explore the relationship between the observed a_c and ANS function.

Methods

A mixed sample of 17 adults, including eight individuals with mTBI [4F/4M, mean (SD) 35 (11) years] and nine healthy controls [5F/4M, mean (SD) 33 (8) years], provided informed written consent for this IRB approved study. All mTBI subjects were greater than 3 weeks post-mTBI and still symptomatic.

Each participant walked for two-minutes at their self-selected pace around a custom course containing 45, 90, and 135 degree turns. Inertial measurement units (IMUs) (APDM Opals, Portland, OR) on their feet, lumbar, chest, forehead, and left wrist collected tri-axial acceleration, angular velocity, and magnetometer data at 128 Hz. The inertial sensors were used to compute the average a_c at each step, which is also a valid correlate of lateral margin of stability.[6]

Separately, continuous beat-to-beat heart rate (HR) and blood pressure (BP) were obtained for each participant during a tilt table test (5 minutes supine, 5 minutes head up tilt, 5 minutes return to supine) to assess autonomic function measured through mean blood pressure (MBP) and heart rate (MHR), and variability in blood pressure (BPCV) and heart rate (HRCV).

Linear mixed models with random intercepts compared a_c values between groups after stratifying for limb and controlling for axial turning velocity. Pearson correlations compared each subject's range of a_c to MHR, MBP, HRCV, and BPCV.

Results and Discussion

Individuals with mTBI exhibited significantly lower magnitudes of a_c for a given axial roational velocity during turning regardless of stance limb ($p < 0.001$). When the stance limb was on the inside of the turn (i.e., spin turn), the mTBI group exhibited a_c near zero, while the control group exhibited centripetal accelerations lateral to the stance limb. Similarly, the mTBI group exhibited lower magnitudes of a_c when the stance limb was on the outside (i.e., step turn). Based on previous validations with respect to margin of stability and lateral inclination,[6] these results suggests the mTBI group adopted a conservative strategy with less lateral inclination into the turn. These results also highlight the reluctance of the mTBI group to exhibit high a_c during a spin turn, when the CoM is outside the base of support.

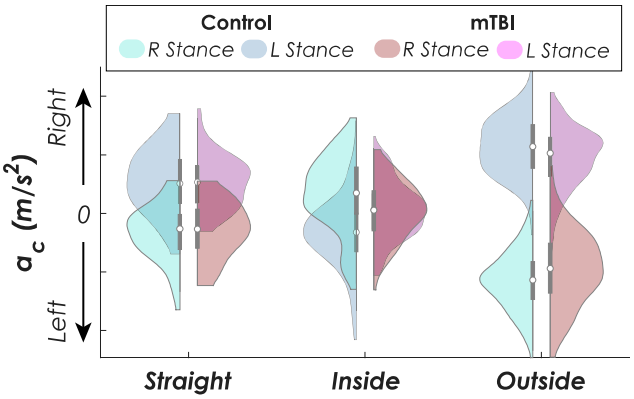

Figure 1: Violin plots centripetal acceleration, a_c, during straight and turning gait. Turning gait results are stratified by stance limb and presented separately for inside limb versus outside limb (e.g., the right limb in stance would be the inside limb during a right turn).

The range of a_c was significantly associated with upright HRCV across all participants ($\rho = 0.56$), and remained associated within each group ($\rho_{Control} = 0.63$; $\rho_{mTBI} = 0.66$). Since HRCV is a measure of the flexibility of the ANS to accommodate different states, these initial results suggest individuals with an inflexible ANS may limit a_c to prevent an onset of symptoms. However, future work should examine this question more directly while considering the role of oculomotor and vestibular function.

Significance

Individuals with persistent symptoms from mTBI exhibit conservative turning behavior beyond slower axial rotation. The physiological mechanisms prompting less inclination and a_c remain unclear, but the role of the ANS should be considered.

References

1. Imai et al. *Exp Brain Res*, 136(1):1-18, 2001.
2. Fino et al. *J Neurotauma*, 35(1):1167-77, 2018.
3. Fino et al. *J Head Trauma Rehabil*, 34(2):E74-E81, 2019.
4. Taylor et al. *Hum Mov Sci*, 24(4):558-73, 2005.
5. Serrador, et al. *Aviat Space Environ Med*, 76(2):91-6, 2005.
6. Fino et al. *IEEE TNSRE*, 28(3):629-36, 2020.

Talocrural Morphology: A Statistical Shape Modeling Multi-Articulation Joint Approach

Amy L. Lenz[1], Nicola Krahenbuhl[2], Andrew C. Peterson[1], Rich J. Lisonbee[1], Beat Hintermann[2], Charles L. Saltzman[1], Alexej Barg[1], Andrew E. Anderson[1]
[1] University of Utah, Salt Lake City, UT, [2] Kantonsspital Liestal, Leistal, Switzerland
Email: amy.lenz@utah.edu

Introduction

Morphometric understanding of the ankle joint has been derived primarily from 2D measurements of conventional radiographs, with little focus given to the fibula and the complete talocrural joint. Volumetric imaging has made it possible to generate 3D reconstructions of the talocrural joint [1]. Weightbearing CT (WBCT) scans provide an added benefit to assess pathology and joint space narrowing that may be overlooked in the absence of load. Statistical shape modeling (SSM) can be used to visualize and analyze morphological differences in 3D and enables the identification of mean bone shapes and shape modes of variation using correspondence particles (mathematically placed points of interest throughout the bone's surface). But, SSM has commonly assessed bone variation independent of joint relationships. The objective of this study was to develop a joint level SSM to evaluate shape differences in combination with joint distance and congruency of the talocrural joint based on WBCT scans.

Methods

Twenty-seven controls (age: 50.0 ± 7.3 years; height: 169.4 ± 6.4 cm; BMI: 25.3 ± 3.8 kg/m2; 7 males) underwent weight-bearing CT scans (0.4 x 0.4 x 0.4 mm voxels) with IRB approval. The tibia, fibula and talus were segmented to generate 3D surfaces (Amira, v6.0.1). Procrustes analysis removed scaling (i.e. size) as a mode of variation in the shape model. Mean shapes for the tibia, fibula, and talus were generated using ShapeWorks (Univ of Utah). Correspondence particles from the SSM analysis were evaluated using principal component analysis (PCA). Significant PCA modes of variation were identified using parallel analysis. Using the 2nd principle of curvature and a joint coverage calculation in PostView (v2.1.0), the articulating surfaces of the tibiotalar (TT), tibiofibular (TiF) and talofibular (TaF) joints were isolated. The surface mesh within the articular regions were used to calculate joint distance. SSM mean shapes were aligned in joint relationships with articular region correspondence particle locations isolated across all participants. Joint distance and congruency were calculated at each common correspondence particle using MATLAB (R2017b, MathWorks, Natick, MA, USA). The congruency index, which begins at 0 mm^{-1} to define perfectly congruent surfaces, was calculated [2]. Joint distance and congruency index values were averaged at common correspondence particle locations.

Results and Discussion

Seven PCA modes were determined to be significant for the tibia, fibula, and talus, which contained 78.2%, 74.8%, and 65.5% of the overall shape variation for the three bones respectively. SSM models showed bone shape variations including: the width of the talar trochlea and curvature in the inferior articulating surface, tibial plafond rate of curvature variations and fibular malleolar fossa angulation. In our healthy population during a weight-bearing position, the TT, TiF and TaF mean joint distances and congruency index are shown (Figure 1). Regardless of joint distance variation, mean congruency indices were consistent across the articular regions, with the TT joint being the most congruent (Table 1). Despite morphological differences, congruency remained very consistent in this healthy population. These findings highlight the necessity to consider anatomical variations in the shape of the tibia, fibula and talus as independent bones along with a joint analysis of the interaction of these bones when evaluating a patient's talocrural joint health, alignment and function. Ideally, the combination of high-resolutions volumetric imaging and 3D morphometrics could be used to improve the treatment of patients suffering from OA and other diseases in the talocrural joint. These tools should provide improved metrics for clinicians to link 3D joint morphology findings to individual bone variability seen on weightbearing CT scans.

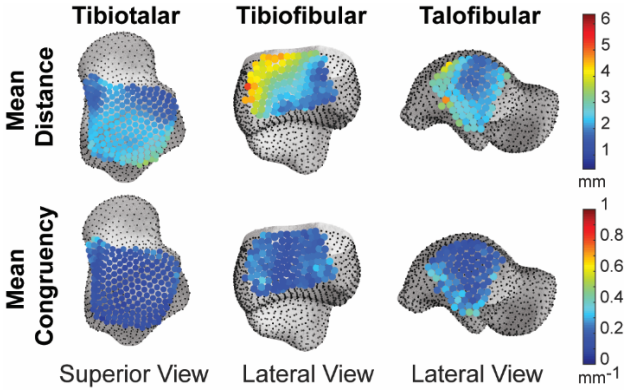

Figure 1: Mean joint distance and congruency for the talocrural joint.

Significance

Results herein established normative measurements of bone shape variation, joint distance and congruency in the talocrural joint. Computational methods presented a new SSM joint analysis approach to apply in other joints and pathological cases.

Acknowledgments

Funding was provided by the National Institutes of Health (R21AR069773, R01EB016701), Stryker/ORS Women's Research Fellowship, and the L.S. Peery Discovery Program.

References

[1] Hayes, A et al., 2006, Iowa Orthop J., 1-4. [2] Ateshian, G. et al., 1992, J of Biomech, 591-607.

Table 1. Joint distance (mm) and congruency (mm^{-1}) averages ± standard deviation with minimums and maximums across the cohort.

	Joint Distance (mm)			Congruence Index (mm-1)		
Joint	Ave ± SD	Min	Max	Ave ± SD	Min	Max
Tibiotalar	2.15 ± 0.41	1.08	3.46	0.15 ± 0.05	0.06	0.38
Tibiofibular	3.36 ± 0.83	2.00	5.38	0.21 ± 0.04	0.12	0.35
Talofibular	2.43 ± 0.56	1.69	4.77	0.22 ± 0.07	0.09	0.44

Bone strain distribution, not magnitude, is affected by execution of a forearm loading task

Megan E. Mancuso[1], Michael S. DiStefano[1], Karen L. Troy[1]
[1]Department of Biomedical Engineering, Worcester Polytechnic Institute, Worcester, MA
Email: ktroy@wpi.edu

Introduction

Exercise can increase bone density 1-3%,[1] but the mechanism of load-driven bone adaptation in humans is not completely understood. Previously, we established an upper extremity loading model of human bone adaptation.[2] Women are instructed to lean onto their palm with their arm vertical, applying cyclic, axial loading to the forearm. Distal radius strain is estimated using validated finite elment (FE) models based on clinical and high resolution computed tomography (HRpQCT).[3] FE models apply forces at the scaphoid and lunate carpals, representing an axial compressive load distributed through the wrist. However, people likely do not perform this task identically. Here, our purpose was to measure the degree to which actual loading direction and distribution vary using 3D motion capture, and to quantify the influence on bone strain by varying FE model boundary conditions. We hypothesized that changes in loading, within the range of measured variability, will affect bone strain distribution but not the overall magnitude of achieved strain.

Methods

Six women ages 21-40 completed this institutionally approved study. Markers were placed on the non-dominant hand and wrist, and 100 cycles of forearm loading were performed on a multiaxis force plate within a six-camera motion capture system. The average angle between the force vector and the forearm, as well as the center of pressure relative to the wrist joint center at the instance of peak force, were determined for each participant.

Based on the motion capture data, four boundary conditions were applied to thirteen multiscale FE models generated from CT scans acquired in a prior study: (1) standard distributed axial loading, axial loading through the (2) scaphoid only or (3) lunate only, and (4) a tilted, distributed load. Energy equivalent strain, ε_{eeq}, was calculated for each element within the cortical and trabecular compartments in the HRpQCT scan region (Figure 1).

Bone strain magnitude was measured as the median ε_{eeq}, and load distribution as the percent of bone volume with ε_{eeq} greater than 75% of the 95th percentile value, where a smaller high strain volume indicates more concentrated, less uniform loading. Strain metrics were compared across the conditions using repeated measures ANOVA with Boneferroni posthoc t-tests (α=0.05).

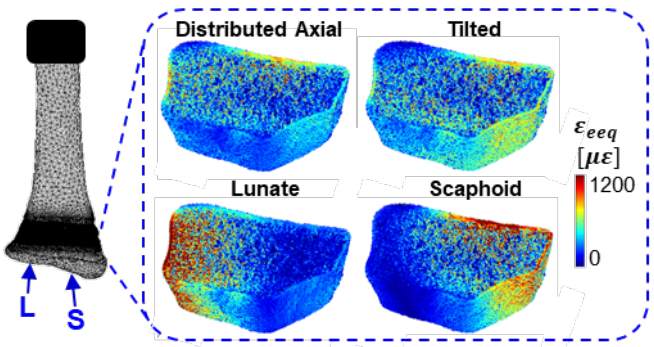

Figure 1: Representative FE model used to simulate forearm loading through the lunate (L) and/or scaphoid (S) to estimate energy equivalent strain, $\boldsymbol{\varepsilon_{eeq}}$, in the HRpQCT distal radius scan region.

Results and Discussion

Across participants, the average force vector was tilted 7.2° in the dorsal-radial direction, relative to the forearm. Within each participant, center of pressure fell either medially or laterally relative to the wrist joint center, at an average distance of 1.4±0.4 cm (mean±sd). Shifting the distributed axial load to the scaphoid only led to a significant, 15.1±3.6% decrease in trabecular strain magnitude (Figure 2). Shifting to the scaphoid or lunate only significantly decreased the volume of bone under high strain in the cortical and trabecular compartments, suggesting less uniform loading compared to the distributed axial condition. Tilting the force vector did not have a significant effect on strain magnitude, but significantly increased the volume of bone at high strains, suggesting more uniform loading compared to to the distributed axial condition. Overall, our hypothesis was generally supported, as strain distribution was more sensitive than strain magnitude to changes in loading condition.

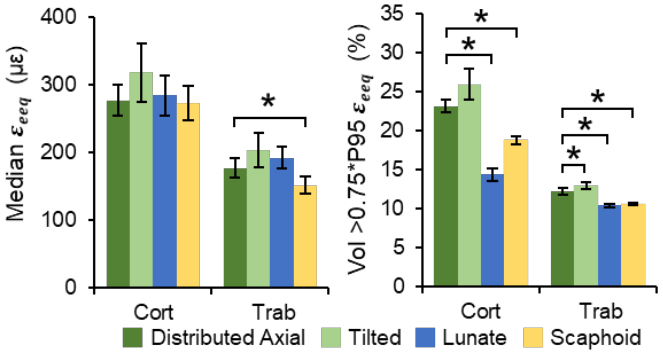

Figure 2: Strain magnitude, measured as median ε_{eeq}, and strain distribution, measured as the percent of bone volume with strain >75% of the 95th percentile, presented as mean±se (n=13). *Indicates a significant post-hoc comparison versus distributed axial loading.

Significance

Our combined experimental-computational approach allows the mechanism of load-driven bone adaptation to be systematically studied in humans. Quantifying the sensitivity of FE-estimated strain to task execution (i.e. loading direction and distribution) helps to identify biomechanical factors that need to be controlled to standardize bone loading across participants, or can be modified to target loading to particular regions within a bone. Ultimately, measuring internal bone loads generated by external forces may enable comparison and optimization of osteogenic exercise programs for specific clinical populations or individuals.

Ackowledgments

This work was funded by the NIH (R01AR063691) and the NSF (DGE 1106756). Computational resources supported by the Academic & Research Computing Group at WPI.

References

[1] Babatunde (2012) *Osteoporos Int.* [2] Troy (2013) *J Orthop Res.* [3] Johnson (2017) *Med Eng Phys.*

Effect of Pelvis Bone Geometry Personalization on Hip Kinematics and Dynamics

Geng Li[1], Mohammad S. Shourijeh[1], Benjamin J. Fregly[1]
[1] Department of Mechanical Engineering, Rice University, Houston, TX
Email: *Geng.Li@rice.edu *include just the corresponding author email

Introduction

Personalized models can represent musculoskeletal systems more accurately in simulating gait movement than generic models that are created by averaging data for a population [1]. We seek model personalization of pelvis as a potential way to address the research need of designing more effective treatments for pelvic sarcoma patients. Kinematics, muscle length and moment arms, and reaction loads at hip joints are all important factors to be considered for such treatment design. Therefore, this study investigates the effect of personalizing a pelvis model on estimation of hip joint kinematics, muscle geometry and joint reaction loads during walking. reaction loads.

Methods

We collected motion capture (Vicon Corp., Oxford, UK), and ground reaction (Bertec Corp., Columbus, OH) data of a subject (male, mass 70 kg, age 48 years) walking on an instrumented split-belt treadmill at a self-selected speed of 1.2 m/s for more than 50 gait cycles. reaction loads.

We used a generic OpenSim musculoskeletal model [2, 3] as the base model to create two separate models to represent the subject. The first model was created using the OpenSim scaling tool. We named this model as the scaled generic model. The second model was created from segmentation of CT images of the subject in the pelvic region using software ITK-SNAP [4]. We then replaced the pelvis in the scaled generic model with the segmented pelvis. We updated the muscle attachment locations on the pelvis by registering published data of attachment locations onto the subject-specific pelvic model using affine transformation function of software NMSBuilder [1]. The second model ws named as the personalized model. reaction loads.

For both models created, we used OpenSim inverse kinematics tool to estimate the joint kinematics from experimental marker data and subsequently used the OpenSim muscle analysis tool to obtain muscle-tendon length (l_{MT}) and moment arms about hip. Muscle forces were estimated using OpenSim static optimization tool. The muscle force estimation was furnished to the OpenSim Joint Reaction analysis to compute the joint reaction loads. reaction loads.

Results and Discussion

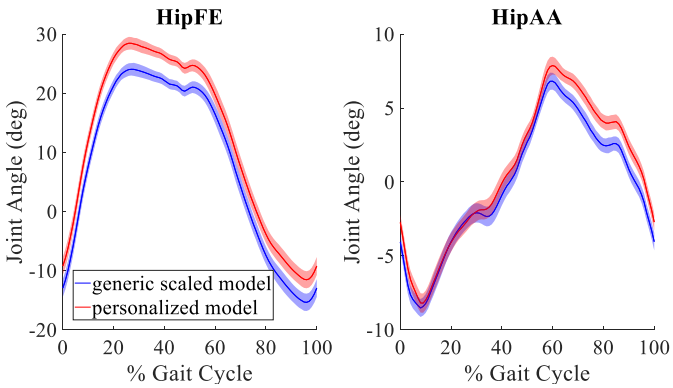

Figure 1: (the A) Hip joint angles, (B) Length and moment arms of hip muscles, (C) Joint reaction loads estimated by two models

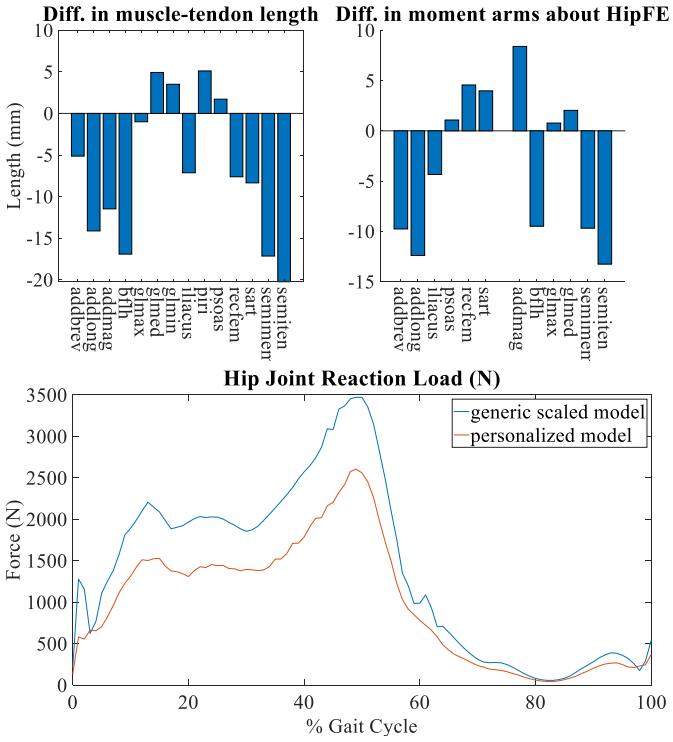

Generic scaled model on average underestimated hip flexion, and adduction by 4º and 1º respectively in comparison to personalized model (Fig. 1A). The personalized model predicted lower l_{MT} for adductor and hamstring muscles. Moment arms about HipFE revealed large inconsistency between the two models. Adductor magnus gained 8 mm while other adductor and hamstring muscles lost approximately 10 mm in moment arms (Fig. 1B). As most hip muscles in the personalized model operated in a lower region of force-length curve than those in the generic scaled model, our simulation predicted less muscle forces generated and hence less hip joint load for the personalized model (Fig. 1C). reaction loads.

Significance

This study highlighted the discrepancy in joint kinematics, muscle lengths and moment arms, and joint reaction loads between a scaled generic model and a personalized one. Imaged-based model should be recommnened for the purpose of achieving more accurate simulation of movement. EMG-driven modelling calibration would be used in future work to model muscle activation and predict joint loads more accurately. reaction loads.

Acknowledgment

This work is supported by Cancer Prevention Research Institute of Texas (CPRIT) funding RR170026. reaction loads.

Reference

[1] Valente et al., *Comput Meth Prog Bio*, 2017. [2] Delp et al., *IEEE Trans Biomed Eng*, 2007. [3] Rajagopal et al., *IEEE Trans Biomed Eng*, 2016. [4] Yushkevich et al., *Neuroiamge*, 2006 .

Estimating Unmeasured Muscle Excitations: NNMF vs Gaussian Process-Based Synergy Models

Reed D. Gurchiek[1], Anna T. Ursiny[1], and Ryan S. McGinnis[1]
[1]M-Sense Research Group, University of Vermont, Burlington, VT, USA
Email: reed.gurchiek@uvm.edu

Introduction

Advances in wearable sensor technology and estimation algorithms point toward a new approach to healthcare that leverages remote observation of a patient's symptoms to detect disease and direct treatment decisions. Critical to this vision are technologies that minimize patient burden. This limits the use of many surface electromyography (sEMG)-based techniques for estimating clinically-relevant joint mechanics, as they require information from a large number of muscles which would require unwieldy sensor arrays. However, it has recently been suggested that sEMG data from a subset of muscles may be able to reconstruct the muscle excitations of a complete set [1,2]. To this end, we recently proposed a novel Gaussian process (GP)-based model of the synergistic relationship between muscles which enables estimation of unmeasured muscle excitations from a measured subset (manuscript under review). In this study, we compare the ability of our new technique to estimate unmeasured muscle excitations to the reconstruction accuracy of a non-negative matrix factorization (NNMF)-based approach [2].

Methods

The sEMG (1000 Hz) of 10 muscles (TA: tibialis anterior, PL: peroneus longus, LG: lateral gastrocnemius, MG: medial gastrocnemius, SOL: soleus, VM: vastus medialis, RF: rectus femoris, VL: vastus lateralis, BF: biceps femoris, ST: semitendinosus) from the right leg were recorded from a single healthy female during a one-minute walking trial (speed: 1.2 ± 0.03 m/s, stride time: 1.11 ± 0.02 s). Data were processed so as to replicate as closely as possible the results presented in [2]. Therefore, all sEMG data were high pass filtered at 30 Hz, rectified, low pass filtered at 6 Hz, and normalized by the maximum value across the walking trial and several muscle specific maximum voluntary contraction (MVC) trials.

Data from 12 seconds (about 10 strides) from the first half of the one-minute walking trial were used to train muscle-specific functions that take as input one-second of sEMG data from each muscle in an 'included' subset (the predictor muscles) and output the excitation value of the corresponding muscle (belonging to the 'excluded' subset) for the time associated with the middle of the one-second input window. This constitutes the GP-based technique and model 'training' amounts to hyperparameter optimization (minimization of the negative log marginal likelihood) and a large matrix inversion [3].

The GP and NNMF methods were compared in their ability to reconstruct the muscle excitations of several 'excluded' subsets for a 12 second interval of the latter half of the one-minute walking trial (different data than were used to inform the GP model). The NNMF-based method is described in [2] where synergy vectors and corresponding excitations were determined using an iterative procedure utilizing both the multiplicative update and alternating least squres NNMF algorithms. Synergy weights for the muscles in the 'excluded' subset were determined using linear least squares regression [2].

Six different 'included' muscle subsets were investigated: (1) TA, LG, RF, BF; (2) TA, MG, ST, VL; (3) TA, MG, ST, VL, SOL; (4) TA, MG, ST, VL, SOL, LG; (5) TA, MG, ST, VL, SOL, LG, RF; and (6) TA, MG, ST, VL, SOL, LG, RF, PL. Subsets (2)-(6) were chosen based on the most informative muscles according to the analysis presented in [2]. Subset (1) was also included as it was used in our original development of the GP model. The 'excluded' subset for each were all muscles not in the 'included' subset. Estimation performance was evaluated using mean absolute error (MAE) and variance accounted for (VAF).

Results and Discussion

The GP-based estimation outperformed the NNMF-based reconstruction across all muscle subsets according to both MAE and VAF (Table 1). The reported error statistics of the NNMF reconstruction essentially represent the training error in that the synergy model was informed partly by the data it sought to reconstruct. For this reason, as noted in [2], the NNMF-based reconstruction does not solve the problem of estimating unmeasured excitations using a measured subset; it only provides insight into the feasibility of doing so. This is in contrast to the proposed approach wherein the GP model was informed by a completely different dataset than it was tested on. To the authors' knowledge, our GP-based model is the only existing method which maps a subset of sEMG data to unmeasured excitations.

Table 1: Comparison of GP estimation and NNMF reconstruction accuracy. Values are mean $\pm$ standard deviation across all muscles. MAE units are % MVC.

	GP		NNMF	
Subset	MAE	VAF	MAE	VAF
1	$2.0 \pm 1.3\%$	$93 \pm 2\%$	$3.5 \pm 3.2\%$	$79 \pm 11\%$
2	$2.3 \pm 1.1\%$	$88 \pm 4\%$	$3.4 \pm 1.8\%$	$78 \pm 7\%$
3	$2.2 \pm 1.2\%$	$88 \pm 4\%$	$2.7 \pm 1.9\%$	$86 \pm 10\%$
4	$1.8 \pm 1.2\%$	$89 \pm 5\%$	$2.4 \pm 2.2\%$	$87 \pm 12\%$
5	$2.1 \pm 1.1\%$	$88 \pm 5\%$	$2.9 \pm 2.3\%$	$84 \pm 14\%$
6	$1.9 \pm 1.5\%$	$86 \pm 7\%$	$3.2 \pm 3.2\%$	$80 \pm 16\%$

Significance

Our results support the use of the GP-based technique for estimation of unmeasured muscle excitations across a range of predictor muscles. This approach may enable the use of sEMG informed estimates of clinically relevant biomechanics in remote environments for continuous monitoring and comprehensive patient characterization.

Acknowledgments

This research was supported by the Vermont Space Grant Consortium under NASA Cooperative Agreement NNX15AP86H.

References

[1] Gurchiek et al. (2019). *Sensors,* **19**(23).
[2] Bianco et al. (2018). *J Biomech Eng*, **140**(1)
[3] Rasmussen and Williams (2006). The MIT Press.

Isometric force-length and isotonic force-velocity properties and Hill-type models contain little information needed to predict *in vivo* muscle forces.

Kiisa Nishikawa[1], Nicole Rice[1], Siwoo Jeong[1], and Monica Daley[2]
[1]Department of Biological Sciences, Northern Arizona University, Flagstaff, AZ USA; [2]Department of Ecology and Evolutionary Biology, University of California at Irvine, USA
Email: kiisa.nishikawa@nau.edu

Background

Isometric force-length and isotonic force-velocity relationships [1-2] are useful as standard measures of muscle contractile properties. However, these measures and models based upon them fail to predict muscle force under dynamic conditions [3-5]. This failure is due in part to absence of history-dependence. The goal of this study was to explore *in vivo* muscle force during perturbed running in guinea fowl [6] using a novel *ex vivo* avatar approach, and to test the ability of a 12-parameter Hill-type muscle model from OpenSim [7] to predict forces observed during dynamic length changes. The results provide insights into muscle mechanical behavior and demonstrate the limitations of Hill-type models and the F-L and F-V relationships on which they are based.

In vivo function of the lateral gastrocnemius (LG) during treadmill obstacle running in guinea fowl

Previous studies [6] demonstrated increased step-to-step variability in muscle force and dissociation of activation and force during *in vivo* treadmill running over obstacles in the LG muscles of guinea fowl (**Fig. 1**).

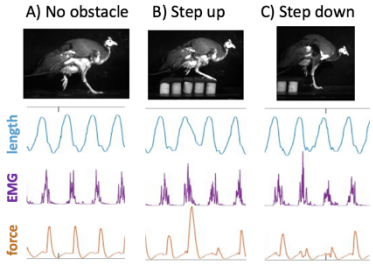

Fig. 1: Variability in length, EMG and force of guinea fowl LG during treadmill obstacle running. **A**) Normal step with no barrier. **B**) Step up onto obstacle. Force is higher despite average EMG. **C**) Step down onto treadmill. Force is lower despite higher EMG.

In addition, there is a long and variable delay (90-150 ms) between EMG onset and force onset (**Fig. 2**).

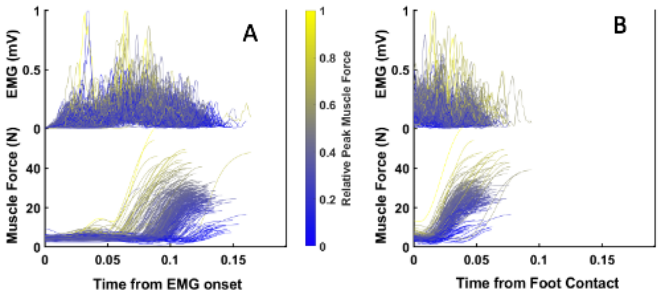

Fig. 2: Decoupling between force and activation. Delay between EMG onset and force onset (**A**) is longer and more variable (90-150 ms) than (**B**) delay between foot contact and force onset (10-40 ms).

The correlation between peak EMG and peak force ($R^2 = 0.34$) is small compared to the correlation between muscle length at foot contact and peak force ($R^2 = 0.63$) (data not shown).

Muscle 'avatar' approach

To further demonstrate decoupling between force and activation, we used *ex vivo* extensor digitorum longus muscles (EDL) of mice as an 'avatar' for the *in vivo* guinea fowl LG. Instead of sinusoidal inputs typically used in work loop experiments, we used strain trajectories matching those from *in vivo* LG recordings as inputs for the *ex vivo* work loop experiments. Work loops recorded from the *ex vivo* EDL using *in vivo* strain trajectories matched the shape of the in vivo workloops of the guinea fowl LG. Both *ex vivo* EDL and *in vivo* LG work loops deviate substantially in shape from traditional *ex vivo* work loop experiments. Hill model simulations (**Fig. 3**) demonstrate that neither the isometric force-length relationship nor the isotonic force-velocity relationship can predict the step-to-step variability in muscle force observed during dynamic *in vivo* movements.

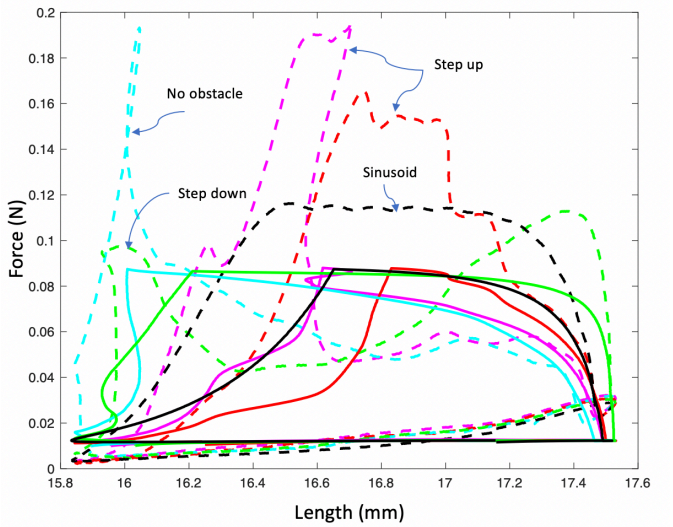

Fig. 3: Hill model predictions (solid lines) of force in EDL avatar steps (dashed lines). R^2 for model ranges from 0.41 for level step (no obstacle, cyan, Fig, 1A) to 0.9 for sinusoidal trajectory (black). The model fails to capture effects of strain trajectories on muscle force.

Conclusions: The isometric force-length relationship and isotonic force-velocity relationship and Hill models based upon them fail to capture the dynamic step-to-step variability of muscle force during dynamic movements.

Acknowledgments - Supported by the National Science Foundation [IOS-1456868], the W. M. Keck Foundation, and the Technology Research Initiative Fund of NAU.

References

[1] Josephson RK (1999) J Exp.Biol 202:3369–75.
[2] Holt NC Azizi E. (2014) Biol Lett 10:20140651.
[3] Perreault EJ et al (2003) J. Biomech 36 :211–218.
[4] Lee SSM et al (2013 J Biomech 46:2288–2295.
[5] Dick TJM et al (2017) J.Exp. Biol 220:1643–53.
[6] Daley M Biewener A (2011) Phil Trans R Soc B 366:1580-91.
[7] Seth A et al (2011) Procedia IUTAM 2:212–32.

Whole Muscle Passive Mechanics Do Not Simply Scale by Architectural Properties

Benjamin I Binder-Markey[1,2] and Richard L Lieber[1,2]
[1]Shirley Ryan AbilityLab & [2]Department of Physical Medicine and Rehabilitation, Northwestern University, Chicago, IL, USA
Email: bbindermar@sralab.org

Introduction

Whole muscle active length-tension properties accurately scale from the sarcomere to the whole muscle level [1], but interestingly, in mammalian muscle, passive mechanical properties do not [1,2]. This is largely because the detailed relationship between the passive mechanical properties of fibers, fascicles, and whole muscles are rarely studied. Only in frog muscle, has uniform passive scaling been demonstrated from the fiber to the whole muscle [3]. We believe that this is because intramuscular connective tissue in frog is very poorly developed compared to mammals [2]. Recent work in rabbit muscle demonstrates that fiber, fiber bundle and fascicle mechanics do not simply scale to whole muscle mechanics [4]. Thus, the purpose of this study was to measure whole muscle passive mechanical properties and use modeling to identify sources that could contribute to non-linear scaling from fascicle to whole muscle.

Methods

Passive mechanical properties from three muscles of varying architecture and function were measured in 12-week C57Bl6 mice: rectus femoris (RF; n=6), semimembranosus (SM; n=6), and tibialis anterior (TA; n=5). Muscles were dissected from origin to insertion, placed in a physiological bath, attached to a 1N force transducer, and lengthened in ~0.5mm increments. Force was recorded after 3-minutes of stress-relaxation. Samples were weighed and physiological cross sectional area (PCSA) was calculated using published architectural properties [5].

Muscle passive force was normalized to PCSA and muscle deformation was converted to fascicle strain using the fiber length-to-muscle length ratio [5], thus creating a passive stress-strain relationship normalized by architectural parameters for each muscle. Each raw and normalized data set was fit to an exponential [3] and all curves were averaged to create a single exponential describing that muscle's passive force-deformation (Fig. 1A) or stress-strain relationship (Fig. 1B). All curve fits were excellent, exceeding r^2 values of 0.96

To investigate potential sources that might lead to the fascicle differences observed in Fig. 1B, we developed three Hill-type models of progressively increasing complexity. **Model 1**: A simple lumped parameter model normalized fascicle property across muscles that has the form $\left(\frac{a}{b}(e^{b\varepsilon}-1)\right)$; **Model 2**: Model 1 plus a muscle-specific parallel element elastic element (c_m) across the whole muscle representing parallel elastic connective tissue differences among muscles; **Model 3**: Model 2 plus a muscle-dependent inter-fascicular shear factor (τ_m) that resists fascicle rotation. For each model, each parameter (a, b, c_m, and τ_m) was optimized in MATLAB by minimizing the sum of the squared error (SSE) between the muscles' modeled force-deformation data and the experimentally collected data (Fig. 1A).

Results and Discussion

Data from all three muscles were well-fit by the exponential stress-strain curve (RF r^2=0.994±0.008 SD, SM r^2=0.991±0.004 SD, RF r^2=0.990±0.012 SD). The RF was the stiffest muscle, followed by the TA (especially at high deformation) and then the SM (Fig. 1A). Accounting for fiber length differences, stress-strain curves became more similar, but not identical (Fig. 1B).

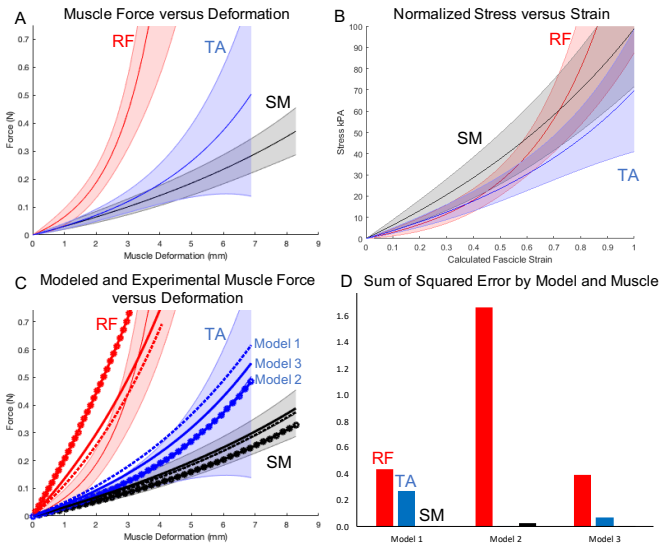

Figure 1: A) Force *vs.* muscle deformation for RF (red), SM (black), and TA (blue). B) Stress-strain relationship for each muscle normalized by architecture. Data shown as average±SD. C) Force *vs.* muscle deformation of the experimental and modeled RF (red), SM (black), and TA (blue) for Model 1 (dashed), Model 2 (circles), and Model 3 (solid). D) SSE for each model and muscle with lower numbers better fit.

The degree to which more complex models explained experimental data were related to the complexity of each muscle (Figs. 1C and 1D). The SM, which is a very simple parallel-fibered muscle with fascicles running from origin to insertion was best fit by the simplest model, Model 1 (SSE=$1.35\text{x}10^{-4}$). The TA, in which fascicles run from a broad proximal tibial origin to a single internal insertion tendon was fit best by the slightly more complex Model 2 (SSE=$3.28\text{x}10^{-3}$). Finally, the RF whose fascicles originate on a central internal tendon and radiate distally to a broad aponeurosis surrounding the muscle was fit best by the most complex model, Model 3. (SSE=0.397).

Significance

These results demonstrate that, to accurately model muscle passive mechanical properties, the model must reflect the complexity of the muscle. To a first approximation, architectural normalization helps (Fig. 1A), but in order to provide high resolution properties, additional terms are needed. The precise structures that represent these mathematical terms are not currently clear and must be the subject of ongoing investigations.

Acknowledgments

The Brinson Fellowship and the Shirley Ryan AbilityLab.

Literature References

[1] Winters *et al.* 2011; [2] Meyer & Lieber 2018; [3] Magid and Law 1985; [4] Ward *et al.* 2020; [5] Burkholder *et al.*1994.

Imaging and Simulation of Inter-Muscular Triceps Surae Contributions to Forward Propulsion During Walking

William H. Clark, Richard E. Pimentel, Jason R. Franz
Joint Department of Biomedical Engineering, University of North Carolina at Chapel Hill &
North Carolina State University, Chapel Hill NC, USA
Email : wihclark@unc.edu

Introduction

Forward propulsion during the push-off phase of walking is largely governed by differential neuromechanical contributions from the biarticular medial (MG) and lateral gastrocnemius (LG) and the uniarticular soleus (SOL) muscles spanning the ankle [1]. However, the relative contribution of these individual muscles to forward propulsion is equivocal, with important implications for the design and control of wearable assistive devices and for targeted therapeutics. We can indirectly estimate these contributions *in vivo* using empirical measurements (e.g., EMG, ultrasound imaging); yet, neither activation nor fascicle kinematics provide direct measurements of muscle force or work. Fortunately, advances in musculoskeletal (MSK) modelling provide the opportunity to estimate the neuromechanical contributions of individual muscles *in silico*. Although empirically driven, biological complexity of MSK modelling is often exchanged for computational performance, potentially yielding reduced specificity to fully characterize inter-muscular differences. Here, we evaluated the agreement between empirical and model-predicted triceps surae contributions to forward propulsion during walking for the first time in the same group of subjects. We tested the null hypothesis that conclusions based on muscle-specific responses derived from empirical measurements would be consistent with those derived from MSK simulations over a range of tasks that alter the demand for forward propulsion.

Methods

We report data for 10 young adults (age: 23.5±3.0 yrs, 5 females). Subjects walked on a treadmill for 1 min each at a range of speeds (0.8, 1.2, 1.6 m/s) and again at 1.2 m/s with: (i) a 5% body weight horizontal aiding force (↓ push-off demand) and (ii) a 5% body weight horizontal impeding force (↑ push-off demand). A 60 mm ultrasound transducer recorded cine B-mode images through the right MG and SOL at 76 fps. Simultaneously, motion capture tracked lower body joint kinematics and wireless electrodes recorded LG and SOL activation. An affine extension to an optic flow algorithm quantified time series of MG and SOL fascicle lengths from 2 strides per condition [2]. Subject-specific, scaled MSK models, driven by measured joint kinematics and ground reaction forces, estimated MG, LG and SOL excitation, force, and positive mechanical work using static optimization [3]. For each muscle, we analysed all data during the "push-off" phase of walking, defined as the second half of stance, ending at the offset of force generation (threshold = 10% peak force) [1]. Two rmANOVAs tested for significant main effects of condition (speed or aiding/impeding) on relative MG and SOL muscle shortening and average MG, LG and SOL kinetics (activation, force, positive mechanical work) during push-off (α=0.05).

Results and Discussion

Our experimental manipulations successfully altered mechanical demand for forward propulsion; peak anterior ground reaction force systematically changed in response to changes in speed and applied horizontal forces ($p \leq 0.05$). *In vivo*, measured MG and SOL relative fascicle shortening were both significantly affected by increasing speed ($p \leq 0.05$). Conversely, in response to horizontal forces, MG fascicle shortening was more sensitive to altered demands for forward propulsion than that of the SOL (**Fig. 1A**). Compared to walking normally, increased propulsive demand elicited greater relative fascicle shortening in MG ($p \leq 0.05$) but not SOL. *In silico*, model-predicted neuromechanical contributions generally supported our empirically-drawn conclusions. Here, speed similarly affected MG, LG, and SOL average muscle force ($p \leq 0.05$) and similarly unaffected positive mechanical work ($p \geq 0.05$) during push-off. Conversely, in response to horizontal forces, only MG and LG force (**Fig. 1C**) and positive mechanical work (**Fig. 1D**) increased significantly to meet the increased demands for forward propulsion ($p \leq 0.05$). Moreover, only measured (LG, **Fig. 1B**) and model-predicted (MG, LG) gastrocnemius muscle activation was affected by both horizontal impeding and aiding forces ($p \leq 0.05$).

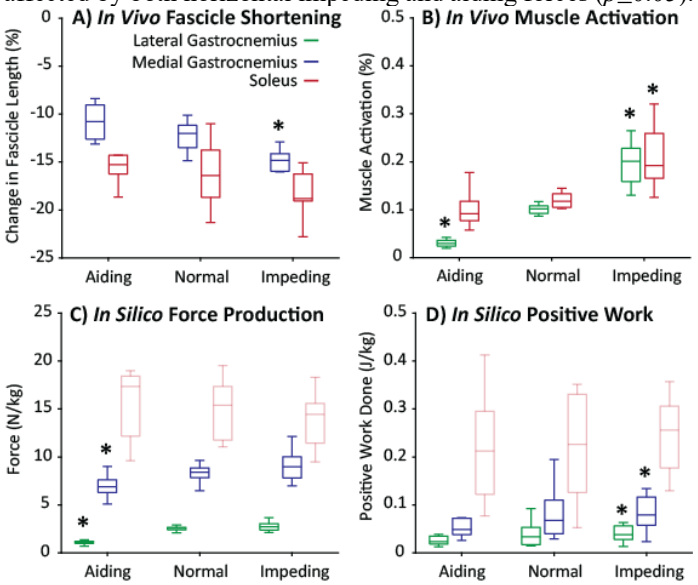

Fig. 1: Muscle specific responses to 5% body weight horizontal aiding and impeding forces at 1.2 m/s. Significant main effect represented by opacity, pairwise comparison vs. normal represented by *, $p \leq 0.05$.

Significance

Based on consistent evidence from empirical measurements and musculoskeletal simulations within the same subjects, we conclude that the biarticular gastrocnemius muscles play a more significant role than the uniarticular soleus in governing forward propulsion during the push-off phase of walking.

Acknowledgments

Supported by NIH (R01AG051748, F31AG060675) and the NCSRR (NIH P2C HD065690).

References

1. Gottschall et al. J Appl Physiol (1985), 2003.**94**(5):p.1766-72.
2. Farris et al. Comput Methods Prog Biom, 2016.**128**:p.111-8.
3. Delp et al. IEEE Trans Biomed Eng, 2007. **54**(11): p.1940-50.

Parametric Analysis and Validation of 3D American Football Faceguard Structural Stiffness Models

William D. Ferriell.[1], Gregory S. Batt[2], John D. DesJardins[1]
[1]Department of Bioengineering, [1]Department of Food, Nutrition and Packaging Science, Clemson University, Clemson, SC
Email: jdesjar@clemson.edu

Introduction

Despite continued efforts to improve American football headgear technology, minimal structural changes have been made to faceguard design in the past 20 years [1]. Although each new helmet system has its own compatible faceguard series, the primary design components have changed little between helmet systems. Additionally, little is known about specific parameters that influence faceguard performance—largely due to variation inherent in laboratory impact testing.

Recently, Bina *et al.* developed a novel testing procedure to analyze the structural stiffness of faceguards independent of the helmet system [2]. The goal of this study was two-fold: to validate a reverse engineering method for developing a library of faceguard models; and to validate the finite element simulation of three common American football faceguards subject to a quasi-static structural stiffness test [2]. This study will result in a validated model to be used in parametric design analysis and computational optimization. Collectively, these studies should inform football athletes, coaches, parents, equipment managers, and headgear manufacturers of design variables relevant to faceguard performance.

Methods

Three common Riddell® (Des Plaines, IL) Speedflex™ faceguard styles (SF-2BD, SF-2BD-SW, and SF-3BD) were modelled using a novel reverse engineering approach. The faceguards were modelled as a stainless steel (E=193 GPa, ν=0.31). Each faceguard mesh converged using a 1.5 mm sizing control with quadratic tetrahedral elements.

Each compression location/direction from the literature was simulated on each faceguard [2]. To simulate the experimental setup, the analysis occurred over a singular step lasting 3 seconds. A displacement of 5 mm was prescribed in the posterior (z) direction. The experimental test allows for coronal plane (x, y) translation at clip attachement locations; thus, the corresponding geometry and boundary conditions were applied. To prevent rigid body motion, two boundary conditions were applied: each faceguard was constrained to not deviate from the midsagittal plane; and program controlled weak springs were applied to the entire model. Constraint reaction forces were measured to ensure each did not artificially stiffen the faceguard model. Validation was determined by comparing experimental averages to computational results using a Pearson Correlation test with a 95% confidence interval (α=0.05).

Results and Discussion

The computational results correlated to the experimental results with statistical significance (p-value=0.001). The Pearson's Correlation coefficient of 0.912 demonstrated a high degree of correlation. Furthermore, a linear regression model $Comp = 0.98 * Exp - 0.07\ N/mm$ further illustrates the near 1:1 comparison between computational and experimental results. Additionally, the weak springs and midline constraint reaction forces were less than 0.01 N and assumed to not have artificially stiffened the faceguard models.

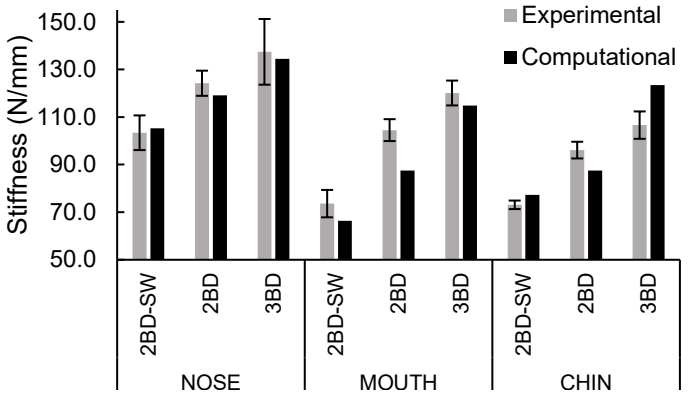

Figure 1: Results comparing experimental data to computational results. Note: The experimental data (n=10) have a standard deviation represented by error bars, whereas computational results (n=1) do not.

The Nose location was the most reliable with an average percent difference from experimental results of 2.7%, compared to 10.8% and 9.9% at the Mouth and Chin locations, respectively, as shown in Fig. 1.

Significance

Many studies utilizing computational models of protective headgear lack reported validation of headgear components. This study has validated the structural stiffness of three common faceguards to be used in future computational analyses. Furthermore, advancements in additive manufacturing technologies have opened the door to increasingly complex faceguard design capabilities; however, little is known about specific parameters that influence faceguard performance. With the models validated in this study, parameterized faceguard models should be used to iterate between design variables and assess the contribution of each variable on faceguard structural stiffness. The goal of this study was to influence faceguard design by informing headgear manufacturers of the specific variables that determine faceguard stiffness to improve headgear technologies and athlete safety.

Acknowledgments

Thank you to industry partners Green Gridiron for continually supporting research in the Clemson Headgear Impact Performance (CHIP) Lab. Thank you to the Clemson Makerspace for allowing the use of their equipment for our research goals.

References

[1] K. L. Johnson *et al.*, "Constrained Topolgoical Optimization of a Football Helmet Facemask based on Brain Response," Materials and Design, vol. 111, pp. 108-118, 2016.

[2] A. Bina *et al.*, "Development of a Non-destructive Method to Measure Football Facemask Stiffness," Journal of Sports Engineering and Technology, 2018

Simulation of Speech Muscle Biomechanics to Explain Differences in Corrective Surgery Outcomes

Vi-Thanh Tran[1], Kazlin Mason[2], Jamie Perry[3], and Silvia Blemker[1]
[1] Department of Biomedical Engineering, University of Virginia; [2] Curry School of Education, University of Virginia
[3] Department of Communication Sciences & Disorders, Eastern Carolina University
Email: ttt9bu@virginia.edu

Introduction

Cleft palate is a common birth defect that affects approximately 1 in 700 live births. Cleft palate disturbs velopharyngeal (VP) closure, in which speech muscles, predominantly the levator veli palatini (LVP) muscle, contracts to elevate the soft palate so that it comes in contact with the posterior pharyngeal wall (PPW). All children with cleft palate undergo primary reconstruction of the soft palate before the age of 12 months; however, many of these children need additional surgeries because the LVP muscle still does not function properly, resulting in hypernasal speech. Sphincter pharyngoplasty is one of the most common surgical treatments for hypernasal speech. The goal of the surgery is to facilitate improved VP closure by augmenting the PPW with a muscle graft (3). Despite its wide use, the outcomes of these surgeries are variable and there remains several questions as to why some surgeries fail. It is still unknown whether differences in muscle biomechanical function influence surgical outcomes. The goal of the study is to (i) develop two subject-specific finite element models of the sphincter pharyngoplasty, the LVP muscle, and associated VP mechanism based on medical image data collected from one successful and one failed surgical outcome case, and (ii) use the model simulations to examine the extent to which differences in muscle biomechanics may explain the differences in surgical outcomes between the two cases.

Methods

Two age-matched male subjects were selected based on the clinically evaluated post-surgical speech outcome to represent a successful and a failed case. A three-dimensional model, including the soft palate, LVP muscle, sphincter graft, and PPW, was developed based on MRI data post sphincter pharyngoplasty surgery. Mechanical properties of muscle and soft tissue were incorporated into the finite element model based on previous studies (2,4). The LVP muscle was activated to simulate VP closure. The reconstructed LVP muscle in the failed case was identified with an asymmetric overlap alignment from original reconstruction. An additional hypothetical simulation with a symmetrical LVP overlap was also modeled to analyze the impact of muscle overlap location on VP closure. The model output of LVP muscle's minimum activation (the amount of muscle effort required for closure) and the amount of muscle fiber shortening (an estimate of how much of the force-length curve the muscle traverses) at initial contact was used to examine the effectiveness of VP closure. Uncertainty quantification for the model was estimated by varying the Young's modulus of the soft palate with the estimated range of values based on material testing and model input data (1,5).

Results and Discussion

The minimum required activation and amount of muscle shortening to achieve VP closure was lower in the successful case (6.39±1.7 % and 13.5±0.6%) compared to the original failed case with asymmetrical (23.6±12.9% and 22.9±1.8%) and the hypothetical symmetrical LVP overlap (13.1±5.9% and 18.60±0.7%). Furthermore, the required activation for VP closure in the successful case falls within range of previously reported data from a healthy population (5), which agrees with the clinical evaluation that the corrective surgery succeeded in reconstructing healthy VP closure mechanics. In contrast, there is no contact between the soft palate and sphincter graft in simulations of the failed surgery case for both asymmetrical and symmetrical LVP overlap. However, lower activation and amount of fiber shortening for closure in symmetrical LVP overlap indicates that alignment of muscle overlap might have influenced the advantageousness of the LVP muscle to achieve closure. Future research includes using the models to simulate hypothesized sphincter location to examine the impact of sphincter location in VP closure and ultimately in surgical outcome. Additional subject will also be added to confirm the model's applicability.

Significance

The computational model illustrated how muscle biomechanical function significantly differs between successful and failed post-pharyngoplasty surgeries. Future work will involve developing a streamlined method for creating subject-specific modeling framework to predict the optimal surgical approach on a subject-by-subject basis. Finally, more generally, we hope that this work illustrates how biomechanical analysis of muscles has a wide variety of applications beyond more traditionally studied limb muscles.

Acknowledgments

We acknowledge NIH grant R21DC014570 and the Hartwell Foundation for providing funding for this project.

References

(1) Birch et al. *Cleft Palate Craniofac J*, 2009**(2)** Blemker SS, et al. *J Biomech*, 2005.**(3)** Chiu et al, *Oper Tech Otolayngol Head Neck Surg*, 2009 **(4)** Inouye, et al. *J Craniofac Surg*, 2015.**(5)** Pelland C. *Doctoral dissertation*, 2019.

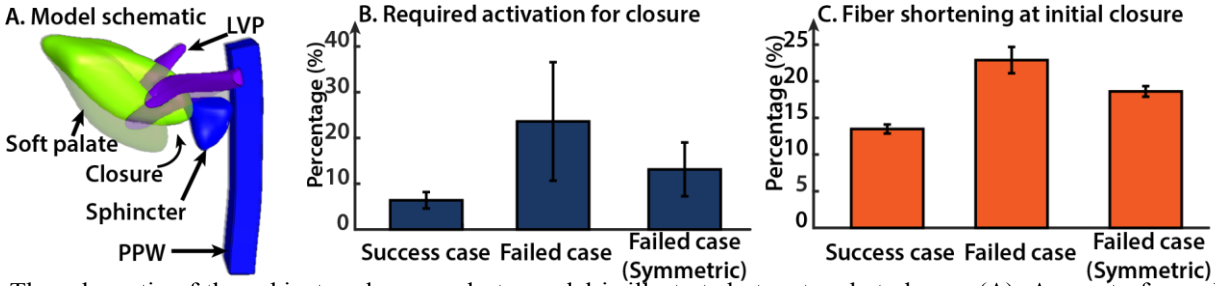

Figure 1:The schematic of the sphincter pharyngoplasty model is illustrated at rest and at closure (A). Amount of muscle activation required for closure (B) and LVP muscle fiber shortening (C) is lower in the success case simulation .

A Split-Belt Rimless Wheel Can Passively Walk Steadily on a Split-Belt Treadmill

Julia K. Butterfield[1], Surabhi N. Simha[2], J. Maxwell Donelan[2], and Steven H. Collins[1]
[1]Department of Mechanical Engineering, Stanford University, Stanford, California, USA
[2]Department of Biomedical Physiology and Kinesiology, Simon Fraser University, Burnaby, British Columbia, Canada
Email: *jbutterf@stanford.edu

Introduction

Split-belt treadmills are commonly used for motor learning experiments [1] and stroke rehabilitation [2], but we are still learning how people adapt to the two belts moving at different speeds. For example, Sánchez et al. [3] recently showed that after sufficient exposure, participants will self-select a gait with wider leg angles and longer steps onto the fast belt, rather than a gait with equal angles and step lengths as had previously been observed. People can extract positive work from a split-belt treadmill [3], and this may be driving split-belt adaptation. But how do choices like leg angles and treadmill belt velocities affect how energy is harvested from the treadmill?

We used a split-belt rimless wheel model to further explore the mechanics and energetics of split-belt walking. A rimless wheel loses energy during its collisions with the ground so must successfully harness energy from the treadmill to walk steadily, an impossible task if the belts are tied. We explored how treadmill conditions and leg angles affect the passive wheel's ability to extract enough energy from the treadmill to walk steadily.

Methods

We simulated a split-belt rimless wheel (Fig. 1A), two identical sets of spokes that are rigidly attached and offset by a small angle. The spokes are arranged such that only one spoke is ever in contact with the ground, and the wheel alternates contacting the fast and slow treadmill belts. The angular offset results in different inter-leg angles at collision onto the fast and slow belts, just as humans adjust their step lengths during split-belt walking to have different leg angles during the fast and slow steps.

We tested combinations of inter-leg angles and belt speed differences to find initial velocities corresponding to steady walking. If a solution existed, we calculated the wheel's average velocity in the slow belt reference frame, which is the slow belt velocity required for the wheel to station-keep.

We designed and built a physical prototype (Fig. 1B) to demonstrate that the simulation model was physically realistic. For the sets of spokes, we used plates with evenly spaced toes. We added stabilizer wheels to the front to prevent leaning and a rudder to prevent turning.

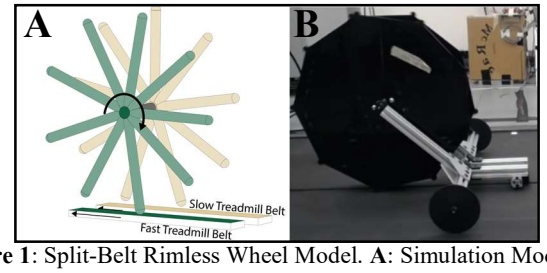

Figure 1: Split-Belt Rimless Wheel Model. **A**: Simulation Model **B**. Physical Prototype

Results and Discussion

We found a wide range of inter-leg angles and belt speed differences for which the split-belt rimless wheel could harness enough energy from the treadmill to walk. During steady walking, energy lost in step-to-step transitions is recovered as energy gained during rotation on the fast belt.

Two asymmetries in the system, the difference in belt speeds and the difference in inter-leg angles at collision, enable energy harvesting during the fast belt rotation. Because of the belt speed difference, the foot has non-zero velocity when viewed from the slow belt reference frame. The contact force on the foot then results in work being done on the wheel. Having a wider inter-leg angle at fast collision ensures the net work done is positive by enabling the wheel to primarily rotate upward during this rotation, with the contact force aligned with the foot's velocity.

A counterintuitive result is that increasing the fast belt's backward velocity increases the wheel's forward velocity in the slow belt reference frame (Fig. 2). With complicated underlying mechanics, the wheel travels further backward while on the fast belt but rotates faster through both steps, thereby achieving a greater forward gain per unit time.

The physical model, with radius 0.25 meters and fast and slow belt collision angles of 31 and 9 degrees, walked steadily for belt speed differences from 0.2 to 1.1 m/s and achieved a maximum speed of 0.2 m/s in the slow belt reference frame.

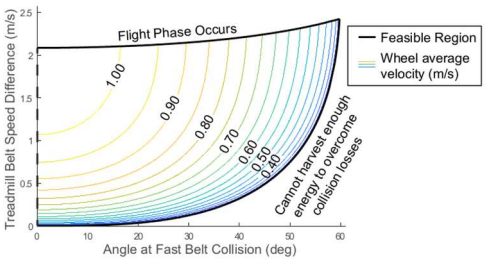

Figure 2. With an infinitesimally small angular offset between the plates such that collision onto the slow belt occurs at nearly vertical, the model can walk steadily with a large range of inter-leg angles and treadmill speed differences. Results look similar as the offset increases as long as the fast collision angle remains significantly wider.

Significance

These results confirm observations from human experiments that extracting positive work from a split-belt treadmill is possible when a wider step is taken onto the fast belt [3]. The belt speed difference, rather than the speeds themselves, is the crucial element contributing to the model's energy-free solutions. Improvements in human split-belt energy economy may be possible, and these results help us understand the limitations of humans' ability to harness energy from a split-belt treadmill.

Acknowledgments

This research is supported by the NSF Graduate Research Fellowship program and NSF Award No. 1734449.

References

1. Malone, et al. (2010) *J. of Neurophys.* **103**:1954-1962.
2. Reisman, et al. (2013) *Neurorehabilitation and Neural Repair* **27**:460-468.
3. Sánchez, et al. (2019) *J. of Physiology* **597**:4053-4068.

An Instrumented Glove to Induce Agency-based Performance of Secure Grasp

Mingxiao Liu[1,2], Samuel Wilder[1,2], Sean Sanford[1,2], and Raviraj Nataraj[1,2]
[1]Department of Biomedical Engineering, Stevens Institute of Technology,
[2]Movement Control Rehabilitation (MOCORE) Laboratory, Email: mliu26@stevens.edu

Introduction

Improving grasp performance for activities of daily living is a key rehabilitation objective following neuromuscular traumas such as stroke, traumatic brain injury or spinal cord injury. Typical rehabilitation protocols involve intensive or repetitive physical training to reformulate motor connections. Few approaches consider cognitive factors to better motivate and engage patients for more efficient rehabilitation. *Sense of agency* is the perception of true authorship over neuromuscular actions and related consequences. Possessing greater *agency* to improve functional movement appears intuitive, but agency has not been a focus of traditional rehabilitation. We have developed an instrumented glove with onboard force and flex sensors, modules for user feedback, and access to computer processing. The glove reliably predicts secure grasp on an object and alerts the user with various sensory cues to induce greater agency via intentional binding [Moore and Obhi 2012]. In this study, we investigated whether sensory feedback from the glove facilitates improved hand grasp performance.

Methods

Fifteen participants performed a functional grasp task while receiving visual (LED) and audio (beeper) feedback onboard our *Cognition Glove* during a training session (**Figure 1**). The functional task involved the participant grasping a small cubic object from one location and placing onto a designated target. A 2-layer feedforward neural network was used to assess secure grasp from flex and force sensor signals based on offline training data. Sensory feedback was provided to the user during training across three distinct conditions: (1) No feedback, (2) 'Instant' feedback provided immediately upon achievement of secure grasp, and, (3) 'Decay' feedback provided at progressively shorter time-intervals (from 1 to 0 sec) after secure grasp. The third condition was intended to facilitate greater agency through intentional binding, whereby one builds a stronger perception to couple action (secure grasp) with a sensory consequence. The primary performance metrics were minimizing the completion time and pathlength in moving the object. Performance was assessed before and after training with the glove. A motion capture system (*Optitrack*, *Prime17W* cameras) was used to track motion of the grasped object.

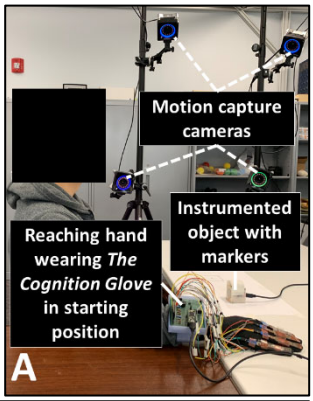

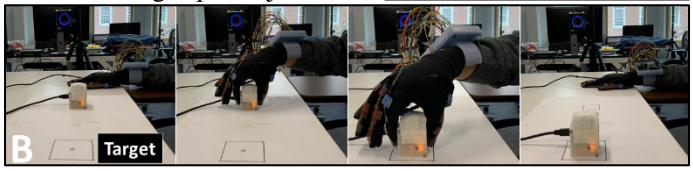

Figure 1: **A)** Experimental setup of the functional grasp task **B)** Participant performing the task while wearing *The Cognition Glove*

Results and Discussion

The change in mean performance (difference between after training and before training) of the functional task after glove training is shown in **Figure 2**. ANOVA indicated significant ($p<0.05$) differences in performance across all three feedback conditions. The greatest reductions in time and pathlength were observed with 'Decay' feedback. These results indicate that providing onboard sensory feedback from an instrumented glove to inform secure grasp can improve grasp performance. Furthermore, providing that feedback with intention to induce greater agency may best accelerate the improvement in grasp performance.

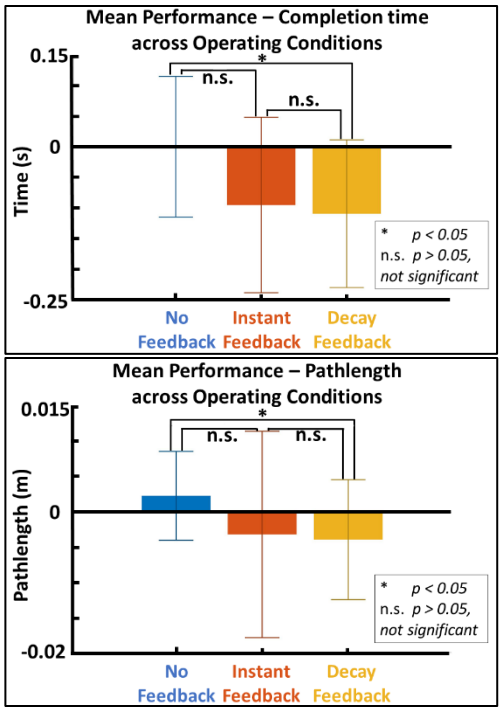

Figure 2: Results of training effects between different sensory feedback on grasp performance – completion time (TOP) and pathlength (BOTTOM).

Significance

This study presents a novel approach to predict and inform about secure grasp during a functional task. It will serve as a potential agency-based rehabilitation platform to accelerate gains in functional grasp performance after neuromuscular traumas. This may foster greater user integration and clinical retention of rehabilitation methods. Future work will incorporate *The Cognition Glove* with virtual reality platforms to create mixed-reality rehabilitation intended to further augment sensory feedback capabilities.

Acknowledgments

The authors would like to acknowledge the Schaefer School of Engineering and Science at Stevens Institute of Technology, Hoboken, NJ, 07030 and research grant (Grant no. PC 53-19) from the New Jersey Health Foundation.

Pose-matching MRI-CT co-registration via dynamic X-ray for creating subject-specific neck musculoskeletal models

Yu Zhou[1], Curran Reddy[2], Bocheng Wan[1], Wei Yin[1], and Xudong Zhang[1,2,3]*
[1]Department of Industrial & Systems Engineering, [2]Department of Biomedical Engineering,
[3]Department of Mechanical Engineering, Texas A&M University, College Station, TX, USA
Email: *xudongzhang@tamu.edu

Introduction

Magnetic resonance imaging (MRI) and computed tomography (CT) are commonly used as the "gold standard" to image soft and hard tissues, respectively. The reconstructed 3D muscular models from MRI and skeletal models from CT must be combined in order to create subject-specific musculoskeletal models. However, this MRI-CT co-registration is challenging for complex structures with a substantial number of degrees of freedom such as the cervical spine, because the poses used in two modalities would not have completely coincided. In addition, due to its complex 3D geometry, vertebral bone models segmented from MRI can be subject to volume loss as compared to CT-based bone models, which further compounds the uncertainty and difficulty in the co-registration process [1]. In this study, we present a novel approach that takes advantage of dynamic X-ray data to identify the best matching pose and employs principal component analysis (PCA) to align the bones, thus optimizing the creation of subject-specific neck musculoskeletal models.

Methods

We used CT and MRI scans of the neck region, and dynamic X-ray captures of a neck flexion-extension motion collected from five healthy subjects (all male, aged 21–32 years). The CT and MRI scans were first segmented in Mimics 20.0 platform to create 3D vertebrae models. A previously validated CT-model-based tracking algorithm was applied to the dynamic X-ray images to obtain the 3D neck vertebral kinematics [2]. The 3D point clouds of the reconstructed vertebrae models were then exported into MATLAB and the vertebral foramen at the middle height of each vertebra was fitted by a circle with a least-squares method. The centroids of the fitted circles at all levels (C1-C7) were then fitted by a cubic polynomial to characterize the cervical spine curvature. The cervical spine curvature in the MRI was compared with the dynamic X-ray series to identify the best matching pose that minimized the curvature discrepancy measured as Fréchet distance [3]. Next, a PCA algorithm was applied to the point clouds of vertebrae models in both modalities to define the orientation of the superior vertebra with respect to the inferior vertebra. Lastly, the differences in 3D vertebral orientation between vertebra models in MRI and the matching dynamic X-ray frame were quantified as the target registration errors (Figure 1). The CT-based skeletal model with the best matching pose identified in the dynamic X-ray series was thus integrated with the MRI-based muscular model to create anatomically accurate subject-specific neck musculoskeletal models.

Results and Discussion

The overall mean curvature discrepancy between the two modalities was 0.34 mm of Fréchet distance. The average 3D orientation difference was greater in flexion-extension (1.28º) than in axial rotation (0.34º) and lateral-bending (0.05º) (Table 1). The greater flexion-extension differences found in the upper (C1-C2 and C2-C3) and the lower (C6-C7) cervical spine may be attributed to a more flattened cervical spine curvature found in the MRI model. The greater axial rotation differences in the upper cervical spine (C1-C2, and C2-C3) could be explained by the fact that the C1-C2 joint is the atlanto-axial joint where C1 and C2 may pivot around one another. In addition, some of the differences in both axial rotation and lateral-bending could be due to that flexion-extension motions captured by dynamic X-ray were performed not strictly in the mid-sagittal plane.

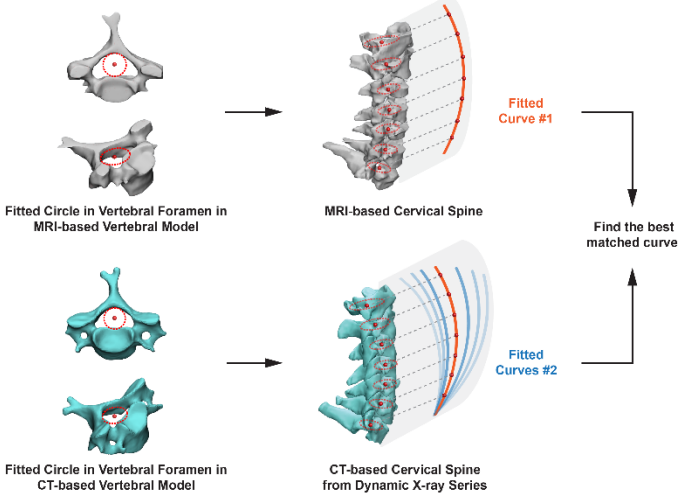

Figure 1: Pose-matching MRI-CT registration process via dynamic X-ray.

Table 1. 3D orientation differences (mean and standard error) between the MRI and best matching CT models. FE, AR, and LB denote flexion-extension, axial rotation, and lateral-bending, respectively.

	C1-C2	C2-C3	C3-C4	C4-C5	C5-C6	C6-C7
FE	3.71	5.00	1.03	0.47	1.49	-4.04
(º)	(1.97)	(0.95)	(2.56)	(1.81)	(2.02)	(2.80)
AR	1.06	1.92	0.26	-0.04	-0.87	-0.29
(º)	(1.93)	(2.17)	(2.99)	(2.93)	(0.56)	(1.50)
LB	-0.89	0.28	-1.06	0.95	-0.69	1.68
(º)	(1.25)	(0.62)	(0.54)	(1.02)	(0.73)	(1.11)

Significance

The proposed approach to MRI-CT co-registration by utilizing dynamic X-ray data provides a novel solution to the problem of pose variation across the modalities, a major obstacle hindering the development of complex yet accurate subject-specific musculoskeletal models.

References

1. Schmid, J., et al. (2011). *Med Image Anal*, *15*(1), 155-168.
2. Bey, M., et al. (2006). *J of Bio Eng,* 128: 604-609.
3. Eiter, T., et al. (1994). *Techical report*.

Trunk Control during Walking with Below-Knee Amputation: Effects of Prosthetic Ankle-Foot Actuation

Adam J. Yoder[1,2], Jonathan R. Gladish[3,4], Ashley D. Knight[1,3,5], Shawn Farrokhi[1,2], John M. Chomack[6], Michael N. Poppo[6], Jason T. Maikos[6], Brad D. Hendershot[1,3,5]
[1]DoD-VA Extremity Trauma and Amputation Center of Excellence, [2]Naval Medical Center San Diego, [3]Walter Reed National Military Medical Center, [4]Henry M. Jackson Foundation, [5]Uniformed Services University of Health Sciences, [6]VA New York Harbor Healthcare System
Email: adam.j.yoder.civ@mail.mil

Introduction

Persons with below-knee amputation (BKA) often exhibit abnormal trunk motion during walking, with associations to low back pain and challenged balance [1–3]. We recently identified that altered mechanics of the affected-limb knee and prosthetic ankle have potential to adversely influence trunk rotational dynamics when walking with BKA [4]. As such, modifying prosthetic ankle-foot mechanics (e.g., torque, range of motion) may be an indirect means to influence trunk control. This preliminary analysis explores this concept by comparing ankle contributions to rotational trunk control while wearing three distinct, prosthetic ankle-foot devices.

Methods

Within scope of clinical trial NCT03505983, one subject with traumatic, unilateral BKA (F, 40yr, 172cm, 63kg, 25 years post-amputation) wore three different ankle-foot prostheses: (1) energy storage and return (ESR, Ossur Proflex XC), (2) ESR with articulation (ART, Ossur Proflex Pivot), and (3) powered with articulation (POW, Ottobock Empower). Each foot was aligned on a replicate socket and granted 1-week daily use acclimation (order: ART/POW/ESR), after which whole-body kinematics and kinetics were measured while walking overground at 1.3m/s. Data processing and simulation mirrored [4]. Briefly, a single patient model was generated by scaling OpenSim Gait2392 to session-averaged anthropometrics. Estimated joint angles and net moments were input to a torque-driven induced acceleration (IA) analysis. Trunk segment rotational accelerations induced by individual joint moments were then compared between prostheses and versus non-BKA normative (NORM) ranges [4].

Results and Discussion

Ankle push-off moment increased 27% with POW versus EST/ART, to within NORM (Fig 1; A*). This coincided with less ipsilateral, frontal ankle-trunk IA in POW (Fig 1, B*), and differed versus NORM for all feet (lesser frontal, greater sagittal). Ankle-trunk IA differences were most apparent during loading response, where earlier peaks above NORM acted to flex the trunk forward and ipsilaterally (Fig 1; C*, D*). This feature, greatest with POW and least with ART, may indicate high sensitivity of trunk stabilization to prosthetic actuation during weight acceptance. If not balanced by opposing IA contributions from other joints, this has potential to destabilize the trunk [2]. This specific subject exhibited stable, net trunk control; attaining measured trunk kinematics within NORM range for all feet.

During push-off, peak lumbar moments were greater than NORM with ESR/ART (+42% frontal, Fig 1, E*; +53% sagittal Fig 1, F*), as were concurrent lumbar-trunk IAs (Fig 1; G*, H*). POW appeared to mitigate this, decreasing moments and IAs to within NORM, which may indicate an improved whole-body strategy; i.e. less necessity with POW to actively modulate dynamic postural control via trunk inertia.

Significance

These observations, albeit patient-specific, highlight that contributions to trunk rotational control can be influenced by varied prosthetic ankle-foot actuation (passive/active power, variable articulation). Further analyses will help determine if similar trends are characteristic of BKA, or individualized. More broadly, this line of inquiry aims to inform new, clinically translatable strategies to modify problematic trunk motion, relevant to mitigating low back pain and dynamic balance [1–3].

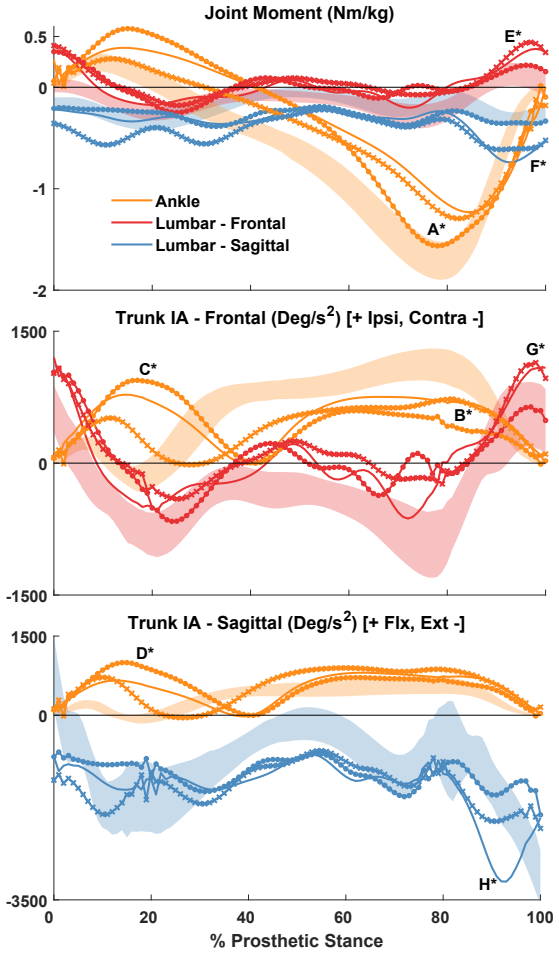

Figure 1: Joint moments (top) and trunk rotational induced accelerations (IA) in the frontal (middle) & sagittal (bottom) planes, for the ESR (solid line), ART (**x**), POW (●) ankle-foot prostheses. Shaded areas are mean±1std non-BKA normative ranges (NORM) [4].

Acknowledgments

Funding support CDMRP W81XWH-17-2-0014.

References

1. Devan, et al. *JRRD*. 2015;52:1–20.
2. Nott CR, et al. *J Biomech*. 2010;43:2648–52.
3. Klemetti, et al. *J Biomech*. 2014;47:2263–8.
4. Yoder, et al. *Scientific Reports*. 2019;9:1–8.

Whole-body angular momentum during walking in persons with unilateral transfemoral amputation

Genki Hisano[1,2], Ryo Amma[3], Matthew J. Major[4,5], Motomu Nakashima[1], Hiroaki Hobara[2]
[1]Tokyo Institute of Technology, Japan, [2]National Institute of Advanced Industrial Science and Technology, Japan, [3]Tokyo University of Science, Japan,[4]Northwestern University Prosthetics-Orthotics Center, Northwestern University Feinberg School of Medicine, USA, [5]Jesse Brown VA Medical Center, USA, Email: hisano.g.aa@m.titech.ac.jp

Introduction

Currently, more than half of lower limb prosthesis users fall at least once each year [1]. Since the greater range of whole-body angular momentum (L) about body center of mass during walking would lead to the greater postural control demands, persons with unilateral transfemoral amputation (TFA) must adequately manipulate the whole-body L to maintain the dynamic stability. Generally, the whole-body L during walking is kept close to zero through segment-to-segment cancellations by segmental angular momenta. Considering that persons with TFA needs to regulate the whole-body L using the passive prosthetic components, the range of L would be different from those of able-bodied (AB) subjects. Therefore, the aim of this study was to investigate the range of whole-body L during walking with unilateral TFA.

Methods

Fourteen persons with unilateral TFA and 14 AB subjects performed level walking at a self-selected speed on a straight 10-m walkway. Three-dimensional kinematic data were collected using reflective markers and an optical motion capture system. Ground reaction forces (GRFs) were recorded using nine force plates. Three-dimensional whole-body L was calculated using a 15-segment model and normalized by body mass, height and walking speed. The range of whole-body L was calculated as the peak-to-peak value through first and second half of the affected (right for AB) limb's gait cycle. Independent t-tests (α=.05) were performed to assess the main effects of group (TFA, AB) on the range of whole-body L.

Results and Discussion

In the sagittal plane, the range of whole-body L was greater in TFA compared to AB subjects through the first half of the affected limb gait cycle (p = 0.035; Figure 1), but differences were non-significant in the second half (p = 0.140). These results indicate that persons with unilateral TFA may require greater demands for maintaining balance during prosthetic limb stance compared to AB subjects. During this phase, persons with TFA must also work to prevent prosthetic knee buckling (i.e., rapid knee flexion), which requires additional postural control demands. If a disturbance due to knee buckling or an external perturbation were to elevate sagittal-plane L on the affected limb, persons with TFA may be more likely to fall if L is not successfully managed.

In the transverse plane, the range of whole-body L in TFA subjects was greater than AB subjects during both the first (p = 0.010) and second (p < 0.001) half of the gait cycle. In the transverse plane, leg angular momentum is counterbalanced to some extent by that of the arms. As a previous study demonstrated no difference in transverse-plane whole-body L between persons with unilateral transtibial amputation and AB subjects [2], our results suggest that persons with unilateral TFA are less able to neutralize angular momentum during gait.

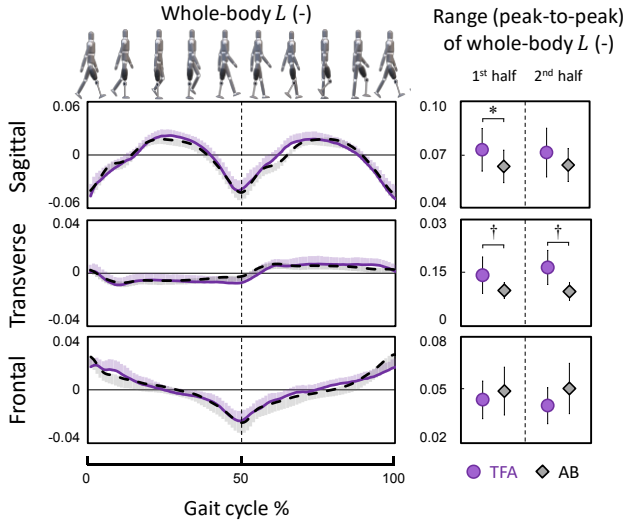

***Figure* 1**: Whole-body L during the gait cycle of the affected (right for AB) limb of walking in TFA (bold purple line) and AB (dashed black line) subjects. The shaded area indicates the standard deviation. Range (peak-to-peak) of whole-body L was compared through first and second half of gait cycle between TFA and AB subjects. An asterisk and a dagger (*,†) denotes significance at p < 0.05 and p < 0.01, respectively.

No significant group effects were observed in the range of frontal plane whole-body L during the first (p = 0.305) or second half (p = 0.056) of the gait cycle, which is different than findings for persons with unilateral transtibial amputation [2]. Since whole-body L in this plane is primarily balanced through lower limbs and abdomen/pelvis motion and affected by GRF peaks [2, 3], these results suggest that persons with unilateral TFA are able to regulate frontal-plane L through these mechanisms similar to AB.

To conclude, persons with unilateral TFA displayed greater ranges of whole-body L than AB subjects to suggest that they would require greater postural control demands to avoid falling in the presence of a perturbation that elevates sagittal and transverse-plane L. For a better understanding of the strategy of segmental cancellation, future research should investigate the segmental contributions to whole-body L.

Significance

Since the successful management of whole-body L during walking is essential for recovering from perturbations and preventing falls, understanding how persons with unilateral TFA control whole-body L can be useful for designing appropriate devices or interventions to enhance gait safety.

References

[1] Kim et al., (2019). *PM R.* 11(4), 344-353.

[2] Silverman et al., (2011). *J. Biomech.* 44, 379-385.

[3] Herr et al., (2008). *J. Exp. Biol.* 211, 467-481.

Effects of exoskeleton assistance in individuals with unilateral transtibial amputation

Alexandra S. Voloshina[1*], Katherine L. Poggensee[1], Julia K. Butterfield[1], and Steven H. Collins[1]
[1]Department of Mechanical Engineering, Stanford University, Stanford, USA
Email: *svoloshina@stanford.edu

Introduction

Unilateral transtibial amputation often leads to increased energy expenditure during gait, as well as larger ground reaction forces on the contralateral side [1, 2]. In turn, this causes a higher prevalence of joint pain and early onset osteoarthritis [3], negatively affecting mobility and reducing overall quality of life of individuals with impairment. Powered prostheses may help mitigate some of these issues (e.g. [4]), but the benefits of increased prosthesis work are uncertain [5]. Past research has largely focused on improving active prosthesis control and design, but it is possible that the potential benefits of active devices are limited by changes in motor learning post impairment [6]. The aim of this study was to identify if people with lower-limb amputation adapt to powered ankle exoskeleton assistance applied to their sound leg similarly to people without impairment. Specifically, we assessed changes in energy expenditure in users with impairment when walking with individualized assistance and no assistance at the ankle.

Methods

We evaluated the benefits of optimized exoskeleton assistance on energy expenditure in individuals with lower-limb amputation by implementing a controller optimization protocol previously shown to lead to an average 24% reduction in metabolic cost in users without impairment [7]. We used an experimental, tethered exoskeleton emulator device to provide plantarflexion assistance during stance (Figure 1A, [8]). To optimize exoskeleton assistance to each user, we used an optimization strategy that continually adapts to changes in user dynamics [7]. This human-in-the-loop approach relies on a standard optimization algorithm to reduce user energy expenditure by systematically updating four parameters that define the exoskeleton torque profile.

Five individuals with unilateral transtibial amputation participated in the study. Each participant walked with their prescribed prosthesis and with the exoskeleton worn on their sound limb. All participants completed 20 optimization bouts, performed over multiple days of testing, with each bout consisting of 8 optimizer-selected control profiles experienced by the user for 2 minutes each. This protocol was longer than in previous studies with unimpaired individuals in order to ensure the optimizer converged and users were fully acclimated to assistance. We performed separate validation trials after 4-6 optimization bouts and at the end of the experiment, measuring user energy expenditure during walking without the device, wearing the unpowered device (zero torque), and with the device providing optimized assistance (optimized).

Results and Discussion

The first evaluation of user energy expenditure in response to assistance occurred after 4-6 optimization bouts, or 1-1.5hrs of walking, and as dictated by participant fitness level. At this time, participants showed only a 3.6% reduction in net metabolic cost when walking with optimized assistance compared to walking with zero torque (2.63 and 2.73 W/kg, respectively; Figure 1B). In contrast, unimpaired users reduced energy cost on average by

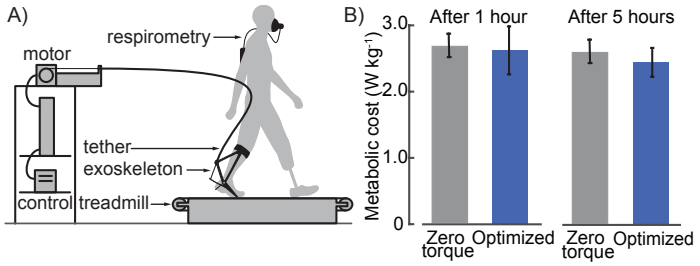

Figure 1: A) Exoskeleton emulator system, with the device worn on the sound limb of people with unilateral amputation. B) Average metabolic cost of users after approximately 1 and 5 hours of optimization, during the zero torque and optimized assistance conditions.

24% compared to walking with zero torque, and after only one hour of optimization [7]. Four participants with amputation completed 20 optimization bouts, or more than 5 hours of walking, and showed just a 5.8% reduction between conditions (2.43 and 2.58 W/kg, respectively). Energetic cost during the zero torque and normal walking conditions differed by less than 2%.

Such differences in metabolic cost reduction in response to assistance between impaired and unimpaired individuals imply that lower-limb amputation presents different motor learning challenges in the context of robotic assistance. In addition, these results further suggest that the benefits of powered prostheses could be significantly limited by learning and biomechanical restrictions caused by impairment. New user training and device assistance approaches are likely needed to significantly assist people with amputation.

Significance

The results of this study show that individuals with amputation adapt to assistive robotics differently from people without impairment. This is likely also true for individuals with other locomotor deficits, such as those following stroke, and advocates for further research into balance, coordination, and learning limitations caused by impairment. In addition, gait rehabilitation protocols post injury likely need to be reevaluated with the introduction of robotic assistive devices.

Acknowledgments

This research is supported by the National Science Foundation [Award No. 1818749].

References

[1] Gailey, R. *et al.* (1994). *Prosth. and Orth. Int.* **18**, 84-91.
[2] Powers, C.M. *et al.* (1994). *Arch. of Phys. Med. and Rehab*. **75**, 825–829.
[3] Hurwitz, D.E. *et al.* (2001). *Cells Tiss. Organs* **169**, 201–209.
[4] Grabowski, A.M. and D'Andrea, S. (2013). *J. of Neuro. and Rehab*. **10**, 49.
[5] Quesada R.E. *et al.* (2016). *J. of Biomech.* **49(14)**, 3452-3459.
[6] Sawers A. *et al.* (2012). *J. of Rehab. Res. and Dev.* **49(10)**. 1431-1442.
[7] Zhang, J. *et al.* (2017). *Science*. **356**, 1280-1284.
[8] Witte, K.A. *et al.* (2015). *IEEE ICRA*. 1223–1228.

Walking to Exhaustion: The Effects of Powered Prosthetic Ankles

Jay Kim and Deanna H. Gates
School of Kinesiology, University of Michigan Ann Arbor, MI
Email: jaywoo@umich.edu

Introduction

People with lower limb amputation often have difficulty walking for long-durations and infrequently perform activities for more than 15 minutes at a time (< 1 per day) [1]. Despite this, few studies have explored the factors limiting long-duration walking in this population. One study found that people with transtibial amputation (TTA) reduced their intact side ankle power during push-off and increased hip power generation on their prosthetic side after 60 minutes of walking [2]. This suggests that people with TTA alter their strategy, potentially in response to fatigue in the intact limb.

Powered prosthetic ankles have been developed to address lack of ankle plantarflexor power in people with (TTA) [3], which may alter joint kinetics during walking [4]. The purpose of this study was to determine if using a powered prosthesis increased walking endurance and altered ankle and hip kinetics.

Methods

10 males (53 ± 11 years old) with unilateral TTA completed two test sessions, one with their prescribed unpowered prosthesis and one with the BiOM T2 (BiONX, Bedford, MA) powered ankle prosthesis in random order. Participants had at least 3 weeks of at-home acclimation time with each device prior to testing. In each session, participants walked overground, on a treadmill until they could no longer continue, and then on level ground again. During overgound trials, participants walked at a fixed speed based on their leg length (1.18 ± 0.08 m/s). The treadmill speed was set as 10% faster than the fixed speed. During overground trials, we recorded kinematics using a motion capture system and kinetics using forceplates. The outcome measures were peak sagittal ankle and hip power during loading response and push-off and peak vertical ground reaction force (vGRF) during the first and second half of stance. We compared the effects of power (unpowered vs powered) and fatigue (pre vs post) using linear mixed models.

Results and Discussion

Participants walked for a similar duration with the powered (13.2 min) and unpowered (14.7 min) prostheses ($p = 0.165$). When using the unpowered prosthesis, participants stopped due to pain in their stump (n=6), phantom limb (n=1), and/or hip (n=1). When using the powered prosthesis, three participants stopped walking due to stump or phantom pain rather than fatigue.

With both unpowered and powered prostheses, there were no changes in intact ankle or residual hip power in the loading response or push-off phase. Our results were not consistent with previous findings on the effects of 60-minute walks in individuals with TTA [2]. An important difference in our study was the increased walking speed (10% faster than the fixed speed). Because of this, our participants walked considerably less than 60 minutes, which might not have been enough time for fatigue-induced muscular or kinetic adaptations to be observed.

The treadmill speed was faster than many participants were accustomed to. This may have led to increased socket pistoning. This is supported by the fact that participants reported stopping due to pain, predominantly in the residual limb. The pain experienced did not result in "off-loading" the prosthetic limb, as the vGRF was not different pre- and post-fatigue.

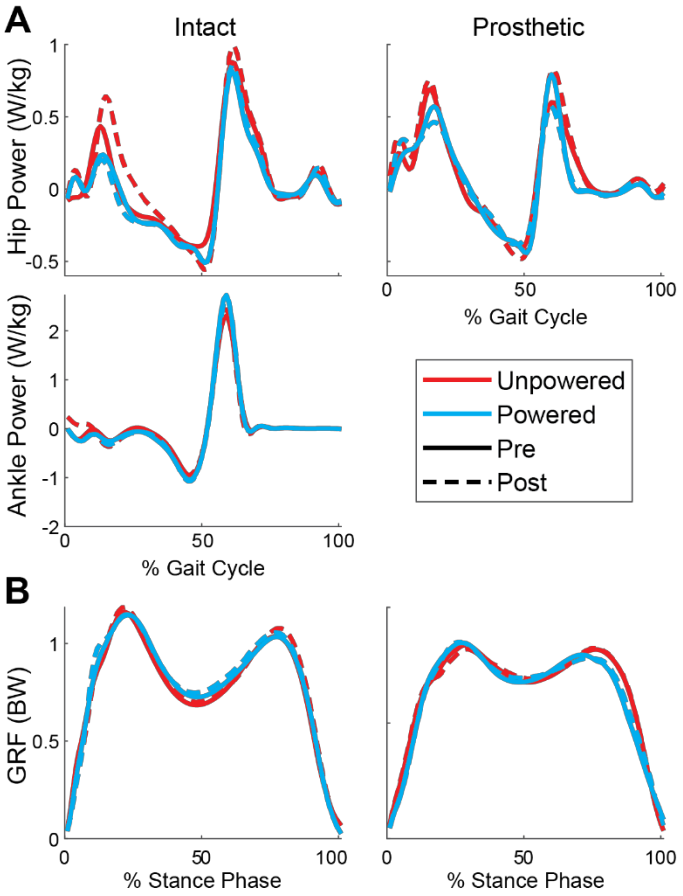

Figure 1: A) Sagittal hip and ankle power. B) vGRF in the intact (left) and prosthetic (right) limbs.

Significance

More participants were limited by pain than fatigue when walking with an unpowered prosthesis compared to walking with an unpowered prosthesis. However, the use of a powered ankle did not enable participants to walk for a longer duration. This may suggest that while pain may be a limiting factor for fast-speed walking with an unpowered prosthesis, there may be different limiting factors for powered ankles.

Acknowledgments

Thank you to Kelsey Ebbs, Luis Nolasco, Kiichi Ash, Manan Anjaria, and the CDMRP (Grant number W81XWH-15-1-0548).

References

[1] Klute, G. Arch Phys Med Rehab 87, 717-22, 2006.
[2] Yeung, L. F. Gait Posture 35, 328-33, 2012.
[3] Herr, H. Proc Biol Sci 279, 457-64, 2012.
[4] Ferris, A. Arch Phys Med Rehab 93, 1911-1918, 2012.

Characterizing Strut Stiffness in Running-Specific Ankle-Foot Orthoses

Kara Ashcraft[1], John Collins[2], Trevor Kingsbury[2], Alena M. Grabowski[1]
[1]University of Colorado, Boulder, CO, USA
[2]Naval Medical Center San Diego, San Diego, CA USA
Email: Kara.Ashcraft@colorado.edu

Introduction

Running is well-characterized by a spring-mass model[1] where the legs are represented by massless linear springs and the center of mass (COM) is represented by a point mass. During ground contact, the leg spring compresses and stores elastic energy until mid-stance, and then returns mechanical energy through the end of ground contact.[2] The magnitude of the stored and returned mechanical energy is inversely related to leg stiffness (k_{leg}), which equals the quotient of the peak applied force (F) and change in leg length[3]: (Δl): $k_{leg} = \frac{F}{\Delta l}$.

Passive-dynamic running-specific ankle-foot orthoses (AFOs) were developed to stabilize the ankle joint of people with salvaged lower-limbs and provide spring-like function. These AFOs include a carbon fiber strut that acts in parallel with the ankle to store and return elastic energy during ground contact (Fig.1).

Figure 1. Passive-elastic running-specific ankle-foot orthoses (AFOs) include a carbon fiber strut that flexes anteriorly at initial heel contact, and posteriorly at toe-off.

During running, ankle joint stiffness is similar across speeds.[4] Wach et al.[5] mechanically tested two running-specific AFO's under compression in a materials testing machine and reported that the AFOs (carbon fiber strut and shank components) have curvilinear force-displacement profiles, suggesting that strut stiffness depends on the force applied. The struts of running-specific AFOs are classified into predetermined stiffness categories, which are based on body mass and/or intended activity (slow or fast running).

AFO strut stiffness affects its function, but the stiffness values of these struts have not been systematically determined. Therefore, we quantified the stiffness values of AFO struts, and hypothesized that each strut stiffness would change by the same magnitude for between each stiffness category (Cat). Based on previous findings that an AFO exhibits a curvilinear displacement profile, we hypothesized that the force-displacement profiles of the carbon fiber AFO struts deflected in the posterior and anterior directions would be curvilinear.

Methods

To evaluate AFO strut stiffness, we constructed a custom three-point bending apparatus to recreate the anterior and posterior deflection that typically occurs during ground contact for running. We applied force to 7 struts in three successive loading and unloading cycles, and reached a maximum deflection of 10° in the anterior direction and 7° in the posterior direction based on a previous study.[6] We measured force with a force transducer (Omegadyne, Stamford, CT), deflection with motion capture (Vicon Nexus, Oxford, UK), and resolved each to be perpendicular with the strut.

We compared average R^2 values from linear and curvilinear force-displacement for all strut categories. We also calculated average stiffness and used a linear regression model to compare stiffness values between strut categories. We used SPSS software (IBM, Chicago, Ill.) and significance of p <0.05.

Results and Discussion

Overall, a linear relationship best characterized the AFO strut force-displacement curves in anterior and posterior directions using a three-point bending apparatus (average R^2 = 0.998). In the anterior direction, stiffness increased 2.01 N/mm for each increase in strut stiffness Cat (Fig. 2A). In the posterior direction, stiffness increased 1.90 N/mm for each increase in strut stiffness Cat (Fig. 2B). The exception was Cat 7, which increased 7.34 N/mm from Cat 6 to Cat 7 in both the anterior and posterior directions.

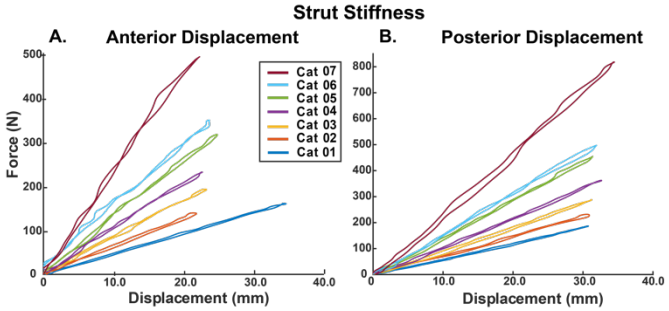

Figure 2. Force versus displacement in the anterior (A) and posterior (B) directions for carbon fiber AFO struts, categories (Cat) 1-7.

Conclusion

Contrary to previous studies, we found that AFO carbon fiber struts exhibit linear force-displacement profiles. This linear relationship suggests that AFO struts have a constant stiffness, much like that of a biological ankle. AFO strut stiffness values changed systematically between categories with on exception. Future research is planned to better understand how a running-specific AFO with different strut stiffness, acting in parallel to the ankle, behaves in dynamic activities such as running.

References

1. Blickhan, R. *J. Biomech.* **22**, 1217–1227 (1989).
2. Alexander, R. M. *J. Exp. Biol.* **160**, 55–69 (1991).
3. Farley, C. T. et al. *J. Exp. Biol.* **185**, 71–86 (1993).
4. Arampatzis, A. et al. *J. Biomech.* **32**, 1349–1353 (1999).
5. Wach, A. et al. *J. Biomech. Eng.* **140**, (2018).
6. Lobb, N. et al. "Influence of strut stiffness category on IDEO flexion and energetics during walking." AOPA. 2019. San Diego, CA.

Acknowledgement

Views expressed do not reflect the views or policy of the Dept of the Navy, DOD, DHA, or US Govt. CDMRPL-17-0-DM170709

Optimized Hip-Knee-Ankle Exoskeleton Assistance at Different Speeds

G. M. Bryan[1*], P. W. Franks[1], R. Reyes[1], S. H. Collins[1]
[1]Department of Mechanical Engineering, Stanford University, Stanford, USA
Email: *gbryan@stanford.edu

Introduction

Exoskeletons have led to significant reductions in user energy expenditure during walking [1]. However, these studies are typically limited to one speed, whereas an effective autonomous device will need to assist at a variety of speeds. Optimal exoskeleton assistance at different walking speeds may mimic biological responses such that joint torque, angle excursion and power increase with speed [2]. To investigate the relationship between walking speed and ideal exoskeleton torque, we optimized assistance with a hip-knee-ankle exoskeleton [3] while the participant walked at slow, medium and fast speeds.

Methods

We optimized multi-joint exoskeleton assistance to reduce user energy expenditure at three speeds with human-in-the-loop optimization [4]. One participant (male, 90 kg, 188 cm) walked with assistance for slow, medium and fast walking (1.0 m/s, 1.25 m/s and 1.5 m/s respectively), while we measured metabolic expenditure, exoskeleton joint angles and ground reaction forces.

Results and Discussion

The participant experienced a 30% reduction in metabolic energy expenditure for slow walking and a 50% reduction for both medium and fast walking (Fig. 1 A). The participant saw the largest absolute reduction at fast walking (Fig. 1 B).

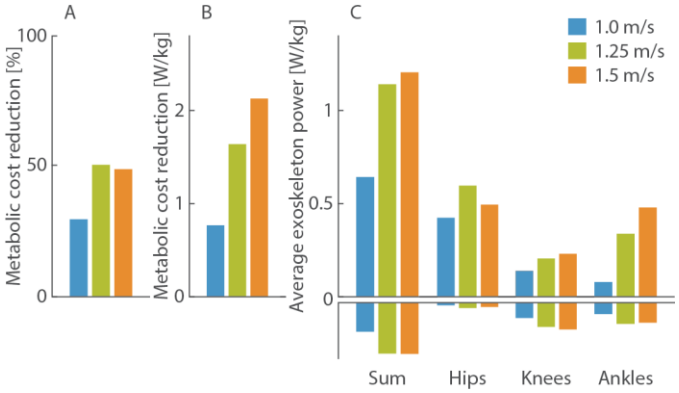

Figure 1: Metabolic reduction and exoskeleton power after optimization. (A) Metabolic reduction normalized to metabolic cost of walking with the device turned off. (B) Absolute metabolic reduction relative to walking with the device turned off. (C) Average positive and negative joint power at the hips, knees, ankles, and sum of all three. The y-axis scale for C is half the scale of B.

Ideal exoskeleton power did not linearly increase with speed like biological power. The exoskeleton provided the least amount of power for slow walking and similar amounts of power for medium and fast walking (Fig. 1 C). In contrast, the absolute reductions in metabolic cost increased with speed (Fig. 1 B). This suggests that exoskeleton power cannot fully explain reductions in energy expenditure.

Unlike biological torques, optimized exoskeleton torques did not increase monotonically with speed (Fig. 2 B). Ankle plantarflexion and knee flexion torque at toe off (60% of stride) were the smallest for slow walking, and all other torque magnitudes were similar independent of speed. Effective torque profiles may work at a range of speeds, but it seems that push-off torque should be lower at slower speeds.

Biological joint angle excursion linearly increases with speed, but the joint angle excursion with assistance did not follow that trend (Fig. 2 A). The hips and ankles saw increased excursion greater than biological around toe-off. With assistance, the knee was relatively straight during stance. However, biological knee excursion during stance increases with speed to reduce the impact from heel strike.

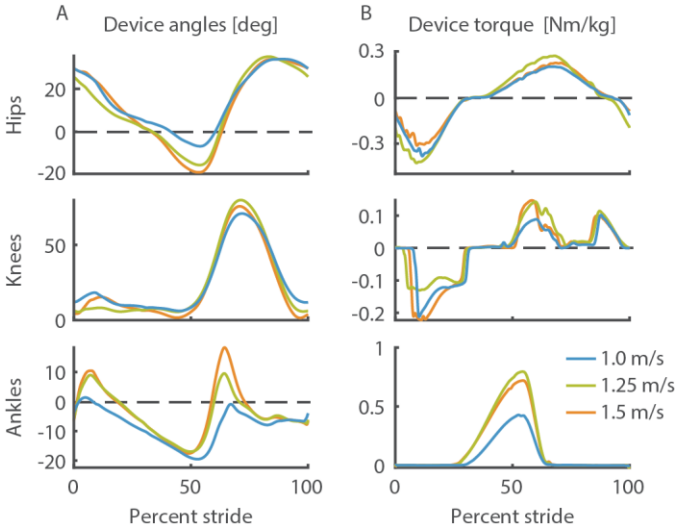

Figure 2: Average exoskeleton joint angles and optimized, exoskeleton torques. (A) Average hip, knee and ankle device angles during optimized torque application. (B) Average applied hip, knee and ankle torque. The applied torques at the hip and ankle are torque- time profiles, and the applied torque at the knee is defined by a virtual spring during stance, time based flexion near toe off a virtual damper during late swing.

Significance

Exoskeletons can reduce the metabolic cost of walking at a range of speeds, with largest improvements seen at faster speeds. Assistance may reduce energy expenditure by replacing positive work done by the muscles, but the positive device power does not fully explain the metabolic reductions.

Acknowledgments

This work is supported by the U.S. Army Natick Soldier Research, Development and Engineering Center (W911QY18C0140).

References

[1] G. S. Sawicki et al, "The exoskeleton expansion" *J. NeuroEng. Rehabil*, 2020.
[2] D. A. Winter, "Biomechanics and motor control" 1991.
[3] G. M. Bryan, P. W. Franks et al, "A hip-knee-ankle exoskeleton" *Int. J. Rob. Res*. in review.
[4] J. Zhang et al, "Human-in-the-loop optimization" *Science*, 2017.

A biomechanical analysis of adaptive assistance strategy for uphill walking using a powered hip exoskeleton

Inseung Kang[1], Dean D. Molinaro[1,2], Gayeon Choi[1], and Aaron J. Young[1,2]
[1]School of Mechanical engineering, Georgia Institute of Technology, Atlanta, GA, USA
[2]Institute for Robotics and Intelligent Machines, Georgia Institute of Technology, Atlanta, GA, USA
Email: ikang7@gatech.edu

Introduction

Over the last decade, research groups have explored methods to optimize different assistance strategies to maximize the human-exoskeleton performance in different environmental settings[1]. However, these studies were often conducted at a specific condition and did not capture what a user would experience in a realistic setting. Our previous study indicates that, for a given environmental setting, there is an optimal assistance to maximize the energetic benefit of using an exoskeleton[2]. To maintain an optimal control strategy for dynamic settings, the effect of adapting exoskeleton assistance across different locomotion intensities needs to be investigated. We utilized a powered hip exoskeleton to evaluate the biomechanical effect of applying adaptive assistance during uphill walking. Our hypothesis is that providing hip assistance during uphill walking that scales relative to the degree of incline will have a greater reduction in the corresponding electromyography (EMG) activation compared to the static assistance strategy.

Methods

One able-bodied subject participated in an IRB approved experiment walking with a preferred walking speed on a height adjustable ramp in four different inclines (7.79°, 9.21°, 10.99°, and 12.42°) while wearing a powered hip exoskeleton (Fig. 1A). Our exoskeleton utilized a state machine-based torque controller providing a hip flexion/extension torque during the region where the corresponding biological hip moment is exhibited. Three exoskeleton conditons were tested: 1) scaling hip extension assistance magnitude relative to inclines, 2) static hip extension assistance across all inclines, and 3) no assistance (exoskeleton controlled to be transparent to the user's movement). Each condition at a given incline consisted of 8 trials of uphill walking. For both scaled and static assistance, flexion assistance magnitude was set constant. We utilized the biological hip moment data during ramp ascent to compute the desired hip extension assistance magnitude (20% of the user's biological hip moment) for different inclines for the scaled assistance condition[3]. For the static assistance condition, we computed the assistance magnitude to be nominal to the scaled assistance across all inclines. During the experiment, we collected motion capture data to analyze the user's kinematic data, instrumented force plate on the ramp for the ground reaction force data, exoskeleton data including the measured joint torque, and EMG data from the user's hip flexor and extensor region.

Results and Discussion

Overall, our exoskeleton's hip extension assistance (for both controllers) was able to alleviate the corresponding biological demand from the user via reduction in joint moment and EMG activation. While our study is preliminary (N=1), biomechanical benefits of using our asstiance strategy were consistent across trials. Across all inclines, scaled and static controllers reduced the average maximum biological hip extension moment (Fig. 1B) by 8.84 ± 2.94% and 4.66 ± 1.30%, compared to no assistance mode, respectively. Additionally, the scaled controller reduced the average maximum Gluteus Medius (GM) EMG activation by 10.98 ± 13.19% compared to no assistance mode. However, across all inclines, scaled and static controllers increased the average maximum Vastus Medialis (VM) EMG activation by 21.76 ± 19.22% and 24.76 ± 23.24%, Rectus Femoris (RF) EMG activation by 15.19 ± 14.18% and 24.08 ± 25.89% compared to no assistance mode, respectively.

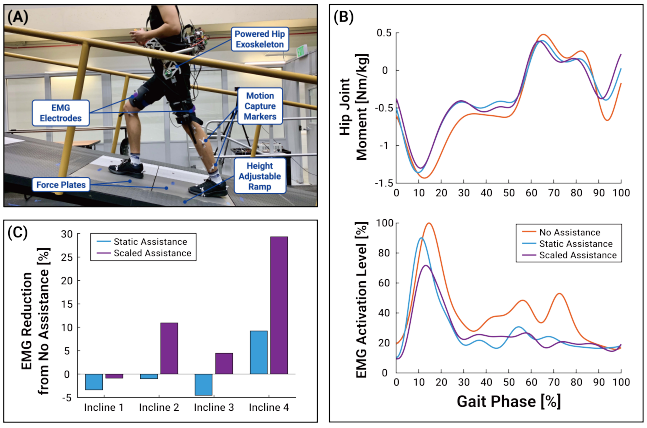

Figure 1: A) Experimental setup for the study. Powered hip exoskeleton provides hip flexion and extension assistance during the gait cycle. B) Biomechanical effects of providing exoskeleton hip extension assistance during uphill walking (incline 4). Hip joint moment (top) and EMG activation for GM (bottom) are shown for scaled (purple), static (blue), and no assistance (red) conditions. C) Maximum GM EMG activation reduction relative to no assistance mode for scaled and static controllers across different inclines.

Significance

Our results indicate that providing hip extension assistance during the early stance phase of the gait cycle can aid the user in reducing the relevant hip extensor EMG activation. While the kinetic results showed similar behavior between two controllers, the effect of these assistances showed significant differences in EMG actviation. Not only did the scaled controller outperform the static controller by reducing a greater hip extensor EMG, it had lesser effects in antagonist muscles. From an energetics perspective (utilizing our analysis in multi channel EMG), our preliminary results illustrate that scalable assistance magnitude for the assistance may further improve the overall exoskeleton performance in uphill walking.

Acknowledgments

The authors acknowledge the NSF Research Traineeship: ARMS Award #1545287 and the NSF NRI Award #1830215 for supporting this work.

References

[1]Sawicki et al. (2020). *JNER,* **17**: 25. [2]Kang et al. (2019). *IEEE RA-L,* **4**: 430-437. [3]Bovi et al. (2011). *Gait & Posture,* **33:** 6-13.

Hip, Knee, Ankle and Multi-Joint Exoskeleton Assistance Can Reduce Metabolic Cost

Patrick W. Franks[1], Gwendolyn M. Bryan[1], Ricardo Reyes[1], and Steven H. Collins[1]
[1]Department of Mechanical Engineering, Stanford University, Stanford, CA, USA
Email: pfranks@stanford.edu

Introduction

It is well known that exoskeletons can reduce the metabolic cost of walking, but what are the best ways to do so and what are the limits? For example, is it better to assist the hip or the ankle joint? Both joints are associated with a large portion of normal energy use [1] and assistance at each has yielded large improvements [2], but direct comparisons have yet to be made. A related question is: can knee-only assistance reduce metabolic cost? Knee musculature consumes significant energy [1], but assistance at this joint has yet to be effective during level walking. Even more interestingly, if we assist all three joints simultaneously, will the benefits be greater than the sum of their parts? The benefits might be greater, because coupled exoskeleton assistance can offload bi-articular musculature [3]. The benefits might be lesser, because assistance at one joint may already indirectly assist muscles at other joints [4]. And when assisting all joints simultaneously in the sagittal plane, how close can we come to completely eliminating the metabolic cost of walking? We can expect that some energy will be required for frontal and transverse functions, and perhaps for baseline muscle activity related to balance, but how much is unknown.

Methods

We used a hip-knee-ankle exoskeleton emulator to conduct human-in-the-loop optimization of exoskeleton torque to minimize measured metabolic cost of walking in a manner similar to [5]. Muscle activity was measured using surface electromyography in a manner similar to [6]. Three participants (2M 1F, 61-90 kg) completed the protocol.

Results and Discussion

Hip-only and ankle-only assistance reduced the metabolic cost of walking by about 26% and 30% respectively (Fig. 1), confirming that both joints are good targets for assistance. Knee-only assistance reduced the cost of walking by 13%, demonstrating that effective knee assistance is indeed possible.

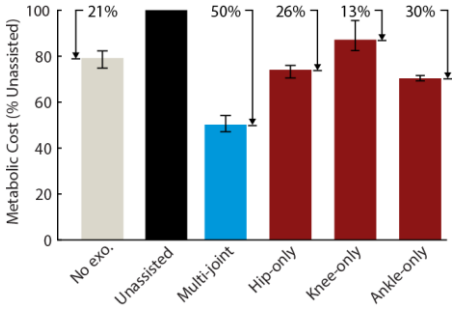

Figure 1: Metabolic cost of walking as a percentage of walking in the exoskeleton with no torque (black) for multi-joint assistance (blue) and each single-joint assistance (red), with bars as mean over three participants and range indicated by whiskers. Metabolic cost of walking is calculated by subtracting out the cost of quiet standing. For each assistance, percent reduction relative to no torque is shown.

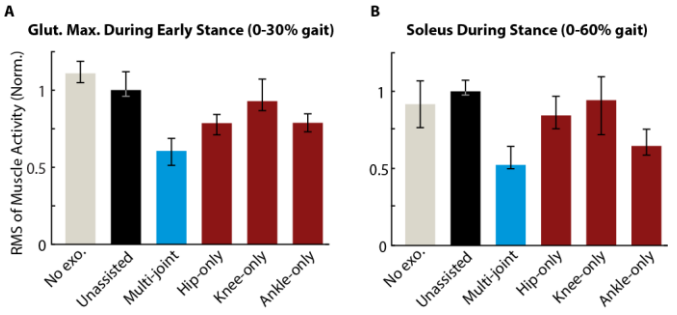

Figure 2: Normalized root-mean-square (RMS) of measured muscle activity for walking without the exoskeleton (gray), in the exoskeleton with no torque (black), with multi-joint assistance (blue) and with each single-joint assistance (red), with bars as mean value and whiskers indicating range. Muscle activity was analyzed for the gluteus maximus (**A**) during early stance, estimated as 0-30% gait, when it is expected to be active, and for the soleus (**B**) during stance, estimated as 0-60% gait.

Multi-joint assistance reduced the cost of walking by 50%, the largest improvement to date, showing that at least half of the metabolic energy expended during walking can be saved through exoskeleton assistance. It remains to be seen whether this limit could be exceeded by assisting additional joint functions, such as hip abduction, or aiding balance. The total energy cost reduction was smaller than the sum of its parts (69%), consistent with the idea that optimal single-joint assistance derives a substantial portion of its benefit from indirectly assisting musculature at other joints. This is supported by the muscle activity of the gluteus maximus (Fig. 2A); activity decreased for hip-only and multi-joint assistance as expected, but also decreased during ankle-only assistance, indicating that the gluteus was indirectly assisted by ankle exoskeleton torque. This effect was less pronounced for the soleus (Fig. 2B), where hip-only assistance only slightly reduced muscle activity.

Significance

Designers of exoskeletons can reduce the metabolic cost of walking by assisting any lower-limb joint in the sagittal plane, but the hip and ankle are the best single joints, and, at least when it comes to energy, all three is better, substantially.

Acknowledgments

This work was supported by the U.S. Army Natick Soldier Research, Development and Engineering Center (W911QY18C0140).

References

[1] B. R. Umberger, *J. R. Soc. Interface*, **7**, 1329-1340, 2010.
[2] G. S. Sawicki et al., *J. NeuroEng. Rehabil.*, **17**, 25, 2020.
[3] P. Malcolm, et al., *Front. Neurosci.*, **12**, 69, 2018.
[4] T. Lenzi et al., *TNSRE*, **21**, 6, 938-948, 2013.
[5] J. Zhang et al., *Science*, **356**, 1280–1284, 2017.
[6] R. W. Jackson et al., *TNSRE*, **27**, 10, 2059-20 69, 2019.

Biomechanics of individuals with and without lower limb amputation during dual-task walking

Sarah R. Bass[1,3], Jonathan R. Gladish [1,2], and Brad D. Hendershot[1,3,4]

[1]Walter Reed National Military Medical Center, Bethesda, MD, [2]Henry M. Jackson Foundation, Bethesda, MD, [3]Uniformed Services University of the Health Sciences, Bethesda, MD, [4]DoD-VA Extremity Trauma & Amputation Center of Excellence

Email: sarah.r.bass3.civ@mail.mil

Introduction

Although walking is considered to be primarily a motor task requiring little cognitive effort, individuals with lower limb amputation (AMP) may utilize additional cognitive resources while walking[1]. This may ultimately result in adaptations that lead to poor gait mechanics and increased risk of falls[2]. Previous research in individuals without AMP has shown reduced gait speed and increased gait variability during dual-task walking[3], as well as variability in spatiotemporal characteristics of gait[4]. Here, we evaluated spatiotemporal features of gait (speed, stride length, and double limb support time) among individuals with and without AMP during dual-task walking, wherein the concurrent task varies in level of difficulty.

Methods

Ten individuals with unilateral AMP (6 transtibial and 4 transfemoral) and thirteen uninjured controls (CTR) completed three N-back memory tasks (zero back [0B], one back [1B], and two back [2B]) while walking at a self-selected pace (4min each). Each task was completed in a virtual hunting environment, where participants were asked to hit a button on a handheld controller for ducks of matching colors. For the 0B task, participants were asked to only hit a duck matching a given color (e.g., red). For the 1B task, participants were asked to hit the ducks that matched the color of the duck displayed one prior (e.g., red, red). Lastly, for the 2B task, participants were asked to hit a duck that matched the color of the duck displayed two prior (e.g., red, blue, red).

All trials utilized a self-paced treadmill speed algorithm within the Computer Assisted Rehabilitation Environment (CAREN; Motekforce Link, Amsterdam, The Netherlands), which modulates belt speed by responding to changes in fore-aft position of the pelvis. Treadmill belt speed (300 Hz) and kinematic data (120 Hz) were collected continuously throughout the trial. Mean, standard deviation, and the coefficient of variation (COV) in gait speed (GS), as well as stride length (SL) and double limb support time (DLS), were computed within 20-second bins and then averaged across the trial. An independent samples t-test was used to compare group differences across tasks ($p<0.05$).

Results and Discussion

SL were larger in the AMP vs. CTR group during the 1B (p=0.014) and 2B (p=0.039) tasks (Fig 1; left), but similar for the 0B task (p=0.064). Across all three tasks, DLS time and GS were not statistically different (0B-GS: p=0.407; DLS: p=0.281; 1B-GS: p=0.294; DLS: p=0.155; 2B-GS: p=0.425; DLS: p=0.385) between the AMP and CTR groups. Although not statistically different (0B-p=0.097; 1B-p=0.397; 2B-p=.0145), GS COV tended to be larger among the AMP group (Fig 1; right).

Overall, the CTR group walked with a more conservative and less variable gait, evidenced by slower GS, shorter SL, and longer DLS; all of which are gait adaptations that have been associated with enhanced balance, improved gait stability, and decreased falls[5]. Faster GS, as well as longer SL, therefore suggest the AMP group may be more susceptible to falls during dual-task walking or in response to a trip-inducing perturbation[5]. Furthermore, greater variability in GS and SL may also be associated with an increased risk of falls.

Alterations in spatiotemporal gait characteristics were observed in both groups, suggesting walking became more unstable as task difficulty increased[3]. This may indicate, as shown previously with electroencephalography, that greater cognitive resources are utilized as (concurrent) task difficulty increases[4].

Significance

The current study extends previous studies suggesting dual-task walking can lead to poor gait mechanics, and may have implications on the rehabilitation of individuals with AMP; specifically, perhaps incorporating dual-task walking into the rehabilitation plan, which may ultimately assist in mitigating falls during community ambulation.

Acknowledgments

This work was supported by the Center for Rehabilitation Sciences Research, of the Uniformed Services University of the Health Sciences (USUHS; award HU0001-15-2-0003). The views expressed are those of the authors and do not reflect the official position of the USUHS, Henry M. Jackson Foundation, Departments of the Army/Navy/Air Force, Defense, nor the U.S. Government.

References

[1] Morgan et al. *Gait Posture* (2017); [2] Beurkins et al. *Neural Plast* (2007); [3] Pruziner et al. *Exp. Brain Res.* (2019); [4] Brach et al. *J Neuroeng Rehabil* (2005); [5] Kang et al. *J. Biomech* (2008).

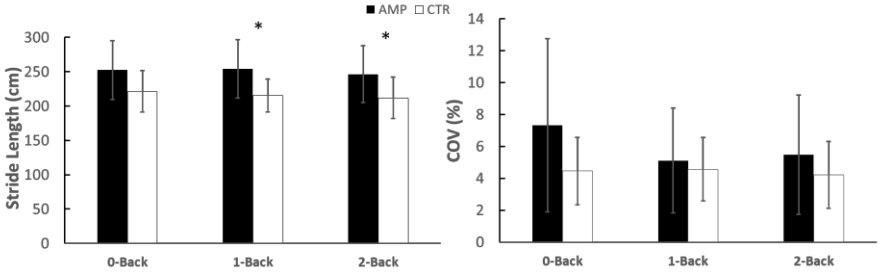

Figure 1. Mean (standard deviation) in stride length (left) and coefficient of variation (COV) in gait speed (right) for individuals with amputation (AMP) and uninjured controls (CTR). *p<0.05

How Training, Adaptation, and Customization Contribute to Exoskeleton Assistance

Katherine L. Poggensee[1] and Steven H. Collins[1]
[1]Department of Mechanical Engineering, Stanford University, Stanford, California, USA
Email: *ktpognc@stanford.edu

Introduction

Human-in-the-loop optimization (HILO) methods can be used to identify customized device parameters to best assist human walking [1]. One of the unique features of these methods is that while the algorithm is identifying the ideal parameters, the human is experiencing a range of possible candidate controllers. The long periods of exposure time as well as the variation in the experienced controllers have been suggested as possible reasons HILO can also be used as a training protocol.

We conducted an experiment to determine how training and customization affect exoskeleton performance. We hypothesize that the extended training will contribute the most to reductions in metabolic cost, while customization will provide additional benefit. We also expect a moderate amount of variation to result in better outcomes than static exposure to a fixed controller.

Methods

Naïve participants (N=15) were randomly sorted into three groups for a six-day protocol. The first day of testing served as a pre-test to determine performance with a generic assistance profile relative to baseline walking trials. On each subsequent day, participants experienced a group-specific adaptation trial for 74 minutes followed by short validation tests. One group (continued optimization) experienced HILO as in [1], where each day was a continuation from the previous day. Another group (static training) experienced the generic assistance for the duration of the adaptation block to decouple the effects of time on training. The final group (re-optimization) experienced HILO with a reset on each day to understand the effects of variation on learning. All groups experienced the generic assistance trial and baseline walking trials during the validation tests. The two optimization groups also experienced their optimized profiles from the end of the adaptation period.

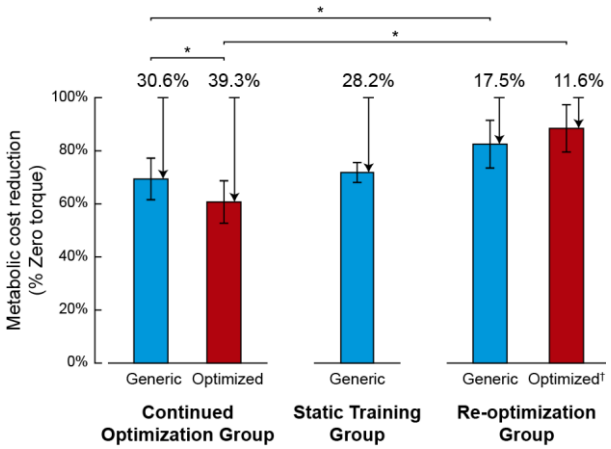

Figure 1: Metabolic costs of exoskeleton walking under different types of training, with respect to a zero torque condition. The optimized assistance for individuals in the continued optimization group resulted in the largest reduction in metabolic cost by any exoskeleton to date. The response to the generic condition was significantly worse for the re-optimization group compared to the continued optimization group, suggesting that too much variation can interfere with training.

Results and Discussion

Initially participants receive very little benefit from exoskeleton assistance, with 10.0±11.0% reduction in energy cost compared to walking in a zero torque condition. By the end of the experiment, the continued optimization group exhibits a 30.6±8.1% energy cost reduction in response to the generic profile and a reduction of 39.3±8.2% for the optimized profile, compared to the zero torque conditions. The latter result is the largest reduction in metabolic cost with an exoskeleton to date. In response to the generic profile, all participants learned to reduce their metabolic cost (Fig. 1).

Participants in the static training group reduced their energy cost by a statistically similar amount by the end of the experiment, though at a slower rate. This result indicates that some amount of variation may speed training. Participants in the re-optimization group were significantly worse at walking with the generic assistance by the end of the experiment than participants in the continued optimization group, indicating that there is a limit to the amount of beneficial variation training. Because this group was not properly trained, their customized profiles were less beneficial.

In addition to reducing the energy cost of walking, participants simultaneously reduced the mechanical power received from the ankle exoskeleton. This result is in contrast with the idea that increasing mechanical power should decrease the metabolic cost of walking with an assistive device.

These results illustrate the importance of training in exoskeleton studies. Customization can also increase the benefits of walking with an assistive device, provided that the user is properly trained. Previous exoskeleton failures may have actually been failures of training.

Significance

Exoskeletons can enhance human mobility, but we still know little about why they are effective. In this study, people learned how to use ankle exoskeletons through different training methods. Their performance was measured to understand the relative importance of training, human adaptation, and device customization. We found large benefits, reducing the energy cost of walking by 39%, of which about half was due to training and a quarter to customizing assistance. Training type had a strong effect on training time and expertise. Our results show that work to improve training could be more important than robot design for developing better gait aids.

Acknowledgments

This research is supported by the National Science Foundation Graduate Research Fellowship Program and National Science Foundation Award No. 1818749.

References

1. Zhang, et al. (2017) *Science* **356**(6344): 1280 – 1284.

Achilles Shear-Wave Tensiometry During Walking With a Passive Exoskeleton: A Proof-of-Concept

Dylan G. Schmitz[1], Darryl G. Thelen[1]
[1]Department of Mechanical Engineering, University of Wisconsin-Madison, Madison, WI, USA
Email: dgschmitz@wisc.edu

Introduction

Passive exoskeletons that can reduce the metabolic cost of locomotion have garnered considerable interest [1,2]. Subsequent studies have probed the biomechanical factors that underlie metabolic improvement by: 1) modeling muscle-tendon actions in the presence of passive assistance [3] and 2) measuring how exoskeletons alter natural gait and muscle-tendon mechanics [4,5]. Such studies have shown that passive elastic torque about the ankle during push-off alters the operating lengths and velocity of the triceps surae and that such effects are speed-dependent [4]. Hence, it is important to understand how such modulations of muscle kinematics affect force production of the muscle-tendon unit when passive assistance is provided. We have begun investigating this question by using shear wave tensiometry to gauge changes in in Achilles tendon force patterns with and without passive assistance.

Methods

We built passive ankle exoskeletons based on the design of Collins et al. 2015 [1]. The clutch was 3D printed from fiberglass-reinforced nylon. The exoskeleton attached to the shank with a calf wrap and to the foot with a fiberglass-reinforced heel cup. A spring was attached in parallel with the clutch (Fig. 1). A healthy young adult walked on a treadmill while wearing the passive exoskeleton bilaterally. After adequate adaptation to walking with the exoskeleton, a grid of three speeds [2.0, 2.5, 3.0 mph] and four stiffnesses [0, 45, 85, 145 N*m/rad] (12 total conditions) were enforced. Shear wave speed was measured at 50 Hz for 10 sec at each condition using a shear wave tensiometer secured over the right Achilles tendon [6].

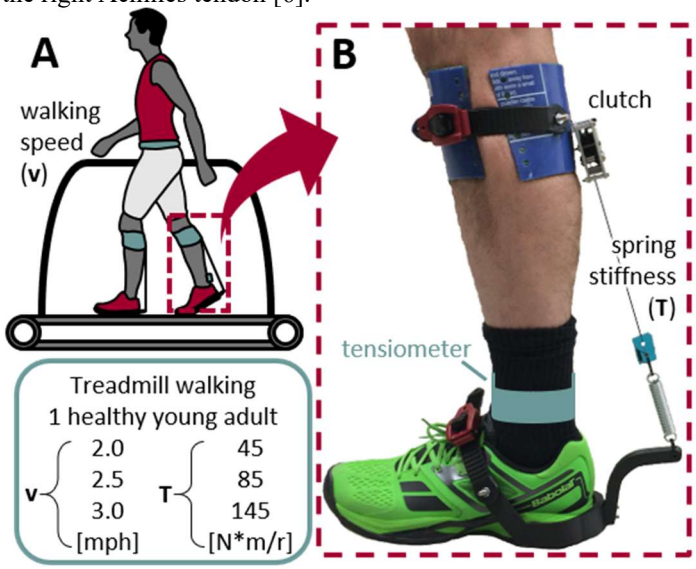

Figure 1: A) Treadmill walking at three speeds and four spring stiffnesses. B) The passive exoskeleton, based on [1].

Results and Discussion

Both walking speed and spring stiffness markedly influenced the tendon wave speed patterns (Fig. 2). For all speeds, tendon wave speed magnitudes decreased with some level of elastic assistance, suggesting that the exoskeleton was successful in offloading the triceps surae. The greatest reduction in tendon loading occurred at an effective ankle spring stiffness of 85 Nm/rad (2, 2.5 mph) or 145 Nm/rad (3 mph), depending on the walking speed. These stiffnesses are lower than that observed by Collins et al. [1], but could result from our calf wrap introducing additional compliance into our system. Achilles tendon wave speeds were most sensitive to spring stiffness at slower walking speeds, which is consistent with subjective assessments and may arise from the slower walking speed being considerably below the subject's preferred speed.

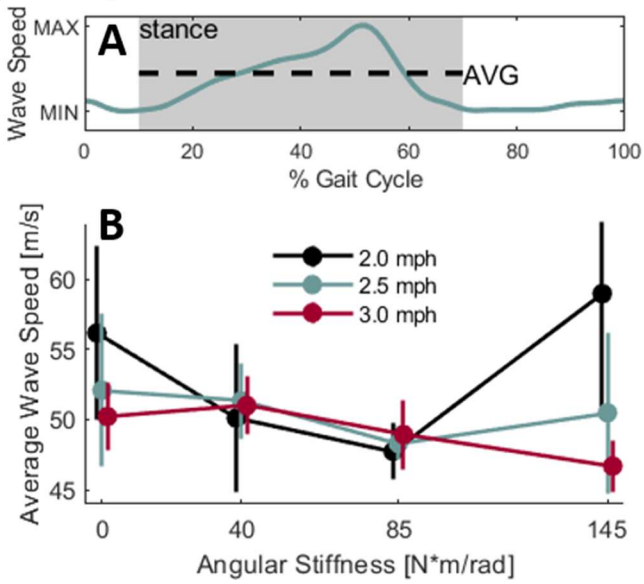

Figure 2: A) Stride-average wave speed profile (2.5 mph, 145 N*m/rad shown). B) Average stance wave speed for each condition (10-70% gait cycle). Standard deviations were computed on per-stride averages within each condition.

Significance

This pilot study demonstrates that shear wave tensiometry can detect changes in tendon loading arising from the use of exoskeletons. The simple noninvase nature of shear wave sensors could be leveraged to track biomechanical adaptations arising from exoskeletons during unconstrained locomotion outside a laboratory. Such usaAge could aid translation by unconvering the benefits and detriments of real-world use of exoskeleton usage, and thereby improve devices designed for gait compensation, rehabilitation, and augmentation.

Acknowledgments

NSF GRFP (DGE-1747503)

References

[1] Collins et al. **2015**, *Nature*. [2] Yandell et al. **2019**, *IEEE Trans Neural Syst Rehabil Eng*. [3] Sawicki & Khan **2016**, *IEEE Trans Biomed Eng*. [4] Nuckols et al. **2020**, *Sci Rep*. [5] Witte et al. **2020**, *Sci Rob*. [6] Martin et al. **2018**, *Nat Comm*. [7] Keuler et al. **2018**, *Sci Rep*.

EFFECTS OF PROSTHETIC SOCKET DESIGN ON RESIDUAL LIMB MOTION USING DYNAMIC STEREO X-RAY

John M. Chomack[1], Michael N. Poppo[1], Kathryn M. Bradley[2], J. Peter Loan[2], Susan E. D'Andrea[3], Jason T. Maikos[1]
[1]Veterans Affairs New York Harbor Healthcare System, New York, NY, USA
[2]C-Motion Inc., Germantown, MD, USA
[3]Department of Kinesiology, University of Rhode Island, Kingston, RI, USA
Email: john.chomack@va.gov

Introduction

A well-fitting prosthesis is essential for individuals with lower extremity amputation (LEA) to achieve functional independence and reduce secondary comorbidities [1]. However, common clinical practices often hold subjective and observable input above objective, quantifiable outcomes during prosthetic fitting and fabrication, which can limit independence. Currently there is little existing data on dynamic, in vivo residual limb-socket kinematics, but an advanced imaging technology, known as Dynamic Stereo X-Ray (DSX), can detect submillimeter in-vivo bone movement in 6 degrees of freedom. The goal of this study was to quantify in-vivo bone movement for individuals with transfemoral amputation (TFA) using two socket types: compression/release and stabilization (CRS) and traditional encapsulation and containment (TRAD). We hypothesized that the CRS socket would provide greater rotational and translational control the the residual femur compared to the TRAD socket.

Methods

Five individuals with unilateral TFA were recruited from Veterans Affairs New York Harbor Healthcare System (VANYHHS) and the Providence Veterans Affairs Medical Center (PVAMC). Participants were randomized to start with either the TRAD or CRS and acclimated to the sockets for 4 weeks each. Participants then received CT scans of their residual limb and sockets and completed DSX and optical motion capture (OMC) testing at Brown University. DSX was utilized to record dynamic X-ray sequences in a 60° antero-posterior orientation simultaneously with OMC for 16 trials of treadmill walking at self-selected (SS) speed (0.36 - 0.80 m/s) recorded at 120fps. CT scans of the residual femur were segmented, creating 3D polygonal mesh objects and a digitally rendered radiographs (DRR) in a DSX suite of software (C-Motion, Germantown, MD). Image data was then calibrated and time synchronized to the OMC data. Residual femur DRRs were matched to two non-coplanar views of the X-ray video sequences. DRRs were manually positioned in each view to match the X-rayed femur which generated an exact bone pose (position and orientation) during the gait cycle. A biomechanical assessment of the DSX bone pose and OMC data was performed in Visual3D (C-Motion, Germantown, MD) producing kinematic motion of the residual bone within the socket. Residual femur movement was expressed as the excursion of the translations and rotations between TRAD and CRS sockets. To assess soft-tissue artifact, a linear fit method (LFM) was used to quantify the agreement between knee kinematics derived from both the DSX and OMC data.

Results and Discussion

The TRAD socket had significantly less axial translation (1.55 ± 0.66cm) compared to the CRS socket (2.03 ± 0.59cm; $P<0.05$) (Figure 1) during SS treadmill walking. No other differences were found in the anteroposterior and medial-lateral translations or rotations in any plane. While the CRS socket was designed to stabilize the residual femur through strategically placed struts in the socket wall, it offered less axial control of the residual limb. It may be necessary to increase the localized pressure of the struts to improve axial control of the femur, but due to the thickness of the thigh, this may not be tolerable to the patient or may severely reduce blood perfusion to the tissue [2]. The LFM analysis was used to determine the agreement of knee kinematics derived from DSX and OMC data. No significant differences in R^2 values for the sagittal, transverse, and frontal planes were found between socket conditions ($P>0.5$). Average R^2 values showed strong agreement between DSX and OMC in the sagittal plane for both the CRS (0.934±0.07) and TRAD (0.922±0.04) sockets, which was in contrast to the R^2 values for the medial-lateral (CRS: 0.502±0.30; TRAD: 0.359±0.25) and axial (CRS: 0.177±0.10; TRAD: 0.259±0.12) planes. These results reinforce OMCs limited capabilities of tracking residual limb movement during gait in non-sagitaal planes, while also demonstrating the capability of DSX to accurately evaluate in-vivo, dynamic bone movement of the residual limb within a prosthetic socket.

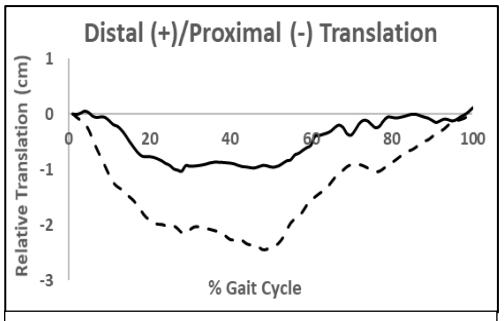

Figure 1: Proximal-Distal translation for each the TRAD and CRS socket types.

Significance

Ensuring a proper socket fit is partially predicated on the analytical and experimental tools that aid in modeling bone pose within a prosthetic socket. DSX demonstrated the ability to detect small changes in bone movement between different socket designs during dyanamic movements. Furthermore, LFM analysis showed the systematic differences between DSX and OMC and the ability of DSX to accurately track underlying residual bone movement. The ability to accurately assess the dynamic interaction between the residual limb and socket is necessary to develop effective, evidence based prosthetic solutions to reduce secondary physical comorbidities and degenerative changes that result from complications of poor prosthetic load transmission.

Acknowledgments

Sponsored by aVA Rehabilitation Research and Development Grant (RX001743-02).

References

[1] Gailey K. et al. J. Rehab/Res & Dev vol. 45 pp.15-30 2008.
[2] Alley R. et al. J. Rehab/Res and Dev vol. 48 pp.679-96. 2011.

Neuromuscular Compensation Strategies Adopted at the Shoulder Following Bilateral Subpectoral Implant Breast Reconstruction

Joshua M. Leonardis[1], Whitney L. Wolff[1], Adeyiza O. Momoh[2], and David B. Lipps[1]
[1]School of Kinesiology, University of Michigan, USA, [2]Section of Plastic Surgery, University of Michigan, USA
Email: jleo@umich.edu

Introduction

Following mastectomy for breast cancer, most women will have a breast reconstruction to return the look and feel of healthy breast tissue. The most popular reconstructive approach is a subpectoral tissue expander and implant, which requires the disinsertion of the pectoralis major muscle from its inferior attachments. The pectoralis major is a primary contributor to shoulder adduction and internal rotation. Clinical practice assumes that the remaining, intact shoulder musculature increase their contributions to shoulder function in the absence of the pectoralis major[1]. However, there is no empirical evidence to suggest this occurs. Therefore, the purpose of this study was to assess how patients adapt their neuromuscular compensation strategies at the shoulder following bilateral subpectoral implant breast reconstruction.

Methods

Fourteen bilateral subpectoral implant breast reconstruction patients (>2.5 years post-operative, mean±SE age: 49±3 yr, height: 1.66±.01 m, weight: 73±4 kg) and 10 healthy controls (age: 55±2 yr, height: 162±.02 m, weight: 62±2 kg) generated maximum voluntary shoulder torques with their dominant and non-dominant arms. Participants then performed 8 submaximal, three-dimensional shoulder torques in 5 arm postures bilaterally. Each arm was assessed in a random order. Surface electromyography recorded activity from 16 shoulder muscles per arm[2]. Non-negative matrix factorization revealed the muscle synergies underlying shoulder torque generation, while the normalized similarity index (SI) assessed between group synergy similarity. An SI ≥0.63 indicated two synergies were more similar than is expected by chance. Neuromuscular complexity was evaluated using the total variance accounted for by the principal (first) synergy (VAF_1) and the number of synergies required to account for more than 95% of variance in experimental data (N_{95}). Group and arm differences in shoulder strength were assessed with linear mixed-effects models. A linear mixed-effects model assessed group and arm differences in VAF_1 while Kruskal-Wallis tests assessed differences in N_{95}.

Results and Discussion

Our experimental groups did not differ with regard to shoulder strength on either arm (all p>0.11). Three-dimensional torque generation was described by three muscle synergies, regardless of group or arm (Figure 1A). These synergies were visually similar to shoulder muscle synergies previously derived from healthy participants[2]. Synergy structure was influenced by subpectoral implant breast reconstruction only on the dominant arm (Figure 1B). Specifically, Synergies 1 and 2 were more similar than expected by chance between the groups on the non-dominant arm, whereas only Synergy 2 was more similar than expected by chance on the dominant arm. Synergy 1 is characterized by primary contributions from the pectoralis major. A reduction in contributions from the sternocostal fiber region of the pectoralis major is likely driving differences in the structure of Synergy 1 between the groups on the dominant arm. This is not surprising given this region of the muscle is most impacted by subpectoral implant breast reconstruction. Interestingly, bilateral subpectoral implant patients do not experience those same adaptations on the non-dominant arm. An assessment of neuromuscular complexity, as measured by VAF_1 and N_{95}, revealed no differences between our experimental groups, regardless of arm (all p>0.07). Combined with our findings regarding muscle synergy structure, these results suggest that subpectoral implant breast reconstruction patients maintain neuromuscular complexity after surgery by altering synergy structure on their dominant arm, and maintaining synergy structure on their non-dominant.

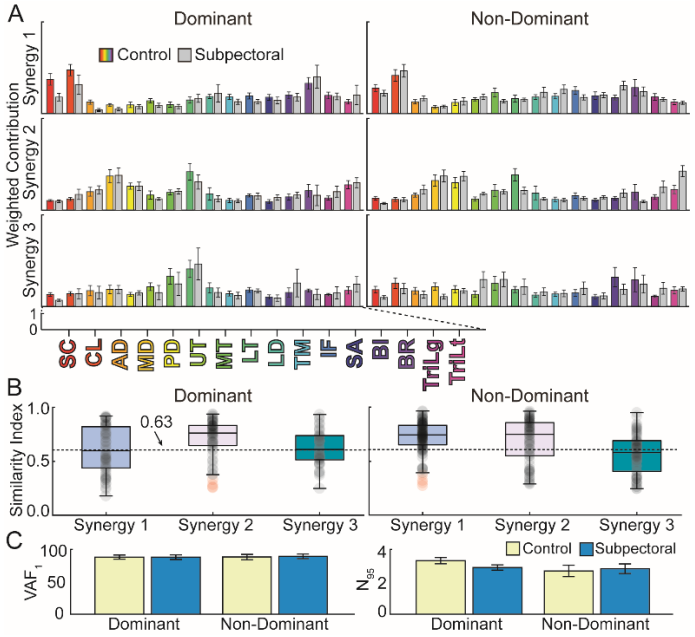

Figure 1: (A) Non-negative matrix factorization revealed the synergies underlying shoulder torque generation on the dominant and non-dominant arms of our experimental groups, while the SI (B) assessed group differences in synergy structure. (C) Neuromuscular complexity was assessed using the total variance accounted for by the principal synergy (VAF_1) and the number of synergies required to account for more than 95% of variance in experimental data (N_{95}). Bars represent mean ± SE, while boxplots represent median ± interquartile range.

Significance

Clinical practice assumes that intact synergist muscles increase their contributions to shoulder function following the disinsertion of key shoulder musculature such as the pectoralis major. The current study provides the first ever evidence of this phenomena, by quantifying changes in shoulder muscle synergy structure and neuromuscular complexity following bilateral subpectoral implant breast reconstruction. The results of this work provide insight into other clinical situations where an otherwise intact nervous system must adapt to the disinsertion of shoulder musculature, such as in the reconstruction of large resections of tissue using latissimus dorsi or serratus anterior muscle flaps[3,4].

Acknowledgements

NIH R03HD097704 and a Rackham Predoctoral Fellowship

References: 1. Spear, *Plast Reconstr Surg*, 2005; 2. J.M. Leonardis, *J Neurophys*, 2020; 3. J.B. McCraw, *Plast Reconstr Surg*, 1978; 4. S. Takayanagi, *Annals Plas Surg*, 1982

Are Gait Kinematics Different in Young Children Who Receive Working Prosthetic Knees?

Mark Geil[1], Colleen Coulter[2], Brian Giavedoni[2], and Zahra Safaeepour[3]
[1]Kennesaw State University, Kennesaw, GA
[2]Children's Healthcare of Atlanta, Atlanta, GA
[3]University of South Carolina Upstate, Spartanburg, SC
Email: mgeil@kennesaw.edu

Introduction

Traditionally, young children with limb loss who require a prosthetic knee joint do not receive a working knee in their initial prosthesis, based on the assumption that a child cannot learn to stand and walk with a knee that can passively flex. An alternative to this "Traditional Knee" (TK) prescription protocol is an "Early Knee" (EK) protocol that provides a working, articulating knee in the first prosthesis, during development of crawling.

The timing of knee provision is controversial. Even within the same medical text, different chapters provide conflicting advice to clinicians.[1] A few previous studies have noted advantages of the EK protocol,[2,3] but no study has characterized gait of separate samples of children in each protocol. The purpose of this study was to describe knee flexion and clearance adaptations in young children at a site where TK is the standard of care and a site were EK is the standard of care, along with age-matched typically developing children.

Methods

This was a multi-site comparison with a convenience sample of 18 children aged 12 months to five years in three groups: six with unilateral lower limb loss at or proximal to the knee at an EK site, six with unilateral lower limb loss at or proximal to the knee at a TK site, and six age-matched typically developing controls without amputations (C). Children with limb loss used their prosthesis daily without assistive devices and had the same knee protocol from the time of their first prosthesis. Fitting and alignment of each prosthesis was performed by an ABC board-certified prosthetist with pediatric experience at each hospital. The protocol was approved by human subjects review boards at each institution, and informed parental consent was obtained.

To ensure inter-lab reliability, a single typically developing four-year-old test subject was assessed at both sites within two weeks in a separate, approved protocol. Both laboratories utilized similar Vicon motion capture systems with identical models and software, and examiners followed standardized video training for marker placement.

Children at each site walked at self-selected speed on a level overground walkway with no external assistive devices. Temporospatial and kinematic data were analysed. Three of the authors reviewed reconstructed 3D motion from each trial for each subject to provide subjective documentation of clearance adaptations. Observers were blinded to condition. The two clinicians (CC and BG) were primary observers, and the third (MG) broke any ties. These results were compared to literature-based numerical calculations for hip hiking, valuting, and circumduction.

Results and Discussion

Two children (one EK and one TK) were excluded from the final analysis. One was the only subject to use crawling as the primary mode of ambulation, and one had recently transitioned from a locked to an articulating knee at the time of the study. Therefore, the data from sixteen children were analyzed. All EK and TK subjects had congenital limb deficiencies. The TK group had a mean age of 25.20 ± 9.04 months, and the reasons for amputation were varied. The EK group had a mean age of 44.60 ± 22.15 months, and all had Proximal Femoral Focal Deficiency (PFFD). Differences between groups affected analysis. An age-matched C was recruited for all TK and EK children, but direct age-matched comparisons between EK and TK were limited. Therefore, analysis focused on description of gait in each group, with consideration of relative levels of development.

All children in the EK group flexed their prosthetic knees during swing (Fig 1). Mean prosthetic peak knee flexion over all steps and all EK subjects was 59.8° ± 8.4°. The mean for the C group was 68.4° ± 3.8°. Contralateral side knee flexion was 69.3° ± 5.8° and 75.0° ± 5.5° for EK and TK, respectively.

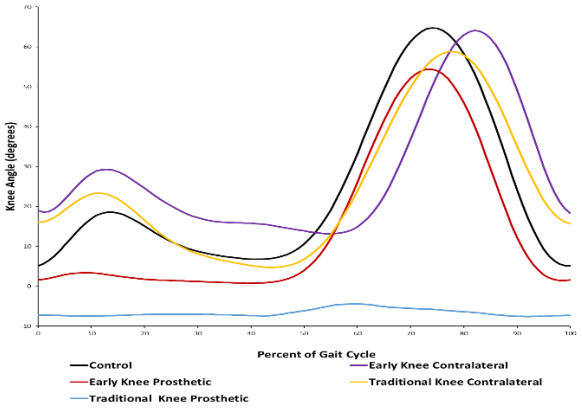

Figure 1: Knee flexion angle (degrees), averaged for right and left for C, and displayed separately for prosthesis side and contralateral side for EK and TK.

Clearance adaptations were present in both prosthesis groups, and some children utilized multiple adaptations. Based on clinical observation, no adaptations were present in the C group, six were observed in the EK group, and twelve in the TK group.

Significance

Young children with limb loss utilize a flexing prosthetic knee joint if it is provided to them. Given that there is often no monetary cost associated with provision of a knee joint in the first prosthesis, and the possibility of improved gait, the Early Knee protocol should be considered as a standard of care, replacing the traditional protocol.

Acknowledgments

This research was supported by a grant from Gerber Foundation (#1828-3236).

References

[1]Atlas of Amputations and Limb Deficiencies. 2016. LW&W.
[2]Geil et al, Prosth Orth Int. 2014;22(1):21-5.
[3]Geil et al, J Prosth Orth. 2013;25(1):22-9.

Preparations for Expected Underfoot Perturbations in Healthy and Concussed Individuals

Nicholas Kreter[1], Bre Dumke[1], Claire Rogers[1], Keith R. Lohse[1], Lee E. Dibble[1] and Peter C. Fino[1]
[1]University of Utah, Salt Lake City, UT, USA
Email: nick.kreter@utah.edu

Introduction

A wide range of abnormal gait parameters have been well documented in concussed populations. While most of the previous research examined gait over flat surfaces[1], uneven terrain is regular in everyday life. Walking over uneven terrain requires constant pre-planning and cortical control of gait. Prior to stepping on uneven terrain, anticipatory adjustments to trunk position are often used to mitigate the effects of the upcoming disturbance.[2] Concussion-related motor deficits may alter the ability to select appropriate motor plans prior to a known gait disturbance. For instance, concussed athletes demonstrate altered trunk motion when crossing a known obstacle.[3] However, such obstacle crossing studies still maintained a flat support surface around the obstacle. Few, if any studies have examined the effects of concussion to underfoot perturbations common in everyday life, such as stepping on a small rock or pebble.

The purpose of our study was to compare anticipatory adjustments to expected overground perturbations delivered by a mechanized shoe in healthy and recently concussed adults. We hypothesized that the concussed and control groups would differ in their preparations for expected perturbations.

Methods

Five healthy [4F, mean (SD) age = 23.8 (4.7) yrs] and five recently concussed [2F, mean (SD) age = 24.6 (5.2) yrs] adults provided informed written consent and participated in this IRB-approved study. Each participant wore a pair of custom mechanized shoes containing a small aluminum block just proximal to the 5th metatarsophalangeal joint.[4] The small block was recessed into the sole of the shoe and could rotate outward, eliciting approximately 12° of eversion when it was deployed.

While wearing the shoes, participants completed several walking trials including walking with and without a perturbation. During 12 of the 36 trials, a single perturbation was delivered to the left foot at a random step in the trial. Half of the perturbation trials contained a loud beep one stride prior to the perturbation to warn the participants of the upcoming disturbance. Four of these expected perturbations occurred within a randomized block consisting of trials with and without the perturbation.

Inertial sensors were placed at the feet, lumbar region, trunk and wrists to collect accelerations, angular velocities and magnetic field potentials during walking. Raw data were collected at a sampling frequency of 128 Hz and filtered with a 4th order recursive low-pass Butterworth filter with a cutoff frequency of 10 Hz. Data was processed with a continuous wavelet transform to identify specific gait events, and for trials with a perturbation, the time of the perturbation. Data for the stride prior to, during and following the perturbation was isolated and each stride segment was time normalized to 200 samples. The standardized mean difference of accelerations between perturbation and non-perturbation trials was calculated for each subject using 1-dimensional statistical parametric mapping (1D SPM). The mean of the standardized difference for the region one quarter of a stride before the perturbation was calculated for the left foot and trunk and a mixed-effects model compared the effect of group and sensor on this mean standardized difference with post-hoc pairwise t-tests.

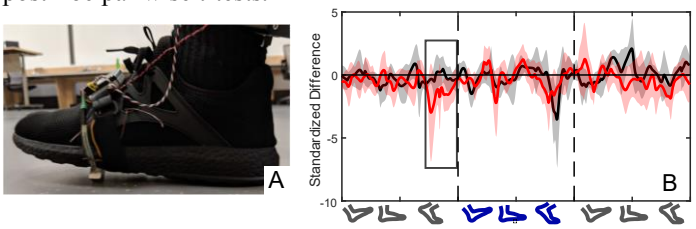

Figure 1A. Example of perturbation delivered from the mechanized shoe. **Figure 1B.** Standardized mean difference of accelerations between expected perturbation and non-perturbation trials for control (black) and concussed (red) subjects. The box indicates the ¼ stride before the perturbation extracted for analysis.

Results and Discussion

The mixed-effects model revealed no difference between groups at the foot sensor. However, there was a difference at the trunk sensor and a group-by-sensor interaction. A post-hoc t-test confirmed the between groups difference at the trunk sensor *(p=0.03, d=-1.64)*. The results indicate that the concussed group prepared by limiting their lateral trunk movement prior to the upcoming perturbation while the control group did not alter their trunk motion relative to a normal stride. A reduction of trunk acceleration increases stability at the trunk during walking and limits the likelihood of a loss of balance. The conservative strategy used by the concussed group is similar to the strategy seen in other neurodegenerative populations, such as older adults, walking over uneven terrain.[5] The reduction of trunk movement prior to the perturbation suggests that the individuals with concussion may overestimate the scale of the perturbation.

The small sample size and reliance on acceleration limit our conclusions. Future work will explore these effects in a larger sample using positional marker data in addition to accelerations.

Significance

Individuals with recent concussion demonstrated anticipatory trunk motion prior to a small expected perturbation. This trunk motion, not observed in controls, may reflect a compensatory strategy to maintain balance when confronted with uneven terrain common to everyday living.

Acknowledgments

Funding support provided by the Medical Research Foundation of Oregon (PI: Fino), University of Utah College of Health (PI: Fino). Special thanks to Drs. James Ashton-Miller and Hogene Kim for their assistance designing the shoes.

References

1. Fino, P. C. et al (2018). *Gait & posture*, *62*, 157-166.
2. Tang, P. F., Woollacott, M. H., & Chong, R. K. (1998). *Experimental brain research*, *119*(2), 141-152.
3. Catena, R. D., et al (2009). *Journal of neuroengineering and rehabilitation*, *6*(1), 25.
4. Kim, H., et al (2013). *Gait & posture*, *38*(4), 853-857.
5. Menz, H. B. (2003). *Age and ageing*, *32*(2), 137-142.

Stress Provides a Lower-Bound Estimate of Shear Wave Velocity in Skeletal Muscle

Tom Sandercock[1], Michel Bernabei[2], Sabrina Lee[3], and Eric Perreault[2,4]
[1]Departments of Physiology, [2]Biomedical Engineering, [3]Physical Therapy and Human Movement Sciences,
Northwestern University, [4]Shirley Ryan AbilityLab, Chicago, IL
Email: t-sandercock@northwestern.edu

Introduction

Shear wave elastography can be used to characterize the mechanical properties of unstressed materials. This technique, which involves measuring shear wave propagation, has been used to study muscle during loaded and unloaded conditions. In many studies of contracting muscle, measurements of shear wave velocity (SWV) have been assumed to be directly related to the material properties of muscle, most commonly stiffness. Some have also used measures of SWV to estimate force, since muscle stiffness and force covary during active contractions. However, few have considered the direct influence of muscle force on SWV, independent of the force-dependent changes in muscle stiffness, even though it is well known that force in a material influences shear wave propagation [2]. We previously used an experimental manipulation to demonstrate that SWV is sensitive to changes in muscle stiffness that occur independent from changes in muscle force [1]. Here we perform a complementary experiment to evaluate the influence of force on SWV. Our purpose was to determine how well changes in muscle force alone can explain measurements of SWV in passive and active muscles.

Methods

Experiments were designed to test the null hypothesis that force alone could be used to predict SWV, comparing experimentally measured changes in SWV to predictions from a theoretical model of shear wave propagation [2]. Data were collected from six isoflurane-anesthetized cats; three soleus muscles and three medial gastrocnemius muscles were tested. Muscle force was measured directly along with SWV, the latter using ultrasound elastography. Measurements were made across a range passively and actively generated forces, obtained by varying muscle length and activation. Some muscle lengths were well beyond physiological lengths. Activation was controlled by stimulating the sciatic nerve. Muscles not being tested were denervated. Measured forces were normalized by physiological cross-sectional area resulting in estimates of stress that could be compared across muscles.

Results and Discussion

We found that the theoretical model of how stress influences SWV predicted our experimental results well for passively stretched muscles (Fig. 1). The errors for this model were not significantly different from zero (0.20 ± 0.22 m/s; mean ± 95% CI; p=0.08). In contrast, this same model significantly underpredicted the SWV in active muscles (2.72 ± 0.44 m/s; p~0). Results were consistent in the soleus and medial gastrocnemius muscles, suggesting our results generalize across muscles with different architectures and fiber types. These findings demonstrate that SWV is sensitive to changes in muscle stress and that a model of how stress influences SWV can be used to predict the SWV in passively stretched muscles. This same model provides a lower bound on the SWV in active muscle, presumably due to activation-dependent changes in muscle stiffness. Together, our results provide further clarity on the factors influencing shear wave propagation in muscle.

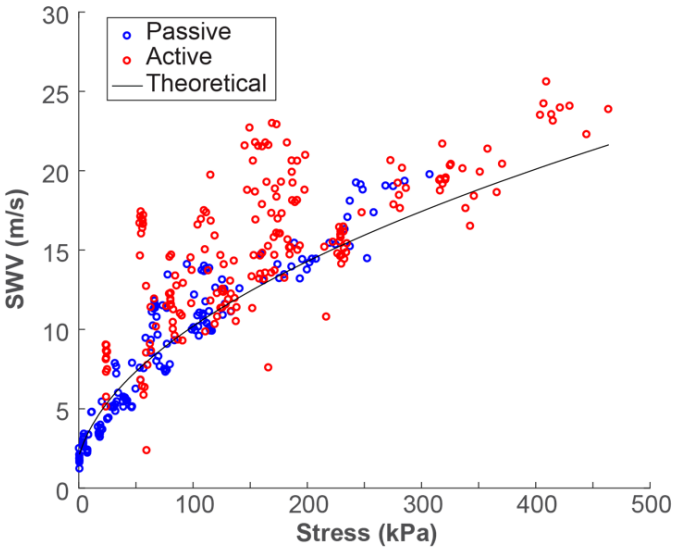

Figure 1. Comparison of experimental data and theoretical model describing stress-dependent changes in shear wave velocity (SWV). Data are from passively stretched and actively contracting soleus and medial gastrocnemius muscles.

Significance

Our results show SWV provides a good measure of passive tension. Active tension is more complex and our results suggest changes in muscle stiffness also contribute to SWV. SWV may provide a good tool to measure muscle properties, but before it can be used in active muscle the souce of the increase in SWV must be understood.

Acknowledgments

Supported by National Institute of Health Grant 5R01-AR-071162-02 to E. J. Perreault..

References

[1] Bernabei M, Lee SSM, Perreault EJ, Sandercock TG. Shear wave velocity is sensitive to changes in muscle stiffness that occur independently from changes in force. J Appl Physiol (1985). 2020 Jan 1;128(1):8-16

[2] Martin JA, Brandon SC, Keuler EM, Hermus JR, Ehlers AC, Segalman DJ, Allen MS, Thelen DG. Gauging force by tapping tendons. Nat Commun 9: 1592, 2018

3D Model of the Soleus Reveals Complex Muscle Fascicle and Aponeuroses Deformations during Passive Stretch

Katherine R. Knaus[1] and Silvia S. Blemker[1]
[1]Department of Biomedical Engineering, University of Virginia, Charlottesville, VA; Email: *ker4e@virginia.edu

Introduction

The soleus muscle is an important generator of the plantarflexion torque required for locomotion. In musculoskeletal simulations, which are widely used to understand typical and pathologic gait, muscle function is predicted using lumped-parameter models. These models assume a simplified representation of 3D muscle fascicle architecture while combining the mechanical behavior of the external tendon and aponeuroses into a single series elastic element. The soleus muscle has complex 3D fascicle architecture comprising multiple compartments with different pennation[1,2] as well as complex aponeurosis morphology with broad and thin interdigitating structures that differ significantly from the thick external Achilles tendon[3]. In the case of the soleus, a lumped parameter model cannot fully represent the interaction of the muscle fascicles and aponeuroses and may not accurately predict this muscles' *in vivo* force generating capacity.

Our goal was to develop a finite element (FE) model of the soleus that represents its complex 3D structure in order to simulate excursion of this muscle during ankle motion. We hypothesize that the model will predict deformations in the aponeuroses and fascicle length changes that differ between the anterior and posterior portions of the soleus and would then be inconsistent with the assumptions of a lumped-parameter model.

Methods

Based on segmentations of high-resolution magnetic resonance images of the lower limb, a 3D geometric model of the soleus muscle was constructed with distinct structures for the anterior and posterior muscle compartments and the anterior and posterior aponeuroses. Fiber directions were assigned for each muscle geometry, using aponeuroses surfaces to define fiber origins and insertions, by performing Laplacian flow simulations[4].

To perform FE simulations, the 3D model was meshed into tetrahedral elements. Muscle was modelled as a transversely isotropic material using the assigned fiber directions, while aponeurosis was modelled as an isotropic Neo-Hookean material. To simulate passive soleus stretch in ankle dorsiflexion, the distal end of the posterior aponeurosis, at the Achilles tendon attachment, was displaced 20 mm distally, while the attachments of the anterior aponeurosis to the tibia and fibula were fixed.

To validate predicted architecture, fascicle tracts were created with streamlines and compared to soleus measurements made with diffusion tensor imaging (DTI)[2]. Fascicle stretch in the posterior and anterior compartments were compared to muscle belly stretch and displacement of the anterior and posterior aponeuroses were determined in proximal-distal directions.

Results and Discussion

Model fascicle tracts were similar in length (posterior: 31.6±12.3 mm; anterior: 25.0±14.0mm) and pennation angle (post: 37.9± 16.7°; ant: 23.2 ±12.9°) to DTI measurements of the soleus (post: 35.8±7.4mm, 36.6±6.2°; ant: 37.6±9.4mm, 24.6±5.0°) [3], giving us confidence that our fluid simulations provided a reasonable representation of soleus muscle architecture for FE simulations.

With a prescribed distal displacement of the soleus MTJ, the muscle belly lengthened by 5.4%. Average stretch in the soleus compartments were very different: posterior fascicles lengthened by 18.1±2.9%, while the anterior fascicles lengthened by 2.5± 0.7%. However, fascicle stretch was highly variable throughout the muscle with greatest stretch in the distal portion, suggesting that fascicle measurements in a single location would not capture full soleus kinematics. We measured aponeuroses displacement by averaging the proximal, middle, and distal portions of each and found the greatest displacement in the distal portions (Fig. 1). The posterior aponeurosis experienced greater displacement and stretch than the anterior, again demonstrating nonuniformity in the soleus muscle-tendon unit, now in the series elastic element.

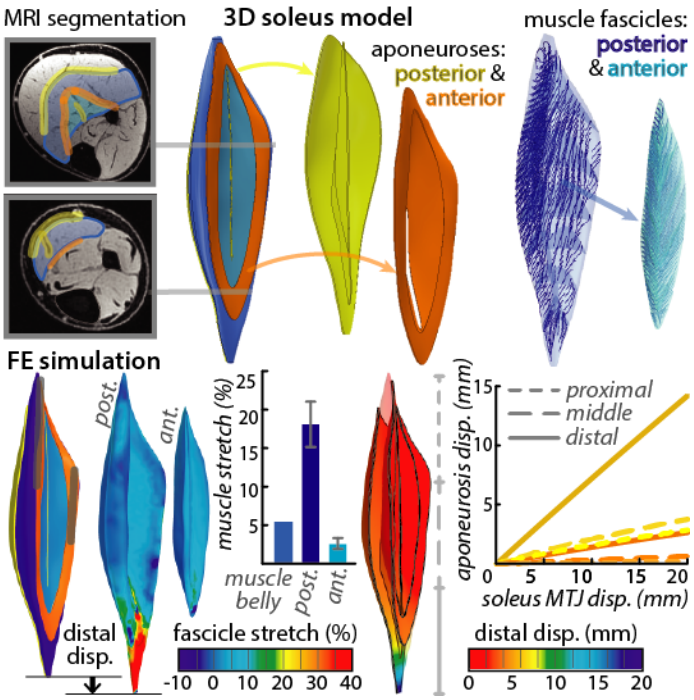

Figure 1: 3D muscle and aponeurosis geometry were constructed based on MRI. Muscle fascicle tracts were computed from Laplacian flow simulation results. FE simulations of passive stretch were performed. Predicted fascicle stretch and aponeurosis displacement are shown.

Significance

Development of this model helps us better understand the role of complex fascicle architecture and aponeurosis morphology in the muscle function. This model improves our ability to predict the *in vivo* force generating capacity of the soleus in order to probe its contributions to human locomotion. Such predictions may be especially important for investigating age-related gait changes, characterized by reduced plantarflexor output, enabling further study of muscle and tendon structure-function relationships.

Acknowledgments

Thanks to Darryl Thelen and NMBL members at UW Madison for collecting the MR images and grant #R01AG051748.

References

[1]Agur et al. (2003). *Clinical Anatomy* **16**:285-293; [2]Bolsterlee et al. (2018). *Peer J*, **6**:e4610; [3]Hodgson et al. (2006). *J Morphology* **267**:584-60; [4]Handsfield et al. (2017). *BMM*, **16**(6):1845-1855

DENSE INTRAMUSCULAR CONNECTIVE TISSUE DRIVES COLLAGEN CONTENT VARIATION WITHIN MUSCLE

Benjamin I Binder-Markey[1,2], Nicole Broda[1], Richard L Lieber[1,2]
[1]Shirley Ryan AbilityLab & [2]Department of Physical Medicine and Rehabilitation, Northwestern University, Chicago, IL, USA
Email: bbindermar@sralab.org

Introduction

Collagen content is often used as a surrogate for connective tissue quantity to infer muscle stiffness and load bearing capacity. However, a single collagen content may not be adequate because collagen content (Fig. 1A) and connective tissue distribution (Fig. 1B) vary throughout a muscle [1]. Determining the relationship between muscle's connective tissue quantity and collagen content would greatly enhance our ability to create biomechanical models that relate collagen content to muscle load bearing. The purpose of this study was to determine how a muscle's intramuscular connective tissue structure impacts collagen content.

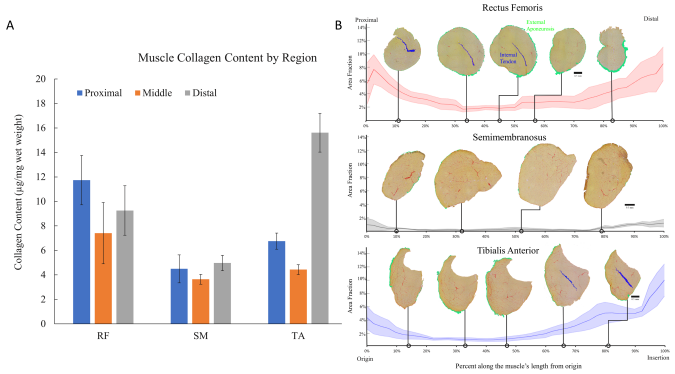

Figure 1: A) Muscle collagen content±SEM variation by region (n=6 muscles/bar) of RF, SM, and TA. B) Average area fraction±SEM (shaded region) along the normalized length of RF (top), SM (middle), and TA (bottom) (n=4/muscle).

Methods

The relationship between collagen content determined via hydroxyproline assay, and dense connective tissue structures (internal tendons and aponeurosis), quantified histologically, was determined from samples of the rectus femoris (RF), semimembranosus (SM), and tibialis anterior (TA) muscles of 12-week old C57Bl6 mice using three independent approaches.

(1) Linear regression analysis used to quantify the relationship between biochemically measured collagen content and histologically measured connective tissure area fraction of cooresponding muscles and regions (Fig. 2).

(2) Predictive modeling to compare experimentally data obtained above to a modeled relationship of total collagen content and connective tissue quantity using a law of mixtures model:

$$Col_{tot,p} = \frac{Col_{ct}V_{ct}\rho_{ct} + Col_m V_m \rho_m}{V_{ct}\rho_{ct} + V_m \rho_m} \qquad (1)$$

where $Col_{tot,p}$, total collagen content, was predicted throughout a range of connective tissue and muscle volume fractions, V_{ct} & V_{ct}, using experimentally measured collagen content values of dense connective tissue (n=21), Col_{ct}, and baseline muscle tissue (n=24), Col_m, and liteterature densities for ρ_{ct} [2] and ρ_m [3].

(3) Non-linear optimization to predict Col_{ct} and Col_m:

$$\min_{Col_{ct,p},Col_{m,p}} \left[Col_{tot}^{M,r} - \frac{Col_{ct,p}V_{ct,m}\rho_{ct} + Col_{m,p}V_{m,m}\rho_m}{V_{ct,m}\rho_{ct} + V_{m,m}\rho_m} \right] \qquad (2)$$

where $Col_{tot}^{M,r}$ is the average collagen content measured in a specific muscle (M) and region (r) and $V_{ct,m}$ is the average summed area fraction of that respective muscle and region.

Results and Discussion:

Using these three approaches, we obtained results strongly suggesting a relationship (r^2=0.89 for both linear regression and non-linear optimization) between a muscle's connective tissue distribution and collagen content that falls within 1 standard deviation of our predicted relationship (Fig. 2). Specifically, we found that muscle collagen content is driven primarily by its dense connective tissue structures due to the extremely high collagen content of connective tissue (204.45 to 276.85 µg/mg) compared to muscle tissue (2.72 to 2.81 µg/mg). As demonstrated in our analyses, for every 1% increase in collagen volume fraction, collagen content is predicted to increase by 2.04-2.77 µg/mg. These are substantial changes in light of the very low baseline muscle collagen content (~3 µg/mg)

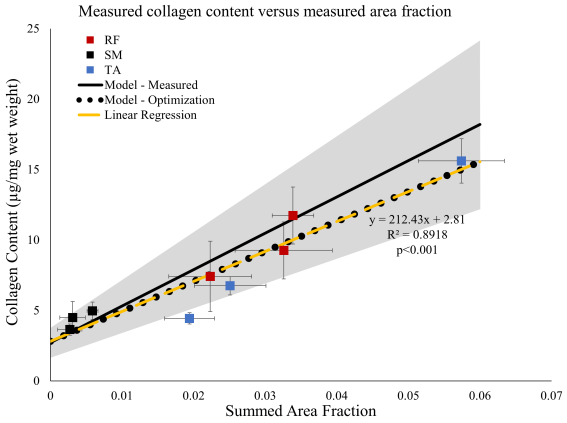

Figure 2: Average measured collagen content±SEM *vs.* summed area fraction±SEM from Figure 1. Linear regression (dashed yellow line), predicted relationship based on the law of mixtures (eq. 1) (solid black line ±1SD shaded region), and relationship using non-linear optimized values of connective tissue and muscle (black dotted line).

These results demonstrate that a single collagen content measurement typically will not accurately represent a muscle's connective tissue structures. However, measured collagen content throughout a muscle will directly reflect the internal connective tissue structures throughout the muscle. Future studies must account for collagen content variation and connective tissue structure location in order to determine more accurate relationships between collagen content measurements and whole muscle passive mechanics.

Significance

This study demonstrates that collagen content variations within and among muscles were driven by the complex connective tissue's distribution within muscle. A consequence of these findings further suggests a single collagen content measurement does not accurately represent the distribution of connective tissue in a muscle and potential load bearing capacity of that muscle.

Acknowledgments

Brinson Fellowship – Shirley Ryan AbilityLab.

References

[1] Binder-Markey et al. 2020 [2] Ker, 1981, [3] Mendes & Keys 1960

In vivo measurement of gracilis muscle-tendon characteristics

Lomas S. Persad[1], Filiz Ates[1], Alexander Y. Shin[1], Richard L. Liber[2], and Kenton R. Kaufman[1]
[1]Department of Orthopedic Surgery, Mayo Clinic, Rochester, MN
[2]Shirley Ryan AbilityLab, Chicago, IL
Email: Kaufman.Kenton@mayo.edu

Introduction

Musculotendon experimental data are needed to develop and validate muscle-driven biomechanical models. Most of these data are obtained from cadavers. The aim of this study was to obtain *in vivo* gracilis muscle-tendon parameters experimentally. These parameters included isometric force-length properties, muscle-tendon unit (MTU) length at various joint configurations, and muscle architectural data. Cadaveric data were also obtained for the gracilis MTU. These included passive force during knee flexion and hip abduction trials, and the gracilis tendon stress-strain relationship. These novel data can help limit assumptions and ensure biological accuracy when modelling the action of the gracilis muscle.

Methods

In vivo data were collected during a free functioning muscle transfer surgery of the gracilis to the upper limb in patients with brachial plexus injuries (n=9). Force-length and MTU length data were obtained from the muscle *in situ*, prior to its removal from the leg. After the muscle was freed, it was weighed and photographed. Muscle-tendon unit dimensions were measured from images of the freed MTU. *In vivo* muscle force was measured by stimulating the muscle via the obturator nerve at 50% of the maximum compound mucle action potention (CMAP) current at 20 Hz. This was repeated for four joint configurations throughout the muscle excursion range. Both *in vivo* and cadaveric force-length data were recorded using a buckle force transducer attached to the gracilis tendon. The gracilis distal tendon was harvested from three cadavers and mounted on a materials testing system where forces from 0N to 200N were applied at a constant strain rate of 25%/s.

Results and Discussion

This study successfully obtained novel *in vivo* gracilis muscle-tendon data (Table 1). *In vivo* gracilis muscle length was similar to values reported by Ward *et al.* and Dziedzic *et al.* Muscle mass was 4 times greater and tendon cross-sectional area was 1.6 times smaller when compared to cadaveric data. Tendon slack length was 11.2 cm which was similar to the 13.9±1.85 cm reported by Dziedzic *et al*. Previous studies have shown tendon slack length strongly affects muscle force generation. Models created by Arnold *et al.* and Rajagopal *et al.* were both based on the same cadaveric dataset where they modeled tendon slack length to be 16.9 cm and 17.2 cm respectively. Our results demonstrate the errors associated with using cadaver data versus *in vivo* data.

Muscle mass (g)	229± 63
Muscle-tendon length (cm)	39.2 ± 2.7
Muscle length (cm)	29.2 ± 3.0
Tendon length (cm)	11.2 ± 2.5
Tendon cross-sectional area (cm^2)	0.2 ± 0.1

Table 1: *In vivo* gracilis muscle-tendon parameters. Values expressed as average ± standard deviation (n=9; height 178±7.8cm, weight 94±19.5kg)

Gracilis fiber length was calculated to be 23.06 cm using a fiber length:muscle length ratio of 0.79 (Ward *et al.*). The measured average tendon length was less than muscle fiber length indicating that the gracilis is a stiff musculotendon unit, meaning the tendon would not stretch greatly.

Force length data demonstrated that when the knee was flexed to 45° while the hip was at 60° and 45° of flexion and abduction respectively, the muscle was at its optimal length (Figure 1). The tendon and muscle lengths at this position were calculated to be 11.34 cm and 36.63 cm respectively. This resulted in an optimal muscle fiber length of 28.94 cm. The data presented here quantify gracilis muscle-tendon compliance, muscle fiber lengths, tendon slack length and optimal fiber length, all of which are important parameters in modeling this muscle.

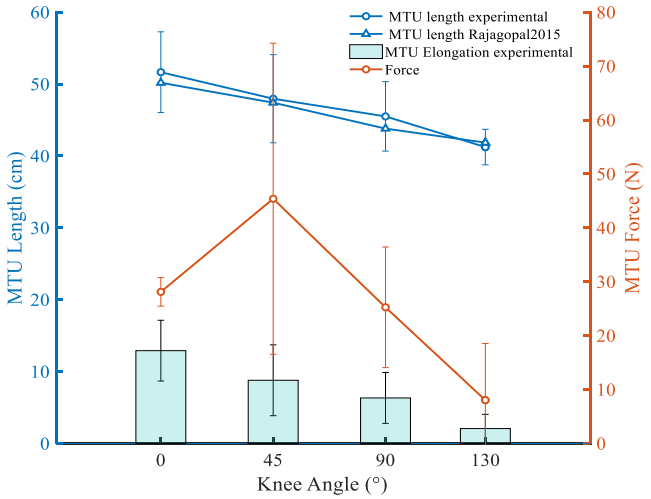

Figure 1:Gracilis force-length data for three subjects. MTU lengths are presented for all nine subjects.

Significance

In vivo muscle length and force data presented here demonstrate that differences exist between experimentally measured parameters and those predicted using current musculoskeletal models. We present these novel *in vivo* data augmented with cadaveric data that can be used to validate musculotendon parameters currently being employed in biomechanical models of the gracilis muscle.

Acknowledgments

Supported by VA funding 1 I01 RX002462

References

[1] Arnold, E.M *et al.* (2010). Ann. Biomed. Eng. 38,269-279 DOI 10.1007/s10439-009-9852-5
[2] Rajagopal, A *et al.*, https://simtk.org/projects/full_body/
[3] Dziedzic, D.W *et al.* (2018). Folia Morphol DOI 10.5603/FM.a2017.0069
[4] Ward, S.R *et al.* (2008). Clin Orthop Rel Res DOI 10.1007/s11999-008-0594-8

Muscle stiffness exceeds tendon stiffness at physiologically relevant levels of muscle activation

Kristen L. Jakubowski, Daniel Ludvig, Sabrina S.M. Lee, and Eric J. Perreault
Northwestern University, Evanston, IL
Email: kristen.jakubowski@northwestern.edu

Introduction

Successfully navigating our environment, such as adapting to uneven terrain and resisting postural disturbances, requires appropriate regulation of joint impedance [1]. The impedance of a joint is strongly dependent upon the mechanical properties of the muscle-tendon units spanning it. While joint impedance has been well characterized [2], it is currently not possible to quantify the contributions from individual muscles and tendons. This presents a critical gap as these structures can be selectively altered by aging, pathology, or injury, resulting in functional impairments. Understanding how these structures contribute to the impedance of the joint over a range of activation levels will provide a clearer understanding of their respective roles in unimpaired and impaired control of posture and movement.

Muscle and tendon stiffness, the static component of impedance, have been estimated *in vivo*. However, most previous estimates have been limited to a range of muscle activations greater than 40% of maximum voluntary contraction (MVC) [3], whereas lower levels of activation are typical in common tasks such as standing (10% MVC) and walking (30% MVC) [4]. These estimates are also mostly restricted to assessing a single structure, limiting our understanding of the interaction between the muscle and tendon. Only one study has simultaneously assessed both muscle and tendon stiffness during standing [5]. However, a combination of experimental and model-based estimates are used and it is unclear if this finding is applicable to other tasks and levels of muscle activation. The lack of experimentally based data across a range of physiologically relevant activation levels hinders our ability determine the respective roles of the muscle and tendon in the control of posture and movement. We recently developed a novel technique using ultrasound to address this gap. We can simultaneously quantify the impedance of the muscle, tendon, and joint. The aim of this study was to quantify the contribution of the muscle and tendon to the impedance of the ankle over a physiologically relevant range of plantarflexion torques.

Methods

Four healthy adults (2 male) were seated with their right foot rigidly secured to a rotary motor with the ankle positioned at 90°. Small, quick, stochastic perturbations of ankle angle were applied while ankle angle and torque were measured. The muscle-tendon junction (MTJ) of the medial gastrocnemius muscle was imaged using B-mode ultrasound. During each trial, subjects generated voluntary isometric plantarflexion torques of either 0, 10, 20, or 30% maximum voluntary contraction (MVC).

We estimated ankle impedance as the dynamic relationship between the imposed ankle rotations and the torque generated in response. We also estimated the frequency response function relating ankle rotations to the resultant MTJ displacements. This relationship represents, when scaled by Achilles tendon moment arm, the ratio of the net musculotendon impedance to muscle impedance, a relationship we refer to as the *impedance ratio*. Achilles tendon moment arm was estimated as the mean across subjects from Clarke et al. [6] with an ankle angle of 90°.

The muscle and tendon were modeled as two impedances in series. Under this assumption, muscle and tendon impedance can be derived from the experimental estimates of ankle impedance and the impedance ratio. We report the stiffness component of the measured and computed impedances due to its relevance in the control of posture and movement. Stiffness values were estimated by averaging the magnitude of each frequency response function from 1.0 to 3.0 Hz, over which they had a constant magnitude.

Results and Discussion

Ankle stiffness increased with voluntary torque, as previously reported [2]. As torque increased, the stiffness ratio decreased, indicating that muscle stiffness increased proportionally faster than muscle-tendon unit stiffness (Fig 1A). Muscle and tendon stiffness increased with volitional torque, but the muscle was stiffer than the tendon for torques greater than ~3 Nm (Fig. 1B). Since ankle stiffness is dominated by the most compliant component within the muscle-tendon unit, our results indicate that ankle stiffness is determined largely by the mechanical properties of the Achilles tendon at almost all tested levels of activation. It is commonly concluded that the increase in ankle stiffness is driven by the increase in muscle stiffness. However, these results indicate that the increase in ankle stiffness is due to the strain-dependent increase in tendon stiffness. This finding is fundamental to our understanding of how muscle and tendon contribute to the control of posture and movement.

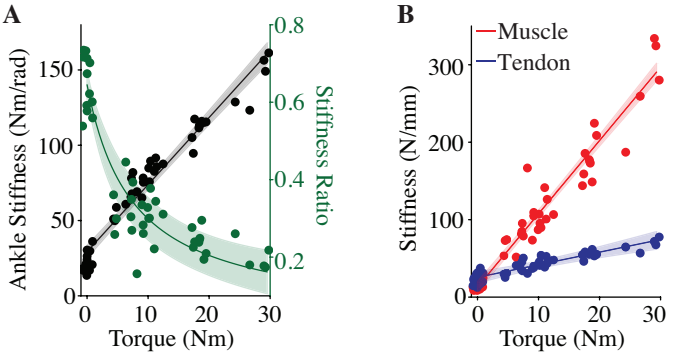

Figure 1 A) Ankle stiffness (black) and the stiffness ratio (green) and **B**) muscle (red) and tendon (blue) stiffness for all subjects across the range of plantarflexion torques. Solid lines represent a fitted model and shaded area represents the 95% confidence interval for the respective model.

Significance

We demonstrated that muscle stiffness exceeds tendon stiffness at almost all physiologically relevant levels of muscle activation, and that the mechanics of the ankle are dominated by the nonlinear mechanics of the Achilles tendon during the isometric conditions of our protocol. Our novel approach that allows for simultaneous assessment of muscle, tendon, and ankle impedance is not only useful for understanding the unimpaired control of movement but may be useful for tracking the mechanisms contributing to altered ankle mechanics with age and injury.

Reference

[1] Whitmore et al (2019) *IEEE T Biomed Eng*. **66**: 2381-2389;
[2] Kearney RE et al (1990) *Crit Reivew Biomed Eng*. **18**: 55-87;
[3] Hauraix et al (2015) *Eur J Appl Physiol*. **115**: 1393-1400.
[4] Nagai et al (2011) *Arch Gerontol Geriat*. **53**: 338-343.
[5] Loram et al (2007) *J Physiol*. **584**: 677-692.
[6] Clarke el al (2015) *Med Eng Phys*. **37**: 93-99.

The Effect of Rotator Cuff Tear Severity on Joint Loading During Dynamic Tasks

Joshua Pataky[1], Sujata Khandare[1], Ali A. Butt[1], Meghan E. Vidt[1,2]
[1]Biomedical Engineering, Pennsylvania State University, University Park, PA, USA
[2]Physcial Medicine & Rehabilitation, Penn State College of Medicine, Hershey, PA

Introduction

Rotator cuff tears (RCT) are common in older adults, which can negatively affect function.[1] RCT severity ranges from a partial thickness supraspinatus tear to a massive tear including tendons of the supraspinatus, infraspinatus, and subscapularis muscles. Previous simulation-based studies observed that with increased RCT severity, glenohumeral joint contact force (JCF) is relatively consistent for a given static posture, but changes across different postures.[2] These outcomes suggest dynamic task performance may alter glenohumeral JCF magnitude and orientation and exacerbate the RCT or lead to development of secondary injury (e.g. subacromial impingement). Our objective was to determine how glenohumeral JCF changes with increased RCT severity during performance of several dynamic tasks.

Methods

A computational musculoskeletal model of the upper limb[3] was developed in OpenSim (v.3.3)[4] to represent mean muscle force-generating characteristics of healthy older adult males[5] (age=75.6yrs; body weight (BW)=81.0kg). The model was modified to represent 8 different RCT severities by systematically reducing peak isometric force of supraspinatus (S), infraspinatus (IS), and subscapularis (SS) muscle paths. Kinematics for forward reach, functional pull, and axilla wash motions measured from a representative healthy older adult male from a prior study were used.[6] With each model and the dynamic tasks kinematics, a series of computational simulations were performed using OpenSim's Computed Muscle Control (CMC)[7] and Joint Force Analyses tools to predict muscle activations and associated glenohumeral JCF, respectively. All combinations of model and kinematics were run, for a total of 21 permutations. The peak resultant JCF was identified for each tear severity and compared to the no RCT model.

Results and Discussion

Results revealed that JCF magnitude and orientation changed with RCT severity during each dynamic task. All tasks had comparable decreases in percent change of JCF at each tear severity when compared to no RCT (Fig. 1). For forward reach, when compared to the no RCT model, JCF magnitude decreased by 21.9% in the most severe (IS25/SS25) RCT model. When using kinematics for functional pull, JCF magnitude decreased by 26.3% in the most severe tear model compared to the no RCT model. For axilla wash kinematics, JCF magnitude decreased by 26.7% in the most severe tear model compared to the no RCT model. When projected onto the glenoid fossa, the resultant JCF vector for forward reach (Fig. 2), functional pull, and axilla wash kinematics were oriented more superiorly for models with greater RCT severity, although all vectors remained within the glenoid rim. Decreased JCF magnitude and superior trend of the orientation are consistent with expectations, as fewer intact muscles contribute to overall force distribution across the joint.

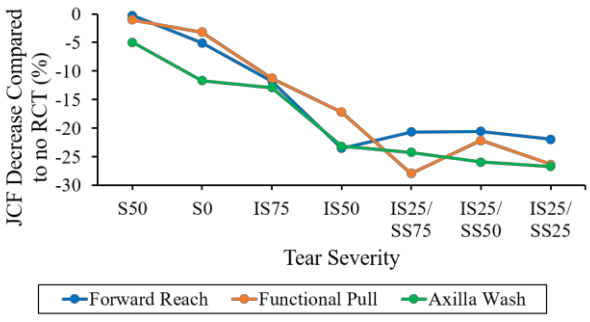

Figure 1. Percent change of peak JCF magnitude for increasing RCT severity for forward reach, functional pull, and axilla wash kinematics.

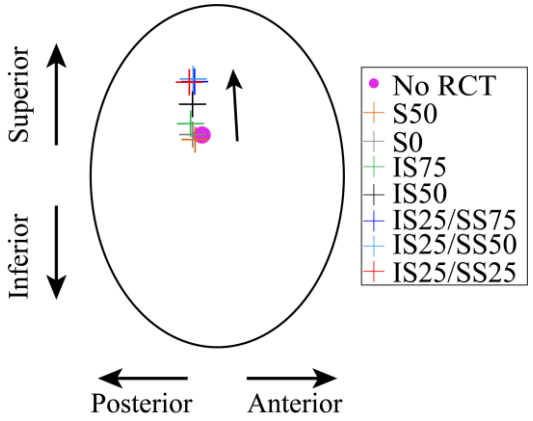

Figure 2. Forward reach kinematics resultant JCF vector projected onto the glenoid fossa across increasing RCT severity. Arrow indicates trend in JCF location observed across tear severities.

Significance

Observed changes in JCF with increased RCT severity support clinical reports of increased risk of secondary injury.[8] Ongoing work continues to explore how JCF magnitude and orientation change with increased RCT severity during dynamic tasks that require a variety of postures to complete. Additional work seeks to examine the compensatory role of uninvolved muscles in the shoulder and how their contribution changes with increased RCT severity.

Acknowledgments

Penn State startup funds (Vidt).

References

1. Lin JC. et al. J. Am. Med. Dir. Assoc. 2008;9(9):626-632.
2. Khandare S. et al. J. Electromyogr. Kinesiol. 2019;(18):30516-9.
3. Saul KR. et al. Comput. Methods Biomech. Biomed. Eng. 2015;18(13):1445-1458
4. Delp SL. et al. IEEE Trans Biomed Eng. 2007;54(11):1940-50.
5. Vidt ME. et al. J. Biomech. 2012;45(2):334-341.
6. Vidt ME. et al. J. Biomech. 2016;49:611-617.
7. Thelen DG. et al. J. Biomech. 2003;36(3):321-328
8. Hsu HC. et al. Acta Orthop. Scand. 2003;74(1)89-94

The Effects of Osteoarthritis and Unicompartmental Knee Arthroplasty on Hip, Knee, and Ankle Joint Kinematics

Sabreen Megherhi[1], Clarissa LeVasseur[1], Tom Gale[1], Ken Urish[1] and Wiliam Anderst[1]
Department of Orthopedic Surgery, University of Pittsburgh, Pittsburgh, PA, USA
Email: SAM454@pitt.edu

Introduction

Total knee arthroplasty (TKA) is one of the most common surgical procedures in the USA, with approximately 600,000 TKA procedures performed in 2014 [1]. TKA is predominately performed due to end-stage osteoarthritis (OA). For eligible patients that have OA in only the medial or lateral portion of the tibiofemoral joint, a unicompartmental knee arthroplasty (UKA) can be a viable alternative. UKA is associated with less post-operative pain, faster rehabilitation, and younger patients who desire high post-operative activity levels [2,3].

Previous studies that compared lower body joint kinematics and kinetics in patients before and after TKA reported changes in joint moments, but not in joint kinematics at the hip, knee and ankle during gait [4]. In contrast, there is a lack of research focusing on bilateral lower body joint kinematics pre and post UKA. The aim of this study is to compare side-to-side differences (SSD) in hip, knee, and ankle joint kinematics during walking, both pre and post-surgery, in patients receiving a UKA. It was hypothesised that pre-operative SSD in the hip, knee, and ankle kinematics would be resolved after UKA.

Methods

Ten patients scheduled to receive a medial UKA consented to participate in this IRB-approved study. Nine patients (age: 62±5 years, 4F, 5M) completed pre-surgical (3 weeks before) and post-surgical (7±2 months) testing. All patients walked across a 7m lab walkway at their self-selected pace for at least 6 separate trials while a 12-camera Vicon motion capture system collected data at 100 Hz. We used a custom set of 31 markers, based on anatomical positions from Visual 3D recommendations and custom tracking markers. An average of 9 steps were included per person per leg each day. Bilateral hip, knee, and ankle joint angles were calculated using Visual 3D. Average bilateral hip, knee, and ankle flexion/extension and ab/adduction were normalized to percent gait cycle and averaged across all trials. Average joint kinematics were calculated for each leg pre and post-surgery. Statistical parametric mapping was used to compare kinematics curves of the UKA and contralateral limbs using a two-tailed paired t-test with significance set at $p < 0.05$.

Results and Discussion

We were unable to identify any significant side-to-side differences in sagittal or frontal plane joint kinematics pre or post-surgery (Figure 1). These results agree with a previous study that found no changes in ankle, knee, and hip kinematics from pre to post-TKA [4]. Interestingly, we did observe trends toward restoration of knee frontal plane kinematics that were accompanied by greater side-to-side differences in ankle kinematics post-surgery (Figure 1). These observed trends suggest the need for larger studies focused on the effect of UKA on adjacent joint kinematics.

Significance

The results of this study suggest that kinematic differences at the hip, knee, and ankle in the sagittal and frontal plane are small prior to and after UKA. Studies using conventional motion capture and large patient cohorts might be able to identify side-to-side differences in frontal plane joint kinematics prior to and after UKA. While UKA may restore native knee kinematics, the effects of UKA on ankle and hip kinematics and kinetics is worthy of further investigation.

Acknowledgments

This work was supported by a research grant from Smith and Nephew.

References

[1] Sloan et al., J Bone Joint Surg, 2018. [2] Rodríguez-Merchán, et al., EOR, 2018. [3] Kleeblad, et al., Knee, 2019. [4] Levinger, et al., J Arthroplasty, 2013.

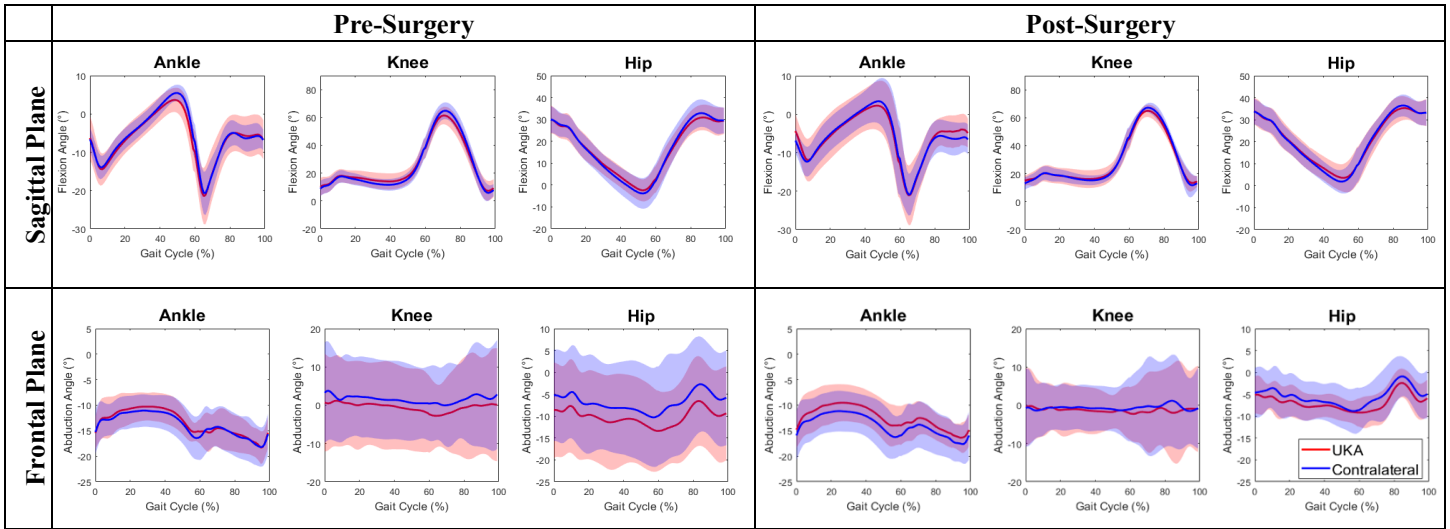

Figure 1: Sagittal and frontal plane kinematics pre and post UKA. Solid lines indicate group means, and shaded areas ±1 SD.

Modular Control and Patient Function in Individuals with Knee Osteoarthritis and Total Knee Arthoplasty

Rebekah R. Koehn[1], Sarah A. Roelker[2], Laura C. Schmitt[1], Ajit M.W. Chaudhari[1], Robert A. Siston[1]
[1]The Ohio State University, Columbus, OH, USA; [2]The University of Texas at Austin, Austin, TX, USA
Email: koehn.19@osu.edu

Introduction

Individuals who undergo total knee arthroplasty (TKA), the end-stage treatment for knee osteoarthritis (KOA), often experience suboptimal outcomes.[1] Multiple studies have been conducted to determine the source of these functional deficits, yet few have explored neuromuscular control. A recent study[2] suggested that neuromuscular control strategy, demonstrated by motor modules (or synergies),[3] may be associated with the range of post-operative functional outcomes. However, it is unknown how modular control may change during recovery or relate to functional outcomes. The purpose of this study was to determine the relationship between function and modular control during gait before and after TKA. We hypothesized that participants who demonstrated better function would demonstrate modular control that was (i) more complex (i.e. more modules) and (ii) resembled healthy age-matched controls.

Methods

36 individuals (38 knees, 19R/19L) with medial compartment KOA provided written informed consent prior to undergoing TKA and were tested before and 6- and 24-months after surgery. During over-ground walking trials, we collected surface electromyography (EMG) data from rectus femoris (RF), vastus medialis and lateralis (VM,VL), medial hamstrings (MH), biceps femoris (BF), medial and lateral gastrocnemii (MG, LG), and soleus (SO) on the TKA-involved limb. Using previously described methods,[4,5] we extracted muscle modules and selected one representative trial for analysis. We defined modular complexity as the number of modules extracted. We defined modular organization as the distribution of significantly active muscles within each module (W_{musc}).[6] Modular organization was only evaluated in participants with 3 modules. We used the 6-minute walk test[7] (6MW) to categorize patients as high- or low-functioning based on published age-, height-, mass-, and gender-specific thresholds.[8]

We performed individual one-way ANOVAs to determine the relationship between modular complexity and function. We compared muscle weights to healthy age-matched controls (HC)[9] using Pearson correlations to define module quality,[10] and performed 2-sample t-tests to determine the relationship between module quality and 6MW performance (all $\propto$=0.05, *a priori*).

Results and Discussion

Modular complexity was not related to function before or after surgery (all $p \geq 0.406$). This contrasts Ardestani et al.,[2] who found that low-functioning patients exhibited fewer modules during gait than high-functioning patients 1-year post-TKA.

Although we did not find a difference in module quality between the high- and low-performing 6MW groups (all $p \geq 0.284$), both groups showed changes in modular organization. The healthy controls demonstrated quadriceps (QUAD), plantarflexors (PF), and hamstrings (HAM) dominated modules (Table 1). In comparison, the 6MW-high group had more significantly active muscles in all modules before surgery and decreased in W_{musc} and W_{musc2} throughout the timecourse of recovery, moving toward healthy organization. However, the 6MW-low group had fewer active muscles before surgery and either increased or remained constant in W_{musc} and W_{musc2}. All 6MW-low modules did not consistently move toward healthy throughout recovery, most notably in the HAM module.

Table 1. Significantly active muscles in high- and low-functioning participants (n) demonstrating 3 modules before, 6-months after, and 24-months after TKA (Pre, 6m, and 24m, respectively) compared to healthy controls (HC). ■: 95% confidence interval (CI) of weights does not include 0; ▨: CI does not include 0, upper bound is <0.25; †: CI includes 0 and 1; W_{musc}: number of ■ & ▨; W_{musc2}: number of ■ & †.

Module & Group			n	W_{musc}	W_{musc2}	Muscle: RF	VM	VL	MH	BF	MG	LG	SO
QUAD		HC	5	4	-	■	■	■					
	Pre	High	17	8	6	■	■	■	■	■	▨	▨	
		Low	4	4	5	■	■	■	■	†			
	6m	High	15	8	7	■	■	■	■	■	▨	■	▨
		Low	3	4	5	■	■	■	†	†			
	24m	High	7	6	5	■	■	■		■		▨	▨
		Low	6	6	5	■	■	■	■			▨	■
PF		HC	5	5	-	■		■			■	■	■
	Pre	High	17	8	5	■	▨	■	▨	▨	■	■	■
		Low	4	3	3						■	■	■
	6m	High	15	7	5	■	▨	▨		■	■	■	■
		Low	3	3	3						■	■	■
	24m	High	7	4	4	▨					■	■	■
		Low	6	4	3						■	■	■
HAM		HC	5	4	-		■		■	■	■	■	
	Pre	High	17	8	5	▨	■	▨	■	■	■	■	▨
		Low	4	2	2		■		■				
	6m	High	15	8	5	■	■	▨	■	■	▨	▨	■
		Low	3	2	2				■	■			
	24m	High	7	3	2			▨	■	■			
		Low	6	5	3		▨	■	■	■	▨		

Significance

Our findings indicate that there may be an underlying relationship between module characteristics and function in this population. The plasticity of modular control, despite not receiving specific neuromuscular control training after 6-months post-TKA, is a novel finding in the TKA population, which may influence functional outcomes in populations with orthopaedic disorders. Such a relationship between modular control characteristics and patient function may open opportunities for further investigations of neuromuscular control as a factor which influences function in populations with orthopaedic disorders and may inform novel rehabilitation protocols to improve patient function.

Acknowledgments

This project was supported by Grant Number R01 AR056700 from the National Institute of Arthritis and Musculoskeletal Skin Diseases and an Ohio State Fellowship (RRK).

References

1 Singh et al. *Osteo Cart.* 18:515-21, 2010. **2** Ardestani et al. *J Electromyogr Kines.* 37:90-100, 2017. **3** Lee. *J Motor Behavior.* 16(2):135-70, 1984. **4** Koehn et al. *Proc ASB*, 2018. **5** Clark et al. *J Neurophysiol.* 103:844-57, 2010. **6** Hayes et al. *Clin Neurophysiol.* 125(10):2024-35, 2014. **7** Enright. *Respir Care.* 48:783-5, 2003. **8** Enright et al. *Am J Respir Crit Care Med.* 158:1384-7, 1998. **9** Roelker et al. *Proc ASB*, 2018. **10** Routson et al. *Gait Posture.* 38(3):511-7, 2013.

Effects of age-related changes on fracture resistance of human cortical bone

Ebrahim Maghami[1], Timothy Josephson[1], Jason Moore[1], Ahmad R. Najafi[1,*]
[1]Department of Mechanical Engineering and Mechanics, Drexel University, Philadelphia, PA 19104, USA
Email: *arn55@drexel.edu

Introduction

During an individual's lifetime, microcracks are formed in the bone tissue due to fatigue and cyclic loading [1]. The formation and growth of the microcracks are affected by the morphology and heterogeneity of the microstructure [1]. However, the bone microstructure and composition undergo significant changes by aging [1]. Aging has a negative impact on the effectiveness of toughening mechanisms acting at different length scales of the bone structure and therefore decreases the fracture resistance of bone [1]. However, the reasons for these age-related changes in bone are complicated and require more extensive investigations.

In the present study, the objective is to investigate the effects of microstructure and bone mechanical characteristics by aging upon fracture phenomenon and the microcrack propagation. In order to capture different toughening mechanisms, we use a brittle model of the phase-field method to analyze the crack growth.

Methods

At the microscale level, the human Haversian (osteonal) cortical bone has been considered as a composite material and modeled as a fiber-ceramic matrix. We consider osteons as fibers and the interstitial tissue as the matrix [1]. We also define the interface between the osteons and interstitial tissue as the cement line. We use human microscopic images obtained from the tibias of female donors (60 and 81-year-old) to create 2D plain-strain models (Figure 1). We investigate the region-dependent fracture behavior of the cortical bone. We also evaluate the influence of mechanical properties of the cement line on crack growth. We adopt a brittle model of the phase-field method developed by Molnár *et al*. [2]. We implement the brittle model into a subroutine using Abaqus software. The boundary conditions of the models are shown in Figure 1.

Results and Discussion

Our results show that aging changes the crack growth trajectory in the cortical bone microstructure. Aging also affects the rate of damage. Our simulations show that the rate of damage increases by aging. This rate is highly dependent on the critical energy release rate of the osteons. The difference between the elastic moduli of the osteons and the interstitial bone also affects damage growth.

We also observe crack branching in our models. Crack branching is determined as one of the toughening mechanisms in the simulations. It happens when there are multiple osteons ahead of the main crack. Our simulations show that sometimes microcracks could reach Haversian channels by passing through cement lines. In this case, reaching microcracks to Haversian channels could lead to catastrophic failure due to the high-stress concentration associated with the channels.

We also evaluate the important role of the cement line in crack deflection. Our results indicate that crack deflection is affected by a decrease in the critical energy release rate of the cement line (i.e., decreasing the resistance of the cement line to fracture). Therefore, the microcrack is arrested along the cement line. The simulations reveal that the crack stops once it enters in a high osteon density bone tissue. We also observe that debonding mostly happens in the cement line where the interstitial bone and osteon are tougher and stiffer than the cement line. Our results also reveal that the toughness of the cortical bone microstructure is dependent on the area density of osteons. An increase in the area density of the osteons leads to an increase in the toughness of the cortical bone microstructure.

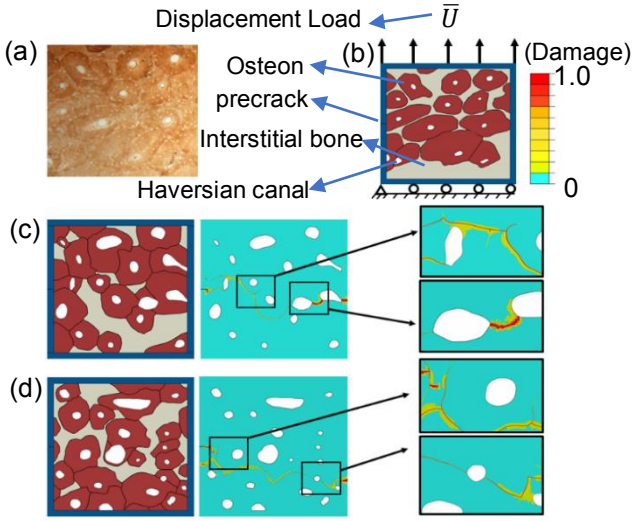

Figure 1: (a) A cross-section of the cortical bone in 60-year-old human tibia, and (b) the 2D model of the cortical bone microstructure. Fracture patterns and 2D models of the anterior region at the same cross-section of the cortical bone for two different ages (c) 60-year-old, and (d) 80-year-old. Damage with 1.0 shows the crack path and the zero value presents that there is no damage.

Significance

The findings of the present study show the region-dependent fracture behavior of the cortical bone in human tibia and this leads to improving the materials used in orthopedic implants. We can also predict the probability of failure in human tibia by monitoring the rate of damage in various regions.

Acknowledgments

The authors acknowledge the high-performance computing resources (PROTEUS: the Drexel Cluster) and support at the Drexel University. We would like to express our special thanks to Dr. Lamya Karim and Taraneh Rezaee for providing us with the cortical bone samples from human tibias. We also thank Dr. Theresa Freeman for using her facilities and providing invaluable support with the staining and imaging process.

References

[1] Najafi AR, et al. *Medical engineering & physics*, 29(6), pp.708-717, 2007.
[2] Molnár G, et al. *Finite Elements in Analysis and Design*, 130, pp.27-38, 2017.

Trabecular bone stiffness and yield are not declined after exposure to *Staphylococcus aureus*

Meir M. Barak.[1], Emily B. Long[2], and Victoria J. Frost[2]
[1]Department of Veterinary Biomedical Sciences, College of Veterinary Medicine, Long Island University, Brookville, NY, USA
[2]Department of Biology, Winthrop University, Rock Hill, SC, USA
Email: Meir.Barak@liu.edu

Introduction

Bone infection (osteomyelitis) due to *Staphylococcus aureus* (*S. aureus*) is challenging to treat due to the difficulty of early diagnosis and growing antibiotic resistance. While the cellular mechanisms of *S. aureus* and osteomyelitis have been studied, little information exists on the biomechanical effects of such infections on bone tissue. With the growing number of osteomyelitis cases diagnosed, and with the increased usage of bone banks as a source of bone graft supply, it is necessary to understand the possible long term effects of *S. aureus* induced osteomyelitis on the mechanical properties of bone. In a recent study conducted in our lab (Kunde et al. 2018), we found that *S. aureus* was able to penetrate cortical bone tissue, yet no significant difference in bone stiffness was found between the test group, exposed to *S. aureus*, and control group, immersed in distilled water (dH_20). Due to the porous nature and increased surface area of trabecular bone tissue, the potential of *S. aureus* to penetrate and negatively affect trabecular bone material properties is markedly increased. Thus, we hypothesized that bone exposure to *S. aureus* for 72 hours would significantly decrease both the stiffness and yield of trabecular bone tissue.

Methods

One hundred and three trabecular cubes (5 mm^3) from the proximal tibiae of nine white-tailed deer were cut, sterilized and then swabbed to confirm sterilization before inoculation with *S. aureus*-ATCC-12600 (test group, n = 51) or sterile nutrient broth (control group, n = 52) for 72 hours. All cubes were tested in compression along the axial direction until yield using an Instron 5942 machine. Structural stiffness (N/mm) and yield (MPa) were calculated and compared between the two groups.

Results and Discussion

Mean axial stiffness of control and test groups were 5561 ± 4027 and 5798 ± 4182 N/mm, respectively (Fig. 1, left). Mean axial yield of control and test groups were 11.0 ± 5.1 and 12.9 ± 4.9 MPa, respectively (Fig. 1, right).

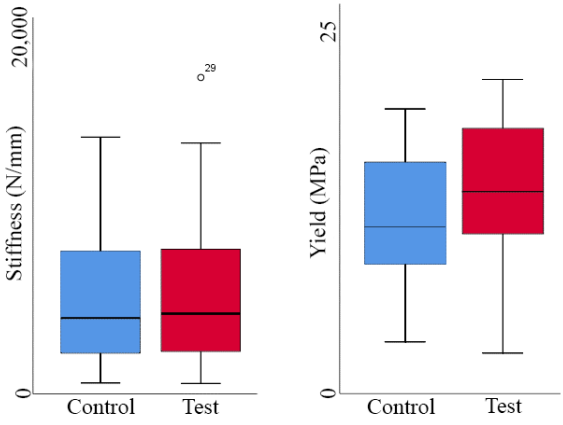

Figure 1: Boxplots comparing stiffness (left) and yield (right) between the control and test groups and the test group.

An ANCOVA (with bone density as the covariate) revealed no significant difference between groups for both stiffness and yield ($P > 0.05$), thus refuting our working hypothesis.

A Spearman's correlation statistical test reveald a significant positive correlation between stiffness and yield ($r = 0.72$, $P < 0.001$; Fig. 2).

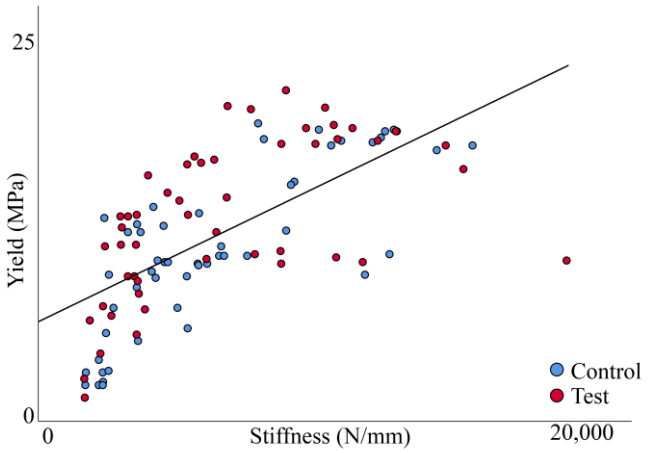

Figure 2: Scatterplot showing significant positive correlation between stiffness and yield ($P < 0.001$).

The axial direction corresponds to the primary physiological direction of loading of the proximal tibia that would occur during normal activities (walking, running, jumping, etc.).Thus, these results indicate that acute exposure to *S. aureus* probably does not adversely affect trabecular bone stiffness or yield during daily compressive loading activities.

Significance

The end-result of untreated osteomyelitis is bone necrosis and destruction of bone structure, which leads to a decrease in the ability of bone to support physiological loads. With the increase usage of bone banks as a source for bone graft supply, it is important to screen for any possible pathology that may affect the bone graft success to function normally in the receiving patient. Currently, according to the FDA's guidelines, eligible bone donors must not have had a diagnosis of sepsis "immediately preceding death," but there is no mention of previous osteomyelitis diagnosis as a donor restriction. Our findings support the current tissue collection screening methods employed by bone-graft banks.

Acknowledgments

This project was supported by the Winthrop University Research Council Grant SC19003.

References

(1) Kunde et al. 2018. J Mech Behav Biomed Mater. 82:329–37.

Joint Acoustic Emissions as a Biomarker for Knee Health Assessment in Loaded and Unloaded Exercises

Sevda Gharehbaghi[1*], Daniel C. Whittingslow[1,2], Lori A. Ponder[2], Sampath Prahalad[2], and Omer T. Inan[1]
[1]Georgia Institute of Technology, Atlanta, GA, United States
[2]Emory University School of Medicine, Atlanta, GA, United States
Email: *sevda@gatech.edu

Introduction

Juvenile idiopathic arthritis (JIA) is the most common childhood arthritis. Diagnosing and treating JIA is challenging due to its highly variable presentation and lack of reliable biomarkers. The knee is commonly affected in JIA which appears with chronic synovitis and inflammation causing damage to the underlying cartilage and bone. The internal friction of articulating joints generates acoustic emissions (AE) which can potentially be used as a digital biomarker of the disease [1]. In this study, knee AEs are compared in loaded and unloaded exercises in patients with JIA as well as healthy controls.

Methods

In this study, knee AEs were acquired from 38 participants under a protocol approved by the Georgia Institute of Technology and Emory University Institutional Review Boards. The participants were divided between two age-matched groups consisting of 18 healthy controls (15 female/3 male, 12.5 ± 3.2 years) and 20 subjects with JIA (17 female/3 male, 12.9 ± 2.5 years). To measure longitudinal changes in the knee AEs during the course of treatment, 10 subjects with JIA had a follow-up recording, 3-6 months after initial measurements.

In this protocol, subjects were asked to perform two sets of exercises as shown in Fig. 1(a): 1) unloaded knee flexion/extensions (flex/extn) while seated, and 2) loaded knee squats while bearing body weight. The joint AEs were divided into individual movement cycles (~ 4 seconds each) and bandpass filtered with a 250Hz–10kHz bandwidth to supress the noise and interference. Each cycle is divided into 200 ms frames with 50% overlap. An automated algorithm was used to detect the rubbing noise accociated with loose microphone contact [2], and the detected frames were excluded from the analysis to increase the reliability and accuracy of the analysis. Next, audio features [1] were extracted for each signal frame, which includes temporal features, band powers, spectral features, and mel-frequency ceptrum coefficients. The mean, median, and standard deviation of these features for cycle frames were calculated and imported to a soft classifier with corresponding subject labels (0 for control and 1 for arthritis). A logistic regression classifier is trained using the top 44 features, selected through a forward-feature-selection process to reduce the possibility of overfitting. The classifier assigns a knee health score for each movement cycle, which is the estimated probability that a given knee signal belongs to an involved knee with JIA (0 for control and 1 for arthritis).

Results and Discussion

The classifier performance is analyzed with leave-one-subject-out cross validation (LOSO-CV) and achieved a subject-wise accuracy of 89%. The outputs of the classifier – knee health scores – are illustrated in the box plot in Fig. 1(b), and the key results are summarized as follows: 1) The post-treatment scores in subjects with JIA were always lower than the pre-treatment scores, which correlates with these subjects' clinically reported

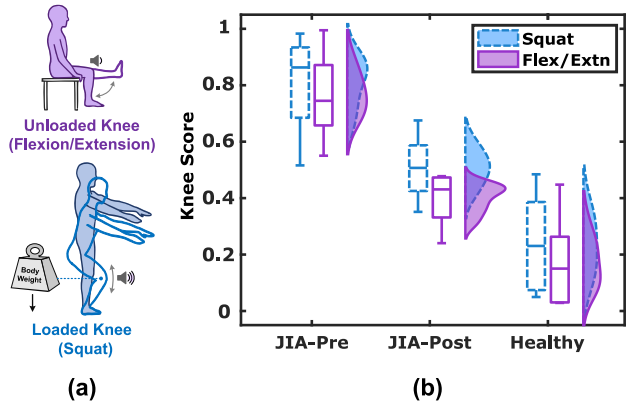

Figure 1: (a) Loaded vs. unloaded knee exercises and (b) knee health score box plots for healthy controls and subjects with JIA (pre/post-treatment).

successful treatment; 2) the median of pre-treatment knee scores in subjects with JIA for squats (loaded) is higher compared to flex/extn (unloaded), suggesting that the squat is more difficult exercise to perform than the flex/extn and AEs associated with JIA are more pronounced in squats; 3) Similarly, the median of post-treatment scores for squats are also higher compared to flex/extn, and the difference is statistically significant ($p < 0.05$ using two sample Kolmogorov-Smirnov test).

In summary, subjects with JIA exhibit significantly different knee AEs compared to healthy controls, and a successful treatment can move AE characteristics of subjects with JIA closer to those of controls. AEs produced during the loaded activity showed less of a trend toward healthy control values than the unloaded activity. We hypothesize that the loaded exercise increases interjoint friction which may make the AEs more sensitive to micro changes in the knee architecture. Future work should investigate longitudinal data taken more frequently and over longer periods of time to determine the kinetics of AEs such that these digital biomarkers can be used to titrate care in JIA.

Significance

The results of this study support the use of knee AEs as affordable and quantitative digital biomarker of knee health assessment in wearable systems. Additionally, analysis and classification of AEs from unloaded and loaded activities reveals that these two exercises contain different, possibly clinically-relevant, information that could be used to further improve this novel assessment modality in JIA.

Acknowledgments

This research was supported by the National Science Foundation under Grant Number 1749677.

References

[1] Semiz et al. (2018). *IEEE Sens J*, **18(22)**: 9128–9136.
[2] Bolus et al. (2019). *Sensors*, **19(12)**: 2683.

Associations Between Daily Steps, Moderate-Vigorous Physical Activity, and Femoral Articular Cartilage Composition in Individuals with Anterior Cruciate Ligament Reconstruction

Hope C. Davis-Wilson[1], A.C. Hackney[1], J. Troy Blackburn[1], Louise M. Thoma[1], Jason R. Franz[1,2], Lara Longobardi[1], Brian Pietrosimone[1]
[1]University of North Carolina at Chapel Hill, Chapel Hill, NC, USA, [2]North Carolina State University, Raleigh, NC, USA
Email: davishc@live.unc.edu

Introduction

Alterations in biomechanical loading may lead to deleterious changes in cartilage composition consistent with the development of early post-traumatic osteoarthritis (PTOA) in individuals with anterior cruciate ligament reconstruction (ACLR).[1] It is unknown how habitual loading, objectively measured via daily steps and time in moderate to vigorous physical activity (MVPA) with an accelerometer, influences changes in cartilage composition post-ACLR. T1rho relaxation times (T1rho) measured with magnetic resonance imaging (MRI) provide an *in vivo* estimate of proteoglycan density in the articular cartilage.[2] Decreased proteoglycan density, or increased T1rho, are indicative of early compositional changes consistent with PTOA development. The primary purpose of this study was to determine the association between T1rho in the femoral articular cartilage and daily steps and MVPA in individuals post-ACLR. Second, we evaluated the modifying influence of sex on these associations.

Methods

Twenty-six individuals (61% female, age: 21±4 years, body mass index: 24.9±2.9 kg/m^2) within 18 months of a unilateral patellar-tendon autograft ACLR were asked to wear an ActiGraph GT9X Link triaxial accelerometer placed over their right-hip for seven consecutive days. A valid wear-period for the ActiGraph was considered a minimum of 4 days (3 weekdays and 1 weekend day) and no less than 10 hours/day. T1rho MRI were acquired on the ACLR and uninjured contralateral limb. The articular cartilage of the medial femoral condyle (MFC) and lateral femoral condyle (LFC) were manually segmented and sectioned into regions of interest (anterior, central, and posterior) based on the location of the meniscus in the sagittal plane. T1rho in the ACLR limb were normalized to values in the same regions of the uninjured limb and presented as interlimb ratios (T1rho of ACLR limb/T1rho of uninjured limb). Separate univariate linear regressions were conducted to analyze the association between separate independent variables (daily steps and MVPA) and separate dependent variables (T1rho in each region of interest). Second, we stratified the analyses by sex.

Results

Greater time in MVPA associated with greater T1rho in the central LFC in the entire cohort (Table 1). Greater daily steps demonstrated greater T1rho in the anterior, central, and posterior MFC, and greater time in MVPA associated with greater T1rho in the anterior, central, and posterior MFC as well as the anterior LFC, in males (Table 1). Greater daily steps, but not MVPA, associated with lesser T1rho in the central and posterior MFC, in females (Table 1). Overall, greater time in MVPA associated with worse MRI outcomes in the entire cohort. Greater daily steps and MVPA associated with worse femoral articular cartilage composition in males, while greater daily steps associated with better cartilage composition in females.

Significance

Personalized targets for habitual loading are needed early following ACLR. Females post-ACLR may benefit from therapeutic interventions aimed at increasing habitual loading.

Acknowledgements

Supported by NIH (R21AR074094) and American College of Sports Medicine Foundation Doctoral Student Research grants.

References

1. Pietrosimone B, et al. (2017). J Orthop Res, 35(10):2288-2297.
2. Regatte R, et al. (2002). Acad Radiol, 9(12):1388-1394.

Table 1. Linear Regressions Between Habitual Loading and T1rho Relaxation Times in Individuals Post-ACLR

	Daily Steps			MVPA		
	Cohort (N=26)	Males (n=10)	Females (n=16)	Cohort (N=26)	Males (n=10)	Females (n=16)
Anterior MFC	ΔR^2=0.02 β<0.001 P=0.48	ΔR^2=0.66 β=0.06 P=0.01*	ΔR^2=0.05 β<0.001 P=0.40	ΔR^2=0.12 β=0.001 P=0.09	ΔR^2=0.75 β=0.056 P<0.01*	ΔR^2<0.001 β<0.001 P=0.98
Central MFC	ΔR^2=0.01 β<0.001 P=0.57	ΔR^2=0.64 β<0.001 P=0.01*	ΔR^2=0.28 β< -0.001 P=0.04 *	ΔR^2=0.001 β<0.001 P=0.88	ΔR^2=0.71 β=0.003 P<0.01*	ΔR^2=0.11 β= -0.002 P=0.22
Posterior MFC	ΔR^2=0.01 β<0.001 P=0.60	ΔR^2=0.57 β<0.001 P=0.01*	ΔR^2=0.30 β<-0.001,P=0.03*	ΔR^2<0.001 β<0.001 P=0.97	ΔR^2=0.45 β=0.002 P=0.03*	ΔR^2=0.12 β= -0.001 P=0.19
Anterior LFC	ΔR^2=0.03 β<0.001 P=0.44	ΔR^2=0.24 β<0.001 P=0.15	ΔR^2<0.001 β<0.001 P=0.95	ΔR^2=0.05 β=0.001 P=0.30	ΔR^2=0.50 β=0.002 P=0.023 *	ΔR^2<0.001 β< -0.001 P=0.98
Central LFC	ΔR^2=0.07 β<0.001 P=0.19	ΔR^2=0.10 β<0.001 P=0.38	ΔR^2=0.04 β<0.001 P=0.47	ΔR^2=0.18 β=0.002 P=0.03 *	ΔR^2=0.35 β=0.003 P=0.07	ΔR^2=0.02 β<0.001 P=0.57
Posterior LFC	ΔR^2=<0.001 β<0.001 P=0.96	ΔR^2=0.02 β< -0.001 P=0.69	ΔR^2=<0.001 β<0.001 P=0.96	ΔR^2=0.01 β<0.001 P=0.62	ΔR^2=0.01 β<0.001 P=0.76	ΔR^2=0.01 β<0.001 P=0.67

*significant association (P ≤ 0.05)

Linear Discriminant Analysis Predicts Knee Injury Outcome from Biomechanical Variables

Nathan D. Schilaty[1], Nathaniel A. Bates[1], Aaron J. Krych[1], Timothy E Hewett[2]
[1]Mayo Clinic Biomechanics Laboratories & Sports Medicine Center, Rochester & Minneapolis, MN, USA
[2]Hewett Consulting, Minneapolis, MN, USA
Email: schilaty.nathan@mayo.edu

Introduction

Continued evidence supports that knee abduction moment is a factor that contributes to non-contact anterior cruciate (ACL) injury,[1-2] with the non-contact mechanism accounting for 70-80% of ACL injury.[3] However, there are also concomitant injuries that occur with non-contact ACL injury, including the medial collateral ligament (MCL) and the medial meniscus. The most commonly damaged structures of the knee are the ACL, MCL, and menisci.

Given that these injuries present as either isolated or concomitant, it follows that these events are driven by specific mechanics versus mere coincidence. This study was designed to investigate the multiplanar mechanisms and determine the important biomechanical and demographic factors that contribute to classification of specific injury outcomes.

Methods

In vivo kinetics/kinematics of 42 healthy, athletic subjects were measured to determine stratification of injury risk (i.e. low, medium, and high) in three degrees of knee forces/moments (knee abduction moment, anterior tibial shear, and internal tibial rotation). These stratified kinetic values were input into a cadaveric impact simulator to assess ligamentous strain and knee kinetics during a simulated landing task.[1] Uni-/multi-axial load cells and implanted strain sensors were utilized to collect mechanical data for analysis. Data analyses were performed on 41 specimens [age 44 (37.5, 47.5) years; 79.3 (64.0, 100.9) kg; 21M:20F]. Of the 41 specimens included in this study, there were 5 different classifications of injury (**Table 1**). Linear Discriminant Analysis (LDA) was utilized to determine classification of injury outcomes from biomechanical variables.

Results and Discussion

Three LDA models were generated: 5-, 10-, and the optimized 11-factor model. The 5-factor model was 14% less accurate than the 10-factor model, but could properly classify 63.4% of injuries [area under the curve (AUC) ≥0.68] with 'excellent' prediction of 4 of 5 injury classifications. The 10-factor model improved accuracy (77.5%; AUC ≥0.94), especially with the ACL+MCL injury group (AUC improved from 0.68 to 0.94). Finally, the optimized 11-factor model improved accuracy (87.5%; AUC ≥0.96, **Fig. 1**). It should be noted that since there are 5 outcomes possible, the random chance for selection of the appropriate outcome would be 1 in 5 (20%). These data demonstrate that these particular knee injuries are not random occurrence, but are determined by specific biomechanical forces/torques at the time of injury.

Utilization of LDA accurately predicted the outcome of knee injury from kinetic data from cadaveric simulations with the utilization of a mechanical impact simulator. Thus, it is possible to use knee joint kinetics to determine clinical risk of injury as well as differentiate the likely type of presentation during knee injury. LDA demonstrates that injury outcomes are largely characterized by specific mechanics that can distinguish ACL, MCL, and medial meniscal injury. Furthermore, as the mechanics of injury are better understood, improved interventional prehabilitation can be designed to reduce these injuries.

Table 1. Confusion Matrix of 11-Factor LDA.

		Predicted Count				
	Injury Group	**ACL**	**ACL+ MCL**	**ACL+ MCL+ Meniscus**	**ACL+ Meniscus**	**MCL**
Actual Count	**ACL**	21	2	0	0	0
	ACL+MCL	2	8	0	1	0
	ACL+MCL+ Meniscus	0	0	1	0	0
	ACL+ Meniscus	0	0	0	3	0
	MCL	0	0	0	0	2

Note: Highlighted boxes demonstrate agreement between predicted and actual values. Values in the diagonals denote correct predictions.

Significance

This study demonstrates that knee injury outcomes are not mere coincidence, but are driven by specific injury mechanics. These specific injury mechanics can *predict* the type of knee injury outcome with high confidence. This classification paradigm is an important step in future production of machine learning algorithms that can rapidly assess complex, covariate data and determine specific risk of musculoskeletal injury.

Figure 1: ROC Curves of the 11-Factor Linear Discriminant model of Knee Injury. The plots demonstrate the AUC and prediction sensitivity/specificity for each injury classification.

Acknowledgments

NIH funding: K12HD065987 and L30AR070273 to NDS, R01AR055563 to NAB and AJK, and R01AR056259 to TEH.

References

1. Bates NA et al. *Clin Bio* (2017) 44:36-44.
2. Bates NA et al. *Am J Sport Med* (2018) 46(9):2113-2121.
3. Schilaty ND et al. *Orthop J Sport Med* (2017) 5(8):1-8.

Mindsets are related to reductions in pain after a gait modification intervention for people with osteoarthritis

Melissa A. Boswell[1], Sean R. Zion, Scott D. Uhlrich, Jennifer L. Hicks, Alia J. Crum, and Scott L. Delp
[1]Department of Bioengineering, Stanford University
Email: boswellm@stanford.edu

Introduction

Psychological factors and the context of an intervention (e.g., personal interactions, beliefs about the outcomes, intervention presentation) can affect outcomes above the direct effects of the intervention alone [1]. For example, telling individuals they have a high-endurance genotype increases their cardiorespiratory capacity during running, regardless of their actual genotype [2]. Mindsets, which are core assumptions about the nature of things and processes in the world, are psychological factors that orient people to a particular set of expectations, explanations, and goals. Patients with more adaptive mindsets about chronic illness (e.g., "my illness may be challenging, but it can be managed") report improved physical and mental health compared to patients with less adaptive illness mindsets (e.g., "my illness negatively impacts all parts of my life") [3].

The relationship between mindsets and biomechanical interventions is unknown, yet likely influences intervention efficacy and patient outcomes. As a first step towards understanding this relationship, we evaluated the association between mindsets about chronic illness and changes in pain after introducing a gait modification for people with knee osteoarthritis, a chronic disease. We hypothesized that a more adaptive mindset about chronic illness would be associated with larger reductions in pain. By studying mindsets and interventions together, we can understand how they influence each other, and how they both influence health.

Methods

Twenty-six individuals with radiographic knee osteoarthritis completed one year of gait retraining aimed at reducing the loading in the medial compartment of their knee (via reducing the knee adduction moment). During 13 visits to the gait lab, participants were trained to adopt their modified gait pattern. Medial knee pain was assessed with the 11-point numerical rating scale (NRS) from no pain (0) to the worst imaginable pain (10). Reduction in pain was defined as the difference in NRS pain score between the beginning and end of the study (where a positive value indicates less pain at the end of the study). At the end of the study, participants' mindsets about illness were assessed with the Illness Mindset Inventory (IMI) [3]. The participants' illness mindsets were calculated as a composite variable (from 1-6) using the catastrophe and manageable subscales of the IMI, with higher scores reflecting the mindset that chronic illness is manageable. We calculated Pearson's correlation coefficient (R) to evaluate the association between illness mindsets and reduction in pain.

Results and Discussion

Illness mindset was positively correlated with pain reduction ($R=0.433$, $p=0.027$), meaning a more adaptive mindset was related to a larger reduction in pain (Figure 1). On average, participants experienced significant reductions in their pain ($p<0.001$) and knee adduction moment ($p<0.001$) with their personalized gait modification. These results suggest that the illness mindset may influence pain outcomes in addition to the reduction in medial knee loading.

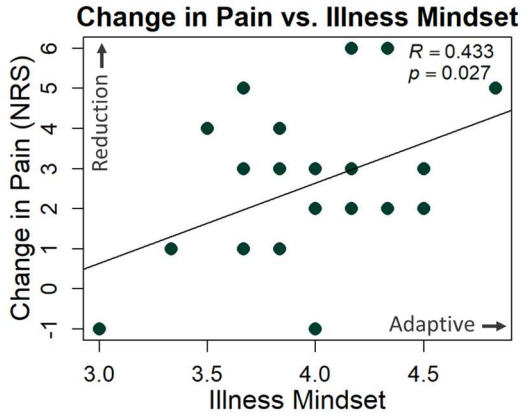

Figure 1: Change in pain vs. illness mindset. A reduction in pain is associated with a more adaptive illness mindset.

Due to the cross-sectional nature of this study, we cannot determine causality. Mindsets at the end of the intervention are likely shaped by the participant's experiences and expectations both before and during the intervention. If biomechanical interventions affect mindsets, we can leverage the influence on mindsets for optimal intervention compliance, design, and outcomes. For example, even if a biomechanical intervention, such as a gait modification, reduces knee loading, patients that do not have the mindset that they can manage their disease may not receive the maximum benefit from the intervention. In addition to psychological improvements, these benefits can include physical improvements as mindsets can influence physiological processes, such as inflammation. On the other hand, mindsets may influence the efficacy of interventions by mediating outcomes, such as changes in pain. This research motivates future work to understand the mechanisms by which biomechanical interventions affect mindsets and vice versa.

Significance

We found that an individual's mindset about chronic illness is related to changes in pain after a biomechanical intervention. By bridging the gap between psychology and biomechanics, we can design traditional biomechanical interventions more effectively. Integrating subtle nudges towards more adaptive mindsets, such as presenting an intervention as an opportunity to manage pain or chronic illness, may improve intervention compliance and health outcomes.

Acknowledgments

This work was supported by the NSF GFRP Grant No. DGE – 1656518, U.S. Dept. of VA Rehab RD Service Merit Review Award No. I01 RX001811, and Stanford Catalyst Project.

References

[1] Zhang W et al. *Ann Int Med,* 163(5). 2015.
[2] Turnwald et al. *Nature Hum Behav,* 3. 2019.
[3] Zion et al. *Soc for Pers and Soc Psych Ann Conf*. 2018.

Isolating the energetic consequences of mechanically imposed reductions in ankle and knee flexion during gait

*Emily M McCain[1], Katherine R Saul[1], Gregory S Sawicki[2], and Michael D Lewek[3]
[1]Department of Mechanical Engineering, North Carolina State University, Raleigh, NC, USA
[2]George W. Woodruff School of Mechanical Engineering, Georgia Institute of Technology, Atlanta, GA, USA
[3]Division of Physical Therapy, University of North Carolina at Chapel Hill, Chapel Hill, NC, USA
Email: *emmccain@ncsu.edu

Introduction

Post-stroke gait is influenced by paretic limb weakness and marked by increases in metabolic cost. Weakness at the ankle is associated with reduced peak ankle power and propulsion, and knee extension is the cornerstone of "stiff-knee gait," which results in compensatory mechanics including hip hiking and circumduction [1]. Post-stroke gait interventions often seek to improve paretic ankle and knee function thereby reducing the need for the compensations assumed to contribute to increased metabolic cost [2, 3]. *However, the design of these interventions is limited since ankle and knee flexion are interrelated, making the independent roles of ankle and knee dysfunction on metabolic efficiency difficult to discern*. Using a knee brace and custom 3D printed ankle stay, this study isolated the contributions of unilaterally reduced ankle flexion, knee flexion, and ankle+knee flexion on walking outcomes and energetics. Our hypotheses are: (h1) reduced ankle and knee flexion will result in decreased propulsion and increased circumduction, respectively, (h2a) Reduced ankle + knee flexion will yield the highest metabolic cost, and (h2b) limiting ankle flexion will be more metabolically expensive than limiting the knee.

Methods

Data were recorded for 15 (7M/8F) unimpaired controls walking ($0.8ms^{-1}$) for 7 mins in the following conditions: braced control (*unlocked*), unilaterally fixed ankle (*uni-ank*), unilaterally fixed knee (*uni-knee*), and unilaterally fixed ankle and knee (*uni-a+k*). We converted recorded rates of oxygen consumption and carbon dioxide production to metabolic powers [4]. A motion analysis system recorded 3D positions of markers placed on the pelvis and lower limbs. Simulations performed in OpenSim (v3.3) used a lower limb model adapted from a full-body model and scaled to participants [5]. Inverse kinematics, inverse dynamics, and analysis tools were used to compute joint angles, moments, and powers, respectively. Limb circumduction was calculated as maximum lateral foot displacement during swing [1]. Ground reaction forces measured on an instrumented dual-belt treadmill were used to identify peak propulsion. Outcome measures were averaged over 10 consecutive gait cycles, and statistical significance between conditions was determined by paired t-tests ($p<0.05$) with Bonferroni correction for multiple comparisons.

Results and Discussion

Peak propulsion on the locked limb (**Fig 1a.**) was significantly decreased in *uni-ank* and *uni-a+k* conditions compared to *unlocked,* demonstrating that restricting the ankle limited subjects' capacity to propel forward. Additionally, hip circumduction (**Fig 1b.**) was significantly higher in *uni-knee* and *uni-a+k* conditions as compared to *uni-ank* condition, reinforcing the interaction between reduced knee flexion and circumduction. These results support h1 and demonstrate the effectiveness of mechanical bracing to elicit compensatory strategies characteristic of post-stroke gait.

While metabolic cost (**Fig 1c.**) in the *uni-a+k* condition was significantly higher than *unlocked* and *uni-knee*, it was not significantly higher than the *uni-ank* condition, so we reject h2a. Additionally, the *uni-ank* condition was not significantly ($p=0.17$) more metabolically expensive than *uni-knee* condition; therefore, we reject h2b. However, we note that both the *uni-ank* and *uni-a+k* conditions are significantly higher than the *unlocked* condition, indicating that regardless of restrictions in knee flexion, any direct restriction on the ankle is metabolically detrimental. Further, the significant increase in metabolic rate between *uni-knee* and *uni-a+k* suggests that combined restriction of the ankle and knee is more metabolically detrimental than restriction of the knee in isolation.

Significance

These results confirm that the combined impacts of reduced ankle and knee flexion are more detrimental metabolically than reduced knee flexion alone, providing support for the potential of ankle-based rehabilitative technologies in persons post-stroke to provide a metabolic benefit.

Acknowledgments

NIH grant F31 HD097872-01 to EMM

References

[1] Lewek, M et al (2012). *Arch Phy M & R* **93**(1): p. 123-128.
[2] Awad, L et al. (2017) *Science* **9** (400).
[3] Chen, G et al. (2015) *G&P* **22** (1): p. 57-62.
[4] Brockway, J. (1987) Hum Nutr Clin Nutr 41(6): p. 463-71.
[5] Rajagopal et al. (2016). *IEEE T Biomed Eng.* **63:** 2068-207.

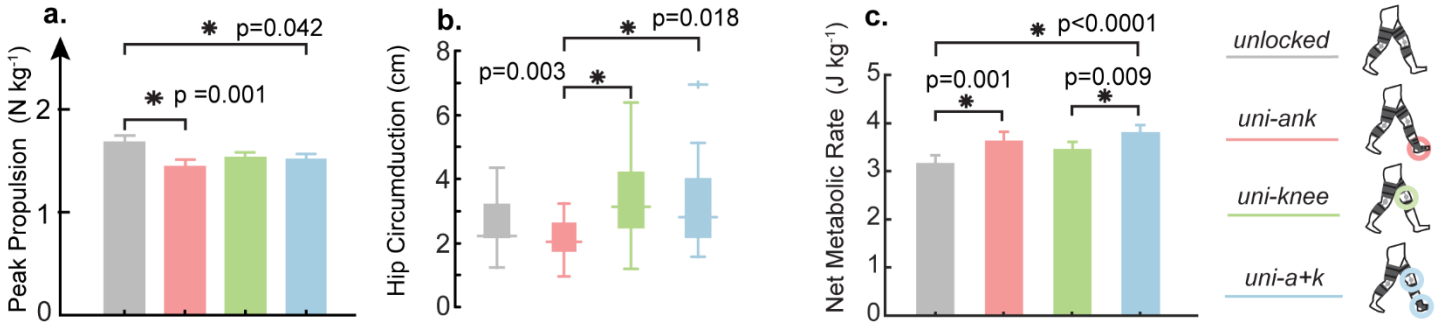

Figure 1. Subject averaged **(a)** locked limb peak propulsion, **(b)** locked limb hip circumduction, and **(c)** net metabolic rate are shown with standard errors for *unlocked*, *uni-ank*, *uni*-knee, and *uni-a+k* conditions.

Real-Time Gait Biofeedback Enhances Dynamic Ankle Stiffness and Propulsion in Healthy and Post-Stroke Participants

Nicole K. Rendos[1], Jeffrey D. Simpson[2], Zahin Alam[1], Amit Grewal[1], Annie Goldman[1], Sophie Hart[1], Benjamin M. Rogozinski[1], Trisha M. Kesar[1]
[1]Emory University School of Medicine, Atlanta, GA; [2]University of West Florida, Pensacola, FL
Email: nrendos@emory.edu

Introduction

Individuals with post-stroke hemiparesis demonstrate decreased propulsive force generation from the paretic leg during late stance, measured as anteriorly-directed ground reaction force (AGRF).[1] Reduced paretic AGRF adversely impacts gait speed, inter-limb symmetry, and walking function.[1,2] Gait interventions such as treadmill training, functional electrical stimulation, and gait biofeedback have shown improvements in paretic AGRF.[3-6]

Gait biofeedback (BF) provides the user with instantaneous, quantitative information regarding a targeted gait variable with the intent to improve gait impairments. Previously, we showed that a single session of real-time AGRF BF improves peak AGRF in post-stroke and young able-bodied individuals, with concomitant short-term improvements in gait variables such as plantarflexor (PF) moment and trailing limb angle.[5,6]

PF moment and ankle power generation during the mid- to late stance phase of gait contribute to propulsive force generation, which is crucial for normal stance-to-swing transition, and are reduced in individuals post stroke.[2] Dynamic ankle-joint stiffness (DAS) during gait is the resistance to an applied moment, with contributions from both active and passive mechanisms.[7,8] DAS can be modulated in response to mechanical demands of walking and contributes to propulsion.[9] The relative contributions of active (e.g. PF moment and power) versus more passive (e.g. stiffness) factors to gait propulsion are poorly understood, especially post-stroke. The purpose of this study was to examine the contributions of peak PF moment and DAS on BF-induced increases in AGRF in able-bodied and post-stroke individuals.

Methods

Baseline gait data were collected on 9 individuals with post-stroke hemiparesis (6 M, 3 F, 63 ± 9.8 y, 44.9 ± 36.0 months post-stroke) and 9 able-bodied individuals (2 M, 7 F, 24.6 ± 3.0 y) as they walked at a self-selected pace on an instrumented treadmill (Baseline). Next, during a BF trial at matched speed (AGRF-BF), participants were provided audiovisual feedback to increase peak AGRF in the paretic (stroke) or right (healthy) leg by 25% compared to baseline.[5,6]

Gait biomechanics data were collected with (AGRF-BF) and without (Baseline) AGRF biofeedback. Dependent variables included peak AGRF, peak PF moment, and DAS of the targeted limb. DAS was calculated as the average of ankle moment-ankle angle slopes during dorsiflexion during the stance phase of gait.[7,8] Repeated measures ANOVAs and % change scores (AGRF-BF versus Baseline) were calculated to examine the effects of AGRF-BF. Correlation analyses evaluated relationships among % change scores for each combination of dependent variables.

Results and Discussion

As intended, BF targeting peak AGRF successfully increased peak AGRF during stance of the target leg in both post-stroke and control subjects by 150.7% and 61.6%, respectively. ($F_{(1,17)}$ = 44.78, $p < .001$). AGRF-BF increased PF moment in both paretic (stroke) and right legs (able-bodied) with increases of 15.9% and 11.0% respectively ($F_{(1,17)}$ = 26.06, $p < .001$). Similarly, AGRF-BF increased DAS in both the paretic (post-stroke) and right leg (control), with increase of 17.1% and 31.8%, respectively ($F_{(1,17)}$=9.22, p = .007). Although AGRF-BF induced significant increases in peak AGRF, PF moment, and DAS, correlations among these % change scores were weak (R^2=0.03-0.2).

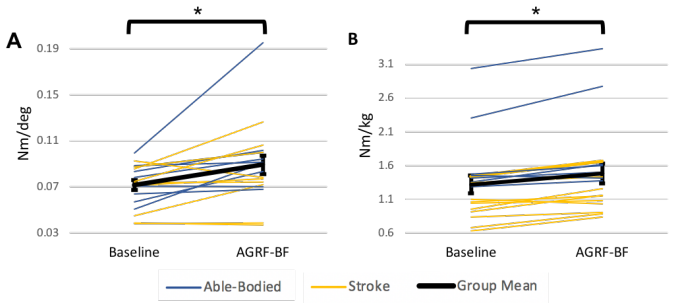

Figure 1. (A) DAS and (B) Peak PF moment data. *indicates significant increase between Baseline to AGRF-BF.

While both stroke and able-bodied groups showed significant improvements in both DAS and PF moment during AGRF-BF versus baseline, smaller increases in DAS were observed in the paretic limb post-stroke (17.1%) than in able-bodied individuals (31.8%). We speculate that post-stroke, there may be greater contributions of passive versus active mechanisms to DAS[8], explaining smaller BF-induced increases in DAS on the paretic leg post-stroke compared to controls, in contrast to similar improvements in PF moment (15.9% vs. 11.0%). Additionally, lack of correlation among % change scores may reflect variable movement strategies as participants develop individualized biomechanical solutions to achieve greater propulsion during BF.

Significance

Our results take a step toward elucidating potential contributions of passive and active mechanisms to propulsion during late stance in individuals post-stroke, using gait biofeedback as a probe. Future studies will investigate intrinsic factors contributing to DAS during gait in able-bodied versus post-stroke individuals, by concurrent measurement of joint excursion and angular velocities, EMG, and clinical measures. This work has potential clinical implications for gait rehabilitation targeted at enhancing propulsion and gait speed in individuals post-stroke.

Acknowledgements

NIH NICHD R01 HD095975, K01 HD079584, R21 HD095138 (Kesar)

References

[1] Bowden MG. *Stroke*. 2006; 37(3): 872. [2] Awad LN. *Neurorehabil Neural Repair*. 2015; 29(6): 499. [3] Awad LN. *Arch Phys Med Rehabil.* 2014; 95(5): 840. [4] Awad LN. *Neurorehabil Neural Repair*. 2016; 30(7): 66. [5] Genthe K. *Top Stroke Rehabil*. 2018: 25(3): 186. [6] Schenck C. *J Neuroeng Rehabil*. 2017; 14(1): 52. [7] Davis RB. *Gait Posture*. 1996; 4(3): 224. [8] Lamontagne A. *Arch Med Phys Rehabil*. 2000; 81(3): 351. [9] Bayram H. *J Foot Ankle Surg*. 2018; 57(4): 668.

Using visual guidance to acquire work from the treadmill during split-belt walking does not accelerate adaptation

Camille Grandjean*[1], Noah Tristan*[1], Surabhi N. Simha[2], J. Maxwell Donelan[2], James M. Finley[1,3], and Natalia Sanchez[3]
*Equal contribution. [1]Department of Biomedical Engineering, University of Southern California, Los Angeles, CA, 90089
[2]Department of Biomedical Physiology and Kinesiology, Simon Fraser University, Burnaby, British Columbia, Canada V5A 1S6
[3]Division of Biokinesiology and Physical Therapy, University of Southern California, Los Angeles, CA, 90033

Introduction

Human gait patterns are influenced by our surroundings, and when introduced to potential sources of assistance, our neuromotor system adapts our gait to take advantage of this assistance. We recently found that split-belt treadmills can act as assistive devices by performing positive work on the body during walking [1]. During initial split-belt adaptation, step lengths are longer with the leg on the slow belt, but as time progresses, people lengthen the steps on the fast belt [2] and gradually reduce the mechanical work performed by the legs [3] and metabolic cost [4]. As people bring their fast leg further forward to walk with longer steps on the fast belt, they generate net negative work with the legs such that people can exploit the work done by the treadmill to reduce the positive work by the legs [1]. However, the emergence of this gait requires at least three times longer than is typically allotted in adaptation experiments [5]. Whether instructing individuals to walk with a gait that minimizes the amount of positive work by the legs would change the timescale of the adaptation process has yet to be determined. We hypothesized that providing people with guided experience of a gait that exploits positive work from the treadmill will accelerate adaptation toward a less energetically costly gait [6].

Methods

Eight people walked on an instrumented split-belt treadmill with left and right belts moving at 0.5 m/s and 1.5 m/s, respectively. We measured ground reaction forces and the location of ankle markers. We defined step lengths as the distance between ankle markers at heel strike and step length asymmetry (SLA) as fast minus slow step length, normalized by the sum. Participants used visual feedback to maintain an SLA of +15% for five minutes (SplitFBK), and after five minutes, we turned the feedback off (SplitNoFBK) without stopping the treadmill and participants walked for an additional 10 minutes. We calculated the mechanical work rate using the individual limbs method [3,7]. We compared fast limb placement at heel-strike and fast leg work rate for the first minute (1st min) of SplitFBK and the first and last minute after feedback was turned off (SplitNoFBK) to data at the same time-points (6th and 15th min) from a previous unguided adaptation study [5] using independent samples t-tests.

Results and Discussion

During SplitFBK, participants rapidly increased forward placement of the fast leg compared to unguided adaptation (Fig. 1A & B, $p=6.69\times10^{-6}$). This increase in forward foot placement led to a positive SLA (0.08 ± 0.05). Initially, during SplitNoFBK, limb placement remained further forward compared to unguided adaptation (6th min, p=0.020). By the end of adaptation, limb placement was not different between participants who experienced guided vs. unguided adaptation [8] (15th min, p=0.090). The initial increase in forward foot placement was accompanied by a lower positive work rate by the fast leg during SplitFBK compared to unguided adaptation (Fig. 2A, p=0.039 1st min). Thus, participants acquired and accepted positive work by the treadmill to reduce the work by the legs at initial exposure to the split-belt treadmill. However, after removing feedback, participants generated similar amounts of work as seen in unguided adaptation (Fig 2B, 6th and 15th min).

Results suggest that short-term, guided experience with a less energetically costly gait can aid in increasing external assistance, but is not sufficient for people to retain this gait when guidance is removed. Therefore, performance using guided experience is not an indication that individuals have learned how to adjust their gait to accelerate energetic optimization.

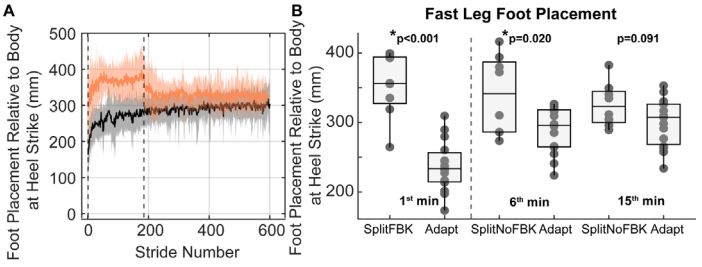

Figure 1. Foot placement on the fast belt relative to the body. A) Timeseries. Off-red: Guided adaptation. Black: Data from previous adaptation study. Vertical lines: start of SplitNoFBK trial. B) Foot placement at specific timepoints during our study and a previous unguided adaptation study (Adapt).

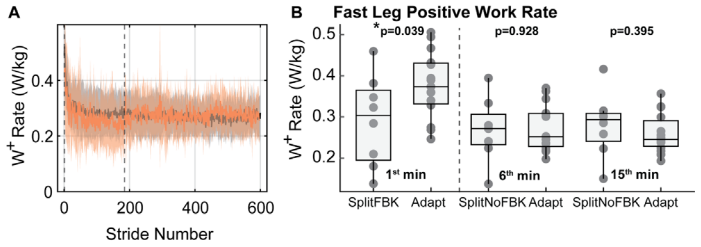

Figure 2. Positive work rate by the fast leg. A) Timeseries. B) Positive work rate at specific timepoints.

Significance

The success of assistive devices for reducing energy cost depends not only on their design but also on the neuromotor system's ability to adapt coordination to take advantage of external assistance. Accelerating adaptation to assistive devices will lead to more effective implementation of these systems both in healthy and pathological populations. Here, we show that despite the effective use of external assistance with guided feedback, individuals do not retain coordination patterns that allow them to effectively take advantage of assistance in the absence of feedback. Therefore, short exposure with less energetically costly gaits is not enough to accelerate adaptation of locomotion to use external assistance.

References: [1] Sánchez et al. J Physiol 2019. [2] Reisman et al. JNeurophysiol 2005. [3] Selgrade et al. J Exp Biol 2017. [4] Finley et al., JPhysiol 2013. [5] Sánchez et al. Dyn.Walk., 2019. [6] Selinger et al., CurrBiol 2015. [7] Donelan et al. JBiomech 2002. [8] Roemmich et al. CurrBiol 2016.

Step time asymmetry optimizes energy cost of split-belt treadmill walking

Jan Stenum[1,2] and Julia T. Choi[3]
[1]Center for Movement Studies, Kennedy Krieger Institute, Baltimore, MD 21205
[2]Department of Physical Medicine and Rehabilitation, The Johns Hopkins University School of Medicine, Baltimore, MD 21205
[3]Department of Applied Physiology and Kinesiology, University of Florida, Gainesville, FL 32611
Email: jstenum1@jhmi.edu

Introduction

Hemiparetic and amputee gaits are often asymmetric and uneconomical [1]. Consequently, asymmetry has been thought to explain the added cost of pathological gait. But it is also possible that gait asymmetry may be adopted if it is energetically optimal.

Adaptability of gait asymmetry is often shown using a split-belt treadmill. Following an adaptation period, step lengths return to symmetry while step times become asymmetric [2]. Recent studies have estimated the energetically optimal value of step length asymmetry [3], but it is unknown how step time asymmetry affects energy cost of split-belt treadmill walking.

Here, we tested the hypothesis that the preferred asymmetry in step times and step lengths adopted during split-belt treadmill walking are selected to optimize energy cost. We tested this hypothesis in 3 speed-difference conditions in which the average speed was kept constant at 1.25 m s^{-1} while speed-differences were set at 0.5 m s^{-1}, 1.0 m s^{-1} and 1.5 m s^{-1}.

Methods

We recruited 10 healthy, young participants that walked on a split-belt treadmill in 3 speed-difference conditions (Δ0.5 m s^{-1}, Δ1.0 m s^{-1} and Δ1.5 m s^{-1}) on separate days. Speed-differences between the belts were set at 0.5 m s^{-1}, 1.0 m s^{-1} and 1.5 m s^{-1} while the average belt speed was constant at 1.25 m s^{-1}. During each visit, participants walked: 1) with tied-belts at 1.25 m s^{-1}; 2) in an adaptation trial with belts split to assess preferred asymmetry; and 3) in cost mapping trials with belts split. Cost mapping consisted of one set of trials with step time asymmetry enforced to −0.10, −0.05, 0, +0.05 and +0.10 of the preferred value (obtained during adaptation) and another set of trials with step length asymmetry enforced to −0.10, −0.05, 0, +0.05 and +0.10. Asymmetry is calculated as the difference between the 2 steps divided by their sum. We express metabolic cost as the percentage of net metabolic power of split-belt walking relative to its value during tied-belt walking. Energetically optimal values of asymmetry were estimated for individual participants from the cost mapping trial with minimal metabolic cost. We used paired *t*-tests to test if the preferred asymmetry in step times and step lengths were different from the energetically optimal value of asymmetry.

Results and Discussion

Participants increased their preferred value of step time asymmetry with greater speed-differences between belts (Fig. 1A; 0.080, 0.178 and 0.282, $F_{2,18}$=288.1, P<0.001; post-hoc tests P<0.001). Participants' preferred value of step time asymmetry tracked the energetically optimal values (Fig. 1B; 0.082 for Δ0.5 m s^{-1}, P=0.407; 0.183 for Δ1.0 m s^{-1}, P=0.545; 0.302 for Δ1.5 m s^{-1}, P=0.096). This suggests that participants adopted asymmetric step times in order to optimize energy cost.

Participants' preferred values of step length asymmetry remained constant, and nearly symmetric, with greater speed-differences (Fig. 1C; −0.024, −0.034 and −0.047, $F_{2,18}$=4.0, P=0.037; post-hoc tests P≥0.168). In contrast to step time asymmetry, preferred values of step length asymmetry were not energetically optimal (Fig. 1D; 0.036 for Δ0.5 m s^{-1}, P=0.001; 0.061 for Δ1.0 m s^{-1}, P<0.001; 0.086 for Δ1.5 m s^{-1}, P<0.001). While modifying step length asymmetry may lead to energy savings during the adaptation period [2,3], our results suggest that the preferred value of step length asymmetry is not selected in order to optimize energy cost.

Our findings show that humans will adopt an asymmetric gait to optimize energy cost and suggest that energy optimization of gait asymmetry is associated with the control of temporal gait asymmetry.

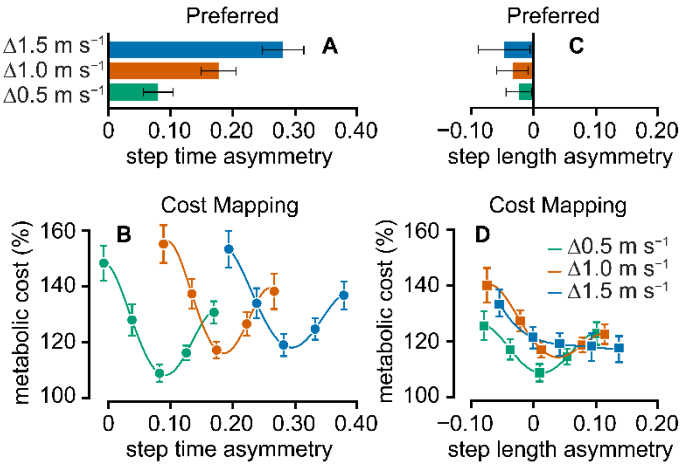

Figure 1: Preferred asymmetry and cost mapping during split-belt treadmill walking. Preferred step time asymmetry (A) and step length asymmetry (C) obtained from adaptation trials (error bars are S.D.). Metabolic cost of step time asymmetry (B) and step length asymmetry (D) from cost mapping trials (error bars are S.E.M.). Metabolic cost is net metabolic power relative to its value in tied-belt walking at 1.25 m s^{-1}.

Significance

We have shown that healthy humans adopt asymmetric step times during split-belt treadmill walking that are energetically optimal. Our results support the idea that gait asymmetry may be adopted if asymmetry is energetically optimal. This suggests that the gait asymmetry commonly seen in clinical populations may be adopted because it is an economical gait pattern for these individuals and that enforcing a symmetric gait pattern will result in increased energy cost. Of special notice is whether gait asymmetry is manifested in the spatial or temporal domain since our results suggest that it is only the control of temporal gait asymmetry that is associated with energy optimization.

References

1. Waters, RL and Mulroy, S. (1999). *Gait Posture* **9**, 207–31.
2. Finley, JM, et al. (2013). *J Physiol* **591**, 1081–95.
3. Sánchez, N, et al. (2019). *J Physiol* **597**, 4053–68.

The Effects of Age and Locomotor Demand on Foot Mechanics During Walking

Rebecca L. Krupenevich[1*], Samuel F. Ray[2], William H. Clark[1], Kota Z. Takahashi[2], Howard E. Kashefsky[3], Jason R. Franz[2]
[1]UNC Chapel Hill and NC State University, Chapel Hill, NC
[2]University of Nebraska Omaha, Omaha, NE
[3]UNC Hospitals, Chapel Hill, NC

Email: *rlkrup@email.unc.edu

Introduction

Older adults exhibit a substantial reduction in push-off intensity during walking that is often attributed to deficits in mechanical output from the plantarflexor muscles. Yet, muscle strengthening has been generally unsuccessful in improving habitual gait performance [1], indicating the plantarflexors are not the sole source of age-related reductions in push-off intensity. Recent studies have revealed an important role for foot structures in governing push-off power during walking [2]. The structures of the foot (e.g. plantar aponeurosis and intrinsic muscles) are uniquely suited to function as both a stiff lever for push-off and an elastic energy storage and return system[3] for economical locomotion. However, the effect of age on foot mechanics during walking is unclear. The purpose of this study was to quantify age-related differences in foot mechanical work during walking. Consistent with evidence of age-related decreases in the stiffness of elastic tissues spanning the foot and ankle [4], we hypothesized that (i) older adults would exhibit less positive foot work and more net negative foot work compared to young adults – effects that would (ii) increase with locomotor demand.

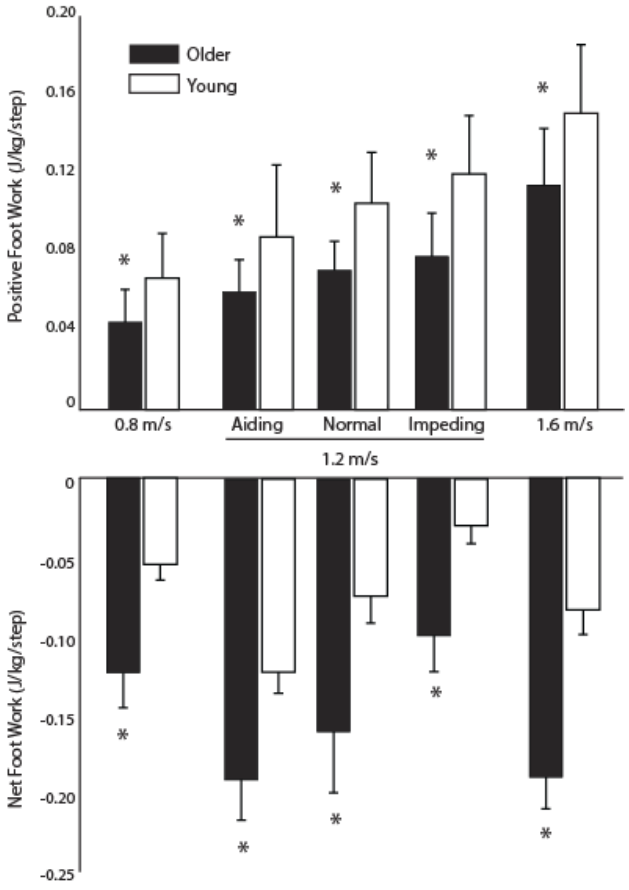

Figure 1. Group means (SE) for positive (top) and net (bottom) foot mechanical work during walking. *age effect, p<0.05

Methods

9 young (24±3 yrs, 76.5±10 kg, 1.7±0.1 m, 5M/4F) and 9 older adults (73±4 yrs, 69.3±6.8 kg, 1.7±0.1 m, 5M/4F) walked barefoot on an instrumented treadmill at three speeds (0.8, 1.2, and 1.6 m/s). Subjects also walked at 1.2 m/s while wearing a waistbelt connected to a motor that prescribed constant horizontal pulling forces (impeding or aiding) equal to 5% body weight. Lower limb kinetics and kinematics were recorded during all walking trials. We calculated foot work in Visual3D using a unified deformable foot model, accounting for contributions of structures distal to the hindfoot's center-of-mass [5]. Two mixed-factor ANOVAs were performed to test for the effect of age and speed (0.8, 1.2, 1.6 m/s) or horizontal pulling force (1.2 m/s, aiding, impeding) on positive and net foot work.

Results and Discussion

Consistent with our first hypothesis, we found that older adults generated, on average, 38% less positive and 76% more net negative foot work across speeds (W^+: p=0.007; W^{net}: p=0.014) and pulling forces (W^+: p=0.001; W^{net}: p=0.007) compared to young adults (Fig. 1). Contrary to our second hypothesis, the effect of age on positive and net foot work did not change with increasing speed (age×condition, W^+: p=0.527; W^{net}: p=0.108) or pulling force (age×condition, W^+: p=0.251; W^{net}: p=0.543). Although both age groups responded similarly to changes in locomotor demand, greater energy losses via foot structures would appear to place older adults at more of a mechanical disadvantage to young adults during walking tasks with greater demand for power generation; specifically, impeding forces are functionally analogous to accelerating or walking uphill.

Significance

Age-related differences in foot mechanics may contribute to reduced push-off intensity - directly via foot mechanical energy loss, and indirectly via the misappropriation of ankle power output. Moreover, mechanical energy losses via the foot may have metabolic consequences with additional functional relevance. Ultimately, these findings emphasize the need for broader perspective in our biomechanical understanding and thus clinical management of walking ability limitations in our rapidly aging population.

Acknowledgments

This work was supported by a grant from the NIH (R01AG058615)

References

[1] Franz (2016). *Exer Sport Sci Rev*, 44(4):129-136
[2] Zelik and Honert (2018). *J Biomech*, 75: 1-12
[3] Kelly et al. (2019) *J Appl Physiol*, 126(1): 231-238
[3] Onambele (2006). *J Appl Physiol*, 100: 2048-2056
[4] Takahashi et al. (2017), *Sci Rep*, 7(1): 15404

On the Use of Shear Wave Speed to Assess Tendon Loading in Children with Cerebral Palsy

Anahid Ebrahimi[1*], Michael Schwartz[2], Tom Novacheck[2], and Darryl Thelen[1]
[1]University of Wisconsin-Madison, Madison, WI, USA
[2]Gillette Children's Specialty Healthcare, St. Paul, MN, USA
Email: *aebrahimi2@wisc.edu

Introduction

Children with Cerebral Palsy (CP) often exhibit contractures, spasticity and impairments in selective motor control [1], which collectively contribute to inappropriately timed and modulated muscle forces during walking. This can result in severe gait disorders that make daily activities challenging and exhausting [2]. Treatments for gait disorders in children with CP, e.g. spasticity treatments, muscle lengthening procedures, and tendon transfers, are intended to alter muscle-tendon mechanics. However, conventional gait analysis cannot be used to infer the underlying muscle-tendon mechanics, particularly in pathological gait. We are exploring the use of shear wave tensiometry [3] to directly gauge muscle actions during gait in children with CP. In this study, we tested the hypothesis that tendon shear wave patterns would be distinct from joint torques.

Methods

Nine children with CP (cases) and fifteen typically developing children (controls) participated in this study. The cases were all GMFCS levels 1 or 2 and had previously received one or more orthopaedic treatments. Shear wave tensiometers were secured over the Achilles and patellar tendons of the more affected limb of the cases, and on the right limb of the controls. Tendon wave speeds were measured at 50 Hz during preferred speed walking. We normalized wave speed to the peak value and subtracted the minimum wave speed (which approximated a zero-load state). Lower extremity kinematics and EMG activities were measured bilaterally throughout [4]. Sagittal knee and ankle torques were calculated using inverse dynamics and normalized to body mass.

We calculated both the Pearson correlation and mutual information (MI) index [5] between patellar or Achilles tendon wave speeds and knee or ankle torques, respectively. MI values were normalized such that 0.0 would indicate no synchrony between the two variables and 1.0 would indicate that the two variables covary exactly together. Monte Carlo resampling (100) was used to determine significant MI values [6].

Results and Discussion

We found a high correlation between Achilles tendon wave speed and ankle torque in both the cases and controls (Table 1). The mutual information between Achilles tendon wave speed and ankle torque was significant in 8/9 cases (MI range: 0.1-0.5) and 13/15 controls (MI range: 0.1-0.3). It is notable that the corresponence was evident across the varied gait patterns seen in the patients with CP. For example, equinus gait gives rise to early triceps surae loading that is visible in both the Achilles tendon wave speed and ankle torque signals (Fig 1).

Table 1: Mean (SD) linear correlation coefficient between tendon wave speed and joint torque.

	Cases	Controls
Patellar/Knee	0.70 (0.37)	0.76 (0.13)
Achilles/Ankle	0.97 (0.02)	0.96 (0.03)

Relative to the ankle, there was significantly less (p<0.01) and more variable correlation between patellar tendon wave speed and knee torque (Table 1). The mutual information index was significant in 8/9 cases (MI range: 0.1-0.4) and 8/15 controls (MI range: 0.1-0.4). We noted in individual trials periods of high patellar tendon wave speed and low knee torque (Fig 1), which can arise from co-contraction of the knee extensors and flexors.

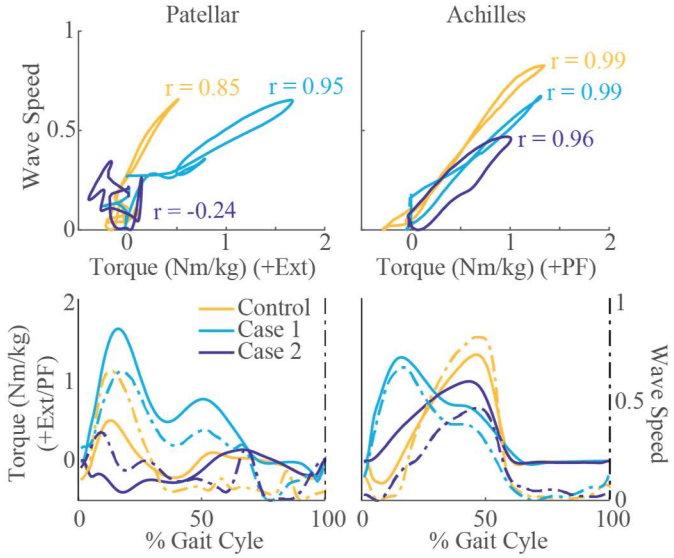

Figure 1: Representative data shows strong correspondence between Achilles tendon wave speed and ankle torque, even in cases where temporal patterns differ. Correspondence between patellar tendon wave speed and torque is more variable.

Significance

We are assessing whether shear wave tensiometry can be used to guide treatments of gait disorders in CP. Our data shows that Achilles tendon wave speeds can capture the net ankle loading seen in pathological gait. Patellar tendon wave speeds were shown to both track periods of knee extensor loading and may also capture periods of co-contraction. We note that our current analysis has been limited to patients with CP who are GMFCS levels 1 and 2 and who exhibited relatively mild gait disorders. Ongoing testing is evaluating whether these results extend to more severe gait disorders and to evaluate how tensiometry can be used to evaluate specific treatments.

Acknowledgments

Funding provided by NIH HD092697.

References

[1] Wren, et al. *J Pediatr Orthop,* 2005
[2] van den Hecke, et al. *J Pediatr Orthop,* 2007
[3] Martin, et al. *Nat Commun,* 2018
[4] Schwartz, et al. *J Biomech,* 2008
[5] Ardón, et al. *Elementa,* 2017
[6] Cazelles, *Ecol Lett,* 2004

Effects of Ankle Weights During Overground Walking Using a Bodyweight Support System

Skyler M. Levine, Patrick M. Costello, Mhairi K. MacLean, and Daniel P. Ferris
[1]University of Florida, Gainesville, Florida, USA
Email: skylerlevine@ufl.edu

Introduction

Bodyweight support can be used in biomechanics research to study the relationship between weight support and joint dynamics. Bodyweight support is also widely used as a rehabilitation therapy after neurological injury. Increasing the amount of harness bodyweight support decreases peak extensor moments of the ankle, knee, and hip [1]. One possible way to alter lower limb joint flexor muscle loading is to add ankle weights, a strategy used in strength training and rehabilitation. Given past debates about the role of plantar flexion power at the end of stance [3], we decided to investigate how ankle weights would affect joint dynamics during walking with and without bodyweight support. If plantar flexor power contributes substantially to accelerating the trailing limb for swing, then adding ankle weights would lead to increased plantar flexion peak power regardless of bodyweight support level.

Methods

Twelve participants (5 male, 7 female, 26±4 years old, 70±8 kg in mass) walked across an overground walkway at a speed of 1.2 m/s. Participants were supported at 100%, 76%, 55% and 31% gravity (G) via a harness connected to constant force springs which were attached to a trolley mounted on a ceiling I-beam. At all support levels, participants walked with and without 1.81 kg (4-pound) weights attached at the bottom of each shank. 3 force plates along the walkway and a motion capture system were used to record both kinetics and kinematics.

We used Visual3D to model and calculate joint angles, moments and powers. To account for the mass added to the shank, we made a second Visual3D model for each participant with modified mass, center of mass, and moment inertia properties for the shank. We normalized data to body mass, stride, and averaged across participants.

Results and Discussion

The angle, moment, and power of the lower limb joints were all affected by level of bodyweight support (*Fig. 1*). Increased bodyweight support decreased the magnitude of flexor and extensor moment and power for all joints. The impact of the ankle weights on joint kinetics was generally small, but varied by joint and gravity level. In particular, ankle weights led to a larger decrease in the plantar flexion peak power at lower gravity levels (higher bodyweight support) than at 1.0G (*Fig. 1*).

The large burst in ankle plantar flexion power at the end of stance contributes both to redirecting the center of mass to vault over the stance limb and to accelerate the trailing limb into swing [2]. Our findings show a large decrease in ankle push-off power with increased bodyweight support at the torso, which is in agreement with the theory that ankle push-off contributes to moving the center of mass. We also found that push-off power increased with the addition of ankle weights, supporting the theory that ankle push-off contributes to acceleration of the trailing swing leg. These results support both interpretations of ankle plantar flexor mechanical power at the end of the stance phase.

Significance

The results from this experimental intervention supports the theoretical effects of ankle joint function during human walking [2]. It also provides some useful data for considering how to use bodyweight support and ankle weights to target specific muscle groups and gait deficiencies during rehabilitation after neurological injury. Lastly, with the development of powered lower limb prostheses and robotic lower limb exoskeletons, having a good understanding of how mass added to the lower limb affects walking biomechanics can be useful for future assistive technology design.

Acknowledgments

We thank Angel Bu and Han Nguyen for their assistance collecting and processing the data.

References

[1] Apte et al., 2018, *J Neuroeng Rehabil*, **15**(1):53.
[2] Zelik & Adamczyk, 2016, *J Exp Biol*, **219**(23):3676–3683.

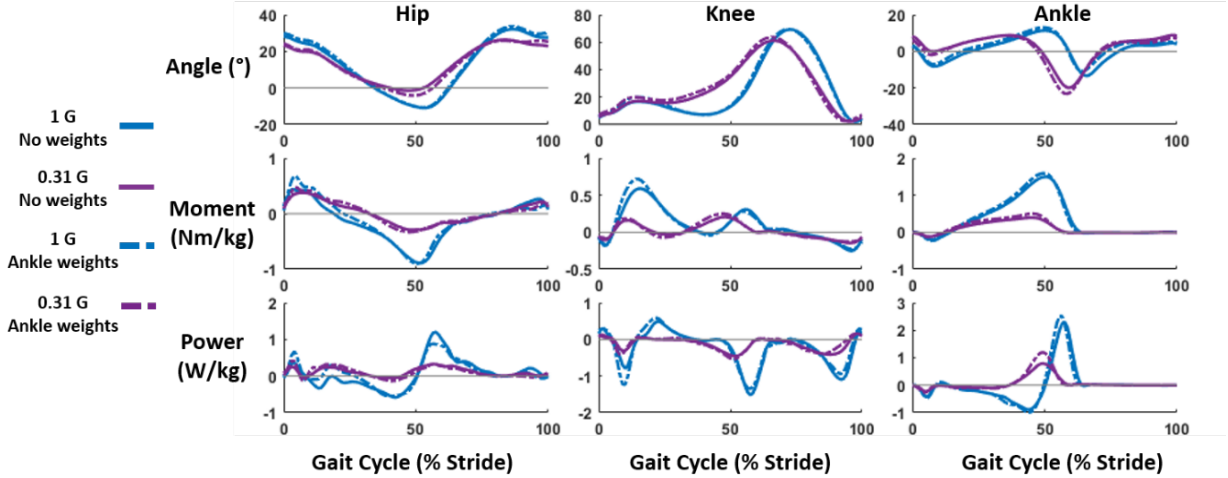

Figure 1: Angle, moment, and power for the hip, knee, and ankle joints during the gait cycle Ankle weights at 0.31G have a larger effect on ankle plantar flexor power than at 1.0G.

Split-belt walking against resistance increases walking propulsion asymmetrically

Hurt CP, Kuhman D, Baumann A, Jiang W, Marsh K,
[1]University of Alabama at Birmingham, Birmingham, AL, U.S.A.
Email: *cphurt@uab.edu

Introduction

Progression of walking requires the generation of positive work on the center of mass in the direction of travel, which is primarily generated by locomotor propulsive forces applied by the stance limb. Symmetric lower extremity propulsive force production is a hallmark of normal gait and related to similar positive work production between limbs as well as relatively low energetic cost of walking[1]. In certain patient populations with kinematic limb asymmetry (e.g., persons post-stroke), this compensatory gait adaptation is related with slower gait speed, higher energy utilization and asymmetric lower extremity force production[2]. Interventions to mitigate asymmetries have primarily focused on modifying kinematic strategies to reduce step length asymmetry using a split-belt walking paradigm whereby one belt goes faster than the other. It is unclear if increased propulsive forces account for the reported improved symmetry. Other novel interventions encourage greater propulsive force output using impeding forces[3]. We performed a study whereby we combined split-belt treadmill walking with increasing impeding forces (hill walking) in young healthy individuals to assess the ability to specifically target increased force output in given limb.

Methods

We recruited 10 healthy, young adults to participate in this study (mean age: 25.3; mean height: 1.72 m; mean mass: 72.27 kg). Individuals were excluded if they had any lower extremity injury within 6 months prior to participation. We collected kinematics and ground reaction forces (GRF) simultaneously using an 8-camera motion capture system (Vicon) and a dual-belt, force instrumented treadmill (Motek), respectively. Data was processed in Visual 3D and Matlab. Participants walked under the following belt speed configurations: both belts tied at 0.5 m/s and at 1.0 m/s, belts split, with the left belt at 1.0 m/s and the right belt at 0.5 m/s for all participants. After each split-belt trial the participant walked with the belts tied at 1.0 m/s to serve as a "wash out" trial. These conditions were performed in the order listed above at 0 degrees, +5 degrees, and +10 degrees of treadmill incline. Thus, each participant performed a total of 11 walking trials. The "wash out" trials were collected until the participants felt that their gait had normalized and visually appeared to have returned to a normal gait pattern. Brief periods of rest were provided between each trial. For this abstract, only split-belt data on the 0 degrees, +5 degrees, and +10 degrees of incline are presented. Prior investigations have used multiple measures to assess asymmetric force production such as peak propulsive force, peak power production, propulsive impulse and positive ankle work generation[4]. A repeated measures ANOVA was used to assess the effect of limb and incline on these measures with a Bonferoni post hoc analysis.

Results and Discussion

For propulsive GRF impulse, we observed an interaction effect of belt speed and slope ($p < 0.001$, Figure 1A) where the GRF impulse of the limb on the slow belt increased at a greater rate than the fast belt. Stance time did not change with slope ($p=0.546$) but was different between limb($p<0.001$) however

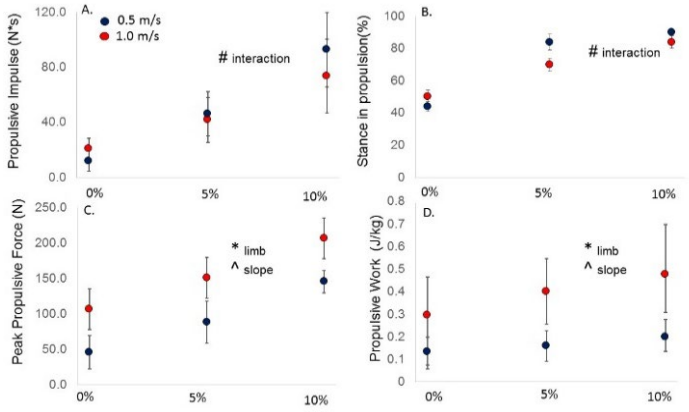

*Figure 1. Result of the split belt incline conditions. 1A Propulsive impulse with incline 1B % stance with respect to split-belt and incline, 1C Peak propulsive force with respect to split-belt and incline 1D propulsive work with respect to split belt and incline #significant interaction, *significant effect of limb, ^significant effect of slope*

the interaction was not significant (0.818), suggesting that this variable did not explain the interaction effect on propulsive impulse. Time spent in propulsion (i.e. positive GRF) however, increased with slope to a greater amount for the slow limb compared to the fast limb ($p<0.05$ interaction) explaining the propulsive impulse finding. Peak propulsive GRF forces for both limbs increased at the same rate ($p<0.001$ main effect of slope) and the limb on the fast belt generated a larger peak GRF ($p<0.001$ main effect of limb Figure 1C), with no significant interaction ($p=0.939$). Ankle joint work increased with slope ($p<0.01$) while the limb on the fast belt performed 70% more positive work than the limb on the slow belt ($p<0.01$ Figure 1D). This data may suggest that under these conditions increased propulsive impulse may relate to increased time spent in the stance phase on the slow belt supporting body weight, whereas the increased positive ankle work by the limb on the faster belt is in response to an increased propulsive stimulus to that limb (faster belt+increased resistive forces via treadmill belt incline). It would be of interest to extend this analysis to the hip extensors as well.

Significance

Split-belt treadmill walking paradigms may create opportunities to improve asymmetric gait adaptations that negatively impact walking in patient populations. Addition of resistive force (e.g., incline walking) to forward progression showed that, depending on the variable used, different decisions can be made about which limb to put on the fast belt and which limb to put on the slow belt to improve kinetic asymmetric gait adaptations. This requires an assessment of goals for the training be carefully laid out.

References

1.Ellis et al. Proc R Soc B 2013. **2**. Awad et al. NNR 2014. **3**. Hurt et al.. JNER 2015. 4.Kuhman D, Hurt CP Hum Mov Sci 2019.

Muscle coordination retraining reduces knee contact force during gait

Scott D. Uhlrich[1], Rachel W. Jackson[1], Ajay Seth[1], Julie A. Kolesar[1], Scott L. Delp[1]
[1]Stanford University, Stanford, CA, USA
email: suhlrich@stanford.edu

Introduction

Reducing knee contact force (KCF) during gait is the target of many non-surgical interventions for knee osteoarthritis[1]. Muscle forces are responsible for 50-75% of KCF during walking[2], but most joint-offloading interventions do not target the muscle contribution to KCF. Musculoskeletal simulations suggest that minimizing the activation of the gastrocnemius muscle, without changing joint-level kinetics, could reduce the second peak of KCF[3]. However, it is unknown what muscle compensations are necessary to walk without activating the gastrocnemius and whether humans can change the relative activation of redundant muscles during a complex task like walking. The aims of our study were to identify the coordination changes necessary to walk with minimal gastrocnemius activity, to test whether healthy individuals could learn this new coordination pattern with biofeedback, and to evaluate if the intervention reduced the second peak of KCF.

Methods

To investigate the differences between natural and "gastrocnemius avoidance" coordination patterns, we simulated walking in OpenSim[4] with two static optimization objective functions: one that minimized the sum of activations squared and another that additionally penalized gastrocnemius activation. Walking without the gastrocnemius required increased soleus and hamstrings activation to generate the necessary ankle plantarflexion and knee flexion moments.

Based on the simulation results, we chose to retrain the relative activation of the ankle plantarflexors, with the goal of reducing gastrocnemius activity without altering the ankle plantarflexion moment. Ten healthy adults (26±4 years old, 4 female) performed five 6-minute walking trials on an instrumented treadmill: a baseline trial, three feedback trials, and a retention trial. During all feedback trials, a real-time bar plot instructed participants to reduce their gastrocnemius to soleus activation ratio, which we defined as the ratio of the average electromyogram (EMG) linear envelopes. During the final two feedback trials, participants were given additional feedback (bar color) to reduce average gastrocnemius EMG. No feedback was given during the retention trial. To evaluate the effect of gastrocnemius avoidance gait on KCF, we simulated five gait cycles from the baseline and retention trials using a custom static optimization algorithm that minimized activations squared while constraining the simulated gastrocnemius to soleus activation ratio to match the ratio from EMG.

Muscle activity and KCF were compared between trials using t-tests (α=0.05) with a Benjamini Hochberg correction. We compared average ankle moments using a TOST equivalence test with equivalence bounds of 1 baseline standard deviation. Average values are reported as mean ± standard deviation.

Results and Discussion

During the retention trial, participants reduced their gastrocnemius to soleus activation ratio by 25±15% (p=0.003) and their average gastrocnemius activation by 17±19% (p=0.036, Fig. 1a). The average ankle plantarflexion moment during the retention trial trended towards being equivalent to baseline (p=0.063, Fig. 1b). These results demonstrate that when provided with interpretable EMG biofeedback, healthy individuals can quickly learn to change the activation of redundant muscles while maintaining normal joint kinetics.

The 8 participants who retained a reduction in gastrocnemius activation reduced their second peak of KCF by 0.41±0.34 bodyweights (12%, p=0.011) compared to baseline (Fig. 1c). This KCF reduction is similar to the effect of losing 20% of bodyweight[5], suggesting that gastrocnemius avoidance gait may be a promising new intervention for knee osteoarthritis.

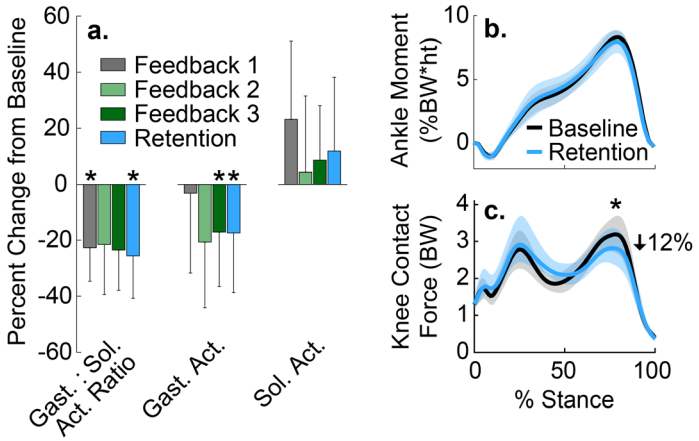

Fig. 1: **(a)** During the retention trial, participants reduced their gastrocnemius to soleus activation ratio (p=0.003) and average gastrocnemius activation (p=0.036) compared to baseline **(b)** without substantially changing their average ankle moment (p=0.063 equivalent to baseline). **(c)** The 8 participants who retained a reduction in gastrocnemius activation reduced the simulation-estimated second peak of knee contact force by 12% (p=0.011). (* p<0.05)

Significance

Simulation-guided coordination retraining is a promising tool for reducing joint contact force in the knee as well as in other redundantly-actuated joints that often experience osteoarthritis, such as the hip. More generally, we show how simulations and biofeedback can be coupled to design coordination retraining interventions that achieve non-intuitive but clinically-meaningful objectives. This approach may allow individuals to optimize muscle coordination for a variety of rehabilitation, injury prevention, and sports performance applications.

Acknowledgments

This work was supported by an NSF Graduate Fellowship (DGE-114747) and a Stanford Graduate Fellowship.

References

[1] Andriacchi et al., 2004. *Ann Biomed Eng* **32**.
[2] Windby et al., 2009. *J Biomech* **42**.
[3] Demers et al., 2014. *J Orhop Res* **32**.
[4] Seth et al., 2018. *Plos Comput Biol.*
[5] DeVita et al., 2016. *Gait Posture* **45**.

Peak Knee Joint Forces During Asymmetric Split-Belt Treadmill Walking: A Preliminary Study

E. Dan Syrett[1], Carrie L. Peterson[1], and Benjamin J. Darter[1]
[1]Virginia Commonwealth University
Email: syretted@vcu.edu

Introduction

Certain pathologies, such as lower limb amputation or stroke, can cause individuals to walk asymmetrically. An increase in knee joint contact forces (KJCF) may be a consequence of gait asymmetry and is hypothesized to contribute to osteoarthritis (OA) development.[1] Musculoskeletal modeling and simulation provides a means to non-invasively estimate KJCF.

A previous simulation study showed that changes in symmetry affect KJCF in a 2D model based on normative data.[2] However, no study has used data from *in vivo* collections where gait symmetry is manipulated to inform simulations and estimate KJCF. A split-belt treadmill (SBTM) is a unique tool that utilizes two belts moving at different speeds to provoke gait asymmetries (most robustly in step length) in a systematic manner. The purpose of this preliminary study was to determine the effect of provoked step length (SL) asymmetry during a SBTM walking program on peak KJCF in healthy individuals.

Methods

The analyses were conducted on previously collected data from 15 healthy adults who completed a standardized SBTM test.[3] The test consisted of Baseline slow walking (both belts 0.5 m/s), a Split adaptation period with a random belt-limb assignment ("Fast" belt speed 1.5 m/s, and "Slow" belt speed 0.5 m/s), and a Post "wash out" period after the Split condition (both belts 0.5 m/s). Of significance, the limb assigned to the Fast belt for the Split condition has a longer SL relative to the limb assigned to the Slow belt during the Post condition. As such, SL is symmetric during Baseline walking but more asymmetric early in the Post condition.

Full-body motion capture data (100 Hz) and SBTM-integrated force plate data (1000 Hz) were collected with analyses completed on 5-second epochs from late in the Baseline condition and early in the Post condition. Using OpenSim's suggested workflow and the gait2392 model, muscle activation patterns were determined using computed muscle control and KJCF was calculated. Axial KJCF curves for each limb were created and normalized to the subject's body weight (BW) and to the gait cycle. SL (in meters) and peak KJCF (peak force) were calculated then averaged for each condition. A symmetry value for SL (SLSym) and peak force (PFSym) were calculated using a previously established method[3] for each walking condition in which 0 reflects perfect symmetry.

Paired t-tests were used to compare SL, peak force, SLSym and PFSym values between belts and walking conditions. A Pearson correlation between PFSym and SLSym was also calculated to examine their association.

Results and Discussion

SLSym and PFSym values revealed symmetric SL and peak force values during the Baseline condition and asymmetric SL and peak force values during the Post condition (Table 1, both comparisons $p<0.01$). SL/SLSym values behaved as expected for this testing paradigm.

There was a significant negative correlation between SLSym and PFSym values (Figure 1, $r=-0.64$, $p<0.01$). This indicates that as the relative SL of the Slow belt limb compared to the Fast belt limb decreases, the peak force experienced on the Slow belt limb compared to the Fast belt limb increases.

Table 1. Average values for SL, peak force, SLSym, PFSym for each walking condition and paired t-test significance results.

Variable	Belt	Baseline	Post	p
SL (m)	Fast	0.41±0.04	0.44±0.06	0.02*
	Slow	0.39±0.03	0.20±0.08	<0.01*
SLSym		0.02±0.04	0.40±0.15	<0.01*
Peak Force (BW)	Fast	3.28±0.40	2.62±0.33	<0.01*
	Slow	3.29±0.38	3.51±0.45	0.10
PFSym		-0.00±0.06	-0.14±0.09	<0.01*

(mean±SD), *=p<0.05

These preliminary results suggest that an increase in SL asymmetry may be associated with an increased asymmetry in peak knee joint forces between limbs during gait in healthy individuals. When SL asymmetry occurs, the limb with a shorter SL appears to demonstrate higher peak knee force.

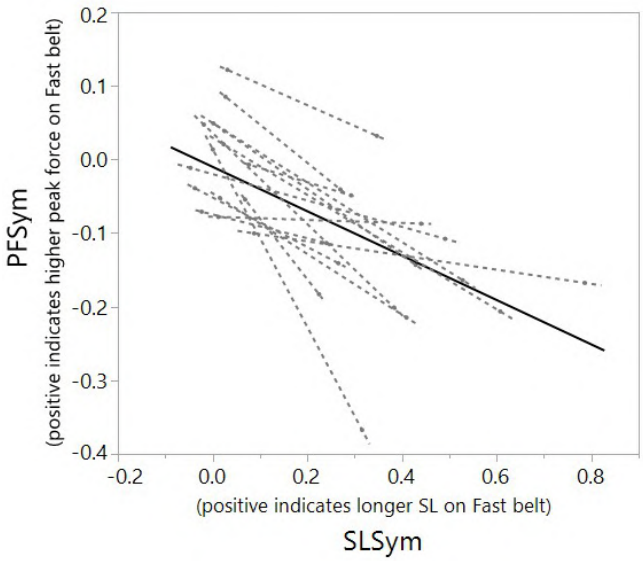

Figure 1. Negative correlation between PFSym and SLSym. Solid line indicates overall best fit. Dashed lines indicate fit between Baseline and Post for each subject.

Significance

This study suggests that step length asymmetry may correlate with peak knee joint forces during gait, a modifiable factor thought to contribute to the increased prevalence of knee OA seen in certain clinical populations.[4,5] If these preliminary results hold, rehabilitation techniques may consider addressing gait symmetry to mitigate the development of knee OA.

References

1. Morgenroth DC. (2012). PM&R, 4(5 Suppl.), 20–27.
2. Koelewijn AD (2016). Gait Posture, 49, 219–225.
3. Darter, BJ (2018). Gait Posture, 62(March 2018), 86–91.
4. Silverman AK (2014). J Biomech, 47(11), 2556–2562.
5. Struyf PA. (2009). Arch Phys Med Rehab, 90(3), 440–446.

Surface stiffness affects knee joint kinetics during decline but not level running

Paul DeVita[1], Joey Casadonte[1], Nick Murray[1] and John Willson[2]
[1]Department of Kinesiology and [2]Department of Physical Therapy, East Carolina University
Email: *devitap@ecu.edu

Introduction

Running provides numerous health benefits and detriments including increased cardiovascular health and knee joint injuries, respectively. Here we focus on knee joint loading as a potential mechanism for tissue conditioning and knee injury. External loads in running, i.e. GRFs, are affected by surface inclination (1) and surface stiffness (2) with downhill running and stiffer surfaces associated with relatively large GRFs. Since runners increase their lower extremity stiffness with less stiff surfaces (3) the effect of surface stiffness on actual knee loads is difficult to predict (and is not in the literature) as is the interaction of inclination and stiffness. Indeed, we envision the potential of softer surfaces to reduce knee loads in decline but not level running because the displacement of the surface material during runner-surface interactions may be greater in decline running; i.e. the runner's momentum would be directed more along the surface in decline vs level running. We therefore hypothesized an interaction effect between surface inclination and stiffness on knee joint loads: a less stiff surface will reduce knee loads more in decline and less in level running. The purpose of this study was to test the effect of surface stiffness on knee joint loads in decline and level running.

Methods

14 healthy runners (22 yrs, 71 kg, 8 males) provided written informed consent to university approved procedures. Knee joint patello-femoral compression and tibio-femoral compression and shear forces were modelled (4) from GRFs and kinematics during 10° decline and level running at a controlled speed (mean 3.2 ms^{-1}), both with and without a 3 cm thick polyvinyl chloride (PVC) sponge shock absorbing mat (closed cell, Shore 00 65) placed along the entire runway. All trials used a heel-strike pattern. Maximum forces were analysed with 2-way (inclination x surface stiffness) ANOVA followed by Scheffe post hoc tests, all $p<0.05$.

Results and Discussion

Significant interactions were observed for the four forces in figures 1 and 2. Decline running on reduced surface stiffness lowered the posterior GRF 56% and the patello-femoral compression, tibio-femoral compression and shear forces 15%, 6%, 15%, respectively, compared to the stiffer surface, all $p<0.05$. Whereas, surface stifness had no effect on these forces in level running (all $p>0.18$).

Maximum vertical GRF was not affected by inclination angle or surface stiffness (data not shown). We suggest that the mat reduced knee forces in decline but not level running because the impact between runner and surface was more in line with the surface in decline producing a larger displacement of the mat material (thus the reduced Ant/post but not vertical GRF). We note the general similarity between the magnitude of the decline and level forces may have been due to the 10% shorter stride length in decline (means, 2.21 m vs 2.44 m, $p<0.001$)

These data may be specific to the declination angle, running speed, and amount and quality of the cushioning mat surface. At lower and higher angles of decline running smaller and larger differences may have been observed between decline and level running, respectively. At faster speeds, the differences between surface inclinations may be reduced if the given mat could not dissipate the loads sufficiently in decline running. Different mat thicknesses and shore specifications could also yield different results. Given these limitations, we observed support for the hypothesis that reductions in surface stiffness during decline running would reduce knee joint forces more so than during level running.

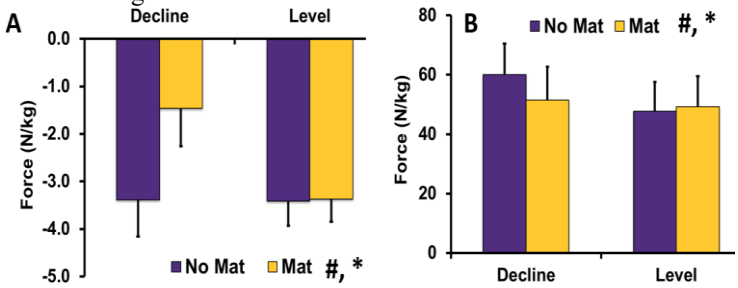

Figure 1: A) maximum posterior ground reaction force, B) maximum patello-femoral compression, #interaction $p<.005$, * decline $p<.05$.

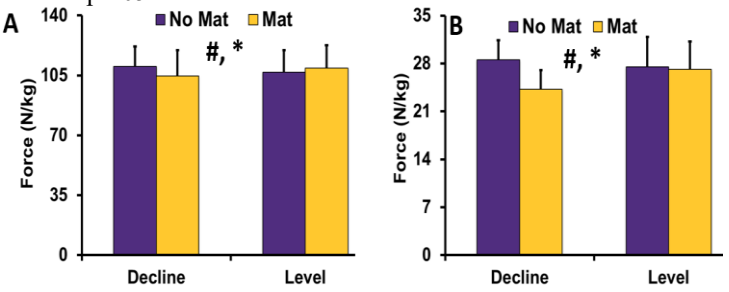

Figure 2: A) maximum tibio-femoral compression, B) maximum tibio-femorial shear, #interaction $p<.005$, * decline $p<.05$.

Significance

We demonstrated that within our limitations, reducing surfaces stiffness does not reduce knee joint loads in healthy, young adults during moderate speed level running. Further, the same reduction in surface stiffness can reduce knee loads during moderate angled decline running. These data provide a basis to hypothesize about tissue conditioning and running injury and the interactions highlight the need for more comprehensive analyses when investigating running biomechanics.

Acknowledgments

The work partially supported by the Department of Kinesiology and the College of Health and Human Performance, East Carolina University.

References

1) Gottschall et al. *J Biomech* 2005;38(3):445-452.
2) McMahon et al. *J Biomech* 1979;12(12):893-904.
3) Ferris et al. *Proc Biol Sci*. 1998;265(1400):989-994.
4) DeVita et al. *J Appl Biomech* 2001;17(4):297-311.

Estimating Knee Joint Load with Joint Acoustic Emissions During Walking

Keaton L. Scherpereel[1], Nicholas B. Bolus[2], Hyeon Ki Jeong[2], Omer T. Inan[2], and Aaron J. Young[1]
[1]Woodruff School of Mechanical Engineering, Georgia Institute of Technology, Atlanta, GA, USA
[2] School of Electrical and Computer Engineering, Georgia Institute of Technology, Atlanta, GA, USA
Email: keaton@gatech.edu

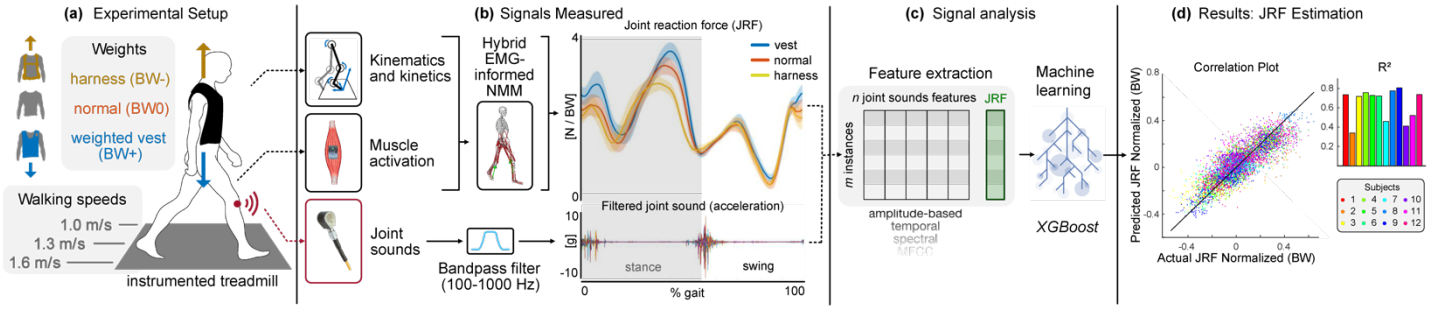

Figure 1: Summary of the experimental setup, data acquisition, analysis, and results.

Introduction

Joint load during dynamic activities is an important metric for understanding the mechanics of knee joint injuries [1], assessing the progression of disease [2], and evaluating rehabilitation and prevention procedures [3]. However, knee joint load cannot be measured directly but instead must be estimated in facilities that have access to advanced data acquisition tools (including motion capture systems, force plates, and often surface electromyography (EMG) sensors) [4]. A wearable solution that could offer continuous monitoring of joint load and be readily integrated into a brace or wearable exoskeleton would offer new possibilities for clinicians to assess rehabilitation procedures and for device designers to incorporate joint load into adaptive control schemes.

Joint acoustic emissions can enable differentiation of healthy and injured knees [5], evaluation of the progress of knee injury rehabilitation [6], and detection of changes in mechanical load during controlled flexion-extension tasks [7][8]. This study investigates whether joint acoustic emissions can be used to estimate joint load, specifically during walking.

Methods

Twelve able-bodied subjects with no history of surgery or symptomatic injury within the past year were recruited to participate in a single day, IRB approved, gait analysis study. The experimental protocol consisted of level ground walking for two minutes on a split-belt force-instrumented treadmill for nine conditions (three loading conditions, three speed conditions). During this study, joint acoustics from two locations on the left knee (Dytran contact accelerometers), EMG for 7 muscles on the left leg (Delsys), kinematics (Vicon motion capture), and ground reaction forces (Bertec) were collected (Figure 1a).

The latter three measures were processed using conventional gait analysis tools (OpenSim) and used to estimate joint reaction forces (JRF) using a hybrid EMG-informed neuromuscular model [9]. The joint acoustic emissions were bandpass filtered between 100-1000Hz, split by gait cycle, and features (time-based, spectral, MFCCs, etc.) were extracted from 50ms windows of stance phase for the instrumented leg (excluding heel strike). Finally, a regression model, based on the machine learning algorithm XGBoost, was developed to estimate joint load from the acoustic features. The data for each condition were split using the first minute of each trial for training and the second minute for testing. A model was developed for each subject (Figure 1b,c).

Results and Discussion

The results show that the joint load for a three-cycle average can be predicted with a root-mean-squared error of 73.2 ± 10.5N and a mean absolute percent error of 3.3 ± 0.4% of the total load. For the correlation plot (Figure 1d), the JRF for each subject was normalized to the normal body weight condition at 1.3 m/s. Ongoing work includes examining the relationship between joint acoustics and varying walking speeds, as well as developing a subject-independent model for estimating joint load. The key result of this study is that joint acoustic emissions contain information about loading that can be extracted during walking in order to estimate joint load.

Significance

Joint acoustic emissions have the potential to estimate joint load accessibly and non-invasively, which may provide clinicians with a wearable means of monitoring joint load outside of a research facility through a cumulative, ambulatory load estimate. Such a device could open possibilites for developing new adaptive device control strategies that respond to the physiological state of patients and for utilizing joint load as a metric to better evaluate the effects of rehabilitation strategies and devices.

Acknowledgments

This material is based upon work supported in part by the National Science Foundation (NSF) / National Institutes of Health Smart and Connected Health Program under Grant No. 1R01EB023808 and NSF NRT Traineeship Program.

References

1. Jung, Y., et al. *J Biomech Eng* 138, (2016); 2. Hunt, M. A., Bennell, K. L. *The Knee* 18, 231–234 (2011); 3. Zheng, N., et al *Journal of Biomechanics* 31, 963–967 (1998); 4. Fregly, B. J. et al. *J Orthop Res* 30, 503–513 (2012); 5. Hersek, S. et al. *IEEE Trans Biomed Eng* 65, 1291–1300 (2018); 6. Inan, O. T. et al. *Journal of Applied Physiology* 124, 537–547 (2017); 7. Bolus, N. B., et al. *Sensors (Basel)* 19, (2019); 8. Jeong, H.-K., et al. *IEEE Trans Neural Syst Rehabil Eng* 26, 594–601 (2018); 9. Pizzolato, C. et al. *J of Biomech* 48, 3929–3936 (2015).

Predictive Modeling of Serious Injury Risk in Frontal Crashes

Zachary Merrill[1*], Omid Komari[1], Kevin Toosi[1]
[1]BioEx Consulting, Pittsburgh, Pennsylvania
Email: *zfmerrill@bioexconsulting.com

Introduction

Previous research has shown differences in the prevalence of serious injuries and fatalities based on obesity, mass, and sex [1-5], particularly for the risk of lower extremity, spine, and head injuries [2,3]. Explanations for these differences include alterations in seatbelt kinematics [4,5], as well as interactions with the steering wheel in frontal collisions [6].

The objective of this study was to use a Bayesian logistic regression approach to further investigate the effects of anthropometric parameters including sex, age, and BMI on the probabilities of serious injury, based on the Abbreviated Injury Scale, or death in frontal car crashes with airbag deployment. This analysis will improve upon existing research [1,2] by observing cases specifically involving airbag deployment, describing the full probability distributions of the outcomes, and validating the predictive abilities of the models. The results will serve as a jumping-off point for future work describing the ranges of probabilities for specific injuries based on accident parameters.

Methods

Car crash and occupant injury data were collected from the National Automotive Sampling System for 2010 through 2015. Variables of interest included occupant age, BMI, sex, restraint use, and injury severity/fatality, as defined by the maximum abbreviated injury score (MAIS), along with the principal direction of force due to impact and airbag deployment status.

Data were filtered to only include cases containing all variables of interest for front seat occupants (N = 3,171), and the 2010 through 2014 data were used as the training data set, while the 2015 data were used for model validation. The analysis was performed using a custom Python script, with a Markov Chain Monte Carlo algorithm to determine the relationships between age, sex, BMI, and restraint use and the probability of serious injury (MAIS 3+) or death over a range of peak longitudinal change in velocity during a crash (delta-V) in the training set.

Outcomes of interest included the odds ratios and credibility intervals of each parameter of interest, as well as the risk of serious injury or death across a range of delta-V for sets of parameter inputs. The logistic models were validated based on the ROC plot and area under the curve (AUC) for the 2015 injury outcomes and predicted injury probabilities.

Results and Discussion

Age, restraint use, and BMI all had significant predictive abilities on the risk of serious injury or fatality in crashes with frontal airbag deployment. The ROC plot (Figure 1) AUC value of 0.851 indicated that the resulting models had excellent accuracy in predicting serious injury risk. The overall results indicate that increased age and BMI, and lack of restraint use are associated with increased risk of serious injury in frontal collisions involving airbag deployment (Figure 2).

While obesity is a known risk for certain types of automobile crash-related injuries [4], this work highlights the specific probabilities of overall serious injury or death depending on anthropometric inputs and crash parameters and quantifies the statistical effects of aging, obesity, sex, and restraint use.

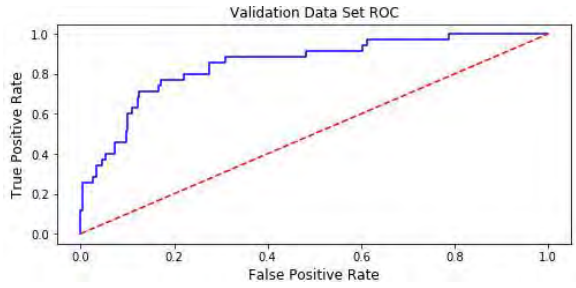

Figure 1: ROC plot for the validation data set. AUC = 0.851.

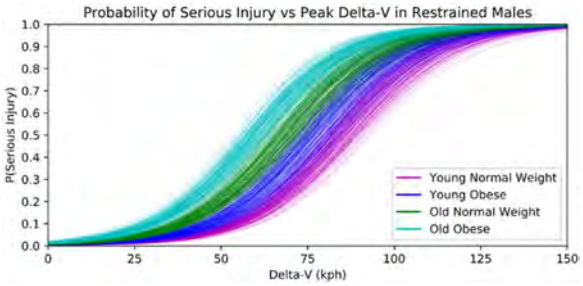

Figure 2: Probability of serious injury or death for restrained front seat male occupants for delta-V ranging from 0 to 150 kph, stratified by age (20 and 60 years) and BMI groups (20 and 40 kg m^{-2}).

Significance

This analysis defines the overall serious injury and fatality risk as it applies to a wide range of occupant age and BMI in frontal crashes involving airbag deployment. Future work will apply this methodology to observe the risk of differing levels of injury severity to various body regions (for example, how spine or lower extremity injury risks related to age and obesity), as well as fatalities and their specific causes from different types of automobile accidents. This work will be particularly useful to the forensics field, where delta-V (and other relevant crash parameters) can be derived from vehicle crush calculations and data from event data recorders, and can be used along with individual occupant information to determine the real-world risk of specific injuries occurring during a given crash. The inclusion of airbag deployment status is especially important for injury prediction due to the lack of clear airbag deployment thresholds based only on the delta-V experienced during an accident [7].

Utilizing a Bayesian approach for predicting injury and death risk will also allow for the future predictive models to incorporate prior knowledge, such as the prevalence of pre-existing conditions within the general population, as well as age, sex, and obesity-related trends in these conditions, and how they may affect the probability of specific injury occurs due to a motor vehicle accident while avoiding the potential statistical disadvantages of previous work [1], which employed a stepwise elimination process [8].

References

[**1**] **Carter** PM, et al. 2014. doi: 10.1016/j.aap.2014.05.024. [**2**] **Rupp** JD, et al. 2013. doi:10.1002/oby.20079. [**3**] **Kim** J-E, et al. 2015. doi:10.1002/oby.21018. [**4**] **Reed** MP, et al. 2005. Report No. DOT HS 812164. [**5**] **Jones** ML, et al. 2017. Effects of High Levels of Obesity on Lap and Shoulder Belt Paths. IRCOBI. [**6**] **Newgard** CD, et al. 2005. doi:10.1016/j.annemergmed.2004.09.011. [**7**] **Wood** M, Earnhart N, Kennett K. 2014. doi:10.4271/2014-01-0496. [**8**] **Harrell** FE. 2001. *Regression Modeling Strategies*. Springer New York, NY.

Force and linear acceleration differences after head impacts with clenched and relaxed neck muscles

Mohammad Homayounpour[1*], Andrew S. Merryweather[2]
[1]PhD. Candidate, Department of Mechanical Engineering, University of Utah, UT, USA
[2]Associate Professor, Department of Mechanical Engineering, University of Utah, UT, USA
Email: m.homayounpour@utah.edu*

Introduction

Concussions in sports occur at an alarming rate, with nearly 4 million concussions in the United States each year [1]. Experimental data are needed first to understand how a person responds to an impact and then to propose strategies to reduce the risk of concussion.

Although muscle activation at the time of impact can be a useful protective mechanism, muscles are not fast enough to fully activate at the time of impact. [1]. Several studies have indicated that stronger necks reduce concussion risk [2], but other literature reports opposing viewpoints [4], [5]. Experimental studies that involve safe impacts on participants in laboratory settings suggested active neck muscles may reduce the risk of injury [2]-[3]. Also, we hypothesized that the peak force of the impact increased when the participants clenched their necks. In this article, we investigate the effect of neck muscle activation on the force profile and linear acceleration of the head during impact.

Methods

Ten male participants (Age: 24.9±3.5 y.o and 72.3±16 kg) were studied using a custom head impact testbed described in prior work [6]. Each participant experienced 50 impacts in four different directions. In 7 of those 50 impacts, 1 second before the impacts, participants were warned with an audio signal and clenched their neck prior to the impact. In 10 control trials, participants did not know about the incoming impact (Unwarned). The direction of the impact was unknown for both conditions. Impact force was measured using an S-type load cell at 2kHz, and the linear acceleration of the head was measured using an instrumented mouthguard at 2 kHz. A linear mixed model was used for statistical analysis and paired t-test used for the post-hoc analysis. P-value<0.05 is considered statistically significant.

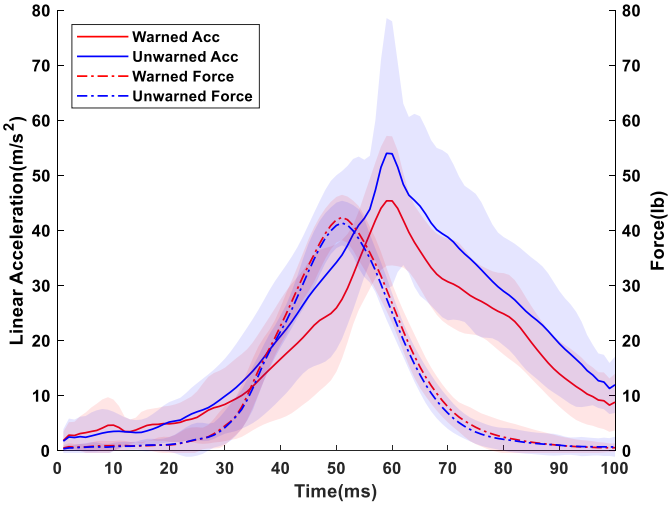

Figure 1: Resultant linear acceleration and applied force to the head at impact.

Results and Discussion

As it is depicted in Figure 1, the resultant linear acceleration of the head shows a significant reduction in the warned condition, 45.6±1.5 m/s^2, compared to 54.3±2.5 (mean±StdErr) m/s^2 in the control condition. The neck muscle contraction reduces the peak resultant linear acceleration by 16%. The participants' strength was not significant in the linear mixed as a fixed factor (p = .7), but it improves the accuracy of the model significantly as a random slope. Peak linear acceleration of the head was not significant in front impact, 45.2±7.5 (mean±Std) m/s^2, versus back impact, 45.7±5.9 m/s^2, but both of them where significant compared to the lateral impacts, 58.1±30.25 m/s^2. These results suggest that there is greater force dampening of an impact in the sagittal plane from the anterior or posterior versus a lateral impact.

The peak force in a warned condition of 42.38±4.1N is not significantly different from the control condition, 41.37±4.0 N, however, the area under the curve for the warned condition, 1.057±.071 N.s, is significantly higher than the control condition, 1.003±.081 N.s. Also, the peak force is not significantly different in lateral impact compared to the front and back impact, but the peak linear acceleration of the head is significantly different in all of these cases. Although we hypothesized that stiffer neck muscles would increase the peak force, we failed to reject the null hypothesis. The flexibility of the headband strap may have contributed to this unexpected finding.

Significance

A reduction in head linear acceleration for the impacts with warning compared to control trials suggests that active neck muscles can help to dampen the force of impact. These results do not suggest there is a benefit of muscle strength in the reduction of linear acceleration. We cannot suggest the elimination of the neck strength program from the training as the forces are concussive level. Also, we would not suggest using the force of an impact as the only predictor for linear acceleration because the direction of the impact and the neck muscle activation significantly affect the resultant acceleration.

Acknowledgments

This research was funded in part by grants from the National Science Foundation (#1622741) and the National Institute of Occupational Safety and Health (NIOSH Education and Research Center Training Grant T42/CCT810426-10).

References

[1] J. J. Leddy, *et al.*, *Br. J. Sports Med.* 2019.
[2] J. T. Eckner, *et al.*, *Am. J. Sports Med,* 2014.
[3] M. Fanton, *et al.*, *IEEE Trans. Biomed. Eng.*, 2018.
[4] J. D. Schmidt, *et al.*, *Am. J. Sports Med.*, 2014.
[5] J. P. Mihalik, *et al.*, *Clin. J. Sport Med.* 2011.
[6] M. Homayounpour, *et al.*, HFES, 2019.

Choosing Mastectomy and Breast Reconstruction or Breast Conserving Therapy: Implications for Pectoralis Major Function

Joshua M. Leonardis[1], Adeyiza O. Momoh[2], and David B. Lipps[1]
[1]School of Kinesiology, University of Michigan, USA, [2]Section of Plastic Surgery, University of Michigan, USA
Email: jleo@umich.edu

Introduction

Traditionally, breast cancer that is localized to the breast is managed with breast conserving therapy (BCT) which refers to the combination of lumpectomy and radiotherapy. A lumpectomy removes the tumor and a small volume of soft tissue, while radiotherapy minimizes recurrence. However, an increasing number of women eligible for BCT are opting for a mastectomy, which is a surgical procedure that removes all of the breast tissue. The majority of women undergoing mastectomy will also have a reconstructive surgery performed to restore volume to the chest with an implant or autologous tissue[1]. The most common breast reconstruction is a two-stage subpectoral implant, which requires the disinsertion of the pectoralis major from its inferior attachments. Pectoralis major function is likely impacted by both BCT and mastectomy with a subpectoral implant breast reconstruction, but there has been no direct comparison of these treatments for managing breast cancer[2,3]. Therefore, the purpose of this study was to assess the effect of subpectoral implant breast reconstruction and BCT on the material properties of the pectoralis major at rest and during the generation of planar shoulder torques.

Methods

Fourteen BCT patients (mean: 602 days post-treatment, age: 54 yr, height: 1.61 m, weight: 69 kg), 14 subpectoral implant breast reconstruction patients (570 days post-operative, age: 50 yr, height: 1.63 m, weight: 71 kg), and 14 healthy, age-matched controls (age: 52 yr, height: 1.64 m, weight: 65 kg) generated maximum voluntary shoulder torques with their treated (BCT and subpectoral implant) or dominant arms (controls). Next, an Aixplorer ultrasound elastography machine measured the shear wave velocity (SWV) of the clavicular and sternocostal fiber regions of the pectoralis major while participants either remained at rest or generated shoulder torques scaled to 10% of their maximal strength in flexion or adduction[4]. When obtained at rest and during active contraction SWV provides insight into a muscles contributions to joint function. Linear mixed effects models assessed group differences in shoulder strength. Separate linear mixed effects models assessed the influence of the experimental group and shoulder torque magnitude on SWV obtained from each fiber region of the pectoralis major.

Results and Discussion

Healthy control participants were significantly stronger during the generation of shoulder adduction, internal rotation, and external rotation torques when compared to BCT patients (all $p \leq 0.02$), and significantly stronger during the generation of adduction torques when compared to subpectoral implant patients ($p=0.004$) (Figure 1A). We observed that in all three groups, SWV within the clavicular fiber region increased with increasing flexion torque magnitude and sternocostal fiber region SWV increased with increasing adduction torque magnitude (all $p \leq 0.037$). This is to be expected based on the anatomy of the pectoralis major, as the clavicular fiber region's largest moment arm is in flexion, while the sternocostal fiber region's largest moment arm is in adduction. However, we found that healthy participants utilize the clavicular fiber region more during the generation of shoulder adduction torques (all $p \leq 0.049$) (Figure 1C) and the sternocostal fiber region more during the generation of flexion torque (Figure 1D) when compared to BCT or subpectoral implant participants (all $p \leq 0.002$). These results suggest that in healthy participants, the entire pectoralis major contributes to shoulder function, whereas the individual fiber regions contribute only to their primary function in BCT and subpectoral implant participants. Finally, we found that the clavicular fiber region increased its contributions to shoulder flexion torques in subpectoral implant patients when compared to healthy controls ($p=0.016$) (Figure 1B). The clavicular fiber region is the only intact fiber region in subpectoral implant participants, so it is not surprising that it increases its contributions to shoulder flexion. Together these results indicate that pectoralis major function is fundamentally altered following BCT and subpectoral implant breast reconstruction.

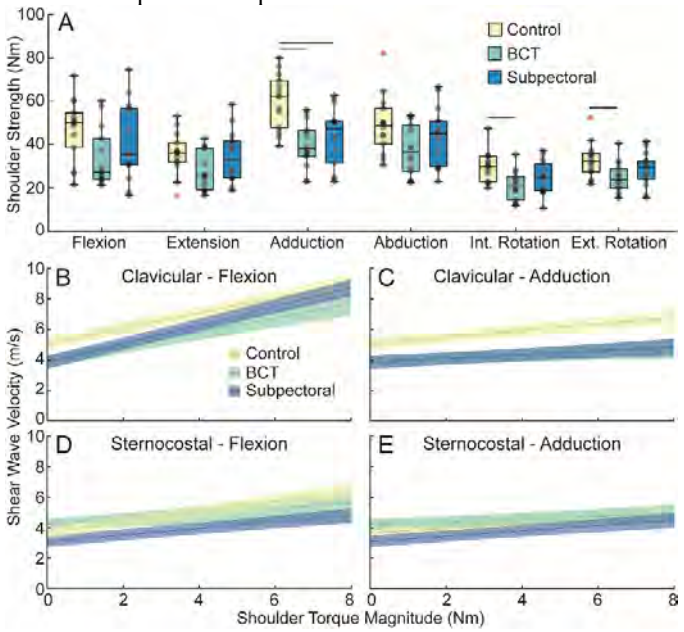

Figure 1: (A) Box plots representing group median ± interquartile range differences in shoulder strength. Individual subject data are presented as transparent black dots, while outliers are presented in red. Horizontal bars signify significant group differences at $p<0.05$. (B-E) The influence of shoulder torque magnitude on mean SWV obtained from the fiber regions of the pectoralis major during the generation of shoulder torques. Lines represent the resultant linear mixed model fits for each experimental group. Shaded regions represent 95% confidence intervals.

Significance

Women who undergo BCT or mastectomy and breast reconstruction may experience significant, long-term shoulder strength deficits. Our results suggest that these deficits are driven in part by fundamental changes to the underlying function of the pectoralis major. Findings from this study will better inform patient choice for BCT eligible women interested in mastectomy and breast reconstruction.

Acknowledgements

NIH R03HD097704 and a Rackham Predoctoral Fellowship

References: 1. K.L. Kummerow, *JAMA Surgery*, 2015; 2. D.B. Lipps, *Sci Rep*, 2019; 3. J.M. Leonardis, *J Orthopaed Res*, 2019; 4. J.M. Leonardis, *J Biomech*, 2017

Quantifying Sternocleidomastoid Material Properties after Definitive Chemoradiation for Head and Neck Cancer

Whitney L. Wolff[1], David B. Lipps[1,2]
[1]School of Kinesiology, [2]Department of Biomedical Engineering, University of Michigan, MI, USA
Email: wolffw@umich.edu

Introduction

Definitive chemoradiation for head and neck cancer is associated with multiple morbidities, including pain, progressive tissue sclerosis, and decreased strength[1]. However, these deficits have not been objectively quantified and there is no post-treatment standard of care for alleviating or preventing these morbidities. Other neck pathologies like chronic neck pain cause the sternocleidomastoid muscle (SCM) to reduce the focus of its neural activity (i.e. increase coactivation)[2] and alters SCM passive material properties[3]. However, it is unclear how chemoradiation for head and neck cancer influences the material properties of the SCM. Therefore, the purpose of this study was to quantify the early changes to SCM material properties following chemoradiation treatment for head and neck cancer. We hypothesized that patients would display increased antagonist SCM contribution and altered material properties of the SCM (increased shear wave velocity) after chemoradiation treatment.

Methods

Four patients prescribed definitive chemoradiation for non-metastatic head and neck cancer participated in this study. Patients completed a baseline visit within 2 weeks prior to starting treatment and a second visit 3 months after starting treatment. Patients were seated with their head secured in a halo attached to a 6 degree-of-freedom load cell. They then generated 3-D neck torques to match 26 targets representing combinations of neck flexion, extension, right/left lateral bending, and right/left axial rotation. During the first visit, four blocks of 26 targets were completed. Two blocks were scaled to 40% maximum voluntary contraction (MVC) in axial rotation, and 2 blocks were scaled to 60% MVC. During the second visit, 2 blocks were scaled to 60% of the participant's current MVC in axial rotation, and 2 blocks were scaled to 60% MVC from the first visit. In total, 108 trials were performed per visit.

Ultrasound shear wave elastography images (Supersonic Imagine Aixplorer, France) were collected bilaterally from the SCM at rest and while they matched the previously described targets. Mean shear wave velocity (SWV) provides insight into the shear modulus of the tissue, with greater SWVs indicating higher shear modulus. SWV for each target was used to calculate the SCM's preferred direction (PD) (representing the azimuth and elevation angles where shear modulus was greatest) and focus (the angular spread of SWV relative to the PD). Paired t-tests were used to compare each variable (PD, focus, mean SWV nearest the PD) from baseline to the 3-month visit.

Results and Discussion

The PD of the SCM was a combination of flexion, ipsilateral bending, and contralateral axial rotation. Neither the azimuth nor elevation angles of the PD were significantly different at the 3-month visit when compared to baseline (all $t_6<0.18$, $p>0.31$). The mean SWV nearest the PD was significantly greater at the 3-month visit (mean±SD: 7.9±2.2 m/s) when compared to baseline (6.3±2.0 m/s) ($t_{13}=-3.4$, $p=0.005$) (Figure 1). This increase in active SWV of the SCM after chemoradiation treatment for head and neck cancer may be a response to pain or deep cervical muscle dysfunction[2].

In contrast, passive SWV of the SCM significantly reduced from baseline (3.2±0.4 m/s) to the 3-month visit (2.8±0.4 m/s) ($t_{13}=4.7$, $p < 0.001$). These results are contrary to increased tissue sclerosis following radiation treatment to the neck. However, the late effects of chemoradiation have likely not developed at our 3-month follow-up. Lastly, the focus of the SCM's PD significantly increased from baseline (0.13±0.07) to the 3-month visit (0.19±0.08) ($t_{13}=-4.6$, $p<0.001$), meaning there was narrower range where the SCM contributed to stability following treatment. Future work is needed to determine if this reduced focus after treatment is indicative of altered behavior of other neck muscles.

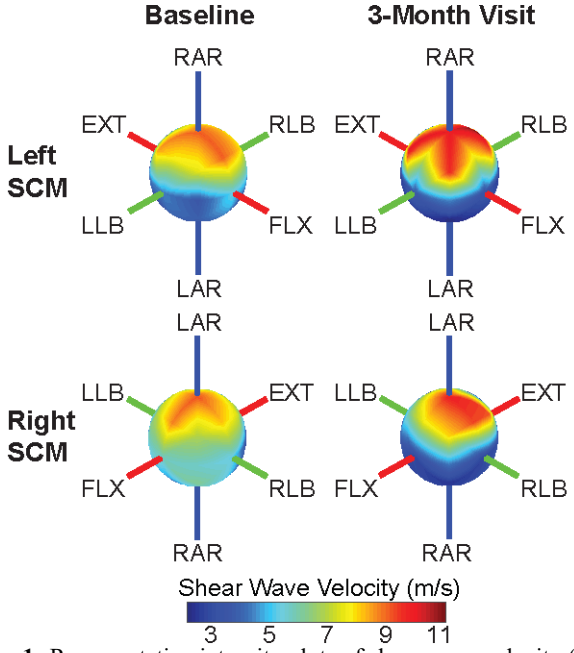

Figure 1: Representative intensity plots of shear wave velocity (SWV) data from both the right and the left SCM from baseline to the 3-month visit. Warmer colors indicate greater SWV magnitude. All targets were scaled to 60% of the axial rotation MVC collected during the baseline visit. FLX=flexion, EXT=extension, RLB, and LLB=right and left lateral bending, RAR and LAR=right and left axial rotation.

Significance

This study provides novel insights into how the material properties of the SCM adapt to definitive chemoradiation treatment for head and neck cancer. The SCM exhibits greater SWV during volitional torque production at the neck. However, we did not observe increased antagonistic contribution or passive SWV. The results of this study highlight the need to quantify the late effects of chemoradiation on neck function to accurately identify patients in need of early physical rehabilitation.

Acknowledgements

U-M CCubed grant and clinical assistance of Drs. Frank Worden, Paul Swiecicki, and Michelle Mierzwa.

References:

[1] Bach, C-A., et al. *Euro Annals Otor.* 129 (2012).
[2] Falla, D., et al. *Clinical Neurophys.* 121 (2010).
[3] Taş, S., et al. *J Manip Phys Ther.* 41 (2018).

Estimating Lumbar Loading with Wearable Sensors over a Broad Range of Manual Lifting Tasks

Emily S Matijevich[1], Peter Volgyesi[1], Karl E. Zelik[1]
[1]Vanderbilt University, Nashville, TN, USA
Email: *emily.matijevich@vanderbilt.edu

Introduction

Low back pain is a disabling condition experienced by 60-85% of adults within their lifetime [1]. High and/or repetitive forces on lumbar muscles and discs are known to be major risk factors. There are numerous opportunities for reducing pain and overuse injury risk if the repetitive forces on the back could be easily monitored in daily life (e.g. via biofeedback).

Wearable sensors are an exciting tool for monitoring human movement non-invasively in daily life. However, there are many complex and intertwined questions involved in using wearable sensors to estimate musculoskeletal loading. The objective of this study was to estimate lumbar moment (torque about the L5/S1 joint) over time using wearable sensors for a diverse range of manual lifting tasks. Specifically, we 1) adapted a machine learning algorithm to estimate sagittal lumbar moment using wearable sensor signals and 2) identified a minimal set of sensor signals necessary for estimation.

Methods

This study involves participants each performing >300 manual lifting tasks in a motion analysis lab; one of the largest data sets of its kind. Here we summarize results from the first participant. Testing is ongoing and multi-subject results will be presented at the conference. Tasks covered a broad range of leaning, twisting, and lateral bending postures while moving boxes of 5-23 kg (**Fig. 1**). Full-body kinematics and ground reaction forces were collected. *Lab-based* lumbar moment was estimated using bottom-up inverse dynamics (M_{lumbar}), and was chosen as the target metric for this study due to its relation to lumbar muscle forces and resulting compressive spine force [2].

Inertial measurement unit (IMU) based kinematics (XSENS) and plantar pressures (Novel Pedar) were collected synchronously with lab-based data. These *wearable* data were normalized and used as feature inputs to a machine leaning model to provide time-series *wearable* lumbar moment estimates (M'_{lumbar}). Wearable features were: lower limb and lumbar joint kinematics, and normal force and center of pressure under each foot. The regression model was built with Gradient Boosted Decision Trees [4] using 200 estimators. The dataset was divided so 85% of samples were used for model training and 15% were reserved for testing. The root mean squared (RMS) error was computed for this test set. Our target accuracy was 10% of the expected peak M_{lumbar}, or <35 Nm, a desired error used by other wearables [3]. The trained model also returns normalized feature importances, indicating how valuable each feature was in estimating lumbar moment.

Results and Discussion

Our *wearable* algorithm estimated sagittal lumbar moment with average RMS error of 20 Nm. $\boldsymbol{M_{lumbar}}$ and $\boldsymbol{M'_{lumbar}}$ were strongly correlated (r^2=0.9). Thus this wearable algorithm distinguishes tasks of lower vs. higher lumbar moment (**Fig. 1**).

Model training identified four features as having a relative importance >5%. Retraining the model using only these key features yielded an RMS error of 21 Nm, a similar error to the model using all the feature inputs. For reference, an error of 20 Nm in lumbar moment equates to ~0.5 bodyweights of error in compressive spine force using a single equivalent muscle approximation. It is promising that a wearable device embedded with just a small set of sensors could estimate sagittal lumbar moment with this accuracy across a broad range of manual lifting tasks.

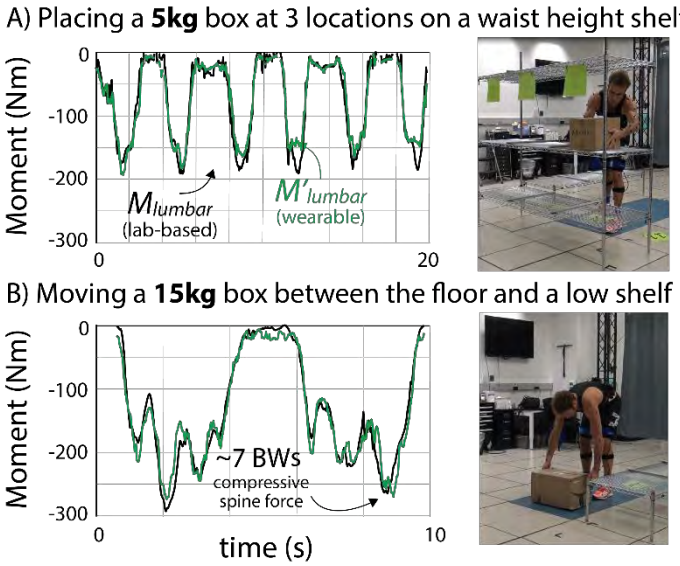

Figure 1: Lab-based (M_{lumbar}) and wearable algorithm (M'_{lumbar}) estimates of sagittal lumbar moment across two subsets (A, B) of the ~300 manual lifting tasks. Of note, subset (A) was part of the test set, and subset (B) was part of the model training set. BWs = bodyweights.

Significance

To the authors' knowledge, this is the first study to synchronously collect both lab-based and wearable kinematic and kinetic data over such a broad range of manual lifting tasks. Errors <21 Nm suggest wearable sensors can be used to estimate lumbar moments outside the lab environment, providing exciting opportunities for understanding lumbar spine loading and preventing low back pain and overuse injury risk.

Acknowledgments

Funding provided by NIH 1R01EB028105-01.

References

[1] WHO. Priority diseases and reasons for inclusion: low back pain. (2013).
[2] McGill & Cholewicki. Mechanical stability of the in vivo lumbar spine. *Clinical Biomechanics*. (1996).
[3] Faber et al. Validation of a wearable system for 3D ambulatory L5/S1 moment. *J Biomechanics*. (2020).
[4] Natekin, Alexey, and Alois Knoll. Gradient boosting machines, a tutorial. *Frontiers in neurorobotics* (2013).

Lower Back Demands During Induced Lower Limb Gait Asymmetries

Jacob J. Banks and Graham E. Caldwell
Department of Kinesiology, University of Massachusetts, Amherst, MA, USA
Email: jbanks@umass.edu

Introduction

Walking is an intrinsic form of exercise and therapeutic relief[1]. For those with asymmetric gait it is also associated with increased prevalence of lower back pain (LBP)[2]. Asymmetric gait can arise from various clinical conditions, but its impact on lower back demands such as joint and muscle kinetics has largely been reported in amputees[2,3]. Lower back demands are reportedly larger for amputees than in able-bodied controls, but these studies were limited by within-group heterogeneity and an absence of an appropriate baseline comparison[2,3]. In addition, lower back demands have generally been estimated with a static optimization approach that may not reflect actual muscle recruitment strategies[4], particularly in those with asymmetries.

An alternative to heterogenous amputee populations and static optimization is to perturb able-bodied participants to artificially induce asymmetry and to include electromyography (EMG) within the optimization algorithm[5]. Such a controlled and participant-specific experiment may provide unique insights into why gait asymmetry is associated with LBP. Therefore, the objective of this study is to investigate how different asymmetric perturbations impact lower back demands as estimated from EMG optimization[5]. We hypothesized that lower back demands would be larger in perturbations inducing greater gait asymmetry.

Methods

A convenience sample of twelve healthy participants consented to the study. Conventional biomechanical techniques were used to record each participant's full-body kinematics (Qualisys AB, Sweden), external kinetics (Treadmetrix, USA), and muscle activity from 12 trunk muscles (Delsys Inc. USA). After a treadmill acclimation period, five different gait conditions were recorded: 1) baseline of normal walking (Control), and walking with 2) a ~1.2 kg ankle weight (AW), 3) a ~2.54 cm "leg lengthener" on the shoe sole (LegL), 4) both the ankle weight and leg lengthener (AW&LegL), and 5) a walking boot that restricted ankle and toe movement (Boot). All perturbations were assigned to the right leg while participants walked at 90% of their self-selected preferred speed. The degree of gait asymmetry between right and left step lengths was quantified by an asymmetry index (AI)[8].

The *in silico* model[7] developed for this study was modified from an existing OpenSim model[8,9]. A MATLAB (Mathworks, USA) custom API[10] was developed to integrate EMG, kinematic and kinetics to estimate lower back demands at L5/S1 via an EMG optimization approach[5]. Bodyweight-normalized peak L5/S1 compressive, peak resultant shear, and AIs from an average of three consecutive strides were used as dependent variables in one-way repeated measure ANOVAs, with Tukey post hoc tests for differences (α=.05) across the five gait conditions.

Results and Discussion

The five gait conditions yielded three unique levels of asymmetry (Fig. 1), with longer left than right steps in the Boot (AI ~-6%), but the reverse in the LegL conditions (AI ~+9%). The AW alone and the control conditions were both approximately symmetrical (AI=~0). Despite these AI differences, the L5/S1 compressive and shear forces were similar across all conditions. These results did not support our hypothesis.

This study is the first to investigate how lower limb perturbations in healthy able-bodied participants can impact lower back compressive and shear forces. Previous work has reported significant changes in EMG and joint kinematics during similar perturbations or the lower back demands of amputees[11,12]. A preliminary analysis of our EMG and kinematic data shows significant between-condition differences, supporting that our AI values reflect gait asymmetry. The similarity in compressive and shear forces across conditions we observed may be due to the choice of the L5/S1 joint or other musculoskeletal limitations.

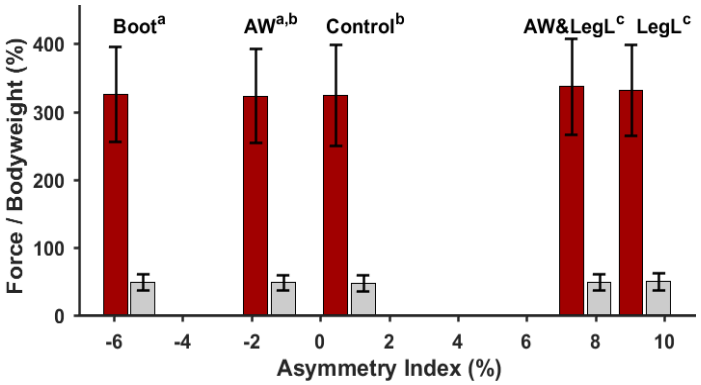

Figure 1: Normalized peak L5/S1 compression (maroon) and shear (grey) forces across different gait conditions and degrees of asymmetry (labeled). A positive asymmetry index represents longer perturbed (right) vs. unperturbed (left) steps. Superscripts following each condition denote post-hoc pairings of asymmetry indexes. There were no significant differences between peak L5/S1 forces across conditions. See Methods for details on each gait condition.

Significance

Our results suggest that the high LBP incidence associated with asymmetric gait[2] may not be the consequence of increased lower back demands during normal level walking. Although non-significant but repeated subtle increases in joint demands could eventually result in tissue injury and lead to LBP, perhaps other gait tasks (e.g. turning, stairs, carrying) or secondary conditions are responsible for the high incidence of LBP in individuals with asymmetric gait.

Acknowledgements

UMass Amherst Kinesiology Travel Grant & Graduate School Dissertation Grant

References

[1.]Morris & Hardman, *Sports Med.* 23(5): 1997. [2.]Deven et al., *Med. Hypo.* 82: 2014. [3.]Sagawa et al. *G&P* 33: 2011. [4.]Davis & Jorgensen, *Occ. Ergo.* 5: 2005. [5.]Cholewicki et al., *JBmch* 28(3): 1995. [6.]Robinson et al., *JMPT* 10(4): 1987. [7.]Banks et al. ISCSB conf: 2019. [8.]Delp et al., *IEEE Trans.* 54: 2007. [9.]Beaucage-Gauvreau et al., *CMBBE* 22(5): 2019. [10.]Lee & Umberger, *PeerJ* 4: 2016. [11.]Hendershot et al., *JBmch* 70: 2018. [12.]Gulgin et al., *G&P* 59: 2018.

Material Properties of Human Testicles under Unconfined Compression and Probing with Varying Strain Rate

Blake Johnson, PhD[1] and Naira Campbell-Kyureghyan, PhD[1,2]
[1]U Department of Industrial and Manfuacturing Engineering, University of Wisconsin-Milwaukee, Milwaukee, WI, USA
[2]Department of Mechanical Engineering, Merrimack College, North Andover, MA, USA
Email: john2742@uwm.edu

Introduction

Knowing the material properties of human tissue can lead to advancements in many fields such as forensics, prostetics, diagnosis, surgical training, etc. The human testicle is an organ that needs advanced understanding of its mechanical behavior as injuries resulting from genitourinary trauma is increasing [1]. Virtually no mechanical testing has been conducted on this organ and characterizing the properties would be valuable for the scientific community.

It has been found that in other human organs the testing methodology and strain rate have been factors that influence material properties [2,3]. To date the stain rate dependencefor the testicles is not known. . It is hypothesized that as strain rate increases the elastic modulus of testicle tissue will increase. It is also hypothesised that the modulusof testicle tissue measured in a probing protocol will be different than in an unconfined compression protocol.

Methods

Six testicles were surgically removed from the scrotum of cadavers, and remained intact for testing. Each testicle was subjected to both nondestrutive probing and unconfined compression protocols at rates of 1%/s to 25%/s. After each non-destructive testing trial the specimen was allowed to relax until initial height was restored. Destructive compression testing was performed at rates from 25%/s to 500%/s. Failure was defined as a 5% reduction in stress or a 3% increase in strain with no increase in stress.

Stress and strain were continuously collected throughout all trials. The secant slope at the most linear portion of the stress-strain curve was used to determine the elastic modulus (E). Failure stress and failure strain were found in each of the destructive testing trials. An ANOVA was performed to test the statistical significance of strain rate on stiffness. A two sample t-test was use to determined if the two non-destructive protocols were statistically different. Alpha was set at 0.05 for all tests. Statistical tests were not performed on failure stress or strain because of the limited sample size.

Table 1: Average (std) elastic modulus from the tested rates of 1%/s to 25%/s for both non-destructive probing and unconfined compression protocols.

	Elastic Modulus (MPa)			
Protocol	**1%/s**	**5%/s**	**10%/s**	**25%/s**
Unconfined Compression	0.0025 (0.0006)	0.0034 (0.0008)	0.0039 (0.0006)	0.0046 (0.0011)
Probing	0.0053 (0.0012)	0.0063 (0.0016)	0.0079 (0.0015)	0.0104 (0.0039)

Table 2: Failure stress and strain from destructive compression testing.

Strain Rate	***Fstress (MPa)***	***Fstrain***
25%/s	0.27	48%
50%/s	0.60	57%
100%/s	0.59	51%
250%/s	0.66	53%
500%/s	0.87 (0.04)	57% (0.03%)

Results and Discussion

Both non-destructive compression and probing modulus (Table 1) increased with increases in strain rate ($p<0.05$). The stiffness from non-destructive testing increased by 36% from 1%/s to 5%/s and from 5%/s to 25%/s. The effect of strain rate was observed to be linear between the rates of 1%/s to 25%/s. An increase in stiffness of 20% was observed between 1%/s and 5%/s, and a 65% increase from 5%/s to 25%/s.

The stiffness measured from the probing protocol was higher at all rates compared to the unconfined compression protocol ($p<0.05$). The largest difference between protocols was a 126% increase from the unconfined compression protocol to the probing protocol with an average of 108% across all rates. An increase in measured modulus in the probing protocol could be due to the smaller compression area. Using a probe will results in increased stiffness as there are parts of the tissue surrounding the probe that is not included in the calculation.

Failure stress was observed to increase as strain rate increases (Table 2). Failure stress was 0.27 MPa at 25%/s and increased by 191% to 0.87 MPa at 500%/s. Failure strain was not affected by strain rate. The failure strain at 500%/s (57%) was only 9% higher than at 25%/s (48%), with the other tested failure strains falling within this range.

Significance

This study characterized the material properties of the human testicle in both unconfined compression and probing protocols. These properties will enable researchers to model the testicle and run various simulations. The models developed can improve surgical simulation, injury diagnosis, forensics, and other areas. The failure threshold has also been established at multiple rates. This study additionally determined how much stress is required to rupture the human testicle which can lead to improvements in protection.

The factors of methodology and strain rate were determined to influence the material properties of the human testicle. Understanding these factors further expands the knowledge of testicle material properties and can lead to improve modelling for this tissue which expands the significance of the results explained above.

Acknowledgments

This study was funded by US Department of Defense grant No. 4892-ARMY-DHP -ELVIS Ph II.

References

1. Janak J, et al. *J. of Urol,* **197,** 414-419, 2017.
2. Kemper A, et al. *J. of Biom. Eng.*, **135**, 1-8, 2013.
3. Umale S, et al. *J. Mech. Beh. Biom. Mat.*, **17**, 22-33, 2010

VERTICAL STIFFNESS ASYMMETRY IN NCAA DIVISION I ATHLETES

Jonathan (FJ) S. Goodwin[1], Mason L. Moore[1], Benjamin T. Ivey[1]
[1]Department of Physical Therapy Education, Elon University, Elon, NC
Email: fgoodwin@elon.edu

Introduction

Athletic injuries are often unavoidable in sport participation and injury rates among NCAA Division I athletes have risen over the past ten years with injury rates reported to be as high as 13.79/1000 athlete-exposures in collegiate athletes [1,2]. Recent efforts have been made to identify a testing battery that can successfully identify athletes who are at an increase for injury [3].

Vertical stiffness (K_{Vert}) is a modifiable biomechanical measurement that is associated with potential lower extremity injury risk [4]. K_{Vert} is the resistance to deformation of the lower limb during the ground contact phase of dynamic movement accounting for relative kinetic load of the lower extremity [5]. K_{Vert} is typically modelled as an inverted pendulum. K_{Vert} asymmetry between limbs is correlated to an increased risk of soft tissue lower extremity injury development within an athletic population during an athletic season [6].

The purpose of this study is to identify if there is a significant difference in K_{Vert} between dominant vs non-dominant limbs among athletes entering intercollegiate Division I athletics.

Methods

Twenty-seven (15f/12m; 18.9±0.87 y.o.; 18-21 y.o. range 71.0±12.2 kg; 1.75±0.09 m) incoming Division I NCAA athletes volunteered for this study. Subjects consisted of 9 women's soccer, 8 men's soccer, 6 women's tennis, and 4 men's football athletes. Subjects were required to be cleared by physician for physical activity and be currently injury-free.

Subjects were fit with retroreflective markers on the torso, pelvis and bilateral lower extremities to collect three-dimensional kinematics. Subjects completed a shod single-leg hopping protocol for 20 seconds at a self-selected frequency on an embedded force plate [7]. This was completed for both limbs in a counter balanced order. During the hopping protocol ground reaction forces and whole-body kinematic data were sampled. K_{Vert} was calculated as the maximum vertical ground reaction force (F_{max}) divided by the vertical displacement of center of mass during ground contact (Δy) and averaged over 10 successive hops ($F_{max}/\Delta y$) (Figure 1) [5]. K_{Vert} values were compared utilizing a dependent t-test between the dominant and non-dominant limb (α=0.05).

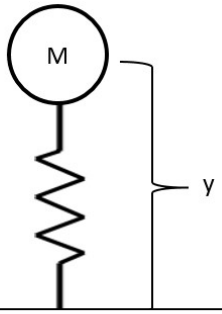

Figure 1: Idealized model for K_{Vert} during hopping.

Results and Discussion

There was an average non-dominant limb stiffness of 16.7±3.1 KN/m and an average dominant limb stiffness of 16.4±3.1 KN/m. There was no significant difference in K_{Vert} between dominant and non-dominant limbs. (p=0.56).

However, the differences between limbs were highly variable with an average difference of 1.5±1.0 KN/m and a range 0.06-3.6 KN/m. This equated to an average difference of 9% in K_{Vert}. Previous literature states that a 4.5% average difference in K_{Vert} has been linked to increased risk for lower extremity soft tissue injury [6]. Given these data, there is a need to screen athletes for lower extremity stiffness before beginning a season and monitor those individuals who displayed higher asymmetries in K_{Vert}.

Significance

Our study built upon previous studies by including both male and females athletes as well as a variety of sports. We believe by screening athletes from a variety of sports this will provide a more robust understanding of K_{Vert} and its utility in injury prevention screenings.

K_{Vert} is a potentially clinically feasible assessment without a significant amount of needed training and resources compared to a typical motion capture laboratory. With greater understanding of its associated injury risk, K_{Vert} assessments could provide a wide variety of health care practitioners the ability to screen for injury risk. This could allow for implementation of preventative rehabilitation techniques to reduce lower extremity soft-tissue injury burden.

References

[1] Kerr ZY, et al. (2015). *MMWR.* 64(48): 1330-36
[2] Hootman JM, et al. (2007). *J Athl Train.* 42(2): 311-19
[3] Chimera NJ, et al. (2016). *World J Orthop.* 7(4): 202-17
[4] Butler RJ, et al. (2003). *Clin Biomech*. 18(6): 511-17
[5] McMahon TA, et al. (1990). *J Biomech*. 23: 65-78
[6] Sporri D, et al. (2019). *J Sports Sci.* 37(21): 2425-32
[7] Padua DA, et al. (2005). *J Motor Behav.* 37(2): 111-25

Optimizing whole-body kinematics using OpenSim Moco to reduce peak non-sagittal plane knee loads and ACL injury risk during single leg jump landing

Dhruv Gupta[1], Cyril J. Donnelly[2,3] and Jeffrey A. Reinbolt[1]
[1]Mechanical, Aerospace and Biomedical Engineering, The University of Tennessee Knoxville, Knoxville, Tennessee, USA
[2]Rehabilitation Research Institute of Singapore, Nanyang Technological University, Singapore
[3]School of Human Sciences (Sport and Exercise Science), The University of Western Australia, Australia
Email: dgupta5@vols.utk.edu

Introduction

Every year over 200,000 anterior cruciate ligament (ACL) injuries occur in the US [1]. Out of these, approximately 60% are non-contact in nature, with >90% occurring during single leg landing or sidestepping [2]. Anterior tibial force in conjunction with non-sagittal plane (valgus, varus and internal rotation) knee moments during the weight acceptance phase has been shown to place the maximum strain on the ACL [3, 4]. We used OpenSim's forward dynamics residual reduction algorithm (RRA) to identify optimal whole-body kinematics that would reduce non-sagittal plane knee moments during side-stepping and single leg jump landing (SLJL) [5, 6]. This process involved two steps: 1) optimise model parameters (all actuators and tracking weights) to generate simulations with near zero residuals and 2) reduce non-sagittal plane knee moments and tracking weights to identify associated optimal kinematic patterns. Each of these steps used RRA and an outer level optimization routine [7, 8]. Although this technique is powerful, it is computationally expensive. Therein, it can take as long as 13 hours to run a single 70 ms simulation, with approximately 90% of the time spent on reducing residuals.

The use of direct collocation [9] is a known method capable of improving the speed of musculoskeletal simulations. OpenSim Moco [10] is a novel software package built to reduce the computational complexity of direct collocation technique. Both RRA and OpenSim Moco find control trajectories of a model's actuators over time, but they use different methodologies to solve for them. RRA finds controls at each time frame and numerically integrates model state derivatives to step forward in time, while direct collocation finds controls simultaneously with model states over an entire movement trajectory, which drastically reduces computational time. This approach also removes the need for model residuals to generate a stable simulation. The purpose of this study was to a) use OpenSim Moco to predict the optimal kinematics linked to reduced non-sagittal plane knee moments during SLJL and b) compare the optimal kinematics generated by OpenSim Moco to those generated using the RRA approach.

Methods

We used data from two participants performing SLJL. We started with the same generic actuators, tracking weights and scaled model. We applied similar constraints and costs to the OpenSim Moco approach as the second step of the RRA approach which were reducing the maximal torque capacity of the knee varus/valgus and int/ext rotation actuators, the sum of squared activation of the actuators and tracking weights of the joint coordinates. We then compared the optimal kinematic solutions and reductions in non-sagittal plane knee moments generated by the two approaches.

Results and Discussion

The mean difference in optimal kinematics generated by the two approaches was 0.8°±0.35° and 0.7°±0.32° for the two participants (P1 & P2). The reduction in peak resultant non-sagittal plane knee moments for each participant pre-to-post optimization were 75% (P1) & 45% (P2) for RRA, and 63% (P1) & 74% (P2) for the OpenSim Moco respectively. Both optimization methods resulted in similar kinematic strategies to reduce the peak non-sagittal plane knee moments, which was to re-positioning the knee towards the GRF vector, effectively reducing its moment arm (Figure 1). OpenSim Moco took 6 hours per optimization and RRA 13 hours.

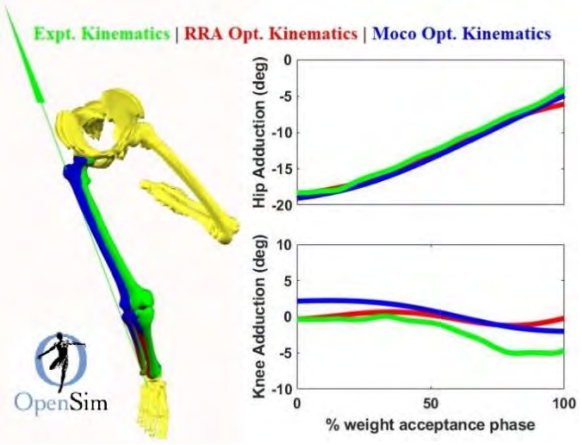

Figure 1: Comparison of Experimental, optimal RRA and optimal Moco kinematics (P2).

Table 1: Comparison of optimization approaches

Similarities	Over 40% reduction in peak non-sagittal plane knee moments Similar post-optimization kinematics
Differences	OpenSim Moco did not require residuals OpenSim Moco takes 50% less time

Significance

The use of OpenSim Moco reproduced the findings of an established forward dynamics approach (RRA) in one half the time. This improvement was accomplished as OpenSim Moco uses direct collocation, which is more computationally efficient than the previous approach. Our results for a high velocity movement like landing suggest that OpenSim Moco may perform even better for low velocity 'real world' applications within time constraints of clinical settings to treat movement disorders.

Acknowledgments

Experimental data was collected under NHMRC grant 400937.

References

1. DeMorat G. et al. Am J Sports Med, 2004; 2. Ekegren CL, et al. J Orthop Sports Phys Ther, 2009; 3. Markolf KL, et al. J Orthop Research, 1995; 4. Cerulli G, et al. Knee Surg, Sport Trauma, Anthro, 2003; 5. Donnelly CJ, et al. J Biomech, 2012; 6. Gupta D, et al. Am Soc Biomech, 2018; 7. Reinbolt JA, et al. Sim. Human Movement, 2011; 8. Weinhandl, et al. Clinical Biomech, 2013; 9.; Hairer E & Wanner G. Springer Series in Comp Math, 2010; 10. Dembia CL, et al. BioRxiv, 2019.

Development of an In-Vivo Ligament Loading Device

Brian J. Diefenbach[1] & Zachary J. Domire[1]
[1]Department of Kinesiology, East Carolina University, Greenville, NC,
Email: diefenbach8@gmail.com

Introduction

Prevention of ACL injuries is important, as ACL injuries are associated long term with the development of knee osteoarthritis, increased pain, functional limitations, and decreased quality of living [1]. Despite the focus on numerous ACL injury prevention mechanisms, ACL injury rates are still on the rise. Investigating a way to strengthen the ACL may be an alternative method to prevent ACL tears.

Traditionally, tissue strengthening would occur through a high magnitude load, applied a limited number of times. However, as ligaments are designed to restrict unhealthy joint movement, high magnitude loading of ligaments is likely non-desirable, making high frequency, low magnitude loading an intriguing possibility. Previous studies have shown that high frequency, low magnitude loading has been very successful in bone. Bone clearly demonstrates the ability to adapt and even strengthen in response to this type of mechanical loading [2], and it would make sense that ligaments, the connective tissue connecting two bones together, would also exhibit similar adaptive properties. However, there is limited research on a typical in-vivo ligament response to mechanical loading. Therefore, the purpose of this study was to develop a device capable of applying an in-vivo, high frequency, low magnitude load to the ACL.

Methods

A custom built device, the RACL Loader (Rabbit Anterior Cruciate Ligament Loader), was used to load the ACL. The motor on the device turns a pulley system, which moves one of two sliders. A spring connects the two sliders, and the second slider is attatched to a cord which pulls on a tibia cast, applying tension to the ACL (Figure 1). The frequency and magnitude of loading can be adjusted through varying spring stiffness and length.

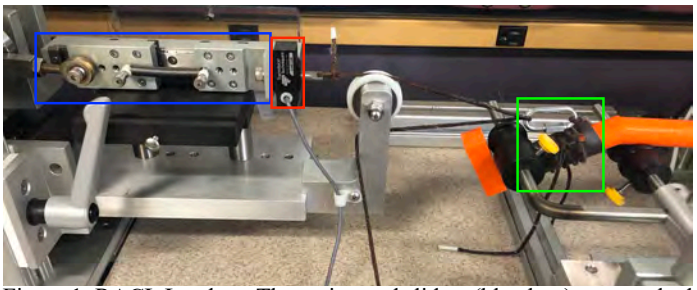

Figure 1: RACL Loader – The spring and sliders (blue box) are attached to a tension/compressive load cell (red box) to measure the tensile force applied to the shank cast/ACL (green box).

The loading parameters from previous successful high frequency, low magnitude bone loading protocols were modified due to differences in material properties between bone and ligament. Therefore, the optimal parameters of ligament loading were determined to be at an oscillating low-magnitude load (~2.0-13 N), and a high-frequency (~15-30 Hz) for 20 minutes [2]. This loading magnitude was determined based on the strain of ligament during normal activity and the percentage of load applied to the knee that would actually translate to the ACL. To ensure the loading occurred along the longitudinal axis of the ACL, the hip was extended, knee positioned at 30° knee flexion, with the device pulling on the tibia at 35-40° to apply tibial anterior translation [3]. As the device is sized to eventually load a rabbit ACL, a 3D printed model rabbit leg was used to test the device. Five springs of varying stiffness and length were tested in the device to determine the which spring would result in the desired high frequency, low magnitude loading.

Results and Discussion

Based on the resulting magnitudes and frequenices from loading the model rabbit leg using each of the five springs, spring C was successful in applying an oscilating loading magnitude from 2-13 N, at a frequency of 15 Hz (Table 1). Additionally, spring C tested during in-vivo loading on the left leg of a New Zealand White Rabbit was successfully able to apply the desired frequency and magnitude of loading on the rabbit's ACL.

Spring	*A*	*B*	*C*	*D*	*E*
Magnitude (N)	2 – 10	2 – 18	2 – 13	2 – 6	2 – 8
Frequency (Hz)	10	15	15	5	6

Table 1: Magnitudes and frequencies produced by the different springs tested in the RACL Loader.

Due to the pulley/gear ratio, the maximum frequency produced by the RACL loader was around 15 Hz. While this loading frequency is on the low end of the desired range, we are confident that this is still a great enough frequency to stimulate a ligament response. This is the first device to our knowledge that is able to load a ligament in-vivo at a high frequency, low magnitude load.

Significance

This device was successful to load a ligament, in-vivo, at the desired high-frequency and low-magnitude parameters. Future studies should perform mRNA-sequencing tests on the extracted ligament following in-vivo loading, to better understand the genetic response to loading. Based on the ligaments genetic response, we can then consider characterization of optimal loading parameters (i.e., loading frequency, magnitude, and duration of load). This technique may be a novel way to tackle a well-establized, ACL injury problem, and may long-term, be the basis for clinical high-frequency, low-magnitude loading as a prevention mechanism to protect against ligament injuries.

Acknowledgments

The authors of this study would like to acknowledge the American Society of Biomechanics for their funding through the ASB Student Grant-In-Aid, and Larry Berglund for the help designing this loading device.

References

[1] Lohmander et al. *Arthritis Rheum,* **50(10),** 3145-52, 2004.
[2] Rubin et al. *J Bone Miner Res,* **17(2),** 349-57, 2002.
[3] Escamilla et al. *J Orthop Sport Phys,* **42(3),** 208-20, 2012

Achilles Tendon Material Properties are Resilient to Variations in Load During Growth

Kavya Katugam[1*], Suzanne M. Cox[1], Matthew Q. Salzano[2], Adam De Boef[1], Tim M. Ryan[3], Stephen J. Piazza[1], Jonas Rubenson[1,2]
[1]Biomechanics Laboratoy, Dept. of Kinesiology, [2]Integrative & Biomedical Physiology, [3]Department of Anthropology
The Pennsylvania State University, University Park, PA, USA
Email: kavya@psu.edu

Introduction

Variations in tendon properties can affect the tendon's strength and safety factor. They can also alter the force capacity and power of muscles, directly influencing performance. However, we do not yet have a clear understanding of how tendons change over time. Material properties of adult tendon responds directly to mechanical load [1,2], but evidence of the plasiticty of tendon in growing individuals is less consistent. Since developmental plasticity can alter adult phenotype, uncovering the influence of activity levels during childhood on musculoskeletal development is necessary to inform variation in adult locomotor capacities.

Given the growing concern of the health consequences of decreases in physical activity in children [3], we investigated the developmental plasticity of tendon to decreases in load. First, we investigated the spring quality of the tendon by assessing the stiffness and modulus of the entire free tendon. Secondly, we assessed the bone-tendon junction, a region which has been shown to be succeptiple to tendon rupture [4].

Methods

To address our questions, we systematically altered the mechanical load environment across the growth span in an avian model (guinea fowl; *Numida meleagris*). Animals were divided at two weeks of age into three groups: 1) a control group permitted to undertake regular exercise (EXE, n = 8); 2) a disuse group restricted from exercise (DIS, n = 8); and 3) a third group that were restricted from exercise and in which the gastrocnemius muscles were partially paralyzed using repeated bouts of bi-lateral Botulinum toxin-A (botox) injections (4 units/kg per leg; BTX, n = 8). At skeletal maturity (27-28 wks) animals were sacrificed for tendon analysis. The left limb was kept fresh and scanned with high-field MRI (Bruker, 7T) from which the cross sectional area of the tendon was quantified in 1 mm incriments. The left limb was kept fresh-frozen and used for material testing (MTS Bionix 858 Mini Bionix II), combining stress-strain loading and digital video capture to assess regional properties.

Results and Discussion

Achilles tendon length, average cross sectional area (CSA), stiffness (***K***), modulus of elasticity (***E***), and hysteresis (***H***) were not statistically different between groups (at α set to 0.05). Tendon stiffness across all animals correlated with modulus (R^2 = 0.743, $p < 0.01$), but not with average tendon CSA (R^2 = 0.007, p = 0.698). Morphological and mechanical properties of the bone-tendon junction found a moderately higher tendon stress in the DIS group, but this, nor tendon strain, were statistically different between groups.

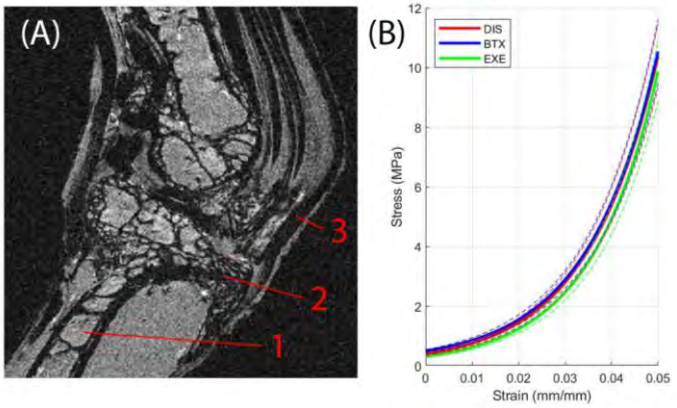

Figure 1: **(A)** Sagittal plane MRI of the guinea fowl ankle joint. 1: TMT. 2: Hypotarsus of the TMT, where Achilles tendon attaches. 3: Achilles Tendon. **(B)** Average loading stress-strain curve by condition. Dashed lines indicate one SD above and below the mean. Red (DIS) and blue (BTX) curves and corresponding SDs are superimposed.

Significance

We found that variations in loading during growth did not significantly alter tendon properties at adulthood, contrary to both of our hypotheses. Our results suggest that either 1) developmental factors override the load-induced remodeling that has been demonstrated in adults of the same species [1] or that 2) plastic changes due to offloading may not be predictable from responses to increased loading. Consistent with these findings, a previous study using botox to alter Achilles loading in growing mice has show similar minimal changes to tendon properties [5]. This resilience to load history during growth suggests that differences in activity level during growth may not greatly affect juvenile tendon development. These results are important for our understanding of musculoskeletal function and tendon health in growing individuals.

Acknowledgments

This study was supported through the NIH grant R21AR071588 and seed grants from the Huck Institutes of the Life Sciences and the Center for Human Evolution and Diversity at Penn State.

References

[1] Buchanan C et al. (2001). J Appl. Physiol, 90: 164-171.
[2] Bohm S et al. (2015). Sports Med. – Open,1186.
[3] Guthold R. et al. (2019). Lancet (Child-Adolescent), 4: 23-5
[4] Wren T A L et al. (2003). Annals Biomed Eng, 31: 710-717.
[5] Eliasson P et al. (2007). J Appl. Physiol, 103: 459-46.

Table 1: Achilles tendons (AT) and bone-tendon junction (BTJ) properties by condition. Values reported as group means ± standard deviation.

	Average AT CSA (mm^2)	***K*** (N/mm)	***E*** (MPa)	***H***	BTJ Strain	BTJ CSA (mm^2)	BTJ Stress (N/mm^2)
EXE	5.63 ± 0.37	51.86 ± 6.92	354.4 ± 61.2	0.24 ± 0.035	0.03 ± 0.03	2.48 ± 0.48	12.89 ± 3.38
DIS	5.69 ± 0.53	51.83 ± 10.19	342.3 ± 106.3	0.24 ± 0.041	0.04 ± 0.02	2.14 ± 0.38	16.13 ± 5.60
BTX	5.53 ± 0.50	50.57 ± 10.32	346.5 ± 69.4	0.23 ± 0.027	0.03 ± 0.02	2.55 ± 0.29	12.83 ± 4.74

Running Exposure is Associated with Achilles Tendon Shear Wave Speed

Matthew C. Ruder[1], Rebekah L. Lawrence[1], Michael J. Bey[1]
[1]Bone and Joint Center, Henry Ford Health System, Detroit, MI
Email: mruder1@hfhs.org

Introduction

Achilles tendinopathy is one of the most common injuries among runners [1]. The etiology of Achilles tendinopathy in runners is not well understood, but is likely influenced by a number of factors. For example, previous research has reported that Achilles tendon injuries are prevalent in high-volume runners [1], which supports the idea of running exposure (i.e., overuse) leading to injury. Previous research has also suggested that increased tendon stiffness may contribute to Achilles tendinopathy [2], supporting the notion that changes in tendon material properties may be a risk factor in the development of Achilles tendinopathy [3]. Lastly, it has also been shown that Achilles tendinopathy is more likely to affect experienced/older runners [1], suggesting that aging may influence the likelihood of a runner developing Achilles tendinopathy. Taken together, these previous studies suggest there are likely complex relationships between age, running experience, running mileage, Achilles tendon stiffness, and Achilles tendinopathy that are not particularly well understood. As an initial step toward understanding these complex relationships, the objective of this study was to use ultrasound shear wave elastography (SWE) – an imaging modality that provides a non-invasive estimate of soft-tissue material properties – to assess the extent to which measures of running exposure are associated with shear wave speed (SWS). We hypothesized that runners with higher running exposure would have higher Achilles tendon SWS.

Methods

Following IRB approval, six male runners (age: 46 ± 8) with no history of Achilles tendinopathy were recruited. Subjects reported their running history as number of years running, average runs per week over the past 3 months, and average weekly mileage over the past 3 months. To assess tendon material properties, each subject first walked on a treadmill for 5 minutes at a self-selected pace to precondition the Achilles tendon. Next, each participant was positioned prone with their lower legs fully extended off the back of an examination table. Five SWE images (Siemens ACUSON S3000) were collected for the free Achilles tendon on both left and right sides.

Data were analyzed using a custom MATLAB program to isolate the Achilles tendon region of interest (ROI) from the remaining tissues on the ultrasound B-mode image. SWS data within this ROI were extracted from the SWE image and then averaged to result in a mean SWS for each trial. Next a mean SWS was calculated across all trials and sides (left, right) to reflect the cumulative effect on both tendons for each subject. Correlation coefficients were calculated between SWS and measures of running exposure (years running, miles per week). The correlation between age and SWS was also examined to assess for the potential confounding relationship between age and running exposure. Significance was set as $p<0.05$.

Results and Discussion

A strong positive correlation was observed between SWS and number of years running (Figure 1, r=0.85, p=0.03). A strong negative association was observed between SWS and weekly mileage, but this did not reach statistical significance (Figure 1, r=-0.74, p=0.09). SWS was not associated with age (r=0.07, p=0.88). Finally, there was a strong negative association between years running and weekly mileage (r=-0.87, p=0.03).

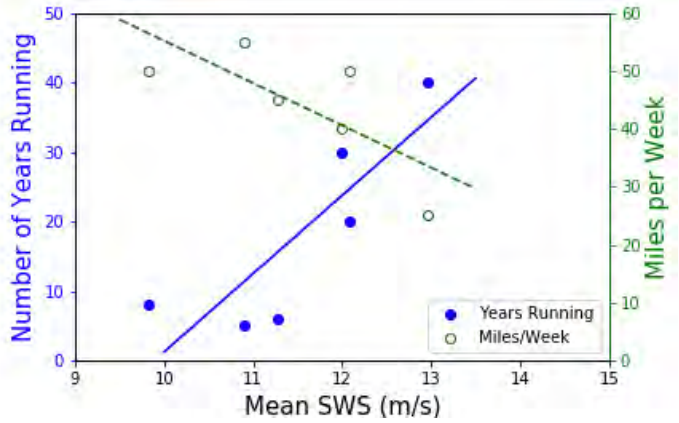

Figure 1: The relationship between Achilles tendon shear wave speed and running exposure (miles per week and years running).

The findings from this preliminary study may lend insight into the development of Achilles tendinopathy in runners. Specifically, low(er) SWS was associated with fewer years running (i.e., less running experience) and higher weekly mileage. Low Achilles SWS is important, because individuals with Achilles tendinopathy have been shown to have lower SWS than healthy subjects [4]. To further understand the significance of low(er) SWS, it's important to recognize that the most experienced runners in this study had the lowest weekly running mileage. Taken together, these findings may suggest that the less experienced, high mileage runners may be at greater risk for Achilles tendinopathy than the more experienced, low mileage runners. Furthermore, these findings may suggest that long-term mechanical loading (i.e., running over several decades) may not necessarily have a negative effect on the Achilles tendon, even though previous research has identified years running as a risk factor for Achilles tendinopathy [1]. However, given the low sample size in this study and without the assessment of tendon pathology, these implications are largely speculative and further research is needed to fully understand the complex relationships between running exposure, Achilles tendon SWS, and the development of Achilles tendinopathy.

Significance

Ultrasound SWE may aid in understanding the role of mechanical loading in the development of Achilles tendinopathy in runners.

References

[1] Taunton JE et al (2002), *Br J Sports Med*, **36**: 95-101.
[2] Lorimer AV et al (2016), *Sports Med.* **46**: 1921-38
[3] Stenroth, L et al (2012), *J App Physiol.***113**: 1537-44.
[4] Coombes, B et al (2018), *Scand J Med Sci Spor*. **28**: 1201-8.

Increased Cervical Spine Musculotendon Strain with Enlarged External Occipital Protuberances in Young Adults

Elizabeth S. Bjornsen[1], Anita N. Vasavada[2], and Kaitlin M. Gallagher[1]
[1]University of Arkansas, Fayetteville, Arkansas
[2]Washington State University, Pullman, WA
Email: kmg014@uark.edu

Introduction

In 2019, 81% of all Americans owned a smartphone, with ownership increasing to 96% for young adults 18-29[1]. Tablet and smartphone use have increased, accompanied by a flexed neck posture during device use[2]. Cervical extensor muscles, including the splenius, semispinalis, suboccipital muscles and superior trapezius, all aid in supporting the head's weight[3]. Any increase in flexion, which is common with device usage, may limit muscle function. Further, increased cervical flexion has been associated with reclined and semi-reclined positions when compared to an upright posture[4].

New research has identified that prominent exostoses at the base of the neck are more prevalent in the young adult population[5]. The presence of an enlarged external occipital protuberance (EEOP) could influence cervical flexion and increase cervical spine musculotendon (MT) strains. Therefore, the purpose of the study was to compare cervical flexion and cervical extensor MT strains between those with and without an EEOP. We hypothesized that:

(1) Individuals presenting with and without an EEOP will have different cervical flexion range of motion.
(2) Cervical extensor MT strains when in full flexion will differ among individuals who present with and without EEOP.

Methods

Twenty-two participants (21.32±1.25yrs) with no history of neck injury had cervical x-rays in neutral and full cervical flexion. The presence of an EEOP was defined by a ≥10mm measurement from the occipital squama to the most distal portion of the protuberance[5]. Cervical flexion in the fully flexed x-ray posture was computed with respect to neutral using individualized landmarks in Image-J (Rasband, WS). Individualized output from a cervical spine biomechanical model (SIMM) calculated 27 MT segment strains in full flexion using the neutral posture as the reference. Between group (presence vs. absence of EEOP) comparisons were conducted using t-tests for MT strain and range of motion (SAS, Cary, NC) with a Bonferroni correction of $p<.0019$ to account for multiple comparisons. Hedge's g effect sizes were computed, recognizing .80 as a large effect[6].

Results

41% (n=9) of participants met the criteria for having an EEOP. Hypothesis 1 was not supported, as cervical flexion range of motion was not statistically different between groups. Cervical flexion was 15.0° ± 2.5° and 16.3° ± 6.7° for EEOP presence and EEOP absence respectively. Hypothesis 2 was partially supported. Five of the twenty-seven MT segments were significantly different between ($p<.0019$) (Table 1). Two of the three deep multifidus MT segments ($p<.002$), two of the three superior multifidus MT segments ($p<.001$) and the semispinalis cervicis observed significant strain differences between groups ($p<.001$). In all cases, higher MT strains were observed for EEOP present individuals.

TABLE 1. Musculotendon Strains (mean ± standard deviation) and Hedge's g effect size for EEOP presence/absence. *p<.0019

MT Segment (name-origin-insert)	Presence	Absence	Effect Size
deepmult-C4/5-C2 *	.3221 ± .0655	.214 ± .0546	1.84
deepmult-C5/6-C3 *	.3192 ±.0540	.195 ± .0661	2.01
deepmult-C6/7-C4	.3304 ± .1272	.2262 ± .0849	1.02
semi_cerv_C2C7 *	.2587 ± .0353	.1793 ± .0457	1.88
supmult-C4/5-C2	.3195 ± .0916	.2355 ± .0682	1.08
supmult-C5/6-C2 *	.3507 ± .0606	.2424 ± .0568	1.86
supmult-C6/7-C2 *	.4054 ± .0561	.2684 ± .0719	2.06

Discussion

The study supports previous findings of EEOP presence in young adults[5]. While not all MT segments had between-group strain differences, all affected MT segments had insertion points on the C2 vertebrae. The multifidus[7], which observed significance in four of six MT segments, and semispinalis cervicis, are responsible for cervical stabilization[8]. None of these MT have insertions on the skull. Muscle attachments near the EEOP are the trapezius (not modelled in this study) and the semispinalis capitis (not significantly different). While it is unclear why other MT segments were unaffected, repetitive mechanical loading, a mechanism for exostoses development[9], at the C2 attachment site could increase MT strain of other tissues in the cervical spine and contribute to exostoses development.

Significance

Technology has transformed society and highlights a new area of clinical concern, especially in young adults. Long-term, cervical flexion associated with smartphone and tablet use may have clinical implications. Therefore, future studies should continue to explore the relationship between hand-held technology use and the presence of an EEOP. Additional research should examine the risk of neck pain development for individuals with an EEOP, potentially reducing the need for clinical interventions.

References

1. Internet and Technology. *Pew Research Center*. (2019).
2. Gold, J. E., et al. *Appl Ergon*. 2012; 43(2): 408–12.
3. Vasavada AN, Li S, Delp SL. *Spine*. 1998; 23(4): 412.
4. Douglas EC, Gallagher KM. *Appl Ergon*. 2018; 70:104–9.
5. Shahar D., Sayers MGL. *Sci Rep*. 2018; 8(1):1–7.
6. Ellis, P.D. *Cambridge University Press*. (2010).
7. Anderson, J. S., et al. *Spine.* 2005; 30(4), E86.
8. Schomacher, J., et al. *Clin Neurophys.* 2011;123(7): 1403-8.
9. Li, J., Muehleman, C. *Clin Anat*. 2007; 20(8): 950-955

Trunk-Pelvic Coordination during Unstable Sitting at Varying Task Demand

Julian C. Acasio[1,2], Maury A. Nussbaum[3], Brad D. Hendershot[1,4,5]

[1]Walter Reed National Military Medical Center, [2]Henry M. Jackson Foundation for the Adv. of Military Medicine, Inc., [3]Virginia Tech, [4]DoD-VA Extremity Trauma & Amputation Center of Excellence, [5]Uniformed Services University of the Health Sciences
Email: bradford.d.hendershot2.civ@mail.mil

Introduction

Unstable sitting is commonly used for evaluating trunk postural control (TPC) [1,2]. TPC measures during unstable sitting are typically derived from center-of-pressure data [3], but these measures do not necessarily quantify the underlying control or movement strategies. Methods that more directly characterize trunk-pelvic coordination, such as vector coding (VC) – which has been used in walking [4], turning [5], and lifting [6] – may provide additional insights into movement control strategies during unstable sitting. The purpose of this study was thus to quantify trunk-pelvis coordination during unstable sitting using VC, and to compare these outcomes across varying levels of task demand. We hypothesized that as task demand increased the frequency of anti-phase movements would increase, with a corresponding decrease in the frequency of in-phase movements.

Methods

Thirteen uninjured individuals (2 female) participated, with mean (SD) age = 28.7 (7.2) yr, stature = 177.1 (6.3) cm, body mass = 74.6 (11.4) kg. Each sat on an unstable chair [1] at four levels of instability, in a random order, relative to each individual's gravitational gradient (∇G) [2]: 100, 75, 60, and 45 %∇G. Three 60-second practice trials were administered to attenuate learning affects, after which one 60-second test trial was completed and analyzed. Trunk and pelvic kinematics were tracked (120 Hz) via an 18-camera motion capture system.

Tri-planar trunk-pelvic coordination was assessed using VC analyses [4], and coupling angles classified movements into: 1) anti-phase (trunk and pelvis move in opposite directions); 2) in-phase (trunk and pelvis move in same direction); 3) trunk-phase (only trunk motion); and 4) pelvic-phase (only pelvis motion). Main effects of instability level (%∇G) were assessed using single-factor ANOVAs ($p<0.05$). Post-hoc Bonferonni-corrected *t*-tests assessed between-condition differences ($p<0.0125$).

Results and Discussion

With decreasing %∇G (i.e., increasing instability), we found [Fig. 1]: increased anti-phase movement in the sagittal ($p=0.011$) and frontal ($p=0.005$) planes; decreased in-phase movement in the sagittal ($p=0.003$) and frontal ($p=0.055$) planes; increased in-phase movement in the transverse plane ($p<0.001$); and increased pelvic-phase movement in the transverse plane ($p=0.003$).

Supporting our hypothesis, increased in-phase motion in the sagittal and frontal planes at lower levels of instability suggests the use of a stiffening strategy, in which the trunk and pelvis move in unison. As the task goal was to minimize chair motions, this strategy likely assisted in limiting extraneous movement and maintaining balance. With increased instability (lower %∇G), participants face larger perturbations and stiffening becomes more difficult. Instead, participants appeared to adopt a strategy involving more anti-phase movements of the trunk and pelvis, which may offset the gravitational effects of each segment and prevent excessive leaning in any one direction.

Significance

VC techniques were able to discriminate between levels of instability during unstable sitting, and thus may serve as useful TPC measures that are more indicative of the underlying movement strategies. Moreover, these results can serve as baseline data for future work investigating populations with impaired TPC (e.g., individuals with low back pain or limb loss).

Acknowledgments

This study was funded by DoD awards W81XWH-14-01-0144 and HU0001-15-2-0003. We also thank Dr. Courtney Butowicz and Mr. Pawel Golyski for assisting with intial data collections. The views expressed are those of the authors and do not reflect the official policy of HJF, USUHS, the Departments of Army/Navy/Air Force/Defense, or U.S. Government.

References

1. Hendershot and Nussbaum 2013, Gait Posture, **38**, 438-42
2. Slota, et al. 2008, Clin Biomech, **23**, 381-86
3. Prieto, et al. 1996, IEEE, **43 (9)**, 956-66
4. Needham, et al. 2014, J Biomech, **47,** 1020-26
5. Golyski and Hendershot 2018, HMS, **58**, 41-54
6. Zehr, et al. 2018, JEK, **39**, 104-13

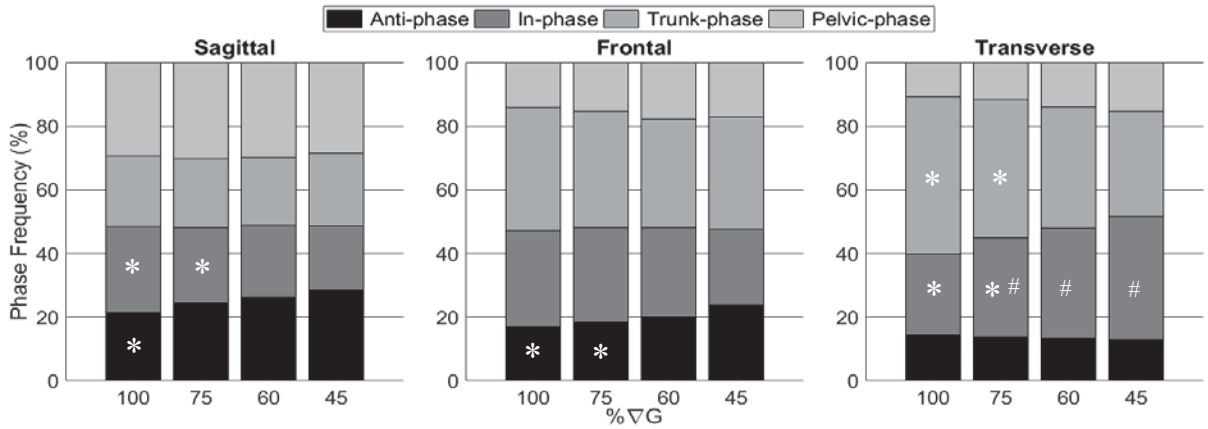

Figure 1: Distribution of phase frequencies in the sagittal (left), frontal (middle), and transverse (right) planes. Within each plane, the symbols (*) and (#) indicate statistical differences relative to 45%∇G and 100%∇G, respectively.

The Impact of Sitting on Active Trunk Stiffness and the Mitigating Effect of Age

Diesbourg, T.L.[1,2], Dumas, G.A.[2,3]
[1]Department of Public and Environmental Wellness, Oakland University, Rochester, MI, USA
[2]School of Kinesiology and Health Sciences, Queen's University, Kingston, ON, CAN
[3]Mechanical and Materials Engineering Department, Queen's University, Kingston, ON, CAN
Email: tdiesbourg@oakland.edu

Introduction

The spine has evolved over time to provide an optimal level of stability to the human body [1]. Researchers have suggested that this stability may be affected by prolonged sitting, which could leave workers at an increased risk for injury, particularly in occupations where dynamic movements immediately follow prolonged periods of seated work [2,3]. To date, this hypothesis has yet to be tested. Numerous methods have been used to assess the dynamic stiffness of the trunk [4,5,6], a variable that represents the trunk's ability to withstand a perturbation, a quality that would be indicative of spinal stability. The purpose of the current study was to determine whether prolonged sitting affects the trunk's ability to react to a perturbation.

Methods

Forty-six individuals (18 males, 28 females) who work sedentary jobs were recruited from three age groups (18 – 28 years: n = 17, 38-48 years: n = 14, and 58-68 years: n = 15). Volunteers were excluded if they were experiencing low back pain, or if they had experienced low back pain significant enough to cause them to seek medical attention or to miss school or work in the past 12 months. Active stiffness of the low back was measured immediately before and after the participants sat in a backless office chair for 60 minutes.

Low back active stiffness was measured through a forward-perturbation protocol as described in literature [4] whereby participants adopted a semi-seated position in a custom apparatus. 15% of their body weight was suspended from the front and back of their torso by way of a chest harness (Figure 1). At a random time and in a random order, one of the two suspended weights was dropped by releasing an electromagnet. The remaining weight caused a perturbation either forward or backward depending on which weight was dropped. The participants were instructed to sit as relaxed as possible prior to the weight dropping, and to return to their upright position as quickly as possible afterwards. For the purpose of this analysis, a faster response and shorter displacement were used to denote an increase in active stiffness.

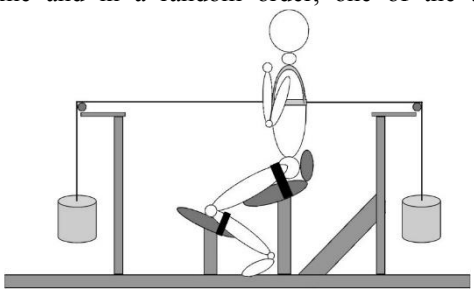

Figure 1: Schematic of custom active stiffness apparatus with participant in neutral position.

Statistical analysis consisted of paired-samples t-tests to identify differences in active stiffness before and after sitting, as well as correlations and one-way ANOVAs with Bonferroni adjustments to identify relationships and associations between age and active stiffness.

Results and Discussion

Paired-samples t-tests revealed a significant difference between variables measured before and after sitting with perturbation displacement ($t(45) = 2.25$, $p = 0.03$) and response time ($t(45) = 3.22$, $p = 0.002$) decreased after a bout of prolonged sitting.

The correlation analysis revealed no relationship between either active stiffness variable before sitting, but a moderate positive relationship between age and perturbation displacement after sitting ($r = 0.245$, $p = 0.02$).

Lastly, the one-way ANOVA showed an interaction between age and both active stiffness variables after prolonged sitting but not before (Figure 3). A post-hoc analysis with Bonferroni adjustments revealed that after sitting, the younger group displaces significantly less than the middle-aged (p = 0.041) and older groups ($p = 0.046$) and responds faster than the middle-aged group ($p = 0.039$).

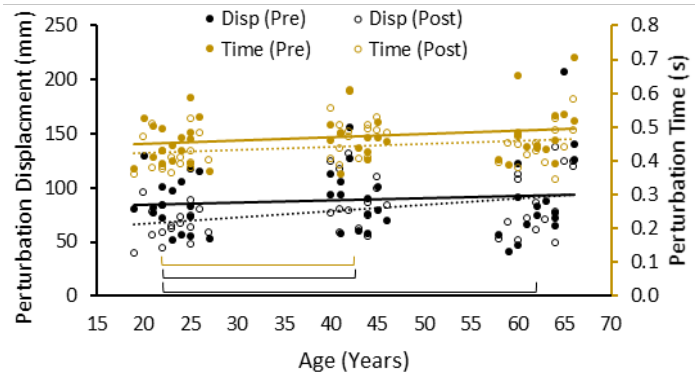

Figure 2: Perturbation displacement (black) and response time (gold) with age before sitting (closed circles, solid trendlines) and after sitting (open circles, dotted trendlines). Between-group differences ($p < 0.05$) after sitting are shown by square brackets at the bottom of the figure.

Significance

The results of the current analysis suggest that contrary to previous beliefs, spine stability appears to increase following a bout of prolonged sitting. This could be a protective mechanism of the spine to prevent injury when dynamic motions are required immediately following a bout of sitting. It also appears, however, that this protective mechanism may be reduced with age, where older individuals do not show an increase in spine stability but rather, maintain their pre-sitting level. This could leave older workers at an increased risk for injury should they be required to lift and/or bend after sitting for an hour or more and further investigation is needed to determine the mechanisms involved. With the average age of the global workforce steadily increasing [7], this research could impact the health of workers everywhere.

References

[1] Reeves et al, 2011; [2] Beach et al, 2005; [3] De Carvalho & Callaghan, 2011; [4] Hodges et al, 2009; [5] Larivière et al, 2010; [6] Bazrgari et al, 2009; [7] Chand & Tung, 2014.

Connecting the Pieces: How Low Back Pain Alters Lower Exremity Mechanics in Active Individuals

Alexa K. Johnson[1], John P. Abt[2], Arthur J. Nitz[3], Nicholas R. Heebner[1], Arnold J. Stromberg[4],and Joshua D. Winters[1]
[1]Sports Medicine Research Institute, College of Health Sciences, University of Kentucky
Email: johnson.alexa@uky.edu

Introduction

More than 80% of individuals experience an episode of low back pain (LBP) at some point during their lifetime.[1] In active populations, up to 37% suffer from LBP,[2] and military populations report 70% higher prevalence than the general population.[3] Further, compensatory movement strategies are often used to alleviate pain and often impact lower extremity loading patterns. Those who suffer from chronic low back pain tend to walk and run slower and with less trunk and pelvis coordination and variability.[4] Individuals with LBP also exbhibit greater knee joint stiffness during walking.[5] Moving with less joint coordination and more stiffness may be potential compensatory movement strategies aimed at avoiding pain. Therefore, the purpose of this project was to determine how individuals who suffer from chronic LBP present with altered patient reported outcomes and lower extremity strength, and biomechanics during landing.

Methods

Individuals who suffer from chronic LBP and healthy controls (CTRL) were recruited for this study. Individuals completed the Knee Injury and Osteoarthritis Outcomes Score(KOOS), a patient reported outcome geared toward understanding an individual's self-perceived knee function, measured in five subscales, Symptoms (SYM), Pain, Activities of Daily Living (ADL), Sports and Recreation (S&R), and Quality of Life (QOL).

Lower extremity mechanics were collected during a drop vertical jump,single leg hop, and crossover hop using motion analysis system with two in-ground force plates. Joint angles at initial contact, and peak joint angles during the landing phase of all tasks were calculated. Peak vertical ground reaction forces (PVGRF) were identified as the maximum vertical ground reaction force during the landing phase of each task. Average loading rate was assessed as the mean of the derivative of the vertical ground reaction force curve from ground contact to PVGRF.

Independent t-tests were used to assess differences in KOOS sub scores, bilateral kinematic and kinetics between LBP and CTRL participants for all tasks. An alpha value of a=0.05 was set for all analyses.

Results and Discussion

Twenty-eight individuals with LBP (mass:72.06±12.1kg; 21F, 7M) and 28 matched indivdiuals in the CTRL group (mass:72.66±13.2kg; 21F, 7M) completed testing. Those with LBP presented with lower self-percieved knee fucntion compared to the CTRL group in four KOOS subscales (Figure 1), including SYM (p=0.007), Pain (p=0.002), QOL (p=0.021), and ADL (p=0.003). There were no significant differences between the two groups in the KOOS Sports and Recreation Score.

Individuals in the LBP group presented with greater non-dominant limb knee valgus angles during initial contact during the single limb hop (p=0.033), crossover hop (p=0.020), and drop vertical jump (p=0.043; Figure 2) compared to the CTRL group.

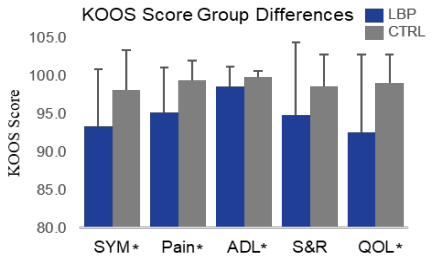

Figure 1: Mean and standard deviation of KOOS scores between groups, * indicating significantly different subscale scores betweent the LBP and the CTRL group.

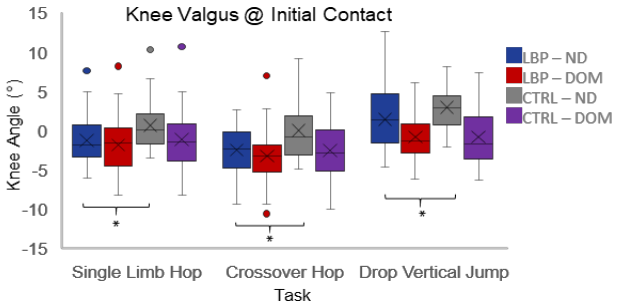

Figure 2: Knee valgus angle at initial contact of all tasks,* indicating significantly different subscale scores betweent the LBP and the CTRL group.

Additionally, during the drop vertical jump individuals with LBP exhibited significantly higher PVGRF (22.15±5.9 N/kg) during landing compared to the CTRL group (19.13±3.3 N/kg; p=0.023). It is possible that individuals with LBP present with worse KOOS scores due to pain avoidance strategies. Overall, pain avoidance may drive mechanical compensations, such as increased knee valgus angles during landing, which over time, could potentially influence how individuals with LBP perceive their knee function.

Significance

Assessing knee function in individuals with LBP may provide the clinician with a more holistic view of overall levels of physical function and performance. While KOOS scores of individuals with LBP are not as severe as those who have recently sustained a knee injury, they are lower than a healthy population. Thus, it may be beneficial for clinicians to assess self-perceived knee function to potentially delay the onset of any further complications.

Acknowledgments

This research was supported by the American Society of Bioemchanics Student Graint-in-Aid. The content is solely the responsibility of the authors and does not necessarily represent the official views of ASB.

References

1. Rubin et al., 2007. Neurologic Clinics.
2. Nadler et al., 1998., Spine.
3. Clark & Hu, 2015. MSMR.
4. Seay et al., 2011. Clin Biomech.
5. Hamill et al., 2009. Res Sports Med.

Thoracolumbar and Pelvis Kinematics are Associated with Paretic Force Production

Donald Prible, PT, DPT[1], Hao-Yuan Hsiao, PhD[1]
[1]The University of Texas at Austin, Department of Kinesiology and Health Education
Email: prible@utexas.edu

Introduction

In individuals with hemiparesis, decreased propulsive force generation and weight bearing ability in the paretic limb are associated with slower walking speeds and increased disability [1]. It has been suggested that the head-arm-trunk system modulates lower extremity force production and foot trajectory during gait [2]. Given that impairments in thoracolumbar strength and coordination exist after a stroke [3] and are predictive of functional outcomes [4], it is conceivable that impairments in thoracolumbar function following stroke interfere with the mechanism of force production during hemiparetic gait. The purpose of this study was to identify relationships between thoracolumbar movement and paretic lower limb force production during stance phase of gait in individuals post-stroke.

Methods

Participants (n = 19) with chronic hemiparesis following stroke walked at their self-selected walking speed on a treadmill (mean speed = 0.76 ± 0.37 m/s) . Kinematics were measured via an 8-camera motion tracking system using a cluster of markers around the sacrum and markers at each acromion. Ground reaction forces (GRFs) were captured via an instrumented split-belt treadmill. Peak vertical and anterior (propulsion) GRFs were calculated and normalized to body weight.

Frontal and transverse plane pelvis position and thoracolumbar angle (thorax relative to pelvis) were calculated in Visual3D. Positions at the start of stance as well as the peak changes during stance were calculated. This generated eight independent variables: (pelvis and thoracolumbar) x (frontal plane and transverse plane) x (initial position and peak change in position).

Pearson's correlation was used to determine relationships between thoracolumbar and pelvis kinematics and GRF variables. Stepwise linear regression was used to identify predictors of peak paretic vertical GRF and propulsion.

Results and Discussion

Peak change in thoracolumbar lateral flexion (LF) during stance phase was correlated with peak paretic vertical GRF and propulsion (Figure 1). It was also the only significant predictor of peak paretic force production (Table 1), indicating that the movement of the pelvis *relative to* the thorax affects weight bearing and forward progression more than movement of the pelvis alone. Additionally, frontal plane kinematics demonstrated significance while transverse plane kinematics did not.

The model predicts that for each additional degree of LF during stance, the propulsive force *increases by 1.34% of body weight*. Given that the maximum propulsive force among participants is approximately 16% of bodyweight, this may suggest that relatively small changes in LF are associated with meaningful changes in force production.

Initial pelvis position independently contributed to the model predicting peak vertical GRF, indicating that altered pelvis position may affect paretic limb weight bearing capacity during stance.

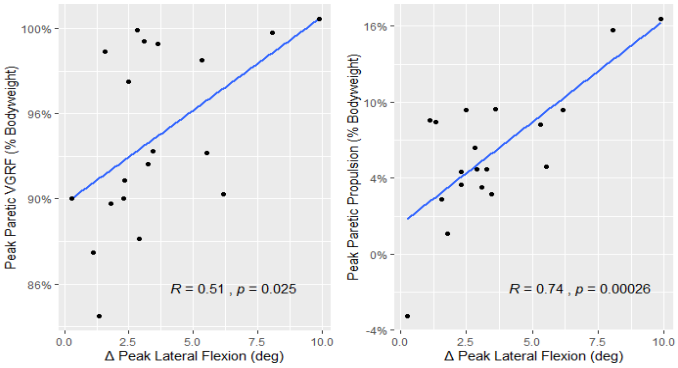

Figure 1: Correlation between peak trunk lateral flexion (degrees) and peak VGRF/propulsion (normalized to body weight) during paretic stance phase at self-selected walking speed.

	Normalized Peak Force During Paretic Stance	
	VGRF	Propulsion
Initial Pelvis Tilt in Frontal Plane	-0.00642 $^{+}$	
Peak Δ Thoracolumbar Lateral Flexion	0.0105 *	0.0134 ***
R^2	0.403*	0.553***

Table 2: Coefficients of linear regression model of peak forces against thoracolumbar and pelvis variables at self-selected walking speed. Significance Level: *** 0.001, *0.05, $^{+}$0.1

Significance

Our findings suggest that thoracolumbar lateral flexion movement during stance is an important factor for functional weight bearing and propulsive force production. This supports a thoracolumbar-mediated mechanism of force production that may inform future rehabilitation strategies.

Acknowledgments

NIH R01 NR010786, we thank Dr. Binder-Macleod for sharing the data.
UT Austin College of Education Recruitment Fellowship

References

[1] Balasubramanian, Chitralakshmi K., et al. (2007). *Archives of Physical Medicine and Rehabilitation* 88 (1): 43–49.
[2] Varraine, E, et al. (2000) *Experimental Brain Research. Experimentelle Hirnforschung. Experimentation Cerebrale* 130 (2): 248–57.
[3] Dickstein R et al. (2004). Arch. Phys. Med. Rehabil., 2004, 85, 261–267.
[4] C.-L. Hsieh CL et al. (2002). Stroke, 33, 2626–2630.

Periacetabular Osteotomy for Hip Dysplasia Alters Dynamic Flexor and Abductor Muscle Moment Arms and Lines of Action

Ke Song[1,2], Molly C. Shepherd[1], John C. Clohisy[3], and *Michael D. Harris[1,2,3]
[1]Program in Physical Therapy, [2]Department of Mechanical Engineering, [3]Department of Orthopaedic Surgery
Washington University in St. Louis, St. Louis, MO, USA
Email: harrismi@wustl.edu *corresponding author

Introduction

Developmental dysplasia of the hip (DDH) is characterized by abnormal bony anatomy, which causes abnormal joint loading and leads to early onset of hip osteoarthritis.[1,2,3] To reduce the risks for joint damage, periacetabular osteotomy (PAO) is commonly prescribed to correct hip anatomy for young adults with DDH. PAO restores femoral coverage and usually relieves symptoms;[2] however, chondral damage has been found in many hips post-PAO,[3] indicating hip loading may still be abnormal after surgery. The bony anatomy of DDH also alters hip muscle moment arm lengths (MALs) and lines of action (LoAs), which affect the muscles' ability to generate forces and may contribute to abnormal hip loading.[4,5,6] However, despite muscles being a key factor in pre- and post-PAO hip mechanics, it is unclear how their force-generating abilities are changed by PAO. Thus, our objective was to compare hip muscle MALs, LoAs and forces during gait before and after PAO using subject-specific musculoskeletal models. We hypothesized that due to the medialization of the lateralized hip joint centers (HJCs) during PAO,[7] hip abductor MALs will be increased, medial LoAs will be reduced, and medial hip loading will be lower than pre-op.

Methods

5 female patients with DDH (25.0 ± 6.8 y/o, BMI: 23.2 ± 1.6 kg/m^2) participated after IRB approval and consent. Gait data were captured for each subject pre-PAO and again post-PAO (4-7 months) using near-infrared cameras, skin markers and an instrumented treadmill. Pre- and post-op MR scans of the pelvis and femurs were both reconstructed in 3D. First, the pre-PAO 3D geometries were added in OpenSim to create models with subject-specific bony anatomy, HJC locations and muscle paths.[8] Then, post-PAO models were created by updating the MR-based post-PAO 3D hemi-pelvis, HJC location, and origin of the rectus femoris muscle (altered by PAO) on the surgical side. Using each pre- and post-PAO model and corresponding gait data, muscle forces over a gait cycle were estimated via static optimization. Dynamic muscle MALs were computed using a generalized-force method;[5] muscle LoAs were extracted as a unit vector with antero-posterior, supero-inferior, and medio-lateral components, which represent the percentage of each net muscle force in these 3 directions.[6] Lastly, hip joint reaction forces (JRFs) were computed from muscle forces. Hip JRFs, muscle MALs, LoAs and forces were compared between pre- and post-PAO models at the times of JRF peaks in early and late stance (paired t or Wilcoxon tests, $\alpha = 0.05$).

Results and Discussion

After PAO, both resultant ($p \leq 0.04$; **Fig. 1**, left) and medial hip JRFs (1.34 vs 0.86 ×BW in late stance, $p = 0.03$) significantly decreased compared to pre-PAO. As past studies found elevated medial JRFs in DDH,[9] current results suggest PAO may be effective for lowering the excessive hip JRFs.

As we hypothesized, hip abduction MALs (**Fig. 1**, center) for gluteus medius increased after PAO ($p \leq 0.05$). Such change may be attributed to medialization of the HJC after PAO (pre: 9.4 mm, post: 8.7 mm from median plane), which reduces the relative distance between HJC and the abductor muscle paths. Consequently, abductor muscle forces decreased (e.g. gluteus medius, 1.59 vs 1.11 ×BW late stance, $p = 0.03$), which supports findings that hip loading is sensitive to HJC medialization.[7]

Due to the repositioned muscle origin of rectus femoris on the reoriented acetabulum, its hip flexion MALs increased markedly (37.6 vs 44.1 mm in early stance, $p = 0.01$). Frontal-plane MAL also changed from near-neutral to abduction (**Fig. 1**, center), which may have affected its net force (0.68 vs 0.33 ×BW in late stance, $p = 0.05$) and contribution to the hip JRFs.

Muscle LoAs were also altered by PAO (**Fig. 1**, right). Medial LoAs became lower in the gluteus maximus ($p \leq 0.05$) and gluteus medius, which supports our hypothesis and means that forces produced by these muscles were oriented less medially, which may have helped reduce the medial hip JRFs.

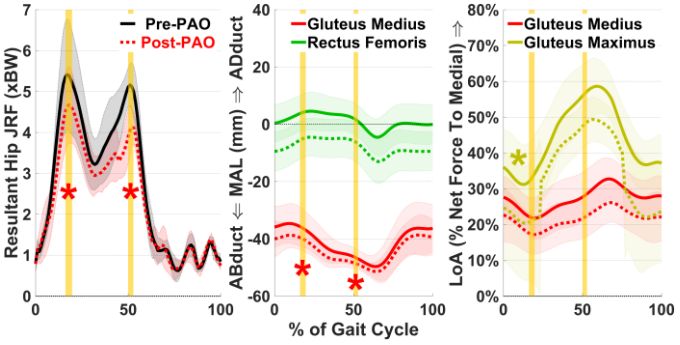

Figure 1: Hip JRFs (left), muscle abduction-adduction MALs (center), and medio-lateral LoAs (right) pre- and post-PAO over a gait cycle.

Significance

PAO considerably influenced the hip muscle MALs and LoAs during gait. Increased hip abduction MALs and reduced medial LoAs lowered resultant and medial hip muscle forces and JRFs. These results elucidate how PAO can help reduce hip loading via modification of the HJC locations and muscle paths, thereby restoring hip muscles' dynamic force-generating abilities.

Because muscles are major contributors to joint loading, identifying the changes in dynamic hip muscle paths and force-generating abilities improves our knowledge of the mechanistic efficacy of PAO for correcting abnormal joint mechanics. This knowledge can inform future surgery and post-op rehabilitation to minimize the likelihood for hip joint damage in DDH.

Acknowledgments

NIH/NIAMS K01AR072072 and P30AR074992.

References

[1] Wyles *Clin Orthop Relat Res* 2017. [2] Bogunovic *Am J Sports Med* 2014. [3] Cvetanovich J *Hip Preserv Surg* 2015. [4] Maquet *Acta Orthop Belg* 1999. [5] Sherman *Proc ASME DETC* 2013. [6] van Arkel *J Orthop Res* 2013. [7] Gaffney *J Biomech* 2020. [8] Song *Comput Methods Biomech Biomed Engin* 2019. [9] Harris *J Biomech* 2017.

Kinetic and Kinematic Comparison of Multiple Hip Pathologies during Sloped and Level Walking

Emily T. Levy[1]*, Jacey Roy[1], Ed Mulligan[2], Avneesh Chhabra[2], Joel Wells[2] and Nicholas P. Fey[1,2]
[1]The University of Texas at Dallas, Richardson, TX
[2]UT Southwestern Medical Center, Dallas, TX
Email: *emily.levy@utdallas.edu

Introduction

Osteoarthritis (OA) is one of the leading causes of ambulatory disability, with symptomatic hip OA affecting at least 4% of Americans over 50 years of age [1]. Developmental dysplasia of the hip (DDH) and femoroacetabular impingement (FAI) are two of the primary causes of premature hip degeneration [2]. These structural deformities hinder the ability of the articular surfaces to properly transfer loads during movement. While anatomical diagnosis of joint morphology can be accomplished using imaging, these lack quantitative assessment during everday tasks.

Several studies have investigated peak measures of gait alterations in level walking biomechanics for FAI and DDH, separately. Yet, this practice excludes other regions in the gait cycle and many researchers suggest more challenging tasks are needed to provide a detailed understanding of both DDH and FAI and inform targeted treatment strategies for each group [3].

The purpose of this study was to quantitatively assess hip kinematics and kinetics during level, incline, and decline walking of individuals with diagnosed DDH and FAI compared with asymptomatic controls. We hypothesized that the DDH patients would show larger differences than controls in decline, while FAI would show larger differences than controls in incline walking, with overall similar behaviour of both groups relative to controls during level walking.

Methods

Thirteen patients with DDH, thirteen patients with FAI, and eight asymptomatic controls (C) provided informed consent, and the 26 patients were scheduled for hip preservation surgery. On the day of scheduled surgery, subjects performed one-minute walking trials at self-selected speeds on level, incline (10°), and decline (-10°). An instrumented splitbelt treadmill (Bertec, Inc.) collected 3D ground reaction forces (GRF, 1000 Hz), and a 10-camera motion capture system (Vicon, Inc.) tracked 46 reflective markers (100 Hz). Kinematic and kinetic data were applied low-pass Butterworth filter (6 Hz cut-off) using Visual3D (C-Motion, Inc.). Statistical Parametric Mapping (SPM) *t*-tests (α=0.05) were computed to compare between group GRF and hip joint angles and moments of the affected leg in sagittal plane, as a function of the gait cycle [4].

Results and Discussion

Some hypotheses were supported and some were not. DDH showed significant ranges of reduced braking and propulsive forces during early and late stance at all slopes, reduced hip extension during middle and late stance at all slopes, and reduced extension moment during early stance for level and incline, possibly due to reduced speed but still suggestive of reduced impact on the joint. Both FAI and DDH showed more flexion-biased moments in pre-swing on the incline, suggesting this may be a protective mechanism that the hip patients used to reduce the range of hip extension. FAI showed lower braking forces, also suggeseting a guarding mechanism. FAI and DDH patients both exhibited gait modifications relative to controls, with the most widespread changes occurring throughout the stride in DDH, especially on the incline.

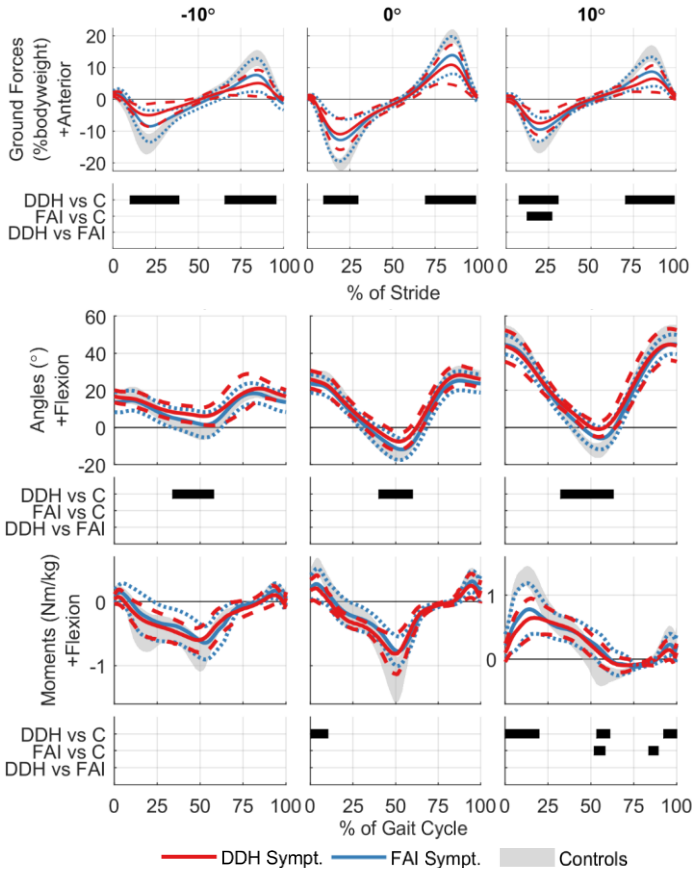

Figure 1: Hip sagittal plane biomechanics. For each subfigure, the top row shows the patient means (solid lines) ±SD (dashed or dotted for DDH or FAI, respectively) and the controls mean ±SD (shaded gray). The bottom row illustrates llustrates solid black bars as regions of statistical significance for SPM t-tests (α=0.05).

Significance

Quantifying gait modifications across multiple tasks shed light on the issues these patients face during daily ambulation that occurs on non-level terrains. Different behaviors relative to control subjects were observed in each group suggesting these data could help diagnose these groups or even inform different options available for therapeutic and surgical treatments [5].

References

[1] Kim, C. (2014) *Arthritis Rheumatol* **66**, 3013-3017
[2] Clohisy, J.C. & et al. (2008) *J Bone Jt Surg* **90**, 2267-2281
[3] Rutherford, D.J. et al. (2018) *Orthop J of Sports Med* **6**, 1-10
[4] Pataky, T.C. et al. (2013) *J Biomech* **46**, 2394-401
[5] Welton, K.L. et al. (2018) *J Bone Jt Surg* **100**, 76-85

Hip Joint Muscle and Contact Forces During Sit-to-Stand and Stand-to-Sit Tasks in Patients with Femoroacetabular Impingement Syndrome

Michael Samaan[1,2], Mia MacDonald[1], Aaron Fain[3], Riham El-Khouli[3], Cale Jacobs[2], Stephen Duncan[2],and Brian Noehren[2,4]
[1]Dept. of Kinesiology & Health Promotion, University of Kentucky
[2] Dept. of Orthopaedic Surgery, University of Kentucky
[3] Dept. of Radiology, University of Kentucky
[4] Division of Physical Therapy, University of Kentucky
Email: michael.samaan@uky.edu

Introduction

Patients with femoroacetabular impingement syndrome (FAIS) exhibit abnormal hip joint morphology and gait mechanics as well as severe hip joint pain and cartilage degeneration[1]. Abnormal hip joint loading patterns within the FAIS population may be due to hip extensor weakness[2]. More specifically, hip extensor weakness is associated with higher anterior hip joint contact forces[3]. Hip extensor weakness may help to explain the utilization of higher hip joint demand during the sit-to-stand task in patients with FAIS[4] yet the effects of hip extensor-related biomechanical abnormalities that occur during the stand-to-sit task within the FAIS population are unknown.

The purpose of this study was to assess hip joint muscle and contact forces (JCF) that occur during the sit-to-stand and stand-to-sit tasks in patients with FAIS and asymptomatic controls. We hypothesized that patients with FAIS will exhibit weaker hip extensors, lower hip extensor muscle force production and higher anterior hip JCF during both tasks compared to controls. We also hypothesized that FAIS patients would perform the sit-to-stand task with lower hip extensor muscle force and higher anterior hip joint contact force compared to the stand-to-sit task.

Methods

Six pre-surgical female patients with FAIS (age: 31.8±12.0years; BMI: 28.0±6.11kg·m^{-2}) and 5 female age- and BMI-matched asymptomatic controls (CONT; age: 36.0±12.9 years; BMI: 26.9±3.20kg·m^{-2}) without clinical indications of hip impingement (negative FADIR test) underwent 3D gait analysis of the surgical (FAIS) or dominant limb (CONT) during the sit-to-stand and stand-to-sit tasks[4]. All participants also underwent unilateral isokinetic strength testing (60°·s^{-1}) to assess concentric hip flexor, extensor, abductor and adductor strength (Nm·kg^{-1}).

Musculoskeletal simulations of both tasks were performed using Opensim[5] utilizing a musculoskeletal model developed for deep hip flexion tasks[6]. Hip flexor, extensor, abductor and adductor muscle forces were estimated using Static Optimization. Hip JCF were computed using Joint Reaction Analysis within OpenSim. The average peak muscle force, anterior, superior and medial hip JCF during both tasks were extracted. Also, the average angle of application and angular distribution of the hip JCF in the sagittal, axial and coronal planes were computed. Both hip joint muscle and JCF were normalized by bodyweight (BW).

Between group differences in muscle strength and hip joint mechanics during both tasks were assessed using independent t-tests ($p<0.05$). Within group differences both tasks were assessed using paired t-tests ($p<0.05$).

Results and Discussion

Patients with FAIS exhibited weaker hip abductors to asymptomatic controls (CONT: 1.33±0.23Nm·kg^{-1}; FAIS: 0.64±0.46Nm·kg^{-1}; p=0.01). No between-group differences were observed in hip muscle forces or JCF parameters during the sit-to-stand and stand-to-sit tasks.

The CONT exhibited significantly lower angular distribution of the hip JCF in the sagittal (Δ= -7.91°; p=0.02) and axial (Δ= -44.3°; p=0.01) planes during the stand-to-sit task compared to the sit-to-stand task. Patients with FAIS exhibited trends of lower hip adductor muscle forces (stand-to-sit: 0.64±0.51BW; sit-to-stand: 0.76±0.53BW; p=0.07) and peak superior hip JCF (stand-to-sit: 2.73±1.64BW; sit-to-stand: 3.44±1.64BW; p=0.09) during the stand-to-sit task compared to the sit-to-stand task. Patients with FAIS exhibited significantly lower angular distribution of the hip JCF in sagittal(Δ= -9.76°; p=0.04), coronal (Δ= -31.4°; p=0.04) and axial (Δ= -49.4°; p=0.03) planes during the stand-to-sit task compared to the sit-to-stand task (Figure 1).

Weaker hip abductors in patients with FAIS may lead to a more adducted hip joint during the stand-to-sit task, which may cause hip joint impingement. Patients with FAIS in this study may reduce the risk of hip impingement and avoid pain during the stand-to-sit task by lowering the hip adductor muscle force and superior JCF yet this neuromuscular compensation causes a more focalized loading pattern on the hip joint articular cartilage, which leads to hip joint cartilage degeneration.

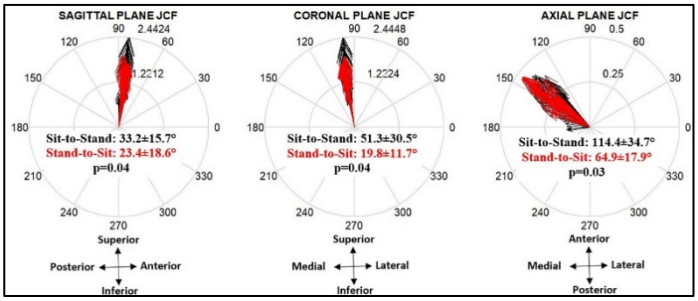

Figure 1: Angular distribution of the hip JCF in all 3 planes within the FAIS group during the sit-to-stand (black) and stand-to-sit (red) tasks.

Significance

Despite our hypothesis being incorrect, the results of this study indicate that the stand-to-sit task may be sensitive in detecting abnormalities in the hip JCF within the FAIS population. Future studies should investigate the effects of hip abductor strengthening interventions in reducing hip JCF abnormalities during the stand-to-sit task in the FAIS population.

Acknowledgments

Funding sources: KL2-TR001996 and UL1-TR001998.

References

1) Ganz et al. 2003. Clin. Orthop. Relat. Res. **417**: 112-120.
2) Kierkegaard et al. 2017. J. Sport Sci. Med. **20**(12): 1062-1067.
3) Lewis et al. 2007. J. Biomech. **40**(16): 3725-3731.
4) Samaan et al. 2017. PM&R **9**(6): 563-570.
5) Delp et al. 2007. IEEE Trans. BME **54**(11): 1940-1950.
6) Catelli et al. 2019. Comp. Meth. Bio. BME **22**(1): 21-24.

Bone-to-bone Distance Changes Are Larger in Patients with Cam Femoroacetabular Impingement Syndrome

Cara L. Lewis[1], Keisuke Uemura[2], Penny R. Atkins[2], Amy L. Lenz[2], Niccolo M. Fiorentino[3], Stephen K. Aoki[2], Andrew E. Anderson[2]
[1]Boston University, Boston, MA, [2]University of Utah, Salt Lake City, UT, [3]University of Vermont, Burlington, VT
Email: lewisc@bu.edu

Introduction

Cam-type femoroacetabular impingement syndrome (FAIS) is a painful, motion-related structural hip disorder. Patients present with a loss of sphericity of the femoral head which may cause the hip to lever- or cam-out as it articulates, leading to instability [1]. However, a quantitative description of hip instability in this patient population is lacking. Traditional motion capture techniques rely on tracking of markers adhered to the skin, and are prone to large errors due to misidentifaction of the hip joint center [2, 3]. We have developed a dual fluoroscopy (DF) system that quantifies in-vivo hip motion through direct imaging of the pelvis and femur during dynamic loading. The primary aim of this study was to apply DF to provide a quantitative description of hip instability. We hypothesized individuals with cam FAIS morphology would have larger changes in bone-to-bone distance as compared to controls, thereby indicating a less stable hip.

Methods

Seven participants diagnosed with cam FAIS (5 males, 2 females; age, 29±7 yrs; height, 179.1±10.1 cm; mass, 78.9±15.2 kg) and eleven asymptomatic individuals with typically-developed anatomy (6 males, 5 females; age, 23±2 yrs; height, 173.3±10.4 cm; mass, 63.8±10.9 kg) provided informed consent for study participation as approved by the University of Utah Institutional Review Board. The femur and pelvis were reconstructed in 3D from CT images (Figure 1, left) (Amira, ThermoScientific). In-vivo hip motion during walking on a level and inclined (5°) treadmill was recorded using DF (see [3] for details). For processing purposes, gait was normalized to 100 time points.

Biomechanists quantify joint translations to measure instability. However, in the case of cam FAIS, the femoral head does not conform to canonical geometry (i.e., sphere, ellipsoid), and thus, measurements of hip translation would be biased. We circumvented this issue by calculating bone-to-bone distances, which are independent of the definition of the hip joint center. Minimum bone-to-bone distance was calculated for six regions of the acetabulum that were divided by 60° increments (Figure 1, left) (PostView 2.0). The change in the minimum distance was quantified as the range of distance values for each time point.

Linear regression with two within-subject factors (*activity, region*) and one between-subjects factor (*group*) was performed in SPSS. We modeled the main effects and interaction terms, and applied a generalized estimating equation correction to account for repeated measures. Significance for all tests was set at $p<.05$.

Results and Discussion

The change in the minimum bone-to-bone distance was larger in the cam FAIS group than controls for all regions except the anterior-superior region (Table 1). In the inferior and posterior-superior regions, the change in minimum bone-to-bone distance was also affected by activity, highlighting the importance of examining multiple activities. The observed differences in bone-to-bone distance are highly suggestive of a less stable hip amongst those with cam FAIS. While it is possible that heterogeneity in the thickness of the cartilage and labrum may have affected the observed results [4], all patients and controls had normal joint spacing as observed on plain film X-rays and CT. We plan to develop finite element models that include cartilage and labrum morphology to better understand interactions between hip instability and chondrolabral damage.

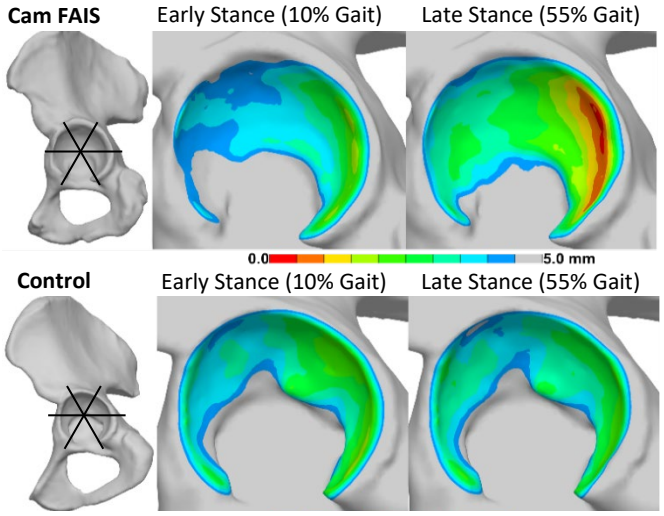

Figure 1. Bone-to-bone distance in representative participants (FAIS and control) at early and late stance.

Significance

The finding that patients with cam FAIS had abnormal hip joint articulation during walking is significant because it suggests that even low-demand activities may cause deleterious biomechanics.

Acknowledgments

Financial support was provided by the National Institutes of Health (K23-AR063235, R21-AR063844, F32-AR067075, S10-RR026565), the National Center for Advancing Translational Sciences under BU-CTSI Grant Number 1KL2TR001411, and the LS Peery Discovery Program in Musculoskeletal Restoration.

References

[1] Canham et al. 2016, Arthroscopy, 203-8. [2] Fiorentino et al. 2016, Gait & Posture, 246-51. [3] Fiorentino et al. 2016, Ann Biomed Eng, 2168-80. [4] Allen et al. 2010, Radiology, 544-52.

Table 1. Mean (standard deviation) change in minimum bone-to-bone distance (mm).

		Region					
Activity	**Group**	Superior*	Anterior-Superior	Anterior-Inferior*	Inferior†§‡	Posterior-Inferior*	Posterior-Superior*§
Walk	Cam	1.56 (.52)	1.86 (.41)	2.07 (.46)	1.38 (.58)	2.17 (.60)	2.54 (.57)
	Control	1.16 (.50)	1.67 (.65)	1.56 (.72)	1.35 (.62)	1.74 (.52)	1.84 (.44)
Incline	Cam	1.68 (.25)	2.12 (.70)	2.22 (.76)	1.96 (.48)	2.03 (.49)	1.97 (.45)
	Control	1.22 (.49)	1.72 (.63)	1.41 (.59)	1.34 (.53)	1.56 (.47)	1.57 (.65)

Significance: †Interaction of Activity and Group; §Effect of Activity; *Effect of Group; ‡Effect of Group for Incline Activity only.

The effect of osteoarthritis on three-dimensional thumb motions and force production

Amber R. Vocelle[1], Gail Shafer[2], and Tamara R. Bush[3]
[1] Department of Physiology and College of Osteopathic Medicine, Michigan State University, East Lansing, MI, USA
[2] Departments of Mechanical and Biomedical Engineering, Michigan State University, East Lansing, MI, USA
[3] College of Human Medicine, Michigan State University, East Lansing, MI, USA
Email: cussenam@msu.edu, reidtama@egr.msu.edu, web: https://www.egr.msu.edu/reidtama/

Introduction

Thumb osteoarthritis (OA) affects one in two aging adults; it causes joint pain, reduced grip strength, and loss of function and independence [1]. Little research has evaluated the effects of OA on thumb strength itself and whether the the loss of thumb force production is uniform or affects forces in some directions more than others. Similarly, although planar motion abilities are reduced in persons with thumb carpometacarpal osteoarthritis, there is limited research investigating the effect of osteoarthritis on three-dimensional (3D) complex thumb motions. As osteoarthritis of the thumb carpometacarpal joint progress, the first webspace contracts and the distal thumb joints become mal-aligned [3]. This aberrant alignment may suggest that the joint's motion and force ability may be asymmetrically compromised. We hypothesize that thumb osteoarthritis causes 1) assymetrical thumb force changes and 2) altered motions during complex 3D movement tasks.

Methods

Participants: All testing occurred under IRB approval. 58 participants were tested: 23 young healthy (22.5 years SD 3.1, 12 males; YH), 11 older healthy (66.3 years SD 8.4, five males; OH), and 21 older with doctor-diagnosed OA (69.4 years SD 5.8, six males; OA). All participants were right handed and their dominant hand was tested.

Testing: Thumb force and motion testing was completed by each participant. Thumb forces during radial abduction (RAB), radial adduction (RAD), palmar abduction (PAB), and palmar adduction (PAD) were measured using a custom built apparatus attached to an AMTI multi-axis load cell (Figure 1a).

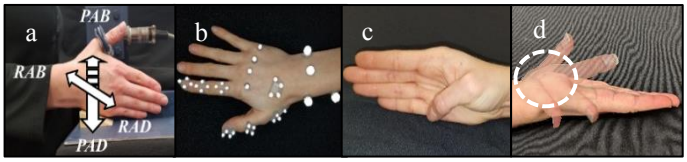

Figure 1: Participant testing. a) Multi-axis load cell with custom built apparatus, b) marker placement for motion testing, c) thumb opposition motion testing, and d) thumb circumduction motion testing.

Thumb motion data were collected using reflective markers (Figure 1b) and a motion capture system (Qualisys): movements included radial and palmar ad/abduction; and complex thumb motions: opposition (Figure 1c) and circumduction (Figure 1d). Force and motion data were analysed using one-way ANOVAs.

Results and Discussion

Forces: All groups had the greatest thumb forces during RAD. OA females produced significantly less RAD and PAD forces than YH females (Figure 2a and b). These data suggest that OA may produce an asymmetrical loss of force production in abduction motions.

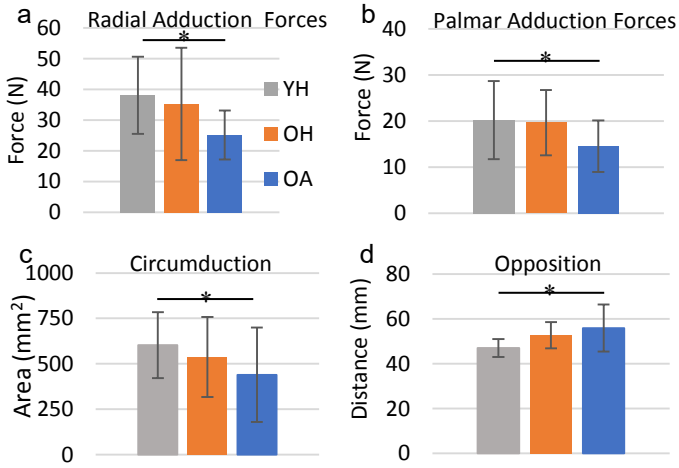

Figure 2: Motion and force data. Female thumb forces during a) RAD and b) PAD. Combined sex data of c) circumduction area enclosed and d) opposition distance from base of fifth finger. * denotes $p<0.05$.

Motions: Both OH and OA groups had a mildly reduced PAD-PAB (OH 42.3º, OA 43.9º, and YH 46.7º; $p>0.05$), but not RAD-RAB (OH 48.2º, OA 47.5º, and YH 47.5º; $p>0.05$) compared to YH. Yet, OA significantly reduced thumb circumduction area ($p=0.0292$) and significantly reduced the ability to reach during opposition ($p=0.0007$) compared to YH (Figure 2c and d). These data suggest OA significantly reduces 3D motion, prior to significant changes in planar motion tasks typically tested.

Our findings are in line with our hypotheses; OA 1) assymetrically reduced thumb forces during adduction motions and 2) reduced thumb motion during 3D complex tasks *prior to* a loss of motion during simple planar tasks. This work suggests that analysis of thumb specific forces and 3D complex motions may provide insight into thumb pathology and should be considered in clinical and reseach testing settings.

Significance

This research indicates valuable information can be gathered through the use of multi-directional thumb forces and motions, beyond what can be obtained using hand grip or planar thumb motions alone. Early 3D complex motion changes have the potential to be early identifiers of OA development and may aid in earlier OA diagnosis [2]. Both thumb forces and multi-directional thumb motions have the potential to act as new therapeutic targets for therapy and surgical intervention.

Acknowledgments

Fundng: Blue Cross Blue Shield of Michigan Student Award and Pearl J. Aldrich Endowment in Aging Related Research.

References

[1] Arden N et al. *Best Pract Res Clin Rheumatol*. 20(1), 3-25, 2006.
[2] Vocelle AR, et al. *Clin Biomech.***73,** 63–70, 2020.

Contact Pattern of Total Wrist Arthroplasty Changes with the Direction of Motion: *In-Vivo* Study

Bardiya Akhbari[1], Amy Morton[2], Kalpit Shah[1, 2], Douglas Moore[2], Arnold-Peter Weiss[2], Scott Wolfe[3], and Joseph Crisco[1,2]
[1]Brown University, Providence, RI, [2]Rhode Island Hospital, Providence, RI, [3]Hospital for Special Surgery, New York, NY
Email: bardiya_akhbari@brown.edu

Introduction

Total wrist arthroplasty (TWA) has a history as long as hip and knee arthroplasty; however, success rates in the wrist are inferior.[1] Current TWA designs have developed empirically, in the absence of rigorous biomechanical studies. Abnormal forces and stresses due to incongruent articulation of TWA components may lead to the carpal component loosening;[2] however, the TWA *in-vivo* pattern of articulation has not been examined to date. Direct methods of measuring contact are mostly invasive, and indirect methods such as biplane video-radiography (BVR) could be used for estimating the contact. Thus, our goal is to use BVR to establish contact pattern of the TWA components and its association with motion.

Methods

Six osteoarthritic patients (74.7 ± 5.6 yrs, 2F, 2R) with size 2 Freedom® TWA implants (Integra LifeSciences) participated in this study. A CT scan was acquired of each wrist (0.39mm × 0.39mm × 0.625mm), and surface models of the TWA carpal component (CC), 3rd metacarpal (MC3), and resected radius (RAD) were generated using Mimics.[3] Models of the radial component and polyethylene cap were constructed using a 3D scanner and were superimposed on RAD and CC, respectively.

BVR (75 kV/80 mA, 200Hz) was used to capture dynamic implant motion while each study participant performed five active tasks of wrist motion. Positions of CC and MC3 were calculated relative to a mathematically fixed RAD in the neutral pose using a 2D to 3D registration software (Autoscoper). Wrist kinematics described relative motion of MC3 with respect to RAD using helical axes of motion. Pure flexion-extension and radial-ulnar deviation positions (positions with secondary wrist motion less than 5% of the maximum range) were selected for further contact processing.

Contact of the polyethylene cap and radial component was calculated using distance fields (D).[4] The distance exclusion threshold (T) was selected using a Monte Carlo simulation that incorporated the accuracy[3] of the BVR. Contact centroid was calculated by weighting the distances by $(T - D)^2$, and it is mathematically alike to the center of pressure. The sensitivity of our approach was evaluated by varying T in 0.05 mm steps.

Linear regression was used to evaluate the association between wrist position and position of the contact centroid.

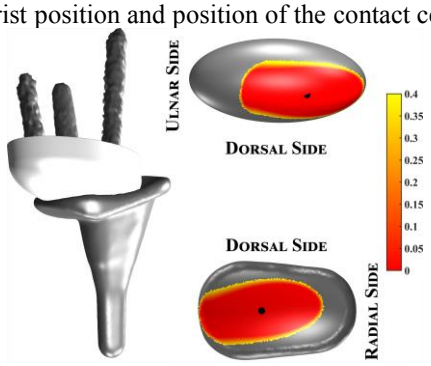

Figure 1: An example of the articulation of TWA components, and the contact patch on both polyethylene cap (top) and radial component (bottom). Black dots demonstrate the weighted contact centroid.

Results and Discussion

Our sensitivity analysis established 0.4 mm as the resolution of our system and thus the lower limit of our contact localization.

The contact centroid moved from dorsal to volar on the polyethylene cap and from volar to dorsal on the radial component during flexion-extension (Fig. 2, Left. $R^2 = 0.80$ and 0.56, respectively), indicating the joint rolls and glides in opposite directions (i.e., forward roll and backward glide). This behavior might result in the impingement and restriction of range-of-motion at certain extreme poses, and it could be due to the structure of surrounding soft tissue or the design of the implant. The contact centroid of polyethylene cap was also located more radially, which shows the components surfaces were not unifromly in contact throughout this *in-vivo* motion.

The contact centroid moved from radial position to ulnar position on the polyethylene cap during radial deviation to ulnar deviation, but its location was essentially constant on the radial component (Fig. 2, Right. R^2= 0.39 and 0.00, respectively) suggesting a purely gliding pattern of articulation.[5]

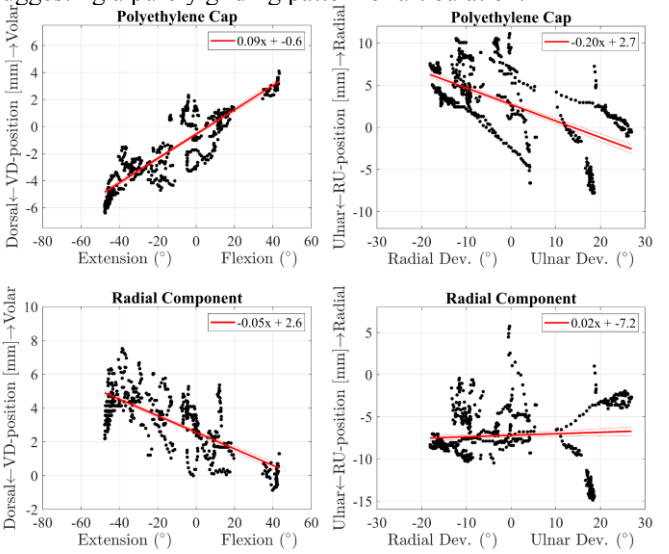

Figure 2: Contact centroid movement for pure flexion-extension (left panel) and pure radial-ulnar deviation (right panel).

Significance

We computed the contact pattern and showed the possibility of localized force concentrations during TWA radioulnar deviation. Our findings could help inform the design and protocols for wear/stress testing of the total wrist arthroplasty implants.

Acknowledgments

This research was funded by NIH P30-GM122732 and AFSH.

References

[1] Halim, 2017. *doi:* 10.1016/j.jhsa.2016.12.004
[2] Kennedy, 2018. *doi:* 10.1177/1753193418761513
[3] Akhbari, 2019. *doi:*10.1115/1.4042769
[4] Marai, 2004. *doi:* 10.1109/TBME.2004.826606
[5] Smith, 2003. *doi:*10.1016/S0003-9993(03)00281-8

Crista Volume Shows a Relationship to Sesamoid Station

AJ Clarke, SF Conti, L Williams , MS Conti , S Ellis, Amr A Fadle, * MC Miller
*Allegheny General Hospital
Email: *mark.c.miller@ahn.org

Introduction

The progression of hallux valgus (HV) deformities results in dislocation of the sesamoids from their position (station) under the plantar surface of the distal first metatarsal. With this dislocation, the crista separating the two sesamoids erodes as the contact of the medial sesamoid with the crista applies pressure with weightbearing. Recently, three dimensional (3D) reconstructions of the metatarsals and first phalanx have demonstrated a means to quantify first metatarsal pronation, showing that three-dimensional models have application to HV problems. The purpose of the current investigation is to examine the relationship of the volume of the crista to pronation, sesamoid station, and intermetatarsal angle (IMA) using three dimensional models. It is hypothesized that crista erosion is directly related to sesamoid subluxation, intermetatarsal angle, hallux valgus angle and first metatarsal pronation in HV deformities

Methods

Twenty five HV patients, sixteen from HSS (NY, NY) and nine from UPMC Passavant (Pgh, PA), and ten normal subjects from UPMC Passavant underwent CT imaging with weightbearing or weightbearing equivalent (WBCT) methods after approval by the relevant Institutional Review Board. Weightbearing images were obtained in a PedCat (CurveBeam, Inc) and WBCT images were obtained with a pedal device in a LightSpeed VCT (GE, Inc.).[1][2] Using the program Mimics, segmentation was performed to create 3D solid models. Pronation, IM angle and HV angle were quantified from the 3D reconstructions.[1] Crista cross-sections in each CT slice were demarcated by slices thickness, the volume was computed. Sesamoid station was quantified using the four stage AOFAS scale. (Figure 1)

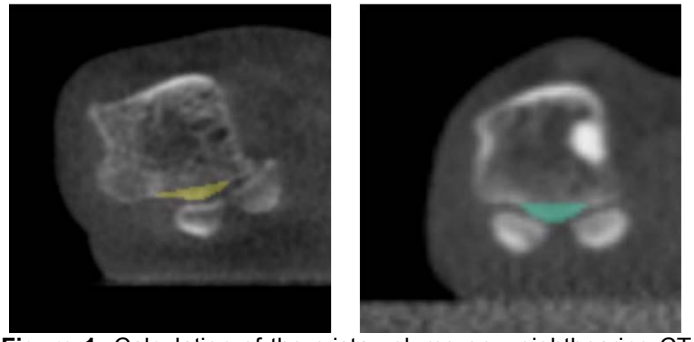

Figure 1: Calculation of the crista volume on weightbearing CT scans. Left: the crista has eroded with the medial sesamoid subluxation. Right: the crista cross-section in a normal subject.

The mean sesamoid station was calculated and the HV and normal stations were compared using a Mann-Whitney test. The sesamoid station was simplified into two categories – mild medial sesamoid subluxation (less than 50% of the medial sesamoid was lateral to the nadir of the crista) and severe medial sesamoid subluxation – and crista volume, IM angle, HV angle and pronation angle between these two groups was compared using a t-test for the HV subjects. Linear regressions were performed to determine if the volume of the crista was associated with the IM angle, HV angle, and the pronation angle.

Results and Discussion

The median sesamoid station in HV subjects was 4 and in normal was 2 and the Mann-Whiney test indicated that the two groups were different. The mean crista volume of HV patients was 86±25 mm^3 and was 148±30 mm^3 in normal patients, with the t-test showing $p<0.001$.

T-tests using simplified sesamoid station to compare crista volumes, IM angle, and HV angle of HV subjects only were all found to be statically significant ($p_{vol} = 0.012$, $p_{IM} = 0.011$, $p_{HV} < 0.001$). However, the t-test using simplified sesamoid station to compare pronation was found to not be statistically significant ($p_{pro} = 0.87$). The regression of crista volume against the IM angle and pronation angle in HV subjects did not show statistical significance ($p_{IM} = 0.09$; $p_{pro} = 0.40$). The regression of crista volumes against the HV angle in HV subjects did show statistical significance ($p = 0.03$, but $r^2 = 0.19$).

In Hallux Valgus, it has been hypothesized that the medial sesamoid erodes the crista resulting in arthritis. This is often overlooked as a source of pain in these patients. Our study found that crista volume, HV angle, and IM angle were all related to a simplified taxonomy of sesamoid position. Pronation of the first metatarsal, however, was not correlated with the sesamoid position.

That sesamoid station appears to be related to IM angle but IM angle does not appear to be related to crista volume needs further investigation. The HV deformity is characterized by the medial angulation of the first metatarsal and the change in sesamoid station reflects that fact. That the IM angle would then not correlate to the crista volume may be a result of a large variance and a sample size of only 25. The relationship between the HV angle and crista volume does, however, agree with expectations because a large HV angle would malposition the sesamoids to cause crista erosion.

The overall results emphasize the need to further analyze 3D data to relate the HV deformity and crista wear. Operative outcomes and early detection of HV offer possible implications for the importance of crista erosion and sesamoid malposition.

Significance

This study is the first to demonstrate that medial sesamoid subluxation as determined by sesamoid station results in erosion of the crista. This supports the hypothesis that sesamoid subluxation, arthritis, and crista erosion are important components of the HV deformity.

REFERENCES

1. Campbell, et al. *Journal of Orthopaedic Surgery and Research*. (2017). 2. Fadle, A, et al. *Foot and Ankle Surgery*. (2019).

Development of Injury Risk Functions for Lisfranc Injury

Zhu J[1*], O'Cain CM[1], Spratley EM[1], Gepner BD[1], Cooper MT[2], Forman JL[1], Kent RW[1,3]
[1] Center for Applied Biomechanics, University of Virginia, Charlottesville, VA
[2] Department of Orthopaedic Surgery, University of Virginia, Charlottesville, VA
[3] Biocore, LLC, Charlottesville, VA
Email: *jz2ru@virginia.edu

Introduction

The Lisfranc joint complex, and the tarsometatarsal (TMT) joints specifically, constitute important structural support of the transverse arch of the midfoot [1, 2]. Injuries to these joints are relatively rare (~0.002%); however, they are significantly higher in football players (~ 4%) yet are missed or misdiagnosed in 1 of every 5 patients. It can severely reduce mobility and diminish performance and can be associated with long-term disability and residual deformity if missed [3]. To date, no study has quantified the precise mechanism or tolerances of Lisfranc ligament injury. Such an injury risk function (IRF) is a necessary predicate for any objective optimization of injury prevention technologies, such as might be implemented in cleats or turf design. Therefore, the objective of this study was to reproduce Lisfranc injury in cadavers using real-world boundary conditions and to subsequently develop an IRF based upon experimental metrics.

Methods

With Institutional Review Board approval, sixteen male cadaveric lower extremities were disarticulated at the knee and tested (mean age=49.1±14.8). During the test, each specimen was secured onto a material testing frame with a custom loading fixture (Figure 1A). Each limb was positioned and supported by a U-bolt through the tibiofibular interosseous hiatus distally, and a heel block below the calcaneus. Bones were affixed with 10 sets of 4-ball retroreflective marker arrays for 3-D kinematics capture (Figure 1B). The Achilles tendon was clamped to resist dorsiflexion imparted by the lowering crosshead. Group 1 (n=7) was loaded in a neutral internal/external rotation posture through a block at the plantar distal first metatarsal. Group 2 (n=9) was similarly tested with the foot maximally externally rotated at the talocrural joint and with the addition of a 100N abducting force at the distal first metatarsal (Figure 1C).

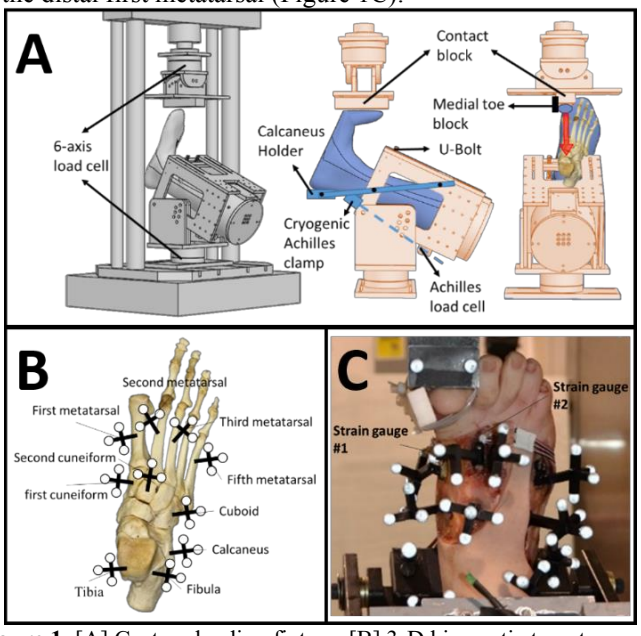

Figure 1: [A] Custom loading fixture. [B] 3-D kinematic targets. [C] Cadaveric specimen instrumented and mounted.

Results and Discussion

Post-test necropsies confirming Lisfranc complex disruption were conducted by a board-certified orthopaedic surgeon with expertise in Lisfranc fixation. Group 1 tests resulted in the midfoot buckling laterally for most specimens and injuries occurring primarily at the tarsometatarsal joints. Group 2 resulted in the midfoot buckling medially for most specimens and injuries occurring primarily along the medial ray of the foot. Injury timing was determined based on the time-synchronized force, strain, and kinematic data. These values were fit using survival analysis (Weibull distribution). Injury risk functions of the Lisfranc ligament injury were developed based on the correlation between injury and four measurable kinematic metrics: 1) resultant force along the long axis of the first metatarsal, 2) change of the foot length, 3) the resultant angle of transverse and sagittal bending and 4) weighted resultant angle.

Table 1: Injury Risk Functions for each injury indicator.

Injury Indicator	Injury Risk Function (IRF)
Resultant force	$P_{Injury}(RF) = \begin{cases} 1 - e^{-\left(\frac{resultant\ force}{3326.96309}\right)^{3.77639}} & x \geq 0 \\ 0 & x < 0 \end{cases}$
Compression Percentage	$P_{Injury}(\%C) = \begin{cases} 1 - e^{-\left(\frac{compress\ \%}{11.00855}\right)^{3.68318}} & x \geq 0 \\ 0 & x < 0 \end{cases}$
Resultant Angle (*M*)	$P_{Injury}(M) = \begin{cases} 1 - e^{-\left(\frac{M}{24.77794}\right)^{9.82709}} & x \geq 0 \\ 0 & x < 0 \end{cases}$ Where $M = acos\ (cos(Transverse\ Angle) * cos\ (Sagittal\ Angle))$
Weighted Resultant Angle (*W. M*)	$P_{Injury}(W.M) = \begin{cases} 1 - e^{-\left(\frac{W.M}{0.9565}\right)^{7.24589}} & x \geq 0 \\ 0 & x < 0 \end{cases}$ Where $W.M = \frac{M}{4.5\left(arctan\left(\frac{Transverse\ angle}{-Sagittal\ Angle}\right)+\frac{\pi}{2}\right)+19}$

Significance

This study is the first to report quantitative, mechanism-based injury risk functions of Lisfranc ligament injury. The results serve as baseline data for evaluation of the Lisfranc injury risk in sports-related scenarios and provide fundamental information needed for the development of countermeasure protection and treatment options for Lisfranc injury. The injury risk functions might also provide enlightenment to rehabilitation program development to minimize re-injuries of Lisfranc joints.

Acknowledgments

The work was supported by the National Football League through a grant from Biomechanics Consulting and Research, LLC.

References

1. Escudero et al., 2018, Foot Ankle Clin.
2. Sivakumar et al., 2018, Orthopedics
3. Llopis et al., 2016, Semin Musculoskelet Radiol.

Step Length Biofeedback with Exoskeleton Assistance Can Improve Walking Function and Gait Mechanics in Cerebral Palsy

Ying Fang.[1], Taryn Harvey[1], and Zachary F. Lerner. [1,2]
[1]Department of Mechanical Engineering, Northern Arizona University, Flagstaff, AZ 86011, USA
[2]Department of Orthopedics, the University of Arizona College of Medicine-Phoenix, Phoenix, AZ 85004
Email: *yf82@nau.edu

Introduction

Many people with cerebral palsy (CP) have impaired walking ability resulting from reduced ankle function [1]. We previously demonstrated that ankle exoskeleton assistance can improve gait mechanics in individuals with CP. However, we also observed decreased muscle activity, which could lead to atrophy [2,3]. Gait training with biofeedback can incentivize people to change their walking behavior [4,5]. Seeking to maximize the benefit of wearable assistance, the **purpose** of this study was to investigate the combined effects of real-time step length biofeedback and exoskeleton assistance on muscle function and gait mechanics in CP.

Methods

Seven participants with CP (Table 1) completed walking trials while wearing shoes (Shod) and while using the ankle exoskeleton [2] with visual biofeedback of step length (Biofeedback-plus-Assistance) (Figure 1B).

We collected motion, force, and muscle activity of the soleus and vastus lateralis for both conditions (Figure 1A). Step length and symmetry index were calculated from the coordinates of the heel markers. Joint angles and moments were derived in OpenSim 3.3 [6]. Average joint power and integrated electromyography (iEMG) were calculated for the stance phase. All parameters were averaged between limbs. Paired one-tailed t-tests ($\alpha \leq 0.05$) were used to assess if outcomes improved with the intervention.

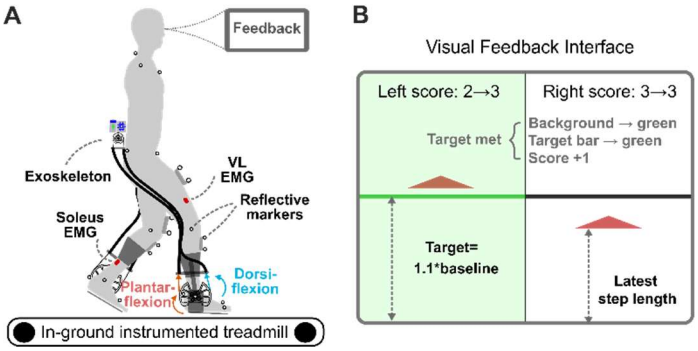

Figure 1: Depiction of the (A) experimental set up and (B) visual interface and algorithm for biofeedback.

Results and Discussion

Walking with Biofeedback-plus-Assistance improved lower-extremity gait mechanics but did not alter muscle activity compared to Shod walking. Participants increased their step length by 20.3%, but decreased step length symmetry when they walked with Biofeedback-plus-Assistance (Figure 2A, B). Combining biofeedback with assistance elicited immediate improvements in gait mechanics by increasing hip (9.7°) and knee extension (7.8°) and ankle (23.3%) and knee power (44.2%) (Figure 2C, D). Soleus peak EMG and iEMG, and VL iEMG were similar during walking with Biofeedback-plus-Assistance compared to Shod, suggesting that the feedback was effective in increasing neuromuscular engagement during assisted walking (Figure 2E).

Table 1. Participant characteristics.

	Age (Years)	Sex	Height (m)	Mass (kg)	GMFCS
P1	13	M	1.51	43.8	I
P2	31	M	1.70	53.3	II
P3	9	M	1.37	31.1	I
P4	10	M	1.39	38.5	I
P5	23	F	1.47	43.8	III
P6	6	M	1.10	17.2	II
P7	6	M	1.18	17.6	I

GMFCS: Gross Motor Function Classification System.

These results demonstrate that step length biofeedback can augment gait outcomes and increase neuromuscular engagement during exoskeleton-assisted walking.

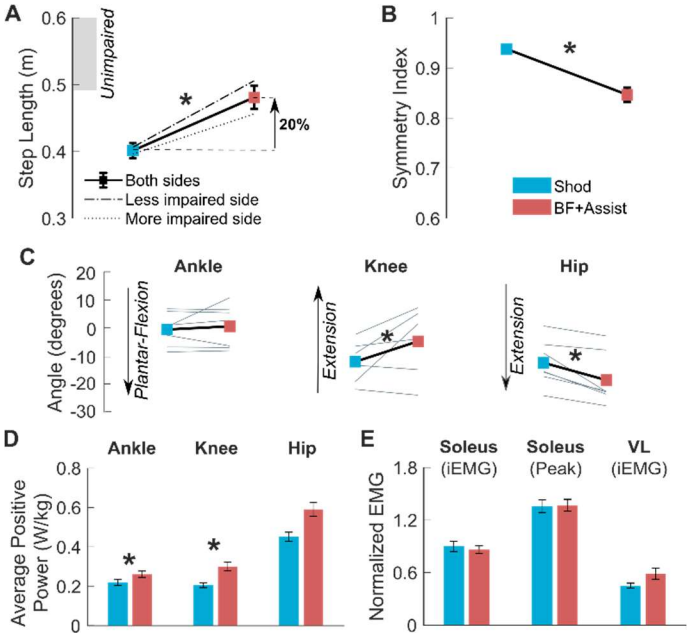

Figure 2: Comparison of all variables between walking with Biofeedback-plus-Assistance (BF+Assist) and shoes (Shod). Error bars indicate standard error of the mean.

Significance

Providing real-time step length biofeedback can increase neuromuscular engagement and improve outcomes during walking with wearable ankle assistance, paving the way for longitudinal investigations with this combined intervention.

Acknowledgments

This project was partially supported by the National Institutes of Health under Award Number R03HD094583.

References

[1] Benner et al. *APMR*, 98, 2017. [2] Lerner et al. *Sci Transl Med*, 9, 2019. [3] Orekhov et al. *IEEE Trans Neural Syst Rehabil Eng*, 1, 2020. [4] van Gelder et al. *Gait Posture*, 2017. [5] Booth et al. *APMR,* 2019. [6] Delp et al. *IEEE T BIO-MED ENG,* 2007.

Estimating Biological Hip Torque During Overground Ambulation: A Machine Learning Approach

Dean D. Molinaro[1,2], Inseung Kang[1], Jonathan Camargo[1,2], and Aaron J. Young[1,2]
[1]Woodruff School of Mechanical Engineering, Georgia Institute of Technology, Atlanta, GA, USA
[2]Institute for Robotics and Intelligent Machines (IRIM), Georgia Insititute of Technology, Atlanta, GA, USA
Email: dmolinaro3@gatech.edu

Introduction

As gait biomechanics research continues to progress, it is important to quantify biological hip torque in unstructured environments, such as those outside of the lab. Wearable sensors provide an opportunity to compute joint dynamics without the need for external sensing. Linked-segment model-based approaches require sensors distal to the joint of interest, such as pressure insoles, which are subject to low resolution GRF measurements and often result in cumbersome, multi-joint sensor suites[1,2]. Machine learning (ML) methods can compute biological joint torque without direct measurement of GRFs by leveraging the limited domain of joint torques during ambulation[3,4]; however, generalizability of these methods to changing ambulation modes remains unknown. Thus, we conducted our study, hypothesizing that hip torque RMSE and peak magnitude and timing error estimated by a neural network (NN) are less than those resulting from an average curve of each ambulation mode.

Methods

Five able-bodied male subjects completed the IRB approved experimental protocol by ambulating over 0°, ±7.8°, ±9.2°, and ±12.4° slopes while wearing a bilateral robotic hip exoskeleton. The hip exoskeleton was used to collect hip encoder and 6-axis thigh-mounted intertial measurement unit (IMU) data during ambulation. Data was transformed into the ML model feature space by computing the mean, standard deviation, and most recent value over a 350 ms sliding time window for each exoskeleton sensor channel. Biological hip torque was computed using the Inverse Dynamics Tool in OpenSim with motion capture and force plate data collected during each trial[5]. A 4 layer NN with 30 nodes per hidden layer was trained using the exoskeleton feature data, labelled by the corresponding hip torque values (Fig. 1A). Additionally, the baseline method was fit as the average hip torque curves for the level ground (LG), ramp ascent (RA), and ramp descent (RD) conditions. The two methods were evaluated using three criteria compared to the ground truth hip torque values: 1) estimation RMSE; 2) peak magnitude error, computed as the absolute difference between the peak estimated and ground truth values; and 3) peak timing error, computed as the absolute difference in gait phase during peak estimated and ground truth values. A paired t-test ($\alpha = 0.05$) was used to compare the NN and baseline methods for each criteria.

Results and Discussion

The estimated hip torque of the NN and baseline methods are shown for an example step during RA in Fig. 1C. On average, the NN model reduced hip torque RMSE, peak magnitude error, and peak timing error by 29.7±12.2%, 32.6±17.4%, and 12.8±13.9% compared to the baseline method, respectively (p=0.015, p=0.057, p=0.117) (Fig. 1B). Thus, the NN model more accurately estimated the shape and magnitude of varying ambulation modes compared to the baseline method as expected; however, both the NN and baseline methods accurately estimated peak torque timing to within 2% of the gait cycle due to the low variability in this metric among ambulation modes. Thus, the NN model is a useful approach for estimating biological joint torques when the estimate must be sensitive to shape and magnitude of the curve, such as in gait analysis and exoskeleton control.

Significance

This study validated an ML algorithm for estimating biological hip torque using only mechanical sensors during various ambulation modes. We demonstrated the benefit of using this model compared to the baseline method of average values due to its improved accuracy and reduced requirement of user state information, such as ambulation mode. Thus, our study provides a promising method for estimating biological joint torque for applications including out-of-lab experiments and exoskeleton control while varying ambulation modes.

Acknowledgments

The authors would like to acknowledge the NSF Research Traineeship: ARMS Award #1545287, the NSF NRI Award #1830215, and the Fulbright Foreign Student Fellowship.

References

[1]Cavanagh et al. (1992). *The Foot,* **4**: 185-194. [2]Forner-Cordero et al. (2006). *Gait Posture,* **23**: 189-199. [3]Jacobs and Ferris (2015). *JNER, **12***. [4]Hahn and O'Keefe (2008). *J. Musculoskelet. Res.,* **11**: 117-126. [5]Delp et al. (2007). *TBME,* **54**: 1940-195

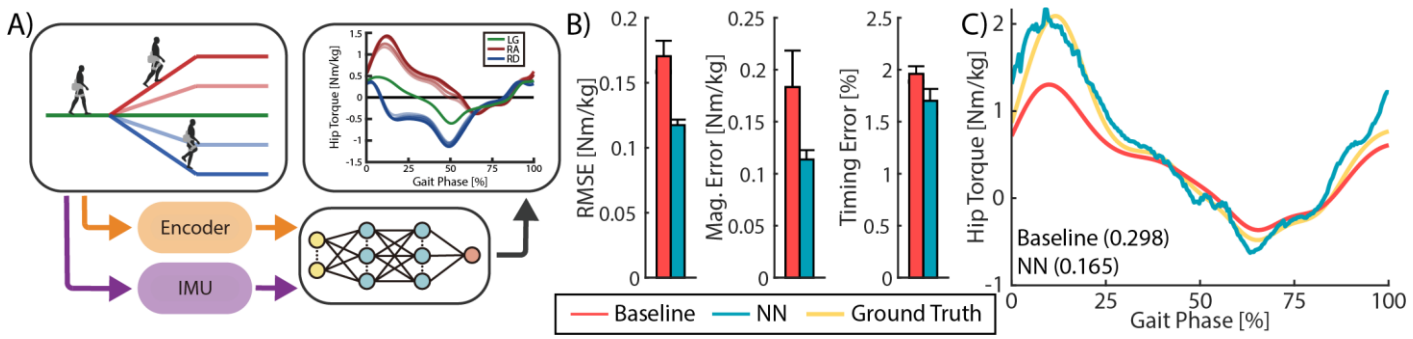

Figure 1: A) A diagram of the neural network based torque estimater is shown. Mechanical sensor data is input to a neural network after windowing and feature extraction. B) Average estimated torque RMSE, peak magnitude error, and peak timing error among ambulation modes is shown for the NN and baseline method. C) Estimated and ground truth hip torque is shown for a single step during the 12.4° incline (RMSE in parentheses).

Reducing Human Energetics Using a Bilateral Knee Exoskeleton

Dawit Lee[1], Bailey McLain[2], Aaron Young[1]
[1]Woodruff School of Mechanical Engineering, Georgia Institute of Technology, Atlanta, GA
[2]Wallace H. Coulter Department of Biomedical Engineering, Georgia Institute of Technology, Atlanta, GA
Email: ldawit127@gatech.edu

Introduction

Incline walking increases the demand of the knee joint positive power generation during the early stance phase of the gait cycle, exhibiting a high extension moment. Assisting the joint during the phase of incline walking using a robotic exoskeleton could yield a metabolic benefit. We previously tested the biomechanical effects of powered assistance using a unilateral knee exoskeleton on able-bodied adults during incline walking, and only half of the participants achieved metabolic reduction with the assistance [1]. The participants who increased metabolic cost with the assistance in the study exhibited biomechanical compensation on the unassisted leg that contributed to the increase. Therefore, assisting the user's knee joints bilaterally would potentially eliminate the issue. In this study, we tested whether bilateral assistance during the early stance phase would lead to metabolic reduction compared to the unassisted condition with three types of controllers: a biological torque controller (BT), an impedance controller (IM), and an adaptive proportional myoelectric controller (PMC). The hypothesis was that the metabolic cost of the user would be reduced with assistance.

Methods

We used a bilateral robotic knee exoskeleton, one degree of freedom (flexion/extension). The tested walking conditions consisted of three assistance conditions and an unassisted condition (UN) on the 15% gradient incline surface (1.1m/s). The biological torque controller is a timing-based controller in which a parabolic shaped assistance profile is generated for the first 30% of the gait cycle. The impedance controller simply behaves like a virtual spring in which the magnitude of the assistance is the stiffness multiplied by the angular deviation of the knee joint angle from the equilibrium angle, 0 degrees. The assistance was active for the first 40% of the gait cycle under IM condition. The PMC used for this study is largely similar to the PMC developed by Koller et. al [2]. We computed activation levels of the Vastus Lateralis and Vastus Medialis, multiplied each activation level by its own adaptive gain to scale it to the assistance magnitude, and averaged the assistance magnitude values between the two muscles. The motor was powered-off under the UN, which yields the RMS interaction torque of 0.4 Nm between the user and the device during walking. Nine able-bodied adults participated in this study. The experiment consisted of two visits. Each subject was asked to practice walking under each assistance condition for 15 minutes during the first visit. Data collection occurred during the second visit where the subjects walked each condition for 5 minutes prior to 6 minutes of data collection. The order of conditions was randomized. After the completion of all walking conditions, the subjects were asked to rank the controllers based on which helped walk with the least amount of effort (rank 1-4 where rank 1 is the best and 4 is the worst). We used repeated measures one-way ANOVA with post-hoc pairwise testing using a Bonferonni correction.

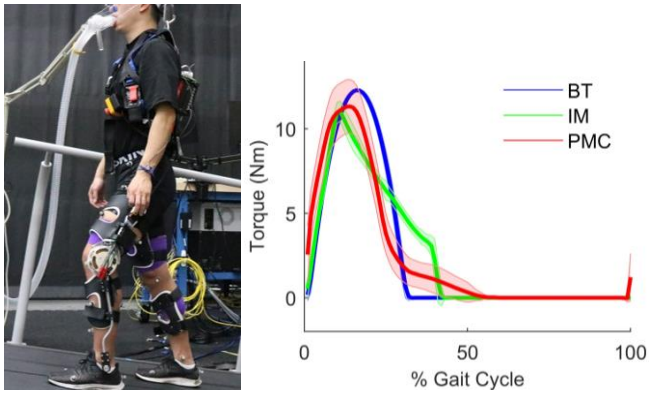

Figure 1: Experimental setup (left) and representative commanded torque profiles of the tested controllers (right). The shaded region represents +/- standard deviation.

Results and Discussion

All assistance conditions had significantly lower metabolic cost than the UN ($p < 0.05$). The metabolic cost was 8.20 ± 0.15 (mean ± standard error of mean) W/kg for UN, 7.95 ± 0.14 W/kg for BT, 7.96 ± 0.18 W/kg for IM, 7.95 ± 0.16 W/kg for PMC. This seems to be resulted largely by removing the role of the unassisted leg that caused an increase in metabolic cost with unilateral assistance [1]. The level of metabolic reduction was very similar across the assistance conditions: 3.1% with BT, 2.9% with IM, and 3.1% with PMC. The user preference rank data also showed that the subjects preferred walking with the conditions with the assistance over the UN condition (UN: 3.9 ± 0.1, BT: 2.0 ± 0.1, IM: 1.7 ± 0.3, PMC: 2.4 ± 0.2). Besides one subject, all subjects ranked the UN as the condition that required the most physical effort among the four walking conditions. The IM condition was preferred the most by the users, and no subject preferred PMC the most.

Significance

This study is one of the few studies exploring energetics with a powered knee exoskeleton. This study shows that bilateral assistance was able to achieve metabolic reduction more consistently than unilateral assistance [1]. The study indicated that early stance phase assistance, regardless of control strategy, had similar metabolic reductions during uphill locomotion. Subjects preferred BT and IM over PMC mostly because walking under the two controllers was more predictable and stable than under PMC during continuous walking at a fixed speed.

Acknowledgments

This work was funded by Shriner's Hospitals for Children, NextFlex NMMI Grant, and in part by the NSF National Robotic Initiative Grant under Award 1830215. The authors acknowledge Sierra Mulrine, Julianne Schneider, Alex Yu, Jeff Cantilag, Nikhil Chattaluru.

References

[1] D. Lee et al. (2020). *IEEE TNSRE*. [2] J. R. Koller et al. (2015) *JNER*

People explore gait dimensions, and reduce this exploration, as they learn to walk with exoskeleton assistance.

Sabrina J. Abram[1], Katherine L. Poggensee[2], Max Donelan[1], and Steven H. Collins[2]
[1]Department of Biomedical Physiology and Kinesiology, Simon Fraser University, Burnaby, Canada
[2]Department of Mechanical Engineering, Stanford University, Stanford, USA
Email: *sabram@sfu.ca

Introduction

The success of assistive devices relies on users learning to take advantage of the assistance [1]. In everyday walking, the nervous system is faced with the dilemma between exploiting, perhaps erroneously, previously learned strategies and exploring new, unknown strategies that may improve its objective [2]. Here we aim to understand how people balance this trade-off when learning to walk with ankle exoskeleton assistance. First, we hypothesized that people explore many candidate gait dimensions as they determine which dimensions are relevant to their objective. Next, we hypothesized that people reduce this exploration with experience as they learn to exploit new strategies.

Methods

We performed a post-hoc analysis of data from Poggensee et al. [3]. In this study, ten participants completed a training session per day for a total of 5-6 days, where they walked on a treadmill while wearing a bilateral, tethered, torque-controlled ankle exoskeleton emulator. Participants completed a validation trial each day where they experienced a generic assistance controller for two, 6-minute trials. They also completed an adaptation trial from Day 2 onwards, where they periodically experienced 2 minutes of generic assistance during a protocol that otherwise differed according to how Poggensee et al. randomly grouped participants. In our current study, we analysed how users learned to walk with this repeated exposure to the generic assistance controller.

In this experimental setup where the pattern of assistive torque was controlled on a step by step basis, users could 1) influence the torque timing by varying their step frequency, and 2) influence the power and work applied to the ankle by varying their ankle kinematics. We determined exploration at the level of the whole movement, the joint, and the muscle by quantifying step-to-step variability along gait dimensions of step frequency, ankle kinematics, and total ankle extensor muscle activity. In all gait dimensions that we measured, we tested how variability changed over multiple days by comparing average variability in the final 3 minutes of the 6-minute validation trial between the first and last day. We also normalized this variability to participant's average variability in normal walking (or zero-torque for ankle angle that was approximated using the exoskeleton) across all days. Finally, we tested for systematic changes along gait dimensions by comparing average adaptation in the final 3 minutes of the 6-minute validation trial between the first and last day.

Results and Discussion

When the nervous system has minimal experience walking with exoskeleton assistance, it explores along many gait dimensions in search of new strategies. We observed higher variability than normal walking at the beginning of the multi-day protocol ($p=6.6\times10^{-5}$, Figure 1A; $p=8.0\times10^{-8}$, Figure 1B; $p=3.6\times10^{-4}$, Figure 1C; $p=1.2\times10^{-4}$, Figure 1D).

The nervous system reduces exploration with experience. Participants had lower step frequency variability ($p=2.0\times10^{-5}$) and ankle angle variability ($p=2.1\times10^{-5}$) on the last day compared to the first day, and reduced this variability with time constants (τ) of 107.8±107.1 minutes and 162.0±204.7 minutes, respectively (mean±SD). They also reduced their total soleus ($p=8.0\times10^{-4}$, τ=20.2±46.1 minutes) and medial gastrocnemius ($p=2.3\times10^{-3}$, τ=25.9±45.9 minutes) variability.

With experience, variability along some gait dimensions converges on the baseline variability observed in the absence of exoskeleton assistance, suggesting that exploration was in part purposeful. Participants' variability converged on their average variability in normal walking for step frequency (p=0.38) and total soleus activity (p=0.68). However, variability in ankle angle ($p=8.0\times10^{-6}$) and total medial gastrocnemius activity ($p=2.2\times10^{-4}$) remained elevated, suggesting that some learning may still be in progress or that there is some added experimental variability.

Exploration only results in systematic changes along some gait dimensions, suggesting that the nervous system did not know a priori which dimensions to adapt. Participants did not have large adaptions in their step frequency (p=0.073, Figure 2A) or ankle angle range during stance (p=0.053, Figure 2B) on the last day compared to the first day; however, they did learn to adapt their total soleus ($p=4.6\times10^{-4}$, Figure 2C) and medial gastrocnemius activity ($p=9.5\times10^{-4}$, Figure 2D).

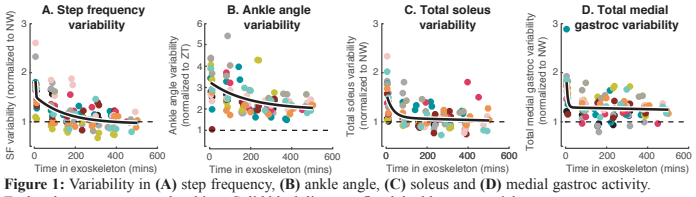

Figure 1: Variability in **(A)** step frequency, **(B)** ankle angle, **(C)** soleus and **(D)** medial gastroc activity. Each colour represents each subject. Solid black lines are fitted double exponentials.

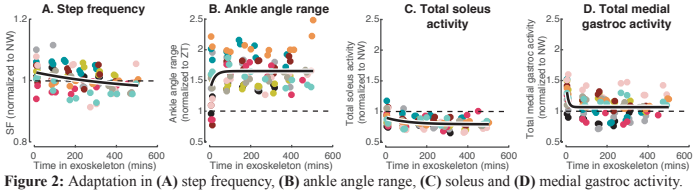

Figure 2: Adaptation in **(A)** step frequency, **(B)** ankle angle range, **(C)** soleus and **(D)** medial gastroc activity.

Significance

Our findings suggest that people balance an explore-exploit trade-off along many gait dimensions as they learn to reduce their metabolic cost of walking with exoskeleton assistance [3]. These insights into the nervous system's algorithms may be beneficial for training older adults and clinical populations to walk with assistive devices. That is, we may customize, and perhaps lower, training time by using baseline variability as a benchmark to indicate when people begin to exploit new strategies.

Acknowledgements

NSERC Michael Smith Foreign Study Supplement (SJA)

References

[1] N. Sanchez, et al. *J Physiol* **597**, 4053-4068, 2019.
[2] R.C. Wilson, et al. *J Exp Psychol Gen* **143**, 2074–2081, 2014.
[3] K.L. Poggensee, et al. *In Prep*.

The Biomechanical Effect of Bilateral Assistance for Hemiparetic Gait Poststroke Using a Powered Hip Exoskeleton

Yi-Tsen Pan, Inseung Kang, Kinsey Herrin and Aaron Young*
School of Mechanical Engineering, Georgia Institute of Technology, Atlanta, GA, USA
Email: *aaron.young@me.gatech.edu

Introduction

The asymmetric nature of hemiplegic walking generally leads to inefficient walking pattern in persons poststroke[1]. A common characteristic of hemiparetic gait is the reduced push-off power on the paretic side, which can significantly limit walking capability. Many assistive devices targeting the ankle joint have been developed, however improvements to gait are not clearly shown[2]. Recent studies have shown that augmenting hip work may provide more energetic benefits with the same amount of power at ankle.[3-4] This study presents a control framework to bilaterally assist hip movement during walking. The aim is to examine the biomechanical effects of hip assistance on hemiparetic walking to identify the optimal assistance strategy between paretic and nonparetic sides. We hypothesize that stroke survivors with unilateral impairment will benefit from the bilateral nature of the hip exoskeleton and thus improve gait performance when optimal assistance is applied on each side.

Methods

A recently developed powered hip exoskeleton (abbreviated as "exo")[4] was used to deliver assistive torque to both the paretic and nonparetic hip during gait. A state machine-based impedance controller was developed to determine the magnitude and onset timing of the assistive profile. The amount of torque was calculated by adjusting the stiffness of virtual torsional springs acting about the hip joint during the hip flexion and extension states. The desired equilibrium in each state was set to a predefined ratio of range of motion (ROM) from the maximum flexion/extension which is the same position that triggers the state transition.

Following informed consent of our IRB approved protocol, three stroke subjects (mean±SD age: 51.6±10.6 years, 3 males) with chronic hemiparesis were evaluated for biomechanical effects of different levels of hip assistance in improving the stroke survivor's gait. All subjects can walk without support at a walking speed greater than 0.4 m/s. Two subjects are right-sided paretic and have aphasia (Subject 1 and 3). Subjects were asked to walk on a force-plate treadmill and a 6-meter instrumented walkway at their preferred speed. Four walking conditions were (1) no exo (baseline); and exo in three different assistance levels: (2) low (3) medium and (4) high, with peak torque corresponding to about 8%, 10%, and 12% of the subject's weight. Hip kinematics/kinetics and gait parameters were recorded and evaluated using VICON motion capture system and an instrumented walkway, respectively. The primary outcome measures are gait asymmetry (ASI) and walking speed. ASI is defined by the difference between the paretic and nonparetic mean step length over one half of the total mean step length on both sides.

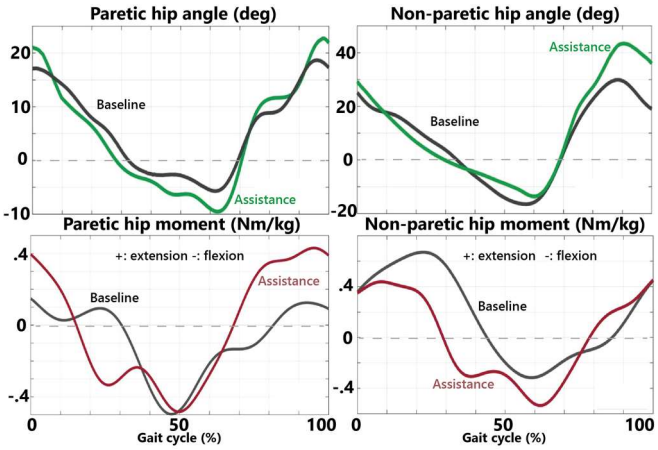

Figure 1: Hip kinematics and kinetics results in 1) baseline (black) and 2) assistance (colored) conditions from representative trials of subject 1.

Results and Discussion

In the medium level of hip assistance condition, ASI reduced (Subject 1: -18.6 cm; Subject 2: -2.1 cm) and walking speeds increased in two of three subjects compared to baseline condition; ASI reduced in the low assistance condition in Subject 1 (-10.6 cm) and 2 (-2 cm) compared to the baseline condition while the same trends were not seen in walking speed. Subjects 2 and 3 increased the ASI (S2: +2.6 cm; S3: +3.4 cm) and Subject 3 decreased speed when the high assistance condition was applied. Overall, with the low and medium levels of hip assistance, subjects demonstrated a trend with improving gait symmetry and step length, while the same trend was not observed in walking speed. Improving gait performance may be associated with the increasing net torque resulted from the exo. In Fig 1, representative trials show increasing hip flexor moments on both sides and hip extensor moments (red lines) on the paretic side with the hip assistance. Range of motion also increased when walking with assistance on both sides. We also found that such hip assistance could vary considerably among subjects, which may be due to different compensatory strategies used by each subject, or the amounts of assistive torque was not efficient on each leg. In conclusion, the current study shows the feasibility of a hip exoskeleton in increasing hip ROM and net torque, resulting in enhanced gait symmetry and walking capability.

Significance

Understanding the hip assistance strategy and how different assistive profiles affect hemiparetic gait will aid the implementation of robotic exoskeletons capable of supporting stroke survivors in community ambulatory activities. Future work will explore optimal assistance ratios between the paretic and nonparetic sides to encourage aid more efficient gait patterns in stroke survivors.

Acknowledgement

This research was funded by NIH R03 (#: 1R03HD097740-01).

References

1. Jonsdottir J et al. *Handbook of Human Motion* p. 1205 2018.
2. Takahashi, K.Z et al. *JNER* **12**(1) p. 23 2015.
3. Young A. et al. *Frontiers in Bioe and Biotech* **5**, p. 4 2017.
4. Kang I. et al. *IEEE RA-L* **4**(2), p. 430 2018

A Case Series Examining the Effects of Wearing a Quantitatively-Prescribed Passive-Dynamic Ankle-Foot Orthosis Compared to Standard-of-Care Ankle-Foot Orthosis

Corey A. Koller[1,2], Darcy S. Reisman[1,3], and Elisa A. Arch[1,2]
[1]Biomechanics and Movement Science Interdisciplinary Program, University of Delaware, Newark, DE, USA
[2] Department of Kinesiology and Applied Physiology, University of Delaware, Newark, DE, USA
[3]Department of Physical Therapy, University of Delaware, Newark, DE, USA
Email: ckoller@udel.edu

Introduction

Individuals post-stroke often have insufficient control of the shank's forward rotation during mid-to-late stance due to plantar flexor weakness [1]. Passive-dynamic ankle-foot orthoses (PD-AFOs) are commonly prescribed to these individuals [2]. PD-AFO bending stiffness is a key orthotic characteristic that can potentially assist the plantar flexors [3] by providing resistance to control the shank's forward rotation [2]. Previous studies have only focused on clinically-prescribed AFOs or AFOs with the same stiffness values for all participants [4,5]. We have developed a prescription model that can quantitatively-prescribe PD-AFO bending stiffness based on an individual level of plantar flexor weakness [6]. For the first time, we provided individuals quantitatively-prescribed PD-AFOs to wear during their daily lives for four weeks. This two-person case series aimed to evaluate the effects on post-stroke gait after four weeks of wearing these PD-AFO compared to wearing the standard-of-care (SOC) AFO. We hypothesized that the participants who improved their mean net peak plantar flexion moment with PD-AFO use would show improvements (toward typical) in biomechanical parameters.

Methods

Two individuals with chronic stroke (> six months post-stroke) underwent an instrumented gait analysis to gather baseline data. From these data, PD-AFO bending stiffness was prescribed by subtracting the participant's mean peak plantar flexion moment from the mean, speed-matched, typical peak plantar flexion moment from our normative database (typical-participant) and then dividing this quantity by the typical average change in ankle angle during stance-phase dorsiflexion (12°) [6]. The individuals then wore the newly prescribed PD-AFO for four weeks. After four-weeks, the individuals underwent another instrumented gait analysis while wearing his/her SOC-AFO and PD-AFO at his/her self-selected walking speed.

Results and Discussion

Two individuals participated in the study (male: 1, age: 64.5 (0.7) yrs, mass: 92.8 (4.2) kg, height: 1.7 (0.1) m). P1 and P2's self-selected walking speed were 0.58 and 1.17 m/s, respectively.

Both participants improved their net peak plantar flexion moment while wearing the PD-AFO compared to wearing the SOC-AFO (Table 1). However, improving net peak plantar flexion moment did not necessarily improve overall gait biomechanics (Table 1). Through examining ankle and hip mechanics, the orthosis in which participants exhibited more of an "ankle strategy" (improved ankle plantar flexor mechanics toward typical to push the limb forward as opposed to pulling the limb forward with the hip flexor muscles) showed improvement in other gait biomechanics. Specifically, P1, who exhibited more of an ankle strategy with the SOC-AFO had increased (toward typical) paretic step length, peak paretic propulsion force, and peak paretic trailing limb angle with the SOC-AFO compared to the PD-AFO. In contrast, P2 exhibited more of an ankle strategy with the PD-AFO and had increased (towards typical) paretic step length, peak paretic propulsion force, and peak paretic trailing limb angle while wearing the PD-AFO compared to wearing the SOC-AFO.

Table 1: Participant's mean ankle plantar flexion kinetics, hip flexion kinetics, and trailing limb angle during the stance phase of gait and step length are shown.

	P1		P2	
AFO Conditions:	SOC	PD	SOC	PD
Kinematics:				
Trailing Limb Angle (°)	11.62	9.73	18.08	20.14
Paretic Ankle Plantar Flexion Kinetics:				
Net Peak Moment (Nm/kg)	-0.88	-0.94	-1.02	-1.25
Peak A/P Force (% BW)	8.90	5.62	12.7	13.3
Angular Impulse (Nms/kg)	-0.53	-0.47	-0.39	-0.43
Peak Power (W/kg)	0.60	0.40	1.40	1.62
Paretic Hip Flexion Kinetics:				
Net Peak Moment (Nm/kg)	0.27	0.30	0.47	0.52
Angular Impulse (Nms/kg)	0.07	0.08	0.09	0.09
Peak Power (W/kg)	0.21	0.24	0.75	0.59
Temporal:				
Step Length (m)	0.53	0.50	0.75	0.79

Significance

These data suggest that the quantitatively-prescribed PD-AFO has the potential to substantially improve gait biomechanics, for some. Further, parameters beyond just the peak plantar flexion moment – specifically use of the hip vs. ankle strategy – may be a better indicator of which AFO is best for a given individual.

Acknowledgments

The Center for Composite Materials and Independence Prosthetic and Orthotics for helping manufacture and prepare the PD-AFOs.

References

[1] Perry J & Burnfield JM. (2010). *Gait Analysis: Normal & Pathological Function*; Slack Inc.
[2] Arch et al. (2015) *Ann Biomed Eng*, **43**: 442-450.
[3] Bregman DJJ et al. (2009). *Gait Posture*, **30**: 144-149.
[4] Bregmann DJJ et al. (2011). *Clin Biomech*, **26**: 955-961.
[5] Kerkum YL et al. (2016). *Gait Posture*, **46**: 104-111.
[6] Arch E & Reisman DS. (2016). *J Prosthetics Orthot*. **28**: 60-67.

Longitudinal Assessment of Gait Quality for Servicemembers with Transtibial Amputation: A Case Series

Tatiana E. Djafar[1], Julianne M. Stewart[1], John D. Collins[1,2], and Trevor D. Kingsbury[1]
[1]Clinical Biomechanics Laboratory, Naval Medical Center San Diego, San Diego, CA, USA
[2]BIOMS, University of Delaware, Newark, DE, USA
Email: tatiana.e.djafar.ctr@mail.mil

Introduction

Persons with amputation often develop secondary musculoskeletal conditions over time, such as knee osteoarthritis in the intact limb and low back pain [1]. Young servicemembers who undergo amputation fortunately have access to specialized programs and advanced prosthetic devices at Advanced Rehabilitation Centers, which results in excellent function early in rehab. However, little is known about their physical function long after they disengage from active rehabilitation.

The purpose of this case series is to longitudinally assess gait quality for patients with transtibial amputation (TTA).

Methods

Three male servicemembers with unilateral TTA (age: 31.7±2.1yrs, height: 1.8±0.1m, mass: 91.2±9.8kg) underwent instrumented 3D gait analyses throughout their rehabilitation (Baseline, 6 months, 1 year) as well as 9 years following their initial baseline study. Variables of interest included self-selected walking speed, anterior pelvic tilt (APT), and knee adduction moment peaks (KAM).

Results and Discussion

Walking speed increased throughout rehabilitation and was maintained at the 9 year study for all patients (Table 1). The sustained speed implies good physical function, which is confirmed by the patients' self-reported occupations and/or hobbies (e.g. police officer, weightlifting, etc.).

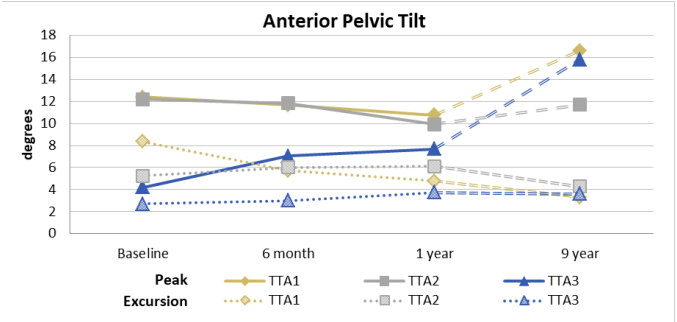

Figure 1: Peak and excursion of APT for each patient over time

APT excursion was maintained or decreased over time for all patients, suggesting good pelvic stability (Figure 1). Peak APT was greater for two patients in their 9 year follow-up, but TTA2 was able to maintain a similar peak as compared to his time during rehab (Figure 1). Anecdotally, per subjective report, TTA2 maintains a focus on core and pelvic stability to be mindful of his low back health, which is reflected in his pelvic motion data. This suggests personal investment can play a large role in minimizing risk of injury.

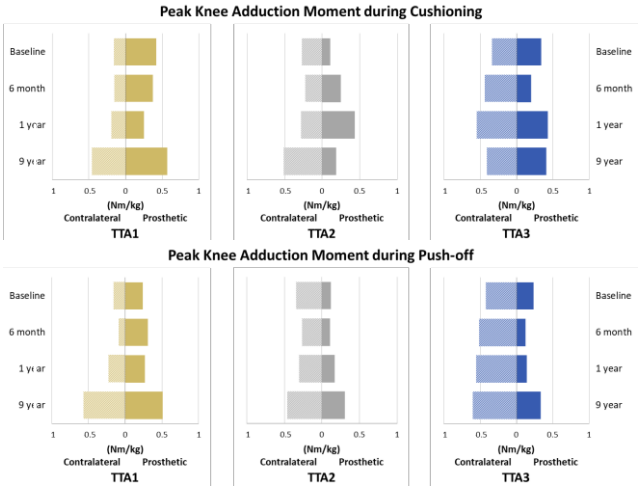

Figure 2a&2b: Peak KAM of both limbs during cushioning (a) and push-off (b) for each patient over time

Peak KAM varied for all patients (Figure 2). TTA1 subverted expectations entirely, loading his prosthetic side more throughout rehab and improving symmetry at his 9 year study. This is likely due to his contralateral limb injuries sustained during initial trauma. TTA2 had a much larger peak KAM in his contralateral limb during cushioning at his 9 year study but was more symmetrical at push-off, while TTA3 was symmetrical during cushioning at his 9 year study with a larger peak KAM in his contralateral limb during push-off. As both patients are highly functional and active individuals, difference in loading symmetry could be due to different compensation strategies and/or different prosthetic devices.

Significance

Few, if any, studies have been published that show longitudinal data for young servicemembers with TTA. Despite exceptional physical function, there is still risk of secondary complications, but being mindful of one's own body may help alleviate risk factors.

Disclosure

The views expressed herein do not necessarily reflect those of the Department of the Navy, Department of Defense, Defense Health Agency, or U.S. Government.

References

[1] Gailey R et al. (2008). *J Rehabil Res Dev*, **45**: 15 – 29.

Table 1: Self-selected walking speed (m/s) for each patient over time

	Baseline	6 month	1 year	9 year
TTA1	1.00	1.30	1.35	1.43
TTA2	1.26	1.40	1.43	1.44
TTA3	1.11	1.38	1.54	1.57

The Effects of Powered Ankles on Gait Initiation and Termination in Daily Life

Jay Kim and Deanna H. Gates
School of Kinesiology, University of Michigan Ann Arbor, MI
Email: jaywoo@umich.edu

Introduction

Individuals with transtibial amputation (TTA) typically do not walk for long durations at a time [1], which suggests that a significant portion of their steps are to initiate or terminate bouts of walking [2]. Transition steps may be more difficult for individuals with TTA as they lack ankle musculature, which contributes significantly to generating and dissipating energy. Powered ankle prostheses have been developed to replace this lost function by generating push-off power during walking [3]. While they have been shown to increase steady-state walking speed [3], their effect on transition steps is unknown. The purpose of this study was to compare the effect of unpowered and powered prostheses during initiation and termination of gait. We examined transition strides by calculating the velocity profile of the foot during late stance and early swing. We hypothesized that the powered ankle would yield greater peak velocity compared to the unpowered prosthesis.

Methods

10 males (53 ± 11 years old) with unilateral TTA and 14 individuals without amputation (13 male; 44 ± 15 years old) participated in this study. All participants wore a foot-mounted inertial measurement unit (IMU) on their prosthetic foot (non-dominant foot for controls) for two weeks. Individuals with TTA completed two weeks of monitoring both with their prescribed unpowered prosthesis and with the BiOM T2 (BiONX, Bedford, MA) powered ankle, in random order.

Walking data were segmented into strides using heel strikes, detected by finding local peaks in the gravity-corrected acceleration signal. This signal was integrated to calculate foot velocity. We included strides with lengths between 0.1 and 2.0 m and examined bouts of walking that consisted of at least 5 consecutive strides. Forward and vertical velocity peaks of the initiation and termination strides were compared between groups (control, unpowered, powered) using a linear mixed model.

Results and Discussion

We analyzed velocity profiles in 730 ± 630 bouts per participant for the unpowered prosthesis, in 930 ± 1070 bouts for the powered ankle, and in 1850 ± 910 bouts for controls.

Compared to controls, participants with TTA had shorter initiation and termination stride times ($p < 0.003$). They also had lower forward and vertical velocity peaks in both initiation and termination strides ($p < 0.003$; Fig 1).

For participants with TTA, there were no differences in stride times between prostheses. Compared to the unpowered prosthesis, the powered prosthesis had a lower first vertical velocity peak during the termination stride ($p = 0.023$) and tended to be lower during the initiation stride ($p = 0.084$).

The first peak of the vertical velocity profile (Fig 1) represents the upward motion of the foot during push-off and early swing, which is facilitated in part by the push-off power at the ankle joint. Unsurprisingly, controls had greater peaks of upward velocity compared to individuals with TTA. This was consistent with a previous study that used ground reaction forces and found greater initiation and termination step velocities in people without amputation compared to people with TTA [4,5].

The powered prosthesis should produce mechanical work at the ankle joint comparable to that of the biological ankle [3]. However, there were no differences in the velocity profiles of the initiation and termination strides. The lower vertical velocity with the powered prosthesis compared to unpowered prostheses suggests that participants may have decreased their push-off to facilitate a more gradual stop. In contrast, control participants produced greater vertical velocities on a quicker termination stride, indicating they tend to stop more abruptly.

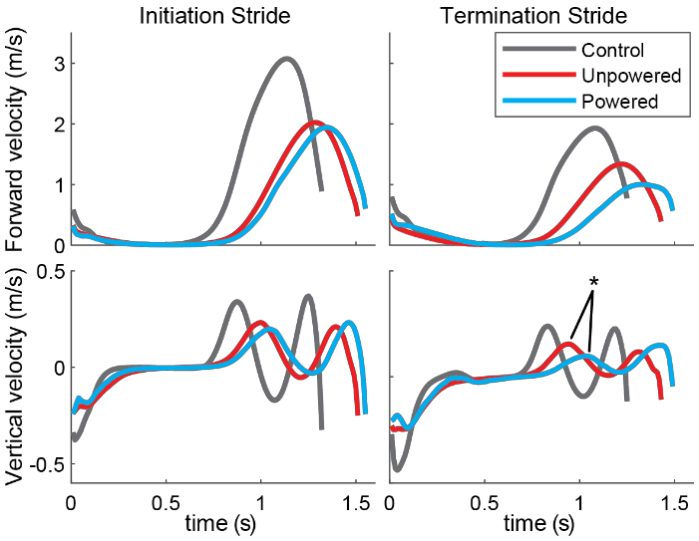

Figure 1: Forward (top) and vertical (bottom) velocity profiles plotted for the initiation (left) and termination (right) strides.

Because our approach uses a single IMU on the prosthetic foot, we do not know whether participants used their prosthetic or intact foot for the first and last steps, though previous studies have found that individuals with TTA usually preferred to initiate with a prosthetic step and terminate gait with an intact step [4,5].

Significance

The powered prosthesis did not normalize the velocity profile of initiation and termination strides to resemble that of controls. Our results suggest that the powered ankle may not be well suited for power absorption during slowing-down transitions.

Acknowledgments

Thank you to Lauro Ojeda, Kelsey White, Luis Nolasco, and the CDMRP Grant number W81XWH-15-1-0548.

References

[1] Klute, G. Arch Phys Med Rehab 87, 717-22, 2006.
[2] Orendurff, M. J Rehab Res & Dev 45, 7, 2008.
[3] Herr, H. Proc Biol Sci 279, 457-64, 2012.
[4] Vrieling, A. Gait & Pos 27, 423-30, 2008.
[5] Vrieling, A. Gait & Pos 27, 82-90, 2008.

Motion of the Residual Femur Within the Socket During Gait is Associated with Patient-Reported Problems in Transfemoral Amputees

Tom Gale[1], Shumeng Yang[1], Richard McGough[1], William Anderst[1]
[1]University of Pittsburgh, Department of Orthopaedic Surgery
Email: thg17@pitt.edu

Introduction

Lower limb amputees are generally found to have reduced mobility and lower quality of life compared to the general population [1], and is believed that poorly fitted prosthetic sockets exacerbate these problems [2-4]. Although a properly fit socket is believed to limit motion between the residual limb and the socket, there is no evidence to confirm that reducing motion between the underlying residual femur bone and the socket will improve patient-reported outcomes.

The purpose of this study was to evaluate the relationship between residual femur motion during gait and patient reported outcomes. A secondary goal was to assess within- and between subject variability in residual femur motion during gait.

Methods

Following Institutional Review Board (IRB) approval, 7 participants (1 female, 6 male; average age: 52.9±7.1 years) gave informed consent to participate in this study. All participants were unilateral transfemoral amputees that were ambulatory using a socket suspension prosthetic.

Up to five trials of synchronized biplane radiographs of the socket/distal femur were collected (100 images/s for 1.0 s) for each participant during treadmill walking at a self-selected speed (avg 0.7 ± 0.2 m/s). Additionally, one neutral standing trial was captured for baseline measurements. Concurrently, skin mounted marker motion capture of the full body was collected (Vicon, UK, 100 Hz), with the thigh markers placed on the prosthetic socket. Ground reaction forces during walking were recorded at 1000 Hz using a dual-belt instrumented treadmill (Bertec Corp, Columbus, OH). After motion testing, a CT scan was collected (0.57x0.57x1.25 mm/voxel resolution) and used to create a subject-specific 3D model of the entire residual femur for each participant. A previously validated volumetric model-based tracking technique was used to match digitally reconstructed radiographs created from the subject-specific CT scans to the biplane radiographs [5].

The coordinate system for the residual femur was established using anatomical landmarks placed on the shaft and femoral head. Surface mounted markers were used to create the socket coordinate system (Fig 1). Euler angle decomposition was used to calculate 6 degree-of-freedom kinematics of the residual femur relative to the socket for all walking trials. All trials were averaged within subject for analysis.

Questionaire for persons with a transfemoral amputation (Q-TFA) was also administered at the time of testing. Correlation of Q-TFA scores with residual femur kineamtics relative to the socket were tested using Spearman's rho (α=0.05).

Results and Discussion

Average rotation ROMs of the femur relative to the socket over full gait cycle were 9.7°±4.2°, 18.3°±3.9°, and 9.0°±5.3° for anterior tilt, internal-external rotation, and varus-valgus, respectively. Average translation ROMs were 17.2mm±9.8mm, 31.1mm±16.2mm, and 30.0mm±13.2mm for medial-lateral, superior-inferior (pistoning), and anterior-posterior directions, respectively. The average within-subject trial-to-trial variability was 1.1°±0.4°, 2.7°±1.2°, and 0.9°±0.3° for anterior tilt, internal-external rotation, and varus-valgus, respectively, and 1.0mm±0.4mm, 1.2mm±0.5mm, and 1.9mm±0.7mm medial-lateral, pistoning, and anterior-posterior directions, respectively.

Although residual femur ROM varied across subjects, consistent patterns of motion were observed across subjects for pistoning, medial-lateral shift, and varus-valgus rotation. All subjects displayed pistoning greater than 20mm, with maximum compression achieved by 20% of gait cycle. Most subjects achieved approximately ±5mm of pistoning relative to the static trial, with one outlier subject achieving >20mm of compression past the neutral position with a ROM of 62mm. All subjects exhibited a lateral shift of the end of the femur as the limb was loaded after foot strike. The residual femur of most subjects started more medial at foot strike relative to the static trial, with one outlier starting more laterally. There was also a consistent pattern of the femur-socket complex going into varus alignment as the limb was loaded after foot strike for all subjects.

Increased medial-lateral motion was strongly correlated to a higher Q-TFA problem score (Fig 2, ρ=0.929, p=0.003), which suggests that residual bone motion is a factor in prosthetic performance and comfort.

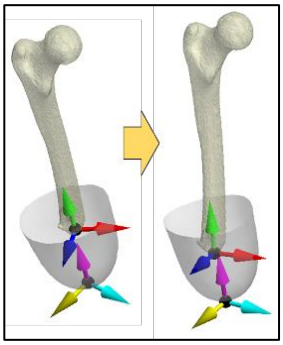

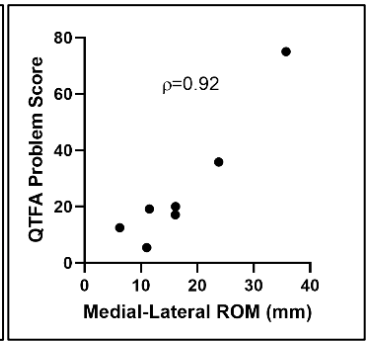

Figure 1: (Left) The femur and socket and their coordinate systems shown at terminal swing and mid-stance for one subject.
Figure 2: (Right) Scatter plot of medial-lateral residual femur range of motion relative to the socket vs Q-TFA Problem Score.

Significance

Residual femur range of motion within the socket during gait is repeatable within subjects, but inconsistent across subjects. Individualized socket modifications that reduce medial-lateral motion between the residual femur and socket may lead to increased performance and comfort for transfemoral amputees.

Acknowledgments

Funded by Univ. of Pittsburgh, Dept. of Orthopaedic Surgery.

References

[1] Davies and Datta, Prosthet. Orthot. Int., 2003. [2] Amtmann et al, Arch. Phys. Med. Rehabil., 2015. [3] Sinha et al, Prosthet. Orthot. Int., 2011. [4] Deans et al, Prosthet. Orthot. Int., 2008. [5] Anderst et al, Med. Eng. Phys., 2009.

The Performance of Implantable Electrodes on the Control of a Myoelectric Prosthesis Over One Year Post-Implantation

Christina Lee[1], Alex Vaskov[1], Philip Vu[1], Alicia Davis[1], R. Brent Gillespie[1], Stephen Kemp[1], Theodore Kung[1], Cindy Chestek[1], Paul Cederna[1], Deanna H. Gates[1]
[1]University of Michigan
Email: chslee@umich.edu

Introduction

Currently available myoelectric upper limb prostheses (MYO) rely on surface electromyography (EMG) recordings to control the terminal device. However, using surface EMG can result in inconsistent prosthetic control due to skin and sweat-based impedances, cross-talk between muscles, and day-to-day differences in electrode placement.[1] Intramuscular recordings have been proposed to address the limitations of surface EMG. We have previously demonstrated the ability to use machine learning algorithms with intramuscular signals to control a prosthesis in a virtual environment with high accuracy.[2] As a next step, it is important to investigate how these algorithms can be used to control a prosthesis in a physical environment, where users may have different muscle activation depending on physical interactions with objects, movement of the limb and differences in arm postures. In this case study, we assessed a person's ability to complete functional assessments using a MYO prosthesis controlled via signals from indwelling electrodes over one year following electrode implantation. Additionally, we explored the movement strategy by quantifying trunk motion as a measure of whole body movement.

Methods

The participant was a 54 year old female with right transradial amputation who used a body-powered prosthesis (BP) at home. One year after amputation, a surgeon implanted five indwelling bipolar EMG electrodes (Synapse Biomedical, Oberlin, OH) into residual muscles of the forearm. One month after surgery, she began real-time control experiments in a virtual reality environment (MuJoCo).[3] A single DOF linear decoder was developed using EMG signals from the index flexor digitorum profundus (FDPI) and the extensor digitorum communis (EDC). This decoder was used to control the tripod grasp of a MYO prosthesis (iLimb Quantum, Ossur, Iceland).

We assessed performance using a modified version of the Box and Blocks Test[4] (MBBT). We placed 16 blocks in an elevated grid and measured how long it took to move all 16 blocks from the ipsilateral to the contralateral side. The assessments were performed standing and repeated 2-3 times per session, depending on participant fatigue. On days 358, 393, and 456 after implantation, we also collected upper limb and trunk motion using a 17-camera motion capture system. From this, we calculated the range of motion (ROM) of segmental trunk angle in all three planes of motion. All tasks were completed with the MYO, intact limb (days 337, 358, 456) and BP (day 483). We assessed changes in these measures over time using linear regression.

Results and Discussion

After one year of implantation, the iFDP and EDC signals still demonstrated a high signal-to-noise ratio (SNR) of 94.1 and 11.3, respectively. The participant was able to complete MBBT with the same decoding algorithm consistently for over 200 days of evaluation ($r = -0.358$, $p=0.09$). She completed the task in 36.6s with her intact hand, 160.3s with her BP, and most recently, 169.6s with the MYO (Fig 1A).

Compensatory trunk motion during the MBBT did not change over time ($0>r\geq-0.569$, $p>0.14$, Fig 1B). ROMs were similar when using the MYO compared to the BP, but both were larger than those when using the intact limb.

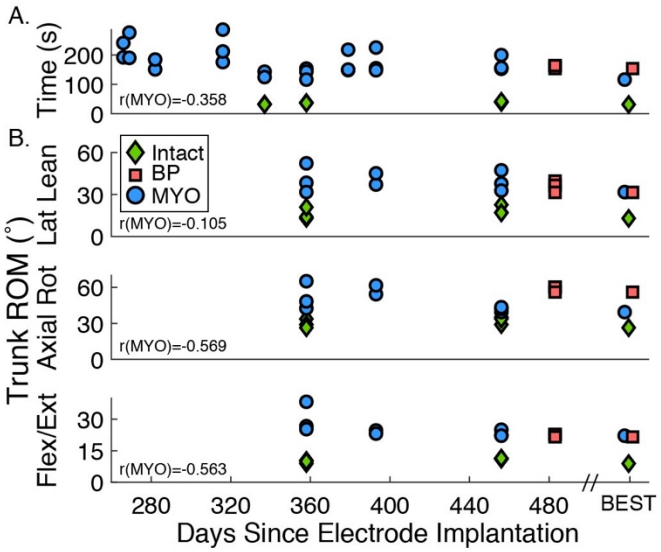

Figure 1: (A) MBBT completion time and (B) segmental trunk range of motion (ROM) during MBBT for the intact limb, BP, and MYO.

Overall, she had similar performance with the MYO that she only used in the lab to her at-home BP. This is notable due to the documented improvements that occur with training,[5] the difference in weight between the prosthesis (BP: 1.1 lb, MYO: 2.25 lb), and differences in prosthesis length. The participant had a small stature (1.41 m) and a medium-length residual limb. As such, the prosthetic side was slightly longer than her intact limb and could not accommodate a wrist flexion unit. Future work will explore the impact of implanted electrodes on the control of multiple degrees of freedom, including wrist motion.

Significance

A participant with upper limb loss was able to perform functional tasks using a control algorithm developed with intramuscular signals from two residual muscles for over one year following implantation. She completed the task with trunk movements similar to those used with her at-home body-powered prosthesis.

Acknowledgments

Thank you to Kelsey Ebbs and Michael Gonzalez. This work was supported by NIH grant number 5R01NS105132-02.

References

[1] Dewald et al. (2019). *J Neuroeng Rehabil*, **16**: 1-13.
[2] Vu et al. (2020). *Sci Transl Med*, **12**: 1-11.
[3] Todorov et al. (2012). *IROS*, **2012**: 5026-5033.
[4] Mathiowetz et al. (1985). *Am J Occup Ther*, **39**: 386-9.
[5] Resnik et al. (2014). *Prosthet Orthot Int*, **40**: 96-108.

Stimulation of residual sensory nerve modulates walking mechanics in the cat with bone-anchored transtibial prosthesis

Alexander N. Klishko[1], Hangue Park, Gina Grenga[1], Celina Zhang[1], Kyunggeune Oh, Kinsey R. Herrin[2],
John F. Dalton IV, Mark Pitkin, Boris I. Prilutsky[1]
[1]School of Biological Sciences, [2]School of Mechanical Engineering, Georgia Institute of Technology, Atlanta, GA, USA
Email: boris.prilutsky@biosci.gatech.edu

Introduction

Previous research has suggested that bone-anchored prostheses provide lower limb amputees with more comfort, range of motion, and osseoperception (Branemark et al. 2014). However, locomotion with a unilateral bone-anchored prosthesis is still assymetric (Jarrell et al. 2018) even if prostheses are powered (Montgomery and Grabowski 2018). In addition, the current solid titanium percutaneous pylons for prosthesis attachment cause a high rate of skin infection (Branemark et al. 2014). A new porous titanium skin & bone integrated pylon (SBIP, Poly-Orth International, USA) has demonstrated a substantial reduction of the skin infection rate in a rat study (Farrell et al. 2014). It could also be used as an interface between the prosthesis and peripheral nerves and muscles for bidirectional prosthetic control (Pitkin et al. 2012) – to drive a prosthesis actuator using EMG from residual muscles and to provide touch perception of prosthesis contact with the external environment by stimulating residual sensory nerves. This bidirectional control is more intuitive and potentially could improve quality of prosthetic locomotion. The goal of this study was to examine effects of stimulation of the residual distal tibial nerve, innervating skin on planar surface of the foot, on joint moments of the prosthetic limb during walking in the cat.

Methods

All experimental procedures were consistent with the Principles of Laboratory Animal Care of the NIH and approved by the Georgia Tech Institutional Animal Care and Use Committee. We recorded kinematics and ground reaction forces during walking of one adult purpose-bred cat that had a bone-anchored, transtibial, powered prosthesis for 29 months; for details see (Jarrell et al. 2018; Park et al. 2016; Park et al. 2018). The proximal stump of the distal tibial nerve was sutured to residuum skin during amputation surgery. An onboard prosthesis stimulator delivered stimulations of the residual nerve during stance phase to modulate muscle activity (Duysens and Pearson 1976). Contact with the ground also triggered prosthetic ankle extension. We investigated intact locomotion before surgery, as well as prosthetic locomotion with and without nerve stimulation.

Results and Discussion

We found that joint moment patterns of the prosthetic limb were similar to the intact patterns (Figure 1), but the moment magnitudes differed significantly. For example, prosthetic peak extension moments at the hip/ankle were higher/lower than in the intact limb ($p<0.05$, Figure 2). Nerve stimulation increased the hip flexion moment peak compared to intact and non-stimulated prosthetic hindlimb (Figures 1, 2). Nerve stimulation also increased peaks of knee flexion and extension moments, positive ankle power and negative hip power, and decreased negative knee power compared with no stimulation. Intact ankle extension moment was greater than the prosthetic ankle extension moment with or without stimulation and was compensated by greater prosthetic hip extension and knee flexion moments. These results indicate that nerve stimulation may change certain aspects of prosthetic locomotion; however, nerve stimulation parameters used in this study (Park et al. 2016) did not eliminate locomotor asymmetry.

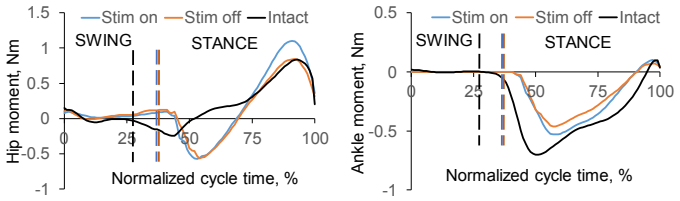

Figure 1: Mean hip and ankle moments during intact and prosthetic stimulated and non-stimulated walking. Negative values - extension.

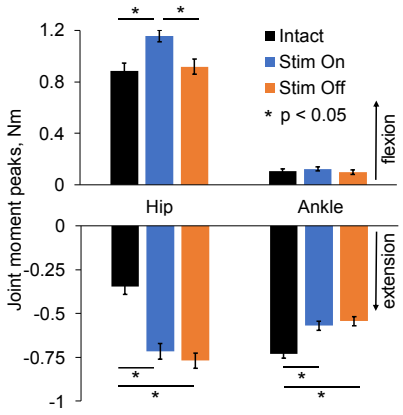

Figure 2: Mean (±SE) peak joint moments of intact and prosthetic limbs.

Significance

The main findings of the study are that (1) the residual distal tibial nerve responds to electrical stimulation 29 months after surgery and (2) stimulation of residual distal tibial nerve, containing mostly cutaneous afferents, modulates kinetic variables of prosthetic walking. Although nerve stimulation parameters taken from (Park et al. 2016) did not eliminate asymmetry of prosthetic walking, it might be possible to optimize stimulation parameters to further modulate locomotor performance (Duysens and Pearson 1976). Additional improvements in symmetry of prosthetic walking could be achieved by using a different operation mode of the prosthesis, in which ankle extension is controlled by both ground contact and EMG activity of a residual extensor muscle (Park et al. 2018).

Acknowledgments

Supported by DOD grant W81XWH-16-1-0791. We thank the T3 Labs for their excellent veterinary assistance.

References

Brånemark et al (2014) *Bone & Joint J* 96-B:106–13.
Duysens, Pearson (1976) *Exp Brain Res* 24: 245-255.
Farrell et al (2014) *J Biomed Mater Res Part A* 102:1305-15.
Jarrell et al. (2018) *J Biomech* 76: 74-83.
Montgomery, Grabowski (2018) *J Roy Soc Interf* 15: 20180442.
Park et al (2016) *IEEE BioCAS Conference*, pp. 95-98.
Park et al (2018) *Front Neurosci* 12: 471.
Pitkin et al. (2012) *J Biomed Materials Res Part B, Appl Biomater* 100: 993-999.

Open Dataset of 18 Above-Knee Amputees Walking at 5 Different Speeds with their Prescribed Prostheses

Sarah Hood[1*], K. B. Foreman[1,2], and Tommaso Lenzi[1]
[1]Department of Mechanical Engineering and Utah Robotics Center, University of Utah, Salt Lake City, UT, USA
[2]Department of Physical Therapy and Athletic Training, University of Utah, Salt Lake City, UT, USA
* Corresponding Author Email: sarah.hood@utah.edu

Introduction

Motion capture is fundamental to improve the understanding of gait abnormalities [1], to assist treatment decision making [2], and to drive the design of new prostheses for individuals with lower-limb amputations [3]. Unfortunately, the use of motion capture is limited by the need for dedicated space, expensive equipment, and specialized technicians, as well as the difficulties in recruiting the patient population. To address these issues, we present the first openly available dataset of 18 above-knee amputee subjects walking at 5 different speeds [4].

Methods

Eighteen individuals with an above-knee amputation (Table 1) were enrolled in this study approved by the University of Utah Institutional Review Board and provided written informed consent. Each participant's walking speed was evaluated to determine their classification as either a limited community ambulator (K2) or full community ambulator (K3) using the threshold of 0.8 m/s [5]. A different set of walking speeds were defined for each group. The K2 speeds were (0.4, 0.5, 0.6, 0.7, 0.8) m/s and the K3 speeds were (0.6, 0.8, 1.0, 1.2, 1.4) m/s.

The biomechanics data was collected in a single visit using a 10-camera Vicon system and a split-belt Bertec Fully Instrumented Treadmill. A modified Plug-in-Gait model consisting of 67 reflective markers was applied to each participant (Figure 1). A static, functional, and joint center calibration was collected for participant specific calibrations. Each participant walked at a single speed to collect 5 dynamic trials capturing 10 full strides and was offered rest between speeds. Participants were encouraged to walk without using the handrails and any handrail use was noted by the experimenter [4].

Table 1: Averages of Patient Demographics

	K2	K3
Number Participants (#)	9	9
Age (Years)	63±9	40±13
Gender (% M-F)	89%-11%	78%-22%
Mass (kg)	97.6 ± 25.6	83.6±18.0
Height (m)	1.72±0.06	1.80±0.11
Age of Amputation (Years)	15±19	13±12

Results and Discussion

Pre-processing was performed on the marker trajectories and gait events using Vicon Software. A low-pass Butterworth filter with a cut-off frequency of 15 Hz and 6 Hz was applied to the force plate data and marker trajectory data, respectively. The kinetics and kinematics were calculated using Visual 3D following the default assumptions for the intact limbs. The knee prosthesis was modelled as 1/3 weight with a center of mass 25% below the knee joint [6]. All raw and processed Vicon data and kinetics and kinematics will be made publicly available [4,7]. Subject specific information, including prosthesis components and patient demographic information, is deidentified. All data can be found in a Figshare database [4,7].

Significance

Many unknowns can be address with motion capture leading to an increased understanding of gait abnormalities in the above knee amputee population. Yet, no dataset is available for the biomechanics community to analyse. By making this dataset openly available to the community [4,7], we expect that researchers, clinicians, and therapists will be able to improve rehabilitation techniques [1], treatment decision making [2], and the design of new technology [3].

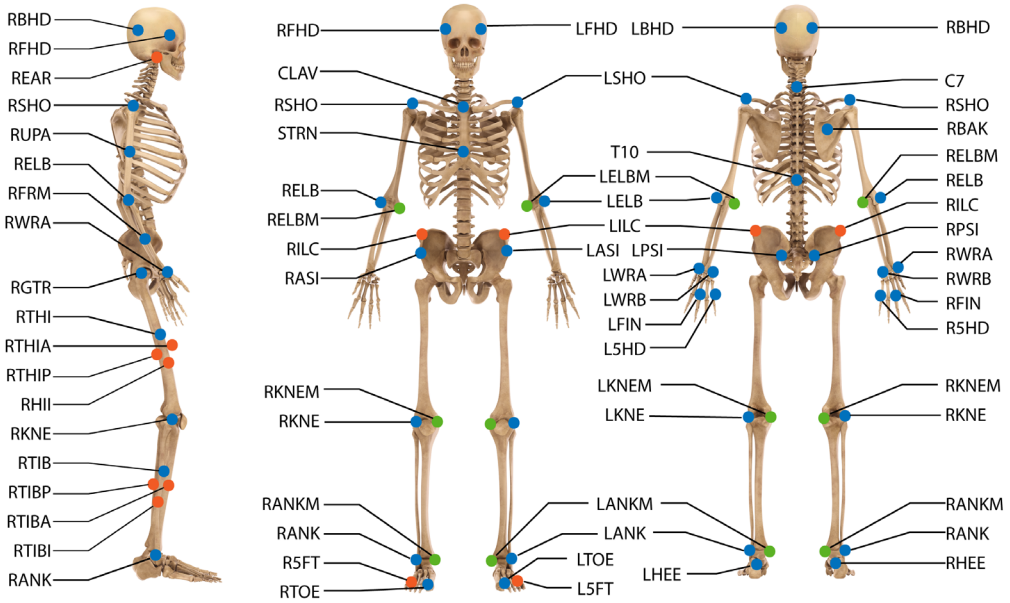

Figure 1: Modified Plug in Gait model, marker locations and names. Markers from original Plug in Gait model are shown in blue. Additional markers to original Plug in Gait model are shown in orange for tracking and green for static calibration.

Acknowledgments

Authors would like to thank Marshall Ishmael, Andy Gunnell and Dr. Colby Hansen, MD.

References

1. Wren et al. *Gait Posture,* **34.2**, 149-153, 2011.
2. Harlaar et al. *Disabil Rehabil,* **20.1**, 29-32, 1998.
3. Tran et al. *IE-EE Trans Rob Autom Letters,* **4.2**, 1186-1193, 2019.
4. Hood et al. *Nat Sci Data*. (under review)
5. Bowden et al. *Neurorehabil Neural Repair,* **22.6**, 672-675, 2008.
6. Mattes et al. *Arch Phys Med Rehabil*, **81**, 561-568, 2000.
7. Hood et al.. DOI: 10.6084/m9.figshare.10308443

Should Baseball Adjust the Mound Height and Pitching Distance?

Glenn S. Fleisig*[1], Alek Z. Diffendaffer[1], Jonathan S. Slowik[1]
[1]American Sports Medicine Institute, Birmingham, AL, USA
Email: *glennf@asmi.org

Introduction

From 2000 to 2015, there was a steady decline in runs scored in Major League Baseball (MLB), causing many fans and experts to call for measures to increase offense. One suggestion was to lower the pitching mound again. (MLB previously lowered the mound in 1969, and offense rose significantly in the following years). Another suggestion was to move the mound farther back, as today's pitchers have higher ball velocity than ever and moving the mound back could give batters more time. Any change enacted by MLB would also be adapted by minor league baseball and most likely by collegiate and high school baseball. A pair of studies were conducted, one varying mound height and one varying pitching distance. The hypotheses tested were that pitching kinematics, pitching kinetics, and ball flight would vary significantly with mound height and pitching distance.

Methods

In the first study, 20 collegiate pitchers were tested pitching five fastballs and five curveballs from four mound heights (15, 20, 25, and 30 cm).[1] Reflective markers on the pitcher were tracked with an 11-camera motion capture system (Motion Analysis Corp, Santa Rosa, CA) while the ball was tracked with a separate system (Rapsodo Inc, Fishers, IN).

For the second study, 26 collegiate pitchers were tested pitching sets of five fastballs from three distances (18.44, 19.05, and 19.41 m).[2] Reflective markers on the pitcher were tracked with an 12-camera motion capture system (Motion Analysis Corp, Santa Rosa, CA) while the ball was tracked with a separate system (SMT, Freemont, CA).

Repeated measures ANOVA were used to test for differences ($p<0.05$) in each study. Pairwise differences were identified with Tukey post-hoc tests ($p<0.05$).

Results and Discussion

Comparison among mound heights showed no significant differences in ball motion, but several differences in pitching kinematics for both fastballs and curveballs. There were no kinetic differences within curveballs, but five differences for fastballs (Table 1). Decreased kinetics with lower mounds was consistent with a previous study finding lower kinetics from flat ground,[3] but were not found in a previous study of adolescent pitchers.[4]

There were no significant differences in fastball pitching kinematics or kinetics associated with pitching distance. However, the ball's duration of flight, horizontal motion, and vertical motion increased with pitching distance (Table 2). A previous study of adolescent pitchers found kinetic changes with pitching distance, but the range of pitching distances were more extreme in that study.[4]

Table 1. Significant differences ($p<0.05$) in fastball kinetics. Mean values shown.

	Mound height				
	15cm	20cm	25cm	30cm	p
Shoulder anterior force (N)	360[a]	360[b]	367[a,b]	365	0.002
Shoulder internal rotation torque (N·m)	90.4	90.4	91.7	91.7	0.013
Elbow proximal force (N)	1011	1009	1023	1020	0.027
Elbow varus torque (N·m)	89.9	89.8	91.0	91.0	0.048
Elbow flexion torque (N·m)	56.9	56.9	58.1	57.8	0.041

Matching superscripts indicate pairwise post-hoc difference

Table 2. Significant differences ($p<0.05$) in fastball motion with pitch distance. Mean values shown.

	Pitch distance			
	18.44m	19.05m	19.41m	p
Ball flight (s)	0.43[a,b]	0.45[a,c]	0.46[b,c]	<0.001
Horizontal break (cm)	2.7[d]	3.3[d]	3.9	<0.001
Vertical break (cm)	15.0[e,f]	16.6[e]	16.8[f]	<0.001

Matching superscripts indicate pairwise post-hoc difference

Significance

Lowering the mound would not increase kinetics and likely would be safe for pitchers, however the current study does not show any benefit for the batters. Increasing pitching distance a moderate amount (1 m or less) would have no significant effect on pitcher kinematics or kinetics. It is unknown if increased distance would help batters (due to longer pitch flight time) or hinder their ability (due to increased ball break).

Acknowledgments

Both studies were supported by grants from MLB.

References

1. Diffendaffer AZ et al. *J Sci Med Sport* 22:858-861, 2019
2. Diffendaffer AZ et al. *J Sci Med Sport* S1440-2440(19)31359-3, 2020
3. Slenker N et al. Am J Sports Med 42(5):1226-1232, 2014
4. Fleisig GS et al. Am J Sports Med 46(12):2996-3001, 2018

Influence of alternative shoe fit configurations on athlete biomechanics

Kate Harrison[1], Bradley Davidson[2], Moira Pryhoda[2], Nick Nelson[2], Brett Vladika[1], and Daniel Feeney[1]
[1]BOA Technology
[2]Human Dynamics Lab, Department of Mechanical Engineering University of Denver
Email: kate.harrison@boatechnology.com

Introduction

The ability to change direction quickly during jumping and cutting is important for sports performance, however, such tasks entail a high risk of injury. Thus, athletic shoe design needs to optimize both performance and injury risk. While the impact of the midsole and outsole of athletic shoes is the focus of much research, little is known about how the upper impacts athlete biomechanics. Shoe uppers specially designed to fit and contain the foot better than a traditional lace system improved key performance measures during rapid direction changes (speed, ground contact time, force generation).[1] However, how the biomechanical mechanisms underlying these performance improvements,[2] as well as the effects on potential injury risk factors,[3,4] are unknown. The purpose of this study was to evaluate how specially-designed shoe fit configurations affect athlete biomechanics during agility and speed drills requiring rapid changes in direction. We hypothesized athletes would produce a greater peak propulsive joint powers and moments, and range of motion in the plane of movement, and decrease motion in other planes of motion in the alternative configurations.

Methods

The dataset from a previous study was reanalysed.[1] Thirty-one NCAA Division 1 and club athletes performed countermovement and skater jumps in four shoe conditions. We prototyped three different fit configurations (Lace replacement, Tri panel, and Y wrap) and tested them against a laced baseline shoe (Figure 1). We instructed each athlete to move as quickly and as forcefully as possible. 3D force and motion data were captured during the agility drills. Ankle and knee range of motion, moments and propulsive powers were compared between footwear conditions using a linear mixed effects model.

Figure 1. Shoe fit configurations.

Results and Discussion

During vertical countermovement jumps and lateral skater jumps, peak ankle and knee concentric power and knee extension moment were greater in alternative shoe fit configurations compared to laces (Table 1). These results help explain improved agility performance during repeated vertical and lateral jumps in these shoes.[1] In countermovement jumps, sagittal plane knee range of motion was greater in alternative shoe fit configurations, while ankle frontal plane range of motion and kinetics were lower. These characteristics are associated with decreased injury risk.[3,4] In contrast, during skater jumps, sagittal plane knee range of motion and peak ankle plantarflexion motion were lower in alternative fit configurations, while frontal plane ankle moments were higher.

Table 1. Biomechanics in alternative shoe closure systems, compared to a baseline laced shoe.

CMJ				
	Lace	**Lace repl.**	**Y wrap**	**Tri panel**
Range of Motion (degrees)				
Ankle inversion/eversion***	20.8	N.S.	-1.9***	-0.8*
Knee flexion/extension***	91.9	2.6***	3.0***	2.0***
Peak Moment (Nm)				
Inversion***	5.5	-0.7*	-1.3***	N.S.
Eversion***	-28.2	1.8*	N.S.	2.4**
Knee Extension***	174.6	10.7***	10.2***	17.3***
Peak Concentric Power (watts)				
Ankle***	2068	53*	45*	87***
Knee***	1918	N.S.	N.S.	80***
Skater Jump				
Range of Motion (degrees)				
Knee flexion/extension***	49.1	N.S.	-1.6**	-1.9***
Peak Moment (Nm)				
Plantarflexion*	-1.1	0.2*	N.S.	0.3 **
Inversion**	35.8	2.1*	2.9**	2.6**
Eversion**	-7.8	N.S.	-1.0*	N.S.
Knee Extension*	191.7	N.S.	7.7**	N.S.
Peak Concentric Power (watts)				
Ankle***	2068	45*	53*	87***
Knee***	1918	N.S.	N.S.	80***

***p<.001, **p<0.01, *p<.05

These results indicate that alternative shoe fit configurations allow athletes to direct force along the intended line of movement without unneeded and uncontrolled joint motion. This helps to explain improved agility performance and biomechanical efficiency previous measured in these athletes.[1]

Significance

Intentional upper design that enhances foot wrapping can help optimize force and motion in such a way to enhance performance in rapid movements by 1-5%,[1] while also mitigating potential injury risk factors. This could be due to mechanical influence of the shoe upper on foot motion, and/or improved proprioception due to better conformity to the foot.

Acknowledgments

Kate Harrison, Brett Vladika, and Daniel Feeney work for BOA Technology.

References

1. Pryhoda M et al. January 2020. doi:10.31236/osf.io/5fr9t
2. Marshall BM, Moran KA.*J Strength Cond Res*. 2015;29(12).
3. Kobayashi T, Gamada K. *Foot Ankle Spec*. 2014;7(4).
4. Alentorn-Geli E et al. *Knee Surg Sports Traumatol Arthrosc*. 2009;17(7).

Performance Evaluation of Rate Activated Tether (RAT) Football Helmet Suspension

Alex J. Lurski[1,2], Ryan J. Neice[1,2], Thomas A. Plaisted[1], and Eric D. Wetzel[1]
[1] CCDC Army Research Laboratory, Weapons and Materials Research Directorate, Aberdeen Proving Ground, MD, USA
[2] Oak Ridge Associated Universities, Oak Ridge, 37831 TN, USA
Email: alexander.j.lurski.ctr@mail.mil

Introduction

Heightened awareness in the football community on sports-related traumatic brain injury has fueled research efforts to improve the performance of helmets. ARL has has developed a rate-dependent strapping material, referred to as rate activated tethers (RATs), that has demonstrated improvements in blunt impact protection for crown impacts [1]. As shown in **Figure 1**, RATs consist of an elastic tube containing two thin ribbons immersed in shear thickening fluid (STF). When pulled in tension the ribbons cause a shearing action in the STF, generating increased resistance with higher extension rates. It is hypothesized that a RAT based helmet suspension will decrease head injury metrics when compared to a conventional padded football helmet.

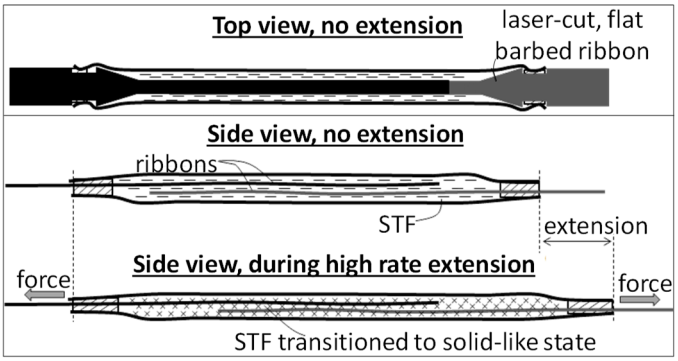

Figure 1: Diagram of rate activated tether (RAT) technology.

Methods

As a proof of concept, the suspension system was focused on reducing the head injury metrics in impacts to the rear of the head. The rear pads in a 2014 Riddell Revolution Speed helmet were removed from the helmet and replaced by a RAT-based helmet suspension system as shown in **Figure 2.** The ends of three RATs were attached to the front of the helmet shell, with the RATs then closely wrapped around the rear of the head. Impacts to the rear helmet shell induce stretching of the RATs. Both conventional padded helmets and RAT-modified helmets were subject to the twin-wire based NOCSAE football helmet test standard for rear impacts [2].

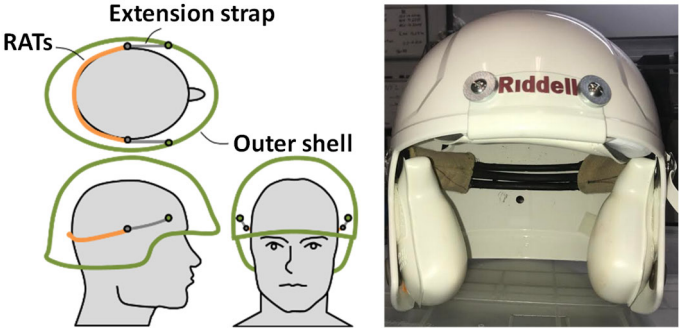

Figure 2: Rate activated tether (RAT) helmet suspension system.

Results and Discussion

		Ambient Temperature		Ambient Temperature		High Temperature	
Parameter	Units	Pads	RAT	Pads	RAT	Pads	RAT
Impact velocity	(m/s)	3.50	3.49	5.67	5.56	6.04	5.57
Peak acceleration	(g)	45.0	39.8	93.5	57.7	80.7	55.7
Severity Index (SI)		99	67	393	190	339	176

Figure 3: NOCSAE twin-wire rear-impact results for both helmets.

As shown in **Figure 3,** the RAT based suspension system decreased both peak acceleration and Severity Index (SI) for each rear impact case in the NOCSAE twin-wire test. At high velocity, the RAT based suspension shows a dramatic improvement in performance.

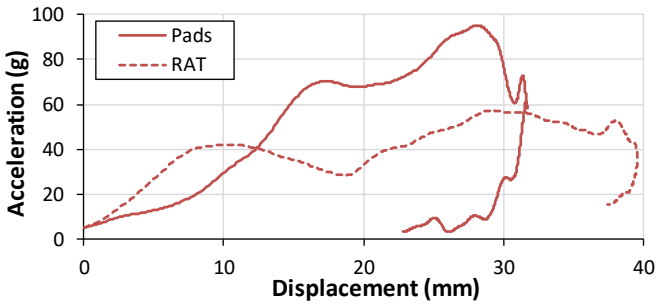

Figure 4: Headform acceleration vs. displacement for both helmets at high velocity and ambient temperature.

Significance

The increased performance of the RAT-based helmet suspension is attributed to three primary characteristics, showcased in **Figure 4**, that differentiate it from traditional padded helmet suspension systems. First, the RAT suspension absorbs energy in a tension over the entire distance (stroke) between the head and helmet shell, while pads do so in compression until the point of densification. Second, the energy attenuating profile of the RAT follows a near square wave energy attenuating response, decelerating the head at a near constant level over the entire stroke, which is inherently more efficient than typical padding. Third, the RAT system decelerates the head earlier in the event compared to the pad system, which is more delayed in its ability to engage the head and decelerate it at a tolerable level. These results show that RATs could fundamentally and disruptively change design concepts and performance expectations for helmets.

Acknowledgments

NTS Chesapeake Testing performed NOCSAE testing reported here. This project was supported in part by an appointment administered by Oak Ridge Associated Universities (ORAU) for ARL through Cooperative Agreement W911NF-16-2-0008.

References

[1] Spinelli et al., *Materials & Design*, May 2018.
[2] NOCSAE DOC (ND)002-13m15

Tibial Bone Strains in Basketball Players During Dynamic Tasks

Chenxi Yan[1], Stuart Warden[2], Mariana E. Kersh[1]
[1]University of Illinois at Urbana Champaign
[2]Indiana University Purdue University Indianapolis
Email: *cyan5@illinois.edu

Introduction

Bone serves a mechanical role; however, repeated loading increases stress fracture risk. Basketball players experience tibial stress fractures. It is crucial to understand tibial loading during basketball activities to develop preventive and management strategies. We hypothesized activities involving rapid direction changes and impact loading would have greater tibial strains relative to walking, and would load different parts of the bone.

Methods

Collegiate-level basketball players (n=11) had biomechanical data recorded during walking, sprinting, a drop-jump task, and lateral sprinting using reflective markers attached to anatomical landmarks (Fig. 1). A force plate recorded ground reaction forces (GRFs). Computed tomography (CT) scans of the tibia, along with density phantoms, were obtained.

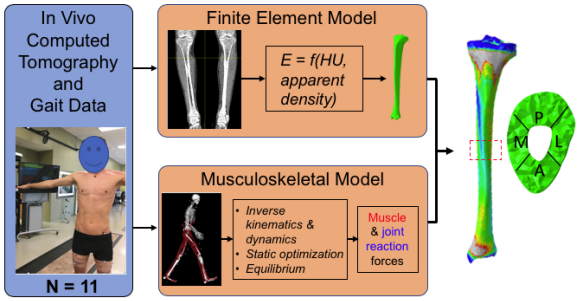

Fig. 1: Pipeline: gait data were applied to musculoskeletal models for finite element analysis of strain at the tibial midshaft.

Marker and GRF data were filtered in Matlab, then run through inverse kinematics, inverse dynamics, and static optimization analyses in OpenSim to obtain muscle and joint force predictions. The tibia was segmented from the CT data and used to create a finite element (FE) model of each subject that included density-based heterogenous material properties. Muscle and joint forces were applied to the tibia using qausi-static FE analyses for the stance phase of each task. The proximal tibia was unconstrained in the proximal-distal direction. Spring elements were used to simulate soft tissue constraints at the distal tibia. Maximum and minimum principal strains of the cross-section and the anterior aspect of the middle diaphysis of the tibia - where fractures have been reported to occur – at the time of peak strains were analyzed.

Results and Discussion

The tibia experienced bending. Minimum principal strains (compressive) were nearly double maximum principal strains (tensile). At the cross-sectional level, sprint and lateral sprint resulted in higher tensile (max principle) strains (133±46%, 90±66%) than walking. However, within the anterior quadrant, landing from a jump resulted in greater tensile strain than walking (146±70%). Meanwhile, sprinting and jumping resulted in significantly greater compressive strain than walking at the cross-sectional level (134±110%, 94±90%). In the anterior quadrant, jumping induced greater compressive strain than walking (155 ± 115%) and lateral sprinting (175±170%) (Fig. 2).

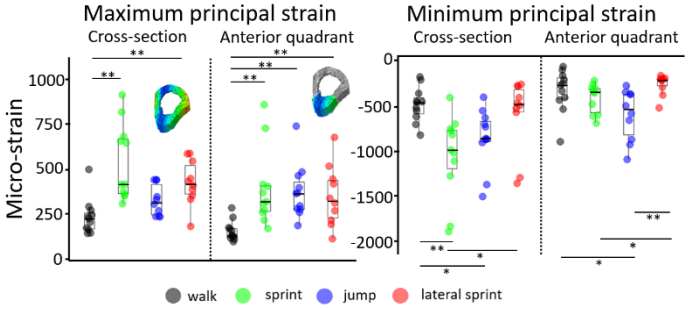

Fig. 2: Principal strains at the entire cross section and anterior aspect (*p<0.05, **p<0.01 between activities).

Peak strains during sprinting occured at 40% of the stance phase which coincided with the time of peak knee flexion (Fig. 3). However, knee flexion is likely not the sole predictor of strain.

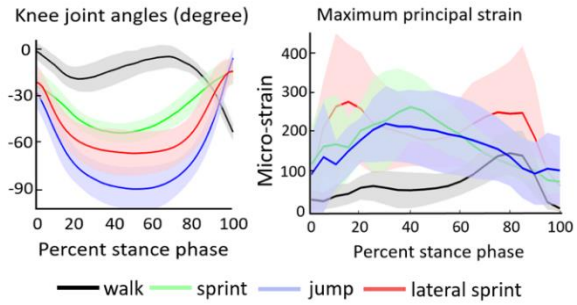

Figure 3: Knee angles, maximum principal strains at anterior quadrant.

Bone is weaker in tension compared to compression. Within the anterior quadrant, all three tasks resulted in increased tensile strains relative to walking. However, fractures seldom occur during sprinting but rather occur during jumping. Our results indicate a modest, but not significant, increase in strains during jumping compared to either sprinting or lateral sprinting tasks possibly explaining the fracture risk associated with jumping.

Significance

Strain gauges were used in the late 90's to measure tibial strains in vivo [1]. However, strain gauging is invasive and limited to small regions. Here, we use for the first time a computational technique to analyse tibial strains during basketball activities. Our results provide insights on tibial loading and the relationship between kinematics and strain. These data may provide direction for the prevention and treatment of stress fractures using biomechanically informed training programs.

Acknowledgments

Funded by National Basketball Association/ General Electric Healthcare Orthopedics and Sports Medicine Collaboration.

References

[1] Burr, David B., et al. Bone 18.5 (1996): 405-410
[2] Yang, Peng-Fei, et al. PLoS One 9.4 (2014)

Racial Differences in Running and Landing Measures Associated with Injury Risk Vary by Gender

Cherice N. Hughes-Oliver [1], Wornie Reed [2], Daniel Schmitt [3], Laura Sands [4], Shawn Arent [5], Robin M. Queen [1]
[1] Department of Biomedical Engineering and Mechanics, Virginia Tech, Blacksburg, VA, USA
[2] Department of Sociology, Virginia Tech, Blacksburg, VA, USA
[3] Department of Anthropology, Duke University, Durham, NC, USA
[4] Department of Human Development and Family Science, Virginia Tech, Blacksburg, VA, USA
[5] Department of Exercise Science, University of South Carolina, Columbia, SC, USA
Email: cnh4ph@vt.edu

Introduction

Running and landing are commonly associated with risk for overuse injuries like stress fractures and impact injuries like tendon ruptures and anterior crucial ligament (ACL) tears. Racial health disparities in the incidence rates of these injuries have been documented between African Americans (AA) and white Americans (WA) [1,2,3,4]. It is unknown whether running and landing mechanics differ between racial groups and whether such differences, if they exist, could result in differential injury risk between racial groups and contribute to racial health disparities.

The purposes of this study were to test the hypothesis that racial differences exist in running and landing mechanics between AA and WA, and that such differences could be explained by a combination of anthropometric, strength, and health status factors in women only as these factors were previously unable to account for racial gait differences in men.

Methods

92 participants equally divided between gender and self-identified race were recruited. 3D motion capture and force plate data were recorded during 7 running (3.2 m/s) and 7 drop vertical jump (31cm box height) trials. Stance time and non-normalized time series data were exported from Visual 3D. Heart rate, blood pressure, stress questionnaires, activity level, anthropometry, lower extremity strength, and blood levels of glucose, interleukin-6, C-reactive protein, and cortisol were also collected. Outcome measures included impact peak, peak vertical ground reaction force (pvGRF), average and maximum loading rate (LR), peak knee flexion (pKFA) and hip adduction angles (pHAdA) during running and pvGRF, average and maximum LR, impulse, pKFA, peak knee abduction angle (pKAbA), and frontal plane knee range of motion (fKROM) during landing.

Univariate ANOVA models determined main and interaction effects of gender and race (JMP Pro 15, α=0.1). Partial eta squared effect sizes were computed for each effect. If interactions or gender effects were observed, separate analyses were run for men and women. For each outcome measure with an observed racial difference, race was locked as a predictor in a stepwise linear regression model. Independent variables that differed between racial groups ($p<0.1$) and were correlated with the outcome measure ($p<0.2$) were included as predictors. If race was no longer significant in the regression model after the inclusion of the independent variable(s), those variables were considered to have explained the effect of race. Landing pvGRF, LR, impulse, and fKROM were log-transformed due to non-normality.

Results and Discussion

Interactions between gender and race existed in stance time [$p=0.073, \eta_p^2=0.040$], pvGRF [$p=0.059, \eta_p^2=0.044$], and pHAdA [$p=0.091, \eta_p^2=0.035$] during running. Landing interactions were found in pvGRF [$p=0.018, \eta_p^2=0.065$], average [$p=0.080, \eta_p^2=0.036$] and maximum LR [$p=0.023, \eta_p^2=0.060$], and fKROM [$p=0.079, \eta_p^2=0.036$]. Smaller pvGRF and pHAdA were found in AA men compared to WA men but were unable to be explained by any assessed factors. AA women had longer running stance times compared to WA women, which was partially explained by higher heart rate and larger crural index. No racial differences were found during landing in men. In women, higher pvGRF, average and maximum LR, and fKROM were found in AA during landing. All racial differences in women were explained by some combination of shorter height, higher levels of chronic perceived stress, higher BMI, and weaker knee flexion strength.

Modifiable factors such as BMI and knee flexion strength may provide targets for interventions aimed at injury prevention and targeted rehabilitation. The direction of the racial differences observed in the current study align with the higher incidence of tendon rupture in AA compared to WA but opposes the lower incidence of ACL injury in AA, which may be explained by lower physical activity levels and potentially limited sport specific landing training in the AA women based on the inclusion criteria. Future investigations should evaluate whether modifiable factors could be targeted to reduce or eliminate racial health disparities in experienced athletes.

These results partly support our hypotheses concerning racial differences, although the possibility for additional factors to explain the observed racial differences in running and landing should be investigated further, especially for men. These findings suggest the need for racially diverse normative running and landing datasets and emphasize the importance of stress control for injury prevention, particularly for racial minorities.

Significance

The impact of race and gender on running and landing measures associated with injuries were explained by innate, modifiable, and environmental factors in women. These racial differences and identified explanatory factors suggest the need for racially diverse normative datasets and targeted interventions focusing on modifiable factors including BMI, strength, and stress management. This data allows development of protocols that could assist in reducing racial health disparities in running and landing related injuries.

Acknowledgments

The Howard Hughes Medical Institute Gilliam Fellowship and the Institute for Society, Culture, and the Environment funded Cherice Hughes-Oliver and this study, respectively.

References

[1] J. Knapik, et al., *Int. J. Sports Med*. 33 (2012) 940–946. [2] D.W.White, et al., *Am J Sport. Med*. 35 (2007) 1308–1314. [3] J.J. Davis, et al., *Mil. Med*. 164 (1999) 872–3. [4] T.H. Trojian, et al., *Am. J. Sports Med*. 34 (2006) 895–898.

Anticipation and an External Target Alter Knee Biomechanics in a Volleyball-Specific Task

Joshua T. Weinhandl[1], Michael J O'Dwyer[1], Lauren E. Schroeder[1],
[1]The University of Tennessee, Knoxville, Knoxville, TN, U.S.A.
Email: jweinhan@utk.edu

Introduction

Noncontact anterior cruciate ligament (ACL) injuries are the most common severe injury in NCAA volleyball, accounting for 26% of severe injuries [1]. Certain sagittal- and frontal-plane knee ACL injury risk factors have been identified during landing [2], especially during landings that involve a rotational movement after landing [3]. Additionally, a primary concern in biomechanics research is the lack of a realistic, game-like environment during data collection. It has been shown that including both external objects [4] and unanticipated tasks [5] in the testing environment can better represent game-like scenarios in the lab. Currently, it is unknown how including both an external object and an unanticipated task affects knee biomechanics during a volleyball-specific block landing.

Therefore, the purpose of this study was to determine the effects of a physical overhead goal and a subsequent unanticipated lateral cut on knee kinematics and kinetics of the dominant-leg during the landing of a volleyball block. It was hypothesized that ACL injury risk factors would increase in both the with-target conditions and unanticipated conditions.

Methods

Fourteen healthy and recreationally active females (age: 21.2±2.7yrs; height: 1.74±0.06m, mass: 68.35±8.86kg), with a minimum of two years high school volleyball experience, completed four volleyball-specific block-and-cut testing conditions – with a target and an anticipated cut after landing (WTA), with a target and an unanticipated cut after landing (WTUA), no target and an anticipated cut after landing (NTA), and no target and an unanticipated cut after landing (NTUA).

3D marker coordinate data were collected using a 12-camera Vicon system (200Hz), and ground reaction forces were collected with two AMTI force plates (2000Hz). A suspended volleyball and volleyball net, set to regulation-standard height, were used in the WT conditions. 3D knee sagittal and frontal plane kinematics and internal moments, normalized to body mass, were calculated. 2×2 (target × anticipation) repeated-measures ANOVAs were perfomed to detect both main effects and interactions between target and anticipation conditions for initial contact (IC) and peak knee angles, and peak knee moments (α=.05).

Results and Discussion

Significant interactions were present for peak knee abduction angle (p=0.021) and peak knee adduction moment (p=0.025, Table 1). Participants demonstrated greater peak knee abduction angles in WTA compared to WTUA (p=0.004). Post hoc comparisons showed no differences for peak knee adduction moment. Significant target main effects were present for IC knee flexion angle (p=0.021), which were decreased in the with-target condition, and peak knee extension moment (p<0.001), which were greater in the with-target condition. Significant anticipation main effects were present for IC knee abduction angle (p = 0.001), which were greater in the anticipated condition, and peak knee flexion angle (p=0.021), which were greater in the unanticipated condition.

Creating a more realistic testing environment by including external targets and unanticipated movements altered knee landing mechanics and may allow for better evaluation of ACL injury risk factors in female volleyball players. Females landed in a more erect posture, as well as experienced greater sagittal plane knee loading when a target was present, giving a potentially better representation of the loads that are sustained during gameplay during a block-and-cut task.

Significance

Changing the testing environment so it better represents gameplay can improve the methods researchers use to find more conclusive evidence in the mechanisms of ACL injury in female volleyball players. While including a target during the block-and-cut movement did result in altered knee biomechanics, using an unanticipated secondary movement resulted in a larger number of biomechanical changes, suggesting that it may be more important to include decision-making tasks in the testing environment to better simulate gameplay.

References

1. Kay et al. (2017) *J Ath Train,* Vol **52**(2), 117-128.
2. Mehl et al. (2017) *Arch Orthop Trauma Surg*.
3. Zahradnik et al. (2017) *Eur J Sport Sci*, Vol **17**(2), 241-48.
4. Mok et al. (2017) *Scand J Med Sci Sports*, Vol **27**(2), 161-66.
5. McLean et al. (2004) *MSSE*, Vol **36**(6), 1008-1016.

Table 1. Mean ± SD knee kinematic and kinetic variables between target and anticipation conditions.

		Anticipated		Unanticipated	
		Target	**No Target**	**Target**	**No Target**
Initial Contact Angles	Knee Flexion (°) *	-12.0±5.5	-13.3±6.2	-10.2±4.1	-11.9±5.1
	Knee Abduction (°) ^	-3.2±3.0	-3.1±2.8	-1.9±3.4	-2.1±3.0
Peak Angles	Knee Flexion (°) ^	-64.5±8.2	-64.9±9.2	-66.1±9.4	-67.4±9.2
	Knee Abduction (°) ^†[a]	-11.0±4.5	-10.3±4.4	-8.7±4.2	-9.4±4.5
Peak Moments	Knee Extension (Nm·kg^{-1}) *	2.04±0.50	1.94±0.52	2.13±0.50	1.90±0.54
	Knee Adduction (Nm·kg^{-1}) †	0.39±0.23	0.38±0.23	0.35±0.20	0.41±0.21

*significant target main effect
^significant anticipation main effect
†: significant target×anticipation interaction (a= WTA is significantly different than WTUA)

Running to a fractal-like stimulus preserves the complexity of stride-to-stride fluctuations

Lauren Biscardi[1], Nelson Cortes[1], João Gomes[2], Joana F. Reis[3], Nicholas Stergiou[4] and João R. Vaz[3]
[1]George Mason University, Sports Medicine, Assessment, Research, and Testing (SMART) Lab
[2]Universidade Europeia, Lisbon
[3]Faculty of Human Kinetics, University of Lisbon
[4]Department of Biomechanics, University of Nebraska at Omaha
Email: ncortes@gmu.edu

Introduction

Pacing strategy during long distance running reflects complex, nonrandom behavior and long-range memory effects in both speed and stride length.[1] It has been reported that self-preferred racing (SPR) displays optimal variability compared to faster and slower running speeds, and imposes the least biological stress on the system.[2,3] Fluctuations in inter-stride-intervals (ISI) during SPR exhibit fractal-like properties and long-range correlations.[2] This suggests an intrinsic physiologic control scheme that purposefully integrates different regulatory systems. The use of periodic metronomes as a pacing strategy during running is common. The long-range correlations of human gait were altered when pacing to a periodic metronome, indicating breakdown of these internal regulatory control processes.[4] Thus, we aimed to investigate the effect of a fractal-like stimulus in running to preserve the natural healthy complexity of the system observed in SPR.

Methods

Thirteen male participants (22.80±3.65yrs, 1.74±0.07m, 67.85±8.96kg, VO_{2max} 49.90±5.45ml/kg/min) completed four 8-minute treadmill running trials (10.38±0.75km/h).

Testing was completed in 3 sessions conducted on separate days. In session 1, participants completed an incremental test to exhaustion to determine peak VO_2, maximal aerobic speed (MAS) and the first ventilatory threshold (VT1). These values were used to determine running intensity for the treadmill trials. In the experimental trials, participants ran in a heavy intensity domain (20 % Δ (VT1 + 0.20 x (MAS - VT1)).

Session 2 began with a SPR condition without a stimulus. The stride time from SPR was used to design individualized stimuli for 3 randomized cued conditions: periodic (PER), random (RND), and fractal (FRC). The stimulus was provided via a moving horizontal bar projected on a screen. Participants were instructed to synchronize their heel strike to the moving bar. The first of 3 randomized trials was completed 45 minutes after the SPR trial. In session 3, participants completed the remaining two randomized trials, separated by 45 minutes rest. Detrended fluctuation analysis (DFA) was used to validate the temporal structure of the FRC and RND stimuli.

An accelerometer (1000 Hz), placed at the ankle, was used to determine gait events. The first 15-seconds of each trial were discarded prior to analysis. A 4th order, zero lag low-pass Butterworth filter with a cutoff frequency of 20Hz was applied. ISI were calculated as the time difference between heel strikes. DFA was used to determine the fractal-scaling exponent from inter-stride intervals (ISIα). ISIα values >0.5 indicate a positively persistent long range correlation, while values <0.5 indicate anti-persistent correlations. A repeated measure ANOVA was used to determine the effects of condition on ISIα, $p<0.05$.

Results and Discussion

A significant main effect for condition was observed for ISIα ($F_{1.60,17.55}=16.04$, $p < 0.05$). Pairwise comparisons showed that ISIα was significantly higher in SPR (0.88±0.13) and FRC (0.85±0.14) conditions than both RND (0.65±0.15) and PER (0.54±0.19). No other significant differences were found ($p>0.05$).

Figure 1: Violin plots generated for data distribution of ISIα for each condition: RND, SPR, FRC, PER. It represents the boxplots with interquartile range, and the distribution of the data.

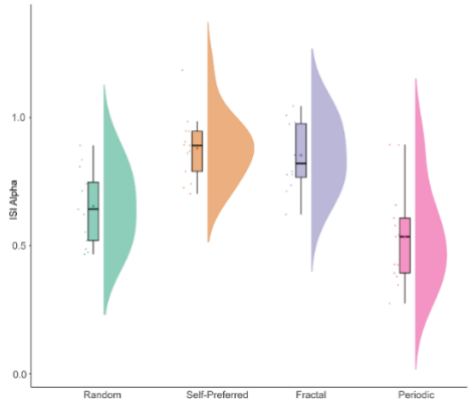

Significance

Pacing to a FRC metronome does not alter the natural system complexity observed in self-paced running, and preserves long-term correlations of the locomotor system during running. Conversely, we found a breakdown in gait complexity with PER and RND metronomes. A viable approach to preserve gait complexity is to alter the metronome temporal structure. The use of PER and RND conditions significantly decreased ISIα, compared to both SPR and FRC conditions. This suggests that the structure of the variability introduced into the temporal structure of the metronome is vital to preservation of long-range correlations in human running gait.

Our findings advocate that structured variability in a metronome pacing stimulus preserves the complexity and long-term correlations observed in SPR running for healthy adults. Thus, a FRC metronome stimulus may be more appropriate than PER metronomes to preserve the natural long-term correlations found in SPR strategy. However, it remains to be determined its impact on running performance (i.e., VO_2).

References

[1] Hoos et al. *Int J Sports Physiol Perform,* 2014;9(3):544-553.
[2] Jordan et al. *Hum Mov Sci,* 2007;26(1):87-102.
[3] Cavanagh et al. *Med Sci Sports Exerc,* 1982;14(1):30-35.
[4] Vaz et al. *Neurosci Lett*, 2019;704:28-35.

Muscle Contributions to Knee Joint Reaction Forces and Moments during Single-leg Landing

Namwoong Kim[1], Todd Leutzinger[1], Brian A. Knarr[1]

[1]Department of Biomechanics, University of Nebraska at Omaha, Omaha, NE, USA
Email: namwoongkim@unomaha.edu

Introduction

Approximately 80,000 to 250,000 ACL injuries occur per year in the United States [1]. Seventy to eighty percent of ACL injuries are caused by a non-contact mechanism such as cutting or landing. Knee joint loading such as tibiofemoral anterior shear force, valgus moments, and internal rotation moments has been associated with an increased risk of ACL injury. Muscles are one of the primary factors in determining knee joint loading during dynamic movements. Therefore, understanding the role of individual muscle contributions to knee joint loading is required. Ultimately, knowledge of individual muscle contributions to the knee joint loading may help to develop interventions that target specific muscles in order to prevent ACL injuries.

Musculoskeletal modeling provides a means to quantify individual muscle contributions to the knee joint loading that have been associated with ACL injuries during dynamic movements. Therefore, the purpose of this study was to identify the role of individual muscle contributions to shear joint reaction forces, valgus moments, and internal rotation moments during single-leg landing. We hypothesized that quadriceps musculature will contribute the most to anterior shear force during single-leg landing. We also hypothesized that hamstring musculature will contribute the most to varus moments and external rotation moments during single-leg landing.

Methods

Ten healthy adults participated in this study (5 females, age: 26.6 ± 1.35 years; height: 1.75 ± 0.7 m, mass: 71.1 ± 14.1 kg). Three-dimensional marker position data were collected at 200Hz using a 3D motion capture system while the participants performed single-leg landings from a height of 45 cm onto a force platform. Each participant performed single-leg landings with their dominant leg until they had 3 successful trials.

Ten subject-specific models were developed in OpenSim for data analysis [1,2]. Each model had a total of 31 degrees-of-freedom (DOF) and 92 musculotendon actuators. Muscle induced ground reaction force was calculated using Induced Acceleration Analysis in OpenSim. A total of 240 Joint Reaction Analysis was performed to calculate individual muscle contributions to knee joint loads by applying muscle force in isolation and corresponding muscle induced ground reaction forces [3]. Our analysis was focused on the weight acceptance phase of landing (from initial contact to peak vertical ground reaction force). Muscles that span the knee joint were analyzed in this study.

Results and Discussion

The lateral gastrocnemius contributed the most to tibiofemoral anterior shear force (961.95 N) during single-leg landing. The medial gastrocnemius provided the greatest contribution to knee varus moment (24.81 Nm). The medial hamstrings (semitendinosus and semimembranosus) also contributed significantly to knee varus moment (17.66 Nm). Although the biceps femoris long head contributed the most to external rotation moment (11.19 Nm), it also made the greatest contribution to knee valgus moment (29.87 Nm). Therefore, further investigation of the biceps femoris is necessary to determine if this muscle has potential to reduce the risk of ACL injury. The medial gastrocnemius and medial hamstrings have great potential to reduce the risk of ACL injury by providing varus moments during single-leg landing. Interventions targeting these muscles may be necessary to prevent ACL injuries because of their ability to resist valgus loading during single-leg landing. Future analysis is required to determine the muscle contributions of non-knee-spanning muscles during landing tasks as these muscle groups have been shown to play an important role in determining knee joint loading during dynamic movements [3].

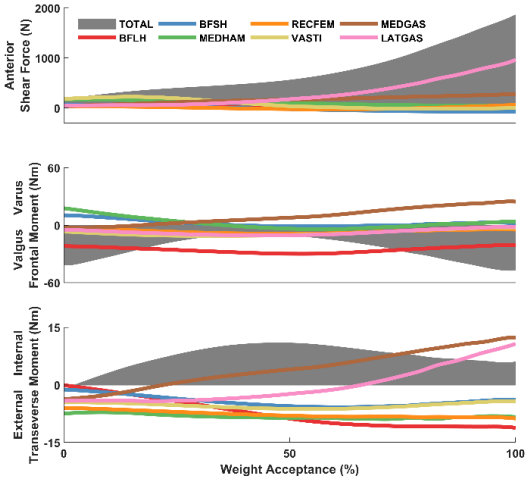

Figure 1: Individual muscle contributions of knee spanning muscles to knee joint loading during single-leg landing. The shaded gray area represents each total reaction load. BFLG: biceps femoris long head; BFSH: biceps femoris short head; MEDHAM: semitendinosus and semimembranosus; RECFEM: rectus femoris; VASTI: vastus medialis, laterals, and intermedius; MEDGAS: medial gastrocnemius; LATGAS: lateral gastrocnemius.

Significance

Knowledge of individual muscle contribution to knee joint loading may help to develop preventative exercises or rehabilitation strategies for ACL injury.

Acknowledgments

R15 HD094194

References

[1] Marks, PH, et al (2006). Am.J.Sports Med. 34:1512-1532

[2] Delp SL, et al. (2007). *IEEE Trans Biomed Eng,* **54**: 1940-1950

[3] Morgan KD, et al. (2014). *J Biomech,* **47:** 3295-3302

[4] Maniar N, et al. (2018). Sci. Rep, 8:1-10

Does Sex Influence Interpretations of Control Complexity via Muscle Synergy Analysis?

Anna T. Ursiny[1], Reed D. Gurchiek[1], and Ryan S. McGinnis[1]
[1]M-Sense Research Group, University of Vermont, Burlington, VT, USA
Email: anna.ursiny@uvm.edu

Introduction

Muscle synergy analysis during gait has been proposed for exploring the effects of neurological impairment on motor control [1,2]. For example, previous research has shown that a lesser number of muscle synergies is required to explain some threshold percentage of the variance accounted for (VAF) in measured muscle excitations for populations with neurological impairment (e.g., Parkinson's disease [1], cerebral palsy [2]) as compared to unimpaired populations. This observation is thought to indicate a less complex motor control strategy attributed to the neurological impairment. These conclusions assume that the observed differences are not confounded by other variables such as sex and age [3]. However, it has been shown that sex can influence observed gait mechanics in impaired populations [4,5] and that sex may impact motor control in activities other than gait [6]. These results provide a basis for questioning the assumption that sex does not influence conclusions concerning motor control complexity via muscle synergy analysis. An understanding of the potential influence of sex on muscle synergy analysis during gait is necessary for clinical interpretation, however, this has not been tested directly. Thus, in this study, we explore the effect of sex on muscle synergy analysis during gait and present preliminary results suggesting the effect of sex is not significant.

Methods

Surface electromyograms (sEMG, 1000 Hz) of 10 muscles (biceps femoris, lateral gastrocnemius, medial gastrocnemius, peroneus longus, rectus femoris, soleus, semitendinosus, tibialis anterior, vastus lateralis, vastus medialis) of the right leg were recorded for 16 unimpaired subjects (10 males: age = 22 $\pm$ 2 yo and 6 females: age = 21 $\pm$ 3 yo) during a one-minute level walking trial on a treadmill at a self selected speed. All sEMG data were high pass filtered at 30 Hz, rectified, low pass filtered at 6 Hz, and normalized by the maximum value across the walking trial and several muscle specific maximum voluntary contraction (MVC) trials. One to nine synergies were extracted from all subjects using non-negative matrix factorization to consider all possible synergy configurations. We compared synergy-based characteristics of motor control complexity between males and females according to statistical techniques that have been used to compare impaired and unimpaired populations [1,2]. To this end, the total VAF across all muscles for each number of synergies extracted was compared between males and females. The normality of the VAF distributions for each group and each number of synergies was confirmed using the Kolmogorov-Smirnov test. Average VAF between males and females was compared for each number of synergies extracted using independent t-tests as seen in [5,6]. Further, following the analysis presented in [1], we also compared muscle specific VAF for the four- and five-synergy configurations using 10 independent t-tests (one for each muscle). Finally, the number of synergies needed to exceed a 95% VAF threshold was compared between males and females using Fisher's Exact Test [1]. The level of significance was set to 0.05 for all statistical tests.

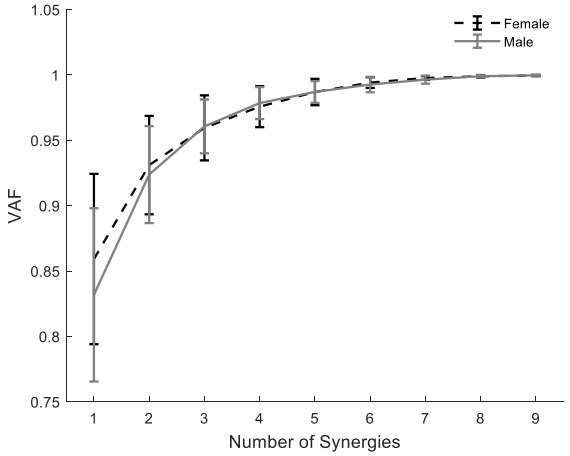

Figure 1: A graphical comparison of total VAF between males and females for each number of synergies extracted.

Results and Discussion

A similar trend for both males and females was observed in the total VAF with respect to the number of synergies extracted and the differences between sexes were not significant for each synergy configuration (Figure 1). The Fisher's Exact Test revealed no differences between males and females in the number of synergies required to exceed the 95% VAF threshold. In similar analyses, others have shown that impaired populations will exceed a given VAF threshold with significantly fewer synergies. This preliminary analysis suggests sex is not a confounding factor using this approach. Further, Rodriguez et al. (2013) found differences between impaired and unimpaired populations on the basis of muscle specific VAF (increased VAF for impaired relative to unimpaired for specific muscles) [1]. However, in this study, the same approach applied to compare males and females revealed no differences in VAF for any muscles for the four- or five-synergy configurations. Thus, this analysis suggests sex does not influence the interpretation of synergy analysis as it relates to motor control complexity.

Significance

Our preliminary analysis suggests that sex does not significantly influence interpretation of motor control complexity via muscle synergy analysis. From a clinical perspective, this is worthy of attention as it eliminates the need to consider sex when assessing a patient's motor impairment. Further work will consist of analyzing a larger sample size and exploring the effect of age on motor control complexity via synergy analysis.

References

[1] Rodriguez et al. (2013) *Clin Neurophysiol,* **124**(7)
[2] Steele et al. (2015) *Dev Med Child Neurol*, **57**(12)
[3] Kibushi et al. (2018) *Front Hum Neurosci*, **12**(4)
[4] Phinyomark et al. (2015) *Scand J Med Sci Sports*, **25**(6)
[5] Webster et al. (2012) *Br J Sports Med*, **46**
[6] Hubley-Kozey et al. (2012) *Hum Movement Sci*, **31**(4)
[7] Bianco et al. (2018) *J Biomech Eng,* **140**(1)

Effect of Transcutaneous Vagus Nerve Stimulation on Visuomotor Skill Learning in Humans

Mitchell St. Pierre[1] and Minoru Shinohara[1]
[1]School of Biological Sciences, Georgia Institute of Technology, Atlanta, Georgia, United States
Email: mstpierre@gatech.edu

Introduction

Loss of functional movement can occur with advanced age and with neuromotor disorders such as stroke and spinal cord injury. Rehabilitative training is commonly employed to help restore motor strength and ability in individuals with such deficits, and pairing neuromodulatory interventions with training may enhance the effects of rehabilitation. In rat stroke models, afferent vagus nerve stimulation (VNS) with implanted electrodes promoted motor recovery when VNS was applied during rehabilitation exercise [1]. While the underlying mechanisms for this efficacy are unknown, it is possible that stimulation of afferent vagus nerve connecting to the locus coeruleus affects neuromodulators in the cortex, and consequently neuromotor performance and adaptation. The applicability of the efficacy of VNS on motor recovery in rats to humans is unknown. Furthermore, implantation of VNS electrodes can be risky and costly, so the viability of transcutaneous VNS (tVNS) in humans must be explored. The purpose of this study was to examine the potential effects of pairing tVNS with motor training on motor skill improvement in healthy young humans. We hypothesized that motor skill improvement due to motor training is altered with tVNS that is paired with the execution of the training task.

Methods

Sixteen healthy young adults completed five days of experimentation. Subjects were assigned to either the tVNS group or Sham group pseudo-randomly to match for initial performance of the motor skill test. Weak electrical stimulation was administered at the tragus for tVNS or at the earlobe for Sham. Over the course of five days, subjects trained for 170 trials of the visuomotor skill task of tracking complex trajectories. The task consisted of accurately tracking complex target trajectories for 20 s with finger forces normalized to their maximum forces (Figure 1). Subjects were instructed to follow the target pattern as close as possible with the abduction forces of their index and little fingers simultaneously while electrical stimulation to the tragus or earlobe was applied concurrently with the task execution during training. Subjects were provided with knowledge of results after each trial, shown as a score based on the inverse of root-mean-square error (RMSE) from the target trace, averaged across fingers. The same visuomotor skill was tested each day without electrical stimulation before and after the training. To assess the progress of skill learning, preliminary analysis was performed on RMSE that was tested before each training. To examine the transfer of learned motor skill, subjects were additionally tested on tracking non-practiced square-wave trajectories on the first and last test days without electrical stimulation.

Results and Discussion

The initial test performance before the training period had comparable RMSE between groups for both complex and square-wave trajectories ($p > 0.05$ for both). RMSE in test trials were normalized to this initial performance to minimize variability between subjects for further analysis.

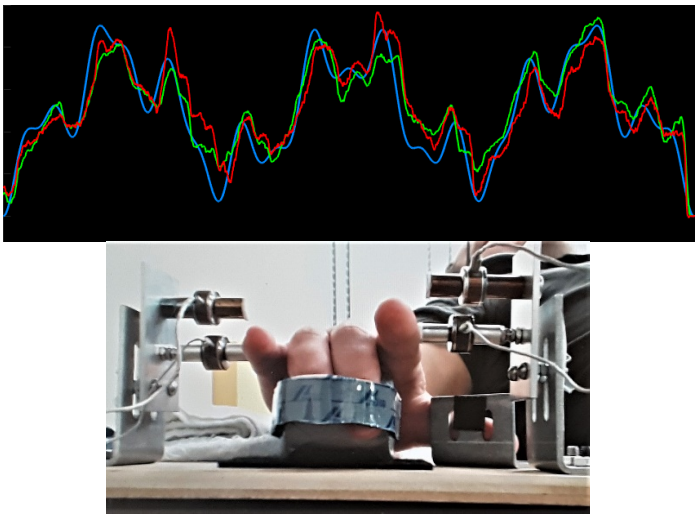

Figure 1: ***Upper,*** visual feedback during the task. Index finger force (green), little finger force (red), and the target trace (blue) were shown. ***Lower,*** subjects used abduction forces of index and little fingers to track the target trajectories

When this normalized test RMSE for the practiced complex trajectories was compared during the subsequent four test days, subjects in the tVNS group showed higher RMSE compared with the Sham group by ~20% across days, on average ($F = 11.78$, $p < 0.01$; main effect of group). This difference was prominent in the initial days but not the final test day. Both groups had significant reductions in RMSE of the practiced trajectories across days ($F = 22.56$, $p < 0.01$; main effect of day). After the training period, the average reduction in RMSE of the practiced trajectories was comparable across groups, i.e. ~56% compared with before training. Average reduction in RMSE of the non-practiced square-wave trajectories was also comparable across groups (~13%, $p > 0.05$). All these trends were observed in both finger forces.

Significance

The results indicate that application of tVNS during visuomotor skill training may delay the initial improvement of practiced skill while the final improvement is comparable to non-tVNS training in healthy young adults. The findings contrary to those of implanted VNS in stroke rats suggest the need to consider the specificity of VNS procedure, species, health/clinical status of subjects, and motor task in understanding and expecting the effect of VNS on motor rehabilitation outcome.

Acknowledgments

The study was funded by National Institutes of Health (1R03NS106088-01A1). The authors thank Steven Wolf and Andrew Butler for consultation on the experimental design.

References

[1] S. A. Hays, et al. (2014). *Stroke*, **45**: 3097

Human Reaction and Movement Enhancement via Audial, Tactile, and Visual Perceptual Cues

A. Bajpai[1], A. Mazumdar[1], and A. J. Young[1]
[1]Department of Mechancial Engienering, Georgia Institute of Technology
Email: abajpai31@gatech.edu

Introduction

The U.S. department of labor cites "equipment contact" as accounting for roughly half of nonfatal occupational injuries that involve days away from work [1]. Improving worker's situation awareness can help them avoid rapidly evolving threats such as moving machines or falling debris. Previous work has quantified how different individual (tactile, audio, and visual) and combined cue modalities affect failure rates and reaction times [2]. However, providing information about the object direction may not be the best approach to inform people of imminent threats. Providing guidance to a safe area, thereby skipping the cognitive evaluation needed for a safe response, would likely yield improved safety in complex environments. However, first we must determine what perceptual cue/cue combination should be used. In this research, experiments were conducted in a virtual reality environment that simulates objects rapidly moving toward the participant. We are interested in how different cues can incite different dodge rates and reaction times.

Methods

Eighteen able-bodied subjects (α = 0.05, Power = 0.8) participated in an experimental protocol, approved by the Georgia Tech Institutional Review Board (IRB H18363) [2]. After the participants give written, informed consent, participants were placed in the virtual environment and oriented with the space (3m x 3m area). Participants wore a custom tethered tactile belt (located on torso), HTC Vive headset and tracker (for COM estimation). After getting oriented to the VR space and an intial training period, the participant was instructed to dodge 27 threats over several conditions (three from each direction) (Fig. 1). The different conditions of this experiment included: 3D audio (A) originating from the object, tactile indicating a safe path (T), and a visual (V) arrow pointing in a safe direction, and combinations of these cues (AT, ATV, AV, TV). The order of the threat speed/direction/width are randomized across conditions, and held constant within subjects (order changes but not the set).

Three metrics used in this study include the hazard avoidance failure rate, reaction time, and movement time. The failure rate is determined per trial block as the percent of the time the participant was hit by a threat. The reaction time is measured by comparing the time the cue(s) were sent to the participant and the time the participant's speed (low-pass filtered at 15 Hz) exceeded twice their nominal speed. Escape time is the time it takes, after the reaction time, for the subject to leave the path of the threat.

Results and Discussion

Three one-way repeated measures ANOVAs with posthoc t tests and bon-ferroni corrections were conducted for the three metrics. Results indicate that there is no statistical difference among cues in terms of escape time but 3D audio yields statistically longer reaction time and higher failure rate ($p<0.01$). Finally, results indicate it is more difficult to escaping sagittal plane threats vs. frontal plane threats.

Conducting a t test of aggregated object information direction vs. escape direction, reveals no statistical difference. This indicates that people can dodge well in the presence of one threat and find safety without guidance. Future work will include incorperating path planning guidance for multiple objects as nonguided performance may decline in more complex situations.

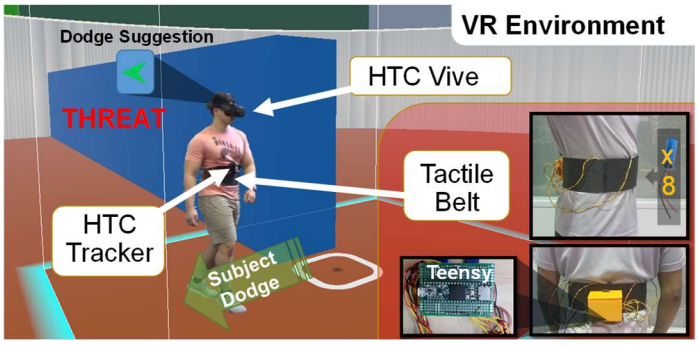

Figure 1: VR Environment. Subject is alerted to an incomming threat (represented by blue walls) from behind and dodges to maintain safety. Objects move at varying rates (8.5, 9.25, and 11 m/s) and come in varying sizes (0.1, 0.35, 0.5 m) from the four cardinal and four intercardinal directions.

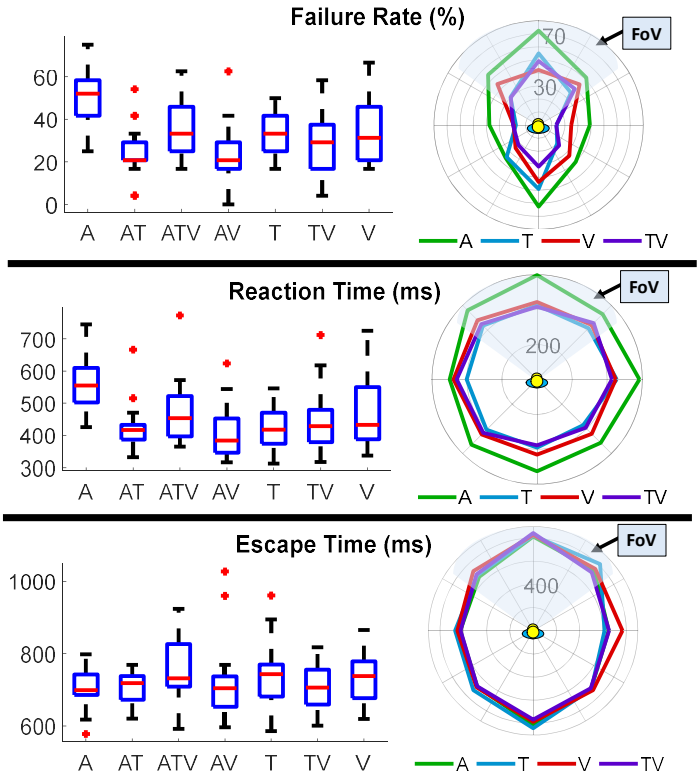

Figure 2: Box and whisker plots of all conditions with accompanying polar plots with selected conditions for (A) dodge failure rate, (B) reaction time, and (C) escape time. Plots omit cue combinations with tactile/visual object information.

Acknoledgements and References

This research is supported in part by the National Science Foundation (NRI) 1830498, (NRT) 1545287, and a NDSEG fellowship.

[1] Bureau of Labor Statistics, USDL-19-1909, Nov. 2019.
[2] Enhancing Physical Human Evasion of Moving Threats Using Tactile Cues. A. Bajpai et. al. Mar. 2020.

Should I stay or should I go? Stability of digit forces is lowered to enhance maneuverability when expecting to move a pinched object

Anvesh S. Naik[1] and Satyajit Ambike[1]
Department of Health and Kinesiology, Purdue University, West Lafayette, Indiana
Email: naik20@purdue.edu

Introduction

Stability of the motor system is the ability to maintain a desired motor state, and maneuverability is the ability to transition between motor states. Stability and maneuverability are antagonistic and animals often trade off stability of the current task to enhance maneuverability [1]. In prehension, maneuverability refers to transitions between different patterns of object manipulation, and it is essential for performing activities of daily living. Yet, the stability-maneuverability tradeoff is not studied in human prehension.

We studied whether the trade-off is evident in the vertical movement of an object held in a pinch grasp (using the thumb and the index finger; Fig. 1A). When an object is moved vertically, the digit forces normal to the digit-object interface increase to compensate for the inertial load due to the object's acceleration. However, these changes depend on movement direction: for upward movement, the digit forces increase before the object accelerates, whereas for downward movement, the digit forces increase after the object accelerates [2]. We leveraged this difference to explore the tradeoff. We computed the stability of the forces during the *foreperiod* of a choice reaction-time task (CRT), when the object is held steady, but the participant expects to move it either upward or downward in response to a visual cue. During the foreperiod, the participant expects to change the digit forces in a somewhat different way depending on the movement direction. We compared the stability during the foreperiod with that computed in tasks when the object is held steady without any expectation of movement (i.e., 'steady' task). We hypothesize that (1) compared to the steady task, the stability would be lower during the foreperiod of the CRT to facilitate the upcoming changes in the digit forces, and (2) greater decline in the stability will be associated with lower response times (RT) in the CRT – which serves as our measure of maneuverability in this study. This association will demonstrate the stability-maneuverability tradeoff in human prehension.

Methods

Healthy young adults (N=11, 4 female, 24.4±5 years) participated in the study. Participants held a vertically-oriented object with a pinch grasp in their dominant (right) hand and tracked a target provided on a computer screen by moving the object vertically. Digit forces were measured using force transducers (Nano-17, ATI), and movement kinematics were measured using a motion capture system (Vicon Vero). Visual feedback of the object's position was provided as a cursor on the screen (Fig. 1B, 1C).

In the steady task, participants were aware that the target will not move, and therefore, they did not expect any object movement in the future. They held the object stationary so that the cursor remained inside the target. The CRT began similar to the steady task, but participants expected the target to jump up or down at any moment. They were required to track the target as quickly as possible by moving the object. Both tasks were performed 15 times. We used the uncontrolled manifold (UCM) method to analyse the digit forces with the object was stationary in the steady trials, and when it was stationary during the foreperiod of the CRT trials. The analysis provides a stability index (ΔV_z), which quantifies the covariation in the digit forces that stabilize the value of an important output variable – the difference between thumb and index finger normal forces in this case. A low value of ΔV_z implies lower stability of the force difference, and vice-versa. RT in the CRT trials was calculated as the interval between the instant when the target jumped to the instant when the object velocity first crossed 5% of the peak velocity during the subsequent movement. A two-sample t-test was used to compare ΔV_z values between the steady task and CRT. A linear regression between $\Delta\Delta V_z$ (the difference between ΔV_z values of the steady task and CRT) and RT across participants was used to asses the stability-maneuverability tradeoff.

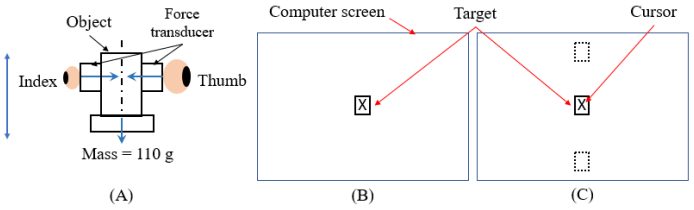

Figure 1: Instrumented object held in a pinch grasp (A), steady task: target does not move (B), choice reaction-time task target jumps at arbitrary time (C).

Results and Discussion

No significant difference was observed between ΔV_z values for the two tasks ($t_{(29)}$=0.1, p>.05). Six out of 11 participants reduced stability while others increased stability in the CRT. However, the regression between $\Delta\Delta V_z$ and RT was significant (p<.05, R^2=0.72; slope=61.4 ms). Participants who reduced stability for the CRT were more maneuverable (lower RT).

Significance

This is a first study demonstrating the stability-maneuverability trade-off in human prehension, and our results are consistent with this trade-off seen in postural control tasks [3]. Our results have implications for understanding the loss of manual dexterity with age, which has a serious negative impact on the quality of life of older adults. Aging leads to slower switching between manual tasks, which arises from system-wide neuromuscular and cognitive changes. This study is the basis for identifying a novel motor mechanism that may also underlie dexterity loss, and may lead to novel interventions for arresting the loss. Finally, individual differences in young participants suggest that our methods could be used for early identification of individuals at a higher risk of dexterity loss with aging.

References

[1] Hasan (2005), *J Mot Behav*, 37: 484-493.
[2] Flanagan and Tresilian (1994), *J Exp Psychol Hum Percept Perform*, 20: 944-957.
[3] Huang and Ahmed (2011), *PLoS One 6*(7): e21815.

Rabbit Hindlimb Ankle Kinematics During Stance Phase of Hopping Gait

Patrick T. Hall[1], Caleb Stubbs[1], Cheryl Greenacre[2], David E. Anderson[2], and Dustin L. Crouch[1]
University of Tennessee, Knoxille (UTK) – Tickle College of Engineering[1] and College of Veterinary Medicine[2]
Email: phall8@vols.utk.edu

Introduction

Animal models are essential tools for conducting musculoskeletal research and translating medical devices. Rabbits are commonly used for testing a wide variety of orthopaedic devices, procedures (e.g. immobilization), and injuries (e.g. tenotomy). For many such cases, the effect of the intervention on sensorimotor function is vital. As with other animals, locomotion is one of the most important tasks for motor function. Before investigating the effect of interventions on locomotor function, there is a need to quantify locomotion variables in healthy rabbits.

Rabbit hindlimb biomechanics during hopping gait was previously reported [1] but required surgical implantation of bone pin markers to track motion. Such invasive methods are able to track the bone motion more accurately but are relatively difficult to implement, may mechanically interfere with movement, or disrupt movement by causing discomfort. Additionally, the prevoius study did not report hindlimb kinematics, only ground reaction forces and joint moments. The goal of our study was to quantify hindlimb ankle kinematics and vertical ground reaction forces during the stance phase of hopping gait using a noninvasive motion tracking technique. We hypothesized that there would be no bilateral difference in kinematics and forces.

Methods

All research presented was approved by the UTK IACUC. Six musculoskeletally mature New Zealand White (NZW) rabbits (weight = 2.70 ± 0.33kgs) hopped through a clear acrylic tunnel when given negative reinforcement (prodding). While rabbits were in the tunnel, we synchronously recorded ground-foot pressures (VHR Walkway 4 pressure mat, Tekscan) and a 60 Hz video (1080P HD Webcam, SVPRO) of motion in the sagittal plane. Immediately prior to testing, we shaved both hindlimbs and marked the approximate joint centers of the metatarsophalangeal, ankle, and knee joints with black ink. Since our set-up permitted measurements from only one hindlimb at a time, we prompted the rabbits to hop across the track ten times in each direction. We extracted the vertical ground reaction force (vGRF) of the contact foot from the pressure recordings. Using morphology-based marker tracking in MATLAB (Mathworks, Natick, MA), we calculated the ankle angle and foot angle (i.e. the angle between the foot and ground) from the videos. We compared the magnitudes of angles and the vGRFs during stance phase between the left and right hindlimbs.

Results and Discussion

Both the foot and ankle angles were similar between hindlimbs (Fig. 1), showing no statistical differences through statistical parametric mapping (SPM) [2]. This indicates that rabbits exhibit symmetric ankle kinematics during locomotion. Future post-intervention testing should analyse both limbs to evaluate if changes in one limb also affect contralateral locomotor function.

Unlike humans, who transition from a negative foot angle during initial contact to a positive angle at toe off [3], rabbits maintain a positive foot angle throughout stance. The ankle dorsiflexed during the loading response phase as the vertical ground reaction force increased. Plantar flexion during terminal stance coincides with and likely contributes to forward propulsion.

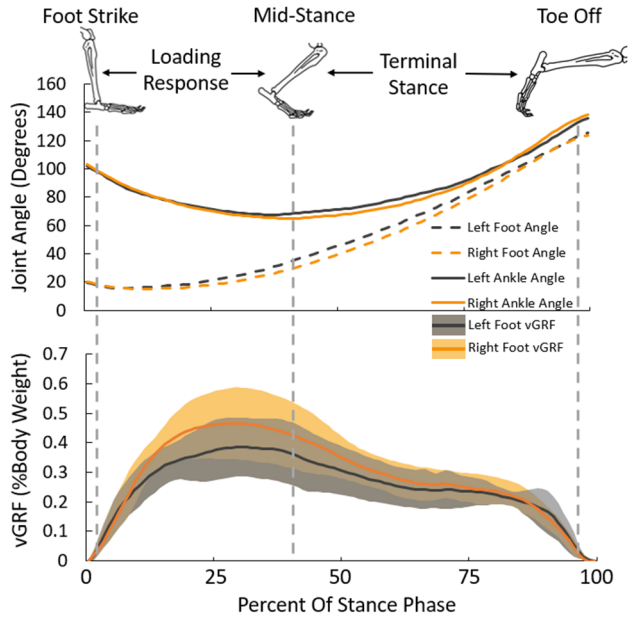

Figure 1: (Top) Sagittal plane joint angles during stance show the foot angle relative to the ground and the ankle angle. Joint angles were similar between limbs. (Bottom) vGRF during stance phase. The right hindlimb hadd qualitatively higher vGRFs. Joint angles and vGRFs are segmented into phases with mid-stance occurring at the lowest ankle angle.

The right hindlimb produced a qualitatively higher vGRF throughout stance. However, SPM revealed that significant bilateral differences occurred only at 48% of stance ($p = 0.047$). Previous studies observed similar vGRF magnitudes and bilateral differences [1], though the cause of bilateral differences is unclear. A limitation of the pressure mat was that we could only measure the vertical force component. Future testing should be conducted with force plates to quantify forces and moments along all six degrees of freedom.

Significance

In this study we quantified healthy rabbit hindlimb ankle kinematics during locomotion based on a noninvasive motion capture approach, the first of its kind reported in rabbits. The data adds to previous data [1] to more fully characterize healthy rabbit hindlimb biomechanics and serve as a baseline for quantifying function following interventions. Noninvasive motion capture is relatively straightforward to implement, which should encourage more researchers to quantify locomotor function in future studies.

Acknowledgments

We thank the Office of Laboratory Animal Care at UTK for providing veterinary care for the rabbits used in this study.

References

[1] D. Gushue, et al. *JOR.* 23: 735-742. [2] T.C. Pataky, *JoB*. 43: 1976-1982. [3] R. Grasso, et al. *JON.* 80:1868-1885.

Gestational Lumbopelvic Postural Changes and Joint Loads in Standing and Walking

Robert D. Catena, W. Connor Wolcott
Washington State University
Email: *robert.catena@wsu.edu

Introduction

Human females have evolved with lumbopelvic morphology that allows them to self-select a more curved spinal posture. These may (contradicting research exists) include such sexual dimorphisms as greater vertebral body wedging ratio[1], lower spinal levels of maximum curvature[2], and zygapophyseal orientations to resist shear forces[3]. These morphological differences were previously hypothesized to mechanically balance the body while carrying a growing abdominal ventral load (fetus during pregnancy) by allowing for gestational-related repositioning of the center of mass over the hip joints[3]. This *Balancing Hypothesis* indicates that lumbopelvic morphology evolved for gestational balance control in standing and walking, which has distinct implications on the evolution of hominin bipedalism. Also based on the *Balancing Hypothesis*, all pregnant women would choose a more curved spinal posture, which isn't the case from our lab observations. The purpose of this study was to determine biomechanical changes associated with self-selected gestational lumbopelvic postural change in both standing and walking. We hypothesized that women with more lumbopelvic curvature change (as compared to those with less change) would benefit most with reduced joint loading during gait.

Methods

Twenty participants were tested in four week intervals between 18 and 34 weeks of gestation. Lumbopelvic angle (LP), the sum of standing pelvis anterior(+) tilt and lumbar lordotic extension(+) angles, was measured at each testing and used as the main independent variable. Joint moments, dynamic balance, and mechanical energy during quiet standing and self-selected pace walking were measured as dependent variables. Dynamic balance and mechanical energy were calculated from center of mass motion, determined from individual center of mass anthropometry for each pregnant woman[4]. Multivariate ANOVAs and hierarchical regressions were employed to test relationships while controlling for confounding variables.

Results and Discussion

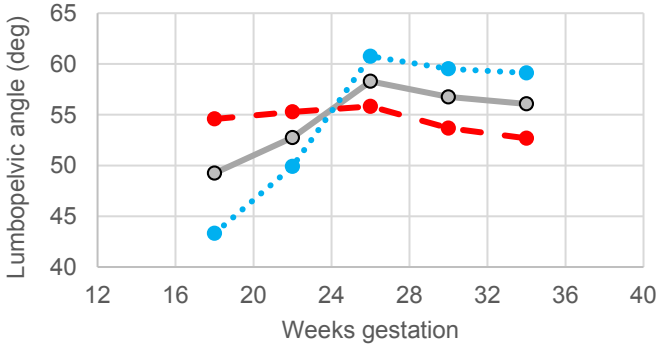

Figure 1: Average lumbopelvic angle (anterior pelvic tilt + lumbar extension) change through gestation. Grey solid line is the average of all participants. Dashed red line (=LP) is the average of the half of the group with the greatest LP beta value. Dotted blue line (ΔLP) is the average of the other half of the group, those with the lowest LP beta value.

On average, LP angle increased through gestation by 8°, but the amount of change is starkly different between pregnant women, with ±30° change through gestation ($p<0.001$) (Fig 1). The two groups (=LP and ΔLP) did not start with different BMIs, nor did they experience different weight gains through pregnancy or have different BMI change through pregnancy, but the ΔLP group was 6cm shorter than the =LP group ($p<0.001$).

There were little significant effects of LP on standing joint loads, standing balance or walking balance.

In walking, LP was positively correlated to walking speed and stride length. Additionally, LP was negatively correlated with torso center of mass motion in the sagittal plane. These indicate a possible positive effects of LP on energy conservation.

The effects of LP change were most apparent during walking in the stance hip (Fig 2), but also seen in the low back, swing hip and swing knee, with joint loads significantly (20-25%) lower in the ΔLP group, even while controlling for body height or normalizing by weight. Increasing LP angle resulted in reduced joint loads in the third trimester of pregnancy. Our results seem to indicate that spinal sexual dimorphisms likely evolved for kinetic aspects of walking rather than balance control.

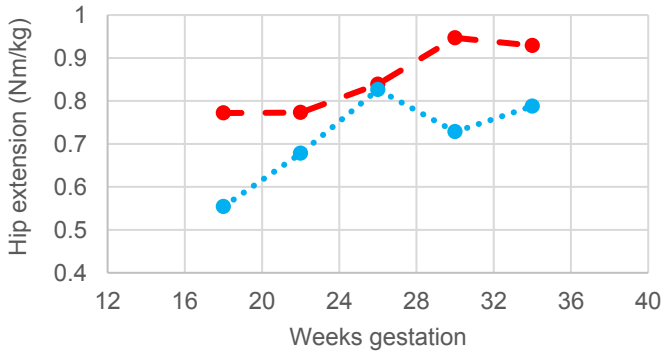

Figure 2: Average hip extension moment (as a percent of body mass at first testing) in loading response phase. Similar significant interaction in midstance phase. Dashed red line is =LP. Dotted blue line is ΔLP.

Significance

This research could have significant impacts on current obstetrics practices and ergonomic product development targeting low back pain during pregnancy. Natural spinal posture changes benefit other joints during walking. We will continue to explore the effects of LP change for groups that can't self-select LP change like pregnant women with pregravid back conditions that prohibit lumbar extension, or with lower extremity conditions that may prohibit anterior pelvic tilt. Our findings may also lead to better understanding of the evolution of hominin sexual dimorphisms, intermediate bipedalism, and dispersal of different hominins.

References

1. Bailey et al. *J Anatomy.* 2016.
2. Zlolinski et al. *Am J Physical Anthropology.* 2019.
3. Whitcome et al. *Nature.* 2007.
4. Catena et al. *J Biomechanics.* 2018.

The effect of active shortening velocity on the ratio of muscle stiffness to muscle force

Siwoo Jeong[1] and Kiisa C. Nishikawa[1,*]
[1]Department of Biological Sciences, Northern Arizona University, Flagstaff, AZ USA
Email: *kiisa.nishikawa@nau.edu

Introduction

It is widely accepted that the ratio of muscle stiffness to muscle force should be relatively constant during isometric contraction at a given muscle length and activation level [1], because both isometric force and stiffness are linearly related to the number of attached cross-bridge [2]. However, Julian and Morgan (1981) found that the stiffness to force ratio was altered during isometric force redevelopment after active shortening at the same muscle length and activation level [3]. Though their study shows the stiffness to force ratio can be altered by active shortening, it remains unknown whether shortening at different velocities affects the ratio. Furthermore, there is no generally accepted mechanism for the difference in the stiffness to force ratio between isometric contraction before vs. after active shortening.

To systematically investigate the effect of active shortening on the ratio of muscle stiffness to muscle force, we designed an experiment in which muscles first develop force isometrically, and are then shortened at different velocities, followed by a period of isometric force development at the same muscle length. If the stiffness to force ratio is determined only by the number of attached cross-bridges, then muscle stiffness should increase linearly with muscle force, with an intercept of zero stiffness at zero force, as observed during force development in a purely isometric contraction,

Methods

Maximal isometric force at 1.05 L_0 was established for whole soleus muscles isolated from wild-type mice (n = 7). The muscles were actively shortened to L_0 at three velocities ($1/8L_0$/s, $1/2L_0$/s and $2L_0$/s) and then held isometrically for four pause durations which allowed isometric force redevelopment (10, 20, 80 and 1000ms). Instantaneous muscle stiffness was measured at the end of the pause by a quick stretch ($0.9\%L_0$ stretch at a speed of $3L_0$/s). For comparison, the muscle stiffness was also measured during isometric contractions at L_0 without active shortening at similar durations after the onset of stimulation (10, 20, 80 and 1000ms).

ANCOVA was used to compare muscle stiffness and muscle force among different shortening velocities. Shortening velocity was the main effect, individual was a random effect nested within shortening velocity, and muscle force was the covariate.

Results and Discussion

During isometric contraction, the stiffness to force ratio was constant with an intercept of zero stiffness at zero velocity as expected (Fig. 1, Yellow). In contrast, significant differences were found for the slopes ($p < 0.01$) and y-intercepts ($p < 0.001$) of the relationship between muscle stiffness and force at different shortening velocities (Fig. 1). At the fastest shortening velocity (red), the slope was similar to that of the purely isometric contraction, but with a larger intercept. The slope decreased with slower shortening velocities. The different slopes and y-intercepts indicate that the ratio of muscle force to muscle stiffness during the isometric for redevelopment period depends on the velocity of active shortening for a same muscle length and activation level.

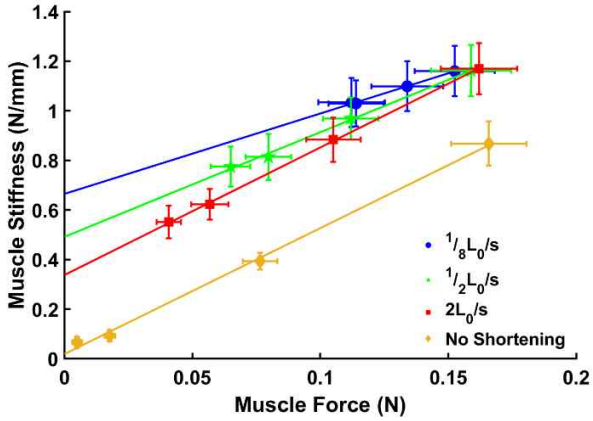

Figure 1. Force vs. Stiffness at different active shortening velocities (n=7). Data points shown are means across mice, with error bars representing SD.

'Stress-induced inhibition' has been invoked to explain the reduction in force that occurs after active shortening [4]. The hypothesized mechanism postulates that weakly bound cross-bridges form in the new overlap zone between myosin and actin filaments that is created during shortening. Although the weakly bound cross-bridges would not produce force, they would contribute to muscle stiffness [5]. Therefore, it contributes to the change in the stiffness to force ratio caused by active shortening.

Another possible explanation of our result is a change in titin stiffness. If muscle stiffness depends exclusively on cross-bridge stiffness and constant titin stiffness, then the ratio after active shortening should be constant at same muscle length. This is due to a muscle having the same titin-actin binding location and the same overlap between myosin and actin filaments at a given length regardless of shortening velocity. Our results cannot be explained solely by cross-bridge and constant titin stiffness. Therefore, it is possible that titin stiffness could be changed by active shortening.

Significance

This study shows that the velocity of active muscle shortening affects the stiffness to force ratio. The sliding filament theory cannot explain the results reported here, Constant titin stiffness in active muscle is also insufficient to explain the observed changes in the stiffness to force ratio of active muscle.

Acknowledgments: Supported by NAU TRIF.

References

[1] Colombini B et al. *Biophys J.* 2010;98(11):2582-2590.
[2] Ford J et al. *J Physiol.* 1979;73(4):453–67.
[3] Julian, F. J. & D. L. Morgan. *J Physiol.* 1981;319:193-203
[4] Mariéchal, G. & L. Plaghki. *J Gen Physiol.* 1979;73:453–67.
[5] Huxley, A. F. *Prog Biophys Chem.* 1957;7:255-31

Shape Characterization of Bighorn Sheep Horns for Bending and Impact Implications

Emma C. Gilmore[1], Luca H. Fuller[1], Aaron M. Drake, Trevor G. Aguirre[2], Aniket A. Ingrole[1], Seth W. Donahue[1], and Benjamin B. Wheatley[3]
[1] Department of Biomedical Engineering, University of Massachusetts Amherst, Amherst MA, USA
[2] Mechanical Engineering Department, Colorado State University, Fort Collins CO, USA
[3]Department of Mechanical Engineering, Bucknell University, Lewisburg PA, USA
Email: b.wheatley@bucknell.edu

Introduction

Male bighorn sheep (BHS) participate in seasonal ramming bouts that can last for several hours, yet they do not appear to suffer major brain injuries from these violent battles [1]. It has been suggested that motion of the horn or its distal portion during and directly following impact plays a significant role in reducing translational brain cavity accelerations, with up to a 50% increase in these accelerations when the distal portion is removed [2]. While the etiology of concussions is not fully understood, translational accelerations of the brain cavity have been correlated with concussion occurrence [3]. The current study aimed to quantify horn shape metrics and their variability from one animal to another to provide insights regarding the role of horn shape in mitigating brain cavity accelerations during impact [2]. We hypothesized that bighorn sheep horns exhibit a transition from having no directional bending preference near the base of the horn to a medial-lateral bending preference at the horn tip to facilitate side-to-side oscillations, which would reduce brain cavity translational accelerations by damping.

Methods

Seven male bighorn sheep skulls provided by The Colorado Division of Parks and Wildlife were scanned using x-ray computed tomography (CT). CT images were segmented with a custom MATLAB script, manually edited and verified as needed, and then converted into a surface geometry (.stl) with open source image processing software (Seg3D, sci.utah.edu). All horn shape characterizations were completed in SolidWorks. Three orthogonal horn views where used to trace an exterior horn shape and to define a horn centerline. The centerline provided a representation of the path of each horn's helicoidal shape from which evenly spaced cross sections were generated. For each cross section, a local coordinate system was defined with a point on the centerline as the origin, a local x-axis parallel to the medial-lateral direction, and a local y-axis perpendicular to the medial-lateral direction and in the plane of each cross section (Fig. 1). Second moment of area was calculated for cross sections about local coordinate systems.

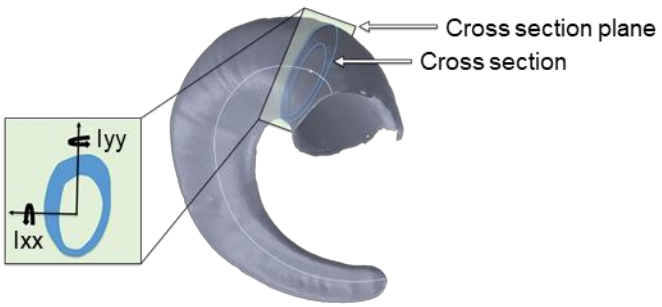

Figure 1: Horn cross section and cross section plane with respective x and y axes. A second moment of area ratio [Ixx / Iyy] greater than 1 indicates a medial-lateral bending preference (ie about y-axis) promoting oscillations of the horn tip.

Results and Discussion

Male BHS horns exhibit a medial-lateral bending preference throughout their length that increases toward the tip, reaching a maximum value at 90% of total length (Fig. 2). The medial-lateral bending preference measured in this study supports medial-lateral oscillations of the horn tip observed in a finite element model of the BHS skull and horns [2]. This model also suggested that removing the horn tip increased brain cavity accelerations during impact [2]. We propose that the gradual cross-sectional variations measured here act to mitigate brain cavity accelerations by inducing damped medial-lateral oscillations.

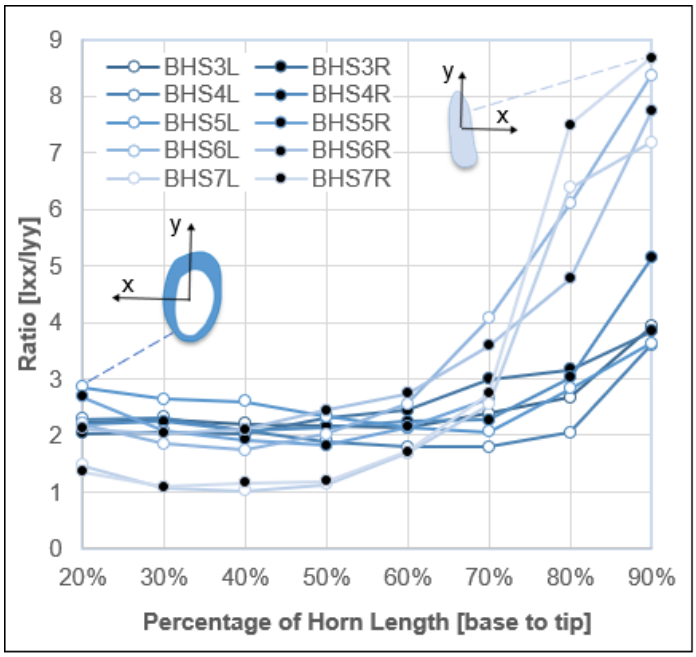

Figure 2: Ratio [Ixx/Iyy] of second moment of areas for all bighorn sheep cross sections. R/L = right/left horn.

Significance

To the best of our knowledge, we have measured bighorn sheep horn second moment of area as a function of horn length for the first time. Results from this study may be used to guide future modeling efforts to better understand the relationship between horn shape, energy dissipation, and reduction of brain cavity accelerations during impact.

Acknowledgments

Authors would like to acknowledge Sai Pranav Rallabhandi at Bucknell for efforts developing horn shape characterizations.

References

[1] Geist (1973). Mountain Sheep. *U Chicago Press*.
[2] Drake et al (2016). *Acta Biomateriala*. **44:**41-50.
[3] Meaney et al (2011). *Clinics in Sports Medicine*. **30**(1):19-31.

Perturbations to the classic force-length relationship of skeletal muscle

Brian Hamilton[1], Carmella Brown[1], Victoria Deyoung[1], Natalie C. Holt[2]
[1]Department of Biological Sciences, Northern Arizona University, 1899 S San Francisco St, Flagstaff, AZ 86011
[2]Department of Evolution, Ecology, and Organismal Biology, University of California, Riverside, Eucalyptus Dr #2710, Riverside, CA 92521
Email: bh558@nau.edu

Introduction

In skeletal muscle, the molecular motors actin and myosin interact to generate force for joint movement and locomotion. Many experiments refer to the classic force-length relationship to predict muscle behavior in a wide variety of conditions[1-3], which states that optimal force is produced at an intermediate muscle length, where overlap of actin and myosin is optimal and peak isometric force is produced. However, muscle performance is known to deviate from the classic muscle force-length relationship under physiologically relevant conditions, such as varying activation level[4,5] and changes in muscle length during contraction[6].

This study looks at the effect of imposing a length change to muscles during fixed-end contractions by adding an elastic element in-series to muscle. If the optimum length of a muscle changes as a result of adding series compliance and the subsequent shortening that the muscle undergoes, then this would suggest that muscle shortening against a compliant element induces an activation-dependent contractile history, which is not currently well understood.

Methods

Sartorius muscles were excised from R. catesbeiana, bathed in an isotonic Ringer's solution, and tied fixed-end to a force transducer either without a series elastic band (isometric "muscle only" condition), or with ("w/ tendon" condition, allowing muscles to shorten approximately 15% of their starting length before reaching isometry). Muscles were stimulated tetanically at various starting lengths and differences in optimum length (L0) and peak force (F0) between "muscle only" (iso) and "w/ tendon" conditions were found and plotted. Differences between tetanus and twitch stimulation will also be found in both conditions to quantify the amount of force-length shift that is due to the activation-dependent contractile history rather than a calcium-dependent shift.

Results and Discussion

Preliminary results suggest that adding an artificial tendon in-series with skeletal muscle causes a decrease in both optimum length (0.91L0iso ± 0.06, n=4) and peak force (0.62F0iso ± 0.08, n=4). The observed shift in optimum length and peak force support that the classic force-length relationship of skeletal muscle may not always be reliable when predicting muscle behavior *in vivo*, where elastic connective tissue interactions are common. When muscles actively shorten against an in-series compliant element, they are subjected to contractile history that causes a decrease in optimum length and peak force, and this activation-dependent contractile history is hypothesized to change the force and length properties of muscle at the sarcomere level. This sarcomere-level change is hypothesized to increase with additional compliance.

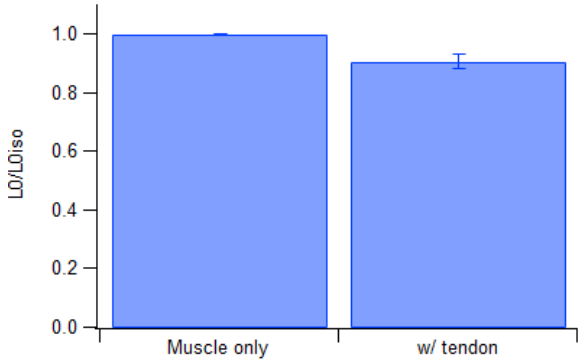

Figure 1. Adding compliance to the muscle setup causes an approximate 9% decrease in optimum length.

Significance

Many clinical and biomedical applications rely on the accuracy of theories in muscle physiology. Muscle modelling, robotic exoskeletons, and powered prosthetics are emerging as some of the most rapidly advancing technologies in biomedicine, but their advance is being slowed by outdated muscle theories. Research like ours brings attention to the need for updates to our understanding of muscle physiology so we can enhance treatment for disabled individuals and reach a better understanding of biological systems as a whole.

Acknowledgments

I would like to thank Dave Williams, Kiisa Nishikawa, and Tim Becker for insightful discussions. Funding was provided by NAU and UCR start-up funds.

References

[1]Delp et al (2007). *IEEE Trans. Biomed. Eng.* 54(11): 1940-50.
[2]Azizi & Roberts (2010). *Proc. Roy. Soc. B.* 277: 1523–1530.
[3]Rubenson et al (2012). *J. Exp. Biol.* 215: 3539-3551.
[4]Rack & Westbury (1969). *J. Physiol.* 204: 443-460.
[5]Holt & Azizi (2014). *Biol. Lett.* 10: 20140651.
[6] Rassier & Herzog (2004). *J. Appl. Physiol.* 96: 419-427.

Impact of surface grade on hindlimb muscle function in desert kangaroo rats (*Dipodomys deserti*)

Brooke A. Christensen[1], M. Janneke Schwaner[1], David C. Lin[2], and Craig P. McGowan[1, 3]
[1]Comparative Neuromuscular Biomechanics Lab, Department of Biological Sciences, University of Idaho, Moscow, ID, USA
[2]Voiland School of Chemical Engineering and Bioengineering, Washington State University, Pullman, WA, USA
[3]WWAMI Medical Education Program, Moscow, ID, USA
Email: chri4094@vandals.uidaho.edu

Introduction

For terrestrial organisms, the ability to navigate complex environments is critical to survival. As habitat conditions vary, animals must modify speed, angle, and direction of travel. These deviations are inherently linked to changes in mechanical demand, providing downstream insight into the functional plasticity of vertebrate muscle. As limb performance fluctuates, it remains unclear whether mechanical demands are satisfied via differential coordination across muscle groups, or if individual muscles vary in their mechanical roles. In the present study, we explore this idea through quantifying the contractile behavior of two hindlimb muscles from *D. deserti*, a bipedal rodent, when hopping on surface inclines of 0°, 10°, and 20°.

Methods

Data were collected as animals (n = 3) hopped at 1.6 m s^{-1} on a motorized treadmill. Electromyography (EMG) and sonomicrometry (SONO) were used to reveal patterns of muscle activation and fascicle strain in the lateral gastrocnemius (LG), a biarticular ankle extensor and knee flexor, and the vastus lateralis (VL), a knee extensor. Video data were recorded at 200 frames s^{-1} with a high-speed camera (Xcitex Inc, Woburn, MA, USA) and digitized using DeepLabCut [1]. EMG, SONO, and kinematic data were analyzed with a customized MATLAB script (2015a, MathWorks, Natick, MA, USA).

Results and Discussion

The LG exhibited similar strain and EMG activation patterns across grades, undergoing low-magnitude shorten-stretch-shorten cycles during stance (Figure 1). Alternatively, a stretch-shorten-stretch cycle was seen during stance in the VL. Unlike the LG, the VL expressed fascicle strain variation across grades, with an increase in both lengthening and shortening strain during incline hopping. As surface grade increased, VL strain fluctuations were accompanied by a decreased period of EMG activity, as well as a delayed onset time.

The strain patterns seen in the VL, particularly the increase in net lengthening, highlight its role in energy absorption as well as its capacity for functional modulation in response to a shifting environment. On the other hand, the statistically homogeneous behavior of the LG across experimental conditions suggests the muscle is not involved in balancing the increased work requirements of incline locomotion. Additional research involving a broader range of *D. deserti* hindlimb muscles, as well as assessments of regional variation within these muscles, will provide further insight into the undefined mechanisms accommodating mechanical demand variance during natural locomotion.

Significance

By determining *in-vivo* patterns of functional deviation across locomotor conditions, we can begin to outline the adaptability of vertebrate muscle in response to variable mechanical demands. Subsequently, a concrete definition of this environment-dictated plasticity will provide a foundation on which to advance navigation capability in legged robotic models.

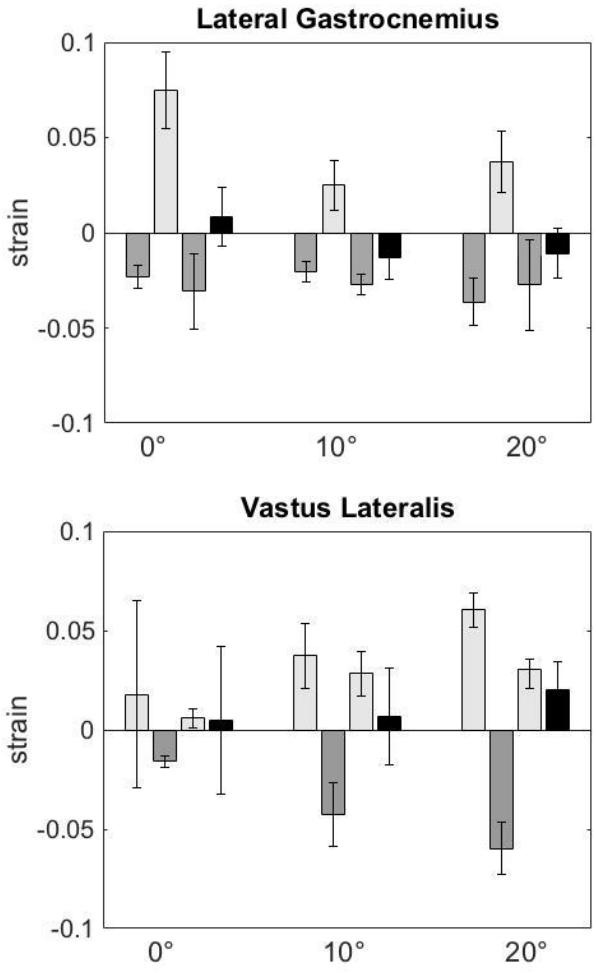

Figure 1. Mean (± s.e.m.) lengthening (light grey), shortening (dark grey), and net (black) strains recorded in the VL and LG during stance phase (n = 3).

Acknowledgements

This research was funded by NSF grant 1553550 (CPM) and ARO grant 66554-EG (CPM and DCL). All experimental protocols were approved by the University of Idaho Institutional Animal Care and Use Committee (IACUC).

References

1. A. Mathis, et al. (2018) Nature Neuroscience.

Dynamic changes in force modulate pennate muscle architecture

Jarrod C. Petersen and Thomas J. Roberts
Brown University, Providence, RI, USA
Email: jarrod_petersen@brown.edu

Introduction

Muscles change shape and experience an array of dynamic forces during a contraction. In pennate muscles, the oblique orientation of the muscle fibers is important in determining the force and speed output of the muscle. Recent studies have shown the important functional implications of this oblique orientation and changes in muscle thickness with a phenomenon known as muscle gearing [1, 2]. Muscle gearing describes the observation that a pennate muscle belly can achieve higher velocities than the fibers, and that this phenomenon is variable depending on the load [1].

While several studies highlight the importance of load for muscle shape change and gearing during a contraction, few show the effect of variable force. Here we use an *in-vitro* isolated muscle prep in conjunction with high speed videography and marker tracking to demonstrate the effects of variable force on pennation angle and muscle thickness. We show that dynamic changes in force result in corresponding changes in pennation angle and muscle thickness and these changes may act on elastic elements located within the muscle belly [3] (Fig. 1). Our results suggest that dynamic force modulates muscle shape change and pennate muscles are capable of storing and releasing internal elastic strain energy.

Methods

The flexor digitorum superficialis brevis (~20mm x 10mm) was isolated from the legs of bullfrogs (*Rana catesbeiana*) and black polyethylene microspheres (350µm) were placed at the ends of fibers and the muscle belly (Fig. 1A). The muscle was submerged in oxygenated ringers solution, fixed to a rigid mount, and attached via stainless steel chain to a muscle servomotor within a clear rectangular housing. The muscle was filmed with one camera at 250 fps, and points were later tracked from this video in XMAlab.

Results and Discussion

During a frog jump, as the muscles in the leg contract, the mechanical advantage at the knee joint improves, providing a latch mechanism with which stored elastic energy is released quickly [4]. We used a control signal to drop the regulated force of the muscle servomotor to mimic this latch, an exaggerated one of which, an instantaneous drop, is shown in Fig. 1. When force declined from 80% to 10% of peak isometric force, there was a concurrent and notable increase in pennation angle and thickness (Fig. 1). An increase in pennation angle is expected with fiber shortening, however, the large increase in pennation angle following the force drop was ~6X the magnitude of pennation angle change for an equivalent amount of fiber shortening prior to the force drop. Based on these observations, the large changes in pennation angle and thickness seem to correspond with the drop in force more so than fiber shortening.

A control signal inducing a more gradual decline in force, much like what typically occurs *in* vivo, also showed what we observe in the instantaneous drop. We suggest these data provide evidence that muscle thickness is modulated by force in pennate muscles. Additionally, we interpret the sharp rise in pennation angle and thickness to mean that elastic energy is being released from within the muscle belly itself, due to the rapid expansion of a transverse spring (T; Fig. 1A) which was initially compressed during force rise [3].

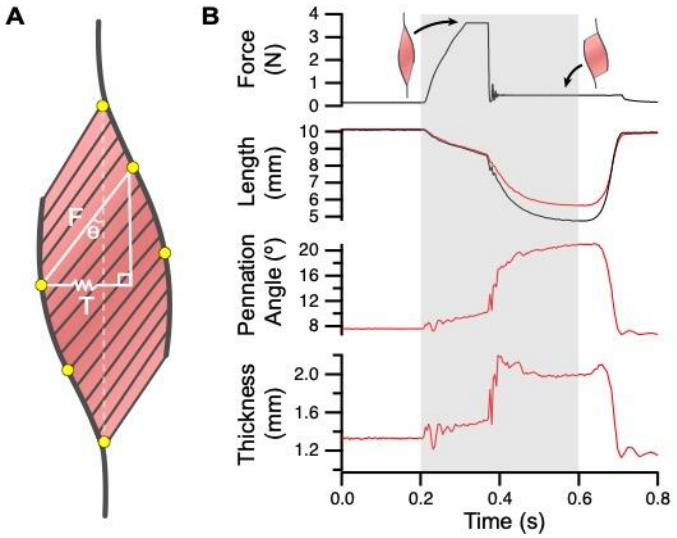

Figure 1: **(A)** Our model of internal elastic energy storage (white) superimposed on an illustration of a unipennate muscle with markers (yellow) used to calculate fiber length (F), muscle thickness (T), and pennation angle (Θ) relative to muscle line of action (dashed line). **(B)** Experimental data shows immediate increases with pennation angle and thickness, indicators of muscle belly shape change, of the muscle fiber (red), and whole muscle (black) in response to a drop in force. Two insets on the force trace show approximate muscle shape before and after the drop in force, the duration of stimulation is highlighted (gray).

Significance

The present results provide evidence that force is a determinant of pennation angle and thickness change in muscle. We find that sudden changes in muscle belly shape occur during force decline, and may allow for internal elastic energy storage and recovery in muscle. These internal elastic elements may augment muscle performance in similar ways to in-series elastic elements, and may do so through changes in muscle shape during variable force.

Acknowledgments

We are grateful to Richard Marsh and Mary Kate O'Donnell for helpful comments and assistance. This work was supported by NIH Grant (AR055295) and NSF Grant (1832795).

References

1. Azizi, E. et al. (2008). *Proc Natl Acad Sci USA* 105, 1745-50.
2. Barinerd, E. & Azizi, E. (2005). *J Exp Biol* 208, 3249-3261.
3. Eng, C. et al (2008). *Int Comp Biol* 58, 2, 207-218.
4. Astley, H. & Roberts, T. (2014). *J Exp Biol* 217, 4372-4378.

Landing on Compliant Surfaces: Lessons from an animal model of landing control

Alex Duman[1] and Emanuel Azizi[1]
[1]Department of Ecology & Evolutionary Biology at the University of California, Irvine
Email: aduman@uci.edu

Introduction

Locomoting in the real world requires us to interact with different surfaces that vary in height, compliance, and damping. This introduces complexity that challenges both humans and animals to modulate their motor behaviour to move effectively [1,2]. Landing and decelerating also pose a greater risk of injury to the musculoskeletal system than takeoff since muscles undergo lengthening contractions while functioning as brakes. Therefore, surface properties may dramatically alter deceleration strategy.

We are interested in exploring how organisms coordinate decelerations when landing on surfaces that differ in stiffness and damping. Toads offer a unique model to study coordinated landing as they can jump several times their own body length, producing relatively large impact forces and energy, while still landing effectively across a wide range of environmental conditions. Here we report on our findings of how joint work, key muscle activity and many other kinematic and kinetic variables change with surface stiffness and damping.

Methods

We used the cane toad, *Rhinella marina*, as a model for probing coordinated decelerations. With high-speed videography, force plate ergometry and electromyography we collected and analyzed joint work across the forelimb using inverse dynamics and patterns of forelimb muscle activity in preparation for and during landing. Toads jumped from a rigid platform 1.5 times their body length onto a platform that recorded impact force and could be locked in place or attached to springs to test how toads responded to landing on a surfaces with varying compliance (0, 2.5, 5 or 10 mm BW^{-1}). To include damping we altered the inertia of the platfrom by changing the mass from 123g to 725g.

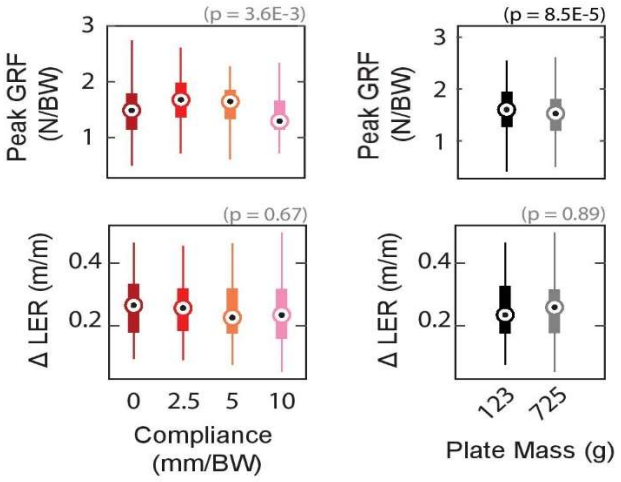

Figure 1: Peak ground reaction forces and change in limb extension ratio (LER) across surface compliance and inertial masses. We observed little change in kinetics and kinematics across surface compliance and damping. Center points indicate the median; box shows upper and lower quartile; and lines indicate min and max values. Statistical results from ANOVA are provided for each variable on the top right of each plot, and significant values are darkened.

Results and Discussion

Our findings suggest compliance and surface damping minimally affect landing in cane toads (Fig. 1). We did observe significantly reduced impact forces and joint work on compliant surfaces. There was also a trend across compliance treatments of more proximal forelimb joints like the shoulder and elbow (as opposed to distal joints like the wrist) doing a greater proportion of work to slow the animal upon impact.

We also observed substantial variation in forelimb extension prior to impact, which lead to certain individuals crashing into the platfrom with their torso, or effectively coordinating a landing with their forelimbs. The crashing and coordinated landing behaviors are not only distinct in forelimb kinematics, but differ in impact force and energetics of the forelimb muscles as well. These results are highly suggestive of varying tolerances for crashing behavior and imply that there are two distinct strategies for dealing with impacts.

Our electromyographic results further support these assertions. We found that platform compliance had little impact on forelimb muscle activity, yet the amount of activity in key muscles was correlated with the use of a crashing strategy. This suggests cane toads have a robust control strategy for landing across a wide range of surface stiffnesses that is likely not influenced by proprioceptive feedback from the forelimbs.

It appears cane toads don't alter landing behavior due to varying surface stiffness and damping, unlike humans [3]. However, cane toads may be an insightful model for understanding mechanisms that coordinate robust movement in complex environments without relying on contact limb proprioceptive feedback.

Significance

Cane toads do not seem to change their motor behaviour in response to changes in the mechanical properties of landing surfaces. While these findings suggest cane toads may not be the best model for exploring neuromuscular control of landing behaviour in humans, they do provide a system to probe control paradigms that may allow robotic devices to locomote effectively over varying terrain conditions with simple commands and without the need for real-time sensory integration.

Acknowledgments

We would like to ankowledge the Army Research Office for financial support.

References

1. Daley MA & Biewener AA. 2006. *PNAS.*
2. Ferris DP, Liang K & Farley CT. 1999. *J Biomech.*
3. McNitt-Grey JL, Yokoi T & Millward C. 1994. *J Appl Biomech.*

EXPLORING HOW FUNCTIONAL IMPROVEMENT IS RELATED TO INTERACTION BETWEEN CHILDREN WITH CEREBRAL PALSY AND HORSES DURING EQUINE-ASSISTED THERAPY: A PILOT STUDY

Yonghee Lee[1], Priscilla Lightsey[2], Nancy O'Meara Krenek[2], and Pilwon Hur[1]
[1]Department of Mechanical Engineering, Texas A&M University, College Station, TX, USA
[2]ROCK (Ride On Center for Kids), Austin, TX, USA
Email: {yongheelee87[1],pilwonhur[1]} @tamu.edu, {priscilla[2], Nancy[2]} @rockride.org

Introduction

The prevalence of cerebral palsy (CP) is 3.3 per 1,000 births in the United States and is the most common cause of motor disability in children [1]. One treatment strategy that may benefit persons with CP is Equine-Assisted Therapy (EAT) utilizing equine movement controlled by the therapist [2]. A few researchers provided kinematic evidence-based effects of EAT, but no one has studied the effects of EAT on kinetics. Thus, we hypothesize the following: 1) the functional mobility of children with CP would improve as the number of EAT sessions increased, 2) there exists the kinetics-related interaction between the rider and the horse during EAT sessions.

Methods

Four children with CP aged 3 - 12 years participated. Eight 20-minute sessions of EAT treatments were conducted, with data collection on sessions 1, 4, and 8. Functional mobility was measured using the Timed Up and Go (TUG) test for 3 subjects and 10-Meter walk (10MW) test for 1 subject, all performed before and after EAT on data collection days. Kinetic measurements were done with acceleration representing force normalized by mass. The acceleration data of the children and horses during EAT sessions were measured using 6 Inertial Measurement Units (IMU). The trends of acceleration data were determined using frequency domain and time domain analyses. For frequency domain analysis, Fast Fourier Transform (FFT) was performed to display a repetitive pattern of each signal and dominant frequencies. Besides, the differences between the frequency spectrum of the horse's back and subject were calculated to study the correlation in the frequency domain. For time-domain analysis, correlation by a time shift between the horse's back and the subject's movement was studied and the time delay between their movements was characterized.

Results and Discussion

Functional Mobility

As the number of sessions increases, TUG or 10MW significantly improved over the course of the study (Figure1). From those results, it might be said that there would be positive changes in the functional mobility of children with CP as the therapy progressed.

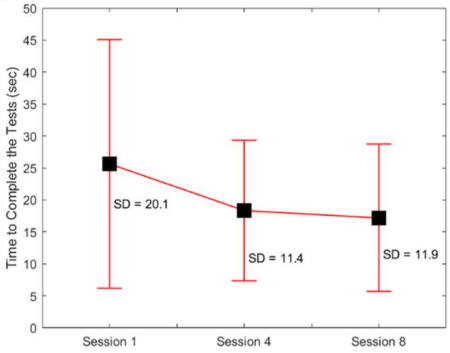

Figure 1: The outcomes of functional mobility tests with error bars. Black points indicate the means of the test results. SD stands for standard deviation. [3].

Kinetic-Related Interaction

The mean values and variation in the difference between the frequency spectrums dropped significantly as EAT sessions progressed (Figure 2), suggesting that the dominant frequencies of the movement of children with CP synchronized with those of horses. The results of correlation by a time shift also showed that there was an increase in the correlation between the horse's back and the subject as therapy progressed.

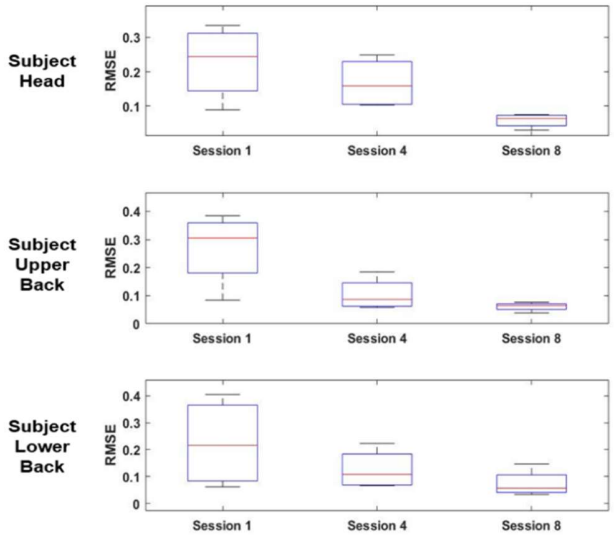

Figure 2: The boxplot of difference between frequency spectrums of the horse's back and subject each session [3].

With continued EAT sessions, participants appeared to become more familiar with the horse's movement pattern. Participants seemed to learn automatic postural responses since the subject's movement tended to synchronize with the horse's movement as EAT progressed. Therefore, this study showed that positive kinetic interaction between the movements of children with CP and a horse might occur during EAT.

Significance

This study showed : 1) that children with CP were able to produce synchronize their movement with the horse's movement and 2) the existence of kinetic interactions between the child and the horse. EAT has the potential to be a valuable treatment intervention that maximizes the functional mobility of children with CP potentially due to the progressive synchronous interaction between the rider and the horse. This study is expected to lay the foundation for a better understanding of the interaction between children with CP and horses.

References

[1] Kirby et al., *Research in Development Disabilities* **32**: 462-469, 2011
[2] MacPhail et al., *Pediatric Physical Therapy*, **10**: 143-147, 1998
[3] Yonghee Lee, MS Thesis, Texas A&M University, 2019

Limb joint mechanics during quadrupedal walking in alligators

Adrien A. Arias.[1], Alexander J. Duman[1], Emanuel Azizi[1]
[1]Dept. of Ecology & Evolutionary Biology, University of California, Irvine
Email: adriena@uci.edu

Introduction

Most limb-level analyses of quadrupedal walking have focused on a small subset of animal models that are cursorial (with limbs adapted for running) and exert negligible mediolateral forces during stance phase of walking [1-3]. These studies have been instrumental in understanding the mechanics of limbed locomotion on land, but have largely ignored the more complex walking strategies used by non-cursorial animals. Previous work in alligators show they exert large laterally-directed forces [4] and have complex limb joint kinematics outside of the parasagittal plane during walking [5,6]. Therefore, the assumptions used by standard 2D inverse dynamics models (e.g. mediolateral forces are negligible, kinematics are parasagittal) are not true in alligators or other non-cursorial walkers. Here we use a quaternion-based inverse dynamics model [7] to estimate the mechanical work done by hindlimb and forelimb joints during steady-state walking in alligators. We expect hindlimb joints will perform net positive work during stance phase of walking and forelimb joints will perform net negative work, similar to other quadrupedal animals studied so far. Results from inverse dynamics and previously published anatomical data [8] will be used to identify representative hind- and forelimb muscles to examine *in situ*, in an attempt to link non-parasagittal body mechanics to the mechanical properties of limb muscles.

Methods

Five juvenile American alligators (523.1 ± 87.9 g) were trained to walk across a custom-built trackway instrumented with two high-speed video cameras (200 frames s^{-1}) and a small circular force plate (16cm^2) flush-mounted with the ground. This allowed analysis of isolated limb strikes of either the hindlimb and forelimb on a given trial. Only trials where alligators walked at a constant speed were analyzed (0.14 ± 0.06 m s^{-1}). Kinematic and kinetic data were synchronized with an external trigger and imported into MATLAB (R2019b). A custom inverse dynamics script calculated instantaneous joint power and work from 3D kinematic and kinetic data using quaternion algebra and inverse dynamics.

Results and Discussion

When normalized to mass of the functional group at each joint [8], we find that peak joint moments were greatest in the ankle joint of the hindlimb and elbow joint of the forelimb. All forelimb and hindlimb joints experienced negative and positive power, but every limb joint analysed performed positive net work during stance phase (Figure 1). Based on patterns observed in other quadrupedal animals walking, we originally hypothesized that forelimb joints would perform more negative work than hindlimb joints. Our results do not support this hypothesis, likely because the non-parasagittal forces and kinematics dominate limb joint function in alligators. We find the greatest muscle mass-specific power and work in the elbow and ankle joints, which are both associated with bipennate, biarticular, limb muscles, therefore it is possible that proximal energy transfer from larger muscles may be an important feature of non-cursorial limbed locomotion .

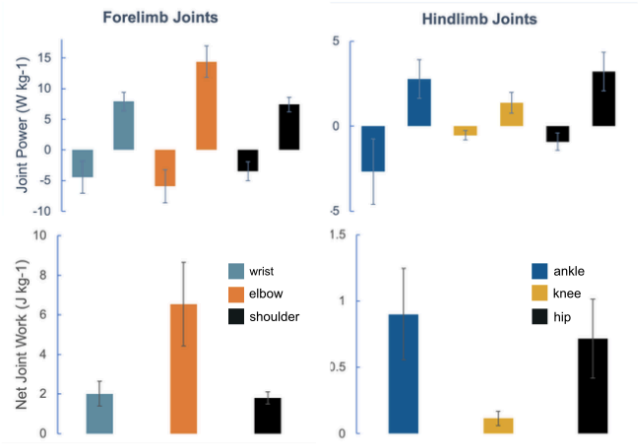

Figure 1: Average peak joint powers (top row) and average net joint work (bottom row) during stance phase of walking in alligators-- normalized to mass of the functional group at each joint. Bars represent means ± sem.

Significance

Detailed analyses of locomotion in a diversity of animals is necessary to understand the evolution of complex integrative movements like walking and can help us identify which components of quadrupedal walking (e.g. joint mechanics, muscle mechanics) are significant to whole-body mechanics. Alligators serve as a model organism for studying walking in non-cursorial animals because they exert large mediolateral forces and have non-parasagittal kinematics. Additionally we benefit from past research on alligator whole-body mechanics (i.e. center-of-mass dynamics in vertical and horizontal directions), musculoskeletal anatomy, and electromyographical activity during walking. This allows us to test joint-level— and eventually muscle-level— hypotheses about functional and mechanical features of locomotion in non-cursorial quadrupeds.

Acknowledgments

The authors like to VM Galicia-Madrid, KM Arreguin, and T Movsesyan for help with data collection.

References

[1] Cavagna, GA, et al. (1977). *Am J of Phys, 233*(5), R243-261.
[2] Clayton, HM, et al. (2000). *Eq Veterinary J*, 32(4), 295-300.
[3] Cronin, NJ et al. (2013). *J of Biomech*, *46*(7), 1383-1386.
[4] Willey, JS et al. (2004). *J of Exp Bio, 207*(3), 553-563.
[5] Baier, DB & Gatesy, SM (2013). *J of Anatomy, 223*(5), 62-9
[6] Reilly, SM, et al. (2005). *J of Exp Bio*, *208*(6), 993-1009.
[7] Dumas, R et al. (2004). *Com Met in Biomech & Biomed Engin*, *7*(3), 159-166.
[8] Allen, V, et al. (2010). *J of Anatomy, 216*(4), 423-445.

DeepLabCut Increases Markerless Tracking Efficiency in Bi-Planar X-Ray Video Analysis of Rat Kinematics

Nathan J. Kirkpatrick.[1], Megha Tippur[2], Robert J. Butera[1,2], and Young-Hui Chang[1,3]
[1]Coulter Department of Biomedical Engineering, Georgia Institute of Technology & Emory University, Atlanta, GA, USA
[2]School of Electrical and Computer Engineering, Georgia Institute of Technology, Atlanta, GA, USA
[3] School of Biological Sciences, Georgia Institute of Technology, Atlanta, GA, USA
Email: NK@gatech.edu

Introduction

Although researchers rely on the measurement of rat locomotion to better understand injury rehabilitation, diseases and more (1-3), existing workflows present a bottleneck that reduces study sample sizes, increases costs, and slows down the scientific process. Rodents present unique challenges with regards to kinematics measurements; their loose hindlimb skin makes optically tracking skin-mounted markers inaccurate (4), and their bones are too small to track surgically implanted markers via x-ray video (5). Currently, researchers interested in whole limb kinematics of rats have two options, both of which rely upon the collection of biplanar x-ray videos: manually track skeletal landmarks (4), or align μCT-derived 3D bone models for each bone of interest (rotoscoping, 6). Both of these options are tremendously time consuming and require sophisticated software and expertise to implement.

We aimed to increase the efficiency of rodent kinematic analysis by combining tools created for x-ray video analysis with DeepLabCut, a deep learning-based tool for markerless body part tracking designed for use with traditional optical video (7).

Methods

Biplanar, high speed x-ray video (41-44kV, 80mA, 5ms, 100 fps) was taken of one Lewis rat with right sciatic nerve injury performing treadmill locomotion (17 cm/s) in accordance with a protocol approved by Georgia Institute of Technology's IACUC. A total of 17 strides from two collection sessions were captured and analysed. 3D calibration and undistortion reference images were captured during each session as well (5).

Training data was generated in XMALab (5) by identifying 19 skeletal landmarks (Fig 1B) in 319 pairs of x-ray video frames. Frames were randomly chosen for labelling to ensure a broad representation of the entire gait cycle. Data fidelity was maintained by minimizing the reprojection error between the paired points. Undistorted trial video frames and corresponding 2D pixel coordinates were exported from XMALab. ImageJ was used to losslessly convert these undistorted frames into video files to accommodate DeepLabCut's input requirements.

Model training was performed on the undistorted x-ray videos in Google Colab with DeepLabCut until performance plateaued. A single model was trained on both x-ray cameras.

Outlier machine-labelled points were identified using a combination of DeepLabCut's reported likelihood score, the jump distance to a given 3D point from its predecessor, and the reprojection error between the two cameras' points. Outliers were manually refined in XMALab. 3D points were low-pass filtered at 7 Hz, after which they can be exported and used for a variety of kinematic analyses (Fig 1C).

Results and Discussion

After training for over 600,000 iterations on 95% of the labelled data, DeepLabCut reported a training error of 2.3 pixels, and a test error of 4.2 pixels.

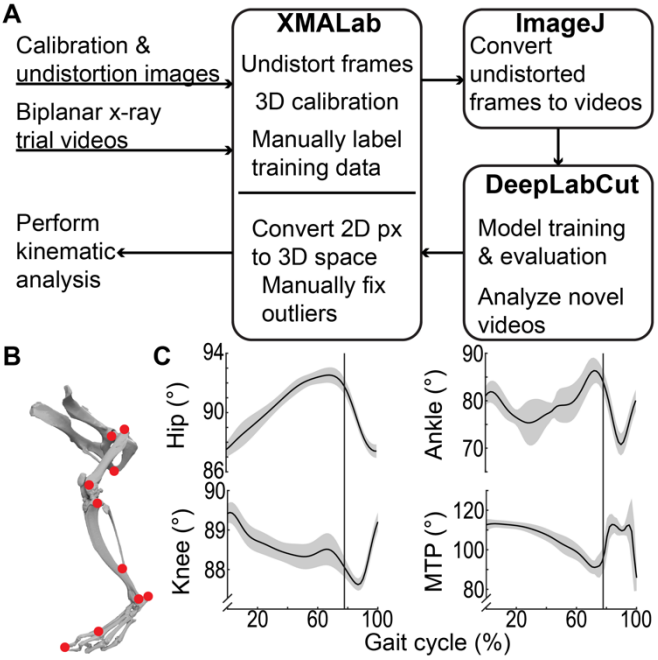

Figure 1: **A**, flowchart of pipeline for biplanar x-ray videos. **B**, diagram of tracked skeletal landmarks. All landmarks are tracked on both hindlimbs except for pubic symphysis. **C**, Pooled data (N=17 gait cycles) of left limb sagittal plane joint angles derived from DeepLabCut and filtered at 7 Hz. SD error bars.

Previous studies measuring rat locomotion analysed kinematics at 3 time points during the gait cycle due to time and resource constraints (3). With our combination of DeepLabCut and XMALab, 600 frames of new video can be analysed by DeepLabCut in ~2 minutes, and outliers can be refined in XMALab in roughly 30 minutes. However, performance is only as good as the training data, so generate it with care.

Significance

Reducing the analytical burden for rodent kinematic analysis can reduce costs, increase sample sizes and expand the possibility for new research collaborations to answer new questions.

Acknowledgments

We would like to thank the Comparative Neuromechanics Laboratory for their help and support.

References

1. J. M. Bauman, Y. H. Chang, *Biol Lett*. **9**, 1-5 (2013).
2. K. D. Allen, et al., *Arthritis Research & Therapy*. **14**, 1-14 (2012).
3. L. C. Tsai, et al., *Osteoarthritis & Cartilage.* **27**, 1851-1859 (2019).
4. J. M. Bauman, Y. H. Chang, *J Neurosci Methods.* **186(1),** 1-19 (2010).
5. B. J. Knörlein, et al., *J Exp Biol.* **219**, 3701-3711 (2016).
6. S. M. Gatesy, et al., *J Exp Zool.* **313**, 244-261 (2010).
7. A. Mathis, et al., *Nat Neuro*. **21**, 1281-1289 (2018).

How do Leg Joint Stiffness Affect Dynamics of Backward Falling: A Simulation Work

Mu Qiao[1,*] and Feng Yang[2]
[1]Department of Kinesiology, Louisiana Tech University, Ruston, LA 71272
[2]Department of Kinesiology and Health, Georgia State University, Atlanta GA, 30303
Email: *mqiao@latech.edu

Introduction

Falls are a serious concern among older adults. Most of the falls experienced by older adults are backward falls, which are more dangerous than other types of falls (such as forward falls and sideways falls) because the visual input cannot be used to plan quick and adequate protective reaction. Little is known about the dynamics of backward falling, such as the falling duration, the impact severity, and how the falling dynamics are affected or controlled by the lower limb joints, in particular, the stiffness. We investigated the influence of the rotational stiffness of individual leg joints on the dynamics of a backward falling after the loss of consciousness in terms of the falling duration and impact velocity.

Methods

We assumed the backward falling occurs in the sagittal plane, and the movements are symmetric between left and right body sides. The same torsional spring with the same time series of angles and moments was applied to each pair of bilateral lower limb joints. We locked joints in the upper body by increasing the stiffness in its joint to a relatively large number to simplify the simulation work. We then constrained the moments at each leg joint (*i.e.*, hip, knee, and ankle) in the sagittal plane to be equal to moment generated by the torsional springs. For each joint, the stiffness of the torsional spring changed between 0 and 8.73 Nm·deg^{-1} (*i.e.*, [0, 500] Nm·rad^{-1}). When the joint's angle was beyond the normal range of motion, the stiffness of the torsional spring increased by 10 times pulling the joint back to its normal range.

Results and Discussion

Both the falling duration and the impact speed are affected by the stiffness of lower limb joints, especially the hip and knee (Fig. 1). The falling duration, head impact speed, and hip impact speed ranged between 0.27 and 0.63 s, 2.6 and 7.9 m·s^{-1}, and 0.35 and 3.4 m·s^{-1} when the stiffness of leg joints changed within their limits. Additionally, hip stiffness is the most influential one affecting both variables (i.e., the falling duration and impact speeds). Knee stiffness also affected both variables when < 4 Nm·deg^{-1}. Ankle stiffness showed little influence on the falling dynamics.

Significance

The influence of the joint stiffness on the falling dynamics (falling duration and impact speeds) is comparable between hip and knee. Whereas, ankle stiffness showed little influence on the falling dynamics. Because the hip and knee are the primary joints controlling the falling dynamics, training on proximal joints may be considered to reduce falling risks. Our findings could also inform the design of protective devices to prevent impact-induced injuries after a fall in individuals with high risk of falls.

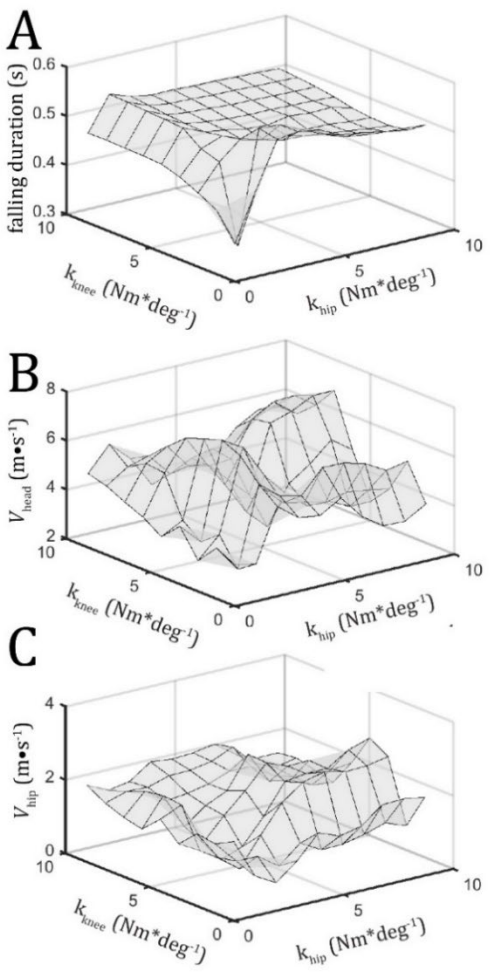

Figure 1: The effect of the stiffness of knee and hip on (A) falling duration, (B) the head speed, and (C) the hip speed at impact.

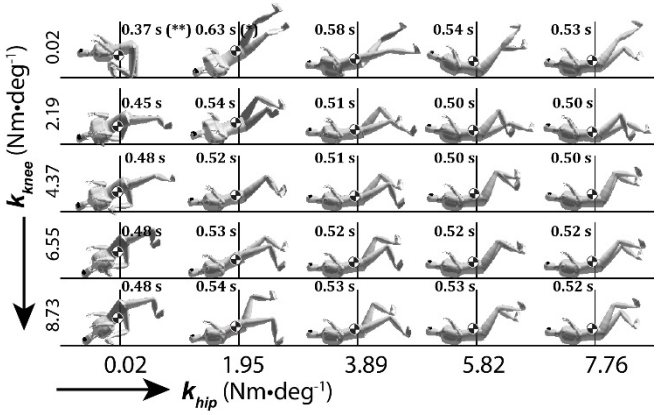

Figure 2: Body postures at impact at selected stiffness of ankle (k_{ankle}), knee (k_{knee}), and hip (k_{hip}).

Evaluation of an app for vestibular rehabilitation of older adults with motion controlled games and remote monitoring

Paulien Roos[1], Michael Rossi[1], Austin Mituniewicz[1], Katherine Marschner[1], Nathan Pickle[1], Timothy Zehnbauer[1], and Susan Whitney[2]
[1]CFD Research Corporation, Huntsville AL.
[2]Department of Physical Therapy, University of Pittsburgh, Pittsburgh PA.
Email: paulien.roos@cfdrc.com

Introduction

About half of people aged over 60 experience vestibular dysfunction [1]. Vestibular rehabilitation has been proven effective in reducing dizziness and falls [2]. However, adherence remains a major problem and can be below 50% [3]. Clinicians typically rely on self-reporting to assess adherence and do not know if exercises were performed correctly at-home. Therefore, this research aimed to develop an app with gaming elements and remote monitoring to improve adherence of older adults to vestibular rehabilitation.

Methods

A mobile (smartphone or tablet) app containing games for the vestibular ocular reflex (VORx1) exercise was developed using Felgo (FELGO GmbH). The app allows exercise prescription and assesses dizziness and balance (Dizziness Handicap Inventory (DHI) [4], Activities based Balance Confidence scale (ABC) [5]; Figure 1). Games are controlled by an Inertial Measurement Unit (IMU; SensorTag, Texas Instruments) placed on the head using an elastic band. Sensor orientation (roll, pitch, yaw) was computed using the Madgwick algorithm [6]. Assessment measures are calculated using IMU data and sent to a cloud-based database for further analysis. Six females aged over 65 undergoing vestibular rehabilitation used the app after providing written informed consent (IRB approval by University of Pittsburgh). Head range of motion and velocity during VORx1 were recorded while participants performed the exercises with and without the app. Participants then answered a questionnaire to evaluate ease of use, enjoyment, motivation, use intention, and usefulness of the app.

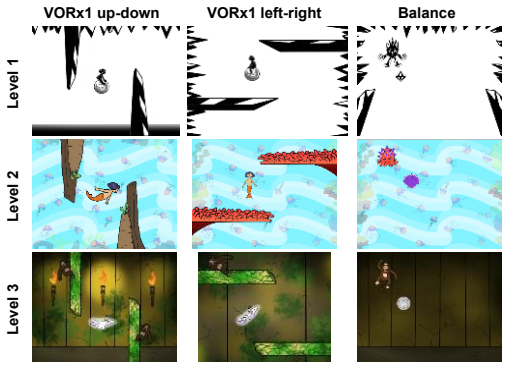

Figure 1: Three different levels of exercise for VORx1 in the pitch and yaw direction plus for a balance exercise. The various levels of visual stimuli are tailored to vestibular dysfunction severity.

Results and Discussion

DHI scores ranged between 24 and 72 (mean: 46, SD: 18.5). Questionnaire responses (Figure 2) showed half the participants felt the app was useful and would motivate them to do their exercises. They reported they enjoyed the app and would use it again. The more negative responses came from the same three individuals, whose DHI scores (mean 44) did not differ from the overall group. Anecdotal feedback from these individuals suggested the negative responses were due to frustration playing the games and not knowing what to expect. This will be addressed in the future by adding a slower speed practice game. Sensor data demonstrated participants performed exercises with similar head range of motion and velocity with and without the app (Table 1).

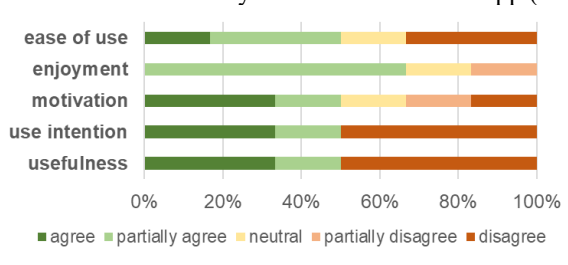

Figure 2: Overview of evaluation of the vestibular app by six older adults undergoing vestibular rehabilitation.

Table 3: Comparison of sensor data of the six older adults performing exercises with the app and traditionally (mean ± standard deviation).

	Angle (°)		Velocity (°/s)	
	App	Traditional	App	Traditional
Flexion	19±5	22±6	106±42	91±41
Extension	26±9	25±6	94±44	97±44
Left	23±6	25±1	85±31	98±45
Right	24±7	32±5	102±16	98±47

Significance

This study demonstrated that patients performed their vestibular rehabilitation similarly with an app and traditional care. Evaluation highlighted areas for improvement and showed that elderly female participants enjoyed having their rehabilitation delivered in the form of a gaming app. Although some gaming approaches have been used successfully with older adults, this is the first study to demonstrate feasibility of this approach for those with vestibular problems and rehabilitation specific games.

Acknowledgments

Research reported in this publication was supported by the NIDCD (NIH Award R43DC017408). The content is solely the responsibility of the authors and does not necessarily represent the official views of the NIH. We also thank our clinical collaborator, Dr. Karen Skop from the James A Haley VA hospital in Tampa FL.

References

[1] Agrawal et al., *Arch. Intern. Med.*, 169(10), p. 938, 2009.
[2] Whitney, et al., *Curr. Treat. Options Neurol.*, 18(3), p. 13, 2016.
[3] Yardley *et al.*, *BMJ*, 344, p. e2237, 2012.
[4] Jacobson and Newman, *Arch. Otolaryngol. Head. Neck Surg.*, 116(4), pp. 424–7, 1990.
[5] Powell and Myers, *J. Gerontol. A. Biol. Sci. Med. Sci.*, 50A(1), pp. M28-34, 1995.
[6] Madgwick, "An efficient orientation filter for inertial and inertial / magnetic sensor arrays.", 2010.

Analysis of Coherence between Electromyographic (EMG) signals of Tibialis Anterior, Soleus and Gastrocnemius during Standing Balance Tasks: A Pilot Study

Anuj Ojha[1], Gordon Alderink[2], John Farris[1], Samhita Rhodes[1]
[1]School of Engineering, Grand Valley State University, Grand Rapids, MI, USA
[2]Department of Physical Therapy, Grand Valley State University, Grand Rapids, MI, USA
Email: ojhaa@mail.gvsu.edu

Introduction

Balancing a large mass over a small Base of Support (BOS) is a major challenge for humans in bipedal stance. It is important that the Center of Mass (COM) remain within the BOS in order to maintain the balance. [1] Postural stability testing provides a valuable tool for objectively evaluating the motor domain of neurologic functioning. [2] Analysis of coherence between EMG signals provides a means of examining the characteristics of common neural inputs to co-contracting muscles during voluntary contraction. EMG-EMG coherence helps to determine the oscillatory input to the muscle. [3]

The primary objective of this project was to analyze the coherence between the pairs of EMG signals from the lower leg in different frequency bands to examine the common neural input characteristics to the muscles during tandem stance balance test.

Methods

Six healthy individuals (3 males; age: 24.1±3.5 yrs; Ht.: 167.4±5.5 cm; Wt.: 71.1±5.5 Kg) participated. Approval was obtained from the Grand Valley State University Human Research Review Committee (IRB#18-246-H). Employing a full body Plug-in-Gait model, 16 Vicon MX cameras (120 Hz) and Nexus motion capture software were used to track anatomical marker trajectories. Ground reaction forces were collected at 1200 Hz, using floor embedded AMTI force platforms. The EMG signals from the lower legs; Anterior Tibialis (AT), Medial Gastrocnemius (MG) and Soleus (SOL) were collected at 1200 Hz using Motion Lab System.

Data were collected with participants standing with arms crossed on two force plates under four different conditions – feet together eyes open (FTEO), feet together eyes closed (FTEC), tandem eyes open (TanEO) and tandem eyes closed (TanEC). The tandem standing position was done with the dominant foot (right foot dominant if right-footed) placed on a rear force plate and the non-dominant foot placed on the fore force plate with knees extended and maintaining equal distribution of weight on each force plate. Data were collected for 30 seconds and five trials were collected under each condition.

The raw EMG signals were used for further analysis to examine the intermuscular coherence between pairs of muscles in different neural frequency bands i.e. gamma (30–100 Hz), beta (13-30 Hz), alpha (8-13 Hz), theta (4-8 Hz) and delta (1-4 Hz) using wavelets and magnitude squared coherence. A time-frequency coherence analysis was performed between different muscle pairs.

Results and Discussion

Strong coherence was found at all frequency bands between the MG and SOL muscle on the right leg, particularly in the delta band (Figure 1). The coherence between the muscle pairs from the same leg were significantly greater during the eyes closed and least stable postures. Previous research also demonstrated stronger coherence between the lower leg muscles within the same leg at the lower frequencies. [4] Dispersion (i.e., standard deviation) of mean muscular coherence was increased in the lower frequency bands and during more complex stability postures. Maximum dispersion for all muscle pairs was observed in the tandem, eyes closed condition. The time frequency analysis also showed greater coherence for muscle pairs RMG and RS in the right leg for the tandem stance posture (Figure 2).

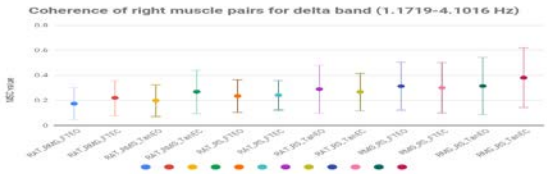

Figure 1: Mean coherence of the right muscle pairs with standard deviation for delta frequency band

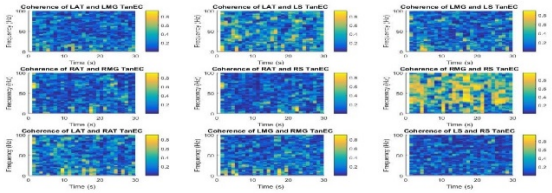

Figure 2: Time-Frequency coherence spectrogram of different muscle pairs for TanEC

Significance

The result of this study might help to provide a benchmark to compare the neural function of athletes who have suffered from concussive damage to our normal, healthy control subjects.

Acknowledgements

Grand Valley State University and all the participants for the study.

References

1. Winter, D. (1995). Gait & Posture, 3(4), pp.193-214.
2. Erratum. (2010). Clinical Journal of Sport Medicine, 20(4), p.332.
3. Grosse, P. (2002). Clinical Neurophysiology, 113(10), pp. 1523-1531.
4. Boonstra, T. (2015). Scientific Reports, 5(1), 17830.

Human-human hand interactions assist walking balance by acting more like a "brake" than a "motor"

Mengnan Wu[1], Luke Drnach, Sistania M. Bong, Yun Seong Song, and Lena H. Ting[1]
[1]The Wallace H. Coulter Department of Biomedical Engineering, Emory University and Georgia Institute of Technology
Email: *mengnan.wu@emory.edu

Introduction

A human can improve another person's balance during walking through haptic interaction by holding hands, but it is unknown *how* these interactions affect balance. The current study characterized the effects of hand contact with a partner during a balance-challenging walking task and examined how hand forces were used to assist balance.

We hypothesized that mechanical power transfer at the hands is used to assist balance during partnered beam-walking, characterized by braking or propulsion. Previous work showed that hand interaction forces were small during a partner-dance task and likely used only for communication[1], but the task did not challenge balance and thus did not require significant physical assistance.

We further hypothesized that the forces at the hand can be directly related to the beam-walker's balance performance through a linear mass-spring-damper model. If so, kinematics and kinetics of the interaction point at the hands could be used to predict task performance of the individual.

Methods

We measured whole-body kinematics and hand forces in 12 pairs of healthy young adults. During the main experimental condition, one person walked on a narrow (2 cm wide) balance beam with a partner walking by their side overground (Fig. 1a). Each partner held one end of a custom handle that measured interaction forces.

We compared balance performance of the person walking on the beam during the partnered condition vs. when they walked on the beam solo. We quantified performance by the beam-walker's lateral sway, distance completed on the beam, and mean forward walking speed.

We compared force and mechanical power at the interaction point (Fig. 1a) during partnered beam-walking vs. during partnered overground walking to examine energy exchange for balance assistance.

Finally, we fit the interaction force to the beam-walker's clavicle displacement, velocity, and acceleration as a mass-spring-damper system (Fig. 1a) in the mediolateral direction during the partnered beam-walking condition.

Results and Discussion

Our results show that all balance performance metrics improved during partnered beam-walking vs. solo beam-walking ($p<0.05$). Lateral sway decreased by 4.2cm and mean forward walking speed increased by 0.24m/s. The mean distance completed during solo beam-walking was 1.8m while every person completed the entire beam length (3.7m) during every partnered beam-walking trial.

Magnitudes of mediolateral interaction forces and power were small during partnered beam-walking: ~2N and ~0.1W, respectively. They were, however, 1.2N and 0.073W larger, respectively, than during partnered overground walking ($p<0.05$). Mean force magnitudes during partnered beam-walking were also higher than the 1N threshold for light touch[2] ($p<0.05$). These results suggest that interactions at the hand provide mechanical support for balance assistance.

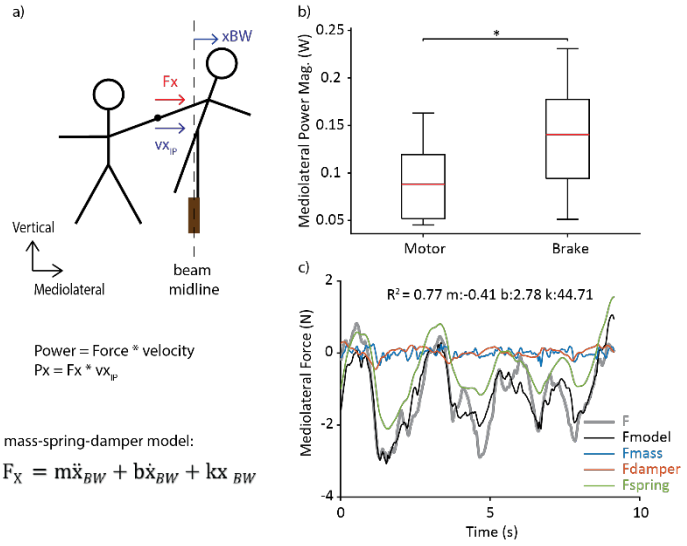

Figure 1: a) Partner (left) and beam-walker (right) during partnered beam-walking condition. Lateral hand interaction force (Fx) and power exchange is calculated at the interaction point (IP). A mass-spring-damper model relates interaction force to beam-walker's lateral displacement (x_{BW}), velocity, and acceleration relative to the beam midline. b) Negative ("braking") power is greater in magnitude than positive ("motor") power for partnered beam-walking across all pairs. c) Measured force, modeled force, and force components from mass-spring-damper model for example "spring-like" pair during partnered beam-walking.

Mean negative power magnitude was greater than mean positive power magnitude during partnered beam-walking ($p<0.05$), indicating that hand contact assists balance during walking by acting more often as a "brake" than a "motor" (Fig. 1b).

Results from the mass-spring-damper model showed that the interaction forces restored balance similar to a passive spring and/or damper in the lateral direction, but some partnerships were more "spring-like" (Fig. 1c) or "damper-like" than others, suggesting different interaction strategies.

Significance

Hand interactions with a partner have low force and affect a person's whole-body balance performance through mechanical power transfer, which is dominated by braking energy. This principle may be used in design of devices and robotic controllers to assist walking balance. Forces at the interaction point in haptic assistance can contain sufficient information for altering balance performance of the individual.

Acknowledgments

Funding: NSF CMMI 1762211 and NSF CMMI 1761679.

References

[1] Sawers, A, et al, J. of Neuroeng. and Rehab., 2017.
[2] Holden, M, et al, J. of Vestibular Research, 1994.

Dance Interventions Improving Balance in Parkinson's Disease: A Systematic Review with Meta-Analysis

Caroline Simpkins MS[1], Jennifer Lees BS[1], and Feng Yang PhD[1]
[1]Georgia State University, Department of Kinesiology & Health, Atlanta, GA
Email: fyang@gsu.edu

Introduction

Parkinson's disease (PD) is a prevalent neurodegenerative disease.[1] Balance, gait, and postural stability impairments are common in people with PD, and this population experiences a higher risk of falling compared to their healthy counterparts.[2] To improve or maintain quality of life (QOL) for people with PD, reducing the likelihood of falling is vital. Dance-based interventions could be an attractive alternative to traditional exercise for people with PD and have shown promise in providing health benefits. Current information about the effect of dance interventions on balance in people with PD is limited due to the small number of articles included in previous reviews. This may negatively impact the deployment of this type of therapy. An updated meta-analysis based on a larger number of randomized controlled trials (RCT) and utilizing a rigorous calculation of effect size (ES) is necessary to advance our understanding of the influence of dance therapy on balance in this population.

The purpose of the current meta-analysis was to analyze the efficacy of dance-based interventions in improving balance among people with PD in comparison to exercise interventions or no intervention. As balance is essential to activities of daily living and closely related to falls, findings from this study could inform the design of dance interventions to reduce falls and heighten QOL among people with PD.

Methods

A systematic literature search was conducted in PubMed, PsycINFO, Cochrane Library, CINAHL, and MEDLINE using search terms "Parkinson" and "danc" and "balance." No restrictions were placed on type of dance or the stage of disease, sex, or age of PD participants. The initial search yielded 175 articles and 94 remained after removing duplications. Remaining studies were checked with the inclusion criteria: 1) peer-reviewed article published in English; 2) conducted among people with PD; and 3) RCT including at least one dance-based intervention arm and a control or placebo arm. Thirteen studies met the inclusion criteria. [3-15] Quality assessment was performed using the Physiotherapy Evidence Database (PEDro) scale.

Information about the article (author(s), publication year), the participants (sex, age, Hoehn and Yahr stage, assessed on/off medication) and interventions (dance type, control type, frequency, duration) were collected from each article. In addition, sample size and balance outcome measures were retrieved. Values for the balance measurement were extracted in the form of means and standard deviations (SD) for both the dance intervention and comparison conditions at two time points (baseline and post-intervention). Changes in balance from baseline to post-intervention and their SD were calculated from the identified means and SD if not given. A meta-analysis was conducted using a random-effects model based on data from all 13 studies within RevMan 5.3 (Denmark).

Results and Discussion

Average PEDro value of the 13 studies was 5.62 ± 0.49 (out of 10). Balance was assessed by Berg Balance Scale, Mini Balance Evaluation System Test, or Fullerton Advanced Balance Scale among studies. The ES varied drastically from -0.14 to 2.00 (Fig. 1). Our meta-analysis on the 16 comparisons yielded a significant and medium ES indicating that dance interventions benefit people with PD to improve balance (ES = 0.62, 95% CI = [0.34, 0.90], $p < 0.0001$). Our results suggest that dance therapy has the potential to safely and effectively improve balance and possibly contribute to lower rates of falls among people with PD.

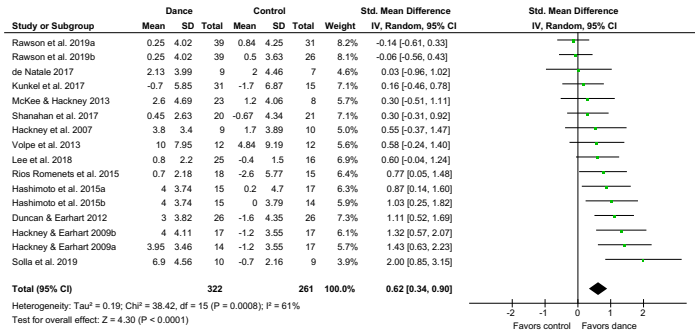

Figure 1: Forest plot of effect sizes (the standardized mean difference) for 16 comparisons between dance interventions and control groups reported by 13 studies assessing the effect of dance-based interventions on balance in people with Parkinson's disease.

Significance

Our findings could inform future studies for designing and deploying effective dance-based balance training and fall prevention programs specific to PD. More high-quality RCT with large sample sizes are needed to further explore the effects of various dance types in improving balance compared to other modes of exercise. The retention effects of dance-based therapies among people with PD should also be addressed in future studies.

Acknowledgments

This study was funded in part by the Brains & Behavior Fellowship (Neuroscience Institute, Georgia State University).

References

1. Pringsheim, *Movement Disorders*, 2014, 13, 1583-1590.
2. Nutt, *Movement Disorde*rs, 2011, 26(6), 166-1174.
3. de Natale, *Neurorehabilitation*, 2017, 40(1), 141-144.
4. Duncan, *Neurorehabil Neural Repair*, 2012, 26(2), 132-143.
5. Hackney, *J Neurol Phys Ther*, 2007, 31(4), 173-179.
6. Hackney, *J Rehabil Med*., 2009, 41(6), 475-481.
7. Hashimoto, *Complement Ther Med*., 2015, 23(2), 210-219.
8. Kunkel, *Clin Rehabil*., 2017, 31(10), 1340-1350.
9. Lee, *Explore*, 2018, 14(3), 216-223.
10. McKee, *Journal of Motor Beha*vior, 2013, 45(6), 519-529.
11. Rawson, *J Neurol Phys Ther*., 2019, 43(1), 26-32.
12. Rios Romenets, *Complement Ther Med*., 2015, 23, 175-184.
13. Shanahan, *Arch Phys Med Rehabil*., 2017, 98, 1744-1751.
14. Solla, *J Altern Complement Med*., 2019, 25(3), 305-316.
15. Volpe, *BMC Geriatrics*, 2013, 13(1), 54.

Margin of Stability during Tandem Stance with Dominant Limb Placed Back or Forward: A Pilot Study

Gordon Alderink[1], Yunju Lee[1,2], Diana McCrumb[2], Samhita Rhodes[2],
[1]Department of Physical Therapy, Grand Valley State University, Grand Rapids, MI, USA
[2]School of Engineering, Grand Valley State University, Grand Rapids, MI, USA
Email: aldering@gvsu.edu

Introduction

Balancing a large mass over a small base of support (BOS) is a challenge for humans in bipedal stance. To maintain control of balance, the center of mass (COM) must remain within the BOS [1]. Center of pressure (COP) displacement and velocity parameters are commonly used to measure static [2], and dynamic balance [3]. Winter et al. demonstrated high correlations between net COP and partitioned right and left limb COPs during tandem standing and medio-lateral control of balance [4]. More recently, postural stability has been measured using the margin of stability (MOS), which accounts for COM velocity [5]. MOS has not been used to examine control of balance during tandem, i.e., heel-to-toe, stance. The primary objective of this project was to examine range and velocity in the COP and range of MOS under four conditions during tandem standing. We hypothesized that the COP and MOS range would increase under the eyes closed condition, but there would be no difference in COP and MOS when foot positons were changed.

Methods

Six healthy individuals (4 females; 24.8±3.3 yrs; 170.8±10.5 cm; 71.0±13.5 kg) participated. Approval was obtained from the Grand Valley State University Human Research Review Committee (#18-246-H). Employing a full body Plug-in-Gait model, 16 Vicon MX cameras (120 Hz) and Nexus motion capture software v2.9.2 (Oxford Metrics) were used to track anatomical marker trajectories. Ground reaction forces were collected at 1200 Hz, using floor embedded AMTI force platforms (Advanced Mechanical Technology Inc). Data were collected with participants standing, with arms flexed, hands touching shoulders, on two force plates under four conditions: 1) eyes open (EO) dominant foot on rear plate; 2) eyes closed (EC) dominant foot on rear plate; 3) eyes open dominant foot on fore plate; and 4) eyes closed dominant foot on fore plate. Participants were asked to stand with knees extended, while maintaining equal distribution of weight on each force plate. Data were collected for 30 seconds and five trials were collected under each condition. Vicon Nexus software was used to determine location of the COM. Custom MATLAB code (MathWorks) was used to determine the combined (from the rear and fore force plates) COP location and MOS [5]. A repeated measures variance of analysis (2 factor rm-ANOVA within subject) was used to test the effect of vision and foot placement ($p<.05$) for range (the maximum distance between any two points) and velocity of COP and range of MOS in antero-posterior (AP) and medio-lateral (ML) directions.

Results and Discussion

The main effect of vision on range and velocity of COP and range of MOS, in both AP and ML directions demonstrated significant differences ($p<.001$) (Figure 1), i.e., increased under the EC condition. These findings are consistent with select findings from Thomson et al. [2].

The foot position affected only COP velocity in the AP direction. Interaction effects were found in range and velocity of COP and in range of MOS in ML direction. Although we instructed participants to maintain equal weightbearing on the front and back feet, we noticed a tendency to bear more weight on the rear plate regardless of dominance. It is possible that leg dominance itself is not as important as vision to control standing balance; however, leg dominance might affect tandem standing in ML direction.

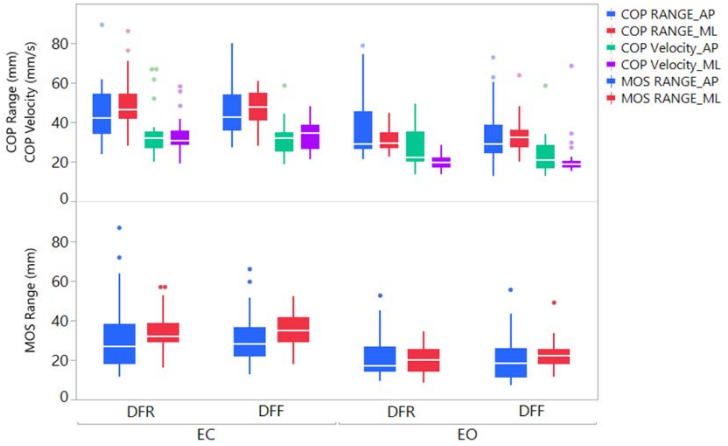

Figure 1 : COP and MOS in antero-posterior (AP) and medio-lateral (ML) directions. DFR = dominant foot rear; DFF = dominant foot fore; EC = eyes closed; EO = eyes open. Y axes include range in mm and velocity in mm/sec.

Significance

It is clear that there are differences in COP displacement and velocity between healthy and concussed athletes in standing balance tasks when eyes are open or closed [6,7,8]. It has also been shown that MOS may better capture dynamic balance because it accounts for the inherent velocity of the COM, i.e., extrapolated COM [5]. Our results also show that both COP and MOS range are increased under EC, a less stable position. Our data suggest that MOS may also be useful to measure residual central nervous system impairment in balance following concusion.

References

1. Winter, D. (1995). *Gait Posture*, 3, pp.193-214.
2. Thomson, LA et al. (2017). *Sports*, 5, p. 86.
3. Parker, T. et al. (2006). *Med. Sci. Sports Exerc*., 38, pp. 1032-1040.
4. Winter, D. et al. (1996). *J. Neurophysiol*., 75, pp. 2334-2343.
5. Hof, AL et al. (2005). *J. Biomech*., 38, pp.1-8.
6. Guskiewicz, KM. (2001) *Clin. J. Sports Med*., 11, pp. 182-189.
7. Powers, KC et al. (2014) *Gait Posture*, 39, pp. 611-614.

Coordination responses to a change in walking speed do not differ with age or knee osteoarthritis

Jocelyn F. Hafer[1] and Ronald F. Zernicke[2]
[1]University of Delaware, [2]University of Michigan
Email: jfhafer@udel.edu

Introduction

Aging and knee osteoarthritis (OA) are associated with changes in gait. These age- or OA-related changes may coincide with altered coordination during gait, potentially indicating a limited ability to adapt to new situations. An inability to adapt to challenges during gait could partially explain the higher incidence of falls in older vs. young adults [1] and those without vs. with knee OA [2]. Testing responses to a challenge such as walking faster may reveal differences in how age or knee OA affect the motor system's ability to adapt and may indicate a need for different interventions by patient population. We sought to determine whether older adults who were asymptomatic or who had knee OA had different coordination responses to an increase in walking speed compared to each other and to young adults. We hypothesized coordination would change differently between participant groups when they walked faster.

Methods

Three groups were recruited: young (28±5 yrs, n=10), older asymptomatic (72±3 yrs, n=10), and older with knee OA (69±5 yrs, n=9). Pelvis, thigh, shank, and foot angular velocities were collected with inertial measurement units as individuals walked on a treadmill at preferred and faster speeds (i.e., young walked faster than older and knee OA (+0.3 m/s) but all groups increased speed similarly (+0.3 m/s) from preferred to faster). Angular displacements about each segment's primary axis of rotation during gait (≈sagittal) were estimated using functional calibration and a zero-velocity update algorithm [3]. Coordination was calculated between adjacent segments using a modified vector coding technique for 100 strides of data [4]. Coordination phase angles were compared between groups and speeds across sub-phases of swing and stance using circular 2-way ANOVAs with α=0.05. Post-hoc comparisons were made with 1-way ANOVAs.

Results and Discussion

Contrary to our hypothesis, there were no significant interactions between group and speed. However, there were significant main effects of group and speed (p-values for significant group effect post-hocs and significant speed effects reported below).

During terminal swing, young adults and adults with knee OA had different phase angles for the thigh v pelvis ($p=0.04$) and shank v thigh ($p=0.05$) (Fig 1). Despite these differences, all groups had similar phase angle patterns for thigh v pelvis (distal segment phase) and shank v thigh (proximal segment phase) during terminal swing. For the foot v shank couple, adults with knee OA had different phase angles from young adults during terminal swing ($p<0.01$) and from young and older asymptomatic adults during early stance ($p<0.01$ and $p=0.05$, respectively). Here, young adults had distal phase patterns (81±44°) while adults with knee OA had anti-phase patterns (134±98°) during terminal swing, and young and older asymptomatic adults had in-phase patterns (208±6° and 204±6°) while adults with knee OA had proximal phase patterns (198±8°) during early stance.

Coordination also changed with increased walking speed for the shank v thigh and foot v shank during terminal swing, and for the foot v shank during early stance (all $p<0.01$). At the thigh v shank, phase angle patterns were the same between speeds. At the foot v shank, phase angle patterns shifted from anti- (140±79°) to distal phase (75.7±49.3°) in terminal swing and from proximal (201±7°) to in-phase (206±7°) in early stance with faster speed.

While we did not find a differential effect of walking speed on coordination across age or musculoskeletal pathology, we did identify consistent differences in coordination at the transition between swing and stance. Because this time in the gait cycle may be a naturally unstable transition, differences in coordination between groups may be an indicator of instability or fall risk.

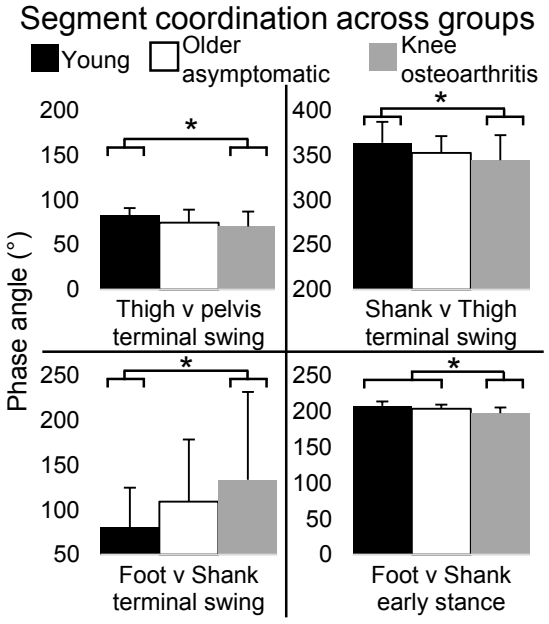

Figure 1. Segment coordination phase angles averaged by group across speeds. *Indicates significant post-hoc difference between groups.

Significance

Differences in coordination patterns between young adults and older adults with knee OA around the transition from swing to stance phase could be an indicator of or risk factor for falls. In this study, we did not assess fall history and so we cannot determine whether differences in coordination are a predictor of future falls or a correlate of fall incidence. Interestingly, the same couples that differed by age or knee OA status shifted towards young coordination patterns with faster walking speed. Greater effort during faster walking may have required a shift to adopt younger coordination patterns. While contrary to our hypothesis that groups would respond differently to the challenge of faster walking, this response may be useful in interventions to reduce instability or falls risk.

References

1. Rubenstein, *Age Aging* 2006, 35(Suppl 2):ii37-ii41
2. Prieto-Alhambra et al., *Ann Rheum Dis* 2013, 72(6):911-7
3. Hafer et al., *J Biomech* 2020, 1095
4. Chang et al., *J Biomech* 2008 41:3101-5

Effects of Sole Thickness on Recovery from an Unexpected Slip during Standing

Jiyun Ahn[1], Meng-Wei Lin[1], Jennifer Lees[1], Kelsey Clark[1], Feng Yang[1]
[1]Department of Kinesiology and Health, Georgia State University, Atlanta, GA 30303, USA
Email: jahn12@gsu.edu

Introduction

Wearing inappropriate footwear has been identified a risk factor of falls [1]. Among the mechanical properties of shoes, the sole thickness is highlighted as a major contributor to falls. Previous studies indicated that the thicker the sole, the greater the risk of falls [2,3]. One possible explanation is that a thick sole impedes the detection of an external perturbation, delays the reactions to the balance disturbance, and thus reduces the likelihood of a successful recovery from a balance loss. Although this theory seems intuitive, no study has specifically inspected how sole thickness alters postural balance maintenance and the likelihood of falls after an unexpected perturbation. The purpose of this study was to explore how the sole thickness impacts the body's reactions to a stance-slip. It was hypothesized that increased shoe sole thickness delays the body's reactions to the slip perturbation.

Methods

Nine young adults (25.3 ± 1.5 y/o) were recruited and evenly randomized into three groups: barefoot (0 mm sole thickness), thin (5 mm), and thick sole (10 mm). The barefoot group underwent the protocol without footwear. The thin/thick group wore a pair of 5/10 mm foamboards secured by tape to their soles during the experiment. The foamboard was individually cut to fit each participant's sole.

After about 5-min familiarization (walking with respective footwear condition over ground), each participant stepped onto the ActiveStep treadmill (Simbex). They put on a safety harness connected to overhead arch through ropes. Following five standing trials on the treadmill, each participant experienced an unexpected stance-slip [4]. The slip distance and acceleration were respectively 36 cm and 4 m/s^2. Full-body kinematics during the slip trial were captured from reflective markers attached to the body using a motion capture system (Vicon). A marker was also applied to the treadmill belt to identify the onset of the treadmill belt movement. The paths of the markers were filtered and used to determine the liftoff and touchdown of the recovery step after the slip occurrence, and three outcome variables: the step latency (the interval from the belt slip onset to the liftoff of the recovery step), step duration (from liftoff to touchdown), and step length (the anteroposterior distance between heels at recovery foot touchdown). Analysis of variance, followed by independent *t*-tests, was adopted to compare the outcomes among groups (0 vs. 5 vs. 10 mm). All analyses were conducted using SPSS 24 (IBM) with an $\alpha = 0.05$.

Results and Discussion

The step latency ($p < 0.01$, Fig. 1a) and length ($p = 0.01$, Fig. 1c) showed a significant overall group-related difference. The step duration was not different among groups ($p = 0.74$, Fig. 1b). Post-hoc tests revealed that both the thin and thick groups exhibited a significantly longer step latency than the barefoot group. Additionally, the thick group showed a longer step latency than the thin group. Similarly, the recovery step length was significantly greater among the thin and thick groups than in the barefoot group.

The results overall support our hypothesis that a thick sole could hinder the body's reactions to an unexpected slip perturbation. Specifically, the thicker the sole, the longer the step latency, indicating more time is needed to sense the perturbation and to plan the recovery step. The aftereffects of the same slip perturbation become more intense as sole thickness increases due to the increasingly delayed initiation of the recovery step. To arrest the backward falling trunk induced by the slip, individuals with thicker soles must take a larger recovery step to regain the body's balance, evidenced by the lengthened recovery step as the thickness of the sole rises. As timely reactions are critical for one to reestablish balance and reduce the chance of falling, thick soles could increase one's risk of falls should an external perturbation occur. Although the step duration did not differ among groups, a trend emerges that the step duration increases as the sole becomes thicker (Fig. 1b). This could be explained by the fact that individuals with thicker soles, in comparison with those with thin or no soles, need to spend longer time to execute the recovery step in order to achieve a longer step length which can effectively regain the body's balance. One limitation in our study is the small sample size. We postulate that non-significant results could be reversed with a larger sample size.

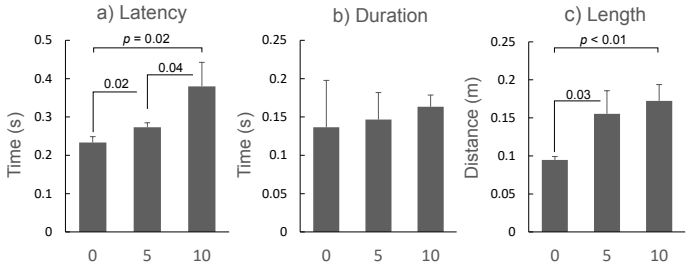

Figure 1. Comparisons of a) latency, b) duration, and c) length of the recovery step in response to an unexpected stance-slip among the three groups: barefoot (0 mm), thin (5 mm), and thick (10 mm).

Significance

This study will enhance our understanding of the effects of the sole thickness on the risk of falls. The results could furnish some references for physicians prescribing appropriate footwear to individuals with high risk of falls. In addition, our findings could inform the design of fall-resistant footwear from the perspective of the sole thickness.

Acknowledgments

The authors thank Shreya Kulkarni and Phum Tuntiansin for assisting with the data collections.

References

[1] Menant, et al. *J Rehabil Res Dev*, 2008. 45(8): 1167-1181.
[2] Robbins, et al. *J Am Geriatr Soc*, 1992. 40(11): 1089-1094.
[3] Tencer, et al. *J Am Geriatr Soc*, 2004. 52(11):1840-1846.
[4] Yang, et al. *J Biomech*, 2018. 72: 1-6.

Muscle activation pattern during a fall from standing height

Kwang Jun Lee[1], Ki-taek Lim[1], Jisoo Jang[1], Woochol Joseph Choi[1]
[1]Injury Prevention and Biomechanics Laboratory, Department of Physical Therapy, Yonsei University, Wonju, South Korea
Email: wcjchoi@yonsei.ac.kr

Introduction

Pre-impact fall detection algorithms have been proposed based on threshold values of velocity, acceleration and/or angle changes of body segments during a fall. However, the practical use of the algorithms is limited due to incomplete sensitivity and specificity [1].

We propose to use lower extremity muscle activation pattern to detect a fall prior to impact, and the first step is to confirm whether there exists a special muscle activation pattern, which is not affected by a variety of fall kinematics. Therefore, we conducted falling experiments with humans to measure lower extremity muscle activation, and examined how this was affected by fall direction and knee position at landing.

Methods

Twenty individuals mimicked older adults' falls and landed sideways on a 30 cm thick gymnasium mattress (Figure 1). Falling trials were acquired with three initial fall directions: forward, backward or sideways. Trials were also acquired with three knee positions at the time of hip impact, where the landing-side knee was being contacted the mat (KOM), the contralateral knee (KOK), or free of constraint (KF). Electrodes of surface electromyography (EMG) (TeleMyo DTS, Noraxon Inc., AZ, USA) were placed on the belly of iliopsoas (Ilio), adductor longus (ADDL), gluteus medius (Gmed) and gluteus maximus (Gmax). Fall kinematics and kinetics were monitored through a motion capture system (Vicon Motion Systems, Oxford, UK) and a forceplate placed under the mat (AMTI, model OR6-7-2000, Waltham, MA, USA), respectively.

Outcome variables included time to onset, activity at the time of hip impact, and timing of peak activity with respect to the time of hip impact. ANOVA was used to test if these outcome variables were associated with fall direction (3 levels) and knee position at the time of hip impact (3 levels).

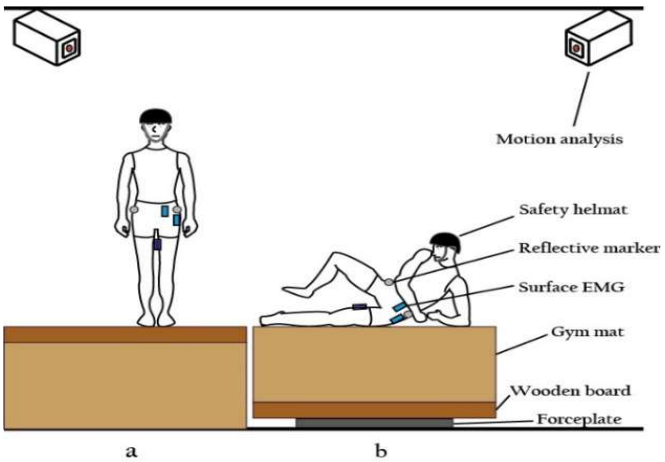

Figure 1: Experimental setup. (a) Participants self-initiated falls and (b) landed sideways on a 30 cm thick mattress.

Results and Discussion

On average, given time available during a fall (941 ms, time between fall initiation and hip impact), lower extremity muscles started to contract at 393 ms after fall initiation, and reached maximum contraction at 39 ms prior to the hip impact. Furthermore, the lower extremity muscles contracted 49% of their maximum when the hip impacted the mat (Figure 2). These baseline measures should be informative for the development of myoelectric pre-impact fall detection algorithms.

For each lower extremity muscle, none of outcome variables were associated with fall direction and knee position, except activity at the time of hip impact of Gmed and ADDL, where Gmed was associated with fall direction and knee position ($F = 5.57$, $p = 0.013$; $F = 4.08$, $p = 0.027$, respectively) and ADDL was associated with fall direction ($F = 5.28$, $p = 0.011$). This is an important finding as pre-impact fall detection through lower extremity muscle activity pattern may provide 100% of sensitivity and specificity in detecting falls, no matter how they fall and land. Since activation patterns of gluteus medius and adductor longus muscles were affected by fall types, gluteus maximus and/or iliopsoas muscles could be a good target to be used for pre-impact fall detection.

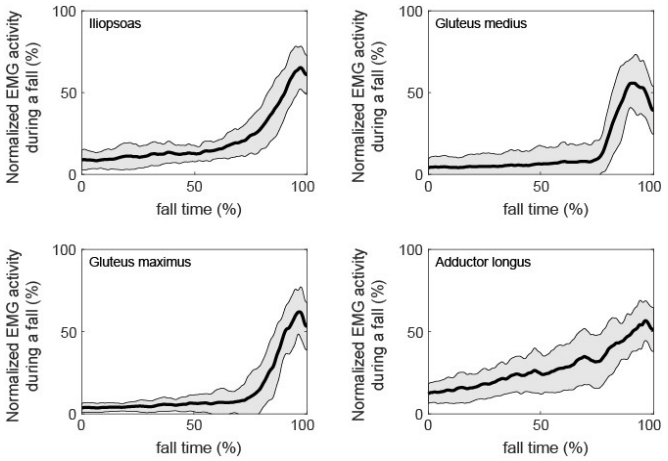

Figure 2: Average EMG activity (thick line) across all 540 falling trials with +/- 1 standard deviation (thin line).

Significance

A special activation pattern of lower extremity muscles exists during a fall, informing the development of prevention strategies for fall-related injuries in older adults (i.e., pre-impact fall detection, balance recovery).

Acknowledgments

This work was supported, in part, by Yonsei University Mirae Campus Future-Leading Research Initiative (#2019-62-0023).

References

[1] Hu and Qu, 2016. Pre-impact fall detection. Biomedical engineering online 15:

Speed of Walking, as well as Walking Mode (Treadmill vs. Overground), can affect Margin of Stability

Farahnaz Fallah Tafti[1], Arash M. Gonabadi[1], Kaeli Samson[2], Carolin Curtze[1], Jennifer M. Yentes[1]
[1]Department of Biomechanics, University of Nebraska at Omaha, Omaha, NE USA
[2]Department of Biostatistics, University of Nebraska Medical Center, Omaha, NE USA
Email: ffallahtafti@unomaha.edu

Introduction

To maintain stability during walking, the body's center of mass (COM) must be controlled effectively within the base of support provided by the feet. In general, margin of stability (MOS) is defined as the distance between the extrapolated COM (i.e. a point on the floor at a distance from the COM that is directly proportional to the COM velocity) with respect to the limits of the base of support during walking in the anterior posterior (AP) and mediolateral (ML) directions [1, 2].

Decreased dynamic stability can be described by decreasing the mean and/or increasing the variability of MOS. During unperturbed walking conditions, dynamics of stepping are expected to result in a similar trend of stability outcomes during walking at different speeds for both overground and treadmill walking. The aim of this study is to determine if walking on a treadmill vs. overground will affect MOS at heel contact during three, speed-matched conditions.

Methods

Twelve healthy young participants, (24.8±5.1 years; 73.0 ±11.8 kg; 1.74±0.07 m) without any disorders that would cause abnormal gait control were recruited to this study. Participants walked on a treadmill and overground at slow, preferred, and fast speed-matched conditions, while kinematic (marker) data were collected. Four participants' data were not included due to insufficient number of speed-matched steps across modes of walking.

The mean and variability (standard deviation) of the MOS in AP and ML directions at heel contact were calculated for 18 right and left steps during overground and treadmill trials. All models were adjusted for preferred speed. ML mean models were adjusted for step width. AP variability models were adjusted for step speed standard deviation. ML variability models were adjusted for step width standard deviation. To identify the main effect of walking mode (treadmill vs. overground) and speed conditions (slow, preferred, fast), and the possible interaction between walking mode and speed, generalized linear model were used. The significance threshold was α=0.05.

Results & Discussion

No significant effect of walking mode was found for MOS AP mean; however, walking faster led to more negative MOS AP mean in both walking mode conditions ($p<0.0001$). This indicated that the extrapolated COM was further anterior to the base of support as they walked faster, thereby reducing stability. There was a significant interaction between speed and walking mode ($p<0.0001$) for MOS AP variability, where overground was more variable than treadmill walking for fast and preferred walking speeds, but not slow speeds. (Figure 1). Greater variability of MOS AP when walking faster may be the result of natural fluctuations during overground walking, while on the treadmill, variability remained consistent due to a more repetitive pattern of stepping.

MOS ML mean during fast and preferred speed was significantly narrower compared to slow (adjusted p's < 0.0001) indicating less stability. This could be due to maintenance of frontal plane stability in the presence of more challenges to the motor control system in the presence of increased COM displacement at slower speed [3]. MOS ML mean during treadmill walking was wider than overground ($p=0.01$) indicating more stability. In the absence of natural optic flow during treadmill walking, as well as different proprioceptive input (legs being pulled back during treadmill versus remaining stationary during overground), subjects may employ strategies to increase stability. A significant interaction for MOS ML variability was found, however, no significant pairwise comparisons were found upon post hoc analysis.

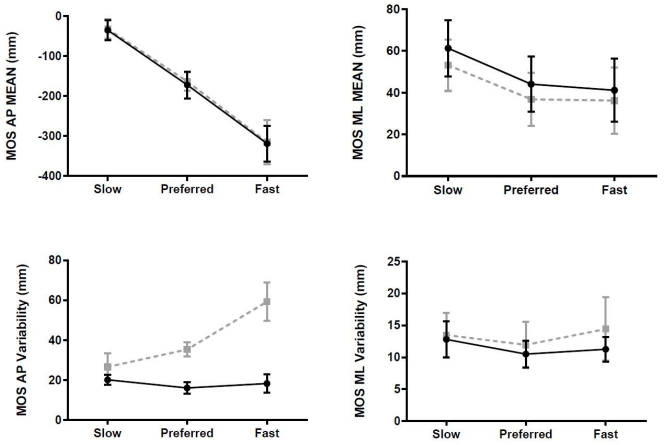

Figure 1: MOS mean (top) and variability (bottom) values in AP (left) and ML (right) directions. Treadmill is represented by black solid lines and overground by gray dashed lines.

Significance

Walking mode matters when we look at the variability, while the trend for absolute mean values stays the same, although they are scaled differently in the ML direction. Walking faster is more variable (overground) and less stable than slower walking (narrower MOS).

Acknowledgments

Funding provided by the National Institutes of Health (P20 GM109090), the Department of Veterans Affairs (I21RX003294) to Dr. Yentes. The authors have no conflicts to disclose.

References

1. Hof et al., *J Biomech*, 38(1), 1-8, (2005).
2. Hollman et al. *Gait Posture*, 43, 204-209, (2016).
3. Orendurff et al. *J REHABIL RES DEV,* 41,829-834, (2004).

Ranking Algorithm for ANN-Based Post-Fall Detection

Bummo Koo[1], Haneul Jung[1], Taehee Kim[1], Jongman Kim[1], Yejin Nam[1] and Youngho Kim[1]
[1]Department of Biomedical Engineering and Institute of Medical Engineering, Yonsei University, Korea
Email: *younghokim@yonsei.ac.kr

Introduction

Falls become significant health risks of death or injury for the elderly. Although the post-fall detection system is unable to prevent falls, it can help victims quickly. The performance of post-fall detection of various classifiers could be improved by selecting feature vectors based on T-score ranking algorithm [1]., 13 ranking algorithms have been introduced and evaluated for the clasification [2]. This study aimed to determine the performance of post-fall detection based on a subset of feature vectors using different ranking algorithms.

Methods

Thirty healthy volunteers performed 9 simulated falls and 14 ADL movements (Table 1). 3-axis accelerations and 3-axis angular velocities were measured using an IMU sensor attached to the middle of LASI and RASI. ANN was applied to IMU data to determine fall and non-fall. Eight different feature vectors were introduced as shown in Table 2 and ranked using five Ranking algorithm: ReliefF[3], T-score[4], Correlation[5], Fisher Score[4] and mRMR[6]. Each ranking algorithm was evaluated by absolute errors (AE). Then, feature vector subsets were created according to the number of feature vectors and applied to the ANN classifier. Data from 10 subjects were used to train the ANN classifier and data from the remaining 20 subjects were used to test the classifier.

Table 1: Experimental Protocol

	Motion
Fall	slip-backward fall, walk-trip-forward fall, jogging-trip-forward fall, sit down-backward fall, sit- backward fall, forward fall, backward fall, lateral fall, and twist fall
ADL	walking, jogging, squat, waist bending, stumble while walking, Jogging in place, jumping, stairs up and down, slowly sit and up in stool, quickly sit and up in chair, trying to get up and collapse in to a chair, lying, slowly sit and up in low height mattress, and quickly sit and up in low height mattress

Table 2: Feature Vectors

Feature	Equation
ASVM	$C_1[k] = sqrt(a_x^2[k]+a_y^2[k]+a_z^2[k])$
ASVMHP	$C_2[k] = sqrt(a_x^2[k]+a_z^2[k])$
TA	$C_3[k] = atan2(sqrt(a_x^2[k]+a_z^2[k]),-a_y[k])$
Jerk	$C_4[k] =(a_x[k]- a_x[k-1])/(t[k]-t[k-1])$
GSVM	$C_5[k] = sqrt(w_x^2[k]+w_y^2[k]+w_z^2[k])$
GSAM	$C_6[k] = abs(w_x^2[k])+abs(w_y^2[k])+abs(w_z^2[k])$
ACM	$C_7[k] = nthroot(abs(a_x[k]\times a_y[k]\times a_z[k]),3)$
AVCM	$C_8[k] = nthroot(abs(w_x[k]\times w_y[k]\times w_z[k]),3)$

Results and Discussion

Figure 1.a) showed the predicted and actual rankings for 5 different ranking algorithm. 'Actual' refers to the classification performance using each feature vector (C_2>C_3>C_5>C_1>C_6>C_8>C_7>C_4).

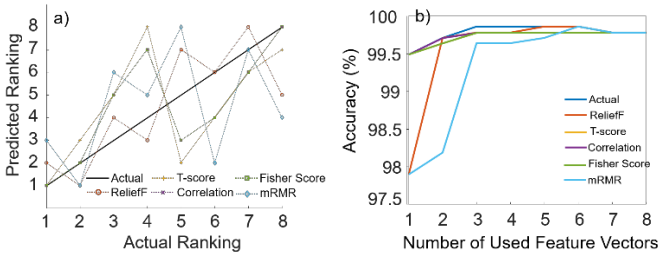

Figure 1: a) Actual Ranking and Predicted Ranking
b) Accuracy according to number of feature vectors

Table 3 showed AE of the ranking algorithm. ReliefF inferred the best ranking and mRMR was the worst. Since ReliefF was the only time-dependent algorithm, it predicted relatively accurate ranking. On the other hand, mRMR aimes to minimize redundancy and maximize relevance. Therefore, if the redundancy of the feature vector was low, the feature vector was evaluated with high rank even though the relevance was relatively lower than other feature vectors.

Table 3: AE of Ranking Algorithms

	ReliefF	T-score	Correlation	Fisher Score	mRmR
AE	10	14	12	14	18

Figure 1.b) showed the accuracy according to the number of feature vectors. When the actual ranking was applied, the best accuracy (99.86±0.65) was obtained by using three characteristic vectors. ReliefF and mRMR achieved the best accuracy (99.86±0.65) when using 5 and 6 feature vectors, respectively. mRMR showed large AE but high accuracy. This might be due to the fact that it minimized redundancy and avoided overfitting.

Significance

The ranking algorithm showed effectiveness in clustering-based classifiers in some studies, but was not effective for post-fall detection using ANN as shown in this study. It is thought that the ranking algorithm might not be suitable for time-dependent data. In addition, it was shown that high accuracy could be obtained with smaller number of feature vectors depending on the selection of feature vectors.

Acknowledgments

This research was supported by the Technology Innovation Program (20006386) funded by the Ministry of Trade, Industry & Energy (MOTIE, Korea).

References

[1] Vallabh et al., IEEE SoftCOM., 1-9, 2016
[2] Vasan et al., IJCAT., 55(4):298-307, 2017
[3] Kononenko et al., ECML PKDD., 171-182, 1994
[4] Zhao et al., ASU feature selection repository., 1-28, 2010
[5] Hall et al., ICML., 1-8, 2000
[6] Peng et al., IEEE TPAMI., 27:1226-1238, 200

Biomechanical Response to Altered Foot-Placement during Steady-State Walking

Lydia G. Brough[1], Glenn K. Klute[2,3], Richard R. Neptune[1]
[1]Walker Department of Mechanical Engineering, The University of Texas at Austin
[2]Department of Veterans Affairs, Puget Sound Health Care System, Seattle, WA, USA
[3]Department of Mechanical Engineering, University of Washington, Seattle, WA, USA
Email: lydia.brough@utexas.edu

Introduction

The ability to maintain dynamic balance is critical for participating in activities of daily living. Dynamic balance in the frontal plane is largely controlled through foot placement (e.g. [1]). To compensate for imposed errors in mediolateral (ML) foot placement individuals often use a hip strategy [2, 3], a lateral ankle strategy that shifts the center of pressure (COP) [3], and/or a stepping strategy [4]. The ankle plantarflexors are important contributors to balance control during steady-state walking [5] and are used to restore balance in response to visual perturbations [6]. However, it is unclear if the plantarflexors provide a biomechanical response to foot-placement perturbations.

The purpose of this study was to identify the biomechanical response to perturbations in ML foot-placement in young healthy individuals. We hypothesized that subjects would compensate for medial (lateral) foot-placement errors with 1) a decreased (increased) hip abduction moment, 2) a lateral (medial) COP shift, and 3) an increased (decreased) ankle plantarflexion moment.

Methods

Kinematic and kinetic data were collected from fifteen healthy volunteers (9 female, age: 25 ± 3 years). Twenty 30-second walking trials were performed at a standard (1.0 m/s) and self-selected speed. Foot-placement perturbations were applied to random steps during 10 of the 20 walking trials using a custom pneumatic device, with each subject experiencing 40 perturbations. The pneumatic device used an inertial measurement unit to identify gait events and triggered a solenoid valve to release compressed air. The air applied a 15N force to the ankle to move the foot an average of 3.2 (3.7) cm medially (laterally). Participants were not aware of the perturbation timing or direction.

Motion capture data were processed using Visual 3D software (C-Motion, Germantown, MD) to perform inverse dynamics analyses. We used the range of frontal plane whole-body angular momentum (H_R) to assess balance control, which was calculated by summing the angular momentum of each body segment about the body's center of mass. Differences between perturbed and unperturbed steps were evaluated using a linear mixed effects models.

Results and Discussion

In agreement with our hypothesis and previous work [2, 3], H_R increased (decreased) following medial **(**lateral**)** perturbations ($p<.001$). Hip abduction moment impulse also decreased following medial perturbations ($p<.001$) Maxiumum COP excursion increased laterally **(**medially**)** following medial **(**lateral**)** perturbations ($p<.001$), which was correlated with decreased **(**increased**)** ankle inversion moments ($p<.001$**,** $p=.001$**)**(Fig. 1A*)*. We hypothesized that ankle plantarflexion moment would increase after medial perturbations to counteract increased H_R . However, peak plantarflexion moments were not significantly different between conditions (Fig. 1B). Moreover, ankle plantarflexion moment impulse increased after lateral perturbations and decreased after medial perturbations during single leg stance ($p=.001$, $p<.001$). This unanticipated result may be due to ankle inverters and everters also having plantarflexion moment arms. Thus, as the lateral ankle strategy is enacted, those muscles may have a small but significant contribution to the plantarflexor moment. Future modeling work will investigate individual muscle contributions to the 3D ankle moments.

In summary, participants used a combination of strategies to maintain balance following perturbations in medial and lateral foot-placement. Stance-leg hip abduction moment decreased after medial perturbations, and a lateral ankle strategy shifted the COP laterally (medially) after medial (lateral) perturbations. Unexpectedly, plantarflexion moment impulse decreased (increased) after medial (lateral) perturbations.

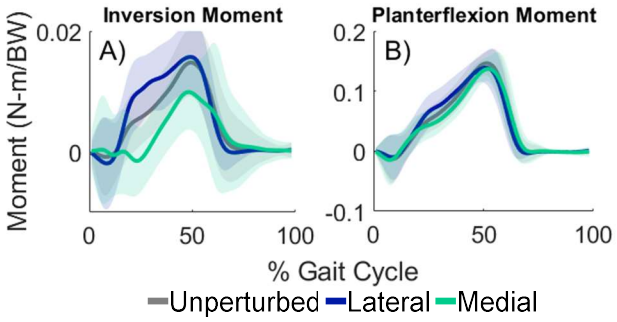

Figure 1: A) Average stance-leg inversion (+) and eversion (-) moment and B) Average stance-leg plantarflexion (+) and dorsiflexion (-) moment ± 1 SD for unperturbed, laterally and medially perturbed gait cycles.

Significance

This work assessed joint-level responses to mediolateral foot-placement perturbations. Characterizing these responses to foot-placment perturbations in healthy individuals can provide a basis for comparison for those with neurological deficits and impaired balance control.

Acknowledgments

This project was supported in part by the NSF GRFP and VA grant RX002974.

References

1. MacKinnon, C.D.and Winter, D.A. *J Biomech.* 26, 633-644, 1993.
2. Miller, S.E. et al. *J Biomech.* 76, 61-67, 2018.
3. Segal, A.D. et al. *J Biomech.* 48, 3982-3988, 2015.
4. Segal, A.D. and Klute, G.K. *J Biomech.* 47, 2911-2918, 2014.
5. Neptune R.R. and McGowan, C.P. *J Biomech.* 49, 2975-2981, 2016.
6. Reimann, S.A. et al. *Front. Physiol.* 9, 2018

Advancing Stages of Pregnancy on Postural Sway Range in Healthy Females

Heather R. Vanderhoof[1], Christian N. Sanchez[1], Jeffrey D. Eggleston[1]
[1]Department of Kinesiology, University of Texas at El Paso, TX, U.S.A.
Email: hvanderhoof@miners.utep.edu

Introduction

One in four pregnant females experience a fall while performing daily tasks, which is a rate similar to that of the elderly[1]. Ten percent of pregnant fallers seek medical attention due to injury and/or fetal complications[1]. As gestational mass gain (GMG) primarily occurs anteriorly about the torso, the center of mass (COM) shifts outside of the standing base of support (BOS)[2]. This may contribute to greater postural instability and increased risk of falling. GMG may also increase the moment of inertia of the body and create an imbalance in displacement between the mediolateral (ML) and/or anteroposterior (AP) center of pressure sway range displacement (COPD)[4]. Recent literature observed that larger COPD in the ML directions were correlated with higher incidences of falls in the elderly[5]. While previous research found that decreasing BOS, by narrowing stance width, created greater ML sway variables in the pregnant population[4]. However, research has not been performed on single-limb support in pregnant and postpartum females.

Thus, the aim of this study was to quantify COPD in ML and AP directions during bilateral standing (BL) and single-limb support (SLS) conditions when comparing 2nd trimester (2T), 3rd trimester (3T), and postpartum (POST), to non-pregnant females (NP). It was hypothesized that the 2T and 3T females would have greater AP COPD compared to NP females to compensate for the asymmetrically distributed GMG.

Methods

Five females in 2T (25.6 ± 4.7 years, 1.6 ± 0.1 m, 76.3 ± 11.9 kg), three females in 3T (25.3 ± 4.2 years, 1.7 ± 0.1 m, 85.7 ± 19.2 kg), three POST (27.7 ± 2.5 years, 1.6 ± 0.1 m, 72.9 ± 16.2 kg), and two NP females (24.5 ± 0.7 years, 1.6 ± 0.1 m, 64.55 ± 14.2 kg) participated in this study. Postural stability**,** was quantified by examining postural sway from COPD data, wherein greater COPD correlates to decreased postural stability[3]. Postural sway was measured in three static standing conditions for 30s per condition: 1) BL; 2) right limb; and 3) left limb, all on a single force platform (1,000 Hz, AMTI. Watertown, MA, USA). BL width was controlled for and consistent for all groups. COPD data were exported to MATLAB and filtered with a digital low-pass Butterworth filter (12.5 Hz). Results from a pilot study revealed no SLS differences existed between right and left limbs, thus limbs were collapsed per participant across the groups in the current study. Variables of interest included: bilateral anteroposterior (BLAP), bilateral mediolateral (BLML), single-limb support anteroposterior (SLSAP), and single-limb support mediolateral (SLSML) COPD were compared to note differences created by a decreased BOS. ML and AP COPD was calculated by the absolute maximum and minimum ML (X) and AP (Y) coordinate data from the following equations: ML = $(Xmax - Xmin)$ and AP= $(Ymax - Ymin)$ in mm^2.

A four (condition) by four (group) factorial ANOVA (α=0.05) was used to test for statistical significance for COPD. If no interaction was detected, variable and group main effects were examined after applying the Sidak adjustment.

Results and Discussion

Results revealed there was not a significant group by limb condition interaction ($F(9, 36)=0.73$, $p=0.68$), nor was there a group main effect ($F(3, 36)=0.53$, $p=0.67$). However, there was a limb condition main effect ($F(3, 36)=16.89$, $p<0.01$). BLAP was significantly greater than BLML (**a**; $p<0.05$) and BLAP was significantly smaller than SLSAP (**b**; $p<0.001$), but not significantly different from SLSML ($p=0.17$). BLML was significantly smaller than SLSML (**c**; $p<0.001$), however, SLSAP and SLSML were not significantly different from each other ($p=0.173$) **(Figure 1).** BL conditions being characterized by smaller COPDs than SLS conditions was expected, as the BOS is greater during BL. BLAP being greater than BLML supported the hypothesis that the increased amount of GMG anteriorly could create AP imbalances. It was expected that significantly larger COPDs may occur with advancing pregnancy, however, this was not reflected in the results. Interestingly, SLS, while larger than BL, was relatively similar in both directions. While pregnant females and the elderly have similar fall rates, pregnant females are likely not falling due to static standing balance tasks. SLS being uniform in AP and ML directions may be important when conducting daily tasks, such as stair locomotion, that rely heavily on SLS.

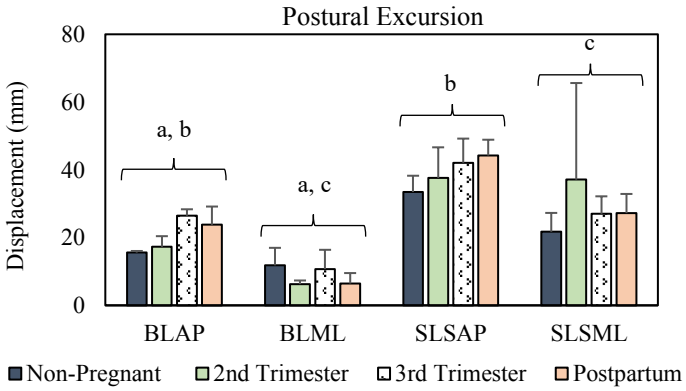

Figure 1: Means and standard deviations for COP displacement (mm) by limb condition and direction (bilateral anteroposterior, bilateral mediolateral, single-limb support anteroposterior, and single-limb support mediolateral) between groups. a, b, c indicates $p < 0.05$.

Significance

The reason behind high fall rates during pregnancy is still not well understood. The current study aims to understand adaptations to static postural control throughout pregnancy prior to considering dynamic postural control. Additionally, it provides evidence of evenly distributed postural stability during SLS which may correlate to dynamic functional movements.

References

1. Dunning, K., et al. (2010). *Mat and Child Health Jrnl, 14*(5).
2. Whitcome, K. et al. (2007). *Nature, 450*(7172).
3. Callahan, R.T. (2017). COPE During a Single Leg Standing Test in Ambulatory Children with Cerebral Palsy.
4. Oliveira, L.F., et al. (2009). *J of OBGYN Repro Bio, 147*(1).
5. Melzer, I., et al. (2010). *Clinical Biomechanics, 25*(10).

The Potential Implications of Co-Contraction Index of Neck Muscles on Traumatic Brain Injuries

Tyler A. Wood[1]*, Christopher M. Hill[1], Dong Jae Park[1], Manuel E. Hernandez[2], Jacob J. Sosnoff[2]
[1]Northern Illinois University, DeKalb, IL, 60115, USA
[2]University of Illinois at Urbana-Champaign, Urbana, IL 61801
Email: *twood1@niu.edu

Introduction

Traumatic brain injuries (TBIs) are a major cause of morbidity and mortality in adults over the age of 75 years [1,2]. It is estimated that ≥80% of TBIs in this population are attributed to head impact during same level falls [2]. Fall-related TBIs are a serious health concern for older adults, and there is a need for investigation of potential modifiable risk factors.

A potential modifiable risk factor may be neck muscle activation in response to prelibation [3,4]. In a recent study, older adults were found to have significantly greater neck muscle activation latency than young adults in response to a postural perturbation [4]. These findings suggest older adults may have reduced ability to support the head during a fall leading to head impact and consequently are at a greater risk of fall-related TBIs [4]. However, it remains to be seen if the neck muscles' response to perturbation can be changed with repeated exposure to perturbations. Thus, the purpose of this study was to examine the effect of repeated postural perturbation on co-contraction index between the right sternocleidomastoid (SCM) and right upper trapezius (UPT).

Methods

Adults between the age of 18 – 30 years and 70 – 90 years were recruited; participants were grouped based on age. Participants were excluded if they reported any history of neck or back pain or dysfunction. Participants underwent dynamic posturography on the Smart Equitest Research System (Natus Medical Inc. Pleasanton CA, USA) with wireless electromyography (EMG) sensors (Trigno wireless system, Delsys Inc, Natick MA, USA) affixed to the right SCM and right UPT. EMG sensors were affixed per manufacturer instructions. Participants stood with their feet shoulder-width apart while staring straight ahead and arms at their side. Participants were exposed to 3 unexpectedly timed anterior translations of 6.35 cm at a velocity of 20 cm/sec on the Equitest System (Figure 1). Participants were not given practice tests.

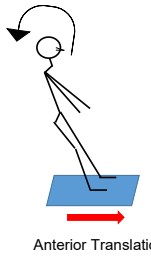

Figure 1: Illustration of anterior translation with body movement.

EMG data was processed using the Teager-Kaiser Energy Operator, followed by a high-pass 6th order Butterworth filter, a low-pass 2nd order zero phase shift Butterworth filter, and full wave rectified. Co-contraction index was calculated using the following equation: EMGS/EMGL*(EMGS+EMGL), where EMGS is the mean muscle activity of the muscle with the least activity and EMGL is the mean muscle activity of the muscle with the highest activity [5].

Results and Discussion

12 young adults (age 22.4±1.6 years; 7 females) and 12 older adults (age 79.7±1.6 years; 8 females) were included in this study. Co-contraction index for each of the three trials are displayed in Figure 2. Repeated-measures ANOVA revealed a significant effect of time; both groups displayed decreases in co-contraction index over the trials ($F(2,44)=3.702$, $p=0.033$). Yet, there was no significant interaction between time and group ($F(2,44)=0.558$, $p=0.576$).

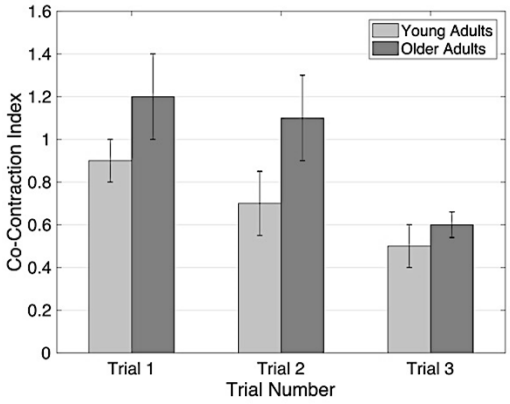

Figure 2: Co-Contraction Index per trial as a function of group.

The lowered co-contraction indexes with each subsequent trial suggest a more selective activation of the muscles [5]. The more selective muscle activations may indicate the ability of the neck muscles to change control strategy with repeated exposures.

Significance

Current fall-prevention exercise programs do not target the neck muscles. However, the decrease in co-contraction index with repeated exposure to postural perturbation may indicate an ability of the neck muscles to be trained. These results have further implications which suggest a potential effectiveness of rehabilitation protocols to improve neck activation during falls. With the ability to appropriately activate during falls, the neck muscles may have the capability to prevent head impact and ultimately prevent fall-related TBIs. Nevertheless, more research is needed to understand the direct effects of neck activation on the head kinematics during a fall.

References

[1] Fu WW, Fu TS, Jing R, McFaull S R, & Cusimano MD. *PLoS One* **12**, 2017.
[2] Taylor CA, Bell JM, Breiding MJ, & Xu, L. *MMWR Surveill Summ* **66**, 1-16, 2017.
[3] Wood TA, Morrison S, Sosnoff JJ. *Frontiers in Medicine*, 2019.
[4] Wood TA, Hernandez ME, Sosnoff JJ. *J Electromyogr Kinesiol* **17**, 2020.
[5] Rudolph KS, Axe MJ, Snyder-Mackler L. *Knee Sug, Sports Traumatol, Arthrose* **8**, 262-269, 2000.

The Effect of a Reduced Marker Set on the Margin of Stability During Gait

Michael S. Christensen.[1], James B. Tracy[1], and Jeremy R. Crenshaw[1]
[1]University of Delaware, Newark Delaware, USA
Email: crenshaw@udel.edu

Introduction

The margin of stability (*MoS*) is a measure of dynamic gait stability that considers the position and velocity of the whole-body center of mass (COM_{body}) relative to the edge of the base of support [1]. This measure is proportional to the perturbing impulse that causes a loss of stability, and it is altered in populations at risk of falling [2,3,4]. Typically, the *MoS* is calculated using a COM_{body} determined from a full-body marker set. However, in clinical gait laboratories, lower-limb marker sets are often used. If an accurate *MoS* can be calculated from a partial marker set, then we may evaluate stability in clinical contexts using an extensive dataset of past gait analyses.

The purpose of this study was to evaluate the agreement between using a full-body marker set and partial-body marker set to calculate the *MoS*. We hypothesized that *MoS* values will show acceptable levels of agreement.

Methods

Fifteen unimpaired participants (6M/9F, mean (SD) Age: 21.0 (3.2) years; BMI: 21.3 (2.5) kg/m^2) were recruited to walk at a self-selected, preferred speed while wearing a full-body marker set. The COM was determined from all segments (COM_{body}), only the lower body segments (COM_{lower}), and the pelvis center (COM_{pelvis}) [6]. Each COM variant was used to determine (1) the anterior *MoS* at midswing ($AMoS_{midsw}$), defined as the anterior distance between the stance toe and the extrapolated COM when the contralateral limb was in midswing and (2) the minimum lateral *MoS* ($LMoS_{min}$), defined as the minimum lateral distance between the stance toe and the extrapolated COM. Each MoS value was averaged across limbs.

Previous studies have identified several sources of bias associated with using partial marker sets to determine *MoS* [5]. Notably the pendulum height was one of the largest sources of bias, as the height of the COM is affected by using a reduced marker set. We addressed this bias by estimating pendulum height as a ratio of leg length [1].

Using Bland-Altman plots (mean [limits of agreement]) and intraclass correlations ($ICC_{2,1}$), the MoS values from the reduced marker sets were compared to those from the full-body marker set (representing the "gold standard") to assess validity.

Results and Discussion

For $AMoS_{midsw}$, COM_{lower} was slightly biased towards less stability (0.71 [-1.10 to 2.51] cm) (Fig. 1A) and showed excellent agreement (ICC = 0.98), while COM_{pelvis} was biased towards more stability (0.39 [-0.68 to 1.46] cm) (Fig. 1B) with less desirable agreement (ICC = 0.64). For $LMoS_{min}$, COM_{lower} was biased towards more stability (-1.01 [-2.27 to 0.24] cm) (Fig. 1C), while COM_{pelvis} was biased towards less stability (0.92 [-0.77 to 2.61] cm) (Fig. 1D). Both methods showed poor agreement to the gold standard (ICC = 0.46).

Our results indicate that a simplified predictor of the COM, using lower-extremity segments, may have utility in estimating anterior *MoS*. Models from the lower-extremities had better validity than models using only the pelvis. This disparity is likely the result of the velocity component of the swing limb not being accounted for by COM_{pelvis}, as evidenced by the bias of the COM_{pelvis} calculation towards less stability.

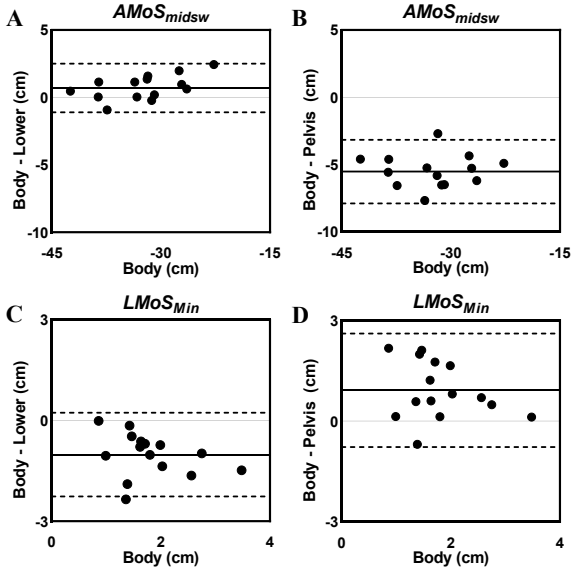

Figure 1: Bland Altman plots showing limits of agreement for COM_{lower} (A & C) and COM_{pelvic} (B & D) for the variables $AMoS_{midsw}$ (A & B) and $LMoS_{min}$ (C & D).

Reduced-model estimates of $LMoS_{min}$ had poor agreement with full-body calculations. This result is likely due to the minimum being determined at different temporal points of stance between conditions. For example, COM_{body} identified $LMoS_{min}$ earlier (25.54 (5.09) %Stance) than COM_{lower} (35.05 (8.30) %Stance). We suggest that lateral stability values at distinct timepoints in the gait cycle (e.g. foot strike) may have better agreement. Futher assessment of lateral MoS during midswing and at ipsilateral heelstrike supported this. At midswing, both COM_{lower} and COM_{pelvis} showed strong agreement (ICC = 0.85 and ICC = 0.79). At ipsilateral heelstrike, both COM_{lower} and COM_{pelvis} also showed improved agreement (ICC = 0.59 and ICC = 0.76).

Significance

Clinical gait laboratories often use a lower-extremity marker set, limiting estimations of the COM used to evaluate dynamic stability. Anterior *MoS* values and lateral *MoS* values occurring at a specific gait event, can be accurately estimated using lower-extremity marker sets. This validation informs the manner in which retrospective analyses of gait data may assess the effects of impairment, rehabilitation, or surgery on gait stability.

References

[1] Hof et al. (2005). *J Biomech*, **38:** 1-8
[2] Peebles et al. (2016). *J Biomech*, **49**: 3949-55
[3] Stegemöller et al. (2007). *Arch. Phys. M.*, **93**: 703-09
[4] Tracy et al. (2019). *Gait Posture*, **72**: 182-187
[5] Havens et al. (2018). *Gait Posture*, **59**: 162-167
[6] Dempster. (1995). *WADC,* 55-159

Association between activities-specific balance confidence, dynamic gait index, and physical activity in people with Parkinson's disease

Junmo An[§1], Jiyeon Kim[§1], Eugene C. Lai[2], and Beom-Chan Lee*[1]
[1]Department of Health and Human Performance, University of Houston, Houston, Texas, USA
[2]Department of Neurology, Houston Methodist Neurological Institute, Houston, Texas, USA
Email: *blee24@central.uh.edu; [§]Authors An and Kim contributed equally to this study.

Introduction

Parkinson's disease (PD), which commonly affects people between the ages of 50 and 60, is a progressive and neurodegenerative disorder associated with the dysfunction of dopamine-producing neurons in the substantia nigra pars compacta of the midbrain [1]. Dopamine acts as a lubricating oil in the neural circuits that coordinate exercise; when an 80 percent or greater of the dopamine-producing neurons (dopaminergic neurons) are depleted, the resulting symptoms of dyskinesia, such as tremor, rigidity, stiffness, bradykinesia, and postural instability, interfere with walking, climbing stairs, etc [2]. Thus, neurologists recommend exercise on a daily or weekly basis to help people with PD reduce dyskinesia and possibly delay the progression of PD [3]. In this study, we tracked the physical activity (i.e., number of steps) of people with PD for 10 weeks, used the Activities-specific Balance Confidence (ABC) scale and the Dynamic Gait Index (DGI), and assessed their physical activity. The objective is to understand the relationship between stepping as a representative physical activity and the ABC and DGI scores.

Methods

Seven individuals (age 68.57 ± 12.47; 6 males and 1 female) with PD were recruited. The inclusion criteria were: age between 50 and 75 years and a diagnosis of idiopathic PD (stages 2 to 4 of the Hoehn and Yahr scale). The study protocol was approved by the University of Houston Institutional Review Boards Prior to the study, a written consent form was obtained from each participant.

The experimental protocols consisted of three laboratory-based assessments of the first, sixth, and tenth weeks. The ABC scale and the DGI, standard clinical tools for assessing gait, balance, and fall risks, were used to assess participants' physical activity. Participants wore a smartwatch (Versa 2, Fitbit, Inc., San Francisco, CA) every day for ten weeks to track daily physical activity (steps). Statistical analyses were conducted with SPSS 21.0 software (IBM Corp., Armonk, NY). Pearson's linear correlation coefficients were used to measure the relationship between the ABC and DGI scores and physical activity.

Results and Discussion

Figure 1 shows that higher physical activity positively correlated with higher ABC ($r = 0.475$, $p = 0.030$) and higher DGI ($r = 0.550$, $p = 0.010$) scores, respectively. Although there were only seven participants, the results imply that people with PD who have higher physical activity may have higher balance control ability and/or lower risk of falling during daily life.

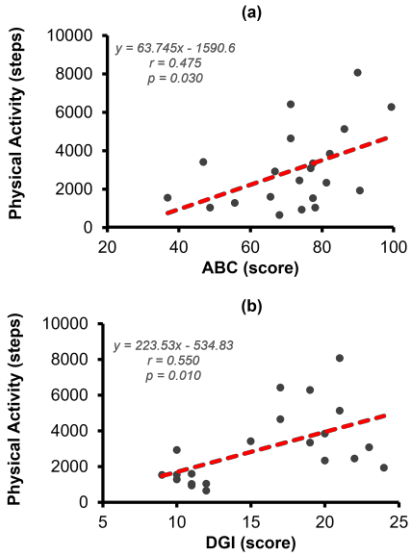

Figure 1: Scatterplots of the relationship between seven participants' physical activity. (a) Activities-specific Balance Confidence (ABC) scale. (b) Dynamic Gait Index (DGI). Red dashed lines indicate the linear regression fits.

Significance

Increased daily physical activity (stepping) may reduce the symptoms of dyskinesia and possibly delay the progression of PD. Physical activity enhancement is expected to be an effective strategy to delay the decline of physical/motor functions and decrease the risk of falling in individuals with PD.

Acknowledgments

This study was supported by the Eunice Kennedy Shriver National Institute of Child Health and Human Development (NICHD) of the National Institutes of Health (NIH) under award number [1R21HD099242]. The authors thank Emily Song and Richard Huh for assistance with data acquisition.

References

[1] De Rijk, M. C., et al. "Prevalence of Parkinson's disease in the elderly: the Rotterdam Study," *Neurology,* vol. 45(12), pp. 2143-2146, 1995.

[2] Haas, Bernhard M., Marion Trew, and Paul C. Castle. "Effects of respiratory muscle weakness on daily living function, quality of life, activity levels, and exercise capacity in mild to moderate Parkinson's disease," *Am J Phys Med Rehabil,* vol. 83(8), pp. 601-607, 2004.

[3] Speelman, Arlene D., et al. "How might physical activity benefit patients with Parkinson disease?," *Nat. Rev. Neurol*, vol. 7, pp. 528–534, 2011

The Effect of Advancing Pregnancy on Postural Sway Velocity in Bilateral and Unilateral Standing

Bianca Tovar[1], Heather R. Vanderhoof[1], and Jeffrey D. Eggleston[1]
[1]Department of Kinesiology, University of Texas at El Paso, TX, U.S.A.
Email: btovar1@miners.utep.edu

Introduction

One in four females fall during pregnancy, which may result in maternal or fetal injury and/or fetal death[1]. During pregnancy, the female body undergoes many hormonal and anatomical alterations, correlating to musculoskeletal adjustments which may affect postural stability[2]. If static posture is altered during pregnancy, then daily activities may be impaired and risk of falling may increase[2]. The utilization of force-plate posturography, such as postural sway velocity (SV), can accurately assess postural instability[3]. Previous research found that greater SV during static posture relates to a decreased balance ability[4], thus leading to an increased incidence of falls[5]. Examining the safety of single-limb dependent activities (e.g., stair locomotion, walking, running) is of importance in pregnant females as these activities may pose an increased risk of falls due to the decreased base of support and increased single-limb support time.

The present study aims to analyze static SV across pregnancy stages (2nd trimester, 3rd trimester, and postpartum) during bilateral (BL) and unilateral (UL) conditions when compared to non-pregnant females. This study further addresses the following research questions: will postural sway velocity be different throughout advancing pregnancy during 1) BL static standing and 2) UL static standing? We hypothesized that SV would be greatest in the third trimester group and the least in the control group for both standing conditions. Furthermore, we expected postpartum SV to be similar to that of the non-pregnant control group for both standing conditions.

Methods

Five 2nd trimester (25.6 ± 4.7 years, 1.6 ± 0.1 m, 76.3 ± 11.9 kg), three 3rd trimester (25.3 ± 4.2 years, 1.7 ± 0.1 m, 85.7 ± 19.2 kg), three postpartum (27.7 ± 2.5 years, 1.6 ± 0.1 m, 72.9 ± 16.2 kg), and two non-pregnant (24.5 ± 0.7 years, 1.6 ± 0.1 m, 64.55 ± 14.2 kg) females participated in this study. Postural SV was measured in three conditions, 30 seconds per condition: 1) bilateral; 2) right limb; and 3) left limb. Data were obtained with one force platform (1,000 Hz, AMTI, Watertown, MA, USA) and filtered with a digital low-pass Butterworth filter (12.5 Hz).

Pilot data supported that right and left limb single-limb stance were not significantly different from one another. Therefore, right and left limb data were collapsed across participants for UL stance trials. SV was calculated as the time-derivative of center of pressure excursion (COPE).

A two (condition: BL, UL) by four (group: NP, 2T, 3T, POST) factorial ANOVA (α=0.05) was used to test for statistical significance for SV. If no interaction was detected, variable and group main effects were examined after applying the Sidak adjustment.

Results and Discussion

There was no significant group by condition interaction ($F(3, 18)=0.96$, $p=0.43$), nor was there a group main effect ($F(3, 18)=0.41$, $p=0.75$), however there was a condition main effect ($p<0.001$). When comparing the two standing conditions (UL vs. BL), UL SV was significantly greater than BL SV across all groups ($p<0.001$) (**Figure 1**).

The results did not support the stated hypothesis due to SV being similar among the stages of pregnancy. Furthermore, there were no significant differences created by a reduction in base of support between the four groups. Therefore, from these results, pregnant and postpartum women displayed similar sway velocities to non-pregnant women in both limb conditions, indicating no significant alterations in stability throughout advancing pregnancy.

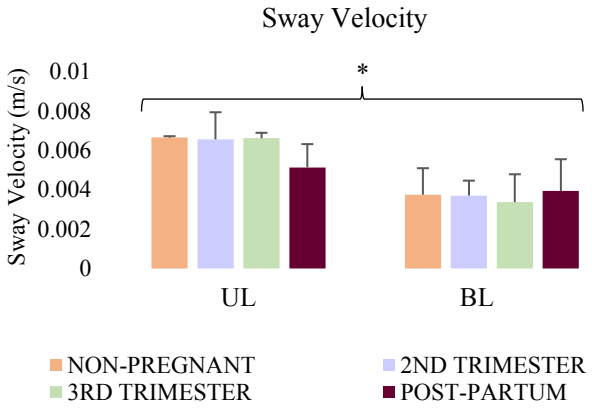

Figure 1: Means and standard deviations for sway velocity (m/s) between group (non-pregnant, 2rimester, 3rd trimester, and post-partum) and limb condition (unilateral, bilateral). * indicates $p<0.001$.

Significance

The current study's findings were aimed to gain insight on the relationship between postural control (via SV) in pregnant and non-pregnant women and the size of base of support. This study infers that postural control of pregnant women did not significantly change across pregnancy stages nor significantly differ from non-pregnant women despite a reduction in base support by standing on a single limb. Thus, SV may not be a key factor in determining the safety (i.e., risk of falls) of single-limb support activities in later stages of pregnancy. Additionally, it can be inferred that physical changes during pregnancy do not pose a significant decrease in balance ability in pregnant females. Hence, the reason behind high fall rates during pregnancy remains unknown.

References

1. Dunning, K., et al. (2010). *Mat & Child Hlth Jrnl*, *14*(5).
2. Moccellin, S. A., et al. (2015). *Brzl J Motor Bhvr*, *9*(5).
3. Blaszczyk, W. S. (2016). *Gait & Posture, 44*.
4. Hye-Sun, N. et al. (2017). *J Kor Phys Ther, 29*.
5. Cho, K. et al. (2014). *J Phys Ther Sci, 26*.

Behavioral risk predicts maximum lateral reach during a roof gutter clearing task

Erika M. Pliner[1,2*], Daina L. Sturnieks[2], Kurt E. Beschorner[1], Christopher L. Deschler[1] and Stephen R. Lord[2]
[1]Department of Bioengineering, University of Pittsburgh, Pittsburgh, USA
[2]Falls, Balance and Injury Research Centre, Neuroscience Research Australia, Sydney, AUS
Email: *empliner@gmail.com

Introduction

Ladder falls are a problem in the domestic setting with injury rates highest among older adults [1]. Ladders aid individuals in completing tasks at elevated levels (e.g. clearing a roof gutter), but individuals often overreach during ladder use. Overreaching has been reported to cause the majority of ladder falls that occur while an individual is working from the ladder [2]. Lateral reach on a ladder is influenced by environmental factors, that is, ladder use acclimation and task motivation [3]. However, there is a lack of knowledge on individual factors that influence lateral reach on a ladder. Understanding individual characteristics that influence lateral reach can assist in identifying individuals at risk of overreaching on a ladder, particularly among older adults.

Similar to ground level reaching [4], lateral reach distance on a ladder may be dependent on the behavioral risk the individual is willing to accept to complete a task. In addition to behavioral risk, greater grip strength and better balance may provide a higher capacity for reaching. Thus, grip strength and balance may also predict how far an individual is willing to reach. We hypothesized that everyday risk-taking behavior, grip strength and balance would predict an individual's maximum lateral reach distance during a roof gutter clearing task on a straight ladder.

Methods

Lateral reach was assessed from 94 healthy older adults (73.0 ± 5.6 years old; 49 females) during a roof gutter clearing task on a straight ladder. Individuals were asked to climb to the third step of a straight ladder to clear a 5.8 m long gutter completely filled with tennis balls as quickly and as safety as possible. Individuals were allowed to reposition the ladder as often as needed to clear the length of the gutter. Maximum reach during the task was the calculated distance in the medial-lateral direction from the distal end of the 3rd metacarpal to the center of the ladder. Maximum task reach was normalized to arm span length. Behavioral risk was assessed from an everyday risk-taking questionnaire [5], where a higher score was associated with greater behavioral risk. Maximum grip strength was assessed from a hydraulic hand dynamometer. Balance was assessed from quiet standing sway: eyes open, on foam. Human research ethics approval and informed consent was obtained.

A multiple linear regression was performed with maximum task reach as the dependent variable. Everyday risk-taking, grip strength, sway, age and gender were entered into the model as predictor variables. A square root transform was performed on grip strength and sway to ensure a skewness of < 1.

Results and Discussion

The mean (standard deviation) maximum task reach was 51.8 (9.7) % of arm span. Greater everyday risk-taking was associated with a farther maximum task reach (standardized $\beta = 0.423$; $t_{87} = 4.16$; $p < 0.001$) (Figure 1). Thus, individuals who take greater everyday risks, may be taking greater risks during ladder use by reaching farther. This suggests risk-takers to be at greater risk of a ladder fall due to overreaching. Grip strength (standardized $\beta = 0.046$; $t_{87} = 0.32$; $p = 0.750$) and sway (standardized $\beta = -0.151$; $t_{87} = -1.35$; $p = 0.180$) were not associated with maximum task reach. This suggests that individuals do not adjust their amount of reach based on their grip strength and balance capabilities during a roof gutter clearing task. Furthermore, maximum task reach was not significantly influenced by age (standardized $\beta = 0.161$; $t_{87} = 1.33$; $p = 0.187$) and gender (standardized $\beta = -0.084$; $t_{87} = -0.61$; $p = 0.546$).

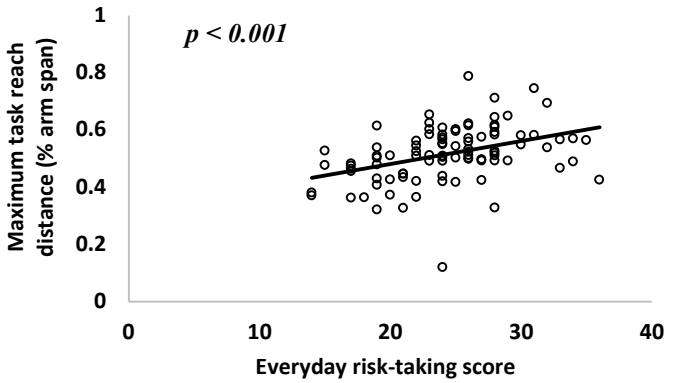

Figure 1: Maximum task reach distance by everyday risk-taking score.

Maximum task reach was predicted by behavioral risk, but not grip strength, balance, age and gender. Behavioral risk is a potential predictor of ladder fall risk if a greater maximum task reach increases ladder fall risk. Furthermore, maximum reach during ladder use may be dependent on an individual's perception of risk more than physical ability. Additional work is needed to investigate the influence of other psychological (e.g. anxiety, fear) and physical (e.g. proprioception, reaction time) factors on maximum reach during ladder use.

Significance

This study found that a simple risk-taking screen predicted reaching behavior during a common ladder task among older adults. The use of this screen, along with educational programs may help prevent ladder falls due to overreaching in this population.

Acknowledgments

This work was supported by the NSF Graduate Research Fellowship Program and Graduate Research Opportunities Worldwide (NSF GRFP 1247842).

References

[1] Faergemann, C., & Larsen, L.B. *Accident Analy. Prev.* 2000.
[2] Faergemann, C., & Larsen, L.B. *J Safety Research.* 2001.
[3] DiDomenico, A.T., et al. *Professional Safety.* 2013.
[4] Butler, A.A., et al. *J Gerontology: Medical Sciences.* 2010.
[5] Butler, A.A., et al. *J Gerontology: Medical Sciences.* 2014.

Characterization of posturography and sensory loss in lower-limb amputees.

Bailey A. Petersen[1], Patrick Sparto[1,2], and Lee Fisher[1,3]
[1]Department of Bioengineering, University of Pittsburgh, Pittsburgh, PA, USA
[2]Department of Physical Therapy, University of Pittsburgh, Pittsburgh, PA, USA
[3]Department of Physical Medicine and Rehabilitation, University of Pittsburgh, Pittsburgh, PA, USA
Email: bap87@pitt.edu

Introduction

An estimated 1.5 million people in the United States are living with a lower-limb amputation[1]. These individuals can suffer from a wide variety of functional deficits and, consequently, a higher risk of falls than the average population. In fact, 52.4% of community dwelling adults with lower-limb amputation reported a recent fall[2]. Determining the factors that influence fall risk in this population is critical. One theory is that lack of sensory feedback from the amputated limb, and the contralateral limb in the case of peripheral neuropathy, may contribute to abnormal postural control. **The purpose of this study is to determine the extent to which impaired sensation affects postural control in individuals with lower-limb amputation.**

Methods

In this study, we collected measures of sensory impairments and balance control in fifteen lower-limb amputees, regardless of level or nature of amputation. Somatosensory integrity of both the intact and residual limb was assessed by a trained physical therapist. These tests included monofilament threshold, light touch and protective (pinprick) sensation, vibration sense, two-point discrimination and joint position sense.

To quantify balance, we used the Sensory Organization Test (SOT) using the NeuroCom Equitest. In the SOT, participants stand on a force platform while either visual (eyes closed, sway-referenced surround rotation) or somatosensory feedback (sway-referenced platform rotation) are altered across six conditions. Each condition consists of three 30-second trials. Standard measures of posturogrpahy (excursion, sway velocity, 95% confidence interval ellipse of sway area and sample entropy) were calculated for each trial. In addition, clinical measures including equilibrium scores and somatosensory ability (ratio of equilibrium scores in conditions with and without vision) were recorded. Equilibrium scores indicate a participant's ability to stay within a normative 12° anteroposterior sway envelope. Regression analyses were performed across all measures of sensation and balance.

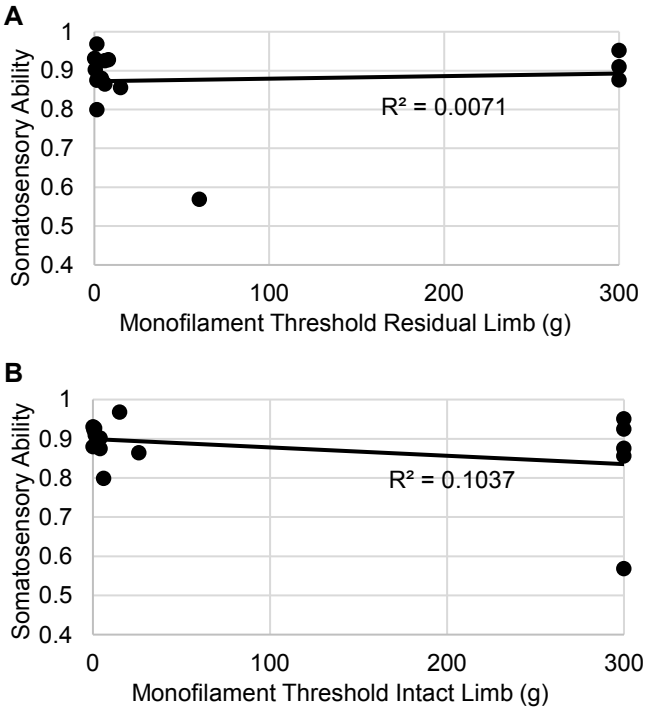

Figure 1: Somatosensory ability versus monofilament thresholds. Somatosensory ability (ratio of equilibrium score in conditions without vision to conditions with vision) shows no relationship to sensory impairments in the residual limb (A) or the intact limb (B).

Results and Discussion

From our preliminary results, lower-limb amputees have significantly lower equilibrium scores across all conditions than controls, and this difference is most pronounced in the static condition without vision (80.1±6.6 vs 92.0±2.9 respectively). Despite the clear balance impairments in this group, we have found no significant relationship between quantitative measures of sensory impairment (monofilament threshold) and posturography measures across all conditions of the SOT.

As expected, area of sway and sample entropy both increased without visual feedback, as was seen in previous studies. However, these changes showed no significant correlation to any measures of severity of sensory impairment ($p<0.05$). In addition, the ratio of sway with vision to without vision (somatosensory ability) shows no correlation with clinical tests of sensation (Figure 1). This lack of correlation could be due to the ceiling effect (maximum 300g) in monofilament testing, especially with the bimodal distribution of sensory loss in our data (Figure 1) or may indicate that lower-limb amputees are able to compensate for loss of tactile sensation in the limbs in static balance.

Significance

This lack of relationship between tactile sensation and balance is surprising, given the spinal reflexive pathways that are activated by tactile stimuli when balance is perturbed. With respect to assessing sensory loss, the ceiling effect seen here calls for a more robust measure of sensory ability across impairments or an alternative test of balance that is sensitive to sensory impairments. On a broader scale, the question of the effects of sensation for postural control remains and, as a field, we may need to shift our focus to tasks that can demonstrate the relative importance of proprioception versus tactile sensation in balance.

References

[1] Ziegler-Graham K, MacKenzie E, …, Brookmeyer R. (2008) Estimating the prevalence of limb loss in the United States: 2005 to 2050. *Arch Phys Med Rehabil*, **89(3)**:422-429.
[2] Hunter SW, Batchelor F,…, Payne M. (2017) Risk Factors for Falls in People With a Lower Limb Amputation: A Systematic Review. *PM R,* **9(2)**:170-1

Influence of Object Characteristics on Patient Safety and Stability During Ambulation

Dorien Butter[1,2], S. Chaeibakhsh[1], M. Homayounpour[1], RS Novin[1], K. Bo Foreman[1,2], and Andrew Merryweather[1]
[1]Mechanical Engineering Department, University of Utah, UT, USA
[2]Deptartment of Physical Therapy, University of Utah, UT, USA
Email: dorien.butter@utah.edu

Introduction

Each year between 700,000 and 1,000,000 patient falls occur in U.S. hospitals, with 33% resulting in injury [1]. Most efforts directed at reducing patient falls have focused on bed alarms, monitoring, and education to raise awareness. Longer term interventions have focused on exercise and balance training [1]. Aspects in room design and environment, often referred to as extrinsic risk factors for falls, have been identified based on fall incident reports [2]. The limited research that exists related to fall risk and room design has focused on individual factors such as flooring and lighting, [3, 4] often missing the complex interactions between the patient and environment.

The purpose of our survey was to investigate how healthcare professionals view object characteristics and their influence on patient safety and stability during ambulation.

Methods

A diverse group of 66 healthcare professionals completed our voluntary online survey (IRB #00099410). Study data were collected and managed using REDCap electronic data capture tools hosted at the University of Utah [5, 6]. In order to participate in the survey, respondents must have interacted with individuals with mobility impairement in a place of employment in the last 5 years. All potential respondents were recruited by email.

The survey presented the following 5 scenarios describing individuals with mobility impairments ambulating without assistive devices: proactively seeking out objects for support during walking (**PW**), reaching for objects after becoming unstable during walking (**RW**), proactively seeking out objects for support during a 180-degree turn (**PT**), reaching for objects after becoming unstable during a 180-degree turn (**RT**) and, completing a sit-stand-sit (**STS**).

Respondents were asked to assign a score between 1 (low) and 5 (high) to the level of influence an object characteristic has on a patient's safety and stability during each scenario. General object characteristics included: Height, Movability, Grasp-ability. Sub-charecteristics included: Compliance of Surface (**COS**), Resistance to Movement (**RTM**), Type of Grasp (**TOG**), Smoothness of Grasp (**SOG**), Seat-pan Height (**SH),** Armrest/rail Height (**AH**) and Backrest Height (**BH**).

Wilcoxon signed-rank test, with an alpha of 0.01 was used to compare scores between characteristics. Only charecteristics in the same group were compared.

Results and Discussion

Table 1 summarizes the distribution of healthcare professionals who responded to the survey. Based on the preliminary results and an α level of 0.01, Wilcox signed-rank test showed no significant difference ($p > 0.01$) between Height/Grasp-ability, Height/Movability, and Grasp-ability/Movability for PW, RW, PT, and RT, suggesting that Height, Movability and Grasp-ability characteristics are equally important for tasks involving gait.

For STS, the Wilcox signed-rank test indicated that Movability (4.05 ± 1.01) and Height (4.29 ± 0.74) were significantly different than Grasp-ability (3.17 ± 1.16), $p < .001$, suggesting that Movability and Height are more influential in providing safety and stability than Grasp-ability. Additionally, the SH (4.56 ± 0.64) and AH (4.05 ± 0.77) ratings were significantly different from BH (2.67 ± 1.07), $p < .001$, and SH was also statistically different from AH, $p < .001$. Therefore, SH may be the most important characteristic contributing to a a patient's safety and stability during STS.

For all scenarios TOG was statistically different than SOG, $p < .01$, and RTM was significantly different from COS, $p < .001$. Therefore TOG, and RTM may be more influential in providing safety and stability than SOG and COS respectively.

Table 1. Distribution of survey respondents

Profession	% Response	Count
Physical Therapist	50.0	33
Physician/Medical Doctor	15.1	10
Nurse/Nurse Assistant	13.6	9
Occupational Therapist	9.1	6
Other Healthcare Professional	12.1	8

Significance

Based on the preliminary results there appears to be a consistent trend in ratings across walking and turning scenarios (PW, RW, PT, RT), suggesting that tasks involving gait require similar object characteristic for safety and stability. Tasks involving sitting, may require slightly different object characteristics.

The results from this survey will provide valuable insight into the way healthcare professionals perceive how different object characteristics influence the safety and stability of a patient with mobility impairment. This insight will provide a starting point for future research into object characteristics, and their influence on safety and stability during ambulation. These data may also impact the future of fall prevention research, shifting the focus more towards room design. Data collection for the survey will continue until 100 responses have been achieved.

Acknowledgments

This research is supported by AHRQ (R18HS024143-01) and the Center for Clinical and Translational Sciences grant (8UL1TR000105).

References

[1] Currie, L.M., Annual review of nursing research 24(1) (2006): 39-74.
[2] Tzeng H.M., et al., J of Nursing Care Quality 23(3) (2008): 233-241.
[3] Simpson, A. H. R. W., et al., Age and ageing 33(3) (2004): 242-246.
[4] Figueiro, M. G.,et al., BMC geriatrics 11(1) (2011): 49.
[5] Harris, P. A., et al., J of biomed info 42 (2) (2009): 377-381.
[6] Harris, P. A., et al., J of biomed info 95 (2019): 1032

Evaluation of the Four Square Step Test as an outcome measure in a fall prevention program

Claire Z. Zai[1], Trevor D. Kingsbury[1], John-David Collins[1], Julianne Stewart[1], Riley Sheehan[2-3], Brad D. Hendershot[4], Christopher L. Dearth[4], Kenton Kaufman[5]

[1]Naval Medical Center San Diego, San Diego, CA; [2]Henry M Jackson Foundation for the Advancement of Military Medicine, Bethesda, MD; [3]Center for the Intrepid, Brooke Army Medical Center, JBSA Ft. Sam Houston, TX, USA; [4]DoD-VA Extremity Trauma & Amputation Center of Excellence, Walter Reed National Military Medical Center & Uniformed Services University of the Health Sciences, Bethesda, MD, USA ; [5]Mayo Clinic, Rochester, MN

Email: claire.z.zai.ctr@mail.mil

Introduction

The Four Square Step Test (FSST) assesses dynamic balance with predictive validity for fall risk in a variety of clinical populations[1]. The FSST was previously used to assess changes in fall risk in a multi-site study aimed a utilizing a training program to decrease fall incidence in Service members (SM) with severe lower extremity (LE) trauma[2]. This secondary study of a larger intervention evaluated the use of the FSST to assess fall risk during a clinically-focused fall prevention program. It was hypothesized that SMs who successfully completed the program would show faster FSST times.

Methods

SMs (n=24) with major LE trauma who utilize an Intrepid Dynamic Exoskeletal Orthoses (IDEO) or prosthesis for high level activities were recruited across three Medical Treatment Facilities (MTFs) and signed informed consent approved by the NMCSD IRB (NMCSD.2016.0077). Subjects (Age: 35.1±8.7 years, time since injury: 5.0±4.2 years) completed a total of 5 FSST as described previously[3] (Baseline; Two-week Baseline Retest; Post-Training; 3Mo; and 6Mo Follow-up) over a 7-month period in conjunction with a training program designed to improve their ability to recover from falls. After the completion of the training program each subject reported any falls via an electronic survey distributed every 2 weeks during the 6 months following training completion. Patients who reported one or more falls post-training were categorized as fallers (F) (n=14), those that reported no falls were categorized as non-fallers (NF) (n=10). A two-way repeated measures ANOVA was used to determine the effect of the training program on FSST times and the tests ability to predict falls in the following 6 months (α=0.05).

Results and Discussion

Mean FSST at Baseline was 6.2 ± 1.4 s for all participants. The average reduction in time for all participants was 0.90 ± 0.93s. There was no decrease across all time points in the FSST score times (*Power*=0.81). Neither the completion of the training program nor time reduced the FSST scores. Furthermore, F reduced their FSST time by 0.89 ± 1.1s and NF reduced their FSST time by 0.88 ± 0.72s; there were no differences (p>0.05) in FSST times between F and NF, nor at any time point (Table 1).

It has been reported that a threshold of 8.49s can differentiate fallers and non-fallers[4]. However, all subjects were below this threshold time at the completion of the training program and yet 14 (58%) still reported falling post-training. This may be indicative of a ceiling effect in the FSST in this population as these participants performed similarly to uninjured military controls[6]. Additionally, the reduction in mean FSST group scores was not greater than the minimally detectable change of 1.41s for either F or NF[5]. SM participating in this study do not represent the typical LE injury patient seen in the civilian sector. Of the 24 participants, 67% reported a walking capacity of more than 5 miles and an additional 13% could walk between 2 -3 miles indicating a high level of fitness. There was also no difference in the time since injury between either F and NF group.SM have greater access to rehabilitative services compared to civilian counterparts which may contribute to lower FSST scores. Other tests, such as the Narrowing Beam Walking Test, have been shown to be a valid measure in similar populations and may be a more appropriate test for this population[6].

Significance

Historically, the FSST has been used to assess fall risk in some populations with LE trauma. This study has demonstrated that high-performing individuals may require a different assessment tool due to a possible ceiling effect. When evaluating fall risk in highly functional patients with lower extremity trauma, test selection is an important and evolving process.

Acknowledgments and Disclaimers

The view(s) expressed herein are those of the author(s) and do not reflect the official policy or position of the U.S. Army Medical Department, U.S. Army Office of the Surgeon General, Department of the Air Force, Department of the Army, Department of the Navy, or the Department of Defense, The Henry Jackson Foundation, or the U.S. Government. Funded by Department of Defense Grant No. W81XWH-15-2-0071.

References

1. Balk et al 2(2019) *Arch Phys Med Rehabil.* Dec;100(12):2354-2370
2. Sessoms et al (2014) *J. Biomech* Jan 3;47 (1): 277-80
3. Wilken et al 2018 *J Orthop Trauma.* Apr;32(4): 183-189
4. Sawers et al (2020) *PM R* Jan;12(1):16-25
5. Wilken et al (2012) *J Am Acad Orthop Surg.* 2012;20 Syook 1:S42-7
6. Sawers et al 2018 *J Rehabil Med* May 8;50 (5): 457-464

Condition	Baseline	2-week Test-retest period	2-week Baseline Retest	Training (~4 weeks)	Post-Training Assessment	3Mo Follow-Up Assessment	6 Mo Follow-Up Assessment
All subjects	6.2±1.4		6.1 ± 1.2		5.8 ± 1.2	5.6 ±1.3	5.3 ±1.1
Non-Fallers (NF)	5.7 ± 1.4		5.6 ± 1.3		5.3 ± 1.1	4.9 ±1.1	4.9 ±1.1
Fallers (F)	6.6 ± 1.5		6.4 ± 1.3		6.0 ± 1.3	6.0 ±1.4	5.9 ± 1.2

Table 1. Four Square Step Test (FSST) times for both Fallers and Non-Fallers. Shaded areas indicate time between Baseline and Retest. Times are listed in seconds (Average ± Standard Deviation). There was no significant difference between groups at any time point or over time within a group.

Causes of increased step incidence in response to perturbations in older adults

Tom Van Wouwe.[1], Lena Ting[2], Friedl De Groote[1]
[1]Department of Movement Sciences, KU Leuven, Leuven, Belgium
[2] W.H. Coulter Department of Biomedical Engineering Emory University and Georgia Tech
Email: tom.vanwouwe@kuleuven.be

Introduction

When perturbed by unpredictable backward support-surface translations during upright standing while trying to keep the feet in place, healthy older adults (OA) step more frequently than young adults (YA). Different possible causes for the increased step frequency in OA compared to YA have been suggested. First, alterations in the musculoskeletal system are thought to underlie this increased step frequency. Reduced plantarflexor strength and rate of force development might reduce the potential to use the ankle strategy to restore balance. Use of the ankle strategy can be quantified by observing the shift of the center-of-pressure (COP) within the base-of-support (BOS, defined by the feet) following a perturbation. However, the relation between muscle strength and stepping frequency is unclear [2]. Other changes in the musculoskeletal system (e.g. reduced hip and lumbar mobility/flexibility) impair performing hip strategies to counteract the effect of a perturbation. Use of the hip strategy can be quantified by observing the trunk lean trajectories during the postural response. Second, the initial COP position is related to the occurance of stepping responses [3], and therefore increased postural sway in OA might explain increased stepping incidence. Third, a change in neural control strategy might favor stepping strategies at less threatening situations in OA, leading to initiation of a step strategy at lower extrapolated center-of-mass (xCOM) deviations. We confirm that (a) OA step more frequently than YA at the same perturbation magnitude and we test three hypotheses about increased step frequency in OA: (b) COP movement is altered due to less effective use of the ankle strategy in OA, (c) anterior initial COP increases step incidence and is more prevalent in OA, (d) older adults initiate steps at lower xCOM.

Methods

We measured the kinematic response of 10 healthy young (20-27y) and 14 healthy older adults (72±3.13y) standing on a movable platform. Subjects were instructed to maintain balance without taking a step. Backward support-surface translations with six different magnitudes were administered randomly five times each within a set of multi-directional perturbations. Motion capture and force plate data was processed to analyze the trunk lean angle, the body COM kinematics, the COP motion and the step incidence during the responses to backward translations.
We compared (a) step incidence between YA and OA (t-test), (b) COP trajectories and trunk lean trajectories between YA and OA (statistical parametric mapping; t-test), (c) initial COP location between stepping and non stepping responses (t-test) and between YA and OA (t-test) and (d) xCOM position at step initiation (instant at which at least one foot leaves the ground) between YA and OA (t-test).

Results and Discussion

OA stepped more often than YA (Fig. 1a). The most plausible hypothesis for this increased step incidence in OA is that OA shift to a stepping strategy at less balance threatening conditions, i.e. at lower xCOM (Figure 1d). OA shift their COP similar to YA, and thus the increased step incidence is not a coping mechanism for a reduced ability to perform an ankle strategy (Fig. 1b). We confirmed that the mobility to properly use a hip strategy is intact in OA as trunk lean trajectories do not differ between OA and YA (not shown). Overall, initial COP is more anterior for step responses (Fig. 1c), but OA do not exhibit higher variability in initial COP (not shown in figure; p>0.1). An important finding is that variability in OA COP trajectories, xCOM at step initiation and trunk lean trajectories (not shown) is higher.

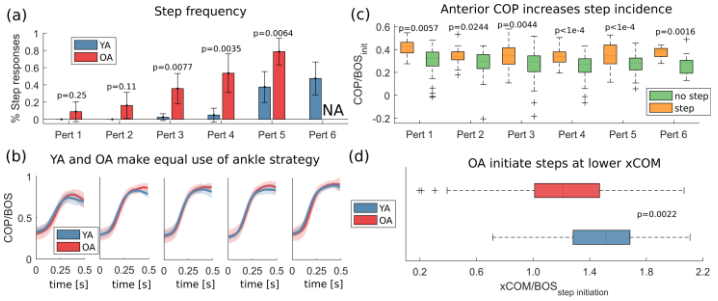

Figure 1 - (a) OA step more often than YA, (b) COP/BOS trajectories are not different for OA and YA. (c) Initial COP is more anterior for step responses. (d) xCOM at step initiation is lower in OA than in YA.

The initial response to the perturbation, which relies on the development of ankle torque to move the COP within the BOS is similar in OA and YA. Yet, OA step more often and our results suggest that this is due to an altered strategy were steps are initiated at a more stable position. The underlying reasons for this shift in strategy needs further investigation. Increased movement variability, originating from sensorimotor noise at different levels of the neuromotor system, might play a role in selecting a more robust strategy. But alternative explanations, such as increased fear of falling are plausible as well.

Significance

OA might adapt movement strategies in order to cope with subtle changes in neuromotor function rather (e.g. increased sensorimotor variability) than with obvious specific declines (e.g. reduced muscle strength) if these don't limit the performance of a specific task. We believe that further research is necessary that focusses on causal interaction between changes in the neuromotor system and adaptations of the central nervous system to cope with these. We will do this by combining simulations with experiments as this is a valuable approach to understand causalities.

Acknowledgments

We acknowledge FWO fellowship: 1S82320N

References

[1] F. Horak, J. Neurophysiol., 1986
[2] M. Fujimoto, Gait & Posture, 2013
[3] Van Wouwe, 2020 (in preparation)
[4] T. J. Welch, J Neurophysiol., 2008
[5] Y. C. Pai, J. Biomech., 2000

Locomotor Response of Older Persons with and without Transtibial Amputation to a Trip Disturbance

Claire Martin[1], Paul Hammond II[2], Rebecca Stine[2], and Matthew J. Major[1, 2, 3]
[1]Department of Biomedical Engineering, Northwestern University, Evanston IL
[2]Jesse Brown VA Medical Center, Chicago IL
[3]Department of Physical Medicine and Rehabilitation, Northwestern University, Chicago IL
Email: matthew-major@northwestern.edu

Introduction

Falls pose a significant health risk to persons with major lower limb loss throughout the rehabilitation process, commonly resulting from trips [1]. Fall risk is already elevated for older individuals due to neuromotor decline [2], and so risk is of greater concern for older lower limb prosthesis users (PUs). Characterizing the motor response of persons to gait disturbances is a useful methodology to understanding the factors related to falls [3]. While this technique has been applied to younger PUs [4], it has not been implemented with their older counterparts. The study aim was to characterize the locomotor response of older PUs to a trip disturbance and compare this response to able-bodied controls. As analysis is ongoing, we present initial results from two age-/gender-matched control and PU participants.

Methods

After obtaining written informed consent, lower extremity muscle strength was measured with a handheld dynamometer (Lafayette Systems, IN). Participants then completed two trials of steady-state data collection while walking on a custom-built treadmill (Motek Forcelink, the Netherlands) at their self-selected speed and 0.8 m/s (steady-state speed used for perturbation trials). Following baseline collections, participants completed 12 perturbation trials. For each perturbation trial, participants first achieved steady-state walking at 0.8 m/s, then at the moment of foot initial contact received a rapid, symmetric treadmill belt acceleration and deceleration (6.5 m/s^2) back to 0.8 m/s. The perturbation occurred at a random stride (n=11-20) after reaching steady-state walking. The trial ended 20 strides after the perturbation occurred. Six trials for each foot side (right, left) initial contact were collected in a randomized order. Participants were instructed to recover from the disturbance and continue walking. Kinematic data were collected with an optical motion capture system (Motion Analysis, CA) and custom marker set. Visual 3D (C-Motion, MD) was used to estimate sagittal-plane whole-body angular momentum (*WAM*), trunk inclination (*TI*), and trunk inclination velocity (*TV*) *PRE*- and *POST*-perturbation.

Results and Discussion

The control participant (70 years, 173.0 cm, 82.8 kg, male) and PU participant (69 years, 180.5 cm, 78.8 kg, male) completed all trials and successfully recovered from the perturbations without a fall (partial harness arrest). A representative temporal WAM profile is displayed in Fig. 1, and Table 1 reports *PRE* and *POST* values for maximum WAM (normalized by subject mass, height, and treadmill speed), TI, and TV across trials for each limb side.

PRE TI and TV were similar for both participants, but the PU displayed a higher maximum WAM during steady-state walking at baseline. As expected, WAM increased *POST*-perturbation, but the control participant experienced a greater increase relative to their *PRE* levels than the PU, as well as greater WAM on both limb sides respectively compared to the PU. This result suggests greater postural control demands of the control participant to regulate higher WAM post disturbance.

Maximum TI and TV increased *POST*-perturbation as participants rotated their trunk forward during recovery, which may help explain the increase in *POST* WAM (Fig. 1). However, while *POST* TI was nearly equivalent for both participants and limb sides, maximum TV was noticeably different. TV increased *POST*-perturbation for controls in a way that aligned with the relative increase in WAM (higher non-dominant than dominant), this trend was the opposite for the PU. Furthermore, the sound-side *POST* TV was considerably higher than control values, while prosthetic-side TV was lower than control values. Even though *POST* sound-side TV was the largest, the WAM was the smallest. Results suggest different postural control strategies between the control and PU to regulate WAM during perturbation response. Future work will assess contributions of other body dynamics.

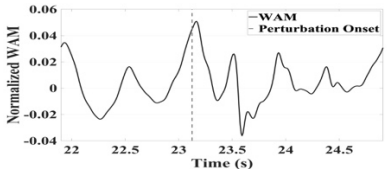

Figure 1: Representative graph of PU normalized WAM approximately one stride pre-perturbation onset and two strides post-perturbation.

Table 1: Maximum WAM, TI and TV (mean±SD) across trials for each perturbed side, control Non-/Dominant and PU Sound/Prosthetic.

Perturbed Limb side	*WAM (PRE)*	*WAM (POST)*	*TI (°) (PRE)*	*TI (°) (POST)*	*TV (°/s) (PRE)*	*TV (°/s) (POST)*
Control, Dom	0.033 ± 0.001	0.053 ± 0.005	6 ± 1	16 ± 3	21 ± 1	73 ± 27
Control, Non-Dom	0.034 ± 0.001	0.065 ± 0.005	6 ± 1	17 ± 2	19 ± 2	90 ± 15
PU, Sound	0.038 ± 0.002	0.050 ± 0.005	7 ± 3	18 ± 2	20 ± 4	113 ± 17
PU, Prosthetic	0.037 ± 0.001	0.053 ± 0.003	7 ± 3	17 ± 2	22 ± 4	67 ± 5

Significance

Initial results suggest different motor control strategies between older able-bodied individuals and PUs when recovering from a trip. This work will help understand mechanisms underlying fall risk in older PUs, and potential strategies to minimize this risk.

Acknowledgments

Work supported by the US Dept of VA (#5IK2RX001322). We thank Jenny Kent for assistance with the biomechanical model.

References

[1] Kim J. PM R, 2018; 11(4): 344-353.
[2] Hausdorff JM. Arch Phys Med Rehabil, 2001; 82: 1050-6.
[3] Owings TM. Clin Biomech, 2001; 16: 813-9.
[4] Crenshaw JR. Gait Posture, 2013; 38: 534-6.

Balance Control and Muscle Asymmetry in Persons with Lower-limb Amputation During Yoga Poses

Nicole M. Stoehr, Pranavi Depur, Andrew St. Julien, Rosa M. Angulo-Barroso Ph.D. and Jacob W. Hinkel-Lipsker Ph.D.
Move-Learn Lab, Department of Kinesiology, California State University, Northridge
Email: Nicole.stoehr.721@my.csun.edu

Introduction

People with lower limb amputation (LLA) commonly experience chronic orthopedic disabilities (e.g. low back pain) and comorbidities (e.g. obesity) partially due to reduced activity levels[1]. Yoga could potentially improve quality of life by increasing muscular strength, flexibility, and overall activity levels[2]. However, the poses commonly performed during general yoga practices are designed for healthy individuals, without considering the compromised balance and musculature for those with LLA.[3,4] Therefore, we seek to assess how individuals with LLA maintain balance during static yoga poses. We hypothesize that people with LLA will experience greater balance challenges, as demonstrated by an increased center of pressure (COP) sway in the medio-lateral (ML) and anterior-posterior (AP) directions. We further hypothesize that these balance challenges will be accompanied by heightened asymmetric behaviors in the trunk and hip muscles.

Methods

Five individuals with LLA and five healthy matched control participants (able-bodied; AB) are being recruited in this ongoing study. Pilot data for n=1 for each group are presented here. Participants were instrumented with eight electrodes placed bilaterally on the belly of the lower rectus abdominus (RA), external obliques (EO), erector spinae (ES), and gluteus medius (GM) for collection of electromyographic data (EMG). They were also fitted with six reflective markers placed on the feet to define their base of support (BOS). Participants partook in a yoga warm-up, followed by a randomized sequence consisting of seven poses that required neutral pelvic orientation and parallel feet, each foot on top of a force plate. Each pose was held for 50 seconds and the sequence was repeated three times. During the sequence, EMG data were recorded at 2000 Hz, COP data were collected using two force plates at 2000 Hz and 3D marker coordinate data were collected at 100 Hz using a 10-camera motion capture system. The root mean square (RMS) for each EMG signal was normalized to the dominant side during standing in anatomical pose (baseline; BL) and the difference between the right and left side was computed as a measure of muscle asymmetry. Using the measured vertical ground reaction force and COP from each force plate, we implemented a novel approach that expresses a combined center of pressure (COPc) from both feet in the global coordinate system. Lastly, we expressed COP sway in each direction (ML, AP) as a percentage of the corresponding BOS width for each direction.

Results and Discussion

Preliminary results from one participant with and one without amputation are presented here. The LLA participant has a unilateral transfemoral amputation (left) but is otherwise healthy. Compared to the AB participant, this individual experienced greater difficulty maintaining balance in the AP direction, with the greatest difficulty in poses with flexed knees (chair and back bend) (Figure 2). In addition, the LLA participant had a pattern of muscle activation across all poses that showed heightened muscle activity towards the amputated side only in the EO group (Figure 1). Such results potentially indicate that the LLA may be using the left EO to stabilize the trunk and may be compensating for the missing lower extremity muscles on the amputated side. These results partially support our hypotheses as asymmetry was only observed on one set of muscles. Furthermore, sway was only increased in the AP direction and decreased in the ML direction for some poses. Data collection is in process and will help to further elucidate these findings.

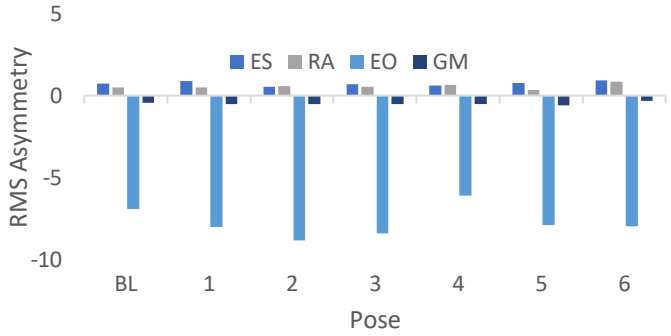

Figure 1: *RMS EMG Asymmetry for a single unilateral transfemoral LLA participant. (+)= greater activation on intact side and (-)= greater activation towards amputated side.*

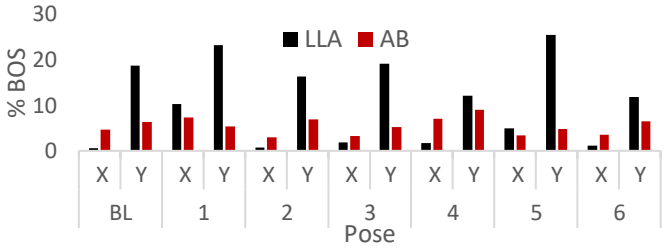

Figure 2. *COP sway in the ML (X) and AP (Y) directions as a percentage of BOS across yoga poses.*

Significance

Findings from this study indicate that the LLA has increased AP instability while performing common yoga poses. Practitioners and clinicians should be mindful of this additional challenge when prescribing these poses to those with LLA. The noted muscle recruitment asymmetries from the LLA demonstrate that the more proximal trunk musculature on the amputated side compensate for the lack of lower limb muscles—indicating that static exercises may be beneficial for training of core stabilization muscles. Further study is warranted to determine how these strategies differ across various subcategories within the LLA population (e.g. type of amputation). In total, performance of these yoga postures were feasible and has the potential to improve quality of life for individuals with LLA.

References

[1] Paxton et al. 2016 [2] Thompson et al. 2011
[3] Gaffney et al. 2018 [4] Nederhand et al. 2012

Segment Angular Momenta in People with a Unilateral Transtibial Amputation During 90-degree Turns

Luis A. Nolasco[1], Jenna Livingston[2], Anne K. Silverman[3], and Deanna H. Gates[1]
[1]School of Kinesiology, [2]Department of Mechanical Engineering, University of Michigan, Ann Arbor, MI
[3]Department of Mechanical Engineering, Colorado School of Mines, Golden, CO
Email: lnolasco@umich.edu

Introduction

People with a transtibial amputation (TTA) have difficulty regulating angular momentum compared to people without amputation during straight-line walking [1], suggesting decreased balance control. In daily life, ~35% of indoor steps are turns [2]. Turns may pose a greater risk for loss of balance as they require greater generation of segment angular momentum compared to straight-line walking in people without amputations [3]. Further, the inability to actively control the ankle in people with TTA may result in altered strategies to regulate segment angular momenta used during turning. The purpose of this study was to compare upper and lower limb segment angular momenta during 90° turns between people with and without TTA and determine the influence of turn direction.

Methods

Eight people with TTA (1F/7M; 52±15 years; 99.5±17.9 kg; 1.77±0.08 m) and 8 controls (2F/6M; 39±15 years; 80.7±19.5 kg; 1.77±0.09 m) performed left and right 90° step turns. Full body kinematics were tracked at 120 Hz using a 20-camera motion capture system. Kinematics were low-pass filtered using a 4th-order Butterworth filter (f_C = 6 Hz). A 13-segment model was developed in Visual3D; the mass and inertial properties of the prosthesis were adjusted for people with TTA [4]. We summed the foot, shank, and thigh, and separately, the upper arm and forearm angular momenta about the body center of mass to calculate the angular momentum (**H**) for each limb (Outside Leg, Inside Leg, Outside Arm, Inside Arm). We normalized limb **H** by body height, mass, and speed across each stride. **H** was defined in the center of mass reference frame. We divided the turn into initiation and termination strides. Turns for people with TTA were grouped for analysis by whether the prosthesis was on the inside (P_{in}) or outside (P_{out}) of the turn. The dependent measures were the four average limb **H** values. We compared measures between groups and turn direction using a doubly multivariate analysis. Significant main effects and interactions were explored using Estimated Marginal Means with a Bonferroni correction.

Results and Discussion

There were group × turn interactions for limb **H** during initiation in the frontal plane and during termination in the sagittal plane ($p < 0.009$). Here, we focused on significant interactions in the transverse plane as this plane is critical for turning and there were differences during both initation and termination.

During initiation and termination in the transverse plane, the P_{in} condition had greater outside leg **H** toward the inside of the turn compared to controls ($p < 0.037$) and P_{out} ($p < 0.001$). Also during initiation, the P_{in} condition had greater inside leg **H** toward the inside of the turn compared to P_{out} ($p < 0.001$). During termination, the P_{in} condition had smaller inside leg **H** toward the outside of the turn compared to P_{out} ($p < 0.001$) while the P_{out} condition had greater **H** compared to controls ($p = 0.013$).

For people with TTA, the **H** generated by the leg to complete the turn depended on whether the prosthesis was on the inside or outside of the turn. Overall, outside leg **H** values were greater during P_{in} relative to P_{out}. Reduced muscle control and range of motion on the prosthetic leg may require greater velocities (and therefore momentum) from the outside leg to complete the turning task. While people with TTA were able to complete 90° turns, greater **H** generation compared to controls suggest that the regulation of **H** between limbs during turning may be more challenging for people with TTA. In addition, prostheses capable of transverse plane movement [5] may influence turning strategy and the associated limb **H**.

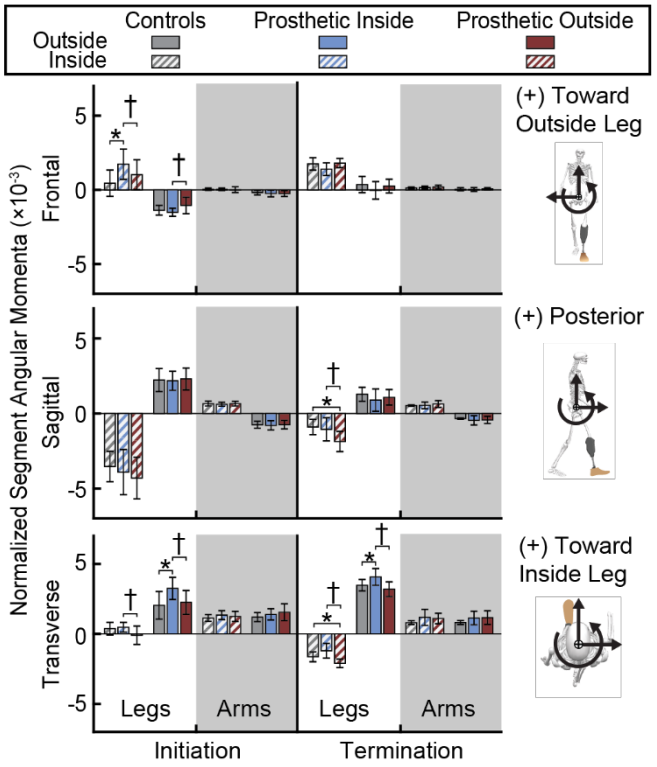

Figure 1: Average limb **H** over the initation and termination strides. ('*' $p \leq 0.05$ between groups; '†' $p \leq 0.05$ between turn types)

Significance

Turning with the prosthesis on the inside may be more challenging for people with TTA as it requires greater leg angular momentum. Thus, prosthetic rehabilitation should focus on generating momentum with other segments to regulate outside leg momentum when turning with the prosthesis on the inside. Future work should explore the role of other body segments and different types of prostheses on angular momentum during turns.

References

[1] Silverman AK, et al. J Biomech, 44, 379-385, 2011
[2] Glaister BC, et al. Gait Posture, 25, 289-294, 2007
[3] Nolasco LA, et al. Gait Posture, 70, 12-19, 2019
[4] Ferris A, et al. J Biomech, 54, 44-48, 2017
[5] Pew C, et al. J Biomech, 96, 109330, 2019

Relationship Between Postural Control and Lower Body Physical Function in Children with Cerebral Palsy

Sydni Wilhoite[1], Katelyn S. Campbell[1], Li Li[2], Karl M. Newell[1], Gavin Colquitt[2], Barbara Weissman[3], Joshua Vova[3] and Christopher Modlesky[1]
[1]Department of Kinesiology, University of Georgia, Athens, GA
[2]Department of Health Sciences and Kinesiology, Georgia Southern University, Statesboro, GA
[3]Children's Healthcare of Atlanta, Atlanta, GA
Email: christopher.modlesky@uga.edu

Introduction

Cerebral palsy (CP) is a neurological disorder often characterized by deficits in postural control.[1] The deficits are often assessed by center of pressure (COP) motion during quiet stance using a single force platform. However, assessing COP motion of each limb using two separate platforms might be beneficial due to the asymmetrical nature of the pathology.

Balance impairments may cause limitations in functional mobility; however little is known about the relationship between balance measures and functional movement measures in children with CP. The purpose of this study was to assess the relationship between COP motion of individual limbs and combined limbs during quiet stance and measures associated with lower body physical function. We hypothesized that compared to COP movements of combined limbs, COP movements of the individual limb will exhibit a stronger association with lower body physical function.

Methods

Eighteen ambulatory children (5-11 y; Gross Motor Function Classification System I-II) with spastic CP were studied. Two force platforms (Bertec, Columbus, OH, 100 Hz) were used to assess COP from more (MAL) and less affected limb (LAL) during quiet stance. Net COP was calculated by combining MAL and LAL data from both platforms.[2] Participants completed 3 trials of quiet stance for 30 seconds each. COP data were filtered using a 5 Hz 8th order Butterworth low pass filter. Linear (i.e., sway distance and velocity) and nonlinear (i.e., sample entropy (sampEn)) COP variables were calculated for both anteroposterior (AP) and mediolateral (ML) directions. Outcome variables presented as the average of the 3 trials. A progressive lateral step up test (LSUT) was conducted to assess lower body physical function. The test consisted of 3 trials of with the MAL on the step and the LAL raised onto and lowered off the step as many times as possible in 20 seconds. Each trial corresponded with an increase in step height (i.e., 10, 15, and 20 cm). A composite score was calculated based on step height and the number of steps completed. Pearson correlations were used to assess the relationship between COP variables for individual and combined limbs and LSUT score.

Results and Discussion

The MAL's AP and ML sway velocity were inversely related to LSUT score (r=-.602, p=.008 and r=-.555, p=.047, respectively; Figure 1A and D). However, none of the LAL's COP variables were significantly related with LSUT score (r range=-.255 to .139, p>.30). The Net AP and ML sway velocities were inversely related to the LSUT score, although the relationships were weaker (r=-.432, p=.073 and r=-.474, p=.047, respectively; Figure 1C and F) than the relationships observed with the more affected limb.

The relationships between sway velocity and LSUT score suggest that assessment of COP using a single force platform may predict lower body functional ability on the more affected side in children with CP. However, the prediction may not be as robust as an assessment of COP using 2 force platforms. Further research should be conducted to examine the relationship between individual limb COP measures and measures of physical function beyond LSUT for individuals with CP and other conditions that may lead to more prominent effects on one side.

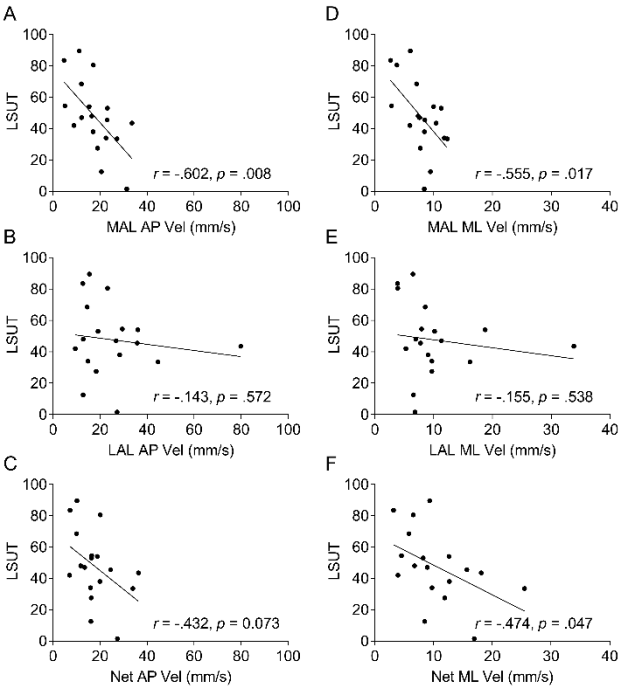

Figure 1. Relationship between COP sway velocity in the anteroposterior (AP) and mediolateral (ML) directions for the more (MAL) and less affected limb (LAL), and combined limbs (Net) and lateral step up test (LSUT) score.

Significance

Postural control assessment using a single force platform is common, but compared to postural control assessment using dual force platforms is likely less representative of the functional deficits in children with CP.

Acknowledgments

This research study was funded by the National Institutes of Health (HD090126).

References

1 Pavão et al. (2013). *Res Dev Disabil*, *34*(5), 1367-1375.
2 Wang & Newell (2014). *Neurosci Biobehav, Rev, 47*, 194-202.

Effects of Foot Structure on Postural Stability in Healthy Young Individuals

Michael J. Jayson[1], Daniel J. Davis[1], Paul L. Juneau[2], and John H. Challis[1]
[1]Biomechanics Laboratory, The Pennsylvania State University, University Park, PA, USA
[2]Division of Biostatistics, NIH Library, Office of Research Services, National Institutes of Health, Bethesda, MD, USA/Contractor – Zimmerman Associates, Inc., Fairfax, VA, USA
Email: jhc10@psu.edu

Introduction

Various structural components of the human foot stabilize the body during upright standing to maintain postural control. Center of pressure (COP) is often used as an index of postural stability in standing [1]. Previous studies have found associations between static foot structural measures and plantar pressures in healthy individuals, but to date no study has investigated the associations between foot structure and metrics of COP motion [2].

This study sought to determine if there is an effect of foot structure on postural stability in healthy young individuals. It was hypothesized that foot structure has an effect on postural stability in this population.

Methods

Measurements of foot structure and postural stability were measured for 10 subjects (5 male, 5 female; age 21.5 ± 0.5 yrs; mass 71.4 ± 19.8 kg; height 1.70 ± 0.11 m) who gave informed consent to procedures which had been approved by the institutional review board.

The subtalar joint of participants' dominant foot was placed in subtalar neutral position defined as equal palpation of the medial and lateral talar head in the frontal plane. Measurements of navicular height (NH), medial longitudinal arch angle (LAA) and Feiss line (FL) were made using an ink pen, a six-inch plastic ruler, and a six-inch plastic goniometer. FL was measured as the perpendicular distance from the navicular tuberosity to a line connecting the medial malleolus to the medial aspect of the first metatarsal head [3]. If the navicular tuberosity was above the line, FL was positive; if below, FL was negative. Measurements were repeated with the foot in subtalar resting position. Differences between neutral and resting measures were used to calculate range of motion (ROM). Foot arch and ROM measurements were then classified using cut-off values from Nilsson et al., 2012 [4].

Indices of COP motion from a force plate were measured at 100 Hz during quiet standing for four trials of 30 seconds each under each of three conditions: eyes open normal (EON) stance, eyes closed normal (ECN) stance and eyes open tandem (EOT) stance (one foot directly in front of the other).

Each COP measurement was modelled, by condition, as a function of foot structure, trial and their interaction via a mixed model employing an unstructured covariance structure to accommodate within subject effects. Hochberg's multiple comparison adjustment was applied to accommodate multiplicity of statistical inference within each condition.

Results and Discussion

The COP metrics produced values comparable to values in the literature [1]. Analysis of the effect of foot structure on COP metrics indicated significant relationships. Incidents of significant interaction effects were found; therefore, Hochberg's multiple comparison adjustments were made (Table 1). Adjusted values show no statistically significant relationships between any of the foot measures and COP metrics (Table 1). These findings do not support the original hypothesis that foot structure has an effect on postural stability in healthy young individuals.

Significant interactions across condition and trial may exist between foot structure and postural stability such that metrics of COP motion are not uniform across trials but rather change over time. Future studies may want to examine two groups with extreme differences in foot structure (e.g. severely high arch vs low arch) to expand upon these findings.

Conclusions

These results suggest that when comparing postural stability between individuals of varying foot structure there is no need to account for foot structure in healthy young individuals.

Acknowledgments

This research was supported by The Pennsylvania State University Department of Kinesiology Marie Underhill Noll Endowment for Undergraduate Research in Exercise and Sport Science.

References

[1] Prieto, TE, et al. *IEEE Trans Biomed Eng* **43**, 956-966, 1996
[2] Jonely H, et al. *Clinical Biomech* **26,** 873-879, 2011
[3] Langley B, Cramp M, and Morrison SC. *J Foot Ankle Res* **9**, 45, 2016
[4] Nilsson KM, et al. *J Foot Ankle Res* **5**, 3, 2012

Table 1: Effect of levels of foot structure on metrics of COP motion within trials

Condition	Trial	Arch/ROM measurement	Arch/ROM classification comparsion	COP measurement	p-value	Hochberg's adjusted p-value
EON	3	FL	Low arch and normal arch	SDx	0.02	0.30
EON	4	FL	Low arch and normal arch	SDx	0.03	0.30
EON	4	FL	Normal arch and severely high arch	SDx	0.03	0.31
EOT	1	FL	Low arch and normal arch	SDx	0.03	0.88
EOT	1	NH	High arch and low arch	Fractal dimension	0.02	0.25
EOT	2	NH	High arch and normal arch	Fractal dimension	0.03	0.32
EON	2	ROM LAA	Normal ROM and rigid ROM	Fractal dimension	0.047	0.19

Note: SDx refers to the standard deviation of the COP motion in the anterior-posterior direction.

The Effects of Golf Specific Footwear on Postural Perturbations

Samuel J. Wilson[1], Jessica A. Mutchler, Paul T. Donahue, Charles C. Williams, Jacob R. Gdovin, John C. Garner
[1]Georgia Southern University, Department of Health Sciences and Kinesiology, Statesboro GA.
Email: sjwilson@georgiasouthern.edu

Introduction

Within a golf swing, one aspect that stands out in each phase is the ability to maintain balance. Previous reports suggest that extrinsic factors such as footwear and intrinsic factors such as muscular exertion level have detrimental effects on human postural control. However, no studies have examined the effects of modern golf footwear on muscle activity of the lower extremity. Thus, the purpose of this study was to examine differences in muscle activity when walking for extended durations in golf footwear

Methods

Six healthy male adults completed the study (age: 23.4±2.2 years; height: 181.5±9.0 cm; mass: 95.8±18.6 kg). Participants were tested in three types of golf-specific footwear including the dress shoe (DS), tennis shoe (TS), and casual spike-less shoe (CAS), as well as a barefoot condition (BF). Participants were instructed to walk at their self-selected walking speed and path throughout a 4 hour testing duration on the artificial turf that was laid throughout the lab. Reactive balance was assessed prior to the start of walking, and again every hour for 4 hours using the Motor Control Test (MCT), that can translate in the backward and forward directions to create two testing conditions, which include backward translations [medium (BWM)/large (BWL)] and forward translations [medium (FWM)/large (FWL)]. During balance tests, muscle activity was examined for two lower extremity muscles of the right leg: the tibaialsi anterior (TA), and the medial gastrocnemius (MG). Raw EMG data were collected at 1,500 Hz, band-pass filtered (20-250Hz) and rectified prior to analysis. Peak EMG, and time-to-peak (TTP) EMG were calculated for each muscle of interest. The EMG parameters were analysed using a 4 x 5 [4 (Footwear – DS, TS, MIN, BF) x 5 (Time – Pre, 60, 120, 180, 240)] repeated measures analysis of variance (ANOVA) independently for each of the MCT tests. Post hoc pairwise comparisons using a Tukey's LSD were performed if main effect significance was found for footwear types, and simple effects were calculated if significant interactions were found. Partial eta squared (η^2) effect size and F statistic are reported. For all analyses, significance was set at an alpha level of $p < 0.05$ and all statistical analyses were performed using the SPSS 22 statistical software package.

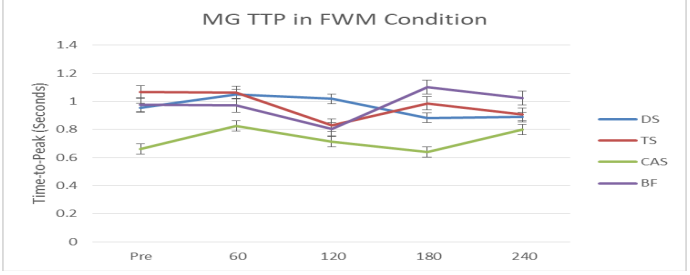

Figure 1: Time to peak EMG in the MG during the FWM condition. Bars represent stand error.

Results and Discussion

A significant interaction was found for the MG peak EMG during the BWL condition ($F(12,60) = 2.016$, $p = 0.03$, $\eta = 0.207$), suggesting that at hour 4, TS peak EMG was greater than the CAS. Time main effect for the TA TTP in the BWL condition ($F(4,20) = 3.62$, $p = 0.02$, $\eta = 0.420$), with increased TTP at hours 3 and 4 compared to hour 2. Finally, a footwear main effect was found for MG TTP in the FWM condition ($F(3,15) = 4.16$, $p = 0.025$, $\eta = 0.454$), suggesting that the DS and TS had increased TTP compared to the CAS.

The findings herein suggest, as expected, that reactive balance decrements would present over time. Specifically, decrements were observed after the second hour of standing and walking. Primarily, footwear differences were observed as decrements in muscle activity wearing the dress shoe and tennis shoe styles relative to the casual styles. Our findings over time corroborate with previous work, where balance deficits are observed after 2 hours of an extended workload (1). While footwear differences are likely due to structural differences between footwear. Previous work has suggested an increase in footwear mass, causes an increased workload in the lower extremity, and may lead to increased muscle activation and balance decrements (2). Currently, the TS and DS, both had a higher mass than the CAS, possibly explaining the balance decrements observed.

Significance

These findings are important, because, while maintaining postural control is a relatively simple process for the CNS under healthy conditions, when alterations to sensory input begin to disrupt the postural control system this task becomes more difficult. Further, as maintaining postural control becomes more difficult, it can affect any second tasks that are being done (3), such as the golf swing. Therefore, if footwear are causing adverse effects on postural control, it could also lead to decrements in golf performance. Based on the current findings, golfers should seek footwear that is lightweight and has relatively thin sole/midsole thickness in order to mitigate postural control deficits and decrease workload on the lower extremity.

References

1. Chander H, Garner JC and Wade C. Impact on balance while walking in occupational footwear. *Footwear Science* 2014; 6: 59-66.
2. Jones BH, Toner MM, Daniels WL, et al. The energy cost and heart-rate response of trained and untrained subjects walking and running in shoes and boots. *Ergonomics* 1984; 27: 895-902.
3. Woollacott M and Shumway-Cook A. Attention and the control of posture and gait: a review of an emerging area of research. *Gait & posture* 2002; 16: 1-14

Preliminary Investigation of Limb Load Symmetry During Quiet Stance & Sit-to-Stand

Sara Elnahhas[1], Nicole Stark[2], Robin M. Queen[2], Sara L. Arena[2]
[1]Mechanical Engineering, Virginia Tech
[2]Biomedical Engineering and Mechanics, Virginia Tech
Email: sarae@vt.edu

Introduction

Understanding human postural control is critical to assessing musculoskeletal and neurological pathologies. Postural control can be characterized by quantifying limb symmetry during various tasks [1]. Thus, limb symmetry is an important factor in evaluating balance performance of numerous populations such as those with Parkinson's Disease [2], or patients who have undergone knee anterior cruciate ligament reconstruction [3] and ankle anthroplasty [4]. Limb symmetry is also affected by everyday, environmental disturbances, and hence performing asymmetry assessments in non-research settings is important to capture a realistic prespective on human balance.

The purpose of this study was to examine load asymmetry during quiet stance in a healthy population, and if that relates to a functional, sit-to-stand, task in a non-laboratory environment.

Methods

This institutional review board approved study was conducted at the Biomedical Engineering Society annual meeting (2019, Philadelphia, PA) . Participants were included based on criteria in self-reported questionnaires that looked for injuries or conditions that may affect their ability to balance or load symmetrically. Each participant completed a quiet stance (QS) task and five sit-to-stand (STS) trials. Two PASCO force platforms (Roseville, CA) recorded vertical ground reaction forces during 30 second, eyes open, bilateral QS and STS.

In MATLAB, load symmetry was quantified using the Normalized Symmetry Index (NSI) [5]. The NSI performs best with multiple trials. Consequently, the middle 20-second interval of the QS task for each participant was broken up into three sub trials, and the five STS trials were used to calculate the NSI. Both calculations were computed with reference to the subjects dominant leg, as self-reported by answering "Which leg would you kick a soccer ball with?". Symmetry differences between tasks was assessed using a paired t-test and the association between tasks was determined usingPearson's correlation (p<0.05).

Results and Discussion

Data from sixty-three healthy, adults (25.9 ± 6.8 years old, 170.3 ± 9.1 cm, 68.0 ± 14.3 kg, 34 females, 29 males) were collected and analysed. Despite a visually large difference in the range of NSI between that for QS (0.692 ± 10.7, mean ± s.d.) and STS (0.824 ± 4.45) as indicated by the standard deviations, the values were not statistically different between tasks, suggesting a similar magnitude of asymmetry between the tasks. (Figure 1, p=0.9191).

This is further confirmed through the Pearson's correlation and the correlation plot (Figure 2). The NSI of QS and STS demonstrated a weak significant positive correlation (r = 0.291, p=0.021).

One goal of this study was to collect asymmetry data in real-world settings, which could also be considered a limitation of this work. The testing took place in a noisy, visually stimulating conference environment disturbing subjects' performance, with limited control over clothing or shoes worn, which restricts capturing the maximum bounds of human balance.

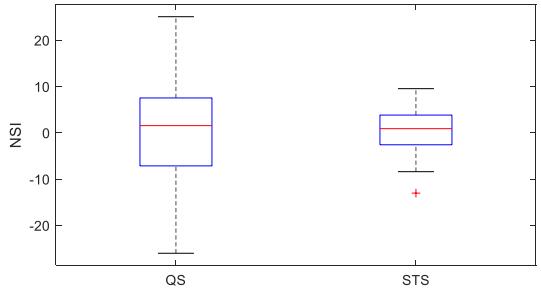

Figure 1: Boxplot comparing NSI values for QS and STS tasks; p-value 0.9191.

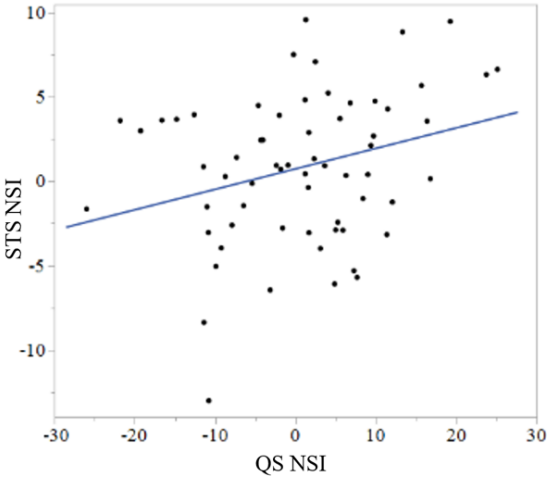

Figure 2: Correlation plot for the QS and STS tasks.

Significance

This study demonstrated that limb load asymmetry was consistent between QS and STS. The large range in asymmetry of QS has been found in a similar study [6]. Compared to NSI of STS, this difference is hypothesized to be associated with the ease of the balance task. QS requires less muscle activation and postural control to maintain balance than a five-time STS, and subjects may displace their weight more asymmetrically due to the reduced risk of falling. Hence, in a healthy population, asymmetry is to be expected within a relatively large range in typical, non-research settings. Future studies should seek to verify load asymmetry in relation to ease of task, and aim to establish the normal bounds of balance in larger populations.

References

[1] L. C. Anker et al. *Gait Posture,* vol. 27, Apr. 2008.
[2] F. A. Barbieri et al., *Hum. Mov. Sci.*, vol. 63, Feb. 2019.
[3] A. Gokeler et al., *Orthop.Trauma.Surg.Res.*, vol. 103, Oct. 2017.
[4] J. R. Gladish et al., *J. Biomech.*, vol. 83, Jan. 2019.
[5] R. Queen et al., *J. Biomech.*, vol. 99, Jan. 2020.
[6] J. Stodółka et al., *Acta Bioeng. Biomech.,* vol. 19, 20

Physical and Perceived Abilities and Motor Planning of Older Adults During A Virtual Beam-Walking Task

Meghan E. Kazanski.[1*], Jonathan B. Dingwell[1]
[1]Department of Kinesiology, The Pennsylvania State University, University Park, PA, USA
Email: *mek79@psu.edu

Introduction

Lateral balance control is critical to remaining upright while walking and maneuvering [1, 2]. In addition to physical stepping ability, we must also consider how perceived ability and motor planning impact responses to lateral balance challenges. Older adults demonstrate discrepencies between perceived and actual balance ability [3] and motor planning ability degrades with age [4]. Older and younger adults respond similarly to continuous lateral perturbations [5]. However, lateral balance challenges that require more motor planning and highlight discrepencies between actual vs. perceived ability may more-comprehensively demonstrate how age-related deficits impact lateral balance.

Here, young and older adults faced competing lateral balance challenges: stay on a continually narrowing beam or make a lateral transition to an adjacent beam. We hypothesized that older adults' physical and perceived abilities to beam walk would be less than those of younger adults, and that older adults would require more motor planning to execute lateral transitions.

Methods

Eighteen healthy older (OH; ages 65+) and 18 younger (YH; ages 18-27) adults performed 35 repetitions of treadmill walking on virtual beams. They began each repetition walking on a constantly-narrowing beam, and chose when to transition to an adjacent, wider beam, trying to avoid stepping errors (Fig. 1). Participants received auditory feednack of stepping errors that occurred whenever a foot landed outside of the beam boundaries. Transitions from the narrowing beam were identified when the center of mass (COM) crossed the z-axis.

For each beam, the number of errors made prior to transition (*Error Count*) quantified task compliance (to minimize step errors). At narrower beam widths, more stepping accuracy is required to stay within the beam bounds. Thus, beam width at the first error instance (w_{error1}) quantified the physical ability to maintain stepping accuracy. The beam width at transition ($w_{transition}$) quantified perceived ability. The change in beam width between first error and transition (w_{diff}) quantified motor planning ability, as it directly related to the time and distance required to execute the transition following the first error.

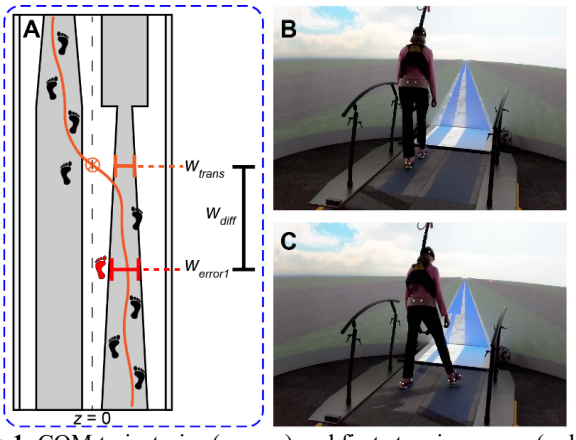

Figure 1: COM trajectories (orange) and first stepping errors (red foot) were recorded (**A**) as participants walked on a narrowing beam (**B**) and transitioned to a wider beam (**C**).

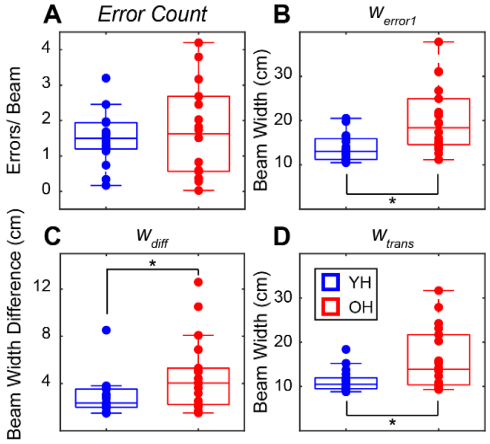

Figure 2: Task compliance (**A**), stepping accuracy (**B**), motor planning (**C**) and perceived abilities (**D**) were compared between groups.

Results and Discussion

Young and older adults made 1.50±0.71 and 1.65±1.29 errors prior to transition (p=0.662), respectively (Fig. 2A). Thus, particpants in both groups generally followed task instructions.

OH adults made initial stepping erorrs (w_{error1}) at greater beam widths (13.8±3.1cm) than YH adults (20.2±7.5cm), respectively (p=0.003; Fig. 2B). OH adults required wider beams to retain their stepping accuracy. This was expected, as older adults generally prefer wider steps and age reduces step accuracy [6].

Beam width changes (w_{diff}) between first error and transition were higher for OH (4.7±3.1cm) than for YH adults (2.9±1.2cm), respectively (p = 0.031; Fig. 2C). OH required slightly more time and distance to respond to errors, likely for processing and motor planning. This was predicted, as these increase with age [4].

OH adults transitioned from the narrowing beam (w_{trans}) at greater beam widths (16.1±7.0cm) than YH adults (11.3±2.5cm), respectively (p = 0.011; Fig. 2D). Thus, OH adults not only demonstrated a reduced physical ability to maintain stepping accuracy, but also appeared to perceive this reduced ability.

Significance

Responses to lateral balance challenges not only require the physical ability to execute walking and maneuvering tasks, but also rely on perceived ability and motor planning. Further, age-related deficits reduce the physical and perceived abilities and increase the motor planning required to execute lateral balance challenges, such as narrow beam walking and lateral transitions.

Acknowledgments

NIH / NIA Grant #: R01-AG049735.

References

1. Bauby CE et al. *J. of Biomech.* 33(11), 1443-40, 2000.
2. Hsieh KL et al. *Gait and Posture.* 61, 466-72, 2018.
3. Butler AA et al. *J. of Geront.* 70(5), 628-34, 2015.
4. Stockel T et al. *Front Aging Neuro.* 9, 283, 2015.
5. Kazanski ME et al. *J. of Biomech.* 2020.
6. Alexander NB et al. *J. of Geront.* 60(12), 1558-62, 2005.

Step Width Variables are not Meaningfully Correlated with Stumble or Fall Incidence in a High Functioning Population with Lower Limb Trauma

Riley Sheehan.[1,2], Mark Grabiner[3], Trevor Kingsbury[4], Brad Hendershot[5], and Kenton Kaufman[6]
[1]Henry Jackson Foundation, [2]Center for the Intrepid, [3]University of Illinois at Chicago, [4]Naval Medical Center San Diego, [5]Extremity Trauma and Amputation Center of Excellence, [6]Mayo Clinic
Email: riley.c.sheehan.crt@mail.mil

Introduction

Individuals with lower limb trauma (LLT) have an elevated risk of falling [1]. Fall risk is the intersection of the likelihood of stumbling and the likelihood of successfully recovering from a stumble. While both of these factors contribute to overall fall risk, the underlying causes and potential interventions are different. It is important to be able to assess these different fall risk features in order to determine the specific stability deficits and most effective interventions.

Individuals with LLT often walk with a wider, more variable step width. A wider step width increases the frontal plane base of support and potentially reduces the likelihood of balance loss. Step width variability has been related to balance control [2] and, thus, may be associated with the likelihood of recovering from a stumble.

The purpose of the study was to determine if step width and step width variability assess different aspects of fall risk. Specifically, we hypothesized that step width would be correlated with the incidence of balance loss and step width variability would be correlated with the stumble recovery rate.

Methods

This is a secondary analysis of fourteen Service Members (age: 35±6 yrs, height: 1.81±0.06 m, mass: 92.1±13.7 kg, 13 males) with LLT who participated in a larger trip-prevention training study. For this analysis, all data are collected prior to receiving any training. Participant's injuries included limb preservation for which custom ankle foot orthoses were worn (4), unilateral below-knee amputation (7), and bilateral below-knee amputation (3). Particpants completed a questionaire that reported the number of stumbles, uncontrolled falls, and controlled falls during the previous four weeks. The total number of balance losses (stumbles plus falls) reported was used as our measure of incidence of balance loss. The stumble recovery rate was calculated as the number of stumbles divide by the total number of balance losses.

Participants walked on a treadmill for 10 minutes at a speed scaled to leg length and injury severity. The position of markers on the heels was used to calculate the step width mean and variability (standard deviation) over the trial. Spearman correlations were used to separately characterize the relationships between the step width variables (mean and variability) and the fall variables (incidence of balance loss and recovery rate).

Results and Discussion

Contrary to our hypotheses, there were no significant correlations between step width or step width variability and the reported balance and fall variables. The strongest correlations were with stumble recovery rate for both step width (Rho=0.19, p=0.51) and step width variability (Rho=0.31, p=0.28). The average step width (160±36 mm) was 66% greater than previously reported able-bodied individuals evaluated at the same facility (96 mm) **[3]**. However, the step width variablility (29±7 mm) was comparable (30 mm) to those same able-bodied individuals **[3]**. Notably, the study cohort was comprised of individuals with LLT, who are young Service Members with an overall high level of fitness and function that may decrease the extent to which they are representative of the typical civilian LLT population. For example, two participants reported the ability to walk a mile and the remainder reported the ability to walk greater than 5 miles. This suggests an overall high level of function for these participants.

Despite the overall high level of physical ability, the participants still reported losing balance and falling. On average, over the previous four weeks, paticipants reported balance losses 8±5 times, reported having fallen 2±3 times, and had a stumble recovery rate of 77±20%. While the small size and diverse makeup of our sample may have limited our ability to identify a significant correlation, the results may also be related to a limitation of the step width variables characterizing fall risk. Many falls occur as a result of trips or slips (balance loss in the saggital plane) and measures of step width and step width variability may not be associated with the capacity to perform compensatory stepping responses following typical balance loss. Further, many of the participants reported that they fell the most on challenging surfaces (e.g. high curbes, uneven terrain, wet floors). Thus, for this more high functioning LLT population, it may be more relevant to look at measures relating to step length and foot clearance in order to more accurately evaluate fall risk.

Significance

This study was not able to identify a meaningful relationship between typical step width metrics and stumble and fall incidences in a high functioning LLT population. However, the high reported stumble and fall incidences suggests the need to evaluate other measures that may be more associated with fall risk in this population.

Acknowledgments and Disclaimer

Funded by Department of Defense Grant No. W81XWH-15-2-0071. The view(s) expressed herein are those of the author(s) and do not reflect the official policy or position of Brooke Army Medical Center, the U.S. Army Medical Department, the U.S. Army Office of the Surgeon General, the Department of the Air Force, the Department of the Army, Department of the Navy, or the Department of Defense, The Henry Jackson Foundation, or the U.S. Government.

References

1. Miller (2001). *Arch. Phys. Med. Rehabil.* **82**.
2. Gabell (1984). *J. Gerontol.* **39**.
3. Rábago (2015). *PLoS ONE* **10**.

Early Testing of a Real-Time Balance Sonification System In Single Leg Stance

Mitchell Tillman[1], Luke Dahl[2], Christopher B. Knowlton[3], and Antonia Zaferiou[1]
[1]Stevens Institute of Technology, Department of Biomedical Engineering, Hoboken, NJ
[2]University of Virginia, Department of Music, Charlottesville, VA
[3]Rush University Medical Center, Department of Orthopedic Surgery, Chicago, IL

Email: MTillman@stevens.edu

Introduction

Fall-related injuries due to loss of balance are a leading cause of injury and mortality for older adults [1]. For those with compromised balance abilities, balance training can be assisted with external biofeedback. An emerging area of biofeedback for clinical applications is called sonification, which maps real-time measurements through sound. Existing systems have been shown to assist balance in static upright stance using an inverted pendulum model [2]. We are in the initial stages of developing a task-independent balance training sonification system, building on previous works [2,3]. This system sonifies margin of stability (MOS) [4], base of support (BOS) area, and total body center of mass (TBCM) location. We hypothesize that sonified biofeedback of balance metrics will increase the MOS in single leg stance compared to before biofeedback in young healthy adults.

Methods

Five participants (two female; age 24 ± 2.65 yrs) volunteered for this study after providing informed consent. They performed five repetitions for one minute each of a single leg stance task, alternating between left and right for five trials. They repeated this in blocks, Before and During sonified biofeedback. Time to move freely and verbal instructions were provided for participants to become familiar with the sound design.

Optical motion capture (Optitrack, OR), Matlab (Mathworks, MA) and MaxMSP (Cycling '74, CA) enabled real-time sonification of three metrics: TBCM location within or outside of the BOS boundaries (boolean value), BOS convex hull area (defined by foot markers in contact with the ground; Fig. 1), and MOS (horizontal distance from the TBCM position to the closest edge of the BOS). The sonification design consisted of a synthesizer that produced continuous oscillatory pulsing sounds (shown here) [adapted from 3]. Decreasing MOS increased pulse speed. Decreasing BOS area increased brightness. Dissonance was added if the TBCM was outside of the BOS.

Within-subject, Cliff's analog of the Wilcoxon-Mann-Whitney test was used to compare mean, median, and max MOS Before vs. During biofeedback (α=0.05).

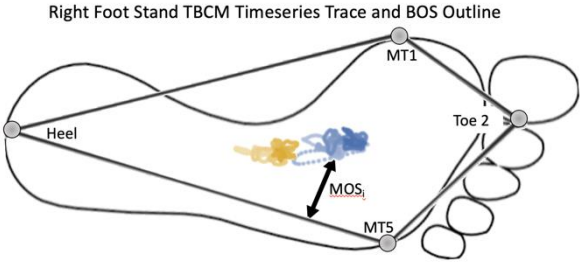

Figure 1: Representative (Subject 4) TBCM trajectories Before (yellow) and During (blue) sonified biofeedback, shown on a right foot BOS convex hull. Light to dark indicates forward progression of time. MOS is labelled at one timepoint. Labelled gray circles are motion capture markers; foot illustration is included for reference.

Results and Discussion

During biofeedback, two of five participants significantly increased their maximum, mean, and median (Fig. 2) MOS vs. Before biofeedback (p=0.032 for all three metrics and both subjects). No subjects displayed the opposite trend between conditions. BOS area was constant throughout given the nature of the single leg stance task. Additionally, the TBCM was only outside of the BOS boundary at any time for Subject 2.

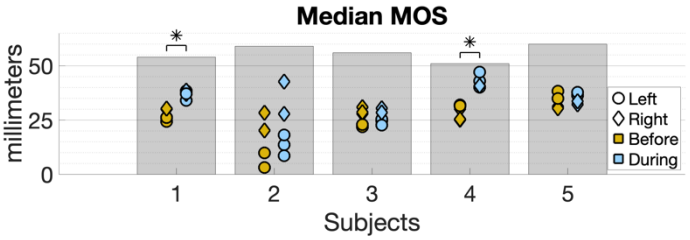

Figure 2: Median MOS in Before (yellow) and During (blue) sonified biofeedback conditions for each subject during single leg stance of the left (circles) and right (diamonds) legs. Gray bar displays the range of possible MOS values per subject-specific base of support geometry.

Due to the differences observed between right and left stance legs (Fig. 2 circles vs. diamonds), future single leg balance research will be restricted to comparisons of the right or left leg support separately. We also acknowledge that our current BOS model is biased medially relative to the foot surface (as in Fig. 1).

Our hypothesis was partially supported by significant changes in two of five subjects' median, mean, and maximum MOS. However, it is unclear whether these changes are practically significant as the TBCM movement is small relative to the BOS size (Fig. 1). Further, maximizing MOS in single-leg stance may not be functionally helpful. Despite the maximum MOS decreasing, posterior TBCM placements can take advantage of underlying musculoskeletal structure that may reduce the need for active balance control.

Significance

This work shows promise towards developing a task-independent optical motion capture-based sonified biofeedback system to assist balance training. We are developing practices to inform future experiments including ways to analyze cognitive load and psychosocial aspects of human computer interaction that can affect who learns most from this biofeedback modality. Next, we will expand towards sonification of balance metrics during dynamic over-ground movements. Our long-term goal is to assist clinical practice to remediate balance deficits.

References

[1] Stevens et al. (2008), *J. of Safety Research,* **39**; 345-349
[2] Schaffert et al. (2019), *Frontiers in Psych*, **10**:244
[3] Dahl et al. (2019), *ACM Int. Conf. Proc. Series*
[4] Hof et al. (2005), *J. of Biomechanics,* **38**; 1-8

A novel measure of standing balance coordination demonstrates greater consistency than traditional measures

Kreg G. Gruben.[1], Jennifer N. Bartloff.[2]
Depts. Kinesiology[1,2], Biomedical Engineering[1], & Mechanical Engineering[1]
Univ of Wisconsin-Madison, Madison Wisconsin, USA
Email: kreg.gruben@wisc.edu

Introduction

Postural imbalance and falls increase with age and disease, incurring substantial social, economic, and medical costs. A key impediment to preventing falls is insufficient understanding of the foundational coordination mechanisms that enable humans to remain upright while standing. Measures of balance ability, such as those related to the center of pressure (CP) of the ground on foot force (F), demonstrate changes with age- and disability-related declines in balance, but are inadequate to quantify angular momentum control, a primary aspect of maintaining one's balance. Also, imprecision in joint torque and muscle activity estimations are unable to capture the subtle adjustments that maintain posture.

Our approach relates directly to sagittal-plane translational *and* angular body motion. We quantify the relationship between CP and the ratio of F horizontal to F vertical as the height of an emergent intersection point (zIP)[1].

Hypotheses:

1. zIP is a more consistent and repeatable metric within a subject compared to traditional measures of balance.
2. zIP has higher discriminatory value across age than traditional measures.

Methods

We examined standing trials from a public dataset of human posturography assessments to analyze force of the ground on the feet during quiet standing on a rigid horizontal surface (3 60s trials)[3]. Subjects were divided into two groups: young (n = 86) and old, defined as >60 years (n = 72). Ground on feet forces in the anterior-posterior horizontal (Fx) and vertical (Fz) directions were bandpass filtered in 0.2 Hz wide bands centered every 0.2 Hz from 0.4 to 7.2 Hz. The slope of the relationship between the bandpass filtered xCP and Fx/Fz was determined with principal components analysis to calculate zIP according to this formula:

$$\frac{1}{zIP} = \frac{(Fx/Fz)}{xCP}$$

For each frequency bin, we used Student's t-tests to compare the mean zIP of the two samples using a Bonferroni correction.

Results and Discussion

Clustering analysis showed that the function of zIP across frequency had a high degree of similarity within the multiple trials of a subject relative to the trials of other subjects, which exceeded that observed for the traditional measures of: variance of (CM acceleration, Fx, & CP), root-mean-square of CP velocity, and CP path length ($p < 0.001$). The zIP in the old was found to be elevated compared to the young ($p<0.0001$). Traditional measures failed to show an age difference.

Standing requires coordinated activation of muscles across multiple joints (sagittal plane). Previously described muscle synergies during standing support the concept of fixed weightings[4] that produce IP's appropriate for the various kinematic modes of falling[5]. Our results of conserved zIP across an individual subject's multiple trials is consistent with fixed weightings of the synergies. zIP is shown to have higher discriminatory value across age than traditional measures.

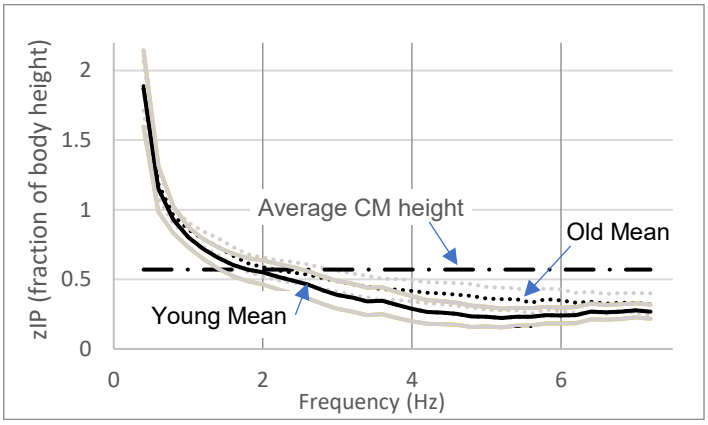

Figure 1: Older individuals have a higher zIP at most frequencies.

An elevated IP provides a greater moment about the CM that induces more angular acceleration toward the desired upright posture. This could be a compensation for aging-related deficits in other components of the postural control system (e.g. sensory degradation, processing delays, modified muscle properties).

Significance

Our findings suggest that zIP is a metric of balance capacity that could have clinical value as a screening and therapeutic feedback tool. A next step is to determine the extent to which IP is associated with fall risk and is able to track balance training improvements in older individuals and those with neurologic impairment. Assessment of zIP can be performed in under a minute with only a force plate and thus could be deployed broadly.

Acknowledgments

Support was provided by the NSF (NRI 1830516), Virginia Horne Henry Fund, and the UW School of Education Grand Challenges Award.

References

1. Boehm, et al. "Frequency-dependent contributions of sagittal-plane foot force to upright human standing." J Biomech 83 (2019): 305-309.
3. Santos, and Duarte. "A public data set of human balance evaluations." PeerJ 4 (2016): e2648.
4. Wojtara, et al. "Muscle synergy stability and human balance maintenance." J Neuroeng and Rehab 11.1 (2014): 129.
5. Blenkinsop et al. "Balance control strategies during perturbed and unperturbed balance in standing and handstand." Royal Society open science 4.7 (2017): 161018.

Spatiotemporal recovery responses used to combat translational platform perturbations during walking

Jennifer K. Leestma[1,2,*], Gregory S. Sawicki[1,2,3], and Aaron J. Young[1,2]
[1]George W. Woodruff School of Mechanical Engineering, [2]Institute for Robotics and Intelligent Machines, [3]School of Biological Sciences, Georgia Institute of Technology
Email: *jleestma@gatech.edu

Introduction

Robust bipedal locomotion is required to traverse the unpredictable and non-uniform environment that exists outside of the lab. However, we know much less about locomotion in these kinds of non-steady-state environments in comparison to steady-state ones. Previous studies have used perturbations to cause instability during gait, revealing information about recovery strategies, step responses, and muscle contributions used to maintain balance [1]. However, much of this work has not evaluated the interplay between many independent variables, which would improve our understanding of highly unpredictable reactions to gait perturbations that occur in real-world environments. In this study, we establish an experimental protocol to investigate how perturbation *magnitude* and *direction* affect locomotion stability. Specifically, we focus here on how perturbation magnitude and direction affect step response.

Methods

One subject walked at 1.25 m/s on a treadmill mounted on a Stewart platform and we applied translational perturbations in the mediolateral and anteroposterior directions. We applied 288 perturbations that varied in direction (8 directions, 45° increments) and magnitude (5, 10, 15 cm), creating 24 conditions. We collected lower body motion capture.

We lowpass filtered marker data at 6 Hz. We identified gait events using a kinematic coordinate method [2]. We identified the step length (SL) and step width (SW) at the heel contact at the beginning of each step using the distance between heel markers, shown in Figure 1. We examined the mean SL and SW for each of the 24 conditions for the perturbed step (S_0) and the five subsequent steps (S_1-S_5), shown in Figure 1.

Results and Discussion

The steady-state SL and SW were 0.661 m and 0.096 m, repectively. SL was affected by perturbation direction, but only for a single step after the perturbation. In the S_1 step, platform movement lateral or posterior to the stance foot resulted in a SL decrease. Similarly, platform movement medial or anterior to the stance foot resulted in a SL increase. These changes in SL also increased with the magnitude of the perturbation. Following the S_1 step, magnitude and direction do not appear to influence SL. SW was also affected by direction, with effects lasting for three steps following the perturbation. Platform movement medial to the stance foot caused a SW decrease in the S_1 step and a SW increase in the S_2 and S_3 steps. Similarly, platform movement lateral to the stance foot caused an SW increase in the S_1 step and a SW decrease in the S_2 and S_3 steps. Similar to SL, perturbation magnitude also scaled the severity of SW changes. The simultaneous influence of both perturbation magnitude and direction on SL and SW responses confirm the importance of considering both of these independent variables when analyzing locomotion stability. Future work will also evaluate the interplay between perturbation timing and the two independent variables tested here.

Significance

Understanding how balance during bipedal locomotion is resilient to unsteady environments is imperative for designing rehabilitation therapies, assistive devices, and bipedal robots. Our results provide a foundation to understand how a diverse set of perturbations affect locomotion dynamics. Additionally, these data provide a biomechanical reference for researchers and engineers who are designing advanced devices for use in non-steady-state environments.

Acknowledgments

This work was funded by the NSF Research Traineeship: ARMS Award #1545287.

References

[1] D. Tokur, et al., *Hum Movement Sci* 69, (2020)
[2] J. A. Zeni, et al., *Gait Posture* 27, (2018)

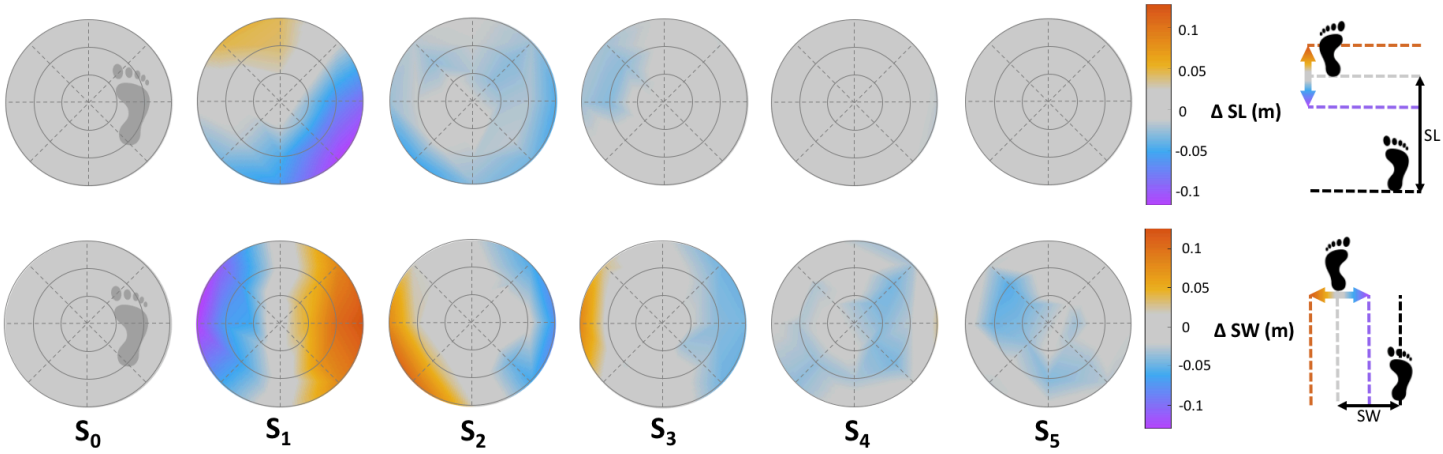

Figure 1: Circular axes represent perturbation magnitude (5, 10, 15 cm) and radial axes represent the direction of platform movement. Perturbations on the right or left foot are normalized and displayed as though the right foot was the perturbed step (S_0), shown by the footprint. The colors show the mean SL and SW deviations from steady-state for each step.

Implementing A Double-Limb Slip Training Protocol To Reduce Falls And Improve Slip Recovery: A Pilot Study

Abderrahman Ouattas[1], Corbin M. Rasmussen[1] & Nathaniel H. Hunt[1]
[1]Department of Biomechanics, University of Nebraska at Omaha, Omaha, NE USA
Email: *aouattas@unomaha.edu, web: https://www.unomaha.edu/college-of-education/cobre/

Introduction

Falls are the second leading cause of accidental death in older adults, and account for 17 million serious injuries worldwide, e.g. bone fractures, head trauma, and bruises[1]. Slips alone account for 25% of overall falls[2]. Traditional fall prevention exercise interventions peak at 30% reduction in falls[3], possibly due to lack of transfer to motor tasks such as trips and slips. Slip training has been previously addressed and shows high promise in reducing falls during slips in the short (1-week) and long term (12 months)[4]. Yet, such methods still lack two factors that may hinder clinical improvement and further recution in overall falls: 1) laboratory induced slips that mimic slips in real world environments (e.g. unknown slip time and location, low friction surface, double limb slips); 2) identifying reliable biomechanical variables that predict the causation or prevention of falls. This study aims to investigate the aftereffects of a 3 session double-limb slip training protocol (12 slips/session) on reducing falls and describe the specificity of reactive responses to slips in younger and older adults using a novel slipping method. We hypothesized that 1) participants who will experience falls in the first session will not experience falls in the last session, and 2) their reactive response will significantly improve.

Methods

Two young adults (28.5 ± 0.7 years; 85.82 ± 8.47 kg, 1.75 ± 0.04 m) participated in the study. The study is a registered clinical trial and we anticipate collection 21 participants in each group (old & young). The study is approved by the University of Nebraska Medical Center IRB. Participants completed 3 sessions of 12 double limb slips each within one week (36 slips in total) that were triggered using an in-lab built Wearable Apparatus for Slip Perturbations (WASP)[5] (Fig 1-H). The WASP induced slips to both limbs simultaneously while participants walked at a fixed gait speed of 1.3±0.2 m/s on a 10 m walkway (Fig 1). Slips were delivered to the dominant foot at 3 separate slip onsets; 1) early stance, 2) mid-stance, 3) late stance. Falls were identified if participants applied more than 30% of body weight to the harness, which was measured using a load cell[6]. Full body kinematics were recorded using a 17-camera motion capture system (Motion Analysis Corp., Santa Rosa, CA) and sampled at 100 Hz.

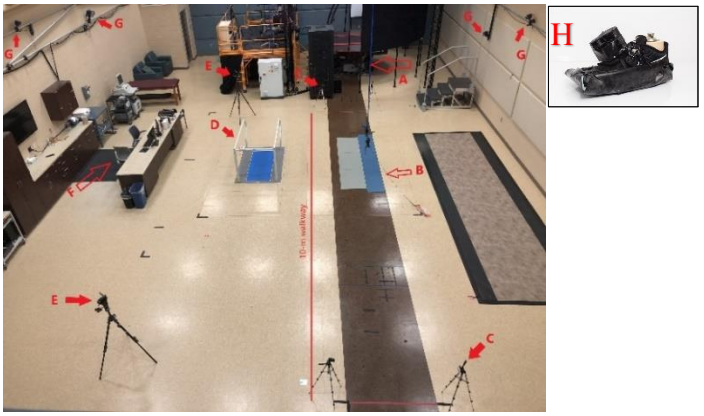

Figure 1: A. Harness and load cell. **B**. 10-m wakway and force plates. **C.** Dashr timing. **D.** AMTI Treadmill. **E.** Cameras. **F.** Control Station. **G.** 17-Camera Motion Capture. **H.** WASP

All data were analysed from slip onset until feet reached a velocity of 0, except for shank angle, which was measured at slip onset. Anterioposterior (AP) and mediolateral (ML) minimum Margin of stability (MOS_{min})[7] were used to analyze dynamic stability. Peak shoulder and trunk angles were used to quantify upper body slip recovery. Slip velocity and diplacement, in addition to shank angle relative to the floor were used to quantify slip severity. A simple paired t-test was used for each outcome variable to measure the differences between the first and last slips for each slip incidence.

Results and Discussion

Only late stance slip incidence on the dominant leg yielded a fall in the first slip trial of the 2nd participant, and the last slip showed reduction in harness assistance (Fig 2).

Interestingly, MOS_{min} increased to reach positive values during all subjects and slip incidences after the slip training protocol (Table 1), which indicates that participants became more stable as negative values indicate instability which requires a compensatory mechanics to recover stability. All other variables did not show any significant differences.

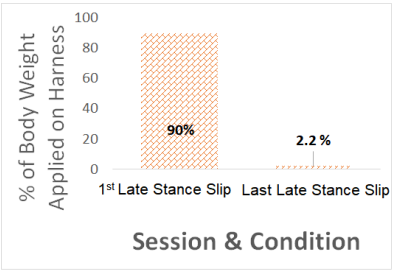

Figure 2: Load Cell results for 2nd participant .

Significance

Based on these preliminary findings, one can conclude that our novel method is a valid tool in disrupting dynamic stability in both legs, but late stance slips induced to the dominant leg may yield more severe balance disruptions compared to other slip incidences. However, more data is needed to support these conclusions, specifically since covariables such as muscle strength or activation may change the recovery behaviour.

Acknowledgments

NIH 2P20 GM109090-06; NIH R15AG063106-01

References

1. WHO. *J Women's Hist*, **15**, 2007.
2. Berg et al. *Age Ageing*, **26**, 261-268, 1997.
3. Owings M et al. *Clin Biomech,* **16**, 813–819, 2001.
4. Pai C et al. *Journals of Gerontology,* **69**, 1586–1594, 2014.
5. Rasmussen C & Hunt N. *J Neuroeng Rehabil*, **16**, 118, 2019.
6. Yang F & Pai Y. *J of Biomech*, **44**, 2243–2249, 2011.
7. Rosenblatt N & Grabiner M. *Gait Posture*, **31**, 380–384, 2010.

Table 1: Kinematic and Kinetic Findings

Groups	Trials	MOS_{min} (cm)			
		AP		ML	
		DM	ND	DM	ND
S001	1st Three	*-31 ± 24	*-30 ± 17	^-17 ± 17	-22 ± 18
	Last Three	20 ± 1	19 ± 0.8	8 ± 0.8	-9 ± 8
S002	1st Three	^2 ± 12	^-3 ± 14	1 ± 6	^0.7 ± 4
	Last Three	17 ± 8	21 ± 2	3 ± 1	8 ± 1

*p=0.05, ^ Trend p=0.05-0.2. DM : Dominant. ND :Non-Dominant.

Acute Effects of Virtual Reality Treadmill Training on Gait and Cognition in Older Adults

Lisa A. Zukowki[1], Faisal D. Shaikh[1], Alexa V. Haggard[1], and Renee N. Hamel[1 2]
[1]Department of Physical Therapy, High Point University, High Point, NC
[2]School of Physiotherapy, University of Otago, Dunedin, NZ
Email: lzukowsk@highpoint.edu

Introduction

Older adults commonly fall while walking in everyday life, which involves simultaneous performance of cognitive tasks (i.e., dual-tasking). Conventional fall prevention interventions aim to improve strength, gait speed, and/or coordination but not impaired cognition. Interventions that incorporate simultaneous physical and cognitive training demonstrate improved dual-task walking performance and reduced fall prevalence.[1–3] Further, a single cognitively-demanding, visually-interactive exergaming session can result in acute cognitive performance enhancement.[4] An exercise intervention utilizing immersive virtual reality on a treadmill may be especially beneficial in mimicking the distractions and demands of everyday walking, but cognitive benefits of this training have not been explored.

The purpose of this study was to identify the acute effects of a single session of immersive virtual realtiy treadmill training (IVRTT) on cognitive and gait performance. We hypothesized that compared to a single session of conventional treadmill training (CTT), after a single session of IVRTT, older adults would demonstrate greater improvements in reaction time and accuracy on cognitive tasks, and greater reductions in dual-task costs on gait and cognition relative to pre-training performances.

Methods

Sixty healthy older adults were recruited and randomized to complete a single IVRTT (experimental) or CTT (active control) exercise session. Participant demographics, baseline cognition, motor abilities, and community participation were assessed.

Exercise sessions were 30 minutes and completed on a treadmill with integrated, immersive virtual reality (GRAIL, Motek). IVRTT incorporated audiovisually-interactive self-paced and set-pace walking challenges. CTT required participants to perform similar motor tasks, but with oral instructions rather than audiovisual components. Participants performed 3 trial conditions before and after the exercise session: 1) single-task walking (ST_{gait}), 2) dual-task walking (DT), and 3) single-task cognitive (ST_{cog}). Gait was recorded with 6 Opal sensors (128 Hz, APDM). A visuospatial reaction time test was utilized for the cognitive test. Stimuli were produced and recorded using DirectRT (Empirisoft) via wireless headphones.

The dependent variables were cognitive response reaction time (ST_{cogRT} and DT_{cogRT}), cognitive response accuracy (ST_{cogAcc} and DT_{cogAcc}), gait speed (ST_{gait} and DT_{gait}), DT effect on gait speed ($DTE_{gait,}$ % = 100*[ST – DT]/ST), and DT effect on cognition (DTE_{cog}, combined reaction time and accuracy). An independent samples t-test was used to compare demographics and baseline abilities of the groups. A multivariate repeated measures ANOVA was used to compare the dependent variables before and after the exercise session for each group (Time x Group).

Results and Discussion

The groups did not differ in demographics, baseline cognition, motor abilities, or community participation (all $p>0.05$). In accordance, there was no Group effect ($p>0.05$) on measures of gait or cognition. Therefore, differences in gait and cognitive performances can be attributed to the exercise interventions.

Both IVRTT and CTT groups improved performances from pre- to post-exercise session. There was a main effect of time ($p<0.001$) with both groups exhibiting an 81.1 ms quicker ST_{cogRT} and 314.2 ms quicker DT_{cogRT}, 0.04 m/s faster ST_{gait} and 0.09 m/s faster DT_{gait}, 14.5% less DTE_{cog}, and 3.9% less DTE_{gait} during post-exercise testing, relative to pre-exercise testing. ST_{cogAcc} and DT_{cogAcc} did not change from pre- to post-exercise testing. These results provide evidence that both exercise interventions acutely improved visuospatial reaction time and gait speed in ST and DT trial conditions and align with previous research providing evidence of improvements in cognitive performance with a single session of dual-task exergaming and aerobic exercise.[4,5]

Contrary to our hypothesis, there was no Group x Time interaction effect ($p>0.05$). The CTT in this study may have been equally cognitively-demanding as IVRTT and more cognitively-demanding than typical exercise because it required participants to interact with instructions from a trainer. Therefore, both exercise interventions may have resulted in gait and cognitive improvements, only differing in terms of the audiovisual input and feedback. Although these results do not provide evidence for the superiority of IVRTT relative to CTT, they still support that IVRTT can result in key acute improvements in gait and cognition. This is important because if IVRTT were administered in a multi-week exercise program, it could result in significant, more permanent improvements in gait and cogntion.[1]

These results support that IVRTT is effective in acutely improving gait and cognition in older adults. IVRTT is a safe way to execute a multimodal exercise intervention that combines simultaneous motor control, attention, planning, visual input, and auditory processing. Results of this study may be used in the design of a multi-week exercise training aimed to safely increase physical activity and reduce fall prevalence in older adults.

Significance

This study is the first analysis of the benefits of IVRTT. The results of this study lay the foundation for the development of a new fall prevention exercise program that aims to address the safe performance of motor tasks in real-life situations with the associated cognitive distractions that contribute to many falls.

Acknowledgments

This project was supported by a University Research Advancement Grant from High Point University.

References

1. Anderson-Hanley et al. Am J Prev Med. 2012;42(2):109-119.
2. Eggenberger et al. Clin Interv Aging. 2015;10:1711-1732.
3. Falbo et al. Biomed Res Int. 2016;2016:5812092.
4. Monteiro-Junior et al. Aging Clin Exp Res. 2017;29:387-394.
5. Peiffer et al. J Sports Sci Med. 2015;14(3):574-583.

Identification of specific somatosensation and location to predict postural control outcomes

Riley J. Horn[1], Meardon[2], O'Brien[3], DeVita[1], and Lin[2]
[1]Department of Kinesology, East Carolina University, Greenville, NC, USA
[2]Department of Physical Therapy and [3]Department of Biostatistics, East Carolina University, Greenville, NC, USA
Email: hornr19@students.ecu.edu

Introduction

Postural control is a complex motor skill requiring interaction of dynamic sensorimotor processes receiving information from the visual, vestibular, and somatosensory systems. Somatosensation has been reported to account for 50-70% of postural control performance in older adults and 30-40% in young adults.[1] Deficits in somatosensation are known to reduce postural control.[2] Somatosensation measures such as touch pressure sensation threshold (PT) and vibration perception threshold (VT) have been used to identify people with somatosensory deficit in the clinic. However, the appropriate threshold, site on the foot, and modality has not been established in relation to postural control.

Postural control can be assessed using the sensory organization test (SOT) and the motor control test (MCT) using the EquiTest platform.[3] The SOT weighs the individual's use of the visual, vestibular, and somatosensory inputs for postural control through manipulation of the individual's visual surrounding and support surface to determine an equilibrium score. The MCT computes the time for postural recovery after backward and forward translations to determine a latency score. Studies have shown people with postural control deficit have lower equilibrium and latency scores.[4] The purpose of this study was to identify the most relevant sites of somatosensation for postural control. We hypothesized that specific sites of the foot and ankle would have significant associations with equilibrium and latency scores.

Methods

In this study, 49 healthy adults (22M, 27F; mean age 42.0 ± 13.8 (SD) y.o.) were evaluated for postural control and somatosensory measures. Subjects with fall history, vestibular, orthopedic, or neurological disorders, knee or hip replacement, abnormal dizziness, low visual acuity, or using an assistive device for ambulation were excluded from this study. Subjects with abnormal SOT scores were excluded from this preliminary analysis.

PT was evaluated using a set of Semmes Weinstein graded monofilaments (Touch-Test Sensory Evaluator, North Coast Medical Inc., Morgan Hill, CA, USA). VT was evaluated using a handheld biothesiometer (Bio-Medical Instrument Co., Newbury, OH, USA). PT and VT were measured at 14 sites on the foot: the plantar surface of the great toe, 1st metatarsal, 3rd digit, 3rd metatarsal, 5th digit, 5th metatarsal, medial arch, lateral arch, the mid heel; the medial and lateral malleoli; and the dorsal surface of the 1st metatarsal, between the 1st and 2nd metatarsal, and the 5th metatarsal. A Smart-EquiTest platform (NeuroCom, Clackamas, OR, USA) was used for the SOT and MCT.

Bivariate correlations were used to quantify the relationship between postural control variables and somatosensory inputs. Linear regression modeling using the backward method was used to identify the most relevant site(s) for postural control outcomes. Data were assessed for muli-collinearity and the model that optimized the variance accounted and standard error of the estimate was identified ($p < 0.05$).

Results and Discussion

A total of 35 subjects were included in our analysis; 14 out of 49 were excluded due to abnormal SOT scores. The final linear regression model demonstrated the PT on the right 1st dorsal metatarsal and VT on the right 3rd metatarsal predicted the equilbrium score ($F(2, 32) = 4.28$, $p < .02$), with an R^2 of .21 (Figure 1). The PT on the right 1st metatarsal, left middle toe, left medial arch, left 5th dorsal metatarsal, and the VT on the left middle toe predicted the latency score ($F(6, 28) = 5.42$, $p < .01$), with an R^2 of .54 (Figure 1).

Somatosensory thresholds were moderately correlated to equilibrium and latency scores in healthy adults. The somatosensory system is only one component in postural control and is expected to only explain a portion of variance in postural control performance. This study provides baseline data for somatosensory measures in healthy adults and gives insight to somatosensory inputs of the foot relevant to postural control.

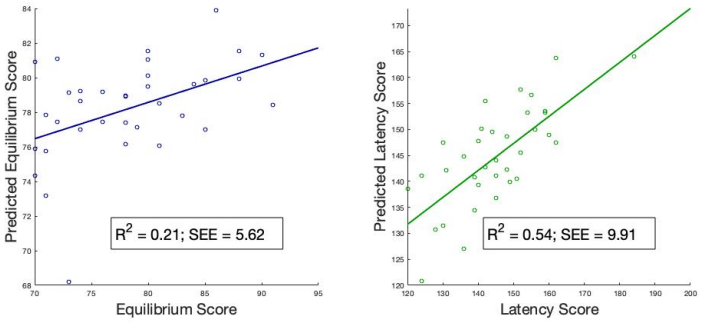

Figure 1: Equilibrium Score vs. Predicted Equilibrium Score and Latency Score vs. Predicted Latency Score.

Significance

This report is part of an ongoing study investigating the potential cut-points of PT and VT for predicting balance dysfunction in older adults and individuals with peripheral neuropathy to improve clinical fall screening algorithms. Future analyses will examine relationships in atypical populations as well as confounding influences of sensory re-weighting.

Acknowledgments

This project is supported by the NIH R15 (1R15AG058228-01A1). We would also like to acknowledge E. Blount, S. Kenny, and A. Skutka for their help in data collection.

References

[1] Simoneau G. et al. (1995). *Gait Posture*, **3**: 115-122.
[2] Horak F. et al. (1995). *Exp. Brain Res*, **82**: 167-177.
[3] Vanicek N. et al. (1990). *J. Vis. Exp.,* **82**.
[4] Whitney S. et al. (2006). *Arch. Phys. Med. Rehabil.*, **87**, 402-407.

Mediolateral Margins of Stability of Older Adults During A Virtual Beam-Walking Task

Meghan E. Kazanski.[1*], Jonathan B. Dingwell[1]
[1]Department of Kinesiology, The Pennsylvania State University, University Park, PA, USA
Email: *mek79@psu.edu

Introduction

Mediolateral stability is critical to remaining upright while walking and maneuvering [1, 2]. Many lateral balance tasks encountered while walking, such as executing lateral maneuvers or modulating step width, require trade-offs in mediolateral stability [2,3,4].

Age-related deficits may affect how older adults adjust their mediolateral stability to successfully respond to lateral balance challenges. Here, young and older participants faced competing lateral balance tasks: stay on a continually narrowing beam or make a lateral transition to an adjacent beam. We hypothesized that older adults would adopt a more cautious tranition strategy that would minimize changes in stability, with more steps required to recover stability following the transition.

Methods

Eighteen healthy older (OH; ages 65+) and 18 younger (YH; ages 18-27) adults performed 35 repetitions of treadmill walking. They began each repetition walking on a constantly-narrowing beam, and chose when to transition to an adjacent, wider beam, trying to avoid stepping errors (Fig. 1A-B). This required participants to plan and execute a lateral maneuver while modulating step width, as both challenge mediolateral stability [2,3]. The transition step (n) from the narrowing beam to the wider beam was identified as the first step after the pelvic centroid crossed the z-axis. The 'transition phase' was defined as 3 preparation steps, one transition step and 3 recovery steps (Fig. 1C). To quantify transition strategy, the mediolateral Margin of Stability (MOS_{ML}) was calculated at the heelstrike of each step during the 'transition phase' for each transition, then averaged.

Results and Discussion

Participants modified their mean MOS_{ML} at steps within the 'transition phase' to perform the lateral maneuver off of a narrowing beam, onto an adjacent beam (Fig. 2). For preparation steps (n-3 to n-1), all participants increased their MOS_{ML} ($p < 0.001$; $p < 0.001$). From step n-1 to step n, participants reduced their MOS_{ML} ($p<0.001$). Following this, the MOS_{ML} was quickly recovered and was similar for recovery steps (steps n+1 to step n+3) following the transition step ($p =0.465$; $p =0.327$; $p =0.860$).

There were no age group differences in MOS_{ML} for the preparation steps ($p = 0.050$, $p = 0.475$, $p = 0.684$) or recovery steps ($p = 0.978$, $p = 0.841$, $p = 0.536$). The only significant age group difference in MOS_{ML} occurred at the transition step n ($p = 0.032$), where OH adults retained slightly higher MOS_{ML} (100±15 mm) compared to YH adults (87±20 mm).

All participants of both age groups adopted a clear strategy when performing the lateral maneuvering task. This strategy involved increases in MOS_{ML} to prepare for the transition, and a rapid return to consistent MOS_{ML} from the very first step following the transition. Similar MOS_{ML} modulation strategies have been adopted by young, healthy subjects navigating constant-width lane changes [2].

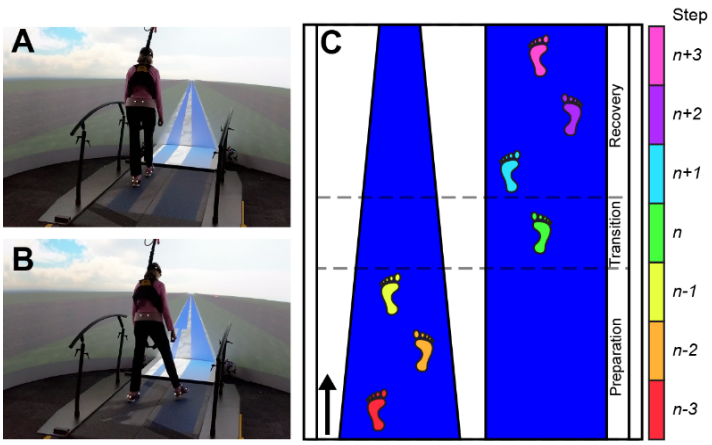

Figure 1: Participants walked on a narrowing beam (**A**) and transitioned to an adjacent, wider beam (**B**). A 'transition phase' from the narrowing beam to the adjacent beam is defined (**C**).

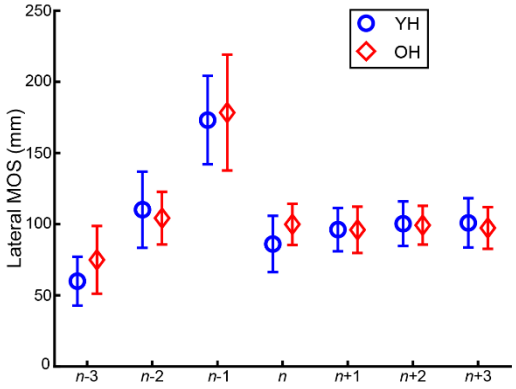

Figure 2: Mean MOS_{ML} plotted for steps in the 'transition phase.'

OH adults chose to transition off of the narrowing beam sooner, at wider beam widths ($p = 0.011$; see accompanying abstract). Thus, while we expected older adults to adopt a more cautious strategy reflected in *how* they modulated stability throughout the transition, it seems this caution was rather applied to *when* they performed the transition. Likely, lateral transitions were perceived as less hazardous than narrow walking.

Significance

Here, competing lateral balance tasks provided insights into older adults' preferences for and execution of these challenges. These preferences may emerge in an effort to retain a maneuvering strategy that modulates stability similar to that of young adults.

Acknowledgments

NIH / NIA Grant #: R01-AG049735.

References

1. Bauby CE et al. *J. of Biomech.* 33(11), 1443-40, 2000.
2. Hsieh KL et al. *Gait and Posture.* 61, 466-72, 2018.
3. Acasio J et al. *Gait and Posture.* 52, 172-77, 2017.
4. Donelan JM et al. *J. of Biomech.* 37,827-35, 2004.

Effect of multicomponent home-based training in older adults with hip fracture: a randomized control trial

Mei Zhen Huang[1], Douglas Pizac[1], Mark Rogers[1], Ann L. Gruber-Baldini[2], Brock Beamer[3], Denise Orwig[2], Marc Hochberg[3], Robert Creath[1], Douglas Savin[1], Vincent Conroy[1], Li-Qun Zhang[1,4], Jay Magaziner[2]
Departments of [1]Physical Therapy & Rehabilitation Science, [2]Epidemiology, [3]Medicine, [4]Orthopaedics, University of Maryland, USA
Email: L-Zhang@som.umaryland.edu

Introduction

Restoration of gait performance is a major rehabilitation goal after hip fracture. Several studies have indicated that relatively high intensity exercise and endurance training beginning six-months post-fracture could benefit gait performance. However, gait characteristics of post hip-fracture recovery are still poorly understood. As an ancillary study of the Community Ambulation Project [1], this study aimed to investigate the effect of a multicomponent home-based rehabilitation training on gait characteristics quantified by spatiotemporal variables, including rhythm, phase, pace and asymmetry [2,3]. We hypothesized that, at the end of the intervention, participants in the multi-component intervention group, compared to the control intervention group, would have greater improvements in gait characteristics.

Methods

Subjects were part of the Community Ambulation after Hip Fracture (CAP) randomized clinical trial Mechanistic Pathways (CAP-MP) ancillary study. In CAP-MP, 40 subjects with hip fracture were randomly assigned to either the multi-component home-based physical therapy intervention (PUSH) that focused on lower extremity strength, endurance, balance and function or an attention control intervention (PULSE) that included active range of motion (AROM) exercises and sensory level TENS to the lower extremity. Of these 40 participants, 27 had gait measures. There were n=14 in PUSH (9 women, mean age=77.6.5±8.1 years, days after fracture: 112±36), and n=13 in PULSE (7 women, age=79.8±6.8 years, days after fracture: 111±32). Both PUSH and PULSE groups did their respective home-based training over 16 weeks.

The GAITRite® System was used to assess gait characteristics and balance. Participants walked across an 8-meter long instrumented GAITRite® walkway under 2 conditions: preferred steady state (normal) speed and at their safe fastest speed to determine spatial and temporal parameters of gait. Each subject completed 2 trials of each condition with a short rest period between trials for a total of 4 trials (i.e., 2 trials x 2 conditions). For each condition, values were averaged over the two trials. Walking aids were permitted only when the participant was unable to walk without assistance. Data were sampled at 120 Hz and processed using GAITRite® Platinum software.

Data were analysed using SAS studio (basic version 3.8). All 27 particpants with at least one baseline value were included. The effect of training on the gait outcome improvements from baseline to 16 weeks was compared between the PUSH and PULSE groups using a general linear mixed-effect model fitted by restricted maximum likelihood. Participants with partial missing data were included in the analysis.

Results and Discussion

Overall, there was no significant difference in the measured gait parameters over the 16-week training between the PUSH and PULSE groups. Thus, our hypothesis was rejected. Results of within group comparison are shown in Table 1. Both PUSH and PULSE groups showed significant improvements in most gait rhythm and pace parameters (p<0.05). The normal walking speed was 0.741 m/s and 0.698 m/s for PUSH and PULSE at 16-weeks, respectively, which was much lower than age-matched healthy adults (e.g., 1.10-1.20m/s reported in the literature) [2]. The PUSH group but not the PULSE group showed improved postural control for normal speed walking and decreased asymmetry between the fractured and non-fractured sides for fast speed walking (P<0.05).

Domain	Gait parameters	PUSH		PULSE	
		Normal	Fast	Normal	Fast
Rhythm/ pace	Walking speed (cm/s)	17.00(4.56)*	13.57(4.95)*	13.6(5.12)*	13.10(5.77)*
	Step time_fracture side (s)	-0.07(0.02)*	-0.04(0.02)*	-0.10(0.03)*	-0.08(0.02)*
	Step time_non-fracture side (s)	-0.07(0.02)*	-0.03(0.02)*	-0.09(0.02)*	-0.04(0.02)*
	Swing phase_fracture side (%)	1.62(1.01)	0.52(0.57)	0.91(1.12)	-1.08(0.67)
	Swing phase_non-fracture side (%)	3.60(1.35)*	2.00(0.82)*	3.15(1.45)*	1.05(0.95)
	Double support phase (%)	-0.13(0.05)*	-0.06(0.02)*	-0.16(0.05)*	-0.07(0.02)*
	Double support phase(%)	-0.12(0.05)*	-0.06(0.02)*	-0.16(0.05)*	-0.06(0.02)*
Postural control	Step length_fracture side (cm)	6.11(2.66)*	4.18(2.05)*	0.85(2.97)	-0.08(2.37)
	Step length_non-fracture side (cm)	6.28(2.69)*	5.29(2.65)	4.11(2.96)	4.09(3.78)
	Heel-to-heel width_fx side (cm)	0.35(0.89)	1.06(1.05)	-0.19(0.99)	0.96(1.20)
	Heel-to-heel step with_nfx side (cm)	0.32(0.90)	0.94(1.06)	-0.14(1.01)	1.10(1.21)
Asymmetry	Single support time assymetry	-6.90(4.04)	-6.1(2.44)*	-5.87(4.24)	-4.77(2.69)
	Step length assymetry	-6.90(4.04)	-6.21(2.55)*	-5.87(4.24)	-4.76(2.69)

Table 1. Changes (standard errors) from baseline to 16-weeks for PUSH or PULSE groups at the normal and fast walking conditions. * indicates significant change between the 16-weeks and baseline (p<0.05).

Significance

The effect of a 16-week multicomponent home-based rehabilitation training is comparable with active control on gait performance for people with hip fracture, starting at 3-months post-fracture. Both PUSH and PULSE interventions provided beneficial effects on gait rhythm and pace for older adults after hip fracture. Moreover, until 7-months post-fracture, the gait performance of the individuals with hip fracture was still inferior to that of age-matched healthy adults. Long-term intervention would be warranted for people to regain their ambultation function after hip fracture.

Reference

[1] Magaziner, J., et al. (2019).

[2] Hollman, J. H., et al. (2011).

[3] Thingstad, P., et al. (2015).

Improvement of Shock Absorption Performance of Construction Helmet using Air-bubble Cushioning- A Preliminary Study

John Z. Wu*[1], Christopher S. Pan[1], Mahmood Ronaghi[1], Bryan M. Wimer[1], Uwe Reischl[2]
[1]National Institute for Occupational Safety and Health, Morgantown, WV, USA.
[2]Boise State University, Boise, ID, USA. *Email: jwu@cdc.gov

Introduction

The industrial helmet is considered as the most common and effective personal protective equipment to reduce work-related traumatic brain injuries [1, 2, 3]. The Type I construction helmet is the most commonly used model in construction and manufacturing. A representative Type I helmet consists of a hard shell and a suspension system. The suspension system, which typically consists of synthetic woven webbing and bands of molded nylon or vinyl, plays an important role in shock absorption and impact force redistribution. In the current study, we tested our hypothesis that adding air bubble cushioning into the suspension system of a Type I industrial helmet will enhance its shock absorption performance.

Methods

The current study was performed only via Type I impact tests, i.e., the impact on the top crown of the helmet shell [4]. Typical off-the-shelf Type I construction helmets were utilized in the study. Helmet drop impact trials were performed using a commercial drop tower test machine (HP. White Laboratory, MD, USA), complying with the ANSI Z89.1 standard [5]. The impactor had a mass of 3.6 kg and was dropped from six different heights from 2.00 ft (0.59 m) to 6.34 ft (1.86 m). The transmitted impact forces to the base of the headform were measured at a sampling rate of 25 kHz. The effects of the air bubble cushioning on the helmets' shock absorption performance were evaluated via two test groups: group I (unmodified helmets) and group II (helmets with air-bubble cushioning). The air-bubble cushioning consists of two layers of typical air-bubble cushioning wrap sheets (Blue Hawk, Gilbert, AZ). The air-bubble cushioning was placed between the headform and the helmet. Four replication trials were performed in each of the drop impacts. A fresh helmet and a fresh cushioning sheet were used for each replication trial.

Results and Discussion

The peak impact forces have been identified from the force-time curves of each drop impact trial. The peak impact forces as a function of the drop height for groups I and II are shown in Fig. 1A. The ANOVA analysis shows that the peak transmitted forces between the two test groups are significantly different ($p < 0.002$) when $h \geq 1.83$ m. For tests in group I, the peak force values increase gradually with the increase in drop height for $h < 1.73$ m (5.68 ft); when $h > 1.73$ m (5.68 ft), peak force values increase dramatically. For tests in group II, the peak force values increase gradually and evenly with the increase in drop height for the entire range of the tested drop height. The ratio of the peak force with the air bubble cushioning to that without air bubble cushioning ($\boldsymbol{\eta = F_{\max,air}/F_{\max,no-air}}$) is shown in Fig. 1B. It is seen that the force reduction ratio (η) varies little for $h < 1.63$ m, and it then decreases dramatically with increasing drop height. At smaller drop heights ($h < 1.63$ m), the air bubble cushioning has little effect on the impact force reduction (i.e., $\eta \approx 100\%$), whereas for higher drop heights ($h > 1.63$ m), adding the air bubble cushioning to the existing suspension system substantially reduces the transmitted peak impact force (i.e., $\eta \ll 100\%$).

Significance

Our results demonstrate that adding an air bubble cushioning layer to a basic Type I construction helmet would substantially enhance the shock absorption performance at high impact forces, providing better protection. The concept of air bubble shock reduction may be introduced to the helmet industry to improve the helmets' shock absorption performance, especially for Type I helmets.

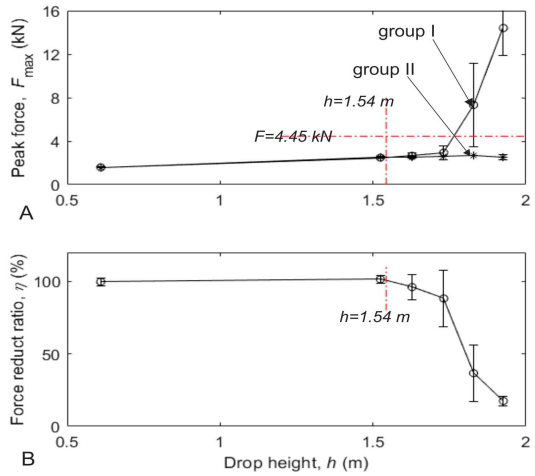

Figure 1. Peak forces for test group I (without air bubble cushioning) compared with those for test group II (with air bubble cushioning). A: Peak force. B: Peak force reduction ratio.

Acknowledgment and Disclaimer

This project was made possible through a partnership with the CDC Foundation. We want to express our gratitude to Turner Construction Company, Liberty Mutual Insurance, Zurich Insurance, and Chubb Insurance for their generous contributions to this project via the CDC Foundation.

The findings and conclusions in this report are those of the authors and do not necessarily represent the official position of the National Institute for Occupational Safety and Health, Centers for Disease Control and Prevention. Mention of any company or product does not constitute endorsement by the National Institute for Occupational Safety and Health, Centers for Disease Control and Prevention.

References

[1] Hino, Y., 2012. Work 41(Suppl 1):3339–42.
[2] Tiesman, H. M., Konda, S., Bell, J. L., 2011. Am J Prev Med 41(1):61–7.
[3] Kim, S., Ro, Y., Shin, S., Kim, J., 2016. Int J Environ Res Public Health 13:1063–78.
[4] Wu, JZ, Pan C.S., Wimer, B.M., 2018. 42th Annual Meeting of American Society of Biomechanics (ASB-2018). Rochester, MN. Aug. 8-11.
[5] ANSI, 2014. ANSI/ISEA Z89.1: American National Standard for Industrial Head Protection.

Assessment of Surgeon Muscle Fatigue during Microsurgery using a Rat Model

Emily J. Miller[1], Stacy R. Loushin[1], Christopher S. Graffeo, MD[2], Avital Perry, MD[2], Kenton R. Kaufman, Ph.D.[1]
[1]Motion Analysis Lab, Department of Orthopedic Surgery, Mayo Clinic, Rochester, MN, USA
[2]Department of Neurologic Surgery, Mayo Clinic, Rochester, MN, USA
Email: miller.emily@mayo.edu

Introduction

Surgical training is often supplemented with simulated procedures using animal models. Representative animal models have been developed to simulate difficult procedures and prepare surgeons for real-time patient surgical operations [1]. The goal of these simulated procedures is to challenge the surgeon, both mentally and physically, above the standard, baseline procedure. Challenging surgical procedures may require additional time to complete and lead to increased muscular fatigue [2]. Muscle fatigue can be detected by quantifying muscle activity frequency. A decrease in the median muscle frequency is indicative of muscle fatigue [2]. The purpose of this study was to validate the increased difficulty of an experimental artery and vein anastomosis rat model by demonstrating that surgeons experience muscular fatigue compared to the standard, control model.

Methods

One seventh year neurosurgery resident was evaluated. The participant performed two procedures, first with the control model followed by the experimental model. Surface electrodes were placed bilaterally on the following muscles: thenar group (TG), flexor digitorum profundus (FDP), and extensor carpi radialis (ECR). EMG signals were obtained using a standalone system (MA-720 system Motion Lab Systems Motion Lab Systems, Inc., Baton Rouge, LA) and collected at 2400Hz for 30 seconds at two minute intervals over the entire procedure. Raw data files were converted to ASCII format files (RData2, Motion Lab Systems Motion Lab Systems, Inc., Baton Rouge, LA) before processing with custom Matlab (Mathworks, Natick, MA) software routines.

For each data collection epoch, the median frequency was calculated for 500 ms blocks for each muscle using non-stationary signal analysis [3]. These slope of median frequencies over time was calculated for each 30 second data collection for each muscle. The procedure was divided into four time blocks: basic exposure, vessel isolation, clamp 1 and clamp 2. The overall slopes during each time block for each time block and condition was determined.

Results and Discussion

The control and experimental procedures lasted 90 and 84 minutes, respectively. Bilaterally, the median frequency for the FDP and the ECR did not change between time blocks or across conditions, which may be due to the surgeon's posture. The forearms were supported for both procedures. Notably, for the surgeon's dominant hand (right side), there was a difference in the median frequency for the TG during the vessel isolation portion of the procedure between the experimental and control conditions (Figure 1). The experimental model was designed to be more challenging during the vessel isolation portion due to increased scaring.

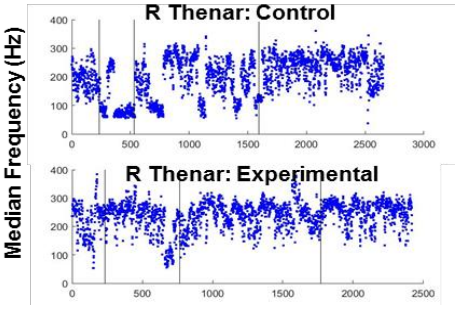

Figure 1: Each data point represents the median frequency for a 500 ms block for right thenar group (dominant hand) for the control (top) and experimental (bottom) conditions. The vertical lines divide the procedure into time blocks (in order): basic exposure, vessel isolation, clamp 1, and clamp 2

Comparison of the slopes of the median frequency during vessel isolation between conditions (control=-0.0805, R^2=0.0087; experimental=-0.3689, R^2=0.8742) demonstrated a decrease in frequency during the experimental condition compared to the control condition (Figure 2).

.

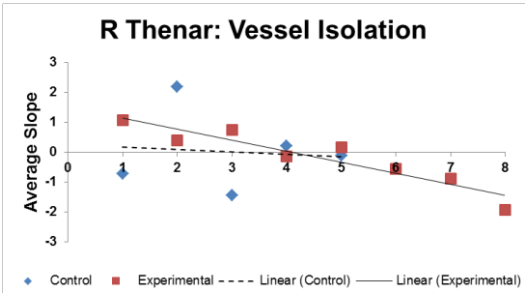

Figure 2: Each data point represents the average slope of the median frequencies for 500 ms blocks during a 30 second data collection during the vessel isolation. The dashed line is the overall slope of the control condition and the solid line is the overall slope of the experimental condition during the vessel isolation.

The decrease in frequency of the TG during vessel isolation demonstrated that there was muscle fatigue during this portion of the procedure. The presence of TG fatigue supports the hypothesis that the experimental model was more challenging than the control model.

Significance

The presence of dominant hand TG muscle fatigue demonstrated that the experimental condition was more difficult than the control condition. This technique can be used to study ergonomics during surgical procedures.

References

[1] Perry, A. et al. Neurosurg Focus 46 (2):E17, 2019.
[2] Slack, P. et al. Ann R Coll Surg Engl 90:651, 2008.
[3] Slack, P. et al. Proc. 29th IEEE EMBS Conf: 4822.

Non-linear analysis of effects of inertial properties on hammer movement variability

Joseph E. Langenderfer[1], Mara R. Thompson[2]
[1]School of Engineering and Technology, [2]Department of Physical Therapy
Central Michigan University, Mt. Pleasant, Michigan
Email: j.langend@cmich.edu

Introduction

Hammers have different inertial properties including overall rotational inertia and the symmetry of inertia. The relationship between the overall inertia and symmetry influences object effectiveness as a hammering tool [1]. Hammering is repetitive, but with variable movement. It is unknown if how the hammer movement varies is different for different hammers.

The purpose of this study was to use recurrence quantification analysis (RQA) to quantify the non-linear dynamics of the hammer movement in order to determine if the predictabily and complexity of movement variance are related to hammer rotational inertia properties. RQA has been used previously to analyse the structure of hand motion variability in experts compared to novice hammerers [2], and to analyse motion when objects were wielded with intention to perceive object dimension compared to no intention [3]. The objective here was to examine the role of hammer inertia and symmetry of inertia. The hypothesis was that hammers with greater rotational inertia symmetry would result in a swinging movement that is more regular but more complex.

Methods

Marker data were collected with VICON from male subjects (N=23) repetitively swinging hammers (Fig. 1). Overall rotational inertia for pairs of hammers (H1-H2 and H3-H4, respectively) was approximately equal. Inertia symmetry of H2 and H4 were 3 and 7 times, respectively, the symmetry of H1 and H3 (approximately equal).

Angular velocity of the hammer swing waveform was analysed with RQA. For 3 hammer swings from each trial, the phase space was constructed using the optimal lag (4 samples) and embedding dimension (m=2), determined from a trial-and-error process [4]. Recurrence plots were constructed using a radius of 10% of the maximum Euclidean norm between data points in the reconstructed phase space with at least two points defining a line segment required for determinism.

Recurrence plots (Fig. 1c) are created by darkening pixels when the waveform revisits the same neighbourhood in phase space. Recurrence rate (%REC), percent determinism (%DET) and Entropy measures the pattern of darkened pixels. RQA measures were assessed with ANOVA and t-tests with Bonferroni correction for pairwise comparisons.

Figure 1: Repetitive swinging (a) of hammers (b); Recurrence plot (c).

Results and Discussion

Pairs of hammers with similar overall inertia demonstrated different RQA parameters. %REC of hammer swinging motion was different between H2 and H3 (p=0.0001) and H3 and H4 (p=0.003) (Fig. 2). %DET was different between H2 and H3 (p=0.003). For Entropy, there was a difference between H2 and H3 (p=0.002) and H3 and H4 (p=0.001).

The greater %REC found for the more inertia symmetric but shorter handled hammers indicates that that movement is more non-linearly autocorrelated, i.e. movement is more regular. Higher %DET indicates the recurrence is more predictable. Entropy is a measure of complexity in the deterministic structure of the time series. Increased Entropy for shorter handle hammers indicates the recurrence is more disordered, with greater adaptability of the movement to meet task demands.

The movement of shorter handle, more inertia symmetric hammers was more regular, less random and of greater complexity. The lack of significant differences between H1 and any other hammer, combined with the lack of differences between H2 and H4, suggests that inertia symmetry does not uniquely affect how hammer movement varies. Rather, handle length, possibly combined with familiarity with the tool and its inertia, may be a more important influence of how the movement varies.

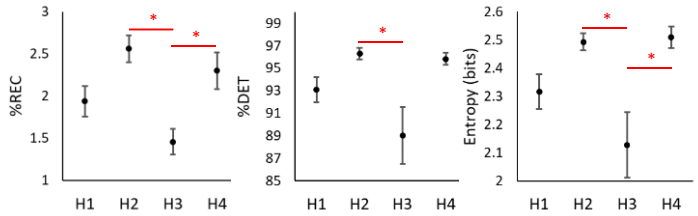

Figure 2: RQA measures for hammers 1-4. * significant difference.

Significance

Results suggest resiliency of motor control to altered inertial properties (overall inertia and symmetry). Handle length likely affects how the hammer movement varies more so than inertia symmetry. Similar techniques may be useful for understanding how subjects move objects differently including tools for manual labor, prostheses, or implements used in sport.

Acknowledgments

Sumaya Ferdous and Nilanthy Balendra were instrumental in data collection.

References

1. Fitzpatrick, P et al. *Zeitschrift Psycholog* 220, 23–28, 2012.
2. Nonaka, T et al. *Hum. Move. Sci.* 31, 55-77, 2012.
3. Riley, MA et al. *Percept. & Psychophysics* 31, 481-510, 2002.
4. Riley, MA et al. *Gait Posture* 9, 65-78, 1999.

Office Workers Maintain Decreased Sitting Time Long Term When Provided Sit-Stand Workstations

Erika Nelson-Wong, Ingrid Carlson, Jack Corrigan, Tara DiRocco, Brianna Hall-Nelson, Stephanie Kutcher, Patrick Mertz
School of Physical Therapy, Regis University, Denver, CO, USA
Email: enelsonw@regis.edu

Introduction

Long periods of sitting have many detrimental health effects, yet American adults still spend an average of 6.4 hours/day seated [1]. Many companies have adopted sit-stand desks (SSDs) in the workplace as an attempt to promote employee health, decrease sedentarism, and reduce musculoskeletal ailments. It is unknown whether intervention approaches directed towards decreasing sedentary behaviors through SSD prescription result in long-term behavioral changes in office workers. While previous studies have noted decreases in sitting time from SSD adoption in the short term [2,3,4] whether these changes last in the long-term is ambiguous. If SSDs are poised to serve as a solution to office place sedentarism, data on long-term SSD utilization is critical.

Previous work investigated the impact of a structured program for transitioning from seated to standing work, with SSDs provided to office workers [4]. The current study seeks to explore whether participants in the previous study maintained decreased sitting time long-term through a follow-up survey. We expected participants to have similar sitting minutes/day to those reported upon completion of the previous study.

Methods

Individuals who had formerly completed a previous study investigating effects of a targeted intervention on standing tolerance were invited to participate in the current follow-up study. Study participants were required to be employed full-time (> 32 hours/week) in an office setting at a primary desk job.

Qualtrics^{XM} survey software (Provo, UT) was used for this study. Pattern of use information including number of hours worked and percentage of time spent sitting and standing during the previous 7 days using the Occupational Sitting and Physical Activity Questionnaire (OSPAQ) [4].

Sitting minutes per day from the follow-up survey were compared with the baseline sitting minutes and final (end-point of previous study) sitting minutes. Sitting minutes were entered into a repeated measures ANOVA for the 3 time-points with Bonferroni corrected paired *t*-tests for post hoc multiple comparisons.

Results and Discussion

Of the 32 original participants, 20 agreed to participate and 12 were lost to follow-up for a response rate of 62.5%. One participant no longer had their SSD, this participant's data was excluded. Time since completing the original study was 19.8 ± 4.2 months (range 12-24 months).

Prior to enrollment in the original study (baseline), participants reported sitting 461.7 ± 86.6 min/day. At study completion, participants reported sitting 289.0 ± 96.3 min/day. In this follow-up survey, participants reported sitting 342.0 ± 111.9 min/day. As reported previously [4], participants in the original study decreased their sitting time by 30-50% during the 12-week study period. While participants increased their daily sitting time 12-24 months after study completion, this was not significant ($p = .13$). Sitting time at follow-up remained significantly lower ($p < .001$) than participants' baseline values prior to SSD implementation.

Limitations of this study include the small sample and the low response rate/loss to follow up. Participants were also highly motivated to use SSDs and were provided the workstations as an incentive for participation in the original study. The original study included a control group and an intervention group (received a structured approach to increasing their standing time over the 12-week period and a home exercise program), however those groups are not analyzed separately here due to the small group sizes.

These findings suggest that the decreased sitting time observed when office workers are provided with SSDs persists over time, even in the absence of continued encouragement and/or structured instruction.

Significance

While beneficial effects have been found in the short-term with standing workstation implementation in office settings, the longer term benefits have been unclear. Findings from this study demonstrate office workers maintain decreased sedentary behaviors at work for a period of 12-24 months following adoption of standing work solutions. Office workers who are motivated to try standing desks at work can be expected to benefit through decreased sitting time long-term.

Acknowledgments

The authors would like to thank VARIDESK for providing the sit-stand desk units for this study. VARIDESK was not involved in study design, analysis, or interpretation of findings. This study was funded by the Regis University Research and Scholarship Council.

References

1. Katzmarzyk P, Church T, Craig C, Bouchard C. *Med. Sci. Sports Exerc*. 2009;**41**(5):998–1005.
2. Dutta N, Walton T, Pereira M. *Prev. Med. Rep*. 2019;**13**:277-280.
3. Graves E, C Murphy R, Shepherd S, Cabot J, Hopkins N. *BMC Public Health*. 2015;**15**:114.
4. Nelson-Wong, E, Gallagher K, Johnson E, et al. *Ergonomics*. 2020, revised and in review.

Surgeon Hand Tremor during Microsurgery using a Rat Model

Stacy R. Loushin[1], Emily J. Miller[1], Avital Perry, M.D.[2], Christopher S. Graffeo, M.D. [2], Kenton R. Kaufman, Ph.D.[1]
[1]Motion Analysis Lab, Department of Orthopedic Surgery, Mayo Clinic, Rochester, MN, USA
[2]Department of Neurologic Surgery, Mayo Clinic, Rochester, MN, USA
Email: loushin.stacy@mayo.edu

Introduction

Development of sophisticated microsurgical skills can be obtained through training with animal models. A rodent model has been developed to simulate the physical and psychological challenges inherent to operating under subarachnoid haemorrhage conditions [1] with the goal of preparing surgeons for a high-stakes procedure at the end of a fatiguing event. Individuals with normal upper-extremity physiology will have a tremor at an 8-12 Hz frequency during times of stress, anxiety and physical exertion [2-3]. This tremor can be used to identify surgeon fatigue. The purpose of this study was to validate the increased difficulty of an experimental artery and vein anastomosis rat model by demonstrating that surgeons experience increased hand tremor compared to the standard, control model.

Methods

In this pilot study, a sixth year neurosurgery resident was evaluated. The subject performed two surgeries: artery and vein anastomosis on a control and experimental rat model. Tremor measurements were acquired using two single axis piezoelectric accelerometers (Type 8640A, Kistler, Novi, MI) affixed to each thumb on the dorsum of the distal third aspect of the 1st metacarpal. The accelerometers were attached to a piezotron coupler (Type 5114, Kistler, Novi, MI) and the data was acquired continuously at 100 Hz (NI-USB-6225, National Instruments, Austin, TX,).

Median and low pass filters were applied to the raw piezoelectric signals to remove noise and separate the acceleration components due to gravity and bodily motion (BA) [4]. The BA was low-pass filtered at 20Hz and a 512-point Fast-Fourier transform (FFT) was calculated. Power spectral densities (PSD) were calculated from the FFT and median frequency was found for each data block. The procedure was divided into four categories: basic exposure, vessel isolation, clamp 1 and clamp 2. The median frequencies for both left and right hands were assessed over time for the control and experimental condition. For each surgical category, the proportion of time above 8Hz was calculated. A Z-test statistic was calculated to determine if there was a difference in the portion of time between the experimental and control procedures. Significance was set to $p<0.05$.

Results and Discussion

The experimental procedure lasted longer than the control (93 and 71 minutes, respectively), with the vessel isolation portion taking 4 times longer in the experimental procedure (28 and 7 minutes, respectively). The surgeon experienced tremor bilaterally, with tremors occurring during the vessel isolation, clamp 1 and clamp 2 portions for both surgeries. There was a statistically significant increase in the median frequencies above 8Hz during the experimental conditions for the surgeon's dominant hand (right) during the clamp 1 ($p<0.00001$) and clamp 2 ($p=0.005$) portions of the surgery (Figure 1).

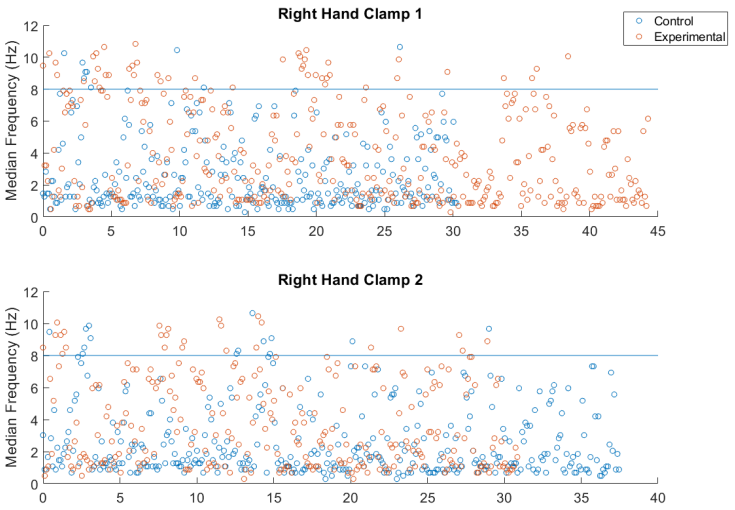

Figure 1: Median frequency of thumb tremor over time for control and experimental conditions. Each data point represents the median frequency for a 512 ms block for the Clamp 1 and 2 portions of the control (blue) and experimental (red) surgeries. Frequencies above the vertical line at 8 Hz indicate fatigue induced tremor.

The experimental model increased scar tissue formation, resulting in more challenging vessel isolation, indicated by the increased time spent on this portion of the procedure. While differences in median frequencies were not found during vessel isolation, the increased scarring of the experimental model acted as a fatiguing event for the subsequent Clamp 1 and Clamp 2 steps.

Significance

An experimental animal model has been design to replicate the physical and psychological challenges to a neurosurgeon performing a high stakes surgical procedure. The efficacy of the model is documented by the increased surgeon tremor compared to the control model. The ability to quantify surgeon fatigue allows for the quantitative assessment of model fidelity and analysis of a surgeon's ergonomic profiles throughout surgical tasks.

References

[1] Perry, A. et al. *Neurosurg Focus.* 2019;46 (2):E17.
[2] Wade P. et al. *Arch Neurol.* 1982;39:358-362.
[3] Gillespie MM. *J Neurosurg Nurs*. 1991;23(3):170-174.
[4] Karantonis DM. et al. *IEEE T Inf Technol*. 2006;10(1):156-167.

Verifying Joint Space-Based Metabolic Energy Expenditure Models

Jazmin M. Cruz[1] and James Yang[1]*
[1]Department of Mechanical Engineering, Texas Tech University, Lubbock, TX, USA
Email: *james.yang@ttu.edu

Introduction

Walking, running, sitting, and sleeping all require some amount of metabolic energy consumption in humans. Naturally, humans prefer to optimize their energy consumption when performing a task because doing so means less energy is required, thus allowing the human to maximize the available energy they have left.

In the past half century, metabolic energy expenditure (MEE) models that estimate energy expenditure have been developed by either using muscle states or by using joint dynamics [1,2]. A recent comparison between energy models was performed by Koelewijn et al. (2019) and found that muscle-state-based models performed better than the joint-based model [3]. It appears that the muscle-based metabolic models are more reliable, but they require muscle information.

If muscle information is not available, the joint space-based MEE offers a more convenient option when calculating energy consumption. Therefore, the objective of this work is to compare the energy consumption calculation accuracy among two versions of a joint-based energy consumption model. It is expected that the latest model will perform better than its predecessor.

Methods

This study uses experimental data provided by Koelewijn et al. (2019). The study recruited 12 individuals (sex: 6 males to 6 females; age: 24 ± 5 y; weight: 70 ± 12 kg; height: 1.73 ± 0.08 m) and measured metabolic cost using indirect calorimetry while walking at two paces (0.8 m/s and 1.3 m/s) during three inclines (0%, 8% , and -8%). This data is available for download online.

In the literature there are two joint space-based MEE models (Kim and Roberts, 2015; Roberts et al., 2016). In Koelewijn et al. (2019), the older joint space-based model (Kim and Roberts, 2015) calculated MEE values based on the experimental scenerios. In this study, MEE values from the new joint space-based model (Roberts et al., 2016) were also calculated. In the calculation, the following inputs are needed: task duration, joint torques, joint velocities, and maximum knee torque. All inputs were available to us except for maximum knee torque. An estimated average maximum knee torque value of 212.4 Nm and 107.6 Nm was used for men and women, respectively. The energy cost was normalized by dividing the energy cost (W) by the participant mass (kg) and speed (m/s). A root mean squared error (RMSE) calculation was used to assess how well each model performed. All scenarios used n = 12, but n = 11 was used for downhill walking at 1.3 m/s because one subject did not have experimental data for this case.

Results and Discussion

The results in Figure 1 show the calculated MEE from the two models and the measured metabolic cost. Table 1 contains the RMSE values for each model during each scenario. Kim's model is more accurate than Robert's model when performing level and uphill walking at both paces. However, when walking downhill, Roberts has a better estimation. The experimental metabolic cost has a steady increase as the incline increases from downhill to uphill, which is intuitive. Yet, it appears that both models do not adjust well to the incline change, where each of the graphs in Figure 1 have very little difference in magnitude and do not follow the steady increase in energy cost as seen in the experimental data.

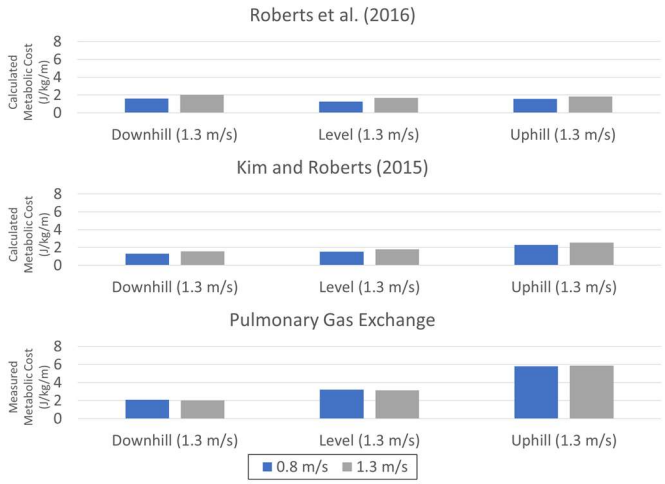

Figure 1: Calculated and measured metabolic cost.

Table 1: Root mean square error (J/kg/m) between the calculated and measured metabolic cost for both models. (The bolded numbers 0.8 and 1.3 are the speed of walking in m/s.)

Model	Downhill		Level		Uphill	
	0.8	**1.3**	**0.8**	**1.3**	**0.8**	**1.3**
Roberts	0.51	0.32	2.05	1.51	4.34	4.04
Kim	0.98	0.57	1.82	1.43	3.59	3.34

Significance

The primary advantage to the joint space-based MEE approach is that there is no need for muscle information, which can be helpful when analyzing full body motion with limited muscle information. It is important to verify whether the published joint space MEE models accurately predict metabolic energy cost for various applications. The findings in this work demonstrate that there was some improvement in the joint-based MEE modelling, but there is still a need to further develop the joint space-based model which can account for incline.

Acknowledgments

This research was funded by the Texas Tech University Presidential Fellowship.

References

[1] Roberts D Hillstrom H and Kim JH, (2016). *PLoS One*, **11**(12): e0168070.
[2] Kim JH and Roberts D, (2015). *Int. J. Numer. Method. Biomed. Eng.*, **31**(9): e02721.
[3] Koelewijn AD Heinrich D and van den Bogert AJ, (2019). *PLoS One*, **14**(9): e0222037.

The Effects of Posterior Shank/Thigh Contact on the Knee Joint Loading during Deep Squatting

John Z. Wu*, Erik W. Sinsel, Robert E. Carey, Liying Zheng, Christopher M. Warren, Scott P. Breloff
National Institute for Occupational Safety and Health, Morgantown, WV, USA. *Email: jwu@cdc.gov

Introduction

In some occupational or sport activities, workers or athletes need to make repetitive deep squatting motions or maintain deep squatting postures for extended periods of time. These unfavourable knee postures may cause excessive loading in the knee joint, thereby leading to the initiation and development of osteochondritis dissecans (OCD) and osteoarthritis (OA) [1,2]. During deep squatting motions, the posterior aspect of the shank comes into contact with the posterior thigh, which will result in a compressive force within the soft tissues. The goal of the current study is to quantify *in vivo* knee joint loading during deep squatting using a dynamic biomechanical model that includes the effects of the interface contact between posterior thigh and shank.

Methods

Inverse dynamical analysis was performed based on the data collected from a healthy male subject (mass 70 kg, height 1.68 m), who performed five deep, heel-up squatting tasks at a self-selected pace (Fig. 1a-b). A 14-camera system (Vicon) captured marker trajectories at 100 Hz, and the ground reaction forces were collected at 1,000 Hz via two force plates (Bertec). The interface contact pressures between the posterior thigh and shank were measured using a pressure sensor film (TekScan) (Fig. 1a). An existing, whole body model with detailed anatomical components of the knee (AnyBody v7.0) has been customized to fit the current study (Fig. 1b). The knee model includes bony segments of the tibia, femur, and patella (Fig. 1c). The motions of the tibiofemoral (TF) and patellofemoral (PF) joints are represented by 11-degrees-of-freedom (DOF), in which TF joint has six-DOF and PF joint has five-DOF. The model includes a total of 159 muscles in the lower extremity.

Results and Discussion

The calculated normal contact forces in PF and TF joint are shown in Fig. 1d and 1e, respectively. The curves represent the average values obtained from five squatting cycles. The model prediction shows that, at the deepest squatting posture (knee flexion of 120 degrees), the maximal PF and TF joint contact forces including the posterior thigh/shank contact are approximately 58% and 43%, respectively, of those that ignore the posterior thigh/shank contact. The model prediction shows that the PF contact force, without considering the posterior thigh/shank contact effects, reached about 3.80 times BW at a deep squatting posture, which is consistent with previous studies [3]. The measured peak thigh/shank contact force at each leg was approximately 43% BW in the current study, which is comparable to a previous study [4].

There was no direct validation for the model. We tried to validate our model indirectly with the experimental observations in two aspects. First, at a static upright standing posture (i.e., knee flexion = 0 degree), the model prediction on one-leg TF contact force was about 0.5 BW, which is physiologically reasonable. Secondly, the predicted time histories of the ground reaction forces agree reasonably well with the experimental measurements (results not shown). The ground reaction force fluctuation during the squatting task is caused by the dynamic mass inertial effects of the body segments and by the muscular forces that are needed to maintain the dynamic balance. The maximal difference between the predicted and measured ground reaction force was approximately 0.01 BW, indicating the agreement between the model predictions and the experiments.

Significance

We demonstrated via the biomechanical modelling that, in a deep knee flexion posture, the contact between posterior thigh and shank will result in a compressive force within the soft tissues around the joint, substantially affecting the joint loading. The model prediction supports the epidemiological observations that occupational or sports activities that require extended squatting are associated with higher prevalence of knee OCD and ORS.

Disclaimer

The findings and conclusions in this report are those of the authors and do not necessarily represent the official position of the National Institute for Occupational Safety and Health, Centers for Disease Control and Prevention.

References

[1] McElroy, M.J., Riley, P.M., Tepolt, F.A., Nasreddine, A.Y., Kocher, M.S., 2018. J Pediatr Orthop 38(8), 410-417.
[2] Accadbled, F., Vial, J., Sales de Gauzy, J. 2018. Orthop Traumatol Surg Res 104(1S), S97-S105.
[3] Komistek, R.D., Kane, T.R., Mahfouz, M., Ochoa, J.A., Dennis, D.A., 2005. Knee mechanics: a review of past and present techniques to determine in vivo loads. J Biomech 38(2), 215--28.
[4] Zelle, J., Barink, M., De Waal Malefijt, M., Verdonschot, N., 2009. J Biomech 42(5), 587-93.

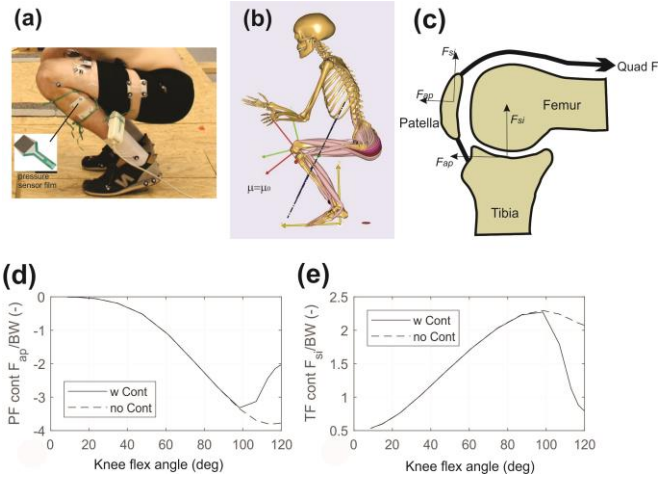

Figure 1. Experimental set-up, biomechanical model, and model predictions. (**a**). Measurement of shank/thigh contact pressure in human subject tests. (**b**). Biomechanical modelling to calculate the joint loading during squatting. (**c**). The definitions of the force directions in PF and TF joints. (**d-e**) Calculated PF (**d**) and TF (**e**) contact force as a function of knee flexion. The solid lines ("w Cont") and the dashed lines ("no Cont") are the results including and without including the effects of the posterior thigh/shank contact, respectively. The joint contact forces are normalized using the body weight (BW).

Evaluation of a Powered Lumbar-Support Exoskeleton during a Pace-Controlled Lifting Task: A Pilot Study

Liying Zheng*, Ashley L. Hawke, Robert E. Carey, Kevin Moore, John Z. Wu
Health Effects Laboratory Division, National Institute for Occupational Safety and Health, Morgantown, WV, USA.
*Email: lzheng2@cdc.gov

Introduction

Back injuries are prominent in work-related musculoskeletal disorder (MSD) cases, especially among those who regularly and manually handle materials [1]. In aim to reduce fatigue and prevent MSD-related injuries at workplace, passive exoskeletons have been developed and adopted in the industries involving material handling, while powered back-assist exoskeletons are still at the early development stage worldwide. In this preliminary study, we evaluated a Japanese powered lumbar-support exoskeleton during a pace-controlled lifting task, where the users' muscle activities, heart rate, cerebral oxygenation and rating of perceived exertion (RPE) were assessed.

Methods

In this pilot study, two subjects (age = 46 ± 25 years old; height = 167.9 ± 0.2 cm; weight = 73.4 ± 11.9 kg) performed 30 times of pace-controlled lifting movements—lifting a 20-lb wooden tray from ankle to hip height at a pace of one lift per 10 seconds guided by a metronome. The subject repeated the 30-lifting task for two conditions: without wearing the exoskeleton (NoExo) and while wearing the powered lumbar-supoort exoskeleton (Exo). The activations of 16 major leg and torso muscles (vastus lateralis, biceps femoris, semitendinosus, thoracic erector spinae, lumbar erector spinae, multifidus, latissimus doris and abdominal external oblique on both sides) were measured by a wireless surface electromyography (EMG) system (Noraxon U.S.A. Inc., Scottsdale, AZ). The heart rate was recorded by a 3-lead Biomonitor (Noraxon U.S.A. Inc.,Scottsdale, AZ). The cerebral oxygenations were measured by a 8-channel functional near-infrared spectroscopy system (fNIRS) (OctaMon+, Artinis Medical Systems B.V., Netherlands). Six long fNIRS channels with 30-mm inter-optode distances were positioned over the prefrontal cortical areas acoording to the international EEG 10-20 system (left: Fp1, F3 and F7; right: Fp2, F4 and F8). Two short separation channels with 10-mm inter-optode distances measured solely the extracerebral signals and were used to remove the "noisy" components from the long channels. Additionally, RPE scores (0: no exertion, 10: exhausted) were collected at the end of the lifting task in each condition.

Results and Discussion

The average heart rate during the 30-lifitng task was reduced 6% in the Exo condition compared to the NoExo condition for both subjects. The effects of wearing the powered exoskeleton on the users' muscle activities, cerebral oxygenation and self-reported RPE values varied between the two subjects. Although both subjects reported samller RPE values (less perceived effort) for EXO condition compared to the NoExo condition, the reduction in the RPE scores is much larger in Subject A (4 vs. 8) than in Subject B (3 vs. 4). Compared to the NoExo condition, reductions in leg and back muscle activations were also found to be more pronounced in subject A (ranged from -3% to -26%). The oxyhaemoglobin (O2Hb) values of Subject A in the left prefrontal cortical area increased in the Exo condition compared to the NoExo condition, while the O2Hb values decreased in the Exo condition for Subejct B.

This pilot study showed promising results of using a powered lumbar-support exoskeleton during a repetitive lifting task. Besides the common evaluation measurements such as muscle activity and heart rate, the cerebral oxygenation demonstrated a possible measure to assess performance of exoskeletons. The prefrontal cortex oxygenation appeared to respond to the subject's perceived effort, which was similar to findings in a previous study [2]. The variations of the user experience and product performace were observed in this small pilot study. More comprehensive evaluations in a large subject pool are expected in the future.

Significance

Our results demonstrate promising applications of powered exoskeletons in industries involving manual material handling. Along with muscle activity and heart rate, cerebral oxygenation manifests the potential to complement the evaluations of the effectiveness of exoskeletons.

Figure 1. A subject performed 30 lifts of a 20-lb box from ankle to hip height at a rate of one lift per 10 seconds. The muscle acitivies, heart rate and cerebral oxygenation were measured simultaneously by EMG, Biomonitor and a fNIRS system.

Disclaimer

The findings and conclusions in this report are those of the authors and do not necessarily represent the official position of the National Institute for Occupational Safety and Health, Centers for Disease Control and Prevention.

References

[1] Bureau of Labor Statistics, *The Economics Daily*, 2016
[2] Thomas R. and Stephane P., Eur J Appl Physiol, 102: 153-163, 2008

Comparison of a Mid-Seated Posture with Seated and Standing Postures

Archana Lamsal[1], Garrett Weidig[1] and Tamara Reid Bush, PhD[1]
Teresa Bellingar, PhD[2]
[1]Michigan State University, East Lansing, MI, USA, [2]Haworth, Holland, MI, USA
email: reidtama@egr.msu.edu

Introduction

Prolonged inactivity during work hours is a major factor that leads to various health issues in office workers [1]. Frequent movement is essential to promote blood and nutrient flow, especially in the intervertebral discs as they are avascular organs [2]. Standing desks promote movement, however, standing for long periods of time has been associated with musculoskeletal disorders, pain, and discomfort of the feet and legs [3]. Current research suggests a need for other positions which can provide changes in body posture without subjecting the legs to large loads. The goal of this study was to compare the joint angles, joint moments and loading on the body between seated, a new type of mid-seated posture and standing.

Methods

Twenty consenting participants (ten males and ten females) were recruited. An 11-camera motion capture system and force plate were used for this study. Reflective markers were attached on various anatomical landmarks. The participants were asked to conduct a computer task in three different postures, spending fifteen minutes in each posture. The postures were: seated, mid-seated, and standing. The mid-seated posture was with a slightly bent knee, in an elevated chair with their feet on the ground. Marker position and force data were collected for every posture and during transition between postures. Data for all postures and motions were collected for 20 participants. Additionally, a sub-set of three participants returned to the lab to conduct movements directly from seated to the standing position.

Pelvic tilt (angle between the pelvic plane and horizontal) and openness angle (angle between the thorax and pelvis) were calculated for all postures (Figure1). Inverse dynamics was used to compute joint moments at the ankle, knee and hips in the sagittal plane for transition between three postures, also referred to as dynamic motions. The motions were: seated-to-mid-seated (Sit-M), mid-seated-to-standing (M-S), and seated-to-standing (Sit-S). Anthropometric data for calculating joint loads were taken from Winter [4].

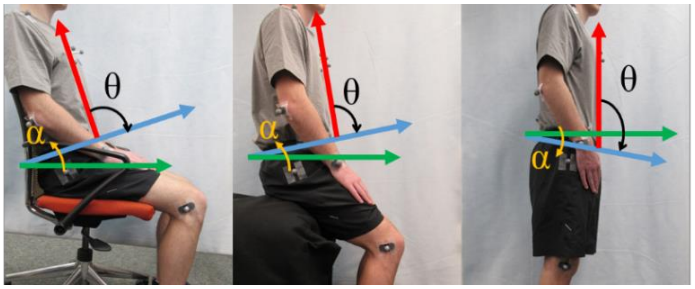

Figure 1: Vector overlay diagram of pelvic tilt angle and openness angle in seated, mid-seated and standing postures. The angle between pelvis plane (blue) and horizontal (green) gives pelvic tilt (α) and the angle between pelvis plane and torso (red) gives openness angle (θ)

Results and Discussion

The average ground reaction force expressed as the percent of body weight in mid-seated posture (16.41%) was slightly higher than the seated posture (12.55%) but significantly lower than standing (96.54%). It is interesting to note that even while "seated" in the mid posture, the pelvis was able to be moved to a point halfway between the seated and standing postures. This is shown by the change in pelvic tilt angles and also supports a change in lumbar curvature (Table 1). The openness angle was smallest in the seated posture and largest in the standing posture. Previous research has shown that a larger openness angle is correlated to an increased lordotic lumbar curvature [5]. This change in lumbar curvature is good as it promotes nutrient transport in intervertebral discs which are avascular.

All the maximum joint moments were smaller for M-S motion compared to Sit-S motion. Moving from the mid-seated position to standing put lower load on the joints than standing directly from the seated posture. The Sit-M motion had smaller joint moments in the knee and ankle joints compared to Sit-S motion. However, the hip moment was the largest in the Sit-M motion. The hip moment was largest because participants had to lean forward to move the seat into the second position, which resulted in larger moment arm for the torso weight. Although this may be similar to when people lean forward to adjust seat height.

Table 1 Average joint angles and standard deviations in degrees across the subject pool for each posture

Angles	Seated	Mid-seated	Standing
Pelvic Tilt	15.3 (6.6)	6.3 (6.6)	-8.4 (7.6)
Openness	96.7 (15.7)	102.1 (14.0)	116.5 (17.1)

To summarize, the mid-seated posture provided a pelvic and lumbar posture closer to that of standing, while subjecting the feet to a lower load than in standing. Standing from the mid-seated posture was easier on the joints than from the standard seated posture as it produced lower moments. A mid-seated posture is another possibility for office workers who wish to achieve postural change without increasing loading on the feet or legs.

Significance

Based on our data, one can say that the mid-seated posture provides the benefit of both sitting and standing. It reduces the load on the feet and legs in comparison to standing and is easier to stand from in comparison to the seated posture. Change of position from the seated posture to mid-seated posture also provides motion to the joints and lumbar region. Thus, the mid seated posture provides an excellent additional working posture.

Acknowledgments

This work was supported by Haworth Inc.

References

1. Hamilton MT, et al., *Diabetes*, 2007
2. H Wilke et al., *Spine*, 1999
3. Boussenna, M., et al., *Ergonomics*, 1982
4. Winter, D. A., *John Wiley & Sons.,* 2009
5. Leitkam ST., et al. *Journal of Biomechanics.* 2011

Glenohumeral Joint Motion Variability during Wheelchair Propulsion in Children and Adults with Spinal Cord Injury

Matthew M. Hanks[1], Alyssa J. Schnorenberg[1], Sergey Tarima[2], Vaishnavi Muqeet[2,3], Lawrence Vogel[4], and Brooke A. Slavens[1,3]
[1] Department of Occupational Science & Technology, University of Wisconsin-Milwaukee, Milwaukee, WI, USA
[2]Medical College of Wisconsin, Milwaukee, WI, USA
[3]Clement J. Zablocki Veterans Affairs Medical Center, Milwaukee, WI, USA
[4]Shriners Hospitals for Children, Chicago, IL, USA
Email: hanks@uwm.edu

Introduction

Manual wheelchair use is associated with a high incidence of shoulder pain and pathology [1]. However, previous reports have found that children and adults with pediatric-onset SCI have less pain than adults with adult-onset SCI. Presence of pain is associated with decreased shoulder range of motion (ROM) [2,3], which may suggest why self-reported pain is less prevalent in pediatric wheelchair users than in adult wheelchair users [1,4]. Moreover, increased ROM and within-subject variability in human movement is important for improved function and reducing the risk of overuse injuries [5]; however, differences in these metrics between pediatric and adult manual wheelchair users remain unknown. The purpose of this study was to investigate differences in glenohumeral (GH) joint ROM and subject variability during propulsion in pediatric and adult manual wheelchair users with SCI.

Methods

Fifteen pediatric manual wheelchair users with SCI (12.2 ± 3.8 years) and eleven adult manual wheelchair users with adult-onset SCI (31.4 ± 15.8 years) participated in this study. A 15-camera Vicon T-Series motion capture system (Vicon Motion Systems, Oxford, UK) was used to collect 3-dimensional (3D) kinematic data at 120 Hz. Twenty-seven passive markers were placed on each subject to implement our validated upper extremity inverse dynamics model [6]. Subjects performed multiple trials of manual wheelchair propulsion at a self-selected speed on a level, tile floor using their own wheelchair. Mean GH joint adduction/abduction, internal/external rotation, and flexion/extension ROM was calculated across multiple strokes for each subject. Data were plotted with respect to age using quantile regression models for 0.10 and 0.90 quantile levels to display within- and between-subject variability (Figure 1).

Results and Discussion

GH joint ROM variability significantly decreased in the coronal and transverse planes. Pediatric manual wheelchair users exhibited greater GH joint variability in adduction/abduction and internal/external rotation ROM compared to adult manual wheelchair users (Figure 1). Findings of this study support the notion that movement variability decreases with age [5]. That is, overuse motions increase and may explain the higher prevalence of shoulder pain reported by those with adult-onset SCI compared to pediatric-onset SCI, despite controlling for age and years of wheelchair use [1,4]. Results also support previous research that found pediatric wheelchair users use highly variable upper extremity biomechanics and propulsion patterns compared to adult wheelchair users [4, 7].

Significance

Implications of this research can be largely impactful for manual wheelchair users across the lifespan with SCI. Current recommendations for promoting the preservation of the shoulder are antiquated and are applicable only to adults [8]. This research indicates the necessity for identifying manual wheelchair propulsion best practices for children and across the lifespan to decrease the trend of shoulder pain and pathology. Research is underway with a larger population of children and adults with both pediatric- and adult-onset SCI. Ultimately this will enchance physical and occupational therapy interventions to improve mobility and quality of life for all wheelchair users with SCI.

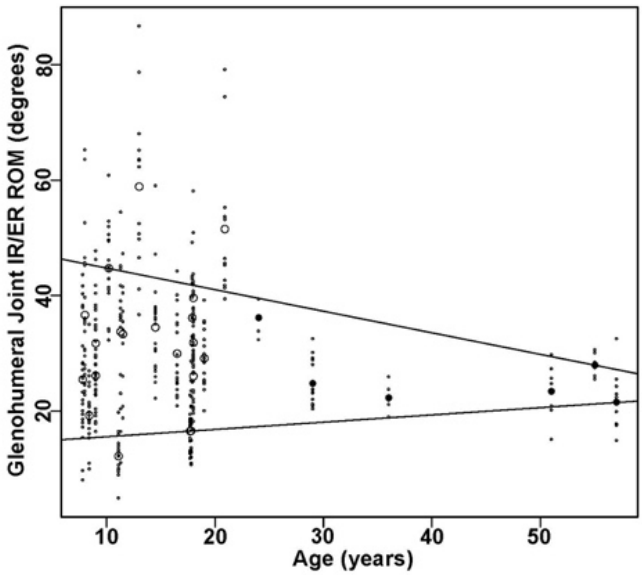

Figure 1: Glenohumeral joint ROM for internal/external rotation with respect to age. Each vertical scatterplot is one subject's data (each stroke is a dot and the subject's mean is the large, open circle (pediatric) and solid circle (adult)). Narrowing of 10% and 90% quantile lines demonstrates the decrease in variability with age.

Acknowledgments

This research was supported by the Eunice Kennedy Shriver National Institute Of Child Health & Human Development of the National Institutes of Health under awards 1R01HD098698 and 2R44HD071653, and the National Institute on Disability, Independent Living, and Rehabilitation Research grant number 90RE5006-01-00.

References

[1] Brose, S.W. et al. (2008) Arch Phys Med Rehabil
[2] Wessels, K.K. et al. (2013) J Rehabil Res Dev
[3] Barnes, C.J. et al. (2002) J Shoulder Elbow Surg
[4] Slavens, B.A. et al. (2015) Front Bioeng Biotechnol
[5] Wilson, C. et al (2016) PLoS ONE
[6] Schnorenberg, A.J. et al. (2014) J Biomech
[7] Boninger, M.L. et al. (2002) Arch Phys Med Rehabil
[8] Paralyzed Veterans of America (2000) J Spinal Cord Med

Neck Kinematic Differences Between Six Computer Monitor Configurations

Caleb C. Burruss, Elizabeth Bjornsen, and Kaitlin Gallagher, Ph.D.
University of Arkansas, Fayetteville, AR, U.S.A
Email: kmg014@uark.edu

Introduction

The average size of a computer screen has increased from 19.5" in 2011 to 21.6" in 2019 [1]. A systematic review on dual monitor usage found that users strongly preferred multiple monitors; however, users may be in non-neutral neck postures while using them [2]. Biomechanics driven studies have also only looked at monitors 15-17" in size [2], which is below the average size used today [1]. The purpose of this study was to determine the effects of computer monitor configuration on neck kinematics. We hypothesized that specific monitor configurations would allow for a neutral neck posture; however, this may be task dependent.

Methods

We recruited 17 graduate students with no current head, neck, back, or upper extremity injuries. Participants came into the lab six different days, and each day used a different monitor configuration (**Figure 1**). Each day, participants completed five tasks [3] consistent with multiple display use: copy/pasting, information comparison, referencing while preparing a document, drag/dropping (not shown), and monitoring information (not shown). Participants' neck rotation was tracked using a motion capture system (Qualysis AB) with markers placed on the head and trunk. The participant performed five 10-minute tasks that were randomized each day. Angles were calculated using Visual3D (v6, C-Motion Inc). Neck rotation angle median and range of motion were calculated using an amplitude probability distribution function. A one-way repeated measures ANOVA was conducted for each task with a factor of monitor configuration. Tukey post-hoc tests were used to evaluate significant main effects. Significance was set at p=.05.

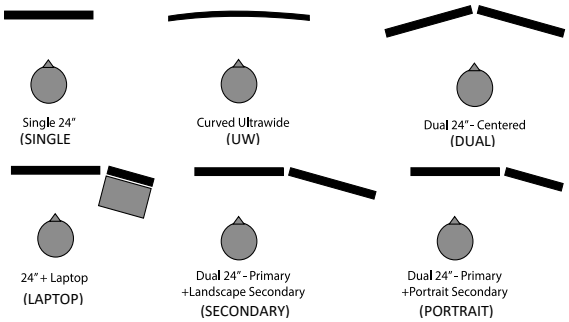

Figure 1: Monitor configurations.

Results and Discussion

There was a main effect of configuration for the median neck rotation angle (p<.001). SINGLE, UW, and DUAL (centered monitors) were significantly different (p<.001) than the off-center configurations (**Table 1**). The UW monitor was never significantly different from SINGLE.

There was a main effect of configuration for range of motion (p<.001) for all tasks. SINGLE and UW had the smallest range of motions for these three tasks (**Table 1**). The other four monitors were significantly different (p<.001) than SINGLE and UW. The UW monitor did not significantly differ from SINGLE. UW had a similar rotation range of motions as SINGLE, and when they differed, it was by less than 5 degrees.

Our results agree with a previous systematic review [2], in that many of the monitors and tasks produced non-neutral neck postures. As hypothesized, the specific task influenced if a person was in a non-neutral neck angle when using a given monitor configuration. Interestingly, the UW monitor had similar median neck rotation and range of motions to SINGLE despite an increased screen area (33" vs. 24" diagonal). The UW monitor also reduced neck rotation median and range compared to other large screen set-ups such as dual monitors and secondary laptops.

Table 1: Median neck angles and neck range of motion values for compare, copy/paste, and reference tasks. Note: Mean (standard deviation) presented. For median, negative = right axial rotation. ^, * denotes significant differences.

	Single	UW	Dual	Laptop	Second	Portrait
Median Neck Rotation						
Compare	7.5	8.7	9.0	1.4*	1.1*	0.0*
	(5.0)	(4.4)	(6.6)	(6.1)	(4.9)	(4.9)
Copy/Paste	-1.9	-2.1	-5.0	-12.0*	-12.8*	-12.8*
	(4.4)	(4.8)	(7.0)	(9.0)	(6.8)	(6.8)
Reference	-0.9	-3.4	-5.8	-11.4*	-15.7*	-13.7*
	(5.0)	(5.1)	(6.8)	(5.1)	(8.5)	(7.0)
Range of Motion						
Compare	10.6	15.3^	21.9*	19.6*	20.2*	19.4*
	(4.9)	(6.5)	(9.5)	(6.8)	(7.6)	(6.8)
Copy/Paste	12.5	16.7	23.2*	24.7*	24.6*	23.7*
	(6.3)	(9.6)	(10.9)	(10.4)	(9.2)	(8.1)
Reference	14.0	16.0	21.4*	22.3*	24.0*	22.3*
	(5.3)	(6.3)	(9.3)	(8.3)	(8.0)	(8.2)

Significance

A larger screen area means more area to scan while working; however, our study found that a 33" UW did not alter neck kinematics compared to a 24" single monitor. As a result, the UW monitor may be more appropriate for office workers compared to one single monitor or two dual monitors. Research on the actual implementation and effect of UW monitors on a user over the course of the day is still limited. As a result, future studies should look at the proper distance for an UW monitor and the potential increase in hand movement when operating a mouse.

Acknowledgements

Funding was received from the Office Ergonomics Research Committee. Herman-Miller provided in-kind equipment.

References

1. IDC. (2015). IDC InfoBrief - Improving Employee Productivity with Dual Monitors.
2. Gallagher, K. M et al. (2019). Human Factors, In press. DOI: 10.1177/0018720819889533
3. Stringfellow, P. F. (2007). Clemson University, United States - South Carolina.

If Sitting Does Not Cause Low Back Pain in Healthy Working Adults, What Does?

Diesbourg, T.L.[1,2], Shaeff, A.[1], Dumas, G.A.[2,3]
[1]Department of Public and Environmental Wellness, Oakland University, Rochester, MI, USA
[2]School of Kinesiology and Health Sciences, Queen's University, Kingston, ON, CAN
[3]Mechanical and Materials Engineering Department, Queen's University, Kingston, ON, CAN
Email: tdiesbourg@oakland.edu

Introduction

For many years, sitting was thought to be a risk factor for low back pain development in sedentary jobs [1,2], however more recently, metanalyses and systematic reviews has suggested that this is not the case [3]. Regardless of whether sitting is the cause of low back pain or not, some individuals will develop low back discomfort while sitting, whereas other people will not [4]. Previous studies describe the complexity of pain and have identified age, sex, and mental health [5], flexibility [6], and health status [7] as predictors of chronic low back pain development however, no study has examined which factors could be used to predict the development of self-reported low back pain in healthy, working individuals.

Therefore, the purpose of the current analysis was to determine whether onset of low back discomfort while sitting could be predicted given some personal characteristics of the worker, and to assess whether this risk could be mitigated through ergonomic recommendations.

Methods

Fifty-four individuals (36 Female, 18 Male) who work sedentary jobs were recruited from three age groups (20 – 25 years, 40-45 years, and 60-65 years). Volunteers were excluded if they were experiencing low back pain, or if they had experienced low back pain significant enough to cause them to seek medical attention or to miss school or work in the past 12 months. Participants completed a battery of physical fitness tests and responded to a comprehensive digital survey which covered areas of health, work history, nutrition, sleep, injury history, mood, depression, anxiety, and stress. Participants sat for 60 minutes in a backless office chair, which was ergonomically adjusted to suit their stature. Every ten minutes during the seated time, the participants were asked to rate their low back discomfort on a digital visual analog scale with "No discomfort" and "Worst discomfort imaginable" as the anchors. A change in perceived discomfort of 10 units of more at any point in the hour was designated as clinically relevant pain development, and those participants were classified as "Pain Developers" (n = 29) [8].

Variables discussed previously as being predictors of pain, as well as those thought to possibly hold a strong association with spine health were selected from the database. These included: age, sex, body fat percentage, grip strength, cardiovascular health, history of joint pain, history of neck and/or back pain, hours of sleep, depression, anxiety, stress, trunk flexibility, hours of exercise per week, and sedentary time per week.

Statistical analysis consisted of binary logistic regression with pain as a binary variable (Pain Developers and Non-pain Developers), and all other variables as binary, categorical, and continuous variables as appropriate. Predicted probabilities from the logistic regressions were used to plot receiver operating characteristic (ROC) curves, and the area under these curves (AUC) identified each factor's ability to group for pain status [9].

Results and Discussion

The binary logistic regression did not identify any significant association between any of the variables of interest and pain status. To determine whether any of these variables could discriminate between pain groups despite their inability to predict the risk of developing pain, the ROC curves were generated and AUCs were calculated. These AUCs are presented in Table 1. None of the variables of interest were found to be discriminatory as far as differentiating those who would develop low back discomfort while sitting from those who would not.

Table 1: AUCs and Significance for all variables of interest. Variable type is presented as: Bin = Binary, Cat = Categorical, or Cont = Continuous.

VARIABLE	AREA UNDER ROC CURVE	SIGNIFICANCE (α = 0.05)
Age (Cat)	0.61	0.18
Sex (Bin)	0.51	0.88
Touch Toes Yes/No (Bin)	0.53	0.68
Percent Body Fat (Cat)	0.56	0.44
Grip Strength (Cat)	0.55	0.51
Trunk flexion (Cont)	0.57	0.41
Cardiovascular Risk (Bin)	0.61	0.17
History of Joint Pain (Bin)	0.53	0.67
Hist. Neck/Back Pain (Bin)	0.54	0.66
Hours of sleep/night (Cat)	0.51	0.87
Sedentary hours/week (Cont)	0.52	0.80
Hours of exercise/week (Cont)	0.51	0.92
DASS 21 - Depression (Cat)	0.50	1.00
DASS 21 - Anxiety (Cat)	0.51	1.00
DASS 21 - Stress (Cat)	0.49	0.94

The lack of any predictive or discriminatory variables just further reminds of the complexity of pain. Without being able to distinguish those at risk for developing low back pain while sitting from those who are less likely to, recommendations should err on the side of caution and treat all workers as possible pain developers by suggesting less time spent sitting for everyone.

Significance

The purpose of this analysis was to identify the risk factors that could be mitigated in order to reduce the risk for developing low back pain while working in seated occupations. Rather, it appears as though, in healthy working adults with no history of chronic debilitating low back pain, the onset of low back discomfort cannot be predicted. This finding (or lack thereof) points to the complexity of pain, and further analysis is required to identify whether there are other previously overlooked factors that could predict the onset of low back discomfort while sitting.

References

[1] Magora, 1972; [2] Andersson, 1998; [3] Hartvigsen et al, 2000.; [4] Dunk & Callaghan, 2010; [5] Hoy et al, 2010; [6] Tekur et al, 2008; [7] Hagen et al, 2006; [8] Nelson-Wong et al, 2009; [9] Cantor et al, 1999.

EMG Based Biomechanical Analysis of the Effect Different Writing Surfaces and Postures Have on Forearm Muscles

Mustafa Ozkan Yerebakan[1], Boyi Hu[1*]
[1]Department of Industrial and Systems Engineering, University of Florida, Gainesville, FL, USA
Email: *boyihu@ise.ufl.edu

Introduction

Writing as we know it has been changing in the past decade. With the introduction of tablet computers, it is possible to write on surfaces other than paper or whiteboards. Although it is being used by millions of people, biomechanical effect of digital device writing is not well understood. Apart from one study that compares different grasp patterns (Almeida et al., 2013), comprehensive studies aim to investigate the effects of posture on writing tasks that have been limited. These two points plus the possible effects of fatigue due to long sessions of notetaking makes it vital to investigate what posture and writing surface are the least damaging to the human body.

Methods

A convenience sample of 5 participants was recruited in this pilot study. The main task of the study was to write randomly selected sentences that included every letter of the English alphabet. There were three writing surfaces (paper, tablet PC and whiteboard) and three writing postures (45-degree angle, horizontal and vertical). The muscle that were selected for EMG data collection were extensor digitorum (ED), extensor carpi radialis (ECR), flexor carpi radialis (FCR), flexor carpi ulnaris (FCU) and flexor digitorum superficialis (FDS). Muscle activity was measured by normalizing the EMG using the values from maximum voluntary contraction (MVC) trials. The EMG signals were recorded with a sampling frequency of 1000 Hz and they lasted for three seconds. Each participant had 9 trials and each trial lasted about 60 seconds.

After data collection was finished the raw EMG signal was pre-processed before normalization was done and median frequency was calculated. Pre-processing involved applying a 3 Hz cutoff frequency filter to the signal, rectification and smoothing by using a 2nd order Butterworth filter. Normalization was done taking the percentage value of the ratio between the average value of the EMG signal and corresponding value from the MVC trial. All of pre-processing and processing was done in Matlab (MATLAB 2019b, Mathworks, Natick, MA).

The data analysis involved a multivariate ANOVA in which the effects of device, posture and interaction was investigated for each of the five muscles. In order to determine the conditions that result in the lowest amount of percentage muscle activation and highest frequency values and further test significance, a Tukey's Honest Significance test was conducted.

Results and Discussion

The muscle activation level results indicate that different surfaces had a more significant effect on both carpi radialis muscles and different postures affected the FCU and FDS more. Looking at these significantly different instances it could be seen that the tablet condition and the 45° posture resulted in the lowest levels of muscle activation. The median frequency values showed the effect of posture being more significant FCR muscle, however it seems there was no significant effect of surface for this variable. A possible reason why the results are limited for the median frequency is the length of the trial.

Significance

This study has investigated the effects of different writing surfaces by using biomechanical tools such as EMG and EMG based signal complexity measures. Although there are studies that compare different writing surfaces (Alamargot and Morin, 2015), all of them utilize kinematics or graphonomics outcomes. This study emphasizes the effects on the human body, specifically the muscles. The results from this study could be used to establish guidelines for tablet usage in both office and recreational usage. Future studies that increases the sample size and lengthen the trial to similar writing fatigue studies (Summers and Catanzaro,2003) would be useful in seeing the effect more clearly.

References

Alamargot et al., 2015.
https://doi.org/10.1016/j.humov.2015.08.011
Almeida et al., 2013.
https://doi.org/10.1016/j.jelekin.2013.04.004
Summers and Catanzaro, 2003.
https://doi.org/10.1046/j.1440-1630.2003.00310.x

Table 1. Average Values (Standard Errors) Average Muscle Activity in Percentage MVC

Muscles	Paper	Tablet	Whiteboard	*p* value*	45°	Horizontal	Vertical	*p* value*
ED	13.9 (0.9)	13.0 (0.6)	14.6 (0.8)	0.070	13.4 (0.7)	14.0 (0.6)	14.2 (0.9)	0.428
ECR	**10.7 (1.5)^{AB}**	**9.0 (1.2)^{B}**	**11.1 (1.4)^{A}**	**0.027**	10.9 (1.5)	10.0 (1.4)	9.8 (1.2)	0.317
FCR	**8.1 (0.4)^{A}**	**7.0 (0.3)^{B}**	**8.7 (0.4)^{A}**	**0.002**	7.3 (0.4)	8.3 (0.3)	8.2 (0.6)	0.079
FCU	10.6 (1.2)	9.6 (0.9)	10.8 (1.1)	0.260	**8.7 (0.6)^{B}**	**10.8 (1.0)^{A}**	**11.6 (1.3)^{A}**	**0.001**
FDS	10.5 (2.4)	9.4 (1.7)	11.0 (2.2)	0.415	**8.1 (1.3)^{B}**	**11.5 (1.8)^{A}**	**11.4 (2.7)^{A}**	**0.009**

Numbers that are bolded indicate significant difference. Numbers that do not share a letter are significantly different where A>B>C

Exoskeleton Usage, Arm Posture, and Tool Weight Changes Shoulder Fatigue Risk

Jason C. Gillette[1*], Shekoofe Saadat[1], and Terry Butler[2]
[1] Department of Kinesiology, Iowa State University
[2] Lean Steps Consulting
Email: *gillette@istate.edu

Introduction

In 2015, shoulder injuries resulted in 23 days median days missed for private industry, the longest recovery time of any body part [1]. It is widely accepted that repetitive overhead arm postures are associated with increased risk of shoulder overuse injuries. Threshold limit values (TLVs) for upper limb fatigue provide a relationship between percent of maximal voluntary contraction (%MVC) and duty cycle [2]. Therefore, the risk of fatigue and overuse injury may be predicted using electromyography (EMG).

The Levitate Airframe is a passive upper body exoskeleton designed to support the arms during elevated shoulder postures. Previous EMG field studies at John Deere and Toyota indicated that the exoskeleton may reduce deltoid fatigue risk [3,4]. The purpose of this study was to determine if fatigue risk changes with exoskeleton usage, arm posture, and tool weight. Our hypothesis was that the exoskeleton would reduce deltoid fatigue risk for shoulder flexion angles 90-135° and tool weights 3-7 lb.

Methods

Twenty healthy young adults (10 male/10 female) participated in this study. Six shoulder flexion angles common to automotive assembly were tested: 60°, 90° out, 90° up (90° elbow flexion), 135°, and 180° (Figure 1). Three tool weights (3 lb, 5 lb, and 7 lb) were created by adding weight to a drill. A frame was adjusted so that the arm postures would be achieved by pressing a button with the drill bit. Participants repeated 4 s movements for 30 s: move to position, press button, move to neutral, and rest.

EMG sensors were placed on the anterior deltoid, biceps brachii, upper trapezius, and right/left erector spinae. Shoulder flexion, shoulder abduction, elbow flexion, and spinal extension were used as MVCs for normalization. Average EMG amplitude was determined while a muscle was active (>5% MVC), and duty cycle was set to time muscle is active divided by task time (30 s). Duty cycle was used to calculate the TLV [2], and the fatigue risk value was calculated as EMG amplitude minus the TLV.

Results and Discussion

Without exoskeleton. Increasing tool weight from 3 lb to 5 lb to 7 lb increased fatigue risk values for all muscles ($p \leq 0.001$). Increasing shoulder flexion from 60° to 90° up to 90° out to 135° increased fatigue risk values for the deltoid ($p<0.001$), while 135° and 180° were similar. In addition, increasing shoulder flexion from 60° to 90° up to 135° increased fatigue risk values for the trapezius ($p<0.001$), while 90° up and 90° out were similar and 135° and 180° were similar.

Exoskeleton vs. without. The exoskeleton reduced deltoid fatigue risk values for all tool weights with arm postures of 90° up, 90° out, and 135° ($p<0.05$, Figure 1), with the exception of 90° up with 7 lb tool weight. Fatigue risk reductions were driven by reductions in EMG amplitudes ($p<0.04$) for these arm posture and tool weight combinations. With one exception, these results support the hypothesis that the exoskeleton would reduce deltoid fatigue risk for shoulder flexion 90-135° and tool weights 3-7 lb.

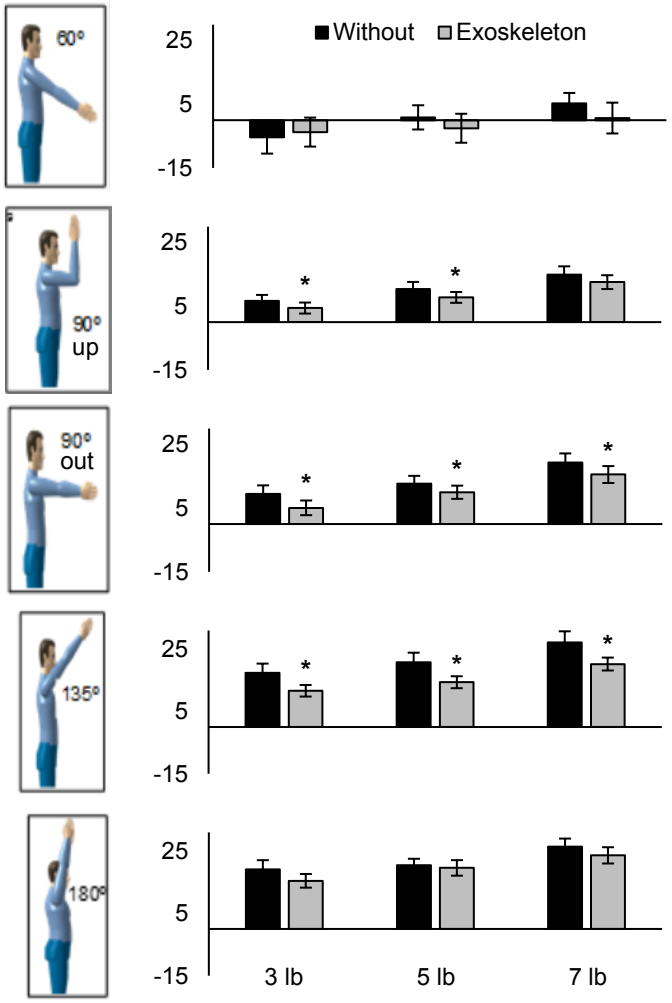

Figure 1: Deltoid Fatigue Risk Values (%MVC). * indicates significant reduction in fatigue risk with exoskeleton ($p < 0.05$).

The exoskeleton is expected to reduce shoulder fatigue for common automotive assembly postures and tool weights. Further testing with the exoskeleton high reach adaptor is recommended for the 180° posture, while the 60° posture has lower fatigue risk.

Significance

Lab tests predict a range of arm postures and tool weights where an exoskeleton is effective for fatigue reduction, which can help ergonomists determine job tasks that may benefit from usage.

Acknowledgments

Levitate Technologies supported this study as a fee-for-service.

References

[1] Bureau of Labor Statistics (2016).
[2] ACGIH (2016). Upper limb localized fatigue.
[3] Gillette & Stephenson (2019). *IISE TOEHF*, 7: 302-310.
[4] Butler & Gillette (2019). *Prof Saf*, 64(3): 32-37.

Effects of a Footrest on the Lumbo-Pelvic-Hip Kinematics and Kinetics, and Low Back Pain during Prolonged Standing Work

Onebin Lim[1], Chunghwi Yi[1]*, Ohyun Kwon[1], Heonseock Cynn[1], Soyeon Park[2], and Wongyu You[3]
[1]Dept. of Physical Therapy, College of Health Science, Yonsei University, South Korea
[2]Dept. of Physical Therapy, College of Health Science, Sangji University, South Korea
[3]Dept. of Physical Therapy, College of Biomedical Science and Engineering, Inje University, South Korea
Email: *pteagle@yonsei.ac.kr

Introduction

Many medical experts recommend the use of a footrest as an ergonomic intervention to reduce low back pain (LBP) during prolonged standing. However, previous research on the effectiveness of using the footrest for prolonged standing were insufficient due to a lack of proper scientific support.

The purpose of this study was to determine the effect of standing with a footrest compared with level standing on lumbo-pelvic-hip kinematics and kinetics, and low back visual analogue scale (VAS) scores between pain developer (PD) and non-pain developer (NPD).

Methods

In total, 30 subjects participated in this study, including 15 classified as PDs, and 15 as NPDs. The subjects were classified as PD if they reported an increase in the low back VAS score greater than 10-mm from baseline on the 100-mm VAS scale during the 2-hour prolonged level standing.

Three-dimensional motion analysis system was used to analyze lumbo-pelvic-hip joint angles, and lumbar flexion-extension moment. The VAS was used to evaluate the degree of low back pain.

Subjects then entered into the 2-hour prolonged level standing task (Figure 1). Subjects visited the laboratory on the second day and performed standing with the footrest. The light simulated tasks, i.e., sorting coins, sorting poker chips, and a simple assembly task, were performed within the subject's shoulder width.

A two-way (2 × 2) mixed analysis of variance with standing positions (level standing, standing with the footrest) as the within-subject variable and groups (PD, NPD) as the between-subjects variable was used to assess the dependent variables.

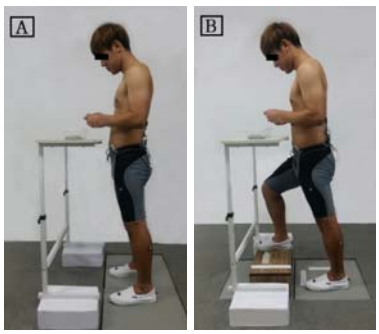

Figure 1: Standing positions (A: Level standing, B: Standing with footrest).

Results and Discussion

The results of this study showed that lumbar flexion angle, posterior pelvic tilt angle, hip flexion angle, and the lumbar flexion moment were significantly higher in standing with a footrest than in level standing ($p < 0.05$) (Table 1).

In PD the group, the low back VAS score was significantly lower during standing with the footrest than during level standing ($p < 0.012$), During level standing, there was a significantly higher low back VAS score in the PD group compared with the NPD group ($p < 0.012$) (Figure 2).

The results of this study indicate that prolonged standing with a footrest can be an effective ergonomic intervention because it increased the lumbar flexion angle, posterior pelvic tilt angle, and lumbar flexion moment, thereby reducing low back pain.

Table 1. Lumbo-pelvic-hip kinematic and kinetic differences

	Level standing	Standing with footrest
Lumbar flexion-extension (°)	-10.48 ± 8.14[a]	-2.62 ± 9.09*
Pelvic tilt (°)	0.07 ± 1.85	-3.42 ± 3.22*
Hip flexion-extension (°)	-1.65 ± 1.99	45.25 ± 6.74*
Lumbar flexion-extension moment (Nm)	-0.02 ± 0.25	1.62 ± 0.37*

[a]Mean ± standard deviation.
*$p < 0.05$ significant difference between standing positions.
Positive values indicate flexion, anterior pelvic tilt, and flexion moment whereas negative values indicate extension, posterior pelvic tilt, and extension moment.

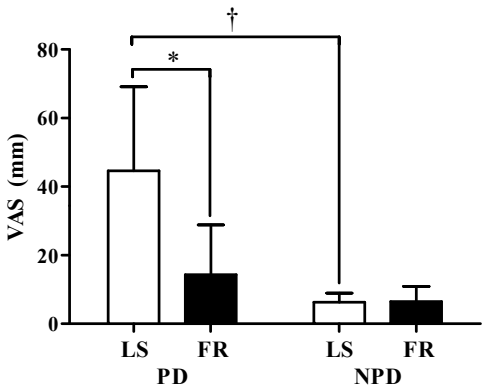

Figure 2. Low back VAS score (PD: Pain developers, NPD: Non-pain developers, LS: Level standing, FR: Standing with the footrest, VAS: visual analog scale *$p < 0.012$ significantly different between standing positions; †$p < 0.012$ significantly different between groups).

Significance

This study is in the field of ergonomics. Through this study, it is a study that proved the effect of the footrest as a biomechanic for people who stand for a long time.

Biomechanics and Ergonomic Analyses of Shoulder Posture in a Seated Position Through the Use of an Avatar

Garrett Weidig[1], Archana Lamsal[1], and Tamara Reid Bush, PhD[1]
[1]Michigan State University, East Lansing, MI, USA
Email: weidigga@msu.edu, reidtama@msu.edu

Introduction

Whether it's playing video games, sitting in class, or working at the computer, posture is always a concern. With teens and young adults interacting with technology more and more, bad habits with respect to posture are perpetuated[1]. This increase in technology use has been shown to cause poor posture, such as slouching with the shoulders or downward neck movement[2]. Poor posture can then lead to back pain and general joint pain- even for teenagers[3]. Ergonomic standards aim to correct poor posture, suggesting that ankle, knee, and hip angles should be at 90°. However, these standards are rarely known and are followed by even fewer individuals. There is a need to quantify good and poor postures. Also, so that these postures can be communicated to others, particularly teens and young adults, a visual representation of these body positions is necessary.

One approach to visually convey biomechanical components (such as numerical data) and deviations from preferred ergonomic postures is the use of an avatar, such as the one in Figure 1. By linking motion data with a human body model, or avatar, differences in posture can be shown visually and these postures can be numerically quantified. Therefore, the goals of this study were twofold. The first was to define and identify poor posture, specifically rounding of the shoulders; and the second was to create an avatar that could serve as a communication medium for postural change.

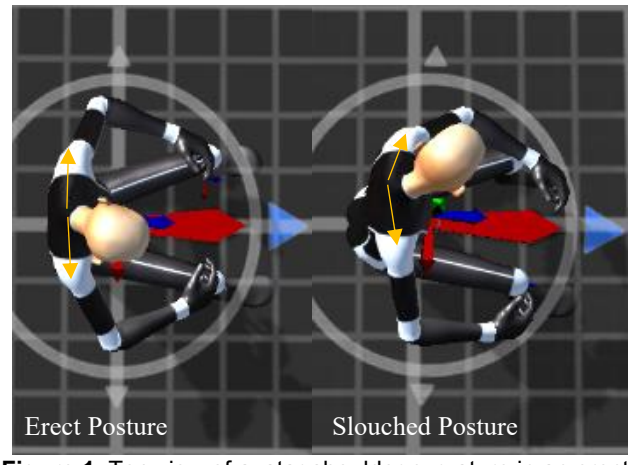

Figure 1: Top view of avatar shoulder curvature in an erect, ergonomic posture (left) and a slouched, non-ergonomic posture (right). The orange arrows represent shoulder curvature.

Methods

Reflective markers were placed on the body and movement data were recorded with an 11 camera motion capture system. Five participants (4 men, 1 woman – average age 20 years SD 1.6) were instructed to type and mouse as they would naturally. At the end of the five minute test, participants were positioned in an erect posture as defined by the ergonomic standards previously noted. The results of this study produced two outputs, the first being engineering definitions for poor posture, specifically related to shoulder curvature. Shoulder curvature was defined by the angle made by the left acromion (shoulder top), 7th cervical vertebra (the top of the spine), and the right acromion. Poor posture was defined by the magnitude of the deviation from the erect posture. The second output from this study was the creation of an avatar from these data sets.

Results and Discussion

The following table provides the averages for the shoulder angle of the participants and the deviation from the erect posture, while mousing, and while typing.

Table 1. Average shoulder angle at erect and slouched postures

Posture	Shoulder Angle(°)	Angle Deviation(°)
Erect	127	-
Slouched Mousing	112	15
Slouched Typing	111	16

The data in Table 1 show that it is possible to define poor posture as a deviation from an erect posture. As of now, there is no spectrum that defines what levels of poor posture are associated with which angles of shoulder curvature. However, these preliminary data show that there is a measurable difference between erect and slouched.

For the second goal of this work, these data were incorporated into an avatar to demonstrate shoulder rounding. Just as there is a difference in the shoulder angle calculation, there is a clear difference in the shoulder rounding appearance in the avatar between the subject's erect and slouched postures.

Significance

The results of this study provided quantitative measures on slouched posture and provided a means to visually present these postural changes. This research has the potential to help in device design such as gaming chairs that provide more support when poor posture is engaged. This also opens up opportunities to create biofeedback devices that, based on duration and magnitude of the poor posture, will tell users how to correct their positioning. With more testing, postural changes between different demographics can be analyzed to further help office/gaming seating companies create optimized designs.

The use of the avatar reveals how people look in these poor postures and the use of the markers can verify the posture. Future work will include more participants, including more activities for participants (such as using a cell phone or playing video games), and include standing.

References

1. Lim C. et al., (2013). *Bridging the Gap: Technology Trends and Use of Technology in Schools*
2. Laeser K. et al., (1998). *The Effect of Computer Workstation Design on Student Posture*
3. N. Quka et al., (2015). *Risk Factors of Poor Posture in Children and Its Prevalence*

Relationship between Joint Stiffness and Limb Stiffness in Running Across Speeds

Li Jin[1], Michael E. Hahn[2]
[1]Department of Kinesiology, San Jose State University, San Jose, CA
[2]Department of Human Physiology, University of Oregon, Eugene, OR
Email: li.jin@sjsu.edu

Introduction

The lower extremity system acts like a spring in the stance phase of running. The loading and unloading characteristics of the leg spring system can be regarded as limb stiffness patterns. Among different stiffness levels, vertical stiffness (K_{vert}) and leg stiffness (K_{leg}) reflect whole body center of mass (COM) and leg spring system loading and response in running stance phase [1]; while joint stiffness (K_{joint}) reflects joint level dynamic loading and response. Little is known about whether connections exist between the lower level system stiffness (K_{joint}) and higher level system stiffness (K_{vert}, K_{leg}) in running across speeds.

The purpose of the study was to investigate whether K_{joint} is associated with K_{vert} or K_{leg} at different running speeds. We hypothesized that K_{joint} would have significant association with K_{vert} and K_{leg} at each running speed.

Methods

Twenty healthy subjects (36.8 $\pm$ 15.3 years, 171.6 $\pm$ 11.2 cm, 68.5 $\pm$ 14.1 kg) were enrolled in the study. Subjects were asked to run on a force-instrumented treadmill (Bertec, Inc. Columbus, OH) at six different speeds, from 1.8 to 3.8 m/s (0.4 m/s intervals), for 75 seconds per stage. Kinematic data were collected at 120 Hz using an 8-camera motion capture system (Motion Analysis Corp., Santa Rosa, CA). Kinetic data were collected at 1200 Hz using the force-instrumented treadmill.

K_{vert} was calculated from peak vertical ground reaction force divided by vertical displacement of the COM from initial ground contact until mid-stance. K_{leg} was calculated as peak vertical ground reaction force divided by leg-spring maximum displacement in stance phase. K_{joint} was calculated as change in sagittal plane joint moment divided by sagittal plane joint angular displacement in the first half of ground contact. Multiple linear regression analysis was conducted to determine potential associations between K_{vert}, K_{leg} and K_{joint} (ankle, knee, hip) for each running speed, using SPSS (V22.0, IBM, Armonk, NY).

Results and Discussion

K_{joint} was associated with K_{vert} at 1.8 m/s and 2.2 m/s (Table 1). At 1.8 m/s, the model accounted for 38.4% of the variance in K_{vert} (R^2 = 0.384, p = 0.046), and K_{knee} had the strongest unique association with K_{vert} at this speed (β = 0.509, p = 0.022). At 2.2 m/s, the model accounted for 49.8% of the variance in K_{vert} (R^2 = 0.498, p = 0.014), and K_{knee} again had the strongest unique association with K_{vert} at this speed (β = 0.553, p = 0.011).

Additionally, K_{joint} was associated with K_{leg} among most speeds, except at 3.0 m/s and 3.8 m/s (Table 1). K_{knee} had the strongest unique association with K_{leg} at 1.8, 2.2 and 2.6 m/s (p = 0.014, p = 0.0004, p = 0.04). K_{hip} also had strong unique association with K_{leg} at 2.2 and 3.4 m/s (p = 0.001, p = 0.009).

Significance

K_{joint} was associated with both K_{vert} and K_{leg} in the multiple linear regression models at slow speeds (1.8 and 2.2 m/s) and K_{knee} had a significant unique association with K_{vert} and K_{leg} at these speeds. K_{joint} was associated with K_{leg} at a wider range of speeds and K_{knee} had a significant unique association with K_{leg} among most speeds. This may be attributed to the observation that in the human leg spring system, under similar loading conditions, the spring with the lowest stiffness (K_{knee} in this case) will undergo the largest displacement and this would have the most influence on the overall leg-spring system stiffness [2]. These findings built a connection between joint stiffness and limb stiffness within certain range of running speeds. K_{knee} may need to be considered as an important factor in future limb stiffness optimization and general running performance enhancement.

Acknowledgments

This work was supported by the Betty Foster McCue Scholarship.

References

[1] Brughelli M and Cronin J., *Sport Med*. 2008.
[2] Farley CT and Morgenroth DC., *J Biomech*. 1999.

Table 1: Multiple linear regression models between joint stiffness and vertical stiffness (first two rows), and leg stiffness (lower four rows). Only the speed conditions with statistically significant associations are shown; n = 20.

Speed	Variable	β_{Kankle}	β_{Kknee}	β_{Khip}	Model Summary
1.8 m/s	K_{vert}	0.246	**0.509**	0.142	β_0 = 8.298, R^2 = 0.384, p = 0.046
2.2 m/s	K_{vert}	0.040	**0.553**	0.338	β_0 = 9.289, R^2 = 0.498, p = 0.014
1.8 m/s	K_{leg}	-0.076	**0.532**	0.323	β_0 = 4.815, R^2 = 0.424, p = 0.028
2.2 m/s	K_{leg}	-0.237	**0.553**	**0.526**	β_0 = 3.210, R^2 = 0.793, p < 0.0001
2.6 m/s	K_{leg}	0.048	**0.456**	0.404	β_0 = 4.512, R^2 = 0.399, p = 0.039
3.4 m/s	K_{leg}	-0.353	0.046	**0.721**	β_0 = 9.760, R^2 = 0.474, p = 0.026

Statistically significant contribution of K_{joint} to predict the models are indicated in bold. $\boldsymbol{\beta_0}$**:** linear regression model constant (y intercept); $\boldsymbol{\beta}$**:** standardized coefficients.

Lower Extremity Support Moment and Distribution of Joint Moments during Sloped Running

Yo Shih, Kathleen Stone, Kai-Yu Ho
Department of Physical Therapy, University of Nevada, Las Vegas

Introduction

Running is a popular exercise for fitness and recreational purposes. However, running injuries are also prevalent and are the main reason a runner temperately or permanently discontinues to run.[1] Previous studies show that runners change their step frequency, step length, lower extremity energetics, and joint moments to adapt to upslope or downslope running surfaces.[2–4] However, how sloped running affects runners' lower extremity loading profiles has not been thoroughly examined. This study aimed to examine the 1) peak total support moment, a variable that incorporates hip, knee and ankle joint moments, and the 2) joint contributions of ankle, knee and hip to the total support moment during level, upslope and downslope running. The data obtained from this work will inform clinical decision making for training lower extremity musculature and/or preventing joint injuries in runners.

Methods

Twenty recreational runners (10 females, age: 24.9 ± 2.4 years, body height: 1.70 ± 0.07 m, body weight 67.0 ± 9.7 kg) were recruited in this study. Each participant ran under three different conditions, including level, 6° upslope and 6° downslope at a standardized speed of 2.3 m/s. Data was collected during three, 20 s trials on an instrumented treadmill. Reflective markers were attached to the trunk and lower extremities. Hip, knee and ankle joint moments were calculated using an inverse dynamics method. Total support moment was calculated as the sum of the hip, knee and ankle joint moments during the stance phase of the running cycle. Each joint's contribution to the support moment was analyzed and presented as a percentage of the total support moment. The primary variable of interest was peak total support moment and the secondary variables of interest were hip, knee and ankle joints' contributions to the support moment at the time of peak total support moment. All variables were examined on the right leg. A one-way ANOVA with repeated measures and post-hoc pairwise comparisons were used to compare the variables among the three running conditions.

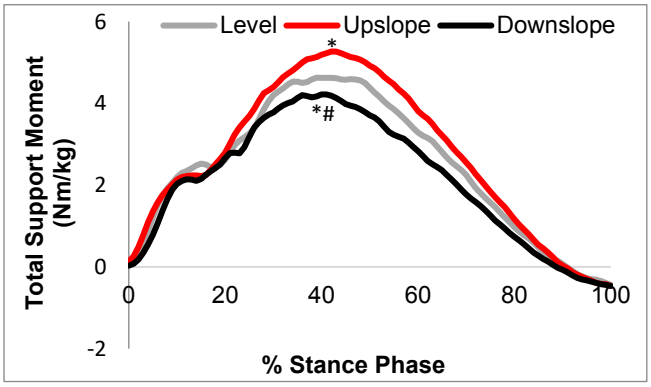

Figure 1. Total support moments of the three running conditions during the 100% stance phase of the running cycle. (* indicates a significant difference from Level; # indicates a significant difference from Upslope)

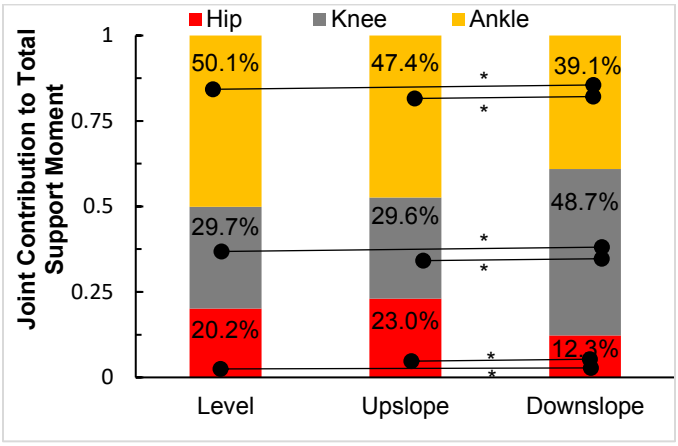

Figure 2. Hip, knee and ankle joint contributions of the three running conditions at the time of peak total support moment (* indicates a significant difference between conditions)

Results and Discussion

Peak total support moment was significantly different among the three running conditions ($p<0.05$). The post-hoc analyses showed that the peak total support moment during upslope running was significantly larger than level and downslope running ($p<0.05$). Also, the peak total support moment during level running was significantly larger than downslope running ($p<0.05$) (Figure 1).

During upslope running, the participants demonstrated no significant difference in ankle, knee, or hip joint contribution to total support moment compared to level running. During downslope running, the participants demonstrated significantly larger knee contribution and significantly less ankle and hip contributions to the total support moment compared to level and upslope running (Figure 2).

Our data suggests that running upslope increased the overall loading of the lower extremity joints, while the increased loading was evenly distributed among the three joints. Running downslope decreased the loading of the lower extremity joints in total as well as the hip and ankle joint contributions. However, the knee joint contribution during running downslope increased 64 % compared to level and upslope running.

Significance

This study shows that different lower extremity loading profiles were used in runners when running on different sloped surfaces. Clinicians and coaches may consider the training slopes for runners based on the training purposes and/or joint conditions of the runners to prevent running injuries.

Reference

1. Taunton, J. E. *et al. Br. J. Sports Med.* **36**, 95–101 (2002).
2. Telhan, G. *et al. J. Athl. Train.* **45**, 16–21 (2010).
3. DeVita, P. *et al. J Biom* **41**, 3354–3359 (2008).
4. García-Pinillos, F. *et al. Gait Posture* **68**, 72–77 (2019).

Training effects on frontal plane kinematics and coordination in novice runners

Kathryn Harrison[1], Adam Sima[2], Benjamin Darter[1], Ronald Zernicke[3], Mary Shall[1], Blaise Williams[4], Sheryl Finucane[1]
[1]Department of Physical Therapy, Virginia Commonwealth University
[2]Department of Biostatistics, Virginia Commonwealth University
3Department of Orthopaedic Surgery, University of Michigan
[4]Nike Sport Research Lab
Email: kate.harrison@boatechnology.com

Introduction

Novice runners appear to be at particularly high risk for knee injury.[1] Position and motion of the hip and ankle in the frontal plane have been linked to development of knee injury,[2,3] potentially because they influence the position and loading of the knee joint.[4]

It could be that runners improve their kinematics over time, leading to reduced risk of knee injury. However, the effect of training on kinematics is not well understood. Further, it is unclear how the ankle and hip may contribute to knee positioning in novice runners. The purpose of this study was to assess changes in frontal plane kinematics as well as ankle and hip coordination in novice runners.

Methods

Eight healthy adult females (30±10 yrs, 28±6 kg/m^2) with no previous running experience performed 8 weeks of walking, followed by 8 weeks of run training. Before and after run training, kinematic data were collected using a 3D motion analysis system while participants ran on an instrumented treadmill at 2.67 m/s. The current analysis compared kinematics immediately before and after the run training period.

Mean frontal-plane ankle, knee, and hip joint angles were calculated throughout the stride for each participant and modelled using cubic splines. The resulting models were compared between pre- and post-training timepoints using a generalized linear model (α=0.05). Confidence intervals (95%) of the mean change in joint angles across the stride were constructed to identify periods where a significant change in joint angle occurred. A modified vector coding technique was used to assess changes in coordination of the ankle and hip in the frontal plane.[5]

We hypothesized that run training would lead to decreased hip adduction, increased ankle eversion, and knee abduction. Further, we expected that training would lead to improved synchronization of hip and ankle motion in the frontal plane.

Results and Discussion

After run training, participants displayed less hip adduction during early and midstance (Figure 1A). This is counter to what has been observed in a cross sectional study,[6] suggesting a prospective design may be more powerful in detecting biomechanical changes with training.

Participants also displayed greater ankle eversion during midstance after training (Figure 1B). Increased eversion has been proposed as injurious to the knee,[7] however the relation between peak eversion and injury is equivocal.[3,8]

The combination of decreased hip adduction and increased ankle eversion appeared to result in less knee abduction during early and midstance (Figure 1C). This may have reduced patellofemoral joint contact force and compression of the medial compartment of the knee.

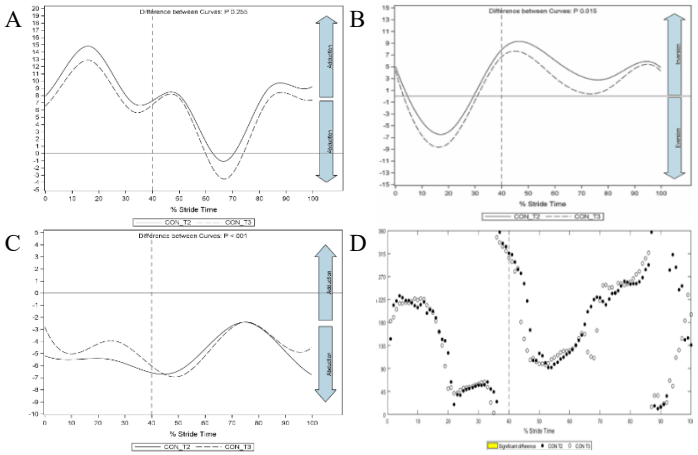

Figure 1: A) Frontal plane hip motion. B) Frontal plane knee motion. C) Frontal plane ankle motion. D) Frontal plane hip-ankle coordination angles. CON_T2=before running, CONT3=after running.

There was no significant change in relative motion of the hip and ankle (Figure 1D). Similarly, it was previously found that coordination of lower extremity joints in the sagittal plane did not differ between novice and experienced runners.[9]

Significance

Run training appeared to alter kinematics related to knee injury, without instruction or supplementary exercise. A reduction in hip adduction and knee abduction during stance may help to explain why experienced runners are at lower risk for knee injury than novice runners. Changes at both the ankle and hip appeared to contribute to improved knee kinematics, and thus may be worth considering in future research.

References

1. Kemler E, Blokland D, Backx F, Huisstede B. *Phys Sportsmed*. 2018;46(4):485-491.
2. Noehren B, Hamill J, Davis I. *Med Sci Sports Exerc*. 2013;45(6):1120-1124.
3. Kuhman DJ, Paquette MR, Peel SA, Melcher DA. *Hum Mov Sci*. 2016;47:9-15.
4. Powers CM. *J Orthop Sports Phys Ther*. 2010;40(2):42-51.
5. Chang R, Van Emmerik R, Hamill J. *J Biomech*. 2008;41(14):3101-3105.
6. Agresta CE, Peacock J, Housner J, Zernicke RF, Zendler JD. *Gait Posture*. 2018;61:13-18.
7. Tiberio D. *J Orthop Sports Phys Ther*. 1987;9(4):160-165.
8. Dudley RI, Pamukoff DN, Lynn SK, Kersey RD, Noffal GJ. *Hum Mov Sci*. 2017;52:197-202.
9. Hafer JF, Peacock J, Zernicke RF, Agresta CE. *Med Sci Sports Exerc*. 2019;51(7):1438-1443.

HOW DO NET MECHANICAL JOINT WORK & STIFFNESS CHANGE ON SLOPES DURING RUNNING

Caelyn Hirschman[1] & Alena M. Grabowski[1,2]
[1]Applied Biomechanics Lab, University of Colorado Boulder, CO USA
[2]Eastern Colorado Healthcare System, Department of Veterans Affairs, Denver, CO USA
email: Caelyn.Hirschman@colorado.edu

Introduction

The spring mass model describes the mechanics of running on level ground, where body mass is represented as a point mass and the legs as massless linear springs [1]. Further, the ankle and knee joints can be characterized as springs with angular stiffness [2], yet the ankle generates net positive mechanical work and knee absorbs net negative mechanical work during level ground running [3].

When running uphill, the leg muscles produce net positive work to lift the center of mass (COM) and overcome gravity [3], mainly due to positive work produced by the muscles surrounding the hip [4]. When running downhill, the leg muscles absorb net negative work to lower and decelerate the COM [5].

We determined ankle and knee net mechanical work and joint stiffness during running on level-ground and uphill/downhill slopes to provide insight into the biomechanics of running and inform the design of running specific leg prostheses (RSPs). We hypothesized, similar to Roberts et al. [4], that the net mechanical work done by muscles surrounding the ankle and knee would not change across slopes during running and that ankle stiffness would increase during uphill and knee stiffness would decrease during downhill compared to level ground running.

Methods

16 runners (11M, 5F; mean ± SD: age 25±5 yrs; 69±7.9 kg; 176±8 cm) provided written informed consent. Subjects reported no cardiovascular, pulmonary, or neurological disease or disorder, or musculoskeletal injuries. Participants ran on an instrumented treadmill (Treadmetrix, Park City, UT) at -6° and 0° at 3 m/s and +6° at 2 m/s. We measured ground reaction forces (GRFs) at 1000 Hz and motion at 200 Hz (Vicon, Centennial, CO) from markers placed bilaterally on the lower extremity. We used a 20 N vertical GRF threshold to determine ground contact and analyzed ≥15 steps from both legs. We used a low pass 4th order Butterworth filter with a 15 Hz cutoff on kinematic and kinetic data. We calculated joint angles (θ) and moments (M) during ground contact using Visual 3D (C-Motion, Germantown, MD). We calculated initial stiffness (K) prior to mid-stance and final stiffness after mid-stance as average $\Delta M/\Delta\theta$. We used a one-way ANOVA and Bonferroni post hoc analyses to determine significant differences.

Results and Discussion

Net positive ankle work decreased during -6° ($p<0.01$) and trended towards increasing during +6° ($p=0.06$) compared to 0° running (Fig. 1). The magnitude of net negative knee work increased during -6° ($p<0.01$) and decreased during +6° ($p<0.05$) compared to 0° running. Thus, we reject our hypothesis that ankle and knee net mechanical work would not change on slopes. Initial K_{ankle} trended towards decreasing at +6° ($p=0.21$) and final K_{ankle} trended towards increasing at -6° ($p=0.20$) compared to 0°. Initial K_{knee} increased at +6° ($P<0.01$) and final K_{knee} increased at -6° ($p<0.01$) compared to 0° (Table 1).

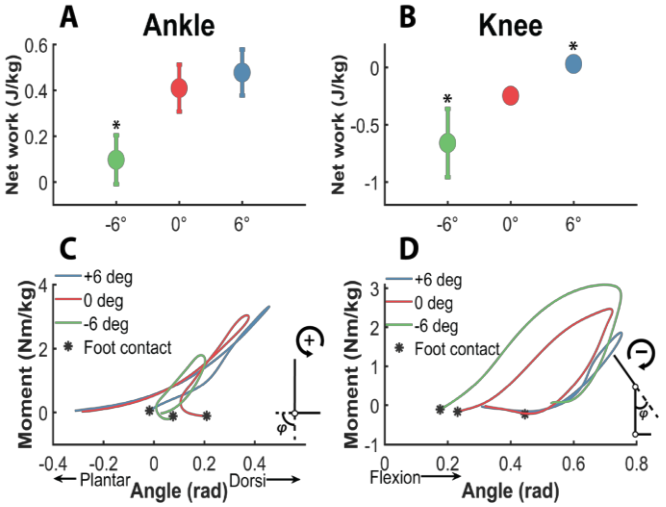

Figure 1. Ankle (**A**) and knee (**B**) net mechanical work during running at 0° and ±6° (* $p<0.05$). Moment versus angle at the ankle (**C**) and knee (**D**) during running at 0° and ±6° for a representative subject. The area within the curve indicates net mechanical work. Positive ankle angles indicate dorsiflexion. Static knee angle is 0 rad and a positive angle indicates flexion. * in (**C**) and (**D**) indicates foot contact and the arrow shows the direction of net mechanical work.

Table 1. Ankle and knee joint stiffness (K in N*m/kg/rad) during running at 0° and ±6°. * indicates $p<0.05$ compared to 0°.

	-6°		0°		+6°	
	Initial	**Final**	**Initial**	**Final**	**Initial**	**Final**
K_{ank}	10.4 ± 4.6	6.7 ± 1.9	10.6 ± 3.6	5.8 ± 1.3	8.3 ± 4.2	5.2 ± 2.3
K_{knee}	6.3 ± 1.3	11.2 ± 4.8 *	6.6 ± 1.3	6.4 ± 1.4	10.4 ± 2.9 *	4.2 ± 1.4

Significance

Our results suggest that during downhill running, a prosthetic knee should absorb more negative work but be stiffer after mid-stance than on level ground and during uphill running, a prosthetic ankle should generate more positive work and be less stiff prior to mid-stance than on level ground. Moreover, joint mechanics and stiffness change on slopes. Future work will determine hip net mechanical work and stiffness on slopes.

Acknowledgments

Work supported by a VA Career Development Award. (VA RR&D A7972-W)

References

1 Blickhan. *J Biomech.* **22**, 1217-1227, 1989
2 McMahon. & Cheng. *J Biomech.* **23**, 65-78, 1990
3 Farris. & Sawicki. *J. Roy. Soc. Interface*. **9**, 110–118, 2012
4 Roberts & Belliveau. *J Exp Biol* **208**, 1963- 970, 2005
5 Buczek & Cavanagh. *J. Med Sci Sports Exerc*. **5,** 669-77, 1990

Beat the Streets: Music-based Stride Length Intervention to Decrease Injury Risk in Runners

Mikaela A Smith[1],
Allison R. Altman-Singles[1,2]

[1] Kinesiology, Penn State Berks, Reading, PA, USA
[2] Mechanical Engineering, Penn State Berks, Reading, PA, USA
Email: mas7377@psu.edu

Introduction

Each year nearly 20 million people participate in running and 65% suffer from an overuse injury due to running mechanics [4]. High impact loading increases the likelihood of injury and over-striding is one factor that contributes to high impact loading [1].

Overstriding is characterized by an increased stride length (SL). At a fixed speed, cadence can be increased to decrease SL. Prior interventions have used a metronome as a cue for foot contact and found it was a good way to decrease SL. One study found that a 5% increase in cadence, decreased impact peak by 34% [2], another found a 15% increase in cadence reduced joint loading by 18% [3]. This study used a controlled music tempo as a cue to increase cadence. As cadence increased and SL decreased it was expected that impact loading characteristics would decrease. Ultimately, this reduction in impact loading could help to reduce running overuse injury risk.

Methods

Active, uninjured runners aged 18-55 were recruited to complete a three-week intervention. Participants were required to run a minimum of 10 mi/wk prior to the study. Participants ran on a treadmill at 2.9m/s to collect cadence. Reflective markers were fixed to the foot to determine SL and impact loading variables overground using a floor-embedded Bertec force plate (Columbus OH) surrounded by the Vicon Bontia camera system (Vicon, Boulder, CO, USA), sampled at 1000 Hz and 200 Hz, respectively. Force data were filtered with a 50 Hz low pass filter.

Cadence from the treadmill was used to determine the target cadence for each week of the intervention. An increase in cadence of 5%, 7.5%, and 10% was targeted each week. Each cadence corresponded to the beats/min of a variety of music. Participants were asked to listen to the music during all runs throughout the intervention, while maintaining their normal mileage.

Cadence, SL, and impact loading characteristics were collected pre and post intervention. Impact peak (IPz), average load rate (ALRz), and instantaneous load rate (ILRz), were extracted from the vertical ground reaction force curve. A paired T-test was used to compare the variables.

Results and Discussion

12 participants entered the study, however, only 11 completed the study. Participants were 29±13 years old, 1.723±0.105 m tall, and 72.2±18.1 kg.

After the intervention, overground SL decreased 3% due to the intervention ($p=0.09$). 8 out of 11 participants responded positively to the intervention showing a 12% decrease in SL, the remaining participants had no change or a small increase. This decrease was associated with a 4% increase in cadence post-intervention ($p=0.012$) measured on the treadmill at a fixed speed (Figure 1). In contrast to the SL, all participants displayed increased cadence on the treadmill after the intervention. Impact characteristics all decreased, but did not reach significance (Figure 1). Among the 8 responders to the study there were decreases in ALRz (12%, $p=0.041$) and IPz (10%, $p=0.073$).

There were some discrepancies between cadence and SL. Speed was fixed on treadmill, but when running over ground, a self- selected speed was used. While SL was trending toward an overall reduction, only 8 participants reduced SL due to the intervention. Compliance and exposure to the intervention were not monitored, and may have limited the effectiveness of the intervention. There was no overall decrease in impact characteristics, however in those who reduced SL, ALRz and IPz were reduced, indicating the intervention was effective for reducing some aspects of impact loading.

Studies using a metronome found 17.6-33.8% reductions in loading with a 5-15% increase in cadence when done at a controlled speed. The current study showed only a 3% reduction in SL overground, which was associated with a non-significant 6.65% reduction in impact loading. In contrast, the 8 responders displayed a 12% reduction in SL, which was associated with a 10.9% reduction in impact loading, which is more similar to the results found in previous studies. It is possible that controlling the overground running speed, increasing compliance, and adding additional participants will yield similar results.

Significance

This intervention was fun for the runners. The use of phone apps encourages ease and compliance. The apps can be used by runners, coaches, trainers, and rehabilitation professionals alike to maximize the potential benefit of the intervention.

References

[1] Edwards et al (2009). MSSE 41(12): 2177-2184.
[2] Heiderscheit et al (2011). MSSE 43(2): 296-302.
[3] Hobara et al (2012) IJ SM. (33): 310-313.
[4] Messier et al (2018) AJSM 46(9): 2211-2221.

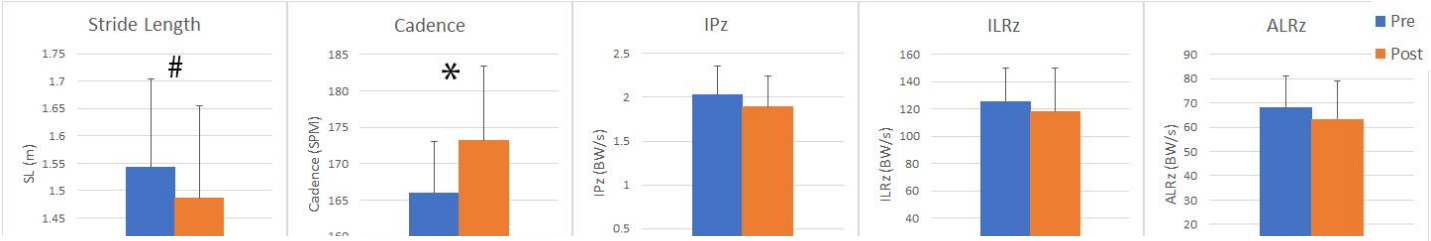

Figure 1. Bars show mean variables of interest with standard deviation error bars. * indicates $p<0.05$ and # indicates $p<0.1$.

Long term training on sand changes foot posture and running kinetics in active individuals with over-pronated feet

AmirAli Jafarnezhadgero[1], Seyed Hamed Mousavi[2], Amir Fatollahi[1]

[1] Department of Physical Education and Sport Sciences, Faculty of Educational Sciences and Psychology, University of Mohaghegh Ardabili, Ardabil, Iran.
*2. University of Groningen, University Medical Center Groningen, Department of Rehabilitation Medicine, Groningen, the Netherlands; Email: s.h.mousavi@umcg.nl

Introduction

Running is one of the most popular sporting activities, but running-related injuries (RRIs) are a major drawback of running which are increasingly ongoing [1]. About 87% of RRIs occur in the knee, lower leg, foot and ankle, with abnormal foot posture as one of the main causes of those injuries [2]. The foot is the only part of the body which is in contact with the ground while running and it is responsible for shock absorption and dispersal of ground reaction force (GRFs) across the foot. Foot overpronation affects running kinetics which is also considered a risk factor for RRIs. Running on sand could be a promising exercise intervention to treat foot pronation because it is easy-to-access worldwide and produces hardly any costs. The present study aimed to evaluate the long-term effect of running on sand on foot overpronation, impact vertical ground reaction forces (GRFs), loading rate, and anteroposterior impulse (impulse y) in active male adults with over-pronated feet compared with controls.

Method and Discussion

Thirty active over-pronated feet male adults as experimental group (EG) and 30 active over-pronated male adults as control group (CG) were enrolled in this study. Participants ran barefoot at pre-defined speed (3.3 m/s) over the level stable ground during both before and after running on sand training protocol. The running training protocol on sand includes continuous jogging, striding, bounding, galloping and short sprints [3]. The CG performed the training protocol for eight weeks (three sessions per week). The training protocol was done during barefoot condition. Each session was started with a warm-up and stretching session for five minutes and ended with a warm-down session for five minutes. Training duration was 50 minutes per session. Foot pronation was measured using navicular drop test. A force plate was included in the 18-m runway to collect GRF data.

Results

In the CG, navicular drop was decreased after running on sand training protocol ($p<0.001$; $d=2.06$). The statistical analysis showed significant group by time interactions for impact vertical ground reaction forces ($p<0.047$, $d=0.71$). In the EG but not the CG, significantly lower Fz_{HC} ($p=0.026$; $d=0.86$) was observed during post-test than that in the pre-test. Also, the statistical analysis showed significant group by time interactions for impulse y and loading rate ($p<0.032$; $d=0.57$-0.77). In the EG but not the CG, significantly lower Impulse y ($p=0.032$; $d=0.39$) and loading rate ($p=0.004$; $d=0.45$) were observed during post-test than pre-test. Both the magnitude and rate of loading have been identified as risk factors for RRIs [4]. Our results show that long-term running on sand resulted in lower navicular drop, impact vertical GRF and lower loading rate. This is in line with a previous study showing that running on sand produces low impact forces [4].

Significance

The results of the current study suggest that running on sand can be considered a training base to modify over-pronated feet and running kinetics. This might lead to reducing the risk of RRIs.

References

[1] R.N. Van Gent et al. (2007). https://doi.org/10.1136/bjsm.2006.033548.

[2] A. Pérez-Morcillo et al. (2019). https://doi.org/10.1016/j.clinbiomech.2018.12.019.

[3] D.B.J. Durai et al. (2019). Effect of sand running training on speed among school boys.

[4] R.S. Barrett et al. (1998). https://doi.org/10.1016/S1440-2440(98)80003-0

Running in the Nike Vaporfly, Saucony Racing Flats, and Own Shoes: Who Wins the Race?

Kim Hébert-Losier[1], Steven J. Finlayson[2], Matthew W. Driller[1], Blaise Dubois[2], Jean-François Esculier[2], Christopher Martyn Beaven[1]
[1]Division of Health, Engineering, Computing and Science, *Te Huataki Waiora* School of Health, University of Waikato, New Zealand
[2]The Running Clinic, Research & Development, Canada
Email: *kim.hebert-losier@waikato.ac.nz

Introduction

Even though multiple factors are involved in running economy and performance, recent World Record performances and research findings from high-calibre runners indicate beneficial effects of the Nike Vaporfly footwear range in runners. In the last year, this particular footwear range has sparked debate regarding whether its use constitutes 'technology doping' and has led to the World Athletic revising their footwear guidelines. It has been proposed that recreational runners might reap greater benefits from wearing the Nike Vaporfly shoes than elite runners; however, laboratory-based data are not available to support this proposition.

Our aims were hence to compare running economy (RE) at relative running speeds and 3-km time-trial (TT) performances of male recreational runners wearing the commercially available Nike Vaporfly 4% (NIKE), Saucony Endorphine Racer 2 lightweight racing flats (FLAT), and their habitual footwear (OWN).

Methods

Eighteen male recreational runners [age: 33.5 (11.9) y, $\dot{V}O_{2peak}$: 55.8 (4.4) $mL \cdot kg^{-1} \cdot min^{-1}$] attended four treadmill-based laboratory sessions. A minimum of four and maximum of seven days separated each session. In the first session, runners completed a $\dot{V}O_{2peak}$ to set RE speeds at 60, 70, and 80% of the speed eliciting $\dot{V}O_{2peak}$. Treadmill RE and 3-km TT performances were examined in the three footwear in a randomised, counterbalanced crossover design in the second, third, and fourth session (**Figure 1**). The two experimental footwear were spray-painted black to minimse the potential for a placebo effect.

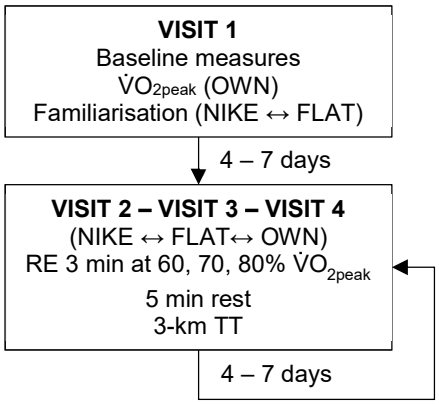

Figure 1: Expertimental study design. ↔, randomized; FLAT, racing flats; NIKE, Nike Vaporfly; OWN, habitual shoes; RE, running economy; TT, time trial; $v\dot{V}O_{2peak}$, speed that elicited $\dot{V}O_{2peak}$.

Results and Discussion

RE was improved in NIKE (3.6 to 4.5%, $p \leq 0.002$) and FLAT (2.4 to 4.0%, $p \leq 0.042$) compared to OWN across intensities, with no significant difference in RE between NIKE and FLAT (1.0 to 1.6%, $p \geq 0.325$). NIKE 3-km TT (11:07.6 ± 0:56.6 mm:ss) was superior to OWN (+16.6 s, 2.4%, p = 0.005) and FLAT (+13.0 s, 1.8%, p = 0.032), with no significant difference between OWN and FLAT 3-km TT times (**Figure 2**). Only five runners, all of whom were rearfoot strikers, were more economical across intensities and faster in NIKE. The four non-rearfoot strikers in our cohort appeared to respond less favourably to NIKE.

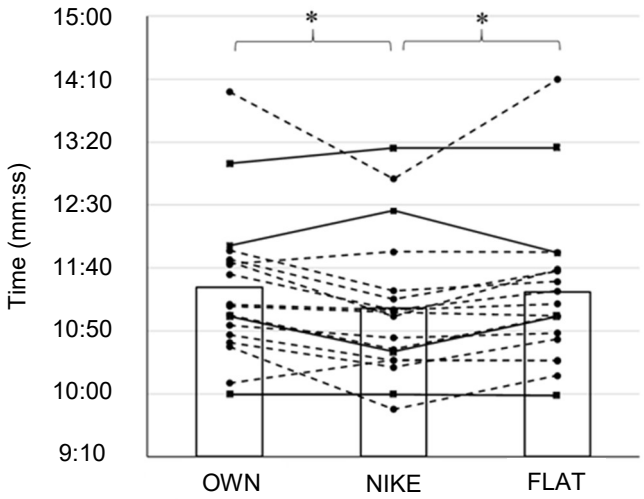

Figure 2: 3-km time-trial time (mm:ss). Bars represent means; circles joined by dashed lines, rearfoot runners; squares joined by black lines, non-rearfoot runners; and asterisks (*), $p \leq 0.05$ during post-hoc tests (significant main effect of footwear). NIKE, Nike Vaporfly; OWN, habitual shoes.

Overall, our findings indicate that NIKE could benefit RE and performance in male recreational runners. However, the high variability in individual RE (-3.1 to 12.1%) and TT (-3.8 to 8.2%) shoe-responses suggests that individualisation of running footwear prescription is warranted. Furthermore, RE was also improved in FLAT versus OWN, consistent with the ~0.7 to 1.0% improvements in RE for each 100 g of ligher mass per shoe[1,2].

Significance

This study provides evidence that NIKE is a viable ergogenic aid in recreational runners; but only 29% of runners were more economical across intensities and faster in NIKE. Given the considerable individual responses, our data does not support a generalised NIKE performance benefit in male recreational runners. Certain runners were more economical or performed better in FLAT. The injury risk associated with changing biomechanical patterns in uninjured runners[3] and transitioning to novel footwear without proper adaptation should also be considered.

References

1. Hoogkamer et al. Med Sci Sports Exerc. 2016;48(11):2175-80.
2. Franz et al. Med Sci Sports Exerc. 2012;44(8):1519-25.
3. Anderson et al. Sports Med. 10.1007/s40279-019-01238-y.

Coordination Variability in Injured and Uninjured Runners: A Systematic Review

Heather M. Hamilton, DPT,[1] Collin D. Bowersock, M.S.[1]
[1]Old Dominion University
Email: hmcco006@odu.edu

Introduction

The study of dynamic systems theory has shown movement variability to be an important characteristic of biological systems, representing the ability for individuals to adapt and respond to environmental changes.[1] Further, decreases in movement variability may be indicative of pathology.[1] Coordination variability, or joint coupling variability, refers to the variability in coordination between joint segments over time and can quantify dynamic coordination throughout the gait cycle.[1] It has been suggested that movement variability is essential for the ability to adapt in a dynamic environment and to decrease the risk for overuse injuries in runners.[2,3]

The purpose of this systematic review was to determine the relationship between coordination variability and overuse injuries in runners. Identifying the association between coordination variability and running injuries may provide information to assist with evaluation, treatment, and prevention of overuse injuries.

Methods

The electronic databases PubMed, CINAHL Plus, and SPORTDiscus were systematically searched in November 2019. The terms "runners" OR "running" AND "coordination variability" OR "joint coupling variability" were used. Reference lists of each included article were hand searched to identify any other appropriate studies. Studies were included that met the following criteria: (1) compared an injured to a healthy control population, (2) measured segmental coordination variability, and (3) included running as the main task. Methodological quality of the included articles was assessed with the Modified Downs and Black Index independently by two reviewers.[4,5]

Results and Discussion

A total of 11 articles met all inclusion criteria and were included in the narrative synthesis. Based on the results of the Modified Downs and Black Index, 2 articles were identified as high quality,[7,12] 7 as moderate quality,[1,3,6,9-11,13] and 2 as low quality.[2,8] There were 3 primary overuse injuries that were reported: patellofemoral pain,[2,6,10] iliotibial band syndrome,[7,9,12,13] and low back pain.[1,11] Of the 11 included studies, 4 studies reported that the injured group demonstrated decreased coordination variability,[1,2,6,8] 2 studies reported that the injured group demonstrated increased coordination variability,[10,13] and 5 studies reported similar levels of coordination variability between the injured and healthy runners.[3,7,9,11,12] The 2 studies with the lowest methodological quality reported decreased coordination variability in the injured group,[2,8] and the studies with the highest methodological quality reported equivocal results between the injured and healthy runners.[7,12]

Overall, moderate quality evidence does not consistently demonstrate altered coordination variability in injured runners compared to healthy controls. Several limitations may affect the interpretation of these results, including inconsistencies in calculating coordination variability, participants running under different conditions, measurement of different joint couplings, and measurement of coordination variability at different points in the gait cycle.

Significance

It is unknown if an optimal amount of coordination variability exists, and whether deviations in either direction are detrimental to performance. There have been no prospective studies to determine if differences in coordination variability lead to injury, or if an injury causes a modification to running mechanics that then alters coordination variability. Further exploration is needed to clarify the role of coordination variability in overuse injuries.[10]

Acknowledgments

No acknowledgements to report.

References

1. Seay JF et al. Low back pain status affects pelvis-trunk coordination and variability during walking and running. *Clin Biomech.* 2011;26:572-578.
2. Hamill J et al. A dynamical systems approach to lower extremity running injuries. *Clin Biomech.* 1999;14:297-308.
3. Ferber R et al. Effect of foot orthotics on rearfoot and tibia joint coupling patterns and variability. *J Biomech.* 2005;38:477-483.
4. Downs SH, Black N. The feasibility of creating a checklist for the assessment of the methodological quality both of randomised and non-randomised studies of health care interventions. *J Epidemiol Community Health.* 1998;52:377.
5. Munn J et al. Evidence of sensorimotor deficits in functional ankle instability: A systematic review with meta-analysis. *J Sci Med Sport.* 2010;13:2-12.
6. Heiderscheit B et al. Variability of stride characteristics and joint coordination among individuals with unilateral patellofemoral pain. *J Appl Biomech.* 2002;18:110-121.
7. Miller RH et al. Continuous relative phase variability during an exhaustive run in runners with a history of iliotibial band syndrome. *J Appl Biomech.* 2008;24:262-270.
8. Maclean CL et al. Influence of custom foot orthotic intervention on lower extremity intralimb coupling during a 30-minute run. *J Appl Biomech.* 2010;26:390-399.
9. Hein T et al. Using the variability of continuous relative phase as a measure to discriminate between healthy and injured runners. *Hum Mov Sci.* 2012;31:683-694.
10. Cunningham TJ et al. Coupling angle variability in healthy and patellofemoral pain runners. *Clin Biomech.* 2014;29:317-322.
11. Seay JF et al. Trunk bend and twist coordination is affected by low back pain status during running. *Eur J Sport Sci.* 2014;14:563-568.
12. Hafer JF et al. Exertion and pain do not alter coordination variability in runners with iliotibial band syndrome. *Clin Biomech.* 2017;47:73-78.
13. Foch E, Milner CE. Influence of Previous Iliotibial Band Syndrome on Coordination Patterns and Coordination Variability in Female Runners. *J Appl Biomech.* 2019;35:1-22.

EVALUATING RUNNING MECHANICS OF SOLDIERS IN VARIOUS ATHLETIC FOOTWEAR

Kari L. Loverro PhD, Victoria Bode MS, Kevin O'Fallon PhD, Jessica Schindler MS
[1]Combat Capabilities Development Command Soldier Center (CCDC SC) Natick, MA USA
Email: *kari.l.loverro.civ@mail.mil

Introduction

US military recruits are issued a single pair of athletic shoes for initial entry training (IET) and used throughout their training timeline (8-22 weeks). These shoes are used across a variety of activities including running, strength training, ruck marching, and fitness evaluation testing as well as on a range of surfaces including gym floors, pavement, grass, sand and gravel. The athletic shoes currently issued are classified as "road running shoes" [1] aimed to reduce running related injuries. The question of whether road running shoes are the proper type of athletic shoe to distribute has arisen, given the breadth of activities being during IET. This program aims to determine if different athletic shoe types effect performance on a variety of activities experienced during training and if the use of a single athletic shoe would effect performance across the training timeline. The preliminary analysis described here aimed to determine if athletic shoe type affects vertical and anteroposterior ground reaction forces (GRF) during running. Future analyses will include the effect of shoe type on performance of other training activities.

Methods

Seven US Army Soldiers (5M, 2F, age: 20.6±3.3 yrs, mass: 70.0±3.1 kg, height: 1.70±0.08 m) completed three running trials in six different athletic shoes: a stability road running, a cushioning road running with an ethyl vinyl acetate (EVA) midsole, cushioning road running with a polyurethane (PU) midsole, trail running, a cross-training and a weightlifting shoe. Soldiers ran an 18m runway at a predetermined speed (4.0±5% m/s) and were positioned to strike a force plate with their dominant limb. Vertical and anteroposterior GRFs were time normalized to the stance phase of each stride and averaged across trials. Peak vertical, braking, and propulsive GRF (normalized to body mass) of the dominant limb were used for analysis. Separate Generalized Linear Models with Generalized Estimating Equations were used to evaluate the affect of shoe type on each dependent variable. Post-hoc pairwise comparisons were performed if factors were significant. (SPSS, IBM Inc.)

Results and Discussion

Shoe type had a significant main effect on all GRF variables ($p \leq 0.002$). Pairwaise comparisons indicate that GRF variables of the weightlifting and cross-training shoes differed significantly from the other shoe types. (Figure 1) Running in the weightlifting shoes significantly decreased peak vertical GRFs compared to all other shoe types ($p \leq 0.026$). While peak braking GRFs were decreased in the weightlifting shoes compared to the cushioning EVA, cushioning PU and stability shoes ($p \leq 0.009$), peak propulsive force was only decreased compared to the cross-training shoes ($p=0.024$). Running in the cross-training shoes also produced greater peak propulsive GRFs than running in the cushioning EVA, cushioning PU, and trail running shoes ($p \leq 0.033$). When running in the cross-training shoes, peak braking GRFs were significantly decreased compared to the cushioning EVA and stability shoes ($p \leq 0.041$). The differences detected between the weightlifting and cross-training shoes compared to the running shoes tested is most likely due structural design differences. The weightlifting shoes have a higher drop height and more rigid sole construction, while the crosstrainers have lower drop and stack heights than the running shoes. The increased drop height of the weightlifting shoes may have forced participants to adjust their foot strike pattern to a more midfoot or forefoot strike, decreasing both the peak vertical and braking GRFs. The flatter construction of the cross-training shoes may have caused the heel to be lower to the ground during the stance phase, resulting in increased propulsive GRFs required to push the foot up into toe-off position.

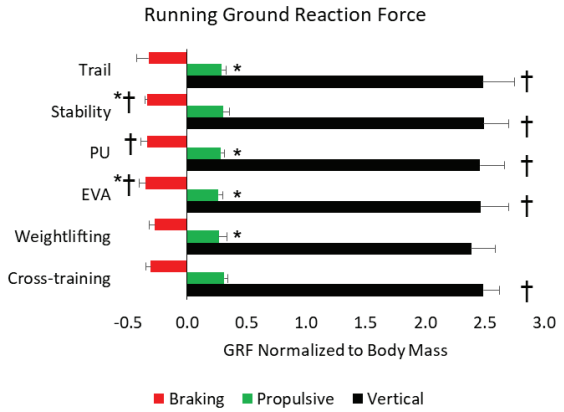

Figure 1: Running GRFs for vertical and anteroposterior directions across shoe type. *Significant difference from the cross-training shoes $p<0.05$ †Significant difference from the weightlifting shoes $p<0.05$.

Significance

When evaluating footwear to be distributed to Soldiers in IET, all aspects of performance must be considered for a variety of tasks. This study is a first step to understanding the influence of different footwear types. Other studies have identified that shoe type can affect GRF parameters during running [2], and our results contribute to this body of knowledge. Running in weightlifting shoes is not frequently evaluated because they are not designed for running activities, but when advising if a single pair of shoes should be distributed in IET it is important to characterize all aspects of the relevant footwear types. Yet it is not surprising that most differences detected were between the weightlifting shoes and the other shoe types. Further analysis of these differences should be conducted to understand any other effects on body mechanics. It is also important to consider the differences identified here when evaluating cross training shoes for IET. This shoe type may seem the natural choice for the diverse activities that Soldiers perform in this environment, but a more complete understanding of the changes in running mechanics demonstrated here is still necessary. Overall, this work makes a start on identifying the ideal footwear for optimal performance or injury mitigation during the diverse tasks of IET.

Acknowledgments

Albert Adams, CCDC SC Soldier Clothing and Configuration Management Team. (Unlimited Distribution: U20-1996)

References

[1] Shorten, MR Book Roy Soc Med Pr pp. 159-169. 2000
[2] Logan et al. J Sp Sci Med 9(1): 147-153. 2010

Novice runners maintain cumulative loads during steady-state running

Jessica G. Hunter[1], Ross H. Miller[1], Irene S. Davis[2]
[1]Department of Kinesiology, University of Maryland, College Park, MD
[2]Department of Physical Medicine & Rehabilitation, Harvard Medical School, Boston, MA
Email: jghunter@umd.edu

Introduction

Previous studies on running injuries have mostly considered training habits and mechanical loads separately. However, an interaction between these two factors leading to running injuries is likely [1,2]. A recent investigation found that cumulative loads associated with tibial stress fracture injuries are higher at slow running speeds than at fast running speeds [3], which may have implications for stress fracture injury risk since popular training programs recommend high proportions of slow running [4]. Prolonged running causes fatigue-induced modifications in running mechanics that may affect the load accumulated throughout a single run or over a volume of running [5]. Therefore, the purpose of this study was to determine if there is a relationship between run distance and cumulative vertical instantaneous loading rate (VILR), run distance and cumulative axial tibial load (TL), and run distance and step frequency (SF) during steady state running to fatigue. The hypothesis was that cumulative loads would increase as running distance increased.

Methods

Twenty novice female rearfoot strike runners ran until they felt they needed to stop at a constant self-selected speed on an instrumented treadmill. Sixteen seconds of kinematic and ground reaction force data were collected at 3 minutes and the end of each kilometer. Data were processed using Visual3D to determine R and L step SF, VILR, and TL. VILR was measured as the greatest change between data points from 20 to 80% of the time between initial contact and impact peak and scaled by body weight. TL was the combined proximal ankle force and Achilles' tendon force. Achilles' tendon force was calculated as the sagittal ankle moment divided by the ankle moment arm, estimated as 5% of foot length. Cumulative load of each kilometer was estimated for VILR and TL by multiplying the number of steps x mean value. A Wilcoxon test determined that outcomes on the dominant vs. nondominant sides were similar, therefore only the dominant side was analyzed further. Spearman's rho was calculated to determine the relationship between run distance and cumulative loads, and run distance and SF.

Results and Discussion

Details on participant demographics and running metrics are shown in Table 1. There was no relationship between run distance and per-kilometer cumulative VILR (r_s = -0.09), cumulative TL (r_s = -0.04) or SF (r_s = 0.04). Figure 1 shows cumulative loads at the beginning to the end of the run. The hypothesis that cumulative loads would increase with run distance was not supported. There was no relationship between run distance and cumulative VILR, cumulative TL, or SF. These results indicate there were no substantial changes to peak loads or the number of loading cycles. Novice runners may be more sensitive to other manifestations of fatigue (physiological or perceptual) and cease running before gait adjustments occur.

Table 1. Participant demographics and run metrics

	mean (SD)	Min.	Max.
age	25 (6)	18	38
miles/wk	12.7 (6.1)	4.5	25
experience (months)	16 (9)	3	36
run speed (mph)	6.1 (0.7)	5	8
run distance (km)	5 (2)	3	8

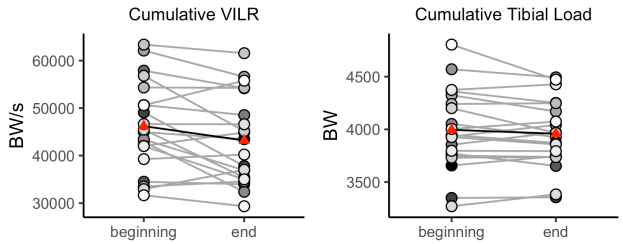

Figure 1: Cumulative loads at the beginning and end of a fatiguing run. Circles show individual subjects, red diamonds show the mean.

Significance

Cumulative load did not increase with run distance, which may be related to differences between the laboratory and runners' typical running environment. Cumulative damage to tissues and subsequent injury risk is not linearly proportional to cumulative load [1] and may be more sensitive to non-significant changes in SF and peak loads. Whether the lack of increase in cumulative load with fatigue translates to an absence of elevated injury risk is unknown. Future studies are required to determine the utility of cumulative load sin running injury risk applications.

Acknowledgments

Funded by the University of Maryland Department of Kinesiology Graduate Research Initiative Program.

References

[1] Edwards, WB (2018). *Exerc Sport Sci Rev*, **46**: 224-231.
[2] Gallagher S & Schall MC, Jr. (2017). *Ergonomics*, **60**: 255-269.
[3] Hunter JG et al. (2019). *Med Sci Sports Exerc*, **51**: 1178-1185.
[4] Hydren J & Cohen B (2004) *J of Str Cond Res,* 29: 3523-3530.
[5] Willson JD & Kernozek TW (1999). *Med Sci Sports Exerc*, **31**: 1828-1833.

Effects of Experimental Anterior Knee Pain on Running Neuromechanics: A Pilot Study

Matthew K. Seeley[1], Justin T. Barker[1], Sunku Kwon[1], Dillon Kunz[1], Hannah Coombs[1], Aubrey R. Odom[2], Shane Huang[2], William F. Christensen[2], and J. Ty Hopkins[1]
Departments of Exercise Sciences[1] and Statistics[2], Brigham Young University, Provo, UT, USA
Email: matt_seeley@byu.edu

Introduction

Patellofemoral pain (PFP), or anterior knee pain (AKP), alters running biomechanics [1]. Altered running biomechanics might affect knee cartilage health [2]. It is difficult to distinguish the independent effects of AKP during running from other simultaneous PFP factors (e.g., joint effusion). The purpose of this pilot study was to test the feasibility of using experimental AKP during a 60-min run in order to clarify the independent effects of AKP during distance running on neuromechanical variables associated with knee cartilage health. We hypothesized that (1) an experimental AKP model could effectively induce perceived AKP throughout a 60-min run and (2) the experimental AKP would alter vertical ground reaction force (vGRF) and quadriceps muscle activation.

Methods

Ten healthy volunteers (5 females; Age = 24 ± 2 yrs; Height = 173 cm ± 11 cm; Mass = 68.4 kg ± 10.3 kg) ran for 60 min on a force-instrumented treadmill on 3 different days. Each day corresponded to a different experimental condition: control, sham, and pain. The pain and sham sessions involved a 75-min hypertonic and physiological saline infusion, respectively, into the right infrapatellar fat pad [3]; this duration included the 60-min run. Surface electromyography (EMG), normalized to reference value specific to each subject and session, was used to quantify activation of the vastus lateralis (VLA) muscle. vGRF and VLA EMG data, during the stance phase of running, were collected and averaged across six 30-s durations (at the end of each 10-min duration throughout the run). Perceived AKP was quantified every 3 min using a 100-mm visual analog scale. vGRF and VLA EMG during the stance phase of running were compared between sessions using a functional data analysis approach. Mean perceived AKP levels were compared between sessions using a mixed-model ANOVA.

Results and Discussion

As hypothesized, mean perceived AKP was greater ($p < 0.01$) during the painful session relative to the control and sham sessions (Figure 1). This is the longest duration (75 min) we have ever utilized this experimental AKP model. As hypothesized, the experimental AKP altered running vGRF and VLA EMG (Figure 2); although Figure 2 does not depict the sham session, to increase clarity. The experimental AKP decreased vGRF as much as 4% of body weight (BW) between 2-9% of stance, and as much as 5% of BW between 27-78% of stance (Figures 2A & 2C). The experimental AKP resulted in decreased and delayed VLA activation: VLA EMG was decreased during the pain session as much as 1 times the EMG reference value during the first 60% of the stance phase, but increased as much as 0.5 times the reference value during the last 40% of stance (Figures 2B & 2D).

These findings fit with previously stated ideas that clinical AKP causes quadriceps weakness [4]. These results show that AKP can independently inhibit quadriceps muscle activation and decrease associated running vGRF during a 60-min run. In combination with previous findings from our laboratory [2], these results also indicate that experimental AKP may influence the acute effects of running on knee articular cartilage; our previous research has shown that altered walking and running biomechanics alter knee cartilage biomarkers [2]. In the future, we plan to observe effects of experimental AKP during distance running on articular cartilage biomarkers, and direct measures of knee articular cartilage morphology and composition.

References

[1] Willson et al. (2008). *Clin Biomech*, 23(2), 203–211.
[2] Denning et al. (2016). *Gait Posture*, 44, 131-136.
[3] Seeley et al. (2013). *J Athl Train*, 48(3), 337-345.
[4] Werner (2014). *Knee Surg Sports Traumatol Arthrosc*, 22(10), 2286-2294.

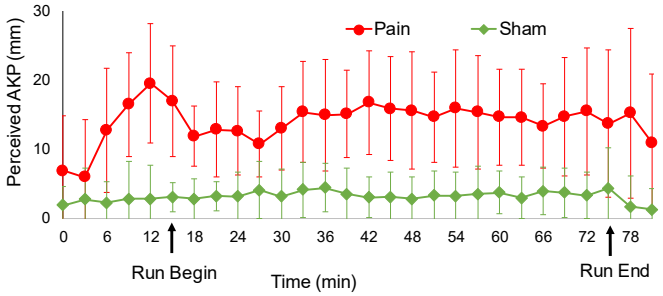

Figure 1. Means and standard deviations for perceived AKP during the pain and sham sessions. No AKP was reported at any time during the control session.

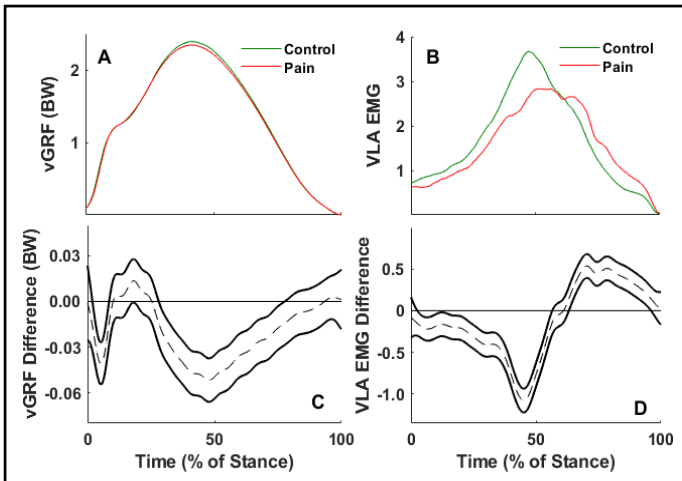

Figure 2. mean vGRF (**A**) and VLA EMG (**B**) across the stance phase during a 60-min run for the pain and control sessions. **C-D:** mean between-session differences (dashed lines) for vGRF (**C**) and VLA EMG (**D**) across the stance phase during a 60-min run; solid lines indicate upper and lower bounds of 95% confidence intervals for the mean differences. Between-session differences existed when the confidence intervals did not overlap zero.

Relationship Between the Single-Leg Step-Down and Lower Extremity Loading in Adolescent Runners

Allison Hoffee[1], Scott Monfort[2], and James Becker[1]
[1]Department of Health and Human Development, [2]Department of Mechanical and Industrial Engineering, Montana State University, Bozeman, MT, USA
Email: james.becker4@montana.edu

Introduction

Previous studies have shown associations between movement screen performance and running kinematics [1]. However, it is still unclear whether movement screen performance is related to injury mechanisms, and by extension, whether they can be used to identify individuals at risk of developing common injuries. Therefore, the purpose of this study was to determine the relationship between performance on the single leg step down (SLSD) movement screen and Achilles tendon (AT) and patellofemoral (PF) joint loads. It was hypothesized that poor performance (i.e. more motion) on the SLSD would be associated with higher AT and PF loads.

Methods

Twenty-one adolescent runners participated in this study (12 M/9 F; age: 12.38 ± 0.79 years; weekly mileage: 23.2 ± 6.4 miles; easy training run pace: 3.25 ± 0.17 m/s). Participants ran for 5 minutes on an instrumented treadmill, after which 10 SLSD trials were performed. 3D motion capture recorded kinematics and kinetics during both running and SLSD. Kinematics during SLSD and kinetics in AT and PF joint were calculated based on previously describe models [2] (Table 1). Principal component analyses were performed for SLSD, AT, and PF variables. Factor loadings were interpreted to create surrogate variables [3] and regressions were performed to determine whether SLSD surrogates predicted AT or PF surrogates.

Results and Discussion

Descriptive statistics for SLSD, AT, and PF loads are shown in Table 1. Three principal components were extracted for SLSD: 1) a hip-rearfoot component, 2) a tibia internal rotation component, and 3) a pelvis-knee component. A single principal component was extracted for AT and PF variables, respectively.

A regression model containing the hip-rearfoot SLSD surrogate predicted AT loading surrogate ($R^2 = 0.277$, $p = 0.014$, Figure 1). Each one unit increase in the hip-rearfoot surrogate resulted in a 3.26 unit increase in AT loading (95% CI 0.73 – 5.79). The tibia rotation ($p = .300$) and pelvis-knee ($p = .447$) surrogates were not significant predictors. None of the SLSD surrogates predicted the PF the surrogate.

Our hypothesis was partially supported as higher SLSD hip-rearfoot surrogate scores predicted higher AT loading surrogate scores. This means adolescent runners with higher hip adduction, hip internal rotation, and rearfoot eversion during the SLSD experience higher AT tendon loads while running. Previous studies have suggested that neuromuscular control at the hip during running is altered in individuals with Achilles tendinopathy [4]. Since the SLSD assesses neuromuscular control of the hip it may be a useful assessment for identifying runners at risk of developing Achilles tendinopathies. Indeed, as we followed this cohort over the course of their running season, the two individuals who performed worst on the SLSD were the ones who developed Achilles inuries. However, future prospective studies are needed to confirm this relationship.

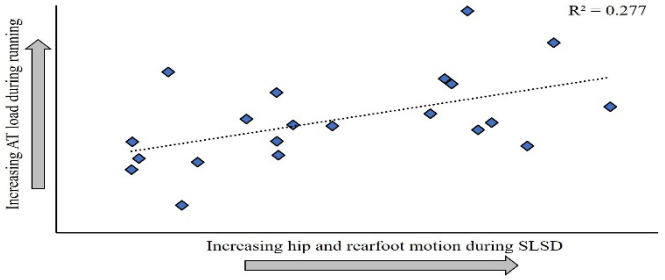

Figure 1. Relationship between SLSD hip-rearfoot surrogate and AT surrogate. The hip-rearfoot motion surrogate is the average of hip adduction, internal rotation, and rearfoot eversion during SLSD. The AT loading surrogate is the average of the peak AT force, loading rate, impulse, and cumulative impulse.

SLSD performance was not, however, associated with PF loads. This is contrary to previous studies that show increases in PF stress in individuals who also have increased hip adduction and internal rotation during both running and SLSD [5]. Whether this is due to the adolescent partipants or other factors requires further research.

Significance

This is the first study to show a relationship between performance on a common movement screen and tissue loading parameters related to the development of common running injuries. This relationship supports the hypothesis that movement screen performance may be beneficial for identifying individuals at risk of developing running overuse injuries.

References

1. Whatman, C. (2011). *Phys Ther Sport* **12**:22-29.
2. Willy, R. (2016). *J Ortho Sport Phys* **46**(8):664-74.
3. Ramsey, F. (2002). *Statistical Sleuth* **2nd ed**:497-524.
4. Creaby, M. (2017). *Med Sci Sport Ex* **49**(3):549-54.
5. Powers, C. (2003). *J Ortho Sport Phys* **33**(11):639-46.

Table 1. Mean and standard deviations for SLSD kinematics (CPD: contralateral pelvic drop, HADD: hip adduction, HIR: hip internal rotation, KV: knee valgus, TIR: tibia internal rotation, RFE: rearfoot eversion), Achilles tendon (AT), and patellofemoral (PF) kinetic variables.

SLSD Variables	Mean Value	AT Variables	Mean Value	PF Variables	Mean Value
CPD (°)	2.61 ± 2.01	Peak force (BW)	7.65 ± 1.41	Contact force (BW)	5.86 ± 1.46
HADD(°)	14.88 ± 4.20	Loading rate (BW/s)	97.97 ± 20.17	Joint stress (MPa)	6.32 ± 2.20
HIR (°)	7.31 ± 5.91	Impulse (BW*s)	0.78 ± 0.14	Loading rate (MPa/s)	162.40 ± 37.14
KV (°)	4.67 ± 2.51	Impulse per km (BW*s*km^{-1})	374.15 ± 72.80	Impulse (MPa*s)	0.56 ± 0.28
TIR (°)	13.18 ± 5.87			Impulse per km (MPa*s/km)	265.14 ± 128.15
RFE (°)	13.92 ± 3.18				

Effect of Increasing Running Cadence on Impact Force in an Outdoor Environment

Taylor L. Musgjerd[1], Jacob D. Anason[1], Thomas W. Kernozek[1], Drew N. Rutherford[1]*
[1]Department of Health Professions, Physical Therapy Program, University of Wisconsin-La Crosse, La Crosse, WI
Email: *drutherford@uwlax.edu

Introduction

Running-related injury prevalence has been reported between 56-80% in U.S. runners (van Gent et al., 2007). A proposed mechanism is high impact loading. Reducing impact forces may be an effective intervention to reduce injury rate (Davis et al., 2010).

Cadence modification was reported to decrease peak vertical ground reaction forces (vGRF) in laboratory settings (Schubert et al., 2014). Increasing cadence while maintaining running pace generally decreases a runner's stride length. Heiderscheit et al. (2011) reported reduced impact loading due to cadence modification during treadmill running (Heiderscheit et al., 2011); however, running over-ground in an outdoor setting may be different.

The goal of this study was to quantify decreases in peak vGRF associated with cadence modification in outdoor running. Additionally, we sought to evaluate the compliance of running cadence modification using an auditory metronome cue.

Methods

Fifteen recreational runners (female n=8 ; male n=7), ages 18-26 (mean=23.5 yrs), with an average mileage of at least 8 miles/week participated. Each completed two outdoor running sessions ≈ 1 week apart. Runners wore wireless sensor insoles (Loadsol, novel gmbh, Munich, Germany) in both shoes interfaced with an iPod Touch for recording data and administering auditory cueing. Vertical ground reaction forces (vGRF) were sampled at 100 Hz and smoothed with a dual-pass Chebyshev filtered with a 30 Hz low-pass cutoff frequency. A GPS watch (Forerunner 25, Garmin International Inc., Olathe, KS) recorded distance and cadence and provided pacing information during runs. Runners utilized their own footwear.

During their Baseline run, participants ran a 2.4 mile (3.9 km) course on a straight, flat asphalt road under their preferred, training pace and cadence. All were instructed to maintain a consistent pace using the GPS watch. During the Follow-up session, runners ran at +10% of their Baseline cadence (Heiderscheit et al., 2011), measured via the GPS watch at the same preferred pace as Baseline. Auditory cueing was provided from the iPod speaker with a metronome application (MetroTimer version 3.3.2, ONYX Apps, US).

Peak vGRF in bodyweight (BW) and cadence data were extracted from one unilateral vGRF time-series for each run. Sensor insole-based cadence data in steps/minute (SPM) were obtained from peak-to-peak timing of vGRF data. Peak force and cadence data were collapsed to mile 1 (1.6 km) and mile 2 (3.2 km) for averages. Two 2x2 repeated measures ANOVA's were performed on time (Baseline, Follow-up) and distance (Mile 1, Mile 2) using IBM SPSS (version 25, Armonk, NY). A separate ANOVA was used for cadence on time and device (Insole, GPS watch). Post hoc testing was performed using Bonferroni correction.

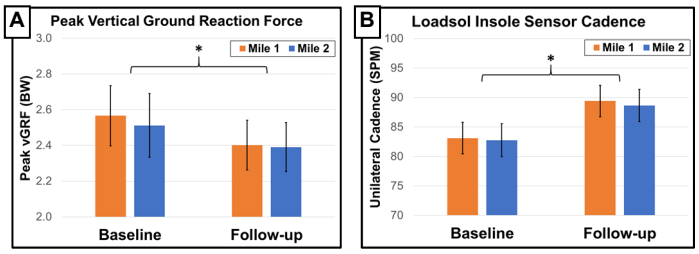

Figure 1: Effects of auditory metronome cueing on peak vGRF (A) and cadence from the pressure insole sensor (B) from Baseline to Follow-up for Mile 1 and Mile 2.

Results and Discussion

Participants demonstrated moderate compliance with the iPod auditory metronome cueing via a 7.3% cadence increase from Baseline to Follow-up ($p<0.001$; Cohen's $d=1.24$). Unilateral peak vGRF decreased 0.15 BW during Follow-Up compared to Baseline (-5.9% ; $p=0.029$; Cohen's $d=0.56$). Treadmill-based studies with cadence increases have reported smaller impact reductions ≈ 2.5% (Heiderscheit et al., 2011; Lenhart et al., 2014); The present study utilized different force sensor technology. Peak vGRF and cadence did not deviate between the first and second mile within each outdoor run.

Cadence reported from the insoles and the GPS watch data showed the two devices were similar ($p>0.05$; 0.5% difference). This may suggest that a commercially available GPS watch can effectively measure cadence while enforcing pace during outdoor running scenarios.

Significance

Runners seeking to lower their impact forces may benefit from the auditory metronome cues for increased cadence and GPS watch to enforce pace. These data support use by clinicians to alter running cadence in an effort to prevent impact-related injury during outdoor running.

Acknowledgments

The authors wish to thank the University of Wisconsin-La Crosse Graduate School for a graduate student research grant funding this work.

References

Davis, I.S., et al. (2010). Do impacts cause running injuries? A prospective investigation. ASB. Retrieved from: http://www.asbweb.org/conferences/2010/abstracts/472.pdf

Heiderscheit, B.C., et al. (2011). Medicine & Science in Sports & Exercise, 43(2), 296–302.

Lenhart, R.L., et al. (2014). Medicine and Science in Sports and Exercise, 46(3), 557–564.

Schubert, A.G., et al. (2014). Sports Health: A Multidisciplinary Approach, 6(3), 210–217.

van Gent, R.N., et al. (2007). British Journal of Sports Medicine, 41(8), 469–480.

Biomechanics during running in Vaporfly shoes with intact vs. cut carbon-fiber plates

Laura A. Healey[1]*, Justin Angelo O. Ortega[1], Dale Haavind-Berman[1], and Wouter Hoogkamer[1]
[1]University of Massachusetts Amherst, Department of Kinesiology
Email: *laurahealey@umass.edu

Introduction

Performance running shoe technology has recently become a polarizing topic, most notably due to the use of carbon-fiber plates. While small benefits of carbon-fiber plates in footwear have been shown before (Roy & Stefanyshyn, 2006), Nike Vaporfly 4% (VF) shoes, which utilize a curved carbon-fiber plate embedded in a compliant and resilient midsole, have been shown to improve running economy by as much as 4% compared to two popular marathon racing shoes (Hoogkamer et al. 2018). In a biomechanical analysis of the VFs, Hoogkamer et al. (2019) determined the clever lever and the stiffening effects of the plate are likely among the main contributors to the 4% energy savings. However, that study compared shoes that differed in both geometry (taller stack height), foam properties (more compliant and resilient) *and* longitudinal bending stiffness (stiffer; carbon-fiber plate). Understanding how the VFs' carbon-fiber plate affects running mechanics is critical to informing optimized shoe design.

Therefore, the aim of this study was to determine how the carbon-fiber plate in the VFs affects ankle and metatarsal-phalangeal (MTP) mechanics. We hypothesized that decreasing the longitudinal bending stiffness would (1) increase MTP angle, moment, and power, (2) decrease ankle angle and moment and (3) increase positive distal rearfoot power.

Methods

To reduce the effectiveness of the carbon-fiber plate six medio-lateral cuts were made in the forefoot of a pair of new VFs through the carbon-fiber plate (Figure 1). Nine male runners (size M9.5, 23±4 years, 67.2±4.7 kg, 174±3 cm) ran over ground across a 100ft runway at 14km/h ± 4% five times in the cut VFs (CVF) and intact VFs (VF). Force plate data (AMTI 2000Hz) and 3D positional data (Qualisys 200Hz) were collected for the right leg and foot. We calculated joint angles, moments, and powers during the stance phase for the ankle and MTP joint, as well as distal hindfoot power (DHFP) (Zelik & Honert, 2018) using a custom Python script. To analyze the entire stance phase, we used one dimensional spatial parametric mapping (SPM) to conduct two-tailed paired t-tests ($\alpha = 0.05$).

Figure 1: Shoe conditions: VF (baseline), CVF (decreased longitudinal bending stiffness)

Results and Discussion

Most differences were found in MTP mechanics, with small changes in ankle moment and distal hindfoot power (Figure 2). MTP angles were more dorsiflexed ($p=0.038$) in the CVF between 0-14% and 72-100% of the stance phase. This was accompanied by increased ($p<0.001$) negative MTP power in the CVF compared to the VF from 68-90% of stance phase. Ankle moment was significantly higher ($p<0.001$) in the CVF from 64-72%. Finally, positive distal hindfoot power was significantly higher ($p=0.027$) in the CVF from 69-72%.

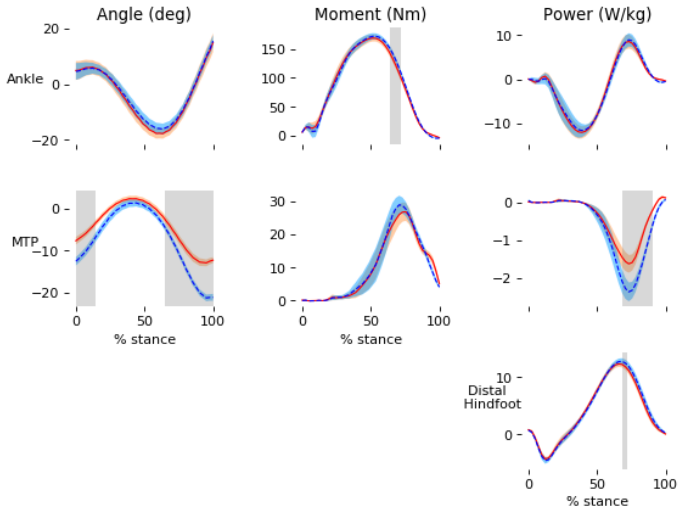

Figure 2: Angle (deg), moment (Nm), and power (W/kg) for the Ankle, MTP, and distal hindfoot in the VF (orange line) and CVF (dashed blue line). Grey areas indicate regions where shoe conditions differ significantly ($p<0.05$).

The results partially support our first hypothesis, that decreasing longitudinal bending stiffness would increase MTP angle and power, however no differences were seen in MTP moments. Interestingly, these differences in MTP mechanics did not translate to the ankle, as few changes were observed. DHFP was calculated to better understand the power contribution from the shoe, including the plate and the foam. In this method only the power fluctuations between the calcaneus and the ground are considered, as treating the whole foot as a rigid segment has been found to be less accurate (Zelik & Honert, 2018). Only a small difference in DHFP was found, suggesting that the carbon-fiber plate does not substantially change the combined power absorption and generation from the shoe foam, plate and foot structures. Overall, our results suggest that the carbon-fiber plate in the VFs has the most influence on the MTP joint.

Significance

As carbon-fiber plates become increasingly popular in running shoe innovation, it is important to understand how they affect joint mechanics, and how this could contribute to improved performance. Outside of performance running, shoes that alter joint mechanics may be beneficial to specialized populations such as older adults or individuals with reduced muscle function.

References

Hoogkamer et al. *Sports Med,* 2018, **48:** 1009-19.
Hoogkamer et al. *Sports Med,* 2019, **49:** 133-43.
Roy & Stephanyshyn. *Med Sci Sports Exerc,* 2006, **38:** 562–9.
Zelik & Honert. *J Biomech,* 2018, ***75:*** 1-12.

The Effect of Carbon-Fiber Plate Racing Shoes on Running Biomechanics

JJ Hannigan & Luisa Westley
San Jose State University, San Jose, CA
Email: jj.hannigan@sjsu.edu

Introduction

Maximal running shoes are loosely defined as shoes that contain greater midsole cushioning from heel to toe compared to a traditional shoe. The effect of maximal running shoes on biomechanical measures related to running injury risk have only recently been investigated, with some studies finding elevated loading rates, impact forces [1,2] and prolonged eversion [2,3] in maximal shoes compared to traditional footwear.

While maximal running shoes were initially designed for training on the road or trails, a new type of maximal shoe has recently become popular for road racing, containing a carbon-fiber plate in the midsole as well as a proprietary new midsole material with high compliance and resilience. Initial findings have demonstrated that shoes in this category may reduce the energetic cost of running by ~4% [4], possibly due to changes in ankle and metatarsophalangeal joint biomechanics [5]. These shoes are in stark contrast to lightweight minimally cushioned shoes that had generally been worn for road racing.

While many running shoe companies have since released a shoe in this category, Nike's Vaporfly 4%, and subsequently the Vaporfly Next%, were the first shoes in this category on the market, and remain the most popular option among runners. While predominately used for racing, these shoes are becoming increasingly popular for use in training, leading to the question of the effect of these shoes on common biomechanical injury risk factors during running. Therefore, the purpose of this study was to compare hip, knee, and ankle biomechanics during running between the Nike Vaporfly Next% and a common minimal shoe.

Methods

Twelve healthy competitive distance runners (age = 21.0 ± 2.5 yrs) participated in this study. Twenty-one reflective markers and six marker clusters were placed on subjects who ran overground in the lab at their marathon pace wearing the a) Nike Vaporfly Next% (NP), and b) New Balance Minimus (NB) in random order. Five successful running trials for each shoe were collected at 200 Hz with a 16-camera 3D motion capture system (Vicon Motion Systems, Oxford UK). Two force plates collected ground reaction forces and were used to determine initial contact and toe-off (Kistler Instrument Corp., Novi MI).

Kinematics were calculated using Visual3D software (C-Motion, Germantown MD). Variables of interest included peak angles and excursions at the ankle (dorsiflexion and eversion), knee (flexion and valgus), and hip (adduction and internal rotation) as well as peak internal moments at the ankle (plantar flexion and inversion), knee (extension and valgus), and hip (abduction and external rotation). Data were compared using paired t-tests with the alpha-level set to 0.05.

Results and Discussion

No significant differences were found between peak angles or excursions at the hip and knee ($p > .05$). At the ankle, peak dorsiflexion (NP: 19.0 ± 3.8°, NB: 25.3 ± 3.7°, $p < .001$) and dorsiflexion excursion (NP: 21.6 ± 4.3°, NB: 25.6 ± 4.2°, $p < .001$) were both significantly lower in the Nike Next% (Figure 1). While there were no differences in peak eversion, eversion excursion was significantly higher in the Nike Next % shoe (NP: 15.1 ± 2.6°, NB: 12.9 ± 2.6°, $p = .001$).

At the ankle, the internal plantar flexion moment was significantly lower in the Next% shoe (NP: 2.4 ± 0.5 Nm/kg, NB: 2.9 ± 0.5 Nm/kg, $p = .001$). At the knee, the internal extension moment was significantly higher in the Next% shoe (NP: 4.4 ± 0.7 Nm/kg, NB: 4.0 ± 0.9 Nm/kg, $p = .01$). Differences between shoes for the internal hip extension moment were close to achieving significance (NP: 1.3 ± 0.6 Nm/kg, NB: 1.1 ± 0.7 Nm/kg, $p = .06$). No other differences were observed for kinetics.

The kinematic results indicated few differences between shoes for important injury risk factors for injury. Greater eversion excursion was observed in the Next% shoe which has been linked to injury, however, these differences were largely driven by slightly greater inversion at initial contact and toe-off.

While not commonly linked to injury risk, less dorsiflexion excursion and peak dorsiflexion were observed in the Next% shoe (Figure 1) in addition to a smaller peak internal plantar flexion moment, which agrees with previous research [5] and may help explain the performance benefits of the shoe. However, this appears to come at a cost, as the internal knee extension moment was significantly higher in the Next% shoe.

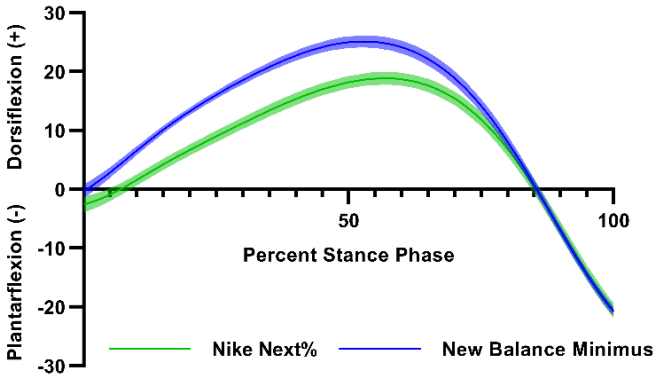

Figure 1. Ensemble curves of sagittal plane ankle kinematics.

Significance

While greater ankle eversion excursion is noteworthy in the Next% shoe, no other kinematic or kinetic risk factors for injury were observed in this shoe, indicating this carbon-fiber plate racing shoe may not substantially increase injury risk. Differences between shoes in ankle biomechanics agree with previous research and may explain the performance benefits.

Acknowledgments

The authors would like to acknowledge Junko Griffith for her assistance and support during data collection.

References

[1] Pollard et al., *Orth J Sport Med* 6(6), 2018.
[2] Hannigan et al., *Am J Sport Med* 47(4), 2019.
[3] Hannigan et al., *J Sci Med Sport* 23, 2020.
[4] Hoogkamer et al., *Sports Med* 48(4), 2018.
[5] Hoogkamer et al., *Sports Med* 49(1), 2019.

Application of automatic segment filtering procedure to the kinematics of running

Daniel J Davis, and John H Challis
Biomechanics Laboratory, The Pennsylvania State University, University Park, PA
Email: djd426@psu.edu

Introduction

The processing techniques used on biomechanical signals can often be as important as the experimental paradigms. The filtering methods of motion capture signals have received considerable attention with respect to estimating signal derivatives in particular. Recently, an automatic filtering procedure which applies a Butterworth low-pass filter with different cut-off frequencies specific to signal sections was proposed [1]. This technique aimed to better filter time-series signals with varying frequency content. It is not clear, however, how this approach would compare to typical filtering procedures when applied to a set of common biomechanical measures which comprise multiple signals. Therefore, the purpose of this investigation was to explore the application of the automatic segment filtering procedure (ASFP) to a publicly available simulated running stride [2].

Methods

The test data of van den Bogert & de Koning (1996) were used as criterion data [2]. This data set consists of lower body segment kinematics and ground reaction forces from computer simulations of running gait. To illustrate the influence of filtering multiple signals in a signal section by section manner, the vertical ground reaction force (vGRF) was estimated from the computed vertical center of mass (COM) acceleration of lower limb segments throughout the stance phase after adding noise to the limb segment coordinates.

Body segment COM displacements and accelerations were estimated ten times using noiseless kinematic signals, and after the addition of noise (0.1 mm root mean square) using three signal processing techniques. 1) The "typical" technique in which all kinematic signals were filtered at a single filter cut-off frequency (the mean of the autocorrelation-based procedure [ABP; 3] cut-off frequencies for the body segment COM displacements), 2) a whole signal ABP technique which saw each body segment COM displacement signal filtered with a cut-off frequency specific to that segment, and 3) the segment filtering technique (ASFP) where the segment COM signals were broken into sections based on the variation in the Teager-Kaise Energy Operator (TKEO) of the estimated vGRF from the "typical" filtering method above [1,4]. In brief, this previously developed segment filtering technique applied the ABP to each section of the given signal to produce a whole signal displacement estimate corresponding to each signal section. These estimates were then joined together such that each section of the final signal contained the acceleration estimate derived from applying the ABP to that signal section.

Results and Discussion

The ASFP was better able to match the impact peak of the simulated vertical ground reaction force than both a typical approach and the ABP as demonstrated by a reduced absolute peak error (Table 1). This was accomplished by allowing for a filter with a higher cut-off frequency during the impact portion of stance. Additionally, the ASFP better attenuated oscillations in lower frequency portions of the signal (Figure 1).

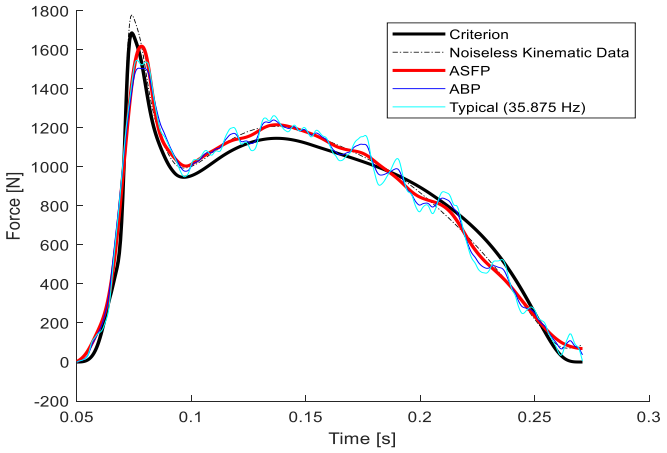

Figure 1: Vertical ground reaction force and estimates from noiseless kinematic signals and three filtering techniques.

Significance

When accurate magnitudes of kinetic and kinematic derivatives are of interest in impact-like biomechanical tasks, removing the appropriate amount of noise in measured signals is of great importance. Commonly, multiple signals are processed with a common Butterworth filter cut-off frequency, potentially inappropriately handling the variation in signal to noise ratio between body segments and signal sections therefore poorly estimating the magnitudes of interest. By implementing processing techniques which are sensitive to changing frequency content, such as the ASFP, more accurate estimation of common measures such as vGRF are attainable.

References

[1] Davis, D. J., & Challis, J. H. (2020). ***Journal of Biomechanics***, 101, 109619.
[2] Bogert, A.J. van den,& de Koning, J.J., (1996). ***Proc. 9th CSB Congress***, pp. 214-215, Burnaby, B.C.
[3] Challis, J. H. (1999). ***Journal of Applied Biomechanics***, 15(3), 303-317.
[4] Kaiser J.F. (1990). ***IEEE ICASSP-90***, 381-384.

Table 1: The percentage root mean square error (%RMSE) for estimating the vertical ground reaction force (vGRF) from kinematic signals and the error in estimating the vGRF impact peak value.

Method	%RMSE	Absolute Impact Peak Error [%]
Noiseless Kinematic Signals	6.0	5.4
ASFP	9.4 ± 1.1	5.1 ± 4.3
ABP	9.6 ± 0.8	11.3 ± 3.3
Typical Filtering	10.18 ± 0.9	8.6 ± 3.4

Visualizing Variation in Vertical Ground Reaction Forces During Running

Bryan P. Conrad[1], Alison L. Sheets-Singer[1]
[1]Nike Sport Research Lab, Nike, Inc.
Email: bryan.conrad@nike.com

Introduction

Ground reaction forces (GRF) provide valuable information about running biomechanics. Variations in speed, foot contact pattern, incline, footwear, etc.[1] can produce a number of distinct patterns. With the many potential variations in the force signal, researcher often aim to find the features that are best able to discriminate different running techniques. Many of the parameters commonly reported from ground reaction forces can be correlated, thus a way to express these differences and their correlations by reducing the dimensionality of the data can be helpful.[2] Using principal component analysis, we aim to quantify the variations in force time series data across a large population and create visualizations that can help researchers understand how these patterns manifest in healthy runnners.

Methods

Ground reaction forces were measured for 198 participants (86 F: mass= 65.2 ± 10.5 kg, age= 33.5 ± 8.7 yrs; 111 M: mass = 78.1 ± 10.8 kg, age= 34.0 ± 6.6 yrs) while running on a Bertec treadmill in neutral running shoes. Data used in this analysis were collected as part of multiple studies implementing different protocols regarding running speed, experimental shoe condition, and treadmill incline. For most of the subjects, multiple conditions were evaluated and included in the analysis. The final data set included a total of 877 trials each consisting of an average of 377 steps. Before data collection, athletes provided informed consent to participate in the research study.

Ground reaction forces were recorded at 1200Hz or higher, and filtered using a low pass Butterworth filter with a 50 Hz cut off. Vertical ground reaction force (vGRF) was normalized to body weight (BW), and stance time was interpolated to 0-100% using 1000 points. Principal component analysis (PCA) was run on the normalized vGRF. Considering the principal components (PCs), the modes of variation can be visualized across the population by transforming PC scroes back into GRF space.

Results and Discussion

The first 3 principal components explain over 90% of the variance between runners. PC 1 predomanintly describes the magnitude of the peak GRF (64% variation explained). PC 2 primarily captures differences in the loading rate of the GRF curve during impact (19% variation explained).

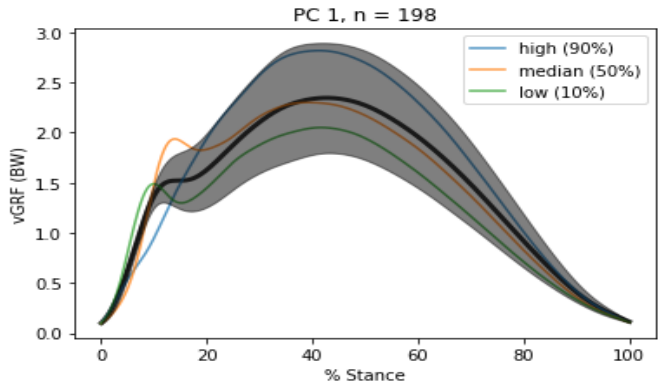

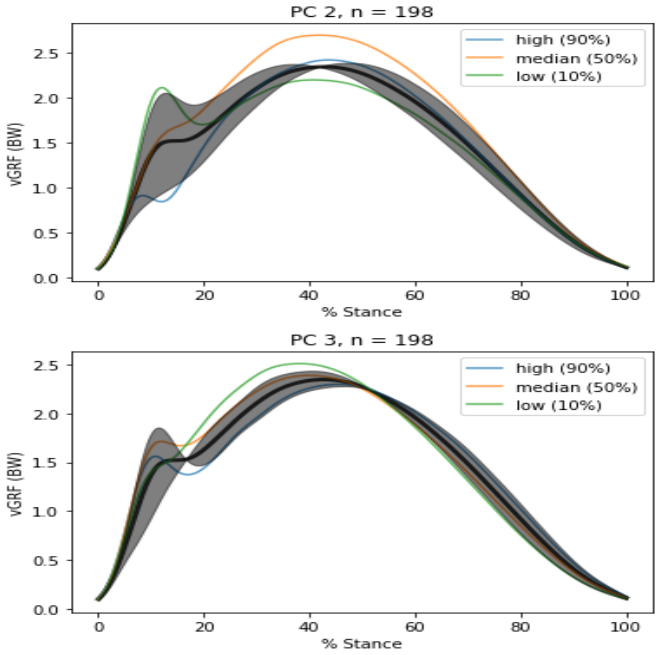

Figure 1: Principal Components 1-3. The black line is the mean ground reaction force (normalized to BW) and the gray band is +/- 2 standard deviations of each Principal Component. Thin lines are representative trials for high and low PC scores.

PC 3 describes the height of the heel impact transient (9% variation explained). Standard deviations for the PC 2-3 are largest during the first 30% of stance. Alternately, after weight acceptance and through push off, standard deviations are smaller. This may indicate that while there are numerous ways to contact the ground during impact (differences in foot strike type being the most obvious), the requirement during mid-stance and push off is more universal: support body weight and propel the body into the air to take the next step. Other factors that affect impact forces include footwear, slope of running surface, and speed, which all also have interactions with foot strike type. Using similar approach, Kiernan showed significant correlations between PC scores and number of running injuries.[3]

Significance

GRF patterns from a wide range of runners can be predominantly described by a small number of features. Researchers can gain a more intuitive understanding for how specific kinetic features relate to running by visualizing PC differences in the time domain.

Acknowledgments

Thank you to the many NSRL researchers who collected the data used for this analysis!

References

[1] Milner, CE. *MSSE.* 38, 2 (2006): 323-328.
[2] Deluzio, KJ. *Gait & Posture*. 25, 1. (2007): 86-93.
[3] Kiernan D, Shim JK, Miller, RH. *ASB Poster* (2015).

Maximum voluntary ankle joint moments are unaffected by extension of the metatarsophalangeal joints

Justin C. Wager[1], John H. Challis[2]
[1]Department of Physical Theraphy and Human Movement Science, Sacred Heart University
[2]Biomechanics Laboratory, The Pennsylvania State University
Email: wagerj4@sacredheart.edu

Introduction

During the push-off phase of walking and running, the ankle plantarflexor muscles provide a large portion of the positive lower-limb power. This power is influenced by the force-generating capacities of the ankle plantarflexors, which are affected by the ankle and knee joint positions and, potentially, the metatarsophalangeal (MTP) joints. The MTP joints may influence the force-generating capacities of the ankle plantarflexor muscles through two possible mechanisms: 1) the multiarticular flexor hallucis longus (FHL) and flexor digitorum longus (FDL), which contribute to ankle plantarflexion and cross the MTP joints, and 2) connections (both anatomical and mechanical) between the plantar aponeurosis and Achilles tendon[1–3], which is a pathway for MTP joint extension to influence the Achilles tendon and triceps surae muscle fibers. As the MTP joints extend during the push-off phase of walking and running, interactions between MTP joint extension and ankle plantarflexion strength could influence the understanding of mechanical power generation during push-off. It was hypothesized that maximum voluntary ankle plantarflexion moments would increase with the MTP joints positioned in extension.

Methods

Eight healthy subjects exerted maximum voluntary isometric ankle plantarflexion contractions on a dynamometer (Biodex Medical Systems, Shirley, NY) in 16 different combinations of knee, ankle, and MTP joint position. The MTP joints were held statically in either a neutral or fully extended position while the knee joint (2 positions: 90 degrees flexion or fully extended) and ankle joint (4 positions: -10, 0, 10, and 20 degrees of plantarflexion) positions were systematically varied. A 3-way repeated measures ANOVA was used to test the effect of the MTP, ankle, and knee joint angles on the maximum voluntary ankle plantarflexion moment. Significance level was set at 0.05.

Results and Discussion

No statistically significant effect of MTP joint extension on the maximum ankle plantarflexion moment was detected (Figure 1). The mean difference between the MTP neutral and MTP joint extended positions (across all knee-ankle configurations) was 2.6 ± 12.8 N·m (p = 0.41). Expectedly, statistically significant effects of ankle joint angle and knee joint angle on the maximum ankle plantarflexion moment were found ($p < 0.001$).

These results do not support our hypothesis that ankle plantarflexion moments would increase when the MTP joints were extended. Further, the results suggest that: 1) the FHL and FDL contribute little to the maximum ankle joint moment, 2) the force-generating capacities of the FHL and FDL are unchanged by MTP joint extension, and/or 3) MTP joint extension has a negligible influence on the force-generating capacities of the gastrocnemius and soleus muscles. While mechanical connections between the toes and the ankle plantarflexors have been shown[3] and the fibers of the plantar aponeurosis seem to continue on to the Achilles tendon in young individuals[1], there does not seem to be an influence of toe position on the strength of the ankle plantarflexor muscles.

Significance

This finding increases understanding of locomotion mechanics by suggesting that if extension of the toes during late stance affects the triceps surae, it is not through direct alterations to the muscle's moment-generating capacity. This understanding may be important clinically, for toe or partial foot amputation, and in sport, for footwear that alters MTP joint mechanics (e.g., by increasing forefoot bending stiffness).

References

1. Snow SW, Bohne WH, DiCarlo E, Chang VK. *Foot Ankle Int*. 1995;16(7):418-421.
2. Stecco C, Corradin M, Macchi V, et al. *J Anat*. 2013;223(6):665–676. doi:10.1111/joa.12111
3. Carlson RE, Fleming LL, Hutton WC. *Foot Ankle Int*. 2000;21(1):18-25.

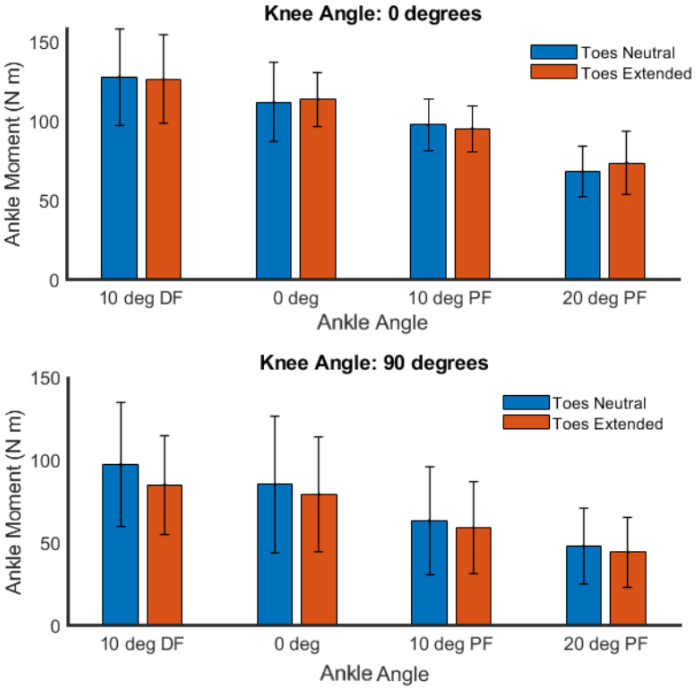

Figure 1: Maximum isometric ankle plantarflexion moments (means across all subjects) with the MTP joints in neutral and extended positions and at various knee (top: knee extended, bottom: knee flexed to 90 degrees) and ankle positions. Error bars show ± 1 standard deviation from the mean. PF: plantarflexion, DF: dorsiflexion.

Assessment of Turning Performance and Muscle Coordination in Individuals Post-Stroke

Lindsey K. Lewallen[1], Steven A. Kautz[2], and Richard R. Neptune[1]
[1]Walker Department of Mechanical Engineering, The University of Texas at Austin, Austin, TX
[2]Department of Healthy Sciences & Research, Medical University of South Carolina, Charleston, SC
Email: lindseylewallen@gmail.com

Introduction

The goal of post-stroke locomotor therapy is to help individuals return to activities of daily living. Straight-line walking has been the primary focus of gait and rehabilitation studies. However, turning steps represent 35-45% of all steps taken during activities of daily living [1]. In addition, nearly four times as many individuals post-stroke report falling while turning compared to healthy adults [2]. Falling while turning can be extremely dangerous, with 70% of those falls leading to injury [3]. Currently, there are no specific exercise protocols for improving turning performance [4]. Thus, there is a need to provide clinicians with evidence-based rehabilitation to improve turning performance for individuals post-stroke. The purpose of this study was to identify relationships between turning performance and muscle coordination, with a focus on two types of turns involved in activities of daily living: 90-degree and 180-degree turns. We hypothesize turning performance will decline for subjects with impaired muscle coordination.

Methods

EMG and full body 3D kinematic data were collected from 20 chronic hemiparetic stroke subjects (20 left hemiparesis) and 20 healthy age-matched controls. Subjects performed 3 tasks including straight over-ground walking, 90-degree turns, and 180-degree turns. For the turning trials, stroke subjects were instructed to turn as quickly as possible towards their paretic side.

Turning performance was defined using two measures: the time to complete the turn and turning smoothness. Time to complete the turn was defined as the time it takes to return to a constant forward velocity. Turning smoothness was assessed using a Velocity Peaks Metric, which was defined as the number of body center of mass (COM) forward velocity peaks over the course of a turn normalized by the number of steps taken. Smoother movement is represented by fewer periods of acceleration and deceleration, leading to fewer peaks in COM velocity. For each subject, muscle coordination was assessed using the number of muscle modules during the straight overground walking task determined by non-negative matrix factorization [5]. We determined differences in turning performance between individuals post-stroke with different number of muscle modules and the age-matched controls.

One-way ANOVAs were used to test for significant differences in the turning performance measures. Tukey's post hoc tests were used to test for differences between each group (controls and individuals post-stroke with 2 modules, 3 modules, 4 modules, and 5 modules).

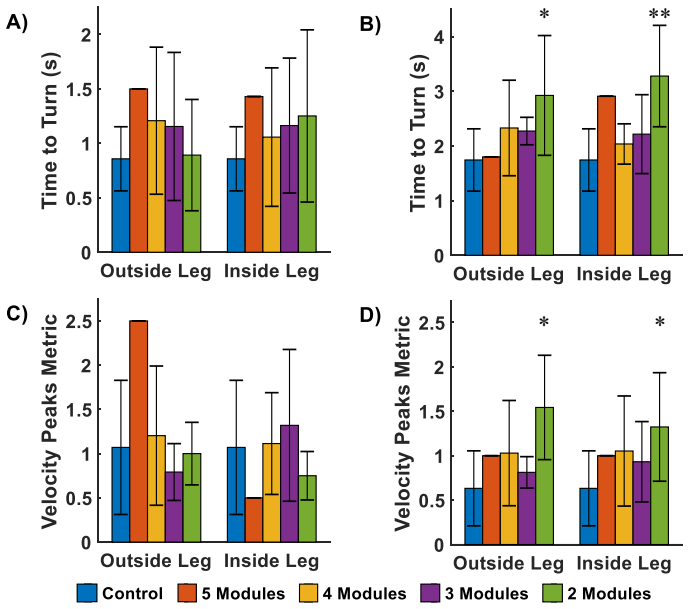

Figure 1: Velocity Peaks Metric and Time to Turn for 90-degree trials (A, C) and 180-degree trials (B, D) grouped by control subjects and the number of modules used in walking for stroke subjects.
*Indicates a significant difference from controls ($p < 0.001$).
**Indicates a significant difference from controls, 2 modules, and 3 modules ($p \leq 0.044$).

Results and Discussion

Differences between groups were only seen in the 180-degree turning performance measures (Fig. 1). Subjects with 2 modules took a significantly longer time to complete the 180-degree turn (Figure 1b) and had a significantly larger velocity peak metric (i.e., were less smooth) during 180-degree turns (Figure 1d). This suggests merged muscle activity is predictive of poor 180-degree turning performance. This is consistent with studies showing the merging of modules leads to impaired walking performance [6] and planar reaching studies showing a lack of smoothness is characteristic of upper limb motor impairment [7]. These results suggest that obtaining independent modules should be an important aim in turning rehabilitation.

Significance

Turning therapy is needed to help individuals post-stroke navigate the complex environments encountered during activities of daily living. These results highlight the relationships between turning performance and impaired muscle coordination and that the time it takes to complete a 180-degree turn is a promising clinical assessment measure of muscle coordination and could be used to help identify impairment levels post-stroke.

Acknowledgments

This work was supported in part by VA RR& D 1I01RX001935.

References

[1] Glaister BC, et al. *Gait Posture.* 2007.
[2] Simpson LA, et al. *PLoS ONE*. 2011.
[3] Talbot LA, et al. *BCM Public Health.* 2005.
[4] Wilkins LW, et al. *ACSM*. 2014.
[5] Ting LH, et al. *J Neurophys.* 2005.
[6] Clark DJ, et al. *J Neurophys.* 2010.
[7] Rohrer B, et al. *J Neurosci*. 2002.

3D Scanned Foot Image: A Potential Biomarker of Spastistic Foot Deformity in Chronic Stroke

Hogene Kim*[1], Ji-Eun Cho[2], Kyung Joon Seo[2]
[1]Department of Clinical Rehabilitation Research, National Rehabilitation Center, Seoul, South Korea
[2]Department of Rehabilitative & Assistive Technology, National Rehabilitation Center, Seoul, South Korea
Email: *hogenekim@korea.kr

Introduction

Stroke causes spastistic foot deformity, equinus foot, which has a foot with more dorsiflexion and inversion at resting condition [1]. It significantly impairs gait and increases trip-related fall risk in chronic stroke. Three dimensional(3D) laser scanning technology is accurate and more economical to identify kinematic differences in clinics compared to magnetic rasonnance imaging or even x-ray[2].

We investigated novel hemiparetic foot parameters that were acquired from 3D laser scanned foot images with non-paretic feet or age-matched normal healthy feet. Several kinematic foot biomarkers were proposed. We hypothized that there are significnat difference in proposed foot parameters between paretic and non-paretic sides.

Methods

Total 30 chronic stroke patients (F/M: 11/19; Age: 65.6±8.7years; Onset: 10.2±8.8years) and 11 age-matched healthy controls(F/M: 7/4; Age: 62.9±5.7years) participated in this study.

Using commercial 3D scanner (Artec Eva, Artec3D, Luxemburg), 3D foot images were acquired from 41 subjects and converted to stl files to measure dimension. Figure 1 shows the definitions of lengths(L_{100F}, L_{10F}, L_{66F}), heights(H_{MM}; H_{LM}:) and angles(θ_{HC}, θ_{MMC}, θ_{LMC}, θ_{MS}, θ_{LS}) in given foot images. θ_{HC} denotes the angle between horizontal line in corronal plane and the line connecting medial and lateral malleoli. After scanning, subjects repeated walking on 10 meter even and uneven surfaces for three times at their self-selected comfortable speed. The gait kinematics were recorded using VICON motion capturing system (Vicon Motion Systems Ltd, United Kingdom). The paired t-test was used to compare between peratic and non-paretic parameters and the t-test with independent samples was used for between group statistic.

Figure 1: Definitions of foot kinematic parameters: (Lengths: L_{100F}, L_{10F}, L_{66F} ; Heights(H_{MM}; H_{LM}:) and Angles(θ_{MH}, θ_{LH}, θ_H, θ_{ML}, θ_{LL})

Results and Discussion

The horizontal tilt angle in corronal plane(θ_{HC}) in paretic foot(17.3º±5.7) was significantly greater than both non-paretic foot(14.6º±5.7, p=0.004) and dominant foot in healthy controls (13.9º±1.3, p=0.024). θ_{LMC} was significantly bigger in paretic side (31.0º±4.4 vs 28.3º±2.7, p=0.007). Foot kinematic paramters showed significant changes in sagittal and coronal planes on paretic foot (H_{MM}:p=0.027; θ_{MMC}: p=0.001; q_{MS}: p=0.001). Table 1 summerizes the kinematic differences in foot parameters between chronic stroke and healthy controls or between paretic and non-paretic sides.

We showed that 3D surface scanning technology is useful to identify the foot kinematic differences using proposed foot kinematic parameters between chronic stroke patients and healthy controls. The proposed foot parameters are possible to be used as foot kinematic biomarkers that may be applied to evaluate the capability to conduct activities of daily livings. Thus further investigation is necessary on the relationship with the proposed foot parameters and gait impairments in chronic stroke.

	Chronic Strokes			**Healthy Controls**	
	Paretic	Nonparetic	vs NP	Dominant	vs HC
H_{MM}	**90.4 ±10.5**	**89.3 ± 6.9**	**0.027**	82.6 ± 6.7	0.627
H_{LM}	68.6 ± 7.4	69.9 ± 5.5	0.303	66.1 ± 5.8	0.472
θ_{HC}	**17.3 ± 5.7**	**14.6 ± 3.1**	**0.004**	**13.9 ± 1.3**	**0.024**
θ_{MMC}	**18.3 ± 5.3**	**20.6 ± 3.8**	**0.001**	22.8 ± 2.2	0.057
θ_{LMC}	31.0 ± 4.4	28.3 ± 2.7	0.094	**28.6 ± 2.4**	**0.007**
θ_{MS}	**63.3 ± 4.8**	**64.2 ± 4.1**	**0.001**	69.0 ± 3.9	0.451
θ_{LS}	73.1 ± 5.5	72.4 ± 3.9	0.092	76.2 ± 3.7	0.556

Table 1: Comparisons in foot parameters with paretic foot (vs NP indicates p-values in non-paretic foot parameters; vs HC indicates p-values in healthy controls foot parameters)

Significance

This study showed potentially useful in clinical fields including physical medicine, orthopaedics etc., to identify pathological conditions that bring kinematic changes in body parts. Especially in the rehabilitation hospital, proposed parameters are used to apply more effective footwears for patients with stroke including ankle foot orthosis.

Acknowledgments

Translational Research Program for Rehabilitation Robots, National Rehabilitation Center, Ministry of Health & Welfare, South Korea (#NRCTR-IN19003).

References

[1] S. Carda et al, *Clinical rehabilitation,* vol. 25, no. 12, pp. 1119-1127, 2011.

[2] Y. Nagata et al, *International Journal of Radiation Oncology Biology Physics,* vol. 18, no. 3, pp. 505-513, 1990

Narrow walking alters qualitative measures of COM movement in TBI vs. Control subjects

Mara R. Thompson[1], Joseph E. Langenderfer[2], and Ksenia I. Ustinova[1]
[1]Department of Physical Therapy, [2]School of Engineering and Technology
Central Michigan University, Mt. Pleasant, Michigan USA
Email: mara.thompson@cmich.edu

Introduction

Traumatic brain injuries (TBIs) can occur during many types of activities and in different populations. As part of recovery, gait intervention may be necessary for patients who have experienced TBI. However, literature on consistently successful techniques is scarce, possibly due to the heterogeneity of the TBI-effected population [1]. More in-depth analysis of gait characteristics could be essential to finding successful intervention techniques. Continued improvements in analysis of gait may better inform and compare intervention techniques for patients who have experienced TBI. Non-linear analysis shows more qualitative aspects of data sets that are missed in typical gait characterization. This abstract uses recurrence quantification analysis (RQA), a non-linear method, to look at center of mass (COM) movement during preferred gait and an interventional gait in TBI patients when compared with a control group.

Methods

Motion capture data was collected at 100 Hz, using a 12-camera Vicon T160 system and standard marker set, from 18 subjects (8 with previous TBI, 10 control). Subjects were directed to walk at their preferred pace and stride length for one of the analyzed trials (Preferred condition). For the Narrow condition, subjects were directed to walk by placing their next foot in a straight line in front of the other, but not required to touch the heel of the front foot to the toe of the standing foot. The COM was calculated by the Vicon Nexus software from collected marker data and anthropometrics (Fig.1a). RQA measures were calculated for the COM virtual marker trajectories for 6 steps in the medial-lateral and superior-inferior directions, using Norbert Marwan's MATLAB CRP Toolbox [2]. Movement in the anterior-posterior direction was not analyzed as it only represents the forward walking of the patients.

RQA measures are quantitative values for data visualization from recurrence plots (Fig. 1b). Recurrence plots show points, known as *recurrent points,* where the 2-D data reenters a section of the phasespace. Determinism (%DET) is the percentage of these recurrent points that form diagonal lines in the plot and maximum line length (LMax) is the inverse of the positive maximal Lyapunov exponent. Paired *t*-tests were performed on the data groups and condition and the critical *p*-value was corrected for multiple comparisons.

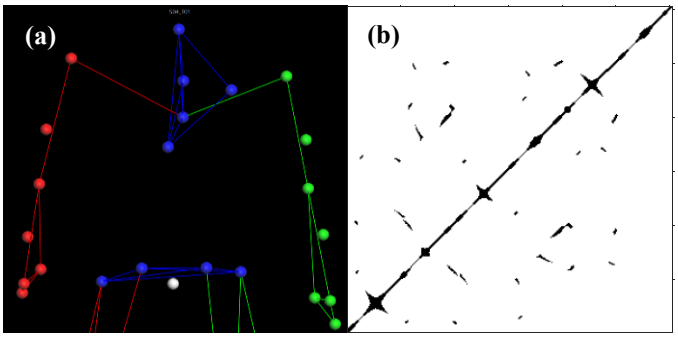

Figure 1: (a) Motion capture markers with COM (white marker) (b) recurrence plot

Results and Discussion

%DET between conditions was not significantly different for the Control group, but a statistically significant difference ($p=0.0032$) was found within the TBI group (Fig 2a). The same is true for LMax with a significant difference ($p=0.0011$) for the TBI group (Fig2b).

%DET measures the predictability of a trajectory and is highest for periodic functions. The predictability of COM movement significantly increased for the TBI group during Narrow walking, showing an improvement in consistency and periodicity across the individual steps. This result may be interpreted as the TBI group gaining better control during narrow walking compared to preferred stride. LMax is a measure of mathematical stability of the data, and larger values show less sensitivity to perturbation [3]. In this case, TBI subjects may have benefited from walking narrowly by decreasing unnecessary movement.

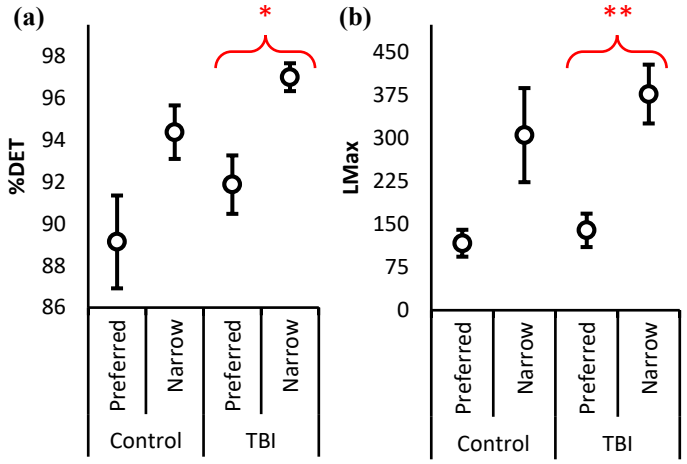

Figure 2: (a) Average determinism values with standard error bars, separated by group and then condition. *Red bracketed pair shows significant difference in mean. (b) Average maximum line length values with standard error bars, separated by group and then condition. **Red bracketed pair shows significant difference in mean.

Significance

Continued research on gait intervention techniques and improved analysis of their success is important to better understand and facilitate the gait recovery process in patients with a history of TBI. Further research could continue to inform clinical practices and help improve quality of life for individuals who have experienced TBI.

Acknowledgments

Hillary Austin and Nilanthy Balendra were instrumental in data collection.

References

1. Bland et al., *Brain Inj*, 2011; 25 (7-8)
2. Marwan et al., *Phys. Rev. E*, 2002; 66 (2)
3. Webber and Zbilut, *Contemp. Nonlinear Method for Behavior. Sci,* 2005; 2 (28)

The relationship between walking coordination and connectivity of motor pathways within lesioned and non-lesioned hemispheres.

Shraddha Srivastava[1,3], Bryant A. Seamon [1, 3], Barbara K. Marebwa[5], Leonardo Bonilha[5], Truman R. Brown[4], Richard R. Neptune[6], Steven A. Kautz [1, 2, 3]
[1] Ralph H. Johnson VA Medical Center, Charleston, SC, USA,
[2] Division of Physical Therapy, College of Health Professions, [3] Department of Health Sciences and Research, College of Health Professions,[4] Department of Neurology, College of Medicine, [5] Department of Radiology and Radiological Science, College of Medicine, Medical University of South Carolina, Charleston, SC, USA.
[6]Department of Mechanical Engineering, The University of Texas at Austin, Austin, TX
Email: srivasts@musc.edu

Introduction

The corticospinal tract (CST) is the major descending motor pathway involved in mediating muscle coordination of skilled movements, but it is possible that CST may not be necessary to control steady-state walking. Previous animal studies support involvement of corticoreticular pathway (CRP) during steady state walking, and CST as well as CRP during skilled movements[1]. It is not clear how damage to the CST post-stroke affects muscle coordination and walking ability. The CRP likely plays an important role in locomotor recovery following stroke when there is CST damage[2]. However, CRP produces mass flexion and extension muscle activation patterns (fewer muscle modules) and fewer modules post-stroke is correlated to poor walking performance. **Therefore, to understand the altered neural control of modules on walking ability, we investigated the relationship of module composition and walking ability of stroke survivors with CST and CRP recovery.**

Methods

We recruited 33 stroke survivors and 17 healthy controls. We collected lower extremity Fugl-Meyer Assessment (FMA), Functional Gait Assessment (FGA), six-minute walk test (SMWT), over-ground self-selected (SS) walking speeds from stroke survivors. Paretic leg EMG data were collected at self-selected walking speeds to compute number of muscle modules using non-negative matrix factorization (Fig 1A). Imaging data for all subjects included T1 and T2-weighted images, and diffusion kurtosis imaging (DKI). Tractography was estimated using FSL's FMRIB's Diffusion Toolbox to evaluate the CST and CRP recovery based on number of streamlines (Fig 1B). Spearman's correlation was used to identify the relationship between motor pathways recovery and functional walking ability. One-way ANOVA was used to identify differences in CST and CRP recovery between stroke survivors with 2, 3, and 4 modules (typically healthy individuals have 4 modules).

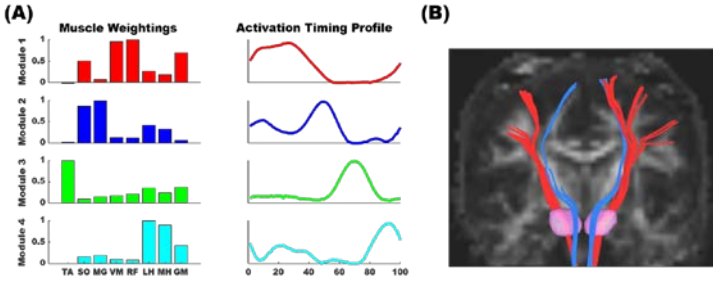

Figure 1: A) Non-negative matrix factorization to identify modules during walking. B) Motor Pathway Connectivity for CST (streamlines between cotex and midbrain cerebral peduncle) and CRP (streamlines between cotex and midbrain reticular formation).

Results and Discussion

We found a positive correlation between CST from the lesioned hemisphere and FGA ($r=0.39$ $p<0.05$); and FMA ($r=0.36$ $p<0.05$). We found a negative correlation between CRP from the non-lesioned hemisphere and FMA ($r=-0.43$ $p<0.05$); and SMWT ($r=-0.37$ $p<0.05$). This suggests that poorer walking ability is related to increased reliance on the non-lesioned CRP following damage to CST. We did not see any significant relation between module number and CST or CRP. However, there was a trend suggesting more CST streamlines on the non-lesioned hemisphere maybe associated with fewer modules ($r=-0.29$ $p=0.09$). There was also an asymmetry in number of streamlines between the hemispheres in stroke population compared to healthy individuals computed as ($Assym_{Stroke=}$ Lesioned/Non-lesioned; $Assym_{Healthy=}$ Right/Left), ($CST_{Healthy}$:1.47, CST_{Stroke}:0.44, $p<0.001$; $CRP_{Healthy}$:1.28, CRP_{Stroke}:0.69, $p<0.01$). In summary, non-lesioned CST and CRP may compensate for the lesioned CST. Furthermore, greater reliance on the motor pathways from the non-lesioned hemisphere is associated with greater impairment of walking ability and poor muscle coordination (fewer modules).

Significance

The current work seeks to extend the understanding of the associations between recovery of motor pathways and steady-state muscle coordination to more complex tasks fundamental to household and community walking, such as speeding up, slowing down, starting, stopping and turning. Results from this work will be used to identify patient-specific deficits in muscle coordination and their impact on limiting household and community walking. We expect clinicians will use this information to understand mobility task requirements and develop individualized targeted therapies.

Acknowledgments

National Institutes of Health (NIH P20 GM109040), VA/ORD Rehabilitation R&D Service (1I01RX001935), PODS I. Any opinions expressed in this presentation are those of the authors and do not necessarily reflect the view of the U.S. Department of Veteran Affairs, NIH or Foundation for Physical Therapy Research.

References

1. Drew et. al (2004)
2. Jang et. al (2013)

Verbal Instructions and Feedback Enhance Motor Learning During Post-Stroke Gait Retraining

Nicole K. Rendos, Laura Zajac-Cox, Rahul Thomas, Sumire Sato, Steven Eicholtz, Trisha M. Kesar
Emory University School of Medicine, Department of Rehabilitation Medicine, Atlanta, GA
Email: nrendos@emory.edu

Introduction

Restoration of walking function is an essential component of neurorehabilitation in individuals who have survived a stroke. Post-stroke gait deficits include reduced paretic propulsion during terminal stance, foot drop during swing, and inter-limb asymmetry with a reduction in gait speed. FastFES, a post-stroke training intervention that combines functional electrical stimulation (FES) delivered to the paretic ankle dorsiflexor (DF) and plantarflexor (PF) muscles during fast treadmill walking, has been shown to induce long-term improvements in gait speed and reduce the energy cost of walking,[1] yet the motor learning processes underlying FastFES are currently poorly understood.

During neurorehabilitation, verbal instructions and feedback regarding motor performance are commonly used to promote motor learning.[2-4] Feedback provides information based on previous movement attempts with the intent to decrease movement errors and facilitate achievement of accurate movement goals.[2] Instructions include statements about how to perform a motor task and/or its desired outcome.[2] The purpose of the study was to determine whether the addition of verbal feedback and individual-specific instructions, which are commonly incorporated during clinical gait training, would augment motor learning of gait patterns induced by FastFES.

Methods

Nine individuals with post-stroke hemiparesis (4 M, 59.0 ± 7.4 y, 35.9 ± 21.1 months post-stroke) completed a crossover study comprising exposure to 2 types of gait training sessions with > 3 weeks between sessions. The first training session involved five, 6-min bouts of FastFES (FF). The second training session was conducted ≥ 3 weeks after FF. Procedures were identical to FF but included the addition of individualized verbal instructions and feedback regarding gait performance from an experienced physical therapist (FF+PT). Non-scripted, individual-specific feedback focused on the variables targeted by FF was provided in a faded schedule throughout the training session.

Gait biomechanics data were measured before (Pre) and immediately after each training session (Post) to evaluate within-session changes, and during a Retention test conducted 24 hours after the training session to evaluate motor learning. A 7-camera Vicon system and a Bertec instrumented treadmill were used for gait analysis. Dependent variables included push-off integral (POI), trailing limb angle (TLA), and ankle angle at initial contact (AAIC) of the paretic limb. Within-Session (Post-Pre) and Retention (Retention–Pre) change scores were calculated to assess online performance and motor learning. Repeated measures ANOVAs examined the effects of training type and time on each variable. Paired samples t-tests were conducted to examine the effects of training type on change scores.

Results and Discussion

For POI, we observed a significant main effect of training type ($F_{(1,8)} = 6.93$, $p = .030$, $\eta_p^2 = .464$), and a significant training type x time interaction ($F_{(2,16)} = 4.66$, $p = .025$, $\eta_p^2 = .368$). Compared to Pre, TLA was significantly greater at Post ($M_{diff} = 2.69$, $SE = .0741$, $p = .007$, g = .30) and Retention ($M_{diff} = 2.39$, $SE = .90$, $p = .029$, $g = .28$) for FF+PT. TLA retention change scores were greater for FF+PT compared to FF ($t(8) = 2.41$, $p = .043$, $g = 1.19$). At Post, AAIC were more plantarflexed than Pre for both FF and FF+PT ($M_{diff} = -1.60$, $SE = 0.62$, $p = .033$).

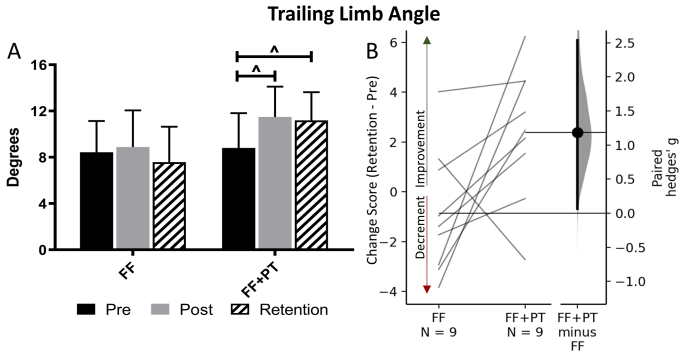

Figure 1. (A) During FF+PT, we found increase in TLA at both Post and Retention compared to Pre, indicating online improvements and motor learning (B) TLA retention change scores were significantly greater for FF+PT versus FF.

Addition of individualized verbal instructions and feedback by a physical therapist (FF+PT) resulted in greater online improvements and motor learning (Retention) of improved gait biomechanics in response to a single training session. Though 12 weeks of FastFES training have been shown to improve walking speed, endurance, energy efficiency, and gait biomechanics post-stroke,[1,5,6] a single session of FF did not induce significant within-session improvements or across-session retention. However, a single session of FF+PT induced significant within- and across-session improvements in TLA and POI, suggesting that addition of individualized verbal instructions and feedback may augment motor learning processes during gait training.

Interestingly, AAIC displayed a within-session decrement for both types of training, which may be related to DF muscle fatigue, further accentuated by non-physiological activation during FES.[7] AAIC is primarily controlled through eccentric contraction of the ankle DF.

Significance

With insurance payers limiting the dosage of gait training sessions, developing clinical strategies to maximize motor learning within each treatment will have significant clinical impact.

Acknowledgements

NIH NICHD R01 HD095975; NICHD K01 HD079584; AHA Scientist Development Grant 13SDG13320000

References

[1] Awad LN, et al. *Arch Phys Med Rehabil.* 2014; 95(5):840-48. [2] Johnson L, et al. *Phys Ther*. 2013; (93)7:957-66. [3] Wulf G, et al. *J Exp Psychol Learn*. 1992; 19(5):1134-50. [4] Durham, et al. *Physiother Res Int*. 2009; 14(2):77-90. [5] Reisman, et al. *J Neurol Phys Ther*. 2013; 37(4): 159-65. [6] Reisman, et al. *Top Stroke Rehabil*. 2013; 20(2): 161-70. [7] Chou LW, et al. *Clin Neurophysiol*. 2007; 118(6): 1387-96.

Combination of Ankle Muscle Functional Electrical Stimulation (FES) & Fast Treadmill Walking Therapy Effect on Post-Stroke Motor Control

Ashley E. Rice*[1], Jill S. Higginson[2], Jeffrey A. Reinbolt[1]
[1]Department of Mechanical, Aerospace, and Biomedical Engineering, University of Tennessee-Knoxville
[2]Department of Mechanical Engineering, University of Delaware
Email: arice22@vols.utk.edu

Introduction

Nearly 800,000 people experience a stroke annually in the US alone [1], and frequently survivors are left with the sudden onset of difficulties completing daily motor tasks [2]. Of particular concern are the dynamic changes that occur to a stroke survivor's gait pattern. Walking is the primary locomotion strategy used by individuals to navigate their environments, and when this ability is compromised, so is the overall quality of life. Gait impairments reflect motor control changes, where unimpaired gait motions are produced by more complex control schemes than impaired ones [3-6]. Unlike common measures of performance following treatments, such as walking speed, step-length symmetry, paretic propulsion, etc., the Dynamic Motor Control (DMC) Index provides insight about the effect of the treatment at the neural level on motor control complexity, and it has successfully been used for analyzing gait in individuals with cerebral palsy [3, 8].

In this study, we sought to answer two questions: 1. *"How does FastFES treatment (combined Fast treadmill walking and Functional Electrical Stimulation) impact post-stroke motor control, as measured by the DMC Index?"* and 2. *"What are the distinguishing pre-treatment gait features between those that responded to treatment and those that did not?"*

Methods

Using OpenSim 3.3, we created forward dynamic simulations tracking gait data of 8 individuals post-stroke [7] with patient-specific musculoskeletal models having 23 degrees-of-freedom and 92 muscles. Computed Muscle Control determined muscle activations of paretic lower-limb muscles, which were then used as inputs to non-negative matrix factorization where only a single module (group of co-activated muscles) was considered [6]. The DMC index is based on the variance accounted for (VAF) by this module in reproducing the original activations signal. A DMC index value of 100 is equal to that of an average unimpaired individual, and smaller DMC index values represent decreased motor control complexity. Following FastFES treatment, individuals were grouped as a *responder* if their DMC index values increased after treatment, and a *non-responder* otherwise.

Distinguishing pre-treatment gait features between the two groups were identified with Statistical Parametric Mapping (SPM), which reduces errors associated with discretized analysis (i.e. selection of instances such as "peak knee flexion") of time-varying data by regarding this data as a single observation [9, 10].

Results and Discussion

The FastFES treatment increased the DMC index in 5 of the 8 individuals (Fig. 1a, green). Interestingly, the 3 non-responders (Fig. 1a, red) had the highest pre-treatment DMC index values. These results suggest that the treatment *is* effective at increasing motor control, but *only if the individual's motor control is sufficiently impaired*. Individuals with moderate motor control impairment may not benefit from this treatment. Furthermore, we identified larger ($p < 0.001$) pre-treatment knee flexion during 20-40% of gait (Fig. 1b, blue) and smaller ($p < 0.001$) support moment (sum of the sagittal-plane moments of the hip, knee, and ankle) [11] between 30-40% of stance (Fig. 1c, blue) in the responders.

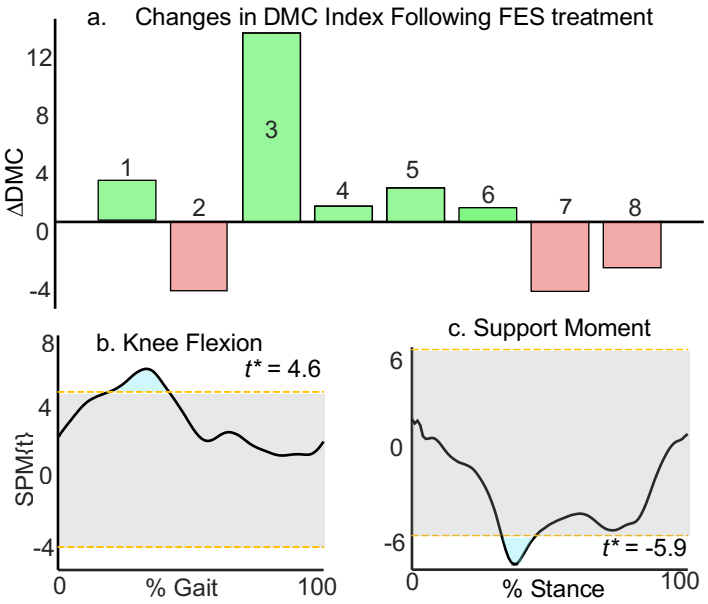

Figure 1: *Variation in treatment response and distinguishing pre-treatment gait features*. a. responders exhibit ΔDMC > 0 and non-responders ΔDMC < 0; b. Responders have larger knee flexion during 20-40% of gait; c. Responders have smaller support moments during 30-40% of stance.

Significance

While our findings are specific to one treatment for post-stroke gait, the approach may be extended to other treatments and disorders. Quantifying treatment response in terms of motor control complexity provides useful information on whether the treatment is targeting the source of the impairment at the neural level. Identifying pre-treatment gait features that distinguish responders and non-responders not only allows for treatment outcome predictions, but clinicians can also learn about what areas to target for specific cases.

Acknowledgments

We would like to acknowledge NIH NR 010786 for funding the collection of the FastFES data.

References

[1] Centers for Disease Control and Prevention.
[2] National Stroke Association.
[3] Schwartz MH, et al. Dev Med and Child Neuro, 2016.
[4] Steele KM, et al. Front Comp Neuroscience, 2013.
[5] Clark DJ, et al. J Neurophys, 2010.
[6] Allen JL, et al. Clinical Biomech, 2013.
[7] Knarr BA, et al. J NeuroEngr and Rehab, 2013.
[8] Steele KM, et al. Dev Med and Child Neuro, 2015.
[9] Donelly CJ, et al. Clinical Biomech, 2017.
[10] Pataky TC. Comp Methods in Biomech and Biomed Engr, 2012.
[11] Winter DA, J Biomech, 1980.

Turning Speed and Performance During a Simulated Urban Patrol Task in People with Mild Traumatic Brain Injury

Peter C. Fino[1], Lee E. Dibble[2], Mark E. Lester[3,4], Lucy Parrington[5], Margaret M. Weightman[6], Laurie A. King[5]
[1]Department of Health, Kinesiology, and Recreation, University of Utah
[2]Department of Physical Therapy & Athletic Training, University of Utah
[3]Department of Physical Therapy, Texas State University
[4]Army-Baylor University Doctoral Program in Physical Therapy
[5]Department of Neurology, Oregon Health & Science University
[6]Courage Kenny Research Center, Allina Health
Email: peter.fino@utah.edu

Introduction

Determining readiness for duty after mild traumatic brain injury (mTBI) is essential for the safety of service members (SM) and their units. Though the ability to perform warrior tasks and battle drills, such as moving under fire while maintaining situational awareness, reacting to contact, and establishing security are critical components of combat effectiveness and survival [1], these aspects are not currently assessed after mTBI. Return-to-duty decisions are based on self-reported symptoms and single-domain clinical tests of function. There is a need for objective tests that are sensitive to mTBI-related deficits, and a need to understand how mTBI affects functional performance in theater.

Turning is an ecologically-relevant task involving coordinated movement of the head and body that can be objectively quantified using inertial measurement units. We have previously found people with mTBI turn slower and have more variable head-body coordination patterns than healthy controls during a clinical turning task [2]. However, the implications of these results remain unclear. Therefore, the purpose of this study was to examine turning behaviour during a task representative of the complex demands a SM may face in theatre. We expected individuals with mTBI to turn slower and to perform significantly worse compared to healthy control subjects.

Methods

Participants included 44 individuals with mTBI [34F/10M, mean age (SD) 33 (10) yrs] and 40 healthy controls [28F/12M, mean age (SD) 31 (10) yrs] across three sites. All mTBI participants were greater than 3 weeks post-injury and reporting residual symptoms. All participants provided informed written consent in accordance with this IRB approved study.

Participants completed a simulated urban patrol task (SUP) that consisted of navigatinga small room containing LED targets representing hostile (red) and friendly (blue) targets. Using a laser-tag weapon, participants were instructed to clear all hostile targets as quickly as possible without tagging friendly targets. Three SUP trials were completed; hostile and friendly targets were changed between trials. Performance was quantified using a hit score (total points / total time).

Inertial measurement units (APDM Opals, Portland, OR) on the lumbar, sternum, and forehead collected angular velocity data at 128 Hz. A $\pm\pi/4$ rad/s threshold identified head, trunk, lumbar, head-on-trunk, and trunk-on-lumbar yaw turns. For each turn, the peak angular rate for each turn was determined. The median of turning speeds at each segment were calculated within a trial and were compared across groups using linear mixed effects regression with random intercepts by subject. Additionally, outcomes were averaged across trials and linear regression models compared the association between turning metrics and task performance after controlling for group using R^2 values.

Results and Discussion

Head-on-trunk ($p = 0.007$) and head-on-lumbar ($p = 0.012$) turns were significantly slower in the mTBI group compared to healthy controls. No between-group differences were observed in other metrics of turning. Compared to controls, the mTBI group completed the task slower ($p = 0.022$) and had lower hit scores ($p = 0.027$). Across all turning measures, slower turning speeds were associated with lower hit rates; lumbar turning speed (adj. $R^2 = 0.37$), head-on-lumbar turning speed (adj. $R^2 = 0.24$), and head-on-trunk turning speed (adj. $R^2 = 0.21$) were most associated with hit rate after adjusting for group.

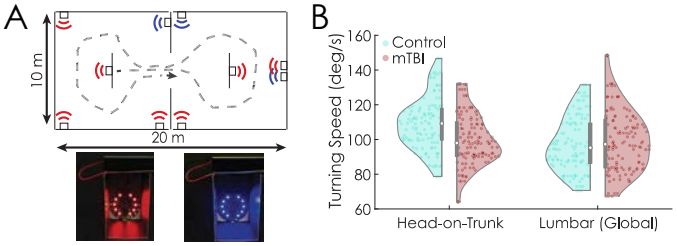

Figure 1: A. Schematic of the testing set-up with sample target configuration. B) Selected results of head-on-trunk and lumbar turning speeds for each group. Head-on-trunk turns were slower in the mTBI group, but lumbar turning speeds did not differ between groups.

The group differences in segmental head-on-turnk and head-on-lumbar turning speeds are consistent with previous reports of slower head turns in acute mTBI [3], but we were surprised overall turning speeds at the trunk and lumbar were not different given previous studies [2]. The group-difference in hit rate suggests the ability to freely move one's head are important for this warfighter tasks and may be impaired in those with mTBI. Future work should examine whether the poorer performance and slower completion times in mTBI participants stem from decreased perceptual awareness due to slower independent head motion.

Significance

Individuals with persisting symptoms after mTBI exhibited performance deficits and slower intersegmental head rotations in a high-fidelity, ecologically relevant task for SMs.

Acknowledgments

Supported by the Department of Defense through the CDMRP under Award No. W81XWH1820049.

References

1. Scherer, et al. Phys Ther, 93:1254-67, 2013.
2. Fino, et al. J Neurotrauma, 35, 1167-77, 2018
3. Fino, et al. J Head Trauma Rehabil, 34, E74-81, 2019

Is Faster Always Better? A Subgroup Analysis of the Effects of Walking Speed on Post-Stroke Gait Biomechanics

Hannah Christianson, Payton Sims, Justin Liu, Brandon Choi, Carol Ann Elliott, Alex Schilder, Benjamin Koke, Trisha M. Kesar
Emory University School of Medicine, Department of Rehabilitation Medicine, Atlanta, GA
Email: tkesar@emory.edu

Introduction

Restoration of walking function is an essential component of stroke rehabilitation. Common post-stroke gait deficits include decreased paretic leg push-off during late stance, foot drop, and inadequate hip, knee and ankle flexion during swing. These deficits lead to compensations such as hip circumduction or pelvic hiking, as well as reduced gait speed, endurance, and energy efficiency, contributing to diminished community participation and quality of life post-stroke[1].

During stroke rehabilitation, clinicians commonly rely on treadmill-based gait training due to the ability to modulate speed and inclination, promote mass stepping practice, and encourage faster walking on a safe, predictable terrain[2]. Previous research suggests that training at faster speeds is an evidence-supported strategy to improve post-stroke gait deficits and function[3-5]. However, gait speed and gait quality may interact in complex ways, which warrants investigation. Here, we comprehensively examined the effect of speed on biomechanics of the paretic leg, non-paretic leg, and inter-limb asymmetry post-stroke.

Methods

Fourteen individuals post-stroke (10 males, 60 ± 11 years, 41 ± 32 months post-stroke) participated in one session of treadmill walking on a dual-belt treadmill embedded with force platforms to enable collection of ground reaction force (GRF) data from each limb. Reflective markers were attached to the trunk, pelvis, and bilateral thigh, shank, and foot segments. Marker data were collected via a 7-camera Vicon system and processed in Visual 3D. Kinematic and kinetic gait biomechanics parameters were measured at 6 different speeds ranging from each individual's self-selected to their fastest walking speed. Dependent variables included ankle push-off (anterior or AGRF), trailing limb angle (TLA), ankle angle at initial contact, peak ankle moment, ankle power, hip power, circumduction, and pelvic hiking. Participants were further sub-grouped into low or high-functioning using gait speed of 0.4 m/s as a cutoff. For each dependent variable, 2-way between-within ANOVAs evaluated the effect of speed (6 speeds ranging from SS to Fast), sub-group (high-functioning, low-functioning), and interaction effects. Planned post-hoc independent t-tests compared each variable between the high- and low-functioning sub-groups at the Fast and SS speeds. Repeated measures ANOVAs were performed to assess the effect of speed separately within each sub-group.

Results and Discussion

For paretic leg push-off, we found a significant main effect for speed ($F=12.312$, $p<0.001$), sub-group ($F=8.833$, $p=0.012$), and a significant interaction ($p=0.001$). A significant main effect of speed for paretic push off occurred in the high-functioning sub-group ($F=21.013$, $p<.001$), but not the low-functioning sub-group ($F=2.198$, $p=.081$). For TLA, both sub-groups showed a main effect of speed, with TLA being greater for the high- than low-functioning sub-groups at both Fast ($p=.012$) and SS speeds ($p=.049$). For ankle moment and power, both groups showed a main effect of speed ($p<0.001$). Ankle moment, ankle power, and hip power were significant larger for high-functioning versus low-functioning sub- group for both Fast ($p<0.01$) and SS speeds ($p<0.02$). There was no main effect of speed for either sub-group on ankle angle at initial contact ($F=1.249$, $p=.240$), but an interaction was present ($p=0.042$). Circumduction worsened as speed increased for both sub-groups ($F=5.690$, $p=.001$), ($F=2.595$, $p=.046$). The high-functioning sub-group failed to show a significant main effect of speed on pelvic hiking ($F=.703$, $p=.625$), but the low-functioning sub-group showed a main effect of speed ($F=3.464$, $p=.014$).

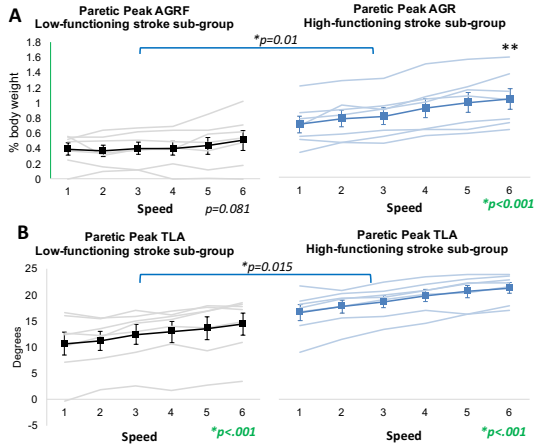

Figure 1. Group (bold lines and symbols) and individual subject data for the 2 stroke sub-groups at 6 different speeds. (A) Peak paretic AGRF did not increase with faster speeds (x-axis) in the low-functioning group ($p=0.081$), but speed did induce AGRF increases in the high-functioning group ($p<0.001$). (B) Both low- and high-functioning individuals increased TLA with faster speed (p's<0.001). Both AGRF ($p=0.01$) and TLA ($p=0.015$ showed a main effect of group.

Interestingly, when stroke survivors were stratified into sub-groups using baseline walking speed, unlike the high-functioning group, for lower-functioning post-stroke individuals, faster gait speeds were not accompanied by improved paretic leg pushoff, and worsened asymmetry and compensatory patterns (circumduction and pelvic hiking).

Significance

We evaluated gait biomechanics across multiple speeds with systematic increments to assess interactions between stroke gait biomechanics and gait speed. Our results demonstrate that baseline walking function influences the effects of gait speed on gait quality (biomechanics). Our findings may have implication for developing individual-specific, data-driven criteria for the selection of training speeds for post-stroke gait rehabilitation.

Acknowledgements

NIH NICHD R01 HD095975; NICHD K01 HD079584 (Kesar)

References

1. Von Schroder HP, et al. *J Rehabil Res Dev.*1995.32(1):25-31.
2. Silver KH, et al. *Neurorehab Neur Rep.*2000.14(1):65-71.
3. Bowden MG, et al. *Neurorehab Neur Rep.*2008.22(6):672-75
4. Awad LN, et al. *Neurorehab Neur Rep.*2015.29(5):416-23.
5. Lamontagne and Fung. *Stroke.*2004.35(11):2543-48

Simulation-based Predictions of Gait Patterns with Muscle Strength Asymmetries

Russell T. Johnson and James M. Finley
Division of Biokinesiology and Physical Therapy, University of Southern California, Los Angeles, CA
Email: rtjohnso@usc.edu

Introduction

Many neuromuscular impairments occur after an individual has a stroke, such as muscle weakness, spasticity, overactivity, and paresis, most of the time primarily affecting one side of the body. These impairments can impact gait performance, as people post-stroke walk slower than controls and display spatiotemporal and kinematic asymmetries [1]. However, since various combinations of these neuromuscular impairments are often present in people post-stroke, it is difficult to determine the relative contributions of these impairments to gait performance.

Musculoskeletal modeling and predictive simulation provide an opportunity to investigate how specific neuromuscular impairments affect gait performance. Our aim was to quantify the spatiotemporal asymmetries and changes in metabolic cost of transport (COT) that emerge from predictive simulation when muscle strength is unilaterally reduced in a musculoskeletal model. This study will allow us to better understand how muscle strength impairments impact gait performance, independent of other neuromuscular changes that occur post-stroke.

Methods

A 2-D musculoskeletal model with 11 degrees-of-freedom and actuated by 42 muscle-tendon units (modified from [2]) was used within OpenSim. The base model was modified by uniformly reducing the peak isometric muscle force in all muscles on the left side of the model by 10, 20, 30, 40, 50, and 60 percent. Optimal control simulations of walking were generated at 1.0 m/s under these seven different conditions using direct collocation with IPOPT [3]. The optimization allowed stride time and length to vary while generating solutions at the set walking speed. The unilateral reduction in muscle strength was intended to model the asymmetry in force generation measured between limbs in people post-stroke. The objective of the optimizations was to minimize the sum of the cubed muscle activations across all muscles, chosen based on its proxy to muscle fatigue.

Outcome measures included asymmetry indices (Asym) for stance time and step length, and were calculated as follows:

$$Asym = \frac{X_{NW} - X_W}{(|X_{NW}| + |X_W|)}$$

Where X_{NW} is the variable for the non-weak limb, and X_W is the variable for the weak limb. Positive values of Asym indicate greater values on the non-weak than the weak side. The other outcome measures were muscle activation cubed (objective function value) and predicted COT based on the Umberger 2010 probe built into OpenSim. The COT was calculated while holding muscle mass constant throughout the conditions.

Results and Discussion

In the optimal control result with the base model (with no strength asymmetry), the model walked with symmetrical stance time and step length. With greater strength asymmetry, the model walked with greater spatiotemporal asymmetry (Fig. 1A, B). The optimal solutions had greater overall muscle activation with greater muscle weakness asymmetry (Fig. 1C), and the metabolic COT gradually increased throughout the conditions. The COT for the model 60 solution was about 10% greater when compared to the solution from the base model.

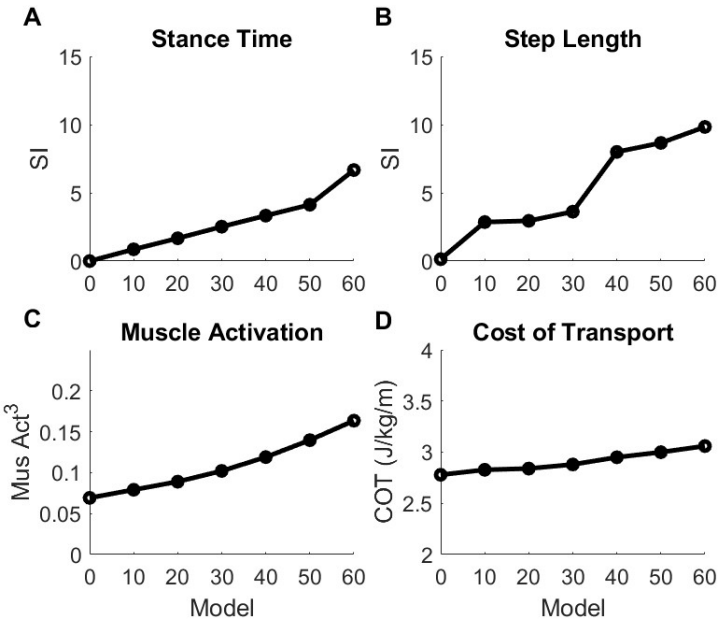

Figure 1: Asymmetry indices (Asym) for the A) Stance Time Asymmetry, B) Step Length Asymmetry. Positive values indicate greater values on the non-weak side than the weak side. C) The sum of muscle activations cubed. D) Cost of transport (COT) computed using OpenSim Umberger probe. Model 0 is the base model, and Model 60 represents a 60% decrease in muscle strength on the left limb.

Our results suggest that the expected level of spatiotemporal asymmetry observed during walking should scale with muscle strength asymmetry. This suggests that independent of other post-stroke impairments, common clinical goals of rehabilitation, which may aim to restore step length and step time asymmetry to patients, may not be energetically optimal if the patient has a lingering strength asymmetry. Furthermore, a unilateral loss in force generating ability may partially explain increases in COT observed in people post-stroke relative to controls [4].

Significance

The most optimal way for people with muscle strength asymmetries to walk is likely not symmetrical, and the level of optimal spatiotemporal asymmetry depends on the level of muscle strength asymmetry between limbs.

Acknowledgments

Funding: NIH NCMRR R01HD091184

References

1. Olney SJ & Richards C, Gait Posture. 4, 136-148, 1996.
2. Porsa S, et al., Ann Biomed Eng. 44, 2542-57, 2015.
3. Lee LF & Umberger BR, PeerJ. 4, e1638, 2016.
4. Finley JM & Bastian AJ, Neurorehab Neural Re. 31, 2. 2017.

Neuromechanical Control of Ankle Joint during Forced Lower Limb Loading in Individuals with Chronic Stroke

Keng-Hung Shen[1], Sunil Prajapati[1,2], James Borrelli[3], Vicki Gray[3], Mark W. Rogers[3], Hao-Yuan Hsiao[1,3]

[1]*Department of Kinesiology and Health Education, University of Texas at Austin, Austin, TX, USA*
[2]*Department of Applied Physiology and Wellness, Southern Methodist University, Dallas, TX, USA*
[3]*Department of Physical Therapy and Rehabilitation Science, University of Maryland Baltimore, Baltimore, MD, USA*

Email: kenghung.shen@utexas.edu

Introduction

Lower limb loading and weight transfer abilities are associated with walking speed and risk of falling in individuals post-stroke (Hsiao et al., 2017; Pavol et al., 2007). Functional weight transfer requires coordination between multiple joints to regulate impact force, prevent limb collapse, and support body weight during loading impact. The ankle joint plays a major role during ground impact energy absorption (Farley et al., 1998). After stroke, deficits in ankle muscle activation and torque production have been documented (Kitatani et al., 2016). It is unclear how these deficits affect loading reactions. Studying lower limb loading capacity in individuals post-stroke is limited partly due to the tendency to avoid fully loading the paretic limb during voluntary movements. Accordingly, a novel perturbation was used to induce rapid loading of the lower limbs in this study. The primary purpose of this study was to characterize the ankle joint torque/power generation capacity and neuromuscular activity during impact absorption in response to imposed unilateral loading in individuals post-stroke compared to able-bodied age-matched controls.

Methods

Fifteen individuals with chronic stroke and fifteen age-matched able-bodied controls participated in this study. Participants stood with each foot on top of a perturbation platform. Five unilateral support surface lowering perturbation trials were delivered at an unpredictable time to each leg in a randomized order.

Kinematic data were collected via a 10-camera motion analysis system (Vicon, UK). Following perturbation onset, sagittal plane average ankle joint torque, angular velocity, power, and work were calculated from maximum plantarflexion to maximal dorsiflexion (impact absorption phase).

Electromyographic data were collected via surface electrodes (Noraxon, US) placed on the Tibialis Anterior (TA) and Medial Gastrocnemius (MG) muscles. Baseline muscle activity is acquired from 200ms - 300ms before perturbation onset, and muscle activation is defined by 3 standard deviation over baseline. Data were averaged across trials for each subject and data from the paretic limb in stroke were compared with non-dominant limb in controls using 2-tailed t-tests.

Results and Discussion

Preliminary results for 11 individuals post-stroke (64.7±8.3 yrs old, 4 females, time since stroke 16.1±13.9 yrs) and 9 controls (66.2±7.0 yrs old, 4 females) were analyzed to date. The duration of impact absorption phase was not different between groups (214.7±75.6 ms in control and 247.5±84.3 ms in stroke). During impact absorption, the stroke group showed reduced ankle work and power production compared to controls (Fig.1), indicating reduced energy absorption by the ankle joint. Ankle plantarflexion torque and angular velocity were similar between groups.

A trend of longer muscle co-activation duration between TA and MG was observed in stroke compared to controls ($p = 0.10$). The prolonged muscle co-activation was likely due to longer activation duration of the TA ($p = 0.12$), while the activation duration of MG was similar between groups (Fig.2). Prolonged co-activation of the ankle muscles may reduce the power production and limit energy absorption ability in the ankle joint after stroke.

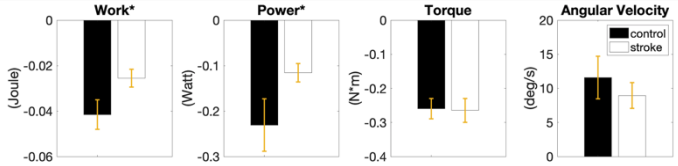

Figure 1: Between-group comparisons of kinetic and kinematic measurements of the ankle joint. For joint torque and angular velocity, negative values indicate ankle plantarflexion. * indicates $p < 0.05$.

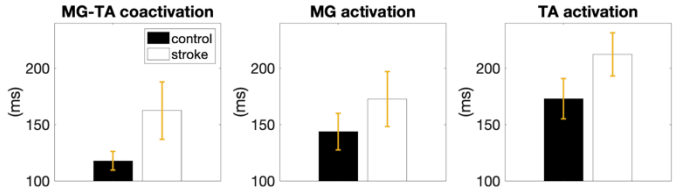

Figure 2: Ankle muscle activation duration during impact absorption.

Significance

A novel approach was used to characterize ankle joint power generation and neuromuscular activity following rapid unilateral lower limb loading. Preliminary results suggest that when impact loading was induced to the paretic limb, individuals post-stroke showed reduced ability to absorb energy with the ankle joint. In addition, prolonged ankle muscle co-activation may have contributed to limited energy absorption. We anticipate that these trends differentiating those with chronic stroke from healthy controls, will be sustained and achieve statistical significance when additional data are analyzed. Future research will determine whether these abnormalities could be modulated through repeated induced limb loading training.

Acknowledgments

[1] NIH 1R21AG060034-01 to VLG and MWR
[2] Texas New Scholar Recruitment Fellowship to K-H S

References

[1] H. Hsiao et al. (2017) *J Biomech.* ***60****:72-78*
[2] M. Pavol et al. (2007) *J Biomech.* ***40(6)****: 1318–1325*
[3] C. Farley et al. (1998) *J Appl Physiol* ***85(3)****:1044-55*
[4] R. Kitatani et al. (2016) *Gait Posture* ***45****:35-40.*

Functional Level Alters the Impact of Assistive Device Use on Propulsive Impulse Post-Stroke

Erica A. Hedrick[1], Russell Buffum[1], Darcy S. Reisman[2], Samuel Bierner[3], and Brian A. Knarr[1]
[1]University of Nebraska at Omaha, Omaha, NE, USA,
[2] University of Delaware, Newark, DE, USA, [3]Nebraska Medicine, Omaha, NE, USA
Email: ehedrick@unomaha.edu

Introduction

Stroke is the primary cause of long-term adult disability in the United States [1]. Walking is a major goal of rehabilitation, and a common intervention is increasing paretic (weak side) propulsion [2]. During rehabilitation, assistive devices such as treadmill handrails or a cane are commonly utilized. Research has demonstrated that these devices alter biomechanics such as step symmetry [3] and energy cost [4] when using handrails, and braking assistance when using a cane [5]. How functional ability affects the interaction of assistive device and propulsive impulse is unknown, and subsequently, there are no quantitative guidelines on how to utilize these devices to maximize a patient's paretic propulsion. Therefore, the purpose of this study is to determine the effect of assistive device use, such as cane or handrails, on propulsive impulse in individuals post-stroke with varying functional levels and experience with assistive devices. We hypothesized that individuals dependent on assistive devices will have increased propulsive impulse with the assistive device and those not device dependent will have increased propulsive impulse without the device. We further hypothesize that assistive device anterior impulse generated on a handrail will be greater than on a cane.

Methods

Six participants (3M, 3F; age 63.33±14.01 yrs.; 1.07±1.00 yrs. since stroke) from an ongoing study with different levels of function were included in this analysis: no history of assistive device use (N=1), past history of an assistive device use (N=2) , and current dependence on an assistive device (N=3). Inclusion criteria included: age 19-80, single-chronic stroke, and ambulatory. Motion capture analysis using a full-body, 65-marker set was done both overground, using in-ground force plates and an instrumented cane, and with an instrumented treadmill and handrails. For the treadmill trials, subjects walked for three walking conditions (3 minutes each): no handrail use, light support handrail use and self-selected handrail device use. For the overground trials, subjects completed three conditions: walking with no cane, walking with a cane using light pressure and walking with a cane comfortably. Real-time feedback of the cane and handrail forces were displayed for the light-support condition on a screen in front of the participant. Two subjects, who were dependent on an assistive device, were only able to complete the handrail and cane conditions. The average paretic propulsive GRF impulse and assistive device anterior force impulse were calculated and were normalized to body weight.

Results and Discussion

The self-selected walking speed was 0.55±0.31 m/s for the overground conditions and 0.38±0.26 m/s for the treadmill conditions. Individuals with a past history of assistive device use tended to produce the most propulsive impulse without a cane, but no assistive device use or current dependence on an assistive device produced more propulsive impulse with the cane (Figure 1). The propulsive impulse generated on the handrail (0.69±0.63% BW) was significantly more than on the cane (0.17±0.12% BW) (p=0.008). For 5 out of 6 subjects, the ratio of cane impulse to propulsive impulse was less than 22%. Conversely, 3 out of 6 subjects (2 device dependent, 1 past history) produced more anterior impulse on the handrails than propulsive impulse from their paretic leg, suggesting these individuals may be utilizing handrails to compensate or replace lower propulsive forces on the paretic limb. These preliminary results suggest that an individual's functional level and experience with the assistive device will change how use of an assistive device will affect propulsive impulse. Further work will include additional subjects and regression modelling based on walking speed and functional level.

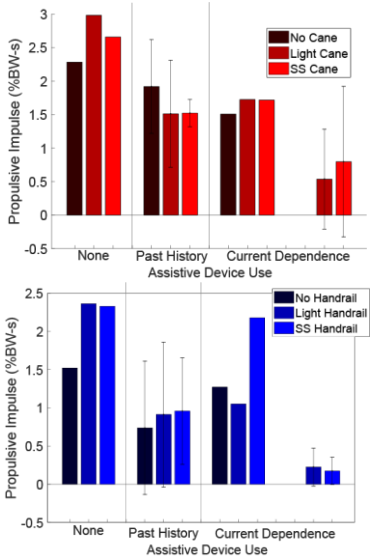

Figure 1: Positive propulsive impulse for assistive device use category, for the overground conditions (red, top) and treadmill conditions (blue, bottom). None (N=1), Past History (N=2), Current Dependence (N=3). Current Dependence are separated because 1 currently dependent subject was able to complete all three conditions, and the other 2 could not complete the no assistive device condition.

Significance

This study aims to provide insight on how best to utilize assistive devices to maximize walking functional recovery for individuals after stroke. Preliminary findings suggest that the amount of propulsive impulse that can be generated with and without an assistive device can inform the amount of assistive device use.

Acknowledgments

This research was funded by the NIH (R15HD094194).

References

1. Duncan PW, et al., *Stroke*,**36**, e100–e143, 2005 .
2. Alingh JF, et al., *Clin. Biomech.*,**71**, 176–188, 2020 .
3. Chen G, et al., *Gait Posture*,**22**, 1, 57–62, 2005 .
4. Ijmker T, et al., *Arch. Phys. Med. Rehabil.*,**94**, 11, 2255–2261, 2013 .
5. Chen CL, et al., *Arch. Phys. Med. Rehabil.*, **82**, 1, 43–48, 2001.

Arm Reaching Controlled by a Tongue-operated Exoskeleton System

Zhenxuan Zhang[1], Maysam Ghovanloo[2], Minoru Shinohara[3], Andrew Butler[4], and Boris I. Prilutsky[3]
[1]School of Electrical and Computer Engineering, Georgia Institute of Technology, Atlanta, GA 30308 USA
[2]Bionic Sciences Inc., Atlanta, GA, USA
[3]School of Biological Sciences, Georgia Institute of Technology, Atlanta, GA 30332 USA
[4]School of Health Professions, University of Alabama, Birmingham, AL 35294, USA
Email: boris.prilutsky@biosci.gatech.edu

Introduction

Stroke is the leading cause of adult disability in the United States [1]. Robotic rehabilitation with self-initiated and assisted movements is a promising technology for upper limb stroke rehabilitation [1]. We have developed a novel tongue-operated robotic system (TDS-KA) for stroke rehabilitation that integrates the tongue drive system (TDS) [3] and a bimanual upper extremity exoskeleton KINARM (BKIN, Canada) [4]. Our working hypothesis is that the voluntary initiation and control of movement in the paretic arm by the normally functioning tongue may help improve arm motor function. The close proximity of brain representations of the tongue and arm may also contribute to arm functional recovery [5]. In order to design appropriate rehabilitation interventions with the TDS-KA system, we characterized arm reaching kinematics of healthy subjects in 4 modes of TDS-KA operation.

Methods

All experimental procedures were approved by the Georgia Tech Institutional Review Board. A group of healthy participants (n=10) of both sexes were instructed to perform multiple accurate and fast unidirectional left-right reaching movements between two anterio-posterior lines with different width and inter-line distances. Four movement modes were tested: (A) the dominant right arm movement (active control), (AV) active control with viscous resistance, (DT) the relaxed arm moved by the TDS-KA system via the tongue motion (discrete tongue control) and (PT) proportional tongue control. Mode A corresponds to a normal arm movement. In mode AV, the robot generates resistive force as a function of the arm endpoint velocity. In mode DT, a discrete command (left or right) is issued by the tongue and the robot moves the arm endpoint in the corresponding direction with an average velocity of 0.1 m/s and bell shaped velocity profile to the end of movement range. When the command is interrupted, the robot will come to a stop as velocity decreases linearly. In mode PT, the instantaneous tongue position is mapped to the force applied to the endpoint of exoskeleton arm.

We recorded tongue tip kinematics using a disk-shaped magnetic tracer glued to the tongue tip and magnetic sensors mounted on a headset. For each subject, a total of 18 trials were collected for each of 4 modes and each reaching distance-target width pair: 24 cm-3 cm, 24 cm-1.5 cm, 12 cm-3 cm, and 12 cm-1.5 cm. Hand kinematics were characterized by throughput [7], arm endpoint jerk cost, conformity to Fitts' Law [7] and symmetry of the arm endpoint velocity profile.

Results and Discussion

The throughput and jerk cost in PT mode were greater than in DT mode and closer to those in A and AV modes although still smaller ($p<0.05$, Figure 1 a, c). The Pearson coefficients of correlation between indeces of difficulty and average movement times were between 0.86 and 0.93 for all modes of operation, confirming Fitts' Law (Figure 1b). Velocity profile of PT mode was comparable to A and AV modes with symmetry relatively close to 0.5 (equal times of the velocity increase and decrease), whereas DT profile was highly assymetric ($p<0.05$, Figure 1d).

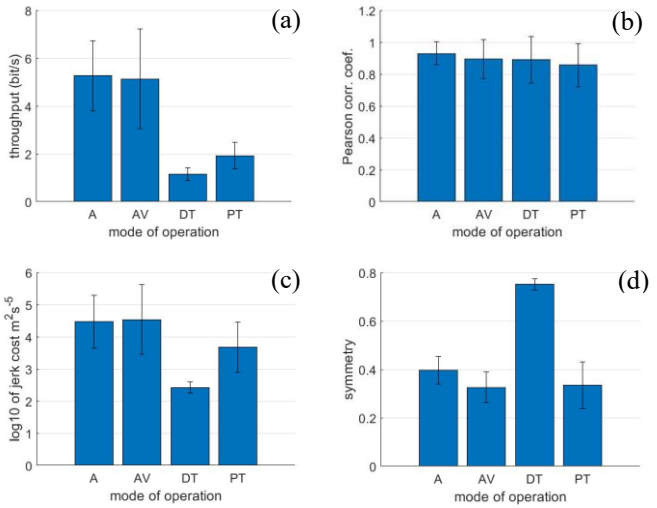

Figure 1: Hand kinematics during reaching movements generated by four control modes of the TDS-KA system. (a) Throughput, (b) Pearson correlation coefficient between indeces of difficulty and average movement times, (c) jerk cost, and (d) hand velocity profile symmetry.

Significance

In this study, we have characterized arm reaching kinematics in 4 modes of TDS-KA operation. We found that the PT mode is more similar to A and AV modes compared to DT. This result indicates that the PT control strategy is a better candidate than the DT for the tongue assisted rehabilitation**.** This study also provides initial insights into possible kinematic similarities between tongue-operated and voluntary arm movements. Furthermore, the results show that the viscous resistance to arm motion does not affect significantly kinematics of arm reaching movements.

In the future studies, we plan to increase the accuracy of the TDS-KA system and to develop a new operation mode of the two-dimentional proportional control by a combination of hardware and algorithm improvements. In addition, we will develop new rehabilitation interventions based on the TDS-KA system and test them in stroke survivals with severe paresis.

References

[1] Benjamin et al. *Circulation*, 136: e229-e277, 2017.
[2] Blank et al. *Curr Phys Med Rehabil Rep*. 2:184-195, 2014.
[3] Kim et al. *Sci Transl Med* 5:213ra166, 2013.
[4] Zhang et al. *Arch Phys Med Rehab* 98: e163, 2017.
[5] Mikulis et al. *Neurology* 5:794-801, 2002.
[6] Funk et al. *NeuroImage* 43:121-127, 2008.
[7] Yousefi et al. *IEEE Trans Inf Technol Biomed 15:747, 2011*.

Abnormal coordinataion of the multiple upper-limb joints during passive movement

Kyung Koh[1], Dongwon Kim[1], Giovanni Oppizzi[1], Li-Qun Zhang[1]

[1]Physical Therapy and Rehabilitation Science, University of Maryland, Baltimore, MD, USA
Email: l-zhang@som.umaryland.edu

Introduction

Motor impairment in upper limb (UL) is one of the most common deficits after stroke. Even though understanding of UL coordination deficits in persons with strokes are crucial for better identification of motor recovery as well as rehabilitation, it is still not clear how stroke affects coordination patterns of multi-joint movements in UL[1]. Here, we investigated kinematic and kinetic coordination patterns of UL after stroke during passive arm movement. We hypothezed that abnormal coordination patterns would be more severe during outward movement (i.e. away from the body) as compared to inward movement (i.e. toward the body) due to stroke accompanied by flexor spastic hypertonia of UL.

Methods

10 stroke surviors (sex (F/M): 2/8; impaired side (L/R): 7/3) and 10 age-matched control subjects (sex (F/M): 2/8) were recruited for this study. All the control subjects were right-handed. Using the rehabilitation robot called IntelliArm, all subjects were asked to sit upright comfortably, and to put the upper arm, forearm and hand on IntelliArm (Fig. 1a) [2]. IntelliArm produces simultaneous passive movements at shoulder, elbow, and wrist joints during inward and outward directions. Each joint was moved until it reaches pre-specified limits for either the joint resistance torque or angular position. Torque and angular position limits were set to be ±3 N·m and 0° to 120° for shoulder horizontal adduction, ±2 N·m and 10° to 90° for elbow flexion/extension, and ±1.5 N·m and -45° to 45° for wrist flexion/extension, respectively. There was 3 seconds holding time at initial position and all movements were performed for 8 repetitions.

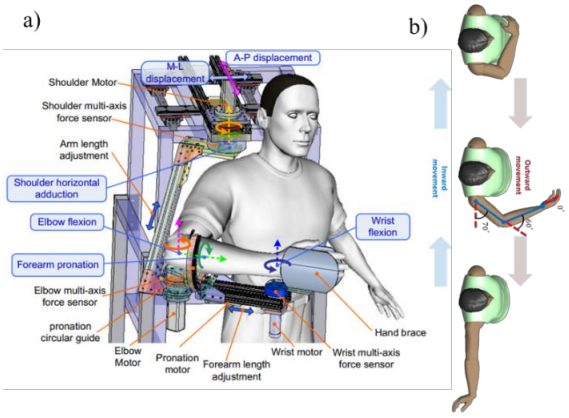

Figure 1: A multi-joint intelligent rehabilitation robot, called IntelliArm was used to control the shoulder, elbow and wrist simultaneously (a). IntelliArm produceed simultaneous movements at shoulder, elbow, and wrist joints, starting to outward direction followed by inward direction.

The uncontrolled manifold (UCM) analysis was used to assess multi-joint coordination patterns in a redundant system by quantifying variability of elemental variables (i.e. joint angles or torques) with respect to changes in performance variable (i.e. position or force or the tip of the end-effector). Using the UCM analysis, we examined how the multiple joints interacted with each other to stabilize the actions of the end-effector in terms of kinematics and kinetics. variability of joint angle and torques were decomposed into task-relevant variability (*TRV*) and task-irrelevant variability (*TIR*), respectively. An index of coordination (*IC*) was defined as $IC=(TIV-TRV)/(TIV+TIV)$.

Results and Discussion

We found no significant *IC* of joint anlges between the groups. However, we found that *IC* of joint torques in Stroke group significantly decreased during outward movement as compared to during inward movement (p=0.003) while *IC* in Control group remained unchanged between movement directions, which was suppored by a repeated measures ANOVA significant interaction *Direction* × *Group* ($F_{1,17} = 5.99$; p=0.026) (Fig. 2). The decreased *IC* in Stroke group was mainly due to the increased TRV of joint torques (TRV_τ) (p=0.001) which was suppored by a repeated measures ANOVA significant interaction *Direction* × *Group* ($F_{1,17} = 5.011$; p=0.038). This result indicates that during passive movement, joint torques were generated in a way that force at the end-effector (i.e. hand) became more variable or less inconsistent during outward movement than inward movement.

In summary, our findings clearly demonstrate that passive UL movements in stroke individuals induces abnormal coordination patterns especially in outward direction. Therefore, the abnormal coordination patterns provide important information for understanding of the motor deficits during passive movements post stroke.

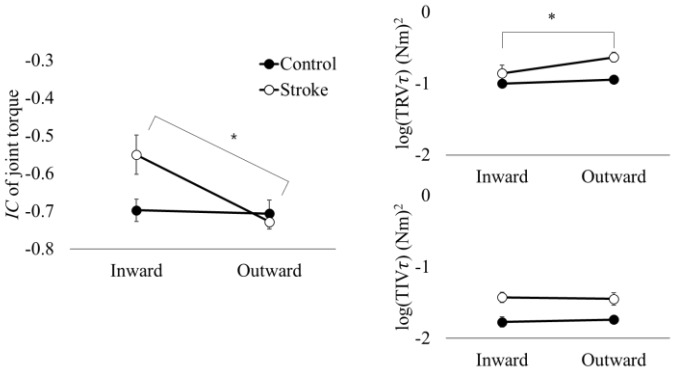

Figure 2: Index of coordination (*IC*), logarithm of task-relevant variability (TRV_τ) and task-irrelevant variability (TIV_τ) of joint torque of during inward and outward directions were compared between stroke group (open dot) and control group (closed dot). The asterisk indicates a significant difference (*: <0.05) between directions in stroke group.

Acknowledgments

This research was supported by NIDILRR grant 90DP0099. Li-Qun Zhang has an equity position in Rehabtek LLC, which received federal grants in developing the robotic device used in this study.

References

1. Vaz, D. V., Pinto, V. A., Junior, R. R. S., Mattos, D. J. S. & Mitra, S. *Gait & posture* (2019)
2. Y. Ren, S. H. Kang, H.-S. Park, Y.-N. Wu, & L.-Q. Zhang, *IEEE TNSRE,* 21:490-499, 2013

Humeral Energy Transfer and Glenohumeral Rotation Strength in Adolescent Baseball Pitchers

Kyle W. Wasserberger, Kevin A. Giordano, Jessica L. Downs, and Gretchen D. Oliver
Sports Medicine and Movement Laboratory, School of Kinesiology, Auburn University, Auburn, Alabama, USA
Email: goliver@auburn.edu

Introduction

During the baseball pitch, the glenohumeral (GH) joint is responsible for transferring large amounts of energy from the trunk to the upper extremity [1]. Due to a lack of bony stability at the proximal end of the humerus, optimization of this energy transfer (ET) is largely dependent on active stabilization provided by the musculature surrounding the GH joint [2]. If weakness of the GH musculature is present, pathological humeral arthrokinematics may develop during arm cocking and arm acceleration; potentially leading to unnecessary increases in ET as pitchers attempt to maintain performance [2].

Active stabilization of the GH joint in baseball pitchers is often assessed in clinical settings using internal (IR) and external (ER) rotation strength tests [3]. Several authors have proposed weakness or imbalance between these muscle groups as a warning sign of future injury [3, 4]. However, the association between clinical GH strength tests and pitching mechanics is still largely unknown. Further investigation into the relationships between clinical strength measures and pitching ET may help elucidate how GH strength impacts the risk of pitching-related injury. Therefore, the purpose of our study was to examine the association between the clinical GH strength and ET to and from humerus during the pitching motion. We hypothesized that increased GH strength would allow pitchers to minimize humeral ET while maintaining a given ball speed.

Methods

A convenience sample of 88 (1.7±0.2m; 59.5±12.9kg; 13.1±2.1yrs) healthy adolescent baseball pitchers were recruited to participate. The Institutional Review Board of Auburn University approved all testing protocols.

Throwing-arm IR and ER strength was assessed using isometric dynamometry in the supine position with the arm abducted 90 degrees in the frontal plane and was normalized to body weight before analysis. Following strength testing, four electromagnetic sensors were affixed to the thorax (T1), throwing arm upper arm, forearm, and hand. A fifth sensor was attached to a moveable stylus for the digitization of bony landmarks consistent with the International Society of Biomechanics recommendations [5]. Participants pitched three fastballs to a catcher at a regulation distance. Kinematic data were collected at 100 Hz using an electromagnetic tracking system.

Energy transfer between the thorax, proximal humerus, and distal humerus was calculated using a segment power analysis similar to that of Howenstien et al [1]. To calculate the total ET, segment power curves were integrated over specific time intervals relevant to the theoretical proximal-to-distal ET patterns of overhead, open-chain, athletic tasks.

Multi-step linear regression was used to estimate the effects of GH strength on predicted humeral ET after accounting for the effects of ball speed. Separate regression equations were developed to estimate ET from the thorax to the proximal humerus during arm cocking (proximal inflow; pIF) and ET from the distal humerus to the forearm during arm acceleration (distal outflow; dOF). Arm cocking was defined as the time between stride foot contact and maximal shoulder external rotation. Arm acceleration was defined as the time between maximal shoulder external rotation and ball release. Statistical analyses were performed in RStudio (R version 3.6.1).

Results and Discussion

Regression analysis showed that pIF was predicted by a linear combination of ball speed and IR strength; accounting for 75% of the variance in pIF. Similarly, dOF was predicted by a linear combination of ball speed and ER strength; accounting for 24% of the variance in dOF. Regression coefficients for pIF and dOF can be found in Table 1.

Table 1
Variables Included in Regression Analyses

		B	Δr^2	p
Proximal IF	Ball Speed	5.93 (0.37)	.73	<.01
	IR Strength	-1.40 (0.59)	.02	<.05
Distal OF	Ball Speed	1.42 (0.29)	.18	<.01
	ER Strength	-1.18 (0.53)	.06	<.05

Glenohumeral IR and ER strength exhibited a small ability to predict pIF and dOF, respectively. In both regression models, GH strength negatively predicted humeral ET, suggesting that, for a given ball speed, increased GH strength may reduce necessary ET. Both models supported our hypothesis that increased GH strength would minimize the amount of ET needed to achieve a given ball speed. This reduction of predicted ET may indicate a protective effect of increased GH strength against unnecessary increases in ET during the pitch.

Although increasing IR and ER musculature strength has long been recommended by the coaching community, data concerning specific mechanisms by which increases in strength may benefit pitchers has been lacking. These data provide initial evidence for reducing ET as a potential mechanism behind the benefits of GH musculature strengthening. Reducing ET is likely to decrease joint loading during the pitch which, in turn, may decrease the risk of mechanical overload to vulnerable tissues in the upper extremity such as the glenoid labrum, rotator cuff musculature, and ulnar collateral ligament.

Significance

Clinically assessed GH strength showed a small ability to predict humeral ET. Our results not only support previous research suggesting strengthening of the IR and ER musculature as a method of decreasing the risk of injury to the throwing arm [4] but also add insight by purposing reduction in ET as a potential mechanism behind the potential benefits of GH muscle strengthening.

References

1. Howenstein (2019). *Med Sci Sports Exerc*. 51(3), 523-531.
2. Urbin (2013). *Am J Sports Med*. 41(2), 336–342.
3. Byram (2010). *Am J Sports Med.* 38(7), 1375–1382.
4. Wilk (2009). *J Orthop Sports Phys Ther*. 39(2), 38-54.
5. Wu (2005). *J Biomech*. 38(5), 981-992.

The relationship between pitch velocity and shoulder distraction force and elbow valgus torque in collegiate and high school pitchers

Kristen Nicholson.[1], Tessa Hulburt[1], Edward Beck[1], Brian Waterman[1], Garrett Bullock[2]
[1]Orthopaedic Surgery, Wake Forest School of Medicine, Winston Salem, NC, USA
[2]Centre for Sport, Exercise and Osteoarthritis Research Versus Arthritis, University of Oxford, Oxford, UK
Email: kfnichol@wakehealth.edu

Introduction

How pitching velocity relates to shoulder and elbow joint loading is not well understood[1,2]. Since medial elbow injuries are linked to excessive elbow valgus torque[3] and peak shoulder distraction force may contribute to rotator cuff injuries[4], understanding the relationship between pitching velocity and upper extremity kinetics can aid in better identification of pitchers at risk for upper extremity injury. Further, these data can provide a foundation for throwing and pitching loading strategies for rehabilitation and return to sport programs following upper extremity injuries. Therefore, the purpose of this study was to determine the relationship between baseball pitching velocity, shoulder distraction force, and elbow valgus torque.

Methods

Data from reports generated as part of a 3D biomechanical pitching evaluation were retrospectively reviewed. A total of 70 baseball pitchers (College: n = 23; High School: n = 47) participated in a pitching evaluation. Inclusion criteria consisted of baseball players, from all competition levels, whom pitcher is their primary or secondary position.

Variables extracted from the pitching reports included pitching velocity, shoulder distraction force, and elbow valgus torque. Shoulder distraction force and elbow valgus torque were normalized by body weight (N) and body weight times height (Nxm), respectively.

Each pitch was considered an individual observation. Multivariable linear regressions with fractional polynomial regressions were used to investigate the relationship between pitch velocity, shoulder distraction force, and elbow valgus torque. Subgroup analyses were then performed for college and high school pitches, and then for pitches that were thrown above 85 mph. R squared (r^2) were utilized to assess model fit.

Results and Discussion

A total of 273 pitches were included in this study. There was a positive linear relationship between pitch velocity and shoulder distraction force (r2 = 0.21, p<0.001) and between pitch velocity and elbow valgus torque (r2 = 0.32, p<0.001) for the entire sample (Figure 1).

Separately, college and high school pitches both exhibited a positive linear relationship between pitch velocity and shoulder distraction force (College: r2 = 0.09, p<0.001; High School: r2 = 0.32, p<0.001), and between pitch velocity and elbow valgus torque (College: r2 = 0.16, p<0.001; High School: r2 = 0.32, p<0.0001).

In pitches that were thrown above 85 mph, there was no relationship between pitch velocity and shoulder distraction force (r2 = 0.005, p=0.500), nor between pitch velocity and elbow valgus torque. (r2 = 0.002, p=0.712). Neither college nor high school pitches thrown above 85 mph exhibited a relationship between pitch velocity and shoulder distraction force (College: r 2= 0.004, p=0.606; High School: r2 = 0.13, p = 0.117). College pitches thrown above 85 mph also did not exhibit a relationship between pitch velocity and elbow valgus torque (r2 = 0.007, p=0.476). However, high school pitches thrown above 85 mph exhibited a positive linear relationship between pitch velocity and elbow valgus torque (r2 = 0.27, p = 0.020).

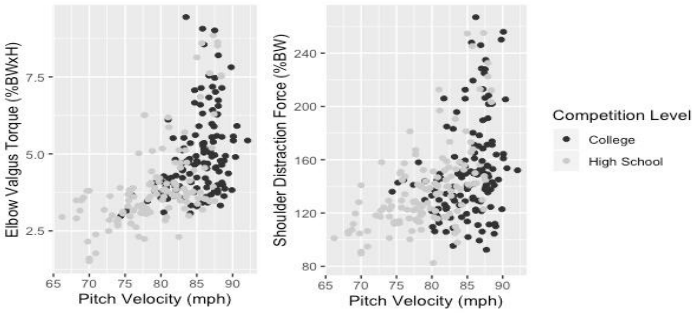

Figure 1: Elbow valgus torque vs pitch velocity and shoulder distraction force vs pitch velocity

Both the high school and college pitchers exhibited significant positive linear relationships between pitching velocity and shoulder distraction force and pitching velocity and elbow valgus torque. After stratification, high school pitchers who threw the fastest experienced greater elbow and shoulder torques. However, this trend did not hold true among the college pitchers. These findings may indicate a survival effect among the elite college pitchers compared with the elite high school pitchers.

It has been shown that pitchers from higher competition levels produce greater pitching velocity and joint forces; but, also have greater pitching mechanical efficiency and skill. These competition level discrepancies between pitching velocity and biomechanical efficiency may potentially attenuate a linear increase between pitch velocity and upper extremity kinetics. The results of this study suggest that these age discrepancies continue to exist, and are more pronounced, among elite or highly skilled pitchers.

Significance

These findings suggest that high school pitchers that throw at high velocities may be more susceptible to pitching injury. There were many successful high velocity pitches from college pitchers who were able to limit stress on the elbow and shoulder. Identifying the mechanics and other meaningful contributors to pitch velocity and arm kinetics among this subgroup would help inform throwing and pitching loading strategies.

References

1. Hurd WJ et al. *Sports health.* 2012;4(5):415-418.
2. Post EG et al. *Journal of athletic training.* 2015;50(6):629-633.
3. Anz AW et al. *The American journal of sports medicine.* 2010;38(7):1368-1374.
4. McLeod et al. *Physical therapy.* 1986;66(12):1901-19

Does Lead and Rear Foot Placement Affect Pitching Biomechanics?

Megan Stewart[1], Ryan Crotin[2], Alek Diffendaffer[1], Jon Slowik[1], Karen Hart[1], Glenn Fleisig[1]
[1]The American Sports Medicine Institute, Birmingham, Alabama, USA
[2]The Los Angeles Angels, Anaheim, California, USA
Email : megan.s.stewart19@gmail.com

Introduction

At the instant of lead foot contact, a variety of biomechanical parameters are associated with an increase in upper extremity kinetics and kinematics [1]. Some of these kinematic parameters include front foot position, shoulder horizontal abduction, and shoulder abduction [1]. While previous studies have indicated that changes in the lead foot position have led to an increase in kinetics and kinematics, minimal studies have investigated the implications of the rear foot placement on the pitching rubber. Therefore, the purpose of this study was to investigate the effects of the rear foot placement on the pitching rubber in relation to both kinematic and kinetic parameters. Our hypothesis was that there would be a significant difference in the kinematics (motions) and kinetics (torques & forces) when pitching from the third base side and first base side of the pitching rubber.

Methods

This was a retrospective review of the American Sports Medicine biomechanics database where four hundred and thirty-three right-handed professional baseball pitchers were determined to fit the criteria for this study. Shoulder and elbow passive range of motion were measured on the participant's dominant and non-dominant arms.

A total of twenty-four kinematic and kinetic parameters were calculated using methods that have already been previously described [2] [3]. All the pitchers were first divided by their third base side or first base side rear foot position. Second, they were sub-divided into having an open or closed front foot position. From these two distinctions, each pitcher was grouped into the following four possible combinations: first base closed (FBC), first base open (FBO), third base closed (TBC), and third base open (TBO).An Analysis of variance (ANOVA) was utilized to detect significant differences among the location of the lead and rear foot placement on the pitching mound.

Results and Discussion

Significance was found in the follow five variables, trunk forward tilt at ball release, trunk forward tilt at maximal internal rotation, shoulder abduction, arm slot, and wrist flexion torque. Our hypothesis was supported that there were significant differences found in the biomechanical parameters between the front foot placement and rear foot location on the pitching rubber. As a baseball pitcher improves their skill, they are better able to adjust their pitching mechanics [5] [7]. Front foot placement on the mound has been shown to increase the coordination and stability of the pitching arm [8]. Although pitch type deception may be improved with a change in foot placement on the pitching rubber, recent research has shown implications of injury to the ulnar collateral ligament with a change of the release point, in relation to the movement on the pitching rubber [9].

Before the conduction of the study, it was thought that when the pitcher had FBO the elbow was put in a compromised posiiton. It was also thought that with a TBC the shoulder would be placed in a compromised position. The results did indicate that there was a significanlty lower arm slot (p-value 0.02) for a pitcher who has a TBC postion when compared to an TBO, however no significant kinetic differences were found. There were no significant findings in relation to the kinematics or kinetics of the elbow with the placement of either the front or rear foot. The implications of this study for baseball coaches will help to increase the ability to change rear foot placement on the pitching rubber with hopes of decreasing the potential incident of injury. Rear foot and lead foot placement drills can be established as part of a training and practice schedule for baseball pitching coaches.

Significance

This study aimed to bring the gap between the incident of injury and foot placement on the pitching mound closer together. The goal for all baseball coaches and pitchers is to stay healthy and decrease the potential risk of injury. Both pitching coaches and players will be better able to adjust their pitching location to increase their likelihood of staying healthy and adjust the above-mentioned biomechanical parameters.

Acknowledgements

The Major League Baseball Organization for access to the professional baseball pitchers.

References

[1] "Baseball Pitching Biomechanics in Relation to Injury Risk and Performance," *Sports Health*

[2] "Differences among overhand, three-quarter, and sidearm pitching biomechanics in professional baseball players," *Journal of Applied Biomechanics ,*

[3] "Kinematic and kinetic compariosn between baseball pitching and football passing," *Journal of Applied Biomechanics*

[5] "Altered stride length in response to increasing exertion among baseball pitching delivery," *Medicine of Science Sports and Exdercise*

[7] "Variability in baseball pitching biomechanics among various levels of competition," *Sport Biomechanics ,*

[8] "Do baseball pitchers improve mechanics after biomechanical evaluations?," *Sport Biomechanics*

[9] "Predictors of ulnar collateral ligament reconstruction in major league baseball pitchers," *American Journal of Sports Medicine*

The Effect of Pronation on Break of The Curveball

Megan Stewart, Alek Diffendaffer[1], Jon Slowik[1], Karen Hart[1], Glenn Fleisig[1]
The American Sports Medicine Institute, Birmingham, Alabama, USA

Introduction

Previous research has indicated that the movement of the wrist and the forearm may have significance on the location of the pitch [1], however, there is no indication of the significance of the amount of wrist supination or pronation with respect to vertical or horizontal break of the baseball. Therefore, the purpose of this study was to investigate the relationship between wrist pronation of a curveball and the horizontal and vertical break.

Methods

This was a retrospective review of the American Sports Medicine database where forty-three baseball pitchers were determined to be eligible. Shoulder and elbow passive range of motion were measured on the participant's dominant and non-dominant arms by the research staff.

Each participant was tested throwing five full-effort curveballs to a target located behind home plate, 18.44 m from the rubber. Horizontal break of the baseball was defined as the maximal horizontal variation from a straight-line path between the release point of the baseball and the point where the baseball crossed the back edge of home plate. Vertical break was defined as the maximal vertical variation from a straight-line path between the release point of the baseball and the point where the baseball crossed the back edge of home plate. A linear regression was utilized to investigate the relationship between forearm pronation and the baseball kinematics (ball velocity, horizontal and vertical break).

Results and Discussion

A statistically significant relationship was found between forearm pronation at foot contact, forearm pronation at foot contact and vertical break, and forearm pronation at ball release, and the velocity of the baseball on both the vertical and horizontal break. These results indicate that the ball velocity (mph) will have a significant effect on the vertical break (up and down) location and horizontal break (side to side) location for the baseball. It was also indicated that the amount of forearm pronation at the instant of foot contact, will significantly affect the amount of pronation at the instant of ball release and the vertical break location. Figure 1 is showing the effect of forearm pronation at foot contact and the vertical break of the baseball.

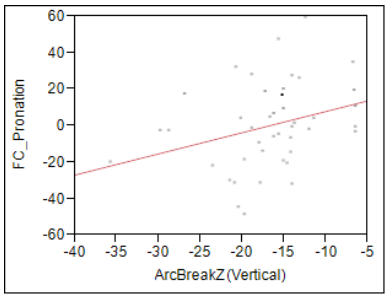

Figure 1: The Relationship Between Pronation at Foot Contact and Vertical Break

Previous research has determined that a baseball pitchers' dominant forearm will have 5^0 more of pronation when compared to their non-dominant forearm [2]. It has been discussed that the ability of greater pronation is a persisting structural difference between position players & pitchers [2] . Even with pitchers having an increase in forearm pronation, it has been seen in some research that the vertical control and horizontal control of the baseball increase with the ability for a pitcher to alter their forearm pronation [2].

There was no significant relationship between the horizontal break of the baseball and the pronation of the forearm at foot contact. However, there was a significant relationship between the velocity of the baseball and the horizontal break. Furthermore, it was found that the amount of forearm pronation at foot contact had a significant relationship (p-value = 0.04) with the amount of forearm pronation at the ball release and the amount of vertical break of the baseball (p-value = 0.05). There is a positive linear relationship between the amount of forearm pronation at foot contact and the location of the vertical break of the baseball. Therefore, as the foot contact pronation at the forearm increases, the vertical break of the curveball increases.

The results of this study indicate that when the velocity of a pitcher is higher there is a significant increase in the horizontal break of the baseball (p-value = 0.02) and the vertical break of the baseball (p-value <0.001). The amount of forearm pronation at the instant of foot contact will have a significant effect on the amount of forearm pronation at the instant of ball release (p-value = 0.04) and the location of the vertical break of the baseball (p-value = 0.05).

Significance

With the ability to manipulate the amount of forearm pronation at foot contact to affect the amount of forearm pronation at ball release, coaches and pitchers will be better adept to adjust their mechanics. The practical applications for coaches and pitchers to implement a training program for foot contact and pronation drills will help to increase the amount of pitch type deception and allow for the potential increase in vertical break of the baseball, which will help to increase the time for the baseball to change positions from the release of the hand. This increase in time and deception will help to generate the potential for more strikeouts and variation in pitch location.

References

[1] "Upper Extremity range of motion and isokinetic strength of the internal and external shoulder rotators in major league baseball players," *The American Journal of Sports Medicine*

[2] "Influence of Pitching Release Location on Ulnar Collateral Ligament Reconstruction Risk Among Major League Baseball Pitchers," *Orthopedic Journal of Sports Medicine*

The Relationship between Fastball Velocity and Elbow Varus Torque in Professional Baseball Pitchers

Jonathan S. Slowik, Kyle T. Aune, Alek Z. Diffendaffer, E. Lyle Cain, Jeffrey R. Dugas, and Glenn S. Fleisig
American Sports Medicine Institute, Birmingham, AL
Email: jons@asmi.org

Introduction

Baseball pitching is a highly dynamic task that involves extraordinary velocities, requiring potentially damaging torque levels, especially in the throwing arm. However, previous studies have been unable to find a strong relationship between ball velocity and elbow varus torque, possibly due to the confounding effects of between-subject differences (e.g., detailed anthropometrics and pitching mechanics) [1,2]. Therefore, the purpose of this study was to examine the relationship between fastball velocity and elbow varus torque in professional pitchers, through both across-subject and within-subject statistical analyses. We hypothesized that ball velocity explains 1) only a small percentage of the across-subject variance in varus torque, but 2) a much higher percentage of the within-subject variance in varus torque.

Methods

From a database of previously collected biomechanical data of baseball pitchers [e.g., 3], we identified 64 professional pitchers meeting the following criteria: 1) threw at least 5 fastball trials, 2) exhibited a velocity range of at least 2.2 m/s (5.0 mph), and 3) had no single pitch trial that accounted for over half of the velocity range. These criteria enabled both within-subject and across-subject statistical analysis methods. We then performed a retrospective review of their fastball data (e.g., ball velocity and inverse-dynamics-based elbow varus torque). We established the across-subject relationship between ball velocity and normalized maximum elbow varus torque using simple linear regression between each subject's mean ball velocity and mean normalized maximum elbow varus torque value. Similarly, we established the within-subject relationship between ball velocity and normalized maximum elbow varus torque using a mixed linear model with random intercepts. An R^2 statistic was calculated for this model by comparing its residual variance against the residual variance of the random intercept alone:

$$R^2 = (ResidualVar_{int} - ResidualVar_{model})/ResidualVar_{int}$$

The significance level α for all tests was set a priori at 0.05.

Results and Discussion

Across all subjects, the mean fastball velocity was 37.6±1.5 m/s (84.1±3.5 mph) and the within-subject range of fastball velocity was 2.8±0.7 m/s (6.4±1.6 mph). The across-subject mean value for normalized maximum elbow varus torque was 5.33±0.74 % body weight*height. The simple linear regression model indicated a statistically significant, but weak positive association between ball velocity and varus torque at the across-subject level ($p=0.03$, $R^2=0.08$). The linear mixed model (with random intercepts) indicated a considerably stronger positive association between ball velocity and varus torque when performing within-subject comparisons ($p<0.001$, $R^2=0.96$). Plots of within-subject normalized maximum elbow varus torque vs. ball velocity are provided in Figure 1.

These results suggest that when comparing two individual professional pitchers, higher velocity may not necessarily indicate higher elbow loading. However, within an individual pitcher, higher ball velocity is strongly associated with higher elbow varus torque. Furthermore, the model suggests that for every 1.0 m/s increase in ball velocity, varus torque increases by 0.092% (body weight*height). For a pitcher with the mean height (1.90 m) and mass (94.6 kg) of the participants, this would equate to a 1.62 Nm increase in varus torque for every 1.0 m/s increase in ball velocity.

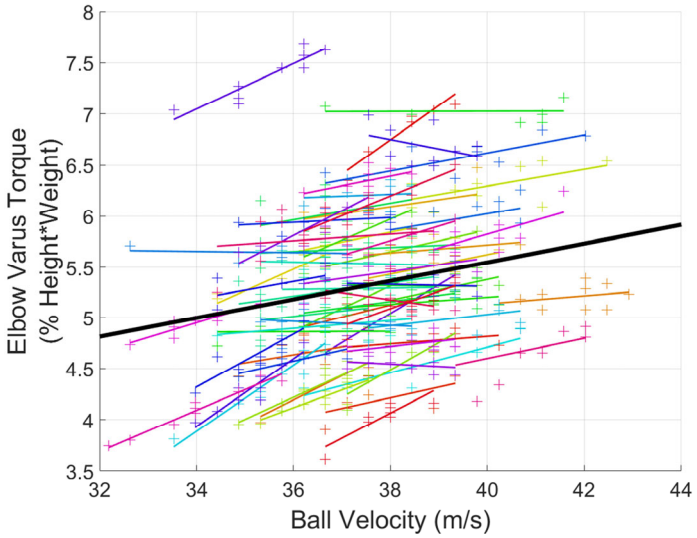

Figure 1: Plot of normalized maximum elbow varus torque vs. ball velocity. Each individual pitcher is represented by a series of points and the best-fit line in one color, while the regression line from the linear mixed model is represented by the thick black line. This model suggested a strong positive within-subject relationship between varus torque and velocity ($R^2=0.96$).

Significance

The results of this study suggest that while between-subject comparisons are obscured by subject-specific attributes, a deliberate reduction in velocity (without compromising mechanics) will likely reduce the load on an individual pitcher's elbow. Considering the fact that many professional pitchers throw over 3000 in-game pitches each season, as well as the extensive research on the dangers of pitch volume and the resulting accumulated load, these results suggest that a pitcher may be able to reduce his elbow injury risk by deliberately varying his velocity from pitch to pitch. Thus, we believe that pitchers should focus on using good mechanics, developing command, determining the minimum level of pitch intensity necessary to obtain the outcome they desire for each of their pitches, and learning to recognize the situations when success requires maximum velocity. Furthermore, professional baseball teams with the ability to recognize when pitchers lack these attributes (i.e., pitchers who require "maximum effort" for success) may be able to avoid potentially costly mistakes by either correcting this weakness, limiting their pitch count, or avoiding signing these players altogether.

References

1. Hurd WJ, et al. *Sports Health* **4**, 415-418, 2012.
2. Post EG, et al. *J Athl Train* **50**, 629-633, 2015.
3. Fleisig GS, et al. *Sports Health* **9**, 210-215, 2017.

Biomechanical Differences between Overhand, Three-Quarter, and Sidearm Baseball Pitching

Jonathan S. Slowik[1], Alek Z. Diffendaffer[1], Glenn S. Fleisig[1], and Rafael F. Escamilla[2]
[1]American Sports Medicine Institute, Birmingham, AL
[2]Department of Physical Therapy, California State University, Sacramento, CA
Email: jons@asmi.org

Introduction

Baseball coaches and trainers frequently summarize a pitcher's delivery by subjectively classifying his arm slot (i.e., orientation of his arm in the frontal plane, at the time of ball release). Arm slots are commonly categorized into one of three groups: overhand (OH), three-quarter (TQ), and sidearm (SA) (Fig. 1). Previous studies have examined quantities that are related to arm slot (e.g., lateral trunk tilt, shoulder abduction), but conflicting results have led to confusion and inconsistent recommendations within the literature [e.g., 1,2]. Therefore, the purpose of this study was to objectively quantify the arm slot angles of professional pitchers, and then investigate the differences in pitching biomechanics between these three arm slot groups.

Methods

From a database of previously-collected biomechanical data of baseball pitchers [e.g., 3], we identified 378 professional pitchers meeting the following criteria: 1) threw at least 5 full-effort fastball trials from the windup position, 2) were healthy at the time of testing, and 3) had not undergone shoulder or elbow surgery in the previous 18 months. Arm slot angle was defined as the angle between a vertical vector and a vector connecting the throwing shoulder joint center to the hand, when viewed from behind the mound (Fig. 1). Three arm slot groups were then defined as follows: OH (≤40° arm slot angle), TQ (50° to 60° arm slot angle), and SA (≥70° arm slot angle). Differences in 37 pitching biomechanics variables were then assessed using a one-way ANOVA. If a significant main effect was found, pairwise comparisons were performed using student t-tests with a Bonferroni correction. The uncorrected significance level for all tests was set at α=0.01.

Results and Discussion

There were no significant between-group differences in age, body mass, body height, or ball velocity. There were significant differences found for 14 biomechanical variables (Table 1). There were large between-group differences in lateral trunk tilt, with OH>>TQ>>SA. A similar trend was seen in shoulder abduction but with smaller differences (OH>TQ>SA). Overall, the kinematic differences between groups suggest that OH moved most in the vertical plane, while the SA moved most in the horizontal plane. In addition, SA had less shoulder anterior force than TQ, while OH had less elbow flexion torque than either TQ or SA.

Table 1: Biomechanical variables (mean ± standard deviation) with statistically significant differences [a]between OH and SA, [b]between TQ and SA, and [c]between OH and TQ.

	OH	TQ	SA
[ab]Max knee height, % height	58±7	60±7	52±14
[ab]Pelvic drift @ MKH, cm	16±5	16±4	20±10
[ab]Foot angle @ FC, deg	8±8	9±9	15±11
[ab]Upper trunk tilt @ FC, deg	13±9	9±6	3±10
[ac]Elbow flexion @ FC, deg	103±15	93±15	94±17
[ab]Max pelvis angular velocity, deg/s	541±68	562±72	645±84
[ab]Max shoulder external rotation, deg	163±12	162±11	169±14
[ab]Elbow flexion @ BR, deg	25±4	25±4	28±3
[ab]Forearm pronation @ BR, deg	22±15	20±15	8±15
[abc]Shoulder abduction @ BR, deg	94±8	88±7	81±8
[abc]Trunk forward tilt @ BR, deg	36±9	33±7	30±7
[abc]Trunk lateral tilt @ BR, deg	32±7	21±6	2±10
[b]Max shoulder anterior force, N	383±71	396±76	346±67
[ac]Max elbow flexion torque, Nm	61±11	67±11	70±13

Significance

The results of this study suggest that arm slot is primarily driven by lateral trunk tilt, with a secondary contribution from shoulder abduction. The greater elbow flexion torque and shoulder external rotation exhibited by SA pitchers may increase their risk of labral injury. Conversely, the lower shoulder anterior force in SA pitchers may indicate lower stress on shoulder joint capsule and rotator cuff.

References

1. Aguinaldo AL, et al. *Am J Sports Med* **37**, 2043-2048, 2009.
2. Solomito MJ, et al. *Am J Sports Med* **43**, 1235-1240, 2015.
3. Fleisig GS, et al. *Sports Health* **9**, 210-215, 2017.

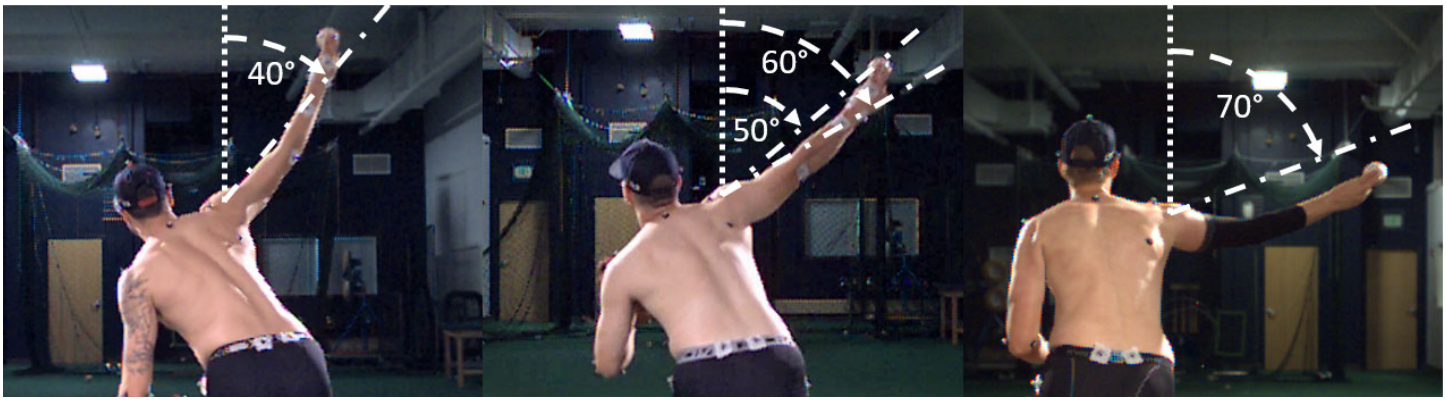

Figure 2: Examples of overhand (≤40°), three-quarter (50°-60°), and side arm (≥70°) deliveries. Arm slot angle is defined as the angle between vertical (dotted line) and a vector connecting the shoulder joint center to the hand marker.

The Relationship between Variability in Baseball Pitching Kinematics and Consistency in Pitch Location

Joshua A. Glanzer[1], Alek Z. Diffendaffer[1], Jonathan S. Slowik[1], Monika Drogosz[1], Nicholas J. Lo[1], and Glenn S. Fleisig[1]
[1]American Sports Medicine Institute, Birmingham, AL
Email: alekd@asmi.org

Introduction

Baseball pitching requires a rapid sequencing of body segment rotations from the windup through ball release. Subtle variations in pitching mechanics may negatively result in decreased ball velocity, increased joint stress, and decreased accuracy. Previous literature has extensively investigated the relationships between pitching mechanics, ball velocity, and joint kinetics [1,2]; however, there has been limited research investigating the relationship between consistency of pitching mechanics and pitch location. Therefore, the purpose of this study was to assess the relationship between variability in pitching mechanics and pitch location. It was hypothesized that lower variability in pitching kinematics would be associated with increased consistency in pitch location.

Methods

From a database of previously-collected biomechanical data, 47 baseball pitchers were identified as meeting the following criteria: 1) threw at least 8 full-effort fastball trials with 3D motion capture and PITCHf/x data being successfully collected and 2) were healthy at the time of testing. For each pitch thrown, vertical and horizontal coordinates of the baseball as it crossed homeplate were measured via the PITCHf/x system. From these coordinates, each pitcher's mean pitch location was calculated. The distances from each pitch location to the mean pitch location were found. A consistency metric was then calculated for each pitcher by averaging these distances. Twenty kinematic parameters were calculated from the motion capture data for each pitch tracked by the PITCHf/x system, which has been previously described [3]. Variability was defined as the standard deviation among the pitches thrown and was calculated for each of the 20 kinematic parameters. A stepwise linear regression analysis using backwards elimination was performed to assess the relationship between kinematic variability and pitch location consistency.

Results and Discussion

At the end of the backwards elimination process ($p < 0.1$), only five parameters remained in the model (Table 1). Three kinematic parameters occurred at foot contact (upper trunk tilt, shoulder abduction, and shoulder horizontal abduction), while two occurred at the time of maximum shoulder external rotation (maximum shoulder external rotation and maximum shoulder horizontal adduction) (Figure 1). The model accounted for 58% of the variance in the consistency metric ($R^2 = 0.58$).

Table 1: Multiple linear regression model resulting from a stepwise linear regression using backward elimination. For each parameter, variability is the standard deviation for the pitches thrown by a pitcher. (B = unstandardized coefficients; SE = standard error, Beta = standardized coefficients)

Parameter	B	SE	Beta	p-value
Constant (cm)	10.08	4.15	-	0.020
Upper Trunk Tilt	2.24	0.78	0.33	0.007
Shoulder Abduction	3.03	1.31	0.26	0.026
Shoulder Horizontal Abduction	-1.64	0.69	-0.29	0.023
Max Shoulder External Rotation	8.86	2.54	0.40	0.001
Max Shoulder Horizontal Adduction	7.71	2.46	0.35	0.003

Significance

The results of this study suggest that a pitcher's ability to locate the baseball is directly dependent on his ability to pitch with consistent kinematics. Four of the above-mentioned parameters involved variability in shoulder kinematics, which has also been proven to significantly contribute to ball velocity and injury risk. In general, pitchers should strive for consistency in shoulder motion and upper trunk tilt to optimize their ability to locate pitches.

References

1. Matsuo T, et al. *J of Applied Biomechanics* **17**, 1-13, 2001.
2. Fortenbaugh D, et al. *Sports Health* **1**, 314-320, 2009.
3. Escamilla RF, et al. *J of Applied Biomechanics* **34**, 377-385, 2018.

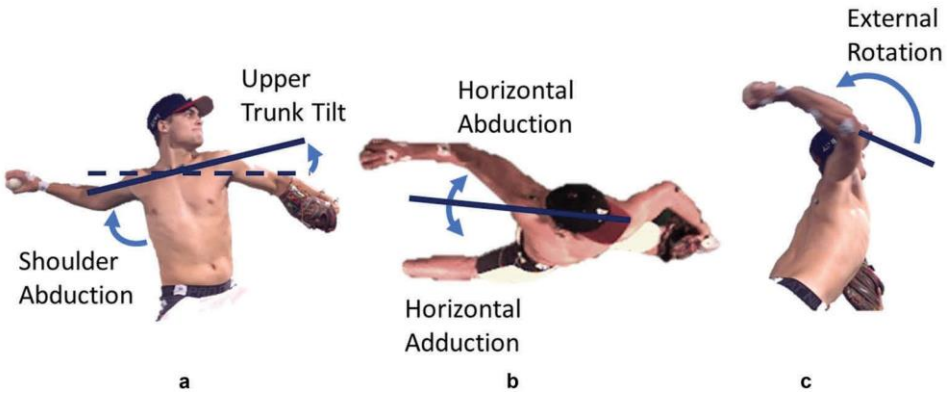

Figure 1: Five parameters remained in the statistical model, accounting for 58% of the variance in consistency of pitch location. (a) shoulder abduction and upper trunk tilt, (b) shoulder horizontal abduction /adduction, and (c) maximum shoulder external rotation

Hip Range of Motion and Isometric Strength Differences Between High and Low Batted Ball Velocity Hitters

Jessica L. Downs, Nicole M. Bordelon, Kenzie B. Friesen, Gretchen D. Oliver
Sports Medicine and Movement Laboratory, School of Kinesiology, Auburn University, Auburn, Alabama, USA
Email: jzd0075@auburn.edu

Introduction

Hitting performance is essential to offensive success in baseball and softball. Specifically, bat speed and batted ball velocity (BBV) are variables coaches analyze when predicting hitting success. Previous hitting research has focused on kinetics and kinematics associated with hand velocity as an indicator of BBV [1,2]; however, there are little to no data regarding the relationship between clinical measures and BBV.

Defensively, hip and shoulder range of motion (ROM) and strength have been correlated with kinetic chain energy transfer, altered throwing mechanics, ball velocity, and potential predictors of injury during the overhand throw [3]. Investigating the relationship between BBV, hip ROM, and hip strength will give coaches and clinicians a field measurement to identify potential musculoskeletal deficits that may influence hitting performance. Therefore, the purpose of this study was to investigate potential differences in hip ROM and strength between low and high BBV hitters in adolescent baseball and softball athletes. It was hypothesized that high BBV hitters will have greater hip ROM than low BBV hitters and that there would be no significant differences between baseball and softball athletes

Methods

Forty-three right-handed adolescent baseball and softball athletes (13.7±2.6yrs, 165.5±15.0cm, 67.2±19.8kg) participated. All participants were deemed free of injury and surgery for at least the past six months.

Passive hip internal rotation (IR) and external rotation (ER) ROM and isometric strength (ISO) of the lead and back leg were collected prior to warm-up. Hip ROM and ISO were measured with a digital inclinometer and a handheld dynamometer, respectively, while the participant was seated with knees flexed at 90°. Isometric strength was normalized to individual participants' body mass.

Participants were given an unlimited amount of time to warm-up from a tee. Once deemed warm, the participants were instructed to execute game effort swings from a tee at a self-selected height and placement for 10 trials. A trial was saved if the hit resulted in a line-drive and if the participant gave verbal feedback that they felt it was a good swing. At least three saved trials were needed for the participant to be included in the analysis. Batted ball velocity was assessed using a radar gun placed behind the participant. The average BBV of the saved trials were used for analysis. Participants were divided into high BBV and low BBV groups. Groups were assigned based on whether their average BBV was above (high) or below (low) the group mean. Participants were also coded based on sport (baseball or softball).

Due to non-normally distributed data, a Mann-Whitney-U test was used to determine differences in IR/ER hip ROM and/or ISO between BBV groups and between sports. To minimize chance of type 1 error, alpha level was set *a priori,* $\alpha = .006$.

Results and Discussion

Results revealed a statistically significant difference in BBV groups for back hip IR ROM ($U = 107.50$, $p = .003$, *effect size* = 0.46), with the low BBV group having significantly greater back hip IR than the high BBV group. There were no other significant differences between BBV groups (Table 1 and 2). When analyzing sport differences, the test revealed a statistically significant difference in lead hip ER ISO ($U = 86.00$, $p = .001$, *effect size = 0.52*). Specifically, baseball athletes had significantly greater lead hip ER ISO than softball athletes. However, the current study did not control for age. Controlling for age is a limitation and may produce different results [4]. There were no other significant differences between sports.

Table 1: Range of Motion Descriptives

Group	n	Batted Ball Velocity	Lead Hip IR	Back Hip IR	Lead Hip ER	Back Hip ER
High	22	33.60	28.04	*25.88	34.68	34.33
Low	21	23.18	33.07	*34.11	36.15	36.67

Note: n=number of participants, IR=internal rotation, ER=external rotation, * denotes significant difference between groups, all range of motion values are reported in degrees, velocity is reported in m/s

Table 2: Isometric Strength Descriptives

Group	n	Batted Ball Velocity	Lead Hip IR	Back Hip IR	Lead Hip ER	Back Hip ER
High	22	33.60	2.21	2.09	2.06	2.03
Low	21	23.18	2.27	2.23	1.94	2.14

Note: n=number of participants, IR=internal rotation, ER=external rotation, all isometric strength values are reported in N/kg, velocity is reported in m/s

The result of increased back hip IR ROM in the low BBV group compared to the high BBV group was not hypothesized. In overhead throwing, there is an optimal range for hip ROM where too little or too much ROM can contribute to increased injury risk [5]. Based on the results of the current study, the same concept of an optimal range may hold true for hitting. It is worth noting however that hip ROM was assessed passively and different results may be found when assessing dynamic hip ROM during the swing.

Significance

The results of this study are important as they are one of the first to analyze the association between hitting performance indicators with passive hip ROM and ISO. These results provide clinical measures that can potentially be used to predict BBV in adolescent baseball and softball atheltes. Future research should be done to investigate if these differences hold true in a collegiate population in addition to the association between dynamic hip ROM and hitting performance.

References

1. Milanovich (2014) *J Sports Sci.* 13(1),180-191
2. Inkster (2011) *Med Sci Sports Exerc.* 43(6), 1050-1054
3. Harding (2018) *J Athl Train.* 53(1), 60-65
4. Picha (2016) *J Athl Train.* 51(6), 466-473
5. Laudney (2010) *Am J Sports Med.* 38(2), 383-387

Movement Patterns of the Torso Predict Upper Extremity Joint Loading in Little League Pitchers

Michael H. Haischer[1,2], Jacob Howenstein[3], Michelle Sabick[4], and Kristof Kipp[1]
[1]Department of Physical Therapy, Marquette University, Milwaukee, WI, USA
[2]Athletic & Human Performance Research Center, Marquette University, Milwaukee, WI, USA
[3]Blast Motion, San Diego, CA, USA
[4]Department of Biomedical Engineering, Saint Louis University, St Louis, MO, USA
Email: michael.haischer@marquette.edu

Introduction

Due to the high forces involved, shoulder injuries are common in baseball pitchers. Despite a number of studies on youth pitching kinematics and kinetics, there is little information about techniques that maximize ball speed and minimize joint loads. Previous work indicates that the sequence of discrete torso movements influence upper extremity joint loading (3). It would also be beneficial to know if dynamic time-series patterns of torso movements relate to pitching performance and joint loads.

One method of analysis that is often used to quantify sport techniques and dynamic movement patterns is principal components analysis (PCA) (2). PCA involves analyzing time series as opposed to discrete values. In the context of pitching, PCA may facilitate a better understanding of how movement patterns throughout the entire pitching motion relate to performance and shoulder joint loads rather than discrete variables at distinct time points. The purpose of this study was to investigate the associations between torso movement patterns extracted via PCA, and shoulder forces, moments, and ball speed.

Methods

Twenty-four little league pitchers were fitted with a full-body marker set consisting of 32 individual markers and 7 marker clusters. Kinematic and kinetic data were recorded at 250 Hz and at 1000 Hz, respectively. Kinetic data were recorded with a two force plates that were built into a pitching mound. A 4th-order, 14 Hz, zero-lag, low-pass Butterworth filter was used on the marker data, while a 4th-order, 300 Hz, zero-lag, low-pass Butterworth filter was used on force plate data. Inverse dynamics equations were used to calculate net joint force and moments (NJM) at the shoulder, and normalized to body mass.

Data from 23 youth pitchers (five trials each) were used for analysis (range: 9-13 years, height: 1.55 ± 0.12 m, body mass: 46.0 ± 11.9 kg). Torso segment orientation data were time-normalized from peak knee height to ball release in three planes and input to a PCA. PC scores for torso forward/backward inclination, lateral tilt, and transverse rotation were calculated for each individual trial, with within-subject averages of PC scores, ball speed, and peak shoulder kinetics (e.g. DistractF: distraction force, HorizAbM: horizontal abduction moment, AdM: adduction moment) analyzed via correlational analysis. Due to the violation of normality, Spearman's rho correlations were used, along with 1,000 replicate sample bootstrapping to increase robustness of the analyses.

Results and Discussion

Mean pitch velocity was 51.6 ± 7.5 mph. The PCA was able to explain 98% of the variance in torso forward/backward inclination angle. PC2 of these data exhibited a significant positive correlation in that a phase shift and delayed transition from backward to forward inclination relates to increased distraction force (Table 1). The PCA accounted for 96.7% of the variance in torso lateral tilt angle, and 96.8% in torso rotation angle. A phase shift to an earlier contralateral tilt (PC2) was related to a greater horizontal abduction moment, and a smaller magnitude of lateral tilt change throughout the movement (PC3) was associated with a greater adduction moment (Table 1). Lastly, a smaller degree of torso rotation for the majority of the movement (PC1) was correlated to reduced ball speed, though the confidence interval for this significant result includes zero (ρ = -0.456, p = 0.029, 95%C.I. = -0.832, 0.037).

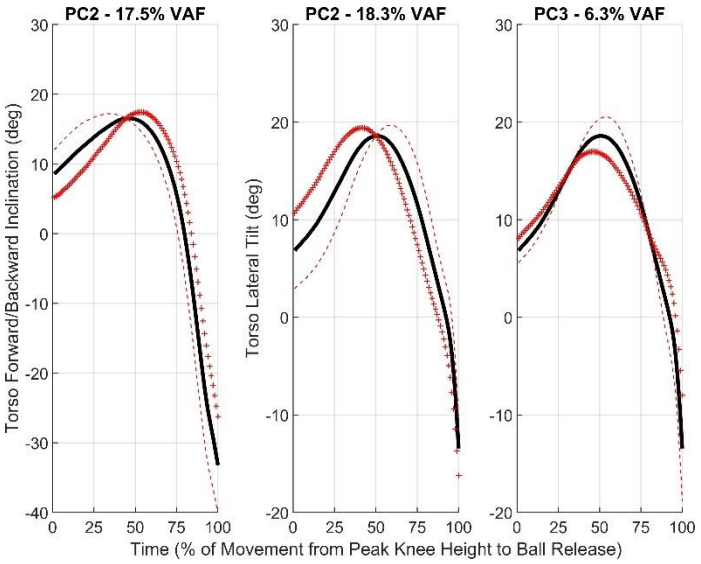

Figure 1: Ensemble average (black line) of time-normalized torso time series data along with the variance accounted for (VAF) and effects of principal components (PC) on the shape of the curves (effects of positive and negative PC scores are illustrated with +/- symbols, respectively).

Table 1: Spearman's Rho Correlations

Torso PCA	*PC*	*Variable*	*ρ*	*Sig.*
Forward/Backward Incl.	PC2	DistractF	0.432	0.040
Lateral Tilt	PC2	HorizAbdM	0.455	0.029
Lateral Tilt	PC3	AddM	0.481	0.020

Significance

Since the kinematic patterns associated with joint loads were not associated with ball speed it may be possible to alter pitching technique to decrease joint loads and retain pitching performance. Future research should investigate this conclusion with an interventional study.

References

1. Howenstein et al. (2019). *MSSE* 51:523–531.
2. O'Connor & Bottum (2009). *MSSE* 41:867–878.
3. Oyama et al. (2014). *Am J Sports Med* 42(9), 2089-94

Shoulder External Rotation ROM During Physical Exam Is Related to the Joint Loading During Baseball Pitching

Hannah L. Stokes[1], Nigel Zheng[1], Koco Eaton[2]
[1]University of North Carolina at Charlotte, NC, [2]Tampa Bay Rays and University of South Florida, FL
nzheng@uncc.edu

Introduction

Baseball pitching is demanding on the shoulder and it is common for injuries to occur. Higher joint loading has been shown to lead to more injury incidences (1). The relationship of shoulder range of motion (ROM) and injury has been studied (2). The shoulder ROM is checked by team physicians regularly.

The purpose of this study is to investigate how shoulder external rotation (SER) ROM measured during a physical exam is related to the shoulder joint loading during pitching. This connection could allow for correction of baseball mechanics and ultimately reduce the risk for injuries. We hypothesize that SER ROM during a physical exam is not related to shoulder forces or torques during baseball pitching.

Methods

The study included 177 college pitchers (height: 186±7.2 cm and weight: 188±19.6 lbs). The study protocol was approved by an institutional board, and all participants gave written informed consent. The maximum SER ROM was previously defined as the end-point angle (EPA), which was recorded during a physical exam using a custom-made wireless device (3). The pitchers were grouped into low (<mean–SD, n=33), medium (mean±SD, n=114), and high EPA (> mean+SD, n=30).

Ten fastball pitching motions were collected at 240 Hz using a motion capture system. Three best pitches were analyzed. A custom MATLAB program was created to calculate: anterior/posterior (AP) force, proximal/distal (PD) force, superior/inferior (SI) force, abduction/adduction (AA) torque, internal/external (IE) torque and horizontal abduction/adduction (HAA) using an inverse dynamics model. One-way analysis of variance (ANOVA) with Tukey pos-hoc tests were performed using SPSS with an alpha set to 0.05. The maximum, minimum and range values and timings or duration of these shoulder kinetics variables were compared among three EPA groups.

Table I: Results p-values for one-way ANOVA, bolded indicates significant, a: Low vs Medium, b: Low vs High, c: Medium vs High (F/T: force/torque, R: Max-Min, %: timing during pitching cycle).

F/T	Max	Max %	Min	Min %	R	R %
AP	0.472	0.432	**0.027^{b}**	0.072	0.082	**0.007^{ab}**
PD	0.093	**0.004^{ab}**	**0.001^{ab}**	0.250	0.374	**0.028^{ab}**
SI	0.885	0.641	0.087	0.167	0.374	0.147
AA	0.144	0.869	**0.005^{bc}**	0.622	**0.015^{b}**	**0.032^{b}**
IE	**0.035^{b}**	**0.030^{a}**	0.325	0.403	**0.026^{b}**	**0.000^{ab}**
HAA	**0.024^{ab}**	0.798	0.243	**0.000^{ab}**	0.067	**0.039^{b}**

Results and Discussion

There was no significant difference in ball speed (Low: 75.7±5.1, Medium: 76.9±4.6, High: 77.7±4.9 mph). The shoulder forces and torques were significantly different among the three EPA groups (Table I). The primary differences appeared in the IE and HAA torque (Fig. 1). The IE torque was significantly different in the maximum value, timing of the maximum value, range and duration between the maximum and minimum values. The HAA torque was significantly different in the maximum value. The PD force was significantly different in the timing of the maximum value.

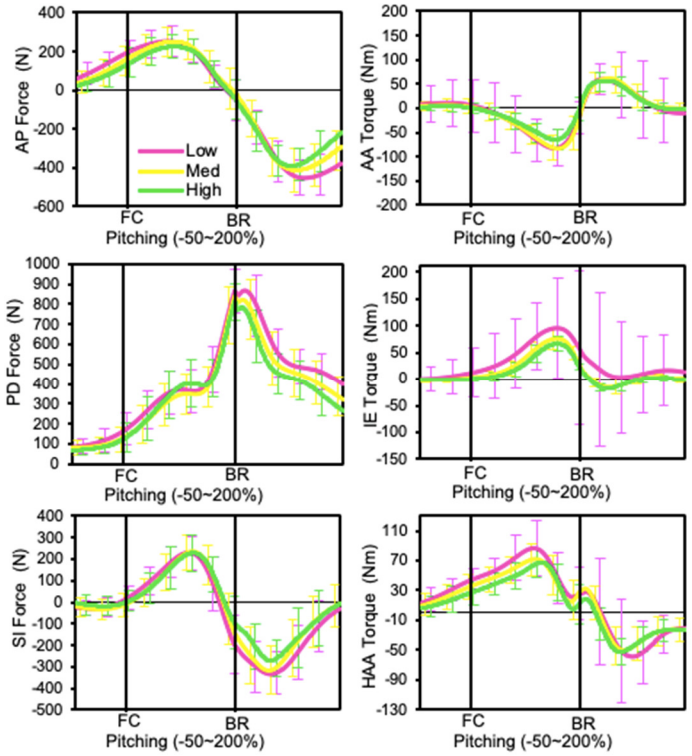

Figure 1: Forces and torques during pitching (mean±SD) normalized from foot contact (FC: 0%) and ball release (BR: 100%).

These findings bridge the gap, showing that SER ROM during exam is related to shoulder joint loading during baseball pitching, aligning with previous work (4). The differences found in the maximums show that lower EPA was associated with higher shoulder forces or torques. The differences found for max, min and range and timings could be contributed to different pitching styles or mechanics, which was similar to a previous study (5). In conclusion, SER ROM during a physical exam is related to shoulder forces and torques during baseball pitching.

Significance

Higher shoulder joint loading leads to more injury incidences. These results show that high EPA is advantageous because it reduces the shoulder joint loading during baseball pitching. The measurement of SER ROM allows team physicians to address and correct those with limited EPA to prevent throwing injury.

Acknowledgments

This study is funded by a Clinical Research Grant from Major League Baseball.

References

1) Oyama S., *JSHS*, 2012. 2) Wilk, *Am J Sports Med*, 2015. 3) Zheng N., *Int J Sports Med*, 2011. 4) Flesig, *Am J Sports Med*, 1995. 5) Urbin M.A., *Am J Sports Med*, 2012.

External Shoulder Flexibility During Physical Exam Is Related to Shoulder Joint Loading During Baseball Pitching

Hannah L. Stokes[1], Nigel Zheng[1], Koco Eaton[2]
[1]University of North Carolina at Charlotte, NC, [2]Tampa Bay Rays and University of South Florida, FL
nzheng@uncc.edu

Introduction

Increased throwing arm flexibility in baseball pitching increases performance but is also a risk factor for throwing-related injuries. A study showed when shoulder laxity worsens then instabilities develop and increase injury incidences (1). Shoulder pain in youth baseball pitchers was shown to be caused by forces and torques on the shoulder joint (2).

The purpose of this study is to investigate how shoulder flexibility measured during a physical exam is related to the shoulder joint loading. This connection could serve as a link between clinical examinations and shoulder joint loading. We hypothesize that shoulder flexibility is not related to the shoulder joint loading during baseball pitching.

Methods

The study included 177 college pitchers (height: 186 ± 7.2 cm and weight: 188 ± 19.6 lbs). The study protocol was approved by an institutional board, and all participants gave written informed consent. The resistive onset angle (ROA) and shoulder rotational flexibility (SRF) during passive ROM exam were previously defined (3). They were measured and calculated during a physical exam using a custom-made wireless device (Figure 1). The pitchers were grouped into low (< mean–SD, n=23,26), medium (mean±SD, n=126,121), and high (> mean+SD, n=28,30) SRF and ROA respectively.

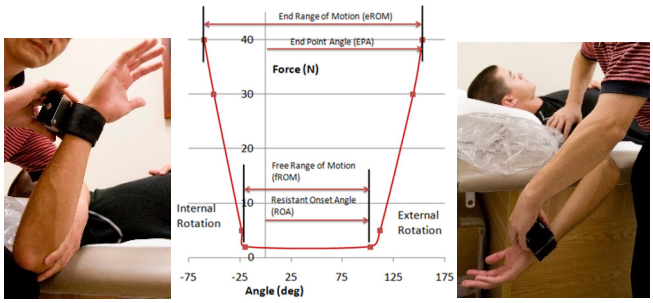

Figure 1: Shoulder rotational laxity test performed during an exam. ROA and EPA were measured and SRF is the slope between the two (3).

Ten fastball pitching motions were collected at 240 Hz using a motion capture system. Three best pitches were analyzed. A custom MATLAB program was created to calculate: anterior/posterior (AP) force, proximal/distal (PD) force, superior/inferior (SI) force, abduction/adduction (AA) torque, internal/external (IE) torque and horizontal abduction/adduction torque (HAA) using an inverse dynamics model. One-way analysis of variance (ANOVA) with Tukey post-hoc tests were performed using SPSS with an alpha set to 0.05. The maximum and minimum values of these shoulder kinetic variables were compared among the three SRF and ROA groups.

Results and Discussion

The maximum value AP force was significantly different among the three SRF groups (Table 1). High SRF leads to low joint loading in PD force, AA torque, and HAA torque at maximum values and AP force, PD force, IE torque, and HAA torque at minimum values. The maximum value IE torque was significantly different among the three ROA groups. High ROA leads to low joint loading for all variables at maximum and minimum values.

Table I: Maximum shoulder forces (N) and torques (Nm) for both SRF and ROA (mean±SD). For post-hoc tests p<0.05, a: Low vs Medium, b: Low vs High, c: Medium vs High.

		Maximum			Minimum		
		L	M	H	L	M	H
ROA	AP	284±83	269±71	268±55	-461±99	-451±96	-436±83
	PD	874±128	861±130	845±94	68±26	67±28	54±27
	SI	259±94	252±79	254±68	-382±120	-372±104[c]	-322±69[c]
	AA	83±57	63±23	65±12	-106±70[b]	-90±26[c]	-71±21[bc]
	IE	86±25[b]	78±19[c]	67±11[bc]	-14±25[ab]	-23±6[a]	-23±5[b]
	HAA	92±44[b]	81±20	76±15[b]	-78±79	-60±21	-63±16
SRF	AP	266±59	265±70[c]	301±76[c]	-468±82	-450±98	-434±85
	PD	874±107	859±127	853±128	74±23	63±30	64±21
	SI	238±59	255±79	261±92	-329±80	-365±103	-390±113
	AA	74±17	71±32	65±27	-83±23	-90±39	-90±32
	IE	75±16	82±73	83±25	-24±6	-22±13	-20±6
	HAA	90±17	82±26	76±22	-63±19	-64±40	-60±24

This emphasizes that shoulder flexibility should be measured and monitored in order to reduce shoulder joint loading during baseball pitching. Both ROA and SRF contribute to the results of shoulder joint loading for EPA. Loss of shoulder flexibility leads to increased shoulder joint loading, aligning with previous work (4). Further, a study showed in youth baseball pitchers that increases in forces and torques of the shoulder can lead to deformation of soft tissue leading to injury over time (5). These differences could be contributed to different age populations and pitching styles or mechanics. In conclusion, shoulder external rotation flexibility measured during physical exam is related to shoulder joint loading during baseball pitching.

Significance

High shoulder flexibility is advantageous in baseball pitchers because it lowers the forces and torques on the shoulder joint. High shoulder external rotation range before any resistance (ROA) may reduce the risk of injury during baseball pitching. Shoulder flexibility could serve as a screening that could aid clinicians and coaches in prospectively identifying players at risk for developing arm injuries during the season.

Acknowledgments

This study is funded by a Clinical Research Grant from Major League Baseball.

References

1) Laudner K., *Am J Sports Med,* 2012. 2) Tanaka H., *Am J Sports Med*, 2018. 3) Zheng N., *Int J Sports Med*, 2011. 4) Oyama, S., *J Sport Health Sci*, 2012. 5) Sabick, M. *Am J Sports Med*, 2005.

Shoulder Rotational Properties During Physical Exam Are Related to Performance and Injury During Baseball Pitching

Hannah L. Stokes[1], Nigel Zheng[1], Koco Eaton[2]
[1]University of North Carolina at Charlotte, NC, [2]Tampa Bay Rays and University of South Florida, FL
nzheng@uncc.edu

Introduction

Increasing both shoulder external rotation and angular velocity during baseball pitching improves performance but also increases the risk for injury. Developing the kinetic chain increases both the shoulder external rotation angle and shoulder angular velocity which increase ball speed and performance (1). A study showed that increasing ball speed also increased the risk for injury (2). Improving performance and reducing injuries are a focus for both coaches and players.

The purpose of this study is to investigate how shoulder rotational properties measured during a physical exam are related to performance and injury during baseball pitching. This connection could create a quantitative measurement and predictor for baseball performance and injury. We hypothesize that shoulder rotational properties during physical exam are not related to shoulder kinematics during baseball pitching.

Methods

The study included 177 college pitchers (height: 186 ± 7.2 cm and weight: 188 ± 19.6 lbs). The study protocol was approved by an institutional board, and all participants gave written informed consent. Self-reported injury questionnaires were filled out when pitchers were tested and then during follow-ups (95 of them were followed at least for one year). The following shoulder rotational properties: end-point angle (EPA), shoulder rotational flexibility (SRF), and resistant onset angle (ROA) were previously defined (3). They were measured and calculated during a physical exam using a custom-made wireless device.

Ten fastball pitching motions were collected at 240 Hz using a motion capture system. A custom MATLAB program was calculated the following shoulder kinematic variables: maximum external rotation angle (ERA), timing of ERA (PERA), maximum internal rotation angular velocity (IRV) and timing of IRV (PIRV) throughout the pitching cycle. Timing variables PERA and PIRV were normalized based on the lead foot contact (0%) and the ball release (100%). One-way analysis of variance (ANOVA) with Tukey post-hoc tests were performed using SPSS with an alpha set to 0.05. The chi-squared test was performed on the follow up injury questionnaires.

Table I: Results from gun speed (mph) of baseball pitch and follow-up injury questionaires (total number of elbow and shoulder surgeries).

	EPA			SRF			ROA		
Group	L	M	H	L	M	H	L	M	H
n	33	114	30	23	126	28	26	121	30
Gun Speed	76 ± 5	77 ± 5	78 ± 5	77 ± 4	77 ± 5	78 ± 5	77 ± 4	77 ± 5	78 ± 5
Surgery	0	12	2	0	9	5	3	10	1
NoSurgery	19	58	18	14	71	10	11	67	17

Results and Discussion

Shoulder ERA, PERA, and PIRV were significantly different among the three EPA groups (Figure 1). Shoulder ERA and PIRV were significantly different among the three ROA groups. No significant difference was found among the three SRF groups. There was no significant difference in gun speed (Table 1). There was a significant difference in follow up surgeries among SRF groups (p=0.02). There was no significant difference in follow-up surgeries among EPA (p=0.13) or ROA (p=0.41) groups.

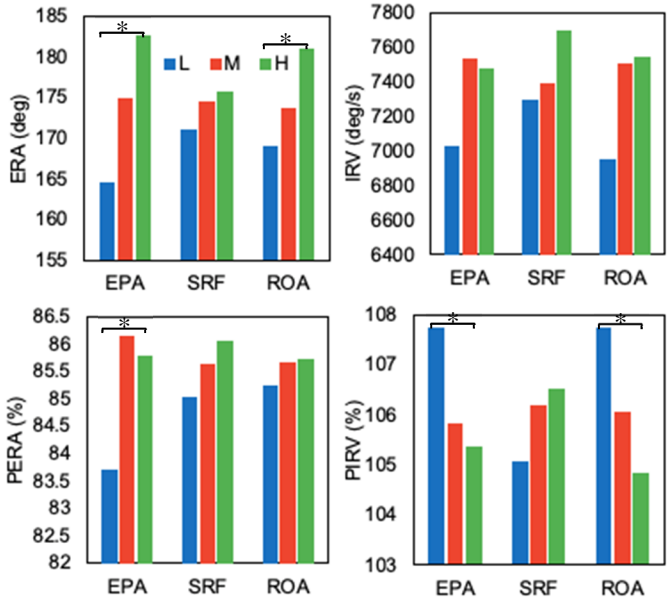

Figure 1: Shoulder rotational properties versus the ERA and IRV values and timings during baseball pitching (* indicates p<0.05).

Findings of this study emphasizes that shoulder rotational properties should be measured and monitored in order to improve performance and reduce injury during baseball pitching. Increased shoulder range of motion increases both ERA and gun speed, aligning with previous work (4). Our results showed many factors influence the incidence of injury, including the following: joint loading, flexibility, experience of pitcher and pitching styles or mechanics, aligning with previous work (5). In conclusion, shoulder rotational properties measured during physical exam are related to both performance during baseball pitching and risks for injuries.

Significance

Greater shoulder external rotation is advantageous in baseball pitching because it reduces joint loading and increases ball speed. Shoulder rotational properties during physical exam should serve as a screening that could aid clinicians and coaches in prospectively identifying players who will perform best and reduce injury throughout the season.

Acknowledgments

This study is funded by a Clinical Research Grant from Major League Baseball.

References

1) Thompson S., *Sports Health*, 2017. 2) Bushnell B., *Am J Sports* Med, 2010. 3) Zheng N., *Int J Sports Med*, 2011. 4) Seroyer S., *Sports Health*, 2010 5) Popchak A., *Am J Phys Med Rehabil*, 2015.

Knee Kinetics in Baseball Hitting and Their Implication for Return to Play After Anterior Cruciate Ligament Reconstruction

Kevin A. Giordano[1], Meredith Chaput[2], Adam Anz[3], James Andrews[3], Gretchen D. Oliver[1]
[1]Sports Medicine and Movement Laboratory, Auburn Universiy School of Kinesiology, Auburn, AL
[2]Ohio University, Athens, Ohio
[3]Andrews Research and Education Foundation, Gulf Breeze, FL
Email: KAG0070@auburn.edu

Introduction

Anterior cruciate ligament (ACL) tears are the most common injury requiring surgery among high school athletes.[1] In baseball, ACL tears are more prevalent in position players than pitchers.[2] Position players are required to complete short bursts of maximal exertion from a static position, often including high rotary movements, like hitting. However, kinetics at the knee in hitting have not been described in the literature.

Despite the large incidence of ACL tears and ACL reconstruction (ACLr), there are very few sport specific measures for return to play (RTP). Therefore, the purpose of this study was two-fold (1) to describe knee kinetics in baseball hitting and (2) to provide clinicians a tool to predict knee kinetics based on easily accessable information to help individualize rehabilitation protocols for safe RTP.

Methods

Nineteen high school baseball athletes (16.3 ± 0.8 yrs, 180.6 ± 5.7cm, 78.4 ± 10.8kg) participated. Participants completed a self selected independent warm up in preparation to give game-effort swings. Participants took ten swings off a tee. The swings with the top three exit velocities were included for analysis. Kinetic data were recorded using an electromagnetic tracking system, normalized to participant mass, and reported as external moements. Position and orientation data were obtained using Euler angle sequences consistent with ISB recommendations.[3]

Linear regressions were used to determine if height, mass, age and exit velocity could predict bilateral knee net, extension, internal (IR) and external (ER) rotation, valgus and varus moments and anterior force. Backwards regressions were chosen to analyse data due to the nature of the predictors being easily accessable by clinicians, who may discard unneeded information.

Table 1: Descriptive Statistics of Maximum Knee Kinetics

Front Knee	
Net Torque	0.32 ± 0.10
Internal Rotation Torque	0.08 ± 0.05
External Rotation Torque	0.09 ± 0.04
Extension Torque	0.20 ± 0.08
Valgus Torque	0.14 ± 0.07
Varus Torque	0.16 ± 0.06
Anterior Force	1.10 ± 0.31
Back Knee	
Net Torque	0.41 ± 0.17
Internal Rotation Torque	0.15 ± 0.09
External Rotation Torque	0.16 ± 0.07
Extension Torque	0.14 ± 0.10
Valgus Torque	0.13 ± 0.06
Varus Torque	0.10 ± 0.06
Anterior Force	0.75 ± 0.20

Torques given in Nm/kg body mass, forces given in N/kg body mass

Results and Discussion

Descriptive statistics of selected kinetic variables are displayed in Table 1 and regression equations in Table 2. Kinetic variables chosen for inclusion were based on their directionality mechanically stressing the ACL.[4,5]

Table 2. Backwards Regression Equations

Front Knee	*F*	R^2	*p*
(IR)' = -0.268 + 0.027(age)	4.51	.163	**0.049**
(ER)' = 1.243 - .007(cm) + .002(kg)	4.74	.294	**0.024**
(Ext)' = 2.371 - .018(cm) + .005(kg) + .043(age)	5.49	.427	**0.010**
(Var)' = 1.331 + .002(EV) - .009(cm) + .003(kg)	3.59	.301	**0.039**
(Ant)' = 10.692 - .082(cm) + .026(kg) + .194(age)	10.44	.611	**0.001**
Back Knee	*F*	R^2	*p*
(Net)' = 0.588 - .016(cm) + .169(age)	3.57	.313	**0.019**
(Vlg)' = 1.552 - .012(cm) + .006(kg) + .020(age)	3.66	.307	**0.037**

' denotes predicted value, IR = internal rotation torque, ER = external rotation torque, Ext = extension torque, Vlg = valgus torque, Var = varus torque, Ant = anterior force, EV = exit velocity in MPH, cm = height in cm, kg = mass in kg, age = age in years

Using predictors age, height, mass and ball exit velocity, we were able to predict IR, ER, extension and varus torques and anterior forces in the front knee. This is clinically meaningful, because our strongest predictor, anterior force, most directly stresses the ACL.[4] In the back knee, we were able to predict net and valgus torques. This is clinically significant as valgus stress is a commonly known risk factor for ACL injury.[6]

To our surprise, ball exit velocity was seldom a predictor of knee kinetics, and height was a negative predictor. Age and mass were positive predictors as expected. These equations can be used by clinicians to predict knee kinetics in baseball players after ACLr and compare to kineitc values of traditional ACL rehabilitation exercises, to safely initiate hitting programs.

Significance

To the author's knowledge, this is the first study describing knee kinetics in baseball hitting. These values can be used by clinicians to determine when it is safe to initiate hitting after ACLr, and adds sport specific measures to general ACLr rehabilitation protocols.

References

1. Rechel JA (2011). *J Trauma.* 71(4).
2. Erickson BJ (2019). *Ortho J Sports Med.* 7(10).
3. Wu G (2002). *J Biomech.* 35(4).
4. Purnell ML (2008). *Am J Sports Med.* 36(11).
5. Peterson W (2007). *Clin Orthop Relat Res.* 454.
6. Hewett (2019) *Journal of Orthopedic Research.* 37(8)

The Relationship between Humeral Segment Energy and Hand Angular Velocity in Softball Hitting

Nicole M. Bordelon.[1], Kyle W. Wasserberger[1], Jessica L. Downs[1], Kenzie B. Friesen[1], Jessica K. Washington[2], and Gretchen D. Oliver[1]
[1]Auburn University, Auburn, AL
[2]Berry College, Mt Berry, GA
Email: goliver@auburn.edu

Introduction

Softball hitting initiates proximal to distal kinetic chain sequencing by transferring mechanical energy sequentially from the lower extremities to the trunk, humerus, forearm, and hand [1]. Based on the summation of speed principle, hand velocity is maximized just before ball contact and is therefore used as an indicator of hitting performance [1, 2]. Although efficient energy transfer is essential to maximizing hand velocity, previous softball hitting research has yet to examine the association between patterns of mechanical energy transfer and hitting performance.

Energy flow analysis can be used to provide a deeper understanding of how energy flows throughout the kinetic chain during hitting. Recent studies examining the baseball pitch and tennis serve have reported relationships between the magnitude of energy flow into the upper extremity and ball velocity [3, 4]. Therefore, the purpose of this study was to investigate the relationship between humeral segment energy flow during the acceleration phase of the softball swing and lead hand angular velocity at ball contact. It was hypothesized there would be a relationship between net and maximum rates of segment energy inflow (IF) and outflow (OF) with hand velocity.

Methods

Twenty-five female collegiate softball athletes (20.4±1.7yr; 166.7±22.0cm; 74.9±15.9kg) participated and were currently active on a playing roster as well as injury free for the past six months. Participants performed three maximum effort swings off a stationary tee placed in the middle of the strike zone. An electromagnetic system and force plate were used to collect kinematic and kinetic data during each swing. Data were analyzed during the acceleration phase, defined as the period from stride foot contact to ball contact.

The rate of work done on or by the humerus at the distal (elbow) and proximal (shoulder) joints were calculated using equations 1 and 2, respectively. The individual joint force power (JFP) and segment torque power (STP) terms were summed to calculate total humeral segment power (SP) using equation 3.

(1) JFP = (joint reaction force) · (linear joint velocity)
(2) STP = (joint moment) · (humeral angular velocity)
(3) $SP = (JFP_{distal} + STP_{distal}) + (JFP_{proximal} + STP_{proximal})$

Total SP was integrated over the acceleration phase to calculate net segment energy transfer. Further, SP was separated into positive (IF) or negative (OF) components to determine net energy gained and transferred out of the humerus, respectively. Pearson product-moment correlations were used to determine relationships between humeral segment IF and OF during the acceleration phase with angular hand velocity at ball contact.

Results and Discussion

The results support the hypothesis indicating a relationship between humeral energy OF and angular hand velocity. Significant negative correlations between humeral OF and hand velocity (r=-.72, p<.01) along with maximum rate of humeral OF and hand velocity (r=-.69, p<.01) (Figure 1a, 1b) were observed. Angular hand velocity increased with increased magnitude of humeral OF. However, the hypothesis for energy IF was not supported.

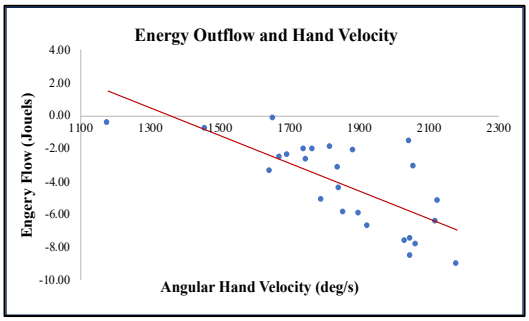

Figure 1a. Outflow and hand velocity

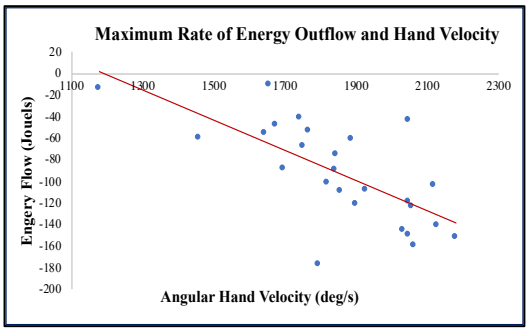

Figure 1b. Maximal OF and hand velocity

Significance

Softball hitting performance is strongly associated with humeral segment energy OF. However, future studies should examine JFP and STP components to more precisely isolate energy IF and OF at the segment's proximal and distal ends in addition to determining the relative linear and angular contributions towards humeral OF..

Efficient energy flow through the kinetic chain is essential to optimizing performance during hitting [1]. This study illustrated a strong relationship between humeral OF and hand angular velocity at ball contact; therefore, energy flow analysis can be used as an additional tool to provide a deeper understanding of how energy is generated, absorbed, and transferred through body segments during softball hitting.

References

1. Welch C, et al. *J Orthop Sports Phys Ther,* 22(5)
2. Washington J, et al. *J Sports Sci*, 38(1)
3. Howenstein J, et al. *Med Sci in Sports and Exerc*, 51(3)
4. Martin C, et al. *Am J Sports Med,* Arthrosc

Segmental components of induced velocity and power of a pitched baseball in collegiate baseball players

Arnel Aguinaldo,[1] Kristen Nicholson,[2] Gordon Alderink[3]
[1]Department of Kinesiology, Point Loma Nazarene University, San Diego, CA, USA
[2]School of Medicine, Wake Forest University, Winston-Salem, NC, USA
[3]Department of Physical Therapy, Grand Valley State University, Grand Rapids, MI, USA
Email: arnelaguinaldo@pointloma.edu

Introduction

In an open kinetic chain such as baseball pitching, the velocity of the throwing arm is affected by the mechanical power through the chain via coordination of proximal-to-distal segmental motion, where muscular torques can induce accelerations of anatomically remote segments through dynamic coupling [1,2]. However, traditional inverse dynamics approaches are insufficient in decomposing the components of segmental motion that contribute to the forward velocity of the pitched ball [3]. Previous researchers have implemented induced acceleration analysis (IAA) models to perform this decomposition in baseball pitching but did not include lower body contributions [1,4]. Hence, the purpose of this study was to use a full-body IAA to examine how muscular and non-muscular torques contribute to the forward velocity of a pitched ball off a mound in collegiate baseball players. A secondary aim was to examine how these components contribute to the induced power of the throwing arm.

Methods

This retrospective study was approved by the institutional review board at Wake Forest University. Data from 17 collegiate pitchers (age = 20.4 ± 1.2 years, height = 1.87 ± 0.05 m, mass = 94 ± 7 kg) were examined from in-season pitching analyses. Each participant threw 12 various types of pitches to a catcher at a regulation distance (18.4 m) away from a mound instrumented with three force platforms (AMTI, Watertown, MA). One representative fastball was extracted for this analysis in which 3D motion data were captured at a sampling rate of 400 Hz using a marker-based motion analysis system (Qualisys, Göteborg, Sweden) [1]. Ground reaction force (GRF) data were collected at sampling rate of 1000 Hz. Ball speed was recorded with a pitch flight analysis device (Rapsodo, Brentwood, MO).

A 14-segment model was configured and implemented in Visual 3D (C-Motion, Germantown, MD). The joint accelerations were estimated using the following IAA equation:

$$\ddot{\boldsymbol{\theta}} = \boldsymbol{I}^{-1}(\boldsymbol{\theta})[\boldsymbol{\tau} + \boldsymbol{V}(\boldsymbol{\theta}, \dot{\boldsymbol{\theta}}) + \boldsymbol{g}(\boldsymbol{\theta})]$$

where $\ddot{\boldsymbol{\theta}}$ = generalized accelerations vector, $\boldsymbol{I}^{-1}$ = inverse of the system inertia matrix, $\boldsymbol{\tau}$ = vector of the net muscular torques, $\boldsymbol{V}(\boldsymbol{\theta}, \dot{\boldsymbol{\theta}})$ = vector due to velocity-dependent (Coriolis, centripetal) forces, and $\boldsymbol{g}(\boldsymbol{\theta})$ = gravitational force. By taking the product of each force or torque component and the corresponding velocity vector, an induced power analysis (IPA) of the throwing arm was performed [1]. All IAA equations were derived in SD/Fast (PTC, Cambridge, MA) and implemented in Visual 3D.

The induced ball velocity was calculated by time-integrating the induced acceleration of each source between the instants of maximum knee height in the stride phase and ball release. Likewise, the mechanical work of the throwing arm was computed via time integration of the induced power between these events. The concurrent validity of the IAA model was estimated with the Spearman rho (ρ) coefficient (α = 0.05) by comparing the induced ball velocity with the ball speed obtained from the pitch flight device.

Results and Discussion

The results of this IAA indicated that the largest contribution to ball velocity came from the shoulder torque followed by velocity-dependent forces (Figure 1).

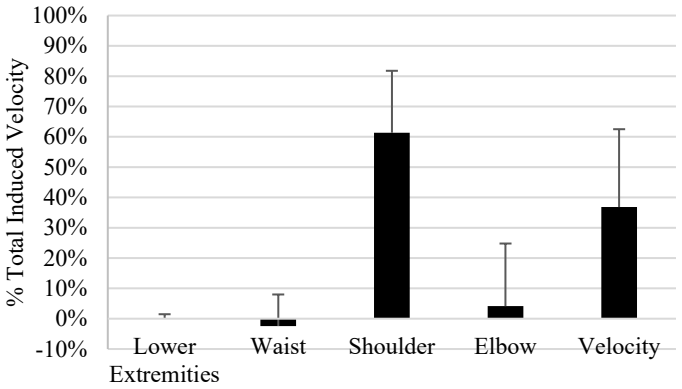

Figure 1: Mean contributions (%) to the induced ball velocity (n=17).

Similarly, the IPA showed that the velocity-dependent torque represented the largest proportion (60%) of the energy transferred to the arm at -0.93 ± 0.62 J/kg. This finding aligns with previous IPA studies which showed how pelvis and trunk motion indirectly accelerate the throwing arm via the velocity-dependent torque [1,3].

The forward velocity of the ball estimated by the IAA model was 32.9 ± 5.4 m/s (73.5 ± 12.1 mph) while the recorded flight speed of the ball was 39.1 ± 0.9 m/s (87.5 ± 2.1 mph), indicating an underestimation error of 16% with low concurrent validity (ρ = -.177, p = .498). This error could be due to the IAA model, which defines the hand and ball as one rigid segment when the ball most likely moves relative to the ball.

Significance

These findings may challenge conventional wisdom regarding training and rehabilitation methods that are based on the current understanding of pitching biomechanics.

Acknowledgements

The authors thank Tom Kepple of C-Motion for the development of the IAA plug-in and for his technical contributions.

References

1. Aguinaldo, A.L., et al. (2020). *Sports Biomechanics*, 1-7, 10.1080/14763141.2019.1696881.
2. Alderink, G., et al. (2008). *Proceedings of the American Society of Biomechanics Meeting*, 5-6.
3. Naito, K., et al., (2011). *Sports Technology*, **4**(1–2), 37-41.
4. Hirashima, M., et al. (2008). *Journal of Biomechanics*, **41**(13), 2874-2883.

Proximal to Distal Sequence is Predicted by the Fibonacci Sequence

Wendi Weimar[1], John Fox[2], Brandi Decoux[3], Christopher Wilburn[1] and Glenn S. Fleisig[4]
[1]Auburn University, Auburn, AL 36849
[2]Other affiliations are optional for the abstract, but will be entered into the submission portal and will be searchable
Email: weimawh@auburn.edu

Introduction

Proximal to distal sequencing is a method of understanding the summation of speed principles proposed by Bunn in 1971. The premise of proximal to distal sequencing is that human limbs will begin in a position that provides for a decreased mass moment of inertia. As the performer progresses through the motion, in this case the overhand throw, the adjacent, more distal segment will extend, thus adding the velocity of the more proximal segment. This progressive increase from proximal segments to distal segments can be seen in many different movements and many theories have been proposed to explain this successive increase in speed, yet a definitive explanation eludes researchers.

In considering an explanation for this increase in speed progression, a mathematical sequence was sought. The sequence that was first to mind was the Fibonacci Sequence as its pattern has been found in other areas of nature. The Fibonacci Sequence starts with the number 1 and proceeds as the sum of the previous two numbers. In this manner, it starts with 1, the second entry is 1+ 0=1, the third entry and 1+1= 2, the fourth entry is 1+2 = 3, and so on. Fascinatingly, the ratio of the adjacent pairs is equivalent to the Golden Ratio which has been identified throughout nature including in the relationship between the variations of lengths of several anatomical segments, such as the length of the upper arm to the forearm. This relationship has also been found in the temporal components of the human gait cycle. However, the correlation of this sequence to velocities remains limited. Therefore, the purpose of the present project endeavoured to determine if the increases in speed associated with proximal to distal sequencing could be predicted by the Fibonacci Sequence.

Methods

Kinematic data collected for an unrelated project on overhand throwing was acquired and served as the measured data for this project. Ten right handed male collegiate baseball pitchers served as participants and kinematic data were captured with a 3D automated tracking system (Motion Analysis Corp.). The right Anterior Superior Illiac Spine (ASIS) was chosen as the beginning of the Fibonacci proximal-to-distal sequence of linear velocities in the direction of throw. As a result, the velocity of the right ASIS formed the initial number in the sequence (the initial "1's" of the previously mentioned sequence). Predicted right shoulder velocity was calculated as the sum of right ASIS and right ASIS. The right elbow predicted velocity was the sum of the velocities of the ASIS and the shoulder. Last, predicted right wrist velocity was calculated as the sum of the shoulder and elbow predicted velocities. A regression analysis was then conducted on the predicted and measured velocities.

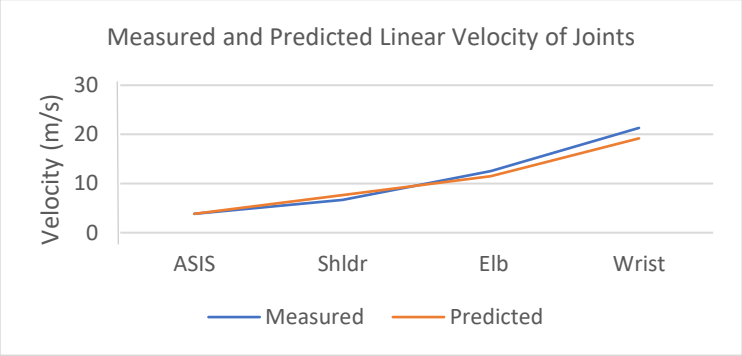

Figure 1: Measured versus predicted velocities of the ASIS, shoulder, elbow, & wrist.

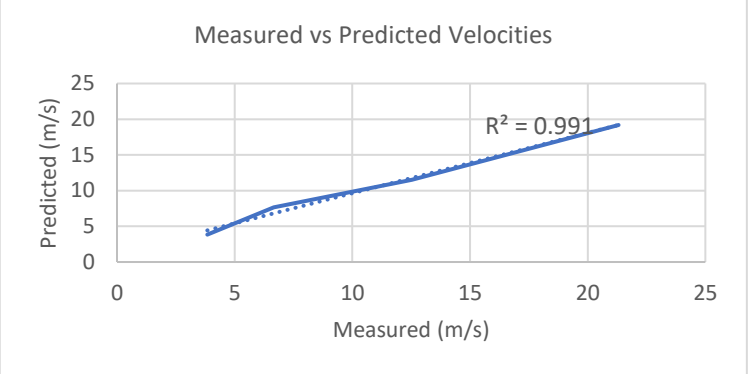

Figure 2: A scatter plot of the predicted values of velocity vs the measured values of velocity for the ASIS, shoulder, elbow and wrist.

Results and Discussion

Figures 1 and 2 present the relationship between the two data sets. The value of Figure 1 is in the pictorial relationship between the two data sets. The value of Figure 2 is in the presentation of the coefficient of determination. Based on the strength of the coefficient of determination, it is clear that there is a strong relationship between the measured and calculated values. Under further scrutiny, two participants deviated from the predicted values to a greater extent than the other participants (not enough to be outliers) and it was revealed that these participants were recovering from injuries. The primary finding of this project is two-fold: (1) the velocity of the wrist can be predicted from the velocity of the ASIS; (2) there is a strong relationship between the peak linear velocity of the ASIS and the wrist velocity of the overhand pitch.

Significance

From a training perspective, the importance of being able to develop pelvic girdle velocity cannot be overstated. Further, the anecdotal finding of being able to identify injured throwers from this analysis may have implications for the prevention of injuries.

References

Bunn, J.W., Scientific Principles of Coaching, Prentice Hall, Inc., Englewood Cliffs, NJ, 1972

Using IMUs to Quantify Throw Counts and Intensities in Youth Baseball Players

Michael J. Rose[1], Katherine A. McCollum[1], Michael T. Freehill[2], and Stephen M. Cain[1*]
[1]University of Michigan, Ann Arbor, MI, USA, [2]Stanford University, Palo Alto, CA, USA
Email: smcain@umich.edu *corresponding author

Introduction

Injuries to the throwing arm, specifically the elbow, in baseball players has reached an epidemic across many age groups [1]. Of particular concern is the frequency of these injuries in younger players who have not reached musculoskeletal maturity. The rise of arm injuries has led to pitch count recommendations and guidelines by age, however, they are made on in-game pitches only and ignore the importance of warm-up throws before the game or at the start of each inning [2]. Further, current methods treat each pitch as equal intensity.

Increased measurement precision of stress on musculoskeletal structures may be possible with recent advances in wearable sensor technology. Small wearable inertial measurement units (IMUs) make it possible to capture every throw during games and practices and utilize IMU-derived data to estimate the amount of musculoskeletal stress via the level of intensity of each throw. The purpose of this pilot study was to develop a methodology to capture total throw count and to estimate the intensity of each throw accrued by adolescent (competitive) baseball players over a season of baseball.

Methods

In our IRB approved study, a local travel 11U baseball team of 11 players (11 males, age 10-11yrs) was recruited for participation in this study. All participants provided informed consent. An inertial measurement unit (GT9X, Actigraph, LLC) and charging station were distributed to each player on the team. IMUs were configured to collect both acceleration (±16 G) and angular rate (±2000 deg/s) continuously at a sampling rate of 100 Hz. IMUs were secured 3-5 cm above the lateral epicondyle of the throwing arm of each participant using a modified protective wrist/forearm guard (EvoCharge, EvoShield, LLC). Participants were instructed to wear their IMUs during any baseball activity (*i.e.* practice and games). Every 1-2 weeks, the IMUs were collected by a study team member to download the data and reinitialize the IMUs.

We developed custom algorithms in MATLAB (The MathWorks, Inc.) to identify and classify the intensity of each throw. Two structured workouts were carried out to develop the throw identification and intensity classification algorithms.

Table 1. Participant data collection and throw data.

Participant ID	Total Days of Data	Days with Throwing	Number of Throws
01	56	30	5,110
02	35	17	3,942
03	14	8	1,020
04	34	13	1,274
05	16	7	759
06	26	5	790
07	15	5	288
08	22	7	660
09	53	18	1,240
10	24	11	2,155
11	8	3	497
		Total	**17,735**

We found that features of the angular velocity signal could be used to accurately distinguish throws from other common baseball movements. For the intensity classification algorithm, a collection of acceleration metrics were calculated for each throw.

Results and Discussion

We were able to successfully utilize wearable IMUs to quantify throw counts and throw intensities over a spring/summer season of baseball. Throughout the study, we identified 17,735 throws from the 11 participants (Table 1). Compliance issues arose as participants were required to keep their own IMUs charged, and many throws were not captured because the IMUs stop collecting data when their battery is depleted.

A linear support vector machine, created from the preliminary structured workout to classify throw intensity, was applied to classify the season-long collection data (Figure 1). The results of this classification in combination with data for when participants pitched during the season suggest counting and assessing the intensity of all throws is more valuable than simply counting in-game pitches in determining player workload and thus mandating rest periods between activities.

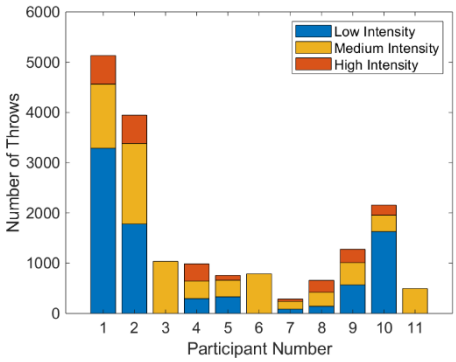

Figure 1: Intensity classification results for full-season data collection.

Significance

A wearable inertial measurement unit (IMU) placed on the throwing arm can be used to more precisely determine musculoskeletal stress (throw count and throw intensity) during a baseball season, which is necessary to reduce injury frequency and severity, particularly in youth athletes. These data can be used to explore the relationship between musculoskeletal stress and structural changes about the elbow joint (measured via clinical tests and imaging).

Acknowledgments

This project was supported by a grant from Major League Baseball. We thank Bethany Ruffino for helping facilitate data collections and thank the participants for diligently wearing the sensors throughout the season.

References

[1] Fleisig GS and Andrews JF (2012). *Sports Health*, **4**.
[2] Zaremski J et al. (2018) *Orthop J Sports Med*, **6**.

Effect of Real-Time Feedback on Baseball Pitching Mechanics Using Inertial Measurement Units

Andrew P. Oliver[1] and Michelle B. Sabick[1]
[1]Saint Louis University, St. Louis, MO
Email: andrew.oliver@slu.edu

Introduction

Overuse injuries in youth pitchers are prevalent and increasing, so prevention is a pressing concern (1). Performing an efficient pitching motion requires optimal activation of musculature and timing of major steps in the motion (2). Correcting flaws in the pitching mechanics could reduce the stress on the elbow and shoulder and possibly prevent many overuse injuries.

This study is important because it collected lower extremity kinetic data in the field using IMUs and it evaluated the effectiveness of real-time feedback given to pitchers. Pitchers threw with increased stride length, decreased stride length, and increased pelvis angular velocity in response to verbal cues. The effect of condition on velocity, ground reaction force, and kinematic measures was quantified. The use of IMUs in the field, the focus on lower extremity contributions to pitching, and the evaluation of real-time feedback are all novel aspects of the study.

Methods

Eleven male baseball pitchers (age: 22.1±1.6ys, ht: 1.8±0.1m, mass: 85.9±12.5kg) were recruited for this study. Kinematic data were recorded with inertial measurement units (IMUs) at 200 Hz, kinetic data of the drive (rear) leg (DL) and stride (front) leg (SL) were sampled at 1000 Hz, and pitch velocity was recorded by a radar gun. Four conditions were tested: baseline (no cue, BL), increased stride length (ISL), decreased stride length (DSL), and increased pelvis angular velocity (PAV). Subjects were told to alter stride length by 10% (~6 inches) and were told to rotate pelvis as hard as was feasible for the PAV condition. The three fastest pitches for each condition were analyzed. Ground reaction force (GRF) data was normalized to body weight (BW). The components of force in the direction of home plate and in the vertical direction were recorded. Variables were compared using Pearson correlation coefficients with the p-value set at 0.05 for all statistical comparisons.

Results and Discussion

The pitch velocity, ground reaction force values (Table 1), trunk angular velocity values, stride length (Table 2), and drive leg impulse values all significantly changed as a result of the real-time feedback cues given to the subjects. This showed that subjects were able to respond to feedback and alter their mechanics in real-time. Many of the ground reaction force variables were highly correlated to increased pitch velocity, increased peak trunk angular velocity, and increased peak pelvis angular velocity (Table 2). In some cases, individual outliers overshadowed the overall trends.

The main takeaways are that feedback can be incorporated in real-time to impact pitching performance and that there are significant differences as a result of this feedback. In addition, pitch impulse was utilized with kinematic variables to better understand the contribution of the lower extremities to pitch velocity in a more holistic way. Drive leg impulse varied significantly among three of the four pitch conditions.

GRF Variable	BL	DSL	ISL	PAV
DL Plate Dir.	56.0 ± 13.3	47.4 ± 9.6	61.3 ± 12.4	57.6 ± 12.3
DL Vertical Dir.	128.4 ± 12.4	120.4 ± 11.6	130.9 ± 12.6	128.7 ± 15.9
SL Plate Dir.	79.8 ± 13.5	84.6 ± 9.5	89.3 ± 19.2	87.3 ± 8.5
SL Vertical Dir.	144.2 ± 27.9	152.5 ± 19.2	160.7 ± 30.5	160.7 ± 26.3
Drive Impulse Plate Dir.	-15.7 ± 4.7	-13.8 ± 3.4	-17.8 ± 4.1	-16.3 ± 3.5

Table 1. Mean (±SD) GRF Values for each Condition (%BW).

GRF Variable	Velocity	Stride Length	Trunk Angular Vel.
BL Plate Direction	**0.534**	**0.619**	0.368
BL Vertical Direction	**0.731**	0.313	0.277
DSL Plate Direction	**0.602**	**0.637**	0.382
DSL Vertical Direction	**0.703**	0.394	**0.523**
ISL Plate Direction	**0.643**	**0.510**	0.283
ISL Vertical Direction	**0.815**	0.351	0.330
PAV Plate Direction	**0.669**	**0.507**	0.192
PAV Vertical Direction	**0.714**	0.474	0.226

Table 2. Correlations between Normalized Drive Leg GRF and Other Pitch Variables. (**Bold** = statistically significant).

Significance

This study demonstrates that simple verbal feedback cues can be used to significantly alter pitching performance, at least over the short term. Most subjects were able to adjust their stride length or pelvis angular velocity, which in turn affected pitch velocity. Therefore, coaches should consider telling pitchers to increase stride length and PAV as two ways of increasing pitch velocity. Significant differences were found in the stride length and pelvis angular velocity when the respective cues were given, showing that pitchers can respond to simple feedback to change their motions. This is one of the first studies to incorporate real-time feedback and its effects on pitching performance.

This study was also conducted completely in the field using IMUs. These versatile tools detected differences in lower extremity mechanics and can be valuable for collecting data outside a typical motion capture laboratory.

In addition, this is one of the first studies to utilize ground reaction force impulse values with other kinematic variables to get a more complete picture of how velocity is generated by pitchers. Future studies should investigate the same variables with a larger subject pool of high level college or professional pitchers to further understand the lower body contributions to pitch velocity.

References

1. Fleisig, G.S. and J.R. Andrews, Sports Health, 2012. 4(5): p. 419-24.
2. Norton, R., et al., AJSM, 2018.

Utilizing Kinematic Motion Capture Data to Visually Improve Lower Extremity Mechanics of a Pitching Motion

Andrew E Bryan[1], Jennifer Mathews, Jacob Howenstein, Michelle Sabick
[1]Biomedical Engineering, Parks College of Engineering, Aviation and Technology, Saint Louis University, St. Louis, MO
Email: andrew.bryan@slu.edu

Introduction

Most adolescent baseball pitchers depend on their coaches and trainers to correct their throwing mechanics. Often, these instructors must rely on visual methods to identify weaknesses and suggest modifications in pitching mechanics. Three easily identifiable variables in a pitching motion are foot placement, pelvis position and pelvis rotation. With maximum shoulder anterior force shown to increase 3.0 N for every centimeter the stride foot lands towards an open position, the need to efficiently and permanently correct stride angle is imperative.[1,2] This study examined the relationship between pelvis orientation at the instant of stride foot ground contact, the change in orientation of the pelvis during the pitch, and the angle between the stride foot and the drive foot, referred to as stride angle. By examining kinematic data obtained from a motion capture system, thoughtful instruction can be relayed to these coaches, so that they have proper and inciteful knowledge as to how to correct potentially long lasting damage to the young athelete or uncover a more efficent manner of pitching.

Methods

After sufficient warm-up, twenty-four male, adolescent baseball players (age: 11.1±1.3 yr) threw 15 fastballs at maximum effort towards a target.[3] Each subject was instrumented with a 32 marker, full-body marker set[3] and threw from a pitching mound. The three fastest pitches thrown for strikes were analyzed. Marker trajectories were tracked using Vicon Nexus Software (Vicon Corp, Oxford, UK) and filtered using a fourth-order, zero-lag, Butterworth filter with a cut-off frequency of 18 Hz using Visual 3D (C-Motion, Germantown, MD). Subjects were modelled using an eleven-segment model to compute kinematics and kinetics of each joint. The data were time-normalized to standardize the four critical phases of the pitching motion; maximum knee height of the stride leg (MKH), ground contract of the stride foot (SFC), maximum external rotation of the throwing shoulder (MIR), and maximum internal rotation of the throwing shoulder (MER). Mean values for the three trials per subject were used for all analyses. Pelvis axial rotation was calculated relative to the home plate direction.[3] The stride foot angle (θ) was calculated using the angle between the two ankles at SFC.

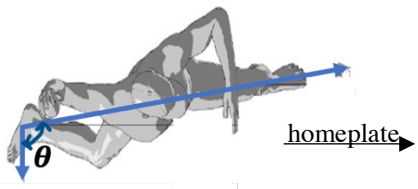

Figure 1: Measuring the stride angle using both ankle joint positions.[1]

Results and Discussion

We hypothesized that the change in axial orientation of the pelvis from MKH to SFC and the final axial angle of the pelvis at SFC would be related to stride angle. Of the 24 subjects, two presented with a θ larger than 90° upon SFC and three were inconsistent within their own trials. For those five subjects, average stride angle was 95.5° ± 4.6. Those with a closed stance averaged a stride angle of 79.0° ± 5.5. A Pearson correlation coefficient (α = 0.05) was caculated for both the change in pelvis orientation from MKH to SFC (Fig. 1) and the pelvis orientation at SFC with respect to the stride angle (Fig. 2). The correlation between the change in pelvis orientation and stride angle was 0.358 ($p=1.55x10^{-14}$) while the correlation between the pelvis orientation and stride angle was 0.017 ($p=3.21x10^{-6}$,). Therefore, both correlations were statistically significant, but practically very weak.

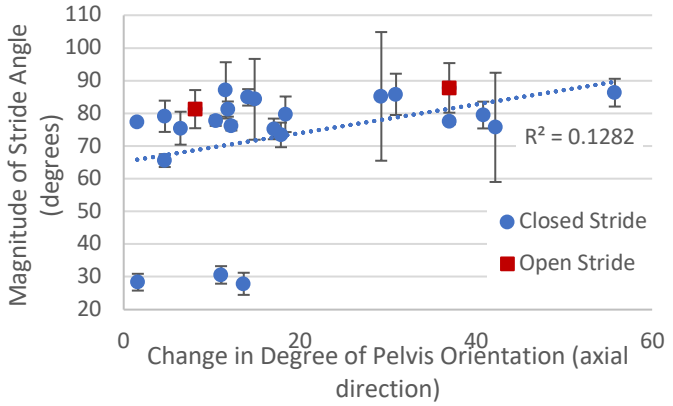

Figure 2: The magnitude of the stride angle compared to the change in pelvis orientation from MKH to SFC yields a weak correlation.

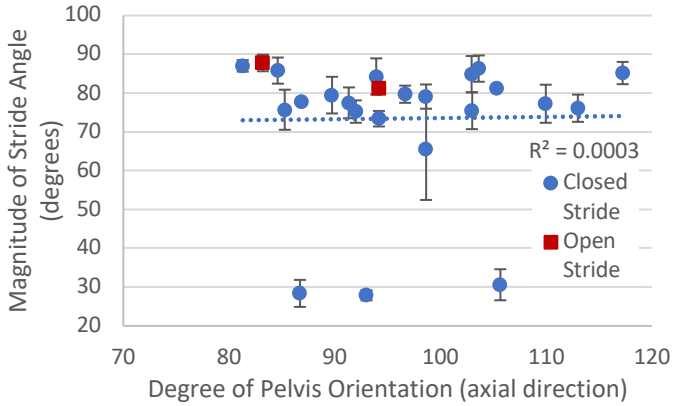

Figure 3: Comparison of the pelivs orientation at SFC and the stride angle yields a weak correlation.

Significance

Observing the change in axial orientation of the pelvis through MKH to SFC or pelvis orientation at SFC is not strongly correlated with the stride angle; therefore, it is not advisable for coaches of the sport to soley fixate on pelvis rotation when trying to correct an inapproriate stride offset. Until future work is completed, instructors of the sport must continue to make direct adjustments to the position of the stride foot at SFC as opposed to observing prior cues and revising those preceding mechanics.

References

1. Whitely Rob. *Baseball Throwing Mechanics as They Relate to Pathology and Performance — A Review*
2. Seroyer Shane. *The Kinetic Chain in Overhand Pitching*
3. Howenstein Jacob. *Energy Flow Through The lower Extremities, Trunk, And Arm In Youth Baseball Pitching*

ASB 2020 ABSTRACT

Christine Walck[1], Quinn Guzman[1]
[1]Embry-Riddle Aeronautical University, Daytona Beach, Florida, USA
Email: guzmanq@my.erau.edu

Introduction

Injuries between the L4-S1 vertebrae are extremely common in the golfing community. This is due to a four times larger compressive load being applied to the L4-L5 during each swing. Sean Foley, world renowned golf coach has reported seeing lower back issues in 80% of his students and claims lower back injuries lead to secondary injuries in the shoulders, wrists, and elbows (Floey,2010). Such injuries are common among those who play a draw-shot due to increases in pelvic angles combined with rotation. Therefore, it is our goal to create a musculoskeletal (MSK) model and simulation of an elite golfer to analyze the golf mechanics during a standard swing to grasp a better understanding of how the lumbar moves through its range of motion. The results from this case study will be used to develop a patient-specific protocol that will be later used to develop a database of relationships between lateral and anterior pelvic tilt with the rotational moments of the L4-L5 vertebrae.

Methods

The subject, a 20 year old male (57.6 kg) collegiate golfer with an official United States Golf Association (USGA) handicap of +1, performed three repetition draw shot swings barefooted. The elimination of shoes was enforced to limit the effects of shoes on the ground reaction forces.

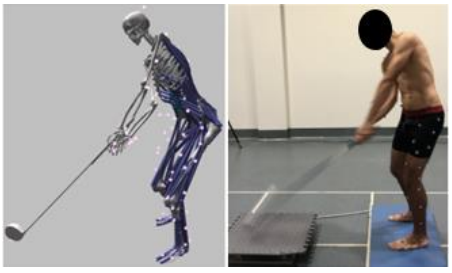

Figure 1: left: OpenSim MSK Model. Right: Subject within the motion capture lab.

Kinematic and kinetic data obtained from the dynamic swing trial was recorded using motion capture system (VICON Nexus, version 2.7; Oxford Metrics Ltd.) and two force plates ((OR6 2000 series; 1000 Hz; Advanced Medical Technologies Inc.). This data was then applied to a modified computational MSK model (Raabe,2016). Within this model, a driver was added as a segment to help scale the virtual driver to the experimental driver (Mahadas,2018). Most drivers are cut to different lengths to accommodate different players so it is important for this segment to be scaled properly. Marker placements followed the marker set from the Raabe model (Raabe,2016). Each segment is defined using 2-3 landmark markers and between 5-6 tracking markers with very heavy focus on the lower extremities given that is where the power is generated in a golf swing. Furthermore, the most common spinal injury for golfers occurs between the L4 and S1 vertebrae. Therefore, additional markers were added to the T10, T12, L3, and L5 vertebrae. The T10 and T12 were chosen since they are the lower portion of the thoracic spine closer to the lumbar. More specifically, the T12 since it is what connects the thoracic to the lumbar regions of the spine. The L3 and L5 were chosen since they are the midpoint and endpoints of the region of interest. The driver also had two markers: one on the driver's grip and the other on the head to aid in scaling. Inverse kinematics and dynamics were then performed to calculate joint angles and joint moments at each instant during the swing cycle. The subject naturally hits a draw shot shape in turn designating him a draw shot player. Although this makes him inherent to injuries between the L4-S1 vertebrae, he is currently free of all known musculoskeletal disorders.

Results and Discussion

A correlation between pelvic tilt and the moments at L4-L5 vertebrae was observed: as pelvic tilt increases the L4-L5 moment also increases as seen in Figure 2. In addition, this same correlation was observed between lateral pelvic tilt and L4-L5 moment. These correlations suggest that the angles of the pelvic griddle in the setup and throughout the swing have an effect on the loads being applied to the lumbar spine.

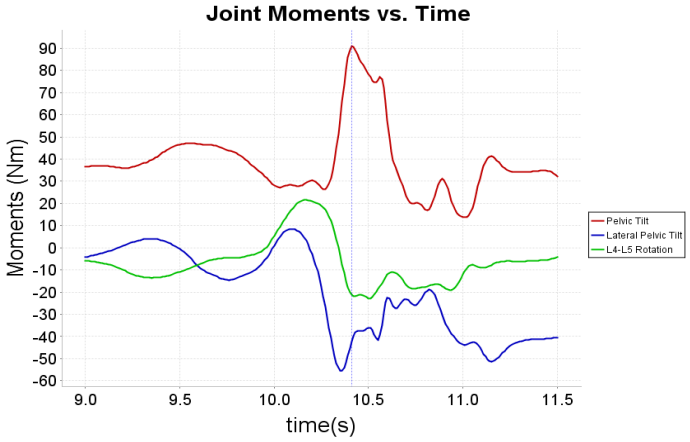

Figure 2: Shows the pelvic tilt and lateral tilt moment, and the L4-L5 rotational moment vs. time during one golf swing.

Significance

The importance of this case study is that it shows the potential for reduction in injuries of the lumbar spine through precision treatment. There is a potential to use these results to reposition the athlete in a less anterior and lateral pelvic tilt. If justified, this could be used by medical professionals, and athletic coaches to prescribe biomechanical adjustments in the golf swing in order to reduce the number of lumbar injuries around the world.

Acknowledgments

This study was conducted in the Embry-Riddle Biomechanical Analysis Laboratory under the assistance of graduate students Yeram Lim Sr. and Tyler Farnese.

References

doi:10.1016/j.jbiomech.2016.02.046.
doi:10.1016/j.compbiomed.2018.12.002.
Simtk-confluence.stanford.edu:8443/display/OpenSim/OpenSim+Documentation.
https://www.golfdigest.com/story/save-your-back-foley
Research, N.C.f.S.i.R. OpenSim User's Guide. 2018 [cited 3.3 2018]; 4.0:[Available from: https://simtk-confluence.stanford.edu:8443/display/OpenSim33/User%27s+Guide.

A Comparison of Filtering Techniques applied to Baseball Pitching Data

Stephen M. Cain
University of Michigan, Ann Arbor, MI, USA
Email: smcain@umich.edu

Introduction

In traditional, lab-based, biomechanics analyses, positions of optical markers on body segments of interest are measured and used to calculate segment positions, orientations, and joint angles. Body segment linear accelerations, angular velocities, and angular accelerations required to estimate joint kinetics via inverse dynamics must be calculated through numerical differentiation of position and orientation data. Position data must be smoothed before differentiation because differentiation can amplify small errors in position data [1]. Proper data smoothing can attenuate the noise content while leaving the true data signal unaffected, whereas improper signal processing can result in large errors in the kinematics calculated by differentiation [2].

Inertial measurement units (IMUs) enable direct measurement of the linear acceleration and angular velocity of any rigid body to which they are attached and therefore provide ideal measurements for evaluating position data filtering techniques. In this study, data collected during a baseball pitch by a wrist-mounted IMU is used to generate position data, which is then used to evaluate common data smoothing approaches.

Methods

In this IRB approved study, a wrist-mounted IMU (Opal, APDM, Inc.) measured the linear acceleration (±200 g) and angular velocity (±2000 deg/s) of the participant's throwing arm using a sampling rate of 800 Hz while the participant (an elite pitcher) completed a 32-pitch bullpen session. Angular velocities that exceeded the measurement range were extrapolated using cubic splines. Position data for a triad of simulated optical markers rigidly attached to the forearm IMU were generated from the measured acceleration and angular velocity by using inertial navigation techniques [3]. The primary marker was placed in the same location as the IMU; the other two markers were placed 0.1 m proximal and lateral from the primary marker, respectively. These noise-free position data were sampled at a range of common motion capture sampling rates (240, 300, and 500 Hz, [4-6]). White Gaussian noise (mean = 0, standard deviation = 0.001 m) was added to the sampled position data to simulate real data. These data were smoothed using 4th order Butterworth low-pass filters with set cut-off frequencies (6, 13.4, and 18 Hz, [4-6]) and a cut-off frequency determined from an autocorrelation-based procedure (ABP [7]), a generalized cross-validatory quintic spline (GCV [8]), and a predicted mean squared error quintic spline (MSE [8]). The smoothed position data were used to estimate the original IMU-measured linear acceleration (a) and angular velocity (ω). The error was quantified by the magnitude of the difference between estimated and measured values starting 200 ms before and ending 100 ms after ball release.

Results and Discussion

Table 1 provides summary data for a simulated motion capture sampling frequency of 500 Hz; lower sampling rates resulted in larger errors. Data from a representative pitch (Figure 1) illustrates the significant errors in estimates of linear acceleration and angular velocity that are created by improper data smoothing. No filtering technique resulted in estimates that were in full agreement with the original IMU-measured data. The results here suggest that employing a quintic spline smoothing algorithm (GCV or MSE) will yield the most accurate estimates of linear acceleration and angular velocity. Other filtering techniques should be explored with the approach above to identify a superior filtering technique for pitching and similar dynamic movements.

Table 1: Root mean squared (RMS) and maximum errors due to data smoothing across 32 pitches for a simulated motion capture sampling frequency of 500 Hz (values = mean (standard deviation)).

Filter	RMS Error		Maximum Error	
	|a| (m/s²)	|ω| (°/s)	|a| (m/s²)	|ω| (°/s)
6 Hz	258 (13)	1502 (71)	851 (40)	3432 (252)
13.4 Hz	183 (12)	647 (76)	581 (40)	1723 (182)
18 Hz	157 (13)	454 (51)	480 (40)	1307 (138)
ABP	72 (7)	128 (19)	270 (34)	438 69)
GCV	55 (6)	68 (6)	206 (32)	244 (39)
MSE	55 (5)	69 (6)	206 (30)	239 (33)

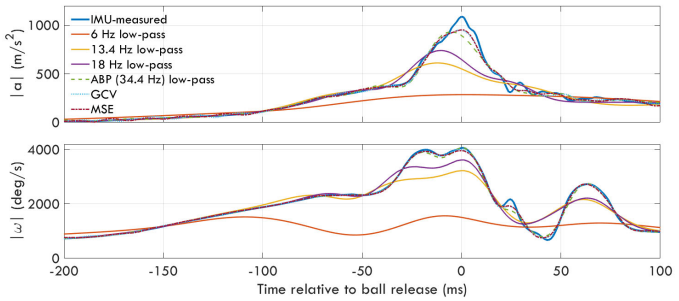

Figure 1: Acceleration (top) and angular velocity magnitudes (bottom) versus time relative to ball release (defined by the time of maximum forearm linear velocity) for one pitch (2-seam fastball, 90.4mph).

Significance

Accurate measurements of body segment linear accelerations, angular velocities, and angular accelerations are critical for calculating joint kinetics dominated by large body segment kinematics. IMUs can provide ideal measurements for accurately calculating joint kinetics as long as the detrimental effects of soft tissue motions between IMUs and bone can be minimized.

Acknowledgments

This research is supported by a University of Michigan Exercise and Sport Science Initiative grant. Thank you to Drs. Jill McNitt-Gray and Antonia Zaferiou for helpful discussions and insights.

References

[1] Derrick TR et al. (2020). *J Biomech* **99**.
[2] Walker JA (1998). *J Exp Biol* **201**.
[3] Titterton D and J Weston (2004).
[4] Hurd WJ et al. (2011). *Am J Sports Med* **39**(6).
[5] Fleisig et al. (2018). *Am J Sports Med* **46**(12).
[6] Aguinaldo A and R Escamilla (2019). *Orth J Sports Med* **7**(2).
[7] Challis JH (1999). *J Appl Biomech* **15**.
[8] Woltring HJ (1986). *Adv Eng Software* **8**.

Comparison of Hip Biomechanics During a Half and Full Golf Swing in Male Amateur Golfers

Christopher S. Wendt[1], Audrey L. Millar[1], Kelly Boss[1], and Chloe Gilgannon[1]
[1]Department of Physical Therapy, Winston-Salem State University, Winston-Salem, NC
Email: wendtcs@wssu.edu

Introduction

Golf has become a very popular sport worldwide, recently growing to approximately 33.5 million participants in the United States alone.[1] According to the National Golf Foundation's 2019 Participation Report, an estimated 15% of beginners in 2018 were over the age of 50. With an increase in middle-aged, committed participants, so does the risk for lower extremity pain, injury and/or surgery. Research has shown that though some participants report hip pain following golfing activities, most are eager to continue to play.[2] This presents a challenge for clinicians to determine the best protocol and progression to allow the patient to safely return to golf.

A common recommendation for those wishing to return to golf after a lower extremity injury or surgery is to use a half swing, however, there is little evidence to support that this significantly reduces the motion or muscular torque at the hip. The purpose of this study was to compare and evaluate the positions and internal torques of the hip during a half and a full golf swing in male amateur golfers.

Methods

Eleven healthy, amateur golfers volunteered to participate in this study. All participants were right-handed males, with a reported handicap of less than 20. Each golfer completed 10 full swings, followed by 10 half swings, instructed by a standardized script. Kinematic and kinetic data was recorded by a 10-camera motion capture system with a force platform under each lower extremity collecting ground reaction forces. A launch monitor recorded ball impact characteristics including club head velocity (CHV).

A 3-D modeling program was used for swing phase identification, data reduction, and standard inverse dynamic calculations to determine internal net joint torques. Participant demographics, internal hip torques (Nm; normalized by %BW*Ht) and hip positions (degrees) in all 6-degrees-of-freedom were analyzed in SPSS (v25). Repeated measures ANCOVAs (full swing CHV in mph as the covariate) and Pearson-Product Correlations were used to compare hip biomechanics during half and full golf swings, with significance level set at $p<.05$.

Results and Discussion

Participants (44±16 years) reported an average handicap of 13±6. Full swing CHV averaged 91±12 mph, consistent with average male amateur golfers. Peak trail hip extensor torque [Figure 1] was the largest internal torque produced in both half (12.04±2.07 Nm/%BW*Ht) and full swings (12.02±1.97 Nm/%BW*Ht). Peak lead hip flexor and abductor, and trail hip abductor torques were next largest, respectively, in both swing styles.

There were no statistically significant differences found in peak internal hip torque production between half and full golf swings when controlling for CHV. With respect to peak hip position, there were no significant differences found between half and full swings, with the exception of peak lead hip flexion ($p=.017$). Correlational analysis showed strong, statistically significant correlations between each half and full swing peak hip torque (ranging from $r=.71$ to $r=.98$) and position (ranging from $r=.85$ to $r=.99$).

Overall, peak hip joint torques and positions during a half golf swing were found to be comparable to those in a full golf swing. This suggests that reducing the length of the backswing may have minimal effect on demands at the hip in male amateur golfers.

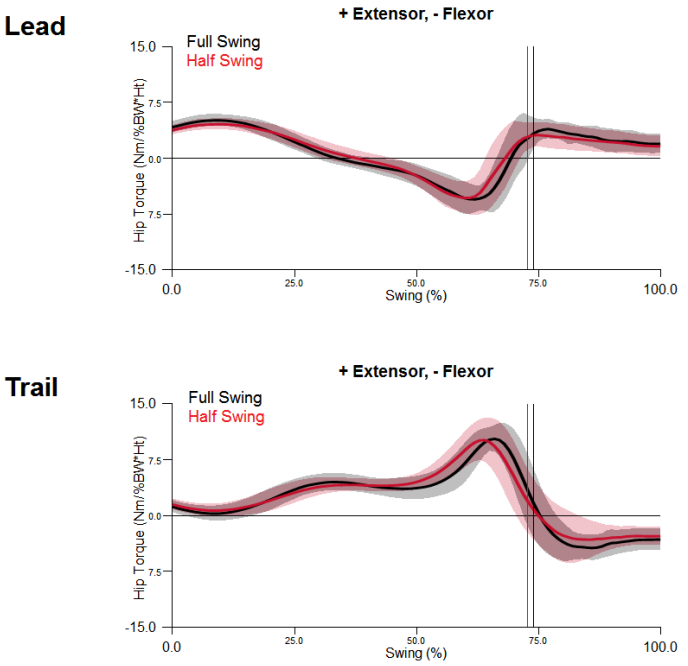

Figure 1: Mean sagittal hip torques (Nm/%BW*Ht) of the lead and trail limbs in a full (black) and half (red) golf swing.

Significance

In the present study, our data revealed no significant reductions in internal torque at either the lead or trail hip when performing a half golf swing, as compared to a full golf swing. Peak muscular torque production around the hip in both swing styles were much higher than reported hip torques for activities of daily living, such as level-walking.[3] These findings suggest that clinicians should use caution in recommending a half versus a full swing for those returning to golf following an injury or surgery.

Acknowledgments

The authors would like to acknowledge Ryan Johnson, DPT, Samantha Cates, DPT, Dustin Sellers and Dexter Perkins for their contributions to the overall, multi-dimensional study.

References

[1] National Golf Foundation. "Golf Participation Shows Positive Trends". Available at: https://www.thengfq.com/2019/06/ngfs-2019-participation-report/. Accessed March 17, 2020.
[2] Chatterji et al. Effect of total hip arthroplasty on recreational and sporting activity. *ANZ J Surg.* 2004.
[3] Moisio et al. Normalization of joint moments during gait: a comparison of two techniques. *J Biomech*. 2003.

Problem-based Learning Improves Student Learning in Undergraduate Biomechanics

Brian J. Wallace[1], Duane Knudson[2], and Naghmeh Gheidi[3]
[1]Department of Kinesiology, University of Wisconsin Oshkosh, USA,[2]Department of Health and Human Performance, Texas State University, USA, [3]Department of Exercise & Sport Science, University of Wisconsin-La Crosse, USA
Email: wallaceb@uwosh.edu

Introduction

Student's anxiety toward the difficult, but important, subject matter of biomechanics requires instructors to develop teaching methods that allow students to most effectively learn course concepts and content. Problem-based learning (PBL) is a primarily concepts-based form of active learning (AL), and closely matches the inquiry-based process of clinicians and researchers in this area of study. It has been successfully utilized in a variety of other subject areas. No studies, however, have quantitatively investigated the effect of PBL on student learning in an undergraduate biomechanics course for kinesiology or exercise and sport science students. Therefore, the purpose of this study was to objectively quantify the effect of PBL on student learning in such a course. A secondary aim was to identify student perceptions of the PBL technique's implementation. We hypothesized that PBL would increase student learning to a similar degree as other AL techniques and that students would view the PBL approach positively.

Methods

Students (n=109) in three introductory biomechanics classes at two comprehensive universities participated. The courses were three credit-hours of effort including lab. The content taught in each class was similar. Ethics approval was obtained prior to any student participation in concurrence with the Declaration of Helsinki and students provided written Informed Consent.

Students took a pre-test consisting of the original Biomechanics Concept Inventory (BCI) (Knudson et al., 2003) on the first day of class, and a post-test on the last day of class. The post-test consisted of the BCI and eight additional questions on student perceptions of the PBL activities.

We implemented PBL assessments as part of the classes across seven different course topics: motions and planes, linear kinematics, angular kinematics, linear kinetics, angular kinetics, mechanics of the skeletal system, and the muscular system. A small number of low-tech AL supplemented PBL. All of the PBL assessments were based off of one or more 2D videos of: depth jumps (drop, land, rebound) and/or drop jumps (drop, land) from 12", 24", and 36" heights.

Gain scores (g), a measure of student learning that incorporates the increase in correct responses between BCI pre and post-tests, were calculated. Descriptive statistics were calculated for the eight questions of student perceptions of PBL. Descriptive statistics of BCI pre-test and learning (g) were calculated for each university, and analyzed with t-tests to compare with data from previous studies. Alpha was set at 0.05.

Results and Discussion

Pre-test, post-test, and gain scores are in Table 1. Student learning (g) was not different (p=0.19) between the two universities (university 1: 0.23 ± 0.11, university 2: 0.26 ± 0.14). The mean (g) scores for all three classes combined were 0.25 ± 0.14, with a 95% CI of [0.22, 0.28]. Student ratings of PBL as helpful in aiding learning were also primarily (83%) positive, however 17% of students disagreed. 95% of students believed that they worked moderately to extremely effectively together in PBL.

Table 1: Pre-test, post-test, and learning scores

	University 1	University 2	Combined
Pre-test*	8.0 ± 1.5	9.5 ± 2.6	8.9 ± 2.4
Post-test*	11.6 ± 2.0	13.4 ± 2.7	12.7 ± 2.6
Learning (g)	0.23 ± 0.11	0.26 ± 0.15	0.25 ± 0.14

Values reported as Mean ± SD. University 1 = University of Wisconsin Oshkosh (n=38), Unviersity 2 = University of Wisconsin-La Crosse (n=71); Pre-test and post-test scores are out of 24 points maximum, g range is between 0 and 1; *Significant difference between universities (pre-test $p = 0.002$, post-test $p = 0.009$).

Learning was greater with the implementation of PBL than what has previously been reported with low-tech AL in similar courses (g=0.15 – 0.22) (Knudson, 2019a,b; Knudson & Wallace, 2019). The PBL exercises by both instructors in this study took up approximately 30 minutes of class time per topic, on average. Reducing low-tech AL and adding PBL increased student learning by 53% with the same instructor (Knudson & Wallace, 2019). PBL seems to have a disproportionately large positive effect on student learning of biomechanical concepts.

Approximately 85% of students "strongly agree(d)" to "agree(d)" that the four individual PBL exercises surveyed (linear and angular kinematics and kinetics) aided their learning of biomechanical concepts, with the rest "disagree(ing)." Students' overall imporession of PBL were similarly positive. These results are encouraging in that not only did students think the PBL aided their learning, they did so even though they required some additional work outside of class with other students.

Significance

PBL was shown to be a highly effective teaching technique for increasing student learning in undergraduate biomechanics. Students also had positive perceptions of the PBL exercise implementation, and thought that it aided in their learning of biomechanical concepts.

Acknowledgments

We thank the students who participated.

References

Knudson, D. (2019a). Active learning and student beliefs about learning. *ISBS Proceedings Archive:* 37: Iss. 1, Article 80. Available at: https://commons.nmu.edu/isbs/vol37/iss1/80

Knudson, D. (2019b). Do low-tech active learning exercises influence biomechanics student's epistemology of learning? *Sport Biomech*, doi:10.1080/14763141.2019.1682650

Knudson, D., & Wallace, B. (2019). Student perceptions of low-tech active learning and mastery of introductory biomechanics concepts. *Sport Biomech*, doi: 10.1080/14763141.2019.1570322

Knudson, D., Noffal, G., Bauer, J., et al. (2003). Development and evaluation of a biomechanics concept inventory. *Sport Biomech*. doi: 10.1080/14763140308522823

Teaching Undergraduate Biomechanics using Project Based Learning: A Case Study

Kayt E. Frisch.[1]
[1]George Fox University, Department of Mechanical, Civil and Biomedical Engineering
Email: *kfrisch@georgefox.edu

Introduction

Project Based Learning (PBL) is a curricular structure that frames students' learning in the context of a real (ill-defined) problem, and then provides resources and guided progression through the relevant information. [1] Used extensively in medical education and increasingly in engineering, it has few application (to date) in undergraduate biomechanics classrooms. [2,3]

Methods

Enrolment & Implementation

During the F2019 semester, 22 mechanical engineering students (with previous course work in dynamics) enrolled in a senior engineering elective course on biomechanics at a teaching-focused university. Groups of 4-5 students completed the project together, submitting team deliverables and receiving a team grade, (individually modified if necessary).

The PBL Statement

The challenge statement was aimed at teaching students do a biomechanical motion analysis:

> One of the "hot topics" at ISB 2019 was wearable sensors as a way to capture motion "in the wild" (e.g. runners on city streets as opposed to on a treadmill in a lab). There is lots of appeal to the idea of being able to do biomechanics analysis in a natural environment but, as with any new technological advance, you need to be sure that you are getting equivalent (or relatable) data and that if you're not the benefits of the tech outweigh the loss. I am very interested in using these sensors in my research studying the swinging motions of volleyball athletes, but I want to know that my set of inertial sensors produce equivalent results to the "gold standard" techniques for a variety of motions (e.g. walking, running, throwing a baseball and hitting a volleyball).

Project Structure & Activities

At the beginning of the 8-week unit, students generated a set of questions based on the PBL statement [4], including two key ones that motivated the learning experience: "what is the "gold standard"?" and "what are IMUs?" These motivated a sequence of class and lab activities to learn the basics of acquiring and analyzing force plates, motion capture, and IMU data. Once familiar with the data they could collect in the lab, students were presented with the requirements for their research project and (with instructor guidance) chose a motion to study. Each group had two 1-hour data collection sessions.

Project Deliverables

The final deliverables were an ISB 2019-style abstract and a "conference" poster (presented in 5-minute quick-talks to a class conference). Scaffolding towards the final deliverables consisted of a literature review, homework on the learning the lab basics activities, and (during the data collection/analysis) group weekly progress reports (including individual learning logs for each member).

Results and Discussion

End-of-semester responses (Table 1) show a favourable student view of PBL as a tool for learning biomechanics. Students felt prepared with adequate foundational knowledge and supported by the assignment framework. Most importantly, based on oral interviews, both students and the instructor believe they learned the subject material.

Table 1: Student responses (N=15) from the end-of-course feedback survey questions relating to the project.

	S.A./A	Neut	D./S.D.
The project created an effective opportunity to learn biomechanics	93%	0	7%
I felt prepared with the knowledge and tools I needed for the IMU project	80%	7%	13%
I had sufficient guidance and resources to complete the IMU project.	93%	0	7%
This course improved my ability to find and interpret information about engineering mechanics from a diverse set of sources.	80%	13%	7%
This course improved my ability to analyze biological problems, particularly relating to human movement and tissue mechanics, using basic mechanics principles.	87%	0%	13%
This course improved my ability to make meaning from a data set	93%	0	7%
Writing the abstract about our data was a valuable learning experience for me and my group.	80%	13%	7%
Creating the poster about our data was a valuable learning experience for me and my group.	67%	27%	7%
My group wrote the abstract before creating the poster.	67%	27%	7%
The in-class peer-review process was valuable for the poster and abstracts.	80%	13%	7%

Significance

This project provides one example of what PBL might look like in a university-level biomechanics course. As with all education innovations, adaptation for other contexts will require flexible use of local resources, however, this case-study shows that the project can be done with a modest number of students, and that all parties believe that the students learned biomechanics from the experience. It is the hope of the author that this example will inspire others to dream about what project-based learning might look like in their classrooms.

Acknowledgments

Thank you to students in ENGB 420 (F19) for experimenting, my dean, Bob Harder for funding, Robin Dorociak for lab facilitation, and the GFU DPT program for access to their lab.

References

[1] Hoffman; Instructional Sci., 1997 Mar, Vol.25(2: 97-115)
[2] Burgess; BMC Medical Education (2018) 18:74
[3] Li; J. Prof. Issuses Eng. Educ. Pract., 2016, 142(3): 04016002
[4] Berger; A More Beautiful Question, ISBN10: 1632861054

The Impact of National Biomechanics Day on Student Perceptions toward Biomechanics: A Multisite Pilot Study

Scott M. Monfort[1*], Kimberly E. Bigelow[2], Srikant Vallabhajosula[3], and Paul DeVita[4]
[1]Montana State University; [2]University of Dayton; [3]Elon University; [4]East Carolina University
Email: *scott.monfort@montana.edu

Introduction

National Biomechanics Day (NBD) is a worldwide celebration of biomechanics that has exposed over 29,000 high school students to biomechanics from 2016 through 2019 [1]. Some initial evidence suggests NBD positively impacts interest, excitement, and perceived importance of biomechanics among the students [2]. These findings were however generated from a single NBD event and their generalizability is unknown in terms of different geographic locations, NBD designs, or assessment tools. We propose that while reaching large student populations is indicative of success, the educational value of NBD needs to be assessed through direct, quantitative tools.

The purpose of this study was to quantify changes in high school students' perceptions toward biomechanics after participating in NBD events held at multiple locations. Our hypothesis was that NBD would increase interest, excitement, and perceived importance of biomechanics.

Methods

High school classes were invited to participate in independent NBD events at two biomechanics laboratories at institutions with different geographical and institutional characteristics (Montana State University and Elon University).

We adapted questions from the STEM Semantics Survey to develop a tool to characterize biomechanics-specific outcomes [3]. Specifically, students were asked to respond to the question "To me, biomechanics is," for four pairs of adjectives: 'appealing vs. unappealing', 'exciting vs. unexciting', 'unimportant vs. important', 'boring vs. exciting', with the last question serving as a reverse-coded validation check. Responses were on a 7-point Likert scale, and students were also given the choice of responding with 'I don't know enough about biomechanics to answer' (IDK), as we anticipated NBD was often students' first exposure to biomechanics. Students also answered questions about their interest in biomechanics-related careers and enjoyment/learning from the NBD event. A combination of Sign Tests (contrast of paired pre-post data) and Chi-Squared tests (unpaired data) were used. Missing and IDK responses were omitted from pairwise comparisons.

Results and Discussion

Data were collected from 112 high school students, although only 109 students (16.5±1.0yr; 63/38 f/m) were included in our analyses as three surveys did not have matched pairs. Ten students provided no or partial demographic information.

Our hypothesis was largely supported as students perceived biomechanics as more exciting and important following the events compared to their paired pre-event responses (all $p<0.015$). The magnitudes of the shift in perceptions were moderate, as paired and unpaired assessments suggested a positive shift in medians of these questions of ≤1 on the 7-point Likert scale. Chi-squared analysis echoed the positive impact of NBD (**Figure 1**). Additionally, number of IDK responses decreased from 114 across the four adjective pairs to a total of one following NBD, which suggests that NBD was effective at helping students form opinions toward biomechanics. While students also seemed more informed regarding biomechanics-related careers (decrease in IDK from 18 to 1), no change was observed in students seeing themselves in a biomechanics career (median = 4). Notably, students resoundingly enjoyed NBD (6.3±1.4 [7 being highest]).

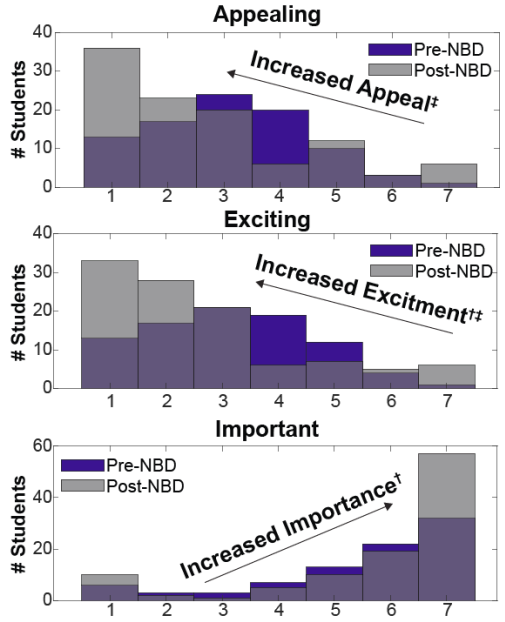

Figure 1: Survey responses from students (omitting IDK) taken before (blue) and after (gray) NBD events (note: dark gray regions reflect overlap in pre/post bars). † indicates $p < 0.05$ for paired Sign Test. ‡ indicates $p < 0.05$ for Chi-Squared test.

The findings of our multi-site pilot study support the generalizability of recent findings by Teeter et al. regarding the positive impact of NBD on student perceptions of biomechanics [2]. Not only did students enjoy NBD, but the event generated excitement and perceived importance in the STEM sub-discipline. The lack of change in perceptions regarding biomechanics-related careers may mark a potential point of emphasis for future NBD events.

Significance

Strengthening the future STEM workforce is a national priority that relies on exciting young students about STEM fields. Our research provides quantitative evidence across two institutions that NBD is well-positioned to support this goal.

Acknowledgments

We would like to thank the many volunteers that contributed to vibrant 2019 NBD events at MSU and Elon University.

References

1. DeVita, P., *J Biomech*, 2018. 71: p. 1-3.
2. Teeter, S.D., et al., *J Biomech*, 2020: p. 109683.
3. Tyler-wood, T., et al., *J Tech Teach Ed*, 2010. 18(2): 341-363.

Teacher Content Knowledge and Confidence in Youth Biomechanics Education

Amelia S. Lanier[1], Anne Karabon[2], Michelle Friend[2], Neal F. Grandgenett[2]
[1]Department of Biomechanics University of Nebraska at Omaha
[2]Department of Teacher Education, University of Nebraska at Omaha
Email: alanier@unomaha.edu

Introduction

Biomechanics plays a prominent role with young children through body and sports connections [1,2] and provides opportunities to teach STEM concepts. To enhance youth STEM fducation, faculty in Teacher Education and Biomechancis organized a 2-week biomechanics focused professional development (PD) workshop for middle and elementary school STEM teachers followed by a 1-week student academy. The student academy introduced students to STEM concepts through the lens of biomechanics. Student participants of the 1-week academy, hosted by the teacher participants, exhibited significant improvements in scientific inquiry skills through the use of a novel assessment tool [3]. This improvement may be due to teacher content knowledge and confidence, which is a crucial factor in student learning, especially in STEM fields [4]. Thus, the purpose of this work was to evaluate teacher STEM self-efficacy and biomechanics content knowledge over the course of the PD. We hypothesized the teachers would exhibit increases in both STEM self-efficacy and biomechanics content knowledge.

Methods

Teacher participants included 13 teachers with elementary teaching licenses from public and private districts. The PD included biomechanics sessions, inquiry based pedagogy sessions, and biomechanics research lectures.

Teachers completed a pre and post PD Teacher Efficacy and Attitudes toward STEM (T-STEM) Survey [5] and pre and post PD interviews. Audio-recorded interview data were transcribed and biomechanics knowledge analysed using NVivo software. Efficacy measures were based on the Personal Teaching Efficacy and Beliefs construct of the T-STEM survey. Eleven questions addressed teachers' confidence in teaching science, on a scale from 1 to 5. A Wilcoxon signed rank test demonstrated significant differences in average self-efficacy score from pre- to post-PD.

Results and Discussion

Findings from this study indicate that teachers' self-efficacy about their ability to teach science significantly increased over the course of PD (Table 1, $p=0.006$). However, a review of transcribed interview data revealed limited changes to teachers' biomechanics definition pre vs. post PD. Almost all teacher participants focused on "body movement" or "how the body moves" in both pre and post responses while a limited number indicated mechanics connections through specific mechanical vocabulary in post responses.

Ideally, teachers would gain both confidence in teaching science and biomechanics content knowledge through this PD, however, this was not the case. Contextual review and analysis of interviews may not be an ideal measure of biomechanical content knowledge for this particular group. Previous work indicates an increase in biomechanics and STEM inquiry skills, which can be related to biomechanics knowledge, post PD using a novel assessement tool [3]. We believe teachers are still gaining biomechanics knowledge which may not be reflected in the interviews and so additional measures will be explored.

Through this biomechanics-focused PD experience teachers gained confidence in teaching biomechanics. These preliminary results from teachers, in combination with previous results showing student learning gains, indicate continued success of the PD model and the ability to integrate biomechanics into elementary and middle school classrooms.

Significance

Biomechanics offers teachers diverse and rich applications to teach STEM concepts in elementary and middle school classrooms. Teachers with pedagogical and scientific confidence engage students in high-quality, child-centered inquiry-based learning experiences. The first steps in integrating biomechanics learning experiences into the classroom must focus on teachers confidence in teaching and knowledge of the field. Through a 2-week PD we are confident in our ability to improve STEM efficacy and hope that this model will be utilized at additional sites.

Acknowledgments

NSF ITEST #1759000 and RMC for evaluation of this project.

References

1. Drazan JF et al. "Biomechanists can revolutionize the STEM pipeline by engaging youth athletes in sports-science based STEM outreach". *Journal of Biomechanics,*2020.
2. Clements DH & Sarama J. "Math, Science, and Technology in the Early Grades". *Future of Children*, 2016.
3. Lanier AS et al. "Assessment of Biomechanics Learning in Elementary and Undergraduate Students Using a Questioning Scenario". *ISB/ASB Joint Meeting*, 2019
4. Fitzgerald EM & Cunningham CM. "Bridging Engineering, Science, and Technology (BEST) for Elementary Educators". *120th ASEE Annual Conference*, 2013.
5. Friday Institute for Educational Innovation. "Teacher Efficacy and Attitudes Toward STEM Survey". 2012.

Table 1: Individual T-STEM Efficacy Scores for teacher participants Pre and Post PD.

Teacher	1	2	3	4	5	6	7	8	9	10	11	12	13	Mean ± STD
Pre	3.64	2.82	4.27	3.82	3.73	4.18	3.73	3.45	3.55	3.55	3.55	3.73	4.27	3.71 ± 0.39
Post	3.55	2.73	4.36	4.36	3.82	4.82	4.18	3.82	3.55	4.00	3.82	4.00	4.36	3.95 ± 0.51

Teaching Methods to FEA of Human Gastrocnemius for STEM Early College Senior Research Project

Shunafrica C. White[1], Matthew B.A. McCullough[2,3], Phung Nguyen[4]
[1]North Carolina A&T State University, Department of Mechanical Engineering
[2]North Carolina A&T State University, Department of Chemical, Biological, and Bioengineering
[3]The Center for Cyber Human Analytics Research for the Internet of Things, North Carolina A&T State University, Greensboro, NC
[4]STEM Early College at N.C. A&T

Email: scwhite@aggies.ncat.edu

Introduction

The STEM Early College at N.C. A&T is an early college designed to serve high-performing students with an interest in science, technology, engineering, and math. In contrast to traditional high school, the STEM Early College exposes students to engineering, technology, and advanced math courses. However, up until their senior year, STEM Early College Students have not applied what they've learn to a real-world problem. Therefore, to address this gap, our lab volunteered to assist students apply their knowledge to an interdisciplinary area of biomechanics. Research in our group includes finite element analysis (FEA) based topographical optimization, soft tissue analysis, and ACL interference screw evaluation. The purpose of this study is to describe the approach used to teach and mentor STEM Early College Students to perform FEA on human gastrocnemius for the investigation of mechanical properties in partial fulfillment of the Senior Internship Graduation Research Project.

Methods

The Senior Research Project equips students with critical, analytical, and problem-solving skills, thus preparing students for post-secondary educational success. Students are expected to participate in Senior Seminars, which cover topics on project deliverables (e.g. annotated bibliography, research paper, oral presentation, and peer review editing). Our lab was entrusted with mentoring students achieve these deliverables. All STEM Early College Students ranked three research topics most suited for their interest. Then based off student's interest, the lab director and manager identified which of the lab's graduate students would be qualified to manage the STEM Early College Student's Senior Research Project. A mechanical engineering graduate student was selected to mentor and teach a STEM Early College Student who identified FEA of soft tissues as their research interest. The central objective of the FEA project was to determine the mechanical properties of human gastrocnemius, which was accomplished using SolidWorks, MATLAB, Excel, and Ansys. A project management sheet via Excel and Monday.com were utilized to identify and assign deliverables needed to complete FEA. The mentor provided references and instructional time to help the student become acclimated with the previously mentioned software products. References included in person step-by-step and video walkthroughs, engineering textbooks, peer reviewed articles, software help websites, and YouTube videos. The purpose of the references was to provide tips for analyzing and interpreting results, performing hand calculations (e.g. normal stress, principal stresses), creating, exporting, and importing gastrocnemius specimen models, techniques for FEA validation (e.g. $\Sigma F = 0$), applying boundary conditions, and generating appropriate meshes.

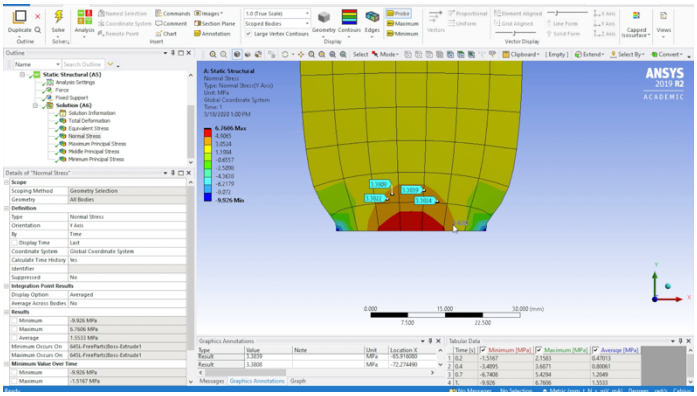

Figure 1: Screenshot of a walkthrough video on how to probe results for normal stress in Ansys as a form of FEA postprocessing.

Results and Discussion

Finite element analysis results of human gastrocnemius were communicated via the research paper and oral presentation for the Senior Research Project. The mentor provided the student references needed to illustrate background knowledge using peer reviewed articles on the mechanical properties and material behavior of calf muscles. The mentor also provided the student with techniques on how to visualize and extract data via contour plots, Excel spreadsheets of hand calculations, and Ansys generated data tables.

Significance

The collaboration between our lab and the STEM Early College intends to encourage more students, particularly minority and female students, to pursue higher education in STEM. Moreover, it challenges instructors and mentors to create rudimental teaching methods that introduce high school students to in depth topics of engineering, such as FEA. Furthermore, the collaboration shows students that a career in the STEM field is attainable for people who do not identify with the majority.

Acknowledgments

We would like to acknowledge B.I.O.F.A.B.B and the STEM Early College at N.C. A&T.

References

1. Shan X, Otsuka S, Yakura T, Naito M, Nakano T, Kawakami Y. *Morphological and mechanical properties of the human triceps surae aponeuroses taken from elderly cadavers: Implications for muscle-tendon interactions*. PLoS ONE 14(2):e0211485. https://doi.org/10.1371/journal.pone.0211485, 2019.
2. Ugural, Ansel C., & Fenster, Saul K. *Advanced Mechanics of Materials and Applied Elasticity, 4th Ed.* Prentice Hall, 2003.

Biomechanics On Our Minds (BOOM): Learnings from a biomechanics podcast

Johanna J. O'Day[1*], Melissa A. Boswell[1*], Scott L. Delp[1], Joseph Hamill
[1]Department of Bioengineering, Stanford University, Stanford, CA, USA
*These authors contributed equally to this work
Email: odayj@stanford.edu

Introduction

Biomechanics is an interdisciplinary field, which is full of diverse perspectives and ideas, both technical and non-technical. Conferences facilitate the exchange of these perspectives and ideas, connect us with the people behind the research, and remind us that science is a human endeavor. Attending conferences is fantastic but requires resources for travel and conference fees and expertise to understand the research. We created the podcast Biomechanics On Our Minds (BOOM) for students and researchers. BOOM was developed with three main goals: increasing access, building community, and improving scientific culture. We discuss our learnings from BOOM and their applicability to other contexts.

Methods

We chose the podcast platform due to its increasing popularity and ability for listeners to learn from any place in the world.

Each episode has three parts: 1) "A Bit of BOOM", which is an overview of new research findings in biomechanics; 2) an interview with a person on a specific topic (Table 1); and 3) "Research Fails," in which we share recent mistakes as learning experiences. Melissa Boswell and Johanna O'Day conduct the interview together starting with the interviewee's path to biomechanics, then exploring the specific topic, and ending with their perspective on the future of biomechanics.

BOOM has included a wide range of topics across biomechanics, career, research, diversity, and support. Running over 2 years, we have released 33 episodes of 45-60 minutes in length. BOOM has had over 16,000 total listens for an average of around 500 listens per episode. It is freely available on Spotify, iTunes, and SoundCloud [1].

Categories	Specific Topics
Biomechanics	exoskeletons, wearables, rehabilitation, prosthetics, orthopedics, impacts, bone, muscle, dinosaur biomechanics, breast biomechanics
Career	paths to biomechanics, academia, industry, graduate school, non-profits, conferences
Research	needs finding, patient-centered research, ambiguity, open-science, collaboration, positive-results bias
Diversity	women in biomechanics, developing countries, internationalization, LGBTQ+
Support	mentorship, mental health, overcoming failure, impostor syndrome

Table 1. Categories and specific topics of BOOM episodes.

Results and Discussion

We discuss our learnings with regard to BOOM's three main goals.

ACCESS. The podcast has been a useful platform for expanding awareness of biomechanics research. One listener shared, *"Thanks to BOOM I've been able to hear from researchers and professors … who I wouldn't otherwise have the opportunity (or know-how) to approach."*

In addition, our conversations provide information that is not typically included in graduate education, such as mental health. We have found that fostering an empathetic and positive environment allows us to navigate sensitive but salient topics. These learnings are transferable; we empower students to conduct interviews with a similar environment and share them through our "Student Voices" series.

COMMUNITY. By leveraging the extensive community already established by the International Society of Biomechanics, we have connected with listeners worldwide; a Dutch listener shared, *"The BOOM podcast has been like a real friend! I literally talk with you guys as I bike across the city."*

CULTURE. Sharing failures and stories of overcoming adversities as learning experiences have proven encouraging and empowering; one student shared, "*My perspective on failing changed as I understood that experts fail.*" Another student shared that, "*Failure makes research successful and meaningful.*" These stories have expanded our perspectives and given us a more holistic picture of the researcher.

We think the most important learnings from BOOM are: empathetic conversations open the door to a wide range of topics, building upon existing communities enables far-reaching impact, and sharing adversities makes us more connected and resilient. These learnings can be applied to other contexts. For the largest positive impact, we encourage listeners to continue these conversations throughout their communities so as to improve our culture.

Significance

BOOM uses the podcast platform to expand awareness of biomechanics research and positively impact accessibility, community, and culture. It has attracted listeners inside and outside of the biomechanics community and serves as an inspiration for others to initiate similar deep, meaningful conversations in their fields

Acknowledgments

The BOOM podcast was started through the International Society of Biomechanics (ISB). We thank the ISB for their continued support, Peter Washington for BOOM's music, and Sanford Health for supporting the Student Voices initiative.

References

[1] Soundcloud. Biomechanics On Our Minds: BOOM. https://soundcloud.com/biomechanics-on-our-minds.

Effects of assistive devices on postural sway during a simulated forward fall

Yunju Lee[1,2], Meri Goehring[2], Rachel Badr[2], Brianna Bove[2], and Patrick Jewett[2]
[1]School of Engineering, Grand Valley State University, Grand Rapids, MI, USA
[2]Department of Physical Therapy, Grand Valley State University, Grand Rapids, MI, USA
Email : leeyun@gvsu.edu

Introduction

Assistive devices are utilized to provide balance and stability to those that may require extra base of support, especially during ambulation or essential functional tasks in activities of daily living [1, 2]. In assistive device use, postural sway is a major factor to consider in the prevalence and prevention of falls [3, 4]. There is a lack of research on assistive devices, such as walkers, regarding measurable outcome variables related to fall risk. Few studies have assessed the effectiveness between walker types on stability during a forward fall [2]. The purpose of this study was to determine how much the postural sway in single limb stance during a simulated forward fall is affected by utilizing three different walker types designed to promote stability.

We hypothesized that the lowest amount of postural sway will be with the standard walker (W1), followed by the front wheeled walker with straight wheels (W2), and the greatest amount of postural sway will be with the front wheeled walker with caster wheels (W3).

Methods

Twenty-three healthy adults (13 females, 10 males; 26.1 ± 4.2 yrs; 76.9 ± 16.3 kg) participated and gave consents. The NeuroCom® SMART EquiTest® system was utilized to simulate forward falls via its moving force plate quickly tipped backward in order to measure postural stability in single limb stance. Each participant experienced a total of 18 simulated falls while the subject was asked to maintain balance. Each trial was completed utilizing random assignment of three different walker types and leg dominance as a standing leg with perturbation. Three trials were collected per condition with two 1-minute seated rest breaks taken every six trials to prevent the fatigue effect.

The two-way repeated measures variance of analysis (rm-ANOVA) were performed to test effect of walker type and leg dominance in SAS JMP ($p<.05$) for the center of pressure's (COP); maximum distance (mm), velocity (mm/sec) in antero-posterior (AP) and medio-lateral (ML) directions. If p value was less than 0.05, we applied Tukey's HSD as post-hoc tests.

Results and Discussion

The ANOVA table 1 showed that the type of walker and the leg dominance in standing limb significantly affected postural sway in a simulated forward fall. The COP maximum distance in AP direction was significantly different under walker type as a main effect however, the rest of variables did not show differences among three walkers in AP direction. As expected, we found that the effect of leg dominance was significant in all variables except velocity in ML direction. There was no interaction effect between walker and stance leg. The post-hoc tests revealed that the standard walker (W1) had the smallest significant maximum distance in AP direction compared to two front wheeled walkers (Fig. 1 left shown as *) while there were no differences between two front wheeled walkers (W2 vs. W3).

The result supported the hypothesis of the relationship between the postural sway and three different walkers during a simulated forward fall. Moreover, the findings provided the evidence to support that a standard walker had best stability when compared to the other two front wheel walkers with wheels.

Table 1. ANOVA table of COP outcome variables.

COP	AP direction		ML direction	
	Max	Velocity	Max	Velocity
Walker type (W1, W2, W3)				
F	6.316	2.348	.856	2.514
p	**.002**	.097	.426	.082
Stance leg (DL vs. NL)				
F	10.797	5.651	122.001	2.795
p	**.001**	**.018**	**<.0001**	.095
Walker x Stance leg				
F	1.239	.837	.336	1.485
p	.291	.434	.715	.228

Significant *p*-values ($p < .05$) are indicated in bold. Key: W1 = Standard Walker; W2 = front wheeled walker with straight wheels; W3 = front wheeled walker with caster wheels; DL = dominant leg; NL = non-dominant leg for a standing limb.

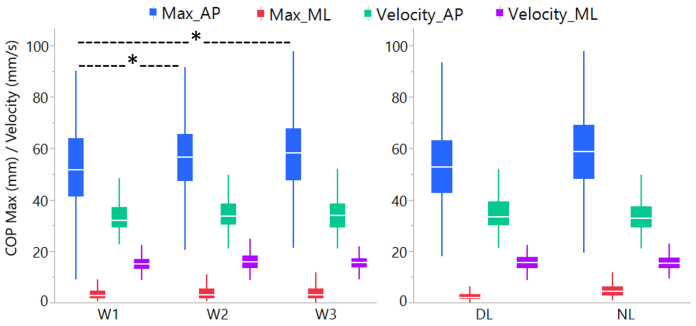

Figure 1: COP Maximum distance and velocity shown by 3 different walker types (left: W1 vs. W2 vs. W3left) and leg dominance in standing limb (right: Dominant leg (DL) vs. Non-dominant leg) in AP and ML directions.

Significance

By investigating the effectiveness of three walker types on postural sway during a simulated forward fall, health care professionals will be provided with clinically relevant information to aide in prescribing appropriate assistive device options for patients that specifically tailor to their stability needs. This is especially important for those who are at a high risk for falls [2, 3]. In addition, walkers are often used for patients who are limited or non-weight bearing on one lower extremity after a lower extremity injury or surgery [1, 2]. Prescribing assistive devices with appropriate stability for a patient's presentation will assist in the effort to decrease falls and therefore minimize fall-related injuries.

Acknowledgments

We thank the study participants for their cooperation.

References

[1] Kaye HS et al. *Disability Statistics Report*. 2006;1-66
[2] Hook FW et al. *American Family Physician*. 2003;1717-1724
[3] Fernie GR et al. *Age Ageing*. 1982;11-16
[4] Stevens JA et al. *Am J Prev Med*. 2012;59-62.

Gait Event Specific IMU-Based Kinematic Metrics are able to Identify Balance Control Deficits in Acutely Concussed Young Adults

Will Pitt[1,2], Suz-Hua Chen[2], and Li-Shan Chou[2,3]
[1]Baylor University – KACH D1 Sports Physical Therapy Fellowship, West Point, NY
[2]Department of Human Physiology, University of Oregon; [3]Department of Kinesiology, Iowa State University
Email: William.j.pitt6.mil@mail.mil

Introduction

Concussed individuals often present with persistent gait balance deficits, identifiable with whole body center of mass (COM) kinematic analysis[1]. Inertial measurement units (IMUs) offer a promising method for clinical assessment of COM-based metrics. Examination of IMU accelerations and angular velocities is necessary to identify metrics indiciative of balance control impairments. The purpose of this study was to identify IMU-baesd kinematic metrics capable of distinguishing concussed from healthy individuals across a two month post-injury period. We hypothesize multiple gait event specific accelerations and angular velocities will be able differentiate healthy from concussed individuals across a two-month post-injury period.

Methods

Eleven acutely concussed individuals (within 72 hours of injury) were matched to 11 healthy controls by sex, age, height, and weight. Individuals with an injury affecting normal gait, a history of permanent memory loss or concentration abnormalities, or who had impaired hearing were excluded. A gait balance control assessment [2] was performed in both single- (ST) and dual-task (DT) conditions at five time points: within 72 hours of injury (72hrs), at one week (1wk), two weeks (2wks), one month (1mo), and two months (2mos) post-injury. Healthy participants were assessed at similar intervals. Participants walked over a seven meter straight level path at a self-selected pace, performed a 180º counter clockwise turn, and returned to the start position. During the DT condition, participants responded to an auditory Stoop task in which the words "high" and "low" were presented in either congruent or incongruent word/pitch combinations. Kinematic data were collected from a single IMU (APDM, Portland, OR) placed over the L5 vertebra. Data were sampled at 128Hz and filtered with a 2nd order low-pass Butterworth filter with a 12Hz cutoff. All IMU measures were analyzed with a 3-way analysis of variance with group (concussed, healthy), condition (ST, DT), and time (72hrs, 1wk, 2wks, 1mo, and 2mos) as independent variables.

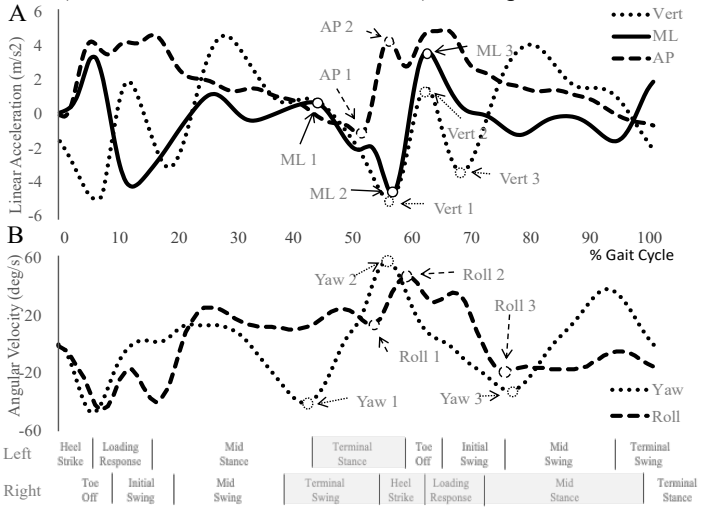

Figure 1: (a) Vert, ML, AP acceleration and (b) Yaw and Roll angular velocity profiles.

Results and Discussion

Eight consistent gait event specific peak accelerations along the medial-lateral (ML), anterior-posterior (AP), and vertical (Vert) axes and six peak angular velocities about the AP (roll) and Vert (yaw) axes were identified. Accelerations and angular velocities were referenced to a left heel strike initiated gait cycle, and occurred at right terminal swing, left terminal stance, right heel strike, right single- to double-support transition (loading response), and right mid-stance (**Fig. 1**). Concussed individuals produced a smaller downward acceleration (Vert2) during loading response, which increased over time in both groups (interaction effect; p=.04), and smaller upward acceleration (Vert3) at the end of terminal stance than healthy participants (main effect of group; p=.02). They also had a slower clockwise angular velocity (Yaw2) at right heel strike which increased over the five assessments (interaction effect; p<.001 [**Fig. 2**]). Non-significant trends of smaller ML accelerations toward the left at right heel strike (ML2) and to the right during loading response (ML3), and a greater peak posterior acceleration from right heel strike to loading response (AP2) were identified in concussed individuals (main effects of group; p=.06, p=.06, and p=.07).

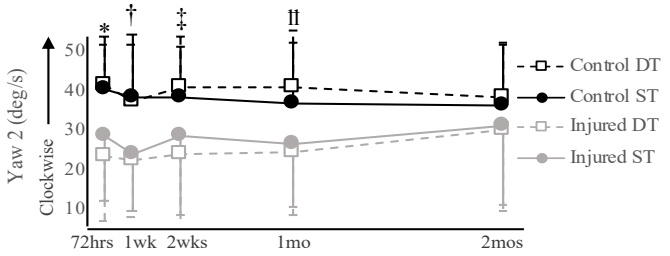

Figure 2: Peak yaw angular velocity (Yaw2). Significant follow-up comparisons (Tukey) between healthy and concussed at 72hrs (*p<.01), 1wk (†p=.04), 2wks (‡p=.01), and 1mo (ǂp=.02).

Significance

Multiple gait event specific peak accelerations and angular velocities collected from a single L5 place IMU were able to detect gait imbalance up to two months post-injury. The timing and magnitude of the metrics suggests a momentum control strategy in which health individuals generate a greater braking acceleration along the AP axis during the loading response phase, resulting in an off-axis shift in energy into the ML and Vert axes. This ability is diminished in concussed individuals suggesting adoption of a more conservative balance control strategy, offering a promising method for identifying individuals with impaired dynamic gait balance control with a clinically feasible instrument.

Acknowledgments

This work was supported by the ACSM Foundation Doctoral Research Fellowship and the Eugene and Clarissa Evonuk Memorial Graduate Fellowship.

References

1. Fino PC, et al., *Gait & Posture*, 62, 157-166, 2018.
2. Pitt W and Chou LS, *Gait & Posture*, 71, 279-283, 2019.

An Investigation of Rambling-Trembling Sway Trajectories with Simulated Somatosensory Deficit

Eryn D. Gerber[1], Camilo Giraldo[2], Paris Nichols[2], Logan Sidener[1], Dr. Carl Luchies[1,2]
[1]Bioengineering Graduate Program, University of Kansas, Lawrence, KS
[2]Department of Mechanical Engineering, University of Kansas, Lawrence, KS
Email: eryngerber@ku.edu

Introduction

Falls in older adults are often multifactorial, but can be primarily attributed to diminished sensation abilities and lowered processing rates due to age-linked neural degeneration.[1,2] A novel method for center of pressure (COP) analysis, called rambling-trembling (RM-TR) decomposition, seeks to understand the underlying feedback loops that modulate balance and has potential to provide new, valuable information about postural sway.[3,4] The purpose of this study is to investigate the effects of of simulated somatosensory deficit on RM-TR-derived measures of the COP during quiet standing. It was hypothesized that RM and TR parameters would show similar trends across deficit severity, but with different magnitudes, and present greater sensitivity to deficit detection compared to traditional COP measures.

Methods

Fifty-two healthy young adults (aged 22.10 ± 1.88 years, 29 male, 22 female) participated in the study. Participants were asked to stand on two force plates (AMTI, Watertown, MA) with a standardized stance and eyes closed. Five randomly-ordered foam thickness conditions (0", 1/8", 1/4", 1/2", and 1", corresponding to F0, F1, F2, F3, and F4, respectively) were used to simulate varying degrees of somatosensory deficit experienced during natural aging. Three 60-second trials were completed for every foam thickness. Foot-floor kinetic data were collected and analyzed using MATLAB software (Mathworks, Natick, MA). Force and moment data were filtered using a 10Hz lowpass Butterworth filter and used to calculate COP, RM, and TR time series, as detailed by Zatsiorsky & Duarte (1999).[3] Velocity, acceleration, and jerk in the mediolateral (ML) and anteroposterior (AP) directions were calculated for RM, TR, and COP time series. In this study, measure sensitivity was used to describe the relative percent change from baseline (F0). MATLAB software was used to perform analyses of variance (ANOVA) with Tukey's HSD post hoc tests with $p<0.05$ to determine statistical significance.

Results and Discussion

Condition F4 showed greatest percent changes from baseline for all assessed parameters, with an upward trend in mean values from F1 to F4 in all measures. In general, standard deviations were very large, likely due to the large sample size and inherent variability in postural sway between healthy young subjects.

Table 1. Mean % change in velocity (vel), acceleration (acc), and jerk from baseline to F4. P-values describe the difference between COP and RM or TR. Significant differences (α=0.05) are bolded.

	COP	RM	*p*-value	TR	*p*-value
VEL_{AP}	43.186	48.687	0.7086	40.766	0.9355
VEL_{ML}	46.526	48.011	0.9776	45.712	0.9932
ACC_{AP}	24.043	**42.380**	**0.0255**	20.425	0.8653
ACC_{ML}	22.009	24.260	0.9376	26.059	0.8118
$JERK_{AP}$	20.329	**43.779**	**0.0161**	**13.860**	**0.0013**
$JERK_{ML}$	5.987	16.344	0.2756	**23.905**	**0.0218**

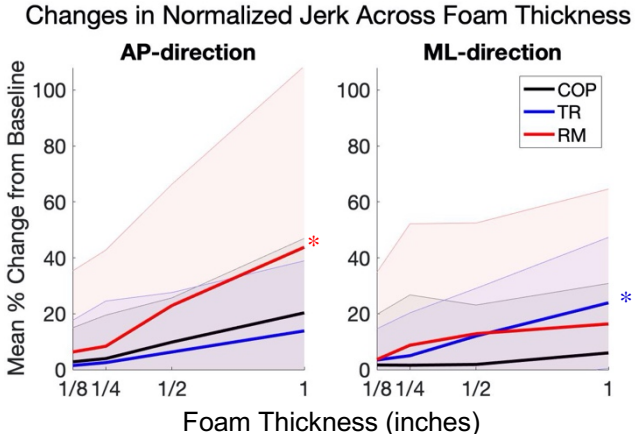

Figure 1. Mean percent changes in normalized jerk across foam thickness. Bold lines represent measurement means with shaded regions depicting the standard deviations.[6] Significant differences between COP and RM or TR are shown with an asterisk (*).

Statistically significant differences between COP and RM or TR acceleration and jerk were found in the F3 and F4 conditions (*Table 1)*. These findings support the hypothesis that COP, RM, and TR measures would show similar trends with variable magnitudes, and RM and TR acceleration and jerk exhibited greater sensitivity to F4 compared to COP.

Much debate surrounds the attribution of physiological mechanisms to RM and TR, but a leading theory suggests that RM trajectories are controlled centrally, while TR trajectories are peripherally-controlled.[5] RM and TR measures showed different behavior in the AP- and ML-direction, with RM greater than COP and TR in the AP-direction, and TR greater than COP in the ML-direction (*Figure 1*). This result is particularly interesting when considering the physiological mechanisms attributed to RM and TR, as these results may suggest that movement is more heavily controlled centrally in the AP and peripherally in the ML.

Significance

Results of this study suggest that RM-TR derived measures may: (1) provide greater deficit detection abilities than traditional COP measures, and (2) reveal previously unknown mechanisms of postural control. Broadening our understanding of postural sway has the potential to alter the way we measure, analyze, and modify balance. From a clinical standpoint, our findings could be used to develop methods that more accurately detect fall risk, inform prevention strategies, and maintain high quality of life with age.

References

1. Speers, R. A., Kuo, A. D. & Horak, F. B. *Gait Posture* **16**, (2002). 2. Wickremaratchi, M. M. & Llewelyn, J. G. **82**, (2006). 3. Zatsiorsky, V. M. & Duarte, M. *Motor control* **3**, (1999). 4. Zatsiorsky, V. M. & Duarte, M. *Motor Control* **4**, (2000). 5. Tahayori, B., Riley, Z. A., Mahmoudian, A., Koceja, D. M. & Hong, S. L. *Motor Control* **16**, (2012). 6. Campbell, R. (2020)

The Effects of Augmented Somatosensory Feedback on Postural Sway and Muscle Co-contraction

Seo-hyun Kim[1], Chung-hwi Yi[2], One-bin Lim[2], Kyung-eun Lee[1] , Jin-seok Lim[1]
[1]Dept. of Physical Therapy, The Graduate School, Yonsei University, Wonju, South Korea
[2]Dept. of Physical Therapy, College of Health Science, Yonsei University, Wonju, South Korea
Email: pteagle@yonsei.ac.kr

Introduction

Postural control is regulated by the visual, vestibular, and somatosensory system. During static standing, augmented somatosensory feedback stimulates the mechanoreceptor to deliver information on bodily position, improving the postural control [1]. The various types of such feedback include ankle-foot orthoses (AFOs) and vibration. The optimal feedback to mitigate postural sway remains unclear, as does the effect of augmented somatosensory feedback on muscle co-contraction. We have compared the effects of feedback-free, AFOs, and vibration on postural sway and muscle co-contraction.

Methods

Fifteen young adults (11 males and 4 females) aged between 21 and 24 participated. The study protocol was approved by the Institutional Review Board at Yonsei University Wonju Campus. The participants stand on the force platform with their feet together and their arms relaxed on both sides of the body. They were instructed to try not to sway during measurements taken over 60 s during all tests.

There were two treatment factors: augmented somatosensory feedback (feedback-free, wearing the AFOs, vibrators on both Achilles tendon) and sensory conditions (eyes open, eyes closed with the head tilted back). Each participants was tested under all six combinations of the two treatment factors in random order.

Postural sway was measured using a force platform (FDMS; Zebris Medical GmbH, Isny, Germany); the mean sway area of the 95% confidence ellipse (AREA) and the mean velocity of the center-of-pressure displacement (VEL) were assessed.

Tibialis anterior (TA) and gastrocnemius (GCM) muscle activities was measured using electromyography (EMG). Co-contraction of TA and GCM converted into a co-contraction index (CI). The CI was calculated using the method of Falconer and Winter (1985) [2].

The two-factor within subjects ANOVA was used to determine the difference in the postural sway and CI among augmented somatosensory feedback (feedback-free, AFOs, vibration). the Bonferroni correction was applied during post-hoc testing.

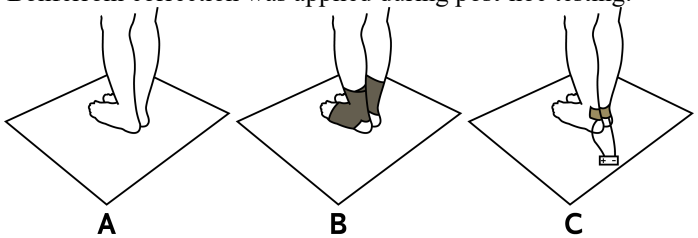

Figure 1: The augmented somatosensory feedback (A: feedback-free, B: ankle foot orthoses, C: vibration).

Results and Discussion

We found significant main effects of the augmented somatosensory feedback on AREA ($F=1.004$, $p = 0.002$), VEL ($F=2.380$, $p<0.001$) and CI ($F=0.747$, $p=0.002$). The sensory conditions exerted significant main effects on AREA ($F=0.680$, $p=0.005$) and VEL ($F=1.061$, $p<0.001$). In AREA and VEL, AFOs resulted in significantly more reduced postural sway than feedback-free ($p=0.014$, $p<0.001$) and vibration ($p=0.024$, $p<0.001$) (Figure 2A,B). In CI, AFOs had significantly better than feedback-free ($p=0.004$). But vibration had not significantly difference with feedback-free in AREA, VEL and CI (Figure 2C). Our results conflicts with a previous finding that vibration reduce the postural sway [3]. In previous studies, the frequency of the vibration to affect the postural sway was 80-100 Hz, whereas in our study, the frequency of the vibration was 1-100 Hz. It is important to set a specific frequency for the vibration to affect the postural control. Our finding that AFOs were better than vibration to improve the postural sway support the previous finding [4]. As the AFOs contact greater proximal stimuli were more effective in reducing postural sway. In addition, We examined that AFOs reduced the CI. During static standing, the plantarflexor are continuously activated and the dorsiflexors are rarely activated, but people with impaired postural control frequently engage the dorsiflexors. AFOs provide adequate somatosensory cues to the ankle dorsiflexors, so the dorsiflexor and the plantarflexor activated properly.

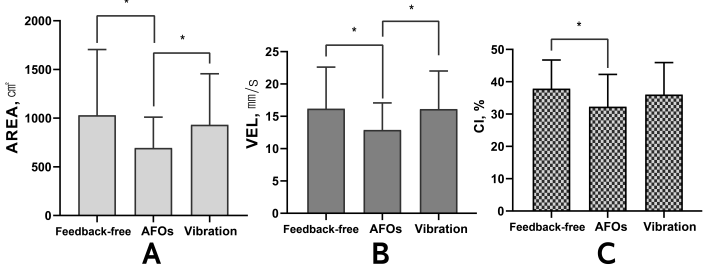

Figure 2: Post-hoc comparison of the effects of the augmented somatosensory feedback (feedback-free, AFOs, vibration) on the AREA, VEL, and CI values during static standing. (AREA: the mean sway area of the 95% confidence ellipse, VEL: the mean velocity of the center-of-pressure displacement, CI: co-contraction index).

Significance

Our finding suggests that AFOs of the somatosensory feedbacks improve postural sway and reduce ankle muscle co-contraction. Such feedback stimulates muscle mechanoreceptors to enhance somatosensory awareness, rather than inducing excessive muscle contractions, and it is particularly sensitive to changes in body movements and position. Therefore, static balance training using flexible AFOs would effectively improve postural control while preventing excessive ankle muscle co-contraction during static standing.

References

[1] Smalley et al. (2018). Gait Posture, 60: 76-80.
[2] Farconer and Winer. (1985). Electromyogr Clin Neurophysiol, 25(2-3): 135-149.
[3] Borel and Ribot-Ciscar. (2016). Exp Brain Res, 234(8): 2305-2314.
[4] Menz et al. (2006). Neurosci Lett, 406(1-2): 23-26.

Effects of vibration training in reducing falls in people with multiple sclerosis

Meng-Wei Lin[1], Jiyun Ahn[1], Feng Yang[1]
[1] Department of Kinesiology and Health, Georgia State University, Atlanta, USA
Email: mlin10@student.gsu.edu

Introduction

Multiple sclerosis (MS) is a chronic central nerve system disease resulting from demyelination. The disease affects both the sensory and motor systems and increases the risk of falls. Numerous efforts have been devoted in developing interventions to reduce falls in people with MS (PwMS). Controlled whole-body vibration (CWBV) training has recently emerged as an alternative fall prevention modality. Previous studies reported that CWBV may reduce the risk of falls by improving body balance, lower limb strengths, mobility, and sensation level (Yang et al., 2016; Yang et al., 2018). As these factors closely relate to falls among PwMS (Finlayson et al., 2006), improving them could lower the likelihood of falls. However, falls in everyday living were not used as an outcome in the previous studies. In addition, prior studies adopted a single-group design. It is impossible to eliminate the potential confounding effects from other factors. The purpose of this study was to further examine the effects of an 8-week CWBV program in reducing falls among PwMS based on a randomized controlled trial. We hypothesized that CWBV reduces falls among PwMS.

Methods

Thrity-one individuals with MS were recruited. They had a less than 7 Patient Determined Disease Steps (PDDS) score, no experience with CWBV training, and no significant relapse within the past 8 weeks. All participants provided a written consent approved by the Institutional Review Board.

Table 1 Between-group comparsion of demographic and disease information prior to training

Group	Intervention	Control	*p* value
Number	24	7	
Males (%)	8 (33%)	0 (0%)	0.081
Age (years)	55.69 ± 14.11	54.63 ± 15.56	0.865
MS duration (years)	10.14 ± 8.57	15.58 ± 10.68	0.228
PDDS (/8)	3.56 ± 1.77	3.93 ± 1.37	0.618

The participants were randomized into two groups: intervention and control groups. The intervention group underwent an 8-week CWBV program on a side-alternating vibration platform (Galileo, Med-L). The vibration frequency and amplitude were 20 Hz and 2.6 mm, respectively. During training, participants were required to stand on the platform with knee bent at 20° and the trunk held upright. Each training session consisted of five CWBV training bouts each followed by a 1-minute rest. The same training session was repeated three times a week over eight weeks. The control group followed the identical protocol except for a 0-mm amplitude. Before the training, the fall incidence in the past year was collected by using a falls-questionaire. During 12 months following the first training session, each particpnat was contacted by research staff members once a month to track whether they have had falls in the past month. Independent *t*-test and chi-square test were used to compare the demographic and disease information between groups prior to the training. Generalized estimating equation (GEE) analysis, with group (CWBV vs. control) and falls data collection period (retrospective vs. prospective) as the two factors in the model, was used to compare the fall incidence between groups over the two 12-month periods. SPSS 24 (IBM) with a significane level of 0.05 wsa used.

Results and Discussion

The demographic and disease information of the two groups were comparable before the training (Tab. 1). GEE results revealed that the two main factors and their interaction had little effect on the fall incidence: group (p = 0.716), session (p = 0.556), and group by session (p = 0.283) on the fall incidence. Although our results did not support our hypothesis, the prospective fall rate over the 12 months after the first training session for the CWBV group was about 17% less than the one for the control group (71% vs. 86%, Fig. 1). Such a reduction could be contributed to the CWBV-induced improvements in fall risk factors as reported by previous studies (Yang et al., 2016; Yang et al., 2018). Our finding may indicate that CWBV training is a clinically-meaningful modality to reduce falls in PwMS. The non-significant results could be due to the small and imbalanced smaple size between groups. A larger scale trial is needed to further confirm the efficacy of CWBV in reducing falls in PwMS.

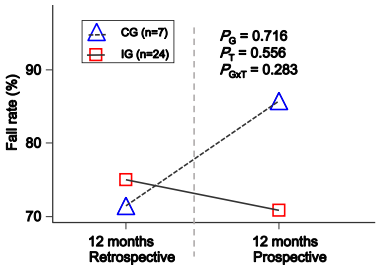

Figure 1. Comparison of the fall rate (12-month retrospective report vs. 12-month follow up) between the intervention (IG) and control groups (CG). p_G: p value for the main factor of group. p_T: p value for the main factor of time (retrospective vs. prospective). $p_{G\times T}$: p value for group by time interaction effect.

Significance

CWBV is an easy, safe, and cost-effective approach to reduce the risk of falls. In addition, it is less physically-demaning in comparsion with other traditional exercise-based intervention for preverntinf falls. Therefoere, CWBV could be an encouraging alternative program to reduce falls in in PwMS.

References

Finlayson, M. L., Peterson, E. W., & Cho, C. C. 2006; *Archives of Physical Medicine and Rehabilitation, 87*: 1274-1279.

Yang, F., Estrada, E. F., & Sanchez, M. C. 2016; *Journal of the Neurological Sciences, 369*, 96-101.

Yang, F., Finlayson, M., Bethoux, F., Su, X., Dillon, L., & Maldonado, H. M. 2018; *Disability and Rehabilitation, 40*, 553-56.

Application of Fuzzy Entropy to Detect Sensory Deficits Through Postural Sway

Paris Nichols[1], Eryn Gerber[2], Camilo Giraldo[1], Logan Sidener[2], Dr. Carl Luchies[1,2]
[1]Department of Mechanical Engineering, University of Kansas, Lawrence, Kansas
[2]Bioengineering Graduate Program, University of Kansas, Lawrence, Kansas
Email: p153n802@ku.edu

Introduction

During quiet stance the human body is unstable and requires constant adjustment from the central nervous system (CNS) to remain upright. Somatosensory deficits, caused by aging, diabetes, or stroke, can create an increased risk of of falling which often results in injury or potentially death.[1] Improving our ability to clinically detect these deficits allows for a better understanding of a patient's need and timing for an intervention.

The center of pressure (COP) time series during quiet stance has been used to detect changes in balance through a variety of parameters.[2] Entropy, a measure of signal predictability, has shown success as one of these parameters.[3] The algorithm used to calculate entropy compares vectors within a signal using the Heaviside function to estimate probability of their occurance. Approximate Entropy (AppEn) and Sample Entropy (SampEn) are two common measures of entropy.[4,5] Recent studies replaced the Heaviside function with fuzzy sets (variation between 0 and 1) leading to the development of Fuzzy AppEn (FAppEn) and Fuzzy SampEn (FSampEn).[6,7] This study tests the hypothesis that fuzzy entropy will improve sensitivity to sensory deficits in COP.

Methods

Testing Procedure: Fifty-two healthy, young subjects (aged 22.10 ± 1.88 years, 29 male, 22 female) stood on two force plates (AMTI, Waterton, MA) with a standard stance and their eyes closed for all trials. Sensory deficits were simulated using five foam thickness conditions (no foam, 1/8", 1/4", 1/2", 1" corresponding to F0, F1, F2, F3, & F4, respectively) applied in a random order. Three 1-minute trials were taken at each condition.

Data Analysis: A subset of ten randomly-selected subjects were used in a parameter study to compare AppEn, SampEn, FAppEn, and FSampEn. MATLAB (Mathworks, Natick, MA) was used to calculate COP in the anteroposterior (AP) from force plate data.[2] All entropy measures were calculated for each trial at varying input parameter, R (0.01 to 1 at a 0.01 step size).[4,5,6,7]

Statistics: Entropy values were averaged across each three-trial set of foam conditions and R input parameter. A paired t-test was run for three pairs of foam condition: (F0,F2), (F0, F4), and (F2,F4). Statistical significance was set at $p<0.05$.

Results and Discussion

All four entropy measures produced significantly different values in the (F0,F4) and (F2,F4) tests at each R. The (F0,F2) test, however, showed varied statistical significance across entropy measures. *Figure 1* demonstrates a trend with AppEn and SampEn p-values >0.05 (likely due to the large variations seen in *Table 1)* while the FAppEn and FSampEn p-values were <.05 as a function of R. Fuzzy entropy values were much smaller in magnitude, but varied less between subjects. The hypothesis was upheld, as both fuzzy entropies studied showed more sensitivity to sensory deficits compared to AppEn and SampEn (due to their statistical significance across almost all values of R).

The results show that there are limitations to the sensitivity of AppEn and SampEn in detecting sensory deficits. Both detected a significant difference on the 1" foam, but the subtle deficit created by the 1/4" foam is only found using the fuzzy entropy values. The difference is likely due to the use of fuzzy sets which create a robustness to random noise. FAppEn and FSampEn were initially developed for use with electro-myography (EMG) signals and successfully reduced the influence of random noise in those signals.[6,7]

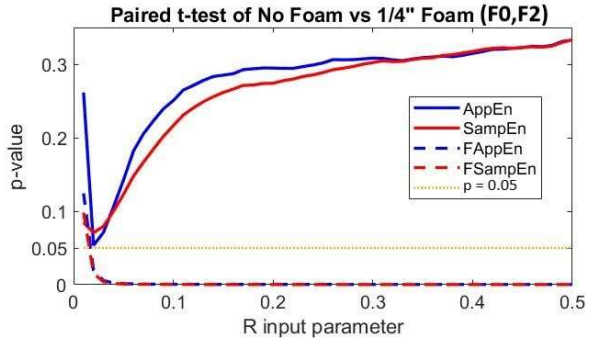

Figure 1. Results of paired t-test (F0,F2). Significance is indicated by the yellow dots at 0.05.

mean ± stdev	R = 0.1		R = 0.3		R = 0.5	
	No Foam	1/4" Foam	No Foam	1/4" Foam	No Foam	1/4" Foam
AppEn	0.379 ± 0.193	0.347 ± 0.172	0.086 ± 0.041	0.081 ± 0.036	0.046 ± 0.020	0.043 ± 0.018
SampEn	0.338 ± 0.177	0.309 ± 0.153	0.081 ± 0.040	0.076 ± 0.034	0.043 ± 0.020	0.041 ± 0.018
FAppEn ($x10^{-3}$)	1.95 ± 0.257	2.03 ± 0.317	0.689 ± 0.087	0.717 ± 0.108	0.419 ± 0.053	0.435 ± 0.065
FSampEn ($x10^{-3}$)	1.92 ± 0.272	2.02 ± 0.293	0.688 ± 0.088	0.722 ± 0.101	0.419 ± 0.053	0.439 ± 0.061

Table 1. Mean and standard deviation (stdev) values for all four entropy measures at select R input parameter values.

Significance

The results of this study demonstrate the potential that fuzzy entropy measures have in detecting postural sway deficits. Potential clinical uses include tracking COP entropy changes over time to track the progression of declining balance. Further analysis is required to understand the relationship between changes in entropy and increased fall risk.

This study shows the versatility of fuzzy entropy for use across a variety of biosignals. It has the potential to improve the sensitivity of analysis outside of EMG and COP signals, uncovering information in biological data that conventional entropy measures cannot detect.

References

1. Peterka, *J Neurophys.* 88 (2002) **2.** Winter et al. *Med Progress through Tech.* 16 (1990) **3.** Ladislao & Fioretti. *Med & Biol Eng & Comp.* (2007) **4.** Pincus. *Proc Natl Acad Sci.* 88 (1991) **5.** Richman & Moorman. *Amer J Physiol*. 278 (2000) **6.** Chen et al. *IEEE – Neural Sys & Rehab Eng.* 12 (2007) **7.** Xie et al. *Applied Soft Comp.* 11 (2011)

Gait changes in young onset Parkinson's disease before and after medication

[1]Klein, S., [2]Savica, R., [1]Kaufman, K.
[1]Motion Analysis Laboratory, Department of Orthopedic Surgery
Mayo Clinic, Rochester, MN
Klein.sara@mayo.edu

Introduction

Young onset Parkinson's disease (YOPD) occurs in people who are between 20 and 50 years of age. Of the one million people with PD in the US, an estimated 4% of them are affected by YOPD [1]. There is a paucity of studies on YOPD available to healthcare providers, leading to poorer patient outcomes. This study was performed to provide objective evidence of changes in the patients' gait patterns with medication.

Methods

Two male patients, ages 48 and 43, were recruited for this study. One patient had been diagnosed with YOPD a year and a half prior, the other six months prior to the study. Both patients were un-medicated for at least seven hours upon arrival for testing. They reported similar impairments, including slowness of movement and difficulty controlling unilateral lower extremity movements. Prior to data collection, a set of 41 retro-reflective markers were placed with respect to bony landmarks on the trunk, pelvis, and extremities using a modified Helen-Hayes marker set. One gait trial was collected prior to the patients orally administering their medication. Thirty minutes were allowed for medication absorption. Then gait trials were collected every five minutes, totaling eight trials. A fifteen minute rest was provided to eliminate the effect of fatigue before a final trial was collected.

Results and Discussion

Each patient demonstrated significant improvements in temporal distance (TD) factors (Figure 1) as a result of subtle improvements in gait kinematics and kinetics. The more involved lower extremity for each patient demonstrated greater improvements than the less involved side. These gait improvements created greater symmetry in support times and step lengths. Overall, the kinematics demonstrated improved muscular control of the limb and foot when on medication, with greater improvement on the more involved side. This was especially apparent in the sagittal plane for both patients, demonstrating increased joint range of motion with longer steps. Similarly, the moments tended toward normal when on medication, with greater improvement on the more-involved side leading to improved gait symmetry. Furthermore, the more-involved side powers were closer to normal on medication, with very little change on the uninvolved side. The improvements in gait kinematics and kinetics resulted in improvements in TD factors including increased velocity (Fig.1), normalized step widths, increased single support times, and increased step lengths. These changes in TD factors, are associated with improved lower extremity support and balance for reduced fall risk [2, 3, 4]. Additionally, the patients' subjective reports of maximal improvement aligned with the time of improved TD measures. Understanding that subjective patient report aligns with objective improvements in gait mechanics is powerful information for practitioners to better manage medications. Overall, TD factors represented medication efficacy and correlated with subjective report.

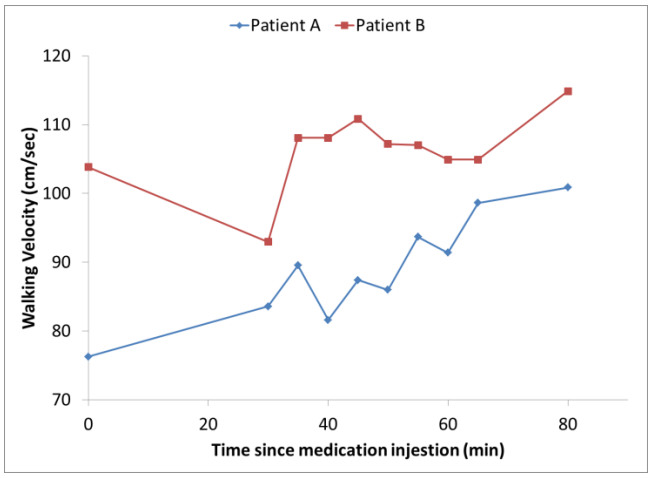

Figure 1: Gait velocity changes over time after administration of PD medication.

Significance

This report is the first to quantify the gait changes of patients with YOPD while off- versus on-medication, and revealed the most important changes were TD measures. This study demonstrates that objective gait measures should be utilized to improve clinical decision making, including medication management. The gait data was used to adjust medication profiles for improved functional outcomes for these patients. Medication adjustments based upon objective measures become especially important in the long term pharmaceutical management of this neurologic disorder where medication intolerance is common. This study provided patient education opportunities, including teaching the patients about their individual gait improvements and the importance of medication adherence to reduce fall risk. There are implications for other healthcare providers as well. With objective gait data, therapists can teach their patients how their PD medications affect their gait, fall risk, and create individualized exercise programs to target patient specific impairments in the off-medication state. Therapists can also use gait data to educate patients and families on activity planning within medication timelines to improve quality of life. Objective gait data should be a standard of clinical practice when treating YOPD for best outcomes.

References

[1] Marras, C., et. al. (2018) *Parkinson's Disease, 4(21)*.
[2] Perry, J. (1992) Gait analysis. Thorofare, NJ: SLACK Inc.
[3] Del Din, S. et. al.(2017) *J Gerontol A Biol Sci Med Sci, 74(4)*, 500–506.
[4] Guimaraes, R. M. and B. Isaacs. (1980) *Int Rehabil Med, 2(4)*, 177-180.

Detecting lingering effects on postural control using linear metrics following TBI

Christian Witkop[1], Nathan Henry[1], Donald Goss[1], Gregory Freisinger[1]
[1]United States Military Academy – West Point

Email: gregory.freisinger@westpoint.edu

Introduction

Traumatic brain injury (TBI) is relatively common and often results in debilitating conditions experienced by military personnel. TBI can negatively influence postural control, which we define as one's ability to maintain a stable posture with their center of mass vertical to their center of support. TBI impairs a patient's ability to maintain this stability which may lead to difficulties during activities of daily living. After recovery from the acute symptoms of TBI, an individual's altered performance may persist. Previous studies have shown that postural control measures are useful in detecting deterioration of balance function following a TBI in the short-term [1,2], however little work has been done on detecting lingering effects outside of this initial timeframe.

The goal of this investigation was to compare linear metrics characterizing postural control between patients with and without a lifetime history of TBI. Significant differences between the two groups may identify lingering effects in postural control due to TBI. This detection would enable clinicians to differentiate between acute effects of a TBI and lingering effects from previous injury.

Methods

253 individuals , 41 with a history of TBI (TBI_hist -age: 18.8 ± 1.1 yr, height: 1.75 ± 0.09 m, mass: 75.3 ± 14.6 kg) and 212 who have no history of TBI (no_TBI - age 18.8 ± 1.1 yr, height: 1.75 ± 0.09 cm, mass: 75.8 ± 12.8 kg) participated in the IRB-approved protocol. For the subjects with a history of TBI, injury occurred at least 6 months before testing. Patient's center of pressure (COP) position data were collected over the course of a Sensory Organization Test (SOT). A SOT consists of six conditions that are a combination of eyes open/closed, platform fixed/sway referenced, and visual surround fixed/sway referenced. This test was performed on a NeuroCom Balance Master [Natus, Pleasanton, CA] which outputs a score representing balance function for each trial based off proprietary algorithm. Raw COP position data were collected at 100 Hz during three trials of each of the six SOT conditions and smoothed with a window size of 10 samples (0.1 seconds).

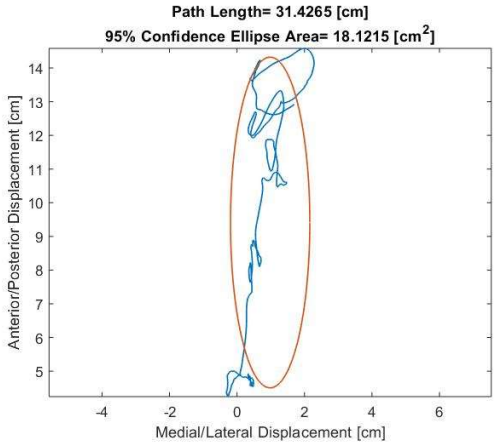

Figure 1: *COP Path overlayed with 95% Confidence Ellipse over a 20 second trial of a Sensory Organization Test (SOT)*

We then calculated the following linear metrics: path length, 95% confidence ellipse area, average speed, average acceleration, and root mean squared medial lateral displacement. Figure 1 shows an example of COP path during a trial and the corresponsing ellipse area. After removals for incomplete and repeated tests, 702 trials of patients with a history of TBI and 4680 trials of never-concussed patients were analyzed. A two-sample T-test was then performed to identify differences between the TBI_hist and no_TBI groups for every metric across each the six SOT conditions, at a significance level of $\alpha < 0.05$. Due to the exploratory nature of this research, a multiple-comparision correction was not applied.

Results and Discussion

No significant differences were observed between subjects in the history of TBI and no history of TBI groups for any of the variables of interest. Table 1 shows results for SOT Condition 1. These findings are in line with work by Buckley et al. that did not observe lingering deficits in postural control characterized by linear metrics outside of the initial post-injury recovery phase from TBI. [2]

Table *2*: Postural control metrics between participants with and without a lifetime history of TBI across all 20 second trials of the Sensory Organization Test (SOT) Condition 1

	History of TBI	**No History of TBI**	
Metric	Mean ± STD	Mean ± STD	P-Value
NeuroCOM Score	83.0 ± 14.7	82.7 ± 15.7	0.81
Path Length	35.6 ± 27.4	37.9 ± 31.2	0.48
95% Ellipse Area	2.30 ± 3.50	2.72 ± 6.55	0.51
Average Speed	1.87 ± 1.52	1.93 ± 1.62	0.72
Average Acceleration	26.7 ± 19.5	27.9 ± 20.1	0.56
RMS Medial-Lateral Displacement	9.91 ± 4.90	10.7 ± 6.85	0.23

Significance

No differences in NeuroCOM functional score or other postural control metrics were observed between individuals with and without a history of TBI. A limitation of this research is that all participants were cadets at the United States Military Academy and passed a comprehensive physical before admittance. Additionally, severity of TBI was not considered in our analysis. Future work should investigate individual SOT conditions and the potential of non-linear metrics to detect lingering deficits between individuals with and without a history of TBI.

Acknowledgments

No funding to disclose.

References

[1] Sosnoff et al. (2011) J. Athl. Train.: 46(1) 85-91

[2] Buckley et al. (2016) J. Sport and Health Sci.: 5(1) 61-69

Correlating postural control metrics with NeuroCOM functional scores

Christian Witkop[1], Nathan Henry[1], Donald Goss[1], Gregory Freisinger[1]
[1]United States Military Academy – West Point

Email: gregory.freisinger@westpoint.edu

Introduction

Traumatic brain injury (TBI) is relatively common among military personnel and may result in debilitating conditions. TBI can negatively influence postural control, which we define as one's ability to maintain a stable posture with their center of mass vertical to their center of support. TBI impairs a patient's ability to maintain this stability which may lead to difficulties during activities of daily living. Current clinical evaluations of postural control rely heavily upon qualitative assessments [1], however these tend to be unreliable and subjective. While commercial computerized posturography systems are becoming more common, they are often cost-prohibitive for widespread use.

The goal of this investigation was to develop metrics to characterize relevant measures of postural control and identify correlations to proprietary commercial posturography output. The non-proprietary algorithms developed from this research would serve as the basis for an inexpensive and effective device to assist clinicians in making return-to-duty decisions for soldiers with TBI.

Methods

253 individuals , 70 females (age: 18.77 ± 1.00 yr, height: 173.55 ± 9.86 cm, mass: 74.89 ± 13.74 kg) and 183 males (age 18.85 ± 1.12 yr, height: 175.66 ± 9.05 cm, mass: 76.07 ± 12.81 kg) participated in the IRB-approved protocol. Patient's center of pressure (COP) position data were collected over the course of a Sensory Organization Test (SOT). A SOT consists of six conditions that are a combination of eyes open/closed, platform fixed/sway referenced, and visual surround fixed/sway referenced. This test was performed on a NeuroCom Balance Master [Natus, Pleasanton, CA] which outputs a score representing balance function for each trial based off a black-box algorithm. Raw COP position data were collected at 100 Hz during three trials of each of six SOT conditions and smoothed with a window size of 10 samples (0.1 seconds). We then calculated the following linear metrics: path length, 95% confidence ellipse area, average speed, average acceleration, root mean squared medial lateral displacement and average rate of heading change. After removals for incomplete and repeated tests, 4240 trials were analyzed. Pearson-R correlations were then calculated to find relationships between the linear metrics and the numerical function score for as determined by the NeuroCom for data in each condition and across the whole SOT (significance level $\alpha < 0.05$). Strong correlations identified where $R > 0.7$.

Results and Discussion

All correlation data between linear metrics and NeuroCom function are shown in Table 1, for each individual condition of the SOT and the combination of all conditions, along with scatter plots for select conditions. The strongest correlation was identified between the NeuroCom function scores and the 95% confidence ellipse area across combined conditions, (R=-0.87; p<0.001). This negative correlation indicates that a larger area covered by the COP during a given trial, is related to a worse NeuroCom function score.

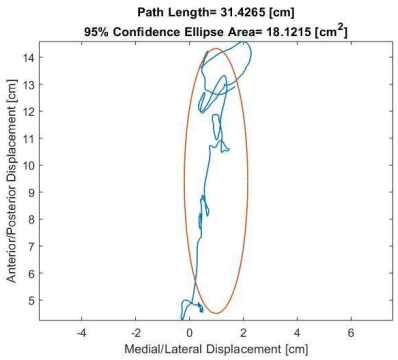

Figure 1: COP Path overlayed with 95% Confidence Ellipse over a 20 second trial of a Sensory Organization Test (SOT)

Path length (R=0.81 p<0.001), average speed (R=-0.81 p<0.001), average acceleration (R=-0.73 p<.001), and RMS ML (R=-.70 p<.001) may be considered as complementary surrogates for the NeuroCom score. Heading change yielded weak correlations indicating that there is little relation between that metric and NeuroCom balance score (R=0.02 p=0.29). Individual condition correlations are less than the total due to the massive number of data points across all conditions. Strong correlations between linear metrics and Neurocom function suggest the possibility of a less expensive system to identify postural control deficits.

Significance

Less expensive, quantitative testing of postural control may assist clinicians in making more informed decisions for TBI patients in smaller clinics. This study laid the groundwork for improving clinical care of TBI without expensive computerized posturography equipment.

References

[1] Marshall et al. (2012). Canadian family physician Medecin de famille canadien, 58(3), 257-267

Table 1. Pearson R and P values for metrics and NeuroCOM scores

	Path Length		95% Ellipse Area		Avg Speed		Avg Acceleration		Avg Heading Change		RMS ML	
Condition	R	P	R	P	R	P	R	P	R	P	R	P
1	-0.61	<.001	**-0.77**	**<.001**	-0.61	<.001	-0.31	<.001	0.02	0.783	-0.53	<.001
2	-0.58	<.001	**-0.78**	**<.001**	-0.58	<.001	-0.36	<.001	0.12	0.065	-0.36	<.001
3	-0.59	<.001	-0.68	<.001	-0.58	<.001	-0.46	<.001	0.04	0.540	-0.50	<.001
4	-0.52	<.001	-0.23	<.001	-0.40	<.001	-0.23	<.001	-0.01	0.847	-0.31	<.001
5	-0.42	<.001	-0.61	<.001	-0.45	<.001	-0.36	<.001	0.15	0.025	-0.42	<.001
6	-0.44	<.001	-0.40	<.001	-0.48	<.001	-0.39	<.001	-0.03	0.625	-0.46	<.001
All	**-0.81**	**<.001**	**-0.87**	**<.001**	**-0.81**	**<.001**	**-0.73**	**<.001**	0.02	0.294	-0.70	<.001

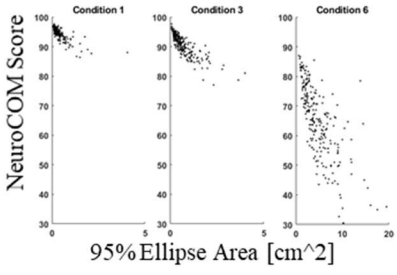

Walking Balance Control is Delayed in Children with Cerebral Palsy.

Ashwini Sansare, Hendrik Reimann, Samuel C.K. Lee, John Jeka
University of Delaware, Newark, DE, USA
Email: ashwini@udel.edu

Introduction

Children with CP are known to be heavily reliant on visual input compared to other sensory modes, as evidenced by increased errors in proprioception when their vision was perturbed in standing[1] and during single plane lower extremity movement[2]. However, it is not known how children with CP use visual information for sensorimotor feedback during walking, an activity where the threat to balance is higher. The aim of this pilot study is to assess how children with CP react to visual perturbations compared to children with typical development (TD). Our hypothesis, based on previous studies on older adults[3], was that children with CP would demonstrate a delayed response to visual perturbations.

Methods

Four subjects with CP between the age of 8-18 years (2 with hemiplegia, 2 with spastic diplegia), Gross Motor Function Classification System (GMFCS) level I-II, were recruited along with four age-matched controls. Subjects walked on a self-paced treadmill in a virtual reality environment. They received a visual fall stimulus in the medio-lateral plane toward the triggering heel strike of either foot, with 12-13 steps intervening steps between stimuli. Randomly determined triggers without stimulus served as controls in the analysis. Each trial lasted two minutes, and was repeated ten times, with intermittent rest breaks.Our primary outcome variables were center of mass (CoM) excursion and velocity.

Results and Discussion

Subjects in both groups reacted to the visual fall stimuli by moving their CoM away from the direction of the perceived fall. The TD group reached the peak average CoM excursion of 5.2±1.7 cm in away direction typically at the 4th post-stimulus step while the CP group demonstrated a more magnified but delayed shift in CoM, with the peak average CoM excursion of 8.3±3.3 cm occurring on the 5th post-stimulus step (Fig 1). The average CoM velocity for the TD group peaked during the 3rd post-stimulus step while that for the CP group peaked during the 4th post-stimulus step. The magnitudes of both peak average CoM excursion and velocity were higher in CP vs. TD group, as evidenced by large effect sizes (Table 1).

Our results suggest that compared to typically developing peers, our cohort of children with CP demonstrated a delayed but magnified balance response to sensory perturbations while walking. This might be suggestive of delayed neural processing and poor sensory integration abilities in children with CP. Previous studies[4] suggest there is a shift from visual dominance towards kinesthetic inputs while mediating postural responses by 6 years of age. A magnified CoM response in an older cohort of children with CP may be indicative of over-reliance on vision, a characteristic seen in younger TD, thus suggesting that CP group's response may not have matured to the level of TD peers. Future research efforts with larger sample size and a wider age range for both CP and TD groups is needed to provide stronger support to the findings of this pilot study.

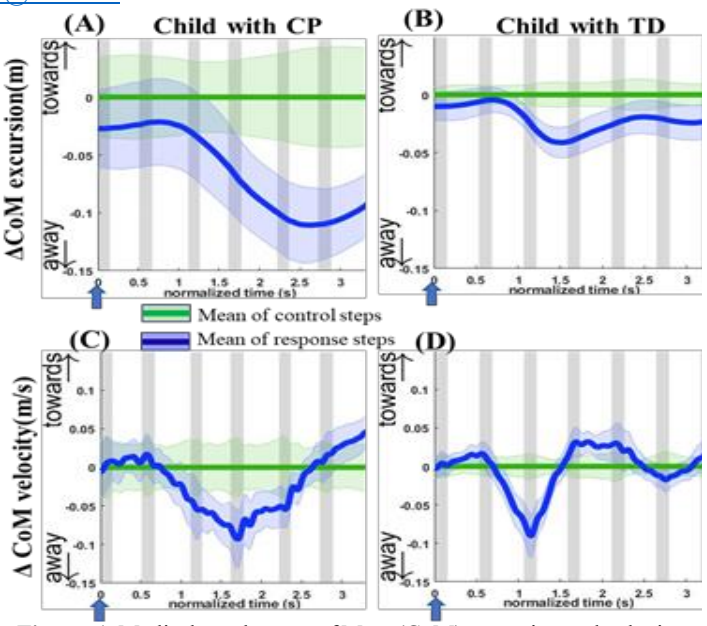

Figure. 1. Medio-lateral center of Mass (CoM) excursion and velocity trajectories in response to visual fall stimuli in one representative subject with CP **(A & C)** and with TD **(B & D)** respectively. Green lines indicate the mean of control (no fall stimulus) steps, which is subtracted from stimulus data, and resulting response is depicted as blue lines. Shaded areas around each line represent one standard deviation. X axis shows 6 steps, time-normalized to 100 timepoints, with double-stance periods shaded gray and single-stance periods white. Arrows at the beginning of each curve mark the triggering visual fall stimulus.

	Peak ΔCoM excursion(m)		Peak ΔCoM velocity(m/s)	
	Mean	**SD**	**Mean**	**SD**
TD	0.05	0.02	0.03	0.02
CP	0.08	0.03	0.04	0.02
Effect Size	1.36		1.03	

Table 1. Mean, standard deviation (SD) and effect sizes for ΔCoM excursion (meters) and velocity(meters/sec) for TD and CP group.

Significance

While most assessments and treatments in CP address motor-related deficits such as weakness, flexibility and spasticity, our results underscore the role of sensory regulation in balance control during walking. These findings are relevant in developing targeted sensory-based treatment protocols to enhance balance control not only in children with CP but also other neurodevelopmental disorders that could benefit from augmented sensory input during walking.

Acknowledgments

Unidel Distiguished Scholars Award research grant.

References

[1] Slaboda et al. IEEE Trans Neural Syst Rehabil Eng;21(2):218-24.
[2] Wingert et al. Arch Phys Med Rehabil. 2009 Mar;90(3):447-53.
[3] J.R. Franz et al. Human Movmnt Sci 40 (2015) 381–392
[4] Shumway-Cook et al (1985). J of Mot Behavior, 17,131–147

Examining Effects of Cognitive Task Difficulty on Postural Stability via Wavelet Transforms

Brittany N. Sommers[1], Douglas A. Wajda[2], Brian L. Davis[1]
[1]Cleveland State University, Department of Mechanical Engineering, Cleveland, OH, USA
[2]Cleveland State University, Department of Health and Human Performance, Cleveland, OH USA
Email: b.n.sommers@vikes.csuohio.edu

Introduction

Multiple sclerosis (MS) affects more than 2.3 million people worldwide and 1 million people in the United States (US) [1]. Symptoms of MS include muscle weakness, poor cognition, and decreased alertness, all impacting upright posture.

The purpose of this study is to examine postural stability mechanisms of MS patients across tasks of increased cognitive demand. Previous work examined the cognitive effects of these tasks [2], but not the dynamic stability effects.

Stability mechanisms were examined through the Hurst exponent (H), a statistical parameter defining long-term correlations in moving systems. H is defined from $0 \leq H \leq 1$, where $H<0.5$ indicates stability and $H>0.5$ indicates instability [3]. H values were calculated with wavelet analyses because this approach can characterize non-stationary signals and provide time-frequency localization of a signal [3,4].

Methods

Four test conditions were: (1) quiet eyes-open standing (EO), (2) quiet eyes-closed standing (EC), (3) perturbed standing with participants leaning to their limits of stability (PRT-LOS), and (4) perturbed standing in a comfortable stance (PRT-STA).

During EO and EC conditions, participants were instructed to stand comfortably for 30s. During the PRT conditions, 20 auditory cues (beeps) were given during each task. Participants were asked to respond as quickly as possible by saying "pop" out loud. They were instructed to maintain their balance on both tasks. Ages for controls (n=33) and MS (n=16) were 62.6±9.1 years and 55.3±11.1 years, respectively.

Anterior-posterior (AP) center-of-pressure (CoP) values were analyzed by a level 12, Symlet 2 wavelet decomposition. To obtain H, log-log plots of the average wavelet coefficients at each decomposition level versus 2^j (j = number of levels) were plotted [3,4]. H values are then calculated as H = slope – ½ [3,4]. Average H values were calculated for both groups.

Results and Discussion

In the AP direction, control $H_{PRT\text{-}LOS}$ values were significantly higher than H_{EO} and H_{EC} ($p<0.001$). Similarly, control $H_{PRT\text{-}STA}$ values were higher than H_{EO} and H_{EC} ($p<0.001$). (Figure 1)

MS did not display significant differences in the AP-directions between conditions. MS were significantly less stable than controls in both the EO ($p=0.019$) and EC condition ($p=0.026$). MS displayed instability on all four conditions ($H>0.5$), whereas controls displayed stability ($H<0.5$) for EO and EC, but instability ($H>0.5$) for PRT-LOS and PRT-STA.

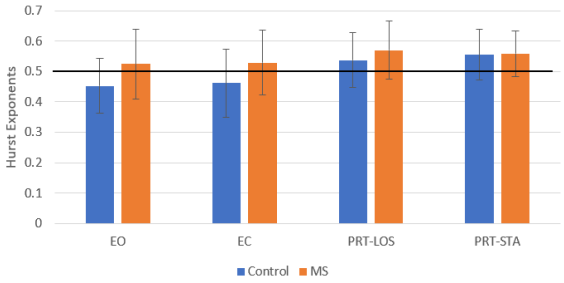

Figure 1: AP Hurst Exponents for Controls and MS. The black line indicates H = 0.05

Controls became less stable on PRT-STA than PRT-LOS, even though the difficulty decreased. MS became more stable on PRT-STA than PRT-LOS. Controls are considered "high hazard estimate, high postural reserve" meaning they are cognitively sound, and have control over their motor output [5]. MS are considered "high hazard estimate, low postural reserve" meaning they are cognitively sound but have poor motor output control [5]. For PRT-STA, controls most-likely spent more time focusing on the cognitive task, as they were more confident in their postural control. As a consequence, their balance suffered. MS participants on the other hand had to focus more on maintaining postural control, and spent less time focusing on the cognitive task as a way to maintain their balance.

Significance

Using wavelets to obtain Hurst exponents allows for the analysis of non-stationary time-series data. Examining dynamic postural changes in neurological disorders is important as it provides information that cannot be seen through cognitive tasks alone. The combination of dynamic and cognitive information can be used by clinicians to enhance rehabilitation methods for patients. The way these different cohorts (control vs. MS) respond to cognitive tasks is connected to their amount of hazard estimate versus postural control.

References

1. National Multiple Sclerosis Society.
2. Wajda D et al. (2019). Journal of Neural Transmission.
3. Simonsen I et al. (1998). Physical Review 58.
4. Schaefer A et al. (2014). Journal of Neuroscience Methods 222, 118-130.
5. Yogev-Seligmann G et al. (2012). Movement Disorders. 27(6).

Leg Joint Mechanics When Hopping at Different Frequencies

Mu Qiao*
Department of Kinesiology, Louisiana Tech University, Ruston LA, 71272, USA
Email: *mqiao@latech.edu

Introduction

Although the dynamics of the center of mass (COM) can be accounted for by a spring-mass model during hopping, less is known about how each leg joint (i.e., hip, knee, and ankle) contributing to the COM dynamics during hopping. This study investigated the function of individual leg joints when humans hopped vertically and unilaterally at four different frequencies (i.e., 1.6, 2.0, 2.4, and 2.8 Hz) (*1*). I hypothesized that 1) all leg joints (i.e., hip, knee, and ankle) maintained the functional as torsional springs and increased their stiffness when hopping frequency increased, and 2) the leg joints are controlled to maintain the same mechanical load when hopping at different frequencies.

Methods

A 3D motion capture system (12 cameras, model Miqus M3, Qualisys, Göteborg, Sweden) was used to record full body kinematics at 120 Hz. A force platform (600 × 900 mm, model 6090-15, Bertec Corp., Columbus, OH, USA) acquired ground reaction forces (GRFs) at 1440 Hz. The stance phase from touchdown (TD) to takeoff (TO) of the left foot on the platform during all cycles in each trial was analyzed. To characterize the leg joint function during hopping, I used previously developed indices decomposing the function of a leg joint into four mutually exclusive and exhaustive components (*i.e.*, strut-, spring-, motor-, and damper- index, Fig. 2).

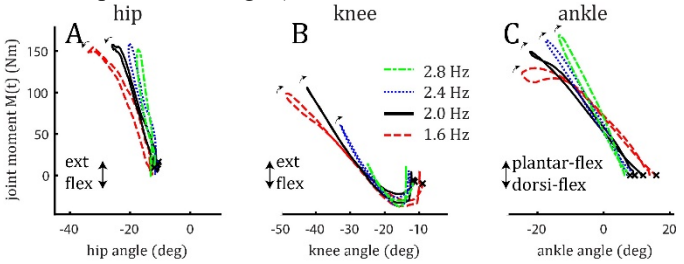

Figure 1: The work loop formed by each leg joint (i.e., hip, knee, and ankle) during stance.

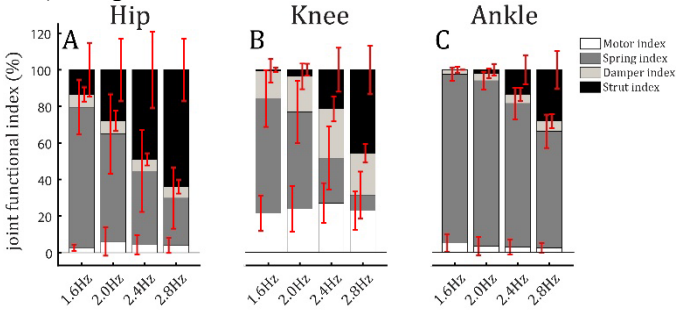

Figure 2: The % of the motor, spring, damper, and strut indices during stance phase of hopping for (A) hip, (B) knee, and (C) ankle.

Results and Discussion

Decomposing the mechanics of leg joints into functional roles supported that, in slow hopping, all leg joints behaved like a spring. The spring indices for the hip (76%), knee (63%), and ankle (93%) were the largest index among motor, spring, damper, and strut indices at 1.6 Hz (Fig. 2).

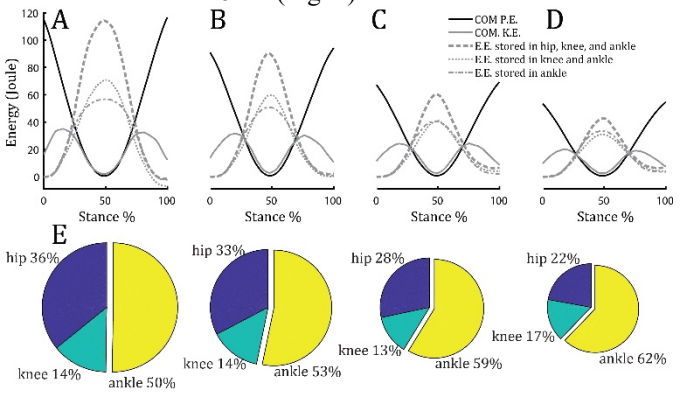

Figure 3: The flow of different mechanical energy during the stance phase of hopping (A) 1.6 Hz, (B) 2.0 Hz, (C) 2.4 Hz, and (D) 2.8 Hz. (E) The % of each leg joint in storage and return mechanical energy in the stance phase.

As hopping fast, leg joints changed their functional roles differently. Specifically, the hip's spring index decreased from 76% at 1.6 Hz to 26% at 2.8 Hz. The decrease of hip's spring index was mainly compensated for by the increase of strut index from 14% at 1.6 Hz to 64% at 2.8 Hz. For the knee, fast hopping required spring index decreased from 63% at 1.6 Hz to 9% at 2.8 Hz and strut index increased from 1% at 1.6 Hz to 45% at 2.8 Hz. Therefore, faster hopping requires hip and knee to change functional roles from spring to strut (Fig. 2). For the ankle, hopping fast mainly decreased the ankle's spring index from 93% at 1.6 Hz to 64% at 2.8 Hz while increased strut index from 0% at 1.6 Hz to 28% at 2.8 Hz. Therefore, hopping fast only required ankle to reduce its primary role as a spring.

For the relative amount of COM mechanical energy's storage and return, the ankle dominated in all hopping frequencies. When hopping frequency increased, the system's mechanical energy decreased (Fig. 3), but ankle's dominance of energy storage and return increased (i.e., from 51% at 1.6 Hz to 65% at 2.8 Hz).

Significance

Understanding the function and control of leg joints in hopping could provide insight into the fundamental principles of legged locomotion of humans. Human hopping is not passive because the functional roles of each leg joints change at different hopping frequencies. The functional change of leg joints could help to understand how the muscles are controlled to achieve task goals.

References

1. Y. H. Chang, R. A. Roiz, A. G. Auyang, Intralimb compensation strategy depends on the nature of joint perturbation in human hopping. *J Biomech* **41**, 1832-1839 (2008).

Methods of Estimating Foot Power in Takeoff Phase of Standing Vertical Jump

Kundan Joshi and Blake M. Ashby
School of Engineering, Grand Valley State University, Grand Rapids, MI, USA
Email: joshik@mail.gvsu.edu

Introduction

Experimental motion capture studies have commonly considered the foot as a single rigid body despite the presence of numerous internal joints and deformable soft tissue. Various approaches have been used to quantify the internal foot power due to rigid body deviations of the foot. Two strategies that can be used with a traditional rigid foot are distal foot power (DFP) [1] and foot power imbalance (FPI) [2] techniques. Another approach for modeling the non-rigid nature of the foot is with a multisegment foot [3]. The purpose of the present study was to compare the internal foot power and work in the takeoff phase of the standing vertical jump (SVJ) using DFP and FPI on a single rigid foot and using a two-segment foot model separated at the metatarsophalangeal (MTP) joints.

Methods

The right-sided lower limb model devised for this study contained a shank and a two-segment foot divided at an MTP joint. A 16-camera motion capture system (Vicon Motion Systems Ltd., Los Angeles, CA) was used to record six physically active participants performing six SVJs from two adjacent force platforms (Advanced Mechanical Technology Inc., Watertown, MA). The participants positioned their feet so that the ground reaction forces (GRF) acting on the foot could be divided at the MTP joints consistent with the protocol introduced by [3].

Using inverse dynamics with a two-segment foot, the total 6DOF power at the MTP joint was calculated and integrated to get MTP work. Using inverse dynamics on a single rigid foot, DFP and FPI were calculated using the equations shown below and integrated to get foot work:

$$DFP = \boldsymbol{F}_{GRF} . (\boldsymbol{v}_G + \boldsymbol{\omega}_{foot} \times \boldsymbol{r}_d) + \boldsymbol{M}_{free} . \boldsymbol{\omega}_{foot}$$

$\boldsymbol{F}_{GRF}$ is the GRF acting on the foot at the center of pressure (COP), $\boldsymbol{M}_{free}$ is the free moment acting on the foot, $\boldsymbol{\omega}_{foot}$ is the foot angular velocity, $\boldsymbol{v}_G$ is the foot mass center (COM) velocity, and $\boldsymbol{r}_d$ is the position vector from the COM to the COP.

$$FPI = \frac{d\boldsymbol{E}_{\boldsymbol{foot}}}{dt} - \boldsymbol{M}_{ank} . \boldsymbol{\omega}_{foot} - \boldsymbol{F}_{ank} . \boldsymbol{v}_{ank}$$

$\boldsymbol{E}_{\boldsymbol{foot}}$ is the foot mechanical energy, and $\boldsymbol{M}_{ank}$, $\boldsymbol{F}_{ank}$, and $\boldsymbol{v}_{\boldsymbol{ank}}$ are the net ankle moment, intersegmental force, and velocity, respectively.

Descriptive statistics for foot power and work were generated. To compare the three methods, one-way within repeated measures ANOVA was implemented (alpha value 0.05).

Results and Discussion

MTP power was basically zero or positive (Figure 1). DFP showed significant power absorption, followed by power generation that peaked lower than the other two. FPI showed lesser power absorption than DFP, with power generation peaking about the same as MTP. The work values were –4.0 ± 1.0 J for DFP, 1.8 ± 1.1 J for FPI, and 5.1 ± 0.5 J for the MTP joint (all significantly different from each other with $p < 0.0001$).

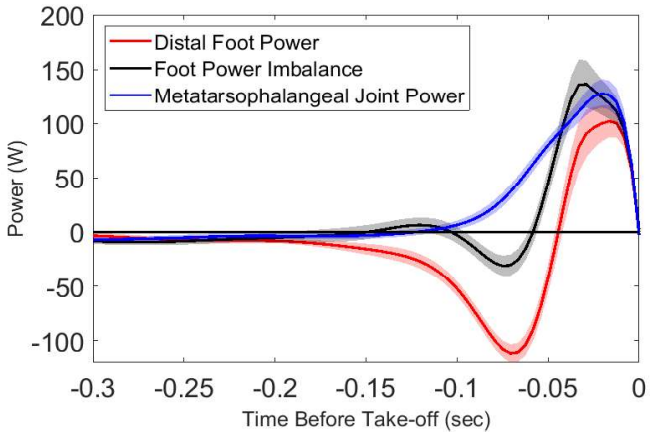

Figure 1: Comparison of least square mean values for DFP versus FPI versus MTP joint power (with 95% confidence interval bands)

All three approaches demonstrate positive power contributions right before takeoff due to structures internal to the foot. The two-segment foot model only calculated the power at the MTP joint, which was almost all positive. The other two approaches, DFP and FPI both demonstrated periods of negative power indicating that areas of the foot other than the MTP joints were absorbing power. The difference between DFP and FPI might be explained by understanding that DFP represents the power due to deviation from the rigid body state only for the portion of the foot between the COM and the COP [4], whereas theoretically, FPI captures the internal power throughout the foot. For both methods, errors can arise from the assumption that the angular velocity of the foot is the same throughout and that the COM can be accurately determined.

Significance

Any of these three methods may be used to quantify internal foot power, but it is important to properly understand the limitations of whichever method is used. Using a multisegment foot may seem like a better approach, but more than two segments is probably required to capture all the internal foot power. Moreoever, apportioning the GRF across multiple segment is rarely practical. DFP and FPI are relatively simple ways of quantifying the power contributions of the foot that can be used with a traditional rigid foot model. The results motivate further research to compare and understand the relative merits of the two methods for movements besides jumping, as well as investigating how to quantify kinetics of a foot model with three or more segments.

Acknowledgments

Special thanks to Gordon Alderink and Yunju Lee.

References

[1] Siegel et al. (1996). J Biomech, 29: 823-827.
[2] Robertson and Winter (1980). J Biomech, 13: 845-854.
[3] Bruening et al. (2012). Gait & Posture, 35: 535-540.
[4] Zhao et al. (2020). J Biomech, 90: 109548

Movement Patterns During Single-Leg Hopping in Individuals with Lower Limb Loss

Joseph G. Wasser[1,2], Julian C. Acasio[1,2], Brad D. Hendershot[1,3,4], Ross H. Miller[5]
[1]Walter Reed National Military Medical Center; [2]Henry M. Jackson Foundation for the Adv. of Military Medicine, Inc.; [3]DoD-VA Extremity Trauma & Amputation Center of Excellence; [4]Uniformed Services University of the Health Sciences; [5]Univ. of Maryland
Email: joseph.g.wasser.ctr@mail.mil

Introduction

For individuals with unilateral lower limb loss, single-leg hopping is often a convenient method of ambulation. However, large and unusual forces presented during single-leg hopping may accelerate degeneration of joint health and integrity compared to walking itself [1]. Therefore, the purpose of this study was to identify the forces and movement patterns used by individuals with unilateral transfemoral (TF) and transtibial (TT) limb loss. With a smaller residual leg, we hypothesize TF vs. TT participants will exhibit larger hip motions.

Methods

Thirty-two males with unilateral lower limb loss (22 TT and 10 TF) participated, with mean (SD) age=36.7 (7.4) yr, height= 178.8 (5.0) cm, body mass=88.7 (13.1) kg. Each hopped on one leg along a 15m walkway, at a self-selected pace. Full-body kinematics were tracked using a motion capture system; ground reaction forces were simultaneously sampled via force platforms.

Kinetic outcomes included features of the knee adduction (KAM) and flexion (KFM) moments; impulse was calculated as the integral of the moment-time series; LR as the slope between 20% and 80% of the time from heel strike to the first KAM peak; and the per-unit-distance (PUD) KAM as the average joint moment across all strides divided by the average stride length[2]. Kinematic outcomes included features of knee, hip, and trunk angles; trunk-pelvic coordination was quantified using continuous relative phase (CRP), computed as the difference between the normalized phase angles of the trunk and pelvis segments [3]. All outcomes were averaged across hops, and kinetic outcomes scaled by body weight and height. Unpaired t-tests assessed differences between TT and TF participants ($p<0.05$).

Results and Discussion

There were no differences in kinetic outcomes between TT and TF participants (Table 1). Although slightly different movement patterns were observed between TT and TF participants, differences in forces applied are compensated with different movement strategies.

Table 1. Single-leg hopping kinetics

	TT (n=22)	TF (n=10)	p(sig)
Peak KAM (BW·Ht)	4.4±2.0	4.4±1.4	0.99
KAM Impulse (BW·Ht)	0.5±0.4	0.5±0.3	0.76
KAM Loading Rate (BW·Ht·s^{-1})	0.5±0.3	0.5±0.3	0.73
Peak KFM (BW·Ht)	14.6±3.4	12.9±3.2	0.19
KAM PUD (BW·Ht·m^{-1})	6.2±2.9	7.9±2.9	0.15

[α]-Values are expressed as mean±SD
*- Statistically significant difference between groups ($p\leq0.05$)

TF participants hopped with increased hip abduction at foot-contact (FC; Table 2). This increased hip abduction indicates dependence on their intact leg for stability, but may also suggest that a longer limb (apparent with TT limb-loss) may provide for counter-weight support during single-leg ambulation. Larger CRPz is indicative of more out-of-phase (or less in-phase) movement, suggesting TF participants are increasing the relative (axial) rotation between the trunk-pelvis to assist with forward propulsion during their hop.

Table 2. Single-leg hopping kinematics.[α]

	TT (n=22)	TF (n=10)	p(sig)
Hop Speed (m/s)	0.50±0.07	0.46±0.04	0.10
Hop Length (m)	0.77±0.24	0.58±0.09	0.02*
Vertical COG Displacement (cm)	1.2±0.1	1.3±0.0	0.08
Knee Flexion ROM(°)	35.1±7.8	31.0±5.1	0.13
Peak Knee Flexion(°)	9.2±6.4	9.7±4.9	0.83
Knee Flexion @FC(°)	13.1±5.8	13.2±5.4	0.90
Knee Adduction @FC(°)	2.0±3.0	4.1±4.9	0.15
Hip Abduction @FC(°)	0.5±3.9	3.9±5.2	0.05*
Trunk Flexion ROM(°)	6.8±3.8	7.6±2.2	0.53
Trunk Tilt ROM(°)	12.7±4.5	10.6±3.6	0.20
Trunk Flexion @FC(°)	3.1±6.2	2.3±6.8	0.76
Trunk Tilt @FC(°)	-0.1±4.7	1.9±5.6	0.29
CRP (sagittal)	57.8±21.2	60.6±23.4	0.74
CRP (frontal)	135.3±15.6	133.8±25.2	0.73
CRP (transverse)	61.3±26.7	84.1±32.8	0.05*

[α]-Values are expressed as mean±SD
*-Statistically significant difference between groups ($p\leq0.05$)

Significance

Identifying movement patterns and associated forces during hopping, unique to the level of limb loss, facilitate development of clinical/movement recommendations and rehabilitative efforts. Future research can utilize the differences in movement patterns to potentially associate them with the high prevalence of knee degeneration in the limb loss population. Moreover, larger axial motions seen in TF may also inform future investigations into other highly prevalent musculoskeletal conditions following limb loss, such as low back pain.

Acknowledgments

This work was supported, in part, by the Center for Rehabilitation Sciences Research, of the Uniformed Services University of the Health Sciences (USUHS; HU0001-15-2-003; PI: Pasquina), and the Extremity Trauma and Amputation Center of Excellence. Views expressed are those of the authors, and do not reflect the official policies of USUHS, HJF, the U.S. Departments of the Army/Navy/Air Force, Defense, nor the U.S. Government. The authors also acknowledge Dr. Alison Pruziner, PT, DPT, ATC and Dr. Rebecca Krupenevich, PhD, for their contributions to idea formulation, project management, and data collection for the primary project from which this data was generated.

References

[1] R. L. Krupenevich, et al. *Med. Sci. Sports Exerc.* 2017
[2] R. H. Miller, et al. *Med. Sci. Sports Exerc.* 2014
[3] J. Hamill, R. E. A. et al. *Clin. Biomech.* 1999

Shorter Muscle Activation Time Increases the Metabolic Cost of Cyclic Force Generation

Owen N. Beck,[1,2] Jonathan Gosyne, Jason R. Franz, & Gregory S. Sawicki

[1]The George W. Woodruff School of Mechanical Engineering, Georgia Institute of Technology, Atlanta, GA, USA
[2]The School of Biological Sciences, Georgia Institute of Technology, Atlanta, GA, USA
Email: obeck3@gatech.edu

Introduction

The biomechanical basis for the metabolic cost of terrestrial locomotion is elusive. That is partly because many parameters change in the same direction as locomotion tasks vary, making it difficult to separate the independent contributions to metabolism. Muscle force generation is presumed to exact a metabolic cost. Yet, it remains unclear how the time-course of force generation affects metabolism [1]. Filling this gap in our understanding is important because reducing the metabolic cost of locomotion may improve performance, mitigate fatigue, and promote physical activity. Thus, we sought to reveal if the time-course of muscle force generation affects the metabolic cost of producing a fixed force-time integral (analogous to stride-Avg muscle force) over periodic activation-deactivation cycles; emulating muscle contractions during steady-state locomotion.

Methods

11 participants performed 6 x 5-minute fixed-end plantar flexion trials on a dynamometer with their right knee and ankle secured at 130° and 90°, respectively. In this position, plantar flexion torque is primarily provided by the soleus. During each trial, participants cyclically generated plantar flexion ankle torque on the fixed-position dynamometer pedal at the downbeat of an audible metronome and then relaxed at the subsequent upbeat (metronome frequency: 0.75 Hz): downbeat-activate, upbeat-deactivate, repeat. During each trial, participants generated a predetermined dynamometer torque (10-30 Nm) over a set duration ($\bar{4}$-$\bar{8}$ s) with the goal of achieving 3 higher and 3 lower torque-time integrals over 3 different activation durations each (Fig. 1). We recorded instantaneous soleus fascicle length and pennation angle, dynamometer torque, muscle activity, joint kinematics, and metabolic data.

Results and Discussion

Consistent with our study design, soleus activation time did not affect total activation-deactivation cycle time-integrated soleus force ($p=0.483$). Greater time-integrated soleus force increased net metabolic power ($p<0.001$). The three higher time-integrated ankle moment trials (Fig. 1: purple symbols) elicited a 51% increased time-integrated soleus force and a 64% greater net metabolic power compared to the targeted lower time-integrated ankle-moment trials (Fig. 1: green symbols). When controlling for time-integrated soleus force, shorter soleus activation time increased net metabolic power ($p=0.002$): every 0.4 s decrease in soleus activation time increased net metabolic power 15.2 Watts.

Greater soleus force-time integrals were associated with increased average and maximum soleus fascicle pennation angles ($p\leq0.029$) and shorter minimum soleus fascicle lengths ($p=0.025$). While controlling the soleus force-time integral, shorter soleus activation times were associated with greater peak soleus fascicle pennation angles ($p\leq0.018$), shorter average and minimum fascicle lengths ($p\leq0.031$), and faster peak fascicle shortening velocities ($p\leq0.005$).

We utilized the relationship between muscle force magnitude and the time-course thereof during steady-state locomotion to study how the time of generating muscle force affects metabolic cost. While controlling other biomechanical parameters that may affect metabolism (*e.g.* activation-deactivation time [2]), the metabolic cost of cyclically generating force depends on the corresponding muscle activation time. Specifically, shorter muscle activations times increase the metabolic cost of generating a force-time integral. This study suggests that when linking biomechanics and metabolism during human locomotion, scientists should consider the time-course of force generation.

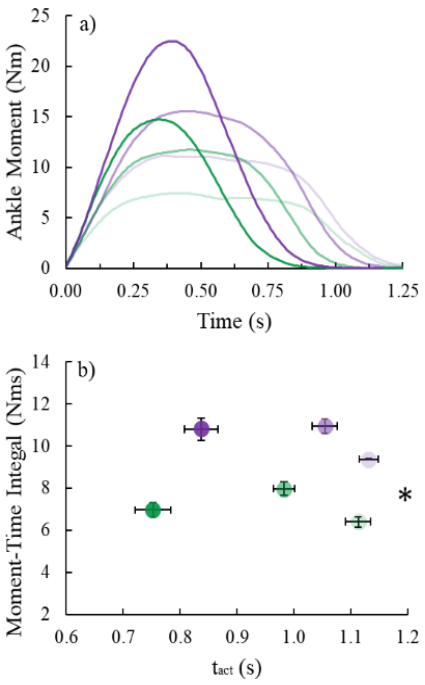

Figure 1. a) Ankle moment versus time for the higher (purple) and lower (green) moment-time integral trials. b) Average (±SE) ankle moment-time integral versus soleus activation time. Lighter to darker color indicates longer to shorter soleus activation time and asterisks (*) indicate statistical significance.

Significance

This study emulated muscle dynamics during steady-state locomotion, controlled for multiple potential co-variables, and revealed that shorter muscle activation times increase metabolic cost. These results may help scientists better link biomechanics to metabolism, which is essential for understanding animal behavior, developing evolutionary hypotheses, and informing interventions that reduce metabolic energy expenditure during terrestrial locomotion (*e.g.* assistive devices, surgical techniques, and training regimens).

References

1. AK Gutmann & JAE Bertram. *J Exp Biol.* (2017) 220, 167-70.
2. J Doke & AD Kuo. *J Exp Biol.* (2005) 210, 2390-98.

Kinetic Energy for Chair Mobility in Individuals with Functional Limitations

A Plot Study for Clinical Validation for the Stand-Up Test –Part II–

Nicholas L. Blonski, BS, SPT[1], Yuri Yoshida, PT, PhD[1], Tzurei B. Chen, PT, GCS, PhD[2],
1: University of New Mexico, Albuquerque, NM, 2: Pacific University, Portland OR
Contact Email: *yyoshida@salud.unm.edu

Introduction

Elderly adults are at an increased risk of falls. A return to sit (RTS) is one of the activities of daily living that is associated with falls and accounting for 12% of falls in elderly at long-term care facilities.[1] Proper quadriceps function are required for efficient RTS completion. A study indicated that experimentally induced muscle damages was found to result in increased knee joint power without differences in knee moment during RTS.[2] Consequently, an altered speed for knee motions relative to the force output should be related to the risk of falls. Considering the sustainability of quadriceps activations during RTS are more inconsistent compared to STS[3], examining movements during RTS should provide clinical insights of alternated performance related to functional limitations. Therefore, the purpose of this study was to investigate biomechanical variables that lead to the decrease in performance during RTS for individuals with and without functional limitations as diagnosed by the Stand-Up Test (SUT). We hypothesized that biomechanical differences in movements during RTS will be revealed in individuals with and without functional limitations as diagnosed by SUT. These differences were not found in our previous analysis for STS despite finding significantly different clinical impairments.[4]

Methods

We analyzed 15 independent community dwelling adults (mean age: 56 years old) who participated in the previously reported study.[5] The participants were categorized into two groups using the SUT: Group 1: non-functional limitations (n=6) and Group 2: the beginning of mobility decline (n=9). Motion data was captured using a 3D Vicon Motion Capture System with 2 AMTI force platforms. The 6-degree of freedom model with using the V3D Composite Pelvis were applied to calculate kinetic energy previously published as a risk of falling. Due to the limited sample size, effect sizes were calculated for between group comparisons.

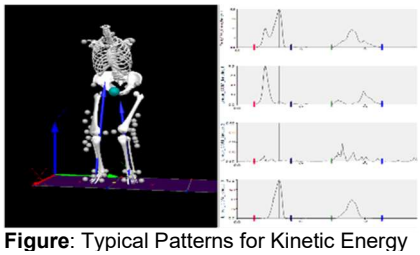

Figure: Typical Patterns for Kinetic Energy

Results and Discussion

Despite our hypothesis, the group differences in kinetic energy were larger in STS (Cohen's d=0.47-1.84) as compared to RTS (Cohen's d=<0.01-2.68). The remarkable differences for STS and RTS between groups were shown in the anterior/posterior (AP) direction. During the RTS, an extremely large effect size (d=2.68) was noted in the linear kinetic energy in the AP direction. A small effect size (d=0.24) was found for differences in the linear kinetic energy in the upward/downward (Vertical) direction. For Group 2, a 49% increase in the AP direction and a 45% decrease in the vertical direction for the kinetic energy was found in RTS when compared to STS. These changes in the kinetic energy distribution could represent altered joint strategies to complete RTS. The overall between-group effect size for the RTS was negligible (d≤0.01) when compared to STS (d=0.53). This may be related to varied patterns of RTS resulted from inconsistent muscle activities or joint-movements strategies when lowering against the gravitational forces.[2,3] Further investigations are needed to explain how muscle functions affect the altered kinetic energy.

Significance

Individuals with subtle functional limitations demonstrated altered RTS by distributing more kinetic energy in the anterior/posterior direction. This altered kinetic energy distribution may improve stability by prolonging the duration of the COG over the feet during RTS. The findings may provide insights to the reasons behind an increased risk of injury and falls due to changes in velocity of a RTS.

Acknowledgments

Supported by the Clinical & Translational Science Center at The University of New Mexico (UL1TR001449).

References

1. Robinovitch S, et al. (2013) Lancet. 381(9860):47-54.
2. Spyropoulos I, et al. (2014) Med Sportiva;10(4):2418-24.
3. Ashford S, et al. (2000) Physiother Res Int. 5(2):111-28.
4. Ogata T, et al. (2015) J Orthop Sci, 20:888-95
5. Yoshida, et al. (2019) Poster: 27th Congress for IBS 2019
6. Chen T, et al (2013) Gait & Posture, 38:696-701

		Total Kinetic Energy*		Linear Kinetic Energy in the AP Direction		Linear Kinetic Energy in the Side-Side Direction		Linear Kinetic Energy in the Vertical Direction	
STS	Group 1	7.11 ± 2.21	d=0.53	7.38 ± 1.18	d=1.84	0.03 ± 0.02	d=0.78	3.92 ± 52.31	d=0.47
	Group 2	9.29 ± 5.27		3.55 ± 2.69		0.05 ± 0.03		5.04 ± 2.48	
RTS	Group 1	5.84 ± 3.7	d<0.01	8.44 ± 0.75	d=2.68	0.06 ± 0.05	d<0.01	1.77 ± 1.76	d=0.24
	Group 2	5.82 ± 3.81		5.28 ± 1.49		0.06 ± 0.03		2.25 ± 2.22	

*Unit for All Kinetic Energy: Joules, d: Cohen's d

Performing Multi-Terrain Transient Locomotion Influence Changes in Joint Coordination of Individuals with Early-Stage Parkinson's Disease

Emma J. Neuendorff[1], Staci M. Shearin[2] and Nicholas P. Fey[1,2]
[1]The University of Texas at Dallas, [2]UT Southwestern Medical Center
Email: emma.neuendorff@utdallas.edu

Introduction

Parkinson's disease (PD) is a neurodegenerative disorder that progressively weakens motor function resulting in symptoms such as tremors, limb stiffness and impaired balance [1]. Daily movement is commonly presented with complex motor tasks, such as changing directions or avoiding an obstacle. Individuals with PD tend to have more difficulty planning and executing these tasks due to lower motor dexterity as the disease progresses. Early detection is important for slowing the progression of PD by beginning exercise programs and other therapeutic interventions [2]. PD is currently diagnosed based on medical history and through an examination performed by a neurologist, but there is no quantitative test for PD diagnosis. Gait analysis using an optical motion capture system is a high-resolution method to examine motor impairments. Detecting changes in gait kinematics in individuals with little to no outward signs of PD relative to control subjects may provide insight into the early signs of disease and promote earlier detection [3]. In this study, we analyzed joint ranges of motion (ROM) of the hips, knees and ankles of individuals with early-stage PD compared to healthy control subjects as they walked continuously on a varying terrain circuit that integrated a level ground walkway, staircase, turn, and ramp. This study hypothesized that since individuals with PD are challenged by self-regulation of their mechanics when presented with complex terrains, subsequent analysis of underlying joint kinematics would reveal differences relative to control subjects, during transitional events between multiple terrains.

Methods

This study consisted of five individuals with PD, Hoehn and Yahr Stage 1 or 2, and five healthy controls that walked on a terrain circuit of a ramp, turn, and four-step staircase. Each subject was equipped with 66 reflective markers attached to 12 body segments of the arms, legs, and trunk. Optical motion data was captured for each subject as they walked through the circuit, performing a total of ten trials each moving from stair ascent to ramp descent and from ramp ascent to stair descent. Lower body joint angles and ranges of motion were calculated for eight transitional terrain events for the ramp and stairs: level-walking to ramp ascent (LW/RA), ramp ascent to turn (RA/T), level-walking to stair ascent (LW/SA), stair ascent to turn (SA/T), turn to ramp descent (T/RD), ramp descent to level-walking (RD/LW), turn to stair descent (T/SD), and stair descent to level-walking (SD/LW). Unpaired, two-sample t-tests were performed across both groups for the transitions (α=0.05).

Results and Discussion

Knee ROM when approaching turns displayed significant differences between PD subjects and controls. PD individuals exhibited less motion in their knees for RA/T and SA/T. Hip ROM was also significantly different for RD/LW. Table 1 reports the ROM and p-values for these transitions. Figure 1 reports knee angle for the SA/T transition.

Terrain Event	PD ROM	Control ROM	p-value
RA/Turn	64.06 (6.48)	68.47 (5.91)	1.91%
SA/Turn	66.92 (6.69)	76.37 (9.91)	0.06%
RD/LW	34.32 (5.81)	42.21 (8.94)	0.08%

Table 1: PD and control ROM with p-values.

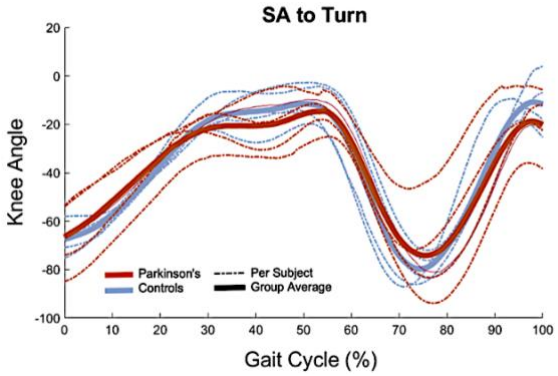

Figure 2: Knee angle during one gait cycle for SA/T. Each subject is shown for PD and control groups, along with an overall group average.

PD subjects decreased their stride length, taking more steps when moving towards the turn, consistent with a festinating gait pattern. We also found that moving from the ramp to level-walking requires a more arbitrary method for task completion compared to moving from the stairs. This is emphasized through decreased hip ROM during RD/LW. We suggest the neuromotor impairment associated with PD is exacerbated by the spatially unconstrained manner of the ramp that presents a less consistent terrain for task planning, evidenced by relatively few changes in coordination during transitions involving the stairs.

Significance

Studying transient locomotion of individuals with mild PD could help diagnose the disease in its early stages, when impairment is not particularly evident during isolated modes of ambulation. Early diagnosis could allow PD individuals to begin therapy to slow the progression of the disease, increasing their chance of continuing to live independently and resume daily activities. The study is also the first to highlighted a significant reduction in joint range of motion when approaching a turn from the stairs or ramps, and even when moving off ramps to level-ground straight-line walking. This suggest that the varying mechanical demands of each task are not necessarily as challenging for these individuals as the issue of neuromotor task planning.

References

1. Morris et al., Clinical Biomechanics 2001, 16:6:459-470.
2. Asburn et al., Journal of Neurology, Neurosurgery & Psychiatry 2007, 78:678-684.
3. Simon et al., Journal of Biomechanics 2004, 37:12:1869-1880

Effects of Gravitational and Inertial Forces on Determinants of Gait Transitions

Nathan G. Frakes[1], Courtney A. Perry[1], and Justus D. Ortega[1]
[1]Department of Kinesiology, Humboldt State University, Arcata, CA, USA
Email: ngf19@humboldt.edu

Introduction

Gait transitions refer to the changing from one mode of locomotion to another [1], e.g., the walk to run (WRT) or the run to walk transitions (RWT). Prior research suggests that gravitational force is pivotal in determining preferred transition speed (PTS) for both WRT and RWT [2], though not much has been researched about the effect of inertial forces on the PTS. By utilizing four key criteria to identify a determinant of the PTS [1,3], prior research suggests that PTS may be triggered across varying conditions by a change in lower limb kinematics [1]. Specifically, it is suggested that when a lower limb kinematic variable adheres to all four criteria, that variable should be considered a key determinant of the PTS.

The purpose of this study was to investigate possible kinematic determinants of PTS for both WRT and RWT across differing levels of gravitational and inertial forces.

Methods

Twelve healthy adults (9 male, 3 female) completed WRT and RWT trials on a motorized treadmill across seven conditions of altered body weight (BW) and body mass (BM) including: 1.0 BM / 1.0 BW; 0.70 and 0.85 BW / 1.0 BM (-GF); 1.15 and 1.30 BM / 1.0 BW (+IF); 1.15 and 1.30 of both BW and BM (+GF+IF) using previously established methods [4]. For each condition, we determined PTS (m/s) by increasing speed (from 1.34 m/s for a WRT) or decreasing speed (from 2.68 m/s for a RWT) 0.09 m/s every 30 sec until a gait transition was achieved. A 9-camera motion analysis system (Vicon) was used to collect (120 hz) lower limb kinematics for each condition. This data was used to calculate the average and peak hip, knee, and ankle joint kinematics (acceleration-α, velocity-ω, and angle-θ) during the gait cycle over the course of 20 strides.

We evaluated three of the four key criteria used to identify if a variable is a determinant of the PTS including 1) an abrupt change in the value of a variable before and after gait transition, 2) a return of the variable to values seen at initial speeds in the previous gait (i.e., at slower walking speeds for WRT or higher speeds for RWT), and 3) the variable reaches a shared critical value just prior to the PTS for all conditions [1]. We assumed that all kinematic variables met the fourth criteria of "needing to act on proprioceptive feedback" [1].

We performed repeated-measures MANOVAs to assess the effects of gravitation force, inertial force and combined forces on determinants of the PTS. We then conducted planned contrasts between speeds of each condition to determine if the variable increases/decreases between speeds and then changed abruptly from before to after transition (Criteria 1). We also used planned contrast to determine if the variable returned to a level observed at a previously slower (WRT) or faster speed (RTW) (Criteria 2). We compared the value of each variable just before transition between all conditions to determine if the transition happened at a similar critical value (Criteria 3). An effect size of <.1 was used to identify a "negligible" difference and thus similar critical value between conditions [1].

Results and Discussion

Walk to Run Transition (WRT)

Criteria 1: In all the WRT conditions, $\alpha_{dorsi\text{-}peak}$, $\omega_{dorsi\text{-}peak}$, and $\theta_{hip\text{-}peak}$ increased between initial and final (before transition) walking speeds ($p < .05$). After the WRT, both $\alpha_{dorsi\text{-}peak}$ and $\theta_{hip\text{-}peak}$ abruptly decreased ($p < .001$) in gravitational and inertial conditions with no significant change in $\omega_{dorsi\text{-}peak}$.

Criteria 2: Following the WRT, both $\alpha_{dorsi\text{-}peak}$ and $\theta_{hip\text{-}peak}$ returned to values observed at initial speeds in the previous gait (66 ± 14% and 77 ± 7% respectively).

Criteria 3: Although each variable ($\alpha_{dorsi\text{-}peak}$, $\omega_{dorsi\text{-}peak}$, $\theta_{hip\text{-}peak}$) shared a similar critical value just prior to the PTS, only $\alpha_{dorsi\text{-}peak}$ and $\omega_{dorsi\text{-}peak}$ had "negligible" effect size (ES) across all conditions (ES = .03; p = .826 and ES = .06; p = .544 respectively).

WRT Summary: Only $\alpha_{dorsi\text{-}peak}$ met the three key criteria used to identify a determinant for the WRT. However, $\theta_{hip\text{-}peak}$ was close to meeting all key criteria. Surprisingly, $\omega_{dorsi\text{-}peak}$ did not meet the criteria required of a determinant for the PTS, contrasting with results found in prior literature [1].

Run to Walk Transition (RTW)

Criteria 1: In all of the RWT conditions, $\alpha_{dorsi\text{-}peak}$ and $\theta_{hip\text{-}peak}$ decreased between initial and final running speeds ($p < .01$). After the RWT, both $\alpha_{dorsi\text{-}peak}$ and the $\theta_{hip\text{-}peak}$ abruptly increased ($p < .0001$ and $p < .02$ respectively) in gravitational and inertial conditions with no significant change in $\omega_{dorsi\text{-}peak}$.

Criteria 2: Following the RWT, both $\alpha_{dorsi\text{-}peak}$ and $\theta_{hip\text{-}peak}$ returned to similar values observed at initial speeds in the previous gait (150 ± 23% and 131 ± 11% respectively).

Criteria 3: All evaluated variables ($\alpha_{dorsi\text{-}peak}$, $\omega_{dorsi\text{-}peak}$, $\theta_{hip\text{-}peak}$) shared a similar critical value just prior to the RWT across all conditions (ES < .1; p >.30).

RWT Summary: Both $\alpha_{dorsi\text{-}peak}$ and $\theta_{hip\text{-}peak}$ met the three key criteria used to identify a determinant for the RWT while $\omega_{dorsi\text{-}peak}$ only met one of the criteria.

Significance

Of the kinematic variables evaluated in this study, only $\alpha_{dorsi\text{-}peak}$ met the three criteria used to identify if a variable is a determinant of PTS for both WRT and RWT while $\theta_{hip\text{-}peak}$ met the criteria for the RWT only. Our results suggest that there are potential differences in mechanical determinant/triggers of gait transition for the RWT compared to the WRT. These results can be used to support the hypothesis that gait transition may occur to prevent overexertion of hip and ankle musculature working maximally at speeds at or near PTS [1].

References

[1] Hreljac, A. (1995). *J. of Biomech.*, 28(6), 669–677.
[2] Kram et al. (1997) *J. of Expr. Bio*, 200(4) 821-826.
[3] Kung et al. (2018). *Hum. Movement Sci.*, 57, 1–12.
[4] Grabowski et al. (2005). *J. Appl. Physiol.*, *98*(2), 579–583

The Effect of Arch Types on Propulsive Forces During Jumping and Hopping Tasks

Christopher M. Wilburn[1], Brandi E. Decoux[2], Portia T. Williams[3], Randy T. Fawcett[4], and Wendi H. Weimar[1]
[1]Auburn University, Auburn, AL
[2] Bridgewater State University, Bridgewater, MA
[3]North Carolina A&T State University, Greensboro, NC
[4]Virginia State University, Blacksburg, VA
Email: czw0043@auburn.edu

Introduction

The intricate and adaptive structure of the medial longitudinal arch (MLA) has a pivotal role in the development of propulsive mechanics during locomotion. Structural alterations within the MLA (i.e. arch type) have been shown to induce maladaptive kinematics and kinetics that modify the generation of adequate foot function and predispose individuals to injury in forward directional movement tasks [1-3]. However, altered bony aliments of lower MLAs may produce biomechanical advantages for locomotive tasks in the mediolateral direction and such investigations remain limited. Thus, the purpose of this study was to examine the influence arch height has on the propulsive phase of directionally specific jumping tasks.

Methods

Twenty-two Division I collegiate male athletes (height: 1.84 ± 0. 06 m; mass: 88.4 ± 12.1 kg) were recruited to participate in this study. All participants indicated their voluntary involvement by signing an informed consent approved by the university's Institutional Review Board. Inclusion criteria for the study included good self-reported health, absence of a lower extremity injury within the last six months, and without any surgical procedure to the foot and ankle.

Prior to completing the locomotive tasks, foot anthropometric measurements were obtained to classify the different arch types [4]. Peak ground reaction forces (GRFs) of the dominant limb were collected with a force platform (Advanced Mechanical Technology, Inc., Watertown, MA, USA), sampling at 1000HZ, during the unilateral stationary hopping(SH), unilateral forward hopping (FH), and lateral jumping (LJ) tasks. The tasks were conducted in a randomize-order. During the SH task, the participants performed nine continuous hops. The three middle repetitions were analyzed to minimize the influence of the initiation and cessation of the task. The FH task consisted of three trials of three consecutive forward hops. The second hop, in which the foot made contact with the force platform, was used for analysis. Within the LJ task, participants began with their dominant foot on the force platform. Participants were then instructed to complete three trials of jumping in the following rhythmic sequence: from the dominant leg to the non-dominant leg, to the dominant leg and back to the non-dominant leg. During this jumping sequence, the participants were instructed to strike the force platform when jumping from the non-dominant leg to dominant leg. Analysis of the foot strike of the dominant leg, back on the force platform was chosen to minimize the influence of initiation and cessation on the data.

Kinetic data were imported into Visual3D (C-Motion, Germantown, Maryland, USA) for the reduction of maximum vertical, anteroposterior, and mediolateral GRFs during the propulsion phases of the jumping and hopping tasks. Data were then transferred to SPSS (IBM SPSS Inc., version 26.0, Chicago, IL, USA) for statistical analysis.

Results and Discussion

The results of the mixed-factorial ANOVAs yielded differences in vertical, anteroposterior, mediolateral GRFs between the LJ, FH, and SH tasks. Specifically, the LJ significantly produced the greatest mediolateral GRFs ($F(1.295, 25.890) = 72.135$, $p = < 0.05$, $\eta 2 = 0.783$), the FH significantly produced the greatest anteriorposterior GRFs ($F(2, 40) = 51.883$, $p = < 0.001$, $\eta 2 = 0.722$) and the least vertical GRFs ($F(1.536, 30.723) = 8.308$, $p < 0.05$, $\eta 2 = 0.293$). Additional findings demonstrated lower arches produced significantly greater mediolateral GRFs in the LJ ($F\ 1, 20) = 4.502$, $p = .047$, $\eta 2 = .184$).

The contributive efforts of the lower extremity during the propulsive phase of locomotion are complex in nature. While the MLA acts a mediator for foot function, skeletal alterations are often deemed pathological. Specifically, changes in the skeletal framework produce modified propulsive mechanisms that provide directional-specific leverage and are often corrected to mend this anatomical dysfunction [3,5]. However, the use of such corrective measures can provide a great hindrance to the overall outcome of the motion. Specifically, the findings of this study suggest that the everted positioning of low arches and production of increase mediolateral GRFs provide a mechanical advantage during propulsion. The novel approach associated with this study suggests the structural alignments and nature of the tasks should be considered when investigating human movement patterns.

Significance

This study demonstrated the complexities of the human body during the propulsive phase of locomotion. More specifically, the arch type differences can induce directional differences in force production during the propulsive phase of locomotive tasks and highlights alternative movement patterns that may be beneficial for movement.

References

[1] Gait Posture. 2009; 30(3): 334–349.
[2] Gait Posture. 2008; 28(1): 29-37.
[3] Gait Posture. 2013; 38(3): 363-372
[4] J AM PODIAT MED ASSN. 2008. 98(2), 102-106.
[5] Gait Posture. 2007 6(2), 219-225

An opensource biomechanics dataset for locomotion in stairs, ramps and level-ground

Jonathan Camargo.[1,2], Aditya Ramanathan[2], Aaron Young[1,2]
[1] Institute for Robotics and Intelligent Machines,
Georgia Institute of Technology, Atlanta, GA, 30332 USA,
[2] Woodruff School of Mechanical Engineering
Email: jon-cama@gatech.edu

Introduction

The biomechanics of locomotion have been profusely studied, stablishing many standards in the field. Winter[1], is the seminal reference of motion capture data used as the standard of biomechanics analysis of walking. Other sources provide insight about the power and torque contribution to locomotion at the joint level [2], [3], [4]. This standard has extended towards other modes of locomotion where ascending and descending stairs and ramps have a major subset of biomechanics research [5], [6]. However, there is a scarcity of databases of locomotion that provide access to raw information from individual trials. Recent efforts have directed towards generating open benchmark datasets that are accessible to public. Hu et al. [7] released the first benchmark database of simultaneous kinematic and EMG data as able-bodied individuals transition between locomotor activities in a circuit consisting of a single of staircase and ramp. Following this established database, we contribute a novel dataset that extends the report of kinematics results by including the joint level moments and powers processed using inverse dynamics from the open-source biomechanics software OpenSim. In addition, we provide access to the kinematics, kinetics and joint power data in conjunction with the data from multiple sources of wearable sensors, including EMG, goniometer, accelerometer and gyroscope signals. The availability of open datasets that link wearable signals to the biomechanics will aid the development of better locomotion assistance techniques.

Methods

The experimental collection consisted of N=22 young healthy adults, age 21±3.4yr, height 1.70±0.07m, weight 68.3±10.83kg, instrumented with 32 motion capture reflective markers. (Vicon Motion Systems Inc, Los Angeles, CA, USA). Ground reaction forces were recorded from an instrumented treadmill (Bertec Corporation, Columbus, OH, USA) and forceplates located in level with the floor, ramp and stairs. In addition, subjects were instrumented unilaterally with 11 EMG (electromyography) 3 goniometers, and 4 six-axis inertial measure units (IMU). The study, approved by the IRB at Georgia Institute of Technology, consisted of subjects performing locomotion tasks in four different terrain types: treadmill, level ground, ramp and stairs. Treadmill walking data was collected at 28 different speeds ranging from 0.5 to 1.85m/s with increments of 0.05m/s. Level ground walking was also collected at three speeds relative to the subject's preferred speeds (slow, normal and fast), and including turns in counterclockwise and clockwise directions. Stairs at four different step heights within the range of ADA accessibility Guidelines [8] 10.16cm (4in), 12.70cm (5in), 15.24cm (6in), 17.78cm (7in). Ramp inclinations corresponded to 5.2°, 7.8°, 9.2°, 11°, 12.4° and 18°. Average profiles are computed from time series data segmented by gait strides. The effect of the terrain context is evaluated at each instant of the gait phase, using linear regression model ($p<0.01$).

Results and Discussion

Kinematic and kinetic profiles for each ambulation are generated, reporting averages at each condition and marking the regions where the context has significant effects ($p<0.01$). For this short abstract, we present the kinematics and joint power for locomotion on treadmill at different speeds, the contribution of energy and the influence of the speed in the modulation of joint power.

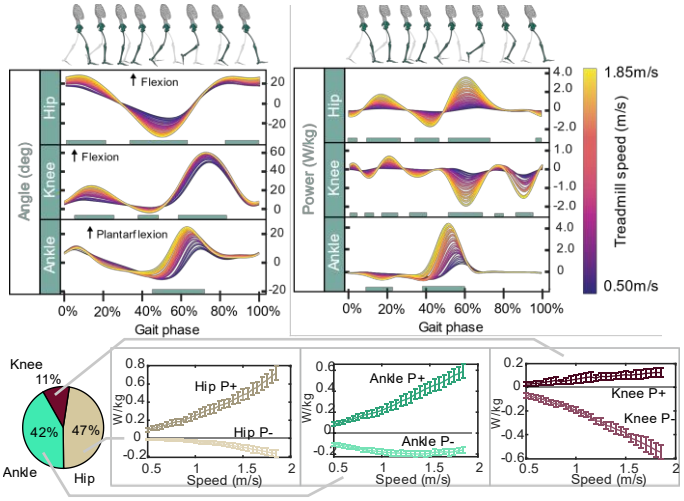

Figure 1: Joint kinematics and instant power during a stride at different walking speeds (0.5m/s – 1.85 m/s). The pie chart represents the contribution of each joint to the average positive power. The sensitivity of joint power is presented as a function of the walking speed, with error bars showing ±std.

Significance

Open biomechanics datasets are beneficial to researchers interested in the development of controllers for assistive devices, where information of joint level state is required to accomplish biomimetic assistance. For this, the access to joint level moment and power at different conditions of locomotion can inform the design of controllers that accommodate for terrain conditions

Acknowledgments

Authors thank the Sensor fusion team at the Exoskeleton and Prosthetic Intelligent Control Lab (EPIC) at GeoriaTech.

References

[1] D. A. Winter, "Biomechanical motor patterns in normal walking," *J. Mot. Behav.*, vol. 15, no. 4, pp. 302–330, 1983, doi: 10.1080/00222895.1983.10735302.
[2] G. W. Lange, et al., "Electromyographic and kinematic analysis of graded treadmill walking and the implications for knee rehabilitation," *J. Orthop. Sports Phys. Ther.*, vol. 23, no. 5, pp. 294–301, 1996,
[3] M. M. Ankarali, et al., "Walking dynamics are symmetric (enough)," *J. R. Soc. Interface*, vol. 12, no. 108, 2015, doi: 10.1098/rsif.2015.0209.
[4] D. J. Farris and G. S. Sawicki, "The mechanics and energetics of human walking and running : a joint level perspective" no. May 2011, pp. 110–118, 2012, doi: 10.1098/rsif.2011.0182.
[5] M. S. Redfern and J. DiPasquale, "Biomechanics of descending ramps," *Gait Posture*, vol. 6, no. 2, pp. 119–125, 1997-
[6] R. Riener,et al. , "Stair AscentAndDescentAtDifferent-Inclinations", Gait Posture vol. 15, pp. 32–44, 2002.
[7] B. Hu, et al., "Benchmark datasets for Bilateral Lower-limb neuromechanical signals from wearable sensors during unassisted locomotion in able-bodied individuals," *Front. Robot. AI*, vol. 5, no. FEB, pp. 1–5, 2018.

Forced Marching Alters Plantar Force Distribution Compared to Running and Walking

Camille C. Johnson[1,2], Kellen T. Krajewski[1], Dennis E. Dever[1], Milad Zarei[2], William J. Anderst[2], Christopher Connaboy[1]
[1]Neuromuscular Research Laboratory, University of Pittsburgh, Pittsburgh, PA
[2]Orthopaedic Biodynamics Laboratory, University of Pittsburgh, Pittsburgh, PA
Email : ccj17@pitt.edu

Introduction

Loaded marches are an important component of military training and operations, and involve carrying combat loads ranging from 20-60+ kg over long distances.[1] Previous studies have identified increases in plantar contact pressure during footstrike while walking with carried loads.[2] Research is required which examines regional plantar forces during the impact phase of loaded walking, running, and forced marching (walking at a velocity above gait transition velocity [GTV]), to further identify potential injurious motion patterns. The purpose of this study was to determine the effect of load magnitude and locomotion pattern on regional plantar forces. It was hypothesized that peak regional force would increase across all regions while running and forced marching compared to walking and with increased carried load.

Methods

Eight healthy physically active females (24.5±2.4 years) participated in this IRB-approved study. Participants wore standard issue military combat boots with Pedar pressure-sensing insoles (Novel Electronics Inc, St. Paul, MN) and an evenly distributed anterior/posterior weight vest. Plantar pressure was recorded during trials of walking, running and forced marching (FM) on a treadmill while unloaded and while carrying an additional 25% and 45% of their bodyweight (+25%: 15.2±1.7 kg +45%: 27.4±3.1 kg). Walking was performed at a velocity 10% below an individuals' GTV and running and forced marching was performed at 10% above GTV. Plantar pressures from the dominant foot (right foot, 23-33 steps) were converted to force, normalized to participant bodyweight, and divided into nine foot regions (medial/lateral heel, medial/lateral arch, medial/mid/lateral forefoot, and greater/lesser toes).[3] Peak regional force (PRF) was determined for each region. Two-way repeated measures ANOVA with post hoc Bonferroni corrections were used to analyze the within-subjects effects of load (no load, +25%, +45%) and locomotion (walk, run, FM) on PRF across the nine foot regions (α=0.05).

Results and Discussion

Effect of load: Additional load increased PRF compared to the unloaded condition at the medial and lateral heel (+25%: p<0.001, p=0.042; +45%: p<0.001, p=0.001) and +45% increased PRF compared to +25% (p<0.001) (Figure 1). Similarly, additional load increased PRF for both the medial and lateral arch regions (+25%: p=0.002, p=0.001; +45%: p<0.001, p<0.001). For the forefoot, +45% increased PRF for for the mid-forefoot (p=0.040) and +25% increased PRF for the lateral forefoot (p=0.044). For the greater toes, an additional +45% increased PRF (p=0.044). Overall, the PRF at the heel was the most sensitive to an increase in carried load. This supports the hypothesis of an increase in plantar forces with increased load, although increases from +25% to +45% were not always significant.

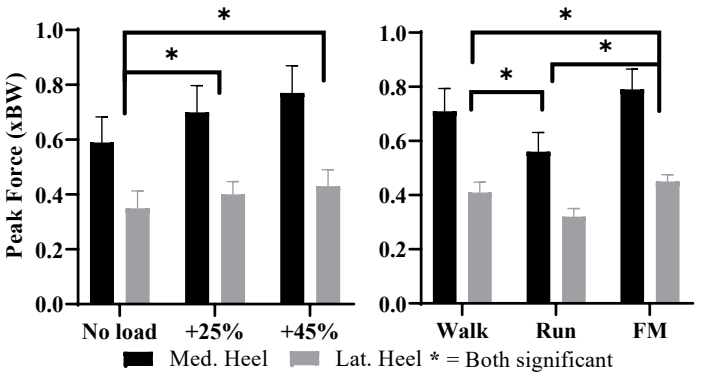

Figure 1: Average normalized peak force for the heel regions.

Effect of locomotion: For the heel, walking increased PRF compared to running (Medial: p=0.010; Lateral: p=0.016), and FM increased PRF compared to run and walk (Medial: p<0.001, p=0.001; Lateral: p=0.002, p=0.001) (Figure 1). For the arch, running and FM increased PRF compared to walking (Medial: p<0.001, p=0.002; Lateral: p=0.001, p=0.006). For the forefoot, running increased PRF compared to walk and FM (Mid: p=0.004, p=0.002; Lateral: p=0.014, p=0.002). Significant interaction between load and locomotion were identified for the medial forefoot and lesser toes (p=0.037, p=0.018). At the medial forefoot, running significantly increased PRF compared to walking (p=0.014, p=0.006) and FM increased PRF compared to running (p=0.010, p=0.027) for the unloaded and +25% conditions. Changes in locomotion type did not affect PRF at the greater toes. Overall, a running gait pattern resulted in higher PRF for the arch and mid/lateral forefoot regions, while forced marching increased the peak forces in the heel, arch, and medial forefoot compared to walking and running.

Significance

This preliminary data suggests that a forced march with additional carried load increases peak force in the heel compared to walking and running. These greater forces during forced marching may increase the risk of injury and long term joint degeneration. The observation that the heel region is most sensitive to increased carried load suggests the heel region is a potential target for intervention such as an orthotic or novel shoe design to reduce heel loading during loaded locomotion.

Acknowledgments

This work was supported by the Freddie H. Fu research award.

References

1) Attwells et al., *Ergonomics*, 2006. 2) Schulze et al., *Sci World J,* 2013. 3) Hong et al., *J Sci Med Sport*, 2012.

Young Adults Recruit Similar Motor Modules Across Walking, Turning, and Chair Transfers

Hannah D. Carey, Daniel Liss, and Jessica L. Allen*
West Virginia University, Morgantown, WV
Email: *jessica.allen@mail.wvu.edu

Introduction

Navigating daily life requires performing diverse movement behaviors. How the nervous system coordinates muscles to successfully perform these behaviors is unknown. We recently showed that recruiting a common set of motor modules (i.e., motor module generalization) across walking and standing balance behaviors is important for successful mobility [1,2]. Here, we investigated whether motor modules are also generalized across walking, turning and chair transfer behaviors using the Timed-Up-and-Go (TUG) test. The TUG test is a common mobility assessment often executed while performing a secondary cognitive task (i.e., counting backwards) [3]. As a first step towards understanding if module generalization across walking, turning, and chair transfers underlies successful daily life mobility, we examined motor modules recruited by young adults in the TUG test. Understanding modular control strategies in young adults will provide a basis for investigating impairments due to aging, disease, and injury.

Methods

Nine young adults (4M, 21.4±1.7 yrs) performed the TUG test with and without a cognitive distraction task (i.e., counting backwards by 3's; avg 18±3.6 trials per condition). To investigate module generalization, we divided the TUG test into 4 subtasks: sit-to-stand, walk, turn, and stand-to-sit. Motor modules from each sub-task were extracted from electromyography collected from 12 muscles spanning the hip, knee, and ankle using non-negative matrix factorization as in [1]. For each subject, modules recruited across subtasks were pooled and clustered using a k-means algorithm to identify the number of unique modules recruited across all TUG subtasks. Motor module generalization was quantified as $\left(1 - \frac{U-M}{S}\right) \times 100\%$, (U: number of clusters, M: smallest number of modules recruited in any subtask, and S: sum of all module numbers) and compared between TUG and TUGC using a paired t-test. To examine whether the cognitive distractive task affected motor module structure, TUG and TUGC modules were compared using Pearson's correlation coefficients.

Results and Discussion

Young adults recruited a small number of structurally similar motor modules across TUG subtasks. Subjects recruited 3-5 motor modules in each subtask (avg 5.3±0.8; Fig. 1a) that were structurally similar across subtasks, illustrated by their high generalization (Fig. 1b). These results suggest that young adults draw upon a small library of motor modules to execute basic actions, such as plantarflexion and stabilization, that are required of walking, turning, and chair transfers. Based on our prior work examining walking and balance [1,2], we expect that motor impaired populations will recruit more task-specific modules across TUG subtasks, contributing to their reduced mobility.

Motor module structure was not affected by concurrent performance of a cognitive task. Neither performance time (t=-1.84,p=0.10) or motor module number (Fig 1c) differed in TUG vs. TUGC. Further, motor modules recruited in TUG vs. TUGC were strongly correlated (Fig. 1d) and generalization across subtasks remained high in TUGC (Fig. 1b). Since motor impaired populations are more affected by dual-task demands than young adults [3], we expect module structure in these populations will exhibit less similarity in TUG vs. TUGC.

Here, we follow-up on our prior studies [1,2] demonstrating the importance of motor module generalization across walking and balance behaviors for daily-life mobility and show that young adults also generalize motor module recruitment across walking, turning, and chair transfer behaviors. Together, these results suggest that young adults recruit a small number of structurally similar motor modules across movement behaviors important for daily life that are unaffected by secondary cognitive demands.

Significance

Identifying how young adults recruit motor modules during walking, turning, and chair transfers is a step towards understanding how motor control strategies are executed across a variety of movements required of daily life. Characterizing modular control strategies in young adults will allow us to more effectively identify deficits resulting from aging and impairment, which may guide the development of more effective and targeted rehabilitation treatments to improve daily life mobility.

Acknowledgments

This work was supported by the WVU Arlen G. & Louise Stone Swiger Fellowship and the WVU Research Corp.

References

[1] Allen et al., J Neurophys. 118:363-73. 2017.
[2] Allen et al., J Neurophys. 122:277-89. 2019.
[3] Porciuncula et al., Aging Clin Exp Res. 121-130. 20

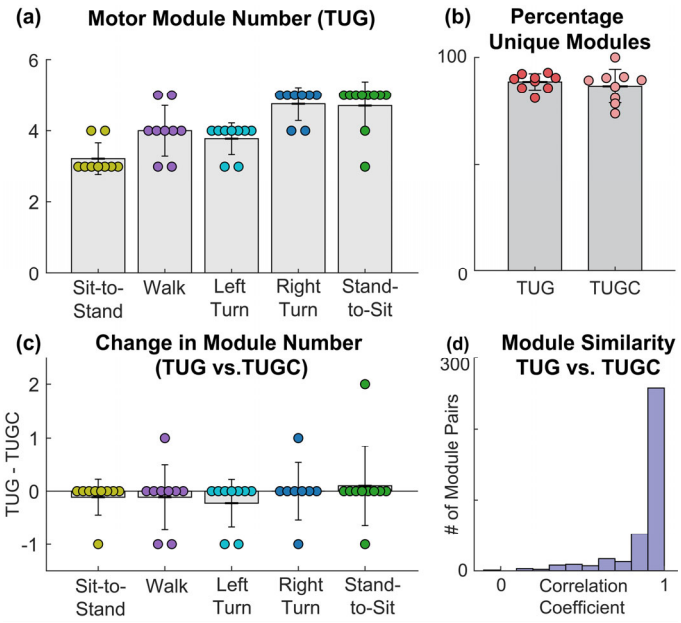

Figure 1: (a) Motor module number in TUG subtasks, (b) Percentage of unique motor modules recruited during TUG and TUGC, (c) Change in motor module number with addition of cognitive task (TUG-TUGC), (d) Similarity in motor module structure between TUG and TUGC.

Association between Foot Thermal Responses and Shear Forces during Turning Gait

Angel E. Gonzalez[1], Ana L. Pineda Gutierrez[1], Andrew M. Kern[1] & Kota Z. Takahashi[1]

[1] Department of Biomechanics, University of Nebraska at Omaha, Omaha, NE USA
Email: agonzalez@unomaha.edu

Introduction

Thermoregulation is a vital function of the nervous system in response to cold or heat stress. Previous studies have demonstrated that foot temperature can significantly increase from pre- to post locomotor activity [1, 2]. Though these temperature fluctuations may not be a problem for healthy individuals, negative consequences may arise for individuals that are unable to properly thermoregulate, such as foot ulcer formations in patients with diabetes [3].

Shear forces have been proposed as potentially having a direct influence in foot temperature responses during walking. Technical challenges associated in measuring shear have hampered further research [4], where adjacent segments within the foot can experience simultaneous opposing shear forces that cannot be measured through a standard force plate. Recent studies utilizing custom shear-sensing force plates have revealed the influence of shear on temperature responses within localized regions of the foot [5]. Another method of potentially exploring this relationship is through curved-path walking, which has been shown to have higher magnitudes of shear compared to straight line walking [6]. Toe-walking on a standard force plate, in particular, may be one method of exploring the shear-thermal relationship while reducing the presence of opposing shear forces from adjacent segments within the foot.

The purpose of this study is to investigate the thermal response of the foot to varying magnitudes of shear forces during barefoot curved-path toe-walking. Due to the mechanical requirement of the task, greater shear forces were expected when turning with a smaller radius, and greater shear was expected on the external foot compared to the internal foot [6]. It was hypothesized that foot temperature increase would be related to a greater shear force. It was also hypothesized that the external foot, due to greater shear forces, would experience higher temperature increase compared to the internal foot.

Methods

14 retroreflective markers were placed on the feet to quantify motion. 18 healthy subjects (9 females) walked barefeet, on their toes for 5 minutes at a speed of 1.0 m/s in three radii of curvature (1.0, 1.5, and 2.0 m in a randomized order). A ground-mounted force plate (AMTI) was used to estimate magnitudes of medial-lateral and anterior-posterior shear forces encountered at the foot. Immediately before and after each trial of walking, we obtained thermal imaging data to quantify changes in foot temperature (ΔT). Using a software (FLIR ResearchIR), we manually traced thermal images with outline of the entire foot, as well as the forefoot region (encapsulating the toes, the first and fifth metatarsal heads). Each trial was separated by 20 minutes of rest.

To compare shear force and ΔT across various radii and between feet, a two-factor repeated measures ANOVA was used. A linear mixed effects (LME) model analysis was used to determine the relationship between shear and ΔT (α=0.05). In order to account for ground contact time, shear impulse (integral of shear force) was extrapolated to the entirety of the 5-minute trial. The LME analysis was thus performed on ΔT as a function of the accumulated shear impulse.

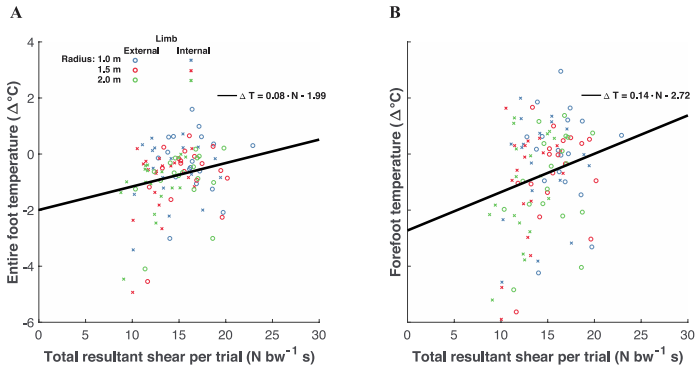

Figure 1: Resultant shear impulse (extrapolated to the 5 minute walking trial) was a significant predictor of entire foot ΔT (Fig. A, $p < 0.001$) and forefoot ΔT (Fig. B, $p < 0.001$). A greater sensitivity of ΔT to shear was found for the forefoot (where shear forces were presumably encountered during toe walking) compared to the entire foot, indicated by the greater slope of the regression line. Walking data were obtained from external (x) and internal (o) limbs, as well as the three different radii: 1.0m (blue), 1.5m (red), and 2.0m (green).

Results and Discussion

Curved-path walking with smaller radius of curvature increased the magnitude of shear impulse ($p < 0.0001$) and increased ΔT of the entire foot ($p < 0.01$) and forefoot region ($p < 0.01$). In support of our hypothesis, shear impulse was positively associated with entire foot ΔT ($p < 0.001$), and forefoot ΔT ($p < 0.001$), in which every unit of increase in shear impulse (normalized to body weight) increased the entire foot and forefoot temperature by 0.08 °C and 0.14 °C, respectively (Figure 1). Also consistent with our hypothesis, the external foot experienced greater ΔT in both the entire foot ($p < 0.01$) and forefoot region ($p < 0.01$). Our findings about shear-temperature relationships are consistent with a prior study that used a specialized shear-sensing force plate [5].

Significance

Using readily available standard force plate, we found a direct link between shear-thermal relationships within the foot. This study may provide a rationale for using turning gait as a simple assessment tool in predicting an individuals' susceptibility to foot temperature elevation due to shear forces, which may inform future diagnoses and/or prevention strategies for diabetic ulcer formations [3].

References

1. Reddy P.N., et al. *Gait Posture* 52, 272-279, 2017.
2. Schmidt D, et al. *Clinical Neuro* 2, 38-43, 2017.
3. Armstrong D.G., et al. *Am J of Med* 120, 1042-1046, 2007.
4. Perry, J.E., et al. *Gait Posture* 15(1), 101–107, 2002.
5. Yavuz M., et al. *J Biomech* 47, 3767-3770, 2014.
6. Orendurff M.S., et al. *Gait Posture* 23, 106-111, 2006.

Are biceps femoris muscle length changes influenced by in-series compliance across locomotor demand?

Pawel R. Golyski[1,2] & Gregory S. Sawicki[1,2,3]
[1] Parker H. Petit Institute for Bioengineering and Biosciences, [2]The George W. Woodruff School of Mechanical Engineering
[3]School of Biological Sciences, Georgia Institute of Technology, Atlanta, GA, USA
Email: pgolyski3@gatech.edu

Introduction

The field of neuromechanics' current view is that terrestrial mammals' lower limbs exhibit a proximal to distal morphology gradient – proximal joints have long parallel muscle fascicles with short, stiff tendons, while distal joints have short pennate muscle fascicles and long, compliant tendons [1]. However, within humans the extent to which in-series compliance (i.e. tendons and aponeuroses) of proximal muscle-tendon units (MTUs) influences muscle and joint mechanics has not been directly quantified during locomotion. This in-series compliance has implications for where on the force-length curve a muscle operates and thus its force generation. We investigated the coupling of ultrasound-measured biceps femoris longhead (BFlh) muscle velocities and OpenSim-generated BFlh MTU velocities across different biomechanical demands (i.e. speeds and slopes) to test the hypothesis that BFlh muscle velocities would be highly positively correlated with MTU velocities, as expected from low BFlh in-series compliance across all locomotor demands.

Methods

One healthy participant (28 yrs, 74.3 kg) completed 2 minute trials at 26 walking and running speed-slope combinations in a randomized order, with motion capture, ground reaction forces, and B-mode ultrasound data collected during the last 20 seconds of each trial. The speeds collected were walking at 1.25 and 2.0 m/s, as well as running at 2.0 and 3.25 m/s. The slopes collected were ±15% grade in 5% grade increments. We did not collect the 3.25 m/s conditions at +15% and -15% grade. BFlh muscle lengths were measured as the product of extrapolated hand-tracked fascicle lengths and cosine of pennation angle. BFlh MTU velocities and joint moments were calculated using OpenSim. A Pearson correlation coefficients quantified coupling between MTU and muscle velocities over the entire gait cycle [2].

Results and Discussion

Loads on the BFlh (approximated by peak hip extension moment) were generally larger with faster speeds and more extreme inclines (Figure 1a). Correlations between BFlh muscle and MTU velocities were generally largest for the slowest walking speed at small slopes, as well as intermediate speed and high slopes, and were smallest for the fastest speed and level slopes (Figure 1b). This suggests that the in-series elasticity of the BFlh may allow for appreciable decoupling between muscle and MTU lengths, in contrast to our hypothesis. Thus, functionally, the in-series compliance of proximal musculature may not always act as a strut in humans during walking and running. Recent experimental work on the human vastus lateralis (VL) may further support this claim – during the period when the VL was active during running, VL fascicles remained approximately isometric while the MTU lengthened, attributable to either series elasticity or changes in pennation [3]. In all, the decoupling of BFlh muscle from MTU we observed during locomotion conditions indicate that in-series compliance of the hamstring group may have real, unappreciated functional implications for human movement, particularly under conditions of high load.

Significance

This is the first direct experimental measurement of BFlh muscle lengths during locomotion in humans. The observed decoupling influence of BFlh series elasticity at high loads suggests: 1) series elasticity of proximal muscles should be carefully reconsidered in musculoskeletal models of movement, 2) the concept of muscle-tendon tuning in elastic exoskeleton design at the ankle may also be useful at the hip, 3) proximal joints may generate force at slower, more economical velocities than previously realized, and (4) since intrafusal fibers may be decoupled from movemens of the entire muscle-tendon, the proprioceptive pathways of proximal muscles should be further explored.

Acknowledgments

PRG is supported by a NSFGRFP: DGE-1650044. This project was supported by the U.S. Army Natick Soldier Research, Development and Engineering Center (W911QY18C0140)

References

[1] Alexander & Kerr. (1990) *Multiple Muscle Systems*.
[2] Sawicki et al. (2015) *J Exp Biol.*
[3] Bohm et al. (2018) *Sci Rep.*

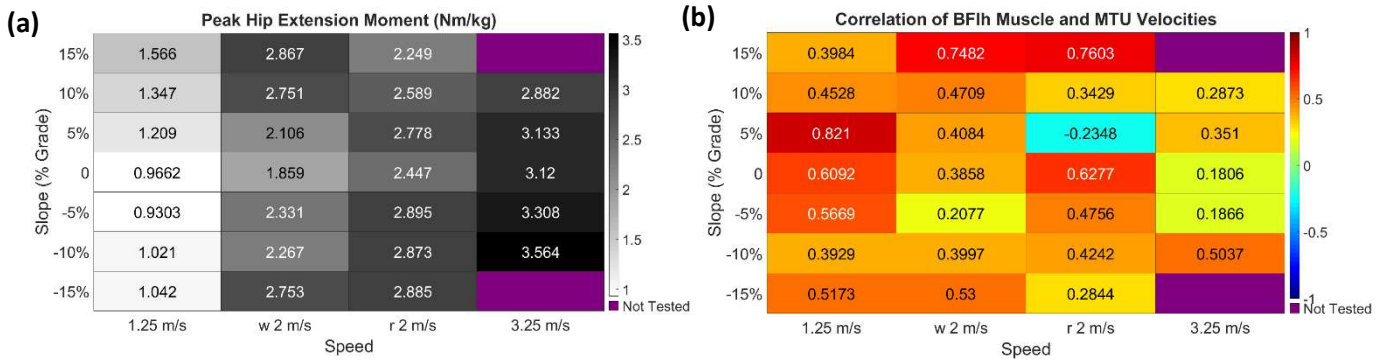

Figure 1: **(a)** Peak hip extension moments and **(b)** Correlation of BFlh muscle and MTU velocities across speeds and slopes

Escape Motions for Real-World Scenarios: A Kinematic and Kinetic Investigation of Rapid, Dynamic Movements

Pooja Moolchandani[1,2], Anirban Mazumdar, PhD[1,2], and Aaron Young, PhD[1,2]
[1]George W. Woodruff School of Mechanical Engineering, Georgia Institute of Technology
[2]Institute of Robotics and Intelligent Machines, Georgia Institute of Technology
Email: pmoolchandani3@gatech.edu

Introduction

Augmentation-based exoskeletons have traditionally addressed the biomechanics behind steady-state locomotion and repetitive tasks; however, rapid and transient human motion has rarely been studied. As environments become more dynamic, so does the type of movement exhibited by the user [1]. Previous work in steady-state walking, running, and sprinting has been a reliable foundation to analyze more targeted, reactive movements. These existing analyses do not address or quantify the kinematic and kinetic behavior employed in quick response time and dynamic movements in all directions, which will be this work's main contribution [2].

This study investigates the biomechanics in escaping threats, or quickly dodging starting from rest. Quantifying this behavior can aid in controlling an agility-enhancing exoskeleton by providing information about user intent and actuation profiles.

Methods

Subjects provide written informed consent for this study that was approved by the Georgia Institute of Technology Institutional Review Board. An experiment is being conducted where subjects, beginning at rest, must escape a pre-defined circle (r = 80 in.) in randomly-chosen directions (8 directions at 45° increments) given a visual instruction, shown in Figure 1. Ground reaction forces and lower limb motion are measured with six force plates (Bertec, Columbus, Ohio, USA) and motion capture (Vicon, Oxford Metric, Oxford, UK).

Results and Discussion

The forward escaping motion (0° direction) was examined for three subjects who exhibited similar escape strategies. The escape strategy is the trailing limb swinging back, making foot contact, and then pushing off. The leading limb swings forwards, makes foot contact, and pushes off. Joint kinematics and kinetics were determined using OpenSim v4.1 and normalized by weight [3]. Figure 2 illustrates subjects' hip, knee, and ankle kinetic results for the trailing limb throughout the described escape strategy. 0% corresponds to when the visual instruction is given and 100% corresponds to the trailing limb's push-off for escaping after the first step. Peak moments and joint speeds, shown in Table 1, were determined during the escape strategy for each limb.

Table 1: Design requirements were found for each limb. Absolute peak values are annotated.

	Trailing Limb		Leading Limb	
	Peak Torque (Nm/kg)	Peak Speed (deg/s)	Peak Torque (Nm/kg)	Peak Speed (deg/s)
Hip	1.11	175	2.19	402
Knee	1.93	373	1.17	390
Ankle	2.96	619	2.33	620

Referring to the peak torques, the dominant limb during quick, transient motions is the trailing limb, where the knee and ankle contribute more than the hip. Regarding joint speeds, the leading limb was uniformly the fastest. These discoveries provide vital information when designing an agility-enhancing exoskeleton by providing peak torque and speed information, and contribute to the understanding of rapid, short movements to assist people in escaping real-world environmental threats. Future work includes completing the experiment and analyzing the 7 other directions.

Significance

This work quantifiably distinguishes kinematic and kinetic behaviors for quick movements from steady-state locomotions and further diversifies what the field traditionally knows about the biomechanics of various locomotion. This effort will heavily contribute to the design of agility-enhancing exoskeletons for use in unstructured environments with dynamic, quick assistances.

Acknowledgments

This research is supported by NSF National Robotics Initiative 1830498, NSF Traineeship Program 1545287.

References

[1] Mero, A., et al (1992). Biomechanics of sprint running. *Sports medicine*, 13(6), 376-392.
[2] Brown, Tyler. "Soldier-relevant loads impact lower limb biomechanics during anticipated and unanticipated single leg cutting movements." *Journal of Biomechanics* 47.14 (2014).
[3] S. L. Delp et al., "OpenSim: Open-Source Software to Create and Analyze Dynamic Simulations of Movement," in *IEEE Transactions on Biomedical Engineering.*

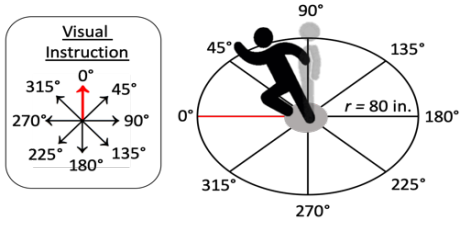

Figure 1: Subjects escape in the direction given in the visual instruction. 0° is annotated here.

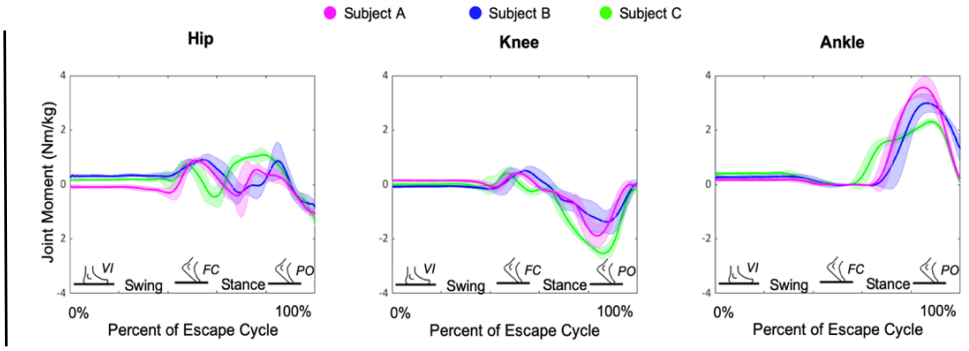

Figure 2: Trailing limb joint moments were found during escape cycle, which is from when visual instruction is given (*VI*), to swing until foot contact (*FC*), to push-off (*PO*) for trailing limb.

Shoulder Kinematics using an Ergonomic Wheelchair

Gaura Saini[1*], Leah Johnson[1], Danilo Harudy Kamonseki[1,2], Melissa Bauer[1], Vivian Hett[1], Swansea Mo[1], Brian Redmond[1], Samantha Wolcott[1], Teresa Bisson[1], and Paula Ludewig[1]
[1]Department of Rehabilitation Medicine, University of Minnesota
[2]Department of Physical Therapy, Universidade Federal de São Carlos
Email: *saini041@umn.edu

Introduction

Traditional manual wheelchairs commonly place the axle of the push rims directly below the user's shoulders. This setup requires users to repetitively move their shoulders through low angles of arm elevation to propel the chair. Concerningly, recent research has found that the subacromial space is smaller in these lower ranges of shoulder elevation compared to higher angles of elevation [1]. Reduced subacromial space may compress the rotator cuff tendons, leading to subsequent tendon degeneration, and development of shoulder pain or rotator cuff tears.

A theorized optimal push rim placement would require the push rim to be placed such that the top dead center of the rim is anterior to the user's shoulder [2]. In a traditional wheelchair, this push rim placement requires the drive wheel to be placed anterior to the user's center of mass, creating posterior instability of the chair. A new wheelchair design - the ergonomic wheelchair - decouples the push rim from the drive wheel, so the push rim can be placed independently without altering stability of the chair. The purpose of this study is to determine how shoulder kinematics and subacromial compression are affected by the wheelchair push rim position.

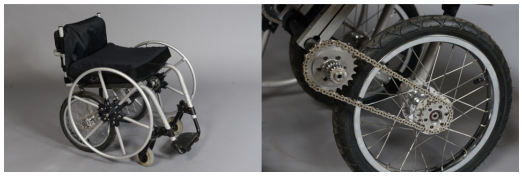

Figure 1: Prototype of the ergonomic wheelchair

Methods

Thus far, data have been collected on four participants without spinal cord injury (SCI) who are not full-time manual wheelchair users. Upper extremity and trunk motion during wheelchair propulsion were captured using an 8-camera Vicon optical motion capture system. The variables of interest were: humerothoracic flexion and abduction; glenohumeral flexion, abduction, and axial rotation; and scapulothoracic internal rotation, upward rotation, and tilt. Data were collected using a custom wheelchair simulator that allowed for individualized placement of the push rims and individualized resistance to replicate the expected amount of inertia the user would experience while propelling overground. The simulator allowed participants to propel without moving out of the capture volume, and a hand switch was used to idenifty hand-to-push rim contact.

Shoulder motions were collected during 10 propulsion cycles in each of the three push rim positions: standard (push rim axle directly below the shoulder), anterior (the theoretical optimal position with the push rim axle anterior to the shoulder), and posterior (push rim axle posterior to the shoulder). For each push rim position, the middle three propulsion cycles were averaged and analysed at three points: initial hand-to-push rim contact, hand at top dead center, and push rim release. Data were analysed using two-way repeated measures ANOVAs.

Results and Discussion

No differences were found in shoulder kinematics across push rim positions. These findings indicate that the theorized optimal anterior push rim position does not alter shoulder kinematics compared to the standard position or even a position in which the push rim is placed posterior to the user's center of mass. However, there were no constraints on hand placement on the push rim. Therefore, rather than altering shoulder kinematics across push rim positions, participants may have altered their push angle - or the arc that the hand travels on the push rim. Despite non-signficiant results and potential changes in push angle, the anterior push rim position generally had more humerothoracic and glenohumeral flexion and less scapular anterior tilt than the standard or posterior positions. Increased flexion and decreased anterior tilt may increase the subacromial space and reduce rotator cuff compression [1,3].

These results reflect the propulsion techniques used by a small number of individuals who are not full-time manual wheelchair users. Upcoming collection will include individuals with SCI who are full-time manual wheelchair users. Additionally, the subacromial space will be quantitatively analysed - using the minimum distance between the coracoacromial arch and the supraspinatus as well as the magnitude of compression when it occurs - through 2D/3D shape matching of subject specific MR bone models on biplane radiography captured during propulsion. This additional data collection will increase our power to detect differences across push rim positions, and the assessment of subacromial space will provide more specific insight into rotator cuff tendon compression than kinematics alone.

Significance

Over 60% of individuals who use manual wheelchairs as their primary mode of mobility report having shoulder pain [4]. Shoulder pain can be devastating for these individuals, as they rely on their upper extremities for critical activities, including wheelchair propulsion. Thus, the design of manual wheelchairs should be updated to protect the user's upper extremities. The results of this study will help guide the redesign of future wheelchairs by describing shoulder kinematics, and eventually subacromial space, while using multiple push rim positions.

Acknowledgments

Thanks to the Minneapolis VA MADE program, Dr. John Looft, and Dr. Andrew Hansen for the ergonomic wheelchair and simulator, and to NIH/NIAMS T32 AR050938 "Musculoskeletal Training Grant" and the Maslowski Charitable Trust for funding.

References

1. Lawrence et al., *J Orthop Res,* 2017; 2. Slowik and Neptune, *Clin Biomech,* 2013; 3. Ludewig and Cook, *Phys Ther*, 2000; 4. Kentar et al., *Spinal Cord,* 2018

The Effect of Frequency on the Energetics of Hopping in Dissipative Terrain

Jonathan R. Gosyne,[1*] Qingyi Lou[2] & Gregory S. Sawicki[1,3]
[1]The George W. Woodruff School of Mechanical Engineering, [2]The Wallace H. Coulter Department of Biomedical Engineering,
[3]The School of Biological Sciences, Georgia Institute of Technology, Atlanta, GA, USA
Email: jonathan.gosyne@gatech.edu

Introduction

Human locomotion on sand requires a higher gross metabolic cost than over hard terrain, however, to date, little has been done to quantify these energetic differences in a laboratory setting [1]. Typically, this metabolic penalty is attributed to the dissipation of mechanical energy into the sand itself during stance, and the added metabolic power required by the muscle-tendon units (MTU's) in the human leg to overcome this extra power requirement [1,2]. As such, this study aimed to quantify the energetic effects of locomotion in sand through the use of a comparative hopping study as a simplification of bouncing gaits. It has been shown that energy consumption of human hopping on hard ground follows a U-shaped relationship, with an energetic minimum between 2.5-2.8 Hz [3]. Due to its highly nonlinear, non-newtownian behaviour, the energy dissipated in a loading cycle on sand depends on the magnitude and rate of the applied ground reaction force as well as the kinematics and surface geometry of the foot. This makes it difficult to predict how metabolic cost of hopping changes on sand. Here, we pose the null hypothesis that hopping in sand would yield a consistent metabolic penalty, shifting the cost up by a fixed amount over a range of frequencies.

Methods

Two male participants (mean ± SD, age = 21.5 ± 0.7 yr, height = 1.82 ± 0.07 m, mass = 80 ± 17 kg) completed two sessions of 4 trails, one on hard ground and one on. Participants were asked to hop to a metronome at four different frequencies (2.2, 2.5, 2.8, and 3.2 Hz), to preferred heights. Gross metabolic power was measured using indirect calorimetry, while hopping frequency and center of mass position were measured using motion capture. Each trial lasted 4.5 minutes, with each ground condition tested on a separate day in order to to minimize fatigue effects due to the physically demanding nature of the protocol. Metabolic data were averaged over the last minute of each trial. The order of conditions and frequencies was randomized. Hard ground hopping was perfomed over a split belt instrumented treadmill, and sand hopping was performed over a custom built sand pit. The sand pit uses dry, loose packed poppy seeds as simulated sand, and allows for self-leveling through a combination of pivot enabled shaker panels that push the sand back toward the middle of the testbed, and airflow to maintain a constant sand depth.

Results and Discussion

We found a U-shaped metabolic curve for the hard ground trials, in agreement with literature (Figure 1; [3]). A quadratic fit to the metabolic data revealed a minimum in metabolic power at 2.7 Hz. This agrees with the findings of Farris et al. which showed that intermediate hopping frequencies values between 2.5-2.8 Hz allow for the lowest level of metabolic power.

Analogous to the hard ground trials, we also found that hopping on sand followed a similar U-shaped curve, with a minimum

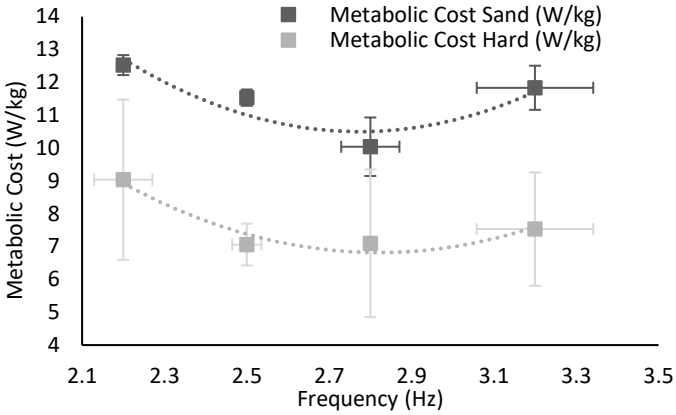

Figure 1: Graph showing metabolic power (W/kg) and frequency relationship for hopping in hard ground and sand. We found a consistent relative increase in metabolic power of 50.1 ± 12% across participants for frequencies from 2.2 Hz to 3.2 Hz

value of approximately 2.8 Hz. Participants reported increased difficulty in trials at 2.2 Hz due to longer ground contact times allowing for significant sinkage and energy dissipation into the sand before the next flight phase. Participants also reported increased sense of effort at 3.2 Hz due to difficulty in achieving a flight phase at all. In this case, brief stance times were not long enough to drive the foot surface into the granular substrate and gain upward momentum. The sinkage time was found to be a constant 0.11± 0.14s across frequencies**.**

Additionally, we found that the best fit metabolic cost curve for sand displayed a constant increase of approximately 50.1 ± 12% from hard ground across frequencies. This is consistent with the initial findings of Lejeune et al, who reported approximate energy expenditure increases of 60% for running on a sand track [1]. Flight time remained consistent across ground conditions for each frequency, (SD ±0.092s), indicating that hop height from rest across conditions was fairly consistent. Thus, the offset may be due to increased muscle activation to overcome excess dissipation while maintaining comparable flight times across variable terrain.

Significance

This experimental protocol is the first frequency-based analysis of the comparative energetics of hopping for sand versus hard ground. It outlines the first step toward the development of a generalized energetic relationship for bouncing gait over complex media. Through this study we begin to develop a more complete understanding of the metabolic effects of locomotion over complex, non-linear substrates. These insights can now be leveraged to design wearable devices that are better suited to "real-world" use over challenging terrain.

References

[1] Lejeune et al. (1998) *J Exp Biol*
[2] Gosyne et al (2018) *SmartTech*
[3] Farris et al. (2015) *J Appl Physio*

Predicting Human Bouncing Behavior from Trajectory Optimization of Minimal Models

Zachary W. Mercer and Christian Hubicki

I. Introduction

Robotic assistive devices hold enormous promise for augmenting and rehabilitating human locomotion (e.g. exoskeletons). However, existing control techniques are heavily dependent on human-in-the-loop optimization [1]. We seek a modeling-driven approach for predicting how human behavior will adapt to forcing from external devices - thereby enabling model-based exoskeleton control. Specifically, we take a reduced-order modeling approach in an effort to find a generalizable framework that is less dependent on subject-specific parameters. This work investigates the efficacy of a variety of minimialistic math models and objective functions of reproducing experimental human behaviors under external forcings. Using trajectory optimization techniques, we systematically examine the effects of differing objectives and mechanical properties on the optimal strategies for completing a model task: human bouncing.

II. Methods

A. Muscle Models

We want to create a general muscle model that can be applied to a variety of specific tasks, constraints, and objectives. Our muscle model is based on a modified Hill-Type structure utilizing a unidirectional contractile element with parallel damping and elasticity in series with an elastic element. This muscle model is structured as the plantar flexor in a 2D bouncing task. We vary the mass of the model to observe trends in optimal bouncing frequency.

B. Locomotion Task Model

Human bouncing, *i.e.* hopping without flight [2], is a simple yet highly constrained movement making it well-suited for generalized analysis. By developing a bouncing optimization problem, we create an optimal control model which can be compared to published human data. Specifically, we task our model to bounce at a series of prescribed frequencies (ranging from 0.5-3 Hz). The optimization solves for the most cost-efficient actuation strategy that bounces at the commanded frequency. Here we analyze the trends in costs as functions of frequency and further pinpoint optimal bouncing strategies which we can compare to human data.

III. Results and Discussion

We implemented a reduced-order muscle model and commanded it to perform a simple bouncing task. Trajectory optimization solved for optimal control strategies over a set of prescribed frequencies and with various changes in physical characteristics (*e.g.* added external mass). Specifically, the optimization solved for control strategies that minimized energetic cost ("force-squared cost" in presented result). The minimum-cost frequencies indicate the optimal bouncing strategy for each physical parameter set (*e.g.* added mass). In the presented results, increasing the body mass consequently shifted optimal bouncing to lower frequencies - a behavior observed qualitatively in human bouncing [2].

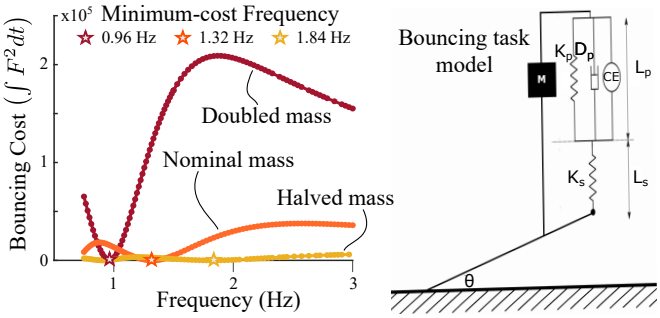

Fig. 1: (Left) Energetic cost of the bouncing model across frequencies. (Right) A schematic of the bouncing model.

IV. Significance

These preliminary results validate a reduced-order model capable of predicting optimal actuation patterns for human movement tasks. This simple model can be freely modified to include external forcing devices (e.g. controlled exoskeletons), with the intention to guide future research into engineering assistive devices aiding human locomotion.

V. Acknowledgements

Supported by Laksh Kumar for advice on the manuscript and technical methods and by the FAMU-FSU Mechanical Engineering Department.

References

[1] Juanjuan Zhang, Pieter Fiers, Kirby A Witte, et al. "Human-in-the-loop optimization of exoskeleton assistance during walking". In: *Science* 356.6344 (2017), pp. 1280–1284.

[2] Jesse C Dean and Arthur D Kuo. "Energetic costs of producing muscle work and force in a cyclical human bouncing task". In: *Journal of Applied Physiology* 110.4 (2011), pp. 873–880.

Quantification of Spatiotemporal Parameter Behavior During Walking Speed Transitions

Claire H. Rodman[1] and Anne E. Martin[1]
[1]Mechanical Engineering, Penn State University Park, State College, PA, USA
Email: chr33@psu.edu

Introduction

Constant speed walking has been rigorously investigated, but healthy humans often walk in short bouts, transitioning between speeds [1]. Starting, stopping [2] and walking to running transitions [3] have been studied, but little is known regarding walking speed transitions and the effect of speed transition magnitude on transition behavior. This work quantified spatiotemporal behavior (step period, length, and speed) in walking speed transitions. We hypothesized that the transition magnitude affects whether divergence occurs only in step period, only in step length, or in both step period and length (H1) and that the transition magnitude affects the number of steps required to perform the transition (H2).

Methods

10 male and 13 female healthy adults (18 to 62 years old, height 163.5 ± 34.4 cm, mass 67.6 ± 11.7 kg) walked on a split-belt, instrumented treadmill at five height-normalized speeds spanning a comfortable walking range (about 1.2 to 1.6 m/s) for one minute each. They then performed ten speed transition trials, in which they walked on the treadmill as it transitioned between the five speeds for a total of 20 transitions. Every 17 steps the treadmill accelerated to the post-transition speed during single support. Three steps prior, subjects were notified of the post-transition speed via a bar chart.

When analyzing the data, to allow for transition behavior after notification but before the speed change, the notification step was step 0, speed change step 3, and so on (Fig. 1). The mean and standard deviation were calculated from the five steps prior to notification to quantify the pre- and post-transition converged states. Independent-sample t-tests were used to determine if the pre- and post-transition converged means were significantly different, indicating that divergence occurred for a given parameter. Number of steps to converge was calculated by subtracting the diverged step (in which the parameter value was beyond two standard deviations of the pre-transition mean) from the converged step (first of three consecutive steps in which the parameter values were within two standard deviations of the post-transition mean). Linear mixed effect models were used to test the significance of transition magnitude on parameter divergence and steps to convergence with fixed and per-subject random effect slopes. Transitions were also grouped into small, medium, and large magnitude categories for qualitative comparisons.

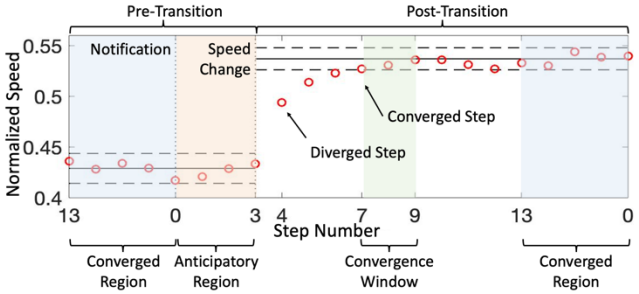

Figure 1 Representative plot of one speed transition showing the average speed (circles), pre- and post-transition means (solid lines), and two standard deviations surrounding the means (dashed lines).

Results and Discussion

Because speed was prescribed, essentially all transitions of every magnitude exhibited divergence in speed, as expected. This was not true for step period and length. As transition magnitude increased, the percentage of transitions that diverged in both step period and length increased ($p < 0.001$, Fig. 2). For small transitions, three divergence behaviors were observed: (1) step period diverged in most transitions, with fewer instances of step length divergence; (2) the converse was true; and (3) divergence in step period and length occurred roughly equally. For large transitions, divergence in both step period and length occurred overwhelmingly. These divergence rates varied across subjects ($p < 0.001$). Thus, both transition magnitude and subject preference influenced divergence behavior.

Small, medium and large transitions resulted in medians of approximately 0, 1, and 2 steps to converge for step period and length and 2, 3, and 3 for speed. At all magnitudes, speed required a greater number of steps to converge compared to step period and length ($p < 0.001$). The transition magnitude fixed effect slope was significant ($p < 0.001$). Across subjects, the effect of transition magnitude on steps to converge for all parameters varied significantly ($p < 0.05$), but all subjects exhibited positive trends with increasing magnitude. So, there is likely a relationship with increasing transition magnitude and steps to converge.

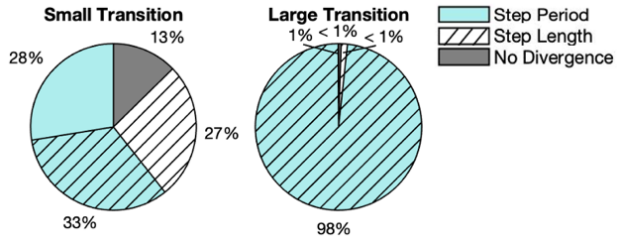

Figure 2 Percentage of small and large transitions that diverged in step period and/or length. The overlap between transitions that diverged in both step period and length increased with increasing transition magnitude ($p < 0.001$).

Significance

This work begins to address the question: what biomechanical behaviors do healthy humans exhibit when transitioning between speeds? Beyond the fundamental understanding gained by pursuing this query, knowledge of desired healthy gait transitions could be applied to improve rehabilitation and assistive technologies for correcting gait impairments.

Acknowledgments

The authors thank Penn State CSTI for StudyFinder. This work was supported by the NSF GRFP under Grant No. DGE1255832.

References

[1] Orendurff MS, et al. *J Rehabil Res Dev* **45**, 1077-1090, 2008.
[2] Jian Y, et al. *Gait Posture* **1**, 9-22, 1993.
[3] Segers V, et al. *Gait Posture* **24**, 247-254, 2006.

A Comparison of Gait Characteristics between Extravehicular Activity Training Environments

Kyoung Jae Kim[1,*], Jocelyn Dunn[1], Eduardo Beltran[1], Omar Bekdash[1], Jason Norcross[1], Andrew Abercromby[2], Meghan Downs[2], Sudhakar Rajulu[2]
[1]KBR, 2400 NASA Parkway, Houston, TX 77058, [2]NASA Johnson Space Center, 2101 NASA Parkway, Houston, TX 77058
Email: *kyoungjae.kim@nasa.gov

Introduction

With the accelerated timeline for NASA's Artemis program, Lunar analog environments are being developed at Johnson Space Center to provide high fidelity extravehicular activity (EVA) simulations and to enable engineering evaluations. The Neutral Buoyancy Lab (NBL) simulates lunar gravity by altering buoyancy and adding weight to subjects underwater to achieve the equivalent ground reaction force of 1/6-G. Another environment, the Active Response Gravity Offload System (ARGOS), uses a computer controlled overhead suspension system programmed to continuously offload a percentage of a subject's weight to simulate partial gravity. The aim of this study is to compare gait characteristics between the EVA training facilities using wireless inertial measurement units (IMUs).

Methods

A subject performed walking tasks in 3 environments: (1) 1-G ground with scuba mask; (2) 1/6-G NBL with scuba equipment; (3) 1/6-G ARGOS with the Mark III spacesuit. The subject was assisted with donning 3 Opal™ IMUs (APDM, USA); 1 on the chest and 2 on the lateral sides of both ankles. For the NBL environment each IMU was inserted in a GoPro waterproof housing and affixed to the subject using an elasticated strap. Before going underwater, the subject walked a measured distance of 10 meters at a self-selected speed on the pool deck (Figure 1). Data were collected at 120 Hz, and the middle 6 meters were analyzed. The subject was then equipped with diving gear and then descended underwater with diver assistance in weighing out subjects to 1/6-G. Once adapted to the 1/6-G weigh-out subjects executed a 10-meter walk on the pool floor at a depth of 12 meters. In the 1/6-G ARGOS environment, 3 IMUs were positioned to the same body segments while wearing the Mark III spacesuit attached to ARGOS via a modified Extravehicular Mobility Unit (EMU) gimbal. Due to the confined testing area, ambulation was performed on a treadmill at 2.0 mph speed for 1 minute and 10 steps were collected in the middle of the trial.

The peaks and troughs of the angular velocity waveform in the sagittal plane (measured from both ankle IMUs) have been associated with specific gait events [1]. Using detected gait events, we segmented the sagittal plane angular velocities into right and left strides (i.e., heel-strike to heel-strike), averaged the segmented gait stride, and normalized to percent gait cycle to compare gait performance between testing environments [2]. The chest IMU measured the torso tilt angle in the sagittal plane [3]. The chest IMU also used to calculate the gait speed [4].

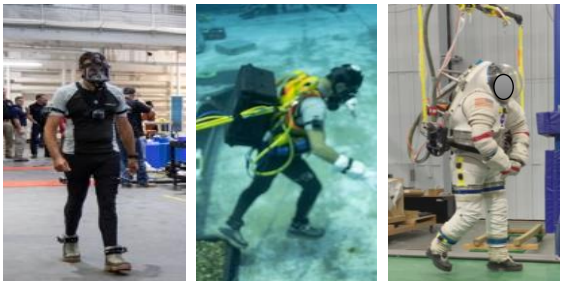

Figure 1: (left) 1-G ground with scuba mask, (middle) 1/6-G NBL with scuba equipment, (right) 1/6-G ARGOS with the Mark III spacesuit.

Results and Discussion

Figure 2 shows the summarized percent gait cycle between testing environments. Table 1 shows the overall gait speed and the averaged trunk tilt angle in the sagittal plane during walking.

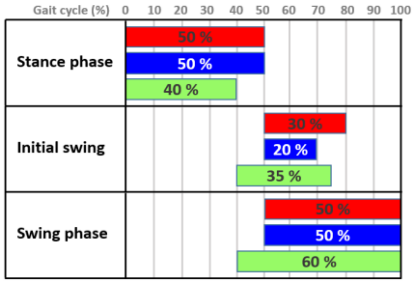

Figure 2: Comparison of percent gait cycles including initial swing, swing phase, and stance phase between the EVA training facilities (red: 1-G ground, blue: 1/6-G ARGOS, green: 1/6-G NBL).

Table 1: Comparison of gait speed and trunk tilt angle.

Variable	1-G ground	1/6-G ARGOS	1/6-G NBL
Gait speed (mph)	2.3 (preferred)	2.0 (prescribed)	0.9 (preferred)
Trunk tilt angle (degree)	6.0	3.1	18.7

The differences in gait strategy found in 1/6-G NBL walking (e.g., forward trunk lean, increased swing phase, reduced gait speed) confirmed the expectation of gait adaptation to increased movement resistance because of underwater drag. At ARGOS, subjects displayed more erect upper bodies and shortened initial swing phases that may be the result of a more realistic 1/6-G environment than NBL. The added support from the offloading system and/or the treadmill could also be contributing factors.

The subject did show the same proportions of swing and stance phases between the 1-G ground and 1/6-G ARGOS conditions. In our previous work with a preceding system, the Partial Gravity Simulator (POGO), an unsuited subject in simulated 1/6-G offload displayed a shorter stance phase than that in 1-G offload that may indicate that the unsuited body may have been relying on the vertical offload forces to assist their upward movement and not producing the necessary propulsive forces in the forward direction [5]. In this study, the increased propulsive force because of the resistance to lower-limb movements of the pressurized suit may be related to the increased stance phase in the ARGOS environment.

Significance

Walking and exploring will be one of the most common tasks during Lunar EVAs for the Artemis program. These Lunar EVA simulations and analog environments enable us to provide potential for developing training protocols and improve the current knowledge of testing environments and limitations in suited Lunar EVAs.

References

[1] Storm FA, et al. (2016). Gait event detection in laboratory and real life settings. *Gait Posture*, 50, 42-46.
[2] Kim KJ, et al. (2018). Exposure to an extreme environment comes at a sensorimotor cost. *Nature npj Microgravity*, 4(1), 1-18.
[3] Madgwick SO, et al. (2011). Estimation of IMU and MARG orientation using a gradient descent algorithm. *Proc. IEEE Int. Conf. Rehabil. Robot.*, 1-7.
[4] Yang S, Li, Q (2012). Inertial sensor-based methods in walking speed estimation: A systematic review. *Sensors*, 12(5), 6102-6116.
[5] Norcross JR, et al. (2010). Characterization of partial-gravity analog environments for extravehicular activity suit testing. *NASA/TM-2010-216139*, 1-60.

Step Length Asymmetry is Associated with Gait Efficiency in Older Women with Hip Osteoarthritis

Chun-Hao Huang [1*], Kharma C. Foucher [1]
[1]University of Illinois at Chicago, Chicago, IL
Email: *chuan26@uic.edu

Introduction

Both aging and hip osteoarthritis (OA) can reduces gait efficiency [1-3]. Consequences may include reduced activity levels to conserve energy and minimize fatigue [4-6]. Only 30% of people who have hip osteoarthritis meet physical activity recommendations[7]. Thus, it is important to understand how hip OA associated factors affect the efficiency of gait so that more effective rehabilitation strategies to improve physical activity for this group. The purpose of this study was to determines how gait efficiency is influenced by step length asymmetry in older women with hip OA. We hypothesized that people with hip OA have statistically significant step length asymmetry which is associated with worse mechanical energy exchange and higher oxygen consumption during walking. We also explored interrelationships among these factors.

Methods

Subjects: Participants gave informed consent to participate in this IRB approved study. 17 women with hip OA (age 59.2±8.6, and BMI 30.6±6.3) were included in the study. *Data collection and processing:* Gait analysis was conducted using standard methods. 2.5 minutes of walking on a treadmill at each subjects' self-selected walking speed was analyzed. Oxygen consumption was measured at the same time using indirect calorimetry. O_2 rate and O_2 cost was extracted from the cardiopulmonary diagnostic software. Step length was determined by the distance between two heel markers. We used Symmetry Index (SI): $[|X_{uninvolved}-X_{involved}|/ X_{uninvolved}] *100\%$ to determine step length asymmetry [8]. We extracted center of mass (COM) by the segmental analysis method [9]. Next, the potential (Ep) and kinetic (Ek) energy were calculated by the equations: $E_p= M_{tot} \times 9.81 COM(z)$, $E_k=1/2 M_{tot} (V_x^2+V_y^2+V_z^2)$ [10]. Finally, mechanical energy exchange, the percent of center of mass energy recovery was calculated by the equation: $\%Recovery= [\Delta^+E_p+\Delta^+ E_k-\Delta^+ E_{tot}]/[\Delta^+ E_p+\Delta^+ E_k]$[11]. %Recovery is the pendulum-like transfer between E_k and E_p and can be considered a measure of gait efficiency. *Statistical analysis:* To test our hypothesis, we used a one sample T-test to determine whether the symmetry index was significantly different from 0, and Pearson correlations to determine whether it was associated with mechanical energy exchange, O_2 rate, and O_2 cost during gait. Next, we used Pearson correlations to evaluate the relationships among mechanical energy exchange, O_2 rate, and O_2 cost during gait.

Results and Discussion

SI for the step length was 5.7±5.4 and was statistically significantly different from zero ($p<0.001$). Mechanical energy exchange was 22.3±5.9 %. Higher (more asymmetric) SI for the step length was statistically significantly correlated with lower (worse) mechanical energy exchange (R= -0.542, p=0.024) (Fig 1). The O_2 rate was 9.6±2.9 ml/kg/min and the O_2 cost was 0.3 ±0.1 ml/kg/m. However, O_2 rate was not statistically significantly correlated with mechanical energy exchange (R=0.44, p=0.079) or SI (R= -0.34, p=0.186). Additionally, O_2 cost was not statistically significantly correlated with mechanical energy exchange (R=0.24, p=0.347) or SI (R= 0.18, p=0.481).

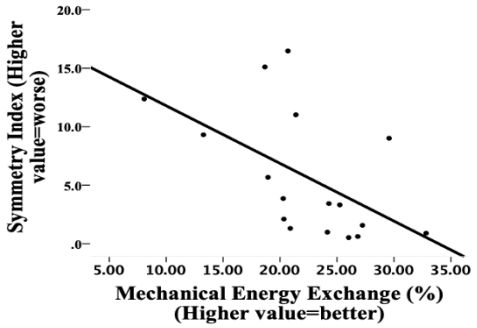

Figure 1: More symmetric step lengths were associated with better mechanical energy

Our hypotheses were partially supported. Statistically significant step length asymmetry was present in hip OA patients. This asymmetry was associated with worse mechanical energy exchange. SI for the step length was significantly lower than the asymptomatic group that has been evaluated using the same method (SI=2.89) (p=0.044)[12]. Contrary to our hypothesis, oxygen consumption (O_2 rate and O_2 cost) was not related to step length asymmetry and mechanical energy exchange. However the O_2 rate was close to significance, with a medium effect size. This was similar to results by Burdett et al.[13], who reported linear relationships between mechanical work energy exchange and energy consumption. More research is needed to explore possible strategies to increase the mechanical energy exchange by modifying step length asymmetry.

Significance

Gait efficiency may be a barrier to physical activity in people with hip OA. This study points to a potential rehabilitation strategy to improve gait efficiency by modifying step length asymmetry.

Acknowledgments

This study was supported by NIH R21 AG052111 grant and the University of Illinois at Chicago Center for Clinical and Translational Science (CCTS) award UL1TR002003. We thank Ike Kabir for his help for the MATLAB coding.

References

1) Larish, D.D., et al., 1988. 2) Waters R.L., et al., 1988. 3) Queen, R.M., T.L. Sparling, and D. Schmitt, 2016. 4) Waters, R.L., Mulroy S., 1999. 5) Schrack J.A, Simonsick E.M., Ferrucci L. 2010. 6) Malatesta D., et al., 2003. 7) Wallis J.A., et al., 2013. 8) Lugade V., et al., 2010. 9) Stagni, R., et al., 2014. 10) Hallemans, A., et al., 2004. 11) Cavagna, G.A., H. Thys, and A.Zamboni, 1976. 12) Blazkiewicz, M.,et al., 2013. 13)Burdett, R., 1983.

Zero power but positive acceleration at the end of a single-support phase in human walking

Seyoung Kim[1*], Cheolhoon Park[1], and Chanhun Park[1]
[1]Department of Robotics and Mechatronics, Korea Institute of Machinery & Materials (KIMM)
Email: *seyoungkim@kimm.re.kr

Introduction

Human walking naturally consists of single- and double-support phases. Although there have been many studies regarding basic understanding of each stage, how the two major sequential phases of walking interact with each other still remains to be clarified. In this study, we investigated the change in walking strategy with increasing walking speed on a local reference frame defined with respect to the direction of a telescoping leg (Fig. 1); we expect that the telescoping directional outcomes (e.g., force and power) at the end of a single-support phase change with walking speed to facilitate the modulation of the push-off work during a double-support phase.

Methods

The telescoping directional force and power are calculated using the compliant walking model shown in Fig. 1 [1,2]. The empirical human walking data for eight healthy young subjects and the corresponding model parameters emulating the human data were used to examine the changing trend of each factor (i.e., force and power) with the increase in speed.

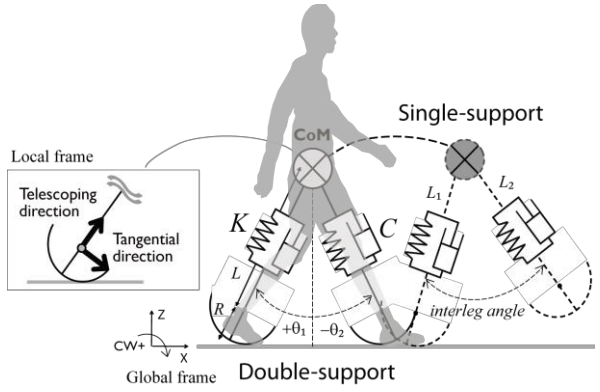

Figure 1: Schematic of the compliant walking model. The human body was modeled as a simple lumped mass with two massless, telescoping legs with curved feet. A local reference frame with telescoping and tangential axes was located at the center of the curved foot (inset).

Results and Discussion

The telescoping directional force ($\boldsymbol{F_{tele}}$) at the end of the single-support phase significantly increased with walking speed (Fig. 2C), whereas the telescoping directional power ($\boldsymbol{P_{tele}}$) remained nearly unchanged at zero for the entire range of walking speeds (Fig. 2D). The positive amount of the telescoping directional force ($\boldsymbol{F_{tele}}$) (i.e., the acceleration force) at the end of the single-support phase (Fig. 2A and C) is a certain preparation for the double-support phase, which can contribute to a larger push-off. Starting with the supportive acceleration force (i.e., $\boldsymbol{F_{adv}}$; force advantage in Fig. 2A and C) in the telescoping direction may help to efficiently increase the total push-off work during the double-support phase in a limited time, when the telescoping directional center of mass (CoM) velocity at the end of the single-support phase is nearly zero (i.e., zero power). Morevoer, it is naturally preferable to have a larger force preparation to reach the increased walking speed because of the CoM velocity redirection cost unavoidably increasing with the speed increase.

Consequently, "zero power (or zero velocity) but positive acceleration depending on the walking speed" would be one possible candidate for describing human-walking strategy during the switching procedure between the single- and double-support phases.

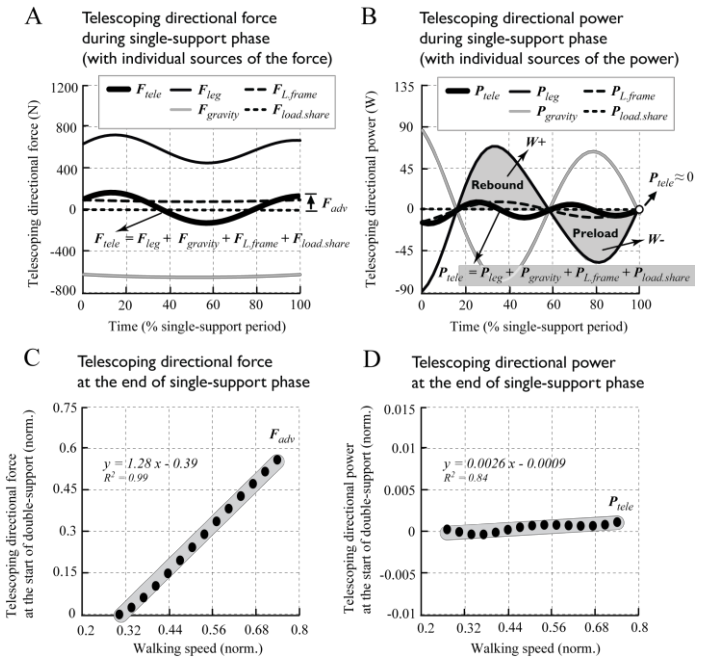

Figure 2: Telescoping directional (A) force (F_{tele}) and (B) power (P_{tele}) during single-support phase at a walking speed of 1.4 m/s, shown with four individual components. (C) Telescoping directional force (F_{tele}) and (D) power (P_{tele}) at the end of the single-support phase, with increasing walking speed.

Significance

This study may contribute to the novel understanding of the human-walking strategy in terms of the role of the phase switching in the telescoping direction, and also can be applied to the clinical measures of walking ability modulating the force advantage with the speed increase.

Acknowledgments

This research was supported by the R&D program of the Korea Institute of Machinery & Materials (KIMM), and the Alchemist project of Ministry of Trade, Industry and Energy (MOTIE).

References

[1] Whittington, B. R., Thelen, D. G., 2009. A simple mass-spring model with roller feet can induce the ground reactions observed in human walking. *J Biomech Eng* 131, 011013
[2] Kim, S., Park, S., 2011. Leg stiffness increases with speed to modulate gait frequency and propulsion energy. *Journal of Biomechanics* 44, 1253-1258

Gait Blanace Control After Fatigue: Effects of Age and Cognitive Demand

Szu-Hua Teresa Chen[1] and Li-Shan Chou[1,2,*]
[1]Department of Human Physiology, University of Oregon, Eugene, OR USA
[2]Department of Kinesiology, Iowa State University, Ames, IA USA
Email: *chou@iastate.edu

Introduction

Studies have reported effects of either fatigue or cognitive demand on gait performance in both young and older adults. However, the study examining how fatigue and cognitive demand interact to affect gait balance control is still lacking. Distracted walking is commonly observed during our daily life and can happen with the presence of fatigue, especially at the end of work or sport activity. Therefore, the purpose of this study was to examine how fatigue affects walking balance control with and without performing a concurrent cognitive task.

Methods

Seventeen young (age: 26.0 ± 5.8) and 17 older (age: 69.5 ± 5.4) adults were tested. Participants were asked to perform three tasks in a random order: 1) walking continuously with a self-selected speed, 2) performing a 3-back task while seated, and 3) walking and concurrently performing the 3-back task (**Figure 1**). During the 3-back test, participants were required to identify the repeated number that was presented three digits before in the sequence of random numbers. Each task lasted for two minutues and these tasks were performed again immediately after finishing a fatigue protocol. A 12-camera motion analysis system was used to record the whole body movement during walking.

A repetitive sit-to-stand (STS) task was selected as the fatiguing protocol [1]. Participants were asked to sit on a regular wooden chair without armrest and perform repetitive STS movements at their comfortable and fixed paces up to 30 minutes. The fatiguing protocol was terminated when 1) participants cannot continue due to exhaustion, 2) when the movement frequency fell below prescribed pace after encouragement, or 3) after raeching 30 minutes. Rating of perceived exertion (RPE) and maximal isokinetic contraction of right knee extensor were examined using a Borg Scale 6-20 scale and a dynamometer, respectively, before and after the fatiguing protocol.

Outcome variables included 1) the medial-lateral center of mass displacement during a gait cycle (***M-L CoM***), 2) ***gait velocity***, and 3) ***accuracy and reaction time*** of 3-back. A 3-way mixed-effect ANOVA was used for statistical analysis with Group (age), Fatigue and Task (single vs. dual) as factors. $\alpha = .05$.

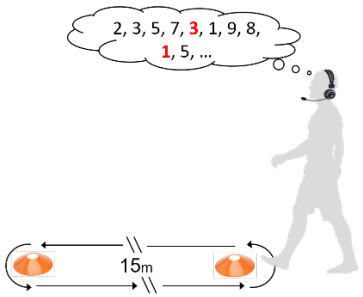

Figure 1: Illustration of dual-task walking (walking task + 3-back test).

Results and Discussion

No significant age-group differences were found for the fatiguing protocol performance in terms of the fatiguing duration (19.2 mins), muscle strength reduction (18%), and increase in RPE (from 7 to 18). From pre- to post-fatigue, a faster gait velocity (103%) was observed during dual-task walking regardless of age, $p = 0.02$, which may be postulated as a strategy to improve stability since the gait stability was shown reaching the best when walking at 100-110% of regular velocity [2]. For M-L CoM, we found an increased body sway at post-fatigue in young but not older adults regardless of task condition (**Figure 2a**). Older participants may have developed adaptability to fatigue, therefore are less susceptible to the fatiguing protocol. Our findings may also be reflective of healthy volunteer effect. Lastly, it is possible that our healthy older adults walked with the body sway closer to their maximum capacity, thus perturbation could not be manifested in the form of M-L CoM after fatigue.

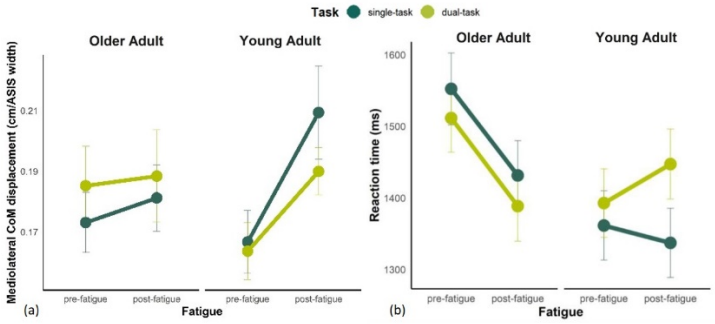

Figure 2: Changes in M-L CoM (a) and reaction time (b) from pre-fatigue to post-fatigue among two age groups (mean ± SEM).

The older adults also improved their cognitive function after fatigue (**Figure 2b**). The result maybe attributed, in part, to learning effect. The differential changes between older and young adults may be speculated from neural substrates for activity-elicited activation, in which older adults dominantly recruit frontopolar area (excitatory) after exercise instead of DLPFC (inhibitory) in young adults [3].

Significance

We found that 1) older adults improve reaction time from pre-fatigue to post-fatigue while maintaining the mediolateral body sway, 2) balance control in young adults become deteriorated at post-fatigue and 3) fatigue effects are not exacerbated during dual-task condition. The results could serve as a scientific evidence and point out another prospective when it comes to prevention of fall accidents in workers whose job requires high physical and/or mental demand.

Acknowledgments

This work was funded by the Northwest Center for Occupational Health and Safety & the Ursula Moshberger Scholarship.

References

1. Barbieri, F.et al. *Gait & Posture* **38**, 702-707, 2013
2. Jordan, K., et al. *Gait & Posture* **26**, 128–134, 2007
3. Hyodo K., et al. *Neurobiology of Aging*, **33**, 2621–32, 2012

Treadmill Walking Does Not Elicit Increased Tripping Risks in Children with Autism

Emily A. Chavez[1], Alyssa N. Olivas[2], Patrick A. Cereceres[1], Pearl Quintero[1], and Jeffrey D. Eggleston[1]
[1]Department of Kinesiology, The University of Texas, El Paso, TX, USA
[2]Department of Biomedical Engineering, The University of Texas, El Paso, TX, USA
Email: eachavez4@miners.utep.edu

Introduction

Children with Autism Spectrum Disorder (ASD) experience obesity at an increased rate (30.4%) compared to controls with neurotypical development (NT; 23.6%) [1]. With the prevalence of ASD increasing to 1 in every 59 children, [2] further research is needed to identify methods aimed at decreasing obesity rates and increasing physical activity in this population. Treadmill (TM) implementation may be a viable option to do so, as previous findings suggest, metabolic requirements were 23% higher in TM walking than overground (OG) walking [3]. However, literatue examining gait mechanics while on a TM in children with ASD is lacking. Specifically, investigating tripping risk or other adverse gait-related events to assess safety and efficacy of TM-use before metabolic measures can be considered. Thus, the purpose of this study was to examine lower extremity (LE) tripping descriptors in children with ASD during OG and TM walking conditions compared to NT controls. It was hypothesized that significant differences will not be identified in the ASD population between OG and TM conditions.

Methods

Two children diagnosed with ASD (1 male [11 yrs], 1 female [10 yrs]) and two age- and sex-matched NT controls were recruited to participate in this study. Participants were outfitted with retroreflective markers on their lower extremities then were instructed to walk over a 10m walkway at a self-selected pace for 12 trials in the OG condition. Afterwards, participants were instructed to walk on a TM at a self-selected pace for a total of five-minutes. Three 30s intervals of three-dimensional LE motion capture data were collected (200 Hz, Vicon Nexus, Ltd., Oxford, UK) following the initial minute on the TM. Raw trajectory data were exported to Visual 3D for processing where a digital low-pass Butterworth filter was applied (6 Hz). The Model Statistic technique (α=0.05) [4] was used to test for statistical significance for tripping descriptors [5]: toe clearance (TC) and peak knee flexion (PKF) in both limbs. Each variable was tested during the OG condition versus the TM condition for each participant.

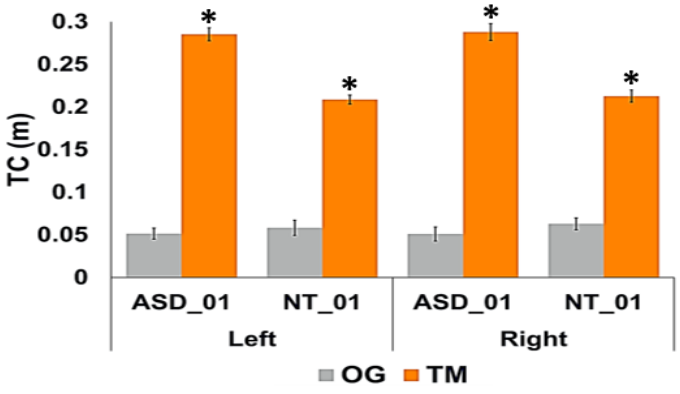

Figure 1: TC values displayed for one matched pair. * denotes significant difference from OG to TM condition; p<0.05.

Results and Discussion

Mean and standard deviation values are displayed in Figure 1. Findings suggest that all ASD and NT individuals displayed more statistically significant differences between OG and TM conditions. Notably, TC in both limbs was signifcantly larger during the TM condition compared to the OG condition for all participants. Right PKF significantly decreased during TM condition in three individuals with the exception of one participant with ASD, who displayed no significant differences between condtions. Left PKF also significantly decreased during the TM condition compared to the OG condition for three participants with the exception of the same ASD participant that displayed a significant increase.

Though there were significant differences observed in this study in all participants, no patterns were identified in the ASD population. This may be due to the heterogenous motor characteristics of the ASD population [6]. Additionally, the magnitude of the TC in all participants may not be considered large enough to increase tripping risk between conditions as no participant experienced an adverse gait-related event during actual data collection. Thus, TM use may be a safe option to implement within the ASD population as an efficient mean of increasing physical activity without increased tripping risks. However, a larger sample size of ASD participants with matched controls needs to be examined to potentially find discernable patterns and further determine if TM use can be utilized in this population.

Significance

Gait mechanics of children with ASD is not fully understood as current literature has only examined overground walking in this population. This study adds to the underpinings of how children with ASD will respond to treadmill walking and asseses the safety of TM intervention as a means to increase energy expenditure. Additionally, treadmill walking may result in reduced obesity rates as well as eliminate the social and physical barriers associated with this population. On a global scale, establishng treadmill walking as a safe intervention, will allow researchers with interdisciplinary concentrations to examine and understand the social, behavioural, neurological, and clinical effecs TM walking has on the ASD population.

Acknowledgments

This work was funded by the Graduate School Dodson Research Grant from The University of Texas at El Paso.

References

1. Curtin et al. (2005). *BMC Pediatrics* **5**: 1-17.
2. Baio et al. (2018) *MMWR Surv. Summ.*. **67**: 1-28.
3. Parvataneni et al. (2009). *Clin. Biomechics.* **24**: 95-100.
4. Bates et al. (1996). *Med. & Sci. Sports. & Ex.*. **28**: 386-391
5. Benson et al. (2018). *Hum. Mov. Sci.,* **62**: 58-66.
6. Dufek et al. (2017). *Med. Sciences*, **5**: 1-11.

Gait adaptations of individuals with limited dorsiflexion ROM during incline walking

Yujin Kwon[1] and Gwanseob Shin[1,*]
[1]Department of Human Factors Engineering, Ulsan National Institute of Science and Technology, Korea
Email: ekwon@unist.ac.kr

Introduction

It is known that individuals who have limited dorsiflexion range of motion of the ankle walk with postural adaptations such as earlier heel lift to compensate for their limited functional capacity of their ankle joints (Johanson, et al., 2006).

Such associations have been observed during level walking, but no research has yet investigated how the dorsiflexion range would affect the gait pattern during inclined walking. As larger amount of dorsiflexion is required on inclined surfaces (Leroux, Fung, & Barbeau, 2002), it is assumed that the effect of limited dorsiflexion range on gait pattern would be more pronounced compared to level walking. Thus, the current study was conducted to investigate the effects of dorsiflexion range on the gait pattern while walking on inclined surfaces.

Methods

Fifteen healthy young participants participated (mean age = 22.2(±1.9)), and grouped into 'Limited' range of motion (ROM) group (3 females, 5 males) and 'Normal' ROM group (5 females, 3 males) by their passive ankle dorsiflexion range in the Weight-Bearing Lunge Test (Table 1).

Table 1: Participant information. Mean(±Standard Deviation)

	Height (cm)	Weight (kg)	ROM (deg)
Limited group (n=8)	170.5(±6.7)	75.1(±6.4)	35.1(±2.9)
Normal group (n=8)	168.6(±12.0)	58.0(±11.4)	46.2(±4.6)

Each participant walked on a treadmill at five inclined slopes (0° (level), 5°, 10°, 15°, and 20°) for 2 minutes each at a self-selected comfortable speed for 20°. During walking, the ankle joint angles of the dominant leg were quantified by tracking reflective markers at 200 Hz using a three-dimensional motion capture system (Optitrack system, USA). The electromyography (EMG) signals of the soleus muscle were also quantified using a surface EMG system at 2,000 Hz (Delsys Inc., USA). The order of the five slopes was randomized between participants.

For each walking trial, the maximum dorsiflexion angle during stance, and foot external rotation and foot pronation angle at the moment of maximum dorsiflexion were identified. From the EMG signals, normalized amplitude (% of the mean amplitude during level walking) of the soleus muscle during stance was computed. The joint angle and normalized EMG data were averaged over 30 gait cycles. Two-way mixed ANOVA and a pairwise comparison with the Bonferroni correction were conducted in R (R studio, USA) to compare the variables between groups and slopes ($p<0.05$).

Results and Discussion

The max dorsiflexion angle and the foot external rotation and pronation angle increased along with the slope angle (Figure 1B-D). Significant between-slope differences in the max dorsiflexion angle were found between 0°, 10°, 15°, and 20° for the limited ROM group, and between 0°, 10°, and 20° slopes for the normal ROM group. For foot rotation, significant difference was only found between 0° and 20° for the limited group. The limited group walked with less dorsiflexion, more foot external rotation, and more pronation during stance compared to the normal group. But significance in the differences was found only at 5° for the foot pronation. The normalized EMG of the soleus muscle during stance increased as the slope angle increased, with significant differences between 0°, 10°, 15°, and 20° for the limited and between 0°, 15°, and 20° for the normal group. The limited group produced significantly higher activity than the normal group at 10° and 15° slopes (Figure 1A).

As hypothesized, the study results show the distinctive gait pattern from those who have limited dorsiflexion ROM when walking on inclined surfaces. The more external rotation and pronation at the moment of max dorsiflexion (late stance phase) would indicate the compensatory response to their limited dorsiflexion ROM when walking on inclined surfaces. The more external rotation at the later phase of stance required the soleus muscle, which is the main muscle of plantarflexion, to produce greater activation for forward propulsion.

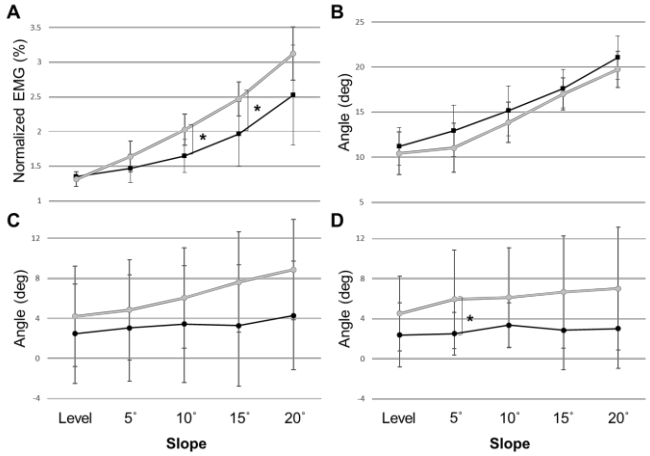

Figure 1: Mean (± SD) of normalized EMG of Soleus (A), Max ankle dorsiflexion angle during stance (B), Foot external rotation angle and Foot pronation angle at max ankle flexion (C,D) of limited (gray) and normal (black) group. *significant difference between groups ($p<0.05$).

Significance

The findings of this study show that the individuals with limited dorsiflexion ROM altered their foot-ankle postures when walking on inclined slopes to compensate for their limitation, and it resulted in the greater activity of the soleus muscle. Such adaptations imply greater risk for muscle fatigue or musculoskeletal problems. The results may provide insight into the development of better walking strategy to prevent injury or exoskeletons for those with limited capacity of ankle joints.

Further research should be conducted with more participants and in more various walking conditions to quantitatively evaluate the risks associated with limited dorsiflexion ROM, and to propose proper interventions to reduce the risks.

References

[1] Johanson, et al. (2006). *J. Athletic Training*, **41:**159–165.
[2] Leroux,Fung,&Barbeau (2002). *Gait and Posture*, **15**: 64-74.

Older Adults Overcome Reduced Triceps Surae Structural Stiffness to Preserve Ankle Joint Quasi-Stiffness During Walking

Rebecca L. Krupenevich[1*], William H. Clark[1], Greg S. Sawicki[2], and Jason R. Franz[1]
[1]UNC Chapel Hill and NC State University, Chapel Hill, NC
[2]Georgia Institute of Technology, Atlanta, GA
Email: *rlkrup@email.unc.edu

Introduction

Ankle joint quasi-stiffness, the slope of the relation between ankle angle and ankle moment, is an aggregate measure of the interaction between triceps surae muscle (TS) stiffness and series elastic Achilles tendon (AT) stiffness [1]. Moreover, activation can regulate joint quasi-stiffness via changes in TS length-tension behavior [2]. However, the extent to which known age-related changes in the structure and functional behavior of the TS and AT alter ankle joint quasi-stiffness is relatively unknown. We hypothesized that, due to a more compliant AT [3], older adults would exhibit lower ankle joint quasi-stiffness than young during: (*i*) walking (Experiment 1) and (*ii*) isolated eccentric contractions at matched TS muscle activations (Experiment 2).

Methods

For experiment 1, 10 young (23±2 yrs, 66.2±10.4 kg, 1.73±0.10 m, 5M/5F) and 12 older (75±5 yrs, 68.6±11.1 kg, 1.51±0.24 m, 5M/7F) adults walked on an instrumented treadmill at their preferred walking speed while we recorded lower limb kinetics and kinematics. We calculated ankle joint quasi-stiffness during the dorsiflexion, dualflexion, and plantarflexion phases of stance as the slope of the best fit line on a moment-angle plot (Fig. 1A). Two-tailed independent samples *t*-tests assessed the effect of age on ankle joint quasi-stiffness during walking. For experiment 2, 9 young (23±3 yrs, 70.7±10.4 kg, 1.76±0.12 m, 4M/5F) and 8 older (72±4 yrs, 69.1±18.6 kg, 1.68±0.09 m, 4M/4F) adults performed a series of eccentric isokinetic contractions at 30 °/s through a 25° range of motion while using biofeedback to match 75% MVIC soleus activation. Ultrasound imaging captured TS muscle fascicle length change. We calculated ankle joint quasi-stiffness and TS muscle stiffness, the latter as the slope of the best fit line on a force-length plot. We used two-tailed independent samples *t*-tests to assess the effect of age on primary outcomes and report effect sizes (Δ) as the difference in means divided by the standard deviation of young adults.

Results and Discussion

Contrary to our first hypothesis, ankle joint quasi-stiffness during walking was unaffected by age [dorsiflexion (p=0.376, Δ=0.43), dual-flexion (p=0.96, Δ=0.04), and plantarflexion (p=0.124, Δ=0.60) (Fig. 1A)]. Our second experiment, performed at a matched activation, removed the potential for activation-dependent modulation of ankle joint quasi-stiffness that could be highly prevalent during a functional task such as walking. As hypothesized, during isolated contractions at a matched activation, older adults exhibited reduced ankle joint quasi-stiffness (p=0.020, Δ=1.04, Fig. 1B), soleus muscle stiffness (p=0.0.38, Δ=0.94, Fig. 1C), and gastrocnemius muscle stiffness (p=0.043, Δ=0.85, Fig. 1D). We offer two inter-related explanations for our findings. First, older adults likely have a scaled down length-tension curve compared to young adults due to a reduced capacity for force generation. Accordingly, we would anticipate a smaller rise in force in older than young adults across a prescribed range of motion which, thereby, would elicit reduced stiffness at the individual muscle and ankle joint levels Second, given evidence of reduced AT stiffness with age [2], the smaller rise in force may be explained by a smaller tendon force contribution to total muscle-tendon unit force. Together, our findings suggest that during normal walking, older adults increase muscle activation to maintain ankle joint quasi-stiffness.

Significance

Ankle joint quasi-stiffness is preserved in elderly gait, an outcome that: (i) persists despite underlying effects of age on triceps surae muscle-tendon structure and function, and (ii) may be governed at least in part via activation-mediated increases in triceps surae muscle stiffness.

Acknowledgments

This work was supported by a grant from the National Institutes of Health (R01AG058615).

References

[1] Shamaei (2013). *PLoS One*, 8(3): e59935.
[2] Onambele (2006). *J Appl Physiol*, 100: 2048-2056.
[3] Clark and Franz (2019) *J Appl Biomech*, 35(3): 182-189

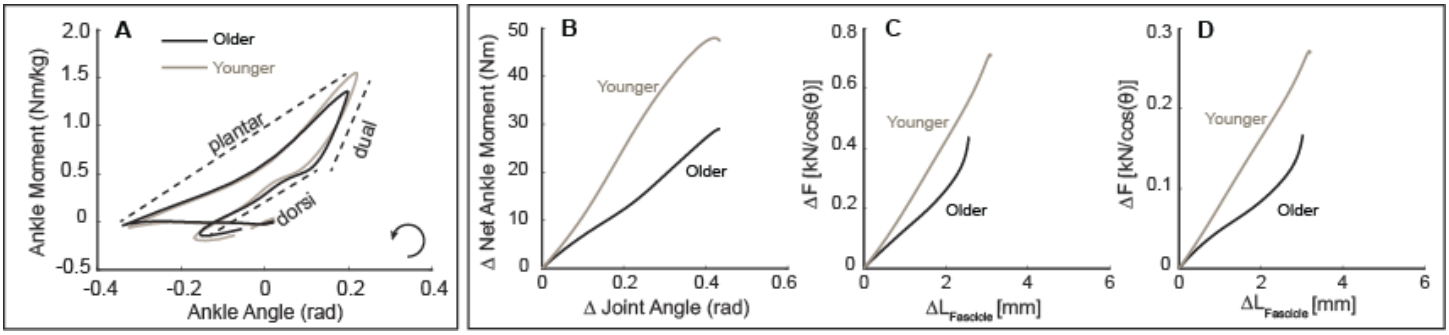

Figure 1: During walking: A) group mean ankle joint quasi-stiffness. Quasi-stiffness was calculated for dorsiflexion (dorsi), dual-flexion, (dual), and plantarflexion (plantar) phases. During isolated contractions: B) Group mean ankle joint quasi-stiffness quantified as the relation between the change in ankle joint angle and net ankle moment, (C-D) group mean soleus and gastrocnemius muscle stiffness quantified via the relation between the change in muscle force (ΔF) and the change in fascicle length (ΔL).

Responses to Incremental Loads in a Weighted Vest in Children with Autism Spectrum Disorder

Alyssa N. Olivas[1], Emily A. Chavez[2], Patrick A. Cereceres[2], Jeffrey D. Eggleston[2]
[1]Department of Biomedical Engineering, The University of Texas at El Paso, El Paso, TX, USA
[2]Department of Kinesiology, The University of Texas at El Paso, El Paso, TX, USA
Email: anolivas4@miners.utep.edu

Introduction

Distinct differences in gait mechanics have been observed when comparing children with Autism Spectrum Disorder (ASD) and neurotypical (NT) peers, including hip, knee, and ankle angular joint positions, as well as vertical and anterior/posterior ground reaction forces [1]. Weighted vests (WV) are a common intervention for children with ASD to help decrease aberrant movements and behaviors linked with the disorder [2]. Recent research has demonstrated a decrease in gait coordination variability [3] and an increase in smoothness of the center of mass while wearing a WV in children with ASD [4]. Previous research analyzing WVs and their effects on movement in children with ASD have examined 15% body mass distributed in the WV; however, this load was previously established with research conducted on NT children. Consequently, a critical mass value for children with ASD has yet to be established [5]. Therefore, the purpose of this study is to investigate potential changes in spatial-temporal parameters for children with ASD during walking with 5, 10, 15, and 20% body mass distributed within the WV, compared to bodyweight. It was hypothesized that spatial-temporal parameters will change with increasing mass, similar to what has been previously observed in NT literature.

Methods

5 children (1 female, 4 males) with a clinical diagnosis of ASD (12.7±3.1 years; 1.6±0.09m; 60.7±10.4kg) participated in the study. Participants walked over-ground for a distance of 9 m, for 12 trials at a self-selected velocity in five conditions: without a WV (baseline), with a WV at: 5, 10, 15, and 20% body mass evenly distributed posteriorly and anteriorly. During all trials, three-dimensional kinematic data were obtained using a 10-camera motion capture system (200 Hz, Vicon Motion Systems, Ltd., Oxford, UK) and exported to Visual 3D (C-Motion, Inc., Germantown, MD, USA) for analysis. Data were smoothed using a low-pass Butterworth digital filter with a cut-off frequency of 6 Hz. Mean and standard deviation values were calculated for right step length, left step length, stride width, stride velocity, and double limb support time. A repeated measures analysis of variance (ANOVA; α=0.05) was conducted to test for statistical significance between conditions. When a significant difference was detected in the omnibus ANOVA test, pairwise comparisons were interpreted after applying the Sidak adjustment.

Results and Discussion

Analysis revealed that children with ASD displayed no statistical difference in spatial-temporal parameters among conditions (Figure 1). The repeated measures ANOVA analysis revealed: left step length: $F(4,16)=1.564$, $p=0.232$, $\eta^2=0.281$, right step length: $F(4,16) = 1.771$, $p=0.184$, $\eta^2=0.307$, stride width: $F(4,16)= 2.101$, $p=0.128$, $\eta^2=0.344$, stride velocity: $F(4,16)= 0.929$, $p=0.472$, $\eta^2=0.189$, double support time: $F(4,16)=1.013$, $p=0.430$, $\eta^2=0.202$. These findings suggest that children with ASD do not modulate their gait with increased weight, rejecting the hypothesis that the spatial-temporal parameters would change with increasing loads. These findings may indicate that children with ASD are not appropriately interpreting the increasing mass while walking, thus, suggesting that children with ASD may not be appropriately interpreting external stimuli. While WVs have shown to decrease hyperactivity and sensory defensiveness in children with ASD [2], the individuals may not be processing the changes of the sensory input and the increasing loads are contributing to the sensory overload that is often observed in this population [6]. Previous research in gait mechanics in children with ASD has described the heterogeneous nature of ASD and how responses may be better understood through single-subject methodology, which could be applied to this project to examine if any individual changes are observed among conditions [7].

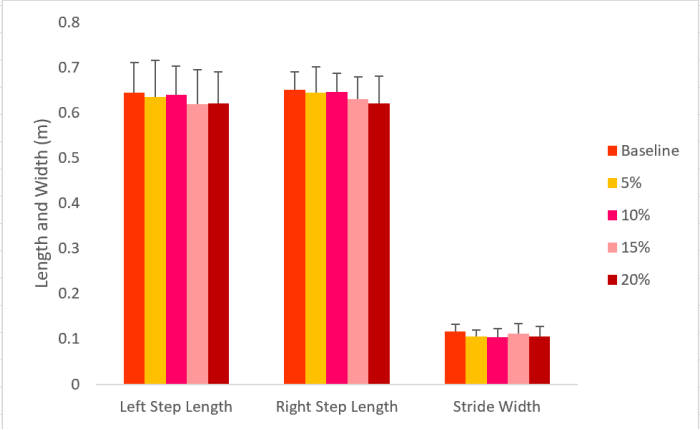

Figure 1: Mean (+SD) left and right step length, and stride width among conditions for children with ASD

Significance

Understanding gait mechanics with an extrenal stimuli present in children with ASD has not been heavily examined. The weighted vest is a common intervention for this population, and it is important to further understand how it can affect the motor deficits that have been observed. This study contributes to further discern how the weighted vest affects gait mechanics in children with ASD. On a global scale, further research in this area could provide a foundation for clinicians to recommend the weighted vest as a multi-use treatment modality for ASD.

Acknowledgments

This research was supported by the University of Texas at El Paso University Research Institute Grant.

References

[1] Eggleston et al. (2017). *Gait & Pos.*, **55**: 162-166.
[2] Olson et al. (2004). *Phys. Occup. Ther. Pedia.*,**24**: 45–60.
[3] Eggleston et al. (2018). *Perc. Mot. Skills,* **125**: 1103-1122.
[4] Harry et al. (2019). *Trans. Jrl. ACSM*, ***4*(10):** 64-73.
[5] Brackley et al. (2004). *Spine*, **29(19):** 2184-2190.
[6] Myles et al. (2004). *Educ. & Train Devlp. Disab.*, 283-290.
[7] Eggleston et al. (2018). *Rsrch Develp. Disab.*, **74**, 50-56.

Spatial Step and Joint Angular Kinematics Differ between Racial Groups

Cherice N. Hughes-Oliver [1], Wornie Reed [2], Daniel Schmitt [3], Laura Sands [4], Shawn Arent [5], Robin M. Queen [1]
[1] Department of Biomedical Engineering and Mechanics, Virginia Tech, Blacksburg, VA, USA
[2] Department of Sociology, Virginia Tech, Blacksburg, VA, USA
[3] Department of Anthropology, Duke University, Durham, NC, USA
[4] Department of Human Development and Family Science, Virginia Tech, Blacksburg, VA, USA
[5] Department of Exercise Science, University of South Carolina, Columbia, SC, USA
Email: cnh4ph@vt.edu

Introduction

Race has rarely been investigated in biomechanics studies despite racial health disparities in the incidence of musculoskeletal injuries and disease [1-3]. Racial differences in gait mechanics could drive disease progression and by examining them it will be possible to identify factors associated with racial health disparities. As race is a social construct, differences in gait mechanics between racial groups could be driven by specific factors other than of racial classification itself.

The purpose of this study was to (1) test the hypothesis that racial differences in fundamental gait measures between African Americans (AA) and white Americans (WA) exist and (2) that these differences would be explained by a combination of anthropometric, strength, and health status factors.

Methods

92 participants were equally divided by gender and self-identified race. Self-selected walking speed was measured and 3D motion capture and force plate data were recorded during 7 walking trials at regular (1.35 m/s) and fast (1.6 m/s) speeds. Step length and width, peak vertical ground reaction force (pvGRF), and peak hip extension (pHEA), knee flexion (pKFA), and ankle plantar-flexion angles (pAPfA) were obtained. Heart rate, blood pressure, stress questionnaires, activity level, anthropometry, lower extremity strength, and blood levels of glucose, interleukin-6, C-reactive protein, and cortisol were also assessed.

Separate multivariate ANOVA models were fit for spatiotemporal, kinetic, and angular measures in both regular and fast walking speed trials to determine main and interaction effects of gender and race (JMP Pro 15, α=0.1). For each significant MANOVA finding, post-hoc univariate ANOVA models were fit, partial eta squared effect sizes were computed for all effects, and student's T effect sizes were computed for pairwise comparisons in each interaction (Table 1). If interactions or gender effects were observed, separate analyses were run for men and women. Stepwise linear regression models were fit including race and all independent variables correlated with the outcome measure ($p<0.2$) and differed between racial groups ($p<0.1$); this was done for each outcome measure with an observed racial difference. If race was no longer significant in the regression model after the inclusion of the independent variable(s), those variables were considered to have explained the effect of race.

Results and Discussion

MANOVA findings were significant for spatiotemporal (*$p<0.001$*) and angular (*regular:$p=0.001$,fast:$p<0.001$*) models, but no for kinetic models (*regular:$p=0.895$,fast:$p=0.200$*). Self-selected walking speed was slower in AA (*$p=0.004$*). Interactions between gender and race existed in step length [*regular: $p = 0.091$, $\eta_p^2=0.03$*], step width [regular: p=0.063, η_p^2=0.04 | fast: p=0.054, η_p^2=0.04], and pKFA [regular: p=0.064, η_p^2=0.04 | fast: p=0.015, η_p^2=0.07]. pHEA [regular: p=0.039, η_p^2=0.05 | fast: p=0.007, η_p^2=0.08] and pAPfA [regular: p=0.012, η_p^2=0.07 | fast: p<0.001, η_p^2=0.14] were smaller in AA. In men, larger step length during regular walking and larger pKFA during fast walking in AA were explained by larger Q-angle and lower interleukin-6 levels, respectively. In women, slower self-selected walking speed in AA was explained by larger Q-angle. Greater step widths during both walking speeds and smaller pAPfA during fast walking in AA women were explained by higher BMI and weaker ankle plantarflexion strength, respectively.

These results support our hypothesis that racial differences in gait mechanics exist and that they can be explained by a combination of anthopometric, strength, and health status factors, however, these observations were only in women. The possibility for additional factors to explain the observed racial gait differences should be investigated further, especially in men. For women, a mix of innate and modifiable factors explained racial differences. Innate metrics such as Q-angle contributing to racial differences suggests the need for racially diverse normative datasets. Modifiable factors such as BMI and ankle plantarflexion strength that are associated with racial differences could provide targets for interventions aimed at injury prevention and optimizing rehabilitation. Identified targets may also be useful in reducing or potentially eliminating racial health disparities in musculoskeletal injury and disease.

Significance

Equivalency in gait measures between racial groups should not be assumed. Racial diversity of study samples should be a priority to enable consideration of racial differences in the development of future research and individualized treatment protocols.

Acknowledgments

The Howard Hughes Medical Institute Gilliam Fellowship and the Institute for Society, Culture, and the Environment funded Cherice Hughes-Oliver and this study, respectively.

References

[1] Allen KD. *Curr Opin Rheumatol*. 2010;22(5):528–32. [2] Cruz-Almeida Y, et al. *Arthritis Rheumatol*. 2014;66(7):1800–10. [3] Faulkner KA, et al. *J Am Geriatr Soc*. 2005;53(10):1774–9.

Table 1: Pairwise comparisons for each significant interaction. AA = African American, WA = white American. † small effect (0.2 < d < 0.39), ‡ medium effect (0.4 < d < 0.59), †† large effect (0.6 < d).

		AA Men vs WA Men	AA Women vs WA Women
Regular Walking	Step Length	0.094 ‡	0.469
	Step Width	0.960	0.008 ††
	Knee Flexion Angle	0.104	0.312
Fast Walking	Step Width	0.825	0.004 ††
	Knee Flexion Angle	0.013 ††	0.325

Using Movement Amplification to Explore the Effect of Walking Speed on Stability in iSCI

Tara Cornwell[1*], Geoffrey Brown, Jane Woodward, and Keith E. Gordon
[1]Northwestern University, Physical Therapy and Human Movement Sciences, Chicago, IL, USA
[*]Email: tcornwell@u.northwestern.edu

Introduction

Individuals with incomplete spinal cord injury (iSCI) often walk slowly to compensate for balance deficits. Walking slowly may allow more time for corrective movements. However, iSCI gait training studies have found a positive correlation between speed and balance[1], suggesting that walking faster can also positively impact balance. The effect of speed on gait stability has been studied in other populations with conflicting results[2,3]. Therefore, our purpose was to examine the interaction between speed and stability. We had individuals with and without iSCI walk at two speeds in a normal environment and in a force field that amplified lateral center of mass (COM) motion. Movement amplification challenges frontal plane control, potentially accentuating the impact of walking speed on stability.

We hypothesized that we would not see significant effects from speed on gait stability in the Null field because challenges to COM control during treadmill walking are relatively small. In contrast, in the Amplification field that dynamically challenges balance, we hypothesized that decreases in stability would emerge at Fast compared to Preferred speeds.

Methods

A total of 12 adults with iSCI and 12 age- and sex-matched participants without iSCI completed the study. We recorded pelvis and foot kinematics during treadmill walking. A cable-driven robot amplified lateral motion during select trials by applying forces to the pelvis that were proportional in magnitude and in the same direction as the participant's real-time lateral COM velocity. Participants performed 4 randomized walking trials of 200 steps. The trials consisted of 2 speeds (Preferred and Fast) performed in 2 force field conditions (Null and Amplification). We calculated short-term Lyapunov exponent of frontal plane COM speed to examine local stability and step width (SW) standard deviation to probe potential control mechanisms.

To evaluate the effect of speed, we created separate linear mixed effects models of Lyapunov exponent and SW standard deviation. Speed, force field, and group were fixed effects and intercepts were random for subjects. Significance was set to $p<0.05$.

Results and Discussion

We hypothesized that individuals would maintain stability across speeds in the Null field, which was supported as there was no significant effect of speed on Lyapunov exponent ($p=0.240$). We also hypothesized that stability would decrease at the Fast speed in the Amplification field, but this was not supported as there was also no significant interaction between speed and field on Lyapunov exponent ($p=0.233$). This suggests that individuals with iSCI can maintain stability at faster speeds, even when balance is challenged. However, we did find an effect of speed on stepping with greater SW variability at the Fast speed ($p=0.031$). See Figure 1 for iSCI group data.

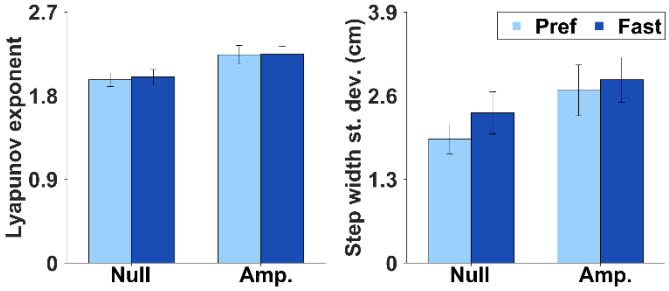

Figure 1: Data for iSCI group. At the Fast speed, Lyapunov exponent (left) did not change, but SW standard deviation (right) increased.

To better understand the significance of higher SW variability, we looked at the relationship between COM motion and foot placement (FP). Previous studies have shown that lateral COM position and speed at midstance predict >80% of lateral FP variance[4]. We created linear mixed effects models for lateral FP with COM position and speed as covariates. We used linear regression to fit the models' predicted values to actual FPs and recorded model fit (R^2). Comparing model fit across trials (Table 1) may suggest a change in mechanics-dependent adjustments to stepping in order to control one's COM.

Table 1: Linear regression model fit values. Higher R^2 values signify a better fit between actual FP and that predicted by COM motion.

Trial:	Null-Pref	Null-Fast	Amp-Pref	Amp-Fast
R^2	0.791	0.813	0.895	0.904

We found R^2 to increase with speed, as well as from Null to Amplification field. This indicates that at the Fast speed, COM dynamics better predicted the next step, adding to a recent study that found this trend in healthy participants[5]. Overall, the findings suggest that individuals with and without iSCI may adapt stepping patterns to accommodate for lateral stability challenges at different speeds.

Significance

Our findings suggest that individuals with and without iSCI can maintain lateral stability at multiple speeds, even when balance is challenged. The increase in stepping variability we observed at the fast speed may have been beneficial for COM control. This could inform iSCI gait training methods and emphasize safely increasing walking speed to encourage practice controlling one's own dynamics.

Acknowledgments

Supported by I01RX001979-01 from the U.S. Department of Veterans Affairs.

References

[1]Alexeeva, N. et al. *The J. of Spinal Cord Med.*, 2011.
[2]England and Granata. *Gait & Posture*, 2007.
[3]Bruijn, SM. et al. *J. of Biomechanics*, 2009.
[4]Wang and Srinivasan. *Biology Letters*, 2014.
[5]Stimpson, K. et al. *J. of Biomechanics*, 2018.

Plantar Force During Walking Is Associated with Arch Structure and Walking Surface

Milad Zarei[1], Elliott Hammersley[1], Naomi Frankston[1], MaCalus Hogan[1], and William Anderst[1]
[1]Department of Orthopaedic Surgery, University of Pittsburgh, Pittsburgh, PA
Email: milad.z@pitt.edu

Introduction

Foot and gait pathologies may be identified by aberrant plantar pressure distribution during gait [1]. Foot pressure distribution is typically measured in clinics and gait labs using a relatively short walkway or a treadmill. It is unknown how well those clinic-based or laboratory-based measurements of plantar pressure reflect "real-world" foot loading that occurs outside the lab. One factor known to affect plantar pressure during gait is foot type (planus, normal, or cavus) [3, 4]. However, it is not clear if foot type differences in plantar pressure are consistent across different walking surfaces.

The goal of this study was to investigate the effects of foot type on plantar forces (PF) during walking on four different surfaces (lab walkway, grass, outdoor pavement, and treadmill). It was hypothesized that participants with planus feet would have higher midfoot plantar forces over all walking surfaces, and that plantar forces would be greater when walking on pavement in comparison to treadmill, grass and laboratory walkway.

Methods

Seventy healthy subjects (41 F/29 M, 43.9±18.2 years old, 71.6±12.6 kg) with no history of foot injury or surgery provided informed written consent prior to participating in this IRB-approved study. All participants wore the same type of shoes (Nike Zoom) and walked at a self-selected pace for at least 5 minutes on four different surfaces: treadmill (TM), 7.8 m laboratory walkway (LW), 80 m outdoor pavement (OP), and 30 m grass (GS) in a random order. A Pedar insole pressure system (Novel Electronics Inc) collected bilateral plantar pressure at 100 Hz using 99 sensors per insole. Overall plantar force during each foot strike was calculated from the pressure recordings, and the first peak (P1: weight acceptance) and second peak (P2: push-off) were identified for each step and used to compare overall foot loading on each surface. The sensors were then partitioned into 9 regions [5] (Figure 1), and the Peak Regional Force (PRF), defined as the peak force within each region, was calculated for each step. These values were averaged over all steps for each surface for each participant. The arch index (AI), determined from footprints [6], was used to classify foot type as planus (low arch), normal, and cavus (high arch) [7]. A 4 way repeated measures ANOVA was utilized to identify differences among walking surfaces and foot types for P1 and P2, and for PRF within each foot region. Significance was set at $p<0.05$ after applying the Bonferroni correction for multiple comparisons.

Results and Discussion

There were 43 planus, 57 normal and 40 cavus feet analyzed. An average of 140 steps per foot from each surface were analysed.

The Effects of Foot Type: Foot type did not affect P1 and P2 (all $p > 0.056$). PRF in the heel (F1 & F2) was greatest in cavus and smallest in planus feet (all $p < .002$) (Figure 2A), confirming the finding of Morag et al [8]. Midfoot PRF (F3 & F4) was greatest in planus and smallest in cavus feet (all $p < .044$) (Figure 2B). Forefoot PRF (F5 & F6) was greatest in cavus and smallest in planus feet (all $p < .031$) (Figure 2C). No differences in toe PRF (F8 & F9) were observed among foot types.

The Effects of Walking Surface: P1 and P2 were significantly higher during OP and GS than during TM and LW (all $p < 0.01$). PRF was affected by walking surface in all foot regions. Differences were most apparent in the heel (F1 & F2), with all PRFs decreasing from OP to GS to LW to TM (all $p < 0.001$). Midfoot PRF was greater during OP than other surfaces (all $p < 0.024$). Forefoot and toe (F5 to F9) PRFs were lower during TM walking in comparison to other surfaces (all $p < 0.003$).

Interaction Between Foot Type and Walking Surface: Significant interactions were found between foot type and walking surface in foot regions F2, F3, F4 and F7 (all $p < 0.04$).

Significance

Plantar forces measured in a controlled environment appear to underestimate peak forces experienced during outdoor walking. Lab or clinical evaluation may therefore fail to identify some potentially harmful loads on the feet. Foot type significantly affects peak regional plantar force and must be considered during any assessment of regional foot loading. Significant interactions within the midfoot suggest that the mechanical response of the arch varies among foot types and walking surfaces.

Acknowlegement

The Albert B. Ferguson Jr., M.D. Orthopaedic Fund of The Pittsburgh Foundation.

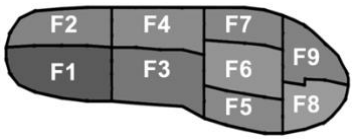

Figure 1: The 9 foot regions.

References

1. Korpelainen et al. (2001) *AJSM*. 2. Kaufman et al. (1999) *AJSM*. 3. Chuckpaiwong et al. (2008) *Gait & Post*. 4. Hillstorm et al. (2013) *Gait & Post*. 5. Hong et al. (2012). *J Sci Med Sport*. 6. Niemhom et al. (2018) *IEEE*. 7. Menz et al. (2012) *JFAS*. 8. Morag et al. (1998) *J. Biomech*.

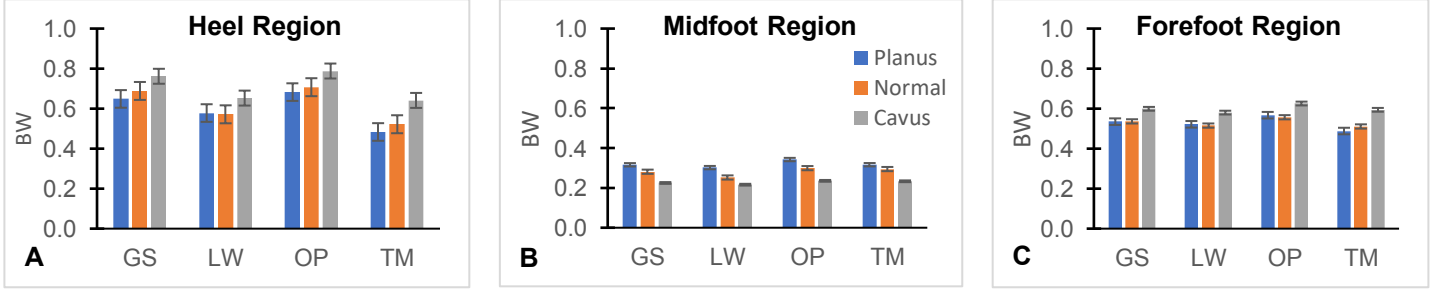

Figure 2: Peak regional force in body weights (BW) in the A) heel area (F1, F2), B) Midfoot (F3, F4) and C) Forefoot (F5, F6, F7) over the four walking surfaces (grass, lab walkway, outdoor pavement, treadmill) for each foot type.

Transient dynamics of energy consumption during walking in cerebral palsy

Nicole L Zaino[1], Andrew J Ries[2], Katherine M Steele[1], and Michael H Schwartz[2,3]
[1]Department of Mechanical Engineering, University of Washington, Seattle, WA, USA
[2]Center for Gait & Motion Analysis, Gillette Children's Specialty Healthcare, St Paul, MN, USA
[3]Department of Orthopedic Surgery, University of Minnesota – Twin Cities, Minneapolis, MN, USA
Email: nzaino@uw.edu

Introduction

The time rate of energy consumption during walking in children with cerebral palsy (CP) averages approximately two times that of their typically developing peers [1]. This elevated demand impacts quality of life, participation, and walking ability [2]. The cause of elevated consumption remains a critical open question, hindering the design of effective clinical treatments. One limitation of current research is the large amount of time required to obtain accurate estimates of consumption. Typically, six minutes of data while walking is collected to obtain a steady-state (SS) measurement. However, this time requirement constrains the number of conditions or treatments that can be examined during an experiment. Future studies would benefit from a method to more rapidly estimate SS consumption.

Previous work in typically developing (TD) adults (n=10) has proposed a method to reduce the time needed to estimate SS consumption [3]. The approach uses the time constant describing the change between resting and the first portion of the transient response when someone starts walking to estimate SS consumption. A time constant of roughly τ = 40 seconds predicted the transient and SS consumption for TD adults and reduced the time required to estimate SS consumption. To our knowledge, the time constant for children with CP has not been studied. Knowing this value could greatly benefit research aimed at understanding elevated consumption in this population. The goal of this research was to determine the time constant for children with CP, and examine its variability with respect to important clinical factors such as age, sex, and functional level.

Methods

We retrospectively identified 815 children with diplegic CP who had previously undergone gait analysis at Gillette Children's Specialty Healthcare (St. Paul, MN, USA) between 2005 and 2020. The testing protocol for each participant consisted of a 10 minute rest period followed by a six-minute over-ground barefoot walking trail at self-selected speed.

Breath-by-breath oxygen consumption was used to determine the time constant (τ) value for each individual according to the model:

$$E(t) = E_{walk} + (E_{rest} - E_{walk})e^{-(1/\tau)\,t}$$

Where E_{walk} is steady-state walking consumption, E_{rest} is steady-state resting consumption, and t is the time from the start of walking (Fig. 1a). We examined the relationship of τ with age, Gross Motor Functional Classification System (GMFCS) level, sex, and SS consumption.

Results and Discussion

The mean time constant for the transient portion of oxygen consumption dynamics in children with CP during walking was 44.0s (SD 16.2) (Fig. 1). These values are similar to TD adults who exhibit a mean time constant of 41.8s (SD 12.1) [3]. This indicates that CP affects SS consumption but not the transient dynamics (time constant). The time constant (τ) for children with CP was not associated with age ($R^2 = 0.008$), SS consumption (E_{walk}, $R^2 = 0.006$), GMFCS levels (GMFCS Level I 46.5(17.0), Level II 43.1(15.4)), or sex (Male 42.5(15.6), Female (46.3(17.0)).

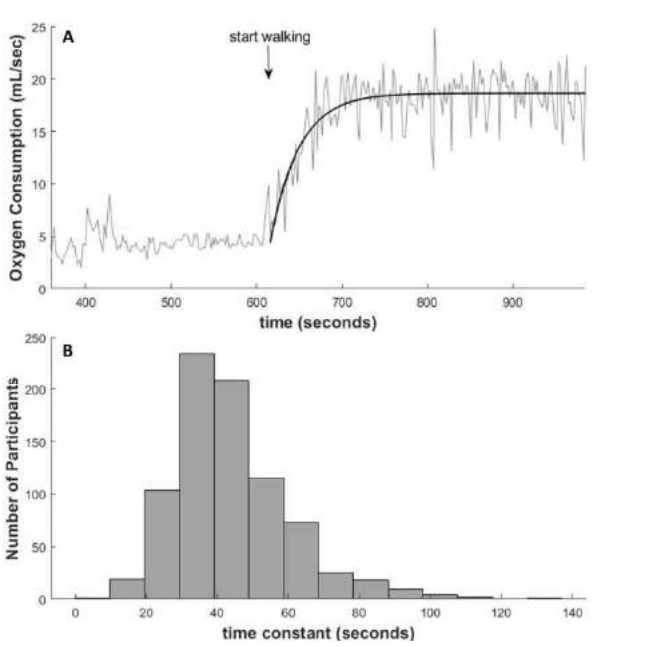

Figure 1: (a) Example of individual breath-by-breath consumption and model prediction during last 3 minutes of resting followed by 6 minutes of walking. (b) Distribution of the time constant across children with CP.

Significance

The time constant and its variability for children with CP was similar to TD adults. The time constant was also found to be independent of age, sex, functional level, or SS consumption. This is the first large scale exploration of the time constant for children with CP. Because the time constant matches TD adults, the results suggest that we can predict SS consumption using less than 6 minutes of walking, as shown by Selinger [3]. By reducing the required testing time for different conditions (e.g. testing various orthoses) we can gain further insight into the underlying causes of elevated consumption and potential treatments to reduce consumption in children with CP.

Acknowledgments

This work was funded by the NIH R01NS091056 and NSF grant CBET-1452646.

References

[1] Norman JF et al. (2004) *Pediatr Phys Ther*, 16: 206-11.
[2] Gross PH et al. (2018) *Dev Med Child Neurol*, 60: 1278-84.
[3] Selinger JC et al. (2014). *J Appl Physiol*, 117: 1406-15.

It's time to start talking about timing of locomotor propulsion

Daniel J. Kuhman[1], Jutaluk Kongsuk[1], Andrew T. Baumann[1], Wei H. Jiang[1], Kathrynne G. Marsh[1], Christopher P. Hurt[1]
[1]University of Alabama at Birmingham, Birmingham, AL, U.S.A.
Email: dkuhman@uab.edu

Introduction

In human walking, the trailing limb generates large forces to propel the body's center of mass upwards and forwards during step-to-step transitions ("locomotor propulsion"). Computational models of bipedal walking suggest that timing of propulsion is crucial for mechanical efficiency [1]. It is possible then that mistimed propulsion contributes to heightened energetic costs in some populations. Propulsion timing also has important implications for designing and controlling powered lower-extremity prosthetic and exoskeletal devices. For example, optimizing actuation timing of a powered ankle exoskeleton could be important for minimizing energetic cost and maximizing user comfort [2]. Gait analyses often quantify magnitudes of propulsion (e.g., peak force or power, mechanical work) but ignore its timing, despite its potential utility for restoring/enhancing walking performance. This abstract describes our current work on propulsion timing – we hope that these data will encourage a broad discussion on this relatively unexplored gait feature at the national meeting.

Methods

This abstract contains data from a series of studies including healthy young (n = 15) and old (n = 8) adults. In both samples, propulsion timing was captured during treadmill walking across a range of speeds. For young adults, we also report propulsion timing across multiple uphill slopes (n = 15) and during split-belt treadmill walking ("SBTW"; n = 8; right belt speed: 0.5ms^{-1}, left belt speed: 1.0ms^{-1} for 2-minutes). Propulsion timing was quantified using two methods: 1) timing of ankle plantarflexor positive power initiation as a percent of the support phase (%), 2) time of contralateral heel strike minus timing of ankle positive power initiation (seconds) [3]. Measuring propulsion timing relative to contralateral heel strike was inspired by the dynamic walking model [1]; positive time values indicate propulsion occurred *prior* to heel strike and negative values indicate it occurred *after* heel strike. Other measures, including timing of aspects related to ground reaction forces and total limb power, were also quantified and would be presented at the meeting (if accepted). We used a 2-way repeated measures ANOVA to compare the effects of age (young, old), walking speed (0.8, 1.2, 1.6ms^{-1}), and their interaction on propulsion timing. We used a repeated measures ANOVA to determine the effects of slope (0°, +5°, +10°) on propulsion timing in young adults. We used a 2-way repeated measures ANOVA to compare the effects of limb (fast, slow), time point (early, mid, late), and their interaction on propulsion timing during SBTW.

Results and Discussion

We found a significant effect of walking speed on both measures of propulsion ($p<0.05$; Fig. 1A & B), but no effect of age. We found a significant effect of treadmill slope on propulsion timing measured as a percent of support (Fig. 1C) and relative to heel strike (both $p<0.001$). Finally, we found a significant effect of limb (fast vs. slow) on propulsion timing ($p<0.001$; Fig. 1D) but no effect of time point during SBTW.

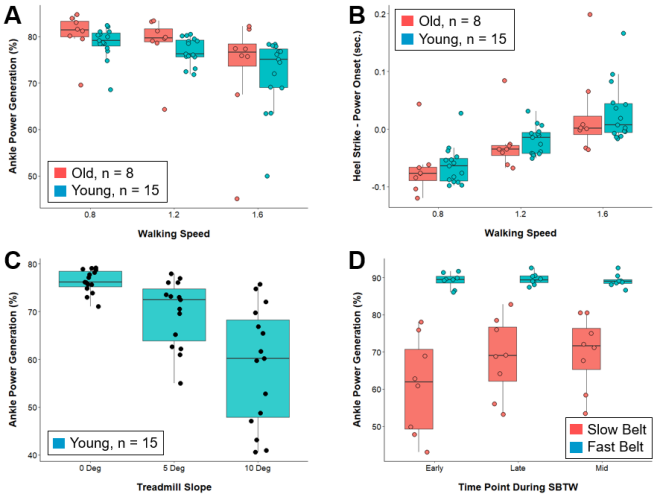

Figure 1: Walking speed had a significant effect on propulsion timing measured as a percentage of support (A) and relative to contralateral heel strike (B) in both young and old adults. As slope increased, propulsion was initiated earlier in support (C). During SBTW, propulsion timing differed between limbs (D).

Significance

Although we found no age-related differences in propulsion timing, more mobility-impaired populations may exhibit mistimed propulsion. If true, interventions seeking to restore walking performance – particularly by lowering energetic cost – may consider targeting proper propulsion timing via gait retraining. We are currently collecting data in individuals with Parkinson's disease walking across a large range of speeds and will include these in the final presentation (if accepted). Altered propulsion timing in response to changes in speed, slope, and SBTW suggest that propulsion timing is an adaptable feature of gait and devices which actively provide or assist propulsion should have the capability of varying actuation timing based on the demands of the locomotor environment. Additionally, between-subject variation in timing appears to change with altered demand, suggesting the need for subject-specific control parameters in these devices. We hope that the data reported here will encourage discussion about propulsion timing at the national meeting, as we believe this gait feature has important implications for a wide range of fields (healthy and impaired gait analysis, rehabilitation, modelling and simulations of locomotion, prosthetics, exoskeletons, robotics, etc.).

References

1. Kuo, *J Biomech Eng* **124(1)**, 113-120, 2002
2. Malcolm et al., *J Neuroeng Rehab* **12(1)**, 2015
3. Kuhman & Hurt, *Hum Mov Sci* **68**, 2019

Interpreting vertical ground reaction force impact spikes using Fourier analysis

Taylor P. Trentadue[1,2,*], Abhinav Goyal[2], and Daniel Schmitt[1]
[1]Duke University Department of Evolutionary Anthropology, Duke University, Durham, NC
[2]Mayo Clinic Medical Scientist Training Program, Mayo Clinic College of Medicine and Science, Mayo Clinic, Rochester, MN
Email: *trentadue.taylor@mayo.edu

Introduction

Human walking gait can be divided into initial contact, weight acceptance, midstance, and toe-off phases. Vertical ground reaction forces (VGRF) include two local maxima separated by a local minimum, sometimes containing impact spikes during weight acceptance. Loading rate is the slope of the VGRF between initial contact and the end of weight acceptance, called the loading response (LR) phase, and it represents time between contact and maximum limb load for that phase.[1] Fourier analysis captures characteristic features and the sinusoidal nature of VGRFs, reflecting loads on the limb and behaviors of the leg spring.[2] The effect of impact spikes, which add a sinusoidal oscillation to the VGRF, has not been systematically evaluated using Fourier analysis.[3,4] Given their influence on lower limb and joint health, impact spike characteristics during LR have strong clinical relevance.[5-7] The goals of this analysis are to (1) determine the effect of leading zeros on modulating VGRF periodicity and (2) detect impact spikes and understand their influence on Fourier analysis.

Methods

From a sample of VGRFs from habitually unshod subjects walking barefoot at self-selected speeds, we selected 10 VGRFs with and 10 without impact spikes. Data were low-pass filtered at 10 Hz with a fourth-order Butterworth filter. We zero-padded steps by appending lagging zeros equal to VGRF length.[2,8] We ran eight-term Fourier analyses with period equal to twice stance phase length on each variation described below.[2] To assess goodness-of-fit between raw VGRFs and Fourier renderings, we computed mean pointwise L^2 distances and compared values with paired t-tests or ANOVAs as appropriate.

To determine how best to capture the very early loading phase, we explored varying levels of leading zero-padding from 0% to 20% VGRF length by 0.5% increments. To characterize the impact spike effect on Fourier reconstruction and facilitate comparison to original curves, we generated two LR component variants for each VGRF: impact LR and complete LR. These, respectively, are a curve with the impact spike component replaced with loading rate from origin to post-impact spike minimum and a curve that replaces LR phase with the loading rate from the origin to the end of weight acceptance (**Figure 1**).

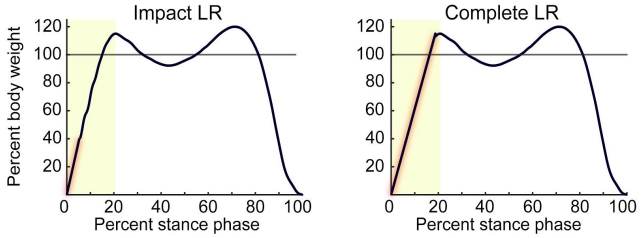

Figure 1: Representative impact spike variants: "Impact LR" in left and "Complete LR" in the right panel. LR phase shaded in yellow. Replaced regions highlighted in red. Grey line is 100% body weight.

Results and Discussion

L^2 distances for leading zero-padding analysis significantly increased from 0.87 (0%) to 1.04 (20%) ($p<10^{-8}$). Thus, we excluded all leading zeros from subsequent analyses. L^2 distances significantly differ among normalized stance subphases, LR variations, and their interaction (2-way ANOVA, $p<10^{-6}$) (**Figure 2; Table 1**). LR of complete LR differs from that of the other two variations ($p<10^{-8}$). Impact loading rates are significantly greater than post-impact loading rates ($p<10^{-6}$). Fourier coefficients a_1, a_3, a_6, a_8, b_2, and b_4 differ between original and impact LR ($p<10^{-2}$).

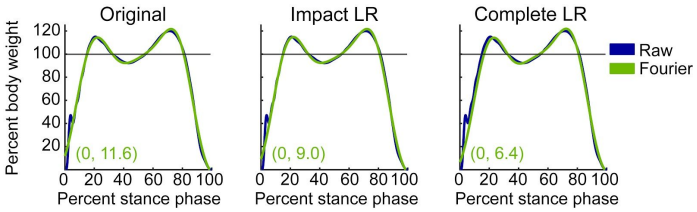

Figure 2: Fourier reconstructions (green) of Original, Impact LR, and Complete LR overlayed on representative raw data (blue). Y-intercepts for Fourier reconstructions labeled. Grey line is 100% body weight.

Table 1: L^2 distances between LR variants and original impact spike VGRFs normalized to stance subphase duration.

	Total	LR	Midstance--toe-off
Original	0.0013	0.0045	0.0016
Post-impact LR	0.0014	0.0049	0.0018
Complete LR	0.0030	0.0111	0.0040

Significance

Impact spikes are associated with acute injury and development of osteoarthritis.[5,6] Our current analysis reveals that representing the LR with a constant loading rate is insufficient and that, within the LR phase, impact spikes have higher loading rates than does the post-impact LR, a pattern that may adversely affect weight-bearing joints.[1,7] We further demonstrate that Fourier coefficients thought to vary with LR frequency[2] differ between LR variants. Standard Fourier analysis effectively models LR in the presence of impact spikes, making it a powerful method able to distinguish clinically-relevant VGRFs without preliminary adjustments to account for variations in LR.

Acknowledgments

Data collection was supported by the Duke University Dean's Research Fellowship (TPT) and Bass Connections Program. TPT is and AG was supported by NIH T32 GM065841.

References

[1]Astephen (2005): Clin Biomech. [2]Trentadue (2017): ASB (abs). [3]Shorten (1992): J Appl Biomech. [4]Castillo (2018): J Exp Biol. [5]Webber (2016): J Exp Biol. [6]Pamukoff (2016): Clin Biomech. [7]Schmitt (2015): Gait & Posture. [8]Lindsten (2010).

Sampling Frequency Influences the Calculation of Temporal, but not Spatial, Regularity of Walking

Farahnaz Fallahtafti[1], Jennifer M. Yentes[1], Shane R. Wurdeman[2]
[1]Department of Biomechanics, University of Nebraska at Omaha
[2]Department of Clinical and Scientific Affairs, Hanger Clinic, Houston Medical Center
Email : *ffallahtafti@unomaha.edu

Introduction

The sampling rate of data acquisition has an effect on time intervals, which are required for recognizing peak points in cyclic data for event detection [1]. The sampling rates derived from the Nyquist theorem may not be appropriate for calculations that are subsequently done in the temporal domain. A low sampling rate will limit the temporal resolution by which gait events may be identified, increasing the chance for aliasing errors in timing of gait events. Low resolution leads to the timing of gait events binning into distinct bins with little variability. Reducing the sampling rate further increases the binning effect, with fewer and fewer bins for the timing of gait events available [2]. The alternative—excessively increasing the sampling rate—will prevent aliasing errors yet increase the capture of high-frequency noise. Decreasing sampling rate is expected to have a greater effect on the temporal gait measures compared to spatial measures, because spatial measures are based on coordinates in space. Coordinates are not limited in resolution based on a moment in time. The purpose of this study was to bring awareness of the effects of sampling rate on mean and regularity of gait variables. Using step time and step length, we examined the averages and sample entropy (i.e. measure of pattern regularity) of data collected from subjects walking on a treadmill.

Methods

Eleven young adults (24.45 ± 2.97 years; 174.15 ±1.52 cm; 74.68 ±12.35 kg), free from any musculoskeletal and neuromuscular disorders, participated in the study. Participants were asked to walk on a treadmill at their comfortable walking speed while lower-extremity kinematic data were recorded at 480 Hz for 10 minutes. Each walking trial was down sampled to 30, 60, 120, and 240 Hz by selecting every sixteenth, eighth, fourth, or second data points, respectively. Right and left step lengths and step times were calculated from the exact same portion of the walking trial (~9 minutes) for all of the sampling rate conditions. A combined time series of right and left SL and ST was calculated for each time series to be used for subsequent analysis. The average and sample entropy (m=2, r=.35*SD, N=756) of SL and ST were then calculated for each time series. Data were inspected for normality. One-way ANOVAs (1x5) were used to compare each gait variable across the five sampling frequencies. Statistical significance was set at alpha=0.05.

Results and Discussion

SL and ST mean were not affected by changing sampling frequencies (Figure 1.a,b). This is credited to linear model statistics that provide us with the central limit theorem, such that 200 steps should provide the average of the population. We did not observe a significant effect of sampling frequency on the sample entropy of SL (Figure 1.c). However, by decreasing the sampling rate and thereby increasing the "binning" effect (Figure. 2), ST was restricted in the spread of values. This led to much less irregularity and a more regular ST as sampling rate decreased ($F(1.463, 14.631) = 21.812$, $p<0.0001$). At 30 Hz and 60 Hz, the ST was significantly more regular compared to all other sampling frequencies ($p<0.01$) (Figure 1.d). When poor temporal resolution and "binning" occurs, the points will likely fall into the tolerance range (r*standard deviation) for sample entropy calculation, and more comparisons will be counted as similar, making a time series appear more periodic.

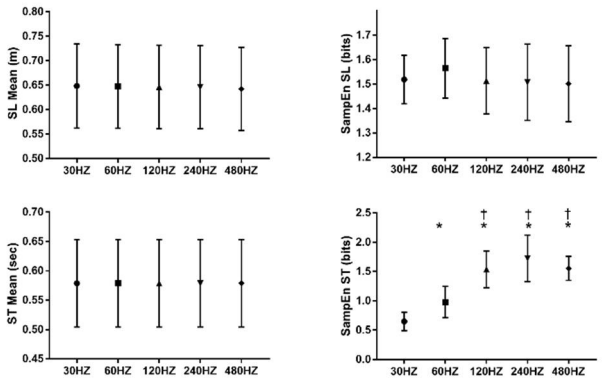

Figure 1. SL and ST mean (a,b) and sample entropy (c,d), † All frequencies significantly differ from 60 Hz, * All frequencies significantly differ from 30 Hz.

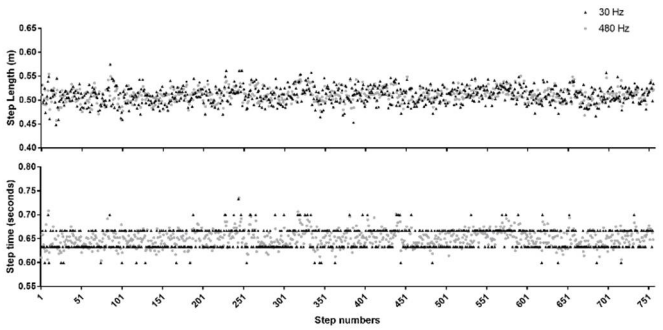

Figure 2. Step lengths (top) and times (bottom) for a single participant

Significance

Sampling rates must be carefully considered when designing studies aimed at understanding regularity of patterns in walking. According to the results of this study it is recommended that gait kinematics should be collected ~ 120 Hz if entropy is to be used. This provides an appropriate compromise between event detection accuracy and processing time.

Acknowledgments

Funding provided by the National Institutes of Health (P20 GM109090), the Department of Veterans Affairs (I21RX003294) to Dr. Yentes. The authors have no conflicts to disclose.

References

1. McCamley et al., Entropy, 20(10), 2018.
2. Marmelat et al., PLoS One, 14(11), 2019.

The Cost and Spring-Like Behavior of Walking: Are Children Scaled Down Versions of Adults?

Vivian L. Rose, CPO and Christopher J Arellano, PhD
Dept of Health and Human Performance, University of Houston, Houston, USA
Email : vlrose@uh.edu

Introduction

Reducing the metabolic cost of walking dysfunction is a main goal of prosthetic and orthotic devices, however, there has been limited success in achieving this goal in children for whom the cost of walking is up to 33% higher than adults, and 2-3 times more for children with a disability [1-2]. Most devices built for children are scaled down versions of adult devices, which is grounded on the assumption that children move in effectively the same way as adults—without accounting for their significant differences in cost. As a first approach in determining the mechanical factors that contribute to a higher cost, we used a simple spring-mass model [3] to compare net cost of transport (COT) and spring adaptation in typically-developing children and in young adults as they walked at their preferred speed, but at varying step frequencies. We tested the idea that when compared to adults, the higher net COT in children can be coupled to differences in how they operate the spring-like behavior of their legs. We hypothesized that when walking at their preferred speed, children would operate their leg at a different spring stiffness than adults. We also hypothesized that when varying step frequencies, children would modulate their spring stiffness in a different manner than young adults.

Methods

Our approach was inspired by a simple bipedal spring-mass model [3], where two independent spring legs attach to the center of mass (COM). The model produces realistic ground reaction force (GRF) patterns at different speeds, which are based on touchdown angle and the leg's spring constant k. The spring constant k can be scaled to a nondimensional $\check{k}$, where $\check{k} = kl_0/mg$. To compare $\check{k}$ empirically, we instructed eight children (5-6 years) and eight adults (18-30 years) to walk on an instrumented treadmill for 5 minutes at 3 step frequencies (75%, 100%, and 125% of preferred) while recording metabolic rate (Parvo Medics) and kinematics (Vicon). We defined a vector from the COM to the center of pressure to represent a 2D spring in the sagittal plane during single support, and then calculated k from the best fit slope of the 2D GRF vs. spring length curve. We used separate repeated measures ANOVAs (α<0.05) to compare net COT, $\check{k}$, and touchdown angle between children and adults.

Results and Discussion

Plots of 2D GRF vs. spring length during single support show typical spring-like behavior. Slopes representing k are within the range of values predicted by the model for adults. However, the spring-like behavior observed in children is less consistent and exhibits more hysteresis (Figure 1). When compared to adults, $\check{k}$ in all conditions was smaller in children (age main effect, p<.001). Our findings support our first hypothesis that children and young adults operate their legs with a different spring stiffness. We also found that children oriented their spring-like legs at higher touch down angles than adults (age main effect, p=.006; step frequency main effect, p<.001). However, when comparing trends across step frequency, children and adults modulated their spring stiffness and touchdown angle in a similar manner (interaction effect, p>0.05), meaning our second hypothesis was rejected. Consistent with previous literature, children walked with a higher net COT across their preferred and non-preferred step frequencies (p=.001).

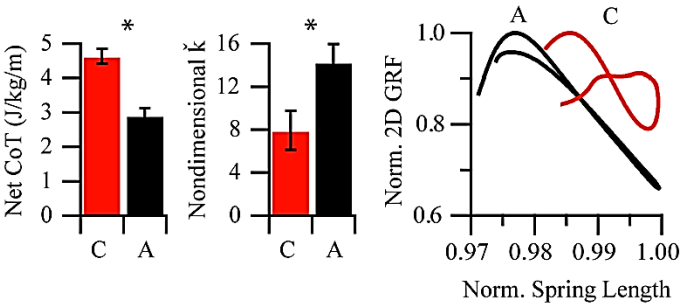

Figure 1. **Left-Middle**. Data show that children walk with a higher net COT (J/kg/m) and a lower $\check{k}$. **Right**. Representative child (C) and adult (A) force-displacement curves normalized to their maximum values. Note that the slope of the curve equals k.

A spring-based model of walking recognizes the importance of storing and releasing energy in the body's elastic elements and has proven useful in scaling for robotic applications and advanced walking simulations of adults [4]. We find a child's leg spring to be more compliant, which seems to be linked to a higher net COT. A spring-based model for walking may prove useful in understanding the biomechanical factors that explain the higher cost in children, and in scaling and tuning prosthetic and orthotic devices to their unique walking mechanics.

Significance

Despite significant differences and changes in physiological and biomechanical development in children, there remains a scientific gap in our effort to model and translate these differences to the design of devices intended to normalize movement in children. Our efforts are aimed at developing a child-specific biomechanical framework that could be used to guide the design and alignment of assistive devices, which would aid physicians, prosthetists, and orthotists in helping children achieve maximum walking function while minimizing cost.

Acknowledgements

The authors would like to acknowledge Anna Larsson, Danny Guevara, and Daisey Vega for assistance with data collection.

References

1. D.DeJaeger et al, "The energy cost of walking in children", Pflug Arch Eur J Phy, 2001.
2. A.J.Ries and M.H.Schwartz, "Low gait efficiency is the primary reason for the increased metabolic demand during gait in children with cerebral palsy", Hum Mov Sci, 2018.
3 H.Geyer et al, "Compliant leg behavior explains the basic dynamics of walking and running", Proc. R. Soc. B, 2006.
4. H.Geyer and H.Herr, "A muscle reflex model that encodes principles of legged mechanics produces human walking dynamics and muscle activities", IEEE Trans Neural Syst Rehabil Eng, 2010

The effects of a 6-week horizontal impeding force training protocol on push-off intensity in older adults

Katie A. Conway[1], Keyaira Crudup[1], and Jason R. Franz[1]
[1]Joint Department of Biomedical Engineering, University of North Carolina Chapel Hill and North Carolina State University
Email: kaconway@unc.edu

Introduction

Walking ability limitations among older adults are extremely prevalent. Diminished push-off intensity, characterized in walking by reductions in peak propulsive ground reaction force (GRF) and ankle joint moment and power generation, is considered an important determinant of slower preferred speeds and thereby age-related mobility loss [1]. Strength gains following conventional intervention (i.e., resistance training) seem to convey benefits during maximum speed walking without improving habitual walking speed or movement biomechanics [2]. One explanation for these disappointing translational outcomes is that resistance training alone is unable to directly encourage access to newfound strength gains. Therefore, there is a vital need for more targeted strategies designed to purposefully enhance push-off intensity during walking. The purpose of this study was to investigate the preliminary efficacy of a 6-week impeding force training paradigm to improve calf muscle strength, walking performance (i.e. preferred and maximum speeds and 6-min walk distance) and push-off intensity (i.e. propulsive GRF and ankle moment and power) in older adults.

Methods

11 healthy but not physically active older adults (age: 76±4 years 6F/5M) participated. Subjects were excluded if they participated in more than 150 minutes of moderate intensity or 75 minutes of vigorous aerobic physical activity per week. Subjects also had no recent neurological or musculoskeletal injuries, and could walk without an assistive device. At baseline ("Pre"), we recorded subjects preferred and maximum safe walking speeds using instrumented 30 m and 2 m walkways, respectively. Subjects then completed a 2 minute walking trial at preferred speed on an intsrumented treadmill (Bertec, OH). We used motion capture (Motion Analysis, CA) and 3D ground reaction force data to estimate ankle joint kinematics and kinetics. Subjects also performed maximum voluntary isometric contractions in a dynamometer (Biodex, NY) at 10° dorsiflexion and a 6 Minute Walk Test (6MWT). After baseline testing, subjects completed 20 minute walking sessions twice per week for 6 weeks. During each session, subjects walked against horizontal impeding forces attached via wastebelt while walking at their preferred speed (**Fig. 1A**). Impeding forces started at 3% bodyweight (BW), and increased by 0.5% BW every 5 minutes based on Rate of Percieved Exertion (RPE, 4-6). After 6 weeks ("Post"), subjects repeated strength, biomechanical, and walking performance testing. In addition, we monitored subjects daily activity levels before and during the 6-week intervention (Fitbit, CA).

Results and Discussion

Subjects completed 100% of their 12 sessions across 6 weeks, and averaged 42 ± 4 days between their Pre and Post sessions. Impeding forces increased from 3% BW to 4.6±1.0% BW on average across the intervention, and subject daily activity (i.e., steps/day) outside of the lab remained relatively constant (p=0.571). Changes that follow characterize the overall effect of the 6-week intervention (i.e., Post vs. Pre). Isometric strength (1.34±0.32 vs. 1.13±0.40 Nm/kg) and maximum walking speed (2.00±0.25 vs. 1.82±0.25 m/s) increased by an average of 18% and 10%, respectively (p-values≤0.002, **Fig. 1B-C**). 6MWT distance also increased by an average of 46±33 m (p=0.001, **Fig. 1D**). Preferred walking speed was generally unaffected (1.30±0.11 vs. 1.25±0.10 m/s, p=0.095), as were habitual propulsive GRF (19.30±2.94 vs. 18.36±2.90 %BW, p=0.148) and stride length (1.37±0.14 m vs. 1.38±0.19 m, p=0.783). However, habitual peak ankle moment (1.35±0.16 vs. 1.23±0.15 Nm/kg, p=0.036) and peak ankle power (3.02±1.00 vs. 2.62±0.69 W/kg, p=0.023) increased by a significant and clinically meaningful 10% and 15%, respectively (**Fig. 1E**).

Significance

The findings of this proof-of-concept intervention study suggest that, following 6 weeks of horizontal impeding force training, older adults exhibit significant strength gains that also translate to improved maximum walking capacity (e.g., maximum speed and 6MWT distance) and habitual walking performance (e.g., greater ankle moment and power output). Moving forward, this paradigm could have broad implications for clinical populations conventionally prescribed strength-based rehabilitation programs (e.g., cerebral palsy, persons following stroke, or older adults).

Acknowledgments

Supported by National Institutes of Health (R01AG051748).

References

[1] Franz JR., *ESSR*, 2016.
[2] Beijersbergen CM. et al., *Gait Posture*, 2017

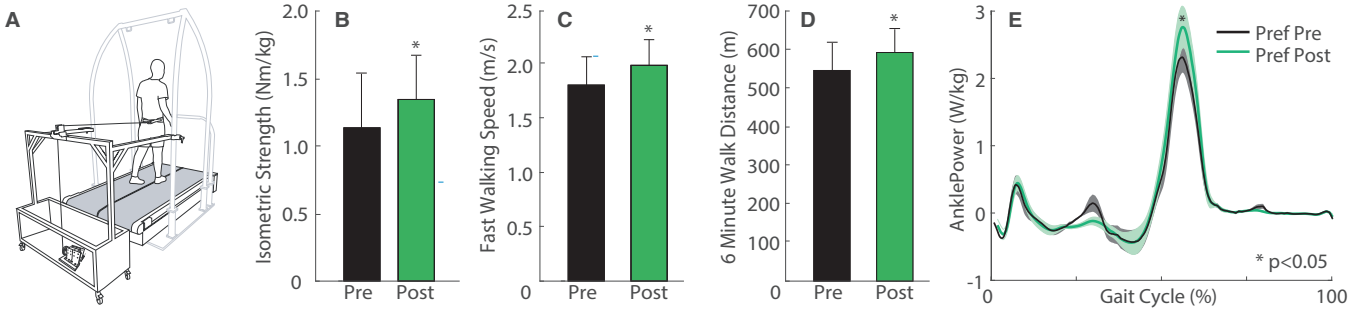

Figure 1 (A) Impeding force system. Mean (SE) values for (B) plantarflexor strength, (C) maximum walking speed, (D) 6 Minute Walk distance, and (E) ankle power for before and after 6 weeks of horizontal impeding force training. Asterisks (*): versus Pre, p<0.05.

Effectiveness of a Gamification Intervention to Limit the Hawthorne Effect in Pediatric Gait Analysis

Mark Geil, Leila Rahnama, Justin Jarrells, Micah Poisal, Erica Sergeant, Kimberly Soulis
Kennesaw State University, Kennesaw, Georgia, USA
Email: mgeil@kennesaw.edu

Introduction

The Hawthorne Effect occurs when individuals alter their behaviour because they are being observed.[1] Anecdotally, the Hawthorne Effect has been observed during gait analysis. Often called "lab gait," individuals walk differently with markers attached and in the presence of camera arrays. Parents often encourage their children to "walk like you do at home" when they observe these atypical gait patterns.

This is problematic in both clinical and research gait analysis, since spontaneous or natural gait provides better knowledge of nervous system function and potential neuromotor abnormalities.[2] Cognitive distraction is sometimes used, but is challenging in many populations. This study tested a low-immersion virtual reality gamification internvention intended to produce more natural gait.

Methods

Typically developing children between the ages of 4 and 12 were recruited to participate in this IRB-approved protocol.

Prior to motion analysis, children were provided a survey of their feelings about the study based on five emotional domains in Walden et al.[3] Next, a standard instrumented 3D motion analysis was conducted with a full-body Vicon Plug-In-Gait marker set during level overground walking at a comfortable self-selected speed. After ten successful trials, we displayed a virtual environment on monitors around the lab using Argonaut software (Idoneus Digital LLC). Children chose an environment (alien planet, city park, castle) and an avatar. The software couples with Vicon marker coordinates to create a real-time 3D animation. Children were free to wander the lab for about ten minutes, seeking objects and exploring the space (Fig. 1). During that time, we collected trials during any straight-line walking in the Vicon system. Next, we turned off the monitors and repeated the initial gait analysis with ten more trials. Finally, we repeated the survey on feelings. Along with survey data, we analysed walking speed, step length, Froude number, arm swing (measured as peak difference in hand bilateral marker coordinates along the axis of progression), and Gait Deviation Index (GDI).

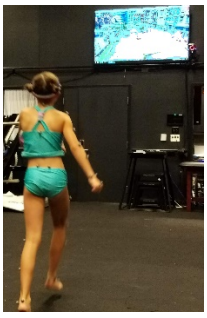

Figure 1: Subject moving through vrtual environment and avatar displayed on monitors around laboratory walls.

Results and Discussion

32 children participated in the study. Although the participants were typically developing children with no orthopaedic or neurological conditions, 81% expressed either diminished feelings of happiness or excitement, or increased feelings of fear in anticipation of the analysis. After the intervention, these feelings improved for 88% of those children. Across all subjects, there were significant improvements in feelings of happiness ($p=0.001$), excitement ($p=0.033$), fear ($p=0.011$), and sadness ($p=0.026$) following the intervention.

As expected, several outcome measures were significantly correlated. As walking speed increased, so did step length and arm swing. Changes were highly variable, which is not surprising, given that the study design could only measure change and could not identify a gait pattern that was more or less "natural." Speed results (Fig. 2) are an example of the variability. While the majority of subjects increased speed post-intervention, this does not necessarily indicate more natural gait.

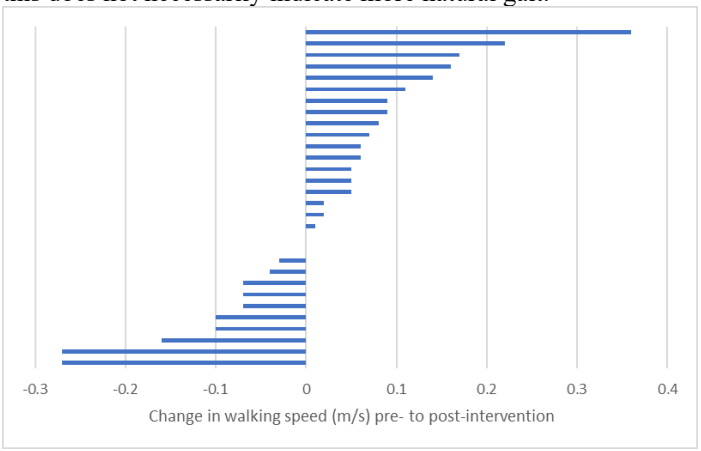

Figure 2: Change in walking speed post-intervention

There was one significant link between changed feelings and changed gait outcomes. Point biserial correlation analysis showed a significant mild correlation between increases in excitement pre- and post-intervention and changes in GDI ($p=0.037$).

Some individual cases do illustrate the potential changes in gait. Subject 25, who changed from "not at all happy" to "totally happy" and from "totally scared" to "not at all scared" post-intervention, showed a 5% increase in GDI and a 36% increase in arm swing.

In summary, the gamification intervention resulted in improved feelings about gait analysis and changed gait patterns. The latter should not be construed as more natural gait, but alterations in gait coupled with improved feelings could imply that conclusion.

Significance

Similar to "White Coat Syndrome," children are often nervous in a laboratory setting, which can lead to altered gait. For example, children with Idiopathic Toe Walking, who walk with initial toe contact most of the time at home, often adopt a heelstrike pattern in the lab, making it difficult to determine the severity of their condition. A simple intervention that reduces anxiety, and leverages the laboratory setting to promote, and not inhibit, natural gait could be helpful in both clinical and research settings.

Acknowledgments

Participant support costs were covered by a small grant from Idoneus Digital. The company had no influence on the study.

References

[1]Fernald et al. *J Am Board Fam Med.* 2012:25(1),83-6.
[2]Sanders et al. *Psychiatry.* 2010:7(7),38-43.
[3]Walden et a. *Psych Assessment.* 2003:15(3),399-4.

Muscle Metabolic Energy Costs While Modifying Propulsive Force Generation During Walking

Richard E. Pimentel, Noah L. Pieper, William H. Clark, and Jason R. Franz
Joint Dept. of Biomedical Engineering, UNC Chapel Hill and NC State University, Chapel Hill, NC
Email: rickypim@live.unc.edu

Introduction

Aging and many gait pathologies are associated with an increased metabolic cost of walking, which negatively affects independence and quality of life. At least in older adults, some theories for this increased metabolic cost, such as maintaining lateral stability or higher total mechanical limb work, have been refuted [1]. Other theories, such as increased antagonist coactivation, leave roughly two-thirds of this increased metabolic cost unexplained [2]. Biomechanically, higher metabolic costs are often accompanied by smaller peak propulsive forces (F_P) generated during push-off and a redistribution of workload from muscles spanning the ankle to those spanning the hip [3]. These are precisely the joint-level responses young adults use when responding to a real-time biofeedback paradigm designed to prescribe changes in F_P during the push-off phase of walking [4]. Indeed, our group has shown that young adults walking with decreased F_P do so by redistributing muscle workload from ankle to the hip without changing total positive mechanical work, mimicking the biomechanics of elderly and pathological gait [4]. It is not feasible to directly measure the metabolic cost of operating individual muscles during walking. Thus, our purpose was to use musculoskeletal modeling simulations to estimate how changes in F_P and changes in the relative utilization of ankle versus hip muscles for power generation in walking influence muscle metabolic cost during walking. We hypothesized that the metabolic costs of operating proximal and distal leg muscles would exhibit different responses to targeting smaller and larger F_P underlying changes in measured whole-body metabolic cost.

Methods

12 young subjects (age: 23.3±3.1 years; 7 female) walked at their preferred speed on a force-sensing, dual-belt treadmill for 5 minutes. Data from the final 2 minutes was analyzed to determine subjects' habitual F_P. At this same speed, participants then completed five 5-min walking trials using F_P biofeedback, where they pushed off the ground with varying vigor to target their typical walking F_P (Norm) and ±20%, and ±40% of Norm in randomized order. We collected bilateral lower body kinematics, ground reaction forces, and expired gases over the final 2 minutes for each condition. For modelling, we analyzed the first left and right strides from a 10-second window with the most accurate biofeedback performance within each condition. In OpenSim, marker trajectories and ground reaction forces drove a scaled musculoskeletal model (gait2392). After residual reductions, we performed computed muscle control and included muscle metabolic probes in our modelling pipeline [5]. Muscle metabolic costs were averaged bilaterally, mass normalized, integrated over gait cycle periods of interest, and summed for muscles spanning the hip and ankle. Repeated measures ANOVA tested for main effects of condition on metabolic cost and LSD post-hoc tests identified pairwise differences versus Norm (α=0.05).

Results and Discussion

Measured whole-body net metabolic power increased by up to 47% and 58%, respectively, when targeting +40% and -40% vs. Norm F_P ($p<0.001$). Simulated whole-body metabolic cost positively correlated with empirical measurements ($r^2=0.336$, $p<0.001$) and individual muscle outcomes supported our hypotheses (Fig. 1). When walking with smaller than usual F_P, stance phase metabolic cost increased for muscles spanning the hip ($p\leq0.017$) and decreased for muscles spanning the ankle ($p<0.001$). Conversely, when walking with larger than usual F_P, stance phase metabolic cost most consistently increased for muscles spanning the ankle ($p\leq0.042$).

Significance

Our experimental manipulations and computational simulations suggest that an increased reliance on muscles spanning the hip, particularly the hip extensors during early stance, may independently increase metabolic cost in walking. This outcome is important for those that routinely exhibit a proximal redistribution of muscle workload (e.g., older adults).

Acknowledgments

This study was supported by a grant from NIH (R01AG058615).

References

1. Ortega, J. D. & Farley, C. T. *J. Appl. Physiol.* **102**, (2007).
2. Hortobágyi, T., et. al. *Journals Gerontol. - Ser. A Biol. Sci. Med. Sci.* **66 A**, (2011).
3. DeVita, P. & Hortobagyi, T. *J. Appl. Physiol.* **88**, (2000).
4. Browne, M. G. & Franz, J. R. *J. Biomech.* **55**, (2017).
5. Umberger, B. R. *J. R. Soc. Interface* **7**, (2010).

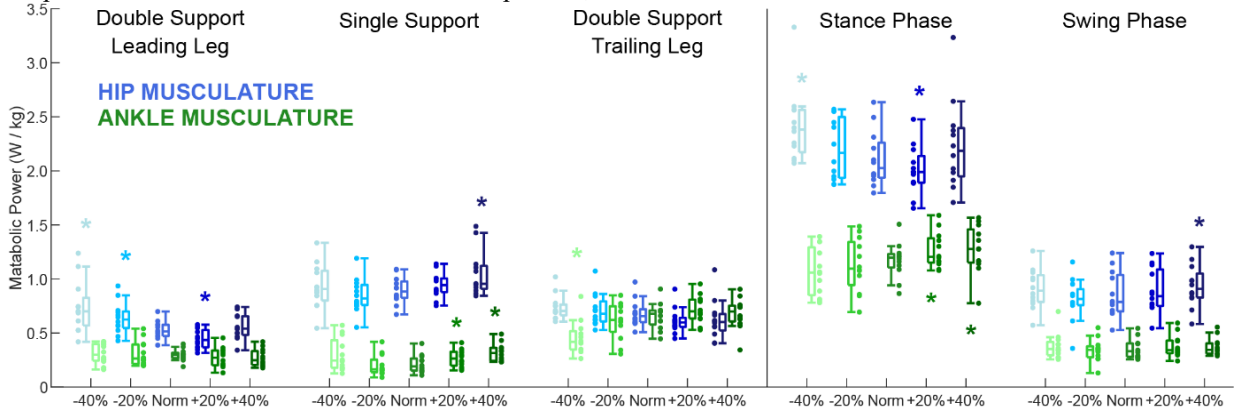

Figure 1. Cumulative metabolic power of muscles spanning the hip (blue) and ankle (green) during normal walking (Norm) and while targeting ±20% and ±40% changes in F_P using real-time biofeedback. Asterisks (*) indicate a significant difference versus normal walking ($p<0.05$).

The relationship between pelvic-hip musculature and functional ambulation in patients with Myelomeningocele

Tasos Karakostas, MPT, PhD[1,2]*; Suruchi Batra[1,3]; Simon Hsiang, PhD[4];
Adriana Ferraz, MD[1]; Vineeta Swaroop, MD[1,2]; Luciano Dias, MD[1,2]
[1]Shirley Ryan AbilityLab, Chicago, IL; [2]Feinberg School of Medicine, Chicago, IL; [3]Northwestern University, Evanston, IL;
[4]University of North Carolina, Charlotte, NC
Email: *tkarakosta@sralab.org

Introduction

Myelomeningocele (MM) is a neuromuscular disorder resulting in muscle paralysis and/or weakness. However, clinical observations suggest that some patients with low lumbar MM (MM2) are independent ambulators (IAs) with the use of orthotics, while others are non-independent ambulators (NIAs) requiring the use of assistive devices (walkers or crutches). To the best of our knowledge, currently, the information explaining the underlying cause of this variability is limited. Thus, the purpose of our study is to investigate how the ambulatory status of MM2 may be related to individual muscle groups and their associated strength.

Methods

This is a retrospective study involving 48 patients, MM2, who underwent 3D gait analysis (3DGA), including a determination of their ambulatory status and a physical exam to assess their lower extremities joint range of motion and muscle strength (manual muscle test [MMT]). Patients were included if they were diagnosed with MM2 and could be classified as IAs or NIAs. Patients were excluded if they had a history of surgery or injury within one year prior to the evaluation.

Based on the grade given from the 5-point clinical MMT scale, muscle strength was converted to a continuous scale from 1 to 24 to allow for statistical analysis (i.e. an MMT score of 3 is a 14 on our continuous scale). Kinematic variables were determined from the 3DGA. Data collected was analyzed using an ANOVA, with $\alpha \leq 0.05$.

Results and Discussion

The purpose of this study was to investigate the relationship between ambulatory status of patients with lower lumbar MM who are IAs or NIAs and their respective muscle strength.

Table 1: Statistical output comparing the muscle strength between patients who ambulate independently and those who do not. Muscles tested: adductors (Add); quadriceps (Quad); iliopsoas (Ilio); sartorius (Sar); gluteus maximus (Glut Max); gluteus medius (Glut Med); hamstrings (Ham). Time-distance characteristics observed: velocity (Vel); cadence (Cad); stride length (Stride Length).

Parameter	Add	Quad	Ilio	Sar	Glut Max
IA Average ± std. dev.	17.83 ± 4.85	21.13 ± 3.20	20.41 ± 3.56	18.6 ± 3.61	11.0 ± 4.22
NIA Average ± std. dev.	17.67 ± 3.98	20.50 ± 3.20	14.81 ± 3.24	14.44 ± 2.40	5.62 ± 2.25
p-value	0.9097	0.5518	*2.6E-05*	*0.0007*	*1.3E-06*

Parameter	Glut Med	Ham	Vel	Cad	Stride Length
IA Average ± std. dev.	8.11 ± 3.60	17.09 ± 2.61	0.798 ± 0.03	0.944 ± 0.02	0.852 ± 0.03
NIA Average ± std. dev.	6.46 ± 2.79	14.21 ± 1.86	0.643 ± 0.03	0.761 ± 0.17	0.833 ± 0.02
p-value	0.1046	*0.0002*	*0.0243*	*0.0049*	0.7504

Table 2: Comparison of the kinematics of pelvic rotation and pelvic obliquity between IAs and NIAs.

Parameter	Pelvic Protraction	Pelvic Retraction	Pelvic Obliquity Upward	Pelvic Obliquity Downward
IA Average ± std. dev.	18.26 ± 7.41	-16.70 ± 8.24	6.74 ± 3.49	-2.88 ± 4.11
NIA Average ± std. dev.	13.74 ± 5.54	-12.54 ± 6.51	8.44 ± 4.42	-6.56 ± 4.90
p-value	*0.0229*	0.0652	0.1997	*0.0178*

Of the muscle groups investigated, the iliopsoas, sartorius, gluteus maximus, and hamstrings were stronger in IAs (Table 1). Additionally, IAs demonstrated higher velocity and cadence (Table 1). Of the kinematic variables assessed, pelvic protraction was greater for IAs, while downward pelvic obliquity was greater for the NIAs (Table 2).

The stronger hip flexors and extensors seen in the IAs group can provide greater hip stability which can facilitate independent ambulation. Furthermore, the greater velocity of the IAs, which, however, appears to be a function of increased cadence, may be further reflective of the improved ability of the IAs to control their gait compared to the NIAs. The greater excursion range for pelvic rotation in the IAs group may reflect that they achieve their stride length, partly, from pelvic rotation. The assisting devices, on the other hand, may be the limiting factor for the decreased pelvic rotation seen in the NIAs group. The decreased pelvic obliquity in the cohort of IAs may suggest that they have greater pelvic control while ambulating. One limiting factor of this investigation may be the discrepancy in sample sizes between the groups (35 IAs versus 15 NIAs). It is possible, therefore, that there may be some outliers influencing the results.

Significance

Currently, to the best of our knowledge, there does not exist any comprehensive motion analysis studies relating the ambulatory status of patients with MM2 to their muscle strength. If this information were known, then more targeted non-invasive thrapeutic interventions could be identified so that NIAs can progress to IAs, a goal of any rehabilitation program..

Acknowledgments

Andrew Moseley-Gholl and Shannon Villegas have been instrumental to this study for the data extraction from patient records.

The study resulting in this presentation was assisted by two grants from the Undergraduate Research Grant Program which is administered by Northwestern University's Office of Undergraduate Research. However, the conclusions, opinions, and other statements in this presentation are the author's and not necessarily those of the sponsoring institution.

Step width and frequency to modulate: Active foot placement control ensures stable gait

A.M. van Leeuwen[1,2], J.H. van Dieën[1], A. Daffertshofer[1,2], S.M. Bruijn[1,2,3]
[1]Department of Human Movement Sciences, Faculty of Behavioural and Movement Sciences, Vrije Universiteit Amsterdam, Amsterdam Movement Sciences, Amsterdam, The Netherlands
[2]Institute of Brain and Behavior Amsterdam
[3]Biomechanics Laboratory, Fujian Medical University, Quanzhou, Fujian, PR China
Email: a.m.van.leeuwen@vu.nl

Introduction

Most of us place our feet, such that we walk without falling over. What we do not fully understand, is how we achieve the required coordination between our center of mass (CoM) and our base of support (BoS). Step-by-step foot placement coordination, relative to the CoM kinematic state, is considered a dominant mechanism aimed at gait stability [1]. Foot placement can be predicted based on CoM state [2]. Such correlation could emerge from the passive dynamics of our body [3]. Yet, recent evidence points towards active control of foot placement [4-6]. CoM kinematic state predicted hip ab-/adductor activity during the swing phase preceding foot placement [4]. In turn, this activity predicted foot placement [4]. Additionally, sensory perturbations elicited predictable foot placement responses [2, 5, 6]. In this study, we identified an actively controlled step-by-step foot placement strategy during steady state walking. It is known that in response to perturbations, this foot placement strategy is complemented by a mediolateral ankle strategy [7]. Similarly, during steady state walking an inverse relationship between the two strategies has been reported [8]. Therefore, we hypothesized that, when constraining the ankle strategy, the degree of foot placement control would increase as a compensation.

Methods

We investigated (active) foot placement control during steady state treadmill walking. We used linear regression models to predict foot placement either by CoM state or muscle activity during the preceding swing phase. We tested the regression coeffients against zero to determine whether the models were significant. We considered the R^2 of the relation between CoM state and foot placement to reflect the degree of foot placement control. We intended to recruit participants until a Bayes Factor indicating strong evidence (BF_{10}> 10) was attained. However, we did not reach this level of evidence for all our outcome measures, leaving us with our predetermined maximum sample size of 30 healthy adults. The participants walked at normal walking speed (1.25 * sqrt(leg length) m/s). A metronome was used to impose a constant stride frequency across conditions. In the steady state walking condition, participants walked for five minutes without any constraints. In the ankle moment constrained condition, participants walked with LesSchuh. This shoe has a narrow support surface, restricting the center of pressure (CoP) shift underneath the stance foot (like a skate), while still allowing for plantar flexion. EMG of the M. gluteus medius and M. adductor longus, ground reaction forces and full body kinematics were recorded. Gait events were derived from CoP data.

Results and Discussion

CoM state and hip ab-/adductor activity significantly predicted foot placement. As such, we identified an active step-by-step control strategy during steady state walking.The degree of foot placement control (R^2) did not increase when the ankle moments were constrained. However, exploratory analysis revealed increased step width (figure 1), and decreased stride time as a general compensatory strategy. Perhaps, with longer exposure to the ankle moment constraint, one can adopt tighter foot placement control and reduce step width. This is in line with repeated exposure to foot placement perturbations [9], and could potentially reduce energy cost [10].

Significance

If training effects occur, LesSchuh could be considered a training tool to enhance the foot placement strategy and mediolateral gait stability. Apart from the foot placement strategy, other (compensatory) strategies, such as the hip strategy might play a role in stabilising gait. Insights in the complementary nature of different gait stability strategies, can help to understand and/or intervene in gait stability in elderly, pathological or prosthetic gait, and may contribute to the control of walking exoskeletons. In a fundamental context, our study contributes to our understanding of neural control of mediolateral gait stability.

Figure 1: Wider steps compensate for limited ankle moments

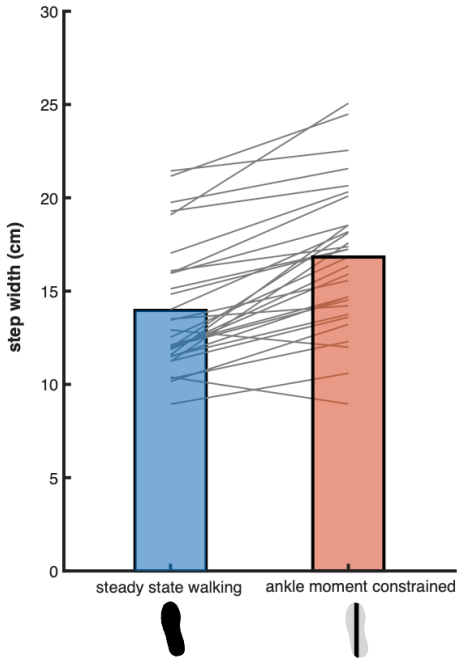

References

1.Bruijn, S.M. and J.H. van Dieën. Journal of The Royal Society Interface, 2018.
2.Wang, Y. and M. Srinivasan. Biology letters, 2014.
3.Patil, N.S., J.B. Dingwell, and J.P. Cusumano, Journal of biomechanics, 2019.
4.Rankin, B.L., S.K. Buffo, and J.C. Dean. Journal of neurophysiology, 2014.
5.Reimann, H., et al. Frontiers in Physiology, 2018.
6.Arvin, M. et al. Frontiers in physiology, 2018.
7. Hof, A. and J. Duysens. Human movement science, 2018.
8.Fettrow, T., et al. bioRxiv, 2019.
9.Reimold, N.K., et al. bioRxiv, 2019.
10.Donelan, J.M., et al. Journal of biomechanics, 2004.

Accuracy of Machine Learning to Determine Gait Events from Electromyography Signals

Natalie L. Egginton.[1], Laura-Anne M. Furlong[1], Baihua Li[2], Paul W. Sanderson[1] and Matthew T.G. Pain[1]
[1] School of Sport, Exercise, and Health Sciences, Loughborough University, UK
[2] School of Computer Science, Loughborough University, UK
Email: n.l.egginton@lboro.ac.uk

Introduction

Determining the swing and stance phase of gait permits calculation of temporal parameters used to evaluate and define rehabilitation goals in clinical populations. Wearable wireless electromyography (EMG) sensors provide information regarding muscle activations during gait but their feasibility to accurately determine temporal aspects of gait is not yet established. This study aims to use machine learning to determine the optimal muscles and features to accurately classify gait phase from EMG during gait.

Methods

Ground reaction force (2000 Hz), marker motion (whole body marker set, 250 Hz) and EMG (2000 Hz) data were recorded during 20 minutes of overground walking at an individual's preferred speed (1.51 ± 0.18 $m \cdot s^{-1}$) from 14 healthy active males (25.5 ± 2.8 years, 82.5 ± 8.6 kg, 1.81 ± 0.07 m). EMG was recorded from tibialis anterior (TA), soleus (SOL), gastrocnemius lateralis (GL) and medialis (GM), rectus femoris (RF), vastus lateralis (VL), semitendinosus (ST), biceps femoris long (BFLH) and short head (BFSH), gluteus maximus (GMAX) and medius (GMED) and erector spinae longissimus (ES); locations were determined with ultrasound.

Ground contact was determined as 6 standard deviations (SD) above baseline mean from force data. EMG signals were trimmed from toe-off (TO) prior to force plate heel strike (HS) to 250 ms post force plate TO. EMG signals from 689 trials were standardised to zero mean and unit standard deviation. Signals were split into 256 ms windows with a 10 ms increment. Fifteen features were extracted within each window; mean absolute value (MAV), mean absolute value slope (MAVS), zero crossings (ZC), slope sign changes (SSC), waveform length (WL), root mean square, variance and 8 histogram bins (equal length bins with a 3 SD threshold). Features were normalised from zero to one within trials. 75% of trials were randomly selected for training data, leaving 25% for test data.

Support Vector Machine Learning (Matlab) with a radial basis function was trained to classify gait phase from the stance limb EMG features. All possible combinations of muscles and features were investigated using a 7 fold cross-validation (CV) of the training data. Algorithm parameters were optimised using the DIRECT method [1] until classification error decreased by less than 0.5% in three iterations. Mean absolute difference between test data HS, TO and ground contact time (GCT) from EMG machine learning and kinematic algorithms (TO, velocity based [2], HS [3]) was calculated using the force plate as the ground truth.

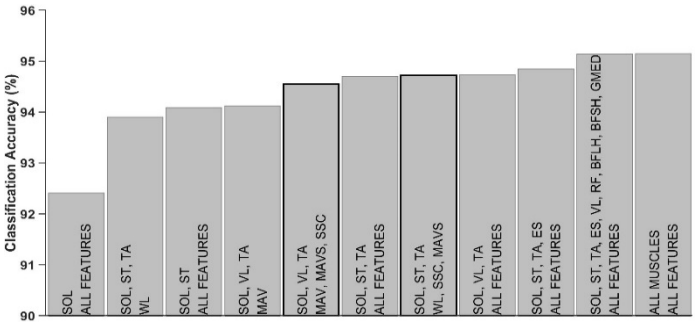

Figure 1: Classification accuracy (%) for optimal muscle and feature combinations. Black outline: combination used with test data.

Results and Discussion

The optimal two muscles with all features were SOL and ST (94.09%). SOL is a better predictor than the gastrocnemii probably due to their biarticular action as knee flexors. Addition of a third muscle improved accuracy by 0.6%. The optimal three muscles with all features were SOL, VL and TA (C_1, 94.73%) or SOL, ST and TA (C_2, 94.70%), with an accuracy less than 0.5% lower than all muscles with all features. Addition of a fourth muscle only improved accuracy by 0.15% (Figure 1).

The optimal features for C_1 (MAV, 94.12%) and C_2 (WL, 93.90%) were similar to Meng *et al.*[4]. Addition of MAVS and SSC to the optimal feature (features used hereafter) for C_1 and C_2 resulted in an accuracy of 94.68% and 94.72%, respectively.

Classification accuracy of C_1 and C_2 when evaluated on the test data was 97.39% and 97.58%, respectively. On average C_1 and C_2 predicted HS and TO time later than the force plate. Machine learning predicted HS and GCT with less mean absolute error than the kinematic algorithms (Table 1). C_2 GCT error was less than half that of the kinematic algorithm.

Significance

Machine learning can accurately predict gait phase and temporal parameters from EMG, permitting assessment of muscle activation without additional gait phase measures.

Acknowledgments

Funded by Engineering and Physical Sciences Research Council.

References

[1] Finkel, D.E. (2003) DIRECT Optimization Algorithm User Guide.
[2] Zeni, J.A. *et al.* (2008) Gait & Posture 27(4): 710 – 714.
[3] De Asha, A.R. *et al.* (2012) Gait & Posture 36(3): 650 – 652.
[4] Meng, M. *et al.* (2010) IEEE ICIA: 852 – 856.

Table 1: Mean absolute difference in heel strike, toe off and ground contact time calculated from electromyography machine learning and kinematic algorithms compared to the force plate (ground truth). C_1: SOL, VL, TA. C_2: SOL, ST, TA. Mean ± SD.

	EMG vs Force plate		Kinematic algorithm vs Force plate
	C_1	C_2	
Heel strike	20.2 ± 42 ms	20.2 ± 42 ms	28.1 ± 40 ms
Toe off	18.0 ± 40 ms	17.6 ± 40 ms	17.4 ± 59 ms
Ground contact time	23.0 ± 17 ms	18.0 ± 15 ms	37.9 ± 46 ms

LSTM Deep Learning and IMU Based Irregular Surface Gait Alteration Recognition

Song Li[1], Boyi Hu[1*]
[1]Department of Industrial and Systems Engineering, University of Florida, Gainesville, FL, USA
Email: *boyihu@ise.ufl.edu

Introduction

Falling injuries pose serious health risks to people of all ages, and knowing the extent of exposure to irregular surfaces will increase the ability to measure fall risk and human biomechanics response during locomotion (Florence et al., 2018). Current gait analysis methods require complex instrumentation and have not tested for external factors such as walking surface type in real-world settings. Artificial intelligence approaches (in particular deep learning networks) to analyze data collected from wearable sensors can be used to automatically identify irregular surface exposure. Among all deep learning models, long short term memory (LSTM) models can not only process single data inputs (e.g. images), but also entire time series of data (e.g. speech) (Hochreiter and Schmidhuber, 1997) which is well suited for human gait alteration recognition using time series data collected from wearable sensors.

Methods

Thirty young adults participated as volunteers in this study. All participants performed 36 walking trials (6 different surfaces with 6 repetitions). Six commonly observed irregular surfaces were included: 1) an even flat surface (FlatEven) , 2) cobblestone pavement (CobbleStone), 3) going up a slope (SlopeUp), 4) going down a slope (SlopeDown), 5) ascending stairs (Upstair), and 6) descending stairs (Downstair). Every participant wear six IMU sensors set on their 1) right wrist, 2) midline of the lower-back, 3-4) left and right thigh, and 5-6) left and right shank.

LSTM network (a kind of special Recurrent Neural Network (RNN) was constructed in TensorFlow. Specifically, in the current study the model first starts with the input data layer. Then add one layer of LSTM unit with 80 filters, we used Relu as activation function in the current study. We inputted the whole reshaped data and returned a sequence of data by the LSTM Unit, followed by another same LSTM layer. Dropout 50% of the neural network unit from the model was then applied. Subsequently, we added another two LSTM layers and a dropout layer but with 100 filters. The model ended with an output layer. We split 80% of the data as training data and save 20% as test data to minimize overfitting.

The performance of the model was evaluated by the result of testing data. The following metrics were used for comparison: 1) overall prediction accuracy, 2) precision, 3) recall, 4) F1-score (harmonic mean of 2) and 3)) (LeCun et al., 2015). A confusion matrix was also created.

Results and Discussion

The accuracy of the model was 0.90. The static standing position had the best performance, with a 0.99 prediction accuracy. The Model also had a great prediction on the upstairs and slope up surface, with accuracy above 0.95. Bank left and Bank right had the worst performance among all, with only 0.76 and 0.75 accuracy. We also repeated the test on the same model to provide a statistically stable result. The results from the repetitions demonstrated accuracy levels varying from 0.84 to 0.91.

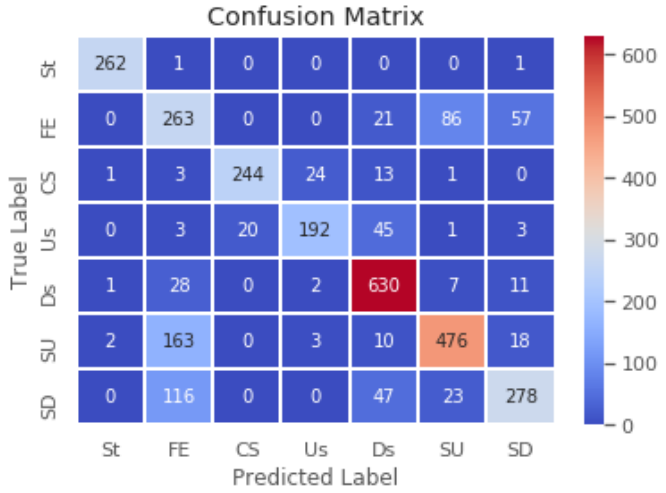

Figure 1: Confusion matrix. St:Standing, FE: FlatEven, CS: Cobble Stone, Us: Upstair, Ds: Downstair, SU: Slope Up, SD: Slope Down.

Significance

In this study we developed deep learning LSTM models to classify human gait patterns when walking on different irregular surfaces using data collected from wearable sensors with satisfactory performance.

The results indicate the strong potential of using LSTM and wearable sensors to track human gait and prevent falling injuries in real-world settings. Furthermore, this method can also be used in numerous biomechanics related settings, such as tele-rehabilitation and physical motion analysis.

Acknowledgments

This investigation was made possible by Grant No. T42 OH008416 from NIOSH.

References

LeCun et al. (2015). Deep learning. nature, 521(7553), 436-444.

Hochreiter, S., & Schmidhuber, J. (1997). Long short-term memory. Neural computation, 9(8), 1735-1780.

Florence, et al. (2018). Medical costs of fatal and nonfatal falls in older adults. Journal of the American Geriatrics Society, 66(4), 693-698.

Do Switched Linear Dynamical Systems Provide Robust Kinematic Predictions of Healthy Treadmill Gait at Different Speeds?

Taniel Winner[1], Trisha Kesar[2], Lena Ting[1,2]
[1]W.H. Coulter Dept. Biomedical Engineering, Emory University and Georgia Institute of Technology, Atlanta, GA, USA
[2]Department of Rehabilitation Medicine, Division of Physical Therapy, Emory University, Atlanta, GA, USA
Email: twinner3@gatech.edu

Introduction

Generalizable models that can characterize each patient's kinematics can provide a more objective gait measure than current subjective clinical ratings used to diagnose and treat gait dysfunction. Machine learning methods can classify different gait patterns, demonstrating that these algorithms can distinguish between different dynamics. Recently, data-driven SLDS models have been used to predict transitions between single and double support gait phases [1]. SLDS models can also predict joint kinematics over relatively long time horizons. However, we do not know whether these models generalize across different walking speeds. Here we tested the ability of SLDS models trained on an individual's kinematic data at a single speed to effectively reconstruct kinematic data of a different gait speed. We show that SLDS representations trained at one speed can identify gait phase from data obtained at a different gait speed. However, prediction of future kinematics over timescales of up to 1 second, require individual- and speed- specific models.

Methods

Two healthy individuals (1 male -28 years, 1 female -28 years) were enrolled in this pilot study. Participants walked on a treadmill at a comfortable self-selected speed and at a fast speed. Kinematic data was collected at 100 Hz using a 7-camera Vicon system and force data was collected at 2000 Hz using an instrumented dual-belt treadmill. We used SLDS to model the bilateral lower limb joint angle trajectories during gait. An SLDS is a set of linear dynamical systems with discrete modes that govern when to switch between the individual linear models using Hidden Markovian model approach. Specifically, we used an autoregressive SLDS, which can be written as in (1).

$$x_{k+1} = A_{z_k} x_k + w_k(z_k) \quad (1)$$

Where $z_k \in \{1, \dots, N\}$ is the discrete mode, x_k is the state vector at time step k, A_{z_k} is the linear system parameters and $w_z(z_k)$ is a zero-mean, Gaussian noise term [2]. We trained an SLDS with four discrete modes on 9 trials of each participant's gait data at one speed and tested the model's ability to predict gait phases and kinematics at different speeds.

Results and Discussion

Despite the ability of SLDS to predict gait phase with high accuracy (>92%) at different speeds, kinematic predictions do not appear to generalize for a different gait speed of the same individual. Fig. 1 shows that it does not have accurate kinematic prediction of a gait speed different to the one it was trained on. Training and testing SLDS models (n=6) on different trials (on subject A) of the same gait speed of 0.9 m/s resulted in an average phase prediction accuracy (aPPA) of 92.8% ± 0.7% and average root mean square error (aRMSE) over all joint angle reconstructions of 3.3˚ ± 0.6˚ (range: 1.2 ˚ - 8.0 ˚). When testing these models on 1.3 m/s speed data trials (n = 9) of subject A, the aPPA decreased by 0.17% and aRMSE increased by 166.9% (range: 4.4˚ – 17.8˚). Training and testing SLDS models (n=6) on different trials (of subject A) of the same gait speed of 1.3 m/s resulted in aPPA of 96.9% ± 0.8% and aRMSE 2.9˚ ± 0.4˚ (range: 1.2˚ -6.6˚). When testing these models on 0.9 m/s speed data trials (n = 9) of subject A, the aPPA decreased by 4.7% and the aRMSE increased by 161.0% (range: 3.8˚-16.5˚).

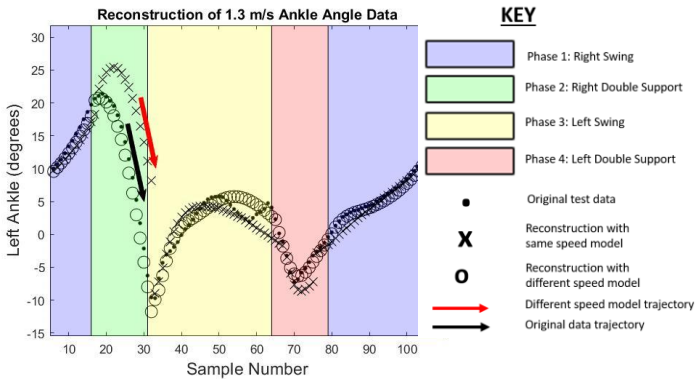

Figure 1: Left ankle reconstructions using different SLDS models tested on 1.3 mps data.

Significance

SLDS models do not appear to generalize across individuals or gait speeds. Perhaps this suggests that SLDS is unable to handle non-linearities within different gaits. SLDS can infer gait phase predictions but not kinematic predictions, and as such, may be used in applications where the determination of changes in the gait phase is necessary (perhaps exoskeleton development). Future studies will evaluate machine learning algorithms to improve the generalizability of these models.

Acknowledgments

This work is supported by the National Science Foundation GRFP to Taniel Winner and M3X CMMI1762211. SLDS code was developed and written by Luke Drnach.

References

[1] Drnach, Luke, et al. 2018, IEEE BioRob and ICRA.

[2] Chiang, J., et al. 2008, IEEE Transactions on Signal Processing

Effect of Unilateral Ankle Loading on Spatiotemporal Gait Parameters during Treadmill Walking

Haneol Kim[1], Matthew Beerse[2], and Jianhua Wu[1]
[1]Georgia State University, [2]University of Dayton. Email: hkim162@student.gsu.edu

Introduction

One has to continuously adapts to changing conditions during walking, including both external and internal disturbances [1]. Unilateral loading has been used to investigate the effects of inertial manipulations on kinematic gait patterns in healthy adults [2]. Step-to-step gait pattern seems to be stable under unilateral loading. However, the effect of unilateral loading on the long-range correlation of spatiotemporal parameters is largely unknown. Long-range correlation may reveal the nondynamic structure of variability of a time-series data.

The purpose of this study was to investigate the effects of unilateral ankle load on spatiotemporal parameters between loaded and unloaded sides in young adults. We hypothesized that with increasing unilateral load, differences between the loaded and unloaded sides may become larger in spatiotemporal parameters and their long-range correlations.

Methods

Twenty healthy young adults (aged 18-35 years, ten males and ten females) participated in this study. Male subjects had higher body mass, height, and leg length than the female subjects. Kinematic data was captured using a Vicon motion capture system. Participants completed treadmill walking at four load conditions in a random order: A0, A25, A50, and A75, representing no load, 0.8%, 1.6%, and 2.4% of body weight, respectively. The load was placed above the ankle of the non-dominant leg, which was not used to kick a ball.

Each participant's preferred overground walking speed was used to set their treadmill speed. Subjects walked on a treadmill for five minutes under each load condition and then rested for five minutes between conditions. Step length was normalized by leg length to minimize the height effect. Step time and foot clearance were also calculated for both loaded and unloaded sides. Detrended fluctuation analysis (DFA) was applied to these gait parameters to investigate long-range correlation embedded in the time-series data.

Table 1: Mean of normalized step length (NSL), step time (ST), foot clearance (FC), DFA alpha of NSL (DFA_NSL), DFA alpha of ST (DFA_ST), and DFA alpha of FC (DFA_FC) at each load condition.

	Side	A0	A25	A50	A75
NSL	Loaded	0.638	0.639	0.646	0.654
	Unloaded	0.647	0.644	0.651	0.653
ST	Loaded	0.525	0.537	0.546	0.555
	Unloaded	0.526	0.525	0.519	0.517
FC	Loaded	2.408	2.347	2.459	2.561
	Unloaded	2.414	2.438	2.476	2.492
DFA_NSL	Loaded	0.770	0.705	0.731	0.732
	Unloaded	0.741	0.734	0.775	0.731
DFA_ST	Loaded	0.798	0.731	0.763	0.736
	Unloaded	0.724	0.724	0.757	0.822
DFA_FC	Loaded	0.724	0.741	0.764	0.808
	Unloaded	0.752	0.682	0.775	0.718

Our preliminary analysis did not demonstrate a gender difference in normalized step length, step time, and foot clearance and their DFA alpha values. Therefore, we collapsed the data from the male and female subjects for further analysis. Two-way (4 condition × 2 side) repeated ANOVA was conducted on these variables at a significant level of α=0.05.

Results and Discussion

Normalized step length increased with unilateral ankle load and the loaded side had a smaller value than the unloaded side. There was a condition effect ($p=0.003$) and a side effect ($p=0.014$). Post-hoc analysis revealed that A0 was different from A50 and A75, and A25 was different from A75.

While step time at the loaded side increased with the load, it decreased at the unloaded side. Statistical analysis demonstrated that there was a condition by side interaction ($p<0.001$). Post-hoc analysis revealed that there was a difference between the loaded and unloaded sides for all the load conditions except A0.

Foot clearance generally maintained similar values between the loaded and unloaded sides regardless of load. Statistical analysis revealed no main effect, nor an interaction. This suggests that unilateral load may affect spatiotemporal parameters more in horizontal than in vertical.

DFA alpha was around 0.75 for all the parameters regardless of load, suggesting these parameters were correlated within the time-series of data. Statistical analysis revealed no main effect, nor an interaction for all the parameters. This indicates that long-range correlation of spatiotemporal parameters was not affected by unilateral ankle load. Therefore, young adults can consistently modulate nondynamic structure of variability of spatiotemporal parameters while changing these parameters to accommodate an external disturbance such as a unilateral ankle load.

Significance

This study indicates that normalized step length and step time are affected by external ankle loading as expected. However, foot clearnance mostly maintained similar values, suggesting the priority of safely clearing the ground while adapting to different ankle loads. In addition, the similar DFA alpha values across load conditions suggest that our neuromuscular system may be robust in maintaining a similar structure of variability (i.e., long-range correlation) while acommodating to an external load. An analysis of long-range correlation can be used for studying movement patterns in clinical populations to understand their movement deficits, or for assessing the effect of physical rehabilitation to improve the rehabilitation design and its outcomes.

Acknowledgments

I would like to sincerely thank all the participants.

References

[1] Bohnsack-McLagan, N. K. et al. (2016). *J Biomech, 49*(2), 229-237.
[2] Kodesh, E. et al. (2012). *Gait Posture, 35*(1), 66-69.

Correlation between forward and backward treadmill walking in school-aged children

Gena Henderson[1,2], Diego Ferreira[1], and Jianhua Wu[1]
[1]Department of Kinesiology & Health, [2]Department of Physical Therapy, Georgia State University, Atlanta, GA
Email: jw11@gsu.edu

Introduction

Backward walking (BW) overground has been characterized as being a simple time-reversal of forward walking (FW). High correlations in joint kinematics between FW and time-reversed BW overground are seen in adults and school-aged children [1]. However, little research has been conducted in children comparing BW and FW patterns on a treadmill even though significant differences in gait patterns have been established between overground and treadmill walking in both adults and children [2]. Thus, we aimed to investigate the correlation between FW and BW kinematics in school-aged children during treadmill walking at different speeds. We hypothesized that kinematic variables would be highly correlated between FW and time-reversed BW on a treadmill at all speeds.

Methods

We recruited 19 typically developing children (10M/9F) aged 6-12 years. Subjects completed bouts of treadmill walking for 2 minutes each; each bout represented a different walking condition. These conditions included FW and BW at 3 speeds: normal (equal to self-selected overground speed), slow (75% of normal), and fast (125% of normal). Kinematic data were collected using an 8-camera Vicon motion capture system. Electromyography (EMG) data were collected from the leg muscles using a Delsys EMG system. Correlations between FW and time-reversed BW [3,4] were calculated at the hip, knee, and ankle for each speed condition (Fig. 1).

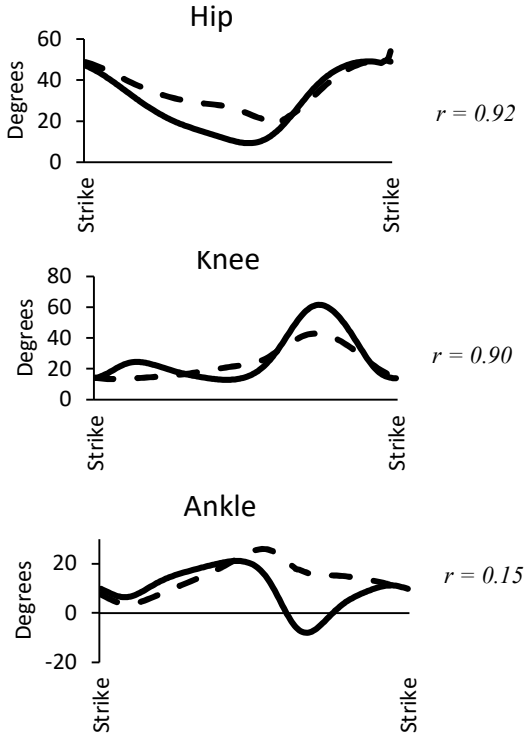

Fig. 1: Representative graphs of the hip, knee, and ankle kinematics during forward (solid line) and time-reversed backward (dotted line) walking on a treadmill at the normal condition.

Results and Discussion

School-aged children demonstrated high coefficients of correlation between FW and BW kinematics at the hip (r=0.83-0.99) and knee (r=0.76-0.99) that were largely unaffected by speed (Fig. 1). At the ankle, however, correlations were much lower at all speeds (r=0.31-0.44). Inter-subject variability was high across all three joints, and the hip and knee joints showed much higher coefficients of determination than the ankle joint across three speed conditions (Table 1).

Table 2: Mean (SD) of correlation of determination (R^2) between forward and time-reversed backward walking.

Speed	Hip	Knee	Ankle
Slow	0.91 (0.07)	0.89 (0.10)	0.25 (0.15)
Normal	0.92 (0.05)	0.87 (0.07)	0.16 (0.18)
Fast	0.92 (0.06)	0.84 (0.09)	0.21 (0.22)

School-aged children adapted their ankle motion differently than adults during BW treadmill walking, limiting their ankle range of motion and utilizing their plantarflexors to a lesser extent. This suggests that although a similar neural control mechanism between FW and BW walking may be present in school-aged children during overground walking, they are not yet able to fully adapt to BW on a treadmill. This is in line with previous findings that treadmill walking patterns continue to mature into adolescence. We suggest that proximal control at the hip and knee may be more advanced by this age, but distal control at the ankle is still under development.

Significance

The decreased motion at the ankle joint during BW walking may result from children minimizing movement at this joint and compensating using adaptations from the hip and knee in order to improve stability on the moving belt. Repetitive treadmill walking is a common intervention technique in pediatric rehabilitation, with clinicians often modulating direction and speed to facilitate desired adaptations in children's gait patterns [5]. Our finding that distal control at the ankle during backward treadmill walking is not yet mature in school-aged children highlights the need to specifically quantify how young children adapt to these conditions on a treadmill so that clinicians can make informed decisions about rehabilitative protocols.

Acknowledgments

The authors wish to thank our subjects and their families for their participation in this study.

References

[1] Meyns et. al (2013). PLoS One. 8:e62747.
[2] Alton et . al (1998). Clinical Biomechanics. 13:434-40.
[3] Grasso et. al (1998). J Neurophysiology. 80:1868-85.
[4] Lee et. al (2013). Gait & Posture. 38:674-8.
[5] Zwicker et. al (2010). Pediatr Phys Ther. 22:361-77.

Physical Activity Affects Rate of Gait Adaptation and Spatiotemporal Adaptation Strategy

Sarah A. Brinkerhoff[1], Patrick G. Monaghan[1], Jaimie A. Roper[1]
[1]Auburn University, Auburn, Alabama
Email: sbrinkerhoff@auburn.edu

Introduction

The nervous system responds to gait perturbations by adapting mechanics of an existing walking pattern (1). Gait adaptation can be altered by individual factors such as injuries to the nervous and the musculoskeletal systems (2,3). Currently, it is unknown how current and past physical activity influences healthy adaptation. The purpose of this study was to examine the influence of physical activity history, weekly amount of activity, and type of activity on gait adaptation in sedentary and recreationally active healthy adults. We hypothesized that activity history and type of activity (non-cyclic, such as team ball sports, and cyclic, such as running) would predict rate of adaptation. Due to the spatial aspects of non-cyclic sports and the temporal aspects of cyclic sports, we also hypothesized that individuals participating in non-cyclic sports would initially adapt their walking pattern using mostly a spatial strategy, while sedentary individuals and individuals participating in cyclic sports would adapt using mostly a temporal strategy.

Methods

Three groups of healthy young adults participated in this study: 14 sedentary, 12 currently participating in cyclic sports, and 11 currently participating in non-cyclic sports. We collected information on activity history via a self-report. Participants walked on a split-belt treadmill (SBT) for ten minutes with their non-dominant leg moving twice as fast as the dominant leg (Adaptation). Gait adaptation was measured by the asymmetry in step lengths taken by the fast and the slow legs. Step length asymmetry (SLA) in the first five strides was measured as initial asymmetry (early SLA). Rate of adaptation was determined from the number of steps each participant took before reaching a plateau in SLA. Additionally, we measured the asymmetry in step position (position of ankle relative to pelvis at foot strike) and step timing (time from one foot strike to the subsequent foot strike, multiplied by the average belt velocity) during early SLA (3). To determine predictors of rate of adaptation, the number of steps to adapt SLA was stepwise linearly regressed on early SLA, group, and activity history. Then, to determine the spatiotemporal strategy used by the sedentary, cyclic, and non-cyclic groups, three (one for each group) stepwise linear regressions regressed early SLA on early step position asymmetry and early step timing asymmetry.

Results and Discussion

Early SLA and activity history, but not activity type, predicted number of steps to adapt SLA. The model explained 22.4% of the variance in rate of adaptation (p=0.013, r=0.473), where early SLA explained 11.9% and step position asymmetry explained an additional 10.5%. As the magnitude of early SLA decreased, fewer steps were needed to adapt. As the number of consecutive weeks spent active increased, more steps were needed to reach a plateau. Against our hypothesis, the type of physical activity did not predict rate of adaptation. However, only 22.4% of the variance in rate of adaptation was explained; additional factors likely influence rate of adaptation in healthy young adults and future research should seek to uncover such factors.

Both step position asymmetry and step timing asymmetry predicted early SLA in the sedentary group and in the cyclic group. In the sedentary group, the model explained 59.2% of the variation in early SLA (p=0.007, r=0.770) where step position asymmetry explained 38.6% and step timing asymmetry explained an additional 20.6%. In the cyclic group, the model explained 87.7% of the variation in early SLA (p<0.001, r=0.937) where step position asymmetry explained 66.0% and step timing asymmetry explained an additional 21.7%. For both groups, as asymmetry in both step position and step timing increased, early SLA decreased. Conversely, in the non-cyclic group, only step position asymmetry predicted early SLA. The model, and therefore step position asymmetry, explained 57.8% of the variation in early SLA (p=0.004, r=0.760); as asymmetry in step position increased, early SLA decreased. Healthy young adults participating in non-cyclic activities use a spatial strategy to combat an asymmetric walking pattern, while those that are sedentary or that participate in cyclic activities use a combination of spatial and temporal strategies.

When assessing spatiotemporal strategies and rate of gait adaptation, it is important to account for physical activity history, current activity level, and current type as confounding factors. The populations studied on a SBT commonly have a mobility disability, such as people with Parkinson's disease, and these populations may be less physically active than healthy populations (4). Resulting differences in gait adaptation may be in part due to differences in current or past physical activity.

Significance

Physical activity history and current type of physical activity influence the rate and the strategy used during early adaptation, respectively. The results of this study will help researchers better understand the individual factors influencing gait adaptation, which is a crucial mechanism in daily life, such as when navigating uneven or changing terrain. It is crucial to understand if physical activity influences gait adaptation in older populations, and if specific physical activity interventions can alter gait adaptation strategies.

Acknowledgments

This study was funded by an Auburn University seed grant. S.A.B. and P.G.M. are each funded by Auburn University Presidential Graduate Research Fellowships.

References

(1) Resiman, D.S. et. al., 2005, *J. Neurophysiol.*
(2) Roper, J.A. et. al., 2016, *Orthop. J. Sports Med.*
(3) Finley, J.M. et. al., 2015, *Neurorehabil. Neural Repair*
(4) Nimwegen et. al., 2011, *J. Neurol.*

CORRELATIONS BETWEEN CLINICAL PAIN MEASURES AND LOWER EXTREMITY KINEMATICS AMONG INDIVIDUALS WITH LOW BACK PAIN

Janki H. Patel[1], Katie Butera[2], Arian Vistamehr[1], Paul Freeborn[1], and Emily J. Fox[1, 2]
[1]Motion Analysis Center, Brooks Rehabilitation, Jacksonville, FL
[2]Department of Physical Therapy, University of Florida, Gainesville, FL
Email: Janki.Patel@brooksrehab.org

Introduction

Chronic pain is a complex, multifactorial nervous system disease [1], often associated with secondary complications, such as movement impairments and disability. Specifically, low back pain (LBP) is a prevalent condition and a leading cause of disability, affecting more than 31 million Americans [1]. Individuals with LBP often demonstrate altered movement or adaptations during walking, such as slower gait speed, or increased trunk and pelvis rigidity [2]. These adaptations may represent compensatory strategies to reduce LBP.

LBP severity and disability are often assessed using self-reported clinical measures. Prior LBP studies have largely focused on trunk and pelvis kinematics during walking with limited emphasis on lower extremity (LE) function. However, there is limited knowledge about the associations between self-reported clinical measures and LE kinematics during walking among individuals with LBP. This is a critical step in understanding the impact of LBP severity and disability on fundamental characteristics of walking function. Therefore, the study purpose was to quantify the associations between peak LE joint kinematics during walking and clinical measures of disability and pain intensity in individuals with LBP.

Methods

Participants were adults with LBP (n=75; 39 females; age: 45 ± 29 years; self-selected walking speed: 1.18±0.19 m/s; fastest comfortable walking speed: 1.88±0.36m/s). Participants self-reported disability (via the Oswestry Disability Index) and pain intensity (via Numeric Pain Rating Scale 0-10). Three-dimensional kinematics were recorded using a 12-camera motion analysis system while participants performed 3 walking trials at a self-selected (SS) pace and 3 trials at a fastest comfortable (FC) pace over ground. LE kinematics were quantified and averaged by the peak sagittal plane hip, knee, and ankle joint angles for the left and right limbs. Associations between peak joint angles, gait speed, and self-reported disability and pain intensity measures were identified using Pearson's correlation (r) and the Benjamini-Hochberg correction was applied for multiple comparisons ($\alpha = 0.05$, q-value = 5%).

Results and Discussion

Higher disability ($r=-0.49$, $p<0.01$;$r=-0.41$,$p<0.01$) and pain intensity ($r=-0.36$,$p<0.01$; $r=0.33$,$p<0.01$) were negatively associated with slower gait speed during both SS and FC walking, respectively. Higher disability was negatively associated with reduced hip extension (($r=0.38$, $p<0.01$; $r=0.37$, $p<0.01$), knee extension ($r=0.30$, $p=0.03$; $r=0.32$, $p=0.01$), ankle plantarflexion ($r=0.30$, $p=0.03$; $r=0.32$, $p=0.01$), and positively associated with greater ankle dorsiflexion during the stance phase ($r=0.37$, $p=0.01$; $r=0.26$, $p=0.02$) during both SS and FC walking, respectively. Higher pain intensity was negatively associated with reduced hip extension ($r=0.45$, $p<0.01$; $r=0.45$, $p<0.01$) during both SS and FC walking, respectively. Higher pain intensity ($r=0.30$, $p=0.01$) was positively associated with greater hip flexion during SS walking. All other correlations between peak joint angles and clinical measures were not significant.

Due to the proximity of the hip joint to the lumbar region, LBP can lead to compensations, such as increased hip stiffness and anterior pelvic tilt, which could result in restricted range of motion [3]. Restricted proximal joint movement is likely related to restricted movement at the distal joints within the kinematic chain. For instance, a reduction in hip joint extension may contribute to reductions in knee extension and ankle plantarflexion during late stance. Restrictions in LE joint motion may also be a movement strategy to compensate for impaired balance or the difficulty maintaining balance during walking due to LBP or anticipated LBP. Additionally, the associations between gait speed and the pain intensity measures align with results from prior studies that indicate individuals with LBP walk slower. Overall, individuals with reduced peak LE kinematics may be adopting this movement pattern as a compensatory strategy to reduce LBP during walking; this compensatory strategy could potentially contribute to greater disability for these individuals.

Significance

Overall, the study results provide evidence of associations between LE kinematics during walking and clinical self-report measures of LBP intensity and disability in individuals with LBP. A common goal of clinical interventions is to restore function, restore normal movement, and reduce pain. These study findings therefore suggest that assessment of LE kinematics may be a valuable component of the clinical examination. Measurement of LE kinematics during walking also may be useful in determining appropriate movement-based interventions for individuals experiencing greater LBP severity and/or pain-related disability. The current results provide support for treating pain as a complex nervous system disease that requires the comprehensive assessment of clinical presentation (pain and disability) alongside performance-based measures of walking function.

Acknowledgments

This work was supported by the Brooks Rehabilitation and University of Florida College of Public Health and Health Professional Research Collaboration.

References

[1] Relieving Pain in America, *National Academies Press*, 2011
[2]Lamoth CJ et al. *Gait & Posture* **23**, 230-239, 2006
[3]Carpes FP et al. *Journal of Bodywork and Movement Therapies* **12,** 22-30, 2008

Normalizing Kinetic Data Alters Conclusions Based on Obesity

Kevin D. Dames*[1], Gary D. Heise[2], and Jeremy D. Smith[2]
[1]Kinesiology Department, SUNY Cortland, Cortland, NY, USA
[2]School of Sport and Exercise Science, University of Northern Colorado, Greeley, CO, USA
Email: *kevin.dames@cortland.edu

Introduction

Normalizing mechanical measures based on anthropometric measures is common in biomechanical gait investigations. Hof suggested that normalization creates unitless measures [1], where linear associations between the normalization metric and the dependent variable are commonly assumed [2]. Ground reaction forces and lower extremity joint moments for obese and non-obese individuals have been reported in absolute terms [3], normalized by body mass [3], or normalized by the product of mass and height [4]. These "normalizations" transform the moment into a new variable, but fail to produce a unitless term and lead to equivocal interpretations of outcomes in the literature [3,4]. Thus, our purpose was to better understand the influence of normalization on data interpretation when participants of various body size (e.g., BMI) were investigated within a single study.

Methods

Ten obese (BMI = 33.8 ±2.9 kg·m^{-2}; 6 Males; age = 26 ±3 years) and twelve non-obese (BMI = 23.6 ±2.2 kg·m^{-2}; 7 Males; age = 23 ±3 years) adults walked overground at 1.5 m·s^{-1} while motion (100 Hz) and force (2000 Hz) data were collected. These data were low pass filtered at 6 and 50 Hz, respectively, and combined to estimate joint reaction forces and moments. Absolute and unitless measures were then developed by dividing forces by bodyweight and moments by the product of weight and height. Linear correlations between the normalization metric and the absolute and normalized measures were investigated based on group: obese only (O), non-obese only (NO), and combined group (N+O). Group outcomes were then compared using independent t-tests for both absolute and unitless measures.

Results and Discussion

When considering both groups together and data in absolute terms, forces and moments were related to body size normalization metrics (i.e., body weight and body weight *height; see Table 1). Once normalized, only one significant correlation remained (i.e., hip extensor moment), but it was opposite in sign from the original correlation. Within the NO group normalization had the desired effect, as no relations were observed between the force or moment measure and the normalization metric. In O, normalized braking force was strongly correlated with bodyweight.

Significance

Given the relationship between the normalized hip joint moment and its normalization metric when group data were combined, data from groups who vary based on body mass index should not be combined for data interpretation in future studies.

References

1. Hof. *Gait Posture,* **4**:222-223, 1996.
2. Wannop et al. *J Appl Biomech*, **28**: 665-676.
3. Browning & Kram. *Med Sci Sports Exer*, **39**: 1632-1641.
4. McMillan, et al.. *Gait Posture*, **32**: 263-268.

Table 1. Correlations between the absolute measures and their normalization metric and comparisons between groups

Parameter	Combined	Obese	Non-Obese	*r* (NO + O)	*r* (O)	*r* (NO)	*t* (NO - O)
Forces (N)							
Propulsive	230.88 (65.29)	287.47 (37.66)	183.72 (40.49)	0.95*	0.94*	0.78*	-6.18*
Braking	-200.77 (53.28)	-252.04 (16.11)	-158.04 (28.75)	-0.89*	-0.46	-0.65*	9.19*
Vertical	1000.67 (258.06)	1230.09 (153.29)	809.49 (142.07)	0.98*	0.95*	0.93*	-6.67*
Moments (Nm)							
Plantar Flexor	137.37 (64.25)	190.88 (56.03)	92.78 (23.25)	0.84*	0.56	0.79*	-5.54*
Knee Extensor	92.37 (42.36	104.35 (46.03)	82.40 (38.11)	0.49*	0.49	0.45	-1.23
Hip Extensor	73.86 (20.51)	78.62 (18.02)	69.89 (22.35)	0.52*	0.33	0.76*	-0.99
Forces (unitless)							
Propulsive	0.27 (0.03)	0.27 (0.01)	0.26 (0.04)	0.07	-0.06	0.07	-0.48
Braking	-0.23 (0.03)	-0.24 (0.03)	-0.23 (0.04)	0.18	0.84*	0.18	0.71
Vertical	1.16 (0.06)	1.16 (0.05)	1.17 (0.07)	-0.15	-0.05	-0.15	0.36
Moments (unitless)							
Plantar Flexor	0.09 (0.02)	0.10 (0.03)	0.08 (0.01)	0.39	0.09	-0.20	-2.67*
Knee Extensor	0.06 (0.03)	0.05 (0.02)	0.07 (0.03)	-0.22	0.11	-0.09	1.28
Hip Extensor	0.05 (0.01)	0.04 (0.01)	0.06 (0.01)	-0.52*	-0.30	-0.02	3.18*

Note: NO = Non-Obese and O = Obese. Normalization metric for ground reaction forces is bodyweight; normalization metric for joint kinetic measures is bodyweight·height. Correlations are between the measure and its normalization metric. *t* is an independent samples test. * indicates a significant result. $p < .05$

Effects of Marker Placement and Body Sizes on Frontal Plane Center of Mass Motion During Walking: A Preliminary Study

Hang Qu, Yu-Pin Liang, Li-Shan Chou
Department of Kinesiology, Iowa State University, Ames, IA, USA
Email: *hangqu@iastate.edu

Introduction

Estimation of the whole-body center of mass (COM) depends on body segment anthropometric measurement and kinematic data measured using a motion capture system with reflective markers adhered to bony landmarks [1]. Various maker sets are commonly employed for motion data collection. However, soft tissue composition and body mass distribution could differ among participants with different body sizes. Therefore, the purpose of this study was to compare the whole-body COM medial-lateral (M-L) kinematics derived from data collected with different marker sets during walking.

Methods

This is an ongoing study. Eleven adult participants were recruited and classified into two groups based on their BMI: the overweight/obese group (4 participants: one female, height: 1.70±0.12 m, weight: 85.66±10.35 kg, BMI: 29.06±3.64 kg/m^2) and normal weight group (7 participants: four females, height: 1.72±0.12 m, weight: 61.15±14.08 kg, BMI: 20.94±2.15 kg/m^2).

A twelve-camera motion analysis system (Oqus 6+. Qualisys AB, Sweden) was used to acquire three-dimensional (3D) Kinematics data. Three whole-body reflective marker sets (MS1, MS2, MS3) were employed in the study. For MS1, a multi-segment trunk, a head, arms, forearms, hands, a coda pelvis, thighs, shanks, and feet were modelled [2, 3]. The MS2 was a modified arrangement based on the Helen Hayes marker set, a head, a trunk, arms, forearms, hands, a Visual 3D pelvis, thighs, shanks, and feet were modelled. For MS3, the segment modelling was similar to the MS2. However, four-marker-mounted clusters were used as tracking markers instead of discrete markers during the dynamic trials [3, 4].

Participants were asked to perform 5 trials of barefoot level walking with their self-selected speeds (average speed ± 5%) when fitted with each marker set. Marker trajectories were smoothed using a 4th order zero-lag Butterworth low pass filter at a cutoff frequency of 12 Hz. All marker data were processed and calculated using the Visual 3D software (6.0, C-Motion, Inc., Germantown, MD). Position of the whole-body COM was computed based on the segmental mass and COM location with weighted-sum method. COM velocity and acceleration were obtained from the first and second derivatives of COM positions using the finite-difference method. The range of COM displacement and peak velocities and accelerations in the frontal plane were identified during a gait cycle, which was defined between two consecutive heel strikes of the right foot.

A 2×3 two-way (Group × Marker set) univariate ANOVA was performed separately to detect differences between groups (overweight and healthy weight) and marker sets (MS1, MS2 and MS3). When an interaction and/or main effect was revealed, a post-hoc comparison with Bonferroni adjustments were used to detect differences between groups and step width conditions. An *a priori* alpha level was set to 0.05.

Results and Discussion

No interactions between body sizes and marker sets were found, thus the selected critical events collapsed by body sizes and by marker sets (Table 1). Although no group differences in gait velocity or M-L COM displacement were detected, overweight/obese group showed a greater lateral velocity right after the initial (~5% % gait cycle) heel strike of the right leg, and greater peak accelerations on both M-L directions (~60% gait cycle), compared to the normal group. These results suggested overweight or obese individuals may control their frontal plane COM motion differently than normal individuals. A faster COM sway velocity or acceleration could impose challenge in momentum control and could lead to a higher risk of sideway imbalance.

All participants demonstrated consistent patterns of M-L COM kinematics among three marker sets. Also, the timing of peak COM velocities and acceleration consistently occurred around the early and end period of the stance phase (~60% of the gait cycle), respectively. Even though the calculation using MS2 may underestimate the peak lateral velocity compared to MS1 (p=.023) and MS3 (p=.041). All three marker sets resulted in a similar COM trajectory in the frontal plane during walking regardless of body sizes.

Significance

Differences in body sizes and variations in marker sets could affect the determination of whole-body COM [5]. It is essential to exam whether the whole-body COM kinematics could be consistently estimated with different marker sets among patients with different body sizes.

Reference

[1].Lee, R.C., et al. (2000) *Am J Clin Nutr*. **72**(3): p. 796-803.
[2].Leardini, A., et al. (2007) *Gait Posture*. **26**(4): p. 560-71.
[3].Cappozzo, A., et al. (1995) *Clin Biomech*. **10**(4): p. 171-178.
[4].Leardini, A., et al. (2011) *Clin Biomech*. **26**(6): p. 562-71.
[5].Peters, A., et al. (2010) *Gait Posture*. **31**(1): p. 1-8.

Table 1: Medial-Lateral (M-L) COM motions during walking: mean±SD.

	Body sizes			Marker sets			
	Normal	Overweight	t test	MS1	MS2	MS3	F test
Gait velocity (m/s)	1.29±0.2	1.48±0.2	p=.161	-	-	-	-
Displacement (cm)	4.0±1.6	3.9±1.3	p=.946	4.0±0.7	4.2±1.6	3.6±1.9	p=.674
Peak lateral velocity (toe off) (cm/s)	12.6±3.2	16.5±8.1	p=.083	14.4±5.2	13.7±6.1	14.0±6.4	p=.935
Peak lateral velocity (heel strike) (cm/s)	-11.6±2.2 *	-15.0±2.6	p<.000	-13.9±2.8	-11.4±2.2 #^	-13.3±3.0	p=.010
Peak left lateral acceleration (cm/s^2)	81.5±40.9 *	121.9±50.2	p=.005	96.2±31.4	95.5±40.3	96.7±51.5	p=.861
Peak right lateral acceleration (cm/s^2)	-82.8±45.5 *	-123.2±55.5	p=.038	-88.8±40.7	-100.3±54.7	-103.4±63.2	p=.687

*: significantly different between body size groups; #: significantly different from MS1; ^: significantly different from MS3.

The Influence of an Expert Audience on Gait Initiation Performance

Patrick G. Monaghan[1], Kenzie B. Friesen[1], Zhaotong Zhang[1], Jaimie A. Roper[1]
[1]Auburn University, Auburn, Alabama
Email: pmonaghan@auburn.edu

Introduction

During gait initiation, postural control strategies are used to achieve stability and efficiency during transition from a static to dynamic posture (1). Changes in gait initiation strategies have been observed in aging populations and populations with neurological disorders (1). However, dynamic postural control strategies have also been shown to be altered by environmental stimuli (3).

Anticipatory postural adjustments (APAs), help to mitigate the threat of postural instability and have been associated with forward progression velocity (4,5). Such control strategies are crucial for successful gait initiation performance and even more so when faced with unfamiliar settings and surroundings (6). The performance of motor tasks in a research setting with a research team present may constitute such an unfamiliar environment.

Indeed, in-laboratory and real-world gait speed have a weak correlation, which may be influenced by the addition of researcher observation (7). Yet, it remains unclear how manipulating a research setting by varying the number of researchers may impact gait initiation performance. Greater understanding of the influence of deliberate and critical observation of researchers contributing to gait initiation performance may enhance our ability to translate laboratory-based findings to 'real world' setting outside of the laboratory.

The aim of this study was to assess the effects of increasing audience size on gait initiation performance and early steady state step parameters. We hypothesized that as audience size increased, the speed of each step would increase along with an increase in APA magnitude.

Methods

Twenty-one college-aged individuals participated in the gait initiation analysis (14 females, 7 males, 21 ± 1 years old, 167.7 ± 16.1 cm, 72.3 ± 15.4 kg). Participants wore 6 wireless inertial sensors and were asked to walk four lengths of a 9.3m walkway at their typical speed (APDM, Portland, OR). Participants completed this protocol in three different conditions: 1) no research audience present, 2) a small audience with two researchers present and 3) a large research audience with 6-10 researchers present. Gait initiation parameters measured included: 1) Peak APA amplitude in the anteroposterior direction (APA-AP) and mediolateral direction (APA-ML), 2) Duration of APA, 4) APA first step duration, 5) After initial foot contact with the lead swing leg, early steady state step speed was also measured. A one-way repeated measures MANOVA was conducted to test for differences in peak APA-AP, peak APA-ML, the duration of APA, APA first step duration and early steady state step speed across each of the no, small and large audience conditions.

Results and Discussion

The multivariate analysis revealed statistical significance between the audience size conditions, $F(14,68) = 2.901$, $p = 0.002$. There was a univariate effect for speed of each of the early steady state steps, first step, $F(2,40) = 17.547$, $p < 0.001$, second step, $F(2,40) = 14.258$, $p < 0.001$ and third step, $F(2,40) = 13.390$, $p < 0.001$. Post-hoc tests revealed significant increases in the speed of steps between the no audience and large audience condition, and between the small audience and large audience conditions. No significant increases in step speed were observed between the no audience and small audience conditions (**Figure 1**). Our findings suggest that participants walked faster when increased number of observers were present. Therefore, it is plausible that in-laboratory findings may conflict with actual performance in a 'real world' setting outside the laboratory environment where such observation and evaluation is atypical.

There was no effect of increasing research audience size on APA-AP, APA-ML, duration of APA or APA first step duration. Gait initiation is a demanding task for the central nervous system compared to straight ahead walking. (6) It is possible that a heightened stimulus may be required to achieve the same magnitude of change as observed in steady-state gait.

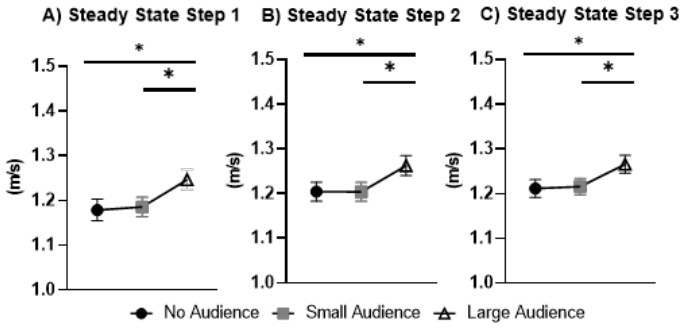

Figure 1: Mean and standard error steady state step speeds across audience conditions. *denotes p < .001.

Significance

Differences in stepping speed were most pronounced in the large audience condition, indicating that participants walked faster when a larger number of observers were present. This is also supported by the lack of difference observed between the no and small audience conditions. However, increasing observation did not impact postural control mechanisms during gait initiation. These results highlight the importance of translation and extrapolation of lab-based findings, as differences in movements produced when under observation, such as in a lab setting, may limit the generalizability to real life settings outside the laboratory. We recommend researchers should keep number of researchers consistent, and or report the number of researchers present during a data collection to acknowledge the impact of observation on performance.

References

(1) Halliday, S.E, 1998, *Gait and Posture*
(2) Naugle, K.M. et. al., 2011, *Emotion*
(3) Polcyn,A.F et al., 1998, Arch Phys Med Rehab
(4) Lepers, R. et. al., 1995, *Exp Brain Res.*
(5) Mirelmani, A. et. al., 2018, *Handbook Cln Neur*
(6) Takayanagi, N. et. al., 2019, *Sci Rep*

Dorsiflexion Restriction Highlights the Role of Early-Stance Modulation of Tibialis Anterior in Forward Body Propulsion

Shakiba Rafiee*[1,2], Joanne Klossner[1], Tim Kiemel[1,2], and Ross Miller[1,2]
[1] Department of Kinesiology ([2] Neuroscience and Cognitive Science Program), University of Maryland, College Park, USA
Email: *shrafiee@umd.edu

Introduction

Our research goal is to identify how the nervous system stabilizes walking by continually making small modulations (adjustments) in the rhythmic pattern of muscle activations. Our previous studies, using a combination of external perturbations and system identification, have suggested a role for early-stance tibialis anterior (TA) muscle modulation in forward body propulsion and speed control[1,2]. However, TA activation in stance has been mostly thought of as a mechanism to prevent foot-slapping or even as a brake on the speed. To clarify the role of early-stance TA modulation, in the current study we added a restriction that limits the contribution of the dorsiflexor muscles to gait and studied the "restricted" gait response to external lower-body mechanical perturbations. We expect that by increasing resistance to dorsiflexion, in response to external perturbations the nervous system would have to adopt alternative strategies to control propulsion and help the subjects maintain balance on the treadmill. The absence of this response would suggest TA modulation is not important for controlling propulsion.

Methods

We have collected data from 7 participants in accordance with University of Maryland IRB. The subjects walked on a treadmill at 1.4 m/s for 12 250-s trials split between 2 conditions: 1) normal and 2) restricted, where dorsiflexion in both ankles was restricted using a traditional Achilles tendon taping method. The subjects were perturbed by small continuously-changing forces applied to their legs through a spring-motor mechanism[2]. Lowpass-filtered white noise signals were used to specify the mechanical perturbation (position of the motor). The kinematic data and surface electromyography were recorded from the legs and trunk. Phase-dependent impulse response functions (φIRFs) were calculated that describe the changes in kinematics and muscle activations in response to brief perturbations applied at any phase of the gait[1,2].

Results and Discussion

The taping method restricted dorsiflexion during late stance and through swing (Fig. 1A). The restriction also significantly decreased the knee flexion during mid stance (Fig. 1B). These changes in kinematics resulted in a significantly shorter step length (not shown) in the restricted condition, compared to the normal condition, which is consistent with the previous findings[3].

With restriction, both the TA and vasti (VAS) muscles saw a significant decrease in their peak activation during early stance, which is also consistent with the ankle orthosis literature[4]. The peak activation of the gastrocnemius (GAS) muscle during late stance also significantly increased in the restricted condition.

In response to the mechanical perturbations during swing that caused a forward perturbation of ankle position, the TA activation increased during early stance in both conditions. The difference between responses during early stance was not significant (Fig. 1C). The VAS muscle activation during early stance increased significantly more in the restricted condition (Fig. 1D). This early stance modulation of VAS is suggested to play a role in forward body propulsion[2]. The mechanical perturbation, applied during swing, increases the length of the same step (not shown). In the absence of the TA contribution to foot-placement correction, the early stance modulation of VAS compensate for the foot being too far in front of the body, by accelerating the center of mass (COM) forward. In response to mechanical perturbations during swing, the contralateral GAS muscle activation during late stance decreased significantly more in the restricted condition (Fig. 1E). This muscle modulation contributes to speed control during push-off. In the restricted condition, in response to the mechanical perturbation, the COM is not propelled forward as much (not shown), the decrease in contralateral GAS muscle activation helps decrease the next step length (not shown) and controls the placement of the contralateral foot relative to the body.

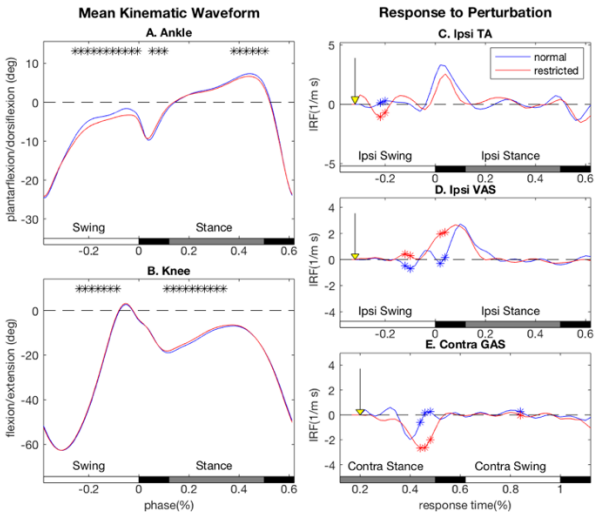

Fig. 1: Average waveforms of kinematics (A-B) and the muscular responses to the mechanical perturbations (C-D) in the normal (blue) and restricted (red) conditions. Asterisks indicate significant differences between conditions ($p < 0.05$). The bars on the horizontal axes indicate gait phase: (white = swing, gray = single support, and back = double support). The yellow arrows indicate the perturbation phase.

Significance

Our study highlights the role of early-stance modulation of TA in forward body propulsion, as when TA's ability to perform work was reduced, the nervous system compensated for this speed control mechanism by modulating the VAS and GAS muscles during early and late stance respectively.

Acknowledgments

Supported by the University of Maryland Kinesiology Graduate Research Initiative Fund to S.R.

References

1. Kiemel, T., Logan, D., & Jeka, J. J. (2016) arXiv preprint arXiv:1607.01746.
2. Rafiee, S. Lower-Body Mechanical Perturbation of Gait to Identify Neural Control. Masters thesis, University of Maryland (2017).
3. Ota, S., et al., *The Knee* **21**, 669–675 (2014).
4. Geboers, J. F., et al., *Arch. Phys. Med. Rehabil.* **83**, 240–245 (2002).

Length vs time: Dominant strategies to increase speed in older adults

Sidney T. Baudendistel, Abigail C. Schmitt, Matthew Terza, Amanda Stone, Chris J. Hass
Department of Applied Physiology and Kinesiology, University of Florida, Gainesville, FL
Email: sbaudendistel@ufl.edu

Introduction

The ability to modulate walking speed is essential to maintaining independence for older adults. Both fastest walking speed (FS) and usual, comfortable speed (CS) decline with age, resulting in a loss of community ambulation. Yet, FS deteriorates more rapidly[1]. The transition of CS to FS can be achieved by decreasing step time and/or increasing step length. Reduced balance, strength, and neuromuscular changes (e.g. redistribution of joint torque) associated with aging may also contribute to the selection of a strategy to increase speed. The strategy chosen to increase speed impacts the kinematic and kinetic signature of the walking pattern[2], but it is unknown why participants may select or prefer one strategy over another.

We investigated the correlates associated with the strategies to increase speed and determined if there were differences between older adults who increase step length compared to those who decrease step time when increasing speed.

Methods

Fifty-seven sedentary older adults at risk for mobility disability completed a biomechanical assessment including walking (5 trials of CS and FS), static balance (eyes open and closed, 3 trials each of 30s), isokinetic dynomometry, and mobility (Short Physical Perfomance Battery's chair stand time).

Length-Time Difference (LTD) is a common measure to quantify the strategy used to increase walking speed[2]. A positive LTD represents an increased step length strategy, a negative LTD represents a decreased step time strategy, and an LTD score of 0 represents equal percent change (%Δ) in step time and length.

$$LTD = \left(\frac{\text{length}^{fast} - \text{length}^{usual}}{\text{length}^{usual}}\right) - \left(\frac{\text{time}^{fast} - \text{time}^{usual}}{\text{time}^{usual}}\right)$$

Since CS is considered a vital clinical sign[3], this analysis includes correlates and comparisons between LTD and both kinetic (peak knee moment, peak hip and ankle power, peak propulsive force and impulse) and kinematic (walk ratio, gait stability ratio, cadence, step length, step time) measures of CS walking. Balance measures included range and velocity in the medial-lateral direction and the 95% confidence ellipse area.

Correlation coeffecients were calculated between outcomes and LTD across all participants regardless of positive or negative LTD group ($p<.05$). T-tests confirmed homogeneity between the two strategy groups including: CS and FS and %Δ speed. Five separate multivariate analyses of variance were used to compare those who had a positive LTD and those who had a negative LTD for strength/mobility, eyes open balance, eyes closed balance, CS kinetics, and CS spatiotemporals ($p<.05$).

Results and Discussion

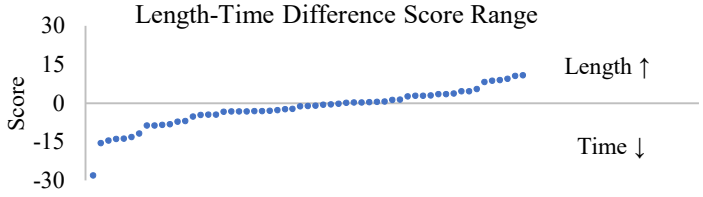

Figure 1. Individual LTD scores across 57 participants

Significant negative correlations were found between three outcomes and LTD (range:-27.87 to 10.97, Figure 1): peak propulsive force ($r=-.357$, $p=.007$), propulsive impulse ($r=-.300$, $p=.026$), and chair stand time ($r=-.273$, $p=.043$). Participants that relied on increases in step length (+LTD) displayed decreased propulsion during CS and reduced chair stand time. No other variables were significantly correlated to LTD.

After categorizing participants by those who used time (n=33, LTD=-6.26±5.98%) vs. length (n=24, LTD= .25±3.52%), no differences were found between CS ($p=.669$), FS ($p=.727$), nor %Δ of speed ($p=.947$). Balance ($p=.322$) and CS kinematics ($p=.352$) were not significant at the multivariate level.

Those who modulated speed with increased step length had significantly better strength ($\Lambda=.816$, $F=3.235$, $p=.031$), with reduced time to complete chair stands (14.16s vs 17.43s, $p=.023$). Peak isokinetic knee ($p=.463$) and ankle ($p=.455$) moments at 60º/s were not different at the univariate level. Kinetic variables were significantly different between groups at the multivariate level ($\Lambda=.781$, $F=2.689$, $p=.032$), driven by peak propulsive impulse ($p=.008$) with no other variables reaching significance. Those who used a step length strategy had significantly less propulsive impulse (20.61N*s vs. 17.35N*s) when walking at their CS than those who modulated step time.

In the current study, we found those who decreased step time during FS were weaker and required more propulsive impulse to create a similar CS. This was reflected with both a significant, continuous correlation and when grouping participants by LTD. This may represent a ceiling of propulsion that limits the ability to increase speed when needed. Comparatively, those who increased step length may have additional "propulsive reserve" to modulate walking speed. Ankle plantarflexion moment and power are functionally limiting factors for older adults[4], thus increasing step length to increase speed may not be possible for those who use more propulsive impulse during CS walking.

In those at risk for future mobility disability, propulsion at a comfortable speed and strength were correlated to the strategy used to increase speed, either increased length or decreased step time. Those who decreased step time to improve speed were weaker but used more propulsive force during comfortable walking, perhaps limiting their ability to modulate speed safely.

Significance

Further investigation of LTD could be helpful in identifying personalized gait interventions and understanding why pathological populations adopt a higher cadence during walking.

Acknowledgments

This work was supported in part by NIH R21 AG048133-01A1 and T32-NS082128

References

1. Ko et al. 2010. *Age Ageing*. 36(6):688-94.
2. Ardestani et al. 2016. *Gait Posture*. 46:118-25.
3. Fritz & Lusardi. 2009. *J Geriatr Phys Ther.* 32(2):2-5.
4. Judge et al. 1996. *J Gerontol.* 51(6):M303-12.

Comparison of Joint Mechanics of the Dominant vs. Non-Dominant Lower Limbs During Locomotion

Stephanie Molitor[1,2*], Karl Zelik[1,2,3], Kirsty McDonald[1,4]
[1]Dept. of Mechanical Engineering, Vanderbilt University
Email: stephanie.molitor@vanderbilt.edu[*]

Introduction

It is common practice for biomechanical analyses of gross, bilateral motor tasks to consider the independent functional role of each lower limb. For example, when kicking a ball, the joints of the dominant limb (hip, knee, and ankle) typically move through a greater range of motion (ROM) and are cumulatively responsible for increased positive power production compared to the non-dominant limb [1]. However, the influence of limb dominance is rarely considered in walking and running research, where biomechanical symmetry between the legs is generally assumed [2]. It remains unclear whether this is a valid assumption, especially at the more distal joints. Recent work from our laboratory found that prosthetic device users who had lost their dominant limb preferred to have a toe joint added to their prosthetic foot, whereas all other participants preferred a prosthesis that lacked toe joint articulation. This suggests a potential link between limb dominance and distal joint kinematics; however, differences in foot kinematics have not been studied in relation to limb dominance in an able-bodied population. The current study therefore aims to compare dominant and non-dominant kinematics and kinetics for the hip, knee, and ankle, as well as foot kinematics (via a multi-segment model), throughout a walking and running stride. We hypothesized that dominant limb joints would move through an increased ROM compared to non-dominant limb joints.

Methods

Able-bodied individuals (N=3 to date, but data collection will resume shortly) completed walking and running tasks (speeds of 0.8-4.0 ms^{-1}) on a treadmill (Bertec) with motion capture (Vicon) markers placed on their lower limbs and feet in accordance with the multi-segment foot model outlined in [3]. After these trials, participants were asked to complete a revised Waterloo footedness questionnaire in order to determine their lower limb dominance as well as the strength of dominance [4].

Kinematic and kinetic data were calculated for the hip, knee, and ankle, as well as foot kinematics (Visual3D). For brevity, we present only metatarsophalangeal joint (MPJ) kinematics, but plan to share more comprehensive results at the conference. Statistical parametric mapping (SPM) analyses will also be employed on the complete dataset (target: N=12).

Results and Discussion

Based on the questionnaire, all three subjects exhibited weak to moderate right-limb dominance. Average differences in MPJ ROM generally fell between 4-6° (Fig. 1). Two subjects displayed a greater ROM on their dominant limb (positive values in Fig. 1), and one subject showed a greater ROM on their non-dominant limb (negative values in Fig. 1). While more testing is required to draw conclusions, we observed small but consistent differences between the dominant and non-dominant limbs of all participants. The differences between the dominant and non-dominant MPJ ROM for individual strides mirrored the average trend for each subject 90% of the time. Differences in ROM were also found between the dominant and non-dominant limb for the ankle, knee, and hip; however, similar to the findings in [5], these differences were smaller in magnitude.

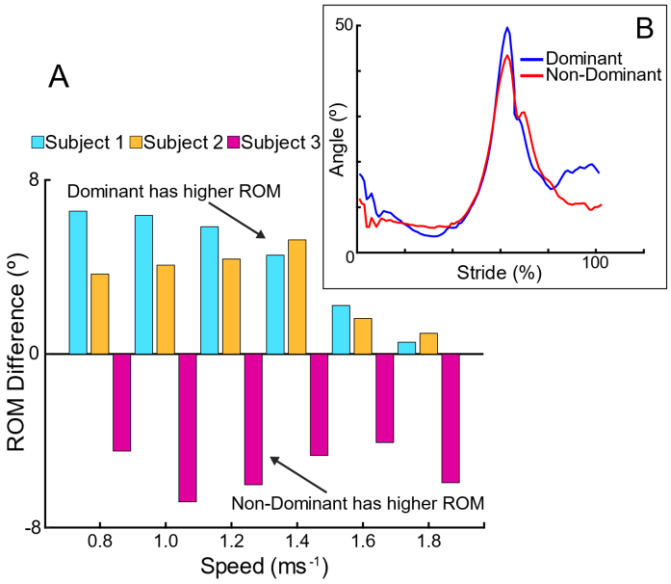

Figure 1: *(A) MPJ ROM differences between dominant and non-dominant limbs. (B) Mean MPJ angle for Subject 1, walking at 1.0 ms^{-1}.*

Upon completion of data collection and analysis, we will have a more holistic view on how limb dominance may affect hip, knee, ankle, and foot biomechanics. Moreover, SPM will allow us to determine where in the gait cycle these differences are most pronounced for both walking and running.

Significance

This study will be the first to statistically analyze continuous time-series data across the gait cycle when characterizing biomechanical differences between the dominant and non-dominant limbs during locomotion. It is expected that results will determine whether limb dominance should be considered in future gait analyses, and could inform the design or prescription of prosthetic feet.

Acknowledgments

The authors thank Dr. Justin Wager for assistance with study design and Mr. David Ziemnicki for help with data collection.

References

[1] Wang, J. et al. (2019). *Adv. Mech.Eng.*, **11**: 5.
[2] Sadeghi, H. et al. (2000). *Gait & Posture*, **12**: 34-45.
[3] Leardini, A. et al. (2007). *Gait & Posture*, **25**: 453-62.
[4] Elias, L. et al. (1998). N*europsychologia*, **36**: 37-43.
[5] Forczek, W. et al. (2012). *J. Hum. Kinet.* **35**: 47-57.

Decreased Balance Confidence Related with Limits Maximum Speed among Older Adults

Jutaluk Kongsuk[1], and Christopher P. Hurt[1]
[1]University of Alabama at Birmingham, Birmingham, AL, U.S.A.
Email: jutalukk@uab.edu

Introduction

Our previous study suggested that older adults become unstable on a step by step basis at slower walking speeds than younger adults[1]. Aspects of the walking performance of older adults related to their balance confidence suggesting an observable link between more cautious behavior and dynamic stability while walking. However, the static measure of balance confidence did not reflect how the individuals'perception was modified by an increasingly challenging task. The purpose of this study was to explore a dynamic range of balance confidence, measured using a novel approach while performing a dynamic walking task and investigate whether decreased balance confidence or decreased dynamic stability while performance of a challenging walking task may be a possible cause of decreased willingness to experience activities.

Methods

Fourteen older participants (68±2.62 years) were asked to complete the Activities Specific Balance Confidence (ABC) Scale, which measures their confidence in performing actives of daily living without losing their balance[2]. Participants were asked to walk on a treadmill at a range of speeds from 0.4 m/s, increasing 0.2 m/s, up to either 2.0 m/s OR a speed they chose to stop. Kinematic data was collected and a measure of gait stability, the margin of stability in the anterior direction at heel strike (MOSAP) was quantified, step-by-step[3]. Prior to increasing each treadmill speed, participants were asked if they wanted to attempt an faster speed and to rate their balance confidence in walking at a faster speed without losing their balance. This measure provided a more dynamic measure of balance confidence compared to the traditional measure. The primary variables assessed were differences of the last two sampled values of balance confidence as well as MOSAP at the last speed attempted, and the quantified slope of the line of the last 3 values between balance confidence and MOSAP. Participants were grouped based on whether they could or could not complete all walking trials. Comparisons between groups were made with Independent T-test and Mann-Whitney U test.

Results and Discussion

Ranges of MOSAP and balance confidence while performing the scaled treadmill speeds between groups are presented in Figure 1. Participants were grouped (n=7 in each group) that they could (70±2.44 years) or could not (67±2.43 years) complete all walking trials. No significant difference was detected in the standard ABC scale and difference for the last 2 values of MOSAP between groups. Significant differences were detected in the maximum speeds achieved between groups, the range of gait stability, as well as the differences on the last 2 values of sampled balance confidence (p=0.005, p=0.001, and p=0.026, respectively). Further, those that could not complete all speeds had a greater slope in the dynamic measure of balance confidence and gait stability compared to those who completed all speeds (p=0.025,Figure 2) .

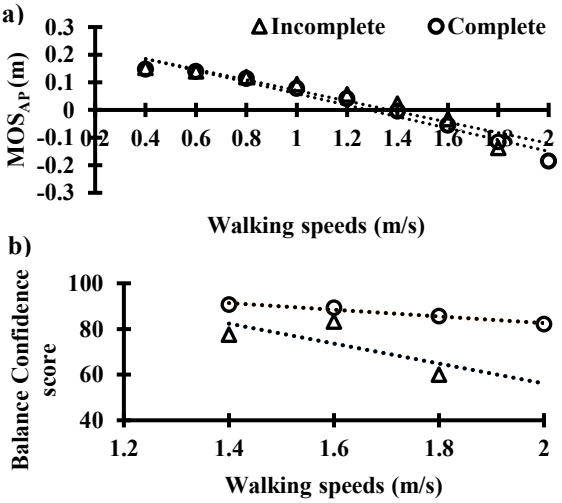

Figure 1: Walking speeds vs a) MOS_{AP} and b) Balance confidence vs for Older adults who could complete and could not complete the entire walking speeds (Note: 0.4-1.2 m/s, n=7; 1.4 m/s, n=4; 1.6 m/s, n=3; 1.8 m/s, n=1 for an incomplete group)**.**

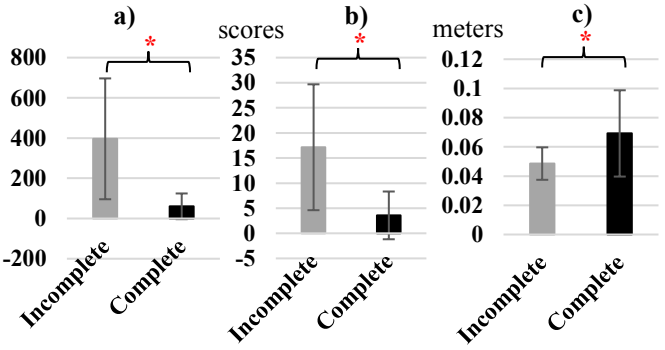

Figure 2: Differences between Older adults who could complete and could not complete the entire walking speeds a) sentivity of MOSAP and Balance confidence b) the last 2 values of Balance confidence, and c) the last 2 values of MOS_{AP}.

Significance

Some older adults who were less willing to experience instability at faster walking speeds on the treadmill might relate with their reduced balance confidence. Sensitivity of dynamic measure of balance confidence may reflect to a perception of loss of stability, this may be an interesting factor in decreased willingness to experience activities for some older adults.

References

1. Kongsuk J, Brown DA, Hurt CP. Gait Posture. 2019;73:86-92. **2.** Powell LE, Myers AM. J Gerontol A Biol Sci Med Sci. 1995;50A(1):M28-34. **3.**Hof A, Gazendam MG, Sinke WE. J Biomech. 2005;38:1-8.

Effects of Smartphone Operation on Pedastrains' Gait Performance: An Outdoor Study

Yue Luo[1], Haolan Zheng[1], Yuhao Chen[1], Wayne C.W. Giang[1], and Boyi Hu[1]
[1]Department of Industrial and Systems Engineering, University of Florida, Gainesville, FL, USA
Email: *boyihu@ise.ufl.edu

Introduction

Smartphone dependency has become a seriou concern for pedastrain safety. In 2010, an estimation of two million smartphone-engaged pedestrian injuries were reported [1]. However, the risk of smartphone use during walking was still underestimated by pedastrains, indicated by the high frequency (84%) of smartphone use been observed on the street [2]. One reason for the risk underestimation maybe that people have no clear understanding of how gait is changed under smartphone usage during public walking. Therefore, the purpose of the study was to investigate the effect of different smartphone operations on gait performance during outdoor walking.

Methods

Eight healthy college students (six females & two males) were recruited from the University of Florida. Participants, with seventeen wearable inertial sensors attached (MVN Awinda) to record gait performance [3,4], were instructed to complete four walking conditions (Walking Only, Walking-Reading, Walking-Tapping, and Walking-Gaming), each with six repetitions. For each trial, participants performed one smartphone operation throughout the 15-meter outdoor walking. Reading refered to a paragraph reading (100-150 words). Tapping referred to number tapping task (ascending order, 1-20). And gaming referred to a number matching game to find number equals to two switches before in a sequence of rapid changing numbers. The order of walking conditions were counter-balanced. All participants used the same smartphone (Moto g6, Motorola) throughout the experiment. Nine kinematics parameters in anterior-posterior plane, including the maximun flexion angle of: 1) C7-T1, 2) T12-L1, 3) L5-S1, 4-5) bilateral hip, 6-7) knee, and 8-9) ankle were extracted for each stride after a 2nd order low-passs Butterworth filter, with beginning and lasting two strides removed [5] (MATLAB R2019b). Univariate repeated-measures ANOVAs and post-hoc pairwise comparison (Fisher's LSD) were then performed (SPSS 26).

Results and Discussion

Table 1 summaries the effects of walking conditions on kinematic papameters. The independent variable was revealed to have significant impact on spinal kinmatic parameters, including C7-T1, T12-L1, and L5-S1 flexion angles ($p < 0.001$). Among lower limb kinematic, hip flexion angles were significantly effected by walking conditions ($p < 0.001$). Similar effect was found in knee flexion angles (left knee: $p < 0.001$, right knee: $p = 0.001$). However, a non-significant difference was observed in ankle flexion angles ($p = 0.057$ and 0.113 for left and right ankles, respectively).

Participants demonstrated larger neck flexion in higher cognitive load tasks (i.e. tapping & gaming) than lower cognitive load task (i.e. reading). It might be the case that, to process information with higher cognitive load, participnats tried to have a closer look at the target on the phone to better perceive the details of the target. However, it might increase the risk of falling or collision injuries because visual detection via peripheral vision was attenuated. Compared with the walking only condition, the restricted lumbar (L5-S1, T12-L1) and hip movement during smartphone-engaged walking indicated body posture adapations to hand-smartphone interaction, probably with the intention to better maintain the core balance of the locomotion system [6]. Tapping, which is a similar task of texting, had most obvious lumbar restriction. The effect of smartphone use on the gait performance, however, was less obvious on knees and ankles, possibly because of the stabilization from the inverted pendulum model of lower limbs during walking. In general, instead of proximal joint movement, smartphone-engaged walking relied more on distal joint movement.

Significance

In order to decrease the smartphone-engaged pedestrian injuries, results from this study could be used as evidence of the recommended levels of phone engagement in public environments. Smartphone application developers could also refer to this study for usage intervention design among pedestrian users.

Acknowledgments

The authors would like to thank Mustafa Ozkan Yerebakan for providing assistance for the data collection.

References

[1] Nasar, J. L., & Troyer, D. https://doi.org/10.1016/j.aap.2013.03.021
[2] AAOS. https://orthoinfo.aaos.org/globalassets/pdfs/aaos-distracted-walking-topline-11-30-15.pdf
[3] Schepers, M. et al. http://doi.org/10.13140/RG.2.2.22099.07205
[4] Hu, B. et al. https://doi.org/10.1016/j.jbiomech.2018.01.005
[5] Mariani, B. et al. http://doi.org/10.1016/j.gaitpost.2012.07.012
[6] Coppola, S. M. et al. https://doi.org/10.1123/jab.2018-0167

Table 1. Kinematic parameters, maximun anterior-posterior flexion angles: Mean (SD) values.

	Walking Only	Walking-Reading	Walking-Tapping	Walking-Gaming	*p*-value
Spinal kinematic parameters					
C7-T1 flexion (deg)	**0.75 (2.34) ^{A}**	**3.45 (3.00) ^{B}**	**4.66 (3.08) ^{C}**	**4.17 (2.87) ^{C}**	**<0.001**
T12-L1 flexion (deg)	**1.18 (1.17) ^{A}**	**0.84 (1.64) ^{B}**	**0.38 (1.65) ^{C}**	**0.65 (1.50) ^{B}**	**<0.001**
L5-S1 flexion (deg)	**2.62 (2.61) ^{A}**	**1.87 (3.67) ^{B}**	**0.84 (3.71) ^{C}**	**1.44 (3.37) ^{B}**	**<0.001**
Lower limb kinematic parameters					
Right hip flexion (deg)	**31.70 (3.84) ^{A}**	**28.11 (4.43) ^{B}**	**29.15 (4.03) ^{C}**	**28.95 (3.54) ^{BC}**	**<0.001**
Left hip flexion (deg)	**31.73 (4.00) ^{A}**	**27.20 (4.11) ^{B}**	**27.70 (4.94) ^{BC}**	**28.12 (4.51) ^{C}**	**<0.001**
Right knee flexion (deg)	**66.58 (3.60) ^{A}**	**67.21 (4.59) ^{AC}**	**68.46 (3.70) ^{B}**	**67.83 (3.76) ^{BC}**	**<0.001**
Left knee flexion (deg)	**67.64 (7.89) ^{A}**	**67.65 (9.02) ^{A}**	**68.70 (8.67) ^{B}**	**68.33 (8.82) ^{B}**	**0.001**
Right ankle flexion (deg)	12.86 (6.14)	12.87 (5.63)	14.74 (5.07)	13.74 (6.78)	0.057, NS
Left ankle flexion (deg)	13.74 (12.32)	11.87 (10.80)	12.52 (10.29)	11.22 (10.20)	0.113, NS

Ankle dynamics during overground walking with bodyweight support

Mhairi K. MacLean.[1], Daniel P. Ferris[1]
[1]University of Florida, Gainesville, Florida, USA
Email: *mmaclean@ufl.edu

Introduction

Bodyweight support is a tool used for gait rehabilitation and can also be used experimentally to better understand human locomotion biomechanics. Providing more bodyweight support decreases vertical ground reaction forces during walking but it is not clear how bodyweight support alters joint dynamics during walking. The ankle displays piece-wise linear relationships between joint moment and ankle angle over the stance phase, sometimes referred to as quasi-stiffnesses [1,2]. The quasi-stiffnesses may be related to inherent musculostendon mechanical properties, allowing individuals to take advantage of stretch and recoil of tendinous structures. Our aim was to test whether the piece-wise linear quasi-stiffnesses of the ankle were similar across a range of bodyweight support levels (simulated gravity levels). The bodyweight support should alter peak joint moments during gait, testing whether there is a relationship between joint moment and quasi-stiffness. We hypothesized that the characteristic linear moment-angle relationships would be similar across bodyweight support levels [3]. Subjects walked at multiple speeds in addition to multiple simulated gravity levels.

Methods

Twelve participants [7 female, 5 male; 26±4 years of age, body mass 70±8 kg, mean±s.d.] walked overground at 1, 0.76, 0.55 and 0.31 gravity (G) at 0.4, 0.8, 1.2, and 1.6 m/s. Bodyweight support was provided by a harness attached to constant force springs mounted to a rolling trolley on the ceiling. We used overground force plates and a motion capture system to measures kinetics and kinematics. We filtered and normalized data to the gait cycle.

We identified 4 key events during stance phase: A – Minimum ankle angle, B – 50% of stance phase, C – maximum ankle moment, and D – toe off. For each participant, we fit a linear model between A-B, B-C, C-D, and A-C. We then calculated R^2 for each fit and averaged across participants.

Results and Discussion

The ankle moment-angle loops changed shape with bodyweight support and speed (*Fig 1)*. The quasi-stiffness of the ankle was also influenced by both simulated gravity level and speed *(Fig 2)*.

The quasi-stiffness of the ankle tended to decrease with reduced gravity across all speeds and linear models *(Fig 2)*. The change was more pronounced between events B-C and C-D. Reduced moments at the ankle could result in less force through the Achilles tendon, moving the tendon mechanics further into the "toe region" and decreasing the stiffness of the musculotendon unit. At lower simulated gravity, relative strength and power increases, allowing subjects to adopt a wider range of gait strategies with fewer constraints.

Significance

These results provide a better understanding of motor adaptation to bodyweight support and reduced gravity locomotion. At lower relative mechanical demand (reduced gravity), humans can alter ankle dynamics as there are fewer biomechanical constraints. This knowledge has application in clinical gait rehabilitation as overground bodyweight support is increasingly be used as a therapeutic intervention. It also provides insight into the physiological determinants of joint quasi-stiffness during walking.

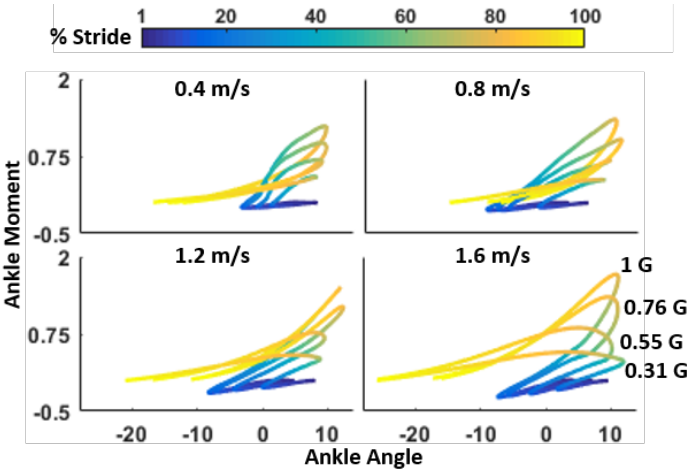

Figure 1: Ankle moment-angle loops during stance phase across speeds and at different levels of bodyweight support. Ankle angle is positive in dorsiflexion and the internal plantarflexion moment is positive.

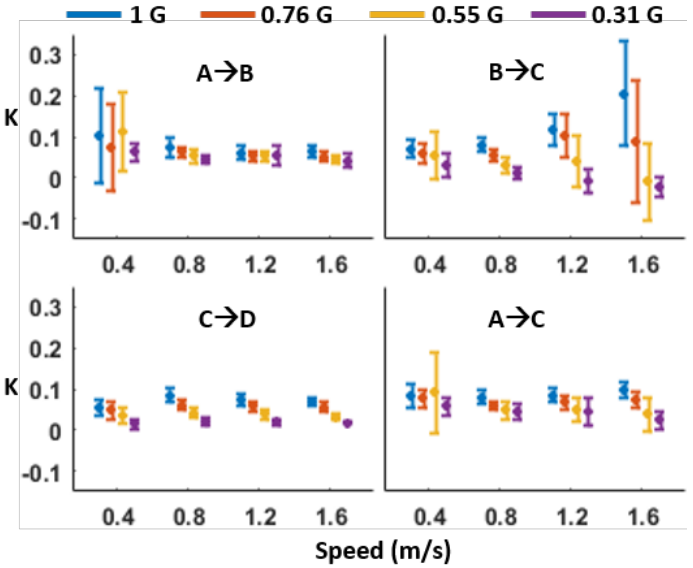

Figure 2: Quasi-stiffness of the ankle as determined by the slope of the best linear fit of ankle moment-angle relationship.

Acknowledgments

We thank Angel Bu, Han Nguyen, Skyler Levine, and Patrick Costello for their assistance collecting and processing the data.

References

[1] Shamaeim K., et al., 2013, *PLoS One*, **8**(3):e59935.
[2] Latash M.L., and Zatsiorsky V.M., 1993, *Hum. Mov. Sci.*, **12**(6):653–692.
[3] He J, et al., 1991, *J. Appl. Physiol.*, **71**(3):863-870.

Real-time Adaptive Treadmill Controller Optimization: A Parameter Sensitivity Study

Kayla M. Pariser, Jill S. Higginson
Department of Mechanical Engineering, University of Delaware, Newark, DE, USA
Email: pariserk@udel.edu

Introduction

Treadmill gait training is a commonly used rehabilitation technique to increase walking speed via increasing paretic limb push-off forces and trailing limb angles.[1] However, fixed-speed treadmills limit natural stide-to-stride variability that is essential for motor learning.[2,3] To address this, researchers have begun to use adaptive treadmills that alter belt speed in real time based on a cost function considering the user's gait mechanics, such as push-off force impulse, step length, step duration, and position relative to the treadmill center, as cost terms.[4]

The *objective* of this study is to conduct a parameter sensitivity analysis to understand how walking speed, cadence, peak push-off forces, and step-length change as the weight on the push-off force impulse in the adaptive treadmill cost function is altered. We *hypothesize* that as the weight on the push-off force impulse term is increased, the users' peak push-off forces will increase without substantial changes in speed.

Methods

Six healthy adults (4 females, 20 ± 2 years, 1.70 ± 0.11 m, 67.17± 10.63 kg) walked on a split-belt instrumented treadmill (Bertec Corp., OH, USA) at their self-selected (SS) comfortable walking speed on five modifications of the adaptive treadmill controller for two minutes each. The adaptive treadmill controller is defined by the following cost function:

$$v_{i+1} = v_i + \alpha * \left(\frac{v_{new,L} + v_{new,R}}{2} - v_i \right) \pm \beta * p^2{}_{com}$$

where α and β are the sensitivity of the treadmill speed to the user's push-off force impulse and their center of mass position relative to the treadmill center respectively.[4] The five conditions were: Half force ($\alpha \approx \frac{1}{2}\beta$), Baseline ($\alpha \approx \beta$), Double force ($\alpha \approx 2\beta$), 2 OM Force ($\alpha \approx 10^2 * \beta$), 4 OM Force ($\alpha \approx 10^4 * \beta$), presented in random order. Walking speed, cadence, and average peak push-off force were calculated using the analog data (2000 Hz) and average step-length from heel marker locations at right heel strike (100 Hz).

Results and Discussion

For all treadmill conditions except the 4 OM Force, average SS walking speed varied ±0.01 m/s from the Baseline condition. In the 4 OM Force condition, speed decreased by 0.07 m/s (Fig 1a). Similarly, cadence decreased by about 2 steps/min with the 4 OM Force condition and between 0-1 steps/min in other conditions. Average change in stride length from Baseline were mostly small (<5% height) and variable. Overall there is quite a bit of variability between participants and seemingly small average changes from the Baseline condition in the aforementioned parameters.

While the treadmill modifications from the Baseline condition do not appear to directly alter the user's speed, cadence, and step length, there were clearer differences observed between average peak push-off forces. Although the sensitivity of the treadmill speed to push-off force impulse was highest in the 4 OM condition, 5/6 participants decreased their push-off force from the Baseline condition by an average of 2.4 ± 3.84% BW. The largest increase in average peak push-off force was achieved with the Half Force condition, 2.22 ± 3.05% BW (Fig 1b). These results suggest that there may be a threshold of force sensitivity where individuals will no longer continue to increase their push-off forces and will select slightly slower walking speeds and cadences. Prior to this threshold, however, modifications in push-off force impulse sensitivity in the treadmill controller can result in increases in average peak push-off forces and maintained walking speed from the Baseline condition. However, the large amount of variation in the gait mechanics strategies of the six participants with each treadmill condition suggests that interventions may need to be designed to be user-specific.

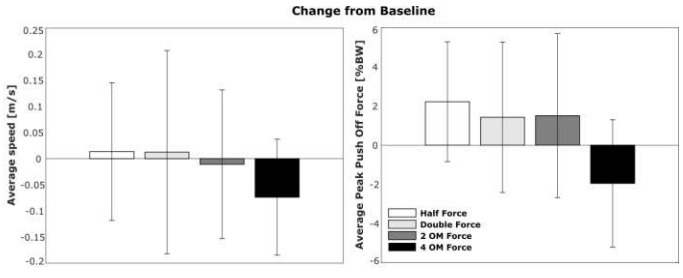

Figure 1. Average ± standard deviation of walking speed (a) peak push-off force (b) changes from the Baseline Condition.

Significance

This preliminary study demonstrates that an adaptive treadmill controller can be optimized to target increased push-off forces, but this must be done on an individual basis to achieve maximum effectiveness. Future work will seek to develop an optimal control simulation framework to understand and predict how a user's gait mechanics will change with modifications to the controller cost function.

Acknowledgments

Funding was provided by the NSFGRFP and the University of Delaware Helwig Mechanical Engineering Fellowship and NIH U54-GM104941.

References

[1] Dickstein R, *Neuro and Nural Repair*, 2008.
[2] Stergiou N et al., *Hum Mov Sci.*, 2011.
[3] Kempski K et al., *Gait Posture*, 2019.
[4] Ray NT et al., *J Biomech*, 2018.

STEP LENGTH SYNERGY DURING ADAPTIVE GAIT TASKS IN YOUNG ADULTS

Ashwini Kulkarni[1], Cho[1], Cui[1], Rietdyk[1], Barbieri[2], Ambike[1]
[1]Department of Health and Kinesiology, Purdue University, West Lafayette, IN, USA
[2]Department of Physical Education, School of Sciences, Sao Paulo State University (UNESP), Bauru, Brazil
Email : *kulkar50@purdue.edu

Introduction

Community ambulation requires navigation of various hazards such as curbs, uneven terrains, and obstacles. Foot placement around a hazard is controlled to satisfy two constraints: allow swing foot trajectories that avoid tripping/stepping on the hazard, and maintenance of stability by providing an appropriate base of support relative to the center of mass movement. Tight control of foot placement prior to obstacle crossing [1], and the relevance of step length stabilization for inferring gait stability for unobstructed walking [2] have been established. However, it is not known whether step length is similarly stabilized while negotiating hazards, specifically with the two legs on either side of a hazard. Therefore, the purpose of this study was to determine whether step length is stabilized during adaptive gait tasks.

Methods

The gait tasks included here were part of separate experiments: experiment 1 (15 young adults, 22.1±5.6 years) performed 15 trials of stepping up and down a curb and experiment 2 (17 young adults, 20.9±1.9 years) performed 15 trials of crossing an obstacle. The curb and the obstacle were placed mid-way on an 8 m walkway. The curb was 4×1×0.15 m (length×width×height). The obstacle was 1×0.008 m (width×depth) and height was 25% of leg length (mean height 0.22 m).

We used the uncontrolled manifold (UCM) approach [3] to quantify the strength of step length synergy. The strength of synergy reflects the negative covariation between the lead and trail foot distances from the curb/obstacle edge that stabilizes their sum, i.e., the step length. A motion capture system was used to identify the distance of the feet on either side of the curb/obstacle edge for each trial. The UCM analysis yields two variance components: one within the UCM (V_{UCM}, or good variance that does not change the step length), and one orthogonal to UCM (V_{ORT} or bad variance that changes the step length). We quantified the synergy index (ΔV) as $(V_{UCM}-V_{ORT})/(V_{UCM}+V_{ORT})$, which was z-transformed (ΔVz) for statistical analysis. $\Delta Vz > 0$ indicates the presence of synergistic covariation in the foot placements on either side of the curb/obstacle that stabilizes step length, with higher positive values indicating stronger synergies. To determine if synergies were present during adaptive gait tasks, one-sample t-tests were performed on ΔVz. One-way ANOVA was performed on (1) ΔVz to determine if the synergy strength was influenced by task, and (2) V_{UCM} and V_{ORT} to determine the changes in the variance components that lead to changes in ΔVz.

Results and Discussion

Synergies were observed for both curb and obstacle crossing ($t \geq 5.97$, $p<.05$; Figure 1A) indicating that step length is stabilized, which likely assists in maintaining gait stability. Step length synergy during curb crossing was lower than obstacle crossing ($F_{2,44}=24.61$, $p<.05$; Figure 1A). The lower synergy resulted from lower good variance (V_{UCM}) ($F_{2,44}=11.24$, $p<.05$; Figure 1B). Lower V_{UCM} indicates that foot placements were more stereotypical for curb crossing, which may result from three possibilities. First, the curb was shorter than the obstacle (15 vs 22 cm), requiring lower muscle activity to cross the hazard, which in turn reduces motor noise and variability. Second, curbs are prevalent in the community, and greater experience with curb crossing may have resulted in lower V_{UCM}. Third, the demand to move the body center of mass to a new height during curb crossing may impose additional foot placement requirements to facilitate the change in potential energy, thereby reducing V_{UCM}. Greater experience with curbs may have resulted in lower bad variance (V_{ORT}; $F_{2,42}=6.04$, $p<.05$; Figure 1C) as well. However, the reduction in V_{ORT} was not commensurate with the reduction in V_{UCM}, resulting in lower synergies for curb crossing.

Significance

While tight control of foot placement prior to an obstacle has been established, we have demonstrated that the step length, with the two legs planted on either side of a hazard is also a control priority while navigating hazards. Furthermore, task-specific differences in the structure of variance (i.e., the variance components) indicate additional constraints that humans impose on their behaviors. Such insights may not be apparent from conventional or clinical gait analyses and measures. Extending this study to include older and pathological populations will potentially help in understanding the etiology of falls during community ambulation.

Acknowledgments

Fulbright scholar program for Barbieri.

References

1. Muir et al., *Gait Posture*, 254-259, 2019.
2. Bruijn et al., *J.R.Soc. Interface*, 15(143), 2018.
3. Scholz et al., *Exp. Brain Res.*, 126(3), 289-306, 1999.

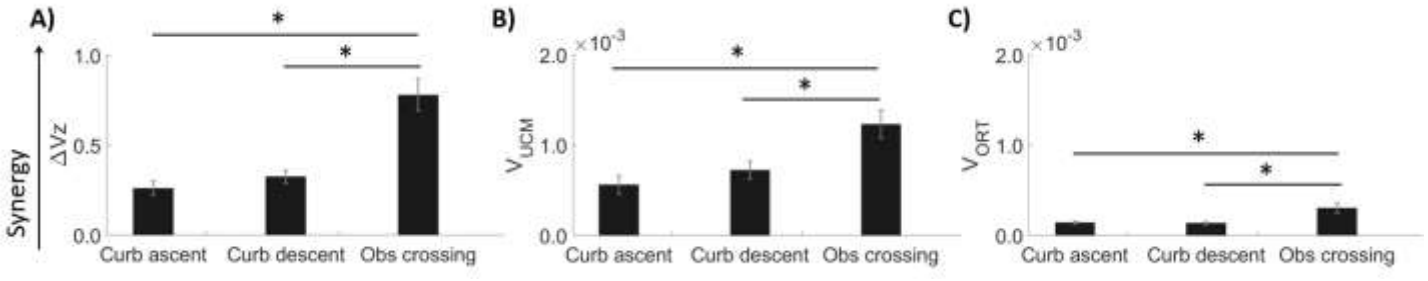

Figure 1: A) Mean ± standard error for synergy index (ΔVz); **B)** V_{UCM} (normalized units); **C)** V_{ORT} (normalized units).

The Effect of Cervical Spondylotic Myelopathy on the Dynamic Stability of Human Gait

Emily Dooley[1], Hamid Hassanzadeh M.D.[2], and Shawn Russell Ph.D.[1,2]
University of Virginia, Departments of [1]Mechanical Engineering and [2]Orthopaedic Surgery, Charlottesville, VA, USA
Email: sdr2n@virginia.edu

Introduction

Cervical spondylotic myelopathy (CSM) is a condition caused by compression of the spinal cord in the neck that results in sensory loss at the extremities due to deterioration of the afferent and efferent nerve pathways. This deterioration results in reduced sensation and motor control of the legs causing difficulty walking due to decreasing dynamic stability.[1] This often presents as a waddling gait with increased step width and time in double support.[2] Angular momentum regulation has been hypothesized as a feedback control mechanism the human body uses to keep itself stable while performing any task. Consequently, angular momentum can be used as a measure of dynamic stability of gait; where greater stability is characterized by minimizing deviation in angular momentum.[3] The aim of this study is to fully characterize the dynamic stability of patients with CSM, resulting in a tool to determine where instability in gait stems from.

Methods

Experimental data was collected for 56 subjects: 24 controls (9M and 15F, 56.2 ± 11.2 y.o.) and 32 CSM patients (15M and 17F, 59.9 ± 10.4 y.o.). Walking trials were collected on a 15m walkway at a self-selected, comfortable walking speed. A minimum of six trials were used from each subject for analysis. Subjects were recorded using 3D motion capture and five Bertec force plates. The Plug-in-Gait model was used to calculate joint kinematics as well as body segment centers, and exported to Matlab for analysis.

The angular momentum of each body segment was computed as the sum of its local angular momentum and angular momentum of segments about the whole-body center of mass (CoM).[4] Whole-body angular momentum is the sum of all of the segments. Upper-body angular momentum is the sum of the arms, thorax, and head segments, and lower-body angular momentum is the sum of the legs and pelvis. Angular momentum was decomposed into sagittal, frontal, and transverse planes for analysis.

Results and Discussion

Angular momentum analysis quantifies clear stability differences between the groups, with CSM patients showing greater angular momentum throughout the gait cycle compared to controls, indicating that they are less stable in all planes of motion.

CSM patients had increased angular momentum in the frontal plane (*Fig. 1, Col. 2*), indicating decreased stability compared to controls in both the upper and lower body. This is reflective of excessive medial-lateral tilting common to the waddling gait pattern seen in this population. Tilting is indicative of rocking from foot to foot over a wider base of support. With this angular momentum analysis it is evident that this decrease of stability is coming from both the upper and lower body rocking in unison, bringing the patient further from stability on each step.

In the sagittal and transverse planes, a phase shift is evident with the patients lagging the control group (*Fig 1, Col 1&3*). This phase shift reflects CSM patients spending more time in double support, a more stable posture; then abruptly moving a leg through the swing phase, a less stable posture. This instability compensation manifests as larger, but delayed, peaks in sagittal momentum, suggesting that CSM patients are able to regulate momentum well through extended periods of double support, but poorly regulate momentum through swing phase.

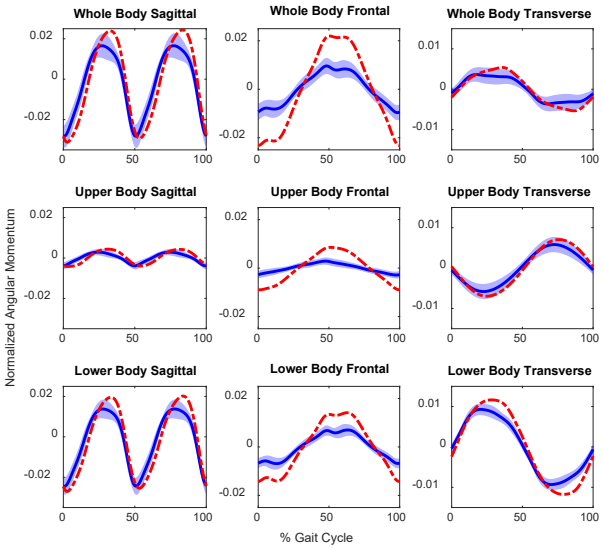

Figure 1. Angular momentum over one gait cycle in the anatomical planes. Control population shown as solid blue line with ±1 S.D. shaded. Mean of CSM patient population shown in dashed red.

Significance

Angular momentum analysis on the three anatomical planes is a useful metric for determining stability of human movement, as it can be related to both biological control processes and observed movement patterns. Deeper understanding of the instabilities of various movements can be gained through decomposition of stability to a segment-by-segment level. Understanding which segments of the body have the largest effects on stability in various movements will allow targeted therapies and rehabilitation procedures to be developed to aid populations with instability pathologies.

Specifically, instability of movement decreases functional ability, increasing inactivity. As CSM patients' ability to function independently decreases they become at greater risk of falling, as well was much more dependent on others to care for them. By gaining an understating as to why they are unstable in motion, therapy and rehabilitation strategies can be developed to counteract the deterioration of function. Ultimately, this would return independence to CSM patients, relieving the impact of the condition on the patients, caregivers, and workforce.

Acknowledgments

This work was funded in part by the OREF.

References

[1] Ono et al. (1977). *Spine*, **2**: 109-25.
[2] Dooley et al (2019). *ISB Conference Proceedings.*
[3] Russell et al. (2011). *J. Applied Biomech,* **27**: 99-107.
[4] Bennett et al. (2010). *H. Movement Sci.*, **29**: 114-2.

Task Challenge Affects Both Gait and Reaction Time Performance in Young Adults

HyeYoung Cho[1], and Shirley Rietdyk[1]
[1] Health and Kinesiology, Purdue University, West Lafayette, IN, USA
Email: * cho273@purdue.edu

Introduction

In daily life, walking is frequently completed with other tasks, and this multitasking typically results in performance decrements [1]. In general, healthy subjects prioritize gait performance over cognitive task performance when there is no specific prioritization instruction [2]. It is well known that more difficult tasks result in greater gait impairment [3]. However, systematic manipulation of the cognitive task difficulty is relatively understudied. Increasing cognitive task challenge increases the demand on cognitive resources and provides a window into capacity interference during multitasking [4]. Thus, the purpose of this study was to examine how level of both gait and cognitive challenge affects task performance while walking.

Methods

Fourteen young adults (age: 20.4±1.1 yrs.) completed fifteen conditions: three levels of cognitive task (simple, choice, and Simon reaction time (RT) tasks), three levels of gait task (no obstacle, 15%, and 30% of leg length obstacle heights), baseline for gait task without RT task, and baseline for cognitive tasks while seated. Twelve trials for each condition were block randomized. The RT task appeared once (i.e. discrete RT task) on the monitor at the end of walkway during the approach phase (1-4 steps before the obstacle). In dual task conditions, participants were not given any specific task prioritization instructions. RT, gait speed for one second after presentation of the RT cue, the number of RT errors, and the number of obstacle contacts were measured. RT and gait speed were analyzed with a two-way ANOVA (obstacle height X RT task).

Results and Discussion

Errors: More obstacle contacts were observed with the highest obstacle (6 vs 17, for 15 vs 30%, respectively), consistent with previous research [5]. The number of obstacle contacts appeared unrelated to the cognitive task. More frequent RT errors were observed with increasing cognitive challenge (1 vs 2 vs 45, for simple vs choice vs Simon, respectively).

A main effect of cognitive task was observed for gait speed ($p<0.01$; Fig. 1A). The slower gait speed for Simon versus baseline indicates that participants only reduced their speed in the most challenging RT task. Gait speed was not affected by the obstacle task ($p=0.37$), likely due to the fact that speed was calculated one second after the RT cue, which occurred on the unobstructed portion of the walkway for all conditions.

Main effects of cognitive and gait task were observed in RT (Fig. 1B). RT was significantly longer for each level of the RT task ($p<0.01$), the increase in RT with RT task was similar for seated, unobstructed walking, and stepping over obstacles (no interaction was observed). RT while obstacle crossing (both 15 and 30% heights) was significantly longer than seated RT tasks ($p<0.01$; Fig. 1B).

In order to complete the task in the most challenging condition (Simon task and the tallest obstacle), participants had the highest RT and the slowest speed. Although young adults changed both RT and gait performance, they demonstrated greater change in RT (up to 22%) than in gait speed (up to 3%), consistent with the posture first strategy [2]. Similarly, the number of RT errors were affected by the RT task, but not the gait errors. Therefore, capacity interference is evident; young adults did not complete both tasks concurrently without a change in performance in both gait and RT measures. Since older adults are more likely to demonstrate greater performance impairment or different task prioritization strategy, such as posture second strategy, future studies will expolore how older adults change performance as a fuction of the level of both gait and cognitive challenge.

Significance

Even though the RT task was only completed once while walking, young adults did not have sufficient cognitive resources to complete the task without modifying performance. Increased demands in both the RT and gait tasks further taxed the cognitive resources. In order to accomplish both tasks, young adults adopted a posture first strategy.

References

[1] Lajoie et al. (1993) *Exp. Brain Res.,* **97**:139-144
[2] Yogev-Seligmann et al. (2012) *Mov. Disord*., **27**:765-770
[3] Bloem et al. (2001) *Gait & Posture*, **14**:191-202
[4] Kahneman (1973) Attention and effort. Englewood Cliffs
[5] Muir et al. (2020) *Gait & Posture*, **77**:100-104

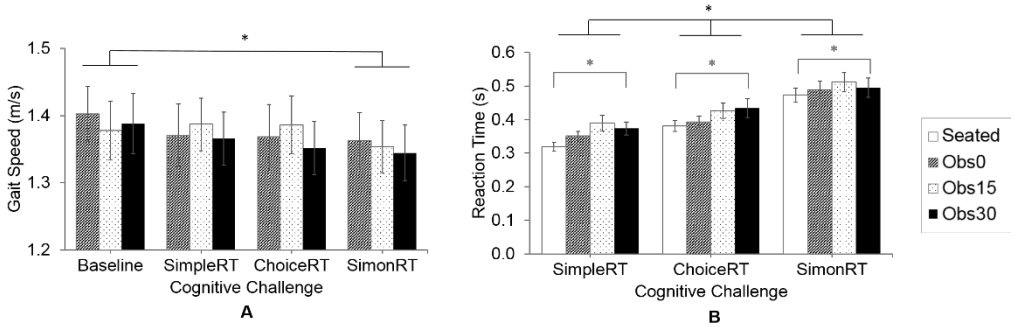

Figure 1. (A) Gait speed for one second after presentation of the RT cue as a function of cognitive challenge. (B) Reaction time as a function of cognitive challenge. Main effects of cognitive (black lines) and postural challenge (gray lines) are shown ($p<0.01$). Error bar represents standard error.

People Can Voluntarily Change Their Lateral Stepping Regulation During Goal-Directed Walking

Anna C. Render[1], Meghan E. Kazanski[1], Joseph P. Cusumano[2], and Jonathan B. Dingwell[1]
[1]Department of Kinesiology, The Pennsylvania State University
[2]Department of Engineering Science & Mechanics, The Pennsylvania State University
Email: *acr313@psu.edu

Introduction

Humans are inherently more unstable in the frontal plane [1]. Thus, appropriate lateral foot placement to stabilize walking from step-to-step is critical to prevent falls. In the frontal plane, humans regulate foot placement over consecutive steps not only to maintain balance, but to achieve other task-relevant goals as well [2]. For normal (unrestrained and unperturbed) walking, healthy humans modulate left and right lateral foot placements (z_{Ln}, z_{Rn}) to trade off regulating some lateral body position (z_{Bn}) and mostly step width (w_n) [3]:

$$\begin{bmatrix} z_{Bn} \\ w_n \end{bmatrix} = \begin{bmatrix} \frac{1}{2} & \frac{1}{2} \\ -1 & 1 \end{bmatrix} \begin{bmatrix} z_{Ln} \\ z_{Rn} \end{bmatrix}. \quad (1)$$

But for real-world walking [4], humans have to continually adapt their stepping regulation. Thus, it is important to quantify how healthy humans regulate lateral foot placements across a range of walking conditions. Here, we determined the extent to which humans can voluntarily modify how they regulate z_{Bn} and w_n from step-to-step when given explicit goal-directed feedback.

Methods

Twenty-four healthy adult men and women (12M/12F; age 23±3) walked on a treadmill in a virtual environment (Fig. 1A) and completed three, 4-minute trials for 3 conditions: normal walking (NOR), maintaining absolute lateral position (POS) on the treadmill, and maintaining constant step width (WID). During POS and WID, participants were instructed to minimize errors with respect to the goal function:

$$F_q = q_n - q^* = 0, \quad (2)$$

where $q \in \{z_B, w\}$ and $q^* \equiv$ the desired goal value. For the POS condition, their goal was to stay at the geometrical center of the treadmill in the lateral direction ($z_B^* = 0$). For the WID condition, their goal was to stay at their own preferred mean w, as calculated from the NOR condition. Participants were given explicit visual feedback of their performance at each step (Fig. 2B). For each condition, stepping time series of z_{Bn} and w_n were extracted. For each time series, variability (σ) and statistical persistence (DFA α; reflecting step-to-step regulation) were calculated.

Results and Discussion

When given POS feedback (Fig. 1C; left), participants significantly decreased ($p<0.001$) variability of z_B compared to NOR. Changes in statistical persistence (α) of z_B also indicated tighter ($p<0.001$) step-to-step regulation of z_B. In addition, α of w significantly *in*creased ($p<0.05$) compared to NOR, reflecting weaker step-to-step regulation of step width when more tightly regulating position.

When given WID feedback (Fig. 1C; right), participants significantly decreased ($p<0.001$) variability of w compared to NOR. DFA α of w remained near α=0.5, reflecting continued tight step-to-step regulation of w. In addition, α of z_B significantly *in*creased ($p<0.001$) compared to NOR, reflecting weaker step-to-step regulation of lateral position when more tightly regulating step width.

In normal walking, humans use multi-objective control of lateral stepping movements to trade-off regulating lateral position vs. step width [3]. Given explicit feedback of task performance relative to the prescribed goal function (2) for each $q \in \{z_B, w\}$, humans increased step-to-step regulation of the prescribed q to decrease variability in that q. In doing so, humans decreased step-to-step regulation of the complimentary (but non-prescribed) lateral stepping variable.

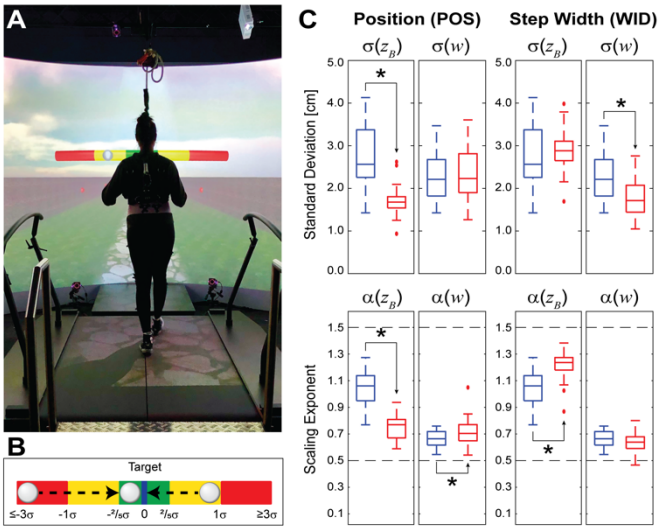

Figure 2: **A**: Participant walking in the virtual environment. **B**: Schematic of visual feedback. **C**: Results for Maintaining Position (left; POS) and Maintaining Step Width (right; WID). Boxplots of variability (top; σ) and statistical persistence (bottom; α) of z_B and w between normal walking (blue) and POS/WID conditions (red). Asterisks denote statistically significant differences ($p < 0.05$).

Significance

To accomplish each prescribed walking task, humans exhibited distinct task-specific tradeoffs between w and z_B. These experimental results are in substantial agreement with predictions from our previously published computational model of lateral stepping regulation [3]. Humans adapt lateral foot placement from each step to the next in systematic and predictable ways that depend on the specific task goals to navigate different and complex environments and task requirements.

Acknowledgments

Funded by NIH Grants 1-R21-AG053470 and 1-R01-AG049735.

References

[1] CE Bauby, AD Kuo, J. Biomech, v. 33, pp. 1433-1440, 2000
[2] SM Bruijn, JH van Dieën, J. Roy. Soc. Interface, v.15, pp.1-11, 2018.
[3] JB Dingwell, JP Cusumano, PLoS Comp. Biol., v.15, pp.e1006850, 2019.
[4] JS Matthis et al, Curr. Biol., v.28, pp. 1224-1233.e5, 2018.

Impact of flip-flops on foot and ankle biomechanics

*Kali Shamaly B.S.[1], , Erica Casto M.S.[1] Katherine Boyer PhD[1]
Department of Kinesiology University of Massachusetts Amherst[1]
Email: kshamaly@umass.edu *

Introduction

Flip-flops are a popular warm weather footwear, its style consists of a thong as the upper portion and a thin-flexible sole. Podiatrists often express concerns about flip-flops' impacts on lower extremity health and that the lack of structure may intensify any muscular or skeletal problems pre-existing in the foot[3]. Prior studies have reported differences in peak ankle plantar- and dorsiflexion angles[1], contact angle and dorsiflexion moments[2]. However, to understand the impact of flip-flops on foot health an analysis of multi-segment foot kinematics is needed. The lack of rigidity of the shoe requires a more detailed analysis to be utilized to fully understand the movements of the foot while walking in flip-flops.

Alterations in foot and ankle kinematics with flip-flops could be attributed to either the lack of an upper or the thin midsole common in a flip-flop[2] but prior work has not considered the effects of these components. For example, the thong of the flip-flop may have an impact on the inter-segmental kinematics of the foot, this may also be attributed to lack of midsole thickness and cushioning in most flip-flips. The purpose of this study was to determine the effect of (H1) the thong of a flip-flop by comparing a closed toe shoe and thick-sole flip-flop with identical soles and (H2) sole thickness and cushioning by comparing a thick-sole flip-flop and a conventional flip-flop on multi-segment foot and ankle kinematics

Methods

Fourteen healthy participants (ages 21-35 years; BMI < 30 kg/m^2) were recruited. All participants were free of lower extremity injury and provided informed consent prior to completing study procedures. Overground gait analysis was completed in four shoe conditions (two flip-flops and two closed toe shoes): Twinpin Flip-flop (Reef), Ooriginal sandal (OOFOs), Ultraboost (Adidas) and the OOmg Low Shoe (OOFOs). Participants were fit with a multi-segment foot marker-set and rigid clusters on the lower leg[4] and then walked at a prescribed speed of 1.3 m/s while markers were tracked by 11 infrared cameras (Qualysis Inc. Sweden). Kinematic and kinetic data was processed in Visual 3D (C-Motion Inc., MD). A low pass Butterworth filter with a cutoff frequency of 8Hz was used to filter raw data. Shank-calcaneus (ankle), hallux-metatarsal and calcaneus-metatarsal 3D angles were calculated. Repeated measures ANOVA was used to test for significant differences between shoes. Post-hoc testing with a least significant difference adjustment was completed where significant main effects of footwear were found.

Results and Discussion

There was a main effect of shoe for the calcaneus-metatarsal peak flexion ($p=0.001$) and inversion-eversion ($p=0.02$) angles, the hallux-metatarsal peak flexion angle ($p = 0.017$) and ankle plantarflexion ($p = 0.032$) and inversion angles at toe-off ($p = 0.016$). There was also a significant shoe effect for peak inversion ($p = 0.028$), plantarflexion ($p < 0.001$) and dorsiflexion ($p = 0.010$) moments. There was a significant effect of the lack of upper (Ooriginal vs low shoe) for the calcaneus-metatarsal and hallux-metatarsal peak flexion angles, ankle plantarflexion and eversion angles at toe-off and peak plantarflexion moment (Table 1). In the flip-flop style shoes (Twinpin vs Ooriginal) there was a significant effect of the midsole structure (H2) on the calcaneus-metatarsal peak flexion and eversion angle, hallux-metatarsal peak flexion angle and ankle plantar-flexion angle at toe-off.

To assess the combined effects of the thong with a structured midsole we also compared the differences between the Ooriginal sandal and low shoe with those of the Twinpin and Ultraboost. For both comparisons there was increased ankle eversion at toe off that is likely related to lack of an upper, this increased joint excursion has previously been associated with overused injuries[1]. However, differences in the peak plantarflexion moment were only found for the OOringial – low shoe comparision suggesting an interaction of midsole geometry and upper style on gait.

Significance

Our data shows that the impact of flip-flops on multi-segment foot kinematics and ankle kinetics results from both the lack of the upper but also the midsole structure. These results suggest that flip-flops with a more cushioned midsole may increase within foot sagital motion and the benefits and consequences of the increased motion should be addressed in future work.

Acknowledgments

Funding provided by Oofos Inc. Braintree MA

References

1. Price et al., (2014). J of Foot and Ankle Res, 7:40
2. Zhang et al., (2013). J Foot Ankle Res 6,45.
3. Shroyer et al., (2008) MSSE 40 (5):S333
4. Leardini et al., 2007. Gait & Posture, 25(3), 453-462

Table 1: Mean foot and ankle kinematic differences between open and closed toe shoe conditions. Significant difference ($p<0.05$ indicated by a. Ooriginal vs. flip-flop b. Ooriginal vs OOmg Low Shoe c. OOmg Low Shoe vs. Ultraboost d. Ultrabost vs Ooriginal e. Ultraboost vs. flip-flop f. OOmg Low Shoe vs. flip-flop

Segment	Variable	Ultraboost	OOmg Low Shoe	Ooriginal Sandal	Twinpin Flip-flop	Significance
Calcaneus-Metatarsal	Flex-ext	4.059	6.404	12.351	10.013	a,b,c,d,e,f
	Inv-ev	1.335	1.750	-1.098	0.125	a,d,e
Hallux-Met	Flex-ext	20.046	27.643	20.281	26.983	a,b,c,e
Ankle	Flex-ext(Toe-off)	-3.217	-4.346	1.516	-0.715	a,b,d
	Inv-ev(Toe-off)	1.095	2.369	4.774	4.460	b,c,d,e,f
Plantarflexion Moment	Peak	-107.441	-104.936	-98.091	-106.106	a,b,d
Dorsiflexion Moment	Peak	14.121	8.034	7.183	13.433	a,c,d,f
Inversion Moment	Peak	-23.266	-18.638	-21.375	-19.339	a,c,d,f

Self-pace treadmill controllers influence gait variability but not average walking speed

Cesar R. Castano*, Helen J. Huang
Department of Mechanical and Aerospace Engineering, University of Central Florida, Orlando, Fl, United States
Email: Castanocesar@knights.ucf.edu

Introduction

Humans walk daily on a variety of slopes and naturally fluctuate their walking speed. Self-pace controllers incorporated into instrumented treadmills allow subjects to walk at their self-selected walking speed while preserving natural gait fluctuations compared to fixed-speed treadmills [1]. These self-pace controllers are typically designed to match a subject's overground walking speed [2], but there are multiple approaches for implementing self-pace controllers. Thus, quantifying the effects of different controllers on gait is imperative. The purpose of this study was to quantify and compare gait parameters (i.e., speed, step length, and step width) using a range of self-pace controllers during uphill, downhill, and level walking. We hypothesized that different self-pace controllers would result in similar average gait speeds, but more sensitive self-pace controllers that change belt speeds more frequently to match the subject's walking speed will produce greater gait variability.

Methods

Ten young adults walked on a self-paced instrumented treadmill (M-Gait, Motekforce Link) at three slopes (+10°, incline; 0°, level; -10°, decline) and with three self-pace controller sensitivities (low, medium, and high) for 5 minutes each. We recorded their movement using a motion capture system (Optitrack) to assess gait kinematics. The self-pace controllers adjusted belt speeds by tracking the pelvis location relative to the center position on the treadmill such that greater sensitivity resulted in more frequent belt speed adjustments. Walking speed was defined as the average velocity of the treadmill belts. We used step length variance and step width variance to quantify gait variability. We also detrended speed from step length and decomposed step length variance according to the identified speed-related trends [3]. The last four minutes of each condition was analyzed. We determined statistical differences in gait parameters using a repeated-measures ANOVA at each slope, followed by a Tukey's honest significance different (HSD) test to identify differences between self-pace controllers.

Results and Discussion

Average walking speeds were similar regardless of self-pace controller sensitivity for each slope (Fig. 1A). The high sensitivity controller, however, had the greatest speed variance, which corresponded with having the most belt speed fluctuations. Not surprisingly, step length variance was also the largest when using the high sensitivity controller, which was observed in all slopes (Fig. 1B). The increased step length variance could simply be the result of increased speed fluctuations. Detrending speed from step length revealed that detrended step length variance was similar for all self-pace controller sensitivities within each slope (Fig. 1B), suggesting that the increase in total step length variance could indeed be largely attributed to the fluctuations in speed. These results supported our hypothesis. Step width variance, however, were not significantly different among the controllers.

Using controllers with different sensitivities resulted in similar average walking speeds. Controllers with greater sensitivity increased speed and step length variability, but not step width variability. These results were consistent across slopes. Previous self-pace studies used self-pace controllers at a level slope and did not detrend speed from gait parameters [1, 2]. Our study indicates that speed fluctuations of self-pace controllers at different slopes need to be accounted for when comparing gait.

Significance

These findings highlight the importance of reporting the speed dynamics of self-pace controlled treadmills at different slopes and the need to use speed detrended gait variabilities to avoid reporting differences in gait that emerge simply as a result of the speed fluctuations of the self-pace controller. These findings also have implications for interpreting energy expenditure and muscle activity for self-pace treadmill walking at different slopes.

Acknowledgments

Partial support from NIH R01AG054621 and a research grant from the Learning Institute for Elders (LIFE) @ UCF.

References

[1] Sloot LH et al. *Gait & Posture*, **2014**, 39(1), 478–484.
[2] Ray NT et al. *J Biomechanics*, **2018**, 78, 143–149.
[3] Collins SH & Kuo AD. *PLOS ONE*, **2013**, *8*(8), e73597.

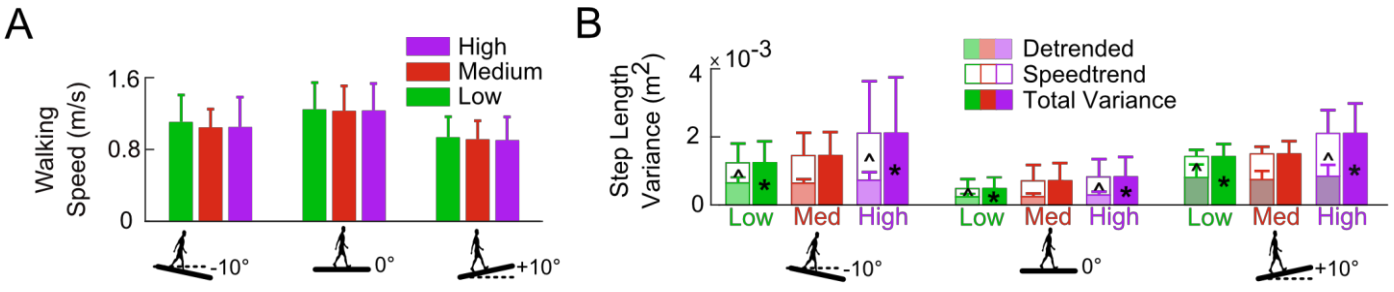

Figure 1: Average walking speed **(A)** and step length variance **(B)** at decline, level, and incline slopes with low, medium, and high sensitivity controllers. Significant (Tukey HSD $p < 0.05$) speedtrend variances (^) and total variances (*) within a given slope. Bars with the same symbol are significantly different from each other.

Roll-over Characteristics Remain Invariant in Patients with Peripheral Artery Disease

Ganesh M. Bapat[1], Jason M. Johanning[2,3], Iraklis I. Pipinos[2,3] and Sara A. Myers[1]

[1]Department of Biomechanics, University of Nebraska at Omaha, NE USA

Email: gbapat@unomaha.edu

Introduction

Lower extremity peripheral artery disease (PAD) is estimated to affect 200 million people globally, including 8-12 million people in the United States [1,2]. Atherosclerosis in the leg arteries obstructs blood flow, causing claudication pain and early fatigue, and this severely reduces walking ability in the affected patients. Our previous work showed that forward push-off is deficient in patients with PAD [3]. Hence, assistive devices such as ankle-foot orthoses and exoskeleton footwear are being developed to help patients with PAD walk further and with less pain. Roll-over shape (ROS) is considered an important design goal for such assistive devices to mimic the equivalent rocker shape generated by healthy lower limbs during the forward progression. ROS remains invariant to walking speed, carrying additional weight and walking with different types of footwear [4]. Our goal is to compare ROS characteristics between patients with PAD during pain-free and pain-induced overground walking and healthy older individuals.

Methods

Gait data of twenty patients with PAD (Age: 64.1 ± 6.6 years) and fifteen healthy older controls (Age: 72.9 ± 5.5 years) were analyzed for ROS parameters from a previously approved study. Gait kinematics and kinetics were recorded using an eight-camera 3D motion capture system and a force plate embedded in the walkway. Three gait trials at self-selected walking speed for the most affected leg during a pain-free and pain-induced overground walking were used. Patients rested between trials to ensure pain-free walking and then claudication pain was induced using a clinical protocol [5] for the pain-induced trials. The leg with lower ankle-brachial index and most symptoms was considered as the most affected.

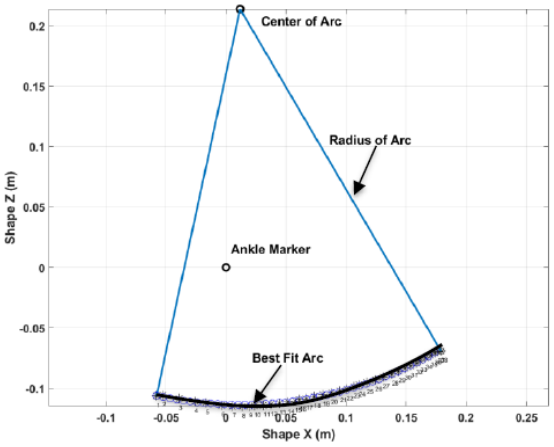

Figure 1: Roll-over shape in a representative patient with peripheral artery disease during overground walking.

The ankle-foot ROS was generated by transforming Center of Pressure (CoP) in the direction of forward progression from the lab-based coordinate system to the shank-based coordinate system. These transformed CoP data points were fit with a circular arc to characterize the ROS using parameters such as radius and arc length as shown in Figure 1. The MATLAB™ based optimization algorithm was used to find the best fitting circular arc. Height normalized ROS radii and arc length were calculated for each subject. Independent t-tests with Bonferroni correction were used to independently compare roll-over characteristics ($p<0.05$) between controls vs. patients with PAD in each walking condition.

Results and Discussion

The mean roll-over radius and arc length were not significantly different when compared between Controls and PAD both in the pain-free (Figure 2; p=0.364 and p=1.00) and in the PAD pain-induced (p=0.208 and p=1.00) walking conditions.

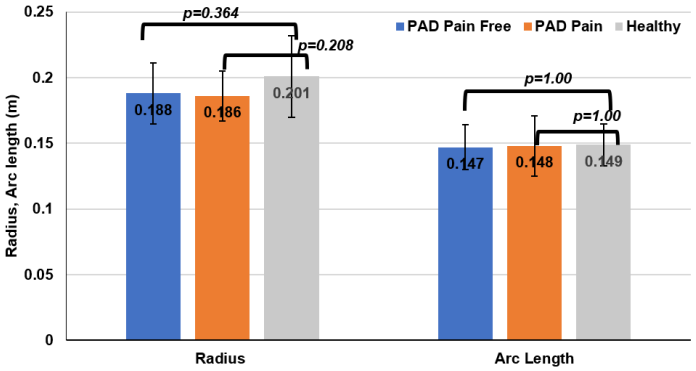

Figure 2: Mean roll-over radius and arc length during pain-free and pain-induced walking in patients with PAD and healthy older individuals. (p values are adjusted for Bonferroni correction)

Our results show that the ROS is preserved in PAD even while patients walk with claudication pain. This finding is in agreement with the general invariance model of ROS during different walking conditions in healthy young individuals [4]. Furthermore, our data support the proposition that preserving ROS is important for forward progression during walking. Literature shows that patients with PAD have modified ankle kinematics while walking with claudication pain compared to healthy older people [5]. Future studies will investigate whether altered ankle kinematics are driven by patients' inherent desire to preserve ROS during walking.

Significance

Invariance of the ROS in patients with PAD makes it a potential design objective for assistive devices that are being developed for them.

Acknowledgments

This research was supported by the NIH (RO1AG034995, RO1HD090333) and UNO UCRCA.

References

1. Fowkes FG et al., *Lancet*, 382, 1329-1340, 2013
2. https://www.nhlbi.nih.gov/health/educational/pad/docs/pad_extfctsht_general_508.pdf (Last Accessed on Mar 12,2020)
3. Chen et al., *Journal of Biomechanics*,41,2506-2514,2008
4. Hansen A. H., *PhD Thesis*, Northwestern University, 2002
5. Celis R. et al., *Journal of Vascular Surgery*,49,127-132,2009

Infant Transportation: Ground Reaction Forces During Gait

Kathryn L Havens[1], Ryan Zerega[1]
[1]Division of Biokinesiology and Physical Therapy, University of Southern California, Los Angeles, CA
Email: khavens@usc.edu

Introduction

The physical demands of new motherhood are extensive yet have not been systematically explored. Infant homo sapiens are born helpless, and caregivers must transport them during early infancy. They may chose to do so in a number of different ways: carrying in their arms, carrying in an infant car seat, wearing on their body in a structured baby carrier, or pushing in a stroller.

Researchers have begun to explore the effects of carrying an infant on biomechanics during walking. Compared to unloaded walking, holding an infant in a babycarrier on the body alters trunk mechanics as well as lower extremity joint loading [1-3]. Interestingly, compared to an unloaded condition, Brown et al. [4] showed that walking using baby carriers yielded an increase in impact peak vertical ground reaction force (GRF), braking and propulsive peak GRF and ground reaction force impulse (GRI).

These studies demonstrate that carrying infants affects gait biomechanics. But it is unclear how this relates to the health of mothers, as only healthy nulliparous young adults have been analyzed. The unique experience of pregnancy and childbirth make the application of these results to mothers unclear.

Therefore, the purpose of this study was to characterize the ground reaction forces of healthy mothers while carrying their own infants in various ways.

Methods

Six healthy mothers (age = 34.3 ± 2.6 yr, height = 1.7 ± 0.1 m, weight = 62.5 ± 7.1 kg) participated. They brought their infants (age = 14 ± 2.4 wk, weight = 6.2 ± 0.8 kg) to the Jacqueline Perry Musculoskeletal Biomechanics Research Laboratory at USC.

Each participant completed 3 trials of overground walking at self-selected speeds under multiple conditions (**Figure 1**): without infant (unload), pushing infant in their own stroller (Stroller - A), holding infant in arms (Arms - B), babywearing by holding infant anteriorly on their body in their own structured baby carrier (Wear - C), and holding infant in an infant car seat (Carseat - D).

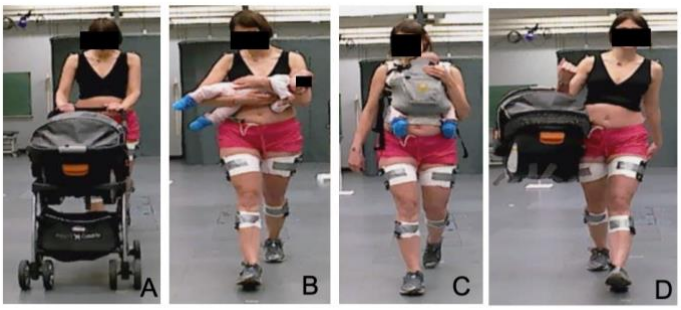

Figure 1: Gait conditions: A) Stroller, B) Arms C) Wear, D) Carseat.

GRFs were collected using AMTI force plates embedded into the lab floor (900Hz). Stance time and peak GRFs were identified. GRI was calculated as the area under the GRF-time curve. GRF variables were normalized to body weight. Custom code (MathWorks, Natick, MA) was written to identify peak GRF, impulse, and timing.

Nonparametric Friedman tests were used to compare variables between gait conditions ($\alpha < 0.05$), and Wilcoxon signed-rank tests were used as a post-hoc analysis ($\alpha < 0.05/10 = 0.005$).

Results and Discussion

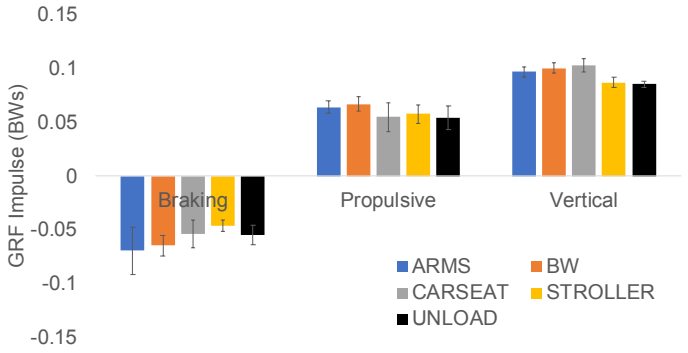

Figure 2: GRF Impulse: Braking, propulsive, and vertical. For visual purposes, vertical impulse was divided by 10.

Vertical GRI ($\chi^2(5) = 17.44$, p=0.002, **Figure 2)** and vertical peak GRF ($\chi^2(5) = 16.48$, p=0.002) differed between conditions. This pilot study was underpowered to identify any post-hoc differences. As carrying an infant is ultimately a load carriage task, the increased vertical forces is not surprising. The weight of the infants represented ~10% of the body weight of participants. Increases in peak vertical force were approximately proportional, with Arms and Wear increasing peak forces by ~15%, and Carseat ~20%. This is consistent with other studies on infant carriage [4, 5] and also backpack loading.

Braking GRI ($\chi^2(5) = 11.36$, p=0.023), peak braking GRF ($\chi^2(5) = 13.6$, p=0.009), and propulsive GRI ($\chi^2(5) = 11.52$, p=0.021) differed between conditions. The time spent braking did not differ. This suggests that braking GRI differences were driven by differences in force magnitude rather than time of force application [4, 5].

Stance time differed between individuals ($\chi^2(5) = 14.56$, p=0.006), indicating that individuals self-selected to perform the tasks at slightly different speeds. This is consistent with previous research [1], but may affect GRF magnitudes.

The results of this pilot study suggest that mothers modulate their forces when carrying their infant. Increased forces indicate that mothers are exposed to additional stresses, which may be delitirious. Additional data is needed to clarify these relationships.

Significance

Approximately 4 million women give birth in the United States each year, and many suffer from persistent low back and pelvic pain even following birth. Increased loads experienced while carrying their infant may place them at greater risk. A better understanding of these loads is the first step to mitigating pain.

References

[1] Junqueira et al., *Gait & Posture,* 2015, [2] Schmid et al., *Gait & Posture,* 2019, [3] Williams et al., *Gait & Posture,* 2019, [4]

Stride Time and Variability in Older Adults Walking on an Uneven Terrain Treadmill

Rohan Gupta[1], Ryan J. Downey[1], Natalie Richer[1], and Daniel P. Ferris[1]
[1]Department of Biomedical Engineering, University of Florida
Email: rohan.gupta@ufl.edu

Introduction

The purpose of this study was to examine the stride time and stride time variability in older adults as they walked over varying levels of uneven terrain on a treadmill. In the real world, humans encounter a range of terrain, some of it having uneven surfaces. We hypothesized that increasing the unevenness of the treadmill surface would result in subjects walking with shorter stride times and greater stride time variability. If the level of terrain unevenness led to greater stride time variability, it would be one indication that the unevenness of the treadmill could be used to increase the difficulty level of walking and decrease gait stability.

Methods

A group of 14 adults (7 females, mean age = 77.2, SD = 3.75 years) walked on a treadmill with four different surfaces to simulate varying levels of terrain unevenness (Fig. 1) [1]. The treadmill speed was adjusted for each individual but remained constant across all four surfaces. Prior to the treadmill trials, subjects walked on an 8-meter overground version of the surfaces to find their self selected walking speeds. The treadmill speed was set to 75% of each person's slowest self-selected walking speed (slowest across all conditions). The average speed for testing across all subjects was 0.58±0.20 m/s (mean±SD). Subjects completed two walking trials per surface lasting three minutes per trial. The order of the surfaces was randomized.

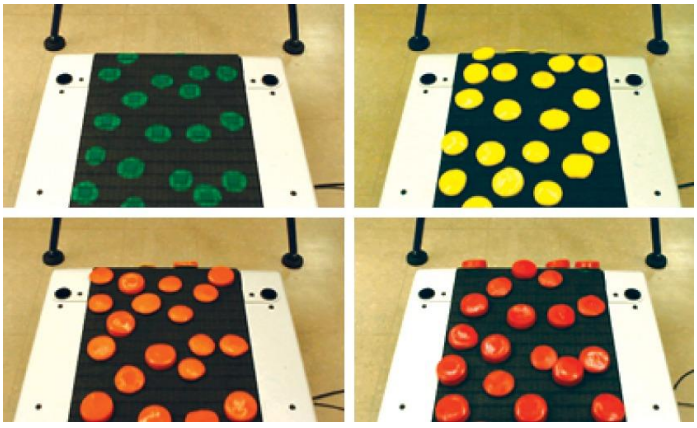

Figure 1: We secured different sized cylindrical hard foam pucks to the surface of a Woodway treadmill using hook-and-loop fasteners. The puck height varied from ~1.3, 2.5, and 3.8 cm, with a diameter of ~10-12 cm. The flat surface (green) had no pucks but flat circles. The surface unevenness level increased from yellow (low) to orange (med) to red (high) pucks.

Subjects wore capacitive insoles to measure foot pressure (loadsol, Novel GmbH, 200 Hz). We used Matlab to identify heel strike events and calculate stride duration kinematics. For each trial, we calculated two outcome variables: the average stride time (in seconds) and the stride time variability (% stride duration). We tested the hypotheses with a repeated measures ANOVA with pairwise comparisons using Tukey's method.

Results and Discussion

As the difficulty of the uneven surface increased, the average stride time decreased ($F_{3,39}$=20.1, p<0.001) and stride time variability increased ($F_{3,39}$=26.7, p<0.001) (Fig. 2).

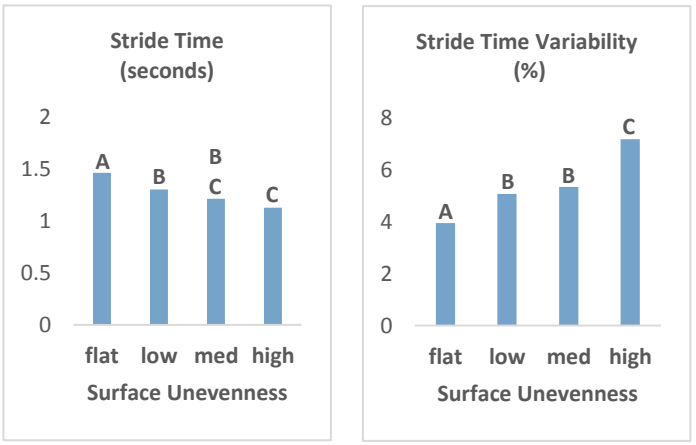

Figure 2: Mean stride time and stride time variability across all subjects. Conditions that do not share a letter are statistically different. An increase in surface unevenness led to shorter stride times and greater stride time variability.

Compared to flat treadmill walking, the most difficult surface unevenness used in this study increased stride variability by 82%. This increase is similar in magnitude to the effect of dual-task walking in elderly participants. Walking while performing a verbal fluency task or a difficult backward counting task led to an increase in stride time variability of 77% and 54%, respectively, compared to single-task walking [2].

Significance

Having a repeatable and robust method for increasing walking difficulty facilitates studying gait biomechanics and control in younger and older subjects. We used treadmill surface unevenness as a means to increase walking difficulty and gait instability. The stride time and stride time variability results suggest the uneven terrain treadmill is effective as an experimental tool for these purposes.

Acknowledgments

This work was supported by a grant from the National Institutes of Health U01 AG061389, and was partially supported by the Older Americans Independence Center at the University of Florida (P30 AG028740).

References

[1] D.J. Clark, T.M. Manini, D.P. Ferris, et al., *Front Aging Neurosci*, vol. 11. Jan. 2020.

[2] M.B. van Iersel, et al., *Arch of Phys Med and Rehab,* vol. 88, no. 2, pp. 187-191. Feb. 2007.

Ankle Power and Stiffness During Gait in Children with Hypermobile Ehlers-Danlos Syndrome

Anahita A. Qashqai[1], Nicole Vigon[1], Alyssa J. Schnorenberg[1], Michael Muriello[2], Donald Basel[2], and Brooke Slavens[1]
[1] University of Wisconsin-Milwaukee, Milwaukee, WI, USA
[2] Medical College of Wisconsin, Wauwatosa, WI, USA
Email: *Anahita@uwm.edu

Introduction

Hypermobile Ehlers-Danlos syndrome (hEDS) is the most frequent subtype of the heritable connective tissue disorder Ehlers-Danlos syndrome [1]. Often, individuals with hEDS report musculoskeletal pain, fatigue, instability, and recurrent dislocations in ankle. These conditions lead to early onset osteoarthritis and osteoporosis [1]. Laxity of tendons and ligaments is considered a major determinant for musculoskeletal complaints in the hEDS population and can be evaluated by measuring joint stiffness [2]. An important question is whether these complications in the ankle joint affect joint dynamics in children during musculoskeletal development. Thus, the aim of this study is to quantify ankle joint dynamics during gait in children with hEDS and compare them to typically developing children.

Methods

Eight children (4 males, 4 females, age: 14.5 ± 2.8 years) with hEDS participated in this study. A modified Newington-Helen Hayes marker set was utilized. A 15-camera Vicon T-Series motion capture system and four AMTI force plates [3] acquired lower extremity (LE) motion and ground reaction forces, respectively. Each subject completed multiple walking trials at a self-selected speed. The Vicon Plug-in Gait LE inverse dynamics model computed 3D joint dynamics. For comparison to typically developing children similar data was obtained from 83 children (age: 10.5 ± 3.5 years) from Schwartz et al. [5].

Ankle dorsiflexion/plantarflexion (degrees), peak ankle moment (Nm), stiffness (Nm/degree), sum of generated power (W), and sum of absorbed power (W) were computed. Ankle joint stiffness was calculated as the deravitive of the ankle moment in the sagittal plane versus the ankle joint angle during the second rocker (from the first relative maximum plantar flexion angle to maximum dorsiflexion angle in stance phase) and a linear regression was fitted [4]. The positive and negative areas under the power curve were measured to determine power generation and power absorption, respectively. The Mann-Whitney U-testwas applied to compare the hEDS and typically developing groups (significance level < 0.05).

Results and Discussion

While the dorsiflexion/plantarflexion range of motion of the hEDS group was similar to the typically developing group, the corresponding ankle moment and power were significantly different (Fig. 1. a-c). Compared to typically developing children, those with hEDS generated significantly more power (30.1 ± 15.4 W vs. 11.6 ± 5.2 W) and absorbed significantly more power (16.9 ± 3.9 W vs. 4.7 ± 0.2 W).

Significantly higher ankle moments (Fig. 1b) and powers (Fig. 1c) were observed in the hEDS group, though there was no significant difference in joint stiffness between the two groups. This may be an indication of increased effort and energy demands in children with hEDS as compared to typically developing children. The ankle joint in children with hEDS generated and absorbed more power during the stance phase compared to healthy children. Additional data collection is underway to enhance our understanding of gait dynamics metrics such as ankle power and stiffness in children with hEDS.

Significance

This novel reseach is one of few quantitative studies of patients with hEDS. We found that children with hEDS appeared to have differences in moments and powers during gait while joint ranges of motion were not significantly different. The long-term goal of this research is to improve hEDS diagnosis and to develop effective therapeutic interventions based on these dynamic joint differences to maximize quality of life for children with hEDS.

References

1. Castori, M. et al. (2010). Am J Hum Genet, A, 152(3), 556-564.
2. Galli, M. et al. (2011). Dev Disabil Res Rev, 32(5), 1663-1668.
3. Kadaba, M. et al. (1990). J Orthop Res, 8(3), 383-392.
4. Davis, R. et al. (1996). Gait & Posture, 4(3), 224-231.
5. Schwartz, M. H. et al. (2008). J Biomech., 41(8), 1639-16

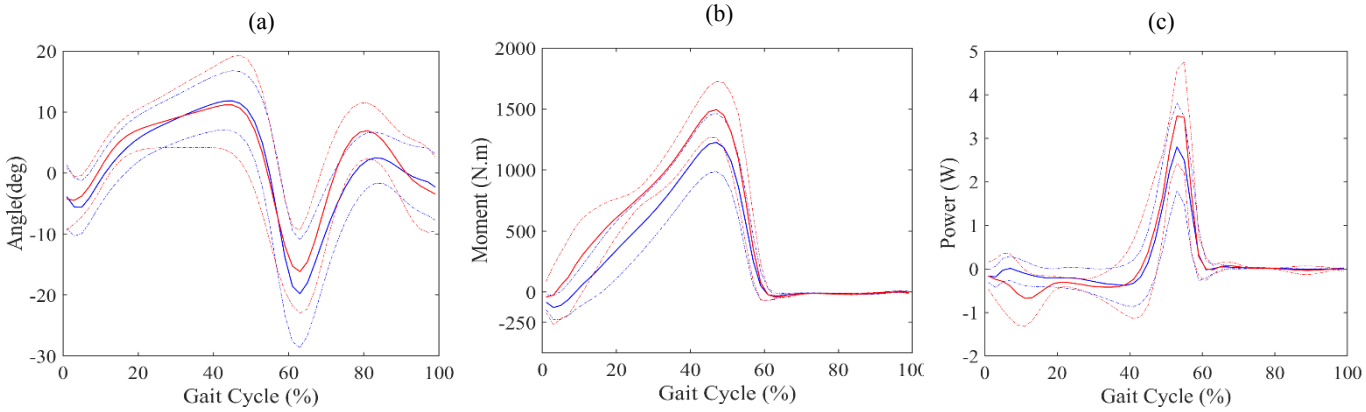

Figure 1: Ankle joint dynamics metrics. (a) Ankle angle, (b) ankle moment, and (c) ankle power during the gait cycle in children with hEDS (red lines; mean ± standard deviation) and typically developing children (blue lines; mean ± 1 standard deviation) on the dominant side.

A Data-Driven Low-Dimensional Optimization Framework Using Dynamical Movement Primitives Produces Human-Like Relationships between Walking Speed and Energetic Cost

Pouria Nozari P.[1], James M. Finley[2,3]
[1] Department of Biomedical Engineering, USC, Los Angeles, CA.
[2] Division of Biokinesiology and Physical Therapy, [3] Neuroscience Graduate Program, USC, Los Angeles, CA.
Email: nozaripo@usc.edu

Introduction

Despite the infinite number of potential strategies for walking, humans tend to walk with a stereotypical pattern. This behaviour is believed to arise, in part, from the optimization of one or more performance criteria related to, for example, energetic cost, stability, or smoothness [1]. However, optimization of motor patterns is a computationally challenging problem if one considers, for example, muscle activations at each time point to be separate decision variables. Solving the control problem in this manner requires high-dimensional trajectory optimization. Also, it is believed that when humans encounter a change or disturbance imposed by the environment the corresponding reactive responsens have a synergistic structure [2].

Dynamical movement primitives (DMPs) have been proposed as low-dimensional control policies to account for the synergistic structure of motor commands [3]. In the present paper, we used positive mechanical cost of transport as the cost function of interest for our optimizations. We hypothesized that we can learn the DMPs for nominal walking kinematic data and, using an energy optimization framework, generalize these motor patterns to different walking speeds and explain metabolic cost measures observed experimentally.

Methods

We constructed an anthropometric biped that waks on a treadmill in the sagittal plane in Matlab SimScape. The biped consisted in three degrees of freedom (DOFs), including hip, knee and ankle flexion/extension on each limb and two translational plus one rotational DOF in the torso. The lower-extremity joints were actuated by motors designed in Matlab Simulink. Also, the biped-treadmill interaction was modelled via viscoelastic elements. We represented each joint angle trajectory as a DMP where we fit the joint angle timeseries from a single participant walking at 1 m/s using locally weighted regression with Gaussian kernels.

The task was for the biped to complete a full stride starting from right push-off. We used positive mechanical cost of transport as the cost function and also added penalties to this cost term to satisfy equality constraints on the initial and final states to ensure a cyclic gait behavior. We used a genetic algorithm to find the energetically optimal walking patterns where the decision variables of interest were the gait period and joint angle amplitudes. These were the two free parameters used to manipulate the DMPs.

Results and Discussion

We found a linear relationship between the positive mechanical energy expenditure and the walking speed squared (Figure 1). These results are similar to those from Ralston [4], which showed that there is a linear relationship between metabolic rate and the walking speed squared.

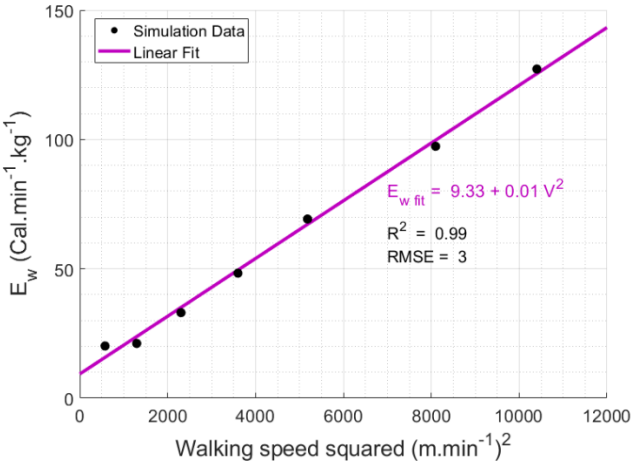

Figure 1: We found a linear relationship between the simulated optimal energy expenditure and the square of walking speed.

After normalizing this relation by the speed, we found the optimal speed of walking to lie around 0.7 m/s. This differed from the corresponding energy optimal speed value in experiments, shown to be ~1.3 m/s [4]. This likely occurred simply because in the literature, the energy expenditure is based on respiratory data, while in our model, there was no energy cost associated with standing still since we did not simulate muscle-like resting energy cost. This could result in having resting state or isometric energy terms ruled out from the modeling. Hence, a next step could be to use a more physiologically plausible model of energetics as the cost function in our optimizations.

Significance

Understanding whether there are quantifiable performance criteria that can explain a wide range of observed human behaviors is a fundamental question of human motor control. A benefit of using a low-dimensional optimization framework is that it will need less number of variables in optimization, thus it will take far less time to find the optimal patterns, compared to full trajectory methods. In addition, it is more consistent with the concept of synergistic control of movement, which may better mimic the physiological constraints on learning and control.

References

[1] Sánchez et al. Scientific reports 7.1 (2017): 7682.
[2] De Groote et al. Frontiers in computational neuroscience, 8 (2014): 115.
[3] Ijspeert et al. Neural computation 25.2 (2013): 328-373.
[4] Ralston, H.J. Internationale Zeitschrift für Angewandte Physiologie Einschliesslich Arbeitsphysiologie 17.4 (1958): 277-283.

Walking biomechanics before and after 30 minutes of walking in young adult women

Jillian L. Hawkins[1], Glenn N. Williams[1], Stella L. Volpe[1], Sinclair A. Smith[1], Dixie L. Thompson[2], and Clare E. Milner[1]
[1]Drexel University, Philadelphia, PA
[2]University of Tennessee Knoxville, Knoxville, TN
Email : jillian.hawkins@drexel.edu

Introduction

Up to 35% of sedentary women get injured, when they start participating in physical activity [1]. Sedentary adults are often encouraged to walk for physical activity, which leads to 25% of all adults getting overuse injuries [1]. Patellofemoral pain (PFP) occurs in 10% to 23% of young adults [2,3]. Thus, sedentary young adult women may be at risk for PFP during walking. The pathomechanical model hypothesizes that small peak knee flexion angle and peak knee extensor moment during walking would likely increase stress on the patellofemoral joint leading to PFP [4]. Additionally, large knee abduction and external rotation angles and hip adduction and internal rotation angles at peak knee extensor moment have also been associated with PFP [4]. The purpose of the study was to determine differences in walking biomechanics associated with PFP following 30 minutes of walking in sedentary and active young adult women.

Methods

Thirty (15 sedentary, 15 active) young adult women (age: 23 (3) years; height: 1.64 (0.08) m; mass: 61.6 (9.6) kg) were recruited and provided written informed consent. Retroreflective markers were placed on the lower extremities and trunk of participants to define joint centers and track body segments [5]. Participants walked across the gait laboratory for five good trials at 1.4 ± 5% m/s. Three-dimensional gait analysis was performed using motion capture sampling at 200 Hz and force plates sampling at 1000 Hz. Next, participants walked for 30 minutes on a treadmill at a self-selected pace where they could "talk but not sing" per Centers for Disease Control and Prevention (CDC) physical activity recommendations [6]. Participants then walked for five additional good trials across the gait laboratory.

Joint angles were determined using joint coordinate systems [5] and joint moment was determined using inverse dynamics. Peak knee flexion angle and peak knee extensor moment were determined during the first 60% of stance. Data were filtered using a low pass fourth-order Butterworth filter at 6 Hz. Means, standard deviations, and effect sizes were determined for all variables of interest. Dependent t-tests were used to compare peak knee flexion angle and extensor moment before and after 30 minutes of walking. A p-value of < 0.05 was considered significant. Findings were also compared to minimum detectable differences (MDDs) determined from laboratory data (Table 1).

Results and Discussion

Sedentary and active young adult women had similar responses to 30 minutes of walking (Table 1). Peak knee flexion angle significantly increased following 30 minutes of walking in the sedentary (p=0.026) and active (p=0.045) groups. However, these increases had small effect sizes and did not increase more than the MDD in either group. Peak knee extensor moment did not change following 30 minutes of walking in the sedentary (p=0.061) and active (p=0.210) groups. These results suggest that the stress on the patellofemoral joint likely did not increase following 30 minutes of walking. These findings are similar to those previously determined for peak knee flexion angle and extensor moment in active young and mid-life adults following 30 minutes of walking [7,8]. The results for knee abduction and external rotation angles and hip adduction and internal rotation angles at peak knee extensor moment further support this finding.

Overall, there were only a few biomechanical changes following 30 minutes of walking in sedentary and active young adult women, none of which were associated with PFP. Therefore, walking for 30 minutes did not increase stress on the patellofemoral joint, indicating no increased risk of PFP in either sedentary or active young adult women.

Significance

Our findings suggest that both sedentary and active young adult women can walk for 30 minutes without detrimental changes to walking biomechanics that may increase their risk of PFP. Thus, sedentary young adult women can safely follow CDC guidelines to walk for physical activity at a pace where they can 'talk but not sing'.

References

1. Howard et al. *J Women's Health.* **22**, 1038-1042, 2013.
2. Dey et al. *BMC musculoskel disord*. **17**, 237, 2016
3. Xu et al. *BJSM*. **19**, 165, 2018.
4. Powers et al., *BJSM*. **51**, 1713-1723, 2017
5. Cole et al. *J Biomech Eng*. **115,** 344-349, 1993.
6. CDC. *Measuring Physical Activity Intensity*, 2015
7. Singh et al., *MSSE*. **49,** 555-562, 2017.
8. Hafer et al., *Gait Posture.* 70, 24-29, 2019.

Table 1: Walking biomechanics before and after 30 minutes of walking in young adult women

	Sedentary (n=15)			Active (n=15)			
	Before walk Mean (SD)	After walk Mean (SD)	Effect size (d)	Before walk Mean (SD)	After walk Mean (SD)	Effect size (d)	MDD
Peak knee flexion angle (°) *	13.7 (5.2)	15.9 (5.5)	0.4	16.8 (4.8)	18.2 (5.6)	0.3	3.6
Peak knee extensor moment (Nm/kg)	0.44 (0.22)	0.53 (0.20)	0.5	0.61 (0.21)	0.64 (0.22)	0.1	0.15
Knee abduction angle (°)	-0.1 (2.1)	-0.1 (2.8)	0.0	0.2 (3.3)	1.0 (3.8)	0.2	1.3
Knee external rotation angle (°)	8.0 (4.0)	6.0 (4.5)	0.5	3.5 (4.4)	0.9 (4.4)	0.6	2.6
Hip adduction angle (°)	9.3 (2.3)	9.2 (2.7)	0.0	8.6 (2.6)	8.6 (2.7)	0.0	1.2
Hip internal rotation angle (°)	6.0 (4.7)	2.8 (5.7)	0.6	5.4 (4.7)	1.6 (4.7)	0.8	1.6

*: p<0.05; Nm/kg: Newton-meters per kilogram; primary variables: bold; secondary variables at peak knee extensor moment: italics

Biomechanical Analysis of Hippotherapy Using 3-D Motion Capture and Surface Electromyography

Anne Marie Holter[1], Nathan Luzum[1], Grace Cassidy[1], Chandler Sizer[1], Jack Lipold[1], John DesJardins, PhD[1]
[1]Clemson University Department of Bioengineering
Email: jdesjar@clemson.edu

Introduction

Hippotherapy is the use of horseback riding as an alternative intervention within physical rehabilitation. This is useful because patients are stimulated to produce 3D movements and muscle excitation patterns that they may not be able to produce on their own[1]. Specifically, it is believed the pelvic motion of the horse is transferred to the rider and generates human kinematics similar to walking, which could be beneficial in the area of gait rehabilitation[2]. The scope of this research is to track horse and rider biomechanics with surface electromyography (EMG) and 3-D video motion capture to monitor horse kinematics and rider biomechanic responses. To further test musculature activation similarities, EMG was paired with motion capture data. It was hypothesized that horseback riding would stimulate similar biomechanic response in the rider compared to healthy gait.

Methods

Ten college aged females (18–22 yr) with no known gait impairments and normal BMI (19–24) were enrolled in this study and divided into two control groups, novice and experienced horseback riders. Reflective biomarkers were placed on anatomical landmarks of the subjects and horse for the 3-D video motion capture (Qualisys, Sweden) tracking. Each subject was also equipped with eight EMG sensors (Biometrics, LTD, United Kingdom). These sensors were placed on four key muscle groups (rectus femoris, biceps femoris, rectus abdominis, erector spinae) on each side of the body. Each subject was analysed while horseback riding and while walking on a treadmill at fixed speeds. Three passes were recorded for ridign and walking, and a single stride was chosen for each pass and were averaged for single stride comparison.

Results and Discussion

A summary of EMG data is shown in **Table 1**. EMG waveform data for the right erector spinae can be seen in **Figure 1**. These waveforms were recorded for each of the four muscles of interest.

Comparison	(α = 0.05)
Novice Average - Walking vs. Riding	N/A
Experienced Average - Walking vs. Riding	R. E.S
Novice Maximum - Walking vs. Riding	N/A
Experienced Maximum - Walking vs Riding	R. E.S

Table 1: EMG Data Statistical Summary - 8 muscle data sets within each comparison group. Only right erector spinae in experienced average signals and maximum signals were considered significantly different.

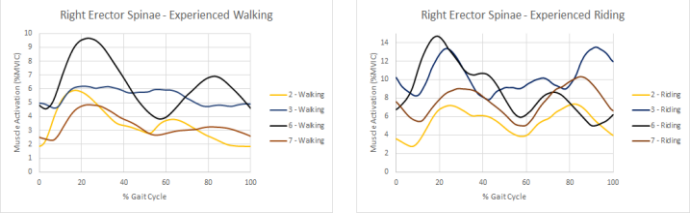

Figure 1: Right Erector Spinae EMG Waveform Data

Overall, very little significant differences existed between the peak and average muscle activity of walking and riding in both control groups (**Table 1**). The right erector spinae (R. E.S.) had significantly greater average and peak contractions in the experienced control group while riding. However, all other muscular activity within groups exhibited no significant differences between walking and riding. The significant activity in the right erector spinae may be due to Rider 6's large peak activity, however, they have not been ruled as an outlier because their kinematic riding patterns may provide further insight. The lack of significant differences between walking and riding suggests that horsebacking riding may stimulate rider musculature similarly to normal, healthy gait.

Sample EMG waveforms exhibited two-peak activity within walking and riding, again referencing their kinematic similarities (**Figure 1**). 3D video motion capture data is still being processed. Rider pelvis and torso Roll, Pitch, and Yaw kinematic patterns will be of interest and angular range of motion will be compared between walking and riding, and further cross correlated to corresponding muscle excitation.

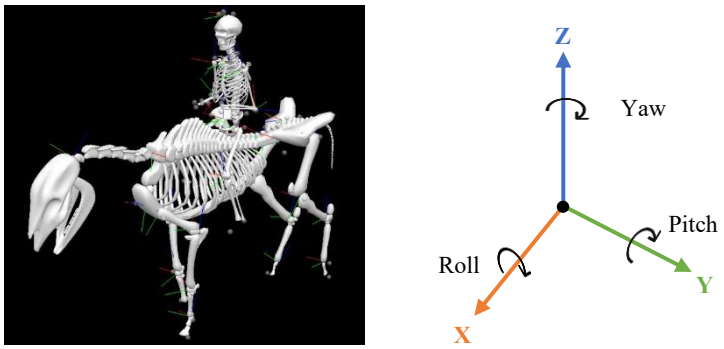

Figure 2: Human and rider skeletal model with reference axis

Significance

Hippotherapy is largely under researched and this data will help lay groundwork for further quantification of horse-ride biomechanical relationships. Specifically, our research group intends to use equine assisted activies as a physical therapy intervention for post-stroke patients, with a focus on gait rehabilitation. This form of physical intervention has the potential to fulfill the need for pelvic movement exercises that stimulate cyclic gait patterns and muscular trunk control.

Acknowledgments

Our research group would like the acknowledge the Clemson University Equine center for their continued assistance and use of facilities.

References

1. Garner BA, Rigby BR. (2015). Human pelvis motions when walking and when riding a therapeutic horse. *Human Movement Science*.
2. Lee CW, Kim SG, Yong MS. (2014). Effects of Hippotherapy on Recovery of Gait and Balance Ability in Patients with Stroke. Journal of Physical Therapy Science.

Developing a Synergistic Control Strategy for Knee and Ankle Exoskeleton Assistance

Safoura Sadegh Pour Aji Bishe[1], and Zachary F. Lerner[1]
[1]Department of Mechanical Engineering, Northern Arizona University, Flagstaff, AZ, USA
Email: SafouraSadeghpour@nau.edu

Introduction

Many studies have been conducted to design exoskeletons in order to assist impaired walking [1], [2]. However, no viable options are available for individuals with moderate-to-severe neuromuscular impairment, like from cerebral palsy (CP), but who are able to walk in some capacity [3]. Commercial full-body exoskeletons, like the EksoGT from Ekso Bionics, are likely too big, bulky and slow to help a child with some walking ability. At the same time, light-duty, single joint exoskeletons may not provide enough assistance for patients with severe CP to walk independently. Therefore, our goal is to design a device that fits in the middle: a lightweight multi-joint exoskeleton where each joint works in coordination with one other.

Our first objective was to develop a simple real-time knee as well as ankle joint moment prediction model and verify our model by comparing the predicted joints moment with the that of estimated by Opensim®. Our second objective was to use the model to create an adaptive control strategy capable of providing synergistic ankle and knee assistance based on real-time joint moment estimation. We validated our synergic controller through comparing the metabolic cost of transportation and ankle as well as knee joints angles with a reference controller by testing on an unimpaired individual.

Methods

We developed a strategy to control a light ankle-knee exoskeleton based on the calculated biomechanical moment of the respective joints. We used Force Sensitive Resistors (FSRs) to estimate ground reaction forces. The ankle and knee joint moments were calculated using inverse dynamics equations. Then, the joint moments were normalized by dividing by the maximum joint moment during baseline walking. The magnitude of the desired moment was set based on the user's preference. The reference controller was a function of time, providing knee assistance during the stance phase and ankle assistance during the mid-late stance phase. An unimpaired subject was asked to walk over a treadmill while wearing our ankle-knee exoskeleton with (1) zero assistance, (2) the reference controller, and (3) the synergic controller.

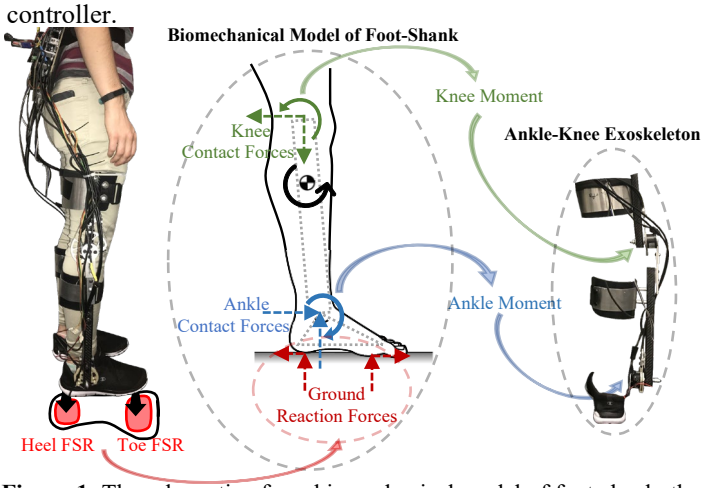

Figure 1: The schematic of our biomechanical model of foot-shank, the control strategy based on this model, and the ankle-knee exoskeleton designed in NAU Biomechatronic Lab.

Results and Discussion

Statistical indices (R^2 of 0.91 and 0.45 as well as root mean square of 0.10 and 0.24 for ankle and knee respectively) shows that our model could predict the ankle plantar flexion moment and stance phase knee moment with reasonable accuracy. The assistance provided by our synergic control strategy reduced the metabolic cost of walking 11.6%, while the reference controller only reduced it by 1.1% relative to zero moment assistance. Our novel control strategy increased the ankle plantar flexion and knee extension angle of the unimpaired subject during the stance about 7.6% and 0.7% respectively, which is less than the increased angles in the case of walking with the reference controller (11.6% and 1.1%). It means that our synergic controller decreased the unimpaired individual's cost of walking without effecting remarkably on her walking pattern.

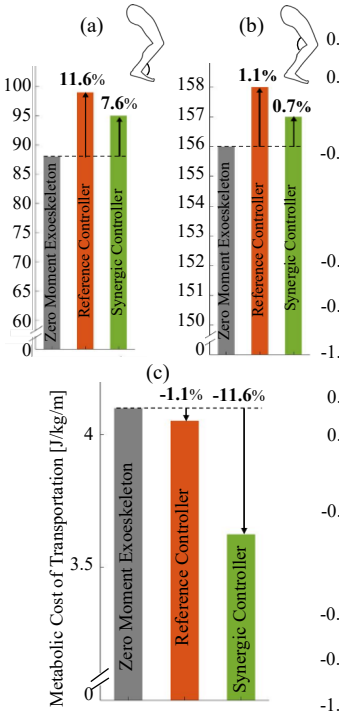

Figure 2: Maximum (a) plantarflexion ankle and (b) knee extension angle during stance phase in degree. (c) Metabolic cost of walking.

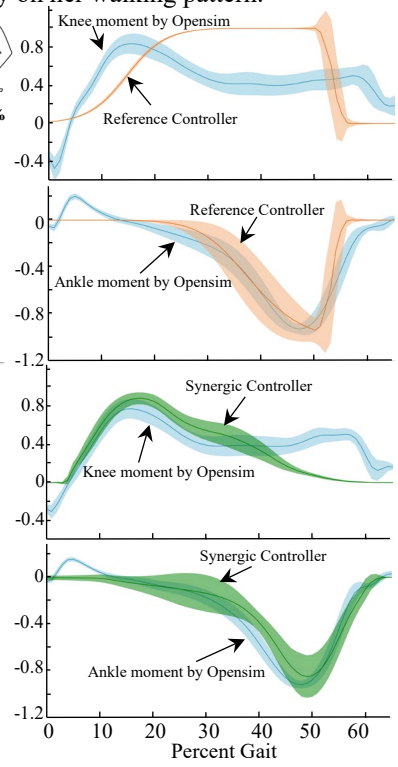

Figure 3: Normalized ankle and knee joint moment estimated by Opensim in compare to the synergic controller and a reference controller during stance phase.

Significance

There have been many studies on control strategies for exoskeletons for patients with CP to overcome their walking restriction, but there is a dearth of research on an exoskeletons adaptive-synergic control strategy for individuals with severe CP, and therefore much research is needed in this area. The ultimate goal of this research is to design a synergic control strategy suitable for assisting individuals with severe CP.

References

[1] M Vukobratovic et al., *Biped Locomotion: Dynamics, Stability, Control and Application*. (Springer Berlin Heidelberg, 2012). [2] G Orekhov et al., IEEE Trans Neural Syst Rehabil Eng 28 (2), 461 (2020). [3] A Joseph, (Scientific American, 2017).

Kinematic Response to Adaptive Speed Treadmill versus Fixed Speed Treadmill Walking in Older Adults

Parker, Sheridan M[1], Hedrick, Erica A.[1], Knarr, Brian A[1]
[1]Department of Biomechanics, University of Nebraska at Omaha, Omaha NE, USA
Email: sheridanparker@unomaha.edu

Introduction

Previous literature has reported that treadmill walking at a fixed speed can lower the joint angle kinematic variability of individuals compared to overground walking, as typically seen in a community dwelling environment [1,2]. It is thought that these changes might be due to differences in neuromuscular control on a fixed speed treadmill as a result of constraining the individual's walking speed [2,3]. This study used a novel Adaptive Speed Treadmill (AST) controller to attempt to emulate overground walking based on kinetic and spatio-temporal walking parameters by including unconstrained walking speed as a factor during treadmill walking [4]. However, the kinematic response between Fixed Speed Treadmill (FST) walking and AST walking is not well understood.

The aim of this study is to determine the kinematic response exhibited between AST and FST walking in older adults. Our first hypothesis is that older adults will walk faster on the AST as the AST more closely emulates overground walking. Our second hypothesis is that older adults will exhibit increased hip, knee, and ankle flexion while walking on the AST as the AST allows for unconstrained walking speeds close to overground walking.

Methods

Sixteen older adult subjects participated in the study (14F, 69.6±4.9 years, 1.6±0.1m, 73.1±12.7kg). The FST condition consisted of three mintues of walking at the participants' self-selected walking speed. The AST condition consisted of three minutes of walking using an adaptive speed treadmill controller. Based on Ray et al. (2018) which found that young healthy adults walk faster on the AST, we have grouped our participants as Responders (RESP), participants who walked faster on the AST, and Nonresponders (NRESP), participants who walked faster on the FST [4]. A 14 camera motion capture system was used to collect hip, knee, and ankle joint kinematics.

Sagittal plane hip, knee, and ankle joint angles were filtered using a 6Hz cut off Butterworth filter. Stride normalized left and right sagittal plane hip, knee, and ankle joint angles were calculated for both FST and AST condtions. Data analysis was performed in Visual 3D and Matlab R2018a.

Our previous analysis reported no statistical differences in peak sagittal joint ankles for FST and AST conditions for this population. Statistical Parametric Mapping (SPM) analysis was performed for sagittal plane hip, knee, and ankle joint angles comparing AST and FST conditions for both the RESP and NRESP groups to determine kinematic differences throughout the gait cycle. Statistical analysis was performed in Matlab R2018a with significance set to $\alpha \leq 0.05$.

Results and Discussion

Twelve participants walked 0.3±0.2 m/s faster on the AST and were included in the RESP group while four participants walked 0.1±0.1 m/s faster on the FST and included in the NRESP. For the RESP group during the AST condition a 3.1° increase in knee flexion, a 3.8° increase in hip flexion and, a 0.8° increase in ankle dorsiflexion during the loading phase (0-20% stance) was exhibited (Figure 1). Additionally, during terminal swing (90-100% stance) a 3.3° and 1.4° increase in hip flexion and ankle dorsiflexion, respectfully, was exhibited during the AST conditon. These values are comparable to previously reported minimal detectable changes for overground walking in older adults [5]. Differences in the loading phase indicates that the RESP group might be changing their kinematic strategy in favor of a more pronounced heel strike and a shorter loading phase due to an increase in walking speed compared to the FST. The 3.3° hip flexion and 1.4° ankle dorsiflexion increases observed during terminal swing may be due to either increases in trunk flexion or earlier activation of the quadriceps and ankle dorsiflexors to increase step length as a result of a 0.3±0.2 m/s increase in walking speed and in anticipation of a shorter loading phase.

There are no significant differences between treadmill conditions for all three sagittal plane joints for the NRESP group, indicating that the NRESP group is not changing their kinematic strategy in response to the different treadmill types. This is potentially due to participants constraining their walking speed.

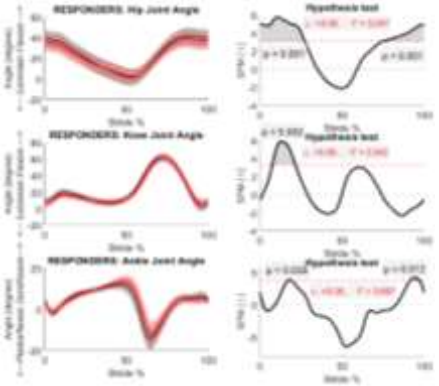

Figure 1: SPM analysis for the RESP particint group. Left graphs depicts stride normalized joint angles for AST (black) and FST (red) conditions. Right graphs show the statistical t-test results for each point during stride.

Significance

These results indicate that including unconstrained walking speed during treadmill walking via an adaptive speed controller may change the kinematic strategy used by individuals that walk faster compared to a fixed-speed treadmill. Future research is needed to compare AST kinematics to overground community dwelling walking kinematics to determine if the AST is a suitable device for research and/or therapy in clinical populations.

Acknowledgments

Funding: R15HD094194, NIHP20GM191090, U54GM115458, UNO GRACA16847

References

[1] Hollman J et al. (2016) *Gait Posture.* **43**:204-209. [2] Dingwel J et al. (2001) *J Biomech Eng*. **123**:27. [3] Kim J et al. (2012) *Conf Proc IEEE Eng Med Biol Soc*. **2012**:3061-3064. [5] Ray N et al. (2018) *J Biomech.* **78**:143-149. [6] Santo Bueno G et al. (2019) *Gait Posture*. **72**:76-81.

Influence of Added Mass on Overground Kinematics and Kinetics in Young Adults

Shanpu Fang[1], Vinayak Vijayan[1], Megan E. Reissman[1], Timothy Reissman[1], Allison L. Kinney[1]
[1]Mechanical and Aerospace Engineering, University of Dayton, Dayton, OH, USA
Email: akinney2@udayton.edu

Introduction

An active gait exoskeleton has the potential to improve a wearer's mobility by providing lower limb torque assistance. To do this, the exoskeleton must have an accurate estimate of the intended gait pattern of its wearer. However, intent recognition with accurate gait estimates is difficult to achieve. As each device creates unique laden mass to the wearer, the wearer will respond with unknown changes to their baseline kinematics. Prior studies have shown that these changes are small but observable [e.g. 1]. Prior results are limited as the subjects were mostly young, healthy males walking on a treadmill, which alters joint kinematics [2]. In this work, we aim to increase understanding of the influence of added mass by presenting the kinematic and kinetic changes of 10 young, healthy participants (6 females and 4 males) who performed overground walking with 6 different conditions of laden mass on their lower body. Our long-term goal is to provide guidance for exoskeleton design which minimizes the estimated changes to the wearer's baseline, or unladen, gait.

Methods

Ten participants (20-25 years of age) who gave written informed consent completed the IRB approved study. Each participant performed overground walking at a self-selected speed with added masses: 2 or 4 pounds on each shank, 2 or 4 pounds on each thigh, and 8 or 16 pounds on the waist. The 6 added mass conditions were randomized, with 5 trials per condition. An 8-camera Vicon motion capture system tracked reflective markers (n=43) placed on the torso, pelvis, and lower limbs and data were post-processed using Nexus 2.9. Ground reaction forces were recorded on 2 Bertec force plates. Kinematics and kinetics were estimated in OpenSim using subject-specific models. Sagittal plane hip, knee, and ankle kinematics and kinetics were averaged across each subject for each condition. Mean differences in kinematics and kinetics relative to baseline were analyzed [3].

Results and Discussion

Added mass at the waist, thigh, and shank caused observable changes (<6°) in kinematics relative to baseline (Fig. 1). Changes in joint kinetics were also observable (<0.2 N-m/kg).

Both levels of added waist mass increased hip flexion during the gait cycle, with the 16 pound mass causing the largest changes of 4-6° (Fig. 1: 8_0_0, 16_0_0). The peak hip flexion moment in late stance was also decreased by up to 0.1 N-m/kg with the 16 pound mass. Despite the larger influence on the hip, changes in both the knee and ankle joints were small for added waist mass. Thus, an exoskeleton design with added waist mass below 8 pounds may reduce changes in walking considerably.

Added thigh mass (Fig. 1: 0_2_0 and 0_4_0) had the smallest overall impact on the joint kinematics. Both levels of added thigh mass caused joint angle changes under 2° relative to baseline. Added thigh mass also influenced the kinetics, with the 4 pound mass decreasing the peak hip flexion moment and the plantarflexion moment in late stance by ~0.1 N-m/kg. This suggests that exoskeleton designs with up to 4 pounds of thigh mass will be well tolerated by young adults in walking.

Added shank mass, particularly the larger 4 pound mass, caused the largest changes in both knee and ankle kinematics relative to baseline (Fig. 1: 0_0_2 and 0_0_4). The 4 pound mass led to the largest changes observed at both the knee and ankle joint. The 4 pound mass increased knee flexion throughout stance and reduced knee flexion during the majority of swing reaching a peak of ~5° at 85% of the gait cycle. The larger shank mass caused relatively small changes in ankle angle during stance, but caused larger changes to the ankle kinematics during swing phase. Both levels of added shank mass increased the hip flexion moment in late stance and caused the largest changes in the ankle moments. Therefore, our younger adults had less ability to adapt to added shank mass that is typical of ankle exoskeletons.

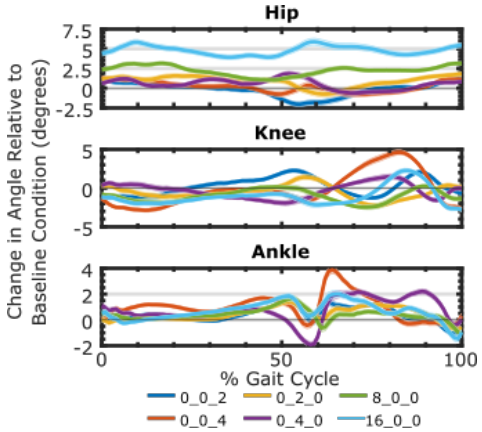

Figure 1. Mean kinematic changes relative to the baseline condition. Shaded bands are the 95% confidence intervals (CI). Regions where the CI bands do not cross zero were considered statistically significant [3]. Legend indicates added waist, thigh, and shank mass in pounds.

Significance

As added thigh mass up to 4 pounds was well tolerated by the younger adults, an exoskeleton design that adds thigh mass will likely induce the smallest changes during walking. Although added mass at the waist caused larger changes at the hip, the smaller 8 pound mass caused minimal alterations at the knee and ankle. Therefore, exoskeletons may be better designed if they limit added mass to below 4 pounds and distribute mass across the thigh and waist. Our results suggest that younger adults have the capacity to adapt to added masses representative of an exoskeleton. However, our results are limited since other potential populations for exoskeleton use, i.e. older adults, likely do not have the same capacity to adapt. Future work will extend this study to observe how older adults (65-85 years of age) respond to added mass during walking.

Acknowledgments

We would like to thank Alice Luanpaisanon for her assistance.

References

[1] Browning RC et al. (2007) *Med Sci Sports Exerc* **39**: 515-525.
[2] Sloot HL et al. (2014) *Gait Posture* **39**: 478-484.
[3] Andrade AGP et al. (2014) *J Appl Biomech* **30**: 348-352.

Treadmill Belt Acceleration Timing Affects Stability During Walking

Esmeralda Vazquez[1,2], Pawel R. Golyski[2], Jennifer K. Leestma[2], and Gregory S. Sawicki[2]
[1]South Atlanta High School, [2]Georgia Institute of Technology
Email: pgolyski3@gatech.edu

Introduction

Balance is a major health problem in the United States, with around 30% of adults over 65 years old falling each year – often caused by trips or slips [1]. In a laboratory setting, treadmill belt accelerations are a reproducible way of emulating slips [2]. Previous research using treadmill belt accelerations looked at the effect of acceleration magnitude on walking stability but overlooked the effect of *when* in the gait cycle the perturbation is delivered [3].

During 15-20% of the gait cycle is when a single foot is flat on the ground during initial support and the body's center of mass is posterior to the foot. This leads us to hypothesize that between 15 and 20% of the gait cycle is when individuals are most vulnerable to losing balance during walking due to a rapid treadmill belt acceleration.

Methods

We had 10 subjects walk on a split-belt treadmill at 1.25 m/s while rapid (15 m/s^2), brief (0.2 sec) accelerations were applied to a single treadmill belt in a randomized order. While the subjects walked, we "slipped" each leg 10 times at 10, 15, 20, 30, 40, and 50% of the gait cycle. We used three metrics to quantify stability of the step before, during, and for four steps after the perturbation. The three metrics we used to quantify balance were mediolateral dynamic stability margin [4], step width, and step length. Increased dynamic stability and step width, as well as decreased step lengths indicated a participant was destabilized. A linear mixed model was used to evaluate the influence of slip timing for each step. Bonferroni-corrected pairwise comparisons were used for post-hoc tests. An alpha≤0.05 indicated significance. All slips that resulted in balance metrics >3x the interquartile range were excluded from analysis (12.7% of the data were excluded).

Results and Discussion

Dynamic stability margins were largest (i.e. subjects were most destabilized) for slips that occurred at 20 and 30% of the gait cycle during the step after the perturbation (Figure 1a). Step widths were larger for 20% slips during the second and third steps after the perturbation (Figure 1b). Step lengths were smaller after slips delivered at 20 and 30% during the second step after the perturbation (Figure 1c). Our results partially support our hypothesis of 15-20% of the gait cycle being sensitive to slips, but slips delivered at 30% of the gait cycle were also destabilizing as measured by dynamic stability margin, step width, and step length. The reason for this discrepancy could be that our hypothesis was based off of static postures throughout the gait cycle, but velocity is also a major contributor to dynamic stability. Additionally, there was a strong mediolateral response to a posterior belt slip. For example, during slips delivered at 20% of the gait cycle, we found a 43% increase in step width, which is substantially larger than responses due to sinusoidal mediolateral translations of the floor (5% increase) or visual field motion (22%) with 5 cm amplitudes [5].

Significance

Despite the wide variety of perturbations used to study stability during walking, the extent to which stability varies as a function of the gait cycle is not understood. We found differences in subject stability responses across 6 treadmill belt acceleration timings, with the largest responses occurring during perturbations applied closer to midstance. This finding suggests that to most effectively quantify a person's limit of stability with a belt acceleration, slips should not be applied during heel strike, as is common in literature, but closer to midstance. Furthermore, wearable robots and training regimens designed to prevent slips/trips during walking may also need to prioritize assisting muscles active during midstance.

Acknowledgments

EV was supported by GT Project ENGAGES, PRG was supported by an NSF GRFP, JKL was supported by a GT ARMS Fellowship.

References

[1] Bergen et al. (2016) *MMWR*
[2] Lee et al. (2017) *EMBC*
[3] Van den Bogaart et al. (2020) *J Biomech*
[4] Hof et al. (2005) *J Biomech*
[5] Terry et al. (2012) *J Biomec*

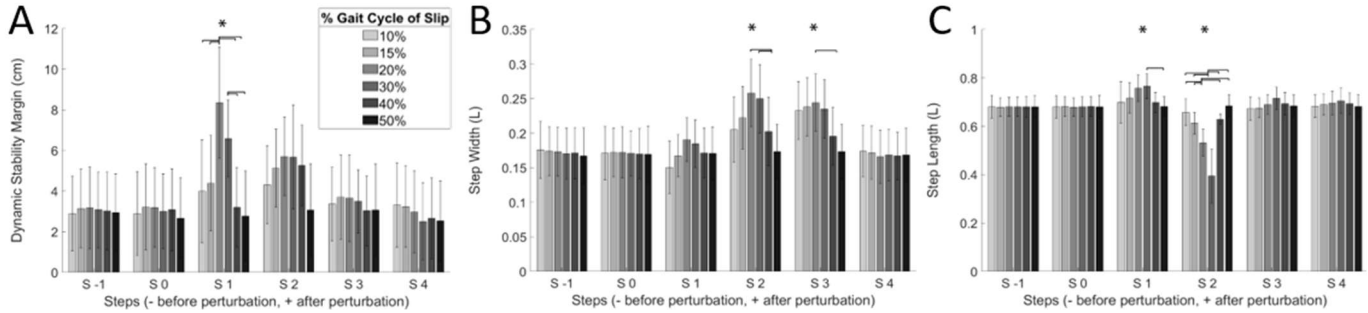

Figure 1: Stability metrics for the step before (S -1), step of (S 0), and 4 steps after belt acceleration. Left and right legs were combined. "L" = normalized to subject leg length. "*" = significant effect of slip timing. Bars = significant pairwise comparisons. Error bars = SD.

FOOT AND ANKLE KINETICS DURING WALKING IN PEOPLE WITH PLANTAR FASCIITIS

John Willson[1], **Erica Bell**[3], Stacey Meardon[1], Stacie I. Ringleb[2], Zachary Domire[3]
[1]Department of Physical Therapy, East Carolina University, Greenville, NC, USA
[2]Department of Mechanical and Aerospace Engineering, Old Dominion University, Norfolk, VA, USA
[3]Department of Kinesiology, East Carolina University, Greenville, NC, USA
email: willsonj@ecu.edu

Introduction

Plantar fasciitis (PF) is one of the most common musculoskeletal pathologies of the foot, affecting 10% of the American population at least once in their lifetime (1). Mechanical factors are believed to contribute to the etiology and exacerbation of PF. The plantar fascia is the principle supporting structure of the medial longitudinal arch, providing storage and release of elastic strain energy during walking due to the windlass mechanism and arch-spring mechanics (2). Despite the relevance of foot mechanics for this common condition, foot and ankle kinetics in people with PF are largely unknown. The purpose of this study was to compare metatarsophalangeal and ankle joint kinetics during walking between people at different stages of PF.

Methods

11 people (51 yr, 8 female) with symptomatic plantar fasciitis (SYMP), 6 people (43 yr, 5 female) with a history of plantar fasciitis but no longer symptomatic (ASYMP), and 10 individuals (31 yr, 5 female) with no history of plantar fasciitis (control) provided informed consent and participated in this study. Bilateral 3D lower extremity kinematics (200 Hz) and ground reaction forces (1000 Hz) were recorded during walking on an instrumented treadmill at 1.3 m/s in standardized footwear. Rigid body inverse dynamics and a multi-segment foot model were used to calculate metatarsophalangeal (MTP) and talocrural (TC) joint peak concentric and eccentric power and work. For the SYMP and ASYMP groups, only the symptomatic (n=17) or formerly symptomatic leg (n=9) were included. Both limbs of the control group were used for analysis (n=20). To account for bilateral observations, a mixed effects model with group as a fixed factor and participant as a random factor was used to test for differences in MTP and TC joint power and work between groups. Cohen effect sizes (d) were calculated to describe the magnitude of the difference between groups.

Results and Discussion

Concentric MTP joint contributions to propulsion occurred following eccentric contractions during the terminal stance phase of walking. Lower mean concentric MTP joint power and work were observed among participants in the SYMP group. Specifically, peak concentric MTP joint power was 37% lower ($p = .02$, $d = 1.26$) than the ASYMP group and 14% lower than the CON group ($p = .16$, $d = .49$). Similarly, concentric MTP joint work in the SYMP group was 46% lower than the ASYMP group ($p = .01$, $d = 1.14$) and 16% lower than controls ($p = .16$, $d = .57$). Eccentric MTP joint power and work were similar between groups. Concentric and eccentric talocrural joint power and work were also similar and within 10% between groups.

The decreased MTP concentric joint power and work during walking reported here for the SYMP group may represent gait adaptations to avoid symptoms, increased energy loss following plantar fascia stretch due to increased hysteresis during the stretch-shortening cycle, or both. Our lab previously identified decreased plantar fascia longitudinal stiffness among people with symptomatic plantar fasciits (3), which may contribute to this observed reduction in MTP joint function during gait.

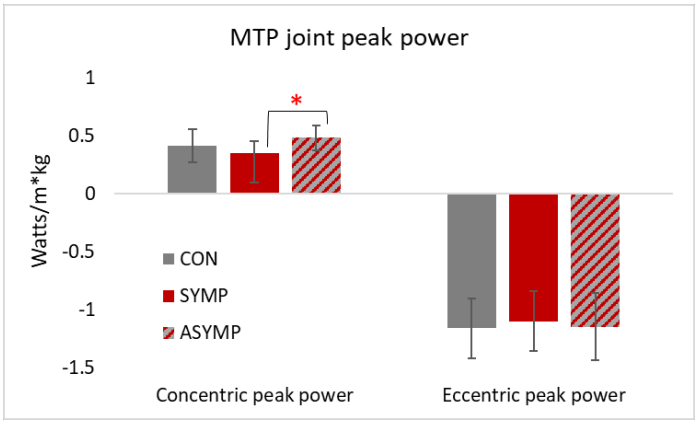

Figure 1. Peak concentric and eccentric MTP joint power during walking in people with symptomatic plantar fasciitis (SYMP), a history of plantar fasciitis but who are no longer symptomatic (ASYMP), no history of plantar fasciitis (CON). Error bars represent ±1 SD.

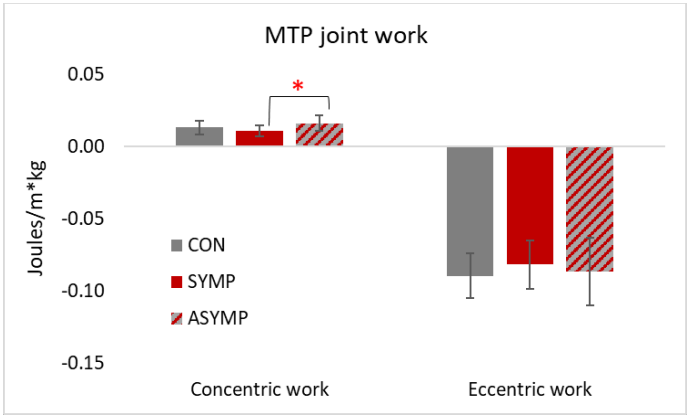

Figure 2. Concentric and eccentric MTP joint work during walking in people with symptomatic plantar fasciitis (SYMP), a history of plantar fasciitis but who are no longer symptomatic (ASYMP), and no history of plantar fasciitis (CON). Error bars represent ±1SD.

Significance

People with symptomatic PF experience lower MTP joint contributions to propulsion during walking than people without PF with no evident redistribution of load to the ankle. These findings may contribute to gait-related disability and low health-related quality of life in persons with symptomatic PF.

Acknowledgments

Data collected with assistance from Madeline Pauley. Funding from the National Science Foundation (EEC-1659796)

References

1) Martin et al. *J Orthop Sports Phys Ther*, 2014; 44(11). A1-33.
2) Welte et al. *JR Soc Interface*, 2018, 15(145): 20180270.
3) Bell et al. ISB 2019 Congress XXVII, Calgary, AB

Gait variability during treadmill walking in older adults with high and low cognitive status

Grace K. Kellaher[1], Tiphanie E. Raffegeau[2], Lori J. Altmann[3], Amanda E. Stone[4], and Chris J. Hass[1]
[1]Department of Applied Physiology & Kinesiology, University of Florida, Gainesville, FL; [2]Department of Health, Kinesiology, and Recreation, University of Utah, Salt Lake City, UT; [3]Department of Speech, Language, and Hearing Sciences, University of Florida, Gainesville, FL; [4]RR&D Center for Limb Loss and MoBility, VA Puget Sound Health Care System, Seattle, WA
Email: gkellaher@ufl.edu

Introduction

As we age, cognition declines. Continuous declines in cognition may lead to cognitive impairments, and older persons with cognitive impairments demonstrate variable and unstable gait patterns while walking overground (1,5). Variable and unstable walking in older adults with cognitive decline could potentially lead to falls (3). Walking on a treadmill at a fixed-speed constrains walking patterns and reduces gait variability during treadmill walking (4). However, it is unknown if cognitive faculties influence the variability of walking patterns during treadmill walking at fixed speeds. The purpose of this study was to investigate if gait variability during treadmill walking is similar for healthy older adults with lower cognitive function compared to healthy older adults with higher cognitive function. We hypothesized older adults with poor cognitive function would exhibit more variable gait patterns while walking on a treadmill compared to older adults with high cognitive function.

Methods

30 age-matched (±2 years) healthy older adults (73±3.5 years; 10 men) were divided into two groups based on their Montreal Cognitive Assessment (MoCA) score, a paper-based test of global cognitive function. 15 participants with a MoCA score ≤ 23 were placed in the "Low Cognition" group (average score: 21±2), while 15 participants with a score ≥ 27 were placed in the "High Cognition" group (average score: 28±1). MoCA scores ≤ 23 are indicative of clinically relevant cognitive impairment (2). Participants with a MoCA score between 24-26 were not included in the analysis. Three-dimensional motion capture technology recorded kinematic data as participants walked on a treadmill for seven minutes at their preferred walking speed. Standard deviation (SD) and coefficient of variation (CV) of gait speed, stride length, cadence, and double support percent during the last 25 cycles of walking were analyzed to quantify gait variability. Stride length, cadence, and double support for each measure of variability were evaluated separately in two, one-way multivariate analysis of variance with average gait speed included as a covariate. SD and CV of gait speed for each group were analyzed in two separate independent t-tests.

Results and Discussion

Independent t-tests revealed both SD ($p = 0.304$) and CV ($p = 0.227$) of gait speed were not different between groups. For SD of stride length, cadence and double support percent, multivariate tests revealed no significant differences ($F(3, 25) = 1.228$, $\lambda = 0.872$, $p = 0.320$) between groups when controlling for gait speed (Table 1). For CV of stride length, cadence, and double support percent, multivariate tests revealed no significant differences ($F(3, 25) = 0.618$, $\lambda = 0.931$, $p = 0.610$) between groups when controlling for gait speed (Table 2). The findings suggest gait variability is not affected by cognitive status when walking on a treadmill. Unlike overground walking where gait variability increases when cognitive ability is impaired (4), the Low Cognition group demonstrated similar variability while walking on the treadmill to age-matched older adults in the High Cognition group. This suggests the constraints of walking at a fixed speed on the treadmill reduces the impact cognitive faculties have on gait variability. Previous studies (6) have shown that while walking overground, executive function is associated with controlling pace (i.e. gait speed, step length). Walking on a treadmill, however, controls these aspects of gait, and is perhaps why no differences in variability were observed between our groups. It is important to note, however, these data were taken from the last 25 cycles of walking at the end of seven-minutes of treadmill walking. It is possible we did not find any significant differences in gait variability between the groups because the participants had acclimated to walking on the treadmill at the time points analyzed. This suggests older adults with low cognitive scores can learn to walk more consistently on a treadmill like older adults with high cognitive scores during short bouts of walking. Future studies should examine gait performance earlier in treadmill walking exposure, or examine changes to gait variability when walking on a treadmill at a fixed speed versus a self-propelled treadmill. This could help us better understand gait variability adaptation in older adults with different levels of cognitive acumen.

Table 1. Measures of variability for the Low Cognition group

	Mean	SD	CV
Gait Speed (m/s)	0.563	0.007	0.013
Stride Length (m)	0.508	0.018	0.036
Cadence (steps/min)	85.793	2.047	0.025
Double Support (%)	30.73	1.173	0.038

Table 2. Measures of variability for the High Cognition group

	Mean	SD	CV
Gait Speed (m/s)	0.642	0.007	0.011
Stride Length (m)	0.545	0.014	0.027
Cadence (steps/min)	91.843	1.662	0.018
Double Support (%)	29.748	1.070	0.036

Significance

Older adults with lower cognitive function exhibit similar variability in gait patterns as age-matched older adults with higher cognitive function when walking on a treadmill. It is possible that having healthy older adults with lower cognitive function practice a less variable walking pattern through treadmill training could lead to reduced variability during overground walking. Reduced gait variability could potentially reduce the incidence of falls in this population.

References

1. Allali et al. (2008). *Dem Geriatr Cogn Disord* 26: 364–369
2. Carson et al. (2018). *Int J Geriatr Psychiatry* 33: 379–388
3. Haudsdorff et al. (2001). *Archives of Physical Medicine and Rehabilitation* 82: 1050–1056
4. Hollman et al. (2016). *Gait & Posture* 43: 204–209
5. Ijmker et al. (2012). *Gait & Posture* 35: 126–130
6. Morris et al. (2016). *Neurosci Biobehav Rev* 64: 326-345

Adaptation to multi-session real-time visual feedback training of knee joint pattern in pediatric cerebral palsy: a case report

Xuan Liu[1,2], Nuno Oliveira[1,2,3], Naphtaly Ehrenberg[1,2], JenFu Cheng[2], Katherine Bentley[2],
Sheila Blochlinger[2], Hannah Shoval[2], Peter Barrance[1,2]
[1]Center for Mobility and Rehabilitation Engineering Research, Kessler Foundation, West Orange, NJ, United States
[2]Children's Specialized Hospital Research Center, New Brunswick, NJ, United States
[3]School of Kinesiology and Nutrition, University of Southern Mississippi, Hattiesburg, MS, United States
Email: pbarrance@kesslerfoundation.org

Introduction

Insufficient knee extension at initial contact (IC) has been identified as clinically frequent and significant among gait deviations in pediatric cerebral palsy (CP). This gait deviation can persist even after a combination of physical therapy, pharmacological, or surgical interventions to improve contracture and spasticity. Biofeedback training that provides participants meaningful cues to augment their inadequate native physiological feedback has shown its potential in gait retraining. However, very few studies have explored biofeedback gait retraining in pediatric CP. In order to help pediatric patients achieve more symmetric and efficient gait, our research team developed a two phase visual kinematic feedback system, and reported a positive effect with one gait retraining session [1]. The current paper reports adaptation to the feedback across multiple training sessions by a pediatric participant with hemiplegic CP.

Methods

Three inertial sensors (MTW Devkit, Xsens, NL) were placed on the participant's thigh, shank and heel. The knee flexion angle (KFA) was defined as the difference between the thigh and shank sensors' rotational orientation about their longitudinal axis. The target knee flexion pattern was selected from typically developing children's patterns. Error metrics were used to drive the feedback display on a computer monitor for the extension and flexion periods via two corresponding needles. A scoring system based on the feedback is incorporated for participant motivation. An adolescent with right hemiplegic CP (male, age 14.7 yrs) who presented with insufficient knee extension at IC and decreased swing phase knee flexion, participated in this study. The participant underwent 5 training sessions over 3 weeks. A baseline trial was recorded during each training day while the participant walked on the treadmill at a comfortable speed. The speed was controlled in four 6-minute training bouts with 3-minutes of rest between bouts. Each training bout included a 3-minute trial with Feedback (FB) and a 3-minute trial with No Feedback (NFB), with the sequence of trials randomized for each bout. For each FB trial, the participant was asked to follow the cues on the monitor and try to modify his knee flexion pattern to rotate the needles towards the target range, whereas for each NFB trial, he was asked to recall and maintain this pattern. The root-mean-square error (RMSE) was calculated from the difference in KFA between the target and the performed patterns. Descriptive statistics were used to describe the changes in KFA at IC, peak KFA, and RMSE across days between FB/NFB conditions.

Results and Discussion

In comparison with the baseline trial on Day 1, the KFA at IC in the FB and NFB trials both decreased markedly on Day 1 and Day 2, increased on Day 3, and remained at around 20° on Day 4 and Day 5, while the peak KFA showed an overall increasing tendency from Day 1 to Day 5 (Fig. 1a). The RMSE in the FB and NFB trials both decreased markedly on Day 1, Day 3, and Day 4 (Fig. 1b). A decreasing trend in RMSE was also observed from Day 2 to Day 5. The decreasing standard deviation (SD) of KFA at IC across days indicated that the participant had started to learn the pattern. The increase of RMSE on Day 2 was caused by overcorrected extension during mid and late stance, which was observed in recorded video and also supported by lower extension scores on Day 2 (FB: 22, NFB: 53) compared with Day 1 (FB: 218, NFB: 145). Starting from Day 2, the RMSE in the FB trials was higher than that in the NFB trials (Fig. 1b), which was attributed to higher peak KFA in FB (Fig. 1a). We expect that increasing the training dosage or number of sessions would help to consolidate adaptation and further reduce error.

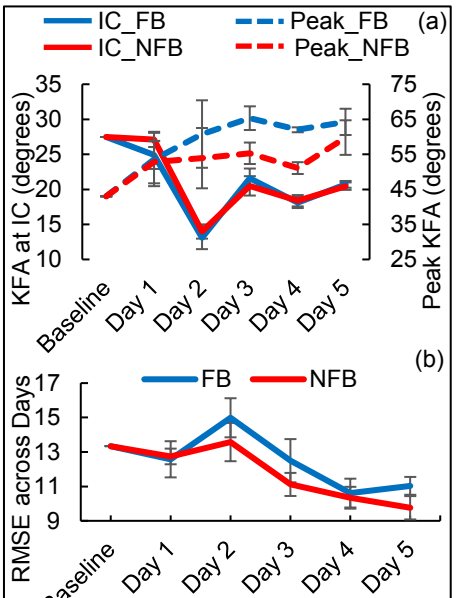

Figure 1: Feedback gait retraining effect. Mean and SD across bouts (error bar) of (a) KFA at IC and peak KFA and (b) KFA RMSE across days for FB and NFB trials.

Significance

The multi-session real-time visual feedback training shifted participant's knee flexion trajectory towards the target, with error reduced across training sessions. This paper highlights the presented feedback training paradigm and its potential applications to clinical practice. Testing of a larger sample with a longitudinal examination of functional measures is ongoing.

Acknowledgments

This study was funded by Children's Specialized Hospital and Kessler Foundation. Patent pending for feedback method.

References

[1] Liu X et al. (2019). *Proceedings of ISB/ASB'19*, Calgary, AB, Canada

Can EMG accurately predict metabolically optimal step frequency

Wendy Nevarez-Sanchez[1], Benjamin A. Shafer[2], Aaron J. Young[2], and Gregory S. Sawicki[2,3]
[1]South Atlanta High School
[2]George W. Woodruff School of Mechanical Engineering, Georgia Institute of Technology, Atlanta, GA
[3]School Biological Sciences, Georgia Institute of Technology, Atlanta, GA
Email: ben.shafer@gatech.edu

Introduction

Measuring metabolic cost is time consuming and cumbersome for both experimenter and participant alike. Despite this drawback, metabolic cost is an important measure for biomechanical studies of locomotion and will continue to be used. Some have estimated metabolic cost using a wide array of measurements such as breathing rate, perspiration, and muscle activity[1]. Others used estimation techniques to approximate steady-state metabolic cost, shortening the duration of collection[2]. As muscles are the primary energy consumers during locomotion and EMG sensors are readily available, it follows that measuring muscle activity could be used to accurately estimate metabolic cost in real-time. One important aspect to metabolic estimation is whether the estimated values follow the same trends as originals (e.g. when walking at a constant speed there is a parabolic trend that determines the metabolically optimal and preferred step frequency (SF)). We hypothesize the metabolically optimal SF will be the same SF to minimize overall EMG activity.

Methods

We measured EMG and metabolic cost of a healthy adult male while walking on a treadmill at 1.3 m/s. The participant walked for 15 minutes to habituate (preferred SF and ±20%), followed by a 35-minute randomized SF sweep between ±30% of preferred SF (7 trials total at 5 minutes each). SF was commanded using an audible metronome. Ground reaction forces (GRFs) were measured to quantify step durations and segment EMG data per gait cycle. The subject had 8 EMG sensors placed on the following leg muscles: Tibialis Anterior, Medial Gastrocnemius, Soleus, Vastus Medialis, Rectus Femoris, Bicep Femoris, Gluteus Medialis, Gluteus Maximus.

Muscle-specific EMG activity of each trial was quantified using 3 mathematical measures: integral (INT), sum square (SS), and waveform length (WL, i.e. geometric length) between 2.5 and 4.5 minutes. For each measurement, the muscle-specific EMG were summed using weights based on relative muscle volume (RMV) or without weights (unweighted; UW). A quadratic fit was made across trials for each EMG measure and the minimum was calculated. The SF where the minimum value occurred was compared to the metabolically optimal SF. EMG adaptation time (time it takes to reach steady-state, i.e. average of last minute of trial) was the first time when three consecutive steps of the EMG measure were within ± 2 std of the steady-state value.

Results and Conclusion

Using the UW sum method, SumSq had the least amount of error (0.5%). WL had the highest absolute error (3.4%). Using the RMV sum method, WL had the least amount of error (0.4%). SumSq had the most amount of error (3.2%).

Based on these preliminary results, these EMG measures and metabolic cost reach their minimum at the same SF of 56 steps/min.

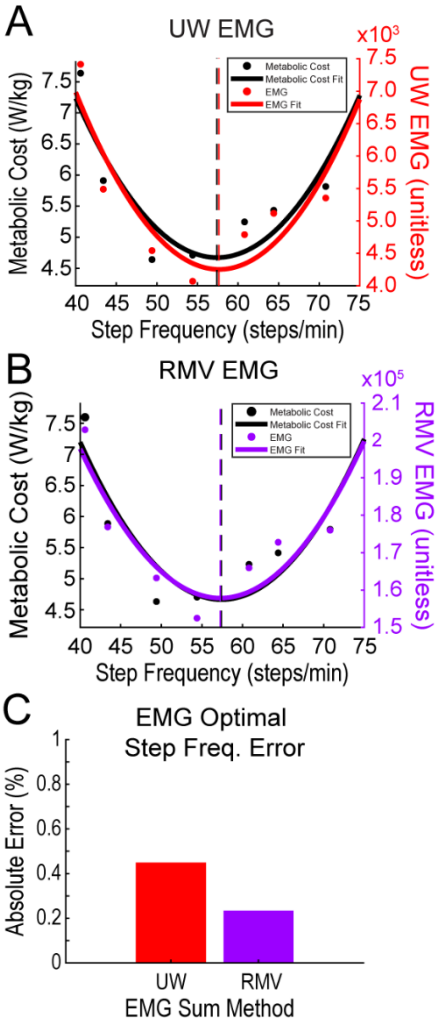

Figure 1: A) Steady-state metabolic cost and UW EMG sums across SFs with quadratic fits. B) Steady-state metabolic cost and RMV EMG sums across SFs with quadratic fits. C) Absolute error between the metabolically optimal SF and EMG optimal.

Significance

This data suggests that EMG has the potential to estimate metabolic cost in real-time while preserving key trends. EMG could be used as a substitute for metabolic measurement, decreasing experimental time and effort. Further, EMG can assist with the optimization of parameters for controls of exoskeletons, as metabolic cost is normally a performance/cost metric. In the future, we plan to investigate how quickly EMG reaches steady-state compared to metabolic cost, directly predict metabolic cost using EMG, and implement this method to optimize exoskeleton control.

Acknowledgments

The authors would like to acknowledge Georgia Tech Project ENGAGES, NSF Research Traineeship Award #1545287, DoD Grant #GR10003831, NSF NRI Award #1830215, U.S. Army NSRDEC (W911QY18C0140), and Lockheed Martin Corp.

References

1. Ingraham et al. (2019) *J Appl Phys*
2. Selinger et al. (2014) *J Appl Phy*

Musculoskeletal Model of Muscle Characteristics with Varied Bodyweight Support

Angel Bu[1], Mhairi K. MacLean[1], Han Nguyen[1], and Daniel P. Ferris[1]
[1]University of Florida, Gainesville, Florida, USA
Email: *angelbu@ufl.edu

Introduction

Bodyweight support can aid gait rehabilitation and provide an experimental perturbation to study human locomotion biomechanics. Increasing bodyweight support causes a decrease in ground reaction forces during walking [1] but it is unclear how bodyweight support affects muscle fiber operating lengths. OpenSim is a predictive musculoskeletal modeling program that can be used for gait analysis in rehabilitation facilities and in research to provide insight into biomechanics [2]. The relationship between muscle activation, velocity, length, and force during movement can be estimated using OpenSim. Our objective was to determine how bodyweight support level during human walking affected muscle activation and muscle fiber length. We hypothesized that muscle activation would decrease with increased bodyweight support and that limb extensor muscle fiber excursion would decrease with increased bodyweight support.

Methods

Eight healthy participants [5 female, 3 male; 24±1 years of age, body mass 69±6 kg, mean±s.d.] walked overground at 1, 0.76, 0.55 and 0.31 gravity (G) at approximately 1.2 m/s. We used a custom bodyweight support system mounted to a rolling trolley on the ceiling. The system was attached to a harness which was pulled up by constant force springs. We used overground force plates, a motion capture system, and unilateral electromyography on the right leg to measure ground reaction forces, kinematics, and muscle activity, respectively.

We used OpenSim 4.0 to compute inverse kinematics and inverse dynamics during right leg stance phase, which we used as inputs for muscle analysis to calculate muscle lengths. For each bodyweight support level, we calculated the average normalized fiber length, defined by OpenSim as fiber length/optimal length, across participants. We normalized the electromyography (EMG) linear envelopes to the maximum EMG value for the subject then averaged across bodyweight condition. The data were processed using the MOtoNMS pipelines [3] and MATLAB.

Results and Discussion

As bodyweight support increased, muscle activation noticeably decreased for all muscles except the biceps femoris which saw an increase in activation (Fig. 1). With increased bodyweight support, every muscle except the biceps femoris long head saw a decrease in normalized fiber length excursion (Fig. 2). Both results were in agreement with our hypotheses.

The bicep femoris showed increased muscle activity with increased support, despite the fiber length excursion showing minimal change. We had expected to find that the increase in muscle activation of the biceps femoris was related to the muscle operating at a different point on the muscle force-length relationship. However, muscle length remained relatively the same.

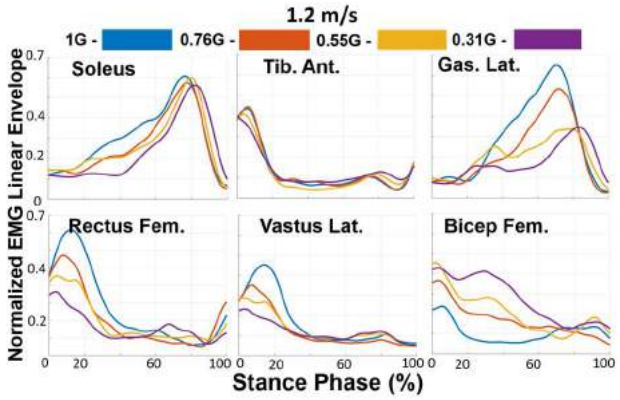

Figure 1: Normalized EMG linear envelopes for 6 muscles at different bodyweight support levels.

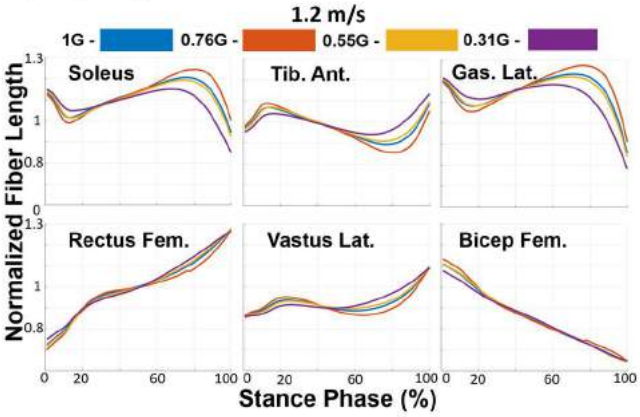

Figure *2*: Normalized fiber length, described as fiber length over the optimal fiber length, calculated during stance phase for 6 muscles at different bodyweight support levels.

Significance

Bodyweight support affects not only ground reaction forces and muscle-tendon forces, but also can affect muscle fiber excursions during walking as well. As expected, we found a decrease in muscle activation and a decrease in the range of muscle fiber excursion with greater bodyweight support levels. These findings provide insight into the muscle mechanical changes that accompany the use of bodyweight support for rehabilitation and scientific study of walking biomechanics.

Acknowledgments

We would like to thank Skyler Levine and Patrick Costello for assisting in data collection and processing.

References

[1] McGowan CP et al. 2008, *J Appl Physiol*, 105:486–94.
[2] Kutilek P et al. 2012, Proc 15th Int Conf Mechatron, 1-6.
[3] Mantoan A et al. 2015, *Source Code for Bio and Medicine* 10:12.

Propulsion timing affects the relationship between paretic propulsion and long-distance walking function after stroke

Andre M. Alvarez[1], Ashley N. Collimore[1], Ashlyn J. M. Aiello[1], Stuart A. Binder-Macelod[2], Louis N. Awad[1*]
[1]College of Health and Rehabilitation Sciences, Boston University, Boston, Massachusetts, USA
[2]College of Health Sciences, University of Delaware, Newark, Delaware, USA
Email: *louawad@bu.edu

Introduction

Stroke is a leading cause of disability that results in neuromotor impairments that contribute to slower and more inefficient walking. As a consequence, walking rehabilitation is a major focus after stroke. The 6-Minute Walk Test (6MWT) is a popular outcome measure used to assess functional walking capacity after stroke; however, the performance-based metrics often evaluated (e.g., the total distance walked) do not identify the underlying neuromotor impairment. Elucidation of the biomechanical contributors to reduced 6MWT performance is necessary for the advance of individualized rehabilitation interventions that target the specific deficits limiting function. Biomechanical variables such as the peak propulsion force (i.e., the peak of the anterior ground reaction force) and the propulsion impulse (i.e., the integral of the anterior ground reaction force) have been shown to contribute to walking function after stroke[1]; however, these magnitude-based metrics do not account for key temporal aspects of propulsion function that may affect walking after stroke—such as the timing of the propulsion peak[2]. The objective of this study was thus to determine how the timing of the propulsion peak relates to 6MWT performance. We hypothesized that propulsion peak timing would contribute to 6MWT performance above and beyond the propulsion magnitude metrics of peak and impulse.

Methods

Data for thirty-four individuals with chronic post-stroke hemiparesis were available for this study. The total distance walked during the 6MWT served as the primary clinical outcome of interest. Metrics related to propulsion magnitude (i.e., peak propulsion and propulsion impulse) and timing (i.e., the timing of the propulsion peak) were extracted from the paretic anterior-posterior ground reaction forces generated during 30 seconds of treadmill walking and then averaged. The propulsion magnitude metrics were expressed as %bodyweight (%bw). Peak propulsion timing was expressed as %stance phase (%sp).

All statistical tests were performed in MATLAB 2019a. Two moderated regression models were examined to evaluate the influence on 6MWT distance of the propulsion magnitude metrics and the timing of the propulsion peak. The first model included peak propulsion, peak propulsion timing, and their interaction. The second model included the propulsion impulse, peak propulsion timing, and their interaction. Significant interactions were evaluated at ± 1 standard deviation of the moderators. Alpha was set to 0.05.

Results and Discussion

Peak propulsion force (R^2 = 0.37, p < 0.01) and propulsion impulse (R^2 = 0.32, p < 0.01) individually contributed to 6MWT distance. Adding peak propulsion timing and its interaction to these models increased the variance explained for both peak propulsion force (R^2 = 0.47, $_{adj}R^2$ = 0.41, $F(3,31)$ = 8.98, p < 0.01) and propulsion impulse (R^2 = 0.45, $_{adj}R^2$ = 0.40, $F(3,31)$ = 8.48, p < 0.01). Significant interactions with peak propulsion timing in each model (ps < 0.05) indicate that the timing of peak propulsion during the stance phase of walking moderates the relationship between the magnitude of propulsion (i.e., both the impulse and the peak) and the distance walked during the 6MWT. More specifically, individuals with lower propulsion magnitudes walked less distances than those with higher propulsion magnitudes; however, among those with higher propulsion magnitudes, individuals with earlier peak propulsion timings walked farther distances (see Figure 1).

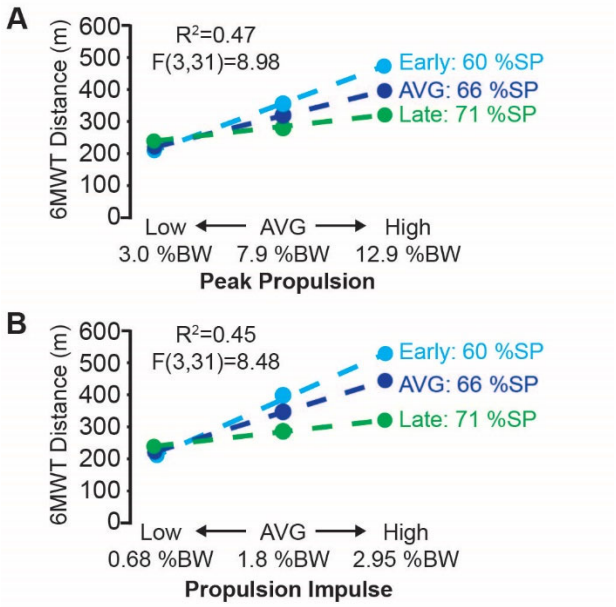

Figure 1: The relationship between propulsion magnitude—both **(a)** peak propulsion and **(b)** propulsion impulse—and 6MWT distance is moderated by the timing of the propulsion peak.

Significance

Deficits in the timing of the propulsion peak may contribute to impaired long distance walking function after stroke. While previous research has highlighted the importance of the magnitude of paretic propulsion to poststroke walking, the present study demonstrates that the timing of the propulsion peak affects the total distance walked during the 6-minute walk test above and beyond the magnitude of paretic propulsion. Post-stroke gait rehabilitation may need to target both the magnitude and timing of paretic propulsion to maximize outcomes.

Acknowledgments

We thank the FastFES study team for data collection; members of the Boston University Neuromotor Recovery Lab for aiding in and reviewing the manuscript; and study participants for their generous time.

References

[1]Awad, L., et al. 2015, *N.N.R*
doi: 10.1177/1545968314554625
[2]Kuhman, D., et al. 2019, *H.M.S.*
doi: 10.1016/j.humov.2019.102524

Plantar Shear Stress Increases with Added Body Mass

Hwigeum Jeong, Spencer R. Petersen, Jared M. Staten, Jordan K. Grover, and Dustin A. Bruening
Brigham Young University, Provo, UT, USA
email: hwiguem@gmail.com

Introduction

Elevated body mass has been shown to increase vertical plantar pressure [1] that presumably contributes to: collapsed arch height, reduced plantar mechanoreceptor sensitivity, postural instability, and altered gait mechanics [2,3,4,5,6]. However, increased body mass may also affect plantar shear that may be further associated with these alterations [6]. For example, in obese subjects, plantar shear likely contribute to tissue spreading, leading to the noted increase in foot contact area [1]. In addition, while plantar pressures are increased with acutely added body mass, foot arch height does not appear to change [7], indicating that kinematic changes likely occur over time secondary to altered pressure and shear. The measurement of these shear may help better understand the effects of body mass on foot mechanics. The aim of this study is to determine the effects of added body mass on plantar shear and arch height during gait.

Methods

Eight healthy male adults (22 ± 3 years, 24 ± 1 BMI) walked across a 5.5 m long elevated walk-way with a pressure and shear sensing system (FootSTEPS, ISSI, 50 Hz, 25 Hz filter) mounted in the center and level with the walkway. A motion capture system (Qualisys, Inc.) was used to capture foot motion (100 Hz, 6 Hz filter) according to a multi-segment foot model using 23 reflective markers with shank and heel clusters [8]. Walking trials were performed with and without a weighted vest (20% of the participants own body weight, evenly distributed front to back) in random order. Three successful walking trials were recorded for each condition while the participants walked at their own set preferred speed with clean foot placement on the FootSTEPS sensing area. Plantar shear forces were analyzed using custom LabView software. Plantar tissue spreading was represented by the difference between total anterior and total posterior forces (AP spreading) and between total medial and total lateral forces (ML spreading) at the mid-stance transition point between braking and propulsion (i.e. when net AP forces are zero). Foot arch height was calculated in Visual 3D software as the sagittal plane angle between the hindfoot and midfoot segments at mid-stance. Metrics were compared between conditions with paired t-tests ($\alpha = 0.05$).

Results and Discussion

The mean walking speed was 1.22 ± 0.28 m/s. ML shear forces showed consistent spreading effects across stance, while AP shear showed primarily unidirectional (i.e. dragging) effects in early and late stance, with spreading effects in mid-stance (Figure 1). The vest condition resulted in higher AP (P =0.008) and ML (P = 0.001) spreading effects compared to the non-vest condition at the mid-stance. For foot arch height, however, there was no statistical difference (P =0.87) in the midfoot joint angle (º) between conditions. These results suggest that the effects of body mass that eventually cause foot deformation may be insidious. In other words, although foot arch height seems intact after acutely increased body mass, soft tissues around the feet are under greater stresses that may cause collapse of both the medial longitudinal and transverse foot arches and/or cause foot injuries as time elapses. In this respect, kinematic data only provide information about the end-result of foot deformation, but not the cause of the consequences. Therefore, kinetic data sensitive to altered mechanical stimuli may be useful to understand and prevent foot deformities.

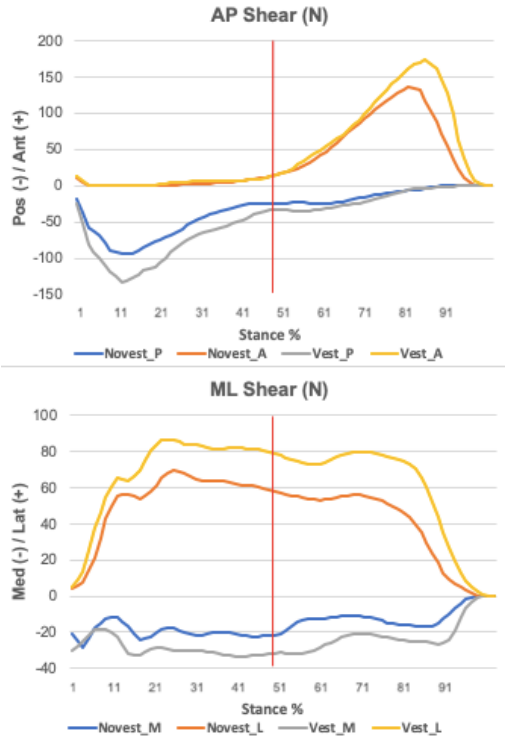

Figure 1. The vertical red line represents the transition point.

Significance

These results suggest that elevated body weight increases plantar tissue shear stress, causing both spreading and dragging effects. While this study only evaluated acute effects, the results, combined with previous studies, suggest that these stresses may be implicated in foot morphology breakdown and decreased mechanoreceptor sensitivity, both of which may contribute to deteriorated postural control and gait mechanics. This is particularly relevant to those who are obese or consistently carry a heavy mass, such as military soldiers, and may be exposed to the potential risks of postural instability and lower limb injuries.

References

1. Hills, et al. *IJO*. 2001.
2. Krishna, et al. *IJIRR*. 2018.
3. Wu & Madigan. *Neurosci. Lett.*. 2014.
4. Lhomond et al. *Front Hum Neur,* 2016.
5. Messier et al. *J. Appl. Biomech*. 1996.
6. Morasso & Schieppati. *Neurophys,* 1999
7. Kern, et al. *PeerJ*, 2019.
8. Bruening, et al. *Gait Posture*, 2012.

Dynamic treadmill walking : asymmetric gait training with a tied-belt treadmill

Michael G. Browne[1,2], Purnima Padmanabhan[3], and Ryan T. Roemmich[1,2]
[1] Center for Movement Studies, Kennedy Krieger Institute, Baltimore, MD 21205
[2] Dept of Physical Medicine and Rehabilitation, Johns Hopkins University School of Medicine, Baltimore, MD 21205
[3] Dept of Neuroscience, Johns Hopkins University School of Medicine, Baltimore, MD 21205
Email: mbrow281@jhmi.edu

Introduction

Walking post-stroke is frequently characterized by slower speeds, due in large part to a precipitous decrease in paretic limb push-off [1]. This decrease in push-off, frequently quantified as the peak of the anterior component of the ground-reaction force vector (FP), often requires persons post-stroke frequently rely on compensatory gait strategies such as vaulting and increased push-off from their healthy leg [2]. A critical target for rehabilitation, therapy frequently aims to elicit volitional improvements in paretic limb push-off with unfortunately lackluster results. Therefore, rehabilitation approaches that do not require volitional changes in gait are needed. To address this need, we aim to develop a novel dynamic treadmill training approach. Our dynamic treadmill controller uses changes in tied-belt treadmill speed to modulate the magnitude of paretic and non-paretic push-off. For example, accelerating the treadmill during paretic push-off should increase the magnitude, as push-off magnitude scales linearly with walking speed [3]. Similarly, decreasing the speed during non-paretic push-off should decrease compensatory push-off from that limb. Importantly, we can customize the treadmill speeds and timing of the speed changes to shape each individual's push-off. As such, we hypothesized that walking in our dynamic treadmill would result in greater push-off from the leg moving quickly during push-off than that moving slowing during push-off in young healthy participants. The results will be used to refine treadmill control for persons post-stroke.

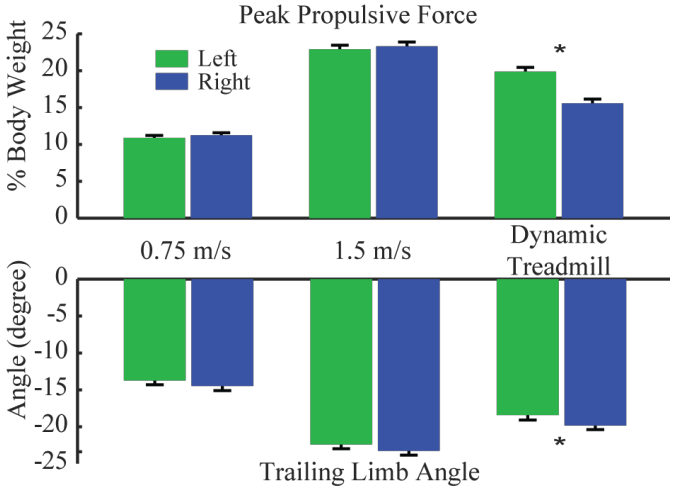

Figure 1: Peak propulsive force and trailing limb angle for left and right legs. During the Dynamic Treadmill condition, treadmill speed was 0.75 and 1.5 m/s at push-off for left (green) and right (blue) legs, respectively.

Methods

10 healthy young adults (mean±SD; age: 22.3±3.6 years, 4M/6F) participated. Subjects first walked normally for 2 minutes each at 0.75 – 1.5 m/s on a dual-belt instrumented treadmill (Motek Medical, Amsterdam, NL) while we collected motion capture and ground reaction force data. Subjects then walked for 10 minutes using our closed-loop dynamic treadmill controller. For all trials, a motion capture system (Vicon Nexus, Denver, CO) recorded the trajectories of markers placed on subjects' pelvis and lower extremities for estimating joint kinetics. Briefly, the dynamic treadmill controller alternated the tied-belt speeds within a gait cycle between 0.75 m/s and 1.5 m/s based on participants' anterior-posterior ground reaction forces. More specifically, the controller set the belt speeds to 0.75 m/s during the braking phase of the right leg then to 1.5 m/s during the propulsive phase of the right leg. Given the tied-belt nature, this resulted in speeds of 1.5 m/s through braking and 0.75 m/s through propulsion for the left leg.

Results and Discussion

Speed linearly modulated bilateral FP and trailing limb angle. The dynamic treadmill condition resulted in 22% greater FP ($p<0.01$) but 8% smaller trailing limb angle ($p=0.02$) in the left leg (when treadmill moved at 0.75 m/s) than the right leg (when treadmill moved at 1.5 m/s).

Our dynamic treadmill controller elicited differential effects in push-off between the left and right legs using only changes in tied-belt treadmill speed. Nevertheless, we completely reject our hypotheses such that a fast treadmill speed actually resulted in significantly lesser push-off than the slow speed. These confounding but exciting results are seemingly due to disruptions to the pendular center of mass mechanics. We look forward to presenting this and follow up experiments specifically exploring joint-level and center of mass mechanics of walking with speed-modulated push-off demands.

Significance

Split-belt treadmill training and robotic and/or exoskeleton-based rehabilitation show great promise for improving walking post-stroke with a big limitation: accessibility. Here, we demonstrate that a single treadmill belt can provide asymmetric gait training solely with appropriately timed within-stride changes in belt speed. This new line of research aims to characterize appropriate speed changes to elicit improved push-off intensity in groups with a unilateral deficit such as that observed in persons post-stroke. These data will support plans to develop standard treadmill controllers for asymmetric gait training.

Acknowledgments

We thank the American Heart Association Postdoctoral Training Fellowship and the NIH T32 (2T32HD007414-26) Postdoctoral Training Fellowship

References

[1] Lewek, et. al. Neurorehabil Neural Repair, 2018.
[2] Farris, et al., J Neuroeng Rehabil, 2015.
[3] Browne and Franz,. J Biomech, 2017. 55: p. 48-55.

Locomotor adaptation to visual cueing of impending mechanical perturbations during treadmill walking

Jinfeng Li[1], Helen J. Huang[1,2]
[1]Mechanical and Aerospace Engineering Department, University of Central Florida, Orlando, FL, USA
[2]Disability, Aging, and Technology (DAT) Cluster, University of Central Florida, Orlando, FL, USA
Email: jinfeng@knights.ucf.edu

Introduction

Understanding how people control and maintain stability during perturbed walking could be beneficial for preventing falls [1]. We have previously shown that brief decelerations of belt speeds applied during right leg midstance of every stride can perturb walking and balance [2]. We found that subjects initially decreased anterior-posterior margin of stability when first experiencing the perturbations but adapted back towards baseline [2]. Visual cueing of the perturbations may increase adaptation because the visual cues may facilitate an anticipatory strategy. A previous study showed that providing visual feedback prior to an upcoming locomotor maneuver enhanced preparatory locomotor adjustments such as decrease margin of stability in the direction of the anticipated maneuver [3]. The aim of this study is to determine whether visual cueing of the magnitudes of impending belt decelerations applied during midstance of every stride facilitates adaptation to the perturbations. We hypothesized that adaptation of anterior-posterior margin of stability will be greater with visual cueing of the impending perturbations compared to no cueing.

Methods

Two healthy young subjects walked on a dual belt treadmill (M-Gait) for 4 trials at a speed of 1.0 m/s while lower body movements were recorded using a motion capture system (OptiTrack). There were 2 cueing conditions (cued or no cue) and 2 perturbation magnitudes (small and large). Each trial started with 2 minutes of unperturbed walking (pre), followed by 4 minutes of perturbed walking (perturbed), and concluded with another 2 minutes of unperturbed walking (post). During perturbed walking, the right belt speed quickly decelerated by either 0.2 m/s or 0.5 m/s for 200 ms during right midstance and then returned to 1.0 m/s. For the cued conditions, a small or large rectangle representing the small (0.2 m/s) and large (0.5 m/s) decelerations were displayed on a monitor placed in front of the subject at left heel strike, ~600 ms before the perturbation at right midstance. No rectangle was shown if there was no perturbation. A no-perturbation catch stride occurred randomly 1 out of every 5 strides during perturbed walking. We calculated margin of stability at every left heel strike as the anterior-posterior distance between the extrapolated center of mass and the toe marker of the leading foot. We calculated the average of the margin of stability for every 5 strides to examine adaptation. Pre was the last 5 strides. Early and late perturbed were the first 3 and last 3 strides during the adaptation period.

Results and Discussion

Both subjects reduced margin of stability from pre to early perturbed for all perturbations except the no cue small perturbation, indicating that the belt decelerations perturbed baseline walking and balance (Fig. 1). The two subjects gradually increased margin of stability from early to late perturbed back towards baseline (pre), indicating that subjects were able to adapt to all perturbations (Fig. 1). Visual cueing increased margin of stability compared to no cueing for the large perturbation, which supports our hypothesis but not for the small perturbation, which opposes our hypothesis. Further, the magnitude of the decrement in margin of stability was greater with cueing compared to no cueing for the small perturbation, which also does not support our hypothesis. For both subjects, the reduction in margin of stability from pre to early perturbed for the large perturbation was larger compared to the small perturbation, regardless of visual cueing, which indicates that larger perturbations were more challenging (Fig. 1). These results partially support our hypothesis and suggest that visual cueing is more beneficial when the mechanical perturbation is more challenging.

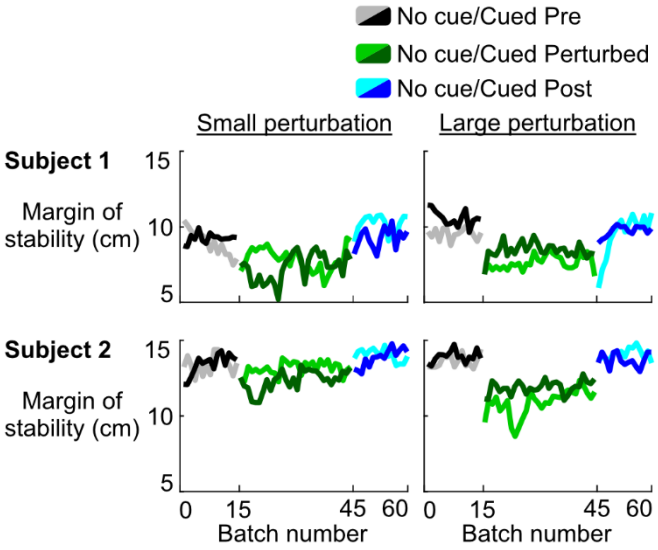

Figure 1. Margin of stability time course for the different visual cueing conditions for both subjects. 1 batch = 5 strides.

Significance

We found that visual cueing does not necessarily improve adaptation to perturbations during gait. These preliminary findings provide additional insight on how visual feedback could be used during gait rehabilitation and fall prevention. We plan to collect more subjects to determine whether this behavior occurs in more subjects and in older adults.

Acknowledgments

Supported by NIH R01AG054621 and a University of Central Florida In-House grant.

References

[1] McAndrew Young PM et al. *J Biomech*. 2012;45: 1053–1059.
[2] Li J and Huang HJ. Dynamic Walking 2019: 47.
[3] Wu M et al. *PLoS One*. 2015;10: e0132707.

Training with ankle resistance improves walking ability in children with cerebral palsy

Benjamin C. Conner[1], Nushka M. Remec[2], Elizabeth K. Orum[3], Emily M. Frank[3], Zachary F. Lerner[1,4]*
[1]College of Medicine – Phoenix, University of Arizona, Phoenix, AZ, USA; [2]Phoenix Children's Hospital, Phoenix, AZ, USA;
[3]College of Health Solutions, Arizona State University, Tempe, AZ, USA; [4] Department of Mechanical Engineering, Northern Arizona University, Flagstaff, AZ, USA; *Corresponding author email: zachary.lerner@nau.edu

Introduction

Children with cerebral palsy (CP) have weaker and poorly coordinated ankle plantar flexors, which likely contributes to their higher metabolic cost of transport and limitations in activity [1]. Despite the significant contribution of this deficit, the current standard of care for improving motor function in CP is not addressing functional ankle performance. We recently developed a novel intervention, wearable adaptive resistance (Fig. 1), with the primary objective of improving ankle plantar flexor function while walking [2].

The purpose this pilot clinical trial was to determine the efficacy of wearable adaptive resistance training for rapidly improving walking ability in children with CP. We hypothesized that a short, four-week training with wearable adaptive resistance would improve neuromuscular function of the ankle plantar flexors for a more efficient gait pattern that would enhance performance on clinical tests of mobility and endurance.

Methods

Six children with CP (hemi- and diplegia, Gross Motor Function Classification System I-II, ages 12 – 17 years, five males and one female) were recruited.

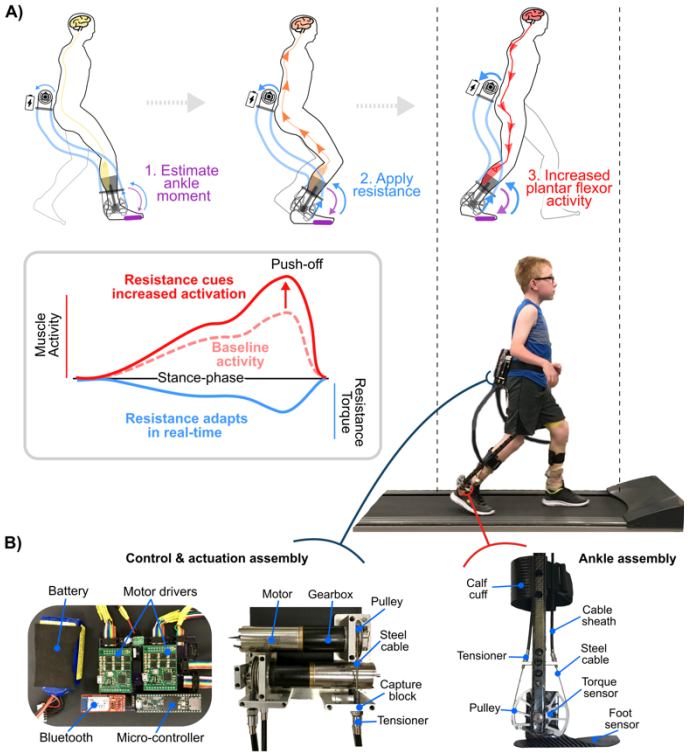

Figure 1: Wearable adaptive resistance A) control mechanism and B) device components.

Pre- and post-assessments included: 1) History and physical by a physical therapist; 2) Gait analysis at a preferred walking speed on a treadmill while measuring full-body 3D kinematics and muscle activity of the soleus; 3) Metabolic cost of transport; 4) Timed up & go (TUG) and six-minute walk test (6MWT).

Participants completed ten, 20-minute training sessions with wearable adaptive resistance over four weeks. Resistance level started at 0.025-0.075 Nm/kg and was increased progressively based on performance and perceived level of exertion.

Paired t-tests with correction for multiple comparisons were run to determine the effect of training on the following primary outcome variables: shape of soleus activation profile, metabolic cost of transport, TUG time, and 6MWT distance.

Results and Discussion

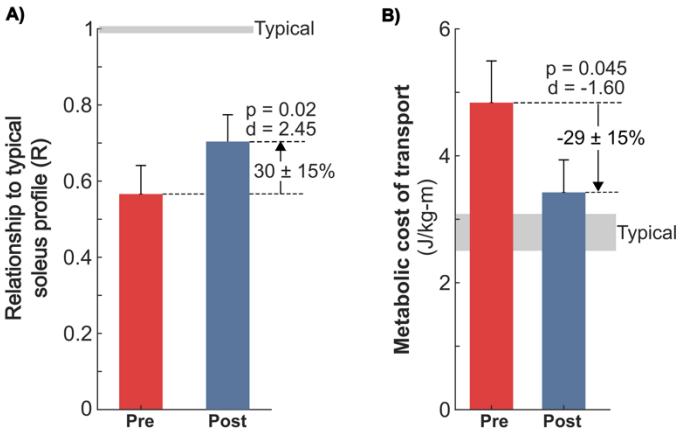

Figure 2: Pre- and post-training A) soleus activation profile shape compared to a typical profile and B) metabolic cost of transport at a preferred walking speed.

Following training, participants displayed a more typical muscle activation profile of their ankle plantar flexors (30 ± 15%, $p = 0.02$, Fig. 2A), leading to improved metabolic cost of transport (29 ± 15%, $p < 0.05$, Fig. 2B), and enhanced performance on tests of functional mobility (TUG, 11 ± 9%, $p = 0.04$) and walking endurance (6MWT, 13 ± 9%, $p = 0.05$). The rate at which wearable adaptive resistance training elicited improved function was 3 – 6 times greater than what has been reported previously for gait training interventions [3,4].

Significance

This relatively low-cost and wearable intervention was designed for translation to both clinical practice and personal use at home. The inherent accessibility of wearable interventions provides individuals with the opportunity to significantly increase the frequency of targeted neuromuscular rehabilitation.

Acknowledgments

Supported in part by the Eunice Kennedy Shriver National Institute of Child Health & Human Development of the National Institutes of Health under Award Number R03HD094583.

References

[1] Graham et al. 2016 *Nat. Rev. Dis. Prim* [2] Conner et al. 2020 *Ann. Biomed Eng.* [3] Provost et al 2007 *Pediatr. Phys. Ther.* [4] Aviram et al. 2017 *Dev. Neurorehabil.*

Compensations during Step Ascent Contribute to Stair Climbing Ability in Multiple Sclerosis

Paul W. Kline[1,2], Cory L. Christiansen[1,2], Emily R. Hager[1,2], and Mark M. Mañago[1]
[1] University of Colorado Anschutz Medical Campus, Aurora, CO, USA;
[2] VA Eastern Colorado Healthcare System, Aurora, CO, USA;
Email: paul.kline@cuanschutz.edu

Introduction

Multiple sclerosis (MS) is a chronic autoimmune-mediated disorder of the central nervous system affecting up to 1 million people in the United States [1]. Numerous studies have demonstrated movement compensations during overground walking involving proximal (trunk and pelvis) and lower extremity kinetics and kinematics [2,3]. However, there is a paucity of evidence on other aspects of physical mobility that relate to functional independence and community participation, including stair climbing. The purpose of this study was to: 1) compare trunk and pelvis motion and lower extremity joint moments during a step ascent task in patients with MS and a matched control group and 2) identify key biomechanical contributors to stair climbing ability in patients with MS.

Methods

Twenty patients with MS (16 F, 49±12 y, BMI: 24.8±5.4 kg/m^2, Expanded Disability Status Scale – EDSS: 1.5-5.5) and 10 matched control participants (7 F, 48±12 y, 23.7±4.2 kg/m^2) were enrolled. All participants underwent 3D motion analysis while ascending a 15.2 cm step in which marker trajectories were recorded using a motion analysis system (Vicon Motion Systems, Oxford, UK) at 100 Hz. Force platform data under and adjacent to the step were simultaneously recorded at 1200 Hz. Three step ascent trials were recorded with each limb as the leading limb. Stair climbing ability was assessed using ascent time during the Functional Stair Test [4]. Participants were instructed to ascend one flight of 4 steps as quickly and safely as possible. Two trials were performed and the mean used for data analysis.

Joint moments were calculated with an inverse dynamics approach and normalized to body mass. Peak joint moments were extracted from the three step ascent trials and averaged to result in a single result for hip, knee, and ankle for each limb in the MS group. A mean of left and right limb values for the control group was used for data analysis. Total sagittal and frontal plane trunk and pelvis angular excursions were determined by subtracting the minimum segment angles from the maximum segment angles during step ascent.

Comparisons between the stronger and weaker limb for the MS group were performed using paired sample t-tests. Comparisons of both limbs (MS group) to the control group were done using independent two-sample t-tests. Pearson correlations were used to assess relationships between step ascent biomechanical variables and stair ascent time. Variables with significant correlations were considered for a multiple linear regression model and a backward stepwise method was used to identify the key biomechanical contributors to stair ascent time.

Results and Discussion

When leading with the stronger limb during step ascent, increased sagittal plane trunk excursion (9.3±3.1 vs 7.6±2.6°, p=.041), greater peak knee extensor moment (1.19±0.29 vs 0.88±0.23 Nm/kg, p=.002), and reduced trail limb peak ankle plantar flexor moment (-1.11±0.17 vs -0.92±0.24 Nm/kg, p=.001) were observed compared to leading with the weaker limb in the MS group. Sagittal plane pelvis (*stronger*: 10.4±4.0 (p=.001), *weaker*: 10.1±5.2 (p=.009), *control*: 5.4±1.8°) and frontal plane trunk excursions (*stronger*: 5.1±2.2 (p=.016), *weaker*: 5.2±2.6 (p=.025), *control*: 3.1±1.4°) were greater when leading with either limb in the MS group compared to the control group, while trail leg peak ankle plantar flexor moments (*stronger*: 1.11±0.17 (p=.032), *weaker*: 0.92±0.24 (p<.001), *control*: 1.26±0.16 Nm/kg) were reduced when leading with either limb compared to the control group. Functional Stair Test time correlated with sagittal (r=.607, p<.001) and frontal plane pelvis excursions (r=.411, p=.008) and trail limb peak ankle plantar flexion moments (r=.418, p=.007). The regression model identified sagittal and frontal plane pelvis excursion to be the primary contributors to Functional Stair Test time (Adj R^2=.458).

The ability to target movement-based interventions for people with MS requires an understanding of movement mechanics during step ascent. The results of this study provide understanding of lower extremity joint moments during a step ascent task in people with MS. Consistent with prior studies demonstrating quadriceps and ankle plantar flexor muscle weakness [5], this study found reduced peak joint moments at the knee and ankle. In addition, larger trunk and pelvis excursions when leading with both the stronger and weaker limbs indicate a potential compensatory movement strategy for reduced peak ankle plantar flexor and knee extensor moments during step ascent tasks in people with MS. Finally, the results of the regression model suggest larger sagittal and frontal plane pelvis excursions may be the primary biomechanical contributors to slower stair ascent time.

Significance

People with MS ascend a step with larger trunk and pelvis excursions, reduced knee extensor moments, and reduced trail limb ankle pushoff compared to matched controls. Increased pelvis motion and reduced ankle pushoff are associated with poorer stair climbing ability and may serve as targets for future interventions designed to optimize functional movement.

Acknowledgments

We thank the University of Colorado Department of Physical Medicine & Rehabilitation Pilot Award for funding this work. The content is solely the responsibility of the authors and does not necessarily represent the official views of the U.S. Department of Veterans Affairs or the U.S. Government.

References

1. Wallin et al. *Neurology.* 2019;92(10):e1029-e1040.
2. Huisinga et al. *J Appl Biomech*. 2013;29(3):303-311.
3. Comber et al. *Gait Posture.* 2017;51:25-35.
4. Fry et al. *Physiother Can.* 2006;58(3):212-220.
5. Wagner et al. *Arch Phys Med Rehabil*. 2014;95(7):1358-1365.

Gait Coordination in Adults with Spinal Cord Injury Receiving Spinal Stimulation

Charlotte D. Caskey[1], Soshi Samejima[2], Chet T. Moritz[2,3], Katherine M. Steele[1]
[1]Department of Mechanical Engineering, University of Washington, Seattle, WA
[2]Department of Rehabilitation Medicine, University of Washington, Seattle, WA
[3]Department of Electrical & Computer Engineering, University of Washington, Seattle, WA
Email: cdcaskey@uw.edu

Introduction

Spinal cord injury (SCI) disrupts the connection between the brain and spinal cord, impacting motor and sensory function. Current rehabilitation treatments cannot recover pre-injury functionality, leaving lasting effects on individuals' mobility and quality of life. Both invasive and non-invasive spinal stimulation have demonstrated the ability to restore voluntary motor control of stepping-like patterns in individuals with complete paralysis after SCI [1]. Non-invasive spinal stimulation research has focused on walking recovery in a gravity neutral condition or with a gait assisting exoskeleton [2, 3]. We investigated the ability of non-invasive transcutaneous spinal stimulation (tSCS), combined with locomotion training to promote recovery of over ground walking in individuals with incomplete SCI. We hypothesized that improvements in functional gait after tSCS would correspond with improvements in subject intra- and interlimb coordination.

Methods

We enrolled 2 males with incomplete cervical SCI. Subject 1 was 64 years old, 3.5 years post injury, and classified as C4 American Spinal Injury Association Impairment Scale (AIS) D at baseline. Subject 2 was 64 years old, 4 years post injury, and classified as C6 AIS D at baseline. Both participants underwent a total of 8-weeks of locomotor training only and 8 weeks of locomotor training combined with tSCS.

Three-dimensional gait analysis and the 6-minute walk test (6MWT) were performed during baseline, throughout the intervention, and up to three months post-intervention. Intralimb coordination was evaluated as the angular component of correlation of correspondence (ACC) of the right leg, which measures the consistency of the knee-hip relationship for all gait cycles [4]. We calculated spatial interlimb coordination as the magnitude of the average difference between the left and right step length divided by the sum of step length for both legs, known as the spatial asymmetry index [5]. Kinematic interlimb coordination was also evaluated using the correlation coefficient and slope comparing joint angles from each side of the body.

Results and Discussion

Both participants increased the distance they could walk during the 6MWT, a change that was sustained at follow-up visits. Subject 1 walked 34 meters (m) at baseline, 88 m after the intervention, and 76 m at 3-months follow-up. Subject 2 walked 199 m at baseline, 377 m after the intervention, and 361 m at 2-months follow-up. We sought to explain the improved functional gait by examining kinematics. Neither intra- nor interlimb coordination, however, changed significantly throughout the study (Figure 1). There were also no significant changes in gait coordination when spinal stimulation was turned on and off on the same day. Previous studies reported that tSCS was able to recover coordinated stepping-like patterns during walking in a gravity neutral device or while wearing an exoskeleton [1, 3]. The lack of change we observed in gait coordination during tSCS may suggest that our participants' improvement in gait was from other factors [4]. At baseline, our participants had high ACC close to one, the ideal intralimb coordination, and relatively low spatial asymmetries close to zero (Figure 1). Since our subjects had high initial coordination, walked overground, and actively loaded their limbs, we may not be able to use gait coordination as a sensitive measure of their functional changes after tSCS.

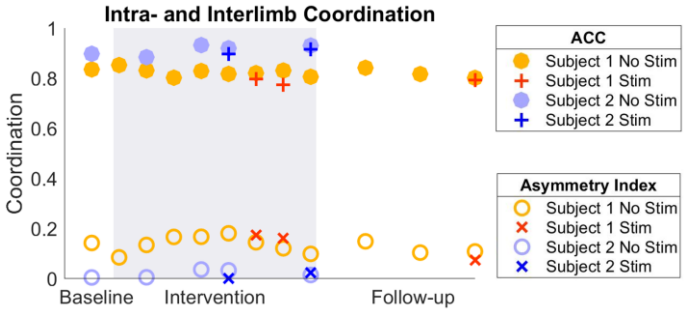

Figure 1. Evaluation of intra- and interlimb coordination was done at baseline, during the intervention (grey box), and up to 3 months follow-up. Gait analysis was always performed with spinal stimulation turned off, but some days it was also performed with the device turned on, marked by x's and +'s.

Further research is needed to expand the study's sample size to evaluate the biomechanical and neuromuscular changes induced by tSCS. Additional work also needs to be done examining the physiological mechanisms of spinal stimulation.

Significance

Stepping and coordination have previously been used to quantitatively describe changes in function as a result of therapy after SCI. However, these results indicate that traditional quantitative measures of gait coordination do not identify changes in coordination with spinal stimulation. Other measures of gait may be needed to systematically evaluate the impact of tSCS on walking function, a critical first step to implementing tSCS in clinical SCI rehabilitation.

Acknowledgments

This work is supported by the UW College of Engineering Dean's Fellowship, NIH NINDS Award R01NS091056, the Center for Neurotechnology, a National Science Foundation Engineering Research Center (EEC-1028725), and Washington State Spinal Cord Injury Consortium.

References

[1] Y. Gerasimenko et al. (2015). J. Neurotrauma, 32: 1968–1980.
[2] Y. Gerasimenko et al. (2015). Ann. Phys. Rehabil. Med., 58: 225–231.
[3] P. Gad et al. (2017). Front. Neurosci, 11.
[4] E. C. Field-fote et al. (2002). Phys. Ther., 82: 707–715.
[5] Y. Thibaudier et al. (2019). Gait Posture, 75: 121–128.

Acute effects of whole-body vibration on stair ascent in children with Down syndrome

Diego M. Ferreira[1] and Jianhua Wu[1]
[1]Department of Kinesiology and Health, Georgia State University, Atlanta, GA, USA. Email: jwu11@gsu.edu

Introduction

Ascending stairs is a common daily activity that is necessary to navigate households and many other buildings. Children with Down syndrome (DS) have lower muscle strength and poorer balance control, resulting in an underdeveloped ability to navigate staircases [1]. Children with DS demonstrate shorter step lengths and slower step velocities when approaching a staircase compared to typically developing (TD) children [1]. Additionally, children with DS demonstrate underdeveloped locomotor adjustments while ascending a staircsae [2].

Whole-body vibration (WBV) is a new intervention and has been shown to improve muscle strength and walking endurance in individuals with DS [3]. However, it is not known if WBV can help improve functional tasks in children with DS. Therefore, this study aimed to investigate the acute effects of a single session of WBV on stair ascent in children with DS. We hypothesized that step length would increase and step time would decrease, resulting in a faster step velocity during the approach and ascent phases after WBV.

Methods

We have recruited five subjects (2M/3F, 11.3±2.36 years) for this study. Subjects completed 5 trials of stair ascent during 3 time points (baseline, pre-WBV, and post-WBV). The lack of a significant difference between the baseline and pre-WBV conditions suggests there might not be a learning or warm-up effect on stair ascent. Each subject walked along a walkway with 2 imbedded force plates to a 3-step staircase with a riser hight of 24 cm, and then ascended the staircase [1]. Rest was given between trials, including a 10-minute break between the baseline and Pre-WBV conditions. The post-WBV condition occurred immediately after the session of WBV.

Subjects completed 10 bouts of 30 seconds on a Galileo side-alternating WBV platform (25 Hz, 2 mm) with 1 minute rest between bouts. An 8-camera Vicon motion capture system was used to collect the spatial-temporal gait parameters for the 2 steps before the stairs (-2 & -1) and 2 steps during stair ascent (step 1 & 2). Gait variables included step length, step time, and step velocity for these four steps. Step length was normalized by each subject's leg length. Step time and velocity were normalized using the equations below [4]:

$$\textit{Normalized step time} = \textit{step time} / \sqrt{leg\ length/g}$$

$$\textit{Normalized step velocity} = \textit{step velocity} / \sqrt{leg\ length * g}$$

where g is the gravitational acceleration (9.81 m/s^2). Two-way (2 step x 3 time) repeated ANOVAs were conducted for the approaching and ascent phases, separately. Post-hoc pairwise comparisons with Bonferroni adjustments were conducted when necessary at a significance level of alpha=0.05.

Results and Discussion

During the approaching phase, step length was shorter but step time was longer and step velocity was slower at step -1 compared to at step -2 (Table 1). There was a step effect on step length, step time, and step velocity (all $p<0.05$). However, there were no differences between before and after WBV (Table 1).

During the ascent phase, step length was longer and step velocity was faster but step time was shorter at step 1 compared to step 2 (Tabel 2). There was a step effect on all three variables (all $p<0.05$). Also, step velocity increased after WBV, particularly at step 2. There was a time effect on step velocity ($p<0.05$). Post-hoc analysis revealed that step velocity at step 2 incresed from baseline to post-WBV.

Table 1. Means (SD) of variables during approaching phase

Variable	Step	Baseline	Pre-WBV	Post-WBV
Step length *	-2	0.51 (0.12)	0.57 (0.08)	0.61 (0.16)
	-1	0.38 (0.17)	0.38 (0.19)	0.43 (0.23)
Step Time *	-2	1.84 (0.09)	1.78 (0.23)	1.77 (0.28)
	-1	1.96 (0.28)	2.12 (0.53)	1.68 (0.18)
Step Velocity *	-2	0.28 (0.07)	0.33 (0.09)	0.36 (0.13)
	-1	0.20 (0.11)	0.20 (0.12)	0.26 (0.13)

Note that * represents a difference between steps

Table 2. Means (SD) of variables during ascent phase

Variable	Step	Baseline	Pre-WBV	Post-WBV
Step length *	1	0.70 (0.09)	0.67 (0.09)	0.68 (0.11)
	2	0.36 (0.05)	0.35 (0.04)	0.36 (0.05)
Step time *	1	2.92 (0.37)	3.59 (1.75)	3.20 (1.01)
	2	6.25 (4.27)	4.30 (1.09)	3.44 (0.70)
Step velocity *‡	1	0.24 (0.05)	0.23 (0.11)	0.23 (0.09)
	2	0.08 (0.04)	0.09 (0.02)	0.11 (0.02)

Note that * represents a difference between steps; ‡ represents a difference between baseline and post-WBV

Significance

These preliminary results suggest that a single session of WBV can modulate neuromuscular function by increasing step velocity while ascending a staircase. Further analysis of joint kinematics and kinetic is needed to determine if WBV provides benefits to other biomechanical aspects of this activity. Since WBV is an easy modality to administer, this would make a modality for children with DS more convenient and less strenuous than typical therapy. The use of WBV training could be implemented in this population's therapy to address motor deficits and potentially improve their daily motor activities and the quality of life.

References

1. Liang et al. *Gait and Posture*. 66: 260-266, 2018.
2. Liang et al. *Gait and Posture*. 63: 46-51, 2018.
3. Eid MA. *Am J Phys Med Rehabil*, 94, 633-643, 2015.
4. Stansfield et al. *Gait and Posture*. 17: 81-87, 2003.

Movement coordination during humeral elevation in individuals with newly acquired spinal cord injury

Margaret Finley, PT, PhD[1], Elizabeth Euiler, MS[1], Shivayogi V. Hiremath, PhD[2], Joseph Sarver, PhD[3]
[1]Department of Physical Therapy and Rehabilitation Science, Drexel University
Email: maf378@drexel.edu

Introduction

Evidence regarding physical impairments during the initial, recovery phase in individuals with spinal cord injury (SCI) is limited to studies on range of motion and gross muscle strength[1], without investigations of shoulder girdle kinematics during overhead reaching. Analysis of this task is critical as alterations have been shown to be sensitive to various chronic musculoskeletal impairments[2] and neurological conditions such as stroke.[3] Kinematic analyses in individuals with long duration SCI is limited to transfers, weight relief maneuvers, wheelchair propulsion and weight bearing tasks rather than overhead reaching. While conducting a larger longitudinal study, we became aware there is a gap in knowledge regarding movement patterns in individuals with newly acquired SCI. Therefore, the goal of this abstract is to present an important novel clinical observation of shoulder girdle kinematics during overhead reaching in individuals with newly acquired SCI. In addition, this exploratory pilot study will describe a novel approach for quantifying scapulohumeral coordination as a potential method for motion classification.

Methods

Adults with newly acquired SCI (n=8) and age and gender matcherd uninjured controls (n=8) completed the Musculoskeletal Pain survey[4], a clinical shoulder evaluation and a kinematic assessment of an overhead reaching task. Three-dimensional kinematics of the trunk, scapula, and humerus of the dominant limb were collected (100 Hz) with The MotionMonitor™ (Ascension TrakStar, Innovative Sports Training, Inc., Chicago, IL).[5] Coordination analysis of scapular upward rotation with humeral elevation (scapulohumeral rhythm) was performed by identifying the linear range of scapular upward rotation during elevation. The humeral elevation angles for initiation and end of the linear range was calculated and expressed as a percentage of maximal humeral elevation.

Differences between groups ($p \leq 0.05$) were assessed for musculoskeletal shoulder pain score, velocity of elevation, plane of humeral elevation, scapular rotations (external, upward, posterior) and thoracic kyphosis at each humeral elevation angle (initiation, 30°, 60°, 90°, 120°, maximum elevation). Effect sizes were calculated for between group measures. Scapulohumeral movement coordination was quantified as the initial and final humeral elevation angle at which scapular upward rotation and humeral elevation were linearly correlated. The initial and final 'linear' elevation angles were averaged for each subject and are reported in both absolute (degrees) and relative (percentage of motion) terms. Group comparisons were analyzed ($p \leq 0.05$). Post hoc correlation analysis revealed a significant inverse association of shoulder pain with maximum elevation ($r=-0.72$, $p=0.04$) in those with SCI.

Results and Discussion

Individuals with SCI had a higher level of shoulder pain per the Musculoskeletal Pain Survey ($p=0.01$, $\delta=1.7$). No difference in velocity or plane of elevation existed, however, the group with SCI had less maximal humeral elevation compared to the control group ($p=0.04$, SCI=117.4°±5.8°; control=132.1°±3.4°). Individuals with SCI had significantly reduced scapular upward rotation at 120° elevation. Movement coordination was altered in those with SCI as the linear relationship started later ($p<0.001$) in the motion (52% compared to 5% for controls) and ended significantly later ($p=0.004$, 93% compared to 68% for controls). Furthermore, the linear relationship spanned a significantly ($p=0.02$) smaller range of humeral elevation for SCI group (16.2° vs 23.2°for controls) (Figure 1).

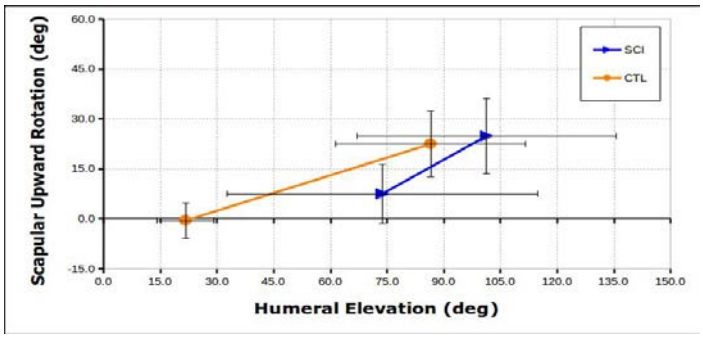

Figure 1: Scapulohumeral movement coupling demonstrated as linear range of scapulothoracic upward rotation during humeral elevation by groups

Significance

This is one of the first studies to demonstrate that individuals with acute SCI have reduced maximal humeral elevation, with only 50% of the sample able to achieve 120° elevation. In a typical day, wheelchair users reach overhead (above 90°) five times more often than able-bodied controls. Coordination/coupling analysis revealed different patterns of motion in this early phase following SCI. Linear relationship of scapular upward rotation to humeral elevation occurred later and had a smaller total range of motion. This delayed upward rotation may predispose individuals to aberrant movement patterns that could lead to development of impairments, such as impingement and/or increased pain.

Acknowledgments

Department of Defense SCIRP Award #W81XWH-17-1-0476

References

1.Eriks-Hoogland I, et al. *Arch Phys Med Rehabil.* 2016;97(1):84-91.
2.Ludewig & Reynolds JF. *J Orthop Sports Phys Ther.* 2009;39(2):90-104.
3.Rundquist PJ, et al. *Disabil Rehabil.* 2012;34(5):402-407.
4.van Drongelen S,e t al. de *Spinal Cord.* 2006;44(3):152-159
5.Wu G, et al. *J Biomech.* 2005;38(5):981-992.

Changes to Walk Speed: Programming Deep Brain Stimulators for Parkinson's Patients

Christopher P Hurt[1], Daniel J Kuhman[1], Carla Rigo Lima[1], Melissa Wade[1], Harrison J Walker[1]

[1] University of Alabama at Birmingham, Birmingham, AL, U.S.A
Email: cphurt@uab.edu

Introduction

Deep brain stimulation (DBS) is an effective therapy for individuals with Parkinson's disease (PD) after pharmacologic interventions no longer optimally control motor symptoms[1]. A recent meta-analysis showed that walk speed improves with DBS, however outcomes varied substantially from large to negligible improvements[2]. However, these measures of gait function were recorded after initial clinical programming sessions. It is possible that gait speed was not measured across all available contacts on the DBS lead suggesting outcomes may not be optimized for gait. Given the clinical and diagnostic utility of walk speed, this measure could provide a simple, objective and integrated clinical tool to assess DBS efficacy for gait, balance, and other motor symptoms if it was assessed during initial programming sessions. The purpose of this study was to investigate clinically meaningful changes in gait function and the reliability of walking speed in participants with PD during a programming session of individuals who have surgically implanted DBS devices.

Methods

Nineteen participants with PD (age 59.1±7.1 years) underwent surgery to implant a multi-contact, directional DBS lead in the subthalamic nucleus. Participants visited the lab one-month after implantation for device activation. Each DBS electrode was tested for clinical benefit with a standardized pulse width of 60 μs and a frequency of 130 Hz by a trained nurse practitioner. The novel DBS device contains six individual contacts and two virtual rings formed by 3 directional contacts each, and individual dorsal and ventral rings. Contacts were tested in random order to avoid an ordering effect. The individuals were tested in the practically defined "OFF" state (>12 hours without PD medicine). Individuals completed four 10m walking trials at a comfortable speed (CWS) with the device OFF and ON for each of the 10 DBS settings (6 directional contacts, 2 virtual rings, 2 individual rings). To determine whether CWS was reliable across trials within each contact, intraclass correlation coefficients (ICC) were quantified for each contact or ring. To determine the efficacy of DBS, maximum and minimum walking speeds captured with the CWS captured prior to device activation using a repeated measures ANOVA. We also categorized changes in walk speed relative to clinical meaningful differences for persons with PD[3]

Results and Discussion

Walking speed differed substantially across directional DBS contact segments, within and across participants ($p<0.001$).

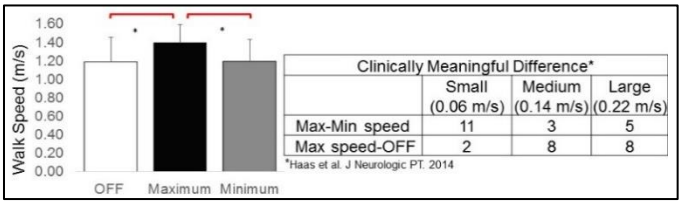

*Figure 1. A) Comparison of walk speed between OFF medicine/DBS and the Maximum and Minimum walk speed per participant across contacts. *denotes significance p<0.05 B) Number of participants experiencing a clinically meaningful difference in walk speed with DBS stimulation.*

Post hoc analyses revealed that the average maximum recorded walking speed with DBS (1.36 ± 20.1 m/s) was significantly faster than both the minimum speed with DBS (1.17± 24.1 m/s) and DBS off (1.18 ± 25.7 m/s, $p<0.000$ for both comparisons, Figure 1A), while no significant difference was detected between DBS off and minimum speed DBS on ($p=1.000$). Across all DBS testing conditions, 18% of the tested rings or contacts actually yielded slower walking speeds however the best contacts tested resulted in at least medium clinically meaningful differences in 89% of particpants (Figure 1B). ICC values for walking speed data were all above 0.949, which suggests excellent reliability (Table 1). When looking at the 95% confidence intervals, the lower limit of the interval was above 0.900 in 8 of the 10 DBS trials, suggesting excellent reliability while 2 of the 10 were greater than 0.883 suggesting good reliability. To the best of our knowledge this is the first study to show that walk speed can be used as a reliable measure to assess gait function while programming DBS and moreover we observed a clinically meaningful speed increase.

Significance

Walking speed is a clinically meaningful, reliable measure that may be used to assess the effect of programming individual DBS contacts to maximize improved gait function in PD. Next-generation directional and closed loop DBS devices have the potential to provide greater improvements in gait and balance by tailoring stimulation parameters to optimize efficacy.

Acknowledgments

Work supported by grant awarded to HW 1UH3NS100553-01.

References

1.Walker HC, et al. Neurosurgery 2009. 2. Roper et al. J Neurol 2016. 3. Hass et al. J Neurol Phys Ther 2014

Table1. ICC values for all contacts tested and OFF condition with 95% confidence intervals.

Contact	1	2	3	4	5	6	7	8	9	10	OFF
ICC	0.975	0.949	0.964	0.964	0.955	0.959	0.96	0.96	0.959	0.971	0.971
95% C.I.	0.936	0.883	0.916	0.926	0.897	0.919	0.911	0.914	0.91	0.937	0.938
	0.99	0.979	0.985	0.985	0.982	0.982	0.984	0.983	0.982	0.988	0.988

Gait and Balance Characteristics for Adults with Degenerative Cervical Myelopathy

Daniel Richie, Arghavan Farzadi, Andrea Hesse, Shelby Miracle, Amy Minnema, Ajit M.W. Chaudhari, Francis H. Farhadi
The Ohio State University, Columbus, OH, USA
Email: daniel.richie@osumc.edu

Introduction

Patients with degenerative cervical myelopathy (DCM) present with a range of motor and sensory symptoms, including poor coordination and loss of balance. When symptoms worsen despite non-surgical treatment, decompression surgery may be recommended. Currently there are no objective criteria to help guide surgical recommendations; therefore, individual patient outcomes have wide variability [1]. Gait parameters, specifically gait speed, stride length and step width, have been postulated to track disease progression as well as response to surgical intervention [2]. However, step width can be difficult to measure in the clinic compared to stride length or speed. Therefore, this study aims to characterize the gait and balance of a pre-operative DCM population and then determine a predictive model for step width from gait speed and stride length that will allow objective assessment of a patient's functional ability during clinical care.

Methods

12 DCM patients (age: 63 ± 13y; 8 female; height 166 ± 9cm) gave informed consent in accordance with procedures of the Institutional Review Board of The Ohio State University. These patients have mild to moderate physical function impairment from DCM (PROMIS Physical Function Score of 40.5 ± 2.2). Patients were tasked with three 30-second, eyes closed standing-balance trials to measure postural sway. Then participants completed four 10-meter walking trials at self-selected pace. Spatiotemporal parameters were extracted from a ten camera Vicon motion capture system with markers placed on both feet. Marker trajectories were low-pass filtered using a 4th order zero-pass Butterworth filter at 6Hz. Spatiotemporal parameters were normalized to height for the predictive model. Standing balance data was collected at 1000Hz using a Bertec balance plate and low-pass filtered using a 4th order zero-pass Butterworth at 20Hz.

Results and Discussion

The balance data was analysed for the root-mean square of the medial-lateral (RMS-ML) sway of the center of pressure. The DCM patient balance data was compared to healthy older adults (N = 38; age: 83 ± 8y; 30 female) [3] and the spatiotemporal gait data was compared to healthy older adults (N = 294; age: 79 ± 5y; 186 female; height 167 ± 6cm) from a separate study [4], shown in Figure 1.

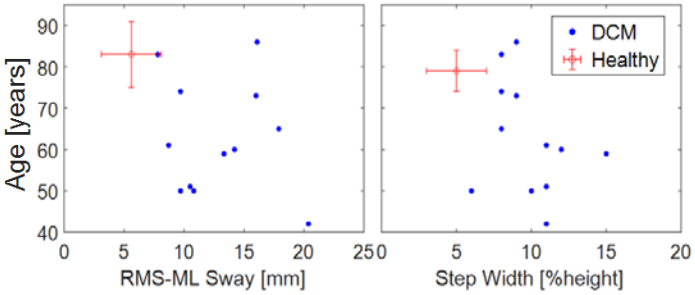

Figure 1: Comparing DCM to Healthy Older Adults

Figure 1 shows the younger DCM group has significantly more medial-lateral sway during standing balance than the healthy, older group. Also shown is the significant increase in step width for the DCM group. Not shown in Figure 1, the younger DCM group had similar gait speed and stride length to the older, healthy adults. To describe a relationship of step width by gait speed and stride length, refer to Figure 2. This relationship shows no significant correlation for step width. This was confirmed with a multivariate least square linear regression for step width predicted by gait speed and stride length (all normalized by height). The regression results in an $R^2 = 0.1$.

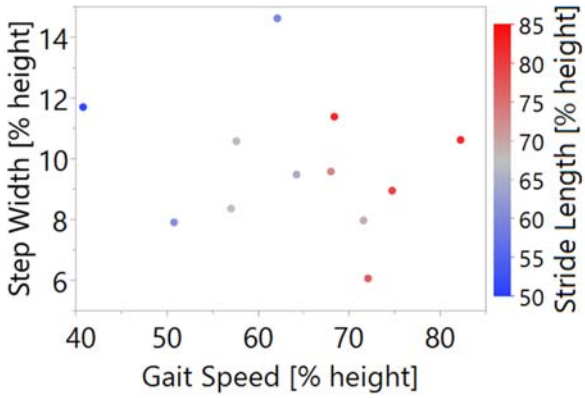

Figure 2: Relationship Between Gait Parameters for DCM

The data presented is significant as it helps to quantify the balance deficits observed in DCM patient groups. The younger DCM group had greater medial lateral sway and step width while walking with the same speed and stride length of older, healthy adults. This leads to the conclusion that the DCM group would show significant balance deficits compared to an age-matched healthy group. By characterizing the balance and gait of the pre-operative DCM population, these parameters can now be tracked post-operatively over time and used to assess the patient's response to surgical intervention.

Significance

This research enforces the importance of a multi-disciplinary approach to improving patient clinic care and leveraging biomechanics to improve surgical outcomes. With this research, the loss of balance observed in DCM patients is quantified and can now be tracked during recovery to inform clinical and surgical decision-making for future patients. The methods used here could be applied to other pathologies where patients experience loss of balance and an intervention is performed. Examples of pathologies include, traumatic brain injuries, cancer, Parkinson's, stroke and other spinal cord injuries.

References

[1] Parker SL, et al. (2017) *Neurosurgery* 80:S61-S69
[2] Siasios ID, et al. (2017) *World Neurosurg* 101:275-282
[3] Reed AC, et al. (2019) *2019 ISB Proceedings*
[4] Hollman JH, et al. (2011) *Gait & Posture* 34:111-118

Gait Variability in Persons with Parkinson's disease after Individualized Physical Therapy

Srikant Vallabhajosula*, Morgan Reich, Krista Nunn, Crystal Ramsey
Department of Physical Therapy Education, Elon University
Email: *svallabhajosula@elon.edu

Introduction

Persons with Parkinson's disease often exhibit deficits with balance and gait. These deficits often put them at a high risk of falling and decreased quality of life. One of the measures of fall risk level is gait variability. Previous research reported increased stride-to-stride variability among individuals with Parkinson's disease.[1] Moreover, recent research has been focused on using backward walking as a challenging assessment of dynamic balance.[2-4] While exercise interventions like Tai Chi have been shown to have mixed results on improving gait[5], literature on the effectiveness of using individualized physical therapy in a group setting to improve gait variability is sparse.

The purpose of this study was to evaluate changes in gait variability of individuals with Parkinson's disease during forward and backward walking after 3 months of individualized physical therapy. We hypothesized that gait variability would decrease.

Methods

Ten individuals with Parkinson's disease (5 females, H&Y score between I and III) aged 60 years and above were recruited.

Participants completed one-hour intervention sessions conducted twice a week for three months. The intervention consisted of a 5-minute warm up, followed by 20 minutes of aerobic activity. Participants self-selected the aerobic activity but were asked to exercise at a rate of perceived exertion level of at least 7/10. Aerobic exercise activity was followed by activities focused on body structures and functions such as dual-tasking, dynamic balancing, obstacle crossing, and walking in different directions which affected the participant's participation goals.

Gait assessment was done before (PRE) and after (POST) the intervention using a 16' pressure-sensor based walkway. Participants walked 5 times at a comfortable pace in forward and backward directions. Within-subject coefficient of variation (CV) was computed for stride length, width, time and stance time. A paired samples t-test was done.

Results and Discussion

For forward walking (Figure below), only stance time variability increased significantly (by 18%; P=0.012).

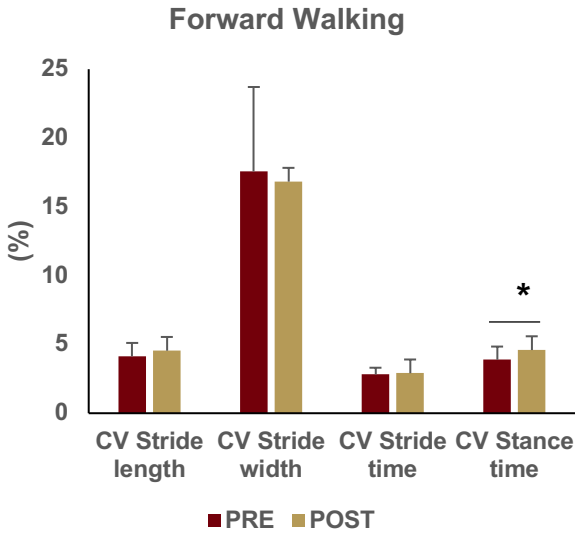

For backward walking (Figure below), there was a significant decrease in variability of stride time (by 23%; P=0.016) and stance time (by 13%; P=0.023). Stride length variability decreased by 14% albeit with a trend towards significance (P=0.063)

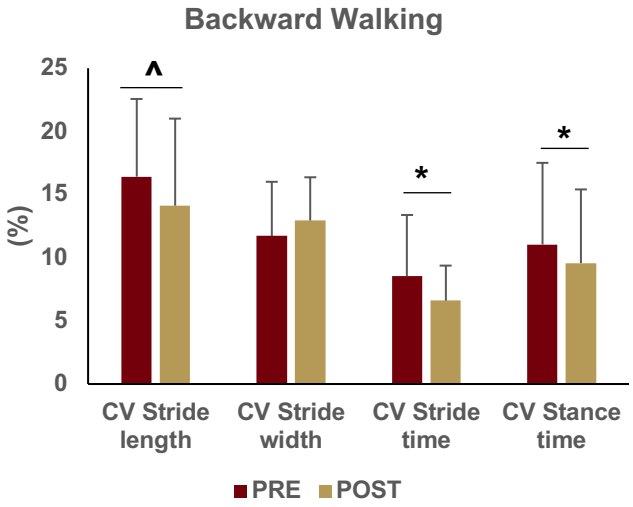

Data from the current study was similar to those reported previously.[3] The results support the hypothesis in the backward walking but not in the forward walking. While it is not entirely clear why variability increased in the forward direction but decreased in the backward direction, specificity of training could have contributed to these findings. Specifically, participants worked on activities like obstacle crossing in forward direction and walking backwards which may have resulted in the results observed.

Significance

Decrease in gait variability during a more challenging task like backward walking could highlight the importance of using individualized physical therapy interventions for individuals with Parkinson's disease. Whether such improvements are related to decrease in fall risk needs to be further evaluated.

Acknowledgments

This study was supported by the Parkinson's Foundation.

References

1. Hausdorff JM, *Chaos*, 2009; 19(2): 026113
2. Hackney ME & Earhart GM, *Mov Disord.*, 2009; 24(2): 218-223
3. Bryant et al, *Acta Neurol Scand.*, 2016; 134(1): 83–86
4. Gilmore et al., *Gait Posture*, 2019; 74:14-19
5. Amano et al., *Parkinsonism Relat Disord.*, 2013; 19(11), 955-6

Differences in Knee Joint Angle between Parkinson's Disease "on" and "off" Medication across Varying Levels of Visual Flow

Zachary Ripic[1], Jeonghoon Oh Ph.D.[2], Dayun Jeon[1], Joseph Signorile Ph.D.[1], and Moataz Eltoukhy Ph.D.[1]
[1]University of Miami, Department of Kinesiology and Sport Sciences
[2]University of Georgia, Department of Kinesiology
Email: zar17@miami.edu

Introduction

Parkinson's Disease (PD) manifests through motor symptoms such as akinesia, bradykinesia, tremor, and rigidity.[1] Additionally, gait disturbances arise with disease progression and as patients transition between medication states. Current efforts seek to reduce this through various cueing interventions that target gait disturbances by extracting discrete spatiotemporal, kinematic, or kinetic variables.

The purpose of this study was to identify differences that occur over the gait cycle between PD patients "on" and "off" medication with and without varying levels of visual flow which may simulate cueing interventions. We hypothesized that differences would be observed in knee joint angle between PD medication groups. Additionally, these differences would be dependent on varying levels of visual flow implemented through carpet patterns displayed on the walking surface.

Methods

Analyses presented in the current study were conducted on de-identified gait data from PD patients "on" medication (PD ON), and PD patients "off" medication (PD OFF). Initially, PD subjects performed gait trials in each medication condition on a control (blank) carpet. The following four visits were randomized for medication condition and four different carpet conditions with varying patterns.

Gait trials were captured with an optoelectronic motion capture system (BTS Bioengineering, Milano, Italy) using the Vicon Plug-in-Gait Model (Vicon Motion Systems Ltd., Oxford, UK). Kinematic trajectories and gait events were processed using Matlab r2019b (MathWorks, Natick, MA). Gait cycles were extracted using subsequent heel strikes. Kinematic trajectories were time normalized to 100 percent of gait cycle and coded for subject and carpet types. Outliers at each time point were removed and normality was checked using Kolmogorov-Smirnov test. Data from each subject and carpet type were averaged across time points and resampled to contain eight observations in each condition (8 x 5 conditions x 2 groups = 80 total observations).

Data were analysed using a statistical parametric mapping (SPM) approach implemented via publicly available spm1d package for Matlab (spm1d.org). Data were analysed using a 2-by-5 factorial ANOVA where significant effects are indicated as exceeding a critical threshold (α = .05) above which only 5% of equally smooth random data would be expected to cross[2,3].

Results and Discussion

Results show a significant effect of medication on knee joint angle during late swing phase. PD ON exhibited significantly less knee flexion from 89-100% gait cycle ($p < .05$) (Figure 1). No significant results were observed for carpet condition or medication-by-carpet condition effects for this sample. Varying levels of visual flow had no effect in or between medication states for these patients. Observed differences in knee joint angle between medication conditions may provide benefit to further cueing interventions. Importantly, research shows PD patients "off" medication walk slower with increased cadence and reduced range of motion in lower limb joints when compared to healthy age-matched controls[4]. Further, others have shown PD fallers also exhibit increased flexion in the swing limb during minimum toe clearance which was thought to be an adaptation to increased knee flexion in the stance limb[5]. Results of the present study indicate, at least during late swing, knee joint angles differ depending on medication state which may be an important target for further developments in cueing interventions that seek to mitigate abnormalities observed during gait in PD populations.

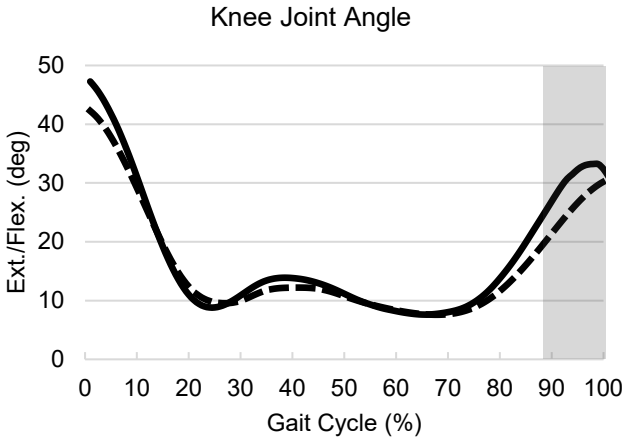

Figure 1: Sagittal plane knee joint angle. Knee joint angle differed between PD ON (- -) and PD OFF (-) from 89-100% of gait cycle indicated by shaded region ($p < .05$)

Significance

The present study offers an alternative method, not strictly as a replacement but an expansion from discrete spatiotemporal, kinematic, or kinetic variables commonly used to quantify gait characteristics in PD populations. Future developments in cueing interventions may benefit by identifying and targeting specific deficiencies that occur during the gait cycle in these patients.

Acknowledgments

This study was funded by the Parkinson's Foundation Leadership Award: PF-PLA-1710

References

1. Moustafa et al., (2016). Neuroscience & Behavioral Reviews, 68, 727-740.
2. Adler, R.J., Taylor, J.E., (2007). Random Fields and Geometry.
3. Nieuwenhuys et al., (2017). Public Library of Science. 12(1).
4. Svehlik et al., (2009). Archives of Physical Medicine and Rehabilitation, 90(11), 1880-1886.
5. Cole et al., (2011). Parkinsonism & Related Disorders, 17(8), 610-616.

A Novel Augmented Reality Platform Delivers Sensory Cues to Improve Parkinsonian Gait

Isaiah J. Lachica.[1], Thomas Chan, Ph.D.[2], Joshua A. Vicente[1], Maria E. Ayala[1], Alex X. Krause[1], Michael A. Weise[1], and Jacob W. Hinkel-Lipsker, Ph.D.[1]
[1]Department of Kinesiology, California State University, Northridge
[2]Department of Psychology, California State University, Northridge
Email: isaiah.lachica.993@my.csun.edu

Introduction

People with Parkinson's disease (PD) often exhibit an atypical gait which is characterized by a decreased step length, increased cadence, and increased gait variability[1]. These gait characteristics can be mitigated by using simple visual (e.g. lines on the floor) and auditory (e.g. beeps from a metronome) cues[1]. Cues such as these are enhanced when they are action-relevant (i.e. related to the task), for instance using footprints instead of lines and recorded footstep sounds instead of beeps[2,3]. However, these cueing strategies are currently limited to the confines of a clinic or laboratory. Recent advances in augmented reality (AR) may allow for these cues to be delivered in a mobile and on-demand fashion. However, literature on AR cueing and Parkinsonian gait remains inconclusive[4]. Studies have also yet to compare the different action-relevant sensory cues to identify which modality is most effective in addressing Parkinsonian gait. As such, the purpose of this study was to compare the effects of AR-based action-relevant sensory cues and to investigate the usability of a novel AR device in providing sensory cues to people with PD. We generally hypothesize that the novel AR platform will acutely improve the gait characteristics of people with PD.

Methods

Ten people with PD are being recruited for this ongoing study. Participants are instructed to complete three walking trials across a 10-meter pathway for each of the following conditions: no cues (NC), action-relevant visual cues (VC), action-relevant auditory cues (AC), and combined action-relevant audio-visual cues (AVC) (Figure 1A). Step length, step length variability, cadence, and cadence variability are acquired at 200Hz from all trials using seven inertial measurement units placed on the legs and pelvis. Step length and cadence are normalized to their mean values from the NC condition while gait variability measures are reported as coefficients of variation (CoV). A Magic Leap One AR headset was used to provide action-relevant sensory cues to the participants (Figure 1B). The System Usability Survey (SUS) is used to assess the feasibility of implementing cues using the platform for this population, where a score greater than or equal to the 68th percentile demonstrates above average usability[6].

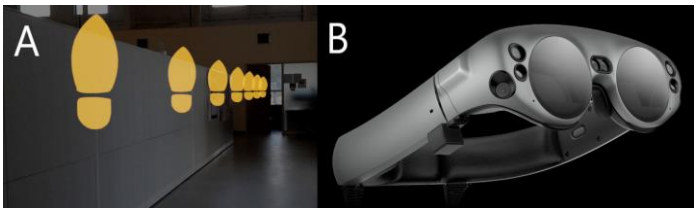

Figure 1: (A) VC condition; (B) Magic Leap One AR Headset.

Results and Discussion

Preliminary data from one person with PD demonstrates that the AVC condition produced the greatest increase in step length and decrease in cadence (Table 1). This is in contrast to a previous study that discussed no additional improvements from combining visual and auditory cues[1]. It is possible that, since the cues combined in the previous study were not relevant to walking, their combination led to a split in attention which has been known to negatively affect people with PD[7]. However, by using action-relevant cues in the current study, competition for attention may have been reduced—leading to the observed improvements. Moreover, none of the cue types used in the current study improved gait variability (Table 1), contrasting with previous action-relevant cueing studies which have demonstrated positive effects on step length and cadence variability[2,3]. This may be attributable to a switch to a more conscious control of walking as the participant attempted to sync each step with the action-relevant sensory cues[6]. The participant also gave the AR platform an above average percentile score in the SUS. The device we are using rated higher than a proprietary one used in a previous study[4], possibly because it weighs less (316g from 530g), has a wider field of view (50° from 45°), and uses action-relevant cues (footprints vs staircase). It seems then that delivering combined action-relevant sensory cues through the Magic Leap One is effective in improving some elements of Parkinsonian gait. More data is currently being collected to confirm these results.

Table 1: Gait measures normalized to mean values from NC condition and SUS score of person with PD.

Condition	Step Length	Cadence	Step Length CoV	Cadence CoV	SUS Score
NC	0.00%	0.00%	8.11%	5.30%	72.50
VC	8.11%	-3.64%	12.50%	9.28%	
AC	8.11%	-1.99%	9.00%	5.74%	
AVC	11.35%	-8.28%	9.22%	6.50%	

Significance

The noted improvements in gait from this study indicate the potential to use AR as a non-pharmacological method for treating the effects of Parkinson's disease on gait. With this device, users can receive visual and auditory cues on-demand during performance of daily living activities. This can lead to positive implications beyond walking ability by increasing opportunities to engage in a more active and social lifestyle.

Acknowledgments

The authors gratefully acknowledge the PAR-D Lab in helping with the development of the software used with the AR headset.

References

[1] Suteerawattananon, M et al. (2004). J Neurol Sci, 219(1-2)
[2] Gomez-Jordana LI et al. (2018). Front Neurol, 9
[3] Young, WR et al. (2014). Neuropsychologia, 57
[4] Janssen, S et al. (2017). Front Neurol, 8
[5] Brooke, J. (2013). J Usability Stud, 8(2)
[6] Vitorio, R et al. (2014). Neuroscience, 277
[7] Peterson, DS et al. (2015). Front Neurol, 6

Intermuscular Coherence within the Upper Limb in Persons with Essential Tremor

DB Free[1], I Syndergaard[1], AC Pigg[1], S Muceli[2], J Thompson-Westra[3], K Mente[4], CW Maurer[5], D Haubenberger[3], M Hallett[3], D Farina[6], SK Charles[1]
[1]Brigham Young University, [2]Chalmers University of Technology, [3]National Institute of Neurological Disorders and Stroke, NIH, [4]Case Western Reserve University, [5]Stony Brook University, [6]Imperial College London
Email: daniel.free816@gmail.com

Introduction

Essential Tremor (ET) affects millions of people, but traditional treatment options leave many patients unsatisfied [1]. Peripheral suppression techniques could prove beneficial to these patients. However, there is uncertainty on the way to apply these techniques because we do not currently know which muscles or joints are most responsible for a given person's tremor.

One difficulty in identifying which muscles are most responsible for tremor is that tremorogenic activations in different muscles are not independent of each other. Previous studies have focused on the relationships between isolated muscle pairs, typically around a single joint [2-3]. To date, no study has characterized the relationship between tremorogenic activity in muscles throughout the arm, from shoulder to wrist. The purpose of this research was to quantify these intermuscular relationships within the upper limb in tremor patients.

Methods

24 ET subjects participated in this study. They performed both postural and kinetic tasks using seven targets in a workspace representative of activities of daily living. Each task was repeated 3 times. Muscle activity was recorded in the 15 major superficial muscles of the arm during these tasks.

The resulting raw EMG signal was processed using the common approach of high-pass filtering (20 Hz), rectification, and low-pass filtering (20 Hz). Next, the coherence between each muscle pair for every subject-task-repetition combination was computed. The maximum of the coherence in the tremor band (4-12 Hz) was then extracted, resulting in a 15-by-15 symmetric coherence matrix for each subject-task-repetition combination.

Our statistical analysis consisted of characterizing the overall pattern of coherence and its variability between subjects and over time, and then calculating the effects of control variables, which included task type (postural, kinetic), arm configuration (target 1-7), and subject characteristics (sex, tremor severity, duration, and onset). To determine the similarity in the coherence patterns between control variables, we calculated the two-dimensional correlation between pairs of coherence matrices corresponding to different control-variable combinations, and then averaged the correlations.

Results and Discussion

Overall, the average maximum coherence in the tremor band was greatest among synergistic muscle pairs (**Figure 1.**).

We found that the coherence patterns between subjects and over time were somewhat correlated ($r = 0.50$ and 0.46, respectively). In addition, we found that while the magnitude of coherence changed significantly between some levels of each grouping (task type, target, and subject characteristics), the patterns of coherence remained largely unchanged (mean $r \geq 0.85$ in all cases). In other words, the distribution of coherence is not significantly influenced by task type, target, or subject characteristics (sex, tremor severity, duration, and onset).

Phase calculations were only reliable for muscle pairs with significant coherence, which were synergists. These muscles pairs were consistently in phase, with a phase difference of $3.5° \pm 26.4°$ (mean ± SD), suggesting a common descending tremor signal for muscle pairs with high coherence.

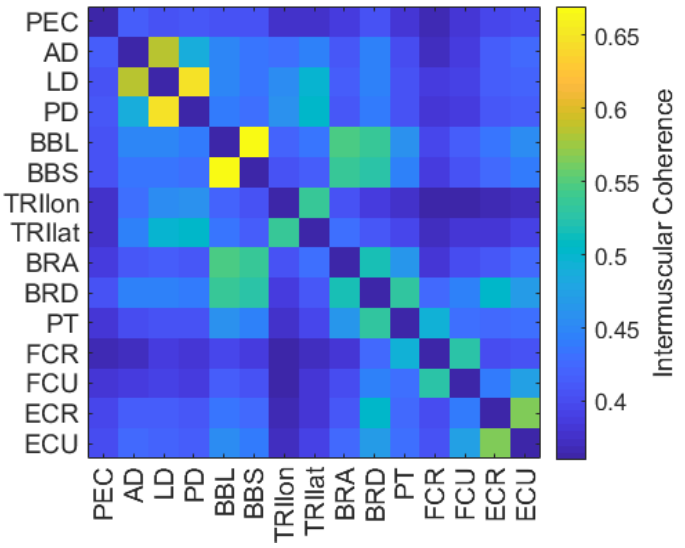

Figure 1: Intermuscular coherence in the tremor band between upper limb muscles, ordered proximally to distally: pectoralis major (PEC), anterior deltoid (AD), lateral deltoid (LD), posterior deltoid (PD), long and short heads of biceps brachii (BBL, BBS), long and lateral heads of triceps (TRIlon, TRIlat), brachialis (BRA), brachioradialis (BRD), pronator teres (PT), flexor carpi radialis (FCR), flexor carpi ulnaris (FCU), extensor carpi radialis (ECR), and extensor carpi ulnaris (ECU). Diagonal values were zeroed to emphasize other elements of the matrix.

Significance

This study is the first to characterize the coherence in tremor-band activity between muscles from the shoulder to the wrist. This characterization is one step in the process of determining which muscles are most responsible for tremor; quantifying the relationships in tremorogenic activity between muscles will allow us to interpret future investigations of the relationships between tremorogenic muscle activity in various muscles and the resulting tremor in the various degrees of freedom of the upper limb.

Acknowledgments

This research was supported by NSF grant 1806056 and the NINDS Intramural Program.

References

[1] Louis ED et al, *Tremor Other Hyperkinetic Mov.*, 2015
[2] van der Stouwe, A.M.M., et al., *Clin. Neurophysiol.*, 2015
[3] Puttaraksa, G., et al., *J. Neurophysiol,* 2019

ECG Artifact Subtraction from Instramuscular Diaphragm EMGs in Humans with Acute Spinal Cord Injuries

Clayton N. Wauneka.[1], Paul Freeborn[1], Emily J. Fox[1,2]
[1]Brooks Rehabilitation Motion Analysis Center, Jacksonville, FL, USA
[2]Deparment of Physical Therapy, University of Florida, Gainesville, FL, USA
Email: clayton.wauneka@brooksrehab.org

Introduction

Intramuscular diaphragm stimulation, also known as diaphragm pacing (DP), is an emerging strategy to promote respiratory function and weaning from mechanical ventilation after severe cervical spinal cord injury (c-SCI). DP involves surgical insertion of wires into the diaphragm that connect to an external pulse generator. Most individuals receiving DP have residual capacity to sustain ventilation without the pacer for short periods, allowing for recording of diaphragm electromyograms (EMGdi). Quantification and analysis of these EMGdi may be valuable for assessment of respiratory function after c-SCI. However, these signals are typically contaminated by electrocardiogram (ECG) artifact which must be removed for subsequent analysis.

The subtraction method is a common approach that subtracts an artifact template from an original, contaminated signal. [1-2]. This approach is most successful if a separate (often unattainable) ECG recording is utilized *and* if the artifact is consistent and has a large amplitude relative to the EMG signal. If these conditions are not met, then the template may be a poor representation. This is particularly evident in recordings in c-SCI patients with severely impared breathing and cardiac function. To address these challenges, we developed an automated modified subtraction method (MSM) to improve template accuracy for artifacts of varying characteristics, without use of a separate ECG recording.

Methods

Step 1 (locate ECG artifacts): Prior methods have required a separate recording of the ECG signal [1] and prior template information [2], and then application of a cross-correlation method to locate ECGs. The MSM approach utilized the Pan-Tompkin method [3] to automatically find *approximate* locations of the ECG artifacts from a single recording that contained EMGdi contaminated with ECG.

Step 2 (create ECG template): To increase efficiency and minimize need for manual selection of isolated ECG artifacts [1-2], an algorithm was developed to identify the location of each isolated ECG. ECG was considered isolated if it occured while the diaphragm was not active (i.e., between breaths). In addition, this method used the maximum number of isolated ECG samples within a recording to create the template.

Step 3 (align and scale ECG template): To improve alignment of the ECG template, the template was cross-correlated with a region of the original contaminated signal (~700 ms) where ECG artifacts were approximately located. The template was then shifted based on the location of the max cross-correlation value. The ECG template was scaled to match varying ECG sizes by multiplying the template by a scale factor (SF):

$$SF = \frac{Artifact\ Max\ Value - Artifact\ Min\ Value}{Template\ Max\ Value - Template\ Min\ Value}$$

A 30 ms region around the ECG peaks (max and min.) was used to determine the SF components. A max SF value was set for each scaling value. The SF values, which were used to scale the template for isolated ECGs, were averaged together to create the max SF.

Step 4 (subtraction): The MSM removed ECG artifacts from the contaminated signal by subtracting the aligned and scaled ECG template from the original signal.

To demonstrate the effectiveness of the MSM, it was applied to the recorded EMGdi from a patient hospitalized for acute traumatic c-SCI (male, age: 59, C3 injury level motor complete; Fig. 1). The patient was receiving mechanical ventilator support and used a diaphragm pacer, which was disconnected during EMGdi recordings (2 kHz sampling rate). The EMGdi power spectral densisty (PSD) was calculated before and after the MSM (Fig. 1c) to quantify which frequency bins contributed most to the signal variance.

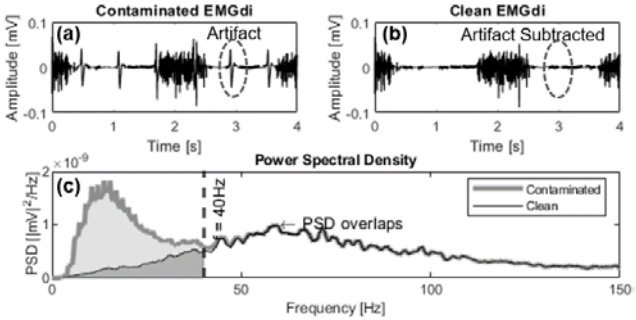

Figure 1: Plot of contaminated EMGdi (a) and clean EMGdi signal (b). Plot of the PSD of both the contaminated and clean EMGdi signal (c).

Results and Discussion

The contaminated and clean EMGdi, Fig. 1a and b , illustrate the reduction of ECG artifact while maintaining EMGdi activity after application of the MSM. Figure 1c demonstrates that nearly 33% of the signal power in the original signal was within the 0–40 Hz spectrum. This was expected since the largest portion of the ECG power lies between 0-25 Hz [2]. Conversely, after applying the MSM, about 12% of the power was within the 0-40 Hz spectrum. This suggests the MSM removed most of the artifact composed of low frequencies while retaining relevant EMGdi signal in the same spectrum. The plots demonstrate (Fig. 1) the effectiveness of MSM to remove ECG from EMGdi signals.

Significance

Applying the MSM may efficiently produce a higher quality EMGdi signal from complex patients such as those with acute c-SCI, where ECG artifacts are particularly challenging to remove. The MSM may be a valuable process in preparing recordings for analysis of diaphragm function and respiratory control in c-SCI patients.

Acknowledgments

Funded by the Craig H. Neilsen Foundation (to EJ Fox).

References

[1] Bloch R. *J Appl Physiol*, 1983; 55(2): 619-23.
[2] Levine S., et al. *J Appl Physiol*, 1986; 60(3): 1073-81.
[3] Pan & Tompkins. *IEEE Bio-Med Eng*, 1985, 32(3), 230-236.

Dynamic task performance for Parkinson's patients with a novel deep brain stimulator

Christopher P Hurt[1], Daniel J Kuhman[1], Carla Rigo Lima[1], Melissa Wade[1], Harrison J Walker[1]
[1] University of Alabama at Birmingham, Birmingham, AL, U.S.A
Email: *cphurt@uab.edu

Introduction

Deep brain stimulation (DBS) is a therapy for individuals with Parkinson's disease (PD) after pharmacologic interventions no longer optimally control motor symptoms[1]. Traditional DBS devices deliver electrical stimulation "omnidirectionally" from circular contact segments (i.e., "ring-mode"). Newer DBS devices include radially oriented contact segments, providing clinicians the ability to steer electrical current and shape the electrical field around the stimulator to maximize therapeutic benefit and minimize side-effects[2]. While these tools promise to maximize efficacy to better treat resistant symptoms of PD it is unclear how these newer devices affect overall movement function. For this initial investigation we sought to quantify the dynamic range in physical performance of DBS to affect physical function by individuals with PD. We further sought to quantify the extent to which individual contacts or circular rings affected quantitative aspects of gait, balance, and upper extremity dexterity during an initial DBS programming session.

Methods

Nineteen participants with PD (age 59.1±7.1 years) underwent surgery to implant a multi-contact, directional DBS lead in the subthalamic nucleus. Participants visited the lab one-month after implantation for device activation. Each DBS electrode was tested for clinical benefit with a standardized pulse width of 60 µs and a frequency of 130 Hz by a trained nurse practitioner. The novel DBS device contains six individual contacts and two virtual rings formed by 3 directional contacts each, and individual dorsal and ventral rings. Contacts were tested in random order to avoid an ordering effect. The individuals were in the practically defined "OFF" state (>12 hours without PD medicine). Individuals completed the following tasks: a10m walking test, a timed up and go (TUG), the 9-hole pegboard test and quiet stance while standing barefoot on force plate for one minute. These tasks represented gait function, mobility, upper extremity dexterity and static balance. All tasks were performed with the device OFF and ON for each of the 10 DBS settings (6 directional contacts, 2 virtual rings, 2 individual rings). Data was ordered from best to worst relative to performance and averaged across participants. To determine whether ring-mode or an individual contact was more effective we performed a repeated measures ANOVA to compare the best contact, the best ring or OFF DBS. Post hoc comparisons were made using a Bonferroni correction.

Results and Discussion

A dynamic range of performance was observed for all measures from improvements that represented clinically significant changes to values that represented worsening of function (Figure 1). This dynamic range suggests that optimizing improvements in movement are possible but may require quantifying task performance during these programming sessions. When comparing the extent to which individual contacts differed compared to ring-mode, a significant

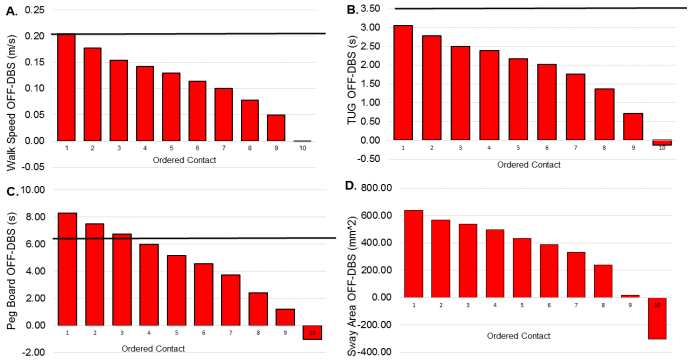

Figure 1. Dynamic Range of tasks when averaged from best to worst performance for A-Walks Speed B-Timed up and go (TUG) C-9-hole pegboard D-Sway area of quiet stance. The solid black line in A) B) and C) represent the minimal clinical difference.

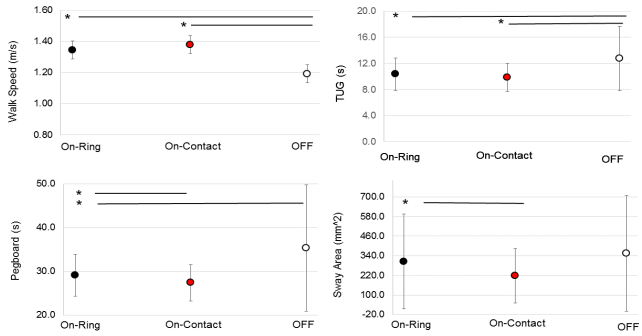

*Figure 2 Comparison of best performance from ring vs. contact vs. OFF deep brain stimulation for walk speed, TUG, Pegboard, and Quiet stance. *Represents significant post hoc difference between conditions highlighted with the line.*

difference was observed. A single contact was as good as a continuous ring (Figure 2) for walk speed (p=0.17) and for Timed up and go (p=0.07) or better for pegboard (p=0.02) and sway area, measured for quiet stance (p=0.02). This suggests a single contact may be effective for improving specific functions and multiple independent contacts may optimize different functional aspects of movement.

Significance

Next-generation directional DBS devices have the potential to provide greater improvements in gait and balance and upper extremity movement by tailoring stimulation parameters to optimize efficacy. This study represents the first step of using quantitative data to optimize and standardize programming for greater clinical efficacy for individual patients with PD who require DBS.

Acknowledgments

Work supported by grant awarded to HW 1UH3NS100553-01.

References

1.Walker HC, et al. Neurosurgery 2009. **2.** Steigerwald Mov Disorder 2016.

Cadaveric ACL Reconstruction Mechanics during Simulated Landings: A Pilot Investigation

Nathan D Schilaty[1], R Kyle Martin[2], Ryo Ueno[1], Luca Rigamonti[1], Nathaniel A Bates[1]
[1]Department of Orthopedic Surgery, Mayo Clinic, Rochester, MN, USA
[2]Department of Orthopedic Surgery, University of Minnesota, Minneapolis, MN, USA
Email: batesna@gmail.com

Introduction

Around half of anterior cruciate ligament (ACL) injures are treated through reconstruction (ACLR), [1] but literature lacks mechanical investigation of these reconstructions in a dynamic athletic task and rupture environment. The objective of this study was to ascertain the feasibility of investigating ACLR mechanics in a rupture environment during simulated landing tasks in a validated mechanical impact simulator. It was hypothesized that the mechanical impact simulator model would generate non-fixation failures in the ACLR grafts and that ACLR grafts would achieve higher peak strain prior to failure than the native ACL, but that the failures would occur with reduced external loading compared to the native ACL.

Methods

This was a descriptive laboratory study. Four cadaveric lower extremities (Age: 41(34.5, 46.8); Mass: 79.6(75.8, 90.8)) were subjected to simulated landing in a previously descrived mechanical impact simulator model. [2] External joint kinetics recorded from an *in vivo* population of 44 healthy athletes were applied to each joint in an increasing stepwise manner. Simulations were repeated until ACL failure was achieved. Strain gauges that continuously recorded ligament strain were implanted on the native ACL and ACLR grafts prior to simulation. Repeated measures design was used to test each specimen in the native ACL and three separate reconstruction states (bone tendon bone (BTB), hamstrings (HT), and quadriceps (QT)). Due to limited sample size, results are presented as medians and interquartile ranges.

Results and Discussion

ACL injures were generated in 100% of specimens. All native ACLs experienced damage to the ligamentous structure, while graft substance damage occurred in 58% of all ACLRs, and in 75% of BTB grafts (Table 1). In the remaining trials, damage occurred to the graft fixation sites. BTB and QT grafts survived greater magnitudes of simulated loading than HT grafts, but smaller magnitudes than the native ACL. 11 of the 12 ACLR grafts tested survived at least one impact trial. BTB grafts most closely represented the native ACL strain response (Figure 1).

The mechanical impact simulator provided a viable construct for mechanical examination of ACLR grafts in a simulated rupture environment. At the time of surgery, ACL reconstruction complexes are weaker than the native ACL when subjected to equivalent loading. BTB grafts most closely resembled the native ligament and provided the most consistent graft substance damage.

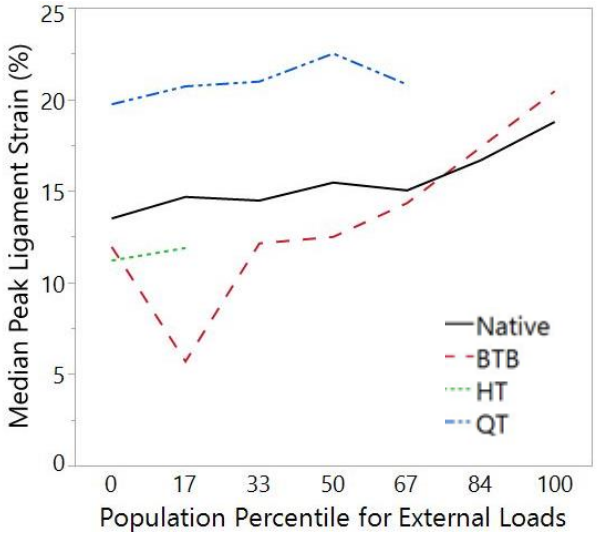

Figure 1: Median peak ligament strain for each ACL state at each magnitude of external loading (0th to 100th percentile of the in vivo cohort) applied to the specimen's knee.

Significance

Mechanical outcomes supported BTB as the clinical standard for mimicking the native ACL. As 92% of ACLRs survived baseline impact, and jump landing generates ~4x the ground contact force of gait, this model advocated ACLR graft ability to sustain force magnitudes generated from immediate weight-bearing during ACLR rehabilitation. Future integration of an animal surrogates to the model would be desireable to quantify ACLR graft performance throughout the healing process.

Acknowledgments

Funding provided by NIH NIAMS grants R01-AR056259, R01-AR055563, L30-AR070273 and NICHD grant K12-HD065987.

References

1. Kim S, et al. 2011. *J Bone Joint Surg*. 93(11):994-1000.
2. Bates NA, et al. 2017. *Clin Biomech*. 44:36-44.

Table 1: Peak ligament strain and failure locations for each structure examined in the mechanical impact simulator.

Ligament	Specimens Tested	Peak ACL Strain (%)	Graft/ Ligament Failures	Graft Failures Peak ACL Strain (%)	Fixation Failures	Fixation Failures Peak ACL Strain (%)	Number of Trials to Failure
Native	4	20.3 (11.6, 24.5)	4	20.3 (11.6, 24.5)	0	N/A	10.0 (4.3, 13.5)
BTB	4	13.5 (4.2, 18.7)	3	9.5 (2.5, 19.1)	2	9.9 (2.5, 17.4)	5.5 (2.8, 6.8)
HT	4	11.9 (6.2, 17.0)	2	11.6 (6.2, 17.0)	2*	11.9	2.0 (1.3, 2.8)
QT	4	24.8 (19.6, 31.3)	2	28.1 (23.3, 33.0)	2	22.4 (18.4, 26.4)	5.5 (2.8, 6.0)

* One fixation failure occurred on the first impact simulated; therefore, strain data was collected from that ACLR graft.

Patellofemoral Kinematics in Patellofemoral Pain Syndrome: The Influence of Demographic Factors

Cameron N. Fick, MS[1]; Rafael Jiménez-Silva, MPH[1]; Frances T. Sheehan, PhD[1]; Camila Grant, PhD[1]
[1] Department of Rehabilitation Medicine, National Institutes of Health, Bethesda, MD, USA
Email: camila.grant@nih.gov

Introduction

Patellofemoral pain (PFP) is prevalent in both the athletic and general populations, reducing quality of life and potentially leading to osteoarthritis[1]. It is a complex multifactorial condition, making it difficult to ascertain the patient-specific etiology of pain. Clinical decision-making is hampered by this lack of granularity into the causes of PFP. Demographics (e.g., sex, height, weight) may play a role in mediating the susceptibility of developing PFP. For example, PFP is more prevalent in females, but the reasons for this have not been well explored. Thus, the aim of this study is to address the potential influence of demographic characteristics on patellofemoral (PF) maltracking, with the specific hypothesis that sex, height, weight, and BMI influence kinematics, whereas age does not.

Methods

As part of an ongoing IRB-approved protocol, this retrospective study included 42 skeletally mature patients with idiopathic PFP and 80 healthy controls, recruited from 2009-2019. The demographic covariates assessed were age, sex, height, weight, and body mass index (BMI). 3D PF kinematics were quantified from dynamic cine-phase contrast MR images. Multiple regression analyses were run to determine the influence of covariates on PF kinematics (R, ver. 3.6.0). To avoid redundancy, for each outcome of interest (PF medial-lateral and superior-inferior shift, tilt, and flexion) was evaluated using two separate models: model_B (covariates: group, age, BMI, sex) and model_HW (covariates: group, age, height, weight, sex). To evaluate the effect of covariates on between-groups differences in PF kinematics, the group variable (PFP vs. controls) was always kept in the model, regardless of its significance. Upon violation of model assumptions, statistical outliers were removed. Significance was set at $p<0.05$.

Results and Discussion

Patellar medial-lateral shift was influenced by weight and by BMI in model_HW and model_B (Table 1). Flexion was influenced by height and weight in model_HW, but not influenced by any covariate in model_B. Superior-inferior shift and tilt were not influenced by any covariates in either model. Age and sex were not significant covariates in either model. Group had a significant effect for flexion and tilt. The lack of group significance in medial-lateral shift was likely due to the fact that the nine outliers (3 controls, 6 PFP) removed from model_HW and 12 outliers (5 controls, 7 PFP) removed from model_B had the most extreme medial/lateral shift, which drastically reduced the difference in shift between groups.

The relationship between weight and patellar kinematics has not been previously explored. However, based on studies[2,3] assessing the quadriceps influence on patellar maltracking, we postulate that with a greater quadriceps force demand, needed to accommodate a heavier leg, the patella flexes and shifts more laterally. Differences in the distal femoral geometry may explain the increased patellar flexion seen in taller individuals. It was surprising that sex did not influence PF kinematics; however, this should be taken with caution, as the higher prevalence of PFP among females led to a smaller cohort of males included in this study. Stratifying age (e.g., pre- and post-bone fusion or time since symptom onset) may help reveal a more nuanced relationship between age and PF kinematics.

Significance

There is a clear influence of key demographic parameters on PF kinematics in patients with PFP and controls. The fact that weight, a modifiable measure, influences both patellar shift and flexion has strong implications for future research and clinical intervention. In our recent review on PF kinematics[4], the majority of included papers did not report cohort weight and/or BMI and, even fewer matched cohorts based on height, weight, or BMI. Clinically, for patients who are overweight and experiencing PFP, weight loss may have a dual benefit of reducing joint stress and maltracking. Lastly, until definitive evidence demonstrates a lack of influence of sex and age on PFP, these characteristics should be taken into account when investigating the etiology of PFP. Controlling for population characteristics is a crucial in research, well beyond our focus on investigating the mechanisms of PFP. Methodology addressing these variables must be adopted moving forward.

Table 1: Multiple Regression Analyses for PF Kinematics

PF Kin.		Reg Coeff	Std Err	CI	P value
		Model_HW			
SHIFT	Intercept	2.75	1.32	0.15, 5.36	**0.039**
	Weight	-0.05	0.02	-0.09, -0.01	**0.011**
	Group	-0.69	0.49	-1.7, 0.29	0.164
	Adj. R^2=0.054				**0.018**
FLEX	Intercept	31.48	8.57	14.50, 48.47	**0.000**
	Weight	0.11	0.04	0.03, 0.2	**0.009**
	Height	-0.18	0.06	-0.30, -0.07	**0.003**
	Group	1.12	0.81	-0.49, 2.72	0.171
	Adj. R^2=0.090				**0.003**
		Model_B			
SHIFT	Intercept	4.48	1.90	0.71, 8.25	**0.0204**
	BMI	-0.23	0.08	-0.4, -0.06	**0.0083**
	Group	-0.61	0.50	-1.6, 0.4	0.2196
	Adj. R^2=0.065				**0.0099**
FLEX	Intercept	7.22	0.46	6.3, 8.14	**<2e-16**
	Group	1.75	0.82	0.12, 3.38	**0.035**
	Adj. R^2=0.032				**0.035**

Acknowledgments

NIH Clinical Center Intramural Research and NIH Medical Research Scholars Program.

References

[1] Conchie H, et al (2016). Knee
[2] Wilson NA, Sheehan FT (2010). J Biomech
[3] Fulkerson (2002). AJSM
[4] Grant C, et al (2020). AJSM

Increased Task Demand Differentiates Knee Muscle Forces after ACL-Reconstruction

Samuel A. Acuña[1], Megan J. Schroeder[2], Chandramouli Krishnan[2,3], and Yasin Y. Dhaher[1,2]
[1] University of Texas Southwestern Medical Center, Dallas, TX
[2] Northwestern University, Evanston, IL [3] University of Michigan, Ann Arbor, MI
Email: samuel.acuna@utsouthwestern.edu

Introduction

Dynamic tasks can magnify kinematic and kinetic differences between healthy knees and those with an anterior cruciate ligament reconstruction (ACLR) [1], likely due to increasing the mechanical loading of the knee during biomechanically challenging tasks. We previously found that individuals with an ACLR exhibited significantly lower peak knee flexion moments than controls when descending stairs, a difference we did not detect during overground walking [2]. Further, we observed that these differences were more pronounced when descending to another step as opposed to descending to the floor, suggesting that the primary driver of differences in joint mechanics between ACLR subjects and controls was an increased locomotor task demand. However, it is yet unknown if this increased task demand could further detect differences in the generated knee muscle forces between ACLR subjects and controls.

The purpose of this study was to examine how increasing locomotor task demand might differentiate estimates of knee muscle forces between healthy control subjects and ACLR subjects with a hamstring tendon (HT) or patellar tendon (PT) autograft. We hypothesized that more demanding locomotor tasks would better discriminate changes in knee muscle forces after an ACL reconstruction. Given that the intrinsic mechanics of the supporting musculature would be affected by the graft type used in the reconstruction [3], we further hypothesized that changes to knee muscle forces after an ACLR would manifest differently based on the graft type.

Methods

We used musculoskeletal modelling and simulation to identify individual knee muscle forces in ACL-reconstructed (n = 9, age = 30 ± 8 yrs, 5 with HT graft,) and control subjects (n = 6, age = 28 ± 4 yrs) when walking overground and descending stairs, derived from motion capture data and ground reaction forces in OpenSim. We restricted our analysis to the stance phase (foot contact through toe-off), yielding 162 separate simulations for overground walking, step-to-floor stair descent, and step-to-step stair descent. Muscle forces were time normalized as a percentage of the stance phase, and amplitude normalized to the maximum isometric force of the generic model scaled by each subject's mass.

We evaluated between-group differences in muscle force using statistical parametric mapping. A one-way ANOVA tested for a main effect (alpha = 0.05) between subject groups (controls, ACLR HT, ACLR PT). Posthoc pairwise comparisons with a Bonferroni correction focused on differences between ACLR subjects vs the controls.

Results and Discussion

Our results support our hypothesis that increased locomotor task demand can differentiate estimates of knee muscle forces in ACLR subjects by graft type, presenting predominantly as changes in quadriceps muscle forces. The quadriceps had long instances during loading and midstance where subjects with an ACLR exhibited significantly reduced muscle forces compared to controls, primarily in the vasti (Fig. 1). These instances within the vasti appeared consistently across all tasks, and grew longer with increased task demand. ACLR HT subjects demonstrated significantly reduced muscle forces during all tasks, but only during the more demanding stair descent task did ACLR PT subjects present significantly reduced muscles forces.

The gastrocnemii exhibited significantly increased gastrocnemii muscle forces for ACLR PT subjects at moments leading up to push-off over level ground (i.e., during walking and stair decent to floor), but we saw no significant differences within peak force production. It was only during the more demanding stair descent to step task did ACLR HT subjects exhibit significant differences in gastrocnemii muscle force from controls, occurring during peak force production within the loading phase.

The few differences in hamstrings muscle force were limited to short instances within the initial loading response or push-off phases, but these differences were not consistent across the tasks.

Significance

Post-surgical rehabilitation strategies employ a variety of dynamic tasks aimed to restore the knee joint [4], and might benefit from therapy targeted at restoring hamstring muscle force. This research also emphasizes the utility of increasing task demand to further detect residual deficits after ACLR, which may provide important clinical metrics of recovery.

References

[1] Tashman, 2007, CORR [2] Schroeder, 2015, Clin Biomech [3] Chouliaras, 2007, AJSM [4] van Rossom, 2018, OSPT

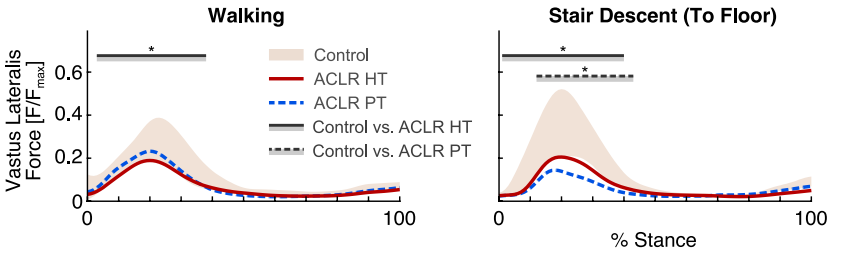

Figure 1 Increased task demand was better able to differentiate ACLR HT and ACLR PT from controls in vastus lateralis muscle force.

Optimal Placement of Suspension Fixation Tunnel to Restore Proximal Tibiofibular Joint Stability: A Finite Element Study

Shangcheng Wang[1], Nahir Habet[1], Tyler L CarlLee[1,2], Olivia M Rice[1], and Claude T. Moorman III[1,2]
[1]Musculoskeltal Institute, Atrium Health, Charlotte, NC, USA
Email: *Shangcheng.Wang@atriumhealth.org

Introduction

The Proximal tibiofibular joint (PTFJ) connects the fibular head to the posterolateral side of the proximal tibia. The anterior and posterior ligament bundles and interosseous membrane are the primary passive structures to stabilize this joint. The injury or rupture of these passive structures, although not common, can lead to PTFJ dislocation or chronic instability and lateral knee pain. When non-operative interventions fail, surgical intervention is needed to restore PTFJ stability. Bicortical suspension fixation (BCSF) is a promising technique and has been very successful in treating distal tibiofibular instability. Unlike screw fixation, it does not require hardware removal after healing and allows physiological motion of the PTFJ which may be important for ligament healing. Unlike anatomic ligament reconstruction, bicortical suspension fixation does not require a harvested tendon graft.

However, the ideal placement of the suture tunnel is still subjective. It is not clear how the variations in tunnel placement can affect the restoration of PTFJ stability. Currently, the joint stability can only be confirmed by pushing the fibular head (anterior shuck test) after the rope is placed and tension is applied. If the PTFJ is still unstable, a second BCSF device is needed [1]. Thus, this study first created a finite element model of an intact PTFJ; virtual ligament resection and tight rope repair were consequently performed. Fourty-eight models of BCSF repair were created by varing the location of the entry point of the guide tunnel on the fibular head and the exit point on anteriomedial tibia. We hypothesized that the location and orientation of the bicortical suspension fixation significantly affects the restored joint stiffness.

Methods

A finite element model of the lower leg including proximal and distal tibiofibular joints was created from MRI data of a female subject in the Visible Human Project (Fig. 1). The anatomic structures of the tibia, fibula, talus, and calcaneous bones were segmented using 3D Slicer software; bones were modeled as rigid bodies. Ligaments and membranes were modelled as tension-only linear springs. The origin and insertion of these ligaments were determined from anatomy atlas and papers. The stiffness and failure strain of each ligament were obtained from several biomechanical papers [2].

The bicortical suspensory fixation was also simulated by a tension-only linear spring. The BCSF was placed through a guide tunnel drilled from the posterolateral fibular head toward anteriomeidal tibia, just medial to the tibial tubercle [1]. Considering the small sizes of the button and suture, six detailed designs of entry point and 8 designs of exit point were created (Fig. 1). The combinations of these designs resulted in 48 BCSF repair models. The stiffness and failure strain of the BCSF were based on mechanical testing of Fiberwire®.

Intact, posterior ligament-resected, and BCSF-repaired models were created by changing the corresponding spring stiffnesses. Anterior shuck test of the PTFJ was simulated for each created model by applying a 100 Newton compression force on the posterior palpable surface of the fibula head. The anterolateral displacement of the fibular head was recorded before any ligament failed. PTFJ stiffness was calculated based on a displacement-force curve.

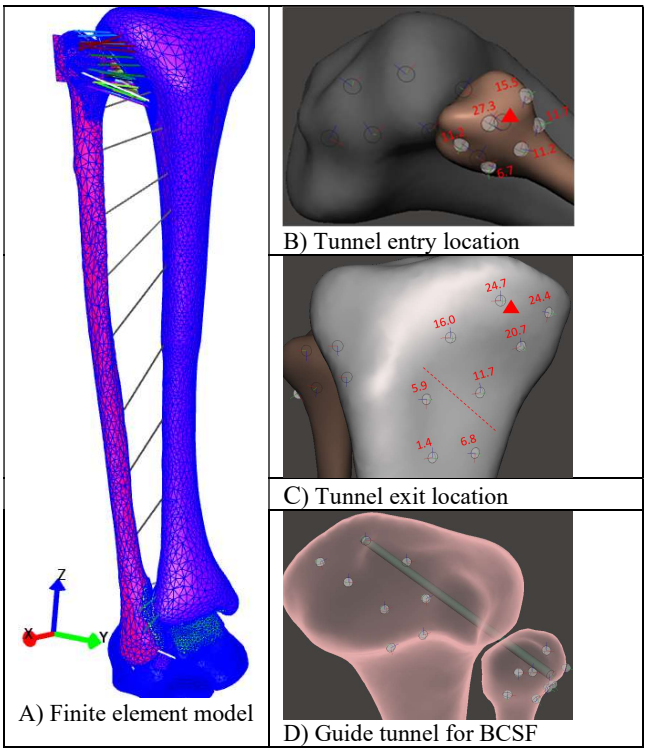

Figure 1: the created finite element model A) and design of tight rope placements, including 6 designs of tunnel entry location on fibular head B) and 8 designs of tunnel exit location on tibia C). One design of BCSF placement is shown in D). The result of average PTFJ stiffness was shown beside each entry/exit point, and the optimal location was marked with a triangle on B) and C).

Results and Discussion

The injury of the posterior ligament decreased PTFJ stiffness from 10 N/mm to 1.6 N/mm, which would make the PTFJ unstable. Paired t-tests revealed that the placement of BCSF affects the restoration of PTFJ stiffness; this confirms our hypothesis. Some placements of BCSF resulted in a PTFJ stiffness less than 10 N/mm. The highest restored stiffness was 53.8 N/mm, with its entry at proximal and posterolateral fibular head (Fig.1 B), and its optimal exit at proximal and medial tibia which is close to the medial collateral ligament attachement area (Fig.1 C).

Significance

PTFJ instability is a very disruptive condition, its relatively uncommon occurrence has prevented a standardized method of repair. This study provides insight on the placement of bicortical suspension fixation devices for the repair of the PTFJ as a standardized method.

References

[1] McNamara et al. 2018 Artho. Tech. 2018, 7(3):271-277; [2] Marchetti et al. 2017, AJSM , 45(8): 1888–189

Risk Factors for Second ACL Injury can be Objectively Measured in a Clinical Setting

Alexander T. Peebles[1], Thomas K. Miller[2], and Robin M. Queen[1, 2]
[1]Granata Biomechanics Lab, Department of Biomedical Engineering and Mechanics, Virginia Tech
[2]Department of Orthopaedic Surgery, Virginia Tech Carilion School of Medicine
Email: *apeebles@vt.edu

Introduction

Reduced knee extension moment symmetry and increased surgical limb frontal plane projection angle (FPPA) range of motion (ROM) during bilateral landing are associated with an increased risk for sustaining a second anterior cruciate ligament (ACL) injury in patients following ACL reconstruction (1). Additionally, low knee flexion ROM symmetry during a unilateral drop landing is prospectively associated with worse self-reported pain and quality of life (2). Recent work has identified clinically feasible methods to quantify these outcomes (3-5). Load sensing insoles have excellent validity (ICC = 0.97) for assing impulse symmetry (3), and can explain 61% of the variance in knee extension moment symmetry (4). Additionally, automated 2D video analysis has excellent validity (ICC > 0.91) for assessing FPPA ROM and knee flexion ROM (unpublished data). The purpose of the present study was to explore the ability of using load sensing insoles and two videocameras to identify landing mechanics deficits in patients who are 6-12 months following ACL reconstruction. We hypothesize that relative to healthy controls, patients following ACL reconstruction would have reduced impulse symmetry and increased surgical limb FPPA ROM during a bilateral landing and reduced knee flexion ROM symmetry in a unilateral landing.

Methods

16 patients recovering from a primary unilateral ACL reconstruction (7 male/9 female) who were between 14 and 30 years old, 6 and 12 months post-operative (9.7 ± 2.0 months), and preparing to return to sports which involved jumping, and 16 healthy control participants (7 male/9 female) who were between 18 and 30 years old and participated in jumping sports signed IRB approved informed consent and particiated in the present study.

All participants completed 7 bilateral forward drop vertical jumps to a distance of half their bodyheight and 7 unilateral drop landings on each limb, all from a 31 cm high box. Plantar impact forces were measured bilaterally using loadsol® sensors (100 Hz, Novel Electronics, St. Paul, MN). Reflective markers were placed bilateral on the lateral thigh, femoral epicondyle, and shank. Frontal and sagittal plane videos were collected using an iPad Pro and an iPhone 6S (240 Hz, Apple, Cupertino, CA). Each marker was automatically digitized throughout each trial using Automated Video Analysis for Dynamic Systems (5). All participants wore standardized neutral cushioned running shoes, but were allowed to wear their own athletic clothing. ACL patients were tested at one of two local rehabilitation centers, and control participants were tested at a university athletic center. Outcomes were chosen based on previous literature that identified risk factors for a second ACL injury (1, 2). Surgical limb or non-dominant limb FPPA ROM and impulse limb symmetry index (LSI) were computed during bilateral landing, and knee flexion ROM LSI was computed during unilateral landing. LSIs were computed as the ratio between surgical (non-dominant) and non-surgical (dominant) limbs. Outcomes and demographics were compared between groups using independent samples t-tests with an alpha level of 0.05.

Results and Discussion

The ACL reconstruction patients were younger than control participants (ACL: 17.1 ± 1.4 years; control: 23.7 ± 2.7 years; $p<0.001$). However, height and weight were similar between groups (both $p>0.135$). Compared to healthy control participants, ACL reconstruction patients had reduced impulse LSI during bilateral landing ($p<0.001$, d=2.14) and knee flexion ROM LSI during unilateral landing ($p=0.004$, d=1.12). However, surgical and non-dominant limb FPPA ROM during bilateral landing was similar between groups (p=0.498, d=0.23).

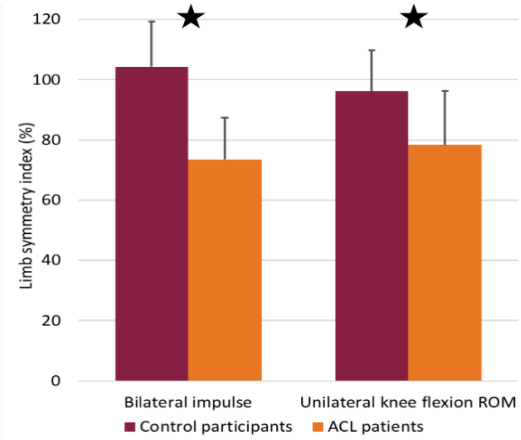

Figure 1: Comparison of LSI outcomes between groups.
Note: * indicates significant (p < 0.05) differences.

The differences observed between groups for impulse LSI and knee flexion ROM LSI are consistent with previous literature. While FPPA has not been previously compared between ACL reconstruction patients and healthy controls, increased FPPA has been prospectively linked to ACL injuries in uninjured athletes (6) and patients following ACL reconstruction (1). Therefore, FPPA is likely an important outcome to assess, despite non-significant differences observed in the present study.

Significance

The present study objectively assessed continuous kinetics and kinematics in a clinical setting, and found landing deficits which have been linked to risk for second ACL injury and greater self-reported pain. These assessment methods could be useful for return to sport testing in patients following ACL reconstruction.

Acknowledgments

This project was financially supported by the Virginia Tech Graduate Student Assembly.

References

(1) Paterno et al., AJSM, 2010; (2) Ithurburn et al., AJSM, 2017; (3) Peebles et al., Sensors, 2018; (4) Peebles et al., JOB, 2019; (5) Peebles et al., In review at ABME; (6) Numata et al., KSSTA, 2017.

Drop-Landing Asymmetries in Young Individuals 6-Months Following ACL Reconstruction

Katie Collins MS[1], Caroline Lisee MEd[1], Thomas Birchmeier MS[1], Ashley Triplett MS[1], Michael W. Straus PA-C[1], Christopher L. Wilcox DO[1], Andrew Schorfhaar DO[1], Sheeba Joseph MD[1], Michael Shingles DO[1], Christopher Kuenze PhD[1]
[1]Michigan State University, East Lansing, MI, USA
Email: colli784@msu.edu

Introduction

Individuals with history of anterior cruciate ligament reconstruction (ACLR) often exhibit aberrant movement patterns compared to their uninjured peers. Asymmetries between limbs during drop vertical jump landing tasks are often utilized as a component of return to sport criteria and patient-reported function.

The purpose of this study was to evaluate limb symmetry indices during a drop vertical jump landing task following ACLR. Secondarily, the purpose of this study was to assess the ability of limb symmetry indices to predict patient-reported activity level and knee function.

Methods

14 recreationally active individuals with history of primary unilateral anterior cruciate ligament reconstruction (ACLR) participated in this study. Participant demographics are included in Table 1.

Participants completed testing 6-months following ACLR. Participants were asked to self-report activity level prior to and following ACL injury and surgery utilizing the Tegner Activity Scale (TAS) and knee function during activities of daily living utilizing the International Knee Documentation Committee Subjective Knee Evaluation Form (IKDC).

Biomechanical assessment of peak vertical ground reaction force (vGRF) and peak knee flexion angle were conducted utilizing three-dimensional motion capture (Vicon Motion Systems, Ltd., Oxford, UK) and two integrated force platforms (Advanced Medical Technology Inc., Watertown, USA).

Clusters with retro-reflective markers were placed bilaterally on participants using tape at the lateral thighs and shanks, navicular of the feet, and the upper thoracic and lumbar spine. A stylus with four retro-reflective markers was utilized to identify major anatomical landmarks in order to estimate joint centers.

Participants were instructed to drop off a 30-cm box, positioned at a distance ½ participant height away from the force platform. Participants were shown the jump-landing task and were instructed to drop from the box and immediately jump upward in order to attain maximal height.

Knee joint biomechanics were processed utilizing a standard inverse dynamics approach. Data were analysed during the descent, landing phase. Limb symmetry index (LSI) was determined by between limb differences of peak knee flexion angle and peak vGRF utilizing the following equation:

LSI = (involved limb value / uninvolved limb value) x 100%

Pearson product moment correlation coefficients (*r)* were utilized to evaluate the relationships between self-reported activity level (TAS), self-reported knee function (IKDC), vGRF limb symmetry (LSI), and knee flexion limb symmetry (LSI).

Table 1. Participant Demographic Information	
Age (Years)	18.9 ± 2.76
Sex (M/F)	6/8
BMI (kg/m^2)	28.27 ± 6.07
Time Since Surgery (months)	6.47 ± 0.98
Graft Type	11 Hamstring/ 2 Patellar/ 1 Hamstring-Allograft
IKDC	82.10 ± 8.48
Tegner Before*	8 [5, 10]
Tegner Current*	5 [1, 8]

Table 1: Participant demographic information is reported as mean ± standard deviation unless otherwise indicated. *median [range].

Results and Discussion

All participants (14) demonstrated limb symmetry surpassing the widely utilized 90% clinical cut-off for knee flexion angle during drop landing (98.99 ± 16.13). However, only 29% of participants (4) met clinical cutoffs for vGRF limb symmetry (71.31 ± 19.24).

Knee flexion LSI and vGRF LSI were moderately correlated (r= 0.597). Knee flexion LSI was not correlated with current self-reported activity (r= 0.190) nor knee function (r= 0.057). vGRF LSI was not correlated with self-reported activity (TAS), r=0.108, nor knee function (IKDC), r= 0.124.

Self-reported activity level (TAS) and knee function (IKDC) were not related to drop vertical jump performance in young individuals 6-months following ACLR. Limb symmetry outcomes, including knee flexion LSI and vGRF LSI were moderately correlated, r= 0.597.

Patient-reported knee function and activity level surveys should be utilized in conjunction with objective outcome measures in order to evaluate function in young individuals 6-months following ACLR. Utilizing subjective measures alone may not provide enough information about knee function following ACLR in order to determine young patients' readiness for return to sport. In addition, the combination of objective and subjective measurements may provide better insight into patient function and prevention of secondary ACL injury.

Significance

The relationship between functional performance and patient-reported survey outcomes has been investigated previously, but the relationship between limb asymmetries during a drop landing vertical jump task and patient-reported knee function and activity level had not been previously investigated. Asymmetries during landing tasks are often associated with increased risk of secondary ACL injury. Importantly, this provides further evidence that there is a need to utilize objective and subjective measures together in order to determine return to play readiness for young individuals with a history of ACLR.

References

Ithburn MP, Paterno MV, Thomas S, Pennell ML, Evans KD, Magnussen RA, Schmitt LC. Change in Drop-Landing Mechanics Over 2 Years in Young Athletes After Anterior Cruciate Ligament Reconstruction. American Journal of Sports Medicine. 2019; 47(11): 2608-2616.

Quadriceps Musculature Motor Unit Characteristics between Injured and Non-Injured Limb after ACL Reconstruction

April L. McPherson[1,2], Nathaniel A. Bates[1], Takashi Nagai[1], and Nathan D. Schilaty[1]
[1]Mayo Clinic, Rochester, MN
[2]United States Olympic Committee, Colorado Springs, CO
Email: april.mcpherson@usoc.org

Introduction

Arthrogenic muscle inhibition (AMI) after anterior cruciate ligament (ACL) injury and reconstruction prevents complete activation of thigh musculature and results in impaired strength recovery [1]. However, it is currently unknown if quadriceps motor unit (MU) characteristics differ between the injured and noninjured limb after ACL injury. It was hypothesized that the injured limb would demonstrate inhibition compared to the noninjured limb. Specifically, inhibition would be demonstrated by smaller MU action potential (MUAP) peak amplitude, lower neural drive, higher recruitment thresholds, and higher average rate coding than the noninjured limb.

Methods

Thirty subjects participated in the study (13 male, 17 female; age: 19.1 ± 3.1 years; height: 172.8 ± 8.8 cm; weight: 77.2 ± 15.1 kg). Subjects were recruited at Pre-Surgery and 6 months post-surgery. Data were acquired at 6 month intervals (± 1 month), resulting in 3 groups (Pre-Surgery, 6 mo, and 12 mo).

Subjects were seated on a HumacNORM dynamometer chair for testing (CSMi; Stoughton, MA). Surface EMG (sEMG) was recorded at 20 kHz (Delsys; Natick, MA). Standard sEMG preparation was performed and electrodes were placed on the vastus medialis (VM) and vastus lateralis (VL) for quadriceps testing according to SENIAM standards. sEMG signals were recorded by a 5-pin array sensor. The signals from the sensor electrodes were differentially amplified and bandpass filtered (20–450 Hz). Three maximal voluntary isometric contraction (MVIC) trials were conducted, and the peak force was determined to establish target forces of 10-50% MVIC. With a randomized protocol, subjects followed a trapezoidal shape, with a 10-second isometric contraction at the target force. EMG decomposition was completed with *Delsys dEMG Analysis* software. MU data was extracted and analyzed with *JMP 14 Pro* (SAS; Cary, NC) statistical software via linear regression (p<0.05) and Tukey's *post-hoc* analyses when appropriate. MU data were normalized to force and mass before analysis. Neural drive is defined as the change in initial rate coding and average rate coding.

Results and Discussion

Injured limb MUAP peak amplitude was higher than the noninjured limb for all three groups (**Fig. 1a**; p<0.001). MUAP peak amplitude was significantly different between all groups and lowest 6 months post-surgery (p<0.001). Injured limb neural drive was lower than the noninjured limb for all three groups and increased from pre-surgery to 12 months post-surgery (**Fig. 1b**; p≤0.02). Injured limb recruitment threshold and average rate coding was higher than the noninjured limb for all three groups (p<0.001). There were significant differences between groups for average rate coding and recruitment threshold, except between pre-surgery and 12 months post-surgery recruitment threshold (p=0.07) and average rate coding for 6 and 12 months post-surgery (p=0.28).

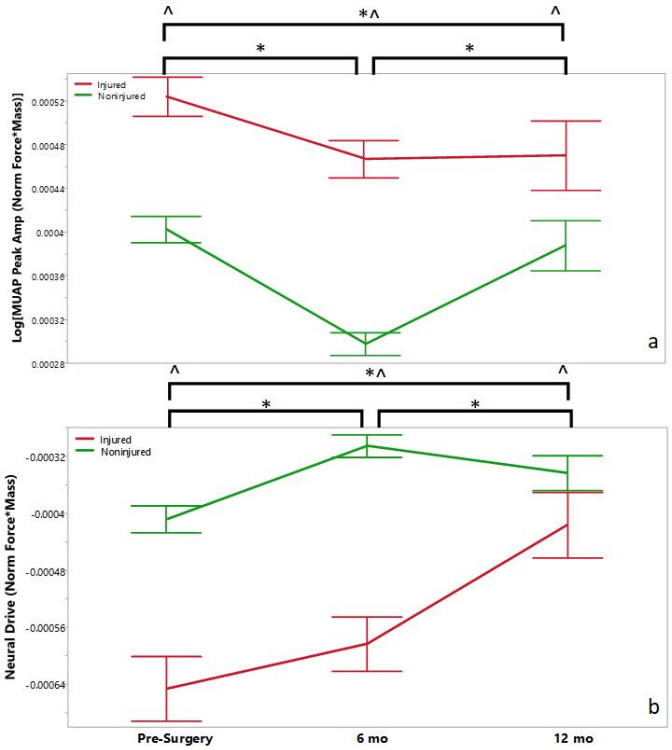

Figure 1: a) MUAP peak amplitude and b) neural drive between groups and limbs. ^ indicates significant difference between limbs; * indicates significant difference between groups

The results partially support the hypothesis. Neural drive was lower and average rate coding and recruitment thresholds were higher in the injured limb, but MUAP peak amplitude was higher in the injured limb. This may suggest that larger MUs are recruited, increased recruitment threshold and average rate coding are a compensatory mechanism following ACL injury to efficiently recruit smaller MUs. Voluntary muscle force production can be controlled by modification of neural and motor control variables, which include MU recruitment, neural drive, recruitment threshold, and average rate coding.

Significance

Current rehabilitation protocols fail to fully restore quadriceps strength and function, as demonstrated by poor return-to-sport testing rates [2]. It may be possible that current rehabilitation methods fail to adequately address the underlying alterations in neural control of muscle function. Thus additional neuromotor strategies should be implemented to address MU inhibition.

Acknowledgments

NIH grants R01AR056259, K12HD065987, L30AR070273, and the Mayo Clinic Ultrasound Research Center.

References

[1]Hart J et al. (2010). *J Athl Train*, **45**(1): 87-97.
[2]Webster KE et al. (2019). *Sports Med,* **49**(6):917-929

Modeling the Effect of Femoral Anteversion on Knee Extensor Muscle Force and Anterior Knee Mechanics

Benjamin B. Wheatley[1], Mark A. Seeley[2]
[1]Department of Mechanical Engineering, Bucknell University, Lewisburg PA, USA
[2]Department of Orthopaedic Surgery, Geisinger Medical Center, Danville PA, USA
Email: b.wheatley@bucknell.edu

Introduction

Severe anterior knee pain limits mobility and is associated with osteoarthritis. High femoral anteversion or excessive torsion of the femur can contribute to joint pain, and in extreme cases is treated surgically with femoral derotational osteotomy. There currently exists no standard to determine the location and extent of de-rotation to optimize patient outcomes. The goal of this work is to develop and employ a computational framework to study the effect of femoral anteversion on patellofemoral joint mechanics.

Methods

A coupled musculoskeletal-finite element modelling approach was developed for this work. In short, an open-source tool designed to simulate surgical intervention for cerebral palsy patients (SimCP) [1] was used to alter femoral anteversion and associated muscle attachment points on the OpenSim FullBodyModel [2]. With freely available motion capture and ground reaction force data [2], inverse kinematics and static optimization methods were used in OpenSim to estimate knee extensor muscle forces during gait for two cases: typically developing lower limb torsion (TD) and increased femoral anteversion by 40° (FA) (Figure 1A).

Scaled knee extensor muscle force vectors (Figure 1B) were then input into four subject-specific finite element models of the patellofemoral joint (Figure 2A). Three models were built from subjects with typically developing patellofemoral joint morphology (S1-S3), while one was built from a subject with a hypoplastic patella (S4). The resulting finite element simulations of peak force during stance across both femoral anteversion conditions provided comparisons of cartilage mechanics.

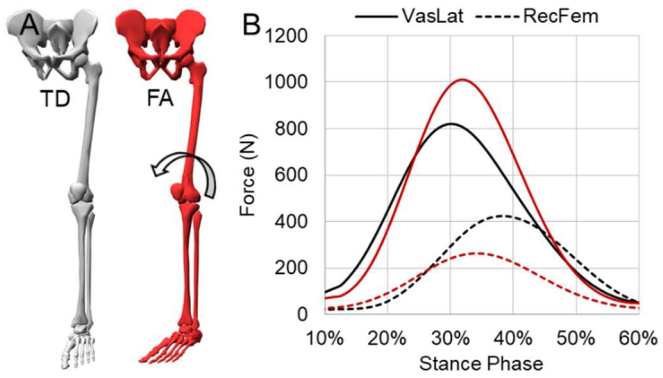

Figure 1: A) Morphological differences between typically developing (TD) and +40° femoral anteverserion (FA) models. B) Vastus lateralis (solid) and rectus femoris (dashed) muscle forces for TD (black) and FA (red) models as a function of stance phase.

Results and Discussion

Increases in femoral anteversion of the musculoskeletal model yielded ~200N changes in muscle force for the vastus lateralis (increase) and rectus femoris (decrease) (Figure 1B). Of the four finite element geoemetries, the hypoplastic subject model (S4) increased maximum cartilage octahedral shear stress and hydrostatic pressure by ~1 MPa with increasing femoral anteversion, while the other models saw negligible changes (Figure 2A). However, increases in mean joint contact pressure were observed across all models (Figure 2B).

Our results suggest that in addition to altered hip kinematics [3], femoral anteversion may alter knee extensor activation patterns and could negatively impact anterior knee cartilage mechanics. Our finite element results generally agree with the observation that patellofemoral cartilage mechanics are sensitive to increases in vastii forces [4]. However, we have suggested that shifting load between knee extensor muscles can also affect cartilage stress, particularly in patients with malformed patellofemoal geometry. However, future pre- and post-surgery clinical data are needed to better understand the interactions between muscle activity, gait dynamics, and patellofemoral mechanics.

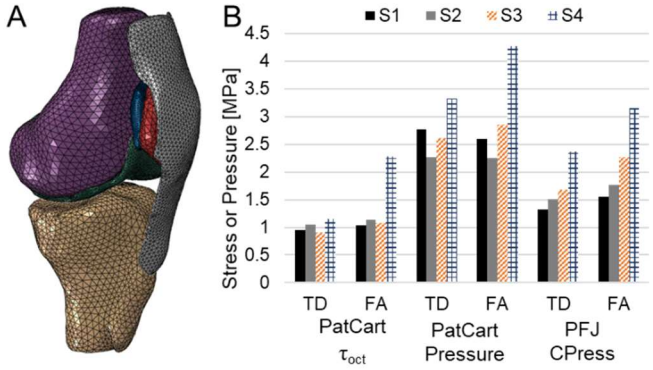

Figure 2: A) Representative finite element model of the patellofemoral joint. B) Finite element modeling results, comparing maximum patellar cartilage octahedral shear stress, maximum patellar cartilage pressure, and mean patellofemoral joint contact pressure for typically developing (TD) and femoral anteversion (FA) muscle forces. Comparisons are made between four subject patellofemoral joint geometries (S1-S4).

Significance

We present a musculoskeletal-finite element modelling workflow that suggests increases in femoral anteversion could alter knee extensor muscle activity and patellofemoral joint mechanics, particularly in patients with malformed patellae. Future clinical data are needed to validate this workflow such that it can be used to aid in patient-specific surgical planning.

Acknowledgments

Authors would like to acknowledge the Bucknell-Geisinger Research Initiative for funding.

References

[1] Pitto et al. (2019). *Front Neurorobot*, **13**(54)
[2] Rajagopal et al. (2016). *IEEE Trans Biomed*, **63**(10)
[3] Alexander et al. (2019). *J Biomech*, **86**
[4] Pal et al. (2019). *Comput Methods Biomech Biom Eng*, **22**(2)

Lower Extremity Muscle Force Adaptation to Increased Q-Factor in Stationary Cycling

Tanner Thorsen.[1], Erik Hummer[1], Joshua Weinhandl[1], and Songning Zhang[1]
[1]The University of Tennessee, Knoxville
Email: tthorsen@vols.utk.edu

Introduction

We have previously shown that as the Q-Factor (QF), inter-pedal width, of a bicycle is increased, the internal knee abduction moment (KABM) increased and the knee extension moment (KEM) remained unchanged [4] . Peak medial pedal reaction force (PRF) also increased while peak vertical PRF did not change. Our recent musculoskeletal simulation results suggest that, with increased QF, the contact force at the medial compartment of knee joint (MCF) increases, yet the total knee contact force (TCF) remains unchanged [3]. It is well known that muscle forces are the key contributor to joint contact forces [2], however, it is unknown if differences in forces produced by knee-joint spanning muscles explain the increased MCF and unchanged TCF. Therefore, the purpose of this research was to identify changes of knee-joint spanning muscle forces as a result of increasing QF during stationary cycling.

Methods

Sixteen recreationally active people (8 male 8 female) cycled on a stationary ergometer at a workrate of 80 Watts and a cadence of 80 rotations per minute at two QF: Normal QF (150mm), and Wide QF (276mm). Wide QF was increased using two pedal extenders. Three-dimensional kinematic data (240 Hz, Vicon) and pedal reaction forces using two custom instrumented bike pedals (1200 Hz, Kistler) were collected. A modified gait2392 model with a knee that includes hinge joints for the medial and lateral compartments [1] was used to estimate muscle forces with static optimization and TCF and MCF with joint reaction analysis (3.3 OpenSim, SimTK, Stanford University).

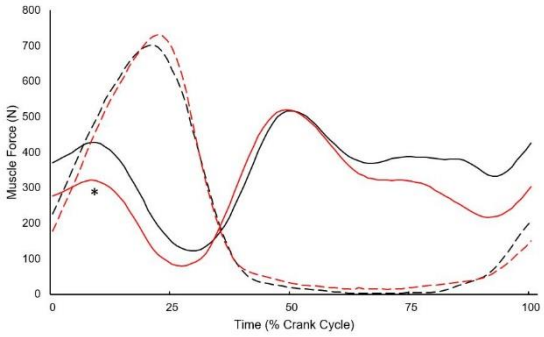

Figure 1: Knee flexor and extensor muscle group forces during cycling with increased QF. Knee Flexors ——, Knee Extensors ---, Wide QF = red . * denotes significance between peaks of same muscle group.

Individual muscle forces as well as two muscle groups (the summed muscle forces of the knee flexors (i.e. the hamstring muscles, sartorius, and the gastrocnemius muscle), and knee extensors (i.e. the quadriceps muscles)) were analyzed. Paired samples t-test and Cohen's d were used to detect differences between conditions.

Results and Discussion

As a group, the knee extensors did not produce different peak forces at Wide QF (Table 1). Individually the rectus femoris produced 60% greater peak force with increased QF. The knee flexor muscles produced 20% less peak force, with the sartorius, and semitendinosus producing lower peak forces. The biceps femoris short head produced 24% greater peak force at Wide QF. Time of peak force production for all muscles and muscle groups remained unchanged.

The trends in peak knee-spanning muscle force production partially suggest that a combined effect of no change in force of the knee extensors (lest a small increase from the rectus femoris muscle) and diminished peak force production of the knee flexors may have contributed to increased MCF. Accounting for the relatively small absolute increase in muscle force for the rectus femoris and sartorius muscles (58.0 N and 6.9 N respectively), solitary analysis of knee-joint-spanning muscles may be insufficient to explain the increase of MCF without increased TCF. Qualitative analysis of hip extensors and hip abductor muscle groups suggest that non-knee-joint-spanning muscle groups may affect MCF.

Table 2: Selected knee joint spanning muscle forces (N) at Normal and Wide QF during cycling. d = Cohen's d.

	Q-Factor			
	Normal QF	Wide QF	p-value	d
Knee Flexors	471.66	378.43	**0.046**	0.45
Knee Extensors	742.81	754.28	0.757	0.06
Rectus Femoris	101.31	159.29	**0.008**	0.80
Semitendinosus	23.56	15.93	**0.012**	0.59
Biceps Femoris	149.65	185.39	**0.002**	0.70
Sartorius	21.23	28.11	**0.001**	0.47

Significance

This study is the first study to identify differences in knee-spanning muscle force production as it pertains to increased QF during cycling. Increasing QF appears to elicit no real change in knee extensor muscles, and, suggests that the knee flexors respond with decreased force. These results do not fully explain the increase in MCF and future work may seek to further identify the effect of non-knee-joint-spanning muscle groups on MCF.

References

1. 1. Lerner, Z. F., et al. (2015). *J Biomech,* **48**, 644-650.
2. Sasaki, K., et al. (2010). *J Biomech,* **43**, 2780-2784.
3. Thorsen, T., et al. (Accepted 2020). *Annual Conf ACSM, San Fancisco, CA.*
4. Thorsen, T., et al. (In Press). *J Sport Health Sci.*

Serum Cartilage Oligomeric Matrix Protein Response to Braced and Non-braced Walking in Individuals with Anterior Cruciate Ligament Reconstruction

Alyssa Evans-Pickett[1], Hope C. Davis-Wilson[1], Christopher D Johnston[1], J. Troy Blackburn[1], Brian Pietrosimone[1]
[1]MOTION Science Institute, Department of Exercise and Sport Science, University of North Carolina at Chapel Hill, Chapel Hill, North Carolina, United States
Email: alyssa7evans@unc.edu

Introduction

Individuals with anterior cruciate ligament reconstruction (ACLR) are at high risk for developing post-traumatic osteoarthritis (PTOA). It is hypothesized that aberrant knee joint loading leads to increased deterioration of tibiofemoral articular cartilage following ACLR.[1] Knee braces are commonly marketed to reduce loading of the tibiofemoral articular cartilage in patients with cartilage injury at risk of PTOA onset. Currently, it remains unknown if knee braces used to reduce cartilage loading benefit articular cartilage health. Cartilage oligomeric matrix protein (COMP) is a biomarker of cartilage breakdown that is associated with osteoarthritis progression and is responsive to mechanical loading during walking. A greater increase of serum COMP following a single walking session may be representative of a worse knee cartilage response to loading in individuals post-ACLR.

The purpose of our study was to determine if acute serum COMP response differs between a braced and unbraced condition following a standardized 3,000 step walking protocol in inidviudals with ACLR.

Methods

30 individuals with ACLR (15 females, 22±4 yrs, 173±8 cm, 72.4±12.8 kg, 52±38 months post-ACLR) participated in a cross-over study. All individuals participated in both loading conditions (Braced Walking and Non-braced Walking) on separate days in a randomized order. For both sessions, participants sat for 45 min prior to the standardized 3,000 step walking protocol. Individuals walked on a treadmill (Bertec, Columbus, OH, USA; Model S020008) at the same self-selected speed in both conditions. During the braced condition, individuals were fitted with the same off-the-shelf brace using the manufacturer's guidelines (Rebound Cartilage; Ossur, Reykavik, Iceland). The brace used in this study is marketed to reduce tibiofemoral loading. Blood was collected from the antecubital region of the arm before and immediately after the standardized walking protocol. Serum was isolated and quantitatively assessed for COMP using a commercially available ELISA kit (R&D systems, Minneapolis, MN, USA). COMP response due to each loading-condition was calculated as the percent change score from pre- to post-walking (%ΔCOMP).

Paired t-tests were used to compare %ΔCOMP between the Braced and Non-braced Walking sessions. A separate *post-hoc* analysis was conducted in a subset of individuals, who demonstrated increased COMP from pre- to post-walking (>0µg/ml increase in COMP during non-braced walking), to determine if differences in %ΔCOMP exsited between condition (n=22, 9 females, 23±5 yrs, 175±8 cm, 75.5±12.8 kg, 58±41 months post-ACLR).

Results and Discussion

There was no significant difference (P=0.196) in %ΔCOMP between the Braced and Non-braced Walking sessions for all 30 individuals. However, there was a significant difference (P=0.036) between Braced and Non-braced %ΔCOMP in individuals who demonstrated an increase in COMP from pre- to post-walking (Figure 1).

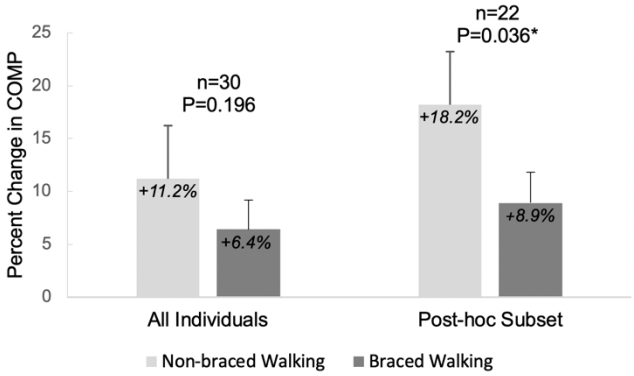

Figure 1: **Percent Change in Cartilage Oligomeric Matrix Protein (COMP) Due to Non-Braced and Braced Walking.** Figure 1 depicts the mean percent change in serum COMP due to walking a standardized 3,000 step walking protocol both with (Braced Walking) and without (Non-braced Walking) a knee brace designed to offload articular tissues both for all indiviudals (n=30) and in a subset of individuals who demonstrated increased COMP (>0μg/ml increase in COMP during non-braced walking; n=22).

Significance

Overall, our results demonstrate that using a brace to reduce tibiofemoral loading during 3,000 steps of walking may not influence acute serum COMP concentrations compared to walking the same number of steps without a brace. Yet, our *post hoc* analysis demonstrates that the braced condition results in decreased serum COMP concentrations in a subset of individuals who demonstrate an increase in serum COMP concentrations following unbraced walking. This suggests that bracing to reduce tibiofemoral loading may produce a beneficial knee cartilage response following ACLR in inidviudals who display an increase in serum COMP following walking Future research is need to elucidate the effect of bracing on the multifaced outcomes associated with PTOA development following an ACLR.

Acknowledgments

The research reported in this publication was supported, in part, by an unrestricted gift from Ossur Americas, Inc.

References

1. Cattano N, et al., *Thera. Adv. in Musculosk. Dis.* **9**, 11-21, 2016.

Biomechanical Evaluation of a Novel, All-Inside Posterior Medial Meniscal Root Repair via Fixation to the Posterior Cruciate Ligament

Nahir A. Habet[1], Bryan M. Saltzman, Marc T. Duemmler[1], David Trofa, Keith T. Corpus, Susan Odum, Juan Carlos Carrillo Garcia[1], Durham Weeks, Patrick Connor, Dana P. Piasecki, James E. Fleishli, Dax Varkey
[1]Atrium Health, Charlotte, North Carolina
Email: Nahir.habet@atriumhealth.org

Introduction

The menisci are integral to normal knee mechanics by dispersing contact forces over a broad area of the tibia through increased congruity of the tibiofemoral articulation.[1] The meniscal root has significant effect on peak loads transferred through the knee.[2] Repair of the meniscal root has been demonstrated to reproduce the ability of the meniscus to effectively recreate the functionality of an intact meniscus suggesting that repairing the root could minimize the progression of joint degeneration seen with meniscectomy or non-operative management of a meniscal root tear.[3,4,5] The purpose of this study was to evaluate the tibiofemoral contact mechanics of a novel, all-inside posterior medial meniscal root repair technique via suture fixation to the PCL, and to compare with that of the intact knee and the knee with a root tear.

Methods

Tibiofemoral contact mechanics were recorded in 8 (4 male, 4 female) fresh-frozen cadaveric knee specimens using pressure sensors that were placed onto the medial and lateral tibial plateaus. Each knee underwent 3 testing conditions related to the posterior medial meniscal root: (1) intact knee; (2) root tear; and (3) all-inside repair via suture fixation to the PCL. Knees were loaded with a 1000-N axial compressive force at 4 knee flexion angles (0°, 30°, 60°, 90°). Calculations were performed for contact area, mean contact pressure, and peak contact pressure in each testing condition.

Results and Discussion

Across all knee flexion angles, there was an overall mean 26.3% reduction in contact area with root tear (vs. intact, p=0.0002), but only a 3.2% reduction with repair (vs. intact, p=0.443). The 31.6% increase in overall mean contact area from root tear to repair was significant (p=0.0297). Across all knee flexion angles, there was an overall mean 24.3% increase in contact pressure with root tear (vs. intact, p<0.0001), and a 5.2% decrease with repair (vs. intact, p=0.696). The 31.1% decrease in overall mean contact pressure from root tear to repair was significant (p=0.0037). Across all knee flexion angles, there was an overall mean 10.6% increase in peak contact pressure with root tear (vs. intact, p<0.0001), and a 1.7% decrease with repair (vs. intact, p=0.9833). The 12.4% decrease in overall mean peak contact pressure from root tear to repair was not statistically significant (p=0.531). The novel repair increased contact area above intact values at all knee flexion angles apart from 0° flexion, dcreased mean contact pressure below intact for angles except for 0° flexion, and decreaed peak contact pressure below intact at 60° and 90° flexion. In most testing conditions and with overall averaging across knee flexion angles, the novel, all-inside posterior medial meniscal root repair with suture fixation to the adjacent PCL fibers restored contact area, contact pressures, and peak contact pressures to that of the intact knee or better (Fig. 1).

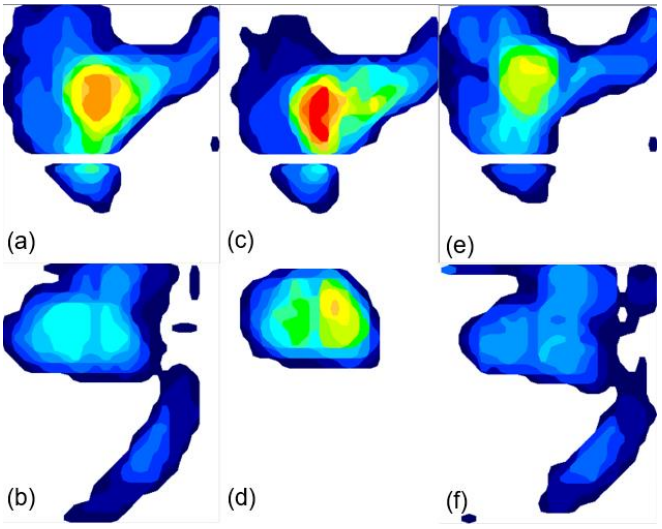

Figure 1: Pressure maps of medial and lateral menisci at 30° knee flexion: (a) lateral meniscus of intact knee, (b) medial meniscus of intact knee, (c) lateral meniscus of torn meniscus root, (d) medial meniscus of torn meniscus root, (e) lateral meniscus of repaired root, (f) medial meniscus of repaired root.

Significance

This new technique provides a posterior medial meniscal root repair construct that restores most tibiofemoral contact mechanics, and offers theoretical benefits of technical ease and reduced demand for an exact 'anatomic' repair location when compared with the current gold-standard transtibial pullout technique for repair.

References

1. Laprade CM, et al. Altered tibiofemoral contact mechanics due to pull-out suture repairs. doi:10.1016/S0021-9355(14)74105-0.
2. Mitchell R, Pitts R, Kim YM, Matava MJ. Medial Meniscal Root Avulsion: A Biomechanical Comparison of 4 Different Repair Constructs. doi:10.1016/j.arthro.2015.07.013.
3. Allaire R, et al. Biomechanical consequences of a tear of the posterior root of the medial meniscus. doi:10.2106/JBJS.G.00748.
4. Woodmass JM, et al. Meniscal Repair: Reconsidering Indications, Techniques, and Biologic Augmentation. doi:10.2106/JBJS.17.00297.
5. Krych AJ, et al. Non-operative management of medial meniscus posterior horn root tears is associated with worsening arthritis and poor clinical outcome at 5-year follow-up. doi:10.1007/s00167-016-4359-

Seasonal Variations in Vertical Stiffness and Jump Height in Ncaa Division-I Soccer Athletes

Michelle E. Ramsey[1*], Brett S. Pexa[2], Kevin R. Ford[3], and Justin P. Waxman[1]
[1]Department of Exercise Science, High Point University, High Point, NC
[2]Department of Athletic Training, High Point University, High Point, NC
[3]Department of Physical Therapy, High Point University, High Point, NC

Email:* mramsey1@highpoint.edu

Introduction

Measures of lower-extremity stiffness are shown to be associated with measures of athletic performance, such as vertical jump height, among others.[1,2] Although some have assessed changes in jump height over the course of an athletic season[3], less is known about seasonal variations in stiffness and the extent to which such variations are associated with changes in athletic performance. Therefore, the purpose of this study was to examine seasonal variations in vertical stiffness and maximum vertical jump performance, and to assess whether seasonal variations in stiffness are associatited with changes in vertical jump height.

Methods

Fifty-eight NCAA Division-I men's (n = 27, 19.6 ± 1.3 yr, 1.8 ± 0.1 m, 75.9 ± 6.9 kg) and women's (n = 31, 19.1 ± 1.1 yr, 1.7 ± 0.1 m, 65.1 ± 6.6 kg) soccer athletes completed vertical stiffness (K_{Vert}) and maximal countermovement jump height (CMJ_{Height}) assessments at two separate time points: pre-season and mid-season. K_{Vert} was assessed via two trials of stationary, double-leg, barefoot hopping on a force platform to the beat of a metronome set at 2.2 Hz. CMJ_{Height} was assessed via three maximal effort CMJ trials on a force platform. Athletes were allowed to swing their arms during CMJ trials. K_{Vert} was later calculated as the ratio of peak vertical ground reaction force to maximal center of mass displacement[4], whereas CMJ_{Height} was calculated via vertical velocity at the instant of takeoff (via numerical integration of the reaction force).[5] Trials were then averaged for use in statistical analyses. Differences in K_{Vert} and CMJ_{Height} were assessed via separate mixed-model ANOVAs, with an a-priori alpha level of ≤ 0.05 used to denote statistical significance. Sex (male or female) was used as the between-subjects factor, whereas time (pre-season or mid-season) was used as the within-subjects factor. Simple linear regression was then used to assess the extent to which pre- to mid-season changes (mid-season – pre-season) in K_{Vert} were associated with changes in CMJ_{Height}.

Results and Discussion

The time-by-sex interaction for CMJ_{Height} was statistically significant, $F(1, 51) = 10.04$, $\eta^2_{Partial} = .17$, $p = .003$. Irrespective of time, CMJ_{Height} for male athletes (mean ± standard error: 39.15 ± 1.00 cm) was significantly greater than that of female athletes (30.03 ± 0.91 cm, $p < .001$); however, the interaction was such that males displayed a reduction in CMJ_{Height} from pre-season to mid-season (40.65 ± 0.98 vs. 37.65 ± 1.68 cm) whereas females displayed an increase in CMJ_{Height} from pre- to mid-season (27.48 ± 0.89 vs. 32.59 ± 1.52 cm). The time-by-sex interaction was not statistically significant for K_{Vert} ($p = .093$); however, there were significant main effects of both time, $F(1, 51) = 10.00$, $\eta^2_{Partial} = .16$, $p = .003$, and sex, $F(1, 51) = 5.99$, $\eta^2_{Partial} = .11$, $p = .018$. The time main effect was such that, irrespective of sex, K_{Vert} significantly decreased from pre- to mid-season (0.44 ± 0.07 vs. 0.42 ± 0.08 kN/m/kg). The sex main effect was such that, irrespective of time, male athletes displayed significantly greater K_{Vert} values compared to female athletes (0.46 ± 0.01 vs. 0.41 ± 0.01 kN/m/kg). Pre-season to mid-season change in K_{Vert} were not associated with changes in CMJ_{Height} ($R = 0.061$, $R^2 = 0.004$, $p = .666$).

Collectively, the main findings of this study show that: (1) male athletes displayed higher K_{Vert} and CMJ_{Height} compared to female athletes, (2) K_{Vert} decreased from pre- to mid-season, (3) although CMJ_{Height} decreased in male athletes from pre- to mid-season, female athletes displayed an increase in CMJ_{Height} over the same period, and (4) although both K_{Vert} and CMJ_{Height} changed from pre- to mid-season, the change in K_{Vert} was not associated with changes in CMJ_{Height}. Future studies examining the effect of workload on such measures, and studies assessing seasonal variations over more frequent time points, appear warranted.

Significance

The findings of this study add to the current body of knowledge regarding changes in vertical stiffness and jump performance that occur during a competitive soccer season. Although both vertical stiffness and jump height changed over time, the noted change in jump was not related to changes in vertical stiffness. Additionally, the findings of this study demonstrate that changes in vertical jump performance during a competitive season are not the same for men and women, suggesting that researchers and clinicians should be encouraged to collect additional data related to workload and fatigue in future studies to better understand potential underlying factors driving such changes. Additional work related to what information the vertical stiffness assessment can provide is needed before having true clinical utility.

References

1. Arampatzis, A., Schade, F., Walsh, M. and Bruggemann, G. P. (2001). Influence of leg stiffness and its effect on myodynamic jumping performance. *J. Electromyogr. Kinesiol.* 11,355 -364.

2. Korff, T., Horn, S.L., Cullen, S.J., Blazevich, A.J. (2009). Development of lower limb stiffness and its contribution to maximum vertical jumping power during adolescence. *J. Experimental Biology*. 212:3737-3742.

3. Thomas, C., Mather, D., Comfort, P. (2014). Changes in spring, changes of direction and jump performance during a competitive season in male lacross players. *Journal of Athletic Enhancement.* 3(5):1-8.

4. McMahon, T.A., Cheng, G.C. (1990). The mechanics of running: how does stiffness couple with speed? *J. Biomech.* 23(Suppl 1):65-78.

5. Street, G., McMillan, S., Board, W., Rasmussen, M., Heneghan, J. M. (2001). Sources of error in determining countermovement jump height with the impulse method. *Journal of Applied Biomechanics*, 17:43–54.

Influence of Baseline Cognitive Function on Knee Mechanics during Dual-Task Sidestep Cutting

Patrick D. Fischer[1], James N. Becker[2], Keith A. Hutchison[3], and Scott M. Monfort[1*]
[1]Department of Mechanical & Industrial Engineering; [2]Department of Health and Human Development; [3]Department of Psychology
Montana State University - Bozeman, MT, USA
Email: *scott.monfort@montana.edu

Introduction

Athletes commonly perform dynamic movements under simultaneous cognitive load (e.g., surveying the field, reacting to an opponent). These scenarios are also associated with increased risk of anterior cruciate ligament (ACL) tears [1]. Cognitive function has been associated with ACL injury risk [2] and has recently been implicated in explaining changes in injury-relevant knee mechanics during a sidestep cut with a sport-specific dual task (i.e., dribbling a soccer ball) in male soccer players [3]. Understanding the spectrum of cognitive-motor relationships regarding altered knee mechanics when adding cognitive tasks during athletic movements may provide novel opportunities for developing injury prevention programs.

The purpose of this study was to determine associations between baseline cognitive function and knee mechanics during sidestep cutting with simultaneous cognitive and/or sport-specific tasks. Our hypothesis was that lower cognitive function would be associated with larger changes in peak knee flexion angle, abduction angle, and abduction moment during dual-task sidestep cutting.

Methods

Thirty female soccer athletes participated in this two-visit study (20.5±3yrs, 62.7±9.1kg, 1.7±0.1m). The first visit consisted of a cognitive test battery to characterize baseline working memory, processing speed (PS), attentional control, and multitasking abilities [4,5]. Composite z-scores represented baseline cognitive ability in these domains, where AC was broken into accuracy (AC_acc) and response time (AC_rt) components, and the multitasking composite score combined performance on concurrent primary and distractor tasks. On a separate day, participants performed a sidestep cut under randomly ordered cutting conditions that included: 1. **baseline**: anticipated direction with no additional task, 2. **ball handling (BH):** while also dribbling a soccer ball, 3. **unanticipated**: reacting to a directional cue (straight or 45° cut) that was provided ~400ms prior to initial contact of the cutting step, 4. **memorization (M)**: a visual array of letters was presented for 1s prior to starting the trial that participants memorized and then recalled a randomly chosen letter after performing the sidestep cut, 5. **memorization + ball handling:** combined M and BH conditions, and 6. **memorization plus visual attention (M+VA)**: the same protocol as M**,** but the letter to be recalled was displayed during the sidestep cut. Kinematic and kinetic data were analyzed for the non-dominant limb during the cutting step.

Changes, relative to baseline, in early stance peak knee abduction angle and moment along with peak knee flexion were the three dependent variables (ΔpKAbA, ΔpKAbM, ΔpKFA). Positive values indicate more abduction and flexion.

All cognitive composite z-scores were entered as candidate predictors for stepwise linear regression (α_{enter}= α_{remove}=0.15) to identify cognitive domains that were associated with ΔpKAbA, ΔpKAbM, or ΔpKFA during the six dual-/multitask conditions.

Results and Discussion

Significant relationships between the cognitive composite z-scores and knee mechanics change scores were observed for the ball handling (BH) condition (**Table 1**). The results suggest that slower processing speed was associated with greater increases in pKAbA while ball handling. Additionally, higher attentional control accuracy (and a trend for faster response times) was associated with less pKFA when ball handling. Other associations (multitasking during the M condition and working memory during the M+VA condition) were observed, but statistical significance depended on a few influential observations.

Table 1: Stepwise regression results for the BH condition indicating the models' R^2 and p-values along with the cognitive composite scores included in the model and the factor p-values.

	Ball Handling (BH) Condition
ΔpKAbA	**R^2** = 17.1%; p=0.026 [PS p=0.026)]
ΔpKFA	**R^2** = 36.0%; p=0.003 [AC_acc (p=0.012), AC_rt (p=0.106)]

The most robust associations between cognitive function and knee mechanics were revealed during a sport-specific dual task of dribbling a soccer ball. Even during this anticipated change of direction task, processing speed was associated with pKAbA. Implicating processing speed as a predictor of cognitive-motor function is consistent with findings from Herman et al. for an unanticipated jump landing task [6]. However, our current findings are somewhat inconsistent with our previous work that found visual-spatial memory being more relevant during the same task, albeit in an experienced male soccer cohort and using different cognitive assessments [3]. Collectively, results from these studies may indicate the dependence of cognitive-motor relationships on population and cognitive assessments.

Significance

Sport injuries are multifactorial in nature and warrant multifactorial preventative strategies. Our results further support cognitive function as a covariate for neuromuscular control during dual-/multitasking movements, which are reflective of common sport scenarios.

Acknowledgments

This work was supported by an NSF Graduate Research Fellowship under Grant No. W7834 (Fischer).

References

1. Krosshaug, T. et al. (2007) *AJSM*, **35**: p. 359-367.
2. Swanik CB et al. (2007) *AJSM,* **35**: 943-948.
3. Monfort SM et al., (2017) *MSSE,* **45**(5S):381.
4. Shipstead Z et al. (2014) *J Mem Lang*, **72**: 16-141.
5. Redick TS et al. (2016) *J Exp Psychol*, **145**: 1473-14.
6. Herman, D.C. and J.T. Barth, (2016) *AJSM*, **44**: p. 2347-53.

Gait Asymmetries are More Apparent at Faster Walking Speeds in Individuals with Acute Anterior Cruciate Ligament Reconstruction

Steven A. Garcia[1,2], Scott R. Brown[3], Mary Koje[3], Chandramouli Krishnan[1,3], Riann M. Palmieri-Smith[1,2]
[1]School of Kinesiology, [2]Orthopedic Rehabilitation & Biomechanics (ORB) Laboratory, [3]Neuromuscular & Rehabilitation Robotics (NeuRRo) Laboratory, Department of Physical Medicine & Rehabilitation, University of Michigan, Ann Arbor, MI, USA
Email: stevenag@umich.edu

Introduction

Abnormal gait biomechanics contribute to post-traumatic osteoarthritis development after anterior cruciate ligament reconstruction (ACLR) [1]. It is suggested that individuals with ACLR exhibit large asymmetries in gait kinetics between limbs and compared to controls [2]. Thus, characterizing gait kinetic asymmetries is vital when monitoring ACLR patients [2]. There is also evidence to suggest task complexity (*i.e.* walking *vs.* stair descent) magnifies biomechanical deficits in ACLR patients between limbs and compared to controls [3]. During gait, altering speed is a means of increasing or decreasing task complexity [4]. Evidence suggests healthy individuals are able to maintain ground reaction force (GRF) symmetry when task complexity is altered (*i.e.* increased or decreased gait speed) [4]. Yet, it is unclear if ACLR patients are similarly able to maintain GRF symmetries across gait speeds. It is possible ACLR patients may have a differential response to altered task complexity compared to controls; information that can be useful for future studies aiming to evaluate gait deficits in those with ACLR.

The purpose of this study was to examine the effects of walking speed demands (100%, 120%, and 80% self-selected walking speed) on resultant GRF limb symmetry indices (LSI) between ACLR patients and healthy individuals. Outcome variables included the 1st and 2nd peak and unloading resultant GRF (*i.e.* GRF between the 1st and 2nd peak).

Methods

Thirty patients 9-weeks post ACLR (Age = 20.6 ± 5.4 yr, BMI = 23.9 ± 3.3 kg/m^2, graft = 25 patellar, 4 hamstring, 1 quadriceps tendon) and 15 healthy control participants (Age = 23.1 ± 4.5 yr, BMI = 23.6 ± 2.7 kg/m^2) were recruited and underwent treadmill walking at three speeds (100%, 120%, and 80% of self-selected walking speed). Self-selected gait speed was determined using a stopwatch while participants walked over-ground across a 20 m walkway. Participants were given one practice trial, then, the average of three trials was used to determine self-selected speed. GRFs were collected at 1000 Hz while participants walked on an fully instrumented Bertec split-belt treadmill. One 65 s trial was collected at each speed (order: 100%, 120%, and 80%). Participants were allowed to familiarize to each speed prior to initiation of the 65 s data recording. Analog force data were analyzed offline using LabVIEW and lowpass filtered using a zerolag 4th order Butterworth filter (100 Hz). Ensemble averages of the resultant GRF were calculated and normalized to body weight (N). Outcome variables from both limbs were used to compute LSI as the ratio of the reconstructed relative to contralateral limb in ACL patients. In controls, the limb with the lowest 1st peak resultant GRF was used as the matched "reconstructed limb" for all speeds. Two (Group) by three (Speed) repeated measures ANOVAs were used to compare LSI between speeds and groups ($\alpha < 0.05$).

Results and Discussion

The Group by Speed interaction was significant for the 1st peak ($F_{2,86} = 12.38$, $P < 0.01$), 2nd peak ($F_{2,86} = 12.55$, $P < 0.01$) and unloading resultant LSI ($F_{2,86} = 9.36$, $P < 0.01$). Post-hoc comparisons (Bonferonni adjusted) indicated all resultant LSI's (1st, 2nd, unloading) differed across speeds in patients with ACL-reconstruction but not controls ($P > 0.05$). At fast speeds, all resultant peaks were different between groups ($P < 0.01$). Only the 1st peak differed between groups at slow speeds. ($P > 0.05$)

Results suggest increasing gait speed magnifies resultant GRF asymmetries while decreasing speed diminishes GRF asymmetries in patients with ACLR. In healthy controls, gait symmetries were maintained regardless of gait speed, supporting previous research [4]. The inability to maintain similar GRF symmetries in patients with ACLR may be partially attributed to underlying neuromuscular dysfunction, like quadriceps weakness, amongst other factors such as pain or kinesiophobia [5]. Nonetheless, our results suggest resultant GRF asymmetries during gait may be partly mediated by gait speed as LSIs were less than 5% asymmetrical at speeds below self-selected. Thus, it may be beneficial to evaluate gait kinetics at speeds above self-selected in order to characterize the extent of gait biomechanical asymmetries in patients with ACLR.

Significance

Walking at fast speeds exacerbated gait asymmetries which may be beneficial when evaluating ACLR individuals in more chronic time periods, when gait deficits may be less pronounced than in early time periods post-surgery. Further research is needed to understand if evaluating gait at faster speeds is beneficial to better detect subtle gait deficits in those several years from ACLR.

Acknowledgments

National Institute of Child Health and Human Development of the National Institutes of Health (Grant # R21 HD092614-02).

References

[1] Andriacchi TP et al. (2004). *Ann Biomed Eng*, **32**:447-457.
[2] Davis-Wilson HC et al. (2019). *Med Sci Sports Exerc*, **Epub.**
[3] Schroeder MJ et al. (2015). *Clin Biomech*, **30**: 852-859.
[4] Rice J and Seeley MK (2010). *Int J Exerc Sci*, **3**:182-188.
[5] Lewek M et al. (2002). *Clin Biomech*, **17**:56-63.

Table 1. Resultant GRF outcome variables as mean (SD). *, indicates speed difference; †, indicates group difference; SS, self-selected gait speed.

	ACLR Patients			Healthy Controls		
	Resultant GRF 1st Peak	Resultant GRF Unloading Peak	Resultant GRF 2nd Peak	Resultant GRF 1st Peak	Resultant GRF Unloading Peak	Resultant GRF 2nd Peak
80% SS	95.35 (0.88)*†	101.44 (0.76)*	96.63 (0.70)*	99.69 (1.24)	100.68 (1.07)	98.97 (1.00)
100% SS	89.71 (1.09)*†	106.63 (1.24)*	93.05 (0.97)*†	97.49 (1.54)	102.50 (1.75)	98.40 (1.37)
120% SS	86.62 (1.28)*†	114.30 (2.12)*†	90.08 (1.01)*†	99.22 (1.81)	102.54 (3.00)	98.99 (1.43)

Asymmetry and Sex Differences in Ankle and Hindfoot Kinematics During Gait

Shumeng Yang[1], Tom Gale[1], MaCalus Hogan[1], William Anderst[1]
[1]University of Pittsburgh, Department of Orthopaedic Surgery
Email: shy41@pitt.edu

Introduction

Recovery progress of patients with lower limb injuries is commonly monitored by measuring differences between the injured and uninjured side. Ankle sprains are the most common injury in sports and recreation and can lead to chronic ankle instability (CAI), which may affect lower limb biomechanics[1]. To properly evaluate the effects of surgery and rehabilitation in CAI and other ankle pathologies, it is first necessary to establish a normative database to characterize typical side-to-side differences in ankle and hindfoot kinematics in healthy adults.

In addition, previous work has identified differences in bony morphology[2] and injury rates[3] between males and females in the ankle and hindfoot. However, only one study, using single-plane fluoroscopy, has investigated ankle and hindfoot kinematics differences between males and females[4].

The aims of this study were: (1) to determine within-subject ankle and hindfoot kinematics differences between the dominant and nondominant sides and (2) identify sex-dependent differences in ankle and hindfoot kinematics over the support phase of gait. We hypothesized that females would have greater tibiotalar and subtalar ROM and that sex-dependent differences would exist in ankle and hindfoot continuous kinematics curves.

Methods

Following Institutional Review Board approval and informed consent, data was collected from 20 participants (10M, 10F; average age: 30.8 ± 6.3 years). All participants were healthy adults with no history of major knee or ankle injuries.

Subjects walked at a self-selected speed on a laboratory walkway. Biplane radiographs of the ankle and hindfoot were collected for 1 second at 100 frames/s. Two walking trials were collected for each side. CT scans were used to create subject-specific 3D models of the distal tibia, talus, and calcaneus. A validated volumetric model-based tracking technique[5] was used to match the subject-specific bone models to the biplane radiographs with a precision of 1.2° and 0.5 mm. Anatomic coordinate systems were created for each bone using an automated algorithm[6] and tibiotalar and subtalar 6 DOF kinematics were calculated for each side using ordered rotations[7].

Joint kinematics were filtered with a 4th order butterworth filter using residual analysis[8] and then interpolated to percent stance phase. The two trials for each side were averaged prior to analysis. Differences in ROM were identified using t-tests, and differences in the continuous kinematics curves were identified using one dimensional statistical parametric mapping (SPM)[9] with significance set at $p < 0.05$ for all tests.

Results and Discussion

The average difference between dominant and nondominant sides in the continuous kinematics curves was 3.9 deg and 1.4 mm or less for all rotations and translations, respectively, at the tibiotalar and subtalar joints. These differences exceeded our measurement accuracy by a factor of 3, suggesting kinematics asymmetry can be commonly detected using this measurement system. No differences between dominant and nondominant side ROM were observed at the tibiotalar (all $p > 0.15$) or subtalar joint (all $p > 0.08$). These results provide a benchmark for comparison when evaluaiting side-to-side differences in patients after surgery or rehabilitation.

Significant differences in the continuous kinematics curves were found between males and females in tibiotalar inversion from 70-90% stance ($p = 0.037$) and from 94-100% stance ($p = 0.049$) (Figure 1, top), and subtalar PD translation ($p=0.003$) and internal rotation ($p<0.01$) (Figure 1, bottom) over the entire stance phase. In contrast to the previous study[4], we did not find greater stance phase ROM in females at the tibiotalar joint (all $p > 0.052$) or the subtalar joint (all $p > 0.10$) (Table 1).

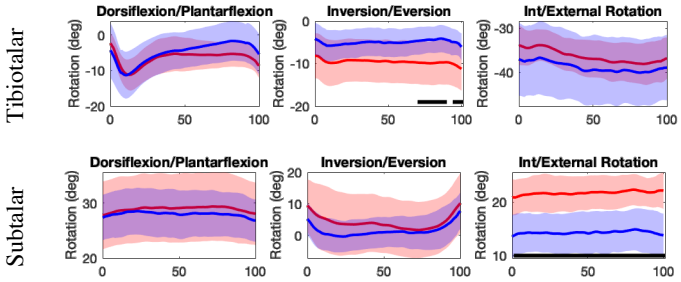

Figure 1: Average (solid line) and standard deviation (shaded regions) of rotational kinematics for the tibiotalar (top) and subtalar (bottom) joints for males (blue) and females (red) during the stance phase of gait. The black line on the bottom of each chart represents periods of significant differences identified by SPM.

Table 1. Average (± SD) ROM during the stance phase of gait for the tibiotalar and subtalar joints. No significant differences were observed.

	Tibiotalar Joint		Subtalar Joint	
	Male	Female	Male	Female
Dorsi/Plantar Fexion	12.2±2.3	10.8±3.8	2.8±1.1	2.5±0.6
Int.Ext Rotation	5.6±2.1	6.8±2.2	3.4±1.3	2.8±1.3
Inv./Eversion	3.1±1.5	3.7±1.6	10.2±2.8	9.6±2.4
AP Trans.	4.5±1.2	3.6±1.2	2.0±0.6	1.9±0.5
ML Trans.	2.1±0.6	1.7±0.5	1.6±0.6	2.0±0.4
PD Trans.	1.2±0.6	1.3±0.5	1.8±0.6	1.7±0.4

Significance

Benchmark data for evaluating ankle kinematics after surgical intervention or rehabilitation was provided. Future studies should account for patient sex when investigating ankle kinematics.

Acknowledgments

Funded by NIH Grant# R44HD066831.

References

[1] Hintermann et al. (2002) AJSM [2] Gabrielli et al (In Press). FAO. [3] Waterman et al. (2010) JBJS [4] Fukano et al. (2018) Hum. Mov. Sci [5] Pitcairn et al (In Press). J. Biomech. [6] Brown et al. (2020). ORS. [7] Grood et al. (1983) J Biomech Eng [8] Winter (2009). Biomech. and Mot. Con. of Hum. Move. (4th Edition) [9] Pataky (2010). J. Biomech.

Use of Nonlinear Dynamics to Characterize Force Control during Leg Press

Lindsey Remski[1], Russell Buffum[1], Amelia S. Lanier[1], Adam B. Rosen[2] and Brian A. Knarr[1]
[1]Department of Biomechanics, University of Nebraska at Omaha, Omaha, NE USA
[2]School of Health and Kinesiology, University of Nebraska at Omaha, Omaha, NE USA
Email: leremski@unomaha.edu

Introduction

Anterior cruciate ligament reconstruction (ACLR) alters strength and neuromuscular control of the quadriceps. Despite meeting current return-to-sport benchmarks after rehabilitation, high re-injury rates still persist[1]. In an effort to better identify patient readiness to return-to-sport and decrease risk of re-injury, novel measures of patient function are being developed[2,3]. An example of one of these novel measures comes from recent work that used Lyapunov exponent (LyE), a nonlinear metric, to describe control of shear ground reaction forces in ACLR patients[3]. Their study found that ACLR patients had diminished control (higher LyE values) compared to healthy subjects, indicating altered function despite meeting majority of criteria for return-to-sport. The ability to measure force control of the quadriceps during a clinically reproducible task, such as the leg press, may be important for further describing patient function and guiding return-to-sport testing. This work aimed to describe a method for measuring force control of the quadriceps during the leg press as well as develop baseline comparative values of force control in healthy individuals. We hypothesized there would be no differences in force control between the dominant limb, non-dominant limb, and both limbs working together in a young, healthy population.

Methods

14 healthy subjects performed continuous repetitions of the bilateral leg press, while the feet remained stationary, for two minutes at 20% of their estimated one repetition maximum (1RM) at 60bpm. Force profiles of dominant and nondominant limb were measured individually using a set of custom, validated force platforms that interfaced with the leg press machine. To describe the total force throughout the task, force profiles of the dominant and non-dominant limb were summed together. Peak force values were extracted from each force profile and normalized to each subject's 1RM. Force control was measured using LyE, which was calculated using Wolf's algorithm [4]. Descriptive statistics were calculated for normalized peak forces and LyE values. A one-way repeated measures ANOVA with a Bonferroni corrected post hoc analysis was performed to compare LyE values from the total, dominant limb, and non-dominant limb force profiles (α=0.05).

Results and Discussion

Our hypothesis that force control (measured as the LyE value calculated from force profiles) would not differ between the dominant limb, non-dominant limb, and total was partially supported with a significant main effect being found ($\eta_p^2 = 0.395$). Force control was not significantly different between dominant and non-dominant limbs. This was expected due to subjects not having a significant history of lower extremity injury and is in agreement with previous work that demonstrated similar force control between limbs during a simulated cutting task [3]. However, contrary to our hypothesis, force control of the dominant limb was diminished compared to the total and may be due the separate roles of the dominant limb as a "driver" and the non-dominant limb as a "stabilizer" during bilateral mobilizing tasks [5].

In summary, this work describes how force control of the quadriceps can be measured in a clinically implementable manner by using low-cost force platforms with nonlinear analysis during the leg press. The baseline values developed through this work may be used as a point of comparison for determining abnormal force control in individuals with ACLR.

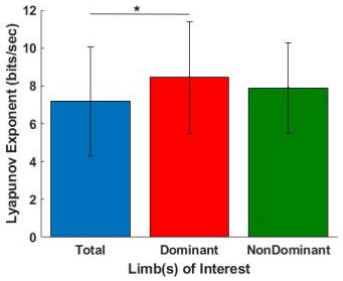

Figure 1: Bar chart of Lyapunov Exponent during the leg press task. *p=0.001.

Significance

This work describes a method for measuring force control of the quadriceps in a manner that may be performed in a clinical setting. Future work will focus on the relationship between force control and return-to-sport outcomes with the intent of developing measures that, when used in conjunction with current return-to-sport benchmarks, further describe patient readiness to return-to-sport and reduce re-injury rates.

Acknowledgments

This project was funded through the University of Nebraska at Omaha's Office of Creative Activity and Research.

References

[1] Wiggins A et al. *American Journal of Sports Medicine* **44**, 1861-1876, 2016.
[2] Moraiti C et al. *Gait and Posture* **32**, 169-175, 2010.
[3] Lanier A et al. *Journal of Orthopaedic Research*, 1-7, 2020
[4] Wolf A et al. *Physica D: Nonlinear Phenomena* **16**, 285-317, 1985.
[5] Peters M. *Psychological Bulletin* **103**, 179-192, 1988.

Table 1: Descriptive statistics for Lyapunov exponent and normalized peak force data from leg press task. *indicates significant difference in Lyapunov exponent values between dominant limb and total force profiles (p=0.001).

FORCE PROFILE	LYAPUNOV EXPONENT		NORMALIZED PEAK FORCE	
	MEAN±SD	95%CI	MEAN±SD	95%CI
TOTAL	*7.185±2.880	5.523-8.848	0.323±0.048	0.295-0.350
DOMINANT	*8.457±2.959	6.479-10.166	0.158±0.032	0.139-0.176
NONDOMINANT	7.902±2.394	6.519-9.284	0.168±0.025	0.153-0.182

Linking Greater Type II Collagen Turnover Following Anterior Cruciate Ligament Injury to a Stiffened- Knee Gait Strategy

Brian Pietrosimone, Alyssa Evans-Pickett, Hope C. Davis-Wilson, J. Troy Blackburn, Lara Longobardi, Richard Loeser, Ganesh M. Kamath, R. Alex Creighton, Jeffery T. Spang
University of North Carolina at Chapel Hill, Chapel Hill, North Carolina, United States
Email: brian@unc.edu

Introduction

Individuals who sustain an anterior cruciate ligament (ACL) injury and undergo ACL reconstruction (ACLR) are at high risk of developing posttraumatic osteoarthritis (PTOA).[1] There is evidence that the biological processes involved in the progression to PTOA, including breakdown of critical components of tibiofemoral articular cartilage (e.g., type-II collagen) begin early after ACL injury. It has been proposed that the persistent aberrant gait biomechanics that are common following ACLR hasten the progression of PTOA by perpetuating abnormal biological tissue changes.[2] A stiffened-knee strategy (i.e. lesser knee flexion angle [KFA] and lesser internal knee extension moment [IKEM],) has been linked to PTOA development. There is a dearth of longitudinal studies to evaluate if early changes in joint tissue metabolism associate with later changes in gait biomechanics. The purpose of this study was to determine if KFA and IKEM differed at 6 months post-ACLR in individuals with the highest synovial fluid (SF) concentrations of type-II collagen turnover (C2C:CPII) compared to those with lowest SF C2C:CPII measured in the first 15 days prior to ACLR.

Methods

Thirty-eight individuals with an ACL injury were initially included in the study (55% females, 20.9±3.5 yrs, 25.2±5.3 BMI) and SF was aspirated 6.9±4.2 days following ACL injury. All individuals underwent ACLR using the same bone-patellar-tendon-bone allograft procedure. Six months following the ACLR, over-ground gait biomechanics were collected at a self-selected comfortable walking speed. A 3-dimentional motion capture system (Vicon, Nexus, Denver, Colorado, United States) was used to collect and integrate marker trajectories with force data collected using 2 force plates (40 × 60 cm, FP406010, Bertec Corporation, Columbus, Ohio, United States) embedded in a 6m walkway. IKEM were normalized to the product of bodyweight (N) and height (m) and KFA was described as the angle of the tibia relative to the femur. Commercial enzyme-linked immunosorbent assays were used to evaluate type-II collagen breakdown (C2C) and type-II collagen synthesis (CPII) concentrations in SF. Greater C2C:CPII ratios were interpreted as greater collagen breakdown compared to synthesis (i.e. greater type-II collagen turnover).[2] Next, we stratified the cohort into quartiles in order to determine the individuals with the highest (1st quartile) and lowest (4th quartile) SF C2C:CPII at the time of injury. Finally, we conducted a functional analysis of variance to determine the mean differences and corresponding 95% confidence intervals in KFA and IKEM throughout stance at 6 months post-ACLR between the highest and lowest SF C2C:CPII groups. The highest and lowest groups were considered to be different at points of stance where mean differences and corresponding 95% confidence intervals (CI) did not cross zero.

Results and Discussion

10 individuals were included in the highest SF C2C:CPII group (5 females, 20.9±3.1 yrs, 25.2±4.4BMI) and 10 individuals were included in the lowest SF C2C:CPII group (6 females, 20.3±4.5 yrs, 26.9±8.4BMI). Individuals in the highest SF C2C:CPII group demonstrated lesser KFA throughout the entirety of stance phase compared to individuals in the lowest SF C2C:CPII group (Figure 1). Similarly, the highest SF C2C:CPII group demonstrated lesser IKEM between 1 and 89% of stance (Figure 2).

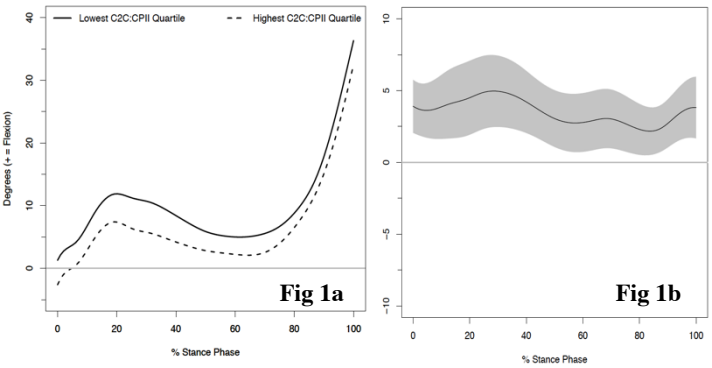

Figure 1: Knee Flexion Angle: (A) The highest SF C2C:CPII group (dotted line) demonstrated lesser KFA throughout the entirety of stance phase compared to the lowest SF C2C:CPII group (solid line), **(B)** as determined by the mean difference and 95% CI not crossing 0 throughout stance.

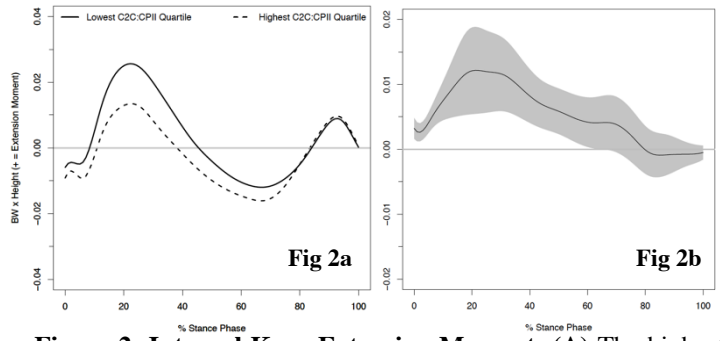

Figure 2: Internal Knee Extension Moment: (A) The highest SF C2C:CPII group (dotted line) demonstrated lesser IKEM between 1 and 89% of stance, **(B)** as determined by the mean difference and 95% CI not crossing 0 for that portion of stance.

Significance

Our study demonstrates that greater SF concentrations of type-II collagen turnover in the first several days following ACL injury are associated with a more stiffened-knee gait strategy 6 months following ACLR (i.e. lesser KFA and IKEM throughout the majority of stance). Future studies may seek to modify early biochemical changes immediately following ACL injury to determine the effect on later changes in gait biomechanics that may perpetuate poor longer-term joint health.

Acknowledgments

Supported by a grant from NIH (R03AR066840).

References

1. Luc, et al., *J Athle Train.* **49**, 806-819, 2014.
2. Pietrosimone, et al., *Am J Sports Med.* **44**, 425-432, 2016.

Does the Pavlik harness treatment cause lower extremity biomechanical changes in infants?

Safeer F. Siddicky[1], Junsig Wang[1], William Hefley III[1], Brien Rabenhorst[1], Elizabeth Aronson[1], Erin M. Mannen[1]
[1]University of Arkansas for Medical Sciences, Little Rock, AR
Email: safeersiddicky@gmail.com

Introduction

Developmental dysplasia of the hip (DDH) occurs in 5.5/1000 full-term babies[1]. The Pavlik harness (PH) non-surgically treats DDH grades 1-3 with 80-92% success[2]. While it is theorized that the mechanism of spontaneous femoral head reduction using a PH is a result of passive abduction of the hip by the weight of the lower limbs during deep sleep[3], the role of active hip movements within the PH in aiding spontaneous reduction has not been explored. Although PH is the best option to achieve closed reduction for babies <6 months, it is restrictive/uncomfortable, requiring 24/7 usage for many weeks; a duration which varies widely based on the severity and among clinicians[4]. Additionally, prolonged harness wear may have negative indications like avascular necrosis or femoral nerve palsy[5]. Therefore, it is critical to better understand the biomechanical impact of closed reduction treatment to improve upon the decades-old PH. The purpose of this study was to measure lower-extremity muscle activity and hip ranges of motion of (1) DDH infants at Pavlik Harness treatment onset and after successful treatment, and (2) infants with mild hip instability who did not require Pavlik harness treatment at the onset of an observation period for dysplasia and after a normal ultrasound. The recorded values were compared to healthy age-matched controls.

Methods

Infants lay supine on a mat for 60 seconds. Surface electromyography (Delsys, 1000 Hz) and motion capture (Vicon, 100 Hz) measured the lower-extremity muscle activity (adductors, quadriceps, biceps femoris, gluteus maximus) and hip range-of-motion of 26 infants. These included DDH infants at PH treatment onset and after successful treatment (n=3), infants with mild hip instability (no PH) at the beginning and end of clinical observation (n=3), and healthy age-matched controls (n=20).

Results and Discussion

The treatment or observation durations were 11 ± 6.3 weeks for infants with DDH and 7 ± 5.4 weeks for infants with mild instability. DDH infants (in the harness at first visit and out of it at follow-up) showed similar muscle activity to controls at both visits, while the mild instability cohort's muscle activity was similar at the first visit but lower at follow-up. At follow-up, DDH infants, as well as the mild instability cohort, showed similar hip range-of-motion to controls, but the mild instability cohort showed lower abduction/adduction ROM. Treatment durations for Pavlik harness treatment fell within the range of values reported in literature, but varied widely (4 to 17 weeks). The lower muscle activity of the mild instability cohort at follow-up may indicate that while the instability is resolved based on ultrasound findings, it is likely that the lower muscle activity may still pose a risk of future instability for these infants. This is also indicated in the lower hip abduction/adduction range of motion at follow up for these infants. Additionally, the mild instability cohort may have lower muscle activity compared to the DDH cohort due to lower opportunity to actively use muscles against resistance (i.e. the Pavlik harness foot strap).

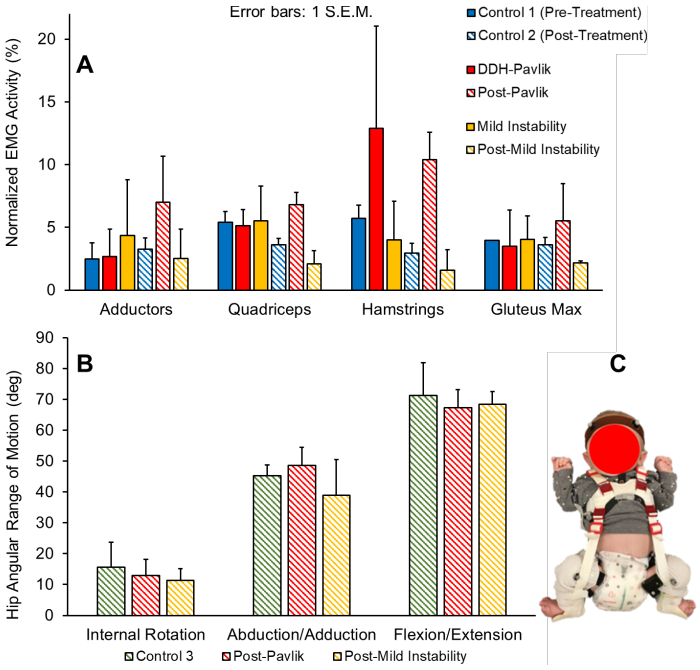

Figure 1. (A) Normalized EMG activity, (B) hip range of motion, and (C) Motion capture markers and EMG sensors on participant.

Limitations of the study include a small sample size in the hip dysplasia population, and a data collection length of only 60 seconds. Future directions include continued enrollment for this study, and utilizing hip ultrasound to examine infants with hip instability in different positions and infant gear. As physicians continue to prescribe the use of the Pavlik harness, further research needs to be conducted on the biomechanical impact of positioning for infants with hip instability, both for treatment and long-term hip health.

Significance

While the Pavlik harness is the gold-standard for closed reduction of DDH in children younger than 6 months, understanding the biomechanical changes infants undergo in such orthopedic devices may educate clinicians' decisions on treatment course and duration.

Acknowledgments

This research was funded by the International Hip Dysplasia Institute, Boba, Inc., and NIH P20GM125503.

References

1. Alsaleem M, et al., Clin Pediatr, 54:921-8, 2015.
2. Huayamave V, et al., J Biomech, 48:2026-33, 2015.
3. Suzuki S, J Bone Joint Surg [Br], 76-B:460-2, 1994.
4. Salduz, et al., Prosthet Orthot Int, 42(3): 299-303, 2018.
5. Swarup I, et al., Curr Opin Pediatr, 30(1): 84-92, 2018.

Estimated Ground Reaction Forces in Stair Climbing After ACL Reconstruction Using a Single Depth Sensor-Driven Musculoskeletal Model

Jeonghoon Oh[1], Moataz Eltoukhy[1], Michael S. Andersen[2], Joseph F. Signorile[1]
[1] Department of Kinesiology and Sport Sciences, University of Miami, Coral Gables, FL, USA
[2] Department of Materials and Production, Aalborg University, Fibigerstraede, Denmark
Email: jxo130@miami.edu

Introduction

Although stair ambulation and other common activities should be included in the rehabilitation of the long-term effects of ACL injury on knee function, most studies have focused on examining ACL deficient during level walking [1]. When compared to level walking, stair climbing produces increasing 12-25 % loading in the knee joint and, consequently, a larger range of external moments. Based on our literature reviews, developing practical laboratory setup as a tool during stair climbing to assist in evaluating the abnormalities in lower extremity that arise from an ACL deficiency.

Therefore, the aim of this study is to develop and validate a full-body musculoskeletal gait model driven by a single depth sensor to estimate the ground reaction forces (GRFs) produced during stairs climbing in patients with ACL reconstruction.

Methods

Fifteen individuals with ACL injury who had undergone reconstructive surgery with Bone-Patellar Tendon-Bone Autograft (BTB) at least one year prior to recruitment where enrolled in this study. GRFs data during stair climbing were collected using a custom-built 3-step wooden staircase without handrails.

The Kinect v.2 depth sensor (Microsoft Corp. Redmond, WA) was located at 2.5 m from the staircase, at a height of 0.75 m from the ground. The subjects performed three trials at their normal walking speeds with barefoot. The depth data was analyzed by subtracting the background depth information and tracking the subjects' movement using anthropometric models in order to extract 26 joint trajectories using a customized Matlab code.

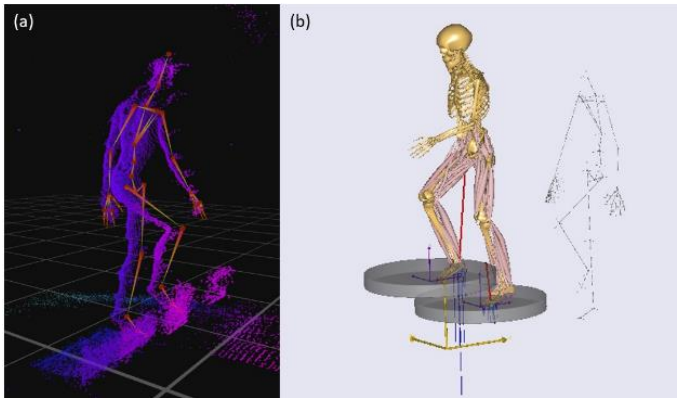

Figure 1: (a) the depth sensor image data with one sample stair climbing task, (b) AnyBody™ musculoskeletal model (KinectAB) including the stick-figure and inverse dynamic analysis with the estimated ground reaction force (red arrows).

The musculoskeletal GaitFullBody model (AnyBody Technology, Aalborg, Denmark), generated the stair climbing GRFs using a modified version of the method proposed by Fluit et al. and Skals et al. [2-3]. This is attained by 25 artificial muscle-like actuators that are placed under each foot. To determine the activation level of each actuator, activation threshold distance was set to -0.01 m, and the activation threshold velocity was set to 1.3 m/sec (Figure 1).

Mean differences between the measured and estimated GRFs were compared using paired samples t-tests in order to establish any significant difference between the measured and predicted values. The ensemble curves and associated 95% confidence intervals (CI95) of the GRFs were compared between both approach.

Results and Discussion

The comparisons between the measured GRFs (force platforms) and the estimated GRFs (AnyBody™ model) at discrete time points during the stair ascent is described in this section. For the ACLR limb, good agreement and consistency were observed for $_{AP}$GRF during the braking (Range ICC: 0.45 ~ -0.86) and propulsive (Range ICC: 0.64 ~ 0.84) phases. Good consistency was also observed for $_{V}$GRF during the propulsive (Range ICC: 0.43 ~ 0.85), while poor agreement and consistency were observed during the braking (Range ICC: 0.41 ~ 0.27) phase. However, there were significant mean differences between the estimated and the measured values during the gait cycle for the vertical braking force (MD: 0.25 ± 0.05) and vertical propulsive force (MD: 0.17 ± 0.01). Fair agreement and consistency were observed for $_{ML}$GRF during the propulsive (Range ICC: 0.43 ~ 0.85) phase.

Generally, investigators have estimated the joint forces and torques from inverse dynamics analysis using kinematic data and GRF measurement from force platforms [4]. However, in the present study, we examined the external validity of this approach to estimate the GRFs during stair climbing that are widely used in the assessment and evaluation of patients with ACL reconstruction. The analysis of the GRFs can give valuable information about basic locomotor mechanisms during gait in patients undergoing orthopedic surgery and provide data which can be used to evaluate the progression of the recovery process in terms of their observed gait patterns.

Significance

This study provided an external validation of a newly developed method to estimate the GRFs during stair ascent that are used in assessment and evaluation of patients who have undergone ACL reconstruction. The ability of the developed model to effectively estimate gait kinetics (e.g. GRFs) was apparent in its ability to effectively assess gait abnormalities due to the ACL injury.

References

[1] Ismail SA et al. (2016). *Clin Biomech*, **35**:68-80.
[2] Skals S et al. (2017) *Multibody Syst Dyn,* **41**(4):297-316.
[3] Fluit R et al. (2014) *J Biomech*, 47(10):2321-2329.
[4] Ren L et al. (2008) *J Biomech,* **41**(3):2750-9.

EFFECT OF SIDE PLANK EXERCISE USING A SLING WITH DIFFERENT HIP ROTATIONS ON TRUNK AND HIP MUSCLES ACTIVATION IN SUBJECTS WITH GLUTEUS MEDIUS WEAKNESS

Seung-Min Baik[1,2], Kyung-Eun Lee[3], Jung-Hoon Choi[1,4], Ji-Hyun Lee[2], Chung-Hwi Yi[3], and Heon-Seock Cynn[1,3]
[1]Applied Kinesiology and Ergonomic Technology Laboratory, Department of Physical Therapy, The Graduate School, Yonsei University
[2]Departement of Physical Therapy, Division of Health Science, Baekseok University
[3]Department of Physical Therapy, The Graduate School, Yonsei University
[4]Rehabilitation 1-team, Severance Rehabilitation Hospital, Yonsei University Health System
Email: cynn@yonsei.ac.kr

Introduction

Among several exercises for activating gluteus medius (Gmed), side plank exercise showed highest-level activation of Gmed in healthy subjects [1]. Also, side plank exercise is one of the weight-bearing exercises that better replicate the functional activities of daily living than the nonweight-bearing exercises [2].

Body weights of individuals can be a resistance for exercise when performing sling-based exercises [3]. Huang et al. (2011) also reported that exercises similar with sling-based exercise are effective in activating the stabilizer muscles such as core muscles [3].

However, it is unclear the effectiveness of side plank exercise using a sling (SPUS) on trunk and hip muscles activation in subjects with Gmed weakness. Therefore, the purpose of this study was to quantify muscle activation of the rectus abdominis (RA), external oblique (EO), lumbar multifidus (LM), Gmed, gluteus maximus (Gmax) and tensor fasciae latae (TFL) during SPUS with three different hip rotations compared to side-lying hip abduction (SHA) exercise.

Methods

Twenty-two subjects with Gmed weakness were recruited. SHA exercise was performed in the same procedure presented in the previous study [4].

For SPUS with three different hip rotations, subjects were positioned side-lying on the treatment table with test leg contact the treatment table first, and then the both legs were suspended on the sling by a principal investigator (SMB). The narrow sling was positioned at the knee joint of test leg and the height of narrow sling was placed at the perpendicular line drawn across the upper shoulder and the foot of the test leg. Thus, the subjects lifted their hip off the table by abducting the test leg until the spine is in neutral position while abducting the top leg about 20% of hip abduction's maximal range of motion. Three different SPUS are SPUS with neutral hip (SPUS-N), SPUS with hip lateral rotation (SPUS-L), and SPUS with hip medial rotation (SPUS-M).

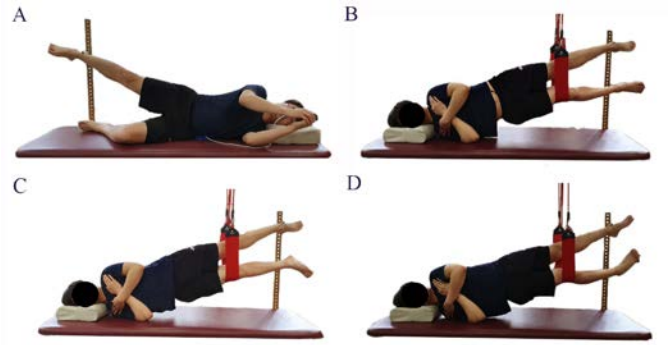

Figure 1: A; Side-lying hip abduction, B: Side plank exercise using a sling with neutral hip, C: Side plank exercise using a sling with hip lateral rotation, D: Side plank exercise using a sling with hip medial rotation

Results and Discussion

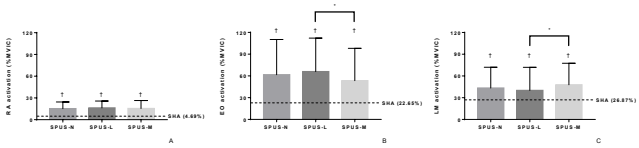

Figure 2: Comparison of trunk muscle activation among four exercises (A: RA; B: EO; C: LM). %MVIC = percentage of maximal voluntary isometric contraction; RA = rectus abdominis; EO = external oblique; LM = lumbar multifidus; SHA = side-lying hip abduction; SPUS-N = side plank using a sling with neutral hip; SPUS-L = side plank using a sling with hip medial rotation; SPUS-M = side plank using a sling with hip lateral rotation. †Significant difference with SHA ($p<.01$). *Significant difference between SPUS subgroups ($p<.01$).

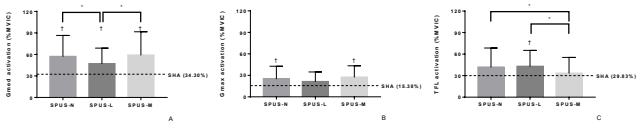

Figure 3: Comparison of trunk muscle activation among four exercises (A: Gmed; B: Gmax; C: TFL). %MVIC = percentage of maximal voluntary isometric contraction; Gmed = gluteus medius; Gmax = gluteus maximus; TFL = tensor fasciae latae; SHA = side-lying hip abduction; SPUS-N = side plank using a sling with neutral hip; SPUS-L = side plank using a sling with hip medial rotation; SPUS-M = side plank using a sling with hip lateral rotation. †Significant difference with SHA ($p<.01$). *Significant difference between SPUS subgroups ($p<.01$).

Three SPUS exercises generally showed significantly higher trunk and hip muscles activation than SHA. SPUS-M showed significantly higher Gmed activation than SBUS-L and significantly lower TFL activation than SPUS-N and SPUS-L. The EO, LM, Gmed activation during three SPUS reached the threshold of 40% to 60% MVIC that can effectively stimulate muscle strength gains.

Significance

Especially, SPUS-N and SPUS-M rather than SPUS-L may be prescribed for patients who have reduced Gmed strength after injuries because they showed significantly higher Gmed activation than SPUS-L. Patients who have Gmed weakness with dominant TFL but have enough trunk stability to prescribe SPUS-M position also may perform SPUS-M because SPUS-M showed significantly lower TFL activation than SPUS-N and SPUS-L.

Acknowledgments

This study was in part supported by the Brain Korea 21 PLUS Project, the Korean Research Foundation for Department of Physical Therapy in the Graduate School of Yonsei University.

References

[1] Reiman MP, Bolga LA, Loudon JK (2012). *PHYSIOTHER THEOR PR*, 28:257-268.
[2] Han HR et al. (2018). *J SPORT REHABIL*, 27:513-519
[3] Huang JS et al. (2011). *J STRENGTH COND RES*, 25:1673-1679
[4] Lee JH et al. (2013). *J SPORT REHABIL*, 22:301-307

EVALUATION OF RUNNING AS A MEANS TO IDENTIFY LIMB SYMMETRY AFTER ACL RECONSTRUCTION

Jacqueline N. Foody[1], Sarah A. Wilson[1], Kimi D. Dahl[1], Matthew T. Provencher[1], and Scott Tashman[1]
[1]Steadman Philippon Research Institute, Vail, CO, USA
Email: stashman@sprivail.org

Introduction

Anterior Cruciate Ligament (ACL) tears are a highly prevalent injury and 30% of patients incur a secondary tear[1]. One proposed method of reducing the risk of secondary injury after reconstruction is through return to play (RTP) testing that measures limb-to-limb symmetry. These differences, however, can be difficult to measure with traditional statistical methods. Statistical Parametric Mapping (SPM) allows for the comparison of entire kinematic curves and can identify key parts of a movement cycle where kinematic dissimilarities exist. The long-term goal of this research is to combine Inertial Measurement Units (IMUs) and SPM to develop more discriminatory tests for determining readiness for RTP. The purpose of the present study was to use IMUs and SPM to determine if limb-to-limb kinematic asymmetries occur in uninjured subjects during various running conditions.

Methods

Thirty-five healthy adults (28±5 years, 72.4±11.4 kg, 1.75±0.08 m, 14 female) were recruited for this study. Participants had no prior injury or surgery to their lower extremities. This study was approved by an IRB, and all participants provided informed consent. Trunk and lower extremity kinematics were captured using eight IMUs (128Hz, APDM). Participants completed an outdoor obstacle course which included flat and downhill running. For the flat running task (FR, 19 participants), participants were instructed to run between 75-100% of their maximum velocity along a roughly 18m flat, concrete path. For the downhill running task, two courses were used: one (DR-woods, 25 participants) was a roughly 25-deg incline with exposed tree roots and compacted soil and the other (DR-gravel, 10 participants) was an approximately 11-deg incline with a mixed grass and gravel running surface. For both downhill courses, participants were instructed to select a speed where they felt comfortable and in control. Four trials of each task were collected for each participant, and gait cycles were determined by assuming heel strikes coincided with the local maxima in the IMU accelerometers on the feet. Sagittal plane kinematics were extracted from one gait cycle per trial, when the participant was not accelerating, using a custom MATLAB script. SPM (spm1d v0.4.3) was used to conduct paired t-tests to evaluate asymmetry during gait cycles.

Results and Discussion

During flat running, no significant kinematic asymmetries were found in the knee, hip, or trunk for healthy volunteers. In the ankle, kinematic asymmetries were seen during maximum plantarflexion (p=0.002) and at the end of the swing phase (p=0.016) (Figure 1a). In an in-lab study using marker-based motion capture, Hughes-Oliver et al found a similar lack of kinematic differences in the sagittal plane in healthy participants during a running task on a 20m walkway using motion capture. This supports the use of IMUs as a fast, reliable way to capture kinematic data.

Similar to flat running, DR-woods showed a significantly greater (p<0.001) amount of plantarflexion (Figure 1b) and an increased amount of peak knee flexion (p=0.019) on the non-dominant limb (Figure 1c). DR-gravel only showed a significant difference between limbs in trunk flexion at roughly 60% of the gait cycle (p=0.041).

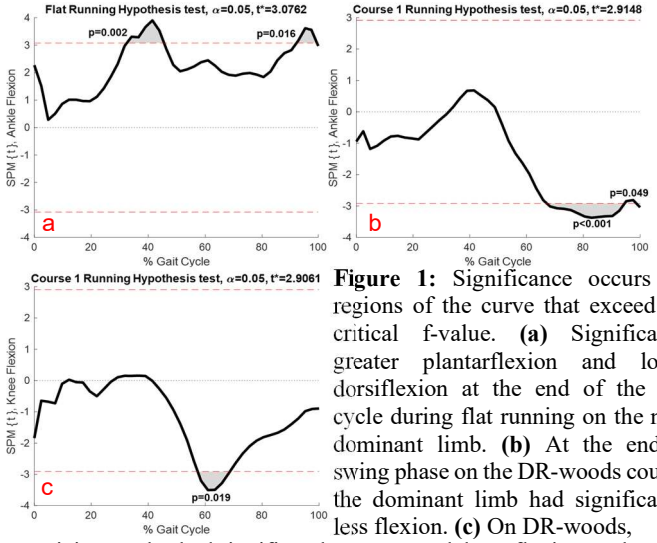

Figure 1: Significance occurs for regions of the curve that exceed the critical f-value. **(a)** Significantly greater plantarflexion and lower dorsiflexion at the end of the gait cycle during flat running on the non-dominant limb. **(b)** At the end of swing phase on the DR-woods course, the dominant limb had significantly less flexion. **(c)** On DR-woods, participants also had significantly greater peak knee flexion on the non-dominant limb.

On all three courses, a large standard deviation in trunk flexion indicated wide variability in movement strategy between participants and trials, so trunk motion may not be an appropriate performance measure in the ACLR group. The increased difficulty of the terrain on the DR-woods course likely resulted in more varied running strategies which increased the standard deviation in the kinematic measures. However, healthy participants showed no limb-to-limb asymmetry in their knee or hip during stance when running downhill, regardless of course.

Significance

Running is an effective task at discerning kinematic similarities in a healthy population, particularly at the knee and hip; however, the terrain should be considered when determining what is normal as symmetry varied between courses. By utilizing SPM, running tasks may have the potential to identify limb-to-limb asymmetries in the ACLR population as part of RTP protocols. Though this has been previously observed in laboratory experiments, this study highlights that an IMU system can be used to identify asymmetries in kinematics in the sagittal plane in more challenging, real-world environments outside of the lab. These devices could potentially assist clinicians in discerning variations in neuromuscular control strategies. Future research will evaluate patient performance in these and other tasks in order to determine their validity as part of an RTP protocol.

Acknowledgments

This project is funded by the Office of Naval Research, Department of Defense.

References

1. Paterno, M et al, DOI 10.1177/0363546514530088
2. Hughes-Oliver, C et al, DOI 10.1123/jab.2018-0392

Latency Between Peak Vastus Medialis Activation and Peak Knee Flexion Moment During Gait is Longer in Knees After Anterior Cruciate Ligament Reconstruction With a Bone-Patellar Tendon-Bone Graft

Naoaki Ito[1,2], Jacob J. Capin, Thomas S. Buchanan[1,3], and Lynn Snyder-Mackler[1,2]
[1]Biomechanics and Movement Science Program, [2]Department of Physical Therapy, and [3]Department of Mechanical Engineering, University of Delaware, Newark, DE
Email: nito@udel.edu

Introduction

Sagittal plane gait alterations after anterior cruciate ligament reconstruction (ACLR) are associated with early osteoarthritis (OA) development.[1] Quadriceps weakness is associated with aberrant gait mechanics[2], and patients with bone-patellar tendon-bone grafts (BPTB) are slower at recovering quadriceps strength compared to those with alternative grafts.[3] Few research studies have evaluated electromechanical delay (i.e., latency) following ACLR.[4] Additionally, the impact of patellar tendon harvest on electromechanical delay is unknown. The purpose of this study was to investigate latency between peak quadriceps muscle activation and external knee flexion moment (pKFM), among patients who received BPTB grafts and those with alternative graft types.

Methods

Sixty-seven participants (19 BPTB / 48 hamstring autograft or soft-tissue allograft) were recruited 6±2 months after primary ACLR. Gait kinetics, kinematics, and electromyography (EMG) data (rectus femoris [RF], medial [VM] / lateral [VL] vasti) were collected during overground walking at self-selected speeds. EMG data were high-pass filtered (2nd order Butterworth at 30Hz), rectified, and low-pass filtered (6Hz) to create a linear envelope. Signal events for peak quadriceps activations and pKFM during the first 50% of stance were created using Visual 3D (C-motion, Germantown, MD), and latency was determined as the time between the events in milliseconds. 2×2 ANOVA (limb by graft type) (α=0.05), adjusted for gait speed as a covariate, was run for our 3 variables of interest (latency between peak RF/VL/VM to pKFM). Demographic variables were evaluated using Pearson Chi-squared tests and T-tests.

Results and Discussion

Our BPTB group was younger ($p<0.01$), had lower quadriceps strength index ($p<0.01$), and had more non-contact ACL injuries compared to contact injuries ($p=0.02$). No differences were observed for time from surgery to testing, height, weight, BMI, sex distribution, and meniscal status.

Variables	Graft type	Latency (ms)		Limb × Graft interaction (p=)
		Involved	Uninvolved	
RF to pKFM	BPTB	69.6 (11.2)	67.5 (15.1)	0.270
	Other	72.3 (18.1)	64.0 (15.3)	
VL to pKFM	BPTB	78.8 (18.2)	70.4 (17.5)	0.434
	Other	73.9 (19.3)	70.1 (17.6)	
VM to pKFM	BPTB	**87.9 (18.9)**	**73.5 (18.1)**	**0.031***
	Other	72.6 (22.7)	72.5 (14.7)	

***Table 1**: Mean (SD) latency and significance (Limb×Graft type interaction effect) for variables of interest.*

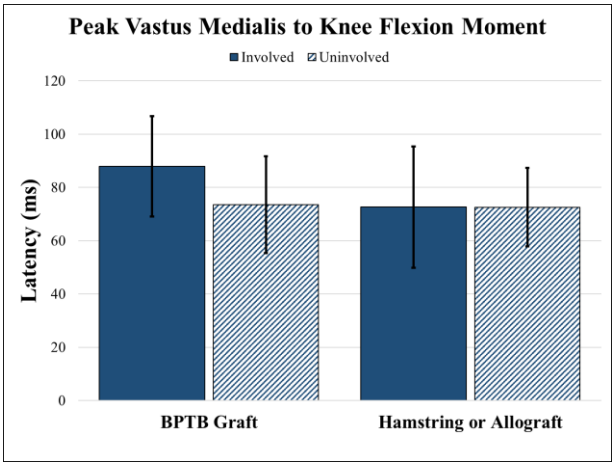

***Figure 2**: Limb-by-Graft type interaction effect ($p=0.03$) was observed;the involved limb in the BPTB group displayed longer latency.*

A limb-by-graft type interaction effect was observed for peak VM to pKFM latency ($p=0.03$), with the BPTB group demonstrating longer latency in their involved versus uninvolved limb. There were no interlimb differences in the alternative graft type group *(Figure 1)*. No significant findings were observed for latency between peak RF or VM to pKFM *(Table 1)*.

The patellar tendon's ability to transfer force following ACLR using a BPTB autograft may be compromised. We found longer latency from peak VM to pKFM in the involved limb of the BPTB group relative to the uninvolved limb of the BPTB group, and both limbs of the hamstring autograft and soft-tisue allograft group. Further investigation including a larger sample size is waranted, as significant differences were not observed for the VL or RF to pKFM latencies. Our preliminary findings, however, suggest BPTB graft harvest may accentuate poor neuromuscular control during activities such as gait (due to the longer time between muscle activation and torque production).

Significance

A graft type specific rehabilitation approach may be necessary to address impairments including altered gait mechanics following ACLR with a BPTB graft. Further research should investigate the role of EMG latency during gait longitudinally after ACLR using larger sample sizes, and the role of patellar tendon morphology[5] on torque production during gait.

Acknowledgments

This work was funded by NIH R01-AR048212, F30-HD096830, R01-HD087459, P30-GM103333, and U54-GM104941.

References

1. Khandha et al., JOR, 2017 2. Shi et al., Gait Posture 2019 3. Smith et al., JOSPT, 2019 4. Freddolini et al., Sports Biomechanics, 2015 5. Gulledge et al., The Knee, 2019

Asymmetries in Patellofemoral Gait Mechanics Are Detectable 3 Months after ACL Reconstruction

Jack R. Williams[1], Kelsey Neal[1], Leah Fisher[2], Abdulmajeed Alfayyadh[1], Ashutosh Khandha[1]
Kurt Manal[1], Lynn Snyder-Mackler[1], Thomas S. Buchanan[1]
[1]University of Delaware, Newark DE
[2]Wichita State University, Wichita KS
Email: jackrw@udel.edu

Introduction

Post-traumatic knee osteoarthritis (OA) following anterior cruciate ligament reconstruction (ACLR) is a well documented phenomenon[1]. Several studies have investigated the development of OA within the tibiofemoral compartment following ACLR. We have associated asymmetries in gait mechanics, including underloading of the involved limb's medial compartment (vs. uninvolved), to the eventual development of knee OA 5 years after surgery[2]. Recent reports, however, suggest that patellofemoral OA after ACLR may be as prevalent as, if not more prevalent than, tibiofemoral OA[3]. Despite this high prevalence of patellofemoral OA, little has been done to investigate the potential mechanisms leading to the disease's development within this compartment. Thus, the purpose of this study is to examine the biomechanical state of the patellofemoral compartment in the early months after ACLR. We hypothesize that asymmetries in patellofemoral mechanics (i.e. peak knee flexion angle [pKFA], peak knee flexion moment [pKFM], and peak patellofemoral contact force [pPCF]) will exist 3 months after reconstruction with lesser values within the involved limb.

Methods

10 participants (7 male, age: 24 ± 6 years, BMI: 25.4 ± 2.3 kg/m^2) completed overground walking trials at their self-selected walking speed 3 months after ACLR. Kinematics, kinetics, and surface electromyography (EMG) were collected bilaterally and used as inputs into a validated, EMG-informed musculoskeletal model[4]. Patellofemoral contact forces, normalized to the subject's bodyweight (BW), were determined using similar methodologies established by Shelburne *et al.* and Yamaguchi *et al.*[5,6]. Three gait trials for each limb were averaged for every subject. pKFA, pKFM, and pPCF were determined for each limb and then averaged across all subjects to get the average pKFA, pKFM, and pPCF in each limb. A one-tailed student's t-test (α = 0.05) was used to compare the peak values for each biomechanical variable across limbs.

Results and Discussion

As hypothesized, asymmetries in pKFA, pKFM, and pPCF were present 3 months after ACLR with the involved limb displaying lesser values compared to the uninvolved limb (Table 1). Of note, significant underloading of the involved limb's patellofemoral compartment (vs. uninvolved) is occurring at this early time point (Figure 1).

Table 1: Involved and Uninvolved Limb Patellofemoral Knee Gait Variables 3 months after ACLR

Variable	Involved	Uninvolved	Significance (p-value)
pKFA (°)	20.11 ± 3.93	21.16 ± 2.36	0.131
pKFM (%BW*HT)	3.72 ± 1.41	5.43 ± 0.81	0.006
pPCF (BW)	1.16 ± 0.51	1.50 ± 0.35	0.023

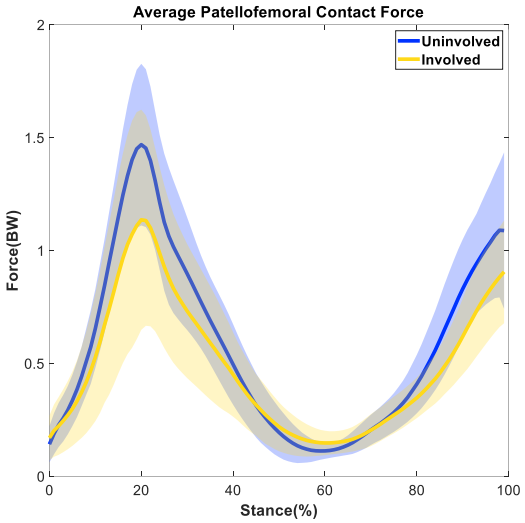

Figure 1: Patellofemoral contact force throughout stance (n=10). Note the involved limb displays a reduced peak compared to the uninvolved limb. [Shaded area = ± 1 standard deviation]

Reduced involved limb loading (vs. uninvolved limb) early after reconstruction has been linked to eventual OA development within the tibiofemoral joint. A similar mechanism could be occurring within the patellofemoral joint. It should be noted that, as this was only three months after surgery, muscle weakness (i.e. reduced quadriceps strength) may be an essential factor driving these asymmetries in mechanics. Future work needs to assess patellofemoral mechanics at later timepoints to see if these asymmetries persist or resolve with time and needs to examine whether or not there is an association between these altered mechanics and early signs of OA development.

Significance

Asymmetries in tibiofemoral gait mechanics early after ACLR have previously been associated with the eventual development of tibiofemoral OA. To our knowledge, this is one of the first studies to examine patellofemoral gait mechanics in the early months following ACLR, particularly with regards to patellofemoral contact force. Asymmetries reported here may be associated with the eventual development of patellofemoral OA. This information could be useful in understanding the biomechanical basis for patellofemoral OA development and may be useful in informing the design of preventative rehabilitation techniques to delay the disease's progression later into life.

Acknowledgments

NIH: R01-HD087459

References

[1] Paschos 2017, [2] Khandha 2017, [3] Culvenor 2013, [4] Manal 2013, [5] Shelburne 1997, [6] Yamaguchi 1989.

3D knee joint angle estimation during drop landing using inertial sensors: Towards ACL injury risk assessment

Bingfei Fan[1], Qingguo Li[2], Peter B. Shull[1]
[1] Department of Mechanical Engineering, Shanghai Jiao Tong University, Shanghai, China
[2] Department of Mechanical and Materials Engineering, Queen's University, Kingston, Canada
Email: bingfeifan@sjtu.edu.cn

Introduction

Anterior cruciate ligament (ACL) injuries are the most common knee injury in sports. The injury usually occurs during landing or cutting tasks, and it can result in immediate knee instability, loss of season and posttraumatic knee osteoarthritis. The biomechanical deficits, such as small knee flexion, excessive knee abduction, are considered to be the risk factors for ACL injury [1]. However, identifying athletes with these biomechanical deficits and training them to move differently is currently done in the biomechanics laboratory which limits the widespread implementation of screening and training. Inertial measurement units (IMUs) are suitable for knee kinematics measurement for their advantages of small size, low cost and portability. Previous approaches using IMUs to assess ACL injury risk during jump landings typically only estimate knee flexion angle [2]. However, the knee abduction angle is also a critical measurement for injury risk assessment [1], though it is challenging to estimate due to its relatively small range of motion. Therefore, the purpose of this study was to develop and validate an algorithm for accurately measuring the 3D knee angle during a landing task.

Methods

Two IMUs were used for 3D knee angle estimation. To estimate the 3D knee angle, we first estimated the sensor orientation ${}^{GS}q$ through a two-step complementary filter. The filter updated the orientation using accelerometer and gyroscope data in the first step and corrected the orientation using magnetometer data in the second step. Finite state machines were used to regulate the filter gain in each step according to the acceleration and magnetic disturbances [3]. Then, we calculated the sensor to body segment rotation ${}^{BS}q$ through Eq. (1), where ${}^{GB}q$ is a known orientation measured in the calibration stage. Finally, we calculated the orientation ${}^{B}q_{TS}$ through the thigh orientation ${}^{GB}q_T$ and shank orientation ${}^{GB}q_S$, as in Eq. (2). The estimated 3D knee angle was the Euler representation of ${}^{B}q_{TS}$.

$$ {}^{GB}q = {}^{GS}q \otimes {}^{BS}q^{*} \quad (1) $$

$$ {}^{B}q_{TS} = {}^{GB}q_T^{*} \otimes {}^{GB}q_S \quad (2) $$

Five healthy subjects (age 32.8±2.8 years, height 174±5.7 cm, mass 63.2±4.8 kg, all male) performed validation drop landing testing while wearing 13 markers on their dominant leg. Two 4-marker clusters were used for motion tracking, and the other five markers were used for segment definition (Fig. 1). An IMU (MTw, Xsens, Netherlands) was aligned and fixed on each cluster. Each subject performed drop landing trials from a 30 cm platform. A sixteen camera motion capture system (Vicon, Oxford, UK) and Visual3D (C Motion, MD, USA) were used for computing reference knee joint angles. The IMUs and Vicon system were electronically synchronized, and the sampling rates were both 100 Hz. Subjects first stood on the platform in a neutral pose for 10 s with the foot aligned with the platform as calibration. We assumed the 3D knee angles were all zero in this state. Subjects then performed 10 consecutive drop landings. Mean and standard deviation of the estimated 3D knee angle of all collected trials were calculated for analysis.

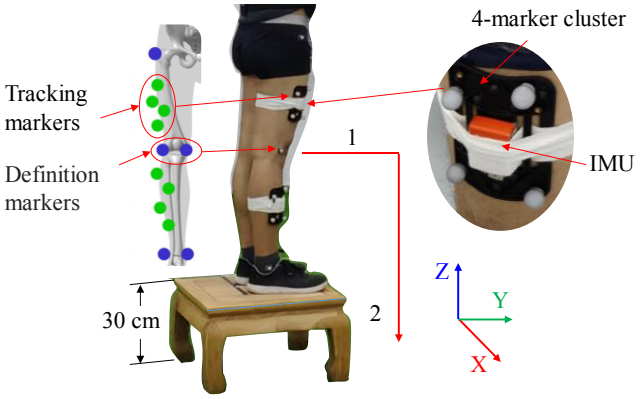

Figure 1: Experimental setup for the drop landing testing.

Results and Discussion

The accuracy of the estimated knee flexion angle, abduction angle and internal rotation angle was 0.17±1.27°, -1.17±1.71° and 3.18±2.76°, respectively (Fig. 2). Knee flexion angle estimation was substantially more accurate than previously reported approaches [2]. Though previous studies haven't reported IMU knee abduction angle accuracy during drop landings, our findings are notably more accurate than previous estimations during walking [4].

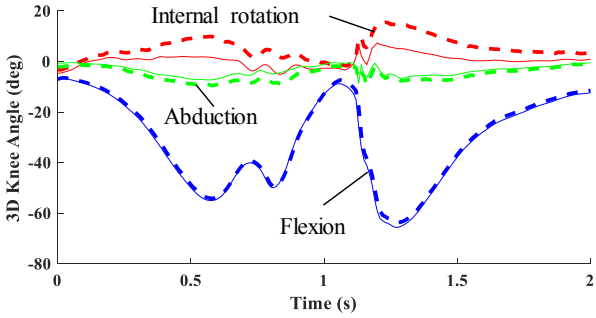

Figure 2: Estimated 3D knee angle for a typical trial. Solid lines indicate IMU estimation, and dotted lines represent motion capture reference values.

Significance

The presented IMU-based 3D knee angle estimation algorithm was relatively accurate in both the sagittal and frontal planes, and could serve as a foundational element to help facilitate in-field biomechanical ACL injury risk assessment.

References

[1] Pappas et al. (2016). Med. Sci. Sport exer. 48(1): 107-113
[2] Dowling et al. (2011). J. Biomech. Eng. 133(7): 071008
[3] Fan et al. (2018). Meas. Sci. Technol. 29: 115104
[4] Schepers et al. (2018). Xsens MVN white paper

Patient-reported Outcomes For Anterior Cruciate Ligament Reconstruction Patients Clustered On Functional and Discrete Walking Biomechanics

Matthew K. Seeley[1], Garritt L. Page[1], Hannah L. Coombs[1], Hope C. Davis-Wilson[2], Christopher D. Johnston[2], J. Troy Blackburn[2], and Brian G. Pietrosimone[2]
[1]Brigham Young University, Provo, UT, USA, & [3]University of North Carolina at Chapel Hill, Chapel Hill, NC, USA
Email: matthewkseeley@gmail.com

Introduction

Walking biomechanics are associated with patient-reported outcomes (PRO) after anterior cruciate ligament reconstruction (ACLR); e.g., vertical ground reaction force (vGRF), knee flexion angle (KFA), and external peak knee adduction moment (KAM). Although associations between walking biomechanics and PRO have been identified, additional complex and still unknown relationships between gait biomechanics and PRO likely exist. Researchers have utilized traditional regression models to investigate associations between discrete biomechanical variables (e.g., peak vGRF) and PRO; yet this approach likely limits the ability to make additional discoveries regarding biomechanical characteristics throughout the entire stance phase of gait for individuals with desirable PRO. The purpose of this study was to test a novel exploratory statistical approach that is capable of clustering ACLR patients based upon functional and discrete walking biomechanics, and then examine potential differences in PRO between the resulting patient clusters. We hypothesized that resulting patient clusters based upon functional and discrete biomechanical measures would differ in PRO and provide direction for future research concerning what biomechanical characteristics are most important in the pursuit of improved PRO for ACLR patients.

Methods

We measured walking biomechanics and Knee Injury and Osteoarthritis Outcome Scores (KOOS) for 131 ACLR patients (Time post-ACLR = 100 ± 10 months; Age = 21 ± 3 yrs; BMI = 24.4 ± 3.7). Subjects were categorized as symptomatic or asymptomatic using KOOS scores [1]. vGRF and KFA curves, across the stance phase of gait, and peak KAM values were clustered using a random partition model as prior distribution for B-spline coefficients in a Bayesian hierarchical model embedded with a predictor dependent partition model [2]. Then, clusters were created using a least squares approach [3]. A chi-squared test was used to test for associations between the resulting patient clusters and frequency of symptomatic and asymptomatic patients.

Results and Discussion

The cluster analysis revealed four distinct clusters of ACLR patients. Clusters 1-4 contained 53, 67, 9, and 2 patients respectively. We chose to omit Cluster 4 from additional analyses due to its small size. As expected, significant ($p < 0.05$) differences existed between clusters for the vGFR and KFA curves (Figure 1), and KAM values (0.022 ± 0.006, 0.022 ± 0.006, and 0.040 ± 0.007 BW·H for Clusters 1-3 respectively). Percentages of symptomatic patients for each cluster were 55, 55, and 33% for Clusters 1-3 respectively; these percentages did not statistically differ, however, this was likely due to the small size of Cluster 3. Although differences in KAM were expected, the direction of these differences is informative: Cluster 3 patients exhibited much greater peak KAM values than the patients in Clusters 1-2.

These results provide a novel view of relationships between functional and discrete walking biomechanics and PRO after ACLR. The patients with similar vGRF and peak KAM values, yet different KFA curves, achieved similar PRO (Clusters 1 and 2). The Cluster 3 patients exhibited greater vGRF during the first 25% of stance, peak KAM values, and KFA excursion during the first 25% of stance; although not statistically significant, these patients trended toward improved PRO. This suggests, perhaps, that increased peak KAM values, or increased vGRF and KFA excursion during the first quarter of stance might lead to improve PRO for ACLR patients. All of these findings can inform future research studies.

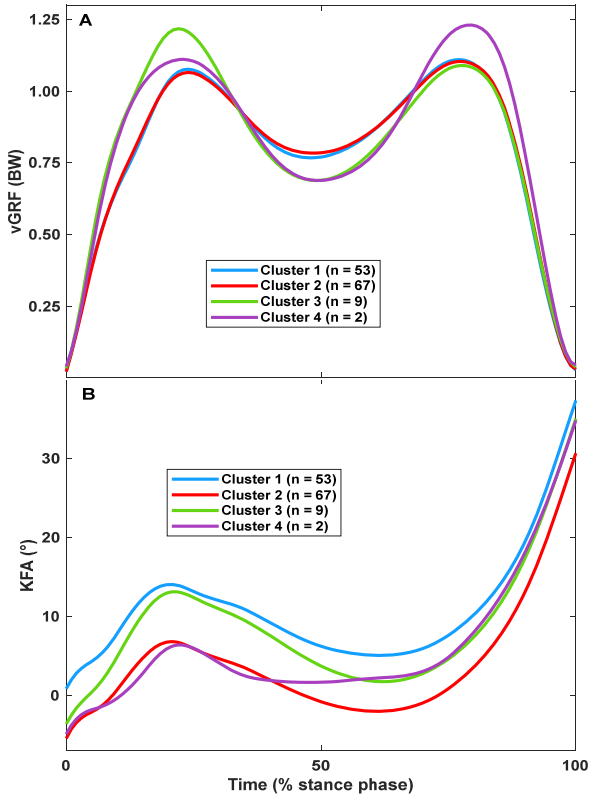

Fig 1. vGRF (A) and KFA (B), plotted across the stance phase of walking, for the four distinct patient clusters.

References
[1] Englund M et al. (2003). *Arthritis Rheum*, 48:2178-2187.
[2] Page GL. (2015) *Bayesian Anal,* 10, 379-410.
[3] Dahl D. (2018). *R Package 1.6,* https://CRAN.R-project.org/package=sdols

The Effect of Antegrade vs. Retrograde Femoral Nailing after Traumatic Femur Fracture on the Kinematics and Kinetics of the Lower Body Through Six-Months of Recovery

John Mead[1], Emily Dooley[2], Michael Hadeed M.D.[3], Seth Yarboro M.D.[3], and Shawn Russell Ph.D.[1,2,3]
University of Virginia, Depts. of [1]Biomedical Eng., [2]Mechanical Eng., and [3]Orthopaedic Surgery, Charlottesville, VA, USA
Email: sdr2n@virginia.edu

Introduction

Femoral nailing is a procedure conducted to repair a fractured femur. There are two main approaches within femoral nailing: the antegrade procedure enters the femur though the hip, while the retrograde procedure through the knee. Antegrade femoral nailing is used for proximal femur fractures. Retrograde femoral nailing optimal for patients suffering from multiple injuries, ipsilateral femoral neck and shaft fractures, and obese paitents[1].

The purpose of this study was to quantify the differences in how well patients recover following surgery. The method used to quantify differences was to evaluate gait by analyzing the moments and angles about the hip and knee of femoral nailing patients, comparing the results of the retrograde versus antegrade procedures. Previous clinical studies comparing the two operations report quadricep atrophy, knee stiffness and knee pain in retrograde patients and, atrophy of the hip abductor muscles and hip pain in antegrade patients[2]. These findings support our hypothesis of decreased range of motion of the knee in retrograde femoral nailing and of the hip in antegrade.

Methods

Experimental data was collected six months after surgery for 6 subjects: 3 antegrade patients (3M; 32±19.08 y.o.) and 3 retrograde patients (2F,1M; 53.67±12.58 y.o.). Subjects were recorded using 3D motion capture and five force plates. Walking trials were collected on a 15m walkway at a self-selected walking speed. A minimum of six trials were analyzed for each subject. The Plug-in-Gait model was used to calculate joint kinematics and kinetics, then exported to Matlab for analysis.

Results and Discussion

Motion analysis revealed key differences between the retrograde and antegrade procedures, mainly at the hip and knee. Retrograde patients had reduced knee flexion during early stance, an increased knee abduction moment, and a decreased knee extension moment. The hip extension moment of retrograde patients also decreased. Antegrade patients displayed a decrease in hip abduction moment and hip adduction angle.

Antegrade patients showed significantly less deviation from the control group than retrograde patients. Minor decreases in hip abduction moment and hip adduction angle were observed. This can be attributed to weakened hip abductor muscles and hip pain[2].

Two of the three retrograde patients had decreased knee flexion during the early stance and a decreased knee extension moment (*Fig. 1*). All of the retrograde patients were observed to have a significantly higher knee abduction moment during the stance phase of their gait (*Fig. 1*). The decreased flexion and extension of the injured knee combined with the decreased hip extension moment indicate that the patient is walking with a straighter injured leg, leading to the increased knee abduction moment. The straight leg gait also puts these patients in a more injury prone position.

Increased knee extension moment observed in the retrograde patients puts these patients at a greater risk of suffering a posterior cruciate ligament (PCL) tear, of which hyperextension is a mechanism of injury. Coupled with the fact that PCL injuries are found to be concomitant with femoral fractures[3], the retrograde procedure likely puts patients at an increased risk of PCL tear.

Significance

The antegrade femoral nailing procedure is the better procedure of the two, from a kinematic and kinetic standpoint. Following the antegrade procedure, patients had a gait that more closely resembled the gait of the control group. Our findings indicate that surgeons should opt to perform the antegrade femoral nailing procedure if the opportunity presents itself. Ultimately, the antegrade procedure will better restore the motion of patients to what it was prior to the injury.

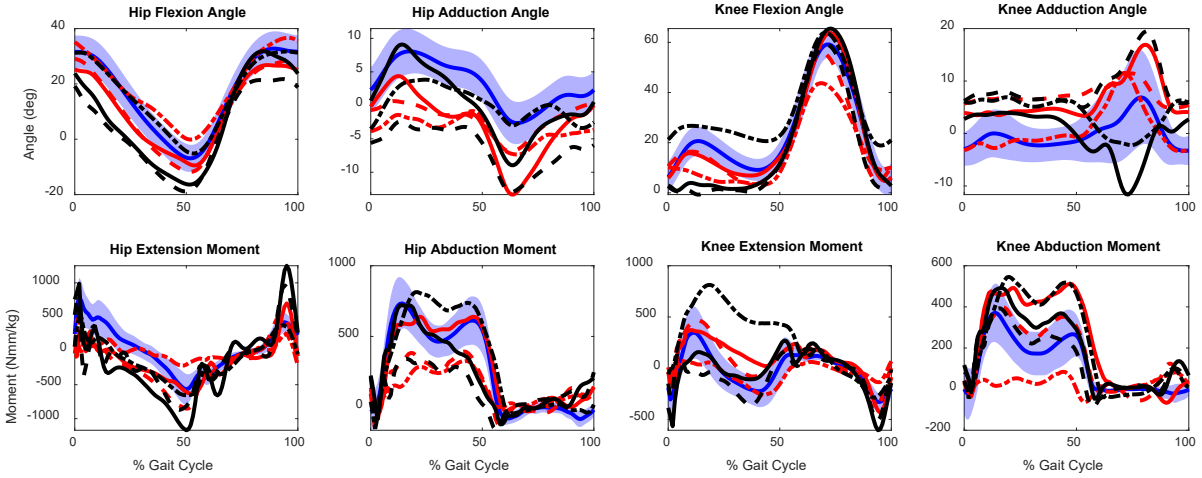

Figure 1. Hip, knee kinematics and kinetics for the injured limb of subjects: antegrade red, retrograde black, normal blue.

Acknowledgments

We would like to thank the following for their support:
UVA Motion Analysis and Motor Performance Laboratory
UVA Department of Orthopaedic Surgery

References

[1] Hussain et al. (2017). *Can. J. Surg,* **60**: 19–29.
[2] Ostrum et al. (2000). *J. Orthop. Trauma,* **14**: 496–501.
[3] Blacksin et al. (1998). *Skeletal Radiol,* vol. 27.

Knee Biomechanical Asymmetries Improve 3 to 6 months After ACLR, but Continue to Persist at 6 Months

Kelsey Neal[1], Jack R. Williams[1], Abdulmajeed Alfayyadh[1], Naoaki Ito[1], Ashutosh Khandha[1]
Kurt Manal[1], Lynn Snyder-Mackler[1], Thomas S. Buchanan[1]
[1]University of Delaware, Newark DE
Email: kaeneal@udel.edu

Introduction

Anterior cruciate ligament reconstruction (ACLR) restores stability to the knee but does not prevent the development of post-traumatic osteoarthritis (PTOA). Gait aberrations in the involved limb, such as reduced peak knee flexion angles, flexion moments, and adduction moments (pKFA, pKFM, pKAM respectively), are commonly reported 6 months after surgery and are associated with PTOA [1,2,3]. Our lab has found that individuals who develop radiographic PTOA 5 years after ACLR display significantly lower peak medial compartment contact forces (pMCF) in their involved knee 6 months after surgery, compared to those who do not develop PTOA[2]. While these asymmetries are present up to 1 year after ACLR, they tend to level out by 2 years[4]. However, regaining symmetry this far after surgery may be too late to help slow the onset of PTOA. It is currently unknown how asymmetries in gait mechanics progress in the early months after reconstruction when modifications may be more beneficial to an individual's long-term health. The purpose of this study was to examine how biomechanical asymmetries progress from 3 to 6 months after ACLR. We hypothesized that individuals will be more asymmetric 3 months after ACLR (vs. 6 months).

Methods

Twenty-two participants (13 males, age: 22 ± 6 years, BMI: 24.5 ± 3.6 kg/m^2) underwent gait analysis 3 and 6 months after ACLR. Individuals walked overground at self-selected speeds while kinematic (120 Hz), kinetic (1080 Hz), and surface electromyography (1080 Hz) data were collected. Walking speed was maintained at both time points. Joint contact forces and muscle forces were calculated using a validated, EMG-informed, subject specific musculoskeletal model[5]. Quadriceps force was calculated by summing the forces of the rectus femoris, vastus medialis, vastus lateralis, and the vastus intermedius during the first 50% of stance. Peak quadriceps force (pEXT), pKAM, pKFM, and pMCF were variables of interest. Interlimb difference (ILD = involved - uninvolved) was calculated for each variable at each time point. A one-tailed Student's t-test ($\alpha = 0.05$) was used to assess significance between knees at each time point.

Results and Discussion

As hypothesized, we found smaller ILDs in all variables of interest at 6 months when compared to the 3-month time point (Figure 1). These trends toward symmetry may be driven by the improved symmetry in peak quadriceps force that is occurring between time points. Of interest, the difference between limbs of many of the biomechanical variables were significantly different regardless of time point (Table 1).

While asymmetries at 6 months after ACLR are linked to the eventual development of OA, this data shows greater asymmetries 3 months after surgery. Asymmetries at 3 months are more pronounced in our cohort, however, it is unknown whether early asymmetries at 3 months initiates long term damage to cartilage and if improving asymmetry between 3 and 6 months after surgery protects the long-term health of the cartilage. Future work will investigate how changes in asymmetries early after surgery affect the long term biochemical health of knee cartilage.

Table 1: Mean involved and uninvolved limb values of knee gait biomechanical variables at 3 and 6 months .

	3 Months			6 Months		
Variable	**Involved**	**Uninvolved**	**p-Value**	**Involved**	**Uninvolved**	**p-Value**
pKFA (Degrees)	17.81 ± 6.83	21.82 ± 5.23	**<0.001**	20.25 ± 4.92	22.88 ± 6.65	**0.006**
pKFM (%BW*HT)	3.36 ± 1.68	5.70 ± 1.61	**<0.001**	4.29 ± 1.71	5.87 ± 2.14	**<0.001**
pKAM (%BW*HT)	2.89 ± 1.18	2.84 ± 0.85	0.42	3.03 ± 1.25	3.04 ± 0.99	0.48
pMCF (BW)	2.69 ± 0.75	3.01 ± 0.43	**0.037**	2.91 ± 0.60	3.13 ± 0.45	0.081
pEXT (BW)	2.03 ± 0.86	2.81 ± 0.70	**<0.001**	2.40 ± 0.70	3.00 ± 0.89	**0.001**

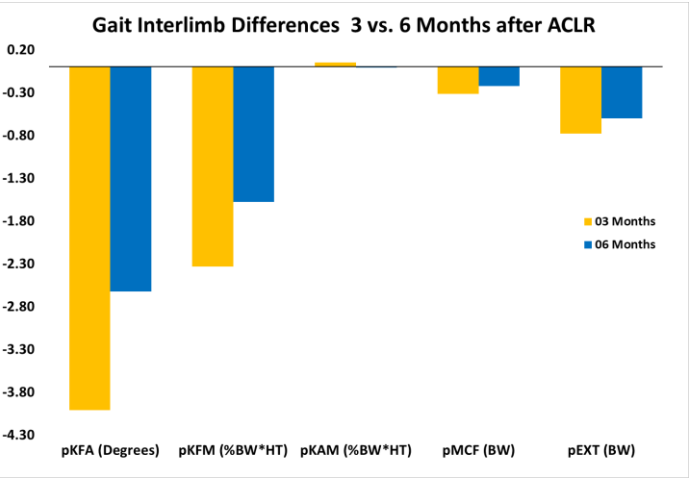

Figure 1: Comparison of 3 month and 6 month interlimb values (ILD = involved – uninvolved). All gait variables had higher levels of asymmetry at 3 months than 6 months after ACLR.

Significance

It is well known that asymmetries after ACLR place an individual at risk for developing PTOA, however it is unclear how early these asymmetries need to be resolved to give someone their best chance at long term joint health. This study found that asymmetries between limbs improves from 3 to 6 months after surgery. While symmetrical gait for many is still not obtained by 6 months, this data shows that individuals can regain symmetry during this time which may be critical in preventing the onset of PTOA. If this is the case further rehab and gait training between 3 and 6 months after ACLR may be needed to help individuals regain symmetry.

Acknowledgments

NIH: R01-HD087459

References

[1] Slater, 2017 [2] Wellsandt, 2016 [3] Khandha, 2017 [4] Hart, 2015 [5] Manal & Buchanan, 2013

Effects of Stroboscopic Vision on Single-limb Postural Stability Measures in ACLR and Healthy Individuals

Nathan J. Robey[1,2], K. Otto Buchholz[3], Shane P. Murphy[4], and Gary D. Hesie[2]
[1]Western Washington University, Bellingham, WA
[2]University of Northern Colorado, Greeley, CO [3]Shenandoah University, Winchester, VA [4]University of Montana, Missoula, MT
Email: nathan.robey@wwu.edu

Introduction

Injury to the anterior cruciate ligament (ACL) is one of the most common knee injuries occurring in sports. Patients often elect to undergo surgical intervention in an effort to return to high-level sports (RTS) activities. However, ACL reconstructed (ACLR) individuals have an increased chance of suffering a second ACL injury after RTS [1]. While mechanical stability may be restored after surgery, lingering somatosensory impairments may still exist after RTS. Somatosensory deficits may encourage sensory reweighting, forcing the central nervous system to rely more on visual feedback during sports activities [2].

Static postural stability measures have previously been used to evaluate an ACLR patient's knee function before RTS [3,4]. Single-limb postural stability assessments of ACLR individuals have demonstrated mixed results [3,4]. The conflicting findings may be the result of a wide variety of testing positions (flexed or extended knee position), surfaces (rigid or compliant), vision (eyes open (EO) or eyes closed (EC)) conditions, as well as center of pressure (COP) measures.

Visual perturbations used to assess static postural stability may be of increased importance for individuals returning from ACLR. However, assessing only the extremes of vision (EO vs. EC) may not appropriate for RTS protocols. Stroboscopic glasses are a clinical tool that offers the assessor increased levels of visual disruption [5]. Therefore, we hypothesized that ACLR individuals will rely on vision more than healthy controls (HC) when testing beyond an EO/EC intervention.

Methods

Thirteen ACLR (F=6, 20±1 years, 1.71±0.09 m, 76.1±8.1 kg, 28.0±9.7 months since surgery) volunteered for this study and were age and sex-matched with recreationally active HC (F=6, 21±2 years, 1.71±0.10 m, 69.5±11.6 kg). During each trial, participants were asked to stand barefoot, on an AMTI force plate (Watertown, MA, USA), under three visual conditions: 1) EO; 2) low visual disruption (LVD); 3) high visual disruption (HVD) using stroboscopic glasses (Senaptec, Beaverton, OR, USA). Ground reaction forces were captured at 1000 Hz for 30s and filtered using a fourth-order, Butterworth low-pass filter with a cut-off frequency of 10 Hz. COP signal calculations for dependent variables were based on previous work [6]. For group comparisons, the ACLR injured limb was compared to the matched limb of the healthy control group. Four two factor (group x vision) ANOVA's ($\alpha = 0.05$) were performed on COP measures (SPSS 26, IBM, USA). Significant main effects were evaluated using pairwise comparisons with Bonferroni correction.

Results and Discussion

The findings of this study were partially in line with our hypothesis. First, we expected to observe an interaction effect between the group and vision conditions; however, our results did not support this hypothesis. Main effects for the group condition were observed only for sway area ($p = .049$). No significant differences were observed for the rest of the group COP variables. However, significant differences were found within visual conditions for each dependent variable, which did support our initial hypothesis (Table 1).

In this study, ACLR individuals demonstrated a ~26% increased sway area (281.26 mm^2/s) when compared to HC (223.93 mm^2/s). These results are similar to Bonfim [7], who found increased postural sway in ACLR limbs during single-leg stance testing. In contrast to previous literature, our study did not find a significant group difference in RMS distance, mean velocity, or mean frequency measures. Mohammadi [3] found a difference between ACLR and HC limbs for both COP velocity and amplitude measures. Our results are in alignment with Bodkin [4], who also found no significant group difference when reporting mean velocity. These conflicting findings may partially be explained by methodological differences in stance position (knee flexed vs. extended).

Significance

ACLR individuals did not perform significantly worse on static postural stability measures than HC, as visual disruption was increased. The findings in this study indicate that individuals with ACLR may not rely on increased visual information during static postural stability assessments as original theorized. However, the knee extended testing position may not be challenging enough to observe changes in static postural stability. Clinicians may consider alternate testing positions before evaluating an ACLR patient's postural stability before RTS.

References

[1] Hui C, et al. (2010). *Am J Sports Med*
[2] Grooms D, et al. (2015). *J Orthop Sports Phys Ther*
[3] Mohammadi F, et al. (2012). *Knee Surg Sports Traumatol Athrosc*
[4] Bodkin SG, et al. (2018). *Gait & Posture*
[5] Kim K, et al. (2017). *J. Sport Rehabil*
[6] Prieto TE, et al. (1996) *IEEE Trans Biomed Eng*
[7] Bonfim T, el al. (2003). *Arch Phys Med Rehabil*

Table 1: Means and standard deviations for visual COP comparisons; a = ($p<0.05$) between EO and LVD; b = ($p<0.05$) between EO and HVD

Measure	ACLR - EO	ACLR - LVD	ACLR - HVD	HC - EO	HC - LVD	HC - HVD
RMS distance (mm)	11.49 ± 2.23[a,b]	15.03 ± 1.10	14.83 ± 2.72	10.49 ± 2.17[a,b]	14.83 ± 2.24	13.22 ±1.56
Mean velocity (mm/s)	48.16 ± 10.17[a,b]	75.10 ± 14.44	73.25 ± 20.40	40.82 ± 10.52[a,b]	65.57 ± 18.62	62.42 ± 13.97
Sway area (mm^2/s)	168.74 ± 51.49[a,b]	338.10 ± 82.69	336.94 ± 141.45	130.0 ± 53.40[a,b]	290.61 ± 101.76	251.18 ± 76.92
Mean frequency (Hz)	0.77 ± 0.18[a,b]	0.91 ± 0.17	0.89 ± 0.17	0.72 ± 0.20[a,b]	0.80 ± 0.20	0.85 0.18

The Relationship among Hip Strength and Hip Kinematics during Single-Leg Tasks: A Systematic Review and Meta-Analysis

Micah C. Garcia[1], Jeffery A. Taylor-Haas[2], Marina C. Waiteman[1,3], and David M. Bazett-Jones[1]

[1]University of Toledo, Toledo, OH, USA
[2]Cincinnati Children's Hospital Medical Center, Cincinnati, OH, USA
[3]São Paulo State University, São Paulo, Brazil

Email: Micah.Garcia@rockets.utoledo.edu

Introduction

Over 8.5 million sports- and recreational-related injuries are reported per year with over 40% of these injuries occurring to the lower extremity [1]. Participation in sports and physical activity oftren require single-leg tasks including running, jumping, and landing. During these tasks, the hip acts to dissipate forces, stabilize the lower extremity, and progress the body forward [2].

During weight acceptance of single-leg tasks, the hip flexes, adducts, and internally rotates to dissipate external moments acting on the hip joint [3,4]. Hip musculature weakness and deleterious hip mechanics have been reported in a variety of injured populations. Due to conflicting results in these studies, the relationship among hip strength and hip mechanics remains unclear. Therefore, the purpose of this systematic review was to gather available research and evaluate the association between hip strength and hip biomechanics during single-leg tasks in healthy populations.

Methods

The protocol of the systematic review was developed using PRISMA guidelines. In November 2019, electronic databases were systematically searched to identify research studies on the relationship among hip strength and lower extremity kinematics during single-leg taks. Inclusion criteria required 1) healthy adolescent and adults, 2) isometric or isokinetic hip strength, 3) single-leg task, 4) two- (2D) or three-dimensional (3D) hip range of motion (RoM) measure during a single-leg task, 5) correlational study, and 6) cross-sectional design.

Two reviewers independently screened the articles for inclusion (MCG, MCW) and quality (MCG, JTH) and then data were extracted. Meta-analyses were conducted using Comprehensive Meta-Analysis Software (Biostat, Inc.; Englewood, NJ) analysing the correlation between hip strength (abduction, external rotation, and extension) and hip RoM (frontal, transverse, and sagittal). Hip strength measures were stratified into either abduction (HABDS), external rotation (HERS), or extension (HEXTS) for subgroup analyses. Significance was set at $p<0.05$.

Results and Discussion

The systematic search returned 14,969 articles. Fifty-seven articles underwent full-text review and 11 were included for analysis. Results from the meta-analysis can be found in Table 1.

No relationship was found among hip strength and frontal plane hip adduction RoM. Stratification of hip strength tests revealed a significant negative relationship between HABDS and frontal plane hip RoM (p=0.037). A significant negative relationship was found among hip strength and transverse plane hip RoM (p=0.006). Stratification of hip strength tests revealed a significant negative relationship among HEXTS and transverse plane hip RoM (p=0.018). No significant relationships were found among hip strength and sagittal plane hip RoM or when hip strength tests were stratified.

Increased frontal and transverse plane hip motion has been implicated with increased patellofemoral joint stress and patellofemoral pain in athletic activites [5-7]. While the meta-analyses calculated statatistically significant correlations, the weakness of the r-values questions the clinical significance of the results and warrants further investigation. A variety of factors may influence the weakness of the relationships. The total sample size was $82 \leq n \leq 302$ for each meta-analysis; however, none of the individual studies had sample sizes larger than n=40. The sample sizes for individual studies may not be large enough for these relationsips to be clinically meaningful. A variety of populations (e.g. males, females, combined sexes) and single-leg tasks were included in this systematic review and meta-analyses. Kinematic motion analysis methodologies (2D or 3D) were also not consistent between studies. Though the meta-analyses showed homogeneity, results should be understood in the context of these limitations. The relationship among hip strength and hip kinematics may be sex-, task-, and/or methodology-specific.

Significance

Results of the systematic review highlight the importance for further investigation among the relationships of hip strength and hip kinematics during single-leg tasks. The current literature is varied regarding task, sex, methodology and lacks adequate sample sizes. Meta-analysis results do suggest lower HABDS and HEXTS are related to greater frontal and transverse plane hip RoM, respectively, while sagittal plane hip RoM is not assocated with hip strength.

References

[1] Sheu Y et al. *National Health Stats Report*. 2016.
[2] Dugan SA et al. *Phys Med Rehabil Clin N Am*. 2005.
[3] Powers CM. *JOSPT*. 2010.
[4] Novacheck TF, *Gait Posture*. 1998.
[5] Liao TC, *Clin Biomech*. 2018.
[6] Souza B, *JOSPT*. 2009.
[7] Noehren B, *MSSE*. 2013.

Table 1. Meta-analyses of relationship between hip strength and hip RoM during single-leg tasks. * indicates significance ($p<0.05$).

Hip Strength	Hip Frontal Plane RoM		Hip Transverse Plane RoM		Hip Sagittal Plane RoM	
	r	*p*	r	*p*	r	*p*
Overall	-0.136	0.092	**-0.134**	**0.006***	-0.007	0.900
HABDS	**-0.169**	**0.037***	-0.106	0.117	-0.020	0.803
HERS	-0.037	0.720	-0.107	0.116	-0.019	0.851
HEXTS	-0.254	0.097	**-0.241**	**0.018***	0.036	0.756

Women Walk With Higher Muscle Co-Contraction Indices 3 Months after Anterior Cruciate Ligament Reconstruction

Abdulmajeed Alfayyadh[1], Naoaki Ito[1], Kelsey Neal[1], Jack R. Williams[1],
Ashutosh Khandha[1], Lynn Snyder-Mackler[1], Thomas S. Buchanan[1]
[1]University of Delaware, Newark DE
Email: fayyadh@udel.edu

Introductions

Gait aberrations after ACL reconstruction (ACLR) are a commonly reported phenomenon[1]. One of the most frequently examined gait biomechanical variables after ACLR is external knee adduction moment which many consider to be representative of medial compartment loading[1,2]. However, these studies fail to account for the possibility of co-contraction between knee agonist/antagonist muscle pairs which may also influence tibiofemoral loading. Muscle co-contraction indices (CCIs), a representative measure of co-contraction, can give insight into the relative amount of co-contraction between muscle pairs; with a higher CCI indicative of more co-contraction[3]. High CCIs of knee muscles are associated with quadriceps weakness[4], and women after ACLR display weaker quadriceps compared to men[5]. Also, sex differences exist in gait mechanics between men and women[6,7], which might alter CCIs among sexes. Despite extensive investigations into altered gait mechanics after ACLR, little is known about CCIs during the early months after surgery. Thus, the purpose of this study was to examine CCIs in the involved and uninvolved limbs for both sexes in patients 3 months after ACLR. We hypothesized that the involved limb would display higher CCIs compared to the uninvolved limb, and women would display higher CCIs compared to men.

Methods

45 participants (27 men, 18 women, age: 22.9 ± 7.0 yrs, BMI: 25.0 ± 3.5 kg/m^2) 3.1 ± 0.6 months after ACLR performed overground walking at self-selected speeds. Electromyography (EMG) data were collected bilaterally for the following muscles: rectus femoris (RF), vastus medialis (VM), vastus lateralis (VL), medial hamstring (MH), lateral hamstring (LH), medial gastrocnemius (MG), and lateral gastrocnemius (MG). EMG data were high-pass filtered at 30Hz, rectified, and low-pass filtered at 6Hz, and normalized to maximum voluntary isometric contractions. CCIs of six muscle pairs: VM-MH, VM-MG, VM-LG, VL-LH, VL-LG, and VL-MG were calculated using Visual 3D (C-motion, Germantown, MD). For each muscle pair, CCIs were defined as the lowest EMG signal divided by the highest EMG signal, multiplied by the sum of these values[3]. The average CCIs between 100ms before heel strike to peak knee flexion angle were reported for each muscle pair[3]. A 2 × 2 (limb × sex) repeated measures ANOVA (α=0.05) was run to compare CCIs between each limb and sex. Demographic variables were compared using t-tests and chi squared analysis.

Results and Discussion

No significant differences in age, graft type, and BMI existed between sexes. Our hypothesis was partially supported; participants tended to walk with higher CCIs in the involved limb (vs. uninvolved limb) with a main effect of limb observed for the VL-LH pair (p = 0.02). Also, main effects of sex were observed for VM-LG ($p < 0.01$) and VL-LG ($p = 0.01$) muscle pairs (Figure 1). In both groups, women had higher CCIs regardless of limb (Figure 1). No other main or interaction effects were observed for the remaining variables of interest.

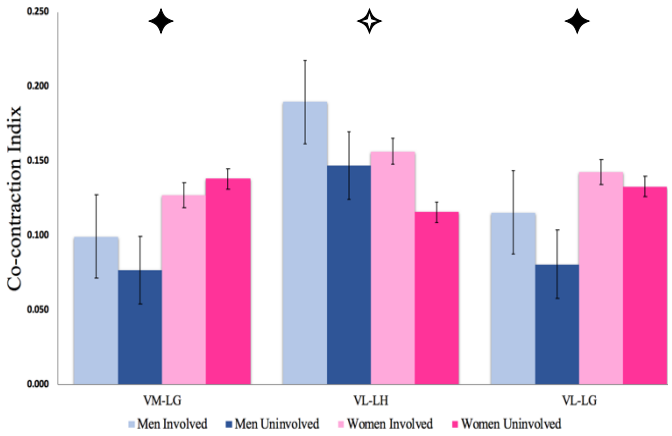

Figure 1: ✦ Main effects of sex for VM-LG ($p < 0.01$) and VL-LG ($p = 0.01$). For both variables, women had higher CCIs regardless of limb. ✧ Main effect of limb for VL-LH ($p = 0.02$). The involved limb had higher CCIs than the uninvolved limb regardless of sex.

Our findings suggest that CCIs after ACLR differ based on sex. However, given that there were no effects of limb for these variables, it is unknown if the findings in sex differences were a result of the ACLR, or if this is reflecting typical sex differences in gait, as this is the first study to assess CCIs grouped by sex. It should be noted that differences in sex only occurred in the muscle pairs containing the lateral gastrocnemius which may indicate that this muscle is being used differently between sexes following reconstruction. The VL-LH pair is more representative of our expected findings with the involved limb displaying high CCIs. Future studies need to investigate CCIs during gait at later time points after surgery and need to examine if there are associations between high CCIs and measures such as quadriceps strength and kinesiophobia that may potentially influence muscle activation patterns during gait.

Significance

This study reiterates the importance of early gait interventions and quadriceps strengthening to address altered gait following ACLR. Our findings between sex add to the current knowledge of gait differences among sexes, and why women may be more likely to develop OA following ACLR[8]. Further research should investigate possible contributors to high CCIs such as kinesiophobia or poor quadriceps strength and activation.

Acknowledgments

NIH: R01-HD087459

References

[1] Slater 2017, [2] Williams 2019, [3] Rudolph 2001, [4] Thoma 2016, [5] Kuenze 2019, [6] Asaeda 2017, [7] Cho 2004, [8] Blagojevic 2010

Joint Angular Impulse and Neuromuscular Control in the Y Balance Test™ in ACLR Individuals

Moore, Logan N.[1] Decker, Meredith N.[1] Ricard, Mark D.[1]
[1]The University of Texas at Arlington, College of Nursing and Health Innovation, Department of Kinesiology
Email: logan.moore@uta.edu

Introduction

The Y Balance Test™ (YBT) is used to measure lower extremity dynamic balance and stability [5]. The YBT is a modified version of The Star Excursion Balance Test (SEBT) looking solely at three reach distances (anterior, posteromedial, and posterolateral) [3, 5]. Dynamic stability tests have been used by clinicians to detect injury risk and as a criterion for return to sport in patients with anterior cruciate ligament (ACL) injuries [2-4]. Patients that have had ACL reconstruction (ACLR) are at a higher risk of reinjury of the ACL and development of osteoarthritis in the knee [1, 2]. Continued dynamic stability tests post rehabilitation could provide insights in the increased risk of reinjury. To our knowledge, there have been no studies focused on neuromuscular control and the joint moments of the lower extremity in patients that are several years out from ACLR. The purpose of this study was to determine if limb to limb differences were present in lower extremity joint moments and neuromuscular control in ACLR patients several years post reconstruction in the anterior direction while preforming the YBT.

Methods

Data collection occurred in one session in the University's Biomechanics Laboratory. Twelve recreationally active adults (male=5, female=7, age=24.7±3.6yrs, mass=76.1±12.3kg, height=168.7±10.1cm) volunteered to participate in this study. All participants had a previous history of unilateral ACLR with an average time of 7±3.1 years post reconstruction. EMG data were recorded at 1000 Hz using DE 2.1 electrodes (Delsys Inc.) for gastrocnemius, gluteus maximus, gluteus medius, biceps femoris, semimembranosus, tibialis anterior, vastus medialis, and vastis lateralis. Participants completed 3 trials of the YBT while being recorded at 100 Hz using Vicon Nexus software and an AMTI force plate (1000 Hz). EMG data was processed by using a critically damped low pass filter and normalized to the maximum amplitude attained during all YBT attempts by muscle. 3D internal joint moments about the hip and knee joints were computed using Visual3D and integrated from 100 ms prior to, and 100 ms after max reach in YBT. Linear mixed-effects were used to determine differences between limbs (affected, unaffected) in joint angles and joint angular impulses with EMG linear envelopes as covariates.

Results and Discussion

There was no significant difference in the anterior reach between the affected 54.92 ± 9.40 cm and unaffected 54.09 ± 9.40 cm, p = 0.23 limbs in the YBT. In the knee joint, the angular impulse for the affected limb was found to have significantly greater abduction impulse, and there was no significant difference found in the knee joint angles (Figure 1). The hip of the affected limb was demonstrated to have significantly greater external rotation and to have greater extension. The angular impulse of the affected limb in the hip was shown to have greater external impulse. While not significant (p=0.08), there was a greater hip abduction impulse in the affected limb.

While there were no significant differences in maximal reach distance, how the reach was obtained did change. To compensate for putative deficiencies in the affected limb, subjects exhibited greater knee joint abduction (valgus alignment) and greater hip external rotation and hip extension to attain the same reach distance, when compared to the unaffected limb. These differences in joint angular impulses and joint angles illustrate dynamic balance asymmetries. Dynamic balance asymmetries may be indicative to having a greater risk of injury in the affected limb. There were no significant differences in the maximal amplitude of the EMG between limbs, however strength measurements could further explain the asymmetries in joint angular impulse and neuromuscular control in ACLR patients.

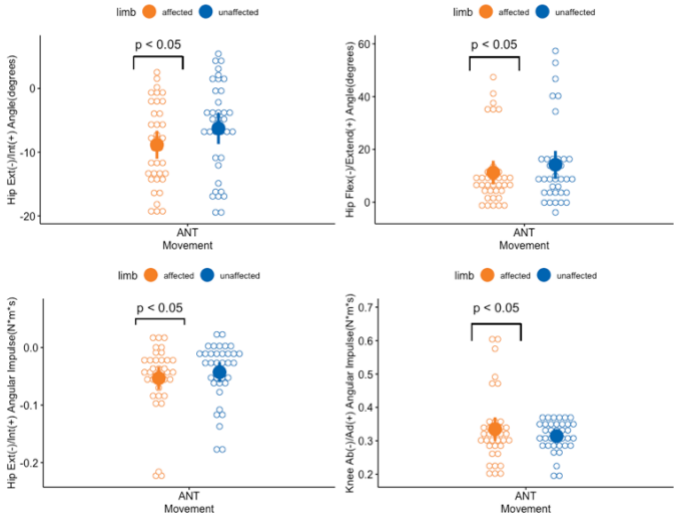

Figure 1: Mean ± 95% CI for hip and knee joint angles and joint angular impulse centered at ± 100 ms at maximum reach by limb (affected, unaffected) in the YBT anterior direction.

Significance

In the anterior direction of the YBT, there were significant differences in the hip and knee joint angular impulses at maximum reach in the affected limb in patients several years post ACLR. There were significant differences in hip joint angles in the affected limb. Continued dynamic stability testing needs to occur post ACLR to identify limb asymmetries and prevent future knee injuries.

Acknowledgements

We would like to thank the University of Texas at Arlington, and all the participants that volunteered for this study.

References

1. Brumitt J, et al. JSAMS, 22:1309-1313, 2019.
2. Cervenka J, et al. *IJES* 11: 817-826, 2018.
3. Hudson C, et al. Phys Ther Sport, 22:61-66, 2016.
4. Plisky P, et al. J Orthop Sports Ther, 36:911-919, 2006.
5. Shaffer SW, et al. Military Med, 178:1264-1270, 2013.
6. Hewett TE, et al. Am J Sports Med, 33:492-501, 2005.

Fiber Splay Obscures Macroscopic Mechanical Measurements of Ligament Stiffness: Implications for ACL Graft Selection

Callan Luetkemeyer[1], Ryan Rosario[1], Jonathan Estrada[1], and Ellen Arruda[1]
[1]Department of Mechanical Engineering, University of Michigan, Ann Arbor, MI
Email: cmluetke@umich.edu

Introduction

Understanding the material properties of ligaments and tendons is important for graft selection, tissue engineered graft design, and computational modeling. However, despite decades of research, even basic material properties like fiber tangent modulus (slope of the uniaxial stress-strain curve) elude scientific consensus. For example, the middle third of a patient's patellar tendon (PT) is a commonly used graft for reconstruction of the anterior cruciate ligament (ACL), but it is debated whether PT material properties are sufficiently similar. Prevailing opinion considers the PT to be a stiffer material than the ACL, since several studies comparing the two have reported a larger tangent modulus for the PT graft [1,2]. Still, others have reported conflicting evidence [3,4].

Collagen fibers tend to spread out, or splay, near the ligament-bone interface. In this study, the influence of fiber splay on the measured (apparent) tangent modulus of the ovine PT and anteromedial (AM) and posterolateral (PL) bundles of the ACL was investigated using experimental, analytical, and computational methods.

Methods

An idealized analytical model of fiber splay was created using the quantities shown in Fig. 1a to describe the splay geometry. Fibers were assumed to be linear elastic. A mathematical relationship between apparent (grip-to-grip) tangent modulus and true material modulus was derived, which we called the "splay ratio."

Results were enhanced with a finite element (FE) model (using material properties published by Marchi et al. [5]) and experimental measurements, depicted in Fig. 1b. Briefly, bone-ligament-bone samples were loaded uniaxially at 0.1 mm/s. Fascicles were removed from the outer edges of the specimen to yield a larger splay ratio, and the mechanical test was repeated. This was repeated 2-4 times to determine the effect of splay ratio on apparent tangent modulus.

Results and Discussion

The analytical model revealed a geometric relationship between the apparent tangent modulus and true material modulus, which we called the splay ratio $\left(\frac{L_0}{w_{max}-w_{min}}\frac{w_{max}}{w_{min}}\right)$. The model predicted that differences in fiber splay geometry would yield different fiber recruitment patterns (see Fig. 1a), causing the PT graft to appear stiffer and more linear than the ACL bundles.

Experimental results confirmed that the apparent tangent modulus increased with increasing splay ratio for the ovine PT and both ACL bundles. The effect of splay geometry on the macroscopic stress-strain curve is illustrated by data collected for a single PT sample in Fig. 1c. As the most splayed collagen fascicles were removed, the average stress in the ligament was larger at the same macroscopic displacement (see traction distribution f in Fig. 1a). Experimentally measured apparent tangent moduli at 5% grip-to-grip strain are plotted against splay ratio for the PT and both ACL bundles in Fig. 1d. Linear and nonlinear regression analysis indicated that the relationship was highly significant, with $p<0.01$ for each group. The 3D FE model produced similar results. Notably, the PT was more compliant than both ACL bundles for similar splay ratios.

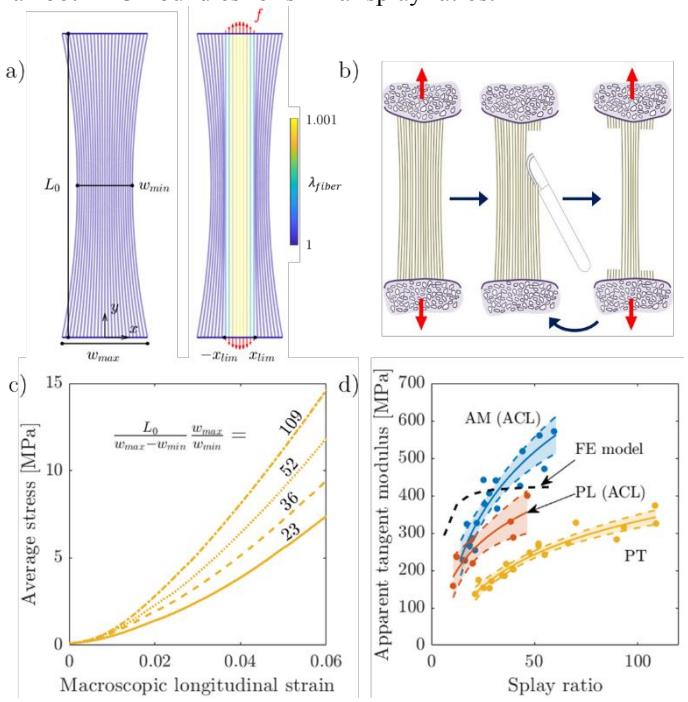

Figure 1: A simplified analytical model (a) was used to derive a relationship between apparent and true material modulus (splay ratio). Uniaxial mechanical tests were performed at multiple splay ratios (b) to examine the validity of the model. Experimental results show that apparent material stiffness increases with increasing splay ratio for the ovine PT (c), and both bundles of the ACL (d).

Significance

Material properties, by definition, are independent of specimen geometry. Therefore, the results of this study suggest that material properties of ligaments are likely not identifiable with macroscopic stress-strain measurements.

The current results suggest that the PT is a more compliant material than the ACL bundles. However, the PT graft (middle third of the PT) is probably a stiffer structure than the ACL. This raises an important question: does an ACL graft need to mimic the a) native ACL material properties, b) force-extension relationship, or c) both? If true material properties are of interest (i.e. for computational modeling), strain heterogeneity can be taken into account with full-field mechanics methods [6].

Acknowledgments

This material was funded by the NSF GRFP Grant No. 1256260.

References

1. Butler, et al. *J Biomech*, 19 (6): 425-432, 1986.
2. Danto, et al. *J Orthop Res*, 11 (1): 58-67, 1993.
3. Butler, et al. *J Orthop Res*, 7 (1): 68-79, 1989.
4. Ristaniemi, et al. *J Biomech*, 79: 31-38, 2018.
5. Marchi, et al. IJSS, 138: 245-263, 2018.
6. Promma, et al. *IJSS*, 46 (3-4): 698-715, 2009.

Kinematics of the foot sesamoids in a cadaver model during simulated activities

Eric Thorhauer,[1,2] Mackenzie French,[1,4] Tadashi Kimura,[1,5] Bruce J. Sangeorzan,[1,3] and William R. Ledoux[1,2,3]
[1]RR&D Center for Limb Loss and MoBility (CLiMB), VA Puget Sound, Seattle, WA; Departments of [2]Mechanical Engineering and [3]Orthopaedics & Sports Medicine, [4]School of Medicine, University of Washington, Seattle, WA; [5]Department of Orthopaedic Surgery, The Jikei University School of Medicine, Tokyo, Japan.
email: ericthor@uw.edu

Introduction

The foot sesamoid bones act as essential shock absorbers, metatarsal head protectors, and tendon moment arm amplifiers during gait. Given these important roles, they are involved directly or indirectly in several toe pathologies, making their study an area of clinical interest [1]. However, due to difficulties in imaging these small bones, 3D kinematic data of normative sesamoid motion is sparse [2]. Additionally, with the recent increased interest in weight-bearing cone-beam computed tomography (CT), we sought to test the feasibility of using a low-dose scanner for reconstructing the sesamoid motion of the great toe. The primary goal of this project was to quantify the normative motion of the tibial and fibular sesamoids in a series of controlled cadaveric experiments.

Methods

Twelve fresh human foot and ankle specimens were prepared and tested in a custom biomechanical testing apparatus assembled around a pedCAT (Curvebeam, USA) weight-bearing cone-beam CT scanner. The device applied axial half-bodyweight load and six tendon forces to produce a range of first metatarsophalangeal (MTPJ1) extension motion in both 1) a standing position and 2) heel rise (simulating terminal stance of gait). Specimens were mechanically loaded into seven poses between a neutral foot position and maximum toe extension. At each static pose, a low-dose CT scan was acquired and used to derive the bone kinematics and anatomical coordinate systems. Coordinate systems were based on distal metatarsal geometry and used to scale motion between specimens of different sizes.

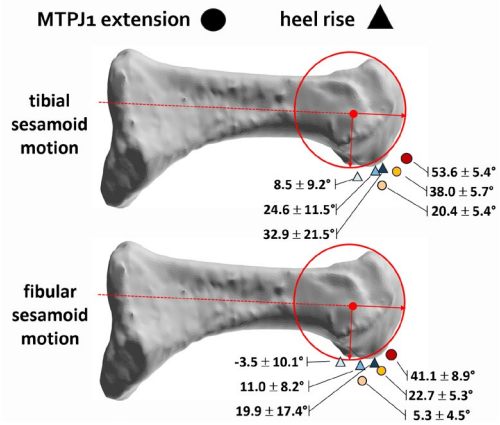

Figure 1: Sagittal plane sesamoid motions for MTPJ1 extension and heel rise positions expressed in a distal metatarsal coordinate system for three poses: neutral, intermediate, and maximum MTPJ1 extension.

Results and Discussion

Both sesamoids moved anterodorsally with toe extension, as expected (Figure 1). Compared to the fibular sesamoid, the tibial sesamoids rotated about the metatarsal medial-lateral axis roughly 12 degrees more in the sagittal plane during heel rise to cover more of the distal metatarsal head (Figure 1). This is most likely related to the more medially directed passage of load through the plantar aspect of the foot during normal gait.

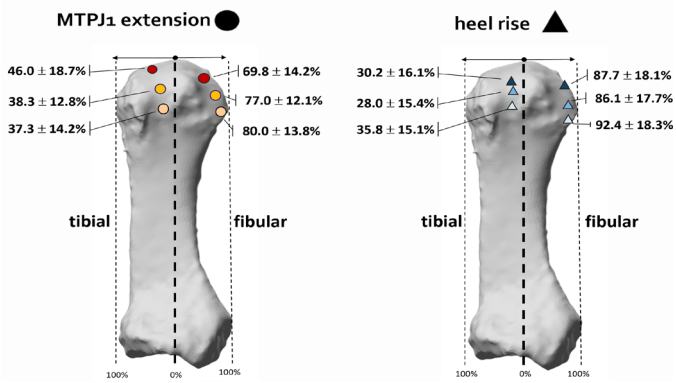

Figure 2: Medial-lateral sesamoid motions for MTPJ1 extension and heel rise positions expressed as a percentage of the metatarsal width for three poses: neutral, intermediate, and maximum MTPJ1 extension.

Along the medial-lateral direction (Figure 2), the sesamoids track together, medially with extension of the MTPJ1. Under the larger axial loading of heel rise, the sesamoids have less medial motion, moving in a plane closer to true sagittal. During heel rise, both sesamoids were shifted more laterally relative to the extension activity; however, the fibular sesamoids shifted to the most lateral margin of its compartment throughout the motion. This apparent shift is likely from the medially-moving metatarsal head with increasing axial load [3]. Contact at the less congruent margins of the joint may put the sesamoid at risk for subluxation.

Significance

The anatomical location and role of the sesamoids make them interesting, but challenging bones to quantify kinematically with imaging. This study demonstrated that low-dose weight-bearing CT scanning could be used to quantify 3D sesamoid motion. The motion patterns of the sesamoids were distinct for each simulated activity. Proper deployment of the sesamoids is essential to the protection of the articular surfaces and for efficient gait. Further investigations into sesamoid-metatarsal joint congruity, morphology, and the feasibility of tracking in vivo sesamoid motion using biplane fluoroscopy are underway. These kinematic data may provide a basis of comparison for clinical diagnosis of sesamoid dysfunction or elucidate how MTPJ1 replacement designs could be improved by considering the contributions of sesamoids to great toe stability and function.

Acknowledgments

Dept. of Veterans Affairs grant RX002357; University of Washington Medical School Scholarship of Discovery Program.

References

[1] Leventen E., Clin. Orthop. Relat. Res, 269:236-40, 1991.
[2] Jamal B., Foot Ankle Surg, 21:22-25, 2015.
[3] Geng X., Foot Angle Surg, 55(1):136-9, 2016.

Iliotibial Band Wave Speed Modulates with Hip Abduction Moments

Stephanie G. Cone.[1], Josh D. Roth[1,2], and Darryl G. Thelen[1]
[1]Department of Mechanical Engineering, University of Wisconsin – Madison, Madison, WI
[2]Department of Orthopedics and Rehabilitation, University of Wisconsin – Madison, Madison, WI
Email: sgcone@wisc.edu

Introduction

The iliotibial (IT) band is a long, complex structure extending proximally from the tensor fascia latae, the gluteus maximus, and the iliac crest and inserting distally primarily on to Gerdy's tubercle on the proximal tibia. As such, active modulation of the IT band is believed to generate abduction and flexion torques at the hip. Inherent stiffness of the IT band may play an important role in providing passive anterolateral stability about the knee. While such mechanical roles are presumed based on anatomy and modelling efforts [1], it is challenging to evaluate *in vivo* IT band loading. Shear wave tensiometry provides a potential solution, given the relationship that exists between wave propagation speed and axial tissue loading in tendons [2]. The objective of this exploratory study was to evaluate whether tensimoters could track IT band wave speed during isometric hip abduction. We also measured IT band wave speeds during walking and running, and compared it to nominal hip abduction torque patterns observed in such tasks.

Methods

Shear wave tensiometers were secured on the IT band approximately 5-10 cm above the femoral condyles unilaterally on 6 healthy adults (3M/3F). Shear wave speeds were measured from the IT band during a standing, isometric hip abduction task. External loads were collected from a uniaxial load cell secured to a cuff about the ankle. Ten second trials of the hip abduction task were performed cyclically in triplicate.

Linear regressions between hip abduction torque and wave speed were performed on individual trials, and goodness of fit was assessed as R^2 values. Multi-way ANOVA tests were performed for the slope of each linear regression with trial, subject, and task as main effects. An overall p-value of 0.05 was considered significant.

Results and Discussion

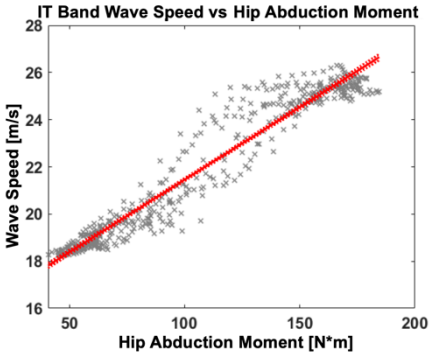

Individual Subject Relationships	
Slope (s/kg*m)	R^2
0.061±0.005	0.934
0.030±0.007	0.407
0.020±0.005	0.360
0.074±0.005	0.710
0.093±0.010	0.587
0.341±0.040	0.715

Figure 1: IT band wave speed modulated with hip abduction moment. Linear regression was used to assess the slope of the wave speed-moment relationship.

IT band wave speeds consistently increased with hip abduction moment for all subjects. The slope of the wave speed-moment relationship was relatively consistent across repeat tasks, but varied considerably ($p<0.05$) across subjects (Figure 1). Linearity of the relationship was also variable, with R^2 ranging from 0.36 to 0.93. Variability was primarily attributable to a subset of individuals exhibiting considerably lower wave speed magnitudes, which could have resulted from differences in ITB band morphology, sensor placement and or wave propagation through subcutaneous tissues. Ascertaining the relative influence of such factors will be important in calibrating the wave speed-tension relationship for individuals.

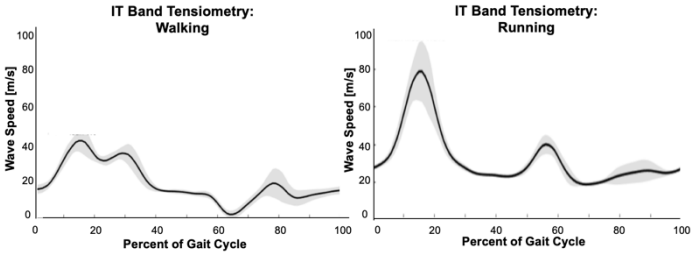

Figure 2: IT band wave speeds measured during walking and running reveal task-specific differences in loading patterns within the tissue both in magnitude and timing. Lines and shaded regions represent mean ± standard deviation over 10 second trials.

IT band wavespeeds during walking and running reveal highly repeatable patterns over the gait cycle (Figure 2). Phases of higher wave speeds during stance are similar to hip abduction moment as ascertained from traditional motion analysis. These results suggest that shear wave tensiometry provides a unique opportunity to ascertain functional IT band loading during walking, running and other locomotor tasks.

Significance

This works shows that shear wave tensiometry may provide a unique opportunity assessing the functional *in vivo* behaviour of the IT band, a complex tissue which is traditionally difficult to study. Tensiometry could provide data for evaluating model predictions of IT band loading, and be used to evaluate IT band function in both healthy and pathologic cases. Potential applications include the evaluation of IT band syndrome in runners, and investigations of orthopaedic procedures that alter IT band geometry (e.g. all-epiphyseal ACL reconstruction) [3].

Acknowledgments

We would like to acknowledge funding from the NIH (NICHD HD092697).

References

[1] Eng CM et al. (2015). *J Biomech;* 48: 3341.
[2] Martin JA et al. (2018). *Nat Commun;* 9: 1592.
[3] Fredericson M et al. (2000). *Clin J Sports Med;* 10: 169.
[4] Kocher MS et al. (2006). *J Bone Joint Surg Am;* 88: 283.

Hamstrings Training Program improves Drop Vertical Jump performance and efficacy of movement in female athletes

Luca Rigamonti[1,2], Nathaniel A Bates[1], Takashi Nagai[1], Ryo Ueno[1], Rena F. Hale[1], Timothy E. Hewet[3], Nathan D Schilaty[1]
[1]Department of Orthopedic Surgery, Mayo Clinic, Rochester, MN, USA; [2]School of Medicine and Surgery, University of Milano-Bicocca, Monza, Italy; [3]Sparta Science, Menlo Park, CA, USA. Email: rigamonti.luca@mayo.edu

Introduction

Lower extremity neuromuscular training programs are utilized to decrease injury risk, with particular reference to the anterior cruciate ligament (ACL) [1]. Training is also used to enhance sports performace. Hamstrings:quadriceps strength ratio (H:Q) is an important estimate of optimal knee function as a H:Q ratio below 0.6 is associated with risk of ligament and muscular injury [2,3]. Further, higher risk of ACL injuries in females can be attributed to poor neuromuscular control and muscular balance [4]. Hamstrings-specific training programs are intended to increase muscular strength and flexibility, improve interaction with quadriceps contraction, and enhance joint movement through neuromuscular control [5]. The objective of this study was to evaluate the impact of hamstrings-specific training on jump performance and biomechanics in female basketball athletes. The hypothesis tested was that athletes who completed training would exhibit better jump performance and biomechanics than controls.

Methods

A total of 43 female high school basketball athletes underwent biomechanical evaluation both before and after their season. Subjects were divided into Control (n=17) and Trained (n=26) groups. Every athlete in the trained group was educated to carry out a specific dynamic hamstrings exercise sequence during their warm-up two times per week throughout the season. The control group did not receive any supplemental exercise beyond their standard team warm-up. The Pre and Post evaluation included drop vertical jump (DVJ) tasks. DVJs can be divided in three phases: the fisrt landing (Land1), the vertical jump (Takeoff) and the second landing (Land2). [3] Change in bodyweight (BW), jump height, vertical ground reaction force (vGRF) from each jump phase, and braking power during landing were collected from each subject. An average of three DVJ trialswas collected for each variable and used for statistical analysis (*Table 1*). The difference between Post and Pre season for each athlete was calculated (*Figure 1*), a simple t-test was used to compare Control and Trained group (P<0.05).

Results and Discussion

Jump height and flight time were both higher in the Trained group (P<0.05). Average vGRF during Land1 was higher in the Trained group, but not statistically significant (P=0.22). This is likely correlated with higher jump performace. During Land2 the vGRF was lower in the Trained group (*Figure 1*) and approached statistical significance (P=0.07). Difference in Braking Power during Land2 was significantly lower in the Trained group (P<0.05). Overall hamstrings-specific training upgraded the efficacy of the movement as jump performance improved in the Trained group without subsequent increase to vGRF on landing, which is a variable that associates with injury risk [4].

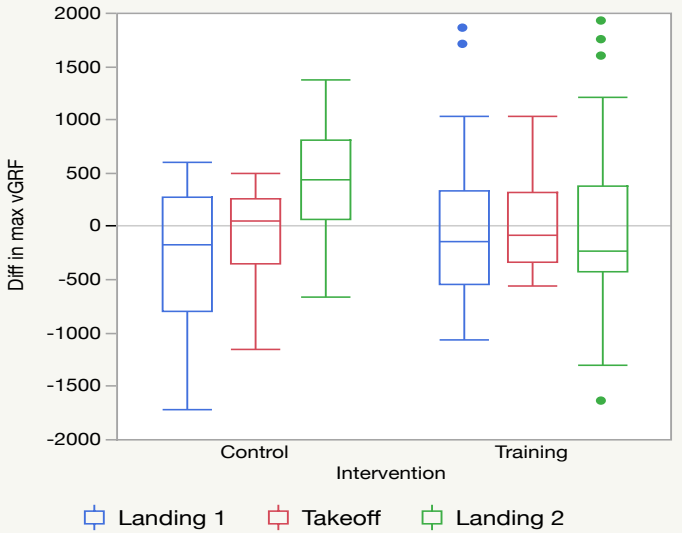

Figure 1: Difference in vGRF between Post and Pre season evaluation in the three different phases of DVJ: Land1, Takeoff and Land2. Lower vGRF in landing phases is related with lower risk of knee injury.

Significance

The current hamstrings-specific training was effective improving jump performance without increasing biomechanical ACL risk factors. Addictionally, we previously demonstrated that the same program was effective improving hamstrings strength and flexibility. Based on these findings, it is highly recommended that female athletes should incorporate hamstrings-specific exercises during their warm-up programs.

Acknowledgments

NBA/GE Collaborative Grant; NIH NIAMS R01AR055563, L30AR070273; and NICHD K12HD065987.

References

1. Webster K, Hewett T. 2018. J Orthop Res; 36(10)
2. Holocomb W, et al. 2007. J Strenght Cond Res; 21(1) 41-47
3. Myer GD, et al. 2009. Clin J Sports Med; 19(1) 3-8
4. Hewett T, et al. 2005. Am J Sports Med; 33(4) 492-501
5. Hewett T, et al. 1996. Am J Sports Med; 24(6) 765-773

Table 1: Summary statistics DVJ

Variables Mean (sd)	Control		Training		
	PRE	POST	PRE	POST	p-value
Body Weight	62.07 (15.55)	61.07 (16.15)	67.13 (12.61)	62.94 (12.49)	0,1876
Jump Height	0.32 (0.06)	0.29 (0.05)	0.28 (0.06)	0.29 (0.05)	0,0004*
vGRF Land1	2809.78 (833.12)	2530.49 (615.72)	2193.35 (671.29)	2197.37 (705.12)	0,2203
vGRF Takeoff	2169.76 (552.11)	2104.12 (499.79)	1749.57 (440.79)	1743.50 (466.58)	0,6572
vGRF Land2	3051.61 (926.99)	3476.23 (1123.97)	2869.45 (975.37)	2852.02 (861.21)	0,0666
Braking Power Land1	4919.16 (2576.60)	5228.44 (3359.93)	3036.92 (1507.98)	3160.46 (1740.75)	0,7734
Braking Power Land2	7615.93 (4141.98)	11738.13 (6531.67)	6249.31 (3269.637)	6049.74 (2918.38)	0,0003*

Ground Reaction Force Distribution Algorithm for a Kinetic Segmental Foot Model

Maxine Wold[1,2], Miriam Hwang[2], Joseph J. Krzak[2,3], Philip Voglewede[1], Gerald F. Harris[1,2], Karen Kruger[1,2]
[1]Marquette University, Milwaukee, WI, [2]Shriners Hospitals for Children, Chicago, IL, [3]Midwestern University, Downers Grove, IL
Email: maxine.wold@marquette.edu

Introduction

Determination of hindfoot, forefoot, and hallux kinetics is important in clinical gait analysis. Several current multi-segmental foot models have the capability to calculate segmental kinetics, however, the complexity of the data collection for these models limits their utility in clinical settings [1-2]. A mathematical algorithm capable of distributing the single composite ground reaction force (GRF) amongst multiple foot segments has been developed. Accurate distribution will allow for segmental kinetics to be determined without the need for additional equipment, additional time spent in the gait lab, or targeted walking by patients.

Understanding the biomechanics of the segmental foot is critical to the proper care of patients with a variety of orthopaedic impairments (e.g., cerebral palsy, Charcot-Marie-Tooth disease) and foot deformities, such as clubfoot, equinovarus, and pes planovalgus. Accurate knowledge of three-dimensional (3D) ankle (hindfoot to tibia) and mid-tarsal (distal-foot to hindfoot) kinetics during walking and other functional activities is essential for identifying the effects of such injury and disease.

Methods

Bilateral data was collected from 10 typically developing pediatric subjects (n=5 male, age=14.1 +-2.1 yrs). Motion capture data was collected using the previously validated kinematic Milwaukee Foot Model (MFM) [4] for the shank, hindfoot, forefoot, and hallux segments.

The algorithm's distribution of the GRF is based upon the three phases in existing models used in induced acceleration analyses. In these models, kinematic constraints are placed on the foot as a function of the center of pressure (COP) as developed by Lin et al (Fig 1) [5]. Phase one, corresponding to heel strike, occurs when the location of the COP is posterior to the axis created by the medial and lateral calcaneus (Axis 1). At this phase, the GRF is acting only on the hindfoot segment. Phase two, corresponding to foot flat, begins as the COP moves past Axis 1. At this point the GRF begins to distribute between the hindfoot (HF) and distal-foot (DF) (forefoot/hallux) segment based on the equation in Fig 1, where d1 is the shortest distance from Axis 1 to the COP and d2 is the shortest distance from Axis 3 to the COP, F_H is the hindfoot force, F_D is the distal-foot force, and F_T is the total force. Phase 3 occurs when the COP approaches Axis 3, d2 approaches zero, and the hindfoot raises from the ground, allotting the entire GRF to the distal foot. An adjustment was made to allocate 10% of the total force to the hindfoot, while the hindfoot is in contact with the ground; the other 90% is distributed using the above equation.

Evaluation of the GRF modeling technique was completed using an RSscan pedobarographic pressure platform synced with an AMTI (GRF) force plate to allow for simultaneous collection of force plate and plantar pressure plate data [2]. Paired t-tests were used to compare peak force, time to peak, and total force for the HF and DF segments as output by the two algorithms (α=0.05).

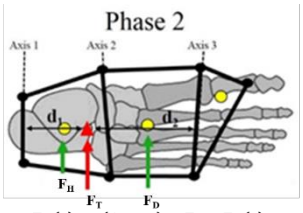

$w = \frac{d1}{d1+d2}$, $F_H(t) = (1-w) * F_T$, $F_D(t) = w * F_T$,

Figure 1: GRF distribution based on COP

Results and Discussion

Fig 2 shows an example trial comparing the force distribution algorithm to the RSscan force distribution. 102 trials were analyzed. No statistical difference was found between the algorithm and the RSscan: HF peak force (p=0.31), HF time to peak (p=0.93), HF total force (p=0.41), DF peak force (p=0.32), DF time to peak (p=0.32), or DF total force (p=0.26).

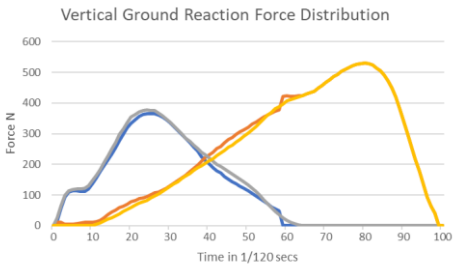

Figure 2:Dark Blue: Algorithm HF, Light Blue: RSscan HF, Dark Orange: Algorithm DF, Light Orange: RSscan DF

The results demonstrate the feasibility of dividing the ground reaction force amongst foot segments with typical motion capture protocols without the need for a plantar pressure plate. An accurate force division allows for calculation of kinetics at the mid-tarsal joint.

Significance

Understanding normal mid-tarsal function is imperative in pathologies such as plantar fasciitis [6]. Our algorithm can be used to understand the moments and power at the mid-tarsal joint. Identifying kinetic corridors for the moments at the ankle and mid-tarsal joints will allow for better comparison and discovery of differences in pathological feet, leading to better management of gait challenges. Future work will be performed to divide the distal foot into forefoot and hallux segments allowing for kinetics at the MTP joint and to validate the algorithm using a population with foot impairments.

Acknowledgments

Shriners Hospital Grant #72002 and OREC (MU/MCW).

References

[1]Bruening et al. Gait Posture 2012;35:535-540 [2] MacWilliams et al. Gait Posture 2003;17:214-224 [3] Vaughan. Human Gait 1999 [4] Long et al. J Exp Clin Med 2011;3(5):239-244 [5] Lin et al. Int J Num Meth BM Eng 2011;27(3):436-449 [6] Bolgla et al. J Athl Trning 2004;39(1):77-82

Weight Bearing CT Detects Early Changes in 3D Joint Space Width after Tibial Pilon Fractures

Erin McFadden,[1] Michael Ho,[1] Kevin Dibbern,[1] Michael Willey,[1] Julie Agel,[2]
Conor Kleweno,[2] Justin Haller,[3] Thomas Higgins,[3] J. Lawrence Marsh,[1] Donald D. Anderson[1]
[1]University of Iowa, Iowa City, IA; [2]University of Washington, Seattle, WA; [3]University of Utah, Salt Lake City, UT
erin-mcfadden@uiowa.edu

Introduction

Post-traumatic osteoarthritis (PTOA) affects over 50% of patients with tibial pilon fractures [1]. PTOA status is most often assessed using KL grade based on arthritic changes seen on plain radiographs including osteophyte formation, sclerosis, and joint space narrowing. KL grading is subjective and lacks sensitivity needed for early PTOA monitoring [2]. The lack of reliable early indicators of PTOA impedes the study of preventive measures. In-clinic weight bearing CT (WBCT) now allows 3D assessment of the ankle in a functional pose, enabling a fuller analysis of degenerative joint changes. This study investigated longitudinal changes in the tibiotalar 3D joint space width (JSW) over the course of 18 months after operative treatment of pilon fractures.

Methods

Sixteen patients with unilateral tibial pilon fractures were enrolled at three institutions under IRB approval. WBCT scans were obtained at 6, 12, and 18 months after operative fixation. 3D triangulated models of tibial and talar subchondral bone surfaces were segmented from WBCT scans using a semi-automated method and then smoothed in Geomagic Design X. The scan data and models from different follow-up times were aligned in 3D Slicer based on image intensities in the talus. Contralateral intact ankle models from 6 month scans were mirrored across a mid-sagittal plane and registered to fractured ankles as a pre-fracture (0 month) stand-in. 3D JSW was computed as the normal distance from the center of each talar mesh face to the nearest point on the tibial surface. The 6-month fractured talus was used as a common datum for all JSW measurements interpolated onto this surface mesh. The JSW distributions were analyzed by measuring the percent joint area under three distance thresholds (T1 = 2.23 mm, the mean intact JSW, T2 = 1.89 mm, 1 standard deviation below the mean, and T3 = 1.55 mm, 2 standard deviations below the mean). The change in 3D JSW (ΔJSW) was also computed for all points with JSW < 4 mm. The ΔJSW from 6 to 12 months on the intact ankles was used to assess measurement reliability.

Results and Discussion

The ΔJSW varied among fractured ankles in magnitude and timing (Figure 1). The intact ankles, used to assess reliability, had ΔJSW equal to -0.01 ± 0.11mm. The fractured ankles saw the most joint space narrowing from 6 to 12 months (ΔJSW = -0.16 ± 0.23 mm), with 14/16 experiencing narrowing. There was also a trend towards narrowing from 0 to 6 months (ΔJSW = -0.12 ± 0.30 mm), with 9/16 decreasing in JSW. From 12 to 18 months, the joints averaged widening (ΔJSW = 0.10 ± 0.19 mm) with only 4 ankles continuing to narrow.

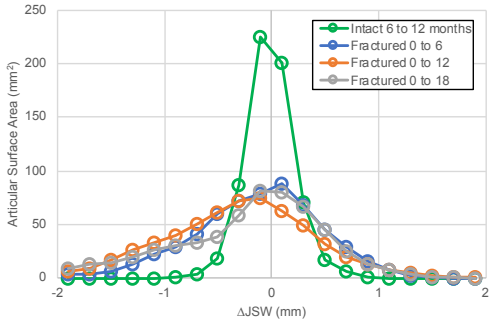

Figure 1: Areas of the articular surface on the fractured ankles have ΔJSW that show substantial narrowing of the joint space.

The intact ankles averaged the least area under all JSW thresholds (T1 = 50%, T2 = 28%, T3 = 10%) (Figure 2). The fractured ankles had similar JSW distributions at 6 months (T1 = 57%, T2 = 38%, T3 = 20%) and 18 months (T1 = 56%, T2 = 35%, T3 = 20%). The joints averaged larger areas of narrow JSW at 12 months (T1 = 65%, T2 = 48%, T3 = 31%). The larger narrowing and higher percentages of narrow regions present in the fractured ankles compared to the intact suggest progressive cartilage degeneration. Variability in the timing and magnitude of these joint changes are consistent with clinical experience that the speed and quantity of cartilage loss varies between fractures, as does PTOA incidence. Future work will examine the extent to which early 3D JSW changes correlate with PTOA development and the onset of clinical symptoms.

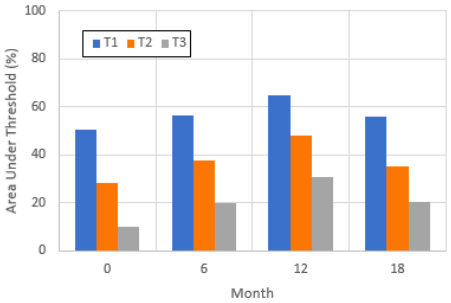

Figure 2: Fracture timepoints show larger regions of narrow joint space as compared to the intact (0 month).

Significance

WBCT scans enable longitudinal analysis of 3D JSW degeneration consistent with PTOA development. From 0 through 12 months post pilon fracture, decreases in average 3D JSW and increases in percent area with low JSW were measured.

Acknowledgments

Aided by a grant from the Orthopaedic Trauma Association. Funds for this grant were provided to the OTA for unrestricted research support by Zimmer.

References

[1] Bourne, et al. (1983). *J Trauma* **23**(7):591-6.
[2] Claessen, et al. (2016). *Knee Surg Sports Traumatol Arthrosc*. **24**:1332-7.

Custom Orthosis Prescription is Needed to Reliably Reduce Harmful Contact Stress after Intra-Articular Fracture

Bryan Tanner, Kirsten Anderson, Jason Wilken, Molly Corlett, Donald D. Anderson
University of Iowa, Iowa City, IA
Email: don-anderson@uiowa.edu

Introduction

Despite operative treatment, the joints of patients with intra-articular fractures (IAFs) of the distal tibia are often subject to elevated contact stresses from residual incongruity that increase the risk for post-traumatic osteoarthritis (PTOA) [1]. Custom dynamic orthoses (CDOs) have been shown to improve function while relieving joint pain in patients after severe lower extremity trauma [2] and may be a suitable adjunct for IAF treatment. CDOs can decrease load transfer across the tibiotalar joint [3], but residual incongruities vary widely, so custom patient-specific prescription may be required. The goal of this study was to investigate whether a custom CDO design prescription would be needed to effectively reduce contact stress exposure in patients.

Methods

A generic musculoskeletal OpenSim model with 92 musculo-tendon actuators (gait2392 model) was scaled to model 7 patients with surgically treated ankle IAFs [4]. Generic motion data were applied to body-weight scaled models, generating ankle joint reaction forces and muscle control matching the kinematic profiles. A coordinate limit force resisting ankle flex/extension and an in-line spring for brace offloading were added to each case. For the generic brace, a rotational stiffness of 4 Nm/rad*kg, 0° neutral angle, and 6000 N/m offloading spring were used. Contact stress exposures were calculated across the segmented post-op tibial articular surfaces using discrete element analysis (DEA) [5]. Then 3 different brace design parameter combinations were tested for each case to determine the one most effective at reducing contact stress exposure compared to the generic design (Table 1). Contact stress exposure distributions were divided into 9 clinically relevant regions on the articular surface of the distal tibia to study the influence of the different CDO designs.

Results and Discussion

The generic brace design substantially reduced the max contact stress exposure in nearly all cases, with the average reduction being 31.5% (Figure 1). The use of a case-specific custom brace design reduced the contact stress exposure an additional 3%, on average, but in some cases the benefit was more substantial, approaching a 20% futher reduction in some regions.

Figure 1: Reduction in contact stress exposure for the generic CDO, averaged over the 7 cases that were studied.

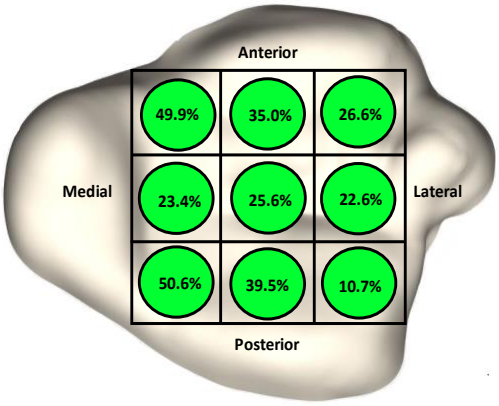

Significance

The data suggest that different brace designs can more or less effectively reduce contact stress exposure at the tibio-talar joint. A single generic brace can predictably reduce contact stress exposure, but differing parameters are necessary to directly address the elevated joint contact stresses of individual patients. Elevated joint contact stress has been linked with an increased risk of PTOA, which if allowed to progress, has damaging affects further down the road. This study provides evidence that custom CDOs would be more effective than generic CDOs in relieving joint contact stress and mitigating PTOA, when regarding the population of IAF patients.

Acknowledgments

Work supported by the Department of Defense, through the Peer Reviewed Medical Research Program, under Award No. W81XWH-18-1-0658. Helpful guidance from Anne Silverman is also gratefully acknowledged.

References

[1] Anderson et al. (2011). *J Orthop Res* **29**(1):33-9.
[2] Patzkowski et al. (2012). *J Bone Joint Surg* **94**:507-15.
[3] Stewart et al. (2017). *41st Annual ASB.* Paper#T6E_1.
[4] Delp et al. (2007). *IEEE Trans Biomed Eng* **54**(11):1940-50.
[5] Kern, Anderson. (2015). *J Biomech* **48**:3427-32.

Table 1: Different brace elements used for custom bracing

	Case 1	Case 2	Case 3	Case 4	Case 5	Case 6	Case 7
Rotational Stiffness (Nm/rad*kg)	4	3.5	5	5.5	5	6	6
Neutral Angle (°)	1	-1.5	-1	1	1	1.5	0
Offloading Stiffness (N/m)	5500	6500	7000	6800	7000	6900	6300

Medio-Lateral Ankle Fluency In People With Chronic Ankle Instability During Dynamic Movement Trials

Nolan King, SPT[1], Tarang Jain, PT, DPT, PhD[2]
Physical Therapy and Athletic Training, Northern Arizona University, Flagstaff, AZ
Email: Tarang.Jain@nau.edu

Introduction

Ankle sprains are a common injury that occurs in the athletic as well as general population. While ankle sprains tend to be discounted in the general public, they have been shown to significantly alter mobility and lifestyle, which increases the risk of developing osteoarthritis after an initial ankle injury.[1] Chronic ankle instability (CAI) is defined as a presence of ankle "giving way" and a feeling of instability that is present for a minimum of one year.[2] CAI has been shown to disrupt postural stablity and neuromuscualr control, and may affect ankle dorsiflexion and fluency during running and jumping activities.[1,3]

Deficits in neuromuscular control in individuals with CAI due to damage to the mechanoreceptors in the ligaments and possibly the muscle spindles have been well documented in the literature.[1,3,4] Specifically, the poor neuromuscular control of the peroneus longus and peroneus brevis is prevalent in those that develop CAI.[4] Our study aims to determine the difference in medio-lateral displacement at the ankle joint during dynamic movement tests in subjects with chronic ankle instability compared to healthy individuals. We hypothesized that people with CAI would demonstrate reduced medio-lateral ankle control compared to healthy controls.

Methods

18 subjects participated in a set of three dynamic movement tests (Table-1). The Cumberland Ankle Instability Tool was used to determine CAI in participants with a cutoff score of less than 25 indicting participants with CAI.[5] For the drop vertical jump (DVJ) test, the subject dropped from a stationary box and immediately upon landing jumped as high as possible vertically and recover on both feet. In the single leg drop (SLD) test the individual hopped off on one foot and landed on the opposite foot. For the crossover drop (COD) test the individual hopped laterally, landing on the opposite leg. All testing was performed in the Human Performance Lab, Northern Arizona Univesity and was approved through the Institutional Review Borad.

Kinematic data were collected at 300 Hz using an eight camera VICON motion analysis system (Oxford Metrics Group Ltd., UK). Reflective markers were placed using the 'Plug-in-Gait' full body marker set. In some trials the the missing data were filled using a custom written program in Vicon BodyBuilder for Biomechanics. Inverse dynamics calculations were performed within VICON Nexus software and data were further processed and analyzed in Matlab R2019a (The Mathworks Inc., USA). Fluency of the ankle movement on the involved/dominant side in the coronal plane was calculated by a method adapted from Smeulders et al. (2001).[6] Two-way Analysis of Variance (ANOVA) with a polynomial first order (linear) contrast post hoc test was used to compare the effects of SLD, COD, and DVJ trials on mean fluency values between the CAI and healthy group. An a priori α-value of 0.05 was used to determine statistical significance for all tests.

	CAI group (n=10)	Healthy group (n=9)
Age, y	25.4 (2.3)	25.8 (7.4)
Gender, M/F	5/5	4/5
Height, cm	167.4 (8.2)	169.1 (11.9)
Mass, kg	66. (7.8)	62.8 (11.6)
CAIT Questionnaire score	18.1 (3.0)	29.3 (0.7)
Ankle 'giving-way' in past 6 months	8.1 (6.1)	0.2 (0.4)

CAIT – Cumberland Ankle Instability Questionnaire
Values are mean (std dev) unless otherwise indicated

Table 1: Demographics of the study prticipants

Results and Discussion

The subject groups were reasonably matched for age, gender, height, mass and ranges of motion (Table 1). CAI group scored on average lower in the CAIT questionnaire, indicating that they had lower ankle function. Fluency of the ankle movement in the coronal plane was significantly different between groups (p=0.023) and demonstrated a significant linear contrast (COD: CAI - 0.10±0.32s vs healthy - 0.19±0.23s (p=.002); SLD: CAI - 0.19±0.49s vs healthy - 0.24±0.28s (p=.06); DVJ: CAI - 0.23±0.29s vs healthy - 0.22±0.23 (p=.41). These preliminary findings suggest that ankle movement in patients with CAI was least fluent in COD and most fluent in DVJ. Patients with CAI also showed larger medio-lateral ankle joint center excursions, which indicates lack of ankle control.

These findings can be interpreted as insufficient motor control during the COD task, or it could be interpreted as a protective strategy, utilized by patients with CAI to avoid further injury. Ankle fluency asymmetry or maladaptive landing technique may explain elevated re-injury rates and the presence of chronic morbidities observed in patients with ankle sprain. The lack of control could arguably result in loading of the articular cartilage on locations that are normally not loaded, which may implicate early development of osteoarthritis.

Significance

To our knowledge, there is no previous literature evaluating ankle coronal plane control during dynamic movement trials in patients with CAI. Ankle rehabilitation strategies should target medio-lateral ankle control to develop optimal neuromuscular control and perturbation exercises for patients with CAI.

References

1 Doherty, C. *et al*. *Sports Med* **44**, 123-140, (2014).
2 Gribble, P. A. *et al*. *J Orthop Sports Phys Ther* **43**, 585-591, (2013).
3 McLeod, M. M. *et al*. *J Athl Train* **50**, 847-853, (2015).
4 Sierra-Guzman, R. *et al*. J. *Clin Biomech (Bristol, Avon)* **54**, 28-33, (2018).
5 Wright, C. J. *et al*. *Arch. Phys. Med. Rehabil*., (2014).
6 Smeulders, M. J. *et al*. *Clin. Rehabil*. **15**, 133-141, (2001).

Higher Volar Tilt and Volar Offset of a Total Wrist Arthroplasty are Associated with Larger Wrist Range-Of-Motion

Bardiya Akhbari[1], Amy Morton[2], Kalpit Shah[1], Janine Molino[2], Douglas Moore[2], Arnold-Peter Weiss[2], Scott Wolfe[3], Joseph Crisco[1,2]
[1]Brown University, Providence, RI, [2]Rhode Island Hospital, Providence, RI, [3]Hospital for Special Surgery, New York, NY
Email: bardiya_akhbari@brown.edu

Introduction

Total Wrist Arthroplasty (TWA) has been used in fewer patients compared to knee and hip arthroplasty mostly due to its high complication rates.[1] Alignment of the knee and hip prostheses strongly correlate with implant performance, and malalignment is a known contributor to implant failure. For TWA, optimal implant alignment has not been defined. More importantly, the effect of implant malalignment on range-of-motion (ROM) has not been studied. Therefore, the aims of this study were to define the alignment of TWA components using three-dimensional (3D) analysis and to determine the influence of alignment on ROM *in-vivo*.

Methods

Six osteoarthritic patients (74.7 ± 5.6 yrs, 2F, 2R) with wrist replacements (Freedom® size 2, Integra LifeSciences) were recruited after IRB approval. None of the patients had a prior radius fracture that would cause the change in radii alignment.

A single CT scan (Lightspeed® 16) was acquired of each wrist (80 kVp/80 mA; 0.39 × 0.39 × 0.625mm^3), and surface models of the carpal component, third metacarpal, and resected radius were generated using Mimics (Materialise).[2,3] A digital model of the radial component was generated using a 3D surface scanner (Artec Space Spider™). Orthogonal coordinate systems were defined for the radial and carpal components based upon geometrical features. Rotational alignments were defined as the orientation between bone's coordinate system and the component's coordinate system as volar-dorsal tilt (VDT) and radial-ulnar tilt (Figure 1). Translational alignments were defined in the same views (e.g. volar-dorsal offset [VDO])

Biplanar videoradiography (75 kV/80 mA, 200Hz) was used to capture dynamic implant motion while each study participant performed active tasks of wrist motion: flexion-extension, radial-ulnar deviation, and circumduction. ROM in each direction of flexion, extension, radial, and ulnar deviation were calculated by tracking the implants using a 2D to 3D registration software (Autoscoper).[2] Motions were described relative to the neutral pose.

Linear regression was used (α-level of 0.10 due to small sample size) to determine the relationship between ROM and alignment parameters.

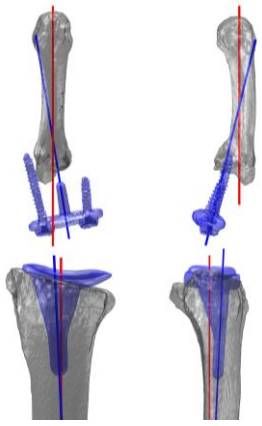

Figure 1. The alignment was defined by radial/ulnar tilt or offset (left) and volar/-dorsal tilt or offset (right).

Results and Discussion

In our cohort, wrist ROM was 49 ± 8° in extension, 27 ± 13° in flexion, 17 ± 5° in radial deviation, and 18 ± 10° in ulnar deviation. Linear regression demonstrated that flexion, radial deviation, and ulnar deviation were significantly ($p = 0.057$, 0.002, and 0.019) higher for patients with larger volar tilt of the radial component. Overall flexion-extension and radial-ulnar deviation were also correlated with the radial component's VDT ($p = 0.047$ and 0.015) and VDO ($p = 0.055$ and 0.050) indicating an increase of 3.7° and 1.6° per degree increase in volar tilt, and 10.8° and 4.2° increase in ROM for every millimeter of volar offset (Figure 2). Previously, the importance of maintaining alignment to obtain good ROM outcome after distal fracture has been reported,[4] and this study reflects similar findings for TWA.

We observed correlations between volar tilt and volar offset of the radial component and ROM in flexion, radial deviation, and ulnar deviation, possibly due to reduced constraint of the polyethylene cap by the radial component when tilted volarly. Interestingly, extension was not correlated with the alignment in our cohort ($p = 0.34$), which suggests that extension is likely constrained by soft tissue envelope of the hand or post-surgical scar, and not the geometry of the implant.

This study was limited by the small cohort of 6 subjects and the single implant's design. Future studies should investigate the impact of malalignment on the functional outcomes.

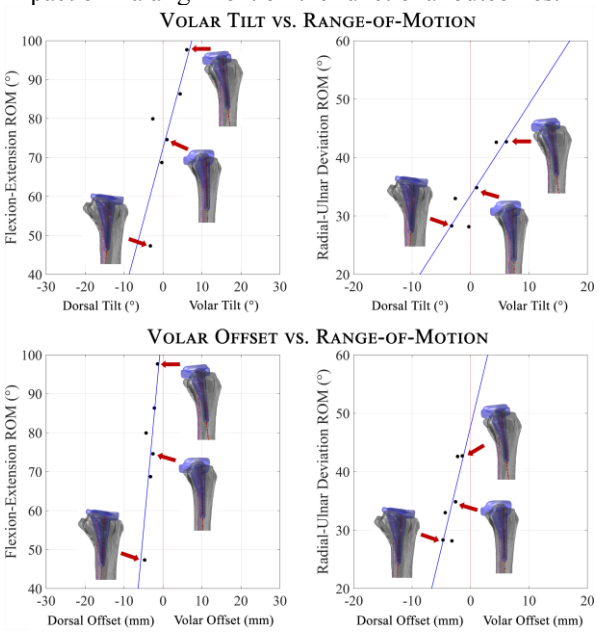

Figure 2. Overall range-of-motion increased as the radial component's volar tilt and volar offset increased.

Significance

We demonstrated that the patients who have a radial component that is more volarly tilted have a higher range of flexion-extension and radial-ulnar deviation motions.

Acknowledgments

This research was funded by NIH P30-GM122732 and AFSH.

References

[1] Melamed, 2016. *doi:* 10.1055/s-0036-1571841.
[2] Akhbari, 2019. *doi:* 10.1115/1.4042769
[3] Moore, 2007. *doi:* 10.1016/j.jbiomech.2006.10.041
[4] Perugia, 2014. *doi:* 10.1016/j.injury.2014.10.018.

Establishing an Age-Matched, Healthy Control Dataset of Joint Kinematics for Comparison to rTSA Patient Joint Kinematics

Tyler Oliver[1], Stacey J.L. Sullivan, PhD[1], Edward G. McFarland, MD[2], Victoria Lilling, MD[3], Kimberly L. Kontson, PhD[1]
[1]US FDA, CDRH, Office of Science and Engineering Laboratories, Silver Spring, MD, [2]Johns Hopkins University, Department of Orthopaedic Surgery, Baltimore, MD, [3]US FDA, CDRH, Office of Product Evaluation and Quality
Email: Kimberly.Kontson@fda.hhs.gov

Introduction

Reverse total shoulder arthroplasty (rTSA) has become an increasingly popular procedure for treating patients with rotator cuff arthropathy and glenohumeral joint disease. Past rTSA studies assessing functional changes using motion capture have used pre- and post-op comparisons, the patient's opposite shoulder, or control groups significantly below the age of the rTSA population[1-3]. A pre- and post-op comparison does not allow for a normative comparison and shoulder studies that have included a representative control population were limited to assessing controlled, in-plane motion[4]. Also, the use of the opposite shoulder may not be representative of an unaffected control[5]. Normative performance during an activity of daily living (ADL) may change with age[6] and average age of an rTSA recipient is approximately 70 years[7]. Therefore, to more accurately characterize the differences between the rTSA and the anatomic joint, a representative healthy subject population is needed. The overall goal of this study is to establish a database comprised of joint kinematics and motion path for 40 healthy, age-matched controls. Preliminary data from n = 6 age-matched, healthy controls are presented.

Methods

All aspects of this study were approved by FDA IRB and all participants gave informed consent. Twelve tasks representative of ADLs were developed from 3 validated patient reported outcome surveys (PROs). Preliminary data from six healthy participants (69.2 ± 4.9 age, 2F/4M) performing three trials of each task were collected. Thirty-three retro-reflective markers were placed on bony landmarks of each participant and tracked in 3D space using a ten-camera Vicon motion capture system. Shoulder joint kinematics were calculated using the Vicon Plug-In-Gait upper body model. Average range of motion and peak angle were calculated for each degree of freedom in the shoulder (flexion/extension, abduction/adduction, and internal/external rotation).

Table 1: Average (standard deviation) of RoM and peak angle

		Range of Motion			Peak Angle		
		Flex/Ext	Ab/Ad	Rot	Flex/Ext	Ab/Ad	Rot
Putting on a Shirt	Average (Std Dev)	70.10 (3.09)	104.38 (2.77)	90.54 (6.41)	48.36 (2.19)	113.39 (1.92)	27.92 (1.27)
Washing Opposite Shoulder		90.47 (1.49)	98.71 (4.78)	131.95 (4.46)	73.59 (1.69)	26.07 (2.18)	144.38 (2.06)
Reach Over-head		81.23 (2.13)	100.80 (1.90)	96.24 (2.76)	59.33 (1.42)	112.05 (1.52)	20.51 (1.44)

Results and Discussion

Here, we focus on three tasks: reaching overhead, washing opposite shoulder, and putting on a t-shirt. Figure 1 shows the average trajectory across all three trials for all participants (Blue) and individual trajectories (Black) for each task and shoulder degree of freedom. Table 1 shows the average and standard deviation of RoM and peak angle values.

Significance

This study will produce the first database inclusive of a wide variety of ADLs for a representative population of TSA patients using a large number of subjects to characterize shoulder motion. With characterization of the healthy control motion path during ADLs, improved understanding of the effect that rTSA implants have on user motion path and function during ADLs may inform rehabilitative outcomes for these patients as well as regulatory evaluation of these types of devices.

Acknowledgements

This project was funded by the FDA Critical Path Initiative. Disclaimer - The mention of commercial products, their sources, or their use in connection with material reported herein is not to be construed as an actual or implied endorsement of such products by DHHS.

References

[1] Langohr, et al., JSES, 2018. 27(2): p.325-332
[2] Maier, et al., Arch Orthop Trauma Surg, 2014. 134(8): p.1065-1071.
[3] Namdari, et al., JSES, 2012. 21(9): p.1177-83.
[4] Roren, et al., Musc Sci Pract, 2017. 29: p.84-90.
[5] Alta, et al., JSES, 2014. 23(9): p.1395-402.
[6] Gulde et al., Exp Brain Res, 2017. 235(5): p.1337-1348.
[7] AOANJRR, AOA: Adelaide, Australia. p. 375.

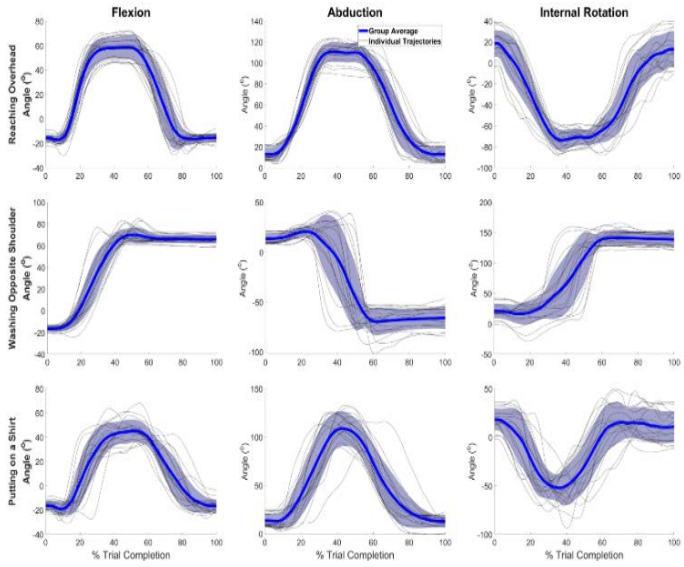

Figure 1: Average kinematic trajectories (blue) and individual trajectories of healthy participants (black)

Effects of sex and vision on shoulder postion sense

Kate A. Spitzley, Kieley Trempy, and Andrew Karduna
Orthopaedic Biomechanics Lab, Department of Human Physiology, University of Oregon, Eugene, OR, USA
Email: kspitzle@uoregon.edu

Introduction

Proprioception is a key component of injury prevention and recovery. Factors with potential influence should be examined in any instance where risk or rate of injury is high. Upper extremity pathologies comprise a high percentage of work-related musculoskeletal disease and women are at significantly higher risk than men when comparing within the same occupation [1]. While it is well known that sex differences exist in skeletal and muscular architecture and factors of motor control [2], differences in proprioception have not been fully elucidated. Further, exploration of this topic is justified by the current conflicting evidence in the field. Some assessments of sex differences in upper limb proprioception have found women to be more accurate at position matching tasks [3], whereas others have found no differences in accuracy [4]. Vision of the proprioceptive target has also varied between studies and therefore the effect has not been fully clarified. The aim of this study was to utilize a joint position sense (JPS) test to assess proprioceptive differences between females and males with and without the aid of vision. It was hypothesized that a) under both visual conditions, females would be less accurate and precise in position matching than males and b) both sexes would be less accurate and less precise without the aid of vision.

Methods

Forty (20F, 20M) healthy, right limb dominant participants completed 4 JPS trials with the right shoulder under both vision (V) and no vision (NV) conditions to a target angle of 90°. Distractor angles were added to mitigate effects of training. A fully immersive virtual reality system was used to provide visual and auditory information to participants and to collect kinematic data. Participant setup is displayed in Figure 1. During trials under the V condition, participants were able to see the position of their upper limb throughout the task, during trials under the NV condition, participants were able to see the position of their upper limb during the presentation phase but not during the replication phase. Angle of the right shoulder was recorded throughout. Independent two-sample t-tests (α=0.05) were used to determine differences between males and females in the V and NV conditions. Dependent two-sample t-tests (α=0.05) were used to determine differences between V and NV in females and males.

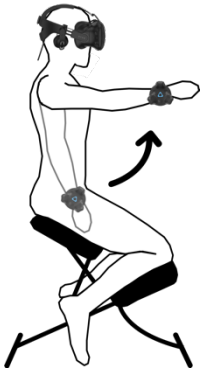

Figure 1: Participant seated in kneeling chair, VR headset with over-ear headphones fitted to their head, tracker affixed to the wrist. Faded arm outline shows starting position of JPS trial, solid arm outline shows target angle of 90°.

Results and Discussion

Under neither visual condition was a difference between sexes found in constant or absolute error, measures of accuracy (Figure 2 a,b). Under the V condition, no difference between sexes was found in variable error, measure of precision, but under NV condition females were less precise than males ($p<0.05$, Figure 2 c). These results refute hypothesis a, indicating that there is no difference in JPS accuracy between sexes and no difference in precision when vision is available. The difference seen in the NV condition indicates that vison contributes more to JPS precision in females than in males.

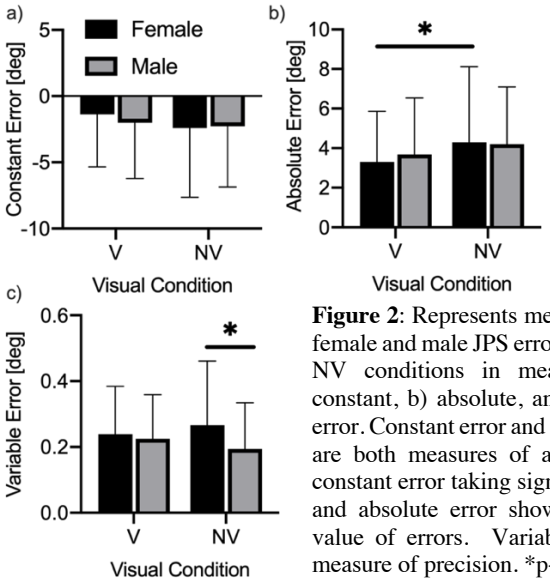

Figure 2: Represents mean and SD of female and male JPS error under V and NV conditions in measures of a) constant, b) absolute, and c) variable error. Constant error and absolute error are both measures of accuracy with constant error taking sign into account and absolute error showing absolute value of errors. Variable error is a measure of precision. *p<0.05

Within the sexes, no differences in constant and variable error were seen (Figure 2 a, c). In males, no difference in absolute error was seen, females displayed higher absolute errors in NV as compared to V conditions ($p<0.05$, Figure 2 b). These results partially refute hypothesis b, as males showed no differences regardless of visual condition whereas females were less accurate without vision than with vision when both undershoots and overshoots of the target were considered equally.

In total, these results indicate a) no sex differences in measures of proprioceptive accuracy, b) lower proprioceptive precision in females without the aid of vision, and c) lower proprioceptive accuracy in females without the aid of vision.

Significance

These findings contribute to the overall picture of sensorimotor distinctions between the sexes. While differences clearly exist in other musculoskeletal and motor control factors, proprioceptive differences are not strongly indicated by these results. However, the apparent reliance on vision in females may contribute to the design of workplace layouts and trainings.

Acknowledgments

This project was supported in part by the O'Day Fellowship in Biological Sciences and the Moshburger Endowed Fellowship.

References

[1] Larsson et al. *Best Pract Res Clin Rheu* 2007
[2] Côté. *Ergonomics* 2012
[3] Sigmundsson et al. *Sex Roles* 2007
[4] Vafadar. *BMC Musculoskelet Disord* 2015

Body Position Effect on Scapulohumeral Rhythm

Matthew J. Petersen[1], Traci Bush[2], David Stapleton[3], Vassilios Vardaxis[2,3]
[1]College of Osteopathic Medicine, [2]Department of Physical Therapy, & [3]Human Performance Lab,
Des Moines University, Des Moines, IA, United States
Email: Vassilios.Vardaxis@dmu.edu

Introduction

Dynamic motion of the shoulder complex predominately occurs at the glenohumeral (GH) and scapulothoracic (ST) joints with concurrent motion at the acromioclavicular and sternoclavicular joints [1]. Scapulohumeral rhythm (SHR) is the coordinated motion occurring at these joints during arm elevation, a clinical parameter affected in most shoulder disorders [1,2]. SHR has been described by Inman [3] as a 2:1 ratio between motion at the GH and ST joints, respectively, and since has been expanded to the illustration of the 3-D motion via three angle-angle plots for arm elevation tasks in the sagittal, scapular, and frontal plane [1] with the trunk in the upright posture (seated or standing). However, functional motion during daily living and occupational tasks, is not performed upright and requires modified/awkward postures with increased risk of shoulder pathology [4]. Body position specific patterns of muscle activation and coordination were elicited for the same task, during rehabilitation protocols on healthy volunteers [5], which may affect the SHR. Thus, this study aims to investigate the effect of seated upright, sidelying, prone, and supine body positioning on the SHR during arm (thoracohumeral) elevations in the frontal and sagittal planes.

Methods

Twenty (20) healthy male participants without any musculoskeletal problems volunteered for the study. Participants completed 5 trials of arm elevation (dominant side) in the sagittal and frontal planes at 4 different body positions (Seated, Sidelying, Prone, and Supine) to ~120 degrees while maintaining a straight arm, with palm on the plane of elevation, and thumb extended. A motion analysis system with 10-cameras (Motion Analysis Corp.) at 120 Hz was used to capture 3D data of reflective markers attached to upper-limb and torso. Reference frames were defined for the thorax, scapula, and humerus and Euler angles were used to compute positioning and 3D rotations of the scapula relative to the thorax, humerus relative to the scapula, and humerus relative to the thorax according to ISB [6].

The SHR was calculated between 16 and 105 degrees of thoracohumeral elevation as the slope between the GH and ST motion. Statistical analysis of the SHR was performed using one-way repeated measures ANOVA on body position, separate for each plane. Paired t-tests were used to assess differences across planes for each body position ($\alpha < 0.05$).

Results and Discussion

The average age and BMI of the participants were: 24.4 ±1.3 years, and 25.6 kg/m² (range 20.4 to 33.4 kg/m²) respectively. The SHR (average ±standard error) values across the 4 different body positions, for each plane separate, are shown in Figure 1. There were significant differences between body positions in the SHR for the sagittal plane arm elevations ($p < 0.001$). In the prone body position the flexion task was performed with limited ST upward rotation and the opposite was true in sidelying compared to other body positions (Figure 1, "!"). In sidelying, while performing the abduction task, the ST upward rotation was the least (reflected as SHR greater than 3:1) and was significantly lower than the flexion task (Figure 1, "*").

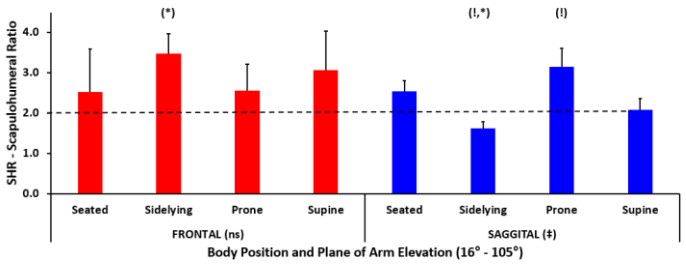

Figure 1: Mean (±SE) of the scapulohumeral ratio (SHR) calculated in 2 different planes (Frontal and Sagittal) at 4 different body positions (Seated, Sidelying, Prone, and Supine). (ns, ‡) One-way ANOVA Repeated Measures $p < 0.05$; (!) Bonferroni adjusted contrast difference from all others (within the plane) $p < 0.008$; (*) Paired t-test difference between planes $p < 0.0125$.

Interestingly, for the frontal plane elevation task the SHR was greater than 2:1 for all body positions, showing greater (non-significant) ratios for the sidelying and supine body positions. The scapula 3D rest/initial orientation also varied, with body position and task, specifically showing significant upward rotation of 11.8 ±7.2° and 14.7 ±7.8° in the supine position for the abduction and flexion tasks, respectively. Despite the considerable limitations of the SHR calculation, ignoring the ST motions in the int/external rotation and the ant/posterior tilt, it reflects differences in task and body position on the GH and ST contribution to thoracohumeral arm elevation [7]. The overall 3D GH and ST motion contribution to arm elevation has been shown to vary with task dynamics [1]. The present study underscores the gravitational vector direction effects relative to the plane of motion and the resting/initial scapular position/orientation.

Significance

Differences in the SHR were observed in non-symptomatic adults between body positions, often used for clinical tests/measures and exercises aiming to assess function and alter the rehabilitation exercise intensity. When restoration of altered kinematics is the therapeutic goal, body position and plane of elevation effects should be considered.

Acknowledgments: Iowa Osteopathic Educational Research for financial support.

References

[1] Ludewig & Reynolds (2009). *JOSPT,* 39: 90-104
[2] Veeger & van der Helm (2007). *J Biomech,* 40: 2119-29
[3] Inman et al (1944). *JBJS*, 26: 1-30
[4] Linaker (2015). *Best Prac & Res Rheum*, 29: 405-23
[5] Cools et al (2007). *Am J Sports Med*, 35: 1744-51
[6] Wu et al (2005). *J Biomech*, 38: 981-92.
[7] De Groot (1999). *Clin Biomech*, 14: 63-6

Glenoid Lateralization Increases Abduction ROM and Strength After Reverse Shoulder Arthroplasty

Clarissa LeVasseur[1], Gillian Kane[1], Alexandra S. Gabrielli[1], Albert Lin[1], and William Anderst[1]
[1]Department of Orthopaedic Surgery, University of Pittsburgh
Email: cll100@pitt.edu

Introduction

Reverse shoulder arthroplasty (RSA) is a common procedure to reduce pain and restore function in patients with rotator cuff arthropathy [1]. Clinical outcomes after RSA are favorable; however, functional outcomes still remain suboptimal. *In vitro* studies suggest that modifications in prosthesis design and surgical technique can improve range of motion and functional outcomes after RSA [1], however controversy still exists as to the best implantation technique and prosthesis geometry for maximizing shoulder function after RSA. This controversy persists due to the lack of quantitative *in vivo* kinematics to guide this debate. In order to achieve the long-term goal of improving functional outcomes after RSA, shoulder kinematics following RSA must be accurately characterized.

The aim of this study is to investigate relationships among surgical technique, prosthesis geometry and functional outcomes (kinematics and strength) after RSA. We hypothesized that lateralization would increase the total work done in the abduction plane and that humeral retroversion would alter the contact center on the glenosphere during abduction.

Methods

12 RSA patients consented to participate in this ongoing IRB approved study (7M, 5F, average age: 66.8±6.3 yrs., time since surgery: 2.5±1.2 yrs.). Lateralization and humeral retroversion were recorded from surgical notes. Isokinetic strength was recorded across each participant's full range of motion for flexion/extension, ab/adduction, and internal/external rotation at 30°/second on a Biodex machine. Additionally, participants performed 3 trials of abduction in the scapular plane while synchronized biplane radiographs of the shoulder were collected at 50 image/s for 2s. Subject-specific models of the humerus and scapula with their respective implants were created from CT scans and matched to the biplane radiographs to measure scapular and humerus motion with sub-millimeter accuracy [2] for 7 of the 12 participants thus far. A 3D CAD model of the polyethylene insert, provided by the manufacturer, was fit into the CT-based humeral tray. The motion of the center of contact between the polyethylene and the glenosphere was calculated. A Spearman's correlation was used to evaluate the relationship between lateralization and peak torque, ROM, and total work done. Significance was set at $p < 0.05$.

Results and Discussion

Six participants had no lateralization and 6 had lateralization between 2mm and 7mm. Retroversion ranged from 20° to 40°.

There was a moderate correlation between the total work done during abduction and lateralization (Table 1, $p = 0.04$), as well as between abduction/adduction ROM and lateralization (Table 1, $p = 0.02$). Total work done and ROM for flexion/extension and internal/external rotation were weakly to moderately correlated with lateralization, however, neither were significant (Table 1, all $p > 0.055$). Our result of a positive correlation between lateralization and abduction ROM confirms previous studies that have found that lateralization increases abduction ROM [3].

Table 1. Correlations between lateralization and strength or kinematics. Bold values indicate significance.

	Peak Torque (Nm)	Total Work (J)	ROM (°)
Abduction	$\rho = 0.45$	$\rho = \mathbf{0.62}$	$\rho = \mathbf{0.67}$
Adduction	$\rho = 0.32$	$\rho = \mathbf{0.57}$	
Flexion	$\rho = 0.36$	$\rho = 0.42$	$\rho = 0.49$
Extension	$\rho = 0.19$	$\rho = 0.54$	
External Rot	$\rho = 0.54$	$\rho = 0.42$	$\rho = 0.51$
Internal Rot	$\rho = 0.25$	$\rho = 0.39$	

The center of contact between the polyethylene insert and the glenosphere varied more in the AP direction than the SI direction between subjects (Figure 1). Subject 2, who had a retroversion angle of 40°, demonstrated a more superior center of contact at similar abduction angles compared to the other six subjects who all had retroversion angles of 20° (Figure 1C). Additional subjects with a retroversion of 40° are needed to confirm that retroversion affects implant contact patterns.

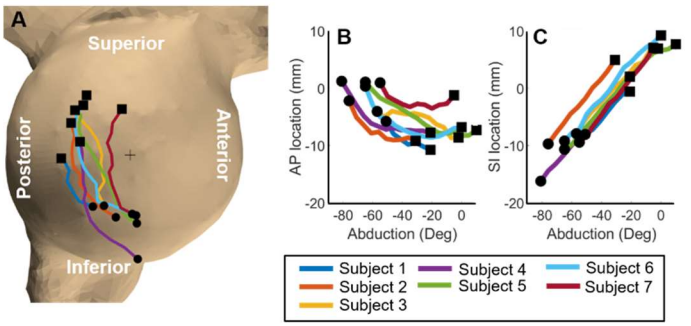

Figure 1. (A) Center of polyethylene contact on the glenosphere during abduction. Circles indicate the start of data collection in lower abduction angles while squares represent maximum abduction. **(B)** AP location of the center of contact with respect to abduction angle. **(C)** SI location of the center of contact with respect to abduction angle.

Significance

This novel dataset improves our understanding of how prosthesis design and surgical technique affect in vivo functional outcome after reverse shoulder arthroplasty. This information help surgeons optimize patient functional outcomes.

Acknowledgments

This work was supported by NIH grant R03AG064417 and by the Pittsburgh Foundation.

References

[1] Churchill and Garrigues, (2016). *JBJS Reviews.*
[2] Bey et al. (2006) *J Biomech*.
[3] Ladermann et al. (2019). *Bone Joint Res.*

Glenohumeral Rotation and Strength Characteristics Related to Shoulder Stress in Collegiate Pitchers

Aaron Trunt, M.S.[1,2], and Lisa MacFadden, Ph.D.[1,2]
[1]University of South Dakota Department of Biomedical Engineering, Sioux Falls, SD
[2]Sanford Sports Science Institute, Sanford Health, Sioux Falls, SD
Email: aaron.trunt@coyotes.usd.edu

Introduction

Overhead athletes are a specific subset of athletes whose sport requires a majority of the movement to occur with the upper arm above the head. Due to the nature of these sports and the repetitive motions and stresses associated with them, overhead athletes are prone to upper extremity injuries[1]. The instability of the shoulder complex coupled with the fact some of these motions, such as the baseball pitch, produce the highest measured velocities recorded in humans place the shoulder at particular risk of injury in overhead athletes. In an effort to mitigate the risk of injury and improve performance in the given sport, an overhead athlete's shoulder undergoes well-documented orthopedic and physiological adaptions[2].

Specifically, baseball pitchers commonly present altered passive range of motion (ROM) and rotator cuff strength in the dominant arm when compared to the non-dominant side[2]. Recent studies have suggested clinical measures of ROM and strength may be related to the amount of stress a pitcher shoulder is subject to during a pitch[3]. The purpose of this study was to describe the relationship shoulder ROM and rotator cuff strength have with shoulder kinetics in the baseball pitch.

Methods

This study was approved by the Sanford Health Institutional Review Board. Twenty-one (n=21) collegiate baseball pitchers participated in the study. Data was collected on two separate occasions prior to the start of the collegiate season. The first session was a clinical evaluation where subject height, weight, arm length, shoulder passive ROM, and rotator cuff strength were collected. After establishing anthropometrics and a brief warmup, glenohumeral internal rotation (IR) and external rotation (ER) was measured passively for each arm using established methods[2]. Isokinetic external and internal rotator cuff strength was measured both eccentrically and concentrically for each arm using a Biodex at three separate speeds (90, 180, and 270 degrees/sec). Peak torque was collected from the Biodex for eccentric and concentric actions of both the external and internal rotator cuff muscles for each arm at all three speeds. Subjects then returned approximately two weeks later for a bullpen session where motion capture data was collected in a biomechanics lab. Fifty markers were applied to each pitcher and tracked with a twelve camera Qualisys motion capture system operating at 300 Hz. Pitchers threw ten fastballs from an artificial mound at a target approximately the size of a strike zone 45 feet from the rubber. The five fastest pitches for strikes were selected and used for analysis.

Biomechanics data was computed in Visual 3D. Pitching shoulder joint moments and forces were estimated in the shoulder joint coordinate system in accordance with ISB recommendations. Kinetics and isokinetic data were normalized to anthropometrics prior to analysis. Peak IR torque and peak shoulder distraction force were the dependent variables chosen as estimates of the amount of stress the shoulder experiences throughout the pitch. Linear regression models were used to assess the relationship between the clinical data and shoulder kinetics (α=0.05).

Results and Discussion

None of the ROM data collected was significantly related to shoulder stress in the pitch. However, a trend was exhibited when comparing peak shoulder IR torque and the amount of increased ER the shoulder undergoes during the cocking phase (active ER) relative to the passive ER measured. A greater difference between active and passive ER approached a significant relationship with increased peak shoulder IR torque ($p=0.07$, $R^2=0.18$).

Bilateral imbalance of the eccentric external rotator musculature was significantly related to peak shoulder distraction force ($p=0.02$, $R^2=0.33$). A greater ratio in dominant/non-dominant arm strength was associated with higher peak distraction force in pitchers when measuring eccentric external rotator strength at 270 degrees/sec. Unilateral imbalance of the eccentric external and internal rotator musculature was significantly related to increased shoulder IR torque ($p<0.05$, $R^2=0.21$). A greater ratio of ER/IR strength was associated with higher shoulder IR torque when measuring eccentric ER and IR strength at 90 degrees/sec.

Clinical measures of ROM were not significantly related to shoulder stress in the baseball pitch even when comparing bilateral differences. Similarly, no single measure of isokinetic rotator cuff strength was significantly related to shoulder stress. Only after assessing strength ratios bilaterally or between muscle groups were significant relationships discovered. These results suggest that evaluating isokinetic strength ratios between arms or agonist and antagonist muscle groups may be more indicative of injury risk than any stand-alone isokinetic strength measure. Further, the results may give clinicians or trainers a better understanding of what to evaluate during a pre-season screen of an overhead athlete's glenohumeral ROM or strength.

Significance

Recent upper extremity literature has struggled to identify specific charactersitcs of an overhead athlete's shoulder complex that are related to increased biomechanical loads during activity. The current study provides insight for clinical measures that can be evaluated without expensive motion capture technology that may be related to increased injury risk in overhead athletes. It is likely that ROM, strength, and mechanics are all interconnected regarding injury risk in these athletes and it is paramount that researchers and clinicians attempt to understand these relationships to ensure the safety of any ballistic athlete.

References

1. Oyama, S., *Baseball pitching kinematics, joint loads, and injury prevention,* J. Sport and Health Science, 2012.
2. Wilk et al., *Deficits in Glenohumeral Passive Range of Motion Increase Risk of Shoulder Injury…,*Am J Sports Med, 2015.
3. Hurd, W., *Glenohumeral Rotational Motion and Strength and Baseball Pitching Biomechanics*, J. Athletic Training, 2012.

Rotator Cuff Tears and Humeral Elevation in Manual Wheelchair Users with Spinal Cord Injury and Able-bodied Controls

Omid Jahanian[1], Brianna M. Goodwin[1], Meegan G. Van Straaten[1], Stephen M. Cain[2], Ryan J. Lennon[1], Jonathan D. Barlow[1], Naveen S. Murthy[1], Melissa M. B. Morrow[1]
[1]Mayo Clinic, Rochester, MN, [2]University of Michigan, Ann Arbor, MI, USA
Email: Jahanian.Omid@mayo.edu

Introduction

The shoulder is the most common site of musculoskeletal pain and pathology in manual wheelchair (MWC) users with spinal cord injury (SCI) [1]. The prevalence and progression rate of shoulder pathology in this population is notably higher than able-bodied individuals [2]. The primary purpose of this study was to compare the progression of rotator cuff (RC) pathology over one year in MWC users with able-bodied individuals. We also aimed to investigate the effects of MWC use on humeral elevation and its contribution to the high prevalence of RC tears in individuals with SCI.

Methods

Under Mayo Clinic IRB approval, 16 MWC users (15 males, age (SD): 37(13) yrs, injury level: C6–L1, median years of MWC use (interqurtile range): 5(4) yrs) and 16 age and sex-matched able-bodied controls were recruited. Bilateral shoulder magnetic resonance images (MRIs) were completed and assessed on two occasions, at baseline visit and approximately one year later using an established rubric [3]. Bilateral humeral elevation angles for a subset of 11 MWC users and controls were calculated throughout one or two typical day(s) (after baseline MRI) from body segment orientations using accelerometry and gyroscope data from three wireless inertial measurement units (Opal, APDM Inc., USA) worn on the bilateral upper arms and anterior torso [4]. McNemar's test was used to compare the prevalence of RC tears between baseline and year 1. Wilcoxon Signed-Rank test was used to compare humeral elevation levels between two cohorts. Differences between participants with and without any tear were compared using Student's two-sample t-test for age and humeral elevation levels. All tests were two-sided with a 0.05 significance level.

Results and Discussion

The bilateral shoulder (14 non-dominant and 15 dominant shoulders) MRI findings indicated that progression of any tears across the RC and the long head of biceps tendons increased for the dominant shoulder of SCI cohort in comparison to the controls; however, the difference was not statistically significant (p = 0.063; Fig. 1A-1B). The progression of the RC pathology was not different between the two cohorts for the non-dominant side. MWC users without tendon tears were significantly younger than those with tendon tears on the non-dominant side at baseline (p = 0.018) and year 1 (p = 0.042), and on the dominant side at year 1 (p = 0.021). The effect of age was stronger for able-bodied participants on both sides and time points ($p < 0.001$).

MWC users spent significantly less time in 0-30º of humeral elevation than the controls (p = 0.050 (dominant); p = 0.011 (non-dominant)). This could be mainly due to resting seated postures in SCI group rather than active movements. MWC users spent more time in other humeral elevations than controls, but the differences were not statistically significant (Fig. 1C-1D). Able-bodied participants without tendon tears on their non-dominant side spent significantly less time in 90-180º of humeral elevation (p = 0.044) than those with tendon tears. There were no significant associations between other humeral elevations and presence of tendon tears for both cohorts.

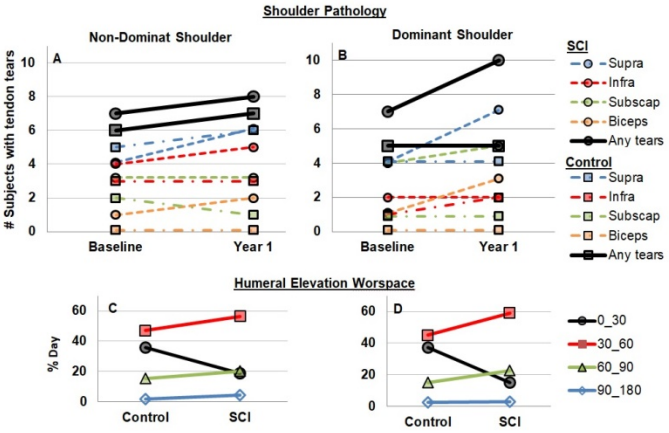

Figure 1. Rotator cuff and biceps tendon tears and humeral elevation angles in MWC usrs with SCI and able-bodied controls. A and B demonstrate the number of participants with any tendon tears (Any tears) or individual muscle tendon teras across the supraspinatus (Supra), infraspinatus (Infra), subscapularis (Subscap), and biceps at baseline and year 1 for MWC users with SCI (circles) and able-bodied controls (squares). C and D demonstrate the percentage of time controls and MWC users with SCI spent in humeral elevation levels for their non-dominant (C) and dominant (D) arms throughout a typical day.

Significance

The higher progression rate of RC pathology in MWC users with SCI than in able-bodied controls indicates that MWC use may predispose individuals with SCI to RC disease beyond intresnsic factors, such as age. The different functional humeral workspace for MWC users compared with able-bodied controls may be a contributor to the observed differences in incidence and progression of RC pathology between these two cohorts. Lack of significant associations between humeral elevations and presence of tendon tears in the SCI cohort might be due to the small sample size. Further investigation with a larger population of MWC users and controls is underway to elucidate the evolution of shoulder pathology and arm use following SCI.

Acknowledgments

This research was supported by NIH Grants R01 HD84423-01 and NCATS UL1 TR002377.

References

[1] Dyson-Hudson, T., et al. (2004). J Spinal Cord Med, 27(1):4-17
[2] Akbar, M., et al. (2010). JBJS (Am), 92(1):23-30.
[3] Morrow, M., et al. (2014). *BioMed Res Int*.
[4] Goodwin B, et al. Proceeding of ISG/ASB'19, Calgary, Canada, 2019

A Comparison of Methods to Estimate Scapular Kinematics for Brachial Plexus Birth Injuries

R. Tyler Richardson[1], Stephanie Russo[2], Matthew Topley[3,4], Ross Chafetz[4], Scott Kozin[4], Dan Zlotolow[4], and James Richards[3]
[1]Pennsylvania State University Harrisburg, Middletown, PA, USA
Email: rtr12@psu.edu

Introduction

Glenohumeral (GH) motion deficits and scapulothoracic (ST) compensations are commonly observed in patients with brachial plexus birth injury (BPBI)[1,2]. Various interventions are employed to improve GH function, however, assessment of GH function in dynamic conditions is lacking due to challenges in measuring dynamic scapular orientation and the inability to distinguish between GH and ST contributions to shoulder motion. The acromion marker cluster with single calibration (S-AMC) has been used to estimate ST kinematics in healthy populations[3] but is unsuitable for BPBI[4]. An updated AMC double calibration method (D-AMC) that interpolates estimated ST orientations based on humerothoracic (HT) elevation[5] is currently recommended[6], but has yet to be assessed in BPBI. A new linear model (LM) approach utilizing measurable HT orientation and acromion process position to estimate ST orientation has been validated in healthy adults[7], but has not been tested in BPBI. This study evaluates the ability of the S-AMC, D-AMC, and LM to estimate ST orientation in static positions across a full shoulder range of motion by comparing against palpation in BPBI. We hypothesized that ST errors between LM and palpation would be less than those of D-AMC and much less than those of S-AMC.

Methods

Trunk and arm orientations of 19 BPBI participants were measured with motion capture. Subjects completed 14 static positions encompassing a full spectrum of shoulder motion. In each position, scapular markers were placed to determine ST orientation. HT and ST angles were calculated. All 14 positions served as test positions for evaluation. For each position, a "leave-one-out" approach was used to create a LM using multiple linear regression on data from the 13 other positions to generate equations that estimated ST angles based on HT orientation and acromion process position. ST angles estimated by each method were compared to palpation and average root mean square errors (RMSE) for each approach were calculated across all participants on each ST axis of motion for each test position.

Results and Discussion

LM and D-AMC produced comparable RMSE values that were generally within established acceptable limits (<10°)[3] for most positions/axes; S-AMC values were occasionally much larger (**Fig. 1**). The percentage of errors >10° for all subjects and positions in this study varied across the three ST axes: LM (9.9-16.0%), D-AMC (1.8-7.3%), S-AMC (2.9-9.2%). Overall, these results do not support our hypotheses.

Estimating ST orientation in BPBI is more challenging than in a healthy population as RMSE values for all methods were close to or beyond the upper ranges reported in all previous healthy analyses[3]. Similar to past findings[5], D-AMC was superior to S-AMC especially on internal/external rotation and anterior/posterior tilt. LM had exceptionally large errors for certain positions that involved HT or ST angle values beyond those of the other 13 positions used to develop the LM; this highlights a LM limitation that should be considered when using this approach. The D-AMC produced acceptable RMSE values for most positions/axes and was the least likely of all methods to produce >10° errors for an individual subject.

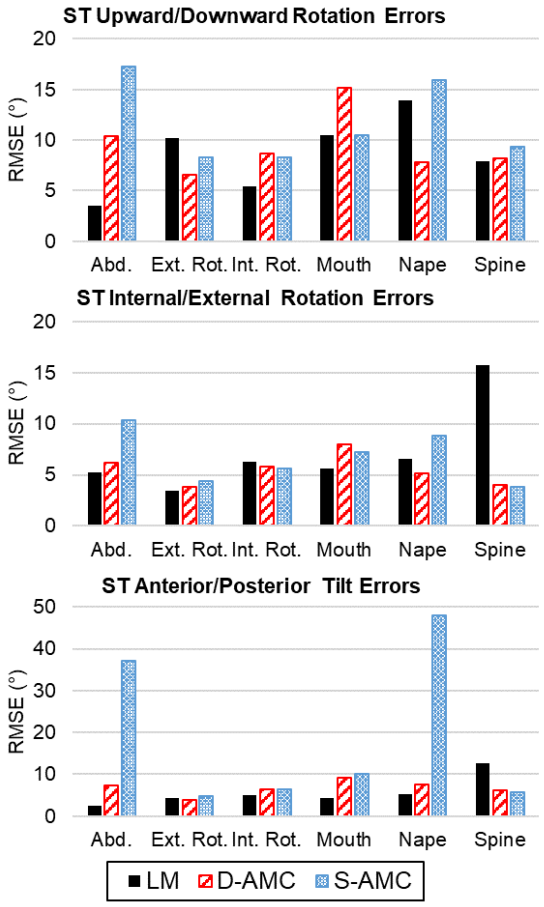

Figure 1: RMSE values for ST orientation at select and representative test positions exemplifying a variety of functional arm postures.

Significance

Current methods for estimating dynamic scapular orientation are less than ideal for BPBI. Use of the D-AMC, however, may be appropriate for certain motions/scenarios and would provide new insights into dynamic ST and GH joint function to ultimately facilitate surgical planning and outcomes assessment in BPBI.

Acknowledgments

Funding provided by a 2017 POSNA Start-Up Research Grant. Thank you to Spencer Warshauer for data collection assistance.

References

1. Hogendoorn, S. (2010) J. Bone & Joint Surg., 92(4):935-942.
2. Duff, S. (2007) Clin. Biomech., 22(6):630-638.
3. van Andel, C. (2009) Gait & Posture, 29(1):123-128
4. Nicholson, K. (2014) J. App. Biomech., 30(1):128-133.
5. Brochard, S. (2011) J. Biomech., 44(4):751-754.
6. Lempereur, M. (2014) J. Biomech., 47(10):2219-2230.
7. Nicholson, K. (2017) J. Biomech., 54:101-105

Macrostructural bone deformity following brachial plexus birth injury cannot be explained solely by limb disuse

Emily B. Fawcett[1,2], Kristen E. Lo[1], Lauren E. Merritt[1], Nikhil N. Dixit[1], Jacqueline H. Cole[1,2], and Katherine R. Saul[1]
[1]North Carolina State University, Raleigh, NC, USA
[2]University of North Carolina, Chapel Hill, NC, USA
Email: ebfawcet@ncsu.edu

Introduction

Brachial plexus birth injury (BPBI) occurs during a difficult childbirth when damage ensues along the brachial plexus nerve bundle [1]. Lifelong arm impairment persists in 30-40% of cases [2], with muscle weakness, limb disuse, and musculoskeletal deformities [3]. Loading at the glenohumeral joint is altered, but the main causes of that alteration are unclear. In addition, nerve injury location can alter outcome severity [4]. In both nerve rupture (*postganglionic*) and nerve avulsion (*preganglionic*), loading alterations could be, in part, due to limb disuse, decreased optimal muscle length, or decreased muscle mass. To determine whether limb disuse may be a major contributor, we compared both postganglionic and preganglionic injuries to a disarticulation model observed to have similar disuse of the affected limb.

Methods

Sprague Dawley rat pups were assigned to three groups (n=16 each): postganglionic neurectomy, preganglionic neurectomy, and elbow disarticulation. Interventions were performed 3-5 days postnatally on one side with the contralateral limb serving as a control. Neurectomies included C5-C6 nerve root excision either distal (postganglionic) [5] or proximal (preganglionic) [6] to the dorsal root ganglion. The disarticulation group underwent amputation of the forearm at the elbow.

Scapulae and humeri were scanned using micro-computed tomography (36 µm, SCANCO µCT 80) and analyzed in Mimics (Materialise). Measurements included glenoid version angle (GVA), inclination angle (GIA), and radius of curvature (GRC), and humeral head thickness (HHT), width (HHW), and radius of curvature (HRC). Affected vs. unaffected limbs were compared within groups with paired t-tests. Group comparisons were made on affected–unaffected differences via one-way ANOVA with Tukey's posthoc tests (normally distributed) or Kruskal-Wallis with Dunn posthoc tests (non-normally distributed). Analyses were performed in GraphPad Prism (α=0.05).

Results and Discussion

Scapula Results: Postganglionic and disarticulation groups both showed changes in affected vs. unaffected limbs, with smaller affected limb GIA (postganglionic: -31%, disarticulation: -83%) and larger (more flattened) affected limb GRC (postganglionic: +119% trend, p=0.064, disarticulation: +374%) (Fig. 1). Compared to disarticulation, postganglionic BPBI tended to have smaller reductions in affected GIA (-96%, p=0.052) and had significantly smaller changes in GRC (-71%), and preganglionic also had smaller changes in GIA (-98%) and GRC (-102%) (Fig. 1). Humerus Results: Preganglionic and disarticulation groups showed deficits in affected vs. unaffected limbs. Preganglionic affected limb tended to have reduced HHT (-11%, p=0.065) and had reduced HHW (-9%) and HRC (-13%), and disarticulation affected limb had reduced HHT (-8%). No group differences were found. Discussion: Similar to our previous study [7], we found primarily humeral head detriments (not scapular) with preganglionic injury but scapular detriments (not humeral head) with postganglionic injury. This study includes disarticulation, which allows assessment of disuse contributions to glenohumeral deformity with BPBI. In the scapula, morphological changes with postganglionic injury were similar, though less severe, than with disarticulation, suggesting limb disuse contributes substantially but is not the only factor. Humeral head morphology, particularly width and curvature, was altered more in affected limbs for preganglionic injury than disarticulation, suggesting limb disuse has little effect and other factors (e.g., other forms of altered loading or the nerve injury itself) drive changes at this site.

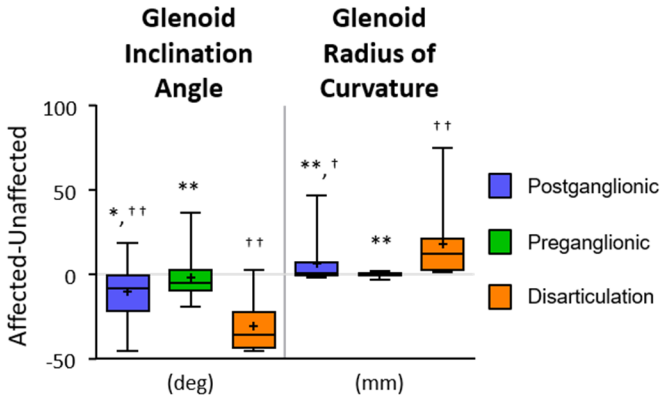

Figure 1. Compared to disarticulation, post- and preganglionic injury had smaller reductions in GIA and less flattening in curvature (*p<0.1, **p<0.05). †p<0.1, ††p<0.05 affected vs. unaffected limbs.

Significance

Our work suggests macrostructural deformities seen in post- and preganglionic BPBI are not due solely to limb disuse. While postganglionic deformity may result partly from limb disuse, it does not display the same severity of deformity as disarticulation. Preganglionic injury has worse humeral deformity in the affected limb than disarticulation and very little alteration of the glenoid, suggesting limb disuse is not a driving factor for preganglionic BPBI. This work allows further exploration of mechanisms of deformity and confirms that limb disuse substantially drives glenoid deformity but not humeral head deformity.

Acknowledgments

Funding: NSF GRFP and NIH R21HD088893. We thank Drs. Danelson and Cornwall for surgical expertise and Dr. Ted Bateman and Eric Livingston for micro-CT support.

References

[1] Geutjens G *et al*. (1996) *J Bone Joint Surg Br* **78**:777.
[2] Pondaag W *et al*. (2004) *Dev Med Child Neurol* **46**:138.
[3] Crouch DL *et al*. (2015) *J Bone Joint Surg Am* **97**:1264.
[4] Al-Qattan MM *et al*. (2003) *Ann Plast Surg* **51**:257.
[5] Li Z *et al*. (2010) *J Bone Joint Surg Am* **92**:2583.
[6] Nikolaou S *et al*. (2015) *J Hand Surg* **40**:2007.
[7] Dixit NN *et al*. (2018) *Orthop Res Soc Annual Meeting*

Adaptations in trabecular bone microstructure following brachial plexus birth injury are not due solely to limb disuse

Emily B. Fawcett[1,2], Lauren E. Merritt[1], Nikhil N. Dixit[1], Katherine R. Saul[1], and Jacqueline H. Cole[1,2]
[1]North Carolina State University, Raleigh, NC, USA
[2]University of North Carolina, Chapel Hill, NC, USA
Email: ebfawcet@ncsu.edu

Introduction

Brachial plexus birth injury (BPBI) results in lifelong arm impairment in 30-40% of cases [1], producing muscle weakness, arm disuse, joint morphological changes [2], and underlying microstructural bone changes in the shoulder [3]. The severity of these consequences differs based on injury location, with nerve rupture (*postganglionic*) producing more severe outcomes than nerve avulsion (*preganglionic*) [4]. Primary underlying drivers have yet to be investigated, specifically, the direct effects of nerve injury versus limb disuse, which occurs following both post- and preganglionic injury. The objective of this study was to compare trabecular bone microstructure for post- and preganglionic BPBI to that for a disarticulation model with similar limb disuse.

Methods

Sprague Dawley rat pups were separated into postganglionic neurectomy, preganglionic neurectomy, and elbow disarticulation groups (n=16 each). Rats received interventions 3-5 days after birth on one arm with the contralateral serving as a control and were sacrificed at 8 weeks. The interventions were C5-C6 nerve root excision distal (postganglionic) [5] or proximal (preganglionic) [6] to the dorsal root ganglion or forearm amputation (elbow disarticulation). Scapulae and humeri were harvested and scanned using micro-computed tomography (10 µm, SCANCO µCT 80). Distal scapula (glenoid) and proximal humerus (epiphysis, metaphysis) regions were analyzed for standard trabecular metrics [7]: bone volume fraction (BV/TV), bone mineral density (BMD), tissue mineral density (TMD), connectivity density (ConnD), trabecular number (Tb.N), thickness (Tb.Th), and separation (Tb.Sp), and degree of anisotropy (DA). Affected and unaffected limbs were compared via paired t-tests; groups were compared for affected/unaffected limb ratios using one-way ANOVA with Tukey's posthoc tests (normal distribution) or Kruskal-Wallis with Dunn posthoc tests (non-normal) in GraphPad Prism (α=0.05).

Results and Discussion

Limb comparisons: Postganglionic and preganglionic groups had significantly less robust trabecular bone in the affected vs. unaffected arm throughout all scapula and humerus regions, with reduced BV/TV, BMD, TMD, ConnD, Tb.N, and Tb.Th, and increased Tb.Sp in the humeral epiphysis of the affected arm (Fig. 1). The disarticulation group also had trabecular deficits in the affected arm throughout the scapula and trends for trabecular deficits (reduced BV/TV, BMD, and Tb.N, and increased Tb.Sp and DA) in the humeral epiphysis but no limb differences in the metaphysis. Group comparisons: Few differences were observed between the neurectomy groups and the disarticulation group in the scapula and humeral metaphysis regions. In the humeral epiphysis, affected/unaffected ratios showed trabecular bone for postganglionic was similar to that of disarticulation, while preganglionic bone had more deficits (Fig. 1). Specifically, preganglionic showed larger reductions than disarticulation in affected BV/TV (ratio 0.64 vs. 0.87), BMD (0.62 vs. 0.86), ConnD (0.71 vs. 0.91), Tb.N (0.74 vs. 0.91), and Tb.Th (0.86 vs. 0.89), and larger increases in Tb.Sp (1.50 vs. 1.12), along with a trend for greater decreased TMD (0.98 vs. 0.99, p=0.098). Discussion: Post- and preganglionic injury both resulted in detriments to affected arm trabecular bone throughout the glenohumeral region, while disarticulation effects were less consistent and more apparent in the scapula than the humerus. Group differences were most prominent in the humeral epiphysis; compared to disarticulation, postganglionic injury had similar effects, while preganglionic injury produced a substantially less robust trabecular microstructure. These results suggest that disuse has a more profound effect on glenoid than humeral trabecular bone and is a stronger driver for trabecular adaptation following postganglionic than preganglionic injury.

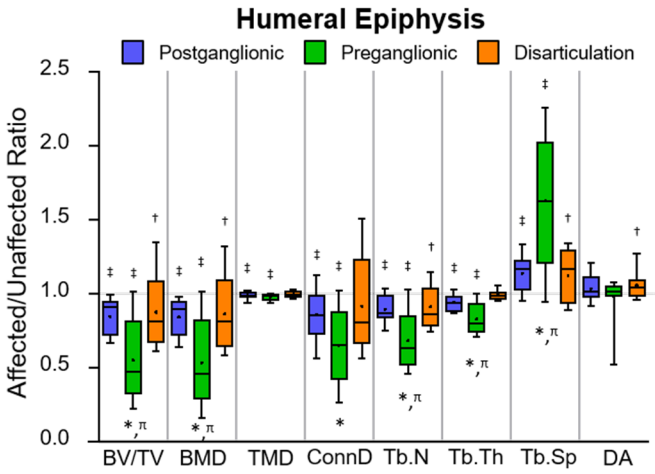

Figure 1. Preganglionic injury resulted in less robust trabecular bone than postganglionic injury ($^{\pi}p<0.05$) and disarticulation ($^{*}p<0.05$). $^{\dagger}p<0.1$, $^{\ddagger}p<0.05$ affected vs. unaffected limbs.

Significance

Disuse has a larger role in trabecular bone adaptations following post- than preganglionic BPBI and is especially detrimental in the glenoid. Severe preganglionic trabecular deficits in the humeral epiphysis are driven by mechanisms beyond limb disuse. Understanding how different factors contribute to microstructural adaptations will inform more effective BPBI treatments.

Acknowledgments

Funding: NSF GRFP and NIH R21HD088893. We thank Drs. Danelson and Cornwall for surgical expertise and Dr. Ted Bateman and Eric Livingston for micro-CT support.

References

[1] Pondaag W *et al*. (2004) *Dev Med Child Neurol* **46**:138.
[2] Crouch DL (2015) *J Bone Joint Surg Am* **97**:1264.
[3] Fawcett E *et al.* (2020) *Orthop Res Soc Annual Meeting*
[4] Al-Qattan MM *et al*. (2003) *Ann Plast Surg* **51**:257.
[5] Li Z *et al*. (2010) *J Bone Joint Surg Am* **92**:2583.
[6] Nikolaou S *et al*. (2015) *J Hand Surg* **40**:2007.
[7] Bouxsein ML *et al*. (2010) *J Bone Miner Res* **25**:1468.

Normalization of Thoracohumeral Kinematics Following Rotator Cuff Repair

Alyssa J. Schnorenberg[1,2], Steven I. Grindel[3], and Brooke A. Slavens[1]
[1]Occupational Science and Technology, University of Wisconsin-Milwaukee, Milwaukee, WI, USA
[2]Biomedical Engienering, Marquette University, Milwaukee, WI, USA
[3]Orthopedic Surgery, Medical College of Wisconsin, Milwaukee, WI, USA
Email: *paulaj@uwm.edu *corresponding author

Introduction

Approximately 300,000 rotator cuff repair surgeries are performed annually in the United States [1]. The goal of post-op rehabilitation is to allow healing of the repaired cuff while restoring function and range of motion [2-4]. It is a prolonged and demanding process [5,6] which can require a full year for the shoulder to feel normal again [5]. Using a patient's asymptomatic contralateral shoulder, normalization of the affected shoulder motion is defined as "changed kinematics toward symmetrical bilateral motion" [7]. While studies have demonstrated the potential for normalization of shoulder kinematics between 1 and 2 years after surgery [7,8], the timing and process for how the normalization occurs is unknown. Thus, the purpose of this study was to perform a biomechanical evaluation of patients with rotator cuff tears pre-op and post-op to elucidate the changes occurring across the rehabilitation process as compared to the non-injured arm.

Methods

Seven adults (mean age 62.0 +/- 5.3 years) with a rotator cuff tear participated in three test sessions: 0-12 weeks prior to surgery, and an average of 3 months and 6 months after surgery. A 15-camera Vicon T-series motion capture system tracked 27 reflective markers on the upper extremity (UE) while the subject performed five trials of maximal thoracohumeral external rotation, from an adducted state with the non-injured arm, followed by the injured arm. A biomechanincal model [9] was applied to calculate the UE kinematics of the thoracohumeral joint over the duration of the task. Group averages and standard deviations were computed for the peak thoracohumeral external rotation angle for both arms at each visit. The Wilcoxon signed rank test was used to compare the non-injured arm to the injured arm at each time ($p<0.05$).

Results and Discussion

Results indicate the peak external rotation of the non-injured arm was significantly greater than the injured arm both pre-op ($p=0.0391$) and at 3 months post-op ($p=0.0156$) (Fig. 1). There was no difference in the peak external rotation achieved by the non-injured and injured arm 6 months post-op ($p=0.5781$). The deficit in motion observed pre-op does not return to a typical amount until 6 months post-op. When examining the pre-op data individually, 4 of the 7 subjects performed the task at a deficit greater than 10 degrees compared with the non-injured arm, with an average of 22.4° (4.9°) less external rotation. At 3 months post-op, 3 of the 7 subjects increased their peak external rotation, but only by an average of 6.0° (5.7°). At 6 months post-op 4 of the 7 subjects still performed the task at a deficit compared to their non-injured arm, with an average difference of 14.2° (3.9°).

Many believe that appropriate rehabilitation, particularly within 3 months postoperatively, is the key to good functional outcomes [4,5]; however the optimal rehabilitation protocol is still being deliberated [3]. Although the goal of most rehabilitation protocols after a rotator cuff repair is to restore active range of motion by 3 to 4 months [6,10], this exploratory study showed that not only was this not achieved by most of the patients by 3 months post-op, but it was not achieved by half of them at 6 months post-op. Further work is underway examining additional joints of the shoulder complex, muscle activation patterns, and functional tasks.

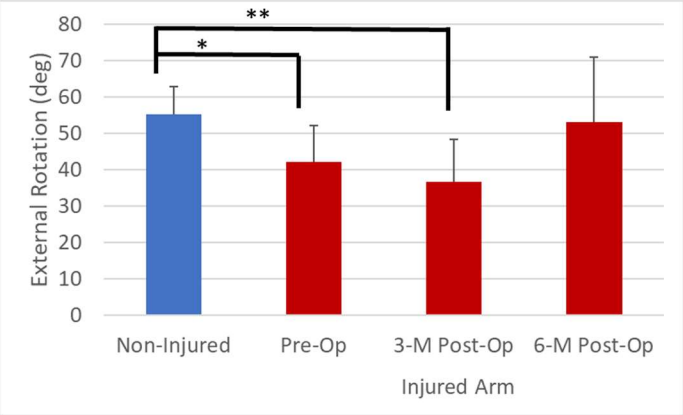

Figure 1: Group average (1 standard deviation error bar) peak external rotation for the injured-arm (red) pre-op and at 3 months and 6 months post-op, and the non-injured arm (blue). Asterisks indicate statistical difference between injured and non-injured arms ($p<0.05$).

Significance

Knowledge of the pre-op alterations and post-op normalization of the movements of the shoulder joint complex compared to the non-injured arm is critical to improve and shorten the post-op recovery process, including more targeted exercises. This work sets the premise for developing targeted rehabilitation interventions by helping to identify critical times during the post-op rehabilitation phases when interventions should be administered.

Acknowledgments

This work was supported by the Medical College of Wisconsin, Department of Orthopedic Surgery Intramural Grant Program and the University of Wisconsin-Milwaukee Mobility Lab.

References

[1] M. Crawford, AAOS Now, 34, 2014.
[2] O. Nikolaidou, et al., Open Orthop J, 11:154-162, 2017.
[3] A. Arshi, et al., Arthroscopy, 31:2392-2399. e1, 2015.
[4] H. Tonotsuka, et al., J Orthop Surgery, 25(3):1-8, 2017.
[5] S. Vollans and A. Ali, Surgery (Oxford), 34:129-133, 2016.
[6] C. Thigpen, et al., J Shoulder Elbow Surg, 25:521-535, 2016.
[7] A. Kolk, et al., J Shoulder Elbow Surg, 25:881-889, 2016.
[8] G. Paletta Jr, et al., J Shoulder Elbow Surg, 6:516-527, 1997.
[9] A. J. Schnorenberg, et al., J Biomech, 47:269-276, 2014.
[10] C. Jung, et al., Obere Extrem, 13:45-61, 2018.

CHARACTERIZING STIFFNESS AND COUPLING AMONG FIVE DIGITS OF THE HUMAN HAND

Oppizzi Giovanni[1, 2], Sanjana Rao[1], Dongwon Kim[1], and Li-Qun Zhang[1, 2]
[1]University Maryland, Baltimore
[2]University Maryland, College Park,
Email: goppizzi@umd.edu

Introduction

Our hand is one of the most complex organs. It is an essential tool for our daily life, so much that a big portion of our motor cortex is dedicated to its control. This being said, it is apparent that a coupling relation exists between the five digits that does not allow us to move them independently from each other. There has been a lack of quantitative characterizations of couplings across the five digits. The purpose of this study was to characterize the coupling relationships that exist across the 5 digits during passive movement.

Methods

To accurately measure the forces and positions of individual fingers, we modified a commercial exoskeletal device, the Hand of Hope (Figure 1). Modifications were made to add force and position measurements of each digit. This allowed us to measure the forces and displacement at each of the five digits. Spacer was placed at the proximal phalanges so that each of the fingers can stretched to the extended position. Five subjects (4 female and 1 male, age 20-60) were evaluated. The subject's hand was strapped into the device and all fingers were extended to the extended position where they were subsequently locked in place. At this point, we asked the subject to relax all digits and started moving them one at a time, while keeping the others locked, for around 10 cycles each at 15mm/s. During the movement, forces and displacement were recorded for each of the 5 digits.

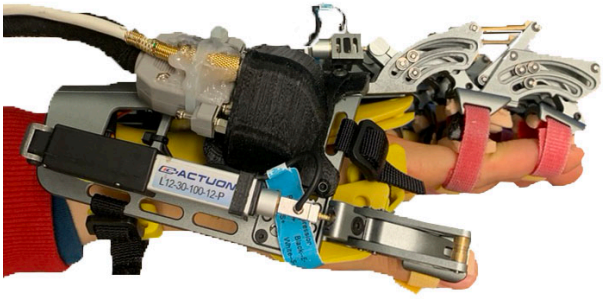

Figure 1: *The modified exoskeleton hand robot. Each digit was equipped with a dedicated servomotor and loadcell. Spacers were added at the proximal phalanges to reach the extended position.*

Results and Discussion

The outcome of these measurements was what was referred to in other publications [1] as the passive stiffness matrix. The diagonal elements of this matrix (local stiffnesses) represent the stiffnesses developed at the finger when moving that specific digit. On the other hand, the off-diagonal elements represent the coupled stiffness recorded at all the other four digits that are kept locked at the extended position. Especially in the case of the local stiffnesses, it was apparent how it is not constant throughout the range of motion, and even at the same position, the value can be different depending on the direction of the passive movement and the position on the force-displacement hysteresis loop. For the purpose of this study, we elected to consider stiffnesses during extension (Fig. 2), in particular we chose to evaluate it at near full extension.

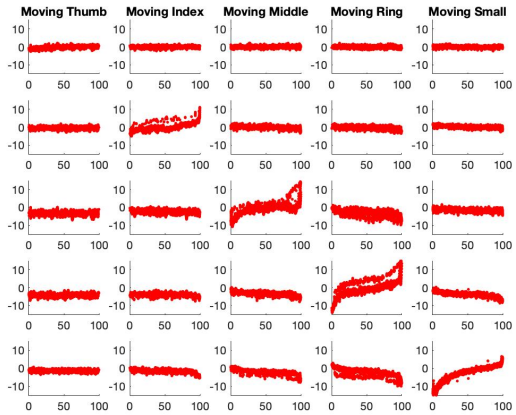

Fig. 2: Stiffness properties across the five digits. On the columns, the results of each trial in which only one finger was moved. On the rows, forces were measured at each digit (thumb, index, middle f, ring f, and small f), respectively. *X axis is ROM% (0 max extension, 100 max flexion), Y axis is stiffness (N/mm)*

What we found was, to start with, higher values for local stiffnesses, and strong coupling in three most lateral fingers (middle finger, ring finger and little finger) across all subjects (Fig. 3).

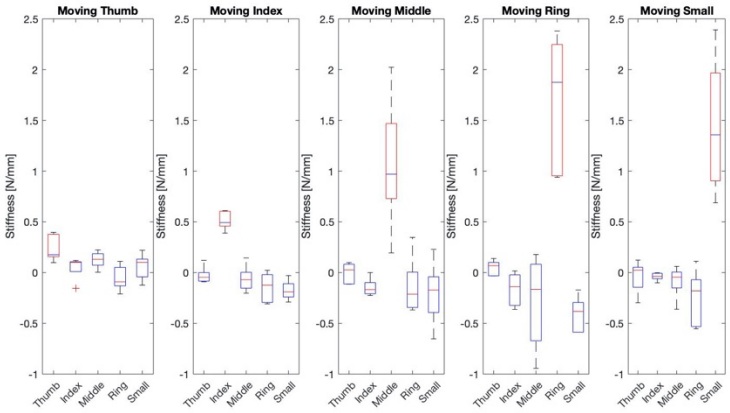

Fig. 3: Local stiffness is highlighted in red and coupled stiffness in black. Note the right 3 columns showed the strong coupling among the 3 most lateral fingers.

Significance

The findings emerged in this study, while interesting on their own, also represent an important foundation for future studies. It will be interesting to evaluate how coupling is affected in patients after stroke, for example.

References

[1] L. Zhang, J. Son, H. Park, S. H. Kang, Y. Lee and Y. Ren, "Changes of Shoulder, Elbow, and Wrist Stiffness Matrix Post Stroke," IEEE TNSRE, 25:844-851, 2017.

Back squat mechanics in persons with a unilateral transtibial amputation: A case study

Kinyata J. Cooper[1,2], AuraLea Fain[1,2], W. Lee Childers, PhD[1,2]
[1]Center for the Intrepid, Department of Rehabilitation Medicine, Brooke Army Medical Center, JBSA Ft. Sam Houston, TX, USA
[2]Extremity Trauma and Amputation Center of Excellence, JBSA Ft. Sam Houston, TX, USA
Email: Kinyata.j.cooper.ctr@mail.mil

"The view(s) expressed herein are those of the author(s) and do not reflect the official policy or position of Brooke Army Medical Center, the U.S. Army Medical Department, the U.S. Army Office of the Surgeon General, the Department of the Army, Department of Defense or the U.S. Government.". "This research was supported in part by an appointment to the Department of Defense (DOD) Research Participation Program administered by the Oak Ridge Institute for Science and Education (ORISE) through an interagency agreement between the U.S. Department of Energy (DOE) and the DOD. ORISE is managed by ORAU under DOE contract number DE-SC0014664. All opinions expressed in this paper are the author's and do not necessarily reflect the policies and views of DOD, DOE, or ORAU/ORISE."

Introduction

Prosthetic users must contend with and adapt to the additional mechanical and physical constraints of a prosthesis to perform a motor task. Persons with unilateral transtibial amputations (TTAmp) have been shown to use hip-dominant strategies compared to persons with intact limbs (INTACT) during various movement tasks such as gait, vertical jumping, and cycling[1,2,3]. Whether this compensatory behavior is a ubiquitous strategy used by TTAmp across all tasks or whether it is task specific is of considerable interest to define mechanisms of motor control in this population. The back squat is a well-defined task with eccentric, energy absorption and concentric, energy generation phases making it suitable to explore a range of compensations. Therefore, this case study was to determine compensation strategies utilized by a TTAmp compared to an INTACT while performing a back squat. We hypothesize that there will be greater relative contribution of hip joint work done in the amputated limb compared to sound limb.

Methods

One male TTAmp (119.8kg) with an Össur VSP foot (energy storage and return component mounted in series with a hydraulic damper) and one male INTACT control (81.4 kg) signed informed consent to participate in this IRB approved study. The participants performed 5 sub-maximal back squats at 75% of their one-rep max (102.3 kg) following a warm-up. Lower limb kinematics and kinetics were quantified for each limb with 39 passive reflective markers using a Full Body PlugInGait model (Vicon, Oxford, UK). Net joint power was calculated using an inverse dynamics approach. The work done at each joint attributed to total limb work (J/kg) was calculated by integration of each of the respective power curves[4] and converted to a percent of total limb work. A two-way RM ANOVA was run to find the main and interaction effects of limb (R vs. L) and amputation status (AMP vs. INTACT) on each joints' percent contribution to total limb positive and negative work. Where significant interactions were observed, simple pairwise comparisons were conducted.

Results and Discussion

The hip contributed significantly more to total limb positive work than the knee and ankle in left ($p<0.001$ and $p=0.001$, respectively) and right ($p<0.001$ and $p=0.001$, respectively) limbs of TTAmp, and the right ($p<0.001$ and $p=0.003$, respectively) limb of INTACT.

While the knee contributed significantly more to total limb negative work than the ankle and hip in the left ($p<0.001$ and $p=0.005$, respectively) and right ($p<0.001$ and $p<0.001$, respectively) limbs of INTACT, similar patterns were not observed in TTAmp. The hip contributed significantly more to total limb negative work than the ankle in the left and right limb of TTAmp ($p < 0.001$). The hip contributed significantly more than the knee in the left limb but not the right limb ($p < 0.001$, $p = 0.349$ respectively) of TTAmp (*Figure 1*).

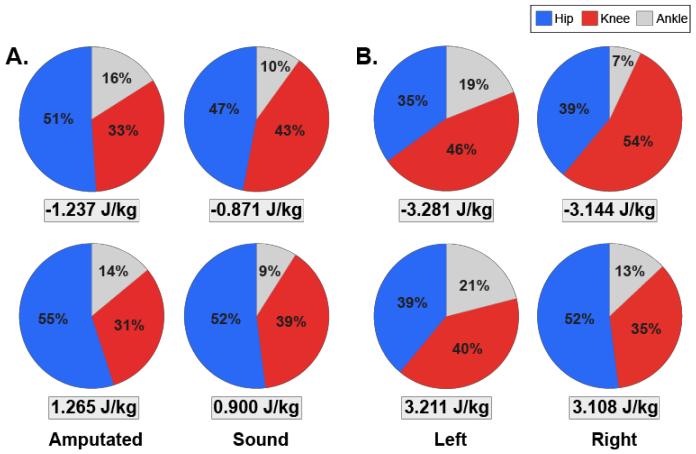

Figure 1: Negative (top row) and positive (bottom row) total limb work per joint in TTAmp (panel A) and INTACT (panel B).

TTAmp utilized a hip dominant strategy to both absorb and generate energy in both limbs whereas INTACT absorbed more energy at the knee. Interestingly, the ankle joint contributed greater negative work than positive work on the amputated and sound limb (15.8% vs 14.2%) suggesting TTAmp loaded the prosthetic foot to get as much energy return as possible allowing the prosthetic side a greater contribution to energy system.

Significance

This case study provided insight on compensation strategies used by prosthetics users during a back squat. Findings suggest greater relative reliance on both hip joints in the amputated and sound limbs vs. asymmetric hip joint work seen during other tasks. These findings may also inform prosthetic foot design and prescription for similar functional weight training tasks. The TTAmp utilized a strategy to load the prosthetic foot during the eccentric phase and was able to utilize the energy returned for the concentric phase, highlighting the benefits of prosthetic feet with high energy storage and return properties for this task. Further work is warranted to define how consistent these strategies are across a larger sample of TTAmp.

References

[1] Schoeman et al. (2012). *JAB,* **28** (4): 438-447
[2] Childers et al. (2014). *J Biomech,* **47**(10): 2306-2313
[3] Prinsen et al. (2011). *Arch phys med rehab* **92**(8): 1311-1325
[4] Czerniecki et al. (1996). *J Biomech,* **29**(6): 717-22

Evaluation of a Passive Knee Exoskeleton for Vertical Jumping

Coral Ben David[1], Barak Ostraich[1,2], Raziel Riemer[1].
[1]Department of Industrial Engineering, Ben-Gurion University of the Negev, Israel.[2] NRCN, Israel.
Email: rriemer@bgu.ac.il; website: http://www.bgu.ac.il/~rriemer/

Introduction

An exoskeleton is a wearable device, designed to enhance physical abilities during human activities. Several exoskeletons have succeeded in assisting walking [1], running [2] and hopping [3]. The goal of these exoskeletons is to reduce the effort expended during aerobic tasks (i.e. the metabolic rate). However, exoskeletons which assist during anaerobic tasks (specifically, vertical jumping) have not yet been thoroughly researched. During countermovement vertical jumping, there is a negative work phase in the knee, followed by positive joint work. Therefore, a passive exoskeleton (based on a spring) can assist knees during a jumping activity.

In this study, we built a passive knee exoskeleton for vertical jumping, and performed an experiment to gain knowledge on exoskeleton-human interaction.

Methods

Eight healthy males (age: 25.1±3.0 years; mass: 71.7±3.6 kg; and height: 1.73±0.02 m) participated in this study. All subjects provided informed written consent before participating in the study. The study was approved by Ben-Gurion University's Human Research Institutional Review Board.

The passive knee exoskeleton consists of aluminium frames, attached to the leg with wide Velcro stripes. Rubber springs provide the assistance torque. The overall device mass is 1.5 kg, for each leg. The subjects performed vertical jumps under five conditions: without the device (No Exo); with the device but with no spring connected (Exo0); with the device and with springs that provide 70 Nm at a 90° knee bend (Exo1); with springs that provide 105 Nm (Exo2); and without the device again (No Exo2). The performance order of the conditions with the device was randomized for each subject. The subjects followed a warm-up routine, and then performed eight vertical jumps under each condition. They were instructed to jump as high as possible, and to keep their hands crossed on their chest. Data was collected from the last five jumps. The subjects rested for 1.5 minutes between jumps, to prevent the effect of fatigue.

Subjects' motion was recorded using 14 cameras (Qualisys), and ground reaction forces were recorded using an instrumented treadmill (Bertec). Invers dynamics was performed using Visual 3D (C-Motion). Rectus Femoris (RF) and Gastrocnemius medialis (GM) muscle activity was measured using surface electromyography (Trigno, Delsys). Next, MATLAB code (Math Works Inc) was used to calculate the difference in the center of mass height (from detachment to maximum jump height) and work performed at each joint (from full bending to detachment).

Results and Discussion

The average height difference from detachment to maximum jump height, for each of the conditions, was normalized by the average height difference gained in No Exo condition, and is presented in Fig. 1. Repeated measures analysis of variance (ANOVA) revealed that the average normalized difference in height for Exo2 was greater by 13± 5% than for Exo0 (P<0.001), and greater by 5 ± 0.1% than for Exo1 (P=0.04). Exo2 was no different from No Exo (P=0.69).

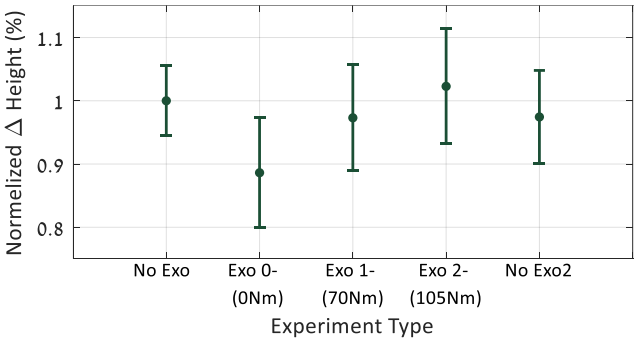

Figure 1: The average height difference from detachment to maximum jump height, normalized by the No Exoskeleton (No Exo) condition

There was no difference between the maximum amplitude of EMG in RF and GM, under all conditions (P>0.05). There was no difference in average ankle joint work between all five conditions. The average total work at the knee joints (i.e. the biological knee work and exoskeleton work) with No Exo2 was greater than all the conditions with the exoskeleton (P<0.01). The work at the hip joints without the exoskeleton (No Exo and No Exo2) was lower than with the exoskeleton (P<0.05, for all the conditions). This might suggest that the subjects changed the way they jump, but that they still did not fully utilize the exoskeleton. In future research, we will train the subjects to better utilize the exoskeleton, by storing more energy in the springs.

Table 1: The average work done by each joint (J)

Condition\ Joint	Ankle	Knee-total	Knee bio	Exo	Hip	All 3 joints
No Exo	128.6	220.3	220.3	-	195.2	544.1
Exo0	129.6	192.3	192.3	-	242.1	563.9
Exo1	139.7	206.6	104.3	102.2	242.6	588.8
Exo2	141.1	192.1	51.3	140.9	247.8	581.0
No Exo2	123.8	239.5	239.5	-	176.5	539.8

Significance

The results contribute to a better understanding of the interaction between an exoskeleton and the human body, and could improve the design of exoskeletons in future.

Acknowledgments

This research was supported in part by the Helmsley Charitable Trust through the Agricultural, Biological and Cognitive Robotics Initiative, and by the Marcus Endowment Fund, both at Ben-Gurion University of the Negev.

References

[1] Collins, S. H et al. (2015). Nature.
[2] Nasiri, R. et al. (2018). IEEE T NEUR SYS REH.
[3] Grabowski, A. M. and Herr, H. M. (2009). J. Appl. Physiol.
[4] Stefanyshyn, J. and Nigg B. M. (1998). J Sports Sci.

Development and Testing of a Linear Adjustable Lower-Limb Prosthesis

Therese E. Parr[1], Dr. Alan R. Hippensteal, MD[2], Sarah K. Thomas[1], Dr. Cody J. Reynolds, PhD[2], Dr. John D. DesJardins, PhD[1]
[1]Clemson University Department of Bioengineering, Clemson, SC, 29634
[2]PRISMA Health Department of Physical Health and Rehabilitation, Greenville, SC, 29615
Email: jdesjar@ clemson.edu

Introduction

Unilateral amputees often experience decreased muscle efficiency during gait as a result of the anatomic asymetries induced with most current prostheses designs. Amputees tend to load 58% of body weight on the intact leg 42% of body weight on the prosthesis.[1] During the prosthesis swing phase, there is higher and prolonged muscle activity seen in the plantar flexion of the intact leg for push-off to ease foot clearance of the prosthesis.[2] During the prosthesis pre-swing phase, transfemoral amputees have a plantar flexion deficiency on the prosthesis, which reduces forward propulsion during pre-swing.[3] This leads to an energy expenditure increase of 60% in transfemoral amputees' gait compared to normal gait, with prosthesis weight and moment of inertia being prime contributors to this issue.[3] The prevalence of falls among lower-limb amputees is estimated to be as high as 52% within a year.[3] Stability issues may be caused by toe clearance, knee-buckling, proprioception, and balance. There is a need to develop a novel lower-limb prosthesis that will focus on foot clearance, forward propulsion, and proprioception.

The proposed lower-limb prosthesis will dynamically lengthen and shorten during gait to improve muscle efficiency and increase the load symmetry between the intact leg and prosthesis. During the prosthesis swing phase, the prosthesis will shorten for easier foot clearance. During the prosthesis pre-swing phase, the prosthesis will extend for increased forward propulsion. The dynamic lengthening and shortening of the prosthesis will result in a reduction of the lateral center of mass and swing inertia to improve proprioception and stability.

Methods

An initial prototype has been developed using an external motor and cam system that uses a cable to affect length adjustment of the prosthesis. (Figure 1) The system was designed telescopically for the cable to pull the top and bottom components together or separate them. The cable is pulled by an arm that follows the cam; as cam diameter increases the cable pulls the components together to shorten the prosthesis and as the cam diameter decreases the prosthesis lengthens. One revolution around the cam represents one gait cycle. Following institutional IRB approval, two transfemoral amputees were able to ambulate with the prototype on a treadmill at a speed that was timed with the speed of cam rotation and prosthesis' dynamic linear motion.

Figure 1. Prototype (left), cam and cable set-up (right)

Results and Discussion

The prototype can support a patient's weight, adjust to the length needed during the gait cycle and shorten to provide foot clearance for swing through. A more compact electromechanical drive system will be needed for a self-contained prosthesis design.

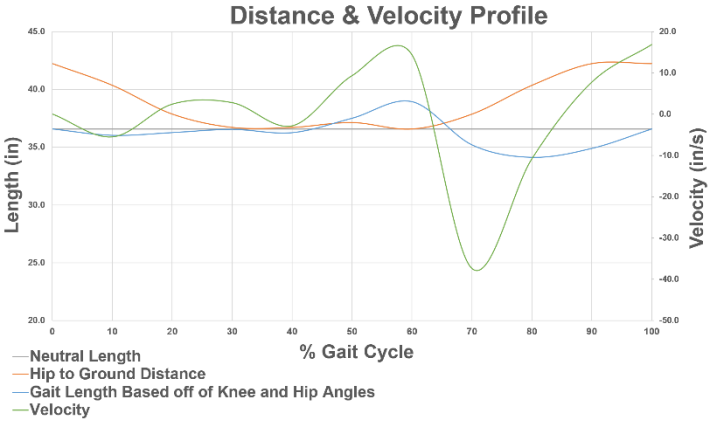

Figure 2. Model of distance and velocity profile during gait

The first prototype proved the concept that a prosthesis with dynamic linear motion can replace the functions of a knee joint. From experimental observation and mathematical modeling of joint angles[4], we will find the optimal weight, and the length and velocity profile of the telescopic system. (Figure 2) This will determine the required power and help conserve energy in a compact electromechanical drive system. The prototype will be tested kinematically to determine foot clearance distance, forward propulsion, and lateral center of gravity displacement.

Significance

There are currently no lower-limb prosthetics on the market that replace the flexion/extension of a knee joint with dynamic linear motion. The dynamic linear adjustable prosthesis is patent pending. The claims of the patent include a prosthesis with a distal and proximal end, where an actuator modifies the distance between ends to alter the length of the prosthesis. The prosthesis can include rotational joints, multiple actuators, springs, shock absorbers, and a control system.

We hypothesize that a dynamically adjusting prosthesis can improve load symmetry through an optimized clearance distance and propulsion force. We anticipate that such a device would improve prosthesis control and quality of life for amputees.

Acknowledgments

This research is funded by the 2020 PRISMA Health Seed Grant.

References

1. Miller WC, et al. *Arch of Physical Medicine and Rehabilitation*. 82(8), 1031-1037, 2001.
2. Wentink EC, et al. *Journal of NeuroEngineering and Rehabilitation*. 10(1), 87, 2013.
3. Howard, D., et al. *Impact* (4), 92–94, 2017.
4. Bowker JH, et al. *Atlas of Limb Prosthetics: Surgical, Prosthetic, and Rehabilitation Principles*. 2002.

Influence of Asymmetry on the Metabolic Costs of Walking

Shane P. Murphy[1], Nathan J. Robey[2], K. Otto Buchholz[3], and Jeremy D. Smith[4]
[1]University of Montana, Missoula, MT, [2]Western Washington University, Bellingham, WA
[3]Shenandoah University, Winchester, VA [4]University of Northern Colorado, Greeley, CO
Email: shane2.murphy@umontana.edu

Introduction

Persons with a unilateral transtibial amputation face a greater metabolic demand during walking than able-bodied individuals [1]. This increase in the metabolic cost of walking may partially explain why the majority of persons with amputations do not engage in a sufficient amount of physical activity to avoid comorbidities of a sedentary lifestyle [2].

Inertial asymmetries in individuals with unilateral lower extremity amputations have been simulated in individuals without amputation by adding mass to one leg [3]. Others replicated asymmetrical gait in able-bodied individuals via an asymmetrical audible metronome [4,5]. In either case of persons with unilateral transtibial amputation or able-bodied individuals asymmetrically manipulated, it is not understood how much the mechanical and spatiotemporal asymmetries contribute to the metabolic cost of asymmetrical walking. Therefore, the purpose of this study was to determine how temporal and inertial asymmetries influence the metabolic costs of walking.

Methods

Ten persons (F = 6, 1.73 ± 0.09 m, 66.5 ± 14.3 kg, 27 ± 2 years, 275 ± 143 min/week of activity) were recruited to participate in two baseline conditions and two subsequent manipulation conditions during a single data collection session. The baseline conditions were designed to represent normal walking in symmetrically unweighted (NLS – No Load Symmetrical) and unilaterally weighted walking (LA – Loaded Asymmetrical). Manipulation conditions were designed to replicate gait manipulations where symmetry (LS – Loaded Symmetrical) or asymmetry (NLA – No Load Asymmetrical) were forced and do not represent the natural gait patterns used in the baseline conditions. Conditions were achieved with the addition of a unilateral 2kg mass attached to the ankle, a symmetrical metronome, or a metronome set to elicit asymmetrical walking at the magnitude caused by the unilateral mass. Spatiotemporal measures were calculated in Visual 3D (C-motion, Germantown, MD) from motion capture data (VICON, Englewood, CO) and ground reaction force data from a tandem-belt instrumented treadmill (AMTI, Watertown, MA), while gas exchange and metabolic cost were measured via indirect calorimetry with a metabolic cart (Parvo Medics, Sandy, UT). A repeated measure ANOVA was performed to determine if the metabolic cost of walking differed between conditions. Two, two factor (load x swing time, load x manipulation) ANOVAs were performed on net metabolic cost of walking data.

Results and Discussion

In general, the findings reveal a significant increase in the net metabolic cost of walking for all conditions compared with the baseline normal walking (NLS) data. There was an interaction between load and swing time symmetries where metabolic costs increased when forcing non-normal swing time symmetry, e.g., a greater cost during NLA compared with NLS and a greater cost during LS compared with LA. This is supported by manipulation conditions (i.e., LS and NLA) resulting in a significantly greater metabolic cost than baseline conditions. In turn, one factor of load or swing time symmetry may not have a greater effect on the metabolic cost of walking, but rather a manipulation from the natural gait pattern symmetry increases the metabolic costs of walking (Figure 1).

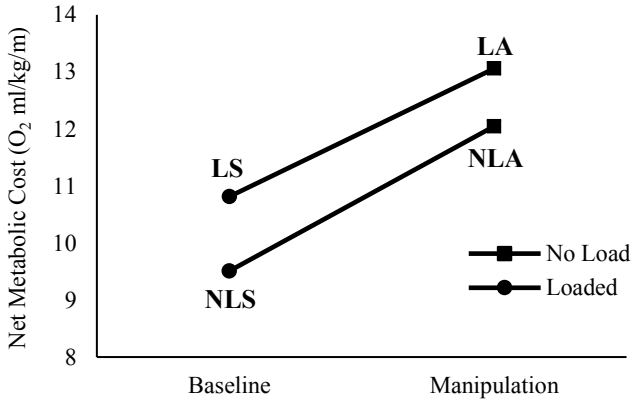

Figure 1: Main Effect of Manipulating Swing Time Symmetry. No interaction was noted between factors of load and manipulation; however, both main effects were found to be significant ($p < 0.05$).

Significance

Both unilateral mass and asymmetrical metronome resulted in an increase in the net metabolic cost of walking relative to unperturbed walking. Further, the factor of manipulating the natural temporal gait patterns that arise from the presence of a unilaterally added mass significantly increased the net metabolic cost of walking. In turn, the attempt to overcome the resulting temporal asymmetry from an interlimb mass asymmetry resulted in a metabolic penalty. To avoid increasing the metabolic demand that persons with a unilateral transtibial amputation are faced with during walking, clinicians should avoid forcing a symmetrical gait pattern. Forcing individuals to walk symmetrically in the presence of a lower extremity inertial asymmetry results in a higher metabolic cost than simply allowing individuals to choose a preferred gait pattern which results in a temporal asymmetry druing walking.

References

[1] Mengelkoch et al. (2014). *Int J Sport Med*
[2] Langford et al. (2019). *Disabil Rehabil*
[3] Smith et al. (2013). *Hum Movement Sci*
[4] Beck et al. (2018). *Eur J Appl*
[5] Ellis et al. (2013). *Proc R Soc B*

Ankle Exhibits Consistent External Quasi-Stiffness Behavior Across Level, Sloped, and Uneven Terrain: Implications for Prosthesis Design

Harrison L. Bartlett[1,2] and Michael Goldfarb[1,2]
[1]Vanderbilt University, Nashville, TN, USA
[2]Synchro Motion, LLC, Franklin, TN, USA
Email: hbarlett@synchro-motion.com

Introduction

Humans regularly encounter sloped and uneven terrain during everyday activities such as walking on a cracked sidewalk or hiking. However, the majority of human walking studies are performed on smooth, level ground. These level-ground studies shed light on the underlying mechanisms of human walking and have also provided insights that guide the design of prosthetic limbs. One such insight commonly utilized in the design of prosthetic feet is the observation that during the mid-stance phase of level-ground walking, the ankle exhibits a spring-like relationship between ankle torque and ankle angle, which will here be called internal quasi-stiffness. Internal quasi-stiffness provides a strong basis for spring-like prosthetic feet that store and release energy during the stance phase of walking. Unfortunately, these level-ground walking behaviors are not consistent on sloped or uneven terrain, and as such, current prosthetic foot designs are suboptimal under those conditions. In order to design prosthetic feet that can accommodate various terrains, the gait of unimpaired individuals should be examined on uneven and sloped terrain to glean design insights.

A previous study on uneven terrain walking observed that during mid-stance, unimpaired individuals maintain a consistent spring-like behaviour between ankle torque and the orientation of the shank in the world coordinate frame (referred to as shank angle)[1], which will here be called external quasi-stiffness. The current study builds upon [1] to determine if this external quasi-stiffness behaviour observed in uneven terrain walking extends to level ground and globally sloped walking.

Methods

Data from [2] were analyzed to assess the degree to which external quasi-stiffness is maintained while walking across globally sloped terrain. The data analyzed consists of ten unimpaired subjects walking on slopes ranging from -6 to 6 degrees in 3 degree increments at a speed of 0.8 m/s. Reflective markers were used to track the motion of limb segments, and joint torques were calculated using inverse dynamics methods detailed in [2]. Ankle torque, ankle angle, and shank angle were computed during mid-stance phase of gait on each global slope. The consistency of internal quasi-stiffness was assessed by examining the slope (internal quasi-stiffness) and torque zero-crossing (internal quasi-stiffness set point) of the ankle torque vs. ankle angle trajectories (Fig. 1a). The consistency of external quasi-stiffness was assessed similarly by examining the slope and torque zero-crossing of the ankle torque vs. shank angle trajectories (Fig. 1b).

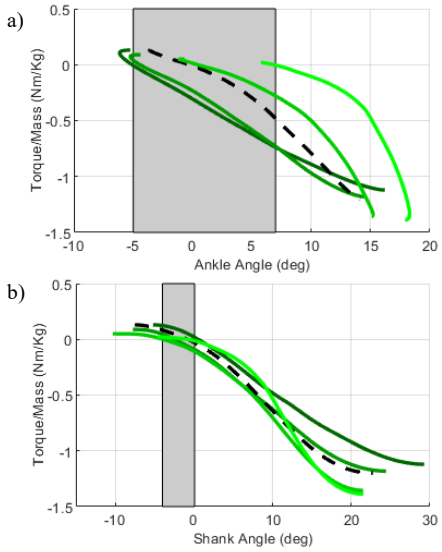

Figure 1: Ankle torque vs. ankle angle during middle stance (a) and shank angle (b) for unimpaired subjects walking on sloped ground ranging from -6 degrees (dark green) to +6 degrees (light green) compared with level-ground (black dashed line). The range of ankle torque zero-crossing values in each plot is indicated with a gray shaded band. Fig. 1a shows the ankle joint internal quasi-stiffness while Fig. 1b shows the ankle joint external quasi-stiffness.

Results and Discussion

The trajectories in Fig. 1 begin at the left-most position and move from left to right, with the magnitude of ankle torque increasing as the individual progresses through stance. Fig. 1a shows that the ankle joint internal quasi-stiffness is relatively inconsistent across various ground slopes. In contrast, the similar trajectories shown in Fig. 1b indicate that the ankle maintains a relatively consistent external quasi-stiffness during sloped walking. This result is consistent with [1], indicating that the external quasi-stiffness behaviour is maintained during mid-stance of walking on level, sloped, and uneven terrain.

Significance

Just as internal quasi-stiffness models of ankle function during level ground walking have inspired the design of current spring-like prosthetic feet, this external quasi-stiffness model of walking on various terrains may be able to lend insights into the design of prosthetic feet capable of walking on sloped and uneven terrain.

Acknowledgments

The authors would like to thank Karl Zelik and Eric Honert for allowing access to the data used in this study.

References

[1] Shultz and Goldfarb (2018), *TNSRE*, **26(4)**: 788-797
[2] Honert and Zelik (2019), *Human Movement Sci.*, **64:** 191-202

Repeated Error-Based Gait Training for Non-Traumatic Amputation: Proof of Concept Study

Paul W. Kline[1,2], Noel So[2], Thomas T. Fields[2], and Cory L. Christiansen[1,2]
[1]University of Colorado Anschutz Medical Campus, Aurora, CO, USA
[2]VA Eastern Colorado Healthcare System, Aurora, CO, USA
Email: cory.christiansen@cuanschutz.edu

Introduction

Chronic gait pattern compensations are common for people with unilateral, non-traumatic transtibial amputation (TTA), and are characterized by asymmetrical step lengths.[1] Such sustained gait compensations likely contribute to secondary musculoskeletal conditions that can affect functional mobility and quality of life.[2]

Error-augmentation gait training (EGT) has demonstrated promise in correcting asymmetrical step lengths after non-traumatic TTA.[3] Using a split-belt treadmill, EGT can be applied by exaggerating step length asymmetry using separate belt speeds under each lower limb. Such an EGT protocol has shown potential for immediate adaptation to greater step length symmetry in patients with non-traumatic TTA.[3] It is unknown if repeated exposure to EGT can lead to persistent adaptation, beyond the immediate response of a single session.

The purpose of this proof-of-concept study was to examine the feasibility and responsiveness of a four-week EGT protocol for people with unilateral, non-traumatic TTA. We hypothesized that repeated EGT sessions over four weeks would be feasible based on protocol fidelity, safety, and participant acceptability. In addition, we hypothesized a small-medium effect of improved step length symmetry 1-week following the intervention.

Methods

Eight participants (8 M, 65±9 years old, 30.8±4.3 kg/m^2, 41±33 months since TTA, 7±3 comorbidities) with unilateral, non-traumatic TTA were enrolled in an EGT protocol using a split-belt treadmill (Bertec Corporation). The intervention included 8, 30-minute sessions delivered over a 4-week period. Each session included five, three-minute sets of EGT at a 2:1 ratio of asymmetrical belt speeds. The faster belt was set to 75% of the participant's self-selected overground gait speed.

Feasibility outcomes included EGT dose goal attainment compared to protocol (protocol fidelity), number and type of adverse events (safety), and Intrinsic Motivation Inventory – Interest/Enjoyment subscale (acceptability). Step length during overground walking at self-selected speeds were assessed at baseline (prior to EGT), once a week during the EGT protocol, and one-week following the last EGT session. Between-limb step length symmetry was calculated using the Normalized Asymmetry Index (NSI).[4] Responsiveness to EGT was evaluated with Cohen's *d* effect size from baseline to one-week follow-up.

Results and Discussion

Seven of the eight participants (87.5%) completed the intervention at the prescribed dose (intensity and duration), with an average overground walking speed of 1.0±0.1 m/s. One participant did not complete the protocol due to a skin blister on their residual limb, which was possibly related to the intervention. This participant completed only one session of EGT, which was deemed insufficient exposure to warrant outcome testing. No falls, musculoskeletal injuries, or increases in pain occured. Participants rated EGT to be acceptable based on scores above 5 on the Intrinsic Motivation Inventory – Interest/Enjoyment subscale (6.6 ± 0.5; mean ± SD).

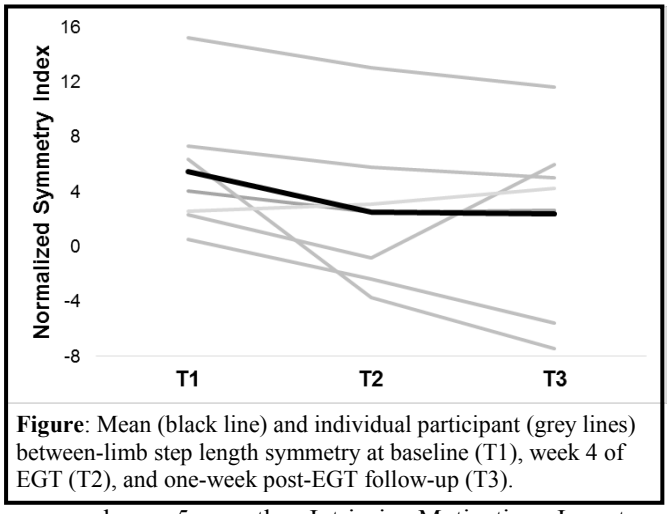

Figure: Mean (black line) and individual participant (grey lines) between-limb step length symmetry at baseline (T1), week 4 of EGT (T2), and one-week post-EGT follow-up (T3).

Average between-limb step length was more symmetrical one-week following EGT (2.41 ± 6.59) compared to baseline (5.47 ± 4.91) indicating a moderate effect size (d=0.52). Individual step length symmetry responses varied (Figure).

The results partially support our hypotheses, demonstrating high protocol fidelity, participant acceptability, and a signal of efficacy for the four-week EGT protocol. The single residual limb skin blister was concerning, as it was possibly related to increased walking exposure. This finding support the idea that neurovascular comorbidities associated with non-traumatic TTA require close attention, including thorough skin tolerance assessment and cautious progression of EGT for this population.

Significance

To date, only single-session EGT studies have been performed for people with TTA, which have demonstrated gait symmetry adaptability.[3,5] Based upon this current study, four weeks of EGT using a split-belt treadmill is feasible for people with unilateral non-traumatic TTA and may modify step length asymmetry up to a week after intervention. The study of EGT efficacy is warranted, in pursuit of intervention to optimize gait patterns and reduce functional limitations with this patient population.

Acknowledgments

Funding: NIH CTSA grant TL1 TR002533.
The content is solely the responsibility of the authors and does not necessarily represent the official views of the NIH, the U.S. Department of Veterans Affairs, or the U.S. Government.

References

1. Isakov E, et al. *Prosthet Orthot Int.* 2000;24(3):216-220.
2. Gailey R, et al. *J Rehabil Res Dev*. 2008;45(1):15-29.
3. Kline PW, et al. *Prosthet Orthot Int*. 2019;43(4):426-433.
4. Queen R, et al. *J Biomech*. 2020;99:epub ahead of print.
5. Darter BJ, et al. *PLoS One*. 2017;12(7)

Effect of Intrepid Dynamic Exoskeletal Orthosis (IDEO) design on knee total joint moment and gait parameters.

Wyatt D. Ihmels[1], Tatiana Djafar[1], Julianne Stewart[1], John Collins[1], & Trevor Kingsbury[1]
[1]Clinical Biomechanics Laboratory, Naval Medical Center San Diego, San Diego, CA, USA
Email: wyatt.ihmels@gmail.com

Introduction

The Intrepid Dynamic Exoskeletal Orthosis (IDEO) provides mechanical compensation for patients with inadequate ankle function [1]. However, this compensation may alter biomechanics up the kinetic chain during gait. In fact, IDEO users exhibit decreased knee sagittal plane range of motion compared to control counterparts [1]. Currently, the impact of the IDEO on knee joint moments during gait compared to an unbraced shod condition is unknown. Additionally, the design of the IDEO has recently been updated from posterior laminated cylindrical rods (Old) to an interchangeable flat strut (New). To our knowledge, comparison of gait parameters between the two brace designs has not yet been performed. Thus, the purpose of this study was to examine temporal-spatial parameters of the two IDEO brace designs and determine the impact of IDEO on the knee total joint moment during gait.

Methods

Participants for this study were identified through a retrospective search of our clinical registry. Inclusion criteria included a completed gait analysis both shod and wearing an IDEO (Old or New). Each gait analysis included the participant walking at a self-selected speed for a series of passes until three successful force-platform foot strikes and five total strides were collected for each condition (IDEO and SHOD). Forty (20 Old; ht: 1.81 ± 0.06 m, wt: 98.8 ± 11.8 kg, age: 35.6 ± 8.1 and 20 New; ht: 1.80 ± 0.05 m, wt: 96.1 ± 15.8 kg, age: 34.2 ± 7.9 years) participants met this inclusion criteria.

During each pass, temporal-spatial parameters and knee biomechanics were quantified from synchronous marker and GRF data. Standard inverse dynamics were used to calculate knee joint moments which were normalized to participant mass (kg) and height (m). MATLAB (Mathworks, Natick, MA.) code was used to estimate knee joint load by calculating peak knee total reaction moment (TKM) using knee flexion, abduction, and internal rotation, moments, as well as TKM sagittal (TKM_{sag}), frontal (TKM_{front}) and transverse (TKM_{trans}) plane components [2].

For analysis, temporal–spatial parameters (velocity, stride length, and stride width), peak stride (0 – 100%) TKM, and TKM_{sag}, TKM_{front}, and TKM_{trans} components were calculated and sent to a two-way RM ANOVA for main effect and interaction analysis ($\alpha = 0.05$) of group (IDEO and SHOD) and brace (Old and New).

Results and Discussion

Use of the IDEO increased velocity 0.11 m/s ($p<0.001$) and stride length 0.14 m ($p<0.001$) compared to the SHOD condition (Table 1), demonstrating an increase in functional recovery [3]. However, no differences were seen in stride width ($p=0.156$). Further, no significant differences in velocity ($p=0.505$), stride length ($p=0.070$), or stride width ($p=0.948$) were evident between Old and New braces, indicating that gait performance may not differ between IDEO designs.

Participants displayed a 19.5% increase in peak TKM with IDEO compared to an unbraced SHOD condition ($p<0.001$; Fig. 1). Greater TKM with IDEO use during gait may lead to reduced overall knee joint health, as higher knee joint loads can induce cartilage degeneration and development of knee osteoarthritis [4]. However, IDEO use also increased TKM_{sag} 6.2% ($p=0.037$) and decreased TKM_{front} 7.2% ($p=0.037$) compared to SHOD. Erhart-Hledik et al. [4] previously reported participants with greater TKM_{sag}, accompanied by reduced TKM_{front}, exhibited a decrease in detrimental cartilage changes compared to participants with greater TKM_{front} contribution. Thus, the shift in TKM components displayed in the current study may represent the most ideal compensation for the increased knee joint load with IDEO use.

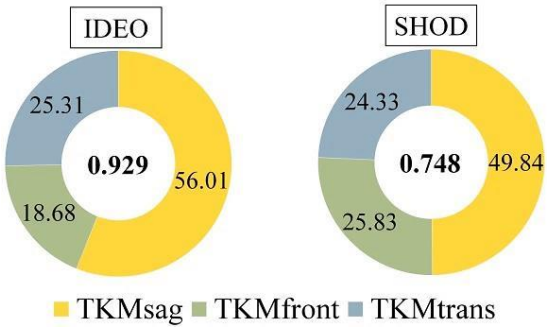

Fig 1: Mean TKM and TKM components (0 – 100%) for IDEO and SHOD conditions

Significance

Wearing an IDEO improved patients' gait parameters and subsequent functional outcomes. IDEO also increased peak TKM and risk of cartilage deterioration, but shifted TKM components in perhaps the least detrimental way possible to accommodate for the heightened knee joint load.

Acknowledgments

The views expressed herein do not necessarily reflect those of the Department of the Navy, Department of Defense, Defense Health Agency, or the U.S. Government. All data were collected under IRB#: NMCSD.2020.0014.

References

[1] Esposito et al. (2014). *J. Ortho & Related,* **10**: 3026-35.
[2] Asay et al. (2018). *J. Ortho Research,* **9**: 2373-79.
[3] Baker & Hewison (1990). *Prosthetics & Orthotics,* **14**: 80-4
[4] Erhart-Hledik et al. (2019). *J. Ortho Research,* **7**: 1546-54.

Table 1: Mean (SD) temporal – spatial parameters during gait at self-selected speed.

	Velocity (m/s)		Stride Length (m)		Stride Width (m)	
	New	Old	New	Old	New	Old
IDEO	1.29 (0.1)	1.31 (0.2)	1.41 (0.2)	1.51 (0.1)	0.36 (0.3)	0.36 (0.3)
SHOD	1.17 (0.2)	1.22 (0.2)	1.31 (0.1)	1.38 (0.1)	0.36 (0.3)	0.35 (0.3)

Effects of Incremental Mass Changes on Wheelchair Motion Using Robotic Tester

Jacob Misch*, Stephen Sprigle PT PhD
Rehabilitation Engineering and Applied Research (REAR) Lab, Georgia Institute of Technology
Email: * mischjp@gatech.edu

Introduction

In an effort to reduce shoulder strain and energetic exhaustion during manual wheelchair (MWC) motion, it is imperative to optimize the vehicle via examination of each design choice. Tire selection and proper maintenance often far overshadow the impacts of mass when using human subjects, even with 10 kg added to the system.[1, 2] However, differences of less than 3 kg separate "standard" from "ultra-lightweight" MWCs, among other criteria. This work showcases a method of using a robotic mechanism[3] to investigate parameters that are hard to precisely control with human subjects.[4] In this study, the robot propelled MWCs with cyclic strokes of torque to replicate the acceleration and coasting that occurs during human motion. We measured the differences in wheelchair motion due to incremental changes in both system mass and weight distribution.

Methods

The Anatomical Model Propulsion System (AMPS) seen in **Figure 1** was employed as a surrogate for testing the MWCs. Torque was applied from motor 'hands' to custom push-rims on the drive wheels. The AMPS applied the standardized torque profile from **Figure 2** to each chair. The trajectory was designed to feature 3 strong "acceleration" pushes followed by 10 identical "steady-state" pushes to maintain velocity. 30 total trials were collected per configuration, with 15 in one heading direction and 15 in the other, to normalize over any inconsistencies in the floor. The analysis period consisted of datapoints between the start of the first push (2.0 s) and the end of the last push (17.0 s).

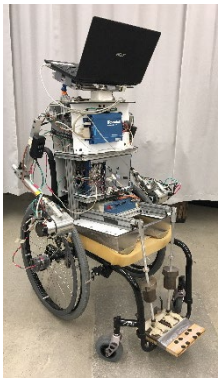

Figure 1. The AMPS.

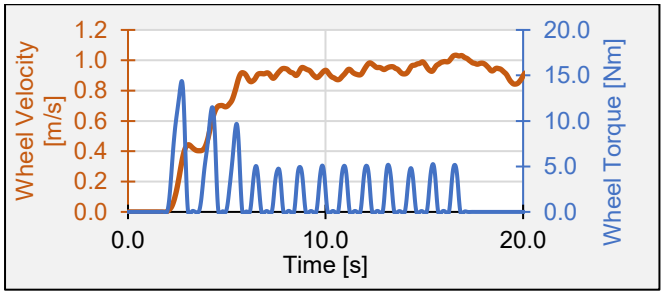

Figure 2: Representative applied torque profile and resulting wheel velocity during a single straight overground trial.

For this experiment, five configurations were used. The AMPS and MWC collectively weighed 93.6 kg with 72% of the weight centered over the drive wheel axle. This was used as the baseline case (+0 kg on the shelf or the footrest, represented as 0S, 0F). A Dibond metal shelf was added under the seat to fasten +2 kg and +4 kg at the center of mass without shifting weight distribution. Moving the weights from the center of mass to the footrest shifted the center of mass forward to 69% over the drive wheels for +2 kg and 66% for +4 kg.

Results and Discussion

The power input to the system was calculated by multiplying torque applied to the wheels with the angular speed of the wheels. Work input, in Joules, was calculated by integrating the power over the duration of the maneuver. One outcome parameter, propulsion cost, was defined as the cumulative sum of work divided by the total distance traveled during the maneuver. A more tangible and descriptive outcome parameter was the total distance travelled by the center of mass during the maneuver.

Table 1: Propulsion costs and distances of each configuration.

	Total Propul. Cost (J/m)				Total Dist. Traveled (m)			
Config	Mean	StDev	Effect Size	% Change	Mean	StDev	Effect Size	% Change
0S, 0F	13.06	0.17	-	-	11.37	0.37	-	-
2S, 0F	13.15	0.14	0.53	+0.65%	10.85	0.45	1.27	-4.61%
4S, 0F	13.21	0.16	0.88	+1.13%	10.58	0.40	2.03	-6.90%
0S, 2F	13.23	0.18	0.93	+1.25%	11.00	0.44	0.91	-3.24%
0S, 4F	13.37	0.17	1.76	+2.34%	10.44	0.45	2.27	-8.21%

The data collected in **Table 1** show only slight differences in propulsion cost across the 5 configurations. The Cohen's *d* effect sizes of medium (0.5) to large (>0.8) imply that the configurations are distinctly grouped, yet the percent differences are less than 2.5%. In contrast, the average total distance traveled by the configurations show much greater difference between groups. All effect sizes are large, and the distances are noticeably different by the human eye. The standard configuration travels at least 0.3 m farther than any other case. Added mass appears to be the dominant factor over weight distribution for travel distance.

Significance

This work demonstrates the importance of examining the MWC system, independent of the human occupant. By mimicking the propulsion torque profile of the human user, the AMPS was able to propel the chairs with high repeatability, and measured small discrepancies in the motion between configurations representing frame masses of standard and ultra-lightweight MWCs.

Interestingly, this study highlights the minimal effect of mass on the propulsion cost and its relatively large effect on distance travelled. The +4 kg configuration rolled nearly 1.0 m less than the standard configuration, an effect that is magnified when the weight distribution is shifted forward over the casters. Thus, despite minute differences in the configurations spanning multiple categories of MWCs, both parameters are optimized at lower masses loaded mostly over the rear wheels.

References

1. de Groot, S., et. al., *Med Eng Phys*, 2013. **35**(10): p 1476-82.
2. Sagawa Jr, Y., et al., *Archives of physical medicine and rehabilitation*, 2010. **91**(8): p 1248-1254.
3. Liles, H., et al., *IEEE Trans Neural Syst Rehabil Eng*, 2015. **23**(6): p 983-91.
4. Sprigle, S., Huang, M., *Assist Technol*, 2015. **27**(4): p 226-35.

Finger Gesture Recognition of Forearm Amputee according to the Sampling rate

Taehee Kim, Jongman Kim, Bummo Koo, and Youngho Kim*
Department of Biomedical Engineering and Institute of Medical Engineering, Yonsei University, Korea
Email: *younghokim@yonsei.ac.kr

Introduction

Surface electromyogram (sEMG) is effective to control prostheses for forearm amputees. Pattern recognition techniques with the selection of some feature vectors have been applied to control various finger gestures. However, sEMG features, especially in the time domain, may vary depending on the sampling rates[1]. In addition, the recognition accuracy also depended on the feature selection. The objective of the study was to determine the effect of the sampling rate and the feature selection of sEMG on the finger gesture recognition for forearm amputees.

Methods

The Non-Invasive Adaptive Prosthetics (NinaPro) datasets[2] was used for the study, in which EMG signals were collected from 11 amputees with a sampling rate of 2,000Hz. In NinaPro datasets, 52 different hand gestures were performed using 12 sEMG sensors (Trigno Wireless, Delsys, USA). In this study, only 7 hand gestures were used: fist, pointing index, thumbs up, 2 finger (index and thumbs) grasp, sphere grasp, cylinder grasp and extention of index and middle finger. Data from only 8 sEMG sensors, equally spaced around the forearm at the height of the radio-humeral joint, were selected for the study. The extracted sEMG data were segmented into 250ms windows with 100ms moving. The segmented data were down-sampled from 2,000 to 50 with divisors of 2,000 (50, 80, 100, 125, 200, 250, 400, 500 and 1,000). All data were low-pass filtered at the cut-off frequency based on the Nyquist sampling theory.

Mean average value (MAV), waveform length (WL), zero crossings (ZC), slope sign changes (SSC) were calculated as sEMG features of artificial neural network (ANN) for every window[3]. The performance of a trained classifier was determined using the cross-validation. MATLAB (Mathworks, USA) was used to analyse the data and Scheffe's post hoc test was performed to determine the statitical differences using SPSS (IBM, USA). A probability of the null hypothesis was set by 0.05.

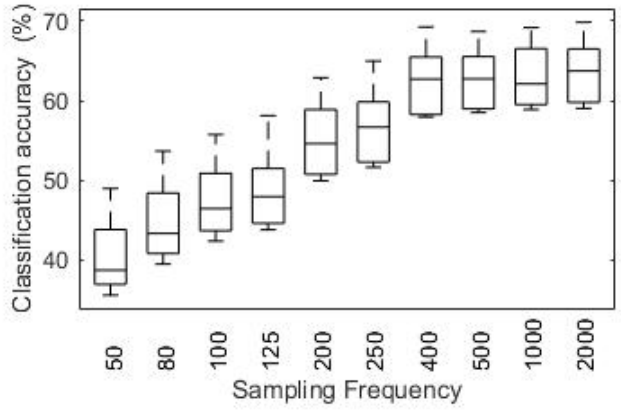

Figure 1: Classification accuracy according to sampling rate.

Results and Discussion

Figure 1 shows the classification accuracy for different sampling rates. In general, the classification accuracy increased with the sampling rate of EMG signals. 2,000Hz sampling showed the highest accuracy (63.47%), but no statistical significance was found in the classification accuracy for different sampling rates from 400Hz to 2,000Hz ($p > 0.407$). However, significantly low classification accuracy was observed in the sampling rates below 400Hz. 50Hz sampling showed the lowest classification accuracy (40.51%).

Table 1 shows that classification accuracy for feature selections with different sampling rates. For every feature selection, the higher sampling rates, the higher accuracies were achieved. 4 features combination showed the highest accuracy (63.47%) in 2,000Hz and ZC showed the lowest (23.23%) in 50Hz.

Tables 1 : Classification accuracy with different EMG feature selections (%).

EMG features	Sampling rate			
	50 Hz	200 Hz	400 Hz	2,000 Hz
MAV	44.7 ± 6.3	54.3 ± 6.2	56.9 ± 5.62	57.5 ± 5.4
WL	42.9 ± 6.4	54.7 ± 6.6	59.0 ± 5.60	60.5 ± 4.4
ZC	23.2 ± 2.3	37.8 ± 3.5	46.7 ± 4.63	46.4 ± 4.3
SSC	31.1 ± 1.5	41.0 ± 4.8	47.5 ± 5.08	42.7 ± 3.3
4 features combination	40.5 ± 4.0	50.9 ± 6.1	58.2 ± 5.06	63.5 ± 4.9

Significance

The present study showed that sampling rate of sEMG clearly affected the accuracy in gesture recognition: Too low sampling rate of sEMG would be inappropriate. In addition, the combinations of some important time domain features would be suitable for the good ANN-based classification performance. Further studies with other amputee subjects would be required to confirm the present results.

Acknowledgments

This research was supported by Bio & Medical Technology Development Program (2017M3A9E2063270) through the National Research Foundation of Korea (NRF) funded by the Minisity of Science and ICT.

References

[1] G Li et al., *Annual Int. Conference of the IEEE Eng. in Medcine and Biology*. IEEE, 2010
[2] M Atzori et al., *Scientific data* 1.1: 1-13, 2014
[3] Hudgins B et al., *IEEE Trans. on Biomedical Eng.* 40.1:82-94, 1993

Modulating Distal Foot Energetics Using A Customized Deformable Foot Orthosis

Adrienne D Henderson[1], Thomas A Hulcher[1], Dustin Bruening[2], Elisa S Arch[1]
[1]University of Delaware, Newark, DE; [2]Brigham Young University, Provo, UT
Email: ahendo@udel.edu

Introduction

Efficient gait is fundamental for independent living. By producing large amounts of positive power late in stance, the ankle has long been considered the primary driver for forward propulsion. Certain pathologies decrease the ankle-foot (A/F) system's power production, leading to less efficient gait. To mitigate this power loss, ankle-foot orthoses (AFOs) are commonly prescribed to enhance a patient's ankle energetics. However, with current AFOs, many patients only have limited gains in ankle power and thus forward propulsion.

Recent research shows the foot does not simply act as a rigid lever but actively contributes to gait energetics.[1] As such, we believe an AFO that seeks to improve foot energetics may enhance user outcomes. Specifically, we hypothesize that a deformable foot orthosis (i.e. AFO footplate) that stores and returns energy could help improve A/F energetics and thus, eventually, gait efficiency. This study's purpose was to determine if a deformable foot orthosis can store and return energy to a typical A/F system in a beneficial way.

Methods

Eight healthy subjects (age: 27.7 ± 4.4 yr, height: 171.1 ± 8cm, weight: 74.7 ± 17.1kg) first performed a baseline barefoot (BF) gait analysis with anthropometric measurements (foot length, width, MTP joint axis) in order to personalize bilateral carbon fiber foot orthoses with a deformable forefoot region. Once manufactured, the subject returned to the lab to walk with two footwear conditions: with minimalist shoes (SH) and with the foot orthoses inside the minimialist shoes (ORTH). Subjects walked at 0.8 statures/sec for all three conditions while kinetic and kinematic data were collected. A three-marker cluster on the superior midfoot was used to track the foot (MFT). Three subjects had three extra markers on their heel to allow ankle power to be calculated when the foot was tracked by the hindfoot, thereby allowing ankle energetics to be discriminated from midfoot energetics. Power curves and work done for the ankle-midfoot (tracked by MFT), ankle (tracked by HFT), distal foot, and A/F complex (ankle-midfoot + distal foot) were extracted for all three conditions. A repeated measures ANOVA with a post hoc test using a Bonferroni correction was used to evaluate changes across conditons for all work metrics except net ankle work (i.e. n=3).

Results and Discussion

The positive distal foot work was significantly greater in the ORTH condition compared to both BF and SH ($p<0.001$) showing the deformable orthosis did indeed return energy. The ankle-midfoot seemed to respond to this by decreasing its net work in the ORTH vs. SH ($p=0.006$). These changes resulted in a relatively equal net A/F complex work across conditions ($p=0.63$). The ankle powers calculated with the MFT tracking likely includes ankle + some midfoot energetics whereas HFT tracking more likely isolates the ankle joint. The ankle powers using HFT tracking were consistently lower than the ankle-midfoot power, supporting the notion that some midfoot energetics were included in the ankle-midfoot parameters. This is further supported by a comparison of ankle-midfoot and ankle peak powers in the BF/ SH with ORTH conditions. The ankle power and work remained relatively consistent cross conditions unlike the ankle-midfoot metrics which see decreases in ORTH. This suggests power from the foot orthosis influences energetics elsewhere in the foot and perhaps is not affecting the ankle.

Significance

Deformable foot orthoses can store then return energy in a beneficial way to the A/F complex for typical individuals. This new technology could prove effective in patients with A/F impairments (e.g. stroke survivors) to enhance A/F energetics and potentially improve gait efficiency.

References

1.Takahashi, K.Z., et al. Sci Rep, 2017. 7(1): 1-9.
2.Arch, E.S., et al. J Appl Biomech, 2016. 32(6):571-577.

Table 1: Work (J/kg) averages measured in all 3 conditions with associated p-values from ANOVA. Measurements used data from all 8 subjects except Net Ankle Work, which had data from 3 subjects.

	Barefoot	Shoe	Orthosis	*p-value*
Positive Distal Foot Work	0.0106	0.0092	0.0397	*<0.001*
Net Ankle-Midfoot Work	0.1779	0.1823	0.1237	*0.005*
Net A/F Complex Work	-0/0089	-0.0200	-0.0512	*0.630*
Net Ankle Work (n=3)	-0.0289	-0.0434	0.0915	

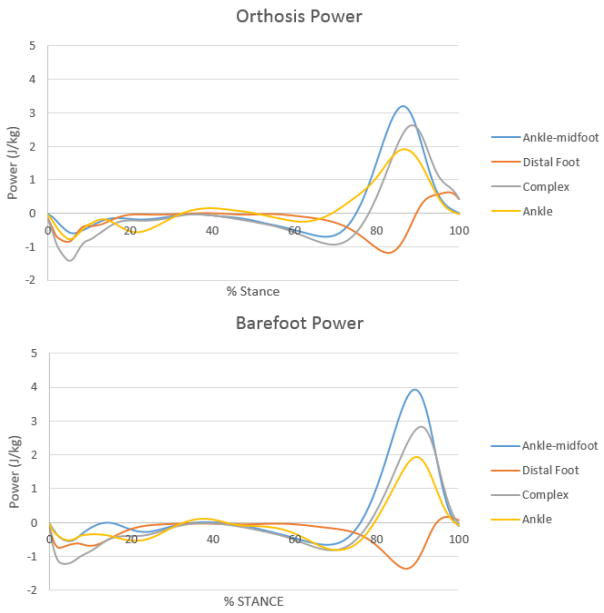

Figure 1: Barefoot and Orthosis power curves. All power curves were calculated from all 8 subjects except for the Ankle, which only used 3. Power curves for Shoe condition not shown due to space limitations, but looked similar to Barefoot.

Impact Biomechanics in Individuals Using a Custom Carbon Fiber Ankle-foot Orthosis during Running

Elizabeth Russell Esposito[1,2,4], Simisola O. Oludare[2,3], Jonathan Elrod[3,4,5], and Kelly Schmitbauer[1,4]
[1]Extremity Trauma and Amputation Center of Excellence
[2]Center for Limb Loss and Mobility, VA Puget Sound Healtcare System, Seattle, Washington
[3]Henry M. Jackson Foundation, Bethesda, Maryland
[4]Center for the Intrepid, Brooke Army Medical Center, San Antonio, TX
[5]Walter Reed National Military Medical Center, Bethesda, MD

Email: Elizabeth.m.russell34.civ@mail.mil

Introduction

Custom carbon ankle-foot orthoses (AFOs) have enabled many individuals with lower limb musculoskeletal injuries to return to high impact activities [1,2]. A rigid footplate acts as a lever to allow the posterior portion of the AFOs to deflect to store and return energy. During activities, such as running, this energy storage and return can be best achieved when using a forefoot strike pattern to utilize the longest lever arm. A forefoot strike pattern has also been reported to reduce impact forces, rate of force development, and impact shock [3] in healthy individuals. Because these impact variables are linked to overuse running unjuries [4], it is important to identify how using an custom carbon AFO for running affects these metrics. Few studies have investigated these devices during running and have found interlimb asymmetry with the unaffected limb having higher loading rates than the AFO side and on the upper end of average values reported in the literature in healthy adults [5]

Methods

Ten individuals (3 female, 37.1±4.4 years, 1.75±0.09 m, 83.0±16.5 kg) with musculoskeletal injuries requiring the use of a passive dynamic AFO (Intrepid Dynamic Exoskeletal Orthosis, IDEO) participated. The IDEO is a custom, carbon fiber AFO with a rigid footplate aligned in plantar flexion, a tibial cuff, and a posterior strut that deforms to store and return mechanical energy. It was required that all participants had worn their AFO for at least 2 months prior to study involvement. Participants ran at a self-selected speed over level ground while kinematic (240 Hz) and kinetic (1200 Hz) data were recorded. Vertical ground reaction forces were recorded from 8 force platforms embedded in the running path and tibial acceleration was recorded from shank-mounted, triaxial accelerometers. Footstrike angle, rate of force development, and peak tibial shock were compared between the sound and AFO limbs using paired t-tests ($p<0.05$).

Results and Discussion

There were no significant differences between limbs for foot strike angle at initial contact or tibial impact shock ($p>0.05$) (Figure 1). These results are contrary to our hypothesis that there would be a decrease in both metrics due to the design of the AFO footplate in plantar flexion, which is intended to encourage a mid- to fore-foot striking pattern at initial contact. Subjects largely adopted rearfoot strike patterns, which is less advantageous for mechanical energy storage and return. These results suggest that the design of an AFO or alignment of an AFO by itself is not sufficient to lead to the desired outcome of encouraging mid to forefoot striking. These results are in line with a recent case study that showed that a biofeedback training protocol was necessary for a participant to use a mid to forefoot strike while running in an IDEO [6].

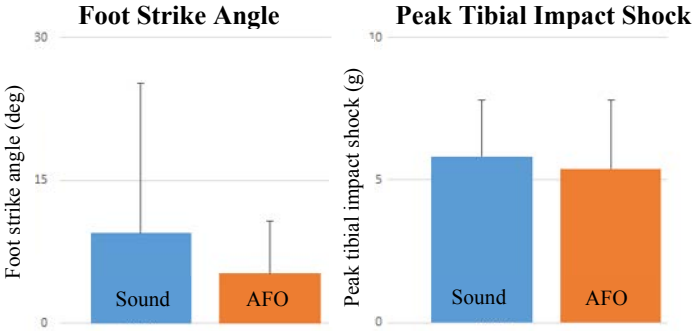

Figure 1: (Left) Foot strike angle and (Right) Peak tibial impact shock are not statistically significiantly different between the AFO and sound limbs. Dorsiflexion is positive for foot strike angle.

The average running speed of subjects in this study (3.08 m/s) was relatively slow. Footstrike angle is known to change with running speed. Thus, it is possible that these results would change with participants who run faster because our outcomes are speed dependent.

Significance

The study results indicate that the design of an AFO by iteself is insufficient to cause an individual to adopt an atypical footstrike pattern. This outcome suggests that a training program may be necessary to encourage running patterns that take better advantage of the mechanical properties of the device and encourage symmetry between limbs.

Acknowledgments

This research was supported by the Telemedicine and Advanced Technologies Research Centers' (TATRC) AMEDD Advanced Medical Technologies Initiative (AAMTI) award.

References

1. Owens et al (2011). *J Trauma*; 71: S120 – S124
2. Patzkowski et al (2011). *J Surg Orthop Adv;* 20: 8-18
3. Lieberman et al (2010). *Nature;* 463
4. Crowell and Davis (2011). *Clin Biomech;* 26:78-83
5. Schmitbauer et al (2019). *Prosthet Orthot Int;* 43:316-32
6. Yoder et al. (2019) Prosthet Orthot Int: 34:447-452

Designing and developing a new semi-rigid bilateral exoskeleton to assist hip joint motion

Arash Mohammadzadeh Gonabadi[1], Prokopios Antonellis[1],
Sara Myers[1], Iraklis Pipinos[2,3], and Philippe Malcolm[1]
[1]Department of Biomechanics, University of Nebraska at Omaha, Omaha, NE USA
[2]Department of Surgery, Veterans Affairs Medical Center, Omaha, NE USA
[3]Department of Surgery, University of Nebraska Medical Center, Omaha, NE USA
Email: *amgonabadi@unomaha.edu

Introduction

Robotic exoskeletons can reduce metabolic cost in healthy individuals restore mobility in patients with peripheral artery disease (PAD) [1]. PAD is a cardiovascular disease produced by atherosclerosis of the leg arteries. The primary symptom of PAD is claudication or pain in the legs during walking, which severely shortens the distance a patient can walk. Up to 40% of the metabolic cost of walking comes from the hip muscles [2]. Different groups have been developing rigid exoskeletons and soft exosuits that assist the hip. Assisting at the hip has the advantage that the exoskeleton mass is positioned close to the center of mass, which minimizes the energy cost of the added mass. Soft exosuits have the advantage that they allow greater freedom of movement. However, soft exosuits often cannot apply the same torque magnitudes as rigid exoskeletons, and they rely on friction with the skin to remain anchored.

The purpose of this work was to develop a semi-rigid hip exoskeleton that can connect to and be powered by an existing actuation unit, to address the limitations of current existing soft exosuits. We evaluated the device performance by analyzing the match between desired and actual torque applied to the hip joint.

Methods

The two pieces of the exoskeleton, anchor to the wearer via friction and compression, but they also stay locked on the body as a consequence of the actuation moment (Figure 1).

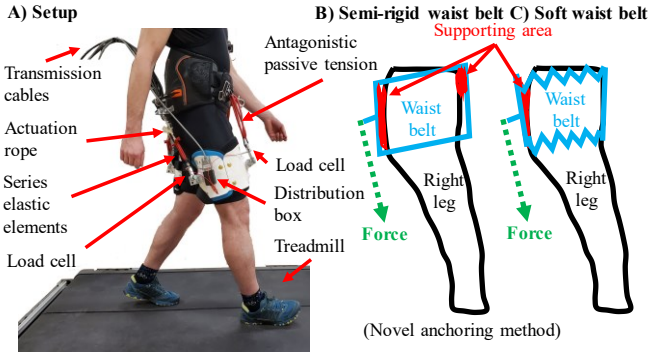

Figure 1: A) Hip exoskeleton setup. The waist belt attaches to a person. The two thigh-braces with the loadcells (Futek) measure the flexion and extension moment. B) Semi-rigid anchoring mechanism. The semi-rigid waist belt anchors to the waist by compression and because it gets stuck when the actuation force tries to rotate the belt. C) A soft waist waist-belt would only be able to anchor based on compression and friction.

We have also developed a high-level temporal controller. This controller enables sinusoidal extension and flexion moment profiles to be applied independently on each leg as a function of the stride cycle percentage. The timings of heel strikes, and toe offs are based on the vertical ground reaction force using an adjustable detection force threshold [3]. Since it is not possible to predict precisely when an ongoing walking step will end, the percentage of the step time is estimated based on the most recent heel contact time and a moving average of previous steps. The low-level controller developed by HuMoTech was used to minimize the error between actual and desired forces [4]. The actuation unit delivers the extension moment. We use a set of antagonistic springs, to deliver the flexion moment [5]

This new design will be tested in experiments aimed at developing faster and more clinically feasible human-in-the-loop optimization algorithms for patients. To measure the moment applied to the hip joint, we multiplied the lever arms by the flexion and extension forces, which allowed the desired sinusoidal profile across each percent of the gait cycle.

Results and Discussion

In preliminary testing, we have found a good match between the desired and actual torque for each leg (Figure 2). To achieve this result, we needed to adjust for proportional, derivative, and damping gains of the controller.

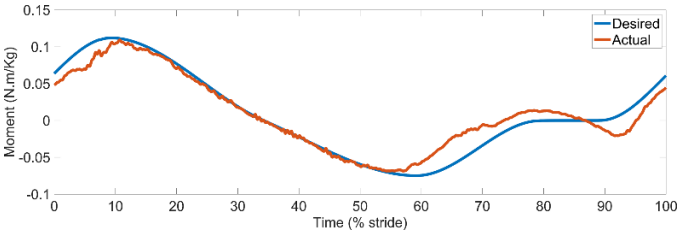

Figure 2: Desired versus actual moment profile. Extension moment is shown as positive, and flexion moment is shown as negative

Significance

The semi-rigid design of our exoskeleton introduces advantages in comfort and efficiency of control in patient populations because it requires less friction and compression than soft exosuits. Our initial work demonstrates a good match between the desired and actual torque the exoskeleton is able to generate for each leg.

Acknowledgments

NIH P20GM109090 and Graduate Research and Creative Activity Award (GRACA) for Arash Mohammadzadeh Gonabadi.

References

1. Nehler MR, et al. *Vasc Med*, 8, 115–26, 2003.
2. Gonabadi AM, Antonellis P, Malcolm P. *Plos Com. Biology*, under rev, 2020.
3. Gonabadi AM, Antonellis P, Malcolm P. *IEEE TNSRE*, 2020.
4. Caputo JM, et al. *J Biomech Eng*, 2014.
5. Kang I, et al. *IEEE Robot Autom Lett*, 4, 430-437. 2019.

Development of a system for assistance at the center of mass

Arash Mohammadzadeh Gonabadi, Prokopios Antonellis, and Philippe Malcolm
Department of Biomechanics and Center for Research in Human Movement Variability
University of Nebraska at Omaha, Omaha, NE USA
Email: *amgonabadi@unomaha.edu

Introduction

Walking can be modeled as an inverted pendulum. However, ankle push-off is needed to redirect the center of mass from the downward phase of one step to the upward phase of the next step which requires metabolic cost. Different groups have been developing devices to reduce metabolic cost. Inverted pendulum models [1] and studies with exoskeletons [2] suggest that timing is important for assisting walking. The purpose of our study was to develop a tether system that could generate horizontal forces with desired force magnitudes and timings.

Methods

We developed a system based on an existing control platform and cable actuation unit (HuMoTech, Pittsburgh, PA, Figure 1).

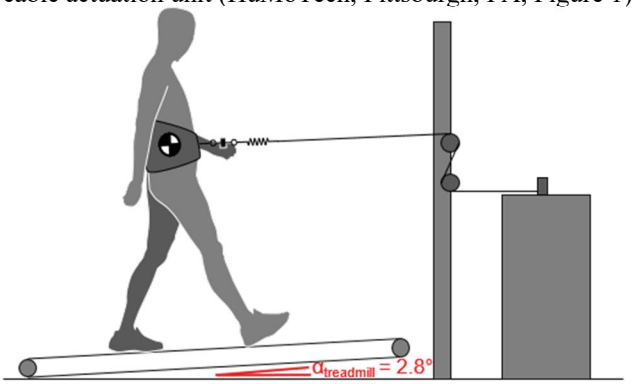

Figure 1: System setup.

The actuation unit produces forces via a direct-drive rotary motor. A force-control algorithm allows to program force profiles that follow a sinusoidal pattern with a desired timing in a repeatable way every step [3]. It is known that adding a series elastic element can improve the tracking of desired forces [4]. High stiffness allows faster response times, however, it might create noise. Intermediate stiffness can enhance force tracking, but it might add delay. A range of stiffnesses was tested by combining multiple loops of Thera-band in parallel. We additionally examined two metal springs.

Results and Discussion

We found that increasing stiffness reduced the root mean square error (RMSE) but this also led to an increase in oscillations in the actual force, characterized using an oscillation metric from [5]. This resulted in an ideal compromise of approximately 3000 Nm^{-1} (Figure 2). The optimal stiffness seems to be of a similar order of magnitude as stiffnesses used in other cable devices (2280 Nm^{-1} [5] and 2500 Nm^{-1} [6]). The steel spring with the highest stiffness (2577 Nm^{-1}) had a within-step RMSE that was about twice as high as the Thera-band spring with similar stiffness. The lowest RMSE value was 1.2% of body weight (BW) which is within the range of a similar tether that has been developed for applying constant forces [7].

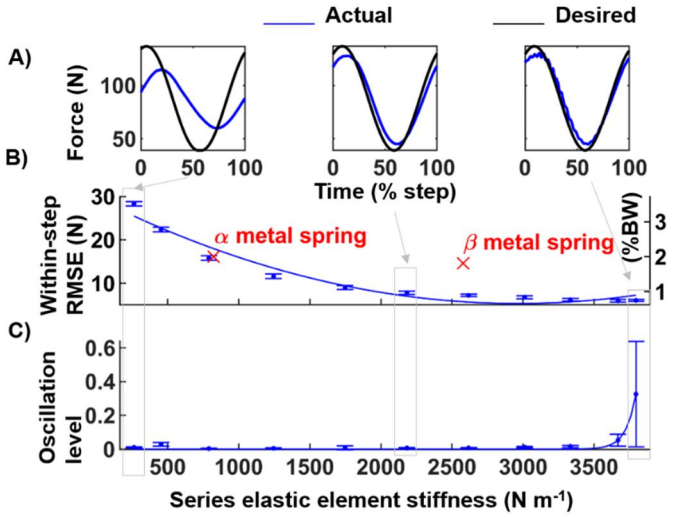

Figure 2: Series elastic stiffness optimization. A) Actual force (blue) and desired force (black) of walking with different series elastic element stiffnesses. B) Within-step RMSE versus stiffness. Dots and error bars show the mean and standard deviations of the steps of all Thera-band conditions. Red crosses show results from two steel springs. The blue lines are curve fits. C) Signal oscillation level.

Significance

By optimizing the series elastic element stiffness, we achieved accurate force tracking. Assisting with a tether that allows to apply forces with accurate timing could lead to greater assistance levels and metabolic cost reductions than exoskeletons, which could be helpful in clinical settings.

Acknowledgments

EPSCoR OIA-1557417 and NIH P20GM109090. Graduate Research and Creative Activity (GRACA) award for PA.

References

1. Kuo AD. *J. Biomech. Eng*, **124**, 113–120, 2002.
2. Malcolm P, et al. *PloS one*, **8**, 2013.
3. Gonabadi A. M., et al., In review TNSRE, 2019.
4. Zhang J, Collins, SH. *Front. Neurorobot*, **11**, 68, 2017.
5. Vashista V, et al. *IEEE ICRA*, 718-723, 2014.
6. Vashista V, et al. *IEEE TNSRE*, **24**, 872–881, 2016.
7. Simha SN, et al. *IEEE TNSRE*, **27**, 1416-1425, 2019.

Biomechanical Evaluation of a Wearable Passive Shoulder Exoskeleton

Morteza Asgari [a*], Dustin L. Crouch [a]
[a] Mechanical, Aerospace, and Biomedical Engineering Department, University of Tennessee, Knoxville
[*] sasgari@vols.utk.edu

Introduction

Movement disability involving the shoulder is associated with orthopedic (e.g. rotator cuff tears [1]) and neurological (e.g. stroke [2]) health conditions. Shoulder impairment can prevent patients from performing activities of daily living and, thus, substantially affect their quality of life and self-esteem. Wearable exoskeletons could meet the need for movement assistance to assist or rehabilitate upper extremity function in patients with shoulder disability. While many exoskeletons are "active" (e.g. motorized), mechanically passive exoskeletons may be a more practical and affordable solution to provide continuous, home-based movement assistance for patients. However, it is imperative to first understand how wearable passive exoskeletons interact with their users prior to clinical translation. We have developed a wearable, passive, cable-driven shoulder exoskeleton (WPCSE) that incorporates a cam wheel gearing component to compensate for part of the shoulder moment due to gravity. The objective of this pilot study was to evaluate how the WPCSE affects the activity of muscles crossing the shoulder during upper extremity movements.

Methods

The study was approved by the University of Tennessee, Knoxville IRB. The WPCSE used in this study was designed to compensate for approximately one-fourth of the shoulder moment due to gravity for a 50th percentile adult male (the design could be customized for individuals in future studies). Four able-bodied participants (3 males, 1 female, age = 27.25(4.45) *years*, height = 173.75(6.65) *cm*, weight = 68.40(5.12) *kg*) performed three different movements: shoulder elevation (from 0° to 90° to 0°) in the sagittal and frontal planes, and shoulder flexion (from 0° to 90° to 0°) in the horizontal plane (i.e. at a constant shoulder elevation angle of 90°). Participants repeated each movement 10 times both with and without the WPCSE. Electromyograms (EMG) of shoulder muscles were recorded at a sampling frequency of 3000Hz using surface electrodes (TeleMyo 2400 G2, Noraxon, AZ, USA). The targeted muscles were anterior (AD), middle (MD), and posterior deltoid (PD), pectoralis major (PM), latissimus dorsi (LD), infraspinatus (ISP), trapezius (TRAP), biceps brachii (BB), and triceps brachii (TB). Prior to data collection, we measured EMG during maximum voluntary contractions (MVCs). Three-dimensional positional data of the arm and thorax were also recorded using a 7-camera infrared motion capture system (OptiTrack). The raw EMG data were rectified, low-pass filtered (4th order Butterworth, cut-off frequency = 3Hz), and normalized to the MVCs. The linear-enveloped EMG signals were divided into positive elevation/flexion and negative elevation/flexion phases, based on the kinematic data. For each movement phase, normalized root mean square (nRMS) was calculated and averaged across five repetitions. Finally, paired t-tests were performed to compare nRMS between movements with and without the WPCSE. In this preliminary study, to identify trends, differences were considered significant for $\alpha \leq 0.05$ without correction for multiple tests.

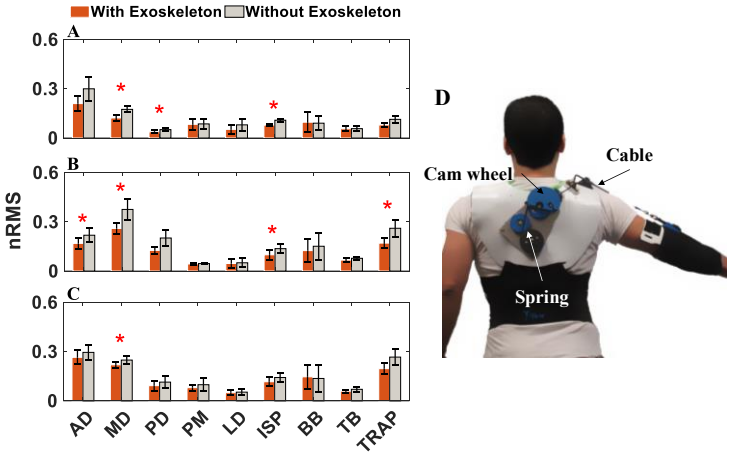

Figure 1: Neuromuscular activity (nRMS) of shoulder complex during shoulder elevation/flexion movements with and without WPCSE. Left column depicts the positive elevation/flexion phase in A) Sagittal plane. B) Frontal plane. C) Horizontal plane. * shows statistically significant differences. D) WPCSE prototype worn by a participant.

Results and Discussion

Our preliminary findings showed that, during positive elevation/flexion, nRMS was lower for trials with the WPCSE (Figure 1). The nRMS difference was significant for the MD, PD, and ISP muscles during sagittal-plane elevation; AD, MD, PM, ISP; TRAP muscles during frontal-plane elevation; and MD during horizontal-plane flexion. During negative elevation/flexion, nRMS was similar between trials with and without the WPCSE. The results demonstrated that the WPCSE can successfully reduce neuromuscular activity at the shoulder during positive elevation/flexion movements without resisting negative elevation/flexion movements. Our future work will focus on testing different levels of assistance to find a desirable range for the exoskeleton assistance for which the WPCSE most enhances shoulder motor function and biomechanics.

Significance

Our promising preliminary results suggest that WPCSEs may be suitable for providing continuous, at-home assistance to patients who suffer from low to moderate shoulder disability.

Reference

[1] "Mechanical strength of repairs of the rotator cuff," *The Journal of bone and joint surgery.* 1994.
[2] "Arm function after stroke. An evaluation of grip strength as a measure of recovery and a prognostic indicator," *Journal of Neurology, Neurosurgery & Psychiatry,* 1989.

Combining an Artificial Gastrocnemius and Powered Ankle Prosthesis: Effects on Transtibial Prosthesis User Gait

David M. Ziemnicki.[1], Kirsty McDonald[12], and Karl Zelik[1]
[1]Department of Mechanical Engineering, Vanderbilt University, Nashville, TN, United States
Email : david.m.ziemnicki@vanderbilt.edu

Introduction

Powered prosthetic ankles can restore the monoarticular function of the soleus muscle during walking, which provides a burst of Push-Off power in late stance. However, the benefits observed from powered ankles (e.g., magnitude of metabolic cost reduction) have often been less than those theorized/expected [1], [2].

One potential explanation is that powered ankles do not restore the biarticular function of the gastrocnemius muscle, which provides a mechanical coupling across the ankle and knee. The gastrocnemius appears to play an important role in transmitting power between proximal and distal body segments. Indeed, simulation [3] and experimental [4] studies provide preliminary evidence that restoring the gastrocnemius ankle-knee coupling to individuals with lower limb amputation (ILLA) may improve walking performance above and beyond restoring soleus function alone. For instance, ILLA demonstrated reductions in prosthesis-side hip and knee joint torques when gastrocnemius function was restored in combination with a powered ankle [4]. However, it is unclear if restoring the gastrocnemius function is only important for prosthetic ankles that generate sufficiently high magnitudes of Push-off power, or whether the gastrocnemius behavior itself (e.g., gastrocnemius stiffness) should to be tuned differently based on the powered ankle behavior. This knowledge gap remains because benefits of an artificial gastrocnemius (AG) have not yet been compared across various levels of powered prosthetic ankle Push-Off.

The objective of this study is therefore to emulate gastrocnemius-like ankle-knee coupling in ILLA, and to characterize its effect on whole-body gait biomechanics across various levels of prosthetic ankle Push-Off power and across various levels of gastrocnemius stiffness. We predict that kinematic and kinetic effects of the artificial gastrocnemius will be larger for higher levels of prosthetic ankle Push-Off power.

Methods

To study the role of the gastrocnemius we are using a robotic emulation system (HuMoTech) that we customized to include: a soleus actuator (to emulate the powered ankle prosthesis), a separate gastrocnemius actuator (to vary behavior of the ankle-knee coupling), a soft conformal leg interface (which attaches to the user's thigh to provide an anchor point for the gastrocnemius), and a foot prosthesis (a modified version of HuMoTech's standard prosthetic hardware, Fig. 1). We have developed a controller that can command the artificial soleus and gastrocnemius in a repeatable, accurate, and precise manner. As subjects walk, we can independently manipulate the dynamics of the soleus and gastrocnemius, in order to systematically analyze how different parameters affect gait.

Otherwise healthy ILLA (N=5) attended an initial familiarization session. Participants then returned for a second session, during which the artificial ankle (soleus) Push-Off power and the artificial gastrocnemius stiffnesses were systematically varied as participants walked at 1.1 $m \cdot s^{-1}$. Ground reaction forces (Bertec), kinematic marker data (Vicon), and electromyography signals (Delsys) were recorded. It is expected that a more complete (e.g., N=10) dataset will be presented at ASB.

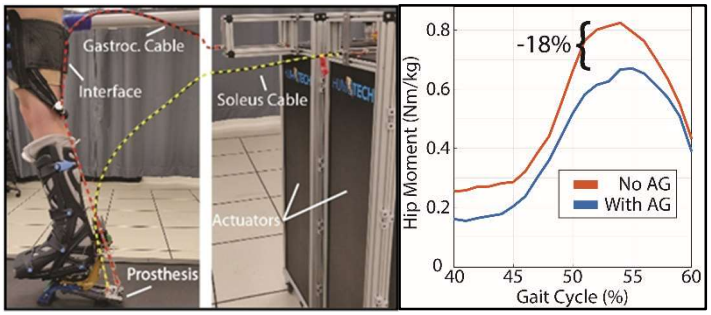

Figure 1: Experimental Set-up (left), Example of Prosthetic Side Hip Torque with vs. without the AG (right).

Results and Discussion

We have verified the controller's ability to emulate different gastrocnemius spring stiffness profiles during walking as well as its ability to provide various levels of ankle (soleus) Push-Off power while working in tandem with the artificial gastrocnemius. We are partway through our data collection and will continue to test unilateral, transtibial ILLA while we sweep across a range of stiffness values for a passive artificial gastrocnemius, and also sweep across different ankle prosthesis Push-Off powers.

Preliminary results confirm that walking with an artificial gastrocnemius has a considerable effect on gait biomechanics, including reducing prosthesis-side hip moments during Push-Off (Fig. 1). Comparison of how the artificial gastrocnemius affects gait kinematics and kinetics for higher vs. lower magntiudes of prosthetic ankle (soleus) Push-off power is presently underway, and the newest results will be presented at ASB.

Significance

The results from this study will provide deeper understanding of the role of the gastrocnemius and how it interplays with soleus behavior during walking, as well as inform how to improve the benefits ILLAs received from powered prosthetic ankles.

Acknowledgments

We thank Dr. Josh Caputo, Dr. Gerasimo Bastas, Dr. Michael Goldfarb and Dr. Steve Collins for their input and advice, and funding from NSF grant 1705714.

References

[1] Herr et al. (2012). Proc. R. Soc. B Biol. Sci.
[2] Quesada et al. (2016). J. Biomech.
[3] Wilson et al. (2015). NW Biomech. Symposium.
[4] Eilenberg et al. (2018). J Robotics.

Leg Muscle Activation Patterns in Persons with a Unilateral Transtibial Amputation Using a Powered Compared to Passive-Elastic Ankle-Foot Prosthesis during Level and Uphill/Downhill Walking

[1]Zane A Colvin, & [1,2]Alena M. Grabowski
[1]University of Colorado, Boulder, CO; [2]Eastern Colorado Healthcare System, Denver, CO
Email: Zane.Colvin@colorado.edu

Introduction

During the single support phase of level ground walking, the mechanics of the body can be modelled by an inverted pendulum that conserves kinetic and potential energy of the center of mass. During double support, the leg muscles generate and dissipate work to retain walking speed [1]. When walking uphill and downhill, the muscle activity of the legs changes to accommodate a net increase or decrease in gravitational potential energy.

People with a transtibial amputation typically use an energy storage and return (ESAR) prosthetic foot to walk. This type of prosthesis acts like a spring but cannot produce net positive work or power. Thus, a biomimetic powered ankle-foot prosthesis has been developed that includes an ESAR prosthetic foot and a battery-powered motor to mimic the muscles surrounding the ankle. Though previous studies have noted compensatory leg muscle activity in people with a transtibial amputation using an ESAR prosthesis, it is unclear how leg muscle activity changes with use of a powered prosthesis [2]. Thus, we measured leg muscle activity during walking on level, uphill and downhill slopes when people with a transtibial amputation used an ESAR and powered prosthesis. We hypothesized that use of a powered prosthesis would reduce leg muscle activity for the affected leg (AL) and unaffected leg (UL) compared to use of an ESAR prosthesis.

Methods

Ten subjects (4 F, 6 M; 79.7 ± 14.97 kg; 1.7 ± 0.075 m) with a transtibial amputation walked on a force measuring treadmill (Bertec, Columbus, OH) at 1.25 m/s using their own ESAR prosthesis and the BiOM powered prosthesis (Ottobock, Duderstadt, Germany). Each subject walked on slopes of 0°, ±3°, ±6°, and ±9° while we measured muscle activity (Noraxon, Scottsdale, AZ) from the biceps femoris (BF), gluteus maximus (Gmax), gluteus medius (Gmed), rectus femoris (RF), and vastus lateralis (VL) of both legs and the lateral gastrocnemius (LG), soleus (Sol), and tibialis anterior (TA) of the UL.

We band-pass filtered (10-499 Hz) raw electromyography (EMG) data using a 4th order Butterworth filter. Then, we rectified, low-pass filtered using a 4th order Butterworth filter with a 10 Hz cutoff, and integrated EMG (iEMG) data over stride time. We determined stride time from subsequent heel strikes within the same leg using a 20 N vertical ground reaction force threshold and analyzed 10 strides for each leg. We normalized iEMG for each muscle and leg to that same muscle's iEMG during level ground walking using the ESAR prosthesis. All analyses were done using custom Matlab scripts (Mathworks, Natick, MA)

We used two-way repeated measures ANOVAs to determine the effect of slope and prosthetic design on iEMG for all muscles and specifically compared iEMG for the BF, VL, and LG because these muscles perform hip extension, knee extension, and ankle plantarflexion, respectively.

Results and Discussion

The iEMG of every muscle increased with slope when subjects walked using an ESAR and BiOM prosthesis with the exception of VL and RF. VL and RF iEMG increased with the magnitude of the slope (Fig. 1). Throughout all tests, the main effect of prosthetic design on iEMG for both legs and all muscles was not significant ($p \geq 0.080$). Therefore, we reject our hypothesis that use of the BiOM would reduce iEMG compared to use of an ESAR prosthesis during walking on level ground and slopes. The main effect of slope on iEMG was significant for the BF, VL, and LG ($p \leq 0.0002$).

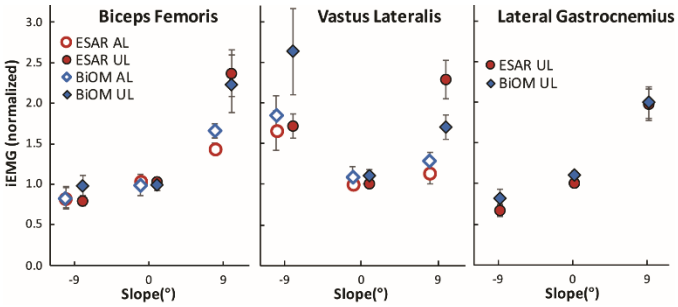

Figure 1. Mean normalized iEMG of the Biceps Femoris, Vastus Lateralis, and Lateral Gastrocnemius of the affected leg (AL) and unaffected leg (UL) during walking on slopes of -9°, 0°, and 9° while subjects used an energy storage and return prosthesis (ESAR) or a powered prosthesis (BiOM). Error bars are standard error.

Significance

We found that use of a powered prosthesis by subjects with a transtibial amputation did not significantly change the iEMG during walking on level ground and slopes compared to use of a passive-elastic prosthesis for any muscle measured in this study. Future research is planned to explore how use of a powered prosthesis affects leg muscle activity magnitude and timing.

Acknowledgments

Work supported by a VA Career Development Award. (VA RR&D A7972-W)

References

1. Lay AN, et al. *J. Biomech.* **40**, 1276-1285, 2007.
2. Winter DA, et al. *J. Biomech.* **21**, 5, 361-367, 1988.

Knee flexion damping affects several key features of the prosthetic limb swing phase

Jenny A. Kent[1], V.N.Murthy Arelekatti[2], Nina T. Petelina[2], W.Brett Johnson[2], John T. Brinkmann[1], Amos G. Winter,V[2], Matthew J. Major[1,3].
[1] NUPOC, Department of Physical Medicine & Rehabilitation, Northwestern University, Chicago, IL.
[2]GEAR Lab, Department of Mechanical Engineering, MIT, Cambridge, MA. [3]Jesse Brown VA Medical Center, Chicago, IL.
Email: jenny.kent@northwestern.edu

Introduction

In the absence of volitional or microprocessor control, the knee of a mechanical transfemoral prosthesis must be configured for two critical behavioral requisites of the limb during the swing phase of gait; shortening via *flexion* to allow the swing limb to pass the stance limb, followed by late phase *extension* to achieve an external moment to passively resist buckling on loading [1]. This behavior may be modified by adjusting the level of swing phase knee flexion damping (KFD_{SW}); higher values of which will attenuate the flexion that occurs shortly after foot-off due to a double pendulum effect. Given that the trajectory of the foot depends on the orchestration of rotations at the hip and ankle in addition to those at the knee, it is unclear how changes in KFD_{SW} in isolation are accommodated holistically during the swing phase. The objective of this study was to systematically explore the effect of adjusting KFD_{SW} on the swing phase dynamics of individuals with a transfemoral amputation during locomotion. We specifically aimed to provide a fuller understanding of the implications surrounding these two primary, yet competing, functional requirements for knee motion, i.e. (i) foot clearance and (ii) knee extension in preparation for foot contact.

Methods

Five individuals with a unilateral transfemoral amputation (2M, 3F; 47.4 ± 18.2 yrs, 1.60 ± 0.10m, 73.6 ± 24.8 kg) were fitted with a passive, single-axis prototype knee [2] that permits adjustment of KFD_{SW} from 0 Nm/rad/s (mechanical friction only) to ~1.80 Nm/rad/s via medial or lateral attachment of a series of lightweight rotary hydraulic dampers. Five damping settings (A-E) were selected for each participant within a range determined based on individual body mass. With each setting, following a brief period of familiarization, participants performed repeat traverses of a motion laboratory at a comfortable self-selected pace. Kinematics of the lower limbs, pelvis and trunk were captured at 120Hz using a motion capture system (Motion Analysis Corp., Santa Rosa, CA). Swing phase toe clearance (TC; vertical distance toe to floor), effective leg length (ELL; distance hip to toe), and knee flexion angle were computed, alongside the sensitivities of vertical toe position to angular displacements at the hip, knee and ankle [3]. Key features of these profiles; selected maxima, minima and their timings, were compared across the 5 damping conditions for each participant. The relationships between KFD_{SW} and each variable were assessed at an individual level by linear and 2nd order polynomial regressions, with R^2 values extracted to measure the amount of variance accounted for by each model fit.

Results and Discussion

Clear quadratic trends ($0.82 \leq R^2 \leq 0.98$) were observed in all variables. With increasing damping coefficient, knee extension occurred earlier in swing phase, promoting a greater timing symmetry. However, minimum TC reduced in magnitude with increased damping, and both minimum TC and maximum ELL occurred earlier (Fig. 1a, b); temporally closer to the instance at which the limb must pass the stance limb, with implications for toe catch. TC became less sensitive to changes in hip flexion (Fig. 1c), suggesting a lesser ability to control toe clearance without employing proximal or contralateral compensations. Further, the pre-swing timing of minimum TC observed with higher damping may limit recovery options should a trip occur at this instance, due to the difficulty of effecting a successful 'lowering' strategy with a transfemoral prosthesis [4].

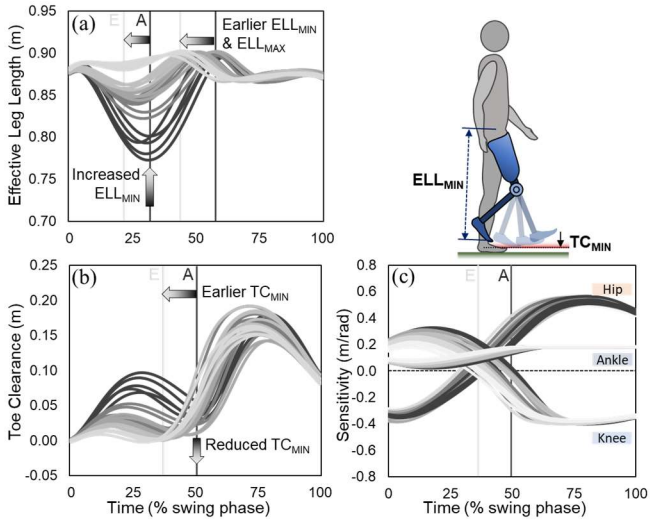

Figure 1: Effect of increasing KFD_{SW} on (a) effective leg length (ELL), (b) toe clearance (TC), and (c) sensitivity of vertical toe position to lower limb joint rotations (positive values: clearance of the toe will be increased by joint flexion). Lines A, E indicate mean TC_{MIN} for lowest and highest damping respectively. Data from a single participant; 5 strides per condition. Shading dark to light in order of increasing damping.

Significance

In addition to highlighting broader implications surrounding swing phase damping selection for the optimization of mechanical knees, this work reveals important design considerations that may be of utility in the formulation of appropriate control strategies for computerized devices.

Acknowledgments

This work was supported by the National Institutes of Health (award #1R03HD092676-01) and Northwestern University Dept. of PM&R. The authors would like to thank R. Stine for her assistance in data collection for this study.

References

[1] Jepson et al. (2008). Prosthet Orthot Int, 32(1), 84-92.
[2] Berringer et al. (2017). ASME, IDETC/CIE, Cleveland, Ohio.
[3] Moosabhoy & Gard (2006). Gait Posture, 24(4), 493-501.
[4] Shirota et al. (2015). JNER, 12, 79-015-0067-8.

A Simple Walking Model to Optimize Prosthetic Knee and Foot Combinations for Prosthetic Limb Stability

Anna Pace[1], David Howard[1], Steven A. Gard[2,3], and Matthew J. Major[2,3]
[1]University of Salford, Manchester, United Kingdom
[2]Northwestern University, Chicago, USA; [3]Jesse Brown VA Medical Center, Chicago, USA
Email: a.pace1@edu.salford.ac.uk

Introduction

Lower limb prosthesis prescription mainly depends on the experience and knowledge of the prosthetist. While the interaction between the prosthetic knee and foot is critical to the safety of transfemoral prosthesis users (TFUs), there are few recommendations guiding their prescription. This interaction is especially important during stance when knee buckling can result in a fall [1,2,3], with significant implications for health [1] and healthcare cost burden [4]. Hence there is a need for a standardized approach to understand how the combination of different prostheses and their mechanical function affects TFUs biomechanics. This study quantified the interaction effect of prosthetic knee alignment and ankle-foot mechanism mechanical function (roll-over shape (ROS)) on stance-phase prosthetic knee stability (prosthetic knee moment) using a walking simlation.

Methods

A numerical sagittal-plane walking model was designed in MATLAB to simulate prosthetic stance phase of TFU gait on level ground based on a single inverted pendulum (IP). Knee center of rotation position modelled knee alignment and was defined by its distance along the IP long-axis from the hip (coinciding with the body center-of-mass) and perpendicular offset from the long-axis. A curved rocker rigidly attached to the bottom of the IP rod modelled foot stiffness and was defined as the ankle-foot ROS (i.e. center of pressure (COP) progression). The hip horizontal trajectory from experimental data was the model input, and outputs were: hip vertical trajectory, knee and COP trajectory, sagittal-plane GRFs, and knee and hip moments.

The model was validated against laboratory TFU gait data [5] by calculating the root mean squared error (normalized by the st. dev.) between model outputs and experimental data. The model was used to predict the effects of varying prosthetic knee alignment and ankle-foot ROS radius within boundaries according to the literature: posterior/anterior knee axis offset of $0.02\ m$ [3]; ROS radius between 0.13 and 0.25 × body height, ranging from a more compliant to a more rigid prosthetic foot [6].

Results and Discussion

Validation results suggest the model adequately simulated TFU gait during prosthetic single-limb support (SS) (RMSE normalized by SD: 0.64 – 4.59), when knee stability is most at risk given reliance on the prosthetic limb and proximal anatomy. Agreement with laboratory data was best when knees with limited or no SS flexion were considered. Fig. 1 displays predicted effects of component intractions on knee moment. During SS, an external extensor moment is necessary at the start and middle to avoid knee buckling, limiting selection of knee alignment and ankle-foot ROS to the solution area beneath the constraint (solid black line) for the SS start (Fig. 1A), while no constraints exist during middle SS (Fig. 1B). At the end of SS (Fig. 1C), transition from a knee extensor to small flexor moment is desirable to facilitate knee break to prepare for swing, denoted by a narrow band (e.g. $10\ Nm$) around a zero moment (between two solid black lines). These constraints combine to create the cross-hatched solution area (Fig. 1D) that limits the selection to posterior to in-line knee alignment combined with low to medium ankle-foot stiffness to maximize SS knee stability. The selection may be further constrained by clinical considerations such as the prescription of a certain prosthetic foot or prosthetic knee alignment. This means operating respectively along a fixed horizontal line or a fixed vertical line in the plots of Fig. 1.

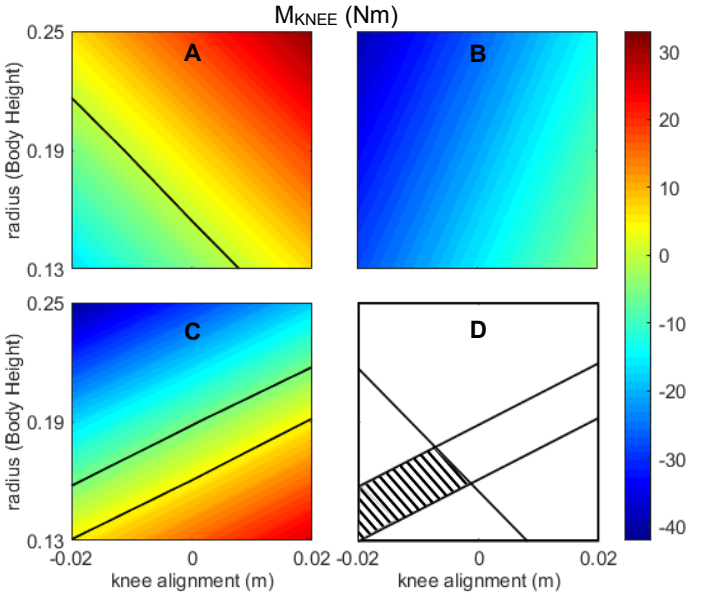

Figure 1: Contour plots displaying predicted prosthetic knee moment (positive values for external flexor moments (Nm)) at the (A) start (solid line corresponding to 0 Nm), (B) middle and (C) end (solid lines defining a hypothetical band of $\pm 5Nm$ around a zero moment) of prosthetic limb SS. (D) Cross-hatched solution area.

In summary, despite the limitation of this IP-based simulation in that it predicts the external knee moment without addressing how this moment is managed by TFUs or their prosthetic knee, the results can inform the selection of the optimal knee alignment and ankle-foot mechanism to maximize TFU stability and safety during SS. Clinicians can work within a band of tolerance derived from the simulation results to optimize the prosthetic system.

Significance

Predictions based on this simple walking model can further inform in-vivo systematic investigations on commercial devices interactions, thereby providing evidence for future Clinical Practice Guidelines on transfemoral prostheses design.

References

1. Kim J, et al. *PM&R* **11**, 344-353, 2019.
2. Highsmith MJ, et al. *Prosthet Orthot Int* **34**, 362-377, 2010.
3. Koehler-McNicholas SR, et al. *J Rehabil Res Dev* **53**, 1089-1106, 2016.
4. Mundell B, et al. *Prosthet Orthot Int* **41**, 564-570, 2017.
5. Fatone S, et al. *J Rehabil Res Dev* **51**, 1217-1228, 2014.
6. Curtze C, et al. *J Biomech* **42**, 1746-1753, 2009.

Characterization of human arm stability in relation to unstable viscous environments

Fatemeh Zahedi, and Hyunglae Lee*
School for Engineering of Matter, Transport, and Energy, Arizona State University
Email: *hyunglae.lee@asu.edu

Introduction

In our daily activities, we sometimes have interaction with unstable environments that challenge the stability of the arm [1]. Many studies have demonstarated how the central nervous system is capable of controlling arm mechanical impedance, in particular arm stiffness, to compensate for the environmental instability [2].

Viscosity or damping is another important component of the mechanical impedance, which is a major energy dissipator that helps achieve limb/joint stability. However, due to technical challenges in reliably estimating arm viscosity, this component has been relatively understudied compared to arm stiffness [3]. Given this challenge, rather than directly measuring arm viscosity, this study investigates how stably the human arm can interact with unstable viscous (damping-defined) environments. In particular, we characterized the lower-bound of viscosity of unstable environments that the arm can stably interact with.

Methods

A 7 degrees-of-freedom robotic arm (LBR iiwa R820, KUKA, Germany) with a 6-axis load cell (Delta IP60, ATI, NC) was used in this study. Two distinct controllers were implemented: a position controller to provide rapid perturbations to disturb the arm posture in either anterior-posterior (AP) or medial-lateral (ML) direction, and an admittance controller to simulate unstable viscous environments. The study was limited to a horizontal plane. Subjects were seated with their trunk securely strapped to a rigid chair, and held the handle connected to the robot end-effector. A visual feedback display (at a distance of ~1 m) helped subjects to complete posture maintenance task by showing current and target hand positions.

Arm stability was evaluated around the neutral posture, defined as follows: shoulder in ~70° of abduction, ~45° of horizontal flexion, and the elbow in ~90° of flexion. Nine evenly distributed points around the neutral posture (±6 cm in AP and ML directions) were tested. Zero stiffness and constant inertia were simulated in the horizontal plane and only viscosity was varied to change level of unstable viscous environments.

In each of the 9 postures, arm stability in both AP and ML directions was tested. For trials in the AP (or ML) direction, the environment viscosity in the ML (or AP) direction was constant at 30 Ns/m. The viscosity in the AP direction was varied from the initial value of -30 Ns/m, and subtracted by 10 Ns/m until the human arm could not stably interact with the simulated viscous enviroment anymore. If the arm failed to stabilize at the initial value, viscosity was added by 10 Ns/m until stable interaction was achieved. From this point, the viscosity was changed based on the bisection method until the difference of the viscosity values for stable interaction and unstable interaction was less than 5 Ns/m. The viscosity for the final successful trial was regarded as the lower-bound of environment viscosity that the human arm could stably interact with. The same algorithm was implemented for the ML direction, except that the initial viscosity was -10 Ns/m and the changing interval was 5 Ns/m. These values were chosen based on preliminary experiments and previous findings on higher arm impedance in the AP direction than the ML [4].

Ten young, healthy subjects participated in this study, which was approved by the Institutional Review Board of Arizona State University (STUDY 00010123).

Results and Discussion

Group analysis on 10 subjects demonstrated that, in average across all 9 testing postures, the lower-bound of environment viscosity that the human arm can stably interact with was -50.3 (2.9) Ns/m for the AP direction and -21.6 (4.0) Ns/m and for the ML direction. Results for each of the 9 testing posture are shown in Fig. 1. Higher arm stability in the AP than ML direction is consistent with previous findings that human arm stiffness is significantly higher in the AP than ML direction. It is also worth to note that the arm has less capability of adjusting to unstable viscous environments when it is closer to the body and when it is laterally displaced for the AP and ML directions, respectively.

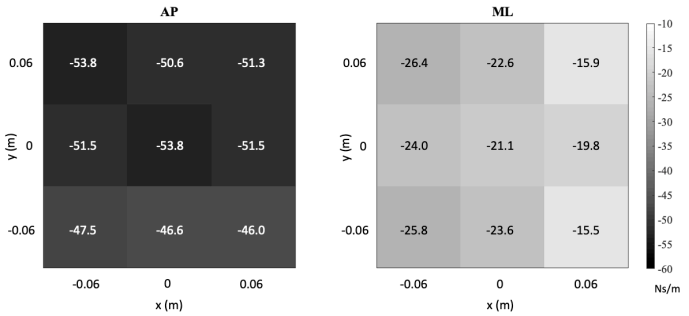

Fig. 1: Lower-bound of environment viscosity that the arm can stably interac with for each of the 9 testing postures for AP and ML directions. The mean of 10 subjects is presented.

Significance

Compared to arm stiffness, arm viscosity has been relatively understudied and this limits the performance of devices (e.g., wearable robots and rehabilitation robots) involving physical interaction between the neuromuscular sysem and surrounding environments. Knowledge on the level of unstable viscous environments that human can stably interact with can be utilized to improve the overall performance of these devices, specifically, transparency and agility, without compromising stability.

Acknowledgments

Research supported by National Science Foundation Awards #1846885 and #1925110.

References

[1] E. Burdet, KP. Tee, and et all (2006) Stability and motor adaptation in human arm movements. Biol Cybern.
[2] M. A. Krutky, R. D. Trumbower, E. J. Perreault (2013) Influence of environmental stability on the regulation of end-point impedance during the maintenance of arm posture. J Neurophys.
[3] E. Burdet, and et all (2000) A method for measuring endpoint stiffness during multi-joint arm movements. J Biomech.
[4] E. J. Perreault, R. F. Kirsch, and P. E. Crago (2001) Effects of voluntary force generation on the elastic components of endpoint stiffness. Exp Brain Res

Ankle Roll-over Shape Comparisons of Different Prosthetic Foot Types

Michael Poppo[1], Andrew Hansen[2,3], John Chomack[1], and Jason Maikos[1]
[1]Veterans Affairs New York Harbor Healthcare System, New York, NY
[2]Minneapolis Department of Veterans Affairs Health Care System, Minneapolis, MN
[3]University of Minnesota, Rehabilitation Science & Biomedical Engineering, Minneapolis, MN
Email: Michael.Poppo@va.gov

Introduction

As the climate of prosthetic devices has evolved, the number of available prosthetic feet has greatly risen. Clinicians have limited guidelines to aid in prosthetic prescription for individuals with lower extremity amputation. Furthermore, most comparative research has been contradictory or non-committal, which makes it difficult for clinicians to understand which devices will maximally benefit a given user. The objective of this study was to examine the dynamic function (radius of curvature (ROC), effective foot length ratio (EFLR), and instantaneous radius of curvature (IROC)) of 3 different types of prosthetic feet: Energy Storing and Returning (ESR), Articulating (ART), and Powered (PWR). This information may be critical in advancing our understanding of the most effective prosthetic designs, which can aid in evidence-based clinical practice and prosthetic prescription guidelines. We hypothesized that the ART and PWR feet would generate similar roll-over shape characteristics that would suggest improved dynamic functionality compared to ESR feet.

Methods

Motion capture and kinetic data were captured for 12 people with unilateral transtibial amputation during overground walking at the Veterans Affairs New York Harbor Healthcare System (VA NYHHS) and Walter Reed National Military Medical Center (WRNMMC). Each patient completed data collection for each of the 3 feet after acclimating to each foot for one week. Center of pressure (COP) data were transformed into the shank coordinate system during single limb stance. EFLR, a measure of the percentage of the foot that is effectively used during a step, was calculated as the distance from the prosthetic heel to the most anterior point of the COP progression divided by the overall length of the foot. Circular arcs of best fit were also applied to the COP data to determine roll-over shape characteristics, such as height-normalized ROC (Hansen, 2003). The IROC was calculated by evaluating the first derivative of COP forward travel with respect to shank angle. The peak IROC is representative of the fastest COP forward travel.

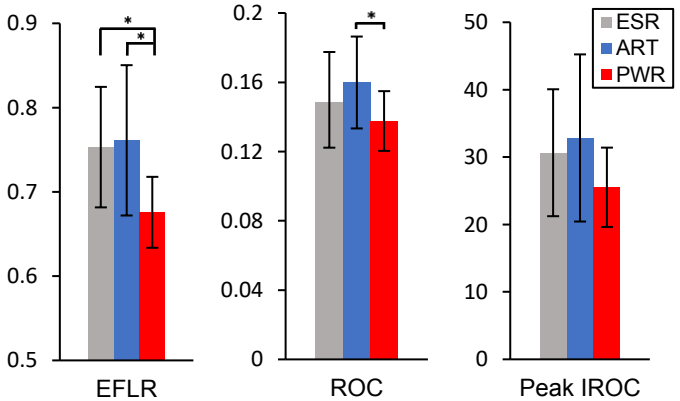

Figure 1: EFLR bar plot (left), height-normalized ROC (center), and peak IROC (cm) (right). * Statistically significant change at $p < 0.05$.

Results and Discussion

Figure 1 shows that EFLR of the PWR foot (0.68±0.04) was significantly lower compared to ESR (0.75±0.07) and ART feet (0.76±0.09) ($p < 0.05$). Reduced EFLR of the PWR device indicates that the COP did not progress as far anteriorly during single leg stance, which can correlate to a reduced ankle lever arm in late stance, decreasing walking efficiency. Furthermore, the PWR group also had a significantly smaller ROC (0.14±0.02) than the ART group (0.16±0.03) ($p < 0.05$), but not compared to the ESR group (0.15±0.03) ($p = 0.24$). Reduced ROC suggests less stability during single leg stance because the foot is rotating about a smaller rocker. However, it is unclear if the small differences found are clinically significant. Lastly, the PWR group had the lowest peak IROC (25.5±5.9 cm) and was trending towards significance compared to the ART group (32.8±12.4 cm) ($p = 0.066$), but not significantly different than the ESR group (30.6±9.4 cm) ($p = 0.11$). Decreased forward travel, as indicated by lower peak IROC, suggests reduced standing stability (Curtze, 2009). Of note, the PWR foot is specifically designed to provide powered plantarflexion at terminal stance and is therefore not active during the single limb stance phase in which this analysis was conducted. We believe the motor could be causing an angular load at the ankle which may play a role in limiting the effectiveness of the passive mechanical components of the foot.

Significance

Prosthetic prescription practices continue to be rooted in anecdotal evidence and manufacturer claims. Clinicians can use the information presented in this study to help prescribe devices that mimic effective rocker shapes to assist in dynamic activities. Manufacturers can design new componentry and prosthetic devices that better approximate the rocker shapes of the physiological ankle-foot complex to reduce interlimb asymmetries (Ferris, 2012). In this investigation, we showed that the PWR foot, while designed to provide biologically normative push-off power, provided less biomimetic function during single-leg stance and utilized less of the effective foot length. As the evolution of prosthetic feet continues, synergy between passive elements and advanced features must be maintained to effectively mimic the physiological ankle-foot complex.

Acknowledgments

This work was supported by a DoD Orthotics and Prosthetics Outcomes Research Program grant (W81XWH-17-2-0014). We would also like to acknowledge our collaborators at Walter Reed National Military Medical Center.

References

Hansen et al. 2003. Roll-over shapes of human locomotor systems: effects of walking speed.
Curtze et al. 2009. Comparitive roll-over analysis of prosthetic feet.
Ferris et al. 2012. Evaluation of a powered ankle-foot prosthetic system during walking.

The Influence of Articulated AFOs on Mediolateral Balance Control and Forward Propulsion during Walking Post Stroke

Arian Vistamehr[1], Christy Conroy[1], Paul Freeborn[1], Gina Brunetti[1], Richard R. Neptune[2], and Emily J. Fox[1, 3]
Motion Analysis Center, Brooks Rehabilitation, Jacksonville, FL, USA
[2] Walker Department of Mechanical Engineering, The University of Texas, Austin, TX, USA
[3] Department of Physical Therapy, University of Florida, Gainesville, FL, USA
email: arian.vistamehr@brooksrehab.org

Introduction

Regulation of dynamic balance and generation of forward propulsion are key requirements for community ambulation, which typically involves adaptability tasks (e.g., obstacles, long steps). Previous studies in healthy adults have shown that the ankle plantarflexors are primary contributors to both of these important biomechanical functions [1-2]. However, individuals post-stroke often have plantarflexor weakness, poor balance control in the mediolateral direction [3-4], and reduced forward propulsion generation by the paretic leg [5]. Further, these individuals commonly use ankle foot orthoses (AFOs) to assist with foot clearance during swing, which may adversely affect their ankle mobility and plantarflexor output during stance. Previous research analyzing healthy adults showed walking with a solid AFO negatively influences forward propulsion generation and balance control [6]. However, it is not clear if AFOs similarly affect individuals post-stroke. Thus, the purpose of this study was to assess the influence of a commonly prescribed articulated AFO on mediolateral balance control and generation of forward propulsion during walking adaptability tasks in individuals post-stroke. We hypothesized that a) walking with an AFO would negatively influence mediolateral balance control and generation of forward propulsion by the paretic leg and b) poor mediolateral balance control would be associated with reduced generation of forward propulsion since the ankle plantarflexors are key contributors to both biomechanical functions.

Methods

Nine individuals with post-stroke hemiparesis (4 left hemiparesis; age: 53.7 ± 11.3 years; 3 female; walking speed: 0.71± 0.44 m/s) were assessed while walking with and without their prescribed articulated AFO. Three-dimensional ground reaction forces (GRFs) and kinematics were collected at 2000 Hz and 100 Hz, respectively, during self-selected (SS), fastest-comfortable (FC), obstacle negotiation (Obst) and long step (LS) walking tasks. Mediolateral balance was assessed as the range of frontal-plane whole-body angular momentum (H) during paretic single leg stance [4]. H was normalized by body mass, height and a term similar to Froude number [4]. Forward propulsion was calculated as the time integral of the anterior GRF (normalized by body weight) during late stance of the paretic leg. Differences between the AFO and NoAFO conditions were assessed using a paired t-test within each walking condition. Relationships between mediolateral balance and forward propulsion were assessed using Pearson's correlation.

Results and Discussion

For all walking tasks, there were no significant differences in mediolateral balance control or forward propulsion generation when walking with and without an AFO ($p > 0.05$; Fig. 1). Thus, our first hypothesis was not supported. These findings contradict our previous observation in healthy adults walking with a solid AFO [6], which is likely due to the articulated AFOs allowing greater ankle mobility and plantarflexor output.

Mediolateral balance control was correlated with forward propulsion during the SS AFO ($r = -0.80$, $p = 0.007$), FC AFO ($r = -0.65$, $p = 0.049$), and FC NoAFO ($r = -0.74$, $p = 0.017$) walking conditions. That is, more impaired forward propulsion generation (i.e., smaller value) was associated with poorer mediolateral balance control (i.e., larger H value), supporting our second hypothesis. This finding was particularly interesting as it highlights the association between forward propulsion in the anterior direction and dynamic balance in the mediolateral direction, which is likely due to the ankle plantarflexors being a primary contributor to both quantities. These findings also highlight that the articulated AFO design does not hinder these key biomechanical functions during stance in both frontal and sagittal planes.

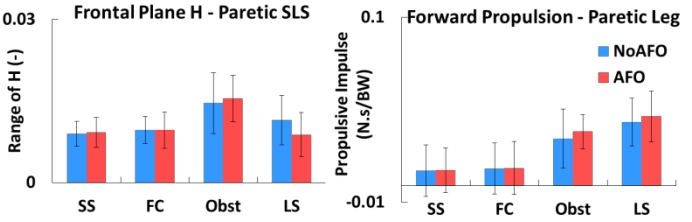

Figure 1: Range of frontal-plane H (during paretic single leg stance) and forward propulsion (generated by the paretic leg) during AFO and NoAFO walking conditions.

Significance

Here, we found that wearing an articulated AFO during a variety of walking (SS and FC) and adaptability tasks (Obst and LS) did not adversely influence mediolateral balance control and forward propulsion in individuals post-stroke. Since these walking tasks require varying amounts of ankle mobility and plantarflexor output, this finding suggests that the articulated AFO allowed for sufficient ankle output across all tasks. Given the widespread use of AFOs post-stroke, it is important to understand the potential influence of AFO use on walking mechanics and motor output as they could encourage adverse gait compensations and accelerate muscle atrophy. Further research is needed to assess the influence of other AFO designs (with more rigid ankle support) on walking machanics and motor output during walking adaptability tasks.

Acknowledgments

This work was funded by Brooks Rehabilitation.

References

[1] Neptune and McGowan. (2016). *J Biomech,* **49**: 2975-2981.
[2] Neptune et al. (2001). *J Biomech*, **34**: 1387-1398.
[3] Nott, et al. (2014). *Gait & Posture* **39**, 129-134.
[4] Vistamehr et al. (2018). *J Biomech,* **74**: 106-115.
[5] Bowden et al. (2006). *Stroke,* **37**: 872-876.
[6] Vistamehr et al. (2014) *Clin Biomech,* **29**: 583-589.

Asymmetry, Instability and Functional Deficits in Transtibial Prosthesis Users During Squatting, Lifting and Sit-to-Stand

Rachel H. Teater, Kirsty A. McDonald, Gerasimos Bastas, and Karl E. Zelik
Department of Mechanical Engineering, Vanderbilt University, Nashville, TN, USA
Email: rachel.h.teater@vanderbilt.edu

Introduction

Lower limb prosthesis users (LLPUs) experience mobility challenges that can impair their ability to carry out activities of daily living, affecting quality-of-life and independence [1]. The vast majority of LLPUs use a passive ankle-foot prosthesis where the ankle joint or foot keel is locked at a fixed angle relative to the shank. Extensive research has characterized the ability of these devices to replicate biological movement and function during walking [2]. However, it is less well understood how conventional prosthetic feet perform during functional transitions and other movements, such as standing up from a chair, picking up an item off the ground, or squatting down. These tasks involve ankle and/or toe flexion in healthy individuals–degrees of freedom that are not included in most passive prosthetic feet. We expect that the lack of ankle and toe joint mobility may contribute to the task performance deficits LLPUs experience. For instance, prosthetic device limitations may lead unilateral LLPUs to perform tasks in a highly asymmetric manner; overloading their intact lower limb and thus contributing to overuse injury or degenerative joint disorder risks. Prosthetic design modifications could potentially improve their comfort, safety, and ability to complete these tasks without overloading their intact lower limb. To investigate this, we aim to (1) characterize lower limb loading asymmetry, stability, and functional deficits of LLPUs during essential everyday movements while wearing their prescribed passive ankle-foot device and (2) investigate if prosthetic design modifications improve symmetry and perceived stability, or overcome functional deficits. We predict that restoring ankle flexion will improve functional movements such as squatting and lifting and toe flexion will assist in lunging and reaching tasks.

Methods

Through reviewing the scientific literature and interviewing local LLPUs, physicians, and prosthetists, we identified several tasks that LLPUs completely avoid or find challenging, and have the potential to be improved by modifying prosthetic ankle-foot design. We are now conducting a comprehensive human movement study evaluating transtibial LLPUs during these identified tasks: sit-to-stand (and stand-to-sit), lifting, squatting, lunging, and reaching. To address the first objective, we are collecting data with users performing variations of all tasks in their prescribed passive prosthesis. We then use the Vanderbilt Powered Ankle [3] to emulate specific device design modifications that are expected to improve the ability of LLPUs to complete these tasks, i.e., adding ankle and/or toe articulation. For each task, we are collecting participant feedback on perceived effort, stability, and comfort in addition to collecting full motion capture (Vicon) and ground reaction force (GRF; AMTI) data.

Results and Discussion

Preliminary vertical GRF data from one participant performing representative sit-to-stand, lifting, and squatting tasks wearing his prescribed prosthesis (Fillauer AllPro) is presented in Figure 1. During each of these tasks, the participant's intact lower limb experienced forces more than twice the magnitude of force on their prosthetic limb. This was consistently seen across multiple trials and variations of these tasks. In pilot testing using the powered prosthesis, there were noteworthy improvements in subjective feedback related to effort, stability and comfort when utilizing increased ankle dorsiflexion during the sit-to-stand task (Fig. 1B). Data collection is ongoing with expanded analyses (e.g., stability, lower limb joint kinematics/kinetics) expected to be completed for multiple subjects prior to the conference.

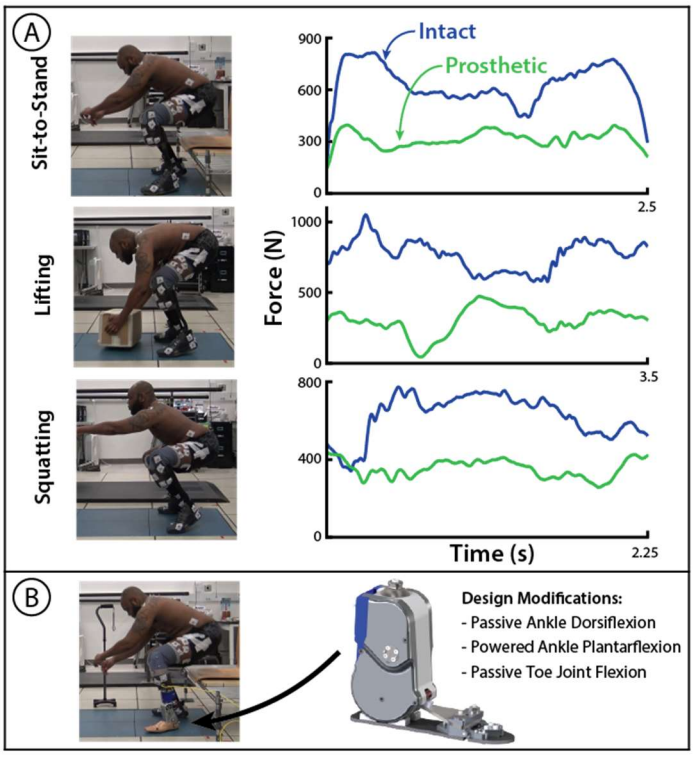

Figure 1: (A) Transtibial LLPU performing sit-to-stand, lifting (10 kg), and squatting wearing his prescribed prosthesis with corresponding vertical GRF. (B) The Vanderbilt Powered Ankle allows us to investigate device modifications by modulating ankle and toe mobility.

Significance

Biomechanical assessments of functional movement deficits in LLPUs are lacking. Understanding how users complete these tasks in their current passive devices and identifying prosthetic design modifications that increase functional ability is an essential step towards improving the standard of care for LLPUs. New devices that increase stability, symmetrical loading, and/or comfort could lead to reduced falls and overuse injuries.

Acknowledgments

This research is supported by NIDILRR (0IFRE0001).

References

[1] Gauthier-Gagnon et al. (1999). *Arch Phys Med Rehabil*.
[2] Versluys et el. (2009). *Disabil Rehabil Assist Technol.*
[3] Shultz et al. (2016). *IEEE Trans Neural Syst Rehabil Eng.*

Myoelectric Control Of An Ankle Exoskeleton In Continuous And Discrete Movements

Rachel L. Hybart[1*] and Daniel Ferris[1]
[1]Human Neuromechanics Laboratory, J. Craton Pruitt Department of Biomedical Engineering, University of Florida, Gainesville, FL
Email: rhybart@ufl.edu *

Introduction

Real world use of lower extremity exoskeletons will require not only assistance for walking but also for discrete motor tasks. Traditional control strategies for exoskeletons usually focus on timing of gait events (heel strike and toe off) [1]. Real world movements include very short bouts of walking with non-steady state transition periods (turning, stopping, starting) [2], and noncyclical motions for discrete tasks.

One control strategy that should work for both continuous and discrete tasks is proportional myoelectric control. Myoelectric control uses electromyography (EMG) from the user to control the exoskeleton motor, allowing smooth transitions between continuous and discrete motions. Past research has shown humans are adept at learning to use proportional myoelectric control of lower extremity exoskeletons during walking [3], but it is not clear how training from walking carries over to noncyclical motor tasks.

The purpose of our study was to determine if subjects practicing walking with robotic ankle exoskeletons would improve their performance on a subsequent noncyclical, discrete motor task compared to subjects that did not practice walking with the exoskeletons. We hypothesized that individuals that practiced walking with the exoskeletons powered would perform better on the subsequent motor task than the subjects without walking practice.

Figure 1: A subject wearing the Dephy Exoboot ankle exoskeleton.

Methods

We adapted a myoelectric controller to control commercially available robotic ankle exoskeletons (ExoBoot, Dephy, Inc.) (Figure 1). The controller used filtered and scaled soleus EMG to enable plantarflexion assistance. 5 participants (3M, 2F) walked on a treadmill at 1.2 m/s while wearing ExoBoots on each leg for 30 minutes, after which they completed a series of discrete force tracking tasks. One group wore the ExoBoots unpowered during walking and powered during the discrete task. The second group wore the ExoBoots powered during both walking and the discrete task. During the discrete task the participants tried to match a target force displayed to them on a screen, with their right leg onto a force plate. The participants applied the force to a force plate for 2-7s, returned to rest, and repeated with a different target force. Participants completed 20 repetitions of force application and returning to rest. The magnitude and duration of each force target varied across the 20 trials.

Results and Discussion

The participants in the powered walking group showed better initial force tracking and faster learning in the discrete task than the unpowered walking group. The group that had powered walking practice had a lower initial root mean square error (RMSE) for the discrete task than the control group. Both groups showed a negative slope of the RMSE between the 1st and 20th repetitions, but the powered walking group had a steeper slope. The steeper slope was indicative of faster learning during discrete force tracking task.

The powered walking group decreased their mean EMG amplitude by 17.54% during the 30 minutes of practice walking with the exoskeletons. That indicated that the subjects showed substantive adaptation to controlling the exoskeletons.

These results suggest that training with robotic ankle exoskeletons during walking carries over to noncyclical, discrete motor tasks. The performance in the subsequent force tracking task was greater for the group that had 30 minutes of walking practice.

Significance

One disadvantage of current lower limb exoskeleton controllers is their inability to easily transition from continuous to discrete tasks. Control strategies focused on steady state, constant speed walking on flat surfaces are limited in their applicability to real world implementation. Discrete movements are important during walking gait transitions such as turning or stopping, and to uneven terrain or obstacles. We found that adaptation to a myoelectric-controlled ankle exoskeleton during walking leads to better performance when using the same device in a discrete motor task.

This research also gives insight into the neural substrates for controlling continuous and discrete tasks. Motor adaptation carryover from walking to noncyclical discrete motor tasks suggests that the neural substrate responsible for the adaptation is used in controlling both tasks. This is particularly important to training and use of robotic exoskeletons intended for real world use for either rehabilitation or occupational reasons.

Acknowledgments

We would like to thank Joseph Dvorak and Elizabeth Sanchez in their help collecting and analysing data.

References

[1] Jiménez-Fabián et al. (2012). *Med. Eng. & Physics*. **34**. 397-408
[2] Orendurff et al. (2008). *JRRD.* **45**. 1077-1090.
[3] Ferris et al. (2009). *IEEE EMBC.* 2119-2124.

The Design and Development of a Wrist Hand Orthosis

Amber Gatto[1,2], Stephen Sundarrao[1,2], and Stephanie L. Carey[1,2]
[1]University of South Florida, Department of Mechanical Engineering
[2]Center for Assistive, Rehabiliation, & Robotics Technologies (CARRT)
Email: ambergatto@usf.edu

Introduction

The most common spinal cord injury (SCI) classification is incomplete quadriplegia (45%-60%); the majority occur in the C5-C7 spinal segments. Studies show the highest priority among individuals with a quadriplegic SCI is restoring grasping ability [1,2]. Patients with an incomplete C5-C7 SCI lose grasping abilities but wrist function is retained [3]. Rehabilitation techniques apply the tenodesis effect, an orthopedic phenomenon that uses wrist extension for grasping and wrist flexion for releasing. Current tenodesis wrist-hand orthoses (WHOs) engage only the thumb and index finger, meaning only 20% of activities of daily living (ADLs) can be completed [3].

Methods

This feasibility study tested a student designed powered WHO on ten able-bodied individuals (avg. age: 42.7 years old). The prototyped WHO utilizes a modified version of the tenodesis effect (wrist flexion for grasping, wrist extension for releasing) to help individuals with an incomplete C6-C7 SCI independently complete ADLs. Subjects used the WHO to complete feeding and grooming tasks in front of a motion capture system. Results were analyzed through OpenSim to get wrist joint angles, which would help determine if someone with a C6-C7 SCI, who likely has limited wrist range of motion (ROM), could use this device [4].

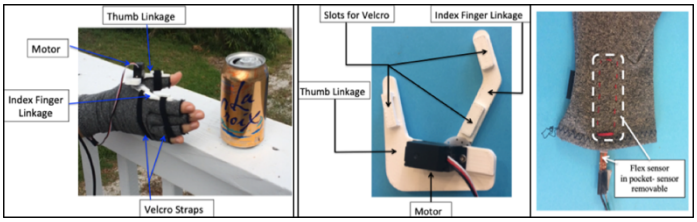

Figure 1: Left: Prototyped WHO. Middle: 3-D printed index finger and thumb linkages. Right: Removable flex sensor housed in pocket.

Results and Discussion

Graphical data shows a greater degree of wrist extension was used versus wrist flexion in the majority of tasks. An exception was the *Full Water Bottle*, which can be considered an outlier due to difficulty picking up this object. Subjects failed to lift this object, and in an attempt to get a more secure grasp they over compensated with more wrist flexion. Figures 2 and 3 show graphs for a single subject.

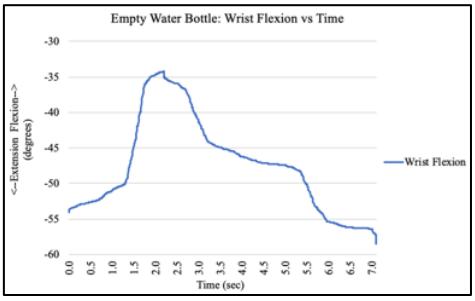

Figure 2: Empty water bottle required more wrist extension

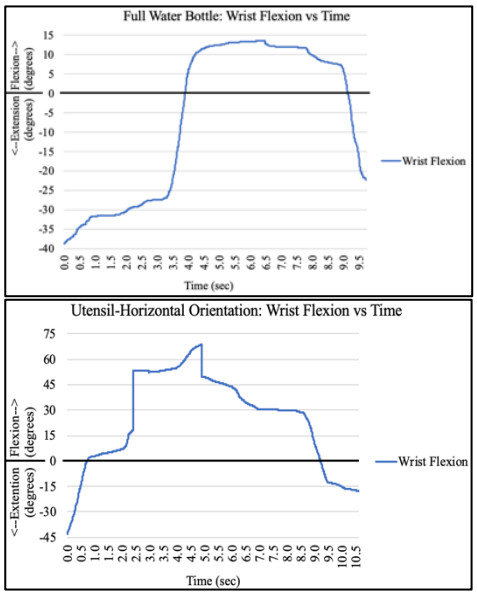

Figure 3: Top: Full water bottle- more wrist flexion than other tasks. Bottom: Utensil-horizontal orientation- maximum wrist flexion.

A greater degree of wrist flexion is required for grasping thin, small diameter (<0.5in) objects. These objects (utensil, brush, toothbrush, razor) in a horizontal orientation require more wrist flexion than in a vertical orientation. The utensil, the thinnest object, in a horizontal orientation requires the most wrist flexion.

Individuals with a C6-C7 SCI (future study), with limited wrist ROM, should still be able to use this device because it can be individually customized such that wrist motion input is disproportionate to finger motion output. For example, the WHO can be programed to output 4° of finger motion for every 1° of wrist motion input. If a user is limited to 10° of wrist extension, the device can be programmed to open the finger linkages 40°.

Significance

This WHO is customizable, lighter, and easier to use than currently available orthoses. Since the operational code can be customized, individuals with limited wrist ROM (e.g. C6-C7 SCI), can still use this device to independently complete ADLs.

Acknowledgments

FL Dept. of Education, Rehab., Engineering & Tech. Program.

References

[1]. National Spinal Cord Injury (SCI) Statistical Center (2016).
[2]. The graded redefined assessment of strength sensibility and prehension: reliability and validity. *Journal of neurotrauma*.
[3]. A noninvasive neuroprosthesis augments hand grasp force in individuals with cervical spinal cord injury: The functional and therapeutic effects. *The Scientific World Journal*.
[4]. Gatto, Amber; 2019 The Design and Development of a Wrist Hand Orthosis. RESNA 2019 Annual Conference, Emerging Technologies

Teleoperation of an Ankle-Foot Prosthesis with a Wrist Exoskeleton

Cara G. Welker[1-2], Vincent L. Chiu[2], Alexandra S. Voloshina[2], Steven H. Collins[2], and Allison M. Okamura[2]
[1]Department of Bioengineering, [2]Department of Mechanical Engineering, Stanford University
Email: cgwelker@stanford.edu

Introduction

When people lose a limb due to amputation, they lose not only motor function, but also sensory information about the state of that limb. A variety of approaches have attempted to reintegrate this sensory information, many of which are invasive [1]. We developed a system that substitutes this missing information from an ankle-foot prosthesis in a noninvasive manner. In our approach, a wrist exoskeleton allows users with amputation to both control and receive feedback from their prosthetic ankle in real time via teleoperation (Fig. 1A).

Methods

System Design: We built a wrist exoskeleton that senses wrist angle with an accuracy of 0.18° and provides up to 1 Nm of wrist flexion or extension torque using a capstan drive mechanism. This exoskeleton interfaces with an existing ankle-foot prosthesis emulator that previously operated only under torque control [2].

Control Schemes: We developed a position control scheme in which the prosthesis angle is commanded to a scaled position of the wrist angle. We tested position control with and without haptic feedback, where a user was able to feel torque at the wrist proportional to the ankle prosthesis torque.

Pilot test: We verified the feasibility and performance of the system with one participant with a transtibial amputation. Eventually we expect that participants will discover their own desired trajectories as they walk, but in this study we dictated desired trajectories to the participant in order to evaluate user ability to control the wrist exoskeleton. Both desired and measured trajectories were displayed on a monitor in front of the participant as they walked on a treadmill. We assessed the ability of the participant to control the prosthesis by measuring error between desired and measured wrist angle. We assessed mechatronic performance of the system by measuring error between desired and measured prosthesis angle.

The participant completed training trials that consisted of following two different desired sine wave trajectories while seated and standing, followed by walking with desired trajectories emulating passive walking or active push-off. Tests were completed over the span of two days, and each training and testing trial lasted five minutes. Data were analyzed for the last 60 seconds of each trial.

Results and Discussion

We achieved good control fidelity of the ankle prosthesis, with error lower than human proprioception (RMSE = 0.8°, compared to ankle proprioception error of 2.3° [3]). Although the subject initially had high errors in wrist trajectory (RMSE = 5.8°), by the end of the second day they were able to control the wrist exoskeleton with accuracy greater than human prioprioception for both desired trajectories (RMSE = 1.6°, compared to wrist proprioceptive error = 2.2° [4]). Results from the second day are shown in Fig. 1B. Qualitatively, the participant preferred the haptic feedback conditions, which they said made position control more intuitive. However, we noticed that providing haptic feedback caused small oscillations in the torque profiles. Future work will investigate the cause of these oscillations and mitigate them.

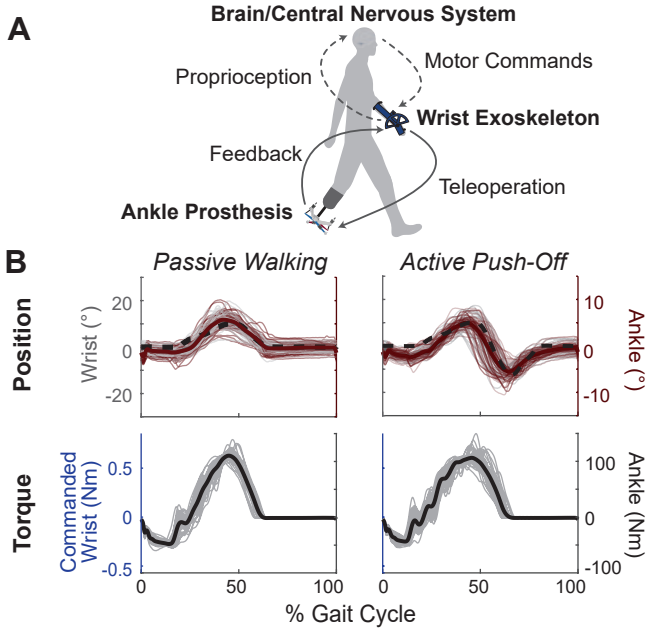

Figure 1: A. We use a wrist exoskeleton to both control and receive haptic feedback from an ankle-foot prosthesis to restore the motor control loop. **B.** The two desired trajectories with haptic feedback are shown, in addition to how well the wrist and ankle matched these trajectories and the resulting torque profiles. The dashed line indicates the desired trajectory, and bold lines indicate averages.

We developed the hardware and control schemes necessary to provide a person with amputation both real-time feedback and control of their prosthesis. We demonstrated the feasibility of this system by validating both our system performance and the ability of a user to voluntarily modulate wrist position in real time with only limited training.

Significance

This teleoperation system will allow testing of novel prosthesis control and feedback strategies that could be used to provide more accurate sensory feedback and facilitate motor learning. Long-term, we aim to discover which parameters amputees intend to optimize during gait, and compare these strategies to those of automated prosthesis control systems.

Acknowledgments

This work was funded by an NSF Graduate Research Fellowship to CGW (DGE-1656518) and an NSF GARDE Grant (CBET-1511177). Thanks to our participant for his time, and S. Stenman, CP, for assistance in fitting the prosthesis to the participant.

References

[1] Petrini et al., *Nature Med* 25(9):1356-63, 2019.
[2] Chiu et al., *TBME* 67(1):166-76, 2020.
[3] Deshpande et al., *Arch Phys Med Rehab* 84(6):883-9, 2003.
[4] Capello et al., *Front Hum Neurosci* 9:198, 2015.

Stumble recovery strategies for healthy individuals and transfemoral prosthesis users

Maura E. Eveld[1], Shane T. King[1], Karl E. Zelik[1], and Michael Goldfarb[1]
[1]Department of Mechanical Engineering, Vanderbilt University, Nashville, TN, USA
Email: maura.e.eveld@vanderbilt.edu

Introduction

Transfemoral prosthesis users (TFPUs) fall 200x more often than healthy individuals [1]. In order to develop interventions (e.g., prostheses) to decrease their fall likelihood, it is important to understand (1) reflexive mechanisms that help prevent falls in healthy populations, and (2) deficiencies in recoveries of the TFPUs.

Concerning (1), it has been established that healthy individuals employ one of three *primary strategies* to recover from a stumble: elevating, lowering, or delayed lowering. However, we have observed that participants used one of two *sub-strategies*: with or without an aerial phase (i.e., jump). Only two prior studies have mentioned an aerial phase [2]; thus the frequency, causes, effects, and implications of these sub-strategies are unknown. This knowledge gap limits how prosthetic interventions are designed/controlled.

Concerning (2), TFPU stumble recovery has been rarely studied. In one study all TFPU participants recovered from perturbations [3], but the perturbation was simulated without a physical obstacle to clear. In the second all TFPUs fell, but stumbles were only elicited at 50% swing. Recovery strategies used/attempted were not consistent between studies, leaving a gap in understanding. A comprehensive characterization of TFPU stumble recovery strategies is needed to identify functional deficiencies of current prostheses, and inform design of next-generation prostheses to help prevent falls.

The overarching goal is to provide a better understanding of both healthy and TFPU stumble recovery by addressing the aforementioned knowledge gaps. Specifically, we aimed to: (1) Characterize the incidence of the aerial phase for each primary recovery strategy in healthy participants, across swing phase, and across speeds, and (2) characterize the recovery strategies of TFPUs for each limb across swing phase.

Methods

For (1), seven healthy participants were stumbled 28 times each at 1.1 m/s using our custom obstacle perturbation system [4]. One participant was tested at two additional speeds, 0.8 and 1.4 m/s. For (2), one TFPU participant was stumbled six times, three times per limb. Testing on additional TFPUs is ongoing and will be presented at the conference. The perturbations were targeted to occur at a range of points in swing phase. Ground-reaction forces and kinematics were collected and joint-level kinematics/kinetics were estimated. For each stumble, the swing percentage of perturbation was calculated and the strategy used/attempted was recorded.

Results and Discussion

Regarding (1), the aerial phase occurred in 40% of recoveries for 1.1 m/s trials. It was used in 92% of delayed lowering strategies, 30% of lowering strategies, and 26% of elevating strategies (Figure 1). For perturbations during 40-70% swing phase, 90% of these resulted in aerial phases. For the single participant tested at multiple speeds, the aerial phase was employed in 92% of 1.4 m/s trials, 32% of 1.1 m/s trials, and 7% of 0.8 m/s trials. Thus the aerial phase was more likely to be used to recover from mid to late swing-phase perturbations and at higher walking speeds. In order to accomplish this aerial recovery with a prosthetic device, an active ankle joint may be required, and device loading capabilities may need to be considered in order to land safely.

Regarding (2), the TFPU participant recovered from all stumbles on his prosthetic side. For the early/mid-swing perturbations, the participant lowered behind the obstacle with the prosthetic limb, followed by a short contralateral step and a hop to clear the obstacle. For the late-swing perturbation, the participant used ipsilateral circumduction to clear the obstacle instead of a hop. On the sound side, the participant attempted an elevating strategy for the early-swing perturbation, and attempted a lowering strategy for mid/late-swing perturbations, but ultimately fell. Thus, sound side stumbles were more dangerous for this TFPU. We are evaluating if this observation holds true in other TFPUs. For stumbling on the prosthesis side, a lack of active knee flexion may contribute to the prolonged recovery (i.e., more recovery steps compared to healthy controls). For stumbling on the sound side, a lack of active plantarflexion and knee flexion may contribute to falls.

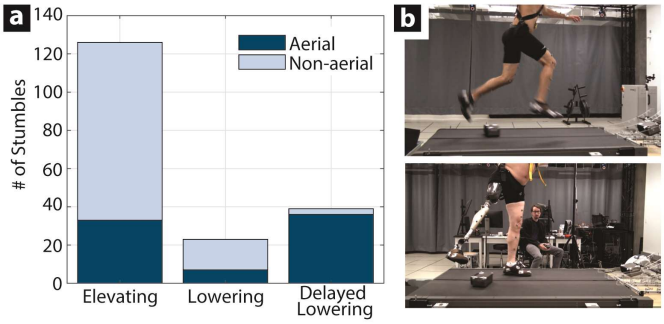

Figure 1: (a) Breakdown of strategies used in healthy stumble study. (b) Aerial phase during recovery for healthy participant (top), and circumduction during recovery for TFPU participant (bottom).

Significance

This is the first study to quantify the prevalence of the aerial phase during healthy stumble recovery, and also the first study to analyze the recovery/falls of a TFPU across a range of swing phase perturbations with a physical obstacle to clear. The insights gained from both healthy and TFPU stumble recovery provide a roadmap for how to successfully design reflexes into a robotic lower-limb prosthesis in order to reduce fall incidence and subsequent injury for this TFPU population (300,000 in U.S. alone).

Acknowledgments

Funding from NIH R01HD088959 and the NSF GRFP.

References

[1] Hafner BJ et al. (2007). *Arch Phys Med Rehab.*
[2] Pijnappels M et al. (2004). *J Biomech*.
[3] Shirota et al. (2015). *JNER.*
[4] Eveld ME et al. (2019). *JNER*.

EMG-Informed Neuromusculoskeletal Model for Knee Joint Load Estimation with a Powered Knee Exoskeleton during inclined walking

Bailey J. McLain[1], Dawit Lee[2], Inseung Kang[2], and Aaron J. Young [1, 2]
[1]Wallace H. Coulter Department of Biomedical Engineering, Georgia Institute of Technology, Atlanta, GA, USA
[2]School of Mechanical Engineering, Georgia Institute of Technology, Atlanta, GA, USA
Email: bmclain3@gatech.edu

Introduction

Of the lower limb joints, the knee joint creates the smallest amount of total positive mechanical work when walking on level ground; however, its role is greater during inclined walking. The knee extension moment increases during uphill walking, which has been correlated to increased knee extensor muscle activation. This can lead to elevated knee joint loads. Therefore, providing assistance at the knee joint during early stance, when the knee exhibits a larger knee moment, has the potential of reducing the knee extensor activation and the knee joint load [1]. Individuals with walking difficulties often exhibit higher tibiofemoral forces compared to able bodied individuals, which can impede mobility and the patient's independence. A previous study has investigated the knee joint load in children with crouch gait, however the methodology exhibited some limitations, involving not considering co-contraction or variations in user's muscle activity [2]. To address this, we utilized an electromyography (EMG) - informed neuromusculoskeletal model to estimate the knee joint reaction load during walking. The following details preliminary results to investigate the capablility of a robotic bilateral knee exoskeleton for reducing the knee joint load in able-bodied adults walking uphill. The primary hypothesis is that the assistance provided at the knee joint during early stance will reduce the quadricep force required for walking and thus decrease the peak knee joint load during early stance compared to the unpowered condition.

Methods

This study was approved by the Georgia Institute of Technology Institutional Review Board. The following displays initial results for one able bodied adult subject. The experiment involved two sessions, training and data collection. The subject walked at 1.1 m/s on a 15% gradient treadmill while wearing the bilateral powered knee exoskeleton. Knee extension assistance was provided by a biological torque controller during early stance, 0-30% of gait cycle. EMG data were collected on six muscles associated with knee extension and flexion (vastus laterilis, vastus medialis, rectus femoris, biceps femoris, semitendinosis, and lateral gastrocnemius) on the right leg. Motion capture, force plate, and device data were also collected. Utilizing MATLAB, Vicon, and OpenSim the collected data were analyzed to calculate the muscle forces and joint reaction load at the knee joint [3][4].

Results and Discussion

During walking with powered assistance, there was a decrease in the peak knee extensor muscle force RMS compared to the unpowered condition. Additionally, it is shown that the muscle force duration is decreased in the powered condition compared to unpowered (**Figure 1A).** This is due to a decreased duration of muscle activation when the assistance is active. There is also a reduction in the peak knee joint force during early stance, where the knee extensor muscles are the largest contribution to the joint load (**Figure 1B)**. These results support the primary hypothesis that the assistance is able to reduce the quadricep forces and the knee joint load during early stance, when the assistance is active. However, there is an increase in the knee joint reaction force later in the gait cycle when the assistance is not active. This increased joint load has been correlated to increased activation of the hamstring muscles as well as the gastrocnemius in assistance mode compared to unassisted for this subject.

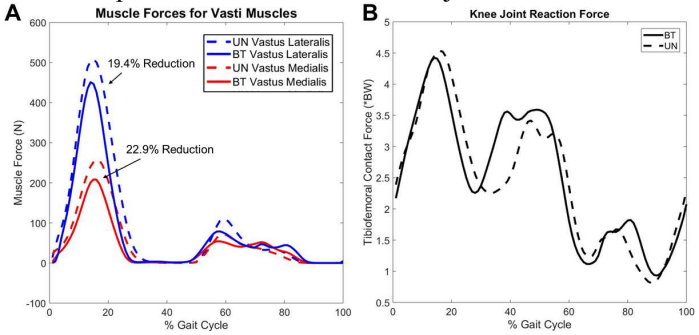

Figure 1: A. Muscle Forces for Vasti Muscles between unpowered (UN) condition and Biological Torque (BT) assistance with the percent RMS reduction labeled**. B.** Knee Joint Reaction Load between unpowered condition (dashed) and Biological Torque assistance (solid). Peak reaction force exhibited a 2.5% *BW reduction when assistance was provided compared to the unpowered condition.

Significance

This study investigated the effect exoskeleton assistance has on the knee joint load of able bodied adults. Our preliminary results show that the exoskeleton assistance is able to reduce the muscle force of the primary knee extensor muscles and reduce the knee joint load when the assistance is active. This analysis method exhibits some limitations, including the optimization weighting may introduce some error in tracking the moment and muscle activation, the muscle force is determined from activation normalized to the maximum voluntary muscle activation of a specific user, which can be difficult to capture even with a detailed protocol, and the results are still an estimate of the actual joint load. In future works, we aim to study the effect exoskeleton assistance has on pediatric patients with walking difficulties due to abnormalities at the knee joint, such as crouch gait or genu recurvatum. The EMG informed method is critical to better estimate the joint loads in these patients, as there is frequently high coactivation while walking.

Acknowledgments

This work was funded by Shriner's Hospitals for Children, NextFlex NMMI Grant, and Georgia Tech Petit Research Scholar Program.

References

[1] D. Lee et al. (2020). *IEEE TNSRE*. [2] KM. Steele et al. (2012). *Gait & posture*. [3] A. Mantoan et al. (2015). *Src Code for Biol and Med*. [4] C. Pizzolato et al. (2015). *J Biomech.*

An automatic human-in-the-loop tuning algorithm for a robotic ankle prosthesis depends on an understanding of gait quality

Kinsey Herrin, Sam Kwak, Audra Davidson, Navya Katragadda, Margaret Berry, Young-Hui Chang

Georgia Institute of Technology
Email : kinsey.herrin@gatech.edu

Introduction

There are more than 1.6 million people living with limb loss, which is expected to more than double by 2050.[1] Powered robotic prostheses may improve metabolic cost, joint loading, and overall mobility[2], but the tuning process associated with a powered prosthesis for an individual user is problematic in that it is: 1. time consuming for busy clinicians and 2. currently completed in clinical settings based on subjective, observational metrics. These problems represent a barrier for access to technology, so efforts to streamline timing towards receipt of a natural physiologically functioning prosthesis would be beneficial both for patients and providers. However, this challenge assumes that there is an ideal, natural physiological gait pattern already defined for humans wearing a powered prosthesis. There are many ways to measure gait, making it challenging to determine a "gold standard" ideal gait for an individual. Studies have attempted to combine biomechanical measures (joint angles, kinetics, etc.) to create indices of gait quality, but it is unclear what measure is most sensitive to changes in gait and which is an optimal "gold standard" for which a device should be tuned against. Therefore, in this preliminary study we test four metrics of gait quality on two human subject groups: healthy controls for whom we have applied systematic joint restraints and an individual with a transtibial amputation using a prosthesis emulator.

Methods

IRB approval for this study was obtained prior to enrollment of subjects. Following informed consent, five healthy control subjects walked in three joint-immobilization conditions including an ankle immobilizer orthosis, a knee orthosis locked in 180º extension, and the combined ankle orthosis and knee orthosis together. Subjects also walked without wearing any restraints as a control condition. One subject with a transtibial amputation walked with his everyday passive prosthesis and a prosthesis emulator[3] while the tuning parameter space was explored for "optimal" gait quality according to current clinical procedures. Gait quality was assessed using the Prosthetic Observational Gait Score (POGS)[4], the Gait Deviation Index (GDI[5]), the Gait Quality Index (GQI[6]), and kinetic data (impulse asymmetry). Data were compared to control values using a repeated measures ANOVA with a significance level set to α=0.05.

Results and Discussion

Data for control subjects showed that impulse asymmetry could discriminate between the ankle immobilized condition and the combined knee and ankle conditions. This trend was followed by the POGS as well. Neither metric could discriminate differences between the knee immobilized condition and the other conditions. The Gait Deviation Index and Gait Quality Index were unable to discriminate between any of the three immobilized conditions. (See Fig 1) This data may indicate that while time consuming, POGS represents an accurate means for determining natural gait. Additionally, load sensors incorporated into a prosthesis to measure impulse could provide valuable information as to proper tuning of a powered device. GDI and

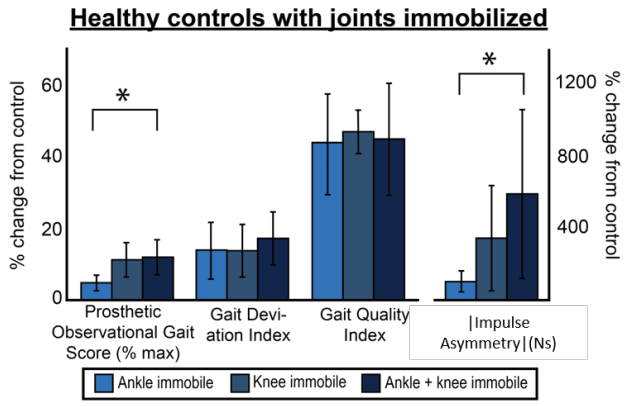

Fig 1. POGS, GDI, GQI and Impulse Asymmetry for healthy controls with systematic joint restraints

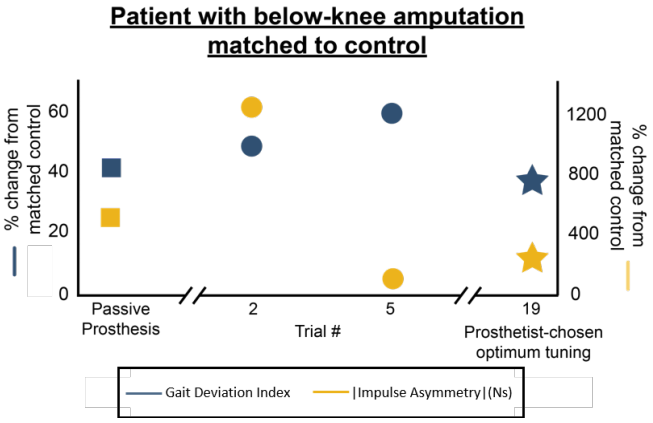

Fig 2. GDI and Impulse Asymmetry for individual with transtibial amputation using everyday, passive prosthesis and powered prosthesis emulator

Impulse Asymmetry were calculated for the passive prosthesis and 19 tuning trials for the powered prosthesis emulator. (See Fig 2) As the device was tuned according to standard clinical procedures, both GDI and Impulse Asymmetry improved with use of the powered prosthesis compared to baseline measures with the subject's everyday prosthesis. Sensors that would allow for this information to be available in vivo could reduce time spent during the initial and follow up tuning processes.

Significance

Broader understanding of what constitutes normal, physiological gait and how to quantify it is imperative for the advancement of prosthetic devices if they are going to be applied clinically.

References

1. Ziegler-Graham, et al.(2008). *Arch. of PM&R*, ***89***(3), 422-429.; 2. Goldfarb, et al. (2013). *Sci. Trans. Med.*, **5**(210). 1-4.; 3. Caputo & Collins (2014). *J Biomech. Eng.,* **136**(3).; 4. Hillman, et al. (2010). *Gait & Post.*, **32**(1), 39-45.; 5. Schwartz, et al. (2008) *Gait & Post.*, **28**(3), 351-357; 6. Marks et al. (2018). *Sci Rep.,* **8**(1), 1-12.

Use of Nearly-Invisible, Non-restrictive Sensory Insoles as Treatment for Idiopathic Toe Walking: A Case Series

Mark Geil[1], Kinsey Herrin[2], Leila Rahnama[1], Cylie Williams[3], Justin Jarrells[1], Micah Poisal[1], Erica Sergeant[1], Kimberly Soulis[1]

[1]Kennesaw State University, [2]Georgia Institute of Technology, [3]Monash University, Melbourne, Australia
Email: *mgeil@kennesaw.edu

Introduction

Idiopathic Toe Walking (ITW) is diagnosed in children three and older who walk on their toes despite no apparent contributing disorders and can result in severe and debilitating loss of ankle range of motion when it persists into childhood[1]. ITW gait is characterized by initial contact with the toe instead of the heel and early heel rise in stance phase. ITW is a diagnosis of exclusion that is only given when all other orthopedic, developmental, and neurological causes have been ruled out[2]. A critical barrier to effective treatment of ITW in children is that current approaches are limited to controlling symptoms by restricting motion of the foot and ankle or manually or surgically altering tendon length. These approaches are variably effective and are focused on orthopedic presentation and not underlying etiologies[3]. Based upon previous studies, we believe that some children with ITW are sensory-seeking[2], and may respond well to in-shoe interventions. In this study, we investigated a novel treatment intended to address tactile stimulation of the plantar surface of the foot, without constraining joint movements.

Methods

Children recruited for the study were between ages 4 and 12, had a clinical diagnosis of ITW, and were at least six months post any treatment (e.g. orthoses, Botox, serial casting, etc.). To be eligible, they also had to display at least 5° dorsiflexion range of motion and screen as possibly or definitely sensory-seeking on the Short Sensory Profile. Following informed consent, subjects were fit with flexible, textured sensory insoles (Fig. 1) and instructed to wear for a four-month period in this IRB approved study. At both initial fitting and final four-month assessment, instrumented 3D gait analysis was conducted in three conditions: shoes and insoles, shoes only, and barefoot. Additionally, the weight bearing lunge test was conducted at each assessment to assess range of motion, and parental feedback was assessed using the Orthotic and Prosthetic User Survey (OPUS).

Figure 1: Flexible, textured insoles (Naboso Technology, Brooklyn, NY)

Results and Discussion

Two subjects have completed the trial to date, a five year old male (A) and a seven year old female (B). Parents of both subjects reported 100% favorable results on the OPUS regarding factors related to device fit, appearance, and durability. These results are somewhat expected given the non-invasive and nearly invisible nature of the insoles hidden inside the child's shoes. Temporospatial parameters with respect to footwear condition (barefoot versus shod with insoles) and time condition (baseline versus follow-up) were inconsistent, but indicate the possibility of improvement. For example, Subject B showed little change in average speed at baseline when the insoles were introduced (1.44 vs 1.40 m/s), but faster walking at follow-up only in the insole condition (1.57 with shoes and insoles, 1.36 barefoot). Gait Variability Index also decreased at follow-up for this subject. Ankle range of motion increased at follow-up in both children, by 5.2 and 5.1 degrees. In both subjects, percent of steps with initial heel contact (not toe contact) improved with insoles at baseline, and improved at follow-up in both the barefoot and insole conditions (Fig. 2). Interestingly, Subject B showed 100% heel contact with the insoles at both baseline and follow up time points, with reduced knee flexion angle at initial contact. In this limited sample, sensory insoles were effective at controlling ITW upon initial donning and after 4 months of wear.

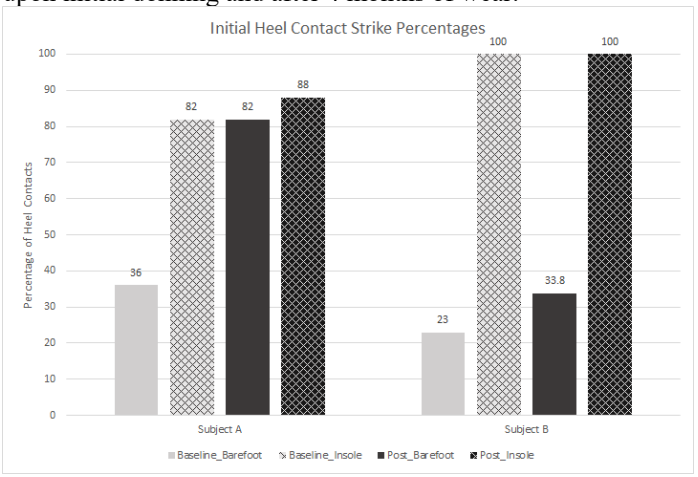

Fig 2: Normal Heel Strike percentage at baseline and follow-up

Significance

While limited in sample size, the results of this study are promising, because current clinical treatments are aimed at mechanically limiting joint motion or even surgically altering tendon length. This treatment addresses a possible etiology for ITW (at least in some children) with the potential to improve our understanding of this unique clinical presentation and remove the term "idiopathic" from the diagnosis.

Acknowledgements

This research was supported by a grant from the Office of Research, Kennesaw State University. Insoles were provided by Naboso Technology, who had no influence on the study.

References

1. Fanchiang HD et al. J Child Neurology. 2015;30(8):1010-6.
2.Williams CM et al. J Foot Ankle Research. 2010;3(1):16.
3.van Kuijk et al. J Rehab Med. 2014;46(10):945-57.

Biomechanics of Women with Transtibial Limb Loss Walking with Heel Height Adjustable Feet

Julia Quinlan[1], Kristin Carnahan[1], Rebecca Stine[2], Jenny Kent[1], Jessica Yohay[1], Andrew Hansen[3], Elizabeth Russell Esposito[4], Matthew Major[1,2,5]
[1]Northwestern University Dept. of Physical Medicine & Rehabilitation; [2]Jesse Brown VA Medical Center; [3]Minneapolis VA Health Care System; [4]EACE/Puget Sound Health Care System; [5]Northwestern University Dept. of Biomedical Engineering
Email: *julia.quinlan@northwestern.edu

Introduction

As of 2005, approximately 35% of the 1.6 million people living with limb loss in the US were women [1]. Compared to men, women with leg amputations experience greater: pain, dissatisfaction with prosthetic fit and appearance, number of prostheses received but also greater rejection rates, and limitations in footwear [2, 3]. Ability to wear appropriate shoes is important for social integration, and while prostheses exist to accommodate different heel heights their effect on walking biomechanics has not been fully studied. The aim of this study was to assess the effects of walking with different heel heights and heel height adjustable prosthetic feet on gait biomechanics of women with transtibial amputation (TTA), as well as the effects of walking with a misaligned prosthetic foot.

Methods

Participants performed over-ground walking trials at self-selected normal speeds wearing footwear with three different heel heights: flat (0 rise), athletic shoe (1.25" rise) and heel (2" rise); and two types of adjustable prosthetic feet: Runway (Freedom Innovations, Irvine, CA), and Accent (College Park, Warren, MI). Prosthetic configurations (prosthesis+shoe) were randomized and participants were blinded to the prosthetic foot.

The prosthesis was first aligned by a prosthetist to the athletic shoe, followed by data collection. The athletic shoe was then switched to a flat shoe, without prosthesis adjustment, followed by data collection. Participants were then allowed to self-align the prosthesis to the flat and heel shoe, followed by data collection for both shoes. An unloaded self-aligned dorsiflexion angle was measured with a goniometer after each realignment. This protocol was repeated with the second prosthesis.

Kinematic data of the lower limbs, trunk and pelvis were collected with a digital motion capture system (Motion Analysis Corporation, Santa Rosa, CA) at 120 Hz. Kinetic data were collected at 960 Hz with six walkway-embedded force plates (AMTI, Watertown, MA). Data were analyzed with Visual 3D (C-Motion, Inc. Germantown, MD).

Results and Discussion

Three female participants (36±9 yrs, 1.62±0.07 m, 64.2±11 kg) with unilateral TTA participated. Time since limb loss was on average 14 (±6) years. All participants accommodated quickly to each condition, despite differences in footwear (heel height and compliance) and limited time to adjust. All participants were able to self-align the foot without difficulty. Findings from only one prosthesis are reported, as both feet had similar results.

Participants maintained consistent prosthetic side kinematics (knee, hip, pelvis obliquity and tilt motion) through ankle joint (set alignment) accommodation. Adaptation of the prosthetic ankle joint allowed for similar ankle motion across heel heights with a shift towards increased dorsiflexion when wearing higher heel heights (Fig 1 A-C). Consistent vertical ground reaction force (GRF) peaks were present across heel heights, however slight delays in second GRF peak occurred with 2" heels, accompanied by longer stance times. Wearing flat shoes with misaligned prosthesis required kinematic adjustments and resulted in an expected shift towards plantarflexion (Fig. 1 C-D). Misalignment led to changes in knee and pelvis motion, and were accompanied by altered first and second GRF peak magnitudes.

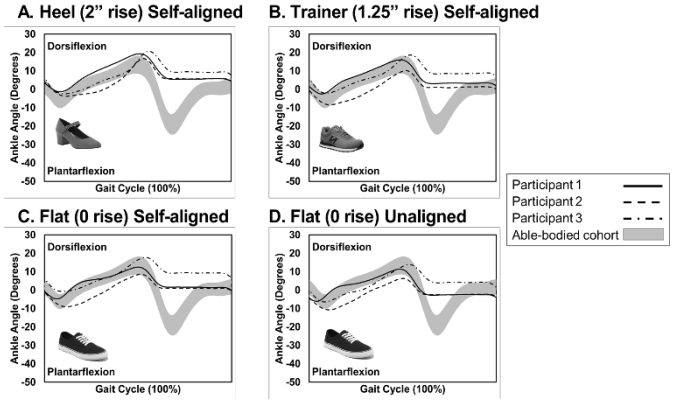

Figure 1: Effects of different heel heights (A-C) and ankle alignment (C-D) on ankle flexion of the prosthetic foot-shoe complex.

Overall, the three prosthesis users adapted to each footwear and alignment condition with minimal changes in kinematics and kinetics. This suggests that using heel height adjustable prostheses can generate consistent gait dynamics without new compensatory mechanisms when walking with different heel height shoes. The participants also expressed the importance of having the option to wear different shoes for daily activity and the need for an adjustable prosthesis. Future work includes expanding cohort size beyond this pilot study, and bench testing of these prostheses with footwear to characterize their mechanical function for aiding interpretation of these results.

Significance

These results may inform on the influence of different shoes on prosthetic gait, and the utility of heel height adjustable prosthetic feet in promoting consistent biomechanics. This study helps address the unique considerations for women with amputation during rehabilitation, and may aid development of more evidence-based, sex-inclusive practice guidelines.

Acknowledgments

This work was supported a Shaw Family Pioneer Award through the Northwestern University Women's Health Research Institute. We thank Clare Severe for her assistance with data processing.

References

[1] Ziegler-Graham et al. (2008). Arch Phys Med Rehabil, 89:422-9.
[2] Elnitsky et al. (2013). Rehabil Nurs, 38:32-6.
[3] Singh R, et al.(2008). *Disabil Rehabil*, 30:122-5.

Effects of material of the 3D printed foot on ankle kinematics/kinetics and toe joint bending during prosthetic walking

Woolim Hong[1], Huijin Um[2], Heonsu Kim[2], Haksung Kim[2,3,§], and Pilwon Hur[1,*]
[1]Department of Mechanical Engineering, Texas A&M University, College Station, TX 77843, USA
[2]Department of Mechanical Engineering, Hanyang University, Seoul, South Korea
[3]Institute of Nano Science and Technology, Hanyang University, Seoul, South Korea
Email: §kima@hanyang.ac.kr, *pilwonhur@tamu.edu

Introduction

Toe joint can impact a gait economy and performance while undergoing substantial flexion/extension during normal walking. To provide the benefits of a toe joint to the amputees, researchers have attempted to mimic human toe joint in their prostheses. [1] proposed a powered toe joint, and [2] applied interchangeable springs to mimic a human toe joint during prosthetic walking, which inevitably require additional parts, and thus more weight.

We previously proposed the structural pattern and material of the 3D printed prosthetic foot in [3]. However, it is not known yet how the joint kinematics/kinetics and toe joint bending are affected by the new design. Thus, in this study, we investigate how the ankle/toe joint kinematics/kinetics vary in accordance with the 3D printed prosthetic foot characteristics while walking.

Methods

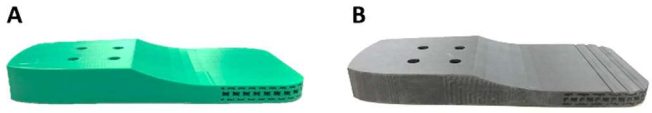

Figure 1: 3D printed prosthetic foot; (A) re-entrant structure using ABS, (B) re-entrant honeycomb with bending zone (BZ) using onyx [3]

Note that there was no stiffness difference between two proposed foot structures (Figure 1) under the small bending conditions according to the simulation result in [3]. Therefore, we focus only on the foot material in this paper.

A treadmill walking experiment was conducted using a powered transfemoral prosthesis (AMPRO II, [4]) with two different feet (ABS and onyx foot), depicted in Figure 1. A healthy subject (male, 31 yrs., 1.70 m, 70 kg) participated using an L-shape simulator and walked at his preferred speed (0.60 m/s). Joint kinematics were recorded by the optical encoders on the prosthesis. Joint kinetics were estimated based on the current from the actuators of the prosthesis. The toe bending was measured using IMUs, defined as the relative angle between the forefoot and midfoot. The control framework adopted was impedance control at the ankle and a hybrid of impedance and tracking control at the knee [4].

Results and Discussion

The onyx foot had lesser ankle dorsi-flexion than the ABS foot (Figure 2A), resulting in lesser ankle joint torque (Figure 3A). However, the difference is minimal. In Figure 2B, the greater toe flexion (2.46 °) was clearly shown when the onyx foot is used, while that of the ABS foot is smaller (0.74 °). Yet, differing from the simulation result (15 °) in [3], this flexion is still small, even in the case of onyx. This may indicate that the toe stiffness of both feet is still too stiff. Also, an insufficient loading condition due to the simulator and less body weight (compared to the simulation) can be another possible reason of a small toe flexion. Further studies should be conducted with a diverse compliant toe.

In Figure 3, the ABS foot shows a slightly larger joint torque and power than the onyx foot, even though not significant.

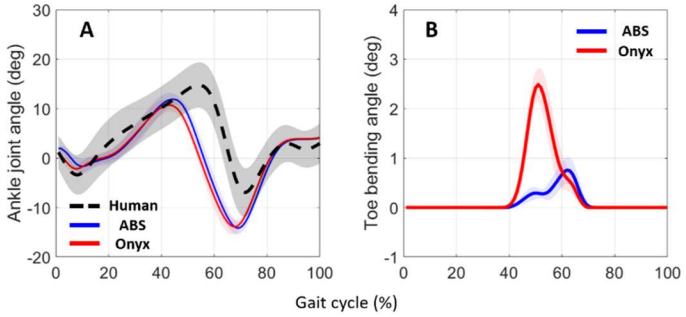

Figure 2: Kinematic comparison between ABS, onyx foot, and human data; (A) ankle joint angle (B) toe joint angle. Bold lines and shaded regions refer to the average and ±1 s.d. of 20 consecutive steps.

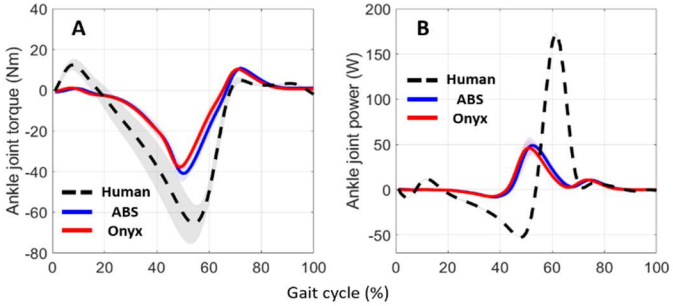

Figure 3: Kinetic comparison between ABS, onyx foot, and human data; (A) ankle joint torque (B) ankle joint power. Bold lines and shaded regions refer to the average and ±1 s.d. of 20 consecutive steps.

Compared to the human data at a faster walking speed of 0.80 m/s [5], both feet show smaller dorsiflexion and earlier push-off, possibly due to a slight mismatch in the timing at the controller. Also, note that the ankle torque and power are smaller due to the restricted torque limit of the actuator on the prosthesis.

In this study, both feet are similar in most measures. However, since onyx foot shows more toe bending, which is more similar to human data, the onyx foot would be a preferred option.

Significance

This study shows the ankle/toe joint kinematics/kinetics using two different 3D printed feet with new structure to replicate the toe joint. Even though there was no significant difference between two proposed feet in most of the measures, still one foot showed relatively significant toe bending. This can be a good starting point for the new consideration of prosthetic foot design. Also, the proposed foot shows almost half weight (540 g) compared to the previous studies [1], [2]. Further designs for toe joint and more realistic loading conditions will be considered to maximize the biomechanical benefits of 3D printable prosthetic feet during walking.

References

[1] J. Zhu, et al. (2014), *IEEE Transactions on Industrial Electronics,* Vol. 61, No. 9
[2] E. C. Honert, et al. (2018), *Bioinspiration & Biomimetics,* Vol. 13, No. 6
[3] H. Kim, et al. (2020), *American Society of Biomechanics*
[4] W. Hong, et al. (2019), *International Conference on Robotics and Automation*
[5] K. R. Embry, et al. (2018), *IEEE TNSRE*, Vol. 26, No. 12

Adjustable prosthetic socket improves symmetry of transfemoral amputees during walking

Joshua R. Tacca[1,2] and Alena M. Grabowski[2]
[1]Dept. of Mechanical Engineering & [2]Dept. of Integrative Physiology, University of Colorado, Boulder, CO, USA
joshua.tacca@colorado.edu

Introduction

Adults with unilateral transfemoral amputation walk using prostheses attached to rigid prosthetic sockets that surround the residual limb. A standard socket used by people with transfemoral amputation is a suction socket that is molded to fit the users residual limb and uses a valve to release air and create a sealed connection between the socket and leg.

During walking, many people with unilateral amputation use a passive prosthesis, which typically results in asymmetric biomechanics such as greater loading of the unaffected (UL) compared to affected leg (AL) [1]. Asymmetry may increase osteoarthritis risk [2] and low-back pain [3] compared to non-amputees. Socket design can influence AL comfort and may change the biomechanics of both legs. Board et al. [4] found that users of a vacuum-assisted suction socket had more symmetric step lengths and ground contact times compared to users of a standard suction socket. An adjustable socket may further improve comfort and biomechanical symmetry during walking. Quorum Prosthetics (Windsor, CO) has developed a socket that uses adjustable panels to provide a custom fit to people with lower limb amputation (Quatro). Due to a better fit, we hypothesize that use of the Quatro socket will decrease contact time and peak ground reaction force asymmetry of people with transfemoral amputation compared to using a suction socket.

Methods

Three subjects (2M, 1F; 46.0 ± 18 yrs; 70.7 ± 5 kg; 1.74 ± 0.01 m) with unilateral transfemoral amputation walked on a force measuring treadmill (Bertec, Columbus, OH) at 0.75 – 1.50 m/s at 0° and at 1.25 m/s at ±3° and ±6°. Subjects walked with a standard suction and an adjustable Quatro prosthetic socket.

We measured perpendicular ground reaction forces (GRFs) at 1000 Hz, filtered them using a 4th-order low-pass Butterworth filter with a 30 Hz cut-off and used a 20 N GRF threshold to calculate contact time (t_c). We also detected 1st and 2nd peak GRFs (f_{z1} and f_{z2}, respectively) of the AL and UL from 10 strides (Matlab, Mathworks, Natick, MA). In addition, we calculated the symmetry index (SI) of each of these parameters using the equation (Eqn. 1) defined by Robinson et al. [5], where X refers to a calculated variable and 0% is perfect symmetry.

$$SI = \left| \frac{X_{unaffected} - X_{affected}}{0.5(X_{unaffected} + X_{affected})} \right| \text{ x } 100\% \quad (1)$$

We constructed a linear mixed effects model ($\alpha = 0.05$) to determine the effect of socket type and speed on each SI when walking on a level treadmill. Then, we constructed a linear mixed effects model ($\alpha = 0.05$) to determine the effect of socket type and treadmill slope on each SI when walking at 1.25 m/s (R-Studio, Boston, MA).

Results and Discussion

For level walking, when using the Quatro compared to suction socket the magnitude of t_c SI decreased by 4.4% ($p = 0.0013$) but for both sockets there was no effect of speed on t_c SI ($p = 0.1037$; Fig. 1a). When walking on slopes using the Quatro compared to suction socket the magnitude of t_c SI decreased by 3.5% ($p = 0.0118$) and for both sockets the magnitude of t_c SI decreased by 0.4% per 1° increase in slope ($p = 0.0133$; Fig. 1b).

During level walking, there was no effect of socket or speed on f_{z1} SI ($p = 0.4175$, $p = 0.9727$; Fig. 1a). Across slopes, there was no effect of socket or slope on f_{z1} SI ($p = 0.0757$, $p = 0.0587$; Fig. 1b). During level walking with the Quatro compared to the suction socket, the magnitude of f_{z2} SI decreased by 5.9% ($p = 0.0083$) and for both sockets f_{z2} SI increased by 17.4% per 1 m/s increase in speed ($p = 0.0001$; Fig. 1a). When walking across slopes using the Quatro compared to the suction socket, the magnitude of f_{z2} SI decreased by 8.1% ($p = 0.0008$) but for both sockets there was no effect of slope on f_{z2} SI ($p = 0.7059$; Fig. 1b).

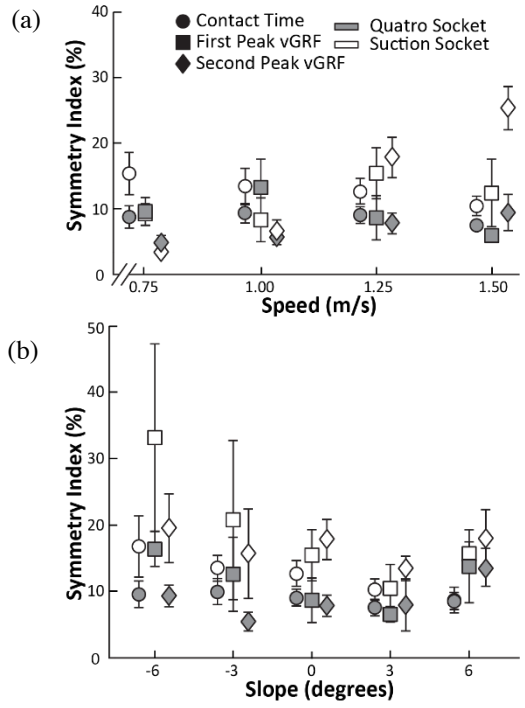

Figure 1. t_c, f_{z1}, and f_{z2} symmetry indices across (a) speeds and (b) slopes. Error bars are SEM. 2 of 3 subjects walked at 1.50 m/s in (a).

Significance

Decreased asymmetry using the Quatro compared to suction socket may be due to improved socket fit and comfort. Future studies will examine prosthetic socket fit by measuring socket pistoning during walking. The results from this study can be used to inform prosthetic socket designs.

Acknowledgments

We thank Joe Johnson and Quorum Prosthetics.

References

[1] Nolan & Lees (2000). *Prosthet. Orthot. Int,* **24:** 117-125.
[2] Kulkarni et al. (1998). *Clin. Rehabil,* **12:** 348-353.
[3] Kulkarni et al. (2005). *Clin. Rehabil,* **19:** 81-86.
[4] Board et al. (2001). *Prosthet. Orthot. Int,* **25**: 202-209.
[5] Robinson et al. (1987). *J. Manip. Physiol. Ther,* **10:** 172-176.

A Comparison of Ground Reaction Forces During Treadmill and Overground Walking in Transfemoral Amputees

Paige Paulus[1,2], Tom Gale[3], Jacob Levy[3], and William Anderst[3]
[1]University of Pittsburgh, Department of Physical Therapy
[2]University of Pittsburgh, Department of Bioengineering
[3]University of Pittsburgh, Department of Orthopaedic Surgery
Email: pap82@pitt.edu

Introduction

As of 2005, 1.6 million people were living with a loss of limb, with this number being projected to more than double by the year 2050 [1]. Poor prosthetic fit increases the likelihood of those who have had an amputation having a secondary complication [2].

Depending upon the setting, a prosthetist could evaluate the fit of their patient's device during treadmill or overground walking. Previous studies have found that peak vertical ground reaction force (GRF) is greater during overground walking compared to treadmill in healthy subjects [3]. Additionally, previous studies have found that those with transfemoral amputations have greater vertical and anterior/posterior (A/P) GRF in their sound limb compared to their prosthetic limb [4].

The aim of this study is to compare GRF of subjects with transfemoral amputations during overground and treadmill walking. We hypothesize that there will be greater GRF on the sound side compared to the prosthetic side and greater GRF during overground compared to treadmill walking.

Methods

Eleven individuals with transfemoral amputations were recruited via clinician referrals and local support groups (age: 24 to 63 years, weight: 59.0 to 130 kg, and height 1.6 to 1.9 m). All participants provided written informed consent prior to participating in this IRB-approved study.

Subjects were fitted with a full body marker set and recorded using a 12-camera Vicon Vantage system to measure gait kinematics. During 10 overground trials, subjects walked across the lab space taking 1-3 steps on the Bertec instrumented treadmill per trial at the midpoint of the walking bout. During the 2 to 10 treadmill trials, 9 to12 steps were recorded per trial, with the speed set to match their self-selected overground speed. GRF data was collected at 1000 Hz for all trials.

GRF data was filtered using a fourth-order Butterworth filter with a 20 Hz cutoff frequency and then normalized to body weight (%BW). Heelstrike and toeoff were determined as the moment when the vertical GRF exceeded and went below 50 N. Output from the Vicon system was reviewed to determine which trials needed to be omitted from the analysis due to the subject crossing over onto the wrong force plate.

GRF variables including A/P (break and peak), medial/lateral (M/L), and vertical (1st and 2nd peak) peaks and impulses were averaged over all trials for each subject and analysed. A paired t-test was performed to compare prosthetic and sound limb outcomes as well as walking surfaces (overground or treadmill) for each GRF parameter [5].

Results and Discussion

Sound side loading was greater than prosthetic side loading during overground and treadmill walking (Figures 1, 2). This supports previous studies which found that those who have an amputation favour putting weight through their sound limb.

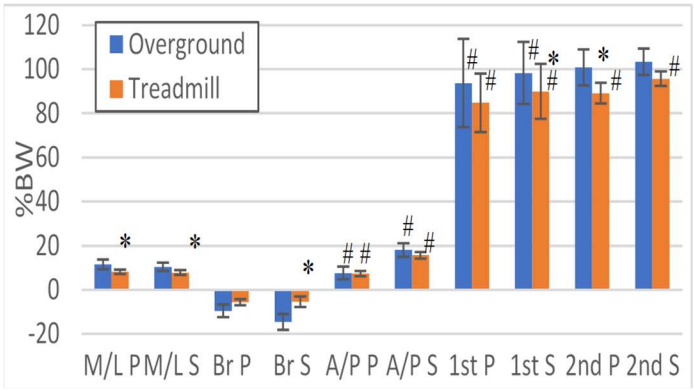

Figure 1: Average peak GRF output in prosthetic (P) and sound (S) limbs across subjects *significant for overground and treadmill trials ($p < 0.05$), #significant between legs ($p<0.05$)

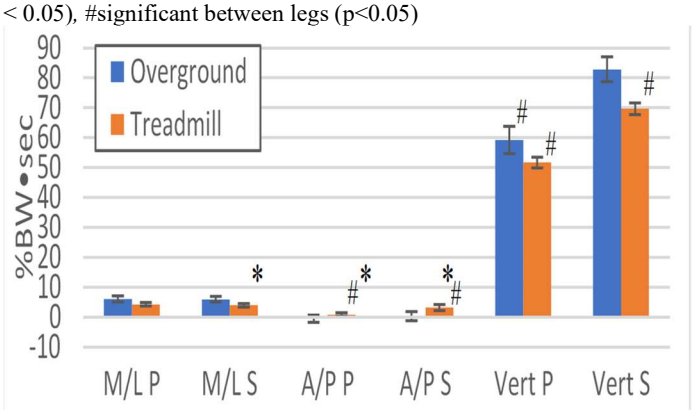

Figure 2: Average impulse in P and S across subjects *significant for overground and treadmill trials ($p < 0.05$), #significant between legs ($p<0.05$).

GRF outputs were greater on average in overground trials compared to treadmill (Figure 1, 2). If the goal is to assess the prosthetic side, M/L peak, 2nd vertical peak and AP impulse will likely be less on a treadmill compared to overground. However, they are correlated (r – 0.63 to 0.69) indicating the treadmill may provide some valuable information that reflects overground walking.

Significance

Given the difference in GRF between overground and treadmill walking, clinicians should be wary of evaluating fit and alignment of prosthetic devices by having their patient walk on the treadmill. Additionally, researchers should be wary of the limitations associated with testing persons with an amputation during treadmill walking.

References

[1] Ziegler-Graham, et al (2008). PM&R. [2] Gailey, R. (2008). JRRD. [3] White, et al (1998). MSSE. [4] Kowal, et al (2018). OTR. [5] Matlab 2019b, The MathWorks, Inc

Restoring Functional Gait of Individuals with Transfemoral Amputation using a Powered Prosthesis

Krishan Bhakta[1], Jonathan Camargo[1,2], William Compton[1], Kinsey Herrin[1,2], Aaron Young[1,2]
[1]Woodruff School of Mechanical Engineering, Georgia Institute of Technology, Atlanta GA, 30332 USA
[2]Institute for Robotics and Intelligent Machines, Georgia Institute of Technology, Atlanta GA, 30332 USA
Email: kbhakta3@gatech.edu

Introduction

When walking, individuals with transfemoral amputation (TFA) use compensatory strategies which often lead to asymmetric joint biomechanics, chronic leg and back pain, joint degradation, increased energetic demands, and increased chance of osteoarthritis.[1,2] Specifically, the hip has to compensate for power lost from missing joints.[3] Powered prostheses are one option of improving gait as they are able to provide similar biological assistance profiles across different walking modes.[4] Our hypothesis is that a powered prosthesis will generate improved bilateral biomechanics than current clinically available passive prostheses, which was initially evaluated based on joint kinematic comparisons.

Methods

Three subjects with a unilateral transfemoral amputation (male, 51 ± 21.1 years old, 1.78 ± 0.07 m, 82 ± 15.5 kg, K3/K4) consented to participate in this IRB approved study. Subjects performed level and sloped walking on an instrumented treadmill (Bertec, Colombus, OH) using their everyday prosthesis and our powered knee and ankle prosthesis at 0 deg, +7.5 deg, and -7.5 deg. Data was collected using a motion capture system (Vicon, Centennial, CO). Analysis was performed using custom built prosthetic models in OpenSim, an open-source musculoskeletal modeling and simulation platform.

Results and Discussion

The results show that the inverse kinematics (IK) were symmetrical to biological signals when using the powered device versus their passive device. Specifically, the ankle kinematics on the prosthetic side show increased pantarflexion for both the level and incline walking trials. Furthermore, the intact side shows a reduction in the amount of plantarflexion explained by the ability of the prosthesis to contribute power to push the user forward. No significant changes were seen in the knee kinematics. It also can be seen that there no major changes in the hip kinematics which may be explained by the additional mass of our prosthetic device as the user may still have to compensate with their hip joint to a certain extent. With the powered prosthesis, the assistance shown during these walking tasks could potentially help reduce the risk of future hip and back related musculuoskeletal pathologies. The key result is that powered prosthetic technology may be helpful in restoring functional gait across multiple ambulation modes.

Significance

Creating smarter powered prostheses for assisting TFA is an important area of research as these devices can restore lost biomechanical function and potentially improve quality of life. For this type of technology to be translated to modern clinical practice, these devices must show improved efficacy over current clinical standards. This is one step in allowing powered prostheses to restore seamless and natural movement to the user.

Acknowledgments

This work was funded by DOD Award No. W81XWH-17-1-0031.

References

1. Highsmith, M. J. *et al. Spine J.* (2018). doi:10.1016/J.SPINEE.2018.08.011

2. Morgenroth, D. C., Roland, M., Pruziner, A. L. & Czerniecki, J. M. *Clin. Biomech.* **55**, 65–72 (2018).

3. Grumillier, C., Martinet, N., Paysant, J., André, J. M. & Beyaert, C. *J. Biomech.* **41**, 2926–2931 (2008).

4. Ingraham, K. A., Fey, N. P., Simon, A. M. & Hargrove, L. J. *PLoS One* **11**, 0147661 (2016).

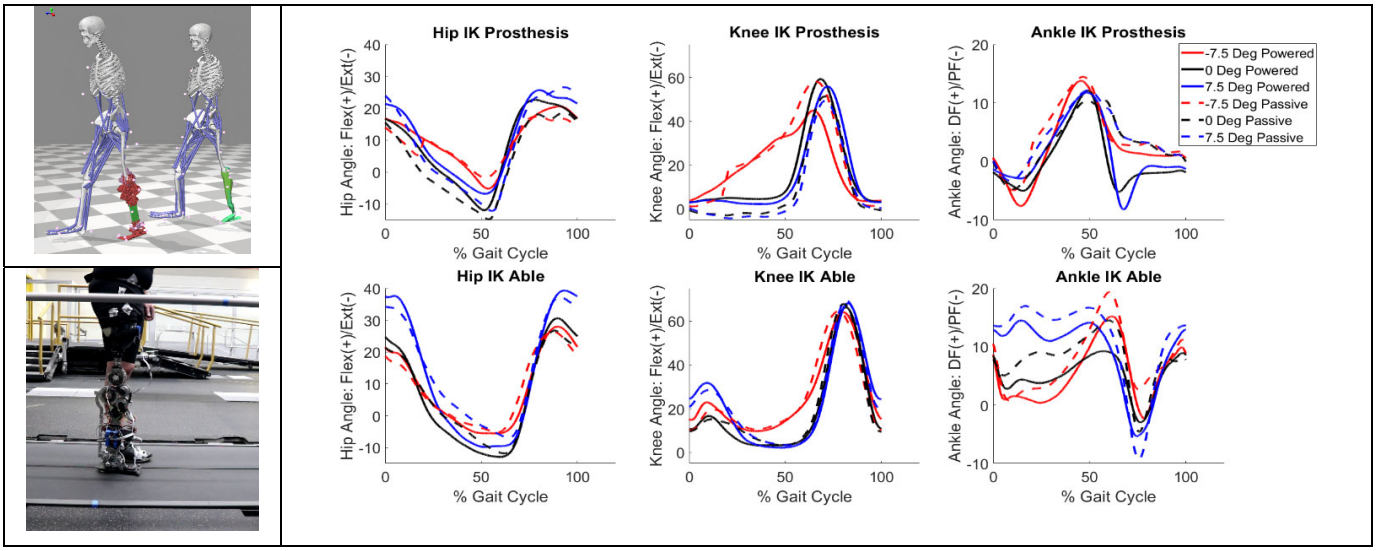

Figure 1: Opensim models of a powered prosthesis and passive prosthesis (top left); one individual wearing our powered prosthesis with motion capture markers placed on both prosthetic and intact side (bottom left); and inverse kinematics for both prosthetic and intact side for three modes of treadmill walking: level ground (0 deg), incline (+7.5 deg), and decline (-7.5 deg).

Leveraging Machine Learning for Real-Time Metabolic Cost Prediction

Matthew Mulligan[1], Kimberly A. Ingraham[1], C. David Remy[1,2], and Deanna H. Gates[1]
[1] University of Michigan, Ann Arbor, Michigan, [2] University of Stuttgart, Stuttgart, Germany
Email: mbmulli@umich.edu

Introduction

Wearable robotic devices have the potential to reduce individuals' metabolic costs during walking. However, the success of these devices depends on the ability to appropriately tune the devices' control parameters on a subject-specific basis. As the optimal parameters will likely vary as the person performs different tasks, this must be performed continuously throughout use. One way to obtain these control parameters is through "body-in-the-loop" optimization or real-time optimization based on human physiological data. This approach has been used successfully to tune assistive devices using a participants' metabolic cost data while they walked on a treadmill at a fixed speed [1-3]. Ingraham et al. expanded on this idea by using data from various sensors and linear regression to predict metabolic costs for a variety of activities [4]. While successful, the predictions had error rates three times that of the minimal detectable change (MDC) of metabolic cost for steady-state walking of 17 W [5]. Here, we expand upon existing work by developing a generalizable model using machine learning to predict metabolic costs for multiple activities and individuals.

Methods

We analyzed data from an open-source dataset [4], which included 8 people performing 22 activities while wearing 15 sensors. We divided our sensor sets into local and global signals. Local signals included data from 6 triaxial accelerometers and 8 surface electromyography electrodes. Global signals included data from an electrodermal sensor and skin temperature monitors, a heart rate monitor and a portable respirometer that collected oxygen consumption, carbon dioxide production, breath frequency, and minute ventilation. The data were filtered and reduced so all resulting features corresponded to one vector per second. This technique assigns a single feature vector to each predicted metabolic cost value on a uniform timescale.

We applied machine learning models including Linear Regression, K Nearest Neighbors (KNN), Bayesian Ridge, a Decision Tree, a Neural Network, and a Random Forest. Each model was built using features from the local signals only, global signals only, and all signals. Additionally, we built a model using only data from a Hexoskin (Hexo) suit, which included global signals and waist accelerometry, to demonstrate performance for a commercially available wearable device. We compared prediction error between each model for each set of data. Model performances were cross-validated using an 80/20 shuffle split, leave one activity out, and leave one subject out.

Results and Discussion

For the shuffle split approach KNN, Decision Tree, and Random Forest models had the lowest error rate regardless of the dataset (Fig. 1). For leave one subject out, Bayesian Ridge and Linear Regression with Global and Hexo signals generated the best performance. For leave one activity out, Neural Network had the best performance with Hexo and Global signals.

Though our results show promise in making predictions, our study was limited by the relatively small number of individuals and activities. Thus, the models made predictions consistent with observed data, as demonstrated in shuffle split, and performed worse in leave-one-out analyses for unseen individuals and data. The appropriate algorithm should be selected based on performance across all three cross-validation techniques as a result. Accordingly, we recommend the use of KNN and Random Forest as they have low errors with shuffle split and their performance is more robust to leave-one-participant and leave-one-subject-out analyses.

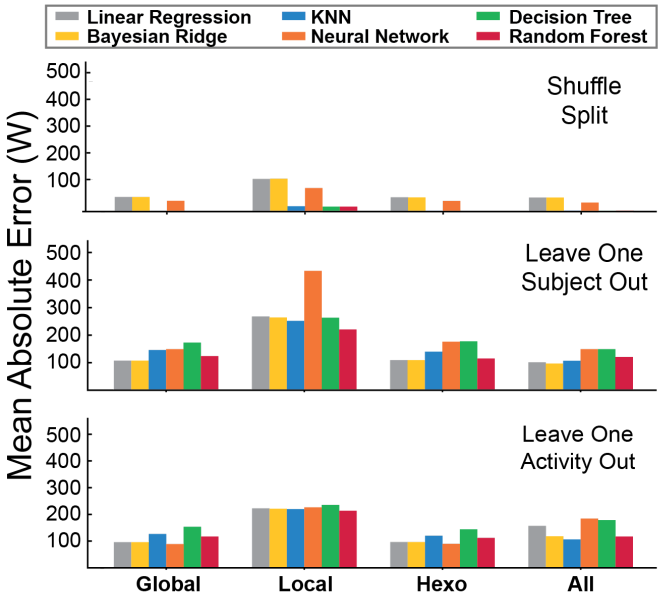

Figure 1: Performance of machine learning models with different sets of sensors and types of validation.

Significance

Machine learning models predicted real-time metabolic cost with low errors (< 2W). These models had moderate errors for unobserved activities (< 89 W) and unobserved participants (< 110 W). Future work will explore feature engineering to determine if these models can be further improved to reduce the prediction error rate.

Acknowledgments

Supported by the NIH under grant #R03 HD092639.

References

[1] Koller, et al. (2016) *Robotics Science & Systems(2016). 1-10*
[2] Zhang et al. (2017) *Science 356(6344). 1280-1284*
[3] Ding, Ye, et al. (2018) *Science Robotics 3(15). eaar5438*
[4] Ingraham, K. et al. (2019) *J Appl Physiol 126(3)*. 717-729
[5] Davidson, A. et al (2016) *Cogent Eng 3(1). eaar1251028*

Impedance Control of the Knee Mechanism of a Transfemoral Prosthetic for Level Walking

Namita Anil Kumar[1], Woolim Hong[1], and Pilwon Hur[1*]
[1]Department of Mechanical Engineering, Texas A&M University, College Station, TX 77843, USA
Email: *pilwonhur@tamu.edu

Introduction

Powered prosthetics have been shown to increase a user's walking efficiency and enable higher walking speeds in comparison to the non-powered counterparts. Yet, powered prosthetics suffer from lack of use owing to poor kinematic compatibility, bulkiness, and low adaptability to changes in the terrain. Additionally, current powered prosthetics mandate tedious calibration and tuning procedures, which prohibit their general usage. A possible approach to some of these problems is to focus on improving user-comfort by replicating able-bodied walking with such prosthetics. Many researchers have done this by adopting impedance control strategies. Under this control scheme, the gait is generally divided into 4-6 phases with a unique set of constant impedance control parameters—stiffness, damping, and equilibrium angles—assigned to each phase [1]. But studies such as [2] have revealed that a healthy human's joint impedance varies continuously throughout the stance phase of the gait cycle. Since the objective of a prosthetic's controller is to mimic able-bodied walking, it stands to reason that control parameters must also be human-inspired. Studies such as [3] have implemented algebraic curves within some phases of the control scheme. While the parameters vary continuously and smoothly within the phases, there are likely non-smooth variations during transitions between phases. Further, the controller proposed in [3] relies on a load cell that measures vertical ground reaction force. Such load cells can be expensive and increase the prosthetic's weight. A prior study by the authors proposes an impedance control scheme that varies the impedance parameters continuously and smoothly throughout the stance phase of the gait cycle [4]. Unlike [3], this scheme does not rely on a load cell. The impedance parameters are estimated using a least squares approach like that used in [1]. In the study, [4], the proposed controller was only implemented on a transfemoral prosthetic's ankle joint. This paper documents preliminary attempts at extending the control scheme to the prosthetic's knee joint.

Methods

The proposed control scheme sections the gait cycle into 4 phases: heel strike (0%) to flat foot (13%), flat foot to heel off (42%), heel off to toe off (62%), and toe off to the end of the gait cycle (100%). The torque generated by the impedance controller is represented as follows.

$$\tau(t) = K(t)\left(\theta(t) - \theta_{eq}(t)\right) + D(t)\dot{\theta}(t)$$

where $K(t)$ and $D(t)$ are the stiffness and damping parameter at the instant t ($0\% \leq t \leq 100\%$). The term θ_{eq} is the equilibrium angle, while $\theta(t)$ and $\dot{\theta}(t)$ represent the joint's position and velocity. Both $K(t)$ and $D(t)$ are represented by 4th order polynomials during the stance phase and a constant value during the swing phase. The polynomials were estimated using a least squares method detailed in [4] and were tuned by scaling and adding an offset. This controller was tested on a transfemoral prosthesis (AMPRO II [4]) with a healthy participant (male, 31 yrs., 1.70 m, 70 kg) using a L-shaped simulator. While the ankle was controlled using impedance control, the knee was controlled using impedance control during the stance phase, followed by trajectory tracking during until 90% of the gait cycle, and low gain PD control during 90%-100% of the gait.

Results and Discussion

The generated kinematics and kinetics have been presented in Figure 1. Both ankle and knee kinematics resemble able-bodied walking. The slightly lessened ankle dorsiflexion during mid-stance can be countered with further tuning. While the ankle torque also followed a humanlike trend, the peak torque is significantly lesser than that of healthy human's. This is due to the torque limitations of the prosthetic's actuators.

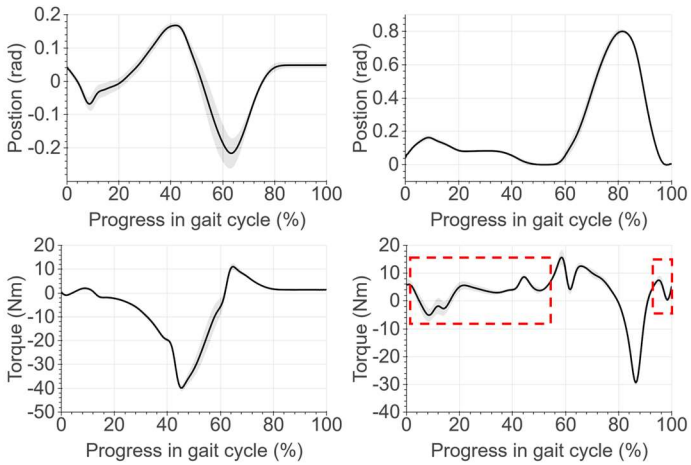

Figure 1: Top left: Ankle position, Top right: Knee position, Bottom left: Ankle torque, Bottom right: Knee torque.

Unlike the ankle, the knee torque deviated from that of a healthy human's. These deviations have been highlighted with red boxes in Figure 1. The first discrepancy is attributed to the controller's high damping parameters. It is believed that the results will improve by constraining the magnitude of damping. The second discrepancy is due to the low gain PD controller.

Significance

In addition to generating near human-like gait, this controller requires lesser tuning. Additionally, the involved tuning process is easy to carry out [4]. With improvements, the proposed control scheme can undoubtedly make prosthetics easier to use for both amputees and therapists/practitioners. Future efforts are directed at eliminating the entire tuning process via auto-tuning methods such as fuzzy-logic.

References

[1] F. Sup, et al. (2011), IEEE Transactions on Neural Systems and Rehabilitation Engineering, vol. 19, pp. 71–78
[2] H. Lee, et al. (2016), IEEE Journal of Translational Engineering in Health and Medicine, vol. 4, pp. 1–7
[3] N. P. Fey, et al. (2014) ,IEEE Journal of Translational Engineering in Health and Medicine, vol. 2, pp. 1–12
[4] N. Anil Kumar, et al. (2019), p. arXiv:1909.09299

THE ASSOCIATION BETWEEN PHYSICAL ACTIVITY PARAMETERS, SELF-EFFICACY, QUALITY OF LIFE AND COMMUNITY PARTICIPATION IN USERS OF UNILATERAL TRANSTIBIAL PROSTHESES

Noah J Rosenblatt[1]*, Sai Yalla[1], Jenny A Kent[2], and Matthew Major[2]
[1]Center for Lower Extremity Ambulatory Research, Rosalind Franklin University of Medicine and Science, North Chicago, IL USA
[2] Northwestern University Prosthetics Orthotics Center, Chicago, IL USA
Email: *noah.rosenblatt@rosalindfranklin.edu

INTRODUCTION

Prosthesis users face unique barriers to physical activity (PA), e.g., socket discomfort, components that poorly accommodate to inclines or uneven surfaces. However, interventions to address these barriers do not always promote PA. For example, changing socket suspension from pin to vacuum, which should increase comfort and mobility[1], reduces steps per day[2]. In addition, while evidence supports the use of microprocessor-controlled knees to increase self-reported mobility, step counts and duration of activity may be unaffected by the type of knee[3]. To some extent these findings may reflect the fact that traditional measures of PA such as step count do not closely relate to changes in community participation or well-being, which may be expected with increase mobility[4], and therefore may not well capture the impact of these interventions. Moreover, traditional measure of PA may not well capture the complexity of PA patterns that may also be impacted. Recent studies using detrend fluctuation analysis (DFA) suggest that daily fluctuations in PA are not random, but rather demonstrate scale invariance (appear similar at short and long time scales). This property is thought to reflect overall motor health, is insensitive to total level of activity and is impacted by disease states such as chronic fatigue that alter the temporal nature of the PA[5]. The purpose of this study was to evaluate the relationship between a number of PA measures derived from activity monitors and self-reported outcome measures associated with well-being, community participation and PA patterns in order to provide insight to guide assessments in future intervention studies.

METHODS

We present data from the first 17 persons with unilateral transtibial amputation recruited into a larger randomized control trial to reduce fear of falling and increase community participation in prosthesis users. To participate, individuals: reported an Activity-specific Balance Confidence (ABC) score <80 and had at least 6 months experience with a definitive prosthesis; they were excluded for: active wounds on weight-bearing surfaces. All participants meeting inclusion were screened by a prosthetist to ensure a well-fitting prosthesis and by a physiatrist to ensure they were safe to engage in low-to-moderate levels of exercise. Participants then completed 6 self-reported measures: ABC; the Fear of Falling Avoidance Behavior Questionnaire (FFABQ) which asks individuals to rate how much fear of falling leads to avoidance of 14 different activities; modified Gait self-efficacy scale (mGES) which asks level of confidence in completing 10 different gait-related tasks; the well-being scale of the Prosthesis Evaluation Questionnaire (PEQ); the Short-form 36 Healthy Survey (SF-36) - we present data from the physical functioning scale only; and the Frenchay Activity Index (FAI) to quantify social participation. Participants wore a Step Watch 3 activity monitor (Modus Health) on their pylon for 1 week, which recorded steps taken in 10 s epochs. From the raw data we calculated 6 PA measures: steps/day (average across all days); median and maximum walking-bout length and number of walking bouts/day, where a bout was defined as ≥5 consecutive steps; the DFA scaling exponent; and the "decay" exponent. For DFA, we followed standard procedures[6]: integrate the time series; plot the average size of the fluctuations (variations about the local trend) of data within windows of increasing size n as a function of n; calculate the slope of the best fit line (α) on a log-log scale. To calculate the "decay exponent" we fit a histogram of the bout data with an exponential decay function and report the exponent; larger values indicate data is skewed toward more short walking bouts. Independent correlations were run to determine the strength of association between the 6 PA measures and 6 self-reported measures. Due to missing data, the number of points differs across correlations.

			SELF-REPORTED MEASURES					
			Self-efficacy and participation				Quality of life	
			ABC	FFABQ	mGES	FAI	PEQ	SF-36
ACTIVITY PARAMETERS	Amount	Steps/day	0.18	0.22	0.22	**0.68 (p=0.004)**	0.50 (p=0.085)	0.28
		Bouts/day	0.01	-0.07	0.06	0.58 (p=0.061)	0.23	0.18
		Median bout length	0.02	-0.08	0.18	0.47 (p=0.064)	0.54 (p=0.058)	0.20
		Maximum bout length	0.22	-0.45 (p=0.096)	0.24	0.45 (p=0.082)	**0.64 (p=0.019)**	**0.55 (p=0.040)**
	Pattern	DFA exponent	0.31	-0.43	0.22	**0.58 (p=0.018)**	**0.66 (p=0.014)**	0.51 (p=0.061)
		Decay exponent	0.40	-0.14	0.10	0.23	0.52 (p=0.068)	0.47 (p=0.089)

Table 1: Correlations between self-reported and PA measures. Grey values correspond to p>0.10; bold values correspond to p<0.05

RESULTS

In general, measures of self-efficacy (ABC and mGES) and related activity avoidance (FFABQ), which, theoretically, should directly relate to PA show nearly no associations with PA measures (Table 1). On the other hand, FAI, a direct measure of participation, as well as quality of life (PEQ) are significantly associated with many PA measure of activity including the DFA scaling exponent. The strongest correlation among all measures was between FAI and the traditional PA measure of steps/day.

CONCLUSION

If activity is an outcome of interest within a prosthetic intervention it may be important to include self-report measures related to activity and quality of life as well as objective measures to asses both amount of activity and pattern of activity to fully understand the impact of the intervention. Additional work is needed to determine the extent to which changes in self-reported measures correspond to changes in PA measures, and vice versa.

SIGNIFICNACE

Prosthetic interventions should include a wide variety of measures to fully understand their impact on the patient.

REFERNCES

1. Rosenblattt et al, JPO, 29:65-72, 2017; ;2. Klute et al, APMR, 92:1570-5, 2011; 3. Sawers & Hafner, JRRD 50:2730314, 2103; 4. Wurderman et al, POI, 42: 498–503, 2018; 5. Paraschiv-Ionescu et al. doi: 10.1038/srep02019; 6. Peng et al 1995

ACKNOWLEDGMENTS

This work was funded by DoD W81XWH-17-1-06

Proportional Myoelectric Control of a Bionic Lower Limb Prosthesis with Series Elastic Actuator

Nicole E. Stafford[1], Lars Wouterse[2], Simon van der Helm[2], and Daniel P. Ferris[2]
[1]University of Florida Department of Mechanical and Aerospace Engineering
[2]University of Florida J. Crayton Pruitt Family Department of Biomedical Engineering
Email: nicolestafford@ufl.edu

Introduction

Robotic lower limb prostheses enable mechanical emulation of human gait biomechanics, but more biomimetic controllers are needed to achieve dynamic and agile locomotion. Traditional state-based controllers offer a finite number of movement options which make it difficult to adapt to different daily activities, postural challenges, and terrain [1, 2]. In contrast, proportional myoelectric control uses signals directly from a prosthesis user to modulate ankle position and mechanical power output [3]. Our purpose was to develop a proportional myoelectric lower limb prosthesis with a series elastic actuator that allows testing of different prosthetic controllers in real-world environments.

Methods

We developed a bionic transtibial prosthesis using a series elastic actuator (Apptronik P170 Orion) controlled by surface EMG mounted on the gastrocnemius within the socket. The controller produced a motor current proportional to rectified, low-pass filtered EMG of the subjects' gastrocnemius. A male subject age 66 with transtibial amputation practiced treadmill walking with the prosthesis under proportional myoelectric control and visual feedback over multiple testing sessions. We collected kinematic, kinetic, and electromyography data across 7 training sessions.

Results and Discussion

With our proportional myoelectric controller, the subject modified their gastrocnemius activity over the course of training to modify the mechanical output of the bionic prosthesis. **Figure 1** depicts the subjects's initial muscle activity walking with the device compared to after seven sessions with visual feedback. The subject learned to produce a large burst of muscle activity during stance to produce ankle plantar flexion.

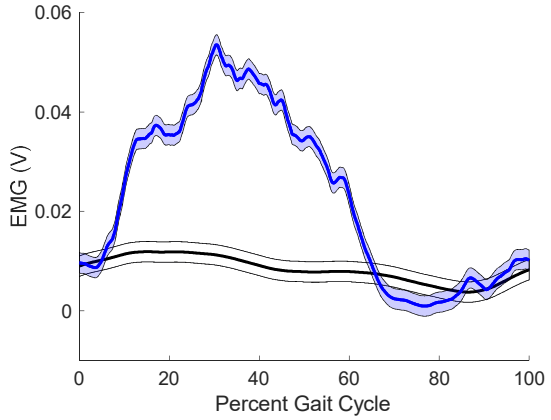

Figure 1: Low-pass filtered gastrocnemius EMG averaged over 10 steps at 0.6 m/s. Black line shows data after 15 minutes practice. Blue line shows data after multiple training sessions with visual feedback. Shaded regions represent 1 SD.

The subject was able to produce plantarflexion pushoff across multiple walking speeds with the prosthesis (**Figure 2**). At 1.0 m/s, the peak plantarflexion at the end of stance occurred earlier than the slower speeds. Walking at faster speeds required training, likely due to the motor adaption in timing of muscle activity. These results suggest that the method of gait training likely plays an important role in learning how to emulate intact lower limb biomechanics with a bionic prosthesis under proportional myoelectric control.

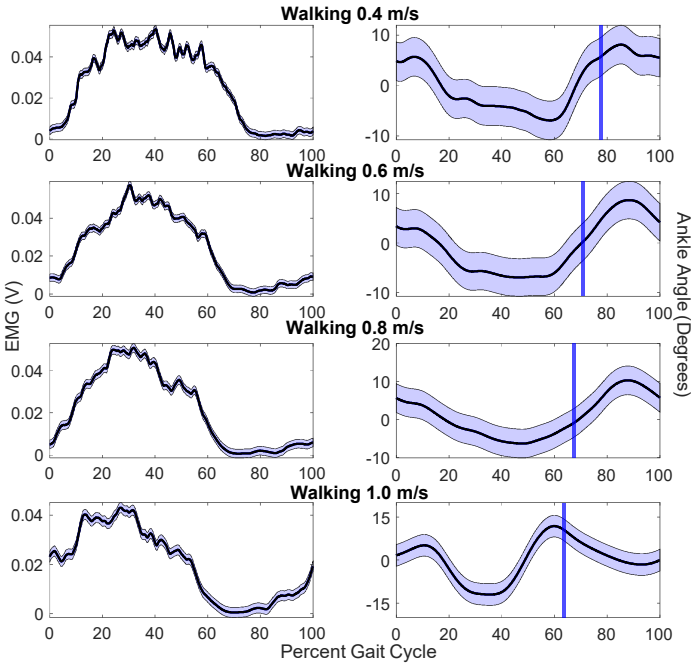

Figure 2: Low-pass filtered gastrocnemius EMG (above left) and prosthesis ankle angle (above right) averaged over five steps across multiple walking speeds (0.4, 0.6 , 0.8 and 1 m/s). For ankle angle, 0 degrees is standing angle and negative is plantarflexion. The vertical blue lines indicate toe off timing for the prosthesis side. Shaded blue region represents 1 SD.

Significance

Three-quarters of daily human walking bouts are less than 40 steps and <1% take more than two minutes [4]. There is a need for bionic prosthesis controllers that can handle non-periodic, volitional movements to enhance maneuverability [1,2]. Adapting feedforward commands from users via proportional myoelectric control allows users to adapt to a wide range of tasks, conditions, and terrain. We are modifying the prosthesis for wireless locomotion outside of lab environments to study how users modify EMG control signals in the real world.

Acknowledgments

We thank Jon Miles and Ryan Jacobs for contributions to the study. Funded by NSF 104772, NIH T32 HD043730, and the Leo, Claire & Robert Adenbaum Foundation.

References

[1] A. Fleming et al. (2019) IEEE Trans Neural Syst Rehabil Eng, 27(7): 1473-1482.
[2] M. Windrich, et al. (2016) Biomed. Eng. Online, 15:140.
[3] S. Huang, et al. (2014) J. Med. Devices, 8(2):024501-024506.
[4] M. S. Orendurff, et al. (2008) JRRD, 45:1077–1090.

Measured Forefoot Stiffness Across Prosthetic Foot Stiffness Categories

Elizabeth G. Halsne, CPO, MS[1,2], Anne T. Turner[2], Carl Curran, MS[4], Josh Caputo, PhD[4], Andrew H. Hansen, PhD[3,5], Brian J. Hafner, PhD[1], and David C. Morgenroth, MD[1,2]
[1]University of Washington, Seattle, WA; [2]Center for Limb Loss and MoBility, VA Puget Sound Health Care System, Seattle, WA; [3]VA Minneapolis Health Care System, Minneapolis, MN; [4]Humotech, Pittsburgh, PA; [5]University of Minnesota, Minneapolis, MN
Email: bhalsne@uw.edu

Introduction

When deciding which stiffness category of a prosthetic foot to prescribe for individuals with lower limb amputation, clinicians often rely on manufacturer recommendations that are focused on patient weight and activity level. However, there is limited evidence and objective data available to guide the selection of the optimal stiffness category that will match each patient's abilities, goals, and the type of environmental terrains that they typically encounter. Knowledge of mechanical properties such as linear stiffness would likely be useful in the prescription process, as it could enable clinicians to select prosthetic feet with the stiffness categories for which their patients are best suited. While prior studies have begun to quantify compressive linear stiffness properties,[1-3] limited data exists measuring linear stiffness across prosthetic foot stiffness categories and foot sizes. Therefore, the purpose of this study was to compare measured forefoot stiffness properties of commonly prescribed prosthetic feet across stiffness categories and to examine whether foot size affected the relationship between stiffness category and measured stiffness.

Methods

Data were collected on the following prosthetic foot models: Trulife Seattle Lightfoot2, Freedom Innovations Walk-tek, Össur Vari-flex, Ability Dynamics Rush HiPro, and Fillauer All-Pro. For each model, sizes 27 and 28cm feet were tested. A range of foot stiffness categories accommodating patient weighing between 100 and 250 lbs were tested for each model and size.

Apparatus: A Mikrolar R2000 robot and an 8-camera Vicon motion capture system were used to collect displacement data. A 6-axis AMTI MC3A load cell was used to collect force data.

Procedures: Each prosthetic foot was shod with a standardized walking shoe and attached to the load cell using a pyramid adapter. The load cell was then fixed to the R2000 robot with neutral alignment in all planes. Procedures included quasi-static testing at a discrete pylon progression angle of +20º to isolate the forefoot component. Using displacement control, the R2000 compressed each foot for six cycles of loading and unloading. A minimum load of 50N of vertical force was maintained prior to the start of loading and between all testing cycles. Because ground reaction force during walking can reach 1.2x body weight in late stance, a maximum force threshold representative of 1.2x the highest body weight recommended by the manufacturer for the tested stiffness category was used. The first three cycles were considered preconditioning and excluded; data from the final three cycles were averaged for analysis.

Results and Discussion

Force vs. displacement curves of prosthetic forefeet were compared across stiffness categories and across sizes 27 and 28cm for each of the foot models. The order of prosthetic foot stiffness categories was at times inconsistent with the order of measured forefoot stiffness for multiple foot models and sizes; there were 8 instances out of 28 total (29%) in which the stiffness categories did not correspond to increasing measured stiffness as expected. For example, in the case of the Rush HiPro, the category 4 had a higher measured stiffness than the category 5 in the size 28cm, though not in the size 27cm feet (Figure 1). Additionally, in both sizes, the lower categories (2 and 3) had nearly the same stiffness. In contrast, the All-Pro models showed consistently increasing measured stiffness across categories, regardless of size. The data suggests that measured prosthetic forefoot stiffness may not increase consistently across categories, as expected, for some types and sizes of prosthetic feet.

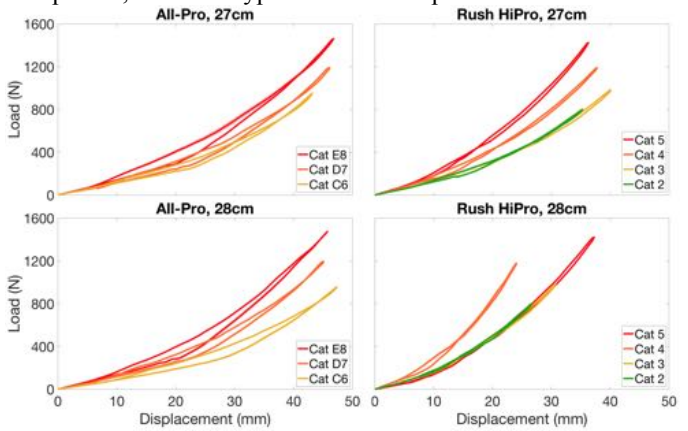

Figure 1: Example force vs displacement data for prosthetic feet in two sizes. While the All-Pro data conform to the expected order of increasing stiffness with increasing category, there are inconsistencies in the Rush HiPro data across categories and across foot sizes.

Significance

Prosthetic foot stiffness can play an important role in functional mobility of people with lower limb amputation. The process by which manufacturers classify the categories of feet is unclear. Some may use mechanical testing to assign the category based on measured properties, while others may designate a category by using the same material layup, without testing after production. These findings suggest variation in measured forefoot stiffness across categories (e.g., a higher category may not actually be stiffer). Furthermore, stiffness across categories varied depending on the size of the foot. These findings suggest the importance of publishing standardized mechanical testing results for commercial prosthetic feet to provide objective data that clinicians could utilize when selecting the ideal prosthetic feet and stiffness categories for patients.

Acknowledgments

This research was supported through Department of Defense award number W81XWH-16-1-0569.

References

[1] Major MJ, et al. Prosthet Orthot Int, 201-7, 2018.
[2] Webber CM & Kaufman K. Prosthet Orthot Int, 463-8, 2017.
[3] Koehler-McNicholas SR, et al. PLoS One, 13(9), e0202884, 2018.

Development and evaluation of a powered knee stumble recovery controller for transfemoral prosthesis users

Shane T. King[1], Maura E. Eveld[1], Leo G. Vailati[1], Karl E. Zelik[1], Michael Goldfarb[1]
[1]Department of Mechanical Engineering, Vanderbilt University, Nashville, TN, USA
Email: shane.t.king@vanderbilt.edu

Introduction

Individuals with transfemoral amputation are 200 times more likely to fall from a stumble [1, 2], which leads to an increase in fall-related injuries and lower community engagement.

The current standard of care is a microprocessor knee prosthesis, which relies upon the user's hip to drive the motion; however, these low-impedance knee joints are easily displaced from their trajectory by an obstacle. A powered device is able to overcome this issue. Inclusion of a motor to drive the knee joint allows the device to actively recover from perturbations.

To test if implementing healthy recovery strategies on a powered prosthesis will reduce users' fall incidence and improve stumble recovery, we have replicated the two primary healthy recovery strategies (i.e., elevating and lowering) [3] on the Vanderbilt Knee (Fig 1, B). However, the most critical component is choosing which strategy to use, which has not been done before. This decision is important because an incorrect selection would lead to a mismatch between the device and the user, making recovery more difficult. We propose that the key to successfully improving stumble recovery for transfemoral prosthesis users is allowing them to drive the actions of the device such that they are able to move together in a coordinated fashion. Thus, the objective of this work is to present the formulation and validation of this controller design.

Methods

The goal of the controller is to follow the initial dynamics of the user's residual limb several milliseconds after the perturbation. This allows the device to ensure its response is in coordination with the user's movement, while still responding quickly enough to recover. For example, if a user continues to flex their hip shortly after the perturbation, then the powered device has time to use an elevating strategy and bring the leg up and over the obstacle as the user continues to swing their leg. However, if the user stops flexing their hip or begins extending, the device must use the lowering strategy to extend the knee, support the user, and assist as they clear the obstacle in the next step.

To determine the initial response of the user's residual limb, an inertial measurement unit (IMU) on the prosthesis shank and an encoder on the prosthesis knee joint are used to observe the user's thigh and shank angle configuration space which forms a portion of an ellipse during swing phase (Fig. 1, A).

The use of this configuration space was piloted with healthy stumble recovery motion capture data that was collected using an in-house treadmill stumble apparatus [3] (Fig. 1, C). The data showed a distinct bifurcation in the response of the configuration space during a perturbation. Perturbations that resulted in an elevating strategy showed the configuration space trajectory exiting from its typical ellipsoid path towards the exterior of the ellipse, while perturbations that result in a lowering strategy showed the configuration space trajectory exiting towards the interior of the ellipse. The controller uses this bifurcation by analyzing the error of the current configuration space trajectory compared to the typical configuration space ellipse trajectory. This allows the device to determine which strategy to use to recover from a perturbation.

Testing with the powered prosthesis was performed on one healthy subject using an able-body adaptor (Fig. 1, A) to determine if the trends were the same when using the powered prosthesis with IMU/encoder signals compared to the healthy motion capture data. Additionally, the controller was tested to see if using the bifurcation to choose the recovery strategy allowed for an improved recovery.

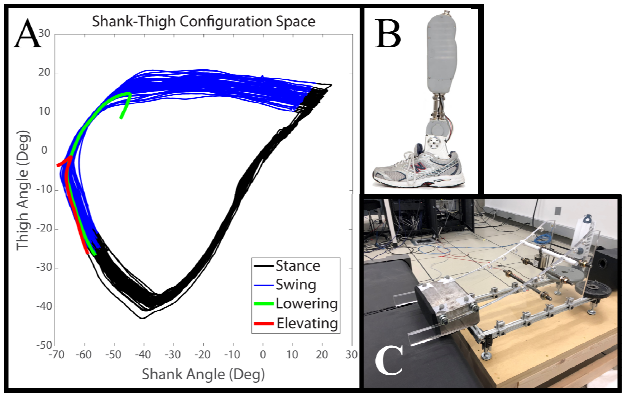

Figure 1: A) Thigh-shank angle configuration space data. **B)** Vanderbilt Powered Prosthesis. **C)** Treadmill stumble apparatus.

Results and Discussion

Preliminary results collected from the healthy subject using an adaptor have matched the initial configuration space trajectory bifurcations of the original healthy stumble recovery data set. An example of this bifurcation is shown in Fig. 1, A. The controller allowed for the subject to successfully recover from stumble perturbations across a range of timings from early to late swing phase using an appropriate stumble recovery strategy. The next step will be testing the controller on transfemoral prosthesis users to ensure the control system is able to coordinate with their current stumble recovery reflex; data from which will be presented at the conference. Metrics will include ability to recover from the perturbation, time to return to steady state walking, and knee angle trajectory comparisons to healthy recovery data to show the benefits of the control system.

Significance

Overall, the control system described herein has the potential to substantially reduce the risk of falling and improve stumble recovery for people with transfemoral amputation. By following the dynamics of the user's body, the controller works in concert with the user's recovery instead of impeding it.

References

[1] Kahle JT et al. (2008). *J Rehabil Res Dev,* **45**: 1-14.
[2] Talbot LA et al. (2005). *BMC Public Health*, **5**: 86.
[3] King ST et al. (2019). *J NeuroEng Rehab*, **16**: 69.

Does the use of a Powered Assistive Ankle Exo Device Augment Cost of Transport?

Leif Hasselquist[1], Meghan O'Donovan[1], Kari Loverro[1], Jonathan Kaplan[1], and Clifford Hancock[1]
[1]Combat Capabilites Development Command Soldier Center, Natick, MA 01760
Email: *leif.hasselquist.civ@mail.mil

Introduction

Our product test identifies a key question when designing an ankle worn augmentation device for healthy populations, how do you provide enough assistance during gait to decrease cost of transport (COT) without disrupting natural gait mechanics enough to incur a significant penalty or increase to COT? The cost of transport (COT) for human (or animal) locomotion is defined as (energy cost)/(body weight × distance traveled). It is a dimensionless quantity to express the energy efficiency of transporting the person (via gait) from point A to point B. [1] Deviations from preferred gait mechanics appear to always incur a metabolic cost (i.e., increased COT). This suggests that preferential gait characteristics are selected in large part to minimize metabolic cost. [2] The goal of this product test was to determine whether a powered, untethered, ankle-worn exoskeleton can produce a measurable metabolic cost reduction that may be linked to a change in gait dynamics during Soldier-relevant locomotor tasks with body-borne loads.

Methods

A total of 12 (11 M, 1 F, age: 26 ± 5 yrs; height: 176 ± 8 cm; weight: 80 ± 8 kg.) active duty infantry Soldiers volunteered as participants. They represented a healthy Soldier population and met all physical and injury screening criteria. Each participant conducted one familiarization session prior to testing. Each test session consisted of four, 7 minute instrumented treadmill (AMTI, USA) trials at a prescribed speed of 1.25 m/s and under two device conditions (Exo, No-Exo). Two load conditions were tested at a 0% grade and at a 4% grade. A No load (NL, 1.5 kg), and approach march load (AML, 42 kg) condition were tested at 0% grade. The AML and a fighting load (FL 27.7 kg), were tested at a 4% grade. To calculate COT we measured the participants' energy cost via an open circuit respirometry system (Cosmed, USA). To determine gait kinetic changes we collected traditional measures of vertical ground reaction force (vGRF) and antero-posterior ground reaction force (A/P GRF). For each condition, the dependent variables of metabolic COT and kinetic measures of peak vGRFs immediately after heel strike and immediately before toe-off, vertical GRF at mid-stance and peak A/P GRF during the braking and propulsive phases of gait were measured. We ran a repeated measures two-way ANOVA to examine the main effects and possible interactions between device (Exo, No-Exo) and load (NL vs, AML at 0% and FL vs AML at 4%), $\alpha = 0.05$. If significant interaction effects were observed between device and load, ($p < 0.05$), tests of simple effects were utilized and a Bonferroni correction was applied.

Results and Discussion

There was a significant main effect of device on mean COT across load at 0% grade ($p = 0.024$) and at the 4% grade ($p = 0.016$). The mean COT at the 0% grade was 11% lower for the Exo condition and 8% lower at the 4% grade for the Exo condition compared to the No-Exo condition (Figure 1). There were no significant interactions between device and load at either grade tested.

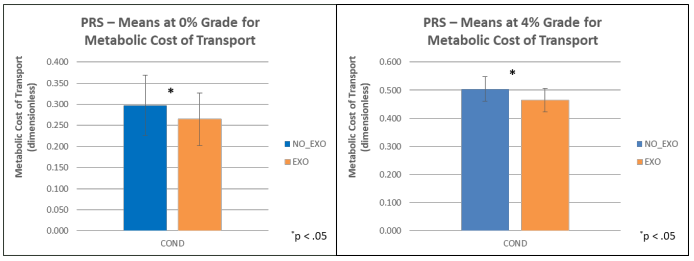

Figure 1: Mean COT for Exo and No-Exo at 0% and 4% grades.

For the kinetic results, the mean vGRF showed no statistically significant differences between Exo and No-Exo conditions at any of the points of interest. There was a significant main effect of device across load on mean peak braking forces at the 0% grade ($p = 0.001$) and at 4% the grade ($p < 0.001$) and propulsive GRFs across load at 0% grade ($p < 0.001$) and at 4% grade ($p = 0.001$). At all points, A/P GRF were higher in the Exo condition compared to the No-Exo condition, indicating an increase in both propulsive and breaking forces while wearing the Exo device. The A/P GRF peak braking force at the 0% grade was 8% higher in the Exo condition and 6% higher at the 4% grade for the Exo condition compared to the No-Exo condition. The peak A/P GRF propulsive force at the 0% grade was 6% higher in the Exo condition and 5% higher at the 4% grade in the Exo condition compared to the No-Exo condition.

Significance

For this product test the Exo ankle system tested appears to significantly reduce the metabolic cost of walking regardless of loads of varying magnitude at multiple grades. Our GRF results demonstrate that this Exo ankle system has little influence on peak vertical forces across the stance phase of gait, but does increase peak A/P forces during braking and propulsive phases. This finding may be attributable to the device's power activation parameters that aim to augment ankle joint moments during walking. There have been few untethered Exo devices that have been able to demonstrate a significant reduction in metabolic cost. Our results indicate that the changes in A/P GRF may be linked to the reduction in metabolic cost for the device tested. It should be noted that our participants demonstrated wide variability in responses to augmentation. Future research in this area, beyond a specific product test, will concentrate on individual variability, adaptation, and acceptance by Soldiers while wearing Exo devices.

Acknowledgments

We recognize the Soldiers from the US Ranger Training Battalion and Natick Soldier Center detachment for their participation.

References

[1] Collins et al., Science, 308, 5178 (2005)
[2] Donelan et. al., Proc. R. Lond. B, 268, (2001)

Reduction of Trunk Extensor Muscle Activation using a Cable-Driven Asymmetric Back Exosuit

Jared M. Li[1], Dean D. Molinaro[1,2], Andrew S. King[1], Anirban Mazumdar[1,2], Aaron J. Young[1,2]
[1]Woodruff School of Mechanical Engineering at Georgia Institute of Technology, Atlanta, GA, USA
[2]Institute of Robotics and Intelligent Machines, Georgia Institute of Technology, Atlanta, GA, USA
Email: jli649@gatech.edu

Introduction

Musculoskeletal disorders of the back are extremely prevalent in the workforce and are often cited as the top workplace health concern in the United States. These injuries are caused by compression of the lumbosacral joint (L5/S1) due to repetitive lifting, especially asymmetric movements[1]. In response to this, wearable exoskeleton devices have been developed to reduce the risk of back injury, often reporting decreased muscle activation as indication of reduced lumbar loading[2,3]. While effective in mainly symmetric lifting, most of these systems lack controllability or are restrictive of asymmetric motions. We designed the Asymmetric Back Exosuit (ABX) to fill this gap with novel active cable-driven actuation. We hypothesized that this would allow ABX to reduce trunk extensor muscle activation during asymmetry.

Methods

ABX was designed in order to achieve the functionality of active muscle activation reduction while allowing the user full freedom of movement. Assistive force is applied to the user through the nylon cables that run from actuators on the thighs up to opposite shoulders on a support vest, creating a crossing pattern along the wearer's back. Active assistance is achieved through pulley-gearbox actuators which are regulated by a microcontroller. An inertial measurement unit (IMU) is used to sense trunk orientation and angular velocity relative to the ground. This allows the exosuit to autonomously apply assistance to the user at lift onset and otherwise slack the cables to allow unimpeded motion.

To examine the exosuit's assistance method, a single-subject experiment was conducted to measure the change in activation of trunk muscle groups when lifting a 23 kg weight from the ground onto a table at waist level with a right-to-left 180° twist for five repetitions. Trials consisted of a sweep of assistive force from 5% to 20% of the subject's bodyweight in 2.5% increments as well as a NO EXO condition in which the subject completed the tasks without wearing the exosuit. Delsys Trigno EMG sensors were used to measure the left and right erector spinae, latissimus dorsi, external obliques, and rectus abdominis muscle groups. RMS of each EMG channel was averaged across repetitions and normalized to max activation per muscle group.

Results and Discussion

As seen in Figure 1, muscle activation reductions of up to 30% and 28% were observed in the left and right erector spinae respectively, as well as 53% for both left and right latissimus dorsi muscles. The trunk flexor muscles (left and right external obliques and rectus abdominis) experienced either a decrease or no increase in activation for most assistance magnitudes. Reduction in activation of erector spinae muscles likely indicates reduced muscular force applied to the L5/S1 joint. This is likely related to decreased joint reaction loads in the lumbar spine.

Because of the cross pattern formed by the actuator cables, assistance that is symmetric in magnitude was supplied to the user asymmetrically, demonstrated by the agonistic muscles (left side) experiencing generally greater activation reduction than the antagonistic (right side). Further studies will examine the biomechanical effects (joint reaction loads, lumbar moments) and investigate the results' sensitivity to changing assistance profiles.

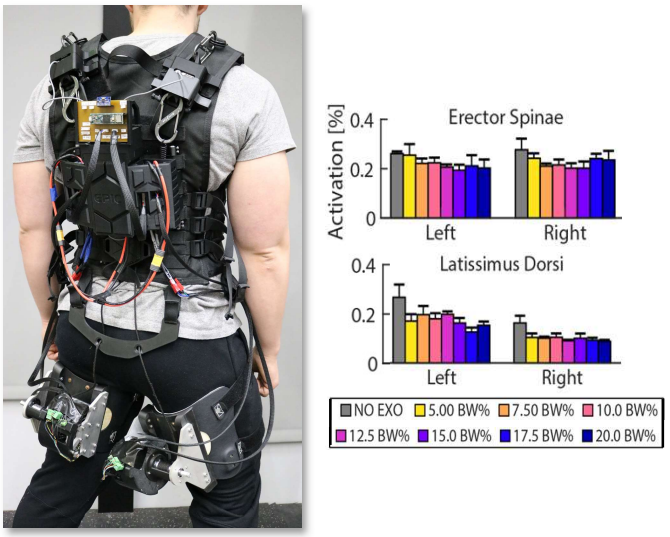

Figure 1: The Asymmetric Back Exoskeleton (left) uses thigh mounted actuators to drive cables attached to opposite shoulders to assist during lifting tasks. RMS electromyography measurements of the erector spinae and latissimus dorsi muscle groups during the asymmetric lift are shown on the right. The results are presented as a function of exosuit assistance by body weight percentage (BW%). The NO EXO condition represents muscle activations without wearing the exosuit. In general, exosuit assistance reduced muscle activation for observed muscle groups.

Significance

Our study presents a novel method of providing active assistance during asymmetric lifting. Asymmetric application of assistance characteristic to this exosuit design allows the cables to naturally follow the twist of the lumbar spine. This method has shown to reduce EMG of the measured trunk extensor muscles, with a larger reduction on the leading side. Because of the prevalence of asymmetric lifting in manual materials handling occupations, this assistance method has the potential to greatly reduce risk factors for back injury during natural lifting movements.

Acknowledgments

The authors would like to acknowledge the NSF Research Traineeship: ARMS Award #1545287 and the NSF NRI Award #1830215.

References

[1]Kelsey et al. (1984). *J. Orthop. Res.*, vol. 2, no. 1, pp.61–66. [2]Toxiri et al. (2018). *Front. Robot. AI*, vol. 5, 2018. [3]Alemi et al. (2019) *J. Electromyogr. Kinesiol.*,vol. 47, pp.25–34.

Design & Control of a novel modular stiffness spring Ankle prosthesis with embedded ball screw powered prosthesis

Sameer Upadhye[1], Ming Liu[2], Xikai Tu[2], Albert Dodson[2], Gregory Buckner[1], He Huang[2]
[1]Department of Mechanical & Aerospace Engineering, NCSU
[2]Joint Department of Biomedical Engineering at UNC Chapel Hill & NCSU
Email: supadhy2@ncsu.edu

Introduction

Over 600,000 people suffer lower-limb amputations in the US every year which significantly affects their quality of life[1]. This has spurred a race in the research & development of lower-limb prosthetic devices, especially powered ankle prostheses[2]. However, it is a real challenge to have a design, which relies on an active actuator and meets the two key requirements: 1) generates large active power needed for locomotion and 2) a small profile, which fits the size of human ankle joint[3]. A common compromise is to involve a passive actuator i.e a passive spring, which is set in parallel with the active actuator and tuned to release power when the power is needed most. Although passive actuators have the capability to generate large torque, its dynamical properties are fixed and often optimized for walking in most of the existing designs. Besides walking, ankle joints play important roles for other tasks beyond level ground walking, such as sit-to-stand (STS) and stairs ambulation, which expect different dynamical properties from the ankle joints. A key question for prosthesis design is whether it is needed to adjust the dynamical properties of the passive actuator for different tasks. Hence, this study presents a powered ankle prosthesis, which includes a passive spring with adjustable stiffness & equilibrium position. This device permits us to study how the properties of passive actuators, such as stiffness (K) and equilibrium angle (θ^e), affect the capability of the amputee-prosthesis-system to conduct various tasks.

Methods

For the purpose of testing, a novel powered ankle prosthesis was developed which employs a motor embedded ball screw design in a four bar linkage mechanism for achieving space reduction[4]. A frameless motor kit (UTH-63-B-18- C-x-000, Rated Torque & Speed:0.268 Nm, 7000 rpm, Celera Motion, USA) and ball screw (SD 12x2R 82/100 G7L-Z-WPR, SKF, Japan) were used. The prosthesis has a peak ankle torque of 138 Nm & range of motion of 30º dorsiflexion & 25º plantarflexion. The mechanical spring design was devised using a slider crank mechanism in conjunction with a stack of Belleville springs as shown in Figure 1 below. The equilibrium angle (the angle when the spring engages & disengages from the prosthetic foot) and mechanical stiffness can be modulated by changing the stack arrangement (different belleville springs can be used and can be arranged in parallel or series & hardened washers can be added for achieving a desired stiffness & spacing characteristics). The spring thus designed gives a angular stiffness range of 0-506 Nm/rad and an allowable equilibrium angle range of 10º plantarflexion to 15º dorsiflexion.

In order to study the effect of the passive springs, we shall conduct a STS scheme for two different passive spring configurations. The first spring configuration will be optimized for walking (K=361 Nm.s/rad, θ^e =0º) and the second one will be optimized for the STS transition (K=0 Nm.s/rad or θ^e =11º for peak angle = 10.7º i.e no spring connected). Both optimizations are based on the Ankle Angle-Torque curves available in literature[5]. The number of sit-to-stand transitions per minute shall be recorded to quantify the performance of the two setups.

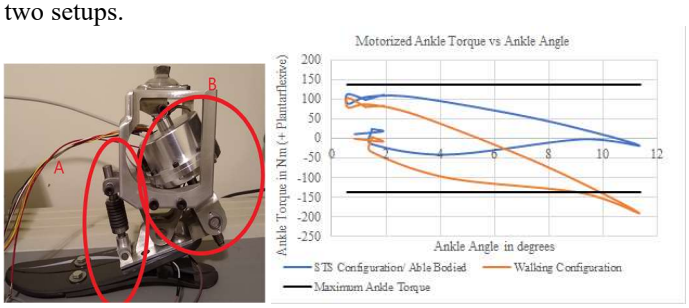

Figure 1. Left (a) The Ankle Prosthesis A-Modular Spring configuration, B- Embedded Ball screw actuator. Right (b) Motorized Ankle Torque vs Angle curves for STS with two configurations & Max Torque.

Results and Discussion

This study expects a significant 40 % reduction in absolute peak torque from the first spring configuration to the second configuration. This is anticipated since the peak ankle torque & peak ankle dorsiflexion do not occur at the same time during STS unlike in walking. Furthermore, it can be seen from Figure 1(b) that the motor shall need to expend an ankle torque of 200 Nm which is greater than maximum allowable torque of 138 Nm to compress the walking spring configuration while the STS configuration poses no such problem. Hence, given that the above estimates hold true, a conclusion could be drawn that the modular spring configuration shows improved characteristics when compared with a fixed stiffness spring configuration for the ankle prosthesis. We also expect that our human subject tests will demonstrate that the second setup will permit the amputee to do sit to stand more quickly.

Significance

This is the first effort to explore the impact of the passive actuator's dynamical properties on the performance of powered prosthetic ankle under different tasks. The results of this study provide the evidence that different passive actuators are needed for different locomotion tasks.

Acknowledgments

This research is partially supported by the National Science Foundation through award 1808898 and the National Health Institute through award 5R01EB024570-02.

References

1. D. Zidarov et al, (2009). Archives of Physical Medicine and Rehabilitation, 90(4):634{45.
2.Cherelle et al, Advances in Mechanical Engineering, Volume 2014, Article ID 984046
3. Au et al, Neural Networks 21 (2008) 654–666
4. Azocar et al "Design & Characterization of an Open-source Robotic Leg Prosthesis", 2019
5. Mak et al , Clinical Biomechanics 18 (2003) 197–206

Powered Knee-Ankle Prosthesis Reduces Effort in Intact Limb During Sit-to-Stand Transitions

Grace Hunt*[1], Sarah Hood[1], and Tommaso Lenzi[1]
[1]Department of Mechanical Engineering and Utah Robotics Center, University of Utah
*Corresponding Author Email: grace.hunt@hsc.utah.edu

Introduction

Standing up is an essential activity of daily life. In non-amputee individuals, standing up involves multiple muscles that span the hip and knee joints. In above-knee amputees, these muscles are severed, and the knee joint is typically replaced with a passive prosthesis, which injects no energy. Thus, above-knee amputees rely on their intact limb and upper body to lift their body during standing[1]. Powered prostheses aim to address this problem by providing positive power at the knee and ankle joints similar to the biological leg. Two previous studies have investigated sit-to stand transitions with a powered prosthesis[2,3]. Both studies found that a powered prosthesis can improve weight bearing symmetry compared to a passive prosthesis, reducing the vertical ground reaction forces (GRF) on the intact side. However, the intact limb's knee power does not seem to be reduced when standing up with the powered prosthesis compared to a passive prosthesis[3]. Thus, it is unclear whether the improvement in weight bearing symmetry observed with a powered prosthesis leads to a reduction of effort.

We hypothesize that if using a powered knee-ankle prosthesis results in the intact limb supporting less of the subject's weight during standing up, then the intact limb's muscle effort will also be reduced. To test this hypothesis, we will ask individuals with above-knee amputation to perform sit-to-stand transitions with their passive prostheses and with an experimental powered knee and ankle prosthesis[4,5], while measuring kinematics, GRF, and intact-leg muscle activations. The goal of this study is to pilot test the experimental protocol with one amputee subject.

Methods

One individual with an above-knee amputation participated in this study, which was approved by the University of Utah Institutional Review Board. The subject provided written informed consent before the experiment started. The participant performed sit-to-stands under two conditions: (1) using their prescribed passive prosthesis device, and (2) using an experimental powered knee and ankle prosthesis[4,5]. The subject was asked to stand up and sit down at their preferred speed without using their hands for assistance. GRF from each foot was recorded using two force plates (Wii Balance Nintendo)[6]. The subject wore an inertial motion analysis system (MTw Awinda, Xsens, Netherlands) to record kinematic data. A surface electromyography (EMG) sensor (13E202=60, Otto Bock, Germany) was placed on an intact-limb quadriceps muscle (Vastus Lateralis) to measure muscle activations. Data were filtered offline using a zero-lag 4th order Butterworth filter. Kinematic and GRF data were filtered at 10Hz, EMG data were filtered at 3Hz. EMG data were normalized to maximum activity during walking with the passive prosthesis.

Results and Discussion

When subjects stood up using the powered prosthesis, the weight supported by the intact limb was reduced by 9.8 kg compared to standing up with passive prosthesis, a 16% reduction. During sitting down, the weight supported by the intact was reduced by 7.2 kg, a 13% reduction. In addition, the subject's

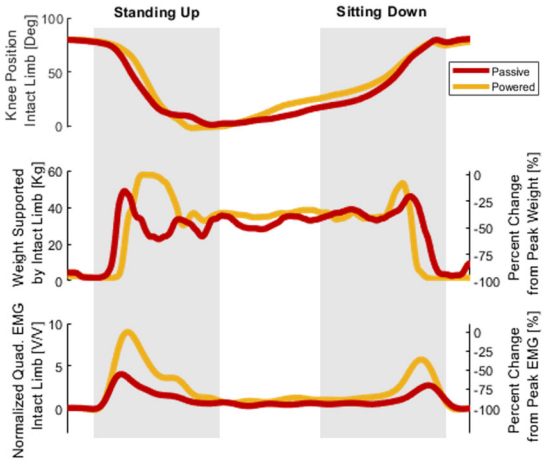

Figure 1: Knee position, weight (GRF), and muscle activation (EMG) data from intact limb of subject with above-knee amputation, during standing up and sitting down using subject's prescribed passive prosthesis (yellow) and experimental powered prosthesis (red).

EMG peak activation during standing up decreased 55% with the powered prosthesis, compared to the passive prosthesis. Similarly, during sitting down with the powered prosthesis, EMG peak activation decreased by 54% compared to sitting down with the passive prosthesis. No notable differences were observed in the intact limb's knee kinematics.

These results show that powered knee-ankle prostheses can reduce both the weight that the intact limb must support, and the muscle contraction effort required during standing-up and sitting-down, without impacting the intact limb knee kinematics. Improvements in weight-bearing have been shown by previous studies[2,3], and our results support these findings. Decreased effort has not been investigated in previous studies. The observed reduction in EMG contraction strongly supports our hypothesis that powered prosthetics can decrease effort during standing up. Future work should include surveys of user-reported effort and fatigue under both conditions, and testing with additional subjects to determine if the observed changes are statistically significant.

Significance

We provided the first demonstration of muscle effort reduction during sit-to-stand transitions with a powered prosthesis. This pilot test will support a future pilot clinical trial aiming to assess the efficacy of powered knee and ankle prostheses in sit-to-stand transitions for individuals with above-knee amputations.

Acknowledgments

This study was funded by NIH grant 1R01HD098154-01A1 and NSF grant 1925371.

References

1 Highsmith, M. J. *et al. Gait Posture* 34, 86–91 (2011)
2 Simon, A. M. *et al. Arch. Phys. Med. Rehabil.* 97, 1100–1106 (2016)
3 Wolf, E. J. *et al. Gait Posture* 38, 397–402 (2013)
4 Tran, M. *et al. IEEE Robot. Autom. Lett.* early acce, 1–1 (2019)
5 Gabert, L. *et al. IEEE Robot. Autom. Mag.* 27, 87–102 (2020)
6 Abujaber, S. *et al. Gait Posture* 41, 676–682 (2015)

Immediate Effects of a Hydraulic Slope Adaptive Prosthetic Foot-Ankle System When Standing on Slopes

Myrriah P. Laine Dyreson[1], Nicole R. Walker[1], Gregory Jacobs[2], Ed Iversen[2], Andrew H. Hansen[1,3], and John M. Looft[1]
[1]Minneapolis VA Health Care System; [2]Motion Control, Inc.; [3]University of Minnesota
Email: Myrriah.LaineDyreson@va.gov

Introduction

In collaboration with the Minneapolis VA Health Care System (MVAHCS), Motion Control, Inc. has developed a hydraulic slope adaptive foot-ankle (SAF) prosthesis. While previous versions of the SAF have been capable of adapting to slopes during walking [Nickel 2014], the SAF's effect on standing posture on varied slopes has not been explored. We hypothesize: **1)** the SAF will more evenly distribute body weight between the user's sound and affected limbs while standing on varied slopes (±5°, ±10°); **2)** using the SAF will decrease observed torques at the ankle and knee joints while standing on varied slopes (±5°, ±10°); and **3)** using the SAF will result in a decrease in perceived exertion during a five-minute standing task on a ±10° slope.

Methods

A 55-year-old male (195 pounds, 73 inches tall, K3 ambulator) with rotationplasty amputation was recruited for this preliminary study. The experimental procedures were approved by the MVAHCS IRB. The subject completed testing using their current prescribed energy-storing-and-returning (ESAR) prosthetic ankle-foot and Motion Control's prototype SAF ankle-foot.

Kinetic and kinematic data were collected simultaneously at 120 Hz using 2 AMTI force plates (AMTI, Watertown, MA) surrounded by a stable walkway, and a 16-camera motion capture system (Qualisys, Gotenburg, Sweden). Reflective markers were placed on the affected limb, pelvis, and trunk.

The subject stood quietly on slopes of 0°, ±5°, and ±10°. Two static trials and three 20-second quiet standing trials for each slope condition were recorded. Single 5-minute trials of quiet standing on ±10° were also recorded. Static trials were recorded with both feet on one force plate while standing trials were recorded with the right and left feet on separate force plates. Following each 5-minute trial, the subject was asked to rate their perceived level of exertion on a 0 (no exertion) to 10 (maximal exertion) scale. These ratings were compared between foot conditions.

All kinematic and kinetic data were processed using Visual3D (C-Motion, Inc., Germantown, MD). Body weight distribution between the affected and sound sides were calculated as a percentage of the total body weight and compared between slope and foot conditions. The angle and torque of the affected side ankle, knee, and hip joints, along with trunk angulation, were also calculated for each standing trial.

Results and Discussion

Ankle and knee torque magnitudes were decreased when using the SAF while standing on slopes of ±5° and +10°. The ankle torque direction was favorably reversed while the knee torque was nearly 0 Nm when standing on a -10° slope using the SAF, as shown in **Figure 1.**

Body weight was more evenly distributed between the sound side and affected side while using the SAF for each slope condition, as shown in **Table 1**. The subject stood with a majority of their body weight on their affected side when standing on a -5° and -10° slope with the SAF.

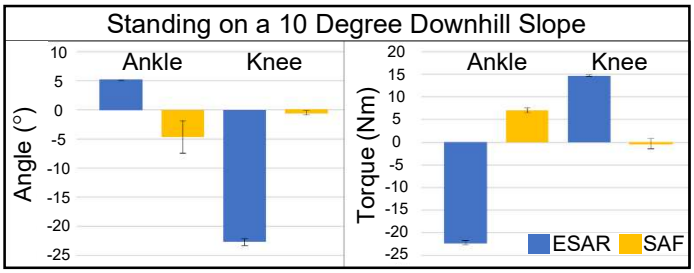

Figure 1: Ankle and knee joint angles (left) and torques (right) when standing on a -10° slope with the ESAR and SAF.

Table 1. Percent difference of body weight supported through sound and affected limbs during 20-second quiet standing trials. Negative values indicate body weight distributed more to affected side than sound side.

	-10 deg	-5 deg	+5 deg	+10 deg
ESAR	11.97%	16.03%	16.92%	7.19%
SAF	-8.02%	-4.55%	6.29%	7.91%

The improvements in torques acting on the ankle and knee when using the SAF create a more stable alignment of the affected limb, particularly when standing on a -10° slope. This improved alignment is believed to be one factor that allowed the subject to stand with more evenly distributed body weight when using the SAF.

The subject's perceived exertion following 5 minutes of quiet standing on a -10° slope were rated as a 6/10 using the ESAR and a 2/10 using the SAF. Perceived exertion was rated a 2/10 and a 7/10 using the ESAR and SAF, respectively, while quiet standing on a +10° slope. Percentage of body weight supported by the sound limb increased for all inclination conditions throughout the 5-minute standing trial. However, at both the beginning and end of the trials, ~10% more body weight was distributed to the affected side when using the SAF compared to the ESAR. Using the SAF allowed the subject to maintain a more even body weight distribution throughout the standing trial.

Significance

Walking and standing on uneven terrain and slopes are notably difficult tasks for persons with lower limb amputations. To complete these tasks, accommodation to slopes is commonly completed through proximal joint adjustments. With the SAF, slope accommodation occurs through slope adaptation of the prosthetic ankle-foot system. This adaptation may increase user stability on slopes, reduce muscular effort and joint stresses, and decrease the likelihood of overuse injuries on the affected side. Improvements to these detrimental effects may allow persons with amputations to increase their community participation.

Acknowledgments

This work was supported by STTR contract number W81XWH18C0314 from the United States Department of Defense and Motion Control, Inc. We would also like to acknowledge Gregory Voss for his efforts to this project.

References

Nickel E, et al. *J Rehabil Res Dev; 51*(5), 803-814, 2014.

Providing Rate-Responsive Bending Stiffness to a Passive Ankle-Foot Orthosis with Shear-Thickening Fluid Elements

Luke Nigro[1], Norman Wagner, PhD, Jill Higginson, PhD, and Elisa Arch, PhD
[1] Department of Mechanical Engineering, University of Delaware, Newark, DE
Email: lnigro@udel.edu

Introduction

Passive-dynamic ankle-foot orthoses (PD-AFOs) are biomechanical assistive devices that help individuals with ankle-foot impairments by providing stability and support to the ankle joint. PD-AFO bending stiffness can be tuned to an individual based on their natural ankle quasi-stiffness (NAS). NAS is typically defined as the linear slope of the ankle joint moment vs. angle curve during the loading phase of stance [1]. However, overall NAS changes across gait speeds [2] and NAS is not constant throughout the loading phase [3]. Thus, AFOs with bending stiffness tuned to a single NAS value may provide inadequate support throughout the entire loading phase, or when walking at different speeds. Novel materials such as shear-thickening fluids may overcome this shortcoming with their rate-dependent properties.

This study's purpose was to investigate the fundamental interactions between a healthy musculoskeletal system and a PD-AFO with a shear thickening fluid (STF) element, known as a rate-activated tether (RAT) [4]. We hypothesized that these novel STF elements used in conjunction with PD-AFOs can provide physiologically appropriate rate-responsive resistance to ankle joint bending.

Methods

Standard 3D motion-capture kinematic and kinetic data were collected from a young healthy subject (25 yrs, 1.75m, 61kg) walking on an instrumented treadmill while wearing a unilateral STF-AFO. Each of the following conditions was performed at 0.8 statures/s and 1.0 statures/s walking speed: 1) no AFO, 2) AFO w/o STF element, 3) STF-AFO w/ low-viscosity STF, and 4) STF-AFO w/ high-viscosity STF. STFs were polyethyleneglycol with colloidal suspensions containing 48% solids (low visc.) and 50% solids (high visc.). The STF elements were secured to a standard hinged AFO at the heel and posterior shank. Ankle joint angle, ankle joint moment, STF element length, and STF element displacement rate were calculated during stance. STF element length and displacement rate were compared to material property testing data to estimate its resistive force during the loading phase of stance (Figure 1). The loading phase was investigated because during it, the ankle-foot-AFO complex resists excessive dorsiflexion and puts the shank in the optimal position prior to push-off.

Results and Discussion

Rate-responsive resistance properties are clearly exhibited when using the STF-AFO. The length, deformation rate, and resistance changed throughout the loading phase of stance.

Overall, the RAT displacement rate followed a unique double-hump profile during the loading phase of stance. Compared to the slow walking speed, the fast walking speed had a higher initial peak displacement rate, but a lower second peak. Peak dorsiflexion angle was also lower for the high-viscosity STF condition compared to the lower-viscosity STF condition. This is also exhibited in the lower deformation lengths for the high-viscosity STF condition (dorsiflexion → STF element extension).

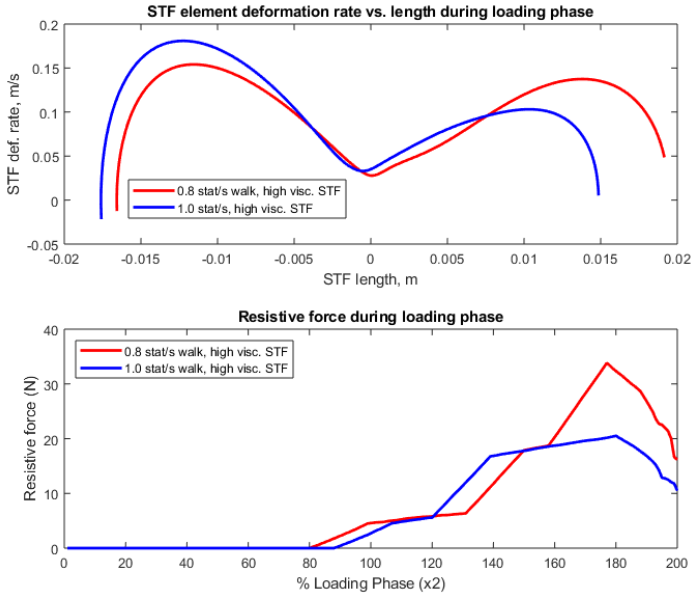

Figure 1: (Top) STF element deformation rate vs. length. Loading phase progresses left-to-right. (Bottom) Resistive force provided by the STF element during the loading phase. Note: STF provides no force during the first ~40% of this phase, since ankle is slightly plantarflexed and the element is slack.

Ankle joint moments and angles during stance did not vary greatly between STFs for either walking speed. However, the STF element is clearly activated and providing resistive force during the loading phase (Figure 1). This indicates that the STF substituted for some ankle joint function during loading.

Significance

This research pushes the state-of-the-art of PD-AFO design forward by evaluating the feasibility of a rate-responsive PD-AFO. To date, PD-AFOs have only been fabricated with a single, unchanging bending stiffness. This simplicity limits the range of activities for which PD-AFOs are useful as they cannot adapt to changes. The STF-AFO tested can provide supportive force that varies depending on the rate of ankle dorsiflexion. A limitation to this work is that the STF element dissipates energy through its damping properties, in contrast to most PD-AFOs that store and release elastic energy. However, more elastic properties may be attainable through more intricate RAT/spring mechanisms.

Acknowledgments

The authors acknowledge Dr. Eric Wetzel, and Alexander Lurski from the Army Research Laboratory in Aberdeen, MD for helping with the design and manufacture of the STF elements and for providing the material property testing data used in this study.

References

[1] Davis & DeLuca, Gait & Posture, 1996.
[2] Collins, Arch, Crenshaw, et al., Gait & Posture, 2018.
[3] Nigro, Koller, Glutting, Higginson, & Arch, Gait & Posture (under review).
[4] Nenno & Wetzel, Smart Mater. Struct., 2014.

Biomimicry of the Gastrocnemius During Gait for Transtibial Amputees.

Gabriel B Rios Carbonell, Hwan Choi PhD
Department of Mechanical and Aerospace Engineering, University of Central Florida
Email : hwan.choi@ucf.edu

Introduction

With an increasing population of amputees in the United States, the adverse effects of prostheses that only mimic a portion of the function of the lost limb are becoming more evident. The majority of people with below knee amputation use passive prostheses, which lack the energy recycling system found in an intact leg made by the gastrocnemius, soleus, and Achilles tendon. During walking, these two muscles and the tendon control the storage and release of the energy into the step, adding to its efficiency. With a passive prosthesis, the storage of energy typically occurs in a carbon fiber blade, but the stored energy mostly returns during mid-stance. Only a small amount of energy contributes to propulsion during terminal stance [1]. This lack of propulsion from the passive ankle foot prostheses leads to additional musculature to accommodate proper walking motion. As a result, this can lead to multiple disadvantages such as increased metabolic cost, gait asymmetry, reduced walking stability, and so on. To regulate the energy storage and release of a passive ankle foot prostheses, we proposed a novel timing module that can control energy release timing [2]. However, it is unclear when the passive ankle foot prosthesis releases energy, making it challenging to determine the appropriate timing, which biological elements that can role of plantarflexion during terminal stance. Thus, we investigated how current passive ankle prosthesis have different energy release timing compared with an unimpaired gastrocnemius muscle which plays an important role in propulsion [3].

Methods

In this study, the behaviour of a passive ankle prosthesis was observed and compared to the activation of the unimpaired limb of a K-4 level participant with transtibial amputation. To analyse the deformation of the prosthesis, a set of six motion capture markers were placed on the ankle foot prosthesis and the unimpaired leg. Measurements of the prosthesis deformation and unimpaired ankle joint were taken with motion capture (Vicon, Oxford, UK), focusing mainly on two markers: one placed on the toe and the second on the tibia. The deformation of a passive prosthesis is quite complex. Using the tibia and toe markers as reference, a virtual string can be created between the two markers. The deformation of this string can be used as a representation of the deformation of the prosthesis. A secondary advantage of using this method to measure the deformation of the prosthesis is that use of the same markers on the unimpaired leg the virtual strings have a similar behaviour. This allows both legs to be compared. The observed behaviour also behaves similarly to that of the ankle angle during gait. The activation of the unaffected side of gastrocnemius was measured using a surface electromyography (EMG) sensor (Avanti™ wireless EMG, Delsys Boston, MA). The participant walked on a treadmill set at a self-selected speed. During walking, we measured the time from maximum ankle dorsiflexion to maximum plantar flexion of the intact ankle and the prosthetic foot. The return of the passive prosthesis to its undeformed was considered as plantar flexion. The peak EMG activation timings of the unimpaired gastrocnemius were identified, and we compared it to the foot deformation of the unimpaired limb.

Results and Discussion

The release of the energy stored by the gastrocnemius is unlike the abrupt deformation return of the prosthesis (Fig. 1). The dorsiflexion to plantar flexion spanned an average of 17% of the gait cycle for the unimpaired limb while the deformation of the passive prosthesis spanned 19% of the gait cycle on average. The unimpaired leg started the push off about 2.5% of the gait cycle after the prosthesis on average. The activation peak of the unimpaired gastrocnemius and plantarflexion of the unimpaired ankle occurred at a similar time in the gait cycle, (62%). These outcomes suggest that passive prosthesis needs to retain the energy release timing by maintaining deformation after peak deformation.

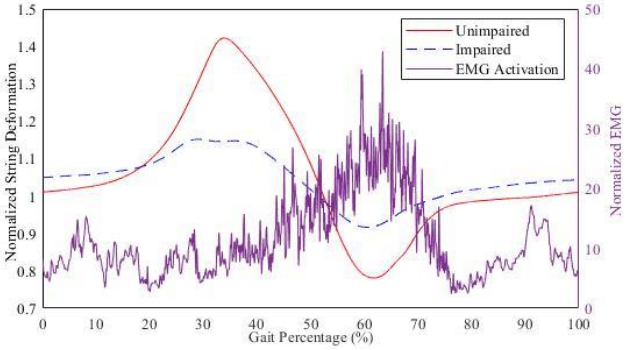

Figure 1: Linear foot deformation compared to the gastrocnemius EMG. All the values were normalized by the values obtained during the anatomic position before the trial

Significance

These results demonstrate that the passive prosthesis was not able to fully replicate the energy recycling system present in the intact limb. With implementation of a timing module, the control of the release timing can be achieved. The two main parameters that need to be considered when replicating motions of the intact ankle into deformations of a foot prosthesis are the total amount of deformation and the deformation rate. With accurate analysis on how the prosthesis foot deforms in the energy return phase, the proper timing can be achieved. Thus, adjustments can be made to the energy release timing to match the energy return of the unimpaired leg. As the timing of its activity is similar, EMG signal from the gastrocnemii could be used to determine the appropriate energy release timing.

Acknowledgments

This research was supported from the University of Central Florida GAP funding (1069239).

References

[1] A. M. Grabowski, J. NeuroEng. Rehabil. vol. 10, 2013
[2] G. B. Rios Carbonell, IEEE Biorob, 2020 (Under Review)
[3] K. M. Steele, J. Biomech, **43** 1387-1398, 2001

Regularity of Center of Pressure Excursion with Proportional Myoelectric Control of a Powered Prosthetic Ankle after Training

Aaron Fleming[1]*, Wentao Liu[1], and He (Helen) Huang[1]
[1]Joint Department of Biomedical Engineering, NC State University and UNC – Chapel Hill
Email: *ajflemin@ncsu.edu

Introduction

For transtibial amputees, the loss of a lower limb results in compromised standing stability and increased attentional demand when controlling standing posture[1]. Recent study seeking to improve amputee function and standing stability have demonstrated promise for the use of descending neural commands (via direct EMG control) to volitionally and continuously modulate prosthetic ankle joint mechanics [2]. However, the loss of normative feedback mechanisms due to amputation raises the concern of the attentional demand of this control paradigm. Thus, in this pilot study we investigate the effect of training on the automaticity of postural control (via sample entropy analysis of center of pressure excursion (CoP) [3]) using dEMG control of a powered ankle prosthesis.

Methods

We asked one transtibial amputee to participate in this preliminary study. The participant provided consent in this IRB approved (UNC-CH) study. We asked the amputee participant to stand quietly with his prescribed device and with a powered ankle prosthesis using direct EMG control[2]. We asked the participant to repeat this task after several days of training with the powered device. The participant stood quietly in different visual (eyes open, eyes closed) and attentional conditions (dual-task, single-task). We conducted 30-second trials and randomized the order of conditions and then repeated trials in reverse order.

We recorded CoP excursion via an instrumented split-belt treadmill. We subtracted the mean, filtered (low-pass, 12.5Hz, 4th Order Butterworth), and normalized all trials individually by their standard deviation. For sample entropy analysis we downsampled all data to 100 Hz (resulting in data lengths of 3000 points), and selected typical template size and tolerances (m = 3, r = 0.2) [3]. We conducted a 3-way ANOVA to test for main and interaction effect of Device (Passive, Powered, Trained), Vision (Eyes Open, Eyes Closed), and Task (Dual-Task, Single-Task) on Sample Entropy of CoP Excursion in the Anterior-Posterior (AP) direction.

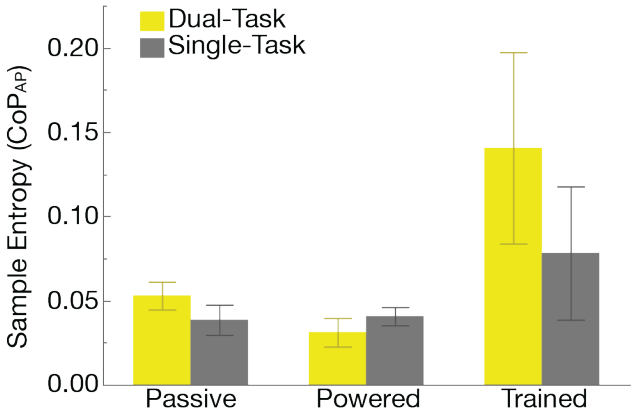

Figure 1: Sample Entropy (Eyes Closed Condition). *Grey)* Single-Task *Yellow)* Dual-Task. Standard error bars are shown.

Results and Discussion

In this pilot study we observed a significant improvement in the automacity (increased sample entropy) of postural control across various quiet standing tasks as a results of training in the dEMG controlled prosthetic ankle (Fig. 1). Statistical analysis showed device as a main effect ($p = 0.0282$), while all other main and interaction effects did not reach significance. We observed the largest change in sample entropy in the trained condition (Fig.1), however sample entropy seemed unchanged between passive and pre-training conditions.

In the trained condition we observed a trending increase in sample entropy (increased automaticity [3]) during dual task conditions, as attention is diverted away from postural control, similar to previous able-bodied study [3]; however, this trend was not visible in the untrained condition (Fig. 1).

We believe regularity of CoP excursion may have potential as a tool for the investigation of attentional demand in postural control for transtibial amputees. In the passive device conditions we noted a trending increase in entropy (decreased regularity) in the dual-task vs. single-task condition (Fig. 1). This measure (often used in able-bodied population) may provide more meaningful information into the automaticity of postural control under attentional demands for amputees compared with typical measures [1].

This preliminary study has demonstrated the potential for an increase in automaticity of postural control using a dEMG control powered prosthetic ankle. Sample entropy appears to be a promising measure for future study involving attentional demands associated with prosthesis wear. This pilot work motivates us to extend this analysis to more amputees to confirm this finding for the general amputee population.

Significance

This is the first study to begin to investigate the potential changes in automaticity of postural control using dEMG control of a powered prosthetic ankle. As far as the authors are aware this is the first study employ entropy measures in the evaluation.

Acknowledgments

Funding for this study provided by NIH NICHD F31HD101285.

References

[1]A. Geurts, T. W. Mulder, B. Nienhuis, and R. Rijken, "Dual-task assessment of reorganization of postural control in persons with lower limb amputation," *Arch Phys Med Rehabil,* vol. 72, no. 13, pp. 1059-64, 1991.
[2]A. Fleming and H. H. Huang, "Proportional Myoelectric Control of a Powered Ankle Prosthesis for Postural Control under Expected Perturbation: A Pilot Study," in *2019 IEEE 16th International Conference on Rehabilitation Robotics (ICORR)*, 2019: IEEE, pp. 899-904.
[3]S. F. Donker, M. Roerdink, A. J. Greven, and P. J. Beek, "Regularity of center-of-pressure trajectories depends on the amount of attention invested in postural control," *Experimental brain research,* vol. 181, no. 1, pp. 1-11, 2007.

The Effects of a Powered Pneumatic Ankle Exoskeleton on Balance Control

Santiago Canete[1] , W. Geoffrey Wright[2,3] and Daniel Jacobs[1]
[1]Department of Mechanical Engineering, [2]Department of Health and Rehabilitation Sciences, [3]Department of Bioengineering, Temple University.
Email: *santiago.canete@temple.edu

Introduction

Robotic exoskeletons have many potential applications to assist in current rehabilitation procedures [1]. While substantial investigations have shown that lower-limb devices can improve walking economy [2], there is limited information on the effects of assistive devices on static and dynamic postural control. One study performed a sensory organization test (SOT) wearing a lower limb exoskeleton but the device was purely passive [3].

This study aims to determine if a pneumatic, myoelectrically controlled, plantarflexion-assist, ankle exoskeleton affects postural control of the user. We aimed to investigate two hypotheses. First, wearing the exoskeleton may negatively affect balance in the anterior-posterior direction because the device is plantarflexion assist only. Furthermore, because the ankle joint's range of motion and predominant control dof is for plantarflexion the device could increase passive stability in the medial-lateral (ML) direction in each ankle while decreasing the bilateral ML control strategy. Second, how the exoskeleton interacts with postural control processes will depend on internally driven sensorimotor control weighting strategies, which will be tested using a modified SOT (mSOT).

Methods

We collected motion capture data (Qualisys), force data (Bertec) from two subjects (1 male and 1 female; Ages: 23-25) with no history of neurological or musculoskeletal impairment.

The experimental protocol was a modified version of the SOT, repeated with and without the exoskeleton. The experimental pairings were: eyes open (EO) vs. eyes closed (EC), stable surface (SS) vs. rocker board (RB), and powered exoskeleton (PE) vs. no exoskeleton (NO). The RB rotation axis was parallel to the plantar flexion rotation axis and perpendicular to the treadmill midline. Each trial lasted 20 seconds. Subjects wore an pneumatically-actuated, myoelectrically-controlled, plantarflexion assist, ankle exoskeleton controlled by the soleus muscle [2].

We collected center of pressure (COP) data for the AP and ML directions. We filtered the COP data (2nd order, 30 Hz). We calculated a single force vector and COP equivalent to the combination of the force and moment data from the treadmill data for the left and right feet. Then we calculated the AP and ML standard deviations (SD), mean velocity, and used a principal component analysis (PCA) to calculate the ellipsoidal sway area for the COP.

Results and Discussion

During the EO-SS trial subjects showed no clear differences between exo-on or exo-off conditions. For the EC-SS trial both subjects saw a reduction in the SD of the COP in the AP direction during the exo-on condition. For both RB trials (EO and EC) with the exo-on, both subjects saw an increase in the mean COP velocity in the AP and ML directions (**Fig 1**).

This study served as preliminary data collection which due to limitations of access to resources and people (COVID-19) tested only 2 participants. The pilot data showed that with the exoskeleton on, both subjects saw an increase in mean COP velocity during both RB trials in the AP and ML directions. The other measures of postural stability were less consistent. There were no conclusive differences in SD of the COP displacement across conditions. With the exoskeleton on, one subject performed better while the other performed worse in the AP direction. In the ML direction SD of the COP displacement stayed consistent between both conditions. Because the area changes were inconsistent but mean COP velocity increased, it may indicate increased joint stiffness when wearing the exoskeleton.

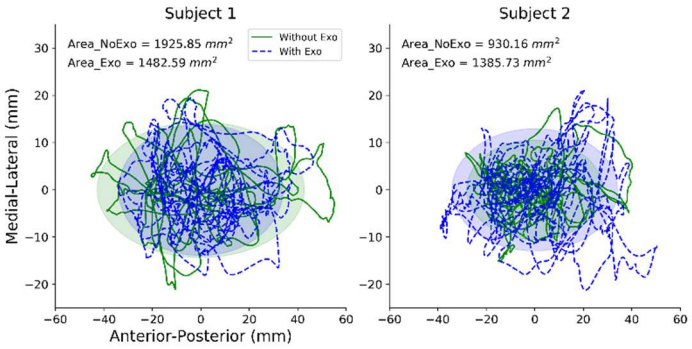

Figure 1: COP displacement (line trace) and sway area (shaded ellipse) in the AP and ML directions for two subjects during the EC-RB trial. When wearing the exoskeleton, Subject 1 showed a reduction, while Subject 2 showed an increase in COP sway area.

Future work will include a larger test sample and a condition wearing an unpowered exoskeleton. This new condition will allow us to determine whether changes in mean COP velocity are related to inertial properties of the exoskeleton and not to the assistive properties. We will also further investigate longitudinal training effects and the role of sensory weighting.

Significance

The effect of exoskeletons on sensory integration in postural control is still largely unknown. This study provides preliminary insights into how assistive devices may modulate the response of postural control and help inform development of novel controllers that enhance both gait and balance.

Acknowledgments

This research was supported in part by the Interdisciplinary Rehabilitation Engineering Research Career Development Program (NIH K12HD073945) to DAJ.

References

[1] Huo W, et al. Lower Limb Wearable Robots for Assistance and Rehabilitation: A State of the Art. IEEE Systems Journal. 2016 Sep;10(3):1068–81
[2] Sawicki GS, Ferris DP. Powered ankle exoskeletons reveal the metabolic cost of plantar flexor mechanical work during walking with longer steps at constant step frequency. Journal of Experimental Biology. 2009 Jan 1;212(1):21–3
[3] Schiffman JM, et al. The effects of a lower body exoskeleton load carriage assistive device on limits of stability and postural sway. Ergonomics. 2008 Oct 1;51(10):1515–2

Sensitivity of Mechanical Outcomes to Various Stiffnesses of Variable Stiffness Foot (VSF)

Kieran M. Nichols*[1], and Peter G. Adamczyk[1]
[1]Mechanical Engineering, University of Wisconsin-Madison, Madison, WI, USA
Email: *knichols4@wisc.edu

Introduction

The Variable Stiffness Foot (VSF) is an energy storage and return (ESR) prosthesis that can passively store and return energy to its users through the deflection of a compliant leaf spring keel in the forefoot [1]. It is a semi-active prosthesis, meaning it does not deliver power (from a motor) during stance phase, but it does adjust the stiffness during swing phase. This adjustment allows the user to have a variety of stiffnesses that can be dependent of the type of activity (standing, flat ground walking, ramp and stairs walking).

The VSF (Figure 1) prototype has a rigid ankle and a compliant forefoot keel whose effective stiffness is modulated by a support fulcrum moved by a motor and belt system. A microcontroller controls the movement to modulate the stiffness during swing phase due to user control or foot trajectory reconstructed by an inertial sensor [1].

Previous studies in prosthetics found that increased range of motion for stairs and ramps are associated with improved gait [3]; stiffer ankles (increased moments for small change of angle) are helpful for standing stability [4]; and a compliant forefoot returns more energy to the rest of the body [2].

This study tested these biomechanical effects of the VSF across level walking under three different stiffness settings. We hypothesized that the decreasing forefoot stiffness would lead toincreasing ankle plantarflexion, decreasing peak ankle moment, and increasing energy returns in push-off .

Methods

Seven persons with trans-tibial amputation were included in this experiment, of whom three are analyzed to date. The participants walked across two force plates (one foot on each plate) in a motion capture lab with twelve cameras. The participants walked with three different VSF stiffness settings (compliant, medium and stiff, scaled to each person's body mass) for 3 trials at 1.1±0.1m/s, with speed tracked using motion capture.

Motion and force data were processed in Visual3D and MATLAB for kinematic and kinetic calculations. We estimated ankle angle and moment according to standard inverse dynamics, and intersegmental power using a deformable body model. Peak values were computed for each stride on the prosthetic side and averaged across the three trials for each stiffness setting.

Results and Discussion

Each subject had similar trends for the angle, moment, and intersegmental power results and there was support for the three hypotheses. The ankle angles (Figure 2) had the largest plantarflexion excursions for the compliant stiffness setting. The ankle plantarflexion moments were smallest for the compliant settings The intersegmental ankle power output tended to be largest close to toe-off (around 60% of stride) for the compliant settings.

Figure 1: side view of the VSF [1]

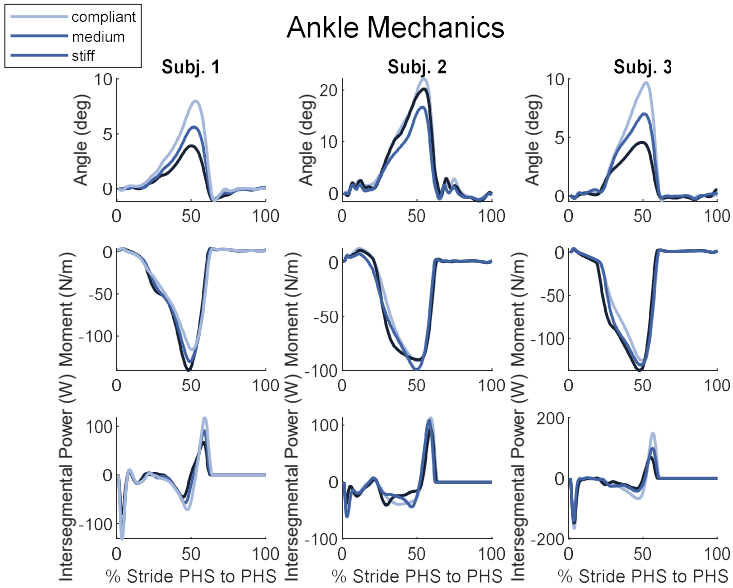

Figure 2: Results showing the angle, moment, and intersegmentatal power related to the ankle joint for each walking stride on the prosthetic side of the participants. Plantarflexion is in the negative direction. PHS: Prosthetic Heel Strike.

Significance

Many prosthetic users are limited to using passive feet that have fixed keel stiffness. This limited variability may be optimal for one function, but will not be suited for many different functions like standing, walking on stairs and ramps, and on uneven surfaces. This VSF can give its users the ability to change the foot stiffness that may increase comfort, adaptability, and help users get closer to functional walking. Future analysis will evalue the ideal stiffness settings for different activities. Semi-active prostheses could also be potentially used in clinics to assess stiffness preferences so prosthetists can better recommend new passive feet.

Acknowledgments

This work was supported by NIH HD074424 and institutional funds from the University of Wisconsin – Madison.

References

[1] Glanzer et. al, IEEE TNSRE 26.12, 2351- 2359, 2018.
[2] Adamczyk et al, IEEE TNSRE, 23, 776-785, 2015.
[3] Torburn et al. Clinical Orthopaedics, 303 185-192, 1994
[4] Hansen et al. Gait & posture 32.2 181-184, 2010

Muscle Response During Interaction with a Variable Damping Controlled Robotic Arm

Connor M. Phillips, Fatemeh Zahedi, Hyunglae Lee*
School for the Engineering of Matter, Transport and Energy, Arizona State University, Tempe, AZ
Email: *hyunglae.lee@asu.edu

Introduction

Current upper limb exoskeletons rely primarily on positive damping controllers (PDCs). This method, although very safe and stable, requires a large force input from the user and greatly reduces agility. In a previous study, our lab developed a variable damping controller (VDC) that manipulates the robotic damping applied to an environment based on the user's intent of movement ($\dot{x}\ddot{x}$). This study showed that subjects using the VDC were more agile in comparison to a PDC and had comparable stability.[1]

Here, we present an electromyography (EMG) study to quantify the difference in muscle activation of our novel VDC compared to fixed positive and negative damping controllers during upper limb physical human-robot interaction (pHRI). There were two hypotheses for this experiment. First, that during the movement phase, the subject would demonstrate less activation in the variable condition compared to the positive, and near equal activation between the variable and negative conditions. Second, that during the stability phase, the subject would demonstrate less activation in the variable condition than the negative, and near equal activation between the variable and positive conditions.

Methods

Six EMG sensors (Trigno Avanti Sensor, Delsys, MA) were used to measure muscle activation of the brachioradialis (forearm), biceps, anterior and posterior deltoids, and longitudinal and lateral triceps. This data was normalized to the maximum contraction (MVC) of each subject.

A seven degrees-of-freedom (DOF) robotic arm (LBR iiwa R820, KUKA, Germany) with a six-axis load cell (Delta IP60, ATI Industrial Automation, NC) was used for the application of all damping-defined environments. Zero stiffness and 10 kg of mass were simulated in the horizontal plane for all experiments. High stiffness of 10^6 N/m was simulated in the vertical plane to constrain vertical movement. Damping of +60 Ns/m was applied for the positive condition and damping of -15 and -20 Ns/m were applied for the negative condition in the mediolateral (ML) and anteroposterior (AP) directions respectively. These quantities were found from a previous human study with the KUKA robot.[1] The range of variable damping was calculated using subject-specific k_p and k_n tuning parameters. These quantities scaled the range of the positive (k_p) and negative (k_n) damping based on the maximum and minimum value of $\dot{x}\ddot{x}$ that the subject could produce.[1] The damping applied during the experiment changed relative to the instantaneous value of $\dot{x}\ddot{x}$.

Subjects were seated with their torso securely strapped to a rigid seat, facing a feedback visual display at ~1 m. This display provided information on neutral and current hand positions to the subject. Subjects held a handle that was connected to the robot's end-effector, with the shoulder in ~70° of abduction, ~45° of horizontal flexion, and the elbow in ~90° of flexion. This starting posture was considered the neutral position for all trials.

Subjects were tasked with moving as quickly as possible to targets shown on the visual feedback display. The position of the target was +/- 0.1 m away from the neutral position, in both the ML and AP directions.

EMG analysis was divided into two components: the movement phase (MP), and the stability phase (SP). The boundaries between phases were determined by the horizontal position of the robot's end-effector in the horizontal plane. The movement phase began at the onset of movement (+/-0.001 m) and ended once the subject reached the target (+/- 0.1 m). The stability phase began directly after the movement phase and ended once the subject was able to keep their marker inside of the target for 0.5 seconds. If the subject was unable to do this, all data post-movement phase was included in the stability phase.

Nine young, healthy subjects participated in this study which was approved by the Institutional Review Board of Arizona State University (STUDY 00010123).

Results and Discussion

Group analysis in the MP revealed that the activation due to the variable condition was less than the positive and near-equal (<1%) to the negative condition in all directions, which directly supports the hypothesis. This was most prominent in the right and upwards directions with differences of 9.94% and 5.11% respectively between the positive and variable conditions. The group results from the SP provide partial support for the hypothesis, as the variable condition is near-equal (<1%) to the positive condition in all directions, while the variable condition is less than the negative in the right (0.52%), down (0.93%), and upwards (0.72%) directions. However, this difference is too small to demonstrate significance.

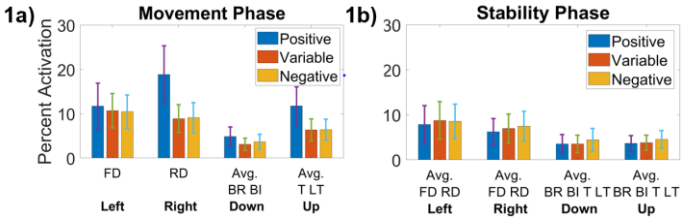

Figure 1: Group averages from the MP (1a) and SP (1b). MP data is the average of agonists in each direction while the SP data is an average of agonists and antagonists. A 95% CI is shown for each condition. Key: FD= Front Deltoid, RD= Rear Deltoid, BR= Brachioradialis, BI=Biceps, T= Lateral Triceps, LT= Longitudinal Triceps.

Significance

These results provide support for further investigation of the variable damping controller in upper limb pHRI, and the expansion of this study into multidirectional movement. A significant reduction in muscle activation was shown during the MP, which supports consideration for the implementation of this technology into industrial settings. However, this pattern must be replicated in conditions more closely resembling real-world pHRI, where the user may move through a larger range of motion.

Acknowledgments

Research supported by National Science Foundation Awards #1846885 and #1925110.

References

[1] T. Bitz, F. Zahedi, and **H. Lee**, "Variable Damping Control of a Robotic Arm to Improve Trade-off between Agility and Stability and Reduce User Effort," *IEEE International Conference on Robotics and Automation* (***ICRA 2020***), May 2020, Paris, France

Biomechanical Design and Preliminary Evaluation of an Ankle-Foot Simulator for Ankle Clonus Assessment Training

Yinan Pei[1], Prateek Garag [1], Kevin Gim [1], Christopher M. Zallek[2] and Elizabeth T. Hsiao-Wecksler[1]
[1] Department of Mechanical Science and Engineering, University of Illinois at Urbana-Champaign, Urbana, IL
[2] Department of Neurology, OSF HealthCare Illinois Neurological Institute, Peoria, IL
Email: ethw@illinois.edu

Introduction

Clonus is defined as involuntary and rhythmic (5-8Hz) abnormal muscle contractions observed during passive stretching and caused by lesions in the descending upper motor neuron pathways. It can be present in patients with spinal cord injury, post-stroke, and other conditions of the brain or spinal cord [1]. Clinically, the ankle joint is the most common site to test for clonus. However, successful triggering of ankle clonus requires mastery of the following technique [2]: 1) correctly position the examining hand on the foot, 2) provide a rapid dorsiflexion at sufficient joint velocity, 3) minimize ankle inversion during test, and 4) maintain appropriate load on the plantar surface of the forefoot to continue the clonus. To master this technique, students need to go through repetitive hands-on training. However, in the traditional education scenario, the availability of practice patients is usually very limited; therefore leaving the trainee skill proficiency questionable. To address this problem, we present a new haptic ankle-foot training simulator to provide healthcare learners more accessable practice opportunities.

Methods

Our goal was to develop a medical training simulator that provides a realistic, safe, and low-noise training environment for the trainees. The series elastic actuation strategy was chosen for its safe human-robot interaction and accurate force control [3]. The specifications of the simulator were derived from the few available quantification studies of ankle clonus [1] and previous devices [4,5]. The simulator, capable of generating a peak ankle torque of 17Nm, was actuated by a 150W Brushless DC motor (M3508, DJI) and a single-stage 3.2:1 timing belt drive (MR5, Misumi). A series spring stiffness (165N/mm) ensured a force control bandwidth of ~14Hz, which was sufficient to replicate oscillatory clonus motion. With known spring stiffness and displacement, interaction force between the examining hand and the simulator were accurately estimated to verify continuous loading needed to maintain clonus.

Fig 1: Ankle-foot simulator prototype

The simulator segment lengths were designed based on a 50th percentile Caucasian male. The principal dorsi/plantarflexion (DF/PF) degree of freedom (DOF) was actuated (available ROM: 20º DF to 55º PF), while the auxiliary inversion/eversion (I/E) DOF was passive (ROM: ±10º). Furthermore, the simulator was equipped with 1) a linear encoder to measure spring deflection, 2) two absolute rotary encoders to measure ankle angular position and velocity in DF/PF DOF and joint angle in I/E DOF, and 3) several force-sensitive resistors on the foot shroud to detect whether the trainee's hand was properly positioned on the forefoot and plantar surface.

The simulator was programmed to initiate ankle clonus when the DF stretch speed was faster than 200º/s. To maintain the clonus behavior, a DF torque of 3Nm must be maintained after the triggering. The frequency of ankle oscillation was set at 5Hz. Sensor signals were sampled at 1000Hz and filtered by a 2nd-order Butterworth filter with a cut-off frequency at 20Hz.

Results and Discussion

The prototype simulator was capable of replicating an experimentally-observed clonus behavior at the ankle with the desired frequency (Fig. 2). Onboard sensors captured the timing of rapid DF stretch and monitored the maintained DF load after clonus was triggered. In the future, these control flow parameters will be iterated based on clinician feedback.

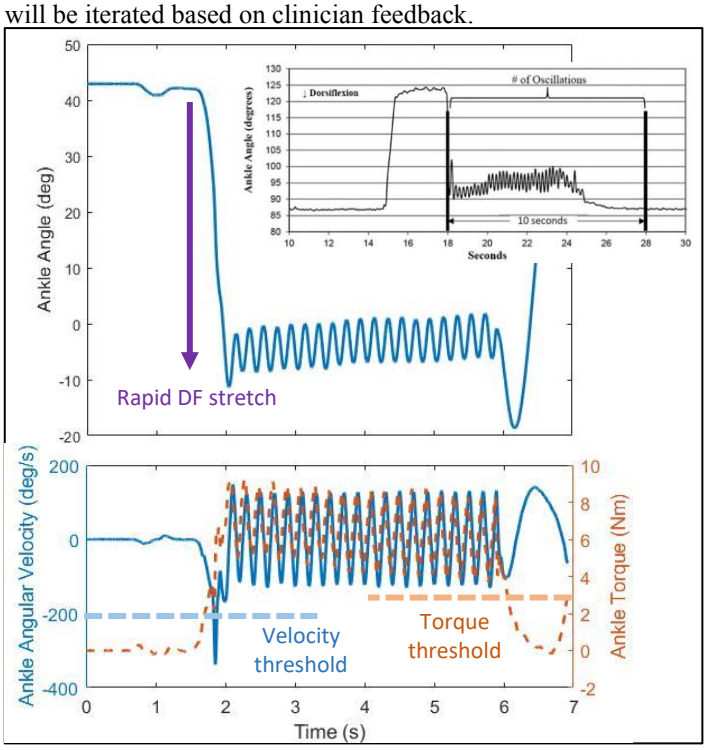

Fig 2: Simulated ankle behavior (blue) compared to experimental clonus behavior from a patient (black) (from [6]). Dorsiflexion is negative.

Significance

Robotic medical training simulators are becoming more accepted as a supplement to the traditional training process. In the case of ankle clonus, there are very few devices for clinicians to train and no commercial product exists. The preliminary results are promising that our device could fill this gap for medical, physical therapy, and other healthcare students.

Acknowledgments

Funded provided by the Jump ARCHES partnership between OSF HealthCare and the University of Illinois.

References

[1] Boyraz, I., et al., 2015, Med. Glas., 12(1)
[2] Campbell and DeJong, 2015, Lippincott Williams & Wilkins
[3] Pratt, J., et al., 2002, Ind. Robot An Int. J., 29(3)
[4] Kikuchi, T., et al., 2010, Adv. Robot., 24(5–6)
[5] Okumura, H., et al., 2015, Haptic Interaction, pp. 209-214
[6] Manella, et al., 2017, J. Neurol. Phys. Ther., **41**(4), pp. 229–238

User- and Speed-Independent Slope Estimation for Lower-Extremity Wearable Devices

Jairo Y. Maldonado-Contreras[1*], Krishan Bhakta[1], Jonathan Camargo[1], and Aaron J. Young[1]
[1]School of Mechanical Engineering, Georgia Institute of Technology, Atlanta, GA 30332 USA
Email: jairoymc@gatech.edu

Introduction

As more powered prostheses and exoskeletons enter real-world settings, it is important to adapt assistance profiles in dynamic environments using slope level information. Adaptive assistance profiles based on environmental information can help wearable devices keep up with real-time changes in human biomechanics and maximize assistance benefits. Advancements in intention recognition (IR) algorithms have enabled wearable devices to autonomously assist users across different terrains (e.g., ramps and stairs) [1]. IR algorithms are capable of classifying ramps of different slope levels without the need for slope level estimations, but assistance profiles typically remain constant or are scaled based on encoded joint trajectories. The inclusion of slope estimation algorithms and torque scaling equations in the control of wearable devices offer a more natural and effective interface between users and their environment.

Numerical solutions for slope estimation using inertial measurement units (IMUs) have been shown to be inaccurate due to sensor drift and variations in walking speed [2][3]. Recent work suggests that machine learning (ML) models trained with electromyography (EMG) and mechanical sensor data can accurately estimate slopes at different speeds (1.3˚ RMSE) [4]. A limitation of this work is that each slope level was estimated for a short range of speeds.

We hypothesize that training a slope estimator with only mechanical sensor data collected on slope levels across a large range walking speeds can accurately estimate slopes independent of the user and walking speed. Our methodology is expected to generate robust slope estimators that could be readily integrated into the control systems of various wearable devices.

Methods

This study focuses on evaluating the performance of ML models in estimating a user's slope level while walking on a speed-varying treadmill. Nine able-bodied subjects were fitted with three 6-axis IMUs (foot, shank and thigh) and three goniometers (ankle, knee, and hip). Thirteen static and five dynamic walking trials were collected for each subject. During static trials, slope levels (-15˚ to +15˚, incremented by 2.5˚) were held constant while walking speeds changed from 0.6 to 1.4 m/s. During dynamic trials, walking speeds of 1.0 and 1.2 m/s were held constant while slope levels changed from 0˚ to 10˚.

Slope estimation algorithms were evaluated for sensor suites commonly found on ankle prostheses, knee-ankle prostheses, and hip exoskeletons. Signals were filtered and segmented into sliding windows of data, incremented by 50 ms. Mean, standard deviation, min, max, and ending value features were extracted from each window. Analyses across different normalization methods, sliding window sizes, gait phases, and ML models were conducted to minimize slope estimation errors. The performance of neural network (NN), XGBoost (XGB), and linear regression (LNR) models were assessed. The phase dependency of the models was explored across four gait cycle types: 1-phase, 2-phase, 3-phase, and 4-phase. Tested window sizes ranged between 200 ms to 500 ms, incremented by 50 ms.

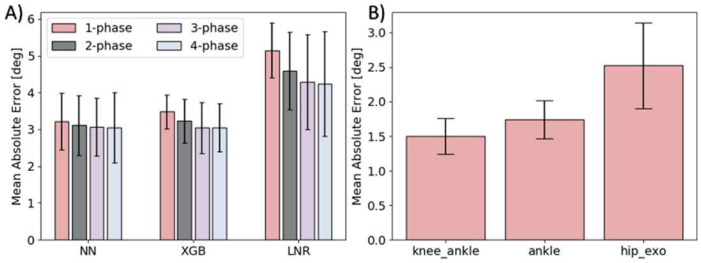

Figure 1: A) Static trial non-optimized model performance across gait cycle types for the knee-ankle case (250 ms window size). B) Optimized XGBoost model performance across all sensor suites using the 1-phase gait cycle analysis method and a 500 ms window size.

Results and Discussion

For static trials, the NN and XGB model similarly outperformed the LNR model across each phase, for each sensor suite, including the knee-ankle case (Fig. 1A). The XGB model was selected over the NN model for hyperparameter optimization due to its lower average MAE variance. Since there was no significant difference between gait cycle types, the 1-phase gait cycle was selected due to its simplicity. With the optimal window size of 500 ms, static trial average MAE errors of 1.500 ± 0.258˚, 1.739 ± 0.276˚, 2.522 ± 0.618˚ were achieved for the knee-ankle, ankle, and hip-exoskeleton sensor suites, respectively (Fig. 1B). Future analyses will test the performance of the proposed ML architectures on the dynamic trials, identify a reduced feature space for each sensor suite, and include a Kalman filter to further reduce errors.

Significance

This user-independent study provides slope estimation solutions that are generalizable to novel users and a variety of wearable devices, including those not explored in this study (e.g., knee exoskeletons). The low errors achieved across dynamic walking speeds and the exclusion of EMG sensors are important steps towards the real-world implementation of slope estimators. Joint torque scaling based on slope level will have a significant impact on the quality of assistance that users receive from lower-extremity wearable devices, which can improve metabolic efficiency, user mobility, and the effectiveness of rehabilitation.

Acknowledgments

The authors would like to acknowledge the NSF Research Traineeship: ARMS Award #1545287. *Supported by an MIT Lincoln Laboratory/GEM Fellowship and Goizueta Fellowship.

References

[1] A. J. Young et al. J. Neural Eng., vol. 11, no. 5, 2014.

[2] Q. Li et al., IEEE International Conference on Rehabilitation Robotics, 2009, pp. 839–844.

[3] J. Kim et al., IEEE International Conference on Rehabilitation Robotics, 2015, pp. 392–397.

[4] I. Kang et al., IEEE International Conference on Rehabilitation Robotics, 2019, pp. 548–553.

Performance Evaluation of a Robotic Knee Exoskeleton

Seth Higgins[1], Nicole Espositio[1], Hannah Sweatland[1], Daniel P. Ferris[1]
[1]J. Crayton Pruitt Family Department of Biomedical Engineering, University of Florida, Gainesville, FL, USA
Email: seth.higgins@ufl.edu

Introduction

Robotic exoskeletons could reduce musculoskeletal loading and energy expenditure in military personnel during their everyday activities. Soldiers often carry loads around 50 kg or more, altering gait biomechanics, increasing metabolic cost, and increasing injury risk [1]. A common way to evaluate an exoskeleton's performance is assessing metabolic cost during movement.

The purpose of this study was to determine if a robotic knee exoskeleton (ONYX, Lockheed Martin) could reduce the metabolic cost of locomotion. Previous research showed a similar lower extremity knee exoskeleton reducing metabolic cost while walking up an incline and wearing a loaded backpack [2]. The ONYX is an altered version of that device. We hypothesized that the ONYX would reduce metabolic cost of walking up an incline and walking up stairs while carrying a load.

Methods

We evaluated the performance of 6 healthy young subjects while walking on a treadmill, and up and down stairs. Subjects walked on a level, inclined (15°), and declined (15°) treadmill at two walking speeds (1.2 m/s and 0.3 m/s for level; 0.6 m/s and 0.3 m/s for incline and decline). Subjects also walked up and down stairs at the University of Florida football stadium at two different cadences set by a metronome (60 steps/min and 40 steps/min). We measured metabolic cost using a wireless device (Cosmed K5) and rate of perceived exertion using a Borg scale (1-10). Subjects completed the tasks with and without the exoskeleton, and with and without a weight vest (18 kg). The exoskeleton used a controller based on a finite state machine tuned to different phases of the movement phase based on kinematic and kinetic sensors. We calculated metabolic cost (W/kg) by using $\dot{V}_{O_2}$ and $\dot{V}_{CO_2}$ measurements and the Brockway equation [3].

Results and Discussion

Metabolic cost increased when wearing the exoskeleton for all conditions (Figure 1 & 2). The knee performs more positive mechanical work during incline walking with a load and stair climbing with a load compared to level and decline walking, and stair descent. As a result, we hypothesized that the exoskeleton would perform the best on inclines and ascents with the load. There was a trend towards a lower percent difference in metabolic cost when walking at an incline and wearing a weight vest, but using the exoskeleton still cost more energy than not using the exoskeleton. Perceived exertion data were in agreement, mostly increasing when using the exoskeleton compared to not suing the exoskeleton. The difference was greater at slower speeds and smaller cadences.

These results suggest that the robotic knee exoskeleton did not benefit the user in metabolic cost or perceived exertion for any of the tasks. Future knee exoskeleton designs should consider how to reduce device mass, increase range of motion and degrees of freedom of motion, and alter the control strategy.

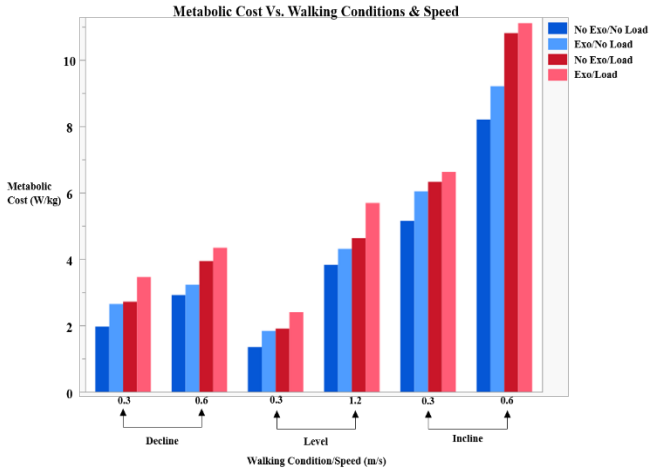

Figure 1: Metabolic cost data for walking conditions.

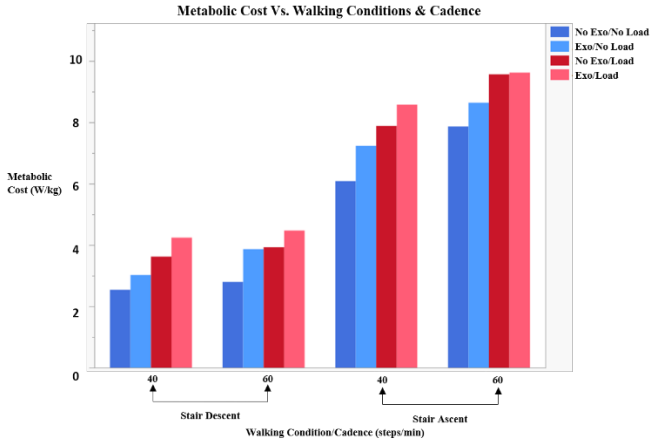

Figure 2: Metabolic cost data for stair conditions.

Significance

Assessing the benefit of wearing a robotic lower extremity exoskeleton is a multi-factorial problem with metabolic energy expenditure and perceived exertion as two factors. These data suggest that the current design of the ONYX robotic knee exoskeleton does not reduce energy cost or perceived exertion for users. The data can provide insight into the biomechanical and physiological aspects that need to be addressed in future exoskeleton designs.

Acknowledgments

Funded by the Lockheed Martin Corporation.

References

[1] Orr et al. (2014) *Int J Inj Contr Saf Promot*, **21**:388–396.
[2] MacLean et al. (2019) *J Appl Biomech*, **35**:320-326.
[3] Brockway et al. (1987) *Hum Nutr Clin Nutr*, **41**:463-471.

Biomechanical Analysis of Device-Assisted Sit-to-Stand Transfers in Young Adults

Shaniel T. Bowen, MS[1], Krystyna Gielo-Perczak, PhD[2]
[1]Department of Bioengineering, University of Pittsburgh, Pittsburgh, PA, USA
[2]Department of Biomedical Engineering, University of Connecticut, Storrs, CT, USA
Email: stb103@pitt.edu

Introduction

Sit-to-stand (STS) transfer is one of the most common activities of independent daily living. The ability to perform this motor task is essential for physical independence and is widely considered as an indicator of postural control and lower-limb strength.[1] This is especially the case for younger adults where injury-related reductions in functional status and capacity have been associated with increased risk of sarcopenia, injury, and obesity.[2] Thus, there is a need for solutions to assist STS transfer. Hence, the aim of this study was to design and evaluate an STS device by assessing postural control during unassisted vs device-assisted STS transfer via force platform analysis.

Methods

Twenty-five college students (18-25 yrs.) with no mobility impairments were recruited from the University of Connecticut, all of whom provided written informed consent as per the IRB-approved protocol. For the experiment, an adjustable bench was used to adjust the seat height such that participants' hips and knees were bent 90° while sitting on the STS device (Figure 1).

Figure 1: STS lifting-seat device on the custom height-adjustable bench.

Participants were instructed to: (1) have their arms crossed against their chest during STS, (2) have their feet shoulder-width apart and flat against the force platform, and (3) to perform STS at a constant, self-selected pace. Three sets of recordings, 5 trials each, were done: (1) unassisted STS (control, C), (2) assisted STS with the device at maximum speed (MS), and (3) assisted STS with the device at an exponentially increasing acceleration (A).

To assess postural control, the (1) average net ground reaction force (F_{NETavg}), (2) mean force development rate (FDR_{mean}), (3) average net ground reaction moment (M_{NETavg}), and (4) mean moment development rate (MDR_{mean}) were calculated. In addition, the (1) average medio-lateral displacement ($ML_{DISPavg}$), (2) average anterior-posterior displacement ($AP_{DISPavg}$), (3) 95% ellipse area ($Ellipse_{95\%}$), (4) average velocity (V_{avg}), and (5) length (L) were measured. All postural control parameters were normalized to body height and weight. The percent reduction between assisted and unassisted STS was used to quantify the efficacy of the device in improving STS performance.

For this study, differences in outcome measures between unassisted and device-assisted STS were compared using the Friedman test. Post-hoc analysis was performed using the Wilcoxon Signed-Rank test with Bonferroni correction to adjust for multiple comparisons (α=.025).

Results and Discussion

The force platform results are shown in Table 1. The STS device significantly reduced the ground reaction forces and moments, and the force and moment development rates. This effect may indicate decreased lower-limb joint loading due to the increased height and lifting force provided by the STS device prior to seat-off, as reported in previous literature.[3] The average COP velocity and average anterior-posterior COP displacement were reduced with device assistance, implying that the momentum needed for STS was lessened. Thus, the STS device was overall successful in enhancing STS performance by reducing the demand on, and instability in, the postural control system during STS.

Parameter	Without Assistance	With Assistance		Percent Reduction		P-Value
	C	MS	A	C-MS	C-A	
F_{NETavg}[1]	65.4 (4.8)	38.7 (5.3)	38.3 (7.2)	40.6 (8.5)	41.4 (12.0)	**<.0001**
FDR_{mean}[2]	258.7 (83.3)	188.2 (59.0)	206.1 (52.6)	20.0 (36.9)	11.4 (35.1)	**.002**
M_{NETavg}[3]	2.53 (1.37)	1.32 (0.58)	1.20 (0.61)	38.4 (18.7)	43.7 (19.9)	**<.0001**
MDR_{mean}[4]	15.7 (4.8)	12.8 (4.3)	12.9 (3.3)	13.5 (31.3)	15.4 (24.9)	**.02**
$ML_{DISPavg}$[5]	0.64 (0.24)	0.78 (0.28)	0.68 (0.25)	-34.8 (57.0)	-1.1 (25.5)	**0.02**
$AP_{DISPavg}$[5]	1.34 (0.20)	1.30 (0.30)	1.27 (0.41)	0.1 (30.4)	2.1 (40.9)	0.93
$Ellipse_{95\%}$[6]	0.21 (0.09)	0.26 (0.09)	0.22 (0.09)	-56.3 (93.1)	-20.9 (72.4)	**0.02**
V_{avg}[7]	8.04 (1.21)	5.17 (0.91)	4.94 (0.09)	36.0 (14.3)	38.7 (14.7)	**<.0001**
L[5]	16.0 (2.5)	29.2 (3.4)	27.6 (4.5)	-83.3 (41.3)	-71.9 (46.1)	**<.0001**

Table 1: Force platform results. *Units: (1) %BW, (2) %BH/s, (3), %BW x BH, (4) %BW x BH/s, (5) %BH, (6) %BH x BH, and (7) %BH/s. P-values: significant overall diff. between assisted and device-assisted STS.*

Significance

These results show that our proposed device was able to lessen the biomechanical effort required for STS transfer. These promising findings reveal the potential benefit the device may give to the mobility impaired.

Acknowledgments

National Science Foundation-funded LSAMP Bridge to the Doctorate fellowship program at the University of Connecticut (Award #: 1400382).

References

1. Whitney, et al., *Phys Therapy*. **85(10)**: 1034-1045, 2005.
2. Lummel, et al., *Sensors*. **18(4)**: 1235, 2018.
3. Munro & Steel, *Phys Therapy Reviews*. **3(4)**: 213-224, 1998.

Gait Phase Estimation of Powered Transfemoral Prosthesis using RNN

Jinwon Lee, Woolim Hong, and Pilwon Hur
Department of Mechanical Engineering, Texas A&M University, College Station, TX, USA
Email: {jinwon, ulim8819, pilwonhur}@tamu.edu Web: http://hurgroup.net

Introduction

The gait phase informs us of the human's progress in the gait cycle. It is widely used to control powered assistive devices like prosthetics and exoskeletons. The controller's desired trajectories or gains are modified depending on the gait phase. Human walking can be divided into heel-strike, flat-foot, push-off, and toe-off [1]. Human gait is considered to consist of two walking phases: i) stance phase when the foot is in contact with the ground and ii) swing phase when the foot is not in contact with the ground. The first 60% of the gait cycle belongs to the stance phase and the next 40% of the gait cycle belongs to the swing phase.

Recently, there were studies using long short-term memory (LSTM) machine learning to estimate the gait phase. LSTM introduced cell state to solve the long-term dependency problem found in Recurrent Neural Networks (RNN). The concept of the cell state is three gates; forget gate, input gate, output gate. Forget gate is to erase unnecessary past information using the sigmoid function. In the input gate, a sigmoid function decides whether to reflect the new information in the cell state. If new information needs to be reflected, the current cell state is updated through the *tanh* function. The output gate determines which part of the information is sent to the cell's output using a sigmoid function. Finally, the output is fed to the input of the next cell state.

Methods

Our network architecture consists of five layers: LSTM (256), bidirectional LSTM (128), LSTM (128), and bidirectional LSTM (64), and fully connected layer. To prevent overfitting, each layer implemented a dropout rate of 0.1 and recurrent dropout rate of 0.4. We used the Adam optimizer with initial learning rate = 0.001, momentum = 0.9, batch size = 128, epochs = 30, and mean squared error (MSE) as the loss function [2, 3].

The data collection experiment had one healthy participant (age:31 years, height:175 cm, weight: 75 kg) who walked on a flat-ground treadmill. The treadmill speed varied from 0.25 m/s to 1.75 m/s. To gather kinematic and force data, we attached two IMU sensor (at the thigh and torso) and one force sensor (at the heel). To train the network's model, we prepared a dataset of 100 steps at three walking speeds (0.75 m/s, 1m/s, and 1.25 m/s). The data was suitably labelled. The refined data consisted of 200 data points per gait cycle. Training on this dataset took 30 minutes to converge with Tensorflow and two RTX 4000 GPU. To verify the model, we collected data for 400 steps at various speeds (0.25 m/s to 1.75 m/s).

Results and Discussion

Figure 1 shows gait phase estimation. Regardless of the speed, the point where the heel strike occurred was accurately predicted. In particular, the gait cycle was accurately predicted at 1.25 m/s. However, there were a few inaccuracies in predicting the gait phase during the stance phase at lower walking speeds. Since the training data used only data from 0.75 m/s to 1.25 m/s, inaccurate predictions can be expected at slow speeds such as 0.25 m/s. Slow walking speeds can increase sensor variation, which can cause data noise.

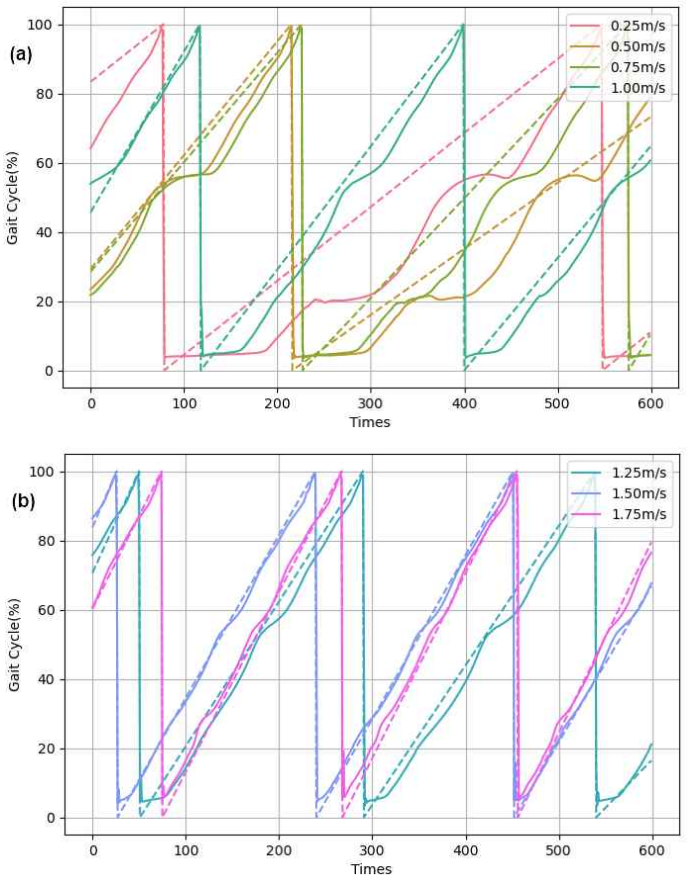

Figure 1: Gait cycle according to low walking speed (a) and hight walking speed (b). Dotted line is ground truth and solid line is predicted cycle.

Significance

Powered lower limb assistive devices rely on the gait phase parameter to determine suitable control inputs. Previously, the gait phase was predicted using multiple sensors and complex calculations. To reduce the prosthetic's weight and battery power efficiency, we must reduce the number of required sensors. In this study, we generated a gait phase estimation model using LSTM. The model requires only two IMUs and one force sensor. Future studies will use the trained gait estimation model to control a powered transfemoral prosthesis.

References

[1] W. Hong et al., International Conference on Robotics and Automation (ICRA), 2019, pp. 2838-2844.
[2] K. Seo et al., IEEE International Conference on Rehabilitation Robotics (ICORR), 2019, pp. 809-815.
[3] I. Kang et al., IEEE Transactions on Medical Robotics and Bionics 2 (1) (2020) 28-37.

Lower Limb Response of Transtibial Amputees Stepping on a Coronally Uneven Surface

Krista M. Cyr[1], Ava D. Segal[2], Richard R. Neptune[3], Glenn K. Klute[1,4]
[1]Dept. of Veterans Affairs Center for Limb Loss and MoBility, Seattle, WA; Depts. of Mech. Engr., [2]Colorado School of Mines, Golden, CO; [3]The University of Texas at Austin, Austin, TX, [4]University of Washington, Seattle, WA
Email: krista.kms@gmail.com

Introduction

Over half of individuals with lower limb amputation experience falls each year [1, 2], and 73% of outdoor falls are due to environmental factors and uneven surfaces [3]. Such falls are three times more likely to result in injury [4]. Navigating uneven surfaces is important for individuals with transtibial amputation (TTA) to enable their participation in community activities. Currently prescribed multiaxial prosthetic feet for individuals with TTA attempt to store and return energy passively in all axes of deformation, which may not be desirable over unexpected coronally uneven surfaces.

The objective of this research was to quantify the biomechanical response of individuals with unilateral TTA wearing their prescribed prosthesis versus healthy controls while taking a step on a coronally uneven and unexpected surface. These findings may elucidate underlying adaptations that could be addressed through therapeutic and prosthetic interventions.

Methods

A 12-camera motion capture system recorded marker trajectories of 8 individuals with unilateral TTA and 8 controls without amputations, while walking at their self-selected speed on a novel instrumented walkway with 5 embedded force plates. The middle force plate could be positioned flush to the surface or rotated ±15˚ in the coronal plane, and could be blinded to participants (Figure 1). Kinematics and kinetics were evaluated during three different surface conditions: unblinded flush, 15˚ blinded inversion, and 15˚ blinded eversion. Coronal hip angle (adduction positive, abduction negative), mediolateral foot position of the recovery step relative to the opposite foot, and ankle energy returned [5] were evaluated between groups with a repeated measures analysis of variance ($p < 0.05$).

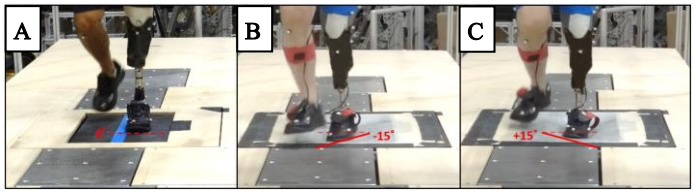

Figure 1: An individual with a TTA stepping on the middle force plate during: (A) the flush condition (unblinded), (B) the blinded eversion condition, and (C) the blinded inversion condition.

Results and Discussion

The TTA group used a more abducted hip strategy (negative coronal hip angles) compared to controls, especially during blinded inversion (Table 1). This is similar to previous findings demonstrating premature activation of hip abductors during unexpected inversion of the ankle for subjects with hypermobility [6], therefore this may be a compensatory response for subjects with altered ankle mobility.

The TTA and control groups had a similar mediolateral foot position of the recovery step during the flush condition, but the TTA group took a significantly wider step following blinded eversion and a slightly narrower step following blinded inversion (Table 1). Individuals with TTA may have less control of their center of mass and balance, resulting in recovery step compensations after a step on a coronally uneven surface.

Less ankle energy was returned for the TTA group, significantly during both blinded disturbances (Table 1). This suggests that currently prescribed prosthetic feet are unable to effectively return stored energy to create the same amount of push-off power as healthy controls. Vickers et al. observed a similar lack of ankle power generation for TTA walking on a sagittal plane ramp while wearing their prescribed prosthesis [7]. Individuals with TTA may need to compensate to maintain forward progression, especially on uneven surfaces.

These results give insight into adaptations used by individuals with TTA when taking a step on a coronally uneven surface. These alterations and compensations could lead to increased energy expenditure and risk of falls during activities of daily living or in the community.

Significance

This study may inform the development of prostheses able to conform to coronally uneven surfaces and rehabilitation therapies for individuals with TTA ambulating on uneven surfaces so they can maintain or increase participation in desired activities.

Acknowledgments

This work was funded by the Department of Veterans Affairs Rehabilitation Research and Development Service, Grants I01 RX001840, RX002357, and RX002974.

References

[1] Miller et al. (2001). *Arch Phys Med Rehabil*, 82(8):1031-7.
[2] Kim et al. (2019). *PM R*, 11(4):344-53.
[3] Li et al. (2006). *Am J Public Health*, 96(7):1192-200.
[4] Kelsey et al. (2012). *Am J Public Health*, 102(11):2149-156.
[5] Takahashi et al. (2012). *J Biomech*, 45(15):2662-7.
[6] Beckman et al. (1995). *Arch Phys Med Rehabil*, 76(12):1138-43.
[7] Vickers et al. (2008). *Gait Posture*, 27(3):518-29.

Table 1: Statistical results within each surface condition (comparing TTA vs. Controls). Bolded *p*-values indicate significance. Abbreviations: (SD) standard deviation, (B) blinded, (C) controls, (ML) mediolateral, (N/A) not applicable.

Metric	Units	Mean (SD)						Pairwise *p*-Values		
		Flush		B. Eversion		B. Inversion		Flush (TTA-C)	B. Eversion (TTA-C)	B. Inversion (TTA-C)
		TTA	Control	TTA	Control	TTA	Control			
Coronal Hip Angle	deg.	0.4 (2.7)	6.5 (2.8)	-0.1 (3.1)	5.9 (3.7)	-2.6 (4.1)	5.1 (3.4)	**0.005**	**0.029**	**0.008**
ML Foot Position	cm	10.5 (3.8)	10.4 (3.1)	14.3 (3.8)	8.3 (3.7)	6.1 (3.7)	8.7 (3.5)	N/A	**0.002**	N/A
Ankle Energy Returned	J/kg	0.22 (0.04)	0.28 (0.07)	0.20 (0.03)	0.31 (0.08)	0.19 (0.03)	0.29 (0.07)	N/A	**0.016**	**0.005**

Comparison of Trunk Muscle Activity during Modified Side-Bridge Exercises and Traditional Side Bridge Exercise

Chi-Whan Choi[1]* PT, MPH, Jung-Wan Koo[2], MD, PhD, Yeon-Gyu Jeong[3], PT, PhD
[1] Department of Rehabilitation Medicine, Seoul National University Hospital, 101 Daehak-Ro Jongno-Gu, Seoul, 03080, South Korea
Email: *cch4105@gmail.com

Introduction

The side-bridge exercise is intended for endurance training and optimal motor control in the early stages of rehabilitation, and many occupational and sporting groups include it as part of injury prevention programs. This exercise helps increase spine stabilization that requires the musculature to be co-contracted for substantial durations. However, there may be some special situations in which it is impossible to tolerate the compressive load on the side supported during the side-bridge, such as in elderly persons with hip or knee replacements and even in athletes with shoulder pain. This leads to three modified side-bridge exercises: both leg lift while side-lying (BLLS), lying on the floor and attempting to raise the legs laterally; torso lift on a 45° bench while side-lying (TLBS), elevating the torso while standing on a 45° bench with the feet anchored; or wall side-bridge (WSB), side-bridge exercises while standing against a wall despite a compromised shoulder, hip, or knee. However, the comparative effects of these traditional side-bridge (TSB) and modified side-bridge exercises on the muscle activities of the lumbar and abdominal wall are not known. The purpose of this study was to examine the effects of three modified side-bridge exercises on the spinal stability muscles such as the external oblique (EO), internal oblique (IO), and quadratus lumborum (QL) compared with TSB for healthy men.

Methods

A total of 20 healthy men with no known neuromuscular, cardiovascular, or orthopedic conditions, especially low back, shoulder, hip, or knee pain were recruited for this study. The participants performed TSB, BLLS, TLBS, and WSB in a random order. Surface electromyography measured the muscle activity of the EO, IO, and QL. A 1-way repeated-measures analysis of variance assessed the statistical significance of the EO, IO, and QL muscle activity. When there was a significant difference, a Bonferroni adjustment was performed.

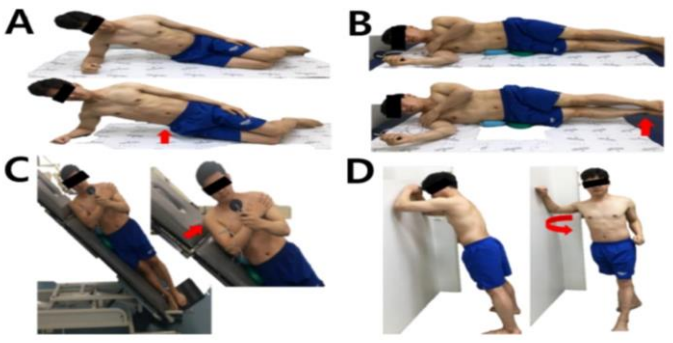

Figure 1: The side-bridge exercise was used in this study. (A) TSB, traditional side-bridge. (B) BLLS, both leg lift on side-lying. (C) TLBS, torso lift on a 45° bench side-lying. (D) WSB, wall side-bridge.

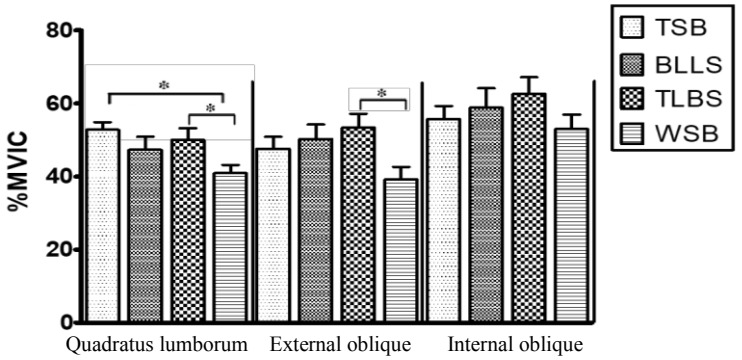

Figure 2: Comparison of the quadratus lumborum, external oblique, and internal oblique muscle activity (%MVIC) for each of the exercises. *p<0.05 using the post hoc Tukey's test.

Result and Discussion

There were significant differences in QL (p<0.001) and EO (p=.007) muscle activity (p<0.001) among the four different exercises. TSB showed significantly greater QL muscle activity (p<0.001) than WSB. TLBS demonstrated significantly greater QL muscle activity (p=.037) than WSB. TLBS showed significantly greater EO muscle activity (p=.017) than WSB. There was no significant difference in IO muscle activity (p=.189) among the exercises. The findings indicate that the effectiveness of BLLS and TLBS was similar to that of TSB in activating the EO, IO, and QL muscles. Given each exercise position of TLBS and BLLS, it is suggested that TLBS may be a practical exercise to activate the EO, IO, and QL in some situations in which it is impossible to tolerate the compressive load on the upper extremity such as for athletes with shoulder pain. BLLS may be effective way for individuals with lower extremities issues including the elderly with hip or knee replacements. In WSB, although it showed significantly less than TSB in activating QL, previous studies recommended WSB for deconditioned patients, implying that in patients unable to perform BLLS or TLBS, EO and IO muscle activity may benefit from WSB. Therefore, three modified side-bridge exercises can be effective therapeutic approaches available for some particular subjects who are unable to perform TSB in clinical practice.

Significance

This study focused on addressing the validity of the modified side-bridge exercises by identifying the activation of the spine stabilization muscles during the exercises. The data suggest that BLLS and TLBS may be effective rehabilitation techniques to activate EO, IO, and QL in those who are unable to perform TSB as spine stability exercises and WSB may be beneficial for patients unable to perform BLLS or TLBS, activating EO and IO.

References

1. Barr KP, Griggs M, Cadby T. Lumbar stabilization: a review of core concepts and current literature, part 2. Am J Phys Med Rehabil. 2007;86(1):72-80.

Semi-Unsupervised Machine Learning System for Gait Event Detection, Locomotion Mode Classification and Prediction

Seth Donahue[1*], Michael Hahn[1]
[1]University of Oregon, Neuromechanics Laboratory, Human Physiology, Eugene OR
Email: *sethd@uoregon.edu

Introduction

Supervised pattern recognition algorithms have become more common recently for identification of gait events, classification and prediction of locomotion mode in control systems for assistive devices. They have been successful in controlled environments with accuracies of ~ 95% [1,2]. Despite their success, these algorithms require large sensor arrays, high sampling frequency and expert user defined feature sets from these data [2].

The purpose of this study was to build a novel semi-supervised machine learning system for idenfitication of gait events, classification and prediction of locomotion mode. We present a two component machine learning system to detect gait events, and then classify and predict locomotion mode. The first component is an unsupervised machine learning algorithm, the Beta Process Auto Regressive Hidden Markov Model (BP-AR-HMM). The second component is comprised of supervised learning algorithms; specifically Long Short Term Memory networks (LSTMs) [3]. Data input into this system were from a single mechanical sensor, and the outputs were gait event detection, classification and prediction of locomotion mode.

Methods

Data were collected from sixteen able bodied participants (8 male and 8 female; 31.1 ± 14.8 years, 173.4 ± 8.5 cm, 66.7 ± 7.7 kg). All analyses were performed offline in custom Matlab programs (Mathworks, Natick, MA). Each participant's dominant foot was determined, and this foot was equipped with an IMU (Vicon, Centennial, CO) mounted on the dorsal aspect. Foot ground contact information was recorded with two different systems during the study. The first three participants were equipped with the Noraxon footswitch Telemyo DTS system (Noraxon, Scottsdale, AZ), and the other 13 participants were equipped with Loadsol inserts (Novel Electronics, St. Paul, MN). Ground contact and IMU data were down-sampled to 25 Hz to simulate a minimally sensorized system embedded in an assistive device.

On the first day of the protocol the subjects preformed 4 locomotion tasks; stair ascent and descent, level ground walking (including slopes <5°) and running. The second day of the study utilized a protocol adapted from Long and Srinivasian [4]. Participants were asked to cross 90 m in a set amount of time. The range of average speeds was 1.3 to 3.0, m s^{-1} (1.30, 1.51, 1.73, 1.94, 2.15, 2.36, 2.58, 2.79, 3.00 m s^{-1}), encompassing typical human locomotion speeds. Trial order was randomized to minimize learning effect.

Gait events were identified from the output of the BP-AR-HMM. Before each gait event a 75 ms window was used to identify the two most frequently occurring states from the BP-AR-HMM. The state counts from the current foot contact were then used as input into one LSTM for classification of the locomotion mode, and the state counts from the previous three foot contacts were used as input into a second LSTM for prediction of pending locomotion mode (Figure 1). The hyperparameters of both LSTMs were optimized utilizing a Bayesian optimization function.

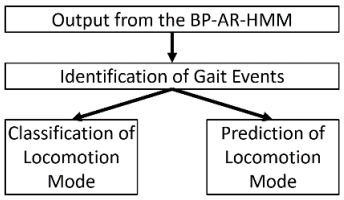

Figure 1: Flow of the data from the BP-AR-HMM to the LSTMs.

Results and Discussion

The output of the BP-AR-HMM identified 100% of the measured gait events from the trials on both days. Initial contact was identified with 4 different states, and toe off was identified with 2 states.

Prediction of locomotion mode is critical for functionally adaptable assisitive devices. However, to make accurate predictions a number of other systems must work, including the identification of gait events and classification of the current locomotion mode. The classification and prediction accuracies from this study are similar to previous work (Table 1) [1,2], with greatly reduced amounts of data needed as input.

Table 1: Classification and prediction accuracies output from two independent LSTMs, combined data from both days.

	Classification (%)	Prediction (%)
Walking	97.8	96.3
Running	92.3	87.8
Stair Ascent	84.2	93.6
Stair Descent	86.1	84.2

A limitation of this study is the system's classifications and predictions do not include ramp output specifically as the ramps the subjects walked on were a maximum of 5% grade, which does not alter limb function enough to elicit a classification difference from level ground walking.

Significance

We have demonstrated that a machine learning system comprised of the BP-AR-HMM (unsupervised) and two LSTMs (supervised) can accurately label gait events from subject independent data, provide classification of locomotion mode and prediction of locomotion mode. The next steps in this work are to implement this system in an assistive device.

References

[1] Joshi, D and Hahn, M., *Ann Biomed Eng,* 44(4):1275-1284, 2016.
[2] Huang, H et al., *J Neural Eng,* 7(5):1-10, 2010.
[3] Fox, E et al, *Ann App Stat,* 8(3):1281-1313.
[4] Long, L and Srinivasian, M., *J R Soc Interface*, 10(4):1-9. 2013

The Impact of Standardized Footwear on Load and Load Symmetry

Adam R. Luftglass[1], Alexander T. Peebles[1], Thomas K. Miller[2], and Robin M. Queen[1, 2]
[1]Granata Biomechanics Lab, Department of Biomedical Engineering and Mechanics, Virginia Tech
[2]Department of Orthopaedic Surgery, Virginia Tech Carilion School of Medicine
Email: adluft@vt.edu

Introduction

Measuring load and load asymmetry during jump-landing tasks has emerged as a promising tool for anterior cruciate ligament (ACL) injury prevention and rehabilitation following an ACL reconstruction. Larger peak vertical ground reaction forces during landing are associated (r = 0.684) with larger peak ACL strains (1) and are prospectively associated with primary ACL injury risk (2). Athletes returning to sport following ACL reconstruction commonly have load asymmetries during landing, which are associated with an increased risk for sustaining a second ACL injury (3). One method to measure load in clinical settings is using force sensing insoles which are wireless, inexpensive, and reliable (4). The loadsol®, a load sensing insole, can measure peak normal force and peak normal force symmetry with high accuracy relative to gold-standard embedded force plates and with high between-day repeatability (4).While load sensing insoles could help translate laboratory biomechanics research into clinical settings, laboratory research typically standardizes footwear across participants, as differences in footwear lead to differences in load outcomes (5). Standardized footwear is likely unavailable in most athletic training and rehabilitation centres, which could pose a challenge when assessing landing kinetics.

Methods

Thirty-seven healthy uninjured participants (20 male/17 female; weight: 68.77 ± 13.49 kg; height: 1.76 ±.08 m) completed 7 bilateral drop vertical jumps from a 30 cm box, jumping horizontally 50% of their body height and 7 unilateral drop landings on each foot, all completed in a randomized order. Participants were asked to bring the footwear that they would normally wear when participating in an athletic activity on a hardwood surface to the testing session. The protocol was completed under 2 conditions in a randomized order: 1) wearing a standard neutral cushioned running shoe (Nike Zoom Pegasus; Nike Inc., Beaverton, OR) and 2) wearing the participant's preferred athletic footwear. Plantar forces were measured bilaterally during each condition using loadsol® sensors sampling at 200 Hz (Novel Electronics, St. Paul. MN). Peak impact force, impulse, peak impact force symmetry (ratio between left and right), and impulse symmetry were computed using a custom-built MATLAB user interface during the first ground impact of both tasks for each condition. All outcomes were normalized to bodyweight and compared between the preferred and standardized footwear conditions using intraclass correlation coefficients (ICC) and paired t-test. Cohen's d was used to quantify the effect size of all observed significant differences.

Results and Discussion

The preferred and standardized footwear conditions showed good to excellent agreement for peak impact force and impulse during both tasks, as well as for peak impact force symmetry and impulse symmetry during the bilateral task (ICC = 0.755 – 0.932, Figure 1. However, agreement was moderate for peak impact force symmetry (ICC = 0.603) and poor for impulse symmetry (ICC = 0.486) during the unilateral landing. Left limb impulse and peak impact force symmetry during the bilateral task and peak impact force during left unilateral landings were significantly different between footwear conditions ($p<0.05$), however the effect size of each difference was small to medium (d = 0.18-0.29). No other significant differences between footwear conditions were observed ($p>0.05$).

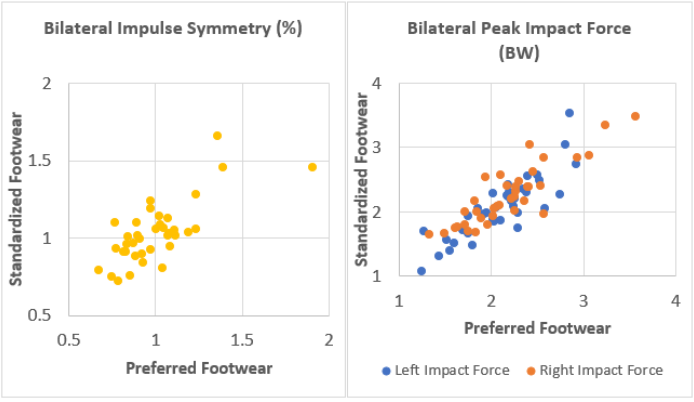

Figure 1: Scatter plots comparing the standardized and preferred footwear conditions. Note: Blue data points represent impact forces for the left limb, and orange data points represent impact forces for the right limb.

The present study found that load outcomes have good to excellent agreement when comparing wearing laboratory-standardized footwear and wearing the participant's own athletic footwear while landing. These results suggest that allowing patients to wear their own footwear when examining landing kinetics in athletic and clinical settings will provide laboratory-relevant landing kinetic information. Load symmetry was not consistent between footwear conditions for the unilateral task, which may reflect increased landing variability during unilateral landing independent of the footwear condition. However, as load and load symmetry during bilateral landing are known risk factors for ACL injuries (2, 3), information pertaining to ACL injury risk could be extracted while using non-standardized footwear.

Significance

The present study demonstrates that quantifying load and load symmetry in settings where standardized footwear is unavailable, will provide relevant information pertaining to the athlete's risk for sustaining an ACL injury.

References

(1) Bakker, et. al, J Orthop, 2016; (2) Leppanen, et. al, AM J Sports Med, 2017; (3) Paterno, et. al, Am J Sports Med, 2010; (4) Peebles, et. al, Sensors, 2018; (5) Queen, et. al, Gait Posture, 2010.

Live Animation Biofeedback Reponses between Children with Autism and Children with Typical Development

Jeffrey D. Eggleston[1], Alyssa N. Olivas[2], Emily A. Chavez[1], Heather R. Vanderhoof[1], Jason B. Boyle[1], Carla Alvarado[3]
[1]Department of Kinesiology, The University of Texas El Paso, El Paso, TX
[2]Department of Biomedical Engineering, The University of Texas El Paso, El Paso, TX
[3]Department of Psychiatry, Texas Tech Health Sciences Center El Paso, El Paso TX
Email: *jdeggleston@utep.edu

Introduction

Recent evidence suggests that nearly 80% of children with Autism Spectrum Disorder (ASD) present with motor impairment [1]. Further evidence suggested children with ASD rely less on visual feedback during movement and rely more on proprioceptive feedback [2]. As such, it has also been observed that children with ASD exhibit greater motor learning when proprioceptive error, not visual error, is present [3]. Given observed motor impairments in this population, motoric output responses to visual live animation biofeedback have largely been understudied.

The purpose of this study was to examine motoric output responses through live animation biofeedback in children with ASD relative to peers with typical development (TD). It was hypothesized that children with ASD will not respond similarly due to deficits in feedback and feedforward processing and sensory stimuli interpretation.

Methods

30 children (15 with ASD and 15 with TD) between the ages of 8 and 17 participated in the study. Parents of children with ASD provided verbal confirmation of ASD diagnosis. Once participant anthropometrics were obtained, participants were outfitted with seven inertial measurement units (IMUs; Noraxon, Scottsdale, AZ) placed on the sacrum, bilaterally on the distal femurs, proximal tibias, and on the dorsal aspect of the feet. Once secured, participants stood still for a 20-sec calibration.

After calibration, participants completed a pre-test consisting of eight bodyweight squats to their preferred depth. Participants were instructed to start with their feet shoulder width apart; no other instructions were provided. Following the pre-test, participants completed a live animation biofeedback training period consisting of five sets of 10 squats while watching an animated skeleton complete a squat. While watching the animation, participants were instructed to replicate the movements of the model. Two-minute rests were given between sets. Then, the post-test was completed consisting of eight bodyweight squats without the animation but to try to replicate the animation as best as possible.

Sagittal plane bilateral hip, knee, and ankle angular joint positions and pelvic position data were exported from Noraxon myoMotion into Visual 3D. Ascent and descent velocity was computed from pelvis data. Mean and standard deviation values for each variable were computed and used for analysis. Dependent t-tests (α=0.05) were used to test for statistical differences between pre- and post-tests values for each individual child. Effect sizes (ES) were also computed and assessed with Cohen's *d*.

Results and Discussion

Statistical significance was observed in nearly every participant when comparing pre- and post-tests angular joint positions (Figure 1). A greater number of ASD participants exhibited statistical significance in lower extremity joint positions, with the exception of the right knee. Examining ES magnitude for lower extremity kinematics, a similar number of large ES (>0.79) were observed in children in both groups.

When comparing ascent velocity pre- and post-test values, a similar number of participants (12 and 13 out of 15, respectively) displayed statistical differences between the groups. Each participant displaying a significant difference also exhibited large ES (>0.79). Descent velocity was the only variable where the number of ASD children was far fewer than children with TD. In total, only 8 of 15 children with ASD displayed statistically significant different descent velocity, compared to 13 of 15 children with TD. Furthermore, all 13 children with TD displayed large ES whereas only 6 of 8 children with ASD displayed large ES.

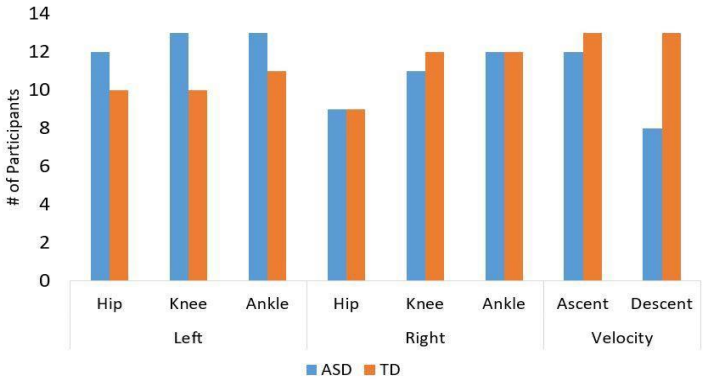

Figure 1. Number of participants who displayed statistically significant differences between pre- and post-tests training.

Significance

Although lower extremity kinematic outcomes were similar between the groups, the differences observed in descent velocity reveal the movement pattern following the live animation biofeedback training, employed by children with ASD was not different than the movement pattern before the training. The limited number of participants with ASD with significant differences in descent velocity are aligned with previously established motor planning impairments [4]. These results support previous findings on learning in the population and expand our understanding on how children with ASD may learn new movements, especially given known motor impairments in the population.

Acknowledgments

This project was funded by the J. Edward Stern and Helen M.C. Stern Foundation and the Department of Kinesiology, UTEP.

References

1. Floris, D.L., et al. (2016), *Molecular Autism*, 7(1), 35.
2. Izawa, J., et al., (2012), *Autism Research*, 5(2), 124-136.
3. Marko, M.K., et al., (2015), *Brain,* 138(3), 363-376.
4. Forti, S., et al., (2011), *Research in ASD*, 5(2), 834-842.

Automated 2D Video Analysis is Reliable for Assessing Knee Kinematics During Landing

Alexander T. Peebles, Sara L. Arena, and Robin M. Queen
Granata Biomechanics Lab, Department of Biomedical Engineering and Mechanics, Virginia Tech
Email: *apeebles@vt.edu

Introduction

Frontal and sagittal plane knee kinematics durng landing are prospectively associated with the risk of sustaining an anterior cruciate ligament (ACL) injury in young athletes and in patients following ACL reconstruction (1, 2). 3D motion capture is not feasible to collect in most non-research settings. Therefore, kinematics are often assessed using 2D video analysis in these settings. There are currently many differences in how kinematics are calculated using 2D video analysis when compared with 3D motion capture. Previous studies visually estimated joint center locations for one or two frames during each landing trial, which is subjectivite and results in reliability issues when comparing 2D video analysis with 3D motion capture during landing (3). Using anatomic markers to estimate joint center locations during a static trial, and automated point tracking software (Automated Video Analysis for Dynamic Systems, AVADS) to digitize markers during movement could improve 2D measurement accuracy (4). This study aimed to explore the validity and repeatability of using automated 2D video analysis to assess frontal and sagittal plane knee kinematics during landing. We hypothesize that 2D video analysis will have good to excellent validity and repeatability.

Methods

24 healthy recreational athletes between 18-30 years of age (12 male/12 female) signed informed consent and participated in this two sessions study. For each session, participants completed 7 forward bilateral drop vertical jumps to a distance of half their bodyheight and 7 unilateral drop landing on each limb, all off a 31 cm box. The first session was completed in a biomechanics lab, where participants wore form fitting athletic clothing and 43 reflective markers. Kinematics were simultaneously assessed at 240 Hz in 3D using a 10-camera motion capture system (Qualisys, Goteborg, Sweden) and in 2D using an iPhone and iPad (Apple, Cupertino, CA). The second session was completed in a university athletic center, where participants wore their own athletic clothing and 6 reflective markers (bilaterally on the lateral aspect of thigh, femoral epicondyle, and shank aligned in the frontal plane). Kinematics were recorded at 240 Hz in 2D only using an iPhone and iPad.

Knee flexion and frontal plane projection angle (FPPA) were computed using the 3D motion capture data (1, 2). Using the 2D video data, two methods were used to estimate joint center locations on the first frame of the static trial. For the first method, termed *2D Manual*, joint centers were digitized manually using visual landmarks (e.g. the patella) (3). For the second method, termed *2D Computed*, joint centers were determined objectively based on anatomically placed markers. Specifically, in the frontal plane, knee and ankle joint centers were estimated as the midpoint between medial and lateral joint markers and the hip joint center was estimated based on the work by Bell et al. (5). In the sagittal plane, the greater trochanter, femoral epicondyle, and malleoli were used to estimate joint centers (4). *2D Manual* was used to estimate joint center locations for each testing session and *2D Computed* was used for the first session only. For both methods, the lateral thigh, knee, and shank markers were used as tracking markers during motion, and were also digitized during the static trial. For both methods, and in both planes, an offset angle between a line connecting estimated joint centers and a line connecting tracking markers was created during quiet stance. The lateral thigh, knee, and shank markers were then automatically tracked throughout each video using AVADS (4), and the offset angle determined during stance was used to compute continuous segment orientation during landing. Outcomes included were peak flexion, peak FPPA (valgus), and knee flexion and FPPA range of motion. Outcomes were compared between 3D motion capture and both 2D methods (validity) and between days for *2D Manual* only (repeatability) using intraclass correlation coefficients (ICC) and paired t-tests.

Results and Discussion

Both methods had good to excellent validity, and *2D Manual* had good to excellent between-day repeatability (Table 1). As the agreement between 3D motion capture and both methods of 2D video analysis were stronger than previously reported (3), we suggest estimating joint centers during quiet stance and using automated software to track segment motion. As validity ICCs were higher for *2D Computed* than *2D Manual*, we suggest using anatomic markers to objectively estimate joint centers. However, as range of motion validity was the same between 2D methods, estimating joint centers is not needed for range of motion. Differences between 3D motion capture and both 2D video analysis methods were observed for each outcome ($p<0.05$), which is consistent with previous video analysis literature (3, 4).

	2D Comp Validity	*2D Manual* Validity	2D Manual Repeatability
Bilateral peak flexion	0.973	0.969	0.915
Bilateral flexion ROM	0.978	0.978	0.950
Bilateral peak FPPA	0.877	0.847	0.760
Bilateral FPPA ROM	0.912	0.912	0.907
Unilateral peak flexion	0.968	0.960	0.929
Unilateral flexion ROM	0.979	0.979	0.938
Unilateral peak FPPA	0.907	0.927	0.889
Unilateral FPPA ROM	0.882	0.882	0.887

Table 1: Validity and between-day repeatability ICCs.

Significance

This study developed a method to assess knee kinematics which is valid, repeatable, and feasible for use in non-research settings.

Acknowledgements

This project was financially supported by the Virginia Tech Graduate Student Assembly.

References

(1) Leppanen et al., AJSM, 2017; (2) Paterno et al., AJSM, 2010; (3) Belyea et al., J Sport Rehab, 2015; (4) Peebles et al., In review at ABME; (5) Bell et al., HMS, 1989.

Discrete Projection and Similarity Analysis in Total Ankle Replacement Patients

Cherice N. Hughes-Oliver [1], Shane Ross [2], Robin M. Queen [1]
[1] Department of Biomedical Engineering and Mechanics, Virginia Tech, Blacksburg, VA, USA
[2] Department of Aerospace and Ocean Engineering, Virginia Tech, Blacksburg, VA, USA
Email: cnh4ph@vt.edu

Introduction

Gait asymmetry has been associated with risk of injury and accelerated disease progression, making it an important area to assess clinically. Data discretization, which is commonly performed when evaluating asymmetry, results in limited interpretation and lost scope of analysis. As opposed to data discretization, analysing continuous data expands the scope of analysis to the entire time series and prevents the loss of potentially important data. Previously developed methods of analyzing continuous data such as the Coefficient of Multiple Correlations[1] and Statistical Parametric Mapping[2] either cannot be used in pathologic populations with abnormal movement patterns or are not defined in concise enough terms to be easily incorporated in clinical care.

The purpose of this study was to develop a method of describing asymmetry in continuous time series data using simple and clinically accessible scores. Total ankle arthroplasty (TAA) patients were used as the clinical test case.

Methods

Pre-operative vertical ground reaction force (vGRF) data from 120 unilateral post-traumatic TAA patients were obtained from a previously collected data set. Additional vGRF data was collected from 54 healthy older adults within the age range of the TAA patients. For computational purposes, we approximated each continuous time series as 101 equally-spaced points. Two scores were developed and computed to assess asymmetry and movement quality: the symmetry score (SS) and closeness-to-healthy score (CTH).

The symmetry score evaluated the similarity of the vGRF between limbs [Eq 1]. Healthy dissimilarity (N) between limbs was computed from the control data as the average Euclidean length of the difference in the vGRF between limbs. TAA and control curves were normalized to the healthy dissimilarity to maximize interpretability of results. The SS was computed as the Euclidean length of the distance between the normalized curves. Small SS indicates greater side-to-side symmetry.

The closeness-to-healthy score evaluated the similarity of the vGRF to that of a healthy population [Eq 2]. First, an average vGRF curve was computed from the control data. The healthy average and vGRF curves on both limbs in TAA patients and controls were normalized by their Euclidean lengths. The CTH score was computed on each limb separately as the dot product of the normalized average healthy curve and the normalized curve of interest subtracted from one. Small CTH scores indicate vGRF similar to what would be expected in a healthy individual.

SS and CTH scores were compared between TAA patients and controls using unpaired t-tests and Cohen's D effect sizes [JMP Pro 15,α=0.05]. Surgical (S) and non-surgical (NS) limbs for TAA patients were compared to non-dominant(ND) and dominant(D) limbs, respectively, for controls.

$$SS = norm\left(\frac{\overrightarrow{vGRF}_{NS/D}}{N} - \frac{\overrightarrow{vGRF}_{S/ND}}{N}\right) \quad [1]$$

$$CTH = \left(1 - \frac{\overrightarrow{vGRF}}{norm(\overrightarrow{vGRF})} \cdot \frac{\overrightarrow{vGRF}_{average\ healthy}}{norm(\overrightarrow{vGRF}_{average\ healthy})}\right) * 100 \quad [2]$$

Results and Discussion

TAA patients had higher SS and CTH scores on both limbs compared to controls [SS: $p<0.001$, $d=0.953$, | CTH (S/ND): $p<0.001$, $d=1.179$, | CTH (NS/D): $p<0.001$, $d=0.986$) (Figure 1). These results align with prior literature demonstrating greater asymmetry and more abnormal gait patterns on the surgical limb pre-surgery in TAA patients[3,4].

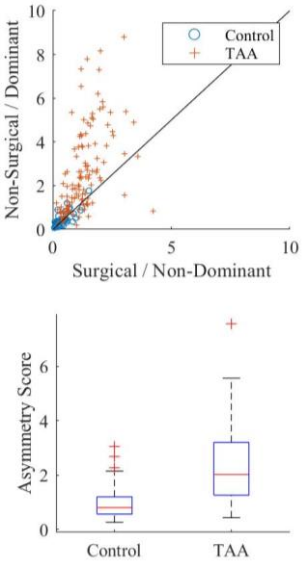

Figure 1: SS and CTH for healthy controls and TAA

Conceptually, the SS and CTH scores have important clinical implications when evaluating disease progression and surgical recovery. Combined with clinically accessible motion analysis methods such as accelerometers or in-shoe pressure sensors, both scores could be used to evaluate patients' movement quality prior to disease diagnosis, throughout disease progression, and during rehabilitation to monitor recovery. Results could be utilized in clinical decision making to assess urgency for surgical intervention and whether a rehabilitation protocol can effectively target specific asymmetries.

Significance

Two scores related to movement asymmetry have been developed and are able to differentiate between healthy controls and TAA patients. These scores could provide clinicians with another tool to objectively assess movement asymmetry and quality from continuous kinetic and kinematic data. These scores could be used to track asymmetry and movement quality throughout disease progression and recovery after surgery.

Acknowledgments

TAA data was initially collected at Duke University. The Howard Hughes Medical Institute Gilliam Fellowship funded Cherice Hughes-Oliver during this project.

References

[1]Kadaba, M. P., et al. (1989). *J. Orthop. Res.*, *7*(6), 849–860. [2]Pataky, T. C. (2010). *J. Biomech.*, *43*(10), 1976–1982. [3]Schmitt, D., et al. (2015). *Gait & Posture*, *42*(3), 373–379.[4]Valderrabano, V., et al. (2007). *Clin Biomech (Bristol, Avon)*, *22*(8), 894–904.

Comparative Effects of Abdominal Breathing and Dynamic Neuromuscular Stabilization Breathing on Diaphragmatic Movement and Pulmonary Function in Chronic Obstructive Pulmonary Disease

Jongseok Hwang[1], JungKi Hoon[1], and Joshua (SungHyun) You[1]
[1] Sports Movement Artificial Robotics Technology(SMART) Institute, Department of Physical Therapy, Yonsei University, Wonju, Republic of Korea
Email: joshuayou@gmail.com

Introduction

Chronic obstructive pulmonary disease (COPD) is a common chronic pulmonary functional impairment and fourth leading cause of death. It is known that diaphragmatic dysfunction is an important deleterious consequence of the progression of the severity of COPD. The purpose of the present study was to compare a novel Dynamic neuromuscular stabilization (DNS) breathing and abdominal breathing (AB) on diaphragm movements and pulmonary functions in patients with COPD.

Methods

10 COPD patients randomly assigned to two groups; DNS breathing group and AB group. The present study used a two group pretest-posttest design. In this research, COPD patients underwent fluoroscopy-guided chest X-ray (Figure 1), pulmonary function tests, and modified Medical Research Council (mMRC) questionnaire in before and after training. Each group underwent comprehensive AB or DNS of pulmonary breathing exercise 5 time per week during 7 weeks (30 minutes per session). A paired t-test and independent t-test and Wilcoxon Signed rank were used to analyze data.

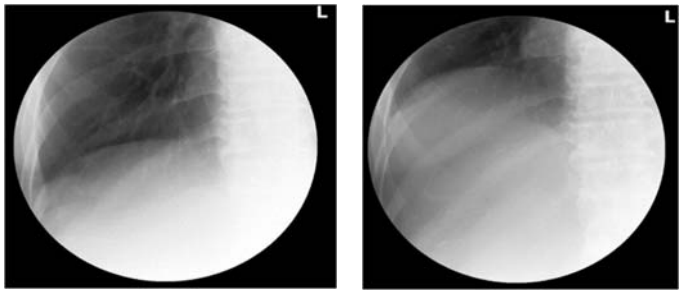

Figure 1: Radiographic image of the area displaced by diaphragmatic movement during inspiration and expiration for the same chronic obstructive pulmonary disease patient

Results and Discussion

There were significant improvements in diaphragmatic movements during full inspiration and expiration in the both group fluoroscopy. (48161.80±25137.42mm² to 75346.00±24394.66mm²; AB Right side P=0.015 and 95027.40±11306.21mm² to 155543.40±50163.74mm²; DNS Left side P=0.033, 69892.60±14686.71mm² to 199941.40±26005.88mm²; DNS Right side P=0.001, respectively) Pulmonary function tests indicated that the only DNS presented statistically significant differences in forced vital capacity (FVC) (%) (P=0.024) and the first second of forced expiration (FEV1) (%) (P=0.000) between pre-test and post-test. The DNS group gained enhanced FVC (P=0.028) and FEV1 (%) (P=0.015) than the AB group. The mMRC score showed significant differences between pre-test and post-test (2.60±0.89 to 1.80±0.44; P=0.016).

This study suggests that the DNS breathing had superior effects compared with the AB in diaphragm movement and pulmonary function in patients with COPD. Our results provide promising evidence that DNS breathing techniques improved diaphragm movement, pulmonary function during pulmonary rehabilitation, and strength while inhale breathing.

Significance

Our results provide promising evidence that DNS breathing techniques improved diaphragm movement, pulmonary function during pulmonary rehabilitation, and strength while inhale breathing.

Acknowledgments

References

[1]Andrade AD, Silva TN, Vasconcelos H, Marcelino M, Rodrigues-Machado MG, Filho VC, et al. Inspiratory muscular activation during threshold therapy in elderly healthy and patients with COPD. J Electromyography Kinesiol. 2005;15(6):631–639.
[2] Begin P, Grassino A: Inspiratory muscle dysfunction and chronic hypercapnia in chronic obstructive pulmonary disease. Am Rev Respir Dis 1991, 143:905-912.
[3] Barreiro E, Bustamante V, Cejudo P, et al. Guidelines for the evaluation and treatment of muscle dysfunction in patients with chronic obstructive pulmonary disease. Arch Bronconeumol 2015;51:384-95.
[4] Breslin EH, Garoutte BC, Kohlman-Carrieri V, Celli BR. Correlations between dyspnea, diaphragm and sternomastoid recruitment during inspiratory resistance breathing in normal subjects. Chest. 1990;98(2):298–302.
[5] Cahalin LP, Braga M, Matsuo Y, Hernandez ED. Efficacy of diaphragmatic breathing in persons with chronic obstructive pulmonary disease: a review of the literature. J Cardiopulm Rehabil. 2002;22(1):7–21.
[6] Eun Mi Chun, Soo Jeong Han, Hitesh N Modi. Analysis of diaphragmatic movement before and after pulmonary rehabilitation using fluoroscopy imaging in patients with COPD. international Journal of COPD. 2015;10(1) 193-199.
[7] F. Lötters, B. van Tol, G. Kwakkel, R. Gosselink Effects of controlled inspiratory muscle training in patients with COPD: a meta-analysis. European Respiratory Journal. 2002 20: 570-577;
[8] Langer D, Hendriks E, Burtin C, et al. A clinical practice guideline for physiotherapists treating patients with chronic obstructive pulmonary disease based on a systematic review of available evidence. Clin Rehabil. 2009;23(5):445

Lower Extremity Biomechanics during Running in Persons Who are Blind: A Preliminary Report

Hunter J. Bennett[1], Kevin A. Valenzuela[2], and Justin A. Haegele[1]
[1]Old Dominion University, Norfolk, VA
[2]California State University Long Beach, Long Beach, CA
Email: *hjbennet@odu.edu

Introduction

Walking and running are the most common modes of physical activity for individuals who are blind (visual acuity <3/60) [1]. Although biomechanics research has extensively examined gait in sighted healthy (from young to old), clinical, injured, and athletic populations, little research has involved persons with blindness [2-4]. Research has found persons with differing levels of visual impairments walk at reduced speeds, with shorter stride lengths, reduced ranges of motion, and with more mechanical work than sighted controls [2-4]. However, no previous research has examined biomechanics of running in persons who are blind. Therefore, the purpose of this preliminary study was to determine if lower extremity kinematics and kinetics differ in persons who are blind compared to sighted controls. We hypothesized persons who are blind would run with shorter strides and reduced joint kinematics.

Methods

Four persons who are blind (ages 14, 23, 28, and 47 yrs.) and four matched sighted controls (age, sex, and body mass index matched) participated in this study. A ten-camera three-dimensional motion capture system and force platforms recorded lower extremity kinematics and ground reaction forces during level running over an 18 m runway. A warmup of walking and running at self-selected speeds was performed by all participants. For testing, persons who are blind ran independently (with/without cane dependeing on preference) at their own comfortable, self-selected speeds. All recorded trials were within ± 5% of their average speeds (group average: 2.7±0.8 m/s). Sighted controls performed running at matched speeds. Marker and ground reaction force data were imported into Visual3d and filtered at 10 Hz using a 4th order butterworth low-pass filter. Stride length and ankle, knee, and hip ranges of motion (max-min) and peak moments were compared between groups using t-tests.

Results and Discussion

Contrary to the shorter stride lengths during walking found in previous reports [2-4], this preliminary study found no differences between persons who are blind and sighted controls when running at matched speeds (1.8±0.7 vs. 2.1±0.5m, respectively, $p>0.05$). As work within the previous literature did not control for speed or anthropometric differences, it is likely previous results are confounded due to these influential measures.

In addition to stride length, we found no differences in ranges of motion or peak moments for the ankle, knee, or hip joints (Figures 1 & 2; all $p>0.05$). Given the lack of differences found in this preliminary study, it appears fundamental lower extremity mechanics are robust even without a history of visual learning. In this respect, research regarding running in persons with congenital blindness could enhance our understanding of the relationships of visual feedback, propriocepton, and central pattern generators with human locomotion.

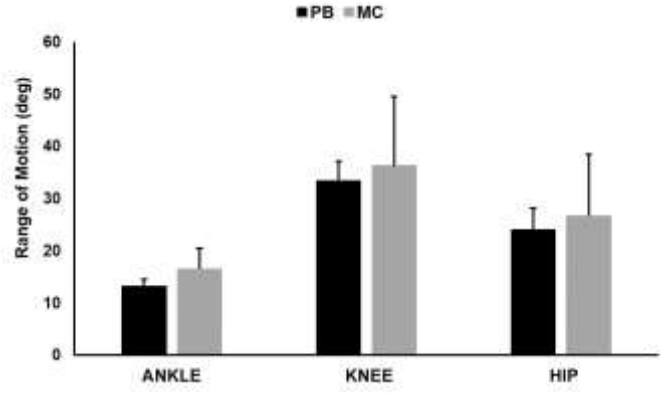

Figure 1: Comparisons of ankle, knee, and hip ranges of motion. PB: particpants who are blind. MC: matched sighted controls. No differences were found for any range of motion variable.

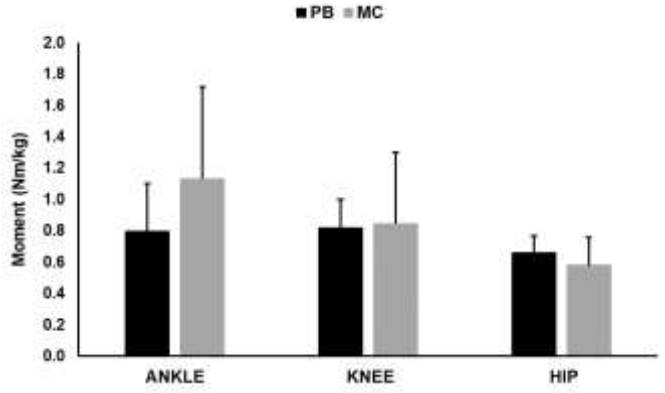

Figure 2. Peak extensor joint moments. For ease of vieiwng, ankle (plantarflexor) and hip moments were plotted as positive. PB: participants who are blind. MC: matched sighted controls. No differences were found in any joint moment.

Significance

Although proper running mechanics are not formally taught in structured physical activity contexts (e.g., physical education settings) for persons who are blind [5], these results suggest only minor therapeutic and rehabilitative intervention programming is actually needed. Programming may only truly be needed to increase a person's comfort and familiarity with running in their environment/surroundings.

References

1. Jaarsma, E.A. et al. 2014; *Adap Phys Activ.* 31
2. Bennett, H. J. et al. 2019; *Hum Mov.* 20
3. Hallemans, A. et al. 2010; *Gait & Posture.* 39
4. Nakamura, T. 2009; *Disabil Rehabil.* 19
5. Holland, K. et al. 2020; *Adap Phys Activ.* In Press

Biomechanics In The Real World: Design and Evaluation of a Clinical Balance Tool

Ajit M.W. Chaudhari, Virginia M. Yazzie, Lise C. Worthen-Chaudhari, and Jennifer H. Garvin
The Ohio State University
Email: Chaudhari.2@osu.edu

Introduction

Falls are a significant source of early morbidity and mortality in the aging population, yet the neurological, sensory, and motor changes that lead to increased fall risk often escape early identification and intervention. Vital signs (VS) are commonly used in clinical settings to (1) establish baseline values when initiating care, (2) screen for increased risk of co-morbidities or diseases, and (3) allow for identification and communication of changes from baseline between health care professionals across time and locations.[1] No VS exists for assessing the balance system. Both clinical tests like the Romberg and quantitative measurements of balance like postural sway have been shown to predict increased fall risk,[2, 3] but they are not common practice in primary care settings. Biomechanists and physical therapists have performed these tests for decades, yet unidentified barriers prevent their use in physician clinics, especially in primary care.

This qualitative research study aimed to identify barriers preventing adoption of a biomechanical, quantitative postural control measurement (qPCM) of balance for fall risk prediction and to identify the design requirements that minimize these barriers to facilitate future use of a quantitative balance tool.

Methods

In this IRB-approved descriptive formative evaluation study, we conducted two rounds of semi-structured interviews in the participants' clinical practice setting. We explored barriers to assessing fall risk and barriers to use of a prototype tool in terms of hardware and software, workflow and communication, and clinical content. We gathered initial information to identify requirements and assess workflow. Participants were able to use an initial and then a modified prototype with clinical scenarios for formative evaluation and usability assessment. Following initial interviews, we modified the prototype and undertook a second set of interviews for further iterative design. We explored the features end users need so that a clinical qPCM tool could be incorporated into a clinical routine for every patient and results used in clinical decision making. We explored alignment of our tool with processes used currently with weight measurement devices. We also assessed the usability of the device in the clinical setting using the System Usability Scale (SUS).[4]

Interview participants were all potential intended users of the device in the medical clinic setting including: (a) medical assistants/physician extenders (n=8), (b) nurse practitioners (n=2), and (c) physicians (n=8) from both academic medical centers and private independent clinics. Five were male and 13 were female. Observations were captured using written notes and audio/video recordings that were later transcribed for analysis.

Results and Discussion

Several common themes and practices emerged from the first round of interviews with the providers. All 18 providers measure weight as a vital sign in some patients, but only 12 reported taking one or more vital signs on every patient at every visit. Only 4/18 reported always asking patients to remove their shoes when measuring weight. While only providers concerned about falls were included, only 9/18 providers reported asking patients specific questions regarding fall risk. 9/18 providers reported watching the patient's gait from the waiting room to the examination room as a primary assessment of fall risk. Half of the participants knew or had heard of one or more of the nationally promoted fall risk algorithms from CDC (STEADI), Johns Hopkins University (JHFRAT), or the American Geriatric Society. No providers reported regularly using a standard functional test such as the Timed Up & Go, 30-second Chair Stand, or 4-Stage Balance Test recommended by the CDC, though one physician who typically treats patients with lower-extremity concerns reported having "all of them stand up and try to balance on one leg, or do a one leg squat, and you can tell pretty quickly if they're unsteady, and then watch them walk."

Several barriers for use were identified from the first round of interviews as well. These included time, space, and interpretation of results. Time was unanimously identified as a barrier, because in these care settings the providers are attempting to manage patients who could have many comorbid conditions and the chief complaint (e.g. hypertension, diabetes, prior injurious fall) often guided the encounter. Importantly physicians and nurse practitioners felt it was practicable to add another test to their patient interaction. Space was also identified as a barrier. 16/18 providers reported that weight was measured at a central "vitals station" or "triage room," and these stations generally were only big enough for a weight scale and chair. Another important barrier was interpretation of a complex set of numbers – several providers preferred a device that reports a single number with a scale to interpret it.

In response to the aforementioned, two prototypes of the clinical balance tool were developed and tested. The final balance tool can take the place of a weight scale at a vitals station, and delivers a single balance score along with the patient's weight after 30 seconds. A quick reference card was designed to assist in administering the test and interpretation. The final tool achieved a mean SUS score of 86.8, the 94th percentile, indicating a system with excellent usability.[5]

Significance

This study demonstrated that a quantitative clinical balance tool can meet the needs of users in a primary care clinic setting and has a strong chance of broad adoption. Current work focuses on determining if the tool informs clinical decision-making.

Acknowledgments

NIA R42AG062065, awarded to Bertec Corporation

References

1. Flaherty JH, et al. J Am Med Dir Assoc. 2007;8(5):273.
2. Agrawal Y, et al. Otol Neurotol. 2011;32(8):1309.
3. Maki BE, et al. J Gerontol. 1994;49(2):M72.
4. Brooke J. In: Jordan PW, et al., eds. Usability evaluation in industry. 1st ed. 1996. p. 189.
5. Bangor A, et al. International Journal of Human–Computer Interaction. 2008;24(6):57

Lower Limb Kinematic Asymmetries and Correlation to Clinical Measures in Individuals with Parkinson's Disease

Graci Finco[1], Sarah Moudy[1], Kendi Hensel[1], Evan Papa[2], Nicoleta Bugnariu[1], Rita M. Patterson[1]
[1]University of North Texas Health Science Center, Fort Worth, TX [2]Idaho State University Health Science Center, Meridian, ID
Malaka.Finco@my.unthsc.edu

Introduction

Gait asymmetries have been directly linked to the development of freezing of gait in individuals with Parkinson's Disease (PD),[1] and freezing of gait has been associated with increased falls.[2] Therefore, reducing gait asymmetries can reduce the development of freezing of gait and decrease fall risk.

Greater gait asymmetry has been shown in kinematic rather than kinetic parameters in individuals with PD.[3] However, previous literature in kinematic asymmetry has focused on spatiotemporal parameters, and has not grouped participants by progressive stages of PD. Investigating range of motion (ROM) asymmetries and their correlation to clinical measures may inform rehabilitation techniques to limit the onset and prevalence of freezing of gait and decrease falls.

This study aimed to: 1) compare kinematic asymmetries in three groups: individuals affected with PD unilaterally (UNI), bilaterally (BI), and matched controls, and 2) correlate asymmetries to scores on three clinical measures: the Hoehn and Yahr (H&Y) scale of progression, Unified Parkinson's Disease Rating Scale (UPDRS) of severity, and Timed Up and Go Test (TUG). We expected greatest asymmetry in UNI participants, and strongest correlations to clinical measures in BI participants.

Methods

Participants with PD and matched controls for age and sex (C) (n=10 each group) ambulated at a self-selected speed for two minutes on a treadmill as part of a larger data set, and kinematics were processed in Visual 3D. PD participants were grouped based on their H&Y score of UNI (1-1.5) or BI (2-3) involvement (n=5 each group). Overall ROM for each joint was averaged from ten steps of each participant's dominant limb (DL) and non-dominant limb (NDL), and waveforms of one gait cycle were averaged for each group (Fig.1). Percent differences assessed interlimb percent asymmetry (IPA), and correlations determined relationships between IPA and clinical measures (Tables 1-2).

Results and Discussion

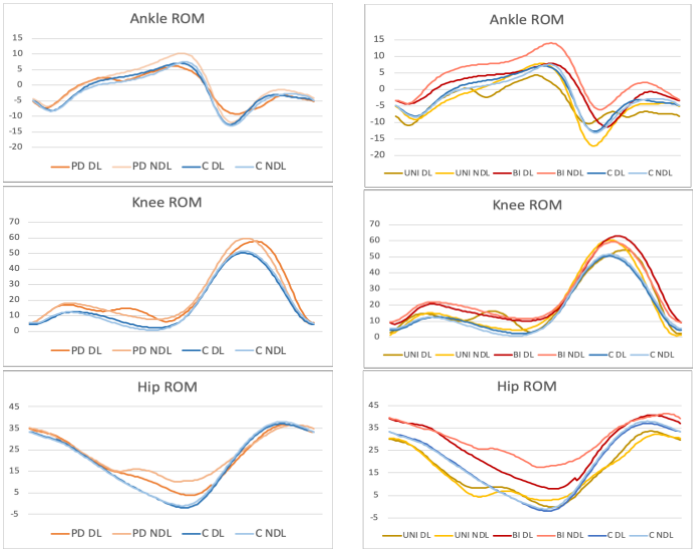

Fig.1A-F: Left: All ten PD participants compared with C participants. Right: UNI and BI PD participants compared with C participants.

Consistent with previous research, participants with PD had greater interlimb asymmetry than matched controls.[4] BI participants had greatest ankle and hip asymmetry, and showed reduced ankle plantarflexion and hip extension compared to the UNI and C groups. Increased plantarflexion and hip extension in UNI compared to BI participants may be explained by the rigidity in the late stages of PD.

UNI PD	Ankle IPA	Knee IPA	Hip IPA	H&Y Score	UPDRS	TUG
Ankle IPA	1					
Knee IPA	-0.424	1				
Hip IPA	0.881	-0.195	1			
H&Y Score	0.783	-0.462	0.817	1		
UPDRS	0.439	0.489	0.684	0.538	1	
TUG	0.694	-0.771	0.663	0.588	-0.081	1

BI PD	Ankle IPA	Knee IPA	Hip IPA	H&Y Score	UPDRS	TUG
Ankle IPA	1					
Knee IPA	0.172	1				
Hip IPA	-0.362	0.519	1			
H&Y Score	-0.514	0.139	0.918	1		
UPDRS	-0.024	-0.381	-0.871	-0.823	1	
TUG	-0.494	-0.013	0.846	0.985	-0.811	1

Tables 1-2: Weak (0-.3), moderate (.3-.7), and strong (.7-1) correlations of IPA to clinical measures in UNI (top) and BI (bottom) participants.

Lower limb IPAs were not strongly correlated with performance on clinical measures, with the exception of strong correlations between hip IPA to clinical measures in BI participants. In UNI participants, ankle and hip IPA were strongly correlated to H&Y score, while knee IPA was strongly correlated to the TUG. Clinical measures were strongly correlated with each other only in BI participants, indicating these measures better reflect the functional mobility of this group.

Significance

Future research of gait asymmetry in this population should consider dividing PD participants into groups based on H&Y score of unilateral or bilateral affectedness, since asymmetries between these two groups had marked differences.

Gait deviations and performances on clinical measures are factors in establishing rehabilitation techniques for individuals with PD and monitoring improvement. Performance in these clinical measures did not accurately reflect gait asymmetry, except in hip IPA with BI participants. Other clinical measures that better reflect overall IPA in both UNI and BI groups need to be determined to target rehabilitation techniques to reduce gait asymmetry, freezing of gait, and fall risk.

Acknowledgments

Thanks to Shelby Alfred and Ty Templin for data collection, and to the American Osteopathic Association for funding this project.

References

[1] Frazzitta et. al. 2012. *J Neurol.* 260(1).
[2] Bloem et. al. 2004. *Movement Disord.* 19(8):871-84.
[3] Villar et. al. 2018. *Sensors.* (18):4224.
[4] Sofuwa et. al. 2005. *Arch Phys Med Rehabil.* (86):1007-13.

Core Stability in Patients Awaiting Hernia Repair

Ajit M.W. Chaudhari, Savannah M. Renshaw, Lindsay M. Breslin, Torri L. Curtis, Melissa D. Himes, Benjamin K. Poulose
The Ohio State University
Email: chaudhari.2@osu.edu

Introduction

The abdominal core serves several functions for balance, movement, and strength. Disruptions or injury to this area, such as ventral hernia and subsequent repair (VHR), can have life-long consequences for patients' quality of life, return to work, pain, and functional status which makes it essential to understand in the VHR disease process.[1] Core stability is a measure of the body's ability to control the torso following perturbations and how well the muscles of the hips, lumbar spine, and abdominal core work together to perform functions of movement.[2] Currently, few methods exist for measuring core stability in the outpatient clinic setting. We developed the Quiet Sitting Test (QST) to evaluate the activation and performance of the core musculature by providing quantitative measures of core stability, separate from core strength, that allow for assessing and tracking core stability for patients over time.[2]

As the next step in the development of the QST, the purpose of this study was to test whether QST scores of patients awaiting hernia repair differ from healthy individuals without a hernia.

Methods

Sixty-three participants were prospectively recruited with IRB consent from individuals at our hernia clinic either as a patient, a companion, or a staff member (Table 1). No companions or staff members had a history of hernia. Data from the first 32 hernia-free control participants were used to establish normative values for the QST, while data from the subsequent 31 participants (with hernia and controls) were used to test the hypothesis.

QST was performed by having participants sit on the rounded surface of a BOSU® balance trainer that had been placed on top of a portable force plate (Bertec BP5046) and situated on a flat, elevated surface. Participants sat unmoving for three 60-second trials with their eyes closed while counting backwards, and the force plate measured sway at 1000Hz. The counting task prevented hyper-focus on staying still, thereby resulting in more accurate measures. Specific QST outcome measures included center of pressure path length (COPexc). After calculating the mean and trial-to-trial variation (i.e. 95% confidence interval of the standard error of measurement, SEM_{95}) of COPexc in the first 32 participants, we calculated a composite core stability score based on the absolute difference from the normative population mean in multiples of SEM_{95}, where 6 represents normal and <6 indicates worsening core stability, as we have previously reported.[3] This score was then calculated for the 31 participants in the test group and the difference between hernia and control groups tested using a nonparametric two-tailed Wilcoxon exact rank sums test.

	N	Median Age, y (Range)	Mean COPexc (mm)	SEM_{95} (mm)
Normative	23F, 9M	45.5 (20-62)	411.6	64.4
Control	13F, 6M	33 (23-62)		
Hernia	3F, 9M	54.5 (38-85)		

Table 1. Demographics of the group used to define QST normative values including mean, SEM_{95}, and composite core stability score; and the two groups tested using the QST.

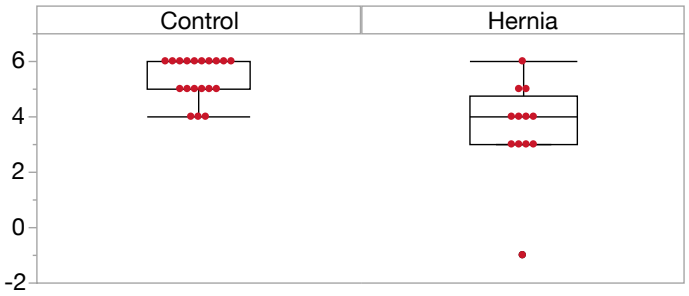

Figure 1: Distribution of QST composite score for control participants and hernia patients awaiting surgical repair. A score of 6 indicates being within normal limits of core stability, while scores <6 indicate poorer core stability.

Results and Discussion

The hernia group demonstrated significantly worse core stability than the control group (Fig. 1, p=0.0004). Ventral hernia disrupts the structure of the anterior abdominal wall in addition to causing pain, so further examination of this group longitudinally is warranted to test the degree to which the poorer core stability is a neuromuscular adaptation to pain or to reduced force-generating capacity of the muscles.

This study also demonstrates the feasibility of quantitatively measuring core stability in the clinic setting. All participants were tested within a fully-operating hernia clinic, and all patients and companions were tested while they awaited their appointment. This confirmation of feasibility in this setting is critical to future exploration of the role of core stability in the natural history of hernia, repair, and rehabilitation, because it would be impracticable to bring large numbers of patients to a research laboratory at multiple timepoints.

We note several limitations to this study. First and most importantly, the normative values we report are not based on function in activities of daily living or quality of life, so validation and minimal clinically important differences must still be established. Second, the gender and age distributions of the groups are a potential source of bias, as the hernia group was more male and older than the other groups (Table 1).

Significance

The QST will be further evaluated as an adequate surrogate marker for improvement in abdominal core related interventions, including hernia repair, that supplements patient-reported outcomes. QST data may also help inform injury prevention and rehabilitation guidelines that can be tailored to the unique needs of VHR patients.

References

1. Poulose BK, et al. Hernia. 2012;16(2):179.
2. Chaudhari AMW, et al. Med Sci Sports Exerc. 2019.
3. Renshaw SM, et al., SAGES 2020; 2020 April 1-4.

Evaluation of Running Biomechanics, CHAMP Performance, and Patient Reported Outcomes of Servicemembers with Lower Extremity Fracture Utilizing an IDEO

Trevor Kingsbury[1], Shian Liu Peterson[1], Tatiana Djafar[1], Julianne Stewart[1], Kevin Kuhn[1]
[1]Naval Medical Center San Diego, San Diego, CA
Email: *trevor.d.kingsbury.civ@mail.mil

Introduction

Fractures represent a high percentage of reported injuries in the US military and can be a substantial threat to a servicemember's (SM) career. A review of literature indicates that fractures represent between 12-65% of combat injuries with a high percentage of open fractures (50%+) and at the tibia/fibula[1]. From 2000-2006, there were 157,096 ankle and 92,581 foot injuries in just the US Army[2]. Many of these SMs have pain and functional deficits after surgery and physical therapy, and some consider amputation. The Intrepid Dynamic Exoskeletal Orthosis (IDEO) has provided an alternative to amputation for patients who wish to continue high level functional activities. Patients complete a 4 week Return to Run (RTR) training program to learn to properly utilize the device. The device is typically worn during high level functional activities to reduce pain and enhance training capacity. **The purpose of this study is to evaluate running biomechanics, functional performance, and quality of life outcomes for SMs prescribed an IDEO for a lower extremity (LE) fracture and compare them to healthy military runners**.

Methods

A retrospective data analysis was conducted utilizing a registry protocol (NMCSD.2014.0026). Patients must have been fit with an IDEO at Naval Medical Center San Diego (NMCSD), have completed the RTR program, and have undergone a 3-D running analysis at a self-selected speed at the completion of the program. Ten SMs with lower extremity fracture who utilize an IDEO for running (29±5 years old, 1.79±0.05 m, 91±12kg) were compared to 15 healthy military runners (32±7 years old, 1.78±0.06 m, 82±8kg). Running time distance parameters, frontal and sagittal plane biomechanics of the trunk and pelvis during running, Short Musculoskeletal Function Assessment (SMFA), 4 Square Step Test (4SST), and CHAMP scores were analysed for all groups. A one-way ANOVA was run to determine differences between the two groups ($p < 0.05$).

Results and Discussion

Descriptive statistics for all running variables are reported in Table 1. Compared to healthy runners, the IDEO patients exhibited significantly less lateral trunk motion during running. IDEO runners also had trends towards shorter step lengths and higher cadence, both of which are taught in the training program. It is noteworthy that IDEO users achieved similar self-selected running speeds and had very low standard deviations in cadence specifically. SMs using an IDEO reported SMFA scores of 23.6±13.9 for Daily Activities, 41.2±19.7 for Emotional, 33.3±18.6 for Mobility, 24.7±12.3 for Function Index, and 25.0±13.6 for Bother Index. These scores are better than the Limb Salvage cohort from the METALs study[3] but significantly worse compared to the controls. This continues to show improved patient reported outcomes for SMs with an IDEO compared to those without. CHAMP performance test consisted of four scores for IDEO SMs: single limb stance (39.2±9.4 s), T-Test (15.4±2.2 s), Illinois Agility test (15.4±1.8 s), and Edgren Side Step test (20.0±3.2 m). While IDEO users performed poorer than controls, they performed similar to the 75th percentile of patients with amputation as reported previously[4]. 4SST (5.3±1.0 IDEO vs 4.5±1.0 control) was not significantly different.

Table 1: Descripive Statistics for Running Biomechanics, significant differences are in bold.

Variable	Group	Mean	StDev	F Stat	Sig
Velocity (m/sec)	$IDEO_F$	3.85	0.23	1.19	0.29
	Control	4.04	0.51		
Cadence (step/min)	$IDEO_F$	177.45	6.69	0.93	0.34
	Control	163.31	45.62		
Stride Length (m)	$IDEO_F$	2.62	0.19	2.49	0.13
	Control	2.77	0.26		
Aff Step Length (m)	$IDEO_F$	1.31	0.09	2.77	0.11
	Control	1.39	0.14		
UnAff Step Length (m)	$IDEO_F$	1.31	0.10	2.96	0.10
	Control	1.39	0.13		
Trunk Lateral Flexion Stance Max	***$IDEO_F$***	***3.30***	***1.77***	***12.69***	***0.00***
	Control	***6.05***	***1.97***		
Trunk Lateral Flexion Total Excursion	***$IDEO_F$***	***7.91***	***2.01***	***8.19***	***0.01***
	Control	***10.82***	***2.76***		
Trunk Forward Flexion Stance Max	$IDEO_F$	14.61	4.88	0.00	0.96
	Control	14.51	4.29		
Peak Pelvic Tilt	$IDEO_F$	23.29	5.52	0.48	0.49
	Control	22.04	3.51		
Pelvic Tilt Excursion	$IDEO_F$	8.07	2.90	1.50	0.23
	Control	7.04	1.26		
Pelvic Obliquity Excursion	$IDEO_F$	14.64	5.04	3.25	0.08
	Control	11.75	3.01		

Significance

Overall, patients who sustained a LE francture and use an IDEO for running and other high level activities are running at similar speeds and with similar biomechanics as their healthy counterparts. They have improved patient reported outcomes compared to limb salvage patients who did not have access to an IDEO. Finally, patients perform near the 75th percentile of their amputee counterparts on the CHAMP performancetest indicating that they have good function and performance in addition to similar running biomechanics to healthy controls. This indicates that the use of IDEO in this population is appropriate and should be continued .

Acknowledgments

The views expressed do not reflect the views or policy of the Department of the Navy, DOD, DHA, or US Government.

References

1. Wheeler (2018). Clin Rev Miner Metab, 16:103-115.
2. Wallace (2011). Mil Med, 176: 283-290.
3. Doukas (2013). JBJS, 95: 138-145.
4. Gailey (2013). JRRD, 50: 905-918.

Effect of body position and external load on knee joint kinematics and muscle activity in healthy young adults during the pendulum test

Diego M. Ferreira[1] and Jianhua Wu[1]
[1]Department of Kinesiology and Health, Georgia State University, Atlanta, GA, USA. Email: jwu11@gsu.edu

Introduction

The Wartenberg pendulum test has been administered in different populations to assess passive stiffness of the knee. While the test is easy to administer, different body positions have been used for this test. Our previous study showed that an external ankle load equalling to 2% of body weight can increase the number of swing cycles and stiffness of the knee during this test [1]. However, it is not known if a higher amount of ankle load can induce further improvements in the test performance.

Additionally, there is limited quantitative analysis of muscle activity within the quadriceps group during this test. The muscles' contribution during each position and load is critical to understand the contributors to increased passive stiffness in certain populations. Therefore, the purpose of this study was to investigate the effect of body position and ankle loading on the knee kinematic performance and muscle activity in healthy young adults. We hypothesized that an increased ankle load would increase the amount of knee kinematics and muscle activity, and a position of lying down would facilitate the pendulum test compared to other body positions.

Methods

Twenty adults (10M/10F, 22.44±3.07 years) sat on a table with their legs hanging over the edge of the table. The dorminant leg was raised so that the knee was in a full extended position. Subjects were instructed to relax their leg, and then the leg was released allowing it to swing freely until it came to a stop. Three body positions were included: sitting upright, sitting reclined at 45 degrees, and lying supine. Three loading conditions were included: without load (NL), an ankle load equaling to 3% of body mass (AL3), and 6% of body mass (AL6). An 8-camera Vicon motion capture system was used to collect kinematic data of the knee (Fig. 1). Electromyography (EMG) was collected using Delsys wireless surface electrodes on the rectus femoris, vastus lateralis, and vastus medialis. Kinematic variables included: the first flexion excursion (A1), number of swing cycles, relaxation index (RI), stiffness coefficient (K1), and a damping coefficient (B1).

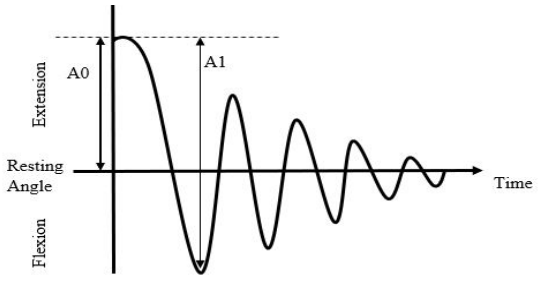

Fig. 1: Knee joint angle during the pendulum test.

RI was calcualed as A1/A0. K1 was calculated using the angular velocity and moment of inertia of the lower leg. B1 was estimated by calculating the damping ratio and natural frequency [1]. The integrated area of EMG during the first flexion excursion was calculated across all the muscles. Two-way (3 position x 3 load) ANOVAs with repeated measures were conducted for the kinematic variables. Three-way (3 position x 3 load x 3 muscle) ANOVAs with repeated measures were conducted for the EMG variable. Post-hoc pair-wise comparisons with Bonferroni adjustments were conducted when necessary at a significance level of alpha=0.05.

Results and Discussion

Our results indicate that body position affects the number of swing cycles and damping coefficient but did not affect A1, K1, or RI. The significant differences were between the upright & supine and upright & incline position ($p<0.05$). The upright position resulted in greater number of swing cycles, but a smaller damping coefficient compared to the other two positions.

While A1, RI and number of cycles increased from the NL to AL conditions, K1 and B1 decreased (Table 1). The addition of the ankle load increased all of the kinematic variables and muscle activity ($p<0.001$). This incidcates that the addition of an ankle load can be used to increase the amount of passive motion about the knee. However, the reduction in K1 and B1 suggests that the knee joint may become less stiff and vicosious under the AL conditions. In addition, muscle activity increased between the NL and AL conditions ($p<0.001$). This response indicates that the quadriceps responded to the increased loads by controlling and slowing down the swings. This suggests that as the external load increased, greater muscle activity tends to accommodate the increased moment of inertia of the leg and improve the stability of the joint. This may correspond with the decrease in damping and stiffness coeffecients.

Table 1. Means (SD) of kinematics and muscle activity.

Variable	NL	AL3	AL6
A1 (deg)	69.35 (9.58)	74.55 (8.63) *	78.37 (8.79) *‡
RI	1.84 (0.11)	1.91 (0.12) *	1.92 (0.17) *
Cycles	6.56 (0.86)	10.08 (1.61) *	12.25 (2.09) *‡
K1 (Nm/rad)	36.17 (7.46)	28.8 (5.47) *	26.35 (5.31) *‡
B1 (Nm*sec/rad)	0.25 (0.06)	0.18 (0.06) *	0.16 (0.06) *‡
EMG (μV*time)	0.06 (0.21)	0.16 (0.50)*	0.26 (0.66)*‡

Note that * represents a difference from NL; ‡ represents a difference from AL3.

Significance

The results indicate that body positions cause small effects on the kinematic pattern of the pendulum test in young adults. Lying down or inclined may provide an alternative position for this test. This may be beneficial to clincical populations who may have difficulty in sitting upright. Additionally, the addition of the ankle load showed increases in passive motion and increased the muscular response. The additional load may be used for developing therapy interventions to address increased passive stiffness of the knee in some clinical populations.

References

[1] Ferreira D, et al. *Gait & Posture*. 76: 311-317, 2020.
[2] Casabona A, et al. *J Appl Physiol*. 113: 1747-1755, 2012.

Kinematics features and experience in differentiating above-knee amputee gait

I-Chieh Lee[1*], Matheus M. Pacheco[2], Michael D. Lewek[3], He (Helen) Huang[1]
[1]UNC-NC State Joint Department of Biomedical Engineering, North Carolina State University and University of North Carolina at Chapel Hill, Raleigh, NC, USA
[2]School of Physical Education and Sport, University of São Paulo, São Paulo, Brazil
[3]Division of Physical Therapy, Department of Allied Health Sciences, University of North Carolina at Chapel Hill, Chapel Hill, NC, USA
Email: * ilee5@ncsu.edu

Introduction

Observe gait is clinically important to allow physical therapists (PT) and clinicians to assess motor deficits in patients. However, the inconsistent results in the skill of visual assessment lead to a question about whether clinicians are accurate and reliable on gait judgment[1]. Also, little is known about which gait features would base accurate judgments. The purpose of this study is to investigate (1) the differences in observational gait analysis skill between those with different level of clinical experience and (2) the informative kinematics features for differentiating amputee gait.

To answer these questions, we introduced a new method that combines biological motion and principal component analysis (PCA) to gradually mesh amputee and typical walking patterns for raters to rank. The synthesized patterns preserved the kinematics features that allow physical therapists (PT), PT students (PTS), and novice raters to discriminate different levels of gait impairment.

Methods

Joint motion of three unilateral transfemoral amputee walkers (Walker A, B and C) and health control walkers were utilized to build three biological motion models through PCA. Each model was based on one amputee walker. We then build 6 videos from each model displaying a synthesized point-light walker varying in weighing from 0, 20, 40, 60, 80 to 100% between healthy walking and the given amputee walking features. These videos were used to test the accuracy in differentiating a range of scaled gait abnormalities for 10 PT, PTS and Novice. The goal was to rank the videos from 1 to 6 based on the weighing within 25 secs (Figure 1). Participants performed a total of 30 trials (3 set*10 repetitions).

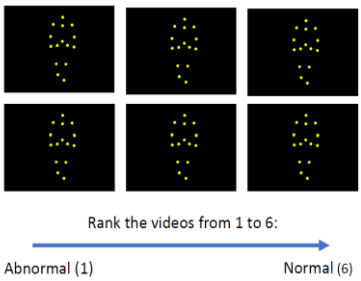

Figure 1. An example of a testing video set for one trial.

Analysis of the first four principle components were used to quantify the amputee gait features that were deviated from normal walking. In addition, the accuracy rate in judging biological videos were used to test the observational gait skill on each rater group.

Results and Discussion

In sum, we quantified the major dissimilar features between amputee and control walkers that allow individuals to perceive and differentiate walker patterns. The quantified features represent the magnitude of medial-lateral body sway, degree of gait asymmetry, and percentage of gait deviation. We postulate that these gait features are the perceptual variables that allow individuals to differentiate between walkers.

A higher degree of spatial asymmetry in gait was presented especially on Walker A and Walker C. Also, the percentage of gait similarity to health walker (Walker A: 38.3 %; Walker B: 75.47% and Walker C: 89.88%) was associated with accuracy rate (negative relationship). A larger medial-lateral body sway was observed in all amputee walkers (Figure 2).

For the comparison of accuracy rate between rater groups, we found that PT and PTS were the same and the both were more accurate than the Novice group. Because greater learning changes occur at the beginning of practice [3], if the PTS can attend to the information that is beneficial to identify gait impairment, they can perform better than Novice and reach comparable levels of as PT. In addition, the minor differences between PT and PTS was found on PT showing equal ability of accuracy for the whole spectrum from normal to abnormal walking patterns in judging Walker C' videos. Considering, Walker C's gait is 89.88% similar to normal walkers but with a relatively larger gait asymmetry, we postulated that PT likely have learned to promptly attend to and sensitive to gait asymmetry.

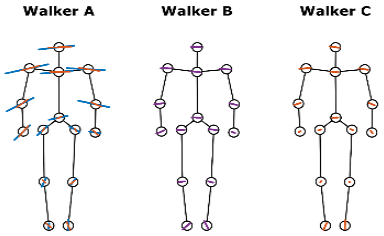

Figure 2. The stick figures of walkers are facing to the viewers. The blue, purple, and red lines indicate the reconstructed joint trajectories of the dissimilar PCs in respected to amputee walker's PC1, PC2, and PC3, respectively.

Significance

We introduced a new method, combining biological motion and PCA, to synthesize gait dynamics between amputees and a control walker. This new method can be used to improve the current way in training/evaluating the observational gait analysis skill for clinicians since it provides flexibility in presenting different level of gait impairment and excludes redundant sources of information that might not relate to gait. In addition, the identified gait features that PTs attended to might inform the future design of automated, clinically relevant gait evaluation and automatic prosthesis tuning algorithm in the future.

Acknowledgments

This work was supported by National Institute of Health (NIH EB024570).

References

[1] F. Ferrarello *et al.*, "Tools for Observational Gait Analysis in Patients With Stroke: A Systematic Review," *Physical Therapy,* vol. 93, no. 12, pp. 1673-1685, 2013.

[2] M. E. Eastlack, J. Arvidson, L. Snyder-Mackler, J. V. Danoff, and C. L. McGarvey, "Interrater reliability of videotaped observational gait-analysis assessments," *Physical therapy,* vol. 71, no. 6, pp. 465-472, 1991.

[3] K. M. Newell, Y.-T. Liu, and G. Mayer-Kress, "Time scales in motor learning and development," *Psychological Review,* vol. 108, no. 1, pp. 57-82, 2001.

Near Infra-Red Spectroscopy Used for Muscles Hemodynamic of Adults with Cerebral Palsy versus Adults with No Physical Impairment

Inbar Kima[1], Ronit Aviram[2], Simona Bar-Haim[2] and Raziel Riemer[1]
[1]Department of Industrial Engineering, Ben-Gurion University of the Negev, Israel
[2]Department of Physiotherapy, Ben-Gurion University of the Negev, Israel
Email: rriemer@bgu.ac.il

Introduction

Cerebral Palsy (CP) is defined as a group of non-progressive motor impairments caused by lesions in the developing brain [1]. However, CP is characterized by muscle spasticity and functional loss later in life [2,3,4]. In this research, we monitored muscle oxygenation and hemodynamics using Near Infra-Red spectroscopy (NIRS), trying to capture for the first time the hemodynamic portion of spastic muscle function. NIRS technology allows for continuous and non-invasive monitoring of muscle oxygen saturation, oxy-hemoglobin, and deoxy-hemoglobin concentrations [5].

Methods

12 participants with CP who were able to walk (4 females, 8 males aged 29.5±7.91 mean±SD) and adults with No Physical Impairment (NPI) (8 females, 6 males aged 26.5±1.51 mean±SD) were evaluated. We measured the change in oxy- and deoxy-hemoglobin concentrations and the muscle saturation (TSI) of Vastus Lateralis (VL) and Rectus Femoris (RF) of the most affected limb using a portable NIRS system (PortaMonand2x Portalite, Artinis, Netherlands). Muscle tissues were continuously recorded at rest and during exercise, while applying venous occlusion (~60 mmHg) to calculate Muscle Blood Flow (MBF) and arterial occlusion (~280 mmHg) to calculate Muscle O2 consumption (mVo2). Participants performed a Maximum Voluntary Contraction (MVC) test, followed by measurements at rest and at one minute of repeated knee extension at 20% and 80% of their MVC. We used a Linear Mixed Model to compare participants with CP and NPI, as well as to compare between the two muscles and between different loads (rest, 20%, 80%). Using the participants' shank length, we calculated the knee extensor torque. Additionally, we calculated muscle efficacy by dividing the MVo2 by the torque (proxy for metabolic energy divided by mechanical work). In all cases, the significance level was $p \leq 0.05$. All statistical analyses were performed using R-Studio.

Results and Discussion

The maximum knee extensor torque was found to be significantly lower in participants with CP compared to participants with NPI (mean $\pm$ SD CP: 19.7± 16.49. NPI 49.61± 16.84N*m) (p=0.00012).

The MBF of participants with CP didn't change in the VL between loads but significantly increased in the RF from rest to 20%MVC and to 80%MVC (p<0.001). In the NPI group, MBF was significantly reduced only for the VL muscle, from rest to 80%MVC (p=0.008), resulting in a significant interaction between the load and group demonstrating 1.45 and 1.69 times greater increase in MBF for participants with CP compared to those with NPI from rest to 20%MVC (p=0.02) and to 80%MVC (p=0.001), respectively. MVo2 of participant with NPI was larger than the mVo2 of participants with CP at rest (p=0.05). In both groups there was a significant increase in mVo2 from rest to 20%MVC and to 80%MVC (p<0.0001). MVo2 to torque was significantly lower for NPI group (P<0.02).

The muscle TSI significantly decreased at 80%MVC compared to 20%MVC, for all participants, with a much greater decrease in NPI than in CP participants [2.3 times vs 1.6 times respectively), resulting in a significant interaction between load (20% to 80%) and TSI (p=0.01)].

Half recovery time in 80%MVC was twice as high in the NPI group as it was for CP participants (p=0.0004). For CP participants, there were no significant differences between loads (p>0.3), whereas for NPI there was a significant increase in half recovery time from 20%MVC to 80%MVC (p<0.0001).

We found a typical reduction of MBF in participants with NPI in the VL muscle at high working loads, a reduction that we attributed to the interference with the MBF, resulting from the massive activation of motor units. In participants with CP, however, the greater force did not restrict MBF in the VL because of a low contractility.

We assume that the MBF increases in the RF due to increased regional MBF coupled with even more limited contraction in the RF muscle. This assumption is reinforced by the fact that the TSI at 80%MVC decreased more in the NPI participants than in participants with CP, suggesting a greater imbalance between oxygen demand and supply in NPI participants. Between the groups, there was no difference in mVo2 at 20% and 80% MVC. Yet, dividing the mVo2 by torque (i.e. muscle efficiency) for NPI participants suggests that the muscle construction is more efficient in the NPI group.

Significance

The NIRS was able to capture differences in muscle hemodynamics and oxygenation in people with CP. These measurements are important to understanding muscle function in order to find treatments and shape training protocols to improve CP lifestyle.

Acknowledgments

This research was supported by Kreitman School of Advanced Graduate Studies Found at Ben-Gurion University of the Negev. The use of NIRS technology was supported by Yogev Koren from Physical Therapy Department at Ben-Gurion University of the Negev.

References

[1] Rosenbaum, P. et al. (2007). *Developmental Medicine & Child Neurology*, *Supplement,* 109 (supplement 109), 8-14.
[2] Day, S. et al. (2007). *Developmental Medicine & Child Neurology*, 49(9), 647-653.
[3] Durstine, J. L. et al. (2000). *Sports Medicine*, 30(3), 207-219.
[4] Shortland, A. (2009). *Developmental Medicine & Child Neurology*, *51*, 59-63.
[5] Jobsis, F. F. (1977). *Science*, 198(4323), 1264-126.

Dynamic Joint Stiffness During Single Leg Drop in FAIS Participants

Jennifer Perry[1], Kate Jochimsen[1], Rich Willy[2], and Stephanie Di Stasi[1],
[1]OSU Sport Medicine Research Institute, The Ohio State University, Columbus, OH, USA
[2]School of Physical Therapy & Rehabilitation Sciences, University of Montana, Missoula, MT, USA
Email: jennifer.perry@osumc.edu

Introduction

Femoroacetabular impingement syndrome (FAIS) preferentially afflicts young, athletic individuals and is associated with functional deficits, pain, and altered movement strategies during functional tasks[3]. Joint stiffness is a valuable tool to assess the interaction between changes in joint torgues and changes in joint motion during loading phases. In other populations with intra-articular pathology, elevated joint stiffness is often observed during dynamic tasks, such as landing. Understanding limb and joint stiffness patterns in FAIS may provide valuable insight into syndrome-specific impairments. As such, the purpose of this study was to compare the total limb and dynamic joint stiffness of the hip, knee, and ankle between the symptomatic and asymptomatic limb of those with FAIS during a single leg drop (SLD) task. We hypothesized that the symptomatic limb would demonstrate greater hip joint and total limb stiffness during landing.

Methods

Twenty athletes with FAIS (22.9±9.1 years old; 11 female) preformed 5 SLDs on each limb from a 31cm box on to a force plate while 3-dimensional motion data were collected. The last 3 trials for each limb were selected for analysis. Dynamic sagittal plane joint stiffness during the initial landing phase was calculated for each joint. Initial landing phase was defined as initial contact to time of peak joint moment. Joint stiffness was calculated as the angular coefficient of the linear regression line when joint moment is plotted as a function of joint angle[3]. Total limb stiffness was calculated from initial contact to lowest center of mass during landing. Total limb stiffness was also calculated as peak vertical ground reaction force divided by vertical displacement of the center of mass during landing (ie. initial contact to lowest center of mass).

Wilcoxon Signed-Rank tests were performed to compare dynamic joint stiffness and total limb stiffness between limbs. Alpha was set to 0.05. Probability of Superiority for dependant measures (PSdep) was defined as the number of observations where the involved limb variable of interest was greater than the uninvolved limb divided by sample size.

Results and Discussion

Subjects with FAIS demonstrated an increased dynamic joint stiffness at the knee on the involved limb compared to the uninvolved limb during a SLD. There was a PSdep of 75% for joint stiffness of the knee, meaning there was a 75% chance that knee stiffness was greater on the involved side. There were no significant differences between limb found at the hip, ankle, or total limb stiffness. However, there was a 70% chance that hip stiffness was greater on the involved side compared to the uninvolved side.

Increased load on the symptomatic limb has been previously reported during gait in those with FAIS[1,2]. The increased dynamic knee joint stiffness on the involved side during the SLD task identified in the current study may be a protective measure employed to adapt to increased joint moments. Alternatively, the increased dynamic knee joint stiffness may be resultant of a decreased sagittal knee excursion. Future studies should evaluate both joint kinematics and kinetics to understand contributing factors to alterations in joint stiffness.

	Limb	Median	IQR	*p*	PS_{dep}	*r*
Hip	Involved	4.82	(3.08, 6.23)	.073	.70	-.283
	Uninvolved	4.28	(3.07, 6.13)			
Knee	Involved	5.08	(4.29, 6.60)	.028	.75	-.348
	Uninvolved	4.75	(4.12, 6.30)			
Ankle	Involved	4.28	(3.51, 5.13)	.737	.45	-.053
	Uninvolved	4.44	(3.41, 5.05)			
Total Limb	Involved	19.31	(14.57, 20.71)	.126	.65	-.242
	Uninvolved	16.70	(15.37, 19.42)			

Table 1: Median dynamic joint stiffness during landing of involved and uninvolved limb for hip, knee, and ankle *(*significant difference for p<0.05)*.

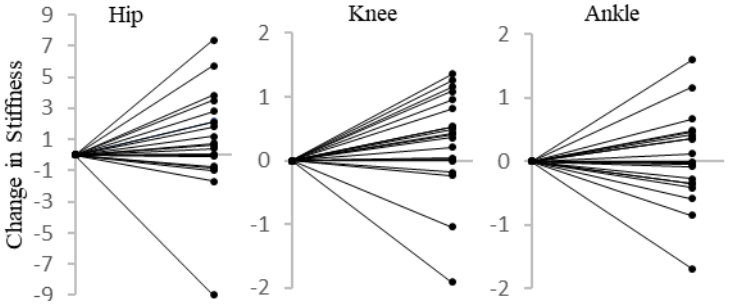

Figure 2: Participant-level limb differences in joint stiffness for hip, knee, and ankle. Positive values indicate higher involved limb stiffness.

Based on participant-level data, some individuals demonstrated higher hip joint stiffness on the symptomatic side. This may or may not correspond with higher knee and/or ankle stiffness; kinematics and joint moments would further explain what is influencing these patterns. With larger samples, including healthy controls, the implication of altered hip stiffness on functional performance can be fully examined. Understanding such strategies may provide critical clinical insight into variations in functional performance and inform rehabilitation strategies.

Significance

Persons with FAIS show asymmetrical dynamic knee joint stiffness between limbs during the dynamic task of SLD. Whether or not this is an effective strategy to maintain sports participation in the presence of hip pain or could negatively impact knee function or furture knee injury is unknown.

Acknowledgments

This study was funded in part by the Legacy Fund of the Sports Section of the American Physical Therapy Association.

References

1. Samaan, M.A. *et al.* (2017) AJSM; 45:4
2. Samaan, M.A. *et al.* (2020) Clin Biomech; 71:214-20
3. Zeni Jr., J.A. *et al* (2009) Clin Biomech; 24:366-71

Are Lower Back Demands Optimal in People with Unilateral Amputation?

Jacob J. Banks[1], Ryan D. Wedge[2], Graham E. Caldwell[1], and Brian R. Umbeger[3]
[1]Department of Kinesiology, University of Massachusetts, Amherst, MA, USA
[2]Department of Physical Therapy, East Carolina University, Greenville, NC, USA
[3]School of Kinesiology, University of Michigan, Ann Arbor, MI, USA
Email: jbanks@umass.edu

Introduction

People with unilateral lower limb amputation (PULLA) often walk asymmetrically with a prosthesis[1]. Asymmetric gaits are usually more inefficient with a greater cost of transport (CoT)[2] and may also be responsible for secondary disorders that impact quality of life[3]. Lower back pain (LBP) is a frequently cited complication, with twice the reported prevalence of the able-bodied population[3]. The increased LBP prevalence coupled with a growing number of amputations[4] have led to studies concerning the demands placed on the lower back during gait in PULLA[2,5].

Lower back vertebral compression forces have been reported to be up to 40% greater in PULLA than in able-bodied controls[5]. These increased spinal demands have been attributed to residual limb and prosthetic limitations that lead to more lateral trunk flexion during stance on the prosthetic leg, greater forward trunk lean, and sustained erector spinae activity[2]. A question of clinical importance is whether these lower back demands could be reduced with more symmetrical gait. To address this question, we compared lower back compression forces in PULLA and able-bodied participants at different levels of enforced (a)symmetry. We hypothesized that compression forces are already optimized at the preferred (natural) gait asymmetry level for both the able-bodied and PULLA, as is the case for CoT[6].

Methods

PULLA and able-bodied participants (Table 1) took part in this study[6], approved by the institutional review board. PULLA were limited to transtibial ambulators capable of variable cadences (i.e. >K3) from non-vascular causes at least 1-year post amputation.

All participants attended two sessions, with the first session used to determine preferred walking speed (PWS), preferred asymmetry level, and to acclimate them to the protocol. Whole-body kinematic data were collected in session 2. During both visits, participants walked on a motorized treadmill with up to eight different conditions of gait (a)symmetry (-15% to 15% in 5% increments [0%=symmetry] and preferred) for five minutes at PWS, with foot targets to aid gait asymmetries. Real-time visual feedback of (a)symmetry performance was provided from insole foot switches. Gait (a)symmetries level was defined as the difference between intact (dominant) and prosthetic (non-dominant) leg stance times relative to the combined stance time[1].

Peak L5/S1 compression forces were calculated for each asymmetry level from a modified full-body OpenSim model[7,8] and expressed relative to bodyweight and PWS. Static optimization[9] was used to estimate individual muscle forces and their contribution to the derived lower back joint moments. For each participant, the minimum L5/S1 compression force across asymmetry conditions was calculated from a quadratic best-fit curve (Fig. 1). For each group, a paired t-test was used to compare (α<.05) the peak L5/S1 compression force at the predicted minimum with the force at the preferred level of asymmetry. A pooled t-test compared the between-group differences at preferred asymmetry levels.

Table 1: Participant (PULLA n=5; able-bodied n=5) demographics by group. Asterisk (*) significant difference between group's preferred walking speeds (PWS).

	Mass (kg)	Height (cm)	Age (years)	PWS (m/s)*
PULLA	84.8±22.0	178.6±10.0	38.6±11.6	1.1±0.3
Able-Bodied	74.1±13.4	177.2±8.3	29.6±6.4	1.4±0.1

Results and Discussion

PULLA preferred to spend more time on their intact leg and therefore exhibited more stance time asymmetry (~4%) than able-bodied (~1%; p=.05), which supports previous work[1,2]. The between group L5/S1 compressive loads were ~20% greater in PULLA for the preferred asymmetry conditions, but this trend was not significant (p=.10) due to a large between-subject variability in the PULLA group. The peak L5/S1 compressive force at preferred asymmetry did not differ from the predicted optimal (Fig. 1) for either group, supporting our hypothesis.

Study limitations include low participant numbers, the use of static optimization to compute muscle forces, variability in task execution strategies, and the brief acclimation to the gait asymmetry conditions compared to the preferred.

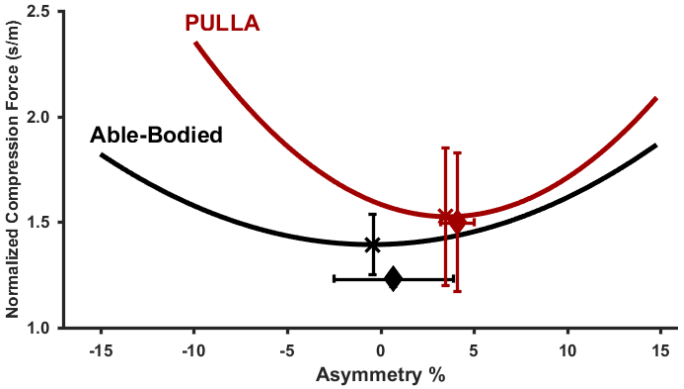

Figure 1: PULLA (maroon) and able-bodied (black) group's normalized peak L5/S1 compression across different (a)symmetric gait conditions. Curves represent the average quadratic fit, crosses the predicted minimum, and diamonds the preferred asymmetry for each group.

Significance

Our results suggest that training PULLA to walk more symmetrically may not reduce lower back demands, as both PULLA and able-bodied participants already locomote at a preferred level of asymmetry that minimizes peak L5/S1 compression forces.

Acknowledgements

UMass Amherst Kinesiology Travel Grant (JJB)
UMass Amherst Graduate School Dissertation Grant (RDW)

References

1. Dingwell et al. (1996) *POI*; **2.** Deven et al. (2014) *Med. Hypo*; **3.** Ephraim et al. (2005) *APMR*; **4.** Zigler-Graham et al. (2008) *APMR*; **5.** Shojaei et al., (2016) *Cl. Bmch*; **6.** Wedge (2019) *UMass*; **7.** Beaucage-Gauvreau et al. (2019) *CMBME*; **8.** Delp et al. (2007) *IEEE Trans*; **9.** Crownsheild & Brand (1981) *JBmch*

Patients Walk Less Mechanically Efficient Following Revascularization Surgery

Alex Dzewaltowski[1], Iraklis Pipinos[2,3], Jason Johanning[2,3] & Sara Myers[1,2]
[1]Department of Biomechanics, University of Nebraska at Omaha, Omaha, NE, USA
[2]Omaha VA Medical Center , Omaha, NE, USA
[3]University of Nebraska Medical Center, Omaha, NE, USA
email: adzewaltowski@unomaha.edu, web: cobre.unomaha.edu

Introduction

Peripheral artery disease (PAD) is a cardiovascular disease that manifests from atherosclerotic blockages in the extremities. Lower extremity PAD results in intermittent claudication, a debilitating leg pain caused by insufficient blood flow to the lower-limb muscles during physical activity. PAD severely impacts patients' ability to complete daily living tasks and negatively affects their quality of life. A key functional limitation caused by PAD is reduced ankle power during late stance compared to healthy, aged-matched adults [1]. Previous literature suggests that this reduced ankle power during late stance could correlate to an increase in negative work during early stance [2]. Work is the amount of energy expended over time with a unit definition of joules. Positive work corresponds towards forward progression while negative work corresponds to braking or slowing of joint rotations[2]. We hypothesized that revascularization surgery to restore blood flow to the affected lower-limbs would lead to improved walking mechanics as demonstrated by increased mechanical walking efficiency. Increased efficiency is defined as increases in positive work produced during late stance and a decrease in negative work produced during early stance.

Methods

Thirty-four patients with PAD were recruited by the Nebraska-Western Iowa Veterans' Affairs Health Care System as well as 24 healthy, aged-matched adults from the University of Nebraska Medical Center. Patients completed over-ground walking trials at their self-selected speed before and 6-months following revascularization surgery. All participants walked over eight in-ground AMTI force plates until six quality foot-to-force plate contacts were recorded for each leg. Three-dimensional kinematics were collected using 17 motion capture cameras (Cortex 5.1, Motion Analysis Corp, Santa Rosa, CA) with retro-reflective markers placed at specific anatomical locations [3].

Lower-limb joint powers were calculated from heel contact to toe-off using Visual3D (Visual3D, Germantown, MD, USA). Ankle, knee, and hip joint work was calculated as the integral of joint power utilizing MATLAB 2018a for each phase of stance. Phases of stance were defined as early (0-28%), middle (29-74%), and late (75-100%) [2]. For each phase of stance, work was summed for the ankle, knee, and hip. A one-way analysis of variance was used to test for significance of summed joint work for each stance phase across groups: patients with PAD at baseline, patients with PAD 6-months following surgery, and healthy adults. A Bonferroni corrected α-level of 0.0167 was used to correct for repeat assessment. As post hoc, Tukey test was implemented to assess significant differences between groups.

Results and Discussion

Contrary to our hypothesis, patients with PAD produced more negative work during early stance and less positive work during late stance following surgery ($p<0.01$). This suggests that patients with PAD walk less mechanically efficient following revascularization. The acute improvement to circulatory blood flow most likely does not translate to immediate improvement in the systemic muscle and passive tissue damage sustained from years of continual and degenerative ischemia.

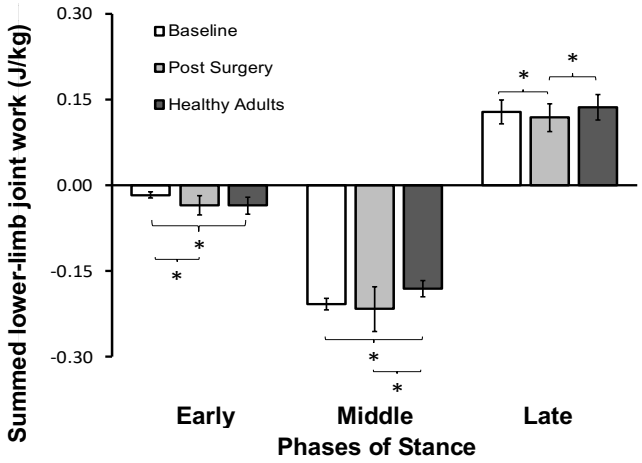

Figure 1: Summed lower-limb joint work performed by patients with peripheral artery disease before and 6-months following revascularization surgery as well as healthy, age-matched participants. Stars indicate statistical significance between groups ($p<0.01$).

Significance

Revascularization did not improve walking gait efficiency 6-months following surgery in patients with PAD. These findings should not diminish the importance of revascularization surgery for patients but instead, should emphasize the need to develop rehabilitation strategies following surgery. These results support further work investigating supplemental therapies such as exercise and assistive devices following revascularization to maximize the circulatory improvement.

Acknowledgments

This work was funded by NIH 1R01HD090333, 1R01AG049868, 1R01AG034995 and by the Veterans' Affairs I01RX000604. Thank you to those who collected data including Mahdi Hassan, Ben Senderling, and Molly Schieber.

References

[1] Wurdeman, Shane R., et al. "Patients with Peripheral Arterial Disease Exhibit Reduced Joint Powers Compared to Velocity-Matched Controls." *Gait & Posture*
[2] Huang, T.-W. P., et al. "Mechanical and Energetic Consequences of Reduced Ankle Plantar-Flexion in Human Walking." *Journal of Experimental Biology*
[3] J. D. McCamley et al., "Gait deficiencies associated with peripheral artery disease are different than chronic obstructive pulmonary disease," *Gait & Posture.*

Spatiotemporal gait characteristics in multiple sclerosis subtypes during brisk walking

Sumire Sato[1,2*], Yeun Hiroi[2], Danielle Zoppo[2], John Buonaccorsi, Jules D. Miehm[2], Caitlin Rajala[2], Jongil Lim, Jane A. Kent[2], Richard E.A. van Emmerik[1,2]
[1]Neuroscience and Behavior program, [2]Department of Kinesiology, University of Massachusetts Amherst, Amherst, MA
Email: *ssato@umass.edu

Introduction

Multiple Sclerosis (MS) has different disease courses that can be broadly categorized into relapsing-remitting (RRMS) and progressive (PMS). Gait impairment is common in MS, and the timed 25-foot walk test (T25FW) is a clinical tool often used to track the level of disability in people with MS. The T25FW is associated with long-term disease outcomes.[1] Interestingly, spatiotemporal gait parameters do not differ between RRMS and primary PMS at preferred speeds when matched for age and disease disability[2], but this has not been examined at the "fast and safe as possible" speeds generally used for the T25FW.[3] There may be spatiotemporal gait performance differences at brisk speeds that may be able to characterize differences in mobility performance (measured by spatiotemporal gait parameters) between MS subtypes.

The objective of this study was to determine if there are group differences in RRMS, PMS, and non-MS healthy controls (HC) in gait performance during T25FW. We hypothesized that gait performance will be more impaired (i.e. shorter steps spatially and longer stride times to increase stability) in PMS compared to RRMS, and in MS groups compared to HC.

Methods

Twenty-four HC (54.8 ± 12.6 yrs), 16 RRMS (52.6 ± 11.0 yrs) and 17 PMS (59.1 ± 6.9 yrs) adults participated in this study. All MS participants walked without any waking aids. Participants completed the T25FWT at a "fast and safe as possible" pace, while wearing inertial sensors on both feet equipped with a tri-axial accelerometer, gyroscope, and magnetometer (Opal, APDM, Inc., Portland, OR; 128 samples/s). Spatiotemporal gait variables were extracted using APDM Mobility Lab (version 2) software. This method has been validated in healthy young and older adults, and in people with Parkinson's disease.[4,5] Our spatiotemporal gait variables were: stride duration (s) double support time (% stride duration), stride length (m), step duration (s), and stance time (% stride duration). One-way analysis of variance and post-hoc independent t-tests with unequal variance were used to examine differences between groups.

Results and Discussion

T25FW time was shorter in HC than RRMS and PMS, but not significantly different between RRMS and PMS (Fig. 1A, Table 1). Similarly, stride duration, double support time, step duration, and stance time were shorter, and stride length was longer in HC than RRMS and PMS, but were not significantly different between RRMS and PMS (Fig. 1B-F, Table 1).

The differences between HC and both MS groups shows that even in persons with MS who walk without aids, speed is slower and spatiotemporal parameters are modified, presumably to increase stability. The lack of differences between MS subtypes in these parameters is consistent with a study by Dujmovic and colleagues that examined spatiotemporal variables at preferred speed.[2] This suggests that even at brisk pace, spatiotemporal gait parameters may not characterize differences between MS subtypes in those walking independently without walking aids.

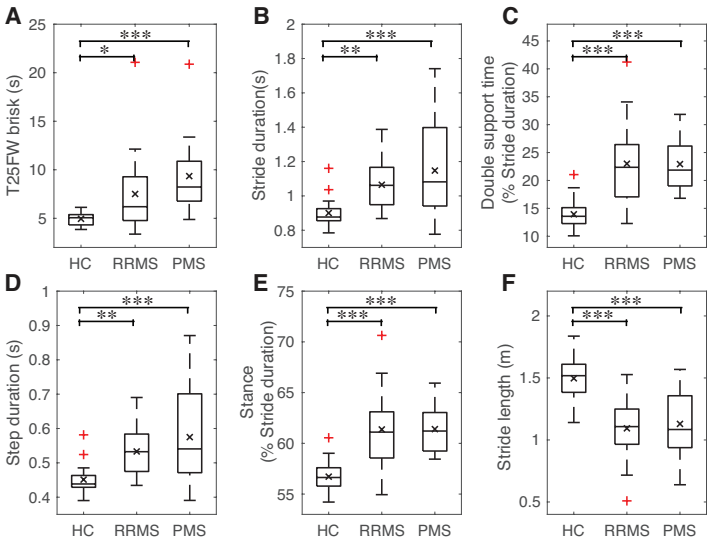

Figure 1: T25FW time (A) and spatiotemporal gait parameters (B-F). Black 'X' indicates mean, and red crosses indicate outliers. ∗: p = 0.010-0.050; ∗∗: p = 0.001-0.009; ∗∗∗: p < 0.001

	ANOVA	HC-RRMS	HC-PMS	RRMS-PMS
T25FW	< 0.001	[-4.4, -0.7]	[-6.3, -2.5]	[-4.4, 0.7]
Stride duration	< 0.001	[-0.2, -0.1]	[-0.4, -0.1]	[-0.3, 0.1]
Double support time	< 0.001	[-13.3, -4.4]	[-11.6,-6.4]	[-4.6, 4.7]
Step duration	< 0.001	[-0.1, -0.04]	[-0.2, -0.1]	[-0.1, 0.04]
Stance time	< 0.001	[-6.9, -2.4]	[-6.1, -3.3]	[-2.4, 2.4]
Stride length	< 0.001	[0.2, 0.6]	[0.2, 0.5]	[-0.2, 0.2]

Table 1. ANOVA p-values and 95% confidence intervals for differences between group means.

Significance

Our results are important because current clinical tests to track disability in MS rely largely on mobility as a key outcome measure. The small spatiotemporal gait differences between independently walking RRMS and PMS demonstrates that gait may not be the best clinical test to characterize MS subtypes. Future analyses should assess the link between these spatiotemporal gait variables and stability in MS subtypes.

Acknowledgments

Supported by the Department of Defense Office of the Congressionally Directed Medical Research Programs grant: #W81XWH-16-1-0351. We also thank the clinicians at University of Massachusetts Medical Center: Dr. Farnaz Khalighinejad and Dr. Carolina Ionete, as well as the participants.

References

[1] Bosma L, et al. 2013;19(3):326-333. [2] Dujmovic I, et al. 2017;13:13-20. [3] Polman CH, Rudnick RA. 2010;74 Suppl 3:S8-15. [4] Morris R, et al. 2019;40(9):095003. [5] Washabaugh et al. 2017;55:87-93.

Force Applied to a Grab Bar During Bathtub Transfers

Manon Guay[1,2], Myriam Vinet[1], Anne-Marie Bombardier[1], Mathieu Hamel[1],
Heidi Sveistrup[4], Louise Demers[5], and Cécile Smeesters[1,3]
[1]Research Centre on Aging, Sherbrooke QC, Canada
[2]School of Rehabilitation and [3]Department of Mechanical Engineering, Université de Sherbrooke, Sherbrooke QC, Canada
[4]School of Rehabilitation Sciences, University of Ottawa, Ottawa ON, Canada
[5]School of Rehabilitation, Université de Montréal, Montreal QC, Canada
Email: Cecile.Smeesters@USherbrooke.ca

Introduction

Fixed grab bars, which must be capable of sustaining a minimum of 1.3kN [1], are recommended to secure bathtub transfers of individuals with chronic mobility impairements. Individuals with a temporary need for assistance (e.g.: post surgery or palliative care) may prefer installing suction cup grab bars.

However, clinicians are reluctant to recommend suction cup grab bars for bathtub transfers because they question their sturdiness. Indeed the forces applied to a grab bar during complete bathtub transfers (step into the bathtub, sit down into the bottom, stand up and step out) are unknown, so an evidence-based decision is impossible.

We thus determined the magnitude and duration of the force applied to a grab bar during complete bathtub transfers, and the factors influencing this force.

Methods

A three factorial repeated measures design was used in an experimental environment including a bathtub, padded walls, instrumented fixed grab bars and a safety harness.

Seven healthy young adults (four women) stepped into the bathtub, sat down into the bottom, stood up and stepped out (three trials), with or without a slippery surface (with or without lubricating gel [2]), grabbing onto four grab bar configurations (vertical, angled, horizontal low, horizontal high).

Maximum force magnitudes and durations applied on the grab bar during complete bathtub transfers were measured by two six degrees of freedom load cells sampled at 2 KHz, for each of the 16 conditions (4 grab bar configurations * 2 surfaces * 2 directions of bathtub transfer).

Separate three-way ANOVAs with repeated measures were used to study main effects and interactions on the magnitude and duration of the force applied to a grab bar. Post-hoc two-way ANOVAs and paired t-tests were then computed.

Results and Discussion

On average, 23.2±6.4% of body weight was applied on the grab bar during complete bathtub transfers.

Maximum resultant forces were not influenced by grab bar configuration, presence of a slippery surface or direction of bathtub transfer (entrance or exit), except for the vertical configuration without a slippery surface. In this configuration, the maximum resultant force was smaller than for the three other configurations, in both directions.

Transferring on a slippery surface also increased the time participants applied a force on the grab bars across all configurations and directions.

Therefore, grab bars used during complete bathtub transfers should be capable of sustaining a minimum of 23.2% of body weight, to which a factor of safety of 1.5 should be added [3], regardless of the grab bar configuration.

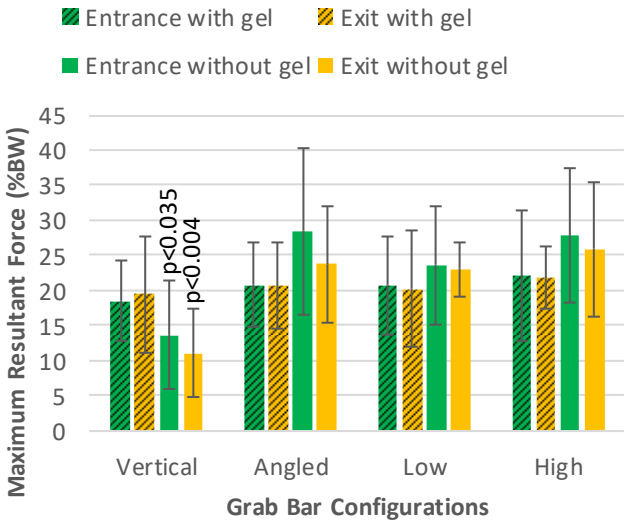

Figure 1: Mean ± standard deviation maximum resultant force applied on the grab bar during complete bathtub transfers (N=7).

For example, a manufacturer whose suction cup grab bar fails at 60kg should claim to sustain a maximum of 60kg / 1.5 = 40kg. Therefore, a 95th percentile male would apply 110.7kg * 23.2% = 25.7kg on the grab bar, which is well below the 40kg of our hypothetical suction cup grab bar and would in fact have a factor of safety of 60kg / 25.7kg = 2.33.

Unfortunately our study cannot confirm the loads that grab bars should be capable of sustaining if a fall occurs, as no falls occurred during testing.

Significance

All grab bars, fixed and removable suction cup grab bars, used during complete bathtub transfers with no loss of balance should be capable of sustaining a minimum of 23.2% of body weight, to which a factor of safety of 1.5 should be added [3], regardless of the grab bar configuration. These results could thus be used to support evidence-based recommendations regarding the safe use of suction cup grab bars to secure bathtub transfers, when it is not feasible or desirable to install a fixed grab bar into the wall.

Acknowledgments

This study was supported by grants from the Research Center on Aging and the Université de Sherbrooke.

References

[1] Standards Council of Canada (2018). *Accessible design for the built environment* (B651-18).
[2] Troy KL and Grabiner MD (2006). *Gait & Posture*, **24**(4), 441-447.
[3] International Organization for Standardization (2016). Assistive products for personal hygiene that support users - Requirements and test methods (17966).

Speed Effects on Knee Joint Loading in People with Unilateral Transtibial Amputation

Ryan D. Wedge[1], Alexander Clark[2] Brian R. Umberger[2], Frank C. Sup[3], John D. Willson[1]
[1]Department of Physical Therapy, East Carolina University (Greenville, NC)
[2]Department of Kinesiology, East Carolina University (Greenville, NC)
[3]School of Kinesiology, University of Michigan (Ann Arbor, MI);
[4]Department of Mechanical and Industrial Engineering, University of Massachusetts (Amherst, MA);
Email: wedger19@ecu.edu

Introduction

People with unilateral lower limb amputation have a greater prevalence of knee osteoarthritis (OA) in the intact limb compared to people without amputation[1]. Greater OA prevalence may be due to greater load magnitude or stance time duration on the intact limb compared with the prosthetic limb[2], leading to greater cumulative loading, which has been linked to OA[3].

Walking speed has opposite effects on knee joint load magnitude and duration. Slower walking speeds reduce peak knee loads[5], therefore that may be why people with amputation generally walk slower than able-bodied people[4] even though it increases stance time. It is unclear how these combined consequences of walking speed affect per-step loads, and loads over a given distance. The purpose of this preliminary study was to understand tibiofemoral joint loading between the prosthetic and intact limbs across gait speeds.

Methods

Four people with unilateral transtibial amputation from non-vascular causes that were either K3 or K4 ambulators (2 female; mass: 65.6 ± 9.1 kg; height 177.2 ± 9.2 cm; years 38.5 ± 9.9 years; preferred walking speed: 1.24 ± 0.04 $m \cdot s^{-1}$) participated in this institutional review board approved study. Participants walked overground at preferred and ± 20% preferred speed with motion capture marker data collected at 240 Hz and ground reaction force data collected at 2400 Hz. Preferred speed was determined by timing 6 m in the middle of a 10 m walk for 3 trials[6].

Tibiofemoral contact forces were estimated with an established model[7]. Briefly, joint kinematics and kinetics were calculated using an inverse dynamics approach. Muscle force estimates for the quadriceps, hamstrings and gastrocnemius were derived from the resulting net joint moments across stance phase using published muscle moment arms as a function of joint angle and muscle cross sectional areas. Muscle forces and joint reaction forces were combined to yield total tibiofemoral joint axial force, which was distributed to the medial and lateral proximal tibia in a manner to achieve the calculated frontal plane knee joint moment. The gastrocnemius was removed when estimating joint contact force on the prosthetic limb because the gastrocnemius does not perform the same biomechanical role after a transtibial amputation. We performed a two way (limb x speed) ANOVA (α=0.05) to test for differences in medial and lateral tibiofemoral joint contact peak force and force impulse.

Results and Discussion

The intact limb had significantly greater peak force ($p<0.001$) and significantly greater impulse ($p<0.001$) than the prosthetic limb during stance across speeds, except for the lateral impulse speed effect ($p<0.508$) (Figure 1a-d). Medial tibiofemoral peak forces had a significant ($p<0.002$) interaction between limb and speed, indicating that intact and prosthetic limb medial

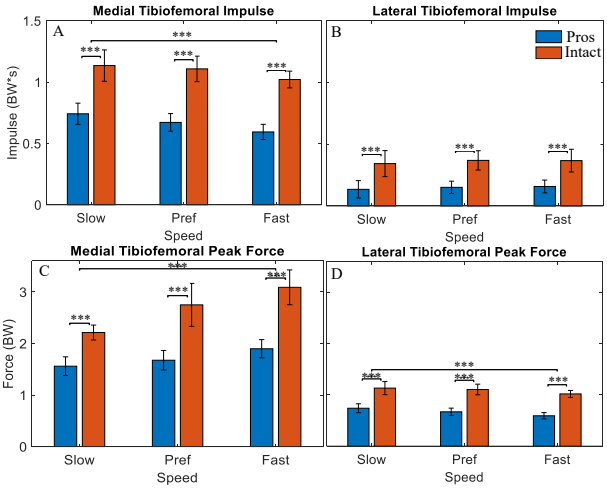

Figure 1: Medial and lateral tibiofemoral stance phase joint force impulse (A & B) and peak force (C & D) for prosthetic (Pros-blue) and intact (orange) limbs across three speeds (slow, preferred (Pref), fast). Braces indicate limb and speed main effects. *** indicates $p<0.001$ The intact limb had greater impulses and forces than the prosthetic limb for both medial and lateral tibiofemoral compartments across three speeds.

compartment peak forces increased with greater speeds, but only for the intact limb (Figure 1C). Greater tibiofemoral peak force and force impulse have been associated with medial knee OA in able bodied[3] and people with unilateral amputation[8]. Based on our preliminary results, people with unilateral amputation generally experience both greater peak force and force impulse on the intact limb than the prosthetic limb regardless of walking speed. Interventions to reduce inter-limb loading asymmetry during walking may reduce this OA risk factor. However, the effects of such interventions on other aspects of walking such as gait stability and metabolic cost of transport require further study.

Significance

People with unilateral amputations utilizing prostheses have greater knee loads on the intact limb that may promote OA onset or progression. Minimizing inter-limb loading asymmetry through gait re-training may prevent secondary disability.

Acknowledgments

Funded through NSF-NRI (IIS-1526986). Data collected with assistance from Andrew LaPre and Mark Price.

References

1. Norvell et al. (2005) *APMR*; **2.** Sanderson & Martin (1997) *G&P*; **3.** Maly et al. (2013) *G&P*; **4.** Waters & Mulroy (1999) *G&P*; **5.** Lenton et al. (2018) *PloS One*; **6.** Johnson et al. (2020) *G&P*; **7.** Barrios & Willson (2017) *JAB*; **8.** Miller et al. (2017) *PeerJ*

Depth of Squat Influences the Two-Dimensional Analysis of Knee, Hip, and Pelvis Frontal Plane Motion in Pain-Free Women

David M. Bazett-Jones[1], Marina Cabral Waiteman[1,2], Neal R. Glaviano[1]
[1]University of Toledo, Toledo, OH, USA
[2]São Paulo State University (UNESP), Presidente Prudente, Brazil
Email: david.bazettjones@utoledo.edu

Introduction

Excessive frontal plane motion of the lower extremity is related to lower limb injuries.[1,2,3] Frontal plane measurements of the lower extremity and trunk during functional motion are easily measured with 2-dimensional (2D) motion analysis and these values are clinically relevant.[3,4] In this context, the squat task is a pratical tool able to evaluate frontal plane motion related to knee injuries development and interventions. However, methodological differences in squat depth are reported and have resulted in varying results.

Studies have reported a minimal depth knee angle (≥60°),[3] a standardized step height (i.e. 21 cm),[4] a knee angle range (45°-60°),[5] and a knee angle that was standardized (i.e. 60°).[6] Each of these methods can result in differing squat depths and resulting knee flexion angles However, it is unkown if frontal plane trunk, pelvis, hip and knee frontal plane motion is influenced by squat depth. Therefore, the aim of this study was to investigate knee valgus (KV), hip adduction (HADD), pelvic drop (PD), and lateral trunk flexion (LTF) at different knee flexion angles during a single-leg squat in pain-free women. We hypothesized that as knee flexion angle increased, all other 2D angles would also increase.

Methods

Twenty pain-free women (age=22.3±1.1 years, height=1.68±0.06 m, mass=63.1±11.7 kg) were recruited from the local university. Markers were placed on the anterior superior iliac spines, greater trochanter and center of the patella. Participants performed three single leg squats to the lowest depth comfortable while keeping pace with a metronome (2s down, 2s up). Frontal and sagittal plane videos were recorded during SLS and images were extracted at 30º, 45º, 60, 75º and 90º of knee flexion. Average values for KV, HADD, PD, and LTF during knee flexion angles were analyzed. Positive values indicate greater KV, HADD, PD, and contralateral LTF. Four repeated measures analysis of variance with Sidak pairwise comparisons were used to investigate differences in frontal plane motion across knee flexion angles. Significance was set to $p \leq 0.05$. Effect sizes (ES) for each comparison were also calculated (Cohen's d <0.40: small effect, 0.41 to 0.70: moderate effect, ≥0.71: large effect).

Results and Discussion

Significant differences for KV ($F=33.95$, $p<0.001$), HADD ($F=67.77$, $p<0.001$), and PD ($F=51.98$, $p<0.001$) among 30º, 45º, 60º, 75º and 90º of knee flexion were found. Post-hoc analyses revealed significant differences for most comparisons. KV significantly inceased at every increase of knee flexion angle ($p \leq 0.05$, ES: 0.54-1.95), as did PD ($p \leq 0.05$, ES: 0.61-3.03). HADD was significantly increased ($p \leq 0.05$, ES: 0.64-3.85) at every knee flexion angle except between 30° and 45° ($p=0.158$, ES: 0.52). No differences in LTF were found ($F=2.73$, $p=0.085$, ES: -0.29-0.08). Means and standard deviations for trunk, pelvis, hip and knee frontal plane motion across knee flexion angles are presented in Table 1.

Our findings show that as knee flexion angles (i.e. squat depth) increase, frontal plane motion of the knee, hip, and pelvis also increased. Analysis of squatting using 2D motion analysis is common among clinicians but no standardized methods for collecting this information have been recommended. More studies investigating the different methodologies of 2D measurement of the single-leg squat seem warranted. Since this study was performed in healthy individuals, future studies should include pathological groups for which front plane motion is important. It could be that groups with pain may limit their motion, thus dampening the relationship found in our study; or it they could demonstrate a greater influence of knee flexion on frontal plane measures. In conclusion, pelvis, hip, and knee motion in the frontal plane are influenced by knee flexion angles during 2D analysis of a single-leg squat task.

Significance

Our results highlight the importance of standardizing squat depth during research and clinical practice ensure appropriate comparisons across time and assessors. Caution would be advised when comparing the KV angles obtained at different angles of knee flexion, both in research and clinical practice.

References

1. Hewett TE et al. 2005 *AJSM*
2. Holden S et al. 2017 *SJMSS*
3. Willson JD & Davis IS. 2008 *JOSPT*
4. Simon M et al. 2018 *Knee*
5. Herrington L et al. 2015 *Manual Therapy*
6. Wyndow N et al. 2016 *J Foot Ankle Res*

Table 1. Trunk, pelvis, hip and knee frontal plane motion across knee flexion angles

Knee flexion angles	30°	45°	60°	75°	90°	F-value	p-value
Lateral Trunk Flexion	13.46 (3.39)	13.36 (3.63)	13.15 (3.98)	13.78 (4.47)	14.44 (4.83)	2.73	0.085
Pelvic drop (°)	2.82 (1.30)	3.89 (1.76)	5.29 (2.70)	8.83 (4.17)	12.11 (4.13)	51.98	<0.001*
Hip Adduction (°)	10.05 (4.21)	12.44 (4.98)	16.01 (6.12)	21.30 (10.03)	29.77 (5.87)	67.77	<0.001*
Knee Valgus (°)	3.95 (2.12)	5.39 (2.95)	7.21 (3.77)	10.32 (5.99)	14.77 (7.55)	33.95	<0.001*

*Represent a significant difference between groups ($p \leq 0.05$).

Muscle Forces of the Lower Extremity During Dynamic Tasks in People With and Without Chronic Ankle Instability

Hoon Kim[1] and Kristof Kipp[1]
[1]Program in Exercise and Rehabilitation Science, Department of Physical Therapy, Marquette University, Milwaukee, WI, USA
Email: *hoon.kim@marquette.edu

Introduction

Ankle ligament sprains are common musculoskeletal injuries, and people who sprain their ankle ligaments may develop chronic ankle instability (CAI).[1] Although people with CAI exhibit neuromuscular deficits, muscle forces have not been studied.[1,2] Although measuring muscle forces directly is difficult, musculoskeletal modelling and simulations can help estimate individual muscle forces. Knowing muscle forces in CAI patients would provide a better understanding of the neuromuscular deficits in people with CAI and may improve targeted rehabilitation protocols. Furthermore, investigating muscle forces would be a first step to understand how muscle forces contribute to the development of ankle osteoarthritis, which is a critical issue in CAI patients.[3] The purpose of this study was to estimate individual muscles forces in the lower extremity and compare these estimates between people with and without CAI during landing, and anticipated and unanticipated cutting tasks.

Methods

Eleven people with CAI and 11 people without CAI participated in this study. Each participant performed a landing, anticipated cutting, and unanticipated cutting task while the position of reflective markers (240 Hz), muscle activity (1200 Hz), and ground reaction force (1200 Hz) were recorded.[4]

A musculoskeletal model was scaled in OpenSim.[5] Inverse kinematics was used to calculate joint angles. Static optimization was used to estimate muscle activity and forces. Results were validated by comparing simulated activations with EMG of the soleus (SL), fibularis longus (FL), tibialis anterior (TA), medial gastrocnemius (MG), and lateral gastrocnemius (LG). Peak muscle forces were normalized by body weight. The SL, MG, LG, TA, FL, TP (tibialis posterior), FB (fibularis brevis), VAS (vastus muscles), RF (rectus femoris), GX (gluteus maximus), GM (gluteus medius), HAMS (biceps femoris long and short heads, semimembranosus, semitendinosus) muscles were considered for statistical analyses. Separate two-way ANOVAs were used to compare muscle forces across group and task. For significant interaction or main effects, Fisher's least significant difference test was used to examine pair-wise differences. The α levels were set to 0.05. Effect-sizes (ω^2) were also calculated.

Results and Discussion

We observed moderate to strong similarity between simulated muscle activation and EMG data for all participants and tasks.

There were no significant group by task interactions for any peak muscle forces. There was, however, a significant group main effect for peak GX force (p = 0.018) with medium effect size (ω^2 = 0.08). Specifically, CAI patients generated approximately 24% greater GX peak force regardless of task compared to the control group.

The result indicates that people with CAI exhibit greater proximal muscle forces (e.g., GX). Similarly, Kim et al. (2019) showed that CAI patients exhibited greater EMG in proximal muscles (e.g., GX) during the eccentric-to-concentric transition phase during jump landing/cutting tasks.[6] In addition, Simpson et al. (2020) reported that CAI patients exhibited greater stiffness in the hip joint than healthy controls.[7] The authors of these studies suggested that greater proximal muscle activations and stiffness compensate for neuromuscular deficits in distal muscles. Collectively, these results suggest that people with CAI cope with distal neuromuscular deficits through proximal compensatory mechanisms aimed to perhaps increase postural control of the larger trunk and upper body segments.

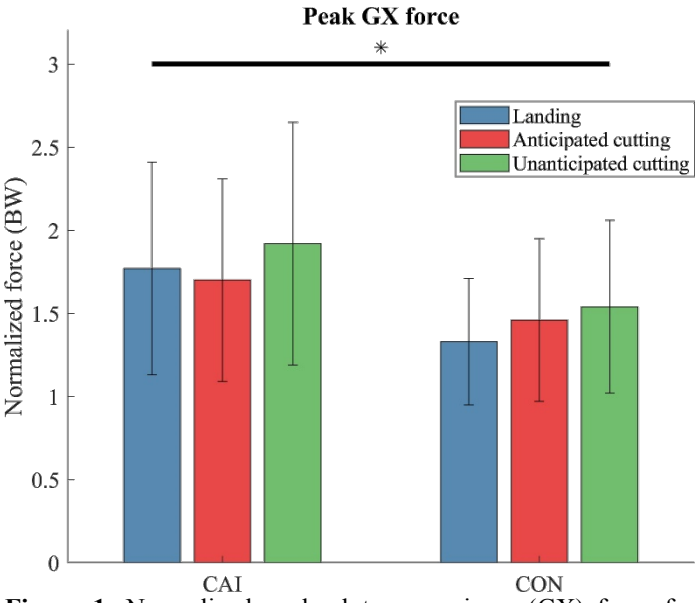

Figure 1: Normalized peak gluteus maximus (GX) force for people with chronic ankle instability (CAI) and control group (CON) during landing, anticipated cutting, and unanticipated cutting tasks.

Significance

The current study is the first to use musculoskeletal modelling to estimate muscle forces in people with CAI. The finding of greater GX muscle force across a variety of tasks agrees with other results. Since ankle osteoarthritis is a critical issue in CAI patients,[3] investigating if and how proximal changes affect ankle joint contact force should be considered in future studies.

References

1. Hertel, J. (2002). J Athl Train, 37(4), 364.
2. Hertel, J., et al (2019). J Athl Train, 54 (6), 572-588.
3. Wikstrom E. A., et al (2013). Sports Med, 43(6), 385-393.
4. Kipp K., et al. (2013). Clin Biomech, 28(5), 562-567.
5. Delp, S. L., et al. (2007). IEEE T Bio-Med Eng, 54(11), 1940-1950.
6. Kim, H., et al. (2019) Scand J Med Sci Spor, 29(8), 1130-1140.
7. Simpson, J. D., et al (2020). Ankle Instability. J Athl Train, 55(2),169-175.

SIMULATION OF A PASSIVE KNEE EXOSKELETON FOR VERTICAL JUMPING

B. Ostraich.[1,2], R. Riemer[2]
[1]NRCN, Israel
[2]Faculty of Industrial Engineering, Ben-Gurion University of the Negev, Israel
Email: * rriemer@bgu.ac.il

Introduction

Research on exoskeletons designed to augment human activities, and the attendant exoskeleton industry, is growing rapidly. However, progress in the field is currently being hindered by a lack of understanding regarding human–exoskeleton interaction. At present, the main method applied understanding this interaction is to build and test prototypes [1] or end-effectors (that simulate the devices) [2], but this is a very time-consuming and costly process. To improve the time and cost inputs for this process, numerical simulation and optimizations were recently used to design an exoskeleton for a standing long jump [3]. In this study, we aimed to simulate passive exoskeleton–human interaction during a vertical jump, with a view to using it as a tool for exoskeletons design.

Methods

Using the simulation, we performed a numerical optimization procedure to determine the muscle excitation and starting postures that would give the maximum jump height. The simulation used a planar 4-DOF dynamic model, where the ankle, knee and hip joints on both sides are considered to be symmetric, and thus each of the joints could be represented by one torque actuator. The torque actuators were modeled on the flexor and extensor muscles of each joint, and passive torque represented the properties of tendons and muscles [3]. We then simulated jumps with a passive knee exoskeleton (two devices) at five different values of maximum torque, with the aim of studying the exoskeletons' effects on jump height. The springs were modeled as linear, with total values of 0,35, 70, 105, and 140 Nm (for both devices), at a 90º knee bend.

The optimal excitation for the maximum jump height was found by using a genetic algorithm (GA). To improve our optimization results, and to test the convergence of the GA solution for each of the five exoskeleton conditions, the GA optimization was performed 500 times (we then used the best solution).

Results and Discussion

The jump heights converged for all five exoskeleton conditions in less than 450 GA runs. The result revealed an increase in jump height as the spring became stiffer (0, 2.8, 5.3, 10.4, 15.1 cm). The analysis of total work for each of the joints revealed that the hip increased by 7.5% and the ankle decreased by 8%; the total knee work increased by 90%, and the biological knee work decreased by 16.5% (Fig. 1). To gain a better understanding of what happens at joint level during a jump, we compared the torque joints with the maximum torque capability of the joint. For the knee, the torque is comprised of exoskeleton torque and biological knee torque (Fig. 2). At the beginning of the jump there is low biological torque, and most of the total knee torque is provided by the exoskeleton. At 0.15 s, the biological torque reaches its maximum value; thus, for the rest of the jump the human knee is working at maximum capacity. This last statement is true for the ankle and hip as well.

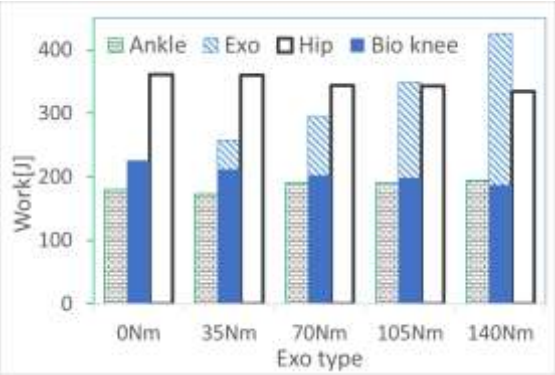

Figure 1: *Work at the joints and at the spring, for each of the spring conditions*

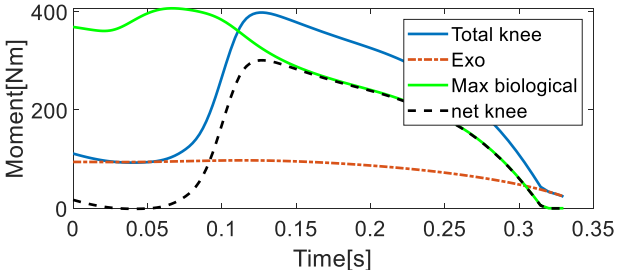

Figure 2: *Torques at the knee with a 70-Nm exoskeleton: total torque and maximum torque available at the given angle and velocity*

Analysis of the exoskeleton work under the 140 Nm condition revealed that 68% of the energy stored in the spring of the exoskeleton was transferred into energy causing an increase in jump height.

Significance

This research shows that a passive spring can enhance human performance for certain physical actions. It can also improve understanding of how to build and utilize (modifying jump technique) such a device.

Acknowledgments

This work was supported in part by Helmsley Charitable Trust through the Agricultural, Biological and Cognitive Robotics Initiative of Ben-Gurion University of the Negev, and by the Israel Science Foundation under Grant 899/18.

References

[1] Collins, S. H et al. Nature, Vol. 522, Issue 7555, pp. 212-215., 2015.
[2] J. Zhang et al., Science ,Vol. 356, Issue 6344, pp. 1280-1284., 2017.
[3] C. F. Ong, J. L. Hicks, and S. Delp, IEEE Trans. Biomed. Eng., Vol. 63, No. 5, pp. 894–903, 2016.
[4] B. M. Ashby, Dissertation, July, 2004.

A Computational Gait Model With Lower Limb Loss and a Semi-Active Variable Stiffness Foot Prosthesis

Michael A. McGeehan[1], Peter G. Adamczyk[2], Kieran M. Nichols[2], Michael E. Hahn[1]
[1]University of Oregon, Eugene, OR; [2]University of Wisconsin-Madison, Madison, WI
Email: mmcgeeha@uoregon.edu

Introduction

Passive energy storage and return (ESR) foot prostheses are the current high-performance standard for mimicking the energy absorptive and propulsive properties of a lost limb. However, the fixed stiffness behavior of these devices contrasts that of the healthy foot-ankle complex, which modulates stiffness in response to varied gait conditions (e.g. velocity and terrain). A recently developed variable stiffness foot (VSF) prosthesis [1] was designed with an actuated keel support fulcrum to semi-actively control sagittal forefoot stiffness and thereby adapt to different gait conditions with low power.

The potential effects of implementing a novel ESR prosthesis may be evaluated using simulations based on computational gait models. Simulations have been used previously to investigate the probable effects of prosthesis design on gait mechanics among persons with lower limb loss [2]. However, these models do not account for the ESR properties of the prosthetic foot, thus limiting their ecological validity. The purpose of this study was to incorporate the variable ESR properties of the VSF in a gait model of a lower limb prosthesis user.

Methods

A model of the VSF was developed in Simscape Multibody (Mathworks, Inc.) (Figure 1). Keel elasticity was modeled as a 16-element lumped parameter cantilever beam. Fulcrum position (i.e. variable stiffness) is controlled through a custom MATLAB script. Foot-ground contact consists of 24 sphere-to-plane contact models parameterized to represent the geometry and dynamics of the VSF's foam base. A least squares optimization approach was applied when determining contact parameters to improve resultant ground reaction force (GRF_R) predictions.

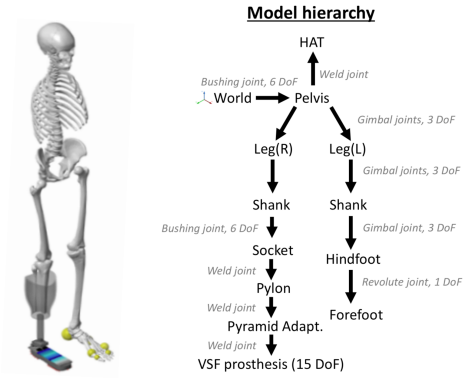

Figure 1: Gait model with the VSF (left) and model hierarchy (right). Sphere-to-plane contact models are depicted in yellow (intact foot) and red (VSF).

An anatomic gait model (Figure 1) was developed in Simscape Multibody using skeletal 3D surface geometry data from Mitsuhashi et al. [3]. Each segment is independently scalable to match subject-specific anthropometrics. The tibia and fibula were transected and encapsulated within a prosthetic socket to represent a transtibial amputation. The residual limb and prosthetic socket were connected via a high stiffness bushing joint to assess 6 DoF socket-residual limb interface dynamics.

Stiffness of the VSF was validated by simulating static compression tests for five discrete fulcrum positions (66, 87, 108, 129, and 151 mm) which span the full continuous range of possible positions. Stiffness was calculated as the slope of the linear fit to the load-displacement data above 200 N [1], and displacement was calculated at the midpoint of this range. Simulation-derived values were compared to those from static compression tests of the physical VSF [1] via correlation and RMSE. To investigate the model's ability to predict GRF_R using joint angles as inputs, a kinematically-driven gait simulation was computed for one male subject with a unilateral transtibial amputation (181 cm, 79 kg, fulcrum position: 66 mm). Simulated kinematics and GRF_R were compared to experimental motion capture data of the subject walking with the VSF [1].

Results and Discussion

Simulated VSF stiffness reproduced experimental stiffness across the five fulcrum configurations ($R^2 = 0.99$, RMSE = 1.31 N/mm). Mid-range displacement also matched well ($R^2 > 0.99$, RMSE = 1.08 mm). Simulated gait demonstrated a similar kinematic profile for all joints (mean $R^2 > 0.98$, mean RMSE = 2.0 deg). Model-predicted GRF_R aligned well in the time domain but showed amplitude discrepancies for both the intact foot and VSF ($R^2 = 0.87$ and 0.97, RMSE = 129 and 56 N) (Figure 2).

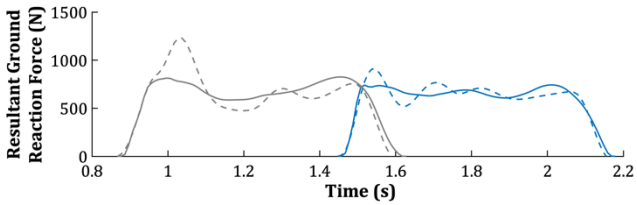

Figure 2: Simulated (dashed) and experimental (solid) GRF_R for the VSF (blue) and intact (grey) sides.

Data from simulated compression tests indicate that the ESR properties of the VSF were modeled with high fidelity. Simulated gait kinematics show that the model is numerically stable when driven by joint kinematics measured during gait with the VSF. However, amplitude discrepancies in GRF_R highlight the need for further optimization of the foot-ground contact models.

Significance

The present results show promise for simulating gait with a VSF prosthesis. Data from these simulations will improve our understanding of how humans interact with foot prostheses and may provide a framework for predictive modeling of human adaptation to variable stiffness. Future efforts include further contact model optimization, validating the generalizability of these methods for additional subjects, and studying how variable stiffness can be used to optimize gait.

Acknowledgments

This work was supported by the Lokey Doctoral Science Fellowship (MM) and NIH grant HD074424 (PA).

References

[1] Glanzer, E and Adamczyk, P, *IEEE TNSRE*, 2018.
[2] LaPré, A et al., *Int J Num Meth BME*, 2017.
[3] Mitsuhashi, N et al., *Nuc Acid Res*, 2008.

Comparison of Vertex Influence Weight Algorithms for Repositioning of 3D Medical Models

Timothy Zehnbauer[1], Austin Mituniewicz[1], Nathan Pickle[1], Gary P. Zientara[2] and Paulien Roos[1]
[1] CFD Research Corporation, Huntsville, AL, USA
[2]US Army Research Institute of Environmental Medicine, Natick, MA, USA
Email: timothy.zehnbauer@cfdrc.com

Introduction

"Rigging" is a technique commonly used in computer animation, which involves computing weights for each vertex in a mesh that govern how the vertices move based on movement of each segment in an associated articulated skeleton, or rig. Rigging methods could be useful for efficient repositioning of finite element (FE; e.g., tetrahedral) meshes representing human anatomy for applications such as thermal analysis or assessment of protective equipment. However, few tools exist to apply rigging methods to FE meshes. We propose a fully automatic method for calculating influence weights for FE meshes. The method is designed to increase the accuracy of deformations in rigged FE meshes. Here, we compare two different methods for computing vertex weights: a material-naïve distance-based method and a novel material-informed distance-based method.

Methods

We start with an articulated FE mesh with labeled materials. We use custom software to load the surface mesh along with a skeleton containing motion data. The skeleton is then rigged by manually placing joint centers at their desired locations and defining segments which connect them. The articulated FE mesh is loaded in at which point distance-based bone-influence weights are calculated one of two ways: using a material-naïve method and a material-informed method where all bone weights are set to the maximum value and Laplacian diffusion is used to ensure a continuous displacement field [1]. The meshes are then morphed into a t-pose, where we examine deformations by comparing change in tetrahedra volume of bone within mesh.

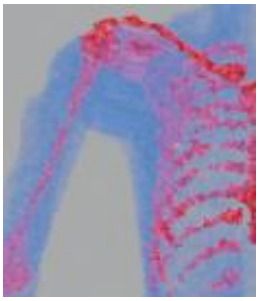

Figure 1: Undeformed bone (red) and muscle (blue) labeled mesh

Results and Discussion

Table 1 shows the mean change in volume for both bone and muscle. Much more deformation occurs in bone when using the material-naïve method as opposed to the material-informed method. However, the difference is less pronounced for muscle.

Mean Change in Material Tetrahedra Volume (mm^3)	Bone	Muscle
Material Naïve	0.99	3.24
Material Informed	0.32	3.20

Table 1: Average change in tetrahedral volume for bone and muscle.

The original undeformed mesh (muscle and bone) is shown in Figure 1. A comparison of naïve and informed weights are shown in Figure 2. Here, we can see that the overall deformation in bone is much less using the informed method than naïve. Using the naïve method results in significant changes in tetrahedral volumes in the torso along with minor changes in volume along the humerus. Additionally, there are large deformations at the edge of the influence of the segment. Large deformations in the informed method only occur near the joint center, leaving much of the humerus and torso bone undeformed.

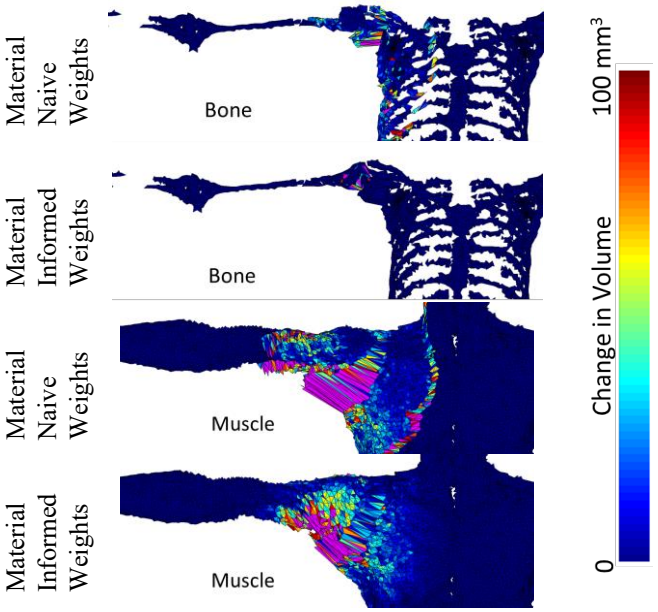

Figure 2: Comparison of change in volume from undeformed pose of tissue naïve and informed methods. Purple indicates change of greater than 100 mm^3.

The overall deformation in muscle does not change much with the use of material-informed weights (Table 1). However, the distribution of deformed tetrahedra in muscle is more desirable with the material-informed method (Figure 2).

Significance

Our results indicate that using material-informed weighting in articulated FE meshes greatly reduces the deformation of specified materials (e.g., bone). This method can be generalized to any FE mesh composed of different materials which are properly labeled. Compared to a material-naïve method, the material-informed method results in more anatomically realistic deformation of 3D medical models for applications such as thermal or projectile penetration analysis.

Acknowledgments

This work is supported by the US Army Medical Research and Material Command under Contract Number W81XWH18C0100. The views, opinions and/or findings contained in this report are those of the authors and should not be construed as an official Departement of the Army position, policy or decision unless so designated by other documentation.

References

[1] Sujar, Aaron et al. "Real-time animation of human characters' anatomy." Computers and Graphics (Pergamon). 2018.

Soleus Weakness Necessitates Increased Control Complexity For Unimpaired Gait

Elijah C. Kuska[1], Naser Mehrabi[1], Michael H. Schwartz[2], and Katherine M. Steele[1]
[1]Department of Mechanical Engineering, University of Washington, Seattle, WA, USA
[2]Center for Gait & Motion Analysis, Gillette Children's Specialty Healthcare, St. Paul, MN
Email: kuskae1@uw.edu

Introduction

Neurological impairments, like cerebral palsy (CP), result in altered motor control as well as secondary musculoskeletal impairments, like contracture and weakness. Combined, these impairments cause abnormal gait patterns that impact function in daily life [1]. However, improving function remains difficult as understanding relative effects neurological and musculoskeletal impairments have on gait, and their implications for treatment, remains challenging [2].

Computational models enable rapid evaluation of hypotheses regarding neuromusculoskeletal impairments and gait [3]. Yet, few frameworks simultaneously consider the impacts of altered motor control and physiology. Recently, a case study using neuromusculoskeletal simulations of a child with CP suggested that musculoskeletal impairments, rather than altered control, played a larger causal role in impaired gait [4]. Whether these conclusions extend to a larger population or prevent individuals with CP from achieving a typically developing (TD) gait pattern remains unknown. We have previously shown that reduced motor control complexity can prevent an unimpaired gait pattern, but only with severe impairment [5]. The goal of this study was to investigate the combined impact of altered motor control and weakness, one of the most common secondary impairments in CP. We hypothesized that muscle weakness would require more complex motor control to achieve TD walking.

Methods

A dynamic sagittal plane musculoskeletal model consisting of seven rigid body segments (thigh, shank, feet, and torso) and 9 degrees-of-freedom was used for analysis [6]. Each limb was actuated by eight Hill-type musculotendon units. Direct collocation optimal control tracked joint trajectories of TD gait while minimizing kinematic error and neural excitation effort.

Simulations were performed with two motor control strategies: individual muscle control (IMC), where each muscle was independently activated, and synergy-based control, where sets of 2-5 synergies dictated which muscles could be activated together in fixed ratios (NNMF). Synergies have been used extensively to model simplified motor control and have been shown to have reduced complexity in CP [7].

Plantarflexor weakness was incorporated by reducing the maximum isometric force of the soleus (SOL), gastrocnemius (GAS), or both plantarflexor muscles (PF). Weakness was varied from 0-100% of nominal TD values and its effect on the model's ability to replicate TD walking was examined with IMC and synergy-based control. We evaluated the amount of weakness the model could tolerate until the optimization no longer identified a feasible set of muscle activations to replicate TD gait.

Results and Discussion

The simplest control (2 synergies) was unable to replicate TD walking (**Figure *1***) with any weakness severity, similar to prior results [5]. The GAS could be completely removed (100% weakness) and still achieve TD gait with all control strategies except 2 synergies. The model was more sensitive to SOL weakness and tolerated less weakness with simplified control: weakened by 59% with IMC but only 50% with three synergies. The model could tolerate less weakness of both PF muscles (33-39%), suggesting that weakness, when severe enough, may prevent unimpaired gait no matter the control complexity.

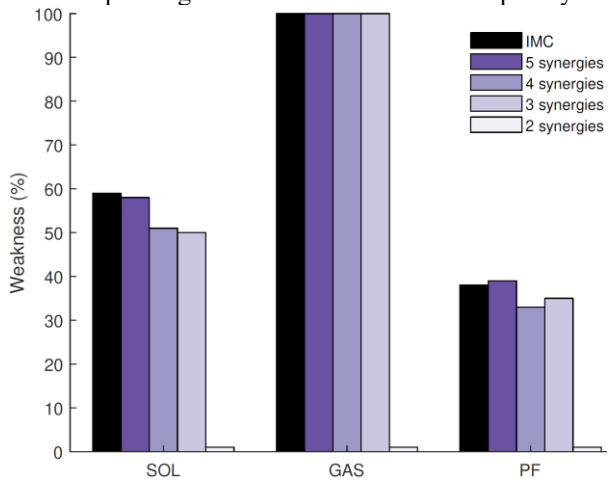

Figure 1: Weakness tolerable in soleus (SOL), gastrocnemius (GAS), and both plantarflexors (PF) for varying levels of control complexity.

Increased plantarflexor weakness required increased motor control complexity eliciting compounding mobility restrictions from interplay between impaired system and control. However, differences in tolerated weakness across control complexities were minimal, indicating that musculoskeletal properties may be a primary determinant of TD walking. Future investigations should examine the combined effects of these impairments across a broader range of impairments and gait patterns.

Significance

This study illustrates that plantarflexor weakness and simplified control, when coupled, create more adverse effects on gait capacity than either alone. Future investigations of populations with neuromusculoskeletal impairments should consider both impaired system and control during predictive simulations. As strength appears to inhibit TD walking, with soleus weakness having a large effect, strengthening may take precedent during therapeutic interventions.

Acknowledgments

This work was supported by NIH Award R01NS091056.

References

[1] H. K. Graham, et al. Nat Rev Dis Prim **2**. 2015.
[2] J. J. Kutch and F. J. Valero-Cuevas. PLoS CB **8**(5). 2012.
[3] L. Pitto, et al. Front Hum Neurosci **14**. 2020.
[4] A. Falisse, et al. Front Neurorobot **13**(54). 2019.
[5] N. Mehrabi, et al. J Biomech **90**(84). 2019.
[6] H. Geyer and H. Herr. IEEE TNSRE **18**(3). 2010.
[7] K.M. Steele, et al. Dev Med Child Neruol **54**(12). 2015.

Moment Arms for Velocity Optimization Vary with Muscle OFL and Resistive Forces

A. C. Osgood[1], G.P. Sutton[2] and S. M. Cox[3*]
[1]Dept. of Physics, Mount Holyoke College, South Hadley, MA 16802
[2]Biological Sciences, University of Bristol, Bristol, UK
[1]Biomechanics Laboratory, Dept. of Kinesiology, The Pennsylvania State University, University Park, PA 16802
Email: *zanne@psu.edu

Introduction

In static conditions, a larger moment arm amplifies the force capacity of a muscle while a smaller moment arm amplifies the output lever displacement. However, in dynamic lever systems driven by muscle contraction, inertia and muscle force-velocity effects confound the relationship between lever geometry and output speed. We hypothesize that in a muscle-driven lever system there is an optimal mechanical advantage above muscle force-velocity properties limit output velocity. Since force-velocity effects are proportional to muscle fiber length[1] and a function of the resistive forces acting on the system, we hypothesize additionally that the optimal mechanical advantage will be a function of muscle optimal fiber length and the inertia of the system.

Methods

To test our hypotheses, we built a computational model of a simple lever system using OpenSim V. 4.0 scripted in Matlab. Our model consisted of an output lever which pivoted around a pin joint, and a muscle acting across the joint with a moment arm defined by the radius of a wrapping surface. The muscle implemented was a Millard2012EquilibriumMuscle muscle model with a non-compliant tendon and a fixed pennation angle of zero. Gravity was not included in the model. We welded a mass to the end of the lever and constrained the range of motion of the lever to 150 degrees with a joint limit force stiffness of 20, damping of 5 and transition range of 2.5°. We generated 3600 modifications of this model with different muscle optimal fiber lengths, OFL, moment arms, starting normalized muscle lengths and driven masses. The volume of the muscle was held constant across changes in OFL such that the muscle force capacity scaled inversely with square root of length. For each modified model, we simulated motion resulting from 100% activation of the muscle model across the full range of motion of the joint in 0.0005 second time steps and extracted the maximum velocity of the driven mass, muscle contractile velocity, normalized contractile distance, total muscle impulse and work.

Results and Discussion

In line with our hypothesis we found that for every muscle simulated, there existed a mid-range moment arm that optimized output speed. We explain the shape of the output velocity-moment arm plot as the interaction of two opposing factors: mechanical advantage and force-velocity effects. At small moment arms, large muscle force capacity is offset by a small mechanical advantage, minimizing torque. At large moment arms, large mechanical advantage is offset by small muscle force capacity due to large muscle contraction velocities.

The optimal moment arm increases linearly with muscle OFL (Fig. 1A). Plotted against normalized moment arm (moment am/OFL), the data collapses to fall along one curve (Fig. 2B). This implies that changes in moment arms can be compensated for by changes in muscle fiber length, as predicted by Zajac [1]. Further, the optimal normalized moment arm increases with driven mass (Fig. 2B) and starting muscle length. Therefore, even for a single individual, changing joint posture (i.e. starting muscle length) or the resistive forces acting on the system (i.e. throwing a different sized ball) can change the moment arm which will maximize output velocity.

Significance

Here we show that the functional consequences of differences in moment arm are dependent on muscle properties and the resistive forces of the system. This suggests that inferences about how variations in moment arm will influence performance could be erroneous if muscle and inertial properties are not accounted for in analyses.

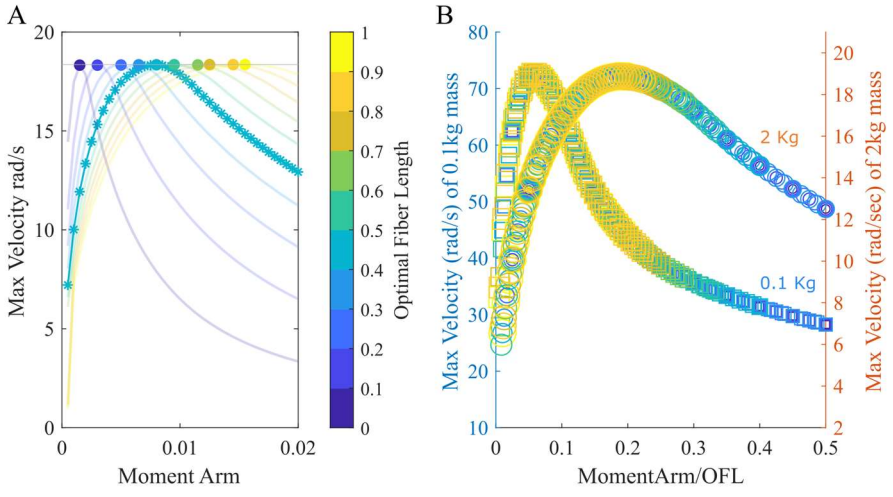

Figure 1: (A) Maximum velocity as a function of moment arm for a system driving a 2 kg mass. There is an optimal moment arm for each muscle and it varies by optimal fiber length. (B) Maximum velocity as a function of OFL normalized moment arm for systems driving both 2kg (circles) and 0.1 kg masses (squares). The data from A collapses such that there is an optimal moment arm/OFL ratio that generates maximum output velocity. That optimum ratio changes with driven mass. In both plots, optimal fiber length is represented by color.

References

[1] Zajac, F (1992). *J.Hand Surgery*, 17(5):799-804.

A Subject-Specific Finite-Element Musculoskeletal Model for Analysis of Lower Limb Biomechanics

Shihao Li[1], Liming Shu[1*], Jiang Yao[2], and Sugita Naohiko[1]
[1] Department of Mechanical Engineering, The University of Tokyo, Tokyo, Japan
[2]Dassault Systemes Simulia Corp., Johnston, RI, USA
*Email: l.shu@mfg.t.u-tokyo.ac.jp

Introduction

Musculoskeletal (MS) modeling is a versatile computational method that gives a great insight into neuromuscular biomechanics of human movement (Delp et al., 1990, 2007). To understand the subject-specific tissue-level mechanics, researchers have developed various workflows that utilize the output of the MS model as the boundary condition of the finite element (FE) model. This unsynchronized feature, however, prevents the detailed changes in the FE model from being reflected into the whole workflow, thus lowering the computation accuracy. In this research, we proposed a subject-specific FE-MS workflow that can concurrently predict the tissue and body level biomechanics.

Methods

The generic FE-MS model developed in Abaqus CAE (Dassault Systems Simulia Corp., Providence, USA) is shown in Figure.1(a). Muscles were modeled as 1D axial connector elements (CONN3N2). The insertion coordinates and parameters of the three-component Hill-type muscle model were obtained from ISB (Delp and Loan, 1995). The model scaling & positioning were executed according to the mass and the marker position extracted from the motion capture data of each subject, thus turning the generic model to a subject-specific model. Then the inverse kinematics & dynamics were implemented using Abaqus Implicit Solver. The whole workflow including scaling & positioning, inverse kinematics & dynamics, and muscle-tendon force optimization was integrated under Isight. While contact and detailed tissues can be easily coupled with the model (Shu et al., 2018), all the joints were simplified as connectors with all the contact ignored in this research. The patient data of JW and DM who underwent total knee replacement with instrumented knee prosthesis from the grand challenge competition (Fregly et al., 2012) were used to verify the proposed model from the aspects of muscle activation, joint kinematics, and joint contact force.

Results and Discussion

The computation time for a single gait cycle on a desktop computer took approximately 30min. The flexion-extension rotations of the knee joint were well predicted, while the prediction for internal-external (IE) and abduction-adduction (Ab-Ad) rotation has failed. The failure might be caused by soft tissue artifact. It is thus necessary to compensate for the Ab-Ad and I-E rotations during the simulation. The muscle activation results of flexor-extensor muscles for both subjects JW and DM showed good consistency on trend with electromyography. Figure 1(b,c,d) shows the comparison of the knee contact force between simulation and experiment. Good agreement on trend and magnitude were found not only in the superior-inferior (SI) tibiofemoral (TF) contact forces but also in anterior-posterior (AP) and medial-lateral (M-L) TF contact forces.

Overall, the proposed subject-specific FE-MS model presented a good prediction accuracy in terms of knee joint kinematics, dynamics, and muscle-tendon forces. It provides an approach for concurrent prediction of the body-level neuro-muscular biomechanics and the tissue-level biomechanics.

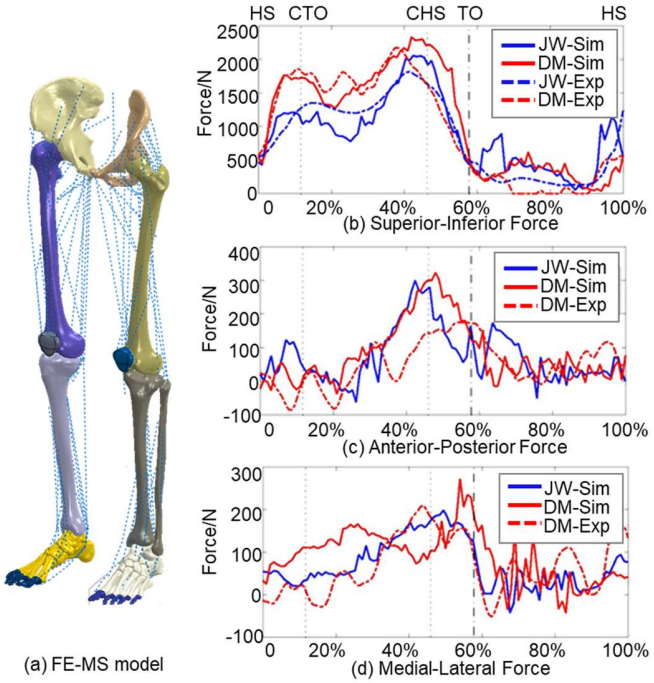

Figure 1: (a) FE-MS model; (b,c,d) knee contact force

Significance

We proposed a finite-element-solver based 3D subject-specific human lower extremity musculoskeletal model which allows synchronized calculation in the FE-MS workflow with reasonable computation time and accuracy. Good agreement on knee joint rotations, muscle-tendon forces, and knee joint contact forces with experimental data indicated that the model has a high potential for the application to investigate the biomechanics of lower extremity, subjective surgical planning and the design of customized prostheses.

References

S.L. Delp. and Loan, J.P. *et al*, 1990. "An interactive graphics-based model of the lower extremity." IEEE Trans. Biomed. Eng. 37, 757–767.

S. L. Delp. *et al*, 2007, "OpenSim: Open-source software to create and analyze dynamic simulations of movement." IEEE Trans. Biomed. Eng. 54, 1940–1950.

S.L. Delp, J.P. Loan, 1995, "A graphics-based software system to develop and analyze models of musculoskeletal structures.", Comput. Biol. Med. 25, 21–34.

B.J. Fregly *et al*, 2012, "Grand challenge competition to predict in vivo knee loads." J. Orthop. Res. 30, 503–513.

Shu, L., et al., 2018, "A subject-specific finite element musculoskeletal framework for mechanics analysis of a total knee replacement." J Biomech, 77, 146-15

Effect of Movement Training on the Location of Acetabular Loading in Developmental Dysplasia of the Hip

Brecca M. M. Gaffney[1], Marcie Harris-Hayes[1], Ke Song[1], John C. Clohisy[1], Michael D. Harris[1]
[1]Washington University School of Medicine in St. Louis
Email: brecca.gaffney@wustl.edu

Introduction

Developmental dysplasia of the hip (DDH) is characterized by altered acetabular and femoral geometries, which result in altered joint loading and increased risk for early hip osteoarthritis (OA) [1-2]. Pre-OA damage in dysplastic hips includes labral tears, which are largely influenced by habitually increased joint loading near the acetabular edge, most commonly in the anterior and lateral regions [3]. Joint loading, whether healthy or pathologic, is dependent on joint kinematics [4]. Movement training to correct kinematics may help normalize both the magnitude and location of joint mechanics without the need for surgery. We recently demonstrated the effect of simulated movement training on hip joint reaction force magnitudes in patients with DDH [5]; yet the direct relationship between altered kinematics and the location of intra-articular joint loading in hips with DDH remains unknown. Using a probabilistic framework, the objective of this study was to identify how kinematic perturbations change the acetabular location of hip joint reaction forces in patients with DDH.

Methods

With IRB approval, MRI (psoas origin to knee) and treadmill gait data were collected from one female patient diagnosed with symptomatic and radiographic DDH (age: 22 y/o; BMI: 25.9 kg/m^2; lateral center edge angle: 7°). An existing musculoskeletal model [6] was modified by including subject-specific pelvis/femoral geometries, hip musculature origins/insertions from MRI, and subject-specific isometric strength values.

The effect of movement training on the acetabular location of the hip JRF was assessed using 2,000 Monte Carlo (MC) simulations and high throughput computing [7]. In each simulation, the sagittal (flexion/extension) and frontal (adduction/abduction) plane hip angles were perturbed by ±10° relative to baseline [4]. Computed muscle control was used to estimate muscle forces throughout the gait cycle, which were used to estimate the hip JRF. The location of the intersection point between the peak hip JRF and the acetabular geometry was determined using a ray-triangle intersection algorithm and expressed relative to the model global origin (mid-ASIS) [8]. Sensitivity factors between the degree of kinematic perturbation and the intersection point coordinates (x-anterior/posterior and z-medial/lateral) were calculated using Pearson correlation coefficients (r) (strong: $0.6 \leq |r| < 1.0$). The slope of each sensitivity factor was multiplied by ±10° to predict the effect of a 10° change in hip angles via movement training on the location of hip joint loading within the acetabulum.

Results and Discussion

The x- and z-acetabular intersection coordinates of the peak hip JRF (12% of gait cycle) were strongly sensitive to perturbations in both the hip flexion/extension (r_x = 0.99 and r_z = 0.83, respectively) and adduction/abduction angles (r_x = 0.98 and r_z = 0.97). Increasing the hip flexion angle by 10° shifted the acetabular intersection location by 4.5 mm posteriorly and 0.8 mm medially. Shifting the hip abduction angle by 10° (i.e. shifted the acetabular intersection location by 1.1 mm anteriorly and 2.6 mm medially (Fig. 1). We have previously shown that increases in hip flexion and abduction angles reduced the overall magnitude of hip JRF by upwards of 30% of the total body weight [5]. The current results indicate that those *magnitude* changes can occur with only minor alteration (<5 mm) to the *location* of peak joint reaction forces within the acetabulum.

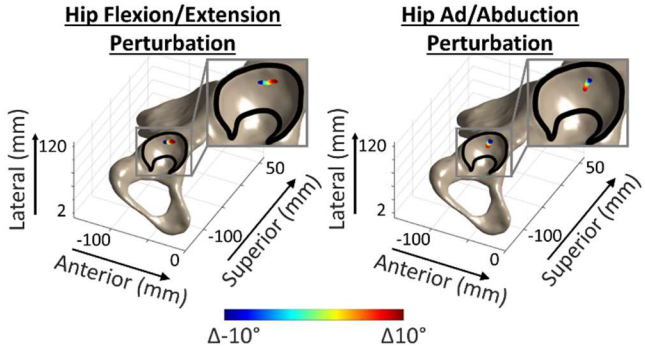

Figure 1. Acetabular intersection location at the point of peak hip JRF in 2,000 MC simulations that perturbed the hip flexion/extension and abduction/adduction angles between +/- 10° relative to baseline.

Significance

We identified that increasing the hip flexion angle during walking shifted joint loading posteriorly, whereas increasing the hip abduction angle shifted joint loading medially. Because the location of acetabular labral tears are most common in both the anterior and superior regions in patients with DDH [3], these results could be used to inform patient-specific intervention planning dependent upon the location of damage. For example, a patient with an anterior labral tear and elevated joint loading near the anterior acetabular edge should adopt increased hip flexion during walking to prevent further labral damage caused by joint overloading. Future work will involve coupling joint reaction force alterations with cartilage contact modelling to clarify how movement training and other nonsurgical interventions may changes articular stress patterns in dysplastic hips.

Acknowledgments

This project was funded by the NIH (K01AR072072, P30AR057235, and F32AR075349) and the L'Oréal USA For Women in Science Fellowship.

References

[1] Cooperman D. (1983). *Clin Orthop Relat Res*, **175**: 79-85.
[2] Reijman M (2005). *Arthritis Rheum*, **52**: 787-793.
[3] Hartig-Andreasen (2013). *Acta Orth*, **84**: 60-64.
[4] Wesseling (2015) *J Orth Res*, **33**: 1094-1102.
[5] Gaffney (2020) *2020 Annual Meeting Orth Res Society*
[6] Lai (2017) *Ann Biomed Eng*, **12**: 2762-2774.
[7] Smith (2019) *J Biomech*, **82**: 124-133.
[8] Tusynksi (2020) *MATLAB Central File Exchange.*

A Comparison of Ligament Strain Estimations Using Bone Pins and Skin Markers

Jeff H. Mettler[1], Erin Ward[2], and Timothy R. Derrick[1]
[1]Department of Kinesiology, Iowa State University, Ames, IA, USA
[2]Central Iowa Foot Clinic, Perry, IA, USA
Email: jmettler@iastate.edu

Introduction

Skin-mounted markers are frequently used to estimate the position, velocity, and acceleration of the underlying bones. However, previous research on the foot has reported significant kinematic differences between skin markers and bone pins [1]. Bone pins are invasive and impractical to use in many situations. Therefore, the purpose of the study is to compare the estimated ligament strains between bone pins and skin markers. A further purpose is to compare the estimated strains to the measured strains from a manual digitizer to validate the current model.

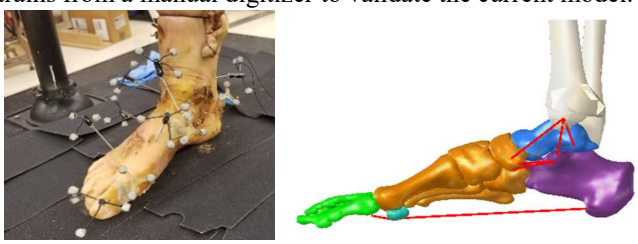

Figure 1: Bone pins and skin markers were used to estimate effects of a tibial axial load on ligament strains using a musculoskeletal model.

Methods

8 cadaver feet were analyzed for the study. An experienced podiatrist dissected the foot to expose the spring and deltoid ligaments, and pins were placed at the origin and insertion of each ligament. Each cadaver was placed with an axial load of 10N on the tibia. A manual digitizer (Microscribe G2, Revware Inc., Raleigh, NC, USA) was used to define the origin and insertion of each ligament. Simultaneously, kinematic data were collected using a 12-camera motion analysis system (Qualisys Oqus 600+, Qualisys NA, Inc., Buffalo Grove, IL, USA). Bone pins and skin marker triads were placed on the calcaneus, navicular, and hallux. Following digitization of the ligaments and the kinematic collection, the axial load was increased to 250N, 500N, 750N, and 1000N, and the process was repeated at each load.

A five-segment model of the foot (calcaneus, talus, forefoot, hallux, and sesamoids) was used to measure the foot position at each load. Movement of the model ankle joint was limited to sagittal plane, and frontal and transverse plane motions at the ankle were attributed to the subtalar joint. Strains of the spring (2 slips) and deltoid (3 slips) ligaments were estimated as the percentage change in length relative to the baseline 10N load condition. Pearson's R correlation coefficients were calculated to investigate the relationship between ligament strains estimated from the model and the strains measured with the digitizer.

Table 1: Pearson's R correlation coefficients between the ligament strains estimated using the musculoskeletal model and the ligament strains measured using the manual digitizer.

Ligament	Digitizer – Bone Pins	Digitizer – Skin Markers
Spring – Superior	0.95	0.96
Spring – Inferior	0.98	0.97
Tibionavicular	0.99	0.85
Tibiocalcaneal	0.60	0.76
Tibiotalar	0.48	0.88

Results and Discussion

Ligament strains estimated using both the bone pins and skin markers were strongly correlated to the ligament strains directly measured by the manual digitizer for both aspects of the spring ligament and the tibionavicular aspect of the deltoid ligament (Table 1). Weaker relationships were noted for the tibiocalcaneal and tibiotalar aspects of the deltoid ligament. Coefficients were larger between the manual digitizer and skin markers than they were between the manual digitizer and bone pins for both the tibiocalcaneal and tibiotalar aspects of the deltoid ligament.

The results show that the ligaments crossing the midtarsal joint of the foot can be estimated using a musculoskeletal model. Furthermore, the high correlations between the strains measured using the digitizer and the strains estimated using skin markers suggest that skin markers placed on the surface of the foot can be used to accurately estimate ligament strain.

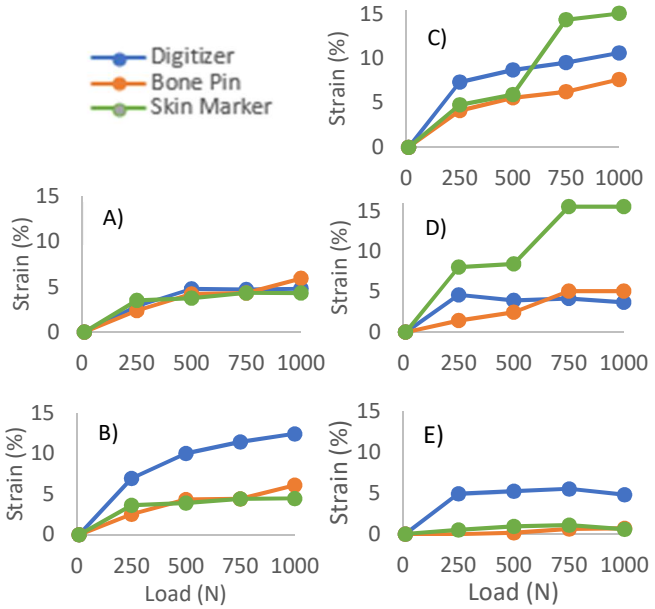

Figure 2: Ligament strains at each axial load for the A) spring – superior, B) spring – inferior, C) deltoid – tibionavicular, D) deltoid – tibiocalcaneal, and E) deltoid – tibiotalar.

Significance

The results from the study will allow us to estimate ligament strains in a living population using a musculoskeletal model. Doing so provides us with the potential to more fully understand soft tissue foot injuries that are related to ligament strains, such as posterior tibial tendon disorder and plantar fasciitis.

Acknowledgments

Richie Technologies, Inc., Seal Beach, CA, USA
KLM Orthotics Laboratory, Valencia, CA, USA

References

[1] Nester C et al. (2007) *J Biomech,* **40**: 3412-3423.

Walking with a cane alters plantarflexor muscle forces during walking in individuals post-stroke

Todd J. Leutzinger[1], Erica A. Hedrick[1], Brian A. Knarr[1]
[1]Department of Biomechanics, University of Nebraska at Omaha, Omaha, NE USA
Email: tleutzinger@unomaha.edu

Introduction

Stroke is the leading cause of prolonged disability in the United States [1]. A prominent issue in gait post stroke is decreased propulsive force generation from the paretic leg [2]. This decreased propulsion force is caused by a reduction in ankle plantarflexor activation [3] and results in metabolically inefficient gait patterns [4] as well as decreased community ambulation, a measure correlated with quality of life [5]. Morever, the use of a cane is prominent in individuals post stroke to help improve balance and overall walking ability. The purpose of the current study was to utilize musculoskeletal modeling to investigate how ankle plantarflexor forces change between walking with versus without a cane post-stroke. Additionally, the authors sought to determine how the model's residual actuators adjusted when the subject walked with a cane, without accounting for the forces of the cane in the model. The authors hypothesized ankle plantarflexor forces would decrease and residual actuator forces would increase with cane use to match the force output of the cane.

Methods

One subject (mass: 101.34 kg, height: 1.8 m) performed walking trials with and without a cane at a self-selected speed across eight in-ground force platforms. Seventeen motion capture cameras sampling at 100 Hz were used to track a full body marker set of 65 retroreflective markers and 6 additional markers placed on the cane. The subject performed four trials in each condition. A single, clean foot contact from the subject's paretic limb was used for analysis in each condition. Data were exported from Visual 3D (Germantown, MD, USA) to OpenSim [6] where all analyses were performed. The model was scaled to fit the subject based on the Visual 3D scale set and inverse kinematics were performed in Visual 3D for both conditions. Residual Reduction Analysis (RRA) was performed to decrease the effects of modeling and marker processing errors. The RRA solution of the cane trial was then compared to the ground reaction forces of the cane. Computed Muscle Control (CMC) was used to calculate the muscle actuator forces used to drive the model forward while tracking the desired kinematics. The medial gastrocnemius (MG), lateral gastrocnemius (LG), and soleus (SOL) muscles of the paretic limb were used for comparison between the two trials.

Results and Discussion

During the cane condition, the average vertical ground reaction force of the cane was within 14% of the average vertical residual force from RRA when the cane was in contact with the force plate. This result is aligned with previous research demonstrating OpenSim's ability to account for handrail use during walking [7]. During the no cane condition, the model displayed a 21.4% and 49.8% increase in peak actuator force of the MG and LG respectively compared to the cane condition. The model also demonstrated a 21.5% decrease in peak actuator force of the SOL compared to the cane condition. Average actuator force in the no cane condition for the MG, LG, and SOL were 27.6%, 56.0%, and 32.6% greater compared to the cane condition, respectively.

The results of this abstract are in accordance with previous literature indicating muscle forces are reduced when walking with versus without a cane in an individual post stroke [8]. Neptune et al. reported that the SOL and MG provide trunk support during early stance and the SOL promotes trunk acceleration during late stance [9]. During early stance, SOL and MG muscle actuator forces are present when not using the cane but are not present when using the cane (Figure 1). This suggests the subject used the cane, not their MG or SOL, to support their trunk. Research has shown canes are able to increase an individual's braking force during walking [10]. The increase in SOL force during the cane condition is likely a result of the subject increasing forces in the SOL to overcome the increased braking force provided by the cane and accelerate the trunk forward.

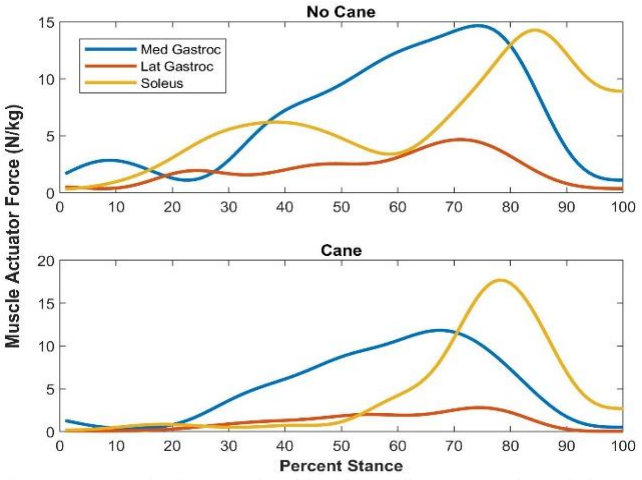

Figure 1: Muscle forces of ankle plantarflexor muscles of the paretic limb when walking with versus without a cane.

Significance

The results of this study indicate ankle plantarflexor muscle force of the paretic leg decreases with the use of a cane, and OpenSim's RRA tool is able to compensate for residual forces not accounted for in the model. Future work is necessary to implement the cane in the simulation to more accurately account for it in the model and determine how the model repsonds to this external force.

Acknowledgments

This work was supported by NIH grant R15HD0941901A1

References

1. Go et al. *Circulation*, 399-410, 2014
2. Bowden et al., *Stroke*, 872-876, 2006
3. Lamontagne et al. *Gait & Posture*, 244-255, 2002
4. Stoquart et al., *Gait & Posture*, 409-413 2011
5. Schmid et al. *Stroke* 2096-2100, 2007
6. Delp et al. *IEEE Trans. Biomed. Eng,* 1940-50, 2007
7. Knarr & Higginson *ASME* 2012
8. Buurke et al. *Gait & Posture*, 164-170, 2005
9. Neptune et al. *J Biomech,* 1387-98, 2001
10. Chen et al. *Arch Phys Med Rehabil,* 43-48 2001

Between-session Reliability of Subject-Specific Musculoskeletal Models of the Spine Derived from Optoelectronic Motion Capture Data

Katelyn A. Burkhart[1], Daniel Grindle[2], Mary L. Bouxsein[1], and Dennis E. Anderson[1]
[1]Center for Advanced Orthopedic Studies, Beth Israel Deaconess Medical Center, Harvard Medical School, Boston MA
[2]Division of Engineering Mechanics, Virginia Polytechnic Institute and State University, Blackburg VA
Email: kburkhar@bidmc.harvard.edu

Introduction

Optoelectronic motion capture data are often used for scaling of musculoskeletal models to an individual's anthropometry. However, there is known error in optoelectronic motion capture due inherent system performance[1] and more notably due to variation in marker placement on anatomical landmarks[2-4]. While these concerns have been well studied in gait models, there has been limited prior investigation into how this variation might affect marker-estimated spine models and spinal loading predictions.

Therefore, the aim of this study was to investigate how variation in the placement of anatomical markers affects the reliability of body segment scaling, estimated spine curvature, and resulting compressive spine loading outcomes when creating subject-specific musculoskeletal models.

Methods

Nineteen healthy participants aged 24-74 years underwent the same set of measurements on two separate occasions. Retroreflective markers were placed on anatomical regions, including C7, T1, T4, T5, T8, T9, T12 and L1 spinous processes, pelvis, upper and lower limbs, and head. We created full-body musculoskeletal models with detailed thoracolumbar spines, and scaled these to create subject-specific models for each individual and each session. Models were scaled from distances between markers, and spine curvature was adjusted according to marker-estimated measurements. Using these models, we estimated vertebral compressive loading from T1 to L5 for five different standardized postures: neutral standing, 45˚ trunk flexion, 15˚ trunk extension, 20˚ lateral bend to the right, and 45˚ axial rotation to the right. Intraclass correlation coefficients (ICCs) and standard error of measurement were calculated as measures of between-session reliability and measurement error, respectively.

Results and Discussion

Of the nineteen healthy subjects, two subjects were excluded from analysis due to non-visible retroreflective markers on the pelvic ASIS or on the L1 vertebra. For body segment scaling, segment lengths were not different between sessions ($p>0.05$). The measurements with excellent reliability (ICC > 0.75) were the head and neck length and width, humeri and radii, spine and foot length and width. All other scaling measurements had fair reliability with ICCs ranging from 0.46 – 0.75. Spine curvature was not different between sessions, however the variability was larger for lordosis than kyphosis. Both measures had excellent reliability with ICCs>0.75. Bland Altman plots of between session measures showed no systematic differences or proportional biases.

Subject-specific spine loading between sessions was not significantly different for all activities. Interquartile ranges and total range of mean difference were similar across all levels of the spine for all simulated activities. Mean difference in compressive spine loading during flexion between sessions is shown in Figure 1. The ICC values of spine loading from T1 to L5 were mostly excellent, with 91% of ICC point estimates being greater than 0.75 for all activities.

This is the first study to determine the reliability of spine loading determined from marker-based subject-specific musculoskeletal models. We found that larger differences in spine loading between sessions (>15%), at any level, were corresponding to larger differences (>10%) in lordosis or kyphosis between sessions. This indicates much of our spine loading differences can be ascribed, at least in part, to differences in spine curvature, and that precise and accurate assessment and implementation of spine curvature is crucial for creating subject-specific musculoskeletal models of the spine.

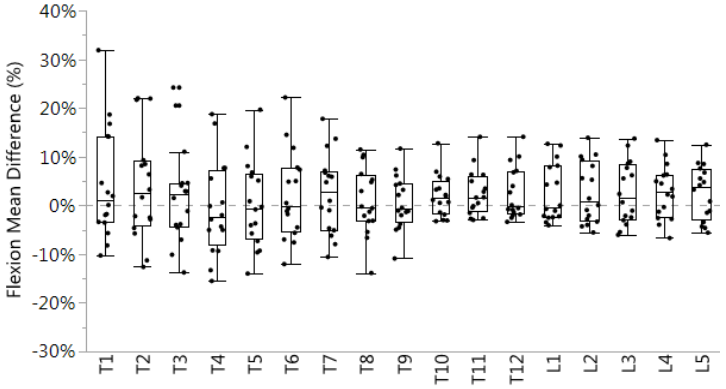

Figure 1: Mean difference in compressive spine loading for flexion between sessions. Box plots show median and inter-quartile range, and black dots represent individual data points.

Significance

Overall, this information is a necessary precursor of using motion capture data to estimate spine loading with subject-specific musculoskeletal models, and suggests that marker data will deliver reproducible subject-specific models and estimates of spine loading**.** This informs the conduct and interpretation of future studies on dynamic spine loading, which are important for gaining insight into mechanisms contributing to back pain, vertebral fractures and other musculoskeletal injuries.

Acknowledgments

Rebecca Tromp and Javad Mousavi contributed to data collection. This work supported by grants from the National Institutes of Health (R00AG042458; R01AR073019), the Department of Orthopaedic Surgery at Beth Israel Deaconess Medical Center, and Harvard Catalyst (UL1 TR001102).

References

1. Richards, J.G., 1999. Hum. Mov. Sci. 18, 589–602.
2. Della Croce et al., 1999. Med. Biol. Eng. Comp. 37(2) 155-61
3. Krumm et al., 2016. Gait Posture. 46, 1-4.
4. Rast et al. 2016. J. Biomech. 49, 807-11.

A self-correcting spiking network model for motor unit coordination during force production

Brianna M. Karpowicz[1], and Lena H. Ting[1,2]
[1] The Wallace H. Coulter Department of Biomedical Engineering at Georgia Tech and Emory University, Atlanta, Georgia 30322-0535
Email: brianna.karpowicz@emory.edu, lting@emory.edu

Introduction

We do not understand how commonly observed and mathematically described properties of motor force output arise from neural circuitry. For example, motor outputs exhibit signal dependent noise, in which force variability increases with force magnitude. Further, the motor system exhibits the ability to robustly maintain a force, such that variability in the output of individual motor units or muscles does not directly affect the variability in force output. This has been extensively described in the motor literature as the "uncontrolled manifold,"[1] or optimal feedback control.[2–3]

Here, we developed a model of a motor neuron pool based on principles of an efficient spiking network, which has been used to understand firing properties of cortical neuronal populations. In an efficient spiking network, the neurons cooperatively produce an output with a balanced distribution of activity across neurons.[4–6] We hypothesize that this balance enables stable force production despite variability in individual neural firing. Provided various desired force trajectories, we tested whether the model output would exhibit signal-dependent noise and robustness to perturbations in its motor neuron firing.

Methods

The model was composed of a network of N=100 leaky integrate-and-fire neurons in an efficient balanced network. The model was given a desired time-varying input force vector x (Fig 1, red). The neurons in the network fire if their firing reduces the error of the system, which is represented by:

$$\mathscr{L} = \langle \|x - \hat{x}\|^2 + \mu \|r\|_2^2 \rangle$$

where $\hat{x} = \sum_i w_i r_i$ is the network's estimated force output, w_i are the fixed weights of the connections between neurons, μ is the cost of firing, and r is the filtered spike train s, where $\dot{r} = -\lambda r + s$ and λ is the neuron's leak coefficient. This loss function minimizes error in the produced force while ensuring that spiking activity is distributed across neurons. A neuron in the network fires when its membrane voltage $V_i = w_i(x - \hat{x}) - \mu_i r_i$ crosses the firing threshold. Each neuron's contribution to $\hat{x}$ is reflected in its inhibitory connections (weighted by w_i) to other neurons. This simulates the effects of interneurons, including Renshaw cells, where each motor neuron inhibits itself and all other motor neurons.

We used this architecture to create two models. First, we simulated a force-sharing network in which the contribution of each neuron to the total force was equal ($w_i = w_j$ for all pairs of neurons i, j), and each neuron had an equal firing threshold. The second model was a motor unit recruitment network; the contributions of each neuron in this network to the total force output increased linearly such that "larger" motor units needed to reach a higher membrane voltage to fire and contributed more to overall force. That is, $w_i < w_j$ for all pairs of neurons i, j such that the size of neuron i is less than the size of neuron j.

We fed time-varying force trajectories to each network and observed the resultant variance and magnitude of the force output to assess the presence of signal-dependent noise. To test the robustness of the model output to neural variability, we created a drastic change in neural firing by silencing a large fraction of neurons and measuring the mean and variance of the force output.

Results and Discussion

Both network models were able to simulate a desired force input (Fig. 1a, b). With respect to signal-dependent noise, only the motor unit recruitment network exhibited an increased variance with an increased magnitude of force output (Fig 1, insets).

Both networks were robust to massive perturbations (Fig 1c), i.e. the destruction of a large fraction of its neurons. Notably, we found that the networks were able to sustain force production by distributing force production amongst the remaining available neurons until the destruction of 60-80% of the neurons (Fig 1d). Across motor pool simulations with successful force production, force output varied by 7%, while the firing of the remaining individual neurons changed by $467 \pm 99\%$.

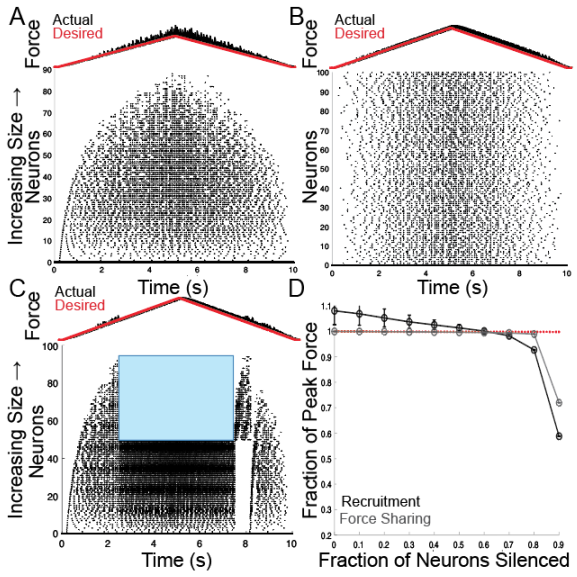

Figure 1: Network Outputs. (A) Raster plot of motor unit recruitment network producing a ramping force. (B) Raster plot of force sharing network producing a ramping force. (C) Representative raster plot showing a fraction of silenced neurons (blue box). (D) Fraction of desired force reached across various fractions of silenced neurons.

Significance

We have developed a biologically plausible model of how motor output may be regulated by a self-correcting network to maintain task level goals despite variability in individual motor neuron output. Such a framework may inform our mechanistic understanding of compensation in debilitating motor impairments.

Acknowledgements

Dr. Sophie Deneve for guidance in implementation. Support to BMK by T32EB025816.

References

1. Scholz and Schoner. Exp Brain Res, 1999. 2. Todorov and Jordan. Nature Neuro, 2002. 3. Todorov. Nature Neuro, 2004. 4. Alemi, et. al. AAAI, 2018. 5. Deneve, et. al. Neuron, 2017. 6. Gutierrez and Deneve. eLife, 2019.

Fracture resistance analysis in human dentin microstructure

Ebrahim Maghami[1], Ahmad R. Najafi[1,*]
[1]Department of Mechanical Engineering and Mechanics, Drexel University, Philadelphia, PA 19104, USA
Email: *arn55@drexel.edu

Introduction

Dentin has a unique hierarchical structure containing mineral crystals embedded in a protein matrix [1]. Fracture behavior in such a biological composite is of great importance for the restorative dentistry. At the microscale level, an important feature is the existence of dentinal tubules. The tubules are surrounded by highly mineralized cylindrical cuffs of peritubular dentin (PTD) [1]. PTDs are embedded in a protein matrix known as intertubular dentin (ITD). The density and diameter of tubules near the pulp tissue are larger than those of near the dentin enamel junction (DEJ) [2]. There is also an increase in the thickness of PTD from the pulp tissue to the DEJ.

The microstructural features have considerable effects on the mechanical resistance of dentin and the hierarchical structure of dentin is associated with various toughening mechanisms [1]. In the present study, we investigate the influence of variations in PTD thickness, the tubules' diameters, and materials properties through dentin on the crack growth. In order to capture different toughening mechanisms, we use a brittle model of the phase-field method to analyze the crack growth.

Methods

At the microscale level, dentin can be considered as a fiber-reinforced composite structure. PTDs are considered as hollow fibers with the inner diameter d_t and thickness t_p and embedded in ITD matrix (Figure 1). To create the models, we use the geometrical information reported by Chu *et al.* [2]. The boundary conditions of the models are shown in Figure 1. We investigate the mechanical response and damage propagation in dentin under 2D plain-strain conditions. To study the region-dependent fracture behavior of dentin, we consider the density and the diameter of dentinal tubules and the PTD thickness at the crown and root parts of dentin. We also evaluate the influence of mechanical properties of ITD and PTD on crack growth. We adopt a brittle model of the phase-field method developed by Molnár *et al.* [3]. We implement the brittle model into a subroutine using Abaqus software.

Results and Discussion

Our results show that microcracking in PTD is found as an effective toughening mechanism in all simulations. The rate of microcracking increases by decreasing the critical energy release rate of PTD. However, microcracking in PTD is not significantly dependent on the elastic moduli of ITD and PTD. We also observe crack branching in our models. Crack branching is determined as one of the toughening mechanisms in the region near to the pulp tissue. Our results also reveal that the toughness of the dentin microstructure is dependent on the density of tubules. Due to a decrease in the density of tubules in the location near to the DEJ, cracks propagate through the ITD matrix with few barriers in head of the cracks in this region (Figure 1).

Our results also indicate that crack deflection is decreased by a decrease in the density of tubules. In this study, we also evaluate the important role of the interface between PTD and ITD in crack deflection. By decreasing the critical energy release rate of the interface (i.e., decreasing the resistance of the interface to fracture), the cracks are arrested along the interface.

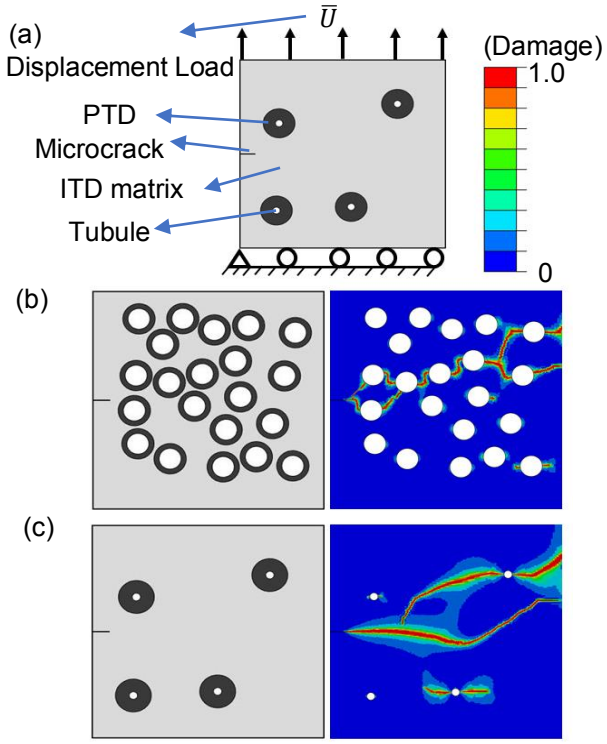

Figure 1: (a) A schematic representation of the microstructural features within dentin including the applied load and the boundary conditions. 2D models of two different locations within dentin and their fracture patterns: (b) near the pulp tissue and (c) near the DEJ. Damage with 1.0 shows the crack path and the zero value presents that there is no damage.

Significance

The findings of the present research show the region-dependent fracture behavior of dentin. This dependency on the regions helps us to develop the dentine-adhesive restorative materials. We can also predict the probability of failure in various regions within dentin. This provides technical information on fracture behavior of dentin for the dental restorations. Our models also enable us to capture various toughening mechanisms such as microcracking, crack deflection and branching in a composite structure.

Acknowledgments

The authors acknowledge the high-performance computing resources (PROTEUS: the Drexel Cluster) and support at the Drexel University.

References

[1] Nalla RK, et al. *Biomaterials*, 24(22), pp.3955-3968, 2000.
[2] Chu CY, et al. *Journal of Dental Sciences*, 5(1), pp.14-20, 2010.
[3] Molnár G, et al. *Finite Elements in Analysis and Design*, 130, pp.27-38, 2017.

MODELING SITE-SPECIFIC WOVEN BONE FORMATION IN RESPONSE TO EXOGENEOUS PURE BENDING OF RAT TIBIA

Ajay Goyal, Jitendra Prasad*
Department of Mechanical Engineering, Indian Institute of Technology Ropar, Punjab, India 140001
*Email: jprasad@iitrpr.ac.in

Introduction

Osteocytes are the mechano-sensors that initiate variety of signaling pathways (such as Ca^{2+}/NFAT, BMP, WNT etc.) within lacunae-canaliculi network in response to exogenous mechanical loading [1]. These signals induce stimuli with in the bone matrix which produces proportionate new bone formation at bone's periosteal and endocortical surface [1]. Induced stimuli must surpass a threshold level to deposit lamellar bone [2]. However, woven bone gets generated in haphazard manner if induced stimuli exceed another higher threshold level [2]. This study presents a mathematical model that fits site-specific woven bone generation for rat tibia mid-section exposed to pure bending. In particular, this model is an extension of an existing model that predicts site-specific lamellar bone for different loading regimens [1]. The model has potential to predict lamellar as well as woven bone distribution for different loading regimens at rat and mice tibial mid-section.

Methods

The current model is an extension of existing mathematical model [1]. Induced strain at location of any osteocyte should surpass a threshold level (ε_1) to allow flow of stimulus to its neighboring osteocyte. Stimuli generated by osteocytic network within lacunae-canaliculi network will reach lining cells and deposit proportionate lamellar bone to stimuli.
However, once lining cell gets differentiated into mature osteoblast and exceeds another higher threshold level of strain (ε_2), then woven bone will be generated in haphazard manner. Therefore, we added that osteoblasts not osteocytes play significant role to predict woven bone when they are exposed to heavy loads. Hence, this modified model can fit both lamellar and woven bone. In addition, osteoblasts behave differently to tensile and compressive loading. Accordingly, the optimization function (f) has been modified as follows:

If ε_{ob_j}-$\varepsilon_2 < 0$

$$f = \sum_{j=1}^{n_{ob}} (t_{ob_j} - kS_{ob_j})^2$$

Otherwise;

$$f = \sum_{j=1}^{n_{ob}} [t_{ob_j} - \{k_i r \left(\varepsilon_{ob_j} - \varepsilon_2\right) (NB)^{1/b}\}]^2$$

ε_{ob_j} , t_{ob_j} and S_{ob_j} represents the induced strain, in-vivo new bone thickness and stimulus from osteocytic network at j^{th} osteoblast located at bone periosteum respectively. N and B represents number of loading cycles/day and number of bouts per week respectively. "k", "b" and "r" are constants adapted from [1]. Proportionality constants "k_i" (i=1, 2) and ε_2 (threshold strain value for woven bone generation) are variables to be optimized.

Results and Discussions

The modified model has been tested at periosteal surface for Sprague Dawley rat tibia mid-section exposed to pure bending [3]. Required input data has been collected/calculated from the literature [3]. Figure 1 shows the in-vivo vs. analytical woven bone distribution. Watson U2 goodness of fit test (p-value = 0.76 and independent two sample Student's t-test (p-value=0.61) suggested a good fit between analytical and in-vivo woven bone distribution.

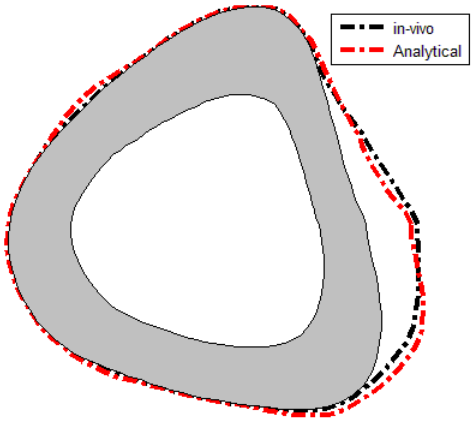

Figure 1: In-vivo vs. analytical woven bone distribution at periosteal surface of 9 months old rat mid-section tibia exposed to pure bending with peak induced strain of 3010με. The loading was done using 504 nos. sinusoidal loading waveform (2Hz) at 64N amplitude in 12 days.

Significance

The model closely predicts site-specific woven bone distribution at least for pure bending cases. The model has potential to predict both lamellar and woven bone distribution for different loading regimens.

Acknowledgements

Defence Research and Development Organisation, India for monthly scholarship to AG.

References

1. Prasad J. and Goyal A. Scientific reports 9.1 (2019): 5890.
2. Anderson HC, et al. Front Biosci 10.1 (2005): 822-837.
3. Turner, CH., et al. Journal of bone and mineral research 9.1 (1994): 87-97.

Contributions of co-contraction and sensory feedback to deal with unstable musculoskeletal dynamics

Tom Van Wouwe.[1], Lena Ting[2], Friedl De Groote[1]
[1]Department of Movement Sciences, KU Leuven, Leuven, Belgium
[2] W.H. Coulter Department of Biomedical Engineering, Emory University and Georgia Tech, Atlanta, USA
Email: tom.vanwouwe@kuleuven.be

Introduction

Robustness of movement in the presence of internal (sensorimotor noise) and external perturbations results from the interaction between neural control and musculoskeletal mechanics. It has been shown that humans use both delayed sensory feedback control [1], and adapt joint impedance by co-contracting muscles [2] to stabilize movement. However, it is yet unclear how those strategies are combined. Simulations might give insight in how task goals and task constraints shape the control strategy. Optimal control explains many features of human movement. However, due to the high computational cost, available approaches require either deterministic open-loop trajectory optimization in case of complex musculoskeletal models, or stochastic feedback control with simpler models and linear [3] or open-loop stable dynamics [4].

We previously proposed an optimal control framework based on direct collocation that enables rapid predictive simulations of movement [5]. Here, we extended our trajectory optimization framework to a generally applicable robust optimal control framework. We then applied the framework to predict muscle co-contraction and sensory feedback for a reaching task in a divergent force field [3].

Methods

Consider a system with dynamics $\dot{\boldsymbol{x}} = f(\boldsymbol{x}, \boldsymbol{u}, \boldsymbol{w})$, with $\boldsymbol{x}$ the states, $\boldsymbol{u}$ the controls and $\boldsymbol{w}$ a set of zero mean Gaussian disturbances (noise). To account for uncertainty, we augment the state-space by adding the state co-variance matrix P. We describe the propagation of the co-variance matrix by the continuous Lyaponuv equation [1]: $\dot{P} = AP + PA^T + C\Sigma_w C^T$, with $A = \partial f(\boldsymbol{x}, \boldsymbol{u}, 0)/\partial \boldsymbol{x}$, and $C\Sigma_w C^T$ the effect of noise with $C = \partial f(\boldsymbol{x}, \boldsymbol{u}, \boldsymbol{w})/\partial \boldsymbol{w}$ and Σ_w the noise co-variance matrix. In our robust optimal control framework, we solve for controls that minimize a task-related cost using direct collocation.

We modeled a reaching task in a divergent force field as performed by Franklin et al. [3]. The musculoskeletal model is a 2-dof planar arm model driven by four mono-articular Hill-type muscles. Muscle excitations (e_m) consist of a feedforward term and linear feedback of the deviation from the optimal hand trajectory: $e_m(t) = e_{ff,m}(t) + K(t) \cdot (p_h(t) - p_h^*(t))$, with p_h the hand's position and velocity in the 2D plane and p_h^* the deterministic trajectory generated by the optimal feedforward controls. We implemented a lumped neuromechanical delay of 100ms. The divergent force field is modelled as an external horizontal force acting on the hand that is dependent on hand position: $F_x = 100[\frac{N}{m}] \cdot x_{hand}$. Sensory noise is modeled as Gaussian noise with standard deviation of 2mm and 4mm/s on respectively hand position and velocity respectively. Motor noise is modeled as Gaussian noise with standard deviation of 0.3Nm added to the shoulder and elbow torques. Starting pose (0,0), end pose (0,0.25m) and movement duration 0.5s are prescribed. We solve for feedforward excitations $e_{ff,muscle}(t)$ and feedback gains $K(t)$ that minimize a trade-off between effort and variance of the end-point position of the hand.

Results and Discussion

We evaluated feedforward muscle excitations, hand trajectories and the end-point error ellipses (95% confidence ellipse resulting from 1000 stochastic forward simulations) under three types of control: (1) feedforward control minimizing effort ('ff nominal'), (2) robust feedforward control minimizing effort and end-point variance ('ff robust') and (3) combined feedforward and feedback control minimizing effort and end-point variance ('ff + fb robust').

Our robust optimal control model predicts co-contraction and delayed sensory feedback as mechanisms to stabilize the musculoskeletal dynamics during a reaching movement in an unstable environment in the presence of sensorimotor noise (Figure 1). Robust feedforward control leads to co-contraction to mitigate the effects of interactions between motor noise and the destabilizing force-field. However, without feedback the motion is not stable and the end-point error ellipse is larger than experimentally observed [3]. Adding sensory feedback leads to end-point variance similar to what is experimentally observed [3]. In agreement with experimental results, co-contraction is still present, due to the limited performance of sensory feedback in presence of delays and noise.

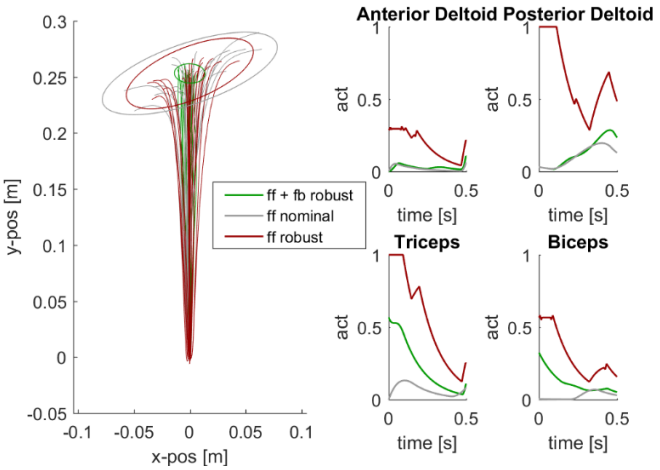

Figure 1: Reaching trajectories and muscle activations for shoulder antagonists (anterior and posterior deltoid) and elbow antagonists (triceps and biceps). Note that co-contraction (simultaneous activity in antagonist muscles) is large in the absence of feedback (red) but still present when feedback is added (green).

Significance

We present a generally applicable robust optimal control framework and demonstrate that optimal control can explain both sensory feedback and co-contraction as strategies to cope with sensorimotor noise in an unstable environment. Importantly, our ability to use complex muscle-driven models allows us to account for the interaction between the intrinsic stabilizing properties of the musculoskeletal system and motor control when studying how uncertainty shapes movement patterns, muscle co-activation, and feedback control.

Acknowledgements

We acknowledge FWO fellowship: 1S82320N

References

[1] Scott S, Nature Reviews Neuroscience, 2004
[2] Hogan N, IEEE Transactions on Automatic Control, 1984
[3] Franklin D, Journal of Neurophysiology, 2004
[4] Todorov E, Proceedings of the American Control Conference, 2005
[5] Falisse A, J. R. Soc. Interface, 2019

3D-Printable Prosthetic Foot with Human Toe-Joint Property

Heonsu Kim[1], Huijin Um[1], Woolim Hong[2], Haksung Kim[1,3,*], and Pilwon Hur[2,*]
[1]Department of Mechanical Engineering, Hanyang University, Seoul, South Korea
[2]Department of Mechanical Engineering, Texas A&M University, College Station, TX 77843, USA
[3]Institute of Nano Science and Technology, Hanyang University, Seoul, South Korea
Email: *kima@hanyang.ac.kr, pilwonhur@tamu.edu

Introduction

In designing a prosthetic foot, the relationship between the mechanical properties (e.g., stiffness and damping) and the gait biomechanics should be considered to have human-like ambulation. One of the critical factors is the toe joint stiffness, which can provide a general feeling of springiness in toe-off step. Several studies have attempted to implement the toe stiffness in the prosthetic foot design; however, their designs were complex to be manufactured [1], [2]. Also, the aforementioned designs usually require an additional mechanical part for the toe joint, leading to the heavier weight of the foot. In this study, we propose the 3D printable foot structure (i.e., re-entrant and honeycomb structure [3]) to mimic human foot characteristics, specifically the toe stiffness. We also propose a composite material, called "onyx", to enhance the elasticity and strength.

Methods

To analyze the toe stiffness properties, two finite element analysis (FEA) models (a: re-entrant, b: re-entrant honeycomb) were established (Figure 1). In Figure 1(a), the re-entrant structure was applied in the forefoot. To investigate the effect of the foot material, two different materials (i.e., ABS and onyx) were compared using the identical structure in the simulation. On the other hand, in Figure 1(b), the combined structure of the re-entrant and honeycomb was applied in the forefoot to release stress concentration of the re-entrant model. Then, to analyze toe bending characteristics, a simulation was conducted with and without the bending zone (BZ). For a toe bending simulation, a rigid plate was placed at the bottom of the forefoot and approached gradually with 10° inclination in the re-entrant model, and 15° inclination in the re-entrant honeycomb model to confirm reinforcement of the latter model. All numerical simulation was done with ABAQUS (v6.14, ABAQUS Inc., Vélizy-Villacoublay, France).

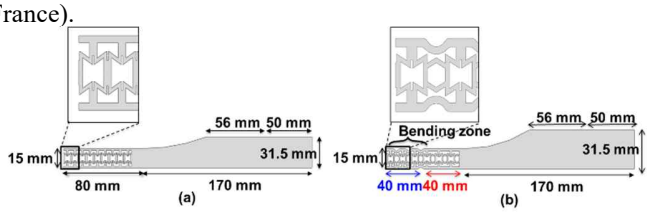

Figure 1: FEA models (a) the re-entrant structure was applied in the forefoot; (b) the combined structure of the re-entrant, honeycomb, and BZ was applied in the forefoot

Results and Discussion

Figure 2 shows the FEA results of the re-entrant model. As it is shown in the force-displacement (F-D) graph (Figure 2(a)), the stiffness (i.e., slope of F/D curve) of the onyx increased while that of the ABS was constant. Note that the nonlinearly increasing toe joint stiffness is desired for the prosthetic foot due to the human gait biomechanics. In addition, the onyx showed lower maximum stress and higher yield strength than the ABS (Figure 2(b)). Since the onyx has high elasticity and strength, it may have performed variable stiffness characteristics while having a proper strength characteristic.

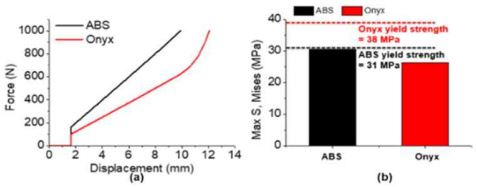

Figure 2: The FEA results of the first model: re-entrant structure (a) F-D graph; (b) maximum stress

However, when the toe bending angle was over 15°, the maximum stress of the re-entrant structure exceeded the yield strength. For this reason, the re-entrant honeycomb model was designed to reduce the maximum stress. Since it resulted in a deterioration of the stiffness characteristics, BZ was used to compensate it. The FEA results are depicted in Figure 3. The characteristics of the stiffness and the strength were enhanced when the BZ is considered. The curved surface of the BZ released the stress concentration, resulting in the enhancement of the bending characteristics.

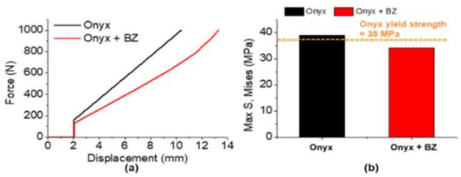

Figure 3: The FEA results of the second model: re-entrant honeycomb structure (a) F-D graph; (b) maximum stress

Significance

This study shows that numerous mechanical properties can be obtained by modifying the structure of the prosthetic foot. Further, the desired characteristics can be obtained by the optimization process. Since the proposed foot is 3D printable, it is easy to manufacture the prosthetic foot while considering individuals' characteristics. We expect that the proposed re-entrant honeycomb structure and onyx will lead to simplicity in manufacturing, the reduction of the cost and the weight, and enhancement of gait biomechanics.

Acknowledgments

This research was supported by the MOTIE (Ministry of Trade, Industry, and Energy) in Korea, under the Fostering Global Talents for Innovative Growth Program (P0008748, Global Human Resource Development for Innovative Design in Robot and Engineering) supervised by the Korea Institute for Advancement of Technology (KIAT)

References

[1] Adamczyk, et al. (2017), *Human movement science*, 54: 154-171.
[2] Honert, et al. (2018), *Bioinspiration & Biomimetics*, 13. 066007
[3] Ingrole, et al. (2017), *Materials & Design*, 117: 72-83

Structural behavior evaluation of prosthetic foot using the auxetic structure via finite element analysis

Huijin Um[1], Heonsu Kim[1], Woolim Hong[2], Haksung Kim[1,3,*], and Pilwon Hur[2,*]
[1]Department of Mechanical Engineering, Hanyang University, Seoul, South Korea
[2]Department of Mechanical Engineering, Texas A&M University, College Station, TX 77843, USA
[3]Institute of Nano Science and Technology, Hanyang University, Seoul South Korea
Email: *kima@hanyang.ac.kr, pilwonhur@tamu.edu

Introduction

In the past years, the design of prosthetic feet has been widely studied for the lower extremity amputees. One of the critical design challenges is the impact reduction at the heel strike [1]. To carefully manage the impact load at the heel strike, a prosthesis design using a lattice structure was considered. The auxetic structure has received an attention due to its excellent mechanical properties, such as increased shear resistance and energy absorption [2]. Specifically, the re-entrant honeycomb structure exhibits an increased energy absorption capacity compared to the conventional honeycomb [3]. In this study, we propose the re-entrant structure for the prosthetic foot to enhance the energy absorption at the heel strike.

Methods

Structural behavior analysis was conducted using ABAQUS (v6.14, ABAQUS Inc., Vélizy-Villacoublay, France). The foot shape was approximated as rectangular with a length of 250 mm and a width of 120 mm. The geometry was meshed with 8-node hexagonal elements and the material properties were set as acrylonitrile butadiene styrene copolymer (ABS). One of the design parameters is the relative density (RD) of a structure, which is the ratio of the volume of all struts in a unit cell to the apparent volume of the unit cell. The finite element analysis (FEA) was conducted using two types of foot with RD of 0.35 and RD of 0.55. In the FEA, the ankle connection part was constrained from moving in the x, y, and z directions. Then, the load was applied normal to the heel (red line in Figure 1 (b)) during the step time of 1 sec as pressure with the total force of 1,000N. All experiments were done numerically in the ABAQUS.

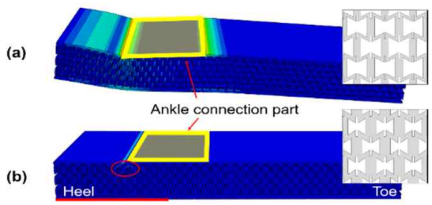

Figure 1: Stress analysis of the prosthetic foot at step time 1; (a) structure relative density of 0.35, (b) structure relative density of 0.55

Results and Discussion

As a result of FEA, the stress distributions of the prosthetic foot are shown in Figure 1. The plastic deformation did not appear in both cases. The stress was evenly distributed in heel part of the foot with RD 0.35. However, in the foot with RD 0.55, the stress was largely concentrated in the area near the ankle connection part. Therefore, the local failure (e.g., brittle failure), not as an elastic deformation, would be expected in foot with RD 0.55. The instability deformations are further described as following. The displacement of the bottom surface of each foot is analyzed as shown in Figure 2. The distance in x-axis means the foot length (0 mm: the end of the hindfoot or heel, 250 mm: the end of the forefoot or toe tip).

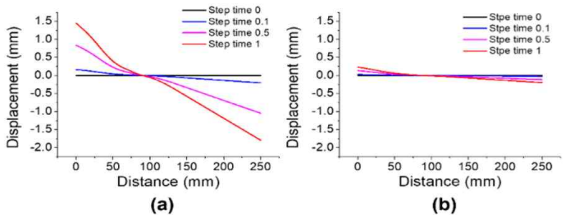

Figure 2: Displacement distribution of prosthetic foot according to the step time; (a) RD 0.35, (b) RD 0.55.

Under the same load condition, the foot with RD 0.35 deformed 6.3 times larger than the foot with RD 0.55. Also, the deformation of the forefoot was much larger in the foot with RD 0.33 than that of the foot with RD 0.55 due to the bending deformation. Through these deformations, the foot with RD 0.35 shows more stable energy absorption. This is because the re-entrant structures exhibit the significant energy absorption capacity at bending deformation [3]. However, with the higher RD (e.g., RD 0.55), the slenderness ratio of the strut increases, which makes the structure more brittle. The brittle properties of the foot with RD 0.55 can lead to instability behaviour, such as local failure due to stress concentration as shown in Figure 1. *Therefore, the decision of an appropriate RD is important to enhance the energy absorption behavior of the prosthetic foot for stable deformation at the heel strike.*

Significance

The longer-term purpose of this study is to manufacture the prosthetic foot using 3D printing technology as a single part. This may make the manufacturing process simpler while enhancing the performance of the prosthetic foot. To achieve the shock-absorbing property at the heel strike, we applied the novel re-entrant structure to the prosthetic foot. Also, we investigated the effect of the structure's RD by comparing two different RD cases in the simulation. We expect that, via biomechanical studies of prosthetic walking, a stable heel strike can be achieved by using the proposed auxetic structure with optimal RD for the prosthetic foot.

Acknowledgments

This research was supported by the MOTIE (Ministry of Trade, Industry, and Energy) in Korea, under the Fostering Global Talents for Innovative Growth Program (P0008748, Global Human Resource Development for Innovative Design in Robot and Engineering) supervised by the Korea Institute for Advancement of Technology (KIAT)

References

[1] S. K. Au, et al. (2008), *IEEE Robotics & Automation Magazine* 15.3: 52-59.
[2] Y. Xue, et al. (2018), *Materials Science and Engineering: A* 722: 255-262
[3] T. Li, et al. (2017), *Composite Structures* 175: 46

Simulations of pendulum test kinematics can estimate underlying parameters to joint hyper-resistance

Jente Willaert[1], Maarten Afschrift[1], Giovanni Martino[2], Anja Van Campenhout[3] , Kaat Desloovere[4], Lena Ting[2], Friedl De Groote[1]
[1]Departement of Movement Sciences, KU Leuven, Belgium;
[2] Neuromechanics Lab, Emory University & Georgia Institute of Technology, USA; [3]Department of Development and Regeneration, KU Leuven, Belgium; [4] Department of Rehabilitation Sciences, KU Leuven, Belgium;
Email: jente.willaert@kuleuven.be

Introduction

A common symptom in neurological disorders is joint hyper-resistance to passive stretch, which results from neural and non-neural contributions. Neural contributions are involuntary muscle activity (muscle tone) and stretch hyperreflexia. Non-neural contributions are due to changes in mechanical tissue properties. However, it is challenging to distinguish these contributions based on clinical tests[1]. Neuromechanical models that explicitely model these contributions may be useful in dissociating the various contributions to joint hyper-resistance in instrumented clinical tests[2]. The pendulum test is such a test where the lower leg is dropped from a horizontal position and features of limb motion are evaluated[3]. The first swing excursion is especially sensitive to the presence of spasticity. We found that it was important to model muscle short-range stiffness (SRS) and its interaction with muscle tone and hyperreflexia to capture the reduced first swing excursion in simulation[2]. SRS is a steep increase in muscle force upon stretch of an isometric muscle that is proportional to muscle tone. Our recent experimental results confirm the contribution of SRS. Moving the leg, which is known to reduce SRS, instead of keeping it isometric before releasing it in the pendulum test increased first swing excursion and reduced reflex activity. Here, we tested whether our model allows identifying individual-specific contributions of hyperreflexia, muscle tone, and damping (resulting from passive tissues) to hyper-resistance based on pendulum test kinematics. To this aim, we assessed (1) the quality of the fit between measured and simulated kinematics, (2) differences in parameters between children with CP and typically developing (TD) children, and (3) whether the effect of pre-movement on pendulum test kinematics could be predicted based on parameters identified from pendulum test kinematics in the isometric condition.

Methods

First, model parameters were identified by fiting pendulum test trajectories for 1 TD child and 4 children with CP (Table 1).

Table 1: Modified Ashworth Scale (MAS) and pendulum kinematics (Measured first swing excursions (FS) (range) and increased FS due to pre-movement (mean),simulated increase due to pre-movement (range)).

	TD1	CP1	CP2	CP3	CP4
MAS (Quadriceps-Hamstrings)	0-0	0-1	0-1	0-1	0-3
Measured FS (°)	106-122	103-104	67-70	26-55	45-54
Measured increase in FS (°)	-4	5	0	22	41
Simulated increase in FS (°)	2-3	3-5	3-10	40-53	19-36

The model consists of a planar lower leg segment actuated with a passive torque, due to damping, and an active torque, representing torque from muscle tone, SRS proportional to muscle tone, and reflex activity modeled as linear feedback from force[2,5]. Parameters (damping, muscle tone and reflex gain) for each child were estimated by tracking 2-3 trials of kinematic data in the isometric condition. Estimated parameters were normalized to leg mass multiplied by leg length. Next, we used these parameters to predict the effect of pre-movement on pendulum test kinematics. Pre-movement was modeled by removing the torque due to SRS from the model.

Results and Discussion

Preliminary results demonstrate that our model can fit a wide range of pendulum test kinematics across children (e.g. Fig 1ab). Damping was variable across subjects (Fig 1c). Muscle tone and reflex activity were higher in children that had a smaller first swing excursion (Fig 1de, CP2-4). The identified parameters have predictive value, as they captured the effect of pre-movement on pendulum test kinematics (Fig. 1ab, Table 1). Although none of the children with CP had quadriceps spasticity according to Modified Ashworth Scores (Table 1), we observed large differences in first swing excursion and the effect of pre-movement on first swing excursion. Our best fit model parameters also suggest different contributions from muscle tone and reflex activity in these children. In CP3 and CP4, reduced first swing excursion might be due to increased muscle tone and reflex excitability, whereas in CP2, reduced first swing excursion might be primarily due to increased damping, consistent with the lack of an effect of pre-movement on first-swing excursion.

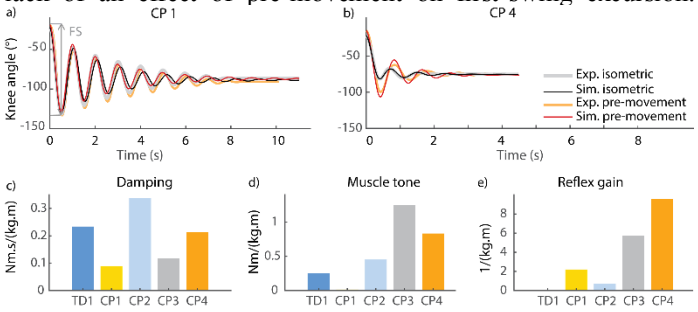

Figure 1: Simulated (no PM: black; PM: red) and experimental (no PM: grey; PM: orange) pendulum trajectories for a child with only minor spasticity (a) and a child with severe spasticity (b). Simulated parameters were damping (c), muscle tone (d) and reflex activity (e).

Significance

Our neuromechanical model combined with an instrumented spasticity assessment revealed abnormal contributions to hyper-resistance that were not identified in clinical tests. Model parameters may be useful to improve diagnosis and guide treatment selection in children with spasticity.

Acknowledgments

FWO (Research Foundation - Flanders) supported this work through fellowship 1192320N to JW and 12ZP120N to MA.

References

1.Van der Noort, EAN, 2017. **2.** De Groote, Plos, 2018. **3.** Fowler, DMCN, 2000. **4.** Willaert, MedRxiv, pre-print, 2020. **5.** Blum, Plos Comput Biol, 2017

Differential effect of spindle gamma drive and reflex gain in passive lower limb movements: a simulation study

Giovanni Martino[1], Brian C. Horslen[1], Friedl De Groote[2], and Lena H. Ting[1,3]
[1]W.H. Coulter Dept. Biomedical Engineering, Emory University and Georgia Institute of Technology, Atlanta, GA, USA
[2]Department of Movement Sciences, KU Leuven, Leuven, Belgium
[3]Department of Rehabilitation Medicine, Emory University, Atlanta, GA, USA
Email: giovanni.martino@emory.edu

Introduction

Spasticity refers to velocity dependent hyperreflexia, where involuntary muscle activation is caused by passive muscle stretch. However, the mechanisms underlying spasticity and its consequences on movement are still unclear.

In a recent study we developed a computational model to simulate pendulum test kinematics in children with spastic cerebral palsy (CP)[1]. The pendulum test is a diagnostic method that consists in evaluating the pattern of lower leg movement after release from the horizontal. Our simulations show that increasing muscle tone and short-range stiffness, with increased reflex strength could explain key kinematic outcomes of the pendulum test that are associated with spasticity in children with CP.

Here, our **objective** was to test the relative contributions of increased muscle spindle sensitivity to stretch versus increased reflex gain to abnormal pendulum test kinematics. We integrated a biophysical model of a muscle spindle[2] with a biomechanical model of the lower limb, increased muscle spindle sensitivity (i.e. sensory signal per unit stretch) is due to gamma motor neuron activity, i.e. gamma drive, increasing tension in intrafusal muscles within the muscle spindle. And reflex gain refers to the transformation of the sensory signal to a motor output within the spinal cord (i.e. reflex torque per unit sensory signal).

We **hypothesized** that increasing gamma drive versus reflex gain would cause different kinematic outcomes in clinical-relevant motor behaviors. Specifically, we simulated two leg motor behaviors commonly used for clinical assessment, the pendulum test and the knee tendon jerk reflex.

Methods

We integrated a biophysical model of muscle spindles[2] with a single-link, torque-driven model of the lower limb[1] with passive damping (Fig. 1). Muscle spindle sensory signals were modeled by simulating cross-bridges in intrafusal muscle and converting the resultant force and yank to simulated afferent neuron driving potentials causing sensory signals. Gamma drive (k_γ) modulates the number of available actin binding sites, increasing the force in the intrafusal fiber. Reflex gain (k_r) modulates the amount of torque produced per unit of muscle spindle sensory feedback.

The knee jerk reflex was simulated by imposing a stretch of the extensor muscle that elicited an initial reflex torque equal to 12Nm in the baseline condition. The pendulm test was simulated as a leg drop from a starting angle of 0°. The number of oscillations (N) and first swing excursion (θ_1) were used to evaluate the effects of increasing k_γ or k_r on kinematics.

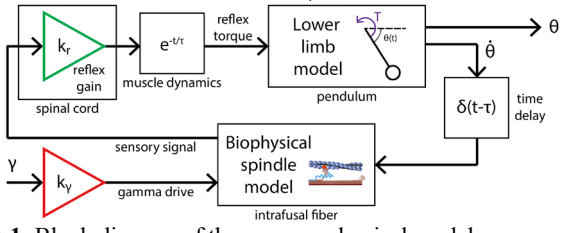

Figure 1: Block diagram of the neuromechanical model.

Results and Discussion

Different limb movements emerged when modulating gamma drive versus reflex gain.

In knee jerk reflex simulations, the reflex torque caused a oscillatory movement of the leg (Fig. 2A). Increasing gamma drive (k_γ) or reflex gain (k_r) increased the first swing excursion, but higher gamma drive *reduced* the number of oscillations whereas higher reflex gains *increased* the number of oscillations.

In pendulum test simulations (Fig. 2B) higher gamma drive *decreased* both first swing excursion and number of oscillations. Higher reflex gain *decreased* the first swing excursion but did not change the number of oscillations. The torque profiles suggest that higher gamma drive causes increased reflex sensitivity to the dynamic component of muscle stretch (narrow peaks), and earlier reflex activity.

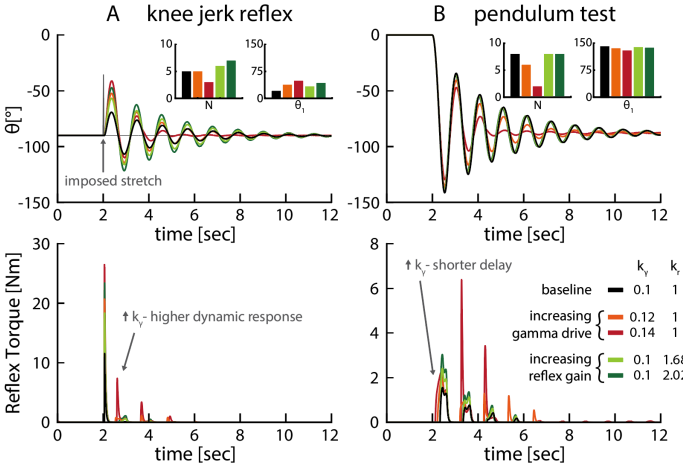

Figure 2: Simulations of knee jerk reflex (A) and pendulum test (B).

Significance

Our neuromechanical simulations including muscle spindle sensory feedback in clinical behaviors provide a framework to dissociate gamma drive from central reflex gain as mechanisms underlying hyperreflexia. Neuromechanical simulations could be used to identify the underlying mechanisms of hyperreflexia from experimental data in patients, understand how physiological and pharmacological factors affect sensorimotor behaviors in health and disease, and guide personalized interventions and novel therapeutic approaches to neurological movement disorders.

Acknowledgments

This work was supported by NIH R01HD046922 to LHT.

References

[1] De Groote et al. (2018). *PLoS One*, 13: e0205763.
[2] Blum et al. (2019). *BioRxiv*, doi:10.1101/858209

Identifying the Role of Residual Gastrocnemius in Isometric Knee Flexion of Below Knee Amputatees

Joseph M Dranetz[1], Sepehr Ramezani[1], Matt S. Stock, Michael Carroll, Michael Varro, Woon-Hong Yeo[2], Yun-Soung Kim[2], Ulas Bagci, Heather Cornnell, and Hwan Choi[1] Email: hwan.choi@ucf.edu

[1]Department of Mechanical and Aerospace Engineering, University of Central Florida, Orlando

[2]George W. Woodruff School of Mechanical Engineering and Institute for Electronics and Nanotechnology, Georgia Institute of Technology

Introduction

The role of residual gastrocnemius in gait for transtibial amputees remains relatively unexamined. During the transtibial amputation surgery, the distal end of the gastrocnemius is typically wrapped around the distal end of the limb. As the apparent role of the muscle changes after an amputation, understanding the characteristics of the residual gastrocnemius and nature of these acquired functions can inform the development of surgical and rehabilitative strategies. Study of the electromyographic activations of the residual gastrocnemius during gait show that activation patterns vary greatly between but not within transtibial amputees.[1] This suggests that transtibial amputees develop different strategies for their gastrocnemius during gait. Developing subject specific models that account for unique physiology of the residual gastrocnemius could better elucidate the character and function of the muscle given the variance observed in electromyographic data.

The goal of this study is to collect data from individual intact and residual gastrocnemii in order to construct subject specific musculoskeletal models in OpenSim. From these models we can assess the character and function of the muscle. In this study we demonstrate that the contribution of the gastrocnemius muscles in knee flexion decrease in an amputated leg.

Methods

A 37 year old male transtibial amputee performed maximal effort isometric knee flexions at knee angles of 0, 30, 60, and 90 degrees in a Biodex System 4 human dynamometer. During these trials, surface electromyographic (EMG) sensors were placed over the muscle bellies of 3 knee flexors and 3 knee extensors, digital goniometers were placed across the knee and ankle joints (if present), and an ultrasound probe was placed over the muscle belly of gastrocnemius muscle. The experiment was repeated done on both the subject's amputated and intact side.

An OpenSim model developed by Rajagopal et al. was adapted to model the seated isometric flexions.[2] Using scaling measurements taken of the subject's segement lengths, an intact model of the subject was created. Next the model was cut at the shank based on subject measurements and all muscles of the shank were removed except for the gastrocnemii, whose paths were modified based on the ultrasound images. New values for tendon slack length, optimal fiber length, pennation angle were modified based on the ultrasound images (isokinetic flexions of the knee were done to identify the optimal fiber length) and the maximum isometric force of the muscle was scaled based on the physiological cross section of subject's muscle.

Static optimization was performed on the model using kinematic data and external forces from the goniometers and the Biodex respectively. Individual muscle contributions are estimated based on their mean activity (and corresponding force contribution) across the duration of the force production. These results are summed and compared to the experimentally measured net knee moment. The EMG data is rectified/filtered and the resultant linear envelope is compared to the predicted muscle activity.

Results and Discussion

On average the moment contribution of the of the medial gastrocnemius dropped from 41% to 11% moment contribution from the unaffected leg to the affected leg, and the lateral gastrocnemius decreased from 12% to 3% moment contribution. The model simulated the experimental net torque with a percent error between 5% and 14% for the affected limb and between 11% and 34% for the unaffected limb. The normalized linear EMG envelopes had a similar shape to the predicted muscle activity curves for most of the muscles, but were less representative in the gastrocnemii in particular.

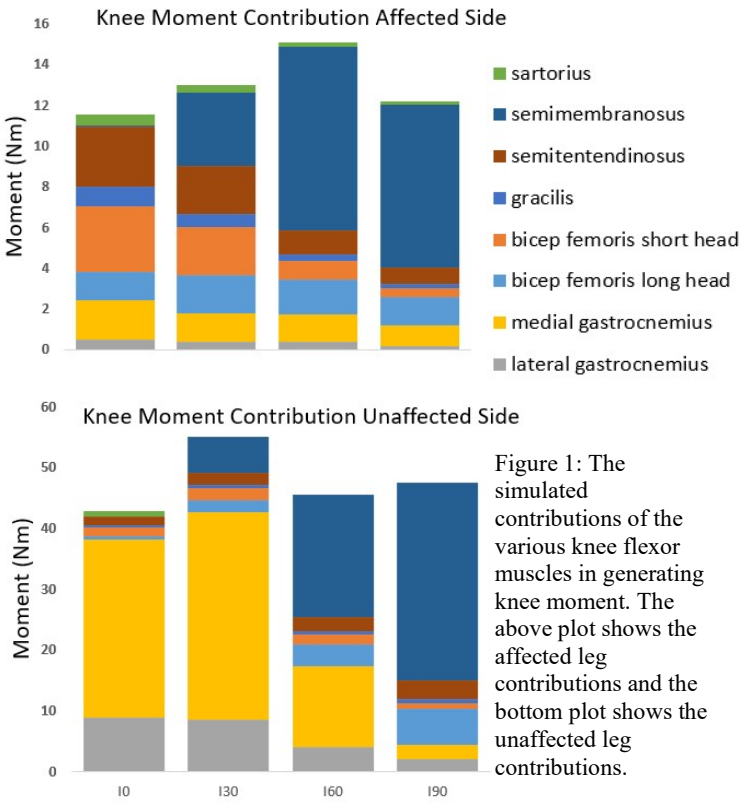

Figure 1: The simulated contributions of the various knee flexor muscles in generating knee moment. The above plot shows the affected leg contributions and the bottom plot shows the unaffected leg contributions.

Significance

The generated model demonstrates the change in relative muscle contribution in knee flexion for transtibial amputees. Through the use of a subject specific model, we were able to account for both macroscopic changes the shape of the gastrocnemii as well as internal changes in muscle properties. The outcome of this study is useful in furthering the understanding of the character of the residual gastrocnemius in dynamic tasks.

References

1. S. Huang, D. Ferris. "Muscle Activation Patterns during Walking from Transtibial Amputees Recorded within the Residual Limb-Prosthetic Interface." doi:10.1186/1743-0003-9-55.
2. Rajagopal, Apoorva, et al. "Full-Body Musculoskeletal Model for Muscle-Driven Simulation of Human Gait." doi:10.1109/tbme.2016.2586891

Effects of End-User and Design Parameters on Shear Wave Propagation: A High-Throughput Parametric Modeling Study

Jonathon L. Blank[1], Darryl G. Thelen[1], and Joshua D. Roth[1,2]
[1]Department of Mechanical Engineering, University of Wisconsin-Madison, Madison, WI
[2]Department of Orthopedics and Rehabilitation, University of Wisconsin-Madison, Madison, WI
Email: jlblank@wisc.edu

Introduction

Shear wave tensiometry is an emerging technique capable of quantifying tendon[1] and ligament[2] loading noninvasively. In shear wave tensiometry, the shear wave propagation speed in the tissue of interest scales predictably with the axial tissue stress. These measurements are made *in vivo* using a handheld or wearable sensor. However, measured shear wave speeds may be sensitive to sensor design and end-user variability in performing these measurements.

We have developed a parametric, dynamic finite element model[3] of a multibody tensiometer that predicts shear wave speeds that agree with an analytical tensioned beam model[1] (FEBio v2.9.1).[4] Using this parametric model, we can vary tensiometer application force, internal tensiometer stiffess, and the tensiometer component mass. Hence, the purpose of this study was to characterize the effect of these parameters on measured shear wave speeds.

Methods

Our parametric model includes a shear wave tensiometer and a fibrous soft tissue structure. We modeled the tissue as a 60-mm long cylinder with a radius of 3 mm. The tissue mechanical behaviour was governed by a transversely isotropic Mooney-Rivlin constitutive relationship with uniformly distributed fibers aligned axially. The tensiometer was modeled using a set of rigid cylinders, representing a piezoelectric tapper and two accelerometers, in contact with the tissue surface (Fig. 1). Each cylinder was prescribed a finite mass and attached to a displacement controlled block by a spring-damper.

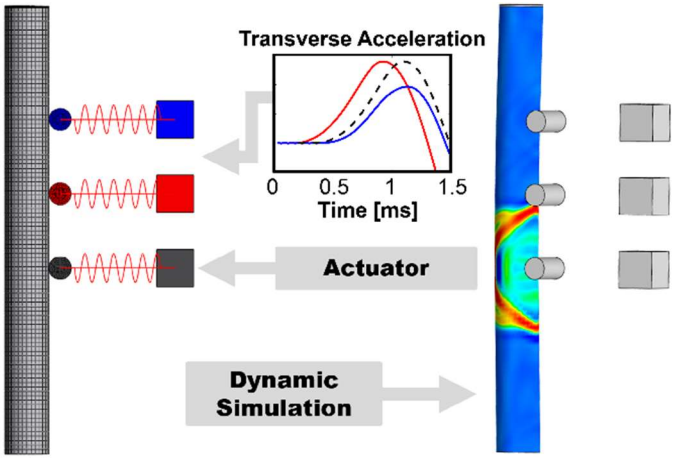

Figure 1: The parametric tensiometer model was used in a dynamic analysis to determine the effects of tensiometer design parameters on measured shear wave speeds.

A shear wave was excited in the tissue via a ramp displacement of the actuator calibrated to the dynamic behaviour of piezoelectric tappers used in our wearable tensiometers.[1] Shear wave speed was calculated using a normalized cross-correlation of the transverse tissue motion at the two accelerometer blocks. Monte Carlo simulations (n = 2,400 at each strain level) were run on a high-throughput computing grid with tensiometer mass (0.2-20 g), stiffness (1-10 N/mm), and application force (1-10 N per component) randomly selected from uniform distributions.

Results and Discussion

The model-predicted shear wave speeds increased with axial tendon strain as predicted by our analytical model.[1] When the tissue was strained to 3%, the shear wave speeds did not scale predictably with tensiometer mass, stiffness, or application force. However, when 6% strain was applied to the tissue, measured wave speeds were highly correlated with application force (R^2 = 0.84), with shear wave speed increasing by 1.02 m/s for a 1 N increase in application force (Fig. 2).

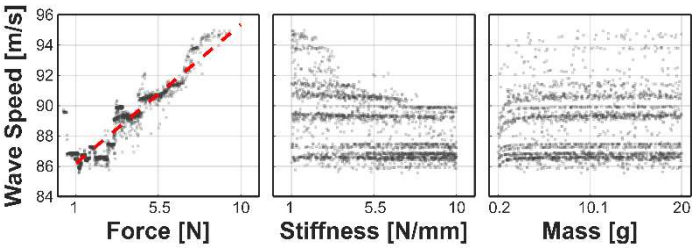

Figure 2: Measured shear wave speeds are sensitive to tensiometer application force at the 6% strain level.

The dependency of measured shear wave speeds on the tensiometer application force could be a result of an increase in the localized tissue stress due to tissue deformation. This would suggest that tensiometer application force should ideally be kept low to mitigate its effect on shear wave propagation within the tissue, which might lead to an over-estimation of the *in situ* stress.

Significance

Shear wave tensiometers enable the noninvasive measurement of ligament and tendon loading. However, the sensor relies on mechanical contact with the tissue of interest, and hence has the potential to alter how waves propagate locally. Our novel parametric model presents a platform by which tensiometer design factors can be studied. High-throughput computing allows us to fully explore the tensiometer design space. The insights gained are important for designing tensiometers that are best suited for targeted applications in orthopedic surgery and wearable kinetics.

Acknowledgments

We gratefully acknowledge support from the NIH (EB024957) and the UW-Madison Center for High Throughput Computing.

References

[1] Martin et al., *Nat. Commun.,* 9:2-10, 2018.
[2] Blank et al., *J. Mech. Behav. Biomed. Mat.,* 103704, 2020.
[3] Blank et al., *Lec. Not. Comp. Vis. Biomech.,* 36:48-59, 2020.
[4] Maas et al., *J. Biomech. Eng.,* 134:1-10. 2012.

Harmonic excitation approach to determine system identification of a mannequin

Muhammad Salman[1*], Edward F. Owens[2], Brent Russell[3] and Ronald Hosek[4]
[1] Department of Mechanical Engineering, Kennesaw State University
[2,3,4] Dr. Sid E. Williams Center for Chiropractic Research, College of Chiropractic, Life University
Email: msalman1@kennesaw.edu

Introduction

An understanding of the resonant frequency of the human body would be beneficial in designing machinery, buildings, and transportation so that exposure to vibrations close to the human body's resonant frequency may be avoided. However, that requires first understanding the mechanical effects and properties of the human body undergoing these vibrations. The human body is a complicated system of interconnected masses, elasticities, and viscous dampers (Coermann 1962). It would be difficult to describe the mechanical properties of this system and almost impossible to find the natural frequency of one part of the body without generating the whole-body resonances (Randall 1997).

The current investigation used a mannequin specially designed for the training of spinal manipulation and has characteristics of human soft tissue, with a 3-D-printed spine, pelvis, and skull connected by anatomically accurate articulating joints and are covered with a silicon skin; stiffness of the lumbar and thoracic regions can be controlled with nylon cords accessible in the chest cavity. This mannequin has been previously examined in static stiffness experiments, to be reported separately. The method of investigation in the present study has been used with inanimate objects and materials; the current investigation is a step in studying its feasibility with humans.

Methods

A vibration fitness machine was used for generating harmonic excitation. The mannequin was laid prone while the data was collected. The machine was run at seven different speed settings corresponding to each hertz reading level, and the mannequin was tested in conditions of "soft", with the cords on slack, and "stiff" with the cords pulled to tension.

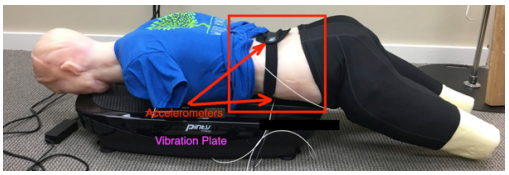

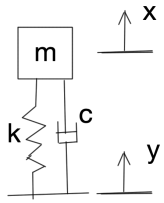

Figure 1: Mannequin lying on top of the vibration plate

Two accelerometers (PCM Model Number 352C65) were used during testing. One accelerometer was attached to the top of the lumbar spine using a strap and the other accelerometer was attached to the base. The machine was turned on and the data was collected from the accelerometers via LabVIEW SignalExpress software. The data collection period was 5 seconds. The calibration factor for the accelerometer is 100 mV/g. The dynamic model of the mannequin is given in Eq. (1) where m is the mass of the lower waist (Lumbar spine region, m = 20.4 kg), c is the damping coefficient, k is the stiffness and y = Y sin(ωt) is the amplitude of the harmonic excitation and ω is the forcing frequency.

$m\ddot{x} = f(t) = c(\dot{y} - \dot{x}) + k(y - x)$ where the velocity, $\dot{x} = -\omega x$ and the acceleration is $\ddot{x} = -\omega^2 x$

The damping coefficient, c was calculated using Eq. (1). The natural frequency, ω_n is found from the largest peak obtained in the power spectrum.

Results and Discussion

The resonance frequency (Fig. 2) of a soft mannequin was 6.4 Hz while the stiffer one had the resonance frequency of 8.6 Hz. This rise in the resonance is in accordance with the Eq. $k = m\omega_n{}^2$. The displacement amplitude is higher for the stiffer as compared to the soft mannequin (Fig. 2). The table shows the stiffness, k, the damping coefficient, c and the damping ratio, ξ. The damping ratio which is the ratio of actual damping to the critical damping is the system property and it is 0.5 which means it's an underdamped system.

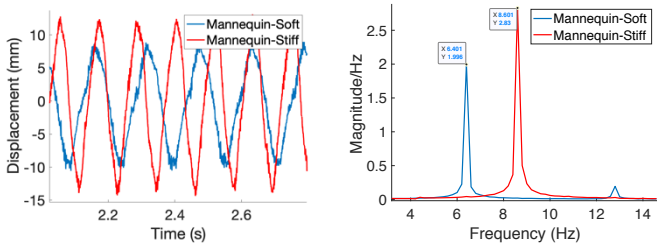

Figure 2: The displacement and the power spectrum

Table: System parameters.

	Stiffness	Damping Coefficient	Damping ratio
Mannequin	**k (N/m)**	**c (N-s/m)**	**ξ**
Soft	32967	820	0.5
Stiff	59528	1103	0.5

Significance

The method was able to differentiate between soft and stiff conditions of the mannequin and thus may be able to assess stiffness for humans with differences in spinal stiffness and body morphology. This method may be used in future studies of human spinal stiffness and outcomes of spinal manipulation.

References

COERMANN R. R. 1962, The Mechanical Impedance of the Human Body in Sitting and Standing Positions at Low Frequencies, *Human Factors: The Journal of the Human Factors and Ergonomics Society,* Vol. **4**, Issue 5, 227 – 253.

RANDALL et al. 1997, Resonant frequencies of standing humans, *Ergonomics*, Vol. **40**, No. 9

Effect of Muscle Passive Force Minimization on EMG-driven Model Calibration

Di Ao[1,*], Mohammad S. Shourijeh[1], Carolynn Patten[2], and Benjamin J. Fregly[1]
[1]Department of Mechanical Engineering, Rice University, Houston, TX, USA
[2]Department of Physical Medicine & Rehabilitation, University of California, Davis, CA, USA
Email: *aodi@rice.edu

Introduction

EMG-driven musculoskeletal modeling uses optimization to calibrate musculotendon model parameter values to subject movement and EMG data. The objective function minimizes the sum of squares of errors between inverse dynamic joint moments and the joint moments estimated by the EMG-driven model. While necessary, this objective function is not sufficient to produce unique model parameter values. Consequently, unrealistic solutions sometimes occur where a muscle generates unreasonably large passive force, even when published passive joint moments for sagittal plane joints are also tracked in the cost function [1]. Previous research has shown that to avoid injury during walking, muscles likely operate primarily on the ascending or early descending region of their active force-length curves, thereby producing relatively low passive forces [2, 3]. To address over-estimation of muscle passive force, this study investigated how EMG-driven model calibration results change through the addition of passive muscle force minimization to the optimization cost function.

Methods

Previously published gait data collected from the non-paretic leg of a subject post-stroke performing treadmill walking were used to scale a generic OpenSim (v3.3; [4]) model and calibrate lower body joint positions and orientations [1]. The OpenSim model possessed $N_m = 35$ muscles controlling $N_J = 5$ degrees of freedom (DOFs) (2 hip DOFs, 1 knee DOF, and 2 ankle DOFs), where muscles were treated as Hill-type models with a rigid tendon. EMG-driven model calibration was performed using 10 gait cycles collected at the subject's self-selected and fastest speeds (5 gait cycles for each speed) by optimizing activation dynamics and Hill-type muscle model parameter values (P). The optimization cost function was formulated as:

$$\min_P J \triangleq (1-\mu)J_{TrackMom} + \mu J_{PassiveF} \quad (1)$$

$$J_{TrackMom} \triangleq \frac{1}{N_J}\sum_{i=1}^{N_J}\left(M_i^{mod} - M_i^{exp}\right)^2 \quad (2)$$

$$J_{PassiveF} \triangleq \frac{1}{N_m}\sum_{j=1}^{N_m}(F_j^{Passive}/F_j^{mo})^2 \quad (3)$$

$J_{TrackMom}$ minimizes for errors in matching joint moments from inverse dynamics, $J_{PassiveF}$ minimizes total normalized passive force cost, and μ is a weighting factor that defines the relative importance of each sub-objective. The sensitivity of the solution to μ was investigated when μ was increased incrementally from 0 to 0.9.

M_i^{mod} and M_i^{exp} represent calculated and experimental joint moments around joint i respectively. $F_j^{Passive}$ defines model-predicted passive force of muscle j, which was normalized to maximal isometric muscle force (F_j^{mo}). For each solution, the resulting joint passive moments for the three sagittal joints were also compared with the passive joint moment measurements reported in the literature [1,5].

Results

A Pareto front (Fig.1 (A)) showed the trade-off between joint moment tracking error and passive force cost, where increasing the weight factor μ led to decreased passive force magnitude and increased joint moment tracking error (Fig.1 (B)). Furthermore, passive moment difference relative to published passive joint moments for different values of μ followed a v-shaped curve with a minimum near $\mu = 0.5$ (Fig.1 (C)), which was close to the elbow of the Pareto front. Passive force minimization reduced passive force cost and joint moment tracking errors simultaneously relative to a solution that tracked published sagittal plane passive joint moments in the cost function (see 'Tracking' in Fig.1 (B)).

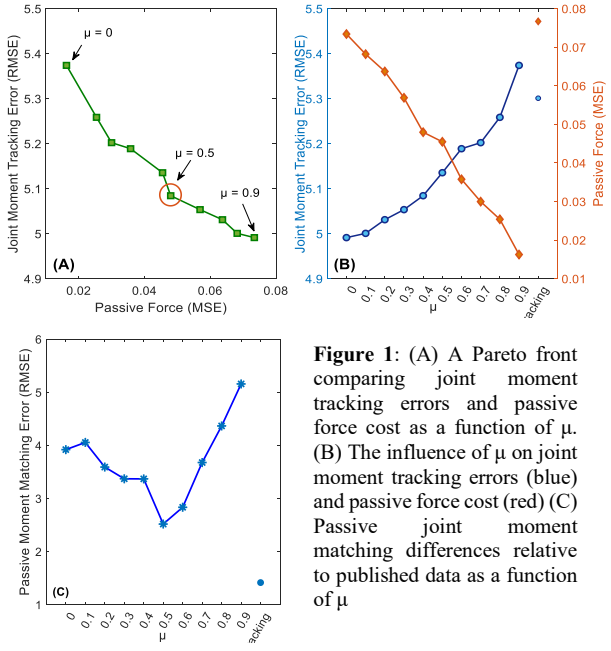

Figure 1: (A) A Pareto front comparing joint moment tracking errors and passive force cost as a function of μ. (B) The influence of μ on joint moment tracking errors (blue) and passive force cost (red) (C) Passive joint moment matching differences relative to published data as a function of μ

Significance

EMG-driven model calibration was influenced by passive muscle force minimization, which tended to increase optimal muscle fiber parameter values while decreasing joint moment tracking errors. Matching published average passive joint moments during model calibration may hinder EMG-driven model calibration [1, 5]. The proposed approach showed the potential to reduce the occurrence of unrealistically high passive muscle forces while simultaneously producing passive joint moments that exhibit trends consistent with published data.

Acknowledgments

This study was funded by the Cancer Prevention Research Institute of Texas (CPRIT) under grant RR170026.

References

[1] A. J. Meyer, et al. (2017), PloS One, 12: e01796.
[2] J. Rubenson, et al. (2012), J. Exp. Biol., 215: 3539–3551.
[3] E. M. Arnold, et al. (2009), Ann. Biomed. Eng., 38: 269–279.
[4] S. L. Delp, et al. (2007), IEEE Trans Biomed Eng., 54: 1940–50.
[5] A.Slider, et al. (2007), J. Biomech., 40:2628-2635

Musculoskeletal Model Calibration Affects Metabolic Cost Estimates for Walking

Marleny Arones[1], Mohammad Shourijeh[1], Carolynn Patten[2], and B.J Fregly[1]
[1]Department of Mechanical Engineering, Rice University, Houston, Texas, USA
[2]Department of Physical Medicine & Rehabilitation, University of California, Davis, California, USA
Email: *ma86@rice.edu

Introduction

Enhancement of human performance while minimizing energy expenditure are common goals for assistive device design. For human-in-the-loop design, a subject's metabolic cost is evaluated as device design and control parameters are varied. However, human-in-the-loop optimization [1] is an inefficient and time/cost intensive process due to several experimental iterations.

Predictive gait optimizations performed using neuro-musculoskeletal (NMS) and metabolic cost models could potentially replace human-in-the-loop optimizations to identify metabolically optimal device designs more rapidly and easily. However, the accuracy of model-based metabolic cost estimates is influenced by the choice of metabolic cost model [2] and possibly by NMS model parameter calibration as well.

This study evaluated how NMS model calibration impacts estimated metabolic cost during walking as calculated using two common metabolic cost models.

Methods

This study analyzed walking data previously collected from high functioning (79 yr, lower limb Fugl-Meyer score of 32) and low functioning (62 yr, lower limb Fugl-Meyer score of 25) male subjects post-stroke with right-sided hemiparesis.

Three modeling approaches were investigated to determine the influence of NMS model calibration on metabolic cost estimates. The first approach used a scaled generic OpenSim model and found muscle activations via static optimization (*SO-Gen*). The second approach used a calibrated EMG-driven model [3] with calibrated functional axes [4] to find muscle activations. The third approach used the calibrated NMS model but found muscle activations via static optimization (*SO-Cal*).

Muscle activation estimates were used to calculate each subject's cost of transport (CoT) at different gait speeds using metabolic cost models published by Umberger [5] and Bhargava *et al*. [6].

The calculated CoT values for the two subjects and two metabolic cost models were compared with experimental CoT values for individuals post-stroke as reported by Finley et al. [7]. That study reported a strong negative linear association between CoT and gait speed (r = -0.98). Thus, for the present study, the Pearson correlation coefficient (r) between CoT estimates and gait speed was calculated for each modeling approach and metabolic cost model.

Results and Discussion

Of the three modeling approaches, the EMG-driven model predicted the strongest negative correlation between CoT and gait speed for both subjects and both metabolic cost models (Table 1). Umberger's model predicted larger CoT estimates but with a higher correlation to gait speed compared to Bhargava's model, where the difference in magnitude was expected as previously observed [1]. Also, Bhargava's model predicted CoT values within the statistical range (±3 SD) of the mean reported in Finley et al. [7].

Significance

Based on these results, we recommend using calibrated EMG-driven NMS models to estimate muscle activations if metabolic cost estimates are to be made. Furthermore, our results suggest that Bhargava's model is the most realistic metabolic cost model since it produced CoT estimates that were of comparable magnitude to published experimental values.

Acknowledgments

Funding provided by the Cancer Prevention and Research Institute of Texas Grant RR170026 and an NSF Graduate Research Fellowship.

References

[1] Ding Y, et al., Science Robotics., 3(15), 2018
[2] R. H. Miller, J. Biomech., 47(6):1373–1381, 2014.
[3] A. J. Meyer, et al., PLoS One, 12(7), 2017.
[4] J. A. Reinbolt et al., J. Biomech., vol. 38, pp. 621–626, 2005.
[5] B. R. Umberger, J. R. Soc. Interface, 7(50):1329–1340, 2010.
[6] L. J. Bhargava et al., J. Biomech., 37(1):81–88, 2004.
[7] J. M. Finley et al., Neurorehab. Neur. Repair, 31(2):168–177, 2017.

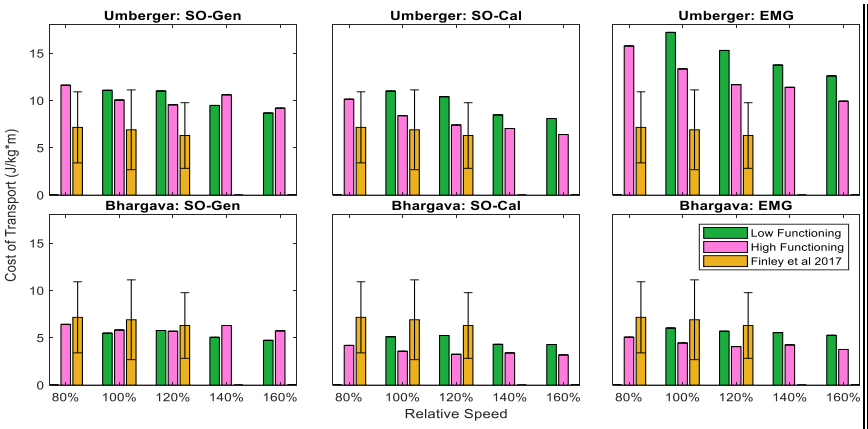

Figure 1: CoT estimates for both metabolic cost models and for all three methods.

Table 1: Pearson correlation coefficients relating estimated CoT obtained from both metabolic models (left: (Umberger [5], right: Bhargava et al. [6]) to gait speed for the low and high functioning stroke subjects.

	High Functioning	Low Functioning
SO–Gen	-0.71, -0.42	-0.95, -0.84
EMG-driven	-0.97, -0.91	-0.99, -0.99
SO–Cal	-0.96, -0.86	-0.96, -0.86

IS MY MUSCULOSKELETAL MODEL COMPLEX ENOUGH?

The Implications of Six Degree of Freedom Lower Limb Joints for Dynamic Consistency and Biomechanical Relevance

Owen D. Pearl[1] and Daniel A. Jacobs[1]
[1]Mechanical Engineering, Temple University, Philadelphia, PA, USA
email: owen.pearl@temple.edu, web: https://sites.temple.edu/rise/

Introduction

In the United States, one in every eight adults suffers from a gait impairment that restricts their mobility **[1]**. Proper diagnosis and treatment of these impairments requires an accurate understanding of an individual's motion and the forces that produce their motion. Musculoskeletal modeling is an essential technique for non-invasively acquiring these kinematic and dynamic estimates **[2]**. At present, most musculoskeletal models assume that the biomechanical effects of soft-tissues like skin, cartilage, and ligaments are negligible **[3]**. However, studies have shown that neglecting soft-tissues in these instances can incite errors known as soft-tissue artifacts (STAs) in estimates of joint kinematics **[4]**, and dynamics **[5]** that limit the accuracy of musculoskeletal models. Research has shown that adding degrees of freedom (DOF) to the joint definitions between the lower limb segments of a human model can improve the estimation of joint forces, work, and power **[5, 6]**. However, the effect of increasing joint DOF on a model's satisfaction of Newton's Second Law of Motion is unclear. Our aim was to determine if increasing the DOF of specific joints reduces the artifical residual wrench applied at the pelvis during inverse dynamics routines to satisfy Newton's Second Law, and whether reductions in these residual forces and moments correlate with walking speed or BMI.

Methods

We recruited ten subjects with no history of neurological or musculoskeletal impairment (8 male, 2 female; age 21.6 ± 2.87 years; BMI 25.1 ± 5.1; mean ± s.d.) and recorded walking data at three speeds normalized by Froude number (Fr) using optical motion capture and an instrumented treadmill. We systematically added DOF to the lower limb joints of OpenSim's 23 DOF lower body and torso model (gait2354). For each model, we calculated the magnitude of the pelvis residual forces and moments for a single, representative subject trial (BMI = 24.0, Fr = 0.15). Finally, we simulated all 30 trials with both models and calculated median differences in residual wrench components using a non-parametric ranked sum test. Then, we tested for correlations using multiple linear regression models. All statistical analyses were completed using JMP Pro.

Results and Discussion

A 35 DOF model (gait3554) resulted in the lowest residuals for the representative subject trial. The gait3554 comprised 6 DOF at each hip, 4 at each knee plus 2 constraints, and 1 at each ankle. Our results showed statistically significant reductions in four of the six residual components with the proposed model **(Figure 1)**. However, for half the subjects, the model did not converge to solutions which respected joint constraints. Incorporating more relevant constraints or including additional modeling elements such as ligaments could improve the effectiveness of the IK algorithm on models with higher DOF. For the subjects where the model converged, the FX and FZ residuals possessed statistically significant (α = 0.05) negative correlations with Fr, while no correlations existed with BMI.

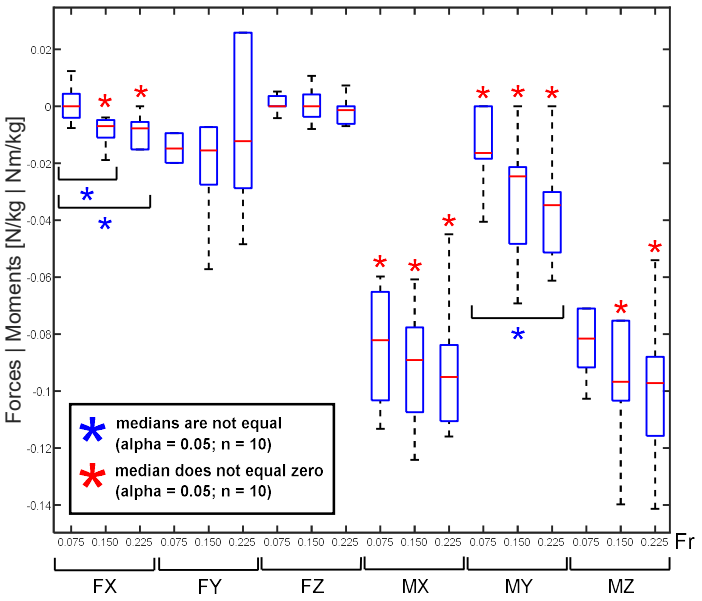

Figure 1: **Average RMS Residual Shifts.** The changes in mean RMS pelvis residuals after switching to the edited model. Each box plot is ten subjects walking at one speed. A negative value indicates a reduction in residuals and an improvement in dynamic consistency. Nonparametric signtests of the medians reveal four of the six residual categories' medians are below zero, while Wilcoxon rank sum tests reveal that slight differences occur due to speed.

Significance

To practically overcome STA by adding DOF, methodologies for subject-specific model tuning must be improved. Adding DOF to the lower limb joints can improve a model's dynamic consistency and biomechanical accuracy, and models of higher speed behaviors are more likely to benefit from adding DOF. Future work will include the development of methods for automatically tuning the inverse kinematics step to better model individuals with higher STA by eliminating the requirement for suboptimal, manual IK tuning for each DOF that is added.

Acknowledgments

This research was supported in part by the Interdisciplinary Rehabilitation Engineering Research Career Development Program (NIH K12HD073945) to DAJ.

References

1. Courtney-Long EA, et al. *CDC MMWR*. 2015. **2.** Delp SL, et al. *IEEE Trans*, 2004. **3.** Fu XY, et al. *Med Sci Sports Exerc.* 2015. **4.** Leardini, A. et al. *Gait & Posture.* 2005. **5.** Zelik KE, et al. *J Exp Bio*. 2015. **6.** Buczek FL, et al. *Gait & Posture.* 2010.

Minimizing Angular Momentum Yields More Robust Walking Trajectories in Five-Link Biped

Christian DeBuys[1] and Pilwon Hur[1]
[1]Texas A&M University
Email: pilwonhur@tamu.edu

Introduction

In the field of humanoid robots, walking motions are typically achieved by calculating desired trajectories and using controllers to help the robot follow those trajectories. The manner in which these trajectories are obtained is critical, since even the best controllers cannot yield a stable walking gait if the trajectories which they track are of poor quality.

In this study, a trajectory optimization via direct collocation is performed to generate desired joint trajectories for a single step of a five-link biped. The trajectories are examined in a forward simulation for their robustness to impulsive disturbances. Prior research has shown that angular momentum H about the whole body center of mass (COM) is highly regulated during human walking [1]. Since human walking is seemingly robust to disturbances and has very low H throughout the gait cycle, it is reasonable to suspect that trajectories with reduced H would be more robust to disturbances than those without. Thus, terms which facilitate the minimization of H are added to the cost function, and the performance of base-line trajectories is compared to the performance of trajectories which also minimize H. It is hypothesized that the trajectories which minimize angular momentum will be more robust to disturbances.

Methods

The simulated walking robot is the five-link biped shown in Figure 1(a). It has dimensions, masses, and inertias similar to that of a human for the shank and thigh, and uses the head-arms-torso (HAT) approximation for the upper body [2].

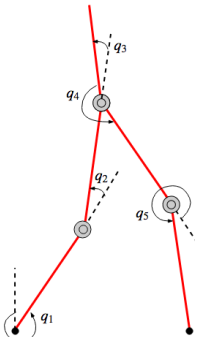

$$\min \sum \tau^2 + \alpha H_{spin}{}^2 + \beta H_{orb}{}^2$$
s.t.
Dynamics = 0
ImpactDynamics = 0
JointRange ≤ 0
TorqueLimit ≤ 0
StepLength ≤ 0
ImpactVelocity = 0

Figure 1: (a) Five link biped **(b)** Optimization formulation. Note that all inequality constraints are expressed with "≤ 0"

The joint trajectories are generated via trajectory optimization using direct collocation, in which the desired optimal trajectories are discretized and used as the decision variables in the optimization [3]. In this case, the accelerations, post-impact velocities, and impact forces are included with the decision variables in addition to those shown in [3]. The optimization is done in Julia (v1.3) using JuMP as an interface and IPOPT as the solver. The Hermite-Spimpson method is used for the direct collocation [3]. The base-line cost function is the sum of the squared joint torques τ^2. This cost function is augmented with the spin angular momentum squared $H_{spin}{}^2$ (i.e., $\alpha = 1$, $\beta = 0$), with the orbital angular momentum squared $H_{orb}{}^2$ (i.e., $\alpha = 0$, $\beta = 1$), or with both $H_{orb}{}^2$ and $H_{spin}{}^2$ (i.e., the total angular momentum squared, $\alpha = 1$, $\beta = 1$). H_{orb} is the angular momentum of a segment COM (point mass) in the reference frame of the whole-body COM. H_{spin} is the angular momentum of a segment about its own COM (in its own reference frame). The optimization includes many constraints such as those for respecting the dynamics, a minimum step length of 0.2 m, periodicity constraints so that the step behavior is repeatable, limits on the joint angles, and impact at the heel strike. A formulation of the optimization with these constraints is given in Figure 1(b). The details of these constraints can be found in [4].

A forward simulation is conducted in which a horizontal impulsive force is applied at 1.0 sec at the hip joint for a duration of approximately 0.4 sec, against the direction of the step. The biped is tasked with walking 10 steps without falling over. A PD controller is used for all simulations to track the trajectories, and center of mass forward progression is used as the phase variable (i.e., time parameterized by state variables).

Results and Discussion

The maximum force the biped withstands without falling over for a given cost function's set of optimal trajectories is reported in Table 1. When the step length was left unconstrained except for the minimum required length of 0.2 m, the optimizer chose this minimum value. To rule out the potential effects of step lengths on the maximum force, trajectories were generated for different fixed step lengths as well.

Table 1: Maximum force (N) of perturbation without falling for sets of trajectories with different cost functions and step lengths.

Step Length [m]	τ^2	$\tau^2+H_{spin}{}^2$	$\tau^2+H_{orb}{}^2$	$\tau^2+H_{spin}{}^2+H_{orb}{}^2$
0.200	222	657	536	536
0.241	221	586	563	551
0.272	unstable	477	570	547

Adding angular momentum into the cost function improved the maximum force tolerated in all cases. For $H_{spin}{}^2$, the maximum force decreased for increasing step length. The opposite trend is seen for $H_{orb}{}^2$. Surprisingly, the maximum force for the cost function with both terms was lower for the shorter two step lengths. These results suggest that it may be advantageous to include one type of angular momentum over the other depending on the desired step length.

Significance

These results support the idea that human walking tends to have low angular momentum because it allows human gait to be more robust to disturbances.

References

[1] Popovic et al., ICRA, pp2405-2411, 2004
[2] Winter, Wiley, 4th ed., 2009
[3] Kelly, SIAM Review, 59(4), pp849-904, 2017
[4] Chao et al., IROS, pp1435-1440, 2019

Sensitivity of simulated grip strength to wrist posture

Daniel C. McFarland[1 2 3], Michael S. Bednar[3 4] and Wendy M. Murray[1 2 3]
[1]Department of Biomedical Engineering, Northwestern University, Evanston, IL
[2]Shirley Ryan Abilitylab, Chicago, IL
[3]Edward Hines, Jr. VA Hospital, Hines, IL
[4]Department of Orthopaedic Surgery and Rehabilitation, Loyola University, Chicago, IL
Email: dmcfarland@sralab.org

Introduction

Grip strength is sensitive to wrist posture, and the preferred wrist posture is extended and ulnarly deviated [1]. Grip strength is significantly reduced as the wrist moves away from this optimal posture [1]. Previous work from our group demonstrated that grip strength in this self-selected posture could be successfully predicted through a forward-dynamic optimization for healthy adults [2]. Before our simulations of grip strength can be generalized to other conditions, we need to validate that our model displays a sensitivity to wrist posture. Our hypothesis is that predicted grip strength would decrease as wrist posture moved away from the optimal posture in any direction.

Methods

A previously developed OpenSim [3] musculoskeletal model of the hand and wrist [1] that incorporated all five digits and 38 Hill-type muscle-tendon actuators (both intrinsics and extrinsics) was used in the simulations. Grip strength was modeled as contact between the skin of the phalanges (cylinders overlayed on the bone geometries) and a massless elliptical cylinder representing the dynamometer. Contact parameters from the literature were used for the skin [4] and the dynamometer. A simulated annealing optimization was used to determine muscle activations that maximized contact force along the long axis of the ellipse during a forward-dynamic simulation. The optimization encourages the wrist to maintain the initial posture with an additional penalty term. A total of 5 wrist postures (self-selected, radially deviated, ulnarly deviated; extended, and flexed) corresponding to postures evaluated in O'Driscoll et al [2] were evaluated to determine the simulations sensitivity to wrist posture.

Results and Discussion

For every wrist posture, the model was able to maintain the initial wrist posture within 0.2°; however, the model's grip capacity was not sensitive to wrist posture. Reductions in predicted grip strength were less than 2kg for 3 of the 4 other postures (Figure 1) whereas experimental reductions ranged from 8 to 13kg [1]. The model predicted the largest reduction for the flexed posture, but this was still above the experimental reduction. This flexed posture had the model's lowest flexion (13.4Nm) and highest extension (29.2Nm) moment capacity at the wrist of all the postures tested (average 28.6 and 13.9 Nm for flexion and extension respectively of other postures). This large difference in moment capacity at the wrist may have contributed to why the largest reduction was seen in the flexed posture. One potential reason why predicted grip strength was not sensitive to wrist posture is that the muscle compartments of flexor digitorum profundus (FDP) and extensor digitorum communis (EDC) were considered as independent actuators. A previous study has shown that voluntary activation of the middle compartment of FDP and EDC causes similar coactivation in the index compartment of the same muscle [5]. For the self-selected posture, the activation of the individual compartments were fairly consistent across these muscles; however, for other postures, the model selectively activated certain compartments while leaving others inactive. For example in ulnar deviation, the model activated the little, ring, and index compartments of FDP (activations of 0.88, 0.51, and 0.55 respectively), but left the middle compartment inactive (activation of 0.16). This ability to selectively activate certain compartments during maximal grip may not be possible *in vivo*. To confirm that involuntary coactivation among muscle compartments would increase sensitivity to wrist posture, we reran the simulations in the self-selected and radial posture with the compartments of FDP and EDC constrained to be within 5% of the activation of the middle compartment. Requiring coactivation reduced grip strength in the radial posture from 40.9 to 34.8 kg, but increased grip strength in the self-selected posture from 41.3 to 43.1 kg.

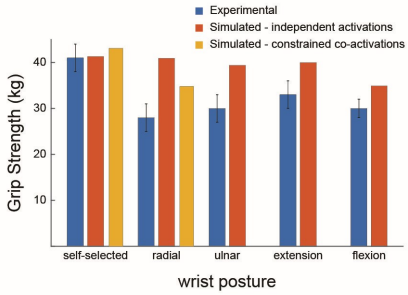

Figure 1: Grip strength measured experimentally (blue) [2] and grip strength predicted by the musculoskeletal model (orange – independent activations, yellow constrained co-activations) .

Significance

Without requiring coactivations of FDP and EDC compartments, the model's predicted grip strength was not sensitive to wrist posture. The constraints on coactivation in the resimulation were simplistic and somewhat arbitray. Furthermore, in actuality, involuntary coactivation of muscles extends beyond individual compartments of singular muscles [5]. Future work is needed to quantify involuntary coactivation of muscles during grasping.

Acknowledgments

This work is supported by NIH T32 HD07418, NIH RO1 HD084009, as well as Merit Review Award #I01RX0019900 from the United States (U.S.) Department of Veterans Affairs Rehabiliation Research and Development Service. This contents do not represent the views of the U.S. Department of Veterans Affairs or the United States Government.

References

[1] O'Driscoll SW. J Hand Surg Am. 1992. 17(1), 169-77.
[2] McFarland DC. BMES 2019. Poster presentation.
[3] Delp SL. IEEE Trans Biomed Engin. 2007. 20(5), 540-549.
[4] Pawlaczyk M. Postepy Dermatol Alergol. 2013. 30(5), 302-6
[5] Birdwell JA. J Neurophysiol. 2013. 110, 1385-92.

An Approach to Simulate Control and Dynamics of Land and Stop Tasks Performed by Humans

Rodolfo Amezcua[1], Jill L. McNitt-Gray [2,3], Henryk Flashner [1]
[1]Departments of Aerospace and Mechanical Engineering, [2]Biological Sciences, [3]Biomedical Engineering
University of Southern California, CA, USA. Email: rodolfo.amezcua@usc.edu

Introduction

Studying complex behavior through the lens of simple models allows fundamental concepts and control strategies used by humans in well-practiced tasks to be revealed. One such well-established example is the spring-loaded inverted pendulum (SLIP) to model walking and running [1] that is used here to capture regulation of linear and angular motion during land and stop tasks. Our aim is to validate the SLIP model with experimental data during a series of landings where the participant intentionally regulated the magnitude of the reaction forces during the initial impact phase of the landing. We expected that the control implemented by the individual could be characterized by determining spring and damper coefficients for the model under each landing condition through an optimization procedure. These spring coefficients, k_ϕ and k_r, along with damping coefficients, c_ϕ and c_r, could then be used as representations of impedance control implemented in the task performance.

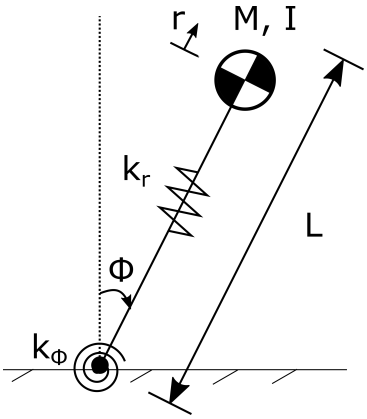

Methods

A female participant with a background in gymnastics provided informed consent and performed a series of land and stop tasks with a range of peak reaction force during the initial impact phase (soft 2.6kN, normal 3.0kN, and hard 4.8kN) from a 0.445 meter platform. Kinematic data in the sagittal plane was captured at 11000 frames per second with a 1.5mm/pixel resolution. Ankle, knee, hip, and shoulder points are tracked with available Matlab software [2]. A cubic smoothing spline is applied to the raw data to attenuate high frequency noise.

Modeling

The dynamics of the SLIP can be described by

$$\mathbf{M}(\mathbf{q})\ddot{\mathbf{q}} + \mathbf{C}(\mathbf{q},\dot{\mathbf{q}})\dot{\mathbf{q}} + \mathbf{G}(\mathbf{q}) = \mathbf{u}$$

where $\mathbf{q} = [\phi,\ r]^T$. By choosing the control to be

$$\mathbf{u} = \mathbf{G}(\mathbf{q}) - \mathbf{K_p}\mathbf{q} - \mathbf{K_d}\dot{\mathbf{q}}$$

where $\mathbf{K_p} = \mathrm{diag}(k_\phi,\ k_r)$ and $\mathbf{K_d} = \mathrm{diag}(c_\phi,\ c_r)$, asymptotic stability of the origin can be analytically shown using Lyapunov theory [3]. To determine the control coefficients $\mathbf{K_p}$ and $\mathbf{K_d}$, the following cost function is minimized.

$$J = \sum_i^n \left(\frac{\phi_{d,i} - \phi_{m,i}}{\phi_{d,range}}\right)^2 + w\left(\frac{r_{d,i} - r_{m,i}}{r_{d,range}}\right)^2$$

where $\phi_{d,i}$ is the ith angular position data value, $\phi_{m,i}$ is the ith angular position model value, $\phi_{d,range}$ is the range of angular position data, and w is a scaling factor. The same notation is used for the deflection coordinate, r.

Results and Discussion

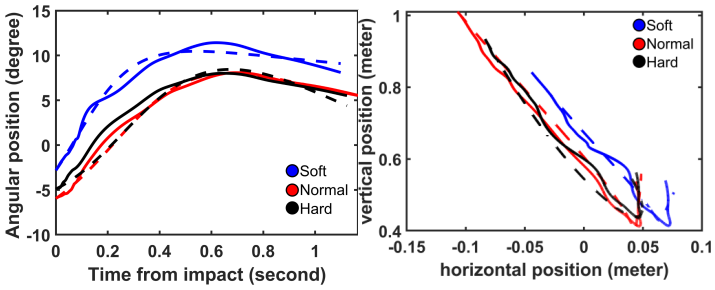

Figure 1: Solid lines: experimental data. Dashed: model. Left: angular position of center of mass (CM). Right: Cartesian position of CM with respect to the ankle.

	k_ϕ (N·m/deg)	k_r (N/m)	c_ϕ (N·m·s/deg)	c_r (N·s/m)
Soft	5.7	173.4	175.7	412.0
Normal	71.7	182.9	107.0	161.2
Hard	116.2	174.8	65.4	288.9

The model satisfactorily reproduces the kinematic behavior of all three impact landing conditions. Also, one can observe the increase of torsional spring coefficient values for the different landing conditions. This demonstrates the ability of the nervous system to modulate the body impedance for drop landings. The translational spring constant does not demonstrate significant difference across landing cases, as seen in the table. Furthermore, all three landing cases exhibit about the same vertical displacement upon landing (Figure 1). This suggests that various impact landing conditions from the same drop height directly affect the angular position more than the vertical displacement of the body center of mass.

Significance

With only two degrees of freedom, the SLIP model can capture the essential kinematics of human drop landings under various conditions. This is of importance because it shows the versatility of the model; it has been used for running, walking, and now drop landings. Previously, drop landings have been modeled as a series of spring-mass systems, performing translational motion and were unable to capture the angular kinematics. Lastly, the control signal consists of a gravity compensation term, linear stiffness and linear damping terms. Thus, allowing for straightforward stability analysis.

Acknowledgements

Ford Foundation and USC DIA Graduate Fellowship to RA.

References

[1] Shahbazi, M. (2016). *IEEE Trans. on Robotics*, 32(5).
[2] Hedrick, T. L. (2008). *Bioinspiration & biomimetics*, 3(3).
[3] Spong, M. W. (2008). *Robot dynamics and control*.

Optimal Bipedal Walking Gaits Found with Different Direct Collocation Settings

Veronica Knisley[1] and Pilwon Hur[1]
[1]Department of Mechanical Engineering, Texas A&M University, College Station, TX
Email: ver96@tamu.edu

Introduction

Applications of bipedal robotics include the navigation of uneven terrain [1] and the development of assistive devices like prostheses [2]. These devices may require an optimal reference trajectory. In order to find such a continuous-time gait, it is helpful to transcribe this problem into a discretized nonlinear program (NLP). One technique, direct collocation, does this by satisfying the system's dynamics at only a few discrete points along the trajectory [3].

This method can be implemented in many different ways. Some studies have compared the specific collocation method chosen in terms of time or accuracy [4], and some have compared differentiation methods in a variety of contexts, including other forms of trajectory optimization [5]. However, such studies have not been completed for the low degree-of-freedom (DOF) bipedal walking models sometimes used by roboticists, such as the two-DOF compass walker and the five-DOF kneed biped with torso. This study [6] addresses this gap in the literature and compares factors such as CPU time for optimal gaits generated with different implementation settings.

Methods

NLPs were developed for finding an optimal trajectory for the two walkers mentioned above. For both models, the objective function was the integral of the sum of squared input torques. Constraints included periodicity constraints, constraints on the initial orientations of the models' legs, and dynamic constraints. For the five-link walker, constraints were also used to prevent the hyperextension of the knees and to ensure foot clearance.

Trapezoidal (TPZD) and Hermite-Simpson (H-S) collocation were used in the objective function and collocation constraints of the compass walker, while only the former was used with the five-link biped. The gradient of the objective and Jacobian of the constraints for the compass walker were found either numerically (ND)—using the central difference approximation—or symbolically (SD). For the five-link walker, these were found using ND, except for the Jacobian of the collocation constraints, which varied in method. Also, for this walker, the joint accelerations were either found numerically or symbolically, or they were included in the decision variables.

Optimizations were performed using the mexIPOPT [7] package for MATLAB. One-hundred optimizations for each of four settings were run for the compass walker with random initial guesses and eleven collocation points. Twenty optimizations were run for each of four settings of the five-link walker. The data were analyzed using an analysis of variance (ANOVA).

Results and Discussion

Figure 1(a) shows the mean and sample standard deviation of two time-related measures for the compass walker. ND was significantly faster than SD, so this differentiation method was considered to be ideal. TPZD was selected over H-S, also for its speed, although there was a slight tradeoff with accuracy.

Similar types of data are shown for the five-link walker in Figure 1(b). It was recommended that accelerations be included in the decision variables due to the rapid per-iteration CPU time

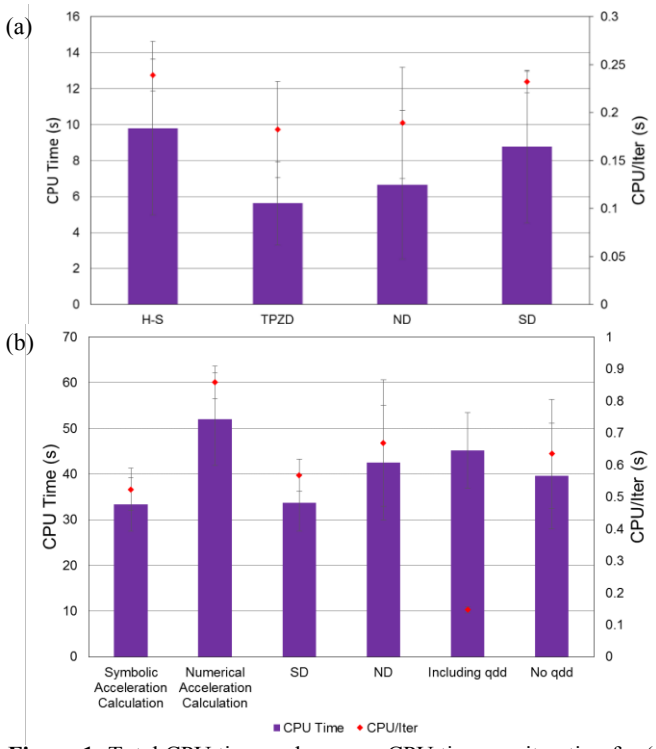

Figure 1: Total CPU time and average CPU time per iteration for (a) compass walker, (b) five-link walker with 21 collocation points. [6]

and a suggested robustness. This was at the expense of the overall CPU time. It was also determined that the joint accelerations should be calculated symbolically due to speed and that ND should be used due to the high complexity of the symbolic expressions required for SD.

In summary, varying the implementation of a direct collocation-based walking trajectory optimization resulted in changes in solution efficiency and, in some cases, accuracy. By analyzing tradeoffs, it was possible to determine potential best practices for performing such optimizations.

Significance

Since many applications of bipedal robotics, such as powered assistive devices, may require a reference trajectory, these results could help to expedite the requisite optimizations. On a wider scale, this study could be combined with those in other fields to see if best practices are similar for multiple types of NLPs with collocation methods. That would extend the value of these results to a far wider range of fields which require the solution of NLPs.

Acknowledgments

The authors would like to thank recent graduate Dr. Kenneth Chao, who introduced one of the authors to direct collocation.

References

[1] H. Dai et al., in *Proc. of the IEEE CDC*, 2012.
[2] V. Paredes et al., in *IEEE/RSJ IROS*, 2016.
[3] M. Kelly in *SIAM Review*, 2017.
[4] D. Pardo et al., in *IEEE Robotics and Automation Lett.*, 2016.
[5] M. Giftthaler et al., in *Advanced Robotics*, 2017.
[6] V. Knisley, MS thesis, Texas A&M University, 2020.
[7] E. Bertolazzi, https://github.com/ebertolazzi/mexIPOPT.

A 3D Computational Model to Simulate 2D Ultrasound Measurements of Medial Gastrocnemius Architecture

Adrienne Williams[1], William H. Clark[2], Jeroen B. Waanders[3], Jason R. Franz[2], and Silvia Blemker[1]
[1]University of Virginia, Charlottesville, VA, USA, [2]UNC Chapel Hill & NC State University, Chapel Hill, NC, USA
[3]University of Groningen, Groningen, the Netherlands. Email: *afw6gf@virginia.edu

Introduction

Real-time two-dimensional (2D) ultrasound (US) is commonly used to non-invasively study skeletal muscle architecture and muscle-tendon interactions *in vivo*. Though informative and fast, the efficacy of 2D US to examine changes in muscle architecture with contraction is limited. For example, these 2D measurements of three-dimensional (3D) architecture capture fascicle length and pennation angle measurements within only a small region of the muscle in the probe's field-of-view (FOV), and rely on identifying a fascicle that appears in the US FOV at a given time.

We aim to examine these limitations by (i) creating a 3D simulation of the medial gastrocnemius (MG) during an isometric contraction, (ii) comparing the model predictions with US measurements, and (iii) analyzing the model to examine how sampling muscle fascicles within the region of an US probe influences fascicle length change predictions.

Methods

MR images were used to create the 3D geometry of a MG muscle. The geometry was scaled to the average thickness of the MG muscles of 6 young adults (age: 23.7±4.9 years, 2 females), then meshed and assigned a muscle material [1] for finite element (FE) analysis. Computational fluid dynamics was used to assign vectors from a laminar flow simulation within the geometry as fiber directions to the model's elements [2]. Based on these fiber directions, streamlines generated (in MATLAB [3]) were used to define representative fascicles (Fig. 1A). Muscle-tendon junction displacement collected by US during a maximum voluntary isometric contraction (MVC) defined the boundary conditions at the distal MTJ. After the FE simulation, we sampled the model fascicles in the region that represented the volume of the muscle that is captured in the FOV of the US probe (L:60mm x W:15 mm x D:24 mm) – Fig. 1B. We assume that the region's thickness is the same as the probe width. Lastly, the 3D trajectories of the fascicles were projected on the 2D plane of the probe (Fig. 1C), to represent what would be visible in the US image.

Results and Discussion

The predicted fascicle arrangement within the probe field of view was qualitatively similar to the ultrasound images (Fig. 1C&D). Of the 367 representative fascicles in the 3D model (Fig. 1A), 86 (23.4%) fascicles at rest and 84 (22.9%) fascicles at MVC had at least two points within the probe volume. Of those 86 fascicles, one fascicle had all points from the 3D model within the probe volume when the muscle was relaxed (Fig 1B,C), while no fascicles were completely within the volume at MVC, as fascicles shifted medially out of the region with contraction. Between rest and MVC, the average length change of all fascicles in the modelled probe region were comparable to the average *in vivo* data, but with a large standard deviation, representing all the fascicles within that image. We see from our model that many fascicles are curved, while ultrasound image analyses typically assume fascicles are straight lines. Future work will account for the curvatures observed in our model fascicles, as we evaluate pennation angles and fascicle curvatures.

Significance

Ultrasound imaging has become a ubiquitous tool in biomechanics to understand *in vivo* muscle function. Our work aims to augment those measurements with 3D modeling to explore the 2D assumptions made with US and investigate issues such as how probe placement (location, tilt, and rotation) influences measurements.

Acknowledgments

We acknowledge funding support from NIH R01AG051748.

References

1. Blemker SS, et al. *J Biomech* **38**, 657-665, 2005.
2. Handsfield, G et al. (2017). *BMMM*, **16**(6):1845-1855
3. Bolsterlee B, et al. *J Appl Physiol* **122** (4), 727-738, 2017.

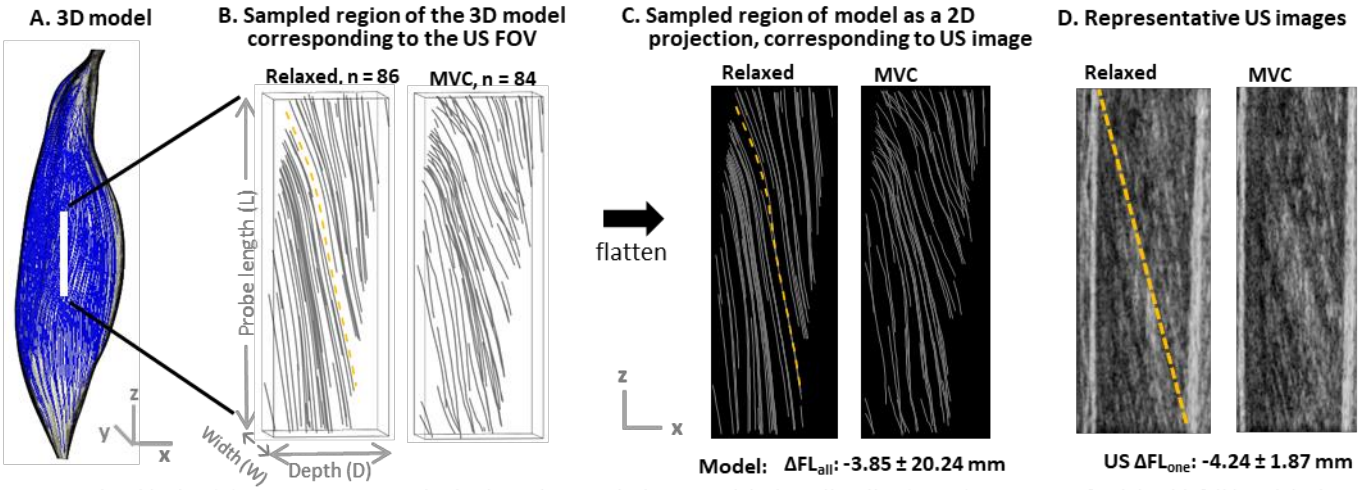

Figure 1: The white bar (A) represents an US probe that is used to sample the 3D model. The yellow line (B,C,D) represents a fascicle with full length in the FOV.

The Contribution of Spinal Erector Muscle Strength and Facet Contact in Reducing Disc Herniation Risk During Forward Bending

Stephanie Rossman M.S.[1,2], Eric Meyer Ph.D.[1], and Steven Rundell Ph.D.[2]
[1]Lawrence Technological University
[2]Explico Engineering
Email: *srossman@explico.com

Introduction

Disc herniations occur in a biomechanical environment consistent with forward bending, i.e. compression and flexion. It is generally believed that facet contact is not relevant in loading modes that place the spine in flexion, such as forward bending. This belief is supported by the use of a compressive follower force to simulate the spine's musculature. This assumes a perfect balance between flexor and extensor muscle activation. However, it is possible, and encouraged by athletic trainers and physical therapists, to activate the spinal extensor muscles during forward bending, i.e., maintaining a flat back.

Activation of these spinal erector muscles during bending may encourage facet contact, which could effectively offset compressive and shear loading from the disc to the facets. This may be an effective way to protect the disc during forward bending activities.

Therefore, the objective of the current study was to utilize a finite element model of a lumbar motion segment to evaluate the association between spinal extensor muscles, specifically the erector spinae (ES) muscle, and facet contact force in reducing disc herniation risk during forward bending. We hypothesized that the presence of intact facets and increased ES muscle force would result in increased sagittal balance and decreased disc pressure, disc stresses, and nuclear extrusion forces compared to no facets.

Methods

A previously developed and validated finite element model of a L4-5 lumbar motion segment was utilized for the current study[3], [6], [7]. Forward bending was simulated by rotating the motion segment 30° and applying 343 N of axial compression 15 mm anterior to the center of the L4 bony endplate. The inferior bony endplate of L5 was fixed rigidly in space. A surface-to-surface contact was established between the L4 and L5 posterior elements. To simulate the removal of facets, the contact between the posterior elements was turned off. The ES was simulated by attaching bi-lateral force elements between the spinous processes approximately 5.5 cm posterior of the joint center. Varying amounts of ES force was applied. The disc pressure, disc 1st principal stress and shear stress, nuclear extrusion forces, facet contact forces, and L4 vertebral x-axis rotations were recorded.

Results and Discussion

Results of the study confirmed our hypothesis that the presence of intact facets resulted in lower disc pressure, disc stresses, and nuclear extrusion forces during forward bending. The greatest reduction in loads on the disc occurred when balance was restored due to increased ES muscle activation. At the point of maximum reduction in disc loads, there was an increase in facet contact force, consistent with the facets offsetting loads in the disc.

Significance

The current study demonstrated the importance of ES muscle strength and facet contact contribution to maintaining a healthy disc environment. This has clinical significance in the surgical realm due to the current practice of removal of facets during decompression techniques for the treatment of disc herniation. Future studies involving the current finite element model may be conducted to evaluate the risk for re-herniation following decompression surgery. Additionally, if the facet joints must be removed, the current study demonstrates increased ES muscle activation may not result in a healthy disc environment, which has many implications in post-surgical physical therapy techniques.

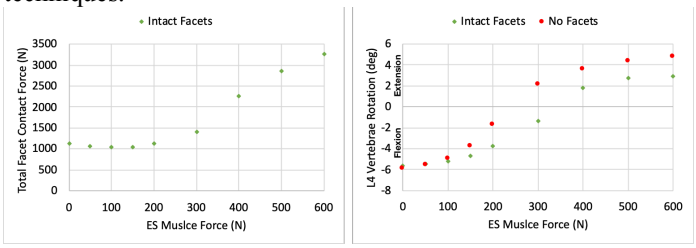

Figure 1: Facet contact force and L4 vertebral x-axis rotations with intact facets and without facets.

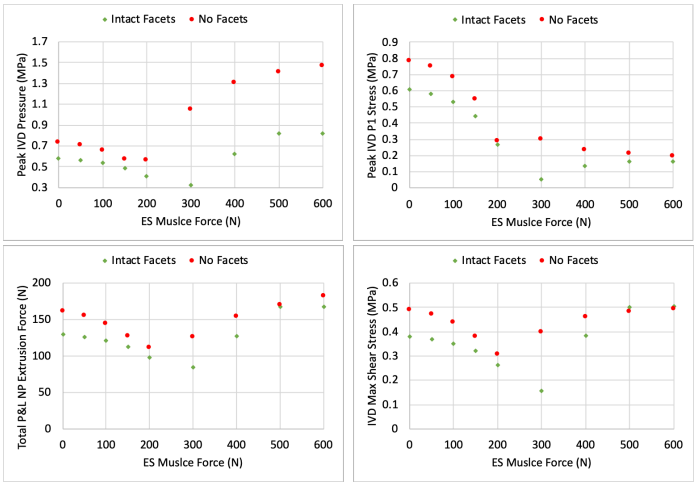

Figure 2: Disc pressure, shear stress, 1st principal stress, and nucleus extrusion force in the posterior and lateral aspect of the disc with intact facets and without facets.

References

[1] D. S. McNally and M. A. Adams, "• Can Intervertebral Disc Prolapse Be Predicted By Disc Mechanics?," 1993.
[2] K. R. Wade, P. A. Robertson, A. Thambyah, and N. D. Broom, "How Healthy Discs Herniate: A Biomechanical and Microstructural Study Investigating the Combined Effects of Compression Rate and Flexion," *2014*.
[3] S. Rossman, E. Meyer, and S. Rundell, "Development of a Finite Element Lumbar Spine Model to Predict Intervertebral Disc Herniation Risk," 2019.
[4] J. P. Callaghan and S. M. McGill, "Intervertebral disc herniation: studies on a porcine model exposed to highly repetitive flexion/extension motion with compressive force," 2001.
[5] K. H. Yang and A. I. King, "Mechanism of Facet Load Transmission as a Hypothesis for Low-Back Pain:," *1984*.
[6] S. A. Rundell, J. D. Auerbach, R. A. Balderston, and S. M. Kurtz, "Total Disc Replacement Positioning Affects Facet Contact Forces and Vertebral Body Strains:," *2008*.
[7] S. A. Rundell, H. L. Guerin, J. D. Auerbach, and S. M. Kurtz, "Effect of Nucleus Replacement Device Properties on Lumbar Spine Mechanics:," *2009*.
[8] M. Bernhardt and K. Bridwell, "Segmental analysis of the sagittal plane alignment of the normal thoracic and lumbar spines and thoracolumbar junction," 1989.

Discrepancy Modeling for Human Locomotion

Megan Auger[1], J. Nathan Kutz[2], and Katherine M. Steele[1]
[1]Department of Mechanical Engineering, University of Washington, Seattle, WA
[2]Department of Applied Mathematics, University of Washington, Seattle, WA
Email: mauger@uw.edu

Introduction

Despite our ability to model the human system, accurately predicting locomotion when idealized musculoskeletal model dynamics differ from reality remains challenging. While first-order, physics-based models describing human motion generally capture salient characteristics of locomotion, physical systems are not ideal. Thus, models are unable to capture the complete dynamics observed in experiment, i.e. simulation does not match experiment [1, 2]. The inability to represent such discrepancies can have significant impact on model predictions.

Discrepancies can arise from a variety of factors often ignored in idealized models, such as with parameter mismatch (subject-specific musculotendon properties, segment mass estimation error) or missing physics (unmodeled body segments, motion artifacts, soft tissue mechanics). These discrepancies are typically unique to an individual and must be learned and quantified as such. Taking inspiration from perturbation theory [3], we develop a mathematical architecture based upon sparse regression that discovers interpretable, data-driven discrepancy models to augment first principles dynamics that may help predictions and guide future experimental studies. To evaluate the feasibility of discrepancy models in human locomotion, we used a simple dynamic walking model in an ideal simuation environment and hypothesized our simulation framework would recover small nonlinear discrepancies from the model's locomotion dynamics.

Methods

The sparse identification of nonlinear dynamics (SINDy) algorithm [1] uses sparse regression to discover a parsimonious representation of nonlinear system dynamics from measurement data. An important assumption about the model structure is that there are only a few salient terms governing the dynamics; this ensures system interpretability and avoids overfitting. Recently, this framework has been used to identify discrepancy models between empirical data and model outputs of a system [2]. Discrepancy models can analogously be thought of as a first-order perturbation model. Our solvable problem (A_0) is an oscillatory 2-link pendulum [4] with collision constraints, and the first-order perturbation solution ($\tilde{A}$) includes small nonlinear contributions to equations of motion $A \approx A_0 + \tilde{A}$ where $\tilde{A} \ll 1$.

We used a simple passive dynamic walking model described by two states: θ *(angle of stance leg w.r.t. vertical)* and φ *(relative angle between legs)* (Fig. 1). N = 1000 trials were performed. Each trial generated a random polynomial discrepancy (max. order 5) and randomly added the discrepancy to a system state. Kinematics were evaluated for stability (10+ steps) before using SINDy to recover the discrepancy model.

Results and Discussion

SINDy recovered first-order physics with high fidelity, correctly identifying 88.6% of the discrepancies. No discrepancy model was identified for the remaining 11.4% due to an inappropreiatly high sparcity regularization parameter. This could be rectified in future analyses via hyperparameter tuning.

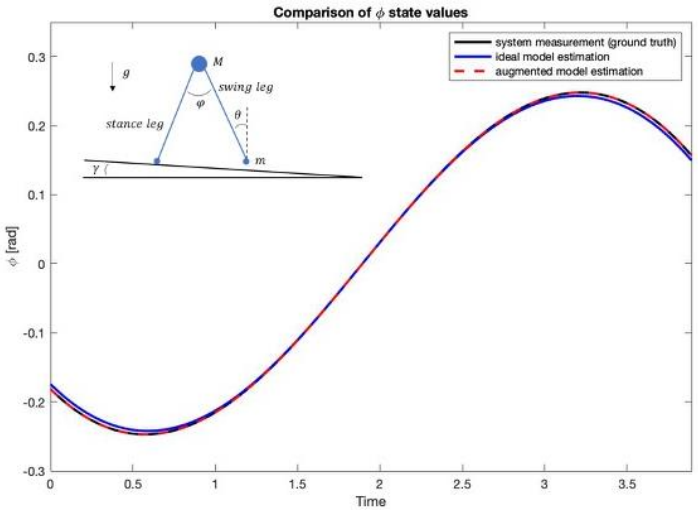

Figure 1: Model parameter φ for one step. Ideal model estimation (blue) fails to fully capture measured system dynamics (black). Discrepancy model augments the ideal model (dashed red) to recover system physics.

While this initial investigation used a simple toy model to investigate the use and accuracy of discrepancy modeling for recovering locomotion dynamics, including system-specific corrections to an idealized model can help close the gap between experiment and simulation.

Significance

This work is a critical first step in improving the integration of heterogeneity into musculoskeletal models to improve prediction accuracy. Developing subject-specific models will be crucial for predicting effects of treatments or interventions computationally. This is especially true when an individual has a motor impairment and does not subscribe to the same assumptions about musculoskeletal properties as unimpaired individuals.

Acknowledgments

This work was supported by NSF GRF DGE-1762114.

References

[1] Brunton, S et al., *PNAS*, 113(13): 3932-3937, 2016.
[2] Kaheman, K et al., *arXiv:1909.08574*, 2019.
[3] Bender & Orzag, *Adv. Math. Methods Sci.,Eng.*, Springer: 1999, 61-145.
[4] McGeer, T, *Int. J. Robot*. Res, 9(2): 62-82, 1990.

Which Muscles are Most Responsible for Tremor? Principles from Computer Simulations

Spencer A. Baker[1], Daniel B. Free[1], Steven K. Charles[1,2]
[1]Mechanical Engineering and [2]Neuroscience, Brigham Young University, Provo, UT
Email: skcharles@byu.edu

Introduction

Tremor is the most common movement disorder. Essential Tremor alone affects approximately seven million people in the United States [1]. Tremor's debilitating effects and lack of satisfactory treatments accentuate the need for new tremor-suppressing methods. Peripheral treatments are possible but are presumably more effective when applied to the muscles that are most responsible for the termor [2]. Determining which muscles cause tremor is a complex challenge. Tremor in the arm "propagates" (spreads) tremorogenic muscle activity to multiple degrees of freedom (DOF), and each muscle-DOF relationship is unique. Past studies have examined tremor propagation from the 15 major superficial muscles of the upper limb [3], but this is only a subset of the muscles capable of causing tremor. The purpose of this research was to expand the previous studies to include all 50 muscles of the upper limb, to discover principles of tremor propagation, and to determine which of these muscles are most responsible for tremor.

Methods

We modeled the upper limb as a linear, time-invariant, multi-input-multi-ouptut system. Inputs are the neural drive in one or multiple arm muscles. Outputs are the displacements in the seven DOF from the shoulder to the wrist. The model simulates tremor propagation in three phases (Figure 1).

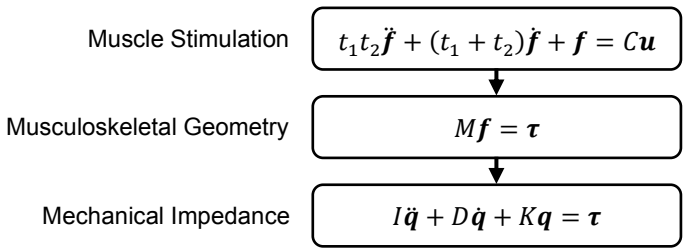

Figure 1: Summary of the model and the relationships between neural drive ($\boldsymbol{u}$), muscle forces ($\boldsymbol{f}$), joint torques ($\boldsymbol{\tau}$), and DOF movement ($\boldsymbol{q}$). Model parameters are the muscle-excitation time constant (t_1), muscle-contraction time constant (t_2), muscle strengths (C), musculoskeleltal geometry (M), inertia (I), damping (D), and stiffness (K). Default parameter values were obtained from prior studies [3-4].

Bode analyses were used to investigate tremor magnitude and spreading on each muscle-DOF relationship in the tremor band (4-12 Hz).

In addition, we conducted a sensitivity analysis to account for error in our parameter values and variability between subjects.

Results and Discussion

Simulations showed that if all muscles had the same amount of tremorogenic input, the proximal muscles produce the most force and joint torque, but the forearm and wrist muscles produce the most tremor (Figure 2). We found that tremor will predominantly affect one or two DOF. The DOF with the most tremor were always distal.

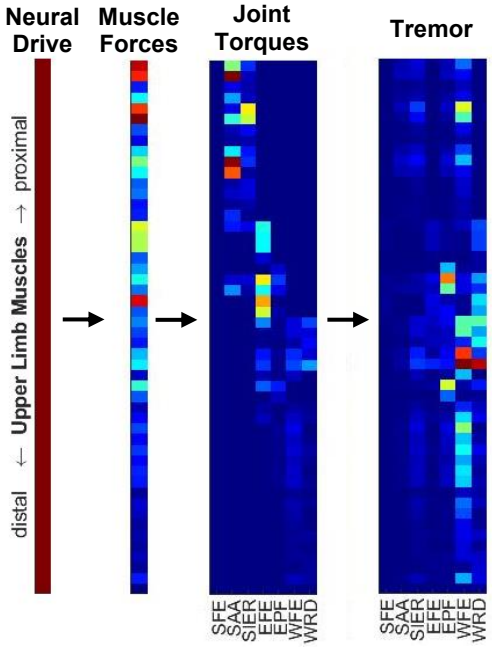

Figure 2: Tremor propagation at 8 Hz from neural drive (plot 1) to muscle forces (plot 2), joint torques (plot 3), and DOF movement (plot 4). The rows represent muscles. The columns in plots 2 and 3 represent the DOF: shoulder flexion-extension (SFE), shoulder adduction-abduction (SAA), shoulder internal-external rotation (SIER), elbow flexion-extension (EFE), forearm pronation-supination (FPS), wrist flexion-extension (WFE), and wrist radial-ulnar deviation (WRUD). Magnitudes are indicated by shades of blue (low) to red (high).

We found that while tremor magnitude depends on exact model parameter values, tremor propagation patterns are robust to parameter errors and subject variability.

Our investigation confirms previous findings that musculoskeletal dynamics spread tremor narrowly (i.e. input in a muscle causes tremor mostly in a small number of DOF) but not necessarily locally (e.g. input in a proximal muscle may cause its greatest tremor in a distal DOF) [1]. We also found that wrist and forearm muscles produce the greatest tremor (for a given tremorogenic input), and that most of the tremor produced (by all muscles together) occurs in the DOF of the wrist and forearm.

Significance

These findings provide principles of propagation for estimating which muscles are most responsible for tremor. This understanding can be used by researchers and clinicians to optimize peripheral tremor-suppression methods, facilitating the innovation of tailored and effective treatments.

Acknowledgments

This research was supported by NSF grant 1806056.

References

[1] E. D. Louis, et al, *Tremor and Hyperkinetic Movements*, 2014
[2] O. Samotus et al, *J. Neuro. Sciences*, 2018
[3] T. H. Corie, S. K. Charles, *J. Biomech.*, 2019
[4] K. R. S. Holzbaur et al, *J. Biomech,* 2006

The Importance of Spinal Erector Muscle Strength and Facet Contact in Establishing Sagittal Balance and Reducing Disc Loads During Standing and Forward Bending

Stephanie Rossman M.S.[1,2], Eric Meyer Ph.D.[1], and Steven Rundell Ph.D.[2]
[1]Lawrence Technological University
[2]Explico Engineering
Email: *srossman@explico.com

Introduction

During normal standing and forward bending, the lumbar spine is exposed to compression and anterior shear due to upper body weight[1]. Additionally, the line of gravity is anterior to the center of the vertebrae resulting in development of a flexion moment. The extensor muscles of the spine, primarily the erector spinae (ES), counter-act the anteriorly biased body weight, and re-establish sagittal balance. Paradoxically, despite the increased amount of loading, it is generally believed that strong spinal extensor muscles provide a biomechanically healthier environment for the discs. We hypothesize that the benefits of extensor muscle activation are the direct result of increased facet engagement. Specifically, strong spinal extensor muscles increase facet force and thereby align the vertebrae, restore sagittal balance, and generally reduce loading on the disc.

The current study involved applying upper body weight (compression, anterior shear, and flexion) to a single finite element lumbar motion segment to evaluate the effect of ES muscle activatio in engaging the facets and re-establishing sagittal balance during simulated standing and forward bending.

Methods

A previously developed and validated finite element model of a lumbar motion segment was utilized for the current study[2]. Axial compression of 343 N was applied 15 mm anterior of the center of the L4 superior bony endplate to simulate standing[3]. Forward bending was simulated by rotating the motion segment 30° and applying 343 N of axial compression 15 mm anterior to the center of the L4 bony endplate. The inferior bony endplate of L5 was fixed rigidly in space. A surface-to-surface contact was established between the L4 and L5 posterior elements. To simulate the removal of facets, the contact between the posterior elements was turned off. The ES was simulated by attaching bi-lateral force elements between the spinous processes approximately 5.5 cm posterior of the joint center. Varying amounts of ES force was applied. The L4 vertebral x-axis rotations, facet reaction forces, and disc pressures were recorded.

Results and Discussion

Results of the study confirmed our hypotheses that an increase in ES force would engage the facets, restore sagittal balance, and decrease loading on the disc. In general, the absence of facet contact resulted in greater mobility of the joint. These results indicate the facet joints play a role in stabilizing the lumbar spine in the sagittal plane. As the ES muscle force increased, an extension moment was created to offset the flexion generated by upper body weight. Facet joint engagement resulted from increased amounts of ES muscle activation, which in turn resisted the compressive and shear components of body weight. The greatest reduction in disc pressure resulted when sagittal balance was restored. Without intact facets, higher ES muscle loads resulted in increased disc pressures and extension rotation suggesting an inherently unstable condition (marble perched on a hill) for spines with jeopardized facets.

Significance

The current study demonstrated the importance of the facet joints and ES muscle strength in maintaining sagittal balance and reducing the loading on the disc. This study provides the foundation for understanding the relationship between the spinal extensor muscles and the facets and the contriubution of these anatomical structures to maintaining a healthy disc environment. This has clinical significance due to the current trend of surgical removal of the facets during decompression techniques used to treat disc herniations. The current finite element model may be used to study the effects of those surgical techniques on disc health and to evaluate how maintaining strong spinal extensor muscles can contribute to disc health after surgical removal of the facets.

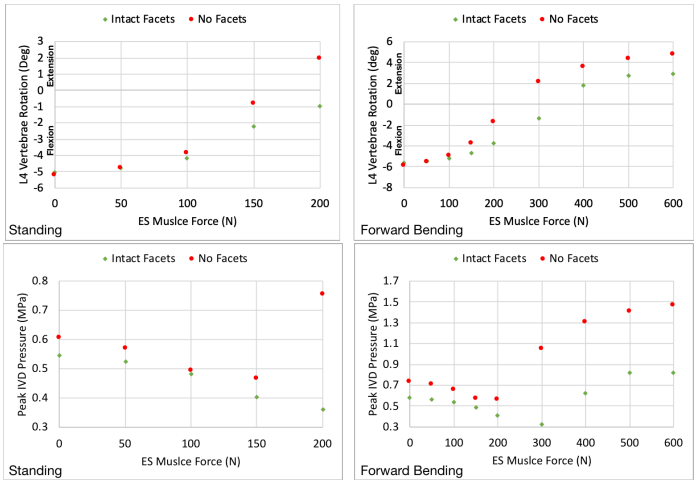

Figure 1: L4 vertebrae x-axis rotations and disc pressures during standing and forward bending, with and without facets, for varying amounts of ES muscle force.

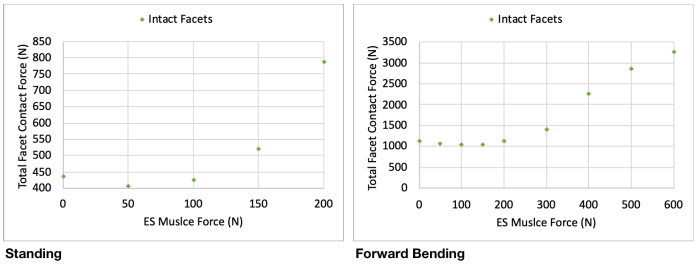

Figure 2: Total facet contact force during standing and forward bending for varying amounts of ES muscle force.

References

[1] B. M. Cyron and W. C. Hutton, "Articular Tropism and Stability of the Lumbar Spine," *SPINE*, vol. 5, no. 2, pp. 168–172, 1980.

[2] S. A. Rundell, J. D. Auerbach, R. A. Balderston, and S. M. Kurtz, "Total Disc Replacement Positioning Affects Facet Contact Forces and Vertebral Body Strains:," *Spine*, vol. 33, no. 23, pp. 2510–2517, Nov. 2008, doi: 10.1097/BRS.0b013e318186b258.

[3] M. Bernhardt and K. Bridwell, "Segmental analysis of the sagittal plane alignment of the normal thoracic and lumbar spines and thoracolumbar junction," *Spine*, vol. 14, no. 7, pp. 717–721, 1989.

Using System Identification to Determine how Tremor Propagates in the Upper Limb

Sydney B. Ward[1], Jing-Song Huang[1], Sadie Cutler[1], C. Paul Curtis[1], Steven K. Charles[1,2]
[1]Mechanical Engineering and [2]Neuroscience, Brigham Young University
Email: Sydney.ward30@gmail.com

Introduction

Essential Tremor (ET) is one of the most common movement disorders, affecting 5% of adults over 60 years old. ET involves involuntary shaking of the hands, arms, head and/or other body parts during voluntary movement and postural stances. Common treatment options include medications and neurotherapy, such as deep brain stimulation and MRI guided focused ultrasound. Unfortunately, the side effects and risks associated with these options cause many people with ET to opt out of treatment altogether. Peripheral tremor suppression options, such as wearable orthotics and weighted utensils, are also available, but one limitation to the effectiveness of these options is we do not currently know where in the upper limb the tremor originates or how the tremor propagates. The purpose of our research is to determine the mechanical origin and propagation of tremor throughout the upper limb.

Methods

Tremor propagation was previously simulated [1] using a linear, time-invariant (LTI) model of the upper limb neuromusculoskeletal system, which takes in muscle activity and outputs joint displacements through a series of three subsystems: muscle activity to muscle force; muscle force to joint torque; and joint torque to joint displacements (Figure 1.A). Also, we previously collected muscle activity and joint displacement data in 15 major superficial muscles and 7 joint degrees of freedom in the upper limb while 24 ET patients assumed multiple postures and performed various movements. Combining the model and measured data would allow us to estimate which muscles are most responsible for a patient's tremor. However, this model includes many unknown patient-specific parameters (muscle time constants, moment arms, joint impedances, etc.). Therefore, we are applying system identification to estimate the physically significant parameters of the upper limb neuromusculoskeletal system based on the model, muscle activity input, and joint displacement output data. We will then apply superposition techniques to the model to determine which muscles are most responsible for each patient's tremor.

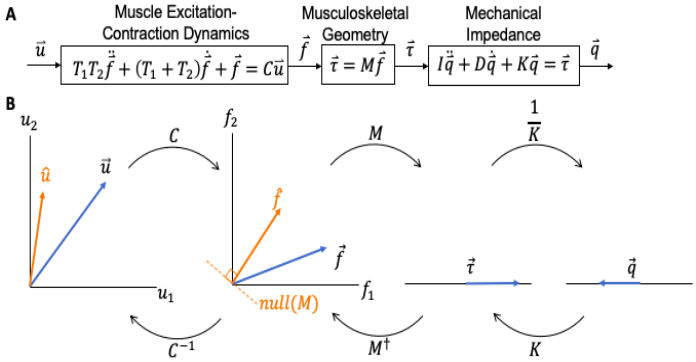

Figure 1: A. LTI model relating tremorgenic muscle activity to joint displacements. u, f, τ, and q represent muscle activity, muscle force, joint torque, and joint displacements; T_1 and T_2 represent muscle time constant diagonal matrices; C and M represent the diagonal muscle gain matrix and the moment arm matrix; and I, D, and K represent positive definite impedance matrices. B. Simplified version of the LTI model (2 inputs, 1 output; derivative terms not included) represented as a series of linear transformations. The inverse transformation from q to u requires the inverse of the wide matrix M. The pseudoinverse of M finds the force vector that is perpendicular to the null space of M, which is not necessarily the true force.

Results and Discussion

We have approached this problem using a least-squares method in the time domain and have faced three significant challenges: 1. Combining the three subsystems into a single system results in a fourth-order ODE that forces least-squares minimization of the residual error of the (very noisy) muscle activity input instead of the residual error of the (smoothed) joint displacement output; 2. Combining the three subsystems into a single system also forces the least-squares solution to perform the inverse transform, which involves calculating muscle forces from joint torques (Figure 1.B); unfortunately, the usual assumptions used to perform this underdetermined inversion (e.g. minimizing effort) do not apply to tremor; 3. The system is linear with respect to the parameter matrices but is not linear with respect to the nonzero, non-repeating elements of the parameter matrices.

Consequently, we are currently investigating other system identification methods to avoid or minimize these three challenges. The issues of minimizing the input residual errors and performing the inverse transform may be resolved by implementing system identification in the frequency domain instead of in the time domain. Frequency domain system identification assumes steady-state, periodic input, which is an appropriate assumption for tremor. The problem of nonlinearities with respect to significant elements of the parameter matrices can be resolved by applying an iterative search method, such as Gauss-Newton, steepest descent, or Levenberg-Marquardt. The drawback of iterative search methods is a more complicated algorithm that carries the risk of getting trapped in local minima when searching for optimal parameters.

Significance

Our work will result in a method for determining the physical parameters of the tremorgenic upper limb neuromusculoskeletal system. We will use parameters generated from this method to determine which muscles are most responsible for a patient's tremor and therefore where peripheral tremor suppression techniques should be applied for maximum tremor reduction.

Acknowledgments

This work was funded in part by NINDS R15NS087447 and NSF 1806056 grants.

References

1. T.H. Corie et al, Journal of Biomechanical Engineering, 2019.

Comparison of Three Unique Foot Models Over One Step

Emily Dooley[1], Watson Spivey[1], W. Brody Hicks[1], and Shawn Russell Ph.D.[1,2]
University of Virginia, Departments of [1]Mechanical Engineering and [2]Orthopaedic Surgery, Charlottesville, VA, USA
Email: sdr2n@virginia.edu

Introduction

Clinical ankle assessment and treatment has become much more sophisticated over the last two decades as treatment for end-stage ankle arthritis has shifted to total ankle arthroplasty (TAA), compared to the traditional ankle arthrodesis (AA).[1] A motivating factor in this is the improvement in the ankle replacements being used in the TAA procedure. However, little work has been done to examine how TAA affects the motion of the foot. This is made difficult by a lack of knowledge of what typical foot motion looks like as well as the lack of technical uniformity between various existing foot models.[2] This case study compares three foot models, all modelling the same step to illuminate differences in the existing models, and propose critical components in the use and development of foot models moving forward.

Methods

3D motion capture data was collected on one healthy, 22 y.o., male subject. Markers were applied to complete the marker sets necessary for the Plug-in-Gait (PiG), Oxford Foot (OXF), and KU Leuven (KUL)[3] models. The subject walked at his self-selected, comfortable walking speed along a 15 m walkway. A single step was isolated and exported to OpenSim 4.0. The 4-segment OXF model was created in OpenSim by fixing the midfoot(MF)-forefoot(FF) joint in the 5-segment KUL model, then replacing all existing joints in the model with ball joints aligned to the anatomical planes. To allow for comparison between PiG, OXF, and KUL the off-axis MF-FF joint of the KUL model was replaced with overlaid revolute joints to report flexion and inversion. With these changes all models report flexion in the sagittal plane, inversion in the frontal plane, and internal/external rotation in the transverse plane. The same step was then modelled by each of the three models. All kinematics were normalized to the static position of the subject standing still. Outputs were compared to Lundgren[4] foot motion for reference.

It is implied that the angles reported by the multi-segment models (OXF, KUL) should converge to the angle reported by the model with the least segments (PiG). The convergence of the models was analyzed by summing all of the joints contributing to flexion and comparing the result to the fewer segment models.

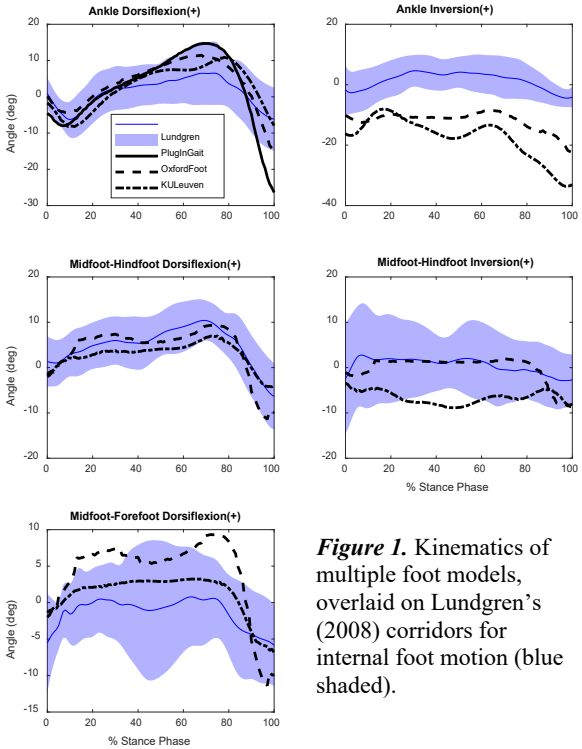

Figure 1. Kinematics of multiple foot models, overlaid on Lundgren's (2008) corridors for internal foot motion (blue shaded).

Results and Discussion

All models represent the total sagittal motion between the ankle and the foot (*Fig. 2*). However, to investigate more degrees of freedom through the foot, it is shown that the PiG model cannot give any more information, as it is only one segment.

Figure 1 shows how the total motion is distributed along the foot. Flexion within the foot is captured by two joints in the KUL model and only one in the OXF model. The result of this is matching reports of the MF-hindfoot(HF) angle between OXF and KUL. However, if the MF-HF angle from OXF is used to capture MF-FF motion, the result falls outside of the Lundgren[4] corridor and varies largely from the result of the KUL MF-FF joint motion (*Fig 1, Row 3*). Lack of uniformity in the midfoot is important to note, as it shows the hypothesis that more segments are necessary to accurately describe the motion of the foot.

When considering the convergence of the models (*Fig. 2*), it can be seen that the models do converge well in the sagittal plane. However, there are still differences seen in the resulting curves, further suggesting that we do not yet have a complete understanding of typical foot motion.

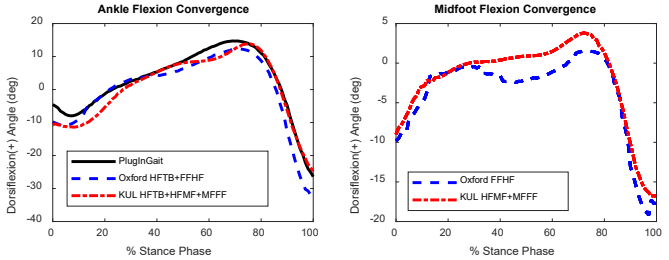

Figure 2. Convergence of joint flexion. PiG solid black. Oxford Foot dashed blue. KU Leuven dot-dashed red.

Significance

We expect the motion of the ankle to change with TAA, so we need a method to analyze this change and ultimately design better ankle replacement mechanisms. These results highlight the importance of a multisegment model for understanding internal foot motion. This comparison also begins to lay the ground work for determining the optimal degrees of freedom needed from a ankle joint model.

Acknowledgments

UVA MAMP Lab & Integra Life Sciences

References

[1] Philippe (2008) F&A Int. [2] Deschamps (2011) G&P.
[3] Malaquias (2017) C.M.B&B.E. [4] Lundgren (2008) G&P.

Static Optimization Personalization for the Muscle Redundancy Problem

Mohammad Shourijeh[1], Marleny Arones[1], Carolynn Patten[2], and Benjamin Fregly[1]
[1]Department of Mechanical Engineering, Rice University, Houston, Texas, USA
[2]Department of Physical Medicine & Rehabilitation, University of California, Davis, California, USA
Email: shourijeh@rice.edu

Introduction

Reliable estimation of muscle forces during human movement could facilitate the development of improved interventions for disorders such as stroke [1]. Muscle forces cannot be measured noninvasively using standard experimental methods, nor can they be computed via rigid body dynamics alone due to the muscle redundancy problem (i.e., more muscles than degrees-of-freedom (DOF) in the human musculoskeletal system). Because of its simplicity, static optimization (SO) is frequently used to resolve the muscle redundancy problem. However, generic musculoskeletal modeling frameworks have shown to be incapable of accurate estimation of muscle activations and, therefore, muscle forces [2].

Model personalization has been applied as one big step forward in personalizing neuromusculoskeletal parameters, especially in pathologic cases, such as stroke [3]. However, to estimate muscle activations/forces more accurately, personalization of the muscle redundancy problem seems necessary. This study explored the customization of the static optimization formulation for an individual post-stroke and how it affects the estimation of muscle activation and force.

Methods

Walking data (Motion, ground reaction, and EMG of 50 trials—5 speeds, 10 trials each) from a previous study of a patient post-stroke were used [3]. A modified OpenSim (v4.0; [4]) model with 31 degrees of freedom (DoFs; 5 per each leg) and 35 leg muscles was used for the initial musculoskeletal analysis, including scaling and inverse kinematics and dynamics. An EMG-driven musculoskeletal model calibrated musculotendon parameters [3]. Standard static optimization was formulated as $\min \sum_{i=1}^{33} a_i^2$, subject to $M_j = \sum_{i=1}^{33} r_{ij} F_i^T (j = 1, \dots, 5)$ and $0 \leq a_i \leq 1$ $(i = 1, \dots, 33)$ where M is joint moment, F^T is musculotendon force, and a is muscle activation. The inverse optimization problem was defined as

$$\max_{w,\, a^{Bg}} \sum_{k=1}^{N} \sum_{i=1}^{33} R_{ij}^2 (a_{ik}, a_{ik}^{EMG})$$

subject to muscle weight parameter $w \geq 0$ and muscle background activation level $0 \leq a^{Bg} \leq 1$ where N is the number of trials, a^{EMG} are the target muscle activations from the EMG-driven model, and activations a are estimated from the inner loop problem, which is a custom SO [4,5]:

$$\min_{a_{ik}} \sum_{i=1}^{33} w_i \left(a_{ik} - a_i^{Bg}\right)^2$$

subject to $M_j = \sum_{i=1}^{33} r_{ij} F_i^T (j = 1, \dots, 5)$ and $0 \leq a_i \leq 1$.

Several sets of trials were used for the inverse optimization problem to assess the sensitivity of the training set on the optimal parameters.

Results and Discussion

The mean of the Pearson correlation between the estimated activations and processed EMG increased from 0.68 for SO to 0.93 for the inverse optimization framework (Figure 1). Optimal weight and background activation parameters resulting from different training sets were robust (R^2>0.95).

Significance

This study showed that personalizing an objective function for the muscle redundancy problem of a patient post-stroke is necessary. Although traditional static optimization is not accurate in estimating muscle activations, we showed that personalized custom static optimization could have the potential to be used for such estimations, which can have a great impact on how the interventions are designed in pathologic populations.

Acknowledgments

Funding provided by the Cancer Prevention and Research Institute of Texas Grant RR170026

References

[1] Erdemir A et al. (2007). Clin. Biomech. **22**: 131–154.
[2] DeMers S et al. (2014) J. Ortho. Research **32.6**: 769-776.
[3] Meyer AJ et al. (2017). PLoS One. **12**.
[4] Delp SL et al. (2007). Biom. Eng. IEEE T. **54**: 1940–1950.
[5] Forster E et al. (2004). J. Biomech. **37.4**: 577-581.

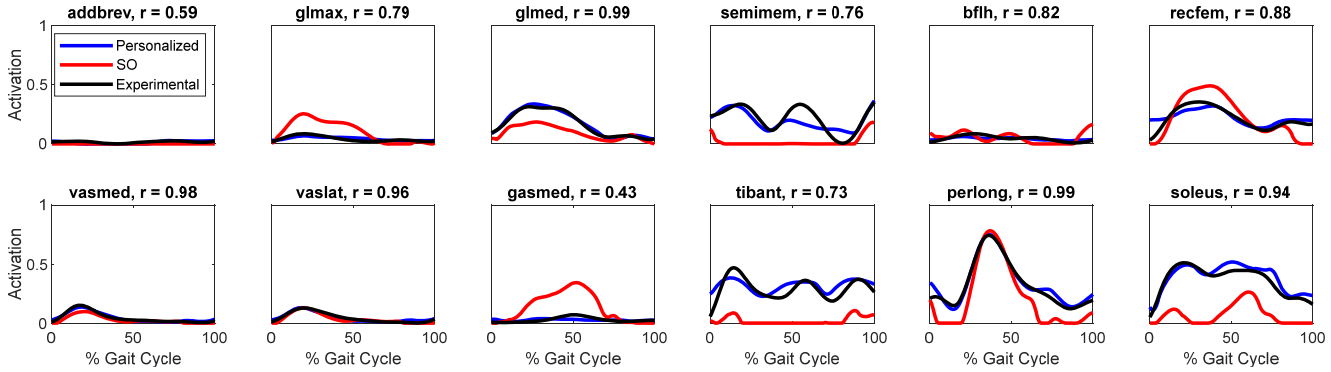

Figure 1: Representative muscle activation estimates of a trial at the self-selected walking speed from the personalized SO versus generic SO and processed EMG for adductor brevis (addbrev), gluteus maximus (glmax), gluteus medius (glmed), semitendinosus, rectus femoris (recfem), vastus medialis (vasmed) and lateralis (vaslat), gastrocnemius lateralis (gaslat) and medialis (gasmed), tibialis anterior (tibant), peroneus longus (perlong), and soleus.

A Framework for Bipedal Walking Research in Biomechanics from Robotics

Pilwon Hur
Department of Mechanical Engineering, Texas A&M University, College Station, TX
Email: pilwonhur@tamu.edu

Introduction

Bipedal walking has been a research topic in biomechanics for many years [1]. After this, many research on human bipedal walking has been conducted. Most common methods require laboratory environments with motion capture systems and force platforms. Measured data were, then, entered into bipedal walking models for further analysis. Even though this method is considered the golden rule in biomechanics, there exist limiting factors including experimental artifacts, time constraints, intractability to change experimental conditions, etc.

In robotics literature, techniques of trajectory optimization have been widely used to produce a set of joint trajectories that minimize a cost function while satisfying constraints. The benefits of these techniques include no need of experiments, no time constraints, ease of changing system parameters, to name a few. Trajectory optimization is beneficial in the biomechanics research for the following reasons. First, no experiments with subjects are needed, which involves with time, cost and, unforeseen safety issues. Second, system parameters can be easily updated without the need of repeated (or paired) experimental design, which is important for research with people with impairments. For example, the optimal reference trajectory for transfemoral amputee patients are not known due to amputation, weakening the usage of the reference trajectory from healthy subjects. Third, perturbation studies and motor control research can be easily conducted. The results from the trajectory optimization can be easily combined with various controllers in the forward simulation to perturb the walking or to test several motor control ideas (e.g., uncontrolled manifold, equilibrium hypothesis, free energy principle). Even though the results from the models need to be validated with the experiments, these can provide the intuition about the human motor control of bipedal locomotion. More importantly, the intuition learned can facilitate the expensive experiments in the more meaningful and successful directions.

In this abstract, we introduce the framework for bipedal walking research that's used in HUR group at Texas A&M University.

Methods

Trajectory optimization: There exist several approaches in the optimal control problems including Pontryagin's minimal principle (MP), dynamic programming (DP), shooting methods (SM), and direct collocation method. Each has its own benefits and disadvantages. While MP, DP and SM can provide accurate solution, they cannot be easily scaled up to cases with higher dimensions and complicated constraints. Direct collocation, however, can provide more efficient computation by discretizing the infinite dimensional domain into lower finite dimensions and using nonlinear programming algorithms (e.g., IPOPT). The compromised accuracy can be remedied by increasing the collocation points or algorithms.

Transcription methods: Both trapezoidal (TPZD) collocation and Hermite-Simpson (HS) collocation methods are used. HS is more accurate than TPZD. However, HS is slower than TPZD. Therefore, depending on the complexity of the model, either method can be selected [2]. Appropriate differentiation methods (e.g., numerical, symbolic, automatic) for dynamics and constraints need to be chosen for the best performance. When the complexity of the model increases, acceleration can be used as separate decision variables.

Dynamic models: Euler-Lagrange (EL) formulation is the usual choice for modeling the bipedal walker. EL formulation can also provide intuitive information including energies in the system, and generalized momenta. If the slipping is required, extra generalized coordinates need to be introduced at the slipping foot (note it can be anywhere in the body) and appropriate constraint dynamics should be formulated by introducing Lagrange multipliers.

Cost functions: Several cost functions have been used in the literature including cost of transport, torque squared. Depending on the complexity, relaxation terms for constraints can be added in the cost. Recently, we reported that adding extra terms (e.g., stepping time uncertainty, angular momentum) in the cost enhanced the robustness of the bipedal walking to perturbation [3,4].

Control in the forward simulation: Once optimal reference trajectories are determined, appropriate controller should be chosen. PD control is the usual choice for tracking the reference trajectories. However, more complicated control schemes are needed in many cases: i) the system is underactuated. ii) perfect trajectory tracking is needed. iii) impedance control is needed, iv) and more. In addition to PD control, we use impedance control, and hybrid zero dynamics (HZD)-based control. Specifically, HZD-based control requires the feedback linearization via desired output functions. HZD approach is useful since it can handle underactuated systems, and provides rapidly exponentially stable trajectory tracking. Lastly, it is more beneficial to use a state-based phase variable (i.e., parameterized time) to track the trajectories rather than time-based control since any perturbed movement will unrealistically correct the errors if time-based control is used. Horizontal whole body COM position normalized by the desired walking speed is a reliable phase variable.

Other considerations: When muscle activation is involved, muscle models should be included in the modeling. Direct collocation can efficiently solve this problem with muscle models included in the optimization due to its strength in scalability. In our research group, muscle models are not considered except the direct EMG measurement. Please refer to OpenSim Moco [5].

Results and Discussion

Using the introduced framework, we could generate human-like walking trajectories for healthy people [6,7] and transfemoral amputees [8,9]. We could also show that human balance and walking tried to minimize the entropy (e.g., H_∞ vs. H_2) due to free energy principle [10]. Robustness to perturbation could be enhanced by appropriate choice of cost function. Optimization performance varied depending on the optimization settings and the complexities of the problems.

Significance

The introduced framework can facilitate the biomechanics and motor control research for human bipedal walking.

Acknowledgments

I would like to thank all my students and colleagues in HUR Group at Texas A&M University.

References

[1] Weber W et al., *Mechanik der menschlichen Gehwerkzeuge*, 1836.
[2] V. Knisley, *MS thesis*, Texas A&M University, 2020.
[3] Chao, *PhD dissertation*, Texas A&M University, 2019.
[4] DeBuys et al., *ASB*, 2020.
[5] OpenSim Moco, https://simtk.org/projects/opensim-moco
[6] Chao et al., *IROS*, pp1435-1440, 2019.
[7] Chao et al., *IROS*, pp4848 - 4853, 2017.
[8] Paredes et al., *IROS*, pp3204-3211, 2016.
[9] Hong et al., *ICRA*, pp2838-2844, 2019.
[10] Hur et al., *Scientific Reports*, 9:16870, 2019

ANALYSYS THE STRAIN OF PLANTAR FASCIA WITH DIFFERENT PLANTAR FASCIA THICKNESS AND TENDON LOADING IN 3-D FINITE ELEMENT FOOT MODEL

Jinhyuk Kim, Stacie I. Ringleb, Sebastian Y. Bawab,
Old Dominion University, Norfolk, VA, USA
email: sringleb@odu.edu

Introduction

The plantar fascia transfers loads from the Achilles tendon to the forefoot during walking [1]. Thus, both Achilles tendon loading and plantar pressure may contribute to the strain in the plantar fascia. In the case of in patients with plantar fasciitis and diabetes, the plantar fascia is typically thicker than healthy asymptomatic [2, 3]. Specifically, the average thickness of healthy plantar fascia is 2.0 ± 0.5mm, while plantar fasciitis and diabetic plantar fascia is 5.71 ± 1.3mm and 3.1 ± 1.0mm [2, 4], respectively. In addition, the properties of plantar fascia are different between healthy and injured or diabetes plantar fascia [5]. However, finite element models of the foot typically keep the plantar fascia at a constant thickness (i.e., 2mm or the cross-sectional area of 3.2mm^2) [1]. The purpose of this study was to examine the strain of the plantar fascia with different plantar fascia thickness and Achilles tendon loading in 3-D finite element foot model.

Methods

A finite element (FE) model was developed using 3DSlicer (Slicer), Geomagic Design X (3D Systems, Rock Hill, SC), Hypermesh (Altair, Troy, MI), and FEBio (FEBio, Salt Lake City, UT) segmented from CT images obtained from one cadaver (Figure 1). The plantar fascia was modeled with three different thickness (3mm, 4mm, and 6mm). The foot was modeled with 4-node quadratic tetrahedral elements (TET4) and homogeneous isotropic elastic materials [6]. Tied surface to surface contact was applied to the bones, cartilage and plantar fascia. A 0 and 700N axial load was applied to the top surface of tibia and fibula, as the Achilles tendon force was increased from zero to 500N to simulate in midstance (Fig 1).

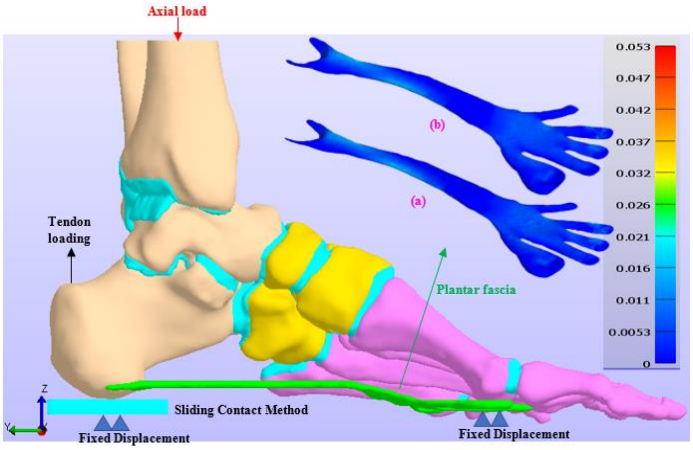

Figure 1 FE model of foot during standing contains; bones, cartilages (aqua), 3mm thickness plantar fascia (green) and strain in. 4mm (a) and 5mm (b) thick plantar fascia.

Results and Discussion

The strain of the 3D FE models, when only the Achilles tendon loading was loaded from 0 to 500N, increased linearly from 0 to 0.0331. In an in vitro experiment with the same loading, the strain increased non-linearly from 0 to 0.023 [7]. Depending on the thickness of the plantar fascia, the difference between the model and in vitro experiment varied by 6-17% before reaching 300 N of loading. Because of the linear elastic properties of the model, the variation increased to 36% difference from 300-500N of Achilles tendon loading at 5mm thickness plantar fascia (Fig 2). With the 700N axial load and for tendoachilles force varying from zero to 500N, the strain value ranged from 0.0214 to 0.0502 (Fig 2), and the percent increase in strain was also calculated 51% at 3mm thickness plantar fascia, 38% at 4mm thickness plantar fascia, and 29% at 5mm thickness plantar fascia. According to the simulation, the strain was decreased more with thicker plantar fascia and Achilles tendon loading. Therefore, further investigation of the characterization of soft tissue in this model must be conducted to analyze the plantar pressure and stress on hindfoot and forefoot. This model was also limited because it was only axially loaded and should be tested with off axis loads, and with non-linear and pathology specific material properties.

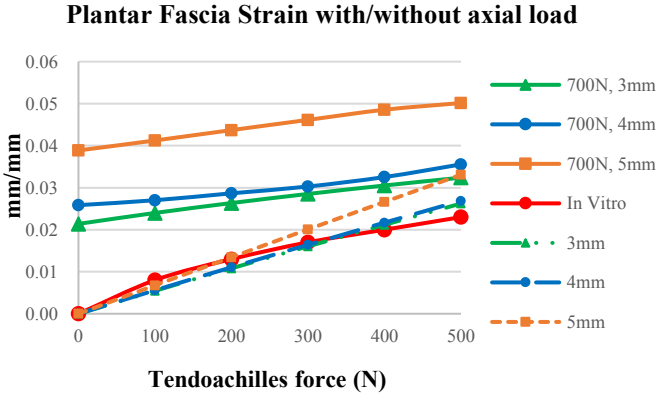

Figure 2 the strain results based on three different thickness plantar fascia compared with an in vitro experiment, with increasing ACH loading, but no axial load.

Significance

A 3D finite element model with varying plantar fascia thicknesses was developed to understand the effect of plantar fascia thickness for a patient with plantar fasciitis and diabetes because a thicker plantar fascia was measured from the patients. Results indicated that, plantar fascia strain decreased with thickness of the plantar fascia, which suggests that this should be further investigated while examining aspects such as plantar pressure and peak stress on the soft tissue. In future iterations of the model, plantar soft tissues will be not included as well as non-linear and pathology specific material properties.

References

[1] A. Erdemir *et al.*, *J Bone Joint Surg*, 2004.
[2] S. Mahowald *et al.*, *J Am Podiatric Med Assoc,* 2011.
[3] F. Ursini *et al.*, *PLoS One,* 2017.
[4] E. D'Ambrogi *et al.*, *Pathophysiology*, 2003.
[5] S. J. Priesand *et al.*, *J DIABETES COMPLICAT,* 2019.
[6] H.-Y. K. Cheng *et al.*, *J. biomech. Eng.*, 2008.
[7] R. E. Carslon *et al.*, *Foot Ankle Int,* 2000.

Investigating Whole-Leg Contributions to Center-of-Mass Acceleration During Gait

Michael C. Rosenberg[1], Katherine M. Steele[1]
[1]Deparmtent of Mechanical Engineering, University of Washington, Seattle, WA
Email: mcrosenb@uw.edu

Introduction

The ability to effectively accelerate the center-of-mass (COM) is fundamental to walking performance and emerges as a combination of musculoskeletal dynamics, motor control, and control objectives [1, 2]. Predicting a clinical intervention's impact on an individual's capacity to accelerate the COM may inform treatment planning. However, the high-dimensional, nonlinear interactions of often-uncertain dynamics and motor control make quantifying intervention effects on an individual's strategy and capacity for controlling COM acceleration challenging, particularly when uncertainty in such parameters exists. "Template" models, which encode high-dimensional COM acceleration strategies in low-dimensional lumped-parameter representations, may facilitate the interpretation of acceleration strategies without assumptions about uncertain physiological parameters [2]. However, if and how template models reflect COM acceleration strategies remains unclear.

We investigated the ability of a template walking model to elucidate whole-leg contributions to COM acceleration in a stroke survivor with left-leg hemiparesis, compared to unimpaired individuals. If an individual accelerates their COM asymmetrically, the template dynamics describing each leg's contribution to COM acceleration should also differ. Therefore, we hypothesized that the dynamics representing the stroke survivor's impaired leg's contributions to COM acceleration would differ from their unimpaired leg, while unimpaired individuals' legs would exhibit similar acceleration dynamics.

Methods

To identify differences in unimpaired and impaired control, we collected marker trajectories and ground reaction forces from seven unimpaired individuals (5F/2M, age = 23.7±2.3 yrs), for whom we expected similar control, and one stroke survivor with left-leg hemiparesis (F, age = 23 yrs), walking at a self-selected speed on a split-belt treadmill for three minutes. We computed COM positions, velocities, and accelerations in OpenSim 3.3 [3].

To identify COM acceleration dynamics for each participant, we used an algorithm that automatically identifies and validates low-dimensional hybrid dynamics capable of explaining, in this study, GRFs from kinematic data [4]. We modeled whole-leg control using variables based on a modified hybrid spring-loaded inverted pendulum: COM position and velocity, leg lengths and leg angles in 3D (Fig. 1) [5]. We identified and compared different candidate dynamics describing COM acceleration strategies (e.g. with or without velocity terms) using a two-minute training dataset and validated on a held-out thirty-second test dataset. Only dynamics with high prediction accuracy and low complexity were considered *plausible* strategies for COM acceleration. We compared the structure of the plausible dynamics over different gait phases across participants.

Results and Discussion

For each phase of the gait cycle, one to two sets of plausible dynamics were identified among over 500 models generated from the training data, supporting that the plausible models best reflected each participants' acceleration strategies, given the candidate model dynamics. Plausible models predicted single-limb support GRFs well (r^2=0.70±0.37) (Fig. 1), though prediction accuracies were reduced (r^2=0.23±0.28) during double-limb support.

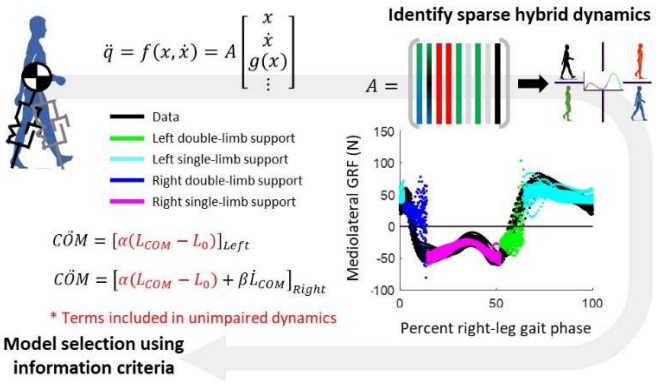

Figure 1: Perimeter: Pipeline for identifying plausible dynamics. Center: Model single-limb support dynamics (left) and predictions (right) for mediolateral COM acceleration in the stroke survivor. L and $\dot{L}$ terms denote position and velocity control, respectively.

The stroke survivor's unimpaired limb's COM acceleration dynamics resembled those of the unimpaired participants, whose dynamics were symmetric. Leg position and velocity variables appeared in 100% and 42% of plausible anterior-posterior and mediolateral single-limb support dynamics, respectively, suggesting a heterogenous reliance on velocity-based control during walking. Interestingly, the stroke survivor's anterior-posterior and mediolateral dynamics included damping only in the unimpaired limb (Fig. 1), suggesting an increased reliance on position-based (elastic) control in the impaired limb. Unimpaired COM acceleration strategies appear to differ between individuals but remain symmetric, while template dynamics reflected asymmetric strategies in the stroke survivor.

Significance

This work supports hypotheses that template models' may elucidate how motor impairments alter COM acceleration strategies. Embedding these template models in physiologically-detailed dynamics may identify mechanisms that are associated with COM acceleration, informing predictions of response to interventions targeting those mechanisms.

Acknowledgments

This work was supported by NSF grant CBET-1452646 and an NSF GRF DGE-1762114.

References

[1] Steele KM, et al., *J Biomech*, 2010.
[2] Full RJ & Koditschek DE, *J Exp Bio*, 1999.
[3] Delp SL, et al., *IEEE Trans Biomed Eng*, 2007.
[4] Mangan NM , et al., *J Royal Soc Proc* A, 2019.
[5] Clever D & Mombaur K, *IEEE-RAS Int Conf on Humanoid Robotics*, 2014.

Bungee Method for Augmenting Human Treadmill Running

John R Rogers[1]
[1]Department of Civil and Mechanical Engineering, United States Military Academy, West Point, NY USA
Email: john.rogers@westpoint.edu

Introduction

Researchers and designers of mechanical augmentation systems will benefit from improved understanding of the benefits and challenges of a simple augmentation system for running, regardless of whether their purpose is to enhance performance, to rehabilitate, or to replace lost function. This abstract describes a mechanical augmentation system that can be modelled in OpenSim to validate simulation-based prediction of metabolic expenditure in the presence of mechanical augmentation.

Methods

This abstract describes methods of a study in progress. Subjects will run on a treadmill both with augmentation and without. Investigators will monitor the subjects' oxygen consumption, forces exerted by the augmentation system, and ground reaction forces detected by the treadmill. Body kinematics will also be monitored using anatomical markers and video motion capture. The experimental protocol will be reviewed by the US Military Academy Collaborative Academic Institutional Review Board. All subjects will provide written informed consent before they participate.

Leg swing during running will be augmented by the forward-acting force of latex rubber surgical tubing ("bungees") attached to the subject above the knees. The opposite end of the bungees will be anchored in front of the runner. The bungees act as springs which assist hip flexion. The subject self-adjusts the spring tension by moving forward or backward on the treadmill, backward to increase force, forward to reduce force (Fig. 1). The above-the-knee location is selected to emulate an exoskeleton prototype that was developed at USMA. The bungee force will vary from zero to a self-selected maximum, approximately 10% of body weight.

Metabolic power will be calculated from VO2 measurements. Motion and force histories collected during trials will be input into OpenSim to simulate the running motion and to calculate the metabolic rate.

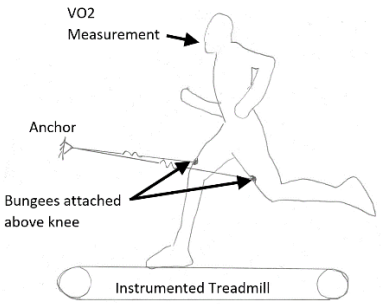

Figure 1: Experimental setup.

Results and Discussion

Pilot data for a 92 kg male running at 3.4 m/s clearly indicate a metabolic benefit similar to running downhill. Metabolic rate in the pilot run was 740 W, 8.0 W/kg augmented, and 1250 W, 13.6 W/kg not augmented. The metabolic difference attributable to augmentation was 510 W. The bungee force (Fig. 2), peaked at 80 N per side; the average sum of left and right was 97 N. The equivalent mechanical work as if over-ground (force * velocity) was 814 W.

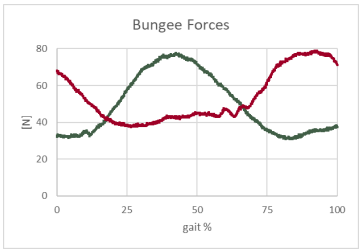

Figure 2: Augmentation force for one gait cycle. Peak force is 9% of body weight. (Pilot data.)

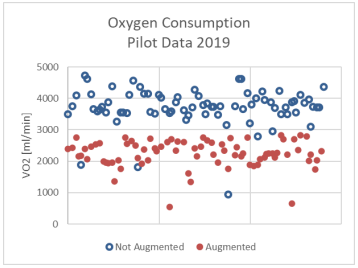

Figure 3: Metabolic data. Two minutes were allowed for VO2 stabilization, then data were collected for five minutes. (Pilot data.)

Data (Fig. 3) show that the bungee cord augmentation provides a substantial metabolic benefit.

Significance

The results of this study are expected to inform researchers, clinicians, and device designers in the field of mechanically-augmented human motion by providing insight about how external work replaces muscle work and thereby contributes to changes in metabolic rate. Robotic-assisted therapy is used in stroke rehabilitation. Exoskeletons and orthoses are used to augment human economy, strength, and endurance. Exoskeletons are used to assist with load carriage.

The project is relevant to any system that modifies human energy expenditure by mechanical means, including robotic rehabilitation. Augmentation could eventually help people with spinal cord injury or stroke to return to running.

Acknowledgments

This project is supported by the USMA-ARL research fund. Thanks to Shane Murphy and Dr. Greg Freisinger of USMA. Additionally, thanks to Dr. Crowell and Mr. Tweedell of ARL.

References

[1] Brockway (1987): Rowett Research Institute, Bucksburn, Aberdeen AB2 9SB, UK.
[2] Gregorczyk et al (2010): Ergonomics, 53:10, 1263-1275
[3] Jackson et al.(2015): Dynamic Walking 2015

Predicted Gait Alterations due to Reduced Paretic Leg Muscle Synergy Complexity

Marleny Arones[1], Carolynn Patten[2], and Benjamin J. Fregly[1]
[1]Department of Mechanical Engineering, Rice University, Houston, TX, USA
[2]Department of Physical Medicine and Rehabilitation, University of California, Davis, CA, USA
Email: ma86@rice.edu

Introduction

Muscle synergies may provide a helpful avenue for predicting patient function following clinical interventions, such as those arising from neurorehabilitation or orthopedic surgery. Theoretically, muscle synergies reduce the achievable control space, making predicted muscle forces and consequently predicted motions more unique. In individual's post-stroke a reduced number of muscle synergies has been associated with a deterioration in walking function [1] and an increase in metabolic cost [2].

This study predicted the effect of reducing the number and complexity of paretic leg muscle synergies on walking function for an individual post-stroke. Walking changes were quantitied using predicted spatiotemporal symmetry measures.

Methods

This study analyzed data from previously collected walking trials from a male subject suffering from stroke walking dysfunctions. The subject's neuromusculoskeletal components were represented using four modeling elements: a kinematic model, an EMG-driven model, a foot-ground contact model, and a motion prediction model using the concept of muscle synergies; see [3] for more details.

The subject-specific neuromusculoskeletal model was used to develop four predictions for how the subject would walk after the number of synergies controlling the paretic leg were reduced from the calibrated case of five to two. In the *first* optimization, the two muscle synergies controlling the paretic leg were free to vary (*FCFW*). In the *second* optimization, the two synergy vectors of the paretic leg were constrained to be a linear combination of the original five synergy vectors while the synergy commands were free to vary (*FCCW*). In the *third* optimization, the paretic leg synergy commands were constrained to be a linear combination of the original five synergy commands while the synergy vectors were free to vary (*FWCC*). In the fourth optimization, the two muscle synergies controlling the paretic leg were constrained to be a linear combination of the original five paretic leg muscle synergies (*CCCW*).

After running all four predictions, the cost of transport (CoT) was calculated using Umberger's model [4] along with ratios describing spatial and temporal symmetry.

Results and Discussion

When walking motion was predicted using two synergies to control the paretic leg, an increase in CoT and a decrease in spatial symmetry were observed (Table 1, read from top to bottom). However, temporal symmetry did not follow the same pattern, consistent with Finley et al.'s 2017 [5] finding that temporal asymmetry was a poor predictor of CoT changes. These findings are consistent with the observation that individuals post-stroke have a more difficult time correcting spatial asymmetry than temporal asymetries [6]. When the model's paretic leg was controlled by two constrained muscle synergies (CCCW, the most limiting case), the model experienced hip hiking, the largest decrease in paretic knee range of motion, and the largest increase in paretic toe drop (Figure 1), which are consistent with clinical observations of hemiparetic gait.

Table 1: Cost of transport, and spatial and temporal symmetry measures

	CoT	Spatial	Temporal
5 Synergies	13.68	0.47	0.52
FCFW	15.89	0.39	0.53
FCCW	17.23	0.37	0.52
FWCC	19.08	0.23	0.42
CCCW	19.14	0.17	0.43

Significance

Our findings support the idea that less complex neural control building blocks may not be the reason for the degeneration of walking function. Rather, constraints on the remaining neural control building blocks may be the main problem.

Acknowledgments

Funding provided by the Cancer Prevention Research Institute of Texas Grant RR170026, and NSF Graduate Research Fellowship

References

[1] D. J. Clark, et al., *J. Neurophysiol.*, 103(2):844-857, 2010.
[2] S. Kramer, et al., *Arch. Phys. Med. Rehabil.*, 97(4):619-632, 2016.
[3] A. J. Meyer, et al., *Front. Bioeng. Biotechnol.*, 4, 2016.
[4] B. R. Umberger, *J. R. Soc. Interface*, 7(50):1329-1340, 2010.
[5] J. M. Finley et al., *Neurorehab. Neur. Repair*, 31(2):168-177, 2017.
[6] L. A Malone., et al,. *J. Neurophysiol.,* 108:672-683, 2012

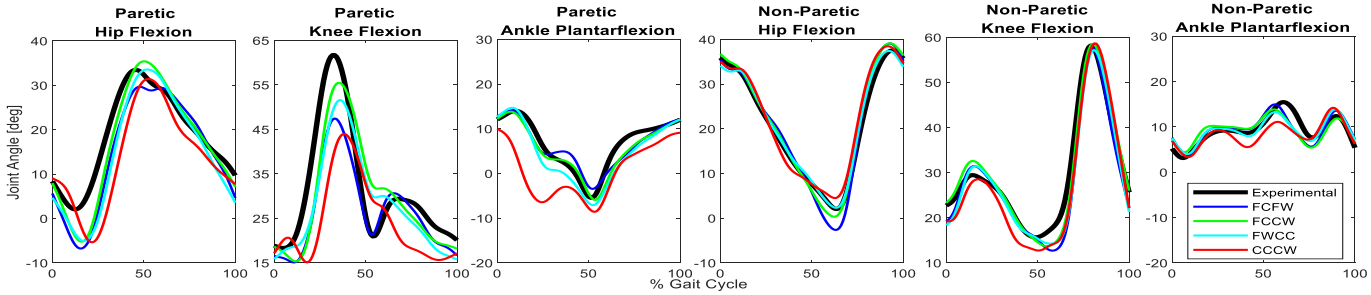

Figure 1: Comparison of joint angles produced between the different control strategies: Calibration-five synergies (black), Free Commands & Weights-FCFW (blue), Free Commands & Constrained Weights-FCCW (green), Free Weights & Constrained Commands-FWCC (cyan), and Constrained Commands & Weights-CCCW (red)

The Influence of Inter-joint Force-dependent Feedback on Whole Limb Impedance Over a Range of Frequencies

Thendral Govindaraj[1], T. Richard Nichols[2], and Gregory S. Sawicki[1,2]
[1]Woodruff School of Mechanical Engineering, Georgia Tech
[2]School of Biological Sciences, Georgia Tech
Email: tgovindaraj3@gatech.edu

Introduction

Neural feedback pathways arise from a variety of sensory receptors. Muscle spindles measure changes in length and velocity, while Golgi tendon organs measure contractile force. Understanding the functions of these pathways is important because they become disrupted in stroke and Spinal Cord Injury. While length and velocity-dependent pathways are relatively localized, force-dependent feedback is asymmetric and can be widely distributed within the limb.

Although the muscle-level distributions of force feedback have been measured under different conditions, it is not known how these distributions regulate limb mechanics (stiffness and interjoint coordination). We analysed the frequency dependent impedance properties and interjoint coordination of a cat hindlimb with intrinsic musculoskeletal impedance. Our hypothesis was that force feedback would reduce whole limb impedance and promote proportional coordination between the knee and ankle.

Methods

We developed a three segment model with realistic lengths and masses [1], with muscles represented as rotational springs and dampers, whose values are based on our physiological best guess, as shown below. The rest angles of the springs were chosen as weight acceptance during landing as defined in [2]. Force feedback was implemented as a generalized torque at the joints in addition to the spring and damper torques, and the values of these torques were calculated at each time step using the following equation, where τ_{fb} is the force feedback torque, [α] is a 3x3 matrix of force feedback gains, [K] is the stiffness matrix, and [B] is the damping matrix:

$$\tau_{fb,n} = [\alpha] * ([K]\{\Delta\theta_{n-1}\} + [B]\{\dot{\theta}_{n-1}\} + \tau_{fb,n-1})$$

We performed a sinusoidal analysis based on the study in [3] adapted here to the whole limb. We applied an endpoint force whose average value was 60N directed at the hip joint center. Using a technique in [4], we calculated the apparent impedance properties and proportionality cost, defined as the integral of $((\theta_k - \theta_{k0}) - (\theta_a - \theta_{a0}))^2$ over time for one sinusoidal cycle, over a range of frequencies for the uni-articular musculoskeletal distribution and two experimentally observed force feedback distributions between the ankle and knee [5].

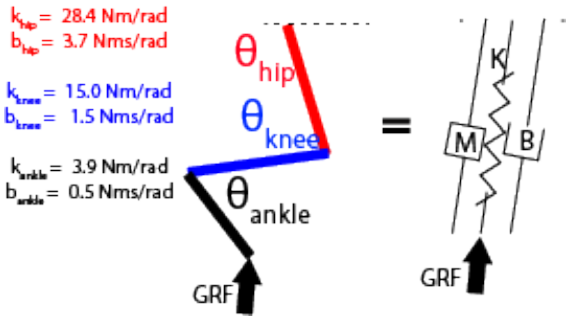

These included a proximal to distal distribution, with inhibition directed towards the toes, and a distal to proximal distribution, with inhibition directed towards the knee.

Results and Discussion

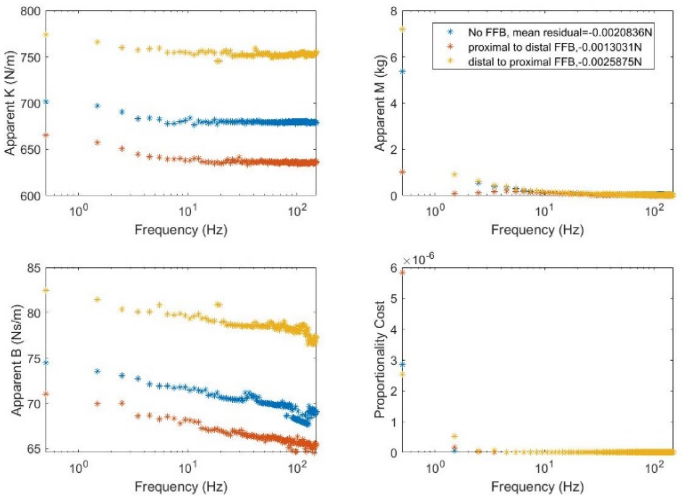

As expected, all of the impedance values were lower for the proximal to distal distribution of force feedback than for the uni-articular musculoskeletal distribution without force feedback. However, contrary to our hypothesis, these impedance values were higher for the distal to proximal force feedback distribution than for the uni-articular musculoskeletal distribution. Examining how force feedback influences the relative contributions of the joint torques to the overall limb force response will elucidate the reason for this outcome. Also contrary to our hypothesis, the proportionality cost was lowest for the uni-articular musculoskeletal distribution without force feedback.

Significance

Patients with stroke and Spinal Cord Injury have impaired knee and ankle coupling compared to able-bodied humans. Therefore, understanding how force feedback influences interjoint coordination, and not only limb impedance, could inform the design of therapeutic and rehabilitation techniques (ex. robotic devices, drug therapies, surgeries).

Acknowledgments

I01 RX002316, R01 NS097781

References

[1] Hoy, MG, et al. (1985). J. Biomech., 18:49-60.
[2] Goslow, GE, et al. (1973). J. Morph., 141:1-42.
[3] Kawai, M., et al. (1980). J. Muscle Research and Cell Motility, 1(3):279-303.
[4] Rouse, EJ, et al. (2014). IEEE Trans Neural Syst Rehabil Eng., 22(4): 870-878.
[5] Lyle, MA, et al. (2018). J. Neurophys., 119(2): 668-678.

A Novel Closed-Loop MIMO Model for Studying the Effect of Spinal Afferents on Tremor

Ian Syndergaard[1], Daniel B. Free[1], Steven K. Charles[1,2]
[1]Mechanical Engineering and [2]Neuroscience, Brigham Young University, Provo UT
Email: ians@byu.net

Introduction

Tremor is the most prevalent movement disorder in the world today; yet despite decades of research, the mechanisms of tremor propagation are not yet fully understood. Recent investigations of the mechanisms of essential tremor generation have provided strong evidence that tremor originates centrally. However, it remains unclear what role spinal afferents play in tremor modification and propagation.

Tremor propagation refers to the way a neural signal in one muscle creates movement in each degree of freedom (DOF) and to the interactions between movement in each DOF. Previous studies have explored the effects of spinal afferents in a single DOF, but did not model interactions between DOF. Other studies have investigated interactions between the DOF of the arm to determine fundamental principles of tremor propagation [1], but did not model afferent feedback. Thus, we present here a novel closed-loop multiple-input multiple-output (MIMO) model of the upper limb, which may provide much-needed insight on the role of spinal afferents in tremor.

Methods

This model expands an open-loop model by Davidson et al. [1] and Corie et al. [2] as summarized in ***Error! Reference source not found.***.

The input to the model is a set of descending neural signals ($u_{descending}$) to the 15 major superficial muscles of the arm. The forward path models the transformation of these descending neural signals to muscle forces (f), then to joint torques (τ), and finally to joint displacements (q) in the 7 DOF of the upper limb.

The inner loop models the effects of the Golgi tendon reflex. The outer loop models the effects of muscle spindles (both type Ia and type II). In the outer feedback path, joint displacements are transformed to muscle stretch (Δλ), which is both multiplied by a reflex gain matrix (representing type II muscle spindles) and by s (to differentiate) and a reflex gain matrix (representing type Ia muscle spindles).

C models the maximum voluntary contraction of each muscle. M represents the muscle moment-arm matrix. I, D, and K model the inertia, damping, and stiffness of the joints, respectively. The G matrices model the reflex gains between homonymous and heteronomous muscle pairs.

Tremor was simulated by feeding the model a synthetic tremorogenic neural signal. An example output is shown in *Figure 2*. Outputs were processed by computing the power spectral density (PSD), then integrated over tremor frequencies (4-12 Hz) to find total tremor power. Reflex gains were multiplied by a range of scalar values and tremor power recalculated to determine the robustness of the simulated findings.

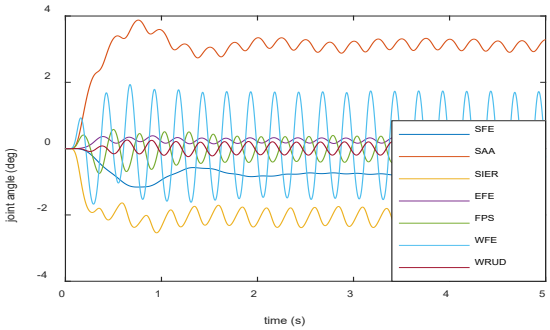

Figure 2 – An example simulation output for a 4 Hz neural signal input in the posterior deltoid.

Results and Discussion

Simulation showed that reflexes generated by Golgi tendon organs did not significantly affect tremor power. The effect of muscle spindles changes depending on the frequency of the descending neural signal. At low input frequencies, spinal afferents tended to greatly attenuate limb motion. However, at tremor frequencies, reflexes between most muscle pairs did not significantly affect tremor. Ongoing research is attempting to identify all muscle pairs which have a reflex relationship that alters tremor at each tremor frequency.

Significance

Optimal tremor treatment requires an understanding of the fundamentals of tremor propagation. This model provides valuable insights on the role of spinal afferents in tremor propagation, and may eventually lead to greater knowledge of where to intervene in the tremor pathway, thus improving tremor treatment and quality of life for those who suffer from this debilitating disorder.

Acknowledgements

This research was supported by NSF grant 1806056.

References

1. Davidson et al, Ann Biomed Eng, 2017
2. Corie et al, J Biomech Eng, 2019

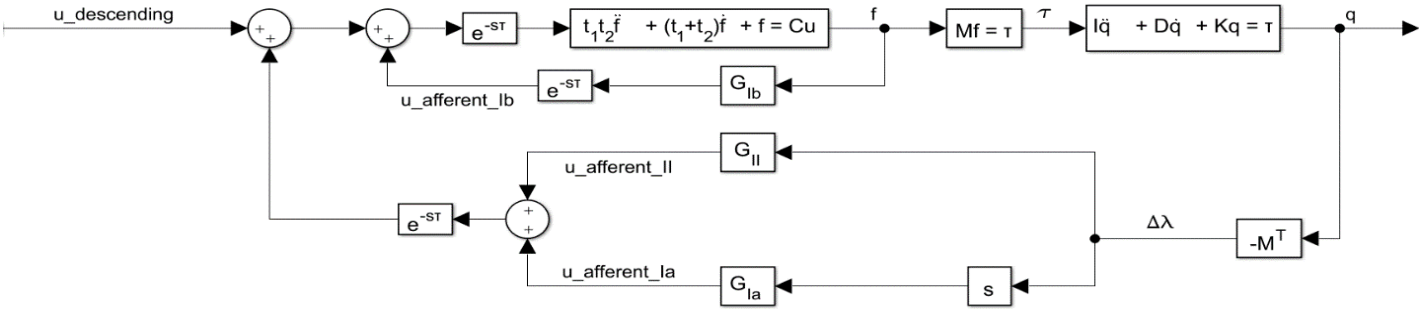

Figure 1 – A novel closed loop multiple-input multiple-output model of the upper limb.

Validation of Musculoskeletal Models Using Single Degree of Freedom Analysis

Sepehr Ramezani[1], Joseph Dranetz[1], Matt S Stock[2], and Hwan Choi[1*]
[1]Department of Mechanical and Aerospace Engineering Department, University of Central Florida
[2]School of Kinesiology, University of Central Florida,
Email: *hwan.choi@ucf.edu

Introduction

Musculoskeletal modeling is known as a non-invasive and cost-effective method for analyzing human motion and musculoskeletal function. Accurate data is required to develop valid models which are representative of the actual test conditions. Additionally, these analyses are extremely challenging due to the complex nature of musculoskeletal function. Thelen et al. measured muscle function and structure from cadavors in order to develop models for musculoskeletal analysis [1]. Although this model represents muscle activity and dynamics during walking reasonably well, there are some discrepancies with certain muscles. More recently, Rajagapol suggested another model which includes: muscle functions from previously conducted muscle experiments, muscle geometry from magnetic resonance image (MRI) of healthy young adults, and improvements to the calculation of muscle force [2]. These models are used to calculate muscle contributions during walking. Because analysis of muscle contribution in walking requires data on the complex motion and contact forces involved, it is difficult to compare the validity of each model. Therefore, in this study, we used two different musculoskeletal models to simulate motion with one degree of freedom, isometric knee flexion, and assessed the contributions of each muscle.

Methods

Experimental data is collected from a 37 year old 196.7 cm height, 104 kg weight male. The subject performed isometric knee flexions at knee angles of 30, 60, and 90 degrees in a Biodex System 4 human dynamometer (Biodex Medical Systems, Shirley, NY). All the trials were randomized. The duration of isometric exercise was 20 seconds in each trial and the participant had 5 minutes resting between trials.

Two musculoskeletal models of Rajagopal et al. and Thelen et al., were used in Opensim to compare knee extensors and flexors in each testing condition. Anthropometric data of the participant were measured and in input into each generic musculoskeletal model for scaling.

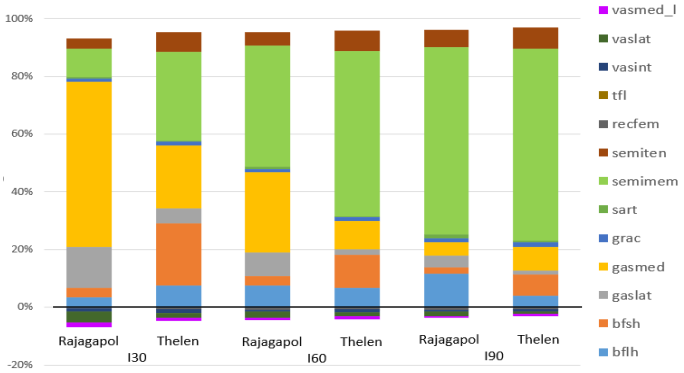

Figure 1: SOP calculation of different muscle torque contribution of the knee joint moment represented in percentages.

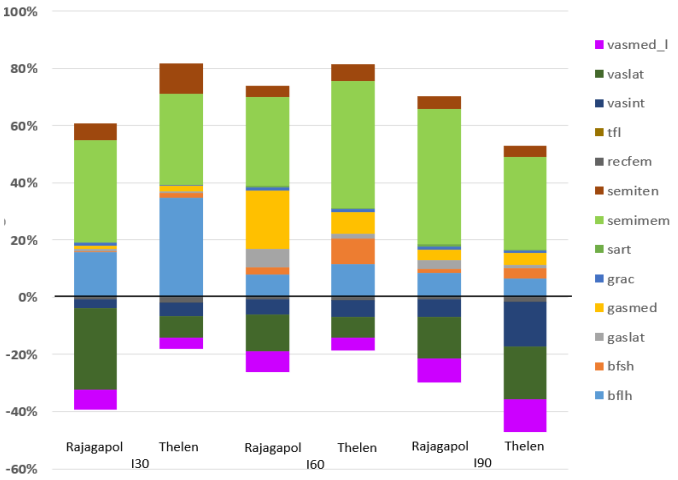

Figure 2: CMC calculation of different muscle torque contribution of the knee joint moment represented in percentages.

Then, we used static optimization (SOP) and computed muscle control (CMC) to calculate muscle forces for the two different musculoskeletal models. For these methods, kinematic data and external force were acquired from goniometer and Biodex respectively.

Results and Discussion

Both models obtained a small residual actuation moment, lower than $3e^{-3}$ Nm, verifying our simulation. In both figures, the positive and negative percentages represent flexion and extension respectively. In figure 2, CMC employed more extensor muscles compare to SOP because CMC calculation uses forward dynamics to simulate muscle co-contraction.

By comparing each of the models in figure 2, the Rajagapol model dedicated a higher percentage of the total torque to extensor muscles in I30 and I60 conditions than the Thelen model. Another significant observation is the increased muscle contribution of the gastrocnemius at I60.

Significance

In this experiment, muscle co-contraction plays a pivotal role in creating muscle forces. It is highly recommended to use the CMC tool when co-contractive muscle forces are expected.

The outcome of this study can be used as a guide for selecting the proper model and method when estimating muscular contribution to torque production.

References

1. Thelen D.G, et al. *J Biomech Eng.* 125(1): 70–77, 2003
2. Rajagopal, Apoorva, et al. *IEEE Trans Biomed Eng*. 63(10): 2068-2079, 201

Experimental Head Injury Investigation of Head Impact Caused by Unsecured Object in Vehicle during Vehicle Frontal Crash

Jaroslav Hruby[1], Brad Parker Wham[2], Aldrich Valerian[3] Zdenek Krobot[4]
[1]Institute of Forensic Engineering, Brno University of Technology
[2]Center for Infrastructure, Energy, and Space Testing, CU Boulder [3]Center for Infrastructure, Energy, and Space Testing, CU Boulder
[4]Department of Combat and Special Vehicles, Brno University of Defense

Email: brad.wham@colorado.edu, aldrich.valerian@colorado.edu, zdenek.krobot@unob.cz

Introduction

Occupant safety in the realistic car crash accident is typically solved as a problem of human body interaction with airbags and vehicle structure (vehicle seats, vehicle body parts, and others). There is also a situation when an unsecured object placed in the vehicle causes the injury of the vehicle occupant. The unsecured object can be described as a bottle, tablet, or laptop.

These unsecured objects are acting in the vehicle during its crash like projectiles, and they have a very significant potential to harm the vehicle occupant if they interact with their bodies.

An experimental investigation was performed to explain what can happen if the unsecured object interacts with the human body and what is the injury risk if this case happens. As a critical human body part was selected human head and as the traffic accident situation was taken frontal vehicle impact.

The hypothesis on which the whole experimental project was build on takes into account: The human head rear part interacts only with the unsecured object and nothing else (airbags, etc.); The seat head restraint is not present; The unsecured object is stiff and has initial speed during the crash similar as the vehicle crash velocity (friction effect is negotiable); The injury effect is blunt.

Methods

Head injury experimental investigation was performed using equipment: Airgun (with pressure vessel and optical measuring barriers); Nilon body projectiles with different mass (0.5 [kg], 1 [kg], 1.5 [kg]) and hard rubber impact part; High-speed camera; Hybrid III 50th percentile male dummy with instrumentation; Vehicle seat with restraint system; DAQ system DEWE A4.

The computation of HIC (see Eq. (1) [2], and Eq. (2)) was done through Software NI DIADEM (Crash Analysis Toolkit).

The symbol a in Eq. (1) represents resultant head acceleration, and it is calculated from Eq. (2) where a_x, a_y, and a_z are representing components of "resultant" acceleration. Symbols t_1 and t_2 are describing a time interval for the HIC calculation process (15 [ms]).

$$HIC=\max_{t_1,t_2}\left\{\left(\frac{1}{t_2-t_1}\int_{t_2}^{t_1} a\,dt\right)^{2.5}(t_2-t_1)\right\} \quad (1)$$

$$a=\sqrt{a_x^2+a_y^2+a_z^2} \quad (2)$$

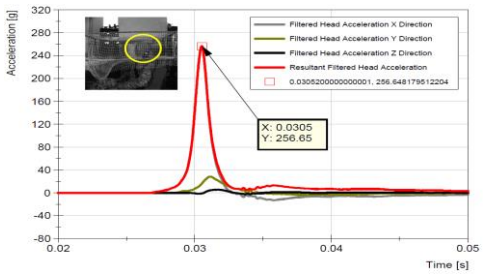

Figure 1: Filtered Impulse from Hybrid III Dummy Head – HIC Input

Results and Discussion

Experimental data show (see Figure 2 and Table 1) that the dangerous speed of an unsecured object in the vehicle during frontal vehicle impact is around 50 [km/h] (HIC = 1000 [-]) [1]. The length of the impulse is short (approx. 1.5 [ms]), and other tools must be used to verify the injury potential calculated through HIC (Blunt Criterion usage).

The results show that the increasing mass (from 0.5 [kg] to 1.5 [kg]) of the unsecured object has a significant effect on the critical object speed (mass increases = dangerous unsecured object speed decreases – see Table 1).

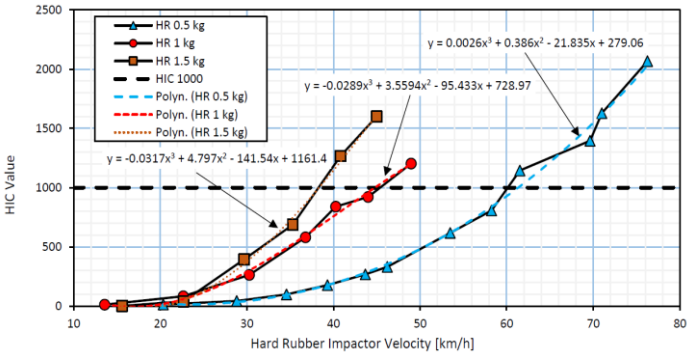

Figure 2: Interpretation of Critical Speeds of Unsecured Object Regarding Computed HIC (15 [ms]) – Comparison with HIC 1000

Projectile Velocity [km/h]	Resultant HIC [-] *Projectile 0.5 [kg]*	Projectile Velocity [km/h]	Resultant HIC [-] *Projectile 1 [kg]*	Projectile Velocity [km/h]	Resultant HIC [-] *Projectile 1.5 [kg]*
58	808	44	921	35	687
62	1144	49	1204	41	1266

Table 1: Critical Speeds of Unsecured Object Regarding Computed HIC (15 [ms]) – Comparison with HIC 1000

The experimental work is focused only on human head interaction (rear part) with unsecured stiff objects. In reality, the transported unsecured objects have different stiffness, and they can act differently than unsecured rigid objects.

Significance

The significance of the experimental research lies in the description of how unsecured objects may act as projectiles during a vehicular crash. Many people are interested only in passive vehicle safety (airbag interaction) and don't care much about the objects they are transporting in the vehicle even that these objects may cause serious injury during the vehicular crash.

References

1. M. Mackay, Sadhana, 397-408, 2007.
2. B. G. Mc Henry, ATB Users Group, 2-8, 20

Evaluation and Modeling of Falls onto Poured Rubber Playground Surfaces

Kyle B. Van Housen[1], Matthew Lara[1], and Sean D. Shimada, PhD[1]
[1]Biomechanical Consultants
Email: *sean@motionsandforces.com

Introduction

It is reported that emergency rooms treat approximately 200,000 playground injuries annually. Three-fourths of these injuries are from falls, mostly affecting the hand and wrist [1]. In recent years, poured rubber (PR) has become a popular choice for surfacing playgrounds. Its smooth look, vibrant coloring, low maintenance, and drainage properties give it clear advantages over other surfacing options, but how effective is it at preventing injuries?

PR is made from two layers: a base layer that provides springiness and a wear layer that protects from abrasion and light damage. Deterioration of the wear layer through overuse can potentially diminish its protective quality, but to what extent? This paper uses a combination of experimental and mathematical methods to determine an estimate for the safe fall heights of children onto PR surfaces both with and without the wear layer intact.

Methods

Experimental

A series of drop tests were performed in order to determine the response of PR to impact forces comparable to those that would cause an injury in children. Because of a lack of available data, Davidson et al. [3] developed an equation to predict fracture tolerance of the distal radius in children. For children ages 3-7, 8-10, and 11-15, the compressive bone strengths calculate to 1390, 1849, and 2738 N, respectively. A metal shotput was dropped onto a Kistler (model 9286BA) force plate with a 15.2x15.2x5.1 cm section of PR securely attatched. The shotput was dropped from heights that exceeded the compressive strengths given above. The force was recorded and the PR was found to closely match the response of a linear spring, where spring stiffness is a function of impact speed ($p < .05$). The wear layer was removed and the experiment was repeated. The spring constants calculated from this experiment were then input into the mathematical model to accurately simulate the PR response for both conditions.

Mathematical

Our model is based on previous work done by Chui and Robinovich [2], who developed a two-mass, spring, and damper system for falls onto an outstretched arm. Our model includes the addition of an extra spring layer that represents the PR surface. Deriving the equation of motion allows us to then make use of the MATLAB Simulink software package to simulate and plot the force on the palm/wrist as it makes contact with the PR.

The model requires inputs for the spring and dampeners that mathematically represent the joints in the arm. These values were experimentally determined by Chiu and Robinovich [2]. The mass m_1 is the weight of the entire arm unit and the mass m_2 is approximately 50% of the total body weight of an average 7 year old. The simulation was run with fall heights ranging from 1.2-1.8 m (4-6 ft) with and without the wear layer (Fig. 1).

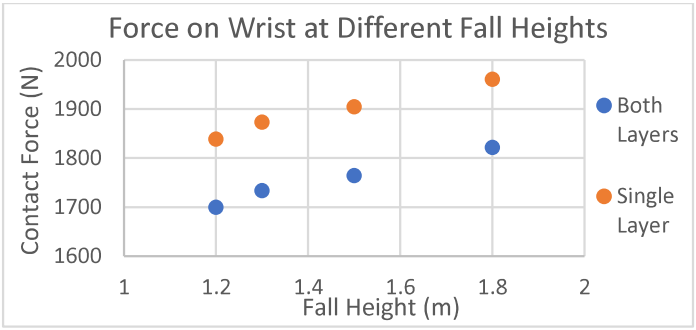

Figure 2: Peak force on the wrist with base and wear layer intact

Results and Discussion

Our mathematical model predicts that falls of the body's center of mass (COM) from heights of 1.2-1.8 m (similar to the height the COM would fall from monkey bars) generate enough force to cause a distal radius compression fracture in children 3-7 years old. When you remove the wear layer, forces were found to increase by approximately 8% for all fall heights. This increase puts the 8-10 year olds at risk for heights exceeding 1.2 m. The wear layer is shown to provide a small but important layer of protection from falls. These results provide a tentative threshold value for safe fall heights onto PR, but are limited because they lack the inclusion of rotational forces and use averaged or mathematically obtained values for physiological properties.

Significance

The mathematical model used here is applied in a novel application to simulate falls onto PR surfacing with an outstretched arm. Values for the stiffness of PR surfacing with and without the wear layer provide information on how the safety of playgrounds change with contant use. These results stress the importance of continual maintenance of playground facilities in order to minimize risk of injury to children. This is only one scenario that can be simulated using this method, by changing spring values and physiological parameters you can simulate falls for a variety of different ages and ground materials.

References

[1] Tinsworth D, McDonald J. Special Study: Injuries and Deaths Associated with Children's Playground Equipment. Washington (DC): U.S. Consumer Product Safety Commission; 2001.

[2] Chiu, J. and Robinovich, S.N. "Prediction of upper extremity impact forces during falls on the outstretched hand", Journal of Biomechanics

[3] Davidson, P.J. and Chalmers, D.J. Stochastic-rheological Simulation of Free-fall Arm Impact in Children: Application to Playground Injuries, Computer Methods in Biomechanics and Biomedical engineering

[4] Chalmers, D.J., *et. al.* (1996) "Height and Surfacing risk factors for injury in falls from playground equipment: a case control study", Injury Prevention 2, 98-104.

The Relationship Between the Hand Pattern Used During Fast Wheelchair Propulsion and Shoulder Pain Development

Shelby L. Walford[1], Jeffery W. Rankin[2], Sara J. Mulroy[2], and Richard R. Neptune[1]
[1]Walker Department of Mechanical Engineering, The Unversity of Texas at Austin, Austin, TX
[2]Pathokinesiology Laboratory, Rancho Los Amigos National Rehabilitation Center, Downey, CA
Email: shelbywalford@utexas.edu

Introduction

Shoulder pain and injuries are prevalent in manual wheelchair users due to the high, repetitive loads required [1]. Weaker shoulder muscles are correlated with shoulder pain development [2] and a recent modeling study found that compensating for weakened shoulder adductors results in increased muscle stress in the rotator cuff muscles [3]. In addition, those that use a single-loop (SL) hand pattern experience the highest overall muscle power and stress compared to the other patterns, particularly in the middle deltoid and rotator cuff muscles [4]. Although previous research found no correlation between hand pattern and future pain development [5], this may have been due to analyzing propulsion at self-selected speeds. Fast wheelchair propulsion may exacerbate underlying poor mechanics due to the higher loads experienced that may not be seen during self-selected conditions.

The purpose of this study was to determine whether the hand pattern used during fast wheelchair propulsion correlates with shoulder pain development. A secondary purpose was to determine whether shoulder adductor strength correlates with the hand pattern used during fast propulsion. We expect that individuals who develop pain use more over-rim (e.g., SL) hand patterns and that weaker shoulder adductors will be correlated with more over-rim patterns.

Methods

Kinematic, kinetic and strength data from 60 individuals with paraplegia (56 men, 4 women; age=35.9±8.31 yrs; time since injury=10.1±5.86 yrs; height=1.74±0.10 m; mass=76.8±16.0 kg) were analyzed from a previously collected dataset [2]. Data were collected at baseline, 18 and 36 months after baseline during propulsion at their fastest comfortable speed. Participants were asymptomatic for shoulder pain at baseline, and self-reported shoulder pain at the follow-up assessments. The no pain group were pain-free at all time points, while the pain group had shoulder pain at only the 36-month time point.

Strength was measured as the maximum isometric torque from the shoulder adductors, abductors, flexors, extensors, internal rotators and external rotators. Hand patterns were quantified using net radial thickness (NRT) and total radial thickness (TRT) of the closed-curve hand path. NRT indicates the hand's displacement above the handrim, and TRT indicates the absolute distance between the hand and handrim [6]. Linear mixed-effects models were used to determine if the hand pattern and shoulder strength were significantly different between the pain and no pain groups. An additional model was created to determine if weaker shoulder adductors correlates to using a more over-rim pattern (e.g., higher NRT values).

Results and Discussion

There was a trend for the pain group to use more over-rim patterns (e.g., SL) than the no pain group (Fig. 1), however there were no signficiant differences between NRT and TRT between groups at any time point. Higher NRT values (e.g., more over-rim patterns) significantly correlated with lower shoulder adduction strength (p=0.042). Of the strength measures, only adduction strength was significantly lower in the pain group (p=0.036). In addition, internal rotation strength significantly decreased over time, regardless of whether they developed pain or not (p=0.004).

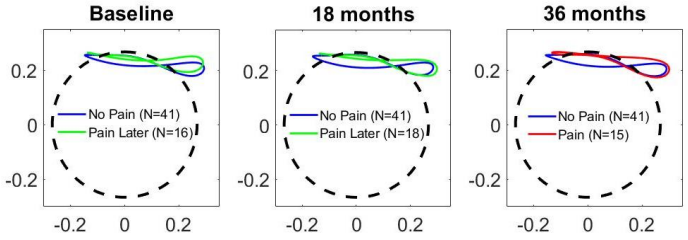

Figure 1: Hand patterns across time for the no pain (blue; NRT for all times = -0.01 ± 0.06 m) and pain (green = pre-pain, red = pain present, NRT for all times = 0.02 ± 0.05 m) groups.

Contrary to our expectations, individuals that developed pain did not use a hand pattern that was more over-rim than the no pain group during fast wheelchair propulsion. Even though the SL pattern requires higher muscle power and stress [4], cadence and handrim forces [7] than other hand patterns, the results of this study suggest that simply changing hand pattern is not sufficient to prevent shoulder pain development. Weaker adductors were significantly correlated to more over-rim hand patterns, which would suggest that the use of the SL hand pattern during fast propulsion may be indicative of shoulder muscle weakness. However, the marginal R^2 value of the correlation between shoulder adductor strength and NRT was low (R^2=0.019), highlighting the large variability across subjects.

Significance

This study showed that the hand pattern used during fast wheelchair propulsion does not predict shoulder pain development. However, more over-rim patterns were correlated to weaker shoulder adductors, although this correlation had large variability. Therefore, further research is needed to verify this relationship before we can use hand pattern as an indicator of shoulder adductor weakness.

Acknowledgments

This study was supported by NIH Grant R01 HD049774.

References

[1] Waring, W., et al. *Paraplegia 29,* 37-42, 1991.
[2] Mulroy, S., et al. *Phys Ther 95*, 1027-38, 2015.
[3] Slowik, J., et al. *Clin Biomech 33*, 34-41, 2016.
[4] Slowik, J., et al. *J Biomech 49*, 1554-61, 2016.
[5] Walford, S., et al. *Clin Biomech 65*, 1-12, 2019.
[6] Slowik, J., et al. *Clin Biomech 30*, 927-932, 2015.
[7] Kwarciak, A, et al. *Disabil Rehabil Assist Technol 7*, 459-63, 2012.

Relationship Between Blood Perfusion and Pressure: A Study with Wheelchair Users and Able-Bodied Individuals

Justin Scott[1] and Tamara Reid Bush[1]
[1]Department of Mechanical Engineering, Michigan State University, East Lansing, USA
Email: reidtama@msu.edu, scottju5@msu.edu

Introduction

Pressure ulcers (PUs) are a pressing issue for wheelchair users, with 47% of individuals affected [1]. PU development is linked to sustained, external pressures. These pressures lead to reduced capillary blood flow, or perfusion, in the loaded tissues [2]. A third of PUs in wheelchair users occur in the buttocks; thus strategies to relieve pressure and increase perfusion to this region are critical [3]. Currently, the most common movements for pressure relief in wheelchairs are recline of the back and whole body tilt [4].

Studies that investigated pressure relieving movements had limitations. No studies investigated changes in pressure *and* blood perfusion in the buttocks while using pressure relieving movements, even though both have been shown to be linked to PUs. Further, most seated load data were collected from able-bodied people, while the majority of people who experience PUs use wheelchairs. Research has shown differences between pressure distributions in wheelchair users and able-bodied individuals, thus it is important the wheelchair user population be included in studies evaluating pressure relieving strategies [5].

Therefore, the goals of this work were to quantify trends in pressure and perfusion data on the buttocks of wheelchair users during three movements: 1) whole body tilt, 2) back recline and 3) isolated seat pan tilt, during which the anterior edge of the seat pan is higher than the posterior edge.

Methods

Twenty able-bodied people (ten males, ten females) and ten male wheelchair users volunteered for this study (IRB#15-889). An articulating chair was created with independent seat pan tilt and back recline to test combinations of the two movements.

Data were gathered on seated participants as the articulating chair moved through nine positions, with three angles of seat pan tilt (0°, 15°, 30°) and three angles of back recline (0°, 10°, 20°). Positions in which there were both a seat pan tilt and back recline created a whole body tilt. A perfusion sensor attached on the skin over the ischial tuberosity collected data in all positions. A pressure mat recorded data on the seat pan for each position, and data were split into two regions, buttocks and thighs (back and front halves of the mat).

Results and Discussion

Trends in perfusion values differed between the two groups. Perfusion in able-bodied people increased with seat pan tilt ($p = 0.0006$) and decreased with back recline ($p = .046$). No significant trends in perfusion emerged in wheelchair users.

The maximum pressures in wheelchair users were larger than those in able-bodied people, but trends in maximum pressures in each region with respect to chair position were consistent in both groups. Maximum pressure in the buttocks increased with recline and decreased with seat pan tilt for both groups ($p < .0001$ for all). Maximum pressures in the thighs decreased with back recline ($p < .0001$ for both) and increased with seat pan tilt in able-bodied people ($p < .0001$).

Table 1: Perfusion values for each group in each seat pan tilt and back recline, normalized by the maximum value within each participant. Perfusion in able-bodied individuals increased with seat pan tilt and mixed trends were seen in wheelchair users.

	Able-bodied			Wheelchair User		
	0° Tilt	10° Tilt	20° Tilt	0° Tilt	10° Tilt	20° Tilt
0° Recline	0.42	0.48	0.69	0.50	0.39	0.50
10° Recline	0.37	0.50	0.53	0.55	0.41	0.46
20° Recline	0.35	0.42	0.52	0.49	0.54	0.46

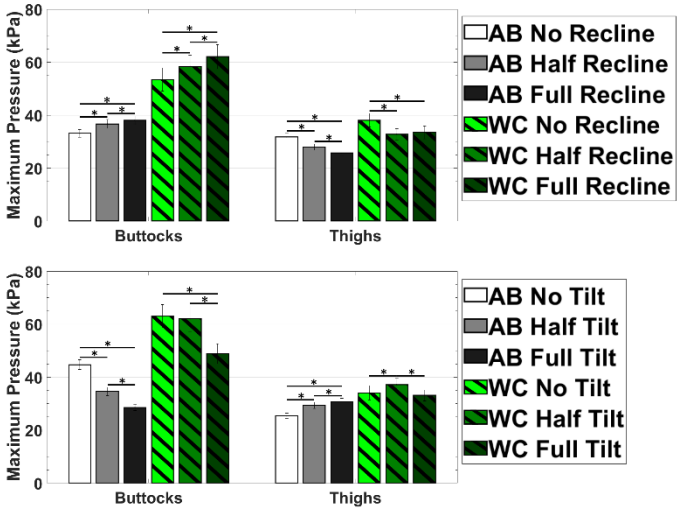

Figure 1: Magnitudes of the maximum pressures, by recline angle (top) and seat pan tilt (bottom). Able-bodied (AB) data are solid bars, and wheelchair user (WC) data are striped. Maximum pressure increased in the buttocks with back recline and decreased with seat pan tilt (* indicates significant differences). Opposite trends were seen in the thighs.

Significance

This work indicated that the movement most commonly used to relieve pressure on the buttocks while seated (i.e., recline) was not effective in relieving pressure or restoring perfusion. However, increasing the seat pan tilt relieved pressure on the buttocks of both groups and increased perfusion in able-bodied individuals. Thus, seat pan tilt has the potential as a strategy for reducing PUs. Because each movement decreased pressure in one area while increasing it in another, these movements may need to be cycled through to reduce overall PU risk in every region.

Acknowledgments

This work was funded by NSF grant CBET-1603646.

References

[1] Cowan, L.J., et al., *Wound Care*, 32:122-130, 2019.
[2] Manorama, A., et al., *Clin. Biomech*., 28:574-578, 2013.
[3] Horn, S.D., et al., *J. Am. Ger. Soc.*, 50:1816-1825, 2002.
[4] Ding, D., et al., *J. Rehab. Res. Dev.*, 45, 2008.
[5] Linder-Ganz, E., et al., *J. Biomech*, 41:567-580, 2008.

Females Exhibit Higher Hamstring Activation Prior to Landing and Reduced Activation After Acute Fatigue

David Phillips, Bridgette Buckalew, Jacklyn S Alencewicz, Bridget Keough
Department of Exercise Science and Physical Education, Montclair State University
Email: phillipsdav@montclair.edu

Introduction

Anterior cruciate ligament (ACL) injuries occur more commonly in females compared to males. Possible intrinsic risk factors can be found in the areas of strength, anatomy, biomechanics (kinematics and kinetics parameters), fatigue, and neuromuscular coordination. The hamstrings receive particular attention as they help counteract the shear forces generated by the quadriceps during landing [1]. This reduces the load borne by the ACL. Because ACL injuries happen rapidly, how athletes activate their hamstrings prior to landing may influence their landing mechanics and injury risk. This activation and coordination can also be affected by the fatigue state of the athlete.

The purpose of this study is to investigate hamstrings activation characteristics prior to landing before and after a fatigue protocol. We hypothesize that males will have a higher hamstrings activation than females and that hamstrings activation amplitude will increase after fatigue.

Methods

Twenty four subjects (13 males, 11 females) participated in the study. Maximum vertical jump was used to estimate peak lower extremity power and quantify fatigue. Subjects performed 3 trials of a drop vertical jump from a 30 cm box onto 2 force plates. Electrodes were placed bilaterally on the biceps femoris muscles. Data were sampled from the force plates and EMG synchronously at 2000 Hz. Subjects then performed a fatigue protocol of bodyweight squats at 60 Hz until exhaustion. Immediately after the fatigue protocol (<1min), subjects performed a maximum vertical jump and 3 successful drop vertical jumps. Two dimensional video was recorded from the sagittal and coronal planes. Dependent variables included max vertical jump power, normalized peak vertical ground reaction force (vGRF), time to peak vGRF, Landing Error Scoring System (LESS), and hamstrings muscle activation 200 ms, 150 ms, 100 ms, 50 ms, & 0 ms before landing.

EMG data was band-pass filtered, 20 Hz – 500 Hz, and smoothed using a 50 ms root-mean-squared window. EMG data were normalized to a MVC contraction and maximum activity measured during the non-fatigue jumps. Force plate and LESS variables were assessed using a mixed 2x2 ANOVA with fatigue (within subjects factor) and sex (between subjects factors). Hamstrings activation was assessed with a mixed 2x5x2 ANOVA with fatigue and time before contact (within subject factors) and sex (between subject factor). The effect of fatigue on peak vertical jump height was assessed with a dependent *t*-test.

Results and Discussion

There was a 63% reduction in max vertical jump height after fatigue ($p < 0.001$). No significant effects were found for normalized peak vGRF or time to peak vGRF. For hamstring activation, there were significant main effects for fatigue ($p = 0.02$), time ($p < 0.001$), and sex ($p = 0.038$) (Figure 1). In both sexes, hamstring activation increased until contact, with males having lower activation compared to females. Fatigue reduced hamstring activation similarly between sexes.

Females had 2.3, 1.7, & 1.4 times the hamstring activation of males at 100 ms, 50 ms, and 0 ms respectively before fatigue. The increased activation remained similar to these amounts after fatigue, but both sexes saw reduced overall activation at 50 ms and 0 ms.

These results are opposite to our hypothesis. We expected females to have lower activation because of the higher incidence of ACL injury. Lower activation would mean less preloading of the hamstrings prior to landing and more shear force being placed on the ACL at landing. Three of the four studies examining hamstring pre-activation, including this study, found higher hamstring pre-activation whereas only one found lower hamstrings pre-activation in females prior to landing [2]. There appears to be a sex-related difference in lower extremity coordination when preparing to land. Acute fatigue affects the landing strategy similarly between sexes with a reduction in hamstring activation.

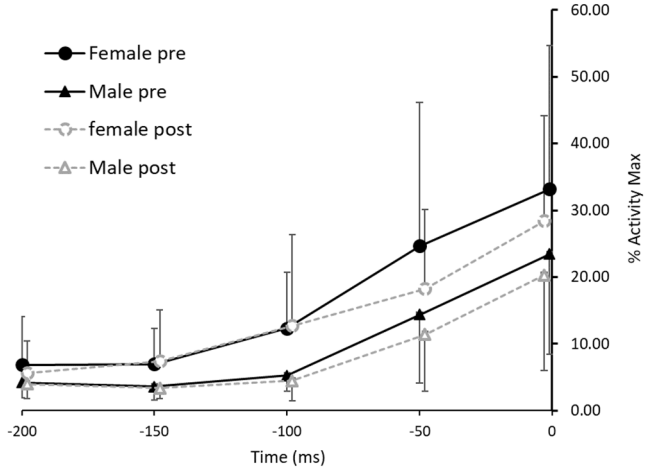

Figure 1: Hamstring prior to landing before and after fatigue, normalized to maximum EMG activity during prefatigue jump landings. Error bars are standard deviation.

Significance

These results support the continued investigation of the hamstrings muscle group as a factor in ACL injuries and as a target for preventative intervention strategies. Caution should be exercised when directly linking to ACL injuries as the activation differences may be due to anatomical differences that require different motor patterns for a landing rather than a pathological origin. As acute fatigue shows an effect on hamstrings activation, clinicians and coaches could choose muscle activation as a potential evaluative method for interventions or training status.

References

[1] MacWilliams et al., (2000). *J. Bone Jt. Surg.* 82(3):86
[2] Bencke et al., (2018). *Front. Physiol.* 9:445

A Threshold-based Algorithm for the Detection of Pre-impact Falls-from-Height

Haneul Jung, Bummo Koo, Yejin Nam, Taehun Kim, Gyoobaek Cho and Youngho Kim*
Department of Biomedical Engineering and Institute of Medical Engineering, Yonsei University, Korea
Email: *younghokim@yonsei.ac.kr

Introduction

The mortality rate of falls-from-height (FFH) is the highest among accidents occurring in construction site. According to BLS data, 366 of 971 construction fatalities were caused by FFH in 2017 [1]. Even though many fall prevention trainings have been provided to workers and supervisors in order to prevent these fall accidents [2,3], they did not reduce fall accidents significantly. Recently, some researches regarding the wearable airbag have been conducted to minimize the damage of inevitable fall accidents [4,5]. Therefore, the algorithm for the detection of pre-impact FFH is essential to guarantee enough lead time (the time interval between the detection and the collision) for inflating the airbag. A threshold-based algorithm for the detection of pre-impact FFH was developed in this study,.

Methods

Totally 20 healthy male volunteers (age: 24.75 ± 1.37 years, height: 174.05 ± 4.86 cm, weight: 73.7 ± 10.05 kg) participated in the study and were equipped with an IMU sensor on thoracic vertebrae 6 (T6). They performed nine different types of non-fall motions and one FFH (Table 1). FFH was performed on a 40cm mattress for the safety. The present study was approved by the Yonsei University Research Ethics Committee (1041849-201911-BM-166-01), and the written informed consent was obtained from every experiment participant.

Table 1: List of experimental motions.

1. Sit quickly and get up	6. Working with pickaxe
2. Sit on the floor and get up	7. Lifting (Front)
3. Stair up and down	8. Lifting (Back)
4. Ladder up and down	9. Lifting (Side)
5. 0.7m height jump	10. 0.7m height forward fall

Due to the safety issue, the actual FFH experiment was performed only from 0.7m height. Instead, a ball-jointed doll was used to perform FFH motions from the heights of 1.5m, 2m and 3m. In addition, Pam-Crash (ESI Group, France) program and human model (HARB) were used to simulate FFH motions in computer. Vertical angle was calculated using the complementary filter with proportional integral controller [6], and vertical velocity was determined by integrating vertical acceleration. Vertical acceleration was obtained by the Euler transformation of 3-axis accelerations [7]. A threshold-based algorithm for the detection of pre-impact FFH is shown in Figure 1.

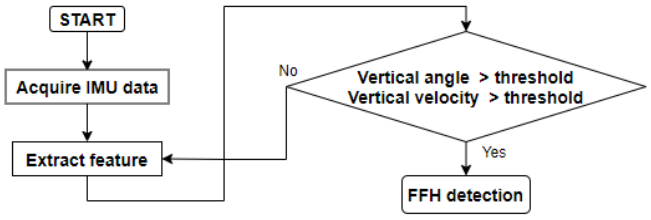

Figure 1. The flow chart of FFH detection algorithm.

The thresholds were set using the receiver operating characteristic curve with randomly selected 10 participants' data. The rest of 10 participants' data was used to test the algorithm.

Results and Discussion

The present algorithm resulted in 100% accuracy of pre-impact FFH detection. Table 2 shows the lead time obtained from the experiment and the simulation for different heights of falls. Since the inflation time of our wearable airbag system was about 200ms [5], it can be said that enough lead time was obtained in this study. In addition, results from the simulation and the experiment were in good agreement.

Table 2: Lead times from the experiment and the simulation (unit: ms).

Fall height	0.7m	1.5m	2m	3m
Experiment	324.3±46.7	380±10.9	462±11.7	592.5±17.8
Simulation	320	340	430	570

However, the number of subjects in this study was relatively small and the number of non-fall motions was insufficient to represent actual activities in construction site. A wearable airbag system to protect workers from inevitable fall accidents has been developed and it is necessary to evaluate the algorithm with various activities in construction site.

Significance

The construction site has many dangerous works and environments. In particular, many activities at high place are inevitable in construction and FFH frequently occurs. Many efforts have been made to prevent these accidents including safety training and installing guardrail and safety net, but a high incidence of FFH still remains. A wearable airbag system has been developed to minimize serious damages caused by FFH. The present threshold-based algorithm for the detection of pre-impact FFH would be essential in developing the wearable airbag system.

Acknowledgments

This research was supported by Basic Science Research Program through the National Research Foundation of Korea (NRF) funded by the Ministry of Science and ICT (No.2018R1D1A1B07048575) and the Technology Innovation Program (20006386) funded by the Ministry of Trade, Industry & Energy (MOTIE, Korea).

References

1. U.S. BLS, https://www.bls.gov/iif/oshwc/cfoi/cftb0321.htm
2. Kaskutas et al., K. Safety Res., 44:111-118, 2013
3. Luz et al., J. Contr. Eng. Manage., 413(8):04017037, 2017
4. Thanh et al., AJSE, 44:3329-3342, 2019
5. Ahn et al., Sensors and Materials, 30(8):1743-1752, 2018
6. Jung et al., Sensors, 20(5):1277, 2020
7. Lee S. et al., KSAS, 11:1422-1425, 2014

A Predictive Model for Stress Fractures in Runners

Yannis K. Halkiadakis*[,1], Helia Mahzoun Alzakerin[1], Kristin D. Morgan[1]
[1]*Department of Biomedical Engineering, College of Engineering, University of Connecticut, Storrs, CT, USA*
Email: *Yannis.Halkiadakis@uconn.edu

Introduction

Up to 50% of all running injuries are attributed to stress fractures [1]. Milner et al. (2006) found that vertical loading rate was greater in female runners with history of tibial stress fractures [1]. Additionally, elevated impact peak has also been reported in individuals suffering from stress fractures [2]. These findings suggest an inability to attenuate tibial shock. While loading rate and impact peak are often analyzed independently, this study explored the relationship between these variables during running to determine if a combined metric could more effectively delineate between those with and without stress fractures. We hypothesized that the relationship between loading rate and impact peak would be a better feature to help differentiate and more accurately classify between runners with and without a history of stress fractures than either feature on its own.

Methods

Fifteen controls (age 19.1 ± 0.8 yrs; height 1.78 ± 0.08 m; mass 64.7 ± 8.7 kg) and 11 individuals with history of stress fractures (age 19.4 ± 0.8 yrs; height 1.77 ± 0.08 m; mass 63.7 ± 6.9 kg) participated in a running protocol. Each participant provided written consent to participate in the study in accordance with the institutional review board. Participants ran on an instrumented split-belt treadmill (Bertec Corporation, Columbus, Ohio). Participants started with a two-minute warm-up period where they ran at 2.5 m/s followed by running at 3.3m/s for 30 seconds. Running parameters were then extracted from the vertical ground reaction force (vGRF) data that was collected at 1200 Hz and low-pass filtered at 35 Hz using a 4th order Butterworth filter.

The variables of interest were impact peak, loading rate and loading rate to impact peak ratio. The impact peak is the first vGRF peak during each stride. The loading rate is the slope between 20 and 80% of the vGRF data between foot strike and impact peak [1]. Both impact peak and loading rate were normalized to individuals body weight (BW). The ratio was created by dividing the loading rate by the impact peak. An unpaired t-test determined if the means of the variables of interest were significantly different between the two groups (α=0.05). Then each single feature was tested as the predictor using a Linear Support Vector Machine algorithm to classify between the two groups. A more advanced model was created by fitting a linear regression model to the control impact peak and loading rate data that provided upper and lower 99% confidence limits. The upper 99% confidence limit served as a dividing line to delineate between the control and stress fracture individuals.

Results and Discussion

Both loading rate and the ratio were significantly greater in the stress fracture individuals than controls ($p<0.01$; $p<0.01$) (Table 1). No significant difference was found in impact peak ($p=0.68$) (Table 1). The assessment of the linear relationship and associated classification line successfully placed 81% of the stress fracture individuals in the injured region (Fig. 1). The overall model accuracy of appropriately classifying individuals in either the stress fracture and control groups was 75%.

The results support the hypothesis that the ratio of loading rate over impact peak is a more impactful feature than loading rate or impact peak on their own. Impact peak showed a 58% classification accuracy (sensitivity = 0.50, specificity = 0.63, AUC = 0.57), loading rate showed a 65% classification accuracy (sensitivity = 0.59, specificity = 0.7, AUC = 0.68), and loading rate over impact peak showed a 71% accuracy (sensitivity = 0.64, specificity = 0.77, AUC = 0.75). This shows that the relationship between impact peak and loading rate can be considered as a more significant feature than either on their own.

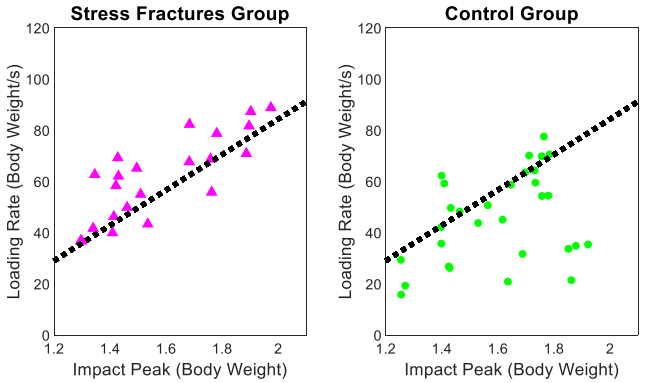

Figure 1. Comparison of the scatter plots of impact peak versus loading rate for the stress fracture and control groups. The line is the stress fracture classification line, which is the upper 99% confidence limit for a linear regression model based on the control individuals.

Significance

This model furthers the understanding of how stress fractures impact the gait patterns of runners and has potential to be used as a real-time, gait retraining tool to help runners lower their risk of stress fractures [3]. A limitation of this study is that it was performed on Division I athletes. Future studies will evaluate how this relationship applies to runners of all levels.

Acknowledgments

We would like to acknowledge Dr. Brian Noehren for providing the data for this study.

References

[1] Milner et al. (2006). *Med. Sci. Sports Exerc.*; 38(02): 323-328.
[2] Pohl, et al. (2008). *J. Biomech.;* 41: 1160–1165
[3] Crowell et al. (2011). *Clin. Biomech.*; 26: 78-83.

Table 1. Comparison of impact peak, loading rate and loading rate to impact peak ratio between the control and stress fracture individuals.

Variable	Controls	Stress Fracture	P-Value
Impact Peak (BW)	1.6 ± 0.2	1.6 ± 0.2	0.68
Loading Rate (BW/s)	45.8 ± 17.6	61.4 ± 16.4	0.002
Loading Rate to Impact Peak Ratio	28.5 ± 10.2	38.5 ± 7.1	<0.001

Pressure Relief in Wheelchair Users with Static Posture Changes

Paige Cordts[1], Justin Scott[1], Tamara Reid Bush[1], PhD
[1]Michigan State University College of Engineering
Email: cordtspa@msu.edu, reidtama@msu.edu

Introduction

Many wheelchair users experience pressure ulcers (PUs), caused by prolonged periods of external loading and high pressures on the body. PUs can result in infections, longer hospital stays, and increased healthcare costs[1]. The seated posture generally produces concentrated pressures around the buttocks, distal thigh, sacrum, and shoulders, thus making these high risk regions for a PU formation[2]. To relieve the pressure on high risk regions of the body, we investigated a large set of postures to identify those that would be able to shift where pressure in concentrated on the legs an back while seated.

Methods

Twenty able-bodied adults (10 male, 10 female) volunteered for this study. A chair was constructed with independently tilting pelvic and thoracic supports on a reclining back, and an independently tilting seat pan. All three supports were mounted on six-axis load cells (AMTI, Watertown, MA) and each driven by independent motors.

Pressures on the thighs, buttocks, and back were measured via pressure mats (Tekscan, Boston, MA) mounted to the seat pan and back of the chair. 27 postures were tested on each participant, each held for one minute to allow settling to occur. These postures were defined by the following angles: (1) back recline 0º (vertical), 15º, 30º, (2) seat pan tilt 0º (horizontal), 15º, 30º, and (3) back posture 0º (vertical) thoracic and pelvic tilt, 5º thoracic tilt and -15º pelvic tilt, 5º pelvic tilt and -15º thoracic tilt. Posture order was randomized for each participant to correct for possible influence from testing fatigue.

Pressure data collected from each of these postures were visually analyzed to determine postures with high and low pressure on specific regions of the body: the distal thighs, buttocks, lower back, middle back, and upper back.

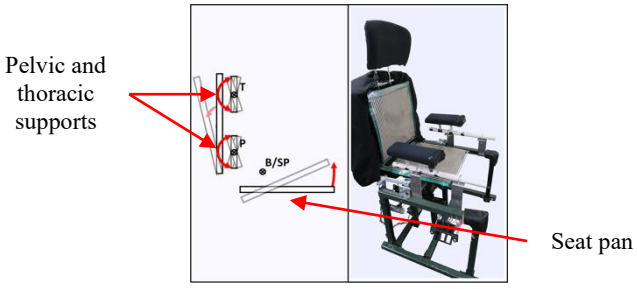

Figure 1: Prototype of the articulating wheelchair used for testing selected postures. Separate motors were used to control the seat pan tilt, recline, and thoracic and pelvic tilts.

Results and Discussion

Areas of highest and lowest pressure were determined for each of the 27 postures. A sample set of postures were identified that could significantly shift pressures from one region to another. Pressure shifts occurred from the butt to distal thigh, and between low, mid, and high back regions. These identified trends were used to determine which static postures would be ideal for offloading specific regions of the body.

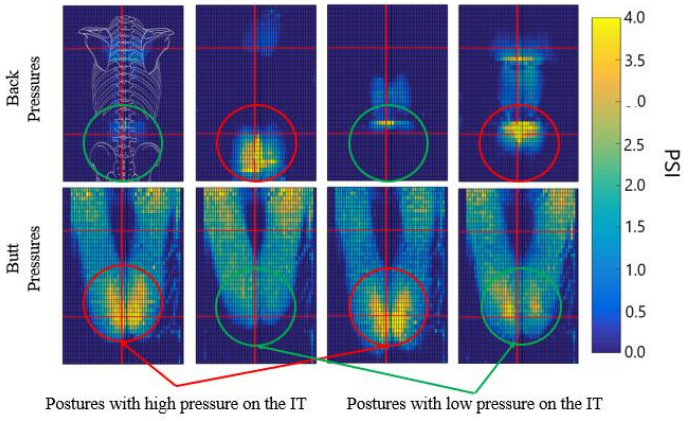

Figure 2: Sample set of postures used to demonstrate areas of high and low pressure. An emphasis was placed on shifting pressure away from commonly loaded areas for a given posture. Areas loaded in each posture are indicated with red circles, while green circles indicate relief or absence of loading in subsequent postures.

Significance

These data are significant for wheelchair design and use, as they show that there is a correlation between position of articulating wheelchair segments and pressure in the buttocks, thighs, and back. With these data, we have identified postures that could be used to offload pressure in a specified region of the body in order to prevent the long periods of external loading that cause PUs. These postures all emphasize placing loading on one region of the body, while attempting to reduce pressure on the other high-risk regions. While the body cannot be completely unloaded while seated, these varying postures reduced loading, thus reducing the likelihood of tissue necrosis and PU formation. Future work will determine how long each posture needs to be held for effective pressure relief.

Acknowledgments

This work was supported by NSF grant CBET-1603646.

References

1. Padula et al. *Int Wound J.* 2019.
2. Groeneveld A, et al. *J Wound, Ostomy, Cont Nurs.* 2004.
3. Chen et al. *Arch Phys Med Rehabil.* 2005.

Bilateral Differences in Lumbopelvic-Hip Complex Kinematics during the CKCUEST

Jeff W. Barfield.[1,]*, Nicole M. Bordelon[2], Kyle W. Wasserberger[2], and Gretchen D. Oliver[2]
[1]Department of Physical Education & Exercise Science, Lander University; Greenwood, SC, 29649
[2]Sports Medicine Movement Lab, School of Kinesiology, Auburn University; Auburn, AL, 36849
Correspondance Email: *jbarfield@lander.edu

Introduction

The closed kinetic chain upper extremity stability test (CKCUEST) is a reliable test used by clinicians and coaches to assess an athlete's recovery from an upper extremity injury by examining lumbopelvic-hip complex (LPHC) and upper extremity stability.[1] In particular, the CKCUEST is a beneficial assessment for overhead athletes participating in unilateral rotational sports which require the body to perform efficiently as a kinetic chain. For example, baseball pitchers repeatedly rotate towards their non-throwing side which, over time, can result in asymmetric LPHC and upper extremity movement patterns.

Clinicians and coaches can benefit from understanding the effect of chronic unilateral rotational motion on LPHC stability, which in turn, impacts upper extremity movement efficiency.[2,3] Therefore, the purpose of this study was to examine how LPHC kinematics differed between dominant and non-dominant hand touches during the CKCUEST in a group of baseball pitchers. We hypothesized that LPHC kinematics observed on a dominant hand touch would differ from the non-dominant hand touch. Specifically, greater compensatory movement patterns, evidenced by increased LPHC kinematic deviation from neutral, would be observed upon a non-dominant hand touch compared to a dominant hand touch.

Methods

Kinematic data from nineteen baseball pitchers (17.71 ±1.98 yrs; 184.92 ± 6.02 cm; 81.75 ±13.78 kg) performing three trials of the CKCUEST[1,4] were collected at 240 Hz with an electromagnetic tracking system. Data from all three trials of the CKCUEST were averaged at the middle touch as determined by Tucci and colleagues.[4] Dominant hand was indicated by the participants' throwing arm. The inverse value of left hip ab/adduction was used for analysis so that data would be relatable to right hip ab/adduction data. Paired samples t-tests were used to assess differences in LPHC kinematics upon dominant and non-dominant hand touching. Specifically, stance width, pelvic axial rotation, and bilateral hip ab/adduction between dominant and non-dominant hand touching were the LPHC kinematics analysed. Cohen's d was used to assess effect size. Testwise error was set at $\alpha = 0.05$.

Table 1: Mean (SD) of dominant and non-dominant LPHC kinematics.

Variable	Dominant	Non-Dominant
Stance Width (m)	0.16 (0.09)	0.15 (0.09)
*Pelvic Axial Rotation (°)	-2.09 (5.73)	-5.58 (6.40)
*Touching Side Hip Abduction (°)	-2.63 (9.64)	-12.76 (10.40)
*Stance Side Hip Adduction (°)	0.40 (9.04)	11.34 (9.74)

*Note: * denotes significant difference at p< 0.05. Stance width = ankle joint center displacement.*

Results and Discussion

Descriptive statistics can be found in Table 1. Differences were observed between dominant and non-dominant hand touches in pelvic axial rotation ($t(18) = 2.45$, $p = 0.025$, $d = 0.56$), stance leg side hip adduction ($t(18) = -3.70$, $p = 0.002$, $d = -0.85$), and touching side hip abduction ($t(18) = 2.91$, $p = 0.009$, $d = 0.67$). Upon dominant hand touch, significantly less pelvic axial rotation, touching side hip abduction, and stance side hip adduction was observed when compared to a non-dominant hand touch. These results support our hypothesis that differences in LPHC kinematics would be observed between bilateral hand touching during the CKCUEST.

During non-dominant hand touching, the pitcher's dominant hand should act to support stabilizing the body on the ground. Interestingly, more LPHC movement was observed in this position compared to when the non-dominant hand was stabilizing. This potentially indicates less LPHC stability while the dominant hand was in a closed chain position. We speculate that experiencing a repetitive unilateral open-chain pitching motion may affect dominant side closed chain stability. However, less LPHC stability during the non-dominant hand touch may be a product of muscular weakness or lack of neuromuscular coordination not related to the pitching motion.

Our results indicate that baseball pitchers appear more stable performing a dominant hand touch as evidenced by decreased kinematic compensations within the LPHC.

Significance

In order to achieve efficient proximal to distal energy transfer, stability of the LPHC is necessary.[2,3] Greater stability was observed during dominant hand touching, indicating a discrepancy between sides that can impact training and rehabilitative programs. Clinicians and coaches should take this information into account when designing programs for baseball pitchers. Since the baseball pitch requires proximal stability for efficient energy transfer, future research should determine whether the observed asymmetry is a result of LPHC or upper extremity instability stemming from the baseball pitching motion. Additionally, future research should examine the effect this asymmetry has on performance and risk of injury.

Acknowledgments

No financial support was received for this project.

References

1. Goldbeck and Davies. Test-Retest Reliability of the Closed... *J Sport Rehabil*. 2000.
2. Oliver et al. Quantitative analysis of… *J Strength Cond Res*. 2018.
3. Putnam. Sequential motions of body segments… *J Biomech*. 1993.
4. Tucci et al. Biomechanical Analysis of Closed… *J Sport Rehabil*. 2015.

ACUTE EFFECT OF AN INTERVENTION TO IMPROVE ANKLE DORSIFLEXION AMONG INDIVIDUALS WHO DISPLAY MEDIAL KNEE DISPLACEMENT

Rebecca Ban[1], Feng Yang[1]
[1]Department of Kinesiology and Health, Georgia State University, Atlanta GA, 30303
Email: rban1@gsu.edu

Introduction

Knee valgus has been identified as an important risk factor for lower extremity injury, specifically non-contact anterior cruciate ligament injury[1]. Dynamic knee valgus is the combination of excessive femoral adduction and internal rotation, and tibial abduction and external rotation[1]. These motions are influenced by joints proximal and distal to the knee, including the hip and ankle[1,2]. Clinically, excessive knee valgus, visually demonstrated as medial knee displacement (MKD), is described as the midpoint of the patella passing medial of the great toe[3].

Recently, numerous studies have reported limited ankle dorsiflexion range of motion (ROM) to be a contributor to excessive knee valgus[2,4]. However, no direct evidence shows an improvement in frontal plane knee motion after an intervention to increase ankle dorsiflexion ROM. The purpose of this study was to examine if an intervention designed to increase ankle dorsiflexion ROM in persons who display MKD acutely reduces MKD in an overhead squat task.

Methods

Sixteen participants were randomly assigned to the intervention (n = 8, mean ± standard deviation age: 21.3 ± 4.7 years, mass: 63.7 ± 16.8 kg, height: 163.2 ± 7.9 cm) or control group (n = 8, age: 22.3 ± 3.3 years, mass: 67.3 ± 12.6 kg, height = 164.3 ± 8.8 cm). All participants were screened using the double-leg squat assessment to verify the presence of MKD[3]. Specifically, the assessment consists of five consecutive squats in a standardized position: feet shoulder width apart, toes pointing forward, arms overhead with elbows locked straight[3]. If MKD is observed, heel lifts are placed under the heels and five additional squats are performed. This movement screen can theoretically differentiate between dysfunction at the hip or ankle as the primary contributor to MKD. If application of the heel lifts rectifies knee alignment, the primary contributor to MKD is reduced ankle dorsiflexion ROM[2].

After screening, qualified participants underwent a pre-test assessment. Ankle dorsiflexion ROM was measured in three conditions: passive straight knee, passive bent knee, and a weight-bearing lunge. Subjects then performed five consecutive double-leg squats in the standardized position and the average was used for analysis. After the pre-test assessment, participants completed the assigned intervention protocol. For the training group, the intervention protocol was developed using procedures from the National Academy of Sports Medicine corrective exercise strategies textbook[5]. Participants used a high-density foam roller embedded with a vibrating motor to perform self-myofascial release of the gastrocnemius and soleus. Participants then performed a weight-bearing static stretch of the gastrocnemius and soleus. Isolated activation of the posterior tibialis and heel raises with the toes internally rotated for two sets of 10 repetitions was completed. Lastly, participants performed single leg squats for two sets of 10 repetitions. Participants in the control group walked on a treadmill at a self-selected speed in lieu of the intervention program. Immediately following the intervention, the measurements performed during the pre-test assessment were repeated for all participants. During the squat task, lower extremity kinematic data were gathered through 23 markers using an 8-camera motion capture system (Vicon, UK).

The changes from the pre-training to the post-training assessments were calculated for each of the four outcomes (ankle dorsiflexion ROM under three conditions and MKD during the overhead squats for the affected leg). Independent *t*-tests were used to compare the changes between groups. SPSS 24 (IBM) was used and a significance level of 0.05 was applied.

Results and Discussion

The intervention group significantly reduced MKD ($p = 0.003$, Fig. 1a), and increased all dorsiflexion ROM measures compared to the control group: passive straight knee ($p < 0.001$), passive bent knee ($p = 0.04$), and weight-bearing ($p = 0.03$) (Fig. 1b). A significant correlation was observed between the changes in ankle dorsiflexion ROM and MKD ($r = -0.548$, $p = 0.014$). Our most important finding was that an increase in dorsiflexion ROM could reduce MKD during an overhead squat task in individuals who displayed MKD that was corrected with a heel lift.

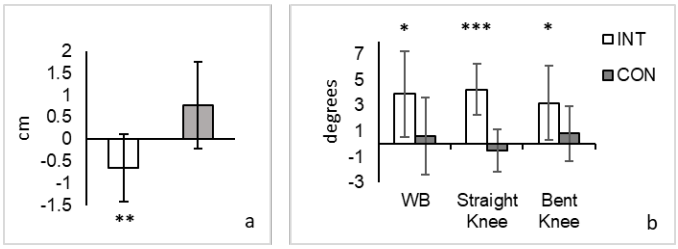

Figure 1 Between-group comparisons for the intervention-induced changes in a) MKD (cm), and b) ankle dorsiflexion ROM (deg) under three testing conditions. WB: weight bearing. *: $p < 0.05$; **: $p < 0.01$; ***: $p < 0.001$ between groups.

Significance

To our knowledge, this is the first study to examine the effects of an intervention aimed to increase ankle dorsiflexion ROM on mediolateral knee motion. Our results indicate that an increase in ankle dorsiflexion ROM has the potential to diminish MKD. Dynamic knee valgus is a modifiable risk factor for knee injury. Intervention programs have previously focused on plyometric training and strengthening hip musculature to reduce knee valgus. Based on our findings, we recommend that interventions to improve dynamic knee valgus include exercises to increase ankle dorsiflexion ROM.

References

[1] Hewett et al. *Am J Sports Med.* 2006; 34:299-311.
[2] Bell et al. *Arch Phys Med Rehabil*. 2008; 89:1323-1328.
[3] Hirth JC, Padua DA. *Athl Ther Today*. 2007; 12:10-14.
[4] Macrum et al. *J. Sports Rehabil.* 2012; 21:144-150.
[5] Clark et al. *Optimum Performance Training for the Health and Fitness Professional*. 2004.

Increased Ankle Range of Motion Reduces Knee Loads during Landing in Healthy Adults

Lauren E. Schroeder[1], Joshua T. Weinhandl[1]
[1]The University of Tennessee, Knoxville, Knoxville, TN, U.S.A.
Email: lschroe1@vols.utk.edu

Introduction

Decreased dorsiflexion range of motion (DROM) has been associated with abnormal knee mechanics during landing [1] and may identify those at an increased risk of anterior cruciate ligament (ACL) injury. Fortunately, DROM can be easily modified using both plantarflexor static stretching (SS) [2] and talocrural posterior joint mobilizations (JM) [3]. Both interventions have shown to produce acute increases in DROM after a single bout and may attenuate known sagittal and frontal plane knee ACL injury risk factors during dynamic tasks. However, it is not known how these interventions compare to each other and how they alter knee landing mechanics.

The purpose of this study was to determine the acute effects of SS and JM interventions on pre to post-intervention DROM measurement changes (ΔDROM) and right-leg drop jump knee landing mechancis. We hypothesized that ΔDROM would be different between interventions, and that there would be favorable knee biomechanical changes after both interventions.

Methods

Seven males (age: 25.1±3.1yrs; height: 1.80±0.08m, mass: 85.69±17.84kg) and 18 females (age: 21.7±2.5yrs; height: 1.65±0.06m, mass: 63.96±8.56kg), all healthy and recreationally active, completed SS on day 1 of testing and JM on day 2 of testing. On both days, right-leg passive and active DROM, the weight-bearing lunge test, the anterior reach portion of the Star Excursion Balance Test, and a motion capture right-leg box landing task were completed both before and after the intervention. For the box landing task, participants stood on a 30cm tall box, placed a distance equal to half of their height away from the center of the force plate, jumped off of their left foot and landed on their right foot until stable.

3D marker coordinate data were collected using a 12-camera Vicon system (200Hz), and ground reaction forces were collected with one AMTI force plate (2000Hz). 3D knee sagittal and frontal plane kinematics and internal moments, as well as peak anterior shear force (ASF), normalized to body mass, were calculated. ΔDROM was calculated as the difference between post and pre-intervention DROM measurements. Pairwise dependent *t*-tests were performed for ΔDROM and 2×2 (time × intervention) repeated measures ANOVAs were perfomed for initial contact (IC) and peak knee angles, peak knee moments, and peak ASF (α=.05).

Results and Discussion

No significant differences were present in ΔDROM between SS and JM interventions (passive: SS = 3.2°, JM = 2.9°, active: SS = 1.9°, JM = 2.2°, WBLT: SS = .86 cm, JM = .84 cm, anterior SEBT: SS = .00 cm, JM = .01 cm, p>.05). There were significant time main effects for peak knee flexion (p=.005, η_p^2=.28) and abduction (p=.004, η_p^2=.30) angles, peak knee adduction moment (p=.001, η_p^2=.40), and peak ASF (p<.001, η_p^2=.42). Additionally, significant intervention main effects were present for IC abduction angles (p=.023, η_p^2=.20) and peak adduction moments (p=.001, η_p^2=.39) (Table 1).

Increases in dorsiflexion measurements did not significantly differ between interventions, indicating both were effective in improving DROM. Peak ASF significantly decreased after both interventions, possibly due to the increased peak knee flexion angles exhibited after both interventions. However participants experienced greater frontal plane excursions after both interventions during the jump landing task, warranting further investigation as to why this occurred.

Significance

Ankle DROM is a potential modifiable ACL injury risk factor that can be improved using either SS or JM interventions. Our results demonstrated that not only were SS and JM interventions effective in increasing DROM, they also improved knee flexion angles and ASF during landing, both of which are known ACL injury risk factors. Plantarflexor SS may be a more practical treatment for those at an increased risk of ACL injury due to the ability to completed the intervention without the assistance of another individual.

References

1. Wahlstedt et al. (2015) *Knee Surg Sports Traumatol,* Vol **23**(11), 3202-3207.
2. Medeiros et al. (2018) *Foot (Edinb)* Vol **34**, 28-35.
3. Maitland (2001) *Maitland's vertebral manipulation* (6th).

Table 1. Mean ± SD knee kinematic and kinetic variables between interventions and pre/post-intervention times.

		Static Stretching		Joint Mobilization	
		Pre	**Post**	**Pre**	**Post**
Initial Contact Angles	Knee Flexion (°)	-9.3±3.8	-9.8±4.3	-9.3±4.8	-9.3±5.0
	Knee Abduction (°) §	1.1±2.9	0.8±3.0	1.5±2.6	1.5±2.8
Peak Angles	Knee Flexion (°) *	-56.3±7.3	-59.2±8.7	-58.2±8.8	-59.6±9.8
	Knee Abduction (°) *	-0.6±3.9	-1.6±3.4	-0.4±3.8	-1.3±4.2
Peak Moments	Knee Extension (Nm·kg^{-1})	2.75±0.45	2.72±0.36	2.70±0.31	2.64±0.37
	Knee Adduction (Nm·kg^{-1}) *§	-0.98±0.29	-0.90±0.26	-0.90±0.22	-0.84±0.27
Peak Anterior Shear Force	ASF (N·kg^{-1}) *	9.43±1.63	9.12±1.36	9.40±1.12	9.02±1.23

*significant time main effect, § significant intervention main effect

Force and Rate Metrics Provide Return-To-Sport Criterion after ACL Reconstruction

Helia Mahzoun Alzakerin[1], Yannis Halkiadakis[1], and Kristin D. Morgan[1*]
[1]*Department of Biomedical Engineering, College of Engineering, University of Connecticut, Storrs, CT, USA*
Email: *kristin.2.morgan@uconn.edu

Introduction

An anterior cruciate ligament (ACL) injury is a common sport's injury that impacts over 250,000 individuals each year and often requires surgical intervention and rehabilitation [1-2]. A goal of post-ACL reconstruction (ACLR) rehabilitation is to restore an individual's neuromuscular control to healthy, pre-injury levels to enable a rapid return-to-sport (RTS) [3]. However, the challenge resides in defining universal benchmarks to quantify the restoration of healthy motor control. Andriacchi et al. (1977) found that gait speed and peak force are linearly related and that this relationship could be used to differentiate between the gait of healthy individuals and those after total knee replacement [4]. Given that elevated peak vertical ground reaction force (vGRF) and linear loading rate are often found to be indicative of altered limb loading, we sought to investigate and exploit the linear relationship between peak vGRF force and linear loading rate to develop a criterion to aid in the individualized assessment of post-ACLR individuals. We hypothesized that there would be a strong linear relationship between the peak vGRF and the linear vGRF loading rate using the data from the healthy controls and post-ACLR non-reconstructed limbs. We will then use the healthy control data to develop a linear regression model to define a region of healthy limb dynamics to aid in the classification of altered limb dynamics in the post-ACLR individuals reconstructed limb.

Methods

Thirty-one post-ACLR individuals (mean ± standard deviation; age: 20.4 ± 6.2 yrs; height: 1.8 ± 0.1 m; mass: 71.7 ± 11.1 kg; running speed: 2.7 ± 0.3 m/s; Tegnar (post-ACLR at 6 months): 6.4 ± 1.8; 16 males and 15 females) and 31 healthy controls (age: 20.9 ± 3.4 yrs; height: 1.7 ± 0.1 m; mass: 65.2 ± 13.8 kg; running speed: 2.7 ± 0.4 m/s; Tegnar: 6.9 ± 1.3; 18 males and 14 females) performed a running protocol. All post-ACLR individuals participated in the study 6 months after surgery and were cleared to RTS by their physician. All of the control participants were injury free for the six months prior to the study and had no history of knee surgery. Participants provided informed written consent prior to their participation.

Participants performed a running protocol where they ran at a self-selected speed on an instrumented treadmill (Bertec Corporation, Columbus, Ohio). Ground reaction force data was collected at 1200 Hz and filtered using a zero-lag, fourth-order Butterworth filter with a 35-Hz low-pass cutoff frequency. Peak vGRF and linear loading rate, defined as the slope from foot strike to peak vGRF were extracted from 10 running strides. A correlation analysis was conducted to measure the strength of the linear relationship between the peak vGRF and linear loading rate for the control right and left and ACLR reconstructed and non-reconstructed limbs. The region of healthy limb dynamics was defined as the upper 99% confidence limit based on the model fit to the control right, control left and ACLR non-reconstructed limb data. All of the statistical analyses were conducted in MINITAB (MINITAB, Version 18, State College, PA, USA).

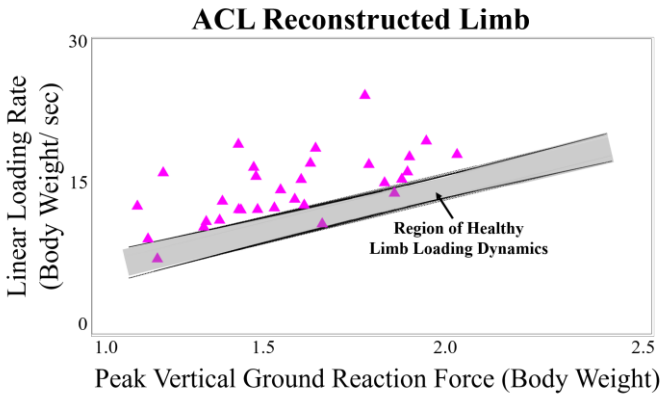

Figure 1: Scatter plot of the peak vertical ground reaction force (vGRF) data versus the linear vGRF loading rate data for ACL reconstructed limbs. The black lines represent the upper and lower 99% confidence limits based on the healthy control and non-reconstructed limb data.

Results and Discussion

There was a strong linear correlation between the peak vGRF and linear vGRF loading rate for the control right (R=0.90), control left (R=0.91) and post-ACLR non-reconstructed limb (R=0.88). A weaker relationship was reported in the post-ACLR individuals reconstructed limb (R=0.61). A linear regression model was fit to the control and non-reconstructed limb data ($R^2 = 0.81$) (Eq. 1).

$$\textit{Linear vGRF Loading Rate} = 0.06 + 7.90 * \textit{Peak vGRF} \quad (1)$$

The 99% upper confidence limit obtained from the linear regression model served as a boundary line to demarcate between the healthy and abnormal limb dynamics (Fig.1). This boundary line successfully classified 90% of the 31 reconstructed limbs as having abnormal limb dynamics. Overall, 83% of the 124 limbs in the study were correctly classified.

The results supported the hypothesis that there was a strong linear relationship between peak vGRF and linear loading rate that could be used to denote abnormal limb dynamics. The deviation from this relationship in the reconstructed limb suggests an inability to properly control the force produced in the that limb which could be attributed to altered neuromuscular control. This analysis is significant because it suggests that there the relationship between these variables can be used as a benchmark by clinicians and researchers to quickly detect individuals with abnormal limb dynamics.

Acknowledgments

We would like to thank Dr. Brian Noehren for providing the data for this study.

References

[1] Boden, et al. (2000). *Physician and sportsmed.;* 28(4): 53-60.
[2] Noehren et al.. (2013). *Med. Sci. Sports Exerc.*; 45(7): 1340.
[3] Palmeri-Smith et al. (2008). *Clin.in Sports Med.*; 27(3): 405-24.
[4] Andriacchi et al. (1977). *J Biomech.*; 10(4): 261-68.

DYNAMIC JOINT STIFFNESS OF THE ANKLE IN CHRONIC ANKLE INSTABILITY PATIENTS

Jaeho Jang[1], Kyeongtak Song[1], and Erik. A Wikstrom[1]
[1]University of North Carolina Chapel Hill, NC, USA
Email: jaeho@live.unc.edu

Introduction

Between 30-40% of patients with a lateral ankle sprain (LAS) experience one or more residual symptoms, which are considered to be hallmark characteristics of a condition referred to as chronic ankle instability (CAI). CAI patients have altered spinal reflex and muscular activity patterns, as well as aberrant movement strategies, which could lead to alterations in joint stability and development of pathomechanical loading at the ankle joint. Consequently, altered joint loading threatens cartilage health and is thought to contribute to the development of ankle posttraumatic osteoarthritis (PTOA).

While decreased dorsiflexion excursion and increased plantar flexion moments during a stance phase of walking are commonly found in CAI patients [1], the interaction between these is not fully understood. This interaction, referred to as stiffness, has been studied during various dynamic activities (i.e. landing and cutting) in CAI patients and thought to reduce joint stability at the ankle [2]. However, little attention has been placed on stiffness during gait, limiting our understanding of how the most common dynamic task during daily life affects ankle cartilage health. Dynamic Joint Stiffness (DJS) is defined as the resistance developed by joint structures during inter-segmental displacement in response to an external moment [3]. DJS is more comprehensive measure than stiffness as it distinguishes ankle behaviors across three distinctive and continuous sub-phases. Thus, DJS is better suited to capture alterations that could modify the visco-elasticity of the joint and lead to reduced joint stability; factors that could facilitate PTOA development. Therefore, the purpose of this study was to compare DJS at the ankle joint between CAI patients and healthy control.

Methods

Forty-five healthy control (age: 20.24 ± 3.90years, weight 67.06 ± 13.18kg, height: 169.32 ± 8.39cm) and forty-five CAI patients (age: 20.71 ± 2.07years, weight 72.65 ± 14.65kg, height: 169.87 ± 7.43cm) participated. CAI inclusion criteria were in accordance with the International Ankle Consortium guidelines. Kinematic (120Hz) and ground reaction force data (1200Hz) were collected while participants completed five gait trials with self-selected speed. The sagittal ankle joint angle and moment during stance phase was normalized to percentages of the stance cycle. Ankle DJS was represented by the slope of the joint moment plotted as a function of the joint angle. The entire curve was split into three sub-phases of ankle behaviors during ground contact: controlled plantar flexion (CPF), controlled dorsiflexion (CDF), and powered plantar flexion (PPF). Least-squares linear regression models were used to determine the corresponding slopes. The coefficient of determination (R^2) was also calculated to determine how accurately data fit a linear model. Average values from the five collected trials were used to compare between groups using independent *t*-tests with the significance level of 0.05.

Results and Discussion

A lower DJS was observed in the CAI group during CPF as seen in Table 1. No group differences were observed during the CDF or PPF phases, and the R^2 was not different across all sub-phases.

CPF is characterized by the initiation of heel contact with a plantar flexion movement and moment. Although CPF is brief, it controls the impact with the ground. The lower slope during CPF in those with CAI is thought to represent their inability to control the plantar flexion moment associated with their plantar flexion excursion. This is consistent with the previous literatures that specified a lack of control of the eccentric contraction of the dorsiflexor muscles in CAI patients [4]. While the exact relationship between kinetic variables and cartilage health remain unknown, the observed DJS alteration might expedite the initiation of ankle cartilage degeneration via increased compressive forces at a more susceptible area of the ankle joint cartilage as muscle force is a contributor to total joint contact force [5].

	CAI (n =45) Mean (SD)	Control (n = 45) Mean (SD)	Differences p-value
CPF (Nm kg^{-1} /°)	0.022 (0.011)	0.028 (0.011)	0.016
CDF (Nm kg^{-1} /°)	0.089 (0.018)	0.093 (0.023)	0.397
PPF (Nm kg^{-1} /°)	0.060 (0.010)	0.062 (0.009)	0.442
CPF – R^2	0.980 (0.028)	0.971 (0.041)	0.256
CDF – R^2	0.904 (0.050)	0.874 (0.113)	0.111
PPF – R^2	0.977 (0.023)	0.982 (0.012)	0.163

Table 1. Dynamic joint stiffness comparison between those with and without chronic ankle instability (CAI); CPF: controlled plantar flexion sub-phase; CDF: controlled dorsiflexion sub-phase; PPF: powered plantar flexion sub-phase.

Significance

Our study indicates that CAI patients have altered ankle DJS during initial ground contact while walking. This inability to control impact with the ground may contribute to cartilage degeneration.

Acknowledgement

This study was partially supported by a Junior Faculty Grant from the University of North Carolina Chapel Hill.

References

[1] Son et al. (2019). *J Athl Train*, 54(6), 684-697.
[2] Kim et al. (2019). *J Athl Train*, 54(6), 708-717.
[3] Davis et al. (1996). *G & P*, 4(3), 224-231.
[4] Sloot et al. (2018). *Springer Int publishing*, 625-643.
[5] Shelburne et al. (2006). *J Ortho R*, 24(10), 1983-19

Kinematic and Kinetic Differences Pre- and Post-Femoral Stress Reaction Injury: A Case Study

Kathryn A. Farina[1], Seth R. Donahue[1], and Michael E Hahn[1]
[1]University of Oregon, Department of Human Physiology, Bowerman Sports Science Clinic, Eugene, OR, USA
Email: kfarina@uoregon.edu

Introduction

Femoral stress fractures account for 10% of stress fractures in runners [1] that are prone to complications and, if left untreated, may require extensive rehabilitation or surgery [2], highlighting the importance of early detection. Stress reactions occur due to repetitive stress, and without rest, may advance to a stress fracture [2], making identification of stress reactions vital to rapid recovery. Few prospective studies have focused on femoral stress reactions or fractures, consisting of case study analysis of imaging, diagnoses, and return to sport [3]. It remains that little is known about how to identify potential risk factors from kinematic and kinetic variables associated with femoral stress injuries. The purpose of this case study was to examine biomechanical variables before and after a femoral stress reaction in a trained female distance runner.

Methods

One collegiate female distance runner suffering a Grade 3 femoral neck stress reaction to the right side was evaluated before and after injury. Assessments were one year apart. Injury occurred roughly two months after the first test. The subject ran at 3.83 m/s for twenty strides on a force instrumented treadmill (f_s=1000Hz) (Bertec, Columbus, OH) while segmental position and orientation data were collected (f_s=200Hz) from both lower limbs (Motion Analysis Corp., Rohnert Park, CA). Inverse dynamics calculations were performed in Visual3D (C-Motion Inc., Germantown, MD). Kinematic and kinetic variables were exported to MATLAB (The MathWorks, Natick, MA), averaged across twenty strides at both time points, and peak values were extracted for analysis. Symmetry Index (SI) was calculated for peak values as $SI = (X_{right} - X_{left})/(0.5(X_{left} + X_{right}) * 100\%$. SI of an uninjured collegiate female runner of similar demographics was included as a healthy control comparison.

Results and Discussion

Sagittal plane peak angles, moments, and powers for the ankle, knee, and hip joints, along with SI, are presented in Table 1. The largest asymmetries pre-injury were ankle angle, knee moment, knee power, and hip power. These discrepancies decreased post-injury, and were more similar to SI values of the healthy control. For example, the knee on the injured side showed an increased angle and moment throughout stance phase prior to injury, but appeared closer in value to the uninjured side post-injury (Figure 1).

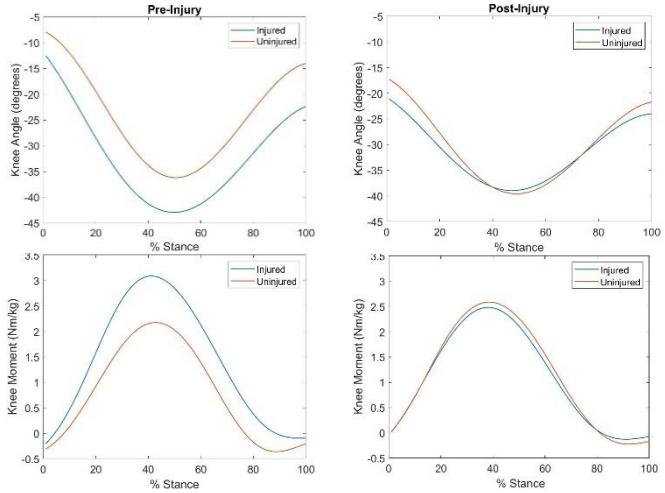

Figure 1. Average sagittal plane knee angle and moment during stance, running at 3.83 m/s: Pre-Injury on left, Post-Injury on right.

Significance

This case study provides a brief examination of sagittal plane mechanics before and after returning from a Grade 3 femoral neck stress reaction. These data indicate a possible link between asymmetry of sagittal plane joint kinematics and kinetics and the development of a femoral stress injury, and demonstrate resolution of asymmetries almost a year after injury. Further study of similar injuries, and variations in limb asymmetry in injured and uninjured runners should provide more insight into the role of asymmetric limb loading on bone stress injuries.

Acknowledgments

This work was supported by a Pac-12 Student-Athlete Health & Well-Being Grant (#3-03 Pac-12-Oregon-Hahn-17-01).

References

[1] McBryde, A. *J of Sports Med,* **3** (5), 212-17, 1976.
[2] McCormick, F. et al. *Clin Sports Med* **31** (2), 291-306, 2012.
[3] Neubauer, T. et al. *Res Sports Med* **24** (3), 283-297, 2016.

Table 1. Sagittal plane peak angles, moments, and powers for the ankle, knee, and hip joints for the right and left limbs running at 3.83 m/s Pre- and Post-injury. Values presented are mean (absolute value) ± standard deviation across twenty strides. Values from a healthy control subject are included. SI = Symmetry Index; DF = Dorsiflexion; PF= Plantarflexion; Ext = Extension; Flx = Flexion; Gen= Generation; Abs= Absorption.

	Pre-Injury			Post-Injury			Healthy Control
	Right	**Left**	**SI %**	**Right**	**Left**	**SI %**	**SI %**
Ankle DF Angle (degrees)	12.92 ± 0.86	9.41 ± 0.93	31.44	12.80 ± 0.96	15.36 ± 0.89	18.18	21.21
Ankle PF Moment (Nm/kg)	2.98 ± 0.05	2.78 ± 0.07	6.94	3.04 ± 0.07	2.82 ± 0.05	7.51	8.60
Ankle Gen Power (W/kg)	11.57 ± 0.50	10.90 ± 0.50	5.96	11.09 ± 0.54	9.51 ± 0.34	15.34	1.02
Knee Flx Angle (degrees)	42.71 ± 1.75	36.54 ± 1.70	15.57	41.35 ± 1.68	42. 10 ± 1.80	1.80	8.51
Knee Ext Moment (Nm/kg)	2.90 ± 0.13	2.17 ± 0.10	26.03	2.69 ± 0.15	2.54 ± 0.09	5.74	3.47
Knee Abs Power (W/kg)	10.63 ± 1.24	6.70 ± 0.80	45.35	9.08 ± 1.28	9.53 ± 0.53	4.84	12.34
Hip Flx Angle (degrees)	50.71 ± 1.48	46.39 ± 1.68	8.90	43.38 ± 1.91	39.55 ± 1.56	9.24	20.20
Hip Flx Moment (Nm/kg)	1.75 ± 0.21	1.57 ± 0.18	10.84	1.43 ± 0.14	1.23 ± 0.19	15.04	17.14
Hip Abs Power (W/kg)	2.00 ± 0.33	3.44 ± 0.42	52.94	2.36 ± 0.58	1.66 ± 0.60	34.83	33.39

Modeling of Feet First Falls into Protective Water Pits in the Context of OCRs

Rachel Tanczos[1], Kyle B. Van Housen[1], Sean D. Shimada, PhD[1]
[1]Biomechanical Consultants
Email: sean@motionsandforces.com

Introduction

Obstacle course races (OCRs) are a relatively new sporting event that involves competitive completion of physically demanding activities or "obstacles." Many of these obstacles utilize a water pit to reduce injury potential from a fall. The buoyant and drag forces of water oppose a person's downward motion, reducing the participant's velocity and ground impact force. The force applied to a falling contestant is principally dependent on the drop height, water depth, and the person's anthropometric characteristics. The purpose of the study is to propose a method to assess lower extremities injury risk during OCR events by determining the ground impact velocity when falling into a body of water.

Methods

This study utilizes calculated estimates for velocity, acceleration, buoyant force (F_b), and drag force (F_d) of a person falling perpendicular to a non-fully submersing body of water. The simulation allows for modification of total fall height, water depths, and a person's anthropometric characteristics. A force balance for a vertically falling body was used to determine the equation for acceleration as seen in (1), where g is acceleration due to gravity and m is the mass of the person. This equation was numerically integrated for velocity and displacement using a time step of 0.005s.

$$a = -g + \frac{F_b}{m} + \frac{F_d}{m} \qquad (1).$$

For the computation of drag force, the cross-sectional area facing the fluid was estimated as the combined area of the subject's feet. The value of the drag coefficient was taken to be the same as a skydiver falling feet first with a closed chute [1]. By implementing these parameters, velocity of the falling body was then used to calculate drag force.

To determine buoyant force, the vertical displacement of the falling body was used to calculate the volume of displaced water, which was estimated based on a geometric representation of a body developed by Hanavan [2]. Anthropometric dimensions were used to model components of lower limbs and torso as either an ellipsoid or conical frustrum. From the displaced volume calculations, buoyant force was then computed.

Results and Discussion

The described method was conducted for a fifty-percentile male falling from a total height of five feet (1.52 m), measured from the ground to the bottom of the subject's feet. Water depths were tested from one foot (0.30 m) to four feet (1.22 m), in one-foot increments. The simulation output revealed a 19.4% decrease in maximum velocity attained between depths of one foot to four feet (Fig. 1).

A threshold velocity for various lower extremity injuries can be determined based on injury tolerances from literature. Funk et al. reports a 50% risk of injury to the foot/ankle complex for an 8.3 kN blunt axial force [3]. Estimating an 88 millisecond time interval of impact [4], the terminal velocity needed to achieve this force (for a fifty-percentile male) is calculated to be 9.9 m/s. With the highest output velocity of 5.13 m/s for the simulated water depth of 1 foot, the simulation suggests low injury risk of the foot/ankle complex for all presented simulation conditions.

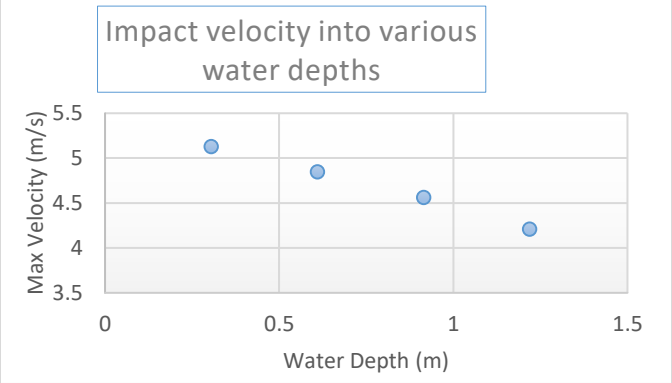

Figure 1: Impact velocity for 1.52 m total fall height into water

Significance

The proposed simulation allows for modification of fall conditions and anthropometric characteristics. The ability to readily conduct analyses for multiple parameters can be used to create safer water pits and obstacles through the evaluation of lower extremity impact velocities and forces.

With OCRs growing in popularity, recent steps have been taken to create safety standards for obstacle implementation. Recently, the World OCR has released guidelines that involve consultation with a qualified medical planner, risk accessor, and engineer [5]. Our simulation could be applied as a standardizing tool by qualified personnel to evaluate obstacle designs and to prepare the level of required medical personnel. Beyond OCRs, the flexibility to change input parameters allow this simulation to be used to model and assess injury risk in other activities such as cliff and splash diving. This analysis is currently limited to feet first, perpendicular water entry; however, future models will include oblique and head first entry to expand applications to platform and swim start diving.

References

[1] OpenStax College Physics, "Drag Forces," *College Physics*, 23-Jan-2012.
[2] A. Seireg and R. Arvikar, *Biomechanical Analysis of Musculoskeletal Structure for Medicine and Sports*. United States of America: Hemisphere Publishing Corporation, 1989.
[3] J. R. Funk *et al.*, "The Axial Injury Tolerance of the Human Foot/Ankle Complex and the Effect of Achilles Tension," *Journal of Biomechanical Engineering*, vol. 124, no. 6
[4] P. Devita and W. A. Skelly, "Effect of landing stiffness on joint kinetics and energetics in the lower extremity:," *Medicine & Science in Sports & Exercise*.
[5] World OCR, "Safety in OCR," *World OCR*, 05-Feb-2020.

Prophylactic Ankle Braces Did Not Elict Changes Associated with Injury or Compromise Performance in Sports Specific Movements

Christian N. Sanchez[1], and Jeffery D. Eggleston[1]
[1]Department of Kinesiology, The University of Texas, El Paso, TX, USA
Email: cnsanchez4@miners.utep.edu

Introduction

Previous research has demonstrated limiting sagittal plane ankle range of motion, such as with a prophylactic ankle brace, causes increased frontal plane knee moments while performing various jumping tasks followed by a secondary movement [1]. Limitting ankle range of motion (ROM) during a landing task increases knee adductor moments which is associated with increased risk of injury during various sporting events [2]. Performing a secondary movement upon landing, such as a countermovement jump (CMJ), may also be associated with increased injury risk [3,4,5]. Currently, frontal plane knee angle and moment have not been quantified at intial peak ground reaction force (vGRF) upon landing followed by a secondary task. The purpose of this study is to examine frontal plane knee angle and moment at peak vGRF, and jump height while performing a jumping task followed by a secondary movement under braced and non-braced conditions to assess injury risk. It is hypothesized that vGRF, frontal plane knee moment and angle would increase while jump height would be decreased in the braced condition.

Methods

3 healthy adults (1 female, 2 males, 23.67±2.08 years of age; 1.70±0.06m; 73.3±3.02 kg) were recruited for participation in this study. Participants performed three standing broad jumps followed by a maximal effort countermovement jump upon landing with and without wearing non-rigid Ankle Stabilizing Orthosis (ASO) braces. During the jumps, simultaneous three-dimensional lower extremity kinematic (200 Hz, Vicon Nexus Ltd., Oxford, UK) and kinetic data (1000 Hz, Advanced Mechanical Technology, Inc. Watertown, MA, USA) were obtained. Raw trajectory and force data were exported to Visual 3D for processing where digital low-pass Butterworth filters were applied (12 and 50 Hz, respectively). Variables of interest include frontal plane knee angle and frontal plane knee moment at vGRF, vGRF, and jump height. Kinetic data were normalized to participants' body mass for comparison. Jump height was computed through the impulse-momentum relationship. A two (limb; left/right) by two (condition; braced/non-braced) analysis of variance (α=0.05) was used to test for statistical significance for each variable. If an interaction was detected, dependent *t*-tests (α=0.05) were used for both unilateral comparisions between conditions and between-condition comparisons. If no interaction was detected, limb and condition main effects were examined after applying the Sidak adjustment. A dependent *t*-test (α=0.05) was used to test for statistical significance for vGRF and jump height between conditions.

Results and Discussion

Frontal plane knee angle did not have a significant interaction ($F(1,8)=0.01$, $p=0.923$, $\eta^2 = 0.00$) or condition or limb main effect (p=0.297 and p=0.661, respectively). Frontal plane knee moment did not have a significant interation ($F(1, 8)=0.40$, p =0.545, η^2 = 0.05) or condition or limb main effect (p =0.896 and p=0.379) (**Figure 1**). Vertical jump height and peak vGRF were not statistically different between conditions (p=0.459 and p=0.562 respectivley). A lack of statistically significant differences indicates that performing braced standing broad jumps followed by a maximal effort countermovement jump may have no adverse effects on knee landing mechanics or jump performance between conditions, as observed in previous literature [1].

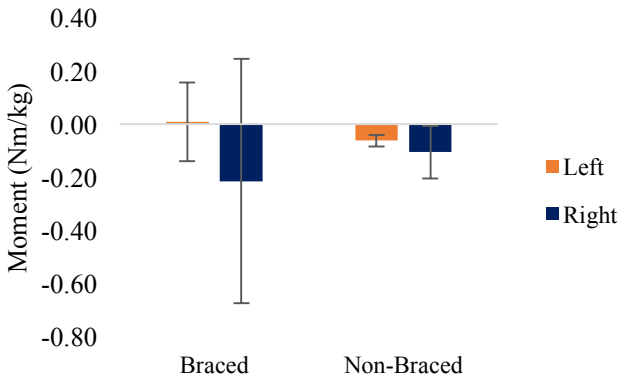

Figure 1: Frontal plane knee moment at peak vGRF during braced and non-braced conditions. Positve knee moment = abduction.

Results indicate that performing a jumping task (broad jump), immediately followed by a secondary movement (CMJ), upon landing while wearing prophylactic ankle braces did not elict changes in frontal plane knee angles or moments, vGRF, or jump height in healthy individuals. This may suggest risk of injury is not elevated when performing a secondary movement upon landing. Additionally, vertical jump height was not significantly different between conditions, suggesting performance was not compromised during braced jumping. Thus, use of ankle braces may provide additional support for the individual without increasing forces on the knee and hindering performance. Specifically, during activities that require various jumping tasks succeeded by secondary task; such as a broad jump immediately followed by a maximal countermovement jump upon landing.

Significance

The effects of restricted ankle ROM on the knee during specific athletic movements are currently unknown. This study contributes to the literature of how the knee may be affected when performing subsequent jump-landing tasks while wearing ankle braces that mimic sport-specific movements during game situations. Understanding jumping and landing mechanics while wearing prophylactic ankle braces may allow individuals to confidently wear them during sporting events without fear of increased injury risk or decreased performance.

References

[1] West et al. (2014) *S J Med Sci Sports,* **24**: 958-963
[2] Sinsurin et al. (2017) *E J Sports Sci,* **17(6)**: 699-709
[3] Farve et al. (2016) *A J Sports Med,* **44(6)**: 1540-1546
[4] Nordin & Dufek. (2019) *R Quart Ex & Sport,* **90(2)**: 190-205
[5] Harry et al. (2018) *J Stre & Condi Researh,* **32(7)**: 1937-1947

EFFECTS OF 15-MINUTE DYNAMIC WARM-UP PROGRAM ON HAMSTRINGS MUSCLE STRENGTH, FLEXIBILITY, STIFFNESS, AND JUMP PERFORMANCE IN HIGH SCHOOL BASKETBALL ATHLETES

Takashi Nagai[1], Nathaniel A. Bates[1], April L. McPherson[2], Rena F. Hale[1], Jun Zhou[3], Alessandro Navacchia[4], Ryo Ueno[1], Luca Rigamonti[1], Timothy E. Hewett[5], Nathan D. Schilaty[1]
[1]Mayo Clinic, USA; [2]United States Olympic & Paralympic Committee, USA; [3]The First Affiliated Hospital of Soochow University, China; [4]Smith & Nephew, USA; [5]Sparta Science, Rocky Mountain Consortium for Sports Research, USA
Email: nagai.takashi@mayo.edu

Introduction

Hamstrings muscle strains (HSMS) are a common musculoskeletal condition for basketball players with high rates of re-injury [1]. Risk factors such as weaker hamstrings (HAM) muscular strength and low flexibility (range-of-motion: ROM) can be mitigated by implementation of targeted dynamic warm-up programs during team practice sessions [2,3]. Recently, additional factors such as ultrasound-based shear wave elastography (SWE) stiffness have been explored [4]. Dynamic warm-up programs for prevention of HSMS commonly consist of eccentric hamstring resistance exercise, balance/core/hip exercise, sprinting/jumping techniques, and active/dynamic stretching [5]. Basketball coaches and players are interested in how such warm-up programs could influence their jump height performance. Therefore, the purpose of this study was to examine the effects of a targeted neuromuscular dynamic warm-up program on HAM muscle strength, ROM, SWE stiffness, and jump performance in high school basketball athletes.

Methods

A total of 31 high school basketball athletes with no recent musculoskeletal injuries (11 females / 20 males, Age: 15.5±1.4years, HT: 176.8±11.3cm, WT: 75.7±22.5kg) from the same high school participated in the study. Pre- and post-intervention tests were conducted at school. For the quadriceps (QUAD) strength testing, subjects sat on a table with the knee flexed to 75°. For HAM strength testing, subjects were prone on a table with the knee flexed to 30°. Subjects were asked to push as hard as they could against a hand-held dynamometer for 3 seconds. Peak force was recorded in kilograms and normalized to their body weight for analyses. Strength ratio of HAM over QUAD (H/Q) was analysed. ROM was recorded using a digital inclinometer (placed on the shaft of the tibia) during passive ROM clinical tests (straight leg raise: SLR and knee extension: KE). For SWE stiffness, the first examiner scanned the biceps femoris while subjects were supine with their hip stabilized at 90° and the second examiner stretched subject's lower leg at 60% and 40% of the maximum KE ROM values. For jump performance, subjects placed their hands akimbo and performed a maximum countermovement jump (CMJ) and drop vertical jump (DVJ) from a 31-cm box onto a force plate. For both jump types, jump height was calculated based on flight time. For all variables, an average of three trials was used for analyses. Descriptive statistics and paired t-tests (or Wilcoxon tests) were used for statistical analyses ($P<0.05$).

An investigator-led dynamic warm-up program was performed twice a week throughout the season (total: 14 wks/28 sessions). Warm-up sessions were 15 minutes in duration at the beginning of practice. It consisted of dynamic stretching (2min), skipping/hopping/jumping exercises in each direction (2min), eccentric Nordic hamstring exercise x 10 rep), balance/hip/core exercises (3min), stretching (3min), and sprinting (3min).

Results and Discussion

Strength and ROM significantly increased after the intervention ($P=0.001$-0.008; **Table 1**). Significance was not seen in SWE stiffness and jump performance ($P=0.100$-0.845).

Table 1. Descriptive statistics and effects of intervention on strength, ROM, SWE stiffness, and jump height performance.

Strength (%BW)	PRE	POST	P
HAM Left	32.3 (7.0)	51.3 (12.4)	0.001
HAM Right	34.0 (8.5)	39.2 (8.6)	0.001
QUAD Left	58.1 (17.2)	72.3 (19.1)	0.002
QUAD Right	58.6 (17.0)	63.0 (15.6)	0.001
H/Q Ratio Left (%)	57.6 (10.8)	73.0 (14.3)	0.001
H/Q Ratio Right (%)	60.0 (12.4)	63.2 (7.3)	0.092
ROM (°)	PRE	POST	P
SLR Left	71.3 (10.1)	73.9 (10.7)	0.008
SLR Right	68.3 (9.8)	71.6 (10.5)	0.001
KE Left	50.9 (7.3)	53.8 (8.1)	0.005
KE Right	52.7 (8.0)	58.1 (8.8)	0.001
SWE (kPa)	PRE	POST	P
SWE 60% Left	69.5 (33.7)	65.0 (38.4)	0.845
SWE 60% Right	83.2 (37.1)	75.2 (36.0)	0.159
SWE 40% Left	70.1 (32.9)	57.6 (29.2)	0.100
SWE 40% Right	63.2 (33.5)	59.8 (29.7)	0.845
Jump Height (cm)	PRE	POST	P
CMJ	29.9 (7.3)	30.3 (6.5)	0.430
DVJ	35.8 (10.1)	34.0 (6.9)	0.109

Significance

Although a lack of control group is a major limitation in the study, the current findings confirm the effectiveness of a simple 15-minute dynamic warm-up on key risk factors of HSMS. There is a trend of less SWE stiffness after intervention; however, clinical significance is not yet known. Prospective studies should follow to examine if such a program could reduce incidence and severity of HSMS.

Acknowledgments

Funding from the NBA & GE Healthcare Orthopedics and Sports Medicine Collaboration.

References

[1] Borowski LA, et al. 2008. AJSM. 2328-2335p.
[2] Witvrouw E, 2003. AJSM. 41-46p.
[3] Orchard J, et al. 1997. AJSM. 81-85p.
[4] McPherson AL, et al. 2020. Skeletal Radiol. In Press.
[5] Al Attar WS, et al. 2017. Sports Med. 907-916p

Impactor Geometry May Obscure The Blunt Impact Performance of a Commuter Bicycle Helmet

Mark Jesunathadas[1], Elizabeth D. Edwards[1], Tiffany L. Landry[1], Trenton E. Gould[1], Thomas A. Plaisted[2], and Scott G. Piland[1]
[1]School of Kinesiology and Nutrition, The University of Southern Mississippi, Hattiesburg, MS, USA
[2]CCDC Army Research Laboratory, Weapons and Materials Research Division, Aberdeen Proving Ground, MD, USA
Email: mark.jesunathadas@usm.edu

Introduction

Blunt impact test methods are an important tool used to examine the ability of helmets to reduce head rotational acceleration and subsequently the risk for brain injury due to blunt force trauma. However, some studies have reported that angular acceleration of the headform can be greater with than without a helmet [1]. Such results are contradictory to those of others [2] and may be influenced by impactor geometry. Thus, the purpose of this study was to investigate the difference in angular acceleration of an anthropomorphic test device (ATD) headform with and without an urban bicycle helmet using a small and large radius impactor. We hypothesized that a larger radius impactor would result in angular accelerations that at some impact locations were greater during blunt impacts with a helmet than without one, but this effect would not be present with a smaller radius impactor.

Methods

A pneumatic linear impactor was used to impact a male 50% Hybrid III head and neck ATD (Humanetics, Huron, OH) outfitted with a nine accelerometer array package [3] at 3 locations (front boss, left side, and rear) at 4 m/s. The bare headform was impacted 6 times at each location with both an impactor that had a small (29.9 mm) and large (127 mm) radius convex impact surface. Both impactors were of similar configuration to that described by ND-081 [4]. Twelve commuter bicycle helmets (CM-1, Retrospec, CA) were also impacted once at each location with a large (n = 6) and small (n=6) radius impactor. Acceleration signals were resolved into peak resultant angular acceleration (PAA) [3]. High-speed video of the impacts (3000 fps; Phantom- V611; Vision Research, NJ) were recorded and used for qualitative analysis (Cineviewer v. 3.3, Vision Research, NJ). A 2 x 2 x 3 (Impactor, Helmet, Location) repeated measures ANOVA was used to make comparisons within groups. Simple effects analyses were used to explain interaction effects. Independent samples t-test were used to compare PAA between the barehead and helmeted condition at each location–impactor condition (SPSS v. 25.0, IBM, NY). We used a modified Bonferroni adjustment to correct the α-level of 0.05 for multiple comparisons ($\alpha = 0.01$). Values are presented as mean ± 1 SD.

Results and Discussion

Highspeed video analysis revealed that for impacts to the front boss location of the bareheadform the large radius impactor made contact with its lower portion. For all other conditions the apex of the impactors made contact with the headform.

A significant interaction between Impactor, Helmet and Location was observed ($p = 0.001$). Simple effects analyses indicated that the small radius impactor had greater PAA values for the barehead condition than the large radius impactor at the front boss ($p < 0.001$) and rear impact locations ($p < 0.001$), but not at the left side impact location ($p = 0.125$).

For impacts with the small radius impactor PAA was less for the helmeted compared to barehead conditions at all locations ($p < 0.001$). For impacts with the large radius impactor PAA was less for the helmeted compared to barehead condition at the front boss ($p < 0.001$) and left side locations ($p < 0.001$). However, for the large radius impactor condition PAA was greater for the helmeted compared to the barehead condition at the rear location ($p = 0.001$). See Figure 1.

These results are similar to Rousseau et al. [1], which showed PAA values were greater in helmeted compared to bare conditions for a subset of helmets and impact locations. The results also support of our hypothesis as we observed that impactor head radius altered whether PAA was greater in the helmeted or barehead condition. This seemed to occur because the smaller radius impactor typically increased the PAA of the barehead condition. However, the reason the large radius impactor produced lower PAA in the barehead than helmeted conditions remains unclear. It is possible such findings are the result of the headform used, which is more rigid than a human head. Future work should explore the influence of headform rigidity and the transfer of force from the impactor to the head as well as the potential for this effect to be observed on other kinematic measures associated with brain injury.

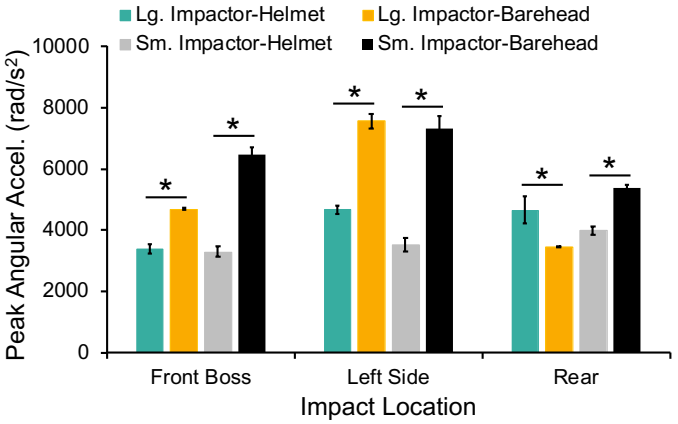

Figure 1: Peak resultant angular acceleration (PAA) for blunt impacts to the ATD headform at three locations. * Indicates significance difference between helmet and barehead condition.

Significance

Our results indicate that impactor geometry has a substantial influence on ATD headform rotational acceleration and should be considered when interpreting blunt impact test results as well as during the design of helmets.

Acknowledgments

This research was funding in part by the Department of Defense and U.S. Army Award #W911NF-18-2-0061.

References

[1] Rousseau et al. *J ASTM* 6, 2008
[2] McIntosh et al. *Traff Inj Prev* 14, 2014
[3] Padgaonkar et al. *J Appl Mech* 42, 1975
[4] NOCSAE Doc ND081-18am-19a

The Influence of Headform Pose on the Blunt Impact Performance of American Football Helmets

Mark Jesunathadas[1], Elizabeth D. Edwards[1], Tiffany L. Landry[1], Scott G. Piland[1], Trenton E. Gould[1], and Thomas A. Plaisted[2]
[1]School of Kinesiology and Nutrition, The University of Southern Mississippi, Hattiesburg, MS, USA
[2]CCDC Army Research Laboratory, Weapons and Materials Research Directorate, Aberdeen Proving Ground, MD, USA
Email: *mark.jesunathadas@usm.edu

Introduction

The position and orientation (pose) of an anthropomorphic test device (ATD) headform has been shown to influence its impact response[1]. However, no study has shown how the pose of the headform influences the impact performance of American football helmets, or if any effect is helmet specific. This is especially important as two main test methods; 1) National Operating Committee on Standards for Athletic Equipment (NOCSAE) method ND-081 and 2) the National Football Leauge (NFL) test protocol, are used to certify and set limits on the performance acceptability of football helmets for use in the NFL, but use different ATD poses [2, 3]. Becauses of differences in the relative location of the neck rotation joint, the poses set forth by NOCSAE put the ATD neck in a flexed position, whereas the NFL protocol often require lateral bending of the neck. Therefore, the purpose of this study was to evaluate the influence of the NOCSAE and NFL poses on the kinematic responses of an ATD donning modern football helmets during blunt impacts test performed at the NOCSAE prescribed locations.

Methods

Two Xenith Shadow and X2E+ (Xenith, Detroit, MI) American football helmets were fit to a medium NOCSAE head attached to a male 50% Hybrid III neck (Humanetics, Huron, OH) outfitted with a nine accelerometer array package [4]. Each helmet was impacted at 6 m/s using a pneumatic linear impactor. Helmets were impacted 4 times at side, rear boss centric (RBCG), rear boss non-centric (RBNC), rear, front boss (FB), and front locations [2]. One set of Shadow and X2E+ helmets were impacted with ATD pose set according to the NOCSAE method, while the other set was impacted with the ATD pose set according to the NFL method. Note, for all impacts the impact location was the same. Acceleration signals were resolved into peak resultant linear and angular accelerations (PLA and PAA) and peak resultant angular velocity (PAV). For each measure the difference between the NOCSAE and NFL methods (NOCSAE – NFL) was calculated. Statistical analyses were performed on these difference scores (dPLA, dPAA, and dPAV). A 2 x 6 (Helmet x Location) repeated measures ANOVA was used to make comparison within groups. Simple effects analyses were used to explain interaction effects (SPSS v. 25.0, IBM, NY). Significance was set at an α-level of 0.05. Values are presented as mean (95% CI) unless otherwise specified. Difference scores whose 95% CI include the zero value indicate no statistical difference exists between the NOCSAE and NFL poses.

Results and Discussion

A significant interaction between Helmet and Location was observed for each dependent variable ($p < 0.001$; $\eta^2 \geq 0.64$). A main effect for helmet was also observed for dPLA ($p < 0.001$; $\eta^2 = 0.92$) and dPAV ($p = 0.004$; $\eta^2 = 0.766$), but not for dPAA ($p = 0.221$; $\eta^2 = 0.24$). Mean difference scores for the dependent variables are reported in Table 1.

Table 1. dPLA, dPAA, and dPAV mean difference scores for each impact location for the X2E+ and Shadow Xenith helmets. * Indicates values in which the 95% CI did not include the zero value.

Loc.	dPLA (g)		dPAA (rad/s²)		dPAV (rad/s)	
	X2E+	Shdw.	X2E+	Shdw.	X2E+	Shdw.
Side	13.0*	18.1*	237*	520*	-2.9*	-2.4*
RBCG	11.1*	-3.4	249	425	-6.5*	-5.3*
RBNC	16.5*	0.8	737*	224	-2.5*	1.2*
Rear	19.0*	-14.5*	424*	-1355*	-6.0*	-5.5*
FB	9.7*	-0.3	718	1561*	2.8*	-8.9*
Front	0.4	-2.8	524*	160	2.5*	1.0

Averaged across impact locations mean dPLA was 11.6 g (9.10 – 14.1 g) for the X2E+, but was 0.34 g (-2.83 – 2.16 g) for the Shadow. At all locations except for the front location dPLA for the X2E+ helmet was greater than zero. However, for the Shadow dPLA was 18.1 g (12.0 – 24.3 g) for the side location, but was -14.5 g (-19.8 – -9.1g) for the rear location. At all other locations dPLA for the Shadow included the zero value.

Averaged across impact locations dPAA was 482 rad/s² (196– 767 rad/s²) for the X2E+, but was 256 rad/s² (-30 – 542 rad/s²) for the Shadow. At the side, RBNC, and rear locations dPAA for the X2E+ was greater than zero. Similarly, at the side and FB locations dPAA was greater than zero, but at the rear location dPAA was -1355 rad/s² (-1611 – -1098 rad/s²) for the Shadow.

In contrast to acceleration values dPAV averaged across impact locations was -2.1 rad/s (-2.6 – -1.6 rad/s) for the X2E+ and was -3.3 rad/s (-3.8 – -2.8 rad/s) for the Shadow. Furthermore, at the side, RBCG, and rear locations both the X2E+ and Shadow helmets dPAV values were below zero.

These results indicate that despite identical impact locations the pose of a headform influences its kinematic response, but differently depending on the model of football helmet worn and location of impact. Furthermore, it seems that while acceleration responses tend to be greater for the NOCSAE style pose, angular velocity was typically greater for the NFL style pose.

Significance

ATD pose is a critical factor in assessing a helmet's ability to manage blunt impact forces and how its performance compares to other helmets. Furthermore, the results highlight the need for ATD pose to be reported in manuscripts and standards.

Acknowledgments

This research was funded in part by the Department of Defense and U.S. Army Award #W911NF-18-2-0061.

References

[1] Walsh et al. *Sports Eng* 13, 2011
[2] NOCSAE ND-081-18am-19a, 2019
[3] Biocore, Helmet Test Protocol, Sept, 2019
[4] Padgaonkar et al. *J Appl Mech* 42, 1975

Loading Asymmetry Before and After Metatarsal Stress Fracture: A Case Study

Ryan S. Alcantara[1] & Alena M. Grabowski[1]
[1]University of Colorado, Boulder, CO, USA
Email: ryan.alcantara@colorado.edu

Introduction

Metatarsal stress fractures are a running-related overuse injury that comprise 23% of all stress fractures affecting collegiate cross country athletes [1]. Stress fracture recovery can take several months, often preventing an athlete from training or competing. Determing biomechanical changes that precede an injury like metatarsal stress fractures could inform coaches and athletes of an increased injury risk.

Previous research suggests that runners with a history of metatarsal stress fractures have similar peak vertical ground reaction forces (vGRFs) as those without a history of injury, but a causal relationship between peak vGRF and metatarsal stress fractures in runners is lacking [2]. A history of running-related overuse injuries may be associated with increased vertical loading rate, but to our knowledge, no prospective work has established an association between increased loading rate and metatarsal stress fractures in runners [3]. We measured peak vGRF and loading rate for each leg over the freshman year of collegiate running during which an athlete sustained a metatarsal stress fracture.

Methods

Data from one male athlete (18 yrs, 75 kg, 1.85 m) were analysed for this case study. The athlete ran on a force-measuring treadmill (Treadmetrix, Park City, UT) at 3 speeds (3.8, 4.1, 5.4 m/s) for 30 seconds each during the fall, winter, and spring competition seasons. The athlete was diagnosed with a Grade 3 bone stress injury of the 2nd metatarsal between winter and spring data collections. The fall data collection was 20 weeks prior to injury, winter data collection was 3 weeks prior to injury, and spring data collection was 11 weeks after injury.

Kinetic data were filtered using a lowpass zero-lag 4th order Butterworth filter with a 14 Hz cutoff. We analyzed the final 10 sec of each trial and used a 30 N threshold to determine stance phase. The athlete was a habitual forefoot strike runner. Peak vGRF was calculated as the maximum value during stance phase. We calculated loading rate as the average slope of vGRF versus time from 10-20% of stance phase because no transient impact peak was visually present.

We calculated the percentage difference in peak vGRF and loading rate for the injured and uninjured leg (Fig. 1). A positive percentage difference indicates a greater magnitude of the given variable for the athlete's injured leg.

Results and Discussion

We observed similar trends across speeds and report the results for the fastest speed (5.4 m/s). We found that the percentage difference between the injured and uninjured leg changed over time for peak vGRF and loading rate (Fig. 1). Peak vGRF of the injured leg was 2.2-3.7% greater than the uninjured leg prior to injury. However, the difference between peak vGRF of the injured and uninjured leg was only 0.6% 11 weeks after metatarsal stress injury (Fig. 1). In addition to these changes in peak vGRF asymmetry, peak vGRF values for the injured and uninjured leg increased 0.2 and 0.3 BW from 3 weeks prior to injury to 11 weeks after injury. Between step variation in peak vGRF was qualitatively similar between legs over the year.

The loading rate of the injured leg was 2.8% lower than the uninjured leg 20 weeks prior to injury, but 6.2% greater than the uninjured leg 3 weeks prior and 8.2% greater than the uninjured leg 11 weeks after metatarsal stress injury. In addition to changes in loading rate asymmetry, loading rate values for the injured and uninjured leg increased 4.7 and 3.2 BW/s from 3 weeks prior to injury to 11 weeks after injury. Between-step variability in loading rate was qualitatively similar for the injured and uninjured leg at 3 weeks prior to injury and 11 weeks after injury, but differed at 20 weeks prior to injury.

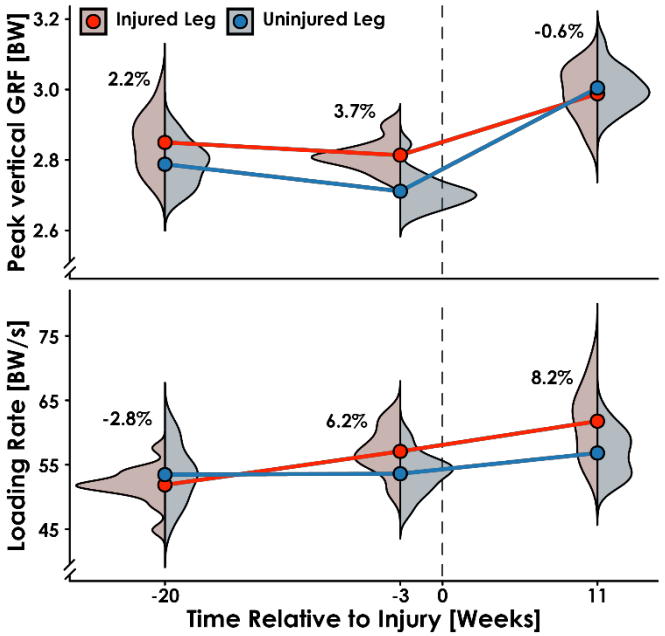

Figure 1. Peak vertical ground reaction force (GRF) and loading rate for the injured and uninjured leg across three data collection sessions. Violin plots illustrate the distribution of values across steps, colored dots represent the mean, with percentage differences between the injured and uninjured leg annotated.

Significance

These preliminary findings suggest peak vGRF asymmetry may differ before and after a metatarsal stress fracture, but it is unclear if loading rate is associated with prospective metatarsal stress fractures. This work provides insight into changes in asymmetry and between-step variability before and after sustaining a metatarsal stress fracture. Future work is planned to quantify how leg-specific external loading metrics predict running-related overuse injuries.

Acknowledgments

Supported by the PAC12 Student-Athlete Health and Well-being Grant Program (#3-03_PAC-12-Oregon-Hahn-17-02).

References

1. Rizzone, K., et al. *J. Athl Training* **52** (10), 966-75, 2017.
2. Bischof, J., et al. *Gait Posture* **31** (4), 502-5, 2010.
3. Hreljac, A., et al. *Med Sci Sport Ex* **32** (9), 1635-41, 2000.

Analysis of a Combat Helmet in a Head-to-Ground Impact Scenario

Ryan J. Neice[1,2], Alex J. Lurski[1,2], Eric D. Wetzel[1], and Thomas A. Plaisted[1]
[1]CCDC Army Research Laboratory, Weapons and Materials Research Directorate, Aberdeen Proving Ground, MD, USA
[2]Oak Ridge Associated Universities, Oak Ridge, TN, USA
Email: ryan.j.neice.ctr@mail.mil

Introduction

Army paratroopers have historically experienced traumatic brain injuries (TBI) at a rate significantly greater than the general soldier population [1]. Paratroopers are particularly vulnerable to posterior helmet-to-ground impact during parachute landing falls. Additionally, helmet-to-ground impacts are a significant risk in recreational football [2]. The purpose of this study was to evaluate head kinematics occurring in a simulated backfall experiment and assess the ability of a standardized rotation-inducing impact method (pneumatic ram) to reproduce the severity of measured backfall head kinematics.

Methods

In the first series of tests, a simulated backfall impact was performed with a Hybrid III anthropomorphic test device (ATD). The ATD torso, arms, neck and head were rigidly attached to pendulum swing arm that falls to ground due to gravity. A 57.5 lb ballast mass was added to the pelvic region of the swing arm to represent the mass of the lower torso. Impact occurs onto a stack of foam and rubber materials that mimic the impulse delivered by an athletic turf field [3]. Head kinematics were measured with 3 linear accelerometers and 3 angular rate sensors.

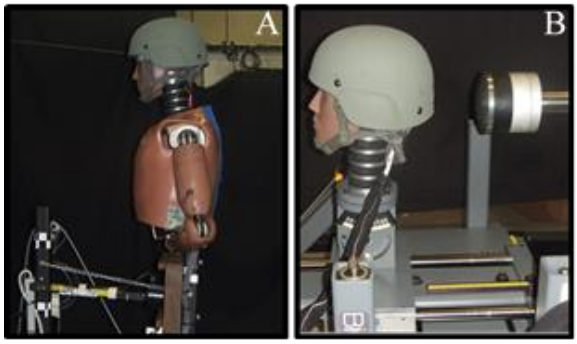

Figure 1: Backfall (A) and pneumatic ram (B) impact setups.

The second series of tests used a Biokinetics pneumatic ram (linear impactor) to determine whether this method could reproduce the severity of head kinematics observed in the backfall test. The pneumatic ram with NOCSAE impact tip was used to impact a Hybrid III neck and head with a nine accelerometer array package. The headform orientation with respect to ground, just prior to impact, was translated from the backfall test to the pneumatic ram setup. Impacts were performed at velocities equal to and greater than the impact velocity observed in the backfall test. A recently developed head kinematic assessment metric that rapidly estimates maximum principal strain (MPS) of brain tissue, DAMAGE, was used to compare the relative severity of each impact [4].

Results and Discussion

The backfall experiment produces severe head kinematics from a combination of intertial and impact loading, illustrated in Figure 2. The headform experiences peak angular velocity as it contacts the ground followed by a change in velocity of 65 rad/s in less than 10 milliseconds as it rebounds from impact. The whipping motion of the head during the backfall test format leads to an increased severity of rotational head kinematics.

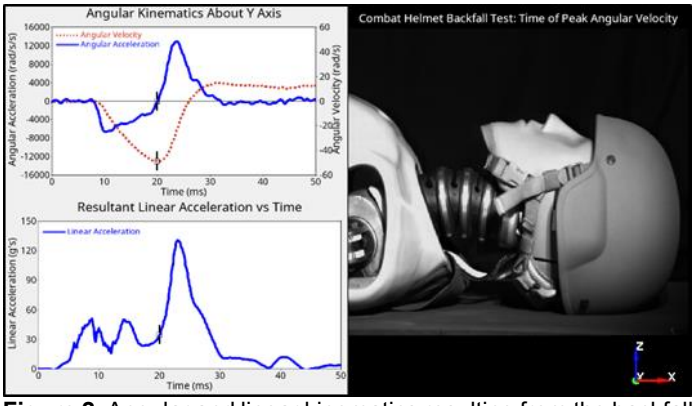

Figure 2: Angular and linear kinematics resulting from the backfall test using a Hybrid III head-neck-torso fitted with a combat helmet.

Measurement	Pneumatic Ram			Backfall
Helmet Impact Velocity (ft/s)	21.9	25.4	29.4	22.0
Peak Linear Acceleration (Res) (g)	152	227	241	132
Peak Angular Acceleration (Y) (rad/s/s)	5,205	5,249	5,973	12,948
Peak Angular Velocity (Y) (rad/s)	36.8	45.3	45.8	49.9
DAMAGE (Predicted Brain MPS)	0.32	0.42	0.43	0.58

Table 1: Results from backfall and pneumatic ram experiments.

In contrast, the pneumatic ram method did not capture the inertial loading of the head-neck that occurs in a backfall test as the torso impacts. Moreover, the peak angular head kinematics in the pneumatic ram format did not reach the same levels as in in the backfall test even as impact velocity was increased (Table 1).

Significance

Head-to-ground impact is a significant source of TBI in the military as well as among athletes. Standardized impact testing methods like the pneumatic ram format, used to certify professional and collegiate football helmets, effectively measure head kinematics resulting from combined linear and rotational loading scenarios. However the pneumatic ram format was not able to replicate the severity of head kinematics or DAMAGE assessment as observed in the backfall test, suggesting a complimentary test specific to head-to-ground impacts may have value in the helmet testing community.

Acknowledgments

The authors acknowledge PEO Soldier Technical Management Division for supporting this research. This project was supported in part by Oak Ridge Associated Universities (ORAU) for ARL through Cooperative Agreement (CA) W911NF-16-2-0008.

References

[1] Ivins et al. *J Traum. 55(4)*, 617-21, 2003
[2] Kent at al. *J Biomechanics, 99*, 2020
[3] Gardner et al. *J Sports Eng. Tech.* 232(9), 197-207, 2018
[4] Gabler et al. *Ann. Biomed. Eng. 47(9)*, 1971-1981, 2019

Kinematic Response of Different Head-Helmet Interface Friction Conditions

Shayne York.[1], Elizabeth D. Edwards[1], Mark Jesunathadas[1], Tiffany Landry[1], Scott G. Piland[1], Trenton E. Gould[1], and Thomas A. Plaisted[2]

[1]School of Kinesiology and Nutrition, The University of Southern Mississippi, Hattiesburg, MS, USA

[2]CCDC Army Research Laboratory, Weapons and Materials Research Directorate, Aberdeen Proving Ground, MD, USA

Email : Shayne.York@usm.edu

Introduction

The purpose of this study was to investigate the influence of friction at the head-helmet pad interface on the rotational kinematic responses of an anthropomorphic test device (ATD) headform when fitted with advanced combat helmets (ACH) with a standard issue foam pad suspension system. We hypothesised that lower head-helmet pad interface friction conditions would illicit lower magnitude angular kinematic responses.

Methods

Five head-helmet pad friction conditions (Polytetrafluoroethylene; PTFE, human hair wig, bald, skullcap, and hook and loop) were used for impact testing on 2 new ACHs. The coefficient of static friction (μ_s) for each condition was determined using the incline plane method [1]. Helmets were fitted to a 50% male hybrid III head and neck (Humanetics, Huron, OH) instrumented with a nine accelerometer array [2] and impacted four times at 7 locations (crown, front, rear, left side, right side, left nape, and right nape) on a pneumatic linear impactor at 14 ft/s [3]. Acceleration signals were resolved to determine peak angular acceleration (PAA), peak angular velocity (PAV) as well as to compute the DAMAGE metric [4]. Separate 5 × 7 (friction condition × location) repeated measures ANOVAs were used to make comparisons within groups (SPSS v25, IBM, NY) for each dependent variable. A Huynh-Feldt adjustment was used when sphericity was violated. Simple effects analyses were used to explain interaction effects. Significance set at α-level of 0.05.

Results and Discussion

The μ_s for each condition is shown in Table 1. Rotational kinematic responses and DAMAGE measure for each condition are reported in Table 2.

Coefficient of Static Friction (μ_s)				
PTFE	Human Hair	Bald	Skullcap	Hook
0.15	0.7	1.38	2.68	∞

Table 1: Average μ_s for each material measured on the incline plane.

An interaction effect was found for friction condition × location for PAA ($p < 0.001$). Significant differences were found between friction conditions at crown ($p = 0.012$) front ($p = 0.006$), rear ($p < 0.001$), and right side ($p < 0.001$). Pairwise comparisons revealed that greater PAA values were not always associated with greater μ_s values. However, at the front location hook resulted in significantly higher PAA compared to wig and PTFE ($p < 0.027$).

An interaction effect was found for friction condition × location for PAV ($p < 0.001$). Significant differences were found for friction condition at all locations. The hook condition was found to have the lowest PAV for all locations but a clear response pattern was not observed for the other friction conditions and locations.

An interaction effect was also found for friction condition × location for DAMAGE ($p < 0.001$). Significant differences were found for friction conditions at all locations. Similar to the PAV results a clear response pattern was not observed for PAV across the friction conditions and locations.

Our hypothesis was not supported. Rotational kinematic responses and DAMAGE varied by location and μ_s, but lower friction conditions did not typically result in lower kinematic or DAMAGE responses.

Significance

Variation in μ_s of the head-helmet pad interface for impacts representative of collisions found in sport did not consistently result in lower magnitude kinematic responses.

Acknowledgments

This research was funded in part by the Department of Defense and U.S. Army Award #W911NF-18-2-0061.

References

[1] ASTM G219-18

[2] Padgaonkar et al. *J. Appl. Mech.*, *42*(3), 552–556, 1975

[3] AR/PD 10-2 with Revision A

[4] Gabler et al. *Ann. Biomed. Eng. 47(9),* 1971-1981, 2018

	Angular Acceleration (rads/s^2)					Angular Velocity (rads/s)					DAMAGE				
	PTFE	Wig	Bald	Skullcap	Hook	PTFE	Wig	Bald	Skullcap	Hook	PTFE	Wig	Bald	Skullcap	Hook
Crown	896	1068	906	1183	879	3	4	2	3	2	0.03	0.05	0.03	0.03	0.02
Front	4195	4099	4457	4475	4801	27	27	27	28	27	0.18	0.18	0.16	0.18	0.16
Rear	2430	2931	2867	2827	2725	31	32	31	32	29	0.27	0.28	0.30	0.30	0.26
LSide	4979	5084	5014	5202	5521	22	21	22	22	21	0.17	0.16	0.15	0.16	0.16
RSide	5185	4814	5153	5139	5972	22	22	23	24	21	0.16	0.16	0.15	0.15	0.16
LNape	4849	5049	4593	4846	5235	26	25	25	25	24	0.21	0.22	0.19	0.19	0.20
RNape	4832	4721	4814	4789	4904	26	27	25	27	25	0.22	0.23	0.21	0.22	0.22

Table 2: Mean angular acceleration, angular velocity, and DAMAGE for each head-helmet pad μ_s condition at each impact location.

Dorsiflexion shoes affect landing mechanics related to lower extremity injury risk

Gina L. Garcia[1]*, Mia Caminita[1], Jessica G. Hunter[1], Ross H. Miller[1], Hyun Joon Kwon[1], Jae Kun Shim[1]
[1]Department of Kinesiology, University of Maryland, College Park, MD, USA
Email: *glgarcia@terpmail.umd.edu

Introduction

Traditional athletic footwear is designed with the heel elevated above the forefoot, putting the ankle in a plantarflexed position (positive drop). Conversely, research suggests that elevating the forefoot above the heel (negative drop), could take advantage of musculotendinous structures in the calf to improve jump height (1). It is unknown, though, if dorsiflexion shoes (negative drop) also affect landing mechanics related to lower extremity injury risk, particularly patellofemoral pain (PFP) and anterior cruciate ligament (ACL) injury which are two of the most common and debilitating injuries experienced in jumping sports (2).

The purpose of this study was to investigate if shoes that vary in midsole drop (negative [NEG], neutral [NTRL], positive [POS]) affect kinetics and kinematics related to lower extremity injury risk during landing. We hypothesized that NEG will illicit jump-landing mechanics associated with PFP and ACL injury compared to NTRL and POS. Decreasing the available ankle dorsiflexion range of motion (ROM) will have a cascading effect on proximal joint ROM, energy absorption, and joint loading. Specifically, peak knee valgus, peak knee abduction moment (KAM), and peak impact forces will be greater in NEG, and sagittal joint displacement and total eccentric work will be less in NEG compared to NTRL and POS.

Methods

Three trials of maximum effort vertical countermovement jumps were performed by 16 females in shoes with negative, neutral, and positive drops (-1.5°, 0°, and 8° respectively) (Figure 1). Kinematic data of the center of mass and at the joint level were collected using a 13-camera motion capture system (VICON, Centennial, CO). Two embedded force plates recorded 3-dimensional GRF data (Kistler, Amherst, NY). A custom Visual3D script (C-Motion, Inc, Germantown, MD) was used for analysis. One-way repeated measures ANOVAs with correction for sphericity determined the main effect. Post-hoc Tukey contracts with a Bonferroni correction assessed differences between conditions. A critical α of 0.01 determined significance.

Figure 1: A lateral view of the three shoe conditions. From the left; NEG, NTRL, and POS. Red lines indicate approximate midsole drops.

Results and Discussion

Peak impact force was similar between shoe conditions. However, shoe condition did affect total eccentric work, where NTRL resulted in significantly less eccentric work than POS. There were no effects of shoe condition on both KAM or knee valgus. Eccentric ankle work was greater in NTRL compared to POS, while knee work was greater in POS compared to both NEG and NTRL. Knee flexion displacement during landing was significantly greater in POS compared to NEG and NTRL, due to greater peak knee flexion in POS (Table 1).

Table 1. Mean ± SD and *p*-value for total (T), ankle (A), knee (K), and hip (H) eccentric work and joint displacement during landing.

	NEG	NTRL	POS	*p*
Eccentric Work (J/kg)				
T	-1.89± 0.51	-1.85± 0.46	-2.02± 0.53	0.029[b]
A	-0.54± 0.27	-0.57± 0.28	-0.47± 0.23	0.005[b]
K	-1.24± 0.44	-1.14± 0.42	-1.42± 0.47	<0.001[ab]
H	-0.11± 0.12	-0.14± 0.17	-0.13± 0.14	0.27
Joint displacement (deg)				
A	60.39± 10.02	58.91± 11.31	58.91± 9.53	0.486
K	-59.57± 12.90	-58.94± 12.72	-63.54± 14.32	0.001[ab]
H	35.79± 14.48	35.5± 14.85	35.49± 14.23	0.963

[a] Significant difference between NEG-POS ($p < 0.05$)
[b] Significant difference between NTRL-POS ($p < 0.05$)

We hypothesized that the dorsiflexion induced by NEG would pose a greater risk for PFP and ACL injury by limiting sagittal joint displacement and energy absorption, which was supported by our results. The greater energy absorption in POS, quantified as eccentric work, was primarily driven by greater knee joint work and peak knee flexion. Peak knee flexion ROM, an active form of impact dissipation, can be used to identify stiff landings (3). Small knee flexion ROM during stiff landings increases the strain on passive joint structures, especially the patellofemoral ligament and ACL, to absorb impact. This and can increase injury risk for athletes whose sport involves repeated jumping (2).

However, our results did not support our hypothesis that knee valgus, knee abduction, and peak impact forces would be greater in NEG. Landing on a negatively sloped surface of -3.6° has previously been shown to increase knee valgus and impact forces, suggesting midsole drops greater than -1.5° are needed to affect knee valgus and external loads (4).

Significance

To our knowledge, this is the first study to examine if dorsiflexion shoes affect landing mechanics related to PFP and ACL injury. We found an immediate effect of of shoe drop on knee joint flexion, joint-level eccentric work, and total eccentric work. These are variables associated with increased strain on ligaments in the knee, but in the absence of increased peak KAM, peak knee valgus, and peak impact forces, athletes can be moderately confident that dorsiflexion shoes with drops of -1.5° or less do not increase risk of knee injury. However, caution is advised if using shoes with greater degress of dorsiflexion as research has yet to determine their effect on injury-related landing mechanics.

Acknowledgments

This research was funded in part by the Korea Institute of Machinery and Materials (KIMM) in 2018 and the University of Maryland's Department of Kinesiology Graduate Student Research Initiative Fund.

References

1. Larkins C, Snabb TE. Clin Biomech. 1999;14(5):321–8.
2. Weiss K, Whatman C. Sport Med. 2015;45(9):1325–37.
3. Leppänen M et al.. Am J Sports Med. 2017;45(2):386–93.
4. Hagins M et al.. Clin Biomech. 2007;22(9):1030–6.

Evaluating Limb Stiffness and Local Dynamic Stability in Cutting and Landing Movements of Female Athletes

Jacob Larson[1], Michael Zabala[1],
[1]Department of Mechanical Engineering, Auburn University, Auburn, AL, USA
Email: jsl0043@auburn.edu

Introduction

It is well established that the risk of anterior cruciate ligament (ACL) reinjury is higher than the initial risk of injury [1]. Additionally, several studies have suggested that high limb asymmetry increases the risk of injury [5]. A previous internal study found that the combined left and right legged local dynamic stability (LDS) of global knee adduction during a repetitive vertical jump was able to effectively identify previously injured subjects when compared to uninjured subjects using a logistic regression, with a receiver operating characteristic (ROC) = 0.8036 [2]. As this study is a continuation of a previous study investigating local dynamic stability, the goal of this experiment was to compare results from the vertical jump tests to cutting and dynamic landing movements, with the hypothesis that limb stability would differ for cutting and landing movements between injured and uninjured subjects.

Methods

This study collected the biomechanics of fourteen female D1 soccer, D1 basketball, and club soccer athletes from Auburn University (height = 171.2 ± 8.9 cm, weight = 66.3 ± 8.6 kg, age = 19.8 ± 1.9 yr). The two main metrics in this study are local dynamic stability and maximum limb stiffness during a trial. Local dynamic stability was calculated using the Rosenstein method [3], and limb stiffness was calculated as the change in virtual leg length divided by the resultant ground reaction force [4]. The Limb Symmetry Index (LSI) of these metrics was analyzed using the following formulation:

$$LSI = \left(\frac{Max(Llimb, Rlimb) - Min(Llimb, Rlimb)}{Llimb + Rlimb} \right) * 100\%$$

Participants were screened into two groups: the first having undergone ACL reconstruction in the past two years, and the second for having no previous history of ACL reconstruction. All subjects were active members of their respective sport who were cleared to participate in their sport at the time of testing. All subjects signed informed consent forms approved by the Auburn University Internal Review Board.

Results

Table 1 shows that the symmetry index of limb stiffness during a landing error scoring system (LESS) jump has a strong and highly significant correlation with the sagittal plane stability of the hip and ankle joints. Additionally, there is a highly significant correlation between the LSI in the right and left limb during a run to cut (RTC) movement.

Discussion

There are several conclusions to be drawn from the results shown in Table 1, namely that local dynamic stability of the hip and ankle are strongly correlated with high limb stiffness symmetry during a landing event. This indicates that individuals with a high limb stiffness symmetry also have high stability in the sagittal plane. This conclusion may be tempered due to how much motion occurs in the sagittal plane during a LESS jump, and this relationship should be further explored during vertical drop landing and single-leg landings in future studies.

The second conclusion which can be drawn from Table 1 is that high limb stiffness symmetry during the RTC indicates a decreased local dynamic stability in ankle inversion. This finding is especially interesting, as it suggests that highly symmetric limb stiffnesses could result in lower dynamic stability during a cutting motion. As most studies find that limb symmetry is beneficial to subject health, and high dynamic stability indicates that a subject has a high degree of control over their motion, this finding seems to conflict with both pieces of information. The explanation behind this correlation is currently unclear to the authors, but the finding should be explored further in future studies.

Table 1. Bivariate correlation between symmetry indices and combined local dynamic stability

		LDS Hip Flexion	LDS Ankle Flexion	LDS Ankle Inversion
LSI LESS	r	**0.5892***	**0.6464***	-0.3085
	P	**0.0266**	**0.0125**	0.2832
LSI RTC	r	0.1703	-0.3569	**-0.6988****
	P	0.5604	0.2103	**0.0043**

** Significance of p<0.01
* Significance of p<0.05

Significance

This research is important to the field of biomechanics because there is much to learn about local dynamic stability, which is seen especially in the correlation between high LSI and low LDS in the ankle. If high LSI and high LDS indicate good subject health, then the negative correlation between these two metrics is one that needs to be reconciled in future studies. Additionally, if this study can further explore correlations between commonly used metrics and local dynamic stability, it will be easier to implement local dynamic stability measures into future research, as well as make the concept of local dynamic stability more easily comprehended to athletes, researchers, and clinicians alike.

References

[1] Wright R et al. (2007) *Am. J. Sports Med.* 35 (7):1131-1135
[2] Larson J, et al. *Annual Meeting of ISB 2019*
[3] Rosenstein, M. et al. (1993) *Physica D.* 65 (1-2): 117-134
[4] Lorimer, A, et al. (2018) *PeerJ.* 6, e5845
[5] Schmitt, L, et al. (2014) *Med. Sci. Sports Exerc.* 47(7)

Mechanical Stimulation as a Non-invasive Tool for Monitoring Meniscus Tear

Mohsen Safaei[1], Daniel C Whittingslow[2], Nicholas B Bolus[2], Hyeon-Ki Jeong[1], and Omer T Inan[1,2]
[1]School of Electrical and Computer Engineering, Georgia Institute of Technology, Atlanta, GA 30308, USA
[2] Department of Biomedical Engineering, Georgia Institute of Technology, Atlanta, GA 30308, USA
Email: msafaei@gatech.edu

Introduction

Disorders and musculoskeletal injuries affecting the knee are common and limit activity in athletes and the eldery [1]. Current technologies used to diagnose knee problems such as computed tomoghraphy and magnetic resonance imaging are limited to clinical environments. Studying the vibratory behavior of the knee when subjected to an external stimulation can reveal information regarding the structure of the joint. Researchers have investigated the vibration characteristics of various parts of the human body such as the skull [2], arm [3], and hip [4]. In this work, vibration transmission through the human knee is used as a tool to determine the presence of meniscus tear in the joint.

Methods

Six fresh frozen cadaver legs with an initial tear on the lateral meniscus were used in this study. The legs were placed on an adjustable frame at a flexion angle of 30˚ and fixed with two Velcro bands. The setup consisted of a permanent magnet shaker (LDS V201, Brüel & Kjær, Nærum, Denmark) equipped with a load cell (Honneywell model 31, Honeywell International Inc., Charlotte, NC) and an impedance head sensor (8001, Brüel & Kjær, Nærum, Denmark) at the driving point. Two accelerometers (3225F, Dytran Instruments Inc., Chatsworth, CA) were placed medial and lateral to the patella proximal to the knee joint. The experimental setup is shown in Figure 1. A frequency-sweep sine excitation signal with frequencies from 100 Hz to 4200 Hz and a total length of 180 sec was sent to the shaker, and the transmitted vibration through the joint was recorded using the two accelerometers. Measurements were carried out at three stages: initial (baseline), after sham surgery, and after a simulated medial meniscus tear. For the sham stage, a 3-cm cut was made just anterior to the medial collateral ligament to expose the medial meniscus. The frequency response function (FRF) of the accelerometers with respect to the input acceleration was calculated and compared for all the legs. Student's t-test was used to determine statistical differences in the measured vibration data between different stages of the tests for all the legs.

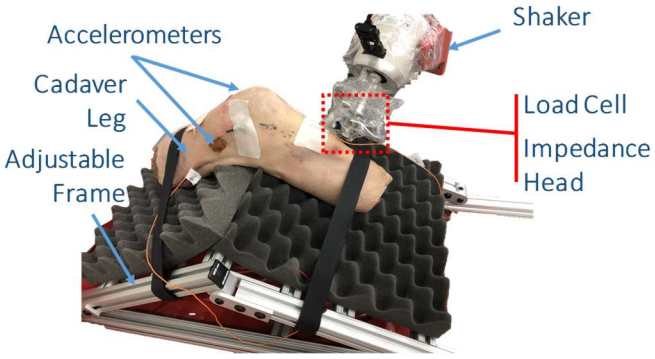

Figure 1. Knee joint vibration stimulation setup.

Results and Discussion

Initial investigation of FRF diagrams revealed a noticeable change in the magnitude of FRF amongst samples at the frequency ranges of 2.8 to 3.2 kHz and 2.2 to 2.6 kHz for the medial and lateral accelerometers, respectively. To measure the differences in FRF results, the root-mean-square deviation (RMSD) values of FRF quantities for the meniscus tear case and the sham case with respect to the initial case were calculated. Results for the six legs are presented in Figure 2. Across-specimen mean values of 0.11 and 0.22 were obtained for the sham and meniscus tear, respectively. The meniscus tear demonstrates a significantly higher RMSD compared to the sham with a p-value < 0.01. The results show that altering the structure of the knee joint by cutting the meniscus results in a significant change in the vibration transmission through the joint. However, the changes are only traceble in specific frequency ranges. Similar behavior has been previously observed in studing the vibration transmission in knee implants with loosening [5].

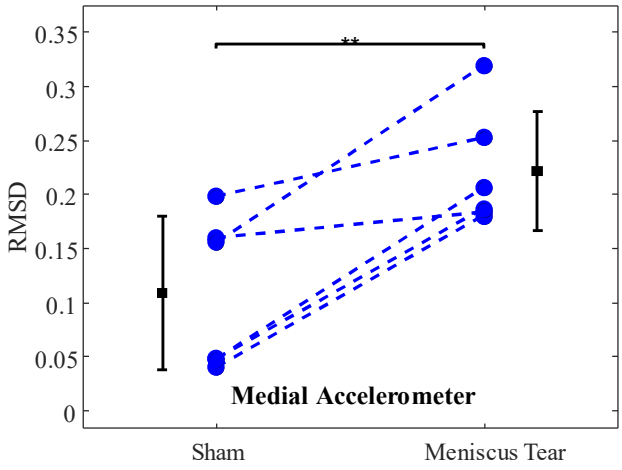

Figure 2. RMSD values for the sham and mesniscus tear stages with respect to the initial stage (** indicates p < 0.01).

Significance

This work demonstrates the promising potential of external vibration stimulation as a noninvasive method of monitoring the structural health of the knee joint. Given the available technologies for miniature vibration actuators, the vibration technique can be used to develop wearable devices capable of tracking joint health outside of clinical settings. In addition, such a measurement system can reduce the cost and inconvenience of current diagnostic technologies.

Acknowledgments

This work was supported by the NSF / NIH Smart and Connected Health Program under Grant No. 1R01EB023808.

References

[1] DK White et al., Arthritis. Care. Res. **66** (9), 1328 (2014).
[2] M Eeg-Olofsson et al., Int. J. Audiol. **47** (12), 761 (2008).
[3] AJ Besa et al., Int. J. Ind. Ergon. **37** (3), 225 (2007).
[4] N Conza et al., J. Biomech. **40** (7), 1599 (2007).
[5] A Arami et al., Ann. Biomed. Eng. **46** (1), 97 (2018).

Kinematic Evaluation of Return-to-Play Hop Tests in a Healthy Population

Kimi D. Dahl[1], Jacqueline N. Foody[1], Sarah A. Wilson[1], Grant J. Dornan[1], Matthew T. Provencher[1], and Scott Tashman[1]
[1] Steadman Philippon Research Institute, Vail, CO, USA
Email: stashman@sprivail.org

Introduction

While return-to-play (RTP) testing is standard practice after ACL reconstruction, there is debate on which tests and criteria to use for effectively assessing an athlete's readiness for safe return to sport [1]. Hop tests remain a standard part of RTP testing batteries. However, passing scores are based only on side-to-side discrepancies in performance (e.g., differences in jump distance); the quality of the movement is rarely assessed. [3] The purpose of this study was to determine the extent of kinematic asymmetry in a healthy population performing standard, RTP hop tests and secondarily to determine the reliability of kinematic measurements from trial to trial.

Methods

Thirty-five healthy adults (28±5yrs; 72.4±11.4kg; 1.75±0.08m; 14 female) were recruited for this study. Participants were pain-free, without any lower extremity or back injury that affected their movement. This study was approved by an IRB, and all participants provided informed consent. Trunk and lower extremity kinematics were captured using eight wearable inertial measurement unit (IMU) sensors (128Hz, APDM). Participants performed three trials of standard-of-care RTP tests, including a single-leg triple hop and a single-leg triple crossover hop for both legs. Consistent with standard test scoring, the trial with the maximum distance achieved from three attempts was used to evaluate asymmetry [2] in the landing phase of the middle hop, and comparisons were made between the dominant and nondominant legs for each test. Correlations and side-to-side difference (SSD) for initial and maximum flexion at both the knee and hip joint were compared. For SSD, legs were considered asymmetric if the measured differences were >10%.

Results and Discussion

The maximum jump distance occurred on the final trial for 57% of participants for the triple hop on both dominant and nondominant limbs. For the crossover, this was 57% on the dominant and 60% on the nondominant limb. This shows a learning effect that may need to be taken into consideration for patient populations.

For both the triple hop and the crossover hop, healthy volunteers had nearly identical maximum hop distances on both the dominant and nondominant legs. However, for both hop tests, a pattern of high kinematic dissimilarity was seen in initial and max flexion at the hip and knee joints. While the max distance jumped on the dominant leg was strongly correlated with that of the nondominant leg (rho=0.96, p<0.001), this correlation was substantially less when assessing kinematic variables (Figure 1). Even though there was dissimilarity between dominant and nondominant legs, there was moderate to good agreement in the reliability of the measurements within a participant between trials for each leg (Table 1). However, the poor symmetry of kinematic variables in this healthy population suggest these measures a) are not the correct metrics to evaluate or b) are not being acquired and identified reliably. In particular, values found at initial landing may be susceptible to variance due to identifying landing timing based only on IMU accelerometer spikes.

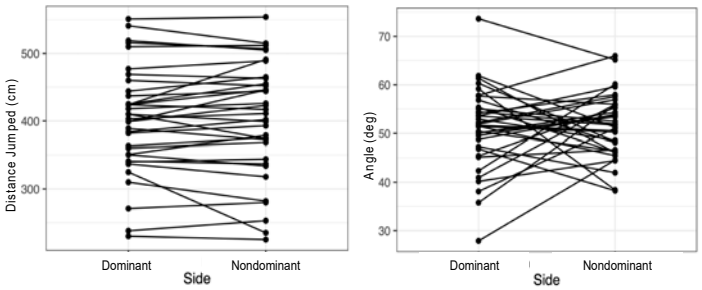

Figure 1: Comparision of dominant to nondominant leg similarity for distance jumped (left) and max knee flexion (right) for the triple jump.

Table 1. Reliability for variables in both hops (ICC [95% CI])

	Limb	Triple Hop	Crossover Hop
Distance Jumped	Dominant	0.94 [0.90-0.96]	0.92 [0.83-0.95]
	Nondominant	0.94 [0.88-0.97]	0.96 [0.93-0.97]
Initial Knee Flexion	Dominant	0.80 [0.68-0.88]	0.81 [0.70-0.89]
	Nondominant	0.77 [0.57-0.88]	0.77 [0.65-0.90]
Initial Hip Flexion	Dominant	0.84 [0.75-0.90]	0.88 [0.78-0.93]
	Nondominant	0.76 [0.61-0.86]	0.83 [0.64-0.90]
Max Knee Flexion	Dominant	0.61 [0.40-0.78]	0.72 [0.57-0.84]
	Nondominant	0.69 [0.55-0.80]	0.66 [0.52-0.80]
Max Hip Flexion	Dominant	0.83 [0.74-0.89]	0.85 [0.75-0.90]
	Nondominant	0.79 [0.58-0.89]	0.83 [0.66-0.89]

Lastly, SSD in initial knee flexion corresponded to SSD in initial hip flexion for both the triple (r=0.58, p<0.001) and crossover (r=0.50, p<0.01) hops. Asymmetry in max knee flexion corresponded to asymmetry in max hip flexion only in the triple hop (r=0.43, p<0.05). These results encourage the inclusion of exercises and tests that address asymmetry not only of the affected joint but also of the surrounding joints.

Significance

RTP testing efficacy has been debated in the literature for patients recovering from an ACL injury. However, the tests used and scoring systems remain largely unchanged. Simple symmetry assessments (e.g., jump distance) did not correlate with kinematic symmetry in a healthy population. Thus, basic movement evaluation may not provide information that is as valuable as clinicians may believe. Instead, this study supports the trend toward whole movement pattern evaluation such as Statistical Parametric Mapping to evaluate overall quality of movement. Furthermore, attention should be given to joints surrounding the injury to ensure additional asymmetries are not present.

Acknowledgments

Funding was received from the Office of Naval Research, Department of Defense.

References

[1] Gokeler, A et al, DOI: 10.1007/s00167-016-4246-3
[2] Kyritsis, P et al, DOI: 10.1136/bjsports-2015-095908
[3] Welling, W et al, DOI: 10.1007/s00167-018-4893-7

Do Power, Strength, and Lower Extremity Kinematics Correlate with Maximum Hop Distance in a Healthy Population?

Kimi D. Dahl[1], Jacqueline N. Foody[1], Sarah A. Wilson[1], Grant J. Dornan[1], Matthew T. Provencher[1], and Scott Tashman[1]
[1] Steadman Philippon Research Institute, Vail, CO, USA
Email: stashman@sprivail.org

Introduction

While return-to-play (RTP) testing is common after ACL reconstructions, there is debate on which tests and criteria to use [1] as well as whether the tests provide a good determination for the patient's readiness to return to sport. Hop tests and strength assessments remain a standard part of RTP testing batteries. However, passing scores are quantitative, and the quality of the movement is rarely assessed. [4] The goals of this study were to determine 1) if kinematic measures from standard RTP hop tests are correlated with maximum jump distance in a healthy population, and 2) if strength and maximum muscle power are correlated with maximum jump distance.

Methods

Thirty-five healthy adults (28±5yrs; 72.4±11.4kg; 1.75±0.08m; 14 female) were recruited for this study. Participants were pain-free, without any lower extremity or back injury that affected their movement. This study was approved by an IRB, and all participants provided informed consent. Trunk and lower extremity kinematics were captured using eight wearable inertial measurement unit (IMU) sensors (128Hz, APDM).

A power test was performed on a leg press machine (Keiser AIR300) with separate foot plates for comparisons between limbs. A hand-held dynamometer was used to measure isokinetic knee extension strength on each leg. Participants also performed three trials of indoor, standard-of-care RTP tests, including a single-leg triple hop and a single-leg triple crossover hop for both legs. Per standard clinical guidelines, [2] a passing score was defined as a maximum dominant versus nondominant limb difference in hop distance of <10%, and consistent with standard test scoring, [3] kinematics were extracted from the trial with the maximum distance achieved from three attempts. Spearman's Rho correlations were made between this, the maximum power output, and the sum of three isometric knee extension repetitions. Correlations were also made between distance jumped and the kinematic variables of initial and max flexion of the hip and knee joints during the landing phase of the middle hop.

Results and Discussion

Based on the 10% asymmetry criterion, three participants (8%) failed the triple hop while eleven failed the crossover hop (31%). In a healthy population, it is expected that most, if not all, of the participants would pass; the high failure rate in crossover hop indicates that a passing score indicating a high degree of limb-to-limb symmetry may poorly represent "normal" function and may not be an ideal measure for readiness to return to play.

For both the dominant and nondominant legs, maximum power and the sum of isometric knee extensions were correlated with maximum distance jumped for both hops (Table 1). While it is not surprising that greater strength and power correlate with a larger hop distance, it does bring into question whether total distance jumped, and the capacity to execute it within 10% of the uninjured leg, are appropriate criteria on their own to clear athletes for return to sport. Instead, since strength and power are moderately correlated with jump distance, RTP tests could *remove* one of these components and add a task that would focus on movement quality. This may allow for diversity in movement strategy to be analyzed and potentially corrected.

There were no strong correlations between knee joint kinematics and maximum hop distance achieved. However, for the triple jump, maximum hip flexion was moderately correlated with jump distance ($r=0.19$, $p<0.05$). For the crossover hop, initial and max hip flexion were moderately correlated with distance jumped on the dominant side ($r=0.19$, $p<0.05$ and $r=0.20$, $p<0.05$, respectively). For the nondominant leg, only max hip flexion was correlated with jump distance ($r=0.21$, $p<0.05$). These results suggest that jumping technique at the hip may be a factor when completing RTP tests. Thus, it may be advantageous to include exercises and tests in physical therapy that address asymmetry not only of the affected joint but also of the surrounding joints Within the same jump for each hop test, initial and max knee flexion were highly correlated for both the dominant and nondominant legs. The same was true for initial and max hip flexion.

Table 1. Spearman's Rho correlation between maximum hop distance and same-side maximum power and isometric knee extension strength.

	Limb	R-statistic Max Power	R-statistic Isometric Extension
Triple Hop Distance	Dominant	0.72 ($p<0.001$)	0.58 ($p<0.001$)
	Nondominant	0.78 ($p<0.001$)	0.58 ($p<0.001$)
Crossover Hop Distance	Dominant	0.64 ($p<0.001$)	0.47 ($p<0.01$)
	Nondominant	0.74 ($p<0.001$)	0.60 ($p<0.001$)

In conclusion, power, strength, and hip kinematics are factors associated with jump distance on RTP hop tests. Within a jump, the total range of motion at the hip and knee joint depends on the initial joint flexion at landing.

Significance

Standard single-leg hop RTP tests are scored on distance symmetry and do not incorporate a kinematic analysis. This study shows that a diversity of kinematic patterns may be employed to pass standard RTP tests. Based on the correlations seen for strength and power, an ACLR patient could use brute force to pass their test, while risk factors in their kinematic pattern at the knee and hip joints could go unnoticed. This study adds to the growing body of literature supporting a more comprehensive approach for determining when a patient is ready to return to sport, using criteria that goes beyond achieving an external pass/fail score and instead looks at the quality of the kinematic movement.

Acknowledgments

Funding was received from the Office of Naval Research, Department of Defense.

References

[1] Gokeler, A et al, DOI: 10.1007/s00167-016-4246-3
[2] Juris P et al, DOI: 10.2519/jospt.1997.26.4.184
[3] Kyritsis, P et al, DOI: 10.1136/bjsports-2015-095908
[4] Welling, W et al, DOI: 10.1007/s00167-018-4893-7

The effect of landing coordination and amputation on high limb loading during bilateral landings

Sarah C Moudy[1,2*], Neale A Tillin[1], Amy R Sibley[1,3], Siobhan Strike[1]
[1]University of Roehampton, London, UK, [2]University of North Texas Health Science Center, Fort Worth, TX, USA, [3]London South Bank University, London, UK, *Email: sarah.moudy@unthsc.edu

Introduction

High impact forces when landing from a jump are thought to be associated with an increased risk of injury [1]. Previous research has suggested that in-phase flexion coordination strategies and increased trunk flexion may be important for mediating forces upon landing [2]. For individuals with unilateral transtibial amputations (ITTAs), ankle joint mechanics and lower-limb coordination strategies are disrupted in the affected limb [3]. The ankle joint is believed to be crucial for attenuating load such that reduced ankle dorsiflexion has been associated with increases in peak vertical ground reaction force (vGRF). As such, ITTAs are discouraged from participating in sports involving jumping. However, it is unclear how the altered affected limb mechanics may effect the landing coordination by the intact limb. There is limited research to suggest that the intact limb experiences a greater load when landing and thereafter is at a greater risk of injury compared to able-bodied controls. **Thus, the purpose of this study was to examine differences in joint coordination and trunk angles between those who experience high versus low load and if the landing strategy is affected by amputation.**

Methods

8 recreationally-active ITTAs and 21 controls hung from a custom hanging bar frame with their heels 30 cm off the ground. Bilateral drop landings were performed with each foot landing on a separate force platform. vGRF was time-normalized to 100% from touchdown to maximal knee flexion in the intact limb or dominant control limb (i.e. absorption phase). Ankle, knee, hip, and trunk flexion angles were extracted and coupling angles (θ) were calculated for ankle-knee, knee-hip, and hip-ankle joint pairs using the following equation:

$$\theta_t = tan^{-1}\left(\frac{Y_{t+1} - Y_t}{X_{t+1} - X_t}\right)$$

where t = time, Y = distal joint angular position, and X = the proximal joint angular position. The average θ value from touchdown to peak vGRF was used in further analysis. Trunk flexion range of motion (ROM) was calculated as the maximum change during the absorption phase. Lastly, the duration of the absorption phase was calculated in seconds.

ITTA and control participants were treated as a single cohort to identify high versus low loaders based on peak vGRF. A 10% threshold around mean peak vGRF was used to identify groups. 3 control participants were within this threshold, identified as a middle group, and removed from further analysis.

Statistical analysis: Independent t-tests were performed between loading groups for each joint pair, trunk flexion, and absorption duration. Hedge's g effect sizes were calculated and interpreted as ≥0.2 = small, ≥0.5 = medium, and ≥0.8 = large.

Results and Discussion

Identification of high and low loaders was confirmed with significant and large effects for peak vGRF (Table 1) suggesting comparisons were made on divergent groups. Low loaders landed with a significantly longer absorption duration (Table 1). Coordination strategies found both groups performed in-phase flexion (Figure 1) with low loaders performing greater flexion in the distal segments (i.e. ankle and knee) and greater trunk flexion. While not all comparisons were significant, medium to large effects were found (Table 1). Results suggest that reduced load can be achieved through increasing the time to attenuate load by increasing trunk flexion and ankle and knee flexion.

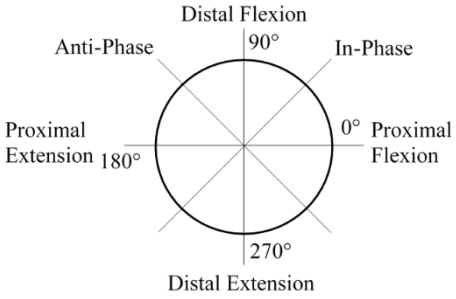

Figure 1. Interpretation of coupling angle values

ITTAs and controls were represented equivalently in both loading groups suggesting that increased vGRF is not dependent on the presence of an amputation rather on landing coordination.

Significance

The results suggest that 1) ITTAs can adapt their intact limb mechanics similar to an able-bodied control, which is consistent with previous research [4] and 2) high limb loading is dependent on landing coordination rather than amputation. Further, it is possible that the intact limb of ITTAs is not at any greater risk of injury than able-bodied controls.

References

[1] Aerts et al. 2013. *Sports Med Phys Fitness*. 53(5): 509-519.
[2] Blackburn & Padua 2008. *Clin Biomech.* 23(3): 313-319.
[3] Schoeman et al. 2013. *J Rehabil Res Dev.* 50(10).
[4] Moudy et al. 2019. *J Appl Biomech.* 27:1-9

Table 1. High and low loading group characteristics based on peak vGRF and differences in joint mechanics of the intact or dominant control limbs during bilateral drop landings. Data presented as mean ± SD.

	n of ITTAs	n of controls	Peak vGRF (N/kg)	Ankle-Knee θ (°)	Knee-Hip θ (°)	Hip-Ankle θ (°)	Trunk ROM (°)	Absorption Duration (s)
High Loaders	3	8	31.6 ± 4.9	52.8 ± 3.7	67.1 ± 1.9	67.6 ± 5.1	8.00 ± 4.4	0.12 ± 0.02
Low Loaders	5	10	17.1 ± 3.7	56.4 ± 6.9	70.8 ± 3.8	73.1 ± 10	12.4 ± 7.5	0.21 ± 0.08
p-value			<0.001	0.125	0.007	0.114	0.095	0.002
Hedge's g			3.31	0.61	1.00	0.63	0.67	1.36

θ = coupling angle coordination value; Hedge's g greater than 1 indicates that differences between groups are larger than 1 SD

Bilateral Asymmetry in Leg Stiffness During Dynamic Activities

William Taylor[1], Abigail Jacobs[1], Jacob Larson[1], Michael Zabala[1]
[1]Department of Mechanical Engineering, Auburn University, Auburn, AL, USA
Email: wat0011@auburn.edu

Introduction

Many of the injuries sustained by athletes in contact sports are preventable soft tissue injuries which occur during deceleration and change of direction movements, such as cutting or landing [1]. Leg stiffness is important to understanding deceleration during these events because an individual's leg stiffness determines the response to generated ground reaction forces in dynamic movement. This study aimed to provide pilot data on tests that involved cutting and landing movements and to identify whether stiffness differences existed between an injured and uninjured population in either movement. A difference in the bilateral limb stiffness between injured and uninjured subjects was expected.

Methods

This study retrospectively reviewed the kinematics of run-to-cut (RTC) and Landing Error Scoring System (LESS) jumps from fourteen female subjects who participated in D1 soccer, D1 basketball, or club soccer teams from Auburn University. To participate in the study, all subjects had to be cleared to participate in their respective sport. Out of the 14 athletes, two had previous bilateral ACL injuries, two had previous unilateral ACL injuries, 3 had other previous surgically repaired knee injuries, and 7 did not have any previous knee injuries. Each subject signed informed consent forms approved by the Auburn University Internal Review Board. Leg stiffness was defined as the resultant vertical ground reaction force divided by the change in the distance between the calculated hip joint center of the leg and the center of pressure of the foot during contact with an AMTI force plate [2]. Paired *t*-tests were used to compare right to left and injured vs uninjured legs.

Results

The *t*-tests showed that the left leg was more stiff than the right leg for all subjects performing the LESS jump, and that the left leg was more stiff than the right in RTC for every subject but one. Data from these tests is shown in Figures 1 and 2. Results did not show significant differences between previously injured and uninjured legs.

Discussion

This study identified a significant difference in bilateral leg stiffness in both LESS and RTC tasks but did not identify any significant difference between injured and uninjured populations. These findings contradict the initial hypothesis and the results of a previous study that found a significant difference in bilateral leg stiffness between injured and uninjured professional Australian football players [3]. The differences in results could be attributed to a different selection in dynamic movement, less specific injury classification, and a small sample size. These issues could be addressed in future studies by comparing affected and unaffected limbs and testing further subjects.

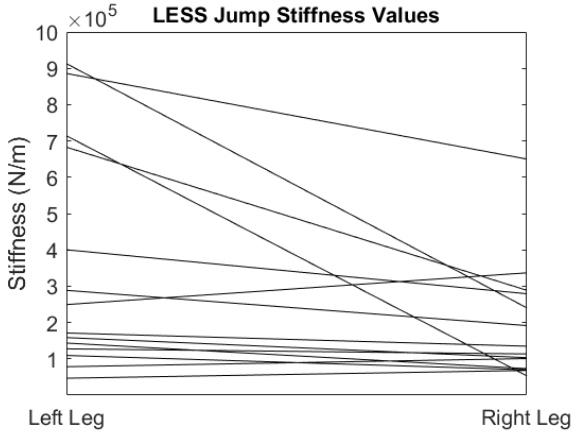

Figure 1: Difference in Stiffness Values for the Left and Right Legs in LESS trial (Mean Difference = 1.81×10^5 N/m; p=0.0278)

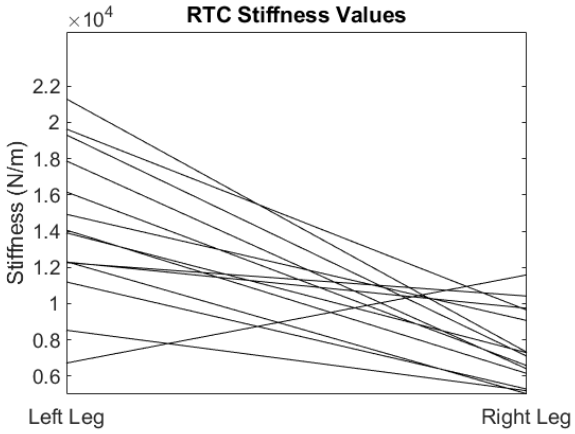

Figure 2: Difference in Stiffness Values for the Left and Right Legs in a RTC Trial (Mean Difference = 7.39×10^3 N/m; p=0.0002)

Significance

This is important to the field of biomechanics because the results in this study contradict those of another and bring up a discussion about whether bilateral limb stiffness is a reliable indicator of injury. This study expected that bilateral limb stiffness would be different for injured and uninjured. However, it did not find that to be the case. Future studies should further investigate the difference in bilateral limb stiffness for injured and uninjured populations performing various movements, and thus determine whether differences in bilateral limb stiffness is indicative of injury.

References

[1] Padua DA, 2018; 53(1):5-19. *J Athletic Training*
[2] Stafilidis S & Arampatzis A, 2007; 25(13):1479-1490. *J. Sports Science*
[3] Elizabeth C. Pruyn 2012; 30(1): 71-78. *J. of Sports Science*

Relationship Between Clinical Assessments of Health and Fitness and Field-Based Physical Fitness Tests in Reserve Officer Training Corps (ROTC) Cadets

Lukas Krumpl[1], Nickolai J. P. Martonick[1], Youngmin Chun[1], Ann F. Brown[1], and Joshua P. Bailey[1]
[1]Department of Movement Sciences, University of Idaho, Moscow, ID, USA
Email: *lkrumpl@uidaho.edu

Introduction

Reserve Officer Training Corps (ROTC) cadets regularly participate in physical training (PF) and physical fitness tests (PFT). PFT are field-based tests evaluate multiple cadets at the same time using minimal equipment, providing scores used by the United States military as an approach to injury prevention [4]. However, the current field-based tests lack the ability to deliver accurate assessments of fitness or predict the likelihood of injury [4]. Meanwhile, clinical assessments of physical health and fitness are considered to be more reliable and valid [4]. The prevalence of lower extremity (LE) injuries with cadets has raised concerns about the efficiency of PT and PFT scores when it comes to injury prevention [1,2,3]. This concern led to a structural adaptation of the PFT in each of the branches. Therefore, the purpose of this study was to evaluate the relationship between traditional field-based PFT scores and clinical assessments of physical health and fitness.

Methods

The study was divided into two sessions. A total of 225 cadets from various ROTC branches were recruited for field assessments similar to the PFT *(Session 1)*. Participants completed a performance test consisting of 2-minute split lunge jumps, 2-minute up-down planks, and a shuttle run. The performance testing was scored by how many split-lunges or plank up-downs the participants completed within two minutes. The shuttle run was timed once and consisted of a back and forth sprinting pattern.

Twenty-eight cadets (*20 males:* 183cm (±5.3), 88.4kg (±12.6), 21.8yrs (± 3.4); & *8 females:* 167cm (±5.2), 59.6kg (± 7.4), 20.7 (± 1.8)) participated in additional clinical and laboratory tests *(Session 2)*. The branches represented were: Air Force (11 cadets), Army (4), Marines (5), & Navy (8). Participants completed a full-body Dual-Energy X-Ray Absorptiometry (DEXA) scan (Hologic, Marlborough, MA), a lower and upper quarter Y-Balance test, and isokinetic testing (CSMi, Stoughton, MA). The isokinetic testing involved five repetitions of bilateral knee flexion/extension (90 & 120°/sec), hip abduction/adduction (60 & 180°/s), and ankle plantar/dorsiflexion (60 & 120°/s). All data were recorded or extracted via Microsoft Excel and imported to MATLAB (MathWorks, Natick, MA) for further analysis. Following session 2, the most current PFT scores were collected from the respective cadre leadership. The PFT (branch specific) consisted of three exercises: push-ups (or pull-ups), sit-ups/curl-ups, and a 1-mile run (or 1.5-mile run).

Pearson product-moment correlation coefficient analyses were conducted to evaluate the relationship between PFT scores and clinical assessments. Statistical analyses were completed via SPSS version 25.0 (IBM, Armonk, NY).

Results and Discussion

The main finding of the present study was the overall weak relationship between clinical assessment scores and ROTC PFT scores. On average, neither Y-Balance, nor DEXA scans, or isokinetic strength test results yielded significant correlations between the three field-tests ($r < 0.5$). Both bone mineral density and lean mass also showed a weak correlation to PFT scores. Similarly, none of the isokinetic strength test results were found to be related to PFT scores. Nevertheless, a significant difference was found between right and left lean mass (kg), as well as relative knee extensor and flexor peak torque (Table 1).

Table 1
Right vs. Left Lower Extremity Differences (Mean & SD)

	Lean Mass (kg)	Extension PT 90°/s (Nm)	Flexion PT 90°/s (Nm)
Air Force	0.34 (± 0.33)†	0.75 (± 0.35)†	0.50 (± 0.22)†
Army	0.32 (± 0.35)	0.72 (± 0.24)†	0.49 (± 0.35)
Marines	0.31 (± 0.2)†	0.75 (± 0.11)†	0.71 (± 0.22)†
Navy	0.34 (± 0.19)†	0.82 (± 0.22)†	0.67 (± 0.32)†

† statistically significant difference ($p < 0.05$)
positive difference shows right LE values greater than left LE values

This finding suggests a discrepancy between the right and left LE and warrant further investigations, specifically regarding the injury rate within the ROTC population. Interestingly, while lean mass and isokinetic knee strength displayed a weak relationship ($r < 0.1$), fat mass and isokinetic knee strength had a moderately strong negative relationship ($r = -0.64$). This implies that the amount of fat mass may affect strength more than the amount of muscle mass.

Overall, the results indicate that clinical assessments are not promising predictors of performance in ROTC field-based physical fitness tests, yet may be useful as additional screening tool for injury prevention.

Significance

The weak relationship between PFT scores and clinical assessments suggests that field-based test scores, such as push-ups, sit-ups, pull-ups, or distance runs may inherently not have the same injury screening capabilities as their clinical counterparts. This was partly shown by the significant bilateral difference in both lean mass and knee extensor and flexor knee torque. Field-based test would not be able to provide such information. Future research should focus on the occurrence of lower extremity injuries and the correlation to bilateral weaknesses revealed by clinical assessments.

Acknowledgments

We would like to thank the Army ROTC, Air Force ROTC, and Navy ROTC cadres of the University of Idaho and Washington State University for their support and willingness to participate in this research study.

References

[1] Kucera et al. (2016). Med and Sci in Sp and Ex, 48(6), 1053.
[2] Ruscio et al. (2010). Am J Prev Med, 38(1), S19-S33.
[3] Scott el al. (2015). Military Med, 180(8), 910-916.
[4] Thomas et al. (2004) J Str and Cond R, 18(4), 904-907.

No Difference in Knee Biomechanics During Landing Between Individuals with and without a History of Concussion

Eric J. Shumski[1], Tricia M. Kasamatsu ATC, PhD[1], Kathleen S. Wilson PhD[1], and Derek N. Pamukoff PhD[1]
[1]California State University, Fullerton; Fullerton, CA
Email: ericshumski@csu.fullerton.edu

Introduction

Recreationally active individuals who are 3 years post-concussion have a higher rate of anterior cruciate ligament (ACL) tear compared to individuals without a history of concussion [1]. Limited research has investigated the effects of concussion on lower extremity mechanics during landings, which are commonly associated with lower extremity injury risk. Individuals with a history of concussion had greater trunk flexion during cutting an average of 124 days post-concussion [2]. Moreover, individuals who were an average of 3.1 years post-concussion exhibited less knee varus and external rotation during a jump cut maneuver compared to individuals without a history of concussion [3].

The purpose of this study was to examine the influence of concussion history on lower extremity biomechanics during a double leg landing. It was hypothesized that individuals with a history of concussion would have greater vertical ground reaction force, greater vertical loading rate, lesser peak knee flexion angle, greater knee abduction angle, and greater external knee abduction moment compared to individuals without a history of concussion.

Methods

Twenty-five individuals with a history of concussion (BMI=24.5 (3.5) kg/m^2; 21.6 (1.5) years), and 25 individuals without a history of concussion (24.8 (3.4) kg/m^2; 21.8 (2.1) years) participated and were matched on sex (13 females, 12 males), age (±3 years), and body mass index (±1 kg/m^2). Participants were included if they were rectionally active and between 18-30 years old. Participants with concussion were included if they had sustained a concussion within the last 6 years [4]. Participants were excluded if they had an acute concussion (preceding 6 months) [3], lower extremity injury in the preceding 6 months, any history of lower extremity surgery and/or traumatic injury, neurological conditions that may alter balance, or currently using medication that may alter balance. Concussion history was assessed via 2 questions: (1) "have you ever been diagnosed with a concussion by a medical professional?" (2) "have you ever sustained a head injury with concussion like symptoms not diagnosed by a medical professional?" If they answered "yes" to either question, they were placed in the history of concussion group [4].

Participants jumped from a standardized 30cm box half the participants' height away from 2 AMTI forceplates. Marker trajectories were sampled at 240 Hz, and force plate data were sampled at 2400 Hz. All data were exported to Visual 3D for model construction. Marker position and force plate data were low pass filtered using a zero-phase lag fourth-order Butterworth filter at 12hz [5]. Peak angle and external moments are reported during the landing phase. Values from both limbs from 3 trials were averaged for analysis. Joint moments were normalized to a product of bodyweight and height (BW*height), and forces were normalized to bodyweight (BW). A one-way multivariate analysis of variance was used to compare landing outcomes between individuals with and without a history of concussion.

Results and Discussion

There was no difference in landing outcomes based on group ($(F_{5, 44})$=0.966, p=0.431, Wilk's Λ=0.898) (Table 1).

Table 1: Summary of Results

Variable	Concussion (mean ± SD)	Control (mean ± SD)
Vertical Ground Reaction Force (BW)	1.89 ± 0.25	1.83 ± 0.28
Vertical Loading Rate (BW/sec)	59.33 ± 13.60	52.39 ± 11.62
Knee Flexion Angle (degrees)	-93.40 ± 11.97	-91.22 ± 9.16
Knee Abduction Angle (degrees)	11.75 ± 6.18	10.41 ± 6.11
Knee Abduction Moment (BW*Height)	0.035 ± 0.019	0.033 ± 0.014

Lynall et al. found that individuals who were 124 days post-concussion had greater trunk flexion compared to individuals without a history of concussion [2]. Additionally, individuals an average of 49.9 days post-concussion had greater hip stiffness, and lower knee and leg stiffness compared to their pre-seaseon baseline scores [6]. The individuals with a history of concussion in this study were an average of 3.3 years post-concussion. It is possible that neuromuscular control is resolved in individuals who are approximately 3 years post-concussion. Previous research found lower knee varus and external rotation during a jump cut manuever in individuals who were 3.1 years post-concussion compared to those without a history of concussion [3], and greater rates of ACL tear have been found 3 years post-concussion [1]. The discrepancy in results may be due to the different tasks performed, or the simultaneous use of a Flanker task [3].

Significance

Individuals with a history of concussion may not have aberrant drop vertical jump biomechanics. Lower extremity injury risk following a concussion may be due to other factors such as the inability to simultaneously process proprioceptive and external stimuli. Future research is needed to determine clinical methods for assessing this inability to process multiple stimuli, and if this deficit may contribute to injury following concussion.

References

[1] McPherson A., et al. (2020). *Sports Med.* Epub ahead of print.
[2] Lynall RC., et al. (2018). *Arch Phys Med Rehabil*. **99**(5): 880-886
[3] Lapointe A., et al (2018). *Int J Psycophysiol.* **132**(A): 93-98
[4] Martini D., et al. (2011). *Arch Phys Med Rehabil.* **92**(4): 585-589
[5] Kristianslund E., (2012). *J biomech.* **45**(4): 666-671
[6] Dubose et al., (2018). *Med Sci Sportx Exerc*. **49**(1): 167-172

Lower Extremity Stiffness is Altered During Decision-Making Drop Jumps in Males and Females

Hillary H. Holmes.[1], Jessica L. Downs[1], Jaimie A. Roper[1]
[1]Auburn University, Auburn, AL, USA
Email: hhholmes@auburn.edu

Introduction

Leg stiffness associates with measures of athletic performance and injuries, making it a versatile and applicable neuromuscular control measure in coaching and rehabilitation (1,2,6). Drop jumps are commonly used to study neuromuscular control mechanisms, like leg stiffness, to identify performance and injury mechanisms (5). However, cognitive constructs important for sports (i.e. reaction time, visual processing speed) may be linked to non-contact injuries and landing mechanics during drop jump protocols simulating cognitive game-like demands (4,8). Thus, adding a cognitive task to drop jump activities may mimic more game-like settings (3,4,6). Importantly, reported sex differences in neuromuscular control of landing indicates reason to analyse sex differences during cognitively loaded drop jump (6). Thus, the purpose of this study was to determine differences in ankle, knee, hip, and leg stiffness among drop jump of varying cognitive demands and between males and females. Secondarily, measures accessible to coaches, clinicians and researchers, like ground contact time and jump height performance, were analysed in relation to leg stiffness to provide potential applicable training and rehabilitation implications.

Methods

Thirty healthy, active young adults (males=12, females=18 age=20±1yr, height=1.7±0.1m, mass=69.8±11.0kg) performed drop jump and drop lands under four conditions from a 0.3m box placed one-half the participant's height from the force plates (7). The standard condition involved asking participants to perform a drop jump or drop land. The choice condition allowed participants to volitionally choose between a drop jump or drop land. Visual and auditory conditions involved decision-making through reactions to visual or auditory cues presented while the participant was in mid-air. Three jumps and one land were randomized in each condition. Leg stiffness equaled the ratio of peak vertical ground reaction force and change in leg length between foot strike and time of minimum leg length. Leg length equaled the distance between the lateral malleolus and greater trochanter. Joint stiffness equaled the ratio of the change in joint moment and angular displacement between foot strike and time of minimum joint angle. All stiffness was normalized to body mass. A 5n threshold identified ground contact time and vertical center of mass position displacement identified jump height. A 2x4 (sex x condition) repeated measures MANOVA with post-hoc Bonferroni adjustments identified differences in lower extremity stiffness and performance outcome variables. Pearson product correlations were performed among dependent variables within conditions.

Results and discussion

There was no significant interaction between sex and condition. There was a significant main effect of condition (Λ=0.703, F(12,206.660)=2.977, p=0.005) and sex (Λ=0.440, F(4,24)=2.977, p=0.008). Standard drop jump ankle stiffness was larger than visual drop jump (p=0.044), and overall leg stiffness was larger during audio drop jump compared to the standard drop jump (p=0.005). Females exhibited lower ankle stiffness compared to males (p <0.001).

Auditory drop jumps exhibited longer ground contact time (0.63±0.13s) compared to visual (0.57±0.09s, p <0.001), choice (0.55±0.11s, p <0.001) and standard drop jump (0.53±0.10s, p<0.001) . Audio drop jump height was lower compared to standard drop jumps (p=0.013), and visual drop jump height was lower compared to choice and standard drop jumps. Males jumped higher than females (p=0.011).

Increased leg stiffness was related to decreased ground contact time during standard drop jump with a large effect relationship (r=-0.523, p=0.003) and decreased choice drop jump with a moderate effect (r=-0.383, p=0.037). However, this relationship was not statistically significant during audio and visual drop jumps.

Our results indicate ankle and leg stiffness are influenced during the drop jump in the presence of reactive decision-making and between males and females. Females are reported to exhibit decreased leg stiffness during hopping (5). Although increased stiffness is related to enhanced athletic performance, too much or too little stiffness, allowing for increased forces or excessive joint motion, may both relate to injury (2,5,6). Our results of decreased ankle stiffness in females during drop jumps support previous findings and may contribute to increased lower extremity laxity postulated to influence injury mechanics (5).

Significance

Differences in drop jump mechanics between different decision-making stimuli and sex have the potential to provide enhanced rehabilitation and coaching tools. Understanding the lack of relationship between ground contact time and leg stiffness during reactive-decision making can allow coaches to monitor ground contact time while implementing auditory and visual stimuli specific to a particular sport. Cues focusing on ground contact time are reported to change leg stiffness (1,2). Thus, considering cues during reactive-decision making drop jumps may contribute to specific stiffness training goals and improve return-to-play protocols specific to a sport. Considering programs that emphasize ankle stiffness in females may benefit both training, rehabilitation and high rates of injuries like anterior cruciate ligament injuries.

Acknowledgments

Auburn University College of Education Seed Grant.

References

1. Arampatzis et al. 2001. *J of Electromyogr Kinesiol*
2. Brazier et al. 2017, *J Strength Cond Res*
3. Helm et al. 2019. *Eur J Appl Physio*
4. Herman & Barth 2016. *Am J Sports Med*
5. Leppänen et al. 2017. *Am J Sports Med*
6. Padua et al. 2005. *J Mot Behav*
7. Padua et al. 2009. *Am J Sports Med*
8. Swanik et al. 2007. *Am J Sports Med*

The Effects of Foot Position on Gluteus Maximus Activation During Jump Tasks

Jason Brunet, Emma Grote, Paige Janka, Tanner Strommen, Mostafa Hegazy
Southwest Minnesota State University, Marshall, MN, USA

Introduction

The primary function of the GMAX during sprinting is trunk and hip control on the stance leg side, as well as decelerating the swing leg [1]. For many individuals the GMAX is often weak or inactive. Inability to properly activate the GMAX has been termed "gluteal amnesia". This phenomenon can be attributed to prolonged periods of sitting [2]. Thus, activation of the GMAX is often the focal point of many training programs. Plyometric tasks involving forward movement stimulate activation of the GMAX in order to stop this forward movement. The use of plyometric training is very popular in sports that involve sprinting such as baseball and softball. It is commonly believed that landing on the heels will produce the greatest amount of GMAX activation. However, there are no studies that have reported this idea. Kovacs et al. (1999) reported no difference in GMAX activation when performing forefoot and heal-toe landing during a drop jump[3]. The Tensor Fasciae Latae (TFL) and Gluteus Medius (GMED) are both hip abductors, however, overactivation of the TFL has been linked to different lower limb disorders. An ideal GMAX exercise would be one that maximizes its activity as well as that of the GMED while reducing activity of the TFL. Thus, the purpose of this study was to determine if foot position during landing affects the activation of the GMAX in Division II baseball and softball players. A secondary purpose was to determine how foot position affects activation of the GMED and TFL.

Methods

Fifteen male baseball players and fifteen female softball players from Division II teams participated in this study. Upon arrival, participants had EMG electrodes (Delsys Trigno Avanti Sensors, Natick, MA) placed on their right and left GMAX, GMED, and TFL. Participants performed three different plyometric tasks, each with three different landings on toes, flatfoot, and on heels with each condition repeated 3 times. The plyometric tasks used were as follows: broad jump (9 trials), forward leap on the right and left side (9 trials per side), and leap with a 90-degree turn on the right and left side (9 trials per side). Task distance was the length of their lower limb for all trials. Muscle activation during landing were calculated as a percent of maximum voluntary contraction. Mixed design ANOVAs with landing type as the within subjects factor and gender as the between subjects factor were conducted.

Results and Discussion

Heel and flatfoots landing led to a significantly greater GMAX activation when compared to toe landings during both right and left forward leaps ($F(2, 56) = 4.038$ ($p<0.05$) and 3.614 ($p<0.05$) for landing on the left and right foot, respectively; Figure 1). Kovacs et al. (1999) reported an increase in plantar flexor activity during drop landings on the toes compared to heel landing [3]. They suggested landing on toes allows the plantar flexors to absorb the impact force. When landing on heels, plantar flexor moment arm is too small for them to be effective, thus control is shifted to the hip, where the GMAX plays a major role. Similarly, it is likely that heel and midfoot landings shifted the load away from the plantar flexors in the forward leap task. Kovacs et al. (1999) did not find a difference in GMAX activation. However, during a forward leap, the GMAX needs to be more active than during a drop jump to control forward trunk flexion.

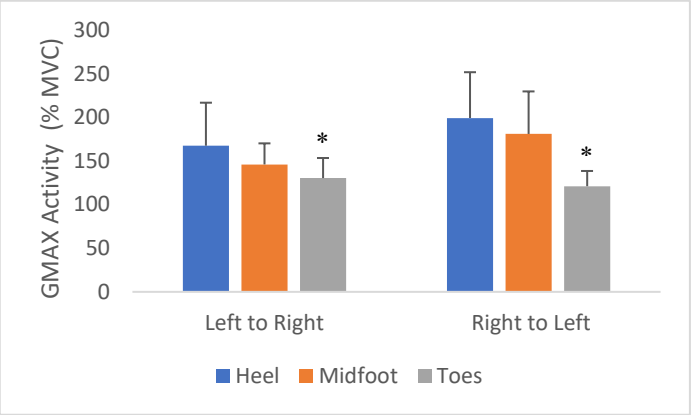

Figure 1: Softball player gluteus maximus activity as a percent of maximam voluntary contraction (%MVC). * Indicates significantly lower activity ($p<0.05$).

Foot placement during landing from the 90 degree-turn leap showed no significant difference in GMAX activation ($p>0.05$). In case of the 90 degree-turn leap, the task is novel for most individuals. Thus, like any new motor skill, participants tended to be stiff during landing regardless of foot placement to reduce degrees of freedom[4]. We hypothesize the outcome may have been different had it been a task participants are familiar with. Foot placement during landing from the broad jump showed no significant difference in GMAX activation ($p>0.05$). Compared to the leap, the broad jump used two feet. Since the distance used was similar in both cases, it is likely forward momentum during the broad jump was not high enough to elicit a difference for this task and perhaps doubling the distance was warranted. There was no significant difference in GMed and TFL activation during all landings for all tasks ($p>0.05$) nor was there a gender difference ($p>0.05$).

Significance

In this study there was evidence found to support the need to land on heels or midfoot during a forward leap when the aim is to maximize activation of the GMAX. We found no evidence to suggest landing on heels or midfoot would increase GMAX activation during a forward leap with a 90-degree turn or during a broad jump. Thus, when performing such task there may be no need to instruct individuals to land on their heels. However, further examining the effect on jump distance and task novelty is warranted.

Acknowledgments

We would like to thank the Southwest Minnesota State University baseball and softball teams their participation.

References

[1] Lieberman, D. E. et al. *J Exp Biol*, *209* (11), 2143-55, 2006.
[2] McGill, S. *Strength Cond J*, *32*(3), 33-46, 2010.
[3] Kovacs et al. *Med Sci Sports Exerc*,*31*(5), 708-716, 1999.
[4]Bernstein N (1967), Pergamon Press, Oxford

Do inclined sleeping surfaces impact infants' upper body muscle activity and movement?

Junsig Wang, Safeer F. Siddicky, John L. Carroll, Brien M. Rabenhorst, David B. Bumpass, Brandi N. Whitaker, Erin M. Mannen
University of Arkansas for Medical Sciences, Little Rock, AR
Email: Jwang3@uams.edu

Introduction

The infant sleep environment has been highlighted due to an increase in the tragic incidence of Sudden Infant Death Syndrome (SIDS). However, commercial infant products evolve quickly, and over the past ten years, infants have been placed to sleep in the relatively new class of Inclined Sleep Products, designed to keep an infant supine at a 10° to 30° incline. Parents are advised to always use restraints in the products and to discontinue use once an infant has the ability to roll over. This implies that the design of infant inclined sleep products may have additional suffocation hazards when infants finds themselves prone in the product. However, no published study has investigated how babies move and use their muscles in different inclined surface conditions. Thus, the purpose of this study was to assess upper body muscle activity and kinematics while normal healthy infants were placed on different inclined crib mattress surfaces (0° vs. 10° vs. 20° vs. 30°) during prone positioning.

Methods

Fifteen healthy full-term infants (age: 17.7±4.9 weeks; 8M, 7F; length: 61.5±4.1 cm; weight: 6.5±1.0 kg) were recruited for this IRB-approved study. The participants were placed prone on the customized crib mattress at 0°, 10°, and 20° for 60 seconds. The 30° incline was excluded since we observed babies were not able to maintain a stable lying posture due to sliding down the incline. Surface EMG (Delsys Inc., Natick, MA; 1000Hz) was recorded from cervical paraspinal, abdominal, erector spinae, and triceps muscles. A motion analysis system with 10 high-resolution cameras (Vicon Nexus, Oxford, UK) was used to collect three-dimensional kinematic data at 100 Hz during each testing condition. Sagittal plane range of motions of neck and trunk as well as the number of neck and trunk angle peaks were calculated. Repeated Measures ANOVAs and Bonferroni post-hoc adjustments were performed to test the effect of incline angles.

Results and Discussion

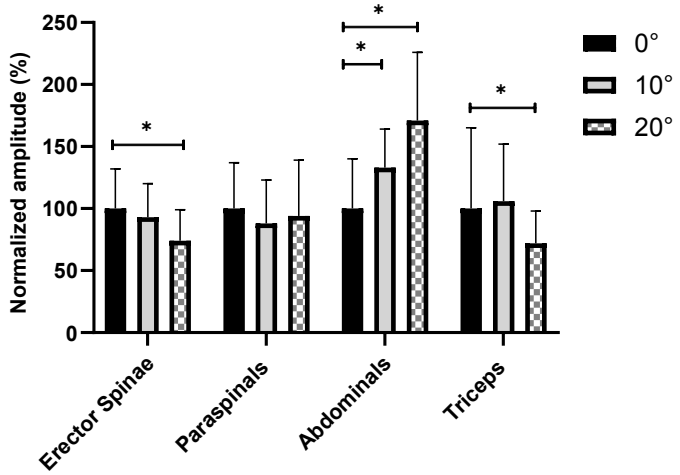

Figure 1: Effect of Incline (0° vs. 10° vs. 20°) on EMG: erector spinae, cervical paraspinals, abdominals, and triceps. * indicates $p < 0.05$ when compared to 0°or 10°.

Table 1. Effect of Incline (0° vs. 10° vs. 20°) on kinematic variables

Variable	0°	10°	20°	Main effect p value
Neck ROM (deg)	40±17	44±15	45±15	0.628
Trunk ROM (deg)	26±11	24±11	26±9	0.678
# of neck peaks per 10s	1.4±0.9	1.5±0.7	1.9±1.7	0.459
# of trunk peaks per 10s	0.7±0.6	1.0±0.8	0.9±0.6	0.453

Erector spinae and triceps muscle activity was decreased by 26% and 28% when comparing to 20° to 0° ($p = 0.019$, $p = 0.036$; Figure 1). Abdominal muscle activity was increased by 33% and 71% when comparing when comparing 10° and 20° to 0° ($p = 0.037$, $p = 0.006$; Figure 1). No significant differences on cervical paraspinal muscle activity and kinematic parameters (neck and trunk ROMs; number of neck and trunk angle peaks) were found (Table 1).

The babies were not moving their heads or trunks more or less often on an inclined surface, yet the muscle activity profile was significantly different. Inclined surfaces (especially 20°) require greater abdominal muscle activity while decreasing erector spinae and triceps muscle activities. The core muscles (abdominals) require 71% more activity to maintain a prone lying position, indicating that muscle fatigue of the abdominals could occur more quickly at an incline (20°) compared to a flat surface (0°). Thus, this situation could likely result in expedited muscle fatigue as the baby attempts to reposition and self-correct.

Significance

The biomechanics of infants is grossly understudied and scarce compared to older children and adults. To the best of our knowledge, this study is the first to determine the effect of different inclined surfaces on infants' upper body and core muscle activity as well as upper body kinematics. During prone positioning, the 20° inclined surface resulted in significantly higher muscle activity of the trunk core muscles (abdominals), which may exacerbate fatigue and contribute to suffocation if infants cannot self-correct.

Acknowledgments

This project has been funded with federal funds from the United States Consumer Product Safety Commission under contract number 61320618P. The content of this publication does not necessarily reflect the views of the Commission, nor does it mention of trade names, commercial products, or organizations imply endorsement by the Commission.

Bone Architecture and Foot Muscle Strength are not Different in Healthy Male Versus Female Runners

Kyle E. Murdock[1], Adam S. Tenforde[2], Irene S. Davis[2], and Karen L. Troy[1]
[1]Worcester Polytechnic Institute, Worcester, Massachusetts
[2]Harvard Medical School, Cambridge, Massachusetts
Corresponding Email: kemurdock@wpi.edu

Introduction

Repetitive mechanical loading of the musculoskeletal system can result in accumulation of damage to bone microarchitecture. These overuse injuries are referred to as bone stress injuries (BSI). BSIs account for virtually 20% of all injuries reporting to sports medicine clinics [1]. BSIs of the metatarsals have been reported to account for 65% of total BSIs in military recruits [2]. In a recent chart review of athletes diagnosed with metatarsal BSI, we found a 2:1 ratio between women and men. BSIs are most frequently found in the second and third metarsals [3]. Several biomarkers for BSI risk have been proposed, including low areal BMD and weakness of intrinsic foot muscles. We hypothesized that female runners have lower bone strength and weaker foot muscles compared to men. In this study, we characterized the bone structure and muscle strength in a group of healthy runners.

Methods

Sixteen runners (9 male, 7 female, age=25±8 yrs) volunteered for participation for this institutionally approved, ongoing study. Subjects were screened for metabolic disorders, previous BSIs, and weekly running distance (≥16 km/week for the past 12 months). Arch strength was assessed using a doming exercise described previously [4, 5]. Quantitative computed tomography (XtremeCT; Scanco, Switzerland) was performed on all subjects. CT images (246 x 246 x 246 μm voxels) were taken of the entire metatarsal volume.

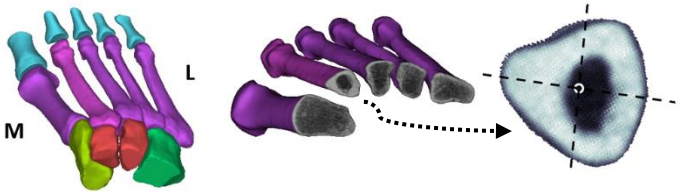

Figure 1: Reconstruction of the forefoot (left) with cross-sectional bone density displayed (middle). Lines show density-weighted center of mass and principal moments of the second matarasal shaft (right).

Integral masks of the right, second metatarsals were imported into MATLAB (MathWorks; Natick, MA). Bones were aligned along the longtidunal axis. Geometric charactersitics were calculated for each individual, including principal moments of interia and a geometric strength index. The strength index (SI) at the mid-shaft was calculated as the ratio of polar moment of inertia and metatarsal width [6].

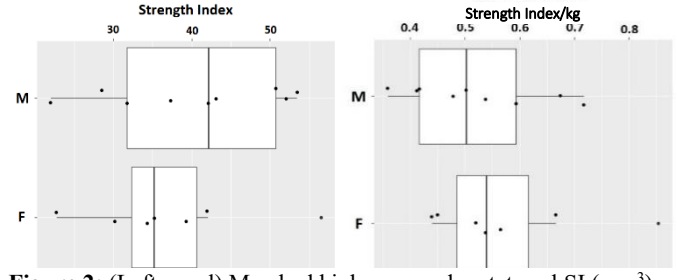

Figure 2: (Left panel) Men had higher second metatarsal SI (mm^3). SI normalized to body mass were similar by sex (mm^3/kg, Right panel).

Results and Discussion

Second metatarsal SI was significantly correlated with body mass (r=0.532, p=0.03). Both raw and normalized SI values to body mass are summarized in the whisker plots in Figure 2. After normalization, SI was not different between men and women (p=0.42). SI is only a single metric calculated at one discrete location, and may not be adequate to discern differences in mechanical integrity of spatially complex shapes such as metatarsal bones.

Arch doming strength was not significantly different between sexes (p=0.06); however, athletes with greater weekly running distance tended to have greater arch muscle strength (Figure 3). Arch strength was not associated with body mass.

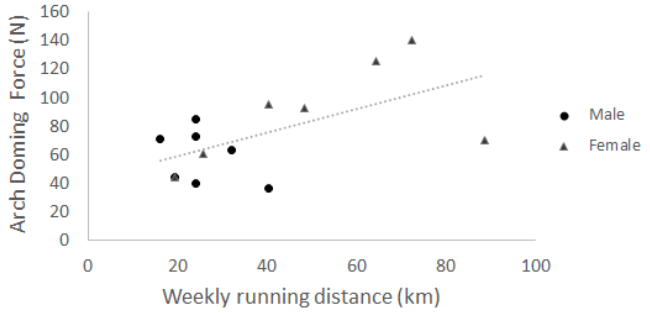

Figure 3: Peak force recorded during maximal voluntary arch doming contraction increased with running activity (R^2 = 0.35, p=0.05).

Neither geometric bone strength nor arch doming strength were different between male versus female healthy runners. Although bone strength scaled with body mass, arch doming strength did not. Collectively, these data support the concept that healthy musculoskeletal systems adapt to the mechanical demands placed on them.

Significance

Our preliminary findings suggest that the increased rate of BSI in female runners cannot be explained by deficits in these measures of bone or muscle strength. In this healthy group, arch muscles were stronger in those who ran more. Applying this method to measure characteristics within athletes with metatarsal BSI may help understand risk factors and management of these injuries.

References

[1] Fredericson M et al, *TMRI*. 17:309–25, 2017.
[2] Wood AM, et al. *Journal of Sports Medicine*. 2014:282980.
[3] Mayer SW et al, *Sports Health*, 6(6)481:491, 2014.
[4] Ridge ST et al, *J Foot Ankle Res*. 10:55, 2017.
[5] Ridge ST et al, *Med. Sci. Sport. Exerc*. 51, 104–113, 2019.
[6] Lang T et al, *JBMR*. 19:1006–1012, 2004.

SEX AND LEG DIFFERENCES IN ACL STRESS DURING UNILATERAL DROP LANDING

Jake A. Melaro & Joshua T. Weinhandl
Department of Kinesiology, Recreation & Sport Studies, University of Tennessee, Knoxville, TN, USA
Email: jmelaro@vols.utk.edu

Introduction

Of the estimated 120,000-400,000 anterior cruciate ligament (ACL) injuries reported annually, roughly 70% are the result of noncontact causes [1]. Athletes consistently exposed to dynamic landing movements are at greater risk of ACL injury. Further, women incur ACL injuries at rates 2-8x greater than men [2]. The link between ACL injury and leg dominance has been investigated but remains unclear. Previous research has shown that non-dominant (ND) compared to dominant (D) leg landings may increase ACL injury risk while being further influenced by sex [3]. The purpose of this study was to investigate the influence of sex and leg dominance on ACL Stress during unilateral landings. We hypothesized that greater ACL stress would be observed in the women and during ND leg landings.

Methods

Forty active participants (20 men, 20 women) performed unilateral drop landings on both their D and ND legs. Participants stepped off a 40 cm box onto a force platform while wearing reflective markers so that force and 3D positional data could respectively be collected. OpenSim static optimization was used to simulate all D and ND leg landing trials whereby specific muscle forces for the quadriceps, hamstrings, and gastrocnemius were estimated and then input into a 3D knee model to estimate ACL stress [4] normalized to body mass. A 2x2 (sex x leg) mixed model ANOVA was run to assess differences in ACL stress. 3D knee joint kinematics and kinetics were also analyzed. Cohen's *d* effect sizes were calculated to determine the magnitude of differences between groups.

Results and Discussion

A significant sex x leg interaction effect was observed for ACL stress (p=.046). Post-hoc comparisons revealed differences between legs in the women (p=.005, d=0.64) but not the men. Women experienced higher ACL stress than men in the D (p<.001, d=2.47) and ND (p<.001, d=1.77) leg.

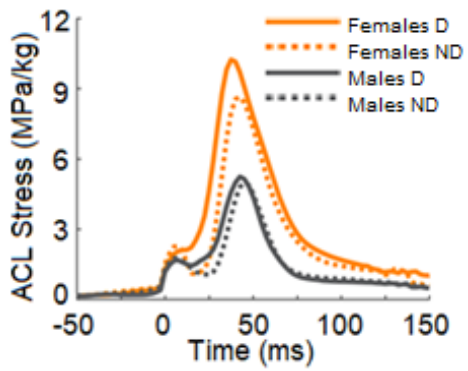

Figure 1: ACL Stress during unilateral drop landings

These results show that women undergo greater ACL stress than men during unilateral drop landings. Further, women experience greater ACL stress during these landings on their D leg. These discrepancies may be due to anatomical differences and different neuromuscular landing strategies that could partially explain why women are at greater risk of noncontact ACL injury than men.

Furthermore, the only leg main effect observed was for knee rotational moments (p=.001) as the ND legs for both men (d=0.57) and women (d=1.00) were subjected to greater peak internal rotation moments than the D legs.

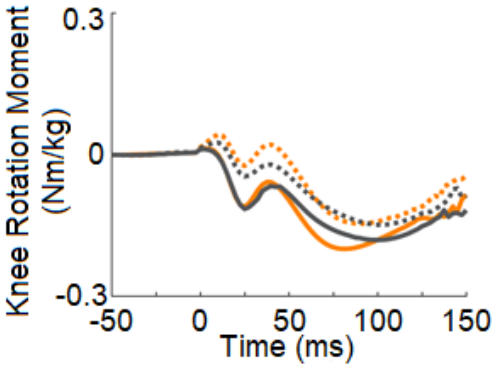

Figure 2: Knee rotation moment during unilateral drop landing

Significance

The magnitudes of the differences observed equated to women experiencing 89 and 71% greater ACL stress during the landings in their D and ND legs, respectively. Further, women were exposed to approximately 17% greater ACL stress in their D leg compared to their ND leg. These data reveal a link between biological sex and leg dominance and their respective influences on ACL stress during single-leg landing tasks. Leg Differences in leg strength, proprioceptive response, and neuromuscular landing strategies between sexes and legs may potentially explain the variance observed in ACL Stress in this study.

References

1. Gornitzky et al., 2016. *Am J Sports Med*, *44*(10), 2716-2723.
2. Yu & Garrett, 2007. *Br J Sports Med, 41 Suppl 1,* i47-51.
3. Negrete et al., 2007. *J Strength Cond Res*, *21*(1), 270-273.
4. Weinhandl et al., 2016. *Comput Methods Biomec*, *19*(14), 1550-1556.

The relationship between Hip and Core Muscular Endurance and Lower Extremity Injuries in Division II Women's Soccer

Macy Violett, Lukas Johnson, Jenna Loch, and Mostafa A. Hegazy, Ph.D.
Southwest Minnesota State Univeristy
Email: Mostafa.hegazy@smsu.edu

Introduction

Soccer is the most popular sport world-wide and has seen recent growth in the United States, which has been associated with increased lower-extremity injuries. Recent studies have investigated the influence of core muscular strength and endurance on sports injuries (Leetun, et al., 2004; Wilkerson, et al., 2012), but only one has done so in soccer players (Abdallah et al., 2019). Considering the majority of injuries occur later in game situations, it is likely that injured athletes generally have the needed muscle strength but are unable to sustain the needed level of force production as games progress, thus, have lower muscle endurance. Specifically, male soccer players with lesser prone- and side- bridge times experienced more injuries (Abdallah et al., 2019). To our knowledge, this type of investigation has never been conducted in female soccer players.

The purpose of this study was to compare pre- and post- season core muscle endurance of Division II female soccer players who sustained injuries during the season to those who did not.

Methods

Twenty-two female Division II soccer players (19.5 ± 1.22 years; 67.4 ± 7.42 kg; 166 ± 4.88 cm) participated in this study. Participants completed a series of four muscular endurance tests: hip abduction, hip external rotation, prone-bridge, and side-bridge. Participants performed repeated hip abduction and external rotation against gravity to exhaustion. These tests were conducted bilaterally with participants performing movements paced using a metronome at 30 bpm. Tests ended once participants were unable to keep pace. The number of repetitions participants were able to perform were recorded. Static side- and prone- bridge tests were conducted with participants maintaining these positions. The length of time participants maintained these positions were recorded. Testing ended when form could not be maintained. All lower limb and trunk injuries that resulted in time away from practice and/or games throughout the season were recorded. One tailed independent t-tests were conducted to compare injured and uninjured players.

Results and Discussion

Eleven players sustained a lower limb and/or trunk injury during the season. Preseason left hip external rotator endurance was significantly lower in injured players ($p<0.05$), while the right external rotator endurance approached significance ($p=0.09$). Postseason right hip external rotator endurance was significantly lower in injured players ($p<0.05$), while the left external rotator endurance approached significance ($p=0.06$). No other significant differences between the groups were observed.

Leetun et al., (2004) were able to predict lower extremity injury status over the course of one season in basketball and track athletes from hip external rotator weakness. In our study, we did not measure muscle force production but we measured muscle endurance. As muscles fatigue, they are unable to continue providing the force needed to maintain stability. This reduced force predisposes players to injuries by altering trunk and lower extremity mechanics (Calston, 2012). Specifically, sufficient external rotator force product can prevent excessive internal rotation, thus, reducing the chance of the knee going into dynamic knee valgus.

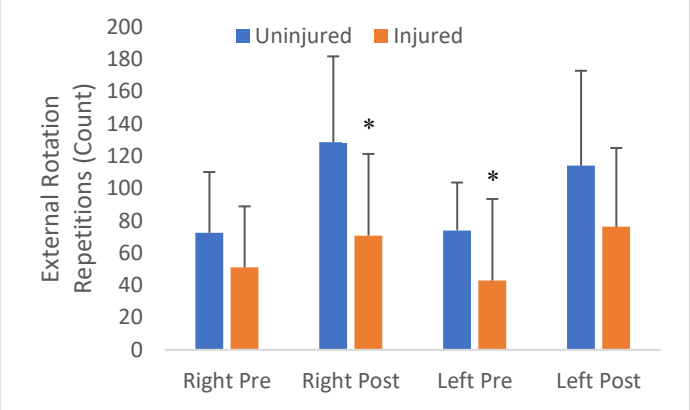

Figure 1. Hip external rotator endurance for injured and uninjured players. * $p<0.05$

Professional male soccer players have been found to experience more injuries when they have lesser side- and prone- plank times (Abdallah et al., 2019). This may be due to structural differences between genders as well as the level of play in our study.

Although not part of the purpose of the study, we noticed that hip external rotation endurance improved over the season, which may have resulted from the season fitness program with emphasis on gluteus maximus muscle endurance. It may also be related to repeated concentric activation of external rotators on the kicking side and eccentric actions of the non-kicking side while controlling pelvic movement during a kick throughout the season.

Significance

Hip external rotator endurance may play a role in reducing injury in Division II women soccer athletes and therefore should be considered by coaches and athletic trainers when designing conditioning programs.

Acknowledgments

We would like to thank the SMSU Soccer team for their participation and efforts in this study. We would also like to thank the SMSU athletic training staff for assistance with injury data collection.

References

Abdallah, AA, et al. *International journal of sports physical therapy*, *14*(4), 525- 536, 2019.

Colston, M. *International Journal of Athletic Therapy & Training* 17, 10-15, 2012.

Leetun, T, et al. *Medicine and Science in Sports and Exercise 36,* 926-936, 2004.

Wilkerson, GB, et al. *Journal of athletic training*, *47*(3), 264-272, 2012.

Pre-Deployment Loading Patterns in Military Personnel with a History of Low Back Injuries

Joshua D. Winters[1], Scott D. Royer[1], Jeremy A Ross[1], Matthew C. Hoch[1], Ryan L. Sheppard[2], and Nicolas R. Heebner[1]
[1]Sports Medicine Research Institute, University of Kentucky, Lexington, KY, USA
[2]United States Marine Forces Special Operations Command, Camp Lejeune, NC, USA
Email: joshua.winters@uky.edu

Introduction

Military training is rigorous in nature placing great demand on the musculoskeletal (MSK) system, resulting in significantly high rates of MSK injuries across all military services.[1] Although MSK injuries may occur as a result of an acute traumatic incident, many result from cumulative loading, or overuse.[2] Overuse injuries, including pain, are commonly reported in the low back.[3] Therefore, the purpose of this analysis was to examine weight bearing asymmetries in active military personnel prior to deployment and compare those with a history of low back injuries to those without a history of MSK injury.

Methods

Loading patterns were collected from 94 Marine Forces Special Operations Command (MARSOC) personnel (age: 28.59 ± 5.17, height: 178.28 ± 6.59 cm, mass: 86.38 ± 12.14 kg) prior to deployment. Weight bearing ratios (WBRs) were calculated from the average of three consecutive unweighted overhead squats performed on a pressure mat (Tekscan, Boston, MA). Pressure was converted to Force (N) and normalized to bodyweight (%BW) for both the dominant (DOM) and non-dominant (NOND) limbs (Figure 1). Participants also completed a self-report injury history questionnaire. Those who reported a previous injury to the back or pain that restricted training for at least one day (LBP, n=10) and those who reported no history of MSK injuries (Controls, n=26) were included in additional between limb WBR analyses.

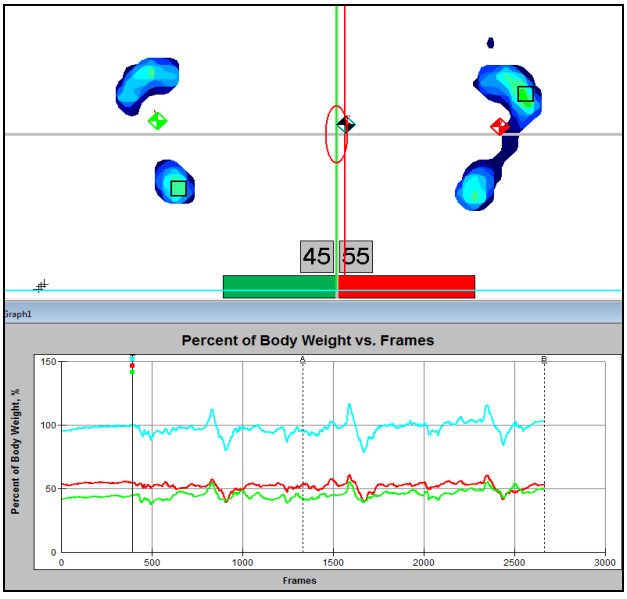

Figure 1. Weight bearing ratios calculated from a pressure mat during an unweighted overhead squat assessment.

Paired samples t-tests were used to evaluate weight bearing asymmetries between the DOM and NOND limbs. Significance level was set at alpha = 0.05. Effect sizes were calculated for all comparisons using Cohen's d.

Results and Discussion

Paired samples t-tests indicated statistically significant pre-deployment WBR asymmetries across all MARSOC personnel ($p<0.001$, $d=0.69$). The LBP group also exhibited statistically significant WBR asymmetries ($p=0.044$, $d=0.738$) but not the control group (($p=0.053$. $d=0.40$), (Figure 2)).

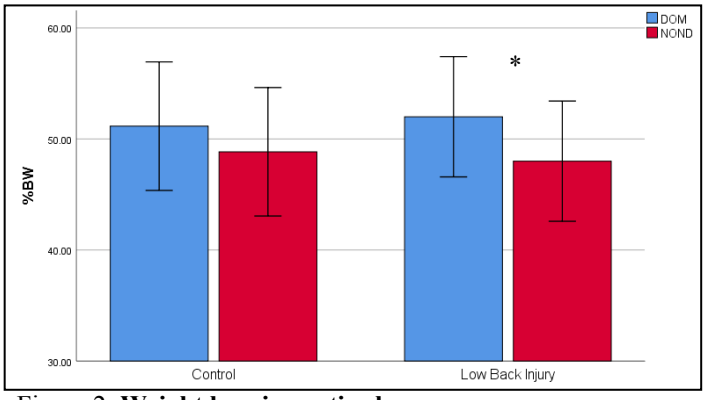

Figure 2. **Weight bearing ratios by group**

Significance

Prior to deployment, MARSOC personnel demonstrated significant asymmetrical WBRs, loading the DOM with 3.66 %BW more on than the NOND during an unweighted squat. These asymmetries were further exaggerated in the LBP group and though the between limb difference was only 4.0 %BW, it was nearly double the 2.3%BW asymmetry in the control group and had a greater effect size (d=0.74 vs d=0.40 respectively). Due to the physicality and cumulative effects of the day-to-day workload during deployment, improving loading symmetry during military training may reduce the warfighter's risk of sustaining a MSK injury while on deployment.

AcknowledgmentsThis research was supported by the Office of Naval Research N00014-18-C-2025.

References

1. Nindl BC, et al. US Army Medical Department journal. 2013.
2. Hauret KG, et al. American journal of preventive medicine. 2010.
3. Knapik JJ, et al. Medicine and science in sports and exercise . 2001

Peak Elbow Angles in Independent Wheelchair Transfer: A Prelim Study

Ashleigh Fults, Stephen Sundarrao MS, and Stephanie L. Carey PhD
Center for Assistive Rehabilitation and Robotics Technologies, University of South Florida
Email: alf3@mail.usf.edu

Introduction

For individuals with spinal cord injuries (SCI) who utilize manual wheelchairs for mobility and recreational wheelchairs for an adaptive sport, it is necessary to transfer into and out of their wheelchairs to compete. These transfers can be easily accomplished with the help of a caretaker or transfer device, but independent transfers, wherein an individual transfers himself or herself unaided using only their upper limbs and torso, have been found to promote rehabilitation and improved mental health over assisted transfers. [1]

Because of the frequency of the transfers, improper movements over time can cause pain, lead to musculoskeletal pathologies, or exacerbate pre-existing damage to the individual's upper limbs. [2] Therefore, it is necessary to develop an optimized transfer technique, especially for transfer into a recreational wheelchair. From the literature, a transfer is broken into three phases. The phase of interest for this study is the lift phase, since it is the weight-bearing phase of transfer. [3] The purpose of this study was to first examine the current transfer technique used by wheelchair athletes to determine if it changes depending on the height of the recreational wheelchair.

Methods

For this study, kinematics were collected using the motion capture system, Vicon Nexus with Nexus 1.8.2 software, and passive, reflective markers adhered to the subject's upper limbs and torso. The recreational wheelchair used was the Top End Eliminator Racing Wheelchair with Open V Cage (Racer). The subject was a 38 year old male manual wheelchair user of more than two years with a SCI at T12 who participates in para ice hockey The subject was asked to arrange and angle his personal wheelchair and the racer as they would in an everyday situation. The subject was instructed to independently transfer from his personal wheelchair into the racer as they normally would three times with the racer seat height equal to, and then 10 centimeters below, that of his personal wheelchair.

Joint angles were calculated with the biomechanics analysis software, C-Motion Visual 3D, and the joint coordinate system used for the elbow was that recommended by the Standardization and Terminology Committee of the International Society of Biomechanics. [4]

Results and Discussion

The start and end of the lift phase was defined as the time at which the subject's pelvis moved off the seat to when subject's pelvis was placed on the seat of the racer. The mean and standard deviation of the maximum and minimum elbow angle was calculated for each arm from the three trials and displayed in Table 1. For the elbow angles reported, 0 degrees is defined as the neutral position with the elbow in neither flexion nor extension. Elbow flexion is reported as positive degrees from the neutral position, and elbow extension is reported as negative degrees from the neutral position.

Descriptive statistics shows a difference between the maximum and minimum elbow angles of the of the leading arm between the two conditions. The elbow angles of the leading arm may be smaller, closer to neutral, when the racer seat is lowered, to compensate for the greater distance that arm must reach from the subject to the racer seat. Since there is no change in the subject's personal wheelchair, the trailing arm shows no difference in maximum and minimum elbow angle.

	Equal Seat Height		Lower Seat Height	
	Leading Arm	Trailing Arm	Leading Arm	Trailing Arm
Max Flex(+)/Ext(-)	51.8 ± 6.0*	34.0 ± 6.8	42.0 ± 2.5*	31.4 ± 6.3
Min Flex(+)/Ext(-)	14.2 ± 3.7*	-1.0 ± 1.4	3.6 ± 6.7*	2.0 ± 2.1

Table 1: Mean ± standard deviation of maximum and minimum elbow angles (˚) during lift phase of transfer for leading arm and trailing arm. *No overlap in mean ± one standard deviation between the conditions

Significance

Although a case study, these results show that there may be some difference in an individual's movement pattern during transfer. Continuation of this study will show if this holds true in additional subjects as well. Furthermore, examining the shoulder and wrist angles during transfer may reveal similar differences. If there are consistent differences in joint angles, the next step is determining if these differences may do the individual harm with repeated occurrences, and, if so, how can the technique be improved to prevent that harm.

Acknowledgments

This study was partially funded by the Florida Department of Education, Rehabilitation Engineering and Technology Program.

References

[1] Gagnon, D., et al. (2003). Biomechanical Analysis of a posterior transfer maneuver on a level surface in individuals with high and low-level spinal cord injuries. *Clinical Biomechanics*. 18, 319-31.

[2] Finley, M. A., et. al. (2005). Scapular kinematics during transfers in manual wheelchair users with and without shoulder impingement. *Clinical Biomechanics.* 20(1) . 41-8.

[3] Koontz, A. M., et. al. (2011). Development of custom measurement system for biomechanical evaluation of independent wheelchair transfers. *Journal of Rehabilitation Research & Development*, 48, 1015-28.

[4] Wu, G., et. al. (2005) ISB recommendation on definitions of joint coordinate systems of various joints for the reporting of human joint motion – Part II: shoulder, elbow, wrist and hand. *Journal of Biomechanics*, 38, 981-99

Influence of Arena Surface Mechanics on Equine Fetlock Joint Motion for a Jump

Christina M. Rohlf[12], Tanya C. Garcia[1], Lyndsey Marsh[1], David Fyhrie[2], Sarah S. le Jeune[1], Elizabeth Acutt[1], and Susan M. Stover[12]
[1]School of Veterinary Medicine, University of California, Davis, CA, USA
[2]Biomedical Engineering Graduate Group, University of California, Davis, CA, USA
Email: cmrohlf@ucdavis.edu

Introduction

Tendon and ligament injuries in the lower limb are a significant cause of poor performance and attrition of show jumping horses [1]. These injuries are typically the result of high cyclic tendon and ligament strains and strain rates [2]. Due to limb anatomy, tendon and ligament strains and strain rates are highly correlated with fetlock joint angle and the rate of change of fetlock angle.

Fetlock joint angle is affected by the force transferred to the limb when the hoof interacts with the ground [3-4]. Relationships between force and gait, force and activity, and force and speed have been quantified for show jumping horses; however, it is unclear how force is modified by properties of the arena surface. This study evaluates relationships between mechanical properties of arena surfaces and biomechanical properties of the fetlock of show jumping horses in order to identify surface property variables which reduce the risk of injury.

Methods

A repeated measures study design was used to collect data from 4 horses jumping 3 times over a 1.1 meter jump on each of 12 arena surfaces (5 dirt and 7 synthetic).

High contrast motion capture markers were placed on the left forelimb of each horse to quantify joint angles at takeoff and landing using monochrome high-speed video. Palpable anatomic landmarks verified by radiographs were used for marker placement. Limb marker positions were digitized using kinematic software to determine maximum fetlock angle (**Figure 1**) and fetlock angular velocity during motion.

Figure 1: Fetlock Angle Definition.

Vertical impact force and horizontal shear force of each arena surface were measured immediately following biomechanical data collection of each horse using a custom designed arena impact device (AID) and quasi-static linear shear tester (STD) respectively (**Figure 2**). The AID features a triaxial accelerometer, 6-axis load cell, and laser displacement sensor and was dropped from a height of 31.3 cm to achieve physiologically equivalent limb accelerations upon landing after a jump. Data were collected at 4,545 Hz. The STD features a single axis load cell, two string potentiometers to measure displacement in horizontal and vertical directions, and a linear transducer. Tests were run under displacement control (0.017 m/s) with data collected for 5 normal loads (50 to 225 lbs) at 1,613 Hz. All data were collected in LabVIEW and processed using custom MATLAB software.

Figure 2: Arena Impact Device (AID) and Quasi-Static Linear Shear Tester Setup (STD).

An analysis of variance accounting for repeated measures was used to assess differences in fetlock motion between takeoff and landing and surface type (dirt, synthetic) and differences in surface properties between surface type (dirt, synthetic). Differences were considered significant at $p<0.05$. Spearman correlation statistics were also examined to determine relationships between fetlock motion and surface properties.

Results and Discussion

Landing exhibited significantly higher maximum fetlock angles (4.8°) than takeoff indicating that tendon strain and injury risk is likely to be maximized during landing. The rate of fetlock extension was also 668°/s higher at jump landing indicating high soft tissue strain rates. Since soft tissues become less elastic at high loading rates (high stiffness and less elongation before failure), high loading rates are predicted to increase the risk of injury to soft tissue structures.

Surface type (dirt, synthetic) exhibited no statistically significant effects on motion at the fetlock. Similarly, ground reaction force and shear force were unaffected by surface type. Historically, the effect of surface type on mechanical properties has involved extremely low sample sizes (one of each type of surface) [5]. Therefore, we believe that categorizing arena surfaces by type does not sufficiently describe the underlying mechanical properties of the surface which affect joint motion and is not a sufficient predictor for injury risk to the horse.

However, this does not mean that mechanical surface properties are not important factors for injury risk. Significant Spearman correlations between arena surface shear forces and rate of fetlock extension were found for both takeoff ($r=0.35$) and landing ($r=0.31$). These results indicate a positive correlation between shear forces and rate of fetlock extension. Thus for the range of shear properties observed in this study injury risk appears to increase as shear forces of arena surfaces increase.

Significance

The results of this study are expected to quantify the relationship between surface properties and joint angle biomechanics of show jumping horses. Since overextension of joint angles correspond to high tendon and ligament strains which are risk factors for injury, results from this study could help determine ideal surface property values that minimize these risk factors and reduce the rate of injury. In this way, the safety of performance horses while training and competing would be improved.

Acknowledgments

Supported in part by the Center for Equine Health with funds provided by the State of California satellite wagering fund and contributions by private donors.

References

[1] Egenvall, et al., Prev Vet Med, 2013(112): p. 387-400.
[2] Lochner, et al., Am J Vet Res, 1980(41): p. 1929-1937.
[3] Meershoek, et al., Equine Vet J, 2001(33): p. 6-10.
[4] Schamhardt, et al., Acta Anat (Basel), 1993(146): p. 123-129.
[5] Setterbo, et al., Am J Vet Res, 2009(70): p 1220-122.

Spatiotemporal Gait Parameters in Middle Age Adults with Persistent Ankle Pain

Mohammed S. Alamri[1], Kazandra M. Rodriguez[2], Emily E. Gerstle[1], and Stephen C. Cobb[1]
[1]Department of Kinesiology, UW-Milwaukee, Milwaukee, WI, USA
[2]Department of Kinesiology, University of Michigan-Ann Arbor, Ann Arbor, MI, USA
Email: msalamri@uwm.edu

Introduction

The prevalence of persistent ankle pain peaks in middle-aged adults and is associated with decreased mobility and health-related quality of life [1,2]. Spatiotemoporal parameters (STPs) during walking gait can be used to evaluate the functional condition of individuals with chronic knee pain and chronic ankle instability (CAI) [3,4]. Further, individuals with chronic foot pain have demonstrated increased double support time compared to those without chronic foot pain [5]. Although the previous studies have improved the understanding of CAI and chronic foot pain, they have primarily focused on young active adults, or defined groups that included both young and middle-age or middle-age and older adults.

The purpose of this study was to investigate walking gait STPs in middle-aged adults with persistent ankle pain. We hypothesized that those with persistent ankle pain would walk with: decreased stride length, uninvolved limb step length, and involved limb single limb stance duration; and increased double limb support time compared to middle-aged adults without persistent ankle pain.

Methods

Nineteen middle-aged (45 – 64 years old) adults participated in the study (Table 1). Persistent ankle pain group participants (PAIN) had a history of at least 1 significant lateral ankle sprain, experienced pain for the previous three months, and complained of at least slightly troublesome ankle pain on most days during the past month [6]. Uninjured participants (CON) were age, sex, and BMI classification matched with PAIN participants, had not had an acute lower extremity injury within the previous 3 mos., had no history of ankle sprain in the previous 12 mos., and no complaints of ankle pain in last 3 mos.

Following written informed consent, each participant performed 10 barefoot overground walking trials at self-selected speeds along a 15 m walkway with 3 embedded force plates sampling at 1000 Hz. The STP variables calculated are defined in Table 2. Independent t-tests were peformed to investigate group differences (SPSS, $\alpha = 0.05$).

Table 1 Study Participant Demographics (Means ± SD).

Group	Age (years)	Sex (F/M)	Height (cm)	BMI (kg/m^2)
Pain	54.4 ± 5.8	9/1	168.0 ± 5.1	27.3 ± 7.1
Control	53.0 ± 5.8	8/1	168.2 ± 6.1	26.5 ± 7.4

Results and Discussion

We postulated that the PAIN group would alter their gait STPs to decrease single limb stance time on the painful limb. The hypothesized differences between groups were not supported (Table 2). The significant decrease in involved limb step length in the PAIN group was not anticipated, but was consistent with a previous study that investigated the influence of CAI on STPs [4] (Table 2). Persistent ankle pain may be associated with the initial ground impact and/or loading rate. If this is the case, a shorter step length of the involved limb may act as compensatory mechanism to decrease the initial impact force and/or loading rate.

With respect to the lack of significant group differences between the other STP variables investigated in the current study and previous studies investigating the effect of CAI or foot pain on gait STPs; the results are consistent with some [7,8] and inconsistent with others [4,5,8]. Comparisons across the studies is difficult given the differences in participant demographics (e.g. age, BMI, activity level), inclusion/exclusion criteria, footwear conditions, and gait speeds.

Table 2 Mean (SD) PAIN and CON Group STPs.

STP	Group		*P*	η^2
	PAIN	CON		
Gait speed (m/s)	1.19(0.1)	1.21(0.1)	.79	.00
Stride length (m)	1.36(0.1)	1.39(0.1)	.20	.09
Cadence (steps/min)	105.2(6.4)	104.0(9.8)	.75	.01
In. Step length (cm)	64.5(6.0)	70.1(4.3)	.03*	.23
In. Single support (%GC)	39.3(1.5)	39.1(1.5)	.76	.01
In. Double support (%GC)	23.2(3.1)	22.6(3.2)	.66	.01
Un. Step length (cm)	71.4(6.6)	69.3(6.9)	.51	.03
Un. Single support (%GC)	37.5(1.8)	38.4(2.0)	.34	.05

In. = Involved limb; Un. = Uninvolved limb
*statistically significant group difference

Significance

Middle-aged adults with persistent ankle pain demonstrate decreased involved limb step length during walking gait. The assessment of STPs may be used to identify the presence of gait dysfunction and as an outcome measure to assess the effectiveness of an intervention aimed at improving the mobility of patients with persistent ankle pain. However, additional research is needed to identify the lower extremity kinematic and neuromuscular function changes that lead to decreased involved limb step length during walking in middle-aged adults with persistent ankle pain.

Acknowledgments

UW-Milwaukee CHS Student Research Grant Award.

References

[1] Al Snih, S., et al. 2001. *J Gerontol A Biol Sci Med Sci*, *56*(7):M400–404.
[2] Adamson, J., et al. 2006. *Ann Rheum Dis, 65*(4):520–524.
[3] Elbaz, A., et al. 2014. *Osteoarthritis & Cartilage*, 22:457–463.
[4] Gigi, R., et al, 2015. *J. Foot & Ankle Research* 8:1–8.
[5] De Kruijf, M., et al. 2015. *Gait & Posture, 42*:354–359.
[6] Parsons, S., et al. 2006. *BMC Musculoskeletal Disorders, 7*:34.
[7] Wright, C. J., et al. 2013. *Athl Train Sports Health Care* 5:201–209.
[8] Kosik, K. B., et al. 2019. *Gait & Posture* 70:403–407.

Effect of Targeted Hamstrings Intervention on Vertical Ground Reaction Force Asymmetries during Takeoff and Landing

Nathaniel A Bates[1], Takashi Nagai[1], Ryo Ueno[1], Luca Rigamonti[1], Rena F. Hale[1], Timothy E. Hewett,[2] Nathan D Schilaty[1]
[1]Department of Orthopedic Surgery, Mayo Clinic, Rochester, MN, USA; [2]Sparta Science, Menlo Park, CA, USA
Email: batesna@gmail.com

Introduction

Side asymmetry, limb dominance, and hamstrings:quadriceps strength ratios are factors associated with increased risk of lower extremity injury during athletic participation. [1,2] Targeted training interventions have proven adept in the reduction of modifiable biomechanical risk factors in high-risk athletes. [3] The objective of this study was to assess the efficacy of a targeted hamstrings training on the reduction of ground reaction force asymmetries in female basketball athletes across a single season. The hypotheses tested was that trained athletes would exhibit less asymmetry compared to controls at the end of the season.

Methods

Female high school basketball athletes (n=43; Age 15±1 yrs; Height = 171±17 cm; Mass = 65.2±12.2 kg) completed both pre- and postseason biomechanical evaluations that were used for analysis. Athletes were divided into intervention groups (control vs. trained) by team. The trained group completed dynamic hamstring exercises twice per week during their standard team warmup throughout the season. The control group received no additional training. Females were selected as they are at higher risk for noncontact lower extremity injury than males. Dominant side was determined by asking which leg an athlete would use to kick a ball. Dual force platforms continuouslly collected vertical ground reaction force (vGRF) separately for each leg at 1000 Hz during countermovement jump tasks. Data was filtered through a lowpass 4th order Butterworth filter with a 50 Hz cutoff and used to calculate rate of force development (RFD) before takeoff and after landing (LAND). RFD was calculated as the peak force divided by the time between this peak and zero force. Side asymmetry was assessed for both RFDs as well as peak force before takeoff and after LAND. Each athlete completed three jump trials and a mean was calculated. The hypothesis was tested via repeated measures ANOVA as collection was repeated pre- and postseason with an intervention (control/trained) factor.

Results and Discussion

For asymmetry in peak takeoff force, a time*intervention interaction effect was significant (P<0.01) as asymmetry shifted toward the non-dominant leg from pre- to postseason in controls (P<0.01; Figure 1), but remained unchanged in trained subjects (P=0.85). For asymmetry in takeoff RFD, no significant effects were observed (P≥0.29). For asymmetry in peak LAND force, a time*intervention interaction was significant (P=0.02) as asymmetry shifted toward the non-dominant leg from pre- to postseason in controls (P<0.01), but remained unchanged in trained subjects (P=0.89). For asymmetry in LAND RFD, a time*intervention interaction effect was not observed (P=0.34).

In basketball, the non-dominant leg is often the launch or pivot limb, which may develop a strength imbalance during the course of a season. This was observed in the current study as control group vGRF asymmetries during takeoff and landing favored the non-dominant leg in postseason testing. This trend was absent in the trained group, which indicated that interventional effects were present. Thus, the hypothesis was supported for a female cohort as development of peak force asymmetries over the course of a season were prevented in the training group.

Significance

These results indicate that targeted hamstrings interventions can influence limb asymmetries during athletic tasks and may be efficacious for high-risk athletes who are predisposed to develop vGRF asymmetries.

Acknowledgments

NBA/GE Collaborative Grant; NIH NIAMS R01AR055563, L30AR070273; and NICHD K12HD065987.

References

1. Paterno MV, et al. 2007. J Orthop Sport Phy Ther; 37(1).
2. Myer GD, et al. 2009. Clin J Sport Med; 19(1).
3. Webster KE, Hewett TE. 2018. J Orthop Res; 36(10).

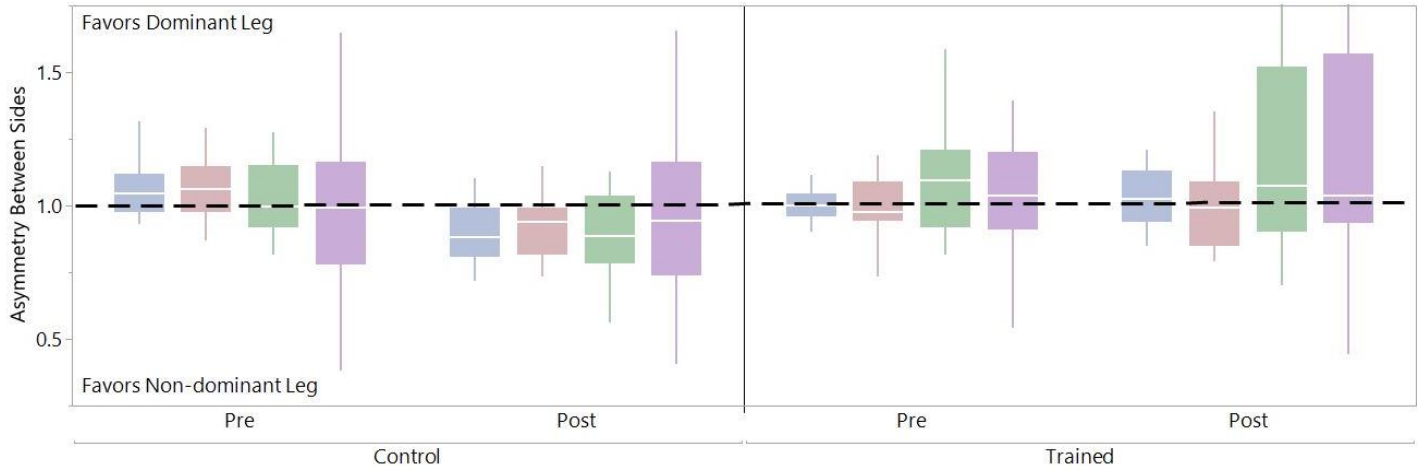

Figure 1: Side to side asymmetry for peak takeoff force (blue), takeoff RFD (red), peak LAND force (green) and LAND RFD (purple). Outcomes are separated by pre-/postseason and intervention. Asymmetry >1.0 indicates favoring of the dominant leg, while asymmetry <1.0 inicates favoring of the non-dominant leg. Increased asymmetry toward the non-dominant leg was observed in controls, but not trained subjects.

Bad vibes? Preliminary data on shock attenuation in injured and uninjured runners

Dovin Kiernan[1] and David Hawkins[1]
[1]University of California, Davis, Davis, CA, USA
Email: dahawkins@ucdavis.edu

Introduction

Running is associated with high injury rates and, with millions of Americans running, preventing these injuries is critical. One proposed injury risk factor is an inability to attenuate the high frequencies imposed on the musculoskeletal system with each step [1]. Some runners may be less capable of attenuating these frequencies or may lose the ability to attenuate these frequencies with fatigue, predisposing them to injury. There is, however, no direct evidence connecting reduced attenuation with injury and the relationship between attenuation and fatigue is equivocal. Here, we investigate whether: (1) shock attenuation changes across a prolonged run, and (2) previously injured runners display altered patterns of attenuation compared to uninjured controls.

Methods

Based on *a priori* sample size calculations, previously injured (n = 15) and uninjured (n = 15) rearfoot strike runners will be recruited. To date, one runner per group has been collected. Inertial measurement units (IMUs; Inertia Technology ProMove MINI; ±100 g, ±2000 deg/s, 1000 Hz) were fixed to runners' distal tibiae and foreheads. Runners performed calibration movements, ran 0.5 km to warm up, then ran for 30 min at their maximum pace. An experimenter biked beside runners to ensure speed remained within ±0.14 m/s (Garmin Edge 520 Plus). Heart rate (HR) was collected continuously (Polar H10) and ratings of perceived exertion (RPE) were collected every 6 minutes [2]. IMU data were rotated to segment local coordinate systems [3] and vertical accelerations from each stance from the 30-min run were isolated [4]. For each stance, the signal was de-trended and -meaned and attenuation was calculated by taking the log-ratio of head and tibia power spectral densities in 1 Hz bins from 0 to 500 Hz [5]. Attenuation was summed across a 10-20 Hz bin of interest and compared across the duration of the run.

Results and Discussion

Current results are preliminary and are limited by sample size but across the 30-min run, runners neared maximal exertion while maintaining relatively constant speeds. Speed remained within a mean absolute difference of 0.14 m/s from target speed. In contrast, HR and RPE increased throughout the run, ending at 190.4±0.2 BPM and 19.3±0.8 RPE, respectively (Fig. 1).

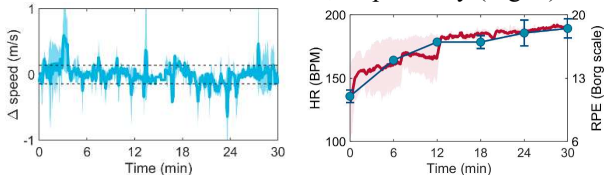

Figure 1: Mean±SD change in speed (left), heart rate (right; red), and Borg rating of perceived exertion (right; blue).

Tibia and head accelerations and signal powers were higher for the injured runner, likely because their target speed was higher (Fig. 2). Attenuation in the 10-20 Hz frequency bin decreased across the run for the uninjured runner while remaining relatively stable for the injured runner (Fig. 3). The stability in the injured runner's attenuation did, however, hide a marked increase in both head and tibia signal power.

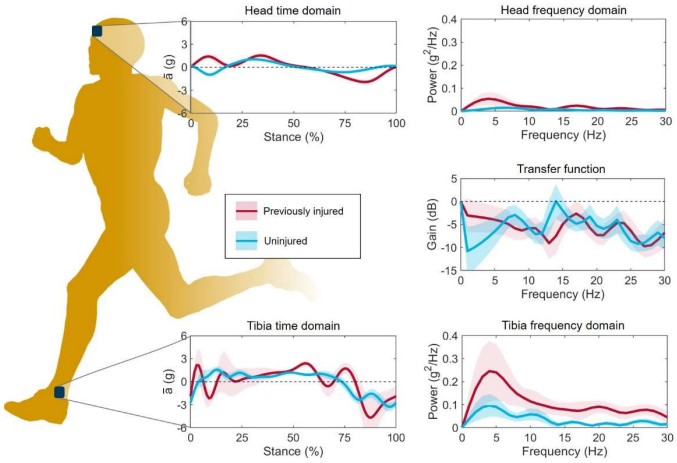

Figure 2: Mean±SD head and tibia de-trended and -meaned vertical accelerations in the time domain (left) with frequency domain and transfer function (right).

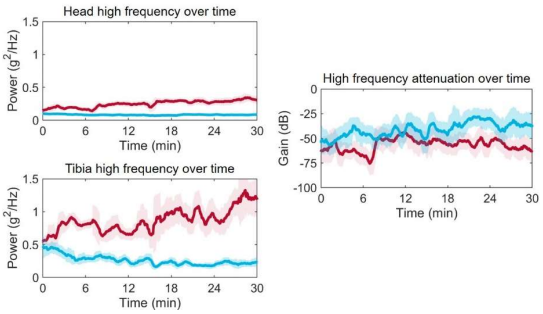

Figure 3: 60-second moving mean±SD sum of signal power in the 10-20 Hz bin for the head (top left) and tibia (bottom left) across the run. Attenuation of the 10-20 Hz bin (right).

Though limited by a small sample and retrospective design, these preliminary results suggest a link between running injury and the propagation of high frequency content up the kinetic chain. Interestingly, attenuation, calculated as the log-ratio of head and tibia frequency content, was not suitable to capture this propagation as both head and tibia high frequency content increased in the injured runner. These results also join an equivocal literature and suggest that fatigue may cause changes to high frequency signal power and/or attenuation. Future work will increase the sample size to further investigate these effects.

Significance

If high frequency content and attenuation are related to running injury and can be non-invasively monitored throughout a run, they may provide a means to monitor runners' injury risk.

Acknowledgments

ASB GIA, NSERC, and the Maury Hull Endowed Fellowship.

References

1. Nigg et al. *Cur Iss in Sport Sci,* **2**, 1-12, 2017
2. Borg. *Med Sci Sports Ex*, **14(5)**, 377-381, 1982
3. McGinnis & Perkins. *Sensors*, **12**, 11933-11945, 2012
4. Benson et al. *Sensors*, **19(7)**, 1483, 2019
5. Hamill et al. *Hum Mov Sci*, **14(1)**, 45-60, 1995

Comparison of trunk neuromuscular control strategies between athletes with and without a shoulder injury

Courtney M. Butowicz[1], Andy S. Camp[2], and Sheri P. Silfies[1]
[1]Department of Exercise Science, University of South Carolina, Columbia, SC
[2]United States Navy, Norfolk, VA
Email: butowicz@mailbox.sc.edu

Introduction

Shoulder injuries account for up to 40% of athletic injuries.[1] It is posited that impairments or variations in trunk control strategies perhaps influence force dissipation and upper extremity movement patterns, contributing to athletic injury. For example, diminished trunk neuromuscular control was associated with an increased risk of injury that resulted in missed days in professional baseball pitchers.[2] However, recent work suggests athletes with shoulder injuries may not demonstrate trunk control deficits when assessing motor performance, thereby challenging established theories of upper extremity injury mechanisms.[3] Trunk neuromuscular control asessments have mainly quantified specific performance parameters (e.g., postural sway, muscle endurance), yet rarely, consider the underlying system control strategy. Thus, the purpose of this study was to compare trunk neuromuscular control strategies between athletes with and without a shoulder injury. We hypothesized that athletes with a shoulder injury would demonstrate altered motor planning and feedback control strategies, corresponding to altered movement timing and accuracy during a goal-directed, unstable sitting task.

Methods

Ten athletes with a current shoulder injury (4 females; age: 22±4 years, mass: 78±19 kg, stature: 174±10 cm) and 10 sex, age, mass, stature, and sport-matched healthy controls consented to the study. Athletes sat on an unstable chair while force platform data were sampled (2400Hz), converted to COP trajectories, and displayed in real-time on a monitor. Athletes were directed to reposition the trunk-pelvis, which tilted the chair, resulting in movement of the COP. Precise changes in trunk-pelvis segments were required to quickly and accurately move the COP trajectory toward 8 targets (radius 35mm). Targets were displayed sequentially (clockwise); after target acquisition (or 12s, whichever occurred first), athletes returned to a central target. Control strategies were defined as (Figure): Motor planning (MP) control bounded by the reaction time (RT) and a local maximum in COP acceleration. Feedback (FB) control began at the end of MP and ended with target acquisition. FB control was further divided into a region that reflected control of movement toward a target (*directional control*) and a region where the goal shifted to target acquisition (*precision control*). A spike in polar velocity was used to separate FB phases. Duration and accuracy in each control strategy were calculated. *MP, FB directional, and precision time* were defined as the duration of the respective regions. *MP accuracy* was defined as off-axis error at the local maxima. *FB directional accuracy* was calculated as normalized RMSE between an idealized (second-order transfer function) and actual COP trajectories. *FB precision accuracy* was quantified with a 50% confidence ellipse area around each target. Performance measues of RT, time to target acquistion (TA), and number for missed targets (MT) were also recorded. Parameters were averaged across targets for each athlete. Independent t-tests were used to determine group differences ($p \leq .05$).

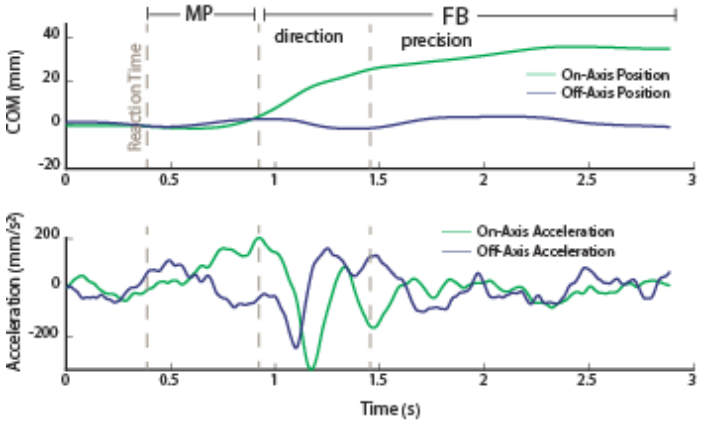

Figure: Representative COP (top panel) trajectory and accompanying COP acceleration data (bottom panel) with control regions identified.

Results and Discussion

Task performance did not differ between groups [*RT* (p=.31), *TA time* (p=.53), *MT* (p=1.0)]. In contrast with our hypothesis, *MP time* (p=.81), *MP accuracy* (p=.60), *FB directional time (p=.62) and accuracy* (p=.94), *FB precision time* (p=.80) and *accurancy* (p=0.27) were not different between groups. These results indicate that trunk control performance, nor underlying control strategies, differed between athletes with and without a shoulder injury. Our findings support recent evidence suggesting isolated trunk neuromuscular control performance does not differ between athletes with and without shoulder injuries.[3] Utilizing a dynamic systems approach to identify trunk control strategies has been previously validated comparing indivdiuals with and without low back pain.[4] Both groups in the current study appear to employ similar control strategies in this the goal-oriented task.

Significance

While trunk neuromuscular control is often incorporated into athletic injury prevention and rehabilitation paradigms, the results of the current study are in concert with recent work suggesting that impairments in trunk control may not associated with shoulder injuries. Assessing trunk control by characterizing strategies for task achievement is a novel approach to identify potential impairments in an athletic population. Though trunk control is likely an important factor in athletic performance, impairments in control may not be present in athletes with a shoulder injury, perhaps challenging the kinetic chain theory.

Acknowledgments

This work was funded by the APTA Legacy Fund.

References

[1] Dick et al. (2007). *J Athl Train*, **42(2)**:183-193.
[2] Chaudhari et al.(2014). *Am J Sports Med,* **42(11):**2734-40.
[3] Pontillo et al.(2020). *Clin Biomech,* **71:**196-200.
[4] Reeves et al.(2018). *J Biomech*, **73**: 33-39.

An investigation into the head accelerations and forces experienced by clay-target shooters

Suzanne M. Konz, Holly Cypert, and Robert O. Powell
Marshall University, Huntington WV, USA
Email: konz@marshall.edu

Introduction

Much attention has focused on the long-term effects of concussion in contact sports. CTE and other degenerative brain disorders have been identified in the brains of contact sport athletes and thought to result from repetitive exposure of the brain to acceleration-deceleration forces. Hunting and trap shooting are popular with the U.S. general population at 4.3 million.[4] School shooting teams are popular, increasing from 60 teams in 2009 to over 32,000 in 2019.[4,5] Clay-target shooters document shooting above 50,000 rounds per year. The military established recoil limits and firearm use protocols, limiting the number of rounds per level of recoil energy to reduce soldier injury risk due to recoil exposure.[1,2] What remains uncertain is the level of recoil energy of the brain during civilian sports. Indeed, the developing brain of high school shooters is of particular concern with the high-frequency head acceleration exposure. Research is needed to understand how high-frequency recoil exposure affects the brain. The purpose of this study was 1) to determine the differences in accelerations and forces encountered by clay-target shooters and 2) to compare the accelerations and forces that the head of clay target shooters' experience to norms from contact sports.

Methods

Subjects (n=35, 82.38±21.142kg) agreed to participate in this IRB approved study. Participants were randomized into a 25-shot or 100-shot group. 100-shot participants were given a 5-minute rest every 25 shots. Firearm and shooter kinematics were determined via inertial movement sensors (IMU's). Participants had an IMU secured behind the ear of the non-shooting shoulder. An IMU was also affixed to the stock of a 12-gauge shotgun. Data was processed using a custom Matlab code. The IMU outcomes of interest were gunstock, shoulder, and head accelerations. Other variables of interest were calculated with custom processing software to include the average and peak shot acceleration, shot force, shot impulse, and shot jerk experienced with each shot as well as the summation of all shots. Descriptive statistics and one-way ANOVA analyzed the day with significance set at the .05 level.

Results and Discussion

The single-shot averages at the gunstock for all shooters were as follows: duration (0.19 ± 0.04 sec), average acceleration (2.32 ± 0.23g), peak acceleration (7.09 ± 0.94g) were minimal, as expected. The accumulated totals at the gunstock for all shooters were as follows: duration (8.63 ± 6.64 sec), average acceleration (106.91 ± 50.34g), and peak acceleration (106.91 ± 84.18g). The gunstock of the 25-shot subjects experienced 2.29 ± 0.22g average acceleration and 7.24 ± 0.89g peak acceleration over 0.20± 0.04 sec while the gunstock of the 100-shot subjects experienced 2.38 ± 0.22g average acceleration and 6.72 ± 0.99g peak acceleration over 0.18 ± 0.05 sec for a single shot.

One-way ANOVA indicated no significance for the single-shot variables from the gunstock, but accumulated gunstock variables were significant.

The single-shot averages for all shooters at the ear was as follows: duration (0.20 ± 0.08 sec), average acceleration (1.34 ± 0.13g), peak acceleration (2.29 ± 0.55g) were minimal, as expected. The accumulated totals at the ear for all shooters were duration (10.27 ± 8.74 sec), average acceleration (68.17 ± 50.34g), and peak acceleration (118.05 ± 96.04g). 25-shot subjects experienced 41.58 ± 29.49g average acceleration and 69.53 ± 53.52g peak acceleration over 7.27 ± 8.32 sec while 100-shot subjects experienced 118.92 ± 42.42g average acceleration and 210.67 ± 92.10g peak acceleration over 15.99 ± 6.57 sec.

One-way ANOVA indicated no significance for the single-shot variables from the ear sensor between the 25-shot and 100-shot groups. But, a one-way ANOVA indicated that the single-shot variables of average force ($F(1,30) = 12.06$, $p = .00$) and peak force ($F(1,30) = 12.70$, $p = .00$) were significant between the shooting groups. The one-way ANOVA determine the accumulated ear sensor variables of duration ($F(1,30) = 9.06$, $p = .01$), average acceleration ($F(1,30) = 36.61$, $p = .00$), peak acceleration ($F(1,30) = 30.35$, $p = .00$), average force ($F(1,30) = 41.39$, $p = .00$) and peak force ($F(1,30) = 29.66$, $p = .00$) were significant.

The significance of the accumulated ear sensor variables between the groups needs to be viewed with caution as an increase in repetition will increase the accumulated accelerations and forces encountered. Football athletes experience peak linear forces at the 50th percentile at 20.3g and 62.2g at the 95th percentile.[3]

Significance

The g-forces encountered by individuals are low for a single shot and are not of concern. However, the accumulated totals for g-forces for all clay target shooters rose to levels where the brain could be influenced due to the repetitive nature of impact and the short duration of the exposure during shooting.

Acknowledgments

The authors received financial support from a NASA WV Space Grant

References

1.Blankenship K, et al. (2004) Army Research Inst
2.Burns BP (2012) Army Research Lab.
3.Crisco, JJ et al. (2012) *J Appl Biomech 28(2).*
4.Foundation NSS. NSSF Facts Sheets. 2020
5.USA High School Clay Target League 2020

The Influence of Concussion History on Reactive Balance Performance

Amanda Morris[1], Benjamin Cassidy[1], Ryan Pelo[2], Lee Dibble[2], Peter C. Fino[1]
Departments of Health, Kinesiology, and Recreation[1] and Physical Therapy and Athletic Training[2], University of Utah, Salt Lake City, UT, USA
Email: amanda.morris@utah.edu

Introduction

Concussion history has been associated with worse outcomes after future injuries, such as increased recovery time [1] and persistent symptoms [2], as well as neurocognitive [3] and motor deficits, such as increased intracortical inhibition [4] and a more conservative gait [5]. Standard clinical testing may be insufficient to detect lingering deficits associated with previous concussions [6].

Athletes frequently need to recover balance after an external disturbance, but little is known about the effects of concussion on reactive balance, and reactive balance is not currently part of standard clinical testing. While some studies have indicated lifetime incidence of concussion (i.e., concussion history) can impair postural control [7], there is little research on reactive balance performance in regard to concussion history. Therefore, the goal of this study was to examine the relationship between concussion history and reactive postural responses in collegiate athletes.

Methods

Reactive postural responses in 107 collegiate athletes (F=48, 19.30 (1.61) years, 23.49 (3.19) kg/m^2) were assessed using the Push and Release (P&R) in four directions (forward, backward, right, left), with eyes closed, under single (ST) and dual task (DT, concurrent cognitive task) conditions. Inertial sensors (Opal, APDM, Portland, OR; 128 Hz) on the sternum, lumbar, right tibia, and feet were used to assess step initiation latency and time to stabilization (TTS). A sensor on the tester's hand was used to determine release time. Participants were sorted into groups based on number of lifetime concussions (Table 1) and time since last concussion (Table 2). ANOVAs (α=0.05) were used to compare latency and TTS, under each condition (ST, DT), between groups.

Table 1. Participants separated by number of lifetime concussions.

	0 (n=69)	1-2 (n=34)	3+ (n=4)
Age mean (SD)	19.19 (1.64)	19.42 (1.48)	20.25 (2.22)
Female (%)	25 (36)	20 (59)	3 (75)

Table 2. Participants with concussion history separated by time since last concussion.

	Within 1 year (n=8)	1-5 years (n=20)	5+ years (n=10)
Age mean (SD)	20.25 (1.91)	18.95 (1.07)	20 (1.76)
Female (%)	7(88)	13 (65)	3 (30)

Results and Discussion

There were no significant differences between groups of lifetime concussions in any of the outcome measures (Table 3). There were also no significant differences between groups of time since concussion in ST latency (p=0.39), ST TTS (p=0.44), or DT latency (p=0.32). However, there was a significant difference in DT TTS (p=0.03) between the group that experienced their last concussion 1-5 years ago and the over 5 years ago group (Figure 1). Similar to previous studies that demonstrated a negative influence of concussion history on physical and cognitive performance, these results suggest that concussion may have long-lasting effects on reactive postural responses.

Table 3: Mean (SD) latency and time to stabilization (TTS) separated by number of lifetime concussions and task.

Number of Concussions	ST Latency (ms)	DT Latency (ms)	ST TTS (ms)	DT TTS (ms)
0	149 (26)	199 (53)	973 (173)	1143 (227)
1-2	150 (28)	200 (43)	1028 (250)	1133 (245)
3+	130 (9)	208 (58)	884 (164)	1040 (125)
p	0.35	0.95	0.23	0.73

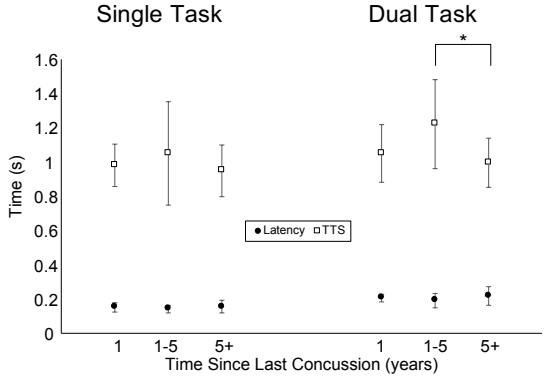

Figure 1: Latency and time to stabilization (mean, SD) separated by time since last concussion and task. *p=0.03

Significance

These findings suggest that lifetime history of concussion may impact reactive balance performance in collegiate athletes. However, the relationship between concussion history and balance performance, especially across sport-relevant tasks, remains unclear. Future research should examine both reactive, dynamic, and static balance performance in relation to acute concussion and concussion history.

Acknowledgments

The project was supported by the Pac-12 Conference's Student Athlete Health and Well-being Initiative (PI: Fino, Dibble). The content is solely the responsibility of the authors and does not necessarily represent the official views of the Pac-12 Conference.

References

1. Guskiewicz (2003) DOI: 10.1001/jama.290.19.2549
2. Zuckerman (2016) DOI:10.3171/2016.1.FOCUS15593
3. Hume (2017) DOI:10.1007/s40279-016-0608-8
4. De Beaumont (2007). DOI: 10.1227/01.NEU.0000280000.03578.B6
5. Buckley (2015). DOI: 10.1016/j.jshs.2015.03.010
6. Iverson (2012). DOI: 10.1155/2012/31657
7. Schmidt (2018) DOI: 10.4085/1062-6050-326-16

Change In Impacts Following a Fatigue Run in Female Runners with Single and Multiple Stress Fractures

Outerleys, J.[1], Popp, K.L., Ackerman, K. E., Tenforde, A.S., Rudolph, S., Loranger, E., Gellman., S., Garrahan, M., Bouxsein, M., Davis, I.S.
[1]Spaulding National Running Center, Harvard Medical School, Cambridge, MA
Email: jouterleys@bwh.harvard.edu

Introduction

Stress fractures are common in female running athletes and military recruits. Risk for stress fracture is multifactorial including both mechanical and biological factors, with high rates for risk of subsequent fracture[1]. Previous research has linked higher external impact loading during running to history of stress in rearfoot strike (RFS) runners[2]. It is unknown, however, if running impact variables differ between those with a history of single versus multiple stress fracture, and relative to controls. In addition, it is unclear how these variables change in response to fatigue, and if individuals with history of stress fracture elicit larger changes. Previous study has reported on increased impact loading with fatigue in the present cohort, however it was difficult to draw conclusions due to heterogeneity in foot strike pattern and it's influence on impact variables with fatigue[3]. The purpose of this study was to investigate change with fatigue between female running athletes who exhibit a RFS with a history of one stress fracture, multiple stress fractures, and those with none. We hypothesized those with a history of stress fracture will show greater changes with fatigue. In addition we hypothesized those with multiple stress fractures to have the largest change.

Methods

Thirty-one female subjects between the ages of 18-40 years who self-reported running a minimum average of 15 miles/week were included in this study. All subjects were classified as RFS using saggital plane 2D digital video (125 Hz) during treadmill running at a standardized speed (2.7 m/s). Subjects were categorized on number of previous stress fractures; no stress fractures (CON, n=11), one (1SFX, n=11), and 3 or more (3SFX, n=9). A fatigue run protocol was conducted on a force instrumented treadmill at a subject determined 5 km race speed and terminated when rating of perceived exertion reached ≥ 18 out of 20. Vertical average (VALR) and instantaneous (VILR) loading rate, along with vertical stiffness during impact (KIL) were calculated at a standardized speed (2.7 m/s) and the subjects' 5 km race speed at the beginning and end of the fatigue run. Change scores (post – pre) were compared separately for both speeds using one-way ANOVAs ($\alpha < 0.05$).

Results and Discussion

All subjects ran faster at their 5 km race speed than the standardized speed (MED: +0.67 m/s, MIN: +0.23 m/s, MAX: +1.79 m/s). No differences were seen between groups in age, mass, miles per week, years running, chosen 5km race speed, or time to fatigue. No differences were detected in impact loading or stiffness change scores at the standardized speed. At the 5 km race speed their was a group effect for KIL, with post-hoc analysis showing the 3SFX group was stiffer than CON ($p = 0.026$, see Table). 3SFX also showed the largest positive changes for VILR and VALR at the 5 km race speed, followed by the 1SFX, but were not statistically significant.

Significance

Our fatigue protocol did not elicit large changes in impact variables between groups, on average. Variation in magnitude and direction of change was observed, suggesting individualized response. It should be noted that "fatigue state" was captured using an exertion scale and not a subjective measure of fatigue, along with a lack of an objective measure of fatigability. This highlights the need for development of validated fatigue protocols and measures specific to running that are linked to the performance changes we expect to observe[4]. Despite this, time to fatigue and race speeds were similar between groups and the 3SFX showed the largest changes as hypothesized, but only during race like speeds. This could potentially be due reduce muscle capacity to attenuate impact loads and stiffness during early stance, resulting in more external loads applied to the skeletal system. This finding could be considered during injury screening and evaluating runners at potentially higher intensity speeds with fatigue. Interestingly, the CON group showed small-to-negative changes at both speeds suggesting an ability to compensate by reducing impacts with fatigue. While further investigation would benefit from being more adequately powered, these results warrant strategies to optimize mechanics and prevent fatigue-induced increases in impacts, particularly in those at risk of subsequent stress fracture.

Acknowledgments

Support provided by the U.S. Department of Defense, Defense Health Program, and Joint Program Committee W81XWH-16-1-0652.

References

[1] Rauh, MJ et al. 2006. MSSE. PMID 16960517.
[2] Milner, CE et al. 2006. MSSE. PMID 16531902.
[3] Outerleys, J et al. 2019. MSSE. doi: 10.1249/01.mss.0000562397.30456.54
[4] Enoka and Duchateau. 2016. MSSE. PMID 27015386.

	Variable	CON (11)	1SFX (11)	3SFX (9)	p (ANOVA)
Change Score at Race Speed	Race Speed (m/s)	3.45 (0.44)	3.42 (0.43)	3.55 (0.33)	0.766
	Time to Fatigue (min)	14.00 (6.93)	13.80 (5.39)	15.56 (6.27)	0.802
	VALR (BW/s)	-0.09 (11.22)	6.77 (12.34)	8.14 (11.50)	0.245
	VILR (BW/s)	0.18 (11.62)	6.23 (13.14)	8.25 (12.07)	0.316
	KIL (N/m)	-2155.54 (5331.41)	2316.21 (4365.19)	4795.10 (6727.26)	0.025

Brace Yourself: Sensitivity of Simulated Ankle Inversion Sprains to Neuromuscular Versus External Factors

Adam J. Yoder[1,2], Yingjun Zhao[3,4], Brittney N. Mazzone[1,2], Tae Hoon Kang[3], Kenneth J. Loh[3], Shawn Farrokhi[1,2]
[1]DoD-VA Extremity Trauma and Amputation Center of Excellence, [2]Naval Medical Center San Diego,
[3]University of California San Diego, Dept of Structural Engineering, [4]Oak Ridge Institute for Science and Education
Email: adam.j.yoder.civ@mail.mil

Introduction

Ankle sprains are a common injury among military Service members, leading to DoD mandated use of semirigid braces during high risk activity [1]. However, conventional designs are inadequate; mechanical response is invariant to task demands, often too restrictive or bulky, and therefore disuse rates are high [1]. Next-generation solutions are needed, although studying injury occurrence is challenging, albeit necessary to assess design efficacy. Dynamic, musculoskeletal simulation has prior been applied to reveal the role of ankle passive flexibility/laxity in sprain occurrence [2], and separately to highlight potential of preparatory co-activation and stretch-reflexes to prevent sprains [3]. This study aimed to estimate likelihood and sensitivity of sprain occurrence during a simulated drop landing within a single framework, given variance in neuromuscular and external loading factors. We expected that co-activation and drop height would be most influential, followed by ankle passive stiffness, reflex strength, and ground surface characteristics, respectively.

Methods

An established framework was adapted for this study [3]. Briefly, authors implemented custom stretch-reflex muscle controllers in a whole-body musculoskeletal model scaled to a single subject (F, 68kg, 1.8m), and tuned control parameters to track experimental kinematics during a 0.4 meter drop onto an inclined surface. After verifying simulation reproducibility, we assigned probability distributions to six model parameters suspected to influence sprain occurrence; with mean equivalent to baseline value, and variance meant to span physiologic neuromuscular ranges or realistic drop heights and surface characteristics (Table 1). Similar to [4], virtual scenarios were instantiated for a 5000-trial Monte Carlo simulation using Latin hypercube sampling (NESSUS, v9.8.0, SwRI), and executed via the MATLAB API (OpenSim v3.3). Since baseline, scaled model anthropometry and posture were kept constant, these scenarios represent a single subject with varied neuromuscular properties and control dropping from different heights onto varied surface stiffness. Peak subtalar inversion angle was extracted and assessed versus a 35±6 degree threshold where ligament failure may initiate [3]. Across all scenarios, subtalar angle cumulative response probability was calculated, as well as Pearson correlation versus each input variable. Scenarios with a response likelihood less than 5% were discarded from consideration. Lastly, probabilistic sensitivity factors were computed for each input 'x' as $(\partial p/\partial x * \sigma/p)$, and averaged over the [29,41] degree sprain range. These factors then identify how sprain likelihood varies with a change in each input's mean (S_u) or variance (S_σ).

Results and Discussion

Across all scenarios, peak subtalar angle ranged 9-46 degrees, and likelihood of a peak greater than [29, 41] degrees was [36, 10]% respectively. Confirming expectations, sprain occurrence was most sensitive to co-activation, indicated by a positive S_μ roughly double that of ankle stiffness (Fig. 1). This indicates increased co-activation decreased sprain likelihood twice as much as an equivalent increase in ankle stiffness. In contrast, reflex gain and ground contact dissipation had negligible influence. This corroborates prior work, which suggested 60% co-activation could prevent a sprain, but even the fastest reflexes could not [3]. Drop height and ground contact stiffness had a similar, but opposite, influence magnitude versus ankle stiffness (S_μ Fig. 1). Sprain likelihood was generally insensitive to input variance S_σ, with exception of co-activation, which had a moderate negative sensitivity, indicating increased co-activation variance increased sprain likelihood, with similar magnitude as increased drop height and ground stiffness over simulated ranges.

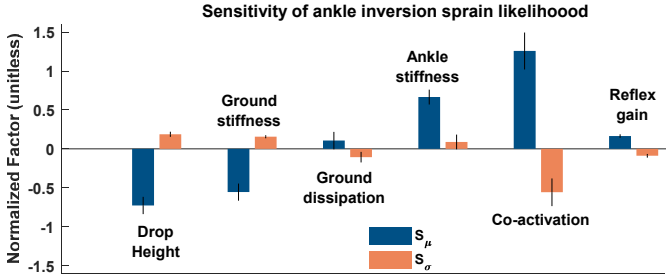

Figure 1: Probabilistic sensitivity factors for peak subtalar angle in response to changes in mean (S_μ) and variance (S_σ) of model input parameters (Table 1). Continuous factor trajectories were reduced to mean(std) over the 35±6 degree range where ligament failure is likely to initiate [3]. A *positive* factor indicates decreased sprain likelihood via a *negative* response correlation (Table 1); *negative* factor vice-versa.

Significance

Our findings suggest relative, theoretical importance of key neuromuscular and external loading factors in sprain prevention. Such data are useful to guide focus of continued simulation and experimental validation studies; ultimately aimed at informing stiffness design requirements for next-generation ankle braces.

References

1. Newman TM, et al. Mil Med. 2017;182:e1596–602.
2. Wright IC. Med Sci Sports & Ex. 2000. 32:260–5.
3. DeMers MS, et al. J Biomechanics. 2017. 52:17–23.
4. Hegarty AK, et al. J Biomech Eng. 2017;139:031009.

Table 1: Probabilistic drop landing simulation inputs and Pearson correlation versus peak subtalar angle across 5000 scenarios.

Model parameter	Distribution	μ	σ	Correlation
Initial drop height (meters)	lognormal	0.30	0.15	**0.36**
Ground contact modulus (MPa\meter)	lognormal	34	15	0.28
Ground contact dissipation (sec\m)	lognormal	5	4	0.04
Ankle passive stiffness (±% scale from baseline)	normal	0%	40%	**-0.39**
Co-activation (invertor/evertor)	lognormal	30%	20%	**-0.63**
Reflex strength (controller gain)	lognormal	5	3	-0.05

Modeling Rodent Gait Compensation Strategies after Lateral Gastrocnemius Volumetric Muscle Loss Injury

W. Brody Hicks[1], Jack Dienes[2], Juliana Amaral Passipieri Ph.D[2], George J. Christ Ph.D[2,3], and Shawn Russell Ph.D.[1,2,3]
University of Virginia, Depts. of [1]Mechanical Eng., [2]Biomedical Eng., and [3]Orthopaedic Surgery, Charlottesville, VA, USA
Email: sdr2n@virginia.edu

Introduction

The rat hindlimb is one of the most highly utilized model systems for pathologies whose healing requires functional recovery. However, most studies focus on indirect functional measurements such as force generation and kinematics of the hindlimb to quantify the quality of their treatment, providing only a partial picture. To fully understand the impact of a treatment on the functional recovery of an animal it is necessary to acquire and compare joint and muscle kinetics.

In order to quantify the effects of volumetric muscle loss on movement function we have previously developed a model and methodology to measure the kinematics and kinetics of rodent gait. We investigated the tibialis anterior (TA) and employed our motion capture approach to evaluate a 20% (by mass) volumetric muscle loss (VML) injury[1]. This work resulted in statistical differences between the injured and healthy animals at all post-surgical timepoints. This was significant considering the low gait impact of the TA, as it is solely responsible for ankle dorsiflexion and toe clearance during swing. We have leveraged that previous work into the investigation of injuries to a major gait contributor in the lateral gastrocnemius (LG). The LG is important, as ankle plantarflexion is the primary means of propulsion in walking. The LG also has the added complexity of being a two-joint muscle.

Methods

8 twelve-week old male Lewis rats were given a 20% by mass VML injury to their right LG with no repair (LGNR). Animals were labeled with motion capture markers and recorded using Vicon Nexus software as they voluntarily walked down an instrumented walkway at -1, and 12 weeks (W12) relative to their surgery date. Before testing sessions, rats were shaved to allow accurate placement of 4mm reflective markers on the bony landmarks. All motion data was normalized to 100% of a complete gait cycle (heel strike), with a minimum of three cycles averaged for each rat. Simulations were performed on subject specific versions of a modified OpenSim 3D rat hindlimb model[1,2] to calculate kinematics, kinetics and muscle length over a gait cycle. Force testing consisted of LG stimulation via a nerve cuff on the tibial nerve, with the distal portion of the LG tethered to a load cell to record maximum isometric torque.

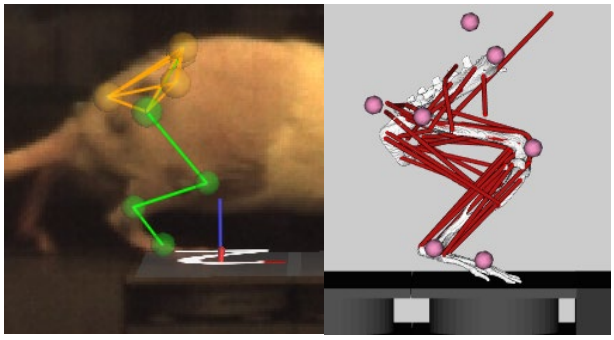

Figure 1: Labeled rat in the walkway (left), OpenSim model scaled to the individual rat (right).

Acknowledgments

We would like to thank the Christ and MAMP Laboratories
This work was supported by Department of Defense Grant W81XWH-18-2-0036 DoD/USAMRAA

Results and Discussion

Force testing at the W12 timepoint showed a significant deficit in the injured vs. contralateral LG muscle's ability to generate force at the ankle. Baseline kinematics[1,3] and GRFs[3] were similar to reported data of normal gait in rats. W12 kinematics showed significant changes in the hip motion in stance and pre-stance, with increased extension, abduction, and external rotation. While not significant, there was a trend at the knee for increased knee extension throughout stance. Surprisingly, there was little difference at the ankle joint. Joint kinetics of the injured limb demonstrated little differences compared to the baseline moments. There was an increased hip abduction and knee extension moments in stance. Again, supprisingly, there was no difference in the moment generated about the ankle.

Post hoc analysis of the medial and lateral gastroc muscletendon unit length adds some insight as to how the rats were able to generate the normal ankle moment with injured LG. Simulations show that the rats LG and MG muscletendon unit was longer at the W12 tests. This moved the force length curve to the right increasing the contributions of the passive portion of the muscle, enabling the rats to generate the required moment with reduced active muscle capacity. This can also be seen in the kinematics where the knee and hip were extended allowing the LG and MG to operate in a more advantageous position.

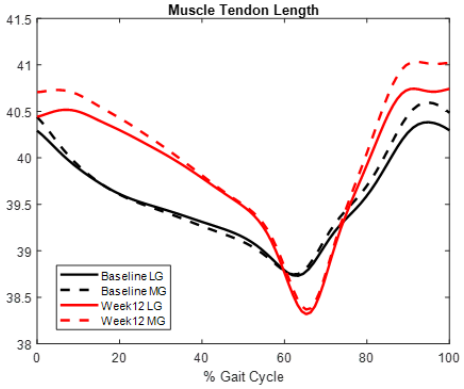

Figure 2: Muscle tendon unit length (mm) over one gait cycle.

Baseline black
Week 12 red

Significance

The development and implementation of robust dynamic models of the Lewis rat musculoskeletal system offers new perspective on how animals adapt to new and novel neuromuscular pathology. Understanding how activation and loads change for a given movement adaptation will help to inform cutting edge methods for VML repair. This includes defining the material properties of engineered regenerated muscle fibers, in addition the models offer a method for testing possible rehabilitation methods to optimized functional recovery.

References

[1] Dienes et al, 2019, Front Bioeng Biotechnol 7:146.
[2] Johnson et al, 2008, J Biomech 41(3) 610-619.
[3] Garnier et al, 2007, Behav Brain Res 186 57-67.

Variability of Spatiotemporal Gait Metrics in Middle-Aged Adults with Persistent Ankle Pain

Stephen C Cobb[1], Kazandra M Rodriguez[2], Mohammed S Alamri[1], and Emily E Gerstle[1]
[1]Department of Kinesiology, University of Wisconsin-Milwaukee, Milwaukee, WI, USA
[2]Department of Kinesiology, University of Michigan-Ann Arbor, Ann Arbor, MI, USA

Email: cobbsc@uwm.edu

Introduction

Persistent ankle pain afflicts an estimated 11.7% of adults over the age of 50 with the prevalence peaking in middle-age [1]. In addition, individuals with ankle pain/ stiffness but no diagnosed OA report similar pain, disability, and decreased Qol as those with ankle OA [2]. Despite the prevalence and adverse impact on Qol, very little research has investigated the influence of persistent ankle pain on gait in middle-aged adults.

Spatiotemporal parameter variability (STPV) may be a sensitive indicator of age- and injury- related changes in the motor control of gait [3,4]. Previous studies have investigated STPV in young adults with chronic ankle instability (CAI) [5] and in middle-old aged adults with chronic lower body joint pain [4], however, persistent ankle pain in middle-aged adults has not been studied.

The purpose of this study was to investigate walking gait STPV in middle-aged adults with persistent ankle pain. We hypothesized that individuals with persistent ankle pain would demonstrate increased spatiotemporal parameter variability.

Methods

Nineteen middle-aged adults (45-64 yo) provided written informed consent to participate in one of two groups (PAIN, CON). PAIN group participants (n = 10; 9 F, 1 M; mean age: 54.4 ± 5.8 y; mean height: 168.0 ± 5.1 cm; mean BMI: 27.3 ± 7.1 kg/m^2) experienced pain for the previous 3 months, complained of at least slightly troublesome pain on most days during the past month [6], and had a history of at least one lateral ankle sprain. CON group participants (n = 9; 8 F, 1 M; mean age: 53.0 ± 5.8 y; mean height: 168.2 ± 6.1 cm; mean BMI: 26.5 ± 7.4 kg/m^2) were matched with PAIN group participants by age (± 5 y), sex, and BMI classification. CON group participants had no complaints of ankle pain in the previous 3 mos., had no history of ankle sprain in the previous 12 mos., and no acute lower extremity injury in the previous 12 mos.

Each participant completed 10 successful self-selected speed barefoot walking trials along a 15 m walkway with 3 embedded force plates (sampling rate: 1000 Hz). For each spatiotemporal metric of interest, variability was expressed as the coefficient of variation (100 x (standard deviation of the metric/mean of the metric) (Table 1). Group differences were investigated using independent t-tests (SPSS, $\alpha = 0.05$)

Results and Discussion

A preliminary analysis of preferred walking speeds revealed no significant differences between the groups (PAIN: 1.19 ± 0.11 m/s, CON: 1.21 ± 0.13 m/s, p = 0.786). The hypothesized increase in PAIN group STPV was supported during double support, but not for the other metrics assessed (Table 1). The increased variability during double support may be the result of decreased strength, changes in neuromuscular function, postural stability, and/or central motor control changes associated with persistent ankle pain [5,7].

The lack of significant difference in stride length and cycle time between the PAIN and CON groups in the current study was consistent with a previous CAI study [5]. Although the results agree, comparison between the studies is difficult given the differing participant ages and inclusion/exclusion criteria. The lack of significant difference in step length variability was inconsistent with a previous study that reported decreased step variability in participants with chronic lower body joint pain [4]. However, the lower body joint pain study included middle-old aged participants with low back, hip, knee and foot pain and suggested the majority of the differences were driven by hip pain. Thus, the effect of chronic pain on STPV may be influenced by the joint(s) affected.

Table 1 Mean (SD) PAIN and CON Group STPV

STPV (%)	Group		*P*	η^2
	PAIN	CON		
Cycle time	2.73 (1.05)	2.67(1.04)	0.904	0.001
Stride length	1.61 (0.56)	1.28 (0.56)	0.222	0.086
Gait speed	2.92 (1.25)	2.81 (0.94)	0.831	0.003
Cadence	2.70 (0.99)	2.63 (0.98)	0.887	0.001
In. Step length	3.62 (1.89)	3.53 (2.77)	0.937	0.000
In. Single support	2.20 (0.85)	2.11 (0.58)	0.794	0.004
In. Double support	4.22 (0.88)	3.13 (0.92)	0.017*	0.292
Un. Step length	3.63 (2.35)	3.33 (1.90)	0.767	0.005
Un. Single support	2.51 (0.73)	2.12 (0.98)	0.339	0.054

In. = Involved limb; Un. = Uninvolved limb
*statistically significant group difference

Significance

Middle-aged adults with persistent ankle pain demonstrate increased variability during double support of walking gait. Further study is warranted to investigate pain-related changes in strength, neuromuscular function, postural stability, and/or central motor control in middle-aged adults with persistent ankle pain that may lead to the increased double support variability during walking gait.

Acknowledgments

UW-Milwaukee CHS Student Research Grant Award.

References

[1] Murray C., et al. 2018. *PLoS One*, *13*(4): e0193662.
[2] Al Mahrouqi M., et al. 2017. *Journal of Science and Medicine in Sport, 20*S:e99
[3] Hausdorff J., et al. 2007. *Hum Mov Sci, 26*(4):555-589.
[4] de Kruijf M., et al. 2015. *Gait Posture, 42*(3):354-359.
[5] Springer S. & Gottlieb U. 2017. *BMC Musculoskelet Disord, 18*(1):316.
[6] Parsons S., et al. 2006. *BMC Musculoskelet Disord, 7*:34
[7] Herssens N, et al. 2018. *Gait Posture, 64*:181-190.

The Effects of Recreational Dance Experience on Landing Mechanics

Cycenas, T. J., Gimberlin, T., Hegazy, M.A, PhD
Southwest Minnesota State University
Email: Taylor.Cycenas@my.smsu.edu

Introduction

Poor landing mechanics expose athletes to increased risk of injury (Harwood *et al*., 2018). However, dancers experience less acute lower limb injuries than non-dance athletes (Turner *et al*., 2018). Specifically, research supports that dancers experience substantially reduced ACL injuries compared to team sport athletes (Liederbach, *et al.,* 2008). Reduced injuries may be a result of the extensive training experienced dancers undergo (Orishimo *et al.,* 2014). Although reseachers have recommended that non-dance athletes may benefit from doing dance training (Turner *et al.,* 2018), it is unknown how much dance training would be needed to gain similar benifits. While research provides evidence that dancers exhibit superior landing mechanics compared to non-dancers, these findings have been conducted in professional and high level dancers who spend at least 12 hours a week practicing (Turner et al., 2018). Competivie athletes typically have time constraints and it is highly unlikely they will engage in dance with the same commitment as professional and high level dancers that spend long hours on a daily basis. It is unknown if recreational dance experience contributes to better landing mechanics. Therefore, the purpose of this study was to determine if recreational level dance experience provided better landing mechanics to that of non-dancers. If so, it is more practical for non-dance athletes to gain a recreational level of dance experience to improve their landing mechanic.

Methods

We compared landing mechanics of noncompetitive college dance team dancers (n=12; weight=61.71±12.53 kg; height=160.66±8.61 cm; years of experience=12.75±4.16; hours/week=10.75±3.44) to those of non-dancers (n=12; weight=80.34±21.13 kg; height= 165.10±5.86 cm). Loadsol insoles (Novel, St. Paul, Minnesota, United States) were inserted into the participant's shoes to measure GRF and Opal inertial sensors (APDM, Portland, Oregon, United States) were secured to the participant's body to collect kinematic data. A 5-minute warmup on an elliptical machine was performed prior to the jumping tasks. Participants then performed 3 maximal countermovement vertical jumps using a vertical jump measuring device, from which their 75%, 50%, and 25% sub maximal values were calculated. Participants then performed three jumps from each submaximal height in a counterbalanced order.

Results and Discussion

No significant differences in normalized peak vertical GRF or peak loading rate were found between groups ($p>0.05$). However, dancers displayed greater peak hip flexion range of motion to peak GRF in both left and right hips with ($F(1, 22) = 5.06$, $p<0.05$ and 11.09, $p<0.05$, for the left and right hips, respectively; Figure 1). In addition, dancers also showed a significantly lesser knee valgus angle than non-dancers with ($F(1, 22) = 4.93$, $p<0.05$ and 4.79, $p<0.05$, for the left and right knees, respectively). Increase in hip flexion during landing increases the moment arm for the ground reaction force vector at the hip and reduces it at the knee. Thus, the demand on hip extensors to control the downward movement increases, while that on knee extensors would decrease (Powers, 2010). Turner et al., (2018) reported that dancers achieved greater gluteus maximus activation and reduced knee valgus angles compared to non-dancers in a drop landing task. However, dancers in their study practiced for a minimum of 12 hours a week and were members of a university dance program. In our study, dance team members with less weekly practice time than typically reported in the literature showed superior landing biomechanics to non-dancers. The landing patterns observed may protect against acute lower extremity injury.

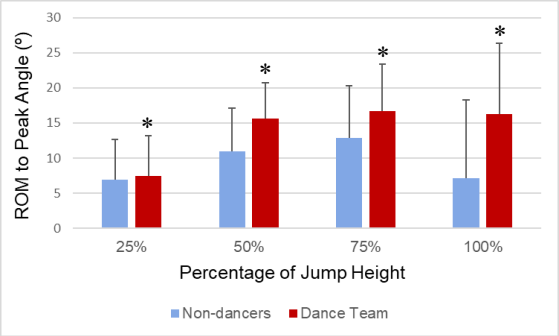

Figure 1: Left hip ROM to peak joint angles of dance team and non-dancers at 25%, 50%, 75%, and maximal jump heights. *$p<0.05$

Significance

In this study we found sufficient evidence to support that non-dance athlete may benefit from implementing dance training at a recreational level. However, dancers in our study spent approximately 10 hours of practice every week, which is less than professional dancers but more than what a typical non-dance athlete may be able to do given time constraints. Thus, future studies should focus on identifying key components of dance training for non-dance athletes to implement. Another direction would be to study landing mechanics of individuals who engage in dance for less than five hours a week. However, finding participants that meet this criteria may prove difficult.

Acknowledgments

We would like to thank the SMSU Dance team.

References

Harwood, A. et al. (2018). *Physical Therapy in Sports Journal*, *32*, 180-186.

Liederbach, M. et al. (2008). *American Journal of Sports Medicine, 36*(9), 1779–1788.

Orishimo, K. F. et al. (2014). *American Journal of Sports Medicine, 42*(5), 1082-1088.

Turner, C. et al. (2018). *Physical Therapy in Sports Journal, 31*, 1-8.

Walter, H. L. (2011). *Journal of dance medicine and science*, *15*(2), 61–64.

Characterization of Activities and Postures during Planetary Extravehicular Activities via Inertial Measurement Units

Kyoung Jae Kim[1,*], Eduardo Beltran[1], Jocelyn Dunn[1], Omar Bekdash[1], Jason Norcross[1], Andrew Abercromby[2], Meghan Downs[2], Sudhakar Rajulu[2]
[1]KBR, 2400 NASA Parkway, Houston, TX 77058, [2]NASA Johnson Space Center, 2101 NASA Parkway, Houston, TX 77058
Email: *kyoungjae.kim@nasa.gov

Introduction

At NASA Johnson Space Center, engineering evaluations of prototype exploration spacesuits and spaceflight analog environments have been led by the Human Physiology, Performance, Protection, and Operations (H-3PO) Laboratory in collaboration with the Anthropometry and Biomechanics Facility (ABF) to advance the current understanding of crewmembers' capabilities and limitations in suited planetary extravehicular activities (EVAs). We have been conducting simulated planetary EVA operations using the Mark III spacesuit [1] in the Active Response Gravity Offload System (ARGOS). While partially offloading subjects' weight to simulate Lunar gravity, 1/6 of Earth's gravity (1/6-G), we are characterizing activities and postures during EVAs to provide both quantitative and subjective data for work-domain and metabolic characterizations as well as engineering evaluations of next-generation spacesuits and tools.

Methods

Subjects conducted EVA-like tasks, such as deploying science experiments on the lunar surface, which enabled efforts toward classifying when subjects were standing, bending over, kneeling, walking, etc. For example, subjects performed each experimental package deployment (i.e., while bending over or kneeling) then ambulated on a treadmill with various incline grades to simulate translation paths to the next deployment site (Figure 1).

For kinematic assessments, we donned 7 Opal™ (APDM, OR, USA) wireless inertial measurement units (IMUs) on the spacesuit: one on the chest; one each on left and right upper hip bearing; left and right mid hip bearing; and left and right ankle bearing. The chest IMU measured the torso tilt angle in the sagittal plane. Specifically, accelerometer, gyroscope, and magnetometer data were fused into quaternion rotation matrices via a gradient descent algorithm [2]. The quaternion rotation matrices were then transformed into Euler angles using custom scripts programmed in MATLAB® (R2019a, Mathworks, MA, USA). The lower limb IMUs discriminated translation (walking), standing activities, and kneeling activities. We utilized an ensemble learning method to capture each activity type. Specifically, activities were first characterized and verified by direct observation using Boris event-logging software [3]. Afterwards, we used ensemble learning on the labeled dataset and enlisted classifier models including linear discriminant analysis and support vector machine that are strategically combined to reduce computational cost while improving the performance compared to a single classifier [4]. We provided a rejection criteria for all pseudo-kinematic motions that were not strictly considered translation (i.e., at least three consecutive gait cycles must be demonstrated for both legs) and kneeling down (i.e., at least three-second kneeling down posture must be maintained).

Results and Discussion

Table 1 and Table 2 show the duration and percentage of each activity type and its corresponding torso tilt angle in the sagittal plane. For example, during a 38-minute experimental package deployment task, the subject spent 32.6%, 50.5%, and 16.9% of the task time translation, standing, and kneeling, respectively.

Figure 1: Examples of activities and postures: (left) translation (walking) on the treadmill, (middle) standing and bending over, (right) non-standing (kneeling with both knees) and bending over.

Table 1: Duration and percentage of each activity (unit: minute [%]).

Total	Translation (walking)	Standing activities	Kneeling activities		
			Both	Right	Left
38.2 (100.0)	12.4 (32.6)	19.3 (50.5)	2.5 (6.6)	3.4 (8.8)	0.6 (1.5)

Table 2: Duration and percentage of the torso tilt angle in the sagittal plane during standing and kneeling activities (unit: minute [%]).

Posture	0-10°	10-20°	20-30°	30-40°	40-50°	50-60°	60-70°	70-90°
Standing activities	9.6 (49.7)	2.8 (14.5)	1.8 (9.3)	1.7 (8.8)	1.7 (8.8)	1.5 (7.8)	0.2 (1.0)	0.0 (0.0)
Kneeling activities	0.4 (5.2)	0.4 (5.2)	0.5 (6.5)	0.6 (7.8)	0.7 (9.1)	1.9 (24.7)	2.2 (28.6)	1.0 (13.0)

Suited subjects were demanded kinematic adjustments during EVA-like tasks at the ARGOS environment, which were depicted by the varying degrees of torso tilt in the sagittal plane (i.e., past 20 degrees). The lack of flexibility in the hard upper torso (HUT) may have caused subjects to increase torso tilt to beyond 60 degrees in the kneeling activities. Advanced materials and joint bearings have allowed room for rotation at the hips and bending of the knees to coordinate these tasks. The modified Extravehicular Mobility Unit (EMU) gimbal limited arm movement during translation, however, subjects could ambulate at a range of speeds and inclination angles without discomfort.

Significance

Mobility and energy expenditure of crewmembers on the lunar surface are of prime interests in any lunar EVA. On Apollo missions, the hopping and falling behaviors were attributed to restricted movement due to the inflexibility of the Apollo suits. However, in this study, the Mark III spacesuit that includes multiple bearings and convolutes at the hip and thigh provided greater mobility. The results should be generalizable to the Exploration EMU (xEMU) for the Artemis astronauts who will be working on the moon. Future work will include the validation study of characterized activities and postures with the xEMU suit. These methods also will be used as part of a metabolic rate task characterization study to determine the physical workload associated with partial gravity EVAs.

References

[1] Cullinane CR, et al. (2017). Mobility and agility during locomotion in the Mark III space suit. *Aerosp. Med. Hum. Perf.*, 88(6), 589-596.
[2] Madgwick SO, et al. (2011). Estimation of IMU and MARG orientation using a gradient descent algorithm. *Proc. IEEE Int. Conf. Rehabil. Robot.*, 1-7.
[3] https://www.boris.unito.it/
[4] Polikar, R. (2006). Ensemble based systems in decision making. *IEEE Circuits Syst. Mag.*, 6(3), 21-45.

Assessing Postural Control with Smartphone Accelerometery in People with Multiple Sclerosis

Katherine L. Hsieh[1] and Jacob J. Sosnoff[1]
[1]Univesity of Illinois at Urbana-Champaign, Urbana, IL
Email: klhsieh3@illinois.edu

Introduction

Falls are a major health concern for people with Multiple Sclerosis (pwMS). One in two pwMS will fall in a three-month period, and up to 50% of falls result in an injury.[1] Impaired postural stability is one of the most important risk factors for falls in MS and affects over 50% of pwMS.[1] Postural stability can be assessed with clinical scales, but these do not always capture underlying balance impairments in pwMS.[2] Technology-based assessments (i.e., force plates, motion capture) can capture minute changes in posture but require expensive equipment.

One alternative solution is to use leverage the power of smartphone technology. Smartphones are embedded with an accelerometer that can potentially be used to assess postural control. Smartphones are also are affordable, ubiquitous, and portable, offering potential for home-based assessments. The purpose of this study was to determine whether smartphone accelerometry can measure postural control in pwMS compared to a research grade accelerometer and force plate measures during standing balance tasks. We also determined whether smartphone accelerometry was capable of discriminating between assisted device users and non-assisted device users, as assisted device usage is a strong predictor of falls in pwMS.[3]

Methods

Twenty-seven individuals with MS participated. All participants underwent static balance assessments while standing on a force plate (Bertec Inc, Columbus, OH) and holding a smartphone (Samsung Galaxy S6, Seoul, South Korea) medially against the chest along the sternum. A research grade accelerometer (Opal, APDM, Portland, OR) was attached to the smartphone.

Two trials of five standing balance tasks were performed on the following order for 30 seconds each: 1) eyes open, 2) eyes closed, 3) semi-tandem, 4) tandem, and 5) single leg. Acceleration from the smartphone and Opal in the mediolateral (ML), anteroposterior (AP), and vertical directions were exported and processed, and Root Mean Square (RMS) acceleration in the ML and AP directions and 95% area ellipse were calculated. Center of Pressure (COP) data from the force plate was exported and processed, and RMS in the ML and AP directions and 95% area ellipse were calculated.

COP and acceleration measures were averaged for the two trials for each condition. Validity between measures derived from the force plate, smartphone accelerometer, and Opal accelerometer were assessed with Spearman's correlations for all balance conditions. Receiving operating characteristic (ROC) curves were constructed and the area under the curve (AUC) was calculated to determine the level of discrimination between assisted device users and non-assisted device users.

Results and Discussion

Of the 27 participants, 12 were assisted device users and 15 were non-assisted device users. Assisted device users had significantly greater Expanded Disability Status Scale scores, suggesting greater disability (p = 0.01). There were no differences in age between groups (p = 0.11).

There were moderate to strong correlations between the smartphone accelerometer and Opal accelerometer for RMS (ρ = 0.66 – 0.97; p = 0.001 – <0.001) and 95% area ellipse (ρ = 0.72 – 0.94; p = <0.001). As anticipated, there were weak to moderate correlations between the smartphone accelerometer and force plate for RMS (ρ = 0.45 – 0.87; p = 0.02 – <0.001) and 95% area ellipse (ρ = 0.48 – 0.72; p = 0.01 – <0.001). These findings suggest that smartphone accelerometry is comparable to measure postural control compared to gold-standard devices in pwMS.

ROC curves were constructed to determine the classification accuracy between assisted device users and non-assisted device users (Fig. 1). For RMS ML, AP and 95% confidence ellipse acceleration from the smartphone, the AUC was statistically significant (p <0.001 – 0.02). For RMS AP and 95% confidence ellipse acceleration from the Opal accelerometer, the AUC was statically significant (p = 0.002 – 0.03). There was no statistical significance for RMS ML from the Opal accelerometer. For COP outputs from the force plate, the AUC was statistically significant (p = 0.004 – 0.05). These results suggest that smartphone accelerometry can be used to classify MS assisted device users and non-assisted device users. Because assisted device usage is a strong predictor of falls and a proxy of postural instability, smartphone accelerometry may provide an insight to understanding those who are at a high risk for falls.

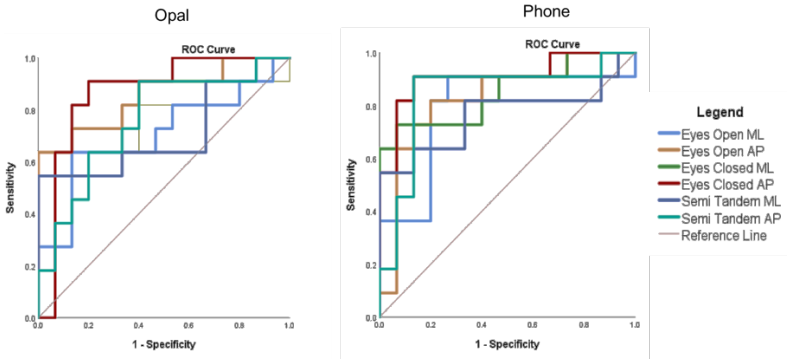

Figure 1. Receiver Operating Characteristic (ROC) curves for Root Mean Acceleration from the Opal and Smartphone.

Significance

There is potential to leverage smartphone accelerometery to provide an objective assessment of standing balance in pwMS. Smartphones are affordable, ubiquitous, and portable, and over 80% of pwMS own smartphones. These finding provide preliminary results to support the development of mobile health app to measure fall risk for those with MS.

References

1. Cameron, MH, & Nilsagard, Y. (2018). Chap 15 - Balance, gait, and falls in MS. *Handbook of Clinical Neurology*. (159, pp. 237-250).
2. Kanekar, N., & Aruin, A. S. (2013). Role of clinical and instrumented outcome measures. *Mult Scler Int.*
3. Peterson, EW, Ben Ari E, Asano M, & Finlayson, ML. (2013). Fall Attributions Among Adults With Multiple Sclerosis. *Archives of PMR, 94*(5), 890-895.

Estimation of Vertical Ground Reaction Forces in a Real World Environment Using Machine Learning

Seth Donahue[1*], Yuta Suzuki[2] Michael Hahn[1]
[1]University of Oregon, Neuromechanics Laboratory, Human Physiology, Eugene, OR, USA
[2]Osaka City University, Research Center for Urban Health and Sports, Osaka, Japan
Email: *sethd@uoregon.edu

Introduction

Machine learning (ML) algorithms for the estimation of biomechanical variables have been implemented in the highly controlled settings of the laboratory. However, one of the ideals of these tools is to take biomechanical analysis into a less constrained environment [1]. In gait biomechanics the accurate measurement of ground reaction forces is crucial for solving inverse dynamics. In the laboratory Inertial Measurement Unit (IMU) data has been input into ML algorithms to estimate ground reaction forces, joint moments and powers [2,3]. These studies have been limited in their real world applicability because only a small number of locomotion modes or speeds were tested.

The purpose of this project was to examine the accuracy of a long short term memory (LSTM) network to estimate the vertical ground reaction force waveform (vGRF) of subjects across multiple locomotion modes (level ground walking, running, ramp and stair, ascent and descent) from data collected in a real world environment. We expect that estimation error, (root mean square error (RMSE)) of the predicted vGRF data will be the lowest for walking, and that running will have the highest RMSE of the locomotion modes.

Methods

Data were collected from 14 subjects (8 male and 6 female, 32.7 ± 15.2 years, 175 ± 7.9 cm, 67.8 ± 9.0 kg) over a two day protocol. All analyses were performed in custom Matlab programs (Mathworks, Natick, MA). Lightweight IMUs (Vicon, Centennial, CO) mounted on the dorsal aspect of each participant's dominant foot and shank recorded linear accelerations and angular velocities at 500 Hz. Vertical ground reaction force data were recorded with Loadsol inserts (Novel Electronics, St. Paul, MN) at 100 Hz.

On the first day of the protocol participants performed 6 locomotion tasks; stair ascent and descent, level ground walking, ramp ascent and descent (slopes <5°), and running. The second day of the study utilized a protocol adapted from Long and Srinivasian [5]. The range of target average speeds was 1.3 to 3.0, m s^{-1} (1.30, 1.51, 1.73, 1.94, 2.15, 2.36, 2.58, 2.79, 3.00 m s^{-1}) on a 90 m course. Participants received feedback at the half-way time point and with five seconds remaining in the trial. Trial order was randomized to minimize learning effect. Vertical ground reaction forces were normalized to body mass. Data were synchronized, resampled to 100 Hz and split into training (70%), validation (15%) and test (15%) sets.

An LSTM network consisting of 4 layers was built to estimate vGRF from IMU data. Inputs to the network were linear aceleration and angular velocity data from single footfalls with swing phase data included from before and after the period of foot contact, from which the network determines gait events. Output from the LSTM was a single vGRF waveform. Ramp, stair and running footfalls were bootstrapped. A Bayesian hyperparameter search was completed to determine optimal hyperparameters for the LSTM. The estimated vGRF waveforms were then filtered with a 6th order low-pass zero lag butterworth filter (f_c=15 Hz). Estimation error of vGRF was quanitifed using RMSE.

Results and Discussion

The overall RMSE for estimation of vGRF was 1.1 N/Kg (Table 1). These are similar to RMSE values reported in previous studies (1-2 N/Kg**)** [3,4].

Table 1: RMSE (N/Kg ± SD) between the measured and estimated vGRF for raw and filtered waveforms.

	Raw RMSE	Filtered RMSE
Walking	1.11 ± 0.49	1.06 ± 0.49
Running	2.18 ± 0.88	2.09 ± 0.88
Stair Ascent	1.02 ± 0.28	0.97 ± 0.28
Stair Descent	1.25 ± 0.45	1.19 ± 0.46
Ramp Ascent	0.99 ± 0.32	0.94 ± 0.32
Ramp Descent	0.99 ± 0.25	0.93 ± 0.25

The results of this study demonstrate that vGRF can be accurately estimated in a real-world environment, across multiple locomotion modes and self-selected speeds. The estimated running vGRFs had the largest RMSE, followed by ramp ascent and descent and then level ground walking. Level ground walking speeds were more variable during the second day of the protocol which may explain why the RMSE is larger for level ground walking compared to ramp walking. Filtering the output vGRF data reduced RMSE, as expected. These filtered outputs can be used to calculate spatiotemporal parameters and gait events with the development of clear rules.

A limitation of this work is that only vGRF waveforms were estimated from the input IMU data. A more complex model may be needed to estimate joint moments across locomotion speeds and modes. For example, other basic measures such as anterior-posterior GRF may be needed for this model to accurately estimate joint forces and moments.

Significance

This work has shown the estimation of a mechanical variable in a real world environment is possible. Our findings can lead directly to the estimation of basic spatiotemporal variables for a variety of locomotion modes and speeds. Additionally, these findings could also inform locomotion mode estimation using IMU data.

References

[1] Anillao, A, et al., *Sensors,* 18, 2564, 2018.
[2] Jiang, X, et al., *Sensors,* 19, 2796, 2020.
[3] Wouda, F, et al., *Front Physiol,* 9:218, 2018.
[4] Komaris, D-S, et al., *IEEE Access* , 7, 2019.
[5] Long, L and Srinivasian, M., *J R Soc Interface*, 10(4):1-9. 2013.

Comparison of Hara and Harrington Hip Joint Center Location and Influence on Hip Moments during Gait

Gordon Alderink[1,*], Yunju Lee[1,2], Lauren Hickox[3]. Jessica Zeitler[1]
[1]Department of Physical Therapy, [2] School of Engineering, Grand Valley State University, Grand Rapids, MI, USA
[3]Department of Mechanical Engineering, Penn State University, State College, PA, USA
E-mail: aldering@gvsu.edu

Introduction

The hip is modeled as a spherical joint with its center (HJC) frequently estimated using predictive [1,2,3,4] or functional methods [5]. Although functional methods are relatively robust, medical imaging is considered the gold standard for determining the HJC [6]. Of the predictive methods, Harrington's (HARR) appears to be most accurate [2,6]. Recently, Hara et al. have provided an alternative algorithm, dependent only on leg length, with HJC results that were comparable to Harrington [4]. Leboeuf et al. compared Hara and Harrington's predictive methods with ultrasound imaging and favored Hara's method because it reduced errors along the anterior-posterior pelvic axis. Leboeuf cautioned that HJC differences influenced hip kinetics [7], as reported elsewhere [8,9], but findings are somewhat discrepant. Therefore, the purposes of this study were to compare Hara and Harrington predicted HJC locations and to examine potential differences in net hip moments during stance in gait.

Methods

Thirty active healthy individuals (13 females; 46.4±26.0 yrs; 1.71±0.01 cm; 69.7±11.5 kg) performed walking trials at self-selected speeds. Approval was obtained from the Grand Valley State University Human Research Review Committee (IRB#14080-H). Eight Vicon MX-T40 cameras (120 Hz) and Nexus software (V2.5, Oxford Metrics) were used to track full-body, modified PIG and Oxford Foot Model trajectories (Woltring filter, MSE 15). Ground reaction forces were collected (1200 Hz, 4th-order, zero lag Butterworth filter, 6 Hz) using floor-embedded AMTI force platforms (Advanced Mechanical Technology, Inc.). Visual3D (v6, C-Motion) was used to determine HJC location and hip kinetics, where the original PIG model was modified to reflect the Hara and HARR derived HJC locations (pelvic frame; +x lateral, +y anterior, and +z superior). Modifications were performed in the commonly used PIG model in order to maintain ancillary model definitions other than HJC calculations.

Right HJC locations and net internal hip moments, from three randomly selected gait cycles, were exported for statistical analysis. Peak stance moments of each pelvic frame were examined. Based on normality testing, paired t-tests for HJC locations and Signed-rank tests for HJC moments (SAS JMP) were used to assess for differences in coordinate positions and net hip joint moments among HJC methods ($p<.05$). Cohen's D method was used to determine effect sizes.

Results and Discussion

There was a significant difference in HJC location along the y-axis ($p<.0001$), suggesting HARR HJCy (red) was more posterior compared to Hara. HJCx (blue) and HJCz (green) locations were similar between the two methods (Figure 1); effect sizes were: HJCx (0.09), HJCy (0.88), and HJCz (0.33).

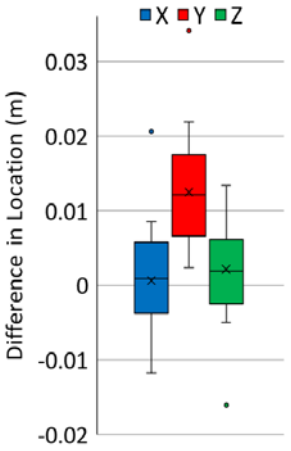

Figure 1. Difference in HJC location between HARR and Hara.

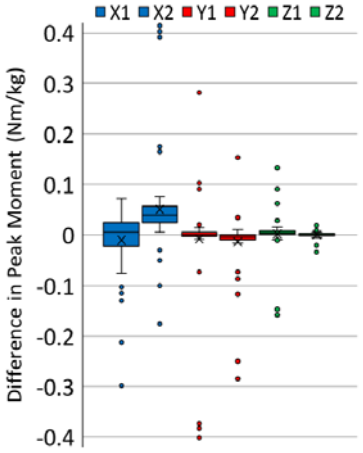

Figure 2. Difference in HJC moments (1st and 2nd peak).

Hara and HARR predictive models have been shown to minimize mean absolute error [4]. Leboeuf et al. demonstrated that HARR's equations were best for medio-lateral HJC location, while Hara's were best in the antero-posterior location [7]. Our data agree with Leboeuf's findings that HARR HJC is more posterior. Leboeuf et al. found that neither Hara nor HARR improved the supero-inferior HJC location. This could be related to the fact that neither method accounts for the pelvic height relationship to HJC [10].

Second peak moments in the sagittal (X2) and frontal planes (Y2), and the first peak in the transverse plane (Z1) were different between the two methods ($p<.0001$) (Figure 2). Our findings are consistent with others [8,9] who have reported differences in hip moments during gait.

Significance

The small significant differences in selected hip moments likely will not impact clinical diagnoses or treatment recommendations. Hara may be the preferred HJC predictive method because of its use of leg length, which minimizes error secondary to soft tissue artefact.

References

[1] Davis RB et al. (1991) *Hum Mov Sci*, 10:575-587.
[2] Kainz H et al (2015) *Clin. Biomech*, 30:319-329.
[3] Harrington ME et al. (2007) *J Biomech*, 40:595-602.
[4] Hara R et al. (2016) *Sci Rep,* 6:37707.
[5] Ehrig RM et al. (2006) *J Biomech*, 39:2798-2809.
[6] Fiorentino NM et al. (2016) *Ann Biomed Eng*, 44: 2168-2180.
[7] Leboeuf F et al. (2019) *J. Biomech, 87:167-171.*
[8] Bennet HJ et al. (2018) *J Biomech*, 81:122-131.
[9] Stagni R et al. (2000) *J Biomech*, 33:1479-1487.
[10] Seidel GK et al. (1995) *J Biomech*, 28:995-998.

Frequency Characterization of Thigh Soft Tissue Artifact During a Relaxed and Activated State

Scot Carpenter[1], Michael Zabala[1], Jacob Larson[1], Anthony Marino[1], and Edmon Perkins[1]
[1]Mechanical Engineering, Auburn University, Auburn, AL, US
Email: zabalme@auburn.edu

Introduction

Marker-based motion capture systems are commonly used for biomechanical analyses to measure human movement by tracking the positions of reflective markers placed on the surface of the skin. A 3-D model of the subject can be created using the data from the markers. This provides an approximate location of the position and orientation of the underlying bones during a particular movement. A well-known limitation of this method of data collection, however, is the relative movement of skin and other soft tissue over the bone [1]. This type of error is known as *soft tissue artifact* (STA). In order to accommodate for this discrepancy, low-pass filters can be used to remove frequencies deemed to be too high for human volitional movement, thus lowering the likelihood of error due to STA. For general data collections, a common method of filtering at 6 Hz has shown to be somewhat effective at removing STA [2] and has been used as the typical low-pass filter. However, the frequency at which data should be filtered has been shown to depend on the movement type as well as various subject characteristics [3]. For this study, we hypothesized that STA frequency will be affected by muscle activation level. Thus, the objective of this study was to analyze how the STA frequencies of the thigh differ based on an activated and relaxed state of the thigh musculature.

Methods

Four human subjects participated in this study, having given IRB-approved informed consent. A 10-camera VICON motion capture system was used during data collection, and reflective markers were placed on each subject using a 79 marker set based on the point cluster technique [4]. The test consisted of subjects standing with their right foot on a platform which was raised to a height such that the knee was at 90 degrees of flexion. The subject was instructed to relax the thigh and perturb the skin by twisting the thigh with one hand about the femoral longitudinal axis to its maximum possible angle and quickly releasing, allowing the soft tissue to oscillate freely. The subject was then asked to repeat the procedure, while activating the musculature of the thigh. Three trials were taken for both conditions. The marker trajectories were gap-filled in Nexus software and further processed in MATLAB by creating an anatomical reference frame on the thigh and tracking movement of the centroid of the 9-marker thigh cluster relative to the origin of the segment. The angle of twist about the femur was calculated for each trial. This data was then converted to the frequency domain with a Fast Fourier Transform (FFT) to analyze the frequency components of the signal.

Results

The angle of twist and frequency plot for a relaxed and activated state in one subject is shown in Fig. 1. The upper left plot shows the time history of the oscillations of the thigh's soft tissue, when it is in a relaxed state. The upper right plot shows the FFT of this data. The lower plots show the same information for an activated thigh. Table 1 shows the mean and standard deviation of frequencies for the activated and relaxed thigh. The mean difference between the two sets of frequencies is shown and is statistically significant with a p-value of 0.022.

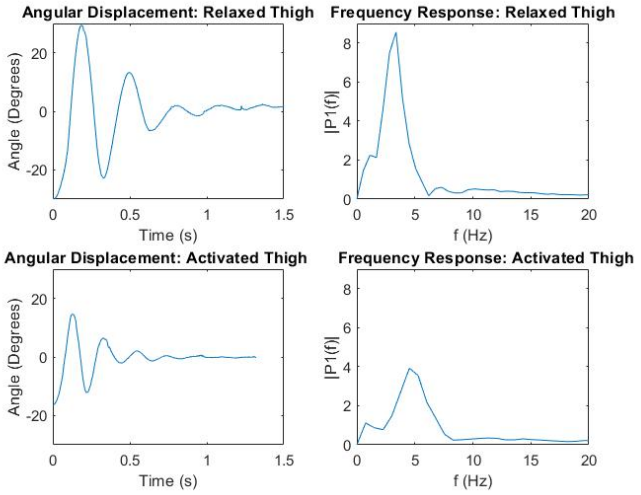

Figure 1: Time history and frequency response plot for a single subject.

Table 1: Frequency statistics based on one data set from each subject.

	Frequency (Hz)	STDEV	Mean Difference
Relaxed Thigh	4.04	0.697	1.55 Hz, P = 0.022
Activated Thigh	5.60	0.749	

The data shows that the average frequency for a relaxed thigh is lower than that of an activated thigh. Also, the maximum angular deflection is much higher in the relaxed thigh, as compared to the activated thigh.

Discussion

The results indicate that the angular frequency of the thigh increased with muscle activation, which can be seen with a higher frequency and a lower maximum amplitude in Fig. 1. More importantly, the average frequency is less than 6 Hz regardless of activation. This means that some STA might not be removed from motion capture data when the typical 6 Hz cutoff frequency is used.

Significance

The results of this study have indicated the possibility of allowing STA into motion capture results while using a 6 Hz lowpass filter. Future work in determing the relationship between STA and physical traits of the subject, such as age, weight, sex, and percent body fat, is needed to further determine STA frequencies for various subject characteristics.

References

[1] Cappozzo A, et al. *Clinical Biomechanics* 1996; 11(2):90-100
[2] Nagano A, et. al. *J Biomechanics* 1998; 31(10):951-955
[3] Peters A, et. al. *Gait and Posture* 2010; 31(1):1-8
[4] Andriacchi, T.P., et. al. *J Biomechanical Engineering* 1998; 120(6):743–749

Application of quadratic regression model in the calculation of lower extremity joint stiffness

Youngmin Chun[1], Joshua P. Bailey[1]
[1]Department of Movement Sciences, University of Idaho, Moscow, ID
Email : *ychun@uidaho.edu

Introduction

Lower extremity stiffness is an effective measure to relate load and deformation characteristics in sport-related activities attempting to evaluate performance [1,2] and identify potential injury risk [3,4]. Investigating lower extremity stiffness can be achieved through a spring-mass model [2,3] calculating leg stiffness or vertical stiffness, or by investigating individual joint stiffnesses in the sagittal planes [1,3]. Traditional methodology for representation of joint stiffness is through the line of best fit using simple linear regression model of the landing phase [1,3,4]. It is debated if this linear regression modelling is the most accurate way to represent such a non-linear relationship of joint position and moments. Therefore, the purpose of this abstract is to demonstrate how using a quadratic regression line of best fit model represents joint stiffness more accurately than a linear regression model. A secondary purpose is to demonstrate the importance of dividing the landing task into phases of interest prior to the identification of the line of best fit regression model.

Methods

Thirty healthy college students participated in this study (15 males: age = 25.8 ± 6.6 yrs, height = 1.82 ± 0.04 m, mass = 82.4 ± 12.1 kg; 15 females: age = 25.2 ± 9.2 yrs, height = 1.71 ± 0.09 m, mass = 64.5 ± 11.2 kg). Fifteen drop vertical jumps from 30 cm of box were collected using 3D motion capture system (Vicon, 250 Hz) synchronized with two force platforms (1000 Hz). The obtained data of preferred limb (kicking limb) were exported to Visual 3D software and lowpass filtered at 15 Hz with 4th order Butterworth filter. The initial contact (IC) was identified if the vGRF of the preferred limb was greater than 20 N. The descending phase (IC to lowest COM position) was divided into loading (IC to peak vGRF) and absorption (peak vGRF to lowest COM position) phases [5]. Sagittal plane joint stiffnesses were calculated using both linear and quadratic regression models. The coefficient of determination (r^2) of each model was also calculated to determine which model represents a better fitted line. Multiple independent *t-tests* ($\alpha < .05$) were performed to compare the r^2 values between models.

Results and Discussion

The r^2 of the quadratic model was significantly greater than the r^2 of linear model in all joints and phases (Table 1). Figure 1 shows the moment-angle mean curves with lines of best fit calculated by both simple linear and quadratic models.

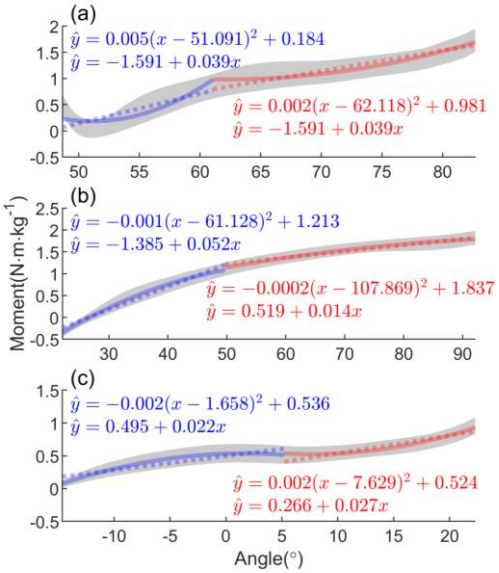

Figure 1. Mean hip (a), knee (b), and ankle (c) sagittal angle-moment graphs with lines of best fit models for each phase. The shaded area with gray color represents mean ± 95% CI of the moment-angle curve, blue and red lines represent the lines of best fit for the loading phase and absorption phase, respectively. *Solid lines* indicate the quadratic models, and *dotted lines* are simple linear models.

Significance

The quadratic regression models provide more accurate lines of best fit than the simple linear models for each joint and each phase. Thus, the given model represents the joint stiffness more accurately. Additionally, the coefficient of x^2 in the quadratic model estimates the slope. Therefore, using this model may indicate changes in joint stiffness.

References

[1] Stefanyshyn DJ & Nigg BM (1998) *Journal of Applied Biomechanics,* Vol **14**, 292 – 299.
[2] Arampatzis et al. (2001) *Journal of Electromyography and Kinesiology*, Vol **11(5)**, 355 – 364.
[3] Padua DA et al. (2005) *Journal of Motor Behavior,* Vol **37(2)**, 111 – 126.
[4] Schmitz et al. (2010) *Journal of Athletic Training*, Vol **45(5)**, 445 – 452.
[5] Harry et al. (2018) *Journal of Applied Biomechanics*, Vol **34(5)**, 403 – 409.

Table 1. r^2 of sagittal lower extremity joint stiffness calculated by simple linear and quadratic regression models

	Loading Phase			Absorption Phase		
	Hip*	Knee†	Ankle*	Hip*	Knee*	Ankle*
Linear	0.46 ± 0.28	0.87 ± 0.11	0.37 ± 0.22	0.36 ± 0.16	0.56 ± 0.23	0.60 ± 0.19
Polynomial	0.88 ± 0.07	0.93 ± 0.04	0.68 ± 0.19	0.60 ± 0.17	0.72 ± 0.16	0.78 ± 0.11

Note. * indicates that significant differences between linear and polynomial regression model ($p < .001$). †indicates that significant differences between linear and polynomial regression model ($p = .002$).

An Investigation of Human Movement IMU Data Compression Methods

David P. Chiasson[1], Junkai Xu[1], Peter B. Shull[1]
[1]State Key Laboratory of Mechanical System and Vibration, School of Mechanical Engineering, Shanghai Jiao Tong University
Email: dchiasso@sjtu.edu.cn

Introduction

Wearable human movement information from inertial measurement units (IMU) is critical for a variety of applications including virtual reality, wearable electronics, physical therapy and human performance. However, techniques for representing this class of multimedia information has received little attention compared with the mature fields of image, audio, and text. Developing compressed representations of kinematic data will allow for higher sampling rates, greater data throughput, more nodes, and more data stored in a limited space. Compression is a key element to enabling previously unfeasible applications particularly those which experience limited transmission bandwidth or data storage. We hypothesised that the most efficient compressed representation format would utilize the interrelated nature of rotation and orientation information in the accelerometer and gyroscope.

Methods

For this study, the Human Gait Database (HuGaDb)[1] is used to meaningfully and repeatably demonstrate the performance of various compression techniques. HuGaDb is a public dataset of six-axis IMU signals collected from six different body segments of 18 healthy subjects performing 12 different movement activities.

Eight lossless compression techniques are proposed and compared with three traditional methods which are already in widespread use. The first six techniques which fall under polynomial regression, are borrowed from the field of audio compression. These techniques extrapolate a polynomial regression of the past n data samples where n is an integer greater than the polynomial degree. The last two techniques are the optimal linear predictors of training data which were computed via Lasso regression. The cross-stream linear compression technique additionally considers past samples of other dimensions and sensor modality. The data collected from three random subjects was designated as training data, and only data from the remaining 15 subjects was used in our results.

The traditional method of comma separated value (CSV) is selected as the baseline size when computing compression ratio (CR). CR is computed by dividing the size of the CSV file by the size of the compressed file. In addition to CSV, two other traditional techniques are included for further context: ZIP compression, and efficient binary representation. All proposed compression techniques are implemented as FIR filters using 16.16 fixed point computation.

Results and Discussion

All proposed compression techniques far outperformed traditional representation methods in size efficiency (Fig. 1). This is likely due to the proposed methods' ability to utilize time auto-correlation and sparsity of the sensor sample space. Delta encoding (zero-degree polynomial) proved to be the best performing polynomial regression technique (CR=19.0), with each additional degree performing worse. This is likely because higher degree polynomial predictors suffer from poor white noise attenuation [2].

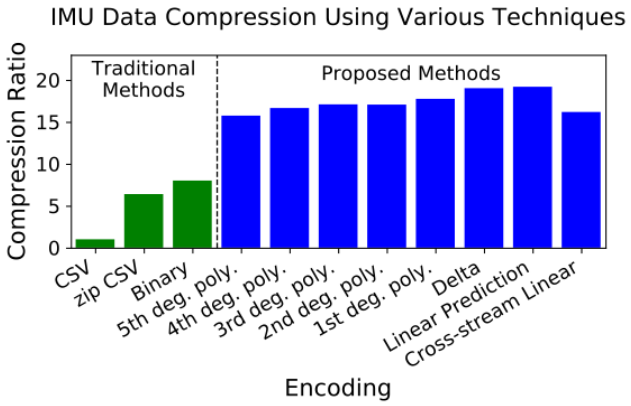

Figure 1: Compression ratios relative to CSV. Higher is better. Proposed methods compressed IMU data 15-20 times more than standard CSV formatting and 2-3 times more than traditional compression methods.

The linear prediction filter (CR=19.2) proved to be slightly better than delta encoding. Investigation of the coefficients showed that the per-stream FIR had learned an approximation of Delta encoding.

Cross-stream linear prediction (CR=16.2) unexpectedly performed significantly worse than linear prediction or delta encoding which fails to support our hypothesis. We expect that this was due to accumulation of error from 16.16 arithmetic. The cross-stream predictor involved two orders of magnitude more computation than delta encoding.

Significance

Using these techniques, kinematic data can be compressed to almost one-twentieth the size of the current de-facto standard. This enables a range of applications which experience stringent requirements such as real-time data streaming, wireless communications, or limited storage space.

Acknowledgments

This work was supported by the National Natural Science Foundation of China (51875347).

References

[1] Chereshnev, R., & Kertész-Farkas, A. (2017). Hugadb: Human gait database for activity recognition from wearable inertial sensor networks. In International Conference on Analysis of Images, Social Networks and Texts

[2] Tanskanen, J. M. A. (2000). Polynomial Predictive Filters : Implementation and Applications. In Electronics.

Magnetometer-Free, Inertial-Sensor-Based Foot Progression Angle Estimation

Tian Tan[1], Zachary A. Strout[1], and Peter B. Shull[1]
[1] State Key Laboratory of Mechanical System and Vibration, School of Mechanical Engineering, Shanghai Jiao Tong University, Shanghai, China
Email: alantantian@sjtu.edu.cn

Introduction

Foot progression angle (FPA) is a critical walking gait parameter for assessment and intervention in a wide variety of movement-related diseases. Measurement of FPA is traditionally performed with an optical motion capture system. Previous approaches to estimate FPA via a foot-worn magneto-IMU (3-axis accelerometer, 3-axis gyroscope, 3-axis magnetometer) typically rely on magnetometer signals to correct the drift in the estimated sensor heading direction [1]–[3], which can be sensitive to magnetic distortion.

The purpose of this study was to develop an FPA estimation algorithm solely based on an inertial sensor consisting of a 3-axis accelerometer and a 3-axis gyroscope. To avoid drift problems, the sensor heading direction was estimated from the peak foot deceleration during the swing phase rather than from gyroscope integration as in previous approaches. We hypothesized that the proposed algorithm would enable accurate estimation of the FPA for normal, toe-in, and toe-out gait patterns.

Methods

Three coordinate systems were used, including a sensor frame *S*, a changing reference frame *C*, and an intermediate frame *F*. The frame *S* is aligned with the foot via sensor placement. The frame *C* is aligned with the foot heading vector and updated after each mid-stance. The Euler angle roll and pitch of frame *F* with respect to frame *C* are both 0, while the yaw is the same as the yaw of frame *S* (sensor heading direction). For each step, the FPA is defined by the angle between the foot vector and the foot heading vector, so it is equivalent to the yaw of frame *F* with respect to frame *C* at mid-stance. The algorithm (Figure 1) consists of three components: 1) roll and pitch angle estimation via gyroscope integration (drift is corrected by the measured gravity vector during mid-stance), 2) estimated orientation conversion into a rotation matrix to transform the foot acceleration from frame *S* to frame *F*, and 3) FPA estimation using the relationship between different acceleration axes in frame *F* as follows:

$$\mathrm{FPA} = \mathrm{yaw} = \arctan\left[\left(a_x^F / a_y^F\right)_l\right], \quad (1)$$

where *l* is the sample with the largest acceleration magnitude during the last 50% of the swing phase.

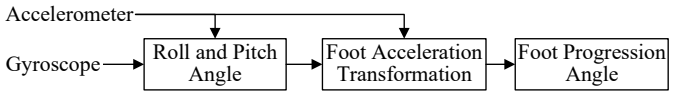

Figure 1: Flow chart of the proposed FPA estimation algorithm.

Twelve healthy subjects (age: 25.8 ± 3.3; height: 1.72 ± 0.07 m; weight: 59.2 ± 8.8 kg, all male) participated in this study after providing informed consent. A motion capture system (Vicon, Oxford, UK) and two reflective markers placed on the calcaneus and the head of second metatarsal were used to collect ground-truth FPA measurements at 100 Hz. A synchronized inertial sensor was embedded in the heel of each subject's left shoe, and inertial data was collected at 100 Hz.

Subjects performed seven walking trials (large toe-in, medium toe-in, small toe-in, normal, small toe-out, medium toe-out, and large toe-out) at a self-selected speed (1.16 ± 0.06 m/s) on a treadmill. A paired t-test was used to determine if there were significant differences between the FPA estimated by the proposed algorithm and the ground-truth FPA for all seven different gait patterns. The level of significance was set to 0.05.

Results and Discussion

The hypothesis was supported that the FPA estimated by the proposed algorithm closely matched the ground-truth FPA (Figure 2). The overall mean absolute error, mean error, and Pearson's correlation coefficient across all walking gait patterns were 3.1 ± 1.3 deg, 0.3 ± 2.7 deg, and 0.99 ± 0.00, respectively. The mean absolute error for large toe-in, medium toe-in, small toe-in, normal, small toe-out, medium toe-out, and large toe-out trial were 2.6 ± 1.2 deg, 2.7 ± 1.3 deg, 2.4 ± 1.0 deg, 2.6 ± 1.1 deg, 3.8 ± 2.4 deg, 3.8 ± 2.5 deg, and 4.0 ± 2.0 deg, respectively. There was no significant difference between FPA estimated by the proposed algorithm and ground-truth FPA for any of the seven gait patterns (Figure 2).

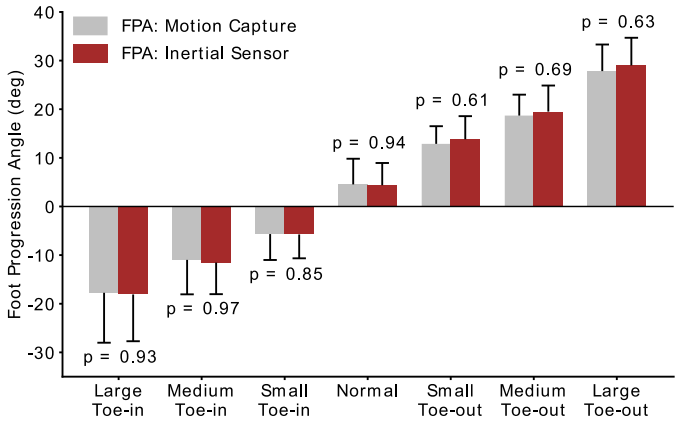

Figure 2: Average FPA grouped by walking gaits. There was no significant difference between FPA: Motion Capture and FPA: Inertial Sensor for any gait pattern.

When based solely on an inertial sensor, regular orientation estimation algorithms are prone to experience drift from angular velocity integration. In our case, the drift in roll or pitch was corrected via the gravity vector measured by the accelerometer, while there was no drift in yaw or FPA because it was estimated via the peak foot deceleration using Equation (1) without integration.

Significance

The orientation of the foot with respect to walking direction can be estimated via a magnetometer-free inertial sensor during gait. The proposed algorithm may be useful for situations requiring wearable FPA assessment that are prone to magnetic distortion.

References

[1] Y. Huang et al (2016). *IEEE TBME.* 63(11): 2278–2285.
[2] H. Xia et al (2017). *J. Biomech.* 61: 193–198.
[3] A. Karatsidis et al (2018). *J. Neuroeng. Rehabil.* 15(1): 78.

Reliability of Wearable Sensors to Assess Impact Metrics during Sport Specific Tasks

Julie P. Burland[1,2,3], Jereme B. Outerleys[2,3], Christian Lattermann[1], Irene S. Davis[2,3]
[1]Brigham and Women's Hospital, Department of Orthopaedic Surgery, Boston, MA, USA
[2]Spaulding National Running Center, Cambridge, MA, USA
[3]Harvard Medical School, Boston, MA, USA
Email : jburland@bwh.harvard.edu

Introduction

Soccer involves various functional movement patterns that require high velocity cutting, pivoting, and acceleration-deceleration maneuvers that can generate large lower extremity accelerations and impacts. Wearable inertial measurement units (IMUs) can capture accelerations of the lower extremity experienced during these high velocity movements. More importantly it can provide clinicians with the ability to estimate lower extremity impact loads during sport related tasks (1).

Previous work has identified the ability of these sensors to reliably measure impact load during running and their ability to predict running related injuries (2-4). To date, there is little information on the reliability of these sensors for capturing impact load metrics during more functional, individual sport specific soccer movements (i.e. cutting, pivoting, kicking). Thus, the purpose of this study is to determine the reliability of the Blue Trident IMU sensors in measuring impact load and step count during a series of soccer related functional tasks to assess its potential use in field-based sporting events.

Methods

Ten healthy individuals (age :27.9 ± 2.18; height: 69.80 ± 4.022; mass: 79.02 ± 13.07; sex: 6 males, 4 females) were recruited and asked to complete a three-visit study where they performed 3 trials of the following standardized tasks during each session: 1) acceleration-deceleration, 2) plant and cut, 3) change of direction and 4) ball kick. Participants were instructed to perform the ball kick task using their dominant limb. Order of tasks was randomized for each participant and tasks were completed in the same order during each session. Test sessions were approximately 7-10 days apart (average 7.95 ± 1.06 days) and all sessions were collected on an outdoor, grass field. All participants currently or had previously participated in recreational ball sport activities (i.e. soccer, basketball, rugby, football etc). Participants were excluded if they had sustained a musculoskeletal injury within the last 6 months or had previous history of lower extremity surgery.

Bilateral impact load and total number of steps during the 4 tasks were collected using two IMUs secured via soft athletic pre-wrap and self-adhesive overwrap to the participant's distal, medial tibia just above the medial malleolus. IMU data was sampled using VICON IMeasureU Blue Trident dual-g sensor (Low-g 1125Hz/High-g 1600 Hz). Impact load was calculated using IMeasureU Step platform where impact load = (#of steps x 1g) + (# steps x 2g) + (# of steps x 3g) + … = Total # of steps * g's. Outcome variables were averaged across the 3 trials during each session and intraclass correlation coefficients (ICC3,1) with 95% confidence intervals were used to assess between day reliability across the 3 sessions.

Results and Discussion

ICC values for right and left impact load during each task are presented in Table 1. ICC values for total impact load were good to excellent (0.743-0.911). ICC values for right, left and total step count were good to excellent during the acceleration-deceleration task (0.728-0.837), change of direction (0.734-0.955) and plant and cut maneuver (0.701-0.866) and fair to good during the ball kick (0.588-0.683).

The high ICC values in the present study demonstrate the ability of the Blue Trident dual-g sensor to reliably measure bilateral lower extremity impact load and step count across an acceleration-deceleration, change of direction, plant and cut and ball kick task. Although the ball kick task demonstrated lower reliability in the number of steps taken, this is likely due to the inherent variability associated with executing the task.

Significance

These results suggest that wearable sensors can reliably measure the cumulative impact load across a variety of athletic functional movements in an outdoor environment. Measuring impact load in the field expands the ability to capture more ecologically valid data. This work can serve as a stepping stone for future research aimed at evaluating impact load metrics over the course of games and practices. This information can help to inform athlete load monitoring strategies targeted towards injury prevention.

References

1. Sheerin, KR et al. Gait and Posture, 67, 12-24, 2019.
2. Van den Berghe, P et al, J Biomech, 86, 238-242, 2019.
3. Sheerin, KR et al. Sports Biomech, 17(4), 531-540, 2018.
4. Milner, CE et al. MSSE, 38(2), 323-328, 2006
5. Cicchetti, DV et al, AJMD, 86(2):127-3 1981)

Table 1. Impact load metrics for left and right limb during each task

Task	Outcome Variable	Limb	Intraclass Correlation Coefficient*	P (95% Confidence Interval)
Acceleration- Deceleration	Impact load	Left	0.879	<0.0001 (0.646-0.967)
		Right	0.890	<0.0001 (0.677-0.970)
Ball Kick	Impact load	Left	0.873	<0.0001 (0.628-0.966)
		Right	0.580	0.056 (-0.230-0.887)
Change Direction	Impact load	Left	0.764	0.004 (0.308-0.936)
		Right	0.853	<0.0001 (0.568-0.960)
Plant and Cut	Impact load	Left	0.745	0.007 (0.254-0.931)
		Right	0.872	<0.0001 (0.624-0.965)

*ICC values were categorized as >0.75 is excellent, 0.60-0.74 is good, 0.40-0.59 is fair, and <0.40 is poor (5).

Description and Validation of a Ground Reaction Force Triggered Treadmill Protocol for Simulation of Tripping Falls

Hui-Ting Shih[1*], Szu-Ting Yi[1], Yo Shih[1], Szu-Ping Lee[1]
[1]Department of Physical Therapy, University of Nevada Las Vegas
Email: *shihh1@unlv.nevada.edu

Introduction

Falls frequently happen during perturbed walking as a result of tripping in community-dwelling middle-aged and older and even in young adults.[1,2] Previous protocols have used concealed obstacles, tether-based obstruction, and the acceleration and deceleration of a treadmill to simulate trips.[3] Each current protocol has its strengths and limitations. The obstacle and tether-based protocol obstructs one limb at a time during swing phase to simulate tripping. However, the timing of the perturbation delivery is difficult to control, leading to less replicable fall trials. The treadmill protocol which utilizes ground reaction force (GRF) to precisely deliver the trips, but so far is mostly limited to perturbing both legs together and therefore less realistic.

The novel protocol examined in our study aims to enables reproducible, unilateral trips. We validated the protocol by examining how the protocol can be used as an assessment tool to differentiate the trunk trip recovery responses[5] between young and middle-aged to older adults.

Methods

The system consists of three main components: 1) Bertec side-by-side split-belt instrumented treadmill (Model ITC-11-20L-4, Bertec Corp., Columbus, OH), 2) VICON motion capture system and Datastream Software Development Kit (SDK) (Oxford Metrics, Oxfordshire, UK), and 3) MATLAB (MathWorks Inc., Natick, MA).

The instrumented treadmill is equipped with one force plate underneath each belt. The force plate data were synchronized with the motion data in real-time and streamed by the SDK. We utilized MATLAB as an interface to communicate between Datastream SDK and the treadmill controller. MATLAB program read the vGRF from Datastream SDK and remotely employed the pre-programmed perturbation to the treadmill via Transmission Control Protocol/Internet Protocol (TCP/IP) port through which the program triggers the tripping perturbation by decelerating/accelerating the treadmill motor.

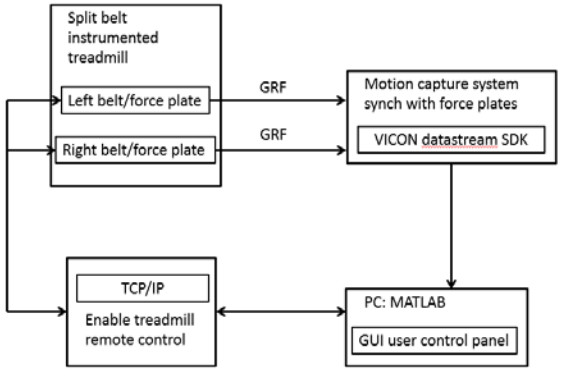

Figure 1: System apparatus.

Triggering criteria were based on the vGRF in order to deliver the perturbation during early stance phase right after initial contact of the tripped limb. First , the vGRF of the tripped side had to be between 20-25% of the person's body weight. Second, the vGRF of the selected frame in criterion 1 had to be greater than the value of the frame that is 10ms before it to ensure the vGRF is in the ascending limb of stance phase.

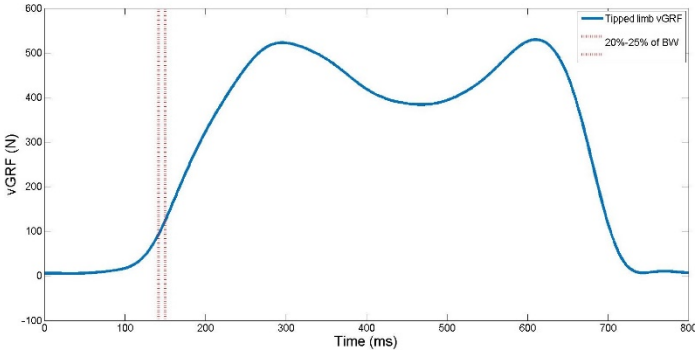

Figure 2: Triggering criteria. Blue vGRF line is from the tripped limb; pink dash lines represent triggering criteria.

During the perturbation, the belt on which the early stance phase occurs, either left or right, would decelerate from the comfortable walking speed (CWS) for 50ms, consecutively accelerate for 270ms, and then decelerate again for 220ms, resuming CWS.[4] Two acceleration levels are used to simulate the more and less severe tripping falls. The acceleration was linearly and positively scaled by the CWS.

Results and Discussion

Of the 12 included participants, 6 were young and 6 were middle-aged to older adults (20.83 vs 58.17 y/o). Significant age group and severity main effects were found in peak trunk flexion angle and velocity, indicating that the protocol was able to discern the two age groups. Besides, both groups exhibited greater response following more severe trips.

	Trunk flexion angle (degree)		Trunk flexion velocity (degree/s)	
	Mild trip	Severe trip	Mild trip	Severe trip
Young (n = 6)	12.10 ± 5.59	23.95 ± 8.17†	81.81 ± 32.68	172.53 ± 61.08†
Old (n = 6)	20.66 ± 7.21*	33.65 ± 11.95*†	98.82 ± 37.80	179.45 ± 55.46†

Table 1: Peak trunk flexion angle and peak trunk flexion velocity in young and middle-aged to older adults.

Significance

Since falling due to external perturbation is one of the most common causes of injury in older adults, having a tool that allows researchers to evaluate fall response and even train the participants under a realistic and safe environment is necessary. Our data show that this protocol can serve as a valid assessment tool for populations with high fall risks.

Acknowledgments

The authors would like to acknowledge the contribution of James Anderson, Catrina Fabian, Samuel Hadley, and Denise Ng.The UNLVPT Student Opportunity Research Grant funds this project.

References

[1]Heijnen et al., 2016. Hum Mov Sci 46, 86-95.
[2]Li et al., 2006. Am J Public Health 96, 1192-200.
[3]Rossignaud et al., 2019. Aging Clin Exp Res, 1-8.
[4]Sessoms et al., 2014. J Biomech 47, 277-80.
[5]Pavol et al., 2001. J Gerontol A Biol Sci Med Sci 56, M428-37.

Combined Deep learning and Top-Down Optimization for Estimation of Kinematics from IMUs

Soyong Shin[1]*, Eric Rapp[1], Reed Ferber[2] and Eni Halilaj[1]
[1]Department of Mechanical Engineering, Carnegie Mellon University, Pittsburgh, PA, USA
[2]Faculty of Kinesiology, University of Calgary, Calgary, Alberta, Canada
Email: soyongs@andrew.cmu.edu

Introduction

One limitation to measuring human movement patterns from inertial measurement units (IMUs) is the susceptibility of magnetometer readings to ferromagnetic interferences. To address this limitation, we recently proposed the use of deep neural networks to predict joint angles directly from inertial data, without relying on noisy magnetometer readings [1]. To further improve the accuracy and generalizability of these models, here we introduce a new framework that combines deep learning with top-down optimization.

Methods

To train the deep neural networks, we used treadmill running data from 586 subjects and walking data from 384 subjects collected at the University of Calgary using an optical motion tracking system. Synthetic IMU data (linear acceleration and angular velocity) were generated by placing virtual IMUs on the segment marker clusters. Sensor noise was modelled synthetically by adding Gausian noise [1], while sensor placement variability was modelled using data augmentation techniques [2]. As a baseline, we built deep neural networks to predict the joint angles, $\boldsymbol{\alpha_i}$ ($\boldsymbol{i} \in \{\mathbf{1}, \mathbf{2}, \mathbf{3}\}$), and orientations of the adjacent segment sensors, $\boldsymbol{q^S} = \{\boldsymbol{q^{S1}}, \boldsymbol{q^{S2}}\}$, from the inertial data.

We then implemented a top-down optimization algorithm, which updated the orientation of each adjacent segment until the discrepancy between the inertial data associated with these predicted orientations and the "true" inertial data from the virtual senors was minimized. The result of the optimization (β_i) was defined as the angle between two optimized sensor orientations. To derive final angle prediction (θ_i), we used weighted average of two prediction results α_i and β_i, where $\theta_i = w_i\alpha_i + (1 - w_i)\beta_i$. We set terminal stance of the predicted angle as zero and express the subsequent predictions as a function of the angle at that pose. We call this process passive pseudo calibration, since it does not require user engagement but is effective in reducing prediction error in subjects with atypical limb alignments.

Results and Discussion

Walking kinematics could be predicted with a mean (± STD) RMSE of less than 2.95° (± 0.82°), while running kinematics could be predicted with a mean RMSE of less than 3.24° (± 1.12°). During walking, flexion/extension was the most accurate degree of freedom, with a mean RMSE of less than 1.07° (± 0.37°) across the ankle, knee, and hip joints, followed by ab/adduction with a mean RMSE of less than 1.98 (± 0.97) and internal/external rotation with a mean RMSE of less than 2.95° (± 0.82°). Similarly, during running, flexion/extension was the most accurate degree of freedom, with a mean RMSE of less than 1.29° (± 0.40°) across the ankle, knee, and hip joints, followed by ab/adduction with a mean RMSE of less than 2.33° (± 0.84°), and internal/external rotation with a mean RMSE of less than 3.24° (± 1.12°). The higher RMSE in internal/external rotation may be explained by the lack of magnetometer data, which, when undisturbed, contribute toward heading estimation. Further, optical motion tracking, which was used as ground truth here, exhibited similar accuracies across degrees of freedom.

Optimization improved prediction of knee flexion by over 15%, hip flexion by over 10%, and ankle flexion by over 15%. When passive pseudo-calibration was applied, optimization had an even larger effect on final kinematics. In this case, prediction of knee flexion improved by over 45%, hip flexion by over 60%, and ankle flexion by over 40%, compared to the neural network outputs. Using this pseudo-calibration framework the predictive accuracy of the algorithms can be tuned passively after a few gait cycles, without requiring attention from the user. Also, because we trained the models on augmented data, sensor placement errors did not significantly degrade the predictive accuracy of the overall framework. While validation with true sensor data is a necessary follow-up step, the accuracy of the presented framework is a promising advance toward prediction of joint kinematics from wearable sensors without relying on ferromagnetic interference, drift-prone algorithms, and/or error-prone calibration techniques.

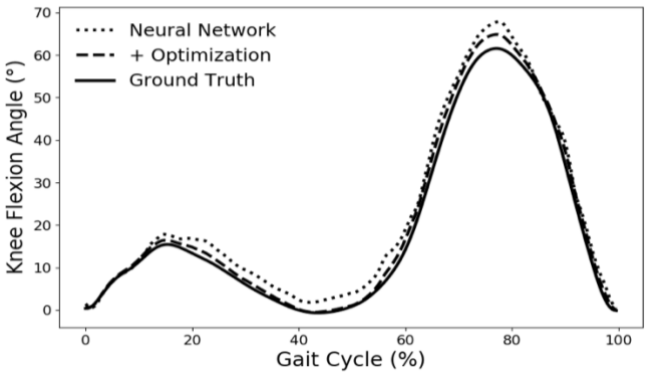

Figure 1: Knee flexion over a representative gait cycle for a test subjet computed from marker data (solid), predicted from a deep neural network (dash), and adjusted with top-down optimization (dotted), demonstrating how optimization improves joint angle estimation.

Significance

Wearable sensors offer a promising alternative for motion analysis in natural environments by overcoming some of the limitations of traditional marker-based techniques: spatial limitation, expensive equipment, and need for human expertise. The hybrid deep learning and top-down optimization approach presented here brings us a step closer toward accurate estimation of kinematics from IMUs. Progress in this direction should enable large-scale studies and new insights into disease progression, patient recovery, and sports biomechanics.

References

1. Thomsen W., Ferber R., Halilaj E.. "Deep neural networks for estimating knee joint kinematics from inertial measurement units." ISB 2019, Calgary, Canada.
2. Thomsen W., Ferber R., Halilaj E. "Predicting Joint Kinematics from Sensors with Varying Body-Segment Alignments." CMBBE 2019, New York, NY

Comparing IMU and Motion Capture Kinematics for Jumping Jacks

Eric D. Brannock[1], Kayt E. Frisch[1]
[1]George Fox University, Department of Mechanical, Civil, and Biomedical Engineering
Email: kfrisch@georgefox.edu

Introduction

Inertial Measurement Units (IMUs) are a promising new tool for biomechanics research, providing the opportunity to move experiments "into the wild." IMU systems have limitations, particularly for short duration motions, that are typically documented by the manufacturers [1], but studies seem to be choosing a system without attention to these details [2]. The goal of this abstract is to compare an IMU system with motion capture (MoCap) for a simple motion which the IMU system is probably not "tuned" for: jumping jacks.

Methods

9 healthy subjects (4 female, 5 male, avg. age 21) took part in the study. Subjects were instrumented with a fullbody XSense Awinda IMU system, and then a full body biomechanics reflective marker set was applied. IMU (60Hz) and MoCap (120 fps, 8-Vicon T40 cameras) data were collected simultaneously while the subject performed two trials of 15 jumping jacks. Center Of Mass (COM) position, hip angle, and shoulder angles were computed for both data sets. MoCap position data was filtered (10Hz, 4th order Butterworth) and angles calculated in the coronal plane using Matlab. All IMU data was based on post-processing calculations performed within the XSENS software.

Results and Discussion

There was a notable difference between the IMU and MoCap data sets. In the jumping jack trials, where both the subject's feet left the ground simultaniously, the IMU system struggled to maintain the correct position in the transverse plane, with the IMU's COM position drifting noticeably compared to the corresponding position of the MoCap LV5 (Fig. 1). Some IMU systems solve this problem by including a GPS system in their sensor suite, though the system used in this study is not one of them [1].

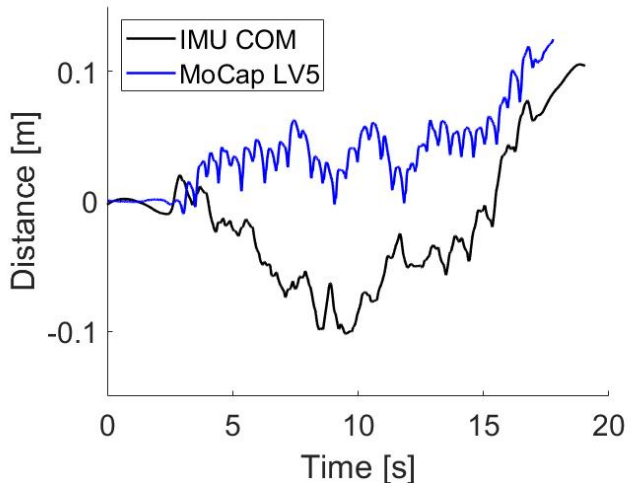

Figure 1: Magnitude of the COM drift distance in the transverse plane over 15 jumping jacks for a single representative subject.

In general the IMU and MoCap joint angles agreed. The greatest divergence occurred at points of impact (Fig. 2), presumably corresponding to high transient accelerations, which would result in data that could not be sampled by a system with a max sampling frequency of 60 Hz. Typical recommendations for data collection rates for high-impact activities (running, and presumably jump jacks landing) is a minimum of 400 Hz [3].

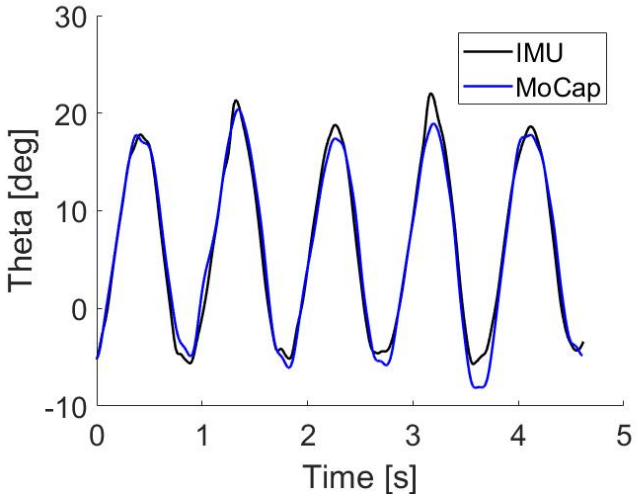

Figure 2: Hip angle over middle 5 jumping jacks for a single subject.

Significance

IMU systems have exciting potential to move biomechanics experiments out of the lab, however, these prelimnary findings suggest that the functionality of the particular system should be carefully considered and matched to the task being analysed. In particular, these specific IMUs seem to be accurate for slow movements, but face challenges for measuring impacts or long-term position tracking. Researchers should take care in selecting a system, paying attention to the sampling rate and tracking limitations as related to their particular context. Using an IMU system in place of motion capture should be done cautiously, and the validity should be checked carefully before a wholesale shift in methodology is adopted.

Acknowledgments

Thank you to students in ENGM420 (F19) especially M.Dyer, G.Lorenzo, C.Lax, and M.Pieper, for help with data collection; Bob Harder for funding; Robin Dorociak for lab facilitation; and the GFU DPT program for lab access.

References

[1] Roetenberg et. al., "6DOF Human Motion Tracking" *XSENS Tech* (2013)
[2] Blair, *J. Biomech* (2018) doi:10.1016/j.jbiomech.2018.03.031
[3] Provot et. al., *Sensors* (2019) doi: 10.3390/s17091958.

sEMG-based Finger Posture Recognition Considering the Electrode Shift

Jongman Kim, Taehee Kim, Bummo Koo, Haneul Jung, Yejin Nam and Youngho Kim*
Department of Biomedical Engineering and Institute of Medical Engineering, Yonsei University, Republic of Korea
Email: *younghokim@yonsei.ac.kr

Introduction

sEMG-based pattern recognition algorithms have been developed to recognize the user's motion or intention. Most previous studies developed sEMG-based gesture recognition systems, and they used sEMG sensors attached to specific muscles to avoid misclassification due to the electrode shift [1]. However, they were difficult to use by non-experts and did not perform well due to the electrode shift when the sensors were worn again in daily life [2]. Furthermore, the selection of feature vectors based on classification performance was not efficient in considering the cost and time to train and evaluate the classifier [1]. This study presents the sEMG-based finger posture recognition algorithm for non-experts and method to select the feature vector considering the electrode shift.

Methods

Ten healthy adults were recruited to perform twelve finger postures in MVC of 20% (rest, spread, V-sign, O.K.-sign, scissor-sign, finger-pointing, thumb-up, palmar pinch, lateral pinch, tip pinch, cylindrical grasp, spherical grasp). Each subject wore a pre-developed armband-type sEMG sensor [3] on the right lower arm, and the electrode of the mainboard was placed on the top of the flexor carpi radialis. The subjects performed each finger posture for five seconds and all finger postures were repeated twice. These sessions were repeated ten times with donning and doffing of the sEMG-based armband sensor. Twenty-one feature vectors in time domain were calculated using the band-passed (10-250Hz) signal. Pearson's correlation coefficients (PCCs) were used to analyse the correlation of inter-gesture and inter-session. In PCCs, the values (r) between $0 < r \leq 0.3$, $0.3 < r \leq 0.7$ and $0.7 < r \leq 1.0$ indicate weak, moderate and strong linear relationship (LR), respectively. An artificial neural network (ANN) classifier with a single feature vector was used to classify finger postures. For each subject, nine sessions were used for training (TRN) the ANN classifier, and the other session for the testing in the MATLAB Neural Network Toolbox.

Results and Discussion

In all feature vectors, the ANN classifier using 9 training data showed higher classification accuracy than the classifier using 1 training data. The accuracy of the classifier was high in the order of WAMP(6.7 ± 6.5%), ZC(66.7 ± 7.3%), WL(65.8 ± 6.1%) in 1 training session, and WL(83.3 ± 7.3%), AAC(82.9 ± 8.7%), IEMG(81.7 ± 6.0%) in 1 to 9 training session. These results mean that the additional training data considering donning and doffing of the sensor can solve the problems of electrode shift. Most feature vectors showed moderate LR of inter-gesture. The feature vectors with high inter-session ($r > 0.8$) showed the classification accuracy of higher than 75%. MYOP and MAVSLP showed mean accuracy of 14.2% and 15.0%, respectively. These feature vectors showed weak LR in inter-gesture and inter-session. PCCs of inter-gesture showed the classification performance of feature vectors. In addition, PCCs of inter-session showed the robustness of the feature vectors regarding the electrode shift by donning and doffing of the sensor. Both of inter-gesture PCCs and inter-session PCCs were important in evaluating the classification performance of feature vectors, but the results showed that the effect of inter-session was greater than that of inter-gesture.
The present study suggested that various finger postures could be recognized using an armband-type sEMG sensor and the problem of electrode shift could be solved using the feature vectors with a high inter-session PCCs.

Table 1: Classification accuracy (CA) and PCCs of inter-session and inter-gesture according to the feature vectors

Feature vectors	CA (%)		PCCs (r)	
	TRN: 1	TRN: 1~9	Inter-gesture	Inter-session
IEMG	60.8±7.4	81.7±6.0	0.477±0.073	0.896±0.055
MAV	61.3±9.8	80.8±7.1	0.477±0.073	0.896±0.055
MAV1	60.4±10.1	78.8±10.7	0.478±0.074	0.897±0.054
MAV2	57.9±9.1	76.3±8.6	0.467±0.072	0.889±0.055
SSI	54.6±7.7	77.9±6.2	0.452±0.071	0.865±0.082
VAR	53.3±11.1	76.7±7.7	0.452±0.071	0.865±0.082
TM3	29.2±9.0	47.9±16.5	0.374±0.040	0.762±0.161
TM4	37.5±11.5	65.0±11.7	0.419±0.071	0.783±0.142
TM5	23.3±7.1	51.3±10.9	0.376±0.044	0.709±0.181
RMS	60.4±10.6	81.7±9.5	0.470±0.069	0.887±0.059
LOG	65.4±10.8	81.7±7.1	0.494±0.077	0.902±0.044
WL	65.8±6.1	83.3±7.3	0.479±0.071	0.896±0.059
AAC	62.9±9.9	82.9±8.7	0.479±0.071	0.896±0.059
DASDV	63.3±9.6	77.9±8.6	0.473±0.068	0.886±0.062
MAVSLP	15.0±5.3	12.1±5.7	0.050±0.004	0.000±0.010
ZC	66.7±7.3	80.8±9.3	0.510±0.075	0.896±0.035
WAMP	66.7±6.5	79.2±11.5	0.507±0.077	0.906±0.039
MYOP	14.2±6.0	18.3±6.6	0.297±0.004	0.219±0.141
SSC	62.1±5.0	81.3±6.0	0.510±0.074	0.890±0.036
AR	29.6±8.0	34.6±10.6	0.331±0.013	0.458±0.072
CC	30.0±5.8	32.9±12.5	0.331±0.013	0.458±0.072

Significance

The robustness on the electrode shift by donning and doffing of the sensor is important in sEMG-based pattern recognition system for non-expert and daily life. In this study, classification performance was improved by the additional training data about the electrode shift in all twenty-one feature vectors. The analysis of PCCs showed that the LR of inter-session is more important than the LR of inter-gesture to improve the finger posture recognition.

Acknowledgments

This research was supported by The Bio & Medical Technology Development Program (No.2017M3A9E2063270) through the National Research Foundation of Korea (NRF) funded by the Ministry of Science and ICT.

References

1. Shi, et al., Biocybern. Biomed. Eng,38(1): 126-135, 2018.
2. Young, et al., IEEE T BIO-MED ENG, 59(3): 645-652, 2012.
3. Kim, et al., INT J PR ENG MAN, 20(11): 1997-2006, 2019.

A comparison of attachment methods of skin mounted inertial measurement units on tibial accelerations

Caleb D. Johnson, Jereme Outerleys, Adam S. Tenforde, Irene S. Davis
Spaulding National Running Center, Dept. of Physical Medicine and Rehabilitation, Harvard Medical School, Cambridge, MA
Email: cdjohnson@mgh.harvard.edu

Introduction

Tibial accelerations (TA) during running have been shown to be a valid surrogate for vertical ground reaction force loading rates [1,2], as well as showing associations with running injury [3]. With their recent proliferation, inertial measurement units (IMUs) containing tri-axial accelerometers, have become a common method of measuring TA. These IMUs often come with manufacturer-provided straps, for easy attachment on the skin. However, early work by LaFortune et al. [4] demonstrated systematically lower TA measured with bone- compared to skin mounted accelerometers, due to signal artefact introduced by soft tissue mounting. However, little attention has been given to the method of attaching skin mounted IMUs and its effect on resulting TA measures. Given the findings of LaFortune, it stands to reason that attaching an IMU more securely to the skin will result in lower mean TA. Further, it may also result in lower stride-to-stride variability and better correlations with vertical loading rates.

Therefore, our purpose was to compare two IMU attachment methods: the manufacturer-provided strap and a combination of tape with a neoprene wrap. We hypothesized that the wrap method would be more secure and therefore show lower mean TA, lower stride-to-stride variability, and higher correlations with vertical loading rates compared to the strap.

Keep Space

Methods

18 runners were recruited as part of an ongoing study (10 men/ 8 women; mean age= 33 ± 11 yrs). An IMU (IMeasureU Blue Trident, Auckland, NZ) was attached to the right distal-medial tibia, 1 cm above the superior border of the malleolus. For the strap attachment method, participants were sized to one of 4 straps provided by the manufacturer for use with the IMU. For the wrap attachment, the IMU was first secured directly to the skin with Kinesio Tape® and then wrapped over top with a neoprene wrap. In both cases, the strap/wrap was secured as tightly as possible without causing significant discomfort.

Participants then ran for 5 minutes at a self-selected pace on an instrumented treadmill (AMTI, Watertown, MA) to warm-up, followed by 16 seconds of data collection (approx. 20 strides). The second attachment method was applied, and these procedures were repeated. Order of attachments was counterbalanced across subjects. Mean comparisons between attachment methods were performed for peak vertical and resultant TA (TA-V, TA-R), the stride-to-stride coefficient of variation for TA-V and TA-R, and vertical and resultant instantaneous ground reaction force loading rates (VILR, RILR). Further, correlations between peak TAs and VILR/RILR were assessed.

Keep Space

Results and Discussion

Results of mean comparisons (Fig. 1) showed significantly lower peak TA-V in the wrap compared to strap condition (p= 0.02, d= 0.34). Mean TA-R was not significantly different between conditions (p= 0.06). Mean VILR and RILR were found to be almost identical between conditions (p> 0.9), indicating that differences in TS-V were due to differences in the IMU attachment, not changes in impact loading. This partially supports our hypothesis, that the wrap condition would more tightly couple the IMU to the skin, resulting in lower peak TAs similar to the results reported by LaFortune [4]. However, the effect size was small.

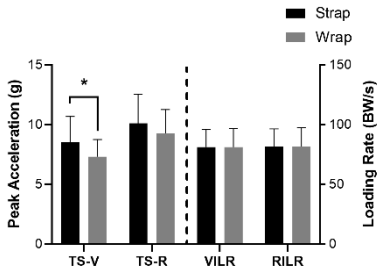

Figure 1: Mean comparisons between strap and wrap conditions

Median stride-to-stride coefficients of variation for TA-V (**Strap:** 8.5%, **Wrap:** 9.6%, p= 0.46) and TA-R (**Strap:** 10.3%, **Wrap:** 10.1%, p= 0.64) were similar. This was counter to our hypothesis, that the wrap condition would also lower stride-level variability in peak TAs.

Finally, our last hypothesis was also not supported. Correlations between TA-V and VILR/RILR were similar for the strap (r_s= 0.91, p< 0.01) and wrap (r_s= 0.84-0.85, p< 0.01) conditions. Correlations were also similar for TA-R (**Strap:** r_s= 0.85, p< 0.01, **Wrap:** r_s= 0.79-0.81, p< 0.01). Our correlations are stronger than those reported by previous studies (r= 0.61-0.82). [1,2] These results indicate that, despite lower mean TAs in the wrap condition, the correlations with ground reaction force loading rates were unaffected by the attachment method.

Keep Space

Significance

Overall, our results provide two key pieces of evidence. For individuals interested capturing the most representative measure of actual TAs during running, a more secure attachment method for skin mounted IMUs may be necessary. This was evidenced by systematically lower peak TA-V in the wrap condition, albeit, with a small effect size. However, many individuals, such as clinicians, may simply be interested in TAs during running as a surrogate for impact loading forces. In these terms, using a simpler method of attaching IMUs (i.e. the strap) appears to be adequate.

Keep Space

References

[1] Van den Berghe, P. (2019). *J Biomech*. **86**: 238-242
[2] Tenforde, A. (2020). *PM&R*. doi: 10.1002/pmrj.12275
[3] Milner, C. (2006). *Med Sci Sports Exerc*. **38**: 323-328
[4] LaFortune, M. (1995). *J Biomech*. **28**: 989-993

Determining Stride Length of Runners using an Ultrawide Bandwidth Local Positioning System equipped with an Inertial Measurement Unit

Pratham Singh[1]*, Michael Esposito[1], Zach B. Barrons[2], Christian A. Clermont[2], John W. Wannop[2], Darren J. Stefanyshyn[1, 2]
[1]Biomedical Engineering Graduate Program, Schulich School of Engineering, University of Calgary, Calgary, Alberta, Canada
[2]Faculty of Kinesiology, University of Calgary, Calgary, Alberta, Canada
Email: *pratham.singh@ucalgary.ca

Introduction

Obtaining running data is crucial for managing an athlete's training load [1]. A gait lab can provide accurate position measurements, but simple wearable technologies are helping athletes reduce their costs and allowing the athlete to remain in a setting that is more representative of their typical gait pattern [2]. In particular, stride length can be obtained with the help of Global Positioning System (GPS) wearables. Unfortunately, a GPS may not be feasible due to the signal being deflected by buildings [3]. An alternative may include a Local Positioning System (LPS) since it is highly accurate, covers a large frequency spectrum (equal to or greater than 500 MHz) and consumes little energy, avoiding the disadvantages of GPS. Despite its advantages, an LPS has its limitations in determining gait events. Sensor fusion may be beneficial in this regard as sensor fusion takes inputs from multiple sensors and combines them into a single output. An Inertial Measurement Unit (IMU) can help characterize a gait event such as stride length. In order to get both good gait event data from the IMU and good position data from the LPS, sensor fusion is required. The objective of the study was to compare stride length obtained from a LPS to a motion capture system (MOCAP), the "gold standard".

Methods

90 recreationally active participants (Age: 27.6 years ± 5.1, Mass: 70.7 kg ± 10.6, Height: 173.8 cm ± 8.7) free of any physical condition that prevents them from running were recruited. The testing session was conducted along a ten-meter running lane. Kinematic data were recorded using reflective markers and eight MOCAP cameras (Vicon, Oxford, UK). The LPS (XCo Tech, Penticton, Canada) consisted of a hub and an IMU sensor equipped with a radio frequency emitter operating in the ultrawide bandwidth (central frequency: 4GHz; bandwidth: 500 MHz). The hub was positioned two meters behind the participant's starting position at a height of one meter. A retroreflective marker was placed on each heel and the IMU was placed on the sacrum. Participants performed three trials at each of a self-selected walk, run and sprint speed. Stride length from the MOCAP was obtained by finding the difference between vertical minima of a heel marker at ipsaleteral heel strikes. Stride segmentation was obtained by finding local peaks in the superior-inferior direction of the IMU data and deeming them as heel strikes [4]. Stride length was then calculated as the difference between position in the anterior-posterior direction obtained from the LPS of the heel strike epoch. The stride length in the last stride was used for analysis. A Bland-Altman plot was used to compare stride length between the LPS and MOCAP systems.

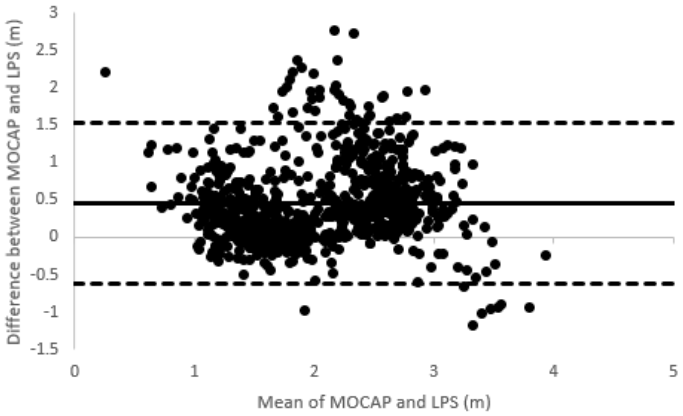

Figure 1: Bland Altman Plot of stride length obtained from the MOCAP and LPS

Results and Discussion

As shown in Figure 1, the bias in the Bland Altman Plot of stride length is 0.46 m, the upper limit of agreement (+1.96 SD) is 1.53 m and the lower limit of agreement (-1.96) is -0.61 m. Out of 810 trials, 46 (5.68%) stride lengths fall outside of the limits of agreement. The Bland Altman plot of stride length showed a large scatter between MOCAP and LPS data.

Significance

An LPS equipped with an IMU and operating in the ultrawide bandwidth may not be a valid method to determine stride length. Additional data processing methods, for example machine learning, should be explored to determine if efficacy can be improved.

Acknowledgments

This project is supported by the NSERC Create We-TRAC Grant and the Mitacs Accelerate Grant.

References

[1] Carling, C. et al. (2008). *Sports Med.*, *38*(10), 839-862.
[2] Higginson, B. (2009). *Curr. Sports Med.*, *8*(3), 136-141.
[3] Hightower, J., & Borriello, G. (2001). *Comput J.*, (8), 57-66.
[4] Lee, J. et al. (2010). *J Sci Med Sport.,* 13(2), 270-273.

A novel use of flexible sensors for ambulatory measurement of gait kinematics

Wei Yin[1], Curran Reddy[2], Yu Zhou[1], and Xudong Zhang[1, 2, 3*]
[1]Department of Industrial and Systems Engineering, [2]Department of Biomedical Engineering,
[3]Department of Mechanical Engineering, Texas A&M University, College Station, TX
Email: *xudongzhang@tamu.edu

Introduction

Optical motion capture systems are often used in studies of human motion and biomechanics but remain expensive and constrained to a calibrated volume. Ambulatory motion sensors are emerging as a cost-effective and mobile alternative. Recent years have witnessed the increasing presence of inertial measurement units (IMUs) in non-laboratory settings for human motion measurement. However, the way these sensors are attached to the human body creates questions concerning subject discomfort, performance interference, and data quality [1]. More recently, a wireless, miniaturized, skin-mounted inertial sensor, BioStampRC (MC10 Inc., Lexington, MA, USA), has been developed, and it overcomes the drawback of conventional IMUs with a soft, flexible design that allows direct body-conforming adhesion to the skin [2]. This sensor integrates an accelerometer, a gyroscope, and a biopotential measurement unit and can be controlled using a tablet without any additional hardware, thus supporting potential ambulatory recording.

This study aimed to establish the viability of flexible sensors for measuring human knee flexion-extension (F/E) kinematics during level walking and develop a corresponding alignment-free auto-calibrating algorithm. We hypothesized that flexible sensors could render joint angle measurement with accuracy comparable to an optical motion capture system. The effects of sensor placement and walking step frequency were also investigated.

Methods

Algorithm

The algorithm first estimates the knee F/E axis of rotation by principal component analysis (PCA) of the gyroscopic data of segments (i.e., thigh and shank) articulating at the knee joint [3]. Then, the knee F/E angular velocity is calculated by subtracting the projection of gyroscopic data of two segments onto the knee F/E axis. Integrating the angular velocity results in knee F/E angle, which unfortunately is subject to significant drift caused by sensors random error. In order to compensate for the drift, an acceleration based sensor position estimation method [4] is employed to predict knee F/E angle of terminal stance phase. Finally, a least squares method is used to estimate the offset to be added to the integrated knee F/E, yielding the ultimate measure.

Experimental Test and Statistical Analysis

Three subjects were recruited and performed level walking across an eight-meter platform with varied step frequency (80, 100, 120 steps/minute). An optical motion capture system, Qualisys (Qualisys AB, Gothenburg, Sweden), was used to record the movements of a set of markers placed on subjects. The marker position data was imported to OpenSim4.0 to derive knee F/E based on individually scaled musculoskeletal models. Three BioStampRC flexible sensors (Figure 1a) were placed on ipsilateral thigh and shank—two on the thigh and one on the shank (Figure 1b&c)—so that knee F/E could be derived using data either from lateral thigh sensor and lateral shank sensor (LTS), or from distal lateral thigh sensor and lateral shank sensor (DTS). Thus, the effect of sensor placement could be investigated. The root mean square error (RMSE) between sensor-measured and OpenSim model-derived knee F/E angle was the response variable in ANOVA. Bland-Altman analysis [5] was also employed to examine the agreement between the sensor-measured and marker-measured (OpenSim-derived).

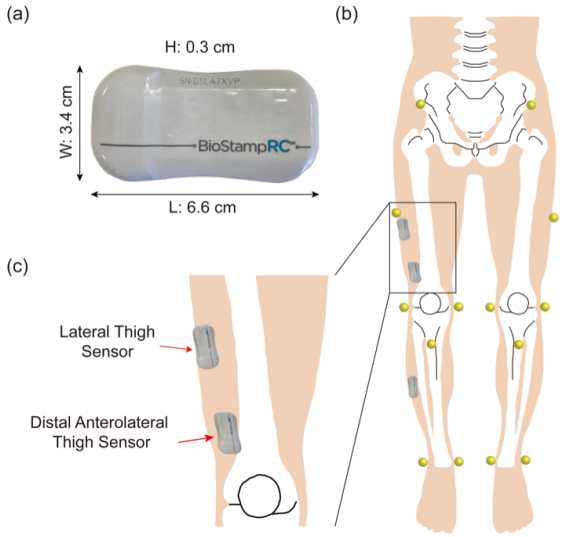

Figure 1: Flexible sensors and reflective markers placement: (a) the dimensions of a BioStampRC flexible sensor; (b) front overall view of flexible sensors and reflective markers placement; (c) detailed view of flexible sensors on the thigh.

Results and Discussion

The overall RMSE were 7.8° and 4.5° for DTS and LTS, respectively. ANOVA indicated that sensor placement had a significant effect on RMSE ($P<0.001$), while no significant effect of step frequency was detected ($P=0.527$). Bland-Altman analysis showed that the r^2 of linear regression between DTS and OpenSim is 0.84, and that between LTS and OpenSim is 0.95. Results demonstrate that flexible sensors, based on the proposed algorithm, can generate comparable results to marker-based measurement, and appear insensitive to varied walking step frequency. A significant sensor placement effect is identified, and a more proximal lateral thigh strategy is recommended.

Significance

Flexible sensors present a novel alternative to acquire human kinematics data in ambulatory or non-laboratory settings, thus extending the capabilities to conduct field biomechanical studies.

References

[1] Sen-Gupta, E., et al., *Digital Biomarkers*, 2019: p. 1-13.
[2] Sun, R., et al., *Digital Biomarkers*, 2018. **2**(1): p. 1-10.
[3] McGrath, T., et al., *Sensors (Basel)*, 2018. **18**(6).
[4] Seel, T., et al., *Sensors (Basel)*, 2014. **14**(4): p. 6891-909.
[5] Bland, J.M., et al., *Lancet*, 1986. **327**(8476): p. 307-310.

Knee Flexion Prediction from a Neural Network Algorithm with Various Sources of Training Data

Michael Zabala[1], Jordan Coker[1]
[1]Mechanical Engineering, Auburn University, Auburn, AL, US
Email: zabalme@auburn.edu

Introduction

Maturation of powered exoskeleton technology would benefit various sectors including military, manufacturing, and healthcare. A key part of this maturity is increased metabolic efficiency of the operator. Most current exoskeleton systems require the operator to "bump into" the device as a means of informing it to move out of the way. However, this impediment of motion is a likely contributor to metabolic inefficiencies [1]. It is critical that the device move prior to contact. In order for this to occur, a prediction of future joint angles is required to actuate the exoskeleton with enough lead time to avoid unneccesary contact with the body. One way to do this is to utilize muscle EMG and current joint angle data in conjunction with trained machine learning algorithms, such as a neural network [2]. However, it is unknown what effect the source of training data has on the prediction error. As such, the purpose of this study was to test the hypothesis that one's own opposite lower-limb used to train a neural network predictive algorithm would produce less error than either a sex-matched independent population or a non sex-matched independent population.

Methods

This study collected whole body biomechanics from ten (5 F, 5 M) healthy participants (21.5 ± 2.0 yrs, 64.5 ± 9.8 kg, 166.9 ± 14.5 cm) during an established gait. A 10-camera Vicon motion capture system was used to capture lower limb kinematics. The marker data was filtered using a 15 Hz lowpass Butterworth filter and knee flexion angle calculated in Visual-3D software. A 6-sensor Delsys Trigno IM set was synchronized to the motion capture system and caputured EMG data for the right and left tensor fasciae latae, rectus femoris, vastus medialis, vastus lateralis, biceps femoris, and semitendinosus. Knee flexion angle and EMG signals were split into three training data sets: the opposite limb of the knee being tested, a population of only males or females (whichever sex match the subject), and a general population that included all other nine test stubjects. Knee flexion angle predictions for the tested knee 50 ms into the future were obtained using a nonlinear input-output time series neural network algorithm trained using Bayesian regularization with a single hidden layer of ten nodes and a feedback delay set to two. This was performed for each knee of all ten subjects. The RMS errors of the predicted angles vs motion capture determined angles were used to compare the accuracy of the neural networks. An ANOVA was conducted to compare the mean RMS errors from each of the sources of training data to determine significant differences. All subjects provided IRB-approved informed consent to be involved in this study.

Results

The RMS error of the predicted knee flexion angle from the three sources of training data are presented in Figure 1 and were as follows: Opposite Limb: 1.7 ± 0.7°, Sex-Matched Population: 3.3 ± 2.4°, and Non Sex-Matched Population: 2.5 ± 1.6° (excluding statistical outliers). The results of the ANOVA analysis (Table 1) showed that there were no significant differences in the RMS error between all three sources of training data.

Table 1: ANOVA results from comparing RMS Error of predicted knee flexion angle for various sources of training data.

ANOVA Table

Source	SS	df	MS	F	Prob>F
Columns	253.28	2	126.64	1.96	0.1509
Error	3692.25	57	64.776		
Total	3945.53	59			

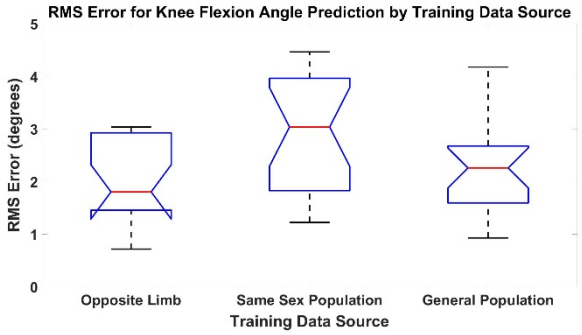

Figure 1: RMS Error for knee flexion angle predicted with data sources of the same subject (opposite limb) and independent populations (same sex, general population). Figure does not represent statistical outliers.

Discussion

The results of the ANOVA disagreed with our hypothesis that one's own opposite knee flexion angle used to train a neural network predictive algorithm would produce less error than either a non sex-matched independent population or a sex-matched independent population. This means that there would not be a significant gain for training on an injured persons' healthy leg to be used on a leg with disabilities.

Significance

The lack of significant difference in the RMS error between all three sources of training data points to a need for further exploring the implementation of the method that would be easiest to enact. In this case, the non sex-matched independent population would see the widest range of success as it would cover any healthy individual. A single, universal algorithm for all exoskeleton users would significantly expidite the acceptance of exoskeleton technology in numerous applications.

References

[1] DP Ferris et al. *International Journal of Humanoid Robotics*, 4(3):507–528, 2007.
[2] Coker J, Zabala M, et al. *Proceedings of the XXVII Congress of the International Society of Biomechanics*, Calgary, Canada, 201

Wearable Tendon Kinetics

Sara E. Harper.[1], Rebecca A. Roembke[2], John D. Zunker[2], Peter G. Adamczyk[1,2], and Darryl G. Thelen[1,2]
[1]Department of Biomedical Engineering, University of Wisconsin-Madison, Madison, WI, USA
[2]Department of Mechanical Engineering, University of Wisconsin-Madison, Madison, WI, USA
Email: seharper@wisc.edu

Introduction

Though wearable movement sensors allow kinematics to be measured in natural environments, it remains challenging to evaluate kinetics outside the laboratory. Instrumented shoes and insoles can be used, but require inverse dynamic models to estimate the underyling tissue loads.[1] This study introduces a wearable sensor for tracking tendon loads during outdoor locomotion. We adapt shear wave tensiometry,[2] based on the relationship between shear wave speed and tension, to a wearable system and assess the viability of tracking fluctuations in Achilles tendon loading during walking on uneven outdoor terrain.

Methods

The tensiometer unit consisted of a piezoelectric actuated tapper, and two miniature accelerometers mounted 8 mm apart within a silicone mold.[2] The actuator was impulsively driven at 100 Hz via a micro-piezo driver. A vibration data logger was used to condition and record accelerometer and timing signals. Cross-correlation analysis of the accelerometer signals after each tap was used to ascertain the wave delay between the two accelerometers,[2] which is then converted into wave speed. The piezo driver, data logger, an inertial measurement unit (IMU), and a battery were all mounted on a waist pack.

Twelve healthy young adults (23.8 ± 2.3 years, 5F/7M) were tested, of whom nine are analyzed to-date. The tensiometer unit was positioned over the right Achilles tendon (Fig. 1-left). Subjects first acclimated to the system while walking on a treadmill. Each subject then walked outdoors at a comfortable speed (~1.5 m/s) over a 1-km course that included level walking, inclines, and declines (Fig. 1-right). Whole-body movement reconstructed from wearable inertial sensors was synchronously recorded throughout. A thresholding technique was used to identify heel strikes from the tensiometer accelerometer signal.

To measure terrain slope, we secured an IMU on a bicycle and recorded both position (GPS) and orientation (IMU) as the bicycle was pushed over the 1-km course. This procedure resulted in a topographical look-up table, used to ascertain terrain slope for each stride of a subject by knowing their position along the course. Strides were binned into slopes ranging from -4 to +4 degrees for averaging (Fig. 2).

To assess sensitivity of tendon wave speed to slope, a linear regression was performed between peak wavespeed and incline angle of each stride. To further illuminate characteristic differences in loading profiles as a function of incline angle, statistical parametric mapping was used to conduct two-sample t-tests between each binned slope condition and level walking.

Results and Discussion

Tensiometry detected characteristic changes in tendon loading with terrain slope. Notably, wave speeds increased during mid-stance on declines, and were amplified at pushoff on inclines (Fig. 2-left). Simple regression between terrain slope and peak wave speed over >5000 strides yielded a highly significant ($p<0.00001$) positive association (Fig. 2-right).

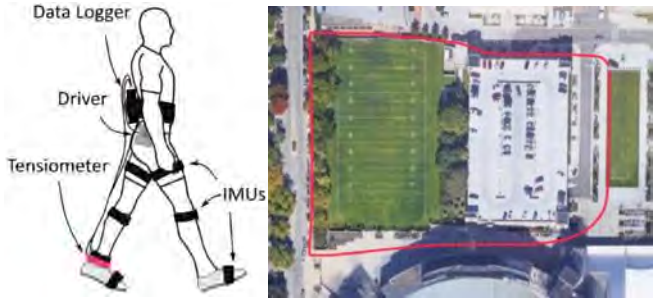

Figure 1: Subjects wore a fully portable version of the tensiometer as well as a lower-body set of IMUs. Aerial view of the outdoor course.

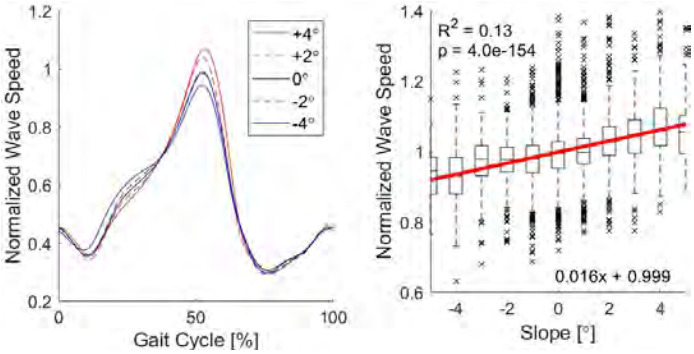

Figure 2: Normalized, mean Achilles tendon loading at binned inclines. A regression of peak loading against slope yielded a positive association.

Slope-dependent variations in Achilles tendon wave speed patterns concur with biomechanical expectations and are generally consistent with lab-based metrics.[3] However, we did observe considerable variability in the slope-wave speed relationship, which likely arises from the other factors (e.g. walking speed, acceleration, obstacles) that affect locomotion outdoors. We are now coupling tensiometry and IMUs to more fully characterize musculotendinous dynamics. Such analyses could prove useful for understanding biomechanical performance and for quantitatively evaluating overuse injury risk, e.g. in military training activities.

Significance

This is the first study to uniquely capture identifiable tendon loading profiles during locomotion in the natural environment. Wearable tensiometry allows the study of tasks and behaviors that are not captured by traditional laboratory measures. These findings validate the motivation for developing and utilizing such tools to study locomotion beyond the lab.

Acknowledgments

Funding provided by WARF Accelerator Program, NIH STTR grant 1R41AR074897-01, and NIH award TL1TR002375.

References

[1] Howell et al. (2013). *IEEE T. Bio-Med. Eng.,* **60**.
[2] Martin JA et al. (2018). *Nat. Commun.,* **9**.
[3] Lichtwark GA et al. (2006). *J. Exp. Biol.*, **209**.

How Accurately Can Motion Capture Identify the Hip Joint Center During Deep Hip Flexion?

Naomi E. Frankston*, Tom H. Gale, William J. Anderst
Biodynamics Laboratory, Department of Orthopedic Surgery, University of Pittsburgh, Pittsburgh, PA, USA
Email: *nef22@pitt.edu

Introduction

Three-dimensional motion capture using skin-mounted markers can be a tool to better understand hip pathology, such as femoracetabular impingement (FAI), as it relates to dynamic motions. However, motion capture is limited in accuracy due to the movement of skin relative to bone, known as soft tissue artifact (1), and errors in marker placement. Dynamic biplane radiography (DBR) evaluates *in vivo* hip kinematics during dynamic tasks with an accuracy of 0.3 mm and 0.8º (2). Previous studies have evaluated the accuracy of motion capture to measure hip kinematics during gait, hip abduction, rotation, and loaded flexion by comparing motion capture with DBR and found errors up to 54 mm and 9.5° (1,3). However, previous studies did not evaluate motion capture accuracy during deep hip flexion, which is an activity that elicits hip pain in FAI patients. The aim of this study was to determine the error in locating the hip joint center using motion capture compared to DBR during deep hip flexion.

Methods

Twelve unilateral FAI patients (9 F/3 M, 31 ± 12 years (20-57 years), 23.5 ± 4.0 kg/m^2) participated in this IRB-approved study. The locations of the bilateral hip joint centers were analyzed during two trials of single-legged standing active hip flexion and two trials of single-legged standing active hip flexion combined with adduction and internal rotation. Motion capture (12-camera Vicon Vantage) and DBR data were captured simultaneuosly at 100 Hz and 30 Hz, respectively. For Vicon data, the hip joint landmarks were estimated in Visual3D from a Coda pelvis and based on regression equations using the ASIS and PSIS marker locations (4). For DBR, the hip joint centers were based on fitting a sphere onto the femoral head on a subject-specific 3D model generated from a CT scan of the hip. DBR and Vicon hip center locations were filtered with 4th and 2nd order Butterworth filters with 3 and 12 Hz cutoffs, repsectively. The hip joint center locations from motion capture were interpolated to yield data synchronized to the DBR data. Hip joint center locations from Vicon were transformed into the DBR coordinate system. Root mean square (RMS) error was used to calculate the average difference in the medial-lateral (ML), anterior-posterior (AP), and superior-inferior (SI) positions of the hip joint centers between Vicon and DBR systems over the period of synchronized imaging. Differences between trials and sides were tested using paried samples t-tests, and repeatability of trials was assessed with Pearson's correlations.

Results and Discussion

A total of 140 movement trials were included in this analysis. Average peak hip flexion angle across all trials was of 92º. RMS errors ranged from 1 to 74 mm across subjects, trials, and anatomical directions. Our findings are similar to, but slightly larger than those reported by Fiorentino et al. (1) who found mean errors ranging from 3 to 54 mm during walking, hip abduction, and hip rotation.

RMS errors were not significantly different between the symptomatic and asymptomatic legs or between the two trials (p>0.05). The repeatability of error between trials of the same motion were high, with an average Pearson's correlation of r=0.77, p=0.02 for all trials.

Although errors were fairly repeatable within subjects for a given motion, RMS error varied between subjects and anatomical direction (Figure 1). The average RMS errors for all subjects and all trials were: ML: 11 ± 8 mm, AP: 26 ± 16 mm, SI: 17 ± 13 mm. While Fiorentino et al. analyzed skin-mounted marker and not hip center locations, our average ML-axis findings for all trials are comparable (11 mm). However, our AP and SI errors are higher than theirs (AP: 18 mm; SI: 12 mm), possibly due to the deep flexion movement we studied. RMS errors were also subject-dependent, with standard deviations of RMS errors ranging from σ=7 to 21 mm.

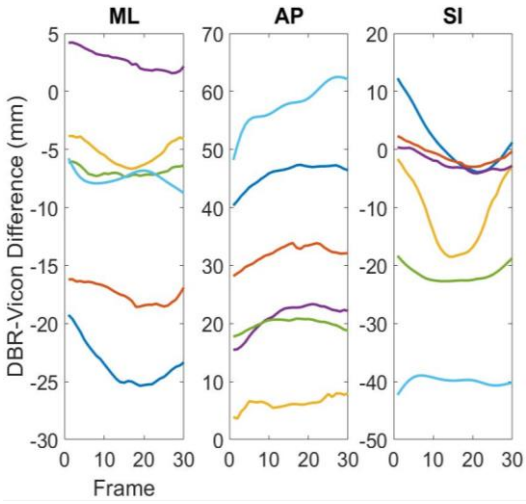

Figure 1: Difference in poistion of hip joint centers between DBR and Vicon systems for 6 representative subjects during right hip deep flexion. (ML: mediolateral, AP: antero-posterior, SI: superior-inferior).

Researchers should be aware that the error in identifying the hip joint center during deep flexion using motion capture is, on average, a factor of 60 times greater than DBR. An important finding of this study is that this error varies among individuals from 1 mm to 74 mm, making it difficult to develop a single algorithm to correct for the errors from both marker placement and skin motion artifact associated with conventional motion capture.

Significance

Skin-mounted motion capture systems have error as high as 74 mm in identifying the hip joint center during deep hip flexion. The magnitude and patterns of error vary considerably between subjects, making it difficult to develop a single algorithm to correct for these errors across many subjects.

Acknowledgments

We thank Camille Johnson, Elliott Hammersley and Jessica Brown for assisting in processing the DBR data.

References

1. Fiorentino NM *G&P,* 2017. 2. Martin DE *J Arthroplasty*, 2011. 3. Zugner R *J Orthop Res*, 2017. 4. Bell AL *Mov Sci*, 1989.

The Accuracy of Machine Learning Models for Detecting Propulsion from an Inertial Measurement Unit Worn on the Arm of Manual Wheelchair Users

Brianna M. Goodwin[1], Omid Jahanian[1], Stefan I. Madansingh[1], Beth A. Cloud-Biebl[1], Kristin D. Zhao[1], Shivayogi V. Hiremath[2], Melissa M. B. Morrow[1], and Emma Fortune[1]
[1]Mayo Clinic, Rochester, MN, [2]Temple University, Philadelphia, PA
Email: Goodwin.Brianna@mayo.edu

Introduction

Manual wheelchair (MWC) users with spinal cord injuries (SCI) are four times more likely to have rotator cuff pathology and can experience unbearable shoulder pain after decades of use [1, 2]. Propulsion and upper extremity weight-bearing tasks likely contribute to the increased pain and pathology in this population.

Monitoring of free-living activity combined with activity classification algorithms has the potential to inform the frequency and duration of tasks to aid in understanding how exposure to specific tasks contributes to shoulder pathology. Machine learning (ML) techniques have been used to detect propulsion in the field using wearable-sensors on the body and MWC; however, this includes passive propulsion such as coasting and being pushed [3, 4]. To understand shoulder health in MWC users, accurate detection models are required to quantify the time the shoulder is engaged in active propulsion. The purpose of this study was to compare the performance of six ML models with three feature selection methods (total of 18 models) to detect MWC propulsion using inertial measurement unit (IMU) data collected from one upper arm of MWC users.

Methods

After IRB approval and informed participant consent, MWC users donned two wireless IMUs (Emerald, APDM, Portland, OR) on their bilateral arms. IMU data (128 Hz) and video data (60 Hz) were synchronized and collected while participants performed six activities of daily living (counter-height reaching, overhead reaching, cross-body lifting, transfers, and level and simulated ramp propulsion on passive rollers). Video data from both arms were coded as propulsion or non-propulsion for each second by two raters; inter-rater reliability: 0.85.

114 normalized temporal and spatial features were calculated from acceleration and angular velocity data for each second for both arms. Data from both arms were used in the model independent of each other. Data were separated into training and testing sets; all data from six of eight randomly selected participants were used as training data (75%), and the data from the remaining two participants made up the testing data. Correlation-based feature selection (CFS), ReliefF (statistical method using k-nearest neighbours), and least absolute shrinkage and section operator (LASSO) were implemented as feature selection methods in MATLAB (Mathworks, Natick, MA). The MATLAB classificationLearner and neural network pattern recognition applications were then used to create the 10-fold classification models: naïve bayes, linear support vector machine (SVM), Gaussian K-nearest neighbour, ensemble boosted tree, logistic regression, and neural network (18 models total). The accuracies of the models were compared.

Results and Discussion

Eight MWC users with SCI (7 males, 39.4±12.6 years, 9.6±11.3 years since injury, C5-T6 injury levels) participated in the study. The highest accuracy was observed for linear SVM with LASSO feature selection (Figure 1). Selected features included spatial and temporal features calculated from the acceleration and angular velocity data. Reported accuracies were slightly higher than a previous study using a neural network model with thirteen manually selected features estimated from the same data as the current study [5]. Future work will incorporate full day free-living data to estimate total daily propulsion time.

Significance

Detection of propulsion in the free-living environment can give insights into the daily exposure of motion and loading experienced by MWC users. As part of another study, authors are currently collecting free-living data alongside shoulder magnetic resonance imaging (MRI). Investigation of the association between daily propulsion time and shoulder MRI findings may lead to better understanding of how MWC propulsion contributes to increased pathology for this population. The models presented in the current study were trained with data collected in the lab and, thus, will be improved with the inclusion of free-living data.

Acknowledgments

This research was supported by the NIH (R01 HD84423) and the Craig H. Nielsen Foundation.

References

[1] Akbar, M., et al. (2010). JBJS (Am), 92(1):23-30.
[2] Divanoglou, A., et al. (2018). J Rehabil Med, 50: 872-878.
[3] Sonenblum, S., et al. (2012). Rehabil Res Pract.
[4] Hiremath, S., et al. (2015). Med Eng Phys, 37(1) 68-76.
[5] Fortune, E., et al. (2019). JEK, 102337.

A

	CFS	ReliefF	LASSO
Naïve Bayes	82.3	87.8	91.0
Support vector machine	90.2	93.4	95.4*
K-nearest neighbor	87.9	91.9	93.6
Boosted tree	92.5	92.9	92.6
Logistic regression	91.0	93.5	94.4
Neural Network	92.8	93.6	95.1

B

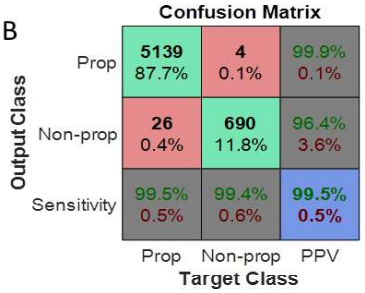

Figure 1: A) The percent accuracy (%) for the 18 tested models using 3 feature selection methods with 6 machine learning models. *denotes the model with the highest accuracy. B) Test data confusion matrix for detection of propulsion (prop) and non-propulsion (non-prop) for the model with the highest accuracy (SVM with LASSO feature selection).

IMU-Based Sit-To-Stand Performance Measurement among Patients with Musculoskeletal Pain

Jake A. Mooney[1], Ruopeng Sun[1*], Amir Muaremi[2], Wei Zhang[3],Ma Ith Agnes[1], Anne Kuwabara[1], and Matthew Smuck[1]
[1]Division of Physical Medicine and Rehabilitation, Stanford University.
Email: *rusun@stanford.edu

Introduction

Patients with musculoskeletal disorders often have difficulty performing daily activities like rising from a chair [1]. Performance on the sit-to-stand (STS) test is influenced by leg strength and power [2], as well as joint limitations caused by musculoskeletal pain [3]. Altered body kinematics (i.e. trunk inclination) and slower transfer speed during STS are reported among patients with musculoskeletal pain [4]. Unfortunately, traditional lab-based assessment methods (3D motion capture, forceplate) are infeasible in the routine clinical setting, and test measurement with a simple stop-watch is not sufficiently accurate for diagnostic use. Alternatively, wearable technology, in particular the inertial measurement unit (IMU), has great potential to provide an accurate and sensitive assessment of body kinematics in a low-cost manner.

This study aims to use a single hip-mounted IMU sensor to evaluate the STS performance between healthy controls (HC) and patients with musculoskeletal pain (Lumbar Spinal Stenosis - LSS and Knee Osteoarthritis - KOA), and to explore the feasibility of using sensor-derived features for better disease phenotyping.

Methods

Thirty participants were enrolled in the study with equal distribution of patients in each of the 3 groups (10 KOA, 10 LSS, and 10 HC, age and gender matched). Each participant completed the 30-second STS test wearing a Shimmer3 IMU sensor (Shimmer, Germany) on the right hip. For each trial, only the first 5 STS cycles were analyzed to ensure signal quality consistency. After IMU orientation correction, the trunk inclination angle (TA), the vertical acceleration, and the sagittal angular velocity were extracted from each STS cycle. The range of each derived measure, as well as the cycle-by-cycle variation of each derived measure (measured by the mean Euclidean distance of the signal profile between STS cycles, using the Dynamic Time Warping method– DTW) were analyzed as the primary outcome measures. The association between each primary outcome and other pertinent clinical outcome measures (i.e. 36-item Short Form health survey,SF-36 [5], etc.) were analyzed using the Pearson correlation. Group difference was analyzed using one-way ANOVA.

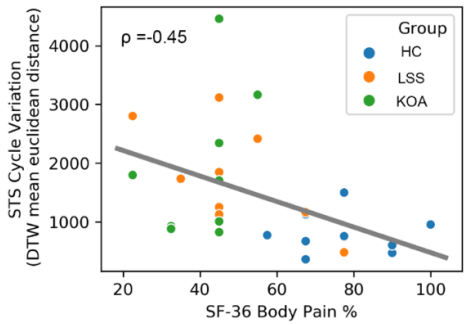

Figure 1: Scatter plot of the STS TA cycle variation (measured by the DTW mean Euclidean distance of TA profile) against the SF-36 Body Pain score (higher score indicates less daily pain reported).

Results and Discussion

As expected, patients with musculoskeletal pain exhibited slower STS movement (longer duration per cycle, smaller vertical acceleration) than HC. An increased TA range per STS cycle was also observed (65.1° ± 20.1° for LSS, 76.2° ± 19.6° for KOA) in comparison with HC (52.9° ± 17.4°, p=0.044). Additionally, the cycle-by-cycle variation (DTW Euclidean distance) for TA was found to be significantly different (p=0.02) between HC (771.6 ±343.5) and patients with musculoskeletal pain (LSS: 1678.8 ± 868.2, KOA: 1901.2 ± 1240.9). Yet the cycle-by-cycle variation for vertical acceleration and saggital gyroscope signal did not reach statistical significance (p=0.08) for group comparison. As shown in Figure 1, the TA cycle-by-cycle variation was also associated (ρ=-0.45, p<0.01) with the perceived pain while doing daily activities (SF-36 Bodily Pain). These findings suggest that the Trunk Inclination Angle as well as its cycle-by-cycle variation during STS, can potentially be used as an additional key parameter for altered mobility detection in patients with musculoskeletal pain. Further work investigating the trunk inclination dynamic to phenotype patients with different musculoskeletal pain mechanisms is underway.

Significance

The results from this work highlight the significance of trunk inclination dynamic during sit-to-stand movement among patients with musculoskeletal pain. The range of trunk inclination and its variation among each sit-to-stand cycles were identified as key features that may be uniquely sensitive to the sit-to-stand test evaluation among musculoskeletal pain patients. These findings could facilitate further feature selection and result interpretation for sensor-based sit-to-stand evaluation in the clinical setting.

References

1. Turcot, Katia, et al. "Sit-to-stand alterations in advanced knee osteoarthritis." *Gait & posture* 36.1 (2012): 68-72.
2. Regterschot, G. Ruben H., et al. "Sensitivity of sensor-based sit-to-stand peak power to the effects of training leg strength, leg power and balance in older adults." *Gait & posture* 39.1 (2014): 303-307.
3. Mizner, Ryan L., and Lynn Snyder-Mackler. "Altered loading during walking and sit-to-stand is affected by quadriceps weakness after total knee arthroplasty." *Journal of Orthopaedic Research* 23.5 (2005): 1083-1090.
4. Coghlin, S. S., and B. J. McFadyen. "Transfer strategies used to rise from a chair in normal and low back pain subjects." *Clinical Biomechanics* 9.2 (1994): 85
5. Ware Jr, John E., and Cathy Donald Sherbourne. "The MOS 36-item short-form health survey (SF-36): I. Conceptual framework and item selection." *Medical care* (1992): 473-483.

Human Motion Monitoring using Smart Nanocomposite Kinesiology Tape

Kenneth J. Loh[1,2,3,]*, Yun-An Lin[1,2], Yujin Park[2,3], and Wei-Hung Chiang[4]
[1]Department of Structural Engineering, University of California San Diego, La Jolla, CA 92093-0085, USA
[2]Active, Responsive, Multifunctional, and Ordered-materials Research (ARMOR) Laboratory, University of California San Diego, La Jolla, CA 92093-0085, USA
[3]Materials Science and Engineering Program, University of California San Diego, La Jolla, CA 92093, USA
[4]Department of Chemical Engineering, National Taiwan University of Science & Technology, Taipei, Taiwan
Email: *kenloh@ucsd.edu

Introduction

In recent years, wearable sensors have attracted considerable interest among the general public due to increased awareness in personal health and wellness management [1]. Technologies as such can be particularly beneficial to industries related to virtual reality, sports performance, military, and healthcare. However, most wearable sensors available today are still based on bulky, inconvenient, electronic devices. Furthermore, they are also limited to discrete sensing at designated points.

On the contrary, sensors in the form of patches are more conformable to the human body and are capable of distributed sensing. For this reason, the objective of this study is to develop a flexible, skin-like sensor capable of continuous physiological and motion monitoring. The approach was to integrate strain-sensitive nanocomposites with commercial kinesiology tape (K-Tape) as the substrate. The sensing properties of these Smart K-Tapes were characterized using a load frame and then tested on subjects performing different activities and movements.

Methods

Wearable Smart K-Tape sensors were fabricated by integrating piezoresistive graphene-based thin films with kinesiology tape. First, graphene nanosheets (GNS) [2] were dispersed in a 2 wt.% ethyl cellulose ethanol solution by ultrasonication. Airbrushing was employed for depositing GNS-EC thin films on commercial fabric transfer, before they were ironed onto K-Tape. Electrodes based on silver paste and conductive threads were formed at opposite ends of the rectangular GNS-EC thin films. These Smart K-Tapes were then mounted in a load frame for characterizing their sensor performance and affixed onto a subject's wrist for validating human motion monitoring.

Results and Discussion

First, Smart K-Tapes were mounted in a Test Resources 100R load frame for characterizing their strain sensing performance. Tensile cyclic strains were applied, while a digital multimeter (DMM) recorded the electrical resistance (R) of the specimen at 2 Hz. Fig. 1 shows a representative resistance time history of a Smart K-Tape specimen, where repeatable and high signal-to-noise ratio sensing response was observed. The strain sensitivity or gage factor was calculated to be ~ 26, which is ~ 13 times higher than the sensitivity of a foil-based strain gage.

Second, Smart K-Tapes (Fig. 2 left) were also mounted onto a subject's wrist. As the subject bent the wrist to different angles and back-and-forth, R of the Smart K-Tape was recorded using the DMM. Fig. 2 (right) plots the resistance time history of the sensor's response. It can be seen that changes in resistance was observed depending on different angles of the wrist, which induced different magnitudes of strain on the Smart K-Tape and its integrated GNS-EC sensing element. The repeatable nature of the sensor signals validated sensor performance and showed promise for applications in human motion monitoring.

Significance

In summary, the results validated that commercially available K-Tape can be engineered with added sensing functionality. The wearable sensors exhibited high strain sensitivities, low-noise, and were highly repeatable over multiple cycles of loading. Not only can Smart K-Tape be used for human and physiological monitoring in various settings, they can also be used for assessing their efficacy from clinical/therapeutical perspectives or if they are even properly applied (or prestretched before affixing) onto the skin.

Acknowledgments

This study was supported by the U.S. Office of Naval Research.

References

[1] S.C. Mukhopadhyay, 2014, "Wearable sensors for human activity monitoring: a review," *IEEE Sensors Journal*, **15**(3): 1321-1330.
[2] K. Manna *et al.*, 2019, "Printed strain sensors using graphene nanosheets prepared by water-assisted liquid phase exfoliation," *Advanced materials Interfaces*, 1900034.

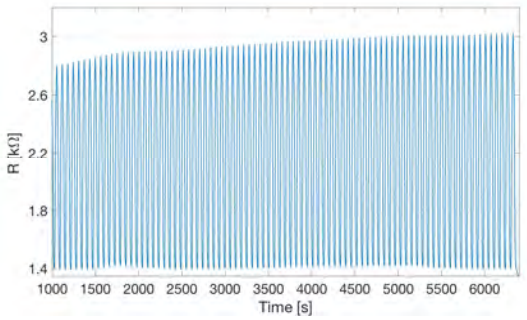

Figure 1: Tensile cyclic load frame testing of a Smart K-Tape specimen and its corresponding resistance time history response

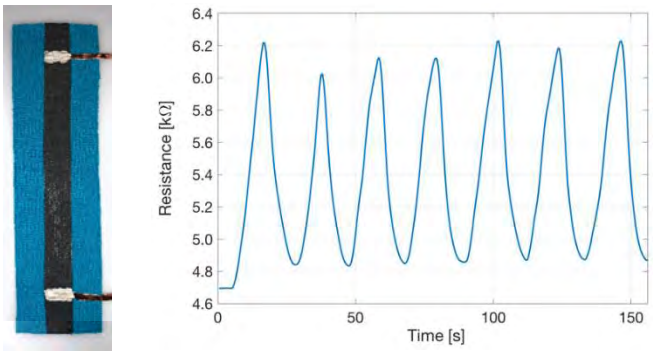

Figure 2: (left) A Smart K-Tape and (right) its resistance response during human motion (wrist) validation tests

IMU-based Kinematic Estimates for a Simplified Model of the Human Lower-limbs: Simulation and Experiment

Michael V. Potter, Stephen M. Cain, Lauro V. Ojeda, and Noel C. Perkins
University of Michigan, Ann Arbor, USA
Email: mvpotter@umich.edu

Introduction

Inertial measurement units (IMUs) present an attractive solution for measuring human kinematics outside of the laboratory due to their small size, portability, low cost, and ease of use. Estimation of kinematics from IMU data requires integration of noisy sensor signals and then correcting the estimates for drift errors. We propose a method for estimating human lower limb kinematics from an array of body-worn IMUs (one on each major segment). As a first step, in this study we present this method for a simplified 3-body model (two legs connected by a pelvis) of the human lower limbs and then assess the fidelity of the estimates via simulation and experiment.

Methods

We utilize an error-state Kalman filter (ErKF) similar to [1] to estimate positions and orientations of the body segments. Kinematic constraints (i.e., joint constraints) are utilized to reduce relative drift between segments [2]. Additionally, known kinematic states (i.e., zero-velocity updates and gravitational tilt corrections) reduce drift errors between the lower-limb system and a fixed world reference frame.

We apply our method to a simplified 3-body model of the lower-limbs (two legs and pelvis) that reveals the key challenges that must be addressed to develop a full 7-body lower-limb model. We first consider noise-free IMU data as created numerically from a walking model. We then add known noise to test the fidelity of the ErKF estimates. The model, created in OpenSim [3] with attached virtual IMUs, generates noise-free IMU data for a 4-minute walk. Noise is then added (commensurate with commercially available IMUs) to generate simulated IMU data. The simulated data is input to the ErKF to yield estimates of lower-body kinematics to compare to the prescribed trajectories of the original model. Because the algorithm requires known sensor-to-segment alignments, we also use OpenSim to investigate the impact of errors in measured sensor-to-segment alignment. In addition to these simulations, we evaluate the performance of this simplified model for a human subject walking overground with stiff legs.

Results and Discussion

Figure 1 shows a comparison of ground truth and estimated right hip joint angles for a representative 20-second sample for the walking simulations. Root-mean-square errors (RMSE) for the joint angles remain below 0.3 degrees on both hips and on all three axes. Additionally, stride parameters were acurately estimated with RMSE of 2% for stride length and 1.3% for stride width. Table 1 summarizes resulting stride width errors with prescribed misalignment between the leg and leg-mounted IMUs about the hip adduction axis. These results demonstrate significant sensitivity of stride width on sensor-to-segment misalignment. Experimental results with stiff-legged human walking also demonstrate good agreement between estimates and ground truth for stride length and stride width (mean errors of -8 cm and -5 cm, respectively). These results will likely improve with improved measurement of sensor-to-segment alignment (as demonstrated in Table 1).

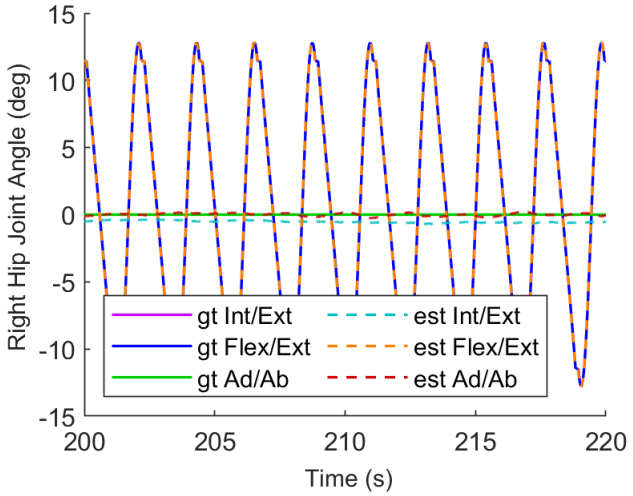

Figure 1: Comparison of ground truth (gt) and estimated (est) joint angles for the right hip over a representative 20-second time sample of walking simulations.

Table 1: Mean and standard deviation (SD) of errors in estimated stride width (SW) due to sensor-to-segment misalignment (from simulation). Misalignment is positive about hip adduction axis.

Misalignment (deg)	-10	-5	0	5	10
Mean SW error (%)	79	40	0	-40	-79
SD SW error (%)	1.0	1.0	1.2	1.0	1.5

Significance

The results presented support extending this approach to a full lower-limb model incorporating seven segments (feet, shanks, thighs and pelvis). Doing so will provide a powerful means to estimate kinematics outside of traditional laboratory environments, thereby enabling research in broad contexts including human health, worker safety, and human performance. Importantly, the method makes no assumptions about the terrain (e.g., ground need not be level) nor is it constrained to low dynamical movement; thus, allowing the method to be used for a wide range of task analyses.

Acknowledgments

This research is supported by the US Army Contracting Command APG, Natick Contracting Division, under contract W911QY15-C-0053 and by the NSF Graduate Research Fellowship Program under Grant DGE 1256260. Any opinions, findings, conclusions, or recommendations are those of the authors and do not necessarily reflect the views of the sponsors.

References

[1] Sola, "Quaternion kinematics...", *arXiv* 2017.
[2] Tuefl, et al. "Validity...", *Sensors* 2018.
[3] Delp, et al. "OpenSim...", *IEEE Trans. Biomed. Eng.* 2007.

The effect of footwear on hindfoot tracking: A marker-based biplane fluoroscopy study

Jing-Sheng Li[1,2], Brittney C. Muir[1,2], Matthew W. Kindig[1], Tadashi Kimura[1,3,4], Bruce J. Sangeorzan[1,3], William R. Ledoux[1,2,3], Patrick M. Aubin[1,2]
[1]RR&D Center for Limb Loss and MoBility, Department of Veterans Affairs, Seattle, WA
Departments of [2]Mechanical Engineering and [3]Orthopaedics & Sports Medicine, University of Washington, Seattle, WA
[4]Department of Orthopaedic Surgery, The Jikei University School of Medicine, Tokyo, Japan
Email: jsli@uw.edu

Introduction

An accurate description of bone motion is essential for understanding motion-related joint pathomechanics. Our in-house, intensity-based centroid detection algorithm for marker-based tracking has been used to track isolated bones using biplane fluoroscopy [1]. However, footwear, which may contain irregular shapes and variable material density, potentially contributes to the image noise level and may influence the tracking performance. The purpose of this study was to use our in-house bead tracking software and evaluate its performance in different footwear conditions. We hypothesized that the tracking performance would be worse in shod and ankle-foot orthoses (AFO) conditions compared to barefoot, as shoes and other devices may attenuate more X-ray compared to the barefoot condition.

Methods

One cadaveric foot specimen (male, 97 years, BMI = 25.1 kg/m^2) without known ankle or foot pathology was used for this study. Extrinsic muscles were dissected and attached to nylon ropes with a Krackow suture (Figure 1A). Ten radio-opaque stainless steel beads (diameter: 3mm) were implanted in the cortices of the tibia (3 beads), talus (3 beads), and calcaneus (4 beads) (Figure 1B). The beads were secured with cyanoacrylate adhesive after implantation. A computed tomography (CT) scan of the specimen was conducted (Siemens Biograph 16, 130kV, variable current, voxel size: 0.867 x 0.867 x 0.7 mm).

A custom designed loading apparatus was used to simulate tibial progression during the stance phase of gait. The cadaveric foot was moved through our biplane fluoroscopic imaging system (Figure 1A), consisting of two modified Philips BV Pulsera C-arm fluoroscopes (Philips Medical Systems, 70-72kV, 19mA) with high-speed cameras (Phantom v5.2, Vision Research, frame rate: 500Hz, exposure time 0.0018s)) [1]. One operator controlled the tibial motion and another operator applied tension through the nylon ropes to the muscles to regulate foot posture (Figure 1A). Four footwear conditions were tested; one barefoot condition and three shod conditions (control shoe or CS (New Balance 928), CS with an AFO (CS-AFO), and rocker bottom shoe (RB)). A strain gauge mounted to the floor was used to indicate when the foot was being loaded; stance phase was determined by a 10% increase in the signal range for each trial. A total of 20 trials (5 for each condition) were collected and analyzed.

The data underwent imaging distortion and flatfield correction, and 3D localization of the system was conducted [1]. Then 3D space frame-by-frame bead (marker) location reconstruction was conducted using an in-house program written in MATLAB (Mathworks, Natick MA). Pairwise intermarker distances were calculated for each bead pair in the tibia, talus, and calcaneus in different footwear conditions. A total of 12 intermarker distances were calculated over at least 885 video frames per condition.The standard deviations for each pair were used to represent the tracking performance.

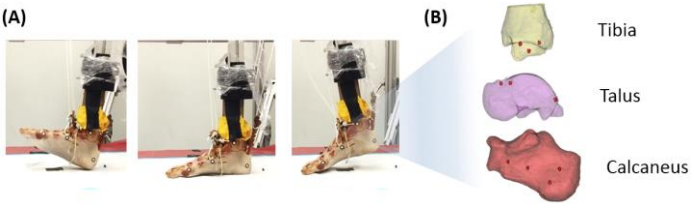

Figure 1: (A) The loading apparatus with a four-bar linkage simulates the tibial progression angle during the stance phase of the gait cycle. Foot positions were controlled through the nylon ropes to the muscles. (B) Ten stainless steel beads implanted in the hindfoot bones.

One-way analysis of variance (ANOVA) was used to test the difference in means of the standard deviation between footwear conditions (barefoot, CS, CS-AFO, RB), with a value of $p < 0.05$ considered significant.

Results and Discussion

The mean of the standard deviation was 0.18 mm (range 0.10-0.33 mm) among all intermarker distances in all testing conditions. For each condition, the standard deviation of the intermarker distances [mean (minimum-maximum)] were 0.20 (0.13-0.33) mm (barefoot), 0.18 (0.13-0.28) mm (CS), 0.15 (0.11-0.22) mm (CS-AFO), and 0.18 (0.10-0.26) mm (RB). The ANOVA showed that there was no significant difference across the footwear conditions ($p = 0.2$), suggesting that the marker tracking performance was not significantly influenced by the selected footwear and orthosis.

Marker-based tracking was used as the gold standard to describe bone motions in other fluoroscopic validation studies [1,2]. However, the effect of footwear on fluoroscopic imaging has not been fully considered. This study is a baseline for our later markerless bone tracking procedures. As we only tested one cadaver, one shoe model, and one AFO, the results may not be generalizable to other footwear designs or conditions.

Significance

Any materials that potentially attenuate X-ray energy may have resulted in worsened fluoroscopic images. The design and materials used in shoes may affect the marker tracking performance. We confirmed that our in-house marker tracker did not perform differently in barefoot and shod conditions. This enables us to use marker-based tracking as the gold standard for subsequent markerless bone tracking analyses.

Acknowledgments

This work was supported in part by the Department of Veterans Affairs Research Rehabilitation and Development grants RX002130, RX002357, RX002278, and I21RX003331.

References

[1] Iaquinto et al. Comput Biol Med. 2018;92:118-127.
[2] Brainerd EL et al. J Exp Zool A Ecol Genet Physiol. 2010;313(5):262-79.

Optimization Tool for the Classification of Human Movement

Kathryn Akmal[1], Corey Pew[1]
[1]Department of Mechanical and Industrial Engineering, Montana State University, Bozeman, MT
Email : *Corey.Pew@montana.edu

Introduction

Classification and prediction of human movement has become an important research topic in the field of biomechanics and health.[1] Quantitative interpretation of an individual's motions in real-time is necessary for the control of robotic prosthetics, orthotics, and exoskeletons and is useful for clinical identification of abnormal gait or adverse events such as falling.[2,3] Body-worn sensors are often used to collect data used to classify human movement, however, the interpretation of data varies considerably among researchers.

Two main hurdles exist when processing sensor data: 1) feature selection and 2) machine learning algorithm selection. First, when processing sensor information, features of the data (such as mean, max, standard deviation, etc.) are analyzed. In addition, these features are often analyzed over time using sliding windows, where the size and overlap of the windows can affect feature usefulness.[4] Second, the processed data is analyzed with machine learning techniques to relate data patterns to varying activity classifications. With a multitude of combinations between feature selection and machine learning methods the same data set can be analyzed in different ways with varying results.[2,4] Finally, the use of machine learning techniques requires the collection of large amounts of human subject data on which to base the algorithm. Often, the collection of human subject data requires significant investment, and the data of multiple researchers is generally incompatible. This makes it difficult to perform new research or to utilize data from others to augment a data pool.

The objective of this project was to create a stand-alone software application to enable automated processing and analysis of data from body worn sensors to accurately classify human movement. In addition, we propose the use of a standardized data format to facilitate data sharing.

Methods

Software development utilized the MATLAB App Designer and the Statistics and Machine Learning Toolbox. The standalone application can upload a single, standardized text file that contains experimental motion data for analysis. The user then guides the application to select data groups and extracts labeled classifications contained within the file. They then choose calculated features (mean, min, max, and standard deviation) that are generated by the application. Calculated features are determined over a time window length and overlap that is optimized as part of the process. The user initially indicates a minimum and maximum time window range and overlap over which the application will analyze the data as well as specified machine learning algorithms they would like to consider. The application then iteratively compares the various combinations of features, time window size, window overlap, and algorithm type to find a setup that produces the highest classification accuracy. Accuracy is calculated using either five-fold cross validation or testing on a percentage of holdout data determined randomly by the application.

Table 1: Comparison of classification accuracy results. **Bold** shows new method had higher accuracy than previous results.

Subject	SVM		KNN		Ensemble	
	Original	New	Original	New	Original	New
A01	96.2	95.0	96.5	**99.7**	96.2	**99.6**
A02	95.2	88.2	94.9	**99.5**	94.8	**99.5**
A03	90.7	**94.0**	90.4	**98.6**	90.3	**93.4**
A04	92.7	**94.2**	92.6	**99.1**	92.1	**99.0**
A05	93.0	**93.9**	94.4	**99.3**	93.8	**99.1**
Pooled	90.5	**93.7**	91.2	**98.9**	90.5	**98.8**

Initial testing of the application utilized pre-existing data used to classify turning in lower limb amputees.[2] In the previous study we looked at data from five amputee subjects (both individually and pooled) and classified whether they were turning or walking straight using data from a single inertial measurement unit simulated using motion capture data. The initial testing compared the efficacy of using support vector machine (SVM), K-nearest neighbor (KNN), and decision tree ensemble (Ensemble) algorithms on the classification accuracy and so we limited the scope of this analysis to those three methods.

Results and Discussion

Results from the previous study compared to the updated analysis are shown in **Table 1**. We found that the new application was able to attain higher classification accuracies (as measured by percentage of correctly predicted data points) than our original analysis for 16 of the 18 conditions. In our original work we also concluded that pooling data resulted in lowered classification accuracy, however, this new method contradicts that with accuracies near 99% for two of the three classifiers using pooled data. The original study made adjustments and accuracy comparisons manually, requiring weeks of work. Our new method ran in 80 minutes for the entire analysis. These results indicate that higher classification accuracies are attainable in far less time using this automated method as compared to manual analysis.

Significance

This work highlights that reported classification outcomes using machine learning to predict human motion from body worn sensors are highly variable depending on the method of analysis. The development of a standardized method to organize and optimize these analyses is greatly needed. This application will provide a standard analysis, and future work will expand the application's functionality and optimization.

References

1) Yang et al., Sensors, 2010, 10(8), 7772-88.
2) Pew, et al., IEEE Trans. Bio. Eng., 2017, 65(4), 789-96.
3) Porciuncula, et al., Phys. Med. Rehab., 2018, 10(9), S220-32.
4) Shell, et al., PloS One, 2018, 13(2), 1-17.

Pennation Angle Changes During Successive Loading Cycles

Josiah D. Mercer.[1] and Benjamin W. Infantolino[1*]
[1]Kinesiology Department, The Pennsylvania State University - Berks
Email: *bwi100@psu.edu

Introduction

Measuring pennation angle changes during muscle contraction has become relatively common and with a number of automated programs being offered for this purpose these types of measures are only getting more common. Antedoteally, in some instances we (and others) have seen what appears to be pennation angle changes throughout time during a cyclical loading protocol. In these instances, the maximum pennation angle during a contraction cycle is larger than the maximum from the previous cycle. Repeated contractions are standard in lifting activities and therefore investigation of this phenomenon in warranted to first see if it actually exists and then if it does to determine what, if any, functional significance it may have.

In the past, pennation angle has been assumed to change in a fixed relationship with joint angle changes. However, recent literature suggests pennation angle change is also dependent on velocity of contraction [1]. This provides some evidence that pennation angle is dependent on more than just joint angle and therefore could change with successive contraction cycles. The purpose of this study was to describe these anomalies previously seen in research.

Methods

Five subjects (2 Female, 3 Male, 21±1 years, 171.7±8.0 cm, 80±21kg) were enrolled in this study. Subjects were asked to plantarflex and dorsiflex through a full range of motion for five cycles while maintaining muscle tension throughout. Subjects maintained a rate of approximately 0.5 Hz while moving through the range of motion. During contractions, ultrasound was used to record the pennation angle of the anterior tibialis and an accelerometer was placed on the dorsum of the foot to verify that the range of motion was consistent throughout all five cycles. Subjects completed three trials each. However, not all trials could be analysed due to ultrasound image quality.

Ultrasound data was processed using a semi-automated custom written Matlab program which identified all fascicle-like objects and then measured the pennation angle for each object. An average pennation angle for each frame of the video was recorded for further analysis. Both accelerometer and pennation angle data were filtered with a first order Butterworth filter with a 2Hz cut-off. The five peaks corresponding to the acceleration vs. time and pennation angle vs. time graphs were selected and a linear regression was used to determine if either peak vs. time regression slope differed from zero.

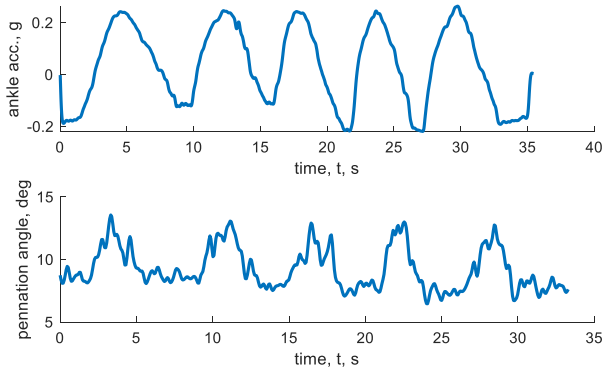

Figure 1: Representative graphs of ankle acceleration vs. time and pennation vs. time graphs for a subject who exhibited a change in pennation angle over time but not in range of motion.

Results and Discussion

Out of a total of 11 trials, two trials showed no difference in ankle angle over time but showed a difference in pennation angle over time. One showed a difference in both ankle and pennation angle over time and one showed a difference in ankle angle but not pennation angle. The rest of the trials showed no difference in either ankle or pennation angle. While many of these results agree with our previous understanding of how muscle behaves throughout a range of motion, a couple trials do seem to suggest something else maybe occurring. Changing cut-off frequency did not change the results, which seems to indicate that the results are not due to an artifact introduced during processing the data.

Some trials showed that pennation angle changed with successive loading cycles even though range of motion did not. This is an important phenomena as so many of our movements involve cyclical loading of our muscles.

Significance

Pennation angle changes during cyclical loading could indicate that the muscle is adjusting to the loading condition with each successive cycle. If this is the case, the mechanism responsible for this adjustment needs to be identified. If this adjustment is advantageous for the muscle(s) completing the task, do all individuals exhibit this adjustment? Additionally, which aspect of muscle contraction is now more advantageous with the adjustment?

References

[1] Azizi, E. et al., *PNAS* **150**(5) 1745-50, 2008

Coordinate Projection vs Unscented Filtering for IMU-based Motion Measurement

Benjamin J. Fregly[1]
[1]Department of Mechanical Engineering, Rice University, Houston, TX
Email: fregly@rice.edu

Introduction

Inertial measurement units (IMUs) are a promising technology for measuring human movement easily and with low cost outside the laboratory. IMUs measure angular velocity and linear acceleration including gravity. IMU-based motion measurement algorithms integrate angular velocity once and gravity-corrected linear acceleration twice to estimate IMU orientation, position, and velocity. This information is then used in some form of a Kalman filter algorithm to estimate joint kinematics in a human body model [1]. The problem with this approach is that noisy IMU measurements amplify numerical integration drift, resulting in violation of kinematic model joint constraints and ultimately inaccurate estimates of model state.

Thus study compares a traditional unscented Kalman filter approach with a novel coordinate projection approach for estimating kinematic model state from noisy IMU measurements. Coordinate projection [2] is a numerical method that maintains joint constraints in a multibody dynamic simulation utilizing absolute coordinates [3], where each rigid body is simulated independently, similar to IMUs. To reduce numerical integration drift further, this study also explores the use of implicit multi-step numerical integration schemes in place of the more common explicit single-step Euler method.

Methods

A planar six degree-of-freedom kinematic model of the pelvis, thigh, shank, and foot was developed in MotionGenesis to evaluate the two state estimation approaches. The pelvis was connected to ground by a planar joint, and the hip, knee, and ankle were modeled as pin joints. One IMU was attached to each model segment. Experimental gait kinematics were input into the model to generate 100 Hz synthetic IMU measurements corrupted with white noise representative of actual IMUs.

Implicit multi-step integrators of orders 1 through 3 were used to integrate the noisy synthetic IMU measurements. Implicit integration used measured IMU quantities from the current time frame to find integrated IMU quantities for the same time frame, allowing estimation of kinematic model joint accelerations as well as velocities and positions. IMU angular acceleration was estimated by backward finite differencing.

Following each numerical integration time step, either an unscented Kalman filter or coordinate projection approach was used to estimate kinematic model state. The unscented filter used integrated IMU orientations, positions, and velocities, measured IMU angular velocities and gravity-contaminated accelerations, and differentiated IMU angular accelerations as measurements for estimating kinematic model state. Coordinate projection used the pseudoinverse to find minimum changes to measured, integrated, and differentiated IMU quantities that satisfied linearized position and linear velocity and acceleration joint constraint equations. Kinematic model state was back-calculated analytically from corrected IMU kinematics. For both approaches, one minute of walking (60 gait cycles) was simulated in Matlab (The MathWorks, Natick, MA), and root-mean-square state errors were calculated for the final gait cycle.

Results and Discussion

Overall, coordinate projection produced more accurate and robust state estimates than did unscented filtering, with accuracy increasing as the order of the implicit integrator was increased (Table 1). Increasing integrator order to 4 did not improve state estimates further. With the 3rd order integrator, both methods produced excellent estimates of not only joint positions (Fig 1 apart from translations) but also joint velocities and accelerations, potentially supporting inverse dynamics analyses.

Compared to unscented filtering, coordinate projection has several advantages. It is faster computationally (25x faster here), requires no tuning of noise variance or other parameters, is more robust to errors produced by low-order integrators, and allows direct calculation of kinematic model state. However, both approaches still require additional measurements to attenuate significant integration drift in joint translations.

Table 1: RMS errors in joint positions for final gait cycle from unscented filter (UF) and coordinate projection (CP) using 1st through 3rd order implicit integrators. Dashes indicate "large" errors.

Solution Method	Integrator Order	q1 (m)	q2 (m)	q3 (º)	q4 (º)	q5 (º)	q6 (º)
UF	1st	----	----	----	----	----	----
	2nd	6.96	2.48	1.47	----	----	----
	3rd	3.59	0.34	0.01	1.26	0.81	1.24
CP	1st	----	1.92	4.13	1.22	----	----
	2nd	3.52	4.83	0.06	0.03	0.18	0.16
	3rd	3.44	0.35	0.04	0.01	0.04	0.08

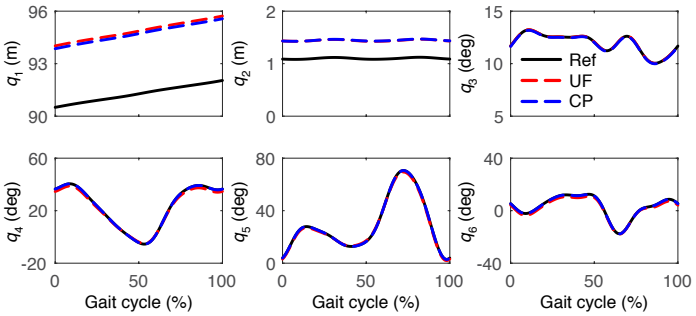

Fig. 1: Joint positions for final gait cycle estimated by unscented filter (UF) and coordinate projection (CP).

Significance

The novel combination of implicit multi-step integration and coordinate projection may improve IMU-based human motion measurement for real-time applications outside the laboratory such as telerehabilitation and remote patient monitoring. The approach does not require magnetometer data to obtain accurate estimates of joint rotations.

Acknowledgments

This study was funded by NSF grant CBET 1805896.

References

1. El-Gohary & McNames (2012) *IEEE Trans Biomed Eng* **59**.
2. Eich (1993) *SIAM J Numer Anal* **30**.
3. Nikravesh (1988) Comp-Aided Analysis of Mech Systems.

Preliminary Assessment of Shoulder Activity after Rotator Cuff Repair

Matthew C. Ruder[1], Rebekah L. Lawrence[1], Roger Zauel[1], and Michael J. Bey[1]
[1]Bone and Joint Center, Henry Ford Health System, Detroit, MI
Email: mruder1@hfhs.org

Introduction

Rotator cuff tears affect about 40% of the population over age 60, with about 250,000 rotator cuff surgeries performed annually [1]. Unfortunately, repair tissue healing after surgery is a major clinical problem, with 42-78% of re-tears occurring within 12 weeks after surgery [2-4]. Risk of repair failure is associated with increasing patient age, tear size, and fatty degeneration, but these factors do not fully explain the high incidence of failure. Another factor that likely influences healing is loading of the repair tissues that occurs during post-operative rehabilitation, but physical therapy accounts for only a small portion of a patient's post-operative life. Moreover, even with the shoulder protected in a sling, activities of daily living (e.g., dressing, self-care, walking) likely results in subtle shoulder motion which may compromise repair tissue healing. However, the extent to which post-operative shoulder activity influences repair tissue healing is unknown. As an initial step toward understanding the relationship between shoulder activity and repair tissue healing, the purpose of this study was to determine if differences in shoulder activity could be detected between rotator cuff repair patients and control subjects using a wearable sensor. We hypothesized that control subjects would have greater shoulder activity than rotator cuff repair patients.

Methods

Following IRB approval, six patients who had undergone rotator cuff repair (age: 56.2±9.0) and six asymptomatic control subjects (age: 61.3±9.4) were recruited. Each participant wore a wrist-based activity sensor (3-axis accelerometer) that collected data at 10 Hz (GENEActiv Original, Activinsights). Patients wore the sensor on their affected side for 1 week within the first 3 months after surgery, while control participants wore the sensor on their dominant wrist for 1 week. Participants wore the activity sensor except when sleeping, bathing, or swimming.

To quantify shoulder activity, the acceleration data were calibrated to 1 *g* (i.e., acceleration due to gravity) [5] and the acceleration magnitude was calculated as the Euclidean norm of the acceleration signals minus one *g*. Next, the volume of activity was estimated by calculating the mean acceleration [6]. To estimate the intensity of activity, we calculated the intensity gradient, defined as the slope of the regression line relating the natural log (ln) of acceleration frequency to the ln of acceleration magnitude in 10 milli-*g* bins [6]. A shallower (less negative) slope of this regression line indicates more high intensity activities, whereas a steeper (more negative) slope indicates fewer high intensity activities. Differences in mean acceleration and intensity gradient between rotator cuff repair and control groups were assessed using a *t*-test. The magnitude of potential differences were also assessed using effect sizes and 95% confidence intervals [7]. Significance was set at $p \leq 0.05$.

Results and Discussion

The difference in activity volume between control subjects (0.022±0.012 *g*) and rotator cuff repair patients (0.008±0.004 *g*) was statistically significant (Fig. 1A, p=0.03, effect size=1.50, 95% CI: 0.15, 2.84). Similarly, the difference in intensity gradient between controls (-2.37±0.22) and rotator cuff repair patients (-2.64±0.20) was statistically significant (Fig. 1B, p=0.05, effect size=1.19, 95% CI: -0.09, 2.48).

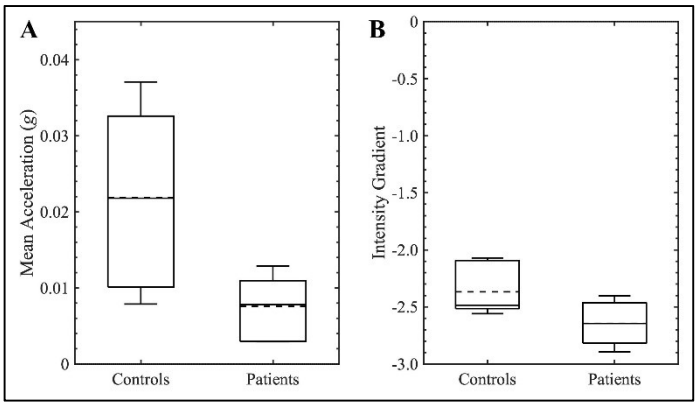

Fig. 1: Control subjects had greater volume (p=0.03, A) and intensity (p=0.05, B) of activity than rotator cuff repair patients.

These findings are encouraging and provide preliminary evidence that differences in activity levels between rotator cuff repair patients and control subjects can be detected using a commercially available wearable sensor. We anticipate that the experimental approach described here will also demonstrate that the volume and intensity of patients' activity will increase over time after surgical repair. However, the six patients whose data are reported here were recruited at various stages after surgery (1 week, 6 weeks, and 12 weeks post-surgery), and therefore this limited sample of patients prevents a rigorous analysis of changes in activity levels over time.

Future efforts will build upon this preliminary work by refining the data processing protocol and recruiting additional patients and control subjects. We expect these efforts will provide objective evidence regarding the role of post-operative shoulder activity on repair tissue healing and clinical outcomes. Understanding the role of shoulder activity on repair tissue healing will decrease the prevalence of failed repairs, improve clinical outcomes, and decrease medical costs associated with this common and debilitating condition.

Significance

This preliminary study is significant, because it provides initial insight into shoulder activity levels in patients during the critical 3-month healing period after rotator cuff repair.

References

[1] Colvin AC, et al. JBJS-Am 94(3), '12.
[2] Barth J, et al. Knee Surg Sports Trauma Arthr 25(7): '17.
[3] Iannotti JP, et al. JBJS-Am 95(11), '13.
[4] Miller BS, et al. AJSM 39(10), '11.
[5] van Hees VT, et al. J Appl Physiol 117(7), '85.
[6] Rowlands AV, et al. Med Sci Sports Exerc 50(6), '18.
[7] Torchiano M. R package version 0.7.6, '19.

Comparison of Dynamic Stability Measures Based on Planar Torque Versus Ground Reaction Force

K. Otto Buchholz[1], Gary D. Heise[2], Nathan J. Robey[3], Shane P. Murphy[4], and Jeremy D. Smith[2]
[1]Shenandoah University, Winchester, VA, [2]University of Northern Colorado, Greeley, CO,
[3]Western Washington University, Bellingham, WA, [4]University of Montana, Missoula, MT
Email: kurt.otto.buchholz@gmail.com

Introduction

Dynamic stability assessment is used to quantify the quality of postural control from a dynamic task to a static posture. Traditional stability measures determine a time to signal stability using the ground reaction force (GRF) only [1,2]. This approach introduces limitations during interpretation, including inferences about the control of the center of mass (COM), the ability to assess simultaneously beyond a single axis, and the potential for the task used to inappropriately influence the measure.

While the GRF fluctuations analyzed in these measures are created by movement of the COM above the base of support, stability measures using the GRF alone can only make inferences about the control of COM motion. Stability assessments could be improved by including the position of the COM in the calculation to better quantify control. Furthermore, incorporating multiple components into the assessment can strengthen observed control mechanisms beyond analysis along a single axis [3]. Finally, varying protocols introduce the possibility that the task influenced the resulting stability measure; a higher landing velocity (LV) may artificially produce higher scores, implying worse dynamic postural control.

Based on this reasoning, the purpose of this study was to develop a dynamic stability measure based on the torque about the COM in the sagittal (T_S) and frontal (T_F) planes during a dynamic task. To validate this torque measure being purely kinetic in nature, kinetic and kinematic estimates of the COM position were compared. Kinetically-derived torque measures were also compared with traditional GRF-based measures. Finally, LV was analyzed for its effect on all measures.

Methods

Sixteen healthy participants [24 ± 3 years, 1.71 ± 0.09 m, 74.5 ± 14.4 kg] performed five, 70 cm hops while barefoot over a 15 cm hurdle. After landing on their dominant leg only, they stabilized for 20 seconds. Landing kinetics were collected using a force plate (AMTI, Watertown, MA) and kinematics of the pelvis COM were collected using motion capture (Vicon, Englewood, CO). The COM position was calculated using GRF by double-integration of the acceleration component of the GRF [4].

Using the kinetic-derived COM position, T_S and T_F were calculated for the 20 second period after landing. To determine the time to stability of the planar torque values, the same determination methods used in sequential estimation (SEQ) [1] and Time to Stabilization (TTS) [2] were applied. For comparison, SEQ and TTS were calculated for the anteroposterior (AP), mediolateral (ML) and vertical (Vert) components of the GRF according to the literature [1,2].

To establish similarity of COM position between the kinetic and kinematic estimates, a correlation was used. SEQ and TTS stabilization times from forces (AP, ML, Vert) and torques (T_S and T_F) were compared using ANOVAs. T_S stabilization time was compared to AP and Vert force times, while T_F time was compared to ML and Vert force times. Finally, LV of the participant was assessed for correlation with all stability measures for potential similarity.

Results and Discussion

Moderate to strong correlations (r_{AP} = 0.89; r_{ML} = 0.60; r_{Vert} = 0.82) were observed between kinetic and kinematic COM positions. Thus, kinetic estimates of COM position were appropriate for use in the torque calculation.

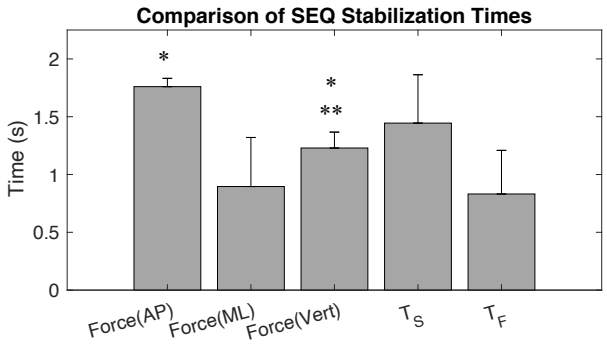

Figure 1: Comparison of all stability times calculated using SEQ methods [1]. Significant differences are noted for GRF stability times from T_S (*) or T_F (**) stabilization time.

Using SEQ, stabilization time of T_S was different from both AP and vertical axis force stabilization times (Fig. 1). T_F stabilization time was different from the time calculated using force along the vertical axis, but not the ML axis. Overall, this indicates using SEQ to calculate the amount of time to stability produces significantly different results with the additional benefit of including the COM position in the calculation of stabilization time. Comparison of force and torque stability times using TTS showed no significant differences.

Finally, LV correlated with the stabilization times of TTS (r = 0.59), SEQ (r = 0.85), and T_F (r = -0.58), but not with T_S (r = 0.02). For T_S, no correlation with LV indicates the stability time provides a measure of stability in the primary plane of motion that is independent from the LV associated with the task.

Significance

This torque-based calculation of stabilization time provides a more complex analysis of dynamic stability, as GRF values are used in tandem with COM motion in the calculation. This measure is also independent from the LV in the primary plane of motion. Removing the effect of LV in this plane allows for postural control analysis with reduced protocol-based influences.

References

[1] Colby et al. (1999). *J Orthop Sports Phys Ther*
[2] Ross et al. (2003). *Athlet Ther Today*
[3] Wikstrom et al. (2005). *J Athlet Train*
[4] Zatsiorsky et al. (1998). *J Biomech*

Knee Joint Acoustic Signatures in Healthy Collegiate Athletes: Sex Differences

Caitlin N. Teague[1] and Omer T. Inan[1,2]
[1]School of Electrical and Computer Engineering, Georgia Institute of Technology, Atlanta, GA 30308
[2]Wallace H. Coulter Department of Biomedical Engineering, Georgia Institute of Technology, Atlanta, GA 30308
Email: omer.inan@ece.gatech.edu

Introduction

Evaluation of knee joint sounds may provide a non-invasive and quantitative method for determining joint health, which could be leveraged as a metric (e.g., "joint score") for tracking progress during rehabilitation following an acute injury or deciding on readiness for return-to-play, for example. Knee injury risk and prevalence in females has been well-studied. Given associated risk factors include biomechanical and anatomical factors, it is imperative that possible male-female differences are studied in the emerging field of non-invasive biomarkers of knee health, including those markers derived from joint sounds.

Methods

The data acquisition protocol is described in [1]. For this work, we analyzed the joint sounds measured from electret microphones placed at the lateral and medial sides of the patella for five seated, unloaded flexion / extension cycles in 49 (N = 15 female) healthy collegiate athletes (male: 28 American football, 6 basketball; female: 7 volleyball, 8 basketball). "Clicks" in the acoustic signal were identified by [1] and used to calculate *b*-value according to the equations in [2]. In total, 196 *b*-values (instances) were found: 49 subjects by two legs (self-reported dominant vs non-dominant leg) at two locations (lateral or medial). A linear mixed effects model was used with sex and leg dominance (LD) treated as fixed effects, subject as a random effect, and microphone location as a covariate (r-project.org). When significant main effects were returned, *a priori* ($\alpha = 0.05$) planned comparisons were completed between (1) sexes at each level of LD and (2) LD at each level of sex using pairwise post-hoc comparisons from the emmeans package in R. These comparisons were repeated for a subset of the data, examining men and women basketball (BB) players (N = 15, 8 females) to complete a direct sport-matched comparison.

Results and Discussion

For *b*-value (Fig. 1), the main effects of sex (collapsed across LD, $p = 0.09$) and LD (collapsed across sex, $p = 0.74$) were not significant. However, the sex by LD interaction was significant ($p = 0.01$). Pairwise comparisons revealed that dominant leg (DL) *b*-values were significantly lower ($p < 0.0001$) in females (1.14 ± 0.23) compared to males (1.44 ± 0.31), while non-dominant leg (NL) *b*-values were not different (male = 1.43 ± 0.25, female = 1.31 ± 0.37, $p = 0.10$). Furthermore, females had a lower *b*-value for the DL compared to NL (by 0.17 ± 0.35, $p = 0.007$), but men did not (-0.014 ± 0.24, $p = 0.75$). Similarly, for the BB player analysis, the main effects of sex (collapsed across LD, $p = 0.20$) and LD (collapsed across sex, $p = 0.48$) were not significant, though the sex by LD interaction was significant ($p = 0.02$). Pairwise comparisons of *b*-values between men (1.34 ± 0.19) and women (1.15 ± 0.24) BB players' DLs did not show a significant difference ($p = 0.08$), and the NL *b*-values were not significant (men = 1.26 ± 0.22, women = 1.39 ± 0.37, $p = 0.23$) as well. Further, women's BB players exhibited smaller *b*-values for the DL compared to NL (by 0.25 ± 0.40, $p = 0.01$), while men's BB players were not significantly different (0.07 ± 0.16, $p = 0.50$).

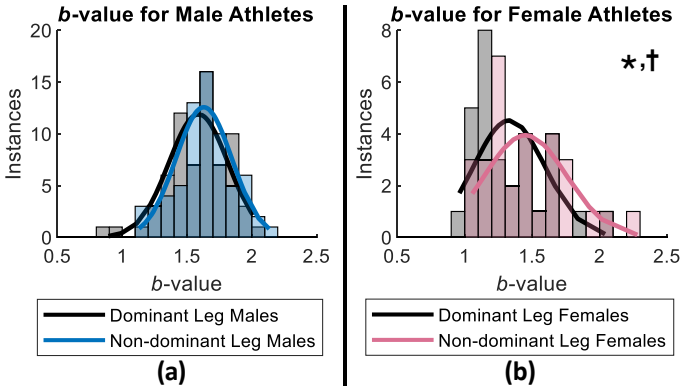

Figure 1: *b*-value for male (a) and female (b) athletes. A significant difference (*$p < 0.01$) was observed between the females' dominant and non-dominant leg. Further, a significant difference (†$p < 0.0001$) was observed between male and female athletes' dominant legs.

Previous studies suggest that a lower *b*-value is associated with a more "unhealthy" knee when comparing within-subject, within-knee measurements for, perhaps importantly, exclusively (or nearly so) male knees [2, 3]. However, it is unclear from these studies if a one-time, singular *b*-value measurement is sufficient to determine joint health—or injury risk—on its own. At this time, we speculate the lower DL *b*-value exhibited in females—specifically those participating in sports involving repetitive jumping—may be, in part, attributed to a larger maximum knee valgus angle during drop vertical jump tasks in females' dominant knee [4]. Notably, models of valgus misalignments show increases in joint contact forces and overall larger and more sustained forces during walking and stair climbing [5], and this larger valgus angle / loading has been associated with increased anterior cruciate ligament (ACL) strain (*in vitro*) [6] and patellofemoral pain as studied in female subjects [7] as well as a potential predictive measure for ACL injury [8].

Significance

Differences in male and female joint sounds were observed as well as female side-to-side differences, supporting existing knee injury literature. Future work (e.g., powering studies, developing joint score algorithms, etc.) should consider sex disparities.

Acknowledgments

DARPA W911NF-14-C-0058 and NIH Grant 1R01EB023808.

References

[1] Teague CN et al. (2016) *IEEE Trans Biomed Eng*, **63**: 1581-90.
[2] Jeong HK et al. (2018) *IEEE Sens Lett*, **2**: 1-4.
[3] Whittingslow DC et al. (2020) *Ann Biomed Eng*, **48**: 225-35.
[4] Ford KR et al. (2003) *Med Sci Sports Exerc*, **35**: 1745-50.
[5] Heller MO et al. (2003) *Langenbecks Arch Surg*, **388**: 291-7.
[6] Withrow TJ et al. (2006) *Clin Biomech*, **21**: 977-83.
[7] Herrington L (2014) *The Knee*, **21**: 514-17.
[8] Hewett TE et al. (2005) *Am J Sport Med*, **33**:492-501.

Beyond walking distance: Evaluating propulsion function during the 6-minute walk test with wearable inertial sensors

Dheepak Arumukhom Revi[1,2], Andre M. Alvarez[1], Lillian R. Braga[1], Conor Walsh[2], Stefano M. M. De. Rossi[1] and Louis N. Awad[1,2*]
[1]College of Health and Rehabilitation Sciences, Boston University, Boston, MA
Email: *louawad@bu.edu

Introduction

The 6-minute walk test (6MWT) is commonly used across clinical diagnostic groups to measure functional walking capacity[1,2]. The total distance walked[1,2] and the distance-induced change in walking speed[2] measured during the 6MWT are strong indicators of real world walking activity. Although demonstrably valuable, distance-based measurements (e.g., across 6 minutes or per minute) do not account for differences in gait quality that may underlie the impaired performance observed in heterogeneous populations, such as people post-stroke. Indeed, as a timed walk test, the ability to both achieve and sustain a fast walking speed underlies 6MWT performance. Given the relationship between propulsion function and short- and long-distance walking speed[3], we posit that measurements of propulsion function during the 6MWT may provide crucial diagnostic data that are currently lacking in the distance-based measurements traditionally extracted from the 6MWT, and that can inform targeted gait therapies. In this study, we present the use of a minimal set of wearable inertial measurement units (IMUs) to provide indirect estimates of propulsion function during the 6MWT.

Methods

Seven individuals with chronic post-stroke hemiparesis completed a 6-minute walk test over a 26.6m walking track instrumented with six forceplates while wearing three IMUs securely attached to the pelvis, thigh, and shank. The forceplates provided direct measurements of the anterior-posterior ground reaction force (AP-GRF) generated during steps with a forceplate strike. In addition, subject-specific models driven by IMU-measured thigh and shank angles and an estimate of body acceleration provided by the pelvis IMU were used to provide indirect meaurements of the AP-GRF generated every step[4]. Peak propulsion point metrics were extracted from the direct and indirect estimates of the anterior portion of the AP-GRF and compared. Moreover, the distance walked per minute of the 6MWT was measured using a measuring wheel. Study participants were dichotomized into endurant and non-endurant subgroups, with non-endurant individuals being those who slow down by more than 0.10 m/s between min 1 and min 6[1]. Peak propulsion medians and 95% confidence intervals are reported.

Results and Discussion

In previous work, we showed that indirect measurements of the AP-GRF time series strongly approximated the direct measurements made by forceplates, with low error and high consistency[4]. The average error between indirect and direct measurements of the peak propulsion magnitude (% bodyweight, %bw) was less than 1.2 %bw—which is lower than the Minimal Detectable Change (MDC) of 1.8%bw[4]. In the present study, four out of seven participants were classified as endurant and the other three were non-edurant. The non-endurant subgroup presented with comparable reductions in speed (-14% [-11%, -16%]) and peak paretic propulsion (-16% [-14%, -38%]) (Ps < 0.05). In contrast, the endurant subgroup did not markedly change speed (0% [-16%, 9%]) or peak paretic propulsion (2% [-8%, 8%]).

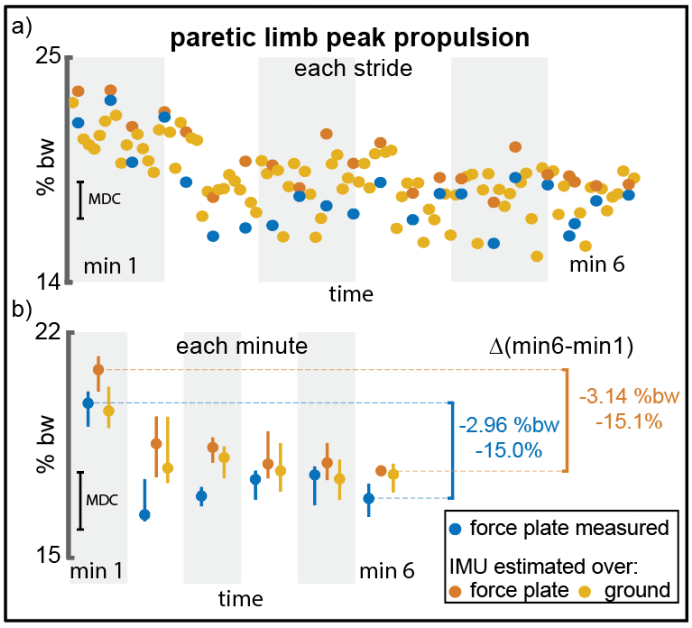

Figure 1: Change in peak paretic propulsion measured by forceplates and estimated by IMUs during the 6-minute walk test for one exemplar, non-endurant participant on a **(a)** step by step basis and **(b)** minute by minute basis. **Minimal Detectable Change (MDC) = 1.8 %bw.*

Significance

Wearable inertial sensors offer a feasible solution to provide clinically-accessible assessments of propulsion function during the 6MWT. We show that individuals post-stroke who reduce their speed over the duration of the 6MWT (i.e., non-endurant individuals) also present with a reduction in paretic limb propulsion (Figure 1). In contrast, individuals who do not reduce their speed (i.e., endurant individuals) do not reduce paretic limb propulsion. This wearable sensor technology has potential to enable clinicians to co-assess changes in propulsion quality with distance-based performance outcomes that are traditionally evaluated, and may thus provide treatment-shaping diagnostic information not currently available in most clinical settings.

Acknowledgment

We thank the Boston University Neuromotor Recovery Lab for assistance with data and our participants for their generous time. Grants: NIH KL2TR001411, AHA 18TPA34170171, AHA 18IPA34170487.

References

[1]Awad, L. N., et al. 2019, *J.N.P.T.* doi: 10.1097/NPT.0000000000000293.
[2]Fulk, D. G., et al. 2017, *Stroke.* doi: 10.1161/STROKEAHA.116.015309.
[3]Awad, L. N., et al. 2015, *N.N.R.* doi: 10.1177/1545968314554625.
[4]Arumukhom Revi, D., et al. 2020, *J.N.E.R* (preprint) https://dx.doi.org/10.21203/rs.2.23757/v1

Center of Mass Accelerations Estimated by Wearable Sensor Technology and Motion Capture System: Are We Measuring the Same Thing?

Yu-Pin Liang, Hang Qu, and Li-Shan Chou
Department of Kinesiology, Iowa State University, Ames, IA
Email: yupinl@iastate.edu

Introduction

Deviations in motion control of the whole body center of mass (COM) during walking could imply motor deficits or balance impairments. Moreover, COM acceleration is reported to better differentiate balance control ability in different populations[1]. However, whole-body COM is traditionally calculated with a whole-body reflective marker set and camera-based motion analysis system, which significantly restricts to laboratory settings. Recent advances in wearable motion sensor technologies offer an opportunity to translate laboratory findings to the clinical environment with similar gait balance measures. Inertial measurement units (IMU) combine accelerometers, gyroscopes, and magnetometers into a single sensor and could be used to estimate COM acceleration. The use of wearable sensors to detect mobility impairments has grown rapidly[2,3] and providing a time-efficient and user-friendly measurement of gait and balance performance. The IMU is placed at a fixed body landmark, such as the 5th lumbar vertebra (L5), as a proxy location of COM. However, such a fixed landmark location does not account for any instantaneous changes in body segment alignment that could result in the relocation of whole-body COM. Although kinematic measures derived from both methods have been successfully used to detect gait imbalance, only limited data are available in the literature for comparison of COM accelerations estimated between the conventional motion capture system and wearable sensor technology. The purpose of this study was to demonstrate and compare patterns of COM acceleration during walking estimated using a wearable sensor and a conventional motion capture approach.

Methods

A total of 11 healthy participants (age: 29.5 ± 13.3 years, BMI: 22.8 ± 4.8 kg/m^2) were recruited so far. Experimental setup for the conventional motion capture system included 12 Oqus infrared cameras (Qualisys AB, Sweden) and forty-nine retroreflective markers placed according to the marker setup[4]. In addition, a single IMU (OPAL, APDM, Portland, OR, USA) was placed at the L5, as the proxy location of COM. Marker trajectory and IMU data of each participant were collected from 10 level walking trials. The whole-body COM position was calculated as the weighted sum of body segments and anthropometric reference data were adopted from the work of Fujimoto[1]. COM acceleration were calculated from the second derivatives of COM positions. For IMU acceleration data, the initial contact (IC) of the gait cycle was determined by transforming the raw acceleration curve to the Gaussian continuous wavelet and identify the maximal value as the point of the start of IC[5]. Data analysis was focused at the time period between 50 and 80% of gait cycle. The 95% confidence intervals for the time when peak accelerations occurred and range of magnitude changes were reported for both approaches.

Results and Discussion

Acceleration data in all three anatomical directions obtained from both methods demonstrated a similar overall pattern**.** However, distinct differences in acceleration magnitudes exist, especially at the time between heel-strike and mid-stance (Figure 1). A smoother and smaller acceleration data from the camera-based system could be a result of data processing, as data were further smoothed during the calculation of velocity and acceleration. There are also timing differences in when peak accelerations occurred between two methods. This could be due to the instantaneous alignment of IMU deviating from the anatomical directions. (Table 1)

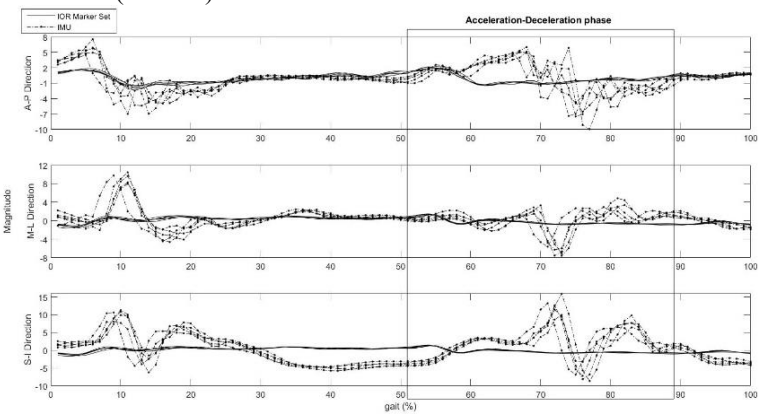

Figure 1: Acceleration from IMU at L5 and COM acceleration from conventional motion capture system during walking (x-axis: normalized by 100% gait phase, y-axis: m/s^2). The anterior, medial and superior direction were denoted as positive values.

Table 1. Timing in peak accelerations occurred and magnitude

	IMU [CI]	QTM [CI]
Timing in when peak (%gait)		
A-P Direction	[54.3, 82.1]	[41.5, 64.7]
M-L Direction	[62.6, 84.5]	[50.1, 68.3]
S-I Direction	[65.3, 87.8]	[52.4, 65.4]
Magnitude range (m/s^2)		
A-P Direction	[15.64, 22.47]	[3.22, 5.76]
M-L Direction	[20.48, 25.02]	[2.63, 3.29]
S-I Direction	[23.11, 28.92]	[2.05, 3.43]

Significance

Consistent COM acceleration patterns and magnitudes during walking could be obtained with marker-based motion system and IMU, respectively. Accelerations obtained by the accelerometer are more sensitive to gait events with ground contact, such as heel-strike, when compared with those calculated from the second derivatives of COM positions. Although kinematic markers derived from both methods have been shown to detect clinical populations, users should be mindful about their inherent differences.

References

1. Fujimoto M, Chou LS. Journal of Biomechanics. 2012;45:543-48.
2. Howell D, Osternig L, Chou LS. J. Biomech. 2015;48(12): 3364–8.
3. Pitt W, Chou LS. Gait & Posture. 2019;71:279-83.
4. Leardini A, Biagi F, Merlo A, Belvedere C, Benedetti MG. Clin Biomech. 2011;26(6):562-71.
5. McCamley J, Donati M, Grimpampi E, Mazzà C. Gait Posture. 2012;36(2):32

Predicting lower limb 3D kinematics during gait using reduced number of wearable sensors via deep learning

Md Sanzid Bin Hossain[1], Youngho Lee[3], Junghwa Hong[3], Hwan Choi[2], and Zhishan Guo[1]
[1] Department of Electrical and Computer Engineering, [2] Mechanical and Aerospace Engineering, University of Central Florida
[3] Department of Control and Instrumentation Engineering, Korea University
Emails: {hwan.choi, zsguo}@ucf.edu

Introduction

Identifying human kinematics is the primary step of biomechanics analyses and clinical evaluation for people with walking disabilities. A typical method for calculating human kinematics is to use a marker-based motion capture system. Such method has a major drawback when capturing motions outside the lab, makes it challenging to measure the various dynamic tasks in daily living. To solve this issue, it has been suggested [1] to use inertial measurement unit (IMU) sensors to capture the motion [1]. However, this method requires attachment of IMU sensors on each body segment. People may feel this is too cumbertom to apply in daily life, limiting the use in real application. Thus, this study aims to investigate the feasibility of capturing the joint angles of lower extremities with a reduced number of IMU sensors using a deep learning algorithm. We hypothesize that if we can train a deep learning model good enough, it can extract the information from a reduced number of IMU sensors for the prediction of kinematics in three dimensions.

Methods

We recruited a young and healthy participant (31 yrs, 1.75 m, and 84 kg). Two IMU sensors were mounted on the dorsal of both feet of the participant. We calculated non-dimensional slow, normal, and fast walking velocity from the participant anthropometric data [2]. Then the participant walked in the treadmill for approximately 1.5 minutes at three different speeds. We collect the data last 1 minute for data analyses. The motion was captured simultaneously by twelve infrared cameras (Vicon, Oxford, UK), and acceleration and gyroscope data were recorded from the IMU sensor (Avanti™ wireless EMG, Delsys Boston, MA). We used OpenSim, which is an opensource musculoskeletal simulation tool to scale the model according to the participant's anthropometric measurements and calculate the hip, knee, and ankle angle using inverse kinematics. We considered five joint angles for each leg, i.e, hip flexion, hip abduction, hip rotation, knee angle, and ankle angle for the prediction. So, we have an input of 12 features and an output size of 10 joint angles for each timestamp. For the learning algorithm, we stacked two bi-directional Long Short Term Memory (LSTM) deep neural networks, followed by a uni-directional LSTM [3]. Five-fold cross-validation was performed to test the efficacy of the model. For the assessment of the result, the root mean square error (RMSE) and the correlation coefficient was calculated between the ground truth of the test set and prediction of the deep learning model.

Results and Discussion

Our algorithm enabled us to estimate the joint angles with high accuracy compared with motion capture system. Figure 1 reports the mean and standard deviation RMSE with for five joint angles for both legs (upper subfigure), as well as their correlations (lower subfigure). The mean RMSE remains very low, ranges from (1.6°±0.25°, 1.42°±0.26°) for hip abduction to (2.51°±0.2°, 2.47°±0.24°) for the knee angles on the sagittal plane for left and right leg. The predicted joint angle shows a higher correlation with the ground truth of the test dataset. However, the correlation was less for hip rotation (0.88±0.024, 0.88±0.028). We believe that increasing the number of data from more participants will result in a better deep learning model, helping to achieve higher accuracy and correlation than what we provided in this study. This is left as future work.

Significance

We have achieved reasonable accuracy with a high correlation using a reduced number of IMU sensors with a specialized deep learning model which supports our hypothesis. Another advantage of our method is to use the dorsal of the foot as the location of the sensor. Reduced number of IMU sensors can be easily mounted to the shoes to monitor kinematics of the athlete and people with gait impairment.

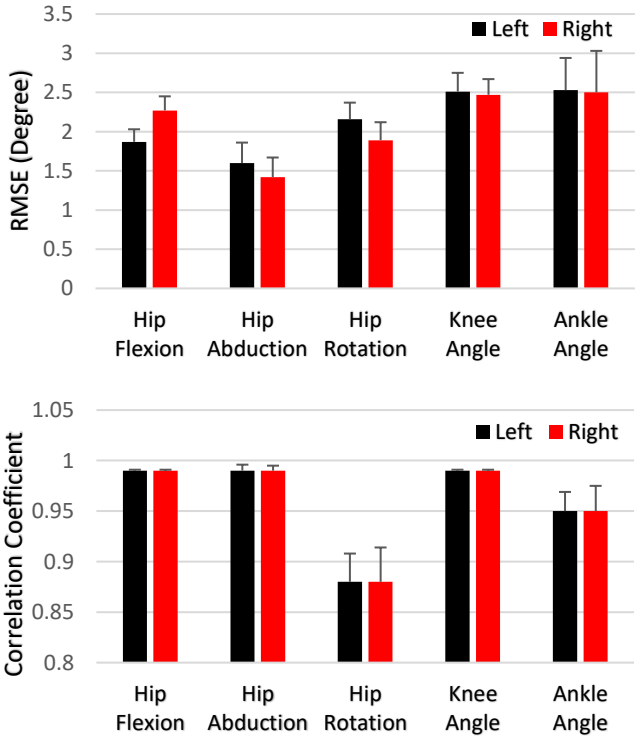

Figure 1: Mean RMSE and Correlation Coefficient with standard deviation for five joint angles for right and left leg.

Acknowledgments

This study was supported by the Institute for Information and Communications Technology Promotion (16268A01).

References

[1] Isabelle Poitras et al., Sensors 2019, 19, 1555
[2] May Q. Liu et al., J. Biomech. 2008, 41 (3243-3252)
[3] Schuster M. et al., *IEEE Trans. Signal Process.* 1997, *45*, (2673–2681)

Soft-tissue Artifact Compensation for Electromagnetic Motion Capture

Zachary Bons[1], Taylor Dickinson[1], Ryan Clark[1], Kari Beardsley[1], and Steven K. Charles[1,2]
[1]Mechanical Engineering and [2]Neuroscience, Brigham Young University
Email: skcharles@byu.edu

Introduction

Motion capture technology is a powerful tool that can be used to create high-fidelity biomechanical models and study movement disorders. Most motion capture systems use sensors mounted to the surface of the skin, and thus suffer from soft-tissue artifact (STA). STA refers to the movement of the skin relative to the skeletal structure. Since the goal of most motion capture efforts is to record the position/orientation of the skeletal structure, measurements from sensors mounted to the skin must be adjusted to better reflect the desired position/orientation of the skeleton.

Understandably, much research has been devoted to STA compensation (STAC); however, most methods have been developed specifically for optoelectronic motion capture systems and, due to inherent differences in methodology, cannot be directly applied to electromagnetic (EM) motion capture systems. To our knowledge there is only one STAC method developed specifically for EM systems [1]; while this method has been shown to be effective, it requires extra data and cannot be applied retroactively to datasets.

The purpose of this research was to develop a STAC method for EM systems that requires no additional experimental procedures or data. Our method adjusts for STA in humeral internal-external rotation (HIER), forearm pronation-supination (FPS), or both, and is based on the method developed by Schmidt et al for optoelectronic systems [2].

Methods

Our STAC method builds on conventional inverse kinematics algorithms (i.e. algorithms that do not compensate for soft-tissue artifact) for determining global upper limb motion in accordance with the ISB recommendations [3]. These inverse kinematics algorithms are described in detail by Clark et al [4]. This process relates four sensor coordinate systems (SCS) to corresponding body-segment coordinate systems (BCS) of the thorax, upper arm, forearm, and hand. Using these relationships, joint coordinate systems (JCS) can be calculated for the thoracohumeral, humeroulnar and radioulnar (grouped), and wrist joints.

STAC for HIER was approximated based on two critical assumptions: 1) the elbow carrying angle is constant, and 2) STA affects only HIER. Based on these assumptions, HIER can be determined from the orientation of the forearm for most of the range of motion. This calculation only becomes unreliable when the arm approaches full elbow extension, in which case we used weighted averages to approximate HIER [2].

We followed a similar approach to compensate for STA in FPS, but relationships were calculated between the forearm and hand. This calculation is reliable over the full range of motion of the wrist.

We tested our STAC method on 10 subjects. Each subject performed 11 simple tasks that explored both the full and functional ranges of motion of the upper limb. We recorded motion using an EM motion capture system (trakSTAR by NDI, Shelburne, VT) and performed inverse kinematics with and without STAC.

Results and Discussion

We found that applying this algorithm significantly changed the approximations of HIER and FPS. As seen in Fig. 1, the average maximum difference of HIER calculated with and without STAC was 29.8° ± 6.6° (mean ± SD). In calculating FPS, relative errors of 1.3° in pronation and 9.3° in supination were identified. This data supports the claims that STA has a large impact on joint angle calculations.

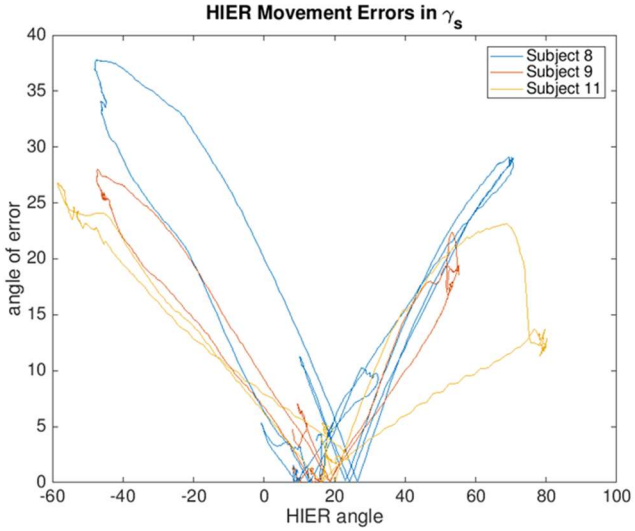

Figure 1: Error due to soft-tissue artifact in humeral internal-external rotation (HIER). As HIER angle increases in either direction, the error also increases significantly.

Since we measured data and calculated joint angles throughout the workspace of the upper limb, we also confirmed that STA varies with joint configuration and quantified the effect of STA throughout the range of motion of the arm.

Lastly, we explored the effect of STAC on other degrees of freedom. Although our STAC assumed that STA directly affected only HIER and FPS, compensating for STA has indirect effects on other DOF. We found that correcting the approximations of HIER and FPS indirectly affects the angle approximations of elbow flexion, as well as wrist flexion-extension and radial-ulnar deviation.

Significance

This research presents an STA compensation method for EM systems that can be applied retroactively. It is a relatively simple method that can improve the accuracy of joint angles calculated from EM motion capture used in analysis of movement impairments, biomechanical modelling, and other research and clinical efforts.

References

[1] Cao et al, J Medical and Dental Sciences, 2007
[2] Schmidt et al, J Biomechanics, 1999
[3] Wu et al, J Biomechanics, 2005
[4] Clark et al, J Biomechanics, 2020

Validity of Peak Tibial Acceleration Obtained from a Wearable IMU during Running

Adriana Miltko[1], Clare E. Milner[2], Max R. Paquette[1]
[1]University of Memphis, Memphis, TN, [2]Drexel University, Philadelphia, PA.
Email: mrpqette@memphis.edu

Introduction

A growing popularity of wearable technology leads companies to create sensors assessing biomechanical parameters including peak tibial acceleration (PTA) during running. Although development of bone injuries is multifactorial, greater PTA using laboratory-grade accelerometers have been observed in runners with a history of tibial stress fractures in comparison to individuals without lower-limb injury history (1).

Since peak tibial acceleration may contribute to risk factors responsible for tibial stress fractures, using measurements of peak tibial acceleration in runners in the field will allow biomechanists to bridge the gap in our understanding of injury development. However, validity of variables obtained from wearable technology relative to "gold-standard" research-grade instruments is necessary. The purpose of the study was to assess the difference in PTA obtained from wearable inertial measurement units (IMU) and a research-grade accelerometer at different running speeds. We hypothesized that with the device's specs, the PTA measured with IMUs would be valid in comparison to a research-grade accelerometer at two different speeds.

Methods

Twenty participants completed 1-2 min treadmill running bouts at 3.0 m/s and 4.0 m/s while wearing standardized footwear. A research-grade tri-axial accelerometer (ACC; PCB Piezotronics) and a 9-axis IMU (Blue Trident, IMeasureU) were secured to the distal tibia to obtain PTA during running. PTA from ACC was obtained while the ACC was placed below and above the IMU (separate trials) at both speeds due to possible position effects. Data were collected for the final 15 seconds of all four running bouts and the average of both positions and both speeds for 10-15 peaks of PTA were used for analyses. Paired t-tests were used to compare mean PTA between sensors at both speeds and the 95% limits of agreement and mean offset was determined 2).

Results and Discussion

At 3.0 m/s, PTA from ACC (4.6±1.5 G) and IMU (4.7±1.9 G; p = 0.97; d = -0.007 were similar. At 4.0 m/s, PTA from ACC (7.0±2.3 G) and IMU (7.1±3.4 G; p = 0.64; d = -0.08) were also similar.

Further, Bland-Altman plots and 95% limits of agreement demonstrate that 95% of PTAs from the IMU were within 0.012 G of PTAs from ACC at 3.0 m/s (p = 0.972; **Figure 1A**) while 95% of PTAs from the IMU were within 0.25 G of PTAs from ACC at 4.0 m/s (p = 0.636; **Figure 1B**).

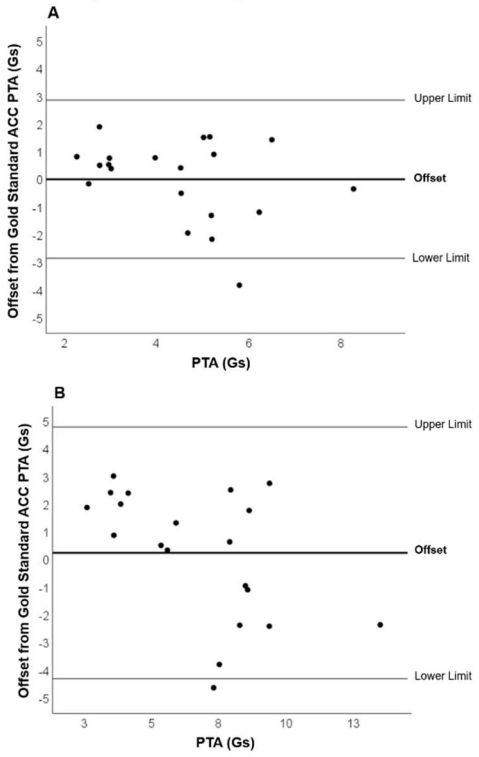

Figure 1. Bland-Altman plots with PTA offset between IMU and ACC including 95% limits of agreement at 3.0 m/s (A) and 4.0 m/s (B).

Significance

Our findings suggest that the tested IMU (Blue Trident, IMeasureU) provides valid measures of PTA in comparison to research-grade 3D accelerometer. Field testing with validated wearable devices such as IMUs will allow for day-to-day analyses of running biomechanics that can provide a more complete picture of typical external loads experienced by runners during study survey periods.

References

1. Bland, J Martin, and Douglas G Altman. 1986. *Lancet*. 1: 307–10.
2. Milner, Clare E. et al. 2006. *Medicine & Science in Sports & Exercise*. 38(2): 323–28.

Uncertainty propagation in validating bone kinematics using biplane fluoroscopy

Eric Thorhauer[1,2] and William R. Ledoux[1,2,3]
[1]RR&D Center for Limb Loss and MoBility (CLiMB), VA Puget Sound, Seattle, WA; Departments of [2]Mechanical Engineering and [3]Orthopaedics & Sports Medicine, University of Washington, Seattle, WA
email: ericthor@uw.edu

Introduction

Biplanar fluoroscopy can be a useful tool for biomechanists quantifying in vivo joint motion, however, given the custom nature of these hardware systems and the challenges inherent in imaging dynamic anatomy, these techniques must be validated to ensure data accuracy for each motion and joint of interest. Validation studies utilize anatomical specimens instrumented with fiducial markers. Borrowing from the fields of optical motion capture and Roentgen stereophotogrammetry, general guidelines of maximizing the embedded inter-marker spacing of the required triads of markers are suggested and degeneracy in marker configurations may be quantified with condition numbers [1]. In biplane studies, kinematic curves derived from model-based tracking are compared to "gold standard" marker-based data. Inter-marker distances in the rigid fiducial clusters of each bone have also been used to quantify tracking performance. Many of the foot bones are so small that embedding them with a non-degenerate marker triad is challenging, and the propagated stream of errors arising from marker localization are exacerbated in these joints. The goal of this work was to understand how the placement of validation markers and errors in their localization affects the "gold "standard" kinematics in the clinically-important first metatarsophalangeal joint (MTPJ1).

Methods

A fresh human foot and ankle specimen was prepared by dissecting the great toe flexors and extensors and embedding a set of three 3.0 mm stainless steel marker beads into both the proximal phalanx and first metatarsal bones. The great toe was actuated through ten cycles while biplanar fluoroscopic data were acquired in a standard gait configuration. A computed tomography scan was used to generate models of the bones, establish anatomical coordinate systems, and to localize the markers. Using these data, the ground-truth kinematics of the joint were determined and then low-pass filtered to yield a smooth, but physiologically accurate model of MTPJ1 motion.

Next, various permutations of three virtual fiducial markers simulating different marker installation strategies were generated in a virtual model of the biplane hardware. Set 1 approximated an ideal distribution of markers in both bones. Set 2 simulated a co-linearity condition of markers in the metatarsal. Set 3 simulated placing two markers in each bone in close confinement to each other, yielding a narrow triangle shape. Using the ideal kinematics to drive the bone models in the virtual biplane software, for each frame of data, the virtual markers were projected onto the camera frames. The centroids of the markers were perturbed with varying degrees of uniformly distributed noise (upper limits of 0.25, 0.50, and 1.0 pixels) representing errors in marker localization and imperfect distortion corrections (pixel size for current camera settings = 0.327mm). The bone positions and kinematics were reconstructed for each trial of noisy markers and compared to the ground-truth. This process was repeated for each set of simulated marker installations.

Results and Discussion

Condition numbers increased as marker distributions became less ideal, with Set 1 having the smallest values (Figure 1). The narrow triangles formed by Set 3's markers led to the largest condition numbers (Figure 1). Except for the 1.0-pixel perturbations, higher condition numbers (Set 2 and 3) were associated with higher kinematic errors (Table 1).

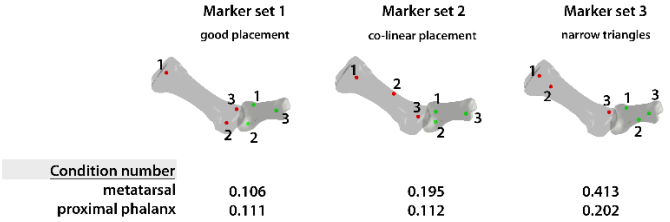

Condition number			
metatarsal	0.106	0.195	0.413
proximal phalanx	0.111	0.112	0.202

Figure 1: Three example marker configurations for the MTPJ1 joint shown (top) and the respective condition numbers for each bone below. Condition numbers increase with worsening marker distribution.

Between the conditions of 0.25- and 0.50-pixel errors, inter-marker distances were consistent across marker sets and conditions (Table 1). Inter-marker distances cannot discriminate between suboptimal marker distributions and are not correlated to kinematic error magnitudes. Therefore, inter-marker distances alone are not an adequate surrogate metric for kinematic accuracy in biplane bone tracking.

	Marker set 1 (good placement)			Marker set 2 (co-linear placement)			Marker set 3 (narrow triangles)		
Perturbation limit (pixels)	0.25	0.50	1.00	0.25	0.50	1.00	0.25	0.50	1.00
RMS inter-marker error (mm)	0.06	0.03	0.65	0.02	0.03	0.06	0.02	0.03	0.06
Std. dev. of error (deg)									
flexion/extension	0.32	0.70	9.47	0.77	1.55	3.56	1.16	2.83	8.75
adduction/abduction	0.22	0.56	3.69	0.31	0.71	2.02	0.39	1.02	3.39
inversion/eversion	0.26	0.65	4.81	0.30	0.74	2.23	0.48	1.33	4.77

Table 1: For each marker set and localization perturbation level, the root-mean-square inter-marker errors (millimeters) and standard deviations of rotational kinematic errors (degrees) are listed for each perturbation range of the marker centroids.

Significance

This study illustrated how localization errors in the assumed "gold standard" marker tracking can propagate into kinematic errors for small joints like MTPJ1. True validity depends on the marker configuration itself. Establishing these marker distributions in small volumes while balancing marker overlap and occlusion in dense, complex anatomic like the foot can benefit from pre-planning and simulation studies to maximize the validity of the derived kinematics and the overall success of the validation study.

References

[1] Kärrholm J. Acta Orthop Scand. 1989 Aug; 60(4):491-503.
[2] Soderkvist I, Wedin PA. J Biomech. 1993;26((12)):1473–7.

SURFACE-EXCITED WAVE DISPERSION IN THE ACHILLES TENDON DURING WALKING

Eli Dawson[1], Dylan G. Schmitz[1], and Darryl G. Thelen[1]
[1]University of Wisconsin-Madison, WI, USA
Email: epdawson@wisc.edu

Introduction

The bulk propagation speed of a shear wave in isolated tendon is well described by a tensioned beam model [1]. This observation led to the development of shear wave tensiometers, which are wearable sensors that excite and record wave propagation as a means of gauging loads in *in vivo* tendons [1]. However, waves measured at the skin surface are dependent on the dynamic interaction of tendon and surrounding tissues. This can result in dispersion due to guided wave behavior within the tendon [2], and interaction of tissues of differing stiffnesses [3]. Inherent tissue viscosity can also induce dispersive behavior in which propagation speed, or phase, depends on the excitation frequency [4]. The purpose of this study was to investigate the dispersive nature of wave propagation in the intact Achilles tendon over a range of excitation frequencies.

Methods

Two subjects walked on a treadmill at 2.5 mph. Each subject also posed statically with their foot in the air and on the ball of their foot to approximate swing-phase unloading and late-stance loading, respectively. A shear wave tensiometer [1] was used to measure wave propagation in the Achilles tendon resulting from Gaussian wavelet excitations (Fig. 1A). Waves were excited using a discrete wavelet frequency for each of 13 walking trials (200-1400 Hz, 100 Hz increments) and an inclusive frequency sweep from 200-1445 Hz for each static trial. Accelerometer signals were bandpass filtered in a narrow range (100 Hz) around each excitation frequency. Wave travel time was computed by finding the lag that maximized the normalized cross-correlation of accelerometer signals [1]. Wave speed was computed by dividing the accelerometer spacing (8 mm) by the travel time. For walking, we detected heel strike from an accelerometer mounted on the treadmill and averaged the wave speed patterns over a minium of 7 strides at each walking speed (Fig. 1B).

Results and Discussion

Wave speeds varied with frequency for both the static-loading frequency sweeps and across walking trials using varied excitation frequencies (Fig. 1C). Both subjects showed frequency-dependence, but the pattern was not identical. The frequency-dependence and subject-specificity is likely a result of differing thicknesses of soft tissue layers surrounding the tendon, including skin, adipose tissue, and muscle. Different tissue thicknesses result in unique wave speed vs. frequency profiles for each subject, which is caused by mode conversion due to guided wave behavior across frequencies. The minimas of the frequency profiles are an approach towards the bulk shear velocity of the stiffest layer at that loading level [3] – in this case the tendon.

Significance

When using wave speed measurements to estimate stress experienced by an individual's tendon, understanding what factors may contribute to subject-specific differences in the wave speed-stress relationship is important. Here, we've shown that measured wave speed is dependent on excitation frequency, especially in the current excitation range used by the tensiometer. Further study of this phenomenon will attempt to link excitation frequency-dependence to subject-specific soft tissue geometry and will guide selection of excitation frequencies that ensure consistent wave speed measurements.

Acknowledgments

Funded by NIH AG051748 and NSF GRFP (DGE-1747503).

References

[1] Martin et Al. *Nat. Comm.* **2018**. [2] Brum et al. *Phys. Med. Bio.* **2014.** [3] Mohan et. al. *Optic Express* **2012.** [4] Cortes et al. *Ultras. Med. Bio.* **2015**.

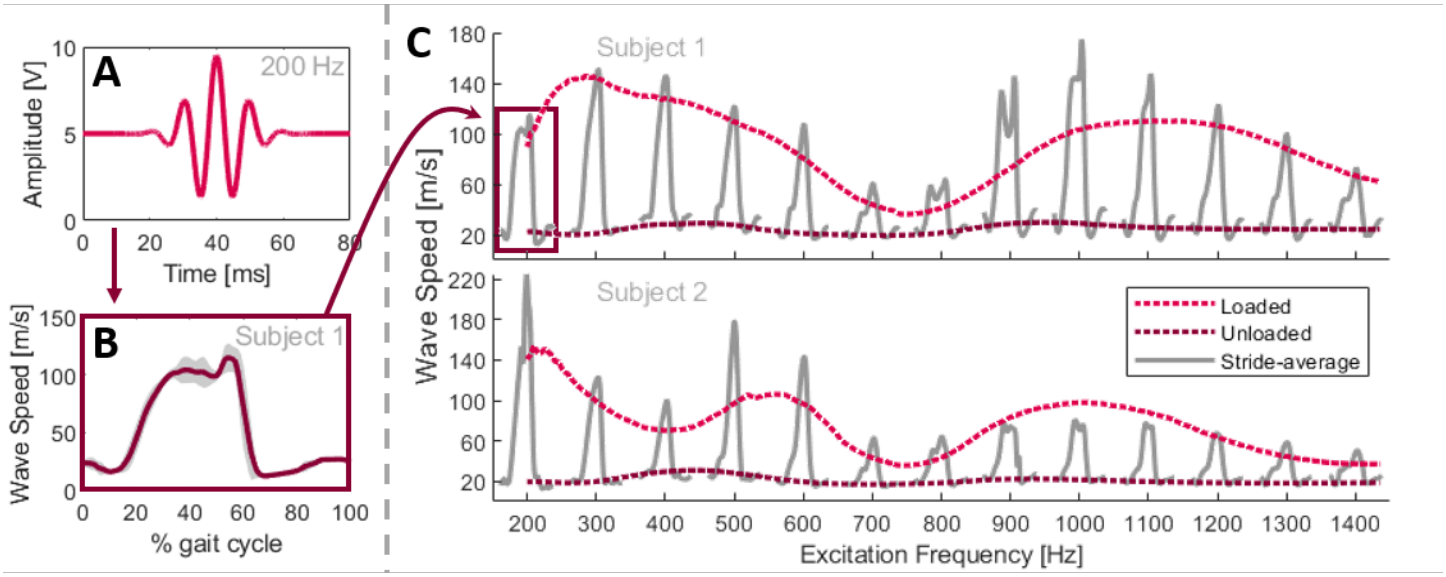

Figure 1. A) Example Gaussian wavelet excitation at 200 Hz. B) Stride-average Achilles tendon wave speed for 200-Hz excitation. C) Loaded and unloaded static trials with swept wavelet frequencies. Each walking trial average (200-Hz example in B) is centered at its excitation frequency.

Validation of IMU-derived knee flexion angle measurements for use in visual kinematic feedback

Peter Barrance[1,2], Xuan Liu[1,2], Naphtaly Ehrenberg[1,2], Nuno Oliveira[1,2,3],
JenFu Cheng[2], Katherine Bentley[2], Sheila Blochlinger[2], Hannah Shoval[2]
[1]Center for Mobility and Rehabilitation Engineering Research, Kessler Foundation, West Orange, NJ, United States
[2]Children's Specialized Hospital Research Center, New Brunswick, NJ, United States
[3]School of Kinesiology and Nutrition, University of Southern Mississippi, Hattiesburg, MS, United States
Email: pbarrance@kesslerfoundation.org

Introduction

Visual biofeedback of joint kinematics has been explored for its potential to enhance retraining of pathological gait patterns in various populations. The most frequently reported modality for kinematic measurement is camera-based optical marker tracking. This presents challenges to adoption in clinical settings, as it requires considerable setup time as well as compatible space and lighting, and is vulnerable to marker occlusions which are likely to occur during therapist-supervised training. We have developed a visual biofeedback system [1] that provides feedback on knee kinematics measured using small lightweight wearable sensors (inertial measurement units / IMUs). We have designed the system specifically to support retraining of gait deviations in children with hemiplegic CP. To ensure that the feedback provided by the system is based on a robust and valid measure of knee flexion, we report a validation study comparing the knee flexion angle calculated by the system with a gold standard (camera-based) measurement of the same angle.

Methods

We collected IMU-derived and camera-based data for this study simultaneously as a participant in our pediatric target population performed treadmill walking in a therapy room typically used for clinical training. The participant was an adolescent female with right hemiplegic CP (age 16.2 yrs, height 1.52 m, weight 44.5 kg). Informed consent was provided by the participant as well as a parent in compliance with the regulations of the local Institutional Review Board. Participant safety during treadmill walking was ensured by a pediatric physical therapist (close supervision). Following standard setup methods, three IMUs (MTW Devkit, Xsens, NL) were placed on the participant's right anterior thigh, posterior shank, and heel while standing. (Note: heel sensor data were not used to calculate knee kinematics). The thigh sensor's longitudinal axis was visually aligned perpendicular to the long axis of the thigh, while the sensor outputs were used to guide alignment of the shank sensor to be parallel to the thigh sensor. The IMU-derived knee flexion angles in our system are defined as the difference between the thigh and shank sensors' rotational orientation about their longitudinal axis ('roll'), which were collected at a rate of 60Hz. For the camera-based measure, reflective markers were placed on the greater trochanter, femoral lateral epicondyle, fibular head, and lateral malleolus of the same limb. A 3 camera motion capture system (Optitrack Trio, NaturalPoint, Inc., Corvallis, OR) was used to collect marker positions, and knee flexion angles were calculated as the 3D angle between a femoral vector (epicondyle to trochanter) and a tibial vector (malleolus to fibular head). Marker data were collected at 120Hz.

Four 30 second treadmill walking trials were recorded in total; two at 0.80 m/s, and two at 1.12 m/s. No special instructions or feedback were provided to the participant during these trials. IMU-derived knee flexion angle data were resampled to 120 Hz and the datasets were aligned in time by the optimization of a variable time offset. Measurement agreement was assessed by linear regressions between the datasets for each trial.

Results and Discussion

Table 1. Trial characteristics and linear regression analysis

Trial number	Speed (m/s)	R^2	Slope (°/°)	Intercept (°)
1	0.8	0.932	1.26	-31.4
2	0.8	0.935	1.27	-32.7
3	1.12	0.966	1.29	-34
4	1.12	0.947	1.28	-34
Mean ± SD			1.27 ± 0.01	-33.0 ± 1.2

The linear regressions illustrated strong convergent validity of the IMU-derived joint angles with the camera-based joint angles, with correlation coefficients varying between **0.932** and **0.966** across the four trials (Table 1). Predictive equations took the form of (IMU-derived angle) = m * (camera-based angle) + b, with the mean values across trials of the slope m and intercept b calculated as 1.27 and -33° respectively. The mean slope indicates that joint angle excursions recorded by the IMU system are somewhat higher than those from the camera data. We observed that this stemmed from movement of the IMUs relative to the overall limb segments. Optical markers are also subject to skin movement artifact, however additional movement of the IMUs may be related to their placement overlying muscles active during gait. During training we used a brief calibration procedure which implements a scaling factor to compensate for this difference and produce appropriate feedback signals. The mean intercept indicates a zero-point measurement offset between the two systems, which is also addressed by the calibration procedure.

Significance

IMUs are compatible with clinical training environments and can provide robust and valid signals for use in visual kinematic feedback. Future work may include further exploration of sensor placement and attachment methods, feedback formulation, and training paradigms.

Acknowledgments

This study was funded by Children's Specialized Hospital and Kessler Foundation. Patent pending for visual feedback method.

References

[1] Liu X et al. (2019). *Proceedings of ISB/ASB'19*, Calgary, AB, Canada

Simple and Low-Cost Methods of Computing Joint Angles Using Inertial Measurement Units Without Magnetometers

Seung Yun Song[1], Yinan Pei[1], and Elizabeth T. Hsiao-Wecksler[1]
[1]Department of Mechanical Science and Engineering, University of Illinois at Urbana-Champaign, Urbana, IL 61801
Email: ethw@illinois.edu

Introduction

Recent progress made in micro-electro-mechanical systems (MEMS) have allowed Inertial Measurement Units (IMUs) to be more compact, affordable, and accurate. IMUs are now becoming a common tool used in movement and gait analysis. Many biomechanics studies have used expensive IMUs with well-developed software packages. Some research groups have tried to create their own IMU system but have not thoroughly validated their system (e.g., [1]). Most studies only validated their methods using arbitrarily defined movement speeds and ranges of motion, a single rotation axis, and/or short test duration (< 2 min) (e.g., [1]). Also, these studies do not provide open-source material, making it difficult for others to replicate their work.

The goals of this study were to: (1) propose a low-cost joint angle IMU-based measurement system, (2) validate and compare common computational methods of calculating joint angle using IMUs for multiple rotation axes, movement speeds and extended collection times, and (3) provide open-source codes and documentation describing the inner workings of these computational methods to help biomechanics researchers develop low-cost IMU systems.

Methods

Our system used two IMUs (MPU-6050, TDK-InvenSense). Each IMU has a 3-axis accelerometer and a 3-axis gyroscope, but no magnetometer, built-in digital low-pass filters, and proprietary Digital Motion Processing (DMP™) algorithm for computing quaternion orientation. This IMU costs ~$10.

We developed a testbed that offered programmable and repeatable rotations to validate the accuracy of our IMU system. The testbed consisted of a stepper motor (NEMA17, 42BY GH3401; Han Ding Motor) with an optical rotary incremental encoder (HEDS-9040#T00; Broadcom). Two microcontrollers were used to ensure consistent data collection at 100 Hz sampling rate (Teensy 3.6; PJRC) and reliable motor control (Arduino Uno; Arduino LLC). One IMU was secured to the motor shaft (moving IMU), and the other IMU was attached to the motor mount (stationary reference IMU). The moving IMU was changed to accommodate rotations about three different axes (yaw, pitch, roll).

Five common methods for computing relative joint angle were investigated: gyroscopic integration (GI), accelerometer inclination (AI), complementary filter (CF), Kalman Filter (KF), and quaternion-based digital motion processing (QDMP). For the QDMP method, we developed a custom calibration and computation protocol, which utilized each InvenSense IMU's DMP-based quaternion data [2]. The other four methods were implemented using previously developed methods from the literature [3]. For yaw calculations, only QDMP, GI methods were used since AI, CF, KF require the rotation axis to be non-parallel to gravity. Open-source code and documentation are available from our group [4].

Nine trials (3 rotation axes x 3 movement speeds (slow 25°/s, medium 100°/s, fast 200°/s)) were performed, each for 25 min and oscillating 180° range of motion. Testing speeds were chosen to replicate a typical walking gait study for analyzing knee joint kinematics. Root-mean-squared-error (RMSE) was used to compare performance of each method to the gold standard joint angle (encoder-derived angle).

Results and Discussion

For pitch and roll angles, the AI, CF, KF, and QDMP methods exhibited highest accuracy (RMSE < 6˚, acceptable maximum RMSE for biomechanical research studies [5]) at all movement speeds* and no signs of drift across the entire duration of testing (Fig 1A). (*AI RMSE = 6.2˚ at fast speed.) The GI method was the least accurate with rapid divergence. These results suggest that four computational methods (AI CF,KF,QDMP) can be used in biomechanical studies to accurately quantify joint angles for movement speeds up to 200˚/s and test durations of 25 minutes.

Computed yaw angles were inaccurate and limiting in terms of available methods (GI, QDMP). After 1.4 and 2.3 minutes, both methods exceeded RMSE 6˚, respectively. These methods can only be used for studies lasting less than one to two minutes.

To minimize error, IMUs should be placed close to the rotation axis, and kinematic data during transient regions with high acceleration/deceleration should be analyzed with caution.

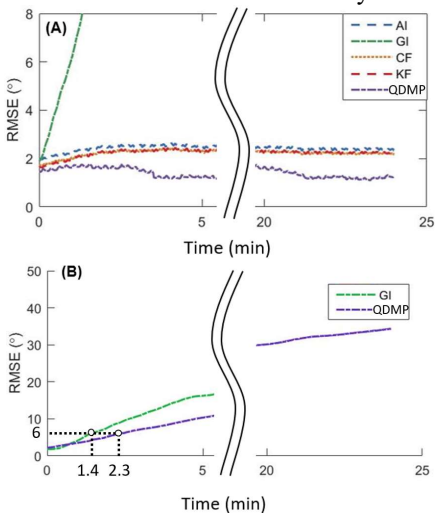

Figure 1: RMSE plots for medium speed for pitch (A) and yaw (B).

Significance

This study provides information about low-cost IMUs and computational methods, so that other biomechanics researchers can develop their own IMU systems.

Acknowledgments

Funded provided by the Jump ARCHES partnership between OSF HealthCare and the University of Illinois.

References

[1] McGinnis, R.S., et al., IMECE. 2014
[2] Song, S.Y., MS Thesis, Mech E, UIUC. 2019
[3] Gui,P., et al., ICIEA,. 2015
[4] https://hdcl.mechanical.illinois.edu/open-source-materials/
[5] Seel, T., et al., Sensors, 14(4):6891-909, 2014

Acceleration Signals and Peaks During Running Vary with IMU Placement

Zachary David Katzman[1], Dovin Kiernan[1], Kristine Dunn[1], and David Hawkins[1]
[1]University of California, Davis, Davis, CA, USA
Email: dahawkins@ucdavis.edu

Introduction

Inertial measurement units (IMUs) provide exciting opportunities to quantify and track biomechanical metrics in the field. To successfully capitalize on these opportunities, however, IMUs must provide repeatable measurements, which may be affected by IMU placement. Understanding the impact of IMU placement is of particular importance when IMUs are placed by end users (e.g. clinicians, coaches, athletes) or where the IMU may move throughout a long data collection. To our knowledge, the effect of IMU placement on repeatability of acceleration measurement during running has not been previously investigated. To address this gap and determine the effects of small changes in IMU placement, we systematically varied IMU placement near several common IMU attachment sites and quantified differences in accelerations.

Methods

Runners (n = 30) ran 25 m overground 60 times at 'slow', 'typical', and 'fast' self-selected speeds while a pair of IMUs simultaneously collected data (Inertia Technology ProMove MINI; ±100 g, ±2000 deg/s, 1000 Hz). IMUs were either placed 'correctly' at one of three commonly used attachment sites (distal tibia, iliac crest, or sacrum) or were 'misplaced' 0.05 m to the upper right ('UR') or upper left ('UL') corner of the correctly placed IMU (Fig. 1).

IMU data were filtered using a 4th order 50 Hz low-pass Butterworth filter. The contribution of gravity to the acceleration signal was removed and signals were rotated to a segment local coordinate system [1]. A single stride was isolated from the middle of each trial [2], when the participant was running at an approximately constant velocity.

For each stride, RMSE values were calculated between correctly placed and misplaced IMU accelerations. Acceleration peak magnitudes and the difference in timing between peaks were then calculated. Paired t-tests were used to evaluate whether magnitude and timing significantly differed between correctly placed and misplaced IMUs ($p < 0.05$; FDR correction).

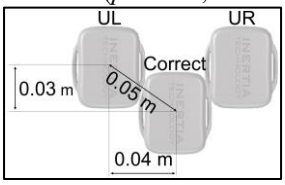

Figure 1: Location of misplaced IMUs in relation to correct placement.

Results and Discussion

The 0.05 m shift in placement led to changes in resultant acceleration signals: RMSE values across a stride were between 0.271 and 0.715 g (Fig. 2). RMSE values were largest for the distal tibia location and smallest for the sacrum location. Magnitude and timing differences were particularly pronounced when accelerations peaked. The largest mean difference in peak magnitude of -0.856 g (correct - misplaced) occurred for UR misplacement at the distal tibia (Fig. 2A), while the largest mean difference in peak timing of -1.46 ms was seen for UR misplacement at the iliac crest (Fig. 2B).

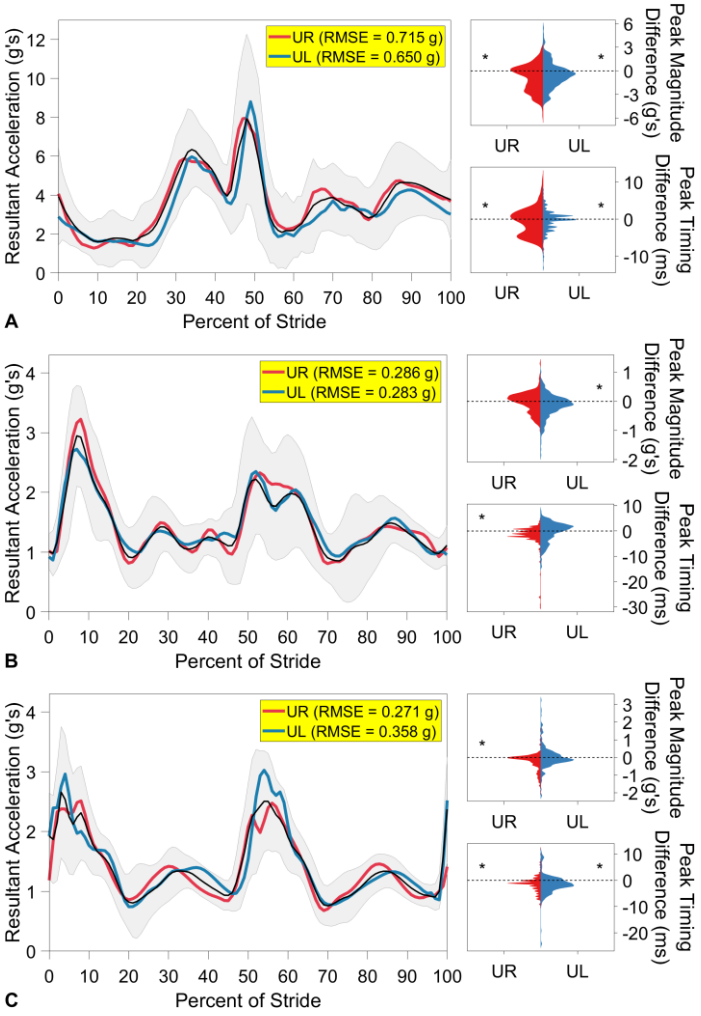

Figure 2: Distal tibia (A), iliac crest (B), and sacrum (C) mean ± SD (black/gray) filtered resultant accelerations, RMSE values across a stride (highlighted in yellow), distributions of correct - misplaced resultant peak magnitude (upper right) and timing (lower right) differences for UR (red) and UL (blue) misplacement. *misplaced significantly different than correct

Significance

Researchers, clinicians, and runners interested in accurately measuring resultant accelerations with error less than 0.271 g across a stride should be conscious of placement, as changes in signals and peaks caused by misplacement may impact the repeatability of acceleration-based measurements. Users should be trained to place their devices before collecting running data. Devices such as IMU belts that minimize IMU movement during long runs should be developed to ensure consistent placement.

Acknowledgments

NSERC, ACSM, Sigma Xi, and the Maury Hull Fellowship.

References

1. McGinnis & Perkins. *Sensors*, **12**, 11933-11945, 2012
2. Benson et al. *Sensors*, **19(7)**, 1483, 2019

IMPROVING CENTER OF PRESSURE ESTIMATION USING A SIMPLE OPTIMIZATION METHOD

Robert A. Creath, Ph.D.
Lewis Human Performance Lab
Department of Exercise Science, Lebanon Valley College
email: creath@lvc.edu.edu

Introduction

Force plates (FPs) are a crucial component of many biomechanics labs. When purchasing a FP, considerable care is spent determining the degree of accuracy and level of precision needed to produce acceptable research data. However, FP accuracy is dependent on proper installation and it can decline in older FPs rendering error into the data.

Factory recalibration is an ideal yet often impractical solution due to the expense of recalibration and lab downtime.

Several *in situ* calibration methods have been published that achieve accurate and reliable results, but require considerable expertise. For example, Collins et al. (2009) used an instrumented pole and inverse dynamics to model FP error. Reported post-calibration FP error was 5 mm rms.

We measured a series of positions using a metric ruler and a weighted metal stylus on two FPs, one new and the other approx. 10 years old. The error values were the differences between measured positions (PMs) and FP data. We assumed the PMs were the desired values and the deviations from true position were the FP data. Error values were reduced by least-squares optimization of a linear function for scaling and offset.

Our goal was to develop a simple yet effective method of optimizing CoP estimation that could be achieved *in situ* and would improve CoP position estimates to levels expected from a factory-installed force plate.

Methods

Nine evenly-spaced position measurements (3x3 grid) were taken on each of two adjacent 400 x 600 mm AMTI FPs using a pointed metal stylus weighted at approx. 20 Kg. The stylus support structure was made from 2x4 lumbar and ¾" plywood. The stylus was moved to each of the measurement points on the FP surface which was covered with contact paper to outline the evenly-spaced grid. Figure 1 shows a schematic of the stylus and support structure.

Figure 1: Point application of weight on force plates

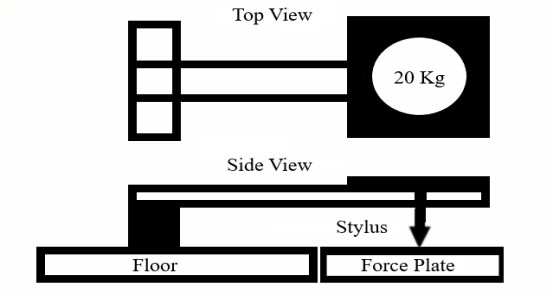

PMs were taken and compared to 10-second FP trials for each measured point using the average value for each trial. Forces and moments were processed according to AMTI User Manual standards. CoP position estimation was calculated according to Kwon (1998).

Measurement error between PMs and FP data was calculated as the average (std.dev.) of the x, y, and radial (Euclidean) position differences.

The FP data positions were optimized to the function

$$X_m = B*X_{FP} + \text{offset} \qquad (1)$$

Where X_m was a vector of the PM values, X_{FP} was a vector of the FP data (10-second trial values), B was the scaling factor, and offset was the difference between the average of X_m and X_{FP}. Y measurements were treated similarly.

Optimization was achieved by the method of least squares using custom MatLab code (fminsearch) with equation 1. The goal was to optimize B and offset so that X_{FP} values were a best fit to X_m. New (optimized) values (OVs) were calculated from X_{FP} using equation 1 and compared to X_m and X_{FP}.

Results and Discussion

Table 1 compares old and new force plates for average radial errors between OV and X_m (Optimized), and between OV and and X_{fm} (Pre-optim.).

Table 1 Comparison (mean (std. dev.)) between optimized and pre-optimized average radial displacements errors.

	Old FP	**New FP**
Optimized	1.0 (0.5) mm	1.6 (1.6) mm
Pre-optim.	6.4 (3.6) mm	12.3 (4.0) mm

In both cases the optimized values were less than the pre-optimized measurements indicating an improvement in accuracy of CoP position estimation.

The large difference errors measured on both plates suggest improper installation which can alter the expected accuracy of the force plates (Collins et al., 2009, AMTI, Inc.). These results suggest the need for professional installation, or as Collins et al. infer, post-installation calibration.

Our goal was to develop a simple, time-efficient *in situ* method to improve CoP position estimation accuracy for embedded force plates. Optimized position estimates were 6.4 to 7.7 times better than the pre-optimization values, but less than AMTI's advertised values of 0.2 mm.

The reader should note this procedure improves CoP position estimates, but not FP forces or moments. For postural control studies, the magnitude of vertical forces far outweighs horizontal forces, so a simple weight calbation could provide adequate ground reaction force values for most studies. If more accurate force and moment values are required, then the method of Collins et al. (2009) should be considered.

References

Collins et al. Gait & Posture, 2009, 29(1):59-64
AMTI User's Manual, AMTI, Inc. Watertown, Mass.
Young-Hoo Kwon, 1998, Kwon3D.com

Estimating Walking Speed in the Wild

[1]Loubna Baroudi, [1]Mark Newman, [2]Elizabeth Jackson, [1]Kira Barton, [1]K. Alex Shorter, and [1]Stephen Cain
[1]University of Michigan, Ann Arbor, MI, USA and [2]University of Alabama, Birmingham, AL, USA
Email: lbaroudi@umich.edu

INTRODUCTION The measurement of physical activity in a clinical setting is often used to predict health outcomes. Hand-timed gait speed, measured during standard clinical gait tests (e.g. 5-meter walk test), is a widespread metric used to quantify physical health. However, there can be measurement noise and bias created by the timing methods and the brevity of these tests. Wearable sensing technologies can be used to complement in-clinic evaluations of movement as they can capture high-resolution kinematic data during free-living. Despite the potential of wearable devices for persistent monitoring, challenges like subject compliance and battery life must be overcome before they can be used regularly in a clinical setting. To address these issues, we use high-resolution measurements of gait kinematics to create subject-specific data-driven models to estimate stride speed from stride frequency. The model is then used to estimate stride speed during daily living from data collected continuously over a week using a low power biologging system.

METHODS To collect data from the free-living environment, we used a lightweight (20 grams) accelerometer-based archival sensor (activPAL) secured to the thigh using a stretch adhesive. This sensor offers 7 days of uninterrupted measurement. Custom algorithms were created to extract steady-state walking bouts and calculate stride frequency f. A data-driven model to estimate stride speed from stride frequency was built using kinematic data estimated from foot-worn inertial measurement units (IMUs) during a prescribed walking task [1]. The walking task consists of a hallway walk, in which a wide range of step frequencies was imposed using a metronome. A power regression model, $d = a.v^b$, was used to describe the relationship between stride length d and stride speed v [2]. Since $f = \frac{v}{d}$, we have the following relationship:

$$f = \frac{v}{d} = \frac{v}{av^b} = \frac{1}{a}v^{1-b} \Rightarrow v = \exp\left(\frac{ln(af)}{1-b}\right) \quad \text{(Eq. 1)}$$

To ensure the model created can be used to accurately estimate speed in the free-living environment, we conducted an experimental verification wearing a foot-worn IMU and the activPAL simultaneously. All protocols used off-the-shelf wearable sensors and were approved by the Institutional Review Board at the University of Michigan.

RESULTS AND DISCUSSION The data extracted from the prescribed walking task was used to identify the parameters {a,b} of Eq 1 and derive a subject-specific model of stride speed vs. stride frequency. The resulting model fits the data well ($R^2 = 0.97$), Fig. 1-a. Speed estimates derived from the thigh worn accelerometer were verified using 14 hours of data collected over 2 days from both a foot-worn IMU and the activPAL. Fig. 1-b. shows the distribution of the speed estimated from the IMU, considered as the true speed, and the estimated speed from the activPAL using our model, as well as their respective fitted Gaussian curves. The mean of the true speed is not statistically different from the mean of the estimated speed ($p \geq 0.01$). These preliminary results support the use of the model to reliably estimate stride speed during daily-living.

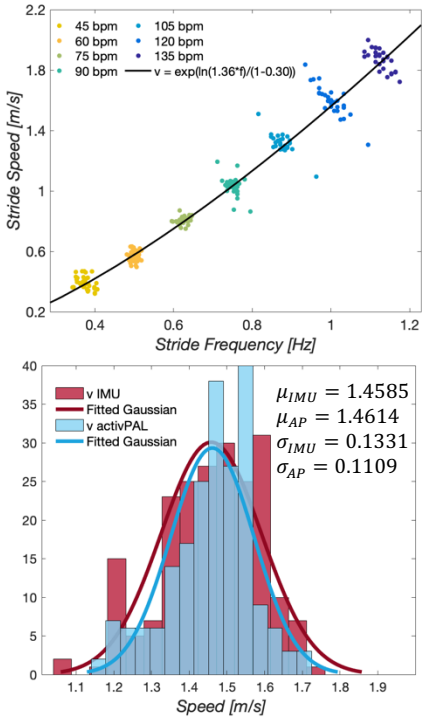

Figure 1: a. Data-driven model of stride speed against stride frequency using pilot data from a single subject extracted from the prescribed walking tests. **b.** Measured speed distribution from the IMU and estimated speed distribution from the activPAL data.

SIGNIFICANCE Week scale data from a minimally invasive biologging instrument on a single charge (activPAL) addresses challenges associated with subject compliance and battery life. However, direct measurement of walking speed cannot be estimated from these data. Using a data-driven modeling approach and combining different temporal timescales and resolutions, we were able to leverage this piece of technology to reliably estimate walking speed during free-living, creating the opportunity for clinicians to gain insight on the physical health of an individual in their natural environment.

REFERENCES

1. Ojeda L, et al. *J of Navigation,* Pages 391-407, 2007.
2. Kuo A, et al. *J Biomech Eng*, Pages 264-269, 2001.

ACKNOWLEDGEMENTS

This research was funded by the Precision Health Investigators Award of the University of Michigan.

Reliability of One-Size-Fits-All In-Shoe Force Sensors Across Various Walking Speeds

Kaleb Burch.[1], Sagar Doshi[1], Erik Thostenson[1], and Jill Higginson[1]
[1]Mechanical Engineering, University of Delaware, Newark, DE 19711
Email: kburch@udel.edu

Introduction

Real-time measurement of ground reaction force (GRF) in unrestricted settings is useful for gait research, clinical assessment, and recreational fitness. One sensing method is the use of force or pressure sensors under the foot. These types of sensor systems can be highly complex, requiring careful sensor placement for each subject [1]. This study seeks to show that one-size-fits-all shoe sensors (SS) can be used to accurately measure both peak GRF and heel strike timing across a range of walking speeds for subjects of various weights and foot sizes.

Methods

The shoe sensor system in this study consisted of 2 fabric-based nanocomposite sensors located on a sandal under the hindfoot and forefoot regions [2]. This system was worn by 10 subjects (age: 23.3 ± 2.5 years; mass: 75.2 ± 18.2; 5 male and 5 female) who participated in calibration trials and walking trials. During calibration trials, subjects performed 3 steps in which they slowly transferred weight onto an individual sensor and then back off the sensor. During walking trials, subjects walked at a given speed (0.5, 1.0, or 1.5 m/s) for 30 seconds. Calibration trials were performed first and then walking trials were performed in a randomized order. Vertical GRF data was collected with an instrumented, split-belt treadmill (Bertec Corp, Worthington, OH, USA) at 2000Hz. Force data was collected from the SS at an average frequency of 28Hz using an Arduino Uno Rev3.

The individual sensors were calibrated against the treadmill during the loading phase of each calibration "step". Since the sensors do not cover the entire foot, they cannot capture the complete force on the foot. This was accounted for by using a weighted combination of the forces measured by each sensor determined based on a least-squares regression [3]. This regression was performed for all trials. The average coefficients across all walking trials were used to obtain the final forces.

For the walking trials, data was segmented into separate gait cycles using heel strikes. The treadmill force plate (FP) identified heel strikes using a 20N threshold [4]. Heel strikes were identified for the SS as zeros of the third order time derivative of resistance after which a threshold (defined by 23% of the subject-specific resistance range during gait) was crossed. Within each gait cycle, cycle time and forces at both GRF peaks were measured for both FP and SS. All forces were normalized to subject body weight. Linear regression was performed to evaluate peak forces in the shoe sensor versus the force plate.

Results and Discussion

The SS demonstrated a consistent increase in peak force (F_{SS}) that correlated with peak forces (F_{FP}) detected by the force plate ($F_{SS} = 0.665F_{FP} + 0.34$, $r^2 = 0.26$, Fig. 1). The SS was accurate across a range of speeds (largest average error over 1 speed for a single subject: 0.5 m/s, 5% BW; 1.0 m/s, 11% BW, 1.5 m/s, 5% BW). The heel strike detection algorithm also matched the treadmill algorithm, accurately reproducing gait cycle duration ($r^2 = 0.996$ when all subjects and trials are included; $r^2 = 0.76$ to 0.8 per subject on average; largest single trial RMSE < 0.012s).

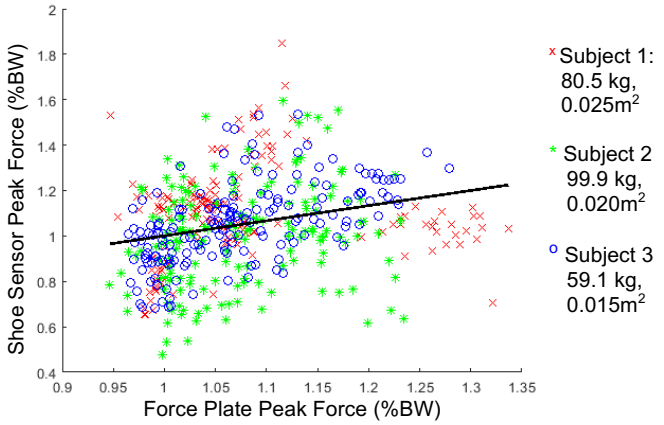

Figure 1: Peak Forces Detected by Shoe Sensor vs. Peak Forces Detected by Force Plate. Peak forces for 3 subjects are depicted, with each symbol corresponding to a different subject. The legend includes subject mass and foot area. The black line represents the linear regression across data from all 3 subjects.

Across speeds and across subjects, the least-squares coefficients were generally not constant (Fig. 2). Nevertheless, taking average values allowed for reasonable force estimates to be obtained.

	0.5 m/s	1.0 m/s	1.5 m/s	Overall
a_1	0.89 ± 0.02	0.89 ± 0.01	1.27 ± 0.01	1.01 ± 0.20
b_1	0.57 ± 0.02	0.47 ± 0.01	0.35 ± 0.01	0.46 ± 0.10
a_2	1.64 ± 0.00	1.88 ± 0.26	1.83 ± 0.17	1.78 ± 0.18
b_2	3.46 ± 0.24	2.99 ± 0.18	3.06 ± 0.41	3.17 ± 0.32
a_3	1.87 ± 0.25	1.98 ± 0.05	1.98 ± 0.02	1.95 ± 0.13
b_3	0.80 ± 0.02	0.74 ± 0.01	0.65 ± 0.00	0.75 ± 0.06

Table 1: Unitless coefficients (mean ± standard deviaton) of linear regression used to calibrate sensors. Subscripts on the coefficients represent corresponding subjects.

With these fabric-based in-shoe sensors, we have demonstrated the ability to estimate peak GRF over a range of walking speeds for a variety of subjects without precise placement of sensors.

Significance

The sensors evaluated in this study have the potential to impact both research and clinical care. The ability to measure GRF for every step allows the researcher to obtain larger data sets without the restrictions of a laboratory setting. In the clinic, it will be useful to physical therapists could monitor how much load is exerted on patients' legs. The low cost and simplicity of the sensor implementation make it practical for use in these settings, where more complex systems would require extra setup.

Acknowledgments

UNIDEL Foundation, Inc.

References

[1] Bamberg, et al. (2008). *IEEE Trans. Info. Tech. Bio,* **12**(4), 413-423
[2] Doshi, et al. (2018). *ACS Sens.* **3**(7), 1276-1282
[3] Zeni, JA et al. *Gait & Posture*, **27**(4), 710-714.
[4] Park, J et al. (2016) *IEEE Int. Conf. Biomed. Robot. & Mech.*

A preliminary study of a motion capture system using smartphones for the ankle joint analysis

Patrick R. Currin[1], Jongyong Park[2], Eunyoung Kim[3], Chiseung Lee[1], Woolim Hong[1], Felipe C.R. Miftajov[1], and Pilwon Hur[1,*]
[1]Department of Mechanical Engineering, Texas A&M University, College Station, TX, USA
[2]Department of Computer Science and Engineering, Texas A&M University, College Station, TX, USA
[3]Department of Aerospace Engineering, Texas A&M University, College Station, TX, USA
Email: pilwonhur@tamu.edu

Introduction

Motion capture systems are used in a number of fields to analyze human movement by collecting data points for motion analysis. Unfortunately, the most widely used motion capture technology (e.g., Vicon) is prohibitively expensive and requires a well-controlled space to be utilized. As a part of an undergraduate education project (i.e., Aggie Challenge at Texas A&M University), in this study, we implemented and verified the feasibility of a design for a smartphone-based motion capture system to analyze the ankle joint kinematics in an easy manner.

Methods

In this study, we used conventional smartphones to capture the object that we desire. The required number of smartphones is dependent on the number of points to capture. In this case, we used two smartphones to capture four ping-pong balls (Figure 1: green) to analyze the ankle joint. In order to calibrate the motion capture system, we used the direct linear transformation (DLT) method, which relates camera images to real world objects using DLT parameters [1]. A 3D calibration bar with 8 ping-pong balls was used as a global coordinate reference for finding the DLT parameters. Based on the recorded data from two different stationary smartphones, two DLT parameter sets were obtained from each camera by a least squares method. These parameter sets allow us to estimate objects' 3D position from their 2D position in the frame of each camera.

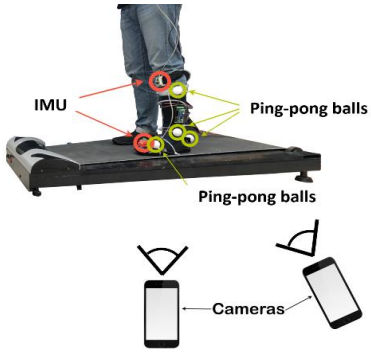

Figure 1: Motion capture experiment setup for the ankle joint angle using two independent capture systems: IMU and smartphone-based system.

To validate the system, a treadmill walking experiment was conducted with a healthy young subject (male, 31 yrs. 1.70 m, 70 kg) in order to capture ankle behavior. The subject was asked to walk at his preferred speed (0.5 m/s). During the experiment, four ping-pong balls and two inertial measurement units (IMUs) were attached to the subject's lower leg and foot as shown in Figure 1. The experiment was recorded with the cameras in the same positions as the calibration process. The resulting videos were time-synchronized in post-processing by cross-correlation of the velocity of a ball located at the heel. The IMU system is commonly used to capture joint kinematics [2] and was used here to verify the proposed smartphone-based system.

After recording the experiment, the movement of each ball was tracked using motion tracking software (OpenCV) to obtain their image plane [u,v] coordinates. Using the DLT parameters from the calibration, the moving image plane data was then converted to three-dimensional coordinates [x,y,z] which were used to calculate joint angles.

Results and Discussion

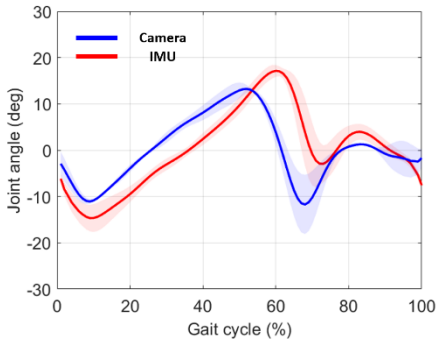

Figure 2: Ankle joint angle estimation from two different methods: IMU system (red) and camera-based system (blue). Bold lines and shaded regions refer to the average and ±1 s.d. of five consecutive steps, respectively.

Figure 2 shows the ankle joint angle in the sagittal plane as measured by the two different methods. This data confirms preliminary feasibility. Compared to the result from the IMU system, the proposed result shows a qualitatively similar trend for the entire gait cycle, especially in showing ankle dorsiflexion and push-off. The discrepancies in angle can be explained by sensitivity to placement both for the IMU sensors and our markers. We expect that we can account for these with modification to the algorithm and marker design, yielding improvements in accuracy. The performance of the improved system will be gauged against the Vicon capture system.

Significance

This study shows the feasibility of using smartphones for motion capture purposes. Once the accuracy of our motion capture system is improved, it can potentially make motion capture experiments easier, portable, and more accessible, since users only require relatively inexpensive phones with minor preparation for the test. Most importantly, this study provided an educational experience for the undergraduate students at Texas A&M University who completed this work.

References

[1] Y. Kwon (1998), http://kwon3d.com/theory/dlt/dlt.html
[2] W. Hong, et al. (2019), *International Conference on Robotics and Automation*

Noninvasive Monitoring of Muscle Metabolic Activity with Near Infrared Spectroscopy and Diffuse Correlated Spectroscopy

Scott Boebinger[1*], Rowan Brothers[1], Sistania Bong, Bharat Sanders, Lena Ting[1], Erin Buckley[1]
[1]Wallace H. Coulter Department of Biomedical Engineering, Georgia Institute of Technology and Emory University
Email: *sboebin@emory.edu

Introduction

Resting rate of oxidative muscle metabolic activity may provide a valuable biomarker to assess muscle tone. Numerous disease states are known to influence muscle tone, including Parkinson's disease, yet we lack reliable assessments that quantify muscle metabolic activity.

Near-infrared spectroscopy (NIRS) provides a low-cost, non-invasive means to measure localized oxidative muscle metabolic activity ($mMRO_2$)[1,2]. While this optical approach is relatively simple to perform, it requires occluding arterial blood flow. The need for arterial occlusion prevents continuous monitoring and limits the measurements to patients who can tolerate occlusion.

Combining NIRS and diffuse correlation spectroscopy (DCS), which measures blood flow, offers an alternative optical approach to quantify a muscle metabolic activity index ($ImMRO_2$) without the need for occlusions. Although NIRS+DCS-measured $ImMRO_2$ has been reported by several groups[1,2] the measurement itself has never been validated against NIRS-measured $mMRO_2$.

We examined the agreement between NIRS ($mMRO_2$) and NIRS+DCS ($ImMRO_2$) measures of muscle metabolism. Additionally, we address common sources of error associated with the occlusion protocol and present methods to mitigate these errors.

Methods

Protocol: Nine participants (4 men, 5 women) were seated with knee extended while the optical sensor was secured to the medial gastrocnemius of their dominant leg. After a 2-minute baseline to ensure hemodynamic stability, a 30-second venous occlusion of the thigh was performed at 90mmHg tourniquet pressure, followed by a release and 2-minute recovery period. Once large hemodynamic variations stabilized, an arterial occlusion of the thigh was performed at 250mmHg tourniquet pressure, followed by a release and 5-minute recovery period. The sensor was removed. The protocol was repeated 5 times (*Figure 1*).

Mucle metabolic activity was measured in two ways; 1) a NIRS-only $mMRO_2$ measure during arterial occlusion and 2) a NIRS+DCS $ImMRO_2$ measure just prior to the arterial occlusion. mMRO2 is quanitified as the mean rate of change from oxy- to deoxy- hemoglobin during the arterial occlusion. Hemoglobin concentrations were calculated using the modified Beer-Lambert Law[1,2]. $ImMRO_2$ is quantified via Fick's law by combining NIRS measures of oxygen extraction with DCS measures of blood flow over a 30s interval prior to arterial occlusion.

Quality Control Criteria: Data were excluded from trials in which arterial leakage occurred. Arterial leakage was quantified as the slope of total hemoglobin concentration during arterial occlusion. Data were excluded if the slope was greater than 10% of the slope of total hemoglobin concentration during the venous occlusion.

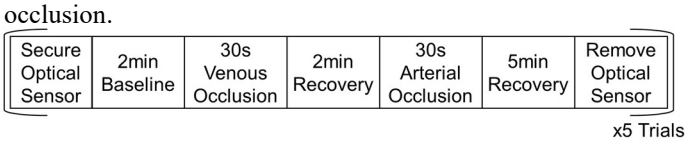

Figure 1: Protocol overview.

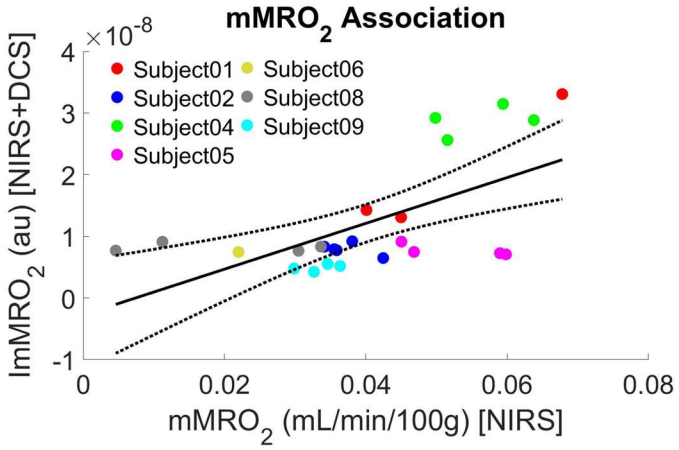

Figure 2: Association between $mMRO_2$ (NIRS) and $ImMRO_2$ (NIRS+DCS). Black line and black dotted line show linear regression and confidence intervals, respectively.

Results and Discussion

Data are reported for 8 out of the 9 participants. Subject 7's data is excluded due to technical difficulties during data collection. Trials 2-5 for subject 6 were excluded as they did not follow the experimental protocol following trial 1.

Out of the 36 trials analyzed 8 did not pass the quality control criterion, none of subject's 3 data passed quality control. Of the eliminated trials there was a significant negative correlation between arterial leakage and metabolic activity for subject 3 ($R^2 = 0.96$, $p < 0.01$). In contrast, there was no significant relation in the reported data in which arterial leakage did not occur. This knowledge could inform future protocols to employ similar quality control criteria to prevent the confounding effect of arterial leakage on $mMRO_2$.

Our values of $mMRO_2$ are similar to those reported in the supine position[1]. Correlations between $mMRO_2$ and $ImMRO_2$ were significant (R^2=0.380, $p<0.01$) (*Figure 2*). We found similar variability between trials for both techniques. However, the differences measured across methods was not significantly correlated (R^2=0.001, p=0.9) (*not shown*). These preliminary relationships need to be validated with a larger sample size.

Significance

To our knowledge we are the first to test the association between $mMRO_2$ and $ImMRO_2$. If an association is found in a larger sample size it would suggest that this index may correspond to physiological units. Therefore, NIRS+DCS may be a promising new modality to continuously monitor oxidative muscle metabolic activity during muscle contraction.

References

1. Henry, B. *J Biomed Opt* (2015). 2. Gurley, K *Biomed Opt* (2012).

Acknowledgments

Funding from NIH R01 HD46922-10

Reliability of Maximium Voluntary Isometric Contractions

Zachary White.[1], Jordyn N. Schroeder[2], Lindsey Trejo[2], Gregory S. Sawicki[2,3]
[1]The B.E.S.T Academy 6-12,
[2]George W. Woodruff School of Mechanical Engineering, Georgia Institute of Technology, Atlanta, GA, USA
[3]School of Biological Sciences, Georgia Institute of Technology, Atlanta, GA, USA
Email: jschroeder9@gatech.edu

Introduction

Maximum Voluntary Isometric Contractions (MVICs) are an integral part to biomechanics research. Muscles have activation dependent behavior that can cascade from muscle level to whole body biomechanics[1]. Many research questions depend on having reliable and repeatable MVIC measurements in one day and over time. However previous studies have found that even at the same location, having multiple evaluators collect MVICs increased variability[2]. The purpose of this study was to assess different methods for collected MVICs from plantar flexors. We hypothesize that using live biofeedback will improve reliability of MVIC measurements, and that increasing the target value higher than subjects can reach will elicit higher activations.

Methods

In this preliminary study, we recruited one participant (N=1). All MVICs were collected on a Biodex Dynamometer during isometric contractions of the right leg with the knee fully extended and the ankle fixed at 0° plantarflexion. Electromyography electrodes were placed on lateral gastrocnemius (LG), and soleus (SOL) muscles, and 3D motion capture markers on the medial knee, ankle axis of rotation and head of the 1st metatarsal. For trials with biofeedback a GUI projected torque value as a ball on a graph with a target line. One baseline condition was collected where subjects were instructed to maximally plantar flex. Then, three conditions with at least 3 trials per condition were randomized:

1) No biofeedback (NBFB), verbal encouragement
2) Biofeedback rampup (RU). The target started as peak baseline torque. Subjects were instructed to beat the target. If they did, the next rampup trial used the new peak torque for the target. This continued until the target could not be beat by more than 5% of the previous trial.
3) High biofeedback (HBFB), target was set to 2X higher than the baseline torque. Subjects were instructed to beat the target.

The participant was given a minimum of a two minute rest between each contraction

Results and Discussion

Preliminary results suggest that the ramp up method elicited the highest torque and activation. Contrary to our hypothesis, there was not a significant difference in the high biofeedback and no biofeedback methods. We anticipate that a target of double the baseline was too high and the participant did not have incentive to reach it. As we get more participants we will be able to draw conclusions on larger scale trends.

Looking to expand these measurements across multiple days, we hypothesize that overtime ramping up will be the best method to produce the highest torques and activations because the participants have a reasonable target to beat. We anticipate that people will get more used to doing contractions so differences between methods will become less apparent overtime.

Although we cannot draw conclusions until the study is complete, results suggest that different tactics even within giving biofeedback yield different results. If a study question relies on MVICs immediately or over time, consideration should be taken on how to collect these data.

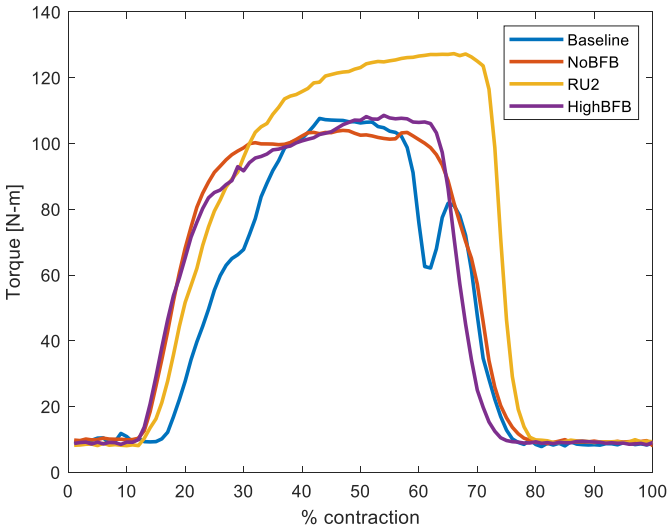

Figure 1: A) Torque values from baseline, no biofeedback, the highest ramp up condition, and high biofeedback

	Normalized Activation
Ramp-Up	1
Baseline	0.899
NoBFB	0.909 +/- 0.035
HighBFB	0.835+/- 0.035

Table 2: LG EMG values normalized to highest condition (Ramp-Up)

Significance

MVICs are a common tool in biomechanics research yet the collection method is not standardized. Our results suggest a need for biofeedback to increase efficacy of these measurements. This study is centered on the plantar flexors but similar standards can be developed for each muscle group. Upon completion, this study can provide guidelines for collecting MVICs, providing consistency across labs, participants, and over time.

Acknowledgments

ZW was supported by GT Project ENGAGES

References

[1] Clark and Franz (2019), *J Appl Biomech.*
[2] Hoagland et al. (1997), *Muscle Nerve.*

Inter-Joint Coordination Variability When Fatiguing With a Repetitive Sit-to-Stand Task

Szu-Hua Teresa Chen[1] and Li-Shan Chou[1,2,*]
[1]Department of Human Physiology, University of Oregon, Eugene, OR USA
[2]Department of Kinesiology, Iowa State University, Ames, IA USA
Email: *chou@iastate.edu

Introduction

The repetitive sit-to-stand (STS) task is often used as a fatiguing protocol when studying fatigue effects on gait. However, little is known about the motor adaptation during such fatiguing course. A recent work has reported an increased variability of continuous relative phase (CRP) after fatigue [1], indicating a reduced motor control or a result of compensation. The purpose of this study, therefore, was to examine changes in variability of both hip-knee and knee-ankle CRPs during the STS course

Methods

Fifteen young (age: 26.7 ± 5.8) and 15 older (age: 69.3 ± 5.7) adults were tested. Participants were asked to sit on a regular wooden chair without armrest and perform repetitive STS movements at their comfortable and fixed paces up to 30 minutes. Participants were instructed to keep their feet in place and not to use arm movements for assisting STS movement during the entire protocol. The repetitive STS fatiguing protocol was terminated when 1) participants cannot continue due to exhaustion, 2) when the movement frequency fell below prescribed pace after encouragement, or 3) after raeching 30 minutes. Rating of perceived exertion (RPE) and maximal isokinetic contraction of right knee extensor were examined using a Borg Scale 6-20 scale and a dynamometer, respectively, before and after the fatiguing protocol. Whole body motion data were collected during each minute of the repetitive STS course. Data from 3 consecutive STS cycles from each minute were extracted, and data in each cycle was normalized to 101 points. Hip-knee and knee-ankle CRPs were calculated using methods previously described [2]. Outcome variable was the ***deviation phase of CRP***, an average value of all standard deviations calculated from 3 CRP curves for each 101 point. Due to individual differences in STS duration, it resulted in various total numbers of trials being recorded from each participant. Thus, STS trial collected from every minute was time normalized to STS duration and dummy coded as five stages: 0-20, 20-40, 40-60, 60-80 and 80-100% of the course (**Figure 1**). A 2*5 mixed-effect ANOVA was used to examine changes in variability during different stages of the course in young and older adults. Alpha level was set at .05.

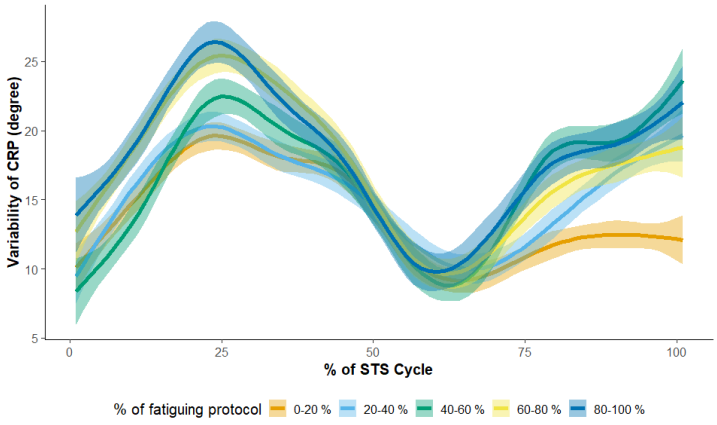

Figure 1: Variability knee-ankle CRP during the STS course.

Results and Discussion

Isokinetic strength was significantly decreased about 18% at post-fatigue with no age-group difference. Both groups demonstrated an increase in RPE from 7 to 18 on average. Older and young adults performed STS protocol to the same degree except for the pace of STS being slower in older adults. No Age x Time interactions were found in neither hip-knee or knee-ankle coordination variability. From sitting to standing, variability of hip-knee and knee-ankle segments did not significantly change along the course nor was there an age effect. In contrast, changes in knee-ankle variability from standing to sitting was dependent on stages, p = .01. Specifically, knee-ankle deviation phase during the late-stage (80-100 %) was higher than that of early-stage (0-20%) regardless of age (**Figure 2**).

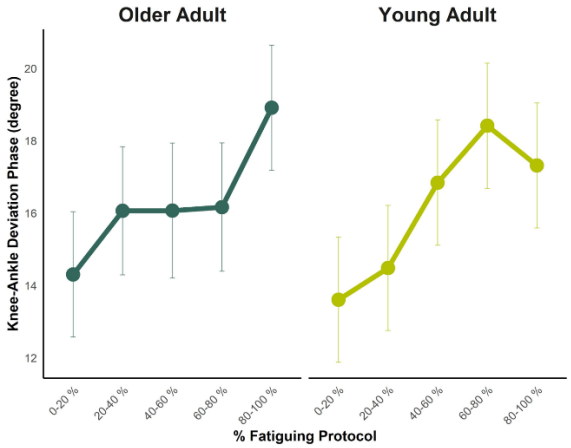

Figure 2: Deviaiton phase of knee-ankle CRP (mean ± SEM).

It is argued that the central nervous system makes efficient use of degree-of-freedom abundance in the human body along the course of fatiguing protocol to compensate for deficit and optimize the performance [3]. Compared to non-goal-orientating task (e.g. standing), a timing error during goal-orientating task (e.g. sitting) was well preserved at the expense of coordinative variability [1].

Significance

The impact of fatigue during repetitive sit-to-stand protocol is not only limited to a decline in force production but also manifested as increasing knee-ankle variability when sitting. Future studies using sit-to-stand movement as a fatiguing protocol could adopt knee-ankle deviation phase as an index of fatigue.

Acknowledgments

This work was funded by the Northwest Center for Occupational Health and Safety & the Ursula Moshberger Scholarship.

References

1. Yang C., et al. *Clinical Biomechanics* **76**, 212–219, 2018.
2. Hamill J., et al. *Clinical Biomechanics* **14**, 297–308, 1999
3. Bonnard M., et al. N*euroscience Letters,* **166**, 101–105, 1994

Autocorrelation and Probability Distributions in Gait-Metronome Synchronization

Ian Sloan[1], Aaron Likens[1], Joel Sommerfeld[1] and Nicholas Stergiou[1]
[1]Department of Biomechanics, University of Nebraska at Omaha, Omaha, NE USA
email: csloan@unomaha.edu

INTRODUCTION

Recent studies have shown that the temporal structure of pacing signals (e.g., visual and auditory metronomes) influences the gait dynamics observed when coordinating with those signals [1,2]. Those studies typically involve pacing signals with interbeat intervals that are either constant over time or 'noisy', with the latter case referring to a class of signals that vary with respect to their autocorrelation function. To-date, however, no studies have directly examined the role that probability distribution functions play in gait-metronome synchronization. This study examines both structure of autocorrelation functions (ACFs) and the shape of probability distribution functions (PDFs) in noisy metronomes as possible sources of information involved in the synchronization process. Pacing signals varied in terms of both ACF decay and PDF shape. Statistical results support the idea that both the ACF and PDF exert independent effects on the temporal structure of gait.

METHODS

Participants. Ten healthy subjects from the University of Nebraska at Omaha volunteered to participate.

Apparatus and Procedure. In this experiment, individual Noraxon FSR SmartLead footswitches (Noraxon USA Inc, Scottsdale, Az) were connected to the heel of each foot of each subject. Then the subject covered the foot switches with their socks and shoes. The footswitches were used to collect stride time intervals. The subject was then instructed to walk around on a track surface for 12 minutes. This baseline trial was self-paced and stride time intervals were collected. The self-paced trial was used to find the average and standard deviation for each subject's preferred walking speed and variability. Computations were performed using custom MATLAB code (MathWorks, Natick, MA).

After performing the baseline condition, subjects walked in four pacing conditions. Trial order was randomized. The trials were Pink-Gaussian, Pink-Uniform, White-Gaussian, and White-Noise. Here, Pink and White refer to long-range and zero autocorrelation, respectively. Gaussian and Uniform refer to standard probability distributions. The noises were delivered as a visual stimulus. A small video screen was attached to a pair of glasses to allow the subject to see the screen with their right eye, and the environment with their left eye. The stimulus screen consisted of two fixed horizontal bars, one on the top and one on the bottom of the display. A third moving horizontal bar was placed between the two bars and moved up and down. When the bar reached the top, the subject was instructed to strike with their right heel while walking. The moving bar timing was based on the mean and standard deviation of the subject's preferred walking speed, and the statistical properties implied by each experimental condition (e.g., Pink-Gaussian). All trials lasted for 12 minutes.

Analysis Strategy. Stride time series were analyzed using Detrended Fluctuation Analysis in order to compute the Hurst exponent, a measure of statistical persistence. Experimental data were analyzed with 2_W(ACF: Pink, White) × 2_W(PDF: Gaussian, Uniform) ANOVA.

RESULTS AND DISCUSSION

That statistical analysis revealed a main effect of ACF, $F(1,9)=93.16$, $p<0.001$, as well as a main effect of PDF, $F(1,9)=6.35$, $p<0.05$. The two-way interaction was not significant. These results show that the Hurst exponents were larger in the Pink condition than in the White condition. Similarly, Gaussian distributions produced larger Hurst exponents than did Uniform conditions.

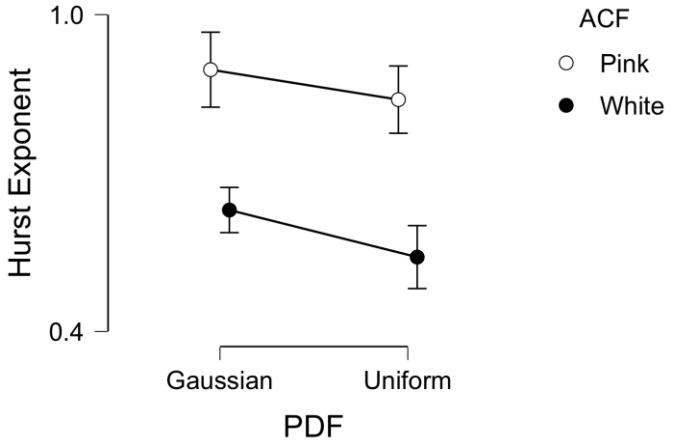

Figure 1: Hurst exponent as a function of autocorrelation and probability distribution functions.

CONCLUSIONS

In this study, we investigated the relative influence of autocorrelation and probability distribution functions on gait variability. These results suggest that both ACFs and PDFs provide relevant information that influences the time-varying structure of stride time intervals. Importantly, these properties appear to exert their influence in a relatively independent manner. Future research will investigate a broader range of ACFs and PDFs and their relevance to pathological gait.

REFERENCES

1. Kaipust, J.P., et al., *Ann Biomed Eng*, **41**(8), 1595-1603
2. Hunt, N., et al., *Sci Rep*, **4**, 5879

ACKNOWLEDGEMENTS

This work was supported by NIH P20GM10909

Sensory Neuroprosthesis Feedback Impacts Movement Planning in Obstacle Clearing

Courtney E. Shell[1*], Hamid Charkhkar[2], Breanne P. Christie[2], Paul D. Marasco[1], and Ronald J. Triolo[2]
[1] Cleveland Clinic and Louis Stokes Cleveland VA Medical Center, Cleveland, OH, USA
[2] Case Western Reserve University and Louis Stokes Cleveland VA Medical Center , Cleveland, OH, USA
Email: *shellc@ccf.org *corresponding author email

Introduction

The nervous system maintains an internal model that predicts outcomes of current motor commands and plans future movement [1]. After limb loss, this model adapts to changes in the limb and sensorimotor feedback, but deficits and sensory misperceptions remain. For example, affected side toe clearance is less than that on the intact side, and has been linked to tripping [2]. Restoring sensorimotor feedback could help reduce deficits and improve internal model predictions. Our team previously developed a sensory neuroprosthesis (SNP) that delivers electrical stimulation to amputees' residual nerves to induce sensations of foot sole pressure [3]. We used a virtual obstacle crossing task to test the hypothesis that amputees would clear obstacles with their prosthesis more similarly to their intact side when receiving restored sensory feedback.

Methods

Two below-knee amputees (Par1, Par2) who had received 16-contact nerve cuff electrodes in their residual limbs walked on a split-belt treadmill at their self-selected walking speed while viewing a virtual path (V-Gait, Motek Medical). Each participants' SNP interfaced with their everyday prosthesis. We identified electrode contacts and stimulation parameters that produced somatosensory percepts in the toes and heel of the missing foot. Sensation onset and intensity were linked to pressure readings from matching locations on instrumented shoe insoles. Body position was recorded using a 10-camera motion capture system (Nexus 1.8.5, Vicon). Obstacles of 3 different heights were presented on one side of the virtual path in a random order a total of 7 times each per trial. Two trials each were collected with obstacles presented on the intact and affected sides, and trial order was randomized. Maximum toe height during steps over obstacles was measured. All trials were repeated with the SNP active and inactive. Statistical comparisons for each participant were made with 3-way ANOVAs (leg, obstacle, SNP active/inactive) with Bonferroni-corrected post-hoc tests.

Results and Discussion

With the SNP off, Par1 stepped higher with his affected limb than with his intact limb, overshooting the obstacles ($p<0.001$, Figure 1). With the SNP on, maximum toe height decreased for both legs, decreasing affected side overshoot of true obstacle height ($p=0.0002$, Figure 1). Par2 undershot obstacles with his affected leg ($p<0.001$), slightly more so when the SNP was turned on (Figure 1).

Both participants decreased their maximum toe height when receiving SNP feedback. Interestingly, Par2 did this despite already undershooting the obstacles. Par1's affected side toe clearance became more similar to that of his intact side. This suggests that with SNP feedback, amputees' perceived ability to clear obstacles improved (i.e., they felt that they could safely step over an obstacle with their foot closer to it). Able-bodied persons balance minimizing energy expenditure and maximizing foot clearance when crossing obstacles [4]. It is possible that the amputees shifted away from seeking additional clearance in favor of decreasing energy expenditure while using the SNP. It would be interesting to measure energy expenditure during this task.

The amount that participants lifted their foot to clear a virtual obstacle could be linked to their perception of their foot's location. Amputees often perceive that their phantom recedes proximally [5] and that the leg is shorter than it truly is. Previously, after a month of receiving sensory stimulation, Par1 reported that his missing foot moved from the end of his stump to the floor; Par2 reported that his foot remained tied to the end of his stump [3]. Par2's perception that his leg is shorter than it is may have caused him to undershoot the virtual obstacles.

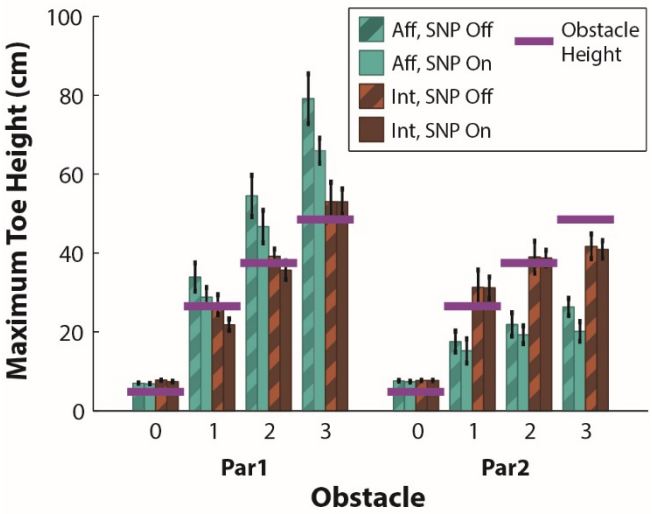

Figure 1: Example toe marker maximum height in unobstructed walking (0) and when stepping over virtual obstacles of different heights (1, 2, 3) for two participants. Results for stepping with the intact leg (brown, Int) and the affected leg (green, Aff) when the SNP was inactive (striped bars, Off) and active (solid bars, On) are shown.

Significance

Sensory neuroprostheses can provide feedback that influences motor control decisions and movement planning.

Acknowledgments

This work was supported by the Defense Advanced Research Projects Agency (DARPA) and Space and Naval Warfare Systems Center Pacific (SSC Pacific) under Contract No. N66001-15-C-4038 and performed using resources and facilities of the Louis Stokes Cleveland VA Medical Center.

References

[1] Wolpert et al., *Science.* 269:1880-2; 1995.
[2] Rosenblatt et al., *Prosthet Orthot Int*. 41:387-92; 2017.
[3] Charkhkar et al., *J Neural Eng*. 15:056002; 2018.
[4] Lu et al. *Gait Posture.* 36:552-6; 2012.
[5] Giummara et al., *Brain Res Rev*. 54:219-32; 2007.

Effects of reinforcement feedback on locomotor adaptation with a 'virtual' split-belt paradigm

Sumire Sato[1], Ashley Cui[2], Julia T Choi[1, 3, 4]
[1]Neuroscience and Behavior program, University of Massachusetts Amherst, Amherst MA, [2]Public Health sciences program, University of Massachusetts Amherst, Amherst MA, [3]Department of Kinesiology, University of Massachusetts Amherst, Amherst, MA, [4]Department of Applied Physiology and Kinesiology, University of Florida, Gainesville, FL
Email: ssato@umass.edu

Introduction

Visuomotor adaptation is a learning process that allows us to maintain movement accuracy (e.g., foot placement). We previously showed that visuomotor adaptation to mismatched visual feedback between two legs (i.e., 'virtual' split-belt) can alter gait symmetry during treadmill walking.[1] The objectives of the current study were to examine the effects of rewarded and punished reinforcement feedback on 'virtual' split-belt adaptation during (1) initial exposure, and (2) re-adaptation 24 hrs after initial adaptation. Based on previous studies using upper limb tasks,[2,3] we hypothesized that rewarded feedback will show greater adaptation and faster re-adaptation compared to those with punished feedback, and those without reinforcement feedback.

Methods

27 healthy young adults (20.4 ± 2.5 yrs) walked with visual feedback of toe position and stepping targets, where the visuomotor gain (VM gain; i.e. relationship between treadmill and screen space) was altered for each leg separately. All participants completed two sessions, ~24 hrs apart. Each session consisted of (1) 5 min familiarization (no visual feedback); (2) 300 steps pre-slow baseline (VM gain 0.9:0.9), (3) 300 steps pre-fast baseline (VM gain 1:1), (4) 600 steps adaptation (VM gain 0.9:1) with targets on the side with lower gain moving slower than the other, (5) 600 steps post-adaptation (VM gain 1:1). Participants were randomly assigned to control (CON; n= 9; did not receive scores), reward (REW; n = 9; received scores that increased by 1 for each accurate step ± 4 cm target), and punishment (PUN; n = 9; received scores that decreased by 1 for each inaccurate step > 4 cm from target) groups. Scores were presented during the adaptation periods.

Normalized step length symmetry was calculated for each stride and averaged across each baseline (first 10 strides), early and late adaptation (first and last 10 strides, respectively), and early and late post-adaptation. We measured the storage of adaptation (i.e., after-effects) as the % ratio between early post-adaptation and late adaptation on day1. The difference (Δ) in symmetry during early-adaptation between day2 and day1 was calculated to quantify difference between initial and re-adaptation.

Results and Discussion

All participants altered step length symmetry during 'virtual' split-belt walking. During adaptation, participants altered their gait mechanics so that the slow leg (VM gain = 0.9) gradually took longer step lengths. During post-adaptation, after-effects were observed, and step lengths gradually returned to symmetry.

Day 1 (initial adaptation): There were no significant group differences in the adaptation of step length symmetry ($F(2,24) = 1.0$, $p=0.4$; Fig. 1a). There were also no significant group differences in %after-effects of step length symmetry ($F(2,24)=2.9$, $p=0.8$; not shown), suggesting reinforcement feedback does not affect the acquisition phase of walking adaptation.

Day 2 (re-adaptation): PUN showed significantly greater step length symmetry on day 2 compared to day 1 ($t(8) = 6.0$, $p<0.001$). This between-session difference in early adaptation was not significant for CON ($t(8)=1.9$, $p = 0.1$) or REW groups ($t(8)=-0.4$, $p=0.7$). Faster re-adaptation in PUN may reflect consolidation of motor adaptation.[4] Δ SL symmetry between day2 and day1 was significantly greater in PUN compared to REW ($p = 0.014$; Fig. 1B). In contrast, previous studies have shown that reward (but not punishment) enhances learning and consolidation of upper extremity motor tasks.[2,3] Our results suggests that reinforcement feedback may affect upper extremity and locomotor adaptation differently.

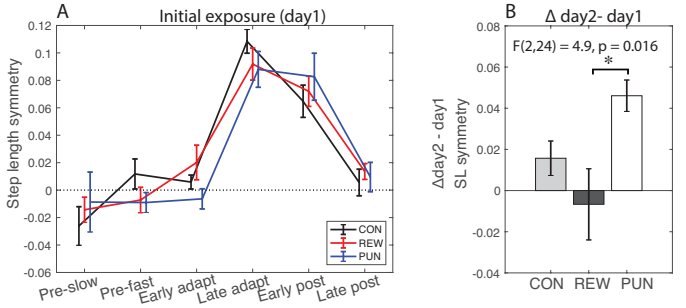

Figure 1: Average SL symmetry during initial exposure (A) and ΔSL symmetry between day2 and day1(B) with SE for CON, REW, and PUN. * indicates group differences $p < 0.05$.

Overall, our results suggest that reinforcement feedback alters re-adaptation, but not initial exposure to visuomotor walking adaptation.

Significance

'Virtual' split-belt paradigm may be a potential alternative intervention to address spatially asymmetrical gait. To maximize the re-learning with repeated exposure to the intervention, it may be beneficial to give punished reinforcement feedback on lower extremity interventions.

Acknowledgments

We thank Yeun Hiroi, Maia Schlechter, and Adam Lee for assistance with data collection, and support from NSF award #1753026.

References

[1] Choi JT, et al. 2014. Adapting gait symmetry with visually guided locomotor training: 'virtual' split-belt walking adaptation. Proceedings of the World Congress of Biomechanics. [2] Wachter T, et al. 2009;29(2):436-443. [3] Abe M, et al. 2011;21(7):557-562. [4] Krakauer JM, Shadmehr R. 2006;29(1):58-64.

Older Adults Retain the Ability to Predict External Perturbations Using Auditory Cues Only

Huaqing Liang, Tippawan Kaewmanee, and Alexander S. Aruin
Department of Physical Therapy, University of Illinois at Chicago, USA
Email: vliang@uic.edu

Introduction

To maintain balance and prevent destabilization, humans utilize anticipatory postural adjustments (APAs) prior to the postural perturbations based on predictions and past experience. APAs involve the activation and inhibition of the trunk and leg muscles and a shift of the center-of-pressure (COP) position [1]. The generation of APAs majorly relies on the availability and accuracy of visual information. However, our previous work showed that young adults could rely on an auditory cue only to generate APAs for an external perturbation similar to that when the visual information was available [2]. Older adults generally have diminished APAs and consequently diminished postural control when postural perturbations occur [3]. In this study, we aimed to train older adults to rely on an auditory cue to generate APAs in response to an external perturbation, and examine the retention of this learning effect after 1 week.

Methods

Five older adults (3M/2F, mean age 70.3±6.6 years) took part in this pilot study. They were instructed to stand on a force plate and be prepared for an pendulum hitting their front shoulders bilaterally. An additional weight (3% of the body weight) was attached to the pendulum. During the first visit, participants received the external perturbation while vision was available (BLV, 5 trials), and while vision was blocked (BLNV, 5 trials). Then they received training (Tr, 50 trials) when vision was blocked but an auditory cue signaling the moment of the pendulum release was provided. After 1 week, retention (Re) was tested when particiapants received the perturbation with the vision blocked but the same auditory cue was provided (10 trials).

The moment of pendulum impact (T0) was identified using an accelerometer attached to the pendulum. Muscle activities were recorded from the right tibialis anterior (TA), medial gastrocnemius (MG), rectus femoris (RF), biceps femoris (BF), rectus abdominus (RA), and erector spinae (ES). Muscle latency was defined as the first time point within a window of 50 ms that the EMG amplitude was consistently greater (activation) than or smaller (inhibition) than its baseline value (-500 to -350ms) ± 2SD. The COP displacements in the anterior-posterior direction at T0 and its peak value after T0 were identified.

Data were organized into 5-trial blocks. Data from the BLV, BLNV, last block of training (Tr10), and two blocks of retention (Re1 and Re2) were used for further analysis. A series of one-way repeated measures ANOVAs were conducted. Statistical significance was set at $\alpha = 0.05$.

Results and Discussion

In BLV condition, latencies of the muscles were detected prior to T0. In the BLNV condition, the latencies were detected mostly after T0. In the Tr10 and Re2 conditions, latencies were comparable to that of the BLV condition. Statistical analysis showed significant differences among conditions for the latencies of TA, MG, RF, BF, and ES (all $p<0.05$).

When vision was available (BLV), older adults moved their COP posteriorly prior to the perturbation impact (APA phase) and demonstrated a small peak displacement after the physical contact of the pendulum. In the BLNV condition, the COP at T0 was close to 0, and the peak displacement was larger. Statistical analysis showed significant differences among conditions for COP peak ($p<0.05$).

These results suggest that after only one session of repetitive training, older adults could learn to generate APAs for an otherwise unpredictable postural perturbation relying on an auditory cue, which also resulted in reduced postural disturbance after the perturbation impact. After 1 week, they partially retained this ability; furthermore, after only 5 repetitions of enforcement, they regained this ability to predict external perturbations relying on an auditory cue only.

Significance

Auditory cues could be used in a training protocol to improve the generation of APAs and consequently to improve overall postural control in older adults.

References

[1] Bouisset & Zattara. J Biomech 20, 735-742, 1987.
[2] Liang et al. Exp Brain Res (In press) 2020. Doi: 10.1007/s00221-020-05738-6.
[3] Kanekar & Aruin. Exp Brain Res 232, 1127-1136, 2014.

Table 1: Mean (SE) of the COP variables and latencies of muscles

	Latencies (ms)						COP (m)	
	TA	MG	RF	BF	RA	ES	COP T0	Peak
BLV	-109 (29)	-204 (40)	-175 (20)	-108 (14)	-43 (35)	-102 (64)	-0.048 (0.010)	-0.192 (0.021)
BLNV	34 (7)	-80 (53)	34 (6)	62 (6)	26 (12)	27 (28)	0.002 (0.006)	-0.275 (0.013)
Tr10	-118 (32)*	-134 (12)*	-96 (29)* ^	-85 (36)*	-14 (31)	-148 (40)*	-0.057 (0.031)	-0.209 (0.016)*
Re1	19 (22) ^	-180 (34)*	-30 (16)* ^	32 (27) ^	-16 (17)	-119 (18)*	-0.025 (0.014)	-0.237 (0.021)* ^
Re2	-47 (26)*	-172 (13)*	-83 (16)* ^	-10 (44)*	-38 (20)	-103 (13)*	-0.041 (0.025)	-0.203 (0.012)*
P value	0.0009	0.0342	<0.0001	0.0005	0.5066	0.0224	0.0809	0.0007

Note: For COP data, positive values represent anterior displacements and negative values represent posterior displacements.* denotes a difference compared to the BL_NV condition, and ^ denotes a difference compared to the BL_V condition.

Young Adults Can Learn to Predict Unexpected Posterior Perturbations Using an Auditory Cue

Huaqing Liang, Tippawan Kaewmanee, and Alexander S. Aruin
Department of Physical Therapy, University of Illinois at Chicago, USA
Email: vliang@uic.edu

Introduction

To reduce the effect of an expected postural perturbation, the central nervous system uses anticipatory postural adjustments (APAs), which include the activation and inhibition of the postural muscles and a slight shift of the center-of-pressure (COP) position [1]. The generation of APAs majorly relies on the availability of visual information, and is learned through past experience. Hence, such protective mechanism to maintain balance is not implemented when perturbation comes from one's back unexpectedly. Our previous work showed that young adults could rely on an auditory cue only to generate APAs for a front perturbation similar to that when vision was available [2]. So the purpose was to evaluate whether adults could learn to generate APAs for an external perturbation coming from the back relying only on an auditory cue.

Methods

Six young adults (mean age 31.5±4.1 years) participated in this pilot study. They were instructed to stand on a force plate, look forward and be prepared for an pendulum hitting their shoulders bilaterally from the back. An additional weight (3% of the body weight) was attached to the pendulum. At first, the participants received perturbation with no cues provided (baseline, BL, 5 trials). Then they received training (Tr, 50 trials) when an auditory cue signaling the moment of the pendulum release was provided via headphones. After a resting period of 5 minutes, they were tested by receiving the perturbation with the same auditory cue (Test, 5 trials).

An accelerometer attached on the pendulum was used to identify the moment of impact (T0). Muscle activities were recorded from the right tibialis anterior (TA), medial gastrocnemius (MG), rectus femoris (RF), biceps femoris (BF), rectus abdominus (RA), and erector spinae (ES). Muscle latency was idefined as the first time point within a 50ms window that the EMG amplitude was consistently greater (activation) than or smaller (inhibition) than its baseline value (-500 to -350ms) ± 2SD. The COP displacements in the AP direction at T0 and its peak value after T0 were identified.

Data were organized into 5-trial blocks. Data from the BL, one block from the beginning (Tr1), middle (Tr5), and the end (Tr10) of training, and the Test were used for further analysis. A series of one-way repeated measures ANOVAs were conducted. Statistical significance was set at $\alpha = 0.05$.

Results and Discussion

In the BL condition, muscle latencies were detected after T0, COP displacement at T0 was close to zero, and the peak displacement was large. These results suggest that no APAs were generated for an unexpected perturbation coming from the back. After some training (Tr5, Tr10, and Test), muscle latencies were detected earlier and prior to the physical impact of the perturbation, which were more noticeable for the dorsal muscles (Figure 1). Additionally, from Tr1 through Test, a slight anterior shift of COP was observed at T0 (APA phase), and the peak displacement gradually decreased (Figure 2).

Statistical analysis showed condition effect for latencies of MG and BF, and COP peak displacement (all $p<0.05$). In Figure 1 and 2, * and ^ denote a difference compared to the the BL and Tr1 condition, respectively.

The activation of frontal muscles and inhibition of dorsal muscles prior to the foreseeable frontal perturbations was reported before [3]. After some training (Tr5, Tr10, and Test), we observed an reverse pattern of early activation of dorsal muscles prior to the impact of the posterior perturbation.

Figure 1

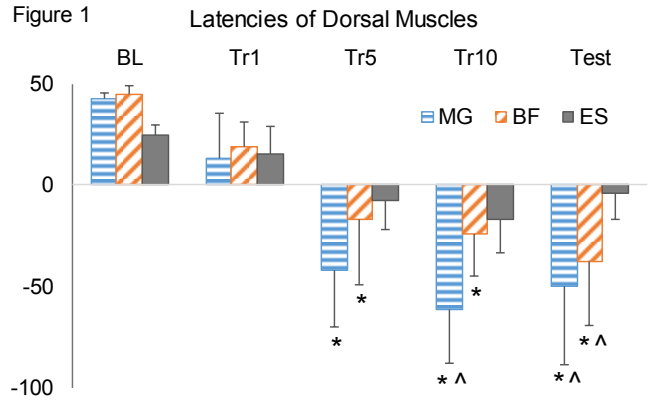

Figure 2

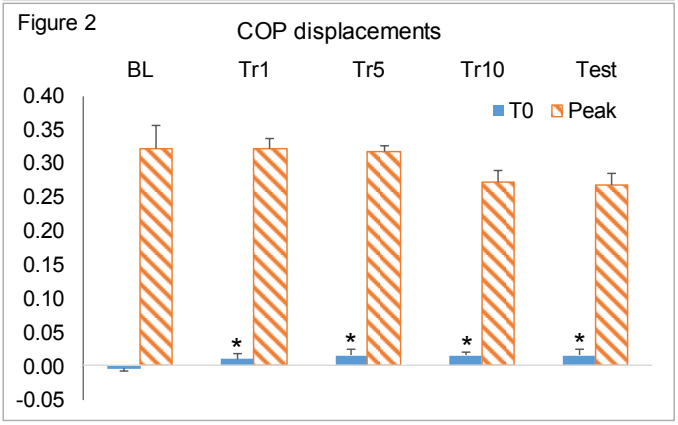

Significance

After only one session of repetitive training, young adults could learn to generate new APA patterns for an unpredictable postural perturbation relying on an auditory cue. Further study will explore the feasibility of using auditory cues for the generation of APAs and reduction of postural destabilization in response to unexpected external perturbations from the back in indivudals with balance problems (i.e. older adults).

References

[1] Bouisset & Zattara. J Biomech 20:735-742, 1987.
[2] Liang et al. Exp Brain Res (In press) 2020. Doi: 10.1007/s00221-020-05738-6.
[3] Massion. Prog Neurobiol 38:35-36, 1992.

Sex Differences of Motor Units Associated with ACL Injury and Arthrogenic Muscle Inhibition

Nathan D. Schilaty[1], April L. McPherson[1], Takashi Nagai[1], Nathaniel A. Bates[1], Timothy E. Hewett[2]
[1]Mayo Clinic Biomechanics Laboratories & Sports Medicine Center, Rochester & Minneapolis, MN, USA
[2]Hewett Consulting, Minneapolis, MN, USA
Email: schilaty.nathan@mayo.edu

Introduction

Females have 4-6x greater risk than males for an anterior cruciate ligament (ACL) injury.[1] ACL injury induces a presynaptic reflex inhibition of joint musculature, termed arthrogenic muscle inhibition (AMI).[2] AMI prevents complete activation of the muscle and may impede long-term recovery. AMI likely manifests differently between sexes and warrants exploration for improved, individualized rehabilitation, especially as females are at higher risk of second injury.[3] The objectives of this study were to determine motor unit (MU) characteristics of thigh musculature between sexes and determine MU adaptations from ACL injury and rehabilitation compared to controls.

Methods

Decomposed electromyography (dEMG) was acquired with a five-pin array sensor (Delsys *Bagnoli*; Natick, MA) placed on four major thigh muscles from 56 subjects [Female (n=32); Control (n=25)]. ACL subjects were longitudinally assessed at Pre-ACL reconstruction (ACLR), 6-mo, and/or 12-mo post-ACLR. Data was acquired at 20 kHz from isometric contractions (quads, hams) with force measured by a custom load cell apparatus (MLP-300). Acquired dEMG data (band-pass filtered 20 – 1750 Hz) was analyzed with *dEMG Analysis* software to extract average firing rate (Avg FR), inter-pulse interval, recruitment thresholds [% maximal voluntary isometric contraction (%MVIC)], and MU action potential (MUAP) from detected MUs (≥90% accuracy, **Fig. 1**). Standard least squares analyses were performed in *JMP Pro 14* on data normalized to Force*Mass (force production dependent on body size). To ensure parametric data for linear regressions, *Cube Root*, *Log*, and *Logit* transformations were selected as appropriate.

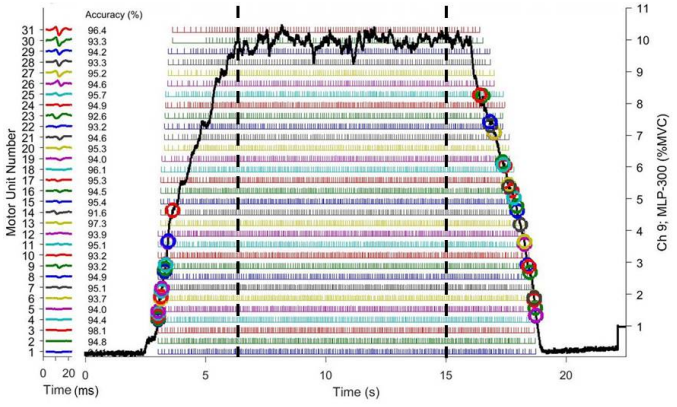

Figure 1: **Isometric Waveform and MU Identification.** With each contraction, the subject followed a trapezoidal waveform with a 3 sec ramp-up, 10 sec hold, and 3 sec ramp-down. The output force is shown (black line). This trial (10% MVC), identified 31 MUs (accuracy ≥ 90%). MU recruitment and derecruitment time are denoted by a colored circle while firing pattern is demonstrated by color-matched spikes. Data for this analysis was specifically windowed during the plateau phase of contraction (7–15 sec; dashed lines).

Results and Discussion

MUs are variably recruited and FR regulated to produce motor control. Regression of Avg FR amplitude by recruitment threshold demonstrated significance of least-squares means for Pre-ACLR, 6-mo, and 12-mo post-ACLR from controls for males and females (p<0.001). Compared to males, females maintained greater Avg FR (**Fig. 2**). Regression of MUAP peak-to-peak amplitude demonstrated significance of higher least-squares means for males at Pre-ACLR (p<0.001) and 6-mo (p=0.02); amplitude was significantly lower for females across all ACLR time points (p<0.001).

Significance

Decreased Avg FR after injury and across rehabilitation was demonstrated by both sexes, but more prevalent in males. As MUAP amplitude is a surrogate for MU size, females demonstrated smaller MUs than controls. Lack of larger MUs likely leaves females susceptible to further injury with higher demand activities. This information is vital to implement more personalized neuromuscular therapy following ACL injury, especially for females.

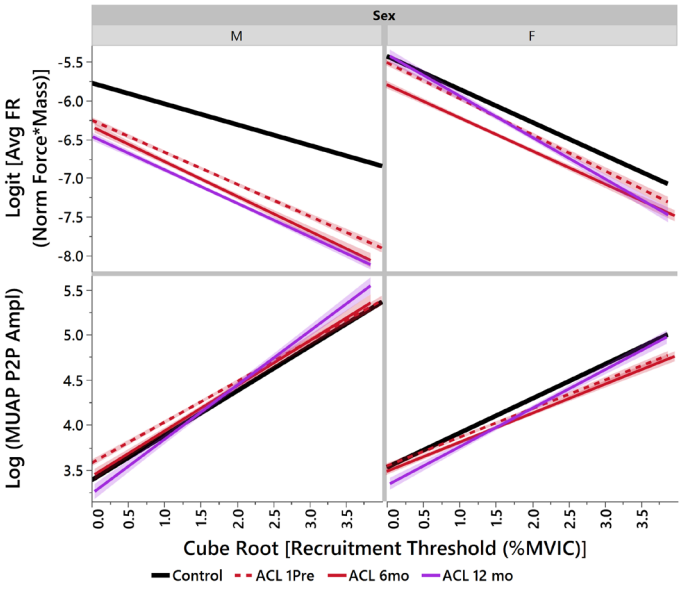

Figure 2: **Sex Differences of Quadriceps Avg FR and MUAP Peak-to-Peak Amplitude by Recruitment Threshold.** All R^2 values range between 0.1 – 0.52. Males demonstrated larger MU recruitment and females smaller MU recruitment than controls (MUAP P2P Ampl).

Acknowledgments

Mayo Clinic Ultrasound Research Center and NIH funding: R01AR055563, K12HD065987, and L30AR070273.

References

1. Hewett et al. *Am J Sports Med* (2006) 34(2):299-311.
2. Hopkins et al. *J Sport Rehab* (2000) 9(2):135-159.
3. Paterno et al. *Am J Sports Med* (2014) 42(7):1567-1573.

Vibrotactile cueing improves kinematic recovery after unexpected slip perturbations induced by a split-belt treadmill

Beom-Chan Lee*[1], Bernard J. Martin[2], Junmo An[1], and Kap-Ho Seo[3]
[1]Department of Health and Human Performance, University of Houston, Houston, USA
[2]Department of Industrial and Operations Engineering, University of Michigan, Ann Arbor, USA
[3]System Control Research Center, Korea Institute of Robot and Convergence, Pohang, South Korea
Email: *blee24@central.uh.edu

Introduction

The design of shoe-based technologies has the potential to detect hazards leading to falls and alert the user to an impending risk via visual, audible, and/or vibrotactile precues (e.g., [1]). Vibrotactile cueing is possibly the most advantageous because it does not interfere with the visual and auditory cues that also monitor walking. This study evaluates the effect of vibrotactile precues on the user's kinematic recovery performance after unexpected slip perturbations induced by a split-belt treadmill.

Methods

Our fall-inducing platform incorporating a programmable split-belt treadmill equipped with two force plates (Bertec Corp.) generated slip perturbations by accelerating one of two belts in the anterior direction [2]. A linear vibrating actuator (C2 tactor, Engineering Acoustics Inc.) was placed on the skin of the left lower leg for vibrotactile cueing. A 12-camera motion capture system (VICON, Vicon Motion Systems Ltd.) captured the whole body kinematics from 35 reflective markers.

A total of ten healthy young adults (5 females and 5 males) completed 6 experimental trials: 2 consecutive trials without vibrotactile cueing and with a slip perturbation (control trials); 3 trials with vibrotactile cueing (2 trials with the slip perturbation (cueing trial) and 1 trial without the slip perturbation (catch trial)); and 1 trial without vibrotactile cueing and with a slip perturbation (post-control trial). During the control, cueing, and post-control trials, the slip perturbation was randomly applied to the left foot between the 31st and 40th step. Each trial included a standing period, walking period, and recovery period from the perturbation onset to the return to normal walking. The three trials with vibrotactile cueing were randomized.

The Nexus 1.8 ran the Plug-in-Gait model to compute the whole body kinematics. MATLAB (MathWorks) was used to compute trunk angular dispersion (AD) and trunk range of motion (ROM) as an average during the three periods in the sagittal plane. The 2 control trials and 2 trials with vibrotactile cueing were averaged as a function of the period for each participant. Statistical analyses were performed using SPSS (IBM Corp.). A two-way ANOVA determined the main effect of the four trial conditions (control, cueing, catch, and post-control), the three periods, and their interactions for trunk AD and trunk ROM. Post hoc analysis was conducted using the Šídák method.

Results and Discussion

Figure 1 shows the results of the trunk AD and the trunk ROM, including the statistical significance from the post hoc multiple comparisons. Post hoc analysis showed that trunk AD and trunk ROM were significantly higher during the recovery period than the standing and walking period for the control, cueing, and post-control trials. Post hoc multiple comparisons of trunk AD and trunk ROM were not significantly different between the walking and recovery periods for the catch trial. Post hoc analysis also showed that trunk AD and trunk ROM were significantly higher during the walking period than the standing period regardless of the trial condition. Post hoc analysis showed that the catch trial had the smallest trunk AD and trunk ROM for the recovery period compared to the other trials.

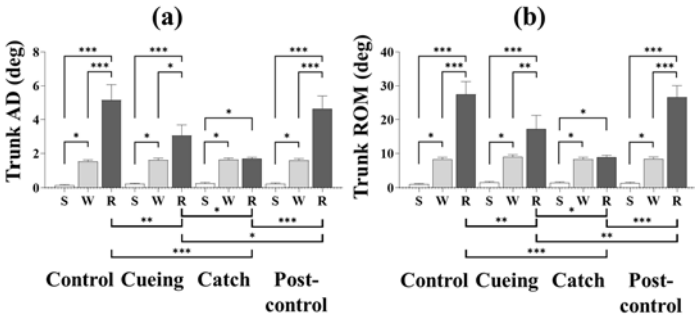

Figure 1: Average trunk AD and trunk ROM as a function of the trial condition and period across all participants. S, W, R indicate standing, walking, and recovery periods, respectively. Error bars indicate standard error of the corresponding mean (* $p < 0.05$, ** $p < 0.01$, and *** $p < 0.0001$).

The results confirmed that vibrotactile cueing facilitates the adequate timing of reactive motor responses after a slip perturbation. We assume that a precue constitutes an alert to prepare for motor action in the brain [3]. The results of the catch trial imply that vibrotactile cueing did not trigger anticipatory motor action because the kinematic behavior is not significantly different during the recovery period and the walking period.

Significance

We believe that our findings can inform the design of wearable technologies that alert users to the risks of falling via vibrotactile cueing, and can assist with developing new gait perturbation paradigms that prompt reactive responses.

Acknowledgments

This work was supported by the ICT R&D program of MSIP/IITP (2017-0-01724). The authors thank Dongyual Yoo for collecting and processing data using the Nexus 1.8.

References

[1] J. Zhang, C. W. Lip, S. K. Ong, and A. Y. C. Nee, "Development of a shoe-mounted assistive user interface for navigation," *Int J Sensor Netw,* vol. 9, pp. 3-12, 2011.
[2] B. C. Lee, B. J. Martin, T. A. Thrasher, and C. S. Layne, "The effect of vibrotactile cuing on recovery strategies from a treadmill-induced trip," *IEEE Trans Neural Syst Rehabil Eng,* vol. 234, pp. 235-243, 2017.
[3] A. Riehle, *Preparation for action: one of the key functions of the motor cortex*. Boca Raton: CRC-Press, 2005.

Perceptual Motor Abilities of Professional eSports Gamers

Haneol Kim.[1], Jianhua Wu[1]
[1]Georgia State University. Email: hkim162@student.gsu.edu

Introduction

eSports is a form of sports primarily using electronic systems (Hamari & Sjöblom, 2017). Players must be able to anticipate a stimulus and react to it as quickly and accurately as possible by manipulating a keyboard and/or a mouse. Playing eSports games demands a high level of perceptual, attentional, cognitive, and fine motor skills (McDermott, et al., 2014). Perceptual motor abilities such as anticipation timing, eye-hand coordination, and peripheral perception are important factors to win a game.

eSports professional players often undergo intensive training at least 10 hours a day. Previous research showed that more experience in playing eSports games enhanced perceptual, attentional, and cognitive skills (Dobrowolski, et al. 2015). However, little is known on the perceptual motor abilities of eSports professional players. Therfore, the purpose of this study was to compare perceptual motor skills between eSports professionals and amateurs. We hypothesized that professionals will show better performance than amateurs in anticipation timing, eye-hand coordination, and peripheral perception.

Methods

Eight male eSports professionals (age 23.8±1.9 years) and eight male amateurs (24.7±2.1 years) participated in this study. Professionals had an eSports professional experience of 3-10 years. A Bassin anticipation timer was used to provide sequential LED light stimuli at various speeds (1mph, 3mph, 6mph, 9mph). Participants were asked to press a button upon the arrival of the moving stimulus at target. A negative anticipation timing means pressing a button before the arrival of the stimulus and a positive timing means after the stimulus. A rotary pursuit device was used to measure eye-hand coordination: (a) under different directions (clockwise, counterclockwise) and (b) under different tasks (triangle, circle, square). Participants tracked the moving target at 30 rpm with the electronic stylus for 30 seconds and time-on-target was obtained in seconds to quantify eye-hand coordination. Peripheral perception was measured in degrees with a Vienna test system which gave random light stimulus from both the left and right sides and participants responded by pressing the foot pedal. A two-way mixed ANOVA was conducted on anticipation timing and eye-hand coordination duration and a t-test on peripheral perception angle at the significant level of alpha=0.05.

Results and Discussion

While amateurs generally decreased the anticipation timing with stimulus speed, professionals maintained negative timings (Fig. 1). There was a group by speed interaction (p=0.023). A post hoc analysis revealed that professionals had a lower timing than amateurs at 1 mph (p=0.001), and amateurs changed the timing from positive to negative from 1mph to 6mph. In general, professional players showed better timing accuracy. Professional eSports players consistently anticipated earlier before the arrival of the stimulus on target across all conditions, which allowed them to defend tactically before the attack of the opponents.

Professionals showed a longer eye-hand coordination duration that amateurs in both clockwise and counter-clockwise directions (p=0.014, Table 1) and across three tasks (p=0.010). Also, professionals had a wider peripheral perception angle than amateurs (p=0.026). The results suggest that multi-year training and playing experience in manipulating a keyboard and/or a mouse rapidly and accurately results in more advanced eye-hand coordination and a wider range of peripheral perception. Overall, the results of this study are consistent with previous studies that professionals show better perceptual motor skills due to their prolonged training and playing.

Fig. 1: Anticipation timing

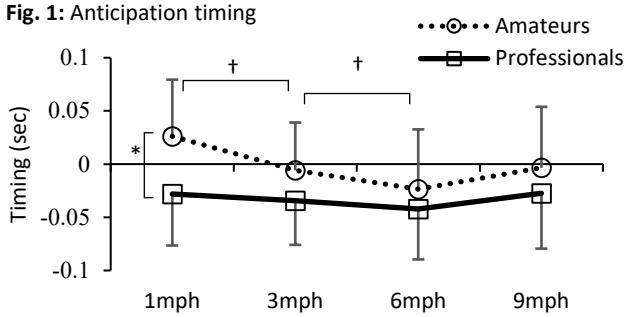

Fig. 1: Means and standard deviations of anticipation timing. Symbol * denotes a group effect and symbol † denotes a speed effect.

Table 1: Mean (SD) of eye-hand coordination & peripheal perception.

		Professional	Amateur
Direction (sec)	CW	28.92 (1.33)	28.11 (0.83)
	CCW	28.93 (0.97)	27.74 (1.10)
Task (sec)	Triangle	28.90 (1.49)	27.55 (1.65)
	Circle	28.67 (1.19)	27.56 (1.10)
	Square	29.20 (1.10)	28.66 (1.02)
Peripheral perception (°)		165.76 (10.17)	151.34 (12.92)

Significance

This study provides evidence on advanced perceptual motor abilities in professional eSports players compared to amateurs. This suggests that perceptual motor skills can be manipulated with the number of years and the intensity of training and playing. The improvement in perceptual motor skills can be found in both visual perception and muscular response to a variety of tasks. It is generally recognized that abundant repetitions of motor task training is key to effective training outcomes for individuals with motor deficits. Playing eSports may thus provide a potential rehabilitation paradigm for individuals with perceptual motor deficits. An eSports setting may help increase the enthusiasm of indviduals with perceptual motor deficits during training, and the emphasis on timing and accuracy in playing may force these individuals to improve their specific perceptual motor skills.

Acknowledgments

We would like to thank all the participants.

References

Dobrowolski, et al. (2015). *Computers in Human Behavior*, 44, 59-63.
Hamari & Sjöblom. (2017). *Internet Research*, 27, 211-232.
McDermott, et al. (2014). *Computers in Human Behavior*, 34, 69-78.

The patterning of local variability during the acquisition of a whole-body continuous motor skill in young adults

Matthew Beerse[1], Kimberly E. Bigelow[1], and Joaquin A. Barrios[1]
[1]University of Dayton
Email: mbeerse1@udayton.edu

Introduction

Initial movement variability when learning a motor skill might enable exploration of the motor space (1). When considering the affect that local variability, e.g. body segment orientation, has on global task variability, e.g. control of center-of-mass (COM), it is possible to partition local variability into two subspaces using an Uncontrolled Manifold (UCM) analysis (2). One subspace of local variability does not affect the global task goal (GEV) and the other subspace of variability affects the global task goal (NGEV). From a motor learning perspective, the GEV represents the implementation of motor solutions to achieve the task goal.

From a motor learning perspective, changes of GEV with practice provide useful interpretations. A reduction of GEV represents a reliance on fewer motor solutions, or exploitation. An increase of GEV represents utilization of more motor solutions. Evidence of both responses have been found, depending on task constraints, for upper limb tasks. However, there is a paucity of evidence for learning whole-body motor skills.

This study aimed to determine how adults modulate local variability during the acquisition of a whole-body continuous motor skill across practice sessions. We evaluated a kettlebell swing because it requires technical proficiency and the hip-hinge motion requires stable COM trajectories across repetitions.

Methods

Twelve young adults (7F/5M), aged 18-35 years participated. Subjects performed kettlebell swings on five separate days, where we collected data on the first and last day, which were one week apart. We collected data before subjects practiced the kettlebell swing (*no practice*) after subjects performed three practice sets (*immediate*) and one week later after three practice days (*short-term*). The data collection sets consisted of three sets of 20 repetitions and the practice sets consisted of five sets of 20 repetitions. Subjects rested for at least three minutes between sets to minimize fatigue.

For instruction, subjects watched an online video. A sagittal plane view was shown of a demonstration by a skilled individual. The video provided cues of the anterior/posterior (AP) motion of the hips and the vertical motion of the body. Subjects were allowed to view the video as often as they wanted. Subjects received no feedback or cues on their performance.

We collected kinematic data using a Vicon Full-Body Plug-In Gait marker set and a Vicon motion capture system (Oxford, UK). For our UCM anlaysis we constructed geometric models relating sagittal plane segment angles to AP and vertical COM position. The model consisted of 16 body segment angles, as well as the kettlebell segment angle. We time-normalized each kettlebell swing cycle and conducted a UCM analysis on every 1% of the cycle. Our referenece configuration was the average position of the COM at each 1% for that condition.

Results and Discussion

The position of the COM was more posterior and vertical during the *short-term* condition compared to the *no practice* condition. Subjects modulated their motor behavior based on the video instruction and in the absence of feedback.

Subjects reduced COM position variance in the vertical direction, but not the AP direction. There might have been a prioritization of the vertical control of the kettlebell swing. Coaching of the kettlebell swing might need to provide cues and feedback on the AP motion, as young adults internally attended to their vertical motion.

Only vertical NGEV decreased from *no practice* to *immediate*. Following initial practice, subjects reduced local variability that affected the vertical COM position, but maintained similar amounts of GEV. This maintenance might represent an exploration of motor solutions that could be beneficial when adapting the motor skill. Interestingly, the subjects who chose to watch the video the most demonstrated the least amount of GEV. This suggests a strategy to adopt a stereotypic movement pattern consistent with the model.

Following *short-term* practice, subjects reduced both AP and vertical GEV. After only a week of practice, subjects began demonstrating a reliance on fewer motor solutions to perform the the kettlebell swing. This result suggests a tendency to exploit preferred motor solutions to perform a whole-body motor skill.

	No practice	Immediate	Short-term
AP NGEV	0.004 (0.002)	0.003 (0.001)	0.002 (0.000)
AP GEV	0.026 (0.020)	0.021 (0.021)	0.015 (0.002)*
V NGEV	0.006 (0.002)	0.004 (0.002)*	0.005 (0.001)*
V GEV	0.026 (0.020)	0.021 (0.021)	0.015 (0.018)*

Table 1: Mean (SD) of the UCM subspaces for the vertical and AP directions across conditions. * indicates a significant difference from the *no practice* condition.

Significance

This study extends the exploration followed by exploitation paradigm, found in motor learning, to a whole-body continuous motor skill. These results could inform motor learning practices for other whole-body tasks, such as locomotion. Considering the tendency for exploitation, identifying techniques to encourage exploration of motor solutions might be pertinent for developing a repertoire of solutions characterized by highly skilled performers (3). In addition, GEV was sensitive to variation of instruction, which would be beneficial when evaluating cueing and feedback techniques for coaching and rehabilitation.

Acknowledgments

This work was funded by the University of Dayton Research Council Seed Grant.

References

1. Dhawale AK, et al. 2017. Annu Rev Neurosci, 40:479-498.
2. Scholz JP & Schöner G. 1999. Exp Brain Res, 126:289-306.
3. Verhoeven FM & Newell KM. 2016. Hum Mov Sci, 49:216-224.

Adaptation of Leg Forces due to Gradually Introduced Split-Belt Walking in People with Trans-Tibial Amputation

Brian P. Selgrade[1,2,*], Young-Hui Chang[1]
[1]School of Biological Sciences, Georgia Institute of Technology, [2]Department of Movement Science, Westfield State University
Email: *bselgrade@westfield.ma.edu

Introduction

People with lower limb amputations exhibit asymmetric step lengths[1], and ground reaction forces [2] during walking. These assymetries may explain the increased risk of overuse injuries like osteoarthritis on the contralateral, intact side[3].

Split-belt treadmill walking, which involves two side-by-side belts moving at different speeds, has been used to correct baseline step length asymmetries in stroke survivors [4]. These studies use error augmentation, in which the split-belt condition exacerbates the walker's baseline asymmetry. After the split-belt condition is removed, symmetry improves.

We used an error augmentation, split-belt paradigm to induce adaptation of ground reaction forces (GRFs) opposite from a person with amputation's baseline asymmetry. Prior work shows aftereffects in braking GRF, but not propulsive GRF [5]. Since people with amputation adapt to split-belt walking similarly to controls [6], we hypothesized people with amputation and their controls would exhibit aftereffects in braking GRF, but propulsive GRF for both groups would return immediately to baseline levels when the split-belt condition was removed.

Methods

Eight people with trans-tibial amputation (body weight=77 kg, intact leg length =88 cm) and eight matched controls (body weight=77 kg, leg length =89 cm) gave written, informed consent before participating in this study.

Participants completed a 2-minute, slow baseline trial with both belts moving at 75% of preferred walking speed (PWS) followed by a 90-second fast baseline trial with both belts at 150%PWS and another 90-second slow baseline trial. People with trans-tibial amputation walked with their prosthetic legs on the slow belt as the fast belt was gradually accelerated to 150%PWS from 75%PWS. Participants then walked for 3 minutes with the fast belt at a constant 150%PWS. After a rest, subjects were immediately exposed to both belts at 75%PWS. We compared GRFs, step length symmetry, double support times and stance times of the first 5 steps of post-adaptation to the last 5 steps of the 75%PWS baseline trials using repeated measures ANOVA and post hoc t-tests with Bonferroni corrections (alpha=0.0167).

Results and Discussion

With the fast (intact) leg, people with amputation and controls had significantly higher peak braking force in early post-adaptation than at baseline (Figure 1), supporting the hypothesis. However, both subject groups also had significantly lower fast leg peak propulsive force in early post-adaptation than at baseline or in late post-adaptation, which does not support the hypothesis and conflicts with previous results on GRF adaptation in healthy people [5]. This indicates that propulsive and braking forces during walking are controlled predictively, and that this control is not impaired by trans-tibial amputation. Thus, this study provides proof of principle that split-belt, error augmentation paradigms can alter kinetic asymmetry in those with amputation.

Overall, people with amputation adapted similarly to their matched controls. Both groups had significant aftereffects of step length symmetry, double support time when the fast leg was leading, and single leg stance time. These data support prior findings that people with amputation adapt to split-belt walking similarly to controls [6, 7] and extend these results to adaptation of temporal, interleg coordination (double support time).

Significance

These findings show that people with amputation can adapt their propulsive and braking forces to split-belt walking. Error augmentation caused lower propulsive and higher braking force aftereffects in the intact leg. This may not be preferable clinically, since the intact side, already at risk for osteoarthritis, increased braking force. Future work should determine joint kinetics associated with these changes in GRFs.

Acknowledgments

NICHD 5T32HD055180, NINDS 5R01NS069655 & NSF ARRA CAREER Award BCS-0847325 supported this research.

References

1. Isakov, et al. 1997. *Scand J Rehab Med* 29:75-9.
2. Engsberg, et al. 1993. *Prosth Orth Intl* 17:83-9.
3. Morgenroth, et al. 2011. *Gait Post* 34:502-7.
4. Reisman, et al. 2013. *Neurorehab Neur Rep* 27:460-8.
5. Ogawa, et al. 2014. *Neurophysiol* 111:722-32.
6. Selgrade, Toney, Chang. 2017. *J Biomech* 53:136-43.
7. Darter, et al. 2017. *PLoS ONE* 12:e0181120.

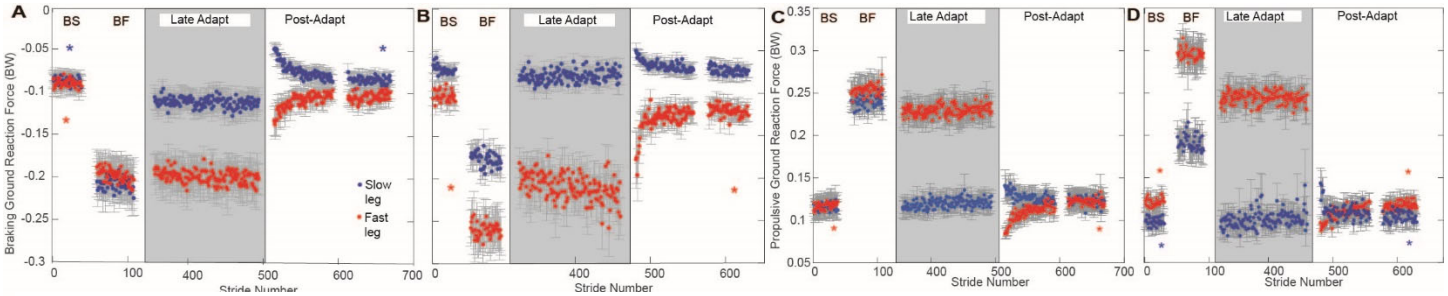

Figure 1: Peak braking GRF for matched control subjects (A) and people with trans-tibial amputation (B); and, peak propulsive GRF for controls (C) and people with trans-tibial amputation (D). * indicates a significant difference from early post-adaptation ($p<0.05$).

Structure of variance in finger forces changes with uncertainty in force tracking tasks

Paige Thompson.[1], Cooper[1], Claxton[1], and Ambike[1*]
[1]Department of Health and Kinesiology, Purdue University, West Lafayette, IN
Email: *sambike@purdue.edu * corresponding author

Introduction

Motor systems are frequently redundant, where numerous input variables contribute to achieve a motor task. Redundant motor systems display compensatory behavior in which errors in some input variables are compensated by changes in others so that the task-specific output variables are stabilized [1]. Such synergistic covariation that stabilizes task variables will also resist any volitional changes in those variables. However, anticipatory synergy adjustments (ASAs) are seen in many tasks: synergies weaken when individuals prepare to voluntarily change their motor state [2]. Furthermore, ASAs occur in response to the mere expectation of an upcoming change, and even when the timing and the nature of the change are uncertain [3]. The mechanisms for weakening a synergy are lower task-preserving covariation in the inputs, increased variability in the inputs that yields higher vriability in the task variables, or both. However, it is not known whether such uncertainty in the upcoming motor change influences the magnitude or the mechanism through which ASAs occur. Therefore, the objective of this study was to compare the ASA magnitude in isometric finger force production tasks with and without uncertainty, and to identify whether the ASAs occur via similar mechanisms in both cases.

Methods

Fourteen right-handed participants (21.6±2.4 yrs) participated in the study. They produced forces with the distal phalanx of their right-hand fingers pressing down on four force sensors (Nano 17, ATI Automation). They produced a total force (F_T) – the sum of the finger forces – to track targets presented on a computer screen in three types of tasks. All tasks began with the participant producing 10% of their maximum voluntary contraction (MVC, measured earlier). In the steady task, a square target appeared at the 10% MVC level and never moved. Participants knew that the target will not move for this task. In the uncertain task, trials began with the target at 10% MVC and began moving vertically after a random time interval. The participants knew that the target will begin to move at any time and in any direction. In the certain task, participants first produced 10% MVC force, and then produced a quick F_T increase after a fixed, predefined time interval. Each task was repeated 15 times.

The finger forces prior to any change in F_T away from 10% MVC in each task were analyzed using the uncontrtolled manifold (UCM) method [1]. The 15 trials for each task yield a distribution in the 4D space of finger forces. The across-trial variance in the forces was partitioned into a component that does not change F_T (along the UCM, V_{UCM}), and another component that changes F_T (orthogonal to the UCM, V_{ORT}). A synergy index was computed as $\Delta V = (V_{UCM}-V_{ORT})/(V_{UCM}+V_{ORT})$, which was then z-transformed (ΔVz) for statistical analysis. $\Delta Vz > 0$ implies $V_{UCM} > V_{ORT}$, and indicates the presence of a synergy (Fig, 1). Higher ΔVz indicates stronger synergy and vice versa. We computed the change in ΔVz for the certain/uncertain tasks relative to the steady task (i.e., the difference variable $\Delta\Delta Vz$). We also quantified the change in the variance components across the certain/uncertain tasks and the steady task: $\Delta V_{UCM\text{-}certain} = (V_{UCM\text{-}certain}-V_{UCM\text{-}steady})/V_{UCM\text{-}steady}$, $\Delta V_{UCM\text{-}uncertain} = (V_{UCM\text{-}uncertain}-V_{UCM\text{-}steady})/V_{UCM\text{-}steady}$, and similarly for V_{ORT}. One-sample t-tests were used to test if the difference variables $\Delta\Delta Vz$, ΔV_{UCM} and ΔV_{ORT} were significantly different from zero. $\Delta\Delta Vz > 0$ will indicate the presence of ASA, and significant changes in V_{UCM} and V_{ORT} will indicate the change in the variance structure - the specific mechanism - that yields $\Delta\Delta Vz$.

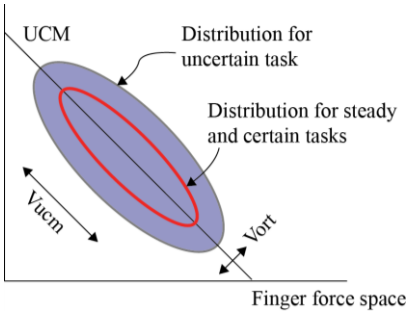

Figure 1: Finger force distributions indicating synergies that stabilize total force. Red ellipse is the distribution for the steady and certain tasks. Large ellipse is the distribution for the uncertain task.

Results and Discussion

$\Delta\Delta Vz$ was not significantly different from zero for either the certain or the uncertain task ($t_{(13)} > 0.23$; $p > 0.22$), indicating that ASA was not observed in our data. This was due to large individual differences, with six of the 14 participants exhibiting ASAs. On the other hand, task uncertainty had a consistent effect on variance structure. V_{UCM} and V_{ORT} for the certain task were not different from those for the steady task ($t_{(13)} > 0.89$; $p > 0.06$). In contrast, they were larger for the uncertain task compared to the steady task ($\Delta V_{UCM\text{-}uncertain}$ and $\Delta V_{ORT\text{-}uncertain} > 0$, $t_{(13)} > 2.79$; $p < 0.02$). Thus, the absence of ASA for the certain task arose from consistent variance components across the two tasks, whereas the absence of ASA for the uncertain task arose from compatible increases in V_{UCM} and V_{ORT} in the uncertain task (Fig. 1). Increased V_{UCM} has been associated with greater flexibility of task performance, and greater V_{ORT} has been associated with lower stability of the current task [1,2,3]. Both these mechanisms likely assist in the preparation for the uncertain change in F_T.

Significance

Investigating the performance of ill-defined or uncertain tasks provides insights about the control of finger forces. In particular, investigating changes in the variance structure (rather than just ASA) is critical for understanding the influence of task uncertainty on finger force production. Changes in variance components and individual differences in ASAs may be relevant for preventing loss of manual dexterity with aging.

References

1. Scholz, J, et al. *Exp Brain Res.* 289-306, 1999.
2. Olafsdottir, H, et al. *Neurosci Lett.* 92-96, 2005.
3. Tillman, M, et al. *J Neurophysiol.* 21-32, 2018.

Effects of asymmetrical footwear height on gait kinetics and kinematics

Sumire Sato[1,2*], Maia Schlechter[2], Adam Lee[2], Wouter Hoogkamer[2]
[1]Neuroscience and Behavior program, [2]Department of Kinesiology, University of Massachusetts, Amherst
Email: *ssato@umass.edu

Introduction

Asymmetrical stance phases and weight-bearing are common in patients with unilateral impairments such as post-stroke.[1,2] Studies have shown that interventions with unilateral shoe inserts may improve weight-bearing and stance time symmetry, and gait speed.[3-5] However, it has not been established whether humans slowly adapt and store kinetics and kinematics with asymmetrical shoe height. If humans are able to adjust to footwear with asymmetrical height and store new gait patterns this may aid in the development of novel therapeutic footwear.

The objective of this study was to examine adaptations in (1) vertical ground reaction force impulse and (2) stance time imposed by asymmetric shoe heights. Based on previous clinical studies, we hypothesized that early during adaptation with asymmetrical shoe height the leg with the shoe insert will (1) exert less force,[4,5] and be in shorter stance phase,[3] but will regain symmetry later during adaptation.

Methods

11 Healthy young adults (21.2 ± 3.1 yrs, 3 males) participated in this study. Participants walked on an instrumented treadmill at 1.3 m/s for four conditions: (1) 5 min with equal shoe height for familiarization on the treadmill, (2) 5 min baseline pre-test with equal shoe height, (3) 10 minutes adaptation with one leg with a 1cm shoe insert in one side (leg with shoe insert = "high leg"; other leg = "low leg"), (4) 10 minutes post-adaptation with equal shoe height. The side with the shoe insert during adaptation was randomized between participants.

To calculate the vertical impulse, ground reaction forces (GRF) were low-pass filtered (15 Hz, 3rd order Butterworth) and normalized to body weight. The integral of GRF were calculated for each stance phase. Stance times were normalized to stride time. The difference (Δ) between legs (low leg – high leg) was calculated for the vertical impulse and normalized stance times to quantify symmetry and then these were averaged across first 50 strides for baseline, first 50 and last 50 strides for adaptation and post-adaptation. To examine between-condition differences, we used a repeated-measures ANOVA with a Bonferroni post-hoc test.

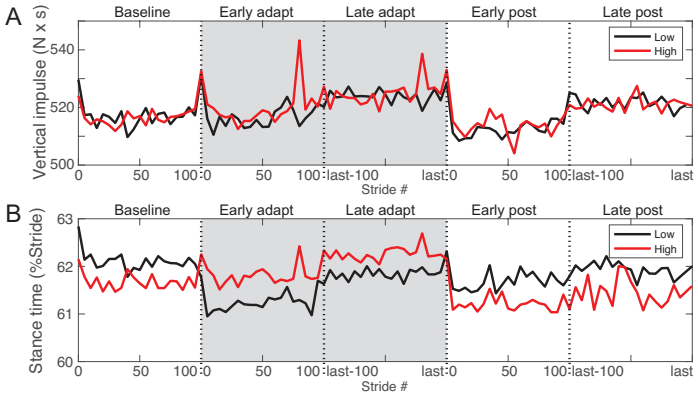

Figure 1: Group average in vertical force impulse (A) and stance time (B) for the low (black) and high leg (red). Shaded area indicates adaptation. Vertical impulse and stance times are averaged across every 5 strides.

Results and Discussion

In general, participants did not alter vertical impulse symmetry, but altered stance time symmetry with asymmetrical shoe heights (Fig. 1). Δ Vertical impulse was not different between conditions ($F(4,40) = 0.73$, $p = 0.580$), but Δ Stance time was different between conditions ($F(4,40) = 14.19$, $p < 0.001$). Δ Stance time during early and late adaptation was lower compared to baseline ($p = 0.005$, Mean difference (MD) = -1.1%; $p = 0.001$, MD = 1.0%), early post-adaptation ($p = 0.031$, MD = -0.9%; $p = 0.021$, MD = -0.8%), and late post-adaptation ($p = 0.009$, MD = -1.1%; $p = 0.025$, MD = -1.0%; Fig. 2).

We were surprised to find that stance time symmetry but not vertical impulse symmetry was significantly different during adaptation compared to baseline. This may suggest that humans prioritize force symmetry and alter stance symmetry to accommodate different shoe height. The immediate change in and nonsignificant difference in baseline and early-post stance symmetry (i.e. little to no aftereffect) suggests that healthy humans may employ reactive strategies to accommodate the change in footwear height.

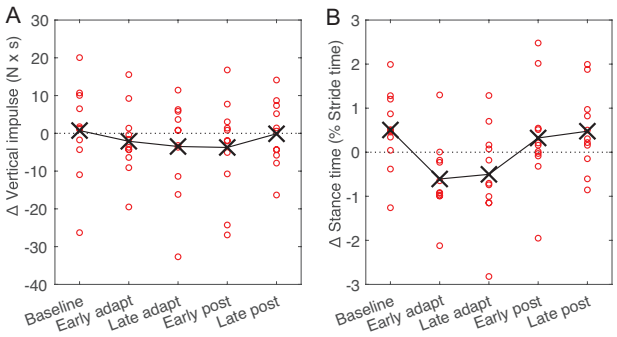

Figure 2: Group mean for vertical force impulse (A) and stance time symmetry (B). Red o's indicate data from each participant. Dotted line at 0 indicates perfect symmetry.

Significance

Asymmetrical footwear may alter temporal gait mechanics, but may not induce long-term neuroplastic changes. However, based on the variability we observed, more studies should be done on long term exposure to different asymmetrical footwear.

Acknowledgments

We would like to thank undergraduate students Yeun Hiroi, Emily Laughlin, Annie Lye, Danielle Zoppo, and our participants.

References

[1] Wall JC, et al. 1986;67(8):550-553. [2] Pattersen KK, et al. 2008;89(2):304-310. [3] Sungkarat S, et al. 2011;25(4):360-369. [4] Aruin AS, et al. 2012;19(6):556-563. [5] Rodriguez GM, et al. 2002;83(4):478-482.

Movement Variability During Dynamic Tasks In Individuals After Anterior Cruciate Ligament Reconstruction

Xenia Demenchuk, Jennifer Perry, Robert A. Siston, Laura C. Schmitt
The Ohio State University, Columbus, OH, USA
Email: demenchuk.1@osu.edu

Introduction

Individuals who undergo anterior cruciate ligament reconstruction (ACLR) often experience suboptimal post-operative outcomes[1] such as high risk of reinjury[5], low levels of returning to former level of sport[1] and increased risk of developing knee osteoarthritis[2]. Abnormal knee motion and movement patterns[3,8] have been observed following ACLR and rehabilitation which may be the cause for these suboptimal results[3] and is not currently considered in return to sport criteria[7]. The dynamic movement theory[3] proposed that there is a preferred range for movement variability; variability that is too high can lead to instability and reduced adaptability to environmental demands while variability that is too low is accompanied by lower ranges of motion. This theory into dynamic movements has been used in gait studies post-ACLR[3,4] but has not yet been used to analyze more demanding dynamic tasks, such as jumping and landing, that are commonly performed by the young, active cohort with ACL injuries. Further understanding of movement variability after ACLR during demanding tasks could provide additional insight into the suboptimal outcomes of this patient population,. Therefore, the purpose of this study was to compare lower extremity movement variability during a single leg drop test between young individuals who have undergone ACLR (ACLR group) and a Control group. We hypothesized that both limbs of the ACLR group would show increased movement variability compared to Controls, and that within the ACLR group, the involved limb would have increased movement variability compared to the uninvolved limb.

Methods

As secondary analysis of an ongoing, prospective study[8], data from a total of 100 participants after primary, unilateral ACLR (ACLR group) (M/F 30/70; 17.65±2.7 y; 168.1±10.4 cm; 66.9±14.8 kg) and 55 uninjured participants (Control group) (M/F 15/40; 17.1±2.3 y; 166.4±8.9 cm; 61.5±12.1 kg) were anaylzed. All participants, or parents/guardians, provided written informed consent. The ACLR group participated within 4 weeks after medical clearance for return to sports. Three-dimensional motion analysis was used to collect lower extremity kinematic data during the single leg drop test; three trials were collected per leg. A 10-camera motion analysis system (240 Hz cameras; Motion Analysis Corp., Santa Rosa, CA, USA) was used to track 37 retroreflective markers on the upper and lower extremities and trunk of each participant. The landing phase, defined as initial contact to lowest position of the center of gravity, was examined. A vector coding technique[3] was used to calculate coupling angles between two adjacent joints to form an angle-angle curve of angular displacements of the proximal and distal joints (Table 1) for each trial. The overall root mean square of the resulting circular standard deviation at each time point across the three trials was computed to represent the within-subject and within-limb variability. A paired Wilcoxon signed-rank test was used to compare the involved/uninvolved sides of the ACL group and a Mann-Whitney U test was used to compare both of the involved and uninvolved sides to the dominant side of Controls.

Results and Discussion

Increased coordination variability was found in both limbs in the ACLR group when compared with Controls which supports our first hypothesis (Table 1). These findings support Devis et al[3] which found increased movement variability in HR/KR, HA/KR and HR/KA for the involved limb during walking and in HA/KR, HR/KR and HR/KA in the uninvolved limb when compared to healthy controls. In this study, more joint couplings showed variability during the single leg drop which suggests that the more demanding movement leads to higher instability and reduced adaptability[3]. We reject our second hypothesis, as there was not a significant difference between the injured limb when compared to the uninjured limb, which only showed an increase in variability in one joint coupling.

Table 1: Difference in Joint Coordination Variability
Symbols indicate statistical difference in: IC – injured leg vs. control; UC – uninjured leg vs. control; IU – injured leg vs. uninjured leg

	Variability (Mean ± STD of RMS)			p-Value
Coupling	Injured	Uninjured	Control	< 0.05
Hip Abduction-Adduction/Knee Abduction-Adduction (HA/KA)	0.835±0.252	0.823±0.273	0.691±0.234	IC, UC
Hip Abduction-Adduction/Knee Rotation (HA/KR)	0.855±0.247	0.835±0.26	0.69±0.248	IC, UC
Hip Flexion-Extension/Knee Abduction-Adduction (HF/KA)	0.821±0.237	0.749±0.251	0.739±0.222	IC, IU
Hip Flexion-Extension/Knee Flexion-Extension (HF/KF)	0.662±0.233	0.607±0.25	0.525±0.228	IC, UC
Hip Rotation/Knee Abduction-Adduction (HR/KA)	0.972±0.227	0.955±0.269	0.863±0.26	IC, UC
Hip Rotation/Knee Rotation (HR/KR)	0.928±0.234	0.918±0.25	0.782±0.262	IC, UC
Knee Abduction-Adduction/Knee Flexion/Extension (KA/KF),	0.704±0.234	0.652±0.222	0.575±0.207	IC, UC
Knee Abduction-Adduction/Knee Rotation (KA/KR)	0.947±0.23	0.913±0.256	0.831±0.247	IC, UC
Knee Flexion-Extension/Ankle Flexion-Extension (KF/AF)	0.598±0.239	0.558±0.246	0.437±0.189	IC, UC

Significance

The increased bilateral movement variability observed may be an indicator for the risk of injury in more dynamic tasks and could contribute to the suboptimal outcomes seen in the ACLR population. Further research needs to be done on the impact that changes in coordinative strategies play on ACLR patients' outcome, which may inform new rehabilitation practices and return to sport criteria

Acknowledgments

This work was funded by the National Institutes of Health grant F32-AR055844; the National Football League Charities Medical Research Grants 2007, 2008, 2009, 2011.

References

1 Ardern et al. *BJSM*, 48(21), 1543–1552. **2** Øiestad et al. *AJSM*., 37 (7) 1434-1443, 2009. **3** Davis et al. *Gait & Posture*, 67, 154–159, 2019. **4** Gribbin, T. C., *Clin Biomech*, *32*, 64–71, 2016. **5** Morrey. *Yearbook of Orthopedics*, *2010*, 163–164. **6** Paterno et al. AJSM 42(7): 1567–1573. 2014. **7** Srinivasan et al. *Clin Biomech*, 53, 37–45, 2017. **8** Schmitt et al. *MSSE*. 2015 Jul;47(7):1426-3

Load Magnitude and Forced Marching Impairs Locomotor System Function in Recruit Aged Females

Kellen T. Krajewski[1], Camille C. Johnson[1,2], Dennis E. Dever[1], Shawn D. Flanagan[1], Qi Mi[1], Nizam U. Ahamed[1], William J. Anderst[2], Christopher Connaboy[1]
[1]Neuromuscular Research Laboratory, University of Pittsburgh, Pittsburgh, PA
[2]Orthopaedic Biodynamics Laboratory, University of Pittsburgh, Pittsburgh, PA
Email : KTK20@pitt.edu

Introduction

Musculoskeletal injuries due to repetitive stress and falls remain a pervasive threat to soldier readiness[1]. A proposed culprit, load carriage, is a common encumberance to military occupational tasks. Soldiers are often required to traverse large distances utilizing a forced march (FM) locomotion pattern, walking at a velocity exceeding their gait transition velocity (GTV), in conjunction with load carriage. A lack of motor variability and gait complexity while executing steady state ambulation may reduce the ability to disperse forces across multiple supportive structures. Moreover, suboptimal organization of the locomotor system components and limited movement solutions impedes adaptability/stability to perturbations. However, there is a paucity of information regarding load carriage and motor control. The purpose of this study was to determine the interactive effect of load magnitude and locomotion pattern on motor variability, stride regulation and gait complexity in recruit-aged females. It was hypothesized that increases in load and FM would reduce motor variability and gait complexity but yield stricter stride regulation.

Methods

Eleven healthy recreationally active females (24.8±2.2 years) participated in this IRB-approved study. Biomechanical data was collected via twelve infrared cameras (Vicon Motion Systems Ltd., Oxford, UK) and an instrumented dual-belt treadmill (Bertec, OH, USA) at 100Hz and 1000Hz respectively. Participants wore standard issue military combat boots and an evenly distributed anterior/posterior weight vest. One minute of running and forced marching (FM) was performed at a velocity 10% above GTV for three load conditions; unloaded (BW), +25% and +45% of their bodyweight. Strides were considered heel strike (50N threshold) to ipsilateral heel strike. Stride length (SL) and stride time (ST) were calculated for a minimum of 120 consecutive strides. Motor variability and stride regulation were assessed with goal equivalent manifold (GEM) decomposition[2]. GEM generates tangential (δ_T) [good] and perpendicular (δ_P) [bad] coordinates of stride variations on a goal manifold based on combinations of observed SL and ST. Relative variability is then calculated as $\sigma\delta_T/\sigma\delta_P$; σ represents standard deviation. Stride regulation was assessed with detrended fluctuation analysis (DFA) of δ_T and δ_P time series, which yields a scaling exponent (α). Gait complexity was assessed with DFA of SL and ST time-series. Suboptimal complexity is $\alpha<.75$ and $\alpha>1.3$, while $\alpha=.75$-1.3 represents optimal. Two-way RMANOVA (load x locomotion) was conducted for relative variability and SL/ST scaling exponents. Three-way RMANOVA was (load x locomotion x direction) conducted on δ_T/δ_P. Post hoc Bonferroni corrected pairwise comparisons were performed for load. Estimated marginal means reported for effects of locomotion and direction (tangential vs perpendicular).

Results and Discussion

Motor Variability: For relative variability, there was a main effect of load (p=.01), with +45% (1.28±.05) having less (p=.02) relative variability than BW (1.55±.07). Additionally, there was a main effect of locomotion (p=.01) with FM (1.53±.08) having more relative variability than running (1.27±.04). Reductions in relative variability indicate an increase in stride fluctuations that impede successful task execution. Further, lower relative variability exhibits a limited movement solution capacity. Alternatively, higher relative variability could represent a task learning behaviour of a novel movement in the form of state-space exploration.

Stride Regulation: There was a main effect of load (p=.002), with BW (.6±.08) exhibiting looser control than +45% (.04±.11). There was a main effect of locomotion (p=.02) with FM (.19±.08) exhibiting stricter control than running (.46 ±.07). There was also a main effect of direction (p<.001) with perpendicular (bad) variability (.18±.07) being controlled more tightly than tangential (good) variability (.47±.06). During the steady-state task at greater load magnitudes stride to stride fluctuations were regulated more tightly or overcorrected quickly each stride, evidenced by $\alpha<.5$ which represents statistical anti-persistence.

Gait Complexity: For SL and ST there was a main effect of load (p=.002, p=.007) with complexity at BW (.69±.08) being greater (p=.02, p=.03) than +45% (.00±.17). There was a main effect of locomotion (p=.02, p<.001) with complexity for running (.68±.09) being greater than FM (.11±.14). During running at BW optimal locomotor system output was exhibited (α=.96). However, FM+45% constrained the system, resulting in less complexity that could result in a negative outcome (fall/injury) with additional perturbations. Therefore, individuals with +45% load may be unable to accommodate a varying terrain or minor injury sustained during mission due to compromised locomotor system component organization (reduced system redundancy).

Significance

There were no significant interactive effects, but load magnitude and locomotion pattern did independently alter motor variability, stride regulation and gait complexity. A load magnitude of +45% diminishes motor variability which may predispose individuals to repetitive stress injuries through a lack of energy dispersion across supportive structures. FM compared to running had increased relative variability but less gait complexity indicating a potential lack of movement stability. A +25% load magnitude failed to illicit significant changes in gait motor variability and complexity. Future research should utilize heavier loads and longer trials to investigate role of fatigue.

Acknowledgments

This work was supported by the Freddie H. Fu research award.

References

1)Le et al., *JAMA* Surg, 2018. 2)Dingwell et al., *PLoS*, 2010.

Interpersonal and interlimb synergies in handling of a heavy object motor task

Mia Caminita[1], Sara Honavar [1,2], Hyun Joon Kwon[1], Yancy Diaz-Mercado[2], Jin-Oh Hahn[2], Tim Kiemel[1], and Jae Kun Shim[1]
[1]Department of Kinesiology, University of Maryland, MD, USA
[2]Department of Mechanical Engineering, University of Maryland, MD, USA
Email: mcaminit@umd.edu

Introduction

Understanding the motor synergies developed between two independent central nervous systems (CNS) could provide critical insight into the underlying mechanisms behind many of our interpersonal interactions and inform the mechanisms for future physical human-robot collaborations (PHRCs). Previous research regarding motor synergies focuses almost exclusively on interlimb synergies or the synergies formed within a single CNS [1,2,3]. The motor behaviors elicited when two individuals work together to complete a motor task without any direct neurological connection is unknown. Additionally, the role of sensory information exchanged between co-workers also remains unknown. Therefore, the purpose of the current study is to examine the synergistic performance of a motor task by co-working partners involving handling a heavy object at both the interpersonal and interlimb levels under two conditions: with visual feedback between co-workers and without visual feedback between co-workers. We hypothesize that both interpersonal and interlimb motor synergies exist during this motor task and removal of visual feedback between co-working partners decreases synergistic performance.

Methods

Twenty-six healthy young adults (23.7 ± 3.7 yrs) participated in the study comprised of 13 gender and height-matched pairs. The pairs performed a motor task which involved working together to lift, move, hold, and place a heavy, table-like object (Fig. 1). The object was instrumented with four 6-dimensional force/torque sensors (ATI Industrial Automation, Apex, NC) to record the forces and moments of force applied to the apparatus by the individual hands of each participant during task performance. The task was performed under two conditions: a) with visual feedback, where partners were able to see each other, and b) without visual feedback, where a screen occluded vision between partners. The analysis presented is limited to the vertical component of forces during the moving phase of the task.

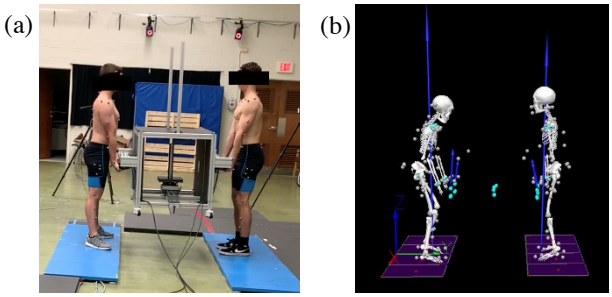

Figure 1: a) Snapshot of co-working partners performing the motor task and b) biomechanical model of the task performance.

Results and Discussion

Examination of the moving phase of the task reveals interlimb motor synergy is present between the hands of individual person. As described in our previous work [4], negative covariance (Table 1b) indicates the presence of a force-stabilizing synergy at the interlimb level between hands. Although a significant synergy exists at the interlimb level in both task conditions, there is no significant difference in the magnitude of the synergy with or without visual feedback between co-workers. At the interpersonal level, the positive covariance (Table 1a) suggests synergy between co-workers to maintain rotational stability of the object during the moving phase of the task. The magnitude of the covariance between the two visual conditions is also not significantly different.

Table 1. Mean ± SD for Covariance: a) between co-working partners (P1 and P2, interpersonal level), and b) between the right (RH) and left (LH) hand of each individual partner (interlimb level).

(a) Interpersonal Level Covariance			
	Visual Feedback	No Visual Feedback	*p*
P1 vs. P2	19.3± 18.41	15.44± 12.30	0.531
(b) Interlimb Level Covariance			
	Visual Feedback	No Visual Feedback	*p*
P1: LH vs. RH	-64.0± 32.9	-66.0± 42.6	0.895
P2: LH vs. RH	-50.9± 36.8	-61.4± 27.7	0.421

On both the interlimb and interpersonal level these findings support our hypothesis that synergies exist at both levels. However, the findings do not support our hypothesis regarding changes in synergistic performance due to the removal of visual feedback between co-working partners. The findings suggest that perhaps the haptic connection between partners moving an object is in fact more critical to successful task completion than the ability to see one another during the moving phase of task at both task levels. Moreover, the lack of a significant difference between visual conditions is fitting on the interlimb level, as one CNS is controlling both hands, and may not need to rely on visual information. At the interpersonal level the formation of a synergy suggests a favoring of moment stabilization and synchronous performance for successful task completion.

Significance

The findings of this study can have far reaching impact in the fields of human movement science, robotics, and engineering. The demand for PHRCs is increasing rapidly in society, and more so today with the current need for social distancing. Understanding how two human partners work together holds the key to suggesting safer, more intuitive, and efficient mechanisms for future human-robot collaborations.

Acknowledgments

This work was supported by the Korea Institute of Machinery and Materials in 2018 [NK210H, Development of core machinery technologies for autonomous operation and manufacturing].

References

1. Karol, S. et al., Exp Brain Res. 2011; 208(2),359-367
2. Kim, Y. et al., Neurosci Lett. 2012; 512(2)114-117
3. Ranganathan, R. et al., Exp Brain Res. 2008;186(4)561-570
4. Koh, K. et al., Exp Brain Res. 2015; 233:2539–2548

Robotic Augmentation of Human Trainers to Investigate the Role of Trainer Manipulative Variability on Patient Learning

Christopher J. Hasson[1,3,4], Min Hyong Koh[1], Sheng-Che Yen[2],
Sarah Gans[6], Keri Sullivan[6], Mansi Badadhe[1,3], Misha Pavel[5], and Lester Y. Leung[6]

[1]Neuromotor Systems Laboratory & [2]Laboratory for Locomotion Research, Dept. of Physical Therapy, Movement & Rehab. Sciences;
[3]Dept. of Bioengineering & [4]Dept. of Biology; [5]Khoury College of Computer Sciences, Northeastern Univ., Boston, MA, USA
[6]Division of Stroke and Cerebrovascular Diseases, Department of Neurology, Tufts Medical Center, Boston, MA, USA
E-mail: c.hasson@northeastern.edu

Introduction

In current practice, the manipulative forces generated by rehabilitation robots are governed by mathematical equations. On the other hand, forces from the hands of a human trainer are regulated by a relatively noisy biological control system, which introduces significant variability into manipulative forces. Self-generated (intrinsic) variability can promote exploration of novel motor actions that can drive learning[1]. Could this also hold for variability injected from an external source, i.e., from a human trainer to a patient? In other words, could the variability from a human trainer be beneficial for patient learning?

Any beneficial aspects of trainer manipulative variability could be masked by trainer fatigue or other sensorimotor encumbrances associated with hands-on manual locomotor training. We address this with a novel approach that robotically augments human trainers, allowing them to physically assist patients with minimal effort, called *Cyberphysical Rehabilitation* (CR). In this approach, a trainer holds onto a small robotic manipulandum that shadows the motion of a locomoting patient (Fig. 1). When the trainer applies a force to the manipulandum, the force is amplified and transferred to the patient with a magnetically-attached robotic arm. We performed a feasibility study that used CR to test the hypothesis that manipulative variability from human trainers promotes patient learning.

Methods

Six patients with prior strokes (P1-P6) undertook a six-day locomotor training program; the goal was to increase the affected leg's step length by 25%. Each patient received CR from one or two robotically-augmented human trainers (separately). The CR system amplified trainer forces by a factor of 18.75 at the maximum transmitted output force of 30 N. An experienced CR trainer (Trainer T1) assisted P1-P3 on all training days except the fifth day, on which a different experienced trainer (Trainer T2) assisted (Trainer T1 was unable to participate). Trainer T2 provided assistance using the CR system for all six sessions for patients P4-P6. Both trainers were familiar with the CR system operation but were not rehabilitation professionals.

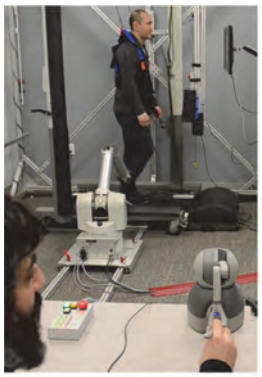

Figure. 1. Robotically augmented human trainer.

Results and Discussion

The magnitude of the assistance force provided by the robotically augmented human trainers was variable between patients, trainers, and days (Fig. 2), in agreement with early work using non-augmented human trainers[2]. One the other hand, the step-to-step variability of trainer forces was, on a relative basis, largely consistent between patients, trainers, and days. This could be a function of the CR system. The human trainers only needed to modulate their force by a small amount to produce large changes in the applied force, e.g., only 1.6 N was required to transmit 30 N to the patient. Thus, trainer forces spanned a small range of their force capability, which constrains variability since human sensorimotor noise scales with motor command magnitude[3]. The relatively low step-to-step variability of trainer manipulative forces makes it difficult to relate this variability to patient learning outcomes at the present time.

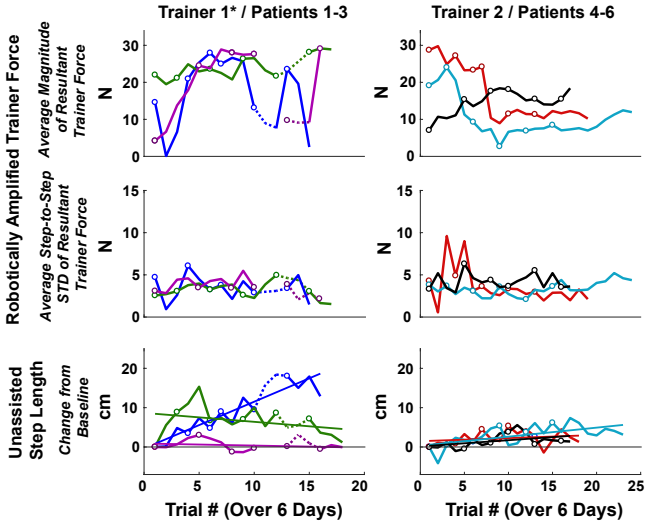

Figure 2. Changes in trainer assistive force magnitude (top row), step-to-step force variability (middle row) and unassisted patient step length (bottom row) across six training days for six individuals who survived strokes. *Patients 1-3 (left) were assisted by Trainer 1 (*except on Day 5 Trailer 2 gave assistance to Patients 1-3, indicated by dashed lines). Patients 4-6 (right) were assisted by Trainer 2. Forces shown are amplified 18.75 times at 30N. (Day 5 data excluded for Patient 3 [purple] because resistance was applied instead of assistance). Step length is relative to Day 1 baseline. Circles = first trial of each day.*

Significance

This new approach, called *Cyberphysical Rehabilitation* (CR), allows robotically augmented human trainers to manipulate a patient's body in real-time during treadmill locomotion. Future work could use CR to modify further how therapist forces are transmitted to patients, with the aim of providing a larger variability bandwidth from which to test the hypothesis that human trainer manipulative variability promotes patient learning.

Acknowledgments

Funded by Northeastern University and the National Center for Advancing Translational Sciences (UL1TR002544).

References

[1] Wu et al., Nature Neuroscience. 2014;17(2):312
[2] Galvez et al., 2005; Proceedings of 9th ICORR.
[3] Harris & Wolpert, Nature. 1998;394(6695):780

Exoskeleton Hip Assistance during Walking: Assisting Flexion or Extension?

Xianlian Zhou*, Neethan Ratnakumar
Department of Biomedical Engineering, New Jersey Institute of Technology
*Email: alexzhou@njit.edu

Introduction

The use of robotic exoskeletons to assist human motion has become one of the most promising approaches to augment human performance or rehabilitate gait disorders. Assistance to lower body joints such as hip, knee, and ankle has been investigated by many researchers. Hip muscles consume the greatest percentage of the total human muscle energy expenditure [1] and thus torque assistance to the hip joint is expected to reduce the metabolic cost of human walking to a great degree.

Hip muscles generate substantial torques for both flexion and extension with similar magnitudes during walking. Exoskeletons have been designed to assist hip in either the flexion [2] or extension direction [3] considering that assisting only one direction can greatly simplify the design and actuation of the exoskeleton. However, there is no clear or conclusive evidence on which assistance direction is better. This study investigates and compares the effects of hip assistance in these two directions through a modelling and optimization approach and aims to provide clues on which one is more efficient in reducing metabolic cost of transport (COT).

Methods

To study human walking, we employed a subject musculoskeletal model that was actuated by sixteen Hill-type muscle tendon units, as shown in Fig. 1(a). The muscle excitations were generated through muscle reflex control whose parameters were optimized with a Covariance Matrix Adaptation Evolutionary Strategy (CMA-ES) method. The optimization was conducted with the SCONE software [4], which used OpenSim[5] to execute single shoot forward dynamics simulations of walking within each optimization iteration. The objective function of this optimization was a weighted combination of multiple motion characteristics, including metabolic COT calculated from a muscle energetics model [6], walking speed range, and penalties for falling, injury, and joint limit violations.

An optimization was first performed to generate a normal walking motion with Self Selected Speed (SSS). Then parameterized hip joint torques (flexion/extension) were directly added to the hip joint for assistance simulations. The assistance torque profile was assumed to take the form of a raise-peak-fall curve [7] and the parameters include the offset time, raise time, fall time, and the peak torque. For flexion assistance, the reference starting time (t=0) for offset is at the middle stance phase whereas for extension the reference time is at the beginning of the swing phase. The peak torque limit was set to be 50 N/m. During optimizations, these assistance parameters were optimized together with the muscle reflex control parameters such that adaptations of muscle reflex and gait were expected.

Results and Discussion

Table 1 compares gait characteristics of normal walking with those of assisted walking, for which the predicted optimal torque profiles are shown in Fig. 1(b). With assistance, the SSS increased by 16.7% and 9.7% for flexion and extension, respectively. Flexion assistance changed the stride length (L) minimally but shortened the stride duration (D) (i.e. increased step frequency) whereas extension assistance increased step frequency further but decreased the stride length. Flexion assistance increased the maximum hip flexion angle by 10.7^{o} and reduced the extension angle by 2.4^{o}. The extension assistance also increased the hip flexion angle slightly (by 1.6^{o}) and decreased the extension angle by 4.5^{o}. In the latter case, the decrease in hip extension angle is likely caused by faster walking with a short stride and the absence of extension assistance during the late stance phase. For both assistances, the COT decreased considerably, by 19.1% for flexion and 11.7% for extension.

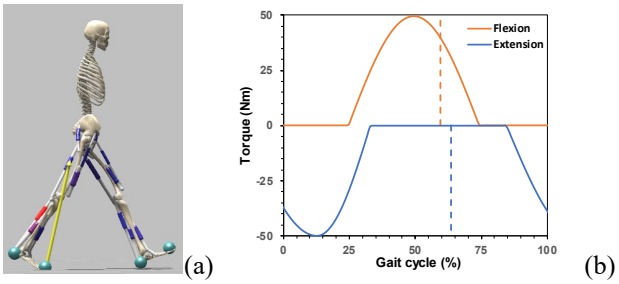

Figure 1: (a) The human subject musculoskeletal model; (b) Predicted optimal hip flexion and extension torque profiles. The gait cycle starts from the heel strike and dashed lines indicate the start of swing phases.

In summary, we demonstrated a computational approach to evaluate the effectiveness of hip assistance to human walking and predicted gait adaptation and change of energetics. We found that the hip flexion assistance performed better than hip extension assistance in terms of COT reduction and caused less changes of gait patterns (stride length and duration).

Table 1: Comparison of gait characteristics for normal and assisted walking. The unit for COT is $J/(kg \cdot m)$; (θ^{o}) is the hip angle range.

	SSS (m/s)	L (m)	D (s)	(θ^{o})	COT
Normal	1.194	1.683	1.41	(-24.2, 41.5)	3.263
Flexion	1.393	1.686	1.21	(-21.8, 52.2)	2.639
Extension	1.310	1.402	1.07	(-19.7, 43.1)	2.881

Significance

Designing wearable exoskeletons is often a trade-off process considering various factors such as power, actuation, cost, weight, and wearability. Knowing how and when to apply assistance to a joint is critical for designing wearable exoskeletons. Our study can provide guidelines for optimal hip actuation (e.g. timing and profiles) and help designers make informed decisions. The method can also be extended to study assistance to other joints.

References

[1] Umberger and Rubenson, Exerc Sport Sci Rev, vol. 39, no. 2, pp. 59-67, 2011.
[2] Quinlivan et al., Sci. Robot, vol. 2, no. 2, pp. 1-10, 2017.
[3] Ding, et al., Science Robotics, vol. 3, no. 15, eaar5438, 2018.
[4] Geijtenbeek, J. of Open Source Softw., vol. 4, no. 38, p. 1421, 2019.
[5] Seth, et al., Procedia IUTAM, vol. 2, no. 0, pp. 212-232, 2011.
[6] Uchida et al., PloS one, vol. 11, no. 3, 2016
[7] Zhang et al., Science, vol. 356, no. 6344, pp. 1280-1284, 2017.

A comparison of kicking kinematics among college students with and without Autism Spectrum Disorder

Kathy Reyes, BS[1], Teri A. Todd, PhD[1], Melissa A. Mache, PhD[2], and Danielle N. Jarvis, PhD, ATC[1]
[1]Department of Kinesiology, California State University, Northridge
[2]Department of Kinesiology, California State University, Chico
Email: danielle.jarvis@csun.edu

Introduction

Autism Spectrum Disorder (ASD) is a neurodevelopmental disorder affecting social communication and interaction skills.[1] Compared to typically developing children, individuals with ASD exhibit poor motor skills at a young age.[2-3] These motor skill deficits in children may contribute to lower levels of physical activity in persons with ASD, leading to a sedentary lifestyle and obesity. However, it is unknown if the motor skill deficits seen in children carry over into adulthood.

Kicking is one gross motor skill commonly performed by children. A proficient kick requires sequential movements of the kicking leg.[4] Forward motion is initiated by rotating the pelvis around the supporting leg and by bringing the thigh of the kicking leg forward while the knee continues to flex backward.[4] Proficient kicking is an essential element of several sports and play activities, such as kickball and soccer. The purpose of this study is to compare the kicking kinematics of college students with and without ASD. It was hypothesized that college students with ASD would exhibit a less proficient kick, demonstrated by decreased peak hip extension in the wind-up, and decreased peak hip flexion and knee extension velocities during the acceleration phase.

Methods

Ten college students with ASD and ten college students without ASD participated in this study (Table 1).

Table 1: Demographic characteristics of participants

	With ASD	Without ASD
Sex (male:female)	8:2	8:2
Age (years)	23.3 ± 3.83	21.70 ± 2.50
Height (cm)	173.10 ± 12.45	171.90 ± 7.75
Body weight (kg)	101.29 ± 23.61	75.82 ± 18.10
BMI	33.88 ± 7.86	25.76 ± 6.08

Note. Values presented as mean ± standard deviation, except for sex which is presented as frequency.

A computer-aided 12-camera video motion analysis system and force plates were used to assess movement patterns. Following a demonstration of the kick, participants were asked to complete five kicking trials where they kicked a ball hard into a net. Hip, knee, and ankle kinematics were calculated. Stance leg peak hip flexion, knee flexion, and ankle dorsiflexion, and kicking leg peak hip extension, knee flexion, hip flexion velocity, and knee extension velocity were extracted and compared between groups using independent t-tests. Alpha level was set at ≤ 0.05.

Results and Discussion

There were no statistically significant differences between groups in stance leg peak hip flexion, knee flexion, or ankle dorsiflexion (Table 2). There were no statistically significant differences in kicking leg peak hip extension or knee flexion during the preparation, or in peak hip extension velocity or knee extension velocity during the kick (Table 3). For all variables, the ASD group had a higher standard deviation than the control group, indicating they may perform kicking with greater variability.

Table 2: Stance leg peak lower extremity joint angles.

Variable	With ASD	Without ASD	*p* value
Hip Angle	39.18±12.46	39.25±11.17	0.989
Knee Angle	55.06±11.00	54.56±8.23	0.908
Ankle Angle	8.28±8.45	7.68±7.00	0.864

Note. Angles reported in degrees, with positive values indicating hip flexion, knee flexion, and ankle dorsiflexion.

Table 3: Kicking leg peak lower extremity kinematics.

Variable	With ASD	Without ASD	*p* value
Hip Extension	10.05±8.45	14.56±7.37	0.219
Knee Flexion	83.36±13.96	85.84±11.85	0.9674
Hip Extension Velocity	496.9±178.8	442.1±92.5	0.401
Knee Extension Velocity	788.7±259.6	935.7±220.5	0.189

Note. Angles reported in degrees and velocities reported in degrees/second. Values presented as mean ± standard deviation.

Significance

There were no statistically significant differences in kicking kinematics between college students with and without ASD. After noting the high kicking leg standard deviations, visual inspection of the data revealed that participants may have approached the kick differently, with some relying more on the hip to drive the kick while others relied more on the knee. It may be possible to break these participants into subgroups for a more detailed analysis to determine if there are differences between groups that were not identified using the present approach. In the future, we also plan to examine the coordination patterns and timing of movements during kicking to determine if differences between groups exist. A detailed analysis of variability may also reveal differences between groups in terms of motor control. While the dependent variables selected for the present analysis did not reveal differences between groups, further work to identify deficits in kicking can contribute to the development of interventions to improve kicking mechanics in individuals with ASD. Improving kicking skills in this population could help with balance and coordination and promote greater participation in physical activity.

Acknowledgments

This study did not have any external funding.

References

1. American Psychiatric Association. 2013.
2. Lim et al. *J Phys Ther Sci.* 2016.
3. Green et al. *Dev Med Child Neurol.* 2009.
4. Kellis & Katis. *J Sports Sci Med.* 2007.

Motor Complexity is Reduced During Emulation of Cerebral Palsy Gait Patterns

Alyssa M Spomer.[1], Robin Z Yan[1], Michael H Schwartz[2], and Katherine M Steele[1]
[1]Department of Mechanical Engineering, University of Washington, Seattle, WA
[2]Center for Gait & Motion Analysis, Gillette Children's Specialty Healthcare, St. Paul, MN
Email: aspomer@uw.edu

Introduction

Muscle synergy analysis has been broadly used to quantify motor coordination during movement, particularly among individuals with neuromuscular disorders. In cerebral palsy (CP), individuals commonly exhibit reduced coordination complexity compared with typically developing peers [1]. It has been hypothesized that this reduction reflects a simplified control architecture stemming from the primary neurologic injury. However, individuals with CP also commonly adopt altered gait patterns (e.g. equinus, crouch gait). Previous studies have suggested that the biomechanical constraints of these gait patterns may limit the feasible solution space for muscle activity, resulting in the reduced complexity observed [2].

Studying the isolated effects of neurologic injury and gait pathology on coordination may elucidate their relative impacts and inform treatment. Prior work has demonstrated that typically developing individuals can replicate common CP gait patterns, but impact of these patterns on motor coordination has not been studied [3-5]. Investigating changes in synergies while unimpaired individuals emulate CP gait patterns provides a unique means of uncoupling the biomechanical constraints from the neurologic injury. We hypothesize that if reduced coordination complexity in CP is primarily neurogenic, then altered mechanical constraints during unimpaired emulation will have minimal impact on synergy complexity.

Methods

Fourteen typically developed participants (7M/7F; 24.1 ± 4.7 yrs) were enrolled. Participants walked at a self-selected speed on a split-belt instrumented treadmill for all trials. Participants performed one, three-minute baseline gait trial (BG) along with three, three-minute emulation trials for the following CP gait patterns: equinus (Eq), equinus-crouch (Eq-Cr), mild crouch (Mi-Cr), and moderate crouch (Mod-Cr). Mi-Cr and Mod-Cr trials were defined as 20° and 30° knee flexion set with a goniometer during standing, respectively [6], and reinforced using a visual aid in-trial. Verbal instruction and researcher demonstration were provided for Eq trials. For Eq-Cr trials, participants adopted the same equinus posture as for Eq trials and knee flexion was set at 20°; a visual aid was again used to reinforce knee flexion.

Kinematic data were collected from a full-body marker set. Electromyography data were collected for a bilateral, eight muscle set spanning the hip, knee, and ankle joints. To reduce learning or fatigue effects, all analyses were performed for 43 strides taken from the middle of one trial for each participant. Muscle synergy decomposition was performed on the concatenated EMG data and total variance accounted for (tVAF) was used to evaluate synergy complexity.

Multiple paired t-tests with Bonferonni correction ($\alpha_{adjusted}$=0.0125) were used to evaluate differences in synergy complexity between BG and each of the emulated gait patterns.

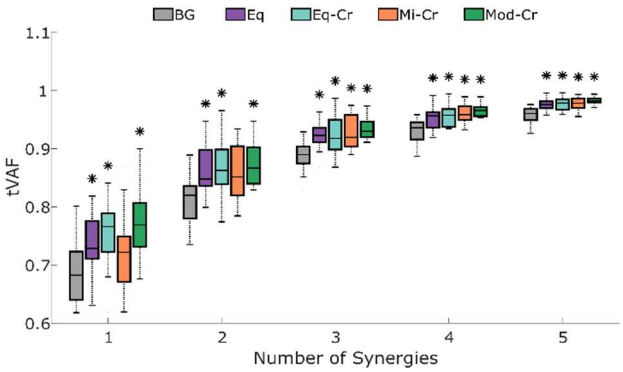

Figure 1: The tVAF during baseline and emulated gait for 1-5 synergies. Larger tVAF for any synergy solution indicates reduced coordination complexity. *Denotes significant difference from BG.

Results and Discussion

Synergy complexity was significantly reduced compared to BG in Eq, Eq-Cr, and Mod-Cr patterns across all synergy solutions ($p < 0.01$). Mi-Cr resulted in significantly reduced complexity for $N > 2$ synergies ($p < 0.002$). Participants demonstrated significant deviations from BG in the joint angles targeted by each emulation pattern; the observed trends were qualitatively similar to CP gait. [3-5].

These data suggest that gait pathology may contribute to reduced synergy complexity seen in CP. However, prior research has shown that changes in kinematics in CP are not associated with changes in synergies [7], suggesting reduced synergy complexity is not entirely biomechanically driven. As such, further work is needed comparing the changes in coordination complexity in these TD emulated gait patterns to a kinematically-matched CP cohort to understand the relative impacts of altered biomechanics and neurology on coordination.

Significanc

Our results suggest that, at least among TD participants, biomechanical constraints reduce synergy complexity. While more work is needed to extend these results to a CP population, this study improves understanding of the factors that impact coordination complexity and may help instigate further research into therapy or other coordination-targeting interventions to improve gait for people with CP.

Acknowledgments

This work was funded under NIH NCATS Award TR002318 and NIH NINDS Award R01NS091056.

References

[1] Steele KM, et al. J Pediatr Rehabil Med. **5**(2). 2012. [2] Kutch and Valero-Cuevas. PLOS Comput Biol. **8**(5). 2012. [3] Thomas SS, et al. Gait Posture. **4.** 1996. [4] Romkes J, Brunner R. Gait Posture. **26**. 2007. [5] Van der Krogt MM, et al. Gait Posture. **26**. 2007. [6] Rozumalski A, Schwartz MH. Gait Posture. **30**. 2009. [7] Shuman BR, et al. J Neuroeng Rehabil. **16.** 2019.

Temporal Hempiparetic Gait Symmetry Altered by a Nonparetic-Leg Weight

Ahmed Ramadan[1,*], Douglas N. Savin[1], Gabriela Lopes Gama[2], and Jill Whitall[1]
[1]University of Maryland, School of Medicine, Department of Physical Therapy and Rehabilitation Science, Baltimore, MD, USA
[2]Institute of Physical Activity and Sport Sciences, Universidade Cruzeiro do Sul, São Paulo, Brazil
Email: *ramadana@som.umaryland.edu

Introduction

Gait adaptation has shown improved symmetry in hemiparetic stroke survivors. Existing methods typically use expensive equipment such as split-belt treadmills or robotic devices, which may make a translation to the clinic less feasible. Using a unilateral leg weight overground may be a more feasible solution.

We hypothesize that adding a weight to either the paretic or nonparetic side may alter spatiotemporal gait symmetry in subjects with stroke and tested both conditions in short-term experiments.

Methods

Five participants with chronic stroke (2 females; 61.4±2.5 years; 93.3±16.1 kg; 171.8±12.5 cm tall) with unilateral hemiparesis were recruited. They walked over ground without a weight, after adding a weight of 3% body weight on participant's ankle, and after the weight (2.67±0.43 kg) was removed (**Figure 1**; BL: Baseline, EA: Early Adaptation, LA: Late Adaptation, ED: Early Deadaptation, LD: Late Deadaptation). During all conditions, participants were instructed to walk at a comfortable speed with their arms free. For safety, the participant wore a gait belt and a researcher walked close and behind the participant.

The participants were assessed over two visits with at least one week between them. Before visit 1's BL, participants walked on a gait mat to find the leg with the shorter step. The weight was placed on this leg in visit 1 and on the contralateral leg in visit 2. Kinematic data were recorded at 120Hz using VICON.

Step legth (SL) and step time (ST) for each leg were calculated using a custom Matlab code. The symmetry index (SI) for a variable X is $SI = (X_{\text{nonparetic}} - X_{\text{paretic}})/(X_{\text{nonparetic}} + X_{\text{paretic}})$. An SI of zero means perfect symmetry. A repeated-measures ANOVA was performed using SPSS. We considered the repeated measures of the testing periods and paretic-perturbed (PP) versus nonparetic-perturbed (NPP). The interaction was assessed in the model.

Results and Discussion

For step-length SI, ANOVA with repeated measures of testing periods and PP-NPP revealed no significant main effect or interaction effect. Therefore, the PP-NPP groups were merged (**Figure 2**, upper panel). An ANOVA with repeated measure of the testing periods revealed no significant effect.

For step-time SI, ANOVA with repeated measures of testing periods and PP-NPP revealed no significant main effects, but a significant interaction (p=0.044). A post-hoc analysis revealed no significant difference between PP and NPP at each testing period. However under NPP only, the BL was significantly different from LA, ED, and LD (p=0.008, 0.033, 0.029, respectively) (**Figure 2**, lower panel).

Taken together, the results suggest that a leg weight does not alter the spatial symmetry of hemiparetic gait, however, it does alter the temporal symmetry when the weight is added to the nonparetic leg. This is a positive outcome since the step time starts asymmetrical in BL (**Figure 2**) and converges to symmetry at the end (LD).

Our results are in line with a study (Khanna et al., 2010) that also reported no change of temporal SI (for % stance duration) when loading on the paretic leg and walking overground. They differ from previous findings on a treadmill with leg swing resistance of 1.25% body weight (Savin, Tseng, Whitall, & Morton, 2013), where step-length SI was altered. This may be due to the different context of a treadmill, the weight perturbation during swing only, or perturbing the leg with the shorter step regardless of being the paretic or nonparetic. These alternative hyotheses need testing in a systematic manner.

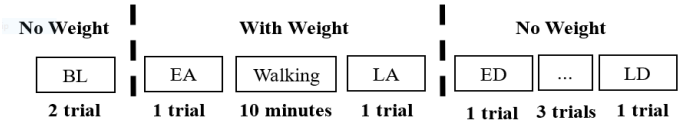

Figure 1: Testing periods. BL=Baseline, EA=Early Adaptation, LA=Late Adaptation, ED=Early Deadaptation, LD=Late Deadaptation.

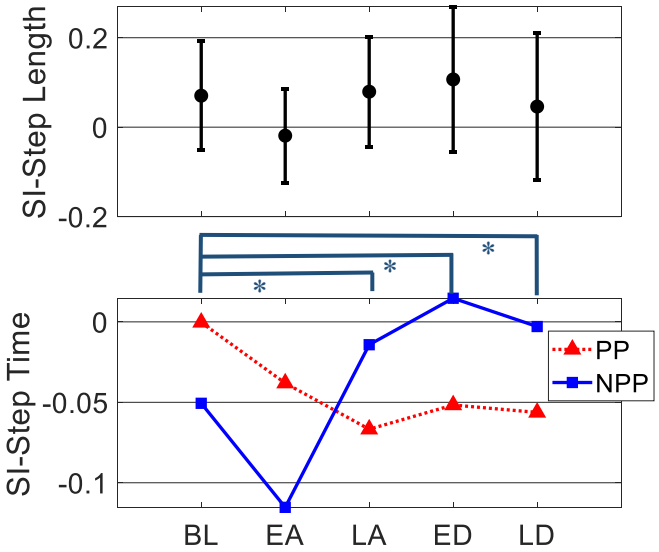

Figure 2: Symmetry index (SI) of step length and time. PP: Paretic Perturbed, NPP: Nonparetic Perturbed. The significant values (denoted by *, p<0.05) are for step-time SI in NPP.

Significance

This study extends the scope of investigating effects of adaptation on overground gait symmetry by testing the effect of perturbing the paretic versus nonparetic sides in individuals after chronic stroke.

References

Khanna, I., et al. (2010). Effects of unilateral robotic limb loading on gait characteristics in subjects with chronic stroke. J. NeuroEngineering and Rehabilitation

Savin, D. N., et al. (2013). Poststroke hemiparesis impairs the rate but not magnitude of adaptation of spatial and temporal locomotor features. Neurorehabilitation and Neural Repair.

Multi-Sensory Feedback for Myoelectric Control

Sean Sanford[1,2], Mingxiao Liu[1,2], Thomas Selvaggi[1,2], and Raviraj Nataraj[1,2]
[1]Department of Biomedical Engineering, Stevens Institute of Technology,
[2]Movement Control Rehabilitation (MOCORE) Laboratory, Email: ssanford@stevens.edu

Introduction

Neuromuscular pathologies can reduce functional capabilities of body extremities. Rehabilitation with the assistance of a myoelectric device is a time-intensive process. We aim to accelerate the rehabilitation process by providing multi-sensory feedback for training of muscle activity [Sigrist 2013]. More consistent muscle activation patterns lead to more effective device control [Huang 2016]. **Our objective** is to develop a rehabilitation platform that applies multi-sensory feedback to optimize myoelectric control after neuromuscular trauma.

Methods

Motion capture system included nine infrared cameras (Prime 17W, Optitrack) to track user head position. Wireless EMG sensors (Trigno, Delsys) were used for measuring muscle activation patterns on up to 14 upper-body muscles spanning the forearm, upper arm, and trunk/shoulder. Machine learning (ML) classification of subject isometric EMG activity will control the subject virtual arm position. Matlab® was used to train and evaluate the ML techniques. The virtual reality environment was created in Unity®. **Multi-sensory Feedback:** *Visual:* Subject and target positions provided with the goal to minimize error between the two. *Haptic:* Vibrotactile feedback to induce more distinct EMG activity for device control.

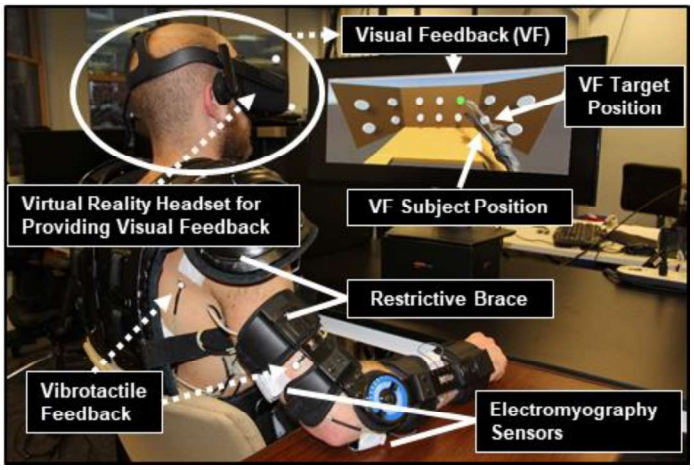

Figure 1: Experimental protocol of a multi-sensory feedback rehabilitation paradigm. Visual and haptic feedback are provided for optimizing myoelectric control of a virtual reality task.

Results and Discussion

Preliminary studies identified 1. The optimal visual feedback (VF) display and 2. The effects of imitated amputee populations on task performance. First, we determined the most effective VF for a multi-segmented movement is presented with body-discernible features. Other VF paradigms presented as abstract cues, or as a single degree of freedom, were less effective for training consistent movement and EMG activity. Therefore, in our rehabilitation paradigm, **Figure 1**, the VF target position was represented as a multi-segmented prosthetic arm. Next, we aimed to identify the effects of reduced muscle sets on myoelectric control by imitating amputee populations. We represented transhumeral and transradial clinical populations by reducing the number of EMG sensors as real-time inputs into the ML classifier. Subjects completed a virtual maze task (**Figure 2**) with EMG input from all 14 muscles, 10 muscles (no forearm, imitated transradial), or 8 muscles (no forearm or upperarm, imitated transhumeral). Two ML methods were evaluated for real-time performance, linear discriminant analysis (LDA) and support vector machine (SVM). For LDA, the set of all 14 muscles had the highest functional task performance measured as completion time and wall collision count (**Table 1**). For SVM, highest performance was found for the 10 muscle set. We concluded that amputees, or participants with reduced muscle capacity, may have high precision myoelectric control in our virtual environment.

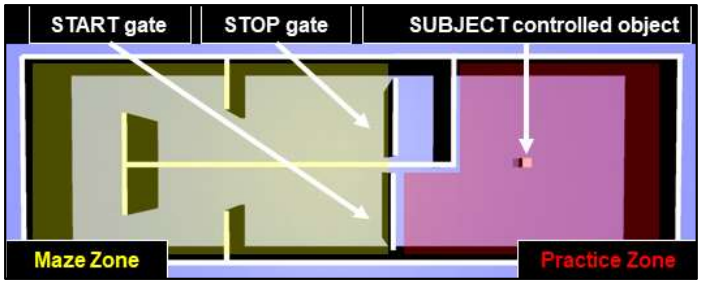

Figure 2: Virtual reality maze task during preliminary study.

Table 1. Results of virtual reality maze task

Completion time (sec)		
(n=5)	**LDA**	**SVM**
14 muscles	9.2 ± 3.6	15.0 ± 18.0
10 muscles	10.9 ± 4.1	7.5 ± 3.0
8 muscles	14.9 ± 14.4	26.4 ± 14.2
Number of collisions with maze walls (#)		
	LDA	**SVM**
14 muscles	2.0 ± 4.6	4.3 ± 1.0
10 muscles	3.3 ± 8.9	1.5 ± 1.7
8 muscles	10.4 ± 34.7	6.2 ± 3.2

Significance

Current rehabilitation programs lack feedback elements informing the subject of task performance beyond verbal cues from clinicians and visual cues from mirrors. Initially, our system will employ motion capture, electromyography, and virtual reality for providing motion and muscle activity performance of a functional task. This can be applied to clinical populations for enhancing current modalities of rehabilitation and training myoelectric device control. Eventually, this system will be commercialized for at-home usage to promote the development of intrinsic mechanisms, such as muscle memory, for greater independent function.

Acknowledgments

Schaefer School of Engineering, Stevens Institute of Technology, Hoboken, NJ 07030

Functional connectivity analysis during direct EMG prosthesis control

Wentao Liu[1]*, Aaron Fleming[1], and He (Helen) Huang[1]
[1] Joint Department of Biomedical Engineering, NC State University and UNC-Chapel Hill
Email : *wliu29@ncsu.edu

Introduction

The study aims to explore the feasibility of functional connectivity analysis to indicate the influence of direct EMG control of robotic prosthetic ankle on neuromuscular control in individuals with lower limb amputations. Powered lower limb prostheses with direct neural control[1] allows amputees to generate control signals using residual muscles and thus partially restore their biomechanics function. How amputee's neuromuscular control mechanism changes under this condition remains unknown. In this study, we assessed and compared multi-muscle function and coordination by performing functional connectivity analysis on surface EMG from an able-bodied person (AB) and a transtibial amputee (TT) during postural sway task. The results might inform a unique way to unveil the potential shift of neuromechanics caused by direct neural control of prosthetic limb, and demonstrate mechanism of neuro control behind it.

Methods

One AB and TT participant were involved in the experiment with IRB approval. All participants was instructed to do forward-backward postural sways following a 0.5 Hz metronome. We collected EMG signals from bilateral tibialis anterior (TA), gastrocnemius (GM), rectus femoris (RF), vastus lateralis (VL), biceps femoris (BF), soleus (SOL), and gluteus medius (GMED). For TT, EMG of SOL on the residual limb was missing.

We applied functional connectivity analysis on EMG data by calculating pair-wise intermuscular coherence for all EMG envelops. To assess muscle coherence under distinct frequency ranges, we decomposed coherence between all muscle pairs by using Non-Negative Matrix Factorization (NNMF)[2]. Basic components and their corresponding factor loadings yield spectral signatures and functional connectivity strength between all muscle pairs.

Results and Discussion

Three major components derived from AB and TT subject (as shown in Fig. 1) indicated different functional connectivity patterns, among which low frequency components are strongly shaped by kinematics of musculoskeletal system, and the influence of motor neural system are expected to be pronounced on the middle and high frequency components.

We observed similarities exist in 'low' frequency component between two subjects, suggesting TT wearing direct neural control prostheses can produce similar kinematics during postural sway task as AB subject. The 'middle' frequency component for TT shifted to a relatively higher frequency range compared to able-bodied person. The pattern of middle and high components are different, and it's obvious that the middle frequency's energy shifted to a higher band area. Raethjen et al's study found corticomuscular transmission of the oscillation between 6-15 Hz to the limbs[3]. The majority of energy in the middle frequency component found in TT's EMG activity concentrates in this band, thus it might reflect active recruitment of supraspinal area during postural sway.

Under each component we pulled out top three pairs of muscles with highest loading, which means these pairs have strongest connection under corresponding component. Based on the topological representation of muscles, they were classified into intra-limb pair or inter-limb pair. The total number of muscle pairs fall under each category is listed in Table 1.

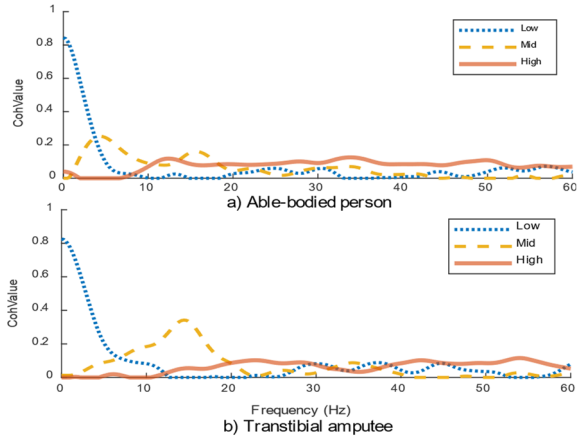

Figure 1: Frequency spectra of three components.

Table 2: Different kinds of intermuscular connectivity observed in AB and TT

	Intra-limb	Inter-limb
Able-bodied person	4	5
Transtibial amputee	7	2

We found AB and TT used different neural control strategy. AB's muscle connection showed more evenly distribute between intra and inter limb, and in contrast TT focused more on intra-limb. The fact that AB has more bilateral connectivity indicated that the functional links are more balanced. However, for TT we found a very strong inter-limb TA-TA connection similar to AB. Perhaps, the motor control system in the CNS has begun to restore the original neural pathway for TA-TA recruitment.

Significance

We demonstrate that functional connectivity analysis for multi-muscle analysis can potentially unveil the neuroplasticity in postural control of lower limb amputees. It will benefit many researches in understanding the neuromechanics of lower limb amputee. Our future study building upon this feasibility study may be used to study the effects of novel prosthetic technology on human neuromuscular control.

References

[1] An experimental powered lowerlimb prosthesis using proportional myoelectric control, J.Med. Devices, S. Huang et al.
[2] Muscle networks: Connectivity analysis of EMG activity during postural control. Sci Rep 5, (2016). Boonstra, T. et al.
[3] Corticomuscular coherence in the 6–15 Hz band: is the cortex involved in the generation of physiologic tremor?, Exp Brain Res (2002). Raethjen, J. et al.

Psychological Readiness is Evident in Motor Unit Action Potentials with ACL Injury

Nathan D. Schilaty[1], April L. McPherson[1], Takashi Nagai[1], Nathaniel A. Bates[1]
[1]Mayo Clinic Biomechanics Laboratories & Sports Medicine Center, Rochester & Minneapolis, MN, USA
Email: schilaty.nathan@mayo.edu

Introduction

Following ACL injury, reconstruction (ACLR), and rehabilitation, only 33-44% of athletes return to their same level of play. [1]. Other psychological responses include: lack of self-confidence, kinesiophobia, depression, and anxiety. Psychological readiness to return to sport is commonly assessed with the ACL-RSI. As psychological readiness can have an affect on motor control, potentially with induction of neuroplasticity [2-3], it is important to understand the motor control deficits related to these psychological responses. This study was designed to assess the effect of psychological readiness on motor control output. Objective demonstration of neural deficits that associate with psychological responses may improve both physical and emotional health outcomes.[4]

Methods

Decomposed electromyography (dEMG) was acquired with a five-pin array sensor (Delsys *Bagnoli*; Natick, MA) placed on four major thigh muscles from 56 subjects [Female (n=32); Control (n=25)]. ACL subjects were longitudinally assessed at Pre-ACLR, 6-mo post-ACLR, and/or 12-mo post-ACLR. Data was acquired at 20 kHz from isometric contractions (quads, hams) with force measured by a custom load cell apparatus. Acquired dEMG data (band-pass filtered 20–1750 Hz) was analyzed with *dEMG Analysis* software to extract average firing rate (AvgFR), inter-pulse interval, recruitment thresholds [% maximal voluntary isometric contraction (%MVIC)], and MU action potential (MUAP) from detected MUs (≥90% accuracy, **Fig. 1**). ANOVA and linear regressions were performed with *JMP Pro 14*. To ensure parametric data for assessment, a *Log* transformation was selected for MUAP. For psychological readiness categorization, an ACL-RSI cutoff value of ≥61 was utilized.[5]

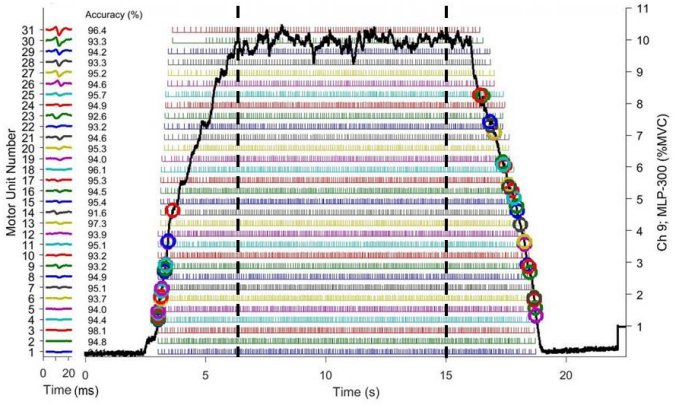

Figure 1: **Isometric Waveform and MU Identification.** With each contraction, the subject followed a trapezoidal waveform with a 3 sec ramp-up, 10 sec hold, and 3 sec ramp-down. The output force is shown (black line). This trial (10% MVC) identified 31 MUs. MU (de)recruitment are denoted by colored circles while firing pattern is demonstrated by color-matched spikes. Data for this analysis was specifically windowed during the 'plateau phase' of contraction (7–15 sec; dashed lines).

Results and Discussion

Linear regressions of MUAP peak-to-peak amplitude (MUAP P2P) demonstrated that the ACL-RSI score <61 group had lower amplitudes with earlier recruited MUs than Controls and ≥61 group. Further, the ACL-RSA <61 group did not achieve MUAP P2P values similar to controls with later recruited units (**Fig. 2**). The ACL ≥61 group demonstrated higher MUAP P2P than controls with later recruited MUs. ANOVA between the ACL-RSI groups demonstrated significantly higher MUAP P2P for quadriceps musculature for the ≥61 group compared to <61 group (p=0.010; **Fig. 2**). Similarly, for the hamstrings, the ≥61 group demonstrated significantly higher MUAP P2P compared to <61 group (p=0.012).

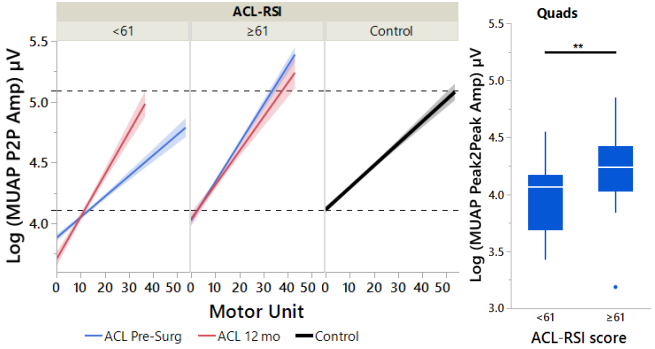

Figure 2: MUAP Peak-to-Peak Amplitude by Recruited MU. Linear regression demonstrates the lower MUAPs utilized by those with lower psychological readiness. Dashed lines represent Control values. The box plot demonstrates the differences of MUAP between ACL-RSI groups for quadriceps.

The MUAP P2P value is a surrogate of MU size.[6] The ability to recruit larger MUs will provide additional control to the musculature. This data demonstrates that those that have lower psychological readiness express MU inhibition across the spectrum of rehabilitation. Those that score higher appear to compensate by recruiting larger MUs.

Significance

This data demonstrates objective results of motor control associated with psychological readiness. These results are important to provide personalized rehabilitation to athletes. Further, it can provide an objective measure to demonstrate effectiveness of psychological counselling to athletes.

Acknowledgments

Mayo Clinic Ultrasound Research Center and NIH funding: R01AR055563, K12HD065987, and L30AR070273.

References

1. Kvist et al. *KSSTA* (2005) 13(5):393-397.
2. Wise. Nat Rev Neurosci (2004) 5(6):483-494.
3. Needle et al. *Sports Med* (2017) 47(7):1271-1288.
4. Schilaty et al. *Sports Med* (2016) 46(3):299-303.
5. McPherson et al. *AJSM* (2019) 47(5):1209-1215.
6. Hu et al. J Neurophysiol (2013) 110(5):1205-1220.

Use-dependent learning, not error-based learning, occurs during perturbed recumbent stepping

Seyed Yahya Shirazi[1*], and Helen J Huang[1,2]
[1]Mechanical and Aerospace Engineering Department, University of Central Florida, Orlando, FL, USA
[2]Disability, Aging, and Technology Cluster, University of Central Florida, Orlando, FL, USA
Email: shirazi@ieee.org

Introduction

Locomotor adaptation is usually an error-based learning experience in which humans modify walking behavior to reduce motor errors in response to perturbations. This adapted behavior often washes out soon after the perturbations are removed [1]. Subjects also initially increase energy cost to respond to the perturbations and then decrease energy cost with adaptation [2]. In seated locomotor tasks (e.g., recumbent stepping), the stakes of an error are lower as the subjects do not need to maintain their balance. Perturbations during seated locomotor tasks, however, likely still engage similar adaptation processes as perturbed walking, which could be beneficial for gait rehabilitation. The purpose of this study was to quantify the motor and mechanical energy responses to brief perturbations during recumbent stepping. We hypothesized that similar to perturbed walking, both stepping error and mechanical energy cost would decrease as subjects adapt to perturbations during recumbent stepping.

Methods

Subjects (n=17) completed four 10-minute trials on a motorized recumbent stepper. Each trial included six minutes of perturbed stepping as well as two minutes of unperturbed stepping at the beginning and the end of the trials. Subject experienced perturbations at either mid-extension or extension onset of the left or right leg as a brief 200 ms increase in stepping resistance. A random no perturbation "catch" stride occurred in every five perturbed strides. We provided a visual pacing cue at one step per second and instructed subjects to step smoothly while matching the pace of the visual pacing cue. We defined stepping error as the maximum difference of the stepping profile from the average unperturbed stepping profile and quantified the stepping mechanical energy cost using the limb forces and stepper speed. We acquired forces from the force sensors in the handles and pedals and the speed from the stepper servomotor.

Results and Discussion

Firstly, subjects were successful at maintaining a stepping pace within ~50 ms of pacing cue during perturbed strides, except for the very first mid-extension perturbed stride. Stepping error decreased significantly during the first perturbed strides of the mid-extension perturbations, indicating fast adaptation to those perturbations and supports our hypothesis (Fig. 1). In contrast, stepping error did not change from early to late during extension-onset trials, indicating that subjects did not adapt and does not support our hypothesis. Interestingly, post-perturbation stepping errors did not wash out and were consistently higher than the pre-perturbation errors for all perturbations. Unlike perturbed walking, stepping mechanical energy cost continuously increased during the perturbations for all trials, which also does not support our hypothesis (Fig. 1). Post-perturbation mechanical energy costs were also higher than the pre-perturbations. During the catch strides, subjects stepped ~200 ms faster than the pacing cue, suggesting they were anticipating a perturbation. Catch strides also had less stepping error than the perturbed strides but did not adapt from early to late perturbation.

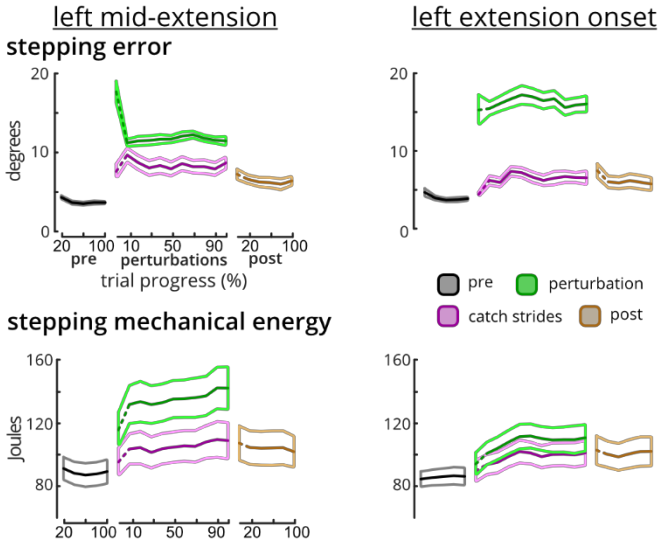

Figure 1: Stepping error and mechanical energy cost of the left mid-extension and extension-onset trials. The light borders indicate standard error. Right-side trials had similar errors and energy costs.

The continuous increase in mechanical energy cost, non-adapting errors, and sustained post-perturbation errors are in line with the use-dependent learning paradigm [3]. When perturbations do not hinder the task goal (here stepping in time), the learning process does not necessarily lead to error reduction. Instead, motor error builds upon the previous instances of the motor behavior and will sustain longer after removing perturbations. The increasing catch stride errors also support this notion of use-dependent learning.

Significance

Brief mechanical perturbations during recumbent stepping enhanced use-dependent learning instead of error-based learning, which resulted in sustained changes during post-perturbation stepping. This aligns with a recent walking study that also reported use-dependent learning and sustained post-perturbation by adding small (and even imperceivable) accelerating perturbations during push-off [4], which is similar to the timing of extension-onset perturbations during recumbent stepping. The sustained motor changes can be particularly beneficial for improving motor impairments and restoring "normal" movement patterns, but further study is needed to determine whether increased energy cost is beneficial or detrimental in rehabilitation.

Acknowledgments

This work was supported by NIH R01AG054621.

References

[1] G. Torres-Oviedo, et al., *Prog. Brain Res.* **2011**, *191*, 65.
[2] J. M. Finley, et al., *J. Physiol.* **2013**, *591*, 1081.
[3] J. Diedrichsen, et al., *J. Neurosci.* **2010**, *30*, 5159.
[4] A. J. Farrens, et al., *bioRxiv* **2020**, 2020.03.27.012591.

OPTIMAL-Based Virtual Reality Feedback to Reduce Dual-Task Balance Cost

Ashley Williams, Samantha Kendall, Jennifer Hogg, Colton Jenkins, Gary B. Wilkerson, and Shellie Acocello
Email: yyb151@mocs.utc.edu

Introduction

Approximately 23-25% of anterior cruciate ligament reconstructed (ACL-R) patients will re-tear the previously injured ACL or contralateral ACL.[1] It is suggested that current ACL rehabilitation practices do not adequately address the demands of real-time competition, resulting in high re-injury rates. Recent evidence indicates that neuromuscular control of the affected limb does not occur in isolation, but is likely governed by central integrative processes of vision, cognition, proprioception, and motor control. The Optimizing Performance through Intrinsic Motivation and Attention for Learning theory (OPTIMAL),[2] a recently developed motor learning framework, shows promise for improving retention of clinical rehabilitation to real-world competition, during which athletes must attend to multiple stimuli simultaneously. Therefore, the purpose of this study was to determine the effectiveness of a motor learning intervention to improve the dual-task cost of adding a cognitive load to a single-leg balance task. We hypothesized that an OPTIMAL-based virtual reality delivered intervention would decrease cognitive-balance task cost immediately after the intervention and at a 24-hour retention test.

Methods

Researchers recruited 21 male and 24 female participants, who were between the ages of 18 and 30 years, and free of concussion, vertigo, lower extremity surgery, and lower extremity injuries within the past 6 months. Participants attended 2 sessions, separated by approximately 24 hours. Participants were randomly assigned to 1 of 3 groups (group 1: control, group 2: autonomy support (AS), group 3: enhanced expectancies (EE)). On force plates sampled at 1000 Hertz, participants completed a single-task balance (20 s) followed by a cognitive-balance task before and after the motor learning intervention on day 1, and for a retention test the following day. The intervention consisted of 5 x 8 single-leg squats on each leg, with adequate rest. Participants wore Virtual Reality (VR) goggles on which was displayed an avatar (control). AS group chose the color of their avatar, and EE group was instructed to keep positive feedback placed on their avatar lit through the duration of each set performed. EE group was instructed to move within pre- determined kinematic thresholds (15° knees valgus and 20° pelvic drop) and received visual feedback via the avatar thresholds.

Dependent variables: Center of pressure(CoP) average velocity cost, Medial lateral(ML) center of pressure standard deviation(SD) cost, Anterior posterior(AP) CoP SD cost, ML Average Velocity Cost, AP Average Velocity Cost. Independent variable was group allocation.

Repeated measures analysis determined change in dual-task cost following intervention and retention. Alpha level was set at .10.

Results and Discussion

On the left side, participants differed over time for CoPAvgVelCost ($p=.05$, $\eta_g^2 = .06$), APCoPSDCost ($p=.02$, $\eta_g^2 = .08$) and APVelAvgCost ($p=.08$, $\eta_g^2 = .04$) and differed between groups for CoPAvgVelCost ($p=.01$, $\eta_g^2 = .04$) and APCoPSDCost ($p=.10$, $\eta_g^2 = .05$). On the right side, participants differed over time for APVelAvgCost($p=.04$, $\eta_g^2 = .03$) and MLVelAvgCost($p=.09$, $\eta_g^2 = .02$). The EE group's average COP velocity decreased by .18 m/s after intervention and remained lower than baseline at retention.

Visual feedback improved postural control and the addition of a cognitive load during stance did not affect the EE group as much. This suggests a favorable central nervous system adaptation, and allowed the participants to maintain a more stable center of pressure.

		Control			AS			EE		
		Pre	Post	Ret	Pre	Post	Ret	Pre	Post	Ret
CoP Avg Vel Cost	L[1]	1.68±7.7	1.26±.8	0.97±0.4	1.71±1.6*	1.22±.7*	1.38±.8*	1.17±.8*	.99±.6*	.84±.6*
	R	1.28±.9	0.96±0.5	1.35±0.7	1.12±.8	1.27±.9	1.26±.8	1.52±.7	.93±.6	1.10±.7
ML Avg Vel Cost	L[1]	2.04±1.0	1.86±1.9	1.18±.8	2.57±2.9*	1.65±1.3*	1.81±1.1*	1.52±1.2*	1.34±0.9*	0.99±1.0*
	R	1.51±.9	1.18±.8	1.85±1.2	1.41±1.2	1.66±1.5	1.67±1.2	2.14±1.3	1.43±1.0	1.66±1.4
MLCoP SD Cost	L	1.01±.6	1.29±1.6	.92±1.3	1.57±1.6	1.22±1.2	2.00±1.2	1.11±1.6	1.36±1.9	0.57±0.8
	R	0.99±.6.6	1.04±.8	1.25±1.0	.90±1.0	.81±.7	.89±1.1	1.22±0.9	0.78±0.7	0.83±0.6
APCoP SDCost	L[1]	1.72±.7	0.93±0.8	.71±0.6	1.90±2.6*	1.17±.4*	1.13±.8*	.96±.7*	0.97±0.5*	0.59±0.8*
	R	1.05±.6	0.78±0.5	1.12±.8	.90±.8	1.12±.8	.80±0.45	1.42±.8	0.77±0.6	0.86±0.7
AP Avg Vel Cost	L[1]	1.30±.5	0.87±0.4	.76±.5	1.02±.8	.91±.4	1.00±.7	.83±0.6	0.63±0.6	0.76±0.6
	R[1]	0.98±.8	0.77±0.7	.82±.5	.78±.4	.83±.6	.88±.5	1.02±0.4	0.51±0.3	0.65±0.4

*= between group differences at .1 level.
[1]= within group differences over time

Significance

Lower extremity/ACL reinjury is a major risk in the athletic/clinical community. An OPTIMAL-based motor learning intervention using visual feedback to improve cognitive-balance control shows promise for reducing dual task cost and improving re-injury outcomes. As this is a pilot study, future work is needed to validate these findings in larger, clinical, and injured cohorts. This work is promising for optimizing ACL rehabilitation and improving transfer of safe motor patterns to real-world sport.

Acknowledgements

This study was funded by THEC Center of Excellence in Applied Computational Science & Engineering (R041302265). We thank Griffin Miller for VR development.

References

Wiggins, A. J., Grandhi, R. K., Schneider, D. K., Stanfield, D., Webster, K. E., & Myer, G. D. (2016). Risk of secondary injury in younger athletes after anterior cruciate ligament reconstruction. *The American Journal of Sports Medicine*

Wulf, G., & Lewthwaite, R. (2016). Optimizing performance through intrinsic motivation and attention for learning: The optimal theory of motor learning. *Psychonomic Bulletin & Review*

Sensory-Motor Assessment of the Lower Extremity in Tibial Rotation: Towards Knee Osteoarthritis Rehabilitation

Ahmed Ramadan*, Raziyeh Baghi, and Li-Qun Zhang
University of Maryland, School of Medicine, Department of Physical Therapy and Rehabilitation Science, Baltimore, MD, USA
Email: *ramadana@som.umaryland.edu

Introduction

Knee osteoarthritis (OA) is the most common cause for disability in older adults [1]. The objective of this preliminary study is to examine lower-limb sensory-motor properties in tibial rotation (stiffness, ROM, and proprioception) and build new insights for a rehabilitation program on a modified elliptical machine [2], [3].

Methods

Four healthy participants (1 male (S2); 28-42 years old) participated in this study. Each subject had their right knee flexed at 90º and the foot mounted onto a footplate of a modified elliptical machine [2], [3]. The footplate rotated horizontally about the long axis of the tibia using a servomotor. The assembly included a 6-axis force/moment sensor whose vertical axis was aligned with the tibial rotation axis.

During the ROM and stiffness test, an ankle brace was used to reduce ankle rotation. Participants were instructed to relax while the footplate rotated at a constant speed 3º/s until a terminal angle (45º) or a peak moment (5Nm except for subject1's 3Nm) was reached for 5 cycles. The most anomalous cycle (by visual inspection) was removed in Matlab. The remaining 4 cycles were divided into descending limbs and ascending limbs, where a 5th order polynomial was fitted to each limb. Polynomial derivatives yielded the rotational stiffness.

For the proprioception test, subjects (S2-S4) closed eyes and the footplate rotated at 0.8º/s in randomized directions until the subject pressed a hand-held switch when motion was detected. Proprioception acuity was measured 4 times in each direction.

Results and Discussion

The female subjects had a less steep hysteresis curves (Figure 1 and 2) compared to the male subject, which agrees with previous study [4]. Each stiffness curve (Figure 2) has an approximate flat region or subtle ramp in the middle. Since this area contains minimum stiffness, we refer to it as the resting stiffness region.

The resting stiffness may reflect the subjects's preference of toe-in, toe-out, or straight-toe during sitting. For example, S1's resting stiffness is approximately from -25º to 5º suggesting this subject prefers toe-out during sitting. Table 1 summarizes these results and the self-reported preferences.

Some knee OA rehabilitation programs target minimizing external knee adduction moment (EKAM) [2], which can be achieved by the foot progression angle (toe in or out). The current test can potentially give rehabilitation programs a proactive subject-specific strategy (what direction of foot progression angle) to reduce EKAM. However, this should be investigated further because of limitations inlcuding: this test is done in a sitting position while EKAM is computed during stepping. The different context (sitting versus standing) may affect the suggested proactive strategy.

The proprioception acuity (Table 2) for female subjects is less than that reported in [3] (3.5º), which may be due to the different context (sitting versus standing with measurements on the weight-bearing side). Improving proprioception acuity through training is an expected outcome as in [3].

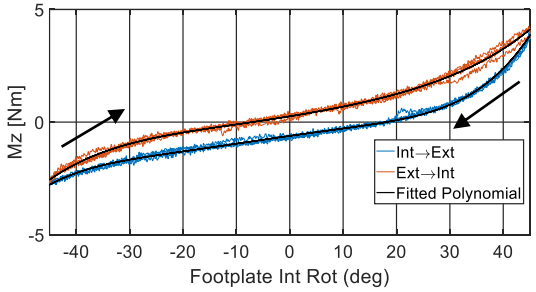

Figure 1: A typical hysteresis curve (for subject#3)

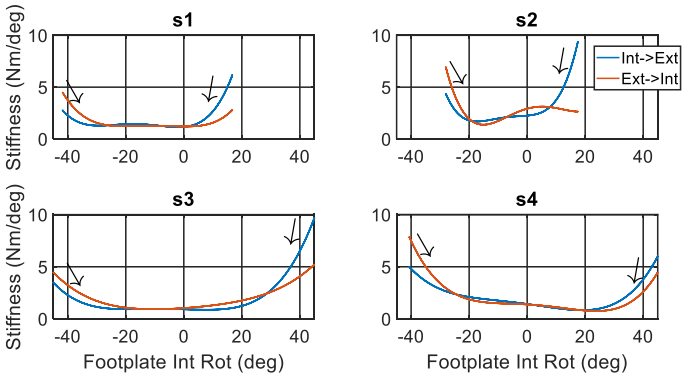

Figure 2: The stiffness curves for each subject

Table 1: Subjects' preference during sitting

	S1	S2	S3	S4
Self-reported	Toe-out	Toe-out	Toe-out	Toe-in
Resting stiffness	Toe-out	Toe-out	Toe-out	Toe-in

Table 2: Subjects' proprioception acuity as mean(SD) in degrees

	S1	S2	S3	S4
External rotate	-	4.35(1.58)	0.94(0.14)	1.64(0.10)
Internal rotate	-	2.75(1.14)	1.20(0.33)	1.64(0.33)

Significance

We suggest a new proactive subject-specific strategy to reduce EKAM via a resting-stiffness principle drived from a sensory-motor assessment of the lower extremity in tibial rotation.

Acknowledgments

L. Zhang has equity positions in Rehabtek LLC, which received federal grants in developing the robotic device used in this study.

References

[1] G. Peat, et al. (2001). "Knee pain and osteoarthritis in older adults: A review of community burden and current use of primary health care," Annals of the Rheumatic Diseases.
[2] S. H. Kang, et al. (2019). "Real-time three-dimensional knee moment estimation in knee osteoarthritis: Toward biodynamic knee osteoarthritis evaluation and training," IEEE TNSRE.
[3] S. J. Lee, st al. (2015) "Pivoting neuromuscular control and proprioception in females and males," Eur. J. Appl. Physiol.
[4] H. S. Park, et al. (2008). "Gender differences in passive knee biomechanical properties in tibial rotation," J. Orthop. Res.

Evaluating activation patterns of the hand and wrist during dynamic tasks using a similarity index

Sarah Agnew[1], Grace Han[1], Yonatan Eshetu[1], and Brad J. Farrell[1]
[1]Georgia State University, Atlanta, GA
Email: jhan39@student.gsu.edu

Introduction

Hand and arm function are vital to recovery following neurological injuries such as those sustained following a brain or spinal cord injury. Inpatient and outpatient rehabilitation provided by Physical Therapists improves motor function acutely, but after discharge from therapeutic care patients often revert to utilizing the uninvolved limb to accomplish tasks. Underutilization of the affected limb results in diminished overall function and patient independence. One way to improve at home care is to utilize the muscle activation patterns to monitor compliance and efficacy of muscle recruitment. The purpose of this study was to determine if the muscle activation patterns can be used reliably to identify the intended movement pattern during dynamic tasks. We hypothesized that a similarity index could reliably identify each dynamic hand and wrist biomechanical movement when prompted by an on-screen video.

Methods

Twenty, non-injured subjects were recruited via a convenience sample. Each subject performed static wrist flexion and extension, radial and ulnar deviation, and hand closing and opening, while electromyography (EMG) data was collected from a low-cost armband around the forearm. Each subject was then asked to perform the tasks in a dynamic fashion, such as repeating wrist flexion and extension, repeating opening and closing of the hand, and a global dynamic pattern task where each movement was prompted by a video in a random order. During each task, EMG data was acquired and streamed via Bluetooth to an Android tablet using a custom software app to quantify and identify the intended movement pattern.

Static and dynamic EMG patterns were compared using a vector similarity index (SI), which ranged from 0 to 1, to evaluate the movements. For the dynamic tasks, a 50 ms moving window was utilized to compare the EMG observed during the dynamic tasks to each static task for identification. A one-way ANOVA was used to evaluate statistical significance.

Results/Discussion

For the non-injured group, similarity index analysis could discriminate between various movements, yielding reproducible and reliable results across subjects (Fig 1). Of the 3 antagonistic movements, wrist flexion and extension and wrist radial and ulnar deviation showed significant differences in SI. However, closing and opening the hand elicited a less reliable SI compared to the others especially wrist extension. For the dynamic tasks, wrist flexion, wrist extension, ulnar deviation, and hand closing were most reliably identified (> 85% time). However, the transition phases between movements or tasks required a thresholding procedure, as no similarity index was appreciably high during this period.

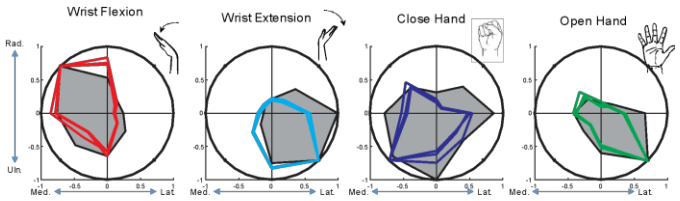

Figure 1: Average patterns (gray) from the 8-sensor EMG armband during specific movements and 3-trials from a representative subject. Note the similarity index for each movement was > 0.95.

Significance

Our hypothesis that muscle activation patterns may be used to differentiatemovement patterns was generally maintained. Therefore, we propose that this similarity index calculation can be integrated into a mobile software app to help delineate dynamic movements during training or natural behavior. Perhaps these movement patterns can also be incorporated as feedback to the participant in an effort to facilitate proper patterning during wrist and hand movements, especially following neurological injury. However, as always, more analysis is needed to fully develop this method.

References

Lee et al. *J ElectromyogrKinesiolo* 2004.
Lim et al. *IEEE Trans Neural Syst RehabilEng* 2004.
McKay et al. *Spinal Cord,* 2011.

Clinical Improvements Relate to Gait Function in Patients with Achilles Tendinopathy

Kayla D. Seymore[1,2], Haraldur B. Sigurðsson[1], Shawn Hanlon[1,2], Brian Honick[1,2], Andrew Sprague[1,2], Karin Grävare Silbernagel[1]
[1]Dept. of Physical Therapy, University of Delaware, Newark, DE, USA
[2]Biomechanics and Movement Science Program, University of Delaware, Newark, DE, USA
Email: seymorek@udel.edu

Introduction

Mid-portion tendinopathy is the most common pathologic condition of the Achilles tendon in adults. In addition to symptoms of pain, Achilles tendinopathy has been shown to significantly alter gait function [1], resulting in lower levels of physical activity and detriments to overall health and well-being [2]. Although full symptomatic recovery is evident after exercise treatments, this does not ensure full functional recovery [3]. Further, it is unknown if changes in patient-reported outcomes of Achilles tendinopathy treatment are related to adaptations in lower limb gait. Thus, the purposes of this study were to (1) evaluate changes in pain, patient-reported outcomes, and gait 24 weeks after initiation of Achilles tendon-loading exercise treatment, and (2) determine relationships between patient-reported outcomes and gait pior to and 24 weeks after initiation of treatment in patients with mid-portion Achilles tendinopathy.

Methods

Twenty-five (11 M, 14 F, 51.2 ± 11.6 yrs) participants with clinically confimed mid-portion Achilles tendinopathy underwent an effective exercise-based treatment program [3]. Pain, patient-reported outcomes, and gait data were collected at baseline and 8-, 16-, and 24-week follow up visits.

Pain was objectively assessed via pain pressure threshold (PPT). Algometer-applied (SBmedic, Solna, Sweden) pressure (kPa) at the Achilles tendon was recorded for 3 trials. Patient-reported outcomes of pain, symptoms, quality of life, and physical activity/sport function were assessed with two validated questionnaires: Victorian Institute of Sport Assessment-Achilles (VISA-A), Foot and Ankle Outcome Score Quality of Life (FAOS-QOL) and Sport and Recreation Function (FAOS-SP) subscales. A MuscleLab IMU system (Ergotest Innovations, Oslo, Norway) was used to collect gait data during a 10-m walk at a self-selected pace. The percentage of time spent in stance, mid-stance, and swing phases over 3 gait trials were calculated.

Average PPT, questionnaire score, and average gait outcomes for the most symptomatic limb were quantified for analysis. Repeated measures ANOVAs were used to test the main effect of time (baseline, week 8, week 16, week 24). Bonferroni corrections were used for post-hoc analysis of significant effects. Pearson's correlations were used to determine relationships between patient-reported outcomes and gait at baseline, and changes over the 24-week period. Alpha was $p < 0.05$.

Results and Discussion

Twenty-four weeks after initiation of Achilles tendon exercise treatment, participants displayed significant clinical and functional improvements in their most symptomatic limb (**Table 1**). PPT increased at 16 and 24 weeks compared to baseline ($p=0.011$; $p=0.001$). Patient-reported outcomes of pain and symptoms measured by the VISA-A ($p<0.001$) improved, while quality of life and physical activity/sport function measured by the FAOS-QOL ($p<0.001$), FAOS-SP ($p<0.001$) increased throughout treatment compared to baseline. VISA-A and FAOS-QOL scores exceeded the minimum clinically important difference/change values [4-5]. Percentage of gait in stance phase decreased ($p=0.039$) and swing phase increased ($p=0.044$) from baseline to week 24 of treatment. After correcting for type I error, there was no effect of time on the mid-stance phase of gait ($p>0.05$).

Table 1: Mean (SD) of outcome measures at baseline and 24 weeks.

	Baseline	Week 24
PPT*	170.9 (67.6)	220.5 (85.5)
VISA-A*	47.2 (20.9)	69.6 (20.9)
FAOS-QOL*	43.0 (18.3)	69.3 (23.3)
FAOS-SP*	58.0 (20.6)	79.4 (17.6)
Stance*	64.5 (2.5)	63.1 (2.8)
Mid-Stance	27.7 (5.2)	26.7 (5.4)
Swing*	35.6 (2.5)	36.9 (2.8)

**significant effect of time ($p<0.05$)*

Gait function displayed a moderate ($\pm0.3<r<\pm0.7$) correlation to patient-reported outcomes at baseline and improvements following the treatment period (**Table 2**). Of clinical relevance, at baseline, lower FAOS-QOL and FAOS-SP scores were correlated to an increased percentage of gait spent in mid-stance ($p<0.01$). Twenty-four weeks after initiation of treatment, higher FAOS-SP scores were correlated to a decreased percentage of gait spent in mid-stance ($p=0.001$).

Table 2: Correlation (r) of changes in patient-reported outcome and gait measures from baseline to 24 weeks.

	VISA-A	FAOS-QOL	FAOS-SP
Stance	0.096	-0.192	-0.031
Mid-Stance	-0.326	-0.116	-0.629*
Swing	-0.088	0.190	-0.036

**significant at $p<0.01$*

Improvements in PPT, patient-reported outcome measures, and gait function were observed in patients with mid-portion Achilles tendinopathy. Patient-reported outcomes and gait were moderately correlated at baseline and 24 weeks after initiation of exercise treatment.

Significance

In patients with midportion Achilles tendinopathy, clinical improvements may be related to functional gait measures during mid-stance 24 weeks after initiation of an Achilles tendon exercise program.

References

[1] Ogbonmwan I et al. (2018). *Gait Posture*, **62**:146-156.
[2] Ceravolo ML et al. (2018). *Clin J Sport Med.,* **1**: doi:10.1097/jsm.0000000000000636.
[3] Silbernagel KG et al. (2007). *Br J Sports Med*., **41**:276-280.
[4] McCormack J et al. (2015). *Int J Sports Phys Ther*., **10**:639-644.
[5] Sierevelt IN et al. (2016). *Knee Surg Sports Traumatol Arthrosc.,* **24**:1339-1347.

Shear Wave Speed Measurement Reliability in the Hamstring Muscles

Scott K. Crawford[1], Christa Wille[1,2], Mikel Stiffler-Joachim[1], Kenneth S. Lee[3], Bryan C. Heiderscheit[1,2]
1. Department of Orthopedics & Rehabilitation, 2. Department of Biomedical Engineering,
3. Department of Radiology; University of Wisconsin-Madison
Email: Crawford@ortho.wisc.edu

Introduction

Ultrasound shear wave elastography (SWE) has been used as a non-invasive method to estimate muscle tissue elasticity [1–3], and may be useful for quantitatively assessing changes in elasticity following acute muscle strain injury. Most studies investigating tissue elasticity with SWE do not report the reliability of their measures [4]. When reliability measures are reported, conflicting evidence exists with larger muscles of the lower extremity, such as the hamstrings, especially in repeat imaging sessions [4,5]. The purpose of this study was to determine the test-retest reliability of shear wave speed (SWS) measures in different regions of the hamstring muscles.

Methods

Ten participants were recruited (18-35 years of age, self-reported regular exercise, no history of lower extremity surgery or hamstring injury) and provided written informed consent.

Participants were asked not to exercise for >3 hours prior to image acquisition. Participants were positioned in prone with their hips and knees in a neutral position, fully supported, and with no active muscular contraction. Locations corresponding to 33, 50, and 67% of the thigh length (proximal, mid-belly, and distal, respectively) from the ischial tuberosity to the midline between femoral condyles were marked bilaterally.

SWS measures were obtained for each hamstring muscle (semimembranosus: SM; semitendinosus: ST; biceps femoris long head: BFlh) at each location along the thigh by an experienced sonographer (5+ years) using the same US system (Aixplorer, Supersonic Imagine). Gel was applied along the length of the thigh and the transducer (SuperLinear, SL 10-2, 38 mm aperture) was applied with minimal pressure. A single image (5 cm depth) was captured at each location and the mean of 3 SWS measurements within the mid-thickness of the muscle (Q-box with 5.0 mm diameter) was calculated. Repeat images were captured bilaterally with 60 s of seated rest between trials.

Intraclass correlation coefficients (ICC(3,1)), standard error of measurement (SEM), minimal detectable change (MDC), and coefficients of variation (CV) were calculated. Reliability was defined as poor (ICC<0.5), moderate (0.5 ≤ ICC < 0.75), good (0.75 ≤ ICC < 0.9), or excellent (ICC ≥ 0.9).

Results and Discussion

Participants (6 females:4 males) had mean ± standard deviation (SD): age 22.7 ± 1.8 years and BMI 22.6 ± 2.2 kg/m^2. Test-retest reliability for most locations across all muscles was moderate to good (Table 1), except at the distal BFlh. SEM ranged from 0.11 – 0.17 (mean: 0.13 m/s) with MDC ranging from 0.31 – 0.48 m/s (mean: 0.35 m/s). The CV across all locations and muscles was less than 9% (range: 4.1 – 8.9%).

Poor reliability at the distal BFlh may be explained by its morphology as it begins to taper and become more tendinous as it joins with the BF short head. This study adds to the current understanding of SWE reliability, as most studies have only imaged at a single location in the muscle [2,5]. Previous studies have reported SWE CV values [kPa] in excess of 15% [5] whereas we found CV values less than 9% across all locations.

Significance

This study indicates SWS measures can be reliable in the hamstring muscles, but care should be taken in extrapolating repeatability measures at a single location (e.g. mid-belly locations reported in many studies) across the whole muscle.

Acknowledgements

Funding provided by NBA & GE Healthcare Orthopedics and Sports Medicine Collaboration and by the Clinical and Translational Science Award Program, through the NIH National Center for Advancing Translational Sciences, grant UL1TR002373 and TL1TR002375.

References

1. Lee et al. *(2016). Clin Biomech, **31**: 20–28.* **2.** Le Sant et al. *(2015). PLoS One, **10**: e0139272.* **3.** Green et al. *(2012). NMR Biomed, **25**: 852–858.* **4.** Dubois et al. *(2015). Ultrasound Med Biol, **41**: 2284–2291.* **5.** Šarabon et al. *(2019). PLoS One, **14**: e0222008.*

Table 1. Reliability of SWS measures between repeat trials.

		Mean (SD)	*ICC [95% CI]*	*SEM (m/s)*	*MDC (m/s)*	*CV (%)*
BFlh	Proximal	2.09 (0.30)	0.80 [0.48, 0.92]	0.14	0.38	6.6
	Mid-belly	1.90 (0.17)	0.55 [0, 0.82]	0.11	0.32	6.0
	Distal	1.93 (0.18)	0.05 [0, 0.62]	0.17	0.48	8.9
ST	Proximal	2.23 (0.26)	0.88 [0.70, 0.95]	0.10	0.25	4.1
	Mid-belly	2.43 (0.30)	0.82 [0.55, 0.93]	0.13	0.35	5.2
	Distal	2.49 (0.27)	0.83 [0.58, 0.93]	0.11	0.31	4.5
SM	Proximal	2.01 (0.27)	0.77 [0.41, 0.91]	0.13	0.38	6.4
	Mid-belly	2.01 (0.24)	0.76 [0.40, 0.91]	0.12	0.33	5.9
	Distal	2.05 (0.23)	0.73 [0.32, 0.89]	0.12	0.34	5.9

Development and Validation of a Finite Element Model of the Cervical Spine

Shadman Tahmid[1] and James Yang[1*]
[1]Human-Centric Design Research Lab, Department of Mechanical Engineering, Texas Tech University
Email: james.yang@ttu.edu

Introduction

The cervical spine protects the spinal cord along with nerve roots, provides structural support and flexibility of movement of the head and neck complex. Injuries to the cervical spine can be fatal [1]. Finite element (FE) model can help understand the injury mechanism and dysfunction in the head and neck complex [2,5]. With the advancement of powerful computational capabilities, FE models are now being widely used as a tool for biomedical applications. There have been a lot of work in modeling cervical spine using finite element technique in the past few decades [2,3,6,7]. Unfortunately, most of these models are not publicly available hence there is a need for building our own model. Verification and validation against experimental study is required for an FE model to be applicable. This study aims to develop a detailed finite element model of the cervical spine and validate the model against existing literature.

Methods

The geometries of the cervical spine finite element model were developed based on CT scan data provided by Texas Back Institute. The three-dimensional model consists of six cervical spine vertebrae (C2 to C7). The vertebral bodies of the model have the cortical bone, the cancellous bone and the posterior bony structure. The spaces between two vertebrae are filled with intervertebral discs. An endplate of approximately 0.1mm thickness is integrated between each disc and vertebra. Each disc is constructed with annulus fibrosus and nucleus pulposus. Five major ligaments (anterior longitudinal ligament (ALL), posterior longitudinal ligament (PLL), ligamentum flavum (LF), interspinous ligament (ISL) and capsular ligament (CL)) are modeled between the vertebrae and discs as shown in Figure 1.

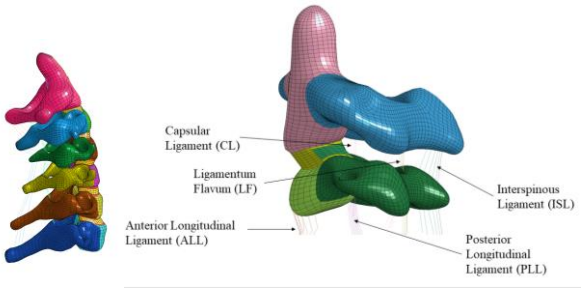

Figure 1. Meshed cervical spine model from C2 to C7 along with the ligaments.

The three-dimensional surfaces of the vertebrae went through a smoothing process using Blender (Blender Foundation, Amsterdam, Netherlands). This procedure removed all spikes and unwanted holes on the surface of the vertebral geometry. Meshing was performed in IA-FEMesh (University of Iowa, Iowa City, IA, USA) using multiblock technique. The intervertebral discs were modeled with concentric layers of elements where the nucleus remains centered. The nucleus is around 40% of the entire disc volume. Nonlinear stress-strain curves were used for the material properties of the ligaments.

Results and Discussion

The complete model was simulated in LS-DYNA. Pure moment (2, 1.5, 1, 0.5 Nm) applied to the C2 vertebrae about x-axis created flexion (+) / extension (-) while all the nodes of the bottom surface of C7 vertebrae were constrained in all degrees of freedom. The model was tested in flexion-extension against experimental data published by Wheeldon et al. [4] and Nightingale et al. [5], and finite element simulation results by Erbulut et al. [6] and Panzer et al. [7]. The range of motion (ROM) of each spinal unit in flexion-extension is in the range of the specified literature as shown in Figure 2. The ROM mostly follows experimental corridor in the literature though a slight stiffness can be noticed in the flexion of C2-C3 spinal unit. For all other spinal units, the result is closer to the studies conducted by Panzer et al. Overall results show an asymmetry in the flexion and extension direction.

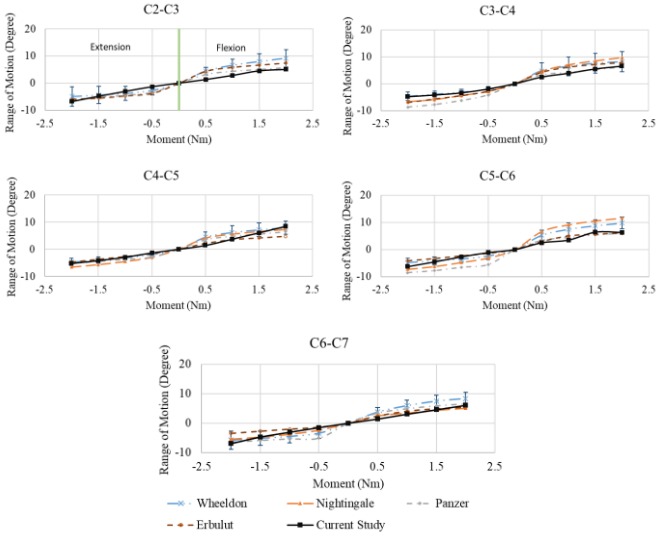

Figure 2. Range of motion during flexion-extension compared with specified literature for different spinal units.

Significance

Finite element models can be applied in medical science to study and simulate real-life situations. Whiplash in car accidents, disc degenerative disease or high-g acceleration during flight maneuvers can injure the cervical spine. These conditions can be studied in detail using this validated finite element model.

References

1. Mustafy, T. et al. (2016). *Journal of the mechanical behavior of biomedical materials,* 53: 384-396.
2. Panjabi, M.M. et al. (1998). *Spine*, 23(24): 2684-2699.
3. Yoganandan, N. et al (1996). *Medical engineering and physics*, 18:569-574.
4. Wheeldon, J. et al. (2006). *Journal of biomechanics*, 39.2: 375-380.
5. Nightingale, R. et al. (2007). *Journal of biomechanics*, 40.3: 535-542.
6. Panzer, M. et al. (2011). *Medical engineering & physics,* 33.9: 1147-1159.
7. Erbulut, D. et al. (2014). *Medical engineering & physics* 36.7: 915-921.

Quadriceps Muscle Morphology Predicts Vertical Ground Reaction Forces Following ACL Injury

Kazandra M. Rodriguez.[1], Steven A. Garcia[1], and Riann Palmieri-Smith[1,2]
[1]School of Kinesiology, University of Michigan-Ann Arbor
[2]Department of Orthopaedic Surgery, University of Michigan Medicine
Email: kazandra@umich.edu

Introduction

Quadriceps weakness is a ubiquitous consequence following ACL injury and reconstruction. Alterations in muscle morphology is one factor theorized to contribute to quadriceps weakness. [1] Features such as muscle cross-sectional area (CSA) and fascicle length determine the force production of muscle. Although greater quadriceps strength is linked to lower peak ground reaction forces, [2] it is unclear whether muscle morphology can predict ground reaction forces. Given that alterations in muscle morphology are associated with deficits in quadriceps force, [3] it is plausible that features such as cross-sectional area and fascicle length may contribute to ground reaction forces during gait. Muscle morphology is a factor that can be modified through interventions such as eccentric exercise [4], thus investigating the relationship between muscle morphology and loading during gait may provide valuable insight into targeting abnormal loading after ACL injury.

Therefore, the primary purpose of this study was to examine the contributions of vastus lateralis (VL) cross-sectional area and fascicle length to vertical ground reaction forces in individuals with ACL injury.

Methods

Fourteen individuals participated in this study (X M/X F; age = Y; time since injury = ZZ). Eligibility criteria included 1) aged 14-45 years of age and 2) an acute ACL rupture. Prior to surgery, 3-D joint kinematics and kinetics were collected during overground walking at 1 m/s using a 10-camera motion capture system (Qualisys; 12 Hz) and two fixed force plates (AMTI; 2000 Hz). Peak vertical ground reaction forces of the ACL-injured leg were extracted from the first half of stance and averaged over 3 trials. Static CSA and fascicle length of the VL were collected using ultrasonography (GE Logiq; 12 MHz, gain 15 dB). Images were assessed using ImageJ and averaged for 3 trials. Cross-sectional area was normalized to body mass (mm/kg) and ground reaction forces were normalized to units of body weight (GRF in N/body mass in N). Linear regressions assessed the contribution of CSA and fascicle length of the VL to peak vertical ground reaction forces. Statistical analyses were performed using R (Version 3.6.1) and level of significance set *a priori* at $p < 0.05$.

Results and Discussion

CSA and fascicle length of the VL significantly predicted peak vertical ground reaction forces of the ACL-injured leg (Adj-R^2_{CSA} = 0.25; Adj-$R^2_{FASCICLE\text{-}LENGTH}$ = 0.27). Greater VLCSA and shorter fascicle lengths were predictive of higher vertical ground reaction forces ($p = 0.04$).

Although the relationship between quadriceps morphology and joint loading after ACL injury has not been studied to date, the current findings are consistent with muscle morphology and its relationship to force production. Pennate muscles like the VL have faciscles oriented at an angle relative to the muscle line of action [5] and result in shorter fascicle lengths. [6] The shorter fascicle lengths allow a greater number of sarcomeres in parallel and greater fascicle rotation, which increases the force production of the muscle. Concurrently, greater CSA would increase the number of sarcomeres in parallel and increase force production further. [7] Thus, individuals with greater GRFs during walking may demonstrate greater quadriceps muscle forces due to larger CSA, shorter fascicle lengths, and greater changes in fascicle rotation. Considering quadriceps strength contributes to tibiofemoral loading during gait, [8] the current findings suggest muscle morphology may present a modifiable parameter to improve abnormal loading following ACL injury.

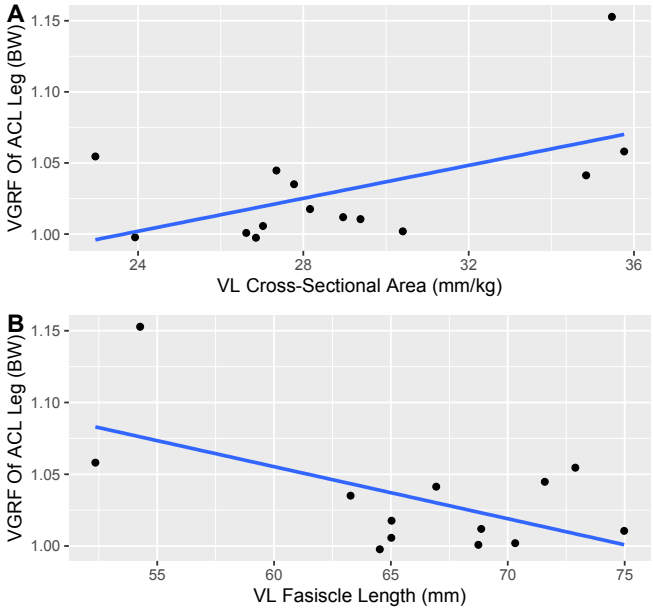

Figure 1: Correlations between **A)** VL CSA of the injured leg and VGRF of the injured leg and **B)** VL fascicle length of the injured leg and VGRF of the injured leg. The line represents the best linear fit.

Significance

Static quadriceps muscle morphology is predictive of joint loading of the ACL-injured leg during gait. However additional research is needed to directly examine the contribution of quadriceps muscle morphology to joint loading during locomotion. Future studies examining joint loading and dynamic muscle morphology during locomotion may provide further insight.

Acknowledgments

This project was funded by the National Institutes of Health (ref. No 1R01HD093626-01A1)

References

[1] Noehren et al. J Bone Joint Surg 2016; 98:1541–1547.
[2] Ward et al. JAT 2018; 53(2):135–143.
[3] Kuenze et al. JOR 2016; 34(9): 1656–1662.
[4] Higbie et al. JAP. 1996; 81(5): 2173–2181.
[5] Gans & Bock Ergeb Anat Entw Gesch 1965; 38:115.
[6] Lieber & Friden Muscle Nerve 2000; 23:1647–1666.
[7] Johnson et al. MSSE 1991. 23(1): 49–55.
[8] Garrison et al. OJSM. 2019; 7(10).

The Effects of Pathology and Surgery on the Instant Center of Rotation in the Cervical Spine

Clarissa LeVasseur[1], Samuel Pitcairn[1], Jeremy Shaw[1], William Donaldson[1], Joon Lee[1], William Anderst[1]
[1]Department of Orthopaedic Surgery, University of Pittsburgh
Email: cll100@pitt.edu

Introduction

Anterior cervical discectomy and fusion (ACDF) is performed approximately 150,000 times per year in the US [1]. However, 14-32% of ACDF patients are symptomatic again within 10 years of the initial surgery [2]. It is unclear whether the new pathology is related to the surgical procedure, which may affect adjacent segment loading and lead to degeneration, or if the new pathology is part of the natural history [3]. Intervertebral range of motion (ROM) is typically used to evaluate adjacent segment kinematics following ACDF, but ROM only provides information regarding the quantity of motion rather than the quality of motion (*i.e.* how the motion occurs). The instant center of rotation (ICR), which incorporates the combined translation and rotation that occurs during movement, has been proposed to evaluate motion quality [4]. The aim of this study was to evaluate (1) the effect of pathology on the ICR, as well as (2) the effect of ACDF on the ICR. We hypothesized are that both pathology and fusion affect the ICR.

Methods

This analysis included 30 middle aged controls (10M, average age 46.3±6.7yrs.) and 45 arthrodesis patients (22M, average age 48.4±7.2yrs.) set to receive either single or double level ACDF at either the C4/C5, C5/C6, or C6/C7 motion segments. All participants consented to participate in these IRB-approved studies. Synchronized biplane radiographs were collected at 30 images/second for 3 seconds as participants moved through three trials of full flexion/extension ROM. Radiographs of the arthrodesis patients were collected before (PRE) and 1 year after (POST) surgery. Six degree-of-freedom kinematics were determined using a validated registration process that matched subject-specific CT-based bone models to the biplane radiographs with sub-millimeter accuracy [5]. The ICR was then calculated using the finite helical axis method, as previously described [6,7]. ICR location was evaluated at every 2° increment of intervertebral flexion/extension from -6° (extension) to +6° (flexion) at each subaxial motion segment. Additionally, changes from before to after surgery in ICR location were analyzed in the arthrodesis patients at the motion segments superior and inferior to the fusion. A Student's t-test was used to identify differences between groups at corresponding motion segments and within the fusion group from PRE to POST with significance set at $p < 0.05$ and a Bonferroni correction applied to account for multiple comparisons ($n = 7$).

Results and Discussion

Eight arthrodesis patients received ACDF at the C4/C5 segment, 37 received ACDF at the C5/C6 segment, and 25 received ACDF at the C6/C7 segment. There were no differences found in either the AP or SI location of the ICR between the controls and PRE arthrodesis patients at the asymptomatic C2/C3 or C3/C4 motion segments (all $p > 0.1$) or the symptomatic C4/C5 or C6/C7 motion segments (all $p > 0.35$, Figure 1). The ICR at the symptomatic C5/C6 was more anterior in the arthrodesis group than the controls at 6° of flexion (purple circle vs triangle, $p < 0.038$, Figure 1). Generally, it does not appear that pathology alters the quality of the intervertebral motion compared to age-matched controls.

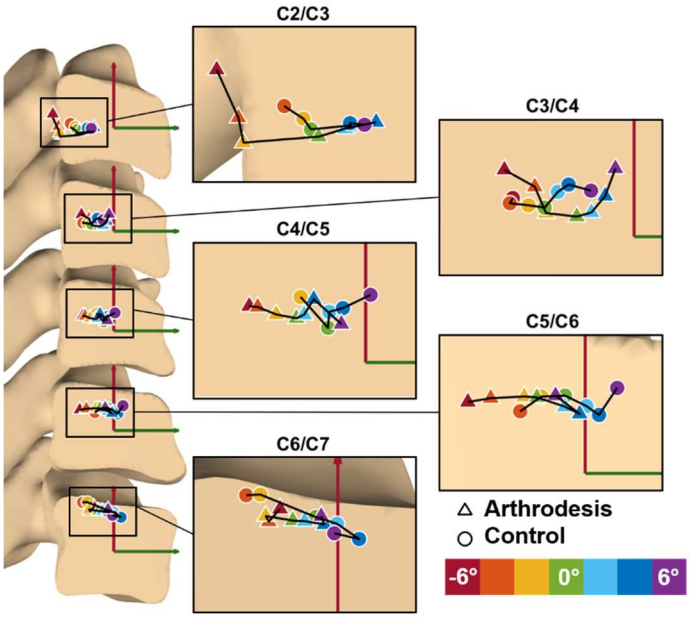

Figure 1. ICR locations from 6° of intervertebral extension (dark red) to 6° of intervertebral flexion (purple) in the arthrodesis (triangles) and control (circles) at each intervertebral level.

There were no changes observed in either the AP or SI location of the ICR at the superior or inferior adjacent segments from PRE to POST (all $p > 0.2$) nor were there differences in the change of ICR location at the adjacent levels following either single or double level fusion (all $p > 0.07$). We found no evidence to suggest that ACDF alters the quality of adjacent segment intervertebral motion at 1 year after surgery.

Significance

Neither pathology nor ACDF surgery appear to alter how motion occurs at the symptomatic or adjacent segments during cervical spine flexion/extension. This finding fails to support the belief that pathology or ACDF surgery alter adjacent segment kinematics.

Acknowledgments

This work was supported by NIH Grant R01 AR069543.

References

[1] Oglesby et al. (2013). *Spine.*
[2] Lawrence et al. (2012) *Spine.*
[3] Riew et al. (2012). *Spine.*
[4] Bogduck et al. (1995). Proc Inst Mech Eng.
[5] Anderst et al. (2011) *Spine.*
[6] Baillargeon and Anderst (2013) *J Biomech.*
[7] Spoor and Veldpaus (1980). *J Biomech.*

Neck muscle size-strength correlation is gender-dependent

Curran Reddy[1], Yu Zhou[2], Bocheng Wan[2], and Xudong Zhang[1,2,3*]
[1]Department of Biomedical Engineering, [2]Department of Industrial and Systems Engineering,
[3]Department of Mechanical Engineering, Texas A&M University, College Station, TX
Email: *xudongzhang@tamu.edu

Introduction

Head injury risk secondary to unsafe head accelerations is a growing concern for athletic populations as new discoveries of adverse effects from even sub-concussive impacts have been made. In order to investigate the potential effects of neck strength on head-acceleration injury risk, previous efforts have used static strength tests and dynamic impact simulations to identify factors that may have injury-prevention implications. While neck strength and muscle size have been shown to have a protective effect in laboratories, their relationships have shown mixed results when used to predict on-field injury rates, stressing the need for a clearer understanding of the muscle size-strength relationship and how it might vary across different conditions and population groups.

Therefore, the purpose of this study was to elucidate the neck muscle size-strength relationships and explore the effects of gender and neck posture on the relationships.

Methods

Thirty healthy adult subjects (13 males, 17 females) underwent neck strength testing and MR imaging of the neck region. In strength testing, the subjects wore a helmet, were strapped into a seat within a custom-built test frame, and performed maximal voluntary exertions (MVEs) by pressing via a helmet-mounted interface against a tri-axial load cell in three different configurations: A) flexion in a neutral posture, B) flexion in a 40° extended posture, and C) extension in a 40° flexed posture. The analysis of MR images (3T clinical scanner, PD-TSE, 3.0mm slice thickness, no gap) involved manual segmentation in MIMICS 20.0 of the following muscles: sternocleidomastoid (SCM), infrahyoids (IH), anterior scalene (AS), longus capitis and colli (LONGUS), semispinalis cervicis and multifidus (DEEP), splenius capitis and cervicis (SPL), longissimus capitis and cervicis (LONGISS), semispinalis capitis (SSC), levator scapula (LS), and trapezius (TRAP).

The following muscle size measures were defined and calculated for each muscle: anatomical cross-sectional area (ACSA) was defined as the single largest cross-sectional area for a given muscle; muscle volume (MV) was calculated by multiplying the sum of segmented areas from all MRI slices by slice thickness; reconstruction-based cross-sectional area (RCSA) was a novel measure of physiologic cross-sectional area calculated by dividing MV by muscle length (ML)—estimated by re-slicing the 3D point cloud reconstruction of a segmented muscle into 3mm axial sections and finding the length of the cubic polynomial fit to the sections' centroids.

Student's t-tests were used to compare anthropometric, strength, and muscle size measures between genders. Linear regression and ANCOVA were used to analyze muscle size-strength relationships and test for gender differences.

Results and Discussion

Males had significantly greater neck strengths than females in all configurations while there were no statistical differences in age, weight, or BMI between the two genders. Female neck strengths showed significant inter-configuration correlations while male strengths did not. ANCOVA models found total superficial flexor (TSF = SCM+AS+IH) and SCM sizes to have significant correlations with flexion strength in the neutral posture, with no gender difference; for males, the SCM was a strong predictor of neck flexion strength in the neutral posture, while the AS muscle was evidently more involved in the extended posture—none of these however held true for females (Fig. 1). Less strength variability was explained by muscle size alone in females than in males. All muscle size metrics yielded nearly identical strength-size relationship results.

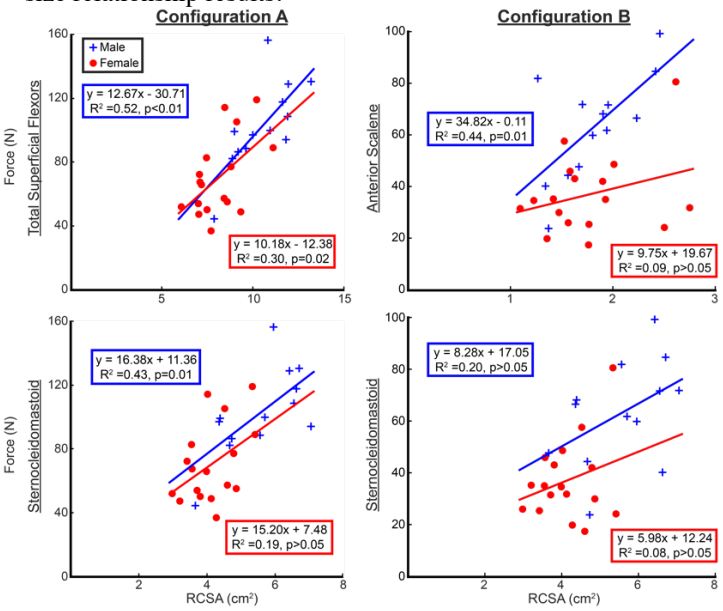

Figure 1: Sample muscle strength-size relationships where statistical significance ($\alpha = 0.05$) was identified for TSF and SCM in config A and for AS but not SCM in config B, for at least one gender.

Significance

Males and females exhibited distinct strength and muscle correlations, highlighting the importance of gender-specific strength data analyses and applications. Such applications may include musculoskeletal modeling, strength prediction for injury prevention, and job design. Muscle strength testing results in the most commonly adopted neutral posture are not good predictors for strengths in deviated neck postures, which may be more relevant to practical or clinical applications. Lastly, there is no readily apparent advantage of one muscle size metric over another when analyzing neck muscle size-strength relationships.

References

1. Bamman MM et al., *Med Sci Sport* 32 (2000): 1307-1313
2. Bruce et al., *Med Sci Sport* 29 (1997): 677-683
3. Holzbaur et al., *J Biomechanics* 40.11 (2007): 2442-2449
4. Schmidt et al., *Am J Sports Med* 42.9 (2014): 2056-2066
5. Tingart et al., *Clin Orth and Rel* 415 (2003): 104-110
6. Vasavada et al., *Spine* 23.4 (1998): 412-422

NECK NEUROMUSCULAR CHARACTERISITCS IN RESPONSE TO MULTIDIRECTIONAL VISUAL CUES IN HEALTHY YOUNG ADULTS: TEST-RETEST RELIABILITY STUDY

Takashi Nagai[1,2], Nathan D. Schilaty[1,2], Ryan W. Chang[3], Valerie Keller[3], Sean T. Stiennon[3], Hanwen Wong[3], Michael J. Stuart[1], David A. Krause[3]
[1]Sports Medicine Center, Mayo Clinic, Rochester, MN, USA
[2]Biomechanical Laboratories, Department of Orthopedic Surgery, Mayo Clinic, Rochester, MN, USA
[3]Department of Physical Medicine & Rehabilitation, Mayo Clinic, Rochester, MN, USA
Email: nagai.takashi@mayo.edu

Introduction

Sports-related concussion (SRC) negatively affects players' neurocognitive function as measured by a simple clinical cognitive test (i.e. the ruler-drop test) [1]. Quicker neck muscle reaction time (RT) against neck perturbations and the rate of muscle force development (RFD) have shown to play a critical role in increasing neck stiffness and reducing potential impacts and severity of SRC [2,3]. In an attempt to examine one's ability to generate neck muscle force in response to specific directions via visual cues, we built a custom neck strength measurement device to measure neck force output (peak force: PF and RFD) [4] in addition to the capability to provide and calculate visual cues with RT. Multidirectional neck muscular characteristics in response to visual cues have not been investigated. Therefore, the purpose of the study was to establish test-retest reliability of an individual's visual-neck muscle RT, PF, and RFD.

Methods

Fifteen subjects (10 females/5 males, Age: 24.5±2.1yrs, HT: 168.1±7.4cm, WT: 70.6±11.3kg) with no history of neck pain/issues participated in the study. Testing was in a research laboratory two times, one week apart. Data was collected with a custom neck strength testing device at 1000 Hz. RT, PF, and RFD were measured for cervical flexion, extension, and lateral flexion. For RT, subjects pushed as hard and quick as they could in response to a black arrow which appeared on a computer screen. The arrow also directed the specific direction of "push" (flexion, extension, right, or left lateral flexion). The trigger time (for the arrow to display) was variable (3-10sec) and the direction of the arrow was randomized. After several practice trials, the average of three trials for each direction were recorded and analysed. RT was the time between the trigger and >5 N at the initiation of responses (in milliseconds:ms). Subjects were verbally encouraged to keep pushing as hard as they could for at least 3 seconds. PF was the highest force output reported during each trial (in Newtons:N). RFD was calculated by dividing the change in neck force over the change in time (in N/sec) from the initiation of responses (~5N) to various points based on the time to pass individual's PF (50% and 90%) and based on actual times (50ms, 100ms, 150ms, and 200ms). Descriptive statistics, test-retest intraclass correlation coefficient (ICC) model (3,1) and standard error of measurements (SEM) were used for statistical analyses.

Results and Discussion

Average RT ranged from 478ms to 533ms. Neck extension PF was higher (187 N) than other directions (115-135 N). Highest RFD was observed at 50%PF and at 100ms (**Table 1**). *Good* to *excellent* ICCs (ICC=0.536-0.957) were reported except for lateral flexion RT and RFD at 90% **(Table 2)**. More subjects and refinement of the protocol will likely improve ICC and SEM by minimizing potential outliers due to missed/delayed responses to visual cues and pushed wrong directions.

	RT (ms)	PF (N)	RFD50%	RFD90%
Flexion	533.5 (44.0)	115.3 (29.2)	502.9 (241.4)	130.0 (121.8)
Extension	513.7 (51.3)	187.4 (53.9)	856.5 (443.6)	217.5 (145.4)
Right LF	478.1 (46.6)	134.0 (31.6)	640.0 (276.8)	148.4 (77.4)
Left LF	495.9 (56.7)	135.1 (32.8)	661.9 (303.4)	131.2 (96.3)
	RFD50ms	RFD100ms	RFD150ms	RFD200ms
Flexion	394.9 (183.3)	484.5 (221.9)	427.6 (163.6)	357.5 (112.9)
Extension	536.8 (240.7)	847.6 (427.0)	764.7 (351.9)	639.8 (249.7)
Right LF	494.3 (212.9)	665.1 (285.1)	582.6 (201.1)	442.7 (122.2)
Left LF	533.4 (295.0)	683.9 (325.2)	598.9 (205.9)	442.8 (118.5)

Table 1. Descriptive Statistics: Means (SD).

	RT	PF	RFD50%	RFD90%
Flexion	0.624 (27.0)	0.798 (13.1)	0.709 (130.2)	0.848 (47.5)
Extension	0.536 (34.9)	0.555 (35.9)	0.738 (227.0)	0.384 (114.1)
Right LF	-0.691 (60.6)	0.709 (17.0)	0.865 (101.7)	-0.141 (82.7)
Left LF	-0.533 (70.3)	0.754 (16.3)	0.959 (61.4)	0.726 (50.4)
	RFD50ms	RFD100ms	RFD150ms	RFD200ms
Flexion	0.706 (99.4)	0.878 (77.5)	0.844 (64.6)	0.910 (33.9)
Extension	0.826 (100.4)	0.741 (217.3)	0.765 (170.6)	0.662 (145.1)
Right LF	0.820 (90.3)	0.900 (90.2)	0.894 (65.5)	0.830 (50.4)
Left LF	0.957 (61.2)	0.935 (82.9)	0.852 (79.2)	0.687 (66.3)

Table 2. Reliability and Precision: ICC (SEM).

Significance

The current findings confirm that most variables related to neck neuromuscular characteristics and multidirectional visual-neck RT can be reliably assessed using the custom-made neck device. Clinical significance of slower RT or lower RFD in individuals with different musculoskeletal conditions such as SRC, neck pain, and whiplash should be examined in future investigations.

Acknowledgments

The neck strength device was built with the financial support by the Mayo Clinic Ice Hockey Research Group.

References

[1] Del Rossi G, 2017, J Athl Train, 766p.
[2] Le Flao E et al., 2018, Sports Med, 2641p.
[3] Schmidt et al., 2014, Am J Sports Med, 2056p.
[4] Nagai et al., 2020, Abstract at Great Lakes Ath Train Meeting

Biomechanical Effect of Valgus/Varus Knee Joint Alignment on ACL Reconstruction Surgery

Byeongchan Cho [1], Tae Soo Bae[1]
[1] Department of Biomedical Engineering, Jungwon University, Goesan-gun, Korea, Republic of Email: *ktroy@wpi.edu *include just the corresponding author email

Introduction

In case of the excessive varus and valgus deformities of the knee joints, they can cause damages to articular cartilage or secondary injuries to peripheral tissue of the knee joint [1]. To maintain the functional balance of the knee joint, the joint alignment should be considered when anterior cruciate ligament reconstruction (ACLR) is performed. However, there were few studies on the varus and valgus deformities of the knee joint in ACLR surgery. Therefore, the aim of this study was to analyze the biomechanical effects of implanted graft in ACLR surgery by calculating the stress which in each surgical site according to the varus and valgus alignment of the knee joint.

Methods

The images of the femur and tibia were obtained through computed tomography of the left knees of four males who have no orthopedic diseases in the musculoskeletal system. Each three-dimensional knee joint model was reconstructed by using an image processing program (Mimics 20.0, Materialize, Belgium). Through multi-flexible body dynamics (MFBD) analyses, von-mises stresses on the implanted graft were calculated during continuous knee flexion and extension motions. In order to apply the continuous knee motion, the knee angle was set by coordinates the movements of the several landmarks on the femur at intervals of 15 degrees. The MFBD analyses were performed for a total of 108 cases were calculated to simulate neutral, varus and valgus deformities (Neutral, +5, +10, +15 and +20 degrees) at three recommended surgical sites (Posteroproximal areas of 5, 10 and 15mm radii on the femoral epicondyle)[2] and then the calculated stresses of implanted graft were compared among them (Figure 1).

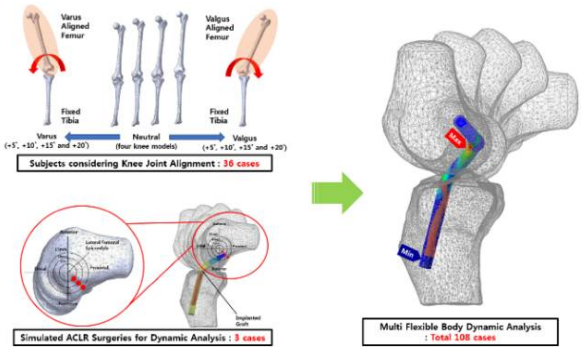

Figure 1: Process of making a 3D varus/valgus knee joint models and recommended surgical sites during MFBD analysis.

Results and Discussion

In the varus and valgus alignment knee joints, the stresses of implanted graft were increased as the knee joint angle decreased. Compared to the stress values (19.53 MPa) of the neutral alignment knee joints at the knee bending angle of 0 degrees, the stress of the the 20-degrees varus alignment knee joints lower by 23% on average. On the other hand, the stress of the 20-degrees valgus alignment knee joints was higher by 32% on average.

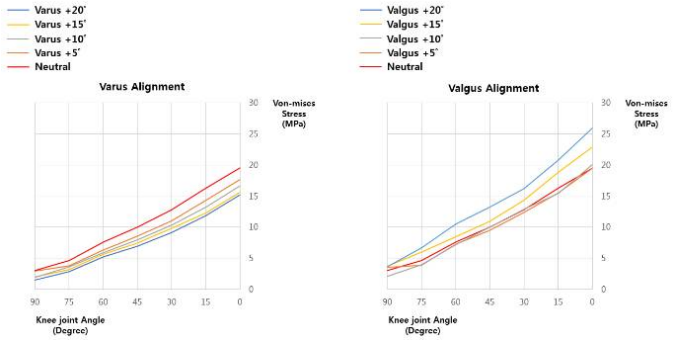

Figure 2: Von-mises stress on implanted graft considering varus and valgus knee joint alignments as knee joint angle.

In the varus alignment knee joints, the stresses of implanted graft were decreased as the alignment angle increased. In the knee joints of 15-degrees and 20-degrees valgus, the stresses of the implanted graft were 22.9MPa and 25.93MPa, which increased slightly (Figure 2).

Significance

Based on the results of this study, we propose that the ACL surgery for severe valgus deformity knee joint (more than valgus deformity of 15-degrees) was implemented after varus alignment of knee joint considering the stress of implanted graft. However, varus and valgus alignments were performed for normal knee models in this study. In the future, we will conduct additional researches for patients' knee models with severe varus and valgus deformities. Furthermore, we will also evaluate the surgical technique that performs ACLR and high tibial osteotomy together.

Acknowledgments

This research was supported by Basic Science Research Program through the National Research Foundation of Korea (NRF) funded by the Ministry of Education (NRF2017 R1D1A3B04033410)

References

1. Ebied Ayman M., Foda Adel Abdel Azim, Journal of Orthopaedics, Trauma and Rehabilitation, Volume 23, December 2017, PP 8-12
2. Kyungmin Kang, Tae Soo Bae, The International Journal of Medical Robotics and Computer Assisted Surgery 5 December 2016

Evaluation of Texture Features from Micro-Computed Tomography of Osteogenesis Imperfecta Bone Specimens

Andrea H. Rossman, Katarina Radmanovic, Gerald F. Harris, Carolyne I. Albert, Peter A. Smith, and Jessica M. Fritz
Medical College of Wisconsin, 8701 W. Watertown Plank Rd., Milwaukee, WI 53226, USA
Email: arossman@mcw.edu

Introduction

Osteogenesis imperfecta (OI) is a genetic, heritable disorder resulting in defective collagen network formation necessary for proper bone formation. Consequently, people born with OI are prone to frequent long bone fractures. There exists a need to better characterize OI bone properties to improve fracture mitigation as well as activity and rehabilitation prescriptions. Volumetric bone mineral density (vBMD) is commonly used to describe bone quality in OI patients [1,2]. However, this density measure does not account for structural differences within the bone. Previous imaging studies have evaluated 3D texture parameters to assess variations in bone texture in OI populations [1,3]. While texture has been studied previously, the use of higher order texture statistics has yet to be investigated. These texture features are used to classify tumors in the field of radiomics [4,5]. We hypothesize that second order texture features (contrast, correlation, energy and homogeneity) derived from micro-computed tomography (CT) images will have higher correlation to mechanical properties than previously used porosity and vBMD values.

Methods

Cortical bone samples taken from two children with OI type III were each machined into eight miniature beams cut in both the transverse and longitudinal directions. There were four beams in each group. The beams were then imaged via micro-CT at a resolution of 10 μm and underwent flexural testing in three-point bending [6]. Porosity and vBMD were calculated using the scanner's SCANCO voxel-counting algorithm. Each beam's modulus of elasticity (E) was calculated from the stress-strain curves of the flexural testing.

A customMATLAB algorithm automatically selected regions of interest (ROIs) from each micro-CT bone scan and calculated four texture variables (Figure 1). For each beam, three ROIs from different levels within the scan were taken. The values from each slice were averaged for use in the analysis.

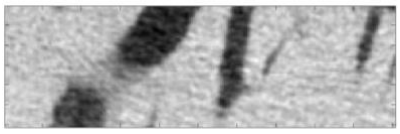

Figure 1: This ROI clearly demonstrates heterogeneous texture throughout its area.

Second order texture statistics (contrast, correlation, energy and homogeneity) derived from the gray-level co-occurrence matrix (GLCM) were calculated to evaluate the bone texture [7]. The GLCM compares the value of pixels to their neighbors, thus encoding spatial information into its derived variables; contrast, correlation, energy, and homogeneity.

The Pearson's Correlation Coefficient was calculated to compare each of the six imaging variables to E for each beam. The longitudinal and transverse beams were analyzed separately.

Results and Discussion

The GLCM-derived variables had higher correlation coefficients than porosity and vBMD for the longitudinal beams (Table 1). However, the E of the transverse beams was most highly correlated to porosity and vBMD. These results indicate that measuring GLCM texture features would be abe to more accurately describe longitudinal bone properties. The small sample sizes of each group and the heterogeneity within each bone sample represent a limitation to the current preliminary study. Continued sample collection and data extraction will increase the power of the analysis.

Table 1: Pearson's correlation coefficients (r) for modulus of elasticity (E) vs. imaging variables, for longitudinal and transverse bone beams.

Variable	r, Longitudinal	r, Transverse
Porosity	-0.43	-0.81
vBMD	0.43	0.73
Contrast	0.63	0.58
Correlation	0.62	0.34*
Energy	-0.71	-0.58
Homogeneity	-0.63	-0.58

* This value based on three samples, as one correlation value was found to be not a number (NaN), and thus was excluded

Significance

The texture parameters show a stronger correlation to E than vBMD and porosity for the longitudinal beams. This demonstrates potential evidence to use additional texture variables other than porosity and vBMD in estimations of mechanical properties from clinical imaging. Highly correlated imaging and mechanical property variables are needed to better inform patient-specific predictive models for OI fracture risk [8]. Clinical decisions in OI for rehabilitation, surgical options, and lifestyle modifications are made based on the presumed fracture risk; therefore, more accurate, patient specific models would allow for personalized medical care to maximize the patients' quality of life.

Acknowledgments

NIH 1R03HD099431-01, Orthopaedic & Rehabilitation Engineering Center, and the Rush MicroCT Histology Core.

References

[1] Folkestead et al (2012). JBMR. 27(6):1405-12
[2] Mikolajewicz et al (2020). JBMR. 35(3):446-459
[3] Abidin et al (2017). Proc SPIE Int Soc Opt Eng. 10134: 1013413.
[4] Lambin et al (2012). Eur J Cancer. 48(4): 441–446
[5] Parekh et al (2016). Expert Rev Precis Med Drug Dev. 1(2):207-226.
[6] Radmanovic et al (2019). ISB/ASB 2019 Proceedings
[7] Haralick et al (1973). IEEE SMC. (6):610–621
[8] Shaker et al (2015). F1000Research. 4:68

Auxetic Behavior of Achilles Tendons while Loading to Failure

Alexander W Hooke[1], Christopher V Nagelli[1], Sebastian A Mueller[1,2], Christopher H Evans[1]
[1]Mayo Clinic, Rochester, MN, USA; [2]University of Basel, Switzerland
Email: hooke.alexander@mayo.edu

Introduction

The Achilles tendon is the largest and strongest tendon in the human body. Scientific understanding of the mechanical and/or biological functions contributing to this exceptional strength remains poorly understood.[3] Previous studies investigated the material properties of the tendon via *ex vivo* testing, but conclusions from these investigations are limited because *in vivo* behavior was not well replicated and the anisotropic stresses and strains along the Achilles' unique geometry were unaccounted for.[1-3] Our team tested Achilles tendons to failure using an anatomically correct fixation and positioning system while measuring the 3D deformations of the entire posterior surface of the tendon using digital image correlation (DIC).

Methods

11 fresh frozen, Achilles tendons were tested. Each specimen's calcaneus was potted in bone cement with the Achilles insertion above the cement and visibile. The muscle-tendon junction was fixed with a cryo-clamp. The tendon's posterior surface was coated with a black and white speckling pattern to enable the DIC system (GOM, Braunschweig, Germany) to record, calculate, and analyze the 3D deformation response. Specimens were mounted to a servo-hydraulic testing machine, oriented to simulate the anatomic position of a plantigrade foot in a neutral position. Tendons were pre-conditioned for 10 cycles then loaded to failure at 5 mm/s.

Results and Discussion

The distribution of the major strain (Fig 1A) was non-uniform and varied by ~20% at the moment before failure. The greatest strain occurs away from the site of failure (Fig 1A,C,D) with a localized strain peak at the failure site occurring only just prior to rupture. The direction of the major strain in a majority of the tissue is not parallel to the loading direction (Fig 1B). Independent examinations of the transverse (Fig 1C) and longitudinal strain (Fig 1D) indicate that the tissue exhibits a negative Poisson ratio, a quality known as auxetic behavior, meaning it becomes wider when stretched. Auxetic materials are recognized for their ability to absorb energy and resist fracture. Previous research on Achilles auxetic behavior shows similar behavior patterns to those identified here, but were limited to a smaller region of the tendon at sub-failure loading.[4,5]

Significance

The strain distribution and extreme degree of auxetic behavior measured in the present study have not been observed before and provide novel insights into the material properties and mechanical behavior of the human Achilles tendon.

Acknowledgments

Supported by the Mayo Clinic Biomechanics Core &The Musculoskeletal Training Grant at Mayo Clinic.

References

1. Louis-Ugbo J, et al., Clin Anat. 2004; 17(1)
2. Wren TA, et al., Ann Biomed Eng. 2003; 31(6)
3. Wren TA, et al., Clin Biomech 2001; 16(3)
4. Gatt R, et al., Acta biomaterialia. 2015; 24
5. Luyckx T, et al., J Exper Ortho. 20

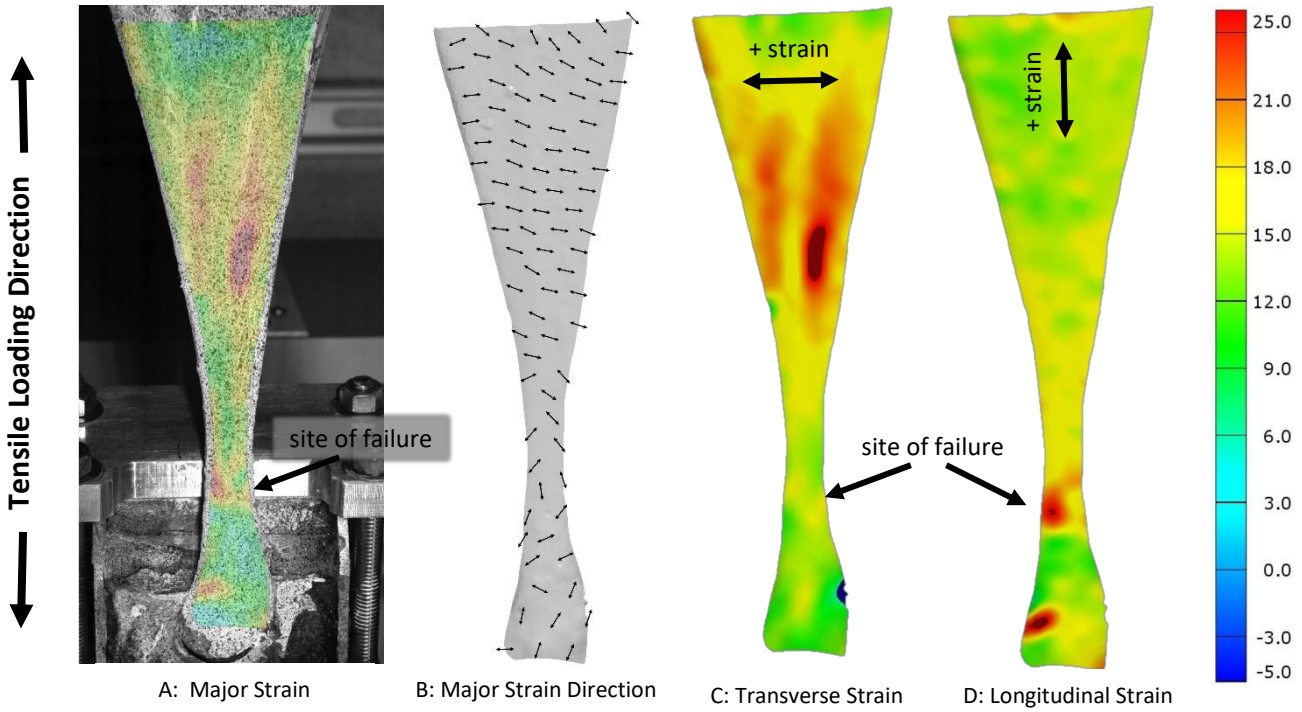

Figure 1: Directional breakdown of technical strain on a human Achilles tendon at the moment prior to rupture. Major strain (A), direction distribution of major strain (B), transverse strain (C), and longitudinal strain (D) are shown.

Material Properties of Bighorn Sheep Horncore Bone for Energy Absorption

Luca H. Fuller[1], Seth W. Donahue[1]
[1]Department of Biomedical Engineering, University of Massachusetts Amherst, Amherst, MA, 01003, USA
Email: swdonahue@umass.edu

Introduction

Professional athletes are commonly diagnosed with concussive injuries due to head trauma sustained through collisions or falls. Recently, evidence of the permanent psychiatric consequences of these injuries has motivated the development of novel technology for concussion prevention [1]. Studying biological injury mitigation mechanisms utilized by animals that experience routine head-impacts may inspire the design of effective head protection systems.

Male bighorn sheep participate in seasonal bouts of intraspecific combat involving high impact head-butting. A lack of symptomatic brain injuries suggests these animals have evolved biological mechanisms for injury mitigation. Computational studies have shown that the bony horncore of bighorn sheep horns plays a key role in absorbing energy during ramming which has clear implications for injury mitigation [2]. Studies of bone tissues from other species have demonstrated that bone has an exceptional ability to adapt its composition and microstructure to provide specialized mechanical functionality [3]. Thus, it was hypothesized that bighorn sheep horncore cortical bone has a reduced mineral content compared to cortical bone from other mammalian species that provides increased energy absorption during loading.

Methods

Cortical bone was extracted from the horncore of 6 bighorn sheep rams that died of natural causes and spanned a wide range of horn size. Three-point bend samples were milled into beams with dimensions of 30 x 3.5 x 2 mm (length x width x depth) and tested to failure with a cross-head speed of 1 mm/s at room temperature under physiological hydration. Engineering beam theory was used to determine the elastic modulus (E), bending strength (BS), and fracture energy (W) of each sample. One half of each fractured specimen was ashed to determine the bone mineral content (BMC) similar to previous studies [4]. Histological sections were stained with toluidine blue and assessed for porosity. Analysis of variance compared the measured parameters to those of cortical bone from black bear tibias [4] and red deer antler [5,6]. Correlations between outcome variables and horn curl length were assessed via regression. Stepwise regression was used to assess the contribution of porosity and BMC to the mechanical properties.

Results and Discussion

The bighorn sheep cortical bone mechanical properties demonstrated positive correlations with curl length, suggesting the older and larger rams have bone with greater mechanical properties. The mechanical properties of horncore cortical bone are all lower than those from black bear tibias and red deer antler (Table 1). The ram horncore and red deer antler have similar BMC, which is lower than black bear tibia BMC. Lower BMC in antler is believed to promote high energy absorption by increasing ductility in these structures that experience impact during combat [3]. Therefore, it was surprising the fracture energy was lower in ram horncore than in red deer antler despite similar BMC levels. However, horncore cortical bone may demonstrate improved energy absorption at the strain rates experienced during ramming, which are several orders of magnitude higher than what was used for this testing [2].

The low fracture energy may also be attributed to the high porosity of horncore bone. Stepwise regression of ram and bear bone indicated that porosity alone was the best predictor of fracture energy. Porosity explained nearly 60% of the variation in fracture energy and demonstrated a negative correlation. Including BMC did not improve the model. It is not clear why ram bone has higher porosity than bear bone, but the porosity of bighorn sheep samples is mainly due to large resorption cavities. One possibility is extreme levels of microdamage develop in ram bone during headbutting and damage-induced targeted bone remodeling leads to high porosity.

Most of the volume inside the keratin horn of bighorn sheep is filled by a porous bone material with a very unique architecture [2]. Previous finite element modeling showed that this porous bone significantly reduces brain cavity accelerations [2]. Therefore, it is possible the horncore cortical bone serves primarily to interface the keratin horn with the high energy absorbing porous bone.

Significance

The energy absorbing mechanisms of bighorn sheep horn and horncore bone have only begun to be elucidated. The mechanical properties measured in this study can be used in future computational models to investigate the role of the porous bone architecture in brain injury mitigation during combat. Additionally, high strain rate testing on cortical and porous horncore bone will further increase our understanding of these unique materials. Ultimately, the mechanical properties and architecture of bighorn sheep horncore bone could influence novel bioinspired designs for injury mitigation devices in humans. [2].

References

[1] Finkbeiner et al. (2016). *Can. J. Psychiatry*, **61**
[2] Drake et al. (2016). *Acta Biomater,* **44**
[3] Currey (1979). *J. Biomech,* **12**
[4] Harvey et al. (2004). *J. Biomech,* **37**
[5] Currey et al. (2009). *J. Exp. Bio,* **212**
[6] Estevez et al. (2008). *Eur. J. Wildl. Res,* **54**

Table 1. *Mechanical properties, BMC, and porosity of cortical bone from the horncore of bighorn sheep, red deer antler, and black bear tibia. Different letters between values in the same column indicate statistically significant ($p < .05$) differences.*

Species	Location	E [GPa]	BS [MPa]	W [kJ/mm^2]	BMC [-]	Porosity [%]	Ref.
Bighorn Sheep	Horncore	9.45 ± 5.65 [a]	140.6 ± 78.0 [a]	8.93 ± 5.15 [a]	0.613 ± 0.045 [a]	26.6 ± 23.3 [a]	Current
Red Deer	Antler	17.50 ± 0.45 [b]	352.2 ± 8.8 [b]	23.4 ± 1.0 [b]	0.618 ± 0.009 [a]		[5, 6]
Black Bear	Tibia	22.85 ± 4.87 [c]	289.5 ± 36.3 [c]	16.1 ± 3.1 [c]	0.660 ± 0.012 [b]	4.4 ± 1.5 [b]	[4]

Padding on the support table affects spinal posterior-to-anterior stiffness measurements

Edward F. Owens.[1], Ronald S. Hosek[1], Muhammad Salman,[2] and Brent S Russell[1]
[1]Sid Williams Center for Chiropractic Research, Life University, Marietta, GA
[2]Kennesaw State University, Marietta, GA
Email: Edward.owens@life.edu

Introduction

Manual therapists use posterior-to-anterior spinal stiffness (PAS) testing as part of routine diagnostic evaluation for low back pain patients. The PAS measurement involves a measure of the bulk displacement of the spine in a prone person lying on a supporting structure subjected to forces directed posterior-to-anterior onto the spine.

While therapists generally use manual palpation in practice, measurements with instruments are considered more objective. Researchers have developed several PAS measurement systems and identified several variables that can affect stiffness measures.[1] Still, the phenomenon itself is poorly understood.

For example, we noticed very different stiffness measures reported in 2 studies of similar patient populations using similar measurement equipment (11 N/mm[2] versus 6 N/mm [3]). One notable difference in the testing apparatus was the presence of padding on the supporting surface of one study and no padding on the other. In the present study we sought to test the hypothesis that table padding could have influenced the stiffness measures.

Methods

We used a custom testing apparatus for this study, which consists of a super-structure supporting a displacement transducer and weights over the prone subject. Forces were directed onto the spinous process of the 3rd lumbar vertebra of subject's spine through a shaft with a load cell affixed to its end. We manually raised and lowered the weights in a series of 10 cycles while recording displacement and applied force.

We used a mannequin as the subject of the study which ensured that there would be no artifacts due to breathing or muscle contraction and no complaints about a long testing session. Moreover, it would not change between readings as a human subject might. We performed the PAS test with the mannequin resting directly on the hard surface of the table, and with two different layers of foam padding. One padding was 3 inches of firm upholstery foam. The other was 2.5" of softer foam.

We calculated stiffness as the slope of the force displacement curve for each cycle in the force range from 55-75 N using linear regression, omitting the 1st and last cycle of each 10 to avoid stopping and starting artifacts. We also omitted outliers in the analysis.

Results and Discussion

Plots of force versus displacement show a non-linear relationship with significant hysteresis on unloading (Figure 1). Six runs of 10 pressure cycles each were perfomed for each of the 3 levels of support conditions. This produced 44 usable data sets yielding the stiffness characteristics shown in Table 1.

We found distinct differences between the stiffness measured when the mannequin was supported on a soft-foam covered table and when there was no foam or stiff foam. Both types of foam would be expected to compress somewhat when the mannequin rests on it. A force plate under the table section supporting the mannequin alone registered 204N. The addition of another 90 newtons during the testing compressed the soft foam further, contributing to the displacement measurement and resulting in apparent lowered stiffness. However, the dense foam did not undergo enough compression during the test to affect results.

Figure 1: A typical plot of load versus displacement for the mannequin.

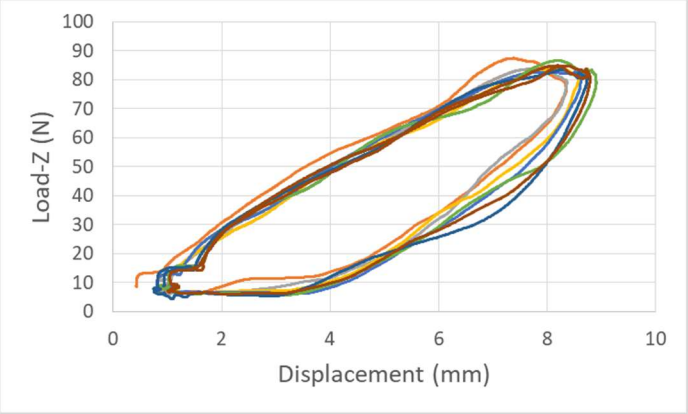

Table 1. Calculated stiffness factors and standard deviation based on 2 trials of 10 loading cycles at each of 3 different support conditions. * Statistically different $p < 0.0001$

	N	Mean Stiffness (N/mm)
No foam	15	12.1 (2.17)
Soft Foam	16	8.8 (1.58)*
Firm Foam	13	13.2 (2.36)

Significance

Foam padding on the patient support structure could have contributed to the differences in PAS reported in the literature on human testing. This suggests that it is important for future researchers to report on the support surface conditions of the testing apparatus used. This is rarely seen in the literature.

References

[1] Wong AYL, Kawchuk GN.. *PM R* 2017;**9**(8):816-830.
[2] Owens EF, et al. *J Manipulative Physiol Ther* 2007;30:493-500.
[3] Wong AY, et al. *Spine* (Phila Pa 1976) 2015;**40**(17):1329-1337.

The Effects of Triceps Surae Muscle Stimulation on Localized Achilles Subtendon Tissue Displacements

Nathan L. Lehr[1], William H. Clark[1], Michael D. Lewek[2], Jason R. Franz[1]
[1]Joint Department of Biomedical Engineering, UNC Chapel Hill & NC State University, Chapel Hill, NC, USA
[2]Division of Physical Therapy, UNC Chapel Hill, Chapel Hill, NC, USA
Email: jrfranz@email.unc.edu

Introduction

A substantial portion of the mechanical power needed to walk is generated by the triceps surae muscles (*i.e.*, medial gastrocnemius [MG], lateral gastrocnemius [LG], and soleus [SOL]) [1]. That power is generated by muscle forces transmitted via interaction with the Achilles tendon (AT), which itself is comprised of distinct subtendons originating from each muscle [2, 3]. During maximal voluntary isometric contractions (MVIC), differences in the magnitude of shortening between the MG and SOL positively correlate with differences in displacement in their associated subtendons of the Achilles. However, complex inter-muscular patterns of volitional activation may confound our interpretation of emergent subtendon tissue displacements. The goal of this study was to leverage electrical muscle stimulation to quantify the effects of activation to individual triceps surae muscles on localized Achilles subtendon tissue displacements at controlled magnitudes of force transmission. We hypothesized that electrical stimulation of individual triceps surae muscles would elicit larger displacements in their associated subtendon.

Methods

We report data for 11 healthy young subjects (age: 22.5±2.9 years, 7 females). Subjects first walked for 6 minutes on a treadmill (Bertec Corp.) at 1.2 m/s to precondition their Achilles tendon [4]. Subjects then sat in a dynamometer (Biodex Medical Systems) and performed MVICs with their knee flexed to 20° and ankle extended to 20° to establish a baseline ankle moment prescribed for all conditions described below. Subjects twice completed 4 separate experimental conditions at each of 3 fixed ankle joint angles (-20°, 0°, 20°): MG stimulation ($Stim_{MG}$), SOL stimulation ($Stim_{SOL}$), combined stimulation ($Stim_{BOTH}$), and a volitional contraction (VOL). We determined stimulation intensities for $Stim_{SOL}$ and $Stim_{MG}$ to individually produce 7.5% of subjects' MVIC ankle moment. $Stim_{Both}$ was designed to produce 15% MVIC ankle moment while preserving the voltage ratio from $Stim_{MG}$ and $Stim_{SOL}$. Finally, for VOL contractions, subjects used real-time biofeedback to match the same 15% MVIC ankle moment. We applied stimulation (Grass Instruments S48 Square Pulse Stimulator) using 11 300 μs pulses at 33 Hz according to published recommendations [5]. In all conditions, we recorded raw radiofrequency ultrasound data from the Achilles free tendon and used 2D cross-correlation to estimate longitudinal displacements of tendon tissue arising from the MG and SOL muscles [6]. We have thus far analysed data for the neutral (0°) and dorsiflexed (-20°) joint postures. A repeated measures ANOVA tested for main effects of condition, while one sample t-tests determined whether differential tissue displacements (i.e., SOL-MG) differed from zero (α=0.05).

Results and Discussion

Consistent with our intended experimental design, we found no significant difference in the elicited peak ankle moment between $Stim_{SOL}$ and $Stim_{MG}$, nor between $Stim_{Both}$ and the VOL contraction (**Fig. 1A**). At both of the analysed ankle joint angles, differential displacement (*i.e.*, SOL subtendon displacement – MG subtendon displacement) was positive for all stimulus conditions (p-values≤0.05), implying larger SOL subtendon tissue displacements than GAS subtendon tissue displacements, independent of individual muscle stimulation (**Fig. 1B**). At the dorsiflexed ankle posture, we found no main effects of stimulus condition for two likely reasons: (i) the much lower force transmission measured at this posture and/or (ii) that subtendon tissue was less receptive to displacements elicited by stimulation in the presence of high levels of baseline passive tension. However, in support of our hypothesis and scientific premise, peak differential displacement (i.e., the relative difference between SOL and GAS subtendon tissue displacement) at the neutral ankle posture was much larger in the presence of SOL stimulation compared to GAS stimulation (p<0.05) despite no different in tendon force transmission (**Fig. 1**). Here also, $Stim_{Both}$ differential displacement was significantly larger than individual muscle stimulation (p-values≤0.05), but no different from VOL.

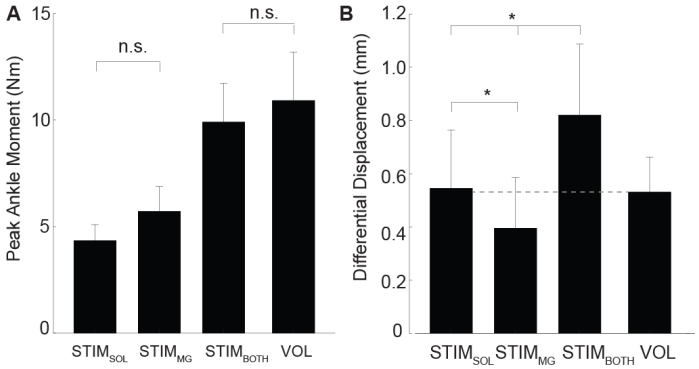

Figure 1. Group average (SE) peak (A) ankle moment and (B) subtendon differential displacements (SOL-MG) for each stimulation condition at the neural ankle posture. Asterisks (*) indicate p<0.05.

Significance

Our results suggest that localized tissue displacements within the architecturally complex Achilles tendon respond in anatomically consistent ways to different patterns of triceps surae muscle activation. Accordingly, this *in vivo* evidence points to at least some neuromechanical independence in actuation between the human triceps surae muscle-tendon units.

Acknowledgments

Supported by grants from NIH (R01AG051748, F31AG060675).

References

1. Farris et al. J R Soc Interface, 2012. **9**(66): p. 110-8.
2. Clark et al. PeerJ, 2018. **6**: p. e5182.
3. van Gils et al. J Foot Ankle Surg, 1996. **35**(1): p. 41-8.
4. Hawkins et al. J Biomech, 2009. **42**(16): p. 2813-7.
5. Merletti et al. Crit Rev Biomed Eng, 1992. **19**(4): p. 293-340.
6. Chernak Slane et al. J Biomech, 2014. **47**(3): p. 750-4.

Regional Differences in Shear Wave Velocity in the Short and Long Head of Biceps Brachii

Grace L. Rozanski[1,2], Tom G. Sandercock[3], Eric J. Perreault[1,3,4], Sabrina S.M. Lee[2],
[1]Departments of Biomedical Engineering, [2]Physical Therapy and Human Movement Sciences, [3]Physiology,
[4]Physical Medicine and Rehabilitation, , Northwestern University, [4]Shirley Ryan AbilityLab, Chicago, IL
Email: s-lee@northwestern.edu

Introduction

Shear wave velocity (SWV) has been shown to be sensitive to changes in the net material properties of the muscle [1] and has also been associated with the net stress in some materials [2]. Howevever, there are regional variations in the material composition, architecture, strain, and stresses within a muscle. [3,4] and it is unclear if SWV is sensitive to these variationsThe biceps brachii muscle is of particular interest as it is comprised of long and short head muscles and has different proximal and distal musculotendinous structures. The distal tendon includes a distal internal aponeurosis that spans approximaltely one third of the length whereas the proximal tendons form external aponeuroses. Thus, our goal was to determine if SWV varies in different regions of the biceps brachii (proximal, belly, and distal), as well as between the short and long head.

Methods

Six healthy youg adults (2 males and 4 females; mean ± std, age: 25.17 ± 2.23 yrs; mass: 59.5 ± 14.98 kg; height: 1.62 ± 0.09 m) participated in this study. Participants were instructed to sit upright in a custom chair with their upper arm resting on a plastic support that was secured to a six-degree-of freedom load cell. Ultrasound data (Aixplorer V9 SuperSonic Imagine) was captured of the biceps brachii (short and long head) at three different locations (proximal, belly, and distal) at a range of elbow flexion angles (90º, 110º, 130º, 150º, 170º). All measurements were obtained under passive conditions. Surface electromyography was placed on the belly of the short and long head of the biceps brachii to verify there was no activation at the time the ultrasound data was captured. For the proximal and distal locations, the region of interest (2cm by 1cm) was placed such that it borderd the musculotendon junction so that the SWV in most proximal and distal regions of the muscle, respectively, could be measured. For the belly location, the region of interest (2cm by 1cm) was placed in the thickest part of the muscle. To provide context of the size of the region of interest relative to the overall muscle lengths, optimal muscle length of the short and long head of the biceps brachii has been reported to be 23.4 and 21.6 cm, respectively [5]. Post-processing included cropping the region of interest to only include muscle or the distal internal aponeurosis. This primarily affected the superficial to deep direction, not the proximal-distal direction. The average SWV of the cropped region was calculated.

Results and Discussion

We observed that SWV increased as elbow angle was increased for all regions in the short and long heads (Fig 1). Shear wave velocity values of the belly region are comparable to previous studies [6]. Shear wave velocity was significantly higher in the short head compared to the long head at the distal location for both the muscle and distal internal aponeurosis (all $p<0.001$), as well as the belly ($p = 0.005$). For the short head, SWV in the distal region was significantly greater than the proximal and belly region ($p = 0.008$ and $p = 0.04$, respectively). Shear wave velocity in the distal interal aponeurosis was 46-63% higher than the muscle at all locations (all $p <0.001$). For the long head, there were no significant differences across the three regions.

These results indicate that SWV is not constant throughout the biceps brachii. Rather, it differs between the short and long head, in particular in the belly and distal regions. This suggests that SWV may be sensitive to heterogeneity of mechanical properties and or force throughout muscle under passive conditions.

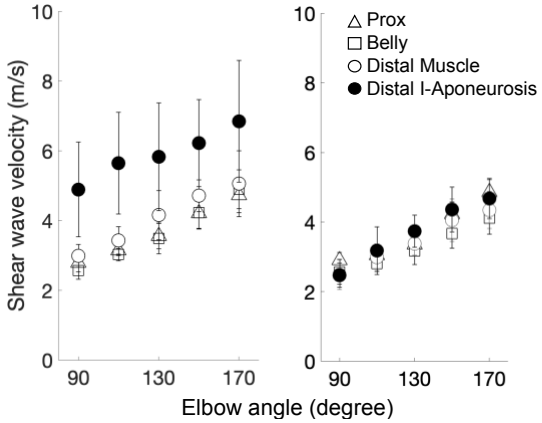

Figure 1: Mean shear wave velocity and standard deviation across elbow angle for short head (left) and long head (right) of the biceps brachii at different locations (prox = proximal, belly, distal muscle, and distal I-aponeurosis = distal internal aponeurosis).

Significance

Our results show that SWV varies depending on region and specific head of the biceps brachii under passive conditions at different lengths. Our results indicate that SWV is sensitive to location.Given that mechanical properties and force vary throughout muscle, shear wave ultrasound elastography is a potential technique for assessing the heterogeneity of such properties and force for which *in vivo* assessment is currently challenging. These findings have implications for muscle models that assume homogeneity and clinically, to better understand how and where musculotendinous injuries occur.

Acknowledgments

Supported by National Institute of Health Grant 5R01-AR-071162-02 to E. J. Perreault.

References

[1] Bernabei et al. (2020) J Appl Physiol 128(1), 8.
[2] Martin JA et al. (2018) Nat Commun 9: 1592.
[3] Pappas GP et al. (2002). J Appl Physiol 92, 2381-2389.
[4] Azizi E, Deslauriers (2014) Front Physiol 5, 303.
[5] Murray et al. (2000) J Biomech 33, 943.
[6] Wang et al. (2019) J Biomech 94, 115.

Preliminary Evaluation of Articular-Sided Supraspinatus Surface Strain for Varying Infraspinatus Loads

Patrick M. Williamson[1,2], Mohammadreza Abbasian[2], Jeremy Johnson,[2] Daron Hamparian[2], Joseph DeAngelis[2], Arun Ramappa[2], and Ara Nazarian[2]
[1]Mechanical Engineering Department, Boston University, Boston, MA
[2]Center for Advanced Orthopaedic Studies, Carl J. Shapiro Department of Orthopaedic Surgery, Beth Israel Deaconess Medical Center, Boston, MA
Email: anazaria@bidmc.harvard.edu

Introduction

Rotator cuff (RC) tears are the most common cause of shoulder disability, representing one of the highest days-away-from-work rates compared to other work-related injuries. (1) Articular-sided rotator cuff tears are common in overhead athletes for whom conservative treatment is strongly recommended, (2) though worse clinical outcomes for articular-sided tears have been reported (3) and return to previous level of play is diminished. (4) Classically, Nakajima *et al* reported that the articular side of the tendon is more vulnerable to tensile load than the bursal side, (3,5) which may be related to the random orientation of collagen fibers in this region.(4) However, no evidence exists to determine which articular-sided tears are stable and which may progress. (6)

Andarawis-Puri *et al.* showed that the supraspinatus and infraspinatus tendons interact mechanically, but the effect of different loads on the infraspinatus tendon were not evaluated. (7) *Our goal was to assess the effect of different infraspinatus loads on the strain of the articular side of the supraspinatus tendon. We hypothesized that increased infraspinatus load would increase the strain on the supraspinatus tendon.*

Methods

A cadaveric, left shoulder specimen (56 y/o; Male) was dissected free of all tissue, leaving the supraspinatus and infraspinatus tendons. The humeral head was resected to allow visual access to the articular-side of the supraspinatus tendon. A 5×3 grid of surface markers (Aluminum beads, 1/32" dia.) was attached to the articular side of the tendon using surgical glue (VetBond, 3M, MN) **Figure 1A.** Three dimensional geometry of the humerus, tendon, and markers were obtained using a computed tomography (CT) machine (XtremeCT, Scanco Medical, Switzerland). A soft-tissue scanning protocol (126mAs, 60 kVp, 0.246 mm slice thickness) was used to visualize the tendon. The specimen was then mounted in the material testing machine (Instron, Norwood, MA) in a custom jig to allow for axial load of the supraspinatus tendon. The supraspinatus tendon was preloaded 5-50N for 10 cycles. (8) The infraspinatus was loaded statically to a series of loads: 1, 2, 3, 4, and 5lbs. Images of the tendon were recorded at 1 Hz using a CMOS camera (PL-B686CU, PixeLINK, CN).

A 3D model of the supraspinatus-infaspinatus complex and markers (MIMICS, 3-Matic) was made using the CT data **Figure 1B**, and imported into the FE Solver (ABAQUS, Dassault Systemes, France). Strain of the supraspinatus tendon was estimated using the FE solver by applying the displacements recorded in the cadaveric setting to the beads. (8)

Results and Discussion

The articular supraspinatus tendon strain increased with increasing infraspinatus load, **Figure 1C**; however, the magnitude of the applied strain to this region is small. This may be due to the condition of the insertion of the tendon in this specimen, which will be evaluated with further samples. Increasing the load on the infraspinatus will allow for evaluation of critical infraspinatus loads.

Significance

This preliminary analysis establishes a method for analyzing articular surface supraspianatus strain, which may prove to be affected by infraspinatus load magnitude.

References

1. "Nonfatal occupational injuries…" US Bureu Labor Statics
2. PMID: 29330670
3. 10.1016/j.jseint.2019.12.002
4. PMID: 29330670
5. PMID: 22959646
6. 10.1177/1758573219864101
7. PMID: 19483078
8. PMID: 31141596

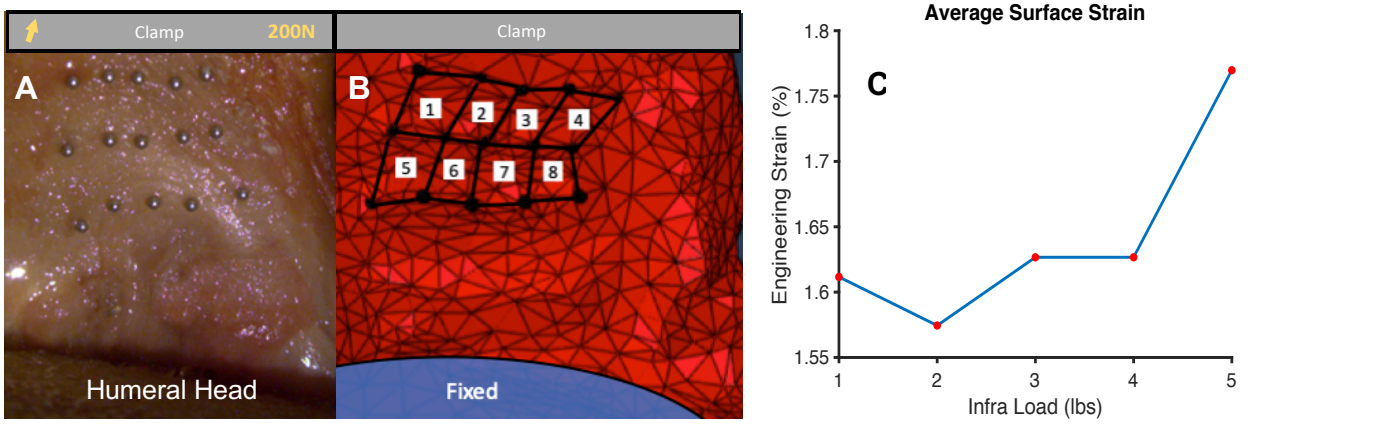

Figure 1. A) Image of the supraspinatus tendon with attached markers. B) Finite element mesh of the supraspinatus (Red), marker geometry (Black Spheres), and insertion on humerus (Blue). Strains during cadaveric testing were estimated by applying displacements to the markers. C) Average engineering (surface) strain of the entire supraspinatus marker grid at 200N for increasing static loads applied to the infraspinatus tendon.

Chronic Neck Pain: *In Vivo* Cervical Spine Kinematics

Craig C. Kage[1], Matthew M. MacEwen[1], Bryan Ladd[1], and Arin M. Ellingson[1]
[1]University of Minnesota, Minneapolis, USA
Email: ellin224@umn.edu

Introduction

Neck pain is the 4th leading cause of years lived with disability [1] and along with low back pain, is the highest US healthcare expense with over $134 billion spent annually [2]. Typical diagnostic imaging techniques are limited to static and/or 2D acquisitions and are unable to capture the dynamic, 3D motion of the cervical spine. Biplane radiography (BR) is able to accurately capture the underlying bony kinematics and provide a quantitative assessment of cervical spine motion [3, 4]. Presently, there is a limited understanding of the underlying, bony-level kinematics for those with chronic mechanical neck pain (MNP). **The purpose of this work was to quantify the underlying bony kinematics of a healthy cohort (CTRL) compared to a cohort with MNP for a flexion/extension task.**

Methods

Eight participants provided informed consent (recruitment ongoing); four without neck pain (27.8±3.8 years | 2M,2F) and four with a history of neck pain >12 weeks (22.0±1.8 years | 1M,3F). Underlying bony anatomy was obtained via CT (100kVp; 0.2×0.2×0.6mm; 1.6mSv, Siemens Biograph, USA). Participants completed three trials of flexion/extension/flexion during BR (160mA, 70-74kV, 3.5ms, 55° IBA, 174cm SID, 30Hz; 0.16mSv/trial). Motions were completed with a metronome (50bpm) for pacing. CT acquisitions were reconstructed (MIMICS Materialise, USA) for levels C3-C6 and anatomic coordinate systems were identified for each vertebrae [4]. Calibration, undistortion, anatomic coordinate identification, and shape-matching were completed in DSX Suite (C-Motion, USA). The final (third) trial was analyzed. Kinematic data were filtered in DSX with a 3.0Hz spline filter and relative kinematics were computed in MATLAB (MathWorks, USA). T-tests were completed in R (R Core Team, Austria).

Results and Discussion

Kinematic variables are presented in Table 1, separated by group, spinal level, and in-plane rotations and translations (flexion/extension (FE) and anterior/posterior (AP)). Kinematics of C4 relative to C5 are displayed for all participants in Figure 1. Those with MNP had significantly greater AP translation at C4/C5 and significantly greater total C3-C6 AP translation. Although not statistically significant, those with MNP demonstrated, on average, greater segmental FE and AP motion components, greater global FE ROM, and lower FE:AP ratio. The trend of the MNP group towards a lower FE:AP ratio implies a greater proportion of AP translation with FE motion (despite a greater FE ROM), which may provide insight into contributions to pain and/or degeneration in those with chronic MNP.

Table 1: Kinematics of controls versus those with chronic MNP

	Flexion/Extension ROM			Anterior/Posterior ROM			Total ROM	Total C3-C6 ROM		Total FE:AP Ratio		
	C3/C4	C4/C5	C5/C6	C3/C4	C4/C5	C5/C6	Vicon	FE(deg)	AP(mm)	C3/C4	C4/C5	C5/C6
CTRL	18.7±4.7	19.4±3.0	20.5±2.0	5.7±1.8	5.6±0.5	5.3±0.3	112.4±15.9	58.6±7.9	16.7±2.5	3.5±0.6	3.4±0.3	3.9±0.5
MNP	22.3±5.8	24.9±4.5	22.6±5.0	7.3±1.2	7.6±0.6	7.1±2.2	130.95±20.8	69.7±9.2	22.0±2.5	3.0±0.3	3.3±0.6	3.3±0.3
p-value	0.37	0.10	0.49	0.20	<0.01*	0.21	0.21	0.12	0.02*	0.37	0.67	0.08

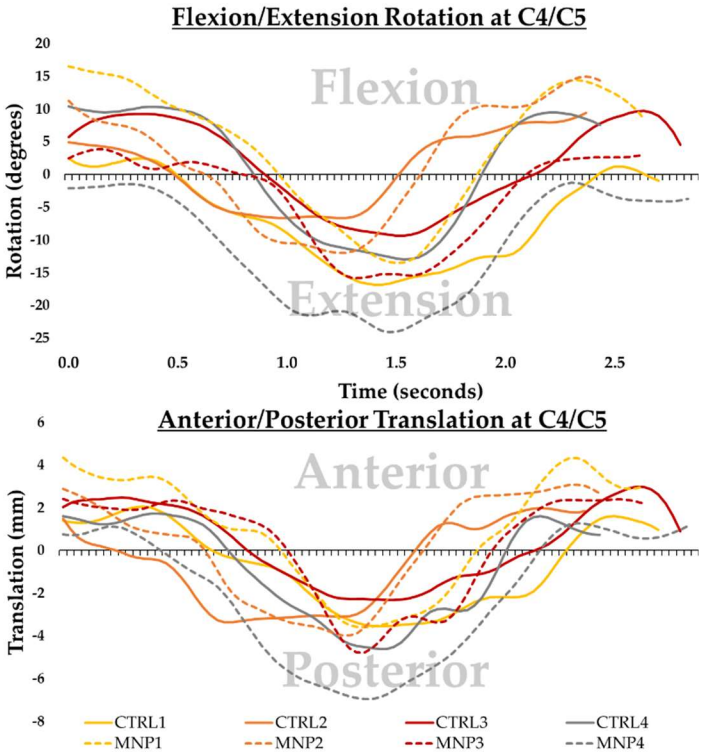

Figure 1: Kinematics of C4 relative to C5 for flexion/extension rotation and anterior/posterior translation components of a FE task.

Significance

Despite the small sample size, we were able to detect significant differences in the kinematics (in particular AP translation) during a FE task in those with chronic MNP compared to a control group. Recruitment efforts are ongoing to achieve sufficient power and additional exploration into multiplanar tasks is underway to better understand the underlying kinematic and coupled differences that may exist in those with chronic MNP.

Acknowledgments

Funding: NIH/NICHD R03 HD09771 and K12 HD073945, Minnesota Partnership for Biotechnology and Medical Genomics (MNP IF#14.02), NIH/NIAMS T32 AR050938 Musculoskeletal Training Grant, and Foundation for Physical Therapy Research (Promotion of Doctoral Studies II).

References

[1]Murray, C.J., et al., JAMA, 2013. [2] Dieleman, J.L., et al., JAMA, 2020. [3] Kage, C.C., et al., PLoS One, 2020. [4] Anderst, W.J., et al., Spine J, 2014.

Skeletal muscle fibrosis involves changes in collagen organization in Duchenne muscular dystrophy

Ridhi Sahani[1], C. Hunter Wallace[1], Silvia S. Blemker[1]
[1]Department of Biomedical Engineering, University of Virginia, Charlottesville, VA, USA.
Email: rs8te@virginia.edu

Introduction

Duchene muscular dystrophy (DMD) is a fatal muscle wasting disease, with no cure or effective treatment to date. Respiratory insufficiency is a leading cause of death in DMD patients, resulting due to dysfunction of the diaphragm muscle[1]. An increase in muscle stiffness occurs with buildup of fibrotic tissue, characterized by excessive accumulation of extracellular matrix (ECM) components such as collagen. Previous studies focus on the impact of increased collagen amount in DMD, but the role of collagen amount on stiffness is unresolved to date[2,3]. Therefore, we are interested in how complex collagen organization is affected in DMD, its impact on passive force production, and how this may lead to respiratory insufficiency. We used scanning electron microscopy (SEM) to capture collagen organization and quantified collagen direction relative to muscle fiber direction as well as collagen straightness parameter. We hypothesized a difference in collagen direction and straightness with the progression of DMD in diseased mice, as well as relative to age matched healthy mice.

Methods

Four samples of diaphragm muscle were collected from each group: 3 (N=2), 6 (N=3), and 12-month (N=2) diseased (*mdx*) and 3 (N=3), 6 (N=4), and 12-month (N=4) healthy (C57BL6) mice. Samples were placed in solution to maintain a relaxed state and collagen structure was isolated by digesting muscle fibers in 10% sodium hydroxide solution[4]. For each sample, an SEM image was taken of collagen fibers (1kX) and fibrils (50kX) in the epimysial layer of the ECM. An image processing algorithm was developed using the Radon transform to measure collagen orientation in local windows for each image in MATLAB. Mean orientation, quantified in degrees relative to muscle fiber orientation, was used to measure collagen fiber (1kX) or fibril (50kX) preferred direction. Collagen straightness parameter (Ps) was determined for collagen fibers (1kX) by measuring the length of a collagen fiber (Lf) and a straight line connecting the ends of the measured fiber (L0) in ImageJ. Collagen straightness parameter (Ps=L0/Lf) was then calculated for three fibers representative of the fibers in each image and averaged. Significance was measured with ANOVA and t test.

Results and Discussion

Differences between diseased and healthy groups were seen, with increased fibril level disorganization at 12 months (Fig 1B). Collagen fibers were straighter in older healthy and all diseased groups: The collagen straightness parameter, measured at fiber level, was significantly different between diseased and healthy groups at 3 and 6-months, as well as between 3 and 12-month healthy and 6 and 12-month healthy groups ($p<0.05$) (Fig 1C). Collagen preferred direction was approximately perpendicular to muscle fiber direction and maintained between fiber and fibril levels. While there was a significant difference between diseased and healthy groups at 3-months at fiber level ($p<0.05$) (Fig 1D), there was no significant difference in diseased groups between ages, with preferred direction ranging from 68-83 degrees at fiber level. Taken together, our results suggest that collagen maintains its orientation relative to the muscle fiber direction, but the waviness seen in young healthy mice is decreased in 12-month healthy mice, and in all ages of diseased mice.

Significance

As collagen fibers lose their waviness, they can take up less strain before being stretched in tension. This results in a shorter toe region on the passive stress-strain curve, with higher stress experienced at lower strains in the elastic region. Therefore, we propose that collagen limits cross-fiber stretch in diaphragm muscle of *mdx* mice. Impairment in respiratory function and fibrosis is reported in *mdx* mice starting at 3 months and reduction in strength and elasticity is reported at 12-18 months[5,6]. Our findings implicate changes in collagen organization on diaphragm function and we will continue to explore the role of cross-fiber stretch on respiratory insufficiency in DMD.

Acknowledgments

Thank you to the National Institutes of Health for funding this project (Grant # U01AR06393).

References

[1]Lo Mauro A. et al, (2016), *Breathe*. [2]Virgilio, K. et al. (2020), *In prep for J. Phys*. [3]Smith LR, et al. (2014), *Am J Phys*. [4]Sleboda, D. et al. (2018), *Soc for Int and Comp Bio Annual Meeting*. [5]Stedman HH, et al. (1991), *Nature*. [6]Huang P, et al. (2010), *Muscle Nerve*

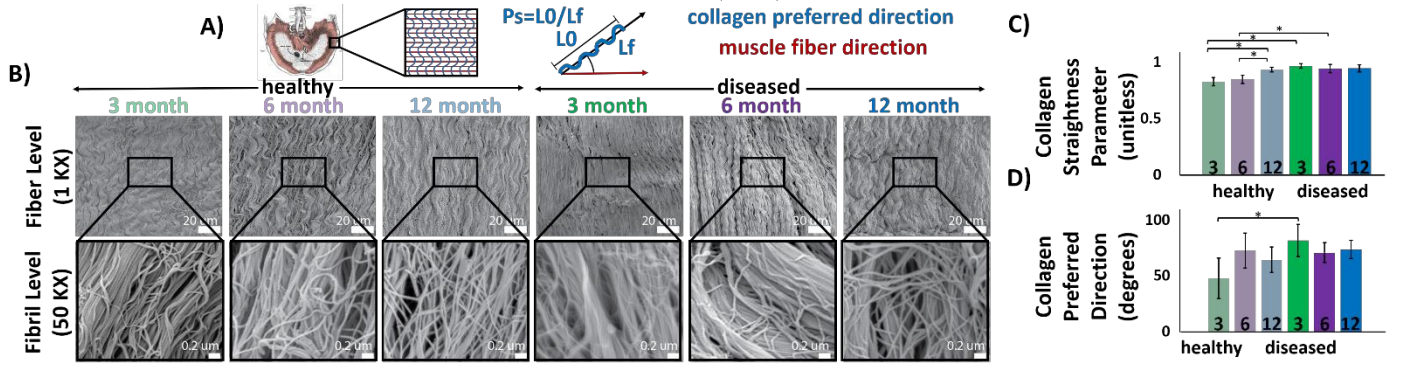

Figure 1: (A) Imaging region and measured values. (B) SEM images of collagen fibers (1kX) and fibrils (50kX), oriented so muscle fiber direction is horizontal. (C) Collagen fiber (1kx) straightness parameter, $p<0.05$ (*). (D) Collagen fiber (1kX) preferred direction relative to muscle fiber direction, $p<0.05$ (*).

Changes in Active and Passive Mechanics of the Diaphragm During the Progression of Duchenne Muscular Dystrophy

C. Hunter Wallace[1], Laura Caggiano[1], and Silvia S. Blemker[1]
[1]Department of Biomedical Engineering, University of Virginia
Email: chw3gr@virginia.edu

Introduction

Duchenne muscular dystrophy (DMD) is a progressive muscle wasting disease that ultimately results in morbidity in the mid-twenties, commonly due to respiratory failure associated with diaphragm muscle degeneration and associated dysfunction[1]. Current assessment of diaphragm function relies on either measuring the changes in the along-fiber properties of individual strips of diaphragm tissue in isolation or imaging movement of the diaphragm as a whole[2,3]. However, the effects of along and cross-fiber changes on *in vivo* diaphragm mechanics and breathing ability are not well understood. In order to address this critical gap, the goals of this study are to (i) design a method of measuring *in vivo* tissue strains both in the muscle fiber direction and transverse to the fiber direction and (ii) use this method to investigate the mechanics of diaphragm function in healthy and dystrophic mice and (iii) relate the measured *in vivo* mechanics to *ex vivo* passive testing.

Methods

Six 6-month-old and 12-month-old healthy (C57Bl6) mice and eight 6-month-old and 12-month old *mdx* mice, a model for DMD, were used in this study. A pair of ultrasound crystals was glued to the muscle in the along-fiber direction and a second pair in the cross-fiber direction and displacement measurements were taken over several continuous breaths (Fig1A). Strains were calculated from the measured displacements and compared between age groups and disease state. Dots were marked on the tissue with dye where the ultrasound crystals were. Following *in vivo* measurements, the mid-costal region of the diaphragm used for sonomicrometry was explanted for biaxial passive testing. Each sample was stretched to 20 percent strain at a strain rate of 1% per second. Starting lengths for passive testing were defined as the point at which passive resistance began and deemed optimum fiber length. Stresses were calculated from the measured forces and areas and compared between age groups and disease state. Finally, to relate *ex vivo* passive measurements to the *in vivo* testing, we divided the *in vivo* resting length by optimum fiber length to determine the resting fiber stretch.

Results and Discussion

We found a decreasing trend in along-fiber strains and a significant decrease in the cross-fiber strains with age in healthy mice. Dystrophic mice had significantly lower strains in both directions compared to healthy mice at 6mo but not at 12mo and no significant changes with age. Strains in young dystrophic mice are indistinguishable from healthy and dystrophic aged mice suggesting a rapid and early degeneration (Fig 1B).

There was a significant increase in along and cross-fiber stresses at all age groups with disease state. No significant changes with aging were found for healthy or dystrophic mice (Fig 1C).

Finally, relating the *in vivo* to *ex vivo* testing, we found a significant change in the aged healthy mice where all other groups are above optimum fiber length while the aged healthy mice are significantly lower (Fig 1D). This shift down the ascending limb of the force-length curve could explain the decrease in *in vivo* strains with age in the healthy mice.

Significance

We have developed a method to measure both along-fiber and cross-fiber strains of the diaphragm *in vivo*. Our results are supported by previous studies[2,3] that found a decrease in diaphragm movement with age and disease. We are now able to connect these findings to alterations in the in vivo fiber behavior and the passive mechanics. Future steps include using our measurements as the basis for a computational model to further investigate the mechanical changes occurring in dystrophic muscle and identify potential targets for therapies.

References

[1] Benedetti et al. (2013). *FEBS J.* [2] Whitehead et al. (2016). *J Physiol.* [3] Pennati et al. (2019) *J Magn Reson Imaging*

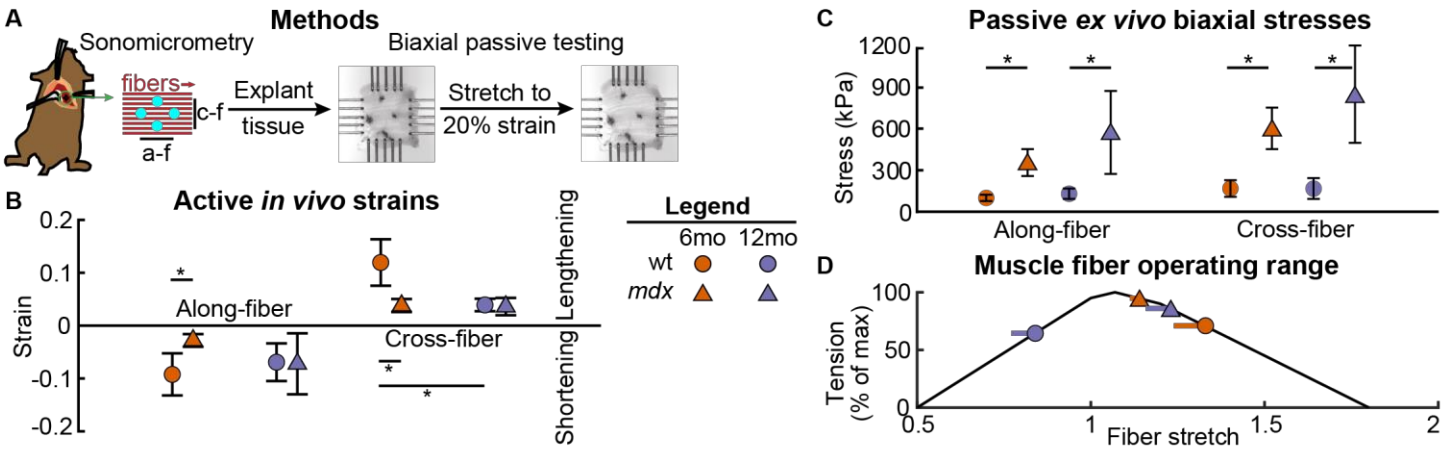

Figure 1: (A) Methods showing along-fiber (a-f) and cross-fiber(c-f) placement of crystals *in vivo* and passive testing. (B) Significant differences in strains were seen between healthy and dystrophic muscle in the along and cross-fiber directions at 6mo but not at 12mo. Healthy muscle also has a significant decrease in cross-fiber strains with age. (C) There is a signicant increase in along and cross-fiber passive stress with disease state in both 6mo and 12mo mice. (D) Most mice are on the plateau or descending limb of the length-tension curve, however 12mo healthy mice are on the ascending limb. Overlayed lines are average strains from sonomicrometry. *p<0.05

Biomechanical Assessment of Bone Staples: Effect of Declining Bone Mechanical Properties

Tanetta L. Curenton[1], Brian L. Davis[1], and Josiah S. Owusu-Danquah[1]
[1]Cleveland State University, Cleveland, OH, USA
Email: j.owusudanquah@csuohio.edu

Introduction

Bone quality changes can occur as a result of aging, inadequate nutrition, and bone diseases. The weakening of bone leads to higher risks of fractures, and poses a greater challenge for fixation due to the declining mechanical strength of bone. Stable internal fixation leading to a quicker return to full weight-bearing activities and adequate bone holding and healing is vital to a patient's quality of life [1].

Internal fixation of bone with diminishing quality can be difficult, with a failure rate ranging from 10% to 25% in osteoporotic bone [2]. Employing an appropriate contact force and contact area to stabilize the bone and prevent malunion or nonunion could lead to higher success rates and better quality of life outcomes. The purpose of this study was to investigate the effects of deteriorating bone mechanical properties on the contact force and contact area of stainless steel and superelastic nitinol staples. A finite element simulation approach was used to vary the Young's Modulus of bone.

Methods

A fracture fixation model consisting of a simple staple surrounding a segment of bone was evaluated using Abaqus 2017 (Dassault Systèmes Simulia, Johnston, RI, USA). The bridge and legs of the staple were 20mm. The staple cross-section was 2mm x 2mm. To simulate post-deployment of the staples, the legs of the stainless steel staple were designed straight while the legs of the superelastic nitinol staple were tilted in by 1mm. (A few data points for nitinol staple legs tilted in by 2mm were also collected). The bone segment was modeled as an 18mm x 16mm block, with the base of the block being 16.50mm. Young's Modulus and Poisson's ratio was set to 205GPa and 0.275, respectively, for the stainless steel staple. The nitinol staple was modeled using a nonlinear user-defined material model [3]. The Young's Modulus of bone varied from 21GPa to 11GPa to indicate the change in the mechanical properties of bone from a healthy state to a diseased state. The simulation procedure involved two loading steps. In the first step, pressure was applied to the staple legs to simulate the opening of the staple before deployment at the fractured site. In the second step, pressure was removed, allowing the staple to establish and maintain contact with the bone.

Results and Discussion

As bone mechanical properties declined, the maximum contact force in steel staples and superelastic nitinol staples decreased (Fig. 1). A 0.02036N decrease occurred in steel staples from the highest elastic modulus to the lowest elastic modulus of bone. A 0.36374N decrease occurred in the nitinol staples tilted in 1mm. A 7.6961N decrease occurred in the nitinol staples tilted in 2mm. The superelastic properties of nitinol and ability to recover more strain play a role in the higher contact forces. Higher contact forces may correlate to improved stabilization of the bone. The greater overall contact force and greater decrease in the contact force for nitinol staples during declining bone mechanical properties could better accommodate bone with diminishing quality. The contact area gradually decreased for steel staples with bone degradation and gradually increased for nitinol staples (Table 1). Larger contact area may reduce stress and contribute to better holding of the fractured bone, which is important in bone with diminishing mechanical properties. Nitinol staples tilted in 2mm had a greater amount of increase in contact area and decrease in contact force compared to the other staples as bone mechanical properties declined. In a study using solid polyurethane foam foot models with the same mechanical properties, Aiyer et al. also reported that nitinol staples have larger contact forces and contact areas and suggested that nitinol staples may be capable of adjusting to gapping and resorption [4]. This study showed that the adjustment of a bone staple, such as pre-deployment opening and post-deployment closure, can impact contact force and area which may be considered to start full weight-bearing sooner and may reduce failure rates in degrading bone if a particular contact force and area may better correlate with particular bone qualities. Material, thickness, curvature, and other properties of fixation devices could be optimized to accommodate cases of diminished bone quality. However, further studies are needed.

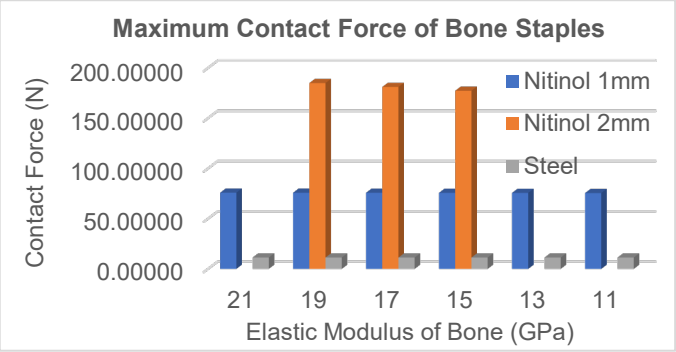

Figure 1: Maximum contact force is highest in nitinol staples.

Table 1: Contact area decreases in steel and increases in nitinol staples with declining bone mechanical properties.

Bone E (GPa)	Steel (mm^2)	NiTi 1mm (mm^2)	NiTi 2mm (mm^2)
19	0.170275	0.942223	0.092224
17	0.170261	0.942224	0.092750
15	0.170244	0.942226	0.093556

Significance

Bone diseases and aging can cause bone properties to decline over time. New fixation device designs optimizing for contact forces and contact areas that accommodate bones of varying quality may improve the short and long-term benefits of fixation in patients with declining bone quality. More regard given to bone quality could be vital for clinical outcomes, particularly if fixation methods could be optimized for a more personalized approach to address diminishing bone mechanical properties.

References

1. von Rüden, C. and Augat, P. *Injury*. 47 Suppl 2:S3-S10, 2016.
2. Cornell, C.N. *J Am Acad Orthop Surg.* 11(2):109-19, 2003.
3. Saleeb, A.F., et al. *Mech. Mat.* 80: 67-86, 2015.
4. Aiyer, A., et al. *Foot Ankle Spec*. 9(3):232-40, 2016.

The OpenArm Project: Exploring Deformation as a Measure of Muscle Force

Laura A. Hallock and Ruzena Bajcsy
Department of Electrical Engineering and Computer Sciences, University of California, Berkeley
Email: lhallock@eecs.berkeley.edu

Introduction

While many musculoskeletal simulation frameworks rely on estimates of muscle force [1], there exists no noninvasive, in vivo method of measuring the force exerted by individual muscles. Instead, forces are estimated based on motion-specific assumptions and/or noisy measures of neural activation. A direct, accurate measure of muscle force would enable improved understanding of dexterity, better quantification of pathology, and safer, more expressive assistive device control. We propose measuring muscle force via *muscle deformation*, a signal that is intrinsically coupled to force production: as muscles shorten and widen during the cross-bridge cycle, tendons lengthen and force increases. In this work, we present *a)* evidence that this deformation is observable during voluntary exertion and (when correctly parameterized) is correlated with joint torque; *b)* preliminary findings on useful signals for force inference; and *c)* the OpenArm project,[1] an open-source collection of data and analysis code to enable study of the force–deformation relationship by the wider research community.

Methods

While deformation is readily observable via 2D ultrasound in the movement of each muscle's surrounding fascia, the observed signal changes substantially based on an individual's morphology, the geometry induced by their joints' kinematic configuration, contact dynamics with other tissue, and sensor location. To enable analysis under this complexity, we developed two exploratory data sets: first, a set of full 3D reconstructions of elbow flexor muscle volumes under varied (static) loading conditions [2, 4], and second, time series data of 2D brachioradialis deformation under isometric time-varying loads and alongside sEMG values [3]. Both sets were collected using ultrasound under multiple elbow angles and for multiple subjects. These data were then analyzed geometrically to establish the relationship between elbow force and various parameterizations of the deformation signal.

Results and Discussion

Example data is shown in Fig. 1. As reflected in the 3D exemplar, the overall shape of the elbow flexors is irregular; however, when cross-sectional area (*CSA*) is measured from a certain range of locations along the biceps brachii, this *CSA* value reliably increases with force exertion, a relationship that generalizes across elbow angles (but varies in magnitude) [2]. These observations confirm the feasibility of measuring force-associated deformation signals and affirm the importance of considering both kinematic configuration and sensor location during their analysis.

Similarly, the exemplar time series data in Fig. 1 — collected from a location along the arm informed by our 3D analyses — show that this static correlation between joint force and muscle *CSA* (and two other deformation measures) extends to dynamic isometric contractions [3]. While these correlations are reliably strong across subjects and most elbow angles, the measure that is most correlated — and even the sign of that correlation — varies by subject. These results confirm that the force-associated deformation studied in our static analyses can be observed (and tracked [3]) over time from a single ultrasound scan; they also highlight the importance of accounting for individuals' morphological variation.

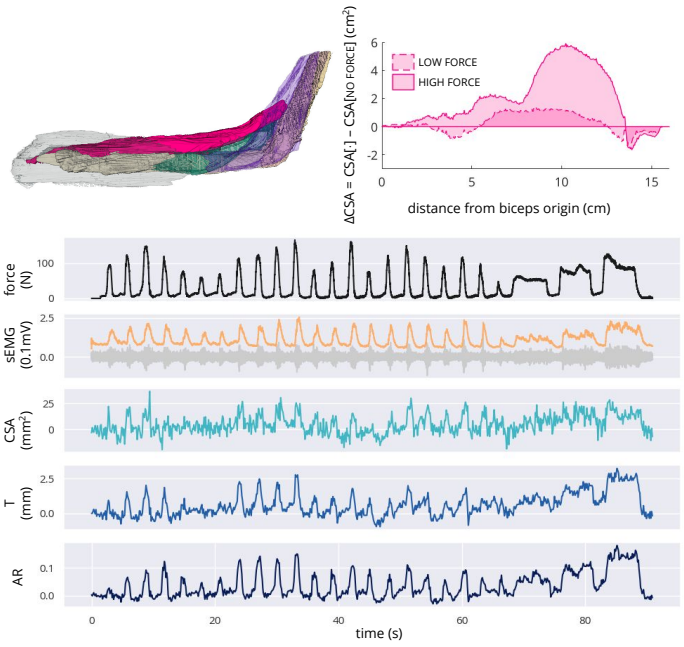

Figure 1: *Top:* Example 3D reconstruction of the elbow flexors (*left*) alongside biceps cross-sectional area (*CSA*) changes under force loading (*right*) [2]. *Bottom:* Time series force and sEMG data alongside three measures of brachioradialis deformation (*CSA*, thickness *T*, and aspect ratio *AR*) during pulsed and sustained isometric contractions [3].

Significance

Our results constitute quantitative evidence that deformation signals are both observable and correlated with joint force under isometric conditions; ultimately, we aim to expand this predictive power to individual muscle forces during natural movement. Identifying good signals for such models will require extensive exploratory data analysis, but will open up new avenues of research in biomechanics, neuroscience, robotics, ergonomics, and even animation. Our system identification efforts use the SimTK OpenArm platform, which contains all data and analyses described here and which we hope will inspire novel collaboration across these domains.

Acknowledgments

This work was supported by the NSF NRI, Siemens Healthcare, NVIDIA, eZono AG, and the NSF GRFP. The authors thank A. Kato, A. Velu, A. Schwartz, G. Kurillo, and D. Kaneishi.

References

[1] S. L. Delp et al. In: *IEEE Tran. Biomed. Eng.* 54.11 (2007).
[2] L. A. Hallock, A. Kato, and R. Bajcsy. In: *ICRA*. 2018.
[3] L. A. Hallock et al. In: *BioRob*. 2020.
[4] Y. Nozik et al. In: *EMBC*. 2019.

[1] https://simtk.org/projects/openarm

Can entropy of muscle synergies help track the gait improvements in ADS patients?

Mohammad Moein Nazifi[1], ,Theodore Belanger[2], MD, Isador H. Lieberman[3], MD MBA FRCSC, Ram Haddas[4], PhD, and Pilwon Hur[1*], PhD
[1]Department of Mechanical Engineering, Texas A&M University, College Station, TX, USA
[2]Texas Back Institute, Rockwall, TX, USA
[3]Texas Back Institute, Plano, TX, USA
[4]Texas Back Institute Research Foundation, Plano, TX, USA
Email: *pilwonhur@tamu.edu

Introduction

Adult degenerative scoliosis (ADS) is a common musculoskeletal problem in older adults affecting up to 68% of the individuals older than 70 years old [1]. ADS causes low back pain and mobility issues. Surgical interventions to restore the original disk spacing remains as one of the treatments for ADS. However, tracking the gait improvements in ADS patients is challenging due to the high inter-subject variations such as affected side, number of the affected disks, and the position of the deformity.

Our prior research extracted a set of *muscle synergies* to explain the walking behavior of ADS patients before and after surgery [2]. Muscle synergies can be thought of as lower-dimensional building blocks of the Central Nervous System (CNS) in controlling motor tasks, where a lower number of required synergies is often associated with less complexity and quality of the motor task [3]. Although our study showed an increase in the number of walking synergies after surgery in ADS patients (i.e. higher complexity), we argue that both the quantity and quality of synergies can reveal gait improvements. Quality of muscle synergies can be examined using the concept of entropy. Higher entropy is associated with more chaotic control while a lower entropy presents more deterministic control (Fig. 1).

We intend to track the walking improvements in ADS patients following surgical procedures by measuring the entropy on their walking muscle synergies. We hypothesize that the entropy of synergies will decrease, indicating a more deterministic control, after surgery.

Methods

Thirteen ADS patients participated in this IRB-approved study. To ensure a comparable severity of their ADS condition, subjects were excluded in case of a Cobb angle greater than 50 degrees. Subjects were asked to walk at their comfortable speed before and 3 months after their surgical interventions. Surface EMG was collected from the following muscles, bilaterally: External Oblique (EO), Gluteus Maximus (GM), Multifidus (MF), Erector Spinae (ES), Rectus Femoris (RF), Semitendinosus (ST), Tibialis Anterior (TA), Medial Gastrocnemius (MG). EMG was collected and processed as described in [2], then fed into a non-negative matrix factorizer to extract seven synergies and their activation.

The summation of all activations in a synergy was then normalized to 1, to enforce each synergy to resemble a probability density function. The entropy of an individual's synergy was defined as:

$$H(W_i) = -\sum_{i=j}^{n} P(j)\log_2 P(j)$$

where H is the entropy, W_i is i^{th} synergy, and $P(j)$ is the normalized activation of a muscle in a synergy. A paired t-test with a significance of 0.05 was performed to find significant differences in entropies pre- and post-surgery.

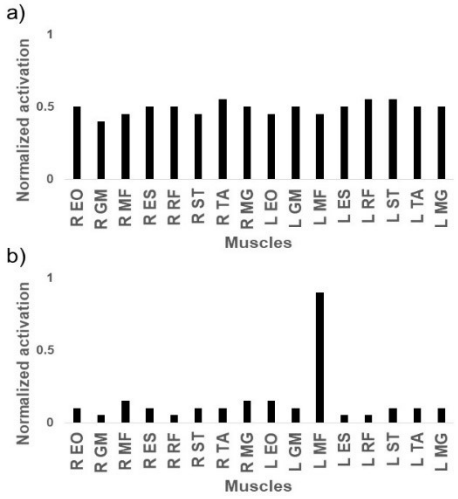

Figure 1: Examples of a high entropy (a) and low entropy (b) muscle synergy. Please note the deterministic control in (b).

Results and Discussion

The entropy values for each individual's synergy was calculated (13×7=91 values), where minimum, maximum, average, and standard deviations were 2.40, 3.76, 3.19, and 0.26, respectively. All seven muscle synergies indicated a significant decrease in their entropy following surgery with p-values < 0.001.

The higher entropy may indicate a more random and chaotic control of the muscles. This shows that surgery is helping ADS patients to have more complex control while walking. In other words, lower entropy may indicate that the CNS is more likely to deliberately choose to activate a muscle to reach a certain kinematic or kinetic goal (Fig. 1). Consistently, researchers claimed that a lower entropy in quiet standing indicated a more deterministic control of the COM to maintain balance [4].

Significance

Using muscle synergies are generally advantageous to kinematic analysis due to its robustness to different conditions. However, synergies can be challenging to interpret due to its numerous dimensions. Specifically, in ADS patients, individuals show improvements on different sides and different muscles due to the nature of the disease. Our introduced method can help track the possible improvements despite the high variation of scenarios in different patients and can be a novel method of assessment.

References

[1] Cho et al. *Asian Spine J.*, **2014**.
[2] Nazifi et al. *ASB (Rochester, MN)*, **2018**.
[3] Clark et al. *Journal of Neurophysiology*, **2010**.
[4] Hur et al. *Scientific Reports*, **2019**.

How do dry needling and high-intensity focused ultrasound affect tendon strain pattern?

Sujata Khandare[1], Ali A. Butt[1], Molly Smallcomb[2], Jacob Elliott[2], Julianna C. Simon[1,2], Meghan E. Vidt[1,3]*
[1]Biomedical Engineering, Pennsylvania State University, University Park, PA, USA
[2]Graduate Program in Acoustics, Pennsylvania State University, University Park, PA USA
[3]Physical Medicine & Rehabilitation, Penn State College of Medicine, Hershey, PA, USA
Email: *mzv130@psu.edu

Introduction

Approximately 14 million tendon and ligament injuries are reported each year in the U.S., costing $254 billion[1]. Injured tendons are mechanically inferior, compromising function and increasing the risk of tendon rupture. Dry needling (DN) is a conservative treatment used to alleviate pain and improve tendon healing. However, it is invasive with mixed success rates[2] due to high inter-practitioner variability. High-intensity focused ultrasound (HIFU) is an emerging therapeutic ultrasound modality that can induce bioeffects in a well-defined focal volume, with the potential to non-invasively enhance tendon healing. The objective of this study is to compare the effect of DN and HIFU treatments on the mechanical properties of *ex vivo* rat Achilles tendons and develop a finite-element model to evaluate their effect on tendon strain pattern.

Methods

Tendons from adult Sprague Dawley rats were randomly assigned to DN, HIFU, or sham, with 5 tendons/group. For DN, a fine-gauge (25G) needle was inserted and quickly removed from central portion of the tendon 5 times over 12 s. For HIFU, the central portion of the tendon was exposed to 10 ms pulses repeated 60 times at 1 Hz with peak +ve pressure >80 MPa and peak -ve pressure >20 MPa. Following DN, HIFU, or sham exposure, mechanical testing was performed using an MTS 858 Mini Bionix (MTS Systems Corp., Eden Prairie, MN) mechanical testing system, using an established testing protocol[3]. Tendon mechanical properties including elastic modulus, stiffness, and percent relaxation were determined. A finite-element model was developed in COMSOL (v.5.4, COMSOL Inc., Burlington, MA) using manual segmentation of magnetic resonance images from a rat. The muscle-tendon unit was modeled as a transversely isotropic material with experimentally measured mean mechanical properties used as model parameters. Loads equivalent to 0.5x (2N), 1x (4N), 2x (8N), 3x (12N), and 4x (16N) mean body weight were applied along the muscle-tendon unit's long-axis. Fifteen computational simulations were performed to predict strain at the tendon-bone interface. Statistical analysis was performed-using a one-way ANOVA in SAS software (SAS Institute, Inc., Cary, NC, v9.4) for the comparison of group mean mechanical properties, with $p<0.05$ considered significant. Linear regression analysis was used to determine the trend of maximum strain across various applied loads.

Results and Discussion

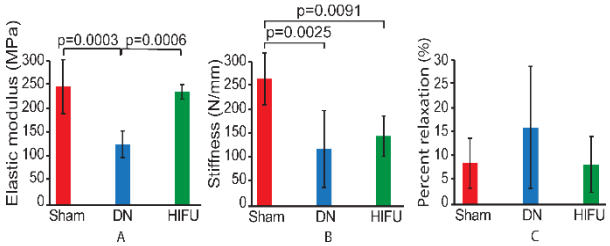

Figure 1: (A) Elastic modulus; (B) stiffness, and (C) percent relaxation of rat Achilles tendons exposed to sham, DN, and HIFU.

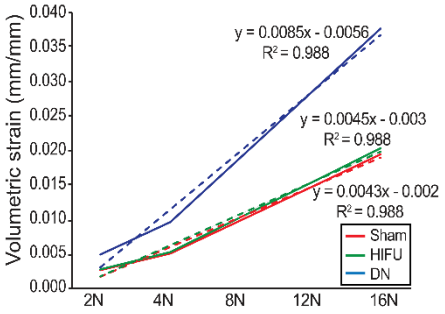

Figure 2: Volumetric strain patterns of sham, DN, and HIFU models for applied loads of 0.5x (2N), 1x (4N), 2x (8N), 3x (12N), and 4x (16N) mean body weight.

Elastic moduli of tendons in the DN (127.7±28.0MPa) group were significantly lower than sham (248.8±56.9MPa; p=0.0003) and HIFU (237.9±15.2MPa; p=0.0006) (Fig.1A); there was no difference in elastic moduli between the HIFU and sham groups (p=0.6573). Stiffness of tendons exposed to DN (116.3±78.9N/mm; p=0.0025) and HIFU (142.9±41.5N/mm; p=0.0091) was significantly lower than sham (260.3±53.5N/mm) (Fig.1B). There was no difference in percent relaxation of tendons exposed to DN (16.07±12.7%; p=0.1981) or HIFU (8.42±5.8%; p=0.9617) compared to sham (8.69±5.2%) (Fig.1C). Predicted maximum strain from the DN model (avg. 19.7e-3mm/mm) was greater than HIFU (avg. 10.5e-3mm/mm) and sham (avg. 10.1e-3mm/mm) models (Fig.2). A linear increase (avg. R^2=0.988) in predicted maximum strain with increased applied load was seen in all models. However, the DN model showed a larger increase (32.9e-3mm/mm) in strain across loading conditions (0.5x body weight to 4x body weight) compared to HIFU (17.7e-3mm/mm) and sham (16.9e-3mm/mm) models.

Results from mechanical tests suggest HIFU has the potential to preserve mechanical properties of tendon better than DN. Modeling results show that strain levels in the DN model were higher near the tendon-bone interface compared to the HIFU model. This suggests that tendons treated with HIFU experience less strain for similar applied forces than DN, making those tendons less susceptible to injury.

Significance

The location of maximum strain from these analyses could inform predictions of location-specific initiation and progression of tendon injuries. This information also could aid in calculating risk of injury and provide insight into injury prevention. Further studies are needed to evaluate the effects of HIFU in animal models to understand if HIFU may be an alternative, non-invasive treatment for tendon injuries.

Acknowledgments

Work funded by the NIH-NIBIB (R21EB027886); NSF Graduate Research Fellowship (Smallcomb; Grant#DGE1255832); and the Penn State College of Engineering Multidisciplinary Seed Grant.

References

1. Praemer A. et al. 1999. AAOS. 182 pp.
2. Myburgh C. et al. 2012. Chiropr. Man. Ther. 20(1):36.
3. Gimbel J. A. et al. 2004. J. Biomech. 37(5):739-49.

Dynamic Arthrokinematic Assessment of the Sacroiliac Joint

Matthew R. MacEwen[1], Andrew L. Freeman[1,2], Arin M. Ellingson[1].
[1]*University of Minnesota, Minneapolis, MN, USA*
[2]*Excelen Center for Bone and Joint Research, Minneapolis, MN, USA*
Email: ellin224@umn.edu

Introduction

Low back pain (LBP) is a leading cause of disability in the world[1]. In particular, pain associated with the sacroiliac joint (SIJ) results in a very low quality of life and contributes to 15-30% of low back pain cases[2,3]. This pain is both intra-articular and peri-articular[4,5]. During abnormal or excessive motion, it is theorized the complementary grooves and ridges of the articular surface no longer conform. Therefore, it is clinically important to understand the arthrokinematics of the SIJ during dynamic activities. **The objective of this study is to quantify the intra-articular distances during induced nutation\counternutation.**

Methods

Two osteoligamentous cadaveric specimens (49F;60F) were obtained and four 1mm tantalum beads were embedded into the sacrum and each ilium to co-register the motion data to the bone models. The pelvises then underwent a CT scan to determine bead location and construct 3D models of the ilium and sacrum (MIMICS Materialise). The L4 vertebral body and the right ischium were potted and loaded into a 6-DOF Spine Tester (MTS 858 Mini Bionix, MTS). Pure moments of up to 7.5 Nm were applied in nutation\ counternutation and kinematics were recorded via 4-camera optical motion capture system (Vicon). Bead location was digitized prior to biomechanical testing. SIJ rotations and translations were calculated with the following anatomical coordinate system: x-lateral bending, y-axial rotation, and z-nutation\counternutation[6]. The minimum distances between the joint surfaces were calculated dynamically. The mean and minimum distances were measured along with the percent differences from the initial neutral position.

Results and Discussion

The results of induced nutation\ counternutation are shown below in Table 1 and Figure 1. The ROM for the primary axis of rotation for each specimen was shown to be comparable at 3.00° and 2.75°, consistent with literature[7]. The proximity of the surfaces shown in Figure 1b indicates the percent difference of the proximity compared to its initial position. There is a greater shift within the first specimen's conformity of surfaces (represented with varying ranges), possibly attributed to the amount of translatory motion in Specimen 1.

The proximity maps help pinpoint regions impacted by the morphological shift of the surfaces. There is a greater change in conformity within the anterior regions of both specimens during counternutation and the inferior concave region during nutation – highlighting regions of potential articular surface contact. Both specimens minimize percent difference in the neutral position during dynamic motion indicating the efficacy this metric to measure conformity changes. Analysis is on going to achieve sufficient power and analyse additional motions and introduce a destabilized experimental condition.

Significance

The results provide insight into the arthrokinematics of the SIJ during macroscale motions. This can ultimately aid in better understanding the SIJ's role in LBP.

Acknowledgements

We would like to thank Excelen for their generous cooperation in obtaining the cadaveric specimens.

References

[1] Dione, Clermont E. *Spine* (2008), [2] Cher, D. *Med Devices (Auckl).* (2014) ,[3] Cohen, SP. *Expert Review of Neurotherapeutics* (2013), [4] Vilensky, JA. *Spine.* (2002), [5] Borowsky, CD. *Arch Phys Med Rehabil.(2008)* [6]Van Hauwermeiren, Liesbeth. *Journal of Orthopedic Research.* (2018) [7] Sturesson, Bergt. *Spine.* (1989)

Table 1: Ranges of Motion and Translations

	# 1	# 2
Nutation\ Counter-nutation	3.00°	2.74°
Axial Rotation	0.27°	0.23°
Lateral Bending	0.38°	0.21°
Medio-lateral Translation	0.69mm	0.31mm
Antero-posterior Translation	1.87mm	0.83mm
Superior Inferior Translation	0.67mm	0.36mm

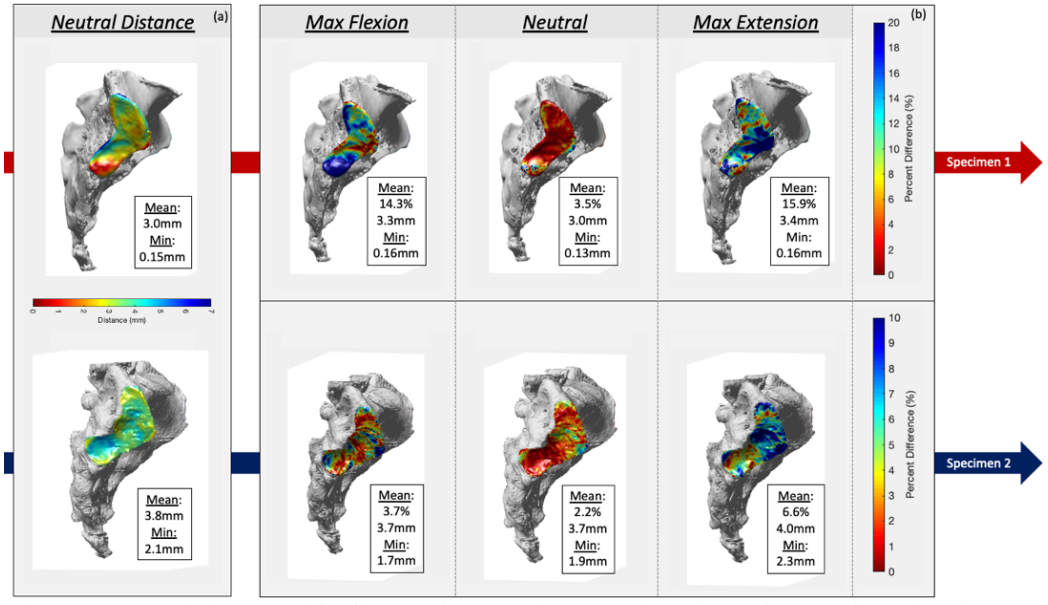

Figure 1: (a) Proximity map of the distances between the two surfaces during the neutral position. (b) Percent differences in distance from neutral position for dynamic motion. Note: scales different between rows

Knee Valgus Angle: MRI versus Motion Capture

Christopher Weathers[1], Taylor Oldfather[1], Michael Zabala[1]
[1]Mechanical Engineering, Auburn University, Auburn, AL, US
Email: zabalme@auburn.edu

Introduction

Precise mathematical methods have been developed to quantify lower limb kinematics in anatomically meaningful ways. In both imaging (particularly magnetic resonance imaging, MRI) and movement analysis, the knee valgus angle (KVA) is commonly measured to determine ACL injury risk and to measure chronic conditions such as knee osteoarthritis [1]. MRI angles are also used for surgery in ACL reconstruction and knee replacement to facilitate normal kinematic functioning of the knee. Knowing how knee angles measured using MRI relate to angles measured during gait, using motion analysis, may help customize knee alignment in total knee replacement surgeries or other repairs. The purpose of this study is to test the hypothesis that multiple knee angles measured with motion capture are related to similar angles measured via MRI.

Methods

A 10-camera Vicon motion capture system (Vicon, Vantage V5 Wide Optics), along with 79 retro-reflective markers placed based on the Point Cluster Technique, was used to collect the biomechanics of nine female student soccer athletes from Auburn University (height = 171.2 +/- 8.9 cm,weight = 66.3 +/- 8.6, kg age = 19.8 +/- 1.9 yr) [2]. The athletes were not excluded based on prior injuries or surgeries. The subjects walked 25 feet at a self-selected pace. The marker data was filtered using a 15 Hz lowpass butterworth filter, and Visual 3D was used to analyze the data. Frontal plane knee angles were measured at maximum knee flexion (KF) during the stance phase of gait. Knee abduction angle (KA) was calculated using the Grood and Suntay joint coordinate system [3]. In addition, KVA was calculated as the angle between the shank and global vertical axis [4]. Secondly, a 7-Tesla MRI machine was used to image both right and left knees using a true fast imaging (TRUFI) sequence. The subjects were placed in the scanner in a comfortable, supine position. The MRI images were segmented in Amira (Thermo Fisher Scientific) to generate 3D point clouds of the distal femur and proximal tibia. Blender software was used to generate local reference frames of both bones with a method based upon that described by Miranda et. al. [5]. The MRI KA and KF were calculated using the Grood and Suntay joint coordinate system [3]. The angles from MRI and motion capture were then compared using a two-tailed Pearson Correlation test with a 95% confidence interval.

Results

Table 1: Mean and standard deviation (SD) of the KF, KA, and KVA measured during walking; and KF and KA measured from the MRI scan.

Activity	Angle	Mean	SD
Walking	KF	1.099507	2.492473
	KA	14.4554	6.379568
	KVA	0.085509	0.037876
MRI	KF	3.085956	6.02223
	KA	0.322674	1.979525

Table 2: The correlation between walking KA, KVA, and MRI KF and corresponding signifance level.

Walking	MRI KF	
Angle	r	P
KA	0.700	0.036
KVA	0.767	0.016

Discussion

The results of this study support the hypothesis that knee angles measured from MRI are related to angles measured using motion capture data. More specifically, the results show a correlation between the resting KF angle measured with MRI with KVA at maximum KF measured from motion capture during the gait cycle. Therefore, KF angle in MRI gives insight to KVA and KA measured with motion capture. This may allow physicians to better understand how surgical alignment of the knee will impact subsequent gait kinematics. The fact that the MRI KF is highly correlated with KVA from motion capture shows that using static measurements for reconstruction alignment is beneficial for the dynamic functions of the knee

Figure 1: A 3D rendering of the femur and tibia from

Future Work

Further correlation between MRI and motion capture angles could be found by using additional subjects and scan types, such as x-ray or functional MRI. Comparing angles at different points in the gait cycle could also be beneficial. It would also be valuable to compare the MRI KA with the motion capture KA at points throughout the gait cycle where KF is equal to the subject's KF from MRI. Additionally, controlling for the amount of knee flexion in the MRI could lead to additional correlations in other angles. Finding a combination of MRI angles and motion capture angles that correlate to one other using these methods has the potential to give more insight to how individuals' knees can be aligned during surgery to result in more natural kinematics during gait.

References

[1] DeFrate et. al. (2006). AM J SPORT MED, 24(8): 1240-1246
[2] Andriacchi et. al. (1998). J. BIOMECH ENG, 120(6):743–749
[3] Grood and Suntay (1983). JOB, 105:136.
[4] Hewett et al. (2005). AM J SPORT MED, 33: 492-501
[5] Miranda et al. (2010). JOB 43.8: 1623-1626.

Graded Loading Challenge test for clinical assessment of foot pain: reliability and validity study.

Gulle H[1], Morrissey D[1,3], Miller S[1], Birn-Jeffrey A[2],
1: Sports and Exercise Medicine, Queen Mary University of London, UK
2: School of Engineering and Materials Science, Queen Mary University of London, UK
3: Physiotherapy, BH NHS Trust, London UK
*Corresponding author email: d.morrissey@qmul.ac.uk

Introduction

Musculoskeletal foot and ankle pain is common and typically aggravated by weight-bearing activity. Examination is usually based on a patient's symptom description, physical examination and imaging findings with severity graded subjectively in the clinical setting using patient reported outcome measures (PROMs). Objective severity grading is challenging to obtain. Therefore, a novel graded loading challenge (GLC) test was devised to grade foot pain severity with an objective measure of potential use in the clinical setting. This study aimed to assess GLC intra-tester reliability and validity, both with respect to patient reported severity and task progression.

Methods

People with foot pain of various kinds (♀=9, ♂=8) and healthy (♀=4, ♂=3) controls were recruited. Prior to performing the tests, all patients completed the Foot Health Status Questionnaires (FHSQ) to severity status. Kinetic and kinematic motion capture were performed during the GLC utilising in-floor force plates (500Hz; 9281CA, Kistler) and an infrared motion analysis system (100Hz; CX-1), respectively. The GLC consisted of four different difficulty levels: 1) normal walking with self-selected speed and step length, 2) walking with a 25% longer step length of participants' original step, 3) normal walking while carrying a load of 25% of body mass (BM), and 4) walking with the 25% longer step length plus the extra 25% load, which is a combination of tasks two and three. There were 10 repetitions of each task. The peak vertical ground reaction force (vGRF) at loading response (first peak), terminal stance (second peak) and rate of peak force development (RFD); Medial longitudinal arch (MLA) and first metatarsophalangeal joint (MTPJ1) angles were calculated at 50% stance and toe off, respectively. A numeric pain rating scale (NRS) was ascertained after each task. GLC score is calculated via the sum of pain values which are multiplying with grade of each task (1,2,3,4) for all levels were then correlated with the participant's score in the FHSQ pain subscale. A two tailed spearman's rank-order correlation test was used for results. Reliability was evaluated with repeated measures of 9 participants on separate days.

Results and Discussion

Each test showed moderate to excellent reliability for intra-rater assessment (ICC: 0.60-0.92 with %95 CI) except for the MLA within the walking with weight task. First and Second Peak Maximum vGRF are significant with linear trend from polynomial contrast, ($F_{1.4, 11.1}=30.8$; $P<0.001$) (Figure 1), ($F_{3, 24}=8.3$; $P=0.001$) respectively. While, MTPJ1 Maximum angles ($F_{2.3, 18.8}=0.40$; $P=0.703$) and MLA Maximum angles ($F_{2.1, 17.1}=2.8$; $P=0.087$) (Figure 1), both are non-significant across the four tasks. Correlations were found between the total GLC score and FHSQ as $r=0.410$, $p=0.065$. The biomechanical measures were repeated and demonstrated similar reliability to published work for kinetics. Kinematic re-test reliability was not as comparable necessitating particular care with marker placement. Results showed that GLC increases in maximum and second peak of GRFs with no progressive change in kinematics. However, the most important parameter of pain provocation during the tasks was seemed to be accumulated effect of the four tasks is suggested to increase the likelihood of achieving a pain response for each patient. The correlation between FHSQ and GLC is supporting the assumption that the GLC can evaluate and quantify the symptoms of patients with foot pain.

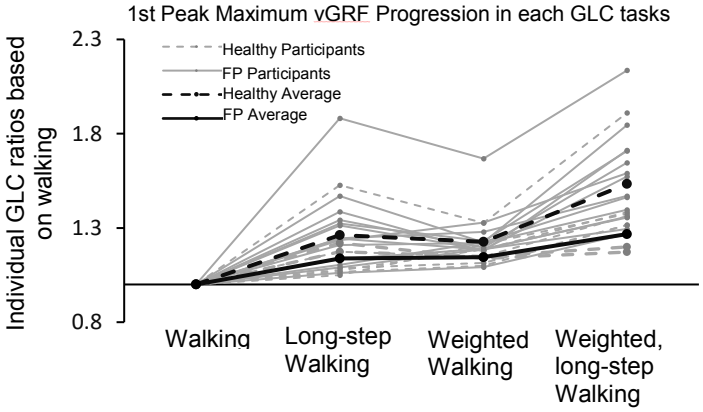

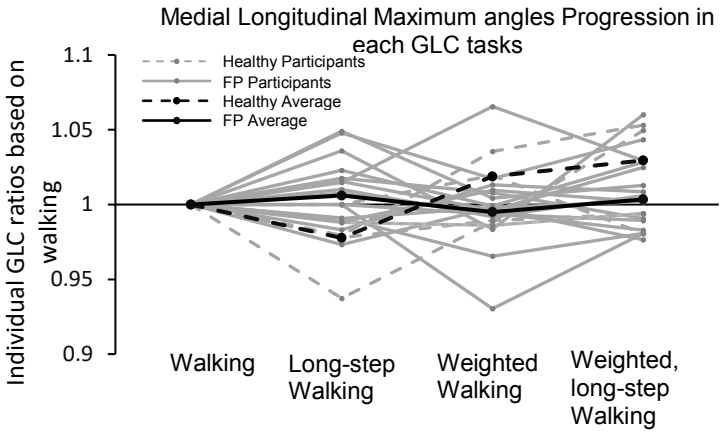

Significance

Specific clinical tests for assessing patients with foot pain facilitate the clinician's understanding of the patient's status, response to intervention, which provide determining of the best treatment option. In this study, easily applied functional tests elicited the patient's relevant foot pain, thus ascertaining a valid clinical assessment. Considering that mechanical overload is thought to be a causal reason for foot pain, and instrumented gait analysis the gold standard, we attempted to construct a graded loading challenge based on previous work to progressively challenge the load-bearing capacity of the plantar fascia by manipulating stride length and carried load. If compressive or tensile load are the biggest aggravating factors for foot pain[1], our results suggest the graded loaded challenge tasks may be a useful indicator of severity, particularly as the kinetic values show a graduated increase with task. The ability of these tests to evaluate changes in the patient's status over time or after therapeutic intervention needs further evaluation.

References

1. *Sullivan, J., Burns, J., Adams, R., Pappas, E., & Crosbie, J. (2015). Plantar heel pain and foot loading during normal walking. Gait & posture, 41(2), 688-693.*

The Utilization of Porcine Ligament Properties as a Substitute for Human Ligaments in a Spinal Finite Element Model

Michael Polanco.[1], Sebastian Y. Bawab[1], Stacie I. Ringleb[1], Michel Audette, Carl St. Remy, James Bennett
[1]Department of Mechanical and Aerospace Engineering, Old Dominion University, Norfolk, VA USA
Email: mpola002@odu.edu

Introduction

Finite element modeling can be used to non-invasively assist in answering pre-surgical questions pertaining to surgical outcomes, which are best answered through input of patient-specific geometric data. However, it is nearly impossible to obtain in-vivo ligament properties and can be difficult to acquire human cadavers for in-vitro experiments. Porcine ligaments are similar in morphology and mechanics when compared with humans [1]. However, porcine spines can behave mechanically different depending on the spinal region of interest [2]. The purpose of this study is to compare the mechanical behavior of a functional unit within the human lumbar spine using porcine ligament stiffness properties with human ligaments.

Methods

Quasi-static analyses were conducted in LS-DYNA (Livermore Software Technology Corporation, Livermore, CA) using an L4-L5 functional spinal unit finite element model (Figure 1). Vertebral and intervertebral disc geometry was obtained from CG Hero (CG Hero Ltd., Manchester, UK) and constructed using HyperMesh (Altair Engineering, Troy, MI). Human material properties for the intervertebral disc and vertebrae were characterized as hyperelastic and linear elastic respectively [3]. Ligaments were characterized as nonlinear tension-only springs. In-vitro porcine ligament data were collected in our lab [4] and human ligament data [5, 6] as well as capsular ligament properties [6] were obtained from the literature. Capsular ligament properties were the same for human and porcine ligament data sets. A pure moment of ±10 N-m was applied in flexion and extension over a rigid body element distributed to the superior endplate and facet processes of L4, while the inferior endplate and facet processes of L5 were fixed. Functional Spinal Unit (FSU) kinematics were assessed with all ligaments intact and then serially removed beginning with spinous ligament removal, followed by facet joint removal, and ending with ligamentum flavum removal in flexion. Only intact and facet joint removal configurations were analyzed in extension. These reflect sequential steps for spinal flexibility gain in a posterior spinal fusion conducted by a surgeon.

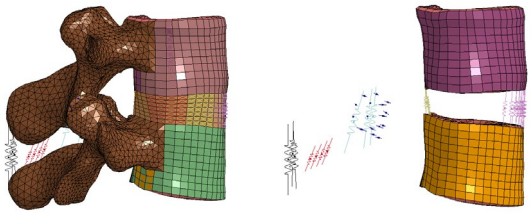

Figure 1. Finite element model of L4-L5 FSU

Results and Discussion

The model showed that the functional unit with porcine ligaments intact matched the in-vitro data [7] more closely than human ligaments (Figure 2), which aligns with similar kinematic assessments [3]. The greatest differences in flexion exist in both cases when the ligamentum flavum is removed from the configuration, because it was stiffer than the other ligaments. In extension, the human and porcine ligament sets guide the FSU to similar behavior while matching in-vitro data with prescribed moments under 5 N-m. Little differences can be found between both sets of kinematics due to the toe stiffness regions of the Anterior Longitudinal Ligament being similar between the porcine and human subjects utilized.

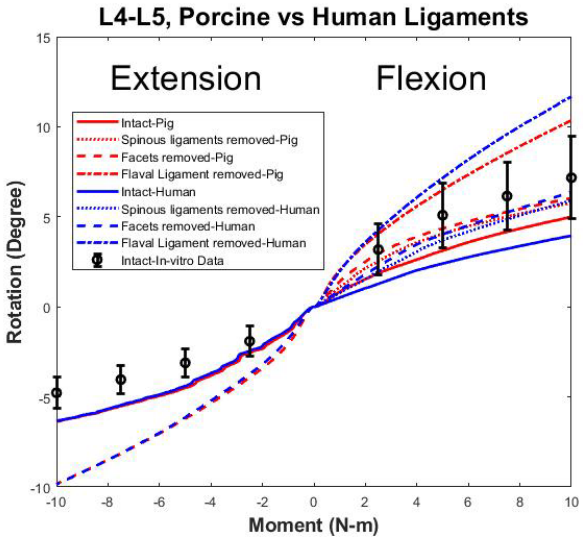

Figure 2. Flexion and Extension-Porcine vs Human

The results only reflect ligament stiffness data for one pig specimen and one FSU from the lumbar region. Future work should incorporate ligament stiffness data from multiple pig subjects while exploring various regions of the spine and human ligament properties.

Significance

As porcine specimens continue to be used as practical alternatives to human subjects because of anatomical similarity and availability, animal ligaments may be sufficient sources for material properties needed for computational modeling. As shown by sagittal kinematics, qualitative behaviour of porcine ligaments in tension may justify their future use as a surrogate for human ligament properties.

Acknowledgments

This work was funded by the SMART Scholarship received by M. Polanco and the Children's Research Foundation. Stephanie Anderson, Matthew Cribb, Cyndal Martell, Robert Martin, and Steve Parasidis collected in-vitro porcine ligament data.

References

[1] Hukins, D.W.L. et al. *Spine* **15**(8), 787-95, 1990.
[2] Wilke, H.J. et al. *Eur Spine J* **20**, 1859-68, 2011.
[3] Naserkhaki et al. *Biomechanics* **70**, 33-42, 2018.
[4] Cribb, M. et al. ASB Conference, Atlanta, GA, 2020.
[5] Chazal, J. et al. *Biomechanics* **18**(3), 167-76, 1985.
[6] Pintar, F.et al. *Biomechanics* **25**(11), 1351-56, 1992.
[7] Heuer, F. et al. *Biomechanics* **40**, 271-80, 2007.

INVESTIGATING ENERGY TRANSFER DUE TO THE WINDLASS MECHANISM: A PILOT STUDY

Lauren R. Williams[1], Dustin A. Bruening[1]
[1]Brigham Young University, Provo, UT, USA
Email: lauren.williams523@gmail.com

Introduction

Metatarsophalangeal joint (MTP) extension exerts tension on the plantar fascia, pulling the midtarsal (MT) joint into plantarflexion and raising the arch[1]. This windlass mechanism has been suggested to redistribute some of the energy absorbed by MTP extension[2], as power generation at the MT joint occurs concurrently with power absorption at the MTP joint.[3-5] However, further investigation is necessary to determine the extent of the power transfer between the MT and MTP joints.

The purposes of this study were twofold: 1. To investigate the relationship between motion at the MTP and MT joints and arch stiffness during three conditions: A) passive MTP extension, B) normal heel raises (Normal), and C) heel raises where MTP extension was altered (ToeFlexed) and 2. To compare MT joint work, as well as distal-to-hindfoot work (DTH; the net contributions of MT and MTP joints and any deformable structures distal to the hindfoot)[5] during both heel raises. We hypothesized that higher arch stiffness would result in more motion at the MTP and MT joints. We also hypothesized that during heel raises, the ToeFlexed condition would result in decreased positive work at the MT joint while DTH work would remain the same.

Methods

Arch stiffness was measured using the arch-height-index measurement system.[6] To measure MT motion during passive MTP extension, the participant's leg rested on a platform while the researcher extended the toes. This was performed 10 times to a metronome (45 bpm). To determine the relationship between motion at the MT and MTP joints, the slope of these two data sets was calculated for each subject and then compared to the subject's arch stiffness.

5 healthy males (age: 29±9.5 years, mass: 86.8±11.0 kg, height: 1.85±0.04 m) participated in this pilot study. The participant's right lower limb was outfitted with a multi-segment foot marker set.[7] In conjunction with a motion analysis system (Qualisys), a force plate (AMTI) was used to collect data during two heel raise conditions. For both conditions, participants performed 2 sets of 10 heel raises to a metronome (45 bpm). Participants were instructed to achieve a maximum height during the heel raise. In Normal, the participant's entire foot was on the force plate. In ToeFlexed, the foot was placed so that the hallux was off the force plate and curled over the edge. ROM at the ankle and MT joints, as well as the work done at the MT joint and DTH work, were calculated for the upward phase of the heel raise (start to peak heel raise). Paired t-tests ($\alpha = 0.05$) were used to identify differences between conditions for each metric.

Results and Discussion

The relationship between MTP and MT motion followed a linear trend with a slope of 14.2±3.9 degrees (i.e. for every 14.2 degrees of MTP extension there is one degree of MT plantarflexion). For 4 out of the 5 subjects, the relationship between this slope and arch stiffness were inversely related. These preliminary results suggest that in individuals with stiffer arches the windlass mechanism is more effective at pulling the MT joint into plantarflexion.

The ROM at the ankle joint was not statistically different between Normal and ToeFlexed ($p=0.33$), verifying that the subjects achieved the same heel raise height. However, the ROM at the MT joint was greater during Normal compared to ToeFlexed ($p=0.02$; 21.7±6.5 degrees vs. 18.9±7.5 degrees, respectively), suggesting that the windlass mechanism was more engaged during Normal compared to ToeFlexed.

The relationship between MTP and MT motion followed a linear trend for both heel raise conditions with a slope of 1.8±0.5 degrees for Normal and 1.7±0.6 degrees for ToeFlexed ($p=0.18$). The slopes for both Normal and ToeFlexed were both substantially lower than passive MTP extension ($p=<.01$), suggesting that much of the motion at the MT joint during heel raises is likely due to active muscle contractions with the windlass mechanism playing a secondary role, but further investigation is necessary to confirm this.

As hypothesized, the work done at the MT joint decreased during ToeFlexed compared to Normal (0.13±0.05 vs. 0.16±0.05; $p<0.001$), while DTH work was not statistically different between conditions (0.21±0.09 vs. 0.21±0.08; $p=0.99$). However, DTH work was higher for both conditions than the work done just at the MT joint. Due to the negative work typically performed by the MTP joint during push-off of walking[5,7] we expected DTH work to be less than MT work. Heel raises may have reduced MTP negative work since the center of pressure does not move as anterior as it does in walking and additional positive work may be performed at joints distal to the MT joint (e.g. Lisfranc joint complex).

Significance

During heel raises, work production and motion at the MT joint are decreased when MTP extension is altered. These results further support previous findings of an energetic interplay between the MTP and MT joints through the windlass mechanism.[2] Further work is needed to fully understand the elevated DTH work relative to gait studies.

Acknowledgments

This material is based upon work supported by the National Science Foundation Graduate Research Fellowship Program under Grant No. 1840996. Any findings and conclusions or recommendations expressed in this material are those of the author(s) and do not necessarily reflect the views of the National Science Foundation.

References

1. Hicks. *J. of Anatomy.* **88**, 25-30, 1954.
2. Bruening, et al. *Gait & Post.* **62**, 111-116, 2018.
3. Zelik, et al. *J Biomech.* **75**, 1-12, 2018.
4. Wager, et al. *J Biomech.* **49**, 704-709, 2016.
5. Takahashi, et al. *Sci. Reports.* **7**, 15404, 2017.
6. Butler, et al. *J Amer. Pod. Med Assoc.* **98**, 102-106, 2008.
7. Bruening, et al. *Gait & Post.* **35**, 535-540, 2012.

Tensile Testing of Spinal Ligaments

Matthew Cribb[1], Stephanie Anderson[1], Robert Martin[1], Steve Parasidis[1], Cyndal Martell[1], Michael Polanco[1], Stacie Ringleb[1], Sebastian Bawab[1]
[1]Department of Mechanical and Aerospace Engineering, Old Dominion University, Norfolk, VA
Email: sringleb@odu.edu

Introduction

Spinal ligaments play a role in stabilizing the spine and preventing excessive motion. Thus their mechanical properties are useful for computational models of the spine [1] frequently used for pre-surgical spinal planning and treatment. However, while human spinal ligaments have been previously tested [2], in-vitro ligament test datasets from literature are limited. Because porcine and human ligaments bear structural and morphological similarities with one another [3], porcine ligaments may be comparable to human ligaments. Additionally, when developing an experimental protocol, a pig is easier to obtain. The purpose of this study is to develop a repeatable method for performing ligament testing and to obtain ligament mechanical properties from a porcine specimen.

Methods

The spine of a 151 lb adult pig was harvested and four vertebral pairs dissected: one lower thoracic (T12-T13) and three lumbar (L1-L2, L3-L4, L5-L6). From each vertebral pair, five bone-ligament-bone (BLB) specimens were isolated, totaling 20, including the anterior and posterior longitudinal ligaments (ALL, PLL), ligamentum flavum (LF), intertransverse (IT), and the interspinous/supraspinous ligament complex (ISL/SSL). The bone ends were potted in a two-part epoxy using a 3D printed clamshell-popsicle potting design that provided adaptability to the various bone geometries. The potted BLB specimens were inserted into a fixation apparatus that adapted to a 10ST tensile testing machine (Tinius-Olsen, Horsham, PA). Specimens were frozen between preparation and epoxy curing stages averaging 10 hours of ambient exposure. All ligaments were preconditioned prior to static loading to failure at 0.01 mm/s from which stiffness data was obtained.

Results and Discussion

Force-deflection curves (Fig. 1) generally reveal characteristics of a ligament loaded in tension, including toe and linear regions up to failure [4]. 15 datasets were included for analysis. Excluding ITL, small standard deviation for each ligament type relative to the mean indicates similar results, regardless of the location in the spine. The ALL registered the highest failure load, followed by LF and PLL. The ISL/SSL ligament complex registered a lower failure load. These patterns are qualitatively consistent with observations made from in-vitro human lumbar ligament experiments. The porcine ligament failure loads were higher than observed in human ALL and flaval ligament specimens with standard deviations of 36.6 Newtons and 40.1 Newtons respectively, while the ISL/SSL complex registered a failure load lower than observed with a standard deviation of 5 Newtons. The PLL failure loads exhibited a standard deviation of 34.2 Newtons; however, the mean was in range of reported failure load values [2]. The differences in failure loads could be attributed to the amount of connective tissue removed from each BLB specimen, which was difficult to distinguish during dissection. Among specimens considered, the ITL failure loads exhibited a standard deviation of approximately 4.3 Newtons due to difficulty in aligning the ligament fibers with the axial load direction, leading to premature lateral tearing. Existing in-vitro ligament testing literature often do not identify testing setup limitations and lack specificity on ligaments isolation. To further refine the experimental protocol and establish statistical significance of the datasets provided, future work includes testing and collecting data from multiple pig spines.

Significance

Porcine ligament specimen testing is a practical alternative to testing human spines for developing robust spinal ligament experimental methods. This is enabled by relatively similar anatomy between porcine and human spine. Therefore, a robust method developed from porcine testing can translate directly to human testing with minor modifications. Furthermore, literature identifies that porcine spinal ligaments have similar qualitative mechanical properties to a human's [5], which could be applicable to human computational studies.

Acknowledgments

The project was funded by the Children's Research Foundation.

References

[1] Tyndyk, M.A. et al. *Acta of Bioengineering and Biomechanics* **9**(1), 35-46, 2007.
[2] Nolte, L.P. et al. *Clinical Implant Materials* **9**, 663-8, 1990.
[3] Hukins, D.W.L. et al. *Spine* **15**(8), 787-95, 1990.
[4] Mattucci, S.F.E. and Conin, D.S. *Mechanical Behavior of Biomedical Materials* **41**, 251-60, 2015.
[5] Kirby, M.C. et al. *Biomed. Eng* **11**, 192-6, 1989.

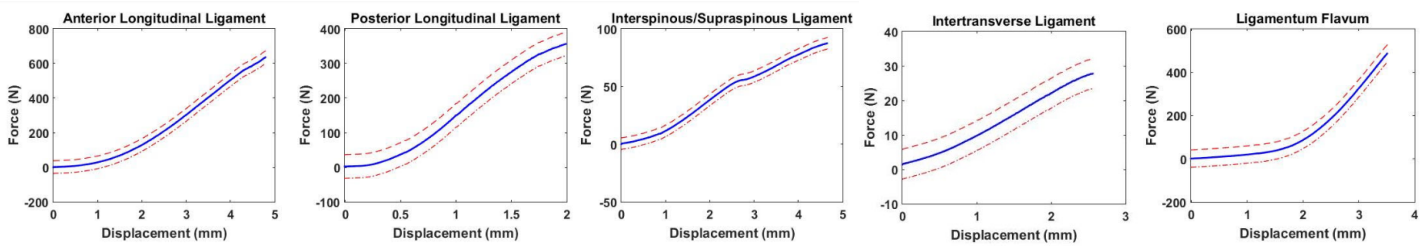

Figure 1. Ligament Test Results, plotted with mean, mean ± 1SD

Relative Contribution of Material and Morphological Properties to Altered Achilles Tendon Stiffness in Aging

Jordyn N. Schroeder[1], Lindsey Trejo[1], Owen N. Beck[1,2], and Gregory S. Sawicki[1,2]
[1]George W. Woodruff School of Mechanical Engineering, Georgia Institute of Technology, Atlanta, GA, USA
[2]School of Biological Sciences, Georgia Institute of Technology, Atlanta, GA, USA
Email: jschroeder9@gatech.edu

Introduction

Both material properties (*e.g.* Young's Modulus (E)) and morphological properties (*e.g.* cross sectional area (CSA) and slack length (l_{slack})) affect tendon stiffness (k_t). While previous studies have observed reduced Achilles tendon (AT) k_t in older adults versus young adults[1,2], the mechanisms for this reduced stiffness are unclear. Some findings suggest decreased E and increased local CSA[1]. Others suggest that increased collagen crosslinking in aging decreases E but increased mechanical stiffness[3]. Differences in methological approaches across laboratories make it difficult to come to consensus about age-related changes in tendon structure-function. The objective of this study was to take comprehensive, functionally relevant measures of AT material and morpohological properties to assess the relative contributions leading to decreased k_t in older adults. We hypothesized that changes in morphology (*i.e.,* lower CSA, longer l_{slack}) would counteract increased E and explain age-realted decreases in AT k_t .

Methods

In this preliminary study, we recruited three young adults (YA: 25.3 +/ 3.2 yrs) and one older adult (OA: 77 yrs). Tendon stiffness (k_t) was measured during isometric contractions of the right leg with the knee fully extended and the ankle fixed at 0°, 15° and 30° plantarflexion. Subjects were instrumented with an ultrasound probe over the medial gastrocnemius (MG) - AT junction, electromyography electrodes over the skin superfiscial to the tibialis anterior (TA), lateral gastrocnemius (LG), and soleus (SOL) muscles, and 3D motion capture markers on the medial knee, medial malleolus,and head of the 1st metatarsal. Measurments of k_t were taken as the slope of the AT force-displacement relationship at a matched absolute force across age groups. AT l_{slack} was measured from the most proximal point of the AT-calcaneus junction to the MG-AT junction at 0 degree angle angle. CSA was measured along the length of the AT, in 10% AT length increments by taking manual measurements from ultrasound images in ImageJ. E for the AT was calculated using the relationship k_t=E*CSA/l_{slack} using the CSA form the most distal measurement location.

Results and Discussion

As expected, the older adult had reduced AT k_t versus the younger adults (Table 1). These preliminary results suggest that in both age groups, CSA increased as you move proximally up the AT. However, differences in older adult vs. younger adults CSA varied depending on the AT location. The older adult had larger CSA near the AT-MG junction but smaller CSA distally.

In partial support of our hypothesis, our results suggest that age-related decreases in k_t may be driven by changes in morphology rather than material properties of the AT. Though our participant sample size is limited, we found that large increases in lslack overshadowed smaller changes in CSA and E to yield a more compliant older AT.

The goal of this study was to understand how age-related trade-offs in AT CSA, l_{slack}, and E contribute to changes in AT k_t in older adults. As we collect more participants, we will apply linear regression models to evaluate the impact of CSA, l_{slack}, and E on AT k_t.

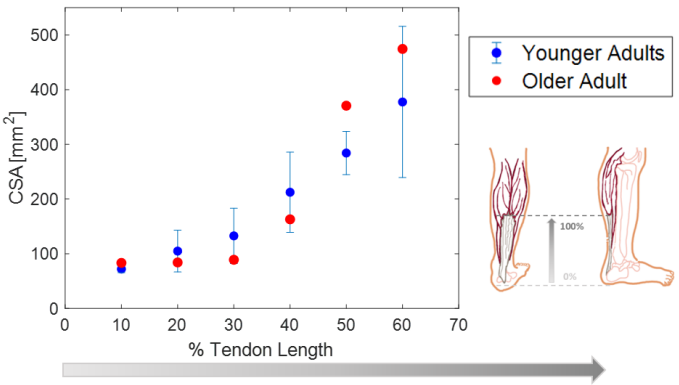

Figure 1: Cross-sectional area (CSA) along the free length of the Achilles tendon (AT). Error bars indicate SD.

	k_t [kN/m]	E [GPa]	CSA [mm²]	l_{slack} [mm]
Younger Adults	136.3 ± 25.2	35.0 ± 8.7	71.9 ± 6.5	18.3 ± 1.7
Older Adult	115.9	32.3	83.2	23.2

Table 2: Achilles tendon (AT) material and morphological properties across age.

Significance

Here, we lay the groundwork to address the key factors that impact AT structure-function across the lifespan. Understanding how changes in morphological and material properties of tendon trade-off in aging is important because therapeutic approaches to alter tendon mechanics, (e.g., drugs, exercise, exoskeletons) often target specific tendon properties.

Acknowledgments

NIH NIA Grant (R0106052017) awarded to G.S.S.

References

[1] Stenroth et al. (2012), *J. Applied Phys.*
[2] Delabastita et al. (2018), *J Aging Phys Act.*
[3] Tuite et al. (1997) *J Med Sci Sports*

Mechanical Testing of System for Anchoring a Synthetic Tendon to Replace the Achilles Tendon in a Rabbit Model

Caleb Stubbs[1], Patrick Hall[1], Remi Grzeskowiak[2], Pierre-Yves Mulon[2], Alisha Pedersen[2], Bryce Burton[2], Cheryl Greenacre[2], David E. Anderson[2], and Dustin L. Crouch[1]
University of Tennessee, Knoxville (UTK) – Tickle College of Engineering[1] and College of Veterinary Medicine[2]
Email: rstubbs1@vols.utk.edu

Introduction

Some musculoskeletal pathologies, such as rotator cuff tear, tendon rupture, and limb amputation, are associated with detachment of muscle-tendons from bone. Reattaching the biological muscle-tendons may not be possible if the tendon is damaged or missing. One group recently developed a synthetic tendon that is intended to replace a damaged or missing biological tendon [1]. The synthetic tendon is composed of a polyester suture that is coated in medical-grade silicon. Previous studies tested the synthetic tendon *in vivo* in a goat model [1] but did not quantify the effect of the synthetic tendon on locomotor function.

We are developing a New Zealand White rabbit model to assess locomotor function after replacing the biological Achilles tendon with a synthetic tendon. In the previous *in vivo* study [1], the synthetic tendon was anchored to bone using a sturdy metallic plate. Alternatively, in a previous surgery, we anchored the synthetic tendon to the calcaneus using a 2.2mm-diameter Arthrex suture anchor (AR-1318FT-40) and a strand of size 4-0 Fiberwire suture. Two weeks after the surgery, we observed that the 4-0 Fiberwire failed, releasing the synthetic tendon. The objective of this preliminary study was to quantify the mechanical strength of our tendon-anchoring system with the previous (4-0 Fiberwire) and two next-larger sizes of Fiberwire suture that are compatible with our anchoring system. We hypothesized that the strength of the 4-0 Fiberwire would be less than the estimated maximum force of the triceps surae muscles during rabbit hopping, while the strength of the larger sutures would exceed the maximum muscle force.

Methods

We use three different sizes of Fiberwire suture: four of size 0, three of size 2-0, and two of size 4-0. Custom-fabricated synthetic tendons were tied, using the Fiberwire sutures, to 2.7mm-diameter Arthrex suture anchors (AR-1319FT), since the 2.2mm anchors are too small for the size 0 Fiberwire suture; the 2.7mm anchors are compatible with our rabbit model. We clamped the suture anchor and proximal end of the synthetic tendon to an Instron tensile tester.

From a biomechanical model of the rabbit hindlimb [2], we estimated the maximum forces generated by the medial gastrocnemius (32.0 ± 8.8 N), lateral gastrocnemius (15.5 ± 2.0 N), and soleus (10.2 ± 0.6 N) muscles during an average gait cycle. We summed the means of the three maximum muscle forces (and rounded up) to approximate the maximum triceps surae force during an average gait cycle as 60 N. We programmed the Instron tensile tester to apply a cyclic (1 Hz, approximate gait cycle duration) 60 N tensile force to the synthetic tendon and suture anchor assembly. In an initial test, we ran two of the size 0 sutures for 1000 cycles; thereafter, we ran all remaining samples for up to 5000 cycles. After the cyclic loading, we applied an increasing pull-out force to the assembly until it failed.

Results and Discussion

All of the size 0 and 2-0 sutures remained intact after 5000 cycles, indicating that the size 0 and 2-0 sutures could withstand the average maximum force of the triceps surae muscles for at least 5000 gait cycles. In contrast, the size 4-0 suture broke during the first cycle of each test, which explains why it failed *in vivo* soon after our first surgery. All assemblies failed at the Fiberwire suture linking the tendon and anchor, just adjacent to where the suture was knotted near the loop in the synthetic tendon.

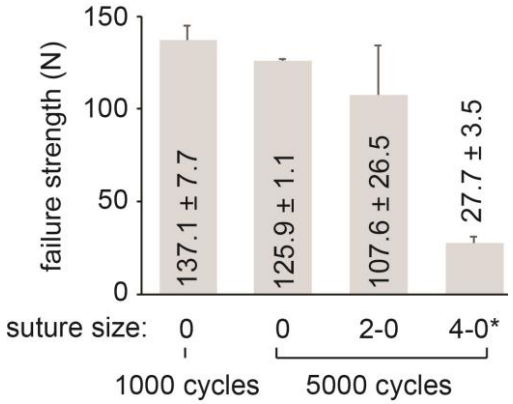

Figure 1: Failure strength of the Fiberwire suture. Values over bars are mean ± standard deviation. *The size 4-0 suture failed during the first load cycle.

The mean failure strength of the size 0 suture was only 18.27 N more than that of the smaller size 2-0 suture, whose failure strength was 47.66 N (or 79%) more than the 60 N maximum muscle force. Therefore, we expect that both the size 0 and 2-0 sutures are suitable for our *in vivo* locomotor function tests. We plan to use the size 0 and size 2-0 sutures with the 2.7mm and 2.2mm suture anchors, respectively, in future surgeries.

For the size 0 suture, the failure strength was 11.22N lower after 5000 cycles than after 1000 cycles (Figure 1), indicating that there is some effect of cycle number on failure strength. If the failure strength trend continued linearly, then the size 0 suture could withstand approximately 26,500 cycles of the 60 N load. We will conduct additional cyclical loading tests to measure the maximum number of cycles that the size 0 and 2-0 sutures can withstand.

Significance

In this study we evaluated the failure strength of the suture connecting the synthetic tendon to the suture anchor. The data shows that the size 4-0 suture is too weak for our rabbit model, and that size 0 or 2-0 sutures should be used in future surgeries. Our data provides critical support for future biomechanical studies of synthetic tendon, a potentially valuable medical device for tendon repair and replacement.

Acknowledgements

This work was funded by the NIH (K12HD073945), NSF (CAREER 1944001), and a University of Tennessee Seed Grant.

References

[1] Melvin AJ, et al. JOR, 30(7):1112-1117, 2012.
[2] Grover DM, et al. J Biomech, 40:2816-2821, 2007.

Factors Influencing Ambulatory Function Following Internal Hemipelvectomy

Yuhui Zhu[1], Nicholas J. Dunbar[1], John E. Madewell[2], Valerae O. Lewis[2], and Benjamin J. Fregly[1]
[1]Rice University, Houston, TX
[2]MD Anderson Cancer Center, Houston, TX
Email: yuhui.zhu@rice.edu

Introduction

Limb-salvage surgery without reconstruction of the pelvis is a promising treatment for type-II pelvic sarcoma. Patients improve in their ability to walk over time despite resection of the native hip joint, loss of surrounding musculature, and significant limb shortening. The exact mechanism for these improvements has not been explained and if determined could lead to optimized treatment planning. The psoas muscle is the only hip flexor preserved after internal hemipelvectomy and likely influences transient gait function. It can undergo atrophy prior to surgery as well as significant shortening after surgery with periods of understretch. Strengthening of the psoas muscle after surgery may explain the improved ambulatory function over time. Since muscle strengthening is indicated by increased muscle size, magnetic resonance (MR) images were retrospectively reviewed for maximum cross-sectional area (CSA) and volume changes at two post-operative time points. The patients with psoas hypertrophy were hypothesized to have improved ambulatory function. Other factors such as superior migration of the femoral head on ipsilateral side of the sarcoma are also thought to affect the ambulatory functions.

Methods

Retrospective imaging and clinical data of 12 patients (10 male, 2 female; mean age at the time of surgery, 28.5 years; range, 13 – 64 years) who underwent internal hemipelvectomy without reconstruction for type-II pelvic sarcoma at the same institution at approximately three months after surgery (patient walking with assistance) and during the patients' most recent clinical visit (patient walking without assistance) were reviewed.

Sectional volume and maximum CSA of each patient's psoas on ipsilateral and contralateral sides of the sarcoma were measured on reconstructed surface geometries built from their T-1 weighted axial MR images. Superior migration of femoral head was measured on MR images and normalized by each patient's height at the time of the visit. The ambulatory function of a patient was indicated by the results of Timed Up and Go (TUG) test and gait speed test during their physical therapy examination and performed within one month of their MR imaging.

Paired t-test of the volume and maximum CSA changes between the ipsilateral and contralateral sides and single t-tests on volume and maximum CSA changes on both sides, normalized migration at 3 months and at latest visit, follow-up time between the two time points, and weight gain (α=0.05) were computed. The coefficients of determination were calculated to measure the linear correlation between each of the different variables and functional measurement improvement. A step-wise linear regression of all variables was computed for each ambulatory function.

Results and Discussion

All 12 patients spent less time to complete the TUG test and walked faster in their gait speed test at the most recent follow-up compared to their 3 month follow-up. The volume of psoas muscle on the ipsilateral side and contralateral side of each patient increased on average by 29% (SD: 47%) and 38% (SD: 43%) respectively; the maximum CSA increased on average by 21% (SD=38%) and 37% (SD=37%) respectively. Paired t-test showed no significance difference of the volume (p=0.46) or maximum CSA change (p=0.24) between the two sides. The single t-tests showed a significant increase of all variables from zero except for ipsilateral side muscle size changes.

Table 1: Single t-test results and correlation coefficients between variables and ambulatory function scores

	p	R with TUG	R with Gait
Ipsilateral side volume change (%)	0.06	0.38	0.72
Ipsilateral side max CSA change (%)	0.08	0.44	0.78
Contralateral side volume change (%)	0.01	0.25	0.38
Contralateral side max CSA change (%)	0.01	0.28	0.39
Normalized migration at 3 months (%)	0.00	-0.66	-0.35
Normalized migration at latest visit (%)	0.00	-0.31	-0.22
Follow-up time (number of months)	-	0.43	0.24
Weight gain (%)	0.02	0.17	0.26

On the ipsilateral side, psoas volume change and maximum CSA were moderately correlated with gait speed improvement and weakly correlated with TUG test improvement. On the contralateral side, psoas volume change and maximum CSA were weakly correlated with both the TUG test improvement and gait speed improvement.

Step-wise linear regression showed that TUG score improvement (R^2=0.59) and gait speed improvement (R^2=0.72) were most sensitive to normalized migration at 3 months, psoas muscle maximum CSA change change on the ipsilateral side, and follow-up time. This suggested that greater ambulatory function improvement was correlated to longer follow-up time, greater psoas muscle strength on ipsilateral side, and less superior migration of the femoral head.

Significance

This study explored whether ambulatory function improvement is correlated to psoas muscle size growth and other factors after limb-salvage surgery for pelvic sarcoma without pelvic reconstruction. Understanding the correlation could lead to optimal treatment planning.

Acknowledgments

This work was supported by the Cancer Prevention Research Institute of Texas (CPRIT) funding RR170026.

Exoskeleton-Assisted Walking Therapy Increases Muscle Volume in People with Spinal Cord Injury (SCI)

Megan P. Pinette[1], Nguyen Nguyen[2], Ricardo A. Battaglino[2], Leslie R. Morse[2], Karen L. Troy[1]
[1]Department of Biomedical Engineering, Worcester Polytechnic Institute
[2]Department of Physical Medicine and Rehabilitation, University of Minnesota

Email: mppinette@wpi.edu, ktroy@wpi.edu

Introduction

Spinal Cord Injuries (SCI) affect 28-55 million people in the United States [1]. Immediately following a SCI, there is rapid muscle atrophy. This loss of muscle can lead to decreased metabolic rate and increased fat storage as well as increased risk of obesity-related injuries, such as cardiovascular disease [2]. Robotic exoskeletons are becoming increasingly available in clinical settings for SCIs. Robotic exoskeletons use motors at the hip and knee, controlled by a computerized control system, to allow for assisted walking and rehabilitation [3]. Exoskeleton assisted gait training is used to deliver controlled repetitive training and reduce physical burden on physical therapists [4]. However, it is unclear whether the passive motion and weightbearing that are associated with exoskeleton-assisted walking in non-ambulatory individuals Here we validated methods to measure changes in muscle density and volume over time using quantitative CT data collected during a clinical trial. We hypothesized that exoskeleton-assisted walking would increase both muscle density and volume in the legs.

Methods

Twenty-four adults with AIS A-C (non-ambulatory) spinal cord injury were enrolled in a 12 month clinical trial (NCT02533713; age: 33.7± 8.8 years, height: 177.8 ± 10.2 cm, mass: 74.8 ± 14.1 kg.) Participants were randomized to either Immediate Gait Training (months 0 to 6) or Delayed Gait Training (months 6-12), with the other 6-month period being observation only/usual activities. Gait training lasted for 1 hour, 3 days a week. Each subject received a CT scan of a 30 cm length surrounding the knees at month 0 (baseline), 6 (midpoint) and 12 (final). The present analysis examined only pre/post gait training data.

Muscle volume and density pre- and post gait training was measured within a 15% limb length region above and below each knee using Mimics v. 18.0 (Materialise, Leuven, Belgium). Density, expressed in Hounsfield units (HU), is an indirect measure of intramuscular adiposity/muscle quality: fat has HU values around -50, water: 0 HU, and muscle/soft tissue up to 200 HU. Using a fixed threshold of -49 to 169 HU, our density and volume measures have %CV of 1.3 and 1.4%, respectively.

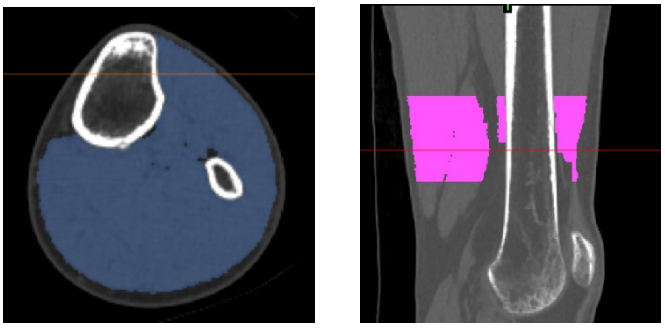

Figure 1: (left) Cross-section of the calf, with muscle highlighted. (right) sagittal plane secion of the thigh, with muscle highlighted.

Paired t-tests were used to compare pre/post measures of muscle volume, density, and a composite measure of volume*density for each participant. Pearson correlations were calculated for demographics and baseline values of muscle volume and density.

Results and Discussion

Baseline muscle volume was significantly correlated with body size (mass and height, $r>0.44$, $p<0.04$). Overall, gait training was associated with significant increases in muscle density*volume (mean change: 102 HU*cm3; $p\leq0.035$). This came from increases to volume, with no change in density (Figure 2).

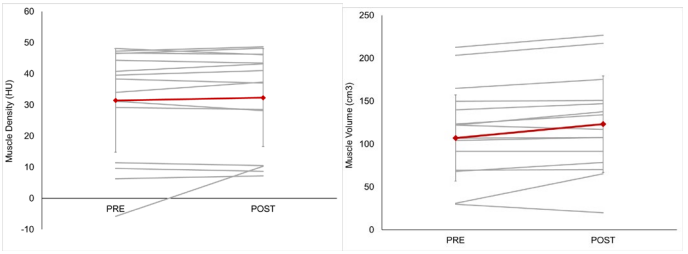

Figure 2 Pre/post changes in muscle density (left) and volume (right). Average muscle density did not change during gait training, but muscle volume increased significantly by 15% (p=0.02). Red bars show the group average at each timepoint (error bars are SD).

Although this exoskeleton-assisted walking intervention did not include any direct stimulation of the muscles, it was associated with significant increases in muscle mass. Exoskeleton walking may benefit leg muscles by placing the individual in a standing position and through passive motion, which can both stretch the muscles and increase circulation.

Significance

Currently, little is known about the musculoekeletal benefits of using an exoskeleton. This research demonstrates that even passive motion generated during exoskeleton-assisted walking may improve muscle quantity in individuals with SCI. This is significant because muscle mass contributes to overall and cardiovascular fitness. These results can be used to develop and evaluate improved rehabilitation interventions for individuals with SCI and other impairments that result in muscle loss.

Acknowledgments

This work was funded by grant W81XWH-15-2-0078 (United States Department of Defense) to Leslie R. Morse. We thank Nguyen Nguyen for assisting with data collection, Leslie Morse for supervising the clinical trial, and all of the individual participants for volunteering their time.

References

[1]J. Mcdonald, et. Al. *The Lancet* 2002 Feb 2;359(9304):417-25 [2] L. Giangregorio, et. al. *J Spinal Cord Med*. 2006;29(5):489-500. [3] S. Banala, S, et. al *IEEE Trans Neural Syst Rehabil Eng.* 2009 Feb;17(1):2-8.[4] C. Tefertiller, et. al. *Top Spinal Cord Inj Rehabil.* 2018 Winter;24(1):78-85.

The Association Between Altered Peak Knee Extensor Moments and Articular Contact Forces during Walking

Amanda E. Munsch[1], Joshua D. Roth[2], Brian Pietrosimone[3], and Jason R. Franz[1]
[1]UNC Chapel Hill and North Carolina State University, Chapel Hill, NC [2]University of Wisconsin, Madison, WI
[3]UNC Chapel Hill, Chapel Hill, NC
Email: aemunsch@live.unc.edu

Introduction

Deficits in voluntary quadriceps activation are considered critical in the biomechanical cascade underlying high rates of osteoarthritis (OA) in individuals with anterior cruciate ligament reconstruction (ACLr) and other knee pathologies [1]. During walking, diminished peak knee extensor moments (pKEM), potentially arising from quadriceps dysfunction [2], may improperly distribute loads accommodated by the articular cartilage in locations and with magnitudes unprotected by prior loading experience [3]. However, little empirical data exist to elucidate the association between changes in pKEM and articular cartilage loading during walking. Our purpose was to leverage novel real-time inverse dynamics in a biofeedback paradigm capable of prescribing systematic changes in pKEM in combination with musculoskeletal simulations to estimate cause-effect changes in knee joint outcomes relevant to the onset of OA.

Methods

Experimental Measurements. Twelve uninjured participants (23.6±2.6 yrs; 6M/6F) completed five treadmill walking trials at their preferred speed. Subjects first walked normally without biofeedback. We immediately analyzed this trial using a real-time surrogate model of the lower limb to extract pKEM targets for use in our biofeedback paradigm. Four biofeedback trials visually cued participants to walk with ±20% and ±40% of normal values. We recorded ground reaction forces (GRFs), 3D motion capture data, and the activity of seven muscles spanning the knee.

Model Predictions. We have completed simulations on one male participant to date (22 yrs, 1.68 m, BMI 22.1). We used measured GRFs and marker trajectories from a representative stride to drive a scaled whole-body muscusloskeletal model embedded with a validated 12 degree-of-freedom model of the knee joint that included representations of 12 ligaments [4]. A concurrent simulation algorithm (i.e., COMAK) predicted secondary knee joint kinematics and muscle, ligament, and articular contact forces necessary to generate the measured motion [4]. Monte carlo simulations accounted for ±30% and ±2% in ligament stiffness and reference strain, respectively, and we report model-predicted variance about the mean. Model outcomes included anterior tibial translation, ACL force, contact force on the medial and lateral tibial plateaus, and vasti (medial and lateral) muscle forces, and all were reported as change relative to usual walking.

Results and Discussion

Biofeedback prescribed pKEM values that ranged from 0.22 to 1.05 Nm/kg. Targeting larger than normal pKEM elicited greater anterior tibial translation and higher ACL force, consistent with quadriceps' classification as ACL antagonists (Fig. 1A) [5]. Conversely, ACL force also increased when targeted 40% smaller than normal pKEM (Fig. 1B), likely due to other secondary knee kinematics and/or diminished mechanical advantage of the hamstrings with increased knee joint extension (not shown). Articular contact forces (Fig. 1C) and the quadriceps muscle forces most responsible for them (Fig. 1D) increased when targeting larger than normal pKEM. However, lateral forces (muscle and contact) were more sensitive to volitional changes in pKEM than medial forces – an outcome consistent with the larger physiological cross-sectional area of the vastus lateralis versus medialis. Targeting smaller than normal pKEM (in this subject by up to 60%), yielded 15% smaller total articular contact forces. This prediction provides convincing evidence that readily-observed gait changes in individuals with ACLr may lower articular contact forces to values below normal physiological loading. Ultimately, these gait changes may disrupt the balance between cartilage breakdown and repair, thereby explaining an increased risk of OA.

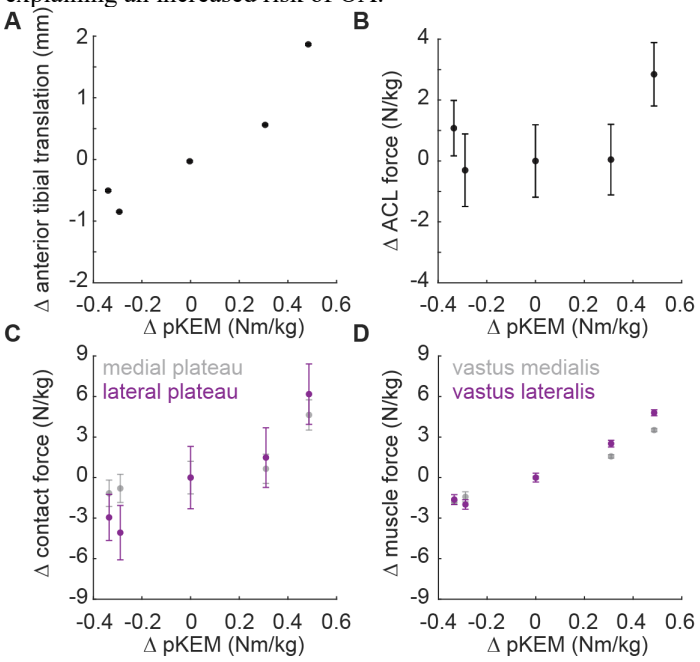

Figure 1. Changes in model-predicted outcomes as a function of those in measured stance phase pKEM prescribed via real-time biofeedback. Zero (0) in all cases represents values during normal walking.

Significance

We demonstrate that changes in pKEM during walking, common to individuals with ACLr and other knee joint pathologies, are accompanied by changes in ACL force, tibia anterior translation, and medial and lateral articular contact forces relevant to the development and progression of osteoarthritis.

Acknowledgments

Supported by a grant from NIH (R21AR074094)

References

[1] Scalan, SF, et al. (2013). *J Biomech*, **46**(5):849-54.
[2] Roewer, BD, et al. (2011). *J Biomech*, **44**(10):1948-53.
[3] Andriacchi, TP, et al. (2004). *Ann Biomed Eng*, **32**(3):447-57.
[4] Brandon SC, et al. (2018). *Handbook of Human Motion*:395-428.
[5] Draganich, LF & Vahey, JW (1990) *J Orthop Res*, **8**(1):57-63

Spatial gait characteristics are related to impaired hip abductor strength in women with hip osteoarthritis

Burcu Aydemir and Kharma C. Foucher
Department of Kinesiology and Nutrition, University of Illinois at Chicago, IL, USA
Email: baydem2@uic.edu

Introduction

Hip Osteoarthritis (OA) is a common condition affecting up to 25% of older adults over a lifetime [1] with a higher prevalence in women. Walking is essential for independent living and it is an exercise that is commonly recommended to people with OA. To be performed safely, walking gait requires sufficient flexibility and stability by the musculoskeletal system. The hip abductor muscles are crucial for stabilization within the frontal plane during single-limb support while the swing leg advances forward to the next step. People with hip OA demonstrate significant hip abductor strength deficits, primarily on the affected side[2]. Any degree of impairment could potentially modulate laterally and anteriorly directed steps consequential to the weakness and instability surrounding the affected hip. Individuals with hip OA also demonstrate altered spatiotemporal gait characteristics compared to adults without OA [3]. However, it remains unclear whether these alterations are related to hip abductor impairment. Our goal was to investigate how impaired hip abductor strength in women with hip OA may be related to commonly reported altered spatiotemporal gait characteristics. We *hypothesized* that *lower* hip abductor strength would be significantly associated with a 1) *shorter* step length on the affected side, 2) *wider* step width, and 3) *slower* gait speed in women with unilateral hip osteoarthritis.

Methods

Fifteen women (age 56.2 ± 6.3 years; BMI 30.2 ± 6.5 kg/m^2) with self-reported unilateral hip OA consented to participate in this cross-sectional study. Hip abductor strength of the affected side was tested in a side-lying position, using an isokinetic dynamometer [Biodex System 4 Pro, Biodex Medical Systems, Inc., Shirley, NY]. Peak isometric torque was measured from three 5 s bouts alternated with 30 s rest and normalized to body mass (Nm/kg). Three-dimensional gait analysis data were collected via an 8-camera motion analysis system (Motion Analysis Co., Santa Rosa, CA) operating at 120 Hz. Subjects were given a 3 min acclimation period to find their preferred walking speed on a split-belt treadmill, followed by a 2.5 min walking trial. Passive markers were placed bilaterally over selected bony landmarks using standard methods. Step length and step width, normalized to body height (%), were defined as the anterior-posterior and mediolateral distances between the heel markers at heel contact, respectively. The average peaks over 10 consecutive steps were processed and extracted using a custom MATLAB algorithm (MATLAB, Natick, MA). The relationships between hip abductor strength, step width, step length, and self-selected gait speed were evaluated using Pearson correlation coefficient (r). Alpha was set at $p \leq 0.05$ for all analyses.

Results and Discussion

The mean self-selected walking speed was 0.67 ± 0.24 m/s. In support of our first and second hypothesis, we found that lower hip abductor strength was associated with a shorter step length of the affected side ($p = 0.036$), and wider step width ($p = 0.038$) (Figure 1). Previous studies similarly reported that people with hip OA tend to walk with shorter [3] and wider steps [4]. Our findings add to the current literature by suggesting hip abductor strength may be a contributor to these altered gait characteristics. These observed stepping strategies could be protective bracing mechanisms adopted due to the weakened hip musculature to place the affected limb in a position that is most stable and reduces loading at the affected hip joint. Contrary to our third hypothesis, hip abductor strength was not significantly associated with gait speed ($r = 0.511$, $p = 0.052$). However, this association may be significant with a larger sample size.

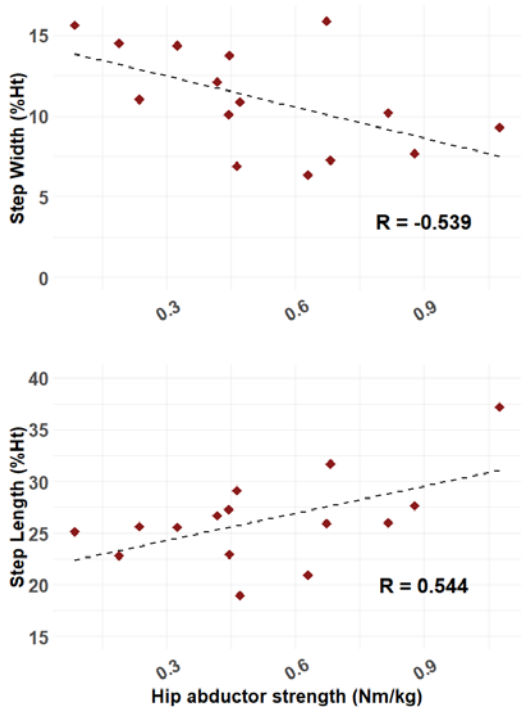

Figure 1: Lower hip abductor strength is associated with higher step width (top) and lower step length of affected side (bottom).

Significance

A better understanding of how hip abductor strength impairments may impact spatiotemporal gait characteristics can lead to effective combined interventions of gait and strength training. Combined therapies aimed at increasing strength and stability in people with lower limb OA may help aide in promoting participation in exercises, such as walking.

Acknowledgments

R21AG052111 (KCF)

References

[1] Murphy LB et al. (2010) Osteoarth Cartil, 18: 1372-9
[2] Zacharias et al. (2016) Osteoarth Cartil, 24: 1727-35
[3] Constantinou M et al. (2017) Gait Posture, 53: 162-67
[4] Lin et al. (2015) Clin Biomech, 30: 874-80

A Classifier for the Categorization of Thumb Carpometacarpal Osteoarthritis

Amy M. Morton[1], Janine D. Molino[1], Douglas C. Moore[1], Joseph J. Crisco[1], Amy L. Ladd[2], Arnold-Peter C. Weiss[1]
[1]Department of Orthopaedics, Brown University and Rhode Island Hospital, Providence, RI, USA.
[2]Department of Orthopaedic Surgery, Stanford University School of Medicine, Stanford, CA, USA
Email: amy_morton1@brown.edu

Introduction

Osteoarthritis (OA) of the thumb Carpometacarpal (CMC) joint is a complex disease of bone and cartilage with highly individualized rates of progression. Radiographic assessment of CMC OA in 2D is hindered by the complex geometry and bony overlap in basal thumb x-rays, and at best delivers a coarse categorical metric.

With advancements in the ability to quantify osteophytes (OPs) from CT images[1], an objective variable of disease state can be calculated. In this study, the magnitudes and rates of OP volume change over a six-year period were combined into a single classifier, with the goal of stratifying CMC OA patients into stable and advanced OA categories. Once categorized, differences in OP volume and dorsal subluxation were evaluated between OA groups and a healthy population over time.

Methods

Following IRB approval, 86 patients with early thumb CMC OA (self-reported pain and radiographic Eaton 0/1 grading) and 22 age-matched asymptomatic heathy volunteers were recruited into an NIH-funded thumb CMC OA biomechanics study.

At enrollment (day 0) and four time points spaced at 1.5-year intervals, data were collected for each OA patient; healthy volunteers returned for only a 6-year follow-up visit. At each visit, CT scans of the affected (patient) or dominant (healthy) wrists were acquired in 11 range-of-motion and task-related positions[2]. At each follow-up visit, the elapsed day count from each subject's day 0 was recorded to measure longitudinal change (Δ/day).

Digital surface models of the trapeziae (TPM) and first metacarpals (MC1) were segmented from CT data. For each day 0 model, coordinate systems (CS) were calculated from manually delineated TMC articular facets[3].

OP volumes were calculated via subtraction of a best-fit bone model[1] from each patient's 1.5, 3, 4.5 and 6-year bone models and via Boolean subtraction of the day 0 models from the 6-year follow-up models in the healthy cohort. The rate of OP growth (mm^3/day) for each participant was determined using linear regression of OP volumes over time. Subluxation was defined as the MC1 CS origin position resolved in the TPM coordinate space in dorsal(-)-volar(+) and radial(+)-ulnar(-)[3] directions for each subject, visit, and CT position. Values were reported as percentage of subject TPM facet area (more negative reflecting greater dorsal subluxation).

Participants were categorized as stable or advanced OA based on thresholds for both magnitude and rate of OP volume growth. The threshold values were defined as the population median of each metric (α=150mm^3 OP volume; β= 0.04 mm^3/day OP growth). Patients were classified as advanced OA if any visit OP volume exceeded α or the subject's rate of OP growth exceed β. Linear mixed models with random intercept and slope were created for the three-way comparison of stable OA, advanced OA, and healthy cohort; evaluating differences in rate of OP growth and rate of subluxation % change.

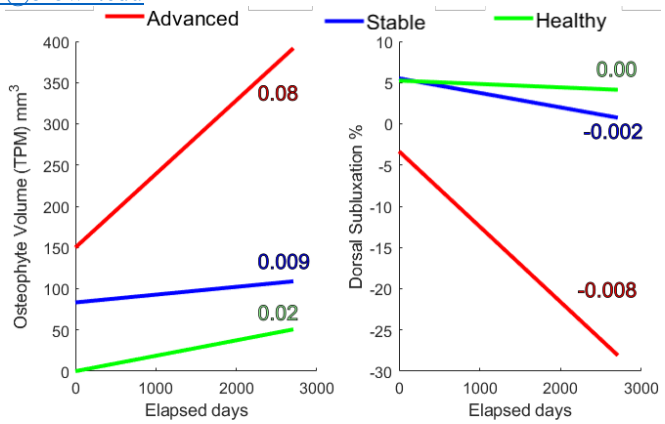

Figure 1: OP volume and subluxation % change over elapsed days from initial visit by TMC OA patient groups: Advanced (49/86) (red), Stable (37/86) (blue) and Healthy subjects (green). Annotated slope values for each group measured in units of mm^3/day (OP volume) and % /day (Subluxation).

Results and Discussion

The rate of OP growth over time was significantly greater in patients with advanced OA than in patients with stable OA ($p<0.0001$) or healthy subjects ($p<0.0001$) (Fig. 1, left). Group differences in subluxation were greatest in thumb flexion. In flexion, the advanced patients' rate of dorsal subluxation was significantly more negative than that of the stable ($p=0.0009$) and healthy subjects ($p=0.0004$), which were alike ($p=0.99$) (Fig. 1, right). Similar trends in subluxation were found for all positions, with a subset (6/11; grasp, grasp-loaded, pinch-loaded, abduction, adduction) also revealing significant differences between stable and advanced OA groups. This indicates that pathological dorsal subluxation may be kinematically coupled, being provoked in some thumb positions more than others.

Patients were successfully grouped into stable or advanced OA by OP volume, allowing group differences in subluxation values to be analysed. In a large longitudinal dataset of patients with suspected disease state heterogeneity, having a robust and objective metric for group differentiation is incredibly valuable. This metric can be improved via sensitivity analysis of α and β threshold modifications on grouping success statistics.

Significance

The ability to differentiate stable patients from within a progressive disease cohort holds promise for the development of predictive tools of thumb CMC OA disease progression.

Acknowledgments

This research was supported in part by funding from NIH AR059185

References

[1] Morton, 2019. doi:10.1002/jor.24569
[2] Halilaj, 2014. doi:10.1109/EMBC.2014.6944588
[3] Halilaj, 2013. doi:10.1016/j.jbiomech.2012.12.002

Image-Based Optimization of Articular Cartilage Material Properties for The Isotropic Poroelastic Cartilage Model with Strain-Dependent Permeability

Kyung Min Kim[1], Joonwon Yoon[1], Yoon Jin Kim[1], Myeong Woo Lee[2], Jung-Ah Choi[3] and Yongnam Song[1*]
[1]School of Mechanical Engineering, Korea University, Seoul, Korea
[2]Inovative SMR System Development Division, Korea Atomic Energy Research Institute, Daejeon, Korea
[3]Department of Radiology, Hallym University College of Medicine, Hwaseong, Korea
Email: *kurtbain@korea.ac.kr

Introduction

The accuracy of cartilage material models is determined by realistic material properties of articular cartilage. However, material properties in conventional confined or unconfined compression tests of a cartilage plug have been shown to be inaccurate in describing *in vivo* cartilage deformations. In this study, we aimed to estimate articular cartilage material properties in porcine hips by comparing cartilage deformation patterns in finite element (FE) analysis with the deformation patterns from CT (computerized tomography) images.

Methods

Loading experiments

Four cadaveric porcine hips were tested. We developed a custom plastic axial loading device. A joint sample was potted in the normal standing position of porcine hips. The direction of joint resultant forces was aligned with the loading axis of the compression device. The joint sample was completely submerged in a PBS solution to avoid dehydration of cartilage tissue. Positions of femoral and acetabular bones were recorded by acquiring CT images (matrix: 512 x 512, FOV: 150 mm, slice thickness: 1 mm) of a joint sample in every 3 min while a 650 N of compressive loading was continuously applied for 15 min.

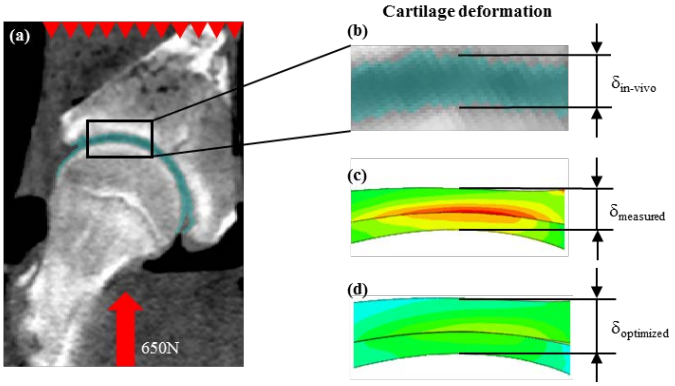

Figure 1: (a) boundary & loading conditions of compression test (b) deformation of compression test (c) FE results with measured material properties (d) FE results with optimized material properties

Finite element modelling with image-based optimization

Cartilage and bone models in femoral and acetabular compartments of the joint sample were created from CT images. An isotropic biphasic poroelastic material model with strain-dependent permeability was used for articular cartilage while the bones are completely rigid. We used C3D8P elements and the femoral bone was subjected to a distributed axial load and the upper surface of acetabular bone was fully fixed (Figure 1.(a)). Fluid flow across an interface was not conceded. We simulated the loading experiment in FE analysis and tried to find optimum material properties (Young's modulus, Poisson's ratio, intrinsic permeability, and permeability constant) to match the cartilage deformation patterns in the FE simulation with the cartilage surface profile in CT images (Figure 1.(b)(c)(d)). This optimization was done by non-linear simulated annealing(SA) algorithm.

Unconfined compression tests of cartilage plugs

We collected multiple cartilage plugs from the joint samples after the loading experiments. Conventional unconfined compression tests were used to measure the material properties of cartilage plugs, which were finally compared with the material property values from image-based optimization process.

Results and Discussion

Articular cartilage material properties for the poroelastic material model in the image-based optimization and unconfined compression tests are shown in Figure 2. image-based optimization estimated significantly greater Young's modulus ($P < 0.05$, student t-test) and Poisson's ratio ($P < 0.05$) than the values in unconfined compression tests. However, we did not find differences in intrinsic permeability and permeability constant valued between both measurements. Fluid flow in *in vivo* articular cartilage is limited by the opposing joint structures and adjacent cartilage tissues. Thus, cartilage deformations in *in vivo* joints would be significantly reduced than the deformations measured in cartilage plug tests.

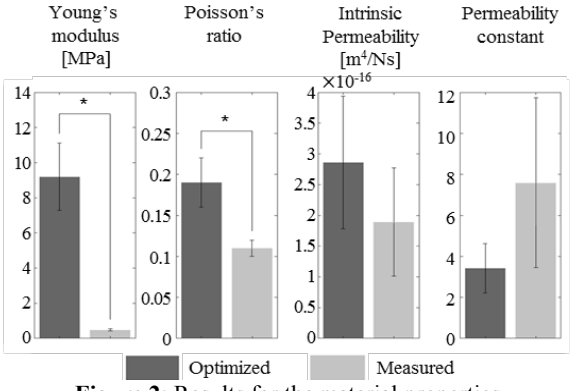

Figure 2: Results for the material properties

Significance

Our results showed that articular cartilage material models with material properties from conventional plug tests may result in greater cartilage deformations than the deformation in *in vivo* articular cartilages. Our image-based optimization technique would be useful to produce accurate articular cartilage material models which describe realistic deformational behaviours in various *in vivo* joints.

Acknowledgments

This work was supported by the National Research Foundation of Korea(NRF) gran funded by the Korea government(MEST) (No. NRF-2015R1C1A1A02037088)

On Computing and Measuring Osteophyte Formation in the Progression of Thumb Osteoarthritis

J.J. Trey Crisco[1], Amy M. Morton[1], Bardiya Akhbari[1], Douglas C. Moore[1], Amy L. Ladd[2] and Arnold-Peter C. Weiss[1]
[1] Dept. of Orthopaedics, The Warren Alpert Medical School of Brown University and Rhode Island Hospital, Providence, RI
[2]Robert A. Chase Hand & Upper Limb Center, Dept. of Orthopaedic Surgery, Stanford University School of Medicine, Stanford, CA
Email: joseph_crisco@brown.edu

Introduction

Osteophyte formation is a critical part of the degeneration of a joint with osteoarthritis (OA). While often qualitatively described, few studies have succeeded in quantifying osteophyte growth over time. A detailed understanding of osteophyte formation is limited in part by the ability to quantify bone pathology. Osteophytes can be quantified relative to pre-osteoarthritic bone, or to the contralateral bone if it is healthy; however, in many cases neither are available as references.

We present a method for computing three-dimensional osteophyte models with a library of healthy control bones with a dissimilarity-excluding Procrustes registration technique (DEP).[1]

We applied DEP to a computed-tomography (CT) image dataset from a longitudinal, observational study of thumb carpometacarpal (CMC) OA. Our aim was to describe osteophyte growth by quantifying location-specific changes in peri-articular bone volume on the first metacarpal (MC1) and trapezium (TPM) over a three-year period in men and women with early OA.[2]

Methods

Our analysis was performed using an existing dataset containing the computed tomography scans of 90 patients with early thumb CMC OA.[2] A corresponding dataset of 46 healthy subjects formed the reference library from which best-fit bones were calculated.[1] Our method best-fit a healthy bone to an OA subject's bone using a dissimilarity-excluding Procrustes registration technique (DEP) that minimized the influence of dissimilar features (i.e., osteophytes).[1] Osteophyte models were then computed via Boolean subtraction of the reference bone models from the OA bone models.

DEP reference bones conformed significantly better to the OA bones ($p < 0.0001$) than finite difference iterative closest point registration (RMS distances 0.33mm ± 0.05mm and 0.41mm ± 0.16mm, respectively). The effect of library size on dissimilarity measure was investigated by leave-k-out cross-validation randomly reducing k from 46 to 1. A library of n >= 31 resulted in less than 10% difference from the theoretical minimum value. To quantify the accuracy and the limitations of the method, a series of artificial osteophytes were generated by extruding the surfaces of healthy control trapezia at different locations around the CMC articular facet and by different heights. Bland-Altman plots were used to evaluate the agreement between the ground truth and computed osteophyte volumes (Figure 1).

The DEP method was applied to study osteophyte formation and progression in 90 patients with early thumb CMC OA (pain, with Eaton 0/1 radiographic changes).[2] All study participants were recruited after IRB approval. Patients with early thumb OA were assessed at enrolment (year 0), 1.5, and 3 years with CT imaging. Osteophyte volume and location on the MC1 and TPM were computed for each patient at each follow-up time point.

Mixed models were used to evaluate differences in osteophyte volume by time and sex. Curves of normalized osteophyte volume (as a percent of total bone volume) were plotted as a function of location about the joint circumference and reported with descriptive statistics (median, 25th percentile, and 75th percentile) at each time point.

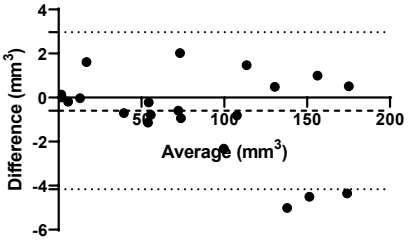

Figure 1: Bland-Altman analysis of the DEP method for computing osteophyte volumes.

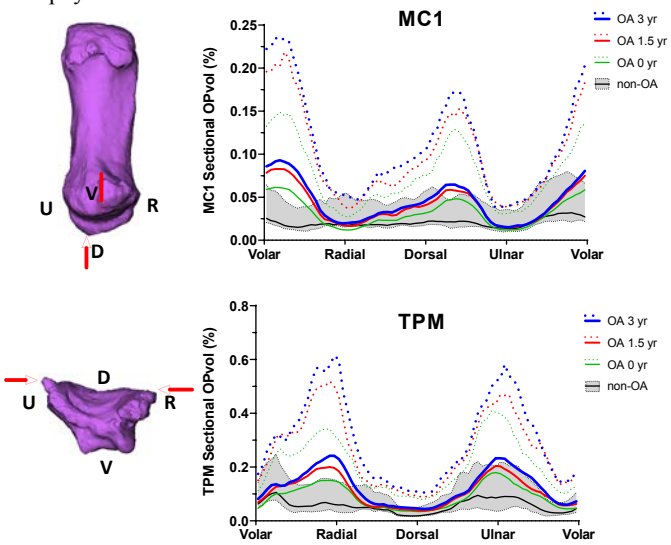

Figure 2: Osteophyte formation occurred at specific non-opposing locations (red arrows) on the MC1 and TPM.

Results and Discussion

We developed an accurate method to compute osteophyte volume and location and to quantify osteophyte progression of patients with OA, whose volume increased significantly over the 3-year follow-up. After normalizing for size, we did not find a statistically significant difference between women and men. Notably, osteophyte formation started and grew fastest at specific locations on the MC1 and the TPM that did not oppose each other (Figure 2).

Significance

Understanding the mechanism behind osteophyte formation that occurred at specific locations may shed insight into OA progression.

Acknowledgments

NIH/NIAMS R01 AR059185

References

1. Morton et al., J Orthop Res. 2019; PMID: 31840852
2. Crisco JJ, et al., Osteoarthritis Cartilage. 2019; PMCID: PMC6702046

The effect of toe-in and toe-out gait on hip moments in people with medial knee osteoarthritis

Kirsten A. Seagers[1], Scott D. Uhlrich[1,2], Julie A. Kolesar[1,2], Amy Silder[1], Madeleine Berkson[2], Gary S. Beaupre[1,2] and Scott L. Delp[1]
[1]Stanford University, Stanford, CA
[2]Department of Veterans Affairs Healthcare System, Palo Alto, CA
Email: kseagers@stanford.edu

Introduction

Individuals with knee osteoarthritis (OA) have a 25% lifetime risk of developing hip OA[1], likely due to mechanical and biological effects of secondary risk factors. Compressive joint loading is related to OA progression[2], but it cannot be directly measured in the native joint. External moments, such as the knee adduction moment, are used as surrogate measures of joint loading[3]. Gait modifications, such as modifying the foot progression angle, aim to decrease the knee adduction moment in order to slow the progression of OA in the medial compartment of the knee[4]. Similarly, the external hip moment can act as a surrogate measure for hip contact force[5]. People with knee OA who adopt an altered foot progression angle often benefit from a reduction in the knee adduction moment, but it is unknown whether this intervention increases external hip moments, thereby altering the loading environment at the hip and placing it at increased risk of OA initiation or progression[6]. The purpose of this study was to determine how altering foot progression angle affects hip moments in individuals with medial compartment knee OA.

Methods

Fifty-four individuals with medial compartment knee OA (grade 1-3 on the Kellgren-Lawrence scale and pain of >3 on the 11-point numeric rating scale) walked on an instrumented treadmill. Participants performed a baseline walking trial followed by 2 foot progression angle modification trials where they were given biofeedback to either toe-in or toe-out by 10° relative to their baseline foot progression angle. The final 20 steps from each trial, from which the participant's foot angle was within 2.5° of their target angle, were analysed.

Hip joint moments from baseline, toe-in and toe-out gait were estimated using OpenSim 4.0. A generic musculoskeletal model[7,8] was scaled to incorporate subject-specific frontal-plane mechanical alignment from a leg-length radiograph and to match marker positions from a standing static calibration pose. We then performed inverse kinematics and inverse dynamics to estimate the hip abduction, extension, and internal rotation moments.

The average moment during 15-20% of stance phase, the typical time of first peak hip contact force[5], was calculated for each step and averaged across all steps in each walking condition. The hip abduction, extension, and internal rotation moments during toe-in and toe-out gait were compared to baseline gait using a Wilcoxon signed-rank test (α=0.05) with a Bonferroni correction for multiple comparisons. Average values are reported as mean ± standard error.

Results and Discussion

The hip abduction moment was reduced by 4.1 ± 1.3% (p=0.025) during 10° toe-in gait compared to baseline (Figure 1). Similarly, the hip abduction moment was reduced by 5.0 ± 1.2% (p=0.003) during 10° toe-out gait. There were no significant changes in hip extension or internal rotation moments compared to baseline. These results demonstrate that foot progression angle modifications that reduce the frontal-plane knee moment have similar effects on the frontal-plane hip moment but do not systematically change sagittal or transverse-plane hip moments.

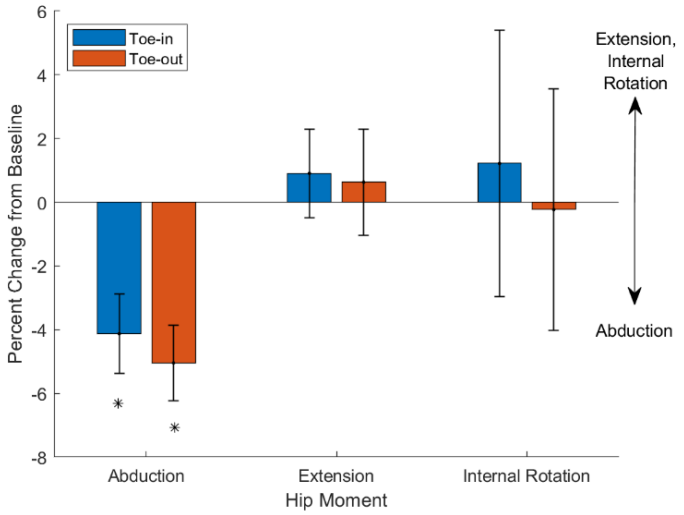

Figure 1: Participants reduced their average hip abduction moment during 15-20% of stance by 4.1 ± 1.3% (p = 0.025) with toe-in gait and 5.0 ± 1.2% (p = 0.003) with toe-out gait compared to baseline.

Significance

Modifying foot progression angle may slow the progression of medial compartment knee OA by decreasing the peak knee adduction moment. Importantly, this gait modification does not statistically increase external hip moments as compared to baseline gait in patients with knee OA. These results suggest that on average, 10° toe-in and 10° toe-out gait modifications may not increase loading in the hip joint. Future work could estimate the effects of foot progression angle modifications on hip contact force estimated from a validated musculoskeletal model.

Acknowledgments

This work was supported by the NSF Graduate Research Fellowship Program and the US Dept. of Veterans Affairs Rehabilitation R&D Service (I01 RX001811).

References

[1] Murphy et al, 2010. *Osteoarthritis Cartilage* **18.**
[2] Andriacchi et al, 2004. *Ann Biomed Eng* **32.**
[3] Miyazaki et al, 2002. *Ann Rheum Dis* **61.**
[4] Shull et al, 2013. *J Orthop Res* **31.**
[5] Wesseling et al, 2015. *J Orthop Res* **3.**
[6] Hall et al, 2019. *J Biomech* **96.**
[7] Rajagopal et al, 2016. *IEEE Trans Biomed Eng* **63.**
[8] Lerner et al, 2015. *J Biomech* **48.**

Total Ankle Replacement Wear Testing: ISO 22622 vs. Previous Wear Testing

Nathan Webb MS[1], Jesse Fleming[1], Emmanuel Lim BS[1], Doug Linton[1], Jon Moseley PhD[1]
[1]Wright Medical Technology, Memphis, TN
Email: *Nathan.webb@wright.com

Introduction

Early Total Hip Arthroplasties (THAs) suffered from buildup of ultra-high molecular weight polyethylene (UHMWPE) wear particles in the joint capsule, and caused reduced bone quality in the area around the implant, leading to loosening. Cross-linking the UHMWPE substantially reduced wear and showed a clinical reduction in the amount of aseptic loosening. Compared to THAs, Total Ankle Replacements (TARs) are geometrically more complex, and move in more degrees of freedom.

Joint simulator studies allow TARs to be evaluated for wear, and approximate the kinematics of a normal walking gait. A set of kinematics representing normal walking gait was adopted from the University of Leeds [1] by most device manufacturers in the United States for previous wear testing. In 2019, however, the International Organization for Standardization (ISO) published a standard for wear testing of TARs, ISO 22622 [2], which differed from the University of Leeds kinematics.

Methods

Two groups of kinematics - the 2007 Leeds version ("Legacy"), and the new ISO 22622 Displacement-controlled version ("ISO") - were applied to a commercially available Total Ankle Replacement device (Inbone, Wright Medical).

Two types of ultra-high molecular weight polyethylene (UHMWPE) inserts were used: Conventional UHMWPE (CPE) and prototype UHMWPE cross-linked with 65 kGy gamma radiation (XLPE). Both kinematic profiles were used on each type of UHMWPE, for a total of four test groups. N=3 inserts for each group were tested in vitro (30% calf serum) in a six-station simulator (Shore Western, Monrovia, CA). The Legacy kinematics were run for 3 million cycles (Mc), while the ISO kinematics were run for 5 Mc.

For command of the wear simulator channels, as based on Legacy kinematics: Flexion and extension were set from -15° to 15°, axial load from -170N to -2800N, anterior to posterior translation from -1.5mm to 1.5mm, while medial to lateral and rotation in varus and valgus were allowed to float freely. The internal/external rotation was set from -2° to 8°, where the toes move towards the midline of the body.

ISO Kinematics used the same endpoints (except for load) but with a different curve shape for each motion. Load in the ISO kinematics ranged from -194N to -2366N.

Lubricant was exchanged every 0.5 Mc; mass loss measurements, dimensional change (by CMM), and wear scar analyses (determination of the modes of wear) were performed every 1Mc.

Results and Discussion

Figure 1 shows a plot of the wear for both sets of kinematics on both materials.With both kinematic profiles, the XLPE material showed a lower wear rate than CPE. Surprisingly, the new ISO 22622 kinematics increased the wear rate by about 30% for both CPE and XLPE. These changes were statistically significant (p = 0.03 XLPE, p = 0.01 CPE, two-sample t-test).

Wear scar analysis (Figure 2) showed that the ISO standard had lower amounts of wear scarring on the surface of the UHMWPE than the legacy kinematics (32% XLPE, 33% CPE vs 22% XLPE, and 25% CPE, respectively). Although the mass lost during wear was higher for the ISO standard group, the wear was distributed over a smaller area of the articular surface. ISO kinematic wear samples also had significantly less amounts of scratching and greater amounts of polishing (burnishing) when compared to legacy kinematics.

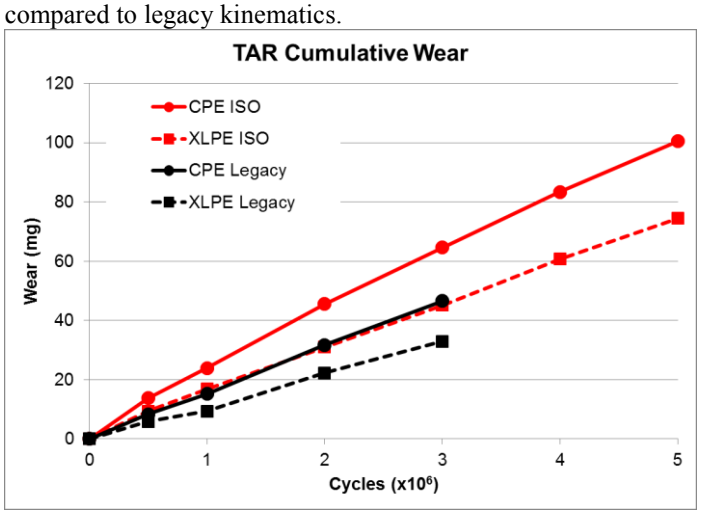

Figure 1: Mass loss vs number of cycles for CPE and XLPE materials. Solid lines are conventional UHMWPE (CPE); dashed lines are XLPE.

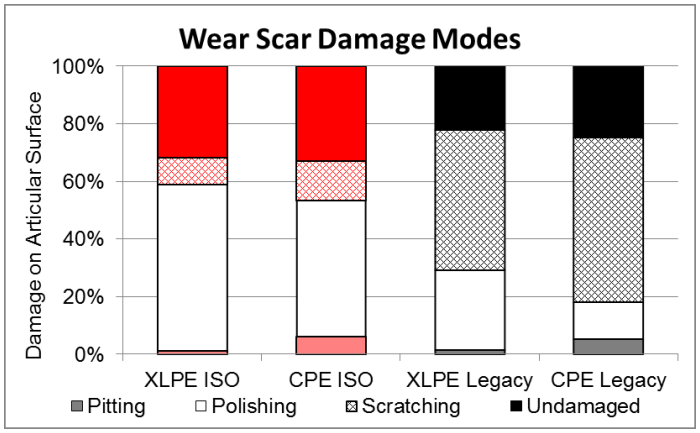

Figure 2: Wear scar analysis graph for XLPE and CPE materials.

Significance

As seen in the gravimetric test results, knowing the kinematics of the ankle joint between the tibia and talus is necessary to properly evaluate a TAR device for use in patients. Minor changes in the motions of the kinematic inputs of the wear test created large changes in the amount and mode of wear scarring observed on the articular surface.

References

[1] Bell, Fisher: "Simulation of Polyethylene Wear in Ankle Joint Prostheses", JBMR B, 2007
[2] ISO 22622:2019: "Wear of total ankle-joint prostheses

Changes in the Plantarflexion Moment Arm of the Achilles Tendon following Total Ankle Arthroplasty

Francesca E. Wade[1], Gregory Lewis[2], Andrea Horne[2], Lauren Hickox[1],
Michael Aynardi[2], Paul Juliano[2], Umur Aydogan[2], and Stephen Piazza[1]
[1]Biomechanics Laboratory, The Pennsylvania State University, State College, PA
[2]Penn State Milton S. Hershey Medical Center, Hershey, PA
Email: few2@psu.edu

Introduction

Following total ankle arthroplasty (TAA), patients have been found to exhibit normal gait kinematics, but deficits persist in gait kinetics [1]. Lack of plantarflexor moment and power in these patients may occur as a result of alterations to joint structure following from TAA. One key structural parameter potentially influenced by TAA is the plantarflexion moment arm of the Achilles tendon (ATma). ATma determines the leverage of the plantarflexor muscles that insert on the Achilles, and therefore is a critical determinant of push-off mechanics during gait [2]. No study to date has quantified how ATma are affected by TAA.

The purpose of this study was to quantify ATma one month prior to TAA and six months post-op in the same patients. We hypothesized that no differences in ATma would be evident between the two timepoints.

Methods

Ten TAA patients (age: 62.86 ± 9.72 y; height: 1.72 ± 0.08 m; body mass: 97.81 ± 20.89 kg; 4 female) underwent our data collection protocol approximately one month pre-op and six months post-op. All procedures were approved by the Penn State Hershey Medical Center Institutional Review Board. ATma was quantified while patients were seated with the knee extended, using a previously published method combining ultrasound imaging of the Achilles tendon with 3D motion tracking of the foot, shank, and ultrasound probe [3].

Sagittal-plane weightbearing radiographs were obtained pre- and post-operatively, and we determined the anterior-posterior distance from the center of the talar dome to the posterior margin of the calcaneus normalized to calcaneus length (d_R). The absolute magnitude of differences in both ATma and d_R were tested to see if they differed from zero using a one-sample t-test. Pre- and post-TAA ATma and d_R were also compared using linear regression. Significance was set at the level of $\alpha = 0.05$.

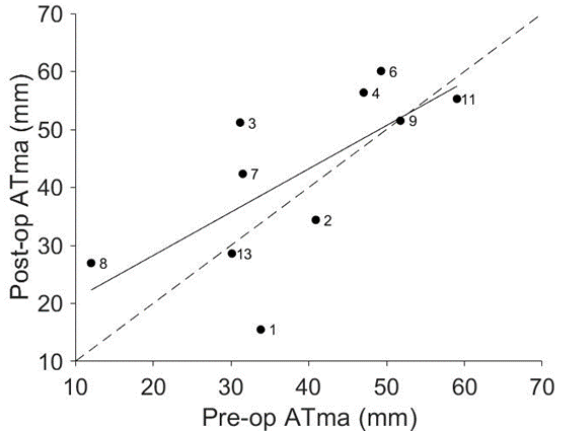

Figure 1: Post-op and pre-op Achilles tendon moment arms were found to be moderately correlated ($r^2 = 0.461$, $p = 0.031$). Participant numbers are beside each marker, and the dashed line indicates y = x.

Results and Discussion

The magnitudes of the differences in both ATma and d_R were both found to be significantly different from zero. For ATma the mean difference was 9.6 ± 6.8 mm ($p = 0.001$) and for d_R the mean difference was 4.6 ± 3.0% of calcaneus length ($p = 0.001$). We therefore rejected our hypothesis that post-op ATma would approximate pre-op values, although on average these values were similar. We found a moderate correlation between pre- and post-op ATma ($r^2 = 0.46$, $p = 0.03$, Figure 1), and between pre- and post-TAA d_R ($r^2 = 0.41$, $p = 0.046$). At the individual level, however, some participants exhibited large and differently-signed changes in ATma. For example, the ATma of Participant 1 was reduced by 54.2% following TAA, whilst the ATma of Participants 3 & 8 were 64.1% and 124.0% greater, respectively, following surgery (Figure 1). When we examined the correlation between change in ATma and change in d_R, 49.7% of the change in ATma was explained by the corresponding change in d_R ($p = 0.023$).

These results suggest that TAA does appear to alter ATma in individual patients, and that the magnitude of this change is related in substantial part to pre-post changes in the anterior-posterior position of the talar dome.

Significance

One implication of our finding that ATma changes following TAA is that ATma some patients may experience benefits related to altered ATma in terms of locomotor function. Longer ATma may augment ankle plantarflexor strength and in this manner permit higher walking velocity. Future work should consider the relationship between the change in ATma following TAA and the corresponding change in gait speed and other measures of mobility. Additionally, a change in ATma may alter the function of the plantarflexor muscles, by changing where they operate on their force-length, and force-velocity curves [4] and may alter the capacity for plantarflexor work and elastic energy storage in the Achilles tendon. Future studies should also consider the extent to which muscles will adapt to altered ATma, especially at follow-up times greater than six months.

Acknowledgments

This work was funded by the Department of Orthopaedics and Rehabilitation, College of Medicine, at Penn State Milton S. Hershey Medical Center.

References

[1] Valderrabano *et al.*, 2007. *Clin. Biomech.* 17:565-85.
[2] Rasske *et al.,* 2017. *Comput. Meth. Biomech. Biomed. Eng.* 20:201-5.
[3] Wade *et al.,* 2019. *J Biomech.* 90:71-7.
[4] Nagano & Komura, 2003. *J Biomech.* 36:1675-81.

Locomotor Function and Pain in Total Ankle Arthroplasty Patients at 6-Months Follow-up

Francesca Wade[1], Gregory Lewis[2], Andrea Horne[2], Lauren Hickox[1], Stephen Piazza[1],
Michael Aynardi[2], Paul Juliano[2], and Umur Aydogan[2]
[1]Biomechanics Laboratory, The Pennsylvania State University, State College, PA
[2]Penn State Milton S. Hershey Medical Center, Hershey, PA
Email: few2@psu.edu

Introduction

Outcomes following total ankle arthroplasty (TAA) are largely positive, with high levels of patient satisfaction, and a return to normal walking kinematics within two years [1]. However, performance on functional clinical assessments has received little attention in TAA patients, and residual pain after the surgery has been identified in up to 60% of cases [2]. While associations between implant kinematics and pain following TAA have been found during walking [3], to date there have been no studies of pain and function during more challenging locomotor tasks.

The purpose of this study was to determine how changes in function experienced by patients receiving TAA are related to pain. We hypothesized that following TAA, improvements in function would be correlated with reductions in pain.

Methods

Complete data sets were obtained for 11 TAA patients (age: 64.04 ± 9.26 y; height: 1.71 ± 0.07 m, body mass: 98.55 ± 20.07 kg; 3 implant designs). All procedures involving human subjects were approved by the Penn State Hershey Medical Center Institutional Review Board. All tasks were performed one month prior to and 6 months following TAA in a motion laboratory. Participants completed the RAND 36-Item Health Survey 1.0 (SF-36), whose global pain score was used in our analysis. Each participant performed three functional tasks: 1) single leg balance task on the involved limb (SLBT), where participants stood with eyes open to a ceiling time of 1 minute or the elevated foot touched the ground; 2) a Timed Up-and-Go test (TUG), where participants stood up from a standardized chair, walked 3m to a cone, pivoted and returned to a seated position; 3) a six-minute walk (6MW) where participants walked in a level hallway, turning every 30 m. From the distance walked, both velocity and a velocity normalized by height were computed. Linear regression analysis was performed to investigate how change in performance on these tasks was dependent on the patients' pre-to-post change in pain (Δpain) and their BMI.

Results and Discussion

Performance on the SLBT improved significantly post-TAA (mean difference: 6.17 s, p = 0.048), but no significant improvements were found for TUG (mean difference: 1.04 s, p = 0.270), 6MW velocity (mean difference: 0.11 m/s, p = 0.072), and normalized 6MW velocity (mean difference: 0.07 statures/s, p = 0.079). Whilst the mean reduction in TUG time we observed (1.04 s) was not significant, a mean reduction of 0.9 – 1.40 s has been identified as clinically important [4].

Linear regression did not predict change in function from Δpain alone, but when BMI and its interaction with Δpain was included, moderate to good fits were obtained (Table 1). Improvements in pain levels (when accounting for BMI) accounted for the majority of improvement in average walking velocity (Adj. R^2 = 0.79, p = 0.003), and might explain up to half of the variation in improvement of TUG, although this was not significant at the level of α= 0.05 (Adj. R^2 = 0.48, p = 0.06).

These results suggested that patients with larger BMI were unable to take advantage of reduced pain, whilst those participants with lower BMI were able to walk faster with reduced pain. The relationship might be weaker for TUG because it is task shorter in duration and thus less affected by pain. Neither Δpain, nor BMI, nor their interaction predicted performance on the SLBT; it is likely that other factors not considered here have more of an influence on balance tasks following TAA.

Significance

To our knowledge, this is the first study relating changes in locomotor function to changes in pain following TAA. Contrary to our hypothesis, we found that changes in pain, as assessed by the SF-36, did not explain variation in observed improvements in function. However, including the interaction between pain and BMI in our regression models, nearly 80% of the changes in 6MW velocity were explained, and approximately 50% of TUG performance change was explained. Despite this, pain and BMI leave substantial variance unaccounted for and other factors, such as changes to the joint structure, might explain some of this unaccounted variance. In conducting investigations of function following TAA, the pain levels and BMI of participants should be taken into account.

Acknowledgments

This work was funded by the Department of Orthopaedics and Rehabilitation, College of Medicine, at Penn State Milton S. Hershey Medical Center.

References

[1] Valderrabano *et al.,* 2007. *Clin. Biomech.,* 22:894-904.
[2] Gougoulias *et al.,* 2010. *Clin. Orth. Relat. Res.,* 468:199-208.
[3] List *et al.,* 2012. *J Foot Ankle Surg.,* 33:883-892.
[4] Mesquita *et al.,* 2016. *Chron. Respir. Dis.,* 13:344-352.

Table 1. Multiple regression output for model predicting change in function from Δpain, BMI, and their interaction

Function	Intercept	Δpain	BMI	Δpain*BMI	Adj. R^2	p-value
6MW Velocity	-3.415***	0.074***	0.103***	-0.002***	0.79	0.003
Normalized 6MW Velocity	-2.098**	0.046**	0.064**	-0.001**	0.75	0.005
SLBT Time	-8.942	1.033	0.279	-0.026	0.26	0.180
TUG	47.393*	-0.937*	-1.414*	0.027*	0.48	0.060

Significance indicated by: '***' $p \leq 0.001$ '**' $p \leq 0.01$ '*' $p \leq 0.05$

Ankle Osteoarthritis Causes Hip Extension Asymmetry Compared to Healthy Controls

Nicole Stark[1], Cherice Hughes-Oliver[1], Robin Queen[1]
[1] Department of Biomedical Engineering and Mechanics, Virginia Tech
Email: *nestark@vt.edu

Introduction

Ankle osteoarthritis (A-OA) has been associated with severe pain and disability and the etiology is post-traumatic in most cases. A-OA has been shown to significantly impact gait mechanics [1, 2] and result in a side-to-side difference in gait mechanics [3]. Asymmetry severity in A-OA patients has not been reported previously. Previous studies have reported an asymmetry of <10% in various gait parameters in healthy adults [4]. The purpose of this study was to determine the degree of gait asymmetry present in A-OA patients and to determine if asymmetry in A-OA patients is significantly different than an age & gender-matched healthy participants.

Methods

Thirty-seven unilateral A-OA [Age 60.16 $\pm$ 10.4 years, BMI 25.41 $\pm$ 3.5, 9 males, 28 females] patients from a previously collected prospective database were age, gender and BMI matched to thirty-seven healthy participants [Age 59.92 $\pm$ 11.7 years, BMI 24.69 $\pm$ 3.3, 9 males, 28 females]. Each participant completed between four and seven walking trials at a self-selected pace while walking speed and motion capture data were collected. Walking speed was measured using timing gates placed 5 meters apart. Motion capture data for A-OA gait mechanics was captured using an eight-camera motion capture system (Motion Analysis Corporation, Santa Rosa, CA; 120 Hz) while the healthy participant group data was captured with a ten-camera motion capture system (Qualisys, Sweden; 120 Hz). The same modified Helen-Hayes marker set was used during all of the testing. The ground reaction forces (GRF) were captured with four AMTI force plates (AMTI, Watertown, MA, 1200 Hz).

Average walking speed and five symmetry variables were compared between the A-OA group and the healthy controls to determine the effects of A-OA on gait symmetry. Gait symmetry was calculated using the Normalized Symmetry Index (NSI) [3]. NSI ranges between -100% to 100% where 0% indicates full symmetry [3]. A-OA and healthy participant data was processed as intact/OA side and dominant/non-dominant respectively. All NSI symmetry measures were calculated using a custom MATLAB script and included knee flexion, hip extension, ankle plantar flexion (PF), knee range of motion (ROM), hip ROM, weight acceptance (early-stage GRF), and propulsion (late-stage GRF).

To compare symmetry measures between the A-OA and healthy participants while accounting for the siginificant difference in walking speed (p=0.0001), an analysis of covariance (ANCOVA) was performed. The statistical analysis was completed using SPSS with an alpha level of 0.05.

Results and Discussion

Participants affected by A-OA had slower average walking speed ($0.88 \pm 0.29\ m/s$) compared to healthy control participants ($1.32 \pm 0.20\ m/s$) indicating gait is significantly affected by A-OA. Hip extension symmetry, weight acceptance symmetry and propulsion symmetry showed a difference between A-OA and healthy participants (Table 1). A reduction in GRF caused a statistical difference in GRF symmetry consistent with previously published findings [4].

Table 1: NSI measures in A-OA and healthy participants.

NSI	A-OA vs Healthy Older Adults				
	A-OA Mean	A-OA SD	Healthy Mean	Healthy SD	p-value
Knee Flexion (%)	2.29	10.88	1.51	11.34	0.678
Hip Extension (%)	15.94	33.14	-6.03	15.57	0.003 *
Ankle PF (%)	11.63	43.52	-10.69	24.25	0.064
Knee ROM (%)	-1.21	15.67	0.36	10.92	0.716
Hip ROM (%)	-5.45	15.03	0.85	5.27	0.107
Weight Acceptance (%)	-0.891	6.302	0.67	7.91	0.026 *
Propulsion (%)	-1.83	4.66	1.08	6.63	0.031 *

* p-value < 0.05

These results demonstrate that the presence of A-OA affects gait mechanics as reported by Schmitt et al., as well as gait asymmetry when compared with healthy control participants. Similar to Schmitt et al., the A-OA participants used greater hip extension to compensate for limitations in ankle motion which most likely resulted in the increase in hip extension asymmetry. The large standard deviation (SD) in ankle motion present in the current study could impact study results and indicates the need for a larger sample to account for this increase in variability between participants. A limitation of this study is that data was collected at two different locations using two different motion capture systems. While this should not impact study outcomes, the differences in marker placement between testing sites could have impacted the study outcomes. Future studies should assess the restoration of symmetry following surgical intervention and develop targeted rehabilitation programs to improve symmetry.

Significance

This study demonstrates that the presence of A-OA increased gait asymmetry compared to a healthy participants. Knowing that hip extension symmetry is effected by A-OA, targeted therapies can be developed to treat patients with A-OA and prevent further injury.

Acknowledgments

A-OA data was initially collected at Duke University. All healthy control data as well as data processing and analysis were completed at Virginia Tech. We would like to acknowledge Laura Dickerson for her help with the collection of the healthy participant data.

References

[1] C.N. Hughes-Oliver et al. *Gait & Posture 65 (2018) 228–233*
[2] Glazebrook, Mark et al. 1 March 2008 *The Journal of Bone and Joint Surgery*
[3] R. Queen et al. 23 January 2020 *Journal of Biomechanics*
[4] D. Schmitt et al. Spetember 2015 *Gait & Posture* Vol. 42

Influence of Pain on Knee Extensor Function in Individuals with Knee Osteoarthritis

Skylar Holmes.[1], Erica Casto[1], Ethan Steiner[1], and Katherine Boyer[1]
[1]University of Massachussetts, Amherst
Email: scholmes@umass.edu

Introduction

Knee extensor (KE) function is important for locomotion, joint stability, and load attenuation during such tasks as walking and stair climbing [1]. KE weakness is commonly exhibited in individuals with knee osteoarthritis (KOA) [2] and may contribute to increased disability in this population. Pain, a primary symptom in KOA, has been suggested as a key contributor to KE dysfunction. However, evidence of the impact of pain and fluctuations in pain on KE function is limited. Previous research has shown that while habitual exercise has a beneficial effect on KOA pain [3], individual bouts of exercise can result in acute pain exacerbations [4]. A better understanding of the impact of exercise-induced pain on KE function is needed to determine the role of pain on mobility limitations in those with KOA. Therefore, the purpose of this study was to investigate the impact of exercise-induced pain on KE function in individuals with KOA. We hypothesized that the peak KE torque and rate of torque development (RTD) would decrease post exercise and be related to the change in pain.

Methods

Eighteen adults with symptomatic KOA (Age: 65.9±5.1 years, BMI: 25.1±3.5 kg/m^2, KOOS pain:71.2±20.6) participated in this study after completing informed consent approved by the University's IRB. Participants completed three maximal isometric KE contractions on an isokinetic dynamometer (Biodex System 4 Pro, Shirley, NY) set at 60° of knee flexion before and after a 20min treadmill walk (20MTW) previously shown to increase pain in KOA [5]. Early (0-100 ms) and late (100-200 ms) rate of torque development (RTD100, RTD200), and peak torque were extracted and normalized to body mass (kg). Perceived pain was evaluated on an 11-point verbal numeric rating scale (vNRS) every two minutes throughout the 20MTW. The pain scores in the first and final 2 min of the 20MTW were used to evaluate change in pain in response to exercise.

Paired samples t-tests were used to compare torque, RTD and pain variables between pre and post 20MTW (α= .05). Participants were also subgrouped into those with and without exercise-induced pain (≥ 1pt on vNRS) to further probe the impact of pain on KE function changes using independent t-tests. Pearson's correlation was used to determine the relationship between baseline strength and the change in pain post exercise (α= 0.05).

Results and Discussion

There was not a significant difference pre to post 20MTW in peak torque in all participants but there was significant decrease in both RTD100 ($t(18)$= -4.95; p<.001) and RTD200 ($t(18)$= -7.43; p<.001) post 20MTW. Similar to prior research [5], close to half (n=8) of participants experienced a significant increase in pain (Δpain= 2.2± 0.5, p<.001) while the remaining participants did not experience a pain change. Baseline peak torque was not correlated to the change in pain (p >0.05). The change in peak torque, RTD 100 and RTD 200 pre to post 20MTW did not differ between those with and without pain (p>.05). These results suggest that exercise to a greater degree than perceived pain may be a sufficient stimulus to induce changes in neural activiation of the KE in individuals with KOA. The lower RTD100 in individuals with KOA post exericse may be indicative of lower motor unit recruitment and firing rate [6]. The lower RTD200 post exercise may suggest a change in recruitment pattern and greater recruitment of type I fibers in early contraction [7].

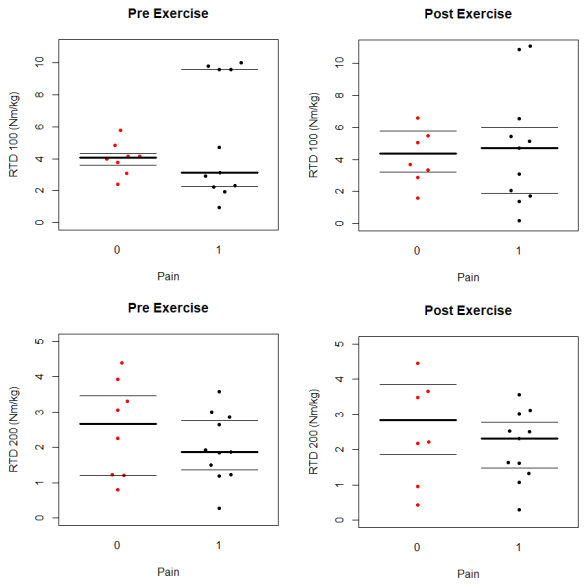

Figure 1. Pre to Post RTD 100 (Top row) and RTD 200 (bottom row). Dark horizontal lines indicate group mean, grey horizontal lines indicate 25th and 75th quartiles, (0=pain, 1=no pain).

Significance

The study findings suggest that RTD rather than peak torque may be a useful screening tool to assses KE dysfunction in individuals with KOA. The RTD changes with exercise may be a result of changes in muscle recruitment pattern and thus may contribute to acute impairments in mobility in this population. The changes in RTD following exercise may also contribute to altered loading of the knee [8] and thus to clinical or structural progression of KOA. The consequences of changes in RTD for mobility and KOA progression should be investigated in future work.

Acknowledgments

Funding provided by a University of Massachusetts- Amherst hMRC Pilot Grant

References

[1] Bennell KL, et al. Rhe Dis Clin North Am. 2013;39:145-76.
[2] Lewek MD, et al. J Orthop Res. 2004;22:110-5.
[3] Focht BC, et al. Ann Behav Med. 2002;24:201-10.
[4] Rejeski WJ, et al. Med Sci Sports Exerc. 1997;29:977-85.
[5] Boyer KA and Hafer JF. BMC Musc Disord. 2019;20(1):107
[6] Maffiuletti NA, et al. Eur J Appl Physiol 2016.
[7] Callahan, DM et al. Exp Gerontol. 2015; 72: 16–21.
[8] Blackburn, J.T, et al. Med Sci Sports Exerc. 2016; 48(9), 1664-16670.

Are Level Walking Knee Biomechanics Different Between Bilateral and Unilateral Total Knee Replacement Patients?

Songning Zhang[1], Derek S. Yocum[2], Harold E. Cates[3]
[1]Department of Kinesiology, Recreation and Sport Studies, University of Tennessee, Knoxville, TN, USA
[2]Department of Kinesiology, Albion College, Albion, MI, USA
[3]Tennessee Orthopaedic Clinic, Knoxville, TN, USA
Email: szhang@utk.edu

Introduction

The number of total knee replacement (TKR) is expected to increase 3.5 million by 2030 [2]. It is rather common to have a second joint replacement after the primary TKR procedure. Limited gait biomechanics research has shown that bilateral TKR patients showed reduced knee ROM and ground reaction force (GRF) [1, 3], and reduced knee extension moment (KEM) [4], compared to healthy controls. To our knowledge, no studies have examined differences of knee biomechanics in gait between the 1st and 2nd replaced TKR limbs in literature. It is unknown if patients with bilateral and unilateral TKRs would have similar knee kinematics and kinetics.

Therefore, the purpose of this study was to examine differences in knee joint biomechanics in both limbs of bilateral TKR patients and replaced and non-replaced limbs of unilateral TKR patients during level walking. It was hypothesized that bilateral TKR patients would have similar peak KEM, KAbM and ROM between the 1st and 2nd replaced limbs, and similar peak KEM and KAbM compared to unilateral TKR patients.

Methods

Fifteen bilateral TKR patients (69.4±5.0 yrs, 1.7±0.10 m, 95.6±15.2 kg) and 15 unilateral TKR patients (68.7±6.2 yrs, 1.7±0.1 m, 87.7±15.7 kg) were recruited. Patients performed 3-5 trials of level walking at their self-selected speed. Kinematic (240 Hz, Vicon) and GRF (1200 Hz, AMTI) data were collected. A 2×2 (Group×Limb) ANOVA was performed to determine differences between groups and limbs. Post-hoc comparisons were performed on significant interactions with the alpha level adjusted using a stepwise Holm adjustment.

Results and Discussion

The bilateral and unilateral TKR patients had similar walking speed: 1.1 vs 1.2 m/s, respectively. There were no differences in knee extension and abduction range of motion (ROM) between the patient groups and limbs. During the push-off, peak vertical GRF showed decreased vertical GRFs in bilateral TKR patients ($p = 0.016$, Table 1). A group×limb interaction ($p = 0.024$) was found for peak loading-response (LR) KEM. Post hoc comparisons showed the 1st replaced limb of bilateral patients had a significantly higher LR peak knee extension moment compared to 2nd replaced limb ($p = 0.024$). The 1st replaced ($p = 0.010$) and 2nd replaced ($p < 0.001$) limbs of bilateral patients were significantly lower than non-replaced limbs of unilateral patients. Furthermore, KEM for the 2nd replaced limb was lower than unilateral replaced limbs ($p = 0.001$). A group main effect difference was identified for the peak LR KAbM ($p = 0.033$) showing that it was lower for the bilateral patients than the unilateral patients. Finally, no differences were found in the range of motion for knee extension and abduction between the 1st and 2nd replaced limbs and between bilateral and unilateral patients.

Our results supported our hypothesis between 1st and 2nd replaced limbs, but not the hypothesis between bilateral and unilateral TKR patients. These results suggest that the bilateral TKR patients still showed greater deficits in the peak KEM and KAbM during level walking even though they had similar knee kinematics and walking speed, and much longer recovery times (71.9 month) compared to the unilateral patients (27.9 month).

Significance

These results indicate that bilateral TKR patients may have produced neuromuscular adaptations that are different compared to unilateral patients, showing similar knee kinematics but deficits in knee joint kinetics. In future studies of TKR gait, bilateral TKR patients should not be combined with unilateral TRK patients.

References

1. Borden, L. S., et al. (1999). *Gait Posture,* **9**, 24-30.
2. Kurtz, S., et al. (2007). *J Bone Joint Surg Am,* **89**, 780-785.
3. Renaud, A., et al. (2016). *Open Orthop J,* **10**, 155-165.
4. Ro, D. H., et al. (2018). *Knee Surg Sports Traumatol Arthrosc,* **26**, 1671-1680.

Table 1. Peak GRFs (N/kg) and knee ROM (Deg), and knee moments (Nm/kg): mean ± STD.

Variable	Bilateral		Unilateral		Group	Limb p	Int. p
	First	Second	Replaced	Non-			
LR Vertical GRF	1.03±0.11	1.05±0.11	1.07±0.06	1.09±0.04	0.195	0.133	0.903
PO Vertical GRF	1.00±0.05	1.01±0.06	1.05±0.06	1.06±0.05	**0.016**	0.095	0.531
LR Extension Moment	0.28±0.23[#,b]	0.18±0.18[a,b]	0.41±0.14	0.53±0.26	**0.001**	0.970	**0.024**
PO Flexion Moment	-0.16±0.13	-0.19±0.16	-0.08±0.14	-0.14±0.13	0.161	0.105	0.481
LR Abduction Moment	-0.35±0.08	-0.38±0.10	-0.46±0.10	-0.45±0.18	**0.033**	0.642	0.731
PO Abduction Moment	-0.29±0.10	-0.26±0.11	-0.32±0.08	-0.36±0.16	0.128	0.604	0.360
Extension ROM	-48.1±4.6	-48.1±4.6	-46.1±5.8	-47.2±6.3	0.511	0.826	0.381
Abduction ROM	3.8±1.9	3.3±1.6	4.3±1.1	3.4±0.9	0.648	0.066	0.856

[#] Significantly different between the 1st and 2nd replaced limbs, [a] Significantly different from Unilateral Replaced, [b] Significantly different from Unilateral Non-Replaced, LR: Loading-Response, PO: Push-off Response, Int.: Interaction.

Knee Joint Kinetic Differences in Bilateral and Unilateral TKR Patients During Stair Negotiation

Derek S. Yocum[1], Harold E. Cates[2], Songning Zhang[3]
[1]Department of Kinesiology, Albion College, Albion, MI, USA
[2]Tennessee Orthopedic Clinic, Knoxville, TN, USA
[3]University of Tennessee, Knoxville, TN, USA
Email: dyocum@albion.edu

Introduction

The high number of current and increased future need for total knee replacements (TKR), as well as a high risk for contralateral TKR following initial TKR, is well established [1,2]. Many researchers have used stair negotiation to investigate the gait of TKR patients. Compared to healthy controls during stair negotiation, unilateral TKR patients have exhibited reduced peak knee internal extension moment (KEM), which may be a sign of a quadriceps avoidance gait [3].

One study found no biomechanical differences at the knee joint between unilateral and bilateral TKR [4]. One study examined bilateral TKR patients with different implants in each knee, and found no differences [5]. To our knowledge, no studies have examined biomechanical differences between 1st and 2nd replaced limbs of bilateral patients during stair negotiation.

This study compared the 1st and 2nd replaced limbs of bilateral patients, and replaced and non-replaced limbs of unilateral patients. We hypothesized that peak KEM and internal knee abduction moment (KAbM) would not be different between limbs of bilateral patients. We also hypothesized KEM and KAbM in bilateral patients would be different than the non-replaced limb of unilateral TKR patients.

Methods

Fifteen bilateral TKR patients (69.40±5.04 years, 1.73±0.09 m, 95.56±15.24 kg) and fifteen unilateral TKR patients (64.93±5.11 years, 1.75±0.09 m, 89.18±17.55 kg) were recruited. Patients performed 3-5 trials of stair ascent and descent. A 2×2 (group x limb) ANOVA was performed to determine differences between limbs and groups.

Results and Discussion

Bilateral patients had similar KEM and KAbM between 1st and 2nd replaced limbs in both ascent and descent, supporting our first hypothesis (Table 1). This shows that both replaced limbs have similar functional capacity and recovery following TKR surgery. Average time since surgery for 1st replaced limbs was approximately 6.33 years, 5.46 years since 2nd replacement, an average of 3.2 years longer than unilateral patients. Given the longer time that bilateral patients have had replacements, any differences in acute adaptations between 1st and 2nd replaced limbs may no longer be present.

During ascent, peak LR KEM of 2nd replaced limbs of bilateral patients was lower than non-replaced limbs of unilateral patients (Table 1). KEM of replaced limbs of unilateral patients was lower than their non-replaced limbs, which was found previously [4].

During descent peak LR KEM moments were lower in 1st and 2nd replaced limbs of bilateral patients, compared to replaced and non-replaced limbs of unilateral patients. PO KEM was lower in both 1st and 2nd replaced limbs of bilateral patients, compared to non-replaced limbs of unilateral patients (Table 1). Significant group differences in KEM may indicate a quadriceps avoidance, seen previously in unilateral patients, which may be more prevalent in bilateral patients. In the frontal plane, no kinetic differences were found during either ascent or descent.

Significance

Implications for this study are that bilateral patients may have functional adaptations that are different than those of unilateral patients. This can be seen in lower KEM in bilateral patients which may be due to decreased muscular strength, and kinesiophobia. Our bilateral patients reported an average 5.47±2.42 days per week of stair usage. Alterations in joint moments in the bilateral group does not inhibit them from using stairs.

References

1. Kurtz et al. (2007). *J Bone and Joint Surgery*, **89**, 780-785.
2. McMahon and Block (2003). *J Rheumatol*, **30**, 1822-1824.
3. Berti et al. (2006). *Clin. Biomechanics*, **21**, 610-616.
4. McClelland et al. (2014). *J Biomechanics*, **47**, 1816-1821.
5. Bolanos et al. (1998). *J Arthroplasty*, **13**, 906-915.

Table 1. Ascent and Descent Knee Extension and Abduction Moments (Nm): mean ± STD.

Ascent	Bilateral		Unilateral		Group p	Limb p	Int. p
	1st Replaced	2nd Replaced	Replaced	Non-Replaced			
LR Knee Ext. Moment	1.00±0.36	0.96±0.31[b]	0.98±0.22[#]	1.27±0.29	0.154	**0.024**	**0.004**
LR Knee Abd. Moment	-0.42±0.16	-0.39±0.22	-0.36±0.11	-0.36±0.18	0.344	0.716	0.739
PO Knee Abd. Moment	-0.32±0.21	-0.19±0.28	-0.27±0.15	-0.32±0.25	0.374	0.617	0.441
Descent					Group p	Limb p	Int. p
LR Knee Ext. Moment	0.32±0.29[a,b]	0.23±0.25[a,b]	0.62±0.33	0.87±0.34	**<0.001**	0.212	**0.011**
PO Knee Ext. Moment	0.79±0.25[b]	0.73±0.25[b]	0.83±0.24	1.07±0.29	**0.027**	0.073	**0.003**
LR Knee Abd. Moment	-0.39±0.24	-0.54±0.23	-0.54±0.26	-0.51±0.24	0.375	0.291	0.173
PO Knee Abd. Moment	-0.32±0.24	-0.47±0.20	-0.38±0.22	-0.35±0.15	0.470	0.387	0.161

[a] Different than Unilateral Replaced, [b] Different than Unilateral Non-Replaced, [#] Within-group difference. LR: Loading-Response, PO: Push-off Response, Int.: Leg×Group Interaction, Bold: p-values indicate significance.

Exploring the Viability of Collecting Joint Acoustic Emissions Around the Wrist

Daniel M. Hochman[1*], Sevda Gharehbaghi[1], Daniel C. Whittingslow[1,2], Omer T. Inan[1]
[1]Georgia Institute of Technology, Atlanta, GA, United States
[2]Emory University School of Medicine, Atlanta, GA, United States
Email: *dmhochman@gatech.edu

Introduction

Joint acoustic emission (AE) sensing has been used to non-invasively quantify knee joint health. This technique employs wide-band, low noise accelerometers placed on the skin above the joint to sense the surface vibrations generated by the dynamic interactions of the underlying anatomy during articulation [1,2]. In this work, we adapt our previously validated knee AE sensing system into one capable of performing measurements around another commonly injured and diseased joint - the wrist.

Methods

For this study, 7 healthy subjects (three male/four female, 24.9 ± 3.5 years, 65.3 ± 8.4 kg, and 168.0 ± 10.1 cm) with no history of major wrist injury or joint disease were recruited. They performed flexion-extension and rotation exercises while wrist AEs were recorded using highly sensitive uniaxial accelerometers (Series 3225f7, Dytran Instruments, Inc., Chatsworth, CA) placed on the skin at 8 locations around the wrist (Figure 1). An inertial measurement unit (BNO055, Adafruit Industries, New York, NY) placed within a custom grip synchronously recorded motion. The accelerometer signal was filtered using a Kaiser-window bandpass filter (150Hz – 20kHz). The signal was separated into individual cycles of motion (~2 sec) and windowed (400ms windows with 50% overlap). Nine previously validated signal features were extracted from each window, and the mean, median, and standard deviation were calculated for each cycle to best quantify the AEs from the wrist. Similarity and repeatability of the AE recordings in healthy subjects are indicative of high recording quality [3] and were assessed using the intraclass correlation coefficient (ICC) and the Jensen-Shannon (JS) divergence of the nine features. Finally, windows of characteristic joint AE clicks and motion artifact were extracted from each recording to calculate signal-to-artifact ratio (SAR) in order to quantify the strength of AE signal in each recording.

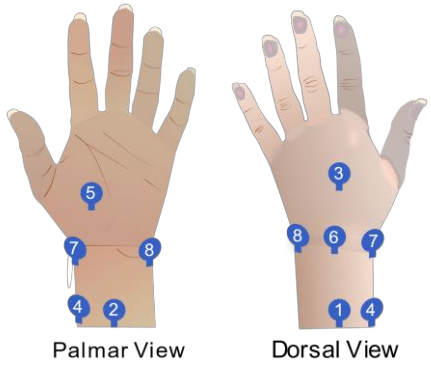

Figure 1: Palmar and Dorsal View of the wrist and marked locations where uniaxial accelerometers were placed to record the AEs excited during wrist flexion-extension and rotation exercises

Results and Discussion

First, a qualitative analysis of the recordings was performed to ensure the system was properly recording AEs. This included visual inspection of the time-series data and listening to the recordings from both exercises at all 8 locations. This perfunctory analysis ensured us that key characteristics of AEs (e.g. signal clicks and grinding sounds) were successfully captured [1-3].

A more thorough quantitative analysis was then performed. Flexion-extension exercises demonstrated high levels of repeatability, with an average ICC of 0.967 (UB/LB at 0.975/ 0.975, p = 0.05). Rotation exercises showed slightly higher repeatability, with average ICC of 0.972 (UB/LB at 0.979/ 0.964, p = 0.05). Both exercises also demonstrated high correlation via JS divergence, indicating that these exercises consistently excite AEs from the wrist joint. With the exercises validated, the optimal location of placement needed to be analyzed.

The location analysis found the signal to be repeatable regardless of location, as repeatability scores via ICC (Figure 2) and JS divergence between each location ranged from an ICC score of 0.972 (UB/LB at 0.985/0.954, p = 0.05) at location 8, to 0.946 (UB/LB at 0.971/0.913, p = 0.05) at location 3. The SAR was calculated (Figure 3) to assess the impact that motion artifacts have on each location. The high SARs at locations 1, 2, and 4 demonstrate that the wrist joint AE signals are less affected by the motion artifacts than other locations, which indicates that accelerometer placement proximal to the end of the radius is better at minimizing motion artifacts within the signal than accelerometer placement distal to or at the end of the radius.

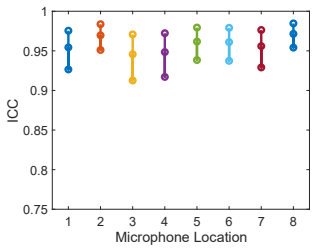

Figure 2: ICC values, upper bounds, and lower bounds with p-value = 0.05 for each of the 8 locations around the wrist

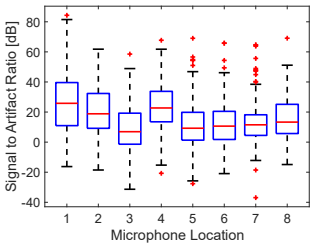

Figure 3: Box-and-Whisker plot of all Signal-to-Artifact Ratios for the 8 locations around the wrist

Significance

High AE signal repeatability as determined with ICC and JS divergence as well as a high SAR demonstrates that it is possible to record high quality and repeatable AEs from the joint. This work supports our hypothesis that flexion-extension and rotation will reliably elicit AEs from the wrist. These AEs have previously been used to noninvasively grade the health of the knee in previous studies. 3 locations proximal to the end of the radius provide the highest repeatability scores in recording AEs while minimizing motion artifacts. This work lays a foundation for future work in using wrist AEs as a biomarker of musculoskeletal pathologies and injury.

Acknowledgements

This research was supported by the National Science Foundation (NSF) under Grant Number 1749677.

References

[1] Whittingslow et al.(2020) *An. of Biomed. Eng,* **48**, 225–235
[2] Semiz et al.(2018) *IEEE Sensors J*, **18**(22), 9128-9136
[3] Hersek et al.(2018) *IEEE Trans. on Biomed. Eng.* **65**(6), 1291-1300

Patient Perceived Pain and Function Measures Are Related to Biomechanical Measures in TKA Patients

C. Avery Callahan[1], Hannah L. Stokes[1], Ronald Singer[2], Michael Bates[2], Nigel Zheng[1]
[1]University of North Carolina at Charlotte, NC, [2]OrthoCarolina at Charlotte, NC
nzheng@uncc.edu

Introduction

Osteoarthritis (OA) is a common joint disease that can typically occur in the knee. At the end stage of OA, total knee arthroplasty (TKA) can deliver pain relief, restore mobility and function and provide quality long-term results. A recent study has shown that subjective measures of function based on patient reported outcome measures (PROMs), directly reflect objective biomechanical measures in TKA patients (1).

The purpose of this study is to investigate how patient perceived measures of pain and ability to perform standard activities are related to biomechanical measures. Previous studies have shown that PROMs could potientially be an indicator of biomechanical function (2). The connection between these measures could help improve the lack of standardization in measuring both patient-perceived function and gait biomechanics following surgery (1). We hypothesize that patient perceived function is not related to biomechanical function.

Methods

The study included 39 subjects with confirmed OA (M/F: 21/16, age: 65±6 years, BMI: 31±4 kg/m^2) who received TKA with posterior stabilized implants. The protocol for the study was approved by an institutional board and all subjects gave written informed consent. All 39 subjects completed PROMs and biomechanical testing before surgery and 19 patients returned to complete both measures six-months post-op.

The PROMs used for this study were pain with level walking (PW) and pain with standard activities of daily living (SA) (The 2011 Knee Society Scoring System). A lower score for PW and a higher score for SA indicates a better subjective measure. Range of motion (ROM) of the knee (flexion-extension) was measured manually using a goniometer. The static and dynamic balance (SB, DB) were tested using the Biodex Balance System. The Timed Up and Go test (TUG) measures the time the subject takes to rise from a chair, walk three meters, turn around, walk back to the chair, and sit down. The averages of three trials were used for SB, DB and TUG. Lastly, one trial of the 10 Time Sit-to-Stand test was performed. A lower value for TUG, S2S, SB and MB and a higher value for ROM indicate a better objective functional measure. Bivariate Pearson correlation tests and paired t-tests were performed using SPSS with an alpha set to 0.05.

Table I: Mean±SD for measures of subjective (PW, SA) and objective (TUG, S2S, ROM, SB and DB) function, * p<0.05 pre-op vs. post-op.

Measures of Function	Pre-Op n=39	Pre-Op n=15	Post-Op n=15
Pain with Level Walking (PW)	5±3	6±3	2±3*
Knee Function with Standard Activities (SA)	13±4	12±5	23±6*
Timed Up and Go (TUG) (s)	11±3.6	11±3.1	11±7.3
10-time St to Stand (S2S) (s)	33.6±10.2	33.6±9.1	27.5±8*
Range of Motion (ROM) (deg)	118±14	122±10	128±7
Static Balance Test (SB)	1.6±1.5	1.9±1.2	1±0.8*
Dynamic Balance Test (DB)	1.6±0.9	1.8±0.8	1.3±0.7

Results and Discussion

Both subjective measures (PW and SA) and two of the objective measures (S2S and SB) were significantly improved following TKA at 6-month post-op (Table I). There were no significant changes for TUG, ROM and DB following TKA at 6-month post-op. Pearson correlation coefficients between subjective and objective measures of function for pre-op, post-op and changes following TKA at 6-month post-op (post-pre) were listed in Table II. For pre-op, both PW and SA were significantly related to SB. SA was also significantly related to TUG. For post-op, there were no significant correlations between subjective and objective measures of function. For changes following TKA at 6-month post-op, both PW and SA were significantly related to ROM and PW was also significantly related to DB.

Table II: Pearson correlation values for measures of subjective (PW, SA) and objective function (TUG, S2S, ROM, SB, MB), * p<0.05.

		TUG(s)	S2S(s)	ROM(deg)	SB	DB
Pre	PW	.285	-.005	-.037	.317*	.136
	SA	-.323*	-.045	.032	-.394*	-.299
Post	PW	.108	.263	-.111	.082	.186
	SA	-.217	-.119	-.369	-.096	-.169
Post-Pre	PW	-.047	-.127	-.609*	-.037	.466*
	SA	-.226	-.117	.613*	-.179	-.254

ROM improvement following TKA is probably a better objective measure than those measured at pre-op and post-op. Relative less change of DB following TKA may be linked to functional deficit when performing more demanding motor tasks. No significant correlations between subjective and objective measures at the 6-month post-op may be linked to small sample size. Small sample size may also contribute to no significant changes following TKA at 6-month post-op for some objective measures. More subjects will be tested in future to improve the sample size. Findings of this study indicate that both subjective and objective measures are important when assessing functional improvement of subjects who undergo TKA. Both pain level with walking and knee function with standard activities contributed to the results of biomechanical measures of function. For some objective measures, changes following TKA are better measures and they should be recorded at both pre-op and post-op.

Significance

A patient's perceived level of pain and function performing standard activities may be used as an indicator for their functional deficits. Objective functional tests are important measures to discover functional deficits.

Acknowledgments

This study is funded by Smith and Nephew through an Investigator Initiated Study award.

References

1) Biggs, P., *Gait Posture*, 2019. 2) Levenger, P., *Knee Surg Sports Traumatol Arthrosc*, 2018.

Invasive and Non-invasive Methods for Humeral Head and Glenohumeral Joint Center Localization

Daniel Kasman[1], Nirmal Maxwell[1], Steven Halvorson[1], David Stapleton[2], Traci Bush[3], James Choi[4], Vassilios Vardaxis[2,3]
[1]College of Osteopathic Medicine, [2]Human Performance Lab, & [3]Department of Physical Therapy, Des Moines University & [4]Iowa Radiology, P.C., Des Moines, IA, United States
Email: Vassilios.Vardaxis@dmu.edu

Introduction

The position of the glenohumeral joint center (GHJC) relative to the scapula is directly linked to the scapulohumeral (SH) muscle moment arms and the kinetics and kinematics of the glenohumeral (GH) joint [1]. The GHJC is often represented by the humeral head center (HHC), considering the congruency of the humeral head and the glenoid cavity curvatures [2], and is used for pre-operative planning and shoulder arthroplasty to regulate the resting tension and the functional capacity of the SH muscles [3]. The GHJC and the HHC location may vary between people based on bony specific characteristics and require advanced imaging and/or mathematical estimates based on scapular/humeral anatomic landmarks. A number of techniques and/or modalities have been used with inherent limitations in terms of accuracy, invasiveness, practicality, and cost.

The aim of the present study was to compare the 3D location of the HHC and the glenoid fossa center (GLF) using CT to ultrasound imaging (US) combined with 3-D motion capture, as well as, the GHJC generated from predictive regression and a functional method.

Methods

Ten (10) right-handed adult males (25.9 ±4.7 years) with no shoulder impairment/pathology participated in this project. The HHC, the GLF and the GHJC position were localized using computed tomography (CT), ultrasound (US) and motion capture (17 reflective marker-set including 3-marker humeral and acromial clusters), via a 10-camera motion capture system. Subjects were supine for the CT scan and seated upright for the US and motion capture sessions with the palm facing medially and thumb anterior. Eight (8) independent great arc US images were taken of the humeral head (2 horizontal & 2 vertical on the anterior and posterior-lateral surface aspects) using a 4-marker cluster equipped US linear probe. Twenty CT points on the humeral head and the glenoid fossa, and forty US humeral head points were least-squares sphere fitted to localize the center of the respective structures. Two additional widely used robust methods, predictive regression (REG) and functional (FNC) were also implemented in determining the GHJC [4,5]. The CT and the probe digitized coracoid process (CP), acromial angle (AA), trigonum spinae (TS), and inferior angle (IA) relative to the acromial cluster, were used to localize the HHC, GLF and GHJC in the ISB scapula coordinate system [6]. One-way repeated measures ANOVA was used to determine between methods differences ($\alpha < 0.05$).

Results and Discussion

Mean and standard deviation values for three orthogonal offsets for all methods are shown on Table 1. There were significant differences between methods for the respective centers in the inferior and anterior direction relative to AA-TS-IA scapula reference frame. Specifically, the FNC-GHJC was the most inferior on the plane of the scapula from AA and it was significantly further from the REG-GHJC. The REG-GHJC was significantly more anterior in the normal to scapula plane direction, than all other methods, while the CT-HHC was the least anterior and significantly farther from the CT-GLF and US-HHC. The CT-GLF sphere fitting radius of the GLF was significantly longer (32.38 ±3.29) than the humeral head radii determined by sphere fitting (24.99 ±1.31 & 22.62 ±2.55) for the HHC obtained by CT and US, respectively [2]. While the values, represented in mm, are comparable to those reported in literature, normalized data will be presented to account for size differences between people [7,8].

Significance

Findings support the utilization of US imaging to localize the HHC as a viable, cost-effective, non-invasive, subject-specific method. The impact of the differences between methods in the GHJC on 3D dynamic GH joint motion will be discussed.

Acknowledgments: Iowa Osteopathic Educational Research & Iowa Radiology, P.C. for their financial support.

References

[1] Mercer D et al, J Shoulder Elbow Surg 2001;20:363-71
[2] Soslowsky L et al, Clin Orthop Relat R 1991;478(3):181-9
[3] Pearl LP, J Shoulder Elbow Surg 2005;14:99S-104S
[4] Meskers CGM et al, *J Biomech*; 1997;31:93-6
[5] Schwartz M & Rozumalski A, *J Biomech*, 2005;38:107-16
[6] Wu G et al, *J Biomech*, 2005;38:981-92
[7] Stokdijk M et al, *J Biomech*, 2000;33:1629-1636
[8] Monnet T et al, *J Biomech*, 2007;40:3487-3492

Table 1: Mean (±SD) values of orthogonal offsets and sphere fitting radius (in mm) for HHC, GLF and GHJC, per ISB scapula coordinate system with the origin coincident with the acromion angle.

	CT-HHC	CT-GLF	US-HHC	FNC-GHJC	REG-GHJC
TS to AA (+ Lateral)	1.39 (3.10)	5.79 (3.91)	-2.41 (5.31)	2.74 (7.25)	1.26 (6.69)
On Plane (+ Inferior) ‡	23.3 (3.7)	24.9 (3.8)	19.8 (5.5)	27.6 (8.1) *	19.0 (4.3) *
Normal to Plane (+ Forward) ‡	39.3 (5.0) *	41.1 (5.6) *	47.3 (6.0) *	45.8 (8.1)	61.5 (9.0) !
Sphere Radius ‡	24.99 (1.31)	32.38 (3.29) !	22.62 (2.55)	N/A	N/A

HHC = Humeral Head Center, GLF = Glenoid Fossa Center, GHJC = Glenohumeral Joint Center, CT = Computed Tomography, US = Ultrasound.
‡ ANOVA Repeated Measures $p < 0.05$, Bonferroni adjusted ($p < 0.005$) contrast difference, ! from all other methods, * between methods

Exercise may Mediate Post-Traumatic Osteoarthritis Through Restoration of Joint Homeostasis

Jarred Kaiser[1,2], Sarvgna Raval[1], Fabrice Bernard[3], Jay McKinney[3], Krishna Pucha[1], Daniel Sok[1], Brandon Dixon[3], Nick Willett[1,2,3]
[1]Emory University, [2]Atlanta Veteran's Affairs Hospital, [3]Georgia Institute of Technology, Atlanta, GA
Email: jarred.kaiser@emory.edu

Introduction

Post-traumatic osteoarthritis (PTOA) is characterized by a chronic state of joint inflammation and cartilage degeneration and remains a significant clinical and socioeconomic challenge. Failure to traffic pro-inflammatory cytokines following traumatic joint injury can propagate chronic inflammation and cartilage catabolism. Joint clearance is regulated via multiple mechanisms, including through blood flow, microvascular permeability, and lymphatic drainage (1). Exercise, the only clinically proven treatment to provide PTOA symptomatic relief, is thought to facilitate joint clearance through increases in blood and lymph flow (2), though if and how this exercise-induced joint clearance occurs remains largely unknown. Understanding the effect of exercise on joint clearance kinetics may provide insight into targeted physical approaches that may be able to restore homeostasis following joint trauma. The goals of these studies were to determine the role of exercise in joint clearance and in treating a preclinical model of PTOA. We hypothesized that exercise will slow PTOA progression by decreasing cartilage degradation and improving joint function in part by expediting joint clearance via venous and lymphatic mechanisms.

Methods

Exercise as a treatment for PTOA

Male Lewis rats received either a sham (medial collateral ligament transection only) or medial meniscus transection (MMT) surgery, with or without exercise (N=6/group). Exercised animals began treadmill walking (10 m/min) 21 d post-surgery, after mild PTOA has developed, and exercised 5 d/wk for up to 30 mins. Gait was measured at 3 and 6 weeks post-surgery. Cartilage and osteophyte morphology and cartilage attenuation (inversely proportional to sGAG content) in the medial tibia were quantified using EPIC-μCT.

Role of exercise in joint clearance rates

Naïve male Lewis rats were acclimated to the treadmill prior to two experiments. On the morning of each experiment, both knees of eight rats received intra-articular injections of a carboxylate modified IRDye800CW and IRDye680RD with 40 kDa polyethylene glycol. The mechanisms of clearance are size-dependent, with the 40 kDa PEG-NIR and free dye clearing via lymphatic and venous systems, respectively (3). NIR images were collected immediately and out to 24 hours after injections. Four rats remained within their cages throughout both experiments. The other four rats underwent treadmill walking (10 m/min for 30 mins) either immediately before or after injection.

Results and Discussion

Exercise as a treatment for PTOA

MMT caused a significant increase in cartilage volume ($p=0.05$) and attenuation ($p=0.01$) in the medial third of the medial tibia plateau at 6 weeks. MMT also caused significant increased in cartilage surface roughness ($p=0.01$) and mineralized osteophyte volume ($p<0.05$). Exercise did not alter any morphological outcomes in sham animals. Exercised MMT animals showed no significant differences in cartilage volume, attenuation, surface roughness, or mineralized osteophyte volume compared to sham animals. Exercise also increased step frequency, decreased step length, and increased duty factor in all animals, regardless of surgery, suggesting a functional modification in these animals. These results suggest that the exercise treatment was largely successful in attenuating PTOA.

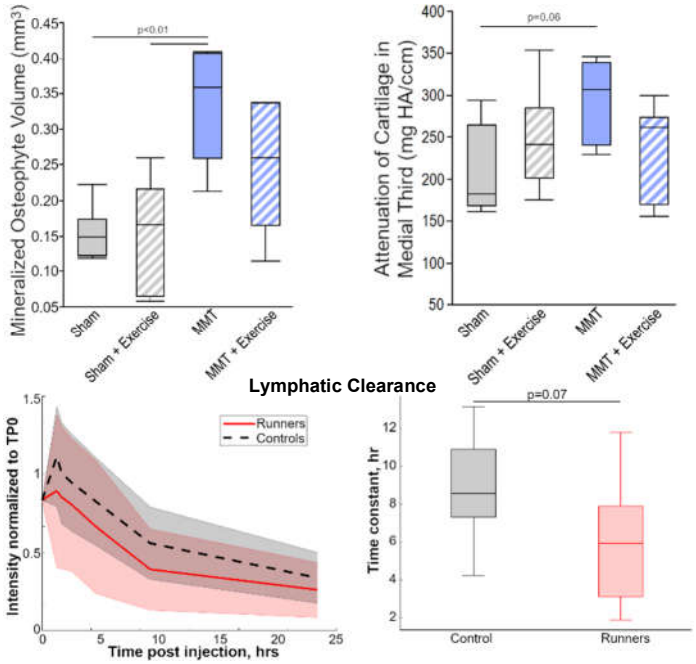

Figure 1: Top: MMT caused an increase in osteophyte volume and attenuation (~loss of proteoglycan) that was not observed in exercised MMT animals. Bottom: NIR clearance and time constants for lymphatic clearance, which was expedited when running after injection.

Role of exercise in joint clearance rates

Exercise immediately prior to NIR injection, which we hypothesized would prime the lymphatic and venous system, had no effect on clearance rates via either mechanism (not shown). Exercise immediately following injection, however, reduced lymphatic clearance time by ~50% ($p=0.07$), with no observed differences in venous clearance (exercise: 2.5 ± 0.4 hrs, none: 2.6 ± 0.7 hrs, $p=0.42$). Notably, both the collagenase sub-group of MMPs and fragmented aggrecan fall into the size range cleared by lymphatics. In the naïve animal, exercise alone can modulate the lymphatic clearance of the knee joint.. While it is unknown if exercise can resolve osteoarthritic dysfunction in clearance, the observations here may provide one potential mechanism by which exercise can effectively modulate disease progression.

Significance

Our results suggest that mild exercise can slow PTOA, potentially by enhancing lymphatic clearance of the knee.

Acknowledgments

Travis Fulton, Thanh Doan, Joseph Shaver, DOD PR171379

Reference (1) Levick JR J Physiol 1980. (2) Ellegaard K et al Rheuma Internat 2013. (3) Doan TN et al Acta Biomat 2019

A Comparison of Modular Control of the Lower Limbs during Gait Following Total Knee Arthroplasty

Rebecca M. Weiss, Rebekah R. Koehn, Laura C. Schmitt, Ajit M.W. Chaudhari, and Robert A. Siston
The Ohio State University, Columbus, OH, USA
Email: Weiss.506@osu.edu

Introduction

Total knee arthroplasty (TKA) is the end-stage treatment for knee osteoarthritis (OA), but one in five patients report poor post-operative function.[1] Recent literature has suggested that altered neuromuscular control patterns may provide insight into functional deficits following TKA.[2] Muscle activations have been found to be symmetric between limbs in healthy individuals[3] and abnormal muscle activation patterns have been observed bilaterally in subjects with knee OA[4] and following TKA.[5] Conversely, asymmetric muscle activations have been observed in subjects with hip OA,[6] suggesting that separate neural circuits might control the limbs independently.[7] However, it is difficult to gain insight into an overall strategy of both limbs with individual muscle activations alone. A recent study[8] found that differences in motor control in a TKA-involved limb, characterized by a higher number of motor modules[9] (or synergistic muscle activations), were related to better patient-reported outcomes. However, it remains unknown whether asymmetric motor control patterns exist bilaterally following TKA and whether the existence of asymmetric motor control is related to patient function.

Therefore, the purpose of this study was to determine if differences in bilateral motor control strategies exist in a cohort of patients 6-months after unilateral TKA and if a relationship exists between functional outcomes and modular control of the operated and non-operated limbs. We hypothesized that (i) asymmetric modular control would be present in a majority of individuals with TKA and (ii) modular asymmetry would be related to poor post-operative function.

Methods

17 participants (M/F 7/10; 59.8±6.6 y; 97.2±20.5 kg; 1.7±0.1 m) provided written informed consent prior to receiving a unilateral posterior-stabilizing TKA. Subjects were tested 6-months post-TKA and completed multiple over-ground walking trials at a self-selected speed. We collected surface electromyography (EMG) data from eight lower extremity muscles, bilaterally: rectus femoris, vastus lateralis and medialis, semitendinosus, biceps femoris, medial and lateral (LG) gastrocnemii, and soleus. We processed the EMGs[10], extracted modules[11], and selected a representative gait cycle for each leg. Patient function was measured using the 6 Minute Walk (6MW) test[12] and was categorized as high- or low- functioning relative to the median.

We compared modular complexity (i.e. number of modules) between limbs. For subjects demonstrating 3 modules in both limbs, we compared muscle weights bilaterally using paired t-tests or Wilcoxon sign-rank tests. We performed a Chi-Square test to examine whether symmetric modular complexity was related to 6MW performance level.

Results and Discussion

We found that 52.9% of subjects had symmetric modular complexity and 47.1% had asymmetric modular complexity. For the operated limb, 2 subjects demonstrated 2 modules, 13 subjects demonstrated 3 modules, and 2 subjects demonstrated 4 modules. For the non-operated limb, we found that 1 subject demonstrated 2 modules, 9 subjects demonstrated 3 modules, and 7 subjects demonstrated 4 modules. Of the 9 subjects with symmetric modular complexity, 1 demonstrated 2 modules 7 demonstrated 3 modules, and 1 demonstrated 4 modules. Of the 7 participants demonstrating 3 modules bilaterally, the only muscle with weighting differences which approached significance was the LG in the plantar flexor-dominated module ($p = 0.076$) and the hamstrings-dominated module ($p = 0.053$). Although there were no significant differences in the other muscle weights (all $p \geq 0.214$), nearly half of the participants demonstrated asymmetric modular complexity, only previously seen in subjects following incomplete spinal cord injury.[7]

Our results did not support our hypothesis that asymmetric modular complexity would be associated with poor function ($p = 0.457$) as measured by the 6MW (Table 1). Our results may be limited by the small sample size and selected measure of function. Future work will investigate modular symmetry before and 2-years following surgery and will examine additional functional measures.

Table 1: Number of participants demonstrating symmetric or asymmetric modular complexity with high or low 6MW performance. Chi-square: $p = 0.457$.

	High 6MW	Low 6MW
Symmetric	4	5
Asymmetric	5	3

Significance

Although our results suggest that the symmetry of modular complexity is not related to patient function 6-months after TKA, the asymmetry of modular complexity demonstrated by nearly half of the participants is a novel finding for a cohort following orthopaedic surgery. Such a finding suggests a need for further investigation into whether those results are present in a larger population over multiple gait cycles. Our work has the potential to inform rehabilitation clinicians on whether or not symmetric muscle coordination during gait is desirable in order to improve patient function after a TKA.

Acknowledgments

This project was supported by Grant Number R01 AR056700 from the National Institute of Arthritis and Musculoskeletal and Skin Diseases and an Ohio State Fellowship (RRK).

References

1 Singh et al. *Osteo Cart.* 18:515-21, 2010. **2** Hubley-Kozey et al. *Clin Biomech.* 25:995-1002, 2010. **3** Burnett et al. *J Electromyogr Kinesiol*. 4:610-5, 2011. **4** Collins et al. *J Electromyogr Kinesiol.* 24(4):497-501, 2014. **5** Thomas, et al. *The Knee*. 21(6):1115-9, 2014. **6** Schmidt et al. *Gait Posture*. 45:187-92, 2016. **7** Reisman et al. *J Neurophysiol*. 94: 2403–15, 2005. **8** Ardestani et al. *J Electromyogr Kines.* 37:90-100, 2017. **9** Lee. *J Motor Behavior*. 16(2):135-70, 1984. **10** Koehn, et al. *Proc ASB*, 2018. **11** Clark et al. *J Neurophysiol*. 103(2):844-5, 2010. **12** Enright. *Respir Care.* 48:783-5, 2003.

Does osteoarthritis impact gait and balance abilities in people with Parkinson's Disease?

Abigail C. Schmitt, Justin N. Daniels, Sidney T. Baudendistel, Chris J. Hass
Department of Applied Physiology and Kinesiology, University of Florida, Gainesville, FL, USA
Email: a.schmitt@ufl.edu

Introduction

Parkinson's disease (PD) is a degenerative neurological disorder that affects over ten million people worldwide[1]. The cardinal signs of PD are motor related, and many patients report gait dysfunction as the most debilitating symptom[2]. These gait impairments include decreased gait velocity, step length, and time spent in single support[3]. Impairments in gait and balance are largely attributed to faulty dopaminergic circuitry. As a result, current therapies often aim towards improving mobility impairments through these mechanisms. Perhaps surprisingly, these interventions remain relatively ineffective in ameliorating gait and balance dysfunction. Underlying comorbidities, that are not being addressed by dopamine targeting therapies, may contribute to the resiliency of gait dysfunction.

Osteoarthritis (OA) is one of the most prevalent comorbidities in individuals with PD, affecting approximately 50% of patients[4]. Knee OA, an inflammatory condition characterized by pain and joint deterioration, is associated with gait alternations such as decreased gait speed, step length, and time spent in single support. Further, individuals with OA exhibit mobility limitations associated with stiff joints, slowness, and inflexibility. Both OA severity and mobility impairments progress over time. These symptoms, limitations, and progression are similar to those reported in PD.

Unfortunately, the extant literature has failed to consider the compound influence that co-occurring OA may have on gait and balance performance in individuals with PD. Understanding this impact, of OA on PD symptomology, is critical to determine the extra burden that OA may contribute to mobility impairment in individuals with PD. Thus, we sought to understand to what extent the presence of OA impacts gait and balance performance in these patients.

Methods

Gait and balance performance was evaluated in 30 individuals with idiopathic PD (23M, 7F, age: 70 ± 5yrs, Hoehn & Yahr score: 2.0 ± 0.5) using a 12-camera 3D motion capture system (Vicon Motion Systems) and 3 embedded force plates (Bertec Corp). Participants received bilateral knee X-rays to determine the presence/severity of knee OA using the Kellgren-Lawrence (KL) classification system.

Overground gait was assessed while participants walked at their typical, comfortable pace and spatiotemporal metrics were analyzed. Quiet stance was measured during: 1) Rigid Surface Eyes Open (RSEO), 2) Rigid Surface Eyes Closed (RSEC), 3) Compliant Surface Eyes Open (CSEO), and 4) Compliant Surface Eyes Closed (CSEC). Ground reaction forces were collected for 30 sec and center of pressure based measures were used to quantify postural steadiness.

Two MANOVAs were used to separately compare the spatiotemporal gait data and the balance data between the PD and PDOA groups (α=.05). Cohen's d was used for effect size, with 0.2, 0.5, and 0.8 denoting small, medium, and large effect sizes respectively.

Results and Discussion

Sixteen of the 30 participants showed radiographic evidence of OA (i.e., KL scores >1) in at least one knee. We observed no significant differences between groups for gait measures (Λ=.802, F=1.543, p=.220), but moderate to large effect sizes suggest meaningful differences exist in gait velocity (Cohen's d= .642), step time (Cohen's d= .529), and time spent in single support (Cohen's d= .844). Specifically, those with PD and OA walk slower, with shorter step times and spend less time in single support on the affected limb (Fig. 1).

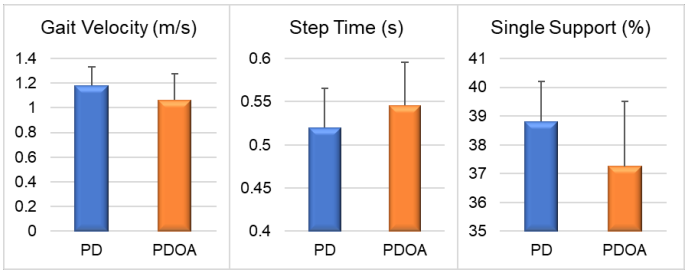

Figure 1: Spatiotemporal metrics between the PD and PDOA groups.

Although there were no significant differences between groups across balance conditions (Λ=.755, F=1.425, p=.254), a significant vision*surface interaction was observed as expected (Λ=.201, F=17.467, p<.001). Regardless of group, all participants decreased postural control as balance conditions became more difficult (Fig. 2).

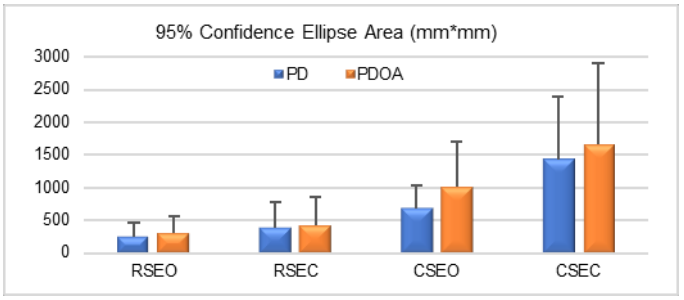

Figure 2: 95% Confidence Ellipse Area across quiet standing conditions.

Significance

Individuals with PD and co-occurring OA appear to have similar balance performance as those with PD alone. The presence of OA is, however, associated with meaningful, but not significant, decrements in gait measures in those with PD.

Acknowledgments

ASB Graduate Student Grant-In-Aid and the Elaine C. Pigeon Neurology Research Fund.

References

[1] Parkinson's Foundation (2018). www.parkinson.org
[2] Nisenzon et al. (2011). *Park Rel Disord*, **17**(2): 89-94.
[3] Hass et al. (2012). *PLoS One*, **7**(8):e42337.
[4] Jones et al. (2012). *Park Rel Disord*, **18**(10): 1073-1078.

AP laxity after TKA does not predict long-term quadriceps strength

Kenechukwu M. Okoye[1], Grant H. Berliner[1] Gregory M. Freisinger[2], Jacqueline M. Lewis[1], Jeffrey F. Granger[1], Andrew H. Glassman[1], Matthew D. Beal[3], Laura C. Schmitt[1], Robert A. Siston[1], Ajit M.W. Chaudhari[1]
[1]The Ohio State University, Columbus, OH; [2] US Military Academy, West Point, NY; [3]Northwestern University, Evanston, IL;
Email: okoye.13@osu.edu

Introduction

Studies have observed reduction in quadriceps activation and weakness in both the knee osteoarthritis (KOA) and post- total knee arthroplasty (TKA) populations as compared to healthy controls, and the mechanism and biomechanical mediators of this loss in function are areas of ongoing study. [1,2] In a set of patients with KOA awaiting TKA, we have shown that perceived instability is predicted by strength, but not varus-valgus laxity of the diseased knee measured intraoperatively [4], supporting previous work [5]. We have also shown that varus-valgus laxity is associated with weaker knee extension strength [6]. Two years post-TKA, these same patients' knee extension strength and stair climbing time both improve [3]. However, the relationship between anterior-posterior (AP) laxity and knee extension strength in either the KOA population or post-TKA remains unknown and has not been studied. Understanding this relationship could provide guidance on both surgical technique, i.e. whether a specific amount of AP laxity should be targeted, and on post-operative rehabilitation.

Therefore, in this study, our purpose was to test the hypothesis that intraoperatively measured knee AP laxity would be negatively associated with normalized quadriceps strength after two years.

Methods

Twenty-one IRB-consented patients (8 male, age 62.6 ± 8.5 years) diagnosed with predominantly medial compartment osteoarthritis and varus knee deformity participated. Potential participants were excluded for revision TKA, BMI > 45, or for requiring an assistive device for ambulation. One patient with bilateral involvement had each knee assessed separately, for a total of 22 knees.

Intraoperatively, a custom navigation system was used by the orthopaedic surgeon to track femoral translation during passive flexion after cruciate ligament excision and implantation of posteriorly-stabilized components (LPS Flex, Zimmer Biomet) [7]. Using the device's optical tracking markers and load cells, AP knee laxity data were collected after cementing in the prosthesis. With the knee straightened, anterior-posterior laxity was collected at +/-100N.

Within 30 days prior to their TKA (21.9 ± 24.8 days), subjects underwent evaluation of their involved limb quadriceps strength using a stationary dynamometer (Biodex, Shirley, USA). Subjects' maximum voluntary isometric contractions (MVIC) were recorded with the patient seated, their knees flexed at 60 degrees over 5 seconds with verbal encouragement throughout the task, then normalized by mass. The subjects returned 24 months post-op (787.4 ± 59.6 days) for the same quadriceps strength evaluation.

Forward stepwise regression was used to determine significant predictors of normalized 24-month post-operative quadriceps MVIC, considering normalized pre-operative quadriceps MVIC and ± 100N AP knee laxity measured intraoperatively.

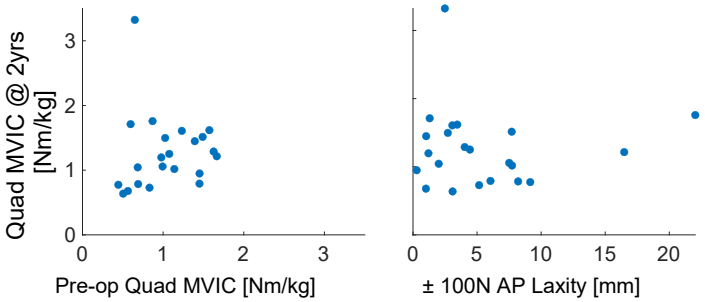

Figure 1: Subjects' pre-operative quadriceps MVIC and ±100N AP knee laxity plotted against two-year quadriceps MVIC.

Results and Discussion

Forward stepwise regression analysis selected neither pre-operative quadriceps normalized MVIC, nor ± 100 N AP knee laxity as significant predictors of 24-month post-operative quadriceps normalized MVIC (p = .817, .987, respectively).

This result differs from the ACL-deficient knee, where AP knee laxity has previously been implicated in quadriceps strength loss [8]. That relationship does not appear to exist in this population even though wide variation in AP laxity was observed (Figure 1). The data suggest the strength improvements observed in our previous study [3] are not driven by anterior-posterior laxity with the leg in extension. Potential limitations to this study include the lack of standardized rehabilitation prescribed to the subjects, the difference between knee flexion angles at which AP laxity and knee extension torque were measured, and small sample size. Further study will examine other aspects of intraoperative knee kinematics and their potential role in knee extension strength, in the context of perceived instability.

Significance

Though previous studies have shown long-term quadriceps strength increases among patients following TKA, AP laxity measured intraoperatively is not associated with quadriceps torque after two years.

Acknowledgments

NIAMS R01AR056700 | The Ohio State University MSTP

References

[1] Skou (2014) *Arthritis Care Res*, **66(5):** 695-701
[2] Stevens-Lapsley JE (2010) *Clin Orthop Relat Res,* **468(9):** 2460-8
[3] Couture G (2019) *J Orthop Sports Phys Ther,* **49(1)**: CSM84
[4] Chaudhari AMW (2019) *J Orthop Sports Phys Ther,* 49(7): 513-7
[5] Schmitt LC (2008) *Phys Ther,* **88(12):** 1506-16
[6] Freisinger GM (2017) *J Orthop Res*, **35(8):** 1644-52
[7] Siston RA et al. (2012) *J Biomech Eng* , **134:**115001
[8] Fossier E (1993) *Rev Chir Orthop Reparatrice Appar Mot,* **79(8):** 615-24

Muscle Forces and Contributions to Acceleration During Chair-Rise in Individuals with Total Knee Arthroplasty

Rachel K Hall[1], Elena J Caruthers[2], Greg M Freisinger[3], Jackie M Lewis[4], Laura C Schmitt[1], Ajit MW Chaudhari[1], & Robert A Siston[1]
[1]The Ohio State University, Columbus, OH [2]Otterbein University, Westerville, OH [3]United States Military Academy, West Point, NY
[4]ARCCA, Inc., Penns Park, PA
Email: siston.1@osu.edu

Introduction

The Sit-to-Stand (STS) transfer is a biomechanically challenging task commonly used to evaluate how individuals after total knee arthroplasty (TKA) rise from a chair[1,2]. Individuals after TKA perform this task more slowly, are more likely to fall, and demonstrate altered kinematics, kinetics, muscle strength and activations compared to healthy older adults[3-6]. Inter-limb differences (asymmetry) in STS kinematics, kinetics, and muscle activations between involved (INV) and uninvolved (UNINV) limbs in individuals with TKA have also been found[1,3], and our previous simulation work indicates that asymmetries in muscles forces and contributions to the acceleration of the body's center of mass (COM) are observed in young healthy individuals, as well[7]. Thus, it is important to investigate both how these variables differ between limbs and how these differences relate to patient function in individuals after TKA. As a result, this study's purposes were to 1) compare muscle forces and contributions to acceleration between limbs in individuals after TKA during a STS transfer and 2) relate chair-rise time, as an indicator of function, to asymmetries in muscle forces and contributions to COM acceleration.

Methods

Nine participants (7F/2M, 80.7±9 kg,1.6±0.1 m, 60.5±8 y) completed a 5-times STS transfer six months after TKA (210±80 days). We collected motion capture, ground reaction, and electromyography data using methods previously described[7].

We used OpenSim[8] to simulate one chair-rise using similar methods to our previous study[7]. We scaled an updated[9] Caruthers Full Body Model[7] with unconstrained knee rotations and strengthened hip and back muscles to match anthropometric data and determined kinematics and kinetics using an inverse dynamics approach. We used Static Optimization to estimate muscle forces by minimizing the sum of activations squared and ran an Induced Acceleration Analysis to calculate each muscle's contributions to horizontal and vertical COM accelerations [7].

For ten muscles, we used separate three-way repeated measures ANOVAs and post hoc Tukey t-tests to examine differences in peak forces (normalized by body weight, xBW) and contributions to acceleration between INV and UNINV limbs across STS phases: flexion-momentum (P1), momentum transfer (P2), and extension (P3)[7,10]. We then used Pearson correlation or Spearman rank tests to determine associations between chair-rise time (STS time) and asymmetries in both peak forces and peak contributions to acceleration (as defined by the percent difference and the absolute value of the percent difference[3]) (α=0.05).

Results and Discussion

Larger peak forces were observed in UNINV limbs than in INV limbs for the vastus lateralis (76±96% larger), vastus medialis (40±33% larger), semimembranosus (79±127% larger, P1 only), tibialis anterior (977±1750% larger, P2 only), and psoas (992±1830% larger, P3 only) ($p \leq 0.048$). Similarly, the UNINV limb had larger peak negative contributions to horizontal acceleration (decelerating the body's COM) in the vastus medialis (21±28% larger, P3 only) and tibialis anterior (318±1990% larger, P2 only) ($p \leq 0.038$) and larger peak contributions to vertical acceleration in the vastus lateralis (90±106% larger) and medialis (57±50% larger) ($p \leq 0.009$).

While some asymmetries were associated with slower STS times, others were associated with faster times. Slower STS times were associated with relatively greater tibialis anterior peak forces in the INV limb and greater relative tibialis anterior peak contributions to vertical acceleration ($p \leq 0.025$) in the UNINV limb in P1. Conversely, faster STS times were associated with greater relative peak contributions to vertical acceleration from the biceps femoris (long head) in the INV limb in P3 (Fig. 1, $p=0.003$), and greater symmetry in semimembranosus peak forces and contributions to horizontal acceleration ($p \leq 0.045$) between limbs in P1. Even though the vasti had significant inter-limb asymmetries and are a common focus of TKA rehabilitation, there were no significant associations between asymmetries in either the vastus lateralis or medialis and STS time ($p \geq 0.286$).

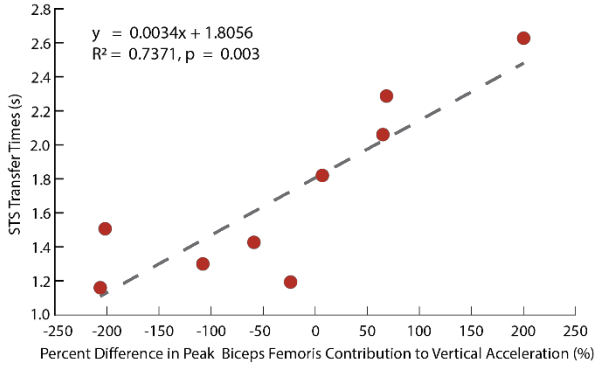

Figure 1: STS transfer time vs percent difference of biceps femoris (long head) peak contributions to vertical acceleration during P3. Negative values indicate that the INV limb was greater than the UNINV limb.

Significance

Understanding asymmetries in muscle forces, contributions to acceleration, and their associations with chair rise times can help inform how physical therapists may tailor rehabilitation protocols in order to help individuals after TKA more efficiently and safely perform activities of daily living, such as rising from a chair.

Acknowledgments

This project was supported by Grant Number R01 AR056700 from the National Institute of Arthritis and Musculoskeletal Skin Diseases.

References

1. Wang, et al. *J Arth* 2019 34: 2494-501. **2.** Su, et al. *Clin Biomech* 1998 13(3): 176-81. **3.** Christiansen, et al. *Arch Phys Med Rehabil* 2011 92: 1624-29. **4.** Boonstra, et al. *Phys Ther* 2010 90(2): 149-56. **5.** Bade & Stevens-Lapsley *J Orth Sports PT* 41(12): 933-41. **6.** Christiansen, et al. *J Orth & Sports* 2015. 45(9): 647-55. **7.** Caruthers, et al. *J App Biomech* 2016 32: 487-503. **8.** Delp, et al. *IEEE Trans Biomed Engr* 2007 54(11): 1940-50. **9.** Catelli, et al. *Comp Biomech and Biomed Engr* 22(1):21-4. **10.** Schenkman, et al. *Phys Ther* 1990. 70(10): 638-48.

Incremental lateral wedging for medial knee osteoarthritis: effects on frontal moment arm of the ground reaction force

Melvin Mejia[1], Jeffrey L. Cole[2], Peter Barrance[1,2]
[1]Center for Mobility and Rehabilitation Engineering Research, Kessler Foundation, West Orange, NJ, USA
[2] Department of Physical Medicine and Rehabilitation, Rutgers, The State University of New Jersey, Newark, NJ, USA
Email: mmejia@kesslerfoundation.org

Introduction

Knee osteoarthritis (OA) is a leading cause of pain and disability associated with diminished quality of life and significant burden to healthcare systems. Laterally wedged footwear insoles have been explored as low cost, conservative interventions having the potential to provide pain relieve and slow disease progression. Clinical evidence for treatment effectiveness has been mixed, and this has motivated studies of biomechanical effects to elucidate treatment mechanisms with a view to optimizing effect. A previous report [1] explored the effect of lateral wedging on the frontal plane moment arm (**MA_{GRF}**), also known as the lever arm, of the ground reaction force (GRF) vector about the knee joint center. The GRF vector usually passes medially to the knee center during the stance phase of walking gait; this is associated with a knee adduction moment which may overload the medial compartment. Lateral wedging lateralizes the center of pressure at ground contact and may thereby reduce this adduction moment. Here we report the effects of three levels of wedging on MA_{GRF} as measured in people with symptomatic knee OA.

Methods

We report results from 11 participants (7M, 4F, 59 ± 9.5 years). Research procedures were approved by the Kessler Foundation Institutional Review Board. Participants had symptomatic, predominantly medial knee osteoarthritis confirmed by physical examination and a standing frontal radiograph. Exclusions included advanced knee OA, more than minimal radiographic signs of lateral OA, and lower extremity joint replacement or recent surgery or viscosupplementation. One knee was assigned as the index knee based on clinical and radiological OA severity, and results are reported for this knee. All participants were tested while walking in standardized walking shoes (New Balance MW577) with lateral wedging of 3°, 6°, and 9°, as well as a neutral ('N') insole. Insoles were prepared by a professional pedorthist; the base insole was constructed of 5/16" thick neoprene, and lateral wedging of 3°, 6°, and 9° was added using cork layers applied to the full width tapering to zero thickness medially. Lengthwise, wedging was applied from the heel to the metatarsal heads.

Data were collected at two walking speeds; here we present data collected at a pace selected by each participant as typical for leisure walking. Testing order within walking speeds was randomized (N/3°/6°/9°). Standard motion analysis (Motion Analysis Corp., CA) and ground reaction force (GRF - Bertec Corp., OH) data collection and reduction methods were used. Walking trials were candidates for analysis if (1) speed was within ±5% of the initially established speed; (2) kinetic data were recorded for the complete stance phase. The peak knee adduction moment at the instant of the first peak of this moment was calculated for all trials, and a standard method for outlier removal was used before averaging across trials to generate final measures. The MA_{GRF} measure was calculated at the same instant using custom developed code to (1) compute the vector from the knee joint center to the closest point on the ground reaction force vector, and (2) compute the norm of the medial/laterally and superior/inferiorly directed components in the laboratory reference frame. Positive MA_{GRF} was computed when the GRF passed medial to the knee. Data were analyzed statistically using a repeated measures ANOVA with lateral wedge level as a repeated factor.

Results and Discussion

While ANOVA testing yielded no significant linear effect of wedge angle on MA_{GRF} ($p=0.220$), a significant quadratic effect ($p=0.016$) was found. The quadratic effect represented initial reduction in MA_{GRF}, followed by a weakening and reversal at higher wedging angles (Fig. 1). Paired t-tests showed MA_{GRF} to be significantly lower for the 3° condition than neutral, whereas the 6° wedge trended lower. Also, an ANOVA test across only the N/3°/6° conditions indicated a trend toward a linear main effect ($p=0.077$), representing reducing MA_{GRF} in this range.

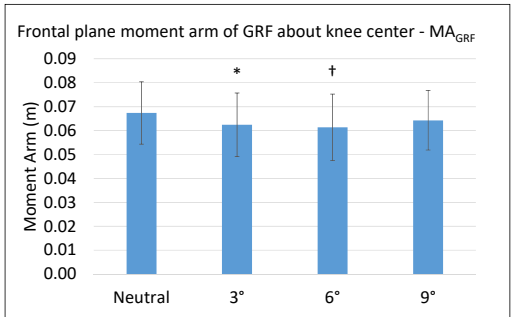

Figure 1: MA_{GRF} for all wedging conditions. *: significant difference for wedged condition relative to neutral wedge ($p=0.002$). †: trend of difference relative to neutral wedge ($p=0.077$).

Significance

The finding of reduced MA_{GRF} with lateral wedging in the range of 3° to 6° is consistent with prior reports on 5° lateral wedging [1]. These results suggest a limitation and potential reversal of effect of wedge level on reduction of MA_{GRF} as the level increases beyond this range. Overall, therefore, the results support a proposition that treatment efficacy across a group may be optimized in the 3° to 6° range. Ongoing work is examining the data for individual-specific responses that may contribute to variability of results in pooled analysis. It is important to recognize that individual patients may benefit most from specifically prescribed lateral wedging levels.

Acknowledgments

This study was supported by NIDILRR grant 90IF0077. Additional funding was provided by Kessler Foundation.

References

[1] Hinman et al. (2012) *Clin. Biomech* 27(1) pp. 27-33

A Biomechanical Processing Comparison between Frontal Plane Kinetics and Kinematics following Total Knee Arthroplasty

Laura M. Linsley.[1], Samantha Andrews[2], Cris Stickley[1], and Cass Nakasone[2]
[1]University of Hawaii at Manoa [2]Straub Medical Center
Email: lmflynn@hawaii.edu

Introduction

High knee adduction moment (KAM) and dynamic varus angle (VA) have been linked to both severity[1] and progression[2-6] of medial knee osteoarthritis (OA). Following total knee arthroplasty (TKA), increased KAM and VA may increase the risk of implant failure[7-8]. However, inconsistent data processing methodologies of previous research evaluating post-TKA changes in KAM and VA has contributed to the inconclusive and often conflicting results. The purpose of the current study was to determine how KAM and VA change over time by processsing method. KAM and VA were compared between Nexus and Visual 3D (V3d). Within V3d, KAM was determined by joint coordinate system (JCS) or segment resolution coordinate systems: thigh (TRCS) and shank (SRCS).

Methods

Nine participants (under 85 and able to walking without an aid) were diagnosed with knee OA and scheduled for unilateral or bilateral TKA by one orthopedic surgeon. Walking gait was assessed pre-TKA and post-TKA at six weeks, three months, six months, and one year. Kinematics (240Hz) of three walking trials were collected with 27 retroreflective markers placed in accordance with a Plug-in Gait model and time synchronized with kinectics (480Hz) collected from a force plate embedded flush with the floor. First peak KAM and VA were determined from Nexus and V3D. A Helen-Hayes model was created in V3D.

Repeated measures ANOVA was performed to compare main effects over time for each processing method. Pairwise comparisons between the factor level means were made using the Fisher's least significant different (LSD) method for multiple comparisons. Paired sample t-tests were used to determine mean differences between the processing methods at the same timepoints. Significance level was set at $p<0.05$.

Results and Discussion

The trend in KAM following TKA was significantly different between Nexus and varying coordinate systems within V3D (Table 1). The trend in VA was also significantly different between Nexus and V3D (Table 2). Of significant clinical importance, changes in KAM and VA appear to be dependent upon the software and coordinate system in which they are derived. Data processed in Nexus yields outcomes indicating an increase in KAM at one year post-TKA and a worsening of VA at six months and one year post-TKA, consistent with previous research[9,10]. Conversely, data processed with TRCS, SRCS, and JCS, suggest an improvement in KAM and VA post-TKA, consistent with previous research[11-13]. SRCS and JCS methods yielded similar results ($p > 0.05$) at each timepoint.

Table 1. KAM (Nm/kg) over time determined by four different processing methods

	Nexus			TRCS			SRCS			JCS		
Pre-TKA	0.66	±	0.18	0.60	±	0.13	0.59	±	0.13	0.5	±	0.27
Post-TKA												
6W	0.50	±	0.12	0.39	±	0.08*†	0.41	±	0.09*†	0.32	±	0.16*†
3M	0.56	±	0.16	0.44	±	0.07*†	0.41	±	0.08*†	0.34	±	0.18*†
6M	0.61	±	0.10	0.50	±	0.13†	0.46	±	0.09*†§	0.37	±	0.19*Ŧ†§
1Y	0.63	±	0.08^	0.50	±	0.09^Ŧ†	0.44	±	0.08*†§	0.39	±	0.22*†

Mean ± Standard Deviation; Nm/kg = Newton meter per kilogram; TKA = total knee arthroplasty; JCS = Joint Coordinate System; W = weeks; M = months; Y= Year
* = significantly different than pre-TKA; ^ = significantly different than 6 weeks post-TKA; Ŧ = significantly different than 3 months.
† = significantly different than Nexus; § = significantly different than Thigh.

Table 2. VA (°) determined by Nexus and V3D

	Nexus			V3D		
Pre-TKA	7.65	±	6.00	7.82	±	4.58
Post-TKA						
6W	0.40	±	4.92*	0.82	±	4.23*
3M	3.64	±	5.93	1.52	±	3.39*
6M	3.56	±	3.50^	1.79	±	3.67*Ŧ
1Y	6.37	±	4.58^	2.93	±	3.37*Ŧ

Mean ± Standard Deviation; TKA = total knee arthroplasty; W = weeks; M = months; Y= Year
* = significantly different than pre-TKA
^ = significantly different than six weeks post-TKA
Ŧ = significantly different than Nexus

Significance

The current study demonstrates that KAM and VA values calculated on the same subects produced significant processing related differences. These markers of TKA outcomes are clinically important; however, variability in outcomes may be due to processing methodology, versus actual changes. Further research is needed to clarify which method is prefered.

References

1. Baliunas AJ, et al. Increased knee joint loads during walking... Osteoarthr Cartilage. 2002 Jul;10(7):573–9.
2. Bennell KL, et al. Higher dynamic medial knee load predicts... Ann Rheum Dis. 2011 Oct;70(10):1770–4.
3. Miyazaki T. Dynamic load at baseline... Ann Rheum Dis. 2002 Jul 1;61(7):617–22.
4. Chang AH, et al. External knee adduction... Osteoarthr Cartilage. 2015 Jul;23(7):1099–106.
5. Woollard JD, et al. Change in Knee... J Orthop Sports Phys Ther. 2011 Oct;41(10):708–22.
6. Brisson NM, et al. Baseline knee adduction moment... J Orthop Res. 2017 Nov;35(11):2476–83.
7. Prodromos CC, et al. A Relationship between Gait... JBJS. 1985 Oct;65a(8):1188-1194).
8. Ritter MA, et al. Preoperative Malalignment... JBJS. 2013 Jan 16;95(2):126–131.
9. Orishimo KF, et al. Does Total Knee Arthroplasty Cha..? Clin Orthop Relat Res. 2012 Apr;470(4):1171–6.
10. Alnahdi AH, et al. Gait after unilateral total knee arthroplasty... J Orthop Res. 2011;29(5):647–52.
11. Mandeville D, et al. The effect of total knee replacement... Clin Biomech. 2008 Oct;23(8):1053–8.
12. Worsley P, et al. Joint loading asymmetries... Clin Biomech. 2013 Oct;28(8):892–7.
13. Hatfield GL, et al. The Effect of Total Knee Arthroplasty... J Arthroplasty. 2011 Feb;26(2):309–18.

Knee Moment Tracking During Elliptical Stepping With Different Foot Progression Angles

Raziyeh Baghi.[1], Ahmed Ramadan [1], Dongwon Kim [1], Li-Chuan Lo [1], and Li-Qun Zhang [1,2,3]
1. Department of Physical Therapy and Rehabilitation Science, University of Maryland, Baltimore
2. Department of Orthopaedics, University of Maryland, Baltimore
3. Department of Bioengineering, University of Maryland, College Park
Email: L-Zhang@som.umaryland.edu

Introduction

Knee adduction moment (KAM) is an indicator of the progression of medial knee osteoarthritis (OA). Higher occurrence of the medial compartment knee OA is attributed to excessive medial compartment compressive overloading, which is closely related to KAM. Therefore, in rehabilitation of patients with medial knee OA, reduction of KAM should be considered. Reduction in KAM could be achieved through a change in foot progression angle (FPA) [1]. However, this modification affects other knee moment components. In this pilot study, we investigate the effects of a change in FPA on total knee moment components while stepping, using a custom-designed elliptical trainer that produces less vertical loading on the knee in comparison to that of over ground walking. Also, the question as to whether the same patterns of KAM reduction repeats in different evaluation sessions days apart is evaluated.

Methods

A customized elliptical trainer with a 6-DOF ankle goniometer was used for the knee moment estimation while stepping on the elliptical trainer. A 6-axis force/torque sensor was mounted underneath each footplate to measure forces and moments in each direction. Footplates of this customized elliptical trainer are modified and can rotate in transverse plane. Five healthy subjects (female; 28-42 years old) with no history of lower limb injury participated in this study. They were asked to perform stepping on the elliptical trainer with their self-selected constant speed in the following order of FPA: neutral position, 5º toe-in,10 º toe-in, 5º toe-out, and 10º toe-out. Each condition lasted 1.5 minutes. Also, the same evaluation was conducted on a second day to examine the repeatability of the FPA that induces minimum KAM in each subject.

Results and Discussion

Results of this study showed a significant difference in KAM, knee flexion moment (KFM), and knee internal rotation moment (KITM) beween different stepping conditions across subjects ($P<0.05$), which is in line with another study [1] (Table.1). Although, all subjects showed reduction in KAM and KFM during multiple stepping conditions, the FPA that demonstrated the greatest decrease in KAM was subject-specific. The only study that evaluated the effect of different degrees of toe-in and toe-out on reduction in KAM for healthy subjects, reported the greatest reduction did not happen in the same position for all subjects [1]. Furthermore, peak KAM and peak KFM values during stepping with different FPAs almost had consisitant patterns between two days. Also, the FPA that induced the minimum KAM was different from the condition that induced minimum KFM in each subject (Fig.1). This observation can be explained by 3-D view of knee moment components (Fig.2). In other words, a decrease in one knee moment component is compensated by an increase in another knee moment component which induces a circular shape of 3-D knee moment components.

Table 1: Mean (SD) values of the knee moment components during stepping with different FPA. Knee moments normalized to the product of body weight (BW) and leg length (LL).

Knee moment component (%BW*LL)	Peak KFM	Peak KAM	Peak KITM	Peak KTM
Regular	13.43 (2.13)	5.17 (3.84)	0.50 (0.32)	8.76 (1.20)
5 toe in	12.49 (2.70)	5.54 (2.29)	0.59 (0.31)	13.78 (2.10)
10 toe in	13.25 (3.65)	3.46 (1.46)	0.48 (0.27)	13.59 (3.74)
5 toe out	12.03 (4.06)	3.22 (0.52)	0.34 (0.12)	12.73 (3.26)
10 toe out	12.66 (3.30)	3.43 (1.63)	0.42 (0.23)	18.97 (3.02)

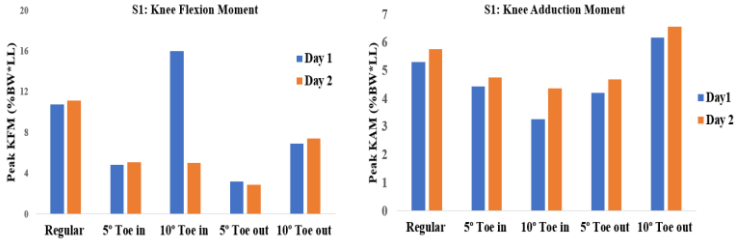

Figure 1: Between-day comparison of the peak KAM and peak KFM during stepping with different FPA in a subject.

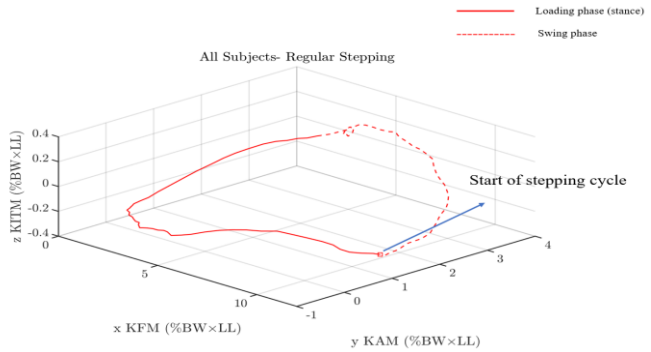

Figure 2: Tracking of three knee moment components among all subjects during regular stepping.

Significance

Our findings suggest the applicability of this modified elliptical trainer in design of a subject-specific rehabilitation program for indivuduals with medial knee OA.

Acknoledgements:

Li-Qun Zhang has equity positions in Rehabtek LLC, which received federal grants in developing the robotic device used un this study.

REFERENCES:

1. S. D. Uhlrich, et al. (2018). “Subject-specific toe-in or toe-out gait modifications reduce the larger knee adduction moment peak more than a non-personalized approach,” J. Biomech.

Countermovement Jump Phase-Specific Differences Between Fast and Slow Jumpers in Division 1 Collegiate Male Basketball Players

John Krzyszkowski[1], Luke D. Chowning[1], John R. Harry[1]
[1]Deptartment of Kinesiology & Sport Management, Texas Tech University, Lubbock, TX, USA
Email: john.krzyszkowski@ttu.edu

Introduction

Countermovement jump (CMJ) time (i.e., time to take off [TTT]) is a variable extracted from the CMJ force-time series to quantify the quickness of the CMJ (2, 3). In addition, TTT and has been used in conjunction with jump height to compute a reactive strength score, referred to as the modified reactive strength index (RSImod) (2). It was suggested that the downward portion of the CMJ be deconstructed into phases that reflect the center of mass (COM) movement effects while also including the predominant muscle action across the involved muscles driving changes in COM movement where appropriate (1). However, phase-specific variables explaining TTT are not well understood in trained populations. This study determined whether quick jumpers, defined by TTT, display superior performance in CMJ phase-specific (a) temporal , (b) yank (i.e., rate of force development), and (c) force production variables.

Methods:

Twenty-two collegiate male basketball players (height: 1.99±0.06m; mass: 93.8±7.5kg; age: 20±2 years) performed 3 CMJs while ground reaction force (GRF) data were obtained (1000 Hz) with two 3D force platforms (OPT464508, Advanced Mechanical Technology, Inc., Watertown, MA, USA). The raw GRF data was exported to Matlab (r2019a; The MathWorks, Inc., Natick, MA, USA) and then smoothed using a fourth-order, dual-pass, low pass Butterworth filter using a cutoff frequency of 50Hz with the order and cutoff before the two passes. Vertical center of mass (COM) acceleration was calculated using Newton's law of acceleration ($a = \Sigma F/mass$), where mass was calculated by dividing body weight (i.e., the average vertical GRF during the first 500 data points of quiet standing before the start of the CMJ trial) by the absolute value of gravitational acceleration (9.81 m/s/s). The vertical COM velocity was obtained by calculating the time-integral of vertical COM acceleration using the trapezoidal rule. The CMJ was deconstructed into unloading, eccentric yielding, eccentric braking, and concentric phases (1). The start of the unloading phase was defined as the instant when the vertical GRF decreased below a threshold equal to 2.5% calculated bodyweight value. The end of the unloading phase and the start of the yielding phase was defined as the local minimum vertical GRF succeeding the start of the unloading phase. The end of the yielding phase and the beginning of the braking phase was identified as the instant of peak negative COM velocity. The end of the braking phase and the beginning of the concentric phase was identified as the instant when vertical COM velocity was greater than 0 m/s after the start of braking phase. The end of the concentric phase was identified as the instant when vertical GRF decreased below 20N after the start of the concentric phase. Phase-specific RFD and force variables were normalized to body mass and calculated as the average RFD (i.e., force at the start and end of each phase divided by the duration of each phase) and discrete force magnitudes within the CMJ phases. The COM depth was calculated as the change in vertical position from the start of the unloading phase to the end of the braking phase. Independent samples t-tests (α=0.05) and Cohen's *d* effect sizes (large≥0.8) were used to compare performance between the fast and slow TTT groups.

Results and Discussion

RSImod (p<0.001, d=1.34), unloading time (p=0.008, d=1.25), unloading RFD (p<0.001, d=2.32), and unloading force (p<0.001, d=1.66), were significantly greater in the fast TTT group when compared to the slow TTT group. (Table 1). The COM depth was not significant (p=0.812, d=0.54) among groups. Since center of mass depth has been shown to influence TTT (4), the differences in TTT and phase durations cannot be attributed to individuals decreasing the depth of their countermovement, which in turn would shorten the duration of each phase and of the jump.

Table 1: Performance, temporal, force, and RFD parameters for the high and low TTT groups.

Variable	Low TTT Group		High TTT Group			
	Mean ± SD	95% CI	Mean ± SD	95% CI	*p*	*d*
Jump Height (m)	0.46±0.07	[0.41,0.51]	0.45±0.04	[0.42,0.48]	0.752	0.16
RSImod* (m/s)	0.66±0.13	[0.57,0.75]	0.52±0.07	[0.47,0.57]	0.005	1.34
COM Depth (m)	-0.26±0.06	[-0.30,-0.22]	-0.29±0.05	[-0.32,-0.26]	0.812	0.54
TTT* (s)	0.70±0.07	[0.65,0.75]	0.88±0.07	[0.83,0.93]	<0.001	2.57
Unload Time* (s)	0.16±0.07	[0.11,0.21]	0.29±0.13	[0.20,0.38]	0.008	1.25
Unload RFD* (N/kg/s)	-50.9±14.7	[-60.8,-41.0]	-21.7±10.1	[-28.5,-14.9]	<0.001	2.32
Unload GRF* (N/kg)	2.40±1.13	[1.64,3.16]	4.22±1.06	[3.51,4.93]	<0.001	1.66

Note: Data are presented as mean ± standard deviation, 95% confidence interval in brackets.
Abbreviations: RSImod, modified reactive strength index; TTT, time to takeoff; COM depth, center of mass depth; RFD, rate of force development; *d*, Cohen's *d* effect size.

Significance

Quick jumpers appear to demonstrate superior (i.e., quicker and more forceful) unloading strategies that slower jumpers in a population of collegiate male basketball players.

References:

1..Harry JR, Barker LA, and Paquette MR. *Med Sci Sports Exerc*, In Press, 2019.
2..Kipp K, Kiely MT, and Geiser CF. *J Strength Cond Res* 30: 1341-1347, 2016.
3..McMahon JJ, et al.*Int J Sports Physiol Perform* 13: 220-227, 2018.
4..Petridis L, et al. *AJSS* 5: 21-26, 2017.

Bivariate Functional Principal Component Analysis of Bar Trajectories during the Snatch

Kristof Kipp[1], Aaron Cunanan[2], and John Warmenhoven[3]
[1]Department of Physical Therapy – Program in Exercise Science, Marquette University, Milwaukee, WI, USA
[2]San Francisco Giants, San Francisco, CA, USA
[3]Australian Institute of Sport, Canberra, Australia
Email: *kristof.kipp@marquette.edu

Introduction

One of the primary biomechanical variables analyzed in the sport of weightlifting is the trajectory of the bar, in part because it captures key aspects related to weightlifting technique and performance [1, 3]. Bivariate functional principal components analysis (*bf*PCA) is a statistical technique that has been used to investigate differences in the shapes of two simultaneously varying time series data [2, 4]. Application of *bf*PCA to barbell trajectory pattern would enable weightlifters, coaches, and sports biomechanists to quantify the shape of, or patterns in, the trajectory throughout the entire snatch and provide a way to analyse these patterns in relation other biomechanical variables related to either weightlifting performance, technique, etc. The purpose of this study was to use *bf*PCA to quantify the patterns of barbell trajectories during the snatch and to correlate these patterns with biomechanical variables related to weightlifting performance.

Methods

The participants of this study consisted of six competitive weightlifters (body-mass: 97.6 kg). Data were collected during the snatch session of a competition with a six-camera motion analysis system at 250 Hz. All three attempts (90-105 kg) from each of the six weightlifters were recorded. The horizontal and vertical position of markers attached to the bar were extracted and smoothed with a 4th order low-pass Butterworth filter at a cut-off frequency of 6 Hz, determined through residual analysis. Peak vertical bar velocities during the second pull were calculated and extracted. Time-normalised horizontal and vertical position data from each lift were centered, concantenated, and pooled into a single matrix and used as input for the *bf*PCA [2, 4]. Correlations between *bf*PC scores and body-mass normalised barbell mass and peak vertical barbell velocity were analysed with Spearman's rho correlations. Bootstrap resampling was performed 100 times to establish 90% confidence intervals for each correlation. The significance level was set to 0.05, and only correlation coefficients where the bootstrapped 90% confidence interval did not cross zero were interpreted as significant.

Results and Discussion

The *bf*PCA extracted bar trajectory patterns related to forward/backward shifts (pattern 1), peak height (pattern 2), and crossing of the vertical reference line (i.e., "0" on the x-axis) (pattern 3). Non-parametric correlation analysis showed that bar mass (normalised to body-mass) of each lift was correlated with pattern 1 (ρ = -0.736) and 3 (ρ = 0.751), whereas peak vertical bar velocity was only correlated with pattern 1 (ρ = 0.580).

Pattern 1 captured a general forward/backward shift in bar trajectory during the entire lift phase. The variation explained by this pattern captured bar path trajectories typically classified as A or B type trajectories (both exhibit initial backward motion, but only A type trajectories cross the vertical reference line) [4]. The results suggest that B type trajectories were associated with better lift performance (i.e., greater bar mass), whereas A type trajectories were associated with greater peak bar velocities.

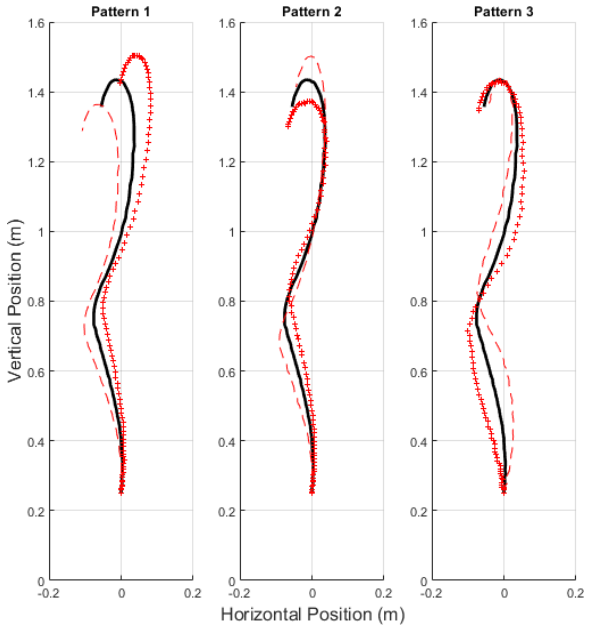

Figure 1: Variations in bar trajectories captured by the three *bf*PCs (i.e., patterns 1-3). Ensemble average bar trajectories are given by the black line, whereas the effect of positive and negative *bf*PC scores on bar trajectories are given by the + and - symbols, respectively.

Pattern 3 captured variation related to the crossing of the vertical reference line in bar trajectories during the first and second pull phases. More specifically, the variation explained by this pattern captured bar path trajectories typically classified as either an A or C type (where A type trajectories exhibit an initial backward motion and C type trajectories exhibit an initial forward motion that crosses the vertical reference line) [4]. The results suggest that in the current sample, better performance (i.e., lifted greater barbell mass) was associated with A type rather than C type trajectories.

Significance

Better weightlifting performance in the snatch was associated with bar trajectories that exhibited an initial backward motion and did not cross the vertical reference line during the second pull. In addition, these trajectories were associated with smaller peak velocities, which may imply a more efficient technique.

References

1. Baumann et al. (1988). *Int J Sport Biomech*, 4, 68-89.
2. Ryan et al. (2006). Sports Biomech, 5, 121-138.
3. Stone et al. (1998). *Strength Cond,* 20, 30-38.
4. Warmenhoven et al. (2019) S*ports Biomech*, 18, 10-27.

The Effects of Isokinetic Testing Speed on Ham:Quad Ratios and Asymmetry Indexes

Ben W. Meyer
Shippensburg University, Shippensburg, PA, USA
Email: bwmeyer@ship.edu

Introduction

The purpose of this project was to examine the ratio between the hamstrings and quadriceps (H:Q ratio) and strength asymmetry index (AI) between right and left legs in isokinetic knee torque testing. Previous literature has examined the effects of training methods on the H:Q ratio and found an increase in the ratio as testing speed increased [1]. A study of intercollegiate athletes showed the same trend in a variety of sporting populations [2]. In male distance runners, the magnitude of the AI increased with increasing speed for flexion, but the magnitude of the AI decreased with increasing speed for extension [3]. It was hypothesized that in a sample of healthy college students, the H:Q ratio would increase and the magnitude of the AI would increase as isokinetic testing speed increased.

Methods

Twelve males and seven females (age = 21 ± 1 yrs; mass = 83 ± 18 kg; height = 1.74 ± 0.11 m) participated in the study. Each participant performed isokinetic knee extensions and flexions on both right and left legs using a Biodex Isokinetic Dynamometer. Three speeds were tested on the dynamometer: 60, 180, and 300 degrees per second. The dynamometer recorded peak extension and flexion torques for both right and left limbs at each speed. Hamstring:quadriceps ratio and strength asymmetry index were computed using standard procedures. A two-way 3 x 2 mixed ANOVA was used to check for the presence of differences. Statistical significance was set at $\alpha = 0.05$.

Results and Discussion

Figure 1 shows the H:Q ratios for right and left legs across the tested velocities. No significant interaction was found for H:Q ratio for velocity $F(2,48) = 0.10$, $p > 0.05$. The main effect of leg was not significant $F(1,48) = 1.18$, nor was the main effect of testing velocity $F(2,48) = 1.79$, $p > 0.05$. Although no significant differences were found, a modest increase in the H:Q ratio was noted as testing velocity increased.

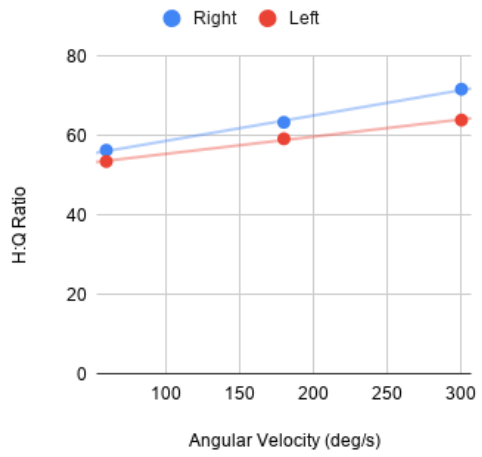

Figure 1: Hamstring:quadriceps ratios for right and left legs across angular velocities of 60, 180, and 300 degrees per second.

Figure 2 shows the AI values across the tested velocities. No significant interaction was found for H:Q ratio for velocity $F(2,48) = 0.19$, $p > 0.05$. The main effect of leg was not significant $F(1,48) = 0.82$ nor was the main effect of testing velocity $F(2,48) = 1.27$, $p > 0.05$. Although no significant differences were found, the AI values were positive at 60 degrees per second but negative at larger angular velocities. In addition, as the testing velocity increased, the magnitude of the AI values also increased.

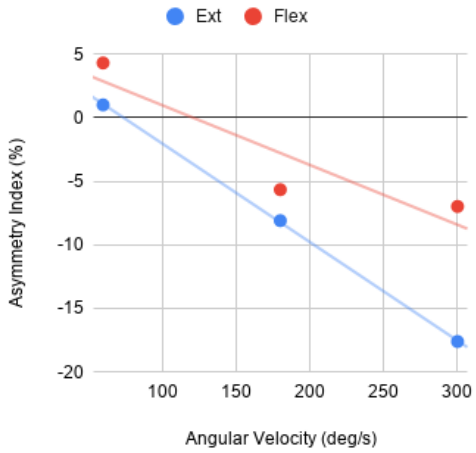

Figure 2: Strength asymmetry indexes for extension and flexion across angular velocities of 60, 180, and 300 degrees per second.

Significance

The H:Q ratios and AI values found in this study fall within the ranges provided in previous literature. The H:Q ratio may be used as a baseline to assess imbalances and those who might be at risk for knee injury [1]. In addition, the changes in AI values across testing speeds, while not significant, do suggest that the symmetry between right and left legs varies with different testing speeds. The functional impact of AI values may vary by sport, and the effects of AI values in excess of 10% on performance need to be examined further [3]. Future research should address the changes in H:Q ratio and AI across testing speeds in larger samples and across broader varieties of participants.

Acknowledgments

The author would like to thank the College of Education and Human Services at Shippensburg University.

References

[1] Bemben MG et al. (2019). *Int J Ex Sci,* **12:** 1080-1093.
[2] Rosene JM et al. (2001). *J Ath Train,* **36:** 378-383.
[3] Dellagrana, RA et al. (2015). *Int J Sp Phy Th,* **10:** 514-519.

Shoulder, hip, and trunk sagittal plane kinematics during stand up paddle boarding

Corina Kaufman and Jamie E Hibbert
Department of Kinesiology, California State University San Marcos, San Marcos, CA, USA
Email: jhibbert@csusm.edu

Introduction

Stand up paddle boarding (SUP) is a growing sport with an increasing number of recreational participants. SUP has been shown to be a good exercise modality to improve cardiovascular fitness [1,2]. Due to the relative simplicity of SUP most recreational participants are self-taught and are not aware of specific techniques that may be helpful for optimizing performance and avoiding injury. There are studies that have been published outlining common injuries sustained by SUP participants [3,4]. Currently, there is only a single study that has been published examining any biomechanical parameters of SUP. This study focused on differences in the SUP stroke between experienced and inexperienced SUP participants [5]. There is still a need to establish kinematic characteristics of SUP technique adopted by injury-free recreational participants.

The purpose of the current study was to analyse sagittal plane kinematics during both standing and kneeling postures commonly adopted by recreational SUP participants. It is also unknown whether there are differences in kinematics between sexes. We hypothesized that there would be greater sagittal plane joint excursion at the trunk and hip while standing, and greater sagittal plane joint excursion at the shoulder while kneeling. We also hypothesized that there would be greater sagittal plane joint excursion at the shoulder in male participants, and greater sagittal plane joint excursion at the trunk and hip in female participants.

Methods

18 self-identified recreational stand up paddle boarders, 7 males and 11 females (22.6 ± 2.15 years), were recruited from the community. All study related procedures were approved by the CSUSM IRB. Informed consent was obtained prior to participation. Participants were fitted with a standard 32 marker set for 3D motion capture (Qualisys, Goenborg, Sweden). Participants performed six paddling trials in both kneeling and standing postures using a stand up paddle board ergometer (SUP ergometer, KayakPro, Miami, FL). Kinematic data were evaluated for differences in shoulder, hip, and trunk excursion in the sagittal plane. The data were also evaluated to determine any sex differences in shoulder, hip, and trunk sagittal plane kinematics. An a priori alpha level was set at α=0.05. All statistical analyses were conducted using paired t-tests (Excel, Microsoft, Redmond, WA).

Results and Discussion

There were significant positive differences in mean joint excursion for both left and right side paddling at the left hip (p=0.005; p=0.007), right hip (p=0.001; p=0.002), and trunk (p=0.008; p=0.01) (Figure 1). There were significant negative differences in mean joint excursion for both left and right side paddling at the left (p=0.0004; p=0.001) and right shoulders (p=0.0002; p=0.0006) (Figure 1).

There were no significant differences noted between sexes in mean joint excursion at the shoulders, hips, or trunk regardless of posture or paddling side.

These data support our hypothesis that sagittal plane joint excursion would be greater at the trunk and hip while standing and greater at the shoulder while kneeling. Our hypothesis that there would be significant differences in sagittal plane kinematics with sex, was not supported by these data. Data collection is ongoing to determine whether any sex-related difference emerge with more equal groups of male and female participants.

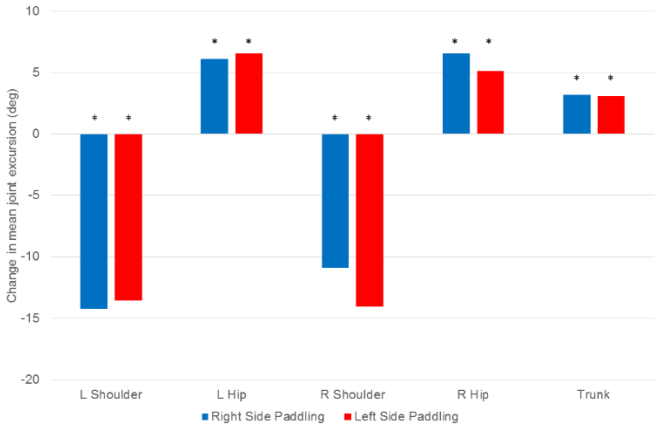

Figure 1: Mean differences in sagittal plane joint excursion between kneeling and standing postures. A negative value indicates greater excursion kneeling. A positive value indicates greater excursion standing. * indicates significance at α=0.05.

Significance

The purpose of this study was to examine the sagittal plane kinematics of stand up paddle boarding in two commonly adopted postures; standing and kneeling. There has not been any previous reporting on kinematics for recreational stand up paddle boarders. These data collected from healthy, pain-free participants may be used in the future to examine differences between healthy and pathological participants to explain the common injuries noted in previous studies [3,4].

These data may also be helpful for developing coaching material for use by self-taught stand up paddle boarders.

Acknowledgments

The authors thank M. Becker for his help on this project.

References

[1] Ruess, C, et al. (2013). *Procedia Eng*, **60**: 62-66.
[2] Schram, B, et al. (2016). *BMC Sports Sci Med Rehabil*, **8(1)**: 32.
[3] Furness, J, et al. (2017).Orthop J Sports Med, **5(6)**: 2325967117710759
[4] Griffin, AR, et al. (2018). *Clin J Sport Med*, **(30)1**: 67-75.
[5] Schram B, et al. (2019). *PeerJ*, **7**: e8006

The Validation of a Portable Dual-Force Plate System for Assessing Countermovement Jump Performance

Grace E. Crowder[1*], Brett S. Pexa[2], Kevin R. Ford[3], and Justin P. Waxman[1]
[1]Department of Exercise Science, High Point University, High Point, NC
[2]Department of Athletic Training, High Point University, High Point, NC
[3]Department of Physical Therapy, High Point University, High Point, NC
Email: *gcrowder@highpoint.edu

Introduction

The analysis of kinetic data recorded via force platforms and their associated software is becoming increasingly common in the sport performance and injury literature, as portable systems allow for greater opportunity to screen athletes on a massive scale. However, understanding the validity of such systems is necessary prior to their widespread use. Therefore, the purpose of this study was to validate the use of a portable dual-force platform against the current gold standard. We hypothesized that the portable system would be a valid measurement tool.

Methods

As part of their pre-season screening, 69 NCAA Division-I athletes (19.5 ± 1.3 yr, 1.8 ± 0.1 m, 79.0 ± 9.1 kg) performed three maximal-effort countermovement jumps (CMJ) on two separate force-plate systems. System #1 (Method A; gold standard) consisted of two laboratory grade in-ground force plates (AMTI, Watertown, MA) sampling at 1200 Hz, whereas system #2 (Method B) consisted of a portable dual-force plate system (Hawkin Dynamics, ME) sampling at 1000 Hz. Both systems were integrated with their respective manufacturer-provided software for data collection and reduction. Athletes were allowed to swing their arms, and were instructed to jump with maximal effort. Three-trial averages were calculated for each athlete's velocity at takeoff and vertical jump height. Validity was assessed via Pearson's correlation coefficients between the two methods. Bland-Altman plots and 95% limits of agreement (LOA) analysis were then used to assess absolute measurement consistency between the two methods.[1,2]

Results and Discussion

Pearson's correlation coefficients indicated strong positive associations between methods for both take-off velocity (r = 0.862, r^2 = 0.743; p < .001) and jump height (r = 0.863, r^2 = 0.745; p < .001). Bland-Altman plots displaying the mean difference between methods for take-off velocity and jump height are shown in Figure 1A and 1B. LOA analyses (absolute measurement error) revealed good agreement between methods with mean differences (Method A – Method B) of 0.03 m/s (95%LOA: 0.24, 0.30 m/s) and 0.26 cm (95%LOA: -7.10, 7.63 cm) for take-off velocity and jump height, respectively. In 95% of the cases, jump height recorded using the portable system (Method B) could be expected to range anywhere from 7.10 cm lower to 7.63 cm higher than that measured by the gold standard (Method A; Figure 1B). In support of our hypothesis, and in agreement with prior work [3], these results indicate that the portable dual-force plate system examined is a valid method for evaluating CMJ performance. Figure 1A,B shows that mean differences are reduced as take-off velocities and jump heights increase, suggesting that the current findings may have been influenced by within-subject factors such as individual effort or level of experience. Allowing athletes to swing their arms during CMJ trials may have also been a factor.

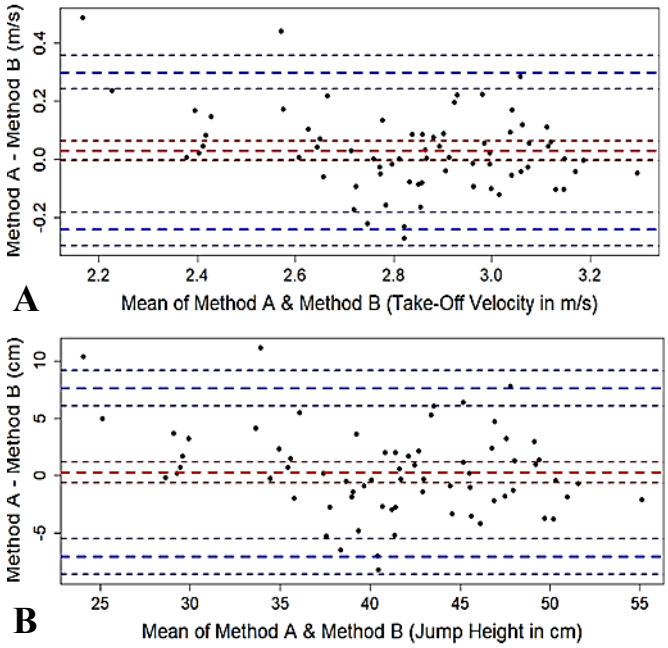

Figure 1. Bland-Altman plot displaying the mean difference and 95% limits of agreement for vertical velocity at takeoff [A] and maximal vertical jump height [B].

Significance

Portable force plates allow for more cost-effective options to screen athletes outside of the laboratory. Although jump mats and other inexpensive pieces of equipment can also be used to assess vertical jump height, a portable dual-force system can provide researchers and practitioners with force-derived metrics in addition to information regarding asymmetrical loading, countermovement depth, rate of force development, etc.; and can thus serve a variety of applications. More on-site athlete screenings may help improve performance techniques and reduce injury risk.

References

1. Altman DG, Bland JK. Measurement in medicine: the analysis of method comparison studies. *Statistician* 1983;32:307-17.

2. Bland JK, Altman DG. Measuring agreement in method comparison studies. *Stat Methods Med Res* 1999;8:135-60.

3. Walsh MS, et al. The validation of a portable force plate for measuring force-time data during jumping and landing tasks. *J. Strength Cond. Res.* 2006,20(4):730-734.

The effects of fatigue on knee mechanics during a landing and cutting task in healthy females: a statistical parametric mapping approach

Shelby A. Peel[1], Jake A. Melaro[1], Joshua T. Weinhandl[1]
[1]The University of Tennessee, Knoxville, Knoxville, TN, U.S.A.
Email: speel@vols.utk.edu

Introduction

Muscular fatigue is a controversial lower extremity injury risk factor, in part due to its complexity. It is thought that when an individual becomes fatigued, the musculature's ability to absorb energy is reduced, leading to decreases in neuromuscular control and altered lower extremity mechanics [1,2]. Few studies have observed the effects of fatigue on lower extremity mechanics in healthy females, which as led to conflicting results. Because fatigue in athletics is unavoidable, a better understanding of its influence on lower extremity mechanics is warranted.

Therefore, the purpose of this study was to determine the effects of muscular fatigue on lower extremity kinematics and kinetics in healthy females using a laboratory-based fatigue protocol. We hypothesized that lower extremity kinematics and kinetics would be different pre- to post-fatigue.

Methods

Six healthy, recreationally active females (23.0 ± 2.7 yrs, 68.2 ± 7.0 kg; 1.65 ± 0.6 m) volunteered to participate in this study. Participants first completed a 5-minute self-selected warm-up, followed by five box land-and-cut trials from a 30 cm box placed ½ their height from the force plates. The box land-and-cut task required participants to jump off the box with their left foot, land on the force plate with their right foot and make a 45° cut to the left. They then completed a laboratory-based fatigue protocol, before returning to the laboratory to perform five additional box land-and-cut trials. Briefly, the fatigue protocol consisted running to 4 different exercise stations and performing various types of body weight exercises. Participants were asked to complete as many rounds as possible, and the protocol stopped when participant maximal jump and reach height decreased 25% during two consecutive jumps.

A 12-camera motion capture system (200Hz, Vicon) and a force platform (2000Hz, AMTI) were used to collect marker coordinate and GRF data, respectively. Visual3D (C-Motion) was used to process and analyze all data. Marker coordinate and GRF data were filtered using fourth-order Butterworth low-pass filters with cut-off frequency of 12 Hz. 3D knee joint kinematics were calculated using a joint coordinate system approach. 3D internal knee joint moments were expressed in the joint coordinate system and normalized to body mass. Pre- and post-fatigue knee kinematics and kinetics were compared across the landing phase with one-dimensional statisticial parametric mapping t-tests (SPM{t}; (α=.05).

Results and Discussion

Participants completed 9 ± 5 rounds of the fatigue protocol (end heart rate: 187.1 ± 7.2 bpm; end RPE: 18.3 ± 1.5) with a decrease in jump height of approximately 14% from pre- to post-fatigue. SPM{t} showed that internal knee abduction moment post-fatigue was significantly greater (mean difference: 0.12 Nm/kg) from 19% to 23% of stance phase compared to pre-fatigue (Figure 1). No statistically significant differences were found between knee flexion, abduction, and rotation angles as well as knee extension and rotation moments pre- and post-fatigue during stance phase of the anticipated box-land-and-cut task.

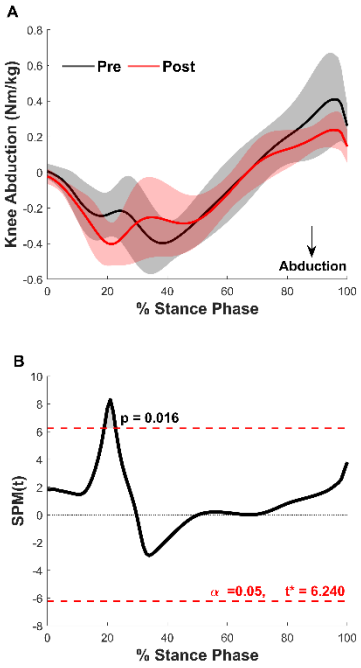

Figure 1: Results from the SPM{t} analysis of knee abduction moment pre- and post-fatigue. A) Black line: pre-fatigue time series, Red line: post-fatigue time series. B) Grey shaded region: supra-threshold cluster representing statistically significant difference.

Significance

Our results indicate that muscular fatigue may play a role in influencing knee kinetics (i.e. knee abduction moment), but not knee kinematics in healthy females. Even more interestingly, by observing the pre- and post-fatigue time series (Figure 1), it appears that fatigue also influences the timing of peak knee abduction moment. During pre-fatigue, peak knee abduction moment occurred at approximately 40% of the stance phase, while post-fatigue peak knee abduction moment transpired at approximately 20% of stance phase. It is plausible that the anticipatory nature of the box-land-and-cut task caused the body's predetermined motor program to adjust muscle mechanics during the stance phase after fatigue [3,4]. Previous research also indicates the body changes optimal movement strategy to perform tasks pre- and post-fatigue [5]. As such, future research is needed to understand this phenomenon.

References

1. Borotikar et al. (2008) *Clin Biomech,* Vol **23**, 81-92.
2. Mair et al. (1996) *A J Sports Med,* Vol **24**, 137-43.
3. Xia et al. (2017) *J Healthc Eng,* 1-8.
4. Kernozek et al.(2008) *Am J Sports Med,*Vol **36**(3), 554-65.
5. Monjo et al. (2015) *Hum Mov Sci,* Vol **44**, 225-33.

Cutting Down on Cutting Injuries: Knee Flexion and ACL Injury Risk at Different Levels of Competitive Women's Ultimate Frisbee

Paul R. Slaughter, Peter G. Adamczyk
Department of Mechanical Engineering, University of Wisconsin, Madison, WI, USA
Email: pslaughter@wisc.edu

Summary:
Ultimate frisbee players have a high rate of ACL injuries. We studied high-risk cutting maneuvers in women's Ultimate across 3 different leagues using lower body wearable motion sensors. More advanced players showed less knee flexion during cut deceleration, suggesting higher ACL strain. This comparison, along with forces and impulses, will reveal at risk populations among different Ultimate leagues.

Introduction:
Injuries in Ultimate, such as anterior cruciate ligament (ACL) tears, are common [1] and occur at higher rates than in other collegiate club sports [2]. In these leagues, women get hurt twice as often as male Ultimate players and are at a greater risk of ACL tears [2]. Despite these high injury risks, Ultimate has rarely been studied in clinical or biomechanical research.

To better evaluate ACL injury risk in Ultimate, we tracked the cutting maneuvers of female players during competition, and then examined their knee kinematics. Cutting was examined because of its high injury risk. Knee flexion angle was used to examine quadriceps dominance, a prominent mechanism of ACL injury: greater quadriceps dominance leads to less knee flexion, causing greater ACL strain [3]. Thus, differences in knee flexion may quantify the relative ACL injury risk experienced by players in different leagues.

Methods:
11 female Ultimate players played in 16 tournament games in three different leagues (intermediate collegiate, advanced collegiate, club) while wearing motion tracking sensors, including a lower body XSens MVN Awinda inertial sensor system (7 segments) and a VX Sport GPS sensor. Movement was reconstructed using the XSens lower-body model, including spatial displacement and bilateral limb pose. For each foot contact gathered during game play, pelvis acceleration and knee rotations were calculated. Cuts were defined as movements beginning from at least 2 m/s running speed, followed by a sequence of 2-7 deceleration (Dec) steps, a 60˚ or greater change in direction, and 2-7 acceleration (Acc) steps, and finally ending at a running speed above 2 m/s again (see Fig 1 for an example).

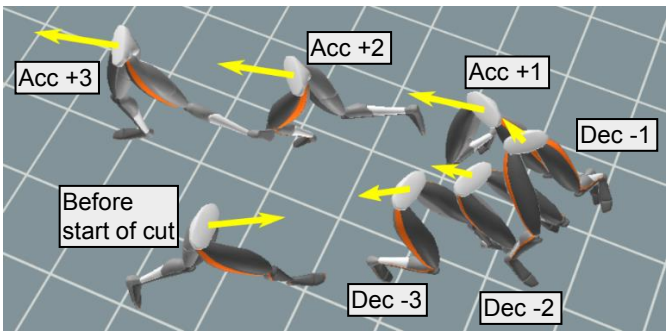

Figure 1: Footfall impulses throughout a cut. This cut features 3 deceleration steps and 3 acceleration steps.

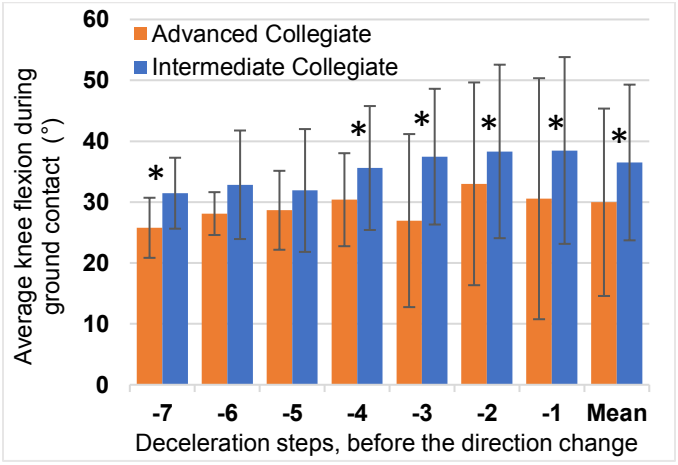

Figure 2: The average knee flexion for the players on the advanced and intermediate collegiate teams. Asterisks represent statistical difference between teams.

Forces and impulses were estimated during cutting maneuvers using pelvis acceleration as an estimate of whole-body center of mass acceleration. To examine quadricep dominance, the average knee flexion during ground contact for each cut deceleration step was calculated.

Results and Discussion:
79 points of play were recorded, lasting a mean of 2.4 minutes and containing a mean of 3.4 cuts. Fig 1 shows an example cut with the impulse for each footfall overlaid on the Xsens kinematic model showing mid-stance body configuration on each step of the cut. Fig 2 shows that players on the advanced collegiate team exhibited less knee flexion than players on the intermediate teams. This suggests that advanced players exhibit greater quadriceps dominance, potentially putting them at a higher risk of ACL injury. This straighter leg among more advanced players correlates with greater deceleration during cutting (1.66 m/s^2) than in intermediate players (1.07 m/s^2).

Significance:
This study is important to the field of sport biomechanics because measuring natural movements during competitive games is more realistic and representative than controlled movements in a laboratory. Additionally, results regarding quadricep dominance, along with impulse data, will help build the foundation for understanding cutting maneuvers in real Ultimate games. Knowing more about the mechanics of cutting in Ultimate will help to develop a preventative training program; such programs have been successful in other sports at reducing ACL injuries [3]. Knowing which leagues are most at risk of ACL injury will help to effectively disseminate this new knowledge.

References:
[1] Hess M et al. (2020) JoAT, **55**: 195-204
[2] Akinbola M et al. (2015) *IJSPT*, **10**: 75-84
[3] Hewett T et al. (2010) NAJSPT, **5**: 234-251

Relationships Between Vertical Stiffness and Jump Performance in NCAA Division-I Athletes

Meghan E. Haser[1*], Brittany M. Warren[1], Kevin R. Ford[2], Brett S. Pexa[3], and Justin P. Waxman[1]
[1]Department of Exercise Science, High Point University, High Point, NC
[2]Department of Physical Therapy, High Point University, High Point, NC
[3]Department of Athletic Training, High Point University, High Point, NC

Email:* mhaser@highpoint.edu

Introduction

It is well accepted that some level of lower-extremity stiffness is necessary to safely stabilize the joints during dynamic activity, with higher stiffness levels generally regarded as being beneficial for athletic performance.[1] To this end, greater stiffness is reported to be associated with greater running economy, running speed, and peak propulsive power, among others.[2] However, this evidence is limited by small sample sizes and a lack of stratified research designs, making it difficult to tease out the true extent to which such measures are related. Therefore, the purpose of this study was to evaluate the extent to which vertical stiffness (K_{Vert}) is related to maximal vertical jump height and peak propulsive power measured during maximal countermovement jumps.

Methods

Ninety-one NCAA Division-I athletes (Baseball = 34, Men's Soccer = 27, Women's Soccer = 30; 19.35 ± 1.24 years, 1.76 ± 0.09 m, 75.87 ± 10.83 kg) performed a series of three maximal-effort countermovement jumps (CMJ) and the K_{Vert} assessment atop a portable dual-force plate system. For the CMJ, athletes were permitted to swing their arms. Maximum vertical jump height (cm) and peak propulsive power (W) were then extracted from each of the CMJ trials and averaged prior to analysis. K_{Vert} was assessed via stationary, double leg, barefoot hopping at a set target frequency of 2.2 Hz. For each hop, initial contact and toe-off were defined as the instants at which the vertical ground reaction force (vGRF) became greater than and less than 10 N, respectively. K_{Vert} was then calculated as the ratio between peak vGRF and maximum center-of-mass displacement (kN/m).[3] As both propulsive power and K_{Vert} are associated with body size, these variables were also expressed, and statistically analyzed, relative to body mass (W/kg and kN/m/kg). Differences in demographics and all other variables of interest were evaluated via a preliminary one-way ANOVA. Relationships between K_{Vert} and CMJ performance were examined via simple regression. All analyses were performed with an a-priori alpha level of ≤ 0.05.

Results and Discussion

Significant differences in body mass, peak vGRF, absolute and normalized K_{Vert}, jump height, and absolute and normalized peak power were identified across sport ($p < .05$). Men's baseball and soccer athletes were taller, had greater body mass, and displayed higher peak vGRFs, absolute K_{Vert}, jump height, and both absolute and normalized peak power compared to women's soccer ($p < .05$; Table 1). Additionally, men's baseball displayed higher jump heights and absolute peak power compared to men's soccer ($p < .05$); however, the difference in peak power was not statistically significant following normalization to body mass ($p = .110$; Table 1). Men's soccer displayed greater normalized K_{Vert} than men's baseball and women's soccer ($p < .05$); however, there was no difference in normalized K_{Vert} between men's baseball and women's soccer athletes ($p = .546$; Table 1). Regression analyses revealed absolute K_{Vert} to be weakly related to jump height ($R^2 = .179$., $p < .001$) and absolute peak power ($R^2 = .310$., $p < .001$) when all athletes were pooled together; however, the relationship between absolute K_{Vert} and absolute power only remained significant in women's soccer ($R^2 = .165$, $p = .026$) when evaluated by sport. Following normalization, K_{Vert} was not found to be related to jump height or peak power for any of the groupings analyzed (R^2 range = .008 - .092, $p > .05$).

Table 1. Descriptive statistics (mean ± SD) by sport.

	M-SOC	M-BASE	W-SOC
Mass (kg)	75.9±6.9	85.3±7.0	65.0±6.7[a]
Height (cm)	179.8±5.6	182.5±6.1	165.7±5.7[a]
Pk vGRF (N)	3111.2±478.9	3204.4±454.8	2461.4 ±371.3[a]
K_{Vert} (kN/m)	34.8±6.6	35.1±6.4	27.2±4.9[a]
K_{Vert} (kN/m/kg)	0.47±0.09	0.41±0.08[b]	0.43±0.06[b]
CMJ_{Height} (cm)	40.7±0.4	44.3±0.5[b]	27.9±0.6[a]
CMJ_{Power} (W)	4590.5±489. 8	5379.3±640.4[b]	3033.2±510.5[a]
CMJ_{Power} (W/kg)	60.9±5.3	62.8±6.5	47.2±7.0[a]

Notes. [a] different from men's soccer and baseball; [b] different from men's soccer ($p < .05$).

Significance

Vertical stiffness, as measured via stationary, barefoot, vertical hopping, does not appear to be associated with measures of athletic performance as assessed during a countermovement jump. These findings contradict the results of previous work,[2] and suggest that additional studies focused on better understanding the various types information that can be gained from the vertical stiffness assessment, as it relates to other characteristics of athletic performance, appear warranted. The findings of the current study are significant in that they should cause researchers and clinicians to question some of the previous evidence supporting a theoretical relationship between vertical stiffness and measures of athletic performance.

References

1. Butler, R.J., Crowell, H.P., Davis, I.M. (2003). Lower extremity stiffness: implications for performance and injury. *Clinical Biomechanics*, 18:511-517.

2. Korff, T., Horn, S.L., Cullen, S.J., Blazevich, A.J. (2009). Development of lower limb stiffness and its contribution to maximum vertical jumping power during adolescence. *J. Experimental Biology*. 212:3737-3742.

3. McMahon, T.A., Cheng, G.C. (1990). The mechanics of running: how does stiffness couple with speed? *J. Biomech.* 23(Suppl 1):65-7

Differences in Vertical Stiffness as A Function of Sex and Sport

Brittany M. Warren[1*], Meghan E. Haser[1], Kevin R. Ford[2], and Justin P. Waxman[1]
[1]Department of Exercise Science, High Point University, High Point, NC
[2]Department of Physical Therapy, High Point University, High Point, NC

Email:* bwarren@highpoint.edu

Introduction

Evidence suggests that an optimal amount of lower-extremity stiffness is required for successful athletic performance, with too much or too little stiffness increasing injury risk; however, this "optimal range" remains elusive.[1] This may be in part due to the large variability in stiffness values displayed by relatively homogenous groups of athletes.[2] Identifying differences in stiffness as a function of sex and sport represents an important first step towards establishing normative ranges to better understand stiffness values and the potential clinical utility of vertical stiffness assessments. Therefore, the purpose of this study was to examine the effects of sex and sport on bilateral and unilateral measures of vertical stiffness (K_{Vert}).

Methods

As part of a larger pre-season screening, vertical stiffness (K_{Vert}) was assessed on a total of 181 athletes from men's high-school football (MFB: n = 47, 15.05 ± 1.41 yrs, 1.74 ± 0.09 m, 80.33 ± 21.88 kg), men's NCAA Division-I baseball (MBB: n = 34, 19.33 ± 1.29 yrs, 1.82 ± 0.06 m, 84.86 ± 6.77 kg), soccer (MSO: n = 27, 19.63 ±1.31 yrs, 1.80 ± 0.06 m, 74.98 ±6.72 kg), and track and field (MTF: n = 13, 19.07 ± 1.04 yrs, 1.78 ± 0.04 m, 72.46 ±25.37 kg), and women's NCAA Division-I volleyball (WVB: n = 18, 19.28 ±1.27 yrs, 1.75 ± 0.08 m, 74.96 ± 10.32 kg), soccer (WSO: n = 30, 19.13 ± 1.12 yrs, 1.66 ± 0.06 m, 63.90 ± 6.60 kg), and track and field (WTF: n = 11, 18.86 ± 1.86 yrs, 1.67 ± 0.06 m, 57.73 ±7.63 kg). Standing barefoot atop a force platform, athletes were instructed to hop (hands on hips) to the beat of a metronome set at 2.2 Hz under bilateral and unilateral (left leg, right leg) conditions. Two trials of 20 hops were recorded for each condition. For each hop, initial contact and toe-off were defined as the instants at which the vertical ground reaction force (vGRF) became greater than and less than 10 N. K_{Vert} was then calculated as the ratio of peak vGRF to maximum center-of-mass displacement.[3] Only trials in which the hops fell within 5% of 2.2 Hz were statistically analyzed. Because K_{Vert} is associated with body size, stiffness was also normalized to body mass. Between-sex differences in absolute and normalized K_{Vert} were evaluated via one-way ANOVA. Separate one-way ANOVAs were used to evaluate differences in K_{Vert} across sport.

Results and Discussion

Between-sex comparisons revealed that men displayed greater absolute K_{Vert} compared to female athletes across all hopping conditions (double: 31.57 ± 7.84 vs. 26.50 ± 4.98 kN/m, $p < .001$; left: 19.89 ± 4.02 vs. 16.75 ± 2.68 kN/m, $p < .001$; right: 19.94 ± 4.02 vs. 16.79 ± 2.54 kN/m, $p < .001$); however, this sex effect disappeared when K_{Vert} values were normalized to body mass (double: 0.41 ± 0.09 vs. 0.41 ± 0.07 kN/m, $p = .928$; left: 0.33 ± 0.09 vs. 0.32 ± 0.09 kN/m, $p = .736$; right: 0.26 ± 0.04 vs. 0.26 ± 0.03 kN/m, $p = .828$). As such, all sport comparisons were conducted using normalized K_{Vert} values. The sport main effect was statistically significant across all hopping conditions ($p \leq .002$). Follow-up pairwise comparisons (Bonferroni) revealed that MFB displayed significantly less double-leg K_{Vert} compared to MSO, WSO, and MTF ($p < .05$, Figure 1). Additionally, WVB displayed less double-leg K_{Vert} compared to MSO, MTF, and WTF ($p < .05$, Figure 1). On the left leg, statistically significant differences in K_{Vert} were observed for all sport comparisons except when comparing AFB to WVB, MBB to MSO and WSO, MSO to WSO, and MTF to WTF (Figure 1). Finally, on the right leg, the only significant finding was that MFB displayed lower K_{Vert} compared to MSO ($p < .001$, Figure 1).

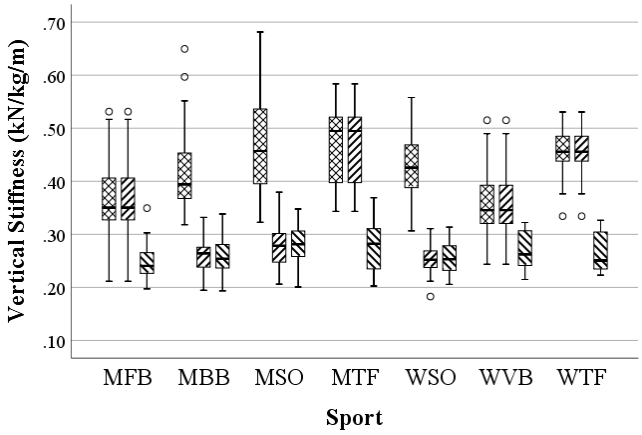

Figure 1. Boxplot displaying normalized vertical stiffness values by sport. Woven pattern = Double Leg; Slant Left = Left Leg; Slant Right = Right Leg.

Significance

To our knowledge, this is the first study to evaluate differences in vertical stiffness (K_{Vert}) as a function of sex and sport using a large and diverse sample of athletes. Our finding that sex differences in stiffness were eliminated after normalization to body mass suggests that between-sex differences in K_{Vert} are primarily due to differences in body size; hence, future studies using between-subject designs are encouraged to use normalized values. Additionally, our findings of significant differences in normalized stiffness among levels of sport suggests that future studies interested in how stiffness relates to injury risk and athletic perofrmance should incorporate sport-stratified analyses.

References

1. Brughelli, M., Cronin, J. (2008). A review of research on the mechanical stiffness in running and jumping: methodology and implications. *Scand J Med Sci Sports*. 18:417-426.

2. Waxman et al. (2018). Female athletes with varying levels of vertical stiffness display kinematic and kinetic differences during single-leg hopping. *J Applied Biomechanics*. 34(1):65-75.

3. McMahon, T.A., Cheng, G.C. (1990). The mechanics of running: how does stiffness couple with speed? *J. Biomech.* 23(Suppl 1):65-78.

Effects of Box Height on Instantaneous Lower Extremity Joint Stiffness during Drop Vertical Jump

Youngmin Chun[1], Joshua P. Bailey[1]
[1]Department of Movement Sciences, University of Idaho, Moscow, ID
Email : *ychun@uidaho.edu

Introduction

Joint stiffness is used to represent the ability of a joint to resist deformation or compliance in response to loads. Traditionally, joint stiffness has been modelled by applying a simple linear model to the moment-angle graph [1,2], but it is unclear that a simple linear model adequately represents the data throughout the whole stance phase. Our lab has proposed that using a quadratic model of best fit is more appropriate to represent this relationship. Thus, the purpose of this study was to investigate the lower extremity joint stiffness changes in subdivided landing phases and due to box height using a quadratic model of best fit.

Methods

Thirty healthy college students participated in this study (15 males: age = 25.8 ± 6.6 yrs, ht = 1.82 ± 0.04 m, mass = 82.4 ± 12.1 kg; 15 females: age = 25.2 ± 9.2 yrs, ht = 1.71 ± 0.09 m, mass = 64.5 ± 11.2 kg). Fifteen drop vertical jumps from each 30 cm and 60 cm of box were collected using 3D motion capture system (Vicon, 250 Hz) synchronized with two force platforms (AMTI, 1000 Hz). The obtained data of preferred limb (kicking limb) were exported to Visual 3D software and lowpass filtered at 15 Hz with 4th order Butterworth filter. The initial contact (IC) was identified if the vGRF of the preferred limb was greater than 20 N. The descending phase (IC to lowest vertical COM position) was divided into loading (IC - peak vGRF) and absorption (peak vGRF to lowest COM vertical position) phases [3]. The phase following absorption phase to TO was defined as propulsion phase. The quadratic regression model was used to calculate the estimates of x^2 for each phase. The instantaneous joint stiffnesses were calculated by the slope of tangent lines using a derivative of the quadratic regression model [$f'(x) = ax + b$] (Figure 1). Two-way repeated measures ANOVAs (box × phase) for each joint were performed to examine changes in estimates of x^2 with .05 α-level. Post-hoc analyses were performed if significant effects were found. Also, ensemble curves were created with mean stiffness ± 95% CI to identify differences of changes in joint stiffness between boxes.

Results and Discussion

Significant phase main effects were observed in estimates of x^2 of all joints (hip: $F_{(2,174)} = 9.911$, $p < .001$; knee: $F_{(2,174)} = 13.902$, $p < .001$; ankle: $F_{(2,174)} = 30.430$, $p < .001$). *Post-hoc* analyses are shown in Table 1. Knee stiffness of 60 cm box was significantly greater than 30 cm box at the beginning of the loading phase (0 – 2%), and ankle stiffness of 30 cm box was significantly greater than 60 cm at 5 - 6, 20 – 43, and 93 – 100% (Figure 1).

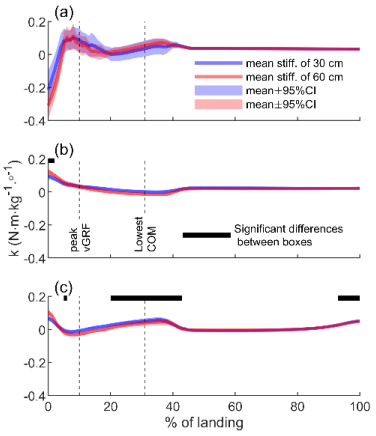

Figure 1. Ensemble curves of instantaneous joint stiffness with mean ± 95% CI. (a) Hip, (b) knee, and (c) ankle joint stiffness of 30 and 60 cm boxes.

Significance

Although there were no box differences when comparing the x^2 coefficients across box heights, the ankle joint demonstrated the greatest change in stiffness between box heights. Ankle joint increased compliance during approximately 30% of the cycle, indicating a potential preferred ankle strategy during the box drop jumps.

References

[1] Padua DA et al. (2005) *Journal of Motor Behavior,* Vol **37(2)**, 111 – 126.
[2] Hamill J et al. (2014) *European Journal of Sport Science*, Vol **14(2)**, 130 – 136.
[3] Harry et al. (2018) *Journal of Applied Biomechanics*, Vol **34(5)**, 403 – 409.

Table 1. Coefficient of x^2 of the quadratic regression models for each phase ($\times 10^{-3}$)

	30 cm			60 cm		
	Hip*,†,‡	Knee*,‡,§	Ankle*,‖,¶	Hip*,†,‡	Knee*,‡,§	Ankle*,‖,¶
Loading	27.20 ± 27.10	-1.12 ± 1.66	-1.30 ± 3.72	43.10 ± 96.00	-1.21 ± 1.95	-2.36 ± 2.68
Absorption	12.60 ± 27.70	-0.69 ± 1.02	3.33 ± 4.13	8.24 ± 21.60	-0.28 ± 1.13	2.02 ± 5.00
Propulsion	0.04 ± 0.30	0.02 ± 0.14	-0.53 ± 0.38	0.05 ± 0.34	-0.01 ± .015	-0.47 ± 0.40

Note. No difference between box heights. * indicates significant phase main effect ($p < .001$). † indicates significant difference between loading and absorption phase ($p = .008$). ‡ indicates significant difference between loading and propulsion phase ($p < .001$). § indicates significant difference between loading and absorption phase ($p = .007$). ‖ indicates significant difference between loading and absorption phase ($p < .001$). ¶ indicates significant difference between absorption and propulsion phase ($p < .001$).

Fabrication of a Hand Brace for a Collegiate Basketball Player Following Surgery: Identification of Hand Forces during Dribbling and Passing

Nicole Arnold[1], Nick Richey[1], Joshua Drost[1], Amber Vocelle[1], Justin Scott[1]
and Tamara Reid Bush[1], PhD
[1]Michigan State University, East Lansing, MI, USA
Email: reidtama@msu.edu

Introduction

Eighty-five percent of all hand fractures that occur in sports happen while playing ball related activities and about two thirds of these hand fractures are in the metacarpals [1]. Many athletes may return to play using a hand brace as long as the fracture is immobilized and protected, even following surgery. Designing proper protection requires an understanding of the forces that will be placed on that body region during play.

In this case study, a college basketball athlete sustained a left 4th metacarpal hairline fracture, which was surgically repaired with fixation using a pin. The athletic trainer asked our engineering team to design a brace that would permit play after surgery and allow the individual to participate in the 2019 Big10 tournament and March Madness. Published data with regard to the forces transmitted into the hand while handling a basketball were not available in the literature. Therefore, the goal of this work was to estimate the loads experienced by the hand during dribbling, an aggressive two-handed single bounce (generally occurring prior to a shot, called a power dribble), a crossover dribble and while receiving a chest pass. These data were then used to assist with brace design and material selection.

Methods

Two male college basketball players, one with the injury and another with similar abilities, served as the participants for this work. Two sets of force data were collected. The first set consisted of data collected during three dribbling styles: normal dribble, crossover, and power dribble. The force plate (Bertec, Columbus, OH) was positioned on the ground, collected forces generated by the ball. The second data set was collected from a chest pass. We placed the force plate on a nearly vertical section of a sports prep table that was mounted to the wall and recalibrated the plate. Basic camera video was also recorded in each trial. A 3D scanner (Sense 3D Scanner, Rock Hill, South Carolina) was used to obtain a scan of the physical features of the injured player's hand, which were used to produce a 3D printed model. The hand was scanned with the thumb side up and hypothenar side resting on the table. Four different hand positions were scanned which included a posture to mimic when the hand was gripping the basketball, a semi-flexed, relaxed hand and the hand in full extension.

Results and Discussion

The maximum force of the ball transmitted into the force plate was used to calculate the maximum pressure experienced by the hand. The maximum force values for a dribble, two-handed dribble, power dribble and chest pass ranged from 1260N-1653N, 1188N-1480N, 1721N-2489N and 540N-1024N, respectively. Based on video evidence, we estimated that the 2nd through 5th proximal and middle phalanges, the 1st distal phalange, the metacarpals, and the distal palm would initially contact the ball. Using the force data and the estimated contact area, the overall pressures were calculated. These data yielded pressure ranges of 11-140kPa.

There are several limitations to this work. These include the estimate of the hand contact area which was based on basic video evidence. Ideally, a high frequency pressure sensing glove would be used to obtain actual contact area and pressure data. Also, we used the force as measured by the force plate which is an overestimation of the force into the hand as it does not account for the force reduction as it moves upwards against gravity. However, when compared to a study of peak hand pressures experienced by softball catchers (269kPa) our peak pressures were less than those by 48-78% [2].

A CAD (computer aided design) file was created from the hand scans and a 3D printer was used to print a full-scale model of the athlete's hand (Figure 1, left). This model was used as a form to mold two composite plates (Figure 1, right). The composite brace was developed from carbon fiber and epoxy which is lightweight, thin and durable. Thus, it was selected as the best material to protect the hand based on our initial load estimates. The brace consisted of two plates each on the palmar and dorsal sections of the hand. The athlete wore this brace, covered with thin foam padding and played in the tournaments. These force data fill a gap in existing literature. Further, by using the 3D hand scans, a brace was personalized for this player.

Figure 1: 3D printed model of injured athlete's hand (left) and composite dorsal and palmar plates developed from carbon fiber and epoxy which is lightweight, thin and durable (right).

Significance

This approach may lead to advances in sports braces with additional customization for the player and injury. This method also allows us to examine and treat those with unusual or specific need cases. Designing a customized brace in this fashion addressed an unmet need of helping athletes who are not able to use an "off-the-shelf" brace system. Also, this work received a tremendous amount of media coverage - linking engineering and athletics is exciting for the K-12, college students and the general public and may be an avenue for exposure of biomechanics to many individuals.

Acknowledgements

A special thank you to Xavier Tillman and Nick Ward for their participation.

References

1. Singletary, S, et al, *J. Hand Ther.*, vpp. 171–179, 2003.
2. Hicks, B, "Analysis of Softball Gloves: e," Thesis, 2015.

Inter-segmental coordination variability during hopping and running on natural and synthetic turf surfaces

Brandi E. Decoux[1], Christopher M. Wilburn[2], and Wendi H. Weimar[2]
[1]Bridgewater State University, Bridgewater, MA
[2]Auburn University, Auburn, AL
Email: bdecoux@bridgew.edu

Introduction

An athlete's performance and musculoskeletal health hinges on their ability to exploit the abundant degrees of freedom in the body and adapt their movement patterns when faced with changes in environmental constraints. Some of the environmental constraints imposed are derived from physical properties of the playing surface, such as firmness and traction. However, research has yet to offer a thorough understanding of the biomechanical response of athletes to synthetic and turf surfaces and whether coordination variability is adjusted as a result [1]. Therefore, the purpose of this study was to investigate lower extremity inter-segmental coordination variability in athletes during two fundamental sport-related tasks, hopping and running, on four turf surfaces—three different synthetic turf surfaces and one natural turf surface.

Methods

Seventeen healthy male recreational athletes (age: 23.1 ± 2.9 years; height: 1.81 ± 0. 06 m; mass: 77.8 ± 9.9 kg) were recruited from the surrounding community to participate in this study. All participants indicated their voluntary involvement by signing an informed consent document approved by the Institutional Review Board prior to participation.

To minimize potential variations induced by differences in cleat models across participants, each individual wore one of two provided models, both of which had the same upper, heel, and shoe plate construction, and stud configuration. Eight wireless inertial measurement unit (IMU) sensors (MTw, Xsens Technologies B.V., Enschede, the Netherlands) were affixed bilaterally to the feet, lower legs, and thighs as well as to the pelvis and trunk. With this inertial motion capture system, kinematic data were obtained at 100 Hz during three hopping trials and three running trials on each of the four surfaces (Xsens MVN Analyze, Version 2019.0, Enschede, the Netherlands). For the single leg hopping trials, participants were instructed to hop in place ten times at a steady, self-selected frequency, on their dominant limb with their hands resting on their hips. For the running trials, the participants were instructed to run 35 m at a steady, submaximal, self-selected frequency.

Data were imported in Visual3D (C-Motion, Germantown, Maryland, USA) for reduction to only the braking and propulsion sub-phases of the hopping and running trials. Braking and propulsion data were then imported into MATLAB® (R2016a, Mathworks, Inc., Natick, MA) in order to compute continuous relative phase (CRP) variability for the following segment couplings of interest: pelvis-thigh, thigh-shank, thigh-foot, and shank-foot sagittal plane couplings and pelvis-thigh and thigh-foot frontal plane couplings

Results and Discussion

Only one significant difference in CRP variability between turf surfaces was found for any of the segment couplings during hopping and running. The single significant finding was observed during the braking sub-phase of hopping (χ^2 (3) = 8.365 p = .037), which is when the body is tasked with resisting downward acceleration of the center of mass. Specifically, the sagittal plane pelvis-thigh coupling demonstrated significantly less CRP variability on synthetic turf 1, which was the firmest of the surfaces, compared to natural turf which was the least firm of the surfaces (55.3° ± 16.8° vs. 67.1° ± 17.2°, p = .03, W = .16).

Movement patterns that allow for greater but not excessive variability between segments are widely considered to be a healthier, more flexible display of adaptive coordination than movement patterns with less variability [2]. Observations of a reduction in variability may place that system at greater risk of injury due to repetitive stress being applied to the same tissues [3]. Evidence of reduced coordination variability in the pelvis-thigh sagittal plane coupling was found in a study comparing CRP measures in people with and without chronic low back pain during free-speed walking [4]. Though not directly observed as a symptom of chronic low back pain and not the cause, the author suggested that a less variable coordination pattern may be indicative of a reduced ability to absorb shock and may lead to further injury [4,5]. Given that low back pain is commonly reported in athletes after playing on synthetic turf [6,7], the reduced coordination variability in the pelvis-thigh sagittal coupling observed on the firmest of the synthetic turfs tested in this study, warrants attention and should be investigated further. Future research should consider the different alignments employed between the trunk, pelvis, and thigh to ascertain whether the altered postures place a greater demand on the trunk extensors.

Significance

This study demonstrated that coordination variability between relative segments, in the dominant limb, is largely unaffected by different turf surfaces. However, the significant reduction in variability observed between the pelvis and thigh may indicate an adverse alternative movement pattern during the braking sub-phase of hopping and warrants further attention.

Acknowledgments

This work was supported by Shaw Industries Group, Inc.

References

[1] J Sport Health Sci. 2016 Sep; 5(3): 355–360.
[2] Sports Med. 2003; 33(4): 245-60.
[3] Clin Biomech (Bristol, Avon). 1999 Jun; 14(5): 297-308.
[4] Hum Mov Sci. 2017 Apr; 52: 55-66.
[5] Clin Biomech (Bristol, Avon). 2001 Mar; 16(3): 213-21.
[6] Clin J Sport Med. 2010 Jan; 20(1): 1-7.
[7] Asian J Sports Med. 2016 Mar 5; 7(1): e28425.

SIMULATED EXERCISE DEVICE VIBRATION ISOLATION SYSTEM FOR SPACEFLIGHT APPLICATIONS

Blocker, A[1], Lostroscio, K[2], Carey, SL[1]*
[1]University of South Florida, Tampa, FL, [2]Johnson Space Center, Houston, TX
*scarey3@usf.edu

Introduction

With future NASA goals including long-duration spaceflight missions, proper countermeasures must be taken to facilitate human health in microgravity environments. Exercise is a vital countermeasure used to prevent bone and muscle loss, among other health interests. An important factor in integrating exercise devices with spacecraft is the vibration isolation component, which allows for exercise to occur on spacecraft without creating unwanted vibrations. This human factor study tested the viability of a vibration isolation system (VIS) by having subjects perform exercise in a simulated VIS environment.

Methods

This study used the Computer Assisted Rehabilitation Environment (CAREN) system to simulate a VIS system. The CAREN (Motek) is a 6-DOF platform with treadmill and force plate capabilities. A Vicon motion capture system, incorporated with the CAREN system, was also used to analyze human kinematics. The VIS System was simulated by applying sine wave inputs to the platform in the heave direction at frequencies of 0.1, 0.35, and 0.6 Hz, as well as a subject-determined baseline frequency. Pitch amplitude was also altered for eight trials, up to 6°, and simultaneous pitch and heave movement was implemented for three trials. Three females and one male were tested from ages 18-44. Height and weight were within range of historical astronaut measurements.

Results and Discussion

Biomechanical analysis of results show that knee, ankle, and hip joint angles are maintained during exercise on the moving platform. Peak joint angles for the knee during the squat exercise center around 95°, indicating that proper squat form was being reached in the knee.[2] Peak hip angle centered around 90° and peak ankle angle centered around 30°, seen in **Figure 1**. These angles are within normal exercise range for the squat exercise.[2] Synchronization with hip and ankle joints with the platform motion indicate that in trials where multiple motion was occurring (i.e. pitch and heave moving at differing frequencies) caused subjects to have difficulty synchronizing to platform motion. This does not indicate that proper exercise form was not being followed, but it may be considered in order to promote astronaut safety and comfort while using the device.

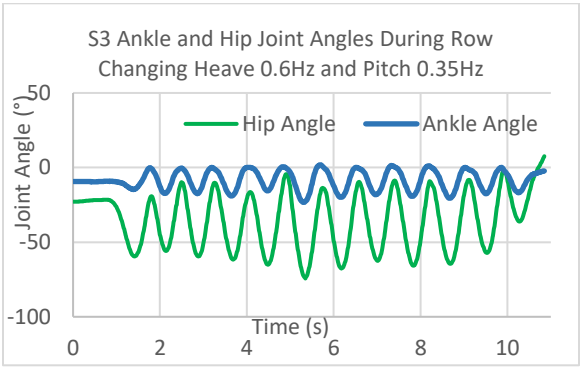

Figure 1 demonstrates how subjects were able to continue exercise and achieve desired peak joint angles even when pitch and heave moved with different frequencies. Pitch amplitude was ±2° and heave amplitude was ±0.04 m.

Significance

The results from this study indicate that further testing may be safely performed using this program and future algorithms to understand the effect of passive and active VIS designs on human exercise. This information will then impact the design and implementation of exercise devices aboard spacecraft, because if a subject is not able to perform exercise completely or get the proper joint loading with the existing design, then the purpose of exercising as a countermeasure to bone and muscle loss will be lost. Future studies will focus on testing human subjects on the additional simulations and analyzing kinetic and kinematic data. Other studies of interest include using motion capture data, joint angles, and/or force data to determine the progression of a squat and move the platform accordingly, as a true VIS might do.

References

1. Lostroscio, K. "Developing Motion Platform Dynamics for Studying Biomechanical Responses During Exercise for Human Spaceflight Applications." 2018.
2. Cronin, J. B., et al. (2007). "Kinematics and kinetics of the seated row and implications for conditioning." Journal of Strength and Conditioning Research. 21(4): 1265-1270.
3. Carey, S., Lostroscio, K., Blocker, A. "Biomechanical Responses During Exercise for Human Spaceflight Applications." 2018. Biomedical Engineering Society Annual Meeting.

Use of Inertial Measurement Units to Quantify Performance in Alpine Skiing

Sarah A. Wilson[1], Scott Tashman[1]
[1]Steadman Philippon Research Institute, Vail, CO
Email: swilson@sprivail.org

Introduction

Inertial Measurement Units (IMUs) offer a promising technique to evaluate athlete biomechanics in sporting environments outside of laboratory constraints. IMU kinematics have been well-validated against video-motion capture in the laboratory [1]; however, use of IMUs in the field remains limited until validated against sport-specific measures that align with coaches' and athletic trainers' "clinical" observations.

Alpine skiing cannot be reproduced in a laboratory, and there have been several attempts to quantify skiing movement with IMUs. Martínez et. al. developed and validated an algorithm using IMU gyroscopes to determine the transition point between turns [2]. This algorithm is based off timing of edge transition, but similar concepts can be applied to additional axes of the gyroscope to quantify skiing performance.

High performance skiing is characterized by simultaneous edge release; equal tipping of the skis; and turning the feet, legs, and skis "gradually and progressively" throughout the turn [3]. This study demonstrates that IMU gyroscope data can quantify these technical characteristics of ski performance, supporting the viability of IMUs as a tool for measuring skiing movements.

Methods

Thirteen intermediate- to expert-level skiers provided informed consent to participate in this IRB- approved research study. Each skier was outfitted with standard ski equipment (Nordica SportMachine boots, Rossignol Experience-84 skis) and IMUs (APDM Opal2, Portland, OR; 128Hz sample rate). Participants skied a twelve-turn giant-slalom style course on moderate terrain twice using a skidded-parallel turn. Skier ability level was assessed on a 9-point scale by three independent, professionally-certified instructors/coaches and was averaged.

IMUs were mounted to the top of both boots between the toe and instep buckles with a rubber backing to reduce vibration. The triaxial gyroscope data were filtered using a 4th-order bidirectional 0.5hz Butterworth filter (Figure 1). The left and right foot roll-axis signals were averaged, and the extrema of the resulting signal were used as the Edge Transition times (ET) [2]. Rotational Transition times (RT) were determined from the zero-crossings of the yaw-axis. The first and last turns were omitted, resulting in five turns each direction per run.

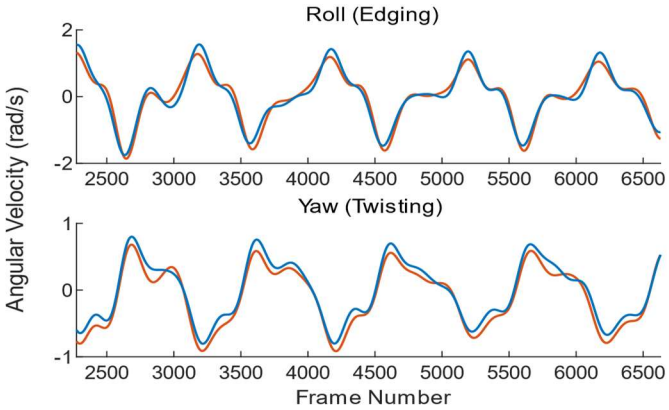

Figure 1: Left (red) and right (blue) filtered gyroscope data from a portion of one run.

Five measures of skier performance were extracted by comparing the edging (roll-axis) and twisting (yaw-axis) gyroscope signals of both feet for each turn cycle, and were averaged. These measures are described briefly in Table 1.

Results and Discussion

Agreement between raters of skier ability level was fair (ICC=0.64). Raters varied with an average range of 1.3 points between the highest and lowest ability score for each skier, with no consistent offset between raters, underscoring the need to identify quantifiable, objective measures of technical skiing ability. Despite this, most of the metrics extracted from the IMU were significantly correlated with skier ability (see Table 1).

Table 1: Correlation of gyroscope metrics with skier ability level

Performance Parameter	R-value	P-value
Edge Synchronicity **(ES)** $\Delta T = \lvert ET_L - ET_R \rvert$	0.64	*0.017
Rotational Velocity at ET **(RV_{ET})**	0.74	*0.004
Max Rotational Velocity (L-R avg) **RV_{Max_Avg}**	0.58	*0.039
Rotational Velocity Symmetry **RVSym** $= (RV_{Max_R} - RV_{Max_L})/RV_{Max_{Avg}}$	0.51	0.073
ET-RT	0.75	*0.003

In a stepwise multiple-regression analysis, no combination of performance parameters outperformed any individual metric. The best regression, Ability = 7.67(RV_{Max_Avg}) - 8.19(RV_{ET}), resulted in an R of 0.75 (p=0.007). This regression considered a change in angular velocity in the ski rotation between ET and maximum, and an acceleration-like parameter could feasibly characterize the "progressive and gradual twisting of the ski throughout the turn." However, this was not better than RV_{ET} or ET-RT, which were each able to account for approximately 56% of the variability between subjects; thus, an additional type of metric or data stream may be necessary to more fully characterize skier performance.

Significance

The ability of IMU metrics to quantify skier ability level supports their use as a functional training and movement measurement tool in skiing. IMUs characterized the simultaneity of edge release and the rate of rotation of the feet throughout the turn to a much higher level of precision than visual observation. These metrics have potential for evaluating the efficacy of interventions for improving skier performance.

Acknowledgments

Funding and in kind support were provided by Lyda Hill Philanthropies, FCFH Lattner Foundation, Double Diamond Ski Shop & Vail Resorts. Concept was proposed by Jeannie Thoren. K.Dahl, K.Dunford, T.Turnbull, M.Koskinen, T.Beauchamp, M.DeClercq, and T.Woolson assisted with this study.

References

[1] Cuesta-Vargas et al., Phys. Ther. Rev., 15.6:462–473, 2010.
[2] Martínez, A et al., fspor, 1:18, 2019.
[3] PSIA Alpine Technical Manual, ASEA, Inc., 2014

Assessing the Generalizability of Dual-Task Effects across Different Movements

Patrick D. Fischer[1], Keith A. Hutchison[2], James N. Becker[3], and Scott M. Monfort[1]
[1]Department of Mechanical and Industrial Engineering, [2]Department of Psychology, [3]Department of Health and Human Performance
Montana State University, Bozeman, MT, USA
Email: patrick.fischer2@student.montana.edu

Introduction

Although jump-landing and sidestep cutting tasks are both sport-specific movements that are associated with non-contact anterior cruciate ligament (ACL) injury[1], they load the knee differently during single-task performance[2]. Cognitive function has been associated with non-contact ACL injury risk[3] as well as high-risk biomechanics during dual-task jump-landing[4] and sidestep tasks[5]. However, it is unknown if dual-task effects are generalizable across these movements. Expanding the understanding of how cognitive-motor function ability transfers between injury-relevant movements would guide injury screening and prevention programs.

The purpose of this study was to investigate the generalizability of athletes' cognitive-motor function across jump-landings and running sidesteps. We hypothesized that dual-task costs (DTC) from cognitive distractions during a jump-landing would positively correlate with DTC from analogous cognitive distractions during a running sidestep.

Methods

Twenty-eight female soccer athletes participated in this study (20±3yrs, 63.5±8.9kg, 1.68±0.05m). On separate, non-consecutive days, participants completed jump-landing tasks[4] and running 45° sidestep tasks off their non-dominant limb. The jumping tasks included a baseline, a working memory task that required participants to memorize and recall the location of six letters on a TV screen (WM_J), that same working memory test with an added challenge of identifying a single stimulus letter during the jump-landing (WM+VA_J), and the WM+VA_J task while reacting to a directional cue (WM+VA+UA_J). The sidestep tasks included a baseline, the working memory task as described above (WM_S), the working memory test with an added letter-identification task (WM+VA_S), and the working memory task while reacting to a directional cue (WM+UA_S).

Motion capture and force plate data were recorded at 250 Hz and 1000 Hz, respectively. Recorded data were filtered using a 4th order, lowpass Butterworth filter at 15 Hz in Visual3D. Peak knee flexion angle (pKFA) and abduction angle (pKAbA) of the non-dominant limb were calculated. Externally defined peak knee abduction moments (pKAbM) were normalized to participant height and weight. Peak values were identified within a 50ms window of participants impacting the force plate[6]. DTC for pKFA, pKAbA, and pKAbM[1] were calculated as the percent change between the multitasking condition and the movement-specific baseline. Spearman's rho correlations tested for relationships between jump-landing DTC and sidestep DTC for analogous cognitive tasks. Significance was set at $p<0.05$ without correcting for the nine comparisons.

Results and Discussion

There was a significant negative correlation in pKFA DTC between WM+VA+UA_J and WM+UA_S (ρ=-0.51, p=0.01); greater decreases in knee flexion in WM+VA+UA_J were associated with greater increases in knee flexion in WM+UA_S (**Table 1**). No other comparisons were significant (all $p \geq 0.17$).

Table 1. Spearman correlations for each DTC between jump landing and sidestepping when performed with a similar cognitive task. Values are: rho (p-value). *indicates (p<0.05)

	pKFA DTC	pKAbA DTC	pKAbM DTC
WM_J vs. WM_S	-0.06 (0.77)	-0.08 (0.71)	0.15 (0.49)
WM+VA_J vs WM+VA_S	-0.01 (0.98)	<0.01 (0.99)	-0.27 (0.17)
WM+VA+UA_J vs. WM+UA_S	**-0.51 (0.01)***	0.04 (0.86)	0.04 (0.84)

The only relationship to reach significance suggested that similar cognitive challenges had opposite effects on neuromuscular control during different movements. This, in combination with the lack of relationships for any other comparisons, suggest that the dual-task conditions cause different neuromuscular responses between the jump-landing and sidestep tasks. Both movements are relevant to injury prevention research[1], but the current findings do not support the idea that dual-task effects are generalizable across injury-relevant movements. Caution should be taken when comparing the effects of similar distractions on different injury-relevant movements. Further research is needed to provide insight into mechanisms that cause task-dependent cognitive-motor relationships.

Significance

Jump landing and sidestep cutting movements are commonly investigated for ACL injury prevention research. The results of this work suggest against generalizing individuals' cognitive-motor function across movement types. They also motivate the need for more comprehensive assessments into the spectrum of cognitive-motor function across cognitive and movement tasks.

Acknowledgements

This material is based upon work supported by the NSF Graduate Research Fellowship under Grant No. W7834.

References

1. Boden BP et al (2000) *Orthop*, **23**: 573-8
2. Kristianslund E and Krosshaug T (2013) *AJSM*, **41**: 684-8
3. Swanik CB et al (2007) *AJSM*, **35**: 943-8
4. Herman DC and Barth JT (2016) *AJSM*, **44**: 2347-53
5. Monfort SM et al (2019) *AJSM*, **47**: 1488-95
6. Krosshaug T et al (2007) *AJSM* **35**: 359-67

DYNAMIC SIMULATION ANALYSIS AND OPTIMIZATION OF A STANDING POWER THROW

Beau Kewley[1], Manoj Srinivasan[2], Gregory Freisinger[1]
[1]United States Military Academy – West Point, [2]The Ohio State University
Email: gregory.freisinger@westpoint.edu

Introduction

With the United States Army's implementation of the Army Combat Fitness Test (ACFT), many different factors are being analysed for their impact on performance in the various events. It is hypothesized that the height of an individual will have a positive correlation to the distance they are able to throw a 10 lb medicine ball during an overhead Standing Power Throw (SPT). This study aims to investigate the effect of limb length on the distance a ball can be thrown, as the multi-link dynamics may provide additional insight compared to strictly looking for relationships to an individual's height.

A dynamic simulation modelling the upper and lower arm as a two-link pendulum was developed and optimized to maximize throw distance. This simulation allows for a controlled way to adjust link length while keeping other factors such as applied torque and release position constant. The results of this work may provide insight into ways to potentially normalize results of Soldier performance based on anthropometric differences.

Methods

A dynamic simulation of simplified human motion utilizing MATLAB [Natick, MA] allowed for optimization based on specified criteria[1]. Optimization was conducted using the *fmincon* function, which takes in multiple subfunctions to provide the constraints and objective function. This was used alongside the equations of motion for a two-link pendulum with a fixed origin representing the shoulder and point masses representing the weight of the upper arm and forearm, hand, and ball, respectively. Joint torque was modelled at the fixed shoulder and elbow joint. Two-link pendulum differential equations were solved using *ode45*. The constraint function set the boundary conditions to only allow motion similar to a human arm during optimization. In this case, the objective was set to maximize the distance a ball can be thrown by a two-link pendulum releasing at an angle of $\pi/3$ radians. MATLAB's *fmincon* iterates from a supplied initial condition until it reaches the set of conditions that meet the objective function within supplied constraints.

We completed optimizations at varied link lengths, where each link was set to either 0.1, 0.5, 1.0, or 2.0 meters (Figure 1). The maximum allowable torques at the elbow and shoulder (75 N-m for each) and point mass of the upper-arm (1 kg) and forearm, hand, and ball (3 kg) remained constant. It is important to note that the chosen values were based on convenience and not an extensive search of the literature. Our main objective was to analyse differences between simulation results, not the accuracy of predicting human performance. Therefore, these values were simplified to ease convergence to an optimal solution.

Results and Discussion

After iterating the 0.1, 0.5, 1.0, and 2.0 lengths, a negative relationship was evident between link length and distance the ball was able to be thrown as shown in Figure 1. These results are contrary to our initial intuition that longer link lengths would increase the throwing distance. However, with the constant torque and mass constraints, it appears that shorter link lengths reduce the system mass moment of inertia therefore increasing the initial velocity of the ball at release. The only exception to this was at length 0.1, where it did not continue to increase the distance thrown. A more extensive parameter analysis would also serve beneficial to further understand how the limb lengths, torque maximums, constraints, and possible other factors each impact the maximum throwing distance.

While these were not the results anticipated, it is possible that with additional links to represent the lower body and torso contribution to a SPT, the linkage lengths may still positively impact the distance thrown. The dynamics of a four-link pendulum provide significantly more operating space for the MATLAB optimization, and the potential for the stronger lower-body joints to create a "whip-like" action at release, which is intuitively our expectation based on observation of human technique.

Significance

This study identified optimal local maximums for a two-link pendulum model of an overhead SPT with varied linkage lengths. Limitations of this model include that it is only a two-link pendulum, and therefore does not fully account for lower limb or torso contribution to an overhead SPT. Future work includes comparing the results of dynamic simulations to the results of the diagnostic tests being conducted by the United States Army. This would serve as an avenue to validate any inferences obtained by this dynamic simulation study.

References

Srinivasan, Manoj. "Computer Optimization of a minimal biped model discovers walking and running," Nature (2006). 72-75.

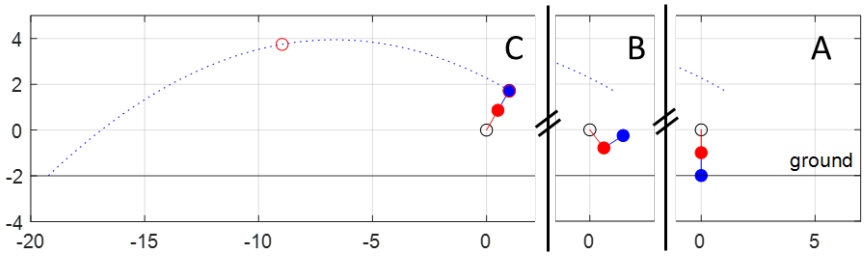

Link Length	MATLAB Iterations	Distance Thrown	Percent Change
0.1	14,903	29.1	+51.6
0.5	6,653	31.1	+61.7
1	18,177	19.2	N/A
2	7,640	10.8	-43.8

Figure 1: Time lapse of dynamic simulation with link length of 1.0 about a fixed shoulder. A) Initial position. B) Mid-throw. C) Final position with ball mid-flight. Table shows the link lengths for the 3 optimizations, along with number of iterations for *fmincon* to converge on optimal solution, distance of ball thrown, and percent change from link length of one.

Elucidating the Spectrum of Cognitive-Motor Relationships during a Sidestep Cut

Patrick D. Fischer[1], Keith A. Hutchison,[2] James N. Becker,[3] and Scott M. Monfort[1]
[1]Department of Mechanical and Industrial Engineering, [2]Department of Psychology, [3]Department of Health and Human Development
Montana State University, Bozeman, MT, USA
Email: patrick.fischer2@student.montana.edu

Introduction

Movement during competitive sport is often done with cognitive distractions, and differences in cognitive ability influence athletes' non-contact anterior cruciate ligament injury risk[1]. Research into the effects of cognitive dual-task challenges during sport-relevant movement is needed to more completely understand musculoskeletal injury risk factors.

The purpose of this study was to quantify the effects of working memory and visual attention tasks on neuromuscular control during a sidestep cut. We hypothesized that introducing cognitive load from various types of stimuli would result in increases in peak knee abduction angles (pKAbA) and moments (pKAbM) and decreases in peak knee flexion angles (pKFA)[2].

Methods

Thirty female recreational soccer athletes (20.5±3yrs, 62.7±9.1kg, 1.68±0.06m) completed running 45° sidesteps off their non-dominant limb under a single-task baseline (BL) and six dual-task conditions. The dual-task conditions were: while dribbling a soccer-ball (BH), reacting to a directional cue instructing them to cut or run straight ahead (UA), with a working memory task of memorizing and recalling letters (WM)[3], the WM task while also dribbling (WM+BH), the WM task with the visual directional cue for unanticipated change of direction (WM+UA), and the WM task with an added visual task of identifying a stimulus letter during the sidestep movement (WM+VA). Approach speed was controlled to participant-specific maximal effort while dribbling a soccer ball. Three good trials of each condition were assessed.

Marker (modified Plug-in Gait) and force data were collected at 250 Hz and 1000 Hz, respectively. Recorded data were filtered using a 4th order, lowpass Butterworth filter at 15 Hz in Visual3D. pKAbA, pKAbM, and pKFA of the plant limb were calculated within 50ms[4] from IC (1st frame of data where the force plate reading exceeded 10N). Externally defined knee joint moments were normalized to subject weight and height.

Linear mixed models were used to test for fixed effects of trial condition on pKAbA, pKAbM, and pKFA, with 'Participant' as a random effect. Post-hoc pairwise comparisons were tested using Tukey tests. Significance was set at $p<0.05$.

Results and Discussion

There was a significant effect of trial condition on pKAbA ($F=2.68$, $p=0.016$). An effect of trial condition on pKFA trended towards significance ($F=1.84$, $p=0.054$). There was no significant effect of trial condition on pKAbM ($F=0.88$, $p=0.51$). (**Table 1**). Post-hoc analysis found that participants experienced greater pKAbA during the UA task compared to the baseline ($p=0.046$) and the WM+VA task ($p=0.017$). No other comparisons reached statistical significance.

Only the comparisons between the UA and baseline and between the UA and WM+VA conditions reached statistical significance, leaving our hypothesis only partially supported. This is in line with previous studies that found similar effects of unanticipated conditions on sidestep cut performance.[5] However, our findings offered no evidence to suggest that the other cognitive challenges were difficult enough to induce detectible effects on neuromuscular control during the sidestep cut. Notably, we previously observed an effect of BH in male competitive soccer players on pKAbA.[6] Additional work is needed to understand the nuances of how factors such as sex, experience level, and cognitive task difficulty influence neuromuscular control during dual task sidestep cutting.

We previously reported that dual-task conditions with divided visual attention (UA, WM+VA,WM+VA+ UA) led to decreased pKFA during a jump-landing task[7] when compared to baseline. We used analogous cognitive challenges during the sidestep study, however we found no such relationship here. This may be because the jump-landing and sidestep tasks load the knee differently, and so the effects observed during one sport-specific movement may not be generalizable to another.

Significance

Cognitive multitasking during dynamic movements is an emerging area of research. Understanding the spectrum of effects of cognitive load on injury-relevant biomechanics during sport-specific movements will help improve the efficacy of injury prevention programs.

Acknowledgements

This material is based upon work supported by the NSF Graduate Research Fellowship under Grant No. W7834.

References

1. Swanik CB et al (2007) *AJSM*, **35**: 943-8
2. Boden BP et al (2000) *Orthop*, **23**: 573-8
3. Shipstead Z et al (2014) *J Mem Lang*, **72**: 116-41
4. Krosshaug T et al (2007) *AJSM* **35**: 359-67
5. Besier TF et al (2001) *MSSE*, **33**(7): 1176-1181
6. Monfort SM et al (2019) *AJSM,* **47**(6): 1488-1495
7. Fischer PD et al (2019) *2019 ISB-ASB Proceedings:* Abs No 913

Table 1. Mean ± SD for biomechanical variables across the sidestep conditions. [a] indicates $p< 0.05$ from BL, [b] indicates $p< 0.05$ from WM+VA

	BL	BH	UA	WM	WM+BH	WM+UA	WM+VA
pKFA (°)	39.1 ± 7.8	37.7 ± 7.2	40.1 ± 6.7	38.6 ± 7.7	38.8 ± 5.7	37.4 ± 8.8	36.7 ± 9.3
pKAbA (°)	7.8 ± 3.7	7.9 ± 3.7	**9.4 ± 4.0** [a,b]	8.2 ± 3.8	8.3 ± 3.8	8.8 ± 4.1	7.7 ± 3.7
pKAbM (%BW*Height)	5.3 ± 4.2	5.7 ± 4.6	5.7 ± 4.3	5.1 ± 3.8	5.0 ± 3.6	5.9 ± 4.6	5.1 ± 3.9

Golf Swing Consistency and Balance Improvements Following an Eight Week Balance Intervention

Meredith K. Owen[1], Julia Gambill[1], Katie Van Damme[1], Jordan Byrd[2], and John D. DesJardins[1]
[1]Department of Bioengineering, Clemson University, Clemson, SC
[2]Department of Athletics, Clemson University, Clemson, SC
Email: mko@g.clemson.edu

Introduction

Golf is a widely played sport with participants ranging across all skills levels. For these golfers, strength, flexibility, and balance are all considered important attributes to successful performance, and these attributes have been studied for direct effect on performance[1-2]. Indeed, many of these skills contribute to increased club head speed or increased driving distance. In addition to single shot improvements, a golfer's ability to consistently replicate the same swing to produce the same output is highly important[3].

While strength, flexibility, and balance have been studied together, balance has yet to be studied in isolation from other training methods. Additionally, few studies have investigated consistency across multiple swings for elite golfers. The purpose of this study was to determine the effects of a golf specific balance training intervention on golf swing consistency. We hypothesized that higher levels of balance would correlate to increased swing consistency measured by decreases in the kinematic range and decreased kinematic variance.

Methods

Eight National Collegiate Athletic Association Division I golfers were assessed for postural stability and golf swing kinematics before and after completing a balance training program. Golfers completed the golf specific balance training program three times a week for eight weeks.

A modified Balance Error Scoring System (BESS)[4] and a 3-axis force plate (AccuSway, AMTI, Watertown, MA) were used to evaluate standing postural stability. Each golfer completed a series of double and single leg stances, with eyes open and closed, while standing on a force plate, and an investigator counted errors according to the BESS scale for each stance. Swing kinematics were assessed using an eight-camera 3D motion capture system (Qualisys AB, Gothenburg, Sweden). A Trackman® launch monitor (Trackman, Scottsdale, AZ) was used to measure swing and ball flight data. Testing was completed before and after competition of the eight week balance training program.

Postural stability was evaluated as deviation in center-of-pressure (COP) measured by the 95% ellipse area of the COP movement during the test period. Modified BESS scores were determined for each stance position. Swing data was analyzed for all 10 swings, and data from 8 swings was included in analysis. Average values, variance, and range for club head speed (CHS), face angle (FA), club path (CP), and pelvis and torso position were determined for each golfer.

Results and Discussion

Postural stability improved for all golfers following the balance training. Significant decreases in BESS scores were noted for both legs for the single leg, eyes closed stance conditions. Changes in COP deviation as measured by the 95% ellipse area were not significant for any stance conditions, but all stance conditions trended towards decreased COP deviation.

CHS, FA, and CP were all unaffected by the balance training. Maximum variance for CHS spanned from a decrease of 4.52 to an increase of 5.43 post-training within the group of golfers. However, average range for the cohort decreased from 9.14 ± 3.53 km/hr to 8.43 ± 1.27 km/hr post-training. Average range decreased slightly for FA (4.67 ± 1.12 to 4.17 ± 1.62) and stayed the same for CP (2.11 ± 0.54 to 2.11 ± 0.61). There were no significant changes for pelvis or torso body segment position consistency for any swing location (Figure 1). Range for the top and half down position for the pelvis and for the half down and impact positions for the torso decreased following the balance training.

Pearson's correlations indicated no relationship between postural stability levels and variance in swing kinematics. Correlations were determined using the 95% ellipse area for the single leg, eyes closed stance position as a representative stance.

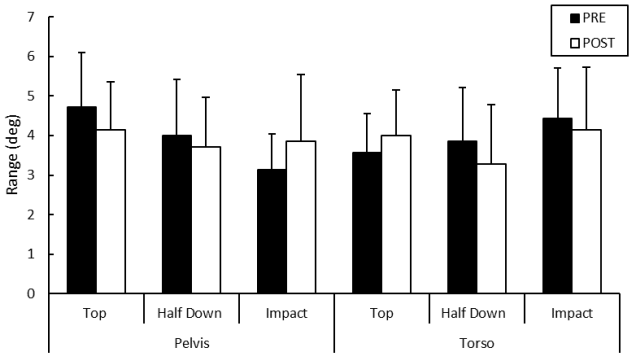

Figure 1: The range of body segment positions (as an angle position) across 8 swings for specific location in the golf swing were determined each golfer.

Significance

Golf performance has been shown to be affected not only by standard skills practice, but also by dedicated strength and conditioning training. Elite collegiate athletes are limited by time constraints, thus understanding the outcomes of dedicated training programs is highly important. The results of this study indicate that isolated balance training ***does*** improve balance, but ***does not*** affect golf swing consistency for elite collegiate golfers.

Acknowledgments

Funding for the study was provided by the Robert H. Brooks Sports Science Institute (RBSSI). The authors would like to acknowledge Thomas Evans for his assistance with developing the balance intervention.

References

1. Parker, J et a., BMC Sports Sci, Med Rehab, 9(21), 2017
2. Fletcher, IM et al., J Strength Cond Res, 18(1), 2004
3. Landdown BL etl al., Sports Biomechanics, 11(2), 2012
4. Balance Error Scoring System (BESS), UNC Sports Medicine Research Laboratory

Coordination of Upper Extremity and Center of Mass Trajectory During Basketball Shots from Varying Distances

Casey Wiens[1] and Jill L. McNitt-Gray[1,2]
Departments of [1]Biological Sciences and [2]Biomedical Engineering, University of Southern California, Los Angeles, CA, USA
Email: cwiens@usc.edu

Introduction

Basketball shooting is a technical skill that requires regulation of ball velocity at release. Due to the strategy and demands of the game, shots are taken at various distances from the hoop. Differences in max angular velocity[1] and timing of max upper extremity joint angular velocities relative to ball release[2,3] across distances has been observed; however, little is known how individuals control their upper extremity in relation to their center of mass (CM) trajectory during the shooting motion. Our aim was to characterize how individual players coordinated their upper body segment shooting motions in relation to their CM trajectory during shots and determine if players use common strategies to regulate ball velocity at release when increasing shot distance. Shot initiation by the upper extremity was hypothesized to occur closer in time to the maximum CM vertical velocity with increases in shot distance.

Methods

Seven male and female basketball players (>10 years of experience, current players in university club and recreational leagues) provided informed consent and volunteered to participate. A minimum of 10 shots were taken from short (<2.5m), mid (4.57m, free throw line), and long (6.02m, high school three-point line) distances. Participants received a chest pass from underneath the hoop and were asked to perform a shot "as if they were in a game." Competition regulation sized balls were used (male: 29.5; female: 28.5).

Two portable force plates (1200Hz, Kistler) measured reaction forces by each leg. Inertial measurement unit sensors (120Hz, APDM) measured arm segment angular velocities in the sagittal plane. Ball trajectories were video recorded (120Hz, Panasonic) and ball kinematics were measured using custom Python code. CM vertical velocity during the shooting motion was calculated using reaction forces and measured body weight. The last positive-minimum value of arm angular velocity (flexion of shoulder joint) and initial instant of negative lower arm angular velocity (extension of elbow joint) defined shot initiation. The angle of the ball CM velocity at release was determined relative to the horizontal (ball release angle). Multiple comparisons using medians on difference scores tested for differences within-participant amongst the timing of upper and lower arm shot initiation between shot distances. p-values were adjusted using the Benjamini-Hochberg method[4].

Results and Discussion

Regulation of ball velocity at release to accommodate for increases shot distance varied across players. Only 14 of 26 shot adjustments involved shot initiation closer to the time of maximum CM vertical velocity during the shooting motion. Upper arm rotation occurred significantly closer to max CM vertical velocity (short-mid: 2/2; short-long: 3/4; mid-long: 2/5; Figure 1) in 7 of 11 significant comparisons. Lower arm rotation occurred significantly closer to max CM velocity (short-mid: 1/3; short-long: 3/6; mid-long: 3/6; Figure 1) in 7 of 15 significant comparisons.

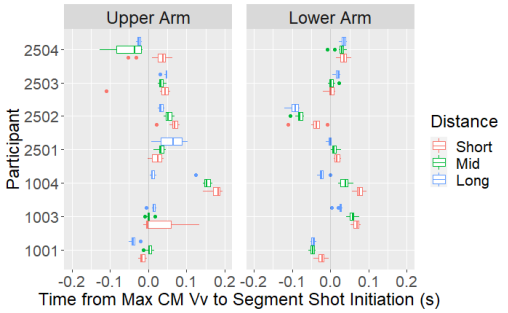

Figure 1: Shot adjustments in upper and lower arm rotation relative to the CM vertical velocity made with progressive increases in shot distance (short, mid, long) made by each participant.

Changes in the timing of lower arm rotation in relation to CM trajectory to accommodate for increases in shot distances were associated with differences in ball release angles. In general, initiating the lower arm shooting motion closer to the max CM vertical velocity was associated with an increase in ball CM vertical velocity and a greater ball release angle (Figure 2). The two players that initiated lower arm shooting motion earliest before max CM vertical velocity had the lowest ball release angles during the mid and long shots. This suggests timing of the upper body shooting motion relative to whole body motion may affect ball release angle, subsequently affecting performance outcomes.

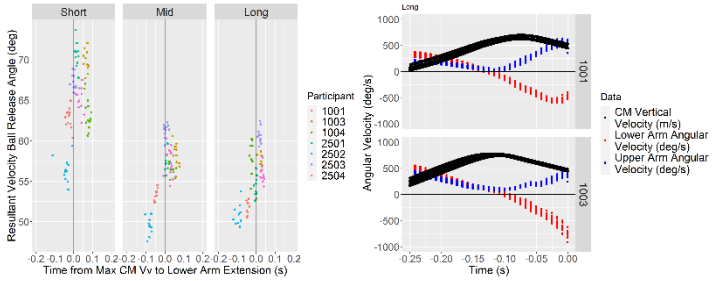

Figure 2: Left: Relationship between ball release angle and coordination between lower arm shot initiation and CM vertical velocity trajectory. Right: Example of how differences in coordination strategies affect ball release angle (top: mean 51.8º; bottom: mean 57.3º).

Significance

Determining how an individual utilizes their capabilities to achieve the mechanical objectives of tasks under progressively more challenging conditions provides meaningful insights as to control priorities as well as modifiable factors that affect task performance.

Acknowledgments

Merit research award from the IEB graduate program.

References

1. Nakano, N., et al. *Sport. Biomech.* 3141, 1–16 (2018).
2. Podmenik, et al. *Kinesiology* 49, 92–100 (2017).
3. Miller, S. & Bartlett, R. M. *J. Sports Sci.* 11, 285–293 (1993).
4. Wilcox, R. (2017). doi:10.1201/9781315154480

Reliability of muscle activity during adaptive rowing: A pilot study

Elizabeth Euiler, MS[1], Margaret Finley, PT, PhD[1]
[1]Drexel University, Health and Rehabilitation Sciences, Philadelphia, PA
Email: ede29@drexel.edu

Introduction

More than 2.7 million people use a manual wheelchair (MWC) for mobility in the United States.[1] MWC users are highly dependent on their upper extremities for activities of daily living and mobility. A secondary injury affecting the upper extremity can negatively impact function, independence, and perceived quality of life.[2,3] Evidence shows that rowing offers several benefits for MWC users including decreased shoulder pain, improved cardiovascular fitness, increased resistance to muscular fatigue, increased muscle strength and lean body mass, as well as providing opportunity for social engagement, participation, recreation and competition, and perceived increase in quality of life.[4,5,6,7]

The purpose of this study was to determine the reliability of upper extremity electromyography (EMG) in MWC users during adaptive rowing. We hypothesized that upper extremity muscle activity would be reliable across multiple trials of submaximal ergometer rowing, regardless of rowing experience.

Methods

Data were collected on 10 individuals (male n=7, female n=3) who use a MWC for at least 50% of community mobility. Participants had a range of rowing experience from no experience to competitive racing. Health conditions of participants included spinal cord injury (n=8), cerebral palsy (n=1), and congenital amputation (n=1). EMG determined muscle activation of seven muscles [upper trapezius (UT), middle trapezius (MT), lower trapezius (LT), latissimus dorsi (LAT), anterior deltoid (AD), posterior deltoid (PD), infraspinatus (IN)] of the dominant upper extremity during the rowing stroke. Following a warm-up and familiarization period, participants completed a 10-stroke maximum effort test for normalization between participants. Next, three submaximal rowing trials (30-35% maximum watts as determined from the 10-stroke maximum) of 20-strokes were completed. The middle 10 strokes of each trial were time normalized (0-100% of the stroke cycle) and mean RMS during of 10% cycle bins determined. Interclass correlation coefficient (ICC) determined intra-person reliability across the three trials.

Results and Discussion

Figure 1 depicts the EMG recording of a full stroke cycle for each of the seven muscles recorded from one representative participant. The stroke is represented from 0 to 100% , where the cycle starts and ends at the catch phase of the stroke (arms fully extended).

As hypothesized, individuals were able to maintain consistent activation patterns across trials regardless of rowing experience. The average reliability across the full stroke cycle was moderate to excellent for each of the seven muscles examined.[8] The UT (ICC=0.90), PD (ICC=0.95), and the IN (ICC=0.90) had excellent reliability, the MT (ICC=0.79), LT (ICC=0.86), and AD (ICC=0.85) had good reliability, and the LAT (ICC=0.67) had moderate reliability. Moderate reliability for the LAT can likely attributed to the EMG sensor coming into contact with the back of the adapted seat during the rowing stroke creating excess noise and inconsistency in the recording. As such, we are investigating alternative methods to collect EMG data of the LAT to reduce this source of error/variability.

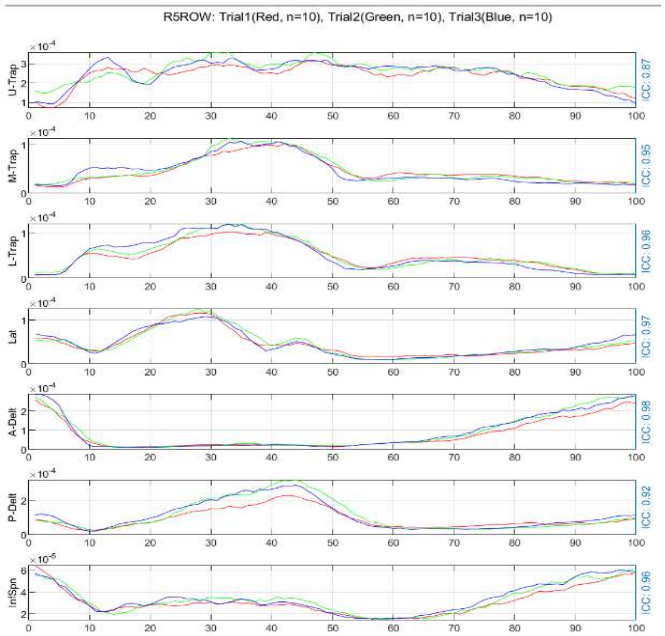

Figure 1: Stroke cycle for one participant, three trials. Interclass Correlation Coefficient (ICC) two-way random effects model, consistency, single rater/measurement. ICC interpretation: <0.5 = poor, 0.5-0.75= moderate, 0.75-0.9= good, >0.9 = excellent.[8]

Significance

Rowing offers the unique benefit of repetitive activation of posterior shoulder muscles which are not primary muscles used during MWC propulsion.[5,9] Although reduced shoulder pain has been reported by MWC users who participated in various rowing-type interventions,[4,5,7] the underlying mechanisms for reduced impairment has not been determined. This pilot data is the first step in a comprehensive look at the biomechanics of the adapted rowing stroke in MWC users. We plan to build a better understanding of the mechanism by which rowing could help to reduce the frequency and intensity of shoulder pain in in MWC users, along with other benefits of participation.

References

1. Steinmetz E. *Americans with Disabilities*, 2002.; 2006. http://www.census.gov/sipp/p70s/p70-107.pdf
2. Eriks-Hoogland IE, et al. *J Spinal Cord Med*. 2014;37(3):288-298
3. Slowik JS, et al. *Clin Biomech*. 2016;33:34-41
4. Olenik LM, et al. *Paraplegia*. 1995;33(3):148-152
5. Wilbanks SR, et al. *J Spinal Cord Med*. 2016(6):645-654.
6. Andrews B, et al. *Artif Organs*. 2017;41(11):E203-E212.
7. Kim D, et al. *Spinal Cord*. 2014;52(8):621-624
8. Portney LG, & Watkins MP. 2000. *Foundations of clinical research: applications to practice.*
9. Hettinga DM & Andrews BJ. *Neuromodulation Technol Neural Interface*. 2007;10(3):291-297.

Blood Flow Restriction Exercise Limb Occlusion Pressure in Hypertensive and Normotensive Participants

Matt J. Wagner[1], Colin W. Bond[1], Sean J. Mahoney[1], Heather A. Evin[1], Benjamin C. Noonan[1], Lisa MacFadden[1]
[1]Sanford Orthopedics and Sports Medicine, Sanford Health, Sioux Falls, SD
Email: matt.wagner@coyotes.usd.edu

Introduction

Low-load blood flow restricted (BFR) exercise has demonstrated the ability to increase muscle size and strength.[1,2] Due to mechanical stress placed on the musculoskeletal system with high-load resistance training, certain clinical populations, such as those post-acute injury, post-operative, or with debilitating chronic conditions, must perform low-load exercise. These populations may benefit from augmenting their low-load exercise with BFR, though they may have other comorbidities such as hypertension. One factor that is presumed to be related to the tourniquet pressure required to occlude the flow of blood is the individual's blood pressure.[1,2,3] In this regard, some clinicians and researchers have prescribed tourniquet pressure relative to the individual's blood pressure (e.g. 1.3 x systolic blood pressure (SBP)).[2,3] One emerging method to determine tourniquet pressure is to identify the individual's limb occlusion pressure (LOP)[1,2] which is defined as the minimum pressure required with a specific type of tourniquet to occlude arterial blood flow into the limb distal to the tourniquet in a specific individual.[2,3] The effects of hypertension on individualized tourniquet pressure has yet to be described. Consequently, the purpose of the present study was to compare LOP, as measured by a commercially available BFR device, between normotensive and hypertensive groups. It was hypothesized that LOP will be similar between hypertensive and normotensive groups.

Methods

The present study was approved by the Sanford Health Institutional Review Board. Thirty nine subjects participated in this study. Twenty-four of the subjects were male and fifteen were female (26 ± 5.2 years, 1.76 ± 0.09 m, 78.9 ± 14.9 kg). After five minutes of rest, participants had their brachial artery blood pressure measured manually on the right arm while they laid in the supine position. Blood pressure was taken in duplicate to ensure accuracy. Participants were then stratified into noromotensive (n = 22) and hypertensive (n = 17) groups using a 120 mm Hg systolic blood pressure threshold. After obtaining each participants' blood pressure, a PTS ii portable tourniquet system designed specifically for BFR and a corresponding tapered, limb circumference specific Easy-Fit Tourniquet (Personalized Tourniquet System for Blood Flow Restriction & Easy-Fit Tourniquet, Delphi Medical, Vancouver, BC, Canada) were used to determine the participant's LOP. The participants laid in the supine position during the LOP assessment. The BFR device progressively increased tourniquet pressure by approximately 10 mm Hg and identified the tourniquet pressure required to eliminate the pressure pulsations in the tourniquet's bladder caused by the underlying arterial flow of blood. LOP was determined on the right leg. Data was analyzed using SPSS (IBM SPSS Statistics v. 26). In order to assess the effect of group on LOP, an independent t-test was performed. Significance was set a priori to $p < .05$.

Results and Discussion

The independent t-test indicated that there was no evidence of a difference ($t(37) = .054$, $p = .957$) in LOP between the normotensive (184.1 ±23.4 mm Hg) and hypertensive (184.5 ±19.4 mm Hg) groups. Furthermore, systolic blood pressure and LOP were found to have an insignificant positive correlation ($r(39) = .20$, $p = .22$). Based on the results of the present study, hypertensive populations do not have a greater LOP than normotensive populations and systolic blood pressure is not associated with LOP. Thus, despite previous assumptions of the significance of blood pressure in determining LOP, the current results indicate that there exists no strong relationship between them. In fact, systolic blood pressure explains just 4.8% of the variance in LOP.

Concerns regarding the limitations of the study may offer a window for further analysis. The present study only included 39 participants, of which only 5 were clinically hypertensive (SBP > 130). Additionally, the hypertensive group was stratified without thorough investigation into their etiology, which may include idiopathic, secondary, or white coat syndrome. Not identifying the cause of elevated blood pressure amongst these participants may have, in part, lead to the lack of the evidence of a difference in LOP between hypertensive and normotensive individuals and association of systolic blood pressure with LOP. The results of this study are important to clinicians. Hypertensive patients will not be exposed to high tourniquet pressures based on their blood pressure alone. Excessively high tourniquet pressures may be dangerous and could lead to disruption of the soft tissues beneath the tourniquet application site.

Significance

Previous BFR literature has not described the effects of hypertension on LOP. The current study provides insight for clinicians using BFR who may work with populations where hypertension is prevalent. The results of this study conclude that there is no significant difference in LOP between hypertensive and normotensive populations. Thus, there is no particular advisement on determining LOP in hypertensive populations compared to normotensive populations.

References

1. Graham, B., et al., *Occlusion of Arterial Flow in the Extremities at Subsystolic Pressures Through the Use of Wide Tourniquet Cuffs.* Clin Orthopod Relat R. 1983. **226**: p. 257-61.
2. Hughes, L., et al., *Blood flow restriction training in clinical musculoskeletal rehabilitation: a systematic review and meta-analysis.* Brit J of Sport Med, 2017. **51**(13): 1003-11.
3. Bond, C. W., Hackney, K. J., Brown, S. L., & Noonan, B. C. *Blood Flow Restriction Resistance Exercise as a Rehabilitation Modality Following Orthopaedic Surgery: A Review of Venous Thromboembolism Risk*. J Orthop Sport Phys, 2019. **49**(1): 17-27

Mass Distribution and Jump Performance

John H Challis[1], and Zachary Domire[2]
[1]Biomechanics Laboratory, The Pennsylvannia State University, University Park, PA 16802
[2]Department of Kinesiology, East Carolina University
Email: jhc10@psu.edu

Introduction

Analysis of maximum vertical jumping with arm swing identifies two mechanisms via which jump height is increased due to the arm swing. One mechanism is that arm swing produces additional vertical energy, and the other is that arm swing slows hip extension which may permit muscles to work on a more favourable region of the force-velocity curve (Domire and Challis, 2010). The second mechanism suggests that a heavier upper body could confer some advantage in maximum vertical jumping compared with jumps with a lighter upper body. Perez-Castilla et al. (2020) examined jump heights with added masses, and while jump height did decrease the decrease with increasing added mass was modest for the lower masses added.

The purpose of this study was to examine the influence of upper body mass on maximum vertical jump performance.

Methods

Two simulation models were used to examine vertical jumping. The first was a simple model comprised of two masses separated by a spring (Figure 1a). With this model the spring was compressed and then released and the model jumped. The mass of the upper body was systematically varied and the jump height for each mass determined. The second model was a previously validated muscle model driven direct dynamics model (Domire and Challis, 2007; Figure 1b). This model comprised four segments and was actuated by eight muscles, each comprised of a series elastic component and a Hill-type muscle model. With this model the lower limb inertial properties were constant but the properties of the upper body (head, arms, and trunk) were systematically varied. The model was an optimal control model where for each set of inertial properties the muscle activations were determined which maximized center of mass height and velocity at the instant of take-off.

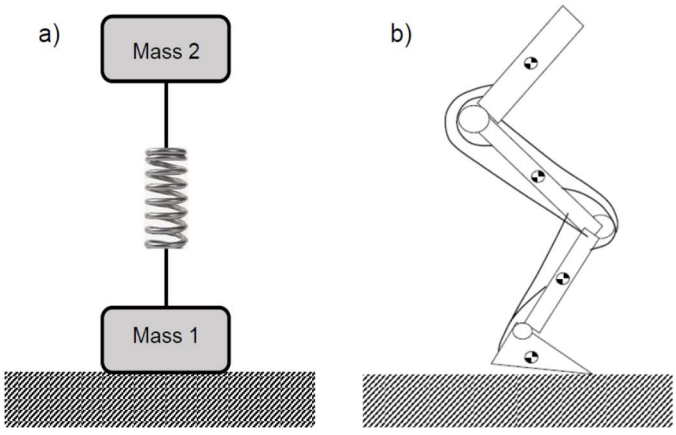

Figure 1: The two models of jumping a) the simple mass-spring-mass, and the b) the direct dynamics optimal control model.

Results and Discussion

For the simple model the same energy was stored in the spring for simulations with a range of masses for the upper segment (Mass 2). Jump height was normalized to maximum jump height. There was a mass which produced optimal jump height, but decreases in upper segment mass decreased jump height at a greater rate than the decrease in jump height with increasing upper segment mass (Figure 2).

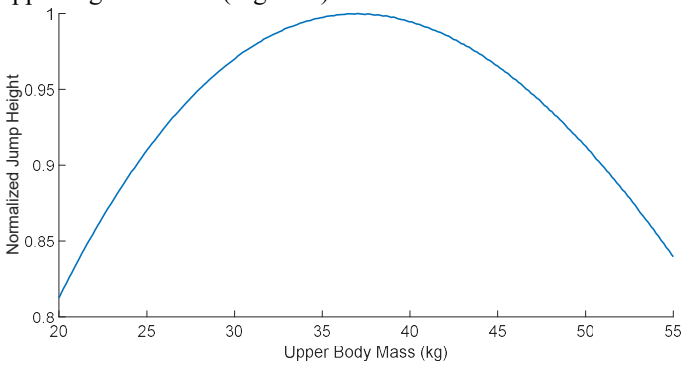

Figure 2: The normalized jump height for the simple model as upper segment model mass is increased.

Simulations were performed with the complex model with variations in the inertial properties of the upper body systematically varied. Similarly to the results from the simple model as upper body inertial properties were either decreased or increased there were corresponding decreases in jump height. When the upper body inertial properties were negligible jump height was approximately 9% lower than the jump height with the original model inertial properties. These results can be explained as with lower upper body inertial properties the body is rapidly accelerated resulted in shorter times to generate jump impulse, in the simulations with a higher upper body inertial properties the jumps take longer allowing the muscles longer time to generate greater force thus obviating some of the constraints due to the greater inertial properties.

Significance

Olympic high jumpers are noted for their gracile physiques (e.g., Khosla and Broom, 1985), these results suggest that simply having a smaller upper body does not necessarily result in increases in jump height.

References

Domire, Z.J., & Challis, J.H. (2007). ***Journal of Sport Sciences***, 25(2), 193-200.
Domire, Z.J., & Challis, J.H. (2010). ***Sports Biomechanics***, 9(1), 38-47.
Khosla, T., & McBroom, V.C. (1985). ***British Journal of Sports Medicine***, 19(2), 96-98.
Perez-Castilla, A., McMahon, J.J., Comfort, P., & Garcia-Ramos, A. (2020). ***Journal of Strength and Conditioning Research***, 34(3), 671-677

An investigation into the release factors of the hammer throw

Suzanne M. Konz
Marshall University, Huntington WV, USA
Email: konz@marshall.edu

Introduction

The ability of a hammer thrower to achieve the distance thrown is based upon the positions the thrower utilizes. Traditionally, the furthest distances are obtained through the optimal use of projectile-based release factors. Release factors include release velocity, release angle, and release height. The importance of release factors has been cited in sports science literature.[2-5] The distance thrown is affected by athlete strength, athlete anthropometrics, and technique.

This study investigated 1) the differences in release variables of American hammer throwers between throw distance groups and sex; and 2) the differences (changes) in release variables over time of American hammer throwers.

Methods

The video from 94 hammer throws (52 female throws and 42 male throws) were analyzed. The footage was captured at the 2016-2019 USA Track and Field Olympic Trials and USA Track and Field National Championships. Two high-speed cameras capturing at 59.94 fps were used to record every throw. Trimmed video was digitized using twenty-four anatomical landmarks on the subject. Bivariate correlation and 1-way ANOVAs analyzed the data. Significance was set at the .05 level. Throw distance groupings (TDG) were delineated as follows: 75m & above, 70-74.99m, 65-69.99m, and below 65m.

Results and Discussion

Correlation analysis indicated relationships among variables exist; however, the correlations were at the moderate to low end of the scale**.**

One-way ANOVA determined that resultant release velocity ($F_{1,3}$ = 9.832, p<.001), vertical release velocity ($F_{1,3}$ = 2.957, p=.011), and lateral release velocity ($F_{1,3}$ = 3.964, p<.001) differed among the TDG. Tukey post-hoc indicated that resultant release velocity for throws for the 75m plus distance (29.02±1.59°/sec) were faster than throws at the 70-74.99m (27.31±2.02°/sec, p=.005), 65-69.99m (26.51±1.65°/sec, p<.001), and below 65m (25.99±0.64°/sec, p=.001) distances. Tukey post-hoc determined that vertical release velocity for throws at the 75m plus (-5.86±6.61°/sec) was significantly different than the 65-69.99m (0.63±7.66°/sec, p<.001).Tukey posthoc indicated that lateral release velocity for throws at the 75m plus (18.52±1.86°/sec) was significantly higher than the 65-69.99m (16.32±2.23°/sec, p<.001).

One-way ANOVA determined that horizontal release velocity ($F_{1,3}$ = 4.206, p<.001), vertical release velocity ($F_{1,3}$ = 15.262, p<.001), lateral release velocity ($F_{1,3}$ = 7.65, p<.001), release angle($F_{1,3}$ = 16.104, p<.001), and release height ($F_{1,3}$ = 6.749, p=.000) significantly differed for the year thrown.Tukey post-hoc testing determined that the horizontal release velocity in 2017 (21.35±1.75m/sec) was significantly faster than the horizontal release velocity in 2019 (20.83±1.57m/sec, p=.034) and 2018 (20.15±2.44m/sec, p=.005); that the vertical release velocity in 2019 (18.16±1.24m/sec) was significantly faster than in 2017 (15.79±1.91m/sec, p<.001) and 2016 (15.02±3.03m/sec, p<.001) and that that the vertical release velocity in 2018 (18.10±1.83 m/sec) was significantly faster than in 2017 (15.79±1.91m/sec, p=.002) and 2016 (15.02±3.03m/sec, p<.001); that 2017 (5.08±14.67m/sec) throws were significantly further to the left of the center of the sector than 2018 (-5.31±7.00m/sec, p<.001) and 2019 (-3.90±4.50m/sec, p<.001); that throw release angle in 2016 (33.69±6.53°) was lower than during 2019 (41.10±2.05°, p=.000), 2018 (42.06±5.35°, p<.001), and 2017(36.54±4.65°, p=.000); and that throw release height was higher in 2016 (1.38±0.34m) than in 2017 (0.99±0.38m, p=.002),2018 (1.10±0.29m, p=.012), and 2019 (1.08±0.15m, p=.002).

One-way ANOVA determined that the vertical release velocity ($F_{1,1}$ =3.924, p=.05), horizontal release velocity ($F_{1,1}$ =11.241, p=.001), release angle ($F_{1,1}$ =10.513, p=.002) lateral release velocity ($F_{1,1}$ =14.675, p=.001) were significantly different between females and males. Females had lower vertical release velocity, greater horizontal release velocity, lower release angles, and a lateral release velocity that placed the hammer further to the right.

Release factor changes indicate that athletes are adopting more strength and power-related strategies to achieve throw distance, forsaking the optimal use of physics principals. Another explanation could be related to the balance of the system as the throw progresses to completion. An athlete who is part of an unbalanced hammer-thrower system will employ countermeasures to keep the throw progressing and legal.

Significance

Hammer throw technique appears to be changing. Athletes are using less than optimal release characteristics.[1] The changes may be the result of athlete strength or the athlete attempting to maintain an unbalanced system until throw release. The hammer throw athlete is unable to affect influence on the implement once released. A suggestion for optimizing the release factors is made to improve throw distance.

Acknowledgments

The author of this paper received financial support from USATF.

References

1.Hubbard, M., et al. (2001). *J Biomech, 34*(4).
2.Konz, S. M. (2006) BYU disertation/thesis..
3.Konz, S. M., & Hunter, I. (2015).*33rd ISBS* Conference Proceedings.
4.Leigh, S. et al. (2008). *Sports Biomech, 7*(2).
5.Linthorne, N. P. (2001). *J Sports Sci, 19*(5).

Head Impact Exposure in Youth Hockey

Abigail G. Swenson[1,2], Logan E. Miller[2,3], Jillian E. Urban[2,3], and Joel D. Stitzel[2,3]
[1]Wake Forest University School of Medicine – Neuroscience
[2]Wake Forest School of Medicine – Biomedical Engineering
[3]Virginia Tech-Wake Forest School of Biomedical Engineering
Email: aswenson@wakehealth.edu

Introduction

An estimated 600,000 youth athletes participate in ice hockey in the United States each year, with rising popularity [1]. Ice hockey has a high incidence of injury; estimated rates of concussion in ice hockey are similar to those of American football [2,3]. Recent increased interest in sports-related concussion has motivated research to better understand the incidence of injury and sport-specific injury mechanisms. While the majority of hockey athletes compete at the youth level, injury studies of pediatric populations are limited [3-6]. This study quantified peak head kinematics and impact, adding to existing knowledge of hockey head impact exposure. The introduction should provide basic information about the field, and additional background with more detail. Include background/context needed to support your hypotheses. Clearly state the general problem that you are addressing with this particular study. If you have hypotheses, state them here. It's ok to use first person.

Methods

This study enrolled male athletes (ages 12-14) participating in a local 14U hockey team for this study. Athletes were fit with a custom instrumented mouthguard to wear for the duration of the season. Each mouthguard features a tri-axial accelerometer and gyroscope embedded within a rigid retainer material bonded to a soft elastomer overlay. Acquisition was triggered when a mouthguard received an impact greater than 5g and a total of 60 ms of data were recorded. This data was paired with time-synchronized video of each corresponding session to identify the contact scenarios associated with the mouthpiece recorded event. Impacts were defined as mouthpiece-recorded events that occurred concurrently with a visually-verified contact scenario involving the instrumented athlete. Analysis of the field data follows the methodology detailed by Rich et al. (2019) [7]. Following data transformation, resultant time histories and summary statistics associated with peak resultant values for linear acceleration, rotational velocity, and rotational acceleration were calculated and compared by contact scenario.

Results and Discussion

A total of 682 contact scenarios were observed from video across all athletes. The three most common contact scenarios observed from video were ice checks (n = 255), board checks (n = 211), and falls (n = 179). Unintentional collisions with the boards (n = 15), punches (n= 9), and other head impacts (n= 13), accounted for the remaining 5.4% of video-verified contact scenarios.

Impact rates were calculated per athlete exposure (AE) for each athlete based on the number of video-verified contact scenarios observed and the number of sessions each athlete attended, with session attendance ranging from 34 total sessions to 49 total sessions (45.14 ± 4.8). Impact rates varied between games and practices (2.93 ± 0.6 and 1.20 ± 0.8 respectively). Of the 682 contact scenarios observed across the complete season, 465 (68%) were classified as "true positive impacts". Board checks (n = 113), falls (n = 152), and ice checks (n = 165) represented 92% of all true positive impacts. Table 1 depicts the median [95th percentile] peak kinematics for the three most common impact types by head contact.

Table 1: Median [95th percentile] linear acceleration (LA), rotational velocity (RV), and rotational acceleration (RA) of the three most common impact types.

	Board Check (n=113)	Fall (n=152)	Ice Check (n=165)
LA (g)	7.01 [27.7]	6.53 [33.2]	7.92 [47.1]
RV (rad/s)	7.75 [18.8]	5.02 [15.3]	8.03 [18.0]
RA (rad/s^2)	544.7 [2613]	391.6 [2798]	606.9 [4243]

Significance

Across 58 total sessions during one 25-week season of play, our instrumented mouthpiece collected 465 video-verified impacts from 682 contact scenarios across seven athletes. The median [95th percentile] linear acceleration, rotational velocity, and rotational acceleration was 7.04 [33.4] g, 6.72 [17.7] rad/s, and 505.5 [3155] rad/s^2 respectively. Overall impact rates ranged from 1.38 to 2.94 impacts per session per athlete and were higher in games than in practices, likely reflecting the role competition plays in athletes' willingness to check. This data represents the first youth study to the authors' knowledge to collect kinematic data using an instrumented mouthpiece, which is associated with improved skull coupling as compared to other wearable head impact sensors [8].

Acknowledgments

The authors thank the Childress Institute for Pediatric Trauma for funding this study and extend their gratitude to the Triad Alliance Hockey Association for participation in this study. Special thanks Konstantina Strates for her efforts in project management and study coordination.

References

[1] USA Hockey, 2018.
[2] Mihalik, J. P., et al., 2008.
[3] Pfister, T., et al., 2016. *Br J. Sports Med.*
[4] Emery, C. A. et al., 2010. *Jama.*
[5] Mihalik et al., *Ann Biomed Eng.* 2012
[6] Miller et al., *J. Biomech. Eng.* 2018.
[7] Rich et al., *Ann Biomed Eng.* 2019

Familiarization time of novel footwear for treadmill running tests

Mei Zhen Huang.[1,2] *, Janet Zhang[1,3], Zoe Chan[1], Shiwei Mo1, Peter Chan[1], and Roy Cheung[1,4]
[1]Gait and Motion Analysis Lab, Department of Rehabilitation Science, The Hong Kong Polytechnic University, Hong Kong
[2]Department of Physical Therapy and Rehabilitation Science, University of Maryland School of Medicine, USA
[3] Department of Integrative Physiology, University of Colorado Boulder, Boulder, USA
[4] School of Health Sciences, Western Sydney University, Australia
Email: mhuang@som.umaryland.edu

Introduction

Treadmill tests have been commonly used in both clinical and research settings for gait analysis. Prior to data collection, participants are often given ample time to familiarize with the treadmill condition and achieve a stable and consistent gait pattern. Familiarization time is thus defined as a state that no significant kinematic or kinetic differences are observed across strides. [1] Meanwhile, different types of running shoes may have a discernible influence on the running biomechanics. Therefore, it is important to ensure that the participant is familiar with the test footwear condition so that errors to the outcomes are avoided. However, due to the lack of evidence, there is no consensus on a suggested treadmill familiarization time when experimenting with a treadmill running condition with different types of running shoes. This study investigated the change in the lower limb kinematics in a group of regular treadmill runners when running in two novel shoe conditions vs. their usual shoes. We aimed to provide evidence suggesting a sufficient treadmill familiarization time for different shoe models. We hypothesized that different treadmill familiarization time would be required when running with different types of running shoes.

Methods

Eleven young adults (age: 26.1±4.1 years) with regular running experience completed three 10-minute running trials at their preferred running speed (8.36±6.36 km/h) on an instrumented treadmill (AMTI, Watertown, MA, USA). Three different types of shoes were used in a randomized order, including their usual running shoes, one pair of minimalist shoes (Brand), which is characterized as minimal amount of foot arch support and low heel-toe drop, and one pair of maximalist shoes (Brand), which provides extra cushioning than usual shoes.

Joint kinematic data from the dominant leg was sampled at 200 Hz using an inertial measurement unit (IMU) based motion-capture system (Noraxon, Arizona, USA) and filtered at 12 Hz [2]. The IMUs were placed on bilateral feet, shanks and thighs, and the pelvic girdle. Synchronized ground reaction force (GRF) was sampled at 1,000 Hz and filtered at 50 Hz.

Time of initial foot-ground contact was defined as the time the vertical GRF exceeded 50 N. [3] Ankle, knee and hip joint angles in the sagittal plane were segmented and time-normalized to each gait cycle, and the first ten gait cycles in every minute running were extracted for further analysis. [2]

We compared the time-normalized ankle, knee, and hip joint angle curve between every two consecutive strides in a given minute by calculating trend symmetry (TS). [4] TS is a quantitative measure of pattern similarity between entire gait cycles, which offers a comprehensive comparison of the kinematic curves between conditions. A value of zero indicates perfect asymmetry, and one indicates perfect symmetry. TS ≥ 0.95 indicates highly symmetrical gait cycles. [2]

Differences in symmetry values for the ankle, knee, and hip were compared using two-way repeated-measures ANOVA [running shoes (3 levels) x time (10 levels)], respectively. If indicated, post-hoc paired t-tests with Bonferroni adjustment were conducted between consecutive minutes. A significance level was set as $p \leq 0.05$.

Results and Discussion

There was no significant interaction effect of running shoes × time, nor the main effect in shoes. A significant main time effect was observed in the ankle, knee, and hip, which suggested that individuals needed time to familiarize the treadmill running regardless of the footwear condition. A paired t-test showed that at least 6 minutes were required to achieve stable kinematics in the lower limb (Figure 1).

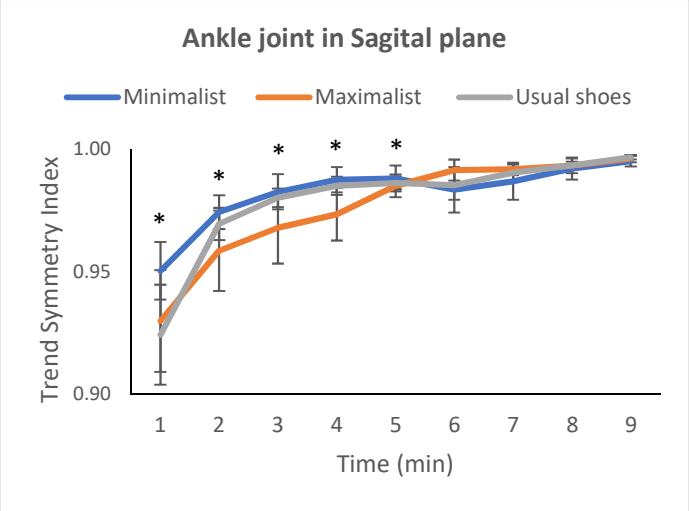

Figure 1: Trend symmetry index of ankle kinematics in the sagittal plane for three running shoes. * indicates significance from paired t-test with Bonferroni adjustment were conducted between consecutive minutes ($p<0.05$).

Significance

Our preliminary results showed that there was no difference in the familiarization period required for different types of running shoes when running a treadmill. At least a 6-minute familiarization time is required for treadmill running regardless of the type of running shoes. Future analysis of changes in 3-dimensional kinematics with larger sample size is warranted.

References

[1] Schieb 1986
[2] Fellin et al., 2010
[3] Crowell and Davis, 2010
[4] Crenshao and Richards, 2006, *Gait & Posture* 24, 515-521

Lower-Extremity Inter-segment Coordination during Ice Hockey Skating Starts

Caitlin M. Mazurek[1], David J. Pearsall[1], Philippe J. Renaud[1], and Shawn M. Robbins[2]
[1]Department of Kinesiology and Physical Education, McGill University, Montreal, QC, Canada
[2]School of Physical and Occupational Therapy, McGill University, Montreal, QC, Canada
Email: caitlin.mazurek@mail.mcgill.ca

Introduction

Quality forward skating starts are essential to ice hockey in order to ultimately out-pace opponents. Skating starts require a distinctive pattern of locomotion in order for skaters to produce sufficient ground reaction forces despite low ice surface friction. It has been established that kinematic differences exist between high-caliber male and female hockey players during skating starts, particularly during the fourth step [1]. Despite the complexity of skating movements, inter-segment coordination during skating tasks is not well established though it may hold implications for more efficient and effective movement patterns.

The objective of this study was to compare lower extremity inter-segment coordination between male and female high-caliber ice hockey players during forward skating starts. It was hypothesized that differences would exist in coordination between males and females, with male players likely more out-of-phase.

Methods

Ten high-calibre female and nine high-calibre male hockey players were recruited. An 18-camera Vicon motion capture system was used to collect forward skating data on an indoor ice surface. Participants began on the blue line and were instructed to perform a forward start, skating with maximal effort to the next blue line (15.3 m). Data were sampled at 240Hz and 30 passive retro-reflective markers were used.

Continuous Relative Phase (CRP) was calculated for the fourth step of each trial, regardless of limb, for shank-*sagittal*/thigh-*sagittal* and shank-sagittal/thigh-*frontal* segments by determining the absolute difference in phase angles of the segments. Phase angles were computed using the Hilbert transform approach with values closer to 180° considered more out-of-phase and values closer to 0° more in-phase. Principal component analysis (PCA) extracted important characteristics from the CRP waveforms called principle components and individual waveforms were scored against these principal components (*PC-scores*). Hierarchical linear model investigated relationships between *PC-scores* and sex after controlling for speed, with individual trial level data entered into the model and clustered within participants to allow for variability to be partitioned both within and between participants.

Results and Discussion

For shank-*sagittal*/thigh-*sagittal* *PC1-scores*, adding sex significantly improved the model (p=0.00). Males were associated with higher *PC1-scores* which indicated a higher CRP (more out-of-phase) throughout the entire stride.

For shank-*sagittal*/thigh-*frontal* *PC3-scores*, the model was significantly improved by adding sex (p=0.019). *PC3* represents the difference in CRP from late stance to recovery. Males had lower *PC3-scores,* indicating that they were more in-phase during late stance.

These results support the hypothesis that differences exist between male and female inter-segment coordination. However, the mode of coordination (more in-phase or out-of-phase) seems to depend on the direction. Males have previously demonstrated significantly wider step widths during step four; a more in-phase mode of coordination of shank-*sagittal*/thigh-*frontal* segments may contribute to this by providing increased stability. Previous studies have suggested that females may have less coordination variability [2] which is reinforced by smaller changes in CRP in late stance/early recovery phases. Males also demonstrated more out-of-phase coordination of shank-*sagittal*/thigh-*sagittal* segments. More out-of-phase coordination is considered more variable and may allow players to more readily adapt to and account for changes in ground reaction force and friction as the player pushes against the ice. The findings of this study can help improve understanding of how males are able to generate greater forward acceleration during their initial skating steps.

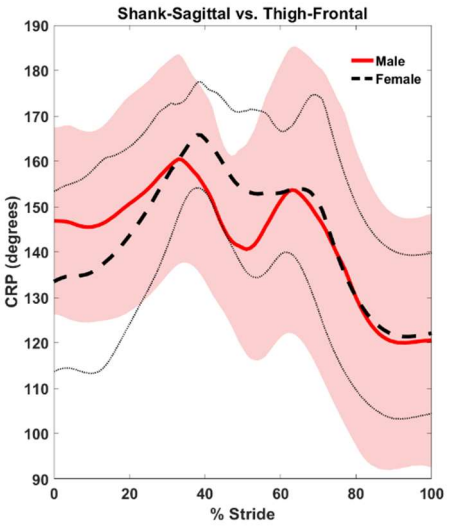

Figure 1: Group means for CRP of shank-*sagittal*/thigh-*frontal* segments during step 4 of a forward skating start for male (red, solid lines) and female (black, dashed lines) groups. The pink shaded area represents one standard deviation for the male group, dotted lines represent one standard deviation for the female group.

Significance

With women's ice hockey steadily growing in popularity, a better understanding of kinematic differences between male and female players is warranted. Training programs better tailored to the needs of these athletes can help to improve skill and raise overall level of play as well as potentially decrease risk of injury, as female hockey players have a higher incidence of injury [3]. Establishing patterns of inter-segment coordination in forward skating will contribute to the overall understanding of human locomotion.

Acknowledgements

This work was financially supported by Bauer Hockey Ltd., and the Natural Sciences and Engineering Resarch Council of Canada (NSERC) under [Grant Number CRDJP 453725-13].

References

[1] Shell JR et al. (2017). *Sports Biomech,* **16**: 313-324.
[2] Dierks TA & Davis I (2007). *Clin Biomech,* **22**(5): 581-591.
[3] Agel J et al. (2007). *J Athletic Training*, **42**: 249-254.

Motor control evaluation of front kick (Ap Chagi) with kinematics pattern executed by professional kyorugi Taekwondo players

Hamidreza Barnamehei[1*], Neda Golfeshan[2], Mohammad Barnamehei[2], and Mohammad Reza Kharazi[3]
[1]Department of Integrative Physiology and Neuroscience, Washington State University, Pullman, WA 99164, USA
[2]Department of Biomedical Engineering, Science and Research Branch of Islamic Azad University, Tehran, Iran
[3]Department of Training and Movement Sciences, Humboldt-Universität zu Berlin, Germany
Email: *h.barnamehei@wsu.edu

Introduction

The front kick in martial arts is a kick executed by lifting the knee straight forward while keeping the foot and shin either hanging freely or pulled to the hip, and then straightening the leg in front of the practitioner and striking the target area [1]. It is desirable to retract the leg immediately after delivering the kick, to avoid the opponent trying to grapple the leg and (unless a combination is in the process) to return to a stable fighting stance. In Taekwondo, the front kick bears the name Ap Chagi. It is distinct from the push kick (Mireo Chagi) in that the power should be delivered instantaneously [2], [3]. The main goal of this study was to evaluate whether there were differences in the front kicking kinematics of lower limb joints (hip, knee, and ankle) executed by professional Kyorugi Taekwondo players.

Methods

Fifteen Taekwondo black belt (M ± SD: age 26.0±3.1 years, mass 69.9±8.7 kg, height 173.6±5.8 cm) executed front kick (Ap Chagi) with their dominant legs [4]. The kinematics and kinetics data were recorded using eight high-speed cameras (VICON, Oxford, UK, 120 Hz). Thirty-nine reflective markers were attached to bony landmarks according to plug-in gait model markers. In order to facilitate the analysis, the time of trials normalized to the percentage. Inverse kinematics was used to evaluate the lower limb kinematics during the front kick. Mean and standard deviation were used to represents the lower limb kinematics during the front kick cycles.

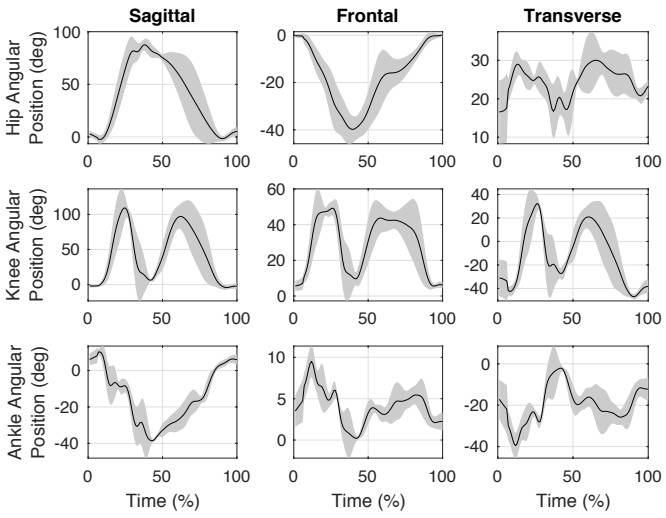

Figure 1: The average of ankle, knee, and hip joint angles during Taekwondo front kick (Ap Chagi). The shaded areas represent one standard deviation.

Results and Discussion

Figure 1 represents lower extremity kinematics variables during the Taekwondo front kick (Ap Chagi). Hip abduction-adduction and hip extension-flexion were observed with one apex at 39% while knee extension-flexion observed with two apexes at 24% and 61% of trial time. Results present maximum hip flexion (87.65°±7.1°) happened at minimum knee extension (3.1°±2.2°) at 39% of front kick normalized time. These results show professional Taekwondo players follow certain kinematics patterns to executed effective and correct techniques. Based on our results, the kinematics relationship between hip and knee can reveal the various characteristics of athletics. In addition, the kinematics characteristics of professional athletics. These patterns can be used as patterns where coaches and physiologists evaluate the amateur and injured athletics, respectively.

Significance

According to our results, kinematics executions strategies for certain movements (front kick) can change motor control and kicking efficacy. Analyzing this kind of research and understanding of motor control patterns can improve the knowledge of athletics and coaches to better performance in training and learning strategies. The recognition of kinematic patterns and coordination between joints can reveal athletics levels of injuries. In addition, this type of study of training strategy and motor control knowledge can reduce sports injuries during matches or training. This study presents the motor control and joint kinematics pattern during Taekwondo front kick (Ap Chagi).

References

[1] H. R. Barnamei and M. R. Kharazi, "Roundhouse kick's TEAKWONDO variability in kinematic coupling assessed by continuous relative phase and vector coding," in *2015 22nd Iranian Conference on Biomedical Engineering (ICBME)*, 2015, pp. 369–374, doi: 10.1109/ICBME.2015.7404172.

[2] H. Barnamehei and M. A. Safaei, "Peak Kinetics and Kinematics Values of Roundhouse Kick in Elite Taekwondo Players TT - Peak Kinetics and Kinematics Values of Roundhouse Kick in Elite Taekwondo Players," *Int. Symp. Taekwondo Stud.*, vol. 2017, no. 0, pp. 222–223, 2017.

[3] H. Barnamehei and M. A. Safaei, "Dimensionless Parameters Based on Motion and Experimental Validation of the Elite and Non-elite Athletes and in Two Groups of Healthy and Injured in Taekwondo Players TT - Dimensionless Parameters Based on Motion and Experimental Validation of the Elite and Non-elite Athletes and in Two Groups of Healthy and Injured in Taekwondo Players," *Int. Symp. Taekwondo Stud.*, vol. 2017, no. 0, pp. 220–221, 2017.

[4] H. Barnamehei *et al.*, "Identification and quantification of modular control during Roundhouse kick executed by elite Taekwondo players," in *2018 25th National and 3rd International Iranian Conference on Biomedical Engineering (ICBME)*, 2018, pp. 1–6, doi: 10.1109/ICBME.2018.8703602.

2D kinematics of skating on a slide board versus skating on a treadmill

Tatiane Piucco[1], Maria Rodriguez[1]
[1]Health and Physical Education Department, Mount Royal University, Calgary, AB T3E 6K6, Canada.
Email: tatipiucco@gmail.com

Introduction

Skating-related exercises have a very specific technique, neuromuscular and physiological responses. The low crouched position during skating and long phase of isometric contraction results in high intramuscular forces and reduced blood perfusion in the working limbs [Foster, 1999]. Despite the importance of this fact, the number of studies investigating skating-specific performance are still limited. The lack of studies could be related to difficulties in reproducing the skating movement in the laboratory, or to control test conditions and measurements on an ice track [Foster et al, 1993]. To overcome this limitation, the use of a slide board to simulate skating movement is a feasible alternative as maximal and submaximal physiological responses on a slide board are similar to real skating [Piucco et al. 2018, 2017a, 2017b]. However, comparison between the skating technique simulated on a slide board and real skating still remains to be established. Therefore, this study aimed to investigate the 2D kinematics of skating on the slide board compared to skating on a treadmill at three different intensities.

Methods

Eleven well-trained speed skaters (17.6 ±0.7 years, 61.6 ± 6.4 kg) performed a skating incremental test to exhaustion on a slide board and on a treadmill. The first and second ventilatory thresholds (VT1 and VT2) and maximal skating intensities (Max) were determined for each athlete. Two video cameras were positioned in the frontal and sagittal views. The athletes skated for 3 minutes at each intensity while 1-minute video was recorded at 120 frames per second. The relative knee flexion (KNE), absolute trunk and hip flexion (TRK and HIP), and the absolute abduction angle of the hip (ABD) for each intensity were analysed using the software Kinovea 0.8.15 (Figure 1).

Figure 1: Knee, trunk and hip angles measured during skating on a treadmill (panel A) and on a slide board (panel B). Values were measured at beginning of gliding phase for 3 strides.

Results and Discussion

Mean values at each intensity are presented in Table 1.

Table 1: Knee (KNE), hip (HIP), trunk (TRK) flexion and hip abduction (ABD) angles for thresholds (VT1 and VT2) and maximal intensities

	Slide Board			Treadmill		
	VT1	VT2	Max	VT1	VT2	Max
KNE	136.4±5	131.1±6*	130.3±7*	131.5±7	123.8±7	118.7±9
HIP	60.5±4	57.3±4*	56.7±5*	59.5±5	53.0±4	47.8±4
TRK	40.0±14	28.9±8	27.4±6	44.7±15	37.6±13	35.2±9*
ABD	48.8±2*	51.0±1*	51.9±1*	35.8±4	42.1±5	46.6±5

* significantly higher values (ES >0.8).

High correlations (r≥0.7) between slide board and treadmill were found for TRK at VT1 and ABD at VT2.

Postural adjustment at each intensity was similar between slide board and treadmill skating as the KNE, HIP and TRK angles decreased and ABD angle increased with increase in workload for both treadmill and slide board skating.

Significance

The results of this work showed that the 2D kinematics of skating on a slide board is similar to real skating at different intensities. These findings support the use of a slide board as an ergometer to evaluate skating-related exercise, such as speed skating, hockey, skate skiing and figure skating, as it mimics the technique and physiological responses of real skating.

This is particularly important for training prescription as physiological and neuromuscular adaptations are specific to the activity itself, and exercise prescription from cycling or running tests results are not suitable for skaters.

Some limitations to this study include the lack of information related to rotational movement, as well as other kinematics parameter such as angular and linear velocities. The muscle recruitment strategy during skating on a slide board versus skating on a treadmill should also be considered in future investigations.

References

Piucco, T. et al. Validation of a maximal incremental skating test performed on a slide board: comparison with treadmill skating. *Int. J. Sports. Physiol. Perform.* 2017a.

Piucco, T. et al. Motor unit firing frequency of lower limb muscles during an incremental slide board skating test. *Sports Biomec.* 2017b.

Piucco, T. et al. Oxygen uptake and muscle deoxygenation kinetics during skating: comparison between slide-board and treadmill skating. *Int. J. Sports Physiol. Perform.* 2018.

Foster, C. et al. Evidence for restricted muscle blood flow during speed skating. *Med. Sci. Sports Exerc.* 1999.

Foster, C. et al. Ergometric studies with speed skaters: evolution of laboratory methods. *J. Strength Cond. Res.* 1993.